



UNIVERSITY OF AGRONOMIC SCIENCES
AND VETERINARY MEDICINE OF BUCHAREST
FACULTY OF LAND RECLAMATION
AND ENVIRONMENTAL ENGINEERING



SCIENTIFIC PAPERS

SERIES E

LAND RECLAMATION, EARTH OBSERVATION &
SURVEYING, ENVIRONMENTAL ENGINEERING

VOLUME XIII



2024
BUCHAREST

SCIENTIFIC PAPERS

SERIES E

LAND RECLAMATION, EARTH OBSERVATION &
SURVEYING, ENVIRONMENTAL ENGINEERING

VOLUME XIII



UNIVERSITY OF AGRONOMIC SCIENCES
AND VETERINARY MEDICINE OF BUCHAREST
FACULTY OF LAND RECLAMATION
AND ENVIRONMENTAL ENGINEERING

SCIENTIFIC PAPERS

SERIES E

LAND RECLAMATION, EARTH OBSERVATION &
SURVEYING, ENVIRONMENTAL ENGINEERING

VOLUME XIII

2024
BUCHAREST

EDITORIAL BOARD

General Editor: Razvan Ionut TEODORESCU

Executive Editor: Ana VIRSTA

Deputy Executive Editor: Mirela Alina SANDU

Members: Augustina Sandina TRONAC, Veronica IVANESCU, Mihaela DRAGOI,
Andreea OLTEANU, Tatiana OLINIC, Constanta MIHAI, Florin NEACSU

PUBLISHERS:

**University of Agronomic Sciences and Veterinary Medicine of Bucharest, Romania -
Faculty of Land Reclamation and Environmental Engineering**

Address: 59 Marasti Blvd., District 1, Zip code 011464 Bucharest, Romania

Phone: + 40 213 1830 75, E-mail: conference@fifim.ro, Webpage: www.fifim.ro

CERES Publishing House

Address: 29 Oastei Street, District 1, Bucharest, Romania

Phone: + 40 21 317 90 23, E-mail: edituraceres@yahoo.com, Webpage: www.editura-ceres.ro

Copyright 2024

*To be cited: Scientific Papers. Series E. LAND RECLAMATION, EARTH
OBSERVATION & SURVEYING, ENVIRONMENTAL ENGINEERING, Vol. XIII, 2024*

*The publishers are not responsible for the content of the scientific papers and opinions
published in the Volume. They represent the authors' point of view.*

Print ISSN 2285-6064, CD-ROM ISSN 2285-6072, Online ISSN 2393-5138, ISSN-L 2285-6064

International Database Indexing:

Web of Science Core Collection (Emerging Sources Citation Index)

Index Copernicus; Ulrich's Periodical Directory (ProQuest); PNB (Polish Scholarly Bibliography);
Scientific Indexing Service; Cite Factor (Academic Scientific Journals) Scipio; OCLC; Research Bible

SCIENTIFIC & REVIEW COMMITTEE

SCIENTIFIC CHAIRMAN

Prof. univ. dr. Sorin Mihai CIMPEANU

MEMBERS*

- Alexandru BADEA - University of Agronomic Sciences and Veterinary Medicine of Bucharest/Romanian Space Agency, Romania
- Ioan BICA - Technical University of Civil Engineering of Bucharest, Romania
- Daniel BUCUR - Iasi University of Life Sciences (IULS), Romania
- Stefano CASADEI - University of Perugia, Italy
- Fulvio CELICO - University of Molise, Italy
- Carmen CIMPEANU - University of Agronomic Sciences and Veterinary Medicine of Bucharest, Romania
- Sorin Mihai CIMPEANU - University of Agronomic Sciences and Veterinary Medicine of Bucharest, Romania
- Maria Jose ORUNA CONCHA - University of Reading, United Kingdom
- Marcel DARJA - University of Agricultural Sciences and Veterinary Medicine Cluj-Napoca, Romania
- Andrea DOMINIJANNI - Politecnico di Torino, Dipartimento di Ingegneria Strutturale, Edile e Geotecnica (DISEG), Torino, Italy
- Claudiu DRAGOMIR - University of Agronomic Sciences and Veterinary Medicine of Bucharest/ National Institute for Research and Development - URBAN-INCERC, Bucharest, Romania
- Eric DUCLOS-GENDREU - Spot Image, GEO-Information Services, France
- Radu Claudiu FIERASCU - National Institute for Research & Development in Chemistry and Petrochemistry - ICECHIM Bucharest/National University of Science and Technology POLITEHNICA Bucharest, Romania
- Jean-Luc HORNICK - Université de Liège, Belgium
- Catalina ITICESCU - „Dunarea de Jos” University of Galati, Romania
- Bela KOVACS - University of Debrecen, Hungary
- Hossein KAZEMi - Gorgan University of Agricultural Sciences and Natural Resources (GUASNR), Gorgan, Iran
- Raluca MANEA - University of Agronomic Sciences and Veterinary Medicine of Bucharest, Romania
- Alina ORTAN - University of Agronomic Sciences and Veterinary Medicine of Bucharest, Romania
- Jovan Br. PAPIC - University „Ss. Cyril and Methodius”, Faculty of Civil Engineering, Skopje, Republic of North Macedonia
- Nelson PÉREZ-GUERRA - University of Vigo, Spain
- Nicolae PETRESCU - Valahia University Targoviste, Romania
- Dorin Dumitru PRUNARIU - Romanian Space Agency, Romania
- Andrei Victor SANDU - „Gheorghe Asachi” Technical University of Iasi, Romania
- Umut Gunes SEFERCIK - Gebze Technical University, Turkey
- Ando SHIN - Tokyo University of Science, Japan
- Jesus SIMAL-GANDARA - University of Vigo, Spain
- Marisanna SPERONI - Centro di Ricerca Zootecnica e Acquacoltura, Consiglio per la Ricerca in Agricoltura e L'analisi Dell'economia Agraria (CREA), Italy
- Razvan Ionut TEODORESCU - University of Agronomic Sciences and Veterinary Medicine of Bucharest, Romania
- Augustina Sandina TRONAC - University of Agronomic Sciences and Veterinary Medicine of Bucharest, Romania
- Ana VIRSTA - University of Agronomic Sciences and Veterinary Medicine of Bucharest, Romania
- Neven VOČA - University of Zagreb, Croatia

**alphabetically ordered by family name*

CONTENTS

ENVIRONMENTAL SCIENCE AND ENGINEERING

1	EVALUATION OF CHEMICAL COMPOSITION OF ESSENTIAL OIL AND TOXIC METAL ACCUMULATION OF LEMONGRASS (<i>CYMBOPOGON CITRATUS</i>) CULTIVATED ON METAL-CONTAMINATED SOILS - Violina ANGELOVA	15
2	DETECTION AND MONITORING OF HYDROCARBON POLLUTION SOURCES IN THE PETROMIDIA REFINERY AREA - Sorin ANGHEL	23
3	RESEARCH ON THE USE OF SLUDGE FROM THE PITEȘTI WASTEWATER TREATMENT PLANT AS FERTILIZER - Gabriela BIALI, Esmeralda CHIORESCU, Maria Cătălina PASTIA, Denis ȚOPA, Iuliana MOTRESCU, Irina Gabriela CARA	30
4	OBTAINING ALKALI ACTIVATED INORGANIC MATERIALS BY RECOVERY OF WASTES - Mihaela CAFTANACHI, Ramona-Elena TATARU FARMUS, Maria HARJA	39
5	TESTING THE INFLUENCE OF EROSION ON SOIL CHEMICAL INDICATORS - Cosmina CANDREA, Marcel DÎRJA, Vasile DODEA	45
6	COMPOSITE MATERIALS FOR ECO-SUSTAINABLE CONSTRUCTIONS - Adrian Alexandru CIOBANU, Aurelia BRADU, Andreea HEGYI	53
7	ECOLOGICAL RESTORATION OF NORWAY SPRUCE STANDS AFFECTED BY DRYING FROM OUTSIDE THE NATURAL RANGE - Cristinel CONSTANDACHE, Ciprian TUDOR, Valentina AGA, Laurențiu POPOVICI	60
8	USING EXPIRED DRUGS AS ENVIRONMENTALLY FRIENDLY CORROSION INHIBITORS - Claudia Alice CRIȘAN, Horațiu VERMEȘAN	67
9	AN INTEGRATIVE APPROACH FOR THE DEVELOPMENT OF ENVIRONMENTAL STRATEGY IN THE CLIMATE CHANGE CONTEXT. THE PERSPECTIVE OF LOCAL PUBLIC AUTHORITIES' ACTION - Anca DRAGHICI, Iudit BERE-SEMEREDI, Gabriela BANADUC, Cornelia BAERA	73
10	ENVIRONMENTAL ASSESSMENT OF THE AREA WITH NATURAL CO ₂ EMISSIONS IN BĂILE LĂZĂREȘTI - Alexandra-Constanța DUDU, Ana Bianca PAVEL, Corina AVRAM, Irina CATIANIS, Gabriel IORDACHE, Florina RĂDULESCU, Naliana LUPAȘCU, Andrei-Gabriel DRAGOȘ, Oana DOBRE, Constantin-Ștefan SAVA	83
11	THE INFLUENCE OF TEMPERATURE ON SOUND WAVES - Bogdan ERGHELEGIU, Mirela Alina SANDU, Daniela IORDAN	93
12	STUDIES REGARDING THE USE OF POURED EARTH IN BUILDINGS - Aurelian GRUIN, Cornelia BAERĂ, Sorin DAN, Bogdan BOLBOREA, Ana Cristina VASILE	101
13	COMPARISON OF METHODS FOR ANTIBIOTIC COMPOUNDS REMOVAL FROM AQUEOUS SOLUTIONS - Diana HANGANU, Lidia FAVIER, Maria HARJA	107
14	ANALYSIS OF GHG EMISSIONS BY SECTORS IN CITY OF VIDIN - Daniela KOSTOVA-IVANOVA	115
15	SMART-ECO-INNOVATIVE COMPOSITE MATERIALS WITH SELF-CLEANING CAPABILITY AND ENHANCED RESISTANCE TO MICROORGANISMS - Adrian-Victor LAZARESCU, Andreea HEGYI, Carmen FLOREAN	125
16	ADVANCED RECOVERY OF VALUABLE MATERIALS FROM E-WASTE - Ștefan-Leontin MARTINAȘ-IONIȚĂ, Gabriela Antoaneta APOSTOLESCU, Maria HARJA	137

17	CARBON FOOTPRINT - IMPORTANT DRIVER OF CLIMATE CHANGE GENERATED BY THE FOOD INDUSTRY - Adelina MOJA, Vasile PADUREANU, Mirabela LUPU, Alina MAIER, Cristina CANJA	143
18	ASSESSING THE EFFICIENCY OF TRANSPORT INFRASTRUCTURE INVESTMENTS IN ROMANIA: A MULTIDIMENSIONAL APPROACH - Petru NICOLAE	150
19	DECARBONIZING IRRIGATION SYSTEMS: INNOVATIVE TECHNOLOGIES FOR ENERGY EFFICIENCY AND SUSTAINABLE WATER RESOURCE MANAGEMENT - Petru NICOLAE, Luminița CHIVU, Raluca Ioana NICOLAE	162
20	CONSISTENCY INDEX OF SOILS, CORRESPONDING TO THE STATE OF SATURATION: AN IMPORTANT PARAMETER IN ANTICIPATING THE BEHAVIOR OF COHESIVE SOILS - Ernest Daniel OLINIC, Tatiana OLINIC	176
21	MICROFLORA OF THE GROUND AIR FROM "HOT POINTS" AND PARK AREAS - Asen PESHEV, Bilyana GRIGOROVA-PESHEVA, Boyka MALCHEVA, Georgi KADINOV	182
22	BUILDING SUSTAINABILITY: INTEGRATING AGRICULTURAL AND INDUSTRIAL SUB-PRODUCTS IN THE BUILDING SECTOR - Cristian PETCU, Claudiu Sorin DRAGOMIR, Andreea HEGYI	189
23	ANALYTICAL FRAMEWORK ORIENTED TOWARDS ENVIRONMENTAL TRIGGERS IN EUROPEAN GREAT CITIES - Stefan-Mihai PETREA, Ira-Adeline SIMIONOV, Alina ANTACHE, Aurelia NICA, Maxim ARSENI, Adrian ROSU, Dragos CRISTEA, Catalina ITICESCU	201
24	NEW POSSIBILITIES OF USING THE ASH RESULTING FROM THE ENERGY RECOVERY OF POULTRY LITTER WITHIN THE CIRCULAR ECONOMY CONCEPT - Luminita Georgeta POPESCU, Roxana Gabriela POPA, Lucica ANGHELESCU, Ramona CAZALBAȘU, Georgeta PREDEANU, Bogdan Stefan VASILE	212
25	A DEEP-LEARNING BASED METHOD FOR WASTE DETECTION - Dan Constantin PUCHIANU	218
26	WASTE CLASSIFICATION USING EFFICIENT NEURAL NETWORKS AND WEB APPLICATION - Dan Constantin PUCHIANU	226
27	PREDICTING THE FUTURE TRENDS OF EUROPEAN AND NATIONAL BENCH-MARKS IN THE MANAGEMENT OF BIODEGRADABLE MUNICIPAL WASTE USING ARTIFICIAL NEURAL NETWORKS - Eda PUNTARIĆ, Lato PEZO, Željka ZGORELEC, Jerko GUNJAČA, Dajana KUČIĆ GRGIĆ, Neven VOČA	234
28	ASSESSING ACCURACY OF LOW-COST COMPACT SYSTEM VERSUS STANDARD AIR QUALITY SYSTEMS - Adrian ROSU, Daniel-Eduard CONSTANTIN, Mirela VOICULESCU, Silvia DRĂGAN, Maxim ARSENI, Stefan-Mihai PETREA, Catalina ITICESCU, Lucian Puui GEORGESCU	244
29	STUDIES ON THE CURRENT CONTEXT OF AIR QUALITY INSIDE EARTHEN BUILDINGS - Vasilica VASILE, Cornelia BAERĂ, Aurelian GRUIN, Adrian-Alexandru CIOBANU, Bogdan BOLBOREA	255
30	ACOUSTIC ABSORPTION CHARACTERISTICS THAT ARE USED IN THE ACOUSTIC DESIGN OF INTERIORS - COMPARISONS BETWEEN SOME CLASSICAL MATERIALS AND NATURAL, ECOLOGICAL MATERIALS - Marta Cristina ZAHARIA, Daniela DOBRE, Claudiu Sorin DRAGOMIR	264

SUSTAINABLE DEVELOPMENT OF RURAL AREA

1	URBAN PARADOX: AN ANALYTICAL PERSPECTIVE RETHINKING SUSTAINABLE LAND AREAS - Gabriela BANADUC, Cornelia BAERA, Anca DRAGHICI	272
---	---	-----

2	STUDY ON THE SOILS OF THE GORJ COUNTY AND THE LIMITING FACTORS OF THEIR QUALITY, IN ORDER TO IMPROVE THEM - Mihaela BĂLAN, Cristian POPESCU	283
3	MODERNIZATION/REHABILITATION OF THE SECONDARY DRAINAGE INFRASTRUCTURE BY REPOSITIONING EXISTING CHANNELS AND BY ASSIGNING THE DUAL ROLE OF DRAINAGE-IRRIGATION - Marin-Vasile ILCA, Teodor Eugen MAN, Robert BEILICCI, Anisoara IENCIU, Daniela Cristina UNTARU, Mariana Antonia PASC	293
4	EXPERIMENTAL RESEARCH OF THE INNOVATIVE ATMOSPHERIC HUMIDITY COLLECTION SYSTEM FOR USE IN CROP IRRIGATION - Dragoș MANEA, Eugen MARIN	305
5	ZOOTECHNICAL WASTE AS RAW MATERIAL FOR BIOGAS PRODUCTION AND AS FERTILIZER FOR AGRICULTURE - Roxana MITROI, Cristina Ileana COVALIU - MIERLĂ, Cristina -Emanuela ENĂȘCUȚĂ, Grigore PSENOVSCHI	313
6	RESEARCHES FOR THE PHYSICO-CHEMICAL CHARACTERIZATION OF SOME GRANULAR FERTILIZERS OBTAINED FROM NATIVE WOOL WASTE, IN ORDER TO USE THEM IN AGRICULTURE - Elena Mihaela NAGY, Teodor Gabriel FODOREAN, Dragoș Vasile NICA, Evelin-Anda LAZA, Teodor VINTILA	320
7	IMPROVING PRODUCTIVITY ON DEGRADED LANDS USING A NOVEL TECHNOLOGY OF CULTIVATING CROPS IN BIODEGRADABLE MULTILAYERED STRUCTURES - Florin NENCIU, Eugen POPESCU, Lorena-Diana POPA, Gabriel NAE, Andreea MATACHE	326
8	DETERMINING GREENHOUSE GAS EMISSIONS RESULTING FROM ENERGY AND WATER CONSUMPTION FOR THE DECARBONIZATION OF CORN PRODUCTION AND DEVELOPING STRATEGIES TO REDUCE THE CARBON FOOTPRINT - Hasan Hüseyin ÖZTÜRK, Bülent AYHAN, Serdar AYGÜN, Ali GÜL, Serkan KARABAĞLI	332
9	SUPERIOR CAPITALIZATION OF VEGETABLE WASTE AND NATURAL AGRO-INDUSTRIAL BY-PRODUCTS BY CREATING INNOVATIVE PRODUCTS FOR CONSTRUCTION. SOCIO-ECONOMIC PREDICTIVE ANALYSES - Irina POPA, Vasilica VASILE, Silviu LAMBRACHE ...	340
10	WATER EROSION OF SOILS IN THE HILLY AREA OF DOLJ COUNTY - ASSESSMENT, CONTROL AND MITIGATION METHODS - Cristian POPESCU, Mihaela BĂLAN, Marius-Nicolae CIOBOATĂ	348
11	FOREST DEBRIS-BASED BIOCHAR APPLICATION IN COMPOSTING PROCESS TO REDUCE GREENHOUSE GAS EMISSIONS: A NATURE BASED SUSTAINABLE SOLUTION - Rupesh SINGH, Henrique TRINIDADE, João Ricardo SOUSA	356
12	EVALUATING GREEN AND BLUE INFRASTRUCTURE IN URBAN AREAS IN ROMANIA: A METHODOLOGICAL APPROACH - Teodora UNGUREANU, Andreea Cătălina POPA, Claudiu-Sorin DRAGOMIR	362
13	INDUSTRIAL WASTES USED AS ADDITIVES IN BUILDING MATERIALS TO REDUCE ENVIRONMENTAL POLLUTION - Mihai VRABIE, Nicolae APOSTOLESCU, Maria HARJA ...	372

DISASTER MANAGEMENT

1	RECYCLING OF STEEL FURNACE SLAGS (SFS) BY EFFICIENT INTEGRATION IN CONSTRUCTION MATERIALS AS AGGREGATE PARTIAL REPLACEMENT - Cornelia BAERĂ, Aurelian GRUIN, Ana-Cristina VASILE, Bogdan BOLBOREA, Alexandru ION, Gabriela BĂNĂDUC	378
2	EFFICACY OF THE SEISMIC ISOLATING SYSTEMS FOR HISTORICAL BUILDINGS UNDER MODERATE SEISMIC FORCES - Stefan Florin BALAN, Bogdan Felix APOSTOL, Anton DANET	390

3	THE INFLUENCE OF EXTREME WEATHER PHENOMENA ON THE MANAGEMENT OF HARDWOOD TREES - Ghita Cristian CRAINIC, Flavius IRIMIE, Flavia Mălina CIOFLAN, Sorin Lucian DOROG, Călin Ioan IOVAN, Eugenia ȘERBAN	397
4	THE EVOLUTION OF THE DYNAMIC CHARACTERISTICS OF THE SOIL-STRUCTURE SYSTEM IN CASE OF A UNIVERSITY BUILDING SEISMIC MONITORING - Daniela DOBRE, Claudiu-Sorin DRAGOMIR, Cornelia-Florentina DOBRESCU, Iolanda-Gabriela CRAIFALEANU, Emil-Sever GEORGESCU, Marta-Cristina ZAHARIA	408
5	THE EFFECT OF URBANIZATION ON CLIMATE CHANGE, THE VULNERABILITY OF URBAN AREAS TO CLIMATE CHANGE AND THEIR CUMULATIVE IMPACT ON STORMWATER - Madalina ENE, Ioan BICA	417
6	MODELING THE STRUCTURAL BEHAVIOR OF A CNC BEARING MEMBER SUBJECTED TO STATIC AND DYNAMIC LOADS - Nicoleta-Adaciza IONESCU, Daniela DOBRE, Claudiu-Sorin DRAGOMIR	425
7	TRANSFORMATION MODEL TOWARDS ENERGY POSITIVE PUBLIC BUILDING - Petar KISYOV	431
8	CONCEPTUAL ANALYSIS ON DISASTER RESILIENCE IN THE CLIMATE VULNERABLE COMMUNITY CONTEXT - Aurelia NICA, Ira-Adeline SIMIONOV, Alina ANTACHE, Catalina ITICESCU, Stefan-Mihai PETREA, Catalin PLATON, Victor CRISTEA	441
9	RICE HUSKS AND THEIR POTENTIAL FOR USE IN CONSTRUCTION - Irina POPA, Cristian PETCU, Daniela STOICA, Alina DIMA	448
10	THE CHALLENGES OF IMPLEMENTING THE GREEN-BLUE INFRASTRUCTURE IN THE METROPOLITAN AREAS OF THE BIG CITIES IN ROMANIA - Oana-Catalina POPESCU, Antonio-Valentin TACHE, Adrian SIMION	456

WATER RESOURCES MANAGEMENT

1	RESEARCH TRENDS IN WATER MANAGEMENT IN CENTRAL AND EASTERN EUROPE IN THE CONTEXT OF CIRCULAR ECONOMY - Alina-Cerasela ALUCULESEI, Nicoleta GUDANESCU, Sorin IONITESCU, George Cornel DUMITRESCU, Simona MOAGAR-POLADIAN	462
2	TEMPORAL VARIATION AND RELATIONSHIP BETWEEN HYDROLOGICAL PARAMETERS AND WATER POLLUTANTS ON THE LOWER DANUBE, ROMANIA - Maxim ARSENI, Valentina-Andreea CALMUC, Madalina CALMUC, Stefan-Mihai PETREA, Adrian ROSU, Eugen BUSILA, Catalina ITICESCU, Puiu Lucian GEORGESCU	473
3	EVALUATION OF MICROBIAL AND CHEMICAL INDICATORS AS A MEASURE OF THE DEGREE OF POTABILITY OF WATER - Aurica Breica BOROZAN, Sorina POPESCU, Delia Gabriela DUMBRAVĂ, Diana-Nicoleta RABA, Mirela Viorica POPA, Corina Dana MIȘCĂ, Carmen Daniela PETCU, Despina Maria BORDEAN, Camelia MOLDOVAN	485
4	PHYSIOLOGICAL AND BIOCHEMICAL RESPONSES OF TWO DURUM WHEAT VARIETIES TO WATER STRESS COMBINED WITH A SLUDGE AMENDMENT - Sonia BOUDJABI, Nawal ABABSA, Haroun CHENCHOUNI, Aya DEBAB, Amna BRAHMI	494
5	ASSESSMENT OF THE SURFACE WATER QUALITY DATA COLLECTED SEASONALLY AT THE DANUBE RIVER BIFURCATIONS (CEATAL IZMAIL AND CEATAL SF. GHEORGHE) - Irina CATIANIS, Adriana Maria CONSTANTINESCU, Dumitru GROSU, Gabriel IORDACHE, Florin DUȚU, Ana-Bianca PAVEL	503
6	ESTIMATION OF RIVERBANK SOIL EROSION RATE - A CASE STUDY - Mihai Teopent CORCHEȘ	515

7	PRINCIPAL COMPONENT ANALYSIS: AN APPROPRIATE TOOL FOR TROPHIC PARAMETERS INTERACTION - APPLICATION IN LARGEST LAKE IN BALKAN - Erdona DEMIRAJ, Irena DUKA, Ferdi BRAHUSHI, Seit SHALLARI	521
8	ASSESSMENT OF PHYSICOCHEMICAL AND BACTERIOLOGICAL QUALITY OF WELL WATER USED FOR DRINKING AND DOMESTIC PURPOSES IN AN INDUSTRIAL AREA OF ELBASAN DISTRICT, ALBANIA - Ariola DEVOLLI, Edlira SHAHINASI, Enkeleida SALLAKU, Marilda OSMANI, Belinda HOXHA, Frederik DARA	527
9	USING HYDROGRAPHIC SURVEYS IN THE STUDY OF WATER BODIES DEPTHS - Levente DIMEN, Silvia Alexandra DREGHICI, Tudor BORSAN	535
10	ASSESSMENT OF THE SEDIMENT (DIS)CONNECTIVITY IN A DELTAIC SYSTEM, DANUBE DELTA, ROMANIA - Florin DUȚU, Bogdan-Adrian ISPAS, Irina CATIANIS, Ana-Bianca PAVEL, Laura DUȚU	541
11	IMPACT OF PHYSICOCHEMICAL PARAMETERS ON ZOOPLANKTON AND BIOCOENOLOGICAL ANALYZES ON ZOOPLANKTON OF MANDRA RESERVOIR, IN SOUTHEASTERN BULGARIA - Eleonora FIKOVSKA, Dimitar KOZUHAROV	550
12	MODERN PROTECTION SOLUTIONS AGAINST COASTAL EROSION - Iulian IANCU, Alexandru DIMACHE, Oana-Stefania BUCUR, Daniel CORNEA	556
13	ANALYSIS OF SOME PARAMETERS OF THE HYDROGRAPHIC BASINS IN THE FOREST FUND - Calin Ioan IOVAN, Nicu Cornel SABĂU, Lucian Sorin DOROG, Florin COVACI, Agneta Rodica IOVAN, Ghiță Cristian CRAINIC	564
14	IRRIGATION CHANGES IN THE MARITSA RIVER BASIN: A CASE STUDY FROM THE PLOVDIV REGION - Krasya KOLCHEVA	572
15	SUSTAINABLE MANAGEMENT OF WATER RESOURCES - Aurelia NICA, Stefan-Mihai PETREA, Ira-Adeline SIMIONOV, Alina ANTACHE, Catalina ITICESCU, Catalin PLATON, Victor CRISTEA	579
16	DRIP IRRIGATION EFFICIENCY IN SOYBEAN CULTIVATION IN SOUTHEAST ROMANIA, A SUSTAINABLE APPROACH TO WATER MANAGEMENT - Oana Alina NIȚU, Ionuț Ovidiu JERCA, Mihaela BĂLAN	585
17	BIODIVERSITY AND ECOLOGICAL ASSESSMENT OF THE CHEPELARSKA RIVER, BULGARIA - Georgi PATRONOV, Diana KIRIN	592
18	VARIATIONS OF PHYSICO-CHEMICAL PARAMETERS IN SULINA BRANCH AND ADJACENT MEANDERS DURING TWO SEASONS IN 2023 - Ana Bianca PAVEL, Florin DUTU, Gabriel IORDACHE, Catalina GAVRILA, Irina CATIANIS, Laura DUTU	600
19	ENABLING SOFT SENSORS FOR WATER QUALITY MONITORING IN MULTI-TROPHIC AQUACULTURE SYSTEMS - Stefan-Mihai PETREA, Ira-Adeline SIMIONOV, Alina ANTACHE, Aurelia NICA, Madalina CALMUC, Valentina CALMUC, Dragos CRISTEA, Puia Lucian GEORGESCU	610
20	VIRTUAL SENSOR FOR AMMONIA ESTIMATION IN AQUACULTURE TECHNOLOGICAL WATER FROM CAMBODIA - Ira-Adeline SIMIONOV, Lin KONG, Samnang PEL, Catalin PLANTON, Domenico CARUSO, Jacques SLEMBROUCK, Stefan-Mihai PETREA	618
21	ASPECTS REGARDING THE ESTIMATION OF THE FLOOD LIMITS USING AN UAV IN ORDER TO HYDRAULIC DESIGN WATER MANAGEMENT WORKS - Alexandru SÎNTU-LĂSAT	626
22	THE INFLUENCE OF THE LAKE HYPOLYMNON DISCHARGE ON THE PHYSICO-CHEMICAL PARAMETERS OF THE RIVER - Lavinia TATARU, Florian STĂTESCU, Nicolae MARCOIE	633
23	SUSTAINABLE APPROACH OF NUTRIENT FILM TECHNOLOGY BASED ON EFFICIENT WATER AND ENERGY USE - INTERMEDIATE RESULTS - Augustina Sandina TRONAC, Dragoș DRĂCEA, Sebastian MUSTAȚĂ, Oana Alina NIȚU	640

24	ADVANCE HYDRAULIC MODELLING FOR IRRIGATION SYSTEMS, CASE STUDY SPP15 IRRIGATION PLOT HOTĂRANI – ROMANIA - Daniela-Cristina UNTARU, Teodor-Eugen MAN, Robert BEILICCI, Mircea VISESCU, Erika BEILICCI, Antonia-Mariana PASC	646
25	DROUGHT MONITORING IN SOUTHEASTERN ROMANIA BASED ON THE COMPARISON AND CORRELATION OF SPEI AND SPI INDICES - Sara VENTURI, Elena MATEESCU, Ana VIRSTA, Nicolae PETRESCU, Daniel DUNEA, Stefano CASADEI	655

POLLUTION CONTROL, LAND PLANNING

1	PHYTOREMEDIATION OF CHROMIUM BY BAD BIRNBACH ROSES IN URBAN AREAS - Aysen AKAY	662
2	<i>SILPHIUM PERFOLIATUM</i> A PROMISING ENERGY CROP FOR PHYTOREMEDIATION OF HEAVY METAL CONTAMINATED SOILS - Violina ANGELOVA, Vera KOLEVA	672
3	IMPACT ASSESSMENT REGARDING POLLUTION WITH NUTRIENTS OF WATER RESOURCES DUE TO THE USE OF FERTILIZERS WITH MICROBIAL BIOMASS - Mihaela BEGEA, Nicoleta RADU, Mariana CONSTANTIN, Roxana ZAHARIA	678
4	ACCUMULATION OF HEAVY METALS IN <i>DACTYLIS GLOMERATA</i> L. PLANTS IN CORRELATION WITH SOIL IN PERMANENT MEADOWS IN THE COPȘA MICĂ AREA OF ROMANIA - Vera CARABULEA, Dumitru-Marian MOTELICĂ, Nicoleta Olimpia VRÎNCEANU, Georgiana PLOPEANU, Bogdan Ștefan OPREA, Mihaela COSTEA, Vasilica LUCHIAN	684
5	GREEN-SYNTHESIZED ZnO NPs AS SUSTAINABLE PHOTOCATALYSTS FOR THE DEGRADATION OF ACETAMINOPHEN - Alexandra Corina COSTANDACHE, Leon Dumitru COVALIU, Anca Andreea ȘĂULEAN, Cristina Ileana COVALIU-MIERLA, Ecaterina MATEI, Razvan TEODORESCU, Valerica TUDOR	692
6	ECOLOGICAL TREATMENT OF WASTEWATER CONTAINING A CATIONIC SURFACTANT POLLUTANT - Leon Dumitru COVALIU, Iuliana PAUN, Vasile Ion IANCU, Ecaterina MATEI, Razvan TEODORESCU, Valerica TUDOR, Gigel PARASCHIV, Cristina Ileana COVALIU-MIERLA	698
7	ENVIRONMENT CONTAMINATION WITH PETROLEUM HYDROCARBONS - Cristian Mugurel IORGA, Puiu Lucian GEORGESCU, Mihaela Marilena STANCU	706
8	SOIL AND SLUDGE SAMPLES CHEMICAL PROPERTIES AND VEGETATION MINERAL COMPOSITION MONITORIZATION ON THE IAȘI SEWAGE TREATMENT-PLANT PONDS PRECINCT (TOMEȘTI) - Mihaela LUNGU, Radu LĂCĂTUȘU, Andrei VRÎNCEANU, Rodica LAZĂR, Ilie CALCIU	712
9	SOIL HEAVY METALS CONTENT VARIATION DEPENDING ON THE DISTANCE FROM POLLUTION SOURCE AND UPTAKE BY THE <i>TRIFOLIUM PRATENSE</i> L. SPECIES HARVESTED FROM COPȘA MICĂ AREA, CENTRAL ROMANIA - Bogdan Ștefan OPREA, Nicoleta Olimpia VRÎNCEANU, Vera CARABULEA, Dumitru-Marian MOTELICĂ, Mihaela COSTEA, Georgiana Iuliana PLOPEANU	719
10	WASTE CLASSIFICATION USING VISION TRANSFORMERS - Dan Constantin PUCHIANU	727
11	GOOD PRACTICES FOR REDUCING LAND POLLUTION IN THE AREA OF SWINE FARMS WITH LIQUID MANURE - Mihaela Alexandra ROTARU, Loredana VĂDUVA, Olimpia Alina IORDĂNESCU, Ioan PETROMAN	734
12	COMPARATIVE ANALYSIS ON AIR POLLUTION LEVEL OF BUCHAREST URBAN AREA DURING THE COVID-19 PANDEMIC - Vasilica VASILE, Cristian PETCU, Alina DIMA, Mihaela ION	742

EARTH OBSERVATION AND GEOGRAPHIC INFORMATION SYSTEMS & TOPOGRAPHY AND CADASTRE

1	RELATIONSHIPS BETWEEN SPECTRAL VEGETATION INDICES (SVIs) AND GROWTH STAGES IN A TABLE GRAPE VINEYARD - Zhulieta ARNAUDOVA, Boyan STALEV	750
2	DETERMINATION OF LAI AT DIFFERENT GROWTH STAGES OF PEPPER PLANTS GROWN IN FIELD - Zhulieta ARNAUDOVA, Dimka HAYTOVA	756
3	PAST AND FUTURE - A PERSPECTIVE OF THE EVOLUTION OF INEU'S FORESTS - Marinela BODOG, Alexandru RACZ, Nicu Cornel SABĂU	762
4	EXPLORING THE TOP 5 DRONES FOR LAND MEASUREMENTS: A REVIEW - Alexandru CĂLIN	770
5	GIS METHODS FOR ESTIMATING SOIL EROSION AND ITS IMPACT ON THE ENVIRONMENT. CASE STUDY: CRIȘUL ALB HYDROGRAPHIC BASIN - Loredana COPĂCEAN, Eugen Teodor MAN, Sorin HERBAN, Luminița COJOCARIU, Cosmin POPESCU	776
6	3D MODELING OF THE CAMPUS OF THE UNIVERSITY OF AGRICULTURAL SCIENCES AND VETERINARY MEDICINE CLUJ-NAPOCA USING ARCGIS PRO - Iulia COROIAN, Diana FICIOR, Tudor SĂLĂGEAN, Silvia CHIOREAN, Ioana Delia POP, Mircea-Emil NAP, Elemer-Emanuel ȘUBA	786
7	ISSUES RELATED TO THE IMPLEMENTATION OF GEOMATIC APPLICATIONS IN THE NATIONAL FORESTRY FUND - Ghiță Cristian CRAINIC	794
8	ANALYSIS OF LANDSAT AND SENTINEL SATELLITE IMAGES FOR ROȘIA POIENI QUARRY AND VALEA ȘESII DECONTATION POND - Sorin HERBAN, Clara-Beatrice VÎLCEANU, Andrei CRIȘAN, Livia NISTOR-LOPATENCO	805
9	EXPLORING THE COSMOS: A WEB-BASED APPLICATION FOR POLLUTION, CONSTELLATION AND MOON PHASE RECOGNITION - Mihai MAFTEI, Iuliana MARIN	813
10	REMOTE ASSESSMENT OF THE FRACTION OF ABSORBED PHOTOSYNTHETICALLY ACTIVE RADIATION (fAPAR) FOR MOUNTAIN GRASSLANDS - Margareta MAGUREANU, Loredana COPACEAN, Despina-Maria BORDEAN, Luminita COJOCARIU	823
11	APPLICATION OF MACHINE LEARNING APPROACHES FOR LAND USE CHANGE MODELLING IN SURINAME - Tamara MYSLYVA, Marciano DASAI, Christiaan Max HUISDEN, Petro NADTOCHIY, Yurii BILYAVSKYI	830
12	THE EFFECT OF THE ALTITUDE GRADIENT ON THE VEGETATION OF THE GRASSLANDS IN THE POIANA RUSCĂ MOUNTAINS, BASED ON NDVI - Monica SFÎRCOCI, Loredana COPĂCEAN, Luminița COJOCARIU	841
13	THE USE OF GEOMATICS FOR THE PLANNING OF A SPORTS COMPLEX - Cornel Cristian TEREȘNEU	851

MISCELLANEOUS

1	REDUCING THE ENVIRONMENTAL IMPACT BY USING A SUSTAINABLE PROTEIN SOURCE IN FISH DIET - INSECT MEAL. A REVIEW - Alina ANTACHE, Ira-Adeline SIMIONOV, Stefan-Mihai PETREA, Aurelia NICA, Catalina ITICESCU, Puiu Lucian GEORGESCU, Catalin PLATON, Alin-Stelian CIOBÎCĂ	857
2	OPTIMISATION OF CULTURE MEDIA FACTORS FOR ACTIVE WINE YEAST BIOMASS PRODUCTION - Iuliana Diana BĂRBULESCU, Raluca Ștefania RĂDOI-ENCEA, Corina DUMITRACHE, Mihaela Violeta GHICA, Mihai FRÎNCU, Mihaela BEGEA, Valerica TUDOR, Elena-Mirela BOROIU, Răzvan Ionuț TEODORESCU	866

3	TRENDS IN "FETEASCĂ REGALĂ" GRAPES YIELD AND SUGAR CONTENT IN SITE SPECIFIC CLIMATE - Octav-Mihai CISMAȘIU, Ioan OROIAN, Marcel DÎRJA, Cristian IEDERAN, Antonia ODAGIU	876
4	TRADITIONAL ROMANIAN CULINARY PRACTICES AND THEIR HISTORICAL AND CULTURAL SIGNIFICANCE - A REVIEW - Carlo Marius DRAGOMIR, Simona-Maria ILIE, Mariana-Atena POIANA, Corina Dana MISCA, Ileana COCAN, Delia-Gabriela DUMBRAVĂ, Camelia MOLDOVAN, Viorica-Mirela POPA, Carmen Daniela PETCU, Claudia ROMAN, Diana-Nicoleta RABA	882
5	SIR JOSEPH WILLIAM BAZALGETTE - THE INGENIOUS CIVIL ENGINEER WHO HAS CHANGED LONDON - Elena NISTOR	890
6	A REFINEMENT OF THE SECOND CRITERIA OF COMPARISON FOR THE CONVERGENCE OF SERIES OR IMPROPER INTEGRALS - Cosmin-Constantin NIȚU	900
7	THE INFLUENCE OF TECHNOLOGY ON CULTURE IN THE PRODUCTION OF LETTUCE IN THE NUTRIENT FILM TECHNIQUE SYSTEM: A REVIEW - Oana Alina NIȚU, Emanuela JERCA, Elene Ștefania IVAN, Marinela GHEORGHE	908
8	EXPLORING THE USE OF WEB APPLICATIONS AND NEURAL NETWORKS FOR CAR PARKING SERVICES - Dan Constantin PUCHIANU	914
9	ROMANIA TOWARDS A GREEN TRANSITION: CARBON BORDER ADJUSTMENT MECHANISM (CBAM) REGULATIONS - Cristiana SÎRBU	921
10	PHYTOCHEMICAL PROFILE OF LEMON BASIL GROWN IN AQUAPONIC CULTURE - Irina TOMASU, Simona MARCU SPINU, Mihaela DRAGOI CUDALBEANU, Constanta MIHAL, Petronela ROSU, Raluca PASCU, Alina ORTAN	927
11	SUSTAINABILITY OF SOME FOREST SPECIES' ASSOCIATIONS ESTABLISHED ON DEGRADED LANDS FROM THE TRANSYLVANIA PLAIN, IN THE CONTEXT OF CLIMATE CHANGE - Alexandru COLISAR, Marcel DÎRJA, Vasile SIMONCA, Steluta Maria SINGEORZAN, Victor SFECLA, Horia Dan VLASIN, Cornel NEGRUSIER, Alina Maria TRUTA, Florin Alexandru REBREAN, Vasile CEUCA	937
12	OPTIMIZING RESOURCES IN AGRICULTURE: A BIBLIOMETRIC ANALYSIS OF ECONOMIC STRATEGIES AND TECHNOLOGICAL ADVANCEMENTS - Iuliana Mirela PINȚĂ	951
13	IMPLEMENTATION OF METHODS AIMED AT SUSTAINABLE DEVELOPMENT THROUGH BIONICS - Cristian-George DRAGOMIRESCU, Victor ILIESCU	958
14	THE LINK BETWEEN CARBON FOOTPRINT SIZE AND PV ENERGY SYSTEM INITIAL INVESTMENT, ESPECIALLY REGARDING STORAGE ELEMENTS AND THEIR EXPLOITATION MODALITY - Mihaita Nicolae ARDELEANU, Emil Mihail DIACONU, Otilia NEDELCU, Sorin IONITESCU	967
15	MODERN STRATEGIES FOR REDUCING POLLUTION IN TRAFFIC CONGESTIONS: A REVIEW OF CARBON FOOTPRINT-BASED METHODS - Mihai ARDELEANU, Emil Mihail DIACONU, Otilia NEDELCU, Marius-Alexandru DINCA, Petru NICOLAE, Sorin IONITESCU	973

EVALUATION OF CHEMICAL COMPOSITION OF ESSENTIAL OIL AND TOXIC METAL ACCUMULATION OF LEMONGRASS (*CYMBOPOGON CITRATUS*) CULTIVATED ON METAL-CONTAMINATED SOILS

Violina ANGELOVA

Agricultural University - Plovdiv, 12 Mendelev Blvd, Plovdiv, Bulgaria

Corresponding author email: vileriz@abv.bg

Abstract

The present study determines the chemical composition of lemongrass oil, content of heavy metals and identifies the possibility of lemongrass growth on soil contaminated by heavy metals. The experimental plots were situated 0.5 km from the source of pollution, the Non-Ferrous-Metal Works (MFMW) near Plovdiv, Bulgaria. Lemongrass is a heavy metal tolerant plant that can be grown on heavily heavy metal contaminated soils (45.0 mg/kg Cd, 1917.9 mg/kg Pb and 2273.1 mg/kg Zn). Pb and Cd accumulate mainly in the above-ground mass, Hg - in the root system, while Zn accumulates approximately in equal amounts in the roots and above-ground mass. Oxygenated monoterpenes (85.57%) predominate in lemongrass essential oil, followed by monoterpene hydrocarbons (8.77%) and oxygenated aliphatic hydrocarbons (3.13%), oxygenated sesquiterpenes (0.84%), sesquiterpene hydrocarbons (0.66%) and phenylpropanoid compounds (0.61%). The content of heavy metals in lemongrass essential oil is lower than the accepted maximum values and meets the requirements for an environmentally friendly product.

Key words: contaminated soils, essential oil, heavy metals, lemongrass.

INTRODUCTION

Lemongrass (*Cymbopogon citratus*) is a tropical herbaceous perennial plant that belongs to the Gramineae (Poaceae) family and the genus *Cymbopogon*.

In tropical climates, lemongrass is grown as a perennial, while lemongrass is grown annually in countries with cold winters. Lemongrass forms tuft with long and tall stems and can reach 1.5 m in height. The leaves are evergreen bluish-green, linear in shape, 1.3-2.5 cm wide and 0.9 m long.

Lemongrass is adaptable to different soil and climatic conditions. It grows best on sunny sites at 20-35 degrees Celsius temperatures, well-drained, nutrient-rich soils with high organic matter content (Sugumaran et al., 2005). Lemongrass can be harvested 4 to 6 months after planting and subsequent harvests at 2 to 3-month intervals (Joy et al., 2006). Harvesting is done by cutting 20 cm above the ground (Sugumaran et al., 2005).

Lemongrass can also be grown successfully in Bulgaria by propagating the tufts. In autumn, the tufts (which have multiple stems) must be removed, transferred to containers, and stored

in light and warm weather (above 15 degrees) during winter.

Lemongrass is a rich source of minerals (Ca, K, Na, P, Mg, Cu, Fe, Zn and Mn), vitamins (vitamin A, vitamin B1 (thiamine), vitamin B2, vitamin B3, vitamin B5, vitamin B6, vitamin C and folic acid) and macronutrients (carbohydrates, protein and small amounts of fat) (USDA National Nutrient Database, 2019). Lemongrass is cultivated chiefly for its essential oil, mainly biosynthesized in the plant leaves (dijAvila et al., 2016). In the amount of 1-2% (Carlson et al., 2001).

Lemongrass leaves and oil have a typical lemony odor, mainly due to the presence of citral. Lemongrass oil is used in the pharmaceutical, cosmetic, food, and perfume industries (Verma et al., 2014). The oil has antiviral, antimicrobial (Bassole et al., 2011), antioxidant (Lawrence, 2015), antifungal (Rajeswara et al., 2015), anticancer (Kumar et al., 2008), sedative, and anti-inflammatory properties (Figueirinha et al., 2010).

Solving soils contaminated with toxic metals using aromatic plants is a promising and sustainable approach. Recently, interest in aromatic plants for essential oil production and

phytoremediation has increased. It has been found that many aromatic plants do not absorb heavy metals from the soil and that heavy metals do not affect the chemical composition of the oil (Zheljazkov et al., 2006). It has been shown that there is the least risk of heavy metal contamination of essential oil obtained by the steam distillation process since the heavy metals remain in the plant and the oil can be marketed. Most promising aromatic plants for phytoremediation of toxic metal-contaminated sites have been identified from the families - Poaceae, Lamiaceae, Asteraceae, and Geraniaceae. Some aromatic grasses such as lemongrass, palmarosa, citronella, vetiver etc. are stress tolerant (Das & Maiti, 2009). Lemongrass has the potential for remediation of highly polluted industrial sites such as landfills (Maiti & Maiti, 2015) and chromite-asbestos mines (Kumar & Maiti, 2015). Lemongrass is recommended for phytoremediation of metal-contaminated sites as it can potentially accumulate the metals Cd, Ni, and Pb (Zakka Israila et al., 2015).

Studies related to the assessment of the phytoremediation potential of lemongrass are limited. There are no studies related to lemongrass cultivation and oil composition.

The present work aims to conduct a comparative study that will allow us to determine the content of heavy metals in the vegetative organs of lemongrass and the quality of essential oil and establish the feasibility of growing it on soils contaminated with heavy metals.

MATERIALS AND METHODS

The experiment was carried out on an agricultural field contaminated with heavy metals, located at a distance of 0.5 from the source of contamination - a Non-ferrous metals plant (NFMW) near Plovdiv, Bulgaria.

The study was conducted using lemongrass as a test plant. Six months after planting, samples of plant material (roots and aerial mass) were collected for analysis. After transporting the plants to the laboratory, scissors separated them into their organs (roots and aerial mass). Samples of roots and above-ground mass (stems and leaves) were dried at room temperature until an air-dry mass was obtained,

after which they were dried at 45°C. The heavy metal content of the roots and above-ground mass was determined. Using a Clevenger-type apparatus, Lemongrass essential oil was obtained under laboratory conditions by steam distillation for 2 hours.

The total metal content of the soils was determined according to ISO 11466. The microwave mineralization method determined the elemental content of the lemongrass and essential oil. Quantitative measurements were carried out by ICP (Jobin Yvon Emission - JY 38 S, France). The Hg content of the samples was determined without prior sample preparation with a mercury analyzer.

Digestion and analytical efficiency of ICP and mercury analyzer were validated using a standard reference material of apple leaves (SRM 1515, National Institute of Standards and Technology, NIST). The chemical composition of the oils in hexane (1:1000) was analyzed on an Agilent 7890A Gas Chromatography system equipped with an FID detector and Agilent 5975C mass spectrometer. The oil's chemical constituents were determined on a 7890A gas chromatograph (Agilent Technologies) and a 5975C mass spectral detector (Agilent Technologies). Compounds were identified by comparing retention times and Kovacs relative indices (RI) with those of standard substances and mass spectral data from the NIST08 library (National Institute of Standards and Technology, USA).

The SPSS for Windows program was used to process the statistical data.

RESULTS AND DISCUSSIONS

Soils

The total content Pb, Zn, Cd, and Hg in soil sampled from NFMW-Plovdiv are presented in Table 1.

The soil used in this experiment was slightly alkaline (pH 7.6), with moderate organic matter content (2.5%). The total content of Zn, Pb, and Cd is high (2273.1 mg/kg Zn, 1917.9 mg/kg Pb, and 40.5 mg/kg Cd, respectively) and exceeds the maximum permissible concentrations (MPC) (400 mg/kg Zn, 100 mg/kg Pb and 3.0 mg/kg Cd). The Hg content in soils was lower than the MPC.

Table 1. The total content of Pb, Zn, Cd (mg/kg) and Hg (ng/g) in soils sampled from NFMW-Plovdiv

Element	Pb	Zn	Cd	Hg
x ± sd	1917.9±4.5	2273.1±3.5	45.0±0.8	574.8±10

x- average value (mg/kg) from 5 repetitions; sd - mean standard deviation
MPC (pH > 7.4) – Pb - 100 mg/kg, Cd - 3.0 mg/kg, Zn - 400 mg/kg, Hg - 1.5 mg/kg

Heavy metal content in lemongrass

Table 2 presents the results obtained for the heavy metal contents in the organs of the essential oil crop studied.

Table 2. Content of Pb, Zn, Cd (mg/kg) and Hg (μg/kg) in lemongrass

Plant organ	Pb, mg/kg x ± sd	Cd, mg/kg x ± sd	Zn, mg/kg x ± sd	Hg, μg/kg x ± sd
Roots	57.2±0.8	11.6±0.5	258.5±1.2	579.9±10
Stems + leaves	149.3±2.4	23.6±1.0	248.8±1.5	96.8±5
Oil	0.11±0.01	nd	0.52±0.05	nd

x- average value(mg/kg) from 5 repetitions; sd - mean standard deviation; nd- non detectable

Pb and Cd accumulate mainly in the above-ground mass, Hg - in the root system, while Zn accumulates approximately equal amounts in the roots and above-ground mass (stems and leaves). The Pb content in the roots of lemongrass grown at a distance of 0.5 km from the NFMW reached 57.2 mg/kg, Zn – 258.5 mg/kg, Cd – 11.7 mg/kg, and Hg – 515.6 μg/kg. The values obtained for the heavy metals (Cd, Pb, and Zn) in the roots were significantly higher than the values considered toxic to plants, 1 mg/kg Cd, 30 mg/kg Pb, and 100 mg/kg Zn (Kabata-Pendias, 2001).

Lemongrass anatomical and biological features can explain the results obtained. The root system of lemongrass has rhizomes and densely furrowed fibrous roots, relatively compact near the soil surface, between 0-20 cm deep, which develop horizontally and gradually penetrate to depth.

Significant translocation and accumulation of Pb, Cd, and Zn have been detected in lemongrass aerial mass. Pb content reached 149.3 mg/kg in the leaves, Cd up to 23.6 mg/kg, and zinc up to 248.8 mg/kg. This is probably due to the anatomical and morphological features of the plant. The significant accumulation of Pb, Cd, and Zn in the above-ground mass is perhaps because the stems and leaves are covered with spiny hairs

(trichomes), which contribute to the fixation of aerosol pollutants and their accumulation there. Hg contamination of plants is due to aerosol pollution (Kabata-Pendias, 2001). The main uptake pathway for Hg is leaves, and the uptake of this element by soil is of secondary importance. Lower levels of Hg were found in the above-ground mass of lemongrass compared to the roots.

The heavy metal content of the essential oil of lemongrass has also been determined. The results showed that most heavy metals in the yellow flowers did not pass into the oil during distillation. Their content in the oil is, therefore, much lower. The Pb content in the essential oil of lemongrass reaches up to 0.11 mg/kg, and the Zn content up to 0.52 mg/kg. The results strongly indicate that most of the Pb, Cd, and Zn in the above-ground mass of lemongrass grown 0.5 km from the NFMW do not pass through into the resulting essential oil. The Pb, Cd, and Hg amounts in the lemongrass essential oil are lower than the accepted maximum values and meet the requirements for an environmentally friendly product (5 mg/kg Pb, 1 mg/kg Cd, 0.1 mg/kg Hg) (Council of Europe, 2021). The extraction of essential oil by steam distillation process may be the main reason for the low concentration of heavy metals in the oil (Zheljazkov et al., 2006). Our result agrees with the finding of Pandey et al. (2020) that despite the high concentration of heavy metals in plant tissues, the content of heavy metals (Cr, Cd, Pb, and Ni) in the essential oil of lion grass is within the WHO recommended limits. Similar results were reported by Khajanchi et al. (2013) and Gautam et al. (2017) in essential oils extracted from lemongrass grown under different irrigation regimes with wastewater and groundwater and treated with red mud, respectively).

Determination of the phytoremediation potential of lemongrass

To definitively answer the question of the ability of lemongrass to absorb heavy metals from soil and to assess its potential for phytoremediation, the bioconcentration factor (BCF) and translocation factor (TF) were calculated. The results obtained for BCF and TF are presented in Figure 1.

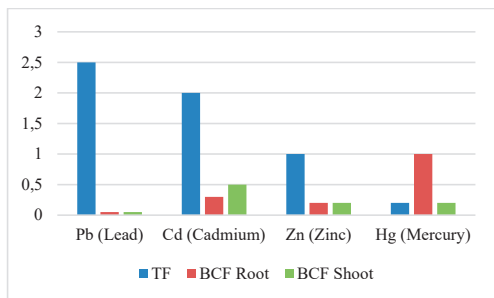


Figure 1. Translocation and bioconcentration factors for lemongrass

The translocation factor (TF) gives information on the ability of plants to uptake heavy metals through the roots and move them to the above-ground mass (leaves). TF values more significant than 1 indicate that the plant is a potential accumulator of heavy metals and can translocate metals efficiently from the roots to the above-ground mass. For Pb and Cd, TF values are more significant than 1. for Zn around 1, and for Hg lower than 1.

Bioconcentration factor (BCF) is the ratio of the heavy metal content in plant organs to the content in the soil. It measures the plant's ability to accumulate metals from the soil. The bioconcentration factor (BCF) is one of the most important indicators for measuring the effectiveness of the phytoremediation process (Adriano, 2001). A plant is an excluder if $BCF < 1$, an accumulator if $1 < BCF < 10$, and if $BCF > 10$, the plant is a hyperaccumulator. Plants with a BCF value > 1 are suitable for phytoextraction. Plants with $TF < 1$ and $BCF_{root-soil} > 1$ is ideal for phytostabilisation.

For Pb, Cd Zn, BCF_{root} , and BCF_{shoot} were < 1 , indicating that their content in the lemongrass does not exceed the amount in the soil. Concerning Hg, BCF_{shoot} was < 1 , while BCF_{root} were 1 (Figure 1).

The BCF_{root} and TF factors of Hg indicate that this element accumulates in the underground mass of lemongrass.

Based on the BCF values, lemongrass can be referred to as an exclusionary plant of lead, cadmium, and zinc and can be used for phytostabilization for Hg. However, according to Pandey et al. (2019), $TF > 1$ for Pb and Ni, while TF was less than 1 for Cr and Cd, and BCF_{shoot} mass was more significant than 1 for Pb and Ni, indicating that metals moved

into the aerial parts of lemongrass. According to Pandey et al. (2020), lemongrass can accumulate Pb and Ni in its plant parts and be exploited as a phytoextractant for the same metals. Soil properties such as pH, EC, and organic carbon content influence the translocation of heavy metals in lemongrass plant parts (Pandey et al., 2020).

Essential oil quality

The results of the chromatographic analysis of the essential oils obtained from the processing of lemongrass leaves grown within 0.5 km of the NFMW are presented in Table 3.

Twenty-nine compounds were identified, constituting 99.58% of the oil (Table 3). The major compounds in the oils were geranial (40.06%), neral (34.45%), myrcene (8.17%), geranyl acetate (2.33%), 6-Methyl-5-heptene-2-one (2.25%), geraniol (2.01%), β -linalool (1.15%). The essential oil mainly contains aldehydes, ketones, alcohol, and esters (Table 3). Table 3 also gives the classification of the identified compounds based on functional groups. Oxygenated monoterpenes (85.57%) were dominant in the oil, followed by monoterpene hydrocarbons (8.77%) and oxygenated aliphatic hydrocarbons (3.13%), while oxygenated sesquiterpenes (0.84%), sesquiterpene hydrocarbons (0.66%) and phenylpropanoid compounds (0.61%) were present in lesser amounts (Table 3).

The major component of lemongrass essential oil is citral. It is a mixture of two geometric isomers. The E-isomer is geranial or citral A, and the Z-isomer is neral or citral B. The content of geranial in the essential oil reaches up to 40.06% and neral up to 34.45% (Table 3), with geranial dominating over neral. The geranial content of lemongrass essential oils is known to range from 20 to 50%, and the neral from 30 to 40% (Schaneberg and Khan (2002); Pandey et al., 2003; Chandrashekar and Joshi, 2006).

The quality of lemongrass essential oil is usually assessed by its citral content.

According to the ISO 3217 (1974) standard, lemongrass oil must contain at least 75% citral to be considered a high-quality product (Barbosa et al., 2008). The quality and quantity of lemongrass essential oil is highly dependent on the time of harvesting of the plants, as the

composition and content of essential oil are related to the stage of development of the whole plant, plant organs, and cells (Verma et al., 2015). The geranial content of lemongrass essential oil increased from 37.58% to 45.95% when lemongrass was harvested at 6.5 months after planting. At later harvest (7.5 months after planting), its content slightly decreased to 42.95%.

Table 3. Composition of lemongrass oil (%)

	Component	RI	% of TIC
1	6-Methyl-5-heptene-2-one	975	2.25
2	Myrcene	990	8.17
3	cis- β -Ocimene	1034	0.4
4	trans- β -Ocimene	1045	0.2
5	6,7-Epoxy myrcene	1088	0.68
6	α -Pinene oxide	1093	0.15
7	β -Linalool	1099	1.15
8	Citronellal	1146	0.7
9	β -Citronellol	1218	0.52
10	Nerol	1227	0.99
11	Neral	1236	34.45
12	Geraniol	1249	2.01
13	Geranial	1266	40.06
14	Methyl nonyl ketone	1274	0.75
15	Methyl nerolate	1283	0.27
16	Geranyl formate	1294	0.49
17	Citronellic acid	1312	0.98
18	Methyl geranate	1320	0.79
19	Geranyl acetate	1377	2.33
20	β -Caryophyllene	1422	0.16
21	β -Copaene	1429	0.22
22	α -Bergamotene	1434	0.17
23	(Z,E)- α -Farnesene	1441	0.11
24	2-Tridecanone	1497	0.13
25	Elemicin	1556	0.1
26	Caryophyllene oxide	1584	0.29
27	Selina-6-en-4-ol	1619	0.43
28	Isoelemicin	1655	0.51
29	Intermedeol	1668	0.12
Oxygenated aliphatic hydrocarbons			3.13
Monoterpene hydrocarbons (MH)			8.77
Oxygen monoterpenes (OM)			85.57
Sesquiterpene hydrocarbons (SH)			0.66
Oxygenated sesquiterpenes (OS)			0.84
Phenylpropanoids			0.61
Total			99.58

RI - Kovacs relative indices

A significant amount of citral indicates high antimicrobial potential and antioxidant activity of lemongrass essential oil.

Myrcene content in the essential oil from the NFMW - Plovdiv reaches 8.17%. Similar is the content of β -myrcene (7.68%) in the essential oil from Vietnam. Studies have shown that myrcene content varies significantly from 0% in essential oil from Benin (Kpoviessi, 2014) and 0.8% in essential oil from Egypt (Mansour et al., 2015) to 25% in essential oils obtained in Brazil (Farias et al., 2019) and Nigeria (Kasali et al., 2001).

Of the alcohols contained in lemongrass essential oil, geraniol has the highest content, ranging widely (from 1.34% in essential oil from South Africa (Mbili et al., 2017) to 21.86% in essential oil from Nigeria (Kasali et al., 2001). The geraniol content in the essential oil we studied reached up to 2.01%.

Of the esters, geranyl acetate predominated (2.33%). Studies have shown that amounts of geranyl acetate vary considerably (0.24% in essential oil from Kenya (Matasyoh et al., 2011) to 3.42% in essential oil from Nigeria (Kasali et al., 2001).

Habitat, genetic variability, climatic conditions, harvesting time, and oil extraction methods can explain these variations in essential oil composition.

The chemical composition of lemongrass essential oil is related to its geographical origin. *C. citratus* essential oil from Africa contains a high amount of myrcene, while the essential oil from Ethiopia contains geraniol (40%), citral (13%), and oxobisal (12%) (Ekpenyong et al., 2014). The major components identified in essential oil from Egypt were geranial (20.90-40.72%), neral (16.20-34.98%), geraniol (8.30%) and linalool (5.60%) (Hana et al., 2012; Mansour et al., 2015), while significant amounts of geranial (37.80%) and neral (33.60%) were found in essential oil from Saudi Arabia (Mansour et al., 2015). The essential oil obtained from Nigeria was poor in citral (0.99%) but rich in geraniol (21.86%), limonene (7.90%), and camphene (7.89%) (Kasali et al., 2001).

Schaneberg and Khan (2002) suggested that geranial, neral, limonene, citronellal, myrcene, and geraniol could be used as marker compounds in lemongrass essential oil. However, some essential oils do not always present limonene, citronellal, and geraniol. In the oil we have studied, limonene is not

present. Some essential oils are rich in limonene (Nigeria 7.90%) (Kasali et al., 2001), while the essential oil from Kenya does not contain this terpene (Matasyoh, 2011).

According to Majewska et al. (2019), citral (neral and geranial) content and β -myrcene content are to be used to distinguish the origin of essential oil. Marker compounds can be used to verify the identity of the essential oil.

The lemongrass essential oils from Brazil, Asia, and West and East Africa have a high geranial content and belong to the geranial chemotype. Two chemotypes of *C. citratus* have been found in Congo - a citral-type and a geraniol-type (Majewska et al., 2019). The oil we studied belongs to the citral chemotype.

CONCLUSIONS

There is a clear pattern in the accumulation of heavy metals in the vegetative organs of lemongrass. Pb and Cd accumulate mainly in the above-ground mass, Hg - in the root system, while Zn accumulates approximately equal amounts in the roots and above-ground mass.

Lemongrass is a heavy metal tolerant plant that can be grown on heavily heavy metal contaminated soils and shows no symptoms of toxicity (chlorosis and necrosis) at a soil content of 45.0 mg/kg Cd, 1917.9 mg/kg Pb and 2273.1 mg/kg Zn.

Lemongrass is an indicator plant and can be used for monitoring of soil and aerosol contamination with heavy metals.

The content of heavy metals Pb, Cd, and Hg in lemongrass essential oil is lower than the accepted maximum values and meets the requirements for an environmentally friendly product. The highest content of oxygenated monoterpenes (85.57%) was found in lemongrass essential oil, followed by monoterpene hydrocarbons (8.77%) and oxygenated aliphatic hydrocarbons (3.13%), oxygenated sesquiterpenes (0.84%), sesquiterpene hydrocarbons (0.66%) and phenylpropanoid compounds (0.61%). Lemongrass essential oil belongs to the citral chemotype.

ACKNOWLEDGEMENTS

This research work was carried out with the support of Bulgarian National Science Fund and also was financed from Project KP-06-H54/7 "Possibilities for limiting the impact of mercury on the environment and human health".

REFERENCES

- Adriano, D.C. (2001). *Trace elements in terrestrial environments: Biogeochemistry, bioavailability and risks of metals*. Springer. New York, 867. <http://dx.doi.org/10.1007/978-0-387-21510-5>.
- Barbosa, L.C.A., Pereira, U.A., Martinazzo, A.P., Maltha, C.R.A., Teixeira, R.R., Melo, E.D. (2008). Evaluation of the chemical composition of Brazilian commercial *Cymbopogon citratus* (D.C) Stapf Samples. *Molecules*, 13(8), 1861-1874.
- Bassole, I.H.N., Lamién-Meda, A., Bayala, B., Obame, L.C., Ilboudo, A.J., Franz, C., Novak, J., Nebie, R.C., Dicko, M.H. (2011). Chemical Composition and Antimicrobial Activity of *Cymbopogon citratus* and *Cymbopogon giganteus* Essential Oils Alone and in Combination. *Phytomedicine*, 18, 1070-1074.
- Carlson, L.H.C., Machado, R.A.F., Spriggo, C.B., Pereira, L.K., Bolzan, A. (2001). Extraction of lemongrass essential oil with dense carbon dioxide. *J. Supercritical Fluids*, 21, 33-39.
- Chandrashekar, K.S., Joshi, A.B. (2006). Chemical composition and anthelmintic activity of essential oils of three *Cymbopogon* species of South Canara, India. *J. Saudi Chem. Soc.*, 10, 109-111.
- Council of Europe. (2021). *European Pharmacopoeia* 10th Edition (with supplements 10.6-10.7-10.8). Strasbourg.
- Das, M., Maiti, S.K. (2009). Growth of *cymbopogon citratus* and *vetiveria zizanioides* on Cu mine tailings amended with chicken manure and manure-soil mixtures: a pot scale study. *Int. J. Phytoremediation*, 11(8), 651-663.
- dijAvila, J.V., Martinazzo, A.P., dos Santos, F.S., Teodoro, C.E.S., Portz, A. (2016). Essential oil production of lemongrass (*Cymbopogon citratus*) under organic compost containing sewage sludge. *Revista Brasileira de Engenharia Agrícola E Ambiental*, 20(9), 811-816.
- European Pharmacopoeia. European Directorate for the Quality of Medicines. Council of Europe: Strasbourg, France, 2007.
- Farias, P.K.S., Silva, J.C.R.L., de Souza, C.N., da Fonseca, F.S.A., Brandi, I.V., Martins, E.R., Azevedo, A.M., de Almeida, A.C. (2019). Antioxidant activity of essential oils from condiment plants and their effect on lactic cultures and pathogenic bacteria. *Ciencia Rural*, 49(2), e2018140.

- Figueirinha, A., Cruz, M.T., Fransisco, V., Lopes, M.C., Batista, M.T. (2010). Anti-inflammatory activity of *Cymbopogon citratus* leaf infusion in lipopolysaccharide-stimulated dendritic cells: contribution of the polyphenols. *Journal of Medicinal Food*, 13(3), 681-690.
- FoodData Central [<https://fdc.nal.usda.gov/>]. Access date: 09.10.2019.
- Gautam, M., Pandey, D., Agrawal, M. (2017). Phytoremediation of metals using lemongrass (*Cymbopogon citratus* (DC) Stapf.) grown under different levels of red mud in soil amended with biowastes. *Int J Phytoremediation*, 19(6), 555–562.
- Hanaa, A.R.M., Sallam, Y.I., El-Leithy, A.S., Aly, S.E. (2012). Lemongrass (*Cymbopogon citratus*) essential oil as affected by dry ing methods. *Annals of Agricultural Sciences*, 57(2), 113-116.
- ISO 11466 (1995). Soil Quality-Extraction of Trace Elements Soluble in Aqua Regia.
- ISO 3217 (1974). Oil of lemongrass (*Cymbopogon citratus*).
- Joy, P.P., Baby, P.S., Samuel, M., Mathew, G., Joseph, A. (2006). Lemongrass: The fame of Cochin. India. *J. Arecanut. Species Med. Plants*, 8(2), 55-64.
- Kabata-Pendias, A. (2001). Trace Elements in Soils and Plants. 3rd ed. CRC Press LLC, Boca Raton, 2001.
- Kasali, A.A., Oyediji, A.O., Ashilokun, A.O. (2001). Volatile leaf oil constituents of *Cymbopogon citratus* (DC) Stapf. *Flavour and Fragrance Journal*, 16(5), 377-378.
- Khajanchi, L., Yadava, R.K., Ravinder Kaurb, D.S., Bundelaa, M. Inayat Khana, Madhu Chaudharya, R.L., Meenaa, S.R., Dara, Gurbachan Singha (2013). Productivity, essential oil yield, and heavy metal accumulation in lemon grass (*Cymbopogon flexuosus*) under varied wastewater–groundwater irrigation regimes. *Industrial Crops and Products*, 45, 270–278.
- Kpoviessi, S., Bero, J., Agbani, P., Gbaguidi, F., Kpadonou- Kpoviessi, B., Sinsin, B., Accrombessi, G., Frederich, M., Mou dachirou, M., Quetin-Leclercq, J. (2014). Chemical composition, cytotoxicity and *in vitro* antitrypanosomal and antiplasmodial activity of the essential oils of four *Cymbopogon* species from Benin. *Journal of Ethnopharmacology*, 151(1), 652-659.
- Kumar, A., Maiti, S.K. (2015). Effect of organic manures on the growth of *Cymbopogon citratus* and *Chrysopogon zizanioides* for the phytoremediation of chromite-asbestos mine waste: a pot scale experiment. *Int. J. Phytoremediation*, 17(5), 437-447.
- Kumar, A., Malik, F., Bhushan, S., Sethi, V. K., Shahi, A. K., Taneja, S. C., Singh, J. (2008). An essential oil and its major constituent iso intermedeol induce apoptosis by increased expression of mitochondrial cytochrome c and apical death receptors in human leukemia HL-60 cells. *Chemico-Biological Interactions*, 171(3), 332-347.
- Lawrence, R., Lawrence, K., Srivastava, R., Gupta, D. (2015). Antioxidant Activity of Lemon Grass Essential Oil (*Cymbopogon citratus*) Grown in North Indian Plains. *Sci. Temper.*, 4, 23–29.
- Maiti, S.K., Maiti, D. (2015)). Ecological restoration of waste dumps by topsoil blan keting, coir-matting and seeding with grass-legume mixture. *Ecol. Eng.*, 77, 74-84.
- Majewska, A., Kozowska, M., Gruczyska-Skowska, E., Kowalska, D., Tarnowska, K. (2019). Lemongrass (*Cymbopogon citratus*) Essential Oil: Extraction, Composition, Bioactivity and Uses for Food Preservation - a Review, *Pol. J. Food Nutr. Sci.*, 69(4), 327-341.
- Mansour, A.F., Fikry, R.M., Saad, M.M., Mohamed, A.M. (2015). Chemical composition, antioxidant and antimicrobial activity of *Cymbopogon citratus* essential oil cultivated in Madinah Monawara, Saudi Arabia and its comparison to the Egyptian chemotype. *International Journal of Food and Nutritional Sciences*, 4(4), 29-33.
- Mansour, A.F., Fikry, R.M., Saad, M.M., Mohamed, A.M. (2015). Chemical composition, antioxidant and antimicrobial activity of (*Cymbopogon citratus*) essential oil cultivated in Madinah Monawara, Saudi Arabia and its comparison to the Egypt tian chemotype. *International Journal of Food and Nutritional Sciences*, 4(4), 29-33.
- Matasyoh, J.C., Wagara, I.N., Nakavuma, J.L., Kiburai, A.M. (2011). Chemical composition of *Cymbopogon citratus* essential oil and its effect on mycotoxigenic *Aspergillus* species. *African Journal of Food Science*, 5(3), 138-142.
- Mbili, N.C., Opara, U.L., Lennox, C.L., Vries, F.A. (2017). Citrus and lemongrass essential oils inhibit *Botris cinerea* on IJGold en Deliciousij, IJPink Ladyij and IJGranny Smithij apples. *Journal of Plant Diseases and Protection*, 124(5), 499-511.
- Moutassem, D., Belabid, L., Bellik, Y., Ziouche, F.B. (2019). Efficacy of essential oils of various aromatic plantsin the biocontrol of Fusarium wilt and inducing systemic resistance in chickpea seedlings. *Plant Protection Science*, 55(3), 202-217.
- Pandey, A.K., Rai, M.K., Acharya, D. (2003). Chemical composition and antimycotic activity of the essential oils of corn mint (*Mentha arvensis*) and lemon grass (*Cymbopogon fl exuosus*) against human pathogenic fungi. *Pharmaceut. Biol.*, 41 ,421–425. doi:10.1076/pbbi.41.6.421.17825.
- Pandey, J., Verma, R.K., Singh, S. (2019). Suitability of aromatic plants for phytoremediation of heavy metal contaminated areas: a review. *International Journal of Phytoremediation*, doi:10.1080/15226514.2018.1540546
- Pandey, J., Verma, R.K., Singh, S. (2020). Trace element accumulation potential in lemongrass varieties (*Cymbopogon species*) and prediction through regression model equations followed by path analysis: a field study. *Chemosphere*, 257, 127-102.
- Rajeshwara Rao, B.R., Adinarayana, G., Rajput, D.K., Kumar, A.N., Syamasundar, K.V. (2015). Essential oil profiles of different parts of East Indian Khilji - Sajid: Phytoremediation potential of lemongrass (*Cymbopogon flexuosus* Stapf.) grown on tannery sludge contaminated soil. *Applied ecology and environmental research*, 18(6), 7703-7715.

- Schaneberg, B.T., Khan, I.A. (2002). Comparison of extraction methods for marker compounds in the essential oil of lemon grass by GC. *Journal of Agricultural and Food Chemistry*, 50(6), 1345-1349.
- Sugumaran, M., Joseph, S., Lee, K.L.W., Wong, K.W. (2005). *Herbs of Malaysia*. Shah Alam, Federal Publication.
- Verma, S.K., Singh, K., Gupta, A.K., Pandey, V.C., Trivedi, P., Verma, R.J., Patra, D.D. (2014). Aromatic grasses for phytomanagement of coal fly ash hazards. *Ecological Engineering*, 73, 425-428.
- WHO. (2007). Guidelines for Assessing Quality of Herbal Medicines with Reference to Contaminants and Residues. Available online: <http://apps.who.int/medicinedocs/documents/s14878e.pdf> (accessed on 1 May 2022).
- Wu, H., Li, J., Jia, Y., Xiao, Z., Li, P., Xie, Y., Zhang, A., Liu, R., Ren, Z., Zhao, M., Zeng, Ch., Li, Ch. (2019). Essential oil extracted from *Cymbopogon citronella* leaves by supercritical carbon dioxide: antioxidant and antimicrobial activities. *Journal of Analytical Methods in Chemistry*, art. no. 8192439.
- Zakka Israila, Y., Edith Bola, A., Casimir Emmanuel, G., Suleiman Ola, I. (2015). The effect of application of EDTA on the phytoextraction of heavy metals by *Vetiveria zizanioides*, *Cymbopogon citrates* and *Helianthus annuus*. *Int. J. Environ. Monit. Anal.*, 3(2), 38-43.
- Zheljazkov, V.D., Craker, L.E., Xing, B. (2006). Effects of Cd, Pb, and Cu on growth and essential oil contents in dill, peppermint, and basil. *Environ. Exp. Bot.*, 58(1-3), 9-16.

DETECTION AND MONITORING OF HYDROCARBON POLLUTION SOURCES IN THE PETROMIDIA REFINERY AREA

Sorin ANGHEL

National Institute for Research and Development on Marine Geology and
Geoecology - GeoEcoMar, 23-25 Dimitrie Onciul, Bucharest, Romania

Corresponding author email: soanghel@geoecomar.ro

Abstract

The detection and spatiotemporal monitoring of hydrocarbon contamination in the geological environment (soil, geological formations, and groundwater) represent the main objective of the study, conducted during the period of 2023-2024. The study focused on areas adjacent to the Petromidia refinery with industrial activity exceeding five decades, located in the vicinity of the city of Navodari. Both 'classic' geophysical techniques (VES - Vertical Electrical Sounding, IP - Induced Polarization) and recently introduced techniques on a global scale (GPR - Ground Penetrating Radar) were employed. Electrical and electromagnetic measurements were complemented by magnetic investigations, drilling works, and geological and hydrogeological observations. The most effective geophysical measurements, both for detecting and monitoring underground hydrocarbon contamination, were the geoelectrical resistivity ones, due to the significant contrast in electrical resistivity between the highly resistive pollutant substances and the affected geological environment, consisting of rocks and fluids with much higher electrical conductivity. The geological and hydrogeological data from shallow boreholes were used for the correct interpretation of geophysical anomalies, while the results of magnetic measurements indicated the routes of buried pipelines, and potential sources of pollution.

Key words: *electrometry, hydrocarbon, pollution, soil.*

INTRODUCTION

Contamination with hydrocarbons of the land and groundwater in the vicinity of refineries, fuel depots, oil wells, and even transportation pipelines, constitutes one of the significant environmental protection issues (Onutu & Tita, 2018). The localization and determination of the spatial-temporal distribution of contamination currently rely exclusively on the use of direct methods of biochemical analysis of soil and water samples taken from the surface or from boreholes.

The information obtained in this way is point-based and therefore cannot provide an overall picture of land and groundwater contamination. Analyses are costly and require an extended period for observations to be made.

The integration of point-based information into a three-dimensional spatial-temporal image of areas contaminated with hydrocarbons and residual waters becomes possible through the appropriate use of geophysical methods, supported by hydrogeological information.

The main objective of the geophysical investigation was to develop a geophysical

monitoring of hydrocarbon contamination resulting from refining, storage, and transportation activities of petroleum products in the vicinity of refinery located in the area of the city of Navodari.

MATERIALS AND METHODS

1. Physical-geographical characterization

The target under investigation is located on the coastal strip separating the Black Sea from the Gargalac (Corbu) and Taşaul lakes, an integral part of the Central Dobrogea Platform.

The relief generally exhibits the characteristics of a high hilly plain, with wide valleys and terraces, reaching heights of up to 100 meters.

The average relief energy is 50 meters. Genetically, the area represents a paneplain (nearly flat land surface resulting from long-continental erosion and denudation) of the Caledonian mountains (Green Shale Formation), covered in the Quaternary by a loess cover.

Beneath this cover of aeolian deposits, patches of eroded Jurassic limestone emerge, featuring karstic landforms such as caves and gorges.

Towards the coastal zone, the relief is lower, featuring lagoons, fluvio-marine estuaries, and sandy coastal barriers.

The climate is typically continental, with the sea exerting its influence over a coastal strip 10-15 kilometres wide. The basin of Lake Taşaul is situated on the contact zone between Jurassic limestone and the Proterozoic substrate of the Green Shale Formation. Along this stratigraphic contact, the course of the Casimcea River has insinuated itself, more active during cold, glacial periods of the Quaternary (Chitea, 2011). From a geomorphological perspective, the studied objective is situated on the "complex barrier beach" (barrier beach) of Taşaul - Corbu, which extends southward to the Mamaia complex barrier beach.

2. Aspects of historical hydrocarbon contamination in the Petromidia refinery area

The pollution phenomenon with petroleum products from industrial areas related to the extraction, transportation, and processing of oil in Romania, noted in the last 40 years, especially through its harmful effects on the quality of some drinking and surface water sources, as well as on the productivity of soil in some agricultural lands, has been the subject of special research initiated in the 1960s.

These studies were prioritized through hydrogeological and geophysical investigations conducted in the vicinity of refineries and fuel transportation pipelines by ISPIF Bucharest and the University of Bucharest starting from 1975. The contamination with hydrocarbons of land, groundwater, and surface water near major pollution sources (refineries, fuel depots, oil and fuel transportation pipelines, oil extraction rigs, petroleum residue ponds, etc.) represents one of the largest and most challenging environmental protection issues in Romania (Paraschiv, 1979). The placement near Navodari city of the country's most important sources of petroleum pollution (the Petromidia refinery, petroleum and fuel depots, and petroleum product transportation pipelines) makes this area the subject of numerous research endeavours and the primary motivation for selecting this perimeter for implementing hydro-geophysical research (Figure 1).



Figure 1. Petromidia refinery

The pollution sources in the Petromidia refinery area are classified as follows:

- systematic losses of petroleum products in the technological processes of extraction, transportation, and storage;
- accidental losses of petroleum products in the transportation and refining processes (explosions, fires, pipeline corrosion, earthquakes, technical accidents, pipeline breakages for fuel theft);
- slow leaks of products through cracks in pipelines, tanks, ponds, basins, sewers;
- losses of petroleum products during long-distance transportation of pollutants through watercourses, rainwater, and wind.

The migration of hydrocarbons, immiscible with water, occurs in two ways:

- a) In unsaturated conditions, under the influence of gravity and meteoric waters (within refinery);
- b) In saturated conditions, at the surface of groundwater in the form of a laminar contamination plume, laterally advancing in the direction of groundwater flow (outside refinery, in the direction of groundwater flow).

An example of contamination in saturated conditions at the level of the groundwater table is represented by the area southeast of the Petrobrazi refinery, where the boundary of the spread of groundwater contamination with petroleum products covered an area of approximately 11 km² in January 1981, separated into two distinct sectors according to the degree of pollution:

A central sector, affected by intense pollution, with significant concentrations of pollutants in the form of a lens-shaped layer above the groundwater, ranging from 1 cm to 5 m in thickness, predominantly spreading within the refinery premises and extending south-eastward

to approximately 2.5 km away; A sector with reduced pollution, with thin films, iridescence, or a specific petroleum smell in the groundwater, with the boundary located approximately 3.5 km from the refinery. In the Petromidia refinery case, the depths of the petroleum layer were frequently recorded at values of 2 - 6 m and are variable over time, depending on the vertical oscillation of local groundwater levels. The general propagation direction of the petroleum pollution front is similar to that of the predominant groundwater flow (NW - SE), but the advancement speed differs from that of water, being slower in the case of petroleum pollutants due to the different physical-mechanical characteristics (higher viscosity and adhesion of petroleum products) and the specific horizontal and vertical migration mechanism of petroleum products (depending on the action of capillary forces in the porous medium).

3. Geoelectric detection of hydrocarbon contamination

The use of various geoelectrical techniques for detecting underground hydrocarbon pollution is an efficient and non-invasive method for soil investigation in search of contamination. Among these techniques are VES (Vertical Electrical Sounding), IP (Induced Polarization), ERT (Electrical Resistivity Tomography), and GPR (Ground Penetrating Radar). Measurements of VES (Vertical Electrical Sounding) conducted with instruments such as AGI MINISTING (Figure 2) is extremely useful in identifying zones of hydrocarbon contamination.

VES involves measuring the electrical resistance of the soil in a vertical manner, allowing for the determination of the vertical distribution of the electrical properties of the subsurface. These techniques are particularly effective when placed on profiles that traverse areas of interest, such as refineries or other potential sources of hydrocarbon pollution.

By combining data obtained from various geoelectrical techniques, a more comprehensive picture of the distribution and characteristics of subsurface contamination can be obtained, which can better guide strategies for remediation and environmental monitoring (Greenhouse, 1993).



Figure 2. Geoelectric data acquisition using Ministing system from AGI

The observation data has been processed and interpreted using specialized software such as Res2DInv, EarthImager, as well as programs developed by the research team members. Analysing the curves of the vertical electrical soundings conducted in the area of the four refineries, it was observed that from a geoelectric standpoint, two main modes of electrical resistivity distribution in depth can be distinguished in the investigated region (Figure 3):

- VES curves representative of type H (for example-yellow colour) in the northeastern area, where the Petromidia refinery is located;
- VES curves representative of type K (for example-blue colour) in the southwestern area, where the Petromidia refinery is located.

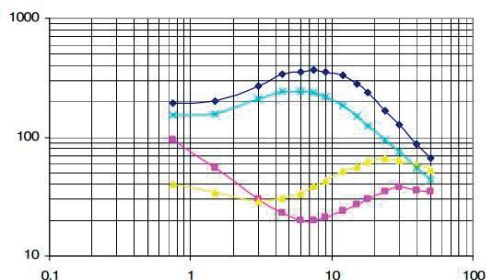


Figure 3. Representative VES curves

The main difference between the two separately identified sectors, with distinct variations in electrical resistivity, lies in the presence of a clay layer electrically conductive at the upper part of the geological structure in the northeastern part of investigated area (type H VES curves), a layer absent in the south-western part of investigated area (type K VES curves). The mentioned clay layer, intercepted in shallow boreholes, largely protects the northeastern area, with hydrocarbon contamination significantly lower compared to the southwestern area. The rapid increase in electrical resistivity in the electrical soundings conducted in the investigated area is due to the presence at shallow depths (1.5-4 m) of the resistive layer containing the pollutant film and geological formations impregnated with petroleum products. The processing and quantitative interpretation of VES data have resulted in obtaining resistivity sections down to a depth of 4 meters along the profiles in the investigated areas. The outlined anomalies of maximum resistivity (Figure 4 - red colour) illustrate the presence of hydrocarbon contamination plumes at depth.

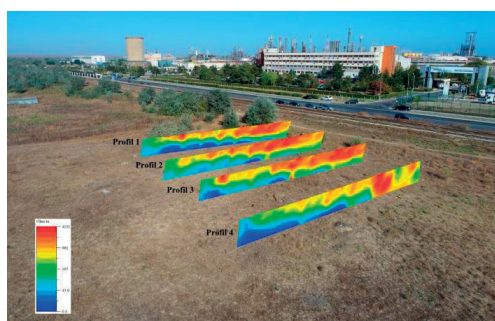


Figure 4. Apparent resistivity sections-Perimeter I

Figure 4 shows the distribution of electrical resistivity along profiles I, II, III and IV (Perimeter I), which traverses the north-south direction of the pollution zone associated with the Petromidia refinery. The elongated anomaly of maximum resistivity located at depths of 1.5-3 meters is interpreted as being due to the presence of the hydrocarbon contamination plume located at the aquifer's surface. Interruptions or variations in the thickness of the resistive layer are interpreted as being caused by

variations in the compaction of the contaminated gravel (Berkowitz, 2008).

The thickness of the resistive layer (Figure 4 - red colour), greater than the contaminant film at the aquifer's surface, also includes that of the gravel impregnated with hydrocarbons during seasonal variations in the hydrostatic level (historical contamination). The interpretation of these resistivity anomalies was supported by direct information from recently executed hydrogeological boreholes and from artisanal excavations present in the immediate vicinity of the investigated perimeters (McNeill, 1980).

In order to obtain detailed information on the distribution of resistivity in depth in areas significant for understanding the relationships between the contaminant and the polluted geological environment, VES measurements were conducted on Perimeter II (Figure 5).

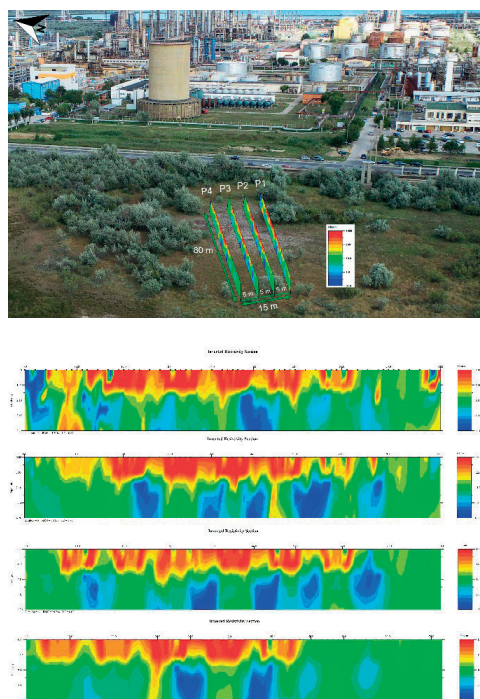


Figure 5. Apparent resistivity sections - Perimeter II

The electrical resistivity section obtained down to a depth of 4 meters illustrates details of anomalies of maximum resistivity associated with the hydrocarbon contamination plume on each profile. Variations in the intensity of resistivity anomalies can be interpreted as

variations in contaminant concentration, while interruptions in the major resistivity maximum anomaly can be attributed to the effects of local tectonic accidents.

4. Georadar detection of hydrocarbon contamination

The georadar investigation at the Petromidia refinery in the southeastern sector revealed some interesting findings. The underground limit interpreted as the water table suggests the presence of groundwater at that depth. Additionally, the zones of weak electromagnetic signal could indicate the presence of a hydrocarbon plume within the upper aquifer. This suggests the possibility of hydrocarbon contamination in the groundwater, which is a concern for environmental and remediation efforts. Further investigation and monitoring would likely be necessary to assess the extent of the contamination and develop appropriate mitigation measures (Fuente, 2021).

In the Petromidia refinery area, 10 longitudinal profiles and 6 transverse profiles were continuously recorded using a 100 MHz antenna (Figure 6).

The analysis of the recordings on the longitudinal profiles shows the existence of a well-defined geophysical boundary located at 0.75 m (Figure 7). The detected interface is practically continuous along the entire length of the measurement profiles. Correlating these observations with archive data obtained from previous boreholes, the following values for velocity and permittivity are obtained:

- a velocity of 6.5-7.6 cm/ns for the medium above the first georadar limit, considering this interface as the water level (Schon, 2004);
- the permittivity varies in the range of 15.58-21.30 (Kapicka, 1997).

Considering that the permittivity of a sandy medium saturated with water is around 25, and the reflection sign is negative, we can conclude that the interface encountered at 0.75 m (Figure 7) is due to the level of petroleum product. Electric permittivity (or dielectric constant) is a quantity, denoted by ϵ , which indicates the resistance to electric polarization of a dielectric material (Tezkan, 2005).

In practice, a dimensionless quantity expressed by the ratio of the permittivity of a medium to that of vacuum is used. The groundwater level is

located at depths of 1.5-2 m. Below the first detected georadar limit, the value of electromagnetic wave velocity decreases due to the presence of water in the propagation medium. By decreasing the velocity, the travel time of the wave increases.

Areas where reflection coefficients have high values and do not allow the delimitation of a reference radar horizon have been interpreted as being due to hydrocarbon intrusions (yellow zones - Figure 8).



Figure 6. Georadar acquisition data with 100MHz antenna

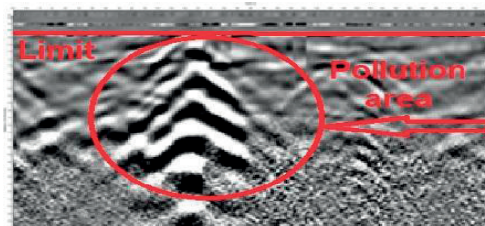


Figure 7. Georadar data (radargram) in the Petromidia refinery area

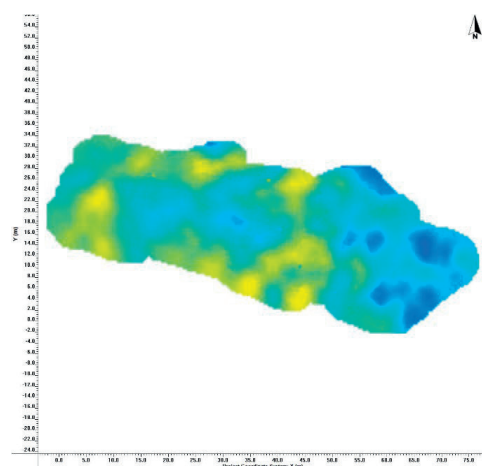


Figure 8. Georadar section

RESULTS AND DISCUSSIONS

Geophysical monitoring of the temporal and spatial evolution of hydrocarbon contamination plumes has been studied in the Petromidia refinery area. The hydrocarbon contamination plume, resulting from the temporal overlay of historical contamination with current contamination, is largely influenced by the regional dynamics of the aquifer. Geoelectrical VES measurements conducted for monitoring has investigated the central part of perimeter I and II.

The results of monitoring measurements were analysed in the form of resistivity pseudo sections to avoid disturbances caused by quantitative interpretation programs. The observed changes in resistivity during monitoring, considered for interpretation, are due to variations in moisture in surface layers (soil, paleosol, loess), fluctuations in the water table level, and some quantities of pollutants recently introduced into the geological environment in the refinery area (Figures 3, 4 and 5). The fragmentation of the major resistivity maximum anomaly is due to active processes of surface water infiltration along a fault system, which affects the geological structure and the soil layer (Figures 3, 4 and 5). The results obtained from the georadar investigation were presented in the form of radargrams or depth sections, which can highlight geological structures at shallow depths, including the localization of tectonic features with local significance, as well as the delineation between hydrocarbon-saturated and unsaturated zones (Manescu, 1994).

CONCLUSIONS

The results of geophysical investigations dedicated to the detection and monitoring of hydrocarbon contamination plumes near the Petromidia refinery have shown that VES geoelectrical resistivity measurements are the most effective. Elongated anomalies of maximum electrical resistivity, located at depths where the first aquifer is localized, illustrate the presence of contamination plumes due to the hydrocarbon film and the geological environment impregnated with contaminants during seasonal variations in the water table

level. Interruptions in the maximum resistivity anomalies are due to variations in the compaction of gravel or local tectonic accidents. The geoelectric monitoring of hydrocarbon contamination plumes was conducted using vertical electrical soundings, through the sequential analysis of resistivity pseudo sections. The geoelectric effect of hydrocarbon contamination is evident even under significantly different seasonal climatic variations, with the maximum resistivity anomaly determined by the presence of hydrocarbons being well delineated through repeated geophysical measurements.

This resilience in detection is particularly significant in delineating the maximum resistivity anomaly associated with subsurface hydrocarbon contamination (Allred, 2010). Repeated geophysical measurements serve as a reliable tool in accurately mapping out these anomalies, aiding in the assessment and management of hydrocarbon contamination in diverse environmental conditions. It's interesting to hear that geophysical investigations near the Petromidia refinery have identified VES (Vertical Electrical Sounding) geoelectrical resistivity measurements as the most effective method for detecting and monitoring hydrocarbon contamination plumes. Geophysical methods play a crucial role in environmental studies, especially when dealing with issues such as pollution and contamination. VES involves measuring the electrical resistivity of subsurface materials at different depths using a vertical electrode array. In the context of hydrocarbon contamination, variations in resistivity can be indicative of changes in the subsurface caused by the presence of hydrocarbons (Vafidis et al., 2014). Here are some reasons why VES geoelectrical resistivity measurements might be effective in this scenario:

Contrast in Resistivity - hydrocarbons generally have a lower electrical resistivity than the surrounding soil or rock. This contrast allows for the detection of hydrocarbon plumes in the subsurface.

Depth Profiling - VES provides information at different depths, allowing for a vertical profile of subsurface resistivity. This can help in understanding the depth and extent of the contamination plumes.

Spatial Resolution - VES can offer good spatial resolution, helping to map the lateral extent of contamination. This information is crucial for effective remediation strategies.

Cost-Effectiveness - compared to some other geophysical methods, VES can be relatively cost-effective, making it a practical choice for large-scale monitoring projects.

Non-Invasive Nature - geoelectrical methods are non-invasive, meaning they don't require drilling or excavation. This minimizes disturbance to the site and provides a more environmentally friendly approach.

Real-Time Monitoring - VES measurements can be conducted periodically, allowing for real-time monitoring of changes in subsurface resistivity. This is important for tracking the dynamic nature of contamination plumes.

It's essential to note that the effectiveness of geophysical methods can vary based on site-specific conditions. Additionally, integrating multiple geophysical techniques can provide a more comprehensive understanding of subsurface conditions.

If VES has proven to be the most effective in this case, it demonstrates the importance of selecting the right geophysical tools for the specific challenges posed by hydrocarbon contamination near the Petromidia refinery. The GPR data was obtained using a NOGGIN system with 100, 250, and 500 MHz antennas. The 100 and 250 MHz antennas provided the best results in terms of spatial resolution and depth, while the shallow groundwater level provided excellent conditions for GPR.

ACKNOWLEDGEMENTS

This research work was carried out with the support of Ministry of Innovation and Digitalization, and also was financed from CORE PROGRAM PN IV - Project PN 23300403.

REFERENCES

- Allred, B.J. (2010). Agricultural Geophysics: Past, Present and Future. *Proceedings of SAGEEP Conference, Keystone, CO.*
- Berkowitz, I., Yaron, B. (2008). *Contaminant Geochemistry. Interactions and Transport in the Subsurface Environment*, Springer-Verlag, Berlin, Heidelberg.
- Chitea, F., Georgescu P., Ioane D. (2011). Geophysical detection of marine intrusions in Black Sea coastal areas (Romania) using VES and ERT data. *Geo-Eco-Marina*, 17, 177–184.
- Fuente, J.V. (2021). Detection and Delineating of Hydrocarbon Contaminants by Using Time and Frequency Analysis of Ground Penetrating Radar, *Journal of Geoscience and Environment Protection*, 9(12.)
- Greenhouse, J., Brewster, M., Schnider, G., Redman D., Annan, P., Olhoeft, G., Lucius, J., Sander, K., Mazzella A. (1993). Geophysics and solvents: The Borden experiment, *The Leading Edge*, 12(4).
- Kapicka, A., Petrovsky, E., Jordanova, N. (1997). Comparison of in situ field measurements of soil magnetic susceptibility with laboratory data. *Studia Geoph. Geod.*, 41, 391–395.
- Manescu, M., Bica, I., Stan, I. (1994). La pollution d'eau souterraine avec des produits petroliers dans la zone de Ploiesti, *Proceedings of the International Hydrogeological Symposium*, Bucharest University Press, pp. 364–388.
- McNeill, J.D. (1980). Electromagnetic terrain conductivity measurement at low induction numbers. *Tech. Note TN-6, Geonics Ltd., Mississauga.*
- Onutu, I. & Tita, M. (2018). Soil contamination with petroleum compounds and heavy metals - case study. *Scientific Papers. Series E. Land Reclamation, Earth Observation & Surveying, Environmental Engineering*, VII, 140-145, Print ISSN 2285-6064.
- Paraschiv, D. (1979). Romanian oil and gas fields, Institute of Geology and Geophysics. *Technical and Economical Studies*, 13(5), 382.
- Schon, J.H. (2004). Physical Properties of rocks: fundamentals and principles of petrophysics. *Elsevier*, 18.
- Tezkan, B., Georgescu, P., Fauzi, U. (2005). Radiomagnetotelluric survey on an oil-contaminated area near the Brazi refinery, Romania. *Geophysical Prospecting*, 53, 311-323.
- Vafidis, A., Soupios, P., Economou, N., Hamdan, H., Andronikidis, N., Kritikakis, G., Panagopoulos, G., Manoutsoglou, E., Steiakakis, M., Candansayar, E., Schafmeister, M. (2014). Seawater intrusion imaging at Tybaki, Crete, using geophysical data and joint inversion of electrical and seismic data. *First Break Journal*, 32(8), 107–114.

RESEARCH ON THE USE OF SLUDGE FROM THE PITEȘTI WASTEWATER TREATMENT PLANT AS FERTILIZER

Gabriela BIALI¹, Esmeralda CHIORESCU², Maria Cătălina PASTIA¹,
Denis ȚOPA², Iuliana MOTRESCU^{2,3}, Irina Gabriela CARA³

¹"Gheorghe Asachi" Technical University of Iasi,
Faculty of Hydraulics, Geodesy and Environmental Engineering,
65 Prof. Dimitrie Mangeron Blvd, Iasi, Romania

²"Ion Ionescu de la Brad" Iasi University of Life Sciences,

Faculty of Agriculture, 3 Mihail Sadoveanu Alley, Iasi, Romania

³Research Institute for Agriculture and Environment, 14 Mihail Sadoveanu Alley, Iasi, Romania

Corresponding author emails: esmeralda_chiorescu@yahoo.com, gbiali@yahoo.com

Abstract

Sludge is a by-product, resulting from wastewater treatment. This study research provides the sludge analysis from the Pitești Wastewater Treatment Plant and the possibility of using this sludge in agriculture in its initial state, resulting from the treatment plant or even after any remediation required or appropriate treatment so that it can be used. For these analyses, we used the services of two laboratories, namely: Iasi Research Institute for Agriculture and Environment - ICAM, from the "Ion Ionescu de la Brad" Iasi University of Life Sciences and WESSLING - testing and consulting laboratory for continuous improvement of quality, safety, environmental protection, and health - the Hungarian laboratory.

The research focused on the presence of heavy metals, antibiotics, and hormones in the sludge and the determination of microplastics in it. The microplastics in the sludge were determined by treating them with 5% HCl sonicated at 25°C and then centrifuging and analyzing the supernatant. The research results show that the sludge obtained from the Pitești Wastewater Treatment Plant cannot be used as fertilizer in agriculture.

Key words: sludge, wastewater treatment.

INTRODUCTION

In the European context, the storage and recycling of sludge generated in wastewater treatment plants are highly contested. Applying sewage sludge to agricultural land can be beneficial as it improves the physical, chemical, and biological properties of soils and enhances crop growth (Dracea et al., 2022). Sludge is a by-product, resulting from wastewater treatment. It is considered a source of energy because it contains elements that must be recycled. Dewatered sewage sludge, depending on stabilization processes, contains on average 50-70% organic matter and 30-50% mineral components (including 1-4% inorganic carbon), 3.4-4.0% N, 0.5-2.5% P and significant amounts of other nutrients, including micronutrients (Fytili & Zabaniotou, 2008; Samolada & Zabaniotou, 2014; Tyagi & Lo, 2013).

Sewage sludge also contains high concentrations of nitrogen and phosphorus and can be considered as a plant fertilizer, but it also contains heavy metals, polychlorinated biphenyls (PCBs), adsorbable organic halides (AOX), pesticides, surfactants, hormones, pharmaceutical products, nanoparticles and many more (Siebielska, 2014; Sandu et al., 2023).

Sludges contain many pathogenic species: bacteria, viruses, and protozoa, which, together with other species of parasitic helminths, can create health hazards for humans, animals, and plants (Fijalkowski et al., 2014; Kacprzak & Stańczyk-Mazanek, 2003).

Currently, sludge is regulated in the European Union legislation as waste resulting from the treatment of domestic and industrial wastewater, which must be treated, recovered, or disposed of.

Sludge management is a complex issue as environmental standards become increasingly restrictive. From this perspective, the wastewater treatment activity must be associated with the usage and/or controlled storage of the sludge resulting from the process. In the European Union, the environmental strategy regarding sludge resulting from wastewater treatment supports the minimisation of production thereof, as well as the implementation of treatment methods with increased efficiency, with a view to recycling. Reusing sludge in agriculture, forestry, or the restoration of degraded lands, although accepted and preferred in many countries of the world, is also a vulnerable and controversial method that still requires numerous interdisciplinary explorations. Although the fertilizing value of sludge is acknowledged, use thereof faces both hygienic and ethical objections due to the unwanted presence of heavy metals and other categories of pollutants, such as hormones, antibiotics, microplastics, etc.

MATERIALS AND METHODS

Location of the studies

The Wastewater Treatment Plant in Pitești is intended for the treatment of the residual water of Pitești and the industrial units within its radius, excluding the petrochemical platform. The industrial wastewater connected to the city network, excluding that of the petrochemical platform, comes from industrial enterprises with a very varied production profile and represents about 60-70% of the total flow.

The plant's location was chosen primarily for relief/landscape considerations. It is at the lowest point in the inner city, which provides the advantage of being supplied with wastewater by gravity; no pumping is necessary.

Also, the minor bed of the Argeș River is only 250 m away. Another consideration for choosing the site was the fact that it is located downstream of the city's water intake.

The wastewater treatment plant in Pitești was built in several stages, along with an increase in the number of inhabitants and industrial development, requiring an increase in the treatment capacity.

The technological process of mechano-biological purification (with a tertiary step) of

wastewater takes place in three main directions: the water line, the sludge line, and the biogas line.

At the present time, the capacity of the Treatment Plant is a maximum flow rate (Q) of 1,138 l/s mechanically, biologically, and chemically treated water. Household, industrial and meteoric water (from the unitary system) are directed to the city's wastewater treatment plant and have approximately the following composition:

- household water - 60%;
- industrial water - 30-35%;
- seepage water - 5-10%.

Table 1. Purification process flow from the Pitești WWTP

Water line		Sludge line
Mechanical treatment:	Biological treatment:	
Mechanical screens (coarse and fine screens) Sludge filter unit and grease separators Retention tanks Sand separators Primary sludge chambers	Secondary sludge chambers Aeration basins FeCl ₃ Dosing	Gravitational thickeners Thickened sludge mixing basins Digester Digested sludge storage tanks Sludge water retention tank Polyelectrolyte dosing systems

Sample collection and analysis

The sludge samples were taken after treatment from the Pitești Wastewater Treatment Plant's drying platform on September 13, 2022, in 3 plastic containers weighing between 0.9 and 2.5 kg each (Figure 1).

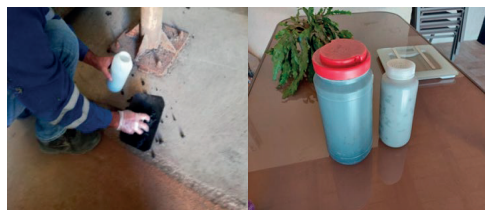


Figure 1. Sampling

RESULTS AND DISCUSSIONS

Analysis of heavy metals presence

As the Analysis Bulletin from ICAM Iași shows, heavy metals were detected in concentrations exceeding the admissible limits according to the legislation in force, as presented in Table 2 for

the following elements: zinc, copper, nickel, and lead. However, the concentration values of the other heavy metals are also not negligible.

Table 2. Analysis Bulletin from ICAM Iași

No.	Test name	UM	Values obtained
1.	pH	-	7.08
2.	Moisture	%	40.2
3.	Total nitrogen	%	0.78
4.	Total phosphorus	%	1.14
5.	Total potassium	%	1.37
6.	Organic matter	%	37.29
7.	Fe	%	2.83
8.	Zn	Ppm	1431
9.	Cu	Ppm	247
10.	Mn	Ppm	415
11.	Cd	Ppm	ND
12.	Co	Ppm	11.2
13.	Ni	Ppm	72
14.	Cr	Ppm	126
15.	Pb	Ppm	57

Contamination of agricultural soils with heavy metals adversely affects plant growth and soil microbiome and it is dangerous for food safety and human health (Wang et al., 2019). If concentrations of heavy metals such as copper (Cu), zinc (Zn), nickel (Ni), iron (Fe), and molybdenum (Mo), which are also essential micronutrients, exceed plant requirements, they become a serious environmental threat (Chen et al., 2014). Although other heavy metals such as lead (Pb), chromium (Cr), mercury (Hg), cadmium (Cd), and arsenic (As) are not essential for plant growth, they can adversely affect soil function, plant growth, and human health (Edelstein & Ben-Hur, 2018; Vardhan et al., 2019).

Heavy metals are dangerous because they tend to bioaccumulate. Bioaccumulation means the increase over time, in biological organisms, of the concentration of the substance in a quantity comparable to the concentration in the environment. Compounds accumulate in living organisms when they are assimilated and stored faster than they are metabolized or disposed of. Heavy metals cannot be degraded or decomposed to reduce their toxicity but can be transformed into non-reactive and less toxic species (Pandey & Keshavkant, 2021).

Once penetrated into plants, heavy metals enter the food chain and undergo specific processes. This circuit has a series of biological barriers, with limited action, which determine a selective bioaccumulation that defends living organisms against excess. However, there is a great risk of increasing the concentration up to toxicity limits

that cause imbalances in the chemical, physical and biological processes in the soil.

Effects of zinc: Zinc is the only metal present in all six classes of enzymes (oxidoreductases, transferases, hydrolases, lyases, isomerases, ligases). It is an essential element for animals and plants. Zinc causes the *phytotoxicity phenomena in contaminated soils*. As the soil pH decreases, the solubility and absorption of zinc increases, and thus, the phytotoxic potential also increases. In acid soils, phytotoxicity is indicated by the presence of ferric chlorosis. The toxicity of zinc can also be caused by the fact that this ion challenges biologically active ions and occupies their binding sites. Typical symptoms in this regard are: *chlorosis, reduction of plant biomass and inhibition of root growth* (Singh et al., 2013).

Effects of copper: Copper – is the metal component of phenol oxidase, ascorbic-acid-oxidase. Copper plays an important role in flowering, fruiting, and ear formation. Copper present in the soil above the natural limits of 1-20 ppm, has negative effects on the percentage of aggregates and the hydro stability of the particles, being susceptible to erosion and compaction. A high concentration of copper causes an increase in the mobile fraction of humus, an increase in hydrolytic acidity, and a reduction in basic cations. In plants, a high Cu concentration (generally > 20 ppm dry matter) reduces the intensity of respiration, slows down the process of chlorophyll formation, and decreases the activity of some ferments.

Effects of nickel: Nickel plays an important role in the life of plants in the synthesis of essential enzymes in the growth and development of plants, such as auxins, cytokines, and gibberellins (Singh et al., 2013). Plants absorb nickel as a Ni^{+2} divalent cation. The required dose is very low, i.e., 1.1 ppm. In excess, nickel is a heavy element and is strongly phytotoxic at a higher concentration. In several plants, Ni produces changes in enzyme activity. The most common symptoms of nickel toxicity in plants are growth inhibition, induction of chlorosis, necrosis, and wilting. Nickel strongly influences the metabolic reaction in plants and has the ability to generate oxygen radicals that can cause oxidative stress. Ni toxicity induces a decrease in the water content of mono- and dicotyledonous species.

Effects of chromium: Chromium compounds are very toxic to plants and act to the detriment of their growth and development. As it is a non-essential element for plant metabolism, chromium does not have specific absorption mechanisms. The toxic effects of chromium are mainly dependent on the metal species, which determines its absorption, translocation and accumulation (Huang et al., 2009).

Effects of lead: Lead in soil negatively influences biological activity by reducing respiratory processes at the root level, as well as by reducing the number of organisms. From the soil, lead passes into plants in amounts directly proportional to the amount of lead available. It acts on: oxidation and photosynthesis processes, limits the amount of water absorbed and intensifies the plant's oxygen requirement, slowing down the pace of crop development, until the crops are compromised (Gisbert et al., 2003).

Effects of cadmium: The toxic effects of cadmium on plant aerial organs include wilting of plants, chlorosis and necrosis of leaves, abnormal stomatal functioning, disruption of gas exchange, hormonal imbalance, production of oxidative stress, and increased peroxidation of membrane lipids. Cadmium usually accumulates in the upper horizons of the soil, in the plowed layer, and migrates with difficulty to the depth. The transition from soil to plants depends on the texture (higher with coarse texture) of the content in organic matter; there is a great affinity for the adsorption of cadmium by organic matter, which can be even 30 times higher compared to mineral soil (Copes et al., 2008; Othman et al., 2009).

The concentration of heavy metals in the sludge is around 0.5 and 2 %, but in some cases, it can increase up to 6% (Vyrides et al., 2017). Over the years, many researchers have studied different processes for the recovery of these heavy metals from sludge. The highest percentages of recovery (> 90%) were obtained using ultrasound (Li et al., 2010). Heavy metals, which are recovered together with proteins, are an inconvenience in the recovery processes, especially if the aim is to use the proteins as nutritional supplements for animals (Tyagi & Lo, 2013; Gherghel et al., 2019). Most studies show that all these heavy elements in the soil are partially transferred by plants to

animals and humans, respectively, leading to health deficiencies.

Analysis of the presence of residues of pharmaceutical substances

Table 3 shows residues of several pharmaceutical substances, some in low concentrations but some in considerable concentrations that depend on the drug from which it comes: antibiotics, analgesics, antimicrobial substances, antidepressants, and contraceptives.

Table 3. Presence of residues of several pharmaceutical substances

No.	Test name	UM	Values obtained
1.	Bisphenol A	mg/kg	0.47
2.	Furosemide	mg/kg	0.02
3.	Ibuprofen	mg/kg	0.03
4.	Triclocarban	mg/kg	0.01
5.	Triclosan	mg/kg	0.02
6.	4-Methoxycinnamic acid 2-ethylhexyl ester	mg/kg	0.21
7.	Amlodipine	mg/kg	0.17
8.	Atorvastatin	mg/kg	0.03
9.	Azithromycin	mg/kg	0.35
10.	Bisoprolol	mg/kg	0.01
11.	Ciprofloxacin	mg/kg	0.14
12.	Diclofenac	mg/kg	0.04
13.	Doxycycline	mg/kg	0.17
14.	Famotidine	mg/kg	0.03
15.	Carbamazepine	mg/kg	0.03
16.	Carvedilol	mg/kg	0.22
17.	Codeine	mg/kg	0.01
18.	Caffeine	mg/kg	0.05
19.	Cotinine	mg/kg	0.01
20.	Levonorgestrel	mg/kg	0.18
21.	Metoprolol	mg/kg	0.09
22.	Miconazole	mg/kg	0.02
23.	Norfloxacin	mg/kg	0.06
24.	Ofloxacin	mg/kg	0.28
25.	Oxytetracycline and 4-Epoxytetracycline	mg/kg	0.09
26.	Progesterone	mg/kg	0.02
27.	Propranolol	mg/kg	0.04
28.	Tetracycline and Epitetracycline	mg/kg	0.18

The substances whose concentration is higher than 0.01 mg/kg are the following:

- **Bisphenol A** is a controversial and highly toxic chemical compound. It comes from plastic products. Being a polymer, polycarbonate is, in turn, composed of several substances (monomers). One of these substances, which is also one of the most used in industry, is represented by **bisphenol A**.

- The **EPA** (*Environmental Protection Agency*) defines **bisphenol A** as "an exogenous chemical substance or combination that alters the structure or function(s) of the endocrine system

and causes adverse effects". A 2014 study shows that bisphenol A (abbreviated BPA) is also used to manufacture aluminium pharmaceutical tubes (for ointments, and creams).

- **Ibuprofen** is a nonsteroidal anti-inflammatory drug (NSAID), a type of drug commonly used to relieve pain and reduce fever. Being a frequently used drug, it is normal to be found in the analyzed sludge.

- **4-Methoxycinnamic acid 2-ethylhexyl ester** is a hormonal treatment. In women, it is used during pregnancy and breastfeeding.

- **Triclosan** is a chemical found in toothpaste, soap, and even some toys, which put American experts on alert after a study has showed that the ingredient is associated with the development of cancer cells and hormonal disorders. Animal studies have shown malformations and problems related to infertility. Human studies have demonstrated the presence of triclosan in urine and blood. This means that there can be negative effects for the mother and for those who have a genetic predisposition to certain diseases.

- **Amlodipine** belongs to the group of medicines called calcium channel blockers. Amlodipine is indicated in the treatment of high blood pressure, angina pectoris or vasospastic angina.

- **Azithromycin** belongs to a group of antibiotics called macrolides. It is used in the treatment of chest, throat, nose, and ear infections. It is a frequently used treatment against the infection with Covid 19 and thus it is understandable why it is found in the list of substances in the studied sludge.

- **Ciprofloxacin** is part of a group of medicines called quinolone antibiotics that have a broad spectrum of activity against microorganisms that can infect the eye and ear.

- **Diclofenac** contains diclofenac sodium as an active substance, which belongs to the class of drugs known as non-steroidal anti-inflammatory drugs (NSAIDs) for local use.

- **Doxycycline** is part of the group of drugs known as systemic antibacterials, tetracyclines. Doxycycline is used to treat respiratory tract infections and bacterial infections, including pneumonia.

- **Carbamazepine** is an antiepileptic with anticonvulsant, sedative and tranquilising properties.

- **Carvedilol** is a beta-blocker which works by relaxing and dilating blood vessels.

- **Levonorgestrel** is a pre-gestational hormone with antiestrogenic action, with various applications in gynaecology. Medicines containing levonorgestrel can be included in the following pharmacotherapeutic classes: emergency contraception, contraceptive pills, and progestogen intrauterine devices.

- **Metoprolol** is a drug from the group of selective beta-blocking drugs. This medicine is used in the treatment of high blood pressure.

- **Norfloxacin** is a new antibacterial derivative from the 4-Quinoline series. It is indicated in the therapy of the upper and lower urinary system.

- **Ofloxacin** is a 2nd generation fluoroquinolone antibiotic. It is used in the treatment of bacterial infections, such as: pneumonia, urethritis, prostatitis and other urinary tract infections.

- **Oxytetracycline** is an antibiotic used in the treatment of various bacterial infections.

- **Progesterone** is a steroid hormone produced by the cells of the ovarian corpus luteum and during pregnancy by the placenta.

- **Propranolol**, the active substance in this drug, belongs to the class of non-selective beta-blocking drugs and is indicated for hypertension.

- **Tetracycline** and **Epitetracycline** are broad-spectrum antibiotics with bacteriostatic action, indicated for the treatment of various infections.

- **Amoxicillin** is an antibiotic that belongs to a group of medicines called "penicillin", the medicine is used to treat infections caused by bacteria.

The treatment of many human and animal diseases relies on access to effective pharmaceutical substances. At the same time, pollution from some pharmaceuticals is an emerging problem, with well-documented evidence of environmental risks. Residues of pharmaceutical products can enter the environment during their manufacture, use and disposal.

Another source of pharmaceutical substances that can end up in wastewater and then in sewage sludge is expired drugs. More than a thousand tons of expired medicines from the population end up either in the sewage system or in the landfill every year.

Current legislation does not provide for minimum or maximum limits because those

sludges in which pharmaceutical substances have been detected are not allowed to be used in agriculture.

The toxic effect of pharmaceutical substances on plant tissues and cells varies depending on the concentration; at high concentrations, the entire growth and development process of the plant can be inhibited. After entering the plant, the pharmaceutical substances will be found in the food chain and are already a danger to human and animal health.

Research on the effects of antibiotics on the anaerobic digestion of sludge has shown that most antibiotics can inhibit methane production and methanogenesis rates at low concentrations. A small number of antibiotics (amoxicillin, metronidazole) have a negative effect on the proportion of methane in biogas because these antibiotics inhibit the activity of methanogenic bacteria that convert VFAs (volatile fatty acids) into methane, the percentage of VFAs converted into methane decreases and the CO₂ content grows. Furthermore, the combined effect of multiple antibiotics also inhibits methane production from anaerobic digestion of sewage sludge. In addition, VFA accumulation increases with the progress of anaerobic digestion, which is mainly due to the toxicity of antibiotics to the methanogenesis phase of VFA consumption. However, a few antibiotics (cephalexin, oxytetracycline, sulfamethoxazole, and kanamycin) can have a positive effect on anaerobic digestion by increasing methane production (Qingdao Wu, 2022).

The rate of antibiotic removal and biogas production during anaerobic digestion of sludge can be improved by adding oxidants (ozone, calcium oxide) and catalysts (zero-valent iron, iron ions).

These pretreatments promote the decomposition of antibiotics by improving complex oxidation reactions and electron transfer or increasing the bioavailability of microbial communities, thus achieving the goal of improving the removal rate of antibiotics and increasing methane production. However, the large-scale application of these pretreatment methods requires further environmental and economic studies to improve the methanogenesis performance of antibiotic-inhibited anaerobic digestion of sludge.

Analysis of microplastic presence

The high content of solid particles in the sample, 50 g of the sample was sampled, which was treated as follows: pre-oxidation with H₂O₂, density separation with CaCl₂ solution 1.3 g/cm³, oxidation with Fenton reaction and filtration on Anodisc inorganic filters that transmit IR.

The filters were analyzed with a Thermo Scientific Nicolet iN10 MX FTIR microscope with a pixel size of 25 µm in the transmission mode; 4 scan numbers and a spectral resolution of 8 cm⁻¹ were applied. The spectral data were evaluated with the "simple" software designed for the analysis of microplastics. The data were compared to a library of reference spectra, and particles with > 70% correlation were considered microplastics.

Microplastics are small particles (< 5 mm) of plastic material dispersed in the environment (Calmuc et al., 2023). They have become a cause for concern as they accumulate in soils, rivers, lakes, and the marine environment and in some foods; within a few decades, they have contaminated all oceans and marine species at all levels, from one pole to the other, and even in the deep sea. These can be fragments of plastic objects or plastic microbeads (spherical plastic particles composed of synthetic polymers) that have been increasingly used in industry, cosmetics, or synthetic fibres and found abundantly in sewage sludge.

Additionally, plastics degrade slowly, often over hundreds if not thousands of years. This increases the likelihood that microplastics will be ingested and embedded in the bodies and tissues of many organisms.

Microplastics enter agriculture through sewage sludge - which, when processed, is used as fertilizer, through plastic films that prevent weed growth or protect seeds, or even intentionally as slow-release fertilizers.

Figure 2 shows the sample prepared for FTIR (Fourier Transform Infrared Spectroscopy) analysis.



Figure 2. Sample prepared for FTIR analysis

Table 4 and Figure 3 show the results of the analysis. The distribution of polymer types is shown in Figure 4, and the distribution of particle sizes in Figure 5.

Table 4. Particle number and polymer type of identified microplastics

Microplastics identified (sum of particles/ sample)		The sum of the particles/ sample	Particles/g Sample dry matter
	Sample mass (g)	50	
	Dry matter content (%)	19.68%	
	PE	149	15.1
	PP	66	6.7
	Polyester	4	0.4
	PA	2	0.2
	Acrylic	3	0.3
	PVC	1	0.1
	PVA	1	0.1
	PVC	4	0.4
	PU	13	1.3
	PS	66	6.7
	ABS	6	0.6
	PTFE	1	0.1
	Cellulose acetate	33	3.4
	Alkyd	130	13.2
	Sum of MPs	479	48.7

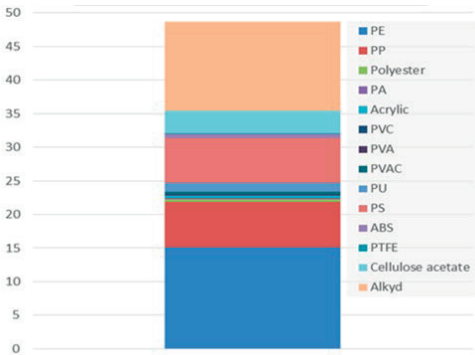


Figure 3. The number of particles and the type of polymer of the identified microplastics

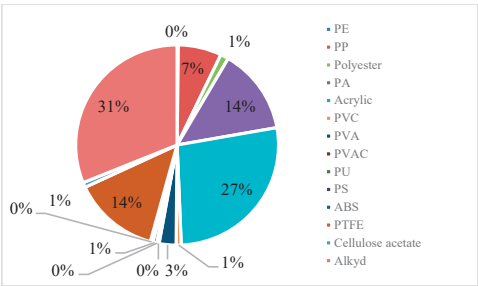


Figure 4. Distribution of polymer types

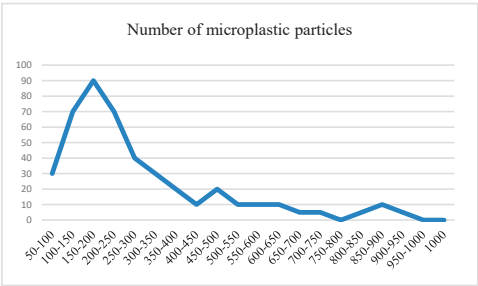


Figure 5. Distribution of particle sizes

Figure 6 present the existence of the types of microplastics detected in the sludge studied and Figure 7 the quantitative and dimensional analysis of the microplastics detected in the sludge studied. Although there are no concrete studies of human ingestion of microplastics, studies of mammals forced in laboratories to ingest these small fragments of plastic have shown that they can pass through cell walls, move through the body, accumulate in the body, and have an impact on the immune system.

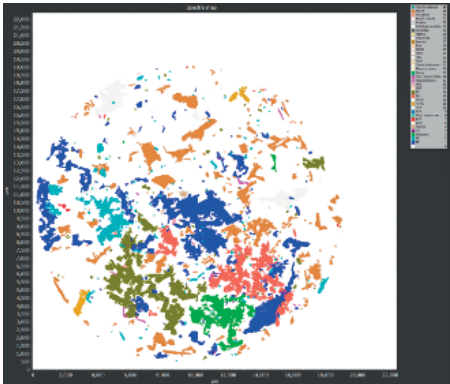


Figure 6. Image with the existence of the types of microplastics detected in the sludge studied

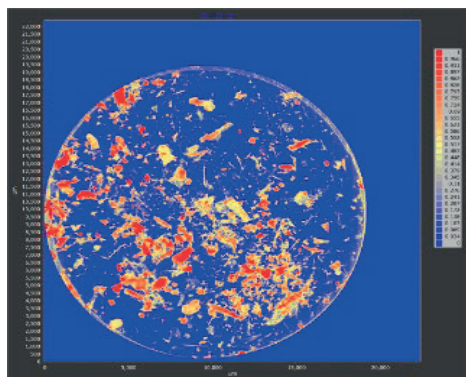


Figure 7. Image with the quantitative and dimensional analysis of the microplastics detected in the sludge studied

The elimination of those small plastic grains from care products (shower gels, face gels, toothpaste), the elimination of single-use plastic products, the ban of plastic films and slow-release fertilisers in agriculture, and companies that produce plastic films should be responsible for their recycling, are among the solutions proposed by specialists, which could solve the problem of microplastics in agricultural land.

CONCLUSIONS

This study research provides for the sludge analysis from the Pitești Wastewater Treatment Plant and the possibility of using this sludge in agriculture in its initial state, resulting from the treatment plant or even after any remediation required or appropriate treatment so that it can be used.

The major objective of sludge treatment in the treatment plant is to avoid the negative impact of environmental pollution and human health. The quality of the sludge differs a lot depending on the origin of the urban wastewater that enters the process, being almost impossible to predict the composition, implicitly their management.

Experimentally, a toxic potential of the anaerobically stabilized sewage sludge could be found at all analyzed levels of organization (prokaryote and eukaryote), especially at high concentrations of use.

Classified as biodegradable waste, anaerobically stabilized sewage sludge is a by-product of sewage treatment plants, whose pathogenic potential presents a health risk for humans but

also for the environment. Ecotoxicological effects can manifest in a short, medium or long time, simultaneously with the bioaccumulation effect of heavy metals or other categories of present pollutants.

Long-term spreading of sludge on agricultural land can lead to the accumulation of contaminants (i.e., heavy metals) in agricultural soil and can affect the entire ecosystems. Even if the level of accumulation might not exceed the currently accepted values, scientific research on soil and flora interactions allows us to understand their risk to the environment.

The final conclusions of this study:

The studied sludge has concentrations for some heavy metals that exceed the values allowed by the legislation to which we refer, i.e., Order no. 344/2004.

The presence of pharmaceutical substances derived from antibiotics and hormones causes high toxicity of the sludge, and its use on agricultural land presents a real danger for the entire food chain: for soil, soil water, plants, animals, and people.

The presence of microplastics in a considerable number and of a great variety in the analyzed sludge leads us to the same conclusion, namely that the analysed sludge from Pitești WWTP cannot be used in agriculture.

REFERENCES

- Calmuc, M., Calmuc, V.A., Condurache, N.N., Arseni, M., Simionov, I.-A., Timofti, M., Georgescu, P.-L., Iticescu, C. (2023). Study on microplastics occurrence in the lower Danube River water. *Scientific Papers. Series E. Land Reclamation, Earth Observation & Surveying, Environmental Engineering*, XII, 303-308, Print ISSN 2285-6064.
- Chen, S., Rotaru, A.-E., Liu, F., Philips J., Woodard Trevor, L., Nevin, K.P., Lovley, D.R. (2014). Carbon cloth stimulates direct interspecies electron transfer in syntrophic co-cultures. *Bioresource Technology*, 173, 82-86.
- Copes, R., Clark, N.A. (2008). Uptake of cadmium from Pacific oysters (*Crassostrea gigas*) in British Columbia oyster growers, *Environmental Research*, 107, 160-169.
- De Carvalho, Gomes, S., Zhou, J.L., Zeng, X., Long, G. (2022). Water treatment sludge conversion to biochar as cementitious material in cement composite, *Journal of Environmental Management*, 306, 114463.
- Dracea, D., Tronac, A., Mustata, S. (2022). Continuous adjustment within wastewater treatment plants operation to meet natural receptors discharge conditions. *Scientific Papers. Series E. Land Reclamation, Earth Observation & Surveying*,

- Environmental Engineering*, XI, 344-349, Print ISSN 2285-6064.
- Edelstein, M., Ben-Hur, M. (2018). Heavy metals and metalloids: sources, risks and strategies to reduce their accumulation in horticultural crops. *Sci. Hortic.*, 234, 431-444.
- Farzadkia, M. & Bazrafshan, E. (2014). Lime stabilization of waste-activated sludge. *Health Scope*, 3(3), e16035. <https://doi.org/10.17795/jhealthscope-16035>.
- Fijalkowski, K., et al., (2014). Occurrence changes of *Escherichia coli* (including O157: h7 serotype) in wastewater and sewage sludge by quantitation method of (EMA) real time - PCR. *Desalin. Water Treat.*, 52, 3965–3972.
- Fytli, D. & Zabaniotou, A. (2008). Utilization of sewage sludge in EU application of old and new methods—a review. *Renew. Sustain. Energy Rev.*, 12, 116–140.
- García-Lopez, J.I., Zavala-García, F., Olivares-Saenz, E., Lira-Saldivar, R.H., Barriga-Castro, E.D., Ruiz Torres N., Ramos-Cortez, E., Vazquez-Alvarado, R., Nino-Medina, G. (2018). Zinc Oxide Nanoparticles Boosts Phenolic Compounds and Antioxidant Activity of *Capsicum annuum* L. during Germination, *Agronomy Journal*, 8, 1-13.
- Gherghel, A., Teodosiu, C., De Gisi, S. (2019). A review on wastewater sludge valorisation and its challenges in the context of circular economy, *Journal of Cleaner Production*, 228, 244-263.
- Gisbert, C., Ros, R., de Haro A., Walker, D.J., Pilar Bernal, M., Serrano, R., Avino, J.N. (2003). A plant genetically modified that accumulates Pb is especially promising for phytoremediation, *Biochemical and Biophysical Research Communications*, 303, 440-445.
- Huang, S-H., Peng, B., Yang, Z.-H., Chai, L.-J., Xu, Y.-Z., Su, C.-Q. (2009). Spatial distribution of chromium in soils contaminated by chromium-containing slag, *Transaction of Nonferrous Metals Society of China*, 19, 756-764.
- Kacprzak, M., Stańczyk-Mazanek, E. (2003) Changes in the structure of fungal communities of soil treated with sewage sludge. *Biol. Fertil. Soils*, 38, 89–95.
- Kisku, G.C., Barman, S.C., Bhargava S.K. (2000). Contamination of soil and plants with potentially toxic elements irrigated with mixed industrial effluent and its impact on the environment, *Water Air Soil Pollut.*, 120, 121–137.
- Li, L., Jing, G., Wu, F., Chen, R., Chen, S., Wu, B. (2010). Recovery of cobalt and lithium from spent lithium ion batteries using organic citric acid as leachant. *Journal of Hazardous Materials*, 176(1–3), 15, 288-293.
- Naja, G.M. & Volesky, B. (2009). *Toxicity an sources of Pb, Cd, Hg, Cr, As and radionuclides in the Environment*. In Heavy Metals in the Environment, (Eds.), CRC Press, Boca Raton, 14-62.
- Nordberg, G.F., Sandstorm, B., Becking, G., Goyer, R.A. (2002). *Essentiality and Toxicity of Metals*. In Heavy Metals in the Environment, Sarkar B., (Eds.), Marcel Dekker, 1-34.
- Olszewski, J.M., et al., (2013). The effect of liming on antibacterial and hormone levels in wastewater biosolids. *J. Environ. Sci. Health Part A.*, 48, 862–870.
- Othman, M., Khonsue, W., Kitana, J., Thirakhupt, K., Robson, M., Kitana, N. (2009). Cadmium accumulation in two populations of rice frogs (*Fejervarya limnocharis*) naturally exposed to different environmental cadmium levels. *Bulletin of Environmental Contamination and Toxicology*, 83, 703-707.
- Pandey, N. & Keshavkant S. (2021). Chapter 1- Mechanisms of heavy metal removal using microorganisms as biosorbents. *New Trends in Removal of Heavy Metals from Industrial Wastewater*, 1–21.
- Qingdan, W., Dongsheng, Z., Xiaochen, Z., Fen, L., Longcheng, L., Zhihua, X. (2022). Effects of antibiotics on anaerobic digestion of sewage sludge: Performance of anaerobic digestion and structure of the microbial community, *Science of the Total Environment*, 846, 157384.
- Samolada, M. & Zabaniotou, A. (2014). Comparative assessment of municipal sewage sludge incineration, gasification and pyrolysis for a sustainable sludge-to-energy management in Greece. *Waste Manag.*, 34, 411–420.
- Sandu, M.-A., Vladasel (Pasarescu), A.-C., Pienaru, A.-M. (2023). Embedding low carbon emission into the water infrastructure. *Scientific Papers. Series E. Land Reclamation, Earth Observation & Surveying, Environmental Engineering*, XII, 52-59, Print ISSN 2285-6064.
- Siebielska, I. (2014). Comparison of changes in selected polycyclic aromatic hydrocarbons concentrations during the composting and anaerobic digestion processes of municipal waste and sewage sludge mixtures. *Water Sci. Tech.*, 70, 1617–1624.
- Singh, N.B., Amist N., Yadav K., Siingh D., Pandey J.K., Singh, S.C. (2013). Zinc Oxide Nanoparticles as Fertilizer for the germination, *Growth and Metabolism of Vegetable Crops*, 3(7), 874-881.
- Spinosa, L., et al., (2011). Sustainable and innovative solutions for sewage sludge management, *Water*, 3(2), 702-717. <https://doi.org/10.3390/w3020702>
- Suciu, N.A., Lamastra L., Trevisan, M. (2015). PAHs content of sewage sludge in Europe and its use as soil fertilizer. *Waste Manag.*, 41, 19–127.
- Tyagi, V.K., Lo, S.-L. (2013). Sludge: a waste or renewable source for energy and resources recovery? *Renew. Sustain. Energy Rev.*, 25, 708–728.
- Vardhan, K., Kumar, P., Panda, R. (2019). A review on heavy metal pollution, toxicity and remedial measures: current trends and future perspectives. *J. Mol. Liq.*, 290, 111-197.
- Vyrides, I. & Stuckey, D.C. (2017). Compatible solute addition to biological systems treating waste/wastewater to counteract osmotic and other environmental stresses: a review. *Critical reviews in Biotechnology*, 37(7), 865–879.
- Wang, S., Cai, L., Wen, H., Luo, J., Wang, Q., Liu, X. (2019). Spatial distribution and source apportionment of heavy metals in soil from a typical county-level city of Guangdong Province, China. *Sci. Total Environ.*, 655, 92-101.

OBTAINING ALKALI ACTIVATED INORGANIC MATERIALS BY RECOVERY OF WASTES

Mihaela CAFTANACHI^{1,2}, Ramona-Elena TATARU FARMUS¹, Maria HARJA¹

¹"Gheorghe Asachi" Technical University of Iasi, Faculty of Chemical Engineering
and Environmental Protection, 73 Mangeron Blvd, Iasi, Romania

²S.C. Gemite RO SRL, 52 S.F. Petru Movila Street, Iasi, Romania

Corresponding author email: maria_harja06@yahoo.com

Abstract

Currently, the large amount of waste produced is a significant problem for the environment and for the people who live near the deposits of by-products obtained from technological processes. Limited storage capacity, as well as the uncontrolled disposal of waste or industrial by-products from landfills, are growing concerns for environmental protection. The recovery of waste can be carried out to obtain new inorganic materials, known under several names, including geopolymers, alkaline activated materials. Aluminosilicate sources can come from industrial by-products such as silica fume, slag, fly ash, etc. In the formulation of this material, the type, ratios and concentrations of the compounds in the mixture are very important to the properties of the new inorganic materials. Prior to synthesis, a compressive analysis of the source materials must be performed to identify the minerals present and their amount relative to the total mass. The aim of this study is the formulation and characterization of new alkaline activated materials with the replacement of cement and establishing the influence of the properties of raw materials over final products.

Key words: aluminosilicate sources, inorganic materials, recovery, waste.

INTRODUCTION

As is well known, Portland cement (OPC) is the most used construction material worldwide due to advantages such as low cost, excellent performance and adaptability. A major impediment to its use would be the process of obtaining it which requires high energy consumption and releases large amounts of CO₂ into the atmosphere thus causing severe environmental pollution. It is estimated that for each ton of cement produced, about 9.5 J of energy is consumed and 0.8 tons of CO₂ are released. Therefore, there is an urgent need to implement alternative green materials with low carbon emissions to replace ordinary Portland cement in the coming years (Alventosa & White, 2021; Cretescu et al., 2018).

The new inorganic materials that are also the subject of the present study are found in specialized literature under various names such as geopolymers, alkaline activated materials. Geopolymers are an alternative material to cement-based materials that have been significantly improved in numerous projects around the world. In this field, research has been intensified to obtain materials with low energy

consumption and friendly to the environment (Aziz et al., 2021; Li et al., 2022). The new materials are synthesized following the geopolymerization reaction between an aluminosilicate material and an alkaline activator alone or composed of the KOH/NaOH solution and the potassium/sodium silicate solution resulting in a three-dimensional and amorphous structure at low temperatures (Prasanphan et al., 2019; Duxson et al., 2007; Arnoult et al., 2018).

The geopolymerization reaction is a complex process consisting of three main stages: dissolution, hydrolysis and polycondensation (De Silva et al., 2007). Numerous factors such as the types of aluminosilicate materials, their chemical compositions and the types and amounts of activators influence the activation mechanism (Mohamed et al., 2021; Nath & Kumar, 2019). From the studies carried out so far, it can be observed that for obtaining geopolymeric materials the most frequently used aluminosilicate by-products are those with a high content of alumina (Al₂O₃) and silica (SiO₂). Si and Al-rich wastes such as power plant fly ash, blast furnace slag are vital wastes in the production of geopolymer material.

Fly ash is grouped into two major classes (class F and class C) which are differentiated by the total amount of SiO_2 , Al_2O_3 , Fe_2O_3 depending on the type of coal burned, cooling conditions and combustion processes. Class C fly ash contains more than 10% calcium oxide, while Class F fly ash has a maximum calcium oxide content of 10% (Alterary & Marei, 2021).

Fly ash and granulated blast furnace slag are not the only wastes that can be activated alkaline thus obtaining materials with promising characteristics, but they are among the by-products that are obtained in large quantities and thus need to be stored. The recovery of larger amounts of waste provides opportunities for recycling and the opportunity for the development of a sustainable and ecological infrastructure (Mohamed et al., 2024).

Fly ash is rich in SiO_2 and Al_2O_3 , while in the case of granulated blast furnace slag the predominant oxides are those of calcium and silicon. Following the alkaline activation of ash and slag waste, we obtain the aluminosilicate gel that gives the newly obtained material high mechanical and chemical resistance (Yong-Sing et al., 2021). The new inorganic materials are obtained following a relatively simple process, a major advantage is represented using industrial waste as a raw material in obtaining them, the materials are made at ambient temperature, thus the alkaline materials are obtained with reduced CO_2 emissions (Caftanachi et al., 2023; Toobpeng et al., 2024).

The aim of this study is the formulation and characterization of new alkaline activated materials obtained from waste by replacing cement. The objective in this work was to obtain an industrial waste-based material with similar mechanical properties to cement-based materials, so that they can be used as construction materials with various applications. At the same time, by reusing this waste produced in large quantities, we contribute to protecting the environment. The recovery of waste leads to the reduction of environmental pollution as well as to the reduction of the costs of their elimination and neutralization.

The large volumes of waste resulting from various industries harm the soil through uncontrolled disposal or unintentional dispersal, as well as air and groundwater pollution, with negative effects on human health (Harja et al., 2023).

MATERIALS AND METHODS

The various wastes: fly ash type F, furnace slag and undensified silica fume were used in this study to obtain the new materials. The slag was purchased from Nanovision Chemicals in Greece. HSH Chemie Romania supplied silica fume undensified. The quartz sand in the composition of the material was provided by S.C. Bega Minerale Industriale SA, with different grain sizes.

The alkaline activator is represented by the mixture of potassium hydroxide solution and sodium silicate solution in different mass ratios. KOH solution with molarities between 7-10 M was prepared from KOH flakes of 98% purity and distilled water. The sodium silicate solution was supplied by PQ Corporation of the Netherlands, having a specific gravity of 1.39 and a modulus ratio (M_s) of 3.3. The raw materials used did not require preliminary purification and mechanical preparation. The chemical composition of the source materials used is shown in the Table 1.

Table 1. Chemical composition of the source materials used in the formulation (%)

Chemical component	SiO_2	Al_2O_3	Fe_2O_3	CaO	MgO	SO_3
Fly ash	51.31	15.01	6.23	5.11	1.06	1.19
Slag	8.81	2.97	21.51	79.15	2.85	-
Silica Fume	93.05	-	-	0.11	-	0.32

Although slag is a vital source of Si and Al, particles must be smaller than $45\ \mu\text{m}$ if used in construction materials.

The use of a percentage of blast furnace slag presents advantages for the material because it is easy to obtain, is chemically resistant and has very good thermal characteristics. Blast furnace slag and class F fly ash are often combined to increase the reactivity of these alkaline binders that possess a low calcium concentration (Vrabie et al., 2023).

Silica Fume contains mainly SiO_2 as can also be seen in Table 1, it has a very high specific surface and acts as a reactive pozzolan, it is used in small quantities compared to the other cementitious materials. Due to the very fine particle size, it greatly improves chemical resistance, minimizes chloride ion penetration,

greatly reduces permeability and reduces material segregation.

SAMPLE PREPARATION

The parameters to be followed in formulating the material are: KOH molarity, sodium silicate/potassium hydroxide ratio, water/binder ratio, alkaline solution/binder ratio, sand/binder ratio. The two formulated materials Sample 1-FA and Sample 2-FA/Slag present molarities between 7-10 M, a sodium silicate/KOH ratio between 1 and 3, the water/binder ratio being in the range 0.3-0.5.

The synthesis of the bicomponent inorganic material takes place in two stages: initially, the powdery part in which we have the source material is mixed with sand and additives, followed by the preparation of the alkaline solution (the KOH solution of established molarity was previously prepared and left at room temperature for cooling). The mixing of the potassium hydroxide solution with the sodium silicate solution took place before the material was made.

To achieve the desired workability and to ensure a complete reaction, mixing was maintained at 10 minutes for both formulations. The powdery part must be free of moisture to reduce the

influence of water on the total mixture. The fresh material is poured into molds, compacted with the help of a vibrating mass to remove air from the material and ensure its uniformity. After 24 hours the material is removed, labeled and aged at room temperature until testing. The samples (three for each experiment) were tested for the apparent densities and mechanical strengths (compressive and flexural strength), these tests being the most used according to the literature. Figure 1 shows the procedure for obtaining the new inorganic material.

The determination of the apparent density of the alkaline activated material was carried out in accordance with the SR EN 12190:2002 standard - Products and systems for the protection and repair of concrete structures.

Determination of compressive strength of repair mortar. This is calculated for each material sample as the ratio of mass to volume. The volume of the samples was calculated by measuring the dimensions of the prism (40 x 40 x 160 mm), the dimensions were measured using an electronic device. The mass of the sample was determined using an analytical balance with a capacity of 620 g and with a precision of 0.001 g under laboratory conditions. Density was determined at 1, 7, 14, 28 days.

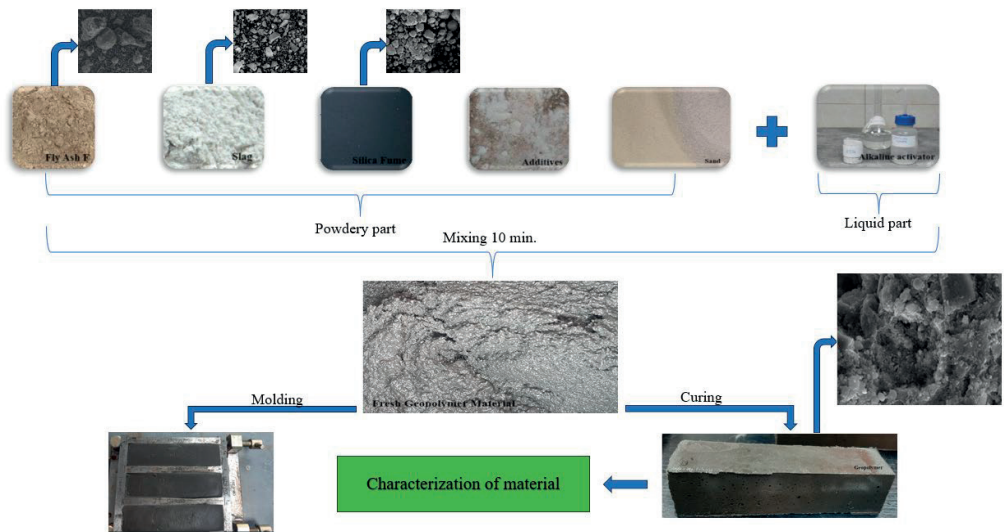


Figure 1. Synthesis of the new inorganic material

RESULTS AND DISCUSSIONS

Density of alkaline activated materials

The density of the cured material influences the mechanical properties of the newly formulated alkali-activated materials.

The graphic representation of the densities for the two material samples is shown in Figure 2.

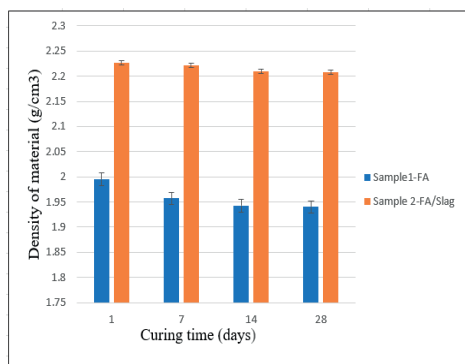


Figure 2. The density of the obtained material

The highest density of the hardened material at 28 days was recorded for Sample 2-FA/Slag, with a value of 2.208 g/cm³. Sample 2 contains 30% slag from the total binder.

Compressive strength

The main design criterion of this new alkaline activated material was to determine the compressive strength as well as the flexural strength. A 15/250kN hydraulic press was used for this test.

In the formulation of this material, the aluminosilicate sources, type, ratios and concentrations of the compounds in the mixture are very important to the properties of the new inorganic material. Prior to synthesis, a microanalysis of the source material was performed to identify the minerals present and their amount relative to the total mass.

The alkaline solution concentration influences the release of Si⁴⁺ and Al³⁺ from the source material during the activation process. High concentration alkaline solution is generally beneficial for achieving high compressive strength but there is an optimum range. The compressive strengths were determined on cube samples of 40 x 40 x 40 mm. Determining the compressive strength of a construction material

is an important characteristic that verifies its quality (Caftanachi et al., 2023).

The compressive strength of a construction material is determined according to the SR EN 12190: 2002 standard. The tests were performed at 7, 14 and 28 days, obtaining the results represented in Figure 3.

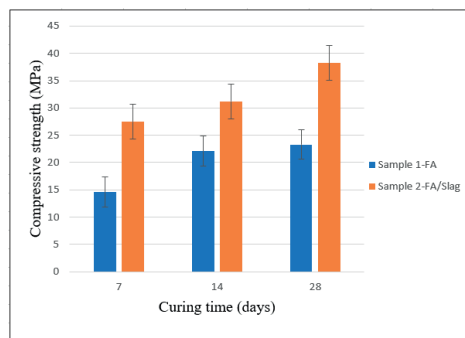


Figure 3. Compressive strength of alkali activated materials

The Sample 1-FA having a low concentration of KOH (7M) records low values in compressive at 28 days, only 23.26 MPa. By adding slag, the compressive strength at 28 days increases at 38.25 MPa.

Flexural strength

Alkali activated material based on fly ash has low flexural strength. A classic method is to incorporate fibers into the material matrix, as this hybridization can improve bond strength and flexural strength. In this way, the resistance to flexural and splitting can be improved. Fibers for the reinforcement of alkaline fly ash-based materials can be polyvinyl alcohol (PVA) fibers (Nematollahi et al., 2015; Sun & Wu, 2008), cotton fibers (Alomayri et al., 2014a; 2014b).

The principle of the test method aims to determine the flexural strength of prismatic specimens with the dimensions of 40 x 40 x 160 mm according to the SR EN 1015-11:2020 standard.

The tests were carried out at 7, 14 and 28 days, obtaining the following results and they were represented in Figure 4.

From the data presented, the following can be concluded: the Sample 1 had 5.04 MPa in flexural respectively, while Sample 2-FA/Slag had a flexural strength over 6.5 MPa.

The low concentration of the potassium hydroxide solution leads to a weak chemical reaction.

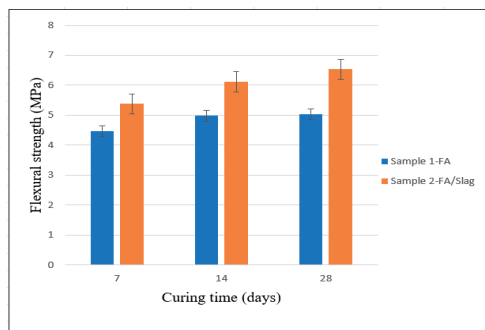


Figure 4. Results for flexural strength

The 10 M molarity of the KOH solution results in a flexural strength of the newly formulated material (Sample 2-FA/Slag) of 6.53 MPa at 28 days. It is observed that the sample presents an optimum alkaline solution concentration, obtaining higher values of flexural and compressive strength. A higher concentration of KOH leads to higher mechanical strengths of material since silicon and aluminum in the source material are dissolved much faster. A 10M concentration of KOH leads to a fast reaction and implicitly to obtaining a denser aluminosilicate gel.

Another parameter that is reflected in the mechanical resistances of the new material is the addition of slag to the amount of binder. The formulation with an addition of 30% slag registers high values in both compressive and flexural strength.

CONCLUSIONS

The main properties of alkali activated materials are related to the precursor type. The Si/Al ratio has a positive influence over mechanical properties of alkali activated materials because increase the amount of silica and the Si-O-Si bonds are stronger than the bonds formed by Si-O-Al or Al-O-Al bonds.

The compressive strength of alkali-activated fly ash material depends on the raw material source, alkali solutions, Si/Al ratios, chemical composition, curing conditions and additives.

When granulated blast furnace slag and fly ash are used together to obtain a composite system,

rapid chemical reactions occur and develop reaction products that contribute to significant changes in setting time, development of material microstructure, improvement of mechanical properties as well as durability of the combined system.

Although fly ash was originally used as a partial replacement for Portland cement to increase durability, reduce costs and lower carbon footprint, alkaline activated material technology using all fly ash or a fly ash/slag mixture as a binder offers an even lower carbon footprint and energy consumption, along with the beneficial use of a larger volume of industrial by-product that is otherwise likely to end up in a landfill with negative effects on the environment.

The obtained new alkaline activated material is economical, environmentally friendly, mechanically durable as seen in its high value of compressive strength: 23.5-38.5 MPa at 28 days, while the flexural strength is in the range of 5.05-6.5 MPa at 28 days, both values above requirements.

Following these obtained results can conclude that this activated alkaline material can be used without problems in the construction materials industry, research remains open to study more industrial by-products for the purpose of incorporation into new materials.

ACKNOWLEDGEMENTS

This research was supported by the Gheorghe Asachi Technical University Doctoral School and POC/163/1/3/Innovative Technology Project, project number 399/390075/17.11.2021, Cod SMIS 2014: 120951.

REFERENCES

- Alomayri, T., Shaikh, F.U.A., & Low, I.M. (2014a). Synthesis and mechanical properties of cotton fabric reinforced geopolymer composites. *Composites Part B: Engineering*, 60, 36-42.
- Alomayri, T., Shaikh, F.U.A., & Low, I.M. (2014b). Effect of fabric orientation on mechanical properties of cotton fabric reinforced geopolymer composites. *Materials & Design*, 57, 360-365.
- Alterary, S.S., & Marei, N.H. (2021). Fly ash properties, characterization, and applications: A review. *Journal of King Saud University-Science*, 33(6), 101536.
- Alventosa, K.M., & White, C.E. (2021). The effects of calcium hydroxide and activator chemistry on alkali-activated metakaolin pastes. *Cement and Concrete Research*, 145, 106453.

- Arnoult, M., Perronet, M., Autef, A., & Rossignol, S. (2018). How to control the geopolymer setting time with the alkaline silicate solution. *Journal of Non-Crystalline Solids*, 495, 59-66.
- Aziz, A., Benzaouak, A., Bellil, A., Alomayri, T., el Hassani, I.E.E.N., Achab, M. & Shaikh, F.U.A. (2021). Effect of acidic volcanic perlite rock on physio-mechanical properties and microstructure of natural pozzolan based geopolymers. *Case Studies in Construction Materials* 15.
- Caftanachi, M., Vrabie, M., Cotofan, A.I., & Harja, M. (2023). Micropilot scale testing of advanced inorganic materials obtained from wastes. *The Bulletin of the Polytechnic Institute from Iași*, 69 (73), 71-80.
- Cretescu, I., Harja, M., Teodosiu, C., Isopescu, D.N., Chok, M.F., Sluser, B.M., & Salleh, M.A.M. (2018). Synthesis and characterisation of a binder cement replacement based on alkali activation of fly ash waste. *Process Safety and Environmental Protection*, 119, 23-35.
- De Silva, P., Sagoe-Crenstil, K., & Sirivivatnanon, V. (2007). Kinetics of geopolymerization: Role of Al_2O_3 and SiO_2 . *Cement and Concrete Research*, 37(4), 512-518.
- Duxson, P., Fernández-Jiménez, A., Provis, J.L., Lukey, G.C., Palomo, A., & van Deventer, J.S. (2007). Geopolymer technology: the current state of the art. *Journal of materials science*, 42, 2917-2933.
- Harja, M., Caftanachi, M., Fanache, M., & Ciobanu, G. (2023). Fly ash waste for obtaining building materials with improved durability. *Scientific Study & Research. Chemistry & Chemical Engineering, Biotechnology, Food Industry*, 24(1), 49-60.
- Li, W., Shumuye, E.D., Shiyang, T., Wang, Z., & Zerfu, K. (2022). Eco-friendly fibre reinforced geopolymer concrete: A critical review on the microstructure and long-term durability properties. *Case Studies in Construction Materials*, 16, e00894.
- Mohamed, O.A., Najm, O., & Zuaier, H.A. (2024). Setting time, sulfuric acid resistance, and strength development of alkali-activated mortar with slag & fly ash binders. *Results in Engineering*, 21, 101711.
- Mohamed, R., Abd Razak, R., Abdullah, M.M.A.B., Shuib, R.K., & Chaiprapa, J. (2021). Geopolymerization of class C fly ash: reaction kinetics, microstructure properties and compressive strength of early age. *Journal of Non-Crystalline Solids*, 553, 120519.
- Nath, S.K., & Kumar, S. (2019). Reaction kinetics of fly ash geopolymerization: Role of particle size controlled by using ball mill. *Advanced Powder Technology*, 30(5), 1079-1088.
- Nematollahi, B., Sanjayan, J., & Ahmed Shaikh, F.U. (2015). Tensile strain hardening behavior of PVA fiber-reinforced engineered geopolymer composite. *Journal of Materials in Civil Engineering*, 27(10), 04015001.
- Prasanphan, S., Wannagon, A., Kobayashi, T., & Jiemsirilers, S. (2019). Reaction mechanisms of calcined kaolin processing waste-based geopolymers in the presence of low alkali activator solution. *Construction and Building Materials*, 221, 409-420.
- SR EN 1015-11. (2020). Methods of testing masonry mortars, Part 11: Determination of flexural strength of hardened mortar.
- SR EN 12190. (2002). Products and systems for the protection and repair of concrete structures, Test methods - Determination of the compressive strength of the repair mortar.
- Sun, P., & Wu, H.C. (2008). Transition from brittle to ductile behavior of fly ash using PVA fibers. *Cement and Concrete Composites*, 30(1), 29-36.
- Toobpeng, N., Thavorniti, P., & Jiemsirilers, S. (2024). Effect of additives on the setting time and compressive strength of activated high-calcium fly ash-based geopolymers. *Construction and Building Materials*, 417, 135035.
- Vrabie, M., Caftanachi, M., Cotofan, A.I., & Harja M. (2023). Wastes used for obtaining sustainable building materials, *The Bulletin of the Polytechnic Institute from Iași*, 69(73), 115-126.
- Yong-Sing, N., Yun-Ming, L., Cheng-Yong, H., Abdullah, M.M.A.B., Chan, L.W.L., Hui-Teng, N., ... & Yong-Jie, H. (2021). Evaluation of flexural properties and characterisation of 10-mm thin geopolymer based on fly ash and ladle furnace slag. *Journal of Materials Research and Technology*, 15, 163-176.

TESTING THE INFLUENCE OF EROSION ON SOIL CHEMICAL INDICATORS

Cosmina CANDREA, Marcel DÎRJA, Vasile DODEA

University of Agricultural Sciences and Veterinary Medicine of Cluj-Napoca,
Faculty of Silviculture and Cadastre, 3-5 Calea Manastur Street, Cluj-Napoca, Romania

Corresponding author email: marcel.dirja@usamvcluj.ro

Abstract

Soil erosion is one of the most widespread forms of soil degradation. The research was conducted with the aim of identifying the influence of erosion on chemical traits of moderately slopy degraded luvisol, using appropriate indicators. The experiment is located in Borod commune, Bihor County. To carry out the study of the level of soil erosion, a bifactorial experiment was organized, with the factors represented by the type of crop (meadow and corn) and the location of the crop (on contour lines and in the hill-valley direction). The biological material consists of alfalfa-dominated grasslands and maize maintained on typical, moderately eroded Luvisol. It is found that for the exploitation of the meadow, the highest values of the nutrient content are recorded, compared to the corn crop. The chemical indicators of soil quality are strongly influenced by the location of the crop, the location of the crop at the base of the slope having the strongest influence, but in the case of pH and mobile phosphorus content, located at the top of the slope.

Key words: differences, dry matter, fertilizer, irrigation, water.

INTRODUCTION

Soil erosion is one of the most widespread and major forms of soil degradation, having a strong impact on the environment as well as an economic one (Govaertes et al., 2006; Sestras et al., 2013). Soil erosion encompasses both geomorphological and land degradation aspects, posing environmental risks that impact human livelihoods (Stavi & Lal, 2011). Detrimental effects of erosion in connection with crop cultivation may encompass constrained root development, diminished water availability, decreased soil fertility, and unfavorable physical circumstances (Cojocaru, 2019; Babur et al., 2016; Havaee et al., 2015; Xiao-Li et al., 2010). In the agricultural sector, it is estimated that approximately 10% of the land surface affected by erosion globally, of which 66.58% is surface affected by water erosion, of which 20.5% with strong and excessive intensity, respectively 33.42% by wind erosion from which 4.7% with strong and excessive intensity, according to the data provided by the International Soil Reference Center (Pintaldi et al., 2018; <https://www.isric.org/>).

The use of appropriate indicators (total degree of structuring of soil aggregates, apparent density,

soil hydraulic conductivity, soil water reserve, water utilization efficiency, soil acid reaction, humus content, mobile phosphorus content, mobile potassium content and productivity corn culture and meadows), makes it possible, through quantification, to highlight the influence of erosion and/or existing crops on the physico-chemical properties of the soil (Abbasi et al., 2007; Imaz et al., 2010; Nael et al., 2004; Biali et al., 2016).

The research was conducted with the aim of identifying the influence of erosion on chemical traits of moderately slopy degraded luvisol, using appropriate indicators.

MATERIALS AND METHODS

The trial was carried on in the Odadei Depression in the west of our country, respectively on the territory of the village of Valea Mare de Criș, which belongs to Borod commune, Bihor County, during 2021-2022. The results are expressed as means by two years. The soil taxonomic unit is the typical moderately eroded Luvosol, loamy/loamy on clays, to which specific morphological characters correspond. Also, the mentioned soil type, in the experimental device, corresponds to

the following particularities (Domuța, 2012): hill area, slope with a slope of 10-15%, W-SW, groundwater depth, 5-10 m, parent material of the soil, clays and medium texture on the surface and fine in depth, slightly acid soil reaction, low humus content in the first horizon and extremely low in the next, very low nitrogen content, extremely low phosphorus content and low potassium content.

The biological material consists of alfalfa-dominated meadows and corn. Pioneer PR38A24 corn hybrid was used. It is part of the FAO 350 group (<https://www.corteva.ro/produse-si-solutii/seminte-corteva/porumb-pioneer-P0217.html>), is included in thermal zone 5 (1000-1200°C), being a semi-early hybrid.

The experiments were carried out in order to study the level of soil erosion and to identify solutions to improve the eroded soil on the slope, according to the method of randomized blocks, in three repetitions, each plot having an area of 50 m². In order to carry out the study of the level of soil erosion, a bifactorial experiment was organized, with the factors represented by the type of crop (meadow and corn) and the location of the crop (on contour lines and in the hill-valley direction).

The experimental variants are: V1 - Control, meadow, peak; V2 - Control, meadow, base; V3 - Culture with maize by level curves, peak; V4 - Culture with maize by level curves, base; V5 - Culture with maize by direction hill-valley, peak; V6 - Culture with maize by direction hill-valley, base.

Soil humus is determined titrimetrically (Tiurin method), pH is determined potentiometrically, mobile potassium and mobile phosphorus are extracted by the Egner-Riehm-Domingo method using an acetate-ammonium lactate solution, phosphorus is measured photocolometrically with blue molybdenum according to the Murphy-Riley method, and potassium is measured flamphotometrically (Domuța & Sabău, 2000).

The Kolmogorov-Smirnov statistic was applied to assess how well the data conforms to a normal distribution. Likewise, a Kaiser-Meyer-Olkin value of 0.732 and Bartlett's test of sphericity, yielding a chi-square value of 677 (with a p-value < 0.0001), affirmed the appropriateness of the data for factor analysis (Merce & Merce, 2009).

RESULTS AND DISCUSSIONS

In addition to the decrease in the quality of the physical properties of the soil, erosion also causes the decrease in the quality of its chemical properties. In the experimental field as it results from the results that will be presented next, results obtained following the laboratory analyzes of the samples collected from the profiles in which the physical analyzes were also performed.

The study of the pH values, reported for the analyzed soil taken from the top and base of the slope, highlights the existence of a slightly acidic character for all the experimental variants. The most pronounced acidic character, located in the value range belonging to the slightly acidic domain, corresponds to pH = 5.49, reported for the soil located at the top of the slope, corresponding to V5. The weakest acid character corresponds to pH = 5.85, reported for the soil located at the base of the slope, corresponding to experimental V5. Between the soil pH evolutions, depending on the experimental variants, according to the LSD5% test, no significant differences are recorded (Table 1). pH values corresponding to surface eroded soil obtained in our study, which frames between 5.49 and 5.85 show an increase of pH in eroded soil, but it is lower compared with values mentioned by Nosarti (2013) of 7.22 or 7.25 depending of use categories. Even though and Bílá et al. (2020) of 7.52 in control soil, and 7.67 in eroded soil, respectively, while Gabbasova et al. (2016) obtained pH values of 7.9 units of pH in moderate eroded light gray forest soils.

At the top of the slope, the humus content of the soil is lower than at the base of the slope, for all experimental variants, but the differences between the humus content at the top and base of the slope, within the three experimental variants, are not statistically significant. Compared to the control variant 1, the humus content is 14.65% for variant 1b, with 10.61% for variant 2b. In the case of the other experimental variants, the humus content is lower: by 4.55% in the case of variant 2a, by 10.10% for variant 2b and by 3.03% for variant 3b.

Between the evolutions of the humus content, no significant differences are recorded. The soil

corresponding to all the experimental variants is characterized as having a medium content of humus (Table 1). The humus content of eroded luvisol identified in our study frames within 1.78-2.27%, which is lower compared with results reported by Rogobete & Grozav (2011) for eroded luvisol (2.38%), or by Gabbasova et al. (2016) who obtained values of 2.77% humus content in moderate eroded light gray forest soils.

The position on the slope differentiates the content of the soil in mobile phosphorus, in a much more obvious way, compared to the previously analyzed soil quality indicators. For variant 1b control, at the base of the slope a content of mobile phosphorus was determined equal to 29.31 ppm (V2) with 61.13% more than

at the top of the slope (V1), the soil here being characterized as poorly supplied with phosphorus. Similar developments are also recorded in the other experimental variants. For the experimental version 2b, at the base of the slope, a content of mobile phosphorus equal to 26.14 ppm was determined, and at the top of the slope, a content equal to 17.58 ppm.

For V6, at the base of the slope, a content of mobile phosphorus equal to 22.34 ppm was determined, and at the top of the slope, a content equal to 14.92 ppm.

Compared to V1, the phosphorus content of the soil is 3.45% lower in the case of V3, and by 17.92% in the case of V5, but by 43.71% higher in the case of V4 and by 22.81% in the case of V6 (Table 1).

Table 1. The soil humus content recorded in eroded arable field according to experimental variants

Issue	pH	%	Humus %	%	P, ppm	%	K, ppm	%
Control experimental variant 1a, meadow, peak – V1	5.61a	100	1.98a	100	18.19ac	100	123.44a	100
Control experimental variant 1b, meadow, base – V2	5.67a	98.94	2.27a	114.65	29.31ca	161.13	129.89a	105.23
Experimental variant 2a cultivated with maize by level curves, peak – V3	5.59a	100.36	1.89a	95.45	17.58ac	96.65	119.46a	96.78
Experimental variant 2b cultivated with maize by level curves, base – V4	5.64a	99.47	2.19a	110.61	26.14ca	143.71	127.62a	103.39
Experimental variant 3a cultivated with maize by direction hill-valley, peak – V5	5.49a	102.19	1.78a	89.90	14.92bd	82.02	112.86a	91.43
Experimental variant 3b cultivated with maize by direction hill-valley, base – V6	5.85a	95.90	1.92a	96.97	22.34c	122.81	121.14a	98.14
Mean	5.64		2.01		21.41		122.41	
CV (%)	2.11		9.36		25.81		4.97	
LSD _{5%}	49.171		8.913		4.294		34.516	
F	0.816 ^{ns}		3.693 [*]		3.582 [*]		4.083 [*]	

CV% – variation coefficient; LSD – Least Significant Differences; F – Fisher coefficient; the means with same letter are statistically insignificant; a - $p > 0.05\%$; b - $p > 0.05\%$.

Soil characterized by poor supply of mobile phosphorus is reported for all experimental variants. Between the evolutions of the content in mobile phosphorus, depending on the experimental variants, according to the test (LSD_{5%}), statistically significant differences are recorded. For all experimental variants, at the top of the slope the content of mobile phosphorus in the soil is lower than at the base of the slope, the differences between the content of mobile phosphorus in the soil at the top and base of the slope, within the three experimental variants, are statistically significant at different

thresholds meaning. The soil is poorly supplied with mobile phosphorus in the case of the experimental variants, but at the base of the slope the recorded values exceed them (Table 1). And in the case of the content in mobile potassium, the position on the slope differentiates the content of the soil in the mentioned element. Mobile phosphorus values corresponding to surface eroded soil obtained in our study, which frames between 14.82 ppm and 29.31 ppm, is much lower compared with values mentioned by Nosarti (2013), of 550 ppm or 590 ppm depending on use categories. Bílá et al.

(2020) also find higher mobile phosphorus content, both in control and eroded soil of 76.8 ppm, and 71.39 ppm, respectively.

For V2, at the base of the slope, a mobile potassium content equal to 129.89 ppm was determined, 5.23% more than at the top of the slope for the control version 1a. For V4, a mobile potassium content equal to 127.62 ppm was determined at the base of the slope, and a content equal to 119.46 ppm at the top of the slope. For V6, a mobile potassium content equal to 121.14 ppm was determined at the base of the slope, and a content equal to 112.86 ppm at the top of the slope.

Compared to V1, soil potassium content is 3.22% lower in V3, 8.57% in V5 and 1.86% in V6, but 3.39% higher in V4. For all experimental variants, the soil is characterized by poor supply of mobile potassium. Between the evolutions of the mobile potassium content, depending on the experimental variants, according to the test (LSD5%), statistically significant differences are recorded.

For all experimental variants, at the top of the slope the content of mobile potassium in the soil

is lower than at the base of the slope, the differences between the content of mobile potassium in the soil at the top and base of the slope, within the three experimental variants, are not statistically significant.

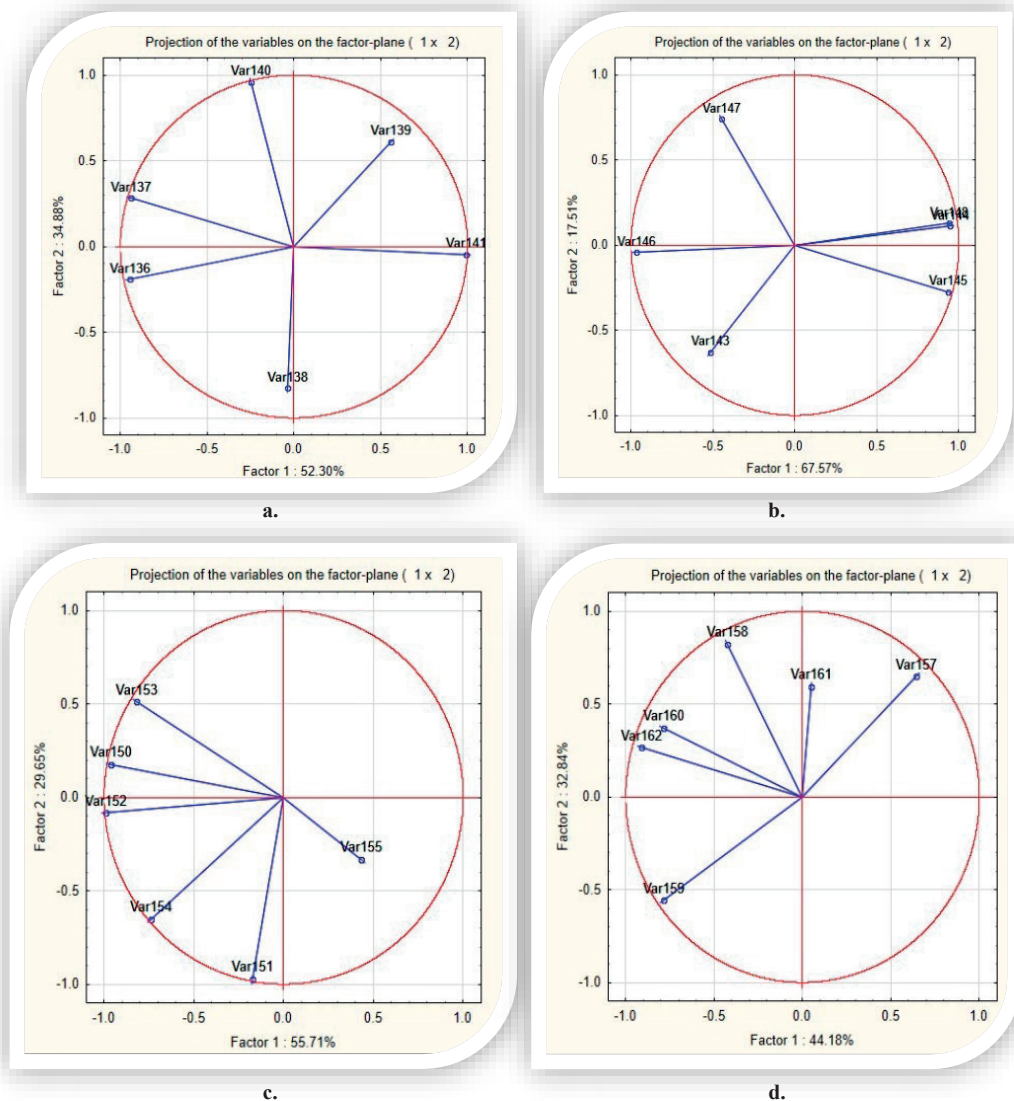
The study highlights the fact that neither the position on the slope nor the crop, or the location on the slope, statistically significantly influences its mobile potassium content (Table 1).

In order to test the feasibility of the analysis of the main components, the intensities of the correlations between the indicators corresponding to the chemical characteristics of the soil important in assessing the level in which the erosion of the land in the experimental field influences the mentioned characteristics are calculated. Due to the fact that in most cases, the intensities of the correlations are medium and strong, the condition of conducting the analysis of the principal components is met (Table 2). Four main factors influencing soil reaction are identified, respectively: experimental variant, location, culture and soil type (Figure 1a - 1d, Table 3).

Table 2. The simple correlations between the chemical soil traits important for assessing the erosion level of slowly arable field according to experimental variants

Issue	Humus, %	Phosphorus, ppm	Potassium, ppm
V1			
Humus, %	R=0.221; R ² =0.048	R=-0.727; R ² =0.528	R=0.215; R ² =0.976
Phosphorus, ppm		R=0.435; R ² =0.230	R=0.832; R ² =0.692
Potassium, ppm			R=0.594; R ² =0.352
V2			
Humus, %	R=0.109; R ² =0.011	R=-0.145; R ² =0.021	R=0.348; R ² =0.121
Phosphorus, ppm		R=0.893; R ² =0.797	R=0.783; R ² =0.613
Potassium, ppm			R=0.676; R ² =0.456
V3			
Humus, %	R=0.190; R ² =0.036	R=-0.748; R ² =0.560	R=0.547; R ² =0.299
Phosphorus, ppm		R=0.331; R ² =0.110	R=0.604; R ² =0.365
Potassium, ppm			R=0.249; R ² =0.062
V4			
Humus, %	R=0.078; R ² =0.006	R=-0.498; R ² =0.248	R=0.264; R ² =0.070
Phosphorus, ppm		R=0.557; R ² =0.310	R=0.402; R ² =0.162
Potassium, ppm			R=0.585; R ² =0.342
V5			
Humus, %	R=0.653; R ² =0.426	R=-0.756; R ² =0.572	R=0.326; R ² =0.106
Phosphorus, ppm		R=0.861; R ² =0.741	R=0.415; R ² =0.172
Potassium, ppm			R=0.482; R ² =0.232
V6			
Humus, %	R=0.455; R ² =0.310	R=-0.773; R ² =0.598	R=0.231; R ² =0.053
Phosphorus, ppm		R=-0.789; R ² =0.623	R=0.489; R ² =0.239
Potassium, ppm			R=0.520; R ² =0.270

R - coefficient of correlation; R² - coefficient of determination; V1 - Control, meadow, peak, V2 - Control, meadow, base, V3 - Culture with maize by level curves, peak, V4 - Culture with maize by level curves, base, V5 - Culture with maize by direction hill-valley, peak, V6 - Culture with maize by direction hill-valley, base.



a - soil reaction (pH); b - humus soil content; c - phosphorus soil content; d - potassium soil content;
 Var 136 - Control experimental variant 1, meadow, peak; Var 137 - Control experimental variant 1, meadow, base; Var 138 - Variant cultivated with maize by level curves, base; Var 140 - Variant cultivated with maize by direction hill-valley, peak; Var 141 - Variant 3 cultivated with maize by direction hill-valley, base; Var 143 - Control experimental variant 1, meadow, peak; Var 144 - Control experimental variant 1, meadow, base; Var 145 - Variant cultivated with maize by level curves, peak; Var 146 - Variant cultivated with maize by level curves, base; Var 147 - Variant cultivated with maize by direction hill-valley, peak; Var 148 - Variant 3 cultivated with maize by direction hill-valley, base; Var 149 - Control experimental variant 1, meadow, peak; Var 150 - Control experimental variant 1, meadow, base; Var 151 - Variant cultivated with maize by level curves, peak; Var 152 - Variant cultivated with maize by level curves, base; Var 153 - Variant cultivated with maize by direction hill-valley, peak; Var 154 - Variant 3 cultivated with maize by direction hill-valley, base; Var 155 - Control experimental variant 1, meadow, peak; Var 156 - Control experimental variant 1, meadow, base; Var 157 - Control experimental variant 1, meadow, peak; Var 158 - Control experimental variant 1, meadow, base; Var 159 - Variant cultivated with maize by level curves, peak; Var 160 - Variant cultivated with maize by level curves, base; Var 161 - Variant cultivated with maize by direction hill-valley, peak; Var 162 - Variant 3 cultivated with maize by direction hill-valley, base.

Figure 1. The projection of the variables involved in the study of the soil traits in the plans of the principal factors

Table 3. The Principal Components Analysis applied to the study of the soil reaction recorded in experimental field

Eigenvalue	Total variance, %	Cumulative Eigenvalue	Total variance cumulative, %	Factor	Factor loading
pH					
3.137	52.296	3.137	52.296	Factor 1 - Experimental variant	-0.944
					-0.941
					-0.037
					0.556
					-0.248
2.092	34.881	5.230	87.1776		0.993
0.740	12.342	5.971	99.520	Factor 2 - Crop placement	-0.190
					0.283
					-0.826
					0.610
					0.958
0.028	0.479	6.000	100		-0.046
Humus					
4.053	67.565	4.053	67.565	Factor 1 - Experimental variant	-0.515
					0.945
					0.934
					-0.965
					-0.450
1.050	17.508	5.104	85.074		0.940
0.878	14.634	5.982	99.708	Factor 2 - Crop placement	-0.629
					0.111
					-0.275
					-0.044
					0.740
0.017	0.291	6.000	100		0.126
Phosphorus					
3.342	55.707	3.342	55.707	Factor 1 - Experimental variant	-0.956
					-0.231
					-0.997
					-0.805
					-0.771
1.778	29.646	5.121	85.3543		-0.956
0.810	13.514	5.932	98.869	Factor 2 - Crop placement	0.253
					-0.960
					-0.020
					0.589
					-0.614
0.067	1.131	6.000	100		0.253
Potassium					
2.650	44.180	2.650	44.180	Factor 1 - Experimental variant	0.641
					-0.426
					-0.783
					-0.784
					0.051
1.970	32.8430	4.621	77.023		-0.909
0.912	15.208	5.533	92.232	Factor 2 - Crop placement	0.648
					0.822
					-0.558
					0.371
					0.594
0.466	7.767	6.000	100		0.265

The experimental variant, which accounts for 52.30% of the variance, is positively correlated with the soil response in the case of corn, both on the level curves and the hill-valley direction

at the soil base. The location of the crop is responsible for 34.88% of the variance and is positively correlated with the soil reaction in the case of: the exploitation of the meadow at the

base of the land, the cultivation of corn on contour lines, at the base of the land and the cultivation of corn on the hill-valley direction, at the top of the eroded land in slope (Figure 1a, Table 3).

For soil humus content, the experimental variant is responsible for 67.56% of the variance and the location for 17.51%. The factor represented by the experimental variant is positively correlated with: the humus content of the soil in the case of the exploitation of the meadow and the plumb in the hill-valley direction, at the base of the land and the plumb on contours, at the top of the land. The location of the culture is positively correlated with the humus content of the soil in the case of the exploitation of the meadow at the base of the land and the plumb in the hill-valley direction, both at the top and at the base of the eroded land on the slope (Figure 1b, Table 3). For the mobile phosphorus content of the soil, the experimental variant is responsible for 55.716% of the variance and the location for 29.65% (Figure 1c, Table 3). The factor represented by the experimental variant is positively correlated with the mobile phosphorus content of the soil for the corn crop in the hill-valley direction, at the top of the field (Figure 1c, Table 3).

The location of the crop is positively correlated with the mobile phosphorus content of the soil in the case of the alfalfa crop at the top of the field and in the case of plum grown on contour lines, at the base of plowed land at the top, as well as at the base of eroded land cultivated on the slope. The experimental variant factor is responsible for 44.18% of the variance and is positively correlated with the mobile potassium content of the soil in the case of alfalfa cultivation, at the top of the land and of maize cultivated in the hill-valley direction, also at the top of the eroded land on the slope (Figure 1d, Table 3).

CONCLUSIONS

The highest pH averages, indicating a slightly acidic reaction, are reported for the soil located at the base of the slope, but they do not differ statistically significantly at the 5% significance level from those reported at the top of the slope. The environments fall within the limits of 5.49 pH units - 5.85 pH units, corresponding to the

corn cultivation technology in the hill-valley direction, both at the top and at the base of the slope.

The highest soil nutrient content averages located in the experimental field are reported for the base of the slope: 1.92 ppm - 2.27 ppm for humus classified as supplied medium, 22.34 ppm - 29.31 ppm for mobile phosphorus classified in the poorly and medium supplied categories and 121.14 ppm - 129.89 ppm for mobile potassium in the poorly supplied category.

Regarding the culture, it is found that for the exploitation of the meadow, the highest values of the nutrient content are recorded, compared to the culture of corn, a fact also explained by the highest degree of water retention in the case of this technology, compared to those of the culture of corn.

Medium and strong correlations are identified between the indicators corresponding to the chemical properties of the soil. Two main factors were considered, namely the experimental variant and the location of the culture. The chemical indicators of soil quality are strongly influenced by the location of the crop, with the mention that, in this case, the location of the crop at the base of the slope has the strongest influence on them, but in the case of pH (soil reaction) and mobile phosphorus content the location at the top of the slope must also be considered.

REFERENCES

- Abbasi, M.K., Zafar, M., Khan, S.R. (2007). Influence of different land-cover types on the changes of selected soil properties in the mountain region of Rawalakot Azad Jammu and Kashmir. *Nutr. Cycl. Agroecosyst.*, 78(1), 97-110.
- Babur, E., Kara, Ö., Susam, Y.E. (2016). Determination of Some Physical and Chemical Properties, and Erodibility Indices of Bare Land Soils. *Journal of Batin Faculty of Forestry*, 8(2), 95-102.
- Biali, B., Cojocaru, P. (2016). Database search in a GIS application intended for mapping the use categories and anti-erosion systems in Antohesti water catchment area, Bacau County. *Scientific Papers. Series E. Land Reclamation, Earth Observation & Surveying, Environmental Engineering*, V, 115-122.
- Bílá, P., Šarapatka, B., Horňák, O., Novotná, J., Brtnický, M. (2020). Which quality indicators reflect the most sensitive changes in the soil properties of the surface horizons affected by the erosion processes? *Soil and Water Research*, 15(2), 116-124.

- Cojocaru, O. (2019). Ecosystem - reproduction of Sustainable structure in agriculture as a factor of soil fertility. *AgroLife Scientific Journal*, 8(1). <https://agrolifejournal.usamv.ro/index.php/agrolife/article/view/418>.
- Domuța, C. (2012). *Agrotechnics*. Oradea Publishing House, Romania [In Romanian].
- Domuta, C., Sabau, N.C. (2000). *Agrotechnics – practical works, part I*. Oradea Publishing House, Romania [In Romanian].
- Gabbasova, I.M., Suleimanov, R.R., Khabirov, I.K., Komissarov, M.A., Fruehauf, M., Liebelt, P., Garipov, T.T., Sidorova, L.V., Khaziev, F.K. (2016). Temporal changes of eroded soils depending on their agricultural use in the southern Cis-Ural region. *Eurasian Soil Science*, 49(10), 1204–1210.
- Govaerts, B., Sayre, K.D., Deckers, J. (2006). A minimum data set for soil quality assessment of wheat and maize cropping in the highlands of Mexico. *Soil and Tillage Research*, 87(2), 163–174.
- Havaee, S., Mosaddeghi, M.R., Ayoubi, S. (2015). In situ surface shear strength as affected by soil characteristics and land use in calcareous soils of central Iran. *Geoderma*, 237–238, 137–148.
- Imaz, M.J., Virto, I., Bescansa, P., Enrique, A., Fernandez Ugalde, O., Karlen, D.L. (2010). Soil quality indicator response to tillage and residue management on semi-arid Mediterranean cropland. *Soil and Tillage Research*, 107(1), 17–25.
- Merce, E., Merce, C. (2009). *Statistics-Consecrated Paradigms and Complete Paradigms* [In Romanian], AcademicPres Publishing House, Cluj-Napoca, Romania.
- Nael, M., Khademi, H., Hajabbasi, M.A. (2004). Response of soil quality indicators and their spatial variability to land degradation in central Iran. *Applied Soil Ecology*, 27(3), 221–232.
- Nosrati, K. (2013). Assessing soil quality indicator under different land use and soil erosion using multivariate statistical techniques. *Environ. Monit. Assess.*, 185, 2895–2907.
- Pintaldi, E., D’Amico, M.E., Stanchi, S., Catoni, M., Freppaz, M., Bonifacio, E. (2018). Humus forms affect soil susceptibility to water erosion in the Western Italian Alps, *Applied Soil Ecology*, 123, 478–483.
- Poesen, J. (2018). Soil erosion in the Anthropocene: research needs. *Earth Surf. Processes Landforms*, 84, 64–84.
- Rogobete, G., Grozav, A. (2011). Methods for assesment of soil erosion. *Research Journal of Agricultural Science*, 43 (3), 174–179.
- Sestras P., Mircea S., Cimpeanu S.M., Teodorescu R., Rosca S., Bilasco S., Rusu T., Salagean T., Dragomir L.O., Markovic R., Spalevic V. (2023). Soil Erosion Assessment Using the Intensity of Erosion and Outflow Model by Estimating Sediment Yield: Case Study in River Basins with Different Characteristics from Cluj County, Romania, *Applied Sciences-Basel*, 13(16), 19.
- Stavi, I., Lal, R. (2011). Variability of soil physical quality in uneroded, eroded, and depositional cropland sites. *Geomorphology*, 125(1), 85–91.
- Xiao-Li Liu, Yuan-Qiu He, H.L. Zhang, J.K. Schroder, Cheng-Liang Li, Jing Zhou, Zhi-Yong Zhang, (2010). Impact of Land Use and Soil Fertility on Distributions of Soil Aggregate Fractions and Some Nutrients. *Pedosphere*, 20(5), 666–673.
- <https://www.corteva.ro/produse-si-solutii/seminte-corteva/porumb-pio-neer-P0217.htm>
- <https://www.isric.org/>

COMPOSITE MATERIALS FOR ECO-SUSTAINABLE CONSTRUCTIONS

Adrian Alexandru CIOBANU¹, Aurelia BRADU¹, Andreea HEGYI²

¹National Institute for Research and Development in Construction, Urban Planning and Sustainable Spatial Development URBAN - INCERC, Iasi Branch, 37 Prof. Anton Sesan Street, Iasi, Romania

²National Institute for Research and Development in Construction, Urban Planning and Sustainable Spatial Development URBAN - INCERC, Cluj-Napoca Branch, 117 Calea Floresti, Cluj-Napoca, Romania

Corresponding author email: bradu_aurelia@yahoo.com

Abstract

This work aims to research and promote construction products based on natural raw materials. The study and promotion of traditional materials can represent an answer to the problem of carbon emissions. More and more specialized studies prove the fact that new, modern constructions can alter both our lifestyle, compromising our physical, mental and emotional health. The conclusions of the studies do nothing but reinforce the idea of the fact that returning to traditional materials, their re-assimilation in current constructive techniques and solutions, represents the right solution both for the environment and for us as individuals. Research involves development and experimental research to check the characteristics and performance of products made from natural raw materials (clay, lime, straw, hemp, wood waste in the form of sawdust) and various additions and/or additives in the lowest possible percentages, by studying some recipes different compositions, in order to optimize them from both a mechanical and hydrothermal point of view, depending on the areas of intended use.

Key words: adobe bricks, clay, sustainable development, traditional composites materials.

INTRODUCTION

Since the dawn of industrialization, technological advances have advanced rapidly, outstripping the ability of the planet's natural resources to support them. In the context of global warming, habitat destruction, poverty and other increasingly urgent socio-environmental problems, it becomes obvious that it is necessary to invest in sustainable development practices. According to the Brundtland Commission, sustainable development is defined as "development that meets the needs of the present generation without neglecting the ability of future generations to meet their own needs".

The renowned environmental analyst Lester R. Brown who introduced the concept of Eco-economy, in the book published in 2001, Eco-Economy: Building an Economy for the Earth, draws attention to the tendency to exhaust natural resources of energy, raw materials and food, consumption of renewable resources at a rate higher than their regeneration capacity and physical damage and pollution of vital environmental factors: water, air, soil, which

supports the need for innovation based on traditional - vernacular sources and the importance of developing the inhabited space in correlation with protecting the environment, Sustainable Development being seen as the "green solution" in the face of the ecological crisis determined by the intensive exploitation of natural resources that caused environmental degradation (Hegyi et al., 2021).

Innovative construction materials developed starting from the traditional - vernacular, find a significant place. Thus, the tendency is encouraged for traditional - vernacular architecture to no longer be seen as obsolete, outmoded, but to become a source of inspiration for innovation, all the more so as the benefits are known both in terms of the quality of constructions, the quality of the environment interior, low construction costs, at the same time with low maintenance costs and an appreciable contribution from the point of view of energy savings for maintaining thermal comfort in the living space. Last but not least, the advantages of this approach are also materialized at the level of the required resources - raw materials that are easily

accessible and can be processed with human resources that do not require special qualifications, allowing both communities from economically developed countries and less developed countries from the point of view economically, an efficient exploitation of own resources benefiting from the knowledge fence that exists worldwide but which can be easily adapted to the local specifics by exploiting the so-called "store of wisdom" of the place.

We can have a healthy life through healthy building materials. According to worldwide studies, we spend between 60 and 90% of our lives indoors, breathing 11,500 litres of air per day, which implies the need to ensure a favourable indoor climate.

The quality of the indoor environment is essential when it comes to the role of buildings on our health. And this indicator is composed of the following elements: natural light, noise, thermal comfort and indoor air quality (Calatan et al., 2014).

Using clay as a building material has many advantages, such as: it balances air humidity, maintains heat, saves energy and reduces environmental pollution, is reusable, reduces costs for materials and transport, is suitable for self-built houses, absorbs polluting agents (Cazac et al., 2011).

An important property of clay is the absorption and release of moisture to a greater extent than other building materials, which influences the balance of the indoor climate. Based on studies (Baughman & Arens, 1996), it was concluded that the humidity level, from the point of view of a healthy environment in inhabited rooms, should be a minimum of 40% and a maximum of 60%. Measurements made over a period of 8 years in a newly built house in Germany, with all external and internal walls made of clay, showed that the indoor relative humidity was consistently 50% throughout the year, with fluctuations between 5% and 10%, which signifies the existence of healthy living conditions with balanced humidity both during summer and winter (Cazac et al., 2011).

In countries whose economy is predominantly agrarian, the use of natural agricultural waste in construction products can have important advantages compared to the use of traditional materials, including reduced environmental impact, lower energy demand, lower costs,

availability at scale wide and good insulation properties (Yaashikaa et al., 2022; Rojas et al., 2019; Sanjay et al., 2018; Asdrubali et al., 2015).

The increase in production and consumption worldwide represents both a significant challenge for waste management and resource use and an opportunity as, by superior recovery of waste materials, industries can reduce waste disposal and related costs, reduce the consumption of conventional resources, thus participating in the development of the circular economy at a regional and global level.

It should also be stated that, not infrequently, the use of vegetable waste, as an addition or as a basic component, determines the obtaining of the new material/product at a lower production price compared to that of the traditional material/product, an important aspect in choosing the option to invest in manufacturing and bringing the innovative material/product to market.

At the national level, directions for the utilization of plant waste in constructions aim, on the one hand, at the superior utilization of some types of waste such as wood fibers or cereal waste, by obtaining innovative materials/products with thermal insulating characteristics, and on the other hand, obtaining bricks or masonry blocks, sound and thermal insulation boards, etc., and making load-bearing or non-load-bearing walls with these materials.

The use of hemp, apart from the general properties of plant fibers, is determined by its main specific characteristics, which include:

- The high growth rate of hemp crops, of 70-140 days depending on the degree of sunshine, are ecological, do not require herbicides, fertilizers or pesticides (Ahlberg et al., 2014);

- It consumes a significant amount of CO₂ during growth, with some studies indicating the existence of CO₂ consumption even after the plant has been put into operation. It is estimated that 1 m² of biocomposite based on hemp fibres, as a result of the carbonation of the lime in the composition, absorbs 14-35 kg of CO₂ over a lifetime of 100 years, actively participating in the reduction of greenhouse gases even during the period exploitation (Ezboziegbe & Mizi, 2013);

- It can be considered an inert material, the amount of CO₂ emitted during lime production being less than or at most equal to the amount of CO₂ consumed by plant growth (Ahlberg et al., 2014);

- Thermal and sound-insulating properties, permeability to air and water vapor and ability to regulate the humidity of the indoor environment, hemp dust - the woody, inner core of the stem, which remains after the fibers have been extracted for textile production - having various uses as building materials/products (Bruijn et al., 2008; Sinka & Sahmenko, 2013; Ahlberg et al., 2014).

Although straw is one of the oldest natural agricultural materials used in traditional Romanian constructions, nowadays they are gaining more and more ground in this field, but being used in modern forms in terms of straw processing technologies, installation techniques of construction, as structures, constructive systems, etc., resulting in straw bale houses - cheap, efficient and sustainable. The characteristics of straws include:

- Very low biodegradability compared to other agricultural residues, due to the high ratio of carbon vs. nitrogen (due to small amounts of nitrogen), especially in the case of rice and wheat straw (Bakker R. et al., 2013);

- Density between 81 - 106.3 kg/m³ for oat and wheat straw bales and between 54.6 - 78.3 kg/m³ for barley straw bales, the optimal density for wheat straw used in construction being 133 kg/m³ and for rice straw, 123.6 kg/m³ (McCabe, 1993; Watts et al., 1995);

- Permeability to vapours and liquid water, thus not needing the use of vapor barrier products. Also, they are a natural, ecological material, without negative effects on people's health.

Wood fibres (sawdust) present a series of general but also specific structural and chemical characteristics for this category of natural materials:

- From a chemical point of view, they are considered to be natural composites with a multilayered cellular structure, having as basic components cellulose - a natural polymer containing glucose units, hemicellulose - in turn a natural polymer made up of several polysaccharides and lignin - a mixture amorphous and heterogeneous of aromatic

polymers and phenyl-propane polymers (Pacheco-Torgal & Jalali, 2010);

-The technical characteristics of this type of vegetable materials vary with the nature of the fibre but, in principle, they have a tensile strength comparable to that of synthetic fibres, although they have a reduced modulus of elasticity (Pacheco-Torgal & Jalali, 2010);

- The structure of plant waste is a basic element of them, generally showing interest.

In the study, recipes were tested based on clay and lime matrices with embedded plant materials: straw, hemp and sawdust. A comparative study of the physico-mechanical characteristics of the obtained mixtures was carried out.

MATERIALS AND METHODS

For the experimentally tested samples, the following stages of raw material preparation were kept: homogenization, formwork preparation, casting, drying and conditioning. The recipes are shown in Table 1.

Table 1. Mixture components

Components	Units	R1	R2	R3
Clay	kg	20	20	20
Lime	kg	20	20	20
Straw	kg	2	-	-
Hemp	kg	-	4	-
Sawdust	kg	-	-	4
Water	l	6	9	9

Ensuring the connection between the fibers of natural insulating material (cereal straw, hemp dust and sawdust) and stabilization against biological degradation, was also achieved by embedding them in solutions of clay, lime and water in quantities established according to the recipes, acting as a binder, of bactericide, bio-preservation, protection and moisture stabilization.

The mixture was made by hand or mechanized (Figure 1), a stage followed by the incorporation of the materials used to cast the thermal insulation boards, based on straw and hemp. The clay solution - slaked lime paste, was obtained by mixing and homogenizing some amount of softened clay and lime paste with water, until a mud-like consistency was

obtained, on top of which the plant materials were added.



Figure 1. Preparation of the straw-based recipe mixture

The samples for the tests were cast in formwork systems made of chipboard, with dimensions necessary for the samples to determine the density, thermal conductivity and compression behaviour (Figures 2 and 3).



Figure 2. Filling the formwork with mixture

The behaviour of composite heat-insulating materials based on plant fibres in clay-lime matrix was studied by performing the following measurements:

- The determination of the density was carried out on samples dried at 80°C by the gravimetric method. The exact dimensions of the samples were measured with an accuracy of 0.01 mm. The mass was determined using a balance with an accuracy of 0.1 g;
- The determination of thermal conductivity and thermal resistance was carried out on samples dried at 80°C by the thermofluxmetric method;
- The determination of the compressive strength was achieved by applying a uniformly distributed and continuously increased load to the samples until failure.

The tests were carried out according to the references for tests specific to heat-insulating products, as well as those specific to masonry elements.



Figure 3. Appearance of cast samples

RESULTS AND DISCUSSIONS

The physico-mechanical characteristics of clay and lime-based mixtures with the addition of vegetable waste monitored in the experimental study are: apparent density, thermal conductivity and compressive strength.

The density was determined according to SR EN 1602:2013 - Thermally insulated products intended for use in buildings. Determination of apparent density.

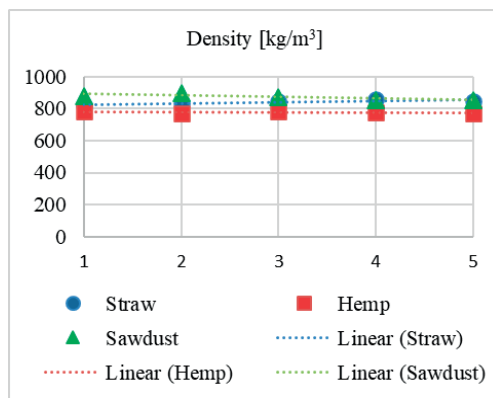


Figure 4. Density of hardened material

The samples were made in the form of cubes with dimensions of 150 x 150 x 150 mm, taken from heat-insulating composite material manufactured in the laboratory, based on lime, clay and the addition of local plant material. The obtained results are shown in Figure 4.

The apparent density (ρ_a) of the straw-added material varied between 820 kg/m^3 and 860 kg/m^3 , with an average of 840.4 kg/m^3 . The standard deviation from repeatability $sr = 18.5 \text{ kg/m}^3$, representing 2.2% of the average value ρ_a .

The apparent density of the material with the addition of hemp recorded the lowest values, these being between 768 kg/m^3 and 781 kg/m^3 , generating an average value of 775.4 kg/m^3 . Standard deviation from repeatability $sr = 5.6 \text{ kg/m}^3$, representing 0.7% of the average value ρ_a .

The highest average apparent density value – 871.8 kg/m^3 was obtained for the mixture with the addition of sawdust, the individual values being in the range of 852 kg/m^3 to 899 kg/m^3 . Standard deviation from repeatability $sr = 19.2 \text{ kg/m}^3$, representing 2.2% of the average value ρ_a .

The conductivity was determined according to SR EN 12667:2002 - Thermal performance of construction materials and products. Determination of thermal resistance by the guarded hot plate method and by the thermoflux meter method. Products with high and medium thermal resistance (Figure 5).



Figure 5. Testing thermal conductivity

Test pieces made in the form of plates with dimensions of $300 \times 300 \times 70 \text{ mm}$ taken from heat-insulating composite material manufactured in the laboratory, based on lime, clay and addition of local plant material. The experimentally determined values are shown in Figure 6.

The average thermal conductivity λ_{10} of the composite with the addition of straw recorded the lowest value of the tested mixtures - 0.1480 W/mK , the standard deviation from repeatability $sr = 0.0157 \text{ W/mK}$, representing 11.3% of the average value λ_{10} .

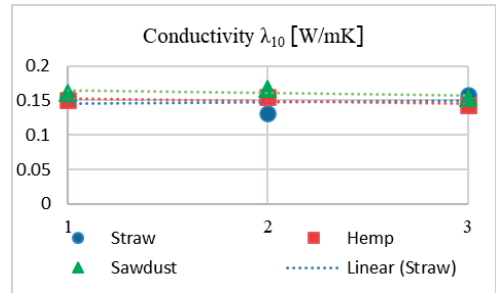


Figure 6. Thermal conductivity

The mixture with the addition of hemp marked a slightly higher average value of thermal conductivity λ_{10} – 0.1493 W/mK , standard deviation from repeatability $sr = 0.0045 \text{ W/mK}$, representing 3.04% of the average value λ_{10} .

The highest average value of thermal conductivity was determined on the samples with sawdust addition - λ_{10} – 0.1609 , the standard deviation from repeatability $sr = 0.0043 \text{ W/mK}$, representing 2.7% of the average value λ_{10} .

The compressive strength was determined according to SR EN 772-1+A1:2016 - Test methods for masonry elements. Part 1: Determination of compressive strength. The samples were subjected to compression with a loading rate of $0.05 \text{ (N/mm}^2\text{)/s}$ (Figure 8), the obtained values are reproduced in Figure 7.

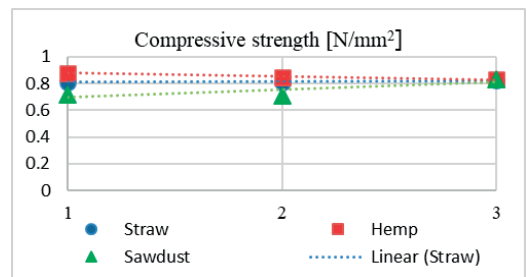


Figure 7. Compressive strength

The average value of the compressive strength (f_b) of the material with straw addition determined experimentally in the laboratory is

0.81 N/mm², the standard deviation from repeatability $sr = 0.004$ N/mm², representing 0.5% of the average f_b value. While the composite with hemp content recorded an average f_b value of 0.85 N/mm², the repeatability standard deviation $sr = 0.25$ N/mm², representing 2.9% of the average value f_b .

The compressive strength determined on the composite with the addition of sawdust marked an average value of 0.753 N/mm², the standard deviation from repeatability $sr = 0.08$ N/mm², representing 1.1% of the average value f_b .



Figure 8. Testing compressive strength

CONCLUSIONS

The use of natural agricultural waste in construction products is both a challenge for the construction materials industry. In this way, ecological materials can be produced, waste disposal costs can be reduced, the consumption of conventional resources reduced, participation in the development of the circular economy at regional and global level.

The utilization of natural agricultural waste in construction products presents a number of advantages compared to the use of traditional materials: reduced environmental impact, lower energy demand, low costs, wide availability and good insulation characteristics.

According to the results obtained in the experimental study, all three types of composites with the addition of vegetable waste: straw, hemp and sawdust presented similar values and a low degree of dispersion of the results.

Lower values of apparent densities specific to hemp-based materials are observed, followed by those based on sawdust, respectively straw.

The thermal conductivity maintains the same tendency of distribution of the results, the lowest values being recorded for materials based on hemp, compared to those from straw, respectively sawdust. Higher compressive

strength values are observed for sawdust-based materials compared to straw and hemp.

ACKNOWLEDGEMENTS

This paper was supported by the Program Advanced research on the development of eco-innovative solutions, composite materials, technologies and services, in the concept of a circular economy and increased quality of life, for a sustainable digitized infrastructure in a built and urban environment resilient to climate change and disasters, "ECODIGICONS", Program code: PN 23 35 03 01: "Integrated system of development and scientific research of constructions and vital infrastructures exposed to extreme seismic and climatic environmental actions and the exploitation of sustainable resources of materials and energy", financed by the Romanian Government.

REFERENCES

- Ahlberg, J., Georges, E., Norlén, M. (2014). The potential of hemp buildings in different climates. A comparison between a common passive house and the hempcrete building system, *UPPSALA University, Sweden*.
- Asdrubali, F., D'Alessandro, F., Schiavoni, S. (2015). A review of unconventional sustainable building insulation materials, *Sustain. Mater. Technol.* 4, 1–17
- Bakker, R., Elbersen, W., Poppens, R., Lesschen, J.P. (2013). Rice straw and Wheat straw - Potential feedstocks for the Biobased Economy, *NL Agency – Ministry of Economic Affairs*.
- Baughman, A., Arens, E.A. (1996). Indoor Humidity and Human Health--Part I: Literature Review of Health Effects of Humidity-Influenced Indoor Pollutants, *UC Berkeley: Center for the Built Environment*.
- Bruijn, P.B., Jeppson, K.H., Sandin, K., Nilson, C. (2009). Mechanical properties of lime-hemp concrete containing shives and fibres, *Biosystems Engineering*, 103, 474-479.
- Calatan, G., Hegyi, A., Mircea, C. (2014). Ecological Materials For Construction, *Geoconference On Nano, Bio And Green - Technologies For A Sustainable Future*, II: 89-96, SGEM.
- Cazac, O., Cazac, V., Sochircă, Ș. (2011). Folosirea lutului în tehnologiile moderne pentru Construcții, *Conferința Universității Tehnice a Moldovei UTM*.
- Eboziegbe, P.A., Mizi, F. (2013). Development of Wood-Crete building materials from sawdust and waste paper, *Construction and Building Materials*, 40, 361-366.
- Hegyi, A., Bulacu, C., Szilagyi, H., Lăzărescu, A.-V., Colbu, D.E., Sandu, M. (2021). Waste management in the context of the development of sustainable thermal insulation products for the construction

- sector, *International Journal of Conservation Science*, 12(1), 225-236, ISSN: 2067-533X.
- McCabe, J. (1993), The thermal resistivity of straw bales for construction. *Master's thesis. Department of Nuclear Engineering University of Arizona, Tucson, AZ.*
- Pacheco-Torgal, F., Jalali, S. (2010). Comenititous building materials reinforced with vegetable fibres: A Review, *Construction and Building Materials*, doi: 10.1016/j.conbuildmat.2010.07.024.
- Rojas, C., Cea, M., Iriarte, A., Valdes, G., Navia, R., Cardenas-R, J.P. (2019). Thermal insulation materials based on agricultural residual wheat straw and corn husk biomass, for application in sustainable buildings, *Sustain. Mater. Technol.* 20.
- Sanjay, M.R., Madhu, P., Jawaid, M., Senthamaraiannan, P., Senthil, S., Pradeep, S. (2018). Characterization and properties of natural fiber polymer composites: a comprehensive re-view. *J. Clean. Prod.*, 172, 566–581.
- Sinka, M., Sahmenko, G. (2013). Sustainable Thermal Insulation Biocomposites from Locally Available Hemp and Lime, *Environment. Technology. Resources Proceedings of the 9th International Scientific and Practical Conference*, 1, 73-77.
- Watts, K.C, Wilkie, K.I., Tompson, K. & Corson, J. (1995). Thermal and mechanical properties of straw bales as they relat to a straw house. *Canadian Society of Agricultural Engineering*, 209.
- Yaashikaa, P.R., Senthil Kumar, P., Varjani, S. (2022). Valorization of agro-industrial wastes for biorefinery process and circular bioeconomy: A critical review, *Bioresource Technology*, 343, 126126.

ECOLOGICAL RESTORATION OF NORWAY SPRUCE STANDS AFFECTED BY DRYING FROM OUTSIDE THE NATURAL RANGE

Cristinel CONSTANDACHE¹, Ciprian TUDOR^{1,2}, Valentina AGA^{1,2}, Laurențiu POPOVICI¹

¹Marin Drăcea National Institute for Research and Development in Forestry,
128 Eroilor Blvd, Voluntari, Ilfov, Romania

²Transilvania University of Brașov, Interdisciplinary Doctoral School, Romania,
29 Eroilor Blvd, Brașov, Romania

Corresponding author email: cipriantudor95@yahoo.com

Abstract

The forest plantations (Norway spruce, pine) installed outside the habitat are fragile, vulnerable ecosystems, exposed to some risk factors, registering significant damages. In the paper, the analysis of the environmental conditions of some lands with Norway spruce stands outside the habitat, affected by intense drying, and the substantiation of their ecological restoration solutions are presented. The results were obtained based on research carried out in 2023 in the area of the Suceava Plateau (Marginea Forest District). The physicochemical characteristics of the soils were strongly altered, having a low content of nutrients and minerals, with a contrasting texture, being poor in bases and heavy drainage, strong acidity, and affected by pseudo-glazing processes. The ecological restoration of Norway spruce stands affected by drying consists of replacing them with species corresponding to the environmental conditions, but only after carrying out special land and soil preparation works to improve its physical and chemical properties. The results obtained are particularly important considering the need for ecological restoration of large areas with Norway spruce stands outside the habitat, strongly affected by drying.

Key words: ecological restoration, environmental conditions, Norway spruce, drying; natural range.

INTRODUCTION

The resinous forest cultures (pines, Norway spruce) installed on the lands outside the natural range occupy important areas, being fragile and vulnerable ecosystems, exposed to some risky factors (drying, ruptures and windfalls, insect attacks and so on), in many situations registering important damages (Constandache et al., 2017; Vacek et al., 2023; Viljur et al., 2022).

These cultures were created starting from 1972 by substituting poorly productive or derived stands (with species of low economic value), being intended for the production of cellulose wood (Norway spruce) or for the production of rosin (pines). The resinous cultures outside the natural range (pure plantations with Norway spruce or pine) are functionally inferior to the substituted ones. The excessive artificialization of forest regeneration has created a certain discordance between the environmental diversity, on the one hand, and the genetic and ecological uniformity of pure resinous cultures, on the other, which reduces their polyfunctional effectiveness. Pure Norway spruce and pine

monocultures were created, endowed with a huge potential for ecological instability, their condition being aggravated by the fact that they were not covered with tending works necessary to strengthen their resistance to adversities (wind, snow, drought and so on) (Constandache et al., 2017).

In the course of their evolution, in the conditions of climate change and of the insufficient scientific substantiation of the afforestation and management works of stands, the risk of them being damaged by the action of disturbing factors appeared and increased before to reach the proposed cycle (Vlad et al., 2019). Some of the stands mentioned were strongly affected, in their youth, by breaks or felling caused by snow and wind. On the other hand, the drought of recent years has greatly worsened the situation of the resinous stands outside their natural range, the drying phenomenon of the Norway spruce being signalled on more and more extensive surfaces, especially after the age of 35-40 years (Constandache et al., 2023). In Central Europe, climate change is making extreme droughts more likely, Norway spruce being particularly

prone to drought-induced mortality through lack of carbon and water, increased susceptibility to pathogens (Rehschuh et al., 2017).

The extent of the damage caused to the resinous stands outside the natural range and the danger that this phenomenon represents in disrupting the ecological balance requires the adoption and application of complex measures aimed at the ecological restoration of the affected stands and the (gradual) return to the natural type of forest (Șenhofa et al., 2020).

The ecological restoration of natural ecosystems has favourable effects in increasing the biodiversity of forest ecosystems, diversifying ecosystem services (Aronson et al., 2006), restoring the landscape, as well as in regenerating and ensuring the continuity of the forest (Constandache & Dincă, 2019).

The replacement of resinous stands installed outside their natural range, must be scientifically substantiated, with great care to avoid new damages (Barbu et al., 2016).

The purpose of the conducted researches was to evaluate the pedological and environmental conditions of some lands with Norway spruce stands from outside the natural range, affected by intense drying and to substantiate their ecological restoration solutions based on the results of the performed research. The results were obtained on the basis of research on the ecological restoration of resinous stands from outside their natural range carried out in the period 2015-2018 and in 2023.

MATERIALS AND METHODS

The research was carried out in research plots, located in representative situations of Norway spruce stands affected by drying. The research plots were located in the area of the Suceava Plateau (Margeia Forest District, Suceava county - Figure 1).

The research consisted of observations, measurements, field data collection, soil analyses, their processing and interpretation. In order to highlight the effect of the limiting factors for forest species, the pedological and environmental conditions were analyzed, starting from the fact that the physical environment of terrestrial ecosystems is the site (ecotope) and the soil represents one of its most important components (Spârchez et al., 2011).

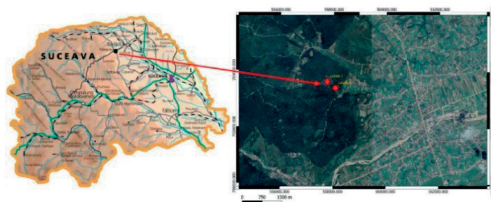


Figure 1. Location of the studied land

For the characterization of the soil in the researched lands, the depth, the groundwater level, the thickness of the horizon with humus (A), the depth at which the horizon C appears, the texture and other characteristics that limit or impose special techniques for the installation and development of new forest cultures were taken into account.

The soil type was determined through field works (soil description on type sheets) and with the help of laboratory analyzes of samples collected on diagnostic horizons from soil profiles.

In order to characterize the soils, main soil profiles and surveys were carried out at distances of approximately 20 to 30 m, in order to determine the change in the soil profile, the plots related to the main profile being delimited. From the main profiles, soil samples were collected on diagnostic horizons. The collected soil samples were analyzed in the "Marin Drăcea" INCDS laboratory, the main chemical and physical properties of the soil being determined: pH, humus, carbonate content, total nitrogen, mobile potassium, degree of saturation in bases (V) and the granulometric fractions which conditionate the trophicity and fertility of the soil. The other characteristics (structure, colour and so on) were determined organoleptically.

The substantiation of the ecological restoration solutions was made based on the analysis of the data related to the relief, lithology, climate, soil and in particular, the limiting factors for the forest vegetation being established in order: the techniques of land and soil preparation, planting of cultures and the species that corresponding with the environmental conditions.

RESULTS AND DISCUSSIONS

The stands/lands studied are located in the north-eastern area of Romania, respectively in

the Suceava Plateau. The forest area of both hill and plateau is interspersed with the mountain-premontane storey of beech stands and the hilly one of oak stands with sessile, Greyish and Hungarian oak. From the analysis of climate data, it follows that the "De Martonne" annual aridity index, having a value of 31.87, corresponds to the humid temperate climate domain, with a humid climate and sufficient precipitation for vegetation and a slight surplus of water from precipitation compared to potential evapotranspiration. This highlights the fact that, from a climatic point of view, the studied territory offers favourable conditions for the development of forest vegetation specific to hill highroads.

In terms of forest vegetation, in the studied area, mostly Norway spruce stands were identified at the border or outside their natural range, but also pure beech and mixed stands with hornbeam, sycamore, Silver fir, Norway spruce (at higher altitudes).

The Norway spruce stands were planted in the 1970s, currently being severe affected by drying (Figure 2).



Figure 2. Norway spruce stands affected by drying
(Unit Production I, Codrul Voievodesei, management unit 16E%)

From previous analyzes it was established that this phenomenon is due to the combined action of severe droughts (from the periods 2011-2012, 2020-2022) and xylophagous insects (*Ips typographus*, *Ips amitinus*, *Ips duplicatus* si *Pityogenes chalcographus*).

The lands from which the stands affected by the drying were extracted are strongly sodded (*Calamagrostis* sp., *Brachipodium* sp., *Poa* sp. and another gramineae) with height over 1 meter

(Figure 3), forming a dense layer of roots in the first 10 to 15 cm of the soil, so that the water from the precipitation below 10 mm is fully retained in the organic substrates on the soil surface. These gramineae species indicate soils poor in bases and rich in acids.



Figure 3. Herbaceous vegetation on the site of the former stands

We identified two representative pedological and environmental situations as follows:

- flat or lowland sites (bumps, low hollows) which it favours the water stagnation during precipitation periods, being predominant (2/3 from the total surface);
- sloped lands or with microrelief having positive and elevated shapes.

The results of laboratory chemical analyzes (Table 1) show that the analyzed soils have a low content of nutrients and minerals, are soils poor in bases, strongly acidic and the physical properties are strongly altered (soils with a contrasting texture, with poor drainage, hardly permeable). Since the external and internal drainage are deficient due to the reduced slope of the land and low permeability for water and air of the Bt (argic) horizon, these soils are frequently affected by the periodic excess of stagnant water, causing the accentuation of pseudogleyization processes. In addition to these unfavorable physical factors, there is also a strong sodding of the soil.

In general, the analyzed soils are both weakly humic in the first horizon (1.46 to 2.02%) and in depth. The same evolution is presented by the nitrogen content (maximum 0.078% being very weakly supplied). Potassium increases steadily on the profile, from 30.03 ppm (weak provision) in the surface horizon (5-25 cm) to 129.10 ppm

(medium insurance) at a depth of over 70 cm. The soil reaction is strongly acidic ($\text{pH} = 4.67\text{--}4.78$) up to a depth of 45–50 cm, after which it becomes moderately acidic ($\text{pH} = 5.18\text{--}5.27$) in depth.

The granulometric analysis (Table 1) shows that the soil texture is Medium (M), Sandy Loam class (S), Dusty subclass (SP) in the first 25–45 cm. Sometimes there is also an intermediate horizon (Ea), where the texture belongs to the Sandy Loam class (S), Sandy-dusty Loam subclass (SS). At a depth greater than 45–50 cm, the texture becomes Fine (F), Clay Loam class (T), Clay and Dusty subclass (TP) (Florea & Munteanu, 2012) where a sudden textural change occurs between horizons (between A/B or Ea and Btw). The clay content increases from 18.2–20% to 25.1%, and in gypses (areas with lower lands) even to 36.7%. At more than 70 cm, the clay content reaches 39.5%, being specific features of the pseudogleyization process. No micro-biological activity was observed.

The characteristics of the soil analyzed in the two profiles determined the inclusion in the class luvisols (argiluvissols), the types of soil being:

1. *Planosol, stagnant subtype* - representative for approx. 2/3 of the land area under study; the light-textured surface horizon becomes hard at dryness, but is not cemented; the sudden change in clay content from the surface horizon to the underlying one is largely caused by the ferrolysis process, respectively a destruction of clay minerals in conditions of alternating wet periods with dry periods. The clay subsoil has a polyhedral structure developed in blocks and prismatic (Figure 4), or it is even massive (destructured). The low permeability of the subsoil is the cause of water stagnation in the surface horizons, which leads to the worsening of internal drainage and aeration conditions, to the accentuation of pseudogleyization processes, considered an important limiting factor.

Chemically, planosols are altered soils: the cationic exchange capacity of the clay fraction in the surface layers and in the eluvial horizon is significantly lower than in the underlying horizons.

2. *Luvisol, the albic-stagnant subtype* (albic pseudogleyized luvisol), for the rest of the plots; they are moderately to strongly texturally differentiated soils, with unfavourable

aerohydric properties on the profile. They are weakly fertile soils, with a low humus content, with a pH of 5 to 5.5, sometimes even 4.5 (in the albic subtypes). The degree of saturation in the bases is lower (60%) and in the Ea horizon it can have values of 15 to 20%.



Figure 4. The structure of soil profiles

The physical and chemical characteristics of the soils have been strongly altered under the effect of Norway spruce stands and as a result of improper silvotechnology. The analyzed soils have a low content of nutrients and minerals, are poor in bases, strongly acidic, have a contrasting texture, poor drainage and are hardly permeable. Since external and internal drainage are deficient due to the reduced slope of the land and low permeability for water and air of the Bt (argic) horizon, these soils are frequently affected by the periodic excess of stagnant water, causing the accentuation of pseudogleyization processes (Btw horizon). Acidity (strongly acidic pH) represents another limiting factor for forest vegetation, in the case of the two soil types determined. On acidic soils, there is a solubilization of aluminium and manganese from the soil in toxic amounts for plants. Another limiting factor is added to these: the strong sodded of the soil following the drying or thinning of the Norway spruce stands. These characteristics determine the need for special works of:

- land preparation (clearing the land of herbaceous vegetation, removing stumps);
- preparation of the soil (scarification at great depths, plowing, discing) for the stimulation of ascending water processes, the limitation of the stagnant one and the improvement of the physical properties of the soil;
- pedo-ameliorative works (application of calcium amendments and complex fertilizers).

The land and soil preparation works have the role of improving the physical properties of the soil, preventing water stagnation and limiting the stagnant water process, ensuring the minimum conditions for the installation of forest cultures and the pedo-ameliorative ones, have the purpose of improving the pH, the structure of the soil, the microbiological activity in the soil, to accelerate the decomposition of the organic matter in the soil and so on.

The ecological restoration of the researched Norway spruce stands, strongly affected by drying, consists in replacing them with species corresponding to environmental conditions, but only after a minimum of one year after carrying out the special land preparation, soil and pedo-ameliorative works.

The degree of correspondence (suitability) of the edificative composition of trees species for certain environmental conditions is expressed by the Ellenberg Coefficient (EQ), calculated according to the formula:

$$EQ = Tw/P * 1000,$$

where:

- Tw is the temperature of the hottest month of the year;

- P is the annual precipitations.

The data presented in the specialized literature show that various EQ values indicate specific climatic conditions for the growth and development of a certain type of forest. The value of this coefficient for the researched area is 33.27 (EQ between 30 and 40), being characteristic of mesophyll oak forests or other species of oaks (Nedealcov et al., 2019). Therefore, mesophilic species from the *Quercus* Genus, with high amplitude and adaptability to climatic conditions, will be associated in the forest composition (Șofletea & Curtu, 2007).

Therefore, the afforestation composition recommended for the ecological restoration of Norway spruce stands affected by drying is with deciduous species corresponding to the phytoclimatic storey and whose ecological requirements can be satisfied by improved pedological and environmental conditions, respectively: 70% Sessile Oak and 30% Wild Pear, Field Maple, Pennsylvanian Ash, shrubs (Pennsylvanian Ash will be introduced into hollow, in biogroups) (MMAP, 2022).

In the hilly sites, characterized by the presence of slight unevenness and small depressions, on slightly inclined slopes, sensible different vegetation conditions are achieved for resinous species, in the sense that the negative microrelief, due to the temporary stagnation of water and pseudogleization phenomena, becomes inappropriate for the introduction of them. This mosaic of environmental conditions leads to a non-uniformity of resinous stands.

The sites where some ecological factors occur in excess (heavy texture, temporary excess of humidity, windy sites) are contraindicated for the installation of intensive resinous cultures, especially with species sensitive to these factors, such as Norway spruce, Douglas fir (Radu et al., 1975). Medium-porosity, well-ventilated, weakly skeletal soils with sufficient moisture are favorable to Norway spruce. Actively draining, stony, sandy soils are much more favorable to it than heavy, slow-draining ones. Even if in the presented situations it supports podzols, it transforms them by accumulating raw humus that is mostly hard to decompose, raising the acidity of the upper horizons of solichides. In fact, due to its litter deposited in thick and felty layers, which decomposes with difficulty and imperfectly, the artificially installed Norway spruce cultures contributed decisively to the acidification of the soils on which it was installed. In these conditions, a large part of the mineral elements remained blocked in the partially decomposed organic substance (Șofletea & Curtu, 2007). The inadequate current state of the Norway spruce stands outside the area was also due to the lack of adaptation to a symbiotic nutrition with mycotrophic fungi for which the environment created by luvisols is unsuitable for their development. The efficiency of the fungus-plant association is determined by the adaptability of the fungal partner to a certain soil pH level. The pH affects both spore germination and their development. The low pH and the low amounts of assimilable phosphorus in the soil resulted in insufficient development of mycorrhizae (Stoian, 2015). Poor soil fertility is one of the limiting factors for the normal development of forest vegetation and the ecological restoration of stands is necessary (Constandache et al., 2022).

Table 1. The chemical and physical characteristics of the soil in Norway spruce stands outside the natural range (Margeia Forest District)

Identification		pH	Ht %	Nt %	Km ppm	SH me/ 100 g	SB me/ 100 g	T me/ 100 g	V %	Granulometry		
Horizon	Depth (cm)									Sand (% gr*)	Silt (% gr*)	Clay (% gr*)
Ao	5-25	4.78	2.02	0.078	30.03	4.5	3.7	8.2	45.1	31.6	53.1	15.3
A/B	26-45	4.67	1.28	0.065	36.70	6.5	5.6	12.1	46.3	27.2	54.6	18.2
Btw1	46-70	5.18	0.55	0.021	94.17	5.5	11.4	16.9	67.5	20.0	43.3	36.7
Btw2	> 70	5.27	0.91	0.035	129.1	5.6	14.8	20.4	72.5	18.2	42.3	39.5
Ao	0-25	4.68	1.46	0.056	26.46	6.9	3.4	10.3	33.2	21.8	53.8	24.4
Ea	26-50	4.70	0.94	0.036	23.69	5.7	3.2	8.9	36.2	30.7	49.3	20.0
Btw1	51-80	5.06	0.41	0.016	37.49	5.6	6.8	12.4	55.1	31.6	43.3	25.1
Btw2	> 80	5.12	0.22	0.008	36.57	5.7	9.0	14.7	61.4	32.8	39.4	27.8

Note: *colloidal clay<0.002 mm; coarse sand = 2.0-2 mm; fine sand = 0.2-0.063 mm; silt = 0.063-0.002 mm; Ht - total humus; Nt - total nitrogen; Km - mobile potassium; SH - the sum of hydrogen cations; SB - the sum of basic cations; T - troficity; V - the degree of saturation in bases.

CONCLUSIONS

The researches carried out highlights the fact that the Norway spruce stands from the outside of the natural range, created during the 70's, are currently strongly affected by drying. The stability of the Norway spruce stands from outside the natural range is threatened by different abiotic (climatic changes, pedological and environmental conditions) and biotic (insects, fungi and invasive plants) factors with great power to destabilize the stands. The magnitude of the damage caused to the resinous stands from outside the natural range and the danger that this phenomenon represents in disrupting the ecological balance, requires the adoption and application of complex measures aimed at the ecology of the affected stands and the (gradual) return to the natural type of forest. The results of the research consisted in the analysis of the pedological and environmental conditions of the lands with Norway spruce stands affected by drying and the scientific substantiation of the afforestation compositions for their ecological restoration. In order to highlight the limiting factors for the forest species that will be introduced, the pedological and environmental conditions were analyzed, starting from the fact that the physical environment of terrestrial ecosystems is the site (ecotope) and the soil is one of its most important components. As limiting factors for the culture of forest species, the following were identified:

- the strong acidity of the soil;
- reduced content of nutrients and minerals;
- the presence of an argic horizon with low permeability for water and air, which hinders

internal drainage and causes the accentuation of pseudoglayzation processes;

- strong weeding of the soil.

The presence of these limiting factors determines the need to apply special works of: land preparation (clearing the land of herbaceous vegetation, removing stumps); soil preparation (scarification at great depths, plowing, discing) for stimulating water processes, limiting the stagnant water process and improving the physical properties of the soil; the application of calcium amendments and complex fertilizers, with the aim of reducing acidity and improving the chemical properties of the soil.

The species recommended for the ecological restoration of Norway spruce stands affected by drying are indigenous deciduous species, predominantly from the *Quercus* Genus, with high amplitude and adaptability to climatic conditions and whose ecological requirements can be satisfied by improved pedological and environmental conditions.

ACKNOWLEDGEMENTS

This research work was carried out with the support of National Forest Administration Romsilva and was financed from Project no. 15.3/2015-2018 (Ecological restoration and regeneration of resinous stands from outside the natural range) and contract no. 16071/03.08.2023/Suceava Forest District (Pedological and environmental study in order to establish the technical afforestation solutions for an area of 14.99 hectares, located in management unit 16E%, 16N% and 16O%,

Production Unit I Codrul Voievodesei – Marginea Forest District).

REFERENCES

- Aronson, J., Aguirre, N., & Muñoz, J. (2010). Ecological Restoration for Future Conservation Professionals: Training with Conceptual Models and Practical Exercises. *Ecological Restoration*, 28(2), 175-181.
- Barbu, I., Barbu, C., Curcă, M., & Ichim, V. (2016). *Adaptation of Romanian forests to climate change*. Bucharest, RO: Forestry Publishing House.
- Constandache, C., Dincă, L., & Tudose, N.C. (2017). The vulnerability to climate changes of pine forest cultures from outside their natural range. In *VIII International Scientific Agriculture Symposium, "Agrosym 2017", Jahorina, Bosnia and Herzegovina, October 2017. Book of Proceedings*, 2605-2610. Faculty of Agriculture, University of East Sarajevo.
- Constandache, C., & Dincă, L. (2019). The management of pine stands situated outside their habitat. *Scientific papers series "Management, Economic Engineering in Agriculture and Rural Development"*, 19(4), 59-65.
- Constandache, C., Tudor, C., Popovici, L., & Dincă, L. (2022). Ecological reconstruction of the stands affected by drought from meadows of inland rivers. *Scientific Papers. Series E. Land Reclamation, Earth Observation & Surveying, Environmental Engineering*, XI.
- Constandache, C., Tudor, C., Popovici, L., & Vlad, R. (2023). The state and behaviour of some forestry cultures installed on degraded lands in the forest-steppe site. *Scientific Papers, Series E. Land Reclamation, Earth Observation & Surveying, Environmental Engineering*, XII, 215-223.
- Florea, N., & Munteanu, I. (2012). *Romanian Soil Taxonomy System (SRTS)*. Craiova, RO: Sitech Publishing House.
- Nedealcov, M., Donica, A., & Grigoraș, N. (2019). Expressing the vulnerability of forests to climate aridification through ecoclimatic indices (case study). „Akademos” Science, Innovation, Culture and Art Magazine, 55(4), 57-63.
- Radu, S. (1975). Establishing the technology for the creation and maintenance of intensive resinous cultures for the production of cellulose wood. *Studies and researches*.
- Rehshuh, R., Mette, T., Menzel, A., & Buras, A. (2017). Soil properties affect the drought susceptibility of Norway spruce. *Dendrochronologia*, 45, 81-89.
- Šēnhofa, S., Katrevičs, J., Adamovičs, A., Bičkovskis, K., Bāders, E., Donis, J., & Jansons, Ā. (2020). Tree damage by ice accumulation in Norway Spruce (*Picea abies* (L.) Karst.) stands regarding stand characteristics. *Forests*, 11(6), 679.
- Spârchez, Gh., Târziu, D., & Dincă, L. (2011). *Pedology*. Brașov, RO: Lux Libris Publishing House.
- Stoian, H.V. (2015). Vesicular and arbuscular mycorrhizal symbioses– a brief review. *Forestry Magazine*, 75-76(3), 19-32.
- Șofletea, N., & Curtu, L. (2007). *Dendrology*. Brașov, RO: "Transylvania" University Publishing House.
- Vacek, Z., Vacek, S., & Cukor, J. (2023). European forests under global climate change: Review of tree growth processes, crises and management strategies. *Journal of Environmental Management*, 332, 117353.
- Viljur, M.L., Abella, S.R., Adámek, M., Alencar, J.B.R., Barber, N.A., Beudert, B., ... & Thorn, S. (2022). The effect of natural disturbances on forest biodiversity: an ecological synthesis. *Biological Reviews*, 97(5), 1930-1947.
- Vlad, R., Constandache, C., Dincă, L., Tudose, N.C., Sidor, C.G., Popovici, L., & Ispravnic, A. (2019). Influence of climatic, site and stand characteristics on some structural parameters of scots pine (*Pinus sylvestris*) forests situated on degraded lands from east Romania. *Range Mgmt. & Agroforestry*, 40(1), 40-48.
- ***MMA, (2022). *Technical norms regarding the compositions, schemes and technologies of forest regeneration and afforestation of degraded lands*, The Order of Ministry of the Environment, Waters and Forests no. 2.533/2022.

USING EXPIRED DRUGS AS ENVIRONMENTALLY FRIENDLY CORROSION INHIBITORS

Claudia Alice CRIȘAN, Horațiu VERMEȘAN

Technical University of Cluj-Napoca, Department of Environmental Engineering and Sustainable Development Entrepreneurship, 28 Memorandumului Street, Cluj-Napoca, Romania

Corresponding author email: claudia.crisan@imadd.utcluj.ro

Abstract

Hazardous waste management is one of the problems our society is facing today. Expired drugs are a type of waste that is not reused in any way, but rather incinerated to be disposed of. These drugs have been proven to act as corrosion inhibitors for different metals and in different corrosive solutions. They are a good alternative to the synthetic inhibitors the industry uses today, due to their environmental friendliness, good corrosion inhibitor efficiency and economic advantages. The present research focuses on expired drugs as corrosion inhibitors for mild steel in concentrated sulfuric acid solution and characterize their inhibitive performance through weight loss measurements, Electrochemical Impedance Spectroscopy (EIS) spectra, and cyclic voltammetry (CV). The drug proved to be effective environmentally friendly corrosion inhibitor for mild steel, being a possible way of recycling expired drugs.

Key words: expired drugs, hazardous waste, green corrosion inhibitor, industrial pickling.

INTRODUCTION

One of the most important steps in mild steel (MS) manufacturing is the surface cleaning process, often done by acid pickling. This process generates an important quantity of industrial waste, exhausted pickling solutions (ESP) that contain high concentrations of metal ions (Gao et al., 2021). The two main solutions used for pickling are hydrochloric and sulfuric acid dilutes with water in a 1:1 ratio (Zaferani et al., 2013). This work focuses on using hydrochloric acid as a pickling liquor.

Literature reports show that the EU generates 0.38 million m³/year compared to the USA's 1.89 million m³/year (Agrawal & Sahu, 2009), managing EPS being a significant environmental concern that the metal manufacturing sector is currently facing. The higher metal concentration within the ESP is caused by the corrosion phenomena that occurs throughout the pickling process. The most common strategy used to manage this phenomenon is to add corrosion inhibitors to the acid solution (Deflorian et al., 2019; Predko et al., 2021).

Due to environmental awareness and stricter guidelines, green corrosion inhibitors have been explored as an alternative to the synthetic chemicals that have been and are presently used

for corrosion inhibition. These synthetic compounds are more expensive and damaging to the environment, while being as effective if not less effective than their eco-friendly counterparts (Chaubey et al., 2021).

Several substances, including plant extracts (Verma et al., 2023), carbohydrates (Seddik et al., 2024), natural polymers (Timothy et al., 2023), ionic liquids (Souza et al., 2023), amino acids (Seddik et al., 2024), and medicinal substances (drugs) (Verma et al., 2021), have been designated as "green corrosion inhibitors". Research shows that adsorption is the main mechanism by which these compounds protect the metal surface, the existence of double bonds, phenyl rings, heteroatoms (N, S, and O) (Quraishi et al., 2021), and other functional groups facilitate their ability to adsorb on the metal substrate effectively inhibiting the corrosion phenomenon, thus lowering the metal ion concentration found the resulted pickling sludge.

There is extended research on expired drugs used as corrosion inhibitors for multiple experimental conditions (e.g. hydrochloric acid, sulfuric acid aluminium, mild steel, copper etc.) (Tanwer & Shukla, 2022). However, the subject is far from being exhausted due to the complexity of the inhibition mechanism of drug

molecules and the limitation of their solubility in polar solvents. Drug molecules prevent corrosion by creating a protective coating by adsorption, however this process is extremely complicated and highly dependent on the characteristics of the metals and electrolyte (Iroha & James, 2019).

In addition, the absence of defined recycling guidelines and procedures has made it difficult to recycle old medications. There are standards for disposing of outdated medications in homes but incinerating them is the only safe way to remove these chemicals which poses concerns to the environment as well (Luo et al., 2021).

There have been reports of metamizole sodium being used as a corrosion inhibitor for carbon steel in 1M hydrochloric acid solution (Salem et al., 2022) and of caffeine being successfully used as a green corrosion inhibitor for copper in 0.1M aerated sulfuric acid solution medium (Souza et al., 2012). However, there have been no reports on the possible synergistic relation between these two substances. The aim of this work is to evaluate the inhibition efficiency of the expired Quarelin drug, which contains metamizole sodium, caffeine and drotaverine hydrochloride (Figure 1) as active substances. The presence of multiple double bonds, sulphur oxygen, nitrogen as well as multiple aromatic cycles shows the multiple adsorption sites through both chemisorption and physisorption. Expired drugs are considered eco-friendly, nontoxic, and non-bioaccumulative which makes Quarelin a good potential green corrosion inhibitor.

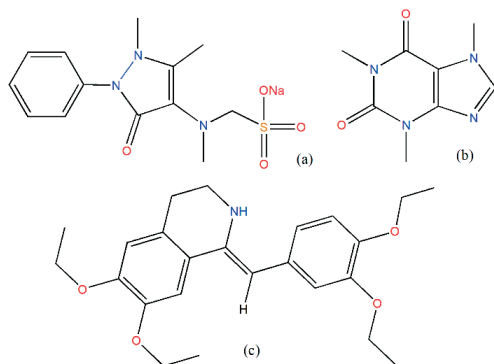


Figure 1. Chemical structure of metamizole sodium (a), caffeine (b), drotaverine hydrochloride (c)

MATERIALS AND METHODS

Expired Quareline since 2021 has been used in this study. It is a pain medication often used in the case of headaches. According to the drug insert one Quarelin tablet contains 400 mg metamizole sodium (an analgesic substance), 40 mg drotaverine hydrochloride (a spasmolytic substance) and 60 mg caffeine as active substances. The drug also contains several excipients such as cornstarch, polyvidone, microcrystalline cellulose, magnesium stearate and talc. In this study three concentrations of expired Quarelin were used and the active substance quantities are presented in Table 1.

Table 1. Active substance quantities

Quarelin conc. (ppm)	Metamizole sodium (mg)	Drotaverine hydrochloride (mg)	Caffeine (mg)
200	8	0.8	1.2
250	10	1	1.5
300	12	1.2	1.8

For the experiments coupon of mild steel were used with the dimension of 25 mm x 25 mm x 0.01 mm. Before the coupons were immersed in the acidic media (HCl:H₂O 1:1, 5.6M) the surface was cleaned, polished with emery sheets, washed with ethanol and dried.

The easiest and cost-efficient method of calculating inhibitor efficiency is the weight loss method, in which the samples are initially weighted, immersed in the acidic media containing different inhibitor concentration for a predetermined time, taken out washed dried and weighted again. For this study, concentrations of 200, 250, 300 ppm of expired Quarelin were used and the immersion time was 8h. Every 2h the coupons were removed from the pickling solution, rinsed with water to remove the corrosion products, dried with hot air and weighted in order to observe the evolution of mass. With the help of this experimental data corrosion rate and inhibitor efficiency calculation were carried out by using Eq. (1) and Eq. (2):

$$CR = \frac{\Delta m}{tS} \quad (1)$$

$$IE_{WL} = \frac{CR_B - CR_I}{CR_B} \times 100 \quad (2)$$

where:

- Δm is the mass loss difference (g),
- t is the time of immersion (h),
- S the surface of the coupon (cm^2),
- CR_B/CR_I the corrosion rate in the absence/presence of the inhibitor ($\text{g}/\text{cm}^2\text{h}$).

The electrochemical system used was a three-cell electrode in which 100 mL of electrolyte solution was used. Working MS electrodes were prepared prior to each experiment by abrading with 1200 emery paper, introduced in an ultrasonic bath in ethanol and dried. As an auxiliary electrode platinum was used and the reference electrode was Ag/AgCl.

Electrochemical impedance spectroscopy (EIS) was carried out with a OrigaFlex 500 potentiostat interfaced with a computer using the OrigaMaster5 software for data acquisition and analysis. The EIS spectra were drawn at a frequency range of 10 kHz to 10 mHz, 5 per decade with an AC amplitude of ± 10 mV. The inhibition efficiency (IE_{eis}) was calculated using Eq. (3) from the polarization resistance determined from the Nyquist plots.

$$IE_{EIS} = \frac{R_p - R_p^B}{R_p} \times 100 \quad (3)$$

where:

- R_p and R_p^B are the polarization resistance with and without the inhibitor present.

Potentiodynamic polarization (PDP) curves were drawn from -500 mV to +500mV vs the corrosion potential. In this case the inhibitor efficiency was calculate with Eq. (4).

$$IE_{Taf} = \frac{I_{corr} - I_{corr(inh)}}{I_{corr}} \times 100 \quad (4)$$

where:

- I_{corr} and $I_{corr(inh)}$ are the corrosion currents in the absence/presence of the inhibitor.

RESULTS AND DISCUSSIONS

The wight loss methos can be used for any metal or alloy that is readily available for purchase, and it is an extremely flexible method of corrosion monitoring. Table 2 shows the change in weight loss between each measurement while Figure 2 shows the corrosion rate evolution.

Table 2. Weight loss experimental data for MS immersed in HCl with different concentrations of expired Quarelin

Time [h]	Expired Quarelin concentration [ppm]			
	Blank	200	250	300
0	4.9574	4.9345	5.0687	5.0489
2	4.9250	4.9136	5.0506	5.0372
4	4.8898	4.8915	5.0332	5.0246
6	4.8607	4.8747	5.0206	5.0124
8	4.8404	4.8664	5.0181	5.0069
IEWL %	-	38.83	51.18	63.81

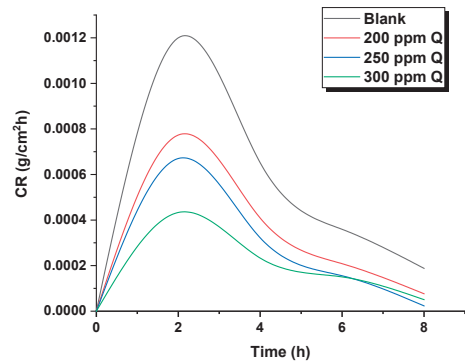


Figure 2. Corrosion rate evolution

The highest inhibitor efficiency was obtained at 300 ppm inhibitor concentration. The reason for this could be that the inhibitor molecules have adhered to the surface of the MS, delaying the metal's breakdown in the corrosive solution. Moreover, the heteroatoms in the molecule enhanced corrosion resistance and facilitated adsorption to the metal surface as other studies have mentioned (Salem et al., 2022).

After the inhibitor has been consumed due to the electrochemical reactions that take place at the metal surface and the repeated batched pickled during and industrial process, the corrosion rate starts to increase. Such increase cannot be seen in the case of this experiment. Further investigations should be carried out with bigger time frames in mind.

The Nyquist diagrams for MS in hydrochloric acid 5.6M with different concentration of expired Quarelin drug are shown in Figure 3 and the equivalent circuit obtained by fitting the EIS data is presented in Figure 4.

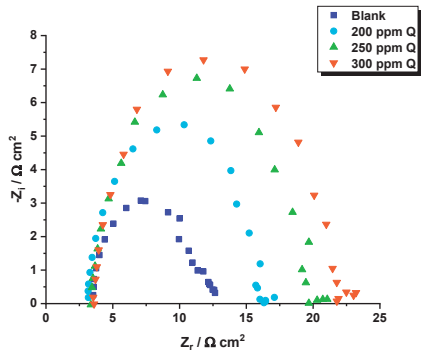


Figure 3. Nyquist plots for MS immersed in HCl solution with different expired Quarelin concentrations



Figure 4. Equivalent circuit used for fitting EIS data

This circuit is composed of a resistance representing the solution (R_s), the polarization resistance (R_p) and a constant phase element (CPE) used instead of a capacitor (C_{dl}) for a better fitting with the help of ZView 3.0 software. The values for the double layer capacitor (C_{dl}) are derived from CPE parameters and were calculated with Eq. (5) and Eq. (6) as previously described by Brug et al. (1984).

$$Z_{CPE} = [Y(j\omega)^n]^{-1} \quad (5)$$

where: $\omega = 2\pi f$ the angular frequency, $j = \sqrt{-1}$ the imaginary unit, Y is the magnitude of the CPE and n is a fitting parameter with values between 0 and 1, which measures the element deviation from the ideal capacitive behavior (in the case of $n = 1$)

$$C_{dl} = (R^{1-n}Y)^{1/n} \quad (6)$$

Using the potentiodynamic polarization (PDP) method, additional electrochemical evaluation of the corrosion of the MS surface in 5.6M HCl with and without expired Quarelin dosage was performed, as illustrated in Figure 5.

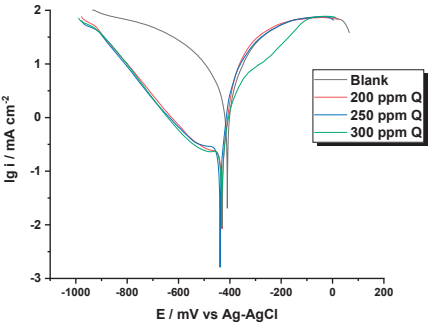


Figure 5. PDP curves for MS in HCl solution with different expired Quarelin concentrations

Table 3 displays the electrochemical parameters for MS immersed in HCl solution when expired Quarelin is added as a green corrosion inhibitor. Calculating the inhibitor efficiency, it is clear that this parameter rises as the concentration of the inhibitor rises, matching the general pattern of most green corrosion inhibitors.

The parameters determined by the Tafel method such as i_{corr} , E_{corr} , β_a , β_c and IE_{Taf} are included in Table 4. The values show that the presence of the inhibitor reduces the corrosion current from 8.86 mA, solution with no inhibitor, to 0.62 mA for the best inhibitor concentration (300 ppm). This further confirms that the inhibitor efficiency of this expired drug is dependent on the concentration used.

Table 3. Electrochemical parameters for MS in HCl solution using expired Quarelin as corrosion inhibitor at different concentrations

C (ppm)	R_s (Ωcm^2)	R_p (Ωcm^2)	CPE ($\mu\text{Fs}^{n-1}\text{cm}^{-2}$)	n	C_{dl} (μFcm^{-2})	IE_{EIS} (%)
Blank	2.975	8.119	875.22	0.7403	1964.626	-
200	3.037	13.46	273.44	0.8623	101.461	39.680
250	3.302	16.44	266.98	0.8417	129.273	50.614
300	3.506	21.81	242.62	0.8454	116.377	62.774

Table 4. Electrochemical parameters determined by Tafel method for MS in HCl solution with different expired Quarelin concentrations

C (ppm)	E_{corr} (mV vs. Ag/AgCl)	i_{corr} (mA/cm ²)	$ \beta_c $ (mV/dec)	β_a (mV/dec)	IE_{Taf} (%)
Blank	-409.85	8.868	328.8	244.6	-
200	-430.13	4.983	319.7	28.2	43.815
250	-436.71	3.768	171.2	18.3	57.514
300	-431.17	2.667	174.1	15.5	69.929

In acidic liquids, there are two different kinds of electrochemical processes: cathodic and anodic. In the former, metal ions in the electrolyte undergo a transition, whereas in the latter, hydrogen ions are released to produce hydrogen gas or decrease oxygen. As a result, the inhibitor is classified as either a mixed type of inhibitor since it affects both processes and as anodic/cathodic type inhibitor because it affects just one of these two processes (Lavanya & Machado, 2024). The Tafel slopes (β_a and β_c) change with the change in inhibitor concentration, both currents decreasing with the increase in inhibitor concentration. This means that expired Quarelin is acting as a mixed type of inhibitor in this case, fact also supported by the change of the corrosion potential (E_{corr}). When the change in value of this parameter is greater than 85 mV it can be classified as a cathodic or anodic type inhibitor (Musa et al., 2012). The largest displacement of corrosion potential presented in this research is approximately 27 mV, showing that expired Quarelin affects both reactions.

The optimal inhibitor concentration for MS immersion in 5.6 M hydrochloric acid, according to all research techniques, the maximum concentration tested, 300 ppm. Even though there is a difference up to 10 percentage points when it comes the different ways of calculating the inhibitor efficiency, the interpretation of the physical phenomena is the same, increasing the inhibitor concentration means increasing its efficiency.

Comparing these results with the already existing research of the inhibition efficiency of metamizole sodium (Salem et al., 2022) and caffeine (Souza et al., 2012), it can be said they are comparable in terms of inhibitor efficiency. Combining these active substances did not increase the inhibitor efficiency in a significant

way as reported in cases of other synergistic relations between compounds (Wang et al., 2023). However this research has focused on the industrial conditions of acid pickling using a more concentrated acidic solution and the results are promising from an industry perspective.

CONCLUSIONS

Hazardous materials such as used pickling solutions and expired pharmaceuticals must be managed and recycled in today's society. One solution for this problem can be expired medications such as Quarelin which was effectively used in this work as a corrosion inhibitor for mild steel immersed in highly concentrated hydrochloric acid. Results have shown that the best inhibition was obtained at 300 ppm concentration.

Electrochemical tests revealed that the efficiency of corrosion inhibition increases with an increase in inhibitor concentration and PDP results demonstrated that expired Quarelin acts as a mixed type of inhibitor. Because the three active ingredients of expired Quarelin are constituted of polar groups, their adsorption on the metal surface serves as the primary mechanism by which the expired medicine inhibits corrosion.

REFERENCES

- Agrawal, A., & Sahu, K.K. (2009). An overview of the recovery of acid from spent acidic solutions from steel and electroplating industries. *Journal of Hazardous Materials*, 171, 61–75.
- Brug, G.J., van den Eeden, A.L.G., Sluyters-Rehbach, M., & Sluyters, J.H. (1984). The analysis of electrode impedances complicated by the presence of a constant phase element. *Journal of Electroanalytical Chemistry and Interfacial Electrochemistry*, 176(1–2), 275–295.

- Chaubey, N., Savita, Qurashi, A., Chauhan, D.S., & Quraishi, M.A. (2021). Frontiers and advances in green and sustainable inhibitors for corrosion applications: A critical review. *Journal of Molecular Liquids*, 321, 114385.
- Deflorian, F., Grundmeier, G., Souto, R.M., Montemor, F., McMahon, M.E., Jr, S.R., Santucci Jr, R.J., Glover, C.F., Kannan, B., Walsh, Z.R., & Scully, J.R. (2019). A Review of Modern Assessment Methods for Metal and Metal-Oxide Based Primers for Substrate Corrosion Protection. *Frontiers in Materials*, 1, 190.
- Gao, Y., Yue, T., Sun, W., He, D., Lu, C., & Fu, X. (2021). Acid recovering and iron recycling from pickling waste acid by extraction and spray pyrolysis techniques. *Journal of Cleaner Production*, 312, 127747.
- Iroha, N.B., & James, A.O. (2019). Adsorption behavior of pharmaceutically active dextetropfen as sustainable corrosion Inhibitor for API X80 carbon steel in acidic medium. *World News of Natural Sciences*, 27.
- Lavanya, M., & Machado, A. A. (2024). Surfactants as biodegradable sustainable inhibitors for corrosion control in diverse media and conditions: A comprehensive review. *Science of The Total Environment*, 908, 168407.
- Luo, Y., Reimers, K., Yang, L., & Lin, J. (2021). Household Drug Management Practices of Residents in a Second-Tier City in China: Opportunities for Reducing Drug Waste and Environmental Pollution. *International Journal of Environmental Research and Public Health*, 18(16), 8544.
- Musa, A.Y., Jalgham, R.T.T., & Mohamad, A.B. (2012). Molecular dynamic and quantum chemical calculations for phthalazine derivatives as corrosion inhibitors of mild steel in 1M HCl. *Corrosion Science*, 56, 176–183.
- Predko, P., Rajnovic, D., Grilli, M.L., Postolnyi, B.O., Zemcenkovs, V., Rijkuris, G., Pole, E., & Lisnanskis, M. (2021). Promising Methods for Corrosion Protection of Magnesium Alloys in the Case of Mg-Al, Mg-Mn-Ce and Mg-Zn-Zr: A Recent Progress Review. *Metals*, 11(7), 1133.
- Quraishi, M.A., Chauhan, D.S., & Saji, V.S. (2021). Heterocyclic biomolecules as green corrosion inhibitors. *Journal of Molecular Liquids*, 341, 117265.
- Salem, A.M., Wahba, A.M., Hossiany, A. El, & Fouda, A.S. (2022). Experimental and computational chemical studies on the corrosion inhibitive properties of metamazole sodium pharmaceutical drug compound for CS in hydrochloric acid solutions. *Journal of the Indian Chemical Society*, 99(12), 100778.
- Seddik, N.B., Achache, M., Zarki, Y., Chraka, A., Bouchta, D., & Raissouni, I. (2024). Computational, theoretical and experimental studies of four amino acids as corrosion inhibitors for brass in 3% NaCl medium. *Journal of Molecular Liquids*, 397, 124113.
- Souza, F.S. de, Giacomelli, C., Gonçalves, R.S., & Spinelli, A. (2012). Adsorption behavior of caffeine as a green corrosion inhibitor for copper. *Materials Science and Engineering: C*, 32(8), 2436–2444.
- Souza, L., Pereira, E., Matlakhova, L., Nicolin, V.A.F., Monteiro, S.N., & De Azevedo, A.R.G. (2023). Ionic liquids as corrosion inhibitors for carbon steel protection in hydrochloric acid solution: A first review. *Journal of Materials Research and Technology*, 22, 2186–2205.
- Tanwer, S., & Shukla, S.K. (2022). Recent advances in the applicability of drugs as corrosion inhibitor on metal surface: A review. *Current Research in Green and Sustainable Chemistry*, 5, 100227.
- Timothy, U.J., Umoren, P.S., Solomon, M.M., Igwe, I.O., & Umoren, S.A. (2023). An appraisal of the utilization of natural gums as corrosion inhibitors: Prospects, challenges, and future perspectives. *International Journal of Biological Macromolecules*, 253, 126904.
- Verma, C., Alfantazi, A., Quraishi, M.A., & Rhee, K.Y. (2023). Are extracts really green substitutes for traditional toxic corrosion inhibitors? Challenges beyond origin and availability. *Sustainable Chemistry and Pharmacy*, 31, 100943.
- Verma, C., Quraishi, M.A., & Rhee, K.Y. (2021). Present and emerging trends in using pharmaceutically active compounds as aqueous phase corrosion inhibitors. *Journal of Molecular Liquids*, 328, 115395.
- Wang, H., Deng, S., Du, G., & Li, X. (2023). Synergistic mixture of Eupatorium adenophora spreng leaves extract and KI as a novel green inhibitor for steel corrosion in 5.0 M H₃PO₄. *Journal of Materials Research and Technology*, 23, 5082–5104.
- Zaferani, S.H., Sharifi, M., Zaarei, D., & Shishesaz, M. R. (2013). Application of eco-friendly products as corrosion inhibitors for metals in acid pickling processes – A review. *Journal of Environmental Chemical Engineering*, 1(4), 652–657.

AN INTEGRATIVE APPROACH FOR THE DEVELOPMENT OF ENVIRONMENTAL STRATEGY IN THE CLIMATE CHANGE CONTEXT. THE PERSPECTIVE OF LOCAL PUBLIC AUTHORITIES' ACTION

Anca DRAGHICI¹, Iudith BERE-SEMEREDI², Gabriela BANADUC¹, Cornelia BAERA¹

¹Politehnica University of Timisoara, 2 Victoriei Square, Timisoara, Romania

²Timis County Council, 17 Revoluției din 1989 Avenue, Timisoara, Romania

Corresponding author email: anca.draghici@upt.ro

Abstract

The present research aims at the identification, characterization, and procedural substantiation of the model for the environmental strategy development (feasible, efficient and effective) to achieve the objective of a sustainable (green) local community, by considering the phenomenon of climate change. Three quantitative studies preceded the qualitative research for the development of the conceptual model: (1) Research on citizens' perception, knowledge, attitudes and behaviour towards climate change with Timisoara citizens; (2) Research on exploring the training needs of public servants (from Timis county) in the knowledge field of climate change and sustainable energy consumption; (3) Research on nature-based solutions and green infrastructure for climate change mitigation and adaptation. We have extended the legal framework of the qualitative study with an inventory of contextual and phenomenological premises given by the European Covenant of Mayors for Energy and Climate and details of the Green European Capitals. The ultimate objective of the presented holistic approach to developing the environmental strategy is a resilient urban community (capable of adapting to change while continuing to function normally and continuously develop itself satisfying citizen needs).

Key words: climate change, conceptual model, environment strategy public authorities, sustainable local community, qualitative research.

INTRODUCTION

Currently, local energy and climate strategies need to fit into European policies in this area, considering the 2030 target of reducing greenhouse gas (GHG) emissions by 40% compared to the 1990 baseline, and more recently by considering the long term aims to be climate-neutral by 2050 (an economy with net-zero greenhouse gas emissions) (European Commission, 2021b; Ulpiani et al., 2024; Petrea et al., 2023). At global level, the effects of climate change are already visible and unavoidable due to the inertia of the climate system, but the actions to reduce emissions can help to decelerate the process of aggressive effects (global warming, depletion of freshwater resources, average global sea level rise, etc.) (Fekete et al., 2021; Scorza & Santopietro, 2024).

As evidenced by the new pledges made by the Covenant of Mayors Europe signatories (Melica et al., 2022) or the number of city actors in the United Nation's Global Climate Action Portal (UNFCCC, 2020), many cities have begun to

adopt the policies required for achieving climate neutrality by the year 2050.

To enjoy the benefits of reduced (GHG) emissions, climate adaptation and resilience, energy poverty eradication, and digitalization, among other things, cities are putting forth their own energy and climate policies and action plans. By testing these solutions, social and digital innovation, creative solutions for climate policy, governance frameworks, and funding schemes that might be replicated or expanded across governance levels, cities are also serving as experimentation and innovation hubs (Ulpiani et al., 2024). Furthermore, for many years, cities have benefited from the methodological advice, technical assistance, exchange of best practices, and chances for peer-to-peer learning provided by voluntary initiatives like the Covenant of Mayors (Melica et al., 2022) also, supporting the Sustainable Development Goals (SDG) target by local communities.

The European Commission established the 100 Climate-Neutral and Smart Cities Mission (hereinafter, the Mission) in 2021 in recognition

of the role that cities play in achieving the European Green Deal goal (European Commission, 2019). The Mission's goal is to deliver at least 100 climate-neutral and smart cities by 2030, thereby serving as a model for other European cities to emulate by 2050. A request for Expressions of Interest (EOI) was sent to communities to choose the cohort of climate neutral cities. The EOI consists of 374 questions that cover every important topic to assess a city's readiness, ability to produce outcomes, and ambition. 362 eligible cities responded to it, making the dataset that was produced the first of its type to show the status of ambitious cities' efforts to mitigate climate change in Europe and beyond (Melica et al., 2022).

In this context, the present study aims at the identification, characterization, and procedural substantiation of the model for the environmental strategy development to achieve the objective of a sustainable (green) local community, by considering the phenomenon of climate change. This is a synthesis of several studies developed in the last five years, most by considering the case of Timisoara city area and the metropolitan surroundings (Romania, West Region). Three quantitative studies preceded the qualitative research for the development of the conceptual model and based on the results achieved there have been designed a holistic approach to develop the environmental strategy is a resilient urban community.

MATERIALS AND METHODS

Research on bibliography and state-of-the-art on topics as "climate change" + "local impact" + "mitigation solutions for local communities" (completed by sourced information on legal aspects and from grey literature, as EU state reports and consulting companies' studies and reports) + "good governance practices" (at the local communities' level, for public bodies) has highlighted those environmental strategies, developed by integrating "climate change" aspects are rare and diverse. Overall, this type of strategies must aim to limit greenhouse gas emissions and their negative effects (Bere-Semerédi & Sirbu, 2022; Bere-Semerédi, 2023b).

From a praxiological point of view, dedicated climate, and energy plans (addressing concepts on the impact of climate change on the natural and anthropogenic environment, potential and residual impacts, vulnerability, adaptation, and resilience) need to be developed integrated with economic, social, and environmental development strategies (Bere-Semerédi, 2023b). The premises of this research are also given by the national legal framework on the development of energy and climate plans related to the National Strategy for Sustainable Development of Romania Horizons 2013-2020-2030 (Ministry of Environment, Water and Forestry, 2018; Ministry of Environment, Water and Forestry, 2020), and those at European level, of the existing guidelines, elaborated under the aegis of the "Convention of Mayors for Climate and Energy", by the SDG as described in the documents, reports and recommendations of the United Nations (UNFCCC, 2020), and which create a global but also local framework on sustainable development. In addition, efficient management of the urban environment requires an understanding of the interactions between policy options/decisions, proposed associated objectives and real processes, covering complex social, economic, technical, and environmental aspects that manifest themselves at local level (of an administrative territorial unit, ATU) (Ministry of Environment, Water and Forestry, 2018; Ministry of Environment, Water and Forestry, 2020).

As a result of these considerations, the approach and resolution of the research theme is linked/determined to the local context Timisoara city, Timis county, Romania, connected to the global one through the normative-legislative dimension. A generic schematisation of the research approach is presented in Figure 1 with details in Table 1. Generally, the proposed approach is based on:

- (1) *Theoretical research* oriented towards the study, characterisation, and analysis of practices (from strategic and tactical level) of local public authorities in Romania, but also of cities (leaders at European and global level), to understand the guidelines, approaches, methodologies specific to this approach and of innovative methods developed (existing best practices). Critical

analysis of good practices will allow the design of a model for developing and implementing a feasible, efficient. Designing an effective approach environmental strategy to achieve the goal of a sustainable local community. Furthermore, research will seek to identify knowledge gaps/skills of staff in public organisations, those involved in development, implementation, monitoring, and evaluation of the results of such strategies (operational level staff) (Burke et al., 2015; Bolsen & Druckman, 2018);

- (2) *Applied research* with the main purpose of conducting a pilot investigation on the level of implementation, implementation of strategic environmental planning (in the context of climate change) at the level of local public authorities. Thus, knowledge capitalisation was achieved in terms of the level of training, responsiveness of employees from various ATUs to adopt and implement the model for developing and implementing a feasible, efficient, and effective environmental strategy for achieving the goal of a sustainable local community (acceptability testing and validation) (Pennycook, 2023).

The research context targeted the national local public authorities, but also public and private organisations in Timisoara and the Growth Pole. The results of the research on climate change will make it possible to compare them with those of other cities (benchmarking), which will help define the research gap and the original innovative approach of the strategic model for environmental protection in the context of climate change for the development of a sustainable community.

The main operational objective of the research was to analyse the concrete ways in which an ambitious environment strategy considering climate change could be developed, by a multidisciplinary team, engaging all stakeholders of the community, including the co-creation and future co-implementation of the plan and action measures for reducing, mitigating and adapting to the effects of climate change; communication (internally and externally) has to be considered, too.

In approaching research, the issue of climate change was the central objective, being the subject of strategic thinking and planning. The secondary objectives pursued by the research were:

A second objective pursued by the research will be dedicated to the need for training of the climate strategy planning team, the theoretical and practical knowledge in the field being incomplete. The lack of formal and informal educational curricula in the field of climate change generates (missing complete in 80% of the higher education specializations), on the one hand, a lack of commitment on the part of the collectives in public or private organisations - employees and coordinators of departments/managers, lack of performance or what is even worse inaction. In the current context of climate change, public administration cannot have a passive attitude, or here we even talk about addressing a second aspect, that of managing change, organizational behaviour and good governance through transparency, accountability, participation, efficiency, and coherence (Bere-Semerédi, 2023b).

A third objective was related to stakeholders' management, but especially considering citizens and groups of citizens. The interest in stakeholder management lies in their importance in the effective implementation of climate change measures and actions. A climate strategy developed with excellence can become unopenable or partially effective without the active involvement of civilian actors. Identifying each group in civil society, assessing knowledge, attitude, perception of climate change and understanding potential inputs in that from the strategic planning phase is essential, otherwise the climate strategy risks being emptied of participatory content (Bere-Semerédi, 2023b).

A fourth objective was related to communication in the phase of strategy development in the climate change context, as a basis for transparency.

Organisational and external communication activity is to be analysed from at least the following perspectives: information, awareness, confidence building, transparency of actions, engagement/activation of stakeholders (Bere-Semerédi, 2023b).

Table 1. Methods and tools used in different stages of the approach

Research stages	Target groups/research context	Methods	Tools
(1) Citizens' perception, knowledge, attitudes, and behaviour towards climate change (Bere-Semerédi & Bere-Semerédi, 2019)	Timisoara citizen (West Region of Romania)	Survey Public debate and consultations	Designed Questionnaire (1) Excel and SPSS software Interview protocol (1) Semantic analysis
(2) Exploring the training needs of public servants in the knowledge field of climate change and sustainable energy consumption (Veliscu et al., 2018; Bere-Semerédi et al., 2020)	Public servants from Timis county, Romania	Survey Debate on public institutions readiness	Designed Questionnaire (2) Excel and SPSS software Interview protocol (2) Semantic analysis
(3) Nature-based solutions and green infrastructure for climate change mitigation and adaptation (Bere-Semerédi et al., 2023a).	References and legal documents 2020-2023	Literature review	WoS, SCOPUS data bases

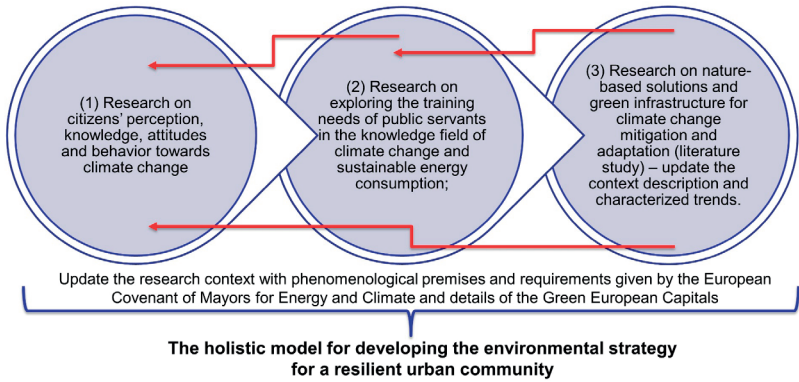


Figure 1. The research methodology

RESULTS AND DISCUSSIONS

In the following sub-chapters are briefly presented some valuable results and conclusions of different research stages.

Results on the citizens' behaviour towards climate change

The complex research scenario together with the results achieved in 2019 are presented in (Bere-Semerédi, & Bere-Semerédi, 2019). In the second research stage of 2020, the same research scenario has been applied with a sample of more than 1200 citizen of Timisoara city (Romania). This research was of great interest for the City Hall of Timisoara - Environmental Directorate that elaborate and implement the "Sustainable Energy Action Plan of the Municipality of Timisoara for 2014-2020" and has responsibilities for designing the Climate

Change Action Plan of the city (being signatory of the Covenant of Mayors for Climate and Energy). Generally, by compared the research results from Timisoara, Romania with those provide by the Climate Action and the Environment Energy Report in 2023 (EC Eurobarometer, 2023) the situation is better, in term of climate change mitigation. One of the main conclusions of study in 2023 was that 40.50% of respondents said that they thought that climate change was the most important issue facing the world. Furthermore, men in the sample are more likely than women (52.6%) to see climate change as the world's most pressing issue (63.4% vs 52.6%). Respondents aged 50 or over, closely followed by those in the 18-25-39 age groups, are the most likely to identify climate change as the single major global problem. Residents of

condominiums and rural homes, as well as those with high levels of education and those who never or almost never have trouble paying their bills, are more likely to identify climate change as one of the most serious problems facing the world at large. Timisoara citizens believe that "climate change" is the most important problem facing the globe (53%), followed by "poverty, hunger, and lack of drinking water" (34%) and "the economic situation" (including international conflicts) (43%).

Respondents recognized that "international terrorism" has been identified as the only worldwide threat, ranking 15.68%. During the study in 2023, Timisoara had a greater percentage of responders (64.6%) identifying "the increasing global population" and "the spread of infectious diseases" as two of the most important worldwide issues; the terms as "armed conflicts" and "proliferation of nuclear weapons" were used less frequently than were identified by the (EC Eurobarometer, 2023). Overall, 94% of the respondents in the research sample have mentioned "climate change" as one of the most serious problems facing the world today. Regarding the responsibility for addressing climate change, nearly 7 out of 10 respondents cite business and industry and regional/local authorities (EC Eurobarometer, 2023). When it came to the response indicating the respondent's personal responsibility for addressing climate change, a high and surprising proportion of 54% was noted. The percentage of respondents who believe that each of the parties on the list has some responsibility for combating climate change was 44%, which is higher than the 2019 survey.

In brief, Timisoara citizens views "climate change" as the world's most pressing issue,

ranking ahead of economic conditions, hunger, poverty, and a shortage of clean drinking water. Most Timisoara residents consider climate change to be a critical issue facing humanity in the present and in the next years, too. These conclusions indicate a higher awareness on the climate change problems and most for responsibility in addressing and managing climate phenomena.

Results on exploring the public servants' training needs for climate change

In the second stage of the research there has been investigated the public servants' readiness for providing a valuable and relevant action on climate change mitigation. First study was developed in 2020 (Bere-Semerédi et al., 2020) and 67 valid questionnaires were processed and recently, the same research scenario has been applied with an extended sample (243 valid answers) at the West Region of Romania (5 counties).

Table 2 shows the research results related to the knowledge domains and subdomains which, highlights the need for specialized courses in some domains (bold figures): "GHG emissions reduction", "energy consumption", "waste management" and "energy efficiency" ("Very strong level of knowledge"). In addition, it was not surprising to see the survey's conclusions about the training materials, techniques, and multiple-choice method of knowledge transfer (Figure 2). "Respondents usually obtain professional information and knowledge (associated with a self-learning process) from scientific resources, legislation (including laws, norms, and standards) and their involvement activities in different projects, with different partners".

Table 2. Methods and tools used in different stages of the approach.

Topics under survey Knowledge Assessment	1	2	3	4	5
	No knowledge	Low level of knowledge	Moderate level of knowledge	Strong level of knowledge	Very strong level of knowledge
	%	%	%	%	%
GHG emissions reduction	2.45	3.43	5.75	52.00	85.00
Climate change adaptation	2.00	4.13	5.65	67.50	25.50
Sustainability concept	0.00	1.25	2.50	2.50	0.00
Water Consumption	0.00	3.96	35.82	44.00	24.50
Energy Consumption	0.00	3.46	37.31	61.00	75.50
Waste Management	0.00	2.97	38.81	63.25	80.44
Circular Economy	0.00	2.00	7.31	6.50	8.96
Energy efficiency	0.00	2.25	37.31	68.50	78.96

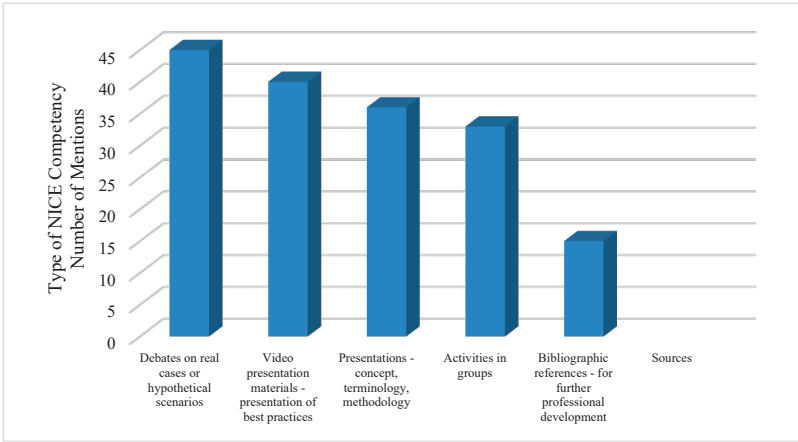


Figure 2. Research results on the adequate training method and information transfer

As the study research result, the debates on actual cases or working on hypothetical scenarios, video presentations of case studies, and the presentation of concepts, terminology, and methodologies followed by group activities (learning, interaction, and work) are the most pertinent training/training methods that could speed up the transfer of information and knowledge of the public servants. The study underlined also, that the public bodies leadership role and the “spirit of organizational learning” were mentioned and most appreciated by respondents as drivers of full filling the knowledge gaps of public servants.

Results on exploring the nature-based solutions and green infrastructure for climate change mitigation

In the last stage of the research there have been developed an inventory of relevant data on nature-based solutions (NBS) and green infrastructure just to identify the most interesting and attractive solutions for climate change mitigation. The main idea was to characterize "good behaviour" in addressing climate change (Bere-Semerédi et al., 2023a). The subject of NBS is multidisciplinary, and complex. Recently, NBS concept and approach have become increasingly appreciated in European cities as a response to addressing urban challenges such as climate change, urban degradation, and obsolete infrastructure;

relevant results on the effectiveness of relevant solutions are still needed.

The bibliographical analysis aims at presenting managerial models or approaches of NBS, in a transdisciplinary manner, by considering actual context of climate change and the related risks. As a result of the research conducted, a consistent bibliographic analysis and synthesis was presented regarding the areas of interest of NBS, key issues addressed and references. All these NBS can be considered and included on the local agenda of local authorities, after a thorough analysis of their effectiveness, with a view to maximising ecosystem benefits. Thus, a problem raised by NBS is co-design and co-participation in implementation to ensure the highest level of community acceptance, after a cost-benefit analysis of possible scenarios (Bere-Semerédi et al., 2023a).

The research on NBS and green infrastructure, as practical ways to mitigate and adapt to the effects of climate change, was approached because of the study of green strategies at the level of European cities/communities, being analysed the candidacy applications of the European Green Capitals. The most relevant common aspect identified in these pioneer cities is that the process of greening, urban regeneration, increasing the quality of life and ensuring the well-being of the inhabitants, for adapting to climate change, is based on NBS.

The model development and testing the public institutions readiness for its implementation

Research results indicate the following key aspects in the strategic planning process:

- (1) The need to involve the citizens in climate actions, by participating as an active and responsible partner, alongside the local public authority. Mitigation and adaptation to climate change and achieving a climate resilient and adapted community status, as a process initiated by the local public authority, supported by the community, through a participatory, transparent planning process and effective climate communication.
- (2) Education for the environment and climate change must be viewed and approached from a double perspective: of information, professional training and increasing administrative (public bodies) capacity at the level of local public administration, organizations, and companies, but also of informing, awareness and increasing the responsibility of the population regarding the new challenges related to environmental issues. Correctly informing citizens contributes to a much firmer commitment and the creation of a critical mass for the voluntary implementation of climate actions at the level of everyone, family and organization and the long-term adoption of a pro-environmental, pro-climate behaviour.
- (3) Communication for environmental protection and climate change plays a crucial role in strategic planning for climate change, being addressed both to climate sceptics and those convinced of the existence and manifestation of the phenomenon at global and local levels. Clear, simple communication based on scientific data and evidence, without exaggeration and with a strong, exemplifying narrative, tends to be one of the success factors of strategic planning, especially if this communication is designed and adapted for each target group and used a greater

diversity of forms and channels of communication.

Finally, as a synthesis of the research results and personal experience in the field, the proposed model for strategic planning for the environment and climate change is presented in Figure 3.

The key elements of the strategic planning model for environment and climate change can be seen in Figure 3. The entire process of strategic environmental planning in the context of climate change is aimed at a bottom-up approach at both the organizational and community level. This aspect must aim at a proactive attitude of public services and civil servants from the specialized departments, with a predilection for the environmental protection departments and the management of emergency situations, so that the triggering factors are those who are aware, supported by the knowledge and understanding of the phenomenon of changes climate, of the risks on the community and in no way generated by a reactive attitude, in response to climate effects manifest at the local level, difficult to control, avoid and with economic and social consequences.

The strategic planning approach must be animated by scientific research data and indisputable evidence on climate change, motivated by the whole context of transforming communities into sustainable, low-carbon urban or rural settlements, the green and energy transition, the opportunity the transformation of public and private spaces through sustainable urban regeneration processes, according to the real needs of the inhabitants. The chance to test and implement innovative investment projects, thanks to European funding, as well as the opportunity to be part of the digital transition that society is currently going through are new arguments to justify the approach of strategic planning for climate change.

The process of initiating strategic planning, supported by political factors, through local elected officials, as well as by the management at the highest level of the organization - mayor, president of the county council, also involves the formation of an action group (Task Force Team), made up of specialists with a good knowledge of the fields of environmental protection, ecosystem services (biology, zoology, environmental engineering) but also of related fields, such as: energy management,

landscape architecture, biology, ecology, spatial development and urban planning, public policies, communication climate and stakeholder engagement, digital solutions and information technology, entrepreneurship and circular economy. This multidisciplinary approach is the key to successful strategic planning for environmental protection, mitigation, and adaptation to climate change by addressing complexities in an integrative way with robust participatory support.

The logical process of the activity must be based on well-defined procedures, in a logic and sequencing of the processes, following well-defined working principles, the role of each team member must be well determined, with

well-defined attributions through the job description, and the resource time allocated to the activity should be sufficient to thoroughly organize and carry out individual and team activities, but also to ensure moments of reflection and evaluation of the implemented actions and measures.

As graphically explain in Figure 3, the strategic vision for mitigating and adapting to climate change and increasing resilience, the mission and specific objectives of the strategic planning approach are to be associated with key energy and non-energy areas relevant at the local level, supported by the analysis of local risks and vulnerabilities.

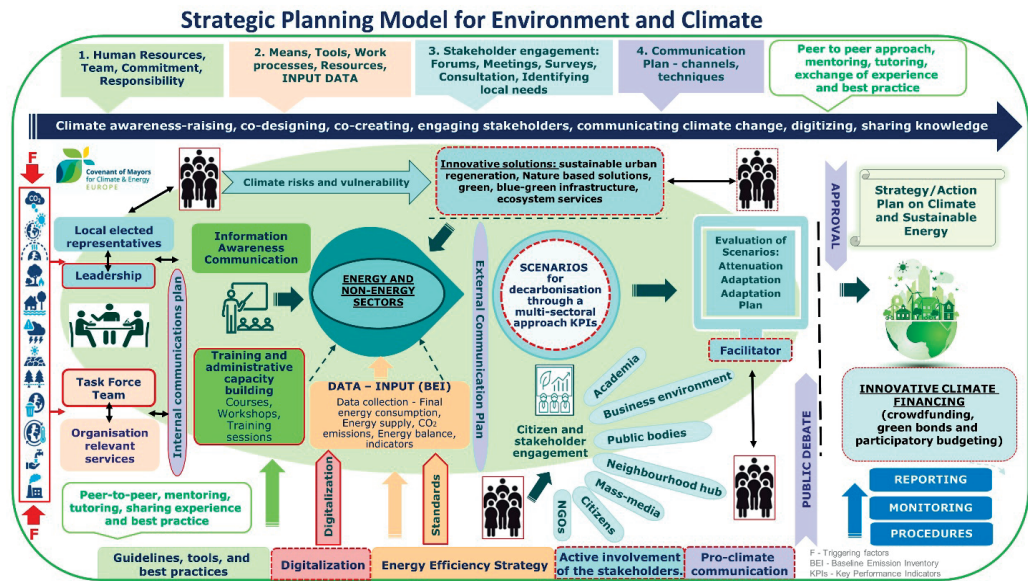


Figure 3. The proposed holistic model for developing the environmental strategy for a resilient urban community

The climate scenarios that will be developed must be based on cost-benefit analyses, and the key indicators for the implementation of strategic actions and measures will be monitored using the Plan-Do-Check-Act cycle, through the collection of climate data, data processing and analysis, results, and information, always having the possibility of adjusting the performance and result indicators.

The internal and external communication process must be permanently supported by clear and strong messages, with robust data and information, through narrative techniques and

the use of communication channels as diverse as possible, adapted to the targeted target groups. For effective communication, making a climate communication plan is very important, connecting this plan with organized climate activities and events is very important.

The pillars that contribute to supporting the strategic planning model for the environment in the context of climate change are: (1) Education for the environment and climate change; (2) Communication on climate change; (3) Engaging stakeholders in strategy co-design and co-implementation of environmental actions; (4)

Digitization and smart solutions in strategic planning for the environment and climate change.

CONCLUSIONS

The presented research was permanently anchored to the praxeological dimension of the environmental, social, and economic phenomena addressed (feed-backs and loops between researchers and practitioners), so that they could be articulated in several recommendations regarding issues such as dilemmas or uncertainties that practitioners may face, as presented in the following:

1. The strategy must be built based on a simple, easy-to-understand structure throughout the development process, including in the case of the environmental strategy in the context of climate change. From this perspective, the success of an environmental strategy depends on two options: the decision of the political decision-makers and that of the local administration to be engaged in the protection of the environment and the urban settlement against climate change and the decision to succeed by reaching the set objectives and targets.
2. The flexibility of strategic documents is the most convenient solution and without being intimidated by the process of developing or revising the strategy, the leadership must take this step, after proper monitoring and evaluation.
3. Testing the logic of strategic thinking and the ongoing analysis of environmental risks are two actions that improve strategic options. Focusing on costs, capabilities, and rigid planning can be pitfalls for the strategy development team, because the planning activity tends to dominate the strategy.

One of the future research opportunities is to extend the research through a longitudinal study that analyses the evolution of the strategy in the implementation process, through the study of strategic environmental management. It will also be appropriate to replicate this study on other local government organizations that wish to develop or update their energy and climate change strategy or environmental strategy,

future research could “test” and develop the results of this research.

ACKNOWLEDGEMENTS

The article is related to the "Education for Plastic in a Circular and Climate Neutral Economy - Preventing Waste from Ending Up in the Environment" (Erasmus+ 2023-1-RO01-KA220-HED-000166242), founded with the support of the European Commission. This paper and the communication reflect the views only of the authors, and the Commission cannot be held responsible for any use which may be made of the information contained therein.

REFERENCES

- Bere-Semerédi, I. & Bere-Semerédi, A.A. (2019). Perception, Knowledge, Attitude and Behaviour Toward Climate Change—A Survey Among Citizens in Timisoara, Romania. In: *Proceedings of the International Symposium in Management Innovation for Sustainable Management and Entrepreneurship*, pp. 199-217. Springer, Cham.
- Bere-Semerédi, I. (2023b). *Research on the Development of Environmental Strategies in the Context of Climate Change*, PhD Thesis, Politehnica University of Timisoara, Romania.
- Bere-Semerédi, I., & Sirbu, R. (2022). Climate Action and Affordable, Clean Energy - A Review on European Sustainable Development Goals Indicators. *Proceedings of the Economic, MakeLearn&TIIM 2023 International Conference: Social and Environmental Sustainability: The Role of Technology and Political Dialogue (779-806)*, 18–20 May 2023 Valetta, Malta & Online (<https://toknowpress.net/ISBN/978-961-6914-30-7/149.pdf>).
- Bere-Semerédi, I., Draghici, A., Fistis, G. (2020). Exploring the Training Needs for Climate Change and Sustainable Energy Consumption in the Case of Public Local Authorities. *Management*, 15(2), 87-97.
- Bere-Semerédi, I., Sirbu, R., & Draghici, A. (2023a). Nature-Based Solutions - A Brief Overview of the Perspective of the Cities in the Light of Climate Change. *Research Journal of Agricultural Science*, 55(1), 20.
- Bolsen, T., & Druckman, J.N. (2018). Do partisanship and politicization undermine the impact of a scientific consensus message about climate change? *Group Processes & Intergroup Relations*, 21(3), 389-402.
- Burke, M., Dykema, J., Lobell, D.B., Miguel, E., & Satyanath, S. (2015). Incorporating climate uncertainty into estimates of climate change impacts. *Review of Economics and Statistics*, 97(2), 461-471.
- EC Eurobarometer (2023). Climate change. Climate Action and the Environment Energy Report. <https://europa.eu/eurobarometer/surveys/detail/2954>.

- European Commission. (2019). COM/2019/640 final - Communication from the Commission to the European Parliament, the European Council, the Council, the European Economic and Social Committee and the Committee of the Regions - The European Green Deal (<https://eur-lex.europa.eu/legal-content/EN/TXT/?uri=CELEX:52019DC0640>).
- European Commission. (2021b). EU mission: climate-neutral and smart cities. https://ec.europa.eu/info/research-and-innovation/funding/funding-opportunities/funding-programmes-and-open-calls/horizon-europe/eu-missions-horizon-europe/climate-neutral-and-smart-cities_en
- Fekete, H., Kuramochi, T., Roelfsema, M., den Elzen, M., Forsell, N., Höhne, N., ... & Gusti, M. (2021). A review of successful climate change mitigation policies in major emitting economies and the potential of global replication. *Renewable and Sustainable Energy Reviews*, 137, 110602.
- Melica, G., Treville, A., Franco De Los Rios, C., Baldi, M., Monforti-Ferrario, F., Palermo, V. et al. (2022). *Covenant of Mayors: 2021 assessment*. Publications Office of the European Union. 10.2760/58412
- Ministry of Environment, Water and Forestry (2018). *National Strategy for Sustainable Development 2030/Strategia Națională pentru Dezvoltare Durabilă a României 2030*, approved by the Government Decision 877/09.11.2018 / MO no. 985/2018.
- Ministry of Environment, Water and Forestry (2020). *National Strategy on Climate Changes / Strategia Națională a României privind Schimbările Climatice 2013 – 2020*. (<http://mmediu.ro/app/webroot/uploads/files/Strategia-Nationala-pe-Schimbari-Climatice-2013-2020.pdf>)
- Pennycook, G. (2023). A framework for understanding reasoning errors: From fake news to climate change and beyond. *Advances in experimental social psychology*, 67(1), 1-85.
- Petrea, A.-M., Simionov, I.-A., Antache, A., Nica, A., Antohi, C., Cristea, D.S., Arseni, M., Calmuc, M., Iticescu, C. (2023). Machine learning-based modeling framework for improving Romanian resilience strategy to greenhouse gas emissions in relation to Visegrad group. *Scientific Papers. Series E. Land Reclamation, Earth Observation & Surveying, Environmental Engineering, XII*, 150-157, Print ISSN 2285-6064.
- Scorza, F., & Santopietro, L. (2024). A systemic perspective for the Sustainable Energy and Climate Action Plan (SECAP). *European Planning Studies*, 32(2), 281-301.
- Ulpiani, G., Vettors, N., Melica, G., & Bertoldi, P. (2023). Towards the first cohort of climate-neutral cities: Expected impact, current gaps, and next steps to take to establish evidence-based zero-emission urban futures. *Sustainable Cities and Society*, 95, 104572.
- United Nation's Global Climate Action Portal (2020). 1,000 cities racing to zero emissions. <https://climatechampions.unfccc.int/1000-cities-racing-to-zero-emissions/>
- Veliscu T.M., Bejinariu A.C., Bere-Semerédi, I., Draghici A. (2018). A Propose Approach for Strategic Performance Management for Public Administration Organizations. In: Abrudan, I. (ed.), *Performance management or management performance? Book Series: Review of Management and Economic Engineering International Management Conference*, pp. 466-477.

ENVIRONMENTAL ASSESSMENT OF THE AREA WITH NATURAL CO₂ EMISSIONS IN BĂILE LĂZĂREȘTI

Alexandra-Constanța DUDU, Ana Bianca PAVEL, Corina AVRAM, Irina CATIANIS,
Gabriel IORDACHE, Florina RĂDULESCU, Naliana LUPAȘCU, Andrei-Gabriel DRAGOȘ,
Oana DOBRE, Constantin-Ștefan SAVA

National Institute for Research and Development on Marine Geology and Geoecology -
GeoEcoMar, 23-25 Dimitrie Onciul, Bucharest, Romania

Corresponding author email: alexandra.dudu@geoecomar.ro

Abstract

Băile Lăzărești, located 16 km north-east from Băile Tușnad, is a representative area for post-volcanic regions where gases emitted at the surface contain over 85% carbon dioxide. Nineteen stations were set up for collecting soil samples for analysis of heavy metals, TOC, carbonates, and lithology and four water stations for nutrient analysis in July and August 2022. The impact of increased CO₂ emissions on the soil is evident through the exceeding normal concentrations of heavy metals such as Cr, Cu, Hg, and Ni in areas with high CO₂ emissions and their reduction in areas with lower volcanic gas emissions. Water sample analysis, all with high CO₂ concentrations, showed elevated levels of nitrites, inorganic phosphorus, and sulphates, classifying the water quality into categories II and III, according to national classification. The impact of high CO₂ concentrations is clearly visible in the vegetation, which is absent at CO₂ concentrations above 20%, predominantly consists of grasses, and shows distinct colorations at concentrations below 20%. These observed and analysed elements could serve as surface indicators for potential CO₂ leaks from anthropogenic storage sites.

Key words: Băile Lăzărești, Băile Tușnad, carbon dioxide emissions, CO₂ impact, soil sampling, water sampling.

INTRODUCTION

Since the 1950s, studies on mineral springs, chemical composition of waters, and emitted gases from post-volcanic gas vents have been conducted in the vicinity of Lăzărești. Various analyses from these studies are mentioned in Artemiu Pricăjan's books "Mineral and Thermal Waters in Romania" (1972) and "Therapeutic Mineral Substances of Romania" (1985). Additionally, Zoltán Rákossy's chapter in the 1974 publication of the People's Council of Harghita County mentions the inventory of 44 mineral water springs in Lăzărești (Karátson et al., 2022). Furthermore, detailed cartography and chemical analyses of carbonated mineral waters and post-volcanic gas vents in the Ciomadul area were carried out between the 1970's and 2000's by geologists and chemists from the Harghita Geological Research and Exploration Company. These findings were later published in various works such as "The Mineral Waters of the Kelemen-Görgényi-Harghita Mountain Range" (2000) by Berner, Z., Csaba Jánosi, C., and Péter, E. Szadeczky, Gy. (1929),

Torok, Z. (1956), Bányai, J. (1929, 1934), Atanasiu, I. (1939), Ianovici, V., Giușcă, D. (1981) and Ghițulescu, P.T. (1975) significantly contributed to deepening the knowledge of the volcanic activity within the Eastern Carpathians. Essential insights into the geological structure of the entire volcanic chain were provided by D. Rădulescu and collaborators. Hydrogeological research in the region was conducted by Pricăjan, A. (1972, 1974, 1985), Pascu, R. (1929), Slăvoacă, D. (Slăvoacă, 1971; Slăvoacă et al, 1978), Lungu, P., Geamănu, N. (1971), Bandrabur, T. (1961) and Vasilescu, Gh. (1964), with a primary focus on mineral waters. The most prominent and active post-volcanic manifestation within the Eastern Carpathians is found in the Gurghiu and Harghita mountain massifs, characterized by predominantly calc-alkaline volcanic activity, resulting in the formation of stratovolcanoes and a complex volcanic chain surrounded by volcanoclastic deposits and monogenetic or polygenetic dome complexes (Airinei & Pricăjan, 1972). Adjacent to the Lăzărești site are parasitic cones or lava domes formed along faults and linked to the

Ciomadu Mare volcanic complex (Seghedi et al., 2019). These domes, with steep or abrupt slopes, rise about 100-250 meters above the general terrain level and develop in various directions, such as from northeast to northwest and from southwest to northeast, including those at Dealul Cetății (1079 m), Haromul Mare (1140 m), and Lăzărești or Haromul Mic (880 m). The Lăzărești site is situated on a succession of deposits ranging from Cretaceous flysch (Sânmartin-Bodoc, Barremian-Albian layers) at the base to terrace deposits. Lăzărești site, with its dry and wet gas vents, can be also considered as a natural laboratory for the study of the environmental impact of a CO₂ leakage from an anthropic reservoir and for testing and designing monitoring strategies. One of the key points of monitoring CO₂ geological storage sites would be to find early indicators of a potential leakage through soil and water sampling and vegetation surveys. Considering Lăzărești to be a suitable site to find these indicators, several field campaigns were conducted in 2022 including measurements of CO₂ concentration, soil and water sampling and vegetation observation. The aim was to correlate abnormal variations of some soil and water parameters and constituents with different CO₂ concentrations and emissions.

MATERIALS AND METHODS

Study area

The study area encompasses the region around Băile Lăzărești, situated approximately 16 km north-east of Băile Tușnad, renowned for its significant post-volcanic activity and characterized by surface emissions with high concentrations of carbon dioxide, exceeding 85%. The site was divided for study purposes in two perimeters, one northern perimeter with high CO₂ emissions and many wet and dry gas vents, including some baths used for therapeutic purposes and one southern perimeter with much lower emissions including only dry gas vents.

Methodology for water and soil analysis

During the field campaigns (conducted in July and August 2022), soil samples were collected from 19 points aligned along two profiles, one with 10 points in the northern perimeter of the

site and one with 9 points in the southern perimeter, for the analysis of heavy metals, total organic carbon (TOC), carbonates, and lithology (Figure 1). The samples were collected in plastic containers, closed with lids, and securely sealed, after measuring CO₂ concentration at the surface. The amount of material collected was approximately 50-100 g, depending on its physical state (solid or with high water content). Measurement of CO₂ concentration at the surface of the sampling points was conducted using a portable gas analyser from West Systems. The soil analysis methods involve determining calcium carbonate (CaCO₃) concentrations through volumetric analysis with 0.5N HCl and 0.5N NaOH, as well as total organic carbon (TOC) using a titrimetric method with K₂Cr₂O₇ and concentrated sulfuric acid (Dean, 1974; Van der Veer, 2006), while elements such as Ti, V, Cr, and others are analysed via energy dispersive X-ray fluorescence spectroscopy for simultaneous qualitative and quantitative determination (Emelyanov & Shimkus, 1986). The sediment samples were analysed for their main lithological components, including water content (WC %), dry matter (DM %), total organic matter (TOM %), total carbonates (CAR %), and siliciclastic fraction (SIL %). The lithological analysis relied on standard techniques and procedures used in sedimentology, specifically employing the Loss of Drying (LOD) method for water content and dry matter estimation, and the Loss on Ignition (LOI) method for determining total organic matter, total carbonates, and the siliciclastic fraction through calcination (Ricken, 1993; ASTM-D2216, 2010). Additionally, 4 surface water samples were collected from the spring (Nagyborvíz) and the wet gas vents - baths (Nyírfürdő) present at the site for nutrient analysis (Figure 1). Nutrient and chlorophyll concentrations were determined by analysing water samples for PO₄³⁻, SiO₄⁴⁻, NO₂⁻, NO₃⁻, and NH₄⁺, which were preserved through freezing (-24°C) using standard methods for water analysis. Analytical methods for nutrient concentrations involved spectroscopic techniques in accordance with HACH water analysis methods.

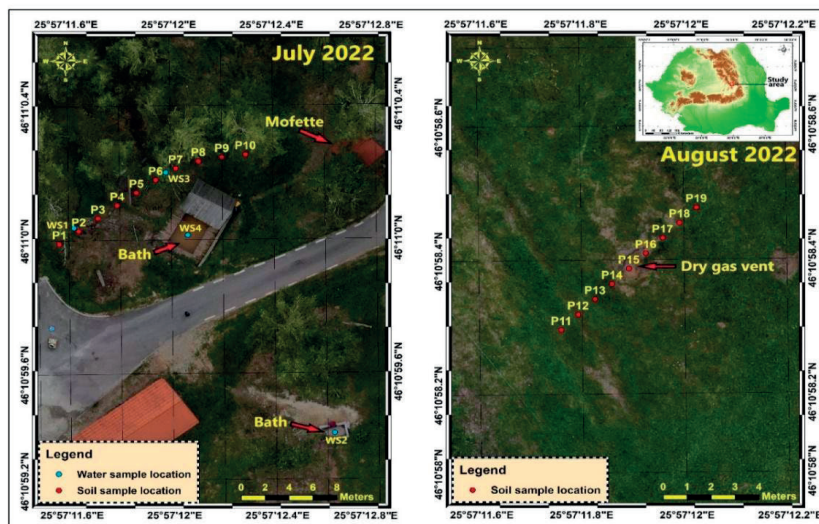


Figure 1. Sampling stations on the Băile Lăzărești area

RESULTS AND DISCUSSIONS

Water analysis

Nitrogen, a crucial nutrient in aquatic ecosystems, enters water through various pathways and exists in multiple forms, including molecular nitrogen, nitrogen oxides, ammonia, ammonium, nitrites, and nitrates (Table 1) (Popa et al., 2022; Sandu et al., 2023).

Nitrate concentrations exhibit high spatial variability in the study area, ranging between 0.02 mg/L and 0.30 mg/L. All nitrate concentration values correspond to Class I water quality in the study area (<1 mg/L). The maximum value of 0.30 mg/L was observed in sample WS3, while the minimum concentration was measured in sample WS2 (0.02 mg/L). Slightly higher values (0.08 - 0.21 mg/L) were recorded in the other two samples from the analysed stations.

Nitrite concentrations, the intermediate form of inorganic nitrogen, varied widely between 0.006 mg/L (WS2) and 0.033 mg/L (WS1). Generally, nitrite values were low, confirming that inorganic nitrogen is the limiting nutrient in primary production. All samples exceeded the threshold value of 0.01 mg/L for nitrites, suggesting classification of the study areas between Class I and Class II water quality, considering the oxidized form of inorganic nitrogen.

Concentrations of *inorganic phosphorus* in the studied sectors exhibited high values, ranging

between 0.08 mg/L and 2.20 mg/L. The highest value exceeding 0.4 mg/L, the limit between Class II and Class III water quality, was determined in sample WS3. However, three out of four values of the samples studied regarding phosphate concentrations fell within the range of 0.1 mg/L to 0.4 mg/L, suggesting, overall, the classification of waters in the study area into Classes I, II, and III in terms of inorganic phosphorus.

Sulphate concentration values exceeded the limit threshold of 60 mg/L according to Order 161/2006. Regarding *silicon*, all samples studied recorded concentrations below the maximum allowable limit according to Order 161/2006. The lowest concentration values of this parameter were recorded in sample WS2 (0.073 mg/L), while the highest value was obtained in sample WS1 (0.140 mg/L). These values indicate the water quality at the studied stations and their classification into Class I according to Order 161/2006.

Soil analysis

The measured CO₂ concentrations at the surface of the sampling points for soil analysis are presented in Tables 2 and 3. As can be seen, on the profile from the northern perimeter, analysed in July 2022, there is a large variation in CO₂ concentrations found, ranging from 485 ppm to 46221 ppm.

Table 1. Nutrient results from water samples

Station	N-NO ₃ ⁻ , mg/L	N-NO ₂ ⁻ , mg/L	PO ₄ ³⁻ , mg/L	SO ₄ ²⁻ , mg/L	SiO ₂ , mg/L	Hg, µg/L
WS1	0.08	0.033	0.08	125	8.34	0.140
WS2	0.02	0.006	0.32	165	8.00	0.091
WS3	0.30	0.012	2.20	210	7.75	0.092
WS4	0.21	0.018	0.21	72.5	10.88	0.073

The smallest CO₂ concentration was found for P10 (485 ppm), while the highest CO₂ concentration belongs to P7 (46221 ppm), near a bath used for therapeutic purposes, followed by P1 (42654 ppm), near the spring. On the profile from the southern perimeter, analysed in August 2022, the variation in CO₂ concentrations is lower than the northern one, ranging from 786 ppm to 3448 ppm. The smallest CO₂ concentration was found for P19 (786 ppm), at the northern end of the profile. As expected, the highest CO₂ concentration was found at the sampling point corresponding to the dry gas vent observed in the field, P15 (3448 ppm). To assess the degree of *soil pollution/contamination*, the values obtained from the analysed samples in July and August were compared with normal reference values, alert thresholds, and intervention thresholds for soils of sensitive use provided by Order 756/1997 of the Ministry of Waters, Forests, and Environmental Protection. The results are presented in Tables 2 and 3. Statistical analysis of the data (Tables 2, 3) revealed slightly variability in all chemical components (CV>20%), with coefficients of variation of concentrations ranging from 18.32% for V to 93.35% for MnO (July 2022) and from 30.97% for V to 53.08% for MnO (August 2022). The higher values of the coefficient of variation for MnO concentrations are due to its high redox sensitivity. As for the other minor component, TiO₂, its relatively high variability (though lower than MnO) (14.38 ppm in July 2022 and 15.67 ppm in August 2022) is likely due to environmental conditions in the analysed area, which may lead to dispersion or concentration of titanium as rutile. Higher TiO₂ values are observed in sample P1 with 4114 ppm (July 2022) and in P16 with 4899 ppm (August 2022). The normal content of chromium in soils (Ord 756/1997) is 30 mg/kg, with an alert threshold of 100 mg/kg and an intervention threshold of

300 mg/kg. Analysing the data obtained for chromium in both campaigns (July and August), exceedances of the normal values of 30 mg/kg are observed in both July and August. Sample P15 (101 ppm - August) even exceeds the alert threshold according to Order 756/1997, while in July the highest chromium values were 78.50 ppm - P5.

Similarly, copper has a normal content in soils of 20 mg/kg, an alert threshold for sensitive uses of 100 mg/kg, and an intervention threshold of 200 mg/kg. The concentrations of copper in the soil at a depth of 0-25 cm for both campaigns are presented in Tables 2 and 3. In the July campaign, exceedances of the normal value were recorded in 70% of the analysed samples. The highest copper concentration was recorded in sample P5 (32.71 ppm), while the lowest copper concentration was recorded in P3 (17.89 ppm), below the normal value of 20 mg/kg. In the August 2022 campaign, the frequency of exceedances compared to the normal value was only 11.11%, compared to July, with only one exceedance of the normal values in sample P15 (96.6 ppm). Thus, for this sample, copper was 4.83 times higher than the normal value.

The lithological analyses conducted in July 2022, on the sediment samples collected revealed significant variations in the main lithological components: total organic matter (TOM%), carbonate content (CAR%), and siliciclastic fraction (SIL%). The analysis results are presented in Table 4. The determined lithological parameters (Table 4) show that the main component of the investigated sediments is represented by organic matter, which has a high proportion, accounting for over 30% of the total weight of the dry sediment in several samples. The range of values is relatively wide, ranging from 3.91 to 76.12 (TOM%), with an average value of 30.76 (TOM%). The carbonate content varies, with values ranging within a narrow interval, namely between 1.55 and 3.18

(CAR%), with an average value of 2.59 (CAR%). The remaining sedimentary material analysed corresponds to the siliciclastic fraction; the values are in the range of 22.33 to 93.63 (SIL%) with an average value of 66.65 (SIL%). Based on the mass percentage content of organic matter ($\geq 15\text{-}30\%$), total carbonate content ($\text{CaCO}_3 \leq 10\%$), and siliciclastic fraction ($\leq 15\text{-}30\%$) from the total weight of the dry sediment, the tested sediments (P3, P4, P5, P6, and P7) can be classified as organic sediments, subordinated to organo-mineral sediments, without a carbonate component (Figure 2 and Figure 3). Similarly, based on the mass percentage content

of the siliciclastic fraction ($\geq 15\text{-}30\%$), total carbonate content ($\text{CaCO}_3 \leq 10\%$), and organic matter ($\leq 15\text{-}30\%$) from the total weight of the dry sediment, the tested sediments (P1, P2, P8, P9, and P10) can be classified as mineral sediments, subordinated to mineralo-organic sediments, without a carbonate component.

The lithological analyses conducted in August 2022 on the sediment samples collected revealed significant variations in the main lithological components: total organic matter (TOM%), carbonate content (CAR%), and siliciclastic fraction (SIL%).

Table 2. CO₂ concentrations and heavy metal content results from July 2022

	P1	P2	P3	P4	P5	P6	P7	P8	P9	P10
CO ₂ , ppm	42654	13162	3199	602	5397	2531	46221	993	631	485
TOC, %	0.03	3.6	6.9	7.14	7.06	7.28	4.99	4.5	3.47	1.63
CaCO ₃ , %	0.57	2.22	2.1	0.51	0.53	0.9	0.1	1.41	1.18	1.05
Na ₂ O, %	0.45	0.47	0.28	0.32	0.33	0.48	1.08	0.41	0.56	0.61
MgO, %	0.41	0.54	0.28	0.36	0.31	0.27	0.33	0.61	0.66	0.65
SiO ₂ , %	22.3	18.08	12.79	17.24	16.75	17.01	19.02	17.92	20.38	20.67
P ₂ O ₅ , %	0.02	0.04	0.07	0.16	0.25	0.03	0.03	0.04	0.08	0.04
K ₂ O, %	1.68	1.65	1.11	1.49	1.35	1.44	1.86	1.61	1.78	1.85
CaO, %	0.42	0.51	0.2	0.29	0.21	0.51	0.79	0.91	0.89	0.63
Ti, ppm	4114	3538	2514	3298	3732	3298	2653	3264	3692	3508
V, ppm	59.1	67.7	57.7	77	94.9	68	49.53	74.7	79	74.3
Cr, ppm	53	59	39.33	59.1	78.5	60.4	38.3	60.7	68.3	64.7
MnO, %	0.008	0.012	0.005	0.007	0.005	0.007	0.012	0.043	0.045	0.042
Fe ₂ O ₃ , %	0.85	1.47	3.53	1.03	0.71	0.52	0.79	2.36	3.22	2.76
Ni, ppm	14.03	20.15	11.48	44.19	24.82	10.94	9.52	22.39	25.64	27.85
Cu, ppm	18.4	19.84	17.89	25.21	32.71	26.69	22.8	23.39	24.72	22.31
Zn, ppm	31.33	49.37	28.26	105	73.5	16.95	20.64	49.79	71	64.8
As, ppm	5.31	7.67	10.04	8.99	9.89	6.18	3.66	7.12	8.23	8.23
Sr, ppm	197	214	180	226	160	213	612	254	245	281
Zr, ppm	314	215	170	165	185	179	179	169	206	199
Sn, ppm	6.82	5	4.36	4.98	6.2	6.24	3.51	4.89	4.58	4.13
Hg, ppm	0.059	0.06	0.056	0.064	0.119	0.078	0.042	0.078	0.093	0.054
Pb, ppm	22.82	26.2	17.64	30.15	30.69	23.89	26.42	26.11	29.07	25.97

Table 3. CO₂ concentrations and heavy metal content results from August 2022

	P11	P12	P13	P14	P15	P16	P17	P18	P19
CO ₂ , ppm	1505	930	977	1609	3448	1457	1174	1520	786
TOC, %	0.98	4.2	2.01	3.49	5.53	0.73	4.91	4.74	4.47
CaCO ₃ , %	0.2	0.83	0.45	0.09	1.04	0.08	0.03	0.63	0.6
Na ₂ O, %	0.73	0.57	0.76	0.74	0.17	0.81	0.55	0.54	0.59
MgO, %	0.9	0.73	0.71	0.76	0.27	0.48	0.55	0.67	0.71
SiO ₂ , %	22.16	17.05	20.46	21.25	13.74	26.12	17.64	18.52	18.61
P ₂ O ₅ , %	0.02	0.03	0.02	0.04	0.02	0.08	0.06	0.04	0.04
K ₂ O, %	1.94	1.58	1.77	1.86	1.91	2.01	1.53	1.65	1.62
CaO, %	0.7	0.8	0.71	0.6	0.03	0.29	0.33	0.69	0.76
Ti, ppm	3725	3291	3756	3712	4550	4899	3281	3294	3330
V, ppm	83.9	66.3	72.7	74.9	143	78.5	62.6	67.3	67.7
Cr, ppm	68.2	61	68.4	62.4	101	75.3	53.9	57.2	58.9
MnO, %	0.027	0.036	0.03	0.03	0.002	0.008	0.014	0.026	0.03
Fe ₂ O ₃ , %	4.34	2.54	2.67	3.07	0.44	1.99	3.11	2.98	3.31
Ni, ppm	33.39	25.72	28.81	28.87	7.86	11.17	19.07	25.13	27.22
Cu, ppm	19.25	17.52	18.55	19.91	96.6	14.09	15.87	18.23	19.88
Zn, ppm	78.1	65.7	62.5	70.8	13.67	22.34	47.49	65.6	71.4
As, ppm	9.67	7.48	7.99	8.56	14.58	18.04	7.64	8.24	9.23
Sr, ppm	315	263	305	304	70.6	227	236	263	254
Zr, ppm	287	220	263	228	117	343	226	243	232
Sn, ppm	5.16	4.5	4.17	4.97	7.66	4.3	4.05	3.86	4.23
Hg, ppm	0.056	0.051	0.043	0.05	0.148	0.037	0.051	0.054	0.055
Pb, ppm	26.6	27.11	27.58	31.22	21.06	43.49	29.83	26.34	29.44

Table 4. The variation of the main lithological parameters analysed in the sediment samples in July 2022 (water content (WC %), dry matter (DM %), total organic matter (TOM %), total carbonates (CAR %), and siliciclastic fraction (SIL %))

Station	WC %	DM %	TOM %	CAR %	SIL %
P1	19.64	80.36	3.91	2.46	93.63
P2	28.11	71.89	18.75	3.18	78.07
P3	39.98	60.02	76.12	1.55	22.33
P4	34.92	65.08	48.89	2.43	48.68
P5	28.62	71.38	36.99	2.64	60.36
P6	29.1	70.9	38.55	3	58.45
P7	21.89	78.11	41.69	1.85	56.46
P8	17.88	82.12	11.47	3.17	85.37
P9	22.64	77.36	17.66	2.65	79.69
P10	17.34	82.66	13.54	2.97	83.49
(n=10)	Min.	17.34	60.02	3.91	22.33
	Max.	39.98	82.66	76.12	93.63
	Media	26.01	73.99	30.76	66.65

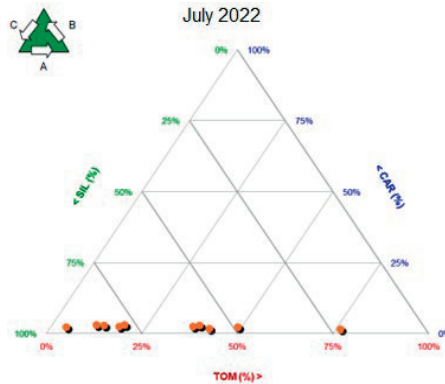


Figure 2. Ternary diagram representing the distribution of total organic matter (TOM %), carbonates (CAR %) and siliciclastic fraction (SIL %), July 2022

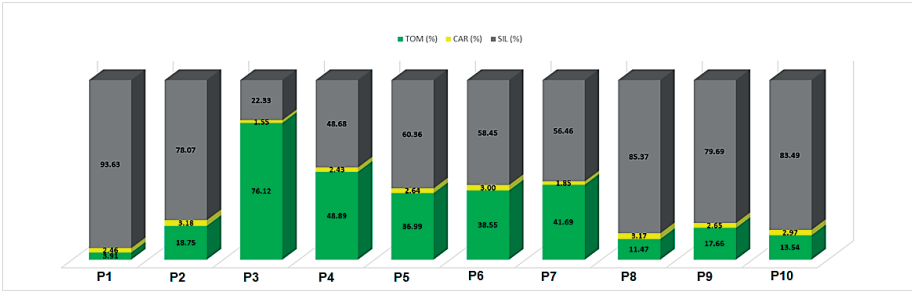


Figure 3. Binary diagram representing the distribution of total organic matter (TOM %), carbonates (CAR %) and siliciclastic fraction (SIL %), July 2022

The analysis results are presented in Table 5. The determined lithological parameters (Table 5) show that the main component of the investigated sediments is represented by the siliciclastic fraction, which accounts for over 30% of the total weight of the dry sediment in most samples. The range of values is wide, ranging between 0.32 and 91.74 (TOM %), with an average value of 72.91 (TOM %).

The carbonate content varies, with values within a relatively narrow interval, namely between 1.59 and 16.20 (CAR %), with an average value of 3.65 (CAR %).

The remaining sedimentary material analysed corresponds to organic matter, with values ranging from 6.34 to 83.48 (SIL %) and an average value of 23.44 (SIL %). Based on the mass percentage content of the siliciclastic fraction ($\geq 15\text{-}30\%$), total carbonate content ($\text{CaCO}_3 \leq 10\%$), and organic matter ($\leq 15\text{-}30\%$) from the total weight of the dry sediment, the analysed sediments (P11, P12, P13, P14, P16, P17, P18, P19) can be included in the domain of

mineral sediments and subordinated to mineralo-organic sediments, without a carbonate component (Figure 4 and Figure 5). However, based on the mass percentage content of organic matter ($\geq 15\text{-}30\%$), total carbonate content ($10\% < \text{CaCO}_3 \leq 30\%$), and the siliciclastic fraction ($\leq 15\text{-}30\%$) from the total weight of the dry sediment, the tested sediment from a single sample (P15) can be included in the domain of organic sediments and subordinated to organo-mineral sediments, with a slight carbonate component.

The impact of increased CO₂ emissions on vegetation was assessed through field observations, combined with measurements of CO₂ concentration at the surface. Complete vegetation absence was observed at points with emissions exceeding 20% CO₂ (Figure 6a). In areas with elevated emissions, with concentrations up to 10% CO₂, the prevalence of simple grasses with increased CO₂ tolerance was observed (Figure 6c).

Table 5. The variation of the main lithological parameters analysed in the sediment samples in August 2022 - water content (WC %), dry matter (DM %), total organic matter (TOM %), total carbonates (CAR %), and siliciclastic fraction (SIL %)

Station	WC %	DM %	TOM %	CAR %	SIL %	
P11	13.65	86.35	6.34	1.92	91.74	
P12	16.81	83.19	14.42	2.21	83.38	
P13	15.59	84.41	14.25	1.78	83.96	
P14	11.05	88.95	16.62	1.72	81.66	
P15	28.22	71.78	83.48	16.20	0.32	
P16	13.42	86.58	8.16	1.64	90.20	
P17	25.09	74.91	19.45	2.12	78.43	
P18	14.49	85.51	20.47	1.59	77.94	
P19	15.05	84.95	27.80	3.64	68.56	
(n=9)	Min.	11.05	71.78	6.34	1.59	0.32
	Max.	28.22	88.95	83.48	16.20	91.74
	Media	17.04	82.96	23.44	3.65	72.91

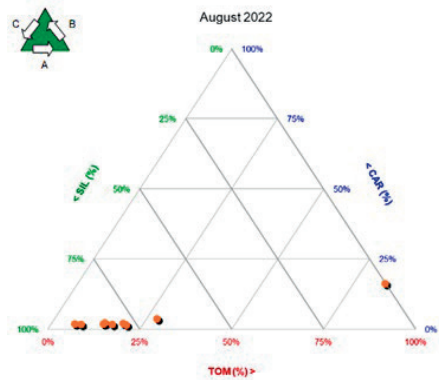


Figure 4. Ternary diagram representing the distribution of total organic matter (TOM %), carbonates (CAR %) and siliciclastic fraction (SIL %), August 2022

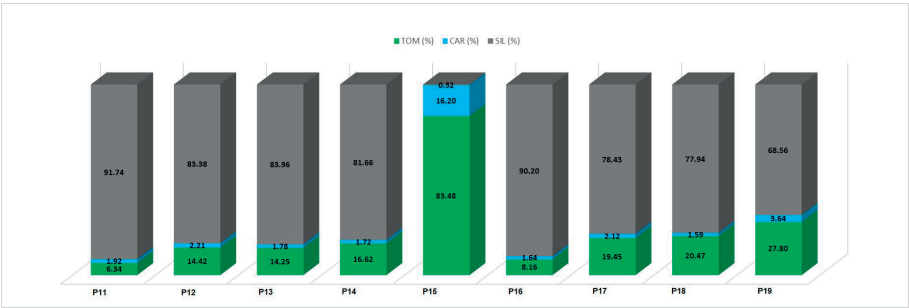


Figure 5. Binary diagram representing the distribution of total organic matter (TOM %), carbonates (CAR %) and siliciclastic fraction (SIL %), August 2022

This phenomenon has been observed in similar sites worldwide and is documented in scientific literature. Additionally, distinct coloration was noted in certain plant species (Figure 6b) at

points with high emissions of CO₂, CH₄, and H₂S. All these observations can serve as surface indicators of potential CO₂ leaks from anthropogenic storage sites.

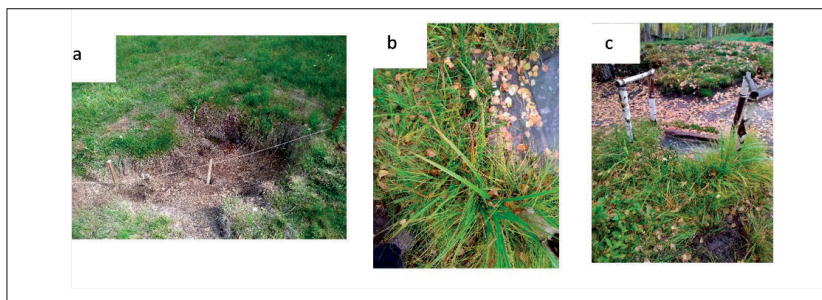


Figure 6. The impact of increased CO₂ concentration on vegetation: a. area without vegetation, b. vegetation with distinct coloration; c - predominance of grasses

CONCLUSIONS

Based on the conducted analyses, it can be concluded that the impact of increased CO₂ emissions on soil manifests in the exceeding of normal concentrations of heavy metals such as chromium, copper, mercury, and nickel at points with high CO₂ emissions, while their levels are reduced at points with lower or normal emissions of post-volcanic gases. Regarding the analysis of water samples, those with high CO₂ concentrations exhibited exceeded levels of nitrites, inorganic phosphorus, and sulphates, suggesting a classification of these waters in quality classes II and III. The influence of high CO₂ concentrations is evident in vegetation, with absence observed at CO₂ concentrations exceeding 20%, predominance of grasses at concentrations below 20%, and distinct coloration noted. These observed and analysed elements could serve as surface indicators of potential CO₂ leaks from anthropogenic storage sites. Consequently, surface monitoring of CO₂ should include periodic sampling of soil and water to monitor exceedances of the aforementioned compounds. Additionally, vegetation monitoring is highly relevant for detecting CO₂ leaks.

ACKNOWLEDGEMENTS

The research leading to these results was made within the projects PN19 20 05 03 "The study of natural CO₂ emission sites in Banat and Harghita for accession to the European ECCSEL network (Studiul siturilor cu emisii naturale de CO₂ din Banat și Harghita în vederea aderării la rețeaua europeană ECCSEL)" and PN 23 30 04 04 "Development of an environmental

monitoring methodology for potential CO₂ storage sites in Romania (Dezvoltarea unei metodologii de monitorizare de mediu pentru potențialele situri de stocare de CO₂ din România)", both financed by the Ministry of Research, Innovation and Digitalization of Romania through the Core Program.

The authors would like to acknowledge and to thank for the support of town hall of Cozmeni who facilitated the access to the site and the smooth running of the campaigns.

We also thank the anonymous reviewers for all suggestions provided for improving the manuscript.

REFERENCES

- Airinei, S., & Pricăjan, A. (1972). Correlations between the deep geological structure and the mofetic aureole in Harghita county, regarding the areas of occurrence of carbonated mineral waters (Corelații între structura geologică adâncă și aureola mofetică din județul Harghita, cu privire la zonele de apariție a apelor minerale carbogazoase). *Geological, Geophysical, Geographical Studies and Research, Geology Series*, 2, 245 –258.
- ASTM-D2216. (2010). *Standard test methods for laboratory determination of water (moisture) content of soil and rock by mass*. West Conshohocken, USA: ASTM International.
- Atanasiu, I. (1939). Regional distribution and genesis of mineral waters in Romania (Distribuția regională și geneza apelor minerale din România), *Rev. Iașul Medical*, 4, Iași, 36-83.
- Bandrabur, T. (1961) Geochemistry of mineral water sediments from the Harghita area (Geochimie des sediments d'eaux minerales de la zone de Harghita). *Asoc. Geol. carp. balc. (Vth Congress 1961)*, 5, 5-16.
- Bányai, J. (1929). *Data on the geology of the mineral waters in Harghita (Daten zur Geologie der Mineralwasser in Harghita)*, Sf. Gheorghe, Romania: Emlékonyv a székely nemzeti muzeum 50-éves jubileumára.

- Bányai, J. (1934). Mineral Waters from Seckler land (A székelyföldi ásványvizek), *Erdélyi Múzeum*, 39, Cluj, 7-12.
- Berner, Z., Jánosi, C., & Péter, É. (2000). A Kelemen-Görgényi-Hargita vonulat ásványvizei” (Mineral waters of Călimani-Gurghiu-Harghita mountain chain). Report for Harghita County Council.
- Dean, W.E. (1974). Determination of carbonate and organic matter in calcareous sediments and sedimentary rocks by loss on ignition: comparison with other methods, *Journal of Sedimentary Petrology*, 44, 242-248.
- Emelyanov, E.M., & Shimkus, K.M. (1986). *Geochemistry and Sedimentology of the Mediterranean Sea*, Dordrecht, N.L.: D. Reidel Publishing Company.
- Geamănu, N., Geamănu, V., Lungu, P., & Lazu, I. (1971). Carbon dioxide manifestations in the underground waters outside the Carpathian flysch between the Valea Tazlăului Mare and the Valea Zăbalei (Manifestări carbogazoase în apele subterane de la exteriorul flișului carpatic între Valea Tazlăului Mare și Valea Zăbalei). *I.G.G. Technical and Economic Studies, E series*, 9, Bucharest, 135-144.
- Ghițulescu, T.P. & Gavăț, I. (1975). The beginnings of Romanian geophysical prospecting (Începuturile prospecțiunilor geofizice românești), *Geophysical Studies and Research*, 13, Bucharest, 15-33.
- Giuşcă, D. (1981). *Studies and researches in geology, geophysics, geography (Studii și cercetări de geologie, geofizică, geografie)*. Bucharest, RO: Publishing house of Academy of R. S. Romania.
- Hakanson, L., & Jansson, J. (1983). *Principles of Lake Sedimentology*. Los Angeles, USA: Springer Berlin Heidelberg.
- Karátson, D., Veres, D., Gertisser, R., Magyari, E.K., Jánosi, C., & Hambach, U. (2022). *Ciomadul (Csomád), The Youngest Volcano in the Carpathians*. Cham, CH: Springer Nature Switzerland.
- Order no. 161/2006. Standard on surface water quality classification for determination of the ecological status of water bodies (Normativul privind clasificarea calității apelor de suprafață în vederea stabilirii stării ecologice a corpurilor de apă), Annex C. Elements and physico-chemical quality standards in water. *Romanian Official Monitor*, I (511 bis), from 13th of June 2006.
- Pascu, R. (1929). Quarries and mineral waters from Ciuc county. (Carierele și apele minerale din jud. Ciuc). *IGR Technical and Economic Studies*, VI(8), Bucharest, 1-53.
- Popa, M., Glevitzky, I., Dumitrel, G.A., Popa, D., Virsta, A., & Glevitzky, M. (2022). Qualitative Analysis and Statistical Models Between Spring Water Quality Indicators in Alba County, Romania. *Scientific Papers-Series E-Land Reclamation Earth Observation & Surveying Environmental Engineering*, 11, 358-366.
- Pricăjan, A. (1972). Mineral and Thermal Waters in Romania. (Apele minerale și termale din România). Bucharest, RO: Technical Publishing House.
- Pricăjan, A. (1974). The dowry of mineral waters and natural gas of Harghita county. (Zestrea de ape minerale și gaze mofetice a Județului Harghita), *Natural Therapeutic Factors from Harghita County*, 7-42.
- Pricăjan, A. (1985). *Therapeutic Mineral Substances of Romania (Substanțele minerale terapeutice din România)*. Bucharest, RO: Scientific and Encyclopedia Publishing House.
- Ricken, W. (1993). Sedimentation as a Three-Component System. Organic Carbon, Carbonate, Noncarbonate. *Geological Magazine*, 132(3), 358-359.
- Sandu, M.A., Virsta, A., Vasile Scăteanu, G., Iliescu, A.-I., Ivan, I., Nicolae, C.G., Stoian, M., & Madjar, R.M. (2023). Water quality monitoring of moara domnească pond, Ilfov county, using UAV-based rgb imaging. *AgroLife Scientific Journal*, 12(1), 191-201. <https://doi.org/10.17930/AGL2023122>
- Seghedi, I., Beșuțiu L., Mirea, V., Zlagnean, L., Popa, R. G., Szakács, A., Atanasiu, L., Pomeran, M., & Vișan M. (2019). Tectono-magmatic characteristics of post-collisional magmatism: Case study East Carpathians, Călimani-Gurghiu-Harghita volcanic range. *Physics of the Earth and Planetary Interiors*, 293, 13 Retrieved 11 November 2022 from https://www.geodin.ro/CUTE/wp-content/uploads/2019/07/Seghedi-et-al_PEPi_2019_v2.pdf.
- Slăvoacă, D. (1971). The genesis of Tușnad mineral waters (Geneza apelor minerale de la Tușnad). *I. G. G. Technical and Economic Studies, E series*, 9, Bucharest, 95-102.
- Slăvoacă, D., Feru, M., Geamănu, V., Simion, G., Goliță, N., & Lungu, P. (1978). Hydrogeological considerations on the natural springs of mineral waters in Romania (Considerații hidrogeologice asupra ivirilor naturale de ape minerale din România). *Technical and Economic Studies, E series*, 13, Bucharest, 5-16.
- Szádeczky, K. G. (1929). *Formation of Székelyland A Székelyföld képződése in Memorial book, Székely National Museum (Emlékkönyv, Székely Nemzeti Múzeum) (pp 491-502)*. Cluj Napoca, RO: Minerva Literary and Printing Institute.
- Török, Z. (1956). Research in the Călimani and Harghita Mountains (Cercetări în Munții Călimani și Harghita). *Reports of the Geological Committee*, 40, 156-160.
- Van der Veer, G. (2006). *Geochemical soil survey of The Netherlands. Atlas of major and trace elements in topsoil and parent material; assessment of natural and anthropogenic enrichment factors*. Utrecht, NL: Netherlands Geographical Studies 347.
- Vasilescu, G. (1964) Hydrogeological research in the People's Republic of Romania (Cercetări hidrogeologice în R. P. România), *Rev. Natura (Geol. Geogr.)* 16(5), Bucharest, 36.

THE INFLUENCE OF TEMPERATURE ON SOUND WAVES

Bogdan ERGHELEGIU, Mirela Alina SANDU, Daniela IORDAN

University of Agronomic Sciences and Veterinary Medicine of Bucharest,
Faculty of Land Reclamation and Environmental Engineering, 59 Marasti Blvd, District 1,
Bucharest, Romania

Corresponding author email: mirela.sandu@fifim.ro

Abstract

Sound waves are mechanical waves in the longitudinal direction that propagate in a variety of solid or gaseous media. The medium for the propagation of sound waves is the atmospheric environment. This medium consists of particles which are influenced by environmental conditions. The purpose of this paper is to show that atmospheric temperature can have an effect on the speed of propagation of sound waves. The measurements on which the study is based were made in the same areas and at the same time intervals, under the same atmospheric conditions, during periods of high and low temperature. The results confirm that the speed of sound waves is influenced by the parameters of the environment in which they propagate. The speed of sound is faster when temperatures are higher.

Key words: environment, propagation, sound waves, temperature.

INTRODUCTION

Noise pollution is an issue of current concern (Baudin et al., 2021; Marquart et al., 2021) and a major problem for the health of the general public (Ertugrul et al., 2021; Liu et al., 2021). Noise pollution is largely a by-product of industrialisation, urbanisation, and modern civilisation. Increasing population and vehicular activity have led to an increase in noise pollution. Traffic noise is a significant source of urban noise, stemming from the movement of people and goods in the city (Hänninen et al., 2014). Excessive exposure to urban noise causes various impairments such as cardiovascular, hearing, or cognitive impairment (Cueto et al., 2017; WHO, 2018). Environmental noise from urban traffic is currently a major health problem in Europe (WHO & JRC, 2011). Approximately 20% of Europe's population is exposed to noise levels harmful to health (EEA, 2019).

Sound is a form of energy. Or we can say that it is a vibration that travels through a medium such as air. Sound even travels through a gaseous medium. It is something that can be heard. The speed of sound is different in different media. A wave is something that carries energy from one place to another through a medium. Sound waves are mechanical waves that propagate through a medium. These waves are created by vibrations, which disturb the molecules in the

medium causing them to oscillate back and forth. The disturbance travels through the medium in the form of a wave, carrying energy with it.

The speed of sound in air does indeed vary with temperature. At higher temperatures, air molecules move faster and can transmit sound more quickly, resulting in a higher speed of sound. Conversely, at lower temperatures, air molecules move more slowly, causing sound to propagate more slowly. This relationship between temperature and the speed of sound can be explained by the kinetic theory of gases, which describes how the motion of gas molecules affects the properties of the gas, including the speed of sound. In air, the speed of sound propagation is 340 m/s at 20°C and 331 m/s at 0°C respectively. The speed of sound is faster when temperatures are higher (Figure 1). The formula used to find the speed of sound in air is as:

$$v = 331 \frac{m}{s} + 0.6 \frac{m/s}{C} \times T$$

where:

- v is the speed of sound;
- T is the temperature of the air.

The case study aims to carry out measurements to determine the influence of environmental conditions - air temperature, on urban traffic noise.

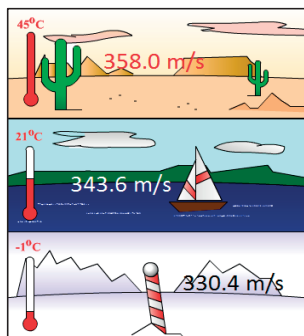


Figure 1. Temperature and the speed of sound
 (<https://www.nde-ed.org/Physics/Sound/tempandspeed.xhtml>)

MATERIALS AND METHODS

In urban areas in Romania there are a significant number of people exposed to high noise levels (Popescu, 2023) especially from traffic (Moscovici & Grecea, 2015) in Bucharest, Romania's capital city (Mihalache et al., 2023; Albu et al., 2019; Tăranu & Ioniță, 2019;

Deaconu & Cioca, 2019; Rusu Boboc et al., 2018; Chiriac et al., 2017).

Romania's capital, Bucharest, is a growing city where noise levels in residential areas during the daytime vary between 55-75 dB, which exceeds the World Health Organization - WHO (WHO, 2018) recommended threshold of 55 dB.

The study area (Figure 2) is located in the south-western part of the city, at the boundary between district 5 and 6, at the intersection of Petre Ispirescu Street, Drumul Sării Street, Antiaeriana Street, Calea 13 Septembrie and Ghencea Boulevard.

The area near the intersection is a mixed area consisting of residential buildings, apartment blocks, houses, shops, restaurants, children's playgrounds, high schools, various institutions, office buildings, busy traffic arteries, as well as streets and pedestrian walkways. It is a congested area of the city with a high level of noise pollution due to heavy traffic, proximity to office buildings and various activities in the area.

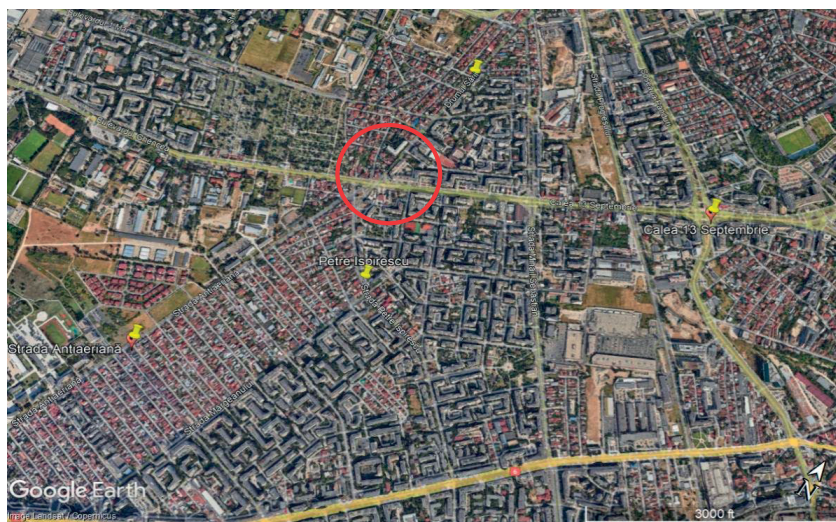


Figure 2. Study area

It was decided to carry out two sets of measurements with similar environmental characteristics, based on forecasts, but to be in two contrasting periods in terms of temperatures, September 2023, and January 2024. In the two measurement periods, September 2023 and January 2024, approximately the same noise sources were

identified; They were mainly produced by public transport in the area, namely buses, trolleybuses and trams that run at approximately equal intervals depending on the time of day or night, intense pedestrian traffic due to existing institutions in the area such as schools, high schools, kindergartens, playgrounds, office buildings, commercial spaces, shops, as well as

various types of vehicles such as motorcycles, bicycles, scooters, etc. In addition to these noises, there are other random sources produced by horns, vehicles that stop suddenly, alarms or various noises of nature, all these sources continuously producing noises.

The environmental conditions at the time of the measurements were as follows: wind speed averaged between 1 and 30 km/h, clear skies, and low precipitation between 0 and 10 mm, atmospheric pressure varied around 1000 hPa. In the first phase, measurements were taken to quantify the noise level and related temperatures and then the measurement sets were compared. The location of the measurements was at the intersection of the Salt Road and the 13 September Road, with measurements taken from the pavement in the immediate vicinity about 30 m from the 13 September Road and about 2 m from the Salt Road. The coordinates of the site, in the 1970 stereographic system, are: East = 584462.00 and North = 324902.00 and Latitude = 44.4189 and Longitude = 26.0591.

Environmental measurements were made using the Lutron sound level meter - Model SL-4012 (Figure 3).



Figure 3. Lutron Sound Level Meter, model SL-4012

The Lutron Sound Level Meter - Model SL-4012 is a high-precision digital instrument with IEC 61672 accuracy class 2, A & C frequency weighting, high-precision condenser microphone and measurement range from 30 to 130 dB. The instrument is designed for measuring urban noise and road traffic. Measurements were made according to the specific requirements for road noise measurements in the immediate vicinity of vehicle traffic at intersections with the

microphone directed towards the main noise source (SR ISO 1996-1 regulation).

The first stage was carried out in September 2023, three times each day at 7 am, 12 pm and 9 pm. The data were taken from the pavement in the immediate vicinity of the intersections mentioned, at a height of 1 metre above the ground. Temperatures at the time of the measurements ranged from a minimum of 8 to 19°C and a maximum of 24 to 34°C.

Depending on the time at which the measurements were taken, they varied as follows: at 7 am temperatures ranged from 10 to 22°C; at 12 noon temperatures ranged from 22 to 31°C; at 9 pm temperatures ranged from 21 to 29°C. As for the ambient noise measurements, they varied according to the time they were taken, as follows: at 7 o'clock, the sound level meter readings ranged from 65.5 dB to 70.4 dB respectively; at 12 o'clock, the sound level meter readings ranged from 63.2 dB to 70.3 dB; at 21.00, the sound level meter readings were between 66.9 dB and 72.5 dB respectively. The second measurement phase was carried out in January 2024, three times a day at the same times 7, 12 and 21. The data were also taken under the same conditions as in the first set of measurements, from the pavement in the immediate vicinity of the intersections mentioned, at a height of 1 metre above the ground. Temperatures at the time of the measurements had minimum values varying between -12°C and 4°C and maximum values between -5°C and 16°C. Depending on the time at which the measurements were taken, they varied as follows: at 7 am temperatures ranged from -9°C to 2°C; at 12 o'clock, temperatures ranged from -2°C to 12°C; at 9 pm temperatures ranged from -6°C to 9°C. The ambient noise measurements varied according to the time of day as follows: at 7 o'clock, the values measured with the sound level meter ranged from 64.9 dB to 69.9 dB respectively; at 12 noon, the sound level meter readings ranged from 62.9 dB to 70.1 dB respectively; at 21.00, the sound level meter readings ranged from 66.6 dB to 71.9 dB. It should be noted that three different times were chosen each being significant because the noise level differs according to the time of day. All the values presented are centralised in Table 1.

Table 1. Measurements taken in September 2023 and January 2024

Date/ Sep.2023	T(C)-max values	T(C)-min values	T(C)-hour 7/2023	noise level(dB)ho ur 7/2023	T(C)-hour 12/2023	noise level(dB)ho ur 12/2023	T(C)-hour 21/2023	noise level(dB)ho ur 21/2023	Date/ Jan.2024	T(C)-max values	T(C)-min values	T(C)-hour 7/2024	noise level(dB)ho ur 7/2024	T(C)-hour 12/2024	noise level(dB)ho ur 12/2024	T(C)-hour 21/2024	noise level(dB)ho ur 21/2024
1	31	14	18	66.5	28	66.6	27	69.8	1	11	-4	-2	65.5	6	66.3	3	69.5
2	32	15	19	68.9	29	65.5	28	70.2	2	11	-2	0	68.6	6	66.4	5	69.1
3	34	13	15	68.9	30	66.5	29	69.9	3	8	-3	-1	68.2	4	66.3	2	69.5
4	26	17	21	67.3	24	65.4	21	68.9	4	14	4	0	67.0	11	65.2	7	68.4
5	28	18	22	69.9	25	65.5	22	69.9	5	16	1	2	69.5	12	65.3	9	69.4
6	30	16	19	70.1	28	65.0	25	69.6	6	12	0	1	69.9	10	64.8	8	69.1
7	31	16	19	66.7	29	65.5	25	68.9	7	8	0	1	66.2	6	65.4	5	68.3
8	29	10	12	65.5	27	64.2	23	70.1	8	3	-5	-2	64.9	2	64.1	1	69.8
9	31	8	10	68.9	28	65.2	22	70.0	9	-2	-8	-6	68.1	0	65.0	-4	69.2
10	29	12	15	68.7	26	66.4	24	69.9	10	1	-9	-6	68.0	0	66.1	-4	69.1
11	29	9	11	70.0	27	64.4	23	69.8	11	3	-7	-4	69.4	0	64.1	0	69.0
12	32	10	14	68.9	28	66.4	25	71.0	12	1	-4	-3	68.2	1	66.2	-2	69.2
13	33	12	15	68.7	30	67.5	27	69.4	13	3	-8	-5	68.1	1	67.1	-3	69.1
14	34	12	14	68.9	31	66.2	27	70.3	14	5	-6	-4	68.2	3	66.0	1	69.5
15	30	18	20	69.6	27	68.1	26	71.1	15	7	-5	-3	68.9	5	67.9	3	70.5
16	24	19	22	70.4	22	68.7	20	72.5	16	8	-4	-2	69.7	7	68.4	3	71.9
17	28	14	18	70.2	26	68.4	23	71.5	17	6	-9	-6	69.5	5	68.1	1	71.0
18	27	11	16	69.7	25	65.3	21	70.5	18	11	-1	0	69.4	10	65.1	6	70.1
19	26	10	14	69.8	25	66.3	20	70.7	19	13	1	2	69.6	11	66.1	7	70.2
20	28	13	16	68.9	26	65.6	23	72.2	20	1	-6	-3	68.2	0	65.2	-1	71.6
21	31	12	14	69.8	29	63.2	25	71.5	21	-1	-10	-7	68.9	-2	62.9	-4	70.8
22	32	14	18	69.9	30	66.3	27	71.2	22	-2	-12	-9	68.1	-2	65.9	-5	70.7
23	34	16	19	68.9	32	67.0	27	71.1	23	-5	-10	-7	68.1	-4	66.7	-6	70.5
24	32	19	22	69.8	30	66.4	26	70.2	24	-2	-5	-2	69.3	-2	66.1	-3	69.8
25	29	16	19	68.5	27	65.6	23	69.7	25	8	-6	-4	68.1	6	65.2	4	69.2
26	30	14	18	66.3	28	67.8	25	69.8	26	7	-3	-1	65.9	6	66.8	4	69.2
27	29	18	21	70.1	26	70.3	24	69.2	27	4	-5	-2	69.8	3	70.1	1	69.1
28	29	14	17	69.2	27	66.6	24	66.9	28	6	-4	-2	69.0	4	66.2	2	66.6
29	30	12	16	66.9	27	61.8	24	69.9	29	5	-5	-2	66.6	4	61.4	2	69.5
30	30	11	15	68.8	27	65.6	25	69.6	30	5	-6	-3	68.4	5	65.2	3	69.2
max	34	19	22	70.4	32	70.3	29	72.5	max	16	4	2	69.9	12	70.1	9	71.9
min	24	8	10	65.5	22	61.8	20	66.9	min	-5	-12	-9	64.9	-4	61.4	-6	66.6
Average	29.9	13.8	17.0	68.8	27.5	66.1	24.4	70.2	Average	5.4	-4.8	-2.7	68.3	4.0	65.8	1.5	69.6

RESULTS AND DISCUSSIONS

Two sets of measurements under similar environmental conditions were carried out for further comparison of the results. The first set of measurements was carried out in September 2023. In terms of temperatures, it was found that the average of the minimum values at which the measurements were taken was 13.8°C and the average of the maximum values was 29.9°C, these varying according to the times at which they were taken, as follows: at 7 am, the average temperature value was 17°C; at 12 noon, the average temperature was 27.5°C; at 21.00, the average temperature was 24.4°C. In terms of ambient noise produced by traffic in the area, it was found that the average of these varied according to the time of day, as follows: at 7 am, the average value was 68.8 dB; at 12 noon, the average value was 66.1 dB; at 21.00, the average value was 70.2 dB. The second measurement phase was carried out in January 2024. In terms of temperatures, it was found that the average of the minimum values at which the measurements were taken was -4.7°C and the average of the maximum values was

5.6°C, these varying according to the times at which they were taken, as follows: at 7 am, the average temperature value was -2°C; at 12 noon, the average temperature was 4°C; at 9 p.m., the average temperature was 1.6°C. In terms of ambient noise produced by traffic in the area, it was found that the average of these varied according to the time of day, as follows: at 7 o'clock, the average value was 68.2 dB; at 12 noon, the average value was 65.8 dB; at 21.00, the average value was 69.6 dB. The systematization of data was achieved by grouping and classifying values into homogeneous groups/classes. For choosing the number of groups/classes we used the relationship:

$$k = 1 + \log_2(n)$$

where:
- n = number of values; for our case resulted a no. of 7 classes.
After ordering the data into classes and calculating the frequencies (number of occurrences of a value), graphical representations were made to analyze noise

levels correlated with the temperatures recorded at the three hours of the day (at 7 o'clock, at 9 o'clock and at 21 o'clock) for the 2 stages of registration (September 2023 and January 2024). Thus, the data obtained were systematized at 7 o'clock/September 2023 - January 2024 (Table 2).

In the same way, the data obtained were grouped at 12 o'clock/September 2023 - January 2024 (Table 3). Similarly, data for the third band were grouped and ordered at 21 o'clock/September 2023 - January 2024 (Table 4).

In order to obtain a spatial image of the data and to highlight the evolution of noise as a function of temperature, the values in (Table 2) found in (Figure 4) were represented. In Figure 4 it is observed that noise values increase at higher temperatures, correlation (interdependence) between the 2 values (temperature/noise) at 7 o'clock/September 2023 - January 2024 is powerful.

Table 2. The grouped results of the period (T (°C)/noise level (dB)/hour 7 sept. 2023 and T (°C)/noise level (dB)/hour 7 Jan. 2024); 7 groups/intervals

T (°C)/hour 7 Sept. 2023	Noise level (dB)/hour 7 Sept. 2023	T (°C)/hour 7 Jan. 2024	Noise level (dB)/hour 7 Jan. 2024
12	65.5	-4	68.2
15	68.8	-3	68.2
18	66.5	-2	69.3
18	66.3	-2	66.6
20	69.6	-1	65.9
21	67.3	0	67.0
22	70.4	1	69.9

Table 3. The grouped results of the period (T (°C)/noise level (dB)/hour 12 sept. 2023 and T (°C)/noise level (dB)/hour 12 Jan. 2024); 7 groups/intervals

T (°C)/hour 12 Sept. 2023	Noise level (dB)/hour 12 Sept. 2023	T (°C)/hour 12 Jan. 2024	Noise level (dB)/hour 12 Jan. 2024
22	68.7	-2	62.9
26	70.3	1	67.1
27	64.4	2	64.1
27	61.8	3	70.1
29	63.2	4	61.4
30	67.5	6	65.4
31	66.2	7	68.4

Table 4. The grouped results of the period (T(°C)/noise level(dB)/hour 21 sept. 2023 and T(°C)/noise level(dB)/hour 21 Jan. 2024); 7 groups/intervals

T (°C)/hour 21 Sept. 2023	Noise level(dB)/hour 21 Sept. 2023	T(°C)/hour 21 Jan. 2024	Noise level (dB)/hour 21 Jan. 2024
20	72.5	1	71.0
20	70.7	2	66.6
21	68.9	3	71.9
23	71.5	4	69.3
23	69.7	5	68,3
24	66.9	7	68.4
25	68.9	7	70.2

This association between variables is given by coefficient of determination $R^2 = 0.9344$ (R-square) (Figure 4). Thus, we can say that (R-square) assign a weight of 93.44% influence of each of the 2 independent variables and 6.56% random factors.

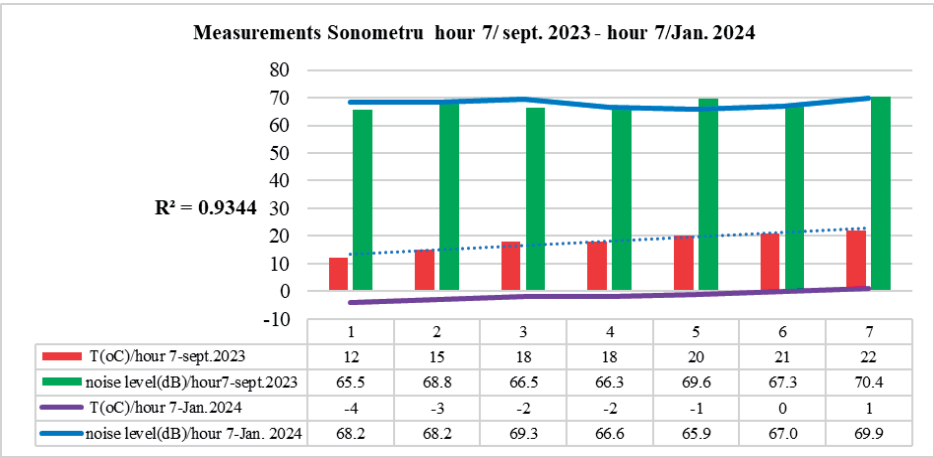


Figure 4. Noise variation as a function of temperature (hour 7/ September 2023 - hour 7/January 2024)

The graphical image of the data (Table 3) is shown in (Figure 5) showing the distribution of noise values according to temperatures. In the graphical representation for grouping data at 12 o'clock/September 2023 - January 2024 also sees the distribution of noise values according to recorded temperatures. The link between the 2 variables (temperature/noise) at 12 o'clock/September 2023 - January 2024 is strong but slightly weaker due to a relatively smaller drop in traffic at 12 o'clock/September 2023 -January 2024. The degree of connection between these 2 variables is given by coefficient of determination $R^2 = 0.9102$ (R-square) (Figure 5). For the data group (Figure 5) (R-square) assigns 91.02% weight to the influence of each

of the 2 independent variables and 8.98% to random factors.

The grouped data (Table 4) can be found in the graphical representation (Figure 6) in which the interdependence between the 2 values (temperature/noise) at 21 o'clock/September 2023 - January 2024 is seen to be strong. Thus, we can say that in this case too, the connection between the 2 variables is related and the dependence is observed in the coefficient of determination $R^2 = 0.9527$ (R-square) (Figure 6). From the representation on the distribution of values (Figure 6) (R-square) assigns 95.27% weight to the influence of each of the 2 independent variables and 4.73% to random factors.

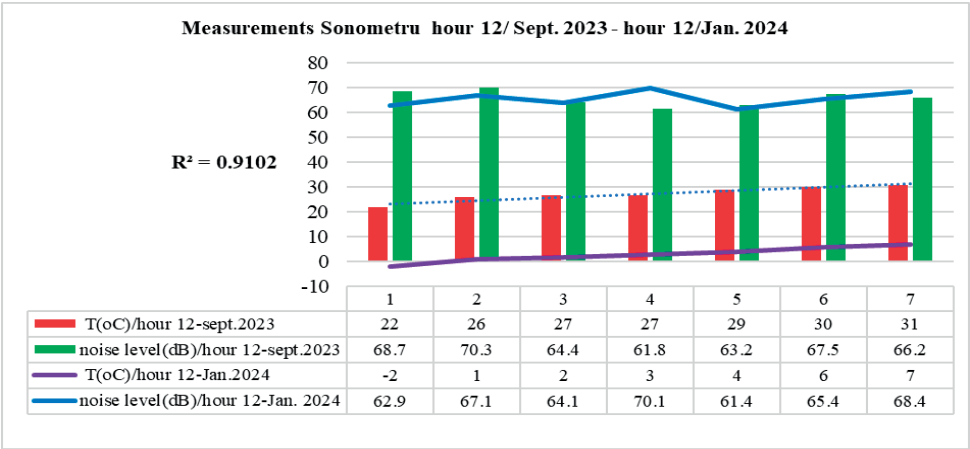


Figure 5. Noise variation as a function of temperature (hour 12/September 2023 - hour 12/January 2024)

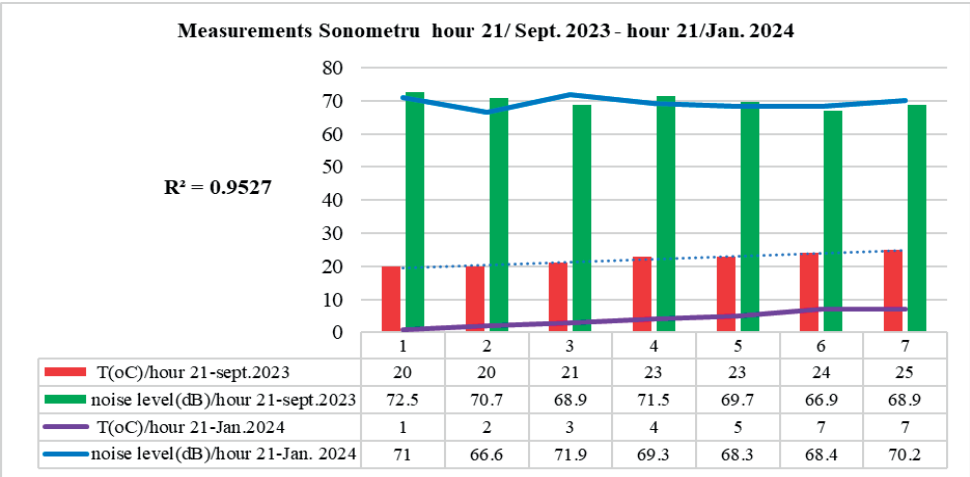


Figure 6. Noise variation as a function of temperature (hour 21/September 2023 - hour 21/January 2024)

In Table 5 are centralized the max./min./average values of the data set used in the study.
With the data grouped in Table 5 we obtained the graphical representation (Figure 7) on the

distribution of max./min./average values that highlight the evolution of noise depending on temperatures for the period September 2023 - January 2024.

Table 5. Max./min./average values of temperatures and noise level - September 2023 - January 2024

(min / max / average) values	T(°C)/hour 7	noise level(dB)/hour 7	T(°C)/hour 12	noise level(dB)/hour 12	T(°C)/hour 21	noise level(dB)/hour 21
max.(T(°C)/(dB)-sep.2023	22.0	70.4	32.0	70.3	29.0	72.5
min. (T(°C)/(dB)-sep.2023	10.0	65.5	22.0	61.8	20.0	66.9
Average/ sep.2023	17.0	68.8	27.5	66.1	24.4	70.2
max.(T(°C)/(dB)-jan 2024	2.0	69.9	12.0	70.1	9.0	71.9
min.(T(°C)/(dB)-jan 2024	-9.0	64.9	-4.0	61.4	-6.0	66.6
Average/ Jan.2024	-2.7	68.3	4.0	65.8	1.5	69.6

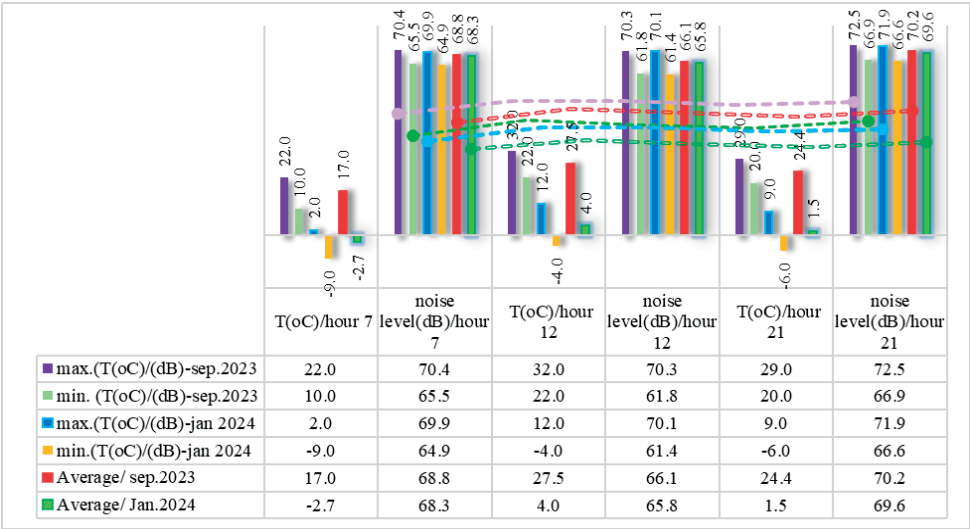


Figure 7. Representation of max./min./average values - September 2023 - January 2024

CONCLUSIONS

Having similar characteristics in both sets of measurements, the values obtained were compared, the aim being to determine the level of traffic noise as a function of ambient temperatures. Also, taking in to account the fact that traffic is different depending on the time of the day, comparisons of the respective values were made according to the period when they fluctuate, being correlated with the corresponding temperatures. From both sets of measurements, it was found that the noise values are lowest around 12 noon, highest in the

morning around 7 am, and highest in the evening around 9 pm. However, it should be noted that the values obtained exceed the threshold recommended by the World Health Organization - WHO (WHO, 2018) of 55 dB. From the point of view of temperatures, it was found that the average temperature varies depending on the time of day, as follows: at 7 am in September 2023, at a temperature of 17°C, a noise value of 68.8 dB was determined. At the same time in January 2024, a noise value of 68.3 dB was determined at an ambient temperature of -2.7°C. Table 1 shows the noise variation as a function of temperature. At 12 o'clock in

September 2023, at a temperature of 27.5°C, a noise value of 66.1 dB was determined. At the same time in January 2024, a noise value of 65.8 dB was determined at an ambient temperature of 4°C. Table 1 shows the noise variation as a function of temperature at 9 pm in September 2023, at a temperature of 24.4°C, a noise value of 70.2 dB was determined. At the same time in January 2024, a noise value of 69.6 dB was determined at an ambient temperature of 1.6°C. If we take the average value of all measurements, for the month of September 2023, for both temperature and noise, we can conclude that at an average temperature of 22.97°C we have an average noise value of 68.4 dB. Similarly, for January 2024, at an average temperature of 0.97°C we have an average noise value of 67.97 dB. Comparing the above values, we can see that at a temperature difference of 22°C between September 2023 and January 2024 respectively, we have a noise difference of 0.43 dB, i.e. at each degree Celsius we have a difference of 0.019 dB. In conclusion, at an average temperature of 22.97°C the traffic noise is more pronounced than at 0.97°C by 0.43 dB. It can therefore be concluded that higher temperatures favour the propagation of sound waves in the atmospheric environment.

ACKNOWLEDGEMENTS

The present paper and the research work included is supported by the Faculty of Land Reclamation and Environmental Engineering, University of Agronomic Sciences and Veterinary Medicine of Bucharest.

REFERENCES

- Albu, C., Olaru, M. & Gavrila, A.G. (2019). Noise pollution in Bucharest: A case study. In *Proceedings of the International Conference on Noise and Vibration Engineering*, pp. 1969-1976.
- Baudin, C., Lefèvre, M., Champelovier, P., Lambert, J., Laumon, B., Evrard, A.-S. (2021). Self-Rated Health Status in Relation to Aircraft Noise Exposure, Noise Annoyance or Noise Sensitivity: The Results of a Cross-Sectional Study in France. *BMC Public Health* 21, 116.
- Chiriac, C.R., Chiriac, A.E. & Popa, V. (2017). Environmental noise monitoring in Bucharest using GIS technology. *Energy Procedia*, 111, 553-562.
- Cueto, J.L., Petrovici, A.M., Hernández, R. & Fernández, F. (2017). Analysis of the impact of bus signal priority on urban noise. *Acta Acustica United Acustica*, 103(4), 561–573. <https://doi.org/10.3813/AAA.919085>.
- Deaconu, S. & Cioca, L.I. (2019). Noise pollution and urban planning in Bucharest, Romania. In *Proceedings of the 16th International Multidisciplinary Scientific GeoConference SGEM*, pp. 63-70.
- EEA Report (2019). Environmental noise in Europe — 2020. ISSN 1977-8449. https://www.courthousenews.com/wp-content/uploads/2020/03/Environment-noise-in-europe-2020_TH-AL-20-003-EN-N.pdf
- Ertugrul, E., Sercan, E., (2021). GIS based mapping and assessment of noise pollution in Safranbolu, Karabuk, Turkey. *Environment, Development and Sustainability*, 23, 15413–15431.
- Hänninen, O. (2014). Environmental burden of disease in Europe: assessing nine risk factors in six countries, *Environmental Health Perspectives*, 122(5), pp. 439-446 DOI: <https://doi.org/10.1289/ehp.1206154>.
- Liu, S., Lim, Y.-H., Pedersen, M., Jørgensen, J.T., Amini, H., Cole-Hunter, T., Mehta, A.J., So, R., Mortensen, L.H., Westendorp, R.G.J. (2015). Long-Term Exposure to Ambient Air Pollution and Road Traffic Noise and Asthma Incidence in Adults: The Danish Nurse Cohort. *Environ. Int.*, 152, 106464.
- Marquart, H., Ueberham, M., Schlink, U. (2021). Extending the Dimensions of Personal Exposure Assessment: A Methodological Discussion on Perceived and Measured Noise and Air Pollution in Traffic. *J. Transp. Geogr.* 93, 103085.
- Mihalache, C., Ergehelegiu, B., Sandu, M.A. (2023). Noise Pollution: A Gis-based approach to mapping and assessment. *Scientific Papers Series E, Land Reclamation, Earth Observation & Surveying, Environmental Engineering, XII*, 2285-6064.
- Moscovici, A.-M. & Grecea, O. (2015). Results of research in noise pollution in urban areas. *AgroLife Scientific Journal*, 4(2).
- Popescu, D.I. (2023). A Study of the Romanian Framework and the Challenges in Implementing the Noise Mapping Legislation. *Archives of Acoustics*, 48(2), DOI:10.24425/aoa.2023.145233.
- Rusu, C.M., Roşu, E., Georgescu, L.P. (2015). Assessment of urban noise pollution in Bucharest, Romania. *Journal of Environmental Protection and Ecology*, 16(3), 1293-1303.
- Tăranu, N. & Ioniță, I. (2019). Mapping noise pollution in Bucharest using GIS technology. *Environmental Engineering and Management Journal*, 18(11), 2593-2601.
- WHO & JRC (2011). Burden of Disease from Environmental Noise - Quantification of healthy life years lost in Europe. <https://apps.who.int/iris/handle/10665/326424>.
- World Health Organization - WHO, (2018). Environmental noise guidelines for the European region, WHO Regional Office for Europe, Copenhagen, <http://www.euro.who.int/en/health-topics/environment-and-health/noise/publications/2018/environmental-noise-guidelines-for-the-european-region-2018>. <https://www.nde-ed.org/Physics/Sound/tempandspeed.xhtml>

STUDIES REGARDING THE USE OF POURED EARTH IN BUILDINGS

Aurelian GRUIN^{1,2}, Cornelia BAERĂ^{1,2}, Sorin DAN²,
Bogdan BOLBOREA^{1,2}, Ana Cristina VASILE¹

¹National Institute for Building Research, Town Planning and Sustainable Territorial Development - URBAN - INCERC, 266 Pantelimon Road, District 2, Bucharest, Romania

²Politehnica University of Timisoara, 2 Victory Place, Timisoara, Romania

Corresponding author email: aurelian.gruin@gmail.com

Abstract

This study explores poured earth construction as an environmentally friendly alternative to conventional cement-based materials. Soil materials, mirroring natural concrete with grains bonded by clay particles, presents environmental benefits, including recyclability, low environmental impact, and effective hygrothermal regulation. The decline in traditional earth construction is associated with industrialization, prioritizing efficiency over traditional methods. The technique involves pouring a mixture of local earth, sand, gravels, and a modest quantity of either Portland cement or additives as alternatives into formworks to fabricate load-bearing and non-loadbearing elements. Despite its potential as a sustainable option, challenges such as shrinkage control and durability persist. Poured earth construction can be a substitute for cement-based materials. Ongoing research and practical applications illustrate feasibility, but further advancements are necessary to enhance productivity and mitigate environmental impact, with additives for stabilization emerging as a prospective way for future development.

Key words: clay, formwork, load bearing, poured earth.

INTRODUCTION

In the pursuit of sustainable development solutions, the use of natural, recyclable, and low-energy-consumption materials, along with building systems and technologies that promote safety, flexibility, and energy efficiency, is becoming increasingly relevant. The thermal performances of buildings, which directly impact energy efficiency, have significant economic, social, and environmental implications. Consequently, the energy consumed throughout a building's lifespan emerges as a key element in the construction sector, underlining the necessity of adopting sustainable and energy-efficient construction practices.

However, the current approach of standards primarily focuses on the objective of energy efficiency, which limits the definition of sustainability and overlooks the specificity of place and relevant cultural and regional aspects. In this context, there is a need to pay greater attention to the social and cultural components of local specificity to develop solutions that enhance the sense of belonging and encourage the formation of communities with common

interests. This can be achieved by leveraging the specific knowledge of the local community in developing sustainable architectural solutions, aiming to strike a balance between energy efficiency and cultural and regional appropriateness.

Vernacular building techniques, inspired by local traditions, represent adaptive ways to the specific conditions of the environment (Özen et al., 2012; Alrashed et al., 2017; Moscoso-García & Quesada-Molina, 2023). Therefore, traditional buildings made with soil materials are capable of meeting a wide range of physical and spiritual needs, seamlessly integrated into the context of the communities in which they are located (Salgin et al., 2017).

Despite the interest shown by the scientific community, the practical use of these materials remains limited. In order to stimulate the interest and usage of soil-based materials in construction (Morel et al., 2021) conducted a study to identify and analyse the latent barriers hindering the adoption of these types of constructions on a large scale, namely: technical, organizational, political and socio-economic barriers. The scientific community is concentrating on the technical aspect in evaluating the performance

of soil-based materials with different additives or waste products (Limami et al., 2020; Makrygiannis & Tsetsekou, 2022; Wolf et al., 2022), especially those containing complex compositions like cob, rammed and poured earth walls with large elements such as gravels, stones, and synthetic or natural fibres (Ojo et al., 2020; Koutous & Hilali, 2021; Sabbà et al. 2021; El Bourki et al., 2023) testing on representative elementary volumes presents challenges (Pinel et al., 2021). Additionally, further investigation is warranted into the actual effects of earth-based materials on thermal behaviour (Mansour et al., 2016; Dao et al., 2018; El Wardi et al., 2022) and indoor air quality (Gomes & Miranda, 2022). Research gaps exist in understanding and controlling the drying kinetics of these walls and their consequential impact on mechanical properties (such as creep and strength) and durability (including resistance to freezing-thawing cycles and fire). Furthermore, there is a need to identify conditions leading to durability issues and develop tools to manage them effectively. Additionally, assessing inhabitant comfort (Ben-Alon & Rempel, 2023) and the influence of earthen walls on it, remains an underexplored technical area deserving future exploration.

The organizational barrier consists of few regulations internationally and especially the lack of standards in Romania to allow the use of earth/clay in the design or execution of constructions. A short review of publications dealing with the construction of rammed or poured earth houses in seismically active zones reveals that most of these documents are designed as instructional publications providing construction specifications to be followed. However, only two of these, namely the work of Arya A.S. (Arya et al., 2014) and the NZS 4297 standard, include formulas for seismic design. Other publications refer to other works to obtain more details on seismic design, such as the NZS 4203 standard mentioned within NZS 4297. Additionally, the design guidelines in NZS 4297 are considered useful by Australian standards as well. In the case of IS 13837, it refers to the IS 1893 part 1:2002 standard for seismic design, while the ASTM E2392-M10 standard specifies the need for seismic design following ASCE 7-16. Although not explicitly mentioned within NBC 204, seismic design is covered by the

Nepalese code NBC 105, which, in turn, recommends application together with the Indian standard IS 4326 - Code of Practice for earthquake-resistant design and construction of buildings. As can be noted, for designing according to the standards and regulations of a construction made of compacted or poured earth, the designer must consult documents from different countries to achieve a structure with seismic action capacity. For Europe, a possible solution to this situation would be to have a unified code, similar to EN 1998-1, Eurocode 8, Part 1 where there are specific rules for steel, concrete, and masonry buildings that analyse specific design criteria for different construction materials, providing detailed information on design calculations to ensure that structures are capable of resisting seismic forces. This may not currently be possible for earthen construction due to the lack of design methods that are not sufficiently researched, correlated, and unified in the form of clear, accepted, implemented, and legislated regulations at the national or European level.

The current study focuses on the use of local raw material for poured earth as a technique of earth building that uses stabilized earth in fluid form, which is then poured into moulds to create durable earthen walls. The earthen material is quarried from Timis County, Romania, an area with a rich tradition in earthen heritage building. Two different soils, fine crushed sand/gravel and additives were mixed and tested to evaluate the pouring settlement, appearance of cracks and strength to further develop a mix for earthen walls.

To achieve the objective, the poured earth must meet in the final stages of the research four main requirements:

It must have high fluidity to be poured/pumpable and ideally self-compacting. At the time of pouring into moulds, it should exhibit a liquid-solid transition behaviour allowing the wall to support its weight after a short drying period. Additionally, the minimum mechanical strength achieved in the wet state should be approximately 0.07 MPa (Pinel et al., 2017), to be obtained in less than 24 hours, a value close to other materials on the market.

It should be formulated with a general formula compatible with the wide variability of earth-based raw materials. To achieve this, besides the

classical analysis of granular correction, the effects on hygrothermal and recycling properties must also be considered, using non-toxic additives.

It should be available at a price that determines costs close to other materials on the market.

MATERIALS AND METHODS

Two types of soils were collected from different areas of Timis County, areas with a rich tradition in earthen heritage building. The grain size distribution of these soils was determined with the combined method according to STAS 1913/5, SR EN ISO 14688-1 and SR EN ISO 14688-2. The results are presented in Table 1. The inclusion in the ternary diagram was made following NP-074:2022 and is presented in Figure 1.

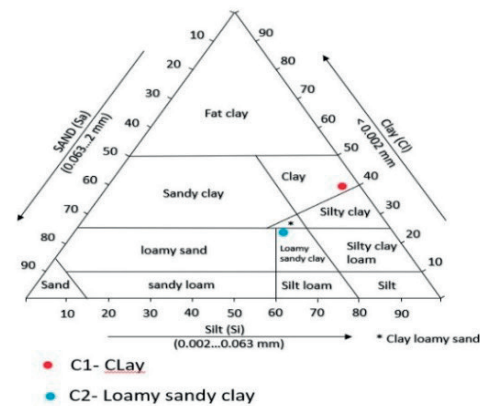


Figure 1. Ternary diagram

Table 1. Determination of grain size distribution through sedimentation

Soil	Clay	Silt	Sand	Gravel
C1	23.50	49.91	26.37	0.22
C2	40.00	56.34	3.66	0.00

The aggregates used are 0/4 mm alluvial silico-limestone, washed sand and 4/8 mm gravel, supplied by a certified quarry.

To reduce the water content and crack a dispersant, Sodium Tripolyphosphate, granular CARFOSEL 996, from Prayon S.A. was used. With the help of the dispersant, the yield stress and viscosity of pastes can be reduced, and the arrangement of clay particles is more regular with the effect of improving the mechanical

strength of clay materials (Rossington et al., 1998).

Normal hydrated lime (HL) was used as a primary additive. Hydrated lime undergoes a chemical reaction with clay particles wherein calcium ions from the hydrated lime displace water molecules and other ions present on the surface of the clay particles upon mixing. This process results in the alteration of soil structure, rendering it friable and granular. Consequently, this transformation enhances the efficacy of soil mixing and compaction processes.

As a secondary additive, calcium lignosulfonate (CL - 48%) concentration and density of 1250 kg/cm³, was used as a catalyst and producer of ion exchanges in the soil structure (Fernandez et al., 2021).

Tap water, with a temperature comprised between 14 and 16°C, was used for all the experiments.

A detailed process of mixing and pouring (vibrating) is presented in Table 2.

Table 2. Work operations

Work operations	Time [min]
Mixing soil and aggregates	5
Adding water	5
Adding dispersant	10
Conducting settlement determination	-
Pouring and vibrating	-
Weighing process (with formwork)	-
Stripping of samples	24 h/3 days

This preliminary research program was conducted in two stages, the first using mostly soil C1 without the use of dispersant. In this stage (R1-R8) water was added to obtain a settlement of 10-15 cm (S3) for each mix. In the second stage (R9-R_{cam}), the mixing water remained fixed at 18% of the material's mass, with the variation being determined by the percentage of aggregates and dispersant.

Metal moulds measuring 40 x 40 x 140 mm were utilized and kept at 20°C and 50-70% air humidity. From visual observations throughout the drying period, multiple cracks appeared in compositions R1, R9 and R14, leading to their exclusion from subsequent tests.

The consistency of the mixtures was evaluated using the compaction method following SR EN 12350 and classification of settlement according to SR EN 206 by analogy with concrete and the results are presented in (Figure 2).

At 24 and 48 hours after casting, it was not possible to demould the samples as the composition adhered to the mould walls. Demoulding was successfully performed at 3 days after casting without damaging the samples. After demoulding, the samples were weighed to monitor the drying period, with the results presented for each composition in Figure 2 as the mass evolution over time and environmental conditions. The proposed compositions, prepared in stage 1 (R1-R8) and stage 2 (R9-Rcam) are presented in Table 3.

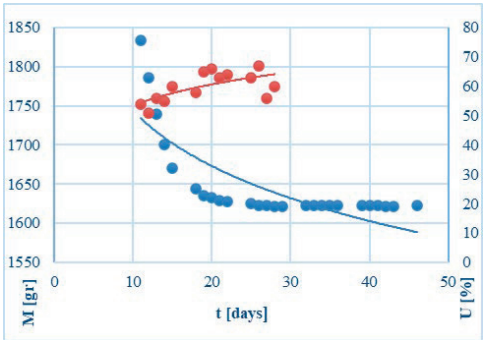


Figure 2. Evolution of drying

Table 3. Compositions

Mix	C1	C2	Sand 0/4 mm	Gravel 4/8 mm	Dispersant % from total mass	Additives %
	%	%	%	%	%	%
R1	-	100	-	-	-	-
R2	75	-	12.5	12.5	-	-
R3	47,5	-	30	17.5	-	-
R4	35	-	30	30	-	5 HL
R5	40	-	30	30	-	-
R6	-	40	30	30	-	-
R7	45	-	20	25	-	10 HL
R8	50	-	25	25	-	-
R9	100	-	-	-	0.2	-
R10	100	-	-	-	0.2	-
R11	75	-	25	-	0.2	-
R12	60	-	40	-	0.2	2 CL
R13	90	-	10	-	0.15	-
R14	-	18	-	-	0.15	-
R _{CAM}	-	25	75	-	-	Straw 1%

After 45 days of drying, for each stage, mechanical tests were carried out to determine flexural and compressive strength by aligning with the mortar standard, using equipment with controlled speed for each determination following SR EN 1015-11, SR EN 196-1.

RESULTS AND DISCUSSIONS

The requirements for pumpable material were met by preparation of mixes R1 to R8 without dispersant with adding water while for the mixes R9 to R13 where percentage of aggregate and the dispersant varies, the compaction goes from S3 to self-compacting.

As shown in Figure 3 the samples were considered dried when the differences between weighing's were lower than 2% taking into consideration the span of air humidity.

The results of the mechanical tests are presented in Figure 4.

In terms of compressive strength, compositions R1 to R9 differentiate based on the percentage of aggregates and the additive (LM) used. The tests from stage 1 indicate the need for the addition of aggregates to complement the compositional matrix and enhance strength, as well as additives that interact with clay particles to form a more stable and stronger matrix.

Using a 10% lime modifier for recipe R7 led to a 100% increase in compressive strength compared to recipe R3. It is essential to investigate the interaction mode of the lime modifier with each soil as well as the saturation curve of clay particles with this additive. In stage 2 the effect of the dispersant on both soil types is highlighted by the increase in strengths across all compositions compared to stage 1 (without dispersant). The addition of additives and fibers resulted in compressive strength values of 2.7 MPa and 1.8 MPa, respectively.

CONCLUSIONS

The study conducted provides evidence of the interest shown by the scientific community for poured earth constructions as a viable alternative to conventional cement-based materials, even in the absence of specific regulations.



Figure 3. Aspects during consistency tests and evaluation of settlement

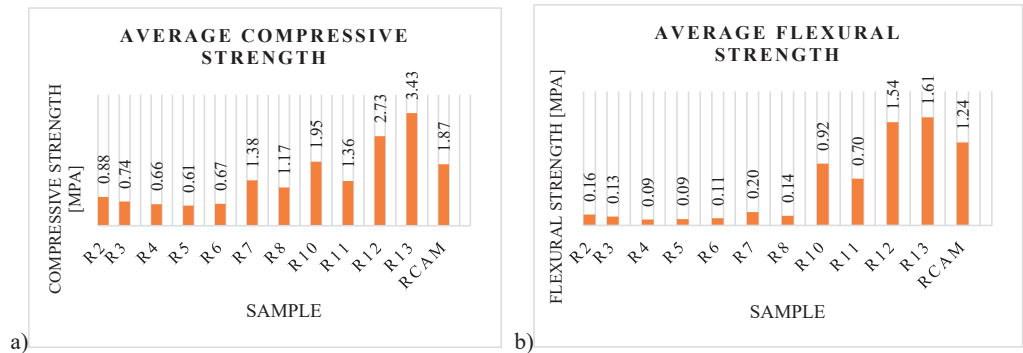


Figure 4. Average a) compressive strength and b) flexural strength

However, further research and development are warranted to establish standardized guidelines and optimize techniques for maximizing the benefits of poured earth construction. The use of the dispersant in earth compositions has led to settlements corresponding to S3-S5 (pumpable) and an increase in mechanical strengths, with the variation in the water/dispersant percentage being subject to further extensive research. The preliminary tests carried out show that lignin plays a stabilizing role, enhancing strengths, the percentage variation of which will be subject to further research. Additionally, a

combination of both soils mixed with additives could be introduced into the composition. Given the conclusions outlined, it is essential to persist in research efforts aimed at evaluating the capabilities of compositions and materials incorporating earth. Specifically, attention should be directed towards assessing their ability to meet the necessary strength requirements for both load-bearing and non-load-bearing elements in construction applications. This ongoing research will offer valuable insights into the suitability and potential utilization of earth-based materials in various construction scenarios

ACKNOWLEDGEMENTS

This work was carried out within Nucleu Programme of the National Research Development and Innovation Plan 2022-2027, supported by MCID, "ECODIGICONS" project no. PN 23 35 04 01: Fundamental-applied research into the sustainable development of construction products (materials, elements, and structures, as well as methods and technologies) that utilizes current national resources to enhance the eco-innovative and durable aspects of Romania's civil and transport infrastructure.

REFERENCES

- Alrashed, F., Asif, M., Burek, S. (2017). The role of vernacular construction techniques and materials for developing zero-energy homes in various desert climates. *Buildings*, 7(1), 17.
- Arya, A. S., Boen, T., Ishiyama, Y. (2014). *Guidelines for earthquake resistant non-engineered construction*. UNESCO.
- Ben-Alon, L. & Rempel, A. R. (2023). Thermal comfort and passive survivability in earthen buildings. *Building and Environment*, 238, 110339.
- El Bourki, A., Koutous, A., Hilali, E. (2023). Fiber-reinforced Rammed Earth: State of the Art and Perspectives. *Civil Engineering and Architecture*, 11(5A), 3162-3174. DOI: 10.13189/cea.2023.110826.
- El Wardi, F. Z., Ladouy, S., Atbir, A., Khabbazi, A. (2022). Study of the thermal and mechanical properties of local clay materials activated with quicklime, Sefrou (Morocco). *Materials Today: Proceedings*, 58, 1423-1430.
- Fernandez, M. T., Orlandi, S., Codevilla, M., Piqué, T. M., Manzanal, D. (2021). Performance of calcium lignosulfonate as a stabiliser of highly expansive clay. *Transportation Geotechnics*, 27, 100469.
- Gomes, M. I. & Miranda, T. (2022). Indoor air quality for sustainability, occupational health and classroom environments through the application of earth plaster. HERITAGE 2022 - International Conference on Vernacular Heritage: Culture, People and Sustainability, September 15th-17th, 2022 Valencia, Spain.
- Koutous, A. & Hilali, E. (2021). Reinforcing rammed earth with plant fibers: A case study. *Case Studies in Construction Materials*, 14, e00514.
- Limami, H., Manssouri, I., Cherkaoui, K., Khaldoun, A. (2020). Study of the suitability of unfired clay bricks with polymeric HDPE & PET wastes additives as a construction material. *Journal of Building Engineering*, 27, 100956.
- Makrygiannis, I. & Tsetsekou, A. (2022). Efficient Recovery of Solid Waste Units as Substitutes for Raw Materials in Clay Bricks. *Recycling*, 7(5), 75.
- Mansour, M. B., Jelidi, A., Cherif, A. S., Jabrallah, S. B. (2016). Optimizing thermal and mechanical performance of compressed earth blocks (CEB). *Construction and Building Materials*, 104, 44-51.
- Morel, J. C., Charef, R., Hamard, E., Fabbri, A., Beckett, C., & Bui, Q. B. (2021). Earth as construction material in the circular economy context: practitioner perspectives on barriers to overcome. *Philosophical Transactions of the Royal Society B*, 376(1834), 20200182.
- Moscoso-García, P. & Quesada-Molina, F. (2023). Analysis of Passive Strategies in Traditional Vernacular Architecture. *Buildings*, 13(8), 1984.
- Ojo, E. B., Bello, K. O., Ngasoh, O. F., Stanislas, T. T., Mustapha, K., Savastano Jr, H., & Soboyejo, W. (2020). Mechanical performance of fiber-reinforced alkali activated un-calcined earth-based composites. *Construction and Building Materials*, 247, 118588.
- Özen, H., Keles, S., Engin, E. (2012). Vernacular building heritage in the eastern black sea region in Turkey. *Journal of Civil Engineering and Architecture*, 6(7), 867.
- Pinel, A., Prud'Homme, E., Charlot, A., Fleury, E., Jorand, Y. (2021). Earthen construction: Demonstration of feasibility at 1/2 scale of poured clay concrete construction. *Construction and Building Materials*, 312, 125275.
- Rossington, K. R., Senapati, U., Carty, W. M. (1998). A Critical Evaluation of Dispersants for Clay-Based Systems. *Materials & Equipment/Whitewares: Ceramic Engineering and Science Proceedings*, 19, 77-86.
- Sabbà, M. F., Tesoro, M., Falcicchio, C., Foti, D. (2021). Rammed Earth with Straw Fibers and Earth Mortar: Mix Design and Mechanical Characteristics Determination. *Fibers*, 9(5), 30.
- Salgin, B., Bayram, Ö. F., Akgün, A., Agyekum, K. (2017). Sustainable features of vernacular architecture: Housing of Eastern Black Sea Region as a case study. *Arts* (Vol. 6, No. 3, p. 11).
- Wolf, A., Rosendahl, P. L., Knaack, U. (2022). Additive manufacturing of clay and ceramic building components. *Automation in Construction*, 133, 103956.

COMPARISON OF METHODS FOR ANTIBIOTIC COMPOUNDS REMOVAL FROM AQUEOUS SOLUTIONS

Diana HANGANU¹, Lidia FAVIER², Maria HARJA¹

¹"Gheorghe Asachi" Technical University of Iasi-Romania, Faculty of Chemical Engineering
and Environmental Protection, 73 Prof. D. Mangeron Blvd, Iasi, Romania

²University of Rennes, Ecole Nationale Supérieure de Chimie de Rennes,
11 Allée de Beaulieu, 7 Rennes Cedex, France

Corresponding author email: maria_harja06@yahoo.com

Abstract

This article presents an in-depth exploration of diverse methodologies for the separation and removal of various classes of antibiotics from water and aqueous solutions. Focusing on recent advancements, the study offers a comprehensive overview of active substances and novel combinations employed in the removal processes. Notably, the role of adsorbents is discussed, emphasizing their high porosity that enables efficient absorption of substantial contaminant doses. Additionally, the financial benefits of employing photocatalysts in contaminant degradation are highlighted, with an emphasis on the growing body of research in this area. The historical significance of exchange resin as one of the pioneering removal methods is acknowledged, alongside a more contemporary examination of electrochemical approaches specifically tailored to the structural and ionic characteristics of antibiotics. Serving as a valuable guide, this article addresses the advantages and considerations associated with diverse methods of separating antibiotics from aqueous solutions, providing insights into emerging technologies and facilitating informed decision-making in environmental remediation efforts.

Key words: antibiotics, adsorption, exchange resin, photocatalysis.

INTRODUCTION

The most frequently detected organic micropollutants in wastewater are pharmaceutically active compounds, either individually or in combination, utilized as medications to treat various diseases (Natarajan et al., 2022). Hospital wastewater stands out as a significant source of antibiotic pollution due to the release of drugs and their metabolites into the environment through the excretion of treated patients (Shen et al., 2022; Sanguanpak et al., 2022). The active substances from medications become part of the ecosystem, affecting the metabolism of wildlife. Even though drinking water treatment plants treat surface water, recent research indicates the presence of traces left behind by the process.

The pharmaceutical compounds are discharged into the environment in their original or metabolized forms (Rusu et al., 2021), often leading to adverse effects as their toxic potency can exceed that of the parent substance (Figure 1). The accumulation of antibiotics in the environment can contribute to the emergence of antibiotic-resistant bacteria, thereby fostering

resistance to drugs in microorganisms. Additionally, this accumulation can result in endocrine disruption, genotoxicity, aquatic toxicity, and the proliferation of pathogenic bacteria resistant to antibiotics. The crucial aspect of separating antibiotics from wastewater primarily revolves around halting or diminishing the process of bacterial antibiotic resistance (Sanguanpak et al., 2022).

Lipophilic molecules reach the adipose tissue of surrounding animals from the water, including the meat intended for human consumption, thus amplifying bacterial resistance to antibiotics. Chloramphenicol and tetracyclines have been identified in significant concentrations, up to 10 mg per 1 kg of vegetables such as tomatoes, cucumbers, lettuce, and carrots, becoming components of the human diet (Wang et al., 2011).

This article will explore several methods for separating drugs from water, each with its own application in nature, while detailing their respective advantages and disadvantages. Many of these methods are particularly effective for removing water-soluble compounds, which are challenging to eliminate from wastewater.

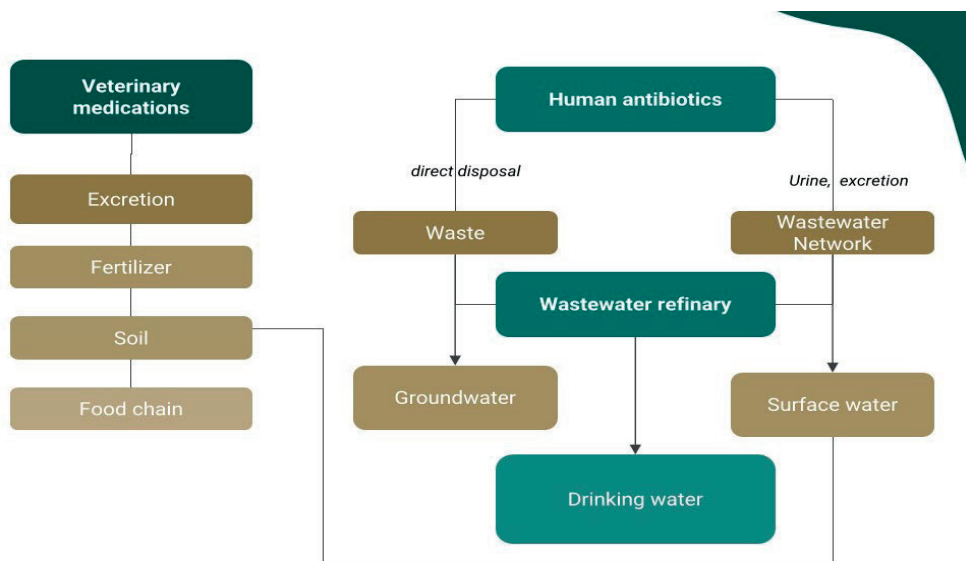


Figure 1. Sources of contamination

While resin exchange, adsorption, photocatalysis, and electrochemical oxidation have shown promising results individually, it is likely that a combination of these techniques will offer the most effective solution for separating a mixture of drugs with diverse chemical structures from aqueous environments.

MATERIALS AND METHODS

Methods for removal antibiotic compounds

The methods that can be used for removal of organic compounds from wastewaters are presented in Figure 2 (Derakhshan et al., 2018; Favier et al., 2023). There are three types of traditional wastewater treatment methods: chemical, physical, and biological.

The chemical processes include neutralization, oxidation, reduction, electrolysis, ion exchange, and catalysis. Two types of properties are associated with chemical wastewater treatment that are considered advantageous: the properties of the reaction products between treated chemicals and contaminants, refer to their volatility, solubility, or other properties related to their inability to remain in suspension and/or water stream; and the chemical characteristics of the pollutants, associated to their ability to interact or react with chemicals designed to treat pollutants. The biological treatments typically are realized with bacteria, nematodes, or other

microscopic organisms, that break down the organic pollutants in wastewater. Using regular cellular processes, converting the biodegradable organic contaminants into simple substances and additional biomass (Phoon et al., 2020; Roşu et al., 2022). Anaerobic digestion, aerated lagoons, activated sludge, fungal treatment, trickling filters, and stabilization are the components of the biological approach. Physical methods of treating wastewater involve removing pollutants through the application of physical barriers and forces found in nature, such as gravity, electrical attraction, and van der Waals forces. The chemical structure of the polluting chemicals is typically not altered by physical treatment. There are, however, some exceptions where the physical state is altered, such as scattered compounds that may have led to agglomeration, as is commonly observed in the filtration and vaporization stages. The physical methods include the following processes: sedimentation, coagulation, membrane treatment, adsorption, distillation, and filtration.

The rate of hydrolysis is crucial for determining how long antibiotics would survive in the environment. Certain organic molecules, such as amides and esters, can undergo substantial breakdown in the environment through a process of hydrolysis.

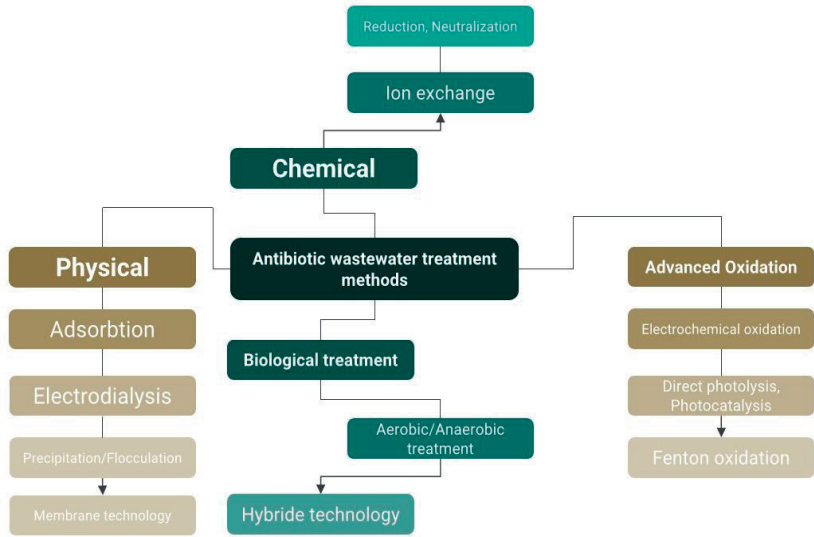


Figure 2. Methods for removing antibiotic substances

Because of their strong polarity, antibiotics containing amides and esters functional groups may be less bio-accumulative (Lin et al., 2007). The most significant environmental variables that affect the rate of hydrolysis are pH and temperature; for example, the rate of hydrolysis usually increases with temperature, on the other hand ionic strength influences hydrolysis.

The adsorption method stands out as a widely used, cost-effective, and non-toxic approach with high regeneration rates for adsorbents. In the process of adsorbing pharmaceutical substances, interactions between the adsorbent and the active compound span various types, including physical bonds, weak chemical bonds, electrostatic interactions, or donor-acceptor interactions.

The selection of a polymer matrix or an ion-exchange column depends on the specific chemical structure of the active substance and its functional groups. To enhance the creation of new active sites, elevate degradation efficiency through accelerated electron transfer, and modify electron density, some research incorporated nitrogen atoms into geopolymers by doping them with nitric acid during polymerization (Huang et al., 2023).

Adsorption can be categorized into physical physisorption, driven by weak intermolecular forces, and chemical chemisorption, involving stronger chemical bond formation such as

electrostatic attraction, ion exchange, van der Waals forces, and hydrogen bonding (Sanguanpak et al., 2022).

Adsorption mechanisms encompass physical adsorption, involving various intermolecular forces like hydrogen bonding and van der Waals forces, and chemisorption, characterized by stronger chemical bond formation such as electrostatic attraction, ion exchange, and hydrogen bonding (Figure 3).

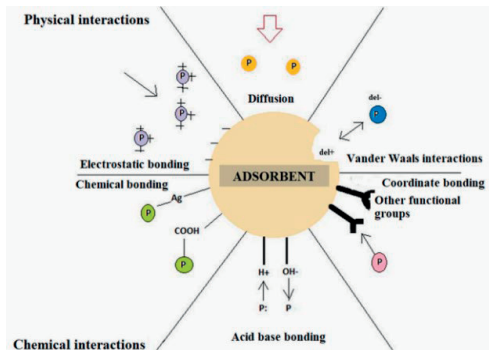


Figure 3. Adsorption mechanism

Other contributing factors include hydrophobic effects, electrostatic interactions, and covalent interactions, including electron acceptor-donor interactions.

Electrostatic repulsion between negatively charged groups from adsorbent and anionic

groups from drugs can hinder effective adsorption. pH plays a crucial role in effective adsorption; when the solution pH is below the pharmaceutical's pK_a value, the drug remains ionized, facilitating greater adsorption onto negatively charged adsorbents through electrostatic linkage (Natarajan et al., 2022).

The characteristics of an adsorbent are crucial for adsorption processes include porosity, high surface area, and functional groups, particularly hydroxyl and amino groups, which facilitate excellent adsorption capabilities. Research have endeavoured to enhance the porosity of adsorbent by employing surface modifiers, including surfactants like cetyltrimethyl-ammonium bromide and sodium dodecyl sulphate, or foaming agents such as hydrogen peroxide and aluminium. This effort aims to facilitate their application as adsorbents for the removal of different types of pollutants (Youssef et al., 2023).

Enhancing the specific surface area of the adsorbent promotes interaction between active adsorption sites and the molecules being adsorbed. This is facilitated by interconnected pores of varying sizes and shapes, providing a larger accessible surface area for molecule adsorption. Materials characterized by fine-grained microstructures, high densities, and low porosities exhibited greater strength compared to those with larger pores and lower densities.

Adsorbents offer various advantages such as stability, affordability, environmental friendliness, ease of preparation, high mechanical strength, durability, mesoporous structure, ion-exchange capacity, physicochemical stability, high durability, acid resistance, good thermal resistance, thermal stability, high mechanical properties, low CO₂ emissions, low energy consumption compared to other separation processes (Youssef et al., 2023). Utilizing adsorption methods a remarkable removal efficiency of 95-100% was achieved for the antibiotic Ciprofloxacin (Natarajan et al., 2022).

Resin exchange is commonly employed in separating antibiotics, while for pharmaceutical adsorption, a different mechanism known as ion exchange can be used. This process involves the exchange of ions between pharmaceutical compounds and protons located on specific

oxygen-containing functional groups within the polymer, such as carboxyl and hydroxyl groups. The pH of the solution plays a main role in this interaction by influencing the quantities of different charged species present (e.g., cations, anions, and neutrals) and their sorptive interactions with the oppositely charged sorbents for ionizable pollutants. Surface complex and electrostatic interactions also impact the adsorption process, particularly in carbon adsorption. Interestingly, the internal charges of the adsorbent material may have a greater impact on adsorption capacity than the surface charges of the adsorbed material. For example, a decrease in the isoelectric point (the pH at which the surface carries no net electrical charge) of the adsorbent's surface from 6 to 4.8 leads to increased electrostatic interactions between the adsorbent and ions.

Resin can also be tailored to encapsulate specific substances or pollutants by analyzing their chemical structure, acting as a framework for a particular template molecule based on its size, shape, and arrangement of functional groups (known as MIPs - molecularly imprinted polymers) (Mokhtari et al., 2022; Mlunguza et al., 2019). These are created using a combination of monomers, crosslinkers, surfactants, solvents, and templates. While they demonstrate a strong foundation in isolating the targeted molecule, their limitation arises when dealing with complex mixtures of antibiotics in water (Mokhtari et al., 2022). In order to delineate the sources of pharmaceutical substances in the environment, MIPs have been developed not only for molecules dissolved in water but also for samples such as human plasma and urine (e.g., albendazole), as well as for determining antibiotics in milk (Liu et al., 2022).

Advanced oxidation process (AOP) is highly efficient in eliminating antibiotics by generating potent oxidizing agents, such as hydroxyl radicals. These radicals dismantle the chemical structure of pharmaceutical substances, yielding non-toxic intermediate products (Carbuloni et al., 2020). Since most pharmaceutical products have a limited biodegradability, the widely utilized wastewater treatment methods are insufficient to fully remove pharmaceutical products from the environment. AOPs are classified into two categories: photochemical

AOPs (such as photolysis, photocatalysis, and photo-Fenton) and non-photochemical AOPs (such as ozonation, Fenton, and electrolysis). Generally speaking, organic pollutants interact with hydroxyl radicals this would result in the formation of a peroxy radical, which would then react with oxygen molecules to produce a variety of oxidation products.

Photocatalysis offers advantages like cost reduction, increased efficacy, and enhanced degradation of active substances (Apostolescu et al., 2023). During advanced oxidation, activated species, primarily hydroxyl radicals, disintegrate pharmaceutical substances into less toxic intermediates or completely oxidize them to CO₂ and H₂O. Titanium dioxide (TiO₂), often immobilized in polymers due to the difficulty of separating fine TiO₂ from wastewater, serves as the most utilized catalyst (Nutescu et al., 2023; Sescu et al., 2018).

(1) Pharmaceutical ingredient + $h\nu \rightarrow e^- + h^+$

(2) $H_2O \rightarrow OH^- + H^+$

(3) $O_2 \text{ (adsorbed)} + e^- \rightarrow O_2^{*-}$

(4) $O_2^{*-} + e^- \rightarrow HOO^*$

(5) $2HOO^* + O_2 \rightarrow H_2O_2$

(6) $H_2O_2 \rightarrow 2OH^*$

(7) $h^+ + OH^- \rightarrow OH^*$

(8) $h^+ + H_2O \rightarrow OH^* + H^+$

(9) $OH^* + RH \rightarrow \text{Less toxic compound}$

(10) Intermediate compound $\rightarrow H_2O + H_2$

Hydroxyl radicals are the predominant oxidizing agents in advanced oxidation processes (Huang et al., 2023). Adsorbents with higher TiO₂ concentrations can bolster active site availability and reactive species production, primarily hydroxyl radicals. However, the presence of organic or inorganic matter in wastewater can hinder oxidant efficiency by attenuating UV light intensity, diminishing photocatalytic degradation performance. Various mechanisms such as size exclusion, molecular sieving, hydrophobic interaction, electrostatic interaction, and adsorption also contribute to pollutant removal.

To enhance the photocatalytic effect, some studies have explored combining TiO₂ (known for its high chemical stability and low cost) with ZrO₂ (characterized by its non-toxicity, reusability, and thermal stability). This combination offers advantages such as improved textural and structural properties, a higher surface area, smaller particle size,

increased anatase phase, and variation in energy band gap (Carbuloni et al., 2020). In any research focusing on the separation and degradation of pharmaceutical substances into intermediary compounds, it is crucial to assess the toxicity of the final molecules (Saravanan et al., 2022). Some studies have utilized *Lactuca sativa* seeds as phototoxicity bioindicators (Carbuloni et al., 2020) or enzymes derived from living organisms and fungal cultures for this purpose (Mlunguza et al., 2019). Mangan-ion-based photocatalysis can effectively manipulate the energy and electronic bands of the catalyst (Wenjing et al., 2023), a process that leads to the removal of up to 88.7% of tetracyclines from water.

In addition to photocatalysis, the oxidation process can also occur electrochemically, with efficiency being enhanced by the use of hydrogen peroxide (Wenjing et al., 2023). Parameters influencing the removal efficiency of antibiotics include the initial concentration of the organic substance, the type of electrolyte, the electrodes used, the electrical intensity applied, and the pH of the solution. Sulfamethoxazole is one of the pharmaceutical substances destroyed in studies through the electrochemical process. Generally, the mechanism of photocatalytic semiconductor unfolds in five main stages: reactant transfer, reactant adsorption, reaction unfolding in the adsorbed phase, product desorption, and removal of products from the intermediate zone.

Membrane treatment was recognized as the key technology for the separation of pollutants. Wu et al. synthesized PVC membrane for UF of antibiotics and the retention can be up to 80% in 2016 (Wu et al., 2016). Weng and co-workers have conducted antibiotics separation by using zwitterionic polyamide NF membranes with the highest antibiotics' retention of 96.5% (Weng et al., 2016).

Studies on **electrochemical separation** techniques for removing molecules from wastewater, such as electrochemical oxidation, electrocoagulation, and electro-flotation, have shown promising results in degrading organic compounds. Electrochemical oxidation can be categorized as direct, where the pollutant is degraded on the anode surface through direct oxidation with the presence of Na₂SO₄, or indirect, where mineralization occurs with

oxidants generated indirectly in the solution, often in the presence of sodium hypochlorite or potassium hypochlorite. Various anode materials are utilized in electrochemical degradation, including platinum, TiO₂, graphite, activated carbon, and combinations like Sn/Sb/Ni, which offer advantages such as low voltage operation, short reaction time, complete mineralization, and sometimes require no pH adjustments (Kurt et al., 2021).

Key aspects of the electrochemical degradation process/experiment include the choice of anode materials, generation of indirect oxidants (e.g., chloride or hypochlorite ions), distance between the anode and cathode, and the electrolyte used to increase conductivity (e.g., NaCl, Na₂SO₄, KCl). Electrooxidation can often be optimized at neutral pH values, which is both easier for researchers and more cost-effective to operate.

The degradation time of molecules is strongly influenced by the type of oxidation process (direct or indirect), the choice of anode material, and the pH of the solution.

Comparative methods: alone or in combination

Advantages and disadvantages of each presented method are presented in Table 1 (Phoon et al., 2020).

In recent studies, research has focused on investigating combinations of antibiotics in aqueous solutions using adsorbents doped with TiO₂ required for photocatalysis. A study conducted a combined approach of adsorption and photocatalysis to separate six antibiotics (amoxicillin, ciprofloxacin, norfloxacin, sulfamethoxazole, tetracycline, trimethoprim) from wastewater (Natarajan et al., 2022).

Table 1. Advantages and disadvantages of methods for antibiotics removal

Treatment process	Main advantages	Main disadvantages
Photocatalysis	Good stability of photocatalyst; high activity and non-toxicity; efficient recovery and recyclability of photocatalyst; low cost, fully destroy the organic pollutant.	Fast electron-hole recombination; poor efficiency for high concentrations; toxic by-products
Fenton	In-situ production of reactive radicals; without sludge; rapid degradation	Formation of unknown by-products; technical constraints; ferrous sludge produced; high concentration of anions.
Ozonation	Destroy antibiotics in a very short period (240–300 s)	
Electrochemical oxidation	Zero-sludge; unselective or selective function of the electrochemical cell	Expensive
Wet oxidation	Converted insoluble organic material into soluble compounds; for effluent too toxic for biological treatment	High pressure and energy conditions; pH dependence; No full mineralization.
Adsorption	High effective process; good ability to separate different contaminants; simple equipment.	Non-selective methods; high cost of regeneration; influenced by pH; further process after adsorption (regeneration). High energy requirements and operation and maintenance costs; limited flow rates; the high cost of investment; fouling effect needs a further process for elimination.
Membrane technology	Large range of applications; high selectivity; simple and efficient; no chemicals required	High energy consumption and operating cost; not digest all type of antibiotics.
Anaerobic treatment	Produces methane as a by-product; Lower biomass yield.	High energy consumption and operating cost; not digest all type of antibiotics.
Aerobic treatment	Higher loading rate; high performance	

A porous material composite membrane, consisting of a semi-crystalline aluminosilicate membrane with two layers, each containing metakaolin, an alkaline activator, and air foam was used. The porous support layer, negatively charged with hydrophobic properties, incorporated aluminium powder, while the dense coating layer contained TiO₂

nanoparticles, rendering it dense with voids and cracks. TiO₂ acted as a filler, densifying the microstructure. This membrane exhibited characteristics of both amorphous gel phase and nanocrystalline zeolite. The maximum degradation achieved was 40% at a TiO₂ concentration of 6% (Natarajan et al., 2022). This study exemplifies effective research into

separating a combination of antibiotics using adsorption and photocatalysis, resulting in enhanced drug degradation in wastewater.

Rimoldi et al. synthesized TiO_2/WO_3 for tetracycline (TC) removal using UV lamp (Rimoldi et al., 2018), Ahmadi et al. investigated TC degradation with UV-C lamps (Ahmadi et al., 2017). Wang et al. evaluated the effectiveness of TC degradation with ZnO under UV irradiation (Wang et al., 2016). Certain studies on photocatalytic TC degradation under UV light have demonstrated good performance; Xu et al. used carbon quantum dots and ZnIn_2S_4 composites was removed more than 80% of TC in 30 minutes (Xu et al., 2018). Acosta et al. reported to have produced active carbon with the TC adsorption capacity of 312 mg/g (Acosta et al., 2016). Besides AC, some other adsorbent materials also have a good performance in TC removal such as, the graphene oxide (GO) that was prepared by Gao et al. in 2012, can achieve 313 mg/g of adsorption capacity (Gao et al., 2012). Zhao et al. (2017) proposed that, the ionic strength of water bodies could affect the adsorption performance.

In an effort to increase the efficacy of wastewater treatment, hybrid systems that combine membrane technology and photocatalysis have drawn interest recently (Sarasidis et al., 2017). The photocatalytic membrane reactor is a type of integrated hybrid system that may be classified into two types: one where the catalyst is dispersed in the wastewater medium and the other where it is immobilized on or in the membrane surface.

CONCLUSIONS

In conclusion, this article offers a comprehensive analysis of various methodologies employed for the separation and removal of antibiotics from water and aqueous solutions. Recent advancements in the field are thoroughly explored, providing insights into active substances and innovative combinations utilized in the removal processes. The pivotal role of adsorbents is underscored, emphasizing their high porosity and efficient absorption capabilities for substantial contaminant doses. Furthermore, the financial advantages of employing photocatalysts in contaminant degradation are highlighted, reflecting the

growing body of research in this domain. Acknowledging the historical significance of exchange resin as a pioneering removal method, the article also delves into more contemporary electrochemical approaches tailored to the structural and ionic characteristics of antibiotics. By offering a valuable guide, this paper addresses the advantages and considerations associated with diverse methods of separating antibiotics from aqueous solutions, thereby providing insights into emerging technologies and facilitating informed decision-making in environmental remediation efforts.

REFERENCES

- Acosta, R., Fierro, V., de Yuso, A.M., Nabarlatz, D., & Celzard, A. (2016). Tetracycline adsorption onto activated carbons produced by KOH activation of tyre pyrolysis char. *Chemosphere*, 149, 168-176.
- Ahmadi, M., Motlagh, H.R., Jaafarzadeh, N., Mostoufi, A., Saeedi, R., Barzegar, G., & Jorfi, S. (2017). Enhanced photocatalytic degradation of tetracycline and real pharmaceutical wastewater using MWCNT/ TiO_2 nano-composite. *Journal of Environmental Management*, 186, 55-63.
- Apostolescu, N., Tataru Farmus, R.E., Harja, M., Vizitiu, M.A., Cernatescu, C., Cobzaru, C., & Apostolescu, G.A. (2023). Photocatalytic removal of antibiotics from wastewater using the CeO_2/ZnO heterojunction. *Materials*, 16(2), 850.
- Carbuloni, C.F., Savoia, J.E., Santos, J.S.P., Pereira, C.A.A., Marques, R.G., Ribeiro, V.A.S., & Ferrari, A.M. (2020). Degradation of metformin in water by $\text{TiO}_2\text{-ZrO}_2$ photocatalysis. *Journal of Environmental Management*, 262, 110347.
- Derakhshan, Z., et al. (2018). Removal Methods of Antibiotic Compounds from Aqueous Environments – A Review. *Journal of Environmental Health and Sustainable Development (JEHSD)*.
- Favier, L., Simion, A.I., Hlihor, R.M., Fekete-Kertész, I., Molnár, M., Harja, M., Vial, C. (2023). Intensification of the photodegradation efficiency of an emergent water pollutant through process conditions optimization by means of response surface methodology. *Journal of Environmental Management*, 328, 116928.
- Gao, Y., Li, Y., Zhang, L., Huang, H., Hu, J., Shah, S.M., & Su, X. (2012). Adsorption and removal of tetracycline antibiotics from aqueous solution by graphene oxide. *Journal of Colloid and Interface Science*, 368(1), 540-546.
- Huang, J., Wang, M., Luo, S., Li, Z., & Ge, Y. (2023). In situ preparation of highly graphitized N-doped biochar geopolymer composites for efficient catalytic degradation of tetracycline in water by H_2O_2 . *Environmental Research*, 219, 115166.
- Kurt, A., et al. (2021). Electrochemical Removal of Cefazolin from Aqueous Media by Novel Composite Anodes: Effects of Electrolytes and Operating

- Parameters. *International Journal of Electrochemical Science*, 16(11).
- Lin, J., Chen, J., Cai, X., Qiao, X., Huang, L., Wang, D., & Wang, Z. (2007). Evolution of toxicity upon hydrolysis of fenoxaprop-p-ethyl. *Journal of Agricultural and Food Chemistry*, 55(18), 7626-7629.
- Liu, P., Wu, Z., Barge, A., Boffa, L., Martina, K., & Cravotto, G. (2022). Determination of trace antibiotics in water and milk via preconcentration and cleanup using activated carbons. *Food Chemistry*, 385, 132695.
- Mlunguza, N., Ncube, S., Mahlambi, P., Chimuka, L., & Madikizela, L. (2019). Adsorbents and removal strategies of non-steroidal anti-inflammatory drugs from contaminated water bodies. *Journal of Environmental Chemical Engineering*, 7, 103142.
- Mokhtari, A., Barati, M., Karimian, H., & Keyvanfar, M. (2022). A molecularly imprinted polymerized high internal phase emulsion adsorbent for sensitive chemiluminescence determination of clopidogrel. *Spectrochimica Acta Part A: Molecular and Biomolecular Spectroscopy*, 265, 120371.
- Natarajan, R., et al. (2022). Understanding the factors affecting adsorption of pharmaceuticals on different adsorbents - A critical literature update. *Chemosphere*, 287(Pt 1), 131958.
- Nutescu Duduman, C., Gómez de Castro, C., Apostolescu, G. A., Ciobanu, G., Lutic, D., Favier, L., & Harja, M. (2022). Enhancing the TiO₂-Ag Photocatalytic Efficiency by Acetone in the Dye Removal from Wastewater. *Water*, 14(17), 2711.
- Phoon, B.L., Ong, C.C., Saheed, M.S.M., Show, P.L., Chang, J.S., Ling, T.C., Lam, S.S. & Juan, J. C. (2020). Conventional and emerging technologies for removal of antibiotics from wastewater. *Journal of Hazardous Materials*, 400, 122961.
- Rimoldi, L., Giordana, A., Cerrato, G., Falletta, E., & Meroni, D. (2019). Insights on the photocatalytic degradation processes supported by TiO₂/WO₃ systems. The case of ethanol and tetracycline. *Catalysis Today*, 328, 210-215.
- Roșu, B., Roșu, A., Arseni, M., Petrea, S.-M., Catalina Iticescu, C., Georgescu, P.L. (2022). The effects of optimizing a simulated wastewater treatment plant on effluent quality. *Scientific Papers. Series E. Land Reclamation, Earth Observation & Surveying, Environmental Engineering*, XI, 367-373.
- Rusu, L., Grigoraș, C.G., Simion, A. I., Suceveanu, E.M., Șuteu, D., & Harja, M. (2021). Application of *Saccharomyces cerevisiae*/calcium alginate composite beads for cephalixin antibiotic biosorption from aqueous solutions. *Materials*, 14(16), 4728.
- Sanguanpak, S., Shongkittikul, W., Saengam, C., Chiemchaisri, W., & Chiemchaisri, C. (2022). TiO₂-immobilized porous geopolymer composite membrane for removal of antibiotics in hospital wastewater. *Chemosphere*, 307(Pt 2), 135760. <https://doi.org/10.1016/j.chemosphere.2022.135760>
- Sarasidis, V., Plakas, K., & Karabelas, A.J. (2017). Novel water-purification hybrid processes involving in-situ regenerated activated carbon, membrane separation and advanced oxidation. *Chemical Engineering Journal*, 328, 1153-1163
- Saravanan, P., Senthil Kumar, S., Jeevanantham, M., Anubha, S., Jayashree, (2022). Degradation of toxic agrochemicals and pharmaceutical pollutants: Effective and alternative approaches toward photocatalysis. *Environmental Pollution*, 298, 118844.
- Sescu, A.M., Favier, L., Ciobanu, G., Cimpeanu, S.M., Teodorescu, R.I., Harja, M. (2018). *Studies regarding photocatalytic degradation of two different organic compounds. Scientific Papers. Series E. Land Reclamation, Earth Observation & Surveying, Environmental Engineering*, VII, 74-77.
- Shen, F., Xu, Y.J., Wang, Y., Chen, J., & Wang, S. (2022). Rapid and ultra-trace levels analysis of 33 antibiotics in water by on-line solid-phase extraction with ultra-performance liquid chromatography-tandem mass spectrometry. *Journal of Chromatography A*, 1677, 463304. <https://doi.org/10.1016/j.chroma.2022.463304>
- Wang, H., Yao, H., Pei, J., Liu, F., & Li, D. (2016). Photodegradation of tetracycline antibiotics in aqueous solution by UV/ZnO. *Desalination and Water Treatment*, 57(42), 19981-19987.
- Wang, Y., et al. (2011). Separation/enrichment of trace tetracycline antibiotics in water by [Bmim]BF₄-(NH₄)₂SO₄ aqueous two-phase solvent sublation. *Desalination*, 266, 114-118.
- Weng, X.-D., Ji, Y.-L., Ma, R., Zhao, F.-Y., An, Q.-F., & Gao, C.J. (2016). Superhydrophilic and antibacterial zwitterionic polyamide nanofiltration membranes for antibiotics separation. *Journal of Membrane Science*, 510, 122-130.
- Wenjing, M., Yan, H., Lihan, K., Xuemin, C., & Leping, L. (2023). Mn-doped geopolymers photocatalysts with sustained-release OH⁻ for highly efficient degradation of malachite green and tetracycline. *Journal of Cleaner Production*, 428, 139467.
- Wu, H., Niu, X., Yang, J., Wang, C., & Lu, M. (2016). Retentions of bisphenol A and norfloxacin by three different ultrafiltration membranes in regard to drinking water treatment. *Chemical Engineering Journal*, 294, 410-416.
- Xu, H., Jiang, Y., Yang, X., Li, F., Li, A., Liu, Y., Zhang, J., Zhou, Z., & Ni, L. (2018). Fabricating carbon quantum dots doped ZnIn₂S₄ nanoflower composites with broad spectrum and enhanced photocatalytic Tetracycline hydrochloride degradation. *Materials Research Bulletin*, 97, 158-168.
- Youssef E., et al. (2023). A state-of-the-art review of recent advances in porous geopolymer: Applications in adsorption of inorganic and organic contaminants in water. *Construction and Building Materials*, 395, 132269.
- Zhao, Q., Zhang, S., Zhang, X., Lei, L., Ma, W., Ma, C., Song, L., Chen, J., Pan, B., Xing, B. (2017). Cation- π Interaction: a key force for sorption of fluoroquinolone antibiotics on pyrogenic carbonaceous materials. *Environmental Science & Technology*, 51(23), 13659-13667.

ANALYSIS OF GHG EMISSIONS BY SECTORS IN CITY OF VIDIN

Daniela KOSTOVA-IVANOVA

University of Food Technologies, 26 Maritza Blvd, Plovdiv, Bulgaria

Corresponding author email: daniela_kostova07@abv.bg

Abstract

The publication presents an analysis of the baseline inventory of greenhouse gas emissions by sector in city of Vidin, based on the assessment of final energy use in the sectors, according to the methodology for developing a Sustainable Energy and Climate Action Plan (SECAP) in the framework of the Covenant of Mayors. The GHG emissions inventory enables local governments to understand the emissions contribution of different activities; to determine where to direct mitigation efforts and to create strategies to reduce GHG emissions and track their progress.

The article presents the results of the analysis of the base inventory of emissions in the city of Vidin, including the description of the methodology and key factors affecting emissions in the sectors "Residential buildings", "Public and Tertiary buildings", "Transport", "Public lighting" and "Industry", considering possible strategies and measures to reduce carbon footprints, including the amount of emissions gases. This analysis aims to provide a basis for developing sustainable policies in the municipality aimed at achieving the goal of reducing greenhouse gas emissions by 40% by 2030 by identifying and planning climate change mitigation and adaptation actions.

Key words: baseline GHG inventory, climate change adaptation and mitigation actions, energy use by sector, GHG emissions, Sustainable Energy and Climate Action Plan.

INTRODUCTION

Climate change will remain the one of the main challenges of the coming decades, shaping the future of the global society and world economy through its huge impacts and the need of our response. The harmful impacts of global warming are increasing in scale and frequency, with devastating effects on people, nature, and economic systems across the globe. The urgent need for stronger action to tackle climate change comes at a time of multiple global crises. In these terms the global emissions rebounded in 2021-2022 and reached a new high in 2022.

A number of scientific studies have been conducted and various actions and initiatives have been taken to address this problem. Kijewska & Bluszcz in 2016 have analyzed the level of differentiation of European Union member states in terms of emissions of four greenhouse gases and identified groups of similar countries based on these criteria. William F. Lamb et al. (2021) provide a sector-by-sector summary of key trends and challenges that collectively shape prospects for a rapid and deep transition and for avoiding dangerous climate change. Csalódi et al. (2022) assess the relationships between time series of GDP per capita and total CO₂ emissions of countries

around the world, discussing the sector's contribution to climate change. Magazzino et al. (2022) examine various drivers of greenhouse gas emissions such as population, economic development, forest density and agricultural practices. Reavis et al. present disclosure and emissions opportunities for the 100 largest global food and drink companies and highlight the urgent need to set truly ambitious, science-based climate targets (Reavis et al., 2022). Minx et al. present a comprehensive and synthetic dataset of global, regional and national greenhouse gas emissions by sector for 1970-2018 with an accelerated extension to 2019 (Minx et al., 2021). Han et al. have explored knowledge structure and boundary trends regarding the IOA model applied to CF research using scientometric visualization analysis (Han et al., 2022). Moiceanu & Dinca have analyzed Romania's GHG emissions under the EU and Romania legislative framework by performing a projected GHG analysis using data from Eurostat and the Romanian National Institute of Statistics (Moiceanu & Dinca, 2021). A number of scientists in Bulgaria have published their research in the field of increasing the energy efficiency of buildings and industrial systems (Iliev et al., 2021; Genbach et al., 2018; Kolev et al., 2017; Komitov et al., 2020; Valchev &

Mihaylov, 2020; Zlateva et al., 2020), but no publications related to the study of GHG emissions by sectors were found.

The European Union is extremely responsible when it comes to activities to deal with the consequences of climate change and also activities to adapt to its adverse effects. All 27 EU countries have committed to making Europe the first climate-neutral continent by 2050.

To achieve this, they have committed, firstly, to reduce emissions by at least 55% by 2030 compared to levels of 1990. In February 2024, the European Commission presented its assessment for a 2040 climate target for the EU (European Parliament Commission Staff, 2024). The Commission recommended reducing the EU's net greenhouse gas emissions by 90% by 2040 relative to 1990. Moreover, the European Green Deal is the key response to the climate challenges, which sets targets for climate neutrality until 2050. It is a strategy that aims to transform the EU into a fair and prosperous society, with a modern, resource-efficient and competitive economy where there are no net emissions of greenhouse gases in 2050 and where economic growth is decoupled from resource use.

As stated in the 100 Climate-Neutral and Smart Cities by 2030 Info Kit for Cities (European Commission, 2021c) the targets of the European Green Deal (namely reducing emissions by 55% by 2030 and becoming the first climate neutral continent by 2050) will be impossible to achieve without cities in the vanguard of concerted efforts. It's obvious that local authorities play a key role in achieving the national energy and climate goals and are leading actors in the implementation of local sustainable energy policies. The greenhouse gases emission commitments are considered that could be fulfilled being the cornerstone of the European deal on climate change (Di Paolo et al., 2023).

Reaching and indeed exceeding national or EU GHG reduction targets, such as those proposed by the EU Green Deal, is not an easy task (Rivas et al., 2021), specially for the small and medium sized municipalities.

It is still relatively difficult for the Bulgarian small municipalities to conduct energy modelling and analysis of final energy consumption, due to lack of capacity and difficult adoption of different energy planning

tools. However, various materials and initiatives have been developed for the benefit of municipalities in terms of tools for energy planning and monitoring.

The energy planning process encompasses a number of elements – institutional arrangements, exemplary guidelines, modelling and forecasting methods, specific methodologies using various scenarios and communication programs. There are well-established planning approaches, but the energy transition creates a need to reassess some aspects of the planning process, especially those related to the construction of an attractive vision and predictability for investments in municipalities (EnEffect, 2023).

Municipal energy planning and energy system modelling, on the other hand, is a research field that has traditionally been de-emphasised in favour of national energy system modelling (Johannsen et al., 2021).

Covenant of Mayors on Climate and Energy provides a framework for energy planning at municipal level and aims to complement national energy and climate plans with a specific initiative to support cities. The initiative aims to gather local authorities to voluntarily commit to implementing sustainability policies in their territories. Local authorities are provided with a harmonized data compilation, methodological and reporting framework to turn greenhouse gas reduction ambitions into reality. One of the possible assessment tools included within the Covenant of Mayors is the GHG emissions inventory, which quantifies the GHG emissions released to the atmosphere (Marchi et al., 2023). The key enabling factor for higher climate ambition in cities is the development of local mitigation actions in line with the results of the baseline emissions inventory; focusing on implementing actions in the most emitting sectors of activity (Rivas et al., 2021).

There is a possibility for Joint SECAP plan, especially in the case of small municipalities in EU countries that lack a national framework for climate planning, which can contribute significantly to building a climate-adaptation strategy (D'Onofrio et al., 2023).

By reducing GHG emissions in their jurisdictions, the local authorities can tackle the root cause of climate change (Papp, 2023).

The Covenant of Mayors includes both climate

mitigation and adaptation aspects and is built around three pillars:

- Actions to mitigate climate change (at least 40% emissions reduction target by 2030 compared to baseline - initially);
- Actions to adapt to climate change;
- Access to secure, sustainable and affordable energy (Bertoldi, 2018a; 2018b).

If the local government has been a signatory of Covenant of Mayors recently, they should comply with "Fit for 55" and the commitment should be 55% reduction by 2030 which can be found quite bold for a lot of cities. If they are members before 2021 the commitment is 40% reduction by 2030.

Municipality of Vidin, as one of the six follower cities in MAKING-CITY project, and has committed to develop a Sustainable Energy and Climate Action Plan, which on the base of comprehensive final energy use analysis and GHG emission inventory defines the main goals, actions and measures for the development of municipal policy for climate change mitigation and adaptation.

The commitment of the Municipality of Vidin is to develop Sustainable Energy and Climate Action Plan in which to present its vision for climate change mitigation - at least 40% emission reduction target by 2030 compared to the baseline year - 2021 and adaptation to climate change (Making-city Consortium, 2023). By developing of Sustainable Energy and Climate Action Plan (SECAP) for a municipality of Vidin they will be offered numerous advantages and benefits, making it a strategic and responsible choice. Vidin's target of reducing emissions by 40% is consistent with the project's goals and is aligned with the near baseline year - 2021.

The plan of Vidin addresses the impacts of climate change by reducing greenhouse gas emissions by identifying climate change mitigation actions the city can significantly decrease a municipality's carbon footprint, contributing to a cleaner and healthier environment.

Moreover, by setting clear goals and strategies for emissions reduction the SECAP of Vidin will play a crucial role in mitigating climate change. The goals will align with the global efforts to limit global warming and help the

municipality to meet international climate agreements like the Paris Agreement.

The energy vision of the city of Vidin until 2030 and until 2050 will help to reduce GHG emissions, increase energy efficiency and improve the quality of life of the local population, while at the same time ensuring sustainable economic development for the city.

MATERIALS AND METHODS

In the preparation of the GHG emissions baseline inventory within the framework of the Sustainable Energy and Climate Action Plan of the city of Vidin, was adopted the methodology of the Handbook "How to develop a Sustainable Energy and Climate Action Plan" Part 1 - The process of development of SECAP, Step by Step towards Low Carbon and Climate Resilient Cities by 2030, which aims to support local authorities in European Union Member States joining the Covenant of Mayors for Energy and Climate.

On the base of the above-mentioned document in the process of establishment of the CO₂ emission baseline inventory within the Sustainable Energy and Climate Action Plan of the city of Vidin, the following key concepts are of utmost importance:

- Local territory analysis: Geographical jurisdiction/administrative territory;
- Assessment of final energy use which covers all energy delivered to end users in all energy consumption sectors: "Municipal buildings"; "Tertiary buildings"; "Residential Buildings"; "Transport"; "Industry";
- Assessment of the sources of greenhouse gases from the energy consumption of the specified sectors.

For each of these sectors, the types of energy sources and the annual quantities used were determined on the base of data collection from different sources.

Sector "Municipal buildings" - The Municipality of Vidin provided a list of all buildings owned by the municipality and state institutions, which includes a total of 88 buildings. The questionnaire was completed for 68 buildings, of which valid data was received for 60 buildings. The Municipality of Vidin has also provided a Report on the average annual

number of resources for heating public buildings for the period 2019-2021, which includes information on 25 buildings in the city of Vidin. Sector "Tertiary buildings" - For the purposes of the research, a reference was made to the website of the Agency for Sustainable Energy Development (SEDA), which includes basic data for the buildings, including total area, energy consumption, availability of a certificate of energy characteristics, etc.

Sector "Residential Buildings" - For the purposes of the research, data were taken from a survey on the project "Improving the quality of atmospheric air in the Municipality of Vidin", which aims to reduce emissions of fine dust particles FPC10 from domestic heating, by means of free replacement of solid fuel appliances (wood and coal) of households with alternative types of heating appliances. A total of 4,825 residents of the Municipality of Vidin took part in the survey conducted for the purposes of the project. The survey was conducted in the period 16.02.2021 - 05.03.2021 and covers the population that uses solid fuel for heating. The survey was conducted to cover more than 25% of homes heated with coal and/or wood.

From the municipal Report on the replacement of stoves in the city of Vidin, it is clear that there are 9181 households using solid fuel for heating. The following statistical data were used to calculate the final energy consumption of households in Vidin:

- Population for 2021 for the city of Vidin – 35,784 people (Population Census for 2021).
- Population for 2021 for the municipality of Vidin – 67,794 people (Population Census for 2021).
- Average number of persons in a household for 2011. 2.3 (National Statistical Institute).
- Number of households in city of Vidin – 15,558.3 units, calculated by dividing the population of city of Vidin by the average number of persons in a household:
- Number of households heating with solid fuel in the city of Vidin: 9,181 units. (Municipality of Vidin, 2021).
- Percentage of households using solid fuel for heating – 59%, calculated as the ratio between the number of households heated with

solid fuel and the total number of households in Vidin.

Sector "Public Lighting" - For the purposes of the research, data were taken from an energy audit of a public lighting system in the city of Vidin, in which the state and type of the street lighting measurement and control system, the energy consumed for the base year, and energy saving measures were analysed.

Sector "Industry" - the final energy use in the industry sector was calculated on the basis of data provided by (Electric Distribution Networks Zapad AD, 2023), which cover the amount of electricity transferred to the company's customers. The amount of electricity for the sectors Public buildings and Street lighting has been removed from the reference for business users on the territory of the municipality.

Sector "Transport" - for the purposes of the survey for used data provided by the Municipality of Vidin regarding Public Transport, Municipal Transport and Private Transport. For public transport, data on reported annual mileage for the base year, valid international passenger transport licenses are provided.

A survey was made on the types of motor vehicles for urban transport and the average fuel consumption on an annual basis.

For municipal transport, data has been provided by the Municipality of Vidin, regarding the number of vehicles by type and fuel as of 31.12.2021, owned by the Municipality of Vidin and municipal enterprises, mileage per year, km or engine changes per year for tractors, and a survey has been made for average consumption of fuel, l/km, l/m.h.

Regarding private vehicles, the following information has been provided by the Municipality of Vidin: Number of vehicles by type and fuel as of 31.12.2021, registered on the territory of the Municipality of Vidin. Average mileage for private vehicles is assumed: 12km/day for 365 days.

To determine the average fuel consumption for the various vehicles, the values from Ordinance No.3 of 25.09.1989 on normalizing the consumption of fuels and lubricants for cars and motorcycles were taken.

At the moment of development of the SECAP of the city of Vidin, no other non-energy sources of

GHG are available.

Local energy sources - the electricity produced by Vidin is obtained from the "Register of Guarantees" system of the Agency for Sustainable Energy Development (SEDA) and includes all installations connected to the electricity network that sell renewable electricity to suppliers in the territory of the city of Vidin.

Local heat/cold production (LPT/C)*, divided into: At the time of the research, there are no local sources of heat or cold energy in the city of Vidin.

Base year selection - the year 2021 has been chosen as the base year for the Municipality of Vidin, as the year in which there is the most up-to-date and complete data on energy consumption by sector, as well as statistical data on the population from the 2021 National Census. To unify the units for the amount of fuel consumed, the following conversion coefficients for the density of fuels were used (Table 1).

Table 1. Density values of different types of fuels (Department for Environment Food & Rural Affairs - Greenhouse Gas Conversion Factor Repository 10)

Density values of different types of fuels	
Fuel type	Conversion factor
Unit	l/t
Gasoline	1,368
Diesel	1,195
Propane-butane	1,957.3
Methane	5,714.29
Oil	1,467

To convert the amount of fuel from natural units (mass or volume) to energy units (calorific value) the conversion values presented in Table 2 were used.

The average fuel use for all types of motor vehicles is taken according to the values specified in Ordinance No. 3 of 25.09.1989 for normalizing the use of fuels and lubricants for cars and motorcycles (Minister of Transport, Ordinance No. 3 of 25.09.1989, 1989), as follows: (Table 3). The amount of fuel consumed (FC) in liters by fuel type and vehicle is calculated according to the equation (1):

$$FC = NV * AAM * FUR \quad (1)$$

where:

- NV is the number of vehicles;

- AAM is the average annual mileage, km;

- FUR is the fuel use rate, l/km.

The amount of energy from fuel consumed is calculated according to the equation (2):

$$FE_{fuel} = (\sum Fuel \text{ in litres} / \rho_{fuel}) * LHV_{fuel} \quad (2)$$

where:

- FE_{fuel} - final energy obtained as a result of fuel combustion, kWh/year;

- ρ_{fuel} - fuel density, l/t;

- LHV_{fuel} - fuel calorific value, kWh/kg.

Table 2. Calorific values of the different types of fuels (Minister of Energy. Regulation on the methodologies for the determination of the national energy efficiency target)

Calorific values of the different types of fuels		
Fuel type	Unit	Net Calorific Value, NCV
Coal	MWh/t	5
Coal briquettes	MWh/t	5.56
Wood	MWh/m ³	3.3 ^a
Pellets, eco-briquettes	MWh/t	4.8
Gasol	MWh/l	11.1
Propane-butane	MWh/kg	12.78
Natural gas	MWh/Nm ³	9.3
Gasoline	MWh/t	12.2
Diesel	MWh/t	11.669
Methane	MWh/t	9.372
Oil	MWh/t	12.211
Electricity	MWh/MWh	1

^a At wood humidity > 30%

Table 3. Norms for use of different types of motor vehicles

Norms for use of different types of motor vehicles	
Vehicle type	Liter per km. mileage/motor hour
Bus	0.35
Car	0.08
Motorcycle	0.05
Motorcycle	0.04
Truck	0.16
Tower	0.25
Motorcycle with basket	0.07
Wheel tractor	16
Three-Wheeler vehicle	0.08

On the base of the above-described methodology, the final energy use for all the mentioned sectors was analysed.

RESULTS AND DISCUSSIONS

The total CO₂ emissions by energy source, calculated on the base of the final energy use in City of Vidin are presented in Table 4.

Table 4. Distribution of greenhouse gas emissions by energy source for 2021

Type of energy source	Final energy consumption	GHG emissions, t CO ₂	Share of total emissions
	MWh/y	t CO ₂ /y	%
Electricity	112,363.31	54,608.57	48%
Natural gas	1,216.2	267.57	0%
Liquefied Gas (LPG)	5,370.6	1,557.4	1%
Liquid fuel for heating	6,918.2	2,006.291	2%
Diesel	99,010.69	28,713.1	25%
Gasoline	43,479.34	12,609.01	11%
Coal	27,942.5	10,059.31	9%
Biomass	107,190.5	4,287.622	4%
Total	403,491.54	114,109	

As it can be seen from Figure 1 the largest contribution to GHG emissions, in the base year 2021, is the consumption of electricity (48%), liquid automotive fuels, respectively diesel (25%), gasoline (11%), coal (9%). Emissions from biomass use are 4% of total emissions from energy use.

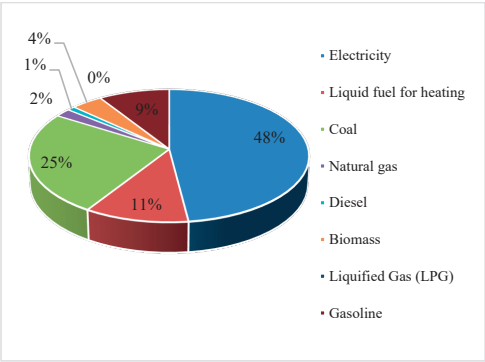


Figure 1. Distribution of GHG emissions by type of energy source for 2021

The distribution of GHG emissions by sector is presented in Table 5.

Sector "Residential buildings" is the sector with the highest percentage of final energy consumption (44%) and contribute significantly to GHG emissions (30%). This emphasizes the

importance of targeting actions for energy efficiency measures and emissions reduction strategies in residential buildings.

The sector with the highest share of GHG emissions (38%) is the Transport sector, which also represents second place in the final energy use with 37%. While industry accounts for 15% of final energy consumption, it contributes a relatively higher percentage (26%) to GHG emissions, due to the main energy source - electricity. Municipal buildings sector accounts for 3% of final energy use and 4% of CO₂ emissions. Sector "Tertiary buildings" and sector "Street lighting" represents 1% each of final energy use and CO₂ emissions (Figure 2).

Table 5. Distribution of final energy consumption and GHG emissions by sector

Distribution of final energy consumption by sector	Distribution of final energy consumption by sector		Distribution of GHG emissions by sector	
	MWh/y	%	t CO ₂ /y	%
Municipal buildings	11,792.1	3%	4,294.2	4%
Tertiary sector	2,838.5	1%	1,379.5	1%
Residential buildings	175,629.8	44%	33,834.5	30%
Street lighting	3,159.1	1%	1,535.3	1%
Industry	61,998.2	15%	30,131.1	26%
Transportation	148,074.0	37%	42,934.3	38%
Total	403,491.5		114,109.0	

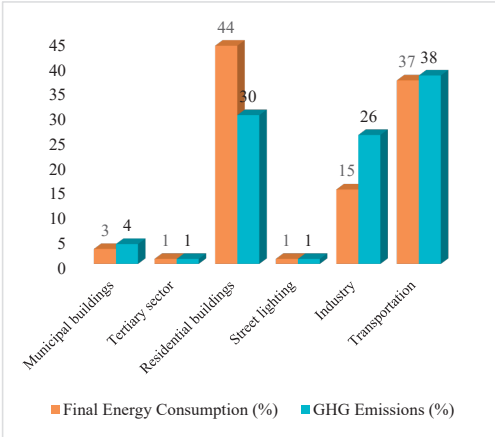


Figure 2. Distribution of final energy consumption and GHG by sector

Figure 2 highlights the need for a multi-faceted approach to assess final the energy use and GHG

emissions. Efforts should be directed towards residential buildings energy efficiency, sustainable transportation solutions, and cleaner industrial practices to achieve a more balanced and sustainable energy consumption. The following sections focus on sector-by-sector greenhouse gas emissions to provide a more in-depth analysis of the energy sources used and their GHG emissions share. An analysis of the final energy use and GHG emissions in the building sector, including residential, municipal and tertiary buildings is shown in Table 6.

Table 6. Distribution of final energy consumption by fuel in the building sector

Energy source	Final energy use	Distribution of GHG emissions	
	MWh/y	t CO ₂ /y	%
Electricity	47,176.6	22,927.85	62,4%
Natural gas	1,032.3	227.11	1%
Liquid fuel for heating	6,918.2	2,006.29	5%
Coal	27,942.5	7,265.06	20%
Biomass	107,190.5	4,287.62	12%
Total	190,260.29	36,713.93	

As can be seen in Figure 3, electricity contributes the largest share (62.4%) of CO₂ emissions in the buildings, followed by coal (20%) and biomass (12%). Liquid fuels represent 5% of the emission sources in the building sector and are used mainly in Municipal buildings. Natural gas is used in a small part of municipal buildings and is a responsible for 1% of the CO₂ emissions.

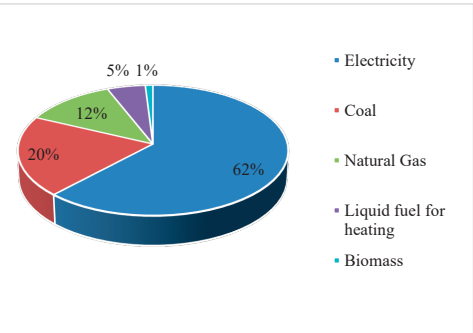


Figure 3. Distribution of greenhouse gas emissions in the building sector by type of energy source for 2021

Sector "Residential buildings" occupy the largest share of GHG emissions in the city of Vidin (Table 7). In turn, the main sources of emissions in the "Residential buildings" sector are electricity consumption (54.8%); coal (30%) and biomass (13%), and liquid fuels contribute 1% of emissions in the sector.

Table 7. Distribution of final energy consumption by fuel in sector "Residential buildings"

Energy source	Final energy use	Distribution of GHG emissions	
	MWh/y	t CO ₂ /y	%
Electricity	39,333.9	19,116.28	56%
Liquid fuel for heating	1,313.4	380.88	1%
Coal	27,931.4	10,055.31	30%
Biomass	107,051.1	4,282.042	13%
Total	1756,29.8	33,834.51	

Electricity, coal and biomass are the main sources of energy in the residential sector (Figure 4). The significant GHG emissions associated with electricity and coal underline the need for strategies to reduce the carbon footprint of this sector. The introduction of energy efficient measures and low emission heating technologies for households can help reduce GHG emissions and sustainably manage the energy needs of residential buildings.

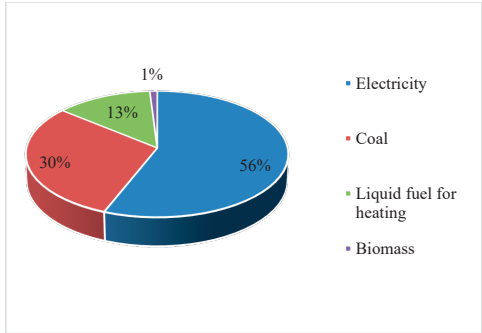


Figure 4. Distribution of greenhouse gas emissions in Sector "Residential buildings" by type of energy source for 2021

The analysis of energy use in Municipal buildings, it can be seen that the largest share of GHG emissions is contributed by electricity (57%), followed by liquid fuels (38%) and natural gas (5%) - Table 8 and Figure 5.

Table 8. Distribution of final energy consumption by fuel in sector "Municipal buildings"

Energy source	Final energy use MWh/y	Distribution of GHG emissions	
		t CO ₂ /y	%
Electricity	5,004.3	2,432.072	57%
Natural gas	1,032.3	227.11	5%
Liquefied Gas	5,604.9	1,625.41	38%
Coal	11.1	4.003	0.09%
Biomass	139.5	5.57	0.13%
Total	11,792.1	4,294.18	

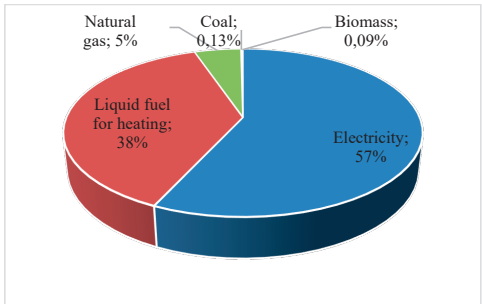


Figure 5. Distribution of greenhouse gas emissions in Sector "Municipal buildings" by type of energy source for 2021

Table 9 provides information on the three sectors - "Tertiary Buildings", "Street Lighting" and "Industry", in terms of their final energy consumption and greenhouse gas emissions in tonnes of carbon dioxide per year.

Table 9. Final energy use and GHG emissions in sectors "Tertiary buildings", "Street lighting" and "Transport"

Sector	Final energy use MWh/y	GHG emissions t CO ₂ /y
Tertiary Buildings	2,838.5	1,379.49
Street Lighting	3,159.1	1,535.3
Industry	61,998.2	30,131.14

Sector "Tertiary buildings" represent 1% of the final energy use in the city of Vidin, and also accounts for 1% of GHG emissions in the city. In the sector, the most significant energy source is electricity. Sector "Street lighting" accounts for 1% of the final energy use and 1% of GHG emissions, respectively.

Table 10 provides information for the energy sources used in Sector "Transport" and its associated greenhouse gas emissions in tons CO₂ per year:

Diesel has the largest share of total GHG emissions in the "Transport" sector (67%), making it a major source of pollution in this sector.

Gasoline follows with a significant share of 29% in total emissions. Liquefied petroleum gas (LPG) and other energy sources (electricity, natural gas/methane) have lower share in the total emissions from "Transport" sector (4%) (Figure 6).

Private motor vehicles have the highest final energy consumption and generate the highest amount of CO₂ emissions (42,466.06 t/year). Urban transport and municipal vehicles use a small amount of energy and generate relatively low emissions but should not be neglected in climate change mitigation actions.

Table 10. Final energy consumption and GHG emissions in the Sector "Transport"

Sector Transport	Final energy use MWh/y	Conversion factor g CO ₂ /kWh	Distribution of GHG emissions	
			GHG emissions t CO ₂ /y	%
Electricity	29.4	486	14.29	0%
Natural gas	183.9	220	40.46	0%
Liquefied Gas (LPG)	5,370.64	290	1,557.49	4%
Diesel	99,010.69	290	28,713.1	67%
Gasoline	43,479.34	290	12,609.01	29%
	148,074.0		42,934.34	

Private motor vehicles have the highest final energy consumption and generate the highest amount of CO₂ emissions (42,466.06 t CO₂/year). Urban transport and municipal vehicles use a small amount of energy and generate relatively low emissions but should not be neglected in climate change mitigation actions.

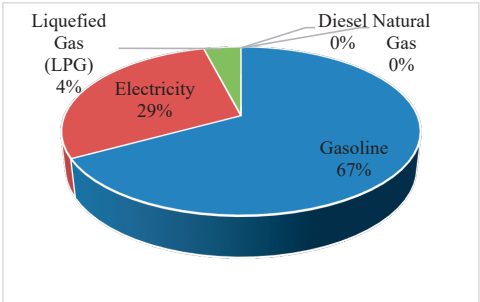


Figure 6. Distribution of GHG emissions in Sector "Transport" by type of energy source for 2021

A summary table (Table 11) is presented to provide an overview of the Vidin's final energy use, as well as greenhouse gas (GHG) emissions across different sectors. on the basis of the presented data, the potential for final energy savings and emission reduction was analysed, as the long-term vision for development of the city

of Vidin was defined until 2030 and until 2050, which considers the medium- and long-term goals and priorities of the regional policy, laid down in the strategic documents at different territorial levels in the country: regional, regional, national level.

Table 11. Summary of final energy use and GHG emissions and 2030 targets by sector

Sector	Distribution of final energy consumption by sector		Distribution of GHG emissions by sector		Final energy usage reduction targets		GHG emissions reduction targets	
	MWh/ y	%	t CO ₂ / y	%	t CO ₂ / y	MWh	t CO ₂ / y	%
Municipal buildings	11,792.1	3%	4,294.2	4%	2,830.1	24%	3,044	71%
Tertiary sector	2,838.5	1%	1,379.5	1%	709.6	25%	344.87	25%
Residential buildings	175,629.8	44%	33,834.5	30%	17,563.0	10%	1,5902.22	47%
Street lighting	3,159.1	1%	15,353	1%	315.9	10%	767.65	50%
Industry	61,998.2	15%	30,131.1	26%	3,719.9	6%	7,532.79	25%
Transport	148,074.0	37%	42,934.3	38%	29,614.8	20%	19,749.8	46%
Total	403,491.5		114,109.0		54,753.3	13%	47,341.32	40%

CONCLUSIONS

To estimate carbon dioxide emissions, a comprehensive analysis of all significant energy consumers in the city of Vidin by sector was implemented.

It was established that the municipality of Vidin lacks a mechanism for energy planning and modelling. There is a lack of tools for analysis and monitoring of energy consumption in the sectors. It was recommended that an energy monitoring system be included in the municipality's strategic energy documents, with the aim of analysing the final energy consumption by sector and evaluating the effect of the implemented measures.

The analysis shows that the residential, transport and municipal sectors are key areas of focus: residential and transport together contribute significantly to final energy consumption and greenhouse gas (GHG) emissions. In addition, municipally owned buildings should serve as an example of increasing energy efficiency.

Based on the analysis, it will be recommended that the Municipality of Vidin focus on the following priority actions to mitigate climate change: reducing final energy consumption in the building sector by increasing the energy efficiency of buildings and municipal infrastructure and modernizing heat sources; increasing the share of renewable energy

sources in final energy consumption, modernizing public, municipal and private transport, creating a favourable business and industrial environment by increasing the competitiveness of local enterprises, creating a better urban environment by building and expanding parks and green alleys in a city, increasing the administrative capacity for energy transition.

The goal of the implementation of the above-mentioned priorities is to achieve the main energy goals of the city: reduction of greenhouse gas emissions by 40% by 2030 and reduction of annual final energy consumption by 13% by 2030.

REFERENCES

Bertoldi, P. (2018a). Guidebook 'How to develop a Sustainable Energy and Climate Action Plan (SECAP) – Part 1 - The SECAP process, step-by-step towards low carbon and climate resilient cities by 2030. EUR 29412 EN, Publications Office of the European Union, Luxembourg. ISBN 978-92-79-96847-1, doi: 10.2760/223399, JRC112986

Bertoldi, P. (2018b). Guidebook 'How to develop a Sustainable Energy and Climate Action Plan (SECAP) – Part 2 - Baseline Emission Inventory (BEI) and Risk and Vulnerability Assessment (RVA), EUR 29412 EN, Publications Office of the European Union, Luxembourg. ISBN 978-92-79-96929-4, doi:10.2760/118857. JRC112986

Csalódi, R., Czvetkó, T., Sebestyén, V., & Abonyi, J. (2022). Sectoral Analysis of Energy Transition Paths

- and Greenhouse Gas Emissions. *Energies*, 15, 7920. <https://doi.org/10.3390/en15217920>.
- D'Onofrio, R., Camaioni, C., & Mugnoz, S. (2023). Local Climate Adaptation and Governance: The Utility of Joint SECAP Plans for Networks of Small–Medium Italian Municipalities. *Sustainability*, 15(11), 8738.
- Department for Environment Food & Rural Affairs - Greenhouse Gas Conversion Factor Repository 10.
- Di Paolo, L., Di Martino, A., Di Battista, D., Carapellucci, R., & Cipollone, R. (2023). The potential of energy planning at Municipality scale: Sustainable Energy and Climate Action Plans (SECAP) and local Energy Communities to meet the energy demand variability. *Journal of Physics: Conference Series*, 2648(1), 012012. IOP Publishing.
- Electric Distribution Networks Zapad AD. <https://ermzapad.bg/bg/>
- EnEffect, Center for Energy Efficiency. Handbook Municipal energy planning and management. Available at: <https://www.eneffect.bg/>
- European Commission (2021c). Info Kit for Cities. Available online at: https://research-and-innovation.ec.europa.eu/system/files/2021-11/ec_rtd_eu-mission-climate-neutral-cities-infokit.pdf
- European Parliament Commission Staff. (2024). Europe's 2040 climate target and path to climate neutrality by 2050 building a sustainable, just and prosperous society. Strasbourg, 6.2.2024 SWD (2024) 63 final.
- Genbach, A.A., Bondartsev, D. Yu., & Iliev, I. K. (2018). Modelling of capillary coatings and heat exchange surfaces of elements of thermal power plants *Bulgarian Chemical Communications* 50 S, 133-139.
- Han, J., Tan, Z., Chen, M., Zhao, L., Yang, L., & Chen, S. (2022). Carbon Footprint Research Based on Input-Output Model - A Global Scientometric Visualization Analysis. *Int. J. Environ. Res. Public Health*, 19, 11343. <https://doi.org/10.3390/ijerph191811343>
- Iliev, I.K., Terziev, A.K., Beloev, H.I., Nikolaev, I. & Georgiev, A.G. (2021). Comparative analysis of the energy efficiency of different types co-generators at large scales CHPs. *Energy*, 221C, 119755.
- Kijewska, A., Bluszcz A. (2016). Analysis of greenhouse gas emissions in the European Union member states with the use of an agglomeration algorithm, *Journal of Sustainable Mining*, 15(4) 133-142.
- Kolev, Z.D., Kadirova, S. & Nenov, T.R. (2017). Research of reversible heat pump installation for greenhouse heating INMATEH. *Agricultural Engineering*, 2, 77-84.
- Komitov, N., Shopov, N. & Rasheva, V. (2020). Model of a building heating system with renewable energy sources. *E3S Web of Conferences*, 207, 02006.
- Johannsen, R.M., Ostergaard, P.A., Maya-Drysdale, D., & Krog Elmegaard Mouritsen, L. (2021). Designing Tools for Energy System Scenario Making in Municipal Energy Planning. *Energies*, 14, 1442. <https://doi.org/10.3390/en14051442>
- Magazzino, C., Cerulli, G., Haouas, I., Onolame Unuofin, J., & Asumadu Sarkodie, S. (2024). The drivers of GHG emissions: A novel approach to estimate emissions using nonparametric analysis. *Gondwana Research* 127, 4–21.
- MAKING-CITY Consortium. (2023). Long-term city plan of Vidin (city vision 2050) – Intermediate version.
- Marchi, M., Capezzuoli, F., Fantozzi, P.L., Maccanti, M., Pulselli, R.M., Pulselli, F.M., & Marchettini, N. (2023). GHG action zone identification at the local level: Emissions inventory and spatial distribution as methodologies for policies and plans. *Journal of Cleaner Production*, 386, 135783.
- Minister of Energy. REGULATION on the methodologies for the determination of the national energy efficiency target
- Minister of Transport. (1989). Ordinance No. 3 of 25.09.1989 on norming the use of fuels and lubricants for cars and motorcycles. Available at: https://www.mtc.government.bg/upload/docs/2016-01/NAREDBA_3_ot_25091989_g_za_normirane_raz_hoda_na_goriva_i_smazocni_materiali_na_avtomobil_ite_i_motoci.rtf
- Minx J.C. et al. (2021). Global greenhouse gas emissions, 1970–2018. *Earth Syst. Sci. Data*, 13, 5213–5252. <https://doi.org/10.5194/essd-13-5213-2021>
- Moceanu, G. & Dinca, M.N. (2021). Climate Change-Greenhouse Gas Emissions Analysis and Forecast in Romania. *Sustainability*, 13, 12186. <https://doi.org/10.3390/su13212186>
- Municipality of Vidin. (2021). Report "Vision for replacing stoves". Available at: Доклад визия Видин. Accessed on: 11.11.2022
- National Statistical Institute. <https://www.nsi.bg/bg>
- Papp, A. T. (2023). The role of the municipalities in achieving the EU's sustainable energy transition. *Észak-magyarországi Stratégiai Füzetek*, 97-109.
- Population Census for 2021. <https://census2021.bg/>
- Reavis, M., Ahlen, J., Rudek, J. & Naithani, K. (2022). Evaluating Greenhouse Gas Emissions and Climate Mitigation Goals of the Global Food and Beverage Sector. *Front. Sustain. Food Syst.*, 5, 789499. doi: 10.3389/fsufs.2021.789499.
- Rivas, S., Urraca, R., Bertoldi, P., & Thiel, C. (2021). Towards the EU Green Deal: Local key factors to achieve ambitious 2030 climate targets. *Journal of cleaner production*, 320, 128878.
- Valchev, S.E. & Mihaylov, I.M. (2020). Analysis of energy efficiency of air handling unit with integrated air to air heat exchanger in heating mode. *E3S Web of Conferences*.
- William, F. Lamb et al. (2021). A review of trends and drivers of greenhouse gas emissions by sector from 1990 to 2018. *Environ. Res. Lett.*, 16, 073005 doi 10.1088/1748-9326/abee4e.
- Zlateva, P., Penkova, N. & Krumov, K. (2020). Analysis of combustion efficiency at boilers operating on different fuels 7th Int. Conf. on Energy Efficiency and Agricultural Engineering (EE&AE), 1-4.

SMART-ECO-INNOVATIVE COMPOSITE MATERIALS WITH SELF-CLEANING CAPABILITY AND ENHANCED RESISTANCE TO MICROORGANISMS

Adrian-Victor LAZARESCU, Andreea HEGYI, Carmen FLOREAN

National Institute for Research and Development in Construction,
Urban Planning and Sustainable Spatial Development - URBAN-INCERC,
Cluj-Napoca Branch, 117 Calea Floresti, Cluj-Napoca, Romania

Corresponding author email: andreea.hegyi@incerc-cluj.ro

Abstract

This research focuses on the development of advanced cementitious composite or geopolymer materials that exhibit smart, eco-innovative properties, including self-cleaning capabilities and heightened resistance to microorganisms. The aim is to address environmental concerns and enhance the durability and functionality of materials in various applications. The composite materials are designed by incorporating novel nanomaterials and eco-friendly additives, leveraging their unique properties. The self-cleaning capability is achieved through the integration of photocatalytic nanoparticles, such as titanium dioxide, which harness solar or artificial light to catalyse the degradation of organic contaminants on the material's surface. The eco-innovative aspect of the research involves the utilization of sustainable components, minimizing the environmental impact of the composite materials throughout their life cycle. The materials are designed to correspond to the Circular Economy and Sustainable Development principles by reducing overall waste generation and the study involves a comprehensive characterization of the mechanisms that allow the production of these type of materials.

Key words: advanced composites, microorganism resistance, photocatalysis, TiO₂ nanoparticles.

INTRODUCTION

Due to the action of external factors, pollutants in the air, water, compounds resulting from the combustion of fuels used for heating and transport, buildings in the urban environment are subject to deterioration and decay. As a result of the growing awareness of environmental and public health issues, the need to manage industrial wastes and by-products from the energy industry, metallurgy, etc. has been identified. More specifically, the global environmental context of drastic reduction of harmful effects related to pollution, destabilisation of ecosystems, global warming and all their related elements, calls for an urgent need to identify possibilities to recycle fly ash, slag and other wastes. The implementation of the Circular Economy cannot be achieved at the level of a single sector of activity and, moreover, this approach would not be successful because if in one sector of activity the product represents waste or an industrial by-product, in another sector the same product may represent a valuable and under-exploited raw material.

Worldwide, in line with the principles of Sustainable Development and the Circular Economy, there is a strong orientation towards reducing the consumption of non-renewable raw materials, increasing sustainability, reducing soil, water and air pollution and, consequently, reducing the volume of waste or identifying possibilities for its recovery. From the point of view of the construction sector, a huge consumption of cement is identified, as it is the main raw material in many technological processes specific to this sector (Zailan et al., 2016). Producing such a large volume of cement/concrete is directly associated with environmental problems - cement production is responsible for about 5-8% of total carbon dioxide emissions (Cembureau, 2023; Aitcin, 2000; Sandu, 2021; Jamaludin et al., 2022). The cement manufacturing industry estimates that, today, applying the best available technologies for producing Portland cement, CO₂ emissions from its production could be reduced by up to 17% (Damtoft et al., 2008; Warid Wazien et al., 2016; Lloyd & Rangan, 2010). At EU level, there are currently specific

documents available for the cement industry that directly address and outline guidelines on reducing environmental impacts: Best Available Techniques (BAT) Reference Document for the Production of Cement, Lime and Magnesium Oxide (BREFs) (Best Available Techniques Reference Document, 2023) and the Commission Implementing Decision of 26 March 2013 setting out the conclusions on Best Available Techniques (BAT) under Directive 2010/75/EU of the European Parliament and of the Council on industrial emissions for the production of cement, lime and magnesium oxide (BAT) (European IPPC Bureau, 2013). In all this context, on the one hand the high pollution potential of the cement manufacturing industry is identified, even applying BAT, and on the other hand two options for the use of fly are identified: the first, less convenient in terms of the degree of environmental impact, would be the use as an auxiliary raw material in the cement production process; the second, also preferable in terms of environmental criteria, being the use as the main raw material in the production of alkali-activated geopolymer materials (Friedlingstein et al., 2010; UNSTATS, 2010).

Research in recent years has shown that one possibility for the efficient management of these types of industrial wastes and by-products is their use in the production of geopolymer composites, so-called "green concrete" or "geopolymer concrete" (Stengel et al., 2009; Weil et al., 2009; Pachengo et al., 2008; Skvara, 2007). In the light of the urgent need to develop environmentally friendly materials that, at some point, will allow the reduction of concrete and, consequently, cement consumption, while at the same time allowing the reuse of waste and industrial by-products, the development of alkali-activated fly ash geopolymer materials present an area of great interest.

On the other hand, the possibility of producing cementitious or geopolymer materials with self-cleaning properties due to the photocatalytic properties of TiO₂ nanoparticles used as an admixture or as a substitute for a cement part is currently reported worldwide (Greibenışan et al., 2023; Janus & Zajac, 2016; Fujishima & Zhang, 2006). It is known that the biocidal mechanism and self-cleaning ability of composite surfaces containing TiO₂ nanoparticles is the result of

two mechanisms, that of superhydrophilicity and that of degradation, destruction of molecules of organic nature, therefore, implicitly of microorganism cells these having a structure of organic nature (Zailan et al., 2017). In this context, it is known that the growth of micro-organisms (moulds, bacteria, viruses, algae, lichens, mites) on building surfaces has negative effects, on one hand on the health of the population, especially if the growth occurs on interior surfaces, and on the other hand on the health of buildings, causing, in addition to an unpleasant appearance, maintenance and repair costs (Haleem Khan & Karuppaiyil, 2012; Ebbehøj et al., 2002; Zeliger, 2013; Andresen et al., 2011).

Life Cycle Assessment (LCA) in the construction sector is a systematic approach to evaluate the environmental impacts of a building or infrastructure project throughout its entire life cycle, from raw material extraction and processing to construction, use, and eventual demolition or disposal. It considers various aspects such as energy consumption, resource depletion, emissions, and waste generation at each stage. LCA in construction industry helps in making informed decisions to minimize the environmental footprint of materials, buildings and infrastructure. It aids in the selection of sustainable materials, energy-efficient designs, and construction practices (Mellado et al., 2014). LCA also supports the development of sustainable infrastructure by providing a holistic view of the environmental performance of materials. It helps inform decision-makers about the environmental consequences of different choices during the planning and design phases and encourages the adoption of more sustainable practices and materials in construction projects. Life Cycle Assessment of geopolymers involves evaluating the environmental impact of geopolymers throughout their entire life cycle, from raw material extraction to production, use, and disposal or recycling and are often considered as a more sustainable option compared to traditional Portland cement (Badurdeen et al., 2018; McLellan et al., 2011; Mellado et al., 2014). Furthermore, the incorporation of recycled aggregates in geopolymer concrete aligns with the growing emphasis on sustainability in the construction industry. This approach addresses

environmental concerns, reduces reliance on virgin materials, and contributes to the development of more eco-friendly construction practices. Proper quality control and mix design considerations are essential to harness the full potential of recycled aggregates in geopolymer concrete applications (Bostanci et al., 2018; Bostanci, 2020; Guo et al., 2018; Lăzărescu et al., 2024).

Several studies indicate that it is not possible to make a simple sustainability comparison on the use of OPC and geopolymers. This is due to the significant impact of reagent transport and variability in the source of energy and technology used to produce the reagents. Costs have been minimized over time for OPC, as it is an established product; however, geopolymers are yet to go through this cycle of scale-up. Large scale geopolymer use is likely to lead to lower costs due to large orders of reagents (McLellan et al., 2011; Chen et al., 2010). To demonstrate the potential variability in the sustainability potential of geopolymer materials compared with OPC a case-by-case investigation must be carried out, considering several parameters regarding local raw materials, availability, location and influencing cost parameters.

The aim of this paper is to present preliminary results on the production of paving block elements produced using the concept of alkaline activation of fly ash and to present results on specific physical and mechanical characteristics. At the same time, to maximize the potential of generating smart-eco-innovative character, different types of aggregates were used to produce these elements, as well as the use of TiO₂ nano-particles into the geopolymer matrix. Finally, the present work aims to highlight an LCA calculation of the resulting CO₂ equivalent emissions by comparison with similar elements produced using traditional materials (cement) and a cost-benefit analysis of the results obtained.

MATERIALS AND METHODS

Several types of alkali-activated fly ash-based geopolymer composites and cementitious composites were designed, prepared and analysed for the aim of the research. In order to assess the LCA, the control samples were

considered the paving blocks produced using only natural aggregates, granular class 0/4 mm with and without the addition of TiO₂.

The following raw materials were selected for the production of the alkali-activated fly ash-based geopolymer paving blocks:

- low-calcium fly ash that was used in this study was obtained from a power plant in Romania and the chemical composition was established by the means of the X-ray fluorescence analysis (XRF analysis) (Table 1). The particle analysis, in terms of cumulative distribution of the fly ash particles was established using a HELOS RODOS/L, R5 instrument capable of dry dispersion in the free aerosol jet for laser diffraction and dynamic image analysis (Figure 1);

- the alkaline activator used in the production of the alkali-activated fly ash-based samples was a combination between sodium silicate solution (Na₂SiO₃ solution) and sodium hydroxide solution (NaOH solution). The chemical composition of the sodium silicate solution is SiO₂=30%, Na₂O=14% and H₂O=56%. The sodium hydroxide solution was prepared by dissolving the NaOH pearls, 99% purity, into water, to obtain the desired concentration of the solution. The NaOH solution concentration was set to 8M;

- granular class 0/4 mm natural aggregates, recycled glass granular class 0/4 mm and micronized quartz were used in this study to produce the alkali-activated fly ash-based geopolymer paving blocks. Particle size distribution of aggregates is shown in Figure 2 and Figure 3;

- TiO₂ nanoparticles of type AEROXIDE® TiO₂ P25, according to the manufacturer's technical data sheet, these TiO₂ nanoparticles are characterized by a purity of 99.5%, containing more than 70% anatase crystalline phase.

Ordinary Portland cement CEM I 52.5 R was used to produce the control samples for the assessment of the LCA.

For all tested mixtures, the introduction of 3% TiO₂ nanoparticles as a percentage of total ash/cement mass was considered to determine the LCA.

The chosen TiO₂ percentage is in accordance with the literature, which shows that for a TiO₂ percentage of 3%, both the physical-mechanical

performance and the resistance to microorganisms' action can be improved.

Table 1. Fly ash chemical composition

Oxides	%
SiO ₂	46.94
Al ₂ O ₃	23.83
Fe ₂ O ₃	10.08
CaO	10.72
MgO	2.63
SO ₃	0.45
Na ₂ O	0.62
K ₂ O	1.65
TiO ₂	0.92
L.O.I.	2.11

Based on the results regarding the possibility of developing such construction elements (Lăzărescu et al., 2022; 2024), the research initially focused on preliminary evaluation of the physical, mechanical and durability characteristics of the obtained products, for the study of their potential, different areas of applicability:

- (1) Apparent density;
- (2) Weathering resistance – total water absorption;
- (3) Weathering resistance – freeze-thaw resistance with de-icing salt;
- (4) Tensile splitting strength;
- (5) Abrasion resistance;
- (6) Slip/skid resistance.

All the test were performed according to norm EN 1388:2004/AC:2006: Concrete paving blocks. Requirements and test methods (ASRO, 2006), which specifies the materials, characteristics, conditions and methods of testing the paving blocks, and it is applicable for the use of pedestrians, vehicles, bicycle lanes, parking lots, roads, highways, industrial areas, etc. To be used in specific applications, they must comply with certain conditions at the time of their declaration as fit for use by the manufacturer.

The Life Cycle Assessment (LCA) was carried out based on a methodology consisting of four steps: setting the objective and defining the scope (1), life cycle inventory (2), environmental impact assessment (3) and interpretation of the results (4) (Figure 4).

For each proposed mix-design the LCA diagram, the main environmental impact element in terms of CO₂Eq was identified. Thus, in the case of geopolymer composites, the heat treatment required for the geopolymerization processes is identified as the main impact element, due to the electricity consumption used to achieve a temperature of 70°C in the heat treatment chamber during the first 24 hours after casting. A possible method to improve the environmental impact in this case is to optimize the heat treatment process or, through compositional optimization, even to eliminate it. In the case of cementitious composites, the main environmental impact in terms of CO₂Eq has been identified as cement, the main raw material.

The LCA has been calculated in terms of price/m², but also in terms of CO₂Eq/m². to produce type I paving blocks (22.5 x 8.8 x 6.0 cm - Figure 5).

RESULTS AND DISCUSSIONS

From the point of view of the physical-mechanical characteristics of the composites analysed the following can be said:

- Geopolymer binder-based composites have a lower density compared to cementitious ones (Figure 6). This parameter is influenced by both the type and nature of aggregates used, with recycled glass aggregates and natural aggregates contributing to the increased density of the composite. On the other hand, the addition of NT contributes to the densification of the material, causing a slight increase in density, through the changes it induces at the microstructural level, especially at the porosity level of the material.

- The use of recycled glass aggregates contributes to reducing the water absorption of the geopolymer composite, a parameter which for the use of natural aggregates or micronized quartz would be close to the water absorption characteristic of cementitious composite. The influence of TiO₂ nanoparticles is also observed this time on the characteristics of the composites, the water absorption reducing with the addition of nanoparticles, both for the geopolymer-bound composites and for the cementitious composite.

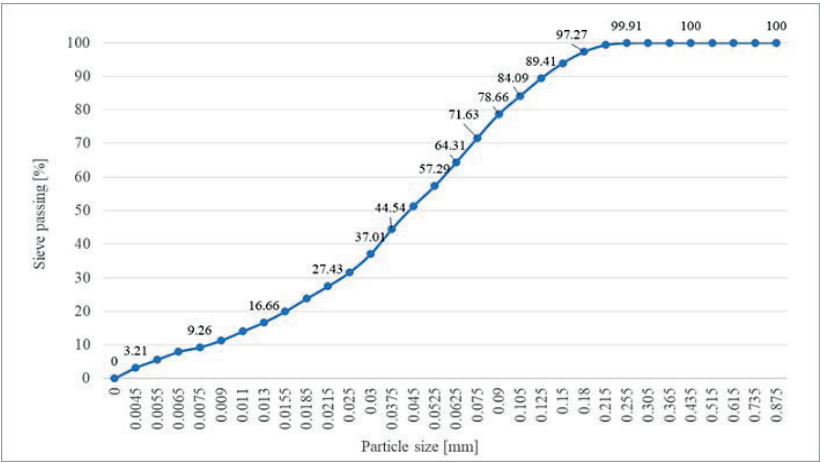


Figure 1. Particle size distribution of fly ash

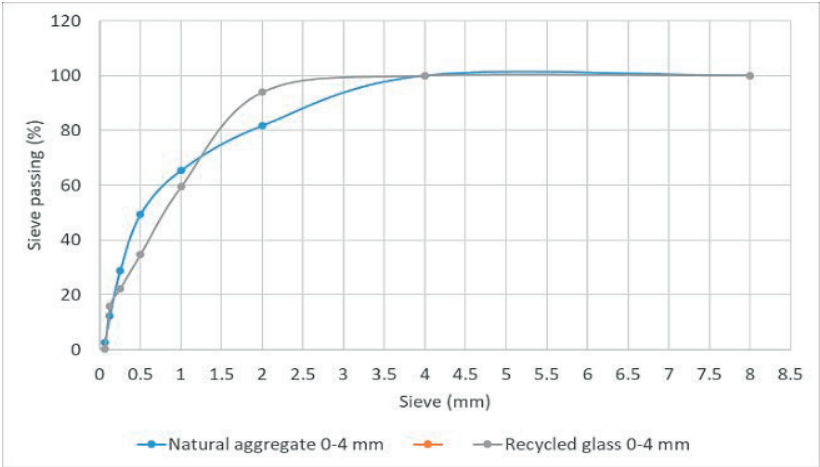


Figure 2. Particle size distribution of natural aggregates granular class 0/4 mm and recycled glass aggregates 0/4 mm

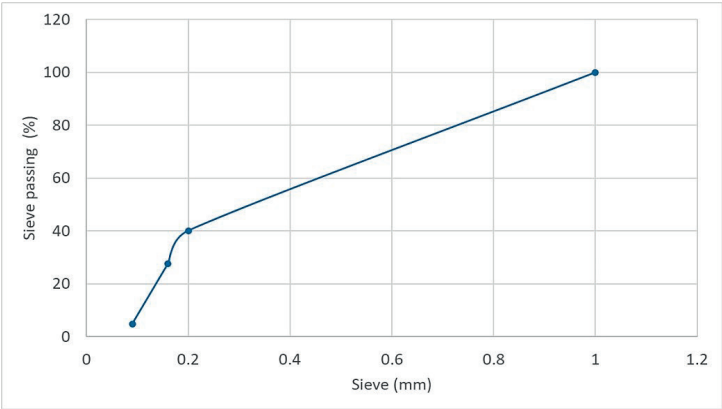


Figure 3. Particle size distribution of micronized quartz

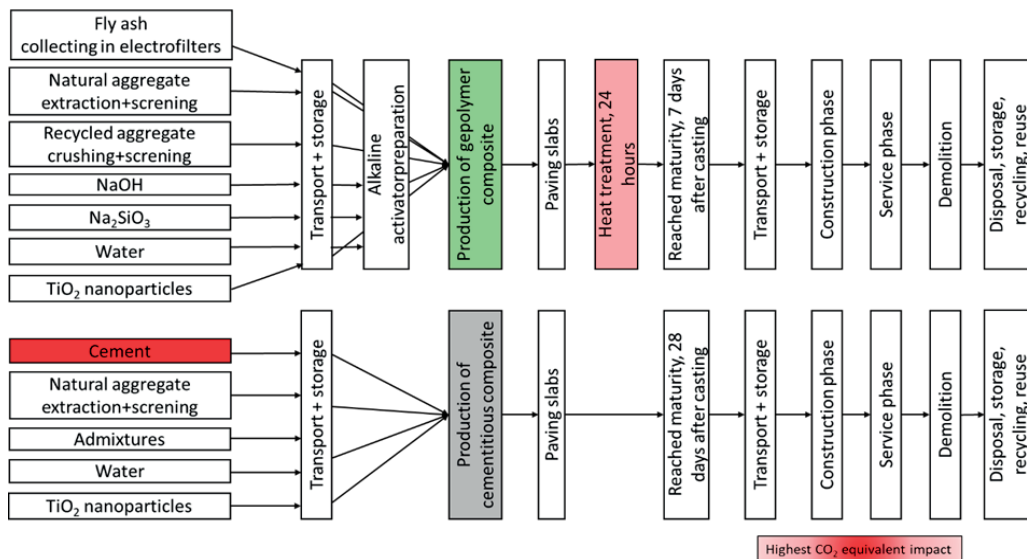


Figure 4. Life Cycle Assessment methodology- Comparative analysis of alkaline activated fly ash geopolimer paving blocks vs. OPC paving blocks



Figure 5. 22.5 x 8.8 x 6.0 cm paving block

By introducing NT as an addition (Figure 7), the water absorption of geopolimer composites decreases by 12.5-15.8% compared to similar materials without NT, and in the case of cementitious composite, the decrease is 10.3%. These changes are beneficial, as a lower water absorption is favourable to increase the resistance of the material to the action of environmental agents and, therefore, to increase the lifetime.

- The abrasion resistance (Figure 8), measured by volume loss, is relatively similar

for geopolimer composites compared to cementitious, but with the introduction of TiO_2 nanoparticles, this volume loss is decreased by 1.1% for cementitious composites and by 5.3-6.2% for geopolimer composites. This time too, the influence of the nature of the aggregates is noticeable, the wear resistance being better for the use of recycled glass aggregates and even micronized quartz.

- As expected, considering the densification of the composites and the reduction of their porosity due to the introduction of NT in the composite matrices, an improvement of the freeze-thaw resistance of both the composites with geopolimer binder (30-50%) and the one with cementitious binder (25%, Figure 9) can be observed, which will again lead to an increase of the lifetime of the products through an improvement of the resistance to the action of environmental factors.

- The splitting strength (Figure 10) is lower in the case of geopolimer material compared to cementitious composite, but this parameter proves to be improvable, on the one hand by compositional changes (type and nature of aggregates), and on the other hand by the introduction of TiO_2 nanoparticles.

- Another important aspect is to reduce the slip potential. As seen in Figure 11, it can also be appreciated that changes at the compositional

level of the geopolymer composite, i.e. changes in the nature of the aggregates, but also the introduction of NT contribute beneficially. Thus, if for the geopolymer composite with natural aggregates the slip potential is classified as "moderate" (USRV 20-39), with the use of recycled glass or micronized quartz aggregates, this potential improves by one class, respectively, reaching the "low" classification (40-74). Also, the introduction of NT in the

composite matrix has the effect of transitioning from the "moderate" class (USRV 20-39) to "low" class (40-74), all of which contributes to increasing the operational safety for users of precast paving products. A beneficial effect of NT is also seen in the case of cementitious composite, with a transition from "moderate" class (USRV 20-39) to "low" class (40-74) also recorded.

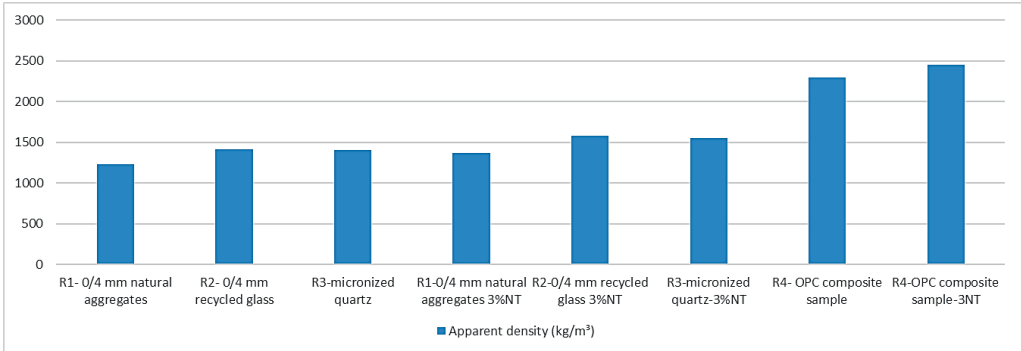


Figure 6. Apparent density of alkaline activated fly ash geopolymer paving blocks and OPC paving blocks

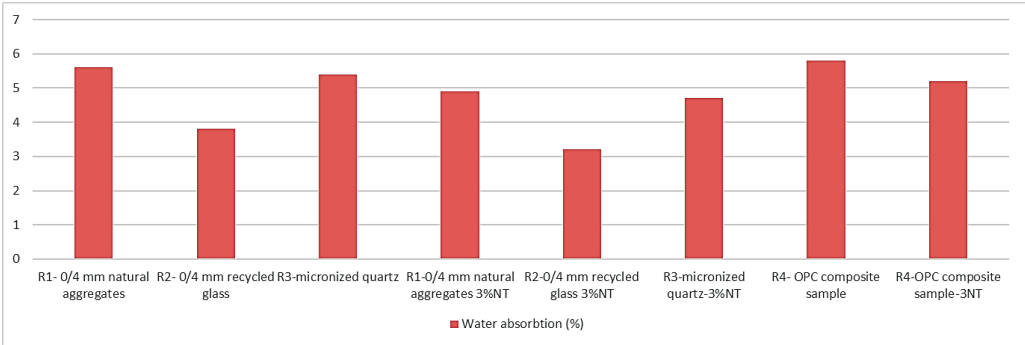


Figure 7. Water absorption of alkaline activated fly ash geopolymer paving blocks and OPC paving blocks

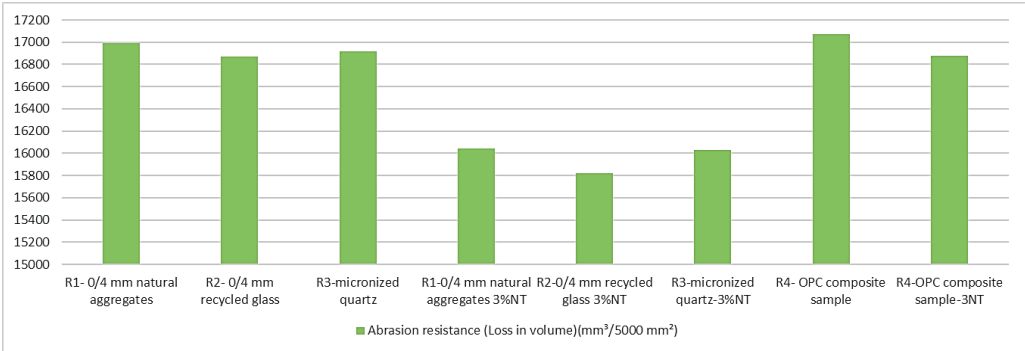


Figure 8. Abrasion resistance of alkaline activated fly ash geopolymer paving blocks and OPC paving blocks

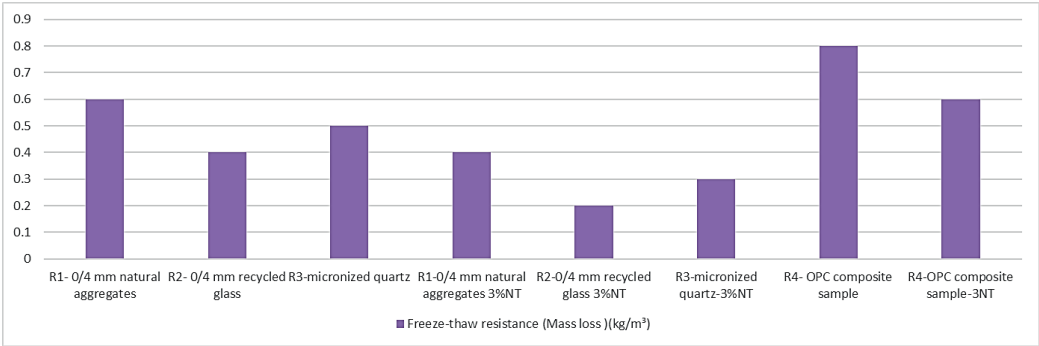


Figure 9. Freeze-thaw resistance of alkaline activated fly ash geopolymer paving blocks and OPC paving blocks

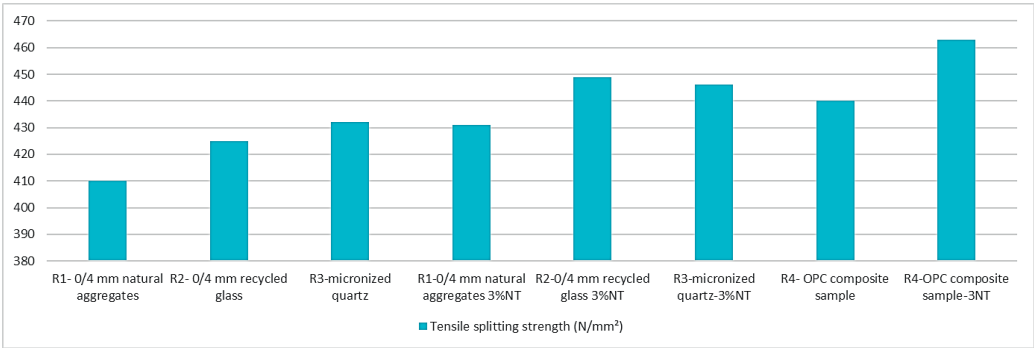


Figure 10. Tensile splitting strength resistance of alkaline activated fly ash geopolymer paving blocks and OPC paving blocks

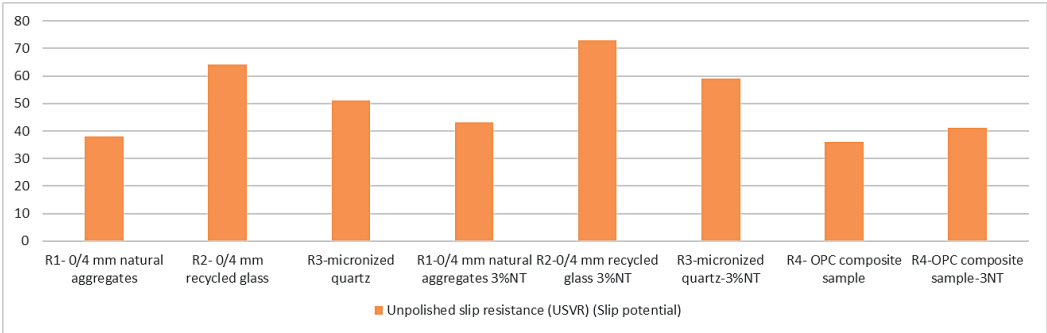


Figure 11. USVR resistance of alkaline activated fly ash geopolymer paving blocks and OPC paving blocks

Analysing each stage of the LCA in turn, the following can be said:

- The raw materials used to produce the geopolymer paving blocks have several advantages in terms of environmental impact: fly ash, the main raw material, is a waste product, collected, by means of electrofilters that consume electricity, but which would otherwise be disposed of/landfilled as waste,

which would have polluting consequences. Similarly, it is considered that the issue of recycled aggregates (glass) should also be addressed. Chemical raw materials (NaOH and Na_2SiO_3) are commonly used materials in various industries, easily accessible, affordable and with medium environmental impact.

- Among the raw materials used in the preparation of the cementitious composite, the

strong polluting impact of cement stands out, while the natural aggregates, used for both variants of composites, contribute equally in terms of $\text{CO}_{2\text{Eq}}$, as well as TiO_2 nanoparticles. However, in the case of TiO_2 nanoparticles, although they contribute their own $\text{CO}_{2\text{Eq}}$ contribution to the final product, their use in composites induces significant benefits on the physical-mechanical characteristics and, consequently, on the increase of the product lifetime and enhanced resistance to microorganisms.

- The phases of transport and storage, production of prefabricated elements (paving blocks), installation, use, maintenance, demolition and disposal, recycling, reuse, being carried out in a similar way for both cases analysed (geopolymer vs. cementitious), have an equal contribution in terms of environmental impact.

- The alkaline activator phase, specific to the preparation of geopolymers, is carried out by simply dosing and dissolving NaOH in water, i.e., subsequent mixing with Na_2SiO_3 , and therefore does not have a significant effect in terms of $\text{CO}_{2\text{Eq}}$.

- The conditioning and maturation stages of the products show some differences, depending on the type of composite. Thus, in the case of geopolymers, the heat treatment phase is identified as the main environmental impact element in terms of $\text{CO}_{2\text{Eq}}$, as previously analysed, followed by an environmental storage phase, which does not represent an environmental impact factor. In the case of cementitious composites, although there is no heat treatment phase, the need for curing is 4 times longer than in the case of geopolymers and under specified conditions (immersion in water) indicates that even in this case, although quantitatively smaller, there is an environmental impact due to the need for handling, with electrically or auto-mechanically operated equipment, of the prefabricated elements and the achievement and maintenance of suitable environmental conditions (water temperature).

- The installation is mostly done by hand, and during the installation there is generally no maintenance/repair work that would induce a $\text{CO}_{2\text{Eq}}$ contribution.

An estimate carried out for the production of prefabricated paving blocks needed to cover a

pedestrian area equal to 1 m^2 , revealed the following (Figure 12):

- as expected, the production of geopolymer composite paving blocks increases the cost price significantly, mainly since the technology is still relatively new and includes the use of more expensive raw materials (NaOH and Na_2SiO_3) to ensure constant product performance;

- partial substitution of natural aggregates with recycled waste glass aggregates does not contribute significantly in terms of price, but has a clear role in reducing the carbon footprint;

- partial substitution of natural aggregates with micronized quartz increases the cost price of geopolymer composite paving blocks, while slightly increasing the carbon footprint;

- the use of TiO_2 nanoparticles induces a price increase, as this material is expensive, and induces some increase in carbon footprint.

All these four observations, at a first analysis, would not seem to encourage the hypothesis of paving blocks produced using geopolymer composite. If all this is analysed in a broader context, on the one hand comparing the carbon footprint with that of cement composite paving blocks and on the other hand comparing the physical-mechanical and durability performance, the results of the analysis are quite different.

Firstly, in all cases the $\text{CO}_{2\text{Eq}}/\text{m}^2$ pavement is much lower for geopolymer composite than for cementitious composite, with 35-50% lower values than for the use of cementitious composite, which is in line with the literature, although the cost price is substantially higher. This is even more so with the use of nanoparticles, which is also consistent with the literature (McLellan et al., 2011).

If the benefits in terms of improved product performance (resistance to environmental agents, wear resistance and mechanical strength) are analysed, it can be indirectly concluded that in terms of geopolymer composite paving blocks, especially with TiO_2 nanoparticle content, further research is desirable, especially with a view to technological optimisation, so that the cost price can be reduced while maintaining the environmental benefits and an extended service life of 10-40%.

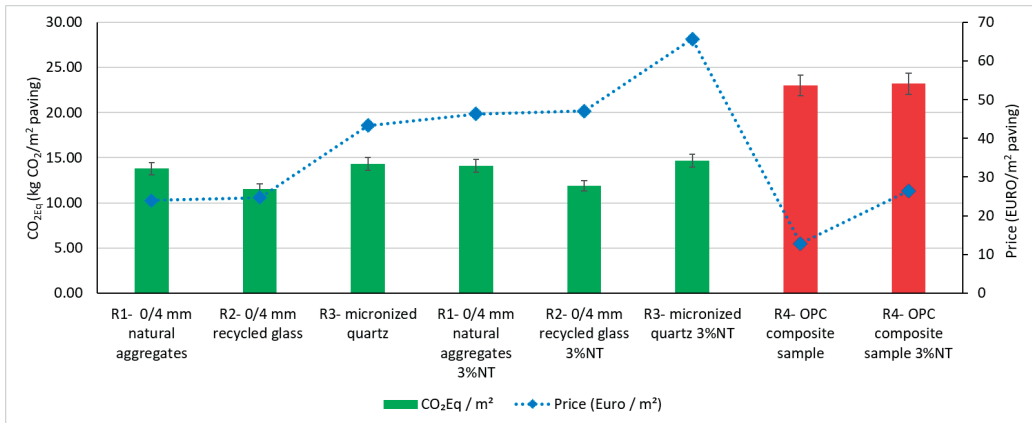


Figure 12. Price and CO₂Eq for the case of 1m² paving blocks produced using alkali-activated fly ash-based geopolymer vs. cementitious composite

CONCLUSIONS

The aim of this paper was to present preliminary results on the production of paving block elements produced using the concept of alkaline activation of fly ash, to present results on specific physical and mechanical characteristics and to highlight an LCA calculation of the resulting CO₂Eq emissions by comparison with similar elements produced using traditional materials (cement) and a cost-benefit analysis of the results obtained.

Conducting a Life Cycle Assessment (LCA) on geopolymer paving blocks provides valuable insights into the environmental performance of this sustainable construction material throughout its entire life cycle. The key conclusions drawn from such an assessment are:

- *Environmental benefits:* Geopolymer paving blocks exhibit the potential for significantly lower environmental impacts compared to conventional paving materials, particularly if they replace traditional concrete. The reduced carbon footprint is a notable advantage, as geopolymer binders typically require lower energy inputs and produce fewer greenhouse gas emissions during production.
- *Raw material savings:* Geopolymers often utilize industrial by-products such as fly ash or slag, diverting these materials from landfills and reducing the need for virgin raw materials. This aligns with principles of sustainable resource management and

contributes to a circular economy by repurposing waste materials.

- *Energy efficiency:* The lower curing temperatures required for geopolymerization contribute to energy savings during the production phase compared to traditional cement-based materials. Reduced energy consumption in the manufacturing process leads to lower overall embodied energy in geopolymer paving blocks.

- *Durability and longevity:* Geopolymer paving blocks have shown promising mechanical properties and resistance to environmental factors, contributing to a longer service life compared to some traditional paving materials. Enhanced durability obtained using TiO₂ nanoparticles can result in reduced maintenance and replacement needs over time, further extending the overall life cycle of the paving blocks.

- *End-of-life considerations:* Geopolymer paving blocks may offer opportunities for end-of-life recycling or reuse, contributing to a more sustainable waste management strategy. Proper disposal methods, such as recycling or utilizing the blocks in other construction applications, can minimize the environmental impact associated with their end-of-life phase.

- *Challenges and opportunities for improvement:* The variability in the quality and availability of raw materials, as well as variations in production processes, can impact

the environmental performance of geopolymer paving blocks.

Ongoing research and development are essential to optimize production processes, improve material consistency, and address any potential challenges associated with the use of geopolymers.

In conclusion, a Life Cycle Assessment of geopolymer paving blocks underscores their potential as a sustainable alternative in the construction industry. While they show positive environmental attributes, ongoing research, standardization, and collaboration within the industry are necessary to optimize their production processes and further enhance their overall sustainability. Additionally, collaboration between researchers, industry professionals, and policymakers is vital to promoting the widespread adoption of geopolymer paving blocks as a sustainable construction solution.

ACKNOWLEDGEMENTS

This research was funded by the Romanian Government Ministry of Research, Innovation and Digitalization, project No. PN 23 35 05 01 “Innovative sustainable solutions to implement emerging technologies with cross - cutting impact on local industries and the environment, and to facilitate technology transfer through the development of advanced, eco-smart composite materials in the context of sustainable development of the built environment”.

REFERENCES

- Aitcin, P.-C. (2000). Cements of yesterday and today, Concrete of tomorrow. *Cem. Concr. Res.*, 30, 1349–1359.
- Andersen, B., Frisvad, J.C., Søndergaard, I., Rasmussen, I.S., & Larsen, L.S. (2011). Associations between Fungal Species and Water-Damaged Building Materials. *Applied and Environmental Microbiology*, 77(12), 4180–4188.
- ASRO (2006). *SR EN 1338:2004/AC:2006 Concrete paving blocks. Conditions and test methods*. Romanian Standard Association.
- Badurdeen, F., Aydin, R., Brown, A. (2018). A multiple life-cycle based approach to sustainable product configuration design. *J. Clean. Prod.*, 200, 756–769.
- Best Available Techniques (BAT) (2023). Reference Document for the Production of Cement, Lime and Magnesium Oxide (BREFs) - <https://eippcb.jrc.ec.europa.eu/reference/production-cement-lime-and-magnesium-oxide> (accessed on 19.01.2024).
- Bostanci, S.C. (2020). Use of waste marble dust and recycled glass for sustainable concrete production. *J. Clean. Prod.*, 251, 119785.
- Bostanci, S.C., Limbachiya, M.C., Kew, H. (2018). Use of recycled aggregates for low carbon and cost-effective concrete production. *J. Clean. Prod.*, 189, 176–196.
- Cembureau. Available online: <https://www.cembureau.eu/library/reports/2050-carbon-neutrality-roadmap/> (accessed on 19.01.2024).
- Chen, C., Habert, G., Bouzidi, Y., Jullien, A. (2010). Environmental impact of cement production: detail of the different processes and cement plant variability evaluation. *J. Clean. Prod.*, 18(5), 478–85.
- Damtoft, J.S., Lukasik, J., Herfort, D., Sorrentino, D., Gartner, E. (2008). Sustainable development and climate change initiatives. *Cem. Concr. Res.*, 38(2), 115–127.
- Ebbehoj, N.E., Hansen, M.O., Sigsgaard, T., Larsen, L. (2002). Building-related symptoms and molds: a two-step intervention study. *Indoor Air*, 12, 273–277.
- European IPPC Bureau (2023). Commission Implementing Decision of 26 March 2013 establishing BAT conclusions pursuant to Directive 2010/75/EU of the European Parliament and of the Council on industrial emissions from the production of cement, lime and magnesium oxide (BAT)- <https://eippcb.jrc.ec.europa.eu/reference/production-cement-lime-and-magnesium-oxide> (accessed on 19.01.2024).
- Friedlingstein, P., Houghton, R.A., Marland, G., Hackler, J., Boden, T.A., Conway, T.J. (2010). Update on CO₂ emissions. *Nature Geosci.*, 3(12), 811–812.
- Fujishima, A., Zhang, X. (2006). Titanium dioxide photocatalysis: present situation and future approaches. *Comptes Rendus Chimie*, 9, 750–760.
- Grebenişan, E., Hegyi, A., Lăzărescu, A.V. (2023). Analysis Regarding the Increase in the Resistance of Cementitious Self-Healing Composites to the Action of Microorganisms by Induced Photoactivation Capacity. *Scientific Papers. Series E. Land Reclamation, Earth Observation & Surveying, Environmental Engineering*, XII, 107–117.
- Guo, M., Tu, Z., Poon, C.S., Shi, C. (2018). Improvement of properties architectural mortars prepared with 100% recycled glass sand by CO₂ curing. *Constr. Build. Mater.*, 179, 138–150.
- Haleem Khan, A.A., Mohan Karuppaiyil, S. (2012). Fungal pollution of indoor environments and its management. *Saudi Journal of Biological Sciences*, 19, 405–426.
- Jamaludin, L., Razak, R.A., Abdullah, M.M.A.B., Vizureanu, P., Bras, A., Imjai, T., Sandu, A.V., Abd Rahim, S.Z., Yong, H.C. (2022). The Suitability of Photocatalyst Precursor Materials in Geopolymer Coating Applications: A Review. *Coatings*, 12, 1348.
- Janus, M., Zajac, K. (2016). Concretes with Photocatalytic Activity, High Performance Concrete Technology and Applications, INTECH.
- Lăzărescu, A.V., Ionescu, B.A., Hegyi, A., Florean, C. (2022). Alkali-activated fly ash based geopolymer

- paving blocks: green materials for future conservation of resources. *IJCS*, 13(1), 175-186.
- Lăzărescu, A.V., Hegyi, A., Csapai, A., Popa, F. (2024). The Influence of Different Aggregates on the Physico-Mechanical Performance of Alkali-Activated Geopolymer Composites Produced Using Romanian Fly Ash. *Materials*, 17(2), 485.
- Lloyd, N.A., Rangan, B.V. (2010). Geopolymer concrete with fly ash. In Second International Conference on Sustainable Materials and Technologies, Zachar, J., Claisse, P., Naik, T.R., Ganjian, E., Eds., Publisher: Università Politecnica delle Marche, Ancona, Italy.
- McLellan, B.C., Williams, R.P., Lay, J., van Riessen, A., Corder, G.D. (2011). Costs and carbon emissions for geopolymer pastes in comparison to ordinary portland cement. *J. Clean. Prod.*, 19(9-10), 1080-1090.
- Mellado, A., Catalan, C., Bouzon, N., Borrachero, M.V., Monzo, J.M., Paya, J. (2014). Carbon footprint on geopolymeric mortar: study of the contribution of the alkaline activating solution and assessment of an alternative route. *RSC Adv.*, 4, 23846.
- Pacheco-Torgal F., Castro-Gomez J., Jalali S. (2008). Alkali-activated binders: A review Part I. Historical background terminology, reaction mechanisms and hydration products, *J. Constr. Build. Mater.*, 22, 1305-1314.
- Sandu, A.V. (2021). Obtaining and Characterization of New Materials. *Materials*, 14, 6606.
- Skvara, F. (2007). Alkali activated material- geopolymer, Department of Glass and Ceramics, Faculty of Chemical Technology, ICT Prague, pp. 661-676.
- Stengel, T., Reger, J., Heinz, D. (2009). Life cycle assessment of geopolymer concrete - what is the environmental benefit? Concrete Solutions 09. Luna Park, Sydney, Australia: Concrete institute of Australia.
- UNSTATS (2010). Greenhouse gas emissions by sector (absolute values). New York: United Nations Statistical Division.
- Warid Wazien, A.Z., Mustafa, M., Abdullah, A.B., Razak, R.A., Rozainy, M.M.A.Z.R., Faheem, M., Tahir, M., Faris, M.A., Hamzah, H.N. (2016). Review on Potential of Geopolymer for Concrete Repair and Rehabilitation. *MATEC Web Conf.*, 78, 01065.
- Weil, M., Dombrowski, K., Buchwald, A. (2009). Life-cycle analysis of geopolymers. In: Provis JL, Van Deventer JSJ, editors. Geopolymers: structures, processing, properties and industrial applications. Cambridge, England: Woodhead Publishing Limited, pp. 194-210.
- Zailan, S.N., Mahmed, N., Al Bakri Abdullah, M.M., Sandu, A.V. (2016) Self-cleaning geopolymer concrete - A review. *IOP Conf. Ser.: Mater. Sci. Eng.*, 133, 012026.
- Zeliger, H.I. (2003). Toxic effects of chemical mixtures. *Archives of Environmental Health: An International Journal*, 58(1), 23-29.

ADVANCED RECOVERY OF VALUABLE MATERIALS FROM E-WASTE

Ștefan-Leontin MARTINAȘ-IONIȚĂ, Gabriela Antoaneta APOSTOLESCU, Maria HARJA

“Gheorghe Asachi” Technical University of Iasi, Faculty of Chemical Engineering and
 Environmental Protection, 73 Prof. D. Mangeron Blvd, Iasi, Romania

Corresponding author email: mharja@tuiasi.ro

Abstract

Due to rising customer demand, the manufacturing of electrical and electronic equipment has expanded dramatically in recent years; nevertheless, because technology is advancing so quickly, the equipment's lifespan has decreased. Consequently, an enormous volume of electronic waste (also known as "e-waste") is produced each day.

The majority of these wastes consist of materials that, in the wrong hands, can have an adverse effect on the habitats they are placed in and, indirectly, the species that live there. Metals, polymers, and refractory oxides are frequently found in these wastes. These materials can be highly valuable economically if they are correctly collected and separated. The main strategies for isolating and recovering valuable components from electrical and electronic waste were examined in this study, along with how successful these approaches were at disposing of waste.

Key words: electronic, metals, pollution, recycle, waste.

INTRODUCTION

In the last decades, a large amount of waste has been generated at an alarming rate, thus electrical and electronic waste has been attracting the attention of scientific communities in recent years, this fact being mainly due to the composition of this waste and the abundant presence of metals in this waste, such as copper (Cu), cobalt (Co), nickel (Ni) or silver (Ag) (Russo et al., 2022). The main component of electrical and electronic waste is represented by printed circuit boards (Fariborz et al., 2022).

It is estimated that the composition of printed circuit boards is composed of 40% metals, 30% plastics and 30% ceramics (Gamez et al., 2019). The printed circuit boards represent a high percentage of all electronic waste, accounting for approximately 3-5% of the total mass (Fariborz et al., 2018). This type of waste metals can exist in different forms, elemental form, various oxides and various alloys (Touze et al., 2020). The complications in the processing of this type of waste come from the fact that it has a multi-metallic composition, and this aspect makes the development of a universal and at the same time efficient recovery process quite difficult (Fariborz et al., 2022).

The concentration of metals depends on the nature of the waste; for example, devices that

require better (faster) connections have higher concentrations of precious metals and devices that contain larger amounts of connections and wiring have higher amounts of elemental copper (Mesquita et al., 2018). Many of these materials are incorporated into printed circuit boards to provide good high temperature insulation properties and high thermal stability of the boards (Qiu et al., 2020).

Fariborz et al. (2022) shows that the composition of printed circuit boards can be different, depending on the nature of the waste. Table 1 (adapted from Fariborz et al., 2022) highlights the composition of printed circuit boards from mobile phones, laptops, televisions and others.

Table 1. PCB elemental metal composition

Types of PCBs	Types of materials					
	Al	Cu	Pb	Ni	Fe	Ag
Mobile phones	0.26	35.50	1.87	3.41	12.49	2100
Laptops	1.47	39.20	1.54	0.64	1.98	165
Television	0.30	11.2	-	0.02	-	48
Old computers	-	34.26	1.11	0.43	2.45	-
Copper-rich PCBs	5.2	34	0.75	-	2.80	-
Mixed PCBs	-	26.82	-	0.20	5.36	530

For an efficient recovery of these metals, several methods have been developed, such as: solvent extraction, ion exchange, membrane separation, compaction, retention on porous polymers, coprecipitation, sequential distillation, precipitation and adsorption, the last one being presented in the literature as the method showing the highest degree of recovery of metals from aqueous solutions (Mokhodoeva et al., 2020).

Metal recovery methods from electrical and electronic waste are chemical precipitation, coagulation and flocculation, ion exchange, membrane filtration, adsorption, electrochemical treatment and photocatalysis (Azmi et al., 2018). These are also the most common methods of metal recovery from electrical and electronic waste (Fan et al., 2018; Martinas-Ionita et al., 2023).

Chemical precipitation is a process of forming insoluble metal precipitates by the reaction of the precipitating agent of hydroxides or sulfides with dissolved metal ions. This technique is the most used treatment method in today's industries by adjusting the pH to basic conditions to reduce the solubility of metal ions in wastewater. The metal precipitates formed are recovered using a solids separation process. The advantages of the method are simple operation and low cost due to their availability and low-cost precipitating agents. The disadvantages are generation of excessive amount of sludge, with negative impact over environment (Azmi et al., 2018).

Coagulation and flocculation are common methods of treating process waters where coagulation is the destabilization of the surface charge of colloids to make flocs and flocculation is the aggregation of these flocs into larger particles. The two methods can significantly improve separation in subsequent treatments such as sedimentation or filtration (Hubert et al., 2024).

In the ion exchange process, the ion exchanger (resin) exchanges its cations with metal ions from the wastewater without any structural modification of the resin. The metal is then recovered by elution with a suitable product after separating the charged resin from the wastewater.

Common cation exchangers are strongly acidic resins with sulfonic acid ($-\text{SO}_3\text{H}$) groups and weakly acidic carboxylic acid ($-\text{COOH}$) resins

where the hydrogen ions in the groups serve as exchange ions with the metal cations in the wastewater (Azmi et al., 2018).

Membrane filtration is an emerging technology for the separation of ions or molecules (Shuaifei et al., 2024). It exhibits high efficiency and low cost, but also has disadvantages such as unsatisfactory selectivity for small ions and short membrane lifetime (Zhao et al., 2021).

Recently, several absorption methods have been developed for the recovery of metals from the leachate in the final stage of the process. These methods include adsorption by various adsorbents, such as chitin, chitosan and activated carbon (Zazycki et al., 2017), membrane-based separation with polymer inclusion, and adsorbent based on biomass derived from agriculture (Rizki et al., 2023).

Electrodeposition precipitates one or more metal ions in leaching solution to achieve ion separation by controlling voltage, current and other influencing factors (Xiaohui et al., 2024). Photocatalysis is a method that couples low-energy ultraviolet light with semiconductor catalyst particles to reduce the metal ions they contain in an electrolyte by photogenerated electrons. Photocatalysis has emerged as a promising alternative approach to conventional pollutant degradation methods. In this method, organic compounds are degraded by the generation and subsequent reaction of hydroxyl radicals and other compounds. The most widely used semiconductor photocatalysts are TiO_2 , ZnO , CeO_2 , CdS and ZnS which are derived from chalcogen compounds (Fernandes et al., 2024).

In addition to these classic methods, in recent years more advanced bio processes have appeared that can lead to the extraction of metals from electrical and electronic waste without polluting the environment. They can also be integrated into classic recovery processes to achieve a higher and faster recovery rate. An example of such an integrated process is the integrated bio- and hydrometallurgical process developed for the extraction of base metals from electronic waste. It is composed of three operation units: biogenic generation of H_2SO_4 , biogenic ferric (Fe^{3+}) generation and non-contact indirect bioleaching of base metals from

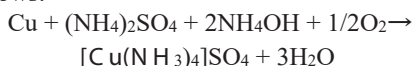
ground waste with biogenic leaching (Yken et al., 2023).

Investigations into the nature and structure of chemical compounds of copper in electrical and electronic waste were carried out by the method of X-ray diffraction analysis.

Since no two chemicals are in the crystalline state where the distance between the reflection planes is identical in all directions, placing a crystal at all possible angles to the X-ray beam produces a characteristic image.

The qualitative analysis is based on the calculation of the d-spacings (lattice constants) for all diffraction lines in the spectrum and their comparison with the d-values given in the literature. A general use in this regard is the ASTM card, with tabular sheets, in which the d values for substances, the relative intensity of the lines (%), relative to the most intense line) and h, k, l are entered indices of the lines. To identify a crystalline phase, the presence of the first 3 intense lines in the spectrum is sufficient. The identification of copper chemical compounds from the obtained spectra is done with the help of A.S.T.M.

Considering that in the electrical and electronic waste analyzed, copper is found in the form of metallic copper and the fact that the other components do not react with the ammonium sulfate solution, the stoichiometric equation of the copper extraction process from the electrical circuit, the electronic waste, in the form of cuproammonia complex can be written as follows:



MATERIALS AND METHODS

In this study, two laptops and two mobile phones presented in Figure 1 were recycled.

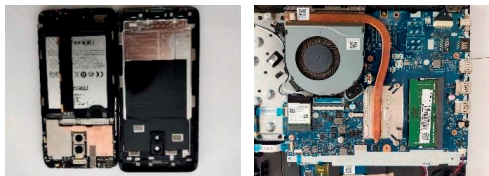


Figure 1. Materials subject to recycling

The first step of this process was to manually disassemble the waste and separate it into

components (case, screen, parts attached to the printed circuit board and printed circuit boards) using different techniques (Kaya, 2016). During disassembly, various components that could be removed were also separated, such as batteries, capacitors and wiring.

RESULTS AND DISCUSSIONS

The main objective of this work is to recycle copper and silver from electrical and electronic waste by passing them into solutions and introducing them into non-polluting chemical processes.

After performing the manual disassembly and separation, a manual mechanical shredding of the printed circuit boards shown in Figure 2 was performed.



Figure 2. Printed circuit boards subjected to the shredding process

The separation of the ferrous metal fraction from the non-ferrous one was achieved by highlighting the magnetic properties of the ferrous metal fraction with the help of magnets, this fact being highlighted in Figure 3.



Figure 3. Separation of the ferrous metal fraction from the non-ferrous metal fraction

In order to reach the smallest possible diameter of the printed circuit boards, grinding was

carried out in a rotating drum mill (Figure 4). A quantity of 200 g of manually shredded waste was prepared for the grinding process. Balls of different sizes (40 g, 50 g, 140 g and 300 g) were added to the mill, their total weight being 3 kg. The grinding time was 2 hours.



Figure 4. Rotary drum mill used in the printed circuit board grinding process

After the grinding process, the metals can be separated by several methods, not before the metals are put into solution. After mechanical processing, the waste is subjected to various metallurgical processes for metal recovery (Ding et al., 2019).

In order to achieve the non-catalytic process that takes place in heterogeneous systems, several preceding steps were carried out. After the grinding process, in the rotary mill, the material was subjected to separation using sieves and a vibrating table. The distribution of the material on the sieves is shown in Table 2.

Table 2. Distribution of the material on the site

Sieve size (mm)	Waste particle obtained (g)
< 2	158.88
< 1 > 2	7.76
< 0.315 > 1	16.1
< 0.250 > 0.315	1.2
< 0.05 > 0.250	12.7
> 0.05	2.58

From the granulometric curve (Figure 5) it can be seen that almost 80% of the amount of waste subjected to the grinding process had dimensions greater than 2 mm, which shows that the grinding in the rotary drum mill did not have a very good yield.

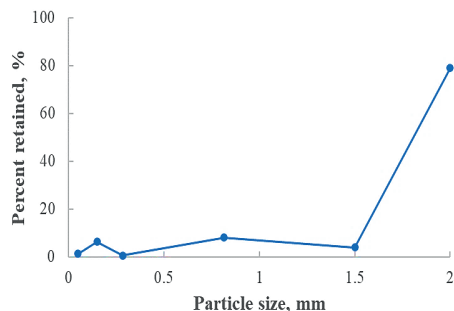


Figure 5. Granulometric curve before pyrometallurgical process

For the process of passing the copper into the solution to be effective, the size of the waste particles must be as smaller. Thus, for this process, a pyrometallurgical separation of copper was achieved. This process was carried out in an electric furnace of the type "S.Y. electric melting furnace Italy" and as a support was used a graphite crucible (Figure 6), so that the adhesion of the melt to the walls of the crucible is as low as possible, and the losses are minimum.



Figure 6. Pyrometallurgy process installation

In this melting process, 30 g of waste was used, previously sorted and shredded by hand. After burning, it was observed that 20.15% of the waste mass considered were volatile substances. In this processing mode, the distribution of particles on the sieve was more uniform (Table 3) and the granulometric curve is represented in Figure 7

Table 3. Distribution of the material on the sieve

Sieve size (mm)	Mass retained (g)
< 1.25	4.278
< 0.5>1.25	4.689
< 0.2 >0.5	3.872
> 0.2	10.877

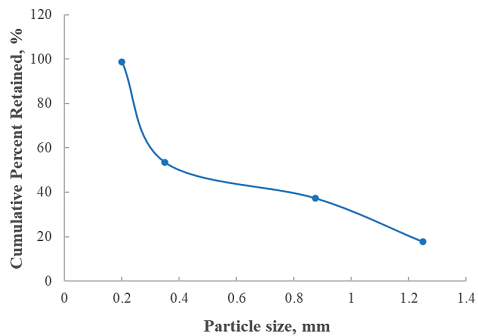


Figure 7. Granulometric curve after the pyrometallurgical process

It is worth noting that following the pyrometallurgical process, metal agglomerates can be observed (Figure 8).



Figure 8. Printed circuit boards after melting

CONCLUSIONS

Different methods can be used for recovery of valuable metals from e-waste. From these, the most common are: chemical precipitation, electrochemical, coagulation, flocculation, ion exchange, membrane filtration, adsorption, pyrometallurgical, etc.

Although have been noticeable advancements in precious metals recovery technologies, there are still certain obstacles to overcome.

There are different factors in order to attain the high recovery rate and environmentally friendly recycling of precious metals. The new technologies have in consideration low emissions, "zero waste", decrease investment and costs. Recovery technologies should be varied and integrated, based on the physical and chemical properties of different materials. Other purpose is higher leaching efficiency, that determine a less pollution. For increase recovery efficiency, different assisted methods or pretreatments are important (ultrasound, microwave, etc.).

As preliminary procedures, reducing particle size is crucial. The particle size of printed circuit boards directly influences the degree of recovery of metals from e-wastes. On the other hand, the environmental pollution is a very important aspect to take into consideration for choosing the better methods for valuable metals recovery, for example in pyrometallurgical processes, volatile materials must not be released into the atmosphere, while in chemical precipitation, flocculation or coagulation processes, no sludge or other waste should result. In this study was demonstrated that for a better yield it is necessary to increase the time of the pyrometallurgical process, the resulting materials being easy to process by grinding. On the base of this study, upcoming technologies for metals recovering can be improved, with higher efficiency, less environmental impact, inferior cost, and advanced recovery rate.

ACKNOWLEDGEMENTS

This research was supported by the Gheorghe Asachi Technical University Doctoral School.

REFERENCES

- Azmi, A.A., Jai, J., Zamanhuri, N.A., & Yahya, A. (2018). Precious Metals Recovery from Electroplating Wastewater: A Review, *IOP Conf. Series: Materials Science and Engineering*, 358. 012024.
- Ding, Y., Zhang, S., Liu, B., Zheng, H., Chang, C.C., & Ekberg, C. (2019). Recovery of precious metals from electronic waste and spent catalysts: A review, *Resources, Conservation and Recycling*, 141. 284-298.
- Fan, C., Li, K., He, Y., Wang, Y., Qian, X., & Jia, J. (2018). Evaluation of magnetic chitosan beads for

- adsorption of heavy metal ions. *Science Total Environment*, 627. 1396–1403.
- Fariborz, F., Golmohammadzadeh, R., Rashchi, F., & Alimardani, N. (2018). Fungal bioleaching of WPCBs using *Aspergillus niger*: Observation, optimization and kinetics. *Journal of Environmental Management*, 217. 775–787.
- Fariborz, F., Rabeeh, G., & Pickles, C. (2022). Potential and current practices of recycling waste printed circuit boards: A review of the recent progress in pyrometallurgy. *Journal of Environmental Management*, 316. 115242.
- Fernandes, S.M., Barrocas, B.T., Nardeli, J.V., Montemor, M.F., Macoas, E., Oliveira, M.C., Carvalho, C.C.C.R., Lauria, A., Niederberger, M., & Marques, A.C. (2024). Maximizing photocatalytic efficiency with minimal amount of gold: Solar-driven TiO₂ photocatalysis supported by MICROSCAFS® for facile catalyst recovery. *Journal of Environmental Chemical Engineering*, 12(2). 112043.
- Gamez, S., Garces, K., De la Torre, E., & Guevara, A. (2019). Precious metals recovery from waste printed circuit boards using thiosulfate leaching and ion exchange resin. *Hydrometallurgy*, 186. 1–11.
- Hubert, M., Meyn, T., Hansen, M.C., Hale, S.E., & Arp, H.P. (2024). Per- and polyfluoroalkyl substance (PFAS) removal from soil washing water by coagulation and flocculation. *Water Research*, 249. 120888.
- Kaya, M. (2016). Recovery of metals and nonmetals from electronic waste by physical and chemical recycling processes. *Waste Management*, 57. 64–90.
- Martinas-Ionita, S.L., Apostolescu, G.A., & Harja, M. (2023). Considerations for recovering valuable materials from electronic waste. *The Bulletin of the Polytechnic Institute from Iasi*, 69 (73). 71–80.
- Mesquita, R.A., Silva, R.A.F., & Majuste, D. (2018). Chemical mapping and analysis of electronic components from waste PCB with focus on metal recovery. *Process Safety and Environmental Protection*, 120. 107–117.
- Mokhodoeva, O., Shkinev, V., Maksimova, V., Dzhelnoda, R. & Spivakov, B. (2020). Recovery of platinum group metals using magnetic nanoparticles modified with ionic liquids. *Separation Purification and Technology*, 248. 17049–17049.
- Qiu, R., Lin, M., Qin, B., Xu, Z., & Ruan, J. (2020). Environmental-friendly recovery of non-metallic resources from waste printed circuit boards: a review. *Journal of Cleaner Production*, 279. 123738.
- Rizki, I.N., Amalina, I., Hasan, N.S., Khusnun, N.F., Abdul Jalil, A., & Firmansyah, M.L. (2023). Functionalized agriculture-derived biomass-based adsorbent for the continuous recovery of gold from a simulated mobile phone leachate. *Chemosphere*, 345. 140455.
- Russo, F., Luongo, V., Mattei, M. R., & Frunzo, L. (2022). Mathematical modeling of metal recovery from E-waste using a dark-fermentation-leaching process. *Scientific Reports*, 12(1). 4274.
- Shuaifei, Z., Akbar, S., Zhuan, W., Pringle, J.M., Yang, Z., & Spas, D.K. (2024). Ionic liquid-based polymer inclusion membranes for metal ions extraction and recovery: Fundamentals, considerations, and prospects. *Chemical Engineering Journal*, 481. 148792.
- Touze, S., Guignot, S., Hubau, A., Devau, N., & Chapron, S. (2020). Sampling waste printed circuit boards: Achieving the right combination between particle size and sample mass to measure metal content. *Waste Management*, 118. 380–390.
- Xiaohui, Z., Shenglong, Y., Chengqing, D., Wentao L., Dinghan, X., Libo, L., Feiyan, L., & Kai, P. (2024). Selective recovery of metals in spent batteries by electrochemical precipitation to cathode material for sodium-ion batteries. *Heliyon*, 10. e27127.
- Yken, J.V., Boxall, N.J., Cheng, K.Y., Nikoloski, A.N., Moheimani, N., & Kaksonen, A.H. (2023). Techno-economic analysis of an integrated bio- and hydrometallurgical process for base and precious metal recovery from waste printed circuit boards. *Hydrometallurgy*, 222. 106193.
- Zazycki, M.A., Tanabe, E.H., Bertuol, D.A., & Dotto, G.L. (2017). Adsorption of valuable metals from leachates of mobile phone wastes using biopolymers and activated carbon. *Journal of Environmental Management*, 188. 18–25.
- Zhao, S., Liao, Z., Fane, A., Li, J., Tang, C., Zheng, C., Lin, J., & Kong, I. (2021). Engineering antifouling reverse osmosis membranes: A review. *Desalination*, 499. 114857.

CARBON FOOTPRINT - IMPORTANT DRIVER OF CLIMATE CHANGE GENERATED BY THE FOOD INDUSTRY

Adelina MOJA, Vasile PADUREANU, Mirabela LUPU, Alina MAIER, Cristina CANJA

Transylvania University, 148 Castelului Street, Brasov, Romania

Corresponding author email: canja.c@unitbv.ro

Abstract

In the context in which one of the biggest problems affecting the environment worldwide is that of global warming, the study of carbon footprint, greenhouse gases and their effects is of utmost topicality. Current statistics show that agriculture and the food industry are some of the sectors with a significant carbon footprint, resulting in the need for conclusive studies to provide solutions to reduce it. The main purpose of this study is to concentrate on the results of research undertaken in this area. Thus, the thorough analysis of studies published in the main databases shows that the food industry contributes significantly to the accumulation of greenhouse gases in the atmosphere, the main sources of emissions being agricultural practices, crop rotation, waste management, etc. The urgency of adopting sustainable practices and mitigation strategies in the food industry to minimize the carbon footprint is underlined. Research not only highlights the urgent need to address the environmental impacts of the food industry, but also provides an essential basis for developing policies and strategies for implementing sustainable agricultural practices.

Key words: agriculture, carbon footprint, food industry, greenhouse gases.

INTRODUCTION

The intensification of climate change is evidenced by a constellation of environmental perturbations, including extreme weather events, deterioration in air quality, diminished agricultural yields, accelerated sea level rise, and the proliferation of infectious diseases. These converging environmental challenges pose a significant threat to the achievement of long-term socio-economic sustainability, particularly in regions with limited adaptive capacity. The preponderance of carbon emissions, primarily driven by anthropogenic activities, is widely recognized as the principal driver of climate change (IPCC, 2013). Extensive international cooperation has led to the prioritisation of reducing carbon emissions at national level. Measuring carbon emissions is essential to ensure sustainable development. The carbon footprint stands out as an effective tool in this regard, providing a scientific way to assess human impact on the environment. Carbon footprint analysis facilitates the identification of significant emission areas, providing a basis for specific measures and regular monitoring. Fighting climate change and promoting sustainable development requires a comprehensive global approach with a focus on

reducing carbon emissions. The carbon footprint plays an important role in this process, providing a solid foundation for strategic decision making (Shi & Yin, 2021).

Connecting different levels of carbon consumption through carbon footprinting provides a unified baseline for diverse research perspectives (He et al., 2019; Shi & Yin, 2021). This is essential to facilitate collaboration and develop a coherent global approach to tackling climate change.

The quantification of carbon footprints offers a compelling rationale for its adoption as a tool to harmonize stakeholder efforts and objectives across diverse sectors. By providing a common unit of measurement, the carbon footprint allows emissions from different sectors and regions to be better compared.

Building upon the concept of ecological footprint, introduced by Rees (1992) and further explored by Wackernagel et al. (1999), the carbon footprint serves as a crucial metric for quantifying greenhouse gas emissions associated with specific activities and products. Challenges associated with a lack of standardized definitions for carbon footprint have been documented by Matthews et al. (2008). Inconsistencies can hinder collaboration and result in difficulties comparing research

findings. To address this issue, the following definition was adopted: carbon footprint is a metric that quantifies the total direct and indirect greenhouse gas (GHG) emissions associated with a product or activity throughout its life cycle.

This definition emphasizes consumer responsibility and considers emissions generated at all stages of a product's life, from production to consumption to disposal. Addressing the carbon footprint is essential to assess the full impact of human activities on the environment and identify opportunities to reduce greenhouse gas emissions (Shi & Yin, 2021).

Food industry: A major contributor to greenhouse gas emissions?

GHG greenhouse gas verification plays a crucial role in assessing an organization's greenhouse gas emissions, providing a detailed picture of its environmental impact. This process includes accurate emission assessment, transparent reporting, and identification of critical emission points through standardised procedures. Companies' awareness of geographically significant emission zones facilitates the implementation of efficient and cost-effective strategies for mitigating their emissions (Clark & Tilman, 2017).

The agricultural and post-production stages of the food system are recognized as prominent contributors to anthropogenic greenhouse gas (GHG) emissions (Tubiello et al., 2022). Emissions occur at various stages, from agricultural and livestock production to food processing, transport, and consumption. (Tubiello et al., 2021) report a noteworthy decline in agricultural land-use emissions between 1990 and 2018. Conversely, energy consumption-related emissions, particularly within the food production sector, are anticipated to rise soon.

To tackle the climate impact of the food system, a holistic approach is needed comprising:

- Implementing sustainable agricultural practices, such as reducing the use of chemical fertilisers and pesticides, can significantly contribute to reducing emissions.
- Reducing energy consumption and food waste in the food industry can significantly reduce GHG emissions.

- Adopting a more sustainable diet with a reduction in meat and dairy consumption can have a significant impact on emissions from the food system.

Thus, a significant increase in emissions from the food industry, especially from energy consumption, is predictable.

Greenhouse gas verification is a process that allows the identification of major sources of emissions and facilitates the implementation of reduction strategies. The international landscape for greenhouse gas (GHG) emissions accounting features a diverse array of established standards. Each standard possesses a distinct focus and scope, catering to specific needs within the emissions management process.

The Greenhouse Gas Protocol (GHG Protocol), being the first protocol developed to do so, provides a comprehensive framework for emissions accounting. The protocol classifies emissions into three categories: Scope 1 (direct emissions), Scope 2 (indirect emissions from purchased energy) and Scope 3 (indirect emissions from the value chain). This classification allows a detailed understanding of emissions throughout the life cycle of food.

ISO 14064 standard (ISO 14064-1, n.d.) is based on the GHG Protocol and provides specific guidelines for quantifying and reporting GHG emissions at the organizational level. ISO 14067 (ISO 14067, n.d.) complements ISO 14064, focusing on quantifying and reporting the carbon footprint of products.

Within the vast array of international standards for GHG accounting, PAS 2050 stands out as a specialized tool for life cycle assessment (LCA) of product emissions. This standard is complemented by STEP 2060 (successor to PAS 2060 according to Liu et al., 2023), which offers a framework specifically designed to achieve carbon neutrality within the context of products or operational activities (PAS 2060 - Carbon Neutrality, n.d.).

The selection of an appropriate standard hinges on an organization's specific objectives, resource constraints, and degree of commitment to sustainability and emissions reduction.

Responsible choices: The environmental impact of food packaging

Packaging serves as a critical element within the food supply chain, safeguarding the integrity of foodstuffs during long-distance transportation.

This multifaceted function encompasses protection against spoilage and contamination, thereby extending shelf life and facilitating efficient handling and distribution.

Packaging materials and weight can significantly influence greenhouse gas emissions. Heavier packaging can lead to higher GHG emissions due to transportation (Xu et al., 2015).

The selection of packaging material is a crucial decision with major environmental consequences. The choice of alternative materials may have less impact. According to a study conducted by (Humbert et al., 2009; Poovarodom et al., 2012) plastic can be a more sustainable option for certain food products, reducing GHG emissions by about 30%, retort cups over metal cans can be a greener alternative to tuna packaging, reducing GHG emissions by 10-22%, and recyclable stainless steel can be a highly sustainable option for beer packaging, reducing GHG emissions by 93-96%, better than glass or plastic.

In addition to the packaging material, its weight also influences the GHG emissions generated. The use of lightweight packaging, such as ultralight glass bottles, can significantly reduce emissions related to production and transport (Martins et al., 2018). Research by Point et al. (2012) demonstrates the potential for significant emissions reduction. For instance, a 30% weight reduction in a wine bottle can lead to a 4-23% decrease in GHG emissions. Material selection also plays a crucial role. While plastic packaging typically generates emissions exceeding 3 kg CO₂-eq/kg (Schenker et al., 2021), cellulose-fibre alternatives boast a lower footprint of less than 1.5 kg CO₂-eq/kg. However, cellulose-based packaging may require combining materials to achieve similar protection levels, potentially negating some weight-related benefits (Schenker et al., 2021). Design optimization, reduced material thickness, and the incorporation of recycled materials present further opportunities to minimize the environmental impact of fibre packaging. In conclusion, strategic selection of packaging materials and weight reduction strategies offer significant avenues for the food industry to lessen its environmental footprint.

MATERIALS AND METHODS

This study investigates the evolution of scientific publications on carbon footprint using the Scopus database. The analysis encompasses articles published between 2012 and 2023, identified through a search string targeting titles, abstracts, and key words containing "carbon footprint" [TITLE-ABS-KEY ("carbon footprint")]. The search retrieved articles published from 2002 to 2024, with a focus on the period 2012-2023 (PUBYEAR > 2012 AND PUBYEAR < 2024). Limiting the document type to research articles [LIMIT-TO(DOCTYPE,"ar")] yielded a total of 18,836 publications. To exclude the possibility of review articles in the analysis, specific query criteria (AND NOT "review") were added, resulting in a result of 3813 articles outside the field of interest of the study.

A systematic review was conducted to analyze the retrieved publications. This review involved a multifaceted segmentation of the data by year, source, author, affiliation, country/territory, domain, and document type. Bibliometric indicators, including total publications, citations, CiteScore, and h-index, were employed to assess and compare the articles.

RESULTS AND DISCUSSIONS

CF Research Impact: An Evaluation Based on Publications and Citations

For a determined period of 10 years, more precisely between 2013 and 2023, a total of 15,023 research articles in the field of carbon footprint were published (Figure 1). There has been exponential growth since 2013, which shows the growing interest of researchers in this field. Carbon footprint research enjoys a significant expansion, with numerous research groups around the world actively involved in various fields. Analysis of the fields reveals the major concern for environmental issues as the focus of carbon footprint studies. This aspect is highlighted by the significant share of publications classified in areas such as: environmental sciences (29.4%), engineering (12%), energy (10.4%) and social sciences (5.2%). Moreover, the multidisciplinary nature of the carbon footprint field is evidenced by the existence of more than 200 classified

publications in fields such as arts and humanities, neurosciences, or dentistry. This demonstrates the significant impact of carbon footprint and greenhouse gas issues across multiple areas of activity.

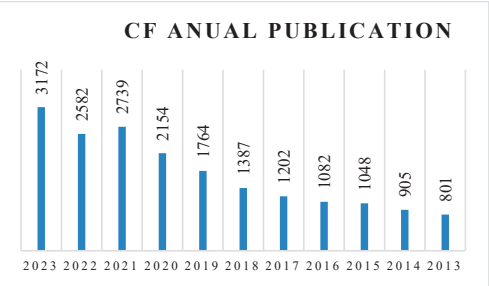


Figure 1. Evolution of the number of publications based on the key word in 2013-2023

The linguistic analysis highlighted the diversity of publications, identifying 22 languages used. English stands out as the dominant language, with a total of 14,619 articles. Chinese (192 articles), German (56 articles), Spanish (54 articles), Russian (41 articles) and French (40 articles) follow. Other languages, such as Portuguese, Polish, Italian, Turkish, Korean, and Japanese, were used in a smaller number of publications.

The journal productivity analysis identified 10 top journals owned by 7 distinct publishers (Table 1). Elsevier stands out as the main editor, with 2 magazines in the top 10, totalling 4 publications. The remaining articles were published by publishers such as Academic Press, American Chemical Society, MDPI, Public Library of Science and Springer Nature.

Table 1. Top 10 most productive carbon footprint journals with their most cited article

Journal	Total publications	Total citations	CiteScore 2022	The most cited article	Times cited	Publisher
Science of the Total Environment	8.468	479.285	16,8	Detection of microplastics in human lung tissue using μ FTIR spectroscopy	326	Elsevier B.V.
Journal of Cleaner Production	4.444	351.758	18.5	The Dynamic Impact of Digital Economy on Carbon Emission Reduction: Evidence City-level Empirical Data in China	184	Elsevier Ltd
Journal of Environmental Management	2.782	102.717	13.4	Combined role of green productivity growth, economic globalization, and eco-innovation in achieving ecological sustainability for OECD economies	142	Academic Press
Environmental Science and Technology	2.100	102.167	16.7	Outside the Safe Operating Space of the Planetary Boundary for Novel Entities	400	American Chemical Society
Sustainability (Switzerland)	13.600	281.274	5.8	A Global Assessment: Can Renewable Energy Replace Fossil Fuels by 2050?	211	MDPI
Resources, Conservation and Recycling	544	42.404	20.3	Challenges toward carbon neutrality in China: Strategies and countermeasures	606	Elsevier
International Journal of Environmental Research and Public Health	7.185	241.049	5.4	Digital Economy Development, Industrial Structure Upgrading and Green Total Factor Productivity: Empirical Evidence from China's Cities	154	MDPI
Plos One	15.413	377.961	6	The mental health of university students during the COVID-19 pandemic: An online survey in the UK	137	Public Library of Science
Waste management	529	33.490	15.1	Opportunities and challenges for the application of post-consumer plastic waste pyrolysis oils as steam cracker feedstocks: To decontaminate or not to decontaminate?	86	Elsevier Ltd

The detailed analysis identified Science of the Total Environment as the most prolific journal, with an impressive 8468 articles. The next positions in the ranking are occupied by Journal of Production Cleaner (4444 articles), Journal of Environmental Management (2782 articles) and

Environmental Science and Technology (2100 articles).

The 2022 CiteScore report highlights a CiteScore greater than 5 for all journals analyzed. The Journal of Cleaner Production has the highest score of 18.5, while the International

Journal of Environmental Research and Public Health has the lowest score of 5.4.

The influence of CiteScore in the decision of authors to select appropriate journals for publication of significant papers is acknowledged. CiteScore, the Elsevier-Scopus alternative to Clarivate Analytics impact factor, provides a measure of journal impact based on citation data from Scopus.

While CiteScore offers valuable insights, it should not be the sole factor guiding author selection. A comprehensive evaluation should also encompass the journal's ability to disseminate research to the targeted readership and its potential to advance the field.

Bibliometric analysis of countries using VOSviewer

Figure 2 illustrates the distribution of countries/territories by region. The visualization within

VOSviewer employs line thickness to depict the collaborative relationships between countries.

Thicker lines indicate stronger collaborative ties between nations positioned closer together within the map. The map contains 68 nodes representing countries. The size of the nodes reflects the number of co-authors in each country. Links between nodes indicate collaboration between countries in scientific publications. The US is the central node, with the largest number of co-authors and links to other countries.

China, Germany, the UK, and France are also important nodes, with large numbers of co-authors and links. There is significant collaboration between countries in Europe, North America, and Asia. There is less significant collaboration between countries in Africa and Oceania.

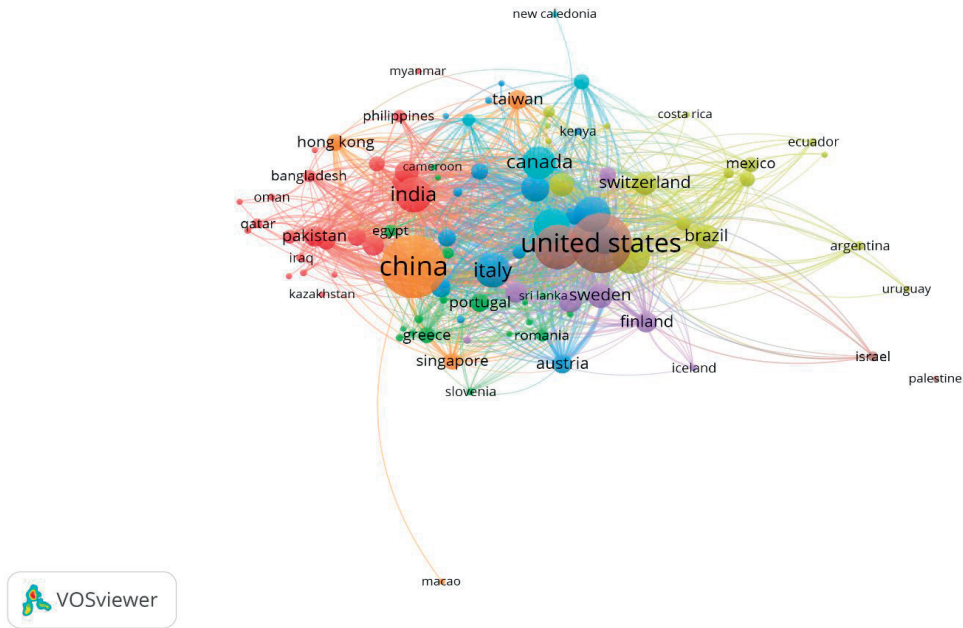


Figure 2. A screenshot of the bibliometric map created based on co-authors with the network visualization

The U.S. is a world leader in scientific collaboration, with an extensive network of co-authors around the world. China, Germany, Britain, and France are also important players in scientific collaboration. There is a significant regional divide in scientific collaboration, with

closer collaboration between countries in similar geographical regions.

In terms of limitations, the map is based on a specific dataset of scientific publications and may not reflect collaboration across all research areas. The size of the nodes reflects only the

number of co-authors and does not consider the quality of the collaboration.

The generated map can be used to identify trends in scientific collaboration over time. For example, an increase in collaboration between Asian countries can be observed in recent years. It can also be used to identify opportunities for collaboration between countries. For example, a country with a small number of co-authors could collaborate with a country with many co-authors to increase its visibility in scientific research. Another use of the map is to identify factors influencing scientific collaboration, such as geographical distance, language, and culture. The VOSviewer map of co-authors by territory provides an overview of scientific collaboration globally.

CONCLUSIONS

The urgent need to reduce greenhouse gas emissions in the food industry is obvious.

Implementing effective strategies along the food value chain is essential to combat climate change. Using sustainable packaging materials and reducing the amount of packaging used can significantly contribute to reducing the carbon footprint generated by the food industry.

Collaborating with research organizations to develop new low-emission technologies is another important direction.

Policymakers have a crucial role to play in promoting the necessary changes. The adoption of policies aimed at reducing emissions from the food industry is essential. Stimulating the development and deployment of low-emission technologies must be a priority. Educating the public about the importance of reducing the carbon footprint of food is another important aspect.

Consumers can play a significant role in reducing the carbon footprint of the food industry. Choosing products with a lower carbon footprint, such as vegetables, reducing food waste and separate collection are actions with major impact.

Interest in the field of carbon footprint has increased considerably in the last 10 years, evidenced by the significant number of publications in the field. The U.S. holds a leading position in global scientific collaboration, with important collaboration also

between countries in Europe, North America, and Asia.

The VOSviewer map provides an overview of scientific collaboration globally. This map can be used to identify trends, opportunities and factors influencing carbon footprint collaboration.

REFERENCES

- Clark, M., & Tilman, D. (2017). Comparative analysis of environmental impacts of agricultural production systems, agricultural input efficiency, and food choice. *Environmental Research Letters*, 12(6), 064016. <https://doi.org/10.1088/1748-9326/aa6cd5>
- He, B., Liu, Y., Zeng, L., Wang, S., Zhang, D., & Yu, Q. (2019). Product carbon footprint across sustainable supply chain. *Journal of Cleaner Production*, 241, 118320. <https://doi.org/10.1016/j.jclepro.2019.118320>
- Humbert, S., Rossi, V., Margni, M., Joliet, O., & Loerincik, Y. (2009). Life cycle assessment of two baby food packaging alternatives: Glass jars vs. plastic pots. *The International Journal of Life Cycle Assessment*, 14(2), 95–106. <https://doi.org/10.1007/s11367-008-0052-6>
- IPCC. (2013). Climate Change 2013: The Physical Science Basis. Contribution of Working Group I to the Fifth Assessment Report of the Intergovernmental Panel on Climate Change (1535).
- ISO 14064-1:2018. (n.d.). ISO. Retrieved February 22, 2024, from <https://www.iso.org/standard/66453.html>
- ISO 14067:2018. (n.d.). ISO. Retrieved February 22, 2024, from <https://www.iso.org/standard/71206.html>
- Liu, T.-C., Wu, Y.-C., & Chau, C.-F. (2023). An Overview of Carbon Emission Mitigation in the Food Industry: Efforts, Challenges, and Opportunities. *Processes*, 11(7), Article 7. <https://doi.org/10.3390/pr11071993>
- Martins, A. A., Araújo, A. R., Graça, A., Caetano, N. S., & Mata, T. M. (2018). Towards sustainable wine: Comparison of two Portuguese wines. *Journal of Cleaner Production*, 183, 662–676. <https://doi.org/10.1016/j.jclepro.2018.02.057>
- Matthews, H.S., Hendrickson, C.T., & Weber, C.L. (2008). The Importance of Carbon Footprint Estimation Boundaries. *Environmental Science & Technology*, 42(16), 5839–5842. <https://doi.org/10.1021/es703112w>
- PAS 2060—Carbon Neutrality. (n.d.). Retrieved February 22, 2024, from <https://www.bsigroup.com/en GB/capabilities/environment/pas-2060-carbon-neutrality/>
- Point, E., Tyedmers, P., & Naugler, C. (2012). Life cycle environmental impacts of wine production and consumption in Nova Scotia, Canada. *Journal of Cleaner Production*, 27, 11–20. <https://doi.org/10.1016/j.jclepro.2011.12.035>
- Poovarodom, N., Ponnak, C., & Manatphrom, N. (2012). Comparative Carbon Footprint of Packaging Systems for Tuna Products. *Packaging Technology and*

- Science*, 25(5), 249–257. <https://doi.org/10.1002/pts.975>
- Rees, W.E. (1992). Ecological footprints and appropriated carrying capacity: What urban economics leaves out. *Environment and Urbanization*, 4(2), 121–130. <https://doi.org/10.1177/095624789200400212>
- Schenker, U., Chardot, J., Missoum, K., Vishtal, A., & Bras, J. (2021). Short communication on the role of cellulosic fiber-based packaging in reduction of climate change impacts. *Carbohydrate Polymers*, 254, 117248.
- Shi, S., & Yin, J. (2021). Global research on carbon footprint: A scientometric review. *Environmental Impact Assessment Review*, 89, 106571. <https://doi.org/10.1016/j.eiar.2021.106571>
- Tubiello, F.N., Karl, K., Flammini, A., Gütschow, J., Obli-Laryea, G., Conchedda, G., Pan, X., Qi, S.Y., Heiðarsdóttir, H. H., Wanner, N., Quadrelli, R., Souza, L.R., Benoit, P., Hayek, M., Sandalow, D., Contreras, E.M., Rosenzweig, C., Moncayo, J.R., Conforti, P., & Torero, M. (2022). Pre- and Post-Production Processes Increasingly Dominate Greenhouse Gas Emissions From Agri-Food Systems. *Earth System Science Data*, 14(4). <https://doi.org/10.5281/zenodo.5615082>
- Tubiello, F.N., Rosenzweig, C., Conchedda, G., Karl, K., Gütschow, J., Xueyao, P., Obli-Laryea, G., Wanner, N., Qiu, S.Y., Barros, J.D., Flammini, A., Mencos-Contreras, E., Souza, L., Quadrelli, R., Heiðarsdóttir, H.H., Benoit, P., Hayek, M., & Sandalow, D. (2021). Greenhouse gas emissions from food systems: Building the evidence base. *Environmental Research Letters*, 16(6), 065007. <https://doi.org/10.1088/1748-9326/ac018e>
- Wackernagel, M., Lewan, L., & Hansson, C.B. (1999). Evaluating the use of natural capital with the ecological footprint. *Ambio*, 28(7), 604–612. Scopus.
- Xu, Z., Sun, D.-W., Zeng, X.-A., Liu, D., & Pu, H. (2015). Research Developments in Methods to Reduce the Carbon Footprint of the Food System: A Review. *Critical Reviews in Food Science and Nutrition*, 55(9), 1270–1286. <https://doi.org/10.1080/10408398.2013.821593>

ASSESSING THE EFFICIENCY OF TRANSPORT INFRASTRUCTURE INVESTMENTS IN ROMANIA: A MULTIDIMENSIONAL APPROACH

Petru NICOLAE

Romanian Academy, School of Advanced Studies of the Romanian Academy, Doctoral School of Economic Sciences, National Institute for Economic Research “Costin C. Kirițescu”,
13 Calea 13 Septembrie, Bucharest, Romania

Corresponding author email: nicolae.petru@gmail.com

Abstract

Transport infrastructure plays a crucial role in the economic development and environmental sustainability of any region. This study focuses on evaluating the efficiency of transport infrastructure investments in Romania, examining their social, economic, and environmental impacts. The research adopts a comprehensive approach, integrating data from national and European sources to assess the long-term effects of these investments. Key findings highlight the need for a balanced investment strategy that considers energy consumption, pollutant emissions, land use and socio-economic inclusion. The study also proposes a methodology for determining the congruence factor, which balances environmental, social, and economic criteria to optimize infrastructure performance. These insights aim to guide policymakers in making informed decisions to promote sustainable development in the transport sector.

Key words: transport infrastructure, investment efficiency, environmental impact, socio-economic development, sustainable development, Romania, congruence factor, policy guidance.

INTRODUCTION

Transport infrastructure, encompassing roads, railways, airports, and waterways, is the backbone of every economic activity, facilitating the movement of goods, services, and people. It plays a pivotal role in regional development, trade, and overall economic growth (Zaman & Geamănu, 2014). However, the development and maintenance of transport infrastructure entail substantial investments, often requiring significant public funds. Therefore, assessing the efficiency of these investments is crucial to ensure that they yield the desired economic, social, and environmental benefits.

In Romania, a country in the midst of economic transition and integration into the European Union policies, the efficient allocation of resources for transport infrastructure is of paramount importance. The country faced challenges related to aging infrastructure, regional disparities in development, and the need to align its transport system with European standards. In this context, a multidimensional approach to assessing the efficiency of transport infrastructure investments is warranted.

This study aimed to evaluate the efficiency of transport infrastructure investments in Romania

by considering their economic, social, and environmental components. It analysed data from national and European sources to assess the impact of these investments on various aspects of Romanian society and the environment. The research also proposed a methodology for determining the congruence factor, a novel concept that aim to balance economic, social, and environmental criteria to optimize infrastructure performance.

The concept of sustainable development, encompassing economic, social, and environmental dimensions, has gained prominence in recent decades (Nidziy, 2017). In the context of transport infrastructure, sustainability implies a balanced approach that considers not only economic benefits but also the social and environmental impacts of projects.

Economic efficiency in transport infrastructure investments is typically assessed using cost-benefit analysis (CBA) and cost-effectiveness analysis (CEA) (Zaman & Geamănu, 2006). These methods quantify the economic costs and benefits of projects, helping decision-makers prioritize investments that yield the highest net benefits. However, they often neglect the broader social and environmental implications not taking in consideration corelated criteria

from local, regional and global needs (Jovovic et al., 2017).

Social impact assessment (SIA) is a methodology used to evaluate the social consequences of projects, including their effects on communities, employment, and quality of life. Environmental impact assessment (EIA) evaluates the potential environmental harm caused by projects, such as pollution, habitat destruction, and resource depletion as well as the adaptation of project characteristics to climate changes in a circular economy concept to eliminate component obsolescence (Latouche, 2017).

In recent years, there has been a growing recognition of the need to integrate economic, social, and environmental considerations into the assessment of transport infrastructure investments. This has led to the development of multi-criteria decision analysis (MCDA) frameworks that incorporate a wider range of criteria beyond economic efficiency (Nicolau et al., 2024).

By financing projects that apply a multiparameter analysis regarding the efficiency of all pillars of the sustainable development concept we can achieve a green future for our future generations (Neaga, 2015).

State of the Art in Transport Infrastructure

Transport infrastructure is a critical component of economic and social development. The efficiency and effectiveness of transport systems directly impact a country's economic growth, regional development, and environmental sustainability. In the European Union, substantial investments have been made to modernize and expand transport infrastructure, focusing on improving connectivity, reducing travel times, and minimizing environmental impacts.

The Europe Union has established two important objectives: to interconnect Europe and achieve neutrality in the context of climate change until the year 2050. However, developing a cohesive transport infrastructure network, particularly at the borders between countries, remains a significant challenge that needs to be addressed. A thorough analysis of cross-border rail infrastructures in Europe, utilizing Geographic Information Systems (GIS), reveals that population size does not significantly influence the presence of these

infrastructures, indicating that many densely populated regions remain unconnected by rail to neighbouring regions across national borders (Theisen & vom Berg, 2024). In the Figures 1 and 2 are presented the major railway and highway infrastructure projects from Europe.

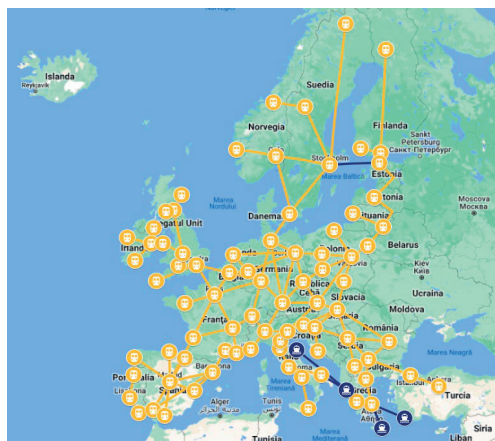


Figure 1. Major European railway lines in exploitation (EURAIL, 2024)



Figure 2. Major European highways in exploitation, extract from European Commission map

The evolving concept of smart highways aims to revolutionize traditional highway systems by integrating advanced sensing, communication, and control technologies to enhance safety, efficiency, and sustainability. Despite the promising potential, the development of smart highways faces significant challenges due to the lack of standardized evaluation criteria and the diversity of regional infrastructure conditions (Li et al., 2024).

Recent studies have quantified the CO₂ emissions from highway construction, revealing

that the total emissions for an entire construction project can reach $10,605.2 \text{ t} \cdot \text{km}^{-1} \cdot \text{lane}^{-1}$. Notably, the raw material production and on-site construction phases contribute 95.2% and 4.8% of these emissions, respectively. These insights underscore the necessity for strategies that incorporate recycled materials and advanced construction technologies to effectively reduce the carbon footprint of transport infrastructure projects (Gao et al., 2024).

In the process of transport infrastructure development, comprehensive planning and assessment methodologies are mandatory to ensure projects are not only economically viable but also environmentally sustainable and socially responsible.

The assessment of transport infrastructure projects involves a multifaceted approach that integrates various studies and methodologies. Recent advancements have highlighted the importance of several critical assessments, including Do No Significant Harm (DNSH) Assessments, Environmental Assessments (EA), Risk Management Plans (RMP), and

Environmental Impact Assessments (EIA), DNSH analysis.

Incorporating considerations of habitat connectivity and biodiversity along road and rail routes is imperative for enhancing ecological coherence.

Road kills pose a significant threat to biodiversity in areas where infrastructure projects are operational. Therefore, it is crucial for specialists to evaluate this criterion for each taxonomic biodiversity group (Nicolae & Stefan, 2022).

Transport corridors can significantly enhance habitat connectivity and support biodiversity, particularly for generalist and open-specialist species that thrive in early to mid-successional habitats. Physiological factors are crucial in determining species' dispersal abilities, emphasizing the need for vegetation management that considers representative communities rather than individual species.

Figure 3 illustrates important aspects in landscape ecology relevant to fragmented landscapes due to infrastructure development.

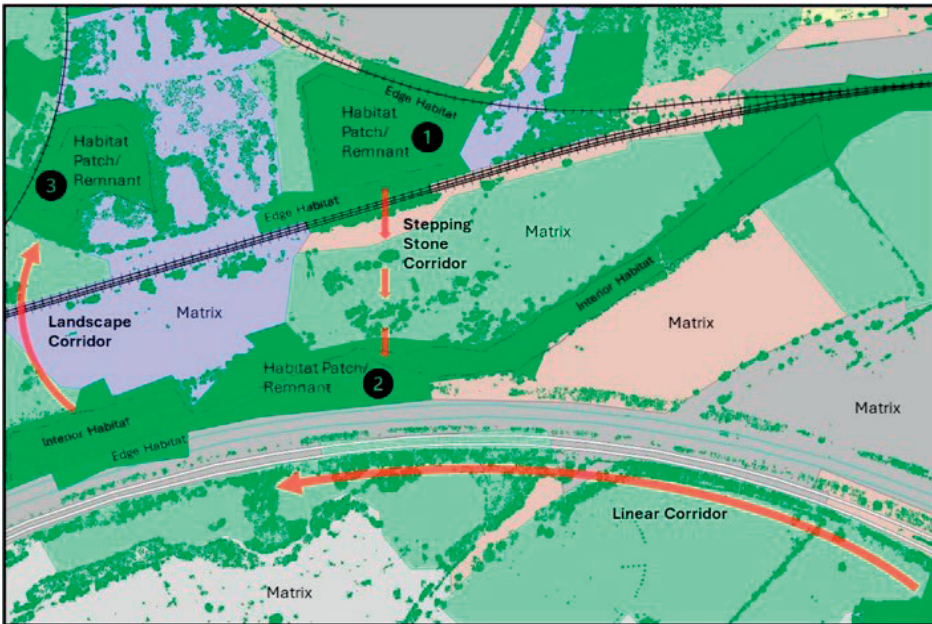


Figure 3. Illustration of Key Terms in Landscape Ecology (Cork et al., 2024)

These assessments evaluate the potential negative impacts, ensure that any adverse effects are minimized, adhering to stringent environmental protection standards, involving a

detailed study of the environmental baseline, the identification of potential impacts, and the proposal of mitigation measures to address these impacts.

Cost-Benefit Analysis (CBA) is a critical tool for analyzing the economic feasibility and benefits of infrastructure projects. This method evaluates the costs of implementation against the expected economic returns, ensuring that resources are allocated efficiently and effectively.

Additionally, Climate Change Adaptation Plans involve measures to adapt infrastructure projects to anticipated climate impacts, addressing vulnerabilities and incorporating resilience strategies to mitigate the effects of climate change on infrastructure.

Traffic Studies analyze the impact of project-related traffic on local transportation networks, helping in understanding and mitigating potential congestion and improving overall traffic flow.

The planning and execution of transport infrastructure projects face several interconnected challenges, including the need for recycling, green infrastructure, renewable energy, biodiversity conservation, population growth.

Addressing these challenges requires a composite and complex approach to evaluation, ensuring that the best options for project development are chosen. This equilibrium can be obtained through meticulous planning and the integration of diverse assessment methodologies, ensuring that infrastructure projects contribute positively to sustainable development goals.

In conclusion, the assessment of transport infrastructure projects involves a multifaceted approach that integrates various studies and methodologies. By addressing the environmental, economic, and social dimensions of sustainability, these assessments ensure that infrastructure development aligns with broader sustainable development objectives. The rigorous evaluation of these factors enables policymakers to make informed decisions, fostering the development of infrastructure that is efficient and sustainable.

MATERIALS AND METHODS

This study utilized a mixed-methods approach, combining quantitative and qualitative data analysis. Quantitative data were obtained from national and European statistical databases,

including Eurostat and the Romanian National Institute of Statistics (INSSE). These data covered various aspects of transport infrastructure, such as investment levels, network length, traffic volumes, energy consumption, and pollutant emissions.

Qualitative data were gathered through a review of the relevant literature on infrastructure projects in Romania. These sources provided insights into the decision-making processes, challenges, and opportunities related to infrastructure investments.

The analysis employed statistical methods to examine the relationships between transport infrastructure investments and economic, social, and environmental indicators. For example, regression analysis was used to assess the impact of investments on GDP growth, while correlation analysis was employed to examine the relationship between infrastructure development and employment rates.

The study also developed a methodology for calculating the congruence factor, which was based on a weighted average of economic, social, and environmental criteria. The weights assigned to each criterion were determined through a literature review and synthesis of expert opinions. The congruence factor formula is as follows:

$$\text{Congruence Factor} = (w_e * E) + (w_s * S) + (w_{env} * ENV)$$

where:

- w_e , w_s , and w_{env} are the weights assigned to economic, social, and environmental criteria, respectively.
- E , S , and ENV are the standardized scores for each criterion.
- w_1, w_2, \dots, w_n are weights assigned to additional attributes A_1, A_2, \dots, A_n to include in the analysis.

Example Attributes (A_1, A_2, \dots, A_n)

Additional attributes can be introduced that are relevant to the efficiency and impact of transport infrastructure investments. These attributes could include:

1. Traffic Flow Impact: Measure of how investments affect traffic congestion and flow efficiency;
2. Accessibility: Measure of improved access to essential services (education, healthcare) due to infrastructure projects;

3. Resilience: Measure of infrastructure's ability to withstand climate change impacts or natural disasters (Nicolae & Nicolae, 2023);
4. Adaptation: Evaluate how the future project can adapt to critical/global events (Fang, 2021);
5. Innovation: Measure of technological innovation or sustainability practices integrated into the infrastructure project.

By expanding the congruence factor formula to include additional attributes with impact weights, the analysis provides a more comprehensive assessment of the efficiency and impact of transport infrastructure investments. The proposed approach allows for an accurate evaluation that considers a broader range of criteria, enhancing decision-making processes for policymakers and stakeholders involved in infrastructure development.

The standardized scores are calculated by dividing the raw value of each criterion by its maximum value, ensuring that all criteria were on the same scale.

RESULTS AND DISCUSSIONS

The following tables present critical data on transport infrastructure and socio-economic impacts across various EU countries, providing a comprehensive overview of the comparative lengths of railway and highway networks and their associated socio-economic benefits. Table 1 highlights the extensive infrastructure in countries like Germany and France, which have substantial railway and highway lengths, facilitating efficient transport and robust economic activities.

Table 1. Comparative data of transport infrastructure in EU Countries

Country	Railway Length (km)	Highway Length (km)
Germany	33,590	13,181
France	29,640	11,882
Italy	16,788	6,957
Spain	15,718	17,228
Romania	10,627	982
Poland	18,515	4,765
Netherlands	7,029	2,758
Belgium	3,607	1,763

In contrast, Romania and Belgium show significantly lower figures, indicating potential areas for infrastructure development and

investment. These disparities underline the varying stages of infrastructure maturity across the EU, with countries like Spain prioritizing highway development, evidenced by its 17,228 km of highways, compared to its 15,718 km of railways.

Table 2 summarizes the socio-economic impacts of transport infrastructure, emphasizing its role in job creation, economic growth, and environmental sustainability. Effective transport networks not only boost GDP by enhancing trade and mobility but also create numerous employment opportunities, fostering socio-economic development. Additionally, well-planned infrastructure can significantly reduce pollution, contributing to environmental sustainability. The data suggest that countries with more developed transport networks, like Germany and France, likely experience higher economic and social benefits compared to those with less extensive infrastructure. This analysis underscores the need for balanced investment in both railways and highways to achieve comprehensive socio-economic development, especially in countries lagging in infrastructure development.

Table 2. Summary of socio-economic impacts

Impact	Description
Employment	Creates jobs
Economic Growth	Boosts GDP
Environmental Sustainability	Reduces pollution

Economic impact

Transport infrastructure investments in Romania yielded mixed results in terms of economic efficiency. While some projects stimulated economic growth and improved connectivity, others were plagued by cost overruns, delays, and underutilization. A key challenge was the need to prioritize projects that aligned with national and regional development goals, ensuring that investments generated the highest possible economic returns.

For instance, the construction of the A2 motorway, connecting Bucharest to Constanța, led to a significant reduction in travel time and transportation costs, boosting trade and tourism in the region. However, other projects, such as the A3 motorway, faced delays and cost overruns, raising questions about their economic viability.

Table 3. Trends regarding the goods transported on the rail and road infrastructure

Year	Rail Transport (thousand tons)	Road Transport (thousand tons)
1990	218828	1934362
1995	105131	616044
2000	71461	262943
2005	69175	306994
2010	52932	174551
2015	55307	198638
2020	49671	266523
2023	48867	321348

Table 3 presents the transport volumes for rail and road transport over selected years. The data illustrates the trends and changes in transport

modes, highlighting the significant differences in volumes transported by rail and road across the years.

The Figure 4 below visually depicts the transport volumes for rail and road transport over selected years. By comparing the two modes of transport side-by-side, the graph provides a clear visual representation of the trends and fluctuations in transport volumes, emphasizing the changes and differences between rail and road transport from 1990 to 2023.

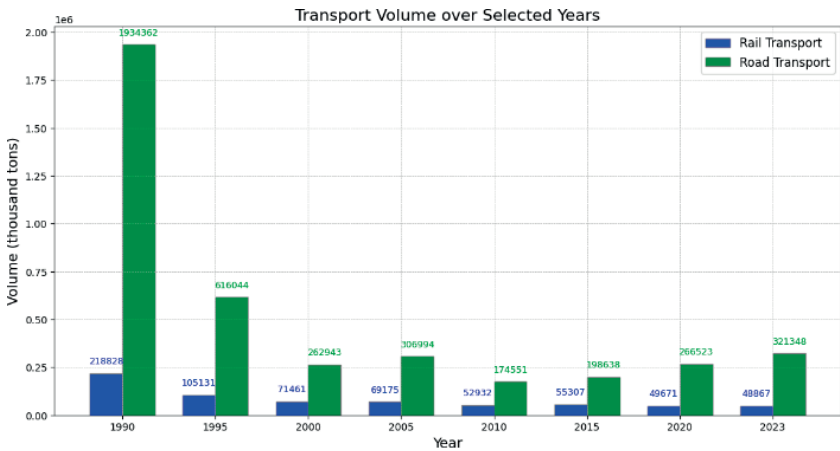


Figure 4. Quantity of goods transported, by types of transport. Time author adaptation from (INSSE, 2024)

The social impact of transport infrastructure investments in Romania was significant, particularly in terms of improved accessibility and mobility for citizens. The development of new roads and railways facilitated access to education, healthcare, and employment opportunities, especially in rural areas. However, there were also negative consequences, such as the displacement of communities and the disruption of social networks due to land acquisition for infrastructure projects.

For example, the construction of the Bucharest Ring Road led to the displacement of thousands of residents and businesses, causing social disruption and economic hardship for some communities (Dyllick & Hockerts, 2002).

The environmental impact of transport infrastructure investments in Romania raised concerns, primarily related to greenhouse gas

emissions, air pollution, and land use changes. The country's heavy reliance on road transport, coupled with the growth in vehicle ownership, contributed to increased emissions and air quality problems (Zubala, 2022).

The relationship between energy consumption and greenhouse gas emissions is a crucial aspect of understanding the environmental impact of transport infrastructure. The methodology for GES evaluation must be in line with the European directives applicable now of the evaluation (IPCC, 2006). The analysis reveals a consistent increase in both metrics over time. Specifically, energy consumption, measured in kilotons of oil equivalent petrol, shows fluctuations but generally trends upwards from 1990 to 2020. Similarly, greenhouse gas emissions from railway and road transport exhibit a continuous rise.

Table 4. Energy consumption and GHG emissions of railway and highway projects

Year	Energy Consumption (kTo eq petrol)	Greenhouse Gas Emissions from Railway and Road Transport (kt CO ₂ eq)	Railway Length (km)	Highway Length (km)
1990	345	11183	11348	72816
1995	396	8179	11376	72859
2000	339	9458	11015	78479
2005	413	12146	10948	79904
2010	407	13677	10785	82386
2015	379	15467	10770	85920
2020	416	18139	10769	86791

The Table 4 presents key data points related to energy consumption, greenhouse gas emissions,

and the lengths of railway and highway networks over selected years. This data is crucial for understanding the trends and relationships between these variables in the context of transport infrastructure.

The Figure 5 shows the relationship between energy consumption and greenhouse gas emissions from railway and road transport. The plot includes a linear regression line, which helps to visualize the correlation between these two variables, offering a clearer understanding of how energy consumption impacts greenhouse gas emissions.

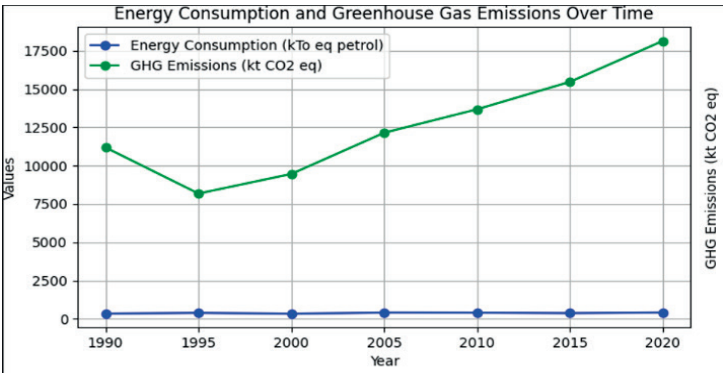


Figure 5. Energy Consumption and Greenhouse Gas Emissions Over Time.
Time author adaptation from (INSSE, 2024)

A detailed scatter plot with a linear regression line underscores this relationship, showing a strong positive correlation (R-value = 0.739). The regression analysis indicates that for every additional unit of energy consumed, greenhouse gas emissions increase by approximately 25.77

kilotons of CO₂ equivalent. This statistically significant relationship (P-value = 0.043) highlights the environmental cost associated with increased energy consumption, underscoring the need for sustainable energy practices.

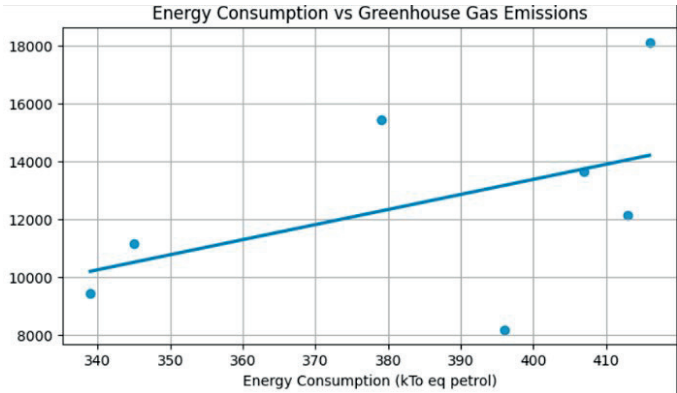


Figure 6. Energy Consumption vs. Greenhouse Gas Emissions. Time author adaptation from (INSSE, 2024)

The Figure 6 above shows the relationship between energy consumption and greenhouse gas emissions from railway and road transport. The plot includes a linear regression line, which helps to visualize the correlation between these two variables, offering a clearer understanding of how energy consumption impacts greenhouse gas emissions.

Our analysis also examines the changes in Romania's transportation infrastructure. The length of railway networks has seen a slight decline from 11,348 km in 1990 to 10,769 km in 2020, possibly reflecting a shift in transportation preferences or investment priorities over the

years. Conversely, highway networks have expanded significantly, from 72,816 km in 1990 to 86,791 km in 2020. This expansion correlates positively with energy consumption ($R\text{-value} = 0.57$), suggesting that increased energy usage is associated with greater investment in road infrastructure.

Figure 7 presents the lengths of railway and highway networks over the selected years. By comparing the two modes of transport infrastructure, this graph provides a visual representation of the changes and growth in both railway and highway lengths, reflecting infrastructure development trends over time.

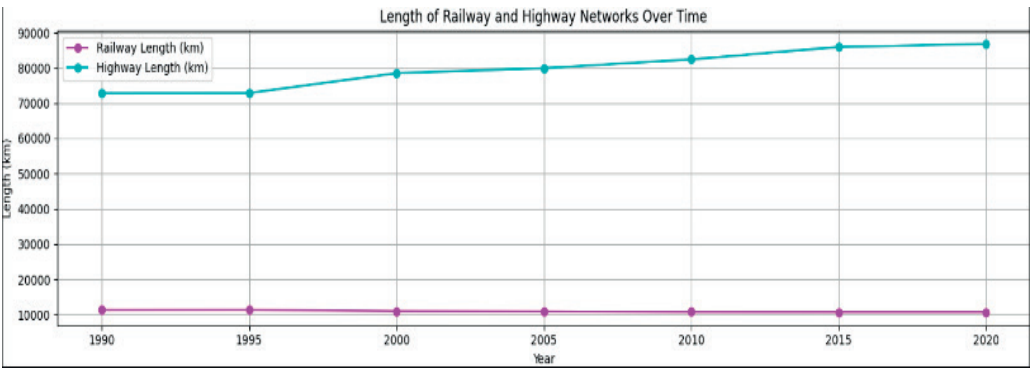


Figure 7. Length of Railway and Highway Networks Over. Time author adaptation from (INSSE, 2024)

The correlation heatmap from Figure 8 provides a visual summary of the relationships between various metrics, revealing key insights. The significant positive correlation between energy consumption and greenhouse gas emissions indicates that Romania's economic development and energy policies significantly impact environmental health. The reduction in railway length and the expansion of highway networks suggest a move towards road-based transportation, which typically has higher energy and environmental costs.

To address these issues, from the analysis we will consider the following projects to be efficient:

- Projects that promote renewable energy: investing in renewable energy sources such as wind, solar, and hydroelectric power can reduce dependence on fossil fuels, thereby decreasing greenhouse gas emissions.

- Projects that enhance public transportation: improving and expanding the railway network can offer a more sustainable alternative to road transport, reducing overall energy consumption and emissions.
- Projects that implement Energy Efficiency Measures: encouraging energy efficiency in industries, buildings, and transportation can lead to significant reductions in energy consumption and emissions.
- Projects that implement solutions for low energy consumption and greenhouse gas emissions reduction: a high positive correlation (0.74) indicates that as energy consumption increases, greenhouse gas emissions also rise.
- Projects that low energy consumption such as railway infrastructure: a moderate negative correlation (-0.51) suggests that increased energy consumption is associated with a reduction in railway length.

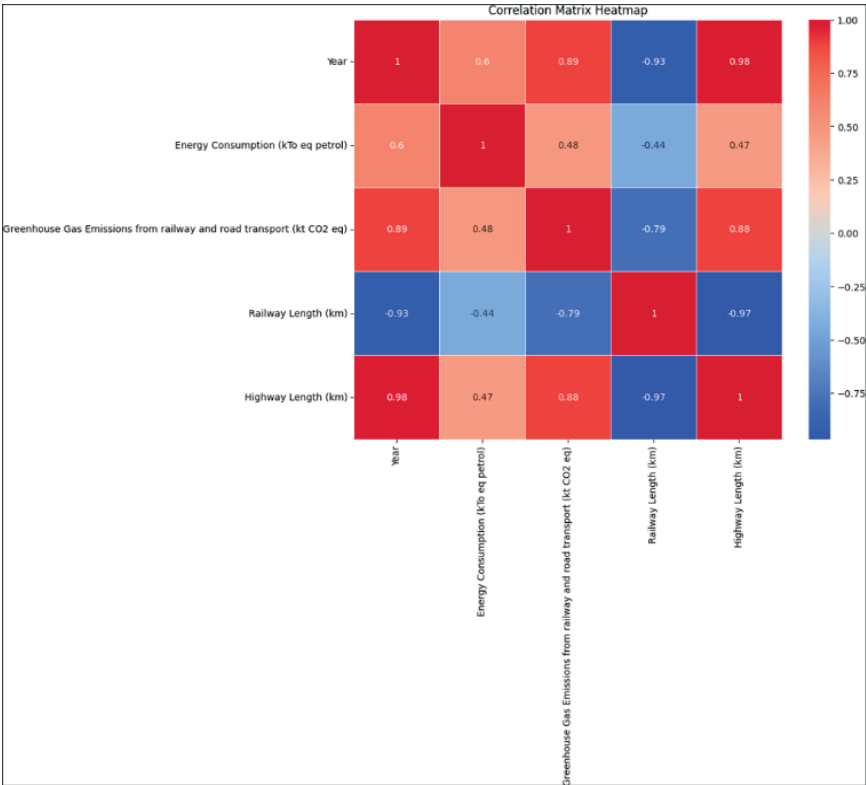


Figure 8. Correlation Matrix Heatmap. Author adaptation from (INSSE, 2024)

A transition towards more sustainable modes of transport, such as rail and clean energy public transport, is essential to mitigate the environmental footprint of the transport sector. As shown in Figure 9, railways currently lead as the least polluting mode of transport in terms of greenhouse gas emissions.

Another explanation for the high emissions generated by road infrastructure is that in Romania, the existing roads are mostly small roads, which does not fill the requirements for a good traffic flow. The polluting emissions will increase in the future, if we continue to use the existing roads, while their rehabilitation and increase its category of use to a sustainable highway provides a downward trend for these emissions (Nicolae et al., 2021).

Carbon management is mandatory for all infrastructure projects, even if we are taking in consideration public transportations, goods and services transportation, or even resource transportation projects, like water transportation infrastructure as it needs to engage all the value

chain to succeed in the neutrality objective (Sandu et al., 2023).

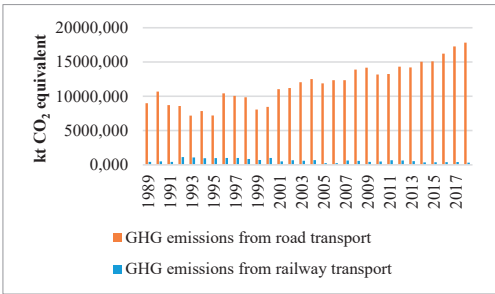


Figure 9. Comparison of emissions from rail transport and road transport over time. Author adaptation from (INSSE, 2024)

The Congruence Factor

To address the multidimensional nature of transport infrastructure efficiency, this study proposed a novel methodology for calculating the congruence factor. This factor represented a holistic assessment of a project's performance

by integrating economic, social, and environmental criteria. The calculation involved assigning weights to each criterion based on their relative importance and then aggregating them into a single score.

The congruence factor methodology was applied to several transport infrastructure projects in Romania, revealing varying degrees of congruence between economic, social, and environmental objectives. Some projects demonstrated high economic efficiency but fell short in terms of social and environmental performance, while others achieved a more balanced outcome.

For example, the A2 motorway project scored high on economic efficiency due to its positive impact on trade and tourism. However, it scored lower on social and environmental criteria due to community displacement and increased emissions. In contrast, the rehabilitation of the Bucharest-Constanta railway line achieved a higher congruence factor by balancing economic benefits with social and environmental considerations.

As it can be seen in the Figure 10 it is easy to understand the graphic representation of a congruence factor analysis performed on a project with a moderately balanced performance across the economic, social, and environmental dimensions, along with a reasonable impact on traffic flow.

1st case study: Moderate Balanced Project

In this case study, the weights and standardized scores are as follows:

Weights:

- Economic: 0.4
- Social: 0.3
- Environmental: 0.2
- Traffic Flow: 0.1

Standardized Scores:

- Economic: 0.75
- Social: 0.65
- Environmental: 0.80
- Traffic Flow: 0.70

The Congruence Factor is calculated as follows:

$$\text{Congruence Factor} = (0.4 \times 0.75) + (0.3 \times 0.65) + (0.2 \times 0.80) + (0.1 \times 0.70) = 0.725$$

In Figure 10 we can observe that the project inclined more towards the economic factor, not

being able to equilibrate the social and environmental factors, in the report with the traffic flow criteria.

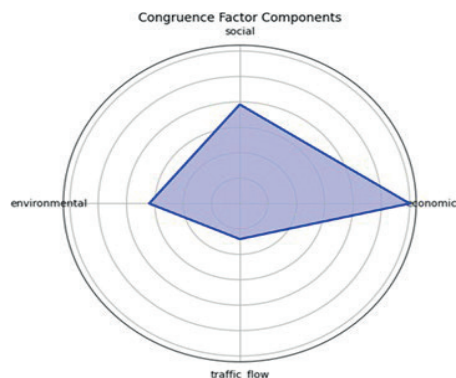


Figure 10. Congruence factor analysis graphic representation for a moderately balanced project

2nd Case study: Highly Balanced Project

In this case study, the weights and standardized scores are as follows:

Weights:

- Economic: 0.3
- Social: 0.3
- Environmental: 0.3
- Traffic Flow: 0.1

Standardized Scores:

- Economic: 0.95
- Social: 0.90
- Environmental: 0.92
- Traffic Flow: 0.88

The Congruence Factor is calculated as:

$$\text{Congruence Factor} = (0.3 \times 0.95) + (0.3 \times 0.90) + (0.3 \times 0.92) + (0.1 \times 0.88) = 0.919$$

This score reflects a project with exceptionally high performance across all dimensions, indicating a well-balanced and highly efficient project, as can be easily observed in Figure 11.

The analysis of Congruence Factors, yielding scores of 0.725 and 0.919 for moderately and highly balanced projects respectively, underscores the critical importance of integrating economic, social, and environmental criteria. This holistic approach ensures that transport infrastructure investments in Romania achieve sustainable development objectives, thereby optimizing their overall efficiency and impact.

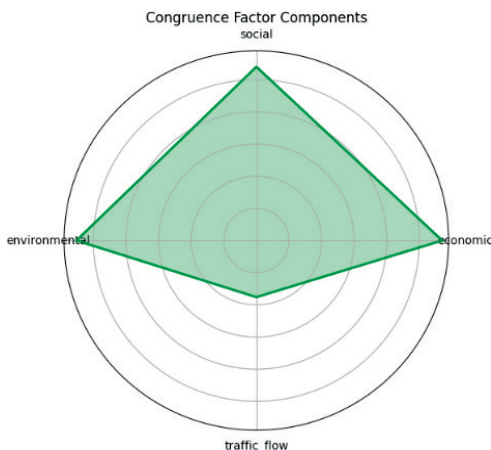


Figure 11. Congruence factor analysis graphic representation for a well-balanced project

CONCLUSIONS

Assessing the efficiency of transport infrastructure investments in Romania required a multidimensional approach that considered economic, social, and environmental impacts. While economic efficiency remains a critical factor, it should not be pursued at the expense of social and environmental well-being. The proposed congruence factor methodology offered a promising tool for evaluating the overall efficiency of infrastructure projects, promoting a more sustainable and balanced approach to development.

Limitations and future research

This study had some limitations. First, the availability of data on certain social and environmental impacts of transport infrastructure projects in Romania was limited. Second, the weights assigned to the criteria in the congruence factor calculation were based on expert judgment and may vary depending on the specific context and stakeholder preferences. Future research could explore the use of more robust methods for determining these weights, such as multi-criteria decision analysis techniques.

In conclusion, this study contributed to the growing body of knowledge on sustainable transport infrastructure assessment. The proposed congruence factor methodology offered a practical tool for policymakers and practitioners to evaluate the efficiency of

transport infrastructure investments in a more holistic and sustainable manner. By considering the economic, social, and environmental dimensions of infrastructure projects, Romania can move towards a more sustainable and equitable transport system that benefits both present and future generations. Future research should focus on expanding the dataset to include a wider range of social and environmental indicators, as well as refining the weighting methodology for the congruence factor. Additionally, the application of the congruence factor to other sectors, such as energy and water infrastructure, could provide valuable insights for sustainable development planning in Romania.

ACKNOWLEDGEMENTS

The work was carried out during the main author's doctoral research activities at the Romanian Academy, National Institute for Economic Research "Costin C. Kirițescu" (INCE).

REFERENCES

- Cork, N.A., Fisher, R.S., Strong, N., Ferranti, E.J.S. & Quinn, A.D. (2024). Corrigendum: A systematic review of factors influencing habitat connectivity and biodiversity along road and rail routes in temperate zones. *Front. Environ. Sci.*, 12, 1445609. doi: 10.3389/fenvs.2024.1445609.
- Dyllick, T. & Hockerts, K. (2002). Beyond the Business Case for Corporate Sustainability. *Business Strategy and The Environment*, 11(2), 130-141.
- EURAIL, <https://www.eurail.com>, site accessed on 11th of May 2024.
- Fang, C. (2021). *Economics of the pandemic. Weathering the Storm and Restoring Growth*. Routledge.
- Gao, S., Liu, X., Lu, C., Zhang, H., Wang, X., Kong, Y. (2024) Quantitative Analysis of Carbon Emissions from Highway Construction Based on Life Cycle Assessment. *Sustainability*, 16, 5897, <https://doi.org/10.3390/su16145897>.
- INSSE, <http://statistici.insse.ro/>, site accessed between January and July 2024.
- Intergovernmental Panel on Climate Change (IPCC). (2006). 2006 IPCC Guidelines for National Greenhouse Gas Inventories. IGES: Japan.
- Jovovic, R., Draskovic, M., Delibasic, M., & Jovovic, M. (2017). The concept of sustainable regional development – Institutional aspects, policies and prospects. *Foundation of International Studies*, 10, 255–266.
- Latouche, S. (2017). *Guaranteed damage planned obsolescence essay*. Seneca Lucius Annaeus Publishing House.

- Li, L., Long, Y., Peng, C. (2024). A Multi-Objective Evaluation Method for Smart Highway Operation and Management. *Appl. Sci.*, 14, 5694. <https://doi.org/10.3390/app14135694>.
- Neaga, F.D. (2015). Concepts of sustainable development. Theoretical - methodological approaches. Romanian Academy - Institute for World Economy.
- Nicolae, R.I., Nicolae, P., Braileanu, A.M. (2021). Reducing greenhouse gas emissions by implementing sustainable infrastructure projects, Conference: GEOLINKS Conference Proceedings.
- Nicolae, R.I., Stefan, C.P. (2022). Study on the correlation between infrastructure projects and wildlife roadkill in Romania, Conference: 22nd SGEM International Multidisciplinary Scientific GeoConference 2022.
- Nicolae, R.I., Nicolae, P. (2023). Climate change vulnerability, mitigation, and adaptation for a large infrastructure project in Romania, Conference: 23rd SGEM International Multidisciplinary Scientific GeoConference.
- Nicolau A.I., Ionitescu S., Moagar-Poladian S., Tilea D.M., Dinu A.M. (2024). Challenges in implementing circular economy strategies in Romania. *Scientific Papers. Series Management, Economic Engineering in Agriculture and rural development*, 24(1), 669-684.
- Nidziy, E. (2017). Financing the construction of transport infrastructure as the basis for sustainable development of the regional economy. In *Earth and Environmental Science*; IOP Publishing: Orlando, FL, USA, vol. 90.
- Sandu, M.A., Vladasel (Pasarescu), A.C., Pienaru, A.M. (2023). Embedding low carbon emission into the water infrastructure. *Scientific Papers. Series E. Land Reclamation, Earth Observation & Surveying, Environmental Engineering*, vol. XII, 52-59. Print ISSN 2285-6064.
- Theisen, P.P., vom Berg, B.W. (2024). *Geospatial Data Processing and Analysis of Cross-Border Rail Infrastructures in Europe*. In: Wohlgemuth, V., Kranzlmüller, D., Höb, M. (eds) *Advances and New Trends in Environmental Informatics 2023*. ENVIROINFO 2023. Progress in IS. Springer, Cham. https://doi.org/10.1007/978-3-031-46902-2_14.
- Zaman, Gh., & Geamănu, M. (2006). *Economic efficiency*. Romania of Tomorrow Foundation Publishing House.
- Zaman, Gh., & Geamănu, M. (2014). *Economic efficiency in terms of sustainable development*. Romania of Tomorrow Foundation Publishing House.
- Zubala, T. (2022). Effect of transport infrastructure development on selected components of the environment of inner-city river valley and the possibility of its revitalization (Lublin, Poland). *Environmental Science and Pollution Research*, 29, 48529–48544. <https://doi.org/10.1007/s11356-022-18964-y>.

DECARBONIZING IRRIGATION SYSTEMS: INNOVATIVE TECHNOLOGIES FOR ENERGY EFFICIENCY AND SUSTAINABLE WATER RESOURCE MANAGEMENT

Petru NICOLAE¹, Luminița CHIVU¹, Raluca Ioana NICOLAE²

¹Romanian Academy, School of Advanced Studies of the Romanian Academy, Doctoral School of Economic Sciences, National Institute for Economic Research “Costin C. Kirițescu”,
13 Calea 13 Septembrie, Bucharest, Romania

²GEOSTUD SRL, 11 Sangerului Street, Bucharest, Romania

Corresponding author email: nicolae.petru@gmail.com

Abstract

Decarbonizing irrigation systems plays a pivotal role in mitigating climate change and promoting sustainable agricultural practices. This paper explores advanced technological solutions to enhance the energy efficiency and sustainability of water resource management in irrigation systems. By leveraging innovations such as floating photovoltaic panels, smart irrigation controls, and the integration of renewable energy sources, this research aims to reduce dependency on fossil fuels and optimize water usage. The analysis encompasses the socio-economic and environmental impacts of these technologies, highlighting significant benefits including reduced greenhouse gas emissions, improved water conservation, and local economic development.

Key words: decarbonization, renewable energy, sustainability, water management, environmental impact.

INTRODUCTION

Irrigation systems are essential for maintaining agricultural productivity, especially in regions with limited rainfall or facing the increasing threat of drought due to climate change (Aspe et al., 2016). However, conventional irrigation practices often rely heavily on fossil fuels for pumping and distribution, contributing to greenhouse gas emissions and exacerbating climate change (Borza & Coste, 2003). Additionally, inefficient water management in these systems can lead to overwatering, water scarcity, and environmental degradation (Baradei & Sadeq, 2020).

The need for decarbonizing irrigation systems has never been more critical. The Food and Agriculture Organization (FAO) projects that by 2050, the world population will reach 9.1 billion, requiring a 70% increase in global food production. Achieving this without further stressing our finite land and water resources demands innovative and sustainable approaches (FAO, 2022).

Ecological farming practices, innovative agricultural techniques that adjust to shifting weather patterns, minimized application of

pesticides, new soil management approaches focused on maintaining soil health and carbon retention through crop cultivation and harnessing atmospheric nitrogen will all contribute to a sustainable agricultural sector that supports the Green Economy principles and delivers healthy food to the population. This aligns with the EU Green Deal's objective for a carbon-neutral Europe by 2050 (Ionitescu, 2023).

In this context, advanced technological solutions such as floating photovoltaic (FPV) panels, smart irrigation controls, and the integration of renewable energy sources emerge as viable strategies to enhance the energy efficiency and sustainability of water resource management in irrigation systems.

To address these challenges, there is a growing need for innovative technologies that can decarbonize irrigation systems and promote sustainable water resource management. This paper explores several promising solutions, including floating photovoltaic (FPV) panels, smart irrigation controls, and the integration of renewable energy sources. These technologies offer the potential to reduce energy consumption, optimize water usage, and

mitigate the environmental impact of irrigation systems (McKuin et al., 2020).

State of the Art in Floating Photovoltaic (FPV)

Floating photovoltaic (FPV) systems represent a future solution in renewable energy, leveraging water bodies to enhance solar energy while conserving the land surface. Notably, FPV systems on irrigation channels offer several advantages, including land conservation, increasing energy efficiency also due to the cooling effect of water, and conserve water resource by reducing evaporation. These systems are particularly beneficial in regions with agriculture where the need for clean energy and food industries are competing for land use. Research employing MATLAB tools has demonstrated that FPV systems on irrigation reservoirs can significantly enhance power generation efficiency. The study highlighted the impact of temperature variations and solar irradiance on the performance of PV panels, emphasizing the improved efficiency of FPV systems over traditional land-based systems (Anbarasu et al., 2024).

Various countries are pioneering the development of floating photovoltaic (FPV) projects and advanced analytical tools to enhance the generation of green and clean energy.

The Fraunhofer Institute for Solar Energy Systems (ISE) has been a leader in FPV research, particularly on artificial water surfaces like pit lakes. Their research demonstrates that FPV systems can outperform land-based systems due to the cooling effects of water, significantly reducing the levelized cost of energy (LCOE) despite higher initial investments (FRAUNHOFER ISE, 2024).

In USA, significant advancements include the development of a global inventory map for FPV systems using satellite imagery. This tool aids environmental assessments and policy management by providing detailed data on FPV installations worldwide. Additionally, technological innovations focus on improving the stability and efficiency of FPV systems in diverse environmental settings, such as pontoon-type structures designed for harsh offshore conditions (Bellini, 2023).

Japan has made significant strides with its Tokyo Bay Offshore Floating Solar Project. This initiative integrates solar energy with electric mobility infrastructure, providing renewable energy for electric vehicles and boats, demonstrating Japan's commitment to local renewable energy generation and sustainability (Oceannews, 2024; Garanovic, 2022).

India has explored the feasibility and benefits of FPV systems in regions like Gujarat and Tamil Nadu. These projects demonstrate significant energy generation and environmental benefits, particularly in areas with limited land availability (Nagababu, 2024).

Brazil's notable FPV projects include the Araucária floating photovoltaic plant and Iberdrola's installation on Fernando de Noronha Island, a site that is declared by UNESCO as a World Natural Heritage Site, part of Brazilian National Marine Park and Environmental Protected Area. These projects aim to develop business models that contribute to decarbonization and sustainable development on an isolated ecosystem (Neves, 2023; Iberdrola, 2024).

In the Netherlands, large-scale FPV parks like the 41.1 MWp Sellingen and 29.8 MWp Uivermeertjes parks have been implemented. These projects generate significant renewable energy while integrating into the local landscape with minimal ecological impact. Researchers from the Netherlands analyzed the effects of floating PV in different climate zones, finding that FPV systems can increase annual energy yield by up to 6% due to the cooling effect of water (Weetch, 2021; Dörenkämper et al., 2021).

Spain's FPV advancements include the Sierra Brava Floating PV Plant, in the reservoir in Cáceres, which covers 12,000 m² and features 3,000 floating solar panels with a total capacity of 1.375 MWp. The project explores various solar module technologies and configurations, supported by new government regulations to boost FPV deployment and includes advanced technologies like hydro-elastic membranes and environmental measures to protect local wildlife (Acciona, 2024).

Romania has initiated significant FPV projects, such as the country's first large-scale floating

PV system by TMK Hydroenergy Power. This 1 MW system, located on a pond in Caras Severin county, is integrated with a hydropower plant, generating power for internal consumption. Additionally, Renera Energy is developing the largest floating photovoltaic park in Romania, with a 50 MW capacity on 37 hectares in Brăila County (Economedia, 2024; Renera, 2024).

The diverse geographical locations, climate challenges, geomorphological and hydrogeological conditions, and opportunities for circular economy practices highlight the necessity for tailored FPV projects. Each project must be thoroughly designed to address the specific context of its implementation area. This requires a comprehensive assessment tool that can accurately evaluate project efficiency by taking into account all relevant factors. Essential documentation, including Do No Significant Harm assessments (DNSH), Cost-Benefit Analyses (CBA), Environmental Impact Assessments (EIA), climate change and immunization studies, social analyses, economic feasibility studies, and technical evaluations, must be integrated into a multi-composite analysis. This holistic approach ensures that all potential limitations and opportunities specific to the implementation area are thoroughly considered. By adopting this method, it becomes possible to declare a project both efficient and financeable, ensuring that all necessary documentation and studies are part of a cohesive and robust evaluation process. This comprehensive strategy is critical for maximizing the project's success and sustainability, particularly in unique and variable environmental contexts.

Giurgiu-Râzmirești case study

The Giurgiu-Râzmirești irrigation system in Romania serves as a compelling case study for the implementation of innovative technologies to decarbonize irrigation and enhance water resource management. This approach represents the key for Romania to achieve the carbon net zero emission in the water-related infrastructure projects (Sandu et al., 2023). This system, covering 19 administrative territorial units (ATUs) across Giurgiu and Teleorman counties, faces challenges related to old infrastructure, inefficient water use, and high energy consumption.

The proposed project aims to address these challenges by installing floating photovoltaic panels on the existing irrigation canals. This dual-use approach not only generates clean electricity to power the irrigation system, but also reduces water evaporation, contributing to water conservation. The project also includes the rehabilitation of existing canals and the implementation of a modern water management system to optimize water distribution and minimize losses (Kleps & Tusa, 1992).

The Giurgiu-Râzmirești project is expected to generate approximately 151.8 GWh of renewable energy annually, significantly reducing the system's reliance on fossil fuels and lowering greenhouse gas emissions. The project's innovative approach aligns with the European Union's RePowerEU plan, which aims to decarbonize industries and increase the use of renewable energy sources (Directive EU, 2018/2001). An environmental impact assessment (EIA) was conducted to evaluate the potential environmental effects of the Giurgiu-Râzmirești project. The assessment considered various factors, including land use change, greenhouse gas emissions, water quality, and biodiversity (Nicolae et al., 2021). Biodiversity field monitoring and studies are essential activities to ensure the durability and sustainability of infrastructure projects. Given that most infrastructure projects occupy large land areas, alter landscapes, or utilize land within or adjacent to environmentally protected areas, which can serve as habitats for protected species, it is crucial for future projects to consider their interactions with biodiversity parameters. This is particularly important for maintaining ecological balance and complying with environmental regulations. Figure 1 illustrates these relationships and the importance of integrating biodiversity considerations into project planning.

The biodiversity criteria to analyse in these projects is mandatory, as infrastructure projects are proven to be a source of multiple environmental impacts, such as roadkill, habitat loss, and habitat fragmentation (Nicolae & Stefan, 2022).

The installation of FPV panels on existing canals eliminates the need for additional land acquisition, thereby minimizing the project's impact on land use. However, the

Environmental Impact Assessment (EIA) estimated that the project would result in the emission of 18,239 tons of CO₂ due to the disturbance of biomass and soil during construction. To offset these emissions, the

project proposes afforestation of 9,600 hectares of degraded land or the establishment of windbreaks on 480,000 hectares of agricultural land.

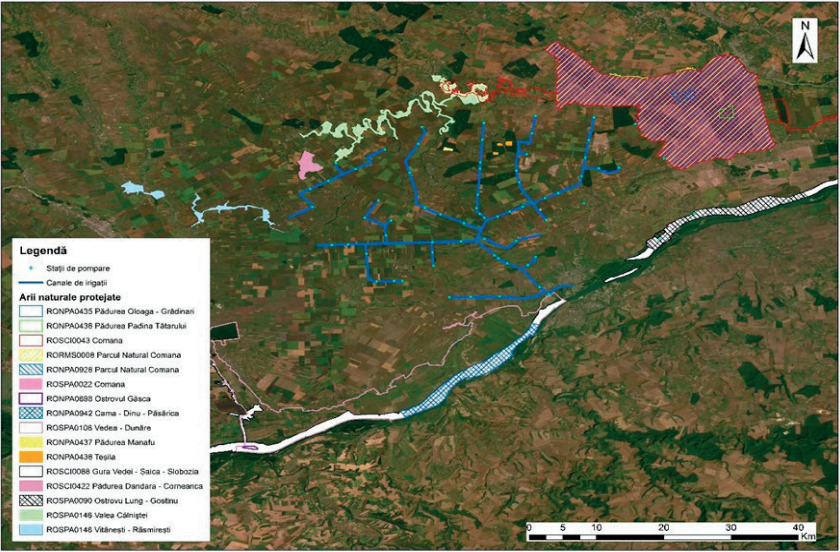


Figure 1. Map of the irrigation project in relation to nearby protected natural areas (GEOSTUD, 2022)

CO₂ Emissions from Biomass Conversion

A comprehensive analysis based on IPCC 2006 guidelines illustrates the significant CO₂ emissions associated with converting different types of land to infrastructure as seen in Tables 1, 2 and 3.

Table 1. Conversion from Pasture to Infrastructure (GEOSTUD, 2022)

Equation 2.15 & 2.16 IPCC 2006	Explanations/IPCC Default Values	Pasture land	Total
$\Delta A_{to \text{ others}}$ (ha)	Area in conversion	19.5	19.5
BAFTER (tDM/ha)	Biomass associated with future use, i.e., biomass stock in the first year after conversion, immediately after conversion	0	-
BBEFORE (tDM/ha)	Biomass associated with previous use, i.e., before conversion	6.1	-
CF	Carbon fraction in dry biomass/IPCC value	0.47	-
ACG (tC/yr)	Increase in stock in the year in question	0	-
ACL (tC/yr)	Carbon loss in the year in question	0	-
Total C stock change, tC		-55.9065	-
Total emissions ("+" /removals ("-"), tCO ₂		204.9905	204.9905

The conversion of 19.5 hectares of pastureland to infrastructure results in approximately 205 tonnes of CO₂ emissions due to the loss of biomass that previously acted as a carbon sink.

Table 2. Conversion from Orchard to Infrastructure (GEOSTUD, 2022)

Equation 2.15 & 2.16 IPCC 2006	Explanations/IPCC Default Values	Orchard	Total
$\Delta A_{to \text{ others}}$ (ha)	Area in conversion	6.5	6.5
BAFTER (tDM/ha)	Biomass associated with future use, i.e., biomass stock in the first year after conversion, immediately after conversion	0	-
BBEFORE (tDM/ha)	Biomass associated with previous use, i.e., before conversion	Calculated	-
CF	Carbon fraction in dry biomass/IPCC value	Generic	-
ACG (tC/yr)	Increase in stock in the year in question	0	-
ACL (tC/yr)	Carbon loss in the year in question	0	-
Total C stock change, tC		-30.55	-
Total emissions ("+" /removals ("-"), tCO ₂		112.0167	112.0167

The conversion of 6.5 hectares of orchard to infrastructure results in approximately 112

tonnes of CO₂ emissions due to the removal of biomass stocks that sequester carbon.

Table 3. Conversion from Arable Land to Infrastructure (GEOSTUD, 2022)

Equation 2.15 & 2.16 IPCC 2006	Explanations/IPCC Default Values	Arable Land	Total
ΔAto_others (ha)	Area in conversion	104	104
BAFTER (tDM/ha)	Biomass associated with future use, i.e., biomass stock in the first year after conversion, immediately after conversion	0	0
BBEFORE (tDM/ha)	Biomass associated with previous use, i.e., before conversion	10	10
CF	Carbon fraction in dry biomass/IPCC value	0.47	0.47
ΔCG (tC/yr)	Increase in stock in the year in question	0	0
ΔCL (tC/yr)	Carbon loss in the year in question	0	0
Total C stock change, tC		-488.8	-
Total emissions ("+")/removals ("-"), tCO ₂		1792.267	1792.267

The conversion of 104 hectares of arable land to infrastructure results in approximately 1792 tonnes of CO₂ emissions, reflecting a significant release due to the loss of carbon-sequestering biomass.

These substantial CO₂ emissions highlight the environmental impact of converting various types of land to infrastructure. Arable lands, in particular, sequester substantial amounts of carbon, and their conversion results in significant greenhouse gas emissions, exacerbating climate change. This underscores the critical need for sustainable land-use practices and policies that mitigate carbon emissions by preserving high-biomass areas and promoting green infrastructure.

By understanding and addressing both the emissions from biomass disturbance during construction and the long-term implications of land-use changes, the project can implement more effective strategies to minimize its environmental footprint (Figure 2).

This comprehensive approach ensures that while the immediate CO₂ emissions are accounted for and mitigated through measures such as afforestation and windbreaks, the broader implications of land-use changes are also considered in the planning and execution of sustainable projects.

The project is also expected to have a positive impact on water quality by reducing evaporation and preventing algal blooms. The rehabilitation of canals will further improve water management and minimize losses due to seepage and infiltration (Kumar et al., 2018).

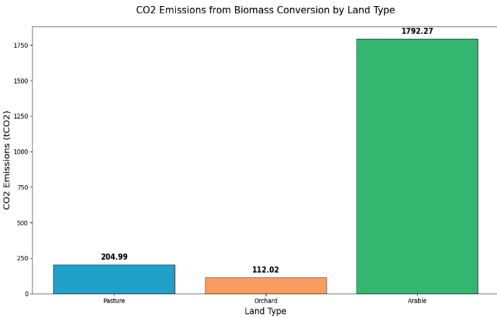


Figure 2. Project's CO₂ emissions from biomass conversion. Adaptation after (GEOSTUD, 2022)

In order to complete the efficiency analysis, a DNSH (*Do No Significant Harm*) study was elaborated according to the European requirements for national funded projects (EC, 2021).

A socio-economic impact assessment (SEIA) was conducted to evaluate the potential social and economic benefits of the project. The assessment considered factors such as job creation, local economic development, and agricultural productivity.

Climate change vulnerability

Data from national meteorological stations indicate that the average annual temperature in 2020 was approximately 13°C. Projecting current trends in temperature increase, we estimate that by 2050, the annual temperature could rise to approximately 22°C. This significant increase underscores the urgent need for optimized water management and conservation of water resources. Moreover, the project must be designed to withstand the impacts of rising temperatures, necessitating the incorporation of more durable and sustainable components. Additionally, it is imperative to address the challenge of diminishing the use water resources, ensuring that the project can adapt to these future climatic conditions (Figures 3 and 4).

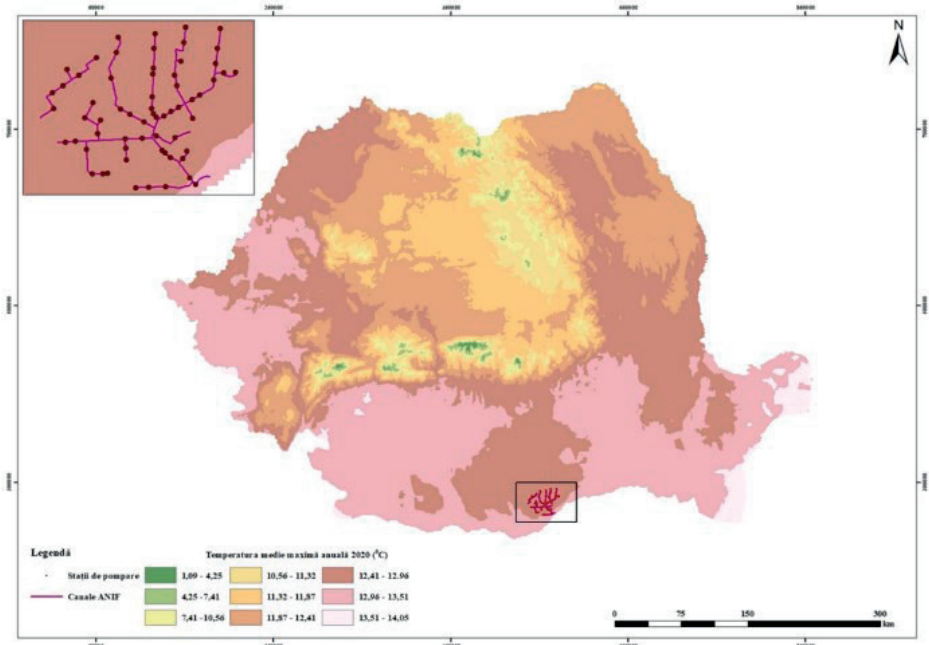


Figure 3. Annual average temperature for the year 2020 - actual situation (GEOSTUD, 2022)

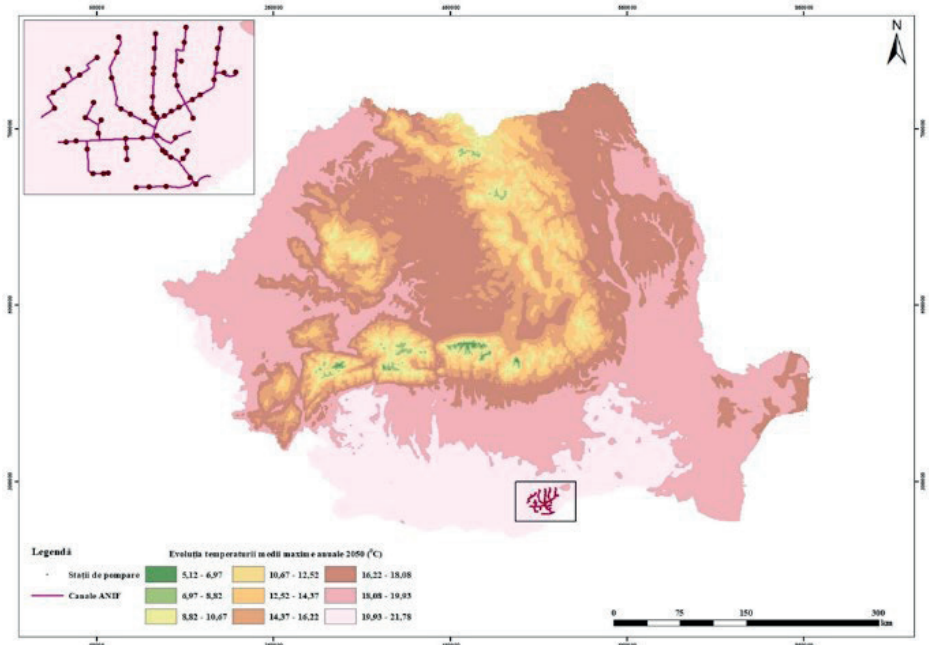


Figure 4. Annual average temperature for the year 2050 - estimated situation (GEOSTUD, 2022)

The project is expected to create new jobs during the construction and operation phases, contributing to local economic development. The improved irrigation efficiency and

increased agricultural productivity resulting from the project are also expected to have positive socio-economic impacts on the local communities (Table 4).

Table 4. Estimated socio-economic benefits of the Giurgiu-Răzmirești project

Impact category	Estimated benefit
Job creation (construction phase)	500 direct jobs, 1,000 indirect jobs
Job creation (operation phase)	50 direct jobs, 100 indirect jobs
Increased agricultural productivity	10-15% increase in crop yields
Reduced water costs for farmers	15-20% reduction in irrigation costs
Increased income for farmers	10-15% increase in farm income

A financial analysis was conducted to assess the economic viability of the Giurgiu-Răzmirești project. The analysis considered the investment costs, operating costs, and revenue generation from electricity sales and water fees. The project's initial investment cost is estimated to be €50 million, with an additional €2 million per year for operation and maintenance. The revenue from electricity sales is projected to be €8 million per year, while the revenue from water fees is estimated to be €4 million per year. Based on these figures, the project is expected to have a payback period of fewer than 10 years and a positive net present value, indicating its economic viability. Table 5 presents the estimated financial performance of the Giurgiu-Răzmirești project over a 20-year period, showcasing its strong economic viability and profitability.

The project generates significant value from energy production, starting at €12,144,000 in the first year and gradually decreasing to €10,260,466 in the twentieth year. Despite this decline, the project consistently produces a high total value. The energy consumed by the project remains constant at €4,100,800 annually, indicating stable operational costs. The surplus energy distributed to the grid, which begins at €8,043,200 and decreases to €6,159,666 by the twentieth year, contributes additional revenue and supports the overall energy supply (Figure 5).

Economic efficiency means obtaining some useful economic effects, under the conditions of spending some resources in a rational and economical way (Zaman & Geamanu, 2006).

Table 5. Estimated profitability of the Giurgiu-Răzmirești project over a 20-year period

Year	Total value generated from energy production (EUR)	Value of energy consumed by the project (EUR)	Value of additional energy distributed to the grid (EUR)	Profitability
1	12144000	4100800	8043200	3942400
2	12044419	4100800	7943619	3842819
3	11946053	4100800	7845253	3744453
4	11846472	4100800	7745672	3644872
5	11746891	4100800	7646091	3545291
6	11648525	4100800	7547725	3446925
7	11548944	4100800	7448144	3347344
8	11449363	4100800	7348563	3247763
9	11350997	4100800	7250197	3149397
10	11251416	4100800	7150616	3049816
11	11153050	4100800	7052250	2951450
12	11053469	4100800	6952669	2851869
13	10953888	4100800	6853088	2752288
14	10855522	4100800	6754722	2653922
15	10755941	4100800	6655141	2554341
16	10656360	4100800	6555560	2454760
17	10557994	4100800	6457194	2356394
18	10458413	4100800	6357613	2256813
19	10358832	4100800	6258032	2157232
20	10260466	4100800	6159666	2058866
TOTAL	224041013	82016000	142025013	60009013

Profitability is a key highlight, starting at €3,942,400 in the first year and remaining positive throughout the 20-year period. This consistent profitability demonstrates that the project effectively covers its operational costs while generating substantial profit. The financial stability of the irrigation system, combined with its environmental and social benefits, underscores its potential as a model for sustainable irrigation and energy management, offering a blueprint for similar initiatives aimed at integrating renewable energy and enhancing resource efficiency.

A complete financial analysis can be performed only by taking in consideration the cost of execution and, the cost of operation and maintenance.

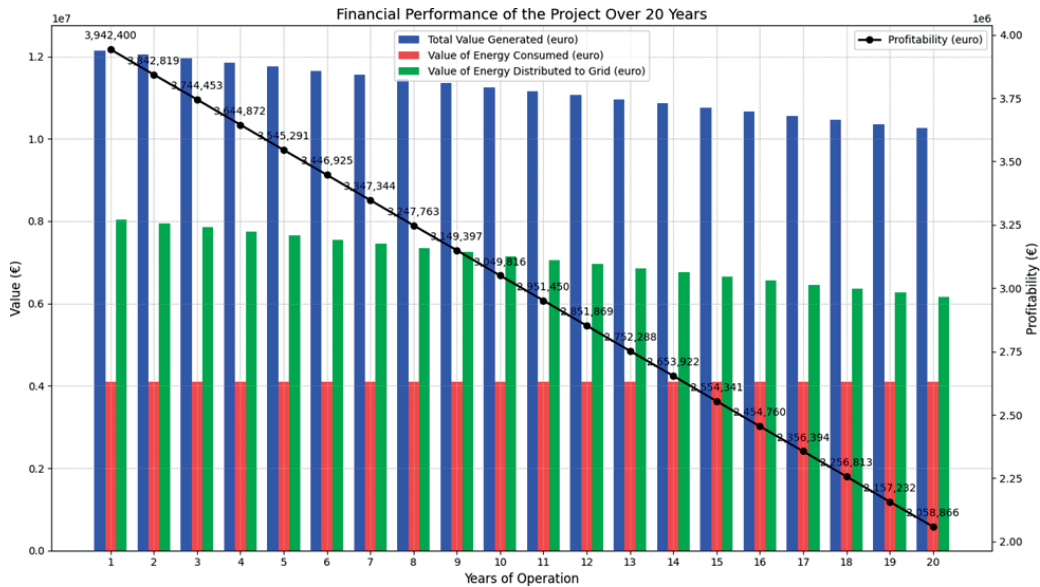


Figure 5. Graphic representation of the project's profitability. Adaptation after (GEOSTUD, 2022)

The analysed hydro-improvement project aims to enhance irrigation efficiency and integrate renewable energy solutions. Below is the summarized data comparing the current scenario without the project and the projected scenario with the project implementation in correlation with the operation cost (Table 6).

Table 6. Operation cost variation of the Giurgiu-Răzmirești project before and after implementation

Specification	Unit	Without the project	With the project
Water volume required at capture point for irrigation	thousand m ³	307,027.69	250,294.32
Electric energy consumed for water pumping	GWh	95.60	58.20
Electric energy consumed for water pumping	kWh	95,600,000.00	58,200,000.00
Renewable electric energy produced by floating photovoltaic panels	GWh	-	138.00
Total operating costs	thousand lei	100,615.22	59,415.64

The volume of water required at the capture point for irrigating the entire area significantly reduces from 307,027.69 thousand m³ to

250,294.32 thousand m³ with the implementation of the project. This indicates a substantial improvement in water use efficiency.

The electric energy consumed for water pumping shows a remarkable reduction from 95.60 GWh (95,600,000 kWh) to 58.20 GWh (58,200,000 kWh). This reduction in energy consumption can be attributed to the enhanced efficiency of the irrigation system and possibly the use of more efficient pumps or techniques.

Additionally, the project introduces the generation of 138.00 GWh of renewable electric energy through floating photovoltaic panels, which not only offsets the energy required for pumping but also contributes to the grid.

The total operating costs are projected to decrease from 100,615.22 thousand lei to 59,415.64 thousand lei. This reduction in operating costs is likely due to the decrease in energy consumption and the integration of renewable energy sources, leading to lower energy costs and improved operational efficiency, as seen in Figure 6.

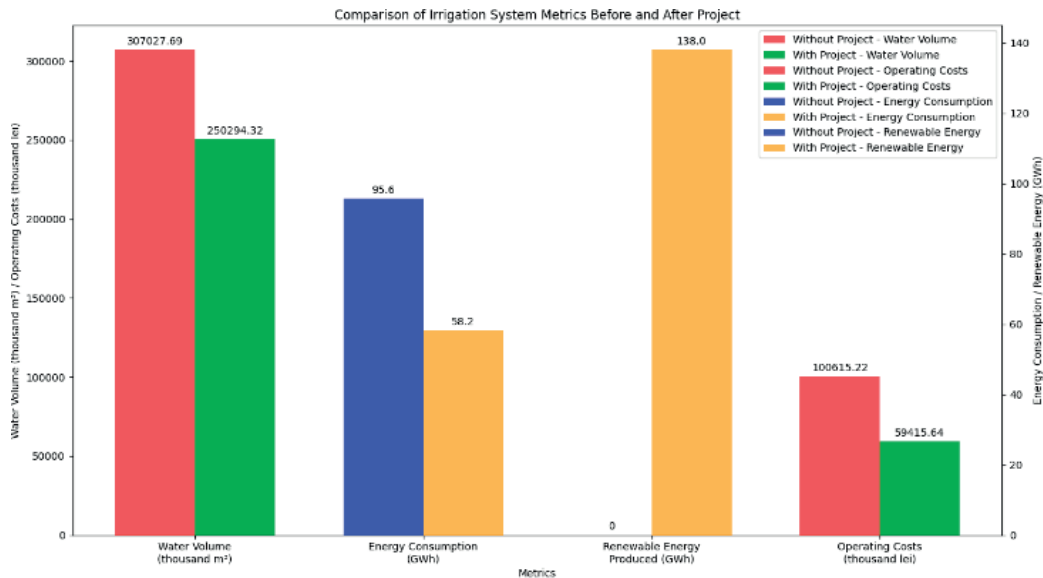


Figure 6. Operation cost with and without the project and the energy produced vs cost.
Adaptation after (GEOSTUD, 2022)

MATERIALS AND METHODS

This study employed a mixed-methods approach, combining literature review, data analysis, and field assessments to evaluate the effectiveness of innovative technologies in decarbonizing the Giurgiu-Răzmirești irrigation system and enhancing its water resource management.

A comprehensive literature review was conducted to examine existing research on FPV panels, smart irrigation controls, and renewable energy integration in the context of irrigation systems (Gallagher et al., 2017). This review provided a theoretical foundation for understanding the potential benefits and challenges associated with these technologies. It also helped identify relevant case studies and data sources for further analysis.

Data collection and analysis

Data on the Giurgiu-Răzmirești irrigation system were collected from the Romanian National Administration for Land Reclamation and Improvement (ANIF) and other relevant national and European sources. This data included information on the system's current energy consumption, water usage, infrastructure conditions, and agricultural productivity.

The collected data were analyzed using various statistical methods to assess the potential impact of the proposed technological interventions. Energy consumption and water usage were modelled under different scenarios, with and without the implementation of FPV panels, smart irrigation controls, and renewable energy integration. The results of these analyses were used to quantify the potential reductions in energy consumption, water usage, and greenhouse gas emissions.

Field assessments were also conducted to evaluate the current state of the Giurgiu-Răzmirești irrigation system and to identify potential sites for the installation of FPV panels. These assessments involved site visits, interviews with local stakeholders, and the collection of environmental data. The findings from the field assessments were used to inform the design and implementation of the proposed technological interventions.

Congruence factor methodology

To assess the overall sustainability of the project, a congruence factor methodology was developed. This methodology integrates economic, social, and environmental criteria into a single metric, providing a holistic assessment of the project's performance. The weights assigned to each criterion were

determined through expert consultation and stakeholder engagement, ensuring that the assessment reflects the values and priorities of the local community.

The congruence factor formula is as follows:

$$\text{Congruence Factor} = (w_e * E) + (w_s * S) + (w_{env} * ENV),$$

where:

- w_e , w_s , and w_{env} are the weights assigned to economic, social, and environmental criteria, respectively.
- E , S , and ENV are the standardized scores for each criterion.

The standardized scores were calculated by dividing the raw value of each criterion by its maximum value, ensuring that all criteria were on the same scale.

The weights and standardized scores are as follows:

Weights:

- Economic: 0.3
- Social: 0.3
- Environmental: 0.2
- Water Conservation: 0.2

Standardized Scores:

- Economic: 0.95
- Social: 0.90
- Environmental: 0.92
- Water Conservation: 0.90

The Congruence Factor is calculated as follows:

$$\text{Congruence Factor} = (0.3 \times 0.95) + (0.3 \times 0.90) + (0.2 \times 0.92) + (0.2 \times 0.90) = 0.922$$

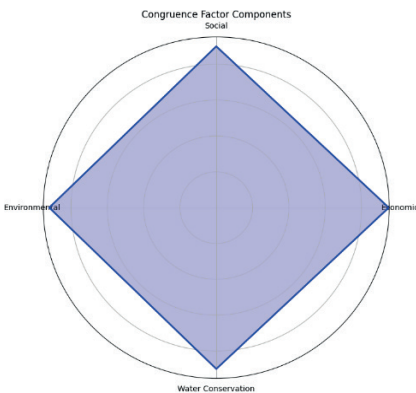


Figure 7. The congruence factor analysis of the Giurgiu-Răzmirești project

The graphical representation of the balanced congruence factor derived from the analysis is

presented in Figure 7. This figure illustrates the integration of various environmental, social, and economic criteria to optimize infrastructure performance.

This score reflects a project with exceptionally high performance across all dimensions, indicating a well-balanced and highly efficient project

Evaluation of project efficiency

The efficiency of the Giurgiu-Răzmirești project was evaluated using a combination of quantitative and qualitative indicators. Quantitative indicators included energy savings, water savings, and greenhouse gas emission reductions. These indicators were calculated based on the data analysis and modelling results.

Qualitative indicators included social acceptance, environmental impact, and technological feasibility. These indicators were assessed through stakeholder interviews, field assessments, and expert consultations.

The overall efficiency of the project was determined by calculating the congruence factor, which integrated the quantitative and qualitative indicators into a single score. A higher congruence factor indicates a more sustainable and efficient project (Neaga, 2015).

RESULTS AND DISCUSSIONS

Floating photovoltaic (FPV) panels are a novel technology that involves installing solar panels on water bodies, such as reservoirs and irrigation ponds. This dual-use approach not only generates clean electricity, but also reduces water evaporation, making it an attractive option for decarbonizing irrigation systems.

The literature review and case studies revealed that FPV systems have the potential to significantly reduce greenhouse gas emissions associated with irrigation. FPV systems can help conserve water by reducing evaporation losses, which is particularly important in arid and semi-arid regions.

However, the implementation of FPV systems also poses some challenges, such as the need for specialized equipment and expertise for installation and maintenance. Additionally, there are concerns about the potential impact of

FPV panels on aquatic ecosystems, although research suggests that these impacts can be mitigated through careful design and management.

Smart irrigation controls utilize sensors, weather data, and advanced algorithms to optimize water delivery to crops. This technology can significantly reduce water waste and improve irrigation efficiency, leading to substantial water savings and reduced energy consumption.

The data analysis revealed that smart irrigation controls can reduce water consumption by up to 50% compared to conventional irrigation methods. This translates to significant energy savings, as pumping and distributing water accounts for a substantial portion of energy use in irrigation systems. Moreover, smart irrigation can improve crop yields by ensuring that plants receive the right amount of water at the right time, further contributing to sustainable agricultural practices.

However, the adoption of smart irrigation controls requires upfront investment in technology and training for farmers. Additionally, the effectiveness of this technology depends on the accuracy and reliability of weather data and sensors, which may be a challenge in some regions.

Integrating renewable energy sources, such as solar and wind power, into irrigation systems can significantly reduce reliance on fossil fuels and lower greenhouse gas emissions. This can be achieved through the use of solar-powered pumps, wind-powered turbines, and hybrid systems that combine multiple renewable energy sources.

The renewable solutions must secure a circular economy approach in order to prevent the inefficient future waste management (Gautam et al., 2021).

The circular solution implies developing a business model that generate a close-loop cycle that will ensure the project sustainability (Contreras-Lisperguer, 2021).

The literature review and case studies highlighted the significant potential of renewable energy integration for decarbonizing irrigation systems.

Additionally, renewable energy can provide a reliable and cost-effective source of power for

irrigation, especially in remote areas where grid electricity may be unavailable or unreliable.

However, the initial investment costs for renewable energy systems can be a barrier for some farmers. Moreover, the intermittent nature of renewable energy sources requires careful planning and design to ensure a stable power supply for irrigation.

The analysis of the irrigation system revealed significant potential for improvement in energy efficiency and water resource management. The implementation of FPV panels is projected to generate a substantial amount of renewable energy, as shown in Table 7.

Table 7. Estimated financial performance of the Giurgiu-Râzmirești project over a 20-year period

Year of operation	Energy production (MWh)	Energy consumption (MWh)	Surplus energy (MWh)
1	151,800	51,260	100,540
2	150,555	51,260	99,295
3	149,326	51,260	98,066
4	148,113	51,260	96,853
5	146,915	51,260	95,655
6	145,733	51,260	94,473
7	144,567	51,260	93,307
8	143,416	51,260	92,156
9	142,281	51,260	91,021
10	141,161	51,260	89,901
11	140,057	51,260	88,797
12	138,968	51,260	87,708
13	137,894	51,260	86,634
14	136,835	51,260	85,575
15	135,792	51,260	84,532
16	134,763	51,260	83,503
17	133,749	51,260	82,489
18	132,750	51,260	81,490
19	131,767	51,260	80,507
20	130,800	51,260	79,540
Total	2,817,242	1,025,200	1,792,042

Figure 8 illustrates the energy dynamics of the analysed irrigation system over a 20-year period. The green line represents the energy production from floating photovoltaic panels, showing a gradual decrease from 151,800 MWh in the first year to 130,800 MWh by the twentieth year. The constant red line indicates the energy consumption of the irrigation system, fixed at 51,260 MWh annually. The blue line, depicting the surplus energy, highlights the difference between energy production and consumption, starting at 100,540 MWh in the first year and gradually

decreasing to 79,540 MWh in the final year. This surplus energy is fed back into the grid, contributing to the overall energy efficiency and sustainability of the project. The consistent energy consumption contrasted with the decreasing energy production underscores the

importance of maintaining high energy efficiency and optimizing renewable energy sources to sustain long-term surplus generation. The figure below illustrates the projected energy production, consumption, and surplus over the 20-year lifespan of the project.

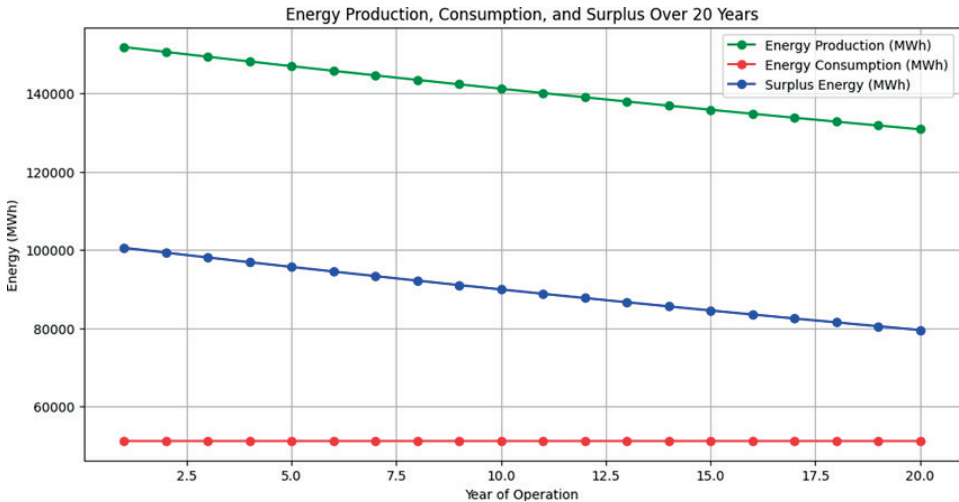


Figure 8. Financial performance of the project. Adaptation after (GEOSTUD, 2022)

The surplus energy generated by the FPV panels can be fed into the grid, providing additional revenue for the project and contributing to the decarbonization of the energy sector. The implementation of smart irrigation controls is expected to result in significant water savings, as shown in Table 8.

Table 8. Estimated water consumption of the Giurgiu-Răzmirești irrigation system with and without smart irrigation controls

Scenario	Water consumption (thousand m ³)	Cost (€)	Savings (€)
Without smart irrigation controls	337,730	23,641,100	-
With smart irrigation controls	275,324	19,272,680	4,368,420
Reduction	62,406	4,368,420	-

The average estimated cost for m³ of irrigation water in Romania was €0.07/m³. This reduction in water consumption not only conserves a valuable resource, but also reduces the energy required for pumping and distribution, further contributing to the project's overall efficiency. The annual cost savings from reduced water

consumption would be €4,368,420, and the cumulative savings over 20 years would be €87,368,400.

The integration of renewable energy sources, such as solar and wind power, is expected to further reduce the project's reliance on fossil fuels and lower greenhouse gas emissions. The combination of FPV panels, smart irrigation controls, and renewable energy integration is projected to achieve a high congruence factor, indicating a balanced and sustainable approach to irrigation system management.

CONCLUSIONS

This study shows that the decarbonization of irrigation systems is possible through the use of innovative technologies such as floating photovoltaic systems, smart irrigation controllers and the integration of renewable energies. In the case of the Giurgiu-Răzmirești irrigation system, these technologies offer significant potential to reduce greenhouse gas emissions, save water and promote sustainable agricultural practices. The implementation of floating photovoltaic panels is expected to

generate a significant amount of renewable energy that exceeds the energy consumption of the system and provides surplus energy to feed into the grid. This not only reduces the system's dependence on fossil fuels, but also generates additional revenue through the sale of electricity. The integration of smart irrigation controllers is expected to result in significant water savings, conserving this valuable resource and reducing the energy required for pumping and distribution. These combined benefits contribute to the overall efficiency and sustainability of the project.

However, the successful implementation of these technologies requires a holistic approach that considers the technical, economic, social, and environmental aspects of irrigation systems. Policymakers, researchers, and industry stakeholders need to collaborate to develop supportive policies, financial incentives, and capacity-building programs to encourage the widespread adoption of these technologies. Future research should focus on expanding the dataset to include a wider range of social and environmental indicators, as well as refining the weighting methodology for the congruence factor. Additionally, the application of the congruence factor to other sectors, such as energy and water infrastructure, could provide valuable insights for sustainable development planning in Romania.

The findings of this study have broader implications for climate change mitigation and adaptation efforts in the agricultural sector. By demonstrating the feasibility and benefits of decarbonizing irrigation systems, this research can serve as a model for other regions facing similar challenges. The integration of renewable energy and smart technologies in agriculture is not only essential for reducing greenhouse gas emissions but also for ensuring food security and resilience in the face of climate change.

ACKNOWLEDGEMENTS

The work was carried out during the main author's doctoral research activities at the Romanian Academy, National Institute for Economic Research "Costin C. Kirițescu" (INCE).

REFERENCES

- Acciona, <https://www.acciona.com/>, accessed at 12th of May 2024.
- Anbarasu, P., Loganathan, N., Narendran, A., Varatharaj, M. (2024). Characterization and Modeling of Floating Photovoltaic Systems using MATLAB to support photovoltaic Sustainable Development. *Journal of Electrical Systems*, 20(3), 2470-2477.
- Aspe, C., Gilles, A., Jacqué, M. (2016). Irrigation canals as tools for climate change adaptation and fish biodiversity management in Southern France. *Regional Environmental Change*, 16 (7, SI), 1975-1984. 10.1007/s10113-014-0695-8. hal-01444648.
- Baradei, S.E., Sadeq, M.A. (2020). Effect of Solar Canals on Evaporation, Water Quality, and Power Production: An Optimization Study. *Water*, 12, 2103. <https://doi.org/10.3390/w12082103>.
- Bellini, O. (2023). Global inventory map of floating photovoltaics, PV Magazine, <https://pv-magazine-usa.com/>, accessed on 10th of May 2024.
- Borza, I., Coste, I. (2003). *Agroecology and sustainable agricultural development*. Eurobit Publishing House, Timișoara.
- Contreras-Lisperguer, R., Muñoz-Cerón, E., Aguilera, J. de la Casa (2021). A set of principles for applying Circular Economy to the PV industry: Modeling a closed-loop material cycle system for crystalline photovoltaic panels. *Sustainable Production and Consumption*, 28, 164-179, ISSN 2352-5509.
- DIRECTIVE (EU) 2018/2001 OF THE EUROPEAN PARLIAMENT AND OF THE COUNCIL of 11 December 2018 on the promotion of the use of energy from renewable sources.
- Dörenkämper, M., Wahed, A., Kumar, A. Jong, M.D., Kroon, J.M., & Reindl, T. (2021). The cooling effect of floating PV in two different climate zones: A comparison of field test data from the Netherlands and Singapore. *Solar Energy Journal*, 219, 15-23.
- Economedia, <https://economedia.ro>, accessed at 05th of May 2024.
- European Commission (2021). Technical Guidelines on the application of the "Do No Significant Harm" principle under the Regulation on the Recovery and Resilience Mechanism, Bucharest.
- FAO. 2022. The State of the World's Land and Water Resources for Food and Agriculture – Systems at breaking point. Main report. Rome. <https://doi.org/10.4060/cb9910en>, ISBN 978-92-5-136127-6.
- FRAUNHOFER ISE, <https://www.ise.fraunhofer.de/en/>, accessed on 10th of May 2024.
- Gallagher, J., Basu, B., Browne, M., Kenna, A., McCormack, S., Pilla, F., Styles, D. (2017). Adapting Stand-Alone Renewable Energy Technologies for the Circular Economy through Eco-Design and Recycling. *Journal of Industrial Ecology*, 23(1), 133-140.
- Garanovic, A. (2022). SolarDuck set to build Japan's first offshore floating solar demonstrator, Offshore energy.biz, <https://www.offshore-energy.biz/>, accessed on 10th of May 2024

- Gautam, A., Shankar, R., Vrat, P. (2021). End-of-life solar photovoltaic e-waste assessment in India: a step towards a circular economy. *Sustainable Production and Consumption*, 26, 65-77, ISSN 2352-5509.
- GEOSTUD, Study regarding decarbonization of irrigation channels, Geostud SRL, 2022.
- Iberdrola, <https://www.iberdrola.com/>, accessed on 07th of May 2024.
- Ionitescu, S. (2023). The role of agriculture in Romania's economy in the period 2013-2022. *Scientific Papers. Series Management, Economic Engineering in Agriculture and rural development*, 23(4), 407-418.
- Klepş C., Tuşa C. (1992). *Water losses on the transport network of irrigation systems and their reduction technologies by using waterproofing films*. Agricultural Technical Publishing House.
- Kumar, N.M., Nallapaneni & Kanchikere, Jayanna & Mallikarjun, P. (2018). Floatovoltaics: Towards improved energy efficiency, land and water management. *International Journal of Civil Engineering and Technology*, 9, 1089-1096.
- McKuin, B., Zumkehr A., Ta, J., Bales, R., Viers, J.H., Pathak, T., Campbell, J.E. (2020). Energy and water co-benefits from covering canals with solar panels. *UC Merced*. <http://dx.doi.org/10.1038/s41893-021-00693-8>
- Nagababu, G., Bhatt, T.N., Patil, P. et al. (2024). Technical and economic analysis of floating solar photovoltaic systems in coastal regions of India: a case study of Gujarat and Tamil Nadu. *J. Therm Anal Calorim*. <https://doi.org/10.1007/s10973-024-12971-6>, accessed on 09th of May 2024.
- Neaga, F.D. (2015). Concepts of sustainable development. Theoretical-methodological approaches. University of Craiova, Faculty of Economics and Business Administration, Romanian Academy - Institute of World Economy.
- Neves I. (2023). New floating PV system design from Brazil, V Magazine, <https://www.pv-magazine.com/>, accessed on 6th of May 2024.
- Nicolae, R.I., Nicolae, P., Braileanu, A.M. (2021). Reducing greenhouse gas emissions by implementing sustainable infrastructure projects, Conference: GEOLINKS Conference Proceedings.
- Nicolae, R.I., Stefan, C.P. (2022). Study on the correlation between infrastructure projects and wildlife roadkill in Romania, Conference: 22nd SGEM International Multidisciplinary Scientific GeoConference 2022.
- Oceannews, <https://www.oceannews.com/>, accessed on 10th of May 2024.
- Renera, <https://renera.energy/ro>, accessed at 15th of May 2024.
- Sandu, M.A., Vladasel (Pasarescu), A.C., Pienaru, A.M. (2023). Embedding low carbon emission into the water infrastructure. *Scientific Papers. Series E. Land Reclamation, Earth Observation & Surveying, Environmental Engineering, XII*, 52-59, Print ISSN 2285-6064.
- Weetch, B. (2021). BayWar.e. commissions floating PV parks in the Netherlands. Energy Global magazine, www.energyglobal.com, accessed on 11th of May 2024.
- Zaman, Gh., Geamănu, M. (2006). *Economic Efficiency*. Publishing House of the Romania of Tomorrow Foundation, Bucharest.

CONSISTENCY INDEX OF SOILS, CORRESPONDING TO THE STATE OF SATURATION: AN IMPORTANT PARAMETER IN ANTICIPATING THE BEHAVIOR OF COHESIVE SOILS

Ernest Daniel OLINIC¹, Tatiana OLINIC²

¹Technical University of Civil Engineering Bucharest,
122-124 Lacul Tei Blvd, District 2, Bucharest, Romania

²University of Agronomic Sciences and Veterinary Medicine of Bucharest,
59 Marasti Blvd, District 1, Bucharest, Romania

Corresponding author email: tatiana.olinic@fifim.ro

Abstract

The physical characteristics of a soil give indication on its mechanical behavior and also offer suggestions in the correct programming of the laboratory tests, which will correctly describe the mechanical behavior of the soil. The plasticity index and the consistency index are two important parameters used to describe the cohesive soils. If the plasticity index is a nature parameter, the consistency index is a state parameter, which describes the state of the soil at its natural moisture content. The consistency index is the difference between the liquid limit and the natural moisture content, divided to the plasticity index. For the calculation of the consistency index corresponding to the state of saturation, the natural moisture content is replaced by the saturation moisture content, a situation in which, for the respective soil, the lowest state of consistency is anticipated in the assumption of its saturation. Beyond the theoretical aspects regarding the definition of this parameter, never previously used in technical literature, being an invention of the authors, the paper presents calculation examples and case studies with an emphasis on collapsible soils and swellings-shrinking soils, which represent difficult foundation conditions.

Key words: collapsible soils, consistency index, degree of saturation, swelling-shrinking soils.

INTRODUCTION

The physical characteristics of a soil give indication on its mechanical behavior and also offer suggestions in the correct programming of the laboratory tests, which will correctly describe their mechanical behavior of the soil. The plasticity index and the consistency index are two important parameters used to describe the cohesive soils. If the plasticity index is a nature parameter, the consistency index is a state parameter, which describes the state of the soil at its natural moisture content. Nature parameters are those who does not depend on moisture content and porosity (or void ratio). As examples, grain size distribution, skeleton density, are not influenced by those two parameters and represents nature parameters. State parameters gives real indications on soil mechanical behavior because the same soil, but with different porosity or moisture content, will behave different and even will have the behavior of a difficult soil under certain circumstances. The highest risk in the case of foundation on

difficult soils is if they are not identified by the elaborator of the geotechnical investigation as difficult foundation conditions. Is there such a risk? It can be explained, both by following the long path of carrying out a geotechnical investigation, as well as through the definition of difficult foundation conditions, defined by NP 074-2022. The geotechnical engineers commonly utilize clay index properties to estimate the geotechnical parameters (Ahmed, 2018).

The elaboration of a technical documentation regarding the geotechnical investigation of a site involves a series of stages, each of them very important: the study of relevant documents and maps, the technical visit to the site, the field investigations, the laboratory tests and the synthesis and interpretation of the results.

The study of relevant documents and maps, especially the geological, geomorphological and hydrogeological characterization of the site, can provide information on the nature and condition of the foundation soil from the site and may even indicate the presence of difficult foundation

conditions. But, the existence of these soils is not always indicated on documents and maps, especially since their scale is sometimes quite small. So, there is a risk that the difficult foundation conditions are not indicated in the relevant documents and maps.

Also, visual observations from the site may not be conclusive regarding the existence of difficult foundation conditions on site.

An extremely important stage in conducting field investigations with sampling is the preparation of the primary borehole log. It must include the preliminary description of the soil, stratigraphy and groundwater table. The greater the operator's experience in the field, the closer the description of the sample will be to the final result and, above that, more useful in the stage of programming the laboratory tests.

It was demonstrated that the increase of groundwater table can cause the saturated loess exhibit a strong strain-softening behaviour, i.e., the soil strength sharply decreases until reaching its critical state around 0 kPa (Xu et al., 2022). Laboratory tests should be scheduled through visual and tactile analysis of laboratory samples. Even in this situation, experience is decisive in correct programming of the tests.

The foundation soils are classified as good, average or difficult and represent the main factor for establishing the geotechnical category. Based on these factors, the frequency and types of field investigations and laboratory tests are established.

Fine soils are classified as foundations soils as follows:

- good if $I_c > 0.75$;
- average if $0.5 < I_c < 0.75$;
- difficult if $I_c < 0.5$.

The classification of fine soils as good, average or difficult, according to the consistency index, drew the attention of the authors of this paper to the parameter that is proposed to have a current use in geotechnical investigation reports.

It is well known that, if the water content increases, the consistency of a fine-grained soil changes from a semi-solid state to a plastic state, and eventually to a liquid state (Dolinar, 2009). The consistency index in its natural state can be higher than 0.75 or 0.5, but if the soil reaches a saturated state, this index can drop below those limits and the classification should be made according to worst case scenario.

In the list of difficult foundation soils, defined by NP 074-2022, there are also the following cohesive soils (to which the paper is addressing):

- collapsible soils (loess);
- swelling and shrinking soils.

These soils require special tests in order to classify them and subsequently, provide the necessary parameters in the geotechnical design. If these tests are not performed, the soil will be classified as medium or even good foundation soils, with major negative implications in the design and execution (Olinic, 2016).

Practically, both types of soils require special tests, including double compressibility tests in the oedometer, both on the sample at natural moisture content and on the initially saturated sample. Of course, these tests extend the execution time of a documentation regarding the geotechnical investigation, which is why it can be useful to use a parameter, which results from the simple tests of identification of physical parameters and which indicate whether it is necessary to carry out these special tests.

It is found that risks are identified in terms of the correct programming of laboratory tests, in all stages of the development of a documentation regarding the geotechnical investigation, and the difficult foundation cohesive soils covered by this paper, can sometimes be difficult to identify only after a visual and tactile analysis.

MATERIALS AND METHODS

Parameters that define swelling and shrinking soils

According to NP 126-2010, for classifying a material in the category of swelling-shrinking soils, the following geotechnical parameters must be determined and calculated, based on laboratory tests:

$A_{2\mu}$ - percentage of clay ($d < 0.002$ mm);

I_P - plasticity index;

I_A - activity index ($I_A = I_P / A_{2\mu}$);

C_P - plasticity criterion [$C_P = 0.73(w_L - 20\%)$];

U_L - free swell;

p_u - swelling pressure.

Depending on these parameters, soils are characterized by low, medium, high and very high activity in relation to water. Unfortunately, the standard does not indicate whether all or only a part of these parameters must include the

soil in those categories. Practically, the regulation requires that, in order to be sure that a cohesive soil is correctly identified as swelling-shrinking soil or not, all these tests must be performed. But, it is found that the first 5 parameters are the parameters of nature. Basically, they indicate the fact that, if the respective soil has certain moisture content and certain porosity, it will be swelling-shrinking soil, without any certainty in this regard. In current practice, especially the activity index provides erroneous information (Olinic et al., 2014).

The swelling pressure is certainly the most important parameter of a swelling-shrinking soil, but NP 126-2010 and STAS 1913/12-88 describe different procedures, for its determination, with positive and negative implications in the results. Worldwide there are several methods for the determination of the swelling pressure.

In some geotechnical problems, the behavior of clay after failure is as much important as the behavior of clay before failure (Atkinson, 1978).

Parameters that define collapsible soils

According to NP 125-2010, to characterize a soil as collapsible (loess), there are 2 criteria related to physical properties and 2 related to mechanical behavior, of which at least one must be met.

In current practice, the physical criteria refers to:
 - silt fraction ($d = 0.002 - 0.062$ mm) to represent de 50- 80% of total dry mass;
 - unsaturated state ($S_r < 0.8$);
 - porosity, $n > 40\%$.

By laboratory tests, the criterion related to the mechanical behavior is that the additional specific settlement index by wetting under the stress of 300 kPa (in the oedometric test), i_{m300} , has a value greater than or equal to 2%. The second mechanical criterion involves tests with the plate load test on the soil at natural moisture content and on saturated soil, a method not currently used in common practice.

Loess is a silty soil in which the constitutive chemical connections are susceptible to degradation by water, resulting in irreversible moisture-related damage (Leng et al., 2021).

It should be relatively easy to identify a loess by visual inspection, especially due to the macropores, the small mass and the yellowish-

brown color. But, there is also within this material a particular risky situation in which it does not stand out as sensitive to water soil: when the soil has $S_r > 0.8$ and the geological stress is lower than the structural resistance, a situation in which, both in the field and in laboratory tests, it will not register additional settlement to wetting but, in the hypothesis of lowering the underground water level, it will become again a collapsible soil.

Structural resistance of a collapsible soil is the minimum pressure for which the behavior (settlement) of the saturated soil is different (higher) than the one at natural moisture content. This value varies between 20 and 250 kPa (cannot be higher than 300 kPa due to the definition of the loess).

RESULTS AND DISCUSSIONS

The definition of consistency index of soils, corresponding to the state of saturation

The consistency index is the difference between the liquid limit and the natural moisture content, divided to the plasticity index (Casagrande, 1948).

$$I_C = \frac{w_L - w}{I_P} \quad (1)$$

For the calculation of the consistency index corresponding to the state of saturation, the natural moisture content is replaced by the saturation moisture content, a situation in which, for the respective soil, the lowest state of consistency is anticipated in the assumption of its saturation.

$$I_C^{sat} = \frac{w_L - w_{sat}}{I_P} \quad (2)$$

For the calculation of the consistency index corresponding to the state of saturation, it is necessary to determine in the geotechnical laboratory, through specific tests: the moisture content (w), the plastic limit (w_P), the liquid limit (w_L), the density in the natural state (ρ) and the density of the mineral skeleton (ρ_s), simple, usual tests and which are not very long time consuming.

From the calculation point of view:

$$I_C^{sat} = f(w_P, w_L, n, \rho_s) \quad (3)$$

From a database that includes 4000 soils from Romania (Figure 1), it appears that w_p varies between 10 and 30%, while w_L varies between 20 and 100%, values also confirmed by technical literature.

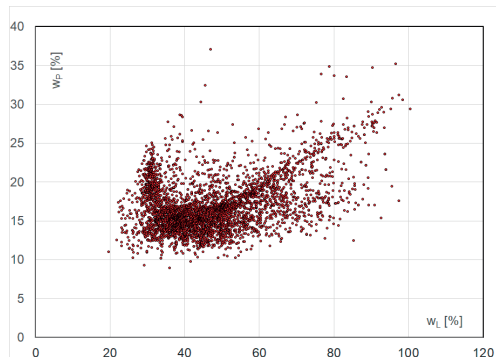


Figure 1. The variation of w_p and w_L obtained for 4000 soil samples from Romania

Figure 2 shows variation graphs of I_c^{sat} depending on soil porosity, for the minimum, intermediate and maximum values of w_p and w_L from the database.

In Figure 2.a and Figure 2.c the variation of I_c^{sat} is represented considering $w_p = 10\%$ and $\rho_s = 2.67 \text{ g/cm}^3$, respectively, $\rho_s = 2.72 \text{ g/cm}^3$. There are typical values for soils with low and average plasticity. For this reason, the lines of $w_L = 70$ and 100% are represented dotted.

It is found that the minimum (theoretical) value of I_c^{sat} is almost -0.4, which corresponds to the liquid state of the soil, a state in which it is impossible to meet a soil in its natural state. But a soil with I_c of a certain value can be encountered and, if for I_c^{sat} values are obtained from very low to liquid consistency, this should be an alarm signal for a more detailed analysis of the respective soil.

With reference to a collapsible soil (loess), it has the porosity between 40 and 55% and, for a plastic limit of 35%, the I_c^{sat} varies between -0.4 and 0.4.

In Figure 2.b and Figure 2.d, the variation of I_c^{sat} is represented considering $w_p = 30\%$ and $\rho_s = 2.67 \text{ g/cm}^3$, respectively, $\rho_s = 2.72 \text{ g/cm}^3$. There are typical values for soils with high and very high plasticity. For this reason, the $w_L = 35\%$ line is represented dotted.

In this case, it is found that a soil, even with a porosity of 55%, in the assumption of its

saturation, will at most reach a soft consistency state.

For porosity in the usual range of cohesive soils, of 35-45%, it is found that, even in a saturated state, the soil has a state of solid consistency. This situation should raise an alarm signal, in the sense that the soil in question is, most likely, in the category of swelling and shrinking soils.

Figure 3 shows the variation of I_c^{sat} depending on the porosity, for a usual value of the liquid limit, $w_p = 20\%$ and $\rho_s = 2.7 \text{ g/cm}^3$. These are average values, often found in current practice. In this graph, the area where swelling-shrinking soils is indicated, respectively, the collapsible soils or soils with very high compressibility.

The graph can be used as an abacus for the quick determination of I_c^{sat} depending on the porosity and the plastic limit of the soil.

The Consistency index of soils, corresponding to the state of saturation, determined on collapsible soils

A database with physical and mechanical determinations made on soil samples collapsible soils (loess) was accessed and I_c^{sat} was determined.

Figure 4 shows the results of several tests performed on loess, respectively, the variation of $I_c - I_c^{sat}$ and im_{300} depending on the porosity. It is noted that, for the selected samples, the I_c in the natural state of the loess is between 0.8 and 1.8, for which the soil is classified as stiff and solid consistency.

In saturated state, the loess reaches a consistency index between -0.44 and 0.58, for which the soil has a consistency from liquid to very-soft, soft and medium-soft.

In the same plot, the additional specific settlement to wetting of the existing soils in the database is also represented.

The results confirm the previously mentioned theoretical aspects.

CONCLUSIONS

In this paper, it is proposed to be implemented the consistency index corresponding to the state of saturation (I_c^{sat}) as a physical state parameter, useful in engineering judgment, in terms of identifying cohesive soils classified as difficult foundations soils, respectively, collapsible soils, swelling-shrinking soils or soils with very high

compressibility which, in their natural state, can register a high consistency index (stiff to solid consistency) but, in the assumption of

saturation, it becomes with soft, very-soft or even liquid consistency, with major implications in reduction of the mechanical behavior.

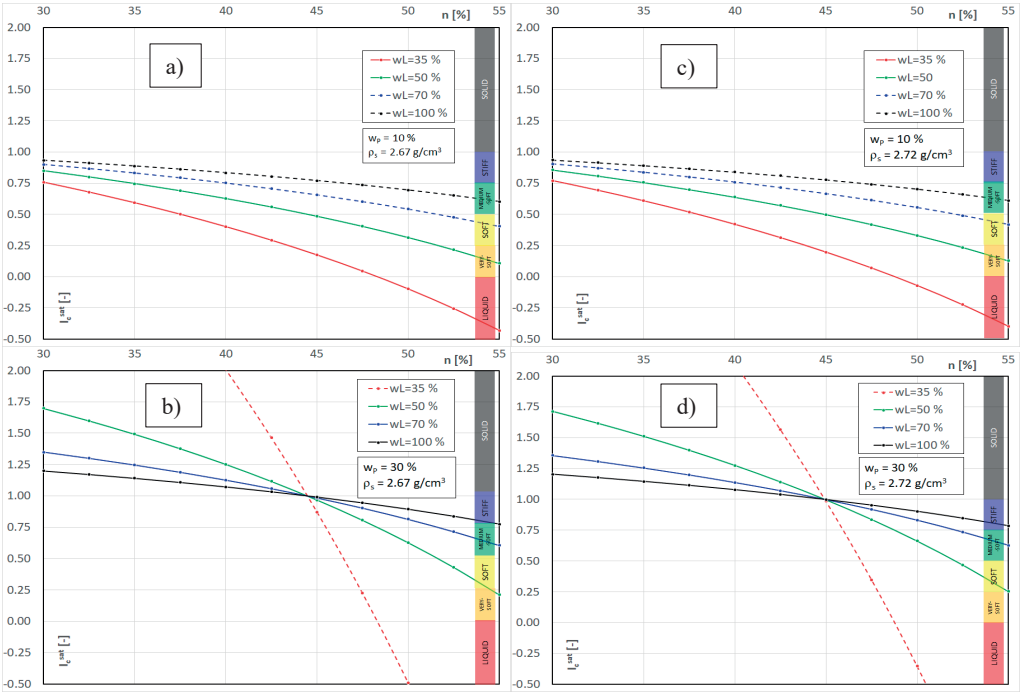


Figure 2. The variation of I_c^{sat} depending on the porosity and plasticity - extreme values

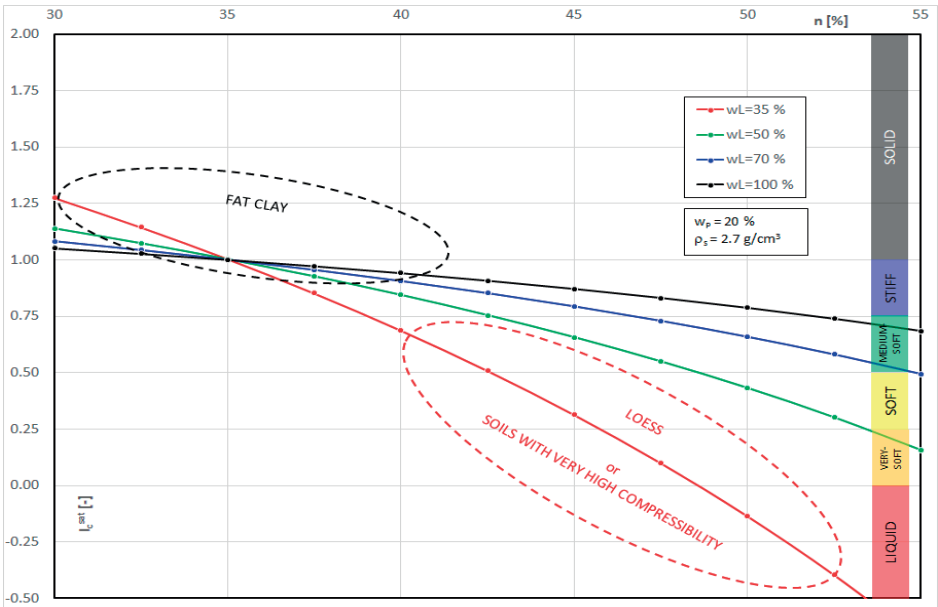


Figure 3. The variation of I_c^{sat} depending on the porosity and plasticity - usual values

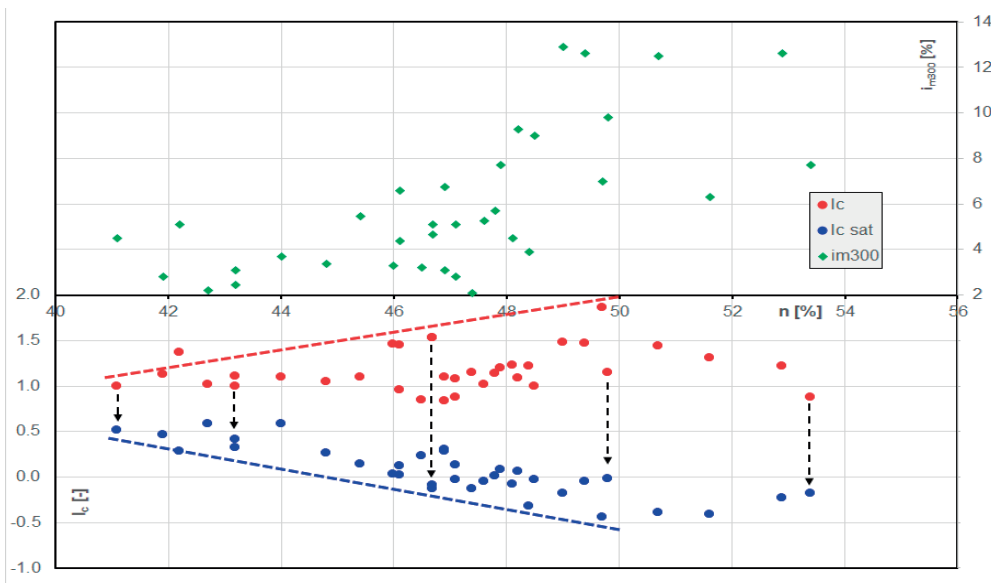


Figure 4. I_c^{sat} for several samples of loess (collapsible soils)

The consistency index corresponding to the state of saturation can be useful, both in the correct programming of laboratory tests, as well as in the expert analysis of some geotechnical documentation in which no difficult foundations were correctly identified.

The classification of cohesive soils as good, medium, or difficult, depending on the consistency index at natural moisture content, as requested in NP 074-2022, should be done according to the consistency index corresponding to the saturation state of the soil (I_c^{sat}).

REFERENCES

- Atkinson, J.H., Bransby, P.L. (1978). *The Mechanics of Soils, an Introduction to Critical State Soil Mechanics*. McGraw-Hill Book Company, England, UK, 375 pp.
- Ahmed, S.M. (2018). Assessment of clay stiffness and strength parameters using index properties. *Journal of Rock Mechanics and Geotechnical Engineering*, 10(3), 579-593.
- Casagrande, A. (1948). Classification and identification of soils. *Transactions of the American Society of Civil Engineers*, 113(1), 901-930.
- Dolar, B. (2010). Predicting the normalized, undrained shear strength of saturated fine-grained soils using

plasticity-value correlations. *Applied clay science*, 47(3-4), 428-432.

- Leng, Y., Peng, J., Wang, S., Lu, F. (2021). Development of water sensitivity index of loess from its mechanical properties. *Engineering Geology*, 280, 105918.
- Olinic, E., Ivasuc, T., Manea, S. (2014). Mechanical behavior of destructured expansive clay. *14th International Multidisciplinary Scientific Geoconference, Science and Technologies in Geology, Exploration and Mining - Conference Proceedings*, Vol. II., 581 -589, Alben, ISBN 978-619-7105-08-7.
- Olinic, E. (2016). Difficult foundation conditions in Romania. *Proc. 25th European Young Geotechnical Engineers Conference*, 37-53, 21-24 June 2016 - Sibiu, Romania, Publishing House Conspress, ISBN 978-973-100-421-1.
- Xu, L., Gao, C., Zuo, L., Liu, K., Li, L. (2022). The critical states of saturated loess soils. *Engineering Geology*, Vol. 307, 106776, ISSN 0013-7952, (<https://doi.org/10.1016/j.enggeo.2022.106776>).
- ***NP 074-2022. Technical norm regarding the geotechnical documentations for constructions.
- ***NP 125-2010. Technical norm regarding the foundation of constructions on soils sensitive to wetting.
- ***NP 122-2010. Technical norm regarding the determination of the characteristic and calculation values of the geotechnical parameters.
- ***STAS 1913/12-88 Foundation soil. The determination of the physical and mechanical characteristics of the swelling and shrinking soils.

MICROFLORA OF THE GROUND AIR FROM "HOT POINTS" AND PARK AREAS

Asen PESHEV, Bilyana GRIGOROVA-PESHEVA, Boyka MALCHEVA, Georgi KADINOV

University of Forestry, Faculty of Forestry, Department of Silviculture,
10 Kliment Ohridski Blvd, Sofia, Bulgaria

Corresponding author email: asenpeshev87@gmail.com

Abstract

The present study aims to track the quantity and distribution of microorganisms in the ground air in "hot points" and park areas of the territory of the city of Sofia. For this purpose, 6 "hot points" were selected, on the territory of boulevards and intersections, and six in the park areas of the capital. The study was carried out using the "Open air" method on suitable solid nutrient media. Each measurement was performed in five replicates. The total microbial number was determined, as well as the amount of the main microbiological groups. The potential presence of streptococci and staphylococci was reported. The data show several times increased levels of the total microflora in the hot spots compared to the green areas. There is also a difference in the percentage participation of the different microbiological groups in the two types of areas studied. In the hot points, fungi represent the main group of microorganisms, followed by bacteria. In green areas, bacteria represent the main group of microorganisms.

Key words: air microorganisms, air microflora, green zone, hot points.

INTRODUCTION

Air pollution represents a significant concern for public health in Europe, as underscored by Annesi-Maesano (2017). Recent findings highlight not only the profound implications of air pollution on human health but also its detrimental effects on ecosystems and the exacerbation of global warming, according to the European Environment Agency (EEA) in 2020. While particulate matter, specifically aerosols, is commonly associated with air pollution, there has been a disproportionate focus on non-biological pollutants, leading to an oversight of bioaerosols (Penner et al., 2001). Bioaerosols are biological particles suspended in the air - such as bacteria, fungi, fungal hyphae, spores, actinomycetes and other microscopic entities such as viruses for example (Kim et al., 2018). Often these bioaerosols are called airborne microorganisms (Chen et al., 2020), although bioaerosols also include fragments of pollen and other organic components.

It is known that fine dust particles represent concentration nuclei for the so-called airborne microorganisms (Aziz et al., 2018). For this reason, fine dust is a suitable environment for

the development and spread of airborne microorganisms (Pepper et al., 2015; Xu et al., 2017). Zhen et al. (2017) established that the air could contain more than 10^6 microbial cells per cubic meter, emphasizing the potential risk posed by fine dust not only through its physical effects but also as vectors for biologically active microorganisms (Klein et al., 2016). These insights highlight the role of fine dust in the attachment and dissemination of microorganisms, including pathogens (Shammi et al., 2021; Chen et al., 2020). Despite their widespread distribution in the atmosphere, the understanding of airborne microbial communities remains limited (Aziz et al., 2018), particularly concerning their concentration in ground air and the influence of environmental factors such as pollution, temperature, climatic conditions, fog presence, vegetation, etc. Ground air is the main part of the atmosphere where airborne microorganisms are concentrated. Studies have been conducted looking for a correlation between the amount of air microflora and various air parameters - such as pollution, temperature, climatic conditions, presence of fog, presence of vegetation, etc. Early studies (Mancinelli & Shulls, 1977) initially suggested a lack of correlation between

air microflora and these environmental parameters. However, further research has identified significant correlations between climatic conditions and microbial air concentrations (Cao et al., 2014; Fang et al., 2018; Chatoutsidou et al., 2023).

Comparative studies between urban and park areas regarding microbial composition and concentration are limited. Mhuireach et al. (2016) delineated differences in microbial communities between urban and green spaces, a finding supported by other researchers examining the influence of vegetation on microbial distributions and pathogen prevalence (Lymperopoulou et al., 2016; Li et al., 2021).

This study aims to explore for the first time the dynamics of total microflora across six hot points and six park areas within Sofia, Bulgaria. For the purpose of the study, the total microbial number of each of the studied samples was determined, as well as the percentage participation of the individual studied microbiological groups.

MATERIALS AND METHODS

The present study aims to track the quantity and distribution of microorganisms in the ground air in "hot points" and park areas within the city of Sofia. For this purpose, six "hot points" (HP) were selected, on the territory of boulevards and intersections, and six in park areas (P) of the capital. The sampling locations are as follows:

- Sample 1: Park Zaimov - green area;
- Sample 2: Crossroad of Evlogii and Hristo Georgievi boulevards and Yanko Sakazov boulevard – hotspot;
- Sample 3: Studentski Grad Park - green area;
- Sample 4: Crossroad of 8 Dekemvri St. and Rosario St. - hot zone;
- Sample 5: Park part on the border with Vitosha Nature Park - green zone;
- Sample 6: Crossroad of Cherni Vrah Boulevard and Ring Road Boulevard - hot spot;
- Sample 7: West Park - green zone;
- Sample 8: Crossroad of Cherni vrah boulevard and Ljubotrun street - hot spot;
- Sample 9: Loven Park - green zone;
- Sample 10: Nikola Vaptsarov Blvd. - hot spot;

- Sample 11: park Borisova Gradina - green zone

- Sample 12: Crossroad Orlov most- Hot Spot.

There is no Bulgarian legislation and guidelines for assessing the quality of the outdoor ground air in relation to the presence of bioaerosols. The study was carried out using the "Open air" method (Nustorova & Malcheva, 2020). The method is based on physical sedimentation of microbial cells under the action of their own weight. The method is based on the axiom that 10 liters of air flow through 100 cm² in 5 minutes, i.e. the microorganisms contained in 10 liters of air settle. For each of the samples, a recalculation to 1 m³ of air was performed. Petri dishes were used with suitable selective nutrient agar media for the studied microorganisms. Meat-Peptide Agar (MPA) was used for the cultivation of bacteria. Cultivation was carried out at a temperature of 2°C, for 48 hours, aerobically; Determination of actinomycetes - on selective medium for actinomycetes: Starch-ammonia agar (SAA). Cultivation was carried out at 28°C for 10 days, aerobically; Capek Dox Agar medium was used for the cultivation of micromycetes. Cultivation was carried out at 28°C for 7 days, aerobically. For the isolation of staphylococci and streptococci, *Staphylococcus* selective agar (48 hours at 35°C, aerobically) and Selective strep agar (48 hours at 35°C, aerobically) were used, respectively.

Each measurement was performed in five replicates, the average value was calculated. The samples were collected during the winter season of 2023-2024. All samples were collected at the same time in all locations at 1 m above the ground. Samples were collected on a non-precipitation day preceded by five non-precipitation days. The reported average air temperature is 11.6°C, relative air humidity-78%, atmospheric pressure 1009 millibars and wind speed 14 km/h from the southeast. The total microbial number was determined, as well as the amount of the main microbiological groups. The potential presence of streptococci and staphylococci was reported. Statistical processing of the microbiological results included calculation of the mean value of five replicates and standard deviation, using the StatSoft Statistica 12 program at significance thresholds of 95%.

RESULTS AND DISCUSSIONS

The results of the microbiological analysis are detailed in Table 1, quantified as colony-forming units (CFU*10³/m³). The study did not detect the presence of streptococci, a genus often linked to a variety of respiratory and other health conditions, typically more prevalent indoors than outdoors (Torrey & Michael, 1941). Staphylococci were found in the lowest concentrations among the analyzed microbial groups. Despite their association with densely populated indoor environments, research has demonstrated a correlation between the levels of fine particulate matter, such as black carbon, and the presence, distribution, and activity levels of specific staphylococci species (Hussey et al., 2017). The analysis presents clear trends, underscoring that urban hotspots exhibit significantly higher microbial numbers compared to green areas, as depicted in Figure 1. This finding is consistent with previous research (Mhuireach et al., 2016). Our study examined green areas of varying sizes: a large park exceeding 5 km² near the Vitosha Natural Park border (sample

5), three medium-sized parks ranging from 1 to 2 km² (samples 7, 9, and 11), and two smaller urban parks under 0.5 km² (samples 1 and 3). Additionally, the maintenance and visitation rates of these parks were considered - whether they were well-maintained and frequently visited (samples 1, 3, 7, and 11) or more akin to natural forest settings with minimal human activity (samples 5 and 9). The study found that parks with fewer visitors and more natural, forest-like vegetation exhibited a markedly lower concentration of airborne microorganisms than their urban counterparts. These observations suggest that the size of the park, coupled with its maintenance level, significantly influences the reduction of fine dust particles and their associated microorganisms. Supporting literature emphasizes the role of specific vegetation types in modulating the distribution and density of airborne microorganisms (Lymperopoulou et al., 2016), as well as vegetation's capacity to lower pathogen levels (Li et al., 2021). When comparing the total microbial count of only the green areas, the above statement is again confirmed.

Table 1. Main microbiological parameters of investigated airborne microorganism

Samples		Coordinate	Total microbial number	Bacteria	Fungi (molds)	Actinomy-cetes	Staphylo-coccus	Streptococcus
1	P	42°41'01" N 23°20'20" E	2.36 ± 10.93	1.57 ± 4.17	0.47 ± 1.36	0.31 ± 2.05	0.00 ± 0.13	--
2	HP	42°41'47" N 23°20'47" E	11.48 ± 8.60	4.09 ± 3.83	7.08 ± 4.34	0.31 ± 1.34	0.00 ± 0.17	--
3	P	42°39'16" N 23°21'05" E	15.90 ± 10.93	8.23 ± 4.17	1.89 ± 1.36	5.46 ± 2.05	0.31 ± 0.13	--
4	HP	42°39'06" N 23°21'11" E	30.04 ± 8.60	9.91 ± 3.83	16.20 ± 4.34	3.77 ± 1.34	0.16 ± 0.17	--
5	P	42°38'28" N 23°18'48" E	1.89 ± 10.93	0.94 ± 4.17	0.63 ± 1.36	0.31 ± 2.05	0.00 ± 0.13	--
6	HP	42°37'29" N 23°18'19" E	30.51 ± 8.60	11.80 ± 3.83	17.77 ± 4.34	0.79 ± 1.34	0.16 ± 0.17	--
7	P	42°40'07" N 23°18'34" E	11.80 ± 10.93	10.85 ± 4.17	0.47 ± 1.36	0.47 ± 2.05	0.00 ± 0.13	--
8	HP	42°40'05" N 23°19'09" E	20.38 ± 8.60	5.82 ± 3.83	12.99 ± 4.34	1.42 ± 1.34	0.16 ± 0.17	--
9	P	42°39'59" N 23°20'09" E	2.88 ± 10.93	2.40 ± 4.17	0.16 ± 1.36	0.31 ± 2.05	0.00 ± 0.13	--
10	HP	42°40'09" N 23°19'52" E	17.41 ± 8.60	6.25 ± 3.83	10.85 ± 4.34	0.31 ± 1.34	0.00 ± 0.17	--
11	P	42°41'03" N 23°20'26" E	12.41 ± 10.93	7.82 ± 4.17	3.72 ± 1.36	0.87 ± 2.05	0.00 ± 0.13	--
12	HP	42°41'25" N 23°20'14" E	32.82 ± 8.60	13.87 ± 3.83	18.05 ± 4.34	0.42 ± 1.34	0.47 ± 0.17	--

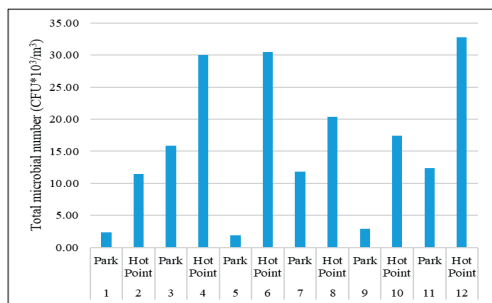


Figure 1. Total microbial number

The study identifies that the samples from the vicinity of Vitosha Nature Park (sample 5) and sample 9 exhibit notably low levels of airborne microorganisms. Similarly, Zaimov Park (sample 1) also shows reduced microbial counts in comparison to other parks. Contrarily, the microbial concentration in the air of the remaining parks is, on average, quintupled. These data show a potential relationship between the number of airborne microorganisms in the ground air of park areas and their anthropogenic load. The specific data here is for Park Zaimov (sample 1), which shows significantly lower levels than the other maintained parks. This data requires additional analyzes of the park territory.

One of the possible reasons for the lower levels of microorganisms in the ground air is that this park is located in the most affluent Municipality of the capital and is frequently cleaned. Part of the cleanup activities include washing the park's walkways, which further minimizes the possibility of lifting dust particles such as condensation nuclei for microorganisms from the ground surface. However, it should not be forgotten that the park is surrounded by boulevards, and it is necessary to analyze other specific parameters that may justify the indicated results.

In sample area 3, the highest total microbial concentration was observed, a finding that can be directly linked to extensive renovation and construction activities in the vicinity, including the development of new residential structures and the execution of infrastructural enhancements within the park itself. This correlation underscores the interaction between elevated dust levels and microbial spread in the atmosphere, where dust particles serve as

aggregation nuclei for microbes (Aziz et al, 2018). It is also important to note the low degree of afforestation of the park. Both in our study and in other similar ones, the positive impact of woody plants on the cleanliness and hygiene of the air is shown (Mhuireach et al., 2016).

Analyzing urban crossroads, identified as significant microbial hotspots, we noted the highest microbial densities at the Orlov Most crossroad (sample 12) - the most traffic-congested point in Sofia. This likely contributes to heightened levels of fine particulate matter, serving as a ground for airborne microorganisms. Intersection points represented by Sample 4 and Sample 6 similarly exhibited pronounced microbial counts, reflecting their heavy traffic congestion. In contrast, Sample 2, located in the vicinity of Park Zaimov, demonstrated markedly lower microbial quantities, with levels significantly reduced compared to other locations under scrutiny. This is due to the cleaning and maintenance regime implemented in this area, underlining the critical role of environmental cleanliness in mitigating microbial presence.

An analysis was conducted to determine the percentage contribution of individual microbiological groups within the total microflora, as illustrated in Figure 2.

The analysis reveals consistent patterns in the distribution of microbial groups within the airborne microflora. Notably, the predominant microbial group differs between high-traffic urban settings and green park areas. Microscopic fungi are the dominant group in urban hotspots, whereas bacterial populations prevail in park environments. This distribution aligns with findings by Barac et al. (2018), who identified fungi as primary agents in various respiratory ailments. This correlation may elucidate the heightened incidence of respiratory issues in populations residing in areas devoid of green spaces. The increased fungi level in the air of urban hot points has been corroborated by additional research (Korneykova, 2021; Pollegioni et al., 2023). Muafa et al. (2024) further established a link between increased vehicular traffic and elevated fungal concentrations in the atmosphere.

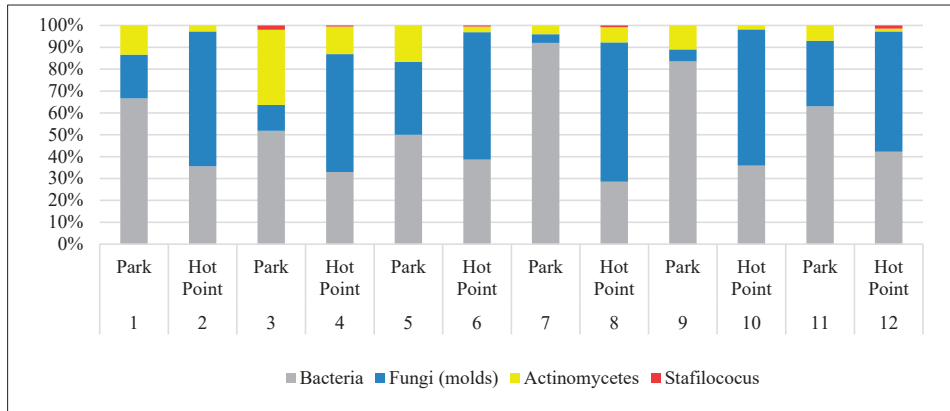


Figure 2. Percentage participation of individual microbial groups to total microbial number

Conversely, studies such as that by Nageen et al. (2021) report no significant disparity in fungal levels between park and urban areas. This discrepancy underscores the necessity for more comprehensive research into the prevalence and intensity of fungal species across various urban contexts, considering their significant impact on respiratory health. Within all green areas analyzed, bacterial populations were predominant. This dominance, while significant in comparison to the overall microflora composition in these areas, still represents a lower bacterial number than those observed in urban hot points, a finding consistent with the observations made by Gang et al. (2007). Following bacteria, fungi emerged as the secondary microbial group in all park areas, with the exception of sample 3, where actinomycetes were more prevalent. This anomaly in sample 3, showing a heightened presence of actinomycetes, could be attributed to the influence of nearby excavation activities. Lloyd (1996) suggested that such activities might facilitate the migration of actinomycetes into adjacent areas, such as we specified, to be present in the territory of the Student City Park.

CONCLUSIONS

This study was initiated to create a basic analysis concerning the total quantity of cultivable microorganisms and to elucidate the proportional representation of microbial groups within selected places. Six green zones and six hot points were selected. The results

demonstrated a higher microbial air load in urban hot points compared to green zones, highlighting the influence of environmental factors such as park size and maintenance practices on microbial prevalence in green spaces. Notably, parks that mimic the conditions of natural forests, both in size and in maintenance approach, exhibited lower microbial numbers in the ground air.

In contrast, the microbial density within urban hot points was significantly shaped by their maintenance standards and the intensity of vehicular traffic. Detailed comparison between two pivotal urban hot points revealed substantial discrepancies in microbial concentrations, with hot point 12 exhibiting microbial levels more than threefold higher than hot point 2. This difference was directly linked to the varying degrees of traffic congestion and the resultant dispersal of fine dust particles, serving as a carrier for microbial dispersal. The data on the distribution of microbial groups show that in hot point the group of fungi predominates, and in park areas the group of bacteria.

The primary goal of this research was to generate a basic dataset that could serve as a reference point for future studies. The outcomes presented herein lay the groundwork for more detailed subsequent investigations into the composition and dynamics of ground-level microflora, offering insights into environmental microbial ecology and its implications for public health and urban planning.

ACKNOWLEDGEMENTS

This research work was carried out with the support of Research Fund of Ministry of Education and Science in Bulgaria, project №: KII-06-H74/5 "Relationships between the amount of fine particulate matter and airborne microorganisms in "hot spots", park areas, urban background areas and control forest areas".

REFERENCES

- Annesi-Maesano, I. (2017). The air of Europe: Where are we going? *European Respiratory Review*, 26(146), 170024, DOI:10.1183/16000617.0024-2017.
- Azis, A., Lee, K., Park, B., Park, H., Park, K., Choi, I. & Chang, I. (2017). Comparative study of the airborne microbial communities and their functional composition in fine particulate matter (PM_{2.5}) under non-extreme and extreme PM_{2.5} conditions. *Atmospheric Environment*, 194, 82-89.
- Barac, A., Ong, D., Jovancevic, L., Peric, A., Surda, P., Spiric, V. & Rubino, S. (2018). Fungi-Induced Upper and Lower Respiratory Tract Allergic Diseases: One Entity. *Front Microbiol*, 9:5863, DOI: 10.3389/fmicb.2018.00583.
- Brooks, P., Gerba, P. & Pepper, L. (2004). Bioaerosol emission, fate and transport from municipal and animal waste. *Journal of Residuals Sci. Technology*, 1, 13-25.
- Cao, C., Jiang, W., Wang, B., Fang, J., Lang, J., Tian, G., Jiang, J. & Zhu, T. (2014). Inhalable microorganisms in Beijing's PM_{2.5} and PM₁₀ pollutants during a severe smog event. *Environ. Sci Technol.*, 48, 1499–1507.
- Chatatoutsidou, S., Saridaki, A., Raisi, L., Katsivela, E., Stathopoulou, P., Tsiamis, G., Voulgarakis, A. & Lazaridi, M. (2023). Variations, seasonal shifts and ambient conditions affecting airborne microorganisms and particles at a southeastern Mediterranean site. *Science of Total Environment*, 892, 164797, DOI: <https://doi.org/10.1016/j.scitotenv.2023.164797>.
- Chen, X., Kumari, D. & Achal, V. (2020). A Review on Airborne Microbes: The Characteristics of Sources. *Pathogenicity and Geography. Atmosphere*, 11(9), 919, DOI: <https://doi.org/10.3390/atmos11090919>.
- EEA Report – Air quality in Europe-2020 report. (2020). Luxembourg, Publication Office of the European Union, ISBN 978-92-9480-292-7, DOI:10.2800/786656.
- Fang, Z., Guo, W., Zhang, J. & Lou, X. (2018). Influence of Heat Events on the Composition of Airborne Bacterial Communities in Urban Ecosystems. *International Journal of Environment Research and Public Health*, 15, 2295.
- Fang, Z., Ouyang, Zh., Zheng, H., Wang, X. & Hu, L. (2007). Culturable Airborne Bacteria in Outdoor Environments in Beijing, China. *Microbial Ecology*, 54, 487-496.
- Friedlander SK. (2000). Smoke, dust, and haze. Fundamentals of aerosol dynamics. Oxford, New York: *Oxford University Press*.
- Hussey, Sh., Purves, L., Allcock, N., Fernandes, V., Monks, P., Ketley, J., Andrew, P. & Morrissey, J. (2017). Air pollution alters *Staphylococcus aureus* and *Streptococcus pneumoniae* biofilms, antibiotic tolerance and colonisation. *Environmental Microbiology*, 19(5), 1868-1880.
- Kim, K., Kabir, Eh. & Jahan, Sh. (2018). Airborne bioaerosols and their impact on human health. *J Environ Sci (China)*, 67, 23-35, DOI: 10.1016/j.jes.2017.08.027.
- Klein, A., Bohannan, B., Jaffe, D., Levin, D. & Green, J. (2016). Molecular Evidence for Metabolically Active Bacteria in the Atmosphere. *Frontiers in Microbiology*, 7, 772.
- Korneykova, M.V., Soshina, A.S., Novikov, A.I., Ivashchenko, K.V., Sazonova, O.I., Slukovskaya, M.V., Shirokaya, A.A., Vasenev, V.I., Vetrova, A.A., Gavrichkova, O. (2021). Microscopic Fungi in Big Cities: Biodiversity, Source, and Relation to Pollution by Potentially Toxic Metals. *Atmosphere*, 12, 1471.
- Li, H., Wu, Zh., Yang, X., An, X., Ren, Y. & Su, J. (2021). Urban greenness and plant species are key factors in shaping air microbiomes and reducing airborne pathogens. *Environment International*, 153, 106539.
- Lloyd, B. (1969). Dispersal of Streptomyces in air. *J. Gen. Microbiology*, 57, 35-40.
- Lymperopoulou, S., Adams, I. & Lindow, E. (2016). Contribution of vegetation to the microbial composition of nearby outdoor air. *Appl. Environ. Microbiol.*, 82, 3822–3833.
- Mancinelli, R. & Shulls, W. (1977). Airborne Bacteria in a Urban Environment. *Applied and Environmental Microbiology*, 35(6), 1095-1101.
- Mhuireach, G., Johnson, B., Altrichter, A., Ladau, J., Meadow, J., Pollard, K. & Green, J. (2016). Urban greenness influences airborne bacterial community composition. *Science of Total Environment*, 571, 680-687.
- Muafa, M., Quach, Z., Al-Shaarani, A., Nafis, M. & Pecoraro, L. (2023). The influence of car traffic on airborne fungal diversity in Tianjin, China. *Mycology*, DOI: 10.1080/21501203.2023.2300343.
- Nustorova, M. & Malcheva, B. (2020). Manual for laboratory exercises in microbiology – in ulgarian. Varna, *IK Gea-Print*, 64-68.
- Penner, J., Andreae, M., Annegarn, H., Barrie, L., Feichter, J., Hegg, D., Jayaraman, A., Leaitch, R., Murphy, D., Nganga, J. & Pitari, G. (2001). Aerosols, their Direct and Indirect Effects-Chapter 5, 300, Cambridge Uk, *Cambridge University Press*.

- Pepper, I., Gerba, Ch. & Genrtru, T. (2015). Aeromicrobiology. *Environmental Microbiology*, 89-110, DOI:10.1016/B978-0-12-394626-3.00005-3.
- Pollegioni, P., Cardoni, S., Mattioni, C., Piredda, R., Ristorini, M., Occhiuto, D., Canepari, S., Korneykova, M., Soshina, A., Calfapietra, C. & Gavrichkova, O. (2023). Variability of airborne microbiome at different urban sites across seasons: a case study in Rome. *Frontiers in Environmental Science*, 11, 1213833, DOI: <https://doi.org/10.3389/fenvs.2023.1213833>.
- Torrey, J. & Lake, M. (1941). Streptococci in air as an indicator of Nasopharyngeal Contamination. *Jama*, 117(17), 1425-1430.
- Xu, C., Ewi, M., Chen, J., Zhu, Chao, Li, J., Lv, G., Xu, X., Zheng, L., Sui, G., Li, W., Chen, B., Wang, W., Zhang, Q., Ding, A. & Mellouki, A. (2017). Fungi diversity in PM2.5 and PM1 at the summit of Mt. Tai: abundance, size distribution, and seasonal variation. *Atmos. Chem. Phys*, 17, 11247-11260.

BUILDING SUSTAINABILITY: INTEGRATING AGRICULTURAL AND INDUSTRIAL SUB-PRODUCTS IN THE BUILDING SECTOR

Cristian PETCU¹, Claudiu Sorin DRAGOMIR², Andreea HEGYI¹

¹National Institute for Research and Development in Construction, Urban Planning and Sustainable Spatial Development - URBAN-INCERC, 266 Pantelimon Road, District 2, Bucharest, Romania

²University of Agronomic Sciences and Veterinary Medicine of Bucharest, 59 Marasti Blvd, District 1, Bucharest, Romania

Corresponding author email: dragomirclaudiusorin@yahoo.com

Abstract

The construction sector demand for thermal insulation materials is rising, to enhance building energy efficiency and indoor thermal comfort. While insulation materials like organic foams (EPS, XPS, PUR, PIR) or inorganic fibers (glass or rock wool) are widely used, there is a shift towards eco-friendly alternatives derived from agro-industrial waste. These sustainable options not only reduce operational energy consumption in buildings but also offset some of their own production energy requirements. Furthermore, using such sub-products as insulation materials presents an ecological advantage, contributing to CO₂ sequestration and offering a greener choice in the construction industry. This paper presents the thermal properties of such insulating materials and compares their values with some of the commonly used insulation materials. The thermal conductivity of the materials was assessed using the λ -Meter EP500e, a guarded hot plate apparatus specialized for such measurements, using the instructions outlined in the SR EN 12667 standard, ensuring accuracy and compliance with established guidelines. The paper aims to elevate awareness about the potential of transforming what is currently viewed as agricultural waste into innovative and environmentally friendly building materials.

Key words: agricultural sub-products, building insulation, thermal conductivity, sustainability.

INTRODUCTION

Taking on and contributing to the achievement of the 17 Sustainable Development Goals is a global and, implicitly, a national priority. In this context, there are four key areas where materials intended for the thermal insulation of buildings have a significant impact: the efficiency of energy consumption that is required to ensure the comfort of the population; the quality of air in living spaces to maintain hygiene and health conditions of the population; sustainable use of natural resources; and environmental impact. Thus, there is a dual focus: on one hand, towards the production of heat-insulating materials with the highest possible performance in terms of thermal insulation, and on the other hand, the increasing need to identify possibilities for creating new, more environmentally friendly heat-insulating materials. These materials should allow for the recycling of industrial waste or by-products and contribute to improving air quality in living spaces. Currently, the market offers a variety of classic

heat-insulating materials, such as expanded or extruded polystyrene, mineral wool, and polyurethane foam, most often available in the form of plates to facilitate installation. Additionally, there are several "niche" materials gaining prominence, made from either vegetable or animal fibers or by recycling waste from various industries (e.g., cardboard and paper waste, cigarette manufacturing waste, wood waste). The specialized literature highlights the following:

- Estimates up to 2020 suggest that buildings account for 30-40% of total global primary energy consumption and over 25% of greenhouse gas emissions (Ricciu et al., 2018; Dodoo et al., 2011; Csanády et al., 2021).
- Thermal insulation based on expanded or extruded polystyrene, polyurethane foam, glass fiber wool, or mineral wool accounts for approximately 87% of the market (Ahlberg et al., 2014; Stevulova et al., 2013).
- Some classic thermal insulation materials, despite their cost-effectiveness and

ease of installation, have disadvantages such as low biodegradability and limited post-use possibilities. Being slightly permeable to gases and water vapors, they could negatively affect indoor air quality by trapping water vapor, volatile organic compounds, radon, or other harmful gases for extended periods. Increased air humidity can also promote the growth of mold on interior wall surfaces, potentially leading to "sick building syndrome" (Maskell et al., 2015; Mølhave et al., 1997; Curling, 2012; Mansour et al., 2016; Salthammer et al., 2010; Takeda et al., 2009). Buildings affected by microbial deposits can experience a decline in indoor air quality due to spore contamination and toxin release. Common mycotoxins found in indoor air and within populations residing in contaminated environments - produced by molds such as *Cladosporium*, *Acremonium*, *Alternaria*, *Periconia*, *Curvularia*, *Stemphylium*, *Penicillium*, *Aspergillus* - include ochratoxin (OCT), aflatoxin B1, and trichothecenes, known for their genotoxic, immunotoxic, hepatotoxic, mutagenic, and potentially carcinogenic effects (Khan et al., 2012; Hope et al., 2013; Zukiewicz-Sobczak et al., 2013; Andersen et al., 2011).

- Research into the production of innovative thermal insulating materials from fibers and agricultural waste, of vegetable or animal origin, or from waste and by-products of other industries, presents new challenges, especially in terms of ensuring satisfactory resistance to micro-organisms and good water behavior, i.e., low absorption in case of accidental immersion (Zach et al., 2013; Vėjeliënė et al., 2011).

- According to national and international regulations, thermal insulation materials must meet specific thermal performance requirements as well as minimum fire resistance standards (Chereches et al., 2021; Ciobanu & Puscasu, 2013; Bode et al., 2023; Simion et al., 2019; Thieblessen et al., 2024; Kušnerová et al., 2018).

- In the case of "niche" heat-insulating materials, the most common antifungal treatments, which also serve to increase fire resistance, include those based on borax, boric acid, aluminum sulfate, or ammonium sulfate (Day et al., 1981; Herrera, 2005), typically applied through wet spraying. However,

research has indicated that these treatments have limited durability, may impact population health, and have a less favorable environmental impact (Papoutsis et al., 2019; Liu et al., 2018; Dai et al., 2022). Moreover, antifungal treatments, like any other treatment intended to enhance durability, fire resistance, etc., must adhere to EU regulations concerning the Registration, Evaluation, Authorization, and Restriction of Chemicals (REACH). This is crucial to prevent threats to human health and the environment.

- Another significant aspect of experimental research concerns the variation in the thermal conductivity coefficient, influenced by either the material's moisture content or the temperature range within which the thermal conductivity coefficient is determined. Vėjeliënė et al. (2006) demonstrated that a 1% increase in hygroscopic moisture content leads to a 1.25%-2% increase in the thermal conductivity coefficient (λ). This finding aligns with earlier research by Sandberg (1992), who formulated a linear equation to describe the variation of the thermal conductivity coefficient as a function of the insulating material's water absorption, as follows:

$$\lambda = 0.037 + 0.0002w \text{ (W/mK)} \quad (1)$$

where:

- w represents the amount of water absorbed per unit volume of cellulose, in kilograms per cubic meter (kg/m^3).

Finally, research by Talukdar (Talukdar et al., 2007) also indicated that the thermal insulation performance, quantified by the thermal conductivity coefficient and measured across a temperature range of 10°C to 30°C , with an average temperature of 22.5°C , varies according to a polynomial function in relation to the moisture content (ϕ). This dependence can be expressed by a non-linear function of the form:

$$\lambda = (a + b\phi + c\phi^{1.5} + d\exp(-\phi)) \quad (2)$$

where:

- a , b , c and d are experimentally determined coefficients, with the values: $a = 0.092482655$, $b = 0.15480621$, $c = 0.066517733$ and $d = 0.1296168$.

The aim of this paper is to conduct a comparative analysis of the resistance of various heat-insulating materials available on the Romanian market to humid environments

and environments contaminated with mold spores. These materials include those found in the category of "classic" materials, such as expanded polystyrene, mineral wool, and polyurethane foam, as well as "niche" materials produced by recycling cellulosic waste and using vegetable or animal fibers.

MATERIALS AND METHODS

The experimental research was conducted at a constant temperature of $23^{\circ}\text{C} \pm (0.25 \text{ to } 0.3)^{\circ}\text{C}$, aiming to evaluate the behavior of certain heat-insulating materials used in construction under conditions of high humidity and/or contamination with mold spores. The selection of these materials aimed to compare classic, commonly used materials (expanded polystyrene, mineral wool, polyurethane foam) with "niche" materials made from raw materials of vegetable origin (wood fiber waste), animal origin (sheep's wool), or by recycling various wastes (acrylic-cellulosic waste from cigarette filters, cellulosic cardboard waste, siliconized paper from printing waste, and aluminized polyethylene film from printing waste). The materials were analyzed as received from the manufacturers, without any further processing or treatment prior to testing. They were coded according to Table 1.

Table 1. Codification and characterization of heat-insulating materials

Sample Code	Installation Method	Raw Material
P1	External cladding in ETICS system	Expanded polystyrene
P2		Mineral wool
P3		Polyurethane foam
P4	Inside the structure, loose-fill, between rigid panels	Processed wood fibers (shredded)
P5		Cellulose acetate, waste from cigarette filter manufacturing
P6		Non-woven sheep wool insulation mat
P7		Cellulose from cardboard waste
P8		Waste from silicone-coated paper printing
P9		Waste from polyethylene film printing
P10		Waste from printed aluminized polyethylene film

The methodology of the work included the following stages:

1. Visual characterization;
2. Determination of apparent density, according to EN 1602;

3. Analysis of water behavior by determining water absorption through the short-term (24 h) partial immersion method, according to EN ISO 29767 for materials with a defined shape (expanded polystyrene, mineral wool, polyurethane foam, and heat-insulating sheep wool mattress). For bulk materials of ligno-cellulosic or animal origin, the sorption-desorption capacity was evaluated according to EN ISO 12571. For waste from the printing industry (silicone paper [P8], polyethylene foil [P9], and aluminized polyethylene foil [P10]), this experimental testing was not applicable as these materials are hydrophobic.

4. Characterization of thermal insulation performance by determining the coefficient of thermal conductivity, λ_{10}^{ct} (W/mK), using a λ -Meter EP500e conductivity meter (Lambda-Messtechnik GmbH, Dresden, Germany) in accordance with EN 12667. Samples were dried to a constant mass in a ventilated oven, and testing was performed at an average test plate temperature of $10^{\circ}\text{C} \pm 1^{\circ}\text{C}$.

5. Characterization of the materials in terms of resistance to mold action, in two test variants:

- Variant 1: Analysis of the risk of mold occurrence in case of exposure to high humidity conditions, following the work methodology specific to the evaluation of the biological resistance of thermal insulation or acoustic insulation materials, made of animal fibers, either manufactured in the factory or in-situ, as indicated in references EAD 040005-00-1201 and EN ISO 846. Accordingly, the samples were exposed in an environment with high humidity resulting from the evaporation of water at normal atmospheric pressure and a constant temperature of $23^{\circ}\text{C} \pm 1^{\circ}\text{C}$, within a closed enclosure, for 28 days. At the end of the exposure period, the samples were analyzed visually without optical magnification and microscopically with the aid of a LEICA SAPO microscope, to identify any signs of mold development. The resistance to the action of microorganisms was quantified by assigning rating classes of fungal growth and categories that indicate the performance in terms of nutrient content conducive to the development of microorganisms, in accordance with EN ISO 846, summarized in Table 2.

- Variant 2: Analysis of resistance to mold when exposed to an environment heavily

contaminated with spores of *Penicillium notatum* and *Aspergillus niger*. To achieve this, culture systems were established: each type of sample was placed in a Petri dish on a nutrient substrate of potato dextrose agar (PDA) (39 g/l). A solution containing spores of *Penicillium notatum* or *Aspergillus niger* (10 µl/10 ml distilled water) was sprayed onto the tested sample and the nutrient substrate, from a perpendicular distance of 100 mm. The entire system was sealed and incubated at a

constant temperature of 23°C ± 1°C in a BIOBASE BOV-D30 incubator. The system was evaluated at regular intervals to monitor the appearance and development of mold and the extent of coverage on the material sample's surface. This was done through microscopic evaluation using a LEICA SAPO microscope. For quantification, a system similar to that used in Test Variant 1 was adopted, as detailed in Table 3.

Table 2. Evaluation of fungal growth and product performance

Class	Fungal Growth Evaluation	Category	Product Performance Estimation
Class 0	No signs of growth under microscopic examination.	0	The material does not provide a nutrient medium for microorganisms (it is inert or fungistatic).
Class 1	Growth not visible to the naked eye, but clearly visible under a microscope.	1	The material contains few nutrients or is so minimally contaminated that it only allows for very limited development.
Class 2	Growth visible to the naked eye, covering up to 25% of the test surface.	2-3	The material does not resist microbial attacks; it contains nutrients that allow their development.
Class 3	Growth visible to the naked eye, covering up to 50% of the test surface.		
Class 4	Growth visible to the naked eye, covering more than 50% of the test surface.		
Class 5	Strong growth covering the entire test surface.		

Table 3. Evaluation of resistance to fungal action in heavily contaminated systems

Classification of the resistance to fungal action	Evaluation
Very High	No signs of growth, with possible punctate signs visible only under a microscope, of mold growth on the analyzed surface.
High	Biofilm covering less than 50% of the analyzed surface, or microscopic analysis reveals visibly intense signs of mold anchoring on the fibers/granules of the material.
Medium	Biofilm covering 50% - 75% of the analyzed surface.
Low	Biofilm covering more than 75% of the analyzed surface.

RESULTS AND DISCUSSIONS

The experimental results concerning thermal insulation performance and resistance to mold action, which have implications for both the compatibility of the materials with their intended use (building insulation) and the quality of indoor air, revealed similarities and differences among the 10 types of materials analyzed. It is believed that these performances are influenced by several factors, with the characteristics of the raw material used to produce the material being the primary element. The apparent density of the materials is a significant characteristic as it has implications including the degree of additional load on the building's structural integrity. As illustrated in Figure 1, generally, this parameter falls within

limits indicating that using these materials for thermal insulation does not significantly stress the structural integrity, with most of them being relatively lightweight. Mineral wool is the densest material among those analyzed, but its density is still far below that of materials typically used for constructing self-supporting walls, such as concrete, which has a density 25 times greater. Short-term water absorption determined by partial immersion, as shown in Figure 3, indicated that all the analyzed materials - those available in defined shapes, such as tiles or mattresses - have values below 1 kg/m². Among these, the sheep's wool mattress (P6) exhibited the highest water absorption rate at 0.6 kg/m². In contrast, the polyurethane foam insulation, due to its closed-cell structure and the material's water-repellent characteristics,

displayed the lowest absorption rate at 0.02 kg/m². This measure is particularly relevant in scenarios where accidental water contact occurs. The sheep's wool mattress, absorbing a larger amount of water, is subject to more significant variations in terms of the thermal conductivity coefficient, which is known to be influenced by the moisture content of the material (Sandberg, 1992). Conversely, polyurethane foam, being minimally affected by water, will consequently demonstrate greater stability in thermal insulation performance, as quantified by the thermal transfer coefficient.

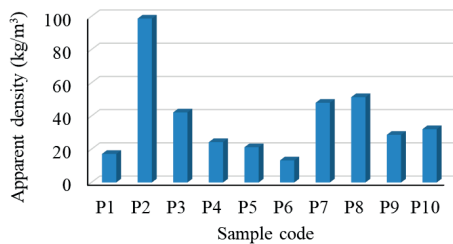


Figure 1. Apparent density

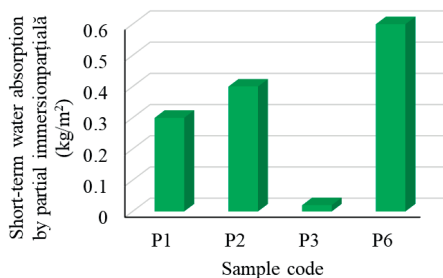


Figure 2. Short-term water absorption by partial immersion

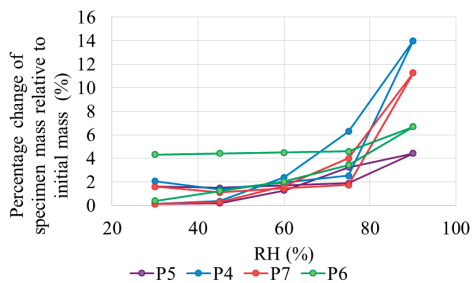


Figure 3. Percentage change in specimen mass relative to initial mass

The hygroscopic nature of the bulk thermal insulation materials (of undefined shape), including the sheep wool mattress, was analyzed using the percentage variation of the specimen's mass relative to its initial mass (representing the amount of adsorbed/desorbed water) as a function of the relative humidity of the air, $w(\%) = f(RH(\%))$, as shown in Figure 3. The four materials analyzed - wood fibers processed by chopping (P4), cellulose acetate from cigarette filter manufacturing waste (P5), non-woven sheep wool mattress (P6), and cellulose from cardboard waste (P7) - demonstrate a relative consistency in the sorption phenomenon, with a slight increasing trend up to an RH of 75%, followed by a marked increase in the sorption phenomenon in the relative air humidity range of 75% - 90%. Examining the desorption diagram for each material type reveals a difficulty in water loss around a real air humidity of 75%. Thus, it is inferred that materials at a 75% relative air humidity retain a larger amount of water, and part of the water adsorbed at the maximum RH (90%) is not released back into the environment when the RH decreases to 75%. Upon examining the sorption/desorption curves (Figure 5) for the bulk materials made from waste (P4, P5, P7), an intersection point between the ascending curve (sorption) and the descending curve (desorption) is observed in the 50%-70% relative air humidity range. For each material, the intersection point is positioned at a specific humidity: about 55% for wood fiber-based material (P4), about 65% for cigarette filter manufacturing waste-based material (P5), and about 67% for cardboard waste-based material (P7). Conversely, for the sheep wool-based material (P6), the characteristic sorption and desorption curves do not intersect, and the sorption curve lies below the desorption curve. This pattern indicates the capacity of the materials to release stored water, although limited. Nonetheless, it suggests that under conditions of indoor air humidity variation (a parameter of indoor air quality), these materials could help regulate this indicator and, by extension, contribute to improving air quality. However, in line with the specialized literature (Rode, 1998; Vrana & Gudmundsson, 2010), the limited ability to release absorbed moisture may lead to moisture

accumulation within the thermal insulation material, potentially fostering conditions conducive to mold growth.

In terms of thermal insulation performance, as depicted in Figure 4, it is estimated that all analyzed materials meet the expectations for their intended use, with the coefficient of thermal conductivity ranging from 0.035 W/mK for mineral wool (P2) to 0.056 W/mK for sheep wool insulation (P6).

Analyzing the two key indicators for the materials - apparent density and the coefficient of thermal conductivity, as shown in Figure 5, it can be first noted that the nature of the material significantly influences these properties. Additionally, advantages and disadvantages can be identified for each specific case. For instance, among the analyzed materials, the sheep wool mattress (P6) has the lowest density but exhibits the least favorable performance in terms of thermal insulation, having the highest value for the coefficient of thermal conductivity. Conversely, mineral wool (P2) possesses the highest density, approximately 7 times higher than that of the sheep wool mattress, yet demonstrates superior thermal insulation performance, with a thermal conductivity coefficient 37.5% lower than that of the sheep wool mattress, which is the highest among the analyzed samples.

The cases of polyurethane foam (P3) and expanded polystyrene (P1) are also notable. Despite its high apparent density - about 3.2 times higher than that of the sheep's wool mattress, the lightest among the analyzed thermal insulating materials - polyurethane foam offers the best thermal insulation performance, with a thermal conductivity coefficient (λ_{10}^{ct}) of 0.022 W/mK. In contrast, expanded polystyrene (P1), while having a low density close to that of the sheep wool mattress and approximately 2.5 times lower than that of polyurethane foam, which is the best performer in this study, exhibits a thermal conductivity coefficient with a value of 0.014 W/mK higher than that of polyurethane foam. Similarly, other thermal insulation materials made from recycled waste (P4, P5, P7-P10) show average thermal insulation performances, with thermal conductivity coefficients ranging from 0.038 to 0.042 W/mK, and intermediate apparent densities ranging from 21.2 to 51.4 kg/m³.

However, when analyzing the interdependence between apparent density and the thermal conductivity coefficient, it appears there is no direct correlation between the two indicators; a function of $\lambda_{10}^{ct} = f(\text{density})$ cannot be clearly identified. This shows that the thermal performance of materials is influenced by multiple factors, not solely by density, and suggests that is impossible to correlate the thermal conductivity value with the materials density, for a range of materials.

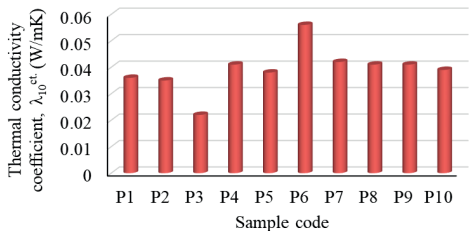


Figure 4. Thermal conductivity coefficient

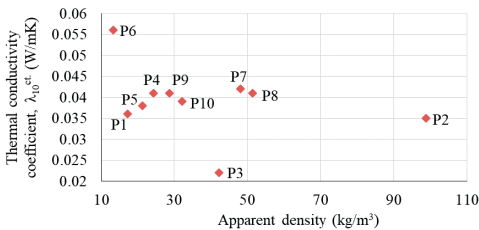


Figure 5. Variation of the thermal conductivity coefficient according to apparent density

Regarding the resistance of materials to the action of molds, significant differences are observed among the species used, influenced by several factors. On one hand, the testing methodology applies different levels of stress on the material. Variant 1 represents a moderate demand method, with a reduced mold spore load, characteristic of a high humidity environment. In contrast, test variant 2 subjects the material to high stress, with the mold spore load significantly increased, by artificial means. On the other hand, the type of material, its nature, and the characteristics of the raw material greatly influence resistance to mold action. Consequently, as shown in Table 4, the heat-insulating materials studied were identified as either belonging to the category that does not provide a nutritious environment

for microorganisms (being inert or fungistatic), such as P2 (mineral wool), P5 (acetate-cellulosic material from cigarette filter manufacturing waste), P6 (non-woven sheep wool mattress), or materials that contain few nutrients or are so minimally contaminated that they only permit very limited mold development under high humidity conditions, like P1 (expanded polystyrene), P3 (polyurethane foam), P4 (wood fibers), P7 (cellulose acetate material from cardboard waste), P8 (silicone paper-type printing waste), P9 (polyethylene film-type printing waste), and P10 (aluminized polyethylene foil-type printing waste).

Table 4. Codification and characterization of thermal insulation materials

Sample code	Fungal growth evaluation (Class)	Product Performance Estimation (Category)
P1	1	1
P2	0	0
P3	1+	1
P4	1+	1
P5	0	0
P6	0	0
P7	1+	1
P8	1	1
P9	1	1
P10	1	1
Note: The "+" sign indicates cases where, although signs of mold existence and growth are not visible to the naked eye, they are more intense/numerous upon microscopic evaluation compared to the density and intensity of samples classified in class 1, without, however, meeting the criteria for classification in class 2 (visible to the naked eye).		

However, it should be noted that while materials P3, P4, and P7 do not meet the criteria to be classified as materials resistant to microorganism attacks (as they contain nutrients that facilitate their development), visible signs of mold appearance and growth cannot be identified through visual examination without magnification. Nevertheless, upon microscopic evaluation, these signs are present either in higher numbers or show more intense development of punctate colonies compared to other materials in the same category. In terms of material resistance in environments heavily contaminated with mold spores, as observed in test Variant 2 (Figures 6-8), specific observations were made for each type of material and mold species. For instance, in cases of contamination with *Penicillium notatum*, mold development was observed on the PDA nutrient substrate after 2 days of exposure, confirming the viability of the

inoculum. Additionally, localized mold areas were identified on some analyzed materials, specifically on the surface of expanded polystyrene granules (P1) and on the edges of the mineral wool sample (P2). More intense signs of mold growth were seen on wood fibers (P4), cellulose acetate threads from cigarette filter manufacturing waste (P5), and cellulosic thermal insulation samples from cardboard waste (P7), with the fibers showing heavier microbiological formations, though these could not be identified without optical magnification. The samples of polyurethane foam (P3), sheep's wool (P6), siliconized paper waste (P8), polyethylene film waste (P9), and aluminized polyethylene film (P10) displayed no signs of contamination. The process of mold colonization and development continued over the 14 days of testing; some samples, like those from cellulosic cardboard waste, ended up being completely covered, while others had 50% - 75% of their surface covered by biofilm (mineral wool, siliconized paper waste, polypropylene foil waste, and aluminized polyethylene foil waste). However, no signs of mold growth were observed on the surface of expanded polystyrene, polyurethane foam, and sheep wool fibers except, perhaps, under microscopic analysis as shown in Figure 6. It's noteworthy that expanded polystyrene, polyurethane foam, and sheep wool fibers exhibited no signs of mold growth on their surfaces.

An interesting observation made during the tests involved expanded polystyrene (P1): initially, after 2 days of exposure in the contaminated environment, slight signs of *Penicillium notatum* mold anchoring were observed on the surface of the polystyrene granules (Figure 7a). However, its growth halted (Figure 7b), indicating that the expanded polystyrene substrate does not support further growth.

The resistance of materials to inoculation with *Aspergillus niger* showed better resilience, at least during the first two days of exposure, with no microscopic signs of mold growth on the surface/fibers/granules of any material. At this stage, signs of mold growth were only identified on the surface of the PDA nutrient substrate, confirming the spore viability.

After 14 days of exposure in a heavily contaminated environment, as shown in Figure 8, the presence of *Aspergillus niger* mold was observed in most of the tested materials. Exceptions, which did not show the

development of this type of mold even after 14 days of contamination, include the polyurethane foam (P3) and the sheep wool mattress (P6).

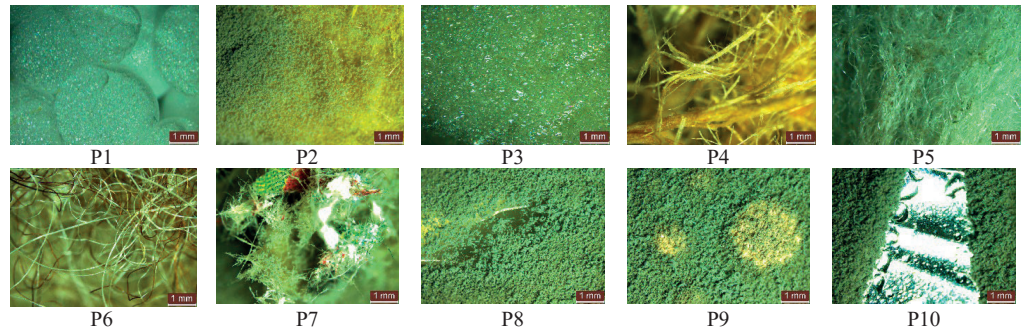


Figure 6. The appearance of the samples exposed in an environment contaminated with *Penicillium notatum* spores, after 14 days of exposure

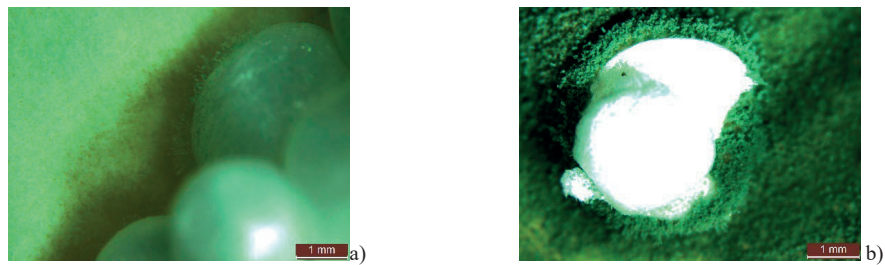


Figure 7. Appearance of the expanded polystyrene sample exposed in an environment contaminated with *Penicillium notatum* spores: a) after 2 days of exposure; b) after 6 days of exposure

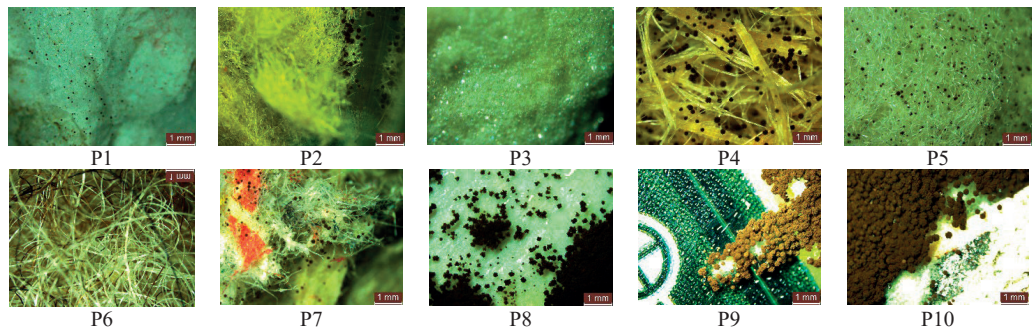


Figure 8. The appearance of the samples exposed in an environment contaminated with *Aspergillus niger* spores, after 14 days of exposure

On the surface of the expanded polystyrene (P1), only a few signs of growth could be identified. The observed differences in the development of biological contamination led to the identification of two distinct behaviors. Thus, on the mineral wool (P2) and the waste

from the printing industry (P8-P10), localized mold colonies were recorded. In contrast, on the heat-insulating materials with a more fibrous structure, such as chopped wood fibers (P4), waste from cellulose acetate used in the manufacture of cigarette filters (P5), and

cardboard waste (P7), mold distribution was relatively even throughout the material, showing good anchorage on the fibers. Based on these experimental results, it is evident that a comprehensive and complex characterization of the analyzed materials can be achieved (Figure 9). This characterization can be extended to a wide range of other

materials intended for thermal insulation of buildings or for protection against other types of potentially contaminating microorganisms. It allows for an analysis that acknowledges the resistance of the analyzed materials to mold action depends both on the material's nature and the exposure conditions.

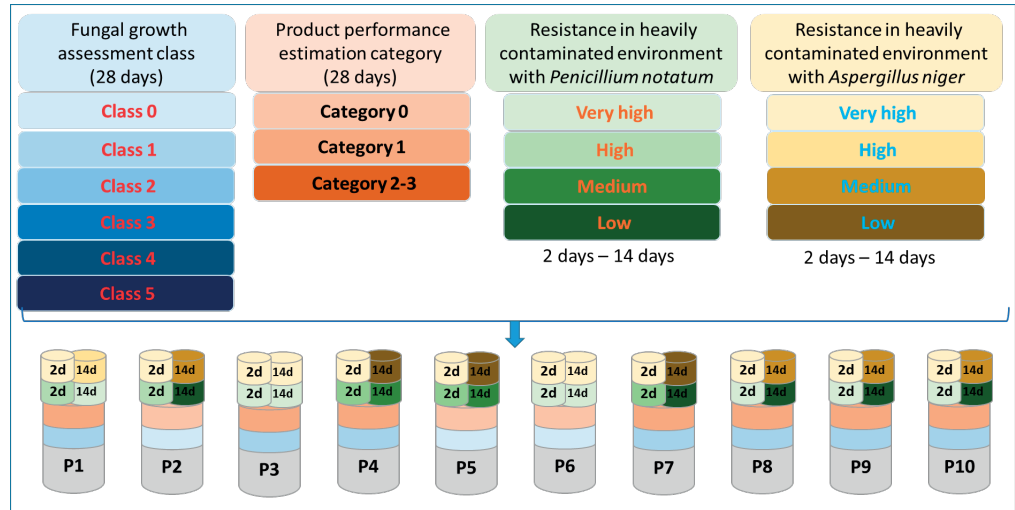


Figure 9. Characterization of materials from the point of view of resistance to the action of mold in an environment with high humidity and in an environment heavily contaminated with spores of *Penicillium notatum*/*Aspergillus niger*

There are cases where the same type of thermal insulation material exhibits good resistance in a humid environment but performs less satisfactorily in an environment heavily contaminated with mold spores, as with mineral wool insulation. Conversely, materials like expanded polystyrene and polyurethane foam, although highly resistant to mold action, are known to restrict "wall breathing" due to their particularly low permeability to water vapor and are also not biodegradable. This can have a less desirable effect on indoor air quality and environmental impact.

A similarly complex situation arises with sheep's wool insulation, which is permeable to water vapor and resistant to mold but has disadvantages in terms of a higher thermal transfer coefficient, indicating lower thermal insulation performance and also has restrictions in order to assure a proper installation method. Regarding thermal insulation materials made from recycled waste, it appears that waste from the cigarette filter manufacturing process

presents the most favorable option, providing an overall less conducive environment for mold development. This is also true for wood fiber waste, which ensures reasonable thermal insulation efficiency.

CONCLUSIONS

The aim of this paper was to analyze the performance and behavior of certain "niche" thermal insulation materials available in the construction market, derived from waste raw materials, in comparison to "classic" thermal insulation materials. The analysis focused on compatibility with their intended use, behavior under humid conditions, and resistance to the risk of mold appearance and development. Based on the research findings, the following conclusions can be drawn:

- From the point of view of the compatibility with intended field of use, all analyzed materials demonstrated thermal conductivity coefficients that classify them as

having thermal insulating properties. It is recognized that their use can significantly contribute to reducing energy consumption by ensuring thermal comfort indoors.

- From the point of view of the behavior in direct contact with liquid water, among the four types of materials tested (those with defined shapes), a notable performance of expanded polystyrene and polyurethane foam was observed due to their granular or closed-cell structure. Conversely, thermal insulation made from animal fibers, such as sheep's wool, exhibited high water absorption due to the organic nature of the fibers. Therefore, special conditions for installation and use are necessary for thermal insulation of animal origin.

- The impact on indoor air quality from the point of view of the ability to regulate air humidity, it has been proven that the materials with an undefined shape (in bulk) analyzed materials possess a capacity for atmospheric humidity sorption and desorption, thus regulating indoor humidity. However, during the desorption process, some of the adsorbed water remains as residual moisture in the material, potentially creating an environment that allows microorganism growth.

- From the point of view of the impact on indoor air quality regarding microorganism contamination, the analysis of mold risk and resistance to mold attacks revealed a generally low risk of mold appearance under high humidity conditions, with mineral wool and sheep's wool insulation showing the best performance. However, when exposed to environments heavily contaminated with mold spores, such as *Penicillium notatum* and *Aspergillus niger*, the resistance of the same insulation materials may vary. For example, mineral wool may perform well in a humid environment but less so in one heavily contaminated with mold spores. Similarly, sheep's wool insulation, while resistant to mold, is highly sensitive to liquid water and has a higher heat transfer coefficient.

Considering all factors for "niche" thermal insulation materials, it is concluded that, regardless of the raw material's nature, antifungal treatment and a proper installation technique are necessary. The antifungal treatment ensures the minimization of microorganism development and, consequently,

a reduction in the negative impact on air quality and public health. Similarly, the use of a properly designed installation method would limit the transfer of air and moisture through the thermal insulation layer, assuring the longevity and effectiveness of the insulation. Proper installation techniques, adapted to the specific characteristics and vulnerabilities of each material, can significantly enhance the material's resistance to environmental stressors, including liquid water, air moisture and thermal cycling. This approach not only maximizes the thermal performance of the insulation but also its durability, contributing to the overall energy efficiency and indoor comfort of buildings. Furthermore, by ensuring that these materials are less susceptible to mold growth, the risk of structural damage and the deterioration of indoor environmental quality over time are greatly reduced. This approach of material selection, correlated with the building design, antifungal treatment, and correct installation practices, forms a comprehensive strategy for improving building sustainability and occupant health, aligning with the broader goals of reducing energy consumption and minimizing the environmental footprint of construction practices.

ACKNOWLEDGEMENTS

This research was conducted with the support of the Technical University of Cluj-Napoca, Faculty of Materials and Environmental Engineering. Undergraduate and master's students contributed to the experimental program as part of their bachelor's thesis and dissertation projects. This research was funded by the Romanian Government Ministry of Research Innovation and Digitization, project No. PN 23 35 02 01 "Synergies of innovation and digitalization in the design of eco materials and multifunctional products for sustainable constructions, with an impact on the environment and the circular economy".

REFERENCES

- Ahlberg, J., Georges, E. & Norlén, M. (2014). The potential of hemp buildings in different climates. A comparison between a common passive house and the hempcrete building system, *Bachelor Thesis, UPPSALA University, Sweden*, 59.

- Andersen, B., Frisvad, J.C., Søndergaard, I., Rasmussen, S. & Larsen, L.S. (2011). Associations between Fungal Species and Water-Damaged Building Materials. *Appl. Environ. Microbiol.*, 77, 4180–4188.
- Bode, F., Simion, A., Anghel, I., Sandu, M., & Banyai, D. (2023). Enhancing Fire Safety: Real-Scale Experimental Analysis of External Thermal Insulation Composite System Façades' Behavior in Fire. *Fire*, 6(12), 451.
- Cherecheș, M.L., Cherecheș, N.C., Ciobanu, A.A., Hudîșteanu, S.V., Țurcanu, E.F., Bradu, A. & Popovici, C.G. (2021). Experimental Study on Airflow and Temperature Predicting in a Double Skin Façade in Hot and Cold Seasons in Romania. *Applied Sciences*, 11(24), 12139.
- Ciobanu, A.A., & Puscasu, I. (2013). Towards low energy building using vacuum insulation panels. Advantages and disadvantages. *Constructii*, 14(2), 56.
- Csanády, D., Fenyvesi, O. & Nagy, B. (2021). Heat Transfer in Straw-Based Thermal Insulating Materials. *Materials* 14, 4408, <https://doi.org/10.3390/ma14164408>.
- Curling, S.F., Loxton, C. & Ormondroyd, G.A. (2012). A rapid method for investigating the absorption of formaldehyde from air by wool. *Journal of Materials Science*, 47(7), 3248–3251.
- Dai, X., Qi, Y., Luo, H., He, Z., Wei, L., Dong, X. & Li, Y. (2022). Leachability and Anti-Mold Efficiency of Nanosilver on Poplar Wood Surface. *Polymers*, 14(5), 884.
- Day, M., Suprunchuk, T. & Wiles, D.M. (1981). The fire properties of cellulose insulation, *J. Build. Phys.*, 4, 157e170, <http://dx.doi.org/10.1177/109719638100400301>
- Dodoo, A., Gustavsson, L. & Sathre, R. (2011). Building energy-efficiency standards in a lifecycle primary energy perspective. *Energy Build*, 43, 1589–97.
- Haleem Khan, A.A. & Mohan Karuppaiyl, S. (2012). Fungal pollution of indoor environments and its management. *Saudi. J. Biol. Sci.*, 19, 405–426.
- Herrera, J. (2005) Assessment of fungal growth on sodium polyborate-treated cellulose insulation, *J. Occup. Environ. Hyg.*, 2, 626e632, <http://dx.doi.org/10.1080/15459620500377667>.
- Hope, J. (2013). A Review of the Mechanism of Injury and Treatment Approaches for Illness Resulting from Exposure to Water-Damaged Buildings, Mold, and Mycotoxins. *Sci. World J.*, 767482.
- Kušnerová, M., Palková, Z., Valíček, J., Harničárová, M., Ionitecu, S. (2018). Heat penetration parameters of newly proposed thermal insulating concretes from the viewpoint of power consumption and environmental impacts. *Scientific Papers. Series E. Land Reclamation, Earth Observation & Surveying, Environmental Engineering*, VII, 37-40, Print ISSN 2285-6064.
- Liu, M., Zhong, H., Ma, E., & Liu, R. (2018) Resistance to fungal decay of paraffin wax emulsion/copper azole compound system treated wood. *International Biodeterioration & Biodegradation*, 129, 61-66.
- Mansour, E., Curling, S., Stéphan, A., Ormondroyd, G. (2016), *Green Mater.* 4(1), 1-7.
- Maskell, D., da Silva, C.F., Mower, K., Rana, C., Dengel, A., Ball, R.J., Ansell, M.P., Walker, P.J. & Shea, A. (2015). Properties of bio-based insulation materials and their potential impact on indoor air quality. *AJCE*, 33(2), 156–163.
- Mølhave, L., Clausen, G., Berglund, B., Ceaurriz, J.D., Kettrup, A., Lindvall, T. & Younes, M. (1997). Total volatile organic 348 compounds (TVOC) in indoor air quality investigations. *Indoor Air*, 7(4), 225–240.
- Papoutsis, K., Mathioudakis, M. M., Hasperuë, J. H. & Ziogas, V. (2019). Non-chemical treatments for preventing the postharvest fungal rotting of citrus caused by *Penicillium digitatum* (green mold) and *Penicillium italicum* (blue mold). *Trends in Food Science & Technology*, 86, 479-491.
- Ricciu, R., Besalduch, L.A., Galatioto, A. & Ciulla, G. (2018). Thermal characterization of insulating materials, *Renewable and Sustainable Energy Reviews*, 82(2), 1765-1773.
- Rode, C. (1998). Organic insulation materials, the effect on indoor humidity, and the necessity of a vapor barrier, *Proceed. Therm. Perform. Exterior Envelope Build.*, VII, 109e121.
- Salthammer T., Mentese S. & Marutzky R. (2010), Formaldehyde in the Indoor Environment, *Chem. Rev.*, 110(4), 2536-2572.
- Sandberg, P.I. (1992). Determination of the effects of moisture content on the thermal transmissivity of cellulose fiber loose-fill insulation, in: Thermal Performance of the Exterior Envelopes of Building III, *ASHRAE/DOE/BTECC/CIBSE Conference* 517e25.
- Simion, A., Dobre, D., Dragomir, C.S. & Anghel, I. (2019). Fire Performance of the Thermo Insulant Facade Systems of the Buildings. In *IOP Conference Series: Materials Science and Engineering*, 603(20, p. 022021). IOP Publishing.
- Stevulova, N., Cigasova, J., Sicakova, A. & Junak J. (2013). Lightweight Composites Based on Rapidly Renewable Natural Resource. *Chemical Engineering Transactions*, 35, 589-594.
- Takeda M., Saijo Y., Yuasa M., Kanazawa A., Araki A., Kishi R. (2009). Int. Arch. Occup. Environ. Health 82, 583.
- Talukdar, P., Osanyintola, O.F., Olutimayin, S.O., Simonson, C.J. (2007). An experimental data set for benchmarking 1-D, transient heat and moisture transfer models of hygroscopic building materials. *Part II: Experimental, numerical and analytical data*, *Int. J. Heat Mass Transf.*, 50, 4915e4926.
- Thieblisson, L.M., Calotă, R., Saca, N., Simion, A., Năstase, I. & Girip, A. (2024). Reaction to fire, thermal, and mechanical properties of materials based on recycled paper granules bound with starch and clay mortar. *Heliyon*.
- Vėjelienė, J., Gailius, A., Vėjelis, S., Vaitkus, S. & Balčiūnas, G. (2011). Evaluation of Structure Influence on Thermal Conductivity of Thermal Insulating Materials from Renewable Resources, *Materials Science (Medžiagotyra)*, 17(2), 208-212.
- Vėjelis, S., Gnipas, I. & Ker_sulis V. (2006). Performance of loose-fill cellulose insulation, *Mater. Sci.*, (MED_ZIAGOTYRA) 12.

- Vrana, K. & Gudmundsson, K. (2010). Comparison of fibrous insulations e cellulose and stone wool in terms of moisture properties resulting from condensation and ice formation, *Constr. Build. Mater.* 24 1151e1157, <http://dx.doi.org/10.1016/j.conbuildmat.2009.12.026>.
- Zach, J., Hroudová, J., Brožovský, J., Krejza, Z. & Gailius, A. (2013). Development of thermal insulating materials on a natural base for thermal insulation systems. *Procedia Engineering*, 57, 1288-1294.
- Zukiewicz-Sobczak, W., Sobczak, P., Krasowska, E., Zwolinski, J., Chmielewska-Badora, J. & Galinska, E.M. (2013). Allergenic potential of moulds isolated from buildings. *Ann. Agric. Environ. Med.*, 20, 500–503.

ANALYTICAL FRAMEWORK ORIENTED TOWARDS ENVIRONMENTAL TRIGGERS IN EUROPEAN GREAT CITIES

Stefan-Mihai PETREA^{1,2,4}, Ira-Adeline SIMIONOV^{1,2,5}, Alina ANTACHE^{1,2,6}, Aurelia NICA¹, Maxim ARSENI^{2,3}, Adrian ROSU^{2,3}, Dragos CRISTEA⁴, Catalina ITICESCU^{2,3}

¹"Dunarea de Jos" University of Galati, Food Science and Engineering Faculty,
111 Domneasca Street, Galati, Romania

²"Dunarea de Jos" University of Galati, REXDAN Research Infrastructure,
98 George Cosbuc Street, Galati, Romania

³"Dunărea de Jos" University of Galati, Faculty of Sciences and Environment,
111 Domneasca Street, Galati, Romania

⁴"Dunărea de Jos" University of Galati, Faculty of Economics and Business Administration,
59-61 Nicolae Balcescu Street, Galati, Romania

⁵"Dunărea de Jos" University of Galati, Faculty of Automatic Control, Computers, Electrical
Engineering and Electronics, 2 Stiintei Street, Galati, Romania

⁶"Alexandru Ioan Cuza" University of Iasi, 11 Carol I Blvd, Iasi, Romania

Corresponding author email: stefan.petrea@ugal.ro

Abstract

The paper aims to develop a comparative and integrated analytical framework (CIAF) that will ensure an in-depth understanding of environmental triggers in Western (W) vs Eastern (E) Great Cities (GC) of the European Union (EU). Parameters corresponding to both environmental (EVD) and economic (ECD) dimensions were selected for each of the first 10 EU WGC and EGC, respectively. The EVD considers the impact of PM2.5. exposure, as well as municipal waste generation and days of strong heat stress, while the ECD considers the GDP, labour productivity, as well as unemployment rate, all connected to the demographical dynamics of the analysed urban areas. A machine-learning methodology, consisting of MLR and XGBoost algorithms, is used for the development of the CIAF. The results indicate significant peculiarities between both WGC and EGC and reveal high accuracy (>85%) in various prediction scenarios. The findings can be used as a basis for the future development of complex decision-support tools, tackling to optimize the environmental management in EU GC.

Key words: environmental triggers, machine learning, great cities, PM2.5, municipal waste.

INTRODUCTION

According to Cristea et al. (2022), environmental triggers and challenges extend their impact on economic and environmental dimensions. Also, Nuță et al. (2021) revealed that industrialization and intensive urbanisation can lead to environmental degradation, thus, affecting the environmental sustainability desideratum. However, the conclusion of the above-mentioned study reveals the hypothesis stating that urbanization may damage the environment only at the early stages, followed by beneficial effects further on.

A previous study (Cristea et al., 2022) emphasizes the peculiarities of various geopolitical blocks (BRICS vs. G7 vs. EU) and geographical regions related to environmental

strategies and triggers. Rapid urban industrialization, transport agglomeration or intensive consumption behaviour can be considered human activity triggers, according to Simionov et al. (2019), that can alter environmental status in terms of water pollution with various contaminants of emerging concern (e.g. microplastics, pharmaceutical compounds) or priority pollutants (e.g. heavy metals) and can increase the air pollution (e.g. increase the concentrations of PM 2.5) according to Andrei et al. (2024), CO₂ emissions according to Nuță et al. (2021) and GHG according to Cristea et al. (2022). Also, Andrei et al. (2024) report a significant correlation between particulate pollution and welfare features in urban areas. According to Petrea et al. (2022), the process of measuring sustainable development at an

aggregate level, requires a broad integration of indicators from various dimensions as economic, environmental, as well as social dimensions, since a symbiotic nexus between these dimensions is required to ensure the long-term development peculiarity.

Economic growth and technological development are revealed by indicators such as labour productivity and unemployment rate, while pollution intensity in urban areas can be estimated by considering air pollution and waste generation, considering the general background of stressors and pressures that create favourable conditions for climate change intensification.

Therefore, an integrated analytical framework that quantifies parameters from both economic and environmental dimensions, considering, at the same time, the climate change impact, can reveal innovative insides related to the conditionalities and relations between the parameters of both dimensions, including climate change.

However, considering that various regions have specific peculiarities possibly generated by their culture, political framework, habits, as well as industrial and technological development background, a comparative study between these regions, in order to identify various triggers that can have significant importance in environmental development strategy, is required.

Thus, the present study aims to develop a comparative and integrated analytical framework (CIAF), based on machine learning algorithms, that will ensure an in-depth understanding of environmental triggers in Western-Central (WC) vs Eastern (E) Great Cities (GC) of the European Union (EU), based the urbanization degree, considering various parameters related to both environment and economical dimensions.

MATERIALS AND METHODS

Data collection and dataset description

The dataset used for training and validation of the resulting models within the present study is structured, as follows:

- Environmental dimension:
 - PM2.5 [$\mu\text{g}/\text{m}^3$], source: www.iqair.com;
 - municipal waste generation (MWG), source: Eurostat.
 - days of strong heat stress (DHS) [no. of days], source: OECD, Eurostat.

- Economic dimension

- GDP, source: OECD, Eurostat.
- labour productivity (LP), source: OECD, Eurostat.
- unemployment rate (UR), source: OECD, Eurostat.

The dataset consists of 63 inputs, no null values, corresponding to both the WCGC and EGC groups. Each of the groups consists of 7 great cities, that were selected considering their geographical position, as well as their urbanization degree and data availability for a 9 years-period. Thus, the WCGC group covers data from Berlin (DE), Rome (IT), Paris (FR), Hamburg (DE), Munich (DE), Milan (IT), and Köln (DE), while the EGC group covers data from Warsaw (PL), Budapest (HU), Sofia (BUL), Krakow (PL), Zagreb (CRO), Wroclaw (PL), Lodz (PL).

Machine learning data-processing methods and workflow

The workflow used in the present study for data processing in order to develop the comparative and integrated analytical framework (CIAF) is presented in Figure 1. Thus, three machine learning-based supervised algorithms were used, namely the multiple linear regression (MLR), XGBoost (XGB) and Random Forest (RF), in order to generate high-metrics predictions for each of the analysed parameters, part of both dimensions. The workflow implies data preparation (a range between 70-80% of the data used for training the models, while the rest of 20-30% is used for validation purposes). This database pre-processing is described by Petrea et al. (2023), while the predictor's standardization was performed as presented by Petrea et al. (2020).



Figure 1. The workflow for CIAF development

The MLR model equation is presented below (eq. 1), according to Petrea et al. (2023):

$$y_{predict} = a_1x_1 + a_2x_2 + \dots + a_nx_n + b + \epsilon \quad (1)$$

where:

- $y_{predict}$ is the dependent variable;
- x_1, x_2, \dots, x_n are the n independent variables (predictors);
- b is the intercept indicating the Y value when all the predictors are zeros;
- a_1, a_2, \dots, a_n are the coefficients of predictors, reflecting the contribution of each independent variable in predicting the dependent variable;
- ϵ is the residual term indicating the difference between the actual and the fitted response value.

According to previous publication (Chen and Guestrin, 2016), the XGBoost model has a core idea to fit and learn the residuals of the previous tree, with the final prediction result being the sum of the effects of all regression trees (eq. 2).

$$Obj = \sum_{i=1}^n l(y_i - \hat{y}_i) + \sum_{k=1}^K \Omega(f_k) \quad (2)$$

where:

- y_i is the measured value;
- \hat{y}_i is the predicted value of each tree; l is the loss function, which is used to measure the total prediction error;
- $\sum \Omega(f_k)$ is the regularization term.

The Random Forest algorithm is presented in eq. 3.

$$RFfi_i = \frac{\sum_{j \in \text{all trees}} normfi_{ij}}{T} \quad (3)$$

where:

- T is the total number of trees;
- $normfi_{ij}$ is the normalized future importance for i in tree j ;
- $RFfi_i$ is the feature i importance, calculated from all the trees in the RF model.

RESULTS AND DISCUSSIONS

MLR models

Considering the WCGC group, it can be observed that the MLR model for predicting the DHS, considering only the environmental dimension, records values of VIF that do not exceed 10, meaning that all parameters are considered suitable to be used as predictors

(Figure 2). The accuracy metrics of the model, presented in eq. 4 record the following values: R-sq 0.54, R-adj 0.53, RMSE 17.30 (Figure 3). It can be concluded that PM 2.5 parameter has the highest influence when predicting the DHS in the case of WCGC. Thus, intensive industrial activity and urbanization, considered triggers of PM2.5. in the great cities, have an immediate impact on climate change, manifested by the increase in the number of days that record temperatures of over 32°C.

$$W-C DHS = -14.39 - 0.001 W-C EU - MWG + 3.55 W-C EU PM2.5 \quad (4)$$

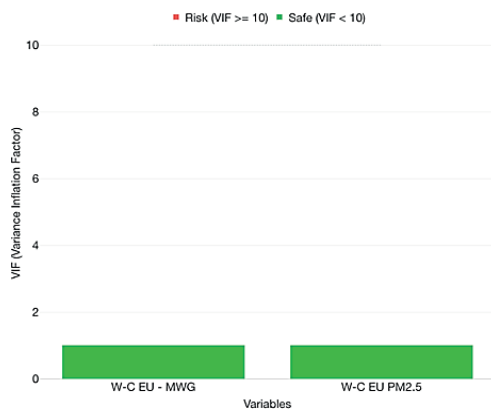


Figure 2. VIF values for the predictors, considering the environmental parameters for W-C DHS prediction

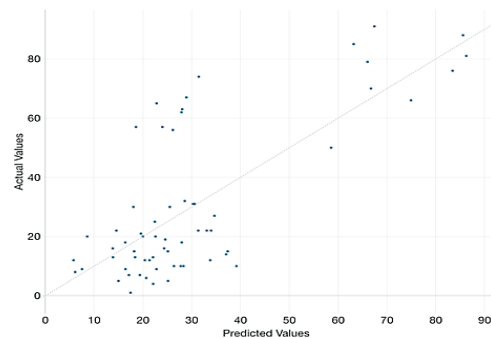


Figure 3. Actual/predicted value for W-C DHS prediction considering the environmental dimension

In the case of EGC group the prediction of DHS model revealed not significant ($p > 0.05$) importance. Thus, the resulting model was considered unfit for the CIAF.

However, the use of economic dimension parameters as predictors in generating the DHS

MLR model, for both WCGC and EGC, is doable. Therefore, the W-C DHS model is presented in eq. 5, while the E DHS model is presented in eq. 6. It can be observed that UR has the main influence in predicting the DHS, a fact valid for both WCGC and EGC. However, the decrease of UR in the WCGC generates an increase in DHS, a fact that may be due to the integration of extra labour in industry and, therefore, the increase of industrial production. The situation is reversed in the case of EGC, emphasizing that although the UR increased, the DHS still records an upward trend, a fact that may be due to the lack of industrial capacity, the labor market being oriented towards other niches with less impact on the environment.

$$W-C DHS = 607.14 - 0.007 W-C EU GDP - 2.907 W-C EU LP - 4.536 W-C EU - UR \quad (5)$$

$$E DHS = 42.69 + 0.002 E EU GDP - 0.407 E EU LP + 1.628 E EU - UR \quad (6)$$

The accuracy metrics of the models, presented in eq. 5 and 6 record the following values: R-sq 0.80, R-adj 0.79, RMSE 11.46 for WCGC (Figure 4) and R-sq 0.56, R-adj 0.53, RMSE 12.01 for EGC (Figure 5).

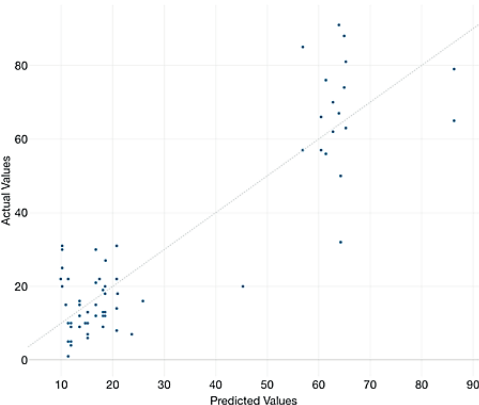


Figure 4. Actual/predicted value for W-C DHS prediction considering the economic dimension

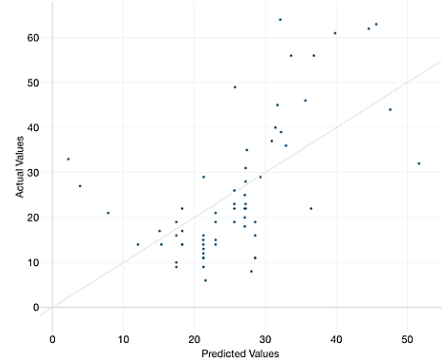


Figure 5. Actual/predicted value for E DHS prediction considering the economic dimension

All predictors were statistically significant ($p < 0.05$) and all VIF values were under 2 (Figure 6) in the case of EGC and under 9 (Figures 7) in the case of WCGC.

When considering the W-C DHS prediction in relation to both economic and environmental parameters (Figure 8), the W-C UR and W-C GDP parameters record VIF values > 10 – thus, these parameters are removed from the framework and the model's training and validation start considering the new formula of predictors. The resulted model is emphasized in eq. 7.



Figure 6. VIF values for the predictors, considering the economic parameters for E DHS prediction

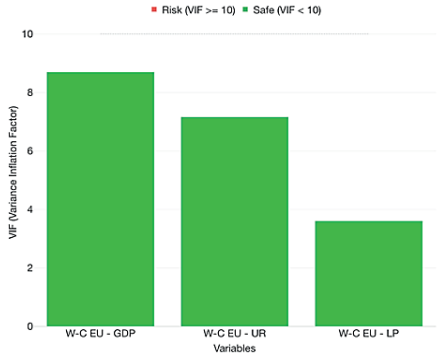


Figure 7. VIF values for the predictors, considering the economic parameters for W-C DHS prediction

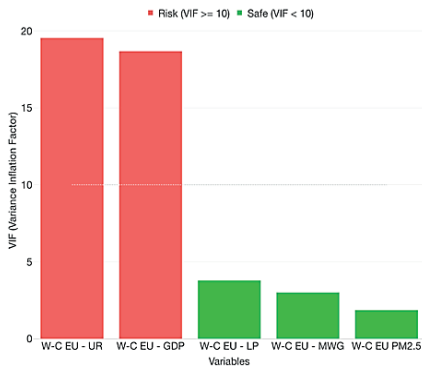


Figure 8. VIF values for the predictors, considering both the economic and environmental parameters for W-C DHS prediction

$$W-C DHS = 614.21 - 5.79 W-C EU LP - 0.004 W-C EU MWG + 1.72 W-C EU PM2.5. \quad (7)$$

The VIF value related to eq. 7 model records values under 2. The accuracy parameters record the following metrics: R-sq 0.80, R-adj 0.79, RMSE 11.38 (Figure 9). All predictors were statistically significant ($p < 0.05$).

The E DHS prediction considering both dimensions (economic and environmental) is emphasized through eq. 8. The values of VIF are under 2 (Figure 10) and all predictors were statistically significant ($p < 0.05$). The model has inferior metrics compared to the WCGC correspondent model, as follows: R-sq 0.57, R-adj 0.52, RMSE 11.94 (Figure 11).

$$E DHS = 28.13 + 0.002 E EU GDP - 0.376 E EU LP + 0.008 E EU MWG + 1.877 E EU - UR + 0.027 E EU PM2.5 \quad (8)$$

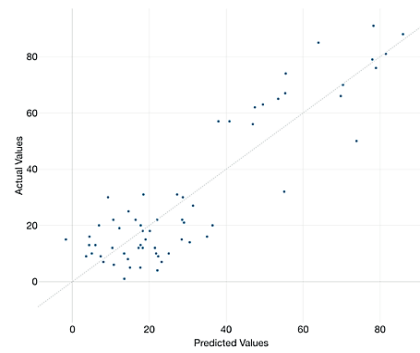


Figure 9. Actual/predicted value for W-C DHS prediction considering both the economic and environmental dimensions

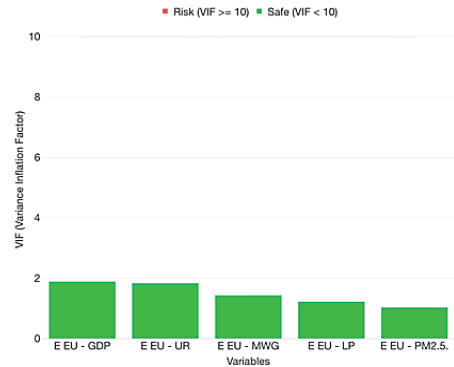


Figure 10. VIF values for the predictors, considering both the economic and environmental parameters for E DHS prediction

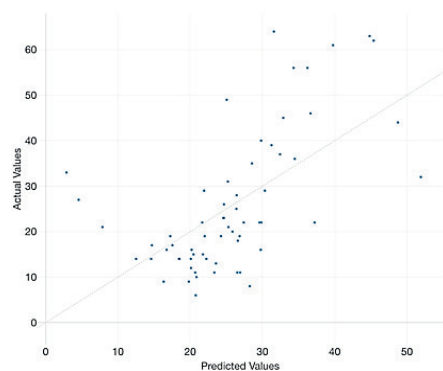


Figure 11. Actual/predicted value for E DHS prediction considering both the economic and environmental dimensions

The PM2.5 prediction, considering the environmental dimension predictors, reveal a not significant model ($p > 0.05$) in the case of EGC, while for WCGC, the model (eq. 9)

confirms the relation between PM2.5 and DHS. The model metrics are as follows: R-sq 0.54, R-adj 0.52, RMSE 3.58 (Figure 12). The VIF values were lower than 10.

$$W-C \text{ EU } PM2.5 = 8.438 + 0.152 \text{ W-C DHS} + 0.00007 \text{ W-C EU -MWG} \quad (9)$$

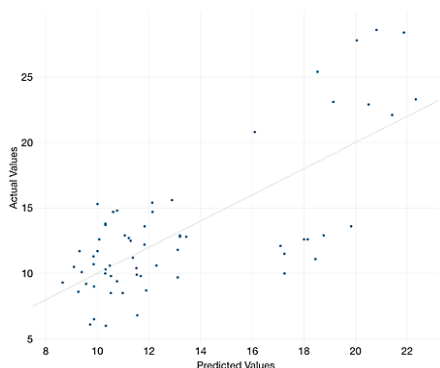


Figure 12. Actual/predicted value for W-C PM 2.5 prediction considering the environmental dimensions

The PM2.5. prediction models considering the economic dimension parameters as predictors were not significant in terms of importance ($p > 0.05$). Thus, this reveals the incapacity of using economic dimension in predicting PM2.5 - however, the number of dataset inputs can be considered a limitation barrier in the process of identifying high accuracy and significant prediction models, considering the above-mentioned background. This situation repeats in when considering the parameters of both dimensions for developing PM2.5 prediction models for EGC and WCGC, as well as in the scenario of developing MWG prediction models considering the environmental dimension parameters as predictors.

The MLR prediction models for MWG that consider the economic dimension parameters as predictors are doable, both in the case of WCGC (eq. 10) and EGC (eq. 11) and emphasize the importance of UR in predicting MWG.

$$W-C \text{ EU } MWG = -15.76 + 0.638 \text{ W-C EU } GDP - 79.89 \text{ W-C EU - LP} + 753.859 \text{ W-C EU -UR} \quad (10)$$

$$E \text{ EU } MWG = 1630.59 - 0.047 \text{ E EU } GDP - 3.641 \text{ E EU - LP} - 28.547 \text{ E EU -UR.} \quad (11)$$

All predictors were statistically significant ($p < 0.05$), except LP in the case of W-C MWG model. All VIF values were under 2 (Figure 13) in the case of EGC and under 9 (Figure 14) in the case of WCGC. The models' accuracy metrics are as follows: Rsq 0.622, Radj 0.600, RMSE 780.26 for W-C MWG and Rsq 0.55, Radj 0.50, RMSE 157.70 for E MWG.



Figure 13. VIF values for the predictors, considering the economic parameters for E MWG prediction

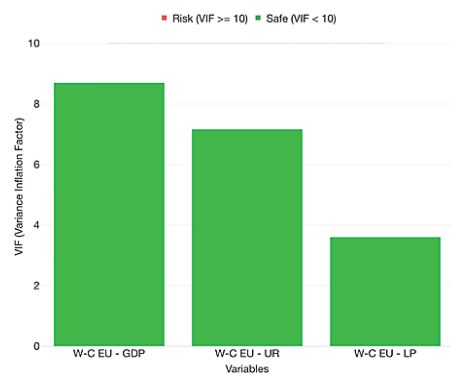


Figure 14. VIF values for the predictors, considering the economic parameters for W-C MWG prediction

If considering all parameters from both dimensions for generating MLR prediction models for W-C MWG and E MWG, it can be observed that in the case of W-C MWG the GDP predictor records a VIF value of 16 (over the limit of 10) and is excluded from the prediction framework. Thus, in terms of statistical significance, in the case of WC MWG the LP and PM2.5 predictors are not significant ($p > 0.05$), while the rest of the predictors are statistically significant ($p < 0.05$). Also, in the case of predicting the E MWG, the predictors

DHS, LP and PM2.5 are statistically not significant ($p>0.05$), while GDP and UR and statistically significant ($p<0.05$). The VIF values are under 4 in the case of WC MWG model (Figure 15), while for E MWG all the VIFs are under 2 (Figure 16).

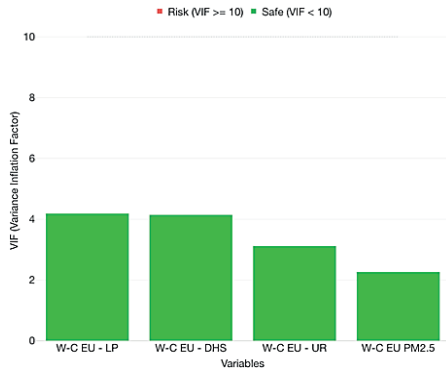


Figure 15. VIF values for the predictors, considering both the economic and environmental parameters for W-C MWG prediction



Figure 16. VIF values for the predictors, considering both the economic and environmental parameters for E-MWG prediction

The prediction of MWG considering all predictors from both dimensions (economic and environmental) reveals LP and UR as main predictors in the case of both WCGC and EGC groups, having the highest weight in predicting the dependent variable. The MWG and LP are in an indirect relation, a fact valid for both groups, while in relation to UR, the predicted variable presents a direct relation for WCGC and an indirect relation for EGC, a situation confirmed also by previous models (eq. 12, 13).

$$W-C \text{ EU } MWG = 11\,867.36 - 44.976 \text{ W-C EU } DHS - 107.036 \text{ W-C EU - LP} + 327.495 \text{ W-C EU UR} - 11.898 \text{ W-C EU PM2.5} \quad (12)$$

$$E \text{ EU } MWG = 1583.27 + 1.480 \text{ E EU - DHS} - 0.050 \text{ E EU - GDP} - 3.010 \text{ E EU - LP} - 0.809 \text{ E EU - PM2.5} - 31.05 \text{ E EU - UR} \quad (13)$$

The models' accuracy metrics are as follows: Rsq 0.513, Radj 0.480, RMSE 885.77 for W-C MWG and Rsq 0.54, Radj 0.50, RMSE 156.64 for E MWG.

The RF and XGB models

The RF and XGB models were applied in predicting each of the environmental dimension parameters, considering the rest of the parameters from both economic and environmental dimensions. A comparative analysis was performed in order to establish which of the algorithms performs better, considering the accuracy metrics associated to the resulted models.

Thus, the XGB model for predicting W-C DHS presents high metrics (Rsq 0.988, RMSE 2.79) and reveals that GDP has the highest feature importance, compared to the rest of the predictors (Figure 17).

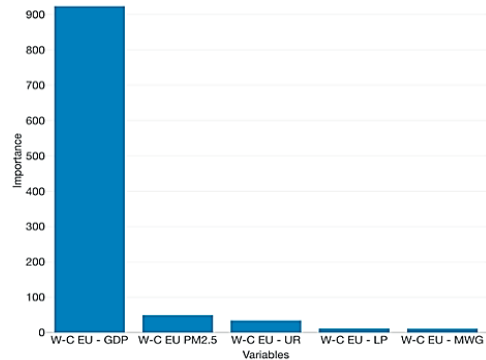


Figure 17. The predictors feature importance when predicting the W-C DHS using the XGB algorithm

This emphasizes the possible impact of economic growth on environmental status, within the WCGC. The RF model reveals that besides GDP, the LP has the highest feature importance (Figure 18), emphasizing a possible conditionality of the economic growth - environmental status relation by the intensity of

the economic activities and, thus, the use of state-of-the-art technologies.

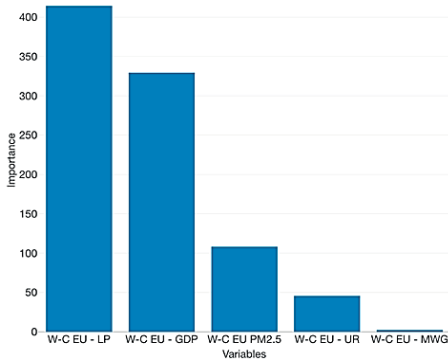


Figure 18. The predictors feature importance when predicting the W-C DHS using the RF algorithm

However, the RF reveals lower accuracy metrics (Rs_q 0.854, RMSE 9.79), compared to XGB. The XGB model for predicting E DHS presents high metrics (Rs_q 0.943, RMSE 44.91) and reveals that UR has the highest feature importance, compared to the rest of the predictors (Figure 19), confirming the results recorded in the MLR models.

This emphasises the low conditionality between the UR and GDP within the EGC, considering, simultaneously, the impact on the environment.

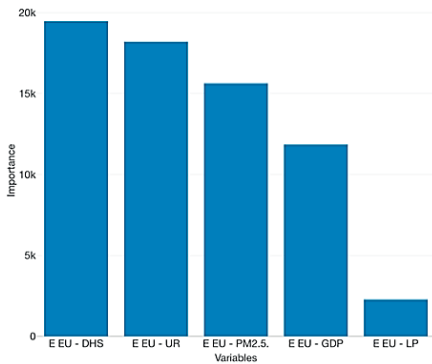


Figure 19. The predictors feature importance when predicting the E DHS using the XGB algorithm

The RF model reveals that E DHS is mostly impacted by LP and, therefore, technological development, in the case of EGC (Figure 20). However, the RF reveals low accuracy metrics (Rs_q 0.58, RMSE 10.88).

The XGB model for predicting W-C PM_{2.5} presents high metrics (Rs_q 0.956, RMSE 1.11)

and reveals that DHS and MWG have the highest feature importance, compared to the rest of the predictors (Figure 21). This emphasises the possible impact of climate change and waste generation on PM_{2.5}. The RF model reveals that besides DHS, the LP has the highest feature importance (Figure 22), thus, confirming the conditionality of the economic growth on environmental status. However, the RF reveals lower accuracy metrics (Rs_q 0.609, RMSE 3.31), compared to the XGBoost W-C PM_{2.5} predictability model.

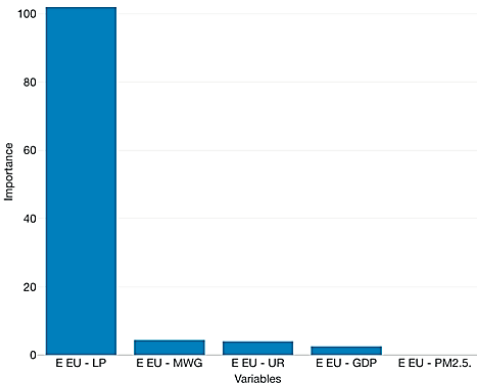


Figure 20. The predictors feature importance when predicting the E DHS using the RF algorithm

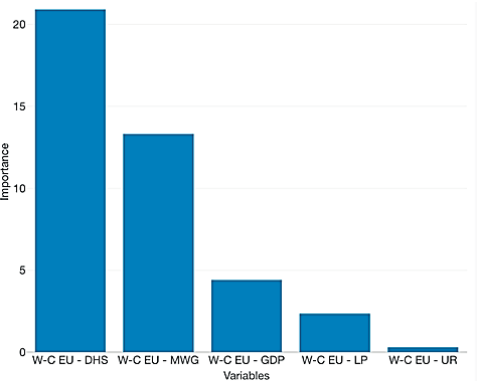


Figure 21. The predictors feature importance when predicting the W-C PM_{2.5} using the XGBoost algorithm

The XGBoost model for E PM_{2.5} (Rs_q 0.853, RMSE 2.08) emphasizes that MWG has the highest feature importance, followed by DHS and GDP, the fact that emphasizes a peculiar problem related to waste management in the eastern bloc, a situation which could be conditioned by the lack of proper legislation or

control in the area of environmental protection (Figure 23).

The E PM2.5 RF model reveals a completely different feature importance ranking among predictors, compared to W-C PM2.5 (Figure 24). Thus, it can be observed (Figure 24) that the first two predictors in terms of feature importance are from the economic dimension (GDP and UR), revealing the conditionality of the economic activities and economic development rate on environmental status and indicating the need to maintain sustainable economic development, limiting the impact on the environment and creating resilience to climate change. However, the RF reveals lower accuracy metrics (Rsqr 0.609, RMSE 3.31), compared to the XGBoost W-C PM2.5 predictability model.

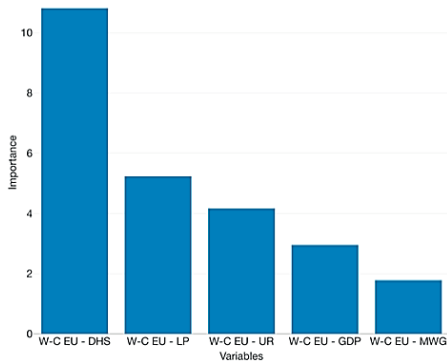


Figure 22. The predictors feature importance when predicting the W-C PM2.5 using the RF algorithm

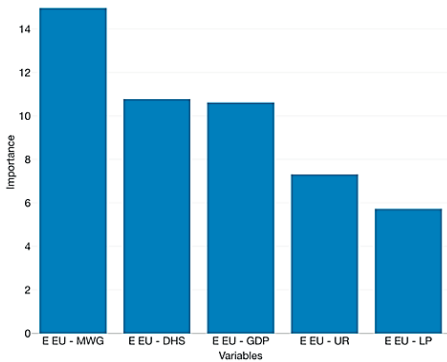


Figure 23. The predictors feature importance when predicting the E PM2.5 using the XGBoost algorithm

The XGB model for predicting W-C MWG presents the best metrics of accuracy from the

present study analytical framework (Rsqr 0.99, RMSE 102.24) and reveals the significant impact of GDP as the main predictor of this model, with the highest feature importance (Figure 25).

The RF model confirms the XGBoost findings (Figure 26) - however, the accuracy metrics are lower (Rsqr 0.75, RMSE 627.02), compared to XGB.

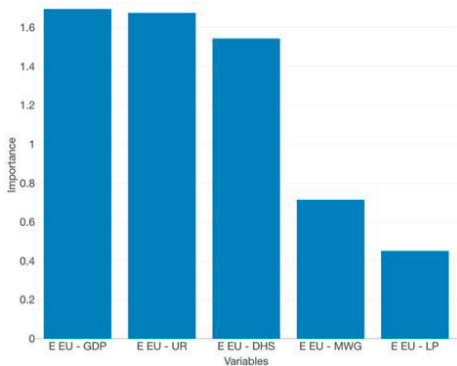


Figure 24. The predictors feature importance when predicting the E PM2.5 using the RF algorithm

The XGB model for predicting E MWG reveals a different framework compared to the one associated with the W-C block (Figure 27). Thus, DHS and UR are the main predictors in terms of the feature importance value. The RF does not perform well in predicting E MWG (Rsqr 0.41, RMSE 145.60) (Figure 28). Thus, even if GDP and PM2.5 are found as predictors with the highest feature importance in determining the E - MWG concentration, their reliability is poor.

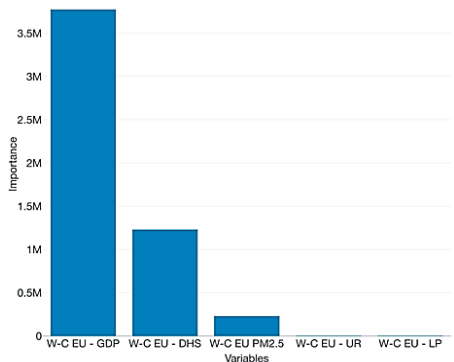


Figure 25. The predictors feature importance when predicting the W-C MWG using the XGBoost algorithm

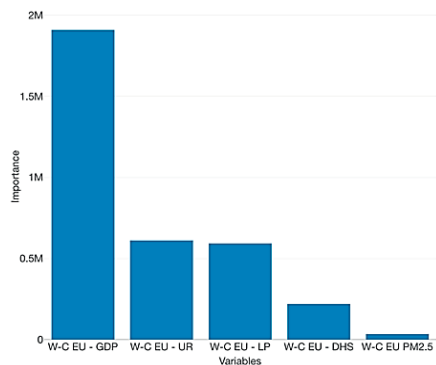


Figure 26. The predictors feature importance when predicting the W-C MWG using the RF algorithm

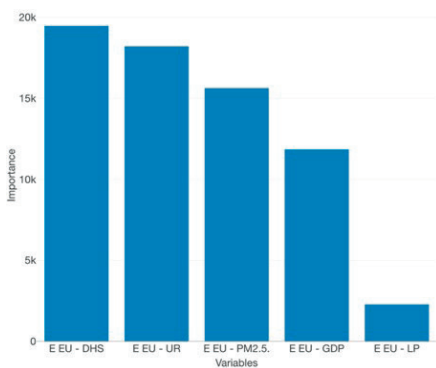


Figure 27. The predictors feature importance when predicting the E MWG using the XGBoost algorithm

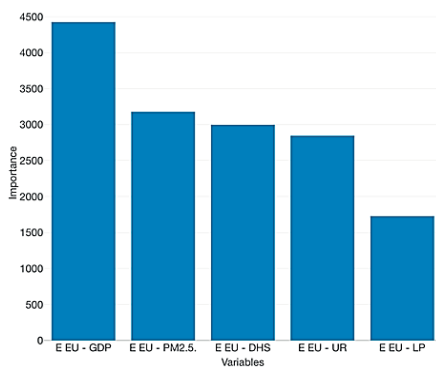


Figure 28. The predictors feature importance when predicting the E MWG using the RF algorithm

Similar to other studies, the present study has also limitations. Thus, firstly, the dataset was conditioned by the existing data – therefore, various GCs from both W-C and E blocks were not included due to the unavailable data. Also, the dataset covers a limited period and limited

parameters that define both dimensions. It is recommended for future studies to extend the dataset to integrate other parameters and, also, to extend the number of dimensions, in order to achieve better ranking in terms of the integrative approach and better understanding in terms of triggers that impact the environmental status.

CONCLUSIONS

The results indicate significant peculiarities between both WGC and EGC and reveal high accuracy (>85%) in various prediction scenarios. The findings can be used as a basis for the future development of complex decision-support tools, tackling to optimize the environmental management in EU GC. The WCGC analytical framework reveals better predictability compared to the EGC.

There is a significant conditionality between the environmental and economic dimensions in both W-C and E GCs. However, it seems that the economic structure and development represent decisive triggers that impact the environmental status. All AI algorithms used for the present study reveal high accuracy metrics – however, it seems that XGB is associated with the best metrics, followed by MLR and RF.

ACKNOWLEDGEMENTS

The present research was supported by the project: "An Integrated System for the Complex Environmental Research and Monitoring in the Danube River Area", REXDAN, SMIS code 127065, co-financed by the European Regional Development Fund through the Competitiveness Operational Programme 2014-2020, contract no. 309/10.07.2021. The present research was supported by the project". Integrated research and sustainable solutions to protect and restore Lower Danube Basin and coastal Black Sea ecosystems, (ResPonSE)", 760010/30.12.2022, component C9. PRIVATE SECTOR SUPPORT, RESEARCH, DEVELOPMENT AND INNOVATION, Investment "I5. Establishment and operationalization of Competence Centers". (specific project no.1 - Decision Support Solutions based on mathematical modeling, for complex ecological systems – CESMoSS).

REFERENCES

- Andrei, J. V., Cristea, D. S., Nuță, F. M., Petrea, Șt. M., Nuță, A. C., Tiron-Tudor, A. & Chivu, L. (2024). Exploring the causal relationship between PM 2.5 air pollution and urban areas economic welfare and social-wellbeing: Evidence from 15 European capitals. *Sustainable Development – Wiley*, <https://doi.org/10.1002/sd.2920>.
- Chen, T., Guestrin, C. & Boost, X.G. (2016). A Scalable Tree Boosting System. In *Proceedings of the 22nd ACM SIGKDD International Conference on Knowledge Discovery and Data Mining (KDD '16)*; Association for Computing Machinery: New York, NY, USA, pp. 785–794.
- Cristea, D.S., Zamfir, C.G., Simionov, I.A., Fortea, C., Ionescu, R.V., Zlati, M.L., Antohi, V.M., Munteanu, D. & Petrea, S.M. (2022). Renewable energy strategy analysis in relation to environmental pollution for BRICS, G7, and EU countries by using a machine learning framework and panel data analysis. *Front. Environ. Sci.*, *10*, 1005806. doi: 10.3389/fenvs.2022.1005806.
- Nuță, F.M., Nuță, A.C., Zamfir, C.G., Petrea, S.M., Munteanu, D., & Cristea, D.S. (2021). National Carbon Accounting-Analyzing the Impact of Urbanization and Energy-Related Factors upon CO₂ Emissions in Central–Eastern European Countries by Using Machine Learning Algorithms and Panel Data Analysis. *Energies*, *14*, 2775. <https://doi.org/10.3390/en14102775>
- Petrea, Ș.M., Cristea, D.S.; Rahoveanu, T.; Zamfir M.M., C.G., Zugravu A., Nancu G.A. (2020). Perspectives of the Moldavian Agricultural Sector by Using a Custom-Developed Analytical Framework. *Sustainability*, *12*, 4671. <https://doi.org/10.3390/su12114671>
- Petrea, Ș. -M., Simionov, I. A., Antache, A., Cristea D. S., Nica, A. & Cristea V. (2023). Analytical framework for the development of water quality virtual sensors in integrated aquaculture systems based on various aquaponics techniques. *IEEE 28th International Conference on Emerging Technologies and Factory Automation (ETFA)*, Sinaia, Romania, pp. 1-5. doi: 10.1109/ETFA54631.2023.10275350.
- Petrea, Ș.M., Costache, M., Cristea, D.S., Strungaru, A., Simionov, I.A., Mogodan, A. et al. (2020). A Machine Learning Approach in Analyzing Bioaccumulation of Heavy Metals in Turbot Tissues. *Molecules*, *25*, 4696.
- Simionov, I.A., Cristea, V., Petrea, S.M., Bocioc Sirbu, E. (2019). Evaluation of heavy metals concentration dynamics in fish from the Black Sea Coastal area: an overview. *Environmental Engineering and Management Journal*, *18*, 5, 1097-1110 <http://www.eemj.icpm.tuiasi.ro/>; <http://www.eemj.eu>

NEW POSSIBILITIES OF USING THE ASH RESULTING FROM THE ENERGY RECOVERY OF POULTRY LITTER WITHIN THE CIRCULAR ECONOMY CONCEPT

Luminita Georgeta POPESCU¹, Roxana Gabriela POPA¹, Lucica ANGHELESCU¹,
Ramona CAZALBAȘU¹, Georgeta PREDEANU², Bogdan Stefan VASILE³

¹Constantin Brancusi University of Targu Jiu, 4 Tineretului Street, Gorj County, Romania

²National University of Science and Technology Politehnica Bucharest,
Research Centre of Environmental Protection and Eco-Friendly Technologies,
1-7 Polizu Street, District 1, Bucharest, Romania

³National University of Science and Technology Politehnica Bucharest,
National Research Centre for Micro and Nanomaterials,
6 Iuliu Maniu Blvd, District 6, Bucharest, Romania

Corresponding author email: luminita.popescu69@gmail.com

Abstract

The increase in domestic poultry production in Romania is a result of the efforts our country is making to limit imports from other countries on one hand, and the development of the poultry sector through domestic investments, on the other hand. In 2022, poultry meat production increased by over 6%, and further increases are expected. In the same dynamic, the amount of aviary waste generated by poultry farms is also increasing, and in these conditions, it is obvious for our concerns to focus on the recovery, recycling, and utilization of avian waste. In this paper, we will present new possibilities for the utilization of ash resulting from the incineration of avian waste. In this case, avian waste is used as fuel, either in addition to biomass or municipal waste, to produce thermal energy.

Key words: circular economy, incineration waste products, poultry litter ash.

INTRODUCTION

According to OECD-FAO Agricultural outlook 2019-2028, in high-income countries, growing awareness of health and sustainability issues is increasingly shaping consumer decisions. This effect has contributed to the rising popularity of lean meats, such as poultry (Korver, 2023). Developed countries are expected to expand per capita poultry food use by nearly 2 kg/capita to reach 31 kg/capita by 2028. Health concerns will motivate corresponding increases in poultry consumption, with Canada increasing per capita food use of poultry by 1.2 kg/capita by 2028, and New Zealand adding 1.6 kg/capita over the same period. Similar substitutions across meat types are projected for the European Union, Norway, Switzerland, and Australia (OECD/FAO, 2019).

Therefore, the production of poultry litter will also increase, potentially aggravating the problems related to management of this waste (Fahimi et al., 2020).

Today, worldwide, several ways of utilizing aviary waste are known, the most common of which include:

- production of organic fertilizers: poultry waste can be composted and turned into nutrient-rich organic fertilizers;
- biogas production: poultry waste can be used in biogas production. In this case, the waste is digested anaerobically, which produces biogas (consisting of methane and carbon dioxide), which can be used to generate electricity and heat;
- thermal energy production: depending on the method of making the poultry bed, the waste can contain a significant amount of organic matter, in which case it can also be used in waste incinerators to produce thermal energy (Lăzăroiu, 2020);
- the production of construction materials: the ash resulting from the incineration of bird waste can be used in the construction materials industry as an additional raw material, either in the manufacture of construction materials made

in the form of burned ceramics, or in the manufacture of construction materials such as concrete.

Organic waste (excrement) from poultry farms is classified as solid organic waste (more than 15% dry matter). Due to the high content of phosphates, these wastes can be used as such as agricultural fertilizers, but the main drawback is the waste of straw, sawdust, etc. which, after spreading on the agricultural soil, can be entrained in the air currents, and thus become the environment polluting factors. In Romania, the recovery of this type of waste is done in such a way that unwanted side effects are partially avoided through preliminary stages of natural drying and fragmentation (shredding), respectively distribution on land in periods preceding the rainy or snowy seasons.

To eliminate the risks of ecological contamination, in many countries it is practiced disposing of aviary waste by incineration, with recovery of produced energy. In this way, the main advantages obtained consist in significant reduction of the waste ash volume resulting after combustion representing less than 30% of the initial volume, as well as the production of thermal energy. The value of agricultural fertilizer does not change essentially (the content of chemical compounds of phosphorus being residual), but the potential for deflation (entrainment in air currents) is considerably reduced.

MATERIALS AND METHODS

This paper presents the results of research activity carried out within the project *Thermal Processing of P-rich ashes aiming for high-grade phosphorus products (PHIGO)*, implemented by a European consortium that also includes the National University of Science and Technology Politehnica Bucharest (UNSTPB). “Constantin Brancusi” University of Targu Jiu (UCB), a subcontractor of UNSTPB, is carrying out research at laboratory level within the project regarding the evaluation of potential use of residues obtained after P recovery through thermal reduction processes. In fact, the purpose of the work carried out in laboratory was to evaluate the potential use of the ash resulting from the combustion of poultry waste after the

extraction of P by reductive heat treatment and to identify areas of use for these waste materials.

The ashes that are the subject of the research within the PHIGO project come from the incineration of poultry litters exhausted after the cycles of use in some poultry farms, and some sewage sludge from Turkey. P-rich ashes were collected from different companies that use poultry litter recovered from the combustion chamber as bottom and fly ash, such as Güres Energy, H29 Energy and Beypi. Additional samples were provided by INEVA and MIMSAN companies that incinerate sewage sludge. The samples used by UCB team in the present study resulted after thermal extraction processes performed by Swerim company, Sweden, the coordinator of the PHIGO project.

To evaluate the potential use of P thermal extraction residues, the Physical-Mechanical Testing Laboratory of UCB team received 12 individual preliminary samples of residual ash accompanied by the sheets containing the results of determinations of chemical oxide composition carried out by X-ray fluorescence analysis (Table 1).

Within UNSTPB, the fixed carbon content of the samples was previously determined following proximate analysis (Table 2). Considering the small amounts of residual samples obtained after heat treatment sent, the cumulation of elementary samples was established, by grouping the initial ones into two series of average samples, depending on the compositional specificity, according to the data entered (Table 3):

- medium sample series 1: ashes with CaO above 40%;
- medium sample series 2: ashes with CaO below 40%.

In addition, with residual ash, the laboratory works also used gray fat clay, which is a mining waste from the excavation work in the lignite quarries in the Gorj area and is currently used as a raw material for the manufacture of building bricks in within MACOFIL S.A. from Targu Jiu. The oxide chemical composition of the gray fat clay (Tables 4 and 5) shows the physical properties of the gray Rovinari clay, Romania (LIFE10 ENV/RO/00079 Project, 2012).

Table 1. Oxide chemical composition of the rezidual ash samples

Sample/oxide	R7	R8	R9	R10	R11	R12	R13	R14	R15	R16	R17	R18
CaO	41.29	43.23	24.63	29.35	33.45	25.28	46.08	44.89	42.91	40.63	44.19	41.72
SiO ₂	30.03	30.27	12.93	20.88	18.08	12.60	14.11	17.45	16.59	13.52	12.98	28.24
K ₂ O	3.18	4.22	25.89	1.83	2.69	20.45	7.74	2.38	8.06	5.45	9.79	5.26
S	3.16	2.42	12.41	2.49	2.26	10.84	6.04	2.08	5.71	1.85	5.96	2.27
P ₂ O ₅	2.59	2.91	9.98	3.11	7.63	9.58	8.82	6.88	6.98	14.52	10.72	4.20
MgO	2.30	2.10	4.01	1.45	3.31	4.50	3.93	4.29	3.59	2.95	3.78	1.99
Al ₂ O ₃	1.33	0.87	1.11	6.51	5.46	2.12	0.64	0.79	0.63	0.58	0.54	0.62
Na ₂ O	0.69	0.74	1.80	0.25	1.10	1.54	1.02	0.69	1.17	1.00	1.06	0.82
Fe ₂ O ₃	0.57	0.35	0.94	6.43	4.95	1.54	0.65	0.67	0.67	0.58	0.60	0.40
TiO ₂	0.05	0.03	0.08	0.75	0.85	0.24	0.04	0.06	0.04	0.05	0.04	0.03
MnO	0.15	0.15	0.42	0.30	0.20	0.47	0.31	0.27	0.31	0.24	0.30	0.16
SrO	0.10	0.02	0.04	0.04	0.11	0.05	0.12	0.11	0.11	0.10	0.12	0.02
Cl	0.04	0.06	5.12	0.05	0.04	1.83	1.45	0.03	1.33	0.33	2.18	0.31
CuO	0.02	0.02	0.05	0.30	0.06	0.05	0.04	0.03	0.04	0.03	0.04	0.02
Cr ₂ O ₃	0.03	0.02	0.02	0.08	0.12	0.03	0.01	0.01	0.01	0.01	0.01	0.01
MoO ₃	0.01	0.01	0.02	0.01	0.01	0.01	0.01	0.01	0.01	0.01	0.01	0.01
NiO	-	-	-	0.02	0.19	0.01	-	0.01	0.01	0.01	0.01	0.00
CdO	-	-	-	-	-	-	0.01	-	-	-	-	-
ZnO	-	-	0.04	-	-	0.01	-	-	-			-

Table 2. Fixed carbon content of the residual ash samples (% wt.)

R7	R8	R9	R10	R11	R12	R13	R14	R15	R16	R17	R18
0.76	0.93	7.78	7.38	6.25	7.56	8.48	8.46	7.41	10.67	9.03	2.77

Table 3. Residual ash samples grouped according to compositional criteria

Series 1		Series 2	
Sample	Weight, g	Sample	Weight, g
R7	15.4	R9	15.3
R8	17.0	R10	12.8
R13	15.8	R11	21.9
R14	17.1	R12	8.5
R15	14.9		
R16	21.1		
R17	16.4		
R18	10.7		

Table 4. Oxide chemical composition of gray fat clay (LIFE10 ENV/RO/00079 Project, 2012)

SiO ₂	TiO ₂	Al ₂ O ₃	Fe ₂ O ₃	MnO	MgO	CaO	Na ₂ O	K ₂ O	P ₂ O ₅	P.C.
65.80	0.68	15.97	5.40	0.11	1.64	0.85	1.86	2.37	0.12	5.35

For the qualitative and quantitative analysis of the samples oxide composition the Thermo Scientific ARL PERFORM'X Sequential X-ray

Fluorescence (XRF) Spectrometer of the UNSTPB was used. Fixed carbon was analysed using STAS 5268: 1990.

Table 5. Physical properties of gray clay
 (LIFE10 ENV/RO/00079 Project, 2012)

Plasticity (I_p)	26-37.8
Consistency (I_c)	0.69-0.86%
Natural moisture (w)	18.6-35.5%
Apparent volumetric weight (γ_a)	(175-194) kPa
Internal friction angle (φ)	13°-26°
Cohesion factor ©	(20-55) kPa

Using the materials presented previously, two experimental mixtures were made in the laboratory, according to the following dosage recipes (% by mass):

1. Compositional variant 1, marked A, with the following content:

- Ashes of Series 1: 85.7%
- Clay: 14.3%

2. Compositional variant 2, marked B, with the following content:

- Ashes of Series 2: 11.5%
- Clay: 88.5%.

At the same time, control/reference samples, marked M, were made from clay only.

From the two mixtures marked A (4 pieces marked A1, A2, A3, A4), B (3 pieces marked B1, B2, B3) but also from clay (3 pieces marked M1, M2, M3), compacted pieces were obtained by pressing in a metal mold, at the nominal pressure of 40 MPa (Figure 1). After compaction, the experimental pieces were kept for 48 hours at ambient temperature, then subjected to the heat treatment of drying in an electric laboratory oven for 8 hours at a temperature of $110^\circ\text{C} \pm 1^\circ\text{C}$. The dry samples were burned in an electric laboratory furnace at a temperature of 1000°C , with a thermal gradient of $5^\circ\text{C}/\text{min}$ and kept for 2 hours at the maximum temperature (Figure 2).

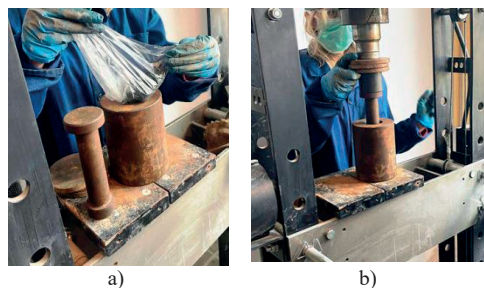


Figure 1. Obtaining of compacted specimens:
 a) Feeding mould; b) Pressing

Both in the raw state and after drying and burning, samples were weighed on a laboratory balance having precision of 0.1 g and measured to the nearest 0.1 mm (Figure 3).

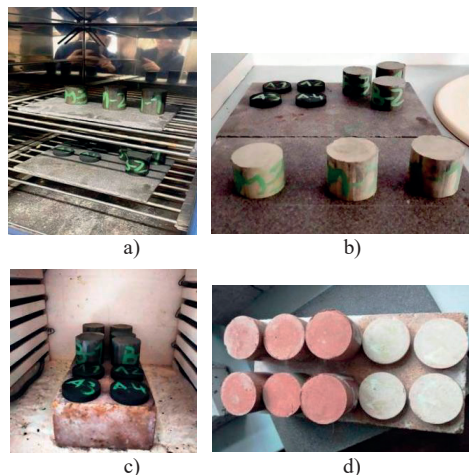


Figure 2. Experimental specimens thermal treatment:
 a) Drying; b) Dried samples; c) Burning; d) Burned samples



Figure 3. Samples weighting and measuring

After burning treatment, the specimens were used distinctly, depending on the predetermined technological destination:

a. Samples marked A were manually fragmented, then ground in the Retsch ring mill to the advanced fineness of a cement powder (Figure 4) and tested to determine hydraulic cold setting ability (Figure 5).

Given the very small amount of processed sample, the hydraulic hardening ability of the ground sample was tested by wetting it with water and making a compact paste of spherical format (Figure 5). The spherical piece was placed on the base of the Vicat device, checking the hardening phenomenon, like the sample for cement paste (Figure 6).

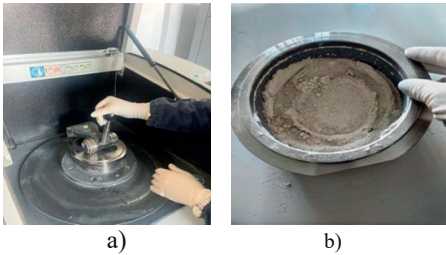


Figure 4. Grinding samples A:
a) Feed mill Retsch; b) Ground sample

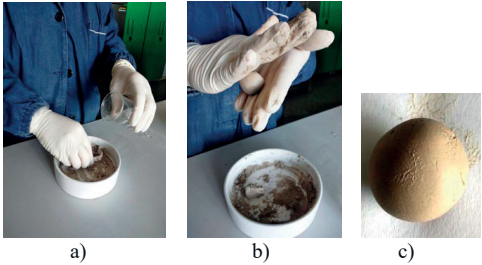


Figure 5. Testing the hydraulic strengthening behaviour:
a) Powder wetting; b) Shaping compacted sample;
c) Spherical piece made from wetted powder

b. Samples marked B and M (burned cylinders) were subjected to the mechanical compressive strength test (Figure 7). The mechanical strength of the samples' marked B was evaluated in accordance with the provisions of Standard R EN 993-5:2001 test methods for dense shaped refractory products. According to it, the mechanical resistance to compression is determined by subjecting the samples to the action of the pressing force between the parallel flat platens of the test press of Accuracy Class 1, with the adjustment of the load loading speed of 2.5 MPa/second (Figure 7).

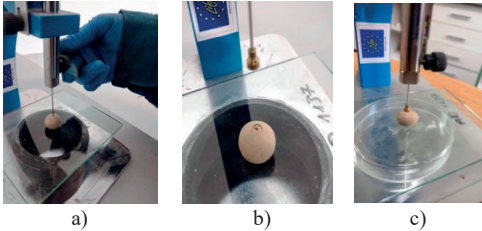


Figure 6. Checking hardening of spherical piece:
a) Socket start; b, c) Socket end

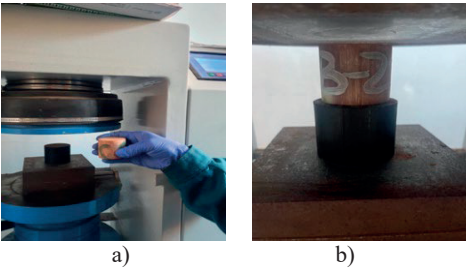


Figure 7. Determination of compression strength:
a) Automat pressing; b) Cylinder pressing

RESULTS AND DISCUSSIONS

At this moment the percentage replacement of natural aggregates such as aviary ash depends only on physical and mechanical characteristics of the final product. Since this is not hazardous waste, there are no concerns regarding the impact on the environment and the human health.

The test carried out on the samples marked A with the Vicat device indicated that the powder obtained by the fine grinding of the samples A burned at 1000°C has the property of cold hydraulic hardening.

The samples marked with B and M were subjected to the mechanical compression resistance test, the results being presented in Table 6.

Table 6. Compression strength of cylindrical specimens burned at 1000°C

Sample	Maximum force applied, MPa	Compression strength, Mpa
B1	48.0	24.47
B2	50.9	25.94
M1	49.5	25.23
M2	52.8	26.88

From data of Table 6, the mechanical strengths of the samples obtained with the addition of de-phosphated ash are like those of the samples without ash (reference samples), which indicates that this type of ash can be used as a degreasing additive in shaping mixtures, in situations where the processed clay (basic raw material) has a too high plasticity.

CONCLUSIONS

This paper presents some scientific preliminary research conducted with the aim of identifying other possibilities of using poultry litter ash than those already known. By finding practical solutions which does not provide leachate, allowing to save chemicals (used in wet methods) and avoid liquid waste, will enable closing the P loop in the EU P-strategy. The most important conclusions are presented below:

a. The residual ash resulting from the thermal treatment of poultry litter waste has a complex chemical composition, like other ashes from incinerated industrial waste. Compared to other waste from agri-food complexes, residual ashes stand out for their high content of calcium and phosphorus oxides.

b. The silico-calcium compositional basis of the ashes suggests the possibility of their utilization as alternative raw materials for the manufacture of Portland cement. An impediment in this direction is the high content of P_2O_5 , a compound that persists with a significant weight even after the thermal processing carried out to recover phosphorus through thermal reduction.

c. Starting from the premise that the negative effect of the presence of phosphorus cannot be avoided in the direction of valorization in clinker, it was aimed to favor the formation of dicalcium silicate by ensuring a CaO/SiO_2 molar ratio of around 2 in the raw material, by mixing the ash with a clay silicate.

d. It was also tested the possibility of using ash as a degreasing additive in the clay raw material on the construction brick manufacturing process, as a substitute for natural quartzite sand in situations where lots of clay with too much plasticity are available.

ACKNOWLEDGEMENTS

Present research received funding from COFUND-ERA-NET ERA-MIN3 contract 310/2022, PHIGO Project.

REFERENCES

- Fahimi A., Bilo F., Assi A., Dalipi R., Federici S., Guedes A., Valentim B., Olgun H., Ye G., Bialecka B., Fiameni L., Borgese L., Cathelineau M., Boiron M.-C., Predeanu G., Bontempi E. (2020). Poultry litter ash characterisation and recovery. *Waste management*, 111, 10-21.
- Korver, D.R. (2023). Review: Current challenges in poultry nutrition, health, and welfare. *Animal*, 17(2), 100755, ISSN 1751-7311, <https://doi.org/10.1016/j.animal.2023.100755>.
- Lăzăroiu G., Ciupageanu D.-A., Mihaescu L., Grigoriu M., Simion I. (2020). Energy recovery from poultry manure: a viable solution to reduce poultry industry energy consumption. *Renewable Energy and Power Quality Journal (RE&PQJ)*, 18, ISSN 2172-038 X.
- LIFE10 ENV/RO/00079 Project, *New building materials by eco-sustainable recycling of industrial wastes – EcoWASTES*, 2011-2014.
- OECD/FAO (2019), OECD-FAO Agricultural Outlook 2019-2028, OECD Publishing, Paris/Food and Agriculture Organization of the United Nations, Rome.
- STAS 5268:1990. *Solid fuels. Volatiles matters, coke and fixed carbon determination*. Romanian Standard Association, Bucharest, Romania, 8 (in Romanian).
- UCB Scientific Report 2023 "Evaluation of the laboratory level potential use of residues/by-products obtained after P recovery. Design of experimental technological schemes". Contract 18948/02.08.2022/3688/PHIGO project.
- UNSTPB contract 310/2022 UEFISCDI COFUND ERA-NET ERA- MIN3 *Thermal Processing of P-rich ashes aiming for high-grade phosphorus products - PHIGO*.

A DEEP-LEARNING BASED METHOD FOR WASTE DETECTION

Dan Constantin PUCHIANU

Valahia University of Targoviste, 13 Sinaia Alley Street, Targoviste, Romania

Corresponding author email: pdantgv@yahoo.com

Abstract

The integration of advanced deep-learning techniques and object detection architectures represents an advanced methodology for waste detection. Considering the importance of recycling and environmental protection in sustainable waste management, automation of such processes becomes an essential task to improve efficiency and accuracy in various industrial and environmental applications. In this study, a system based on convolutional neural networks is proposed for the identification and classification of different types of waste, such as paper, metal, plastic, or glass. An extensive dataset was used to train and evaluate the proposed models using digital RGB images. Following the experimental results, the implementations of this study demonstrated a detection accuracy of over 90%, highlighting the effectiveness of these models and providing modern solutions for correct waste management and manual sorting errors. Efficient recycling is important for ensuring good environmental sustainability practices and automating the process using deep-learning systems is an important step in this direction.

Key words: image processing, object detection, waste management, pollution.

INTRODUCTION

Effective waste management is a critical issue for modern society around the world. In recent years, due to globalization, rapid population growth, excessive consumption has led to the emergence of serious problems represented by the generation of massive amounts of waste (Virsta et al., 2020). Solving these problems requires the adoption of innovative and effective solutions (Abdu & Mohd Noor, 2022; Majchrowska et al., 2022). One of these solutions, which promises to revolutionize this field, is the deep learning development area (Mohammed & Kora, 2023; Petrea et al., 2023). As a branch of machine learning, as a part of the whole set of artificial intelligence, deep learning is based on the integration of deep artificial neural networks with multiple layers and important architectural features (Janiesch et al., 2021). These innovative models are capable of learning complex and abstract features from massive amounts of raw data, eliminating manual intervention to extract the desired information. Based on these characteristics, deep learning architectures demonstrate remarkable performance in recognizing patterns and features of visual data, such as images and videos, being an important research topic (Martin et al., 2013).

The automatic detection and identification of waste is an important field that can capitalize on the modern characteristics of deep learning in the efficient management processes. Quickly identifying the type of waste allows efficient sorting and recycling (L. Zhou et al., 2023). These integrations come in the context of managing a large volume of waste where traditional methods are inefficient, expensive, and time-consuming (Meng et al., 2021). Automating these processes can bring significant efficiency and cost benefits (Zhou et al., 2023).

By optimizing deep learning architectures, applications are numerous in waste detection. A popular research topic in the use of deep learning for waste management focuses on digital image classification for waste identification (Meng et al., 2021). Convolutional Neural Network (CNN) models are the basis of such processes, aiming at training and validating large data sets. Based on these processes, trained models can successfully classify digital images of waste with high accuracy (Feng et al., 2020; Lubura et al., 2022).

Deep learning models such as Faster R-CNN, SSD, and YOLO are popular for detecting garbage objects from digital images and videos (Ren et al., 2022; Zhou et al., 2023). This step involves techniques that allow the identification

and localization of individual objects in digital images and is essential for real-time applications and continuous monitoring (Terven et al., 2023). Unlike traditional methods, deep learning models can process large amounts of visual data much faster and more accurately. This feature brings to the fore more efficient sorting and a higher recycling rate (Mao et al., 2022).

Looking at the state-of-the-art or related works branch, notable works that satisfy waste management problems using up-to-date deep learning technologies are highlighted. Ongoing research highlights the limitations of manual and expensive waste identification and sorting and applies innovative techniques to create automated detection systems.

In the authors' work (Zhou et al., 2023) the detection of SWAD - solid waste detection - from aerial images was pursued. The authors note that manual identification is expensive and inefficient, especially for large images and wide coverage areas. A model named SWDet is presented as part of this study, optimized for the detection of waste from aerial images and integrating an anchor-based object detector. Moreover, the model integrates an ADA-type structure (asymmetric deep aggregation) to extract the image characteristics as best as possible and at the same time efficient attention fusion pyramid network (EAFPN) to solve the problem of image blur of waste, a problem that can appear due to the shapes of irregular waste. The authors proposed a proprietary dataset in this study, and the experiments performed demonstrate notable mAP metrics, with tests also performed on the TACO dataset, surpassing existing research. This study demonstrates the ability of deep learning techniques to extract data from high-resolution images for accurate waste detection.

In another study, the authors (Ren et al., 2022) propose a coastal waste detection model by improving detection speed and small object detection. A proposed model, Multi-Strategy Deconvolution Single Shot Multibox Detector (MS-DSSD), integrates feature fusion, focal loss, and dense block models as an important part of a feed-forward, end-to-end trained network. Focal loss solves the problem of class imbalance, similar to the state-of-the-art RetinaNet model technique, dense blocks improve complex feature extraction, and fusion

modules improve feature extraction for small objects. A data set is proposed for this study, and the obtained results validate the efficiency of the implemented architecture. Finally, optimization methods by growing the data set and by optimizing the fusion method for detection efficiency and speed are noted.

A study by the authors (Fan et al., 2023) leverages the characteristics of a model from the YOLO family for accurate waste identification as part of sorting processes and at the same time by integrating data augmentation techniques. The authors noted a lack of datasets for multi-class debris detection and propose a DCGAN model for image generation using these structures by convolutional adversarial generative networks. At the base of the detection model is a YOLOV4 architecture, modified by introducing an EfficientNet model as a feature extraction network. The proposed implementation had the role of increasing the detection speed and efficiency but also to reduce the number of parameters. In the same context, a feature extraction model with CA - coordinated attention is introduced, reconstructing the classical MBConv model of the architecture. The key points of these implementations are to improve the detection of small and medium objects and increase the generalization and global detection capability of the augmented data model. On the proposed dataset with the mentioned modifications, the model achieves a considerable mAP metric of over 96% and can be successfully applied in automatic waste detection tasks.

The study by the authors (Majchrowska et al., 2022) emphasizes the problem of global pollution as part of the improper management of waste resulting from production activities. The authors analyze important datasets and information related to these issues and present a critical analysis of waste detection methods using deep learning. On the other hand, the authors introduce two datasets named: detect-waste and classify-waste for the tasks of waste detection and classification, analyzing several open-source datasets, covering a vast list of waste classes, with the annotations attached. An EfficientDetD2 detection model is proposed, as well as an EfficientNet-B2 classification model, for seven categories and in a semi-supervised manner. The authors' experiments demonstrate

remarkable performance in multi-class detection and identification, with average accuracy values of 70% for the detection task and 75% for the classification model. The authors note that a quality dataset with properly annotated images, as well as optimized detection and classification models can have a positive impact on the global and modern sustainability of automated waste detection systems of various types.

According to studies dedicated to this field, clear methods of implementing automatic waste detection systems are observed. Datasets for training and validating networks are as important as optimizations to the architectures used for detection. Starting from this aspect, a modern method is presented in the present study and explores the use of deep learning models for waste detection and highlights the benefits and novelty of the methods used. The new, modern YOLO architecture, versions 8, was used for this study and each version was optimized for the associated task. After the introduction part, a materials and methods chapter present the data set used, the proposed models and the settings in which the experiments were performed. In another section, the experimental results and the discussions related to the performances obtained and the methodology approached are presented. At the end of the paper, the conclusions and future research directions are presented.

MATERIALS AND METHODS

To develop a deep learning system for waste detection, several elements and methodologies are considered - a robust and detailed dataset, a high-performance hardware and software architecture, and a series of convolutional neural networks optimized for the object detection task. This chapter presents the details for each individual case.

The dataset for a waste detection system is essential for training and evaluating these detection models, being trained to recognize the various features and information attached to each type of waste. Such a dataset was used for the implementation in the present work and included images captured from various contexts to ensure the detection system's basis, variability, and robustness. The composition of the dataset shows various categories of waste. The dataset used included RGB images in JPEG

and PNG format, with variable resolutions that could simulate various real or usage conditions. Figure 1 shows examples of images from the dataset used for the present work.



Figure 1. Example images from the waste dataset

To standardize the input data, the dataset went through normalization operations and at the same time augmentation techniques to increase the size of the dataset, being applied transformations and various changes such as rotation, contrast and brightness changes and geometric transformations.

Further, the object detection models used were trained on this dataset by tracking the performance of each model at various stages - training, validation, and testing. The division of the dataset was done with respect to these features and included carefully labelled images. The final dataset includes a total of 1300 images: 780 images for the training area (60%), 260 images for validation (20%) and 260 images for testing (20%). Parts of the TrashNet dataset were also analyzed for this study (Thung & Yang, 2016).

The architecture used, YOLOv8, represents one of the new iterations of the YOLO series that brings significant improvements in real-time object detection (Jocher, 2023). The YOLOv8 architecture used includes backbone, neck, and head structures to efficiently extract the characteristics of waste types in the detection process. The YOLOv8 model introduces a neck structure that effectively connects the backbone area to the head that makes the prediction, using a PANet (Path Aggregation Network) module. It is used to combine various information from different abstraction levels of the network. Dynamic settings and anchors are attached to the head area of the architecture to make more accurate detections and to properly adapt to object sizes.

Benefiting from ongoing support and documentation, the YOLOv8 model has been implemented using the PyTorch framework and

following the implementation details from the official developers' Github repo (Jocher, 2023). As part of state-of-the-art deep learning solutions, YOLOv8 stands out for its architecture's ability to cover a wide range of tasks in the field of computer vision, tasks that include object detection, digital image classification and segmentation tasks. The YOLOv8 architecture proposes notable implementations that lean toward the development of network optimization and modification solutions, for better understanding and implementation of solutions. The YOLOv8 version is based on robust and efficient detection modules. Through its modular structure, the architecture can be modified both in width and in depth, being a critical step for implementing the model in various forms and hardware resources. At the same time, changing and optimizing the architecture is done without compromising accuracy and performance, proving scalability and flexibility to match. Like previous models, the YOLOv8 architecture is one-stage, making predictions on images in a single pass, and much more efficiently with the optimizations of this new iteration. In terms of speed and performance, the YOLOv8 architecture was built to improve the ability to detect objects in various lighting and partially visible contexts. At the same time, optimizations are added to this framework to give YOLOv8 the ability to detect objects at very high speeds, ideal for real-time applications.

All the architectures in the YOLOv8 family were implemented for the development of the present study, on the detection task.

In terms of hardware and software, the system on which the models and experiments of the present study were implemented included a custom system featuring a Win 10 Pro operating system, AMD Ryzen 9 5900HS CPU and a GeForce RTX 3060 6GB GPU. The chosen programming language was Python v3.9 and PyTorch as the reference framework.

RESULTS AND DISCUSSIONS

This part of the paper highlights the results obtained in the case of the present study, with notable performances of the detection models chosen and optimized for the present case of waste management and detection. Transfer

learning and fine-tuning was used and the performances that were noted included metrics such as precision, recall, mAP@50, and mAP@50:95. Table 1 and Figures 2 to 6 show the values obtained for each model, after training and validation.

Table 1. Waste detection performances for YOLOv8 models on the validation set (All Class)

Model	Precision	Recall	mAP@50	mAP@50:95
YOLOv8n	0.949	0.926	0.979	0.821
YOLOv8s	0.957	0.920	0.987	0.818
YOLOv8m	0.914	0.968	0.982	0.822
YOLOv8l	0.931	0.885	0.964	0.801
YOLOv8x	0.948	0.913	0.973	0.815

The denoted "All" class represents an average of the results for the dataset classes, a common notation in the object detection area. It was observed that each model demonstrated state-of-the-art object detection performance, that aligns with the overall objective for waste detection systems.

Following this study, the processes attached to waste management using deep learning can present different challenges and limitations. Training models require large sets of labelled data that are often difficult to collect. Moreover, the diversity of the data is essential, as well as its quality, to ensure a high performance of the proposed model. In the same vein, generalization is another challenge resulting from the fact that deep learning models can be sensitive to variations in the input data and can perform poorly in identifying data outside the training process, using new data from real conditions.

The representative classes of the dataset are attached in the following figures, where they are illustrated using bar plots the evolution in the case of each class and metric. The metrics chosen to calculate model performance are global performance indicators that are oriented towards multi-point performance - overall detection, detection of objects of interest, the ability of the models to detect with different confidence thresholds the target objects, and the evolution of detections that deal with important all classes of the data set. Using these metrics provides an overview of each detection model implemented in this study and their ability to identify objects of interest under different conditions.

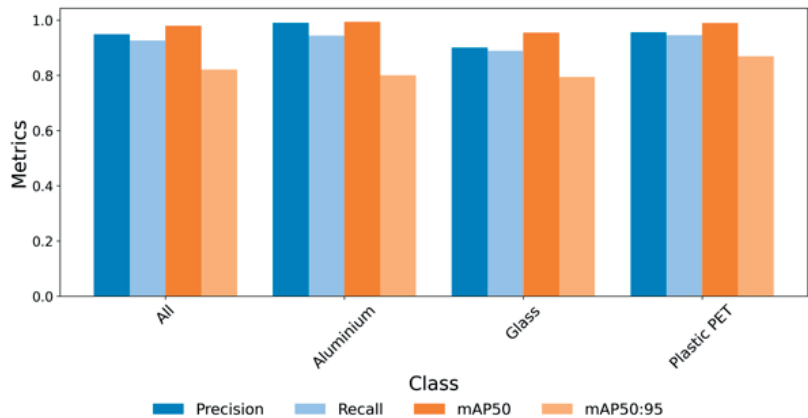


Figure 2. Performance metrics per class for YOLOv8n

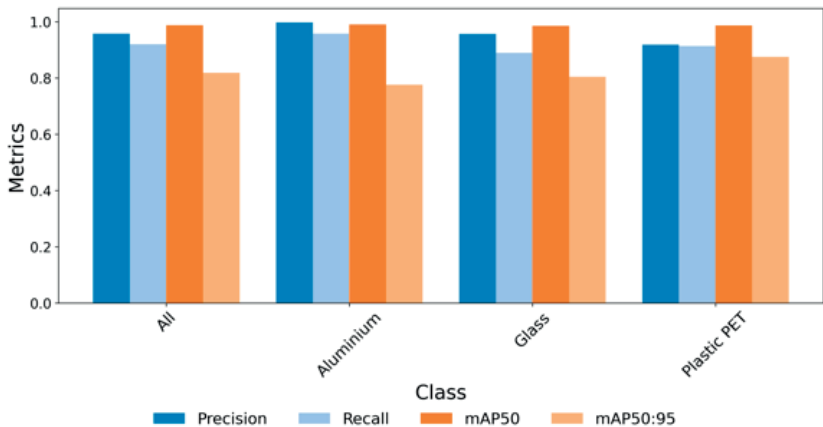


Figure 3. Performance metrics per class for YOLOv8s

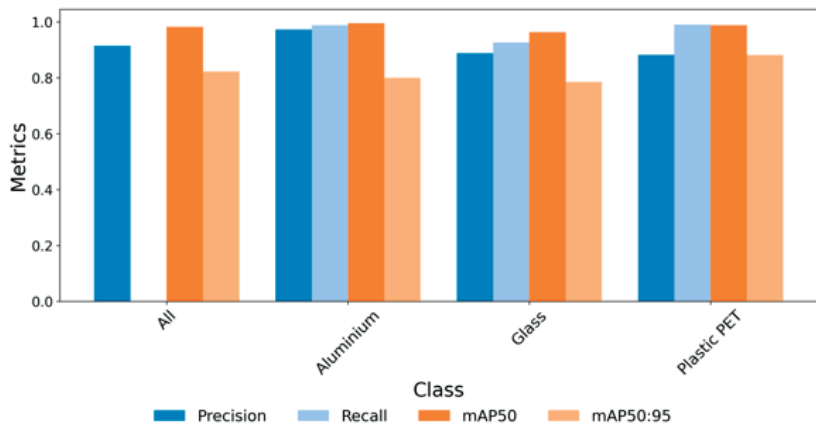


Figure 4. Performance metrics per class for YOLOv8m

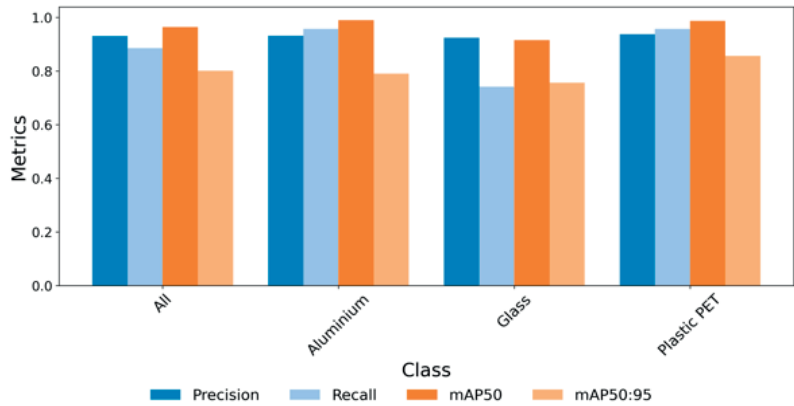


Figure 5. Performance metrics per class for YOLOv8l

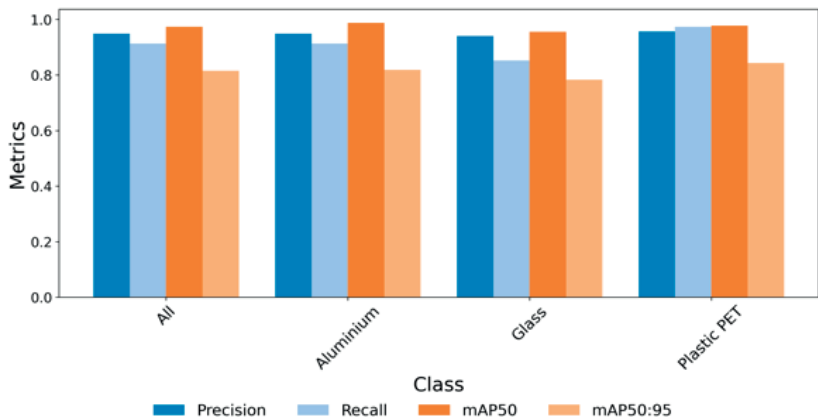


Figure 6. Performance metrics per class for YOLOv8x

Precision is an important indicator that measures the number of correct detections out of the total number of detections performed. A high precision indicates that the model makes few false detections, which is an important metric to isolate the false alarms of a detection model. On the other hand, Recall (sensitivity) measures the ability of the model to correctly identify true instances of a dataset, the reference objects. A high value of Recall describes the model's ability to correctly identify all objects, with as few missed objects as possible. mAP@50 represents the average precision calculated at an IoU threshold of 50%. This Intersection over Union threshold calculates the overlap between the predicted and the actual bounding box. Typically, this indicator summarizes the model's detection capability in easy cases, with moderate overlap, bringing true

detection confidence values above this 50% threshold. In another scenario, mAP@50:95 represents the average of the precision calculated at various thresholds, from 0.5 to 0.95 with a step of 0.05. This indicator presents a more rigorous assessment of detection models, analyzing their detection capability at stricter thresholds. A high mAP of this type indicates the model's true ability to detect instances of interest with high confidence and accuracy. The models proposed for this study stand out as being balanced in terms of the results obtained, with a notable ratio between Precision and Recall, suitable for the proposed application on waste detection. YOLOv8n and YOLOv8s provided good performance for their low complexity, ideal for resource-constrained applications. On the other hand, great metrics are also noted for the medium and large models

of this family, but which come with commensurate complexity and processing power in their development, standing out with accurate detections.

CONCLUSIONS

In this paper, five detection models from the YOLOv8 architecture were presented to solve waste detection and management problems using deep learning. In this sense, the proposed models demonstrated very good performance in relation to the object detection task and the dataset used, observing the effectiveness of the methods, and noting opportunities for research and development for a critical task of modern society.

The obtained performances such as a mAP@50 and a Recall above 90% highlight the ability of the YOLOv8 models as part of automatic waste detection and to identify them with high accuracy in various environmental conditions. The study presented important metrics for the chosen object detection task and underlines the high capability and performance of the models in detecting the objects of interest with confidence. However, as in any other study in this field, limitations and opportunities for improvement were observed, describing a first step of automated waste detection using modern YOLO variants. The present work can be developed by implementing modules and architectures capable of extracting much better information and features in relation to waste detection, researching advanced models involving a larger data set, more classes, complex modified architectures, or a combination of models for a global decision (model ensemble).

REFERENCES

- Abdu, H., & Mohd Noor, M.H. (2022). A Survey on Waste Detection and Classification Using Deep Learning. *IEEE Access*, 12, 128151–128165. <https://doi.org/10.1109/access.2022.3226682>
- Fan, J., Cui, L., & Fei, S. (2023). Waste Detection System Based on Data Augmentation and YOLO EC. *Sensors*, 7, 3646. <https://doi.org/10.3390/s23073646>
- Feng, B., Ren, K., Tao, Q., & Gao, X. (2020). A robust waste detection method based on cascade adversarial spatial dropout detection network. *Optoelectronic Imaging and Multimedia Technology*, VII. <https://doi.org/10.1117/12.2575394>
- Janiesch, C., Zschech, P., & Heinrich, K. (2021). Machine learning and deep learning. *Electronic Markets*, 3, 685–695. <https://doi.org/10.1007/s12525-021-00475-2>
- Jocher, G., Chaurasia, A., & Qiu, J. (2023). Ultralytics YOLO (Version 8.0.0) [Computer software]. <https://github.com/ultralytics/ultralytics>
- Lou, H., Duan, X., Guo, J., Liu, H., Gu, J., Bi, L., & Chen, H. (2023). DC-YOLOv8: Small-Size Object Detection Algorithm Based on Camera Sensor. *Electronics*, 10, 2323. <https://doi.org/10.3390/electronics12102323>
- Lubura, J., Pezo, L., Sandu, M.A., Voronova, V., Donsi, F., Šic Žlabur, J., Ribić, B., Peter, A., Šurić, J., Brandić, I., et al. (2022). Food Recognition and Food Waste Estimation Using Convolutional Neural Network. *Electronics*, 11(22), 3746. <https://doi.org/10.3390/electronics11223746>
- Majchrowska, S., Mikołajczyk, A., Ferlin, M., Klawikowska, Z., Plantykowski, M. A., Kwasigroch, A., & Majek, K. (2022). Deep learning-based waste detection in natural and urban environments. *Waste Management*, 274–284. <https://doi.org/10.1016/j.wasman.2021.12.001>
- Mao, W.-L., Chen, W.-C., Fathurrahman, H. I. K., & Lin, Y.-H. (2022). Deep learning networks for real-time regional domestic waste detection. *Journal of Cleaner Production*, 131096. <https://doi.org/10.1016/j.jclepro.2022.131096>
- Martin, J.W., Stark, T.D., Thalhamer, T., Gerbas-Graf, G.T., & Gortner, R.E. (2013). Detection of Aluminum Waste Reactions and Waste Fires. *Journal of Hazardous, Toxic, and Radioactive Waste*, 3, 164–174. [https://doi.org/10.1061/\(asce\)hz.2153-5515.0000171](https://doi.org/10.1061/(asce)hz.2153-5515.0000171)
- Meng, J., Jiang, P., Wang, J., & Wang, K. (2021). A MobileNet-SSD Model with FPN for Waste Detection. *Journal of Electrical Engineering & Technology*, 2, 1425–1431. <https://doi.org/10.1007/s42835-021-00960-w>
- Mohammed, A., & Kora, R. (2023). A comprehensive review on ensemble deep learning: Opportunities and challenges. *Journal of King Saud University - Computer and Information Sciences*, 2, 757–774. <https://doi.org/10.1016/j.jksuci.2023.01.014>
- Petrea, S.-M., Simionov, I.-A., Antache, A., Nica, A., Antohi, C., Cristea, D.S., Roșu, A., Calmuc, V., Roșu, B. (2023). Prediction models for improving waste decision support management in Romania in association with V4 member countries. *Scientific Papers. Series E. Land Reclamation, Earth Observation & Surveying, Environmental Engineering*, XII, 158–166, Print ISSN 2285-6064.
- Ren, C., Lee, S., Kim, D.-K., Zhang, G., & Jeong, D. (2022). A Multi-Strategy Framework for Coastal Waste Detection. *Journal of Marine Science and Engineering*, 9, 1330. <https://doi.org/10.3390/jmse10091330>
- Terven, J., Córdova-Esparza, D.-M., & Romero-González, J.-A. (2023). A Comprehensive Review of YOLO Architectures in Computer Vision: From YOLOv1 to YOLOv8 and YOLO-NAS. *Machine Learning and Knowledge Extraction*, 4, 1680–1716. <https://doi.org/10.3390/make5040083>

- Thung, G., & Yang, M. (2016). Classification of Trash for Recyclability Status, TrashNet Dataset, <https://github.com/garythung/trashnet?tab=readme-ov-file>
- Virsta, A., Sandu, M.A., Daraban. A.E., Manea, R.M. (2020). Gaps on waste management education in schools and universities from Bucharest. *Journal of Environmental Protection and Ecology*, 21(1), 334-342.
- Zhou, L., Rao, X., Li, Y., Zuo, X., Liu, Y., Lin, Y., & Yang, Y. (2023). SWDet: Anchor-Based Object Detector for Solid Waste Detection in Aerial Images. *IEEE Journal of Selected Topics in Applied Earth Observations and Remote Sensing*, 306–320. <https://doi.org/10.1109/jstars.2022.3218958>
- Zhou, W., Zhao, L., Huang, H., Chen, Y., Xu, S., & Wang, C. (2023). Automatic waste detection with few annotated samples: Improving waste management efficiency. *Engineering Applications of Artificial Intelligence*, 105865. <https://doi.org/10.1016/j.engappai.2023.105865>

WASTE CLASSIFICATION USING EFFICIENT NEURAL NETWORKS AND WEB APPLICATION

Dan Constantin PUCHIANU

Valahia University of Targoviste, 13 Sinaia Alley Street, Targoviste, Romania

Corresponding author email: pdantgv@gmail.com

Abstract

The integration of convolutional neural networks and modern web applications can significantly improve the efficiency of recycling processes. Accurate, rapid identification and separation of waste of various types reduces contamination by marking a process essential to the efficiency of the recycling industry. In this study, a modern approach for classifying recyclable waste using deep-learning techniques based on convolutional neural networks and integrated into a web application developed using ReactJS is presented. Leveraging the features of advanced deep-learning models and modern web interfaces, the present study aims to make a substantial contribution to the field of efficient waste management and environmental protection. Neural network architectures, trained and evaluated on a carefully annotated dataset, demonstrated very good accuracy values outperforming classical state-of-the-art models. Integrating these models with modern web technologies built a web application with an intuitive user interface for real-time classification of waste types, providing immediate feedback. In the same framework, implementations with web technologies also provide educational resources regarding recycling practices and the impact of waste on the environment. The impact on the environment is considerable because the development of such established technologies can reduce the amount of waste managed improperly, improving the recycling rate. Future research can explore optimizing the models and techniques presented in these studies, expanding the dataset, and developing the application to support good sustainability practices.

Key words: waste management, convolutional neural networks, deep learning, web application, reacts.

INTRODUCTION

The path to sustainability and a cleaner future is closely linked to modern and effective waste management practices. Pollution and waste management are major challenges of modern society. The lack of attention in waste management brings critical problems that can affect the environment in which we live and the activities we carry out due to various factors (Guo & Chen, 2022).

Rapid growth in global consumption and population has led to massive accumulations of waste. They can negatively affect public health and the environment in which we live (Bian et al., 2022). The problems of waste management and recycling can be represented by the increase in the amount of waste, the inefficiency of recycling systems through sorting and problematic practices and finally pollution of various forms (Lu et al., 2020). In the absence of effective systems, large amounts of waste end up in landfills and ecosystems, causing substantial damage (Lin et al., 2022; Boldeanu et al., 2023). On the other hand, recycling is an important component of waste management, but it faces

numerous challenges and limitations. A major problem in this context is the incorrect classification of waste. In principle, these errors in recycling processes can affect the efficiency of recycling systems by contaminating the materials that want to be processed, an example being the contamination of plastic and metals through the accidental and erroneous introduction of non-recyclable lots (Qiao et al., 2023; Long et al., 2024).

Waste management, efficient recycling and pollution are areas that can successfully leverage the advanced features of deep learning to solve problems (Zhang et al., 2021).

In recent years, a trend and important research directions have been observed that want to solve these problems through various automatic methods (Alrayes et al., 2023). Deep learning techniques, especially those based on the use of convolutional neural networks (CNN), offer complete solutions in the task of classifying digital images and have applicability in waste management processes (Lubura et al., 2022).

The process of classifying waste using CNN uses models trained on vast datasets capable of classifying images into specific waste categories

such as organic or recyclable, or specific types of metal, plastic, paper, or glass (Sarswat et al., 2024). Throughout studies, such a process involves several steps: collecting data and organizing it into various categories, preprocessing the data, training the models, evaluating the models, and adjusting them (Pitakaso et al., 2024).

The present work aims to implement some convolutional neural network models by creating automatic waste classification systems, in various categories. The systems have been optimized and modified accordingly to extract the details required for superior waste classification performance. Apart from the introduction, the present paper is organized into several sections. A section of materials and methods is introduced to present the methodologies approached in the present research focused on waste classification. Furthermore, an experimental results section presents the obtained performances and discussions based on the implementations. Finally, the paper ends with a conclusion section, presenting a clear summary of the present research.

MATERIALS AND METHODS

The present section notes the methodologies addressed in the waste classification research - the dataset used, the convolutional neural networks implemented, and an overview of the hardware and software area.

As part of the waste classification-oriented research a representative dataset consisting of RGB digital images was used, noting an important part in the training of image classification models.

The dataset used totals 2400 images divided into three parts for training (70% - 1680 images), validation (20% - 480 images) and testing (10% - 240 images). Each part of the dataset illustrates various types of recyclable waste in various poses and scenarios used to train and evaluate convolutional neural network (CNN)-based digital image classification architectures. For the present case, various augmentation techniques were also implemented to increase and diversify the dataset. These included color and geometric transformations: brightness adjustment, contrast adjustment, saturation adjustment, noise

addition, blur, rotation, translation, scaling, shearing, horizontal and vertical flipping, cropping. Transformations of this type are essential in image augmentation processes, contributing to the diversification and robustness of the data set. Thanks to these techniques training CNN models can have robust examples to improve performance and generalization, ultimately able to handle the variations and complexity attached to images in real contexts (Pitakaso et al., 2024; Tian et al., 2024). Representative images of the dataset are attached in Figure 1, as well as representative images of the augmentation processes in Figure 2. Using image resizing the size of the input images of the architectures used was 224 x 224 px.



Figure 1. Example images from the dataset



Figure 2. Example images from the augmented dataset

Commonly used for image classification tasks, convolutional neural networks are complex architectures capable of automatically analyzing and capturing essential visual features. Typically, these CNN structures include convolutional, pooling, and complexly connected layers. Essential convolutional structures apply various filters to extract

important features such as edges and textures, while generating feature maps that bring to the fore essential features of images and objects in these images, such as waste. Over the years several types of architectures have been developed and heavily optimized to better extract these features. As part of the present study, several CNN architectures were implemented and modified to create robust classification systems as part of the waste management domain. Transfer learning and fine-tuning techniques were used to optimize the proposed models, leveraging pre-trained weights.

DenseNet 201 (Huang et al., 2016) is the first model used for this work. The architecture consists of many stars and is designed to streamline the flow of information. Unlike traditional neural architectures, DenseNet connects each layer in a feed-forward manner with dense connections, where each layer has as input the full feature maps of the previous layers. This approach allows the structure to reuse features, adjust the gradient problem, and use efficient parameters. DenseNet201 is a deep variant that excels in classification tasks in various applications and can be successfully assigned to the waste management area.

Another model used for the present study, VGG19, is a state-of-the-art deep network with 19 layers (Simonyan & Zisserman, 2014). The architecture presents a simple and uniform structure that facilitates the extraction of features from digital images based on convolutional layers (3 x 3), pooling layers and fully connected layers. Such a structure is appreciated for its simplicity and efficiency, although it is based on a large number of parameters but involves significant memory and calculation requirements. A batch normalization structure was implemented in this model.

A model that proved a balance between accuracy and computational efficiency, Xception (Chollet, 2016), represents another approach in the present study. The model is described as an extreme structure of the classic Inception model, implementing depth-separable convolutions (in two stages - spatial convolutions and channel convolutions). These implementations aim to reduce the number of parameters but improve

performance with a reduced computational footprint.

Another model used, ConvNext Base, is a convolutional neural network inspired by Vision Transformer (ViT) architectures (Liu et al., 2022). Optimizations to this architecture include large kernel convolutional blocks, hierarchical structures, and Layer Normalization instead of Batch Normalization. At the same time, the gradient vanishing problem and the flow are managed by layering and skip connections. Finally, the ConvNext design demonstrates performance comparable to ViT models, but which preserves the simplicity and efficiency of classical CNN structures.

MNASNet (Tan et al., 2022). is a deep neural network architecture developed for remarkable efficiency and performance among mobile devices. The architecture features a NAS - Neural Architecture Search approach to generate optimal architectures with a balance between complexity and computing resources. The model also features convolutional layers with efficient kernels and inverted moving blocks attached to reduce dimensions and inference times, ideal for computer vision tasks and real-time applications.

A custom system was used to highlight the hardware and software that was the basis of the experiments of the present study. It includes an operating system based on Win 11 Pro, an Intel Core i7-14700HX CPU, 32GB RAM, 1TB SSD and a dedicated NVIDIA GeForce RTX 4070 8GB video card with CUDA support, useful in developing deep learning solutions.

The chosen programming language was Python v3.9, integrating the PyTorch framework, flexible in the implementation and optimization of the chosen architectures.

RESULTS AND DISCUSSIONS

Simple features and complex textures can be extracted as part of waste classification using CNN, demonstrating outstanding performance. Table 1 shows the obtained performances around the accuracy metric and based on images from the test dataset. These images were not seen during the initial training and evaluation process and represent a solid point of testing the architectures using new data.

Table 1. The performances obtained in the case of the classification models

Model	Accuracy	Inference time (ms)
DenseNet201	93.40%	613
ConvNext Base	98.34%	687
Xception	97.38%	553
MNasNet100	90.84%	510
VGG19	94.77%	521

Notable performances were observed in the case of the implemented classification models, noting in some cases points for future development and optimization, based on the graphs of the loss and accuracy functions, from the training and validation side. Figures 3 to 7 show these details, where good convergence and slight fluctuations or differences in the performance of certain models are noted.

The execution time was noted by using a function that takes 5 random images from the test dataset and uses the best saved weights for each model to generate predictions based on these images. The inference times obtained for each model are in the range of 500 - 700ms, Table 1, which marks a fairly good performance on this classification task.

The best accuracy metrics exceed key values of 97% demonstrating superior classification

ability for the presented architectures. At the same time, high performance can be observed in the case of the new state-of-the-art models Xception or ConvNext, superior to classic ones such as DenseNet or VGG. However, in the case of DenseNet, the architecture continues to demonstrate superior performance, and this is due to the complex architecture, capable of extracting essential information using densely connected modules.

The same can be noted in the case of VGG where the well-optimized architecture manages to capture essential details in the classification process. Slightly lower performance can be seen in lightweight architectures where the need for optimization must be higher, with architectures risking losing key details as information is passed and analyzed within layers and structures, in the case of MNasNet.

Table 1 and the illustrated functions highlight key metrics for the classification task: accuracy, loss, and inference time. At their core, each model represents deep, widely used architectures adapted in the present case to waste classification tasks.

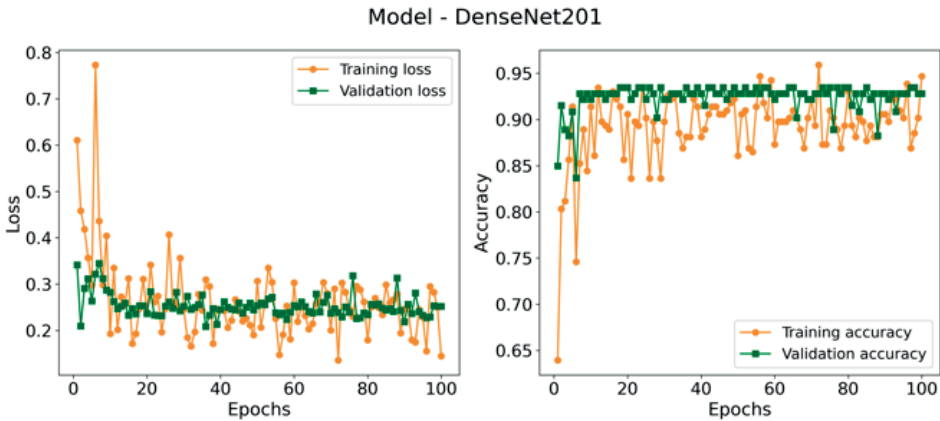


Figure 3. Training and validation performance of DenseNet201 model

Model - VGG19

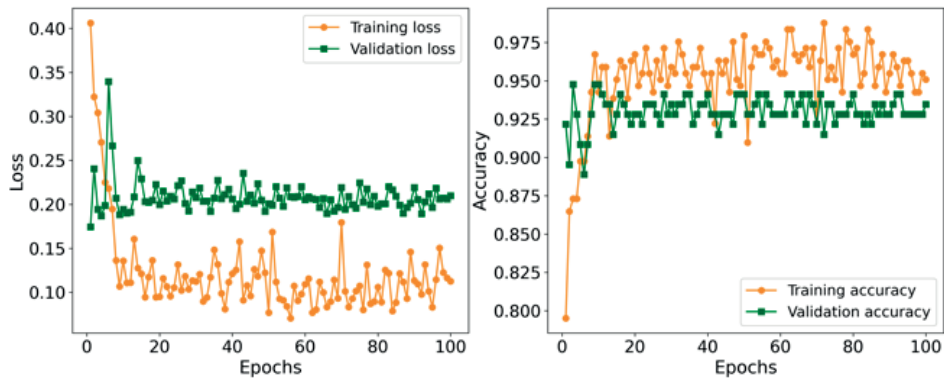


Figure 4. Training and validation performance of VGG19 model

Model - ConvNext Base

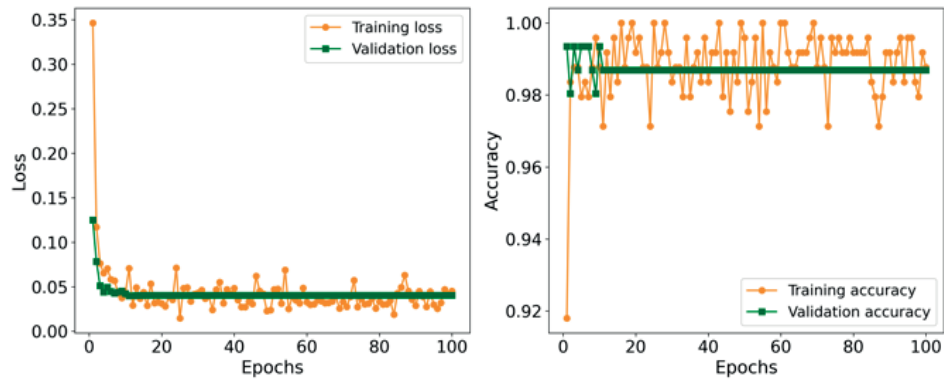


Figure 5. Training and validation performance of ConvNext Base model

Model - Xception

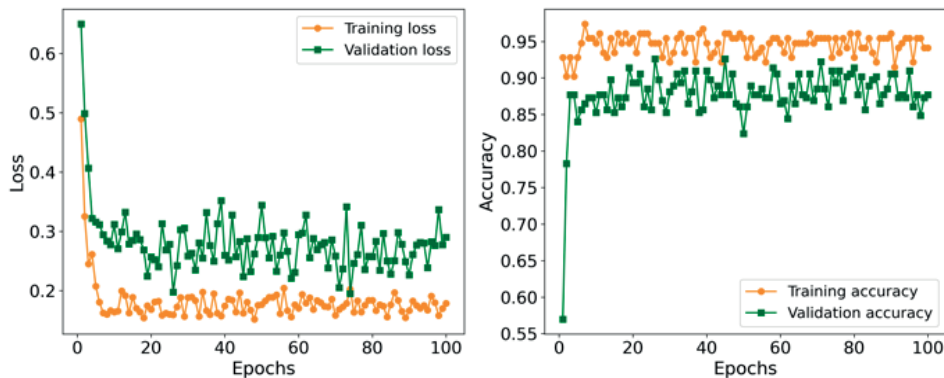


Figure 6. Training and validation performance of Xception model

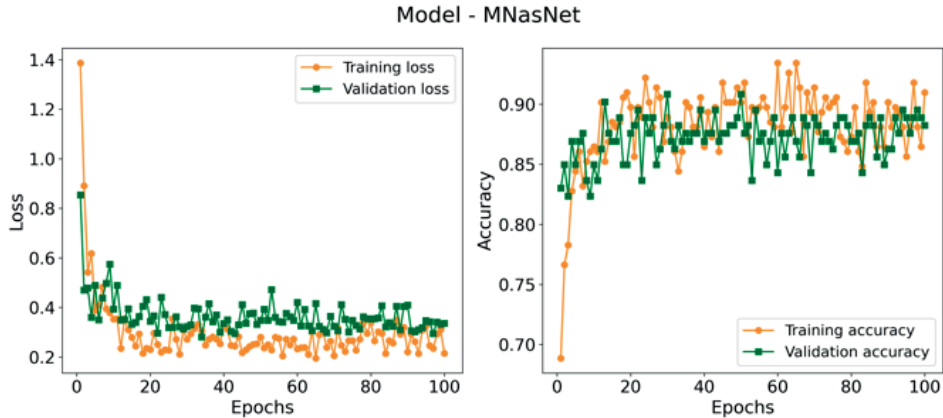


Figure 7. Training and validation performance of MNasNet model

The first model noted, DenseNet201, shows good accuracy with a slightly high inference time. The density of connections and the attached complexity can contribute to a relatively high uptime compared to other better optimized models. The second model, ConvNext Base, describes the best accuracy, but with an equally high inference time due to the associated complexity. The implementation of Layer Normalization modules and large kernels actively contribute to this high performance. Xception shows a slight drop in accuracy compared to ConvNext, but with better inference time due to the reduced complexity associated with using depth-separable convolutions. Designed for efficiency, MNasNet exhibits the shortest inference time, being the fastest in the list of proposed models. This may be due to effective layering in the model architecture. Although the accuracy is lower, the model is an acceptable compromise when developing it for real-time applications on resource-constrained devices. According to the experiments, VGG19 achieves remarkable accuracy being another fast model on the inference side. Although it is an older model, the VGG19 remains competitive due to its simple and deep architecture.

Consequently, choosing the right model depends on the context and application resources where the implementation is needed. In the same context, there must be a focus on accuracy vs inference time, as each model analyzed is suitable for different tasks and different usage

scenarios, offering various advantages or limitations.

To complete the present study a web application. was developed to test the proposed models, using the best weights saved after the training process. In this sense, the web application contains a module that can receive as input a digital image and using the exported weights can automatically generate a prediction in the task of waste classification.

The Javascript language and the React.js framework represented the established web technologies to implement the web application, along with the onnx-runtime-web tool to manage the export of classification models in onnx format, image tensors, attached for the proposed web technologies. Figure 8 illustrates the web application interface as well as an attached prediction example. A web application of this type proves to be a useful tool, with availability, that can capitalize on the characteristics of classification models that can be further integrated as modules of an automatic detection system, performance-oriented and at the same time accessible to users.

The development of the web application was based on the creation of JavaScript and React.js components that consider the characteristics of such a waste classification-oriented web application - web interface modules defined by React components, the basis of this framework. In relation to the classification techniques, the images that can be uploaded and sent to generate predictions go through a processing step so that

the format is known to the classification module, exported in the chosen format.

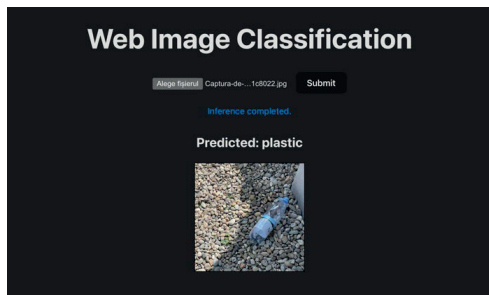


Figure 8. Web application interface

CONCLUSIONS

This study presented a modern method of integrating convolutional neural network architectures with a React.js web application to support the automated waste classification task. Benchmarking of the implemented CNN models revealed notable performance for classification tasks, highlighting strengths and weaknesses for each model, tracking metrics such as accuracy on a test dataset and operation (inference) time. The best models, Xception and ConvNext, demonstrated accuracy values of over 97 and 98%, respectively, which indicates the effectiveness of deep learning techniques adapted as innovative solutions in the field of waste management. However, the observed limitations pave the way for new research and optimization solutions to tune the architectures in achieving maximum performance with reduced inference times. At the same time, it was noted the way to implement such solutions in real-time identification systems and on platforms with limited resources - web applications, mobile hardware.

REFERENCES

- Alrayes, F.S., Mashael, M.A., Mashael, S.M., Mohamed, K.N., Mohammed, R., Azza, E.O., Suhanda, D. & Abu, S.Z. (2023). Waste Classification Using Vision Transformer Based on Multilayer Hybrid Convolution Neural Network. *Urban Climate*, 49, 101483. <https://doi.org/10.1016/j.uclim.2023.101483>.
- Bian, R., Jihong, C., Tingxue, Z., Chenqi, G., Yating, N., Yingjie, S., Meili, Z., Fengbin, Z. & Guodong, Z. (2022). Influence of the Classification of Municipal Solid Wastes on the Reduction of Greenhouse Gas Emissions: A Case Study of Qingdao City, China. *Journal of Cleaner Production*, 376, 134275. <https://doi.org/10.1016/j.jclepro.2022.134275>.
- Boldeanu, G., Gheorghe, M., Moise, C., Dana Negula, I., Tudor, G. (2023). Earth observation techniques applied for land waste detection and monitoring. *Scientific Papers. Series E. Land Reclamation, Earth Observation & Surveying, Environmental Engineering*, XII, 383-388, Print ISSN 2285-6064.
- Chollet, F. (2016). Xception: Deep Learning with Depthwise Separable Convolutions. 2017 IEEE Conference on Computer Vision and Pattern Recognition (CVPR), 1800-1807.
- Guo, S. & Liangliang, C. (2022). Why Is China Struggling with Waste Classification? A Stakeholder Theory Perspective. *Resources, Conservation and Recycling*, 183, 106312. <https://doi.org/10.1016/j.resconrec.2022.106312>.
- Huang, G., Liu, Z., & Weinberger, K.Q. (2016). Densely Connected Convolutional Networks. 2017 IEEE Conference on Computer Vision and Pattern Recognition (CVPR), 2261-2269.
- Lin, K., Tao, Z., Xiaofeng, G., Zongshen, L., Huabo, D., Huanyu, W., Guanyou, L. & Youcai, Z. (2022). Deep Convolutional Neural Networks for Construction and Demolition Waste Classification: VGGNet Structures, Cyclical Learning Rate, and Knowledge Transfer. *Journal of Environmental Management*, 115501. <https://doi.org/10.1016/j.jenvman.2022.115501>.
- Liu, Z., Mao, H., Wu, C.Y., Feichtenhofer, C., Darrell, T., & Xie, S. (2022). A ConvNet for the 2020s. IEEE/CVF Conference on Computer Vision and Pattern Recognition (CVPR), June. <https://doi.org/10.1109/cvpr52688.2022.01167>.
- Long, F., Jiang, S., Bar Ziv, E., & Zavala, V. (2024). Robust Plastic Waste Classification Using Wavelet Transform Multi-Resolution Analysis and Convolutional Neural Networks. *Computers & Chemical Engineering*, 181, 108516. <https://doi.org/10.1016/j.compchemeng.2023.108516>.
- Lu, X., Pu, X., & Han, X. (2020). Sustainable smart waste classification and collection system: A bi-objective modeling and optimization approach. *Journal of Cleaner Production*, 276, 124183. <https://doi.org/10.1016/j.jclepro.2020.124183>.
- Lubura, J., Pezo, L., Sandu, M.A., Voronova, V., Donsi, F., Šic Žlabur, J., Ribić, B., Peter, A., Šurić, J., Brandić, I., et al. (2022). Food Recognition and Food Waste Estimation Using Convolutional Neural Network. *Electronics*, 11(22), 3746. <https://doi.org/10.3390/electronics11223746>.
- Pitakaso, R., Srichok, T., Khonjun, S., Golinska-Dawson, P., Gonwirat, S., Nanthasamroeng, N., Boonmee, C., Jirasirilerd, G., Luesak, P. (2024). Artificial Intelligence in enhancing sustainable practices for infectious municipal waste classification. *Waste Management*, 1887-1900. <https://doi.org/10.1016/j.wasman.2024.05.002>.
- Qiao, Y., Zhang, Q., Qi, Y., Wan, T., Yang, L., Yu, X. (2023). A Waste Classification Model in Low-Illumination Scenes Based on ConvNeXt. *Resources, Conservation and Recycling*, 199, 107274. <https://doi.org/10.1016/j.resconrec.2023.107274>.

- Sarswat, P.K., Singh, R.S., Pathapati, S.V.S.H. (2024). Real time electronic-waste classification algorithms using the computer vision based on Convolutional Neural Network (CNN): Enhanced environmental incentives. *Resources, Conservation and Recycling*, 207, 107651. <https://doi.org/10.1016/j.resconrec.2024.107651>.
- Simonyan, K., & Zisserman, A. (2014). Very deep convolutional networks for large-scale image recognition. arXiv preprint arXiv:1409.1556.
- Tan, M., Chen, B., Pang, R., Vasudevan, V., Sandler, M., Howard, A., & Le, Q.V. (2019). Mnasnet: Platform-aware neural architecture search for mobile. In *Proceedings of the IEEE/CVF conference on computer vision and pattern recognition* (pp. 2820-2828).
- Tian, R., Lv, Z., Fan, Y., Wang, T., Sun, M., Xu, Z. (2024). Qualitative Classification of Waste Garments for Textile Recycling Based on Machine Vision and Attention Mechanisms. *Waste Management*, 183, 74–86. <https://doi.org/10.1016/j.wasman.2024.04.040>.
- Zhang, Q., Yang, Q., Zhang, X., Bao, Q., Su, J., Liu, X. (2021). Waste Image Classification Based on Transfer Learning and Convolutional Neural Network. *Waste Management*, 135, 150–57. <https://doi.org/10.1016/j.wasman.2021.08.038>.

PREDICTING THE FUTURE TRENDS OF EUROPEAN AND NATIONAL BENCH-MARKS IN THE MANAGEMENT OF BIODEGRADABLE MUNICIPAL WASTE USING ARTIFICIAL NEURAL NETWORKS

Eda PUNTARIĆ¹, Lato PEZO², Željka ZGORELEC³, Jerko GUNJAČA³,
Dajana KUČIĆ GRGIĆ⁴, Neven VOČA³

¹Ministry of Environment and Sustainable Development, 80 Radnicka cesta, Zagreb, Croatia

²University of Belgrade, Institute of General and Physical Chemistry,
Studentski trg, 12/V, Belgrade, Serbia

³University of Zagreb, Faculty of Agriculture, 25 Svetosimunska cesta, Zagreb, Croatia

⁴University of Zagreb, Faculty of Chemical Engineering and Technology,
19 Marulicev trg, Zagreb, Croatia

Corresponding author email: latopezo@yahoo.co.uk

Abstract

This research employs Artificial Neural Networks (ANN) to develop predictive models for biodegradable municipal waste at both European and national levels. Leveraging socio-demographic and economic data spanning 25 years across 17 European Union (EU) countries, the models aim to forecast biodegradable waste generation over a five-year period. The primary objective is to examine the influence of socio-demographic and economic factors on waste generation. According to the study's findings, it is anticipated that by 2025, the 17 EU countries will produce approximately 67.4 million tons of mixed municipal waste (MMW), 14.7 million tons of municipal paper and cardboard waste (PCW), 6.4 million tons of municipal wood waste (WW), and approximately 0.6 million tons of municipal textile waste (TW). This substantial volume underscores the pressing need for robust infrastructure covering collection, processing, recycling, and disposal mechanisms. The ANN model demonstrated impressive predictive capabilities for MMW, PCW, WW, and TW. Test predictions spanning 2020 to 2025 revealed R2 values ranging between 0.965 and 0.998 during the training phase for the output variables.

Key words: artificial intelligence, Europe, reduction of municipal waste, quantity estimation, waste generation, waste management.

INTRODUCTION

Biodegradable waste is any waste that undergoes anaerobic or aerobic decomposition (Council Directive 1999/31/EZ; Vis, 2017). Depending on local conditions, climate, energy source, degree of industrialization and consumer habits regarding food and drink consumption, between 60-70% of municipal waste consists of biodegradable municipal waste (food waste, green waste, paper, and cardboard wastes, etc.) (García et al., 2005; Vergara et al., 2012). Proper management of biodegradable waste is particularly important, considering that the amount of greenhouse gases from waste depends on how the waste is treated. Greenhouse gases are released by disposing of biodegradable waste in landfills and its decomposition (Kujawska et al., 2016; Eurostat, 2023). In 2019, waste management was the 4th largest source of

greenhouse gases in the EU and accounted for about 3.3% of greenhouse gases when distributed by sectors (European Parliament. Infographic: Greenhouse gas emissions by country and sector, 2022). Therefore, biodegradable waste (which includes bio-waste) is the key source of greenhouse gas emissions from landfills (EEA, 2018). The above is not surprising if you consider the fact that between 118 and 138 million tons of bio-waste is generated in the EU annually, while only less than 40% is currently recycled into useful products (ECN, 2022). There are also calculations that show that the USA annually disposes almost 300 million tons of organic waste in landfills (Themelis, 2022). Given that large amounts of biodegradable waste are still disposed of in landfills, and keeping in mind that this practice has a negative impact on the environment, it is necessary to urgently apply

alternative methods of managing this type of waste (García et al., 2005). With the aim of preserving the environment, great efforts have been invested in environmentally conscious management of biodegradable waste. In November 2021, a global pledge had been signed in Glasgow, in which more than a hundred countries of the world undertake to reduce emissions of the greenhouse gas methane by 30% by 2030 compared to the amount in 2020 (Le Page, 2021). Just by changing the way biodegradable waste is managed, the USA would be well on its way to reducing methane emissions by 30 percent (Themelis, 2022).

To initiate positive changes, this work aims to create a model for predicting the amount of generated waste of four different components of biodegradable municipal waste using ANNs, which could have a practical benefit in achieving a more efficient waste management system. Proper separation of biodegradable waste would set the pre-conditions for further processing with more environmentally friendly methods, such as composting or anaerobic digestion. In this way, the release of greenhouse gases that occur due to the decomposition of organic material in landfills would be reduced (Wei et al., 2017), and compost and digestate could be used in agriculture as quality soil amendments.

Given that, the mechanism of municipal waste generation is a very complex process and there is a connection between socioeconomic factors and the generation of municipal waste, non-linear regression models like ANN show better accuracy than linear ones. Therefore, the use of neural networks in predicting the generation of waste has recently become more frequent (Wu et al., 2020). As an example, Kulisz and Kujawska (2020) used ANNs to predict municipal waste generation in Poland. Data on waste and socioeconomic data of several municipalities were used for the development of mathematical models. In that re-search, ANN had good predictive quality in terms of determining waste production trends, both in the local context and at the national level (Kulisz & Kujawska, 2020).

Building on the success of previous applications where Artificial Neural Networks (ANN) demonstrated effectiveness in waste generation prediction, this research aims to leverage ANN

to develop models for estimating the generation of mixed municipal waste (MMW), municipal paper and cardboard waste (PCW), municipal wood waste (WW), and municipal textile waste (TW). The focus extends to both national and EU levels, encompassing the analysis of various socio-demographic characteristics, economic factors, and industrial data across seventeen EU countries.

MATERIALS AND METHODS

ANN modelling

Artificial Neural Networks (ANNs) exhibit a unique capability to process extensive datasets, making them an essential tool for deciphering intricate input-output connections within nonlinear systems (Abdoli et al., 2011; Ribić et al., 2019; Agatonovic-Kustrin & Beresford, 2000; Bunsan et al., 2013). Their broad applicability arises from their proficiency in modelling complex nonlinear relationships (Ghazi Zade & Noori, 2008; Noori et al., 2009; Antanasijević et al., 2013). In this research, an ANN model is employed to predict the generation of mixed municipal waste (MMW), municipal paper and cardboard waste (PCW), municipal wood waste (WW), and municipal textile waste (TW). The analysis encompasses socio-demographic, economic, and industrial data across 17 EU countries: Belgium, Croatia, Czech Republic, Denmark, Estonia, France, Hungary, Ireland, Italy, Latvia, Lithuania, Luxembourg, Malta, Netherlands, Slovenia, Spain, and Sweden, spanning the period from 1995 to 2019.

The input variables, comprising demographic data, economic progress, number of employed individuals, education level, tourism, and waste, were extracted from the web site of the statistical office of the EU (Eurostat). Eurostat's website was chosen for its provision of high-quality statistics and data from member states, countries outside the EU, and international organizations. The primary criterion for data selection was the availability of data for a specific variable during the period from 1995 to 2019 or for as long as possible. Total annual data for each country was utilized in model development. After collecting and verifying all data, the construction of the ANN commenced. In the end, 28 input variables were used, including: year (YEAR), population

(POP), LE (life expectancy), EL1 (educational attainment level, less than primary, primary and lower secondary education), EL2 (educational attainment level, upper secondary, post-secondary non-tertiary and tertiary education), EL3 (educational attainment level, upper secondary and post-secondary non-tertiary education), ELT (tertiary education), GDP (gross domestic product at market prices), RGDP (real GDP per capita), TFS (total financial sector liabilities, by sub-sectors, non-consolidated), NED (net external debt), NEER (nominal effective exchange rate), DIRE (direct investment in the reporting economy), TEMP (total employees from 15 - 64 years), URAD (unemployment rate), YUR (youth unemployment rate), MENI (median equalized net income), ATAE (arrivals at tourist accommodation establishments), NSTA (nights spent at tourist accommodation establishments), IGS (imports of goods and services), EGS (exports of goods and services), EOPP (exports of oil and petroleum products by partner country), HPI (house price index, deflated), RRMW (recycling rate of municipal waste), DL (disposal - landfill), GMWK (generation of municipal waste, kilograms per capita) and GMWT (generation of municipal waste, thousand tonnes), and CNT (country, as categorical variable).

Based on the collected input data, ANN model was created with the aim of predicting the output results (four fractions of biodegradable municipal waste in thousands of tons) for the period from 1995 to 2019. There were some missing data in the input database, but at this stage, ANN predicts them as well. Given that the goal of the research was to predict the amount of biodegradable municipal waste that will be generated in the near future, it was necessary to predict the input data for the same period. The above was also done using ANNs. It was necessary to create 26 models based on the variable - time (year) and the categorical variable - name of the country. After that, in the initial mathematical model that was created earlier, the input data were replaced by "new", predicted data. These are the same sociodemographic and economic parameters mentioned earlier, but with data for a different period.

Based on this data, data for 17 member states of the EU will be obtained for 26 input data and four output data for the period from 2020 to 2025.

The database for creating the ANN was divided into three parts: training (60%), cross-validation (20%), and testing (20%) data. The number of hidden neurons in the ANN model, developed as multilayer perceptron, varied from 5 to 30. The optimization process aimed to minimize the validation error, and training was considered successful when the learning and cross-validation curves reached zero after 100,000 training iterations. The Broyden-Fletcher-Goldfarb-Shanno (BFGS) algorithm was employed as a tool for solving unconstrained nonlinear problem in the course of ANN model building. The optimization was based on minimizing the sum of squares (SOS) and accelerating convergence (Taylor, 2006).

The coefficients for the hidden layer were represented by matrices W_1 and B_1 , while the coefficients for the output layer were represented by matrices W_2 and B_2 (Ochoa-Martínez & Ayala-Aponte, 2007):

$$Y = f_1(W_2 \cdot f_2(W_1 \cdot X + B_1) + B_2) \quad (1)$$

where:

- f_1 and f_2 are transfer functions in the hidden and output layers, respectively;
- X is the matrix of input variables.

Global sensitivity analysis

The Yoon interpretation method (Yoon et al., 2017) was applied to determine the relative influence of input data on MMW, PCW, WW and TW, based on the weight coefficients of the developed ANN.

$$RI_{ij}(\%) = \frac{\sum_{k=0}^n (w_{ik} \cdot w_{kj})}{\sum_{i=0}^m \left| \sum_{k=0}^n (w_{ik} \cdot w_{kj}) \right|} \cdot 100\% \quad (2)$$

where:

- w - weight coefficient in ANN model;
- i - input variable;
- j - output variable;
- k - hid-den neuron;
- n - number of hidden neurons;
- m - number of inputs.

The accuracy of the model

Numerical verification of the obtained ANN model was tested using the following commonly used parameters (defined in Eq. 3-8): coefficient of determination (R^2), reduced chi-squared (χ^2), mean bias error (MBE), root mean square error ($RMSE$), mean percentage error (MPE), error sum of squares (SSE), and average absolute relative deviation ($AARD$) (Aćimović et al., 2020):

$$\chi^2 = \frac{\sum_{i=1}^N (x_{exp,i} - x_{pre,i})^2}{N - n} \quad (3)$$

$$RMSE = \left[\frac{1}{N} \cdot \sum_{i=1}^N (x_{pre,i} - x_{exp,i})^2 \right]^{1/2} \quad (4)$$

$$MBE = \frac{1}{N} \cdot \sum_{i=1}^N (x_{pre,i} - x_{exp,i}) \quad (5)$$

$$MPE = \frac{100}{N} \cdot \sum_{i=1}^N \left(\frac{x_{pre,i} - x_{exp,i}}{x_{exp,i}} \right) \quad (6)$$

$$SSE = \sum_{i=1}^N (x_{pre,i} - x_{exp,i})^2 \quad (7)$$

$$AARD = \frac{1}{N} \cdot \sum_{i=1}^N \left| \frac{x_{exp,i} - x_{pre,i}}{x_{exp,i}} \right| \quad (8)$$

RESULTS AND DISCUSSIONS

Two ANN models were developed for the estimation of the main effect of the input variables on network outputs. ANN1 model was used to predict MMW, PCW, WW, and TW, during 1995 to 2019, based on socio-economic data between 1995 and 2019. The in-put database contained some missing data, and ANN1 model was engaged to predict those as well (Figure 1a). To predict socio-economic variables in 2020-2025, it was necessary to create an ANN model based on the known data (1995-2019). The first step was to create the ANN2 model, which could be capable to predict the socio-economic data in 2020-2025, based upon the available data: known socio-economic data (1995-2019), YEAR and CNT (Figure 1b). To obtain better modelling results, 26 separate ANN models were developed instead of just one model, and this set of models would be titled as ANN2 further in the text. The evaluated socio-economic indicators in 2020-2025 (calculated using ANN2 model) were used as inputs in ANN1 model to evaluate MMW, PCW, WW, and TW, in 2020-2025 (Figure 1c). The collected data were presented using descriptive statistics tables. The analysis and mathematical modelling were performed using STATISTICA 10.0.

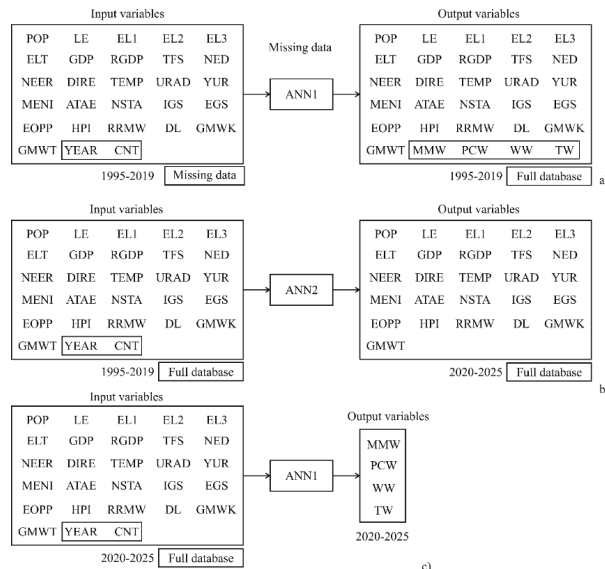


Figure 1. ANN models for prediction of MMW, PCW, WW, and TW, based on socio-economic data

The structure of the ANN, encompassing biases and weight coefficients, as well as the obtained results, is contingent on the initial assumptions of the matrix parameters crucial for building and fitting the ANN to experimental data. Additionally, the behaviour of the ANN model can be influenced by the number of neurons in the hidden layer. To mitigate this concern, each

ANN model topology underwent 100,000 runs to eliminate random correlation arising from initial assumptions and the random initialization of weights. According to this approach, the highest R^2 value throughout the training cycle was achieved when employing n hidden neurons to construct the ANN model (Figure 2a).

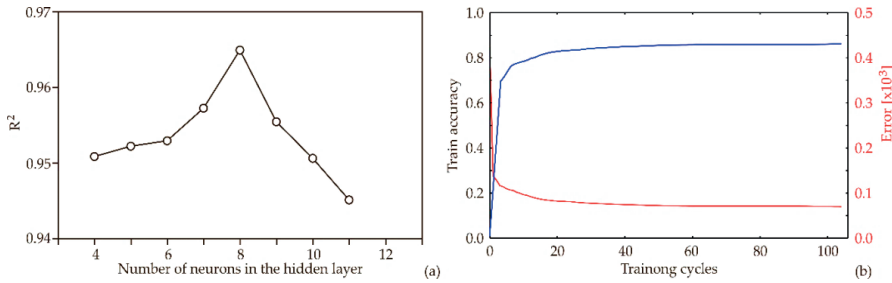


Figure 2. ANN calculation for DIRE variable: (a) The dependence of the R^2 value of the number of neurons in the hidden layer in the ANN model; (b) Training results per epoch

Each ANN model underwent training for 100 epochs, and the training results, including train accuracy and error (loss), are illustrated in Figure 2b. Training accuracy exhibited an increase with increments in the number of training cycles until the 70-80th epoch, reaching an almost constant value. The highest train accuracy and lowest train loss were observed for the 70-80th epoch, beyond which a slight increase in train accuracy and a decrease in train loss were noted, indicative of overfitting. Utilizing more than 80 epochs for training could potentially lead to significant overfitting, while 70 epochs proved sufficient to achieve high model accuracy without incurring the risk of overfitting (Figure 2b). The constructed optimal neural network ANN1 model showed promising

generalization property for the collected database and could be used to accurately predict the settlement waste: 20 (network MLP 44-20-4) to obtain the highest values of R^2 (during the training cycle, R^2 for output variables (MMW, PCW, WW and TW) were: 0.999; 0.998; 0.997 and 0.998, respectively). The obtained ANN models for predicting the outcome variable were complex corresponding to the in-creased degree of nonlinearity in the data. The estimate of the quality of fit between the collected data and the outputs computed by the model, expressed as the ANN power (sum of R^2 between measured and computed output variables) during the training, testing and validation steps, is explained in Table 1.

Table 1. The "goodness of fit" tests for the formulated ANN model

Output variable	χ^2	RMSE	MBE	MPE	SSE	AARD	R^2
MMW	$4.3 \cdot 10^4$	$2.1 \cdot 10^2$	3.5	$1.6 \cdot 10^1$	$9.4 \cdot 10^6$	$4.2 \cdot 10^4$	0.999
PCW	$6.6 \cdot 10^3$	$8.0 \cdot 10^1$	1.2	$6.0 \cdot 10^1$	$1.4 \cdot 10^6$	$1.5 \cdot 10^4$	0.997
WW	$1.7 \cdot 10^3$	$4.1 \cdot 10^1$	-5.1	$9.2 \cdot 10^1$	$3.7 \cdot 10^5$	$1.1 \cdot 10^4$	0.989
TW	$8.9 \cdot 10^1$	$9.4E+00$	1.2	$3.2 \cdot 10^2$	$1.9 \cdot 10^4$	$1.1 \cdot 10^3$	0.992

R^2 - coefficient of determination, χ^2 - reduced chi-squared, MBE - mean bias error, RMSE - root mean square error, MPE - mean percentage error, SSE - error sum of squares, and average absolute relative deviation (AARD).

The ANN models predicted the data sufficiently well for a wide range of process variables. For all ANN models, the predicted values were very close to the measured values in most cases with respect to the R^2 values. The estimated SOS

values of the ANN model were of the same order of magnitude as the errors reported in the literature for output variables (Kollo & von Rosen, 2005), while the lack of fit of the ANN model did not reach a significant level, implying

that the model predicted the output variables satisfactorily. An increased R^2 value indicated that the ANN model fitted the data well.

Future prediction capabilities

The main results of this research were the predicted amounts of waste that will be generated in the period from 2020 to 2025. The waste data are presented below (Table 2).

Table 2 shows the amounts of MMW, municipal PCW, WW and TW that were predicted based on mathematical model created using ANN for the period from 2020 to 2025. The estimated amount of MMW in the 17 observed EU countries in 2025 amounts to 67.4 million tons. In the mentioned period (2020-2025) Spain, France and Italy jump in terms of volumes of MMW. In general, from 2020 to 2025, total volumes of MMW for all 17 countries are declining.

The amount of PCW predicted from 2020 to 2025 slightly decreases (around 15 million tons per year) (Table 2). The countries with the largest amounts of PCW are, as with MMW, Italy, France, and Spain. The amounts of municipal WW with an increase in quantities is predicted, and the quantities range between 5.6 and 6.4 million tons per year. The countries with the largest quantities of municipal WW are France and Italy. In the period from 2020 to 2025, the largest amounts of municipal TW will be generated in Italy, France, and Belgium, and the least in Latvia. In the mentioned period, the quantities range between 0.57 and 0.59 million tons per year (Table 2).

According to the results, it is expected that 411.4 million tons of MMW, 90.3 million tons of PCW, 35.9 million tons of WW and 3.5 million tons of TW will be generated between 2020 and 2025.

Table 1. The amount of waste that will be generated from 2020 to 2025 shown in million tons

Year	MMW	PCW	WW	TW
2020	69.8	15.4	5.6	0.6
2021	69.3	15.3	5.8	0.6
2022	68.8	15.1	5.9	0.6
2023	68.3	15.0	6.1	0.6
2024	67.8	14.8	6.2	0.6
2025	67.4	14.7	6.4	0.6

Global sensitivity analysis - Yoon's interpretation method

The influence of 28 input variables on MMPW, PCW, WW and TW was investigated. The results of the research show that all four outputs are positively affected by POP, GDP, MENI, tourism, EOPP, and NED (Figure 3).

According to Kulisz and Kujawska (2020), the smallest member states of the EU have recorded the lowest level of generated waste, which was confirmed in this study. Malta and Luxembourg had the lowest level of generated waste, while France, Italy, Spain have the largest amount of generated waste. Figure 3 also shows how the number of inhabitants has a positive effect on all four observed types of waste with a relative impact of: 3.26% for MMW, 3.77% for municipal PCW, 1.73% for municipal WW and 1.80% for municipal TW, which is in line with previous research (Kulisz & Kujawska, 2020; Badruddin et al., 2002; Gui et al., 2019).

In addition to the local population, visitors and tourists participate in the generation of municipal waste, which can be seen as an additional population in the context of the generation of municipal waste (Arbulú et al., 2015; Grbeš, 2017). The variable indicating overnight stays in tourist accommodation facilities has a positive effect on all four observed types of waste with a relative impact of: 0.59% for MMW, 1.26% for municipal PCW, 0.07% for municipal WW and 3.94% for municipal TW, which is in accordance with the research of Kumar et al. (2011), Mateu-Sbert et al. (2013) and Arbulú et al. (2015).

The results of this study show that GDP has a positive effect on all four observed types of waste, which is in line with previous research by Kusch and Hills (Kusch & Hills, 2017). A similar study was conducted by Namlisa and Komilisa (2019), whose aim was to investigate the potential impact of four socioeconomic indices on waste generation. In their research, EE waste, paper and wood waste, waste oil, small batteries, scrap metals and tires were positively correlated with GDP, indicating that economic growth directly affects waste generation.

MENI positively affects all four observed types of waste with a relative impact of: 1.57% for MMW, 2.02% for municipal PCW, 6.68% for municipal WW and 4.58% for municipal TW.

The positive impact of net income on waste generation is in accordance with the research of Sabarinah (1997), Bandara et al. (2007), Foday et al. (2012) and Ogwueleka (2013), which show that income has a positive effect on waste generation. In addition, in a study conducted on 39 municipalities in Brazil, a statistically significant linear correlation was observed between income per capita and annual production of municipal waste ($R^2 = 0.391$) (Namlis & Komilis, 2019).

The global dependence on oil, natural gas and coal, as well as the damage that this dependence causes, is well-known, especially nowadays (Lioudis, 2021). It was shown that the ex-port of oil and oil derivatives has a positive effect on all four types of waste with a relative impact of

2.38% for MMW, 2.30% for municipal PCW, 4.74% for municipal WW and 4.53% for municipal TW. The increase in the price of oil positively affects the economy and standard of living, but also leads to an increase in waste generation.

On the other hand, LE, RGDP, TFS and IGS negatively affect all four types of municipal waste. Other observed factors (such as FDI, annual data on URAD, EGS and education) did not give results from which a single conclusion could be drawn. From the above, it could be seen that the accuracy of predicting the amount of biodegradable waste using ANN really depends on the selection of input socio-demographic, economic and industrial indicators.

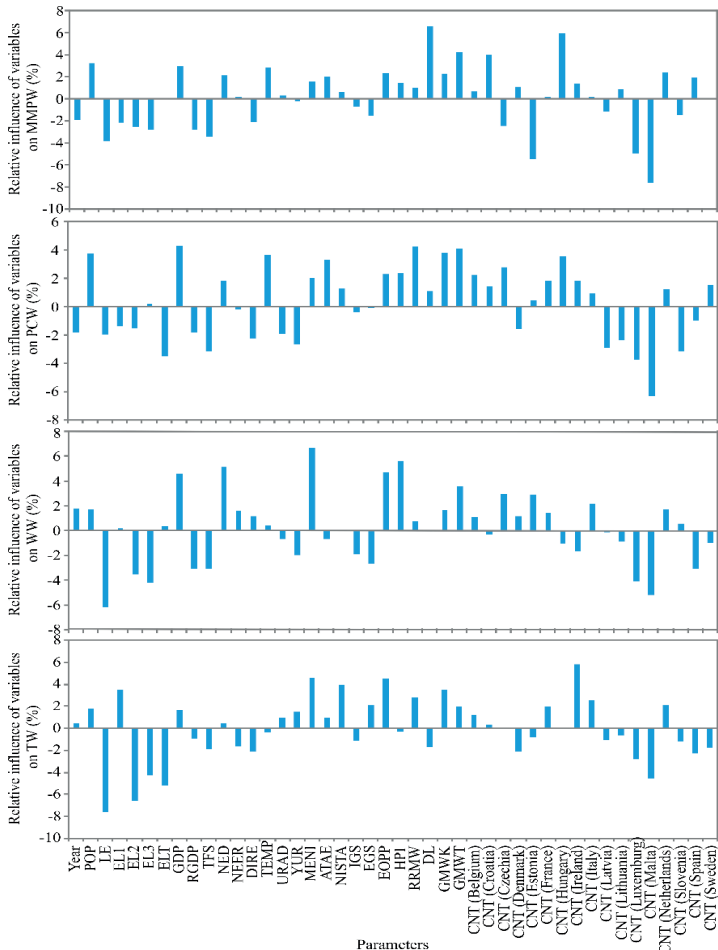


Figure 3. The relative importance of the input variables on MMW, PCW, WW and TW, determined using Yoon interpretation method

Regardless of the satisfactory results and several positive characteristics of ANN, it should be noted that the limitation of this study is the "late" availability of waste data, so future research should upgrade the mathematical model developed in this research with the addition of new data. It could also be assumed that the disease epidemic caused by the coronavirus as well as the war in Ukraine will also affect the amount of waste that will be generated.

CONCLUSIONS

According to the results obtained from this research, it can be expected that in the 17 observed EU countries, the total amount of waste for the four observed fractions (MMW, municipal PCW, WW and TW) in 10 years will increase by approximately 0.5% compared to the data from 2015. It can be also expected that in 2025 in 17 observed EU countries, about 67.4 mil tons of MMW will be generated. The stated amount will include bio-waste that will be unseparated and thrown away as part of MMW. According to the results obtained from this research, it is also expected that in 2025 about 14.7 mil. tons of municipal PCW, 6.4 mil. tons of municipal WW and 0.6 mil. tons of municipal TW will be generated in 17 EU countries. Forecasting the amount of waste generated can help to identify the most appropriate pattern of waste management and at the same time assist decision-makers in updating and modifying legal acts and regulations to enable the transition to a cost-efficient circular economy.

The results also show that all four observed types of municipal waste are positively affected by POP, GDP, TEMP, MENI, tourism, EOPP and NED. On the other hand, LE, RGDP, TFS and IGS negatively affect all four types of municipal waste. From the above, it could be concluded that the accuracy of predicting the amount of biodegradable waste using ANN really depends on the selection of input socio-demographic, economic and industrial indicators. In addition, it can be said that the created mathematical model showed satisfactory properties and possibilities in predicting the amount of MMW, PCW, WW and TW.

In the further research of the topic, it is necessary to expand the research and continue

with innovations in the waste management sector if the ambitious goals of the EU to become the first climate-neutral continent in the world by 2050 are to be achieved. In accordance with all the above, the developed mathematical model could serve as a tool to improve waste management so that the organization is more accurate, simpler, and more economical and environmentally friendly. This model would also ensure that waste management changes in parallel with the change in the socio-economic characteristics of society. In future research, the use of new parameters such as family size, eating habits and the impact of waste prevention is encouraged. In addition, it is proposed to expand the research to other countries and other types of waste. Also, it is suggested to repeat the research with more recent data and to investigate the impact of the corona crisis and the war in Ukraine on waste generation. In addition, it is proposed to expand the research to other countries and other types of waste.

AUTHOR CONTRIBUTIONS

Eda Puntarić: conceptualization, investigation, resources, writing - original draft preparation, writing - review and editing.

Lato Pezo: methodology, software, formal analysis, investigation, data curation, writing - original draft preparation, writing - review and editing, visualization.

Željka Zgorelec: validation, supervision.

Jerko Gunjača: validation, supervision.

Dajana Kučić Grgić: validation, supervision.

Neven Voća: conceptualization, methodology, validation, formal analysis, investigation, resources, writing -original draft preparation, writing - review and editing, supervision, project administration, funding acquisition.

All authors have read and agreed to the published version of the manuscript.

ACKNOWLEDGEMENTS

This paper has been fully supported by Croatian Science Foundation under the project IP-2018-01-7472 Sludge management via energy crops' production.

REFERENCES

- Abdoli, M.A., Nezhad, M.F., Sede, R.S., Behboudian, S. (2011). Long term Forecasting of Solid Waste Generation by the Artificial Neural Networks. *Environ. Prog. Sustain*, 31, 628–636.
- Ćimović, M., Pezo, L., Tešević, V., Čabarkapa, I., Todosijević, M. (2020). QSRR Model for predicting retention indices of Satureja kitaibelii Wierzb. ex Heuff, essential oil composition. *Ind. Crop. Prod.* 154. <https://doi.org/10.1016/j.indcrop.2020.112752>
- Agatonovic-Kustrin, S. & Beresford, R. (2020). Basic concepts of artificial neural network (ANN) modeling and its application in pharmaceutical research. *J. Pharmaceut. Biomed.* 22, 717–727.
- Antanasijević, D., Pocajt, V., Popović, I., Redžić, N., Ristić, M. (2013). The forecasting of municipal waste generation using artificial neural networks and sustainability indicators. *Sustain. Sci.*, 8, 37–46.
- Arbulú, I., Lozano, J., Rey-Maqueira, J. (2015). Tourism and solid waste generation in Europe: A panel data assessment of the Environmental Kuznets Curve. *Waste Manage.*, 46, 628–636.
- Badruddin, M.Y., Othman, F., Hashim, N., Cahaya, Ali N. (2002). The role of socio-economic and cultural factors in municipal solid waste generation: A case study in Taman Perling, Johor Bahru. *Jurnal Teknologi*, 37(F), 55–64.
- Bandara, N.J.G.J., Hettiaratchi, J.P.A., Wirasinghe, S.C., Pilapiya, S. (2007). Relation of waste generation and composition to socio-economic factors: A case study. *Environ. Monit. Assess.*, 135, 31–39.
- Bunsan, S., Chen, W.-Y., Chen, H.-W., Chuang, Y.H., Grisdanurak N. (2013). Modeling the dioxin emission of a municipal solid waste incinerator using neural networks. *Chemosphere*, 92, 258–264.
- Council Directive 1999/31/EZ of 26 April 1999. On the landfill of waste, <https://eur-lex.europa.eu/legal-content/EN/TXT/PDF/?uri=CELEX:01999L0031-20180704&from=EN>, (accessed on 15 September 2022).
- Doumpos, M. & Zopounidis, C. (2011). Preference disaggregation and statistical learning for multicriteria decision support: A re-view. *Eur. J. Oper. Res.*, 209(3), 203–214.
- ECN, Factsheet: Sustainable use of compost and digestate to improve solid organic matter. https://www.compostnetwork.info/download/191129_factsheet-on-sustainable-use-of-compost-and-digestate-to-improve-soil-organic-matter/, (accessed on 29 September 2022).
- EEA, Annual European Union approximated greenhouse gas inventory for the year 2018, EEA Report No 16/2019, European Environment Agency (<https://www.eea.europa.eu/publications/approximate-d-eu-ghg-inventory-proxy-2018>, (accessed on 24 October 2022).
- European Parliament. Infographic: Greenhouse gas emissions by country and sector. <https://www.europarl.europa.eu/news/hr/headlines/societ/20180301STO98928/infografika-emisije-staklenickih-plinova-po-zemlji-i-sektoru>, (accessed on 15 May 2022).
- Eurostat. Greenhouse gas emissions from waste. Greenhouse gas emissions from waste - Products Eurostat News - Eurostat (europa.eu), (accessed on 26 May 2023).
- Foday, P.S., Xiangbin, Y., Alhaji, M.H.C. (2012). A Situational Assessment of Socioeconomic Factors Affecting Solid Waste Generation and Composition in Freetown, Sierra Leone. *J. Environ. Prot.*, 3, 563–568.
- García, A.J., Esteban, M.B., Marquez, M.C., Ramos, P. (2005). Biodegradable municipal solid waste: Characterization and potential use as animal feedstuffs. *Waste Manage.*, 25, 780–787.
- Ghazi Zade M.J. & Noori, R. (2008). Prediction of Municipal Solid Waste Generation by Use of Artificial Neural Network: A Case Study of Mashhad. *Int. J. Environ. Res.*, 2(1), 13–22.
- Grbeš, A. (2017). Odabir varijabli za stvaranje modela obrade krutoga otpada u gradovima i naseljima Hrvatske. *Rudarsko-geološko-naftni zbornik*, 32(3), 55–69. <https://doi.org/10.17794/rgn.2017.3.6>
- Gui, S., Zhao, L., Zhang Z. (2019). Does municipal solid waste generation in China support the Environmental Kuznets Curve? New evidence from spatial linkage analysis. *Waste Manage.*, 84, 310–319.
- Kollo, T. & von Rosen, D. (2005). *Advanced Multivariate Statistics with Matrices*; Springer: Dordrecht, The Netherlands.
- Kujawska, J., Wojciech, C. (2016). Method for Removal of CO₂ from Landfill Gas. *Middle pomeranian scientific society of the environment protection*, 18, 1018–1024.
- Kulisz, M., Kujawska, J. (2020). Predicting of Municipal Waste Generation in Poland Using Neural Network Modeling. *Sustainability*, 12, 10088.
- Kumar, J.S., Venkata Subbaiah, K., Prasada Rao, P.V.V. (2011). Prediction of Municipal Solid Waste with RBF NetWork- A Case Study of Eluru, A.P, India. *International Journal of Innovation, Management and Technology*, 2(3), 238–243.
- Kusch, S. & Hills, C.D. (2017). The Link between e-Waste and GDP - New Insights from Data from the Pan-European Region. *Resources*, 6(2), 15.
- Le Page M. “Make or break” is hardly hyperbole for the climate negotiations due to reach their climax in November in Glasgow, UK. (2021). At the COP26 meeting, nations will have a last chance to really rev up the stuttering motor of climate action and come good on commitments made in Paris in 2015 to limit global warming to a “safe” level of 1.5°C. *New Sci.*, 250(3331), 34–37, 42–45.
- Lioudis, N. *What Is the Relationship Between Oil Prices and Inflation?* Investopedia. <https://www.investopedia.com/ask/answers/06/oilpriceinflation.asp>, (accessed on 8 December 2021).
- Mateu-Sbert, J., Ricci-Cabello, I., Villalonga-Olives, E., Cabeza-Irigoyen, E. (2013). The impact of tourism on municipal solid waste generation: The case of Menorca Island (Spain). *Waste Manage.*, 33, 2589–2593.

- Namlis, K-G. & Komilis, D. (2019). Influence of four socioeconomic indices and the impact of economic. *Waste Manage.*, 89, 190-200.
- Noori, R., Abdoli, M.A., Jalili Ghazizade, M., Samiefard, R. (2009). Comparasion of Neural Network and Principal Component Regression Analysis to Predict the Solid Waste Generation in Tehran. Iran *J. Public Health*, 38(1), 74-84.
- Ochoa-Martínez, C.I. & Ayala-Aponte, A.A. (2007). Prediction of mass transfer kinetics during osmotic dehydration of apples using neural networks. *LWT-Food Sci. Technol.*, 40(4), 638-645.
- Ogwueleka, T.C. (2013). Survey of household waste composition and quantities in Abuja, Nigeria. *Resources, Conservation and Recycling*, 77, 52–60.
- Ribić, B., Pezo, L., Sinčić, D., Lončar, B., Voća, N. (2019). Predictive model for municipal waste generation using artificial neural networks – Case study City of Zagreb, Croatia. *Int. J. Energ. Res.*, 43, 5701-5713.
- Sabarinah, M. (1997). *The Effect of Socio-economy on Municipal Solid Waste Generation: State of Johor*. A Master Thesis. Universiti Teknologi Malaysia.
- Taylor, B.J. (2006). *Methods and Procedures for the Verification and Validation of Artificial Neural Networks* (Springer Science & Business Media. New York).
- Themelis, N.J. Divert Biodegradable Waste From Landfills to Cut Climate-Warming Methane Emissions. <https://news.columbia.edu/news/divert-biodegradable-waste-methane> (accessed on 15 September 2022).
- Vergara, S.E., Tchobanoglous, G. (2012). Municipal Solid Wasteand the Environment: A Global Perspective. *Annu. Rev. Environ. Resour.*, 37, 277–309.
- Vis, M. (2017). *Assessing the Potential From Bio-waste and Postconsumer Wood*. In: Panoutsou C. Modeling and Optimization of Biomass Supply Chains. London
- Wei, Y., Li, J., Shi, D., Liua, G., Zhao, Y., Shimaoka, T. (2017). Environmental challenges impeding the composting of biodegradable municipal solid waste: A critical review. *Resources, Conservation and Recycling*, 122, 51-65.
- Wu, F., Niu, D., Dai, S., Wu, B. (2020). New insights into regional differences of the predictions of municipal solid waste generation rates using artificial neural networks. *Waste Manage.*, 107, 182-190.
- Yoon, Y., Swales, G., Margavio, T.M. (2017). A Comparison of Discriminant Analysis versus Artificial Neural Networks. *J. Oper. Res. Soc.*, 44, 51-60.

ASSESSING ACCURACY OF LOW-COST COMPACT SYSTEM VERSUS STANDARD AIR QUALITY SYSTEMS

Adrian ROSU^{1,2}, Daniel-Eduard CONSTANTIN^{1,2}, Mirela VOICULESCU^{1,2},
Silvia DRĂGAN⁴, Maxim ARSENI^{1,2}, Stefan-Mihai PETREA^{2,3},
Catalina ITICESCU^{1,2}, Lucian Puiu GEORGESCU^{1,2}

¹"Dunarea de Jos" University of Galati, Faculty of Sciences and Environment,
111 Domneasca Street, Galati, Romania

²"Dunarea de Jos" University of Galati, REXDAN Research Infrastructure,
98 George Cosbuc Street, Galati, Romania

³"Dunarea de Jos" University of Galati, Faculty of Food Science and Engineering,
111 Domneasca Street, Galati, Romania

⁴EnviroEcoSmart.S.R.L., 189 Tecuci Street, Galati Romania

Corresponding author emails: rosu_adrian_90@yahoo.ro; adrian.rosu@ugal.ro

Abstract

Air pollution has emerged as a pressing concern in large urban areas, often stemming from sources like intensified traffic and industrial activities within city limits. Addressing this issue requires an understanding of air quality levels, leading to the adoption of low-cost, portable air quality monitoring systems. In our research, we conducted tests using a compact mobile air quality system, SNIFFER 4D (SN), comparing its performance against conventional air quality monitors utilizing standardized methods such as chemiluminescence and spectrometry. The equipment was stationed at the REXDAN research facility situated along one of Galati city's main roads. The primary objective of our study was to evaluate the reliability and suitability of the SN for detailed analysis of trace gases like NO₂, O₃, and PM₁₀, by cross-referencing data with readings from standard instruments capable of measuring individual trace gases. Data collection spanned from August 17 to August 30, 2023. Our findings indicate that the SN system proved to be a stable and sophisticated tool for conducting high-resolution studies on local and regional air pollution, encompassing pollutants such as NO₂, O₃, and PM₁₀.

Key words: Low-cost air quality monitoring systems, air pollution, air quality station, standard air quality system, trace gases, PM₁₀.

INTRODUCTION

Air pollution caused by human activities, such as industry, agriculture, transportation, and other polluting sectors is a worldwide environmental problem. Many studies are performed to illustrate the past, actual level of emissions using in-situ measurements (Hofman et al., 2022; Iannarelli et al., 2022; Leifer et al., 2022; Li K. et al., 2022; Specht et al., 2022; Sturm et al., 2022; Zhao C. et al., 2022), ground-based remote sensing measurements (Constantin et al., 2013; Merlaud et al., 2018; Rosu et al., 2019b; Roşu et al., 2018; 2019a; 2021), satellite instruments (Gupta et al., 2006; Hoff & Christopher, 2009; Leifer et al., 2022; Ung et al., 2021; Zhang et al., 2020; Zhao C. et al., 2022). In general, air pollutants include both gaseous (NO₂, O₃, etc.)

and particulate matter (PM) caused by burning of fossil fuels during different activities (industrial, traffic, warming, etc.) that occur largely in large human agglomerations such as large cities.

Urban air quality has emerged as a critical concern, impacting public health, environmental sustainability, and overall quality of life (Fenger, 1999; Gulia et al., 2015; Hopke et al., 2008; Mocanu et al., 2023). Following, the necessity for the utilization of low-cost air quality systems in urban areas has become increasingly evident. Low-cost air quality systems offer several advantages in urban areas, including affordability, scalability, real-time data availability, and enhanced community engagement. Additionally, their scalability enables the creation of comprehensive monitoring networks across urban landscapes, capturing spatial variations in pollution levels (Kelechi et al., 2022; Li J. et al.,

2020; Morawska et al., 2018; Penza et al., 2017). Real-time data provided by these systems enables timely responses to pollution events, facilitating targeted interventions to improve air quality. However, challenges such as lower accuracy and precision, the need for frequent calibration and maintenance, limited sensor capabilities, and concerns about data quality assurance remain significant disadvantages of low-cost air quality systems (Clements et al., 2017; Idrees & Zheng, 2020; Ikram et al., 2012; Karagulian et al., 2019). Calibrating low-cost sensors is essential to ensure the accuracy and reliability of air quality data collected over time series measurements. Proper calibration involves adjusting sensor readings to match known reference values, minimizing the risk of measurement errors, and ensuring consistency in data interpretation (González Rivero et al., 2023; Han et al., 2021; Ionascu et al., 2021).

In this study, we present the results of a direct comparison of measurements for NO₂ (nitrogen dioxide), O₃ (ozone), and PM₁₀ (suspended particulate matter) using a compact low-cost air quality system with the measurement of the same trace gases using standard air quality equipment deployed near or at the same location for two weeks. The

study aims to evaluate the factory accuracy (errors, correlation factors, etc.) of the low-cost system with respect to standard equipment.

MATERIALS AND METHODS

Study area and localization

The testing of the compact air quality system Sniffer 4Dv2 (SN) data for NO₂, O₃, and PM₁₀ against other standard one-to-multiple trace gas monitors took place at the REXDAN Research Infrastructure (REXDAN), situated on a major thoroughfare in Galati, a city in the SE of Romania (45°26'22"N 28°2'4"E) (98 George Coșbuc Street, Galati, Romania).

This location was selected due to its accessibility for powering the instruments and its proximity to one of the busiest traffic-congested roads in Galati, with high levels of pollution (Roșu et al., 2018; Rosu et al., 2023). Also, the location of the experiment is close to one of the local air quality stations (AQS) GL-2, which is part of a national network for air quality monitoring (Rețeaua Națională de Monitorizare a Calității Aerului - RNMCA), from which data were collected, to be used for comparison of SN data. The map that presents the spatial location of the deployment of equipment along with the position of AQS GL2 is presented in the Figure 1.

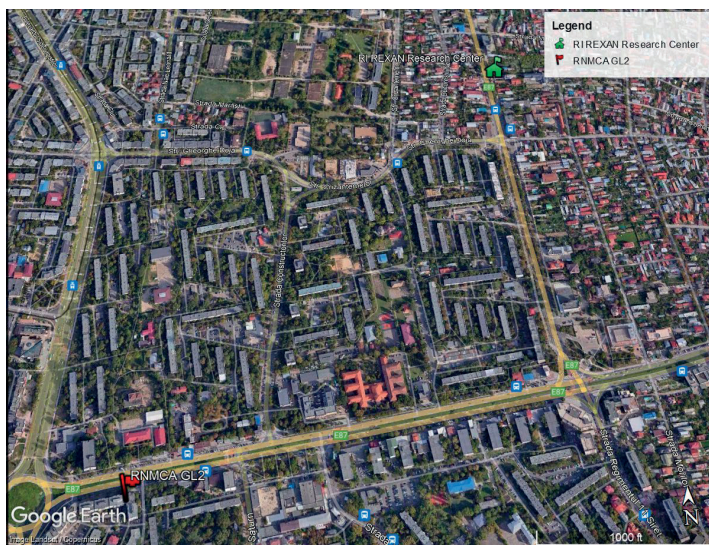


Figure 1. Location of the deployment of the measuring equipment REXDAN RI and the location of the AQS GL2 from RNMCA

We chose to utilize data from GL2 AQS because of the specification about the spatial limit of detection of 5 kilometers around it, thus covering our measurement site, declared by RNMCA and presented in a previous study where we used the SN system to quantify spatial extend of pollution in Galati city (*Calitate Aer | Acasă*, n.d.; Rosu et al., 2023). The period of measurements is from 17 August to 30 August 2023 when all equipment was deployed for synchronous measurement at REXDAN RI inside a climatized box, located in the courtyard as it is presented in the figure from below. The climatized box can maintain a constant temperature while the external air is brought by a pump system with a flow of 5 L/min. We chose this climatized box to remove data drifts of air pollutants caused by temperature variability, especially for electrochemical sensors and other spectroscopic effects that can generate errors in air pollutants measurements.



Figure 2. The temperature-controlled box where all air quality requirements were deployed for consistency of data (removing temperature-driven drifts from data series)

Equipment and data

For our study, we used data collected during 17-30 August 2023 from GL2 RNMCA AQS, and data recorded by each of the following standard equipment: Model 405 nm NO₂/NO/NO_x Monitor (2B NO₂); Sniffer 4Dv2 (SN- the low-cost air-quality system: NO₂, O₃, PM₁₀); Personal Ozone Monitor (POM - 2B O₃). Each of the standard air quality

measurement equipment and AQS are presented in detail below.

The local air quality monitoring network in Galati City is managed by the local administrative office of the Environmental Protection Agency of Galati (Agenția de Protecția Mediului din Galați - APM GL). Comprising four stationary Air Quality Stations (AQS) situated across various areas of the city, each AQS is equipped with monitors and sensors housed within a temperature-controlled container to continuously measure specific pollutants. The parameters measured by each AQS in Galati City encompass a comprehensive array of air pollutants and meteorological data. Of particular interest for our study are the following pollutants, along with their respective determination methods: particulate matter (PM₁₀ - Light Scattering Particle), nitrogen dioxide (NO₂ - chemiluminescence), and ozone (O₃ - ultraviolet photometric analyzer). More information about the equipment that is used at each AQS is presented in Table 1. The data of each AQS can be downloaded from the database available at (*Calitate Aer | Acasă*, n.d.). For our study, we downloaded the data from GL2 RNMCA for the period of the in-situ campaign.

The Personal Ozone Monitor (POM) by 2B Technologies is a lightweight and portable scientific equipment designed for personal exposure monitoring of ozone (O₃) levels. Featuring advanced sensor technology, the POM delivers accurate and real-time measurements of ozone concentrations in ambient air. Its compact design and wearable form factor make it an ideal measurement of ozone exposure, providing valuable insights into air quality and potential health risks associated with ozone exposure. The POM was used in various studies including ship emissions measurements and other studies that present the monitoring of ozone production and emissions sources (In't Veld et al., 2021; Stanier et al., 2021; *What Happens to Ozone Inside a Ship Plume?* | 2B Tech, n.d.). The data of POM (2B O₃) is stored internally and can be downloaded via a USB cable.

The Model 405 nm NO₂/NO/NO_x Monitor by 2B Technologies is a compact and versatile device designed to accurately measure nitrogen dioxide (NO₂), nitric oxide (NO), and nitrogen oxides (NO_x) concentrations. Utilizing advanced 405 nm LED absorption technology, it provides precise and real-time measurements of these key

pollutants in various environmental settings. Its portable design and user-friendly interface make it suitable for both stationary and mobile monitoring applications, enabling efficient and reliable air quality assessments (Dam et al., 2022; Li J. et al., 2021; Rangel et al., 2022). The data of Model 405 nm NO₂/NO/NO_x Monitor (2B NO₂) is stored internally or on an SD card and can be downloaded via a USB cable or by reading the SD card.

The Sniffer 4Dv2 air quality system is a highly portable and compact device, weighing less than 350 grams. This makes the SN system an ideal equipment for mobile (aerial - drone; and car-based measurements) and *in situ* measurements of various pollutants emissions (Rosu et al., 2023). It employs multiple sensors utilizing various determination methods to measure up to nine air quality parameters, including temperature and humidity. Utilizing a pump mechanism, the system draws external air through a frontal inlet to the sensors housed within its main body. Sensors can be configured in different combinations to perform quantitative emissions studies of various air pollutants made by man-made

sources such as industry, traffic, or natural sources, in accord with the desired outcome, such as personal exposure monitoring, urban air quality monitoring, or industrial emissions monitoring (Godfrey et al., 2022; Hay et al., 2023; Kim et al., 2021; Miao et al., 2022, 2024; Rosu et al., 2023; Senarathna et al., 2022). The setup of SN used in our study includes sensors for the measurement of the following air pollutants: NO₂, O₃, and PM₁₀. The data is transmitted in real-time using radiotelemetry (maximum range 1-5 km) that came along with the SN system. An image of the SN system during the test for real-time data transmissions via radio telemetry from outside to the PC located inside the building is presented in the below figure. Representative images of the other deployed equipment and AQS GL2 are presented in Figure 3.

The specifications of each equipment used during the in-situ measurement campaign at REXDAN RI from 17 - 30.08.2023, data availability, type of measured pollutant, method of measurement, the range of detection, and detection limit of each equipment according to manufacturer specifications are presented in Table 1.

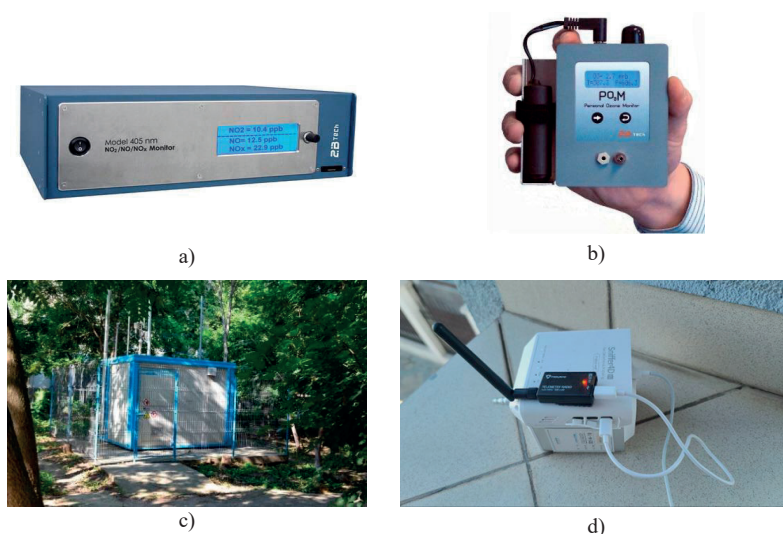


Figure 3. Air quality station and equipment used to measure NO₂, O₃ and PM₁₀ from 17-30.08.2023 at RI REXDAN (including AQS GL2): a) Model 405 nm NO₂/NO/NO_x Monitor - 2B Tech (G. Zhao et al., 2022); b) POM™, Personal Ozone Monitor™ - 2B Tech (He et al., 2022a); c) Local air quality station (RNMCA GL2) (Calitate Aer | Acasă, n.d.); d) Air quality system Sniffer 4Dv2 - Soarability (during the test of data transfer to PC using radio telemetry)

Table 1. Specification of equipment and GL2 AQS during in-situ campaign at REXDAN RI from 17-30.08.2023 (42iQ NO-NO₂-NO_x Analyzer, n.d.; 49iQ Ozone Analyzer, n.d.; 2008. Directive 2008/50/EC of the European Parliament and of the Council of 21 May 2008 on Ambient Air Quality and Cleaner Air for Europe. Vol. 152 - Google Search, n.d.; Model 5028i Continuous Particulate Monitor, n.d.; He et al., 2022; Li J. et al., 2021)

Instrument/ Equipment	Producer	Pollutant measured	Method of measurement	Range of measurement	Detection limit	Data availability during the experiment
RNMCA GL2	Thermo Fisher Scientific	O ₃	Spectroscopy ultraviolet photometric	0 - 200 ppm	0.5 ppb	Available
	Thermo Fisher Scientific	NO ₂	Spectroscopy chemiluminescence	0 - 20 ppm	0.4 ppb	Not available
	Thermo Fisher Scientific	PM ₁₀	Light Scattering Particle	0 - 10000 µg/m ³	0.1 µg/m ³	Available
POM (Personal Ozone Monitor)	2B Tech	O ₃	UV Absorption at 254 nm	0 - 10 ppm	0.1 ppb	Available
Model 405 nm NO2/NO/NOx Monito	2B Tech	NO ₂	Direct absorbance of NO2 at 405 nm	0 - 10 ppm	0.1 ppb	Available
Sniffer 4Dv2	Soarability Technology	NO ₂ +O ₃	Electrochemical	0 - 11 ppm	5 ppb	Available
	Soarability Technology	O ₃	Electrochemical	0 - 11 ppm	5 ppb	Available
	Soarability Technology	PM ₁₀	Laser scattering/Light scattering	0 - 1000 µg/m ³	1 µg/m ³	Available
	Soarability Technology	NO ₂	Electrochemical	0 - 11 ppm	5 ppb	Available

The number of sampled data, time resolution of sampling of each equipment used, and time resolution used for comparison of data recorded during 17-30 August 2023 are presented in Table 2. For comparison, data for all equipment was averaged to an hourly mean. The statistical Pearson correlation factor was produced using the raw data of all equipment and AQS.

Table 2. Sample specifications for each of the equipment used during the in-situ measurement campaign period 17-30 August 2023 at REXDAN RI

Instrument/ AQS	SN	AQS GL2	2B NO ₂ Monitor	2B O ₃ Monitor
Sampling specifications				
Number of Samples	19027	312	9740	9740
The time resolution of sampling	1 s	hourly	5 s	5 s
Average time resolution used for comparison	1 hour	1 hour	1 hour	1 hour

RESULTS AND DISCUSSIONS

Diurnal variations of NO₂, O₃ and PM₁₀

In the first part of our study, we analyzed the data gathered with the SN system, 2B monitors (NO₂ and O₃), and AQS data for the period 17-30 August 2023. The diurnal variation of hourly means, for the entire period of measurements, was compared to the

other equipment for the following air pollutants: NO₂, O₃, and PM₁₀ (Figure 4).

Figure 4 shows that the NO₂ recorded by SN has similar values as the 2B equipment, a maximum value of 71 µg/m³ at 1 AM close to the maximum value of 63 µg/m³ recorded at midnight by the 2B NO₂ monitor with. The high values recorded at the end of each day and past midnight are caused by the compression of the planetary boundary layer (PBL) that captures and concentrates the air pollutants mostly above urban areas where emission sources are more present (Badarinath et al., 2009; Bravo-Aranda et al., 2017; Falasca et al., 2021; Wyngaard, 1988).

Analyzing the general trends of diurnal variation, we observe that both SN and 2B equipment show a descending trend from midnight to 7 AM, when high values are again shown by both equipment's, which are caused mostly by traffic agglomeration during mornings. A decrease in concentrations during morning is observed, probably due to the decompression of PBL and thus a greater dilution of pollution level (Badarinath et al., 2009). Also, another cause can be the fact that NO₂ converts into NO and O₃ by the action of UV and visible solar radiation (Clapp & Jenkin, 2001; Han et al., 2011; Mazzeo et al., 2005). During the afternoon and evenings, both equipment recorded high values, mostly as a cause of decrease in the intensity of solar radiation, thus NO₂ is no longer photochemically converted to O₃ and NO. Also,

this is the time when traffic increases due to the end of the working hours (rush hours). Moreover, the PBL is dropping as a cause of temperature decrease due to lack of sunlight (IR radiation).

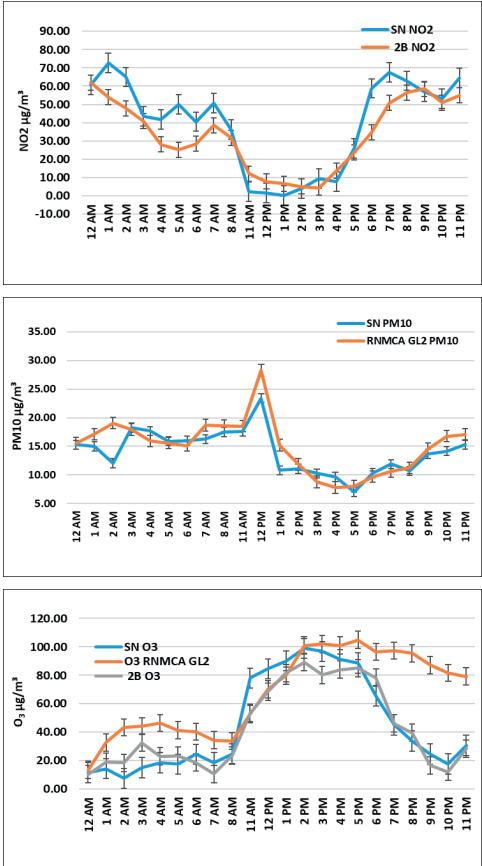


Figure 4. Diurnal variation of NO₂ (top figure), PM₁₀ (middle figure), and O₃ (down figure) recorded by SN versus the other standard equipment (2B NO₂, 2B O₃, AQS GL RNMCA)

A Pearson correlation factor between the two data sets of $R = 0.92$ was found. This shows that SN is a reliable equipment for monitoring local/regional NO₂ emissions (Rosu et al., 2023). Differences between the recorded diurnal values of SN NO₂ diurnal data versus the 2B NO₂ data are presented in Table 3. The SN air quality system records higher values at maximum NO₂ pollution level, with a mean value of $10.04 \mu\text{g}/\text{m}^3$, and underestimates the NO₂ values when the NO₂ pollution is low with a mean value difference between SN data and

2B NO₂ of $-2.46 \mu\text{g}/\text{m}^3$. The mean value of the differences between NO₂ data recorded by SN and 2B NO₂ is $6.35 \mu\text{g}/\text{m}^3$ which is 10 times lower than the maximum values recorded by both equipment's. Therefore, the SN air quality system is suitable and precise equipment for regional and local monitoring of NO₂ pollution level.

The PM₁₀ data (Figure 4) measured with SN and RNMCA GL2, have similar variations. High values are recorded at 12 PM, with $28.3 \mu\text{g}/\text{m}^3$ for RNMCA GL and $23.43 \mu\text{g}/\text{m}^3$ for SN air quality system. Differences between the two data sets are observed when the PM₁₀ pollution is high, with an average difference between $7.01 \mu\text{g}/\text{m}^3$, and $1.89 \mu\text{g}/\text{m}^3$. The small differences between SN and RNMCA GL2 show that our low-cost air quality sensor is a sensitive instrument for PM₁₀ measurements for local to regional areas if we take into account that RNMCA GL2 is an urban background station that has a sampling area of 5 km (*Calitate Aer | Stații*, n.d.). The general diurnal variation is similar for both air quality systems, with an increase from 12 AM to 1 PM, and a decrease during the afternoon. Higher values are recorded by both instruments at noon, possibly due to traffic and to road infrastructure works which intensified in the past months near the study area.

The daily variation for O₃ presented in Figure 4 shows similar trends between SN, 2B O₃, and RNMCA GL2, with high values above $60 \mu\text{g}/\text{m}^3$ of O₃ being recorded by all equipment between 10 AM and 6 PM, due to the photochemical conversion of NO₂ (decrease of NO₂ can be observed in the same period in top graph in Figure 3) plume into O₃ when sun radiance increases during the day. This is backed up by the peak of high O₃ concentration values that can be observed in the data measured by all equipment around 1-2 PM when sun activity reaches its peak and thus more radiation for photo dissociation of NO₂ into O₃ is present. The O₃ measured by RNMCA GL2, is much higher after 4 PM, compared to SN and 2B O₃ data. This may be since emissions in the area around RNMCA GL2 are higher than at the location of our instruments.

The Pearson correlation coefficient for diurnal variations recorded by SN with data recorded by the other standard equipment (2B O₃, 2B NO₂, RNMCA GL2) along with standard deviation (SD), and differences for average, maximum, and minimum are presented in Table 3.

For NO₂ measurements there is a correlation between SN and 2B NO₂ data of $R^2 = 0.97$, which shows that SN is highly sensitive to small variations, like standard NO₂ monitors (2B NO₂).

Table 3. Standard deviation and correlations of SN data with the data from standard equipment, differences between SN and standard equipment for diurnal data

	SN NO ₂	2B NO ₂	SN O ₃	2B O ₃	O ₃ RNMCA GL2	SN PM ₁₀	RNMCA GL2 PM ₁₀
R ² correlation for SN	1.00	0.97	1.00	0.95	0.83	1.00	0.88
SD (µg/m ³)	5.31	4.17	7.14	6.15	6.20	0.80	1.00
Minimum difference SN - standard equipment	0.00	-10.04	0.00	-7.29	-7.55	0.00	-7.01
Average difference SN - standard equipment	0.00	6.35	0.00	2.50	-2.35	0.00	-1.00
Maximum difference SN - standard equipment	0.00	2.46	0.00	2.48	1.75	0.00	1.89

Daily average results

The daily average variation for NO₂, PM₁₀, and O₃ measured by the SN air quality system versus the standard air quality monitors (including RNMCA GL2) are presented in Figure 5.

The NO₂ concentration measured by both SN and 2B-NO₂ have similar daily variation, with a minimum during the first weekend and increased values during the second week, regardless of the day. This may be related to:

- 1) an increased traffic intensity caused by people coming back from vacation since it is the last week of August;
- 2) different meteorological conditions that affect NO₂ concentration (Voiculescu et al., 2020).

Small differences between data from the two equipment are observed, with a mean of 0.16 µg/m³. The differences between the two instrument readings are presented in Table 4 along with the standard deviation of the data sets. Also, the correlation analysis of the two data sets shows a very good agreement with a Pearson correlation coefficient of $R^2= 0.98$. The PM₁₀ daily average observed by both SN and RNMCA GL2 has maximum values on August 28-th and 17-18 August (in the middle of the week). The differences between the two data sets during low PM₁₀ pollution are - 3.51 µg/m³. This shows that the SN system records lower values when the pollution is low, which may suggest that there is a threshold for at low PM₁₀.

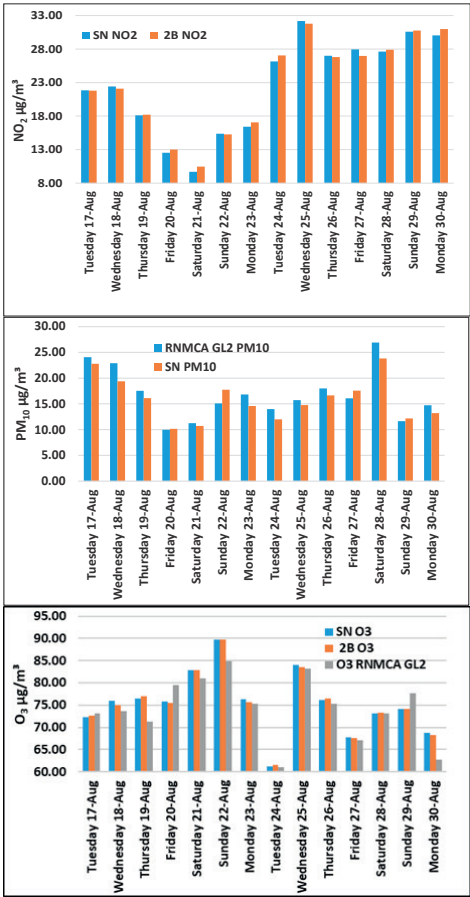


Figure 5. 4 Daily average concentration of NO₂ (top figure), PM₁₀ (middle figure), and O₃ (down figure) recorded by SN versus the other standard equipment (2B NO₂, 2 B O₃, AQS GL RNMCA)

Opposingly, during high PM levels, differences are positive ($2.6 \mu\text{g}/\text{m}^3$), suggesting that the SN system is overestimating the PM_{10} concentration at high levels of pollution.

The average difference between the two data sets is about $-0.92 \mu\text{g}/\text{m}^3$ which indicates that SN is recording a lower value of PM_{10} than RNMCA GL2. This may be due mainly to the fact that the two pieces of equipment are not collocated.

The O_3 daily average recorded by SN, RNMCA GL2, and 2B O_3 are shown in Figure 5. All three datasets show similar behaviour, with the highest value on August 22-nd and 25-th. The differences between daily average concentrations of O_3 recorded by SN and RNMCA GL2 are about $5.62 \mu\text{g}/\text{m}^3$ at high pollution levels and about $-4.08 \mu\text{g}/\text{m}^3$ at low pollution levels. The mean difference between SN O_3 data and RNMCA GL2 is about $1.01 \mu\text{g}/\text{m}^3$, which means that the SN system

measured higher values of O_3 than RNMCA GL2. The correlation factor between SN and RNMCA GL2 for O_3 daily concentration average is $R^2 = 0.87$. Interestingly, a clear absolute minimum during the 2 weeks appears on August 24-th (Tuesday) and shows up for all three equipment.

Small differences between the two data sets are measured at a high level of pollution with a value of $0.94 \mu\text{g}/\text{m}^3$ O_3 and with $-0.38 \mu\text{g}/\text{m}^3$ at a low level of pollution level. These findings support the idea that SN equipment is a very good instrument for the determination of daily average concentration levels with a mean difference of $-0.93 \mu\text{g}/\text{m}^3$ with respect to the values recorded by standard equipment (2B O_3). The correlation for all trace gases recorded by SN along with data recorded by the other standard equipment (2B O_3 , 2B NO_2 , RNMCA GL2) along with standard deviation (SD), and differences for average, maximum and minimum are presented in Table 4.

Table 4. Standard deviation and correlations of SN data with the data from standard equipment, differences between SN and standard equipment for daily averaged data

	SN NO_2	2B NO_2	SN O_3	2B O_3	RNMCA GL2 O_3	SN PM_{10}	RNMCA GL2 PM_{10}
R2 correlation for SN	1.00	0.98	1.00	0.99	0.87	1.00	0.86
SD ($\mu\text{g}/\text{m}^3$)	1.93	1.89	1.90	1.89	1.90	1.12	1.31
Minimum difference SN - standard equipment	0.00	-0.94	0.00	-0.38	-4.08	0.00	-3.51
Average difference SN - standard equipment	0.00	-0.16	0.00	0.10	1.02	0.00	-0.93
Maximum difference SN - standard equipment	0.00	0.96	0.00	0.96	5.63	0.00	2.67

CONCLUSIONS

We have shown that the SN system accurately measures atmospheric pollutants concentration when used for mobile measurements (Godfrey et al., 2022; Li J. et al., 2021; Rosu et al., 2023; Stanier et al., 2021). High correlation coefficients exist between data measured by standard types of equipment, including AQS, when referring to diurnal variation and daily average values. The SN equipment seemingly underestimates concentrations during low pollution events for NO_2 , PM_{10} , and O_3 .

In order to find out with what value the SN is underestimate the value of air pollutants, long term in-situ data is required to accurately find the exact value which will be done in future studies. Also, the SN system can be calibrated, as the manufacturer lets us manipulate the offsets of sensor data, with these data sets to

perform more precise measurements of air pollutants with respect.

These results show that SN equipment is suited for long-term air pollution studies both in-situ and mobile measurements (Rosu et al., 2023) to identify and evaluate the diurnal variation concentration of such air pollutants (NO_2 , O_3 , and PM_{10}) and identification of air pollution emissions sources.

ACKNOWLEDGEMENTS

The present research/article/study was supported by the project An Integrated System for the Complex Environmental Research and Monitoring in the Danube River Area, REXDAN, SMIS code 127065, co-financed by the European Regional Development Fund through the Competitiveness Operational Programme 2014-2020, contract no. 309/10.07.2020.

REFERENCES

- 42iQ NO-NO₂-NO_x Analyzer. (n.d.). Retrieved April 5, 2024, from <https://www.thermofisher.com/order/catalog/product/42iQ>
- 49iQ Ozone Analyzer. (n.d.). Retrieved April 5, 2024, from <https://www.thermofisher.com/order/catalog/product/49iQ>
- Badarinath, K.V.S., Sharma, A.R., Kharol, S.K., & Prasad, V.K. (2009). Variations in CO, O₃ and black carbon aerosol mass concentrations associated with planetary boundary layer (PBL) over tropical urban environment in India. *Journal of Atmospheric Chemistry*, 62, 73–86.
- Bravo-Aranda, J.A., de Arruda Moreira, G., Navas-Guzmán, F., Granados-Muñoz, M.J., Guerrero-Rascado, J.L., Pozo-Vázquez, D., Arbizu-Barrena, C., Olmo Reyes, F.J., Mallet, M., & Alados Arboledas, L. (2017). A new methodology for PBL height estimations based on lidar depolarization measurements: Analysis and comparison against MWR and WRF model-based results. *Atmospheric Chemistry and Physics*, 17(11), 6839–6851.
- Calitate Aer | Acasă. (n.d.). Retrieved April 5, 2024, from https://www.calitateair.ro/public/home-page/?_locale=ro
- Clapp, L.J., & Jenkin, M.E. (2001). Analysis of the relationship between ambient levels of O₃, NO₂ and NO as a function of NO_x in the UK. *Atmospheric Environment*, 35(36), 6391–6405.
- Clements, A.L., Griswold, W.G., Rs, A., Johnston, J.E., Herting, M.M., Thorson, J., Collier-Oxandale, A., & Hannigan, M. (2017). Low-cost air quality monitoring tools: From research to practice (a workshop summary). *Sensors*, 17(11), 2478.
- Constantin, D.-E., Voiculescu, M., & Georgescu, L. (2013). Satellite observations of NO₂ trend over Romania. *The Scientific World Journal*, 2013(2), 261634, DOI:10.1155/2013/261634
- Dam, M., Draper, D.C., Marsavin, A., Fry, J.L., & Smith, J.N. (2022). Observations of gas-phase products from the nitrate-radical-initiated oxidation of four monoterpenes. *Atmospheric Chemistry and Physics*, 22(13), 9017–9031.
- Directive 2008/50/EC of the European Parliament and of the Council of 21 May 2008 on Ambient Air Quality and Cleaner Air for Europe. Vol. 152., Google Search. (n.d.). Retrieved April 5, 2024, from <https://eur-lex.europa.eu/eli/dir/2008/50/oj>
- Falasca, S., Gandolfi, I., Argentini, S., Barnaba, F., Casasanta, G., Di Liberto, L., Petenko, I., & Curci, G. (2021). Sensitivity of near-surface meteorology to PBL schemes in WRF simulations in a port-industrial area with complex terrain. *Atmospheric Research*, 264, 105824.
- Fenger, J. (1999). Urban air quality. *Atmospheric Environment*, 33(29), 4877–4900.
- Godfrey, I., Brenes, J.P.S., Cruz, M.M., & Meghraoui, K. (2022). Using UAS with Sniffer4D payload to document volcanic gas emissions for volcanic surveillance. *Advanced UAV*, 2(2), 86–99.
- González Rivero, R.A., Schalm, O., Alvarez Cruz, A., Hernández Rodríguez, E., Morales Pérez, M.C., Alejo Sánchez, D., Martínez Laguardia, A., Jacobs, W., & Hernández Santana, L. (2023). Relevance and reliability of outdoor SO₂ monitoring in low-income countries using low-cost sensors. *Atmosphere*, 14(6), 912.
- Gulia, S., Nagendra, S.S., Khare, M., & Khanna, I. (2015). Urban air quality management-A review. *Atmospheric Pollution Research*, 6(2), 286–304.
- Gupta, P., Christopher, S.A., Wang, J., Gehrig, R., Lee, Y.C., & Kumar, N. (2006). Satellite remote sensing of particulate matter and air quality assessment over global cities. *Atmospheric Environment*, 40(30), 5880–5892.
- Han, P., Mei, H., Liu, D., Zeng, N., Tang, X., Wang, Y., & Pan, Y. (2021). Calibrations of low-cost air pollution monitoring sensors for CO, NO₂, O₃, and SO₂. *Sensors*, 21(1), 256.
- Han, S., Bian, H., Feng, Y., Liu, A., Li, X., Zeng, F., & Zhang, X. (2011). Analysis of the relationship between O₃, NO and NO₂ in Tianjin, China. *Aerosol and Air Quality Research*, 11(2), 128–139.
- Hay, N., Onwuzurike, O., Roy, S.P., McNamara, P., McNamara, M.L., & McDonald, W. (2023). Impact of traffic on air pollution in a mid-sized urban city during COVID-19 lockdowns. *Air Quality, Atmosphere & Health*, 16(6), 1141–1152. <https://doi.org/10.1007/s11869-023-01330-3>
- He, J., Yin, Y., Pei, J., Sun, Y., Liu, Z., Chen, Q., & Yang, X. (2022a). A model to evaluate ozone distribution and reaction byproducts in aircraft cabin environments. *Indoor Air*, 32(11). <https://doi.org/10.1111/ina.13178>
- Hoff, R.M., & Christopher, S.A. (2009). Remote sensing of particulate pollution from space: Have we reached the promised land? *Journal of the Air & Waste Management Association*, 59(6), 645–675.
- Hofman, J., Do, T.H., Qin, X., Bonet, E.R., Philips, W., Deligiannis, N., & La Manna, V.P. (2022). Spatiotemporal air quality inference of low-cost sensor data: Evidence from multiple sensor testbeds. *Environmental Modelling & Software*, 105306.
- Hopke, P.K., Cohen, D.D., Begum, B.A., Biswas, S.K., Ni, B., Pandit, G.G., Santoso, M., Chung, Y.-S., Davy, P., & Markwitz, A. (2008). Urban air quality in the Asian region. *Science of the Total Environment*, 404(1), 103–112.
- Iannarelli, A.M., Di Bernardino, A., Casadio, S., Bassani, C., Cacciani, M., Campanelli, M., Casasanta, G., Cadau, E., Diémoz, H., & Mevi, G. (2022). The Boundary Layer Air Quality-Analysis Using Network of Instruments (BAQUNIN) Supersite for Atmospheric Research and Satellite Validation over Rome Area. *Bulletin of the American Meteorological Society*, 103(2), E599–E618.
- Idrees, Z., & Zheng, L. (2020). Low-cost air pollution monitoring systems: A review of protocols and enabling technologies. *Journal of Industrial Information Integration*, 17, 100123.
- Ikram, J., Tahir, A., Kazmi, H., Khan, Z., Javed, R., & Masood, U. (2012). View: Implementing low-cost air quality monitoring solution for urban areas. *Environmental Systems Research*, 1(1), 10. <https://doi.org/10.1186/2193-2697-1-10>

- In't Veld, M., Carnerero, C., Massagué, J., Alastuey, A., De La Rosa, J.D., de la Campa, A.S., Escudero, M., Mantilla, E., Gangoiti, G., & García-Pando, C. P. (2021). Understanding the local and remote source contributions to ambient O₃ during a pollution episode using a combination of experimental approaches in the Guadalquivir valley, southern Spain. *Science of the Total Environment*, 777, 144579.
- Ionascu, M.-E., Castell, N., Boncalo, O., Schneider, P., Darie, M., & Marcu, M. (2021). Calibration of co, no₂, and o₃ using airify: A low-cost sensor cluster for air quality monitoring. *Sensors*, 21(23), 7977.
- Karagulian, F., Barbiere, M., Kotsev, A., Spinelle, L., Gerboles, M., Lagler, F., Redon, N., Crunaire, S., & Borowiak, A. (2019). Review of the performance of low-cost sensors for air quality monitoring. *Atmosphere*, 10(9), 506.
- Kelechi, A.H., Alsharif, M.H., Agbaetuo, C., Ubadike, O., Aligbe, A., Uthansakul, P., Kannadasan, R., & Aly, A.A. (2022). Design of a low-cost air quality monitoring system using arduino and thingspeak. *Comput. Mater. Contin.*, 70, 151–169.
- Kim, M.-K., Jang, Y., Heo, J., & Park, D. (2021). A UAV-based air quality evaluation method for determining fugitive emissions from a quarry during the railroad life cycle. *Sensors*, 21(9), 3206.
- Leifer, I., Melton, C., Chang, C.S., Blake, D.R., Meinardi, S., Kleinman, M.T., & Tratt, D.M. (2022). Validation of in situ and remote sensing-derived methane refinery emissions in a complex wind environment and chemical implications. *Atmospheric Environment*, 118900.
- Li, J., Haurlyluk, A., Malings, C., Eilenberg, S.R., Subramanian, R., & Presto, A.A. (2021). Characterizing the Aging of Alphasense No 2 Sensors in Long-Term Field Deployments. *ACS Sensors*, 6(8), 2952–2959. <https://doi.org/10.1021/acssensors.1c00729>
- Li, J., Zhang, H., Chao, C.-Y., Chien, C.-H., Wu, C.-Y., Luo, C. H., Chen, L.-J., & Biswas, P. (2020). Integrating low-cost air quality sensor networks with fixed and satellite monitoring systems to study ground-level PM_{2.5}. *Atmospheric Environment*, 223, 117293.
- Li, K., Bai, K., Li, Z., Guo, J., & Chang, N.-B. (2022). Synergistic data fusion of multimodal AOD and air quality data for near real-time full coverage air pollution assessment. *Journal of Environmental Management*, 302, 114121.
- Mazzeo, N.A., Venegas, L.E., & Choren, H. (2005). Analysis of NO, NO₂, O₃ and NO_x concentrations measured at a green area of Buenos Aires City during wintertime. *Atmospheric Environment*, 39(17), 3055–3068.
- Merlaud, A., Tack, F., Van Roozendaal, M., Constantin, D., Rosu, A., Riffel, K., Donner, S., Wagner, T., Schreier, S., & Richter, A. (2018). Synergetic use of the Mobile-DOAS measurements during CINDI-2. *EGU General Assembly Conference Abstracts*, 18038.
- Miao, C., Cui, A., Xiong, Z., Hu, Y., Chen, W., & He, X. (2022). Vertical evaluation of air quality improvement by urban forest using unmanned aerial vehicles. *Frontiers in Ecology and Evolution*, 10, 1045937.
- Miao, C., Peng, Z.-R., Cui, A., He, X., Chen, F., Lu, K., Jia, G., Yu, S., & Chen, W. (2024). Quantifying and predicting air quality on different road types in urban environments using mobile monitoring and automated machine learning. *Atmospheric Pollution Research*, 15(3), 102015.
- Mocanu, P., Ivanescu, V., Sandu, M.A. (2023). Air emissions inventory from a Romanian construction materials factory. *Scientific Papers. Series E. Land Reclamation, Earth Observation & Surveying, Environmental Engineering*, XII, 342-348, Print ISSN 2285-6064.
- Model 5028i Continuous Particulate Monitor. (n.d.). Retrieved April 5, 2024, from <https://www.thermofisher.com/order/catalog/product/5028i>
- Morawska, L., Thai, P.K., Liu, X., Asumadu-Sakyi, A., Ayoko, G., Bartonova, A., Bedini, A., Chai, F., Christensen, B., & Dunbabin, M. (2018). Applications of low-cost sensing technologies for air quality monitoring and exposure assessment: How far have they gone? *Environment International*, 116, 286–299.
- Penza, M., Suriano, D., Pfister, V., Prato, M., & Cassano, G. (2017). Urban air quality monitoring with networked low-cost sensor-systems. *Proceedings*, 1(4), 573. <https://www.mdpi.com/2504-3900/1/4/573>
- Rangel, A., Raysoni, A.U., Chavez, M.C., Jeon, S., Aguilera, J., Whigham, L.D., & Li, W.-W. (2022). Assessment of traffic-related air pollution (TRAP) at two near-road schools and residence in El Paso, Texas, USA. *Atmospheric Pollution Research*, 13(2), 101304.
- Rosu, A., Arseni, M., Constantin, D.-E., Rosu, B., Petrea, S.-M., Voiculescu, M., Iticescu, C., & Georgescu, L.-P. (2023). Study of air pollution level in an urban area using low-cost sensor system onboard mobile platform. *Scientific Papers. Series E. Land Reclamation, Earth Observation & Surveying, Environmental Engineering*, 12. <https://landreclamationjournal.usamv.ro/pdf/2023/Art16.pdf>
- Roşu, A., Constantin, D.-E., Roşu, B., Calmuc, V., Arseni, M., Voiculescu, M., & Georgescu, L.P. (2019a). Mobile measurements of nitrogen dioxide using two different UV-VIS spectrometers. *Tech. J. New Technol. Prod. Mach. Manuf. Technol.*, 26, 71–76.
- Roşu, A., Constantin, D.-E., Voiculescu, M., Arseni, M., Roşu, B., Merlaud, A., Van Roozendaal, M., & Georgescu, P.L. (2021). Assessment of NO₂ Pollution Level during the COVID-19 Lockdown in a Romanian City. *International Journal of Environmental Research and Public Health*, 18(2), 544.
- Rosu, A., Rosu, B., Constantin, D.-E., Arseni, M., Voiculescu, M., Georgescu, L.P., & Popa, I. (2019b). Overview of tropospheric NO₂ using the ozone monitoring observations instrument and human perception about air quality for the most polluting countries across the world. *Carpathian J. Earth Environ. Sci.*, 14, 423–430.
- Roşu, A., Roşu, B., Constantin, D.-E., Voiculescu, M., Arseni, M., Murariu, G., & Georgescu, L.P. (2018). Correlations between no 2 distribution maps using GIS

- and mobile doas measurements in Galati city. *Annals of the University Dunarea de Jos of Galati: Fascicle II, Mathematics, Physics, Theoretical Mechanics*, 41.
- Senarathna, M., Priyankara, S., Jayaratne, R., Weerasooriya, R., Morawska, L., & Bowatte, G. (2022). Measuring Traffic Related Air Pollution Using Smart Sensors in Sri Lanka: Before and During a New Traffic Plan. *Geography, Environment, Sustainability*, 15(3), 27–36.
- Specht, J.P., Esfahani, S., Xing, Y., Köck, A., Cole, M., & Gardner, J.W. (2022). Thermally modulated CMOS compatible particle sensor for air quality monitoring. *IEEE Transactions on Instrumentation and Measurement*, 71, 1-13, DOI: 10.1109/tim.2022.3141151
- Stanier, C.O., Pierce, R.B., Abdi-Oskouei, M., Adelman, Z.E., Al-Saadi, J., Alwe, H.D., Bertram, T.H., Carmichael, G.R., Christiansen, M.B., & Cleary, P.A. (2021). Overview of the Lake Michigan ozone study 2017. *Bulletin of the American Meteorological Society*, 1–47.
- Sturm, P., Fruhwirt, D., & Steiner, H. (2022). Impact of dust loads in long railway tunnels: In-situ measurements and consequences for tunnel facilities and operation. *Tunnelling and Underground Space Technology*, 122, 104328.
- Ung, A., Wald, L., Ranchin, T., Weber, C., Hirsch, J., Perron, G., & Kleinpeter, J. (2021). *Satellite data for air pollution mapping over a city—Virtual stations*. In *Observing our environment from space*. pp. 147–151. CRC Press.
- Voiculescu, M., Constantin, D.E., Condurache-Bota, S., Călmuc, V., Roșu, A., & Dragomir Bălănică, C.M. (2020). Role of meteorological parameters in the diurnal and seasonal variation of NO₂ in a Romanian urban environment. *International Journal of Environmental Research and Public Health*, 17(17), 6228.
- What Happens to Ozone Inside a Ship Plume?* | 2B Tech. (n.d.). Retrieved April 5, 2024, from https://2btech.io/case_studies/what-happens-to-ozone-inside-a-ship-plume/
- Wyngaard, J.C. (1988). *Structure of the PBL*. In A. Venkatram & J.C. Wyngaard (Eds.), *Lectures on Air Pollution Modeling*, pp. 9–61. American Meteorological Society. https://doi.org/10.1007/978-1-935704-16-4_2
- Zhang, X., Wang, F., Wang, W., Huang, F., Chen, B., Gao, L., Wang, S., Yan, H., Ye, H., & Si, F. (2020). The development and application of satellite remote sensing for atmospheric compositions in China. *Atmospheric Research*, 245, 105056.
- Zhao, C., Zhang, C., Lin, J., Wang, S., Liu, H., Wu, H., & Liu, C. (2022). Variations of Urban NO₂ Pollution during the COVID-19 Outbreak and Post-Epidemic Era in China: A Synthesis of Remote Sensing and In Situ Measurements. *Remote Sensing*, 14(2), 419.
- Zhao, G., Hu, M., Zhang, Z., Tang, L., Shang, D., Ren, J., Meng, X., Zhang, Y., Feng, M., Luo, Y., Yang, S., Tan, Q., Song, D., Guo, S., Wu, Z., Zeng, L., Zhang, Y., & Xie, S. (2022). Current Challenges in Visibility Improvement in Sichuan Basin. *Geophysical Research Letters*, 49(12), e2022GL098836. <https://doi.org/10.1029/2022GL098836>

STUDIES ON THE CURRENT CONTEXT OF AIR QUALITY INSIDE EARTHEN BUILDINGS

**Vasilica VASILE, Cornelia BAERĂ, Aurelian GRUIN,
Adrian-Alexandru CIOBANU, Bogdan BOLBOREA**

National Institute for Research and Development in Construction,
Urban Planning and Sustainable Spatial Development - URBAN-INCERC,
266 Pantelimon Road, District 2, Bucharest, Romania

Corresponding author email: vasile@incd.ro

Abstract

A global problem that affects almost all areas of life is the environmental pollution, and because people stay indoors about 80-90% of their day, it can say that indoor air pollution is most of concerns. The growing attention paid to the use of natural materials has become a current topic among researchers, due to the increasing need to exploit renewable materials, conserve energy and adopt sustainable production methods to create buildings adapted to modern times. Although, earth might be considered, from a current perspective, an ancient building material, between 30 and 50% of the XXI century population lives in dwellings made of earth. In this respect, our studies focused on exploring the current status of worldwide research on air quality inside earthen buildings, in order to establish the performance indicators related to this field. The findings highlight the need to rethink the way in which indoor spaces are designed and operated given the waste generation, resource depletion and climate change, with increasing numbers of people which want to live in environmentally friendly and healthy buildings.

Key words: earthen buildings, health effects, indoor air pollution, performance indicators.

INTRODUCTION

The increasing need to exploit renewable materials, conserve energy and adopt sustainable production methods to create buildings adapted to modern era has led to the increasing importance of using natural materials (Rivera-Gomez et al., 2021). In global terms, current forecasts seem to indicate, that in the next decade, the construction sector will grow continuously at a rapid pace. Although, earth might be considered, from a current perspective, an ancient building material, between 30 and 50% of the XXI century population lives in dwellings made of earth. (Schweiker et al., 2021; Rivera-Gomez et al., 2021). Earthen buildings can be found anywhere on the globe, both in developing countries, it is true most of them, but also in developed countries such as Australia, Brazil, the United States or those of Europe. Because in vernacular buildings can be used climate-adaptive strategies with the possibility of reducing carbon emissions and energy consumption, these have become attractive during the many crises of mankind referring to

environmental pollution and energy shortages (He et al., 2023). Earth is a natural building material, intensively used until now and one of the oldest. Thus, the benefits of earth building materials are seeking by a growing number of people from developed countries and societies, people which wants to enjoy of environmentally friendly and healthy buildings. It is clear that the way buildings are designed, constructed and operated needs to be rethought in light of waste generation, climate change and resource depletion (Schweiker et al., 2021). The subject of many studies is to find solutions to global crisis such as climate change, environmental pollution and energy shortage. There is evidence that vernacular living spaces, by their adapting to the local climate conditions, can become a convenient indoor environment for inhabitants. The key elements in the adjustment of the building's temperature conditions and the occupant's thermal adaptation are the vernacular spaces of the buildings. Analysing the relationships between climate, people and vernacular buildings is a very important topic for understanding and knowing the strategies for sustainable design of

vernacular buildings and for promoting sustainable architecture (Chang et al., 2021). The centuries-long experience of people living in different climates around the world led to the development of vernacular architecture. The environment, the historical background and the culture of the different peoples form the basis for building and design techniques that utilise locally available resources (Chandel et al., 2016).

Clay has several advantages as a building material: It is ecological, economical and can be easily recycled and reused. In addition, clay has good properties for absorbing and releasing water vapour, which has a positive effect on the balance between room temperature and relative humidity, on the air quality of the building and ultimately on the comfort of the occupants (Gomes & Miranda, 2022). A construction technique is rammed earth in which the main components of the earth (gravel, silt, clay and sand), with or without the addition of stabilizers depending on the required strength, are compressed to give it the desired shape, within a set framework (Khadka & Shakya, 2016).

Considering the growing of global population, the request for more resources is increasing every day, causing global warming and all resource exploitation, about 50% of them, being used in the construction industry, one of the least sustainable sectors (Khadka, 2020).

MATERIALS AND METHODS

Given the people spend about 80% of their time indoors (Vijay et al., 2024; Gonzalez-Martin et al., 2021; Karr et al., 2021; Nair et al., 2022; Tsumura et al., 2023; Harb et al., 2018), they being exposed to many different pollutants with high emissions from various sources like furniture, humans and daily activities, construction materials, consumer products, with effects recognized harmful to health (Albertin et al., 2023; Peterson et al., 2023; Petigny et al., 2021; Morin et al., 2019; Arar et al., 2022; Gao et al., 2021; Caron et al., 2016; Santos et al., 2019) our studies focused on exploring the current status of worldwide researches on air quality inside earthen buildings. In order to carry out the proposed aim, a literature review was carried out to

afford a better understanding of pollution from indoor spaces, of the main categories of pollution substances, of the dangerous effects of them on people health, and the direct correlation of these with specific indoor environment of the earthen buildings. At the same time, the studies also focused on the establishing of the performance indicators related to this field of great importance for our daily life.

RESULTS AND DISCUSSIONS

Three main classes of pollutants form the basis for the assessment of indoor air quality: volatile organic compounds (VOCs), inorganic compounds (VICs) and particulate matter (PM). VOCs can be classified into different groups based on their properties regarding molecular structure, polarity and boiling point, most of these compounds being in the focus of several international organizations and countries as essential pollutants for their control (US EPA; Gan et al., 2023). A category of pollutants called aerosols, which group VOCs and PM with polycyclic aromatic hydrocarbons (PAHs) and inorganic pollutants, called gaseous pollutants, from this category being carbon oxides (CO, CO₂), sulphur dioxide (SO₂), nitrogen oxides (NO_x), and ozone (O₃) (Kumar et al., 2023). There are four categories of PM, considering the dimensions (diameter) of them: < 0.01 µm (ultrafine particles - UFP), between 0.01 µm and 2.5 µm, named fine particles, between 2.5 µm and 10 µm, named coarse and more than 10 µm, so-called large particles (Kumar et al., 2023). It is estimated that, globally, only PM_{2.5} are the cause of more than 2 million deaths annually (Teiri et al., 2021). PM_{2.5} can contain various types of chemical substances, such as organic carbon (50%), elemental carbon (3%), sulphates and nitrates (30%), metals (1%), ammonium ions and water (15%) (Kumar et al., 2023). Likewise, PM_{2.5} could have in the component a new category of coming out pollutants namely environmentally persistent free radicals (EPFR) (Chen et al., 2019). These compounds have high toxicity, increased durability and low reactivity. Another component of PM_{2.5}, black carbon, is produced by the incomplete combustion of various types of fuels, and human exposure to

this chemical can lead to strokes and heart attacks, high blood pressure and lung diseases such as asthma and bronchitis. The description

and effects of the pollutants mentioned can be found in Table 1 and their sources in Table 2.

Table 1. Description of main types of pollutants and effects on human health

Type of pollutant	Description	Effects on human health
PM	solid particles and liquid droplets, having different origins sizes, shapes, and chemical compositions, suspended in the air	pulmonary diseases such as bronchitis, asthma, wheezing breath, cardiovascular and neurological problems like high blood pressure, strokes and heart attacks
VOCs	compounds that at room temperature have a low value of boiling point and high vapour pressure, belonging to different classes like alkanes, terpenes, aldehydes (formaldehyde), aromatic compounds, monocyclic like benzene, toluene and xylene or polycyclic, etc.	poor degradability, high volatility and severe toxicity, being able to determine great problems to both humans and environment. Diseases such as nasopharyngeal cancer, lung damage, leukaemia and symptoms related to sick building syndrome can be the results of exposure to formaldehyde on long term
VICs	gases like: sulphur dioxide (SO ₂), carbon monoxide (CO), ozone (O ₃), carbon dioxide (CO ₂), nitrogen oxides (NO and NO ₂)	cardiovascular, respiratory, and neurological problems, besides of dizziness, fatigue, sneezing, eye irritation can be the results of long-term exposure at most of volatile inorganic compounds.

Table 2. Summary of air pollutants sources

Pollutant	Outdoor sources		Indoor Sources
	Natural	Anthropogenic	
PM	gaseous emissions, volcanic eruptions, storms, rock debris, forest fires	fuel combustion, steel industry, mining operations, emissions from power plants, glass manufacturing industry, other types of industrial processes – cement manufacturing, etc	heaters, household burners, fireplaces, household activities (ironing, cooking – frying, cleaning), office equipment (photocopiers), paints, plastics, presence animals of company and different activities of occupants
VOCs	forest fires, volcanic eruptions, etc.	using of fossil fuels, refining, exploitation, transportation, storage, etc.	emissions from different types of materials (construction, finishing/ protection, adhesives, paints), furniture, occupants' activities (cooking, cleaning, etc.), household cleaning products
VICs	world's forests, wetlands, and seas.	ventilated kitchens, garages, greenhouses, tobacco smoke, burning of fossil fuels (furnaces, heaters, stoves)	combustion processes in fireplaces, stoves, furnaces, heaters, gas appliances without ventilation

A significant relationship between excessive exposure to concentrations of indoor air pollutants and the appearance of symptoms that make up the so-called Building-Related symptoms (BRS) or Building-Related Illnesses (BRIs) has identified by previous studies (Chamseddine et al., 2019; Zoran et al., 2020; Shaw et al., 2020; Brown et al., 2021; Suzuki et al., 2021; Gomes and Miranda, 2022; Gan et al., 2023). The two differ because, in the case of SBS, there is not the possibility of the associating the exposure inside the building with symptoms described by the occupants

(Gomes and Miranda, 2022), and the etiology of these symptoms are not known. The range of SBS symptoms varies from red eyes, headache, fatigue, concentration difficulties, dry skin and respiratory irritation (Arar et al., 2022). But researchers agree that the cardiovascular and respiratory illnesses are the most dangerous effects of pollution on humans (Brown et al., 2021; Zoran et al., 2020; Shaw et al., 2020; Arar et al., 2022). The admissible limits of some indoor air pollutants concentrations are presented in Table 3 (Kumar et al., 2023; WHO, 2021).

Table 3. Threshold levels of different indoor air pollutants

Pollutant	Exposure time	Limit value	Measure unit
PM2.5	Annual	5	$\mu\text{g}/\text{m}^3$
	24 h	25	$\mu\text{g}/\text{m}^3$
NO ₂	Annual	10	$\mu\text{g}/\text{m}^3$
CO ₂	24 h	1000	ppm
	-	1600	mg/m^3
SO ₂	Average of 24 h	40	$\mu\text{g}/\text{m}^3$

From the study of the existing specialized literature in the sciencedirect.com and springerlink.com databases, few studies were found in the field of air quality inside earthen buildings, most of them referring to parameters of thermal comfort, namely temperature and relative humidity (Costa-Carrapiço et al., 2023;

He et al., 2023; Chang et al., 2021). Only one study contains data on CO, CO₂ and TCOV pollutant concentration values (Costa-Carrapiço et al., 2023). Only three articles were found related to materials that have an earth composition, namely two ongoing projects on earth plaster (Gomes and Miranda, 2022; Santos et al., 2019), of which one will monitor the emissions of CO, CO₂ and PM_x, and the other study (Darling et al., 2012) looked at the possibility of increasing of inside air quality by studying the ability of a clay plaster to lower ozone concentrations, as well as to lower the concentrations of secondary reaction products. Some details about these studies are presented in Table 4.

Table 4. Details regarding studies carried out in the indoor spaces of some constructions made of earth and on materials that have earth in their composition

Author's/Location/ Material	Study publication year	Monitored parameters/monitoring periods
Studies in indoor spaces of earthen buildings		
Costa-Carrapiço et al., 2023/ Alentejo, Portugalia	2023	air quality (CO, CO ₂ , VOCs), surface temperature, relative humidity, indoor and outdoor air temperature, black body temperature, air velocity, light level, sound level/summer, winter
	2023	wind speed, relative humidity, indoor air temperature, outdoor air temperature, solar radiation intensity /summer, winter
	2021	air speed, relative humidity, air temperature, radiation temperature /summer, winter
Studies on materials containing earth		
Gomes & Miranda, 2022/Earth plaster	2022 (ongoing study)	air temperature, relative humidity, CO, CO ₂ , PM _x (PM2.5 and PM10)/spring, summer, winter
Santos et al., 2019/Earth plaster	2022 (ongoing study)	air temperature, relative humidity
Darling et al., 2012/ Clay plaster	2012	ozone, six aliphatic aldehydes (C5-C10) and two aromatic aldehydes (benzaldehyde and methyl-benzaldehyde)

The study by Costa-Carrapiço and colleagues (2023) analysed a sample of sixty-nine vernacular dwellings in Alentejo, Portugal and sought to evaluate the performance of their inside environment, indoor air quality being evaluated based on the concentrations of CO, CO₂ and VOCs, by the collecting of data on long period of time (summer and winter). In the case studies, the obtained results confirmed that the main sources of indoor air pollution are the emissions from heating and cooking. The minimum values of average concentrations for CO, CO₂ and VOCs (0.1-0.2 ppm) were

obtained in living rooms heated electrically, during no cooking periods of time. VOCs concentrations are 10 ppm near the stove, during cooking activities, but in the living room, this is only 2 ppm. A period of exposure till 15 h results from leaving, in the cold season, the heat working all day, something that more than half of the occupants of the buildings do. Moreover, the health of building occupants can be affected by extended periods with wood heating, this being source of some VOCs like aldehydes (formaldehyde) or aromatic compounds, mono- and polycyclic,

and fine or ultrafine particles. The mentioned chemical substances are harmful in a very small quantities and can have as result serious respiratory problems, by affecting lung's function, even and cancer. Regarding materials that contain earth, Darling et al. (2012) conducted a study to evaluate a clay plaster as a Passive Removal Materials (PRMs) of pollutants to improve air quality by controlling their concentration. This was done by monitoring during the tests of the perceived air quality (PAQ) and quantifying the ozone levels, six aliphatic aldehydes (C5-C10) and two aromatic aldehydes, in two experimental enclosures, which contained eight combinations of an emitting and reactive and pollution source (new textile carpet type floor covering on polyurethane foam support), clay plaster for walls, applied to plasterboard, with and without ozone presence. A commercially available plaster was used for this study, consisting of a proprietary clay mixture (fire clay, kaolin, montmorillonite - an aluminium-rich clay mineral from the group of smectites) and broken marble (size of aggregate: 5-1000 μm). The conclusions of the mentioned study (Darling et al., 2012) can be summarized as follows: clay wall plasters can improve PAQ, especially in the presence of ozone or ozone and textile carpet; perceived air quality was most acceptable and aldehyde concentrations were lowest when only clay plaster or both clay plaster and carpet were present in the ozone-free experimental chambers; addition of clay plaster to the least acceptable PAQ condition (carpet-ozone) considerably decreased both ozone and aldehyde concentrations and significantly improved PAQ.

Obtaining information about existing documents, normative (regulations) or

recommendations (guidelines) regarding the quality of the indoor environment (IEQ - Indoor Environmental Quality) is useful for decision-makers who prepare such documents, as well as for scientists and practitioners operating in different countries (ieqguidelines.org).

In 2018, a members group of International Society of Indoor Air Quality and Climate - ISIAQ discussed the challenges related to the compilation of international guidelines. Challenges include language barriers, varying degrees of quality, and questions about comparing guidelines with many key differences, including health effects, climate, and common building types. To help overcome these challenges, a Scientific and Technical Committee (STC34) was officially launched in September 2020, part of ISIAQ, with three main objectives, namely: congregating and organizing continuously of the information about the global guidelines; realizing of database, functional and open, able to spread information contained in guidelines; updating of guidelines in force and making recommendations. The committee has created an open IEQ guideline database (ieqguidelines.org). This database is organized in fields, including: pollutant name; performance indicators in the form of limit values; average time interval; document category (guideline or regulation); issuing authority (agency, ministry, department of a ministry, etc.); type of effect on human health (acute, chronic, etc.); the type of indoor environment to which it applies (public buildings, schools, homes, etc.). Figures 1-3 show examples of the worldwide performance indicators for some of indoor pollutants, namely TVOC, HCHO and O_3 .

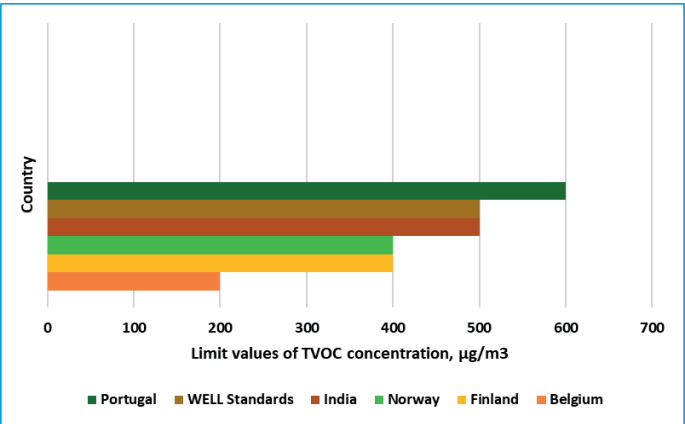


Figure 1. Examples of admissible values of TVOC concentration in different countries

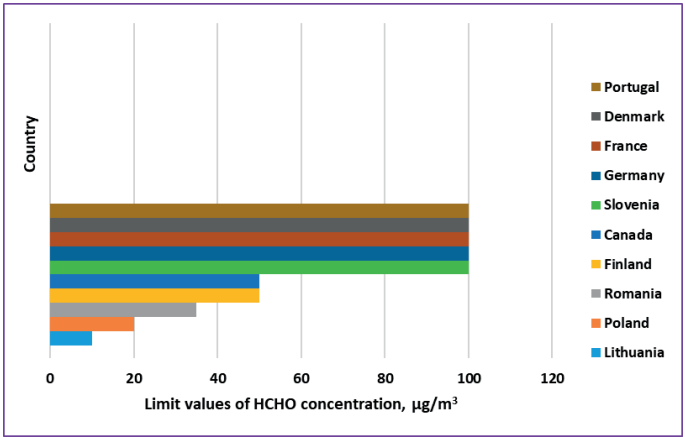


Figure 2. Limit levels of HCHO concentrations, nationally and internationally

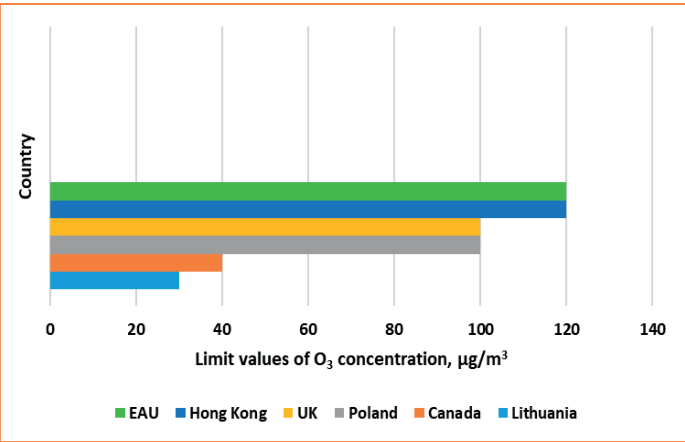


Figure 3. Limit values of O₃ concentrations, internationally

CONCLUSIONS

The conclusions of the bibliographic study carried out to know the current context regarding the air quality inside earthen buildings are:

✓ earth, as a construction material, has several advantages (economic, ecological, easy of reuse and recycling), between 30 and 50% of the world's population living nowadays in dwellings made of earth;

✓ indoor air, where people spend 80 to 90% of their time, contains multiple sources of pollutant emissions, as well as many types of pollutants, leading to ecosystem damage and causing a range of adverse health effects even in the lower detectable concentrations;

✓ air quality of indoor spaces is evaluated mainly having as base the concentration levels of three main categories of pollutants, namely volatile compounds, organic (VOCs) and inorganic (VICs), and particulate matter (PM);

✓ exposure on short or long-term to indoor pollutant concentrations leads to the appearance of symptoms which are part of the categories named sick building syndrome (BRS) or building-related illnesses (BRIs), among which are listed: headaches, fatigue, drowsiness, nausea, irritation of respiratory tract and eyes, dizziness, irritability, nervousness, the most common diseases mentioned being respiratory, cardiovascular, neurological, allergic, etc.;

✓ from the study of the specialized literature existing in the international databases, few studies were found in the field of air quality inside earthen buildings, most of them referring to parameters of thermal comfort, namely temperature and relative humidity. Only one study contains data on CO, CO₂ and TCOV pollutant concentrations, and only three articles were found on earth-based materials, one of which looked at the ability of a clay plaster to improve the quality of indoor air, directly by decreasing reduction the level of ozone, and indirectly by decreasing the levels of secondary products of chemical reactions;

✓ existing documents, normative (regulations) or recommendations (guidelines) regarding the environment quality from inside buildings, have recently been grouped into the ieqguidelines.org database, which contains sixteen types of information, including the

name of the pollutant, performance indicators in the form of admissible limit values, issuing authority and country, etc.

Considering the mentioned conclusions, it is necessary to continue the research with the exploration of the performances of the buildings made of earth and the materials that have earth in their composition, from the point of view of fulfilling the indicators regarding indoor air quality.

ACKNOWLEDGEMENTS

The research paper was carried out within Projects PN 23 35 03 01 and PN 23 35 04 01, financed by the Ministry of Research, Innovation and Digitalization.

REFERENCES

- Albertin, R., Pernigotto, G., & Gasparella, A. (2023). A Monte Carlo Assessment of the Effect of Different Ventilation Strategies to Mitigate the COVID-19 Contagion Risk in Educational Buildings. *Indoor Air*, 9977685, <https://doi.org/10.1155/2023/9977685>.
- Arar, M., Jung, C. & Qassimi, N.A. (2022). Investigating the Influence of the Building Material on the Indoor Air Quality in Apartment in Dubai. *Front. Built Environ.*, 7, 804216, doi: 10.3389/fbuil.2021.804216.
- Brown, L., Barnes, J., & Hayes, E. (2021). Traffic-related air pollution reduction at UK schools during the Covid-19 lockdown. *Science of the Total Environment*, 780, 146651.
- Caron, A., Redon, N., Thevenet, F., Hanoune, B., & Coddeville, P. (2016). Performances and limitations of electronic gas sensors to investigate an indoor air quality event. *Building and Environment*, 107, 19-28.
- Chamseddine, A., Alameddine, I., Hatzopoulou, M., & El-Fadel, M. (2019). Seasonal variation of air quality in hospitals with indoor-outdoor correlations. *Building and Environment*, 148, 689-700.
- Chandel, S.S., Sharma, V., & M. Marwah, B. (2016). Review of energy efficient features in vernacular architecture for improving indoor thermal comfort conditions. *Renewable and Sustainable Energy Reviews*, 65, 459-477.
- Chang, S., He, W., Yan, H., Yang, L., & Song, C. (2021). Influences of vernacular building spaces on human thermal comfort in China's arid climate areas. *Energy & Buildings*, 244, 110798.
- Chen, Q., Sun, H., Wang, J., Shan, M., Yang, X., Deng, M., Wang, Y., & Zhang, L. (2019). Long-life type—the dominant fraction of EPFRs in combustion sources, ambient fine particles in Xi'an. *Atmospheric Environment*, 219, 117059, <https://doi.org/10.1016/j.atmosenv.2019.117059>.
- Costa-Carrapiço, I., González, J.N., & Raslan, R. (2023). Indoor environmental conditions in vernacular

- p dwellings in Alentejo, Portugal.
- <https://ssm.com/abstract=3944793>
- .
- Darling, E.K., Cros, C.J., Wargocki, P., Kolarik, J., Morrison, G.C., & Corsi, R.L. (2012). Impacts of a clay plaster on indoor air quality assessed using chemical and sensory measurements. *Building and Environment*, 57, 370-376.
- Gan, G., Fan, S., Li, X., Zhang, Z., & Hao, Z. (2023). Adsorption, membrane separation for removal, recovery of volatile organic compounds. *Journal of Environmental Sciences*, 123, 96-115, <https://doi.org/10.1016/j.jes.2022.02.006>.
- Gao, M., Liu, W., Hailin, W., Shao, X., Shi, A.; An, X., Li, G., & Nie, L. (2021). Emission factors and characteristics of volatile organic compounds (VOCs) from adhesive application in indoor decoration in China. *Science of the Total Environment*, 779, 145169.
- Gomes, M.I., & Miranda, T. (2022). Indoor air quality for sustainability, occupational health and classroom environments through the application of earth plaster. *HERITAGE 2022 - International Conference on Vernacular Heritage: Culture, People and Sustainability*, September 15th-17th, 2022 Valencia, Spain.
- Gonzalez-Martín, J., Kraakman, N.J.R., Perez, C., Lebrero, R., & Munoz, R. (2021). A state-of-the-art review on indoor air pollution and strategies for indoor air pollution control. *Chemosphere*, 262, 128376.
- Harb, P., Locoge, N., & Thevenet F. (2018). Emissions and treatment of VOCs emitted from wood-based construction materials: Impact on indoor air quality. *Chemical Engineering Journal*, 354, 641-652.
- He, W., Wu, Z., Jin, R., & Liu, J. (2023). Organization and evolution of climate responsive strategies, used in Turpan vernacular buildings in arid region of China, www.sciencedirect.com, accessed on 24.02.2023.
- <https://ieqguidelines.org/>accessed on February 2023.
- Karr, G., Nicolas, M., Maupetit, F., & Ramel, M. (2021). Cleaning product emissions and indoor built environments: Exposure and health risk assessments from experiments under realistic indoor conditions. *Building and Environment*, 206, 108384.
- Khadka, B. (2020). Rammed earth, as a sustainable and structurally safe green building: a housing solution in the era of global warming and climate change. *Asian Journal of Civil Engineering*, 21, 119-136.
- Khadka, B., & Shakya, M. (2016). Comparative compressive strength of stabilized and un-stabilized rammed earth. *Materials and Structures*, 49(9), 3945-3955.
- Kumar, R., Verma, V., Thakur, M., Singh, G., & Bhargava, B. (2023). A systematic review on mitigation of common indoor air pollutants using plant-based methods: a phytoremediation approach. *Air Quality, Atmosphere & Health*, <https://doi.org/10.1007/s11869-023-01326-z>.
- Morin, J., Gandolfo, A., Temime-Roussel, B., Strekowski, R., Brochard, G., Bergé, V., Gligorovski, S., & Wortham, H. (2019). Application of a mineral binder to reduce VOC emissions from indoor photocatalytic paints. *Building and Environment*, 156, 225-232.
- Nair, A.N., Anand, P., George, A., & Mondal, N. (2022). A review of strategies and their effectiveness in reducing indoor airborne, transmission and improving indoor air quality. *Environmental Research*, 213, 113579.
- Peterson, G., Jones, T., Rispoli, D., Haddadi, S., & Niri, V. (2023). Investigation of simultaneous volatile organic compound removal by indoor plants using solid phase microextraction-gas chromatography-mass spectrometry. *RSC Adv.*, 13, 26896.
- Petigny, N., Zhang, J., Horner, E., Steady, S., Chenal, M., Mialon, G., & Goletto, V. (2021). Indoor air depolluting material: Combining sorption testing and modeling to predict product's service life in real conditions. *Building and Environment*, 202, 107838.
- Rivera-Gomez, C., Galán-Marín, C., López-Cabeza, V. P., & Diz-Mellado, E. (2021). Sample key features affecting mechanical, acoustic and thermal properties of a natural-stabilised earthen material. *Construction and Building Materials*, 271, 121569.
- Santos, T., Gomes, M. I., Coelho, F., & Faria, P. (2019). Earth-based and current plasters: assessment of efficiency and contribution to indoor air quality, in: 5th Historic Mortars Conference, Proceedings PRO 130, Álvarez JJ, Fernández JM, Navarro Í, Durán A, Sirera R (ed.), 5-20, 19-21 June 2019, Pamplona, Spain, RILEM Publications S.A.R.L., Paris, France, ISBN: 978-2-35158-221-3.
- Schweiker, M., Endres, E., Gossler, J., Hack, N., Hildebrand, L., Creutz, M., Klinge, A., Kloft, H., Knaack, U., Mehner, J., & Roswag-Klinge, E. (2021). Ten questions concerning the potential of digital production and new technologies for contemporary earthen constructions. *Building and Environment*, 206, 108240.
- Shaw, C., Boulic, M., Longley, I., Mitchell, T., Pierse, N., & Howden-Chapman, P. (2020). The association between indoor and outdoor NO₂ levels: A case study in 50 residences in an urban neighbourhood in New Zealand. *Sustainable Cities and Society*, 56, 102093.
- Suzuki, N., Nakaoka, H., Nakayama, Y., Tsumura, K., Takaguchi, K., Takaya, K., et al. (2021). Association between sum of volatile organic compounds and occurrence of building-related symptoms in humans: A study in real full-scale laboratory houses. *Science of The Total Environment*, 750, 141635, <https://doi.org/10.1016/j.scitotenv.2020.141635> PMID: 32882497.
- Teiri, H., Hajizadeh, Y., & Azhdarpoor, A. (2021). A review of different phytoremediation methods, critical factors for purification of common indoor air pollutants: an approach with sensitive analysis. *Air Quality, Atmosphere & Health*, 1-19, <https://doi.org/10.1007/s11869-021-01118-3>.
- Tsumura, K., Nakaoka, H., Suzuki, N., Takaguchi, K., Nakayama, Y., Shimatani, K., et al. (2023). Is indoor environment a risk factor of building-related symptoms? *PLoS ONE*, 18(1), e0279757, <https://doi.org/10.1371/journal.pone.0279757>.

- US EPA, Introduction to Indoor Air Quality, accessed on 9 March 2023, <https://www.epa.gov/indoorair-quality-iaq/introduction-indoor-air-quality>.
- Vijay, P., Anand, A., Singh, N., Schikowski, T., & Phuleria, H.C. (2024). Examining the spatial and temporal variations in the indoor gaseous, PM_{2.5}, BC concentrations in urban homes in India. *Atmos Environment*, 319, 120287. <https://doi.org/10.1016/j.atmosenv.2023.120287>.
- World Health Organization (2021). New WHO global air quality guidelines aim to save millions of lives from air pollution, <https://www.who.int>.
- Zoran, M.A., Savastru, R.S., Savastru, D.M., Tautan, M.N. (2020). Assessing the relationship between ground levels of ozone (O₃) and nitrogen dioxide (NO₂) with coronavirus (COVID-19) in Milan, Italy. *Science of the Total Environment*, 740, 140005.

ACOUSTIC ABSORPTION CHARACTERISTICS THAT ARE USED IN THE ACOUSTIC DESIGN OF INTERIORS - COMPARISONS BETWEEN SOME CLASSICAL MATERIALS AND NATURAL, ECOLOGICAL MATERIALS

Marta Cristina ZAHARIA^{1,2}, Daniela DOBRE^{1,3}, Claudiu Sorin DRAGOMIR^{1,2}

¹National Institute for Research and Development in Construction,
Urban Planning and Sustainable Spatial Development - URBAN-INCERC,
266 Pantelimon Road, Bucharest, Romania

²University of Agronomic Sciences and Veterinary Medicine of Bucharest,
59 Marasti Blvd, District 1, Bucharest, Romania

³Technical University of Civil Engineering of Bucharest,
124 Lacul Tei Blvd, District 2, Bucharest, Romania

Corresponding author email: marta_cristina_zaharia@yahoo.co.uk

Abstract

In the case of the acoustic design of some rooms, such as audition rooms, classrooms for education, etc., the knowledge of the acoustic absorption characteristics of the materials/products that will be used for the interior surface finishes (walls, floors, ceilings) is of particular importance. Depending on the activity that takes place in the room, it is necessary to obtain a certain value of the reverberation time in order to achieve acoustic comfort. In many research projects, carried out in INCD URBAN-INCERC, INCERC Bucharest Branch, laboratory experiments were carried out on some types of classic materials (polyethylene, felt in plates of basaltic mineral wool) or natural, ecological materials (wool for use in construction, or wooden boards, etc.). The research was carried out in the reverberation chamber in the Building Acoustics Laboratory. The results of the studies are presented in the article as acoustic absorption coefficient in the diffuse field, α_s , in graphical forms of frequency range 100 to 5000 Hz and as the evaluation acoustic absorption coefficient α_w and are compared considering the influence of the physical characteristics of the tested materials.

Key words: absorption coefficients, acoustics, civil buildings, reverberation.

INTRODUCTION

Noise is defined as excessive or annoying sound that can harm human health and the environment. It involves irregular waves that are unpleasant, unwanted, and usually unavoidable, with no meaningful relationship between their amplitude, frequency, and length (Tajic & Ghadami, 2008; Jafari Malekabad et al., 2022). A growing problem in many urban areas, noise affects the physical and mental health of millions worldwide (Mihalache et al., 2023). Because its effects on the population are really worrying, environmental noise is one of the issues that is regulated by an increasingly legal framework, attracting more and more attention worldwide (Titu et al., 2022).

The control of noise in the work environment is crucial to the comfort and efficiency of the individual. Poor acoustic indoor environments have been shown (Kang et al., 2017; Glean et al., 2022) to negatively impact the cognitive

performance and well-being of occupants, thus negatively affecting their productivity. The acoustic design of buildings is a field that ensures the acoustic comfort of people in buildings (Zaharia, 1999; Nowicka, 2020). The acoustic design of the rooms, such as audition rooms, classrooms for education, etc., must be done according to the activities carried out in those spaces, because each type of activity requires ensuring a certain reverberation time, so that that activity takes place in conditions of acoustic comfort for the users (C125, 2013; Zaharia & Delia, 2014; Zaharia, 2020). Reverberation noise is a component of noise in a room, resulting from the reflection of an acoustic wave from the surfaces bounding the room and from objects in it. Thus, it is the noise that is transmitted inside the room and directly affects the room.

Adjusting the reverberation time in a room is done by providing materials/products with sound-absorbing characteristics on the internal

delimiting surfaces (walls, floors, ceilings) (C125, 2013; Zaharia, 1999; Scamoni et al., 2022; Hyung et al., 2015). Various techniques are utilized to control noise in industrial settings, one of this technique is noise absorption materials (Yang & Yu, 2011). To determine the sound absorption characteristics of materials/products that can be used for finishes the inside surfaces of a room, tests are necessary. In the present research, the laboratory tests were conducted on several types of classical materials (polyethylene, felt in plates of basalt mineral wool) or on natural, ecological materials (wool for building, wood panels). The laboratory experiments were carried out in the reverberation chamber of the Building Acoustics Laboratory at INCD -URBAN-INCERC institute (Zaharia et al., 2019; Vasile et al., 2019).

MATERIALS AND METHODS

In Romania, the C125, 2013 - "Normative regarding Acoustics in buildings and urban areas", provides information about the sound absorption coefficient, α_s , in the frequency range 125-4000 Hz, the evaluation sound absorption coefficient, α_w , the sound absorption classes according to α_w , and the form indicators L, M, H. In the same standard there are some stipulations for protection against reverberation in rooms with a high level of reverberation. There are also guidelines on the maximum acceptable reverberation time (T_m , s) of a room. This depends on the volume of the room, $V(m^3)$, and the type of activity that takes place in the room. These are illustrated in Figure 1.

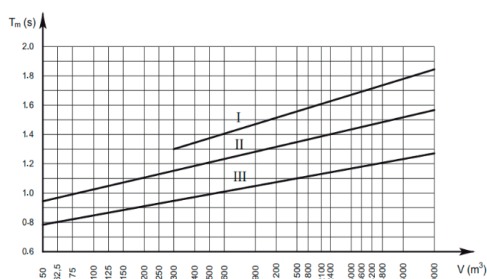


Figure 1. Admissible values of the average reverberation time, T_m , in rooms of different types of buildings:

- I - rooms in industrial buildings;
- II - dining rooms (in restaurants, etc.);
- III - classrooms, amphitheatres, offices

Given that the reverberation time required in a room can be achieved by providing materials/products with specific sound-absorbing characteristics on the interior boundary surfaces, such materials have been investigated. Some materials/products are of the classical type: polyethylene, polyurethane foam, felt in basaltic mineral wool plates, melamine foam. Other materials considered are natural, environmentally friendly, sheep's wool for use in construction, or wooden boards, wood chip boards. A recycled product, uniquely designed within project PN 19 33 03 01, made exclusively from recyclable materials was also analyzed, namely - Plastic bottles (PET) - (wrapped rolls). In this article, nine materials produced by different manufacturers were analyzed. The description and photo of the selected materials/products is presented in Table 1.

The investigations consist of measurements to determine the absorption coefficient of different types of materials according to SR EN ISO 354 "Acoustics - Measurement of sound absorption in reverberation chamber" and SR EN ISO 11654 "Acoustics - Sound absorbers for use in buildings - Evaluation of sound absorption".




According to SR EN ISO 354, 2004, the measurement methodology consists of determining the reverberation times for the empty reverberation chamber, and the reverberation times for the reverberation chamber with the investigated sample. The calculation of sound absorption coefficients is performed according to the specific standards mentioned. The measurement of the reverberation time was carried out by the interrupted noise method, using a broadband signal, of the "pink noise" type.

The measurements were performed in 6 positions of the microphone, with the two acoustic sources located in 2 points. According to the measurement standard, the test specimen shall be made on an area of 10.00 sqm - 12.00 sqm and mounted, depending on the type of material/product, according to the specific mountings in the measurement standard.

The sample may be tested by placing it on one of the side walls of the reverberation chamber or on the floor of the reverberation chamber. The ratio between the sides of the sample shall be $1/L = 0.75-1.0$.

Table 1. Materials analysed description

No.	Type of material	Description of material and photo of the sample mounted in reverberation room
1	felt in plates of basaltic mineral wool	Felt in plates of basaltic mineral wool with a thickness of 100 mm and apparent density of 40 kg/m ³ [7 - Test Report No.: 7/2006]
2	polyethylene	Polyethylene plates with a thickness of 60 mm and apparent density 25 kg/m ³ (PREGIS) [1 - Test Report No.: 9/2009]
3	polyurethane foam	Profiled polyurethane foam sheet N2244, pyramidal profile, white (960 mm x 960 mm x 65 mm) [5 - Test Report No.: 84/2016]
4	polyurethane foam	Profiled polyurethane foam sheet RF2828, pyramidal profile, anthracite grey (960 mm x 960 mm x 60 mm) [8 - Test Report No.: 81/2016]
5	polyurethane foam	ACOUSTICART decorative acoustic panels, lightweight, open-cell polyurethane foam, applied in two layers, with a thickness of 30 mm [2 - Test Report No.: 34/2015]
6	melamine foam	Melamine Foam Plate Basotect G +, gray (615 mm x 615 mm x 60 mm) [4 - Test Report No.: 74/2016]

No.	Type of material	Description of material and photo of the sample mounted in reverberation room
7	sheep wool	Thermal insulating and sound-absorbing wool-based sheep wool, 50 mm thick and apparent density of 30 kg/m ³ [6 - Test Report No.: 58/2018] 
8	Panel of wood chips and mineral wool	DUNAPREF phonoabsorbent panel, 90 mm total thickness, made of: HERAKLITH panels laid on 40mm thick basalt mineral wool, with apparent density aprox. 60 kg/m ³ [3 - Test Report No.: 26/2014] 
9	recycled materials made from PET plastic bottles (wrapped rolled)	Plastic bottles (PET), (rapped rolled), recyclable materials, with an aprox. thickness of 10 to 60 mm [9 - Test within the project no. PN 19 33 03 01] 

RESULTS AND DISCUSSIONS

Between 2006 and 2023, numerous acoustic measurements were carried out in the reverberation chamber for different types of materials and products. The nine selected materials/products are representative, and the measurement results are shown in Figures 2 to 10. These results are given as values of the evaluation sound absorption coefficient ' α_w ', and in graphical form in the frequency range from 100 to 5000 Hz for the diffuse field sound absorption coefficient, ' α_s '.

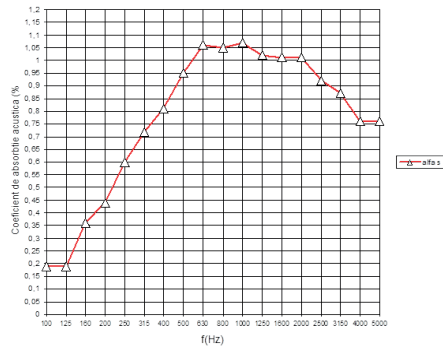


Figure 2. Acoustic results for felt in plates of basaltic mineral wool, $\alpha_w = 1.00$ [7 - Test Report No.: 7/2006]

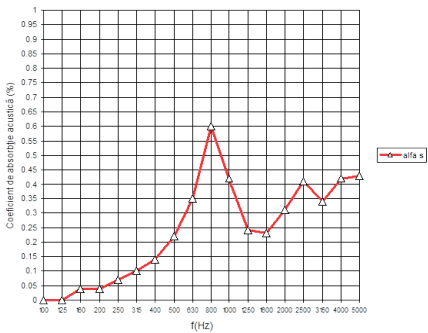


Figure 3. Acoustic results for Polyethylene, $\alpha_w = 0.30$ [1 - Test Report No.: 9/2009]

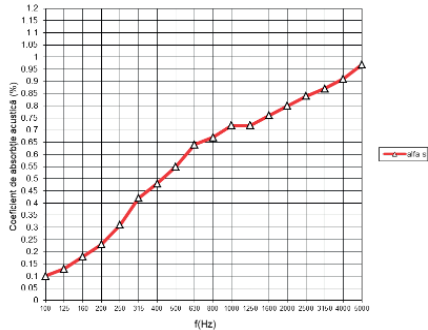


Figure 4. Acoustic results for polyurethane foam $\alpha_w = 0.55$ (H) [5 - Test Report No.: 84/2016]

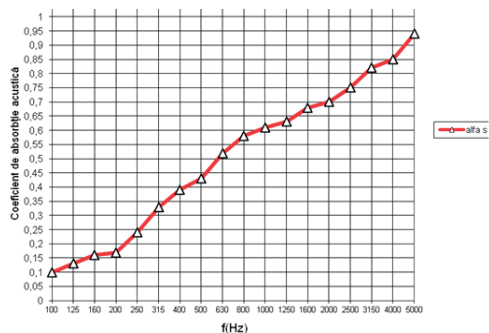


Figure 5. Acoustic results for polyurethane foam
 $\alpha_w = 0.50$ (H) [8 - Test Report No.: 81/2016]

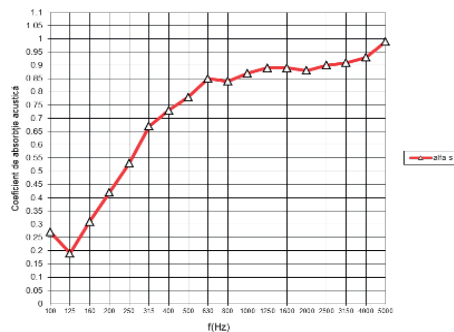


Figure 8. Acoustic results for sheep wool
 $\alpha_w = 0.80$ (H) [6 - Test Report No.: 58/2018]

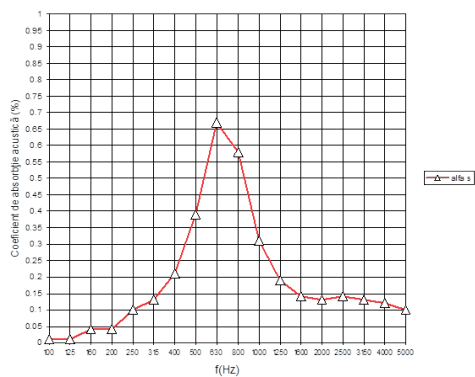


Figure 6. Acoustic results for polyurethane foam
 $\alpha_w = 0.20$ [2 - Test Report No.: 34/2015]

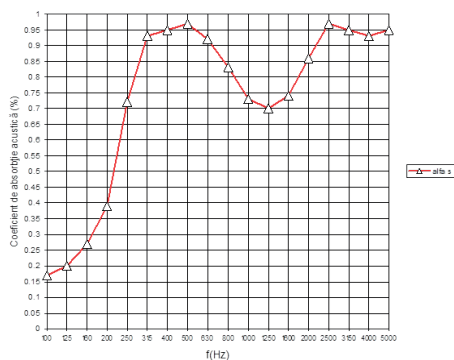


Figure 9. Acoustic results for panel of wood chips and mineral wool
 $\alpha_w = 0.85$ [3 - Test Report No.: 26/2014]

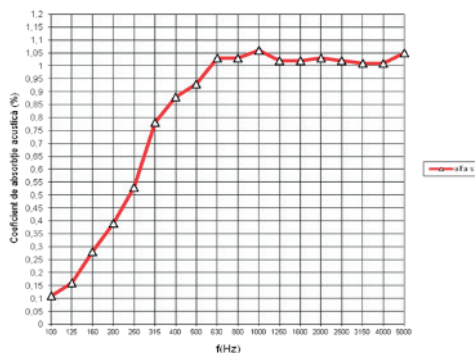


Figure 7. Acoustic results for melamine foam
 $\alpha_w = 0.85$ (H) [4 - Test Report No.: 74/2016]

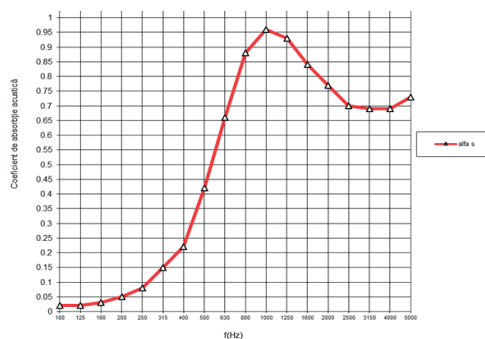


Figure 10. Acoustic results for recycled materials made from PET plastic bottles, $\alpha_w = 0.40$ (M, H) [9 - Test within the project no. PN 19 33 03 01]

When we studied the results of the experiments, we compared the values obtained for the acoustic absorption coefficient considering the influence of the type of material from which they are made (Figure 11), the density of materials (Figure 12) and the geometrical

materials characteristics (Figure 13). We compared the values of diffuse sound absorption coefficient, α_s , as graphs in the frequency range 100 to 5000 Hz, and the evaluation sound absorption coefficient, α_w .

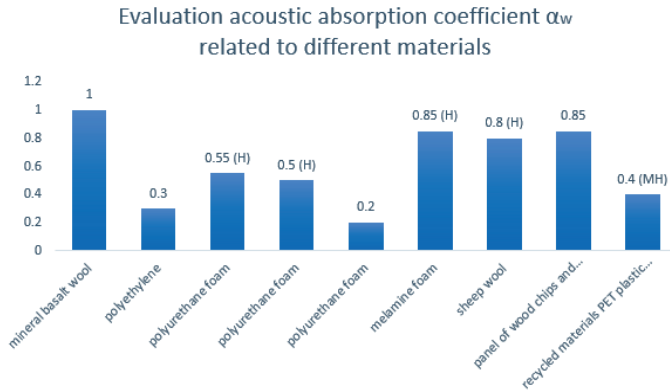


Figure 11. Types of material - acoustic absorption coefficient, relationship

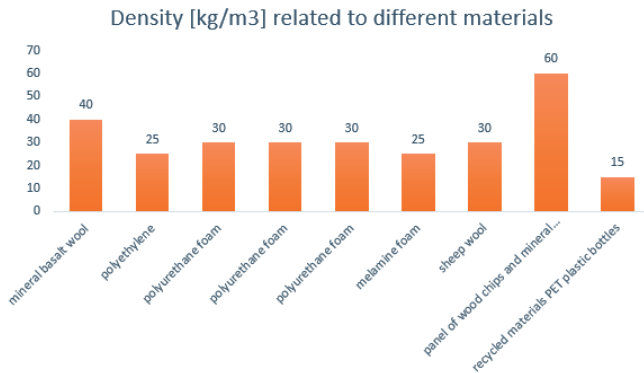


Figure 12. Types of material - density, relationship

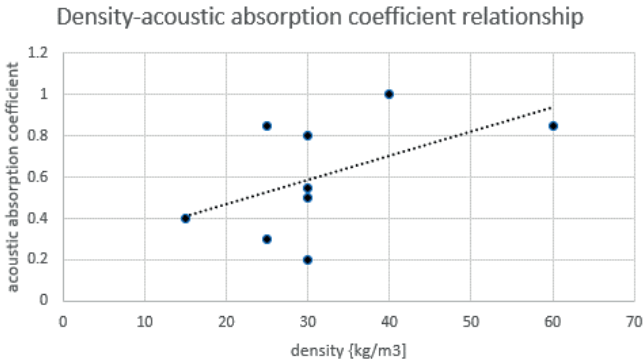


Figure 13. Density - acoustic absorption coefficient, relationship

CONCLUSIONS

The conclusions following from the analyzation of the phono-acoustical results presented above, are:

A) We analyzed materials that have an apparent density between 15 kg/m^3 and 40 kg/m^3 , exception only for the Panel of wood chips which has a higher density, approx. 60 kg/m^3 ;

B) We analyzed materials that have the thickness between 30 mm to 100 mm;

C) In case of materials which have low density, around 30 kg/m^3 , like rigid polyurethane foam and polyethylene, the acoustic absorption coefficient, α_s , in graph forms, have: a) very low values, around zero, in low frequency domain; b) a higher values, with a pick of 0.6..0.65, in the zone of frequency 630 Hz - 800 Hz, and c) low-medium values around 0.35 to 0.15, in the zone of frequency 1250 to 5000 Hz; and the coefficient α_w is between 0.2 to 0.30, depending on the type of thickness and the chemical configuration of the material structure;

D) In case of other materials which have low density, around 30 kg/m^3 , like pyramidal profiled polyurethane foam, the acoustic absorption coefficient, α_s , in graph forms, have: a) very low values, around 0.15 to 0.25, in low frequency domain; b) a linear increase in values, in the medium and higher zone of frequency; and the coefficient α_w is 0.55(H), depending on the type of thickness and the profiled configuration of the material structure;

E) In case of materials with density around 30 to 60 kg/m^3 , like felt in plates of basaltic mineral wool, wood chips and mineral wool, and sheep wool, which are almost natural materials, the acoustic absorption coefficient, α_s , in graph forms, have: a) low values, around 0.15 to 0.25, in low frequency domain, in the zone of frequency 100 Hz - 200 Hz; b) a higher values, around 0.7 to 1.00, in the zone of frequency 400 Hz - 4000 Hz - 5000 Hz; and the coefficient α_w is between 0.80-1.00 depending on the type of configuration of the natural material structure;

F) Melamine foam has the same very good acoustic absorption characteristics, with the coefficient $\alpha_w = 0.85$ (H), because of the chemical configuration of the material structure, which is soft and smooth.

G) From the analysis of the results obtained for the acoustic measurements performed on the

unique sample, made of Plastic Bottles (PET) (rapped rolled), with an approx. thickness of 10 to 60 mm, - respectively from recyclable materials that could be used in different types of rooms with large construction volumes -, tested in the reverberation chamber by the team of researchers, it can be concluded that, from the point of view of the sound-absorbing characteristics of this type of product made of recyclable materials, even if it has a very low density (around 15 kg/m^3), because of the configuration of the spatial pyramidal surface and the geometric interior air cavities of the bottles, it proves to be a very good sound-absorbing material for sounds at medium and high frequencies, with very good performances, comparable to those of some modern materials/products (melamine, etc.) that can be used to adjust the reverberation duration in rooms with specific acoustic requirements, especially for medium and high frequencies.

H) From the statistical analysis that correlates the density of the materials with the acoustic absorption coefficient, combined with the two previous analyses, regarding the type of material, the acoustic absorption coefficient, and the density, it can also be concluded that a particular importance, for obtaining a good absorption of a product, it also has the geometric and texture configuration of the finished part of the product surfaces.

ACKNOWLEDGEMENTS

The authors acknowledge the support of INCD - URBAN-INCERC for the research work that was carried out in institute and acknowledge the financial support from "The Ministry of Research, Innovation and Digitalization (MCID)", "The Ministry of Education and Research (MEC)" and "The Ministry of National Education (MEN)" in the following projects:

- PN 23 35 01 01, "Integrative concept for the digital analysis of data from the large-scale seismic monitoring of the national territory and built environment, aimed for rapid identification of the destructive potential of seismic events occurring in Romania and in the adjacent regions".

- PN 19 33 03 01, "Research to achieve the acoustic and thermal comfort inside the buildings, using an innovative tool for choosing

the optimum structures of construction elements, from classical versus modern materials".

- PN 09-14.04.07, "Methods to combat urban noise. Analysis and multi-criteria solution of the acoustics of buildings and living areas in urban and rural areas exposed to noise".

REFERENCES

- C125, 2013 Normative regarding acoustics in buildings and urban areas [in Romanian language].
- Glean, A.A., Gatland, S.D., II. Elzeyadi, I. (2022). Visualization of Acoustic Comfort in an Open-Plan, High-Performance Glass Building. *Buildings*, 12, 338. <https://doi.org/10.3390/buildings12030338>.
- Hyung, S.J., Ho, J.K., Jin, Y.J. (2015). Scale-model method for measuring noise reduction in residential buildings by vegetation. *Journal Building and Environment*, 86, 81–88. <https://www.sciencedirect.com/science/article/abs/pii/S0360132314004375>.
- Jafari Malekabad A., Zare S., Ghotbi Ravandi M.R., Ahmadi S., Esmaili R., Mohammadi Dameneh M. (2022). The noise absorption prediction of a combined and independent absorber under different conditions and at different frequencies, using the new Engineering Noise Control Software (ENC). *Heliyon*, 8(11), e11556. <https://doi.org/10.1016/j.heliyon.2022.e11556>.
- Kang, S., Ou, D., Mak, C.M. (2017). The impact of indoor environmental quality on work productivity in university open-plan research offices. *Build. Environ.*, 124, 78–79.
- Mihalache, C., Erghelegiu, B., Sandu, M.A. (2023). Noise Pollution: A Gis-based approach to mapping and assessment. *Scientific Papers Series E, Land Reclamation, Earth Observation & Surveying, Environmental Engineering*, XII, 2285-6064.
- Nowicka, E. (2020). The acoustical assessment of the commercial spaces and buildings. *Applied Acoustics*, 169, 107491, ISSN 0003-682X, <https://doi.org/10.1016/j.apacoust.2020.107491>.
- Scamoni, F., Scrosati, C., Depalma, M., Barozzi, B. (2022). Experimental evaluations of acoustic properties and long-term analysis of a novel indoor living wall. *Journal of Building Engineering*, 4(1), 98–16. 103890.
- Tajic, R., Ghadami, A. (2008). The effects of noise pollution and hearing of metal workers in Arak. *Zahedan Journal of Research in Medical Sciences*, 10(4), e94504.
- Titu, A.M., Boroiu, A.A., Mihailescu, S., Pop, A.B., Boroiu, A. (2022). Assessment of Road Noise Pollution in Urban Residential Areas - A Case Study in Pitesti, Romania. *Appl. Sci.*, 12, 4053. <https://doi.org/10.3390/app12084053>.
- Vasile, V., Petcu, C., Meîță, V., Zaharia, M.C. (2019). Innovative Thermal Insulation Products for a Circular Economy. *IOP Conference Series: Earth and Environmental Science*, 290(1), 012037, IOP Publishing Central Europe towards Sustainable Building 2019 Prague (CESB19), <https://iopscience.iop.org/article/10.1088/1755-1315/290/1/012037/pdf>.
- Yang, S., Yu, W.-D. (2011). Air permeability and acoustic absorbing behavior of nonwovens. *J. Fiber Bioeng. Inf.*, 3(4), 203–207.
- Zaharia, M.C. (1999). Contributions regarding the evaluation and combating of urban noise. *Doctoral Thesis*, Faculty of Faculty of Civil Construction and Architecture, Ghe. Asachi Technical University - Iasi, Romania [in Romanian language].
- Zaharia, M.C. (2020). The Influence of the Coefficient of Acoustic Absorption of the Facades of the Buildings from the Street Profiles on the Noise Level from the Urban Road Traffic. *Conference Paper Proceedings Series of the 10th Annual International Conference on Civil Engineering, 22-25 June 2020, Athens, Greece*, ISSN: 2529-167X.
- Zaharia, M.C., Alexe, I.M. (2019). Sound absorption characteristics determined in reverberation room, comparisons between classical and different modern, ecological materials. The 26nd International Congress on Sound and Vibration, - ICSV 26 - Montreal, Canada, *Proceedings of the ICSV26 – The 26th International Congress on Sound and Vibration*, <https://icsv26.sched.com/info>.
- Zaharia, M.C., Delia, M.F. (2014). Chapter 21. Romania, Rasmussen, B., Machimbarrena, M. (Editori). *COST Action TU0901 - Building acoustics throughout Europe, Volume 2, Housing and construction types of country by country*, Echi. COST Office and authors, COST Action - Publisher: Di Script Preimpresion, S.L., 570, e-ISBN: 978-84-697-0159-1, 352-372, www.costtu0901.eu/tu0901-e-books.
- Test reports of Building Acoustic laboratory of INCD URBAN-INCERC, INCERC Bucharest Branch:
- 1 Test Report No.: 9/2009;
 - 2 Test Report No.: 34/2015;
 - 3 Test Report No.: 26/2014;
 - 4 Test Report No.: 74/2016;
 - 5 Test Report No.: 84/2016;
 - 6 Test Report No.: 58/2018;
 - 7 Test Report No.: 7/2006;
 - 8 Test Report No.: 81/2016;
 - 9 Test within the project PN 19 33 03 01.

URBAN PARADOX: AN ANALYTICAL PERSPECTIVE RETHINKING SUSTAINABLE LAND AREAS

Gabriela BANADUC, Cornelia BAERA, Anca DRAGHICI

Politehnica University of Timisoara, 2 Piata Victoriei Street, Timisoara, Romania

Corresponding author email: gabriela.banaduc@student.upt.ro

Abstract

The paper aims to characterize the urban - rural areas relationship in the context of actual urbanization effects. Cities are marked by several social inequalities. These polarized opportunities of the urban environment which are often mirrored in contrast to the rural environment, as patterns of inequality in cities vs rural localities are considerable and generally more widespread. Facing these challenges, accompanied by the determining phenomena of the rapid growth of the urban population, led to extensive debates that had a significant impact on the local development strategy. Thus, a strong movement was generated to reach the clean natural environment, which is called the urban paradox. In the current research, the complex phenomenon of urbanization will be approached from three perspectives: (1) the capacity of cities to open up for including rural landscape as an opportunity to expand sustainable infrastructure; (2) the government ability to promote greener, more sustainable living; (3) the ability to share and provide all urban and rural residents with access to a more sustainable environment (related to the Sustainable Development Goals).

Key words: funds, inclusion, rural area, sustainable development, urbanization.

INTRODUCTION

Nature is experienced as an environment where people can rest and recover from daily stress. There is a growing need for nature as a source of relaxation and recreation (Health Council of the Netherlands and Dutch Advisory Council for Research on Spatial Planning, Nature and the Environment, 2004). In recent years, urban areas have experienced a decline in the quality and quantity of their green spaces. Due to the growth of urbanization and a densification policy, more people are facing the prospect of living in a residential environment with fewer green resources.

Throughout history, rural historical background life in Europe developed amidst a uniquely polycentric pattern of urban structures that emerged in the early Middle Ages (Zonneveld & Stead, 2007). Europe slowly transformed from a largely rural agricultural community into a large urban community: more than half of the European population lived in an urban area by 1950 (United Nations, 2018). In contrast, over 80% of those living in Africa and Asia in 1950 lived in rural areas. While the rhythm of urbanization on these two continents subsequently accelerated, in 2015 their populations, Africa (59.6%) and Asia (51.8%),

continued to live in rural areas. These different levels of urbanization show that, globally, only in the last decade the total number of people living in urban areas has exceeded that of the population living in rural areas (Kotzeva & Brandmuller, 2016).

According to statistical data processed throughout the world (United Nations, Department of Economic and Social Affairs, Population Division, 2018) 70% of global GDP is generated by economic activities located in the urban area and 53% of the total world population lives in the urban area. Moreover, it is estimated that by the year 2050, approximately 70% of the world's population will live in cities (Grimm et al., 2008). Thus, it was recognized that a process of structural transformation of urban areas due to the appearance and expansion of metropolitan areas is being registered worldwide.

The phenomenon of urbanization in Romania, as it is reflected at the level of our country, shows that the rural population in our country is decreasing, while it is estimated that the population in the urban environment will increase considerably, so that by 2050, 70% of the population will be urban. Romania's population will live in the urban environment (United Nations, 2018). An indisputable fact is

that generations to come will be born in cities, generating a huge decrease in rural population (Figure 1 and Figure 2).

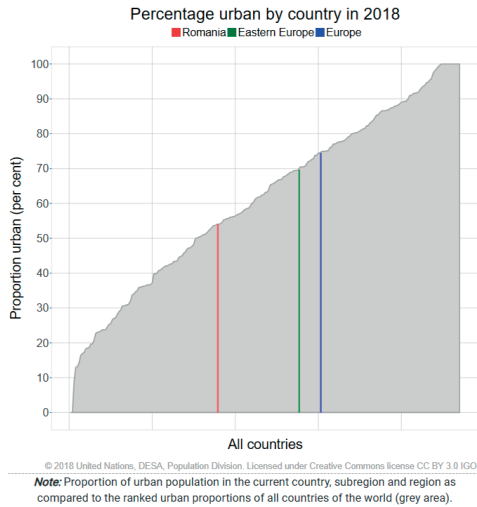


Figure 1. Urban population evolution in Romania, Eastern Europe and Europe in 2018 (by percentage)

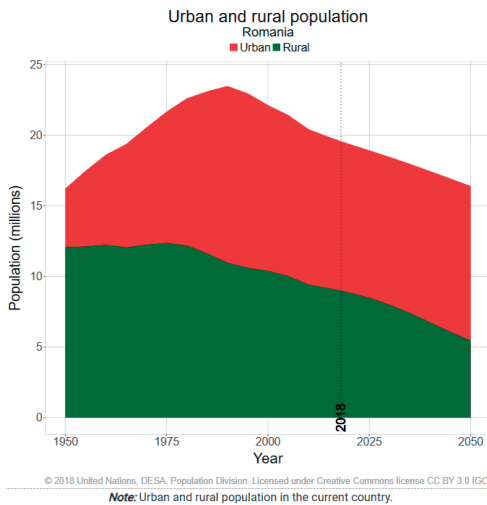


Figure 2. Urban and rural population in Romania in 2018

Most of the literature conceptualizes urbanization as a process of change over time in the size, density, and heterogeneity of human settlements (Cyril et al., 2013).

Urban development strategies are important documents that present the steps towards a more sustainable urban-rural future. It includes

sustainable objectives such as planning for land use and open space for transport coordination (including ITS/TIC systems, electric buses, or electric vehicle charging stations), planning for a better green compact city, controlling green infrastructure, and most importantly preserving agricultural land and promotion of local production. The global development of transport based on internal combustion engines has led to a significant increase in the consumption of fossil fuels produced by the extraction of crude oil from well depths and the refining of it (Simion et al., 2022).

Urban land consumption clearly affects the urban-rural linkages, being one of the biggest challenges of peri-urbanization. The urban network within the city has always formed an important factor in shaping the peri-urban area and the surrounding regions.

The peri-urban interface is formed by complex links of landscapes that cannot be called urban nor rural, but it has features of both and it is in continuous expansion. Much of the rural population depends on the urban area as it provides hospitals, government services, and education. There is a strong positive synergy between rural population and urban population as well as a negative one. The expansion of urban centers because of population growth, influences agricultural land. The peri-urban area is in continuous transformation, and in this transformational process, most of the time the poorest are the most affected. Local decision-making can help avoid neglecting forward and backward links between agriculture services and manufacturing, managers need a coherent, systematic, and scientific approach to sustainable development management (Negulescu et al., 2022). It can also negotiate and regulate the use of natural resources by rural and urban inhabitants and enterprises, otherwise they can become a major cause of conflict (Tacoli, 2003).

An aspect that becomes more and more a certainty is that urbanization is a complex process of change of rural lifestyles into urban ones in Europe (Antrop, 2004). It occurs near cities and in rural areas. It is considered a wave of spread of changing lifestyles, controlled mainly by changing access to places that offer new opportunities.

Urbanization causes space polarization by changing population density, economic activities, and mobility. In addition, cities are often characterized by a number of social inequalities, and it is common for people to enjoy comfortable lives living in close proximity to others who may face considerable challenges, such as housing, poverty, or crime. These polarized opportunities/challenges of the urban environment are often mirrored in strong contrast to the rural environment, as the patterns of inequality in cities versus rural localities are considerable and generally more widespread than those observed for countries.

Cities are recognized by both political factors and public opinion for their significant contribution to wealth creation and human well-being. In the early stage of industrialization and urbanization among developing countries, it is common that rural areas offered support to urban areas. The imbalance between urban and rural leads to serious problems like rural poverty and environmental destruction, which affects the whole environmental and economic development.

Urbanization is also a challenging process for sustainable development of rural territories. One of the most threatened by urbanization pressures is agriculture. The impact consequence of urban expansion generates an increased competition for natural resources in the peri-urban and rural areas where agriculture is the main occupation. This peri-urban zone is associated with the transition from urban structure to that of a rural specific and involves shifts into, out of and across it from both sides, this makes it a priority in understanding the broader regional context and dynamics across the urban-rural environment. Thus, a major challenge for urban planning future is developing the public spaces for an increasing number of people and preserve urban areas sustainable without creating any unnecessary pressure, 'an interconnected network of green spaces that helps stop the loss of biodiversity and enable ecosystems to deliver their many services to people and nature' (Benedict & McMahon, 2012).

Having said this, the search for sustainability involves twin efforts both in cities and in the countryside. The concept of urban-rural areas relationships is discussed both in the academic literature and policy and programming

documents. The concept is being traced back in time (Davoudi, 2002) and mirrored in the present time as cities and villages are two systems that depend on each other, integrate with each other and complement each other (Ji et al., 2019) each deriving different benefits or negative/positive impacts.

Urban-rural relationship can take many different forms but each one enhances urban-rural synergies in a specific way.

The rural areas are not always included in the development processes as it cannot provide a stable income or employment. On the other hand, it provides natural resources, unique natural landscapes and cultural values essential for urban development. In the last years, the linkages between the rural areas and functional urban areas were greatly boosted by structural funds especially in the field of sustainable mobility, public spaces infrastructure, agriculture. These investments are foreseen in the regional, EU Cohesion policy, and echoes in the improvement of communication, social services and economical attractiveness of the rural landscape, strengthening the rural - urban relationship and promoting a smart, sustainable and inclusive growth (Crescenzi & Giua, 2014). Urban-rural partnerships at the European, national, regional level crosses challenging times. To address these challenges the vitality of rural areas due to urbanization development is under decline owed to depopulation and agricultural lack of interest. On the other hand, urban area faces pollution, congestion, and a very intensive development. Also, urbanization has been boosted by large support from rural areas especially natural resources such as energy and food (Kelly-Reif & Wing, 2016) while the rural areas were affected by economic, social and environmental pressure.

In this respect, the paper aims to characterize the urban - rural areas relationship in the context of actual urbanization effects as cities are marked by several social inequalities. The need for structural changes regarding the European policy about funding is in progress.

MATERIALS AND METHODS

The methodological approach applied to study the phenomenon of characteristics of the

urbanization phenomenon in a rural environment consists of three steps (Figure 3). In the first step, the regional territory is classified based on the typology of urbanization pattern from peri-urban and rural areas such as the capacity of cities to open for the inclusion of the countryside as access to city infrastructure (road tolls and integrated public transport systems, reducing pollution, promoting the use of cleaner or renewable fuels, encouraging cyclists/pedestrians or introducing more green spaces). Second, the capacity to foster a greener and more sustainable life living. Third, the capacity to share and provide for the rights of all urban and rural residents, access (to opportunities, places), their capacity to foster a greener, more environmentally sustainable world, to all current and future residents according to the 17 Sustainable Development Goals (SDG) as shown in Figure 3.

RESULTS AND DISCUSSIONS

At EU level, pressure on the EU agriculture resources have increased due to demographics changes as Figure 4 suggestively shows. Furthermore, the growing pressure on the use of natural capital is a reason to increase agriculture productivity in the best sustainable way by involving both urban and rural actors (Figure 5).

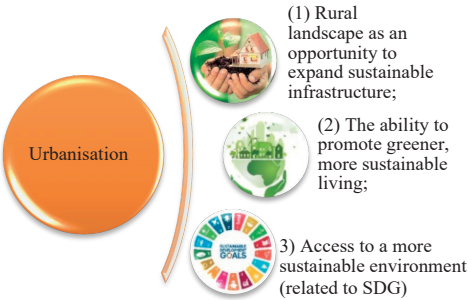
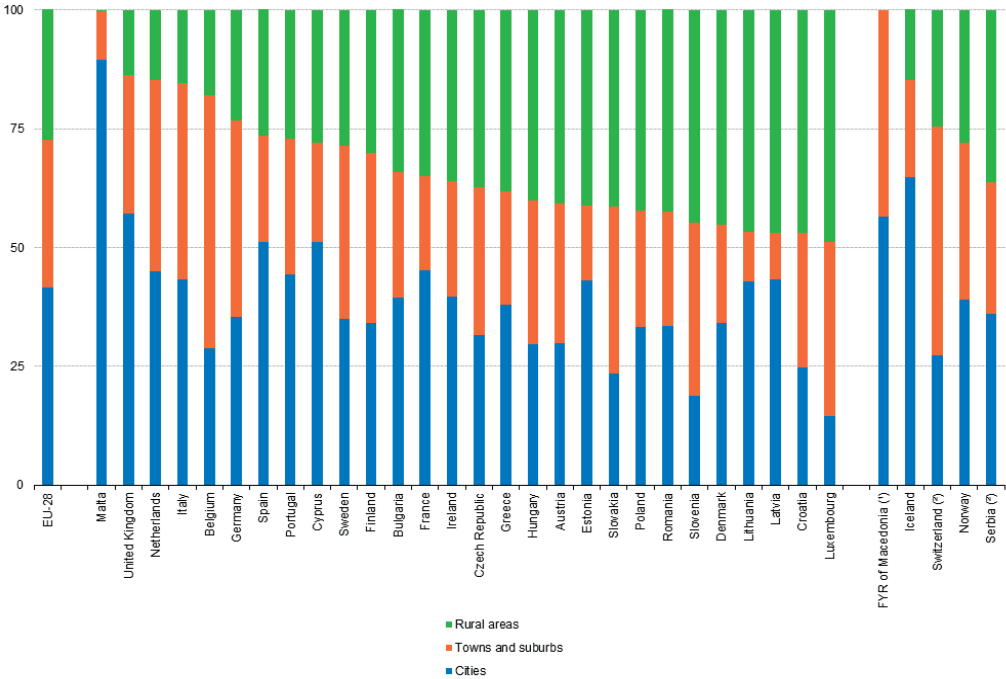


Figure 3. Methodological approach



(*) 2011. Rural areas: low reliability.
(*) 2013.

Figure 4. Population distribution by degree of urbanization, 2014 (% of total population)
(Eurostat online data code: ilc_lvho01)

Rural development is influenced by climate change, high food prices, and endangered biodiversity. Also, there are many changes due to the existing gap between urban-rural area vs. rural-rural areas (limited access to care services, public transport, etc.). The reduction of rural poverty and improvement of rural environment is a process of enhancing the common development of urban and rural areas, and as result, eliminates the imbalance between urban and rural. It is significant to sustainable development, and essential to explore a new urban-rural cooperation mode to address the dual polarization phenomenon (Ji et al., 2019). Common Agricultural Policy (CAP) for 2023-2027 period address the Sustainable Development Goals (SDG) by introducing measures (SDG) as shown in Table 1. These goals support sustainable agriculture, sustainable management of natural resources,

climate action and balanced territorial development, with the aim of conserving nature, such as green payment, focusing on rural areas with anticipated impacts on semi-natural habitats and wild species throughout Europe (Concepción et al., 2020). Rural development is "the set of activities and actions of various actors that, taken together leads to progress in rural areas" (Shepherd, 1998). Details are given in Table 2.



Figure 5. Process of achieving urban/rural sustainable development

Table 1. CAP for 2023-2027 period address sustainable development goals by introducing measures for every sustainable development goal (SDG) (United Nations, 2015)

SDG	Objective	Measures
SDG 1	Ending poverty in all its forms	Reducing inequalities between territories and people
SDG 2	Ending hunger, achieve food security and improved nutrition and promote sustainable agriculture.	Supporting agricultural productivity of small-scale farms, equal access to land, knowledge, farm employment, financial services
SDG 4	Ensure inclusive and equitable quality education and promote lifelong learning opportunities for all.	Enhancing innovation, encouraging research, strengthening advisory services.
SDG 6	Ensure the availability and sustainable management of water and sanitation for all.	CAP strategic plans to reduce nutrient losses and pesticide use by 50% by 2030, thereby protecting water resources
SDG7	Ensure access to affordable, reliable, sustainable and modern energy for all.	Various measures to increase the production of renewable energy, e.g. biogas.
SDG8	Promote sustained, inclusive, and sustainable economic growth, full and productive employment and decent work for all.	CAP promotes income, value-added services, and employment in rural areas.
SDG9	Build resilient infrastructure, promote inclusive and sustainable industrialization and foster innovation.	Improving internet access. Access to government access to information and communication technology services and infrastructure.
SDG12	Ensure sustainable consumption and production patterns.	CAP helps to reduce food loss and waste.
SDG13	Take urgent action to combat climate change and its impacts.	The CAP supports carbon storage and contributes to the prevention and reduction of GHG emissions. GHG emissions from agricultural production decreased from 483 million tons in 1990 to 382 million tons in 2020.
SDG15	Protect, restore and promote sustainable use of terrestrial ecosystems, sustainably manage forests, combat desertification, and halt and reverse land degradation and halt biodiversity loss.	Organic production has increased in the last decade. Organic farming contributes to the promotion of more sustainable farming practices and environmental protection and to the improvement of animal welfare in response to specific consumer demands for sustainable food products.

Table 2. Objectives and results of sustainable agriculture

No.	Objective	Result
1.	Assuring the resilience of agriculture sector.	Long term food security, support family farm income and economic, social and environmental agriculture sustainability
2.	Focus on innovation and research.	A smart productive future farm and a digitalized rural/urban market.
3.	Ensuring a sustainable future for European farmers.	Improve farmer's status developing
4.	Promoting sustainable energy.	Greenhouse gas emission and carbon reduction
5.	Reducing chemical dependency.	Promote sustainable development of natural resources and reducing chemical product in industrial agriculture (biocides, herbicides) synthetic fertilizers.
6.	Preserving habitats and landscapes.	Enhance ecosystem services, reversing biodiversity loss (replanting trees,
7.	Sustainable economic development for the rural areas.	Encourage and support young farmers, new farms, attract new investors.
8.	Promote social inclusion and local development.	Encourage women's participation in rural economic development, gender equality, employment.
9.	Maintain societal needs on food and health.	Encourage high-quality, healthy food produced in a sustainable way, avoiding food waste or animal welfare.
10.	A modern agriculture in rural areas.	Fostering innovation and digitalization, improved access to knowledge, innovation and research, trainings.

Following the methodological approach applied to study the characteristics of the urbanization phenomenon over rural environment, we keep in sight that:

1. Sustainable Infrastructure in Cities Capacity for Inclusion of Rural Areas

Today, human activities have significantly amplified land degradation in both the rural and urban areas. Living standards for the rural population are mostly determined by access to natural resources such as fertile soil or water quality, very affected by urban expansion and associated desertification in the long term (Abu Hammad & Tumeizi, 2012).

Industrialization led to rural land abandonment because of increased cultivation costs, decreased profits, and changes in trade regulations between countries (Atis, 2006), and also, at the same time, the local job market in rural areas connected both to agriculture and tourism became less due to land degradation (urban expansion leading to associated desertification and environmental degradation in time) and land availability, reduced production of the annual harvest.

Rural emigration is probably the most evident example of off-site effects of large-scale urban expansion and socioeconomic development on land degradation (Borrelli et al., 2018).

Socioeconomic development, rural migration, rural land abandonment, and soil erosion are factors that increase the risks of windstorms,

floods, landslides, or other environment deterioration and fully affect rural areas (Seifollahi-Aghmiuni et al., 2022). Different forms of land degradation can affect soil quality and productivity and limit the services of soil ecosystems in certain environmental systems.

Sustainable management and mitigation of land degradation, especially in areas where environmental vulnerability is already a challenge, can improve soil health and structure, support food production and resilience to climate change and human pressures, and provide a regional buffer against climate change and human pressures (Colantoni et al., 2015).

From the perspective of the triple development of urbanization, namely, from the point of view of population, land and economy (Figure 6), the gap between urban and rural areas is easily identified as the degree of influence of population urbanization, industrial urbanization, and land urbanization on the gap between the social economic systems. The living system of residents between urban and rural areas is increasing.

Along with the development of urbanization, the gap between urban and rural financial investments, the remuneration of labor production, the quality of life, and the ability to pay by means of transport will narrow. The key implication of these findings is that relevant future measures and policies should be formulated in the operation of local conditions

to promote the implementation of rural economic development. Urbanization is seen as a double-edged sword, with positive or negative impact on rural development. In addition, different periods or degrees of urbanization will have different mechanisms for developing urban-rural relationships.

How to narrow the gap between urban and rural areas? Strategic documents are the first to predict the step forward a more sustainable urban development (Banaduc et al., 2023) The landscape dynamics are influenced by the polarization territory between urban, rural and accessibility aspects. Urbanization processes are dynamic, multifunctional, and complex; it affects not only cities, but also smaller settlements and remote villages. A detailed inventory of landscape conditions and monitoring is essential to obtain reliable data to fund good decision making.



Figure 6. Triple development of urbanization

The relationship between the city and the countryside is strongly influenced by the transportation infrastructure. Urbanization processes affect main cities but also smaller settlements and even remote rural villages.

2. The Capacity to Foster a Greener and More Sustainable Life Living

Since 2007, Romanian farmers could benefit of some similar rights with European farmers (according to the Romania's accession to the European Union <https://eur-lex.europa.eu/EN/legal-content/summary/the-accession-partnership-with-romania.html>). An important role was played by the funds addressed to agriculture and rural development, an important component of these funds being the allocations financial measures of the National Rural Development Programme (PNDR) 2014-2020. PNDR 2014-2020 represents the programmatic document, in the sense of art. 6 of

Regulation (EU) no. 1305/2013, which provides for the measures and amounts allocated to Romania from the EAFRD, which are approved by the European Commission by decision. From 2021, begun the transition period to the new Community Agricultural Policy (CAP) 2021-2027, and the implementation of a National Strategic Plan. The European model of agriculture is based on competitiveness, such as protecting the environment, offering more convenient residential settlements for the rural population, and the integration of agriculture with the environment and forest. CAP focuses on integrated development of the rural economy and protecting the environment. The EU's rural development policy helps rural areas in the EU to meet the wide range of challenges and opportunities that face them in terms of economic, environmental, and social development. CAP supports the dynamism and economic viability of rural areas through funding actions that support rural development. Sustainable development of rural areas stands up for agriculture by boosting competitiveness of all branches of agriculture, natural resource management, promote food supply chain, restoration, conservation, and development of ecosystems linked to agriculture, social inclusion, and poverty reduction, encourage knowledge transfer and innovation in agriculture to balanced development of rural areas. These objectives are achieved with the help of the European Agricultural Fund for Rural Development (EAFRD) as shown below. The EAFRD budget for Romania the period 2014- 2020 was 12.051.034.359 € out of which were spent 10.150. 481.429 € from the state budget (Figure 7).

Common Agricultural Policy pays more and more attention to rural sustainable development, but in order to formulate appropriate policies and assure the effectiveness of the policy measures, the need to understand these territories is mandatory, and even so, sometimes it is not enough.

Investments in agriculture have a particular impact on the rural economy in general, given that agriculture continues to remain the most important activity in rural areas and an essential source of income for households. The Common Agricultural Programme funds farm activities that improve competitiveness. It points out the

experience of other agricultural systems, from other member states or from other countries that faced the same challenges (political, economic, or environmental).

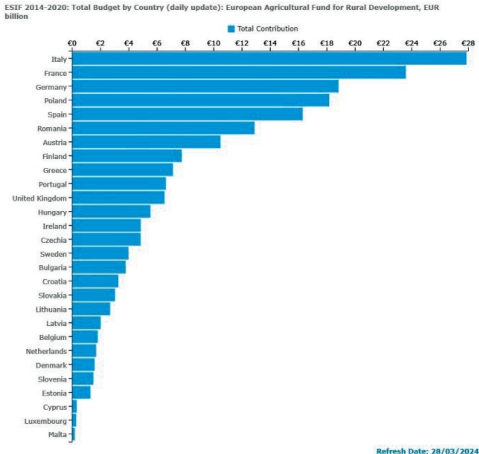


Figure 7. ESIF 2014-2020: Total Budget by Country (daily update): European Agricultural Fund for Rural Development, EUR billion. Retrieved from <https://cohesiondata.ec.europa.eu/funds/eafrd/14-20>

The local landscape change can only be understood when situated in its general geographical context and with all its related dynamics. The patterns of change are different for the countryside near major cities, for metropolitan villages, and for remote rural villages. Planning and designing landscapes for the future requires that geographical context to be understood.

3. Access to a More Sustainable Environment

To maintain and avoid depopulation and degradation of rural communities, it is essential to encourage sustainable rural development and follow the local development strategies step by step. Informed authorities will ensure biodiversity conservation agriculture resilience, innovation and promote sustainable ways of producing energy. Land abandonment related to depopulation changes the vertical and horizontal fuel structure in ecosystems and landscapes, increasing fire hazards (Sil et al., 2019). Abandoned landscapes tend to exhibit higher fire, especially when occurs in conservation areas (Chivulescu et al., 2023).

Adequately planned, sustainable infrastructure projects have developed in the recent years a

governmental proactive promotion of new roads and sanitation, water and electricity supplies, and other types of projects, which contributed greatly to increasing income equality between the poorer and wealthier regions, narrowing the gap between urban-rural economic developments (Ministerul Agriculturii si Dezvoltarii Rurale, 2024). Cultivation of agricultural products, including harvesting, milking, breeding of animals and keeping them for agricultural purposes, maintaining an agricultural area in a condition that makes it suitable for grazing or for cultivation, without any preparatory action that goes beyond the framework methods and usual agricultural machinery (minimum activity), in compliance with the rules of eco-conditionality, represent a proven path on the way to sustainable development or as in the urban-rural migration (Davis, 2011).

Urbanization is associated with dramatic changes in land patterns, demographic structure, types of occupation, and aspects of lifestyle and culture associated with the growth of cities (Popkin, 2017), a complex process of change of rural lifestyles into urban ones (Antrop, 2004).

Government at any level is obliged to provide cities and communities in the urbanization process with the necessary resources to engage in the development of participatory, inclusive policies of involved and informed citizens, to promote investments that ensure access to sustainable jobs, basic services needed for daily living, water, sanitation, transport, green energy, clean, efficient waste management, and pollution reduction, as well as public green spaces and community services (Boc, 2017).

Figure 8 is showing the path on the way to sustainable development in agriculture.

The increase of city population led to question the livability of urban areas. The lack of urban food production, the change in climate and water availability produces consequences making important changes for agricultural land use. Therefore, the distribution of green urban areas in multifunctional way is done by means of implementing sustainable strategies. A smart urban space management supports the economy but also the city aesthetic on its way to a self-sustained community.

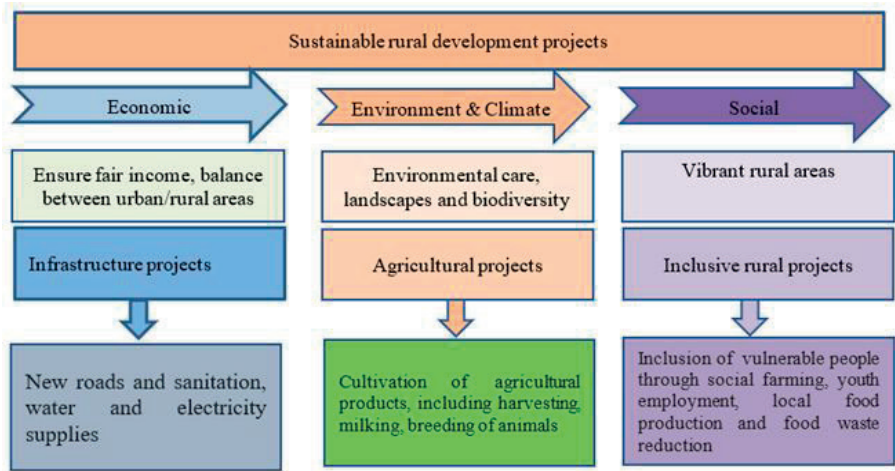


Figure 8. The path on the way to sustainable development

In this respect, the aim of the study is to underline the importance to promote a greener, more sustainable living, shedding light on the importance of smart urbanization. The process follows SDG principles, all under the umbrella of smart governance. The relationship between urban and rural areas, reflected in terms of cooperation and of essential needs as: food, nature, place identity as individual, physical health (Dean et al., 2018) is deepened into the mechanisms of rethinking sustainable land areas, specifically focusing on the potential role of the cities to use every opportunity to expand sustainable infrastructure, sustainable lifestyle and environment. The present study provides insights on sustainable land areas perspectives in accord with SDG 2 (Zero Hunger), SDG 11 (Sustainable Cities and Communities) and SDG 13 (Climate Change), European funds, the dynamic of residential neighbourhoods and green spaces in the context that people are embedded in (Russo et al., 2024; Yu et al., 2024) 2, healthy public spaces (Wood et al., 2017; Jimenez et al., 2021), to promote social cohesion of a healthy resilient city.

The city's capacity for inclusion of rural areas from the point of view of socioeconomic development, industrialization, job market, rural emigration is probably one of the most evident examples of sustainable urbanization. This complex mechanism follows strategic documents (Guvernul Romaniei & Programul Națiunile Unite, 2008) pointing out that conservation and improvement of natural

resources is a priority for increasing economic dynamism of rural areas to maintain social balance through the sustainable development of agriculture, forestry and fishing (Guvernul Romaniei, 2005).

CONCLUSIONS

In recent years, the quality and quantity of green space has declined. Urbanization is a complex process of transforming rural life into urban life. Due to growing urbanization and a policy of spatial planning densification, more and more people are faced with the prospect of living in a residential environment with fewer green resources.

Urban land consumption clearly affects the urban-rural links. Precious land around the city that is used for services and that pollutes the area (waste dumps, treatment plants, etc.), reduces their attractiveness and affects the land market. Natural heritage is misused, valuable natural areas being occupied by aggressive habitation and often incompatible economic functions. The use of the Nature-Based Solutions (BnS) concept proposes the use of nature in addressing urban planning. Most rural populations depend on urban areas because they provide hospitals, government services, and education. Local decision making also negotiates and regulates the use of natural resources by rural and urban residents and enterprises. Cities are recognized by both political factors and public opinion for their significant contributions to the creation of

wealth and human well-being. The impact of urban expansion will result in an increase in competition for natural resources in suburban and rural areas where agriculture is the main occupation.

The urbanization phenomenon in the rural environment consists of three steps:

(1) The capacity of cities to open up for the inclusion of the countryside as access to city infrastructure (road tolls and integrated public transport systems, reducing pollution, promoting the use of cleaner or renewable fuels, encouraging cyclists/pedestrians or introducing more green spaces), channeled by infrastructure projects for new roads and sanitation, water and electricity supplies;

(2) The capacity to foster a greener and more sustainable life living by environmental care of landscapes and biodiversity through agricultural projects;

(3) The capacity to share and provide for the rights of all urban and rural residents, access (to opportunities, places), and their capacity to foster a greener, more environmentally sustainable world for all current and future residents, inclusive rural projects targeting social farming youth employment, local food production or food reduction according to the 17 SDGs).

The EU's rural development policy helps EU rural areas to address a wide range of challenges and opportunities in terms of economic, environmental and social development. The sustainable development of rural areas (Figure 8), is aimed at strengthening the competitiveness of all agricultural sectors, managing natural resources, promoting food supply chains, restoring, conserving and developing ecosystems linked to agriculture, social inclusion and poverty reduction, encouraging knowledge transfer and innovation in agriculture to the development of balanced rural areas. Urban-rural development is considered one of the key pillars of regenerative development, including the economic, social, and environmental balance.

Also, urban-rural development has been regarded as one of the key pillars in driving regenerative development that includes economic, social, and environmental balance. Cultivation of agricultural products, including harvesting, milking, breeding of animals and

keeping them for agricultural purposes, maintaining an agricultural area in a condition that makes it suitable for grazing or for cultivation, without any preparatory action that goes beyond the framework methods and usual agricultural machinery (minimum activity), in compliance with the rules of eco-conditionality, represent a proven path on the way to sustainable development.

Government at any level is obliged to provide cities and communities in the urbanization process with the necessary resources to engage in the development of participatory and inclusive policies of involved and informed citizens.

REFERENCES

- Abu Hammad, A., & Tumeizi, A. (2012). Land degradation: socioeconomic and environmental causes and consequences in the eastern Mediterranean. *Land Degradation & Development*, 23(3), 216-226.
- Antrop, M. (2004). Landscape change and the urbanisation process in Europe. *Landscape and urban planning*, 67(1-4), 9-26.
- Atis, E. 2006, Economic impacts on cotton production due to land degradation in the Gediz Delta, Turkey. *Land Use Policy*, 23, 181–186.
- Banaduc, G., Taucean, I., & Trunk, A. (2023) Towards the Sustainable Urban Development Goal: A Review of Evaluation Tools. *Proceedings of the MakeLearn&TIIM2023 International Conference on Economic, Social and Environmental Sustainability: The Role of Technology and Political Dialogue*, Valetta, Malta (193-200), ToKnow Press. Available at: <https://toknowpress.net/ISBN/978-961-6914-30-7/46.pdf>. Access on 24-01-2024.
- Benedict, M.A., & McMahon, E.T. (2012). *Green infrastructure: linking landscapes and communities*. Island press.
- Boc, E. (2017). Inovare sustenabilă pentru un oras colaborativ, *Revista Transilvana de Stiinte Administrative*, 40(1), 3-12.
- Borrelli, P., Van Oost, K., Meusburger, K., Alewell, C., Lugato, E., & Panagos, P. (2018). A step towards a holistic assessment of soil degradation in Europe: Coupling on-site erosion with sediment transfer and carbon fluxes. *Environmental Research*, 161, 291-298.
- Chivulescu, S., Cadar, N., Hapa, M., Capalb, F., Radu, R.G., & Badea, O. (2023). The Necessity of Maintaining the Resilience of Peri-Urban Forests to Secure Environmental and Ecological Balance: A Case Study of Forest Stands Located on the Romanian Sector of the Pannonian Plain. *Diversity*, 15(3), 380.
- Colantoni, A., Mavrikakis, A., Sorgi, T., & Salvati, L. (2015). Towards a 'polycentric' landscape? Reconnecting fragments into an integrated network of coastal forests in Rome. *Rendiconti Lincei*, 26, 615-624.

- Concepción, E. D., Aneva, I., Jay, M., Lukanov, S., Marsden, K., Moreno, G., ... & Diaz, M. (2020). Optimizing biodiversity gain of European agriculture through regional targeting and adaptive management of conservation tools. *Biological Conservation*, 241, 108384.
- Crescenzi, R., & Giua, M. (2014). The EU Cohesion policy in context: regional growth and the influence of agricultural and rural development policies. *LEQS paper*, 85.
- Cyril, S., Oldroyd, J.C., & Renzaho, A. (2013). Urbanisation, urbanicity, and health: a systematic review of the reliability and validity of urbanicity scales. *BMC Public Health*, 13(1), 1-11.
- Davis, K. (2015). The urbanization of the human population. In *The city reader*, 43-53, Routledge.
- Davoudi, S. (2002). Urban-rural relationships: An introduction and brief history. *Built environment*.
- Dean, J.H., Shanahan, D.F., Bush, R., Gaston, K.J., Lin, B.B., Barber, E., & Fuller, R.A. (2018). Is nature relatedness associated with better mental and physical health? *International journal of environmental research and public health*, 15(7), 1371.
- Grimm, N.B., Faeth, S.H., Golubiewski, N.E., Redman, C.L., Wu, J., Bai, X., & Briggs, J.M. (2008). *Global change and the ecology of cities science*, 319(5864), 756-760.
- Health Council of the Netherlands and Dutch Advisory Council for Research on Spatial Planning, Nature and the Environment, (2004). *Nature and Health. The influence of nature on social, psychological and physical well-being*. The Hague: Health Council of the Netherlands and RMNO 2004; publication no. 2004/09E. Available at: <https://www.healthcouncil.nl/documents/advisory-reports/2004/06/09/nature-and-health-the-influence-of-nature-on-social-psychological-and-physical-well-being>. Access on 12-02-2024.
- Ji, X., Ren, J., & Ulgiati, S. (2019). Towards urban-rural sustainable cooperation: Models and policy implication. *Journal of Cleaner Production*, 213, 892-898.
- Jimenez, M.P., DeVille, N.V., Elliott, E.G., Schiff, J.E., Wilt, G.E., Hart, J.E., & James, P. (2021). Associations between nature exposure and health: a review of the evidence. *International journal of environmental research and public health*, 18(9), 4790.
- Kelly-Reif, K., & Wing, S. (2016). Urban-rural exploitation: An underappreciated dimension of environmental injustice. *Journal of Rural Studies*, 47, 350-358.
- Kotzeva, M.M., & Brandmuller, T. (2016). Urban Europe: Statistics on Cities, Towns, and Suburbs. Publications office of the European Union.
- Ministerul Agriculturii si Dezvoltarii Rurale (2024). Galerie video - Proiecte de success. Available at: <https://www.madr.ro/axa-leader/content/65-galerie-video-proiecte-de-succes.html?start=3>. Access on 24-01-2024.
- Negulescu, O.H., Draghici, A., & Fistis, G. (2022). A Proposed Approach to Monitor and Control Sustainable Development Strategy Implementation. *Sustainability*, 14(17), 11066.
- Popkin, B. (2017). Relationship between shifts in food system dynamics and acceleration of the global nutrition transition. *Nutrition reviews*, 75(2), 73-82.
- Russo, C., Romano, L., Spano, G., Theodorou, A., Carrus, G., Mastandrea, S., ... & Panno, A. (2024). Personal dispositions explain differences in physical health benefits of nature exposure: The role of restorativeness and affect. *Frontiers in Psychology*, 15, 1365512.
- Romaniei, G. (2005). Planul Național de Dezvoltare 2007-2013.
- Romaniei, G., & Unite, P.N. (2008). Strategia Nationala pentru Dezvoltare Durabila a Romaniei Orizonturi 2013-2020-2030. Bucuresti available at <http://www.insse.ro/cms/files/IDDT>, 202012.
- Seifollahi-Aghmiuni, S., Kalantari, Z., Egidi, G., Gaburova, L., & Salvati, L. (2022). Urbanisation-driven land degradation and socioeconomic challenges in peri-urban areas: Insights from Southern Europe. *Ambio*, 51(6), 1446-1458.
- Shepherd, A. (1998). *Sustainable rural development*. Bloomsbury Publishing.
- Sil, A., Azevedo, J.C., Fernandes, P.M., Regos, A., Vaz, A.S., Honrado, J.P. (2019). Wildfire is not an ecosystem service. *Front. Ecol. Environ.*, 17, 429-430.
- Simion, A.F., Găman, A. N., Găman, G. A., Drăgoi, I., & Ghiță, C. (2022). Environmental and ecotoxicological risk assessment of pollution with light crude oil for an oil exploitation field. In *MATEC Web of Conferences*, 354, 00071. EDP Sciences.
- Tacoli, C. (2003). The links between urban and rural development. *Environment and urbanization*, 15(1), 3-12.
- United Nations, Department of Economic and Social Affairs, Population Division, (2018). *World Urbanization Prospects: The 2018 Revision*. Available at: <https://population.un.org/wup/Country-Profiles/> Access on 12-02-2024.
- United Nations, (2015). General Assembly Resolution A/RES/70/1.Transforming Our World, the 2030 Agenda for Sustainable Development. Available at: http://www.un.org/ga/search/view_doc.asp?symbol=A/RES/70/1&Lang=E Access on 10-02-2024.
- World Urbanization Prospects, (2018). Retrieved from: <https://population.un.org/wpp/> Access on 12-02-2024.
- Wood, L., Hooper, P., Foster, S., & Bull, F. (2017). Public green spaces and positive mental health-investigating the relationship between access, quantity and types of parks and mental wellbeing. *Health & place*, 48, 63-71.
- Yu, C., & Kwan, M.P. (2024). Dynamic greenspace exposure, individual mental health status and momentary stress level: A study using multiple greenspace measurements. *Health & Place*, 86, 103213.
- Zonneveld, W., & Stead, D. (2007). European territorial cooperation and the concept of urban-rural relationships. *Planning, Practice & Research*, 22(3), 439-453.

STUDY ON THE SOILS OF THE GORJ COUNTY AND THE LIMITING FACTORS OF THEIR QUALITY, IN ORDER TO IMPROVE THEM

Mihaela BĂLAN, Cristian POPESCU

University of Craiova, Faculty of Agronomy, 19 Libertatii Street, Craiova, Romania

Corresponding author email: popescucristian07@yahoo.com

Abstract

This study aimed at inventorying the soils of the Gorj County, classifying them into quality classes and identifying the limiting factors of their quality. Thus, eight soil classes were identified over an area of 192,405.22 ha and soil complexes and associations over an area of 51,362.78 ha. As far as soil quality is concerned, the soils have been divided into quality classes which were done following the 1:10,000 scale survey. The assessment was made according to soil, relief and climate and it was revealed that the largest agricultural area, i.e. 140,898 ha, which represents 57.8% of the total agricultural area, falls into the fourth quality class, which demonstrates the complexity of the relief and soils in the Gorj County. As far as soil quality limiting factors are concerned, it was found that they can be grouped into three main groups: soil-dependent limiting factors (texture, porosity, reaction, CaCO_3 content, nutrients content); limiting factors dependent on terrain factors <other than soil> (slope, erosion, landslides) and limiting factors caused by anthropogenic activities (pollution).

Key words: land assessment, limiting factors, nutrients content quality, soil.

INTRODUCTION

The Gorj County is located in the south-western part of Romania, on the middle course of the Jiu River. The total area of the county is 560,174 ha, representing 2.35% of the area of the country, ranking 21st in terms of area. The 560,174 ha cover a natural setting of great variability: foothills, lowlands and mountains, which are represented as follows: 243,768 ha agricultural land, 273,868 ha forests, 10,251 ha non-productive land and 25,787 ha other uses (water, roads, construction).

Sustainable land use is very important to maintain its high production capacity and to preserve the quality of the environment (Zafiu & Mihalache, 2021).

Soil quality is influenced by limiting factors, factors which are the same as in the Romanian bonitation system, but which manifest themselves differently depending on geomorphological, lithological, hydrological and climatic specificities (Teaci, 1980).

The limiting factors of soil quality can be divided into three groups:

1. soil-dependent limiting factors (texture, porosity, reaction, CaCO_3 content, nutrient content);

2. limiting factors dependent on terrain - other than soil (slope, landslides, erosion);
3. limiting factors caused by anthropogenic activities (pollution).

With regard to the factors in the first group, several aspects should be mentioned.

Texture is a limiting factor because it cannot be modified in simple ways, directly influencing the hydrophysical properties of the soil.

The effect of the clay fraction is stronger the lower the organic matter content, becoming insignificant when organic matter is present in large quantities (Cochrane & Aylmore, 1994; Thomas et al., 1996).

Soil porosity depends on all soil properties, but is most influenced by texture and structure. Optimum porosity is found in horizons with a glomerular structure, as well as in loose soil, which has non-capillary spaces between aggregates and capillary pores within structural aggregates, with optimum values at: cultivated soils 45%, loamy 47%, clayey 40% (Popescu, 2008).

Soil reaction is a limiting factor of soil quality, being directly related to the degree of base saturation.

In our country, most agricultural plants grow in good conditions at a weak acid to weak alkaline

reaction (pH between 5.81 and 8.40), in this situation the soil reaction (pH) is not a limiting factor for soil quality (Popescu, 2019).

The calcium carbonate (CaCO_3) content of soils becomes a limiting factor when it is present in large (21-25%) and very large (26-40%) quantities. **Nutrient content** can be a limiting factor in soil quality, in particular because important nutrient reserves in soils are in the form of compounds that are inaccessible to plants.

Limiting factors dependent on the land, other than the soil, are given first of all by the configuration of the land - by the slope and the repercussions this has on the soil, namely erosion and landslides - and last but not least by climatic and environmental conditions, which cause excess moisture, or conversely, drought. Slope determines surface and deep erosion. Landslides are induced by abusive and excessive deforestation that leads to soil destabilization, through the removal of roots that provide its stability (Kalmar et al., 2022). Climatic and environmental conditions can act as limiting factors through excess moisture or drought – which occurs in the summer during the vegetation period, being essentially the major abiotic stress that limits crop production (Bonea, 2020) or through the combination of atmospheric and soil drought, which severely affects agricultural crops, significantly reducing or even completely destroying them (Nițu et al., 2023).

Limiting factors caused by human activities are manifested through pollution and soil compaction.

Pollution manifests itself in various forms caused by human activities (agricultural methods, forest management, urbanisation, etc.). Human activities have led to soil degradation, causing a decrease in its productive capacity and affecting surrounding ecosystems (Nițu et al., 2023; Corcheș, 2023).

The main sources of pollution are: mining and quarrying, oil and gas exploitation, the energy industry, agriculture (compaction).

Soil compaction is a process caused by natural or artificial causes, as a result of which the bulk density increases greatly and the total porosity and aeration porosity fall below normal values. In Gorj County, agriculture is of particular importance as an economic branch, primarily to

support the livelihood of the local population. For this reason, it is necessary to know as much as possible about the soil, its fertility status, which influences its productive capacity, but also to identify sustainable, diversified and balanced agricultural technologies that ensure the conservation of both the soil and the surrounding environment, in order to provide high, stable and high nutritional quality productions (Hansen et al., 2006; Patzel et al., 2000).

The decrease in soil fertility should be a wake-up call to limit soil degradation and rehabilitate soils by changing production technologies to improve their physical, chemical and biological properties (Zafiu & Mihalache, 2021). Thus, the identification of soil quality limiting factors is of great importance for the development and implementation of sustainable agricultural technologies (Bouma et al., 2017; Davidson, 2000; Rhodes, 2017; Smith, 2012; Várallyay, 2010) which would ensure that the soil can continue to provide quality goods and services (Doran et al., 2000; Toth et al., 2016; European Commission, 2006; EC Law, 2021), and a healthy environment.

MATERIALS AND METHODS

The aim of this study was to present the limiting factors of soil quality in Gorj County and how they contribute to the degradation of agricultural land quality.

Field research (soil sample collection) and laboratory analysis (determination of nutrient content, soil reaction, CaCO_3) were carried out for this study. During the research, the raw results obtained in the field and laboratory phases were processed and interpreted in the office phase (determination of structural indices). Also, in parallel, statistical data and documents existing at the Gorj O.S.P.A. were studied and analysed in order to highlight the main problems related to soil quality in the county, but also a review of the literature was made in this regard, in order to provide a better understanding of these phenomena and their intensity (Gorj O.S.P.A. Archives, 1979-2010; 1980-2010; 2010; 31/12/2018).

The study also focused on identifying the main measures that could be taken to prevent land degradation and restore degraded land.

RESULTS AND DISCUSSIONS

The distribution of the agricultural area according to the lithological nature of the main parent materials on which the soils of Gorj County evolved is shown in Figure 1. It can therefore be seen that the highest percentage is represented by silts and alluvial deposits (25% each) and the lowest by limestones (2%).

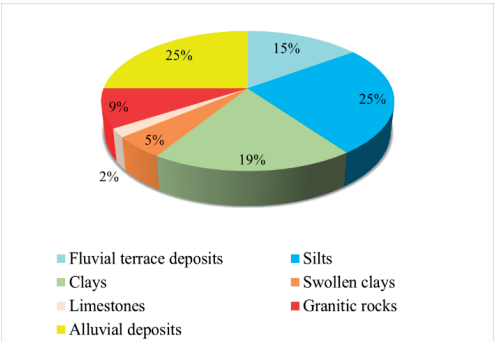


Figure 1. Percentage distribution of lithological materials in the Gorj County

Given the natural framework as well as the environmental conditions existing in Gorj County, a wide variety of soils have evolved and they are divided into the following classes: Protisols, Cernisols, Cambisols, Luvisols,

Spodosols, Pelisols, Hydrisols and Anthrisols (Florea & Munteanu, 2012).

As can be seen, the Gorj County comprises eight soil classes, covering an area of 192,405.22 ha, as well as soil complexes and associations covering an area of 51,362.78 ha (Balan, 2021). Thus, soil classes occupy areas of: 1,395.5 ha cernisols; 71,482.81 ha luvisols; 69,894.36 ha cambisols; 5,131.84 ha spodosols; 3,544.45 ha hydrisols; 8,495.42 ha pelisols; 30,143.80 ha protisols; 2,316.74 ha anthrisols. Soil complexes and associations are found on slopes with uneven slopes greater than 20%, where erosion processes and landslides are more intense.

As far as the distribution of land by quality classes is concerned, this was done following boning, according to soil, relief and climate. Thus, it was revealed that the agricultural area of Gorj county, i.e. 243,768 ha, falls into the fourth quality class with an average score of 36 points, as follows: arable land (101,622 ha) is in the fourth quality class with an average score of 36 points, grassland and meadows (122,070 ha) in the fourth quality class with an average score of 35 points, vineyards (7,604 ha) in the fourth quality class with an average score of 31 points, orchards (12,472 ha) in the fourth quality class with an average score of 32 points (Table 1).

Table 1. Distribution of agricultural area in the Gorj County by quality classes and categories of use

Item No.	Category of use	Surface (ha)	Quality class													
			II			III			IV			V			Class	
			Surface ha	Points No.	%	Surface ha	Points No.	%	Surface ha	Points No.	%	Surface ha	Points No.	%	Average	Points No.
1	Arable	101,622	4,971	65	4.89	26,154	43	25.74	62,502	34	61.50	7,995	18	7.87	IV	36
2	Pastures + meadows	122,070	10,050	67	8.23	27,031	45	22.14	63,891	33	52.34	21,098	17	17.28	IV	35
3	Vines	7,604	216	64	2.84	946	41	12.44	5,465	31	71.87	977	15	12.85	IV	31
4	Orchard - trees	12,472	267	61	2.14	2,105	44	16.88	9,040	31	72.48	1,060	18	8.50	IV	32
5	Agricultural land total	243,768	15,504	65	6.36	56,236	44	23.07	140,898	33	57.80	31,130	17	12.77	IV	36

Soil-dependent limiting factors refer to soil physical properties (texture, porosity) and chemical properties (soil reaction - pH, calcium carbonate content - CaCO_3 and nutrient content).

Texture manifests itself as a limiting factor of soil quality in Gorj County, depending on the parent material on which the existing soil types

evolved. Thus, texture is a limiting factor in soils of the luvisols class (typical preluvisols, typical luvisols, white luvisols), which evolved on clays as parent material, and in vertosols which evolved on swollen clays. These parent materials, having a high clay content and especially colloidal clay, gave the soils in the upper horizons and on the control section a fine

texture (LA-AL-A). Fine texture is a limiting factor on an area of 59,958 ha of which: 47,631 ha soils evolved on clays and 12,327 ha soils evolved on swollen clays.

Coarse and medium-coarse texture is also a limiting factor for soil quality, but to a lesser extent. This texture is found in soils that have evolved on coarse-textured parent materials. Coarse texture affects soil quality on 5,327 ha (NL) and medium-coarse texture 80,487 ha (LN).

The loam texture is not a limiting factor for the quality of soils in the Gorj County, since the grain size fractions have a balanced distribution, and this is found on an area of 104,496 ha, where the soils have evolved on medium parent materials. The medium texture gives the soil favourable physical and chemical properties, i.e. better water permeability of the soil, water retention, accumulation and yield capacity, good porosity, etc.

Total porosity is a limiting factor for the quality of soils in the Gorj County, over an area of:

- 59,958 ha, on fine-textured soils (clayey) in the upper horizon and on the control section, where the degree of subsidence is high and the total porosity low;

- 5,327 ha, on sandy soils, where porosity is high and the soil loose.

In terms of **soil reaction**, soils in Gorj County have a pH between 4.4 (strongly acidic soils) and 9.1 (strongly alkaline soils).

The soils covering the agricultural area of the county are characterized by a wide range of variation (Figure 2) which highlights the difficulties in soil cultivation and choice of uses. Soil reaction is not a limiting factor for soil quality in the Gorj County on an area of 168,638 ha (69.17%) where it falls into the categories of the weakly acid reaction (16.91%), neutral reaction (18.23%) and weakly alkaline reaction (34.03%).

As pH decreases or increases, plants suffer, as soil reaction becomes a limiting factor in soil quality. Thus, soil reaction is a limiting factor in the Gorj County on an area of 75,130 ha (30.83% of the county's agricultural area), of which:

- strong acid reaction occurs on an area of 20,541 ha (8.43% of the agricultural total);

- the moderately acid reaction occurs on an area of 52,570 ha (21.57% of the agricultural total);

- strong alkaline reaction occurs on an area of 819 ha (0.34% of the agricultural total);

- the moderately alkaline reaction occurs on an area of 1,200 ha (0.49% of the agricultural total).

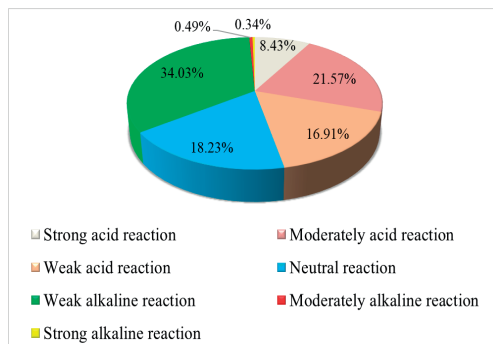


Figure 2. Areas and classes of soil reaction variation on agricultural lands

Knowing the reaction of soils, it is possible to place agricultural crops appropriately, knowing that some plants prefer soils with an acid reaction (potato, lupin, barley, rye) and others prefer soils with an alkaline reaction (alfalfa, asparagus, etc.).

Also, knowing the negative effect of the reaction of soils, the most appropriate measures can be taken for their improvement and rational use. Thus, for the improvement of acid soils, carbonate or calcium oxide-based amendments are used (CaCO_3 , CaO). The amelioration of the strong alkaline reaction is much more complicated and is achieved by the administration of gypsum or phosphogypsum-based amendments, concomitantly with the application of washing and desiccation works.

In the Gorj County **soil calcium carbonate content (CaCO_3)**, is not a limiting factor for soil quality, exceeding normal limits in very rare cases. One of these cases is the regosols, where quantities higher than 20% are found especially in the upper horizons.

As far as **nutrient content** is concerned, in the Gorj County soils they are found in low and even very low assimilable forms.

In order to highlight the nutrient content of the soil, agrochemical mapping was carried out on representative areas under different agricultural

uses. Table 2 shows the agrochemical mapping area by agricultural use.

Nitrogen supply to soils is generally low and medium due to low doses of this macro-element being administered, lack of organic fertilisation, degraded state of soils and also due to low humus content.

The degree of nitrogen supply is determined by the humus content and the nitrogen index. The nitrogen supply situation by nitrogen index is shown in Table 3.

Table 2. Situation of agrochemical mapping areas

Category of use	Total surface area (ha)	Mapped area (ha)	Mapped area (% of total use)
Arable	101,622	80,571	79.28
Pastures - meadows	122,070	88,694	72.66
Orchards - trees	12,472	9,176	73.57
Vines	7,604	4,045	53.20
Total	243,768	182,486	74.86

Thus, of the total agricultural area of 182,486 ha with agrochemical mapping, 175,124 ha (95.97%) are poorly and moderately supplied with nitrogen, 6,640 ha (3.64%) are well supplied and only 722 ha (0.39%) are very well supplied with nitrogen. The arable area of 80,571 ha with agrochemical mapping is as follows: 78,336 ha (97.23%) are poorly and moderately supplied with nitrogen, 2,235 ha (2.77%) are well and very well supplied with nitrogen. Of the 88,694 ha of grassland and meadows with agrochemical mapping, 83,923 ha (94.62%) are poorly and medium supplied with nitrogen, and 4,771 ha (5.38%) are well and very well supplied with nitrogen.

Phosphorus supply to soils in the study area is low due to low humus content, low phosphorus fertilisation, as well as due to the degraded state of soils, and in particular due to soil acidity and mobile aluminium present on 30.82% of the soil surface.

Table 3. Nitrogen supply situation by nitrogen index

Category of use	Mapped area (ha)	Nitrogen supply status according to I.N.											
		Poorly supplied			Averagely supplied			Well supplied			Very well supplied		
		I. N.	Surface	%	I.N.	Surface	%	I.N.	Surface	%	I.N.	Surface	%
Arable	80,571	2	53,930	66.93	3	24,406	30.29	5	1,982	2.46	6	253	0.31
Pastures - meadows	88,694	2	52,430	59.11	3	31,493	35.51	5	4,348	4.90	6	423	0.48
Orchards - fruit trees	9,176	2	5,352	58.33	3	3,579	39.00	5	218	2.38	6	27	0.29
Vines	4,045	2	2,411	59.60	3	1,523	37.65	5	92	2.27	6	19	0.47
Total	182,486	2	114,123	62.54	3	61,001	33.43	5	6,640	3.64	6	722	0.40

Table 4. Soil phosphorus supply status

Category of use	Mapped area (ha)	Phosphorus supply status														
		Very poorly supplied			Poorly supplied			Averagely supplied			Well supplied			Very well supplied		
		P ppm	Surface	%	P ppm	Surface	%	P ppm	Surface	%	P ppm	Surface	%	P ppm	Surface	%
Arable	80,571	8	21,229	26.35	13	20,336	25.24	27.05	18,584	23.07	54.05	12,172	15.11	72	8,250	10.24
Pastures meadows	88,694	8	37,421	42.19	13	22,211	25.04	27.05	14,280	16.10	54.05	7,901	8.91	72	6,881	7.76
Orchards - fruit trees	9,176	8	3,605	39.29	13	2,400	26.16	27.05	1,531	16.68	54.05	978	10.66	72	662	7.21
Vines	4,045	8	1,101	27.22	13	1,279	31.62	27.05	837	20.69	54.05	517	12.78	72	311	7.69
Total	182,486	8	63,356	34.72	13	46,226	25.33	27.05	35,232	19.31	54.05	21,568	11.82	72	16,104	8.82

According to the data in Table 4, the following conclusions can be drawn: out of the total agricultural area with agrochemical mapping of 182,468 ha, 144,814 ha (79.36%) are very

poorly - medium supplied with phosphorus, 21,568 ha (11.82%) are well supplied with phosphorus, and 16,104 ha (8.82%) are very well supplied with phosphorus. Of the total

agricultural area, the agrochemical mapping arable area of 80,571 ha, is as follows: 60,149 ha (74.65%) are very poorly - medium supplied with phosphorus, 12,172 ha (15.11%) are well supplied, and 8,250 ha (10.24%) are very well supplied with phosphorus.

Regarding the area occupied by grassland and meadows, of the 88,694 ha with agrochemical mapping, 73,912 ha (83.33%) are very poorly - medium supplied with phosphorus, 7,901 ha (8.91%) are well supplied, and 6,881 ha (7.76%) are very well supplied with phosphorus. In terms of soil **potassium** supply, it is found that of the total mapped agricultural area of 182,468 ha, 101,508 ha (55.63%) is poorly and moderately supplied with potassium

and 80,978 ha (44.37%) is well and very well supplied with potassium (Table 5).

Poor and medium supply status is caused by irrational, unbalanced fertilisation, lack of organic fertilisation application, as well as soil degradation status.

Of the 80,571 ha of arable land with agrochemical mapping, 44,785 ha (55.58%) are poorly and moderately supplied with potassium and 35,786 ha (44.42%) are well and very well supplied with this element.

Of the 88,694 ha of pasture and meadow area covered by agrochemical maps, 49,393 ha (55.69%) are poorly and moderately supplied with potassium and 39,301 ha (44.31%) are well and very well supplied with this element.

Table 5. Soil potassium supply status

Category of use	Mapped area (ha)	Potassium supply status											
		Poorly supplied			Averagely supplied			Well supplied			Very well supplied		
		K ppm	Surface	%	K ppm	Surface	%	K ppm	Surface	%	K ppm	Surface	%
Arable	80,571	66	11,718	14.54	99,05	33,067	41.04	166.05	21,297	26.43	200	14,489	17.98
Pastures - meadows	88,694	66	14,303	16.13	99,05	35,090	39.56	166.05	21,539	24.28	200	17,762	20.03
Orchards – fruit trees	9,176	66	1,677	18.28	99,05	3,370	36.73	166.05	2,165	23.59	200	1,964	21.40
Vines	4,045	66	748	18.49	99,05	1,535	37.95	166.05	947	23.41	200	815	20.15
Total	182,486	66	28,446	15.59	99,05	73,062	40.04	166.05	45,948	25.18	200	35,030	19.20

Table 6. Anthropogenic degradation processes

Item No.	Specification	Factors and types of pollution									General Total	Str. (%)
		Physical pollution				Chemical pollution and dust						
		Excavations	Waste dump cleaning	Underground activity	Total	Mixed P+A.S	Salt water	Term. powders	Cement powders	Total		
1	Cambisols Class	2,017.38	2,295.10	69.20	4,381.68	68.10	125.30	8,295.00	8,501.00	16,989.40	21,371.08	27.08
2	Luvisols Class	2,394.86	752.50	631.60	3,778.96	291.80	163.70	24,671.00	3,194.00	28,320.50	32,099.46	40.68
3	Pelisols Class	68.01	-	-	68.01	-	195.40	78.00	-	273.40	341.41	0.43
4	Protisols Class	134.75	119.30	-	254.05	29.50	1.00	12,425.00	3,101.00	15,556.50	15,810.55	20.04
5	Soil complexes and associations	2,006.50	514.60	2,030.80	4,551.90	-	-	4,531.00	204.00	4,735.00	9,286.90	11.77
	Total	6,621.50	3,681.50	2,731.60	13,034.60	389.40	485.40	50,000.00	15,000.00	65,874.80	78,909.40	100.00

The main sources of **pollution** in the Gorj County are: day mining, oil and gas natural extraction, industrial and energy activity, non-rational agriculture – compaction.

Anthropogenic degradation processes in the Gorj County are shown in Table 6.

Thus, from Table 6 it can be seen that the most polluted soils are:

- Eutricambosols belonging to the Cambisols class (affected by physical pollution on 4,381.68 ha and by chemical pollution on 16,989.40 ha);

- Luvisols of the Luvisols class (affected by physical pollution on 3,778.96 ha and by chemical pollution on 28,320.50 ha).

The surface area of the Gorj County is affected by pollution sources on 78,909.40 ha of which: physical pollution on 13,034.60 ha (16.52%) and chemical pollution on 65,874.80 ha (83.48%).

The soils most affected by pollution processes are soils of the cambisols class represented by eutricambosols (21,371.08 ha) representing 27.08% of the total area affected by pollution and of the luvisols class represented by luvisols (32,099.46 ha) with a percentage of 40.68%.

Day mining is a source of pollution through the extraction of lignite, which causes physical and chemical pollution. Thus, by excavation and welding, geological deposits of different ages are brought to light, their distribution being different both vertically and horizontally. Thus, the surface affected by mining in the Gorj County is 13,034.60 ha.

Oil and gas extraction is also a source of anthropogenic pollution, generating both physical pollution (through the location of oil equipment) and chemical pollution (with oil and salt water).

Chemical pollution in this case manifests itself on the surface of 874.8 ha. The impacts of oil and salt water pollution are soil salinization, primarily due to sodium chloride and potassium chloride, salt-saturated soils having a chlorine content greater than 12 mg/100 g of soil.

Saltwater pollution occurs during oil and gas drilling. Because of the pressure, salt water gushes out affecting the soils.

The energy sector is the main polluting factor due to ash deposits and the presence of heavy metals from thermal power plants, affecting an area of 50,000 hectares. This corresponds to 79.90% of the territory impacted by chemical contamination and 63.36% of the total polluted areas in the whole Gorj County.

Compaction is a limiting factor for the quality of soils in Gorj County, on an area of 26,580 ha, as a result of the practice of non-national agriculture, which requires deep tillage on an area of 17,718 ha.

In the Gorj County, the distribution of areas according to the **slope of the land** is as follows (Figure 3):

- very gently sloping land (slope between 0 and 5%) or unrestricted land, which covers an area of 104,332.70 ha representing 42.80% of the total agricultural area of the Gorj County;

- gently sloping land (slope between 5 and 10%), or land with reduced restrictions, which is found on an area of 23,864.89 ha, representing 9.79% of the agricultural area;

- moderately sloping land with two slope limits, namely: slope between 10 and 15%, occupying a area of 24,839.96 ha, representing 10.19% and slope between 15 and 25% occupying an area of 37,832.79 ha, representing 15.52% of the total agricultural area, these being severely restricted land;

- steeply sloping land, with a slope of more than 25%, occupying an area of 52,897.66 ha, i.e. 21.70% of the agricultural area in Gorj, which is also land with very severe restrictions.

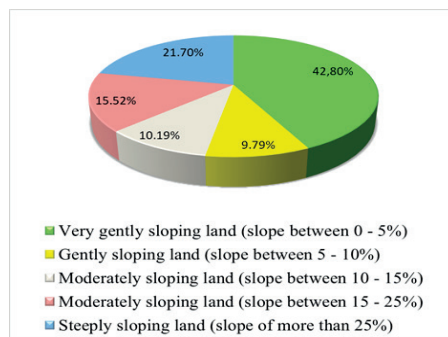


Figure 3. Distribution of agricultural area by slope category

Landslides affect 47,806 hectares, representing 19.61% of agricultural land in Gorj (Table 7). Out of these, stable and semi-stable landslides occupy 43,106 hectares (90.17% of the landslide-affected area), while active landslide areas cover 4,700 hectares (9.83% of the total landslide-affected area).

Excess moisture is manifested on 80,968.27 ha, affecting 33.22% of the agricultural area of the county. As stated above, excess moisture is related to gleization and stagnogleization. Thus, the land affected by gleization occupies an area of 10,628.36 ha (13.13% of the area affected by excess moisture) and the land affected by stagnogleization occupies an area of 70,339.91

ha (86.87% of the area affected by excess moisture).

The most extensive areas affected by excess moisture are found in the northern region of the county, in areas with flat relief, where soils of the Luvisol class predominate and where the phenomenon manifests itself with significant intensity, covering an area of 31,573 ha.

Table 7. Landslides by soil type

Specification	Surface (ha)	Landslides			
		Stable + Semistable	Active	Total (ha)	Str. (%)
Cernisols	1,395	35	-	35	2.51
Luvisols	71,483	9,231	1,200	10,431	14.59
Cambisols	69,894	57	173	230	0.33
Spodosols	5,132	15	-	15	0.29
Hydrisols	3,544	-	-	-	-
Pelisols	8,496	395	840	1,235	14.54
Protisols	30,144	502	133	635	2.11
Anthriscals	2,317	-	-	-	-
Complexes, associations	51,363	32,871	2,354	35,225	68.58
Total	243,768	43,106	4,700	47,806	19.61

Drought is a limiting factor for soil quality during the summer growing season. It is particularly prevalent in the southern part of Gorj County and becomes a limiting factor in years when rainfall is below 520 mm per year.

Due to the uneven distribution of rainfall in one year out of ten, drought sets in from July to October. The lack of rainfall in the southern part of the county, but at the same time its uneven distribution, requires the introduction of irrigation in dry summer periods.

In the Gorj County, **erosion** is the most widespread limiting factor, since 57.2% of the county's agricultural area is on slopes greater than 5%, strongly affecting soil properties and its production capacity. Of the total agricultural area of 243,768 ha, erosion occurs on 139,027.95 ha which represents 57.03% of the agricultural area, of which: surface erosion occurs on 134,940.26 ha, representing 97.06% of the eroded area, and deep erosion on 4,087.69 ha, representing 2.94% of the area affected by erosion (Table 8). Erosion also affects the environment by contributing to the pollution of rivers, lakes, reservoirs, by increasing the percentage of solid silt, i.e. soil or rock particles, transported by surface runoff. Soil types in the Gorj County are affected by surface or deep erosion in different proportions, (Table 8). Thus, the most affected by erosion are spodosols (100%), followed by luvisols (82.37%), then soil complexes and associations (81.03%), cernisols (80.65%), protisols (32.07%), pelisols (31.78%) and cambisols (28.47%).

Table 8. Soil erosion by soil type

Specification	Surface (ha)	Erosion			
		Surface erosion (ha)	Gully erosion (ha)	Total (ha)	Str. (%)
Cernisols	1,395	1,000	125	1,125	80.65
Luvisols	71,483	57,804	1,078	58,882	82.37
Cambisols	69,894	19,420	480	19,900	28.47
Spodosols	5,132	3,397	1,735	5,132	100.00
Hydrisols	3,544	-	-	-	-
Pelisols	8,496	2,700	0	2,700	31.78
Protisols	30,144	9,372	295	9,667	32.07
Anthriscals	2,317	-	-	-	-
Complexes, associations	51,363	41,247	375	41,622	81.03
Total	243,768	134,940	4,088	139,028	57.03

CONCLUSIONS

At the level of the Gorj County, all the limiting factors related to the soil (texture, porosity, pH, CaCO₃ content, nutrient content), soil-

dependent limiting factors (slope, landslides and erosion), as well as limiting factors caused by anthropogenic activities (pollution and compaction, etc.) are manifested, with more or less intensity. The heterogeneous natural

framework at the level of the studied territory has determined the formation and evolution of specific soil classes: protisols, cernisols, cambisols, luvisols, spodosols, pelisols, hydrisols and anthrisols, as well as a complex of soils which, depending on the conditions of their formation and especially their evolution, have undergone degradation processes to varying degrees as a result of the limiting factors listed above. Relief, one of the important factors of soil genesis, is the space in which the degradation process, manifested on the largest surface, i.e. erosion, takes place.

The occurrence of limiting factors on slopes is closely related to exposure, slope gradient and slope shape. In general, soils on slopes are shorter and less evolved, and erosion and landslides are more intense on slopes. The steeper the slope and the lower the vegetation cover of the slopes, the more intense the erosion and landslide phenomena are. Slope shape plays a particular role in the erosion process. Convex slopes are subject to erosion processes and concave slopes favour the accumulation of eroded material.

On uniform slopes, whole soils are found, while on uneven, stepped or unevenly sloping slopes, complexes and associations of soils are found.

Lowlands and terraces are less affected by capacity limiting factors. In the meadows and terraces there are medium-textured soils, unaffected by excess rainfall, with a fairly good degree of fertility. In the microdepression areas of the meadows, where the groundwater is at a shallow depth, gleaming phenomena occur.

Areas in the vicinity of rivers may be affected, but less frequently, by flooding. In the internal depression, more precisely in the secondary depressions of Tismana, Peștișani, Crasna, Novaci, Polovragi, there are soils evolved on fluvial gravels with a strong acidic character, brought from the mountains. In this case, acidity may manifest itself as a limiting factor due to the high hydrogen content. In addition to acidity, these soils contain a high percentage of skeletal material, which manifests itself as a limiting factor by reducing the soil's edaphic volume.

Although texture is a limiting factor, with its high content of fine fractions (clay) and coarse

fractions (sand), this physical property cannot be improved, as it is the most stable property of soil, which does not depend either on human activity or on natural factors acting in the area. It influences soil porosity, (low in the case of clay texture and high in the case of sandy texture), which can be brought to normal parameters, about 50% of soil volume, by applying measures that collaterally improve other soil properties, (i.e. administration of organic fertilizers, which replenish the humus reserve, deep tillage, which improves compaction and application of irrigation that achieves a proper water regime).

Acidity can be improved by administering fertilizers with a physiological alkaline reaction, alkalinity - by using fertilizers with a physiological acid reaction, compaction by deep tillage applied at least once every three years, replenishment of the nutrient reserve - by root fertilisation, replenishing the moisture deficit can be done by building local irrigation systems, especially in the south, where rainfall amounts are lower.

Returning areas of land to the agricultural circuit as a result of day mining, given that large areas of land are taken out of the agricultural circuit every year, by laying the excavated material in separate layers and arranging them in such a way that the surface soil comes from humus-rich material. As this operation is more difficult to carry out in practice, it is beneficial for the Gorj County area, that these terrains be afforested especially with acacia plantations (*Robinia Pseudocacia*).

Preventing and combating erosion involves a range of measures and techniques designed to minimise soil loss and protect water quality and the environment. These include: anti-erosion organisation of the territory, establishing the crop structure according to the degree of erosion and the protection it provides for the soil, the use of a cropping system to reduce the speed, flow and volume of water running down the slopes, shaping the surface of the land to retain as much rainfall as possible, carrying out special hydro-technical works to intercept and drain water from the slopes, maintaining works to combat soil erosion.

REFERENCES

- Bălan, M. (2021). Study on the soils of Gorj County and their quality. *Annals of the University of Craiova - Agriculture, Montanology, Cadastre Series*, 51(1), 199-206.
- Bonea, D. (2020). Screening for drought tolerance in maize hybrids using new indices based on resilience and production capacity. *Scientific Papers Series Management, Economic Engineering in Agriculture and Rural Development*, 20(3), 151-156.
- Bouma, J., Van Ittersum, M.K., Stoorvogel, J.J., Batjes, N.H., Droogers, P., Pulleman, M.M. (2017). *Soil capability: exploring the functional potentials of soils*. In: Field, D.J. e.a. (Ed.), *Global Soil Security*. Springer International Publishing, Switzerland, 27-44.
- Corcheș, M.T. (2023). Land degradation and climate change. *Scientific Papers. Series E. Land Reclamation, Earth Observation & Surveying, Environmental Engineering*, XII, 68-73.
- Cochrane, H.R., & Aylmore, L.A.G. (1994). The effects of plant roots on soil structure. Proceedings of 3rd Triennial Conference "Soils 94", 207-212.
- Davidson, D.A. (2000). Soil quality assessment: recent advances and controversies. *Progress in Environmental Science*, 2, 342-350.
- Doran, J.W., Zeiss, M.R. (2000). Soil health and sustainability: managing the biotic component of soil quality. *Appl. Soil Ecol.*, 15, 3-11.
- Florea, N., & Munteanu, I. (2012). *Romanian Soil Taxonomy System (SRTS)*, Craiova, RO: Sitech Publishing.
- Hansen, L., Noe, E., Hojring, K., (2006). Nature and Nature Values in Organic Agriculture. An Analysis of Contested Concepts and Values Among Different Actors in Organic Farming. *Journal of Agricultural and Environmental Ethics*, 19, 147-168.
- Kalmar, T.M., Dirja, M., A.T., Rădulescu, Măran, P.D., Rădulescu, V.M., Rădulescu, M.C., Rădulescu Gh. (2022). Analysis of the effect of deforestation on land stability by geomatic methods - case study analysed in the geoses project. *Scientific Papers. Series E. Land Reclamation, Earth Observation & Surveying, Environmental Engineering*, XI, 308-315.
- Nițu, O.A., Ivan, E.Ș., Nițu, D.S. (2023). Climate change and its impact on water consumption in the main agricultural crops of the Romanian Plain and Dobrogea. *Scientific Papers. Series A. Agronomy*, LXVI(1), 474-478.
- Nițu, O.A., Mușat, M., Ivan, E.Ș., Burtan, L., Anghel, A. (2023). The determination of the most optimal methods for the irrigation of crops on different soil types. *Annals of the University of Craiova - Agriculture, Montanology, Cadastre Series*, 53(1), 367-374.
- Patzel, N., Sticher, H., Karlen, D. L. (2000). Soil fertility - phenomenon and concept. *Journal of Plant Nutrition and Soil Science*, 163(2), 129-142.
- Popescu, C. (2008). *Ecopedology*. Universitaria Publishing House, Craiova 131-133.
- Popescu, C. (2019). *Pedology*. Sitech Publishing House, Craiova, 236-137.
- Rhodes, C.J. (2017). The imperative for regenerative agriculture. *Science Progress*, 100, 80-129.
- Smith, P. (2012). Soils and climate change. *Current Opinion in Environmental Sustainability*, 4(5), 539-544.
- Teaci, D. (1980). *Agricultural terrains bonitation*. Ceres Publishing House. Bucharest.
- Thomas, G.W., Haszler, G.R., Blevins, R.I. (1996). The effect of organic matter and tillage on maximum compactibility of soils using the proctor test. *Soil Science*, 161, 502-508.
- Toth, G., Hermann, T., Da Silva, M.R., Montanarella, L. (2016). Heavy metals in agricultural soils of the European Union with implications for food safety. *Environment International*, 88, 299-309.
- Várallyay, G. (2010). Role of Soil Multifunctionality in Sustainable Development. *Soil & Water Res.*, 5(3), 102-107.
- Zafiu, C., & Mihalache, M. (2021). Research on the Influence of Technological Systems on Maize Cultivation in the South of the Dolj County, Romania, *Scientific Papers. Series A. Agronomy*, LXIV(1), 180-185.
- ***EU, European Commission (2006). Thematic Strategy for Soil Protection. Commission of the European Communities.
- ***EC Law (2021). Healthy soils – new EU soil strategy.
- *** Gorj O.S.P.A., Tg.-Jiu. Soil studies on municipal scale territories 1:10000, 1:5000, the years 1979-2010, Gorj OSPA Archives.
- *** Gorj O.S.P.A., Tg.-Jiu. Pedology studies for different purposes years 1980-2010 Gorj O.S.P.A. Archives.
- *** Gorj O.S.P.A., Tg.-Jiu. Inventory of degraded land in the Gorj County, 2010 Gorj O.S.P.A. Archives.
- *** Gorj O.S.P.A., Tg.-Jiu. County soil-soil monitoring system for agriculture on 31/12/2018, Gorj O.S.P.A. Archives.

MODERNIZATION/REHABILITATION OF THE SECONDARY DRAINAGE INFRASTRUCTURE BY REPOSITIONING EXISTING CHANNELS AND BY ASSIGNING THE DUAL ROLE OF DRAINAGE-IRRIGATION

Marin-Vasile ILCA¹, Teodor Eugen MAN¹, Robert BEILICCI¹, Anisoara IENCIU²,
Daniela Cristina UNTARU¹, Mariana Antonia PASC²

¹Politehnica University Timisoara, 1A Spiru Haret Street, Timisoara, Romania

²University of Life Sciences "King Mihai I" from Timisoara,
119 Calea Aradului, Timisoara, Romania

Corresponding author email: marin-vasile.ilca@student.upt.ro

Abstract

The paper deals with the need to modernize the existing secondary drainage infrastructure, in an effort to implement new water management strategies, in line with current needs, including a case study that proposes a solution in this sense, by designing a drainage-irrigation system based on the optimization and systematization of the agricultural surface taken into account, the efficiency of the water circuit and last but not least, the achievement of reduced water consumption. Drainage and irrigation systems represent an important element in the complex equation of agriculture, their management being able to make the difference between performance and failure, hence the importance of consolidating the optimal strategy regarding the design, modernization and ensuring their functionality. In geographical areas with excess humidity, it was necessary to build drainage systems to remove excess water from the land to make it arable, through land improvement works as support for agriculture, similar works executed in Romania between 1950-1989 which, especially due to its age, requires restoration/modernization. Considering the modernization of agricultural technologies, the introduction on a larger scale of a new mindset on more environmentally friendly agricultural systems, global climate changes, etc., the rehabilitation and modernization of the secondary infrastructure within the old drainage facilities is currently necessary and timely - drainage, where the technical conditions allow their transformation into complex drainage and irrigation facilities. The paper presents a case study in this sense, from which derives the need to make some legislative changes that will have to be made to facilitate the promotion of such complex facilities desiccation - drainage and irrigation.

Key words: drainage-irrigation canals, repositioning, system modernization.

INTRODUCTION

Land improvement plans in Romania it includes drainage - drainage plans, irrigation plans and soil erosion control. In some cases, there are also complex arrangements that include drainage - drainage and irrigation arrangements, drainage - drainage and soil erosion control arrangements or even drainage - drainage, irrigation, and soil erosion control arrangements.

In Romania, drying, draining and erosion control facilities are owned by ANIF (through the Territorial Branches for County Land Improvements), as well as key infrastructure (basic pumping stations, re-pumping stations and main canals/pipes) that serve the irrigation facilities. In most cases, the secondary irrigation infrastructure has been handed over

to the Irrigation Water User Organizations for management.

MATERIALS AND METHODS

The studied area is a component part of the Teba-Timisat facilities (Figure 1). This is a facility located in the hydrographic basin of the Timis and Bega rivers. In terms of location, the Teba-Timisat drainage-drainage facility has the Bega Canal as its northern boundary, the Sag-Topolovat Complex as its eastern boundary, the Timis River and the settlements of Rudna-Giulvaz and Caraci as its southern boundary, and the border with Serbia as its western boundary. Commissioned in 1962 and completed between 1985 and 1987, the project serves an area of approximately 28,000 ha, of which 285 ha is closed drainage. The area is

divided into three compartments: Dinias (with two drying units), Otelec (with two drying units) and Cruceni (with 8 drying units). For the case study, we narrowed the area to a portion of approximately 1000 ha from the 7144 ha within the Otelec Compartment, the Otelec Vest drainage unit that serves 2420 ha and has a pumping station-Otelec on the left bank-located on the Bega Canal on the left bank km 3+400, with desiccation destination consisting of 5 Brates 600 aggregates with a power of 132 kw and a flow rate of 1.1 m³/s and 2 Flygt type pumps of 110 kw with a flow rate of 1.13 m³/s (ANIF, 2024).



Figure 1. Study area

The drainage network in the studied area totals 45 km of drainage canals of all orders, which at the time of the study were in a deplorable technical condition, requiring restoration, unclogging and repairs/replacement of constructions related to the drainage-drainage arrangements (Figure 2).

The main causes have led to this situation are the lack of maintenance for three decades, the destruction or theft of some components from the constructions related to the arrangements and non-compliance with the exploitation regulations by the farmers with land in the respective area (non-compliance with the safety distance by agricultural works carried out in the immediate vicinity of the banks of the canals, by blocking the section of the canals in order to collect water used for diluting fertilizers and

pesticides, by destroying weirs for the illegal sale of ferrous materials, by filling in sections of the canals in order to increase the surface of the cultivated land, etc.).

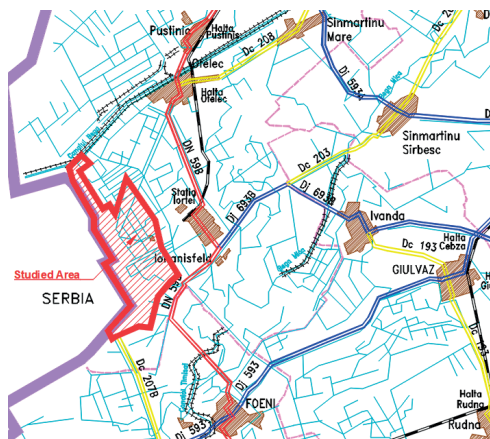


Figure 2. Area of interest, part of the Teba-Timisat improvement

The location of the respective part of the studied secondary drainage infrastructure within the entire complex, as well as the fact that in time a commercial company managed to merge the land in a proportion of 99% on approximately 1000 ha, intending to implement irrigation system projects for large-scale culture and for a hazelnut plantation, determined the initiation of studies for the modernization of the secondary infrastructure of the drainage-drainage and irrigation system.

The following key features were considered when designing:

1. The practice of efficient and modern agriculture will be operated with last-generation agricultural machinery characterized by large dimensions
2. The irrigation system for 2/3 of the surface is sprinkler with Ranger-type linear installations (Plot 1, with water source from the Bega Canal);
3. The irrigation system for 1/3 of the surface is drip fed from a retention basin with water source from boreholes and rainfall (Plot 2);
4. Systematization of soils through modelling, to eliminate micro-depressions and to ensure easier elimination of excess water from precipitation by reorganizing drainage slopes (Man, 2014).

Two options were taken into consideration:

1. Achieving the objectives by maintaining the position and configuration of the existing drainage-drainage channels in the original design of the secondary drainage-drainage infrastructure as it was conceived 60 years ago (in the design of the drainage-drainage facilities, the channels were mostly drawn approximately perpendicular on the line of the greatest slope or with an inclination compared to the level curves to carry out the gravitational evacuation of the surplus water from the respective land and the addition of new irrigation canals, integrated into the old system (Kagalkar, 2017).

2. Achieving the objectives with the repositioning of most of the existing channels (by respecting the names and respectively the geometric and hydraulic elements of the existing channels, without affecting ANIF's patrimony/inventory), the unclogging and/or reprofiling of those channels that do not require repositioning and the construction of new sections (Law 7, 1996; Law 107, 1996; Law 137, 1995; Law 138, 2004).

RESULTS AND DISCUSSIONS

Option 1

For Plot 1, the water source is the Bega Canal, through the gravity intake located at km 0 + 815 m on the left bank and, due to the fact that the water level in the Bega Canal is not constant, especially in the May-September period when irrigation is needed, the outlet being unusable during that period, through a pumping station with four heat pumps. Water for irrigation will be transported using part of the ANIF canals and newly designed canals, with a dual role of drainage and irrigation. Also, in order to preserve the old drainage network, it was necessary to design new hydrotechnical constructions (works of art), in order to be able to use the complex drainage-irrigation system.

Regarding the situation of the ANIF channels included in the system, some of them will be used during irrigation as water transport channels, some will be repositioned to optimize the system. As well as works on them, they almost entirely require unclogging and/or reprofiling. In order to harmonize the system as

a whole with the mode of operation of the new agricultural machinery and modern irrigation installations, the exploitation roads and bridges were also redesigned, bringing - them in sizes that serve the new sizes and technologies. For the second plot (irrigation and drainage Hazelnut plantation 260 ha), the water source is obtained from the rainfall during rainy periods and through 4 shallow boreholes (up to 40 m) that pump water from the lower aquifer layer, in a retention basin, having the following characteristics:

- $S = 2.5$ ha, $V=46000$ m³, land share = 77.40 m, razer share = 75.10 m;
- the average depth of water in the basin is 2 m;
- the inclination of the inner wall of 1:2;
- the elevation of the maximum water level 0.30 m below the elevation of the land;
- the level of the bottom of the basins is located 0.70 m (freezing depth) above water table level;
- the pool will be waterproofed with polyethylene film or geomembrane like this so that the upper aquifer layer is not affected both from a qualitative point of view and also from quantitative point of view.

The excavation volumes will be used to level the local micro depressions on the 263 ha site. The underground drip irrigation system expected to be used to ensure the plantation's water needs was chosen following the optimization (the economy of the water resource by reducing losses through evaporation/watering unproductive land and the direct supply of the reticular system, as well as the necessary fertilization through -a single operation-fertigation-), of the entire system.

The pumps for the four wells will be fed using electric submersible pumps and pumps with thermal or electric motors will be used to take the water from the basin to irrigate the plantation. The necessary electrical energy is obtained by connecting the system to the national electrical energy system, through the mains low voltage nearby. Excess rainwater from the soil will be removed through the existing channels in the secondary drainage system and will follow its designed course, being collected in the emissary, and transported to SP Cruceni, to be discharged into the Timis river. The presence of micro-depressions in the soil - the main cause of quasi-permanent

puddles - requires the remodelling of the land through specific land improvement works, all the more necessary, considering that the area will be prepared for the implementation of an irrigation system (Figure 3). For this classic design model, the following were evaluated as elements that could bring more functionality and financial economy:

1. Reducing the number of hydrotechnical constructions and the necessary works of art;
2. Ensuring a better functionality of the drying system by drawing the drying channels in a straight linear format;

3. Creating optimal conditions for agrotechnical works by systematizing the soils, the straight channels offering regularly shaped soils in an overwhelming proportion;

4. Optimizing water management, maintenance and agrotechnical works.

Pursuing these objectives, a project was developed to reposition the old drainage canals with the integration of the irrigation canal system, resulting in a compact system of canals with the double role of drainage and irrigation, presented in the paper as "Option 2".

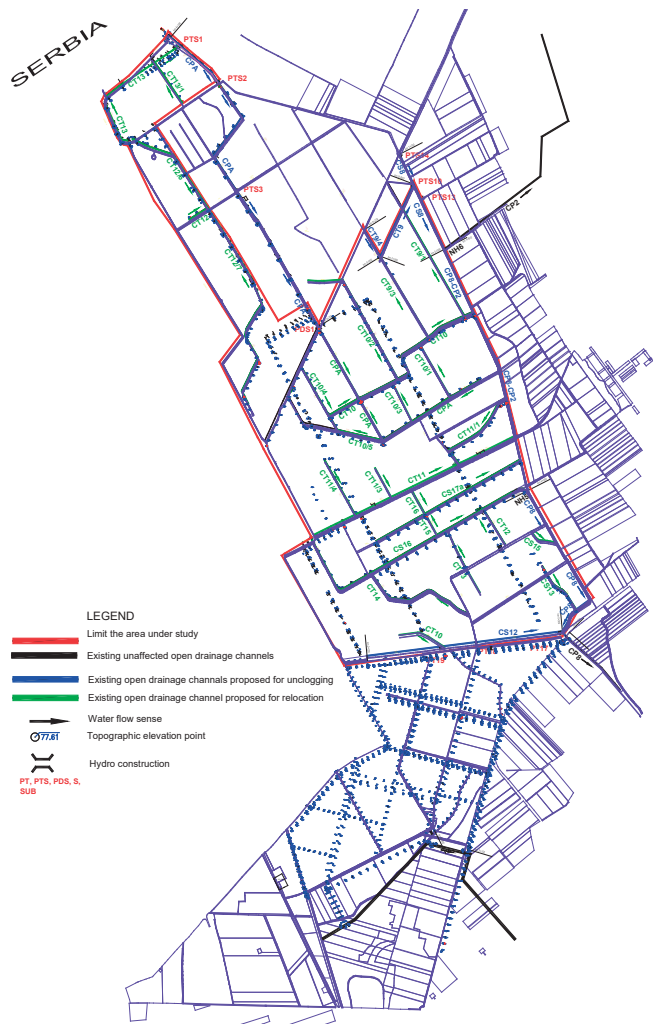


Figure 3. Design option 1

Option 2

The need to find a second option also finds its logic in the current situation stemming from both the new EU policies regarding the CAP and the new direction towards the optimization and sustainability of agricultural practices: reduction of fossil fuel consumption, biodiversity, water management, conservation of natural elements, reduction of carbon emissions, elimination of implementation and exploitation expenses, etc. as well as from strictly pragmatic considerations (economic and resource management). The solution consists mainly in the repositioning of the existing drainage channels and the thickening

of the network of drainage channels to ensure the maintenance of an appropriate water level. This new design solution not only improves the functioning of the entire secondary drainage system, but also assigns it the double role of drainage and irrigation, contributing to the efficiency of logistics and water management, not least, to the reduction of implementation, maintenance, and exploitation expenses. By construction, the new system resystematizes the soils in a way that facilitates specific agricultural technological operations, generating significant savings in time, fuel and money.

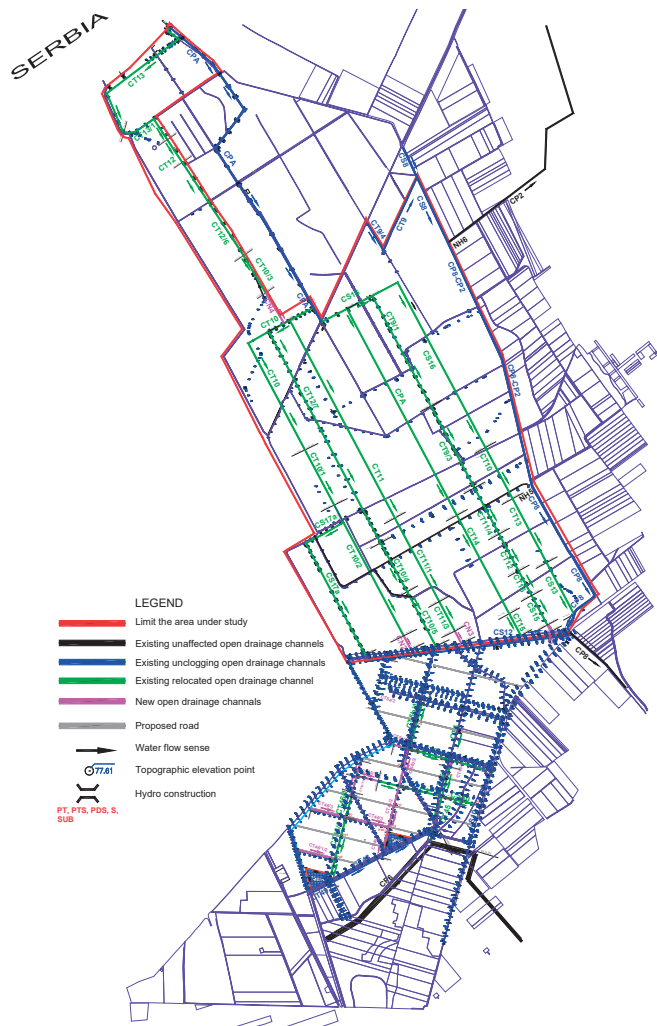


Figure 4. Design option 2

By using the rainwater captured in the drainage canals and led to the reservoir, to reintroduce it into the circuit, the additional pumping costs in the Timis River (in this case), through the Cruci Pumping Station, are reduced. Powering the pumps for extracting water from the groundwater table will be done using green energy generated by a photovoltaic park to be built in the perimeter of the plantation (Figure 4).

The movement of water in channels, beds or partially filled pipes are examples of free-level movements. Generally, for current tubes with free level, the name "channels" is used, respectively the movement in the channels.

The main characteristic geometric and hydraulic elements are:

- S - the cross section of the current (flow section or live section);
- P - the wetted perimeter (the rigid boundary in contact with water in a cross-section of the current);

$$i = \sin\theta = -\frac{dz}{dl}$$

- the (geometric) slope of the eraser;
 $h = h_v = h_R = h_n \cos\theta$

where:

- h_R - normal on the bottom
- $h_n \cos\theta$ - vertical projection
- h_v - vertically

In normal technical conditions (slope $i = \sin\theta \leq 14$), $\cos\theta \geq 0.99$ which justifies the approximation introduced by equating the three depths.

In the following the notation "h" will be used, meaning $h_v, h_R \cos\theta$ or $h_n \cos\theta$, depending on the needs of the studied problem.

$$I_s = -\frac{d(h+z)}{dl}$$

- Q - the flow rate of the liquid stream;
- v - average speed ($v = Q/s$) of the current.

For this case study, only prismatic channels were considered, characterized by the fact that the section is constant for a constant depth along the channel.

$$\frac{dS}{dl} = 0$$

The general equations of the movement of

liquid currents with a free level, in global form, for a current tube segment characteristic of free-level movements are:

- the energy transfer equation;
- the momentum transfer equation.

For the suitability of these equations for practical applications, the following notations and simplifications are considered:

- enter the grades α and β representing the global non-uniformity coefficients of the speed distribution and their turbulent fluctuations;
- is considered $\cos\theta = 1$, that is, the hypothesis small slopes (under 14%);
- the braking influence of the free surface is neglected;
- it is considered that the flow sections S_1 and S_2 are locally orthogonal to the streamlines. With these observations the energy transfer equation becomes:

$$\frac{\alpha V_1^2}{2g} + z_1 + h_1 = \frac{\alpha V_2^2}{2g} + z_2 + h_2 + h_{r12}$$

where:

- V_1, V_2 are the average velocities in the flow sections;
- S_1 and S_2 in the mean turbulent motion;
- h_{r12} represents the energy dissipated and transferred to produce turbulence in the control volume limited by the flow sections and is called the head loss (for turbulent mean motion).

The momentum transfer equation projected along the "l" direction becomes:

$$F(S_x) = \rho Q(\beta_1 V_1 - \beta_2 V_2) + \rho g z_1 S_1 - \rho g z_1 S_2 + G_i$$

where:

- $F(S_x)$ represents the action of the liquid on the rigid boundary S_x .

The continuity equation is added to these equations: $Q = VS$

Introducing the notations:

$i = -\frac{dz}{dl}$ - called the geometric slope

$I_e = \frac{dh_r}{dl}$ - called energy slope (specific dissipation on $\rho g Q$ and the unit of length)

$i_f = \frac{\tau_0}{\rho g R} = \frac{V_*^2}{gR}$ representing the friction slope

where:

- τ_0 wall tension,
- V_* friction speed,

- R the hydraulic radius.

The momentum transfer equation is obtained in the form:

$$i - i_f = \frac{i}{gS} \frac{d}{dl} \left(\beta \frac{Q^2}{S} \right) + \frac{1}{S} \frac{d}{dl} (z_g)$$

The differential forms of the fundamental equations can be put in a more convenient form in order to establish a relationship between the slopes i , i_f , I_e .

To this end it is noted that in the hypothesis of prismatic channels and considering the notations we get:

$$\frac{\partial S}{\partial l} = 0$$

and considering the notations we get:

$$i - I_e = \left(1 - \frac{\alpha Q^2 B}{gS^3} \right) \frac{dh}{dl}$$

$$i - i_f = \left(1 - \frac{\beta Q^2 B}{gS^3} \right) \frac{dh}{dl}$$

It is observed that in general $i \neq I_e \neq i_f$.

In the case of uniform motion, when $h = \text{const.}$, so, $dh/dl = 0$, result:

$$i = I_e = i_f$$

that is, the energy slope (I_e), of friction (i_f) and geometric (i) they're the same.

In case of non-uniform movement

$$\frac{dh}{dl} \neq 0$$

generally, results:

$$i \neq I_e \quad \text{and} \quad i \neq i_f$$

As for the slopes I_e and i_f and they differ in general. It can be seen that they become equal if and only if the coefficients α and β they are equal. The relationship can be established between the two slopes:

$$i_f = I_e \frac{1 - \frac{\beta Q^2 B}{gS^3}}{1 - \frac{\alpha Q^2 B}{gS^3}} + \frac{i(\beta - \alpha) \frac{Q^2 B}{gS^3}}{1 - \frac{\alpha Q^2 B}{gS^3}}$$

However, in current practice it can be considered, with a very good approximation, $\beta = \alpha$, the two slopes i_f and I_e they can be considered practically equal even in the case of non-uniform movement.

Therefore, in contrast to uniform motion, in the case of non-uniform motions the relation:

$$i \neq I_e = i_f$$

It is possible to write based on these relationships:

$$I_e = i_f = \frac{V^2}{gR} = \left(\frac{V_*}{V} \right)^2 \frac{V^2}{gR}$$

where:

- V is the average speed in the flow section.

Using the same notations as in the case of pipes, they are obtained for the energy slope I_e the two types of classical formulas:

- Darcy-type formulas:

$$I_e = \frac{\alpha V_*^2}{\beta gR}$$

$$V = \sqrt{\frac{8g}{\lambda}} \sqrt{RI_e}$$

- Chezy type formulas:

$$I_e = \frac{1}{C^2} \frac{V^2}{R} = \frac{Q^2}{S^2 C^2 R}$$

$$V = C \sqrt{RI_e}$$

where:

- " λ " it is called the Darcy resistance coefficient,

- " C " the Chezy coefficient.

For the calculation of the coefficients λ and C formulas of the same type as in the case of pipes will be used. For λ a general formula of the Colebrook. White type is applied in which D will be substituted by $4R$ (this is due to the connection between the hydraulic radius R and the diameter D in the case of circular pipes $D = 4R$) and a correction coefficient " f " is introduced depending on the shape of the section transverse:

$$\frac{1}{\sqrt{\lambda}} = -2 \log \left(\frac{2.51}{f R_e \sqrt{\lambda}} + \frac{k}{3.71 f 4R} \right)$$

According to Bock, the shape coefficient f has the following expressions.

- for trapezoidal sections:

$$f = \left(1.629 \frac{h}{b} \frac{1 + m \frac{h}{b}}{1 + 2\sqrt{1 + m^2 \frac{h}{b}}} \right)^{0.25}$$

For the coefficient C , it is used as the most common formula:

$$C = \frac{1}{n} R^y$$

with:

$$\frac{y=1}{6} - \text{after Manning} - \text{Stickler}$$

$$y=2.5\sqrt{n} - 0.13 - 0.75\sqrt{R}(\sqrt{n} - 0.1)$$

- or the simplified formulas according to Pavlovski:

$$y=1.5\sqrt{n} \text{ for } 0.1n \leq R < 1.0n$$

$$y=1.3\sqrt{n} \text{ for } 1.0n \leq R < 3.0n$$

The equivalent roughness "k" in the Darcy formulas and the roughness coefficient "n" in the Chezy-type formulas are taken according to the nature of the channel walls (Wehry at al., 1982).

Currents with free level in permanent and uniform motion regime

Uniform movement with free level is achieved in artificial, rectilinear, and prismatic beds (channels, galleries, ditches, etc.)

According to the above, in the case of uniform motion, the relation occurs:

$$i = I_e = i_f$$

that is, the geometric, energy and friction slopes are identical. Considering the definition of the slope of the free surface and this is equal to the others.

Considering the particularities of uniform movement in the general calculation relations, the energy slope will be replaced by the geometric one:

$$I_e = i$$

In general, in technical applications, Chezy-type formulas are currently used:

$$V = C\sqrt{Ri}$$

Associating the continuity equation is obtained for the flow rate:

$$Q = VS = SC\sqrt{Ri}$$

$$R = \frac{S}{P}$$

The hydraulic radius is self-explanatory, and it is obtained:

$$Q = SC \sqrt{\frac{S}{P}} i = \frac{S^{\frac{3}{2}}}{P} C \sqrt{i}$$

By associating the Chezy formula, we obtain for the flow rate:

$$Q = SC\sqrt{Ri} = S \frac{1}{n} R^y \sqrt{Ri} = S \frac{1}{n} R^{y+\frac{1}{2}} \sqrt{i}$$

$$= S \frac{1}{n} \frac{S^{y+\frac{1}{2}}}{P^{y+\frac{1}{2}}} \sqrt{i} = \frac{1}{n} \frac{S^{y+\frac{3}{2}}}{P^{y+\frac{1}{2}}} \sqrt{i}$$

accordingly:

$$Q = \frac{1}{n} \frac{S^{1.5+y}}{P^{0.5+y}} \sqrt{i}$$

By replacing with the Manning relation, we get:

$$Q = \frac{1}{n} \frac{S^{\frac{5}{3}}}{P^{\frac{2}{3}}} \sqrt{i}$$

For the case of trapezoidal sections, it is observed that the area (S) and the wetted perimeter (P) can be expressed in the form:

$$S = bh + mh^2 = (\beta + m)h^2$$

$$P = b + 2\sqrt{1+m^2}h = (\beta + 2\sqrt{1+m^2})h$$

Resulting by substitution:

$$Q = \frac{1}{n} \frac{(\beta + m)^{1.5+y}}{(\beta + 2\sqrt{1+m^2})^{1.5+y}} h^{2.5+y} \sqrt{i}$$

where with m' was noted:

$$m' = 2\sqrt{1+m^2}$$

For example, the Drainage Channel - HCn 23343, identical to CT5 and the P14 bridge (Figure 5).

From the hydraulic calculation breviary carried out for the canals in the case study plot 2 (having the geometric and hydraulic elements shown in Table 1), and the related bridges, having the geometric elements (diameter, length, width) shown in Table 2.

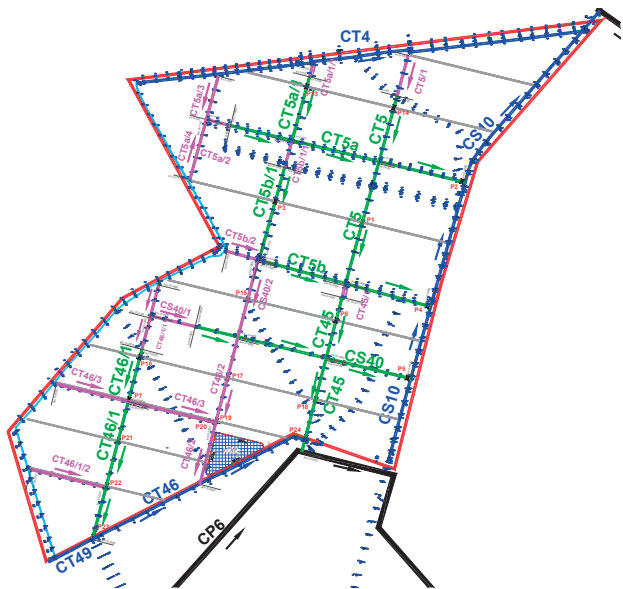


Figure 5. Plot 2 channel CT5, bridge P14

Table 1. Geometric and hydraulic elements

No	Channel name		L channel (m)	Channel section km to km	Confluence	Geometric elements			Hydraulic elements			Bright surface	Protection zone	Excavation/ Digging	
	Cadastral	ANIF			channel	b(m)	m	l 0/00	h _{water} (m)	V (m/s)	Q (m³/s)				
1	HCn 23343	CT5	545	0+000+0+545	CT5b	0.5	1.5	0.6	0.15	0.17	0.02	2725	2180	2248	
1'	HCn 23343	CT5	295	0+000+0+295	CT5a	0.5	1.5	0.6	0.15	0.17	0.02	1475	1180	1217	
2	HCn 23353	CT5a/1	286	0+000+0+286	CT5a	0.5	1.5	0.8	0.2	0.2	0.03	1430	1144	1180	
3	HCn 2341	CT5a	1050	0+000+1+050	CS10	0.5	1.5	0.5	0.25	0.18	0.04	5250	4200	4331	
4	HCn 2335/2	CT5b/1	416	0+000+0+416	CT5b	0.5	1.5	0.8	0.2	0.2	0.03	2080	1664	1716	
5	HCn 2337/1	CT5b	775	0+000+0+775	CS10	0.5	1.5	0.5	0.25	0.18	0.04	3875	3100	3197	
6	HCn 2335/2	CS40	965	0+000+0+965	CS10	0.5	1.5	0.3	0.3	0.21	0.06	4825	3860	3981	
7	HCn 2324	CT45	415	0+000+0+415	CP6	0.5	1.5	0.8	0.2	0.2	0.04	2075	1660	1712	
7'	HCn 2324	CT45	271	0+000+0+271	CS40	0.5	1.5	0.8	0.2	0.2	0.04	1355	1084	1118	
8	HCn 2297	CT46/1	615	0+000+0+615	CT49	0.5	2	0.4	0.3	0.18	0.06	3997.5	2460	3229	
8'	HCn 2297	CT46/1	235	0+000+0+435	CT46/3	0.5	2	0.4	0.3	0.18	0.06	1527.5	940	1234	
TOTAL													30615	23472	25162

Table 2. New bridges proposed

No	Bridge name	Channel name		km	Diameter (mm)	Geometric elements (m)	
		Cadastral	ANIF			Lang	Width
1	P13	CTa/1		0+242	600	5	5
2	P14	CT5		0+244	600	5	5
3	P15	CS40/2		0+171	600	5	5
4	P16	CT46/1		0+203	600	5	5
5	P17	CT46/2		0+478	600	5	5
6	P18	CT45		0+235	600	5	5
7	P19	CT46/2		0+289	600	5	5
8	P20	CT46/3		0+005	600	5	5
9	P21	CT46/1		0+445	600	5	5
10	P22	CT46/1		0+242	600	5	5
11	P23	CT46/1		0+005	600	5	5
12	P24	CT45		0+071	600	5	5

According to the theoretical foundations, the key curves were drawn up for the studied drainage channels. The results are shown in Figures 6 and 7 (Diagram D1 and D2).

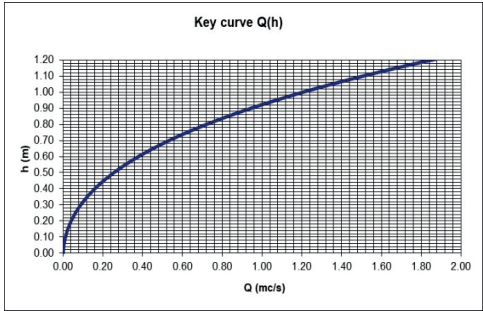


Figure 6. Diagram D1

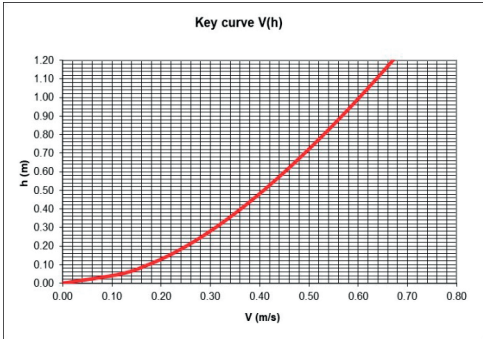


Figure 7. Diagram D2

For the designed flow of channel HCn 23343, identical to CT5 at the designed flow of $Q = 0.02 \text{ m}^3/\text{s}$ the obtained are presented in Table 3.

Table 3. Designed flow of channel HCn 23343

h	V	Q
(m)	(m/s)	(m ³ /s)
0.13	0.22	0.02

Determination of the transport capacity of the proposed tubular bridges.

From the topographical studies as well as the data provided by the beneficiary, respectively the ANIF archive, the slope of the walkways, $i = 0.0006$, $n = 0.021$ and the recommendation

to use tubular walkways DN 600 mm from PEID corrugated pipes result (Pelea, 2021). For the diameter $D = 0.60 \text{ m}$ of the tube, by constructing the curves $Q = Q(h)$, $A = A(\lambda)$ and $B = B(\lambda)$, we obtain Diagram D3 and D4 from Figures 8 and 9.

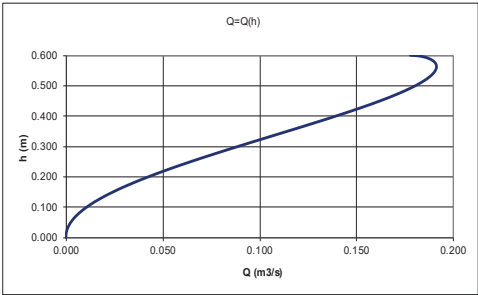


Figure 8. Diagram D3

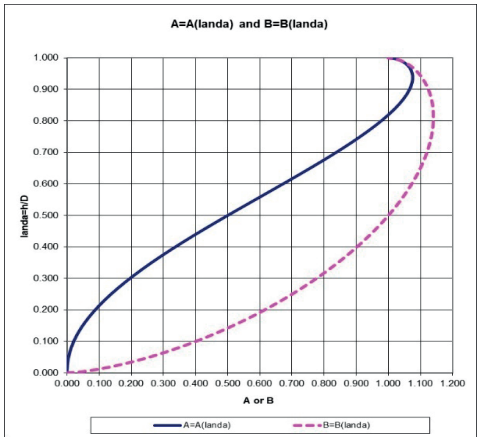


Figure 9. Diagram D4

The diagrams show the flow rates that can be discharged by the proposed tubular bridges with DN 600 mm from PEID corrugated pipes. $Q_{\max} = 0.191 \text{ m}^3/\text{s}$ at $h = 0.56 \text{ m}$. The maximum capable flows far exceed the discharge flows of all channels in the studied site (both relocated and new proposed).

Figure 10 shows one of the dimensioned tubular floors as an example (plan view, sections, reinforcement, and the necessary materials).

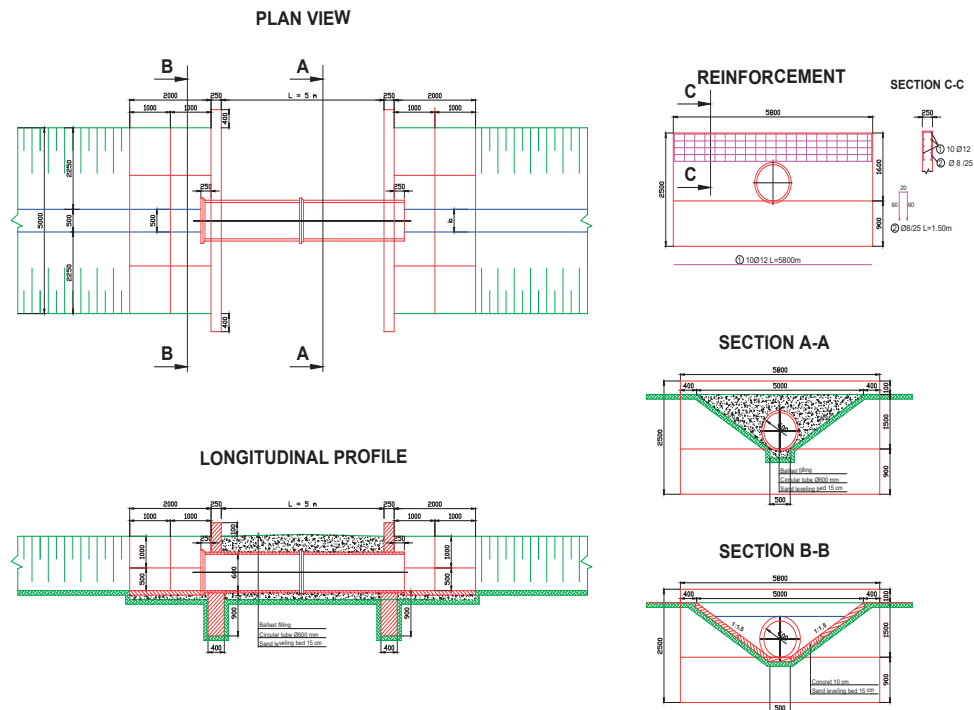


Figure 10. Plan view, sections, reinforcement and the necessary materials

CONCLUSIONS

Although from a technical and functional point of view, Option 2 is clearly superior to the classical option, it is currently facing some difficulties in implementation due to the impediments created by the legislation in force in Romania. This legal problem could be solved by a Government Decision allowing the repositioning of state-owned channels. In this sense, steps were taken, technical memos were presented both to the Ministry of Agriculture and to ANIF Bucharest, presenting solutions for regulation and proposals for procedures that would facilitate the implementation of the new systems of complex drainage-irrigation arrangements.

"Thus, throughout the Procedure reference will be made to the positioning/repositioning of drainage/irrigation channels in development areas with infrastructure improvements land administered by ANIF in the urban/extra-urban localities, for the purpose ensuring their functionality.

The positioning terminology will be used if the channel in question is not tabulated in the land registry system, and the repositioning terminology will be used if the channel in question is tabulated in the land registry, but the course is non-functional or prevents the development of the territory and/ or the urbanization of a site, effectively, and the repositioned course of this channel does not diminish the heritage of the Statute in terms of the inventoried surface.

The ANIF methodology for the issuance of regulatory documents provides for the issuance of approvals for the preparation of PUG, PUZ, PUD, technical approvals for the removal from the agricultural circuit of land located in the outskirts of the towns, technical approvals for obtaining the Construction Authorization for temporary construction works located in the outskirts localities, technical approvals for obtaining the Construction Authorization for the investment objectives located in the urban areas of the localities, technical agreements and specialized approvals." - excerpt from the answer received from MADR-ANIF, regarding

the proposal to modify the procedure regarding the relocation of the ANIF drainage channels-28.12.2022.

REFERENCES

- Kagalkar, A. (2017). Smart Irrigation System, *International Journal of Engineering Research & Technology (IJERT)*, 6(5), ISSN: 2278-0181.
- Pelea, G.N. (2021). Doctoral Thesis: Current management issues in exploitation and maintenance of irrigation systems in western part of Romania, *Politehnica University of Timisoara*, 1(1), 83-90.
- Wehry, A., David, I., Man, T.E. (1982). *Current problems in the drainage technique*. Facla Timisoara Publishing House [in Romanian].
- Man, T.E. (2014). *Drenaje vol I (pp. 383) and II (pp. 574)*. Ed. Orizonturi Universitare Timisoara [in Romanian].
- ANIF (2024) - Administratia Nationala a Imbunatatirilor Funciare, www.anif.ro [in Romanian].
- Law 7/1996, Law on cadastre and real estate advertising [in Romanian]
- Law 107/1996, Water Law. <https://legislatie.just.ro/Public/DetaliiDocumentAfis/8565> [in Romanian].
- Law 137/1995, Environment protection, http://www.cdep.ro/pls/legis/legis_pck.htm_act_text?i=16982 [in Romanian].
- Law 138/2004, Land Improvement Law - with subsequent amendments by GD or Ministerial Orders. <http://legislatie.just.ro/Public/DetaliiDocument/51504> [in Romanian].

EXPERIMENTAL RESEARCH OF THE INNOVATIVE ATMOSPHERIC HUMIDITY COLLECTION SYSTEM FOR USE IN CROP IRRIGATION

Dragoş MANEA, Eugen MARIN

National Institute of Research - Development for Machines and Installations Designed for
Agriculture and Food Industry - INMA Bucharest,
9 Ion Ionescu de la Brad Blvd, District 1, Bucharest, Romania

Corresponding author email: manea_dragos_05@yahoo.com

Abstract

This paper presents the experimental results of an innovative atmospheric humidity collection system for irrigating crops. A humidity and temperature transducer located outside reads the temperature and relative humidity of the atmospheric air. Another transducer located on the indoor unit reads the temperature and humidity of the air leaving the humidification chamber. The controller monitors the temperatures and humidities transmitted by the transducers and when the optimal conditions are met for water to condense on the surface of the external collector, it commands the heating and humidification of the air to start. The system operates until the conditions for humidity condensation are no longer satisfied. The meteorological parameters provided by the local weather station related to the conditions under which water condenses was obtained and led to the adjustment of the automatic algorithm. During the experiments, the following parameters were determined: the flow rate of air pushed by the in-line duct fan, the temperature and humidity of the air jets at the exit from the hot air duct and the volume of water obtained.

Key words: atmospheric humidity, dew point, water.

INTRODUCTION

Considering the seasonal fluctuations in water consumption and availability, recent research found that two-thirds of the global population (4.0 billion people) live under conditions of modest water scarcity for at least one month in a year (Mekonnen & Hoekstra, 2016). Even worse, a half billion people on Earth face severe water scarcity all year round. However, the atmospheric water, which is considered a huge renewable reservoir of water and enough to meet the needs of every person on the planet, is unfortunately ignored (Wahlgren, 2001).

Fog and dew droplets can be confused when occurring upon natural surfaces such as beetle skin (Guadarrama-Cetina et al., 2014), the mechanisms to harvest fog and dew upon an artificial surface greatly differ at a larger scale (Jacobs et al., 2008). Moreover, the dew point depression at the study area seldom is below 0.5°C, the minimum threshold generally considered for fog deposition to occur (Hiatt et al., 2012).

Non-conventional water resources have emerged as means to meet or supplement irrigation demand for reforestation and

agriculture in water scarce regions (Tomaszkiewicz et al., 2017).

In general, any viable atmospheric water-harvesting technology must satisfy five primary criteria: it should be efficient, cheap, scalable, wide-band, and stable enough to operate for a whole year or at last a monsoon season. Currently none of the existing commercial atmospheric water generators meets all these five criteria. From the point of view of thermodynamics, this is mainly due to the energy inefficiency of the process (Tu et al., 2018).

Recently, researchers from the National Institute of Research and Development for Machines and Installations Designed for Agriculture and Food Industry - INMA Bucharest have studied the possibility of obtaining an additional amount of water for crop irrigation by collecting atmospheric humidity (Manea et al., 2021; Mircea et al., 2019; Popa et al., 2021).

This paper presents the experimental results of the innovative atmospheric humidity collection system for irrigating crops, designed and manufactured at INMA Bucharest.

MATERIALS AND METHODS

The innovative atmospheric humidity collection system for use in crop irrigation is mainly composed of: the indoor unit or the air heating and humidification installation, which was located inside the solar house; the outdoor unit or the collector, which was installed outside the solar; the puffer and the automatic control system of the work process parameters (Figure 1). The outdoor unit is connected to the indoor unit by means of a PVC tube buried in the ground and thermally insulated with mineral wool covered with aluminium foil.

The air heating and humidification installation (the indoor unit) is made up of the following elements: recirculation pump model Ferro 32-60-180; warm water heating coil; air humidification chamber; air flow control flap with Belimo CM 230 servomotor; in-line duct fan RUCK ETAMASTER EM 315 EC01; peripheral pressure pump CALPEDA TPM 78; warm water spray system in the form of mist with 5 nozzles; tank with lid and volume of 40 liters, provided with electric float with counterweight model Tecno 2 on the inside; normally closed water solenoid valve, 1/2", 230 V; elastomeric foam insulation with a thickness of 19 mm; insulated flexible tube with a diameter of 315 mm, made of layers of aluminium foil and aluminized polyester.

The air humidification chamber is made of galvanized sheet, in the form of a cube with a volume of approximately one cubic meter. The upper part of the humidification chamber is

sealed with a lid. Under the cover is installed the system of spraying warm water in the form of mist. At the bottom, the humidification chamber is shaped like a funnel, which allows excess water to flow into the tank.

The warm water used for heating and humidifying the air is taken from the puffer with a volume of 500 litres, which is connected to a solar panel.

The collector (the outdoor unit) is made up of the following elements: collector walls; drainage and water collection system; warm air piping; roof. The collector walls are made of stainless-steel sheet profiled in V-shaped alveoli, in order to increase the area for obtaining condensation, at the contact between the cold atmospheric air and the warm and humid air generated by the heating and humidification installation. The collector walls are placed symmetrically left - right in relation to the warm air piping and inclined at an angle of 30° to the horizontal plane (Figure 2).

The warm air piping consists of a horizontal PVC tube with a diameter of 315 mm, made by the linear interconnection of some branched segments in the shape of a T, the branches being arranged in a vertical plane and having a diameter of 110 mm. At one end, the horizontal PVC tube is fitted with an air check valve, and at the other end it is closed with a plug. A double polypropylene branch is mounted on each vertical tube. Both the horizontal tube and the vertical tubes are thermally insulated with elastomeric foam insulation.



the indoor unit and the puffer



the outdoor unit (the collector)

Figure 1. Innovative atmospheric humidity collection system for use in crop irrigation



collector wall



warm air piping

Figure 2. Component elements of the collector

The automatic control system of the work process parameters is made up of the following elements: automatic programmable Mitsubishi AL2-14MR-D; analog output extension module AL2-2DA; 24 Vcc Alpha Power Mitsubishi voltage source; air humidity and temperature transducer 0-10Vdc, located on the tubing at the exit from the humidification chamber; air humidity and temperature transducer 0-10Vdc, located on the frame of the outdoor unit and DRS-201D single-phase digital meter.

The way the system works:

The air humidity and temperature transducer 0-10Vdc, located on the frame of the outdoor unit reads the temperature and relative humidity of the atmospheric air. The other transducer 0-10Vdc located on the indoor unit piping reads the temperature and humidity of the air leaving the humidification chamber.

Through a round-trip circuit, warm water is taken from the puffer and circulated through the warm water heating coil by the Ferro 32-60-180 recirculation pump.

Through a connection located at the top of the puffer, the warm water is transferred to the 40-liter tank located at the bottom of the humidification chamber, from where it is taken over by the peripheral pressure pump CALPEDA TPM 78/A and transferred to the spray system with 5 nozzles mounted in the upper part of the humidification chamber. The water is sprayed as a mist into the warm air stream absorbed by the EM 315 EC01 in-line fan. When the accumulated water in the tank falls below a certain level, the TECNO 2 electric float commands the opening of the 1/2" solenoid valve, the warm water from the puffer

replenishing the level in the tank. When the maximum level in the tank is reached, the TECNO 2 electric float commands the closing of the 1/2" solenoid valve.

The optimal conditions for water from the atmosphere to condense on the surface of the external collector are: the temperature difference between the outside air and the solar air must be greater than a predetermined value (e.g. 10°C); the combination of the temperature and the relative humidity of the outside air, to correspond to reaching the dew point.

The Mitsubishi AL2-14MR-D programmable controller continuously monitors the temperatures and humidities transmitted by the two transducers and when one of the optimal conditions mentioned above is met, commands: starting the warm water recirculation pump Ferro 32-60 180; actuation of the Belimo CM 230 L servo motor to open the air flow adjustment flap; starting the fan EM 315 EC 01; starting the peripheral pressure pump TPM 78/A.

If the temperature difference between the outside and the humidification chamber falls below the preset value, i.e. the air in the humidification chamber does not have time to heat up due to the too high flow of air pushed by the fan, the programmable automatic controls the reduction of the fan speed and the partial closing of the air flow adjustment flap, by actuating the Belimo CM 230 L servo motor.

The system continues to operate until the outside temperature and humidity reach other preset values stored in the PLC, values that no longer satisfy the conditions for condensation

of moisture from the atmosphere. Then the programmable controller commands the system to shut down.

Due to the temperature difference between the flow of warm and humid air from the installation and the atmospheric air, the vapors condense on the surface of the collector walls, the water being drained and stored in the tank from where it can be used to irrigate the crops. The amount of water extracted from the atmosphere increases as the temperature difference between the ambient air and the air in the installation increases. Thus, the best performance can be obtained when the warm water in the puffer is stored during the day and used to heat the air in the installation during the night.

During the experiments, the following parameters were determined: the flow rate of air pushed by the in-line duct fan, the temperature and humidity of the air jets at the exit from the hot air duct and the volume of water obtained.

Determining the flow rate of air pushed by the in-line duct fan:

The determination of the flow rate of air pushed by the in-line duct fan was carried out under the following working conditions: warm water recirculation pump - off; the position of the air flow adjustment flap - maximum open; peripheral pressure pump - off.

Four fan speeds were set from the automatic programmable (25%, 50%, 75% and 100% of maximum speed). For each set speed, the speed

of the air stream at the exit from the terminal tubes was measured with the Anemometer CIH20DL (Figure 3).

The total air flow pushed by the fan, at the exit from the warm air pipe, Q_t , was calculated with formula (1):

$$Q_t = \sum_{i=1}^5 Q_i \text{ (m}^3/\text{h)} \quad (1)$$

where:

- Q_i is the air flow rate pushed through a vertical tube and was calculated with formula (2):

$$Q_i = 3600 \cdot S \cdot (v_{i,l} + v_{i,r}) \text{ (m}^3/\text{h)} \quad (2)$$

where:

- $v_{i,l}$ and $v_{i,r}$ are the speeds of the air current pushed through the left / right branch of a vertical tube, in m/s;
- S is the air outlet section through the terminal tube of the branch, in m^2 .

The measurement of the temperature and humidity of the air jets at the exit from the warm air duct was carried out with the Digital Thermohygrometer P330 for the following working conditions: fan speed - 25%, 50%, 75% of the maximum speed; warm water recirculation pump - on; the position of the air flow adjustment flap - maximum open; peripheral pressure pump - on; the temperature of the hot water in the puffer - 22°C; air temperature inside the solarium - 21°C; the relative humidity of the air inside the solar house - 56% (Figure 4).



Figure 3. Measurement of the speed of the air current at the exit of the terminal tubes, with the Anemometer CIH20DL

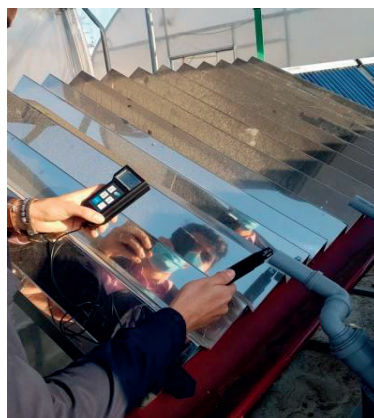


Figure 4. The measurement of the temperature and humidity of the air jets at the exit from the warm air duct with the Digital Thermohygrometer P330

The values of temperature and relative humidity of the air circulated through the heating and humidification installation were measured by the 0-10Vdc transducer located on the piping and displayed on the display of the automatic programmable.

The monitoring and recording of meteorological parameters provided by the local weather station iMetos 3.3 was carried out over three periods (September, October, November 2023) of three consecutive days. The following meteorological parameters were monitored and recorded: air temperature, dew point, relative air humidity, wind speed and precipitation amount.

The collection and measurement of the volume of water obtained during the experiments was carried out in the three periods of three consecutive days, and the averages were calculated. The water was collected in the systems tank, and the measurement of the collected water volume was made with a

graduated cylinder, once a day at the same hour. For each monitored period, a different exit angle of the warm and humid air jets from the terminal tubes was adjusted, in relation to the surface of the collector walls.

The innovative atmospheric humidity collection system was supplied with electricity from an off-grid system with photovoltaic panels.

RESULTS AND DISCUSSIONS

The vertical tubes were numbered from 1 to 5, number 1 being the tube closest to the warm air duct entry. For all four set speeds of the fan (25%, 50%, 75% and 100% of the maximum speed), a relatively uniform distribution of the flow of air pushed through the vertical tubes (Q_i) was observed, so along the warm air duct and implicitly along the length of the collector walls (Table 1).

Table 1. The results obtained when determining the air flow rate pushed by the in-line duct fan

Fan speed (% of max. speed)	No. vertical tube	Measured values		Calculated values	
		inner diameter of terminal tubes: d = 0.028 m		air outlet section: S = 0.0006 m ²	
		Left branch	Right branch	Air flow per vertical tube, Q_i (m ³ /h)	Total air flow, Q_t (m ³ /h)
		Air current speed (m/s)			
		$v_{i,l}$	$v_{i,r}$		
25	1	4.39	4.57	19.35	94.78
	2	4.13	4.45	18.53	
	3	4.33	4.94	20.02	
	4	4.30	4.10	18.14	
	5	4.73	3.94	18.73	
50	1	9.65	9.15	40.61	201.64
	2	8.45	9.20	38.12	
	3	8.95	9.60	42.34	
	4	9.21	9.01	39.36	
	5	10.15	8.93	41.21	
75	1	14.62	14.38	62.64	311.58
	2	13.35	14.65	60.48	
	3	13.65	15.93	63.89	
	4	14.02	14.15	60.85	
	5	15.65	13.85	63.72	
100	1	17.21	17.13	74.17	369.04
	2	15.20	17.87	71.43	
	3	16.25	19.04	76.23	
	4	16.79	16.73	72.40	
	5	18.40	16.23	74.80	

Table 2. The results obtained from the measurements of the temperature and humidity of the air jets at the exit of the warm air duct fan

Fan speed (% of max. speed)	Read values (at inlet)		No. vertical tube	Measured values (at outlet)					
	T (°C)	RH [%]		T [°C]			RH [%]		
				Left branch	Right branch	Average per tube	Left branch	Right branch	Average per tube
25	21.8	95.4	1	13.0	13.3	13.15	89.7	90.6	90.15
			2	13.1	13.1	13.1	90.1	90.9	90.5
			3	12.9	12.9	12.9	90.9	90.5	90.7
			4	12.7	12.8	12.75	91.7	88.8	90.25
			5	12.0	12.3	12.15	91.1	83.9	87.5
			Average			12.81			89.82
50	21.4	92.6	1	15.1	14.7	14.9	91.0	91.4	91.2
			2	15.0	14.5	14.75	91.0	91.3	91.15
			3	14.8	14.5	14.65	91.0	91.3	91.15
			4	14.7	14.7	14.7	91.4	90.9	91.15
			5	14.3	14.3	14.3	91.3	91.3	91.3
			Average			14.66			91.19
75	21.0	90.2	1	16.3	16.6	16.45	89.2	88.9	89.05
			2	16.2	16.6	16.4	89.6	88.9	89.25
			3	16.2	16.5	16.35	89.6	89.3	89.45
			4	16.5	16.4	16.45	89.7	89.3	89.5
			5	15.9	15.9	15.9	90.4	90.0	90.2
			Average			16.31			89.49

Analysing the data in Table 2, the following observations emerge:

- in the condition where the temperature of the warm water in the puffer was 22°C, the air temperature in the heating and humidification installation was maintained in the range of 21°C÷21.8°C; from this it follows that the heat losses of the installation are small, and the thermal insulation is done properly;
- in the condition where the relative humidity of the air inside the solar house was 56%, and the humidity of the air inside the heating and humidification installation was between 90.2% and 95.4%, we can say that the mist water spray system makes a significant contribution to increasing the humidity of the air absorbed through the installation;
- the differences between the temperature of the air entering the pipe (21.8°C, 21.4°C and 21.0°C) and the average temperature of the air leaving the pipe (12.81°C, 14.66°C and 16.31°C), for 3 set fan speeds (25%, 50%, 75% of max. speed) are: 8.99°C, 6.74°C and 4.69°C;
- the differences between the humidity of the air entering the pipe (95.4%, 92.6% and 90.2%) and the average humidity of the air leaving the

pipe (89.82%, 91.19% and 89.49%), for 3 set speeds of the fan (25%, 50%, 75% of the max. speed) are: 5.58%, 1.41% and 0.71%.

- It was observed that these differences decrease with increasing fan speed, both in the case of temperature and in the case of air humidity.

If we compare the air temperature and humidity values measured by the 0-10Vdc transducer located on the pipe with the air temperature and humidity values measured at the exit of the air pipe, the following observations emerge:

- the decrease of the air temperature at the pipe entrance, with the increase in fan speed, while the air temperature at the pipe outlet registers an increase;
- the decrease of air humidity at the pipe entrance, along with the increase in fan speed, while the air humidity at the pipe outlet registers an increase up to 50% of the maximum speed of the fan and then a decrease when the fan speed increases to more than 50% of the maximum speed.

Results obtained from the monitoring and recording of meteorological parameters provided by the local weather station iMetos 3.3:

By monitoring and recording the meteorological parameters provided by the local weather station iMetos 3.3, important information was obtained related to the conditions under which water in the atmosphere condenses, information that led to the adjustment of the data used by the automatic adjustment algorithm of the innovative atmospheric humidity collection system.

- Evolution of meteorological parameters in period 1 (September 2023). The dew point had values in the range of $0.1^{\circ}\text{C} \div 5.6^{\circ}\text{C}$. The minimum dew point (0.1°C) was obtained on 27.09.2023 at 08.00 am, when the average air temperature was 0.14°C and the relative air humidity was 99.98%.

- Evolution of meteorological parameters in period 2 (October 2023). The dew point had values in the range $6.9^{\circ}\text{C} \div 10.8^{\circ}\text{C}$. The minimum dew point (6.9°C) was obtained on 02.10.2023 at 00:00 am, when the average air temperature was 7.04°C and the relative air humidity was 99.98%.

- Evolution of meteorological parameters in period 3 (November 2023). The dew point had values in the range of $7.5^{\circ}\text{C} \div 13.7^{\circ}\text{C}$. The minimum dew point (7.5°C) was obtained on 04.11.2023 at 08.00 am, when the average air temperature was 7.57°C and the relative air humidity was 99.98%.

In all three monitored periods, both the amount of precipitation and the wind speed recorded insignificant values, close to zero.

Table 3. Validation of experimental data

Period/ month	Day no.	Air temperature ($^{\circ}\text{C}$)			Air relative humidity (%)		
		transducer 0-10Vcc outdoor	weather station iMetos 3.3	Difference	transducer 0-10Vcc outdoor	weather station iMetos 3.3	Difference
1 / September	Day 1	0.16	0.14	0.02	98.90	99.98	-1.08
	Day 2	0.85	0.79	0.06	98.80	99.99	-1.09
	Day 3	0.98	0.90	0.08	98.90	99.98	-1.08
2 / October	Day 1	9.30	8.97	0.33	98.90	99.98	-1.08
	Day 2	9.15	8.93	0.22	98.90	99.98	-1.08
	Day 3	8.72	8.56	0.16	98.80	99.97	-1.07
3 / November	Day 1	7.95	7.57	0.38	98.90	99.98	-1.08
	Day 2	8.45	8.03	0.42	98.90	99.98	-1.08
	Day 3	8.86	8.40	0.46	98.80	99.97	-1.07

Table 4. The results obtained from the collection and measurement of the volume of water obtained

Period / month	Day no.	Warm and humid air jet exit angle (°)	Measured water volume (l)	Total water volume (l)
1 / September	Day 1	5	1.87	4.09
	Day 2		1.40	
	Day 3		0.82	
		Average	1.36	-
2 / October	Day 1	10	1.15	3.34
	Day 2		1.35	
	Day 3		0.84	
		Average	1.11	-
3 / November	Day 1	15	1.10	2.44
	Day 2		0.76	
	Day 3		0.58	
		Average	0.81	-

In order to validate the experimental research carried out in the three periods, the values of temperature and relative humidity of the air read by the 0-10Vdc transducer located on the outdoor unit were compared with the values of

temperature and relative humidity provided by the local weather station iMetos 3.3. The readings were taken every day at 08:00 am, and the values are presented in Table 3. The differences obtained are of a maximum of

0.46°C for the air temperature and of a maximum of 1.09% for the relative humidity, which results in a good accuracy of the transducer 0- 10 Vdc (Table 3).

Analysing the results from Table 4, it was found that the largest volume of water collected (4.09 l) was in period 1 (September 2023), for the exit angle of the air jets of 5°.

Comparing periods 2 (October 2023) and 3 (November 2023), which were similar from the point of view of meteorological parameters, it was found that with the increase of the exit angle of the air jets from the piping, the volume of water collected decreases.

If we refer to the average volumes of water collected in each period, related to the total surface of the collecting walls of 5.5 m², we obtain 0.25 l/m²·day for period 1, 0.20 l/m²·day for period 2 and 0.15 l/m²·day for period 3.

CONCLUSIONS

Atmospheric humidity collection is a technology that has greatly evolved in the past decades, but challenges remain to be optimized for efficiency and to ensure the delivery of water with a quality and amount appropriate to its end use. The experimental results presented in this paper demonstrated that atmospheric humidity can be successfully extracted using the innovative atmospheric humidity collection system. By developing and experimenting the innovative atmospheric humidity collection system, an important step was taken to understand the condensation technique.

The research results allow useful recommendations for farmers who are interested in obtaining an additional amount of water needed to irrigate crops in the open field or in protected environments (greenhouses, solariums), by capitalizing on air humidity at a minimum installed energy.

ACKNOWLEDGEMENTS

This research was supported by:

- project *Establishment and operationalization of a Competence Center for Soil Health and Food Safety* – CeSoH, Contract no.: 760005/2022, specific project no.3 with the

title: Fertile and healthy soil through conservation and biological practices, Code 2, financed through PNRR-III-C9-2022 – I5 (PNRR-National Recovery and Resilience Plan, C9 Support for the private sector, research, development and innovation, I5 Establishment and operationalization of Competence Centers).

- a grant of the Romanian Ministry of Research, Innovation and Digitization, through Programme NUCLEU, ctr. nr. 5N / 07.02.2019, project PN 19 10 02 01-Development of innovative technologies inside of Smart Farms.

REFERENCES

- Guadarrama-Cetina, J., Mongruel, A., Medici, M.G., Baquero, E., Parker, A.R., Milimouk Melnychuk, I., Beysens, D. (2014). Dew condensation on desertbeetle skin. *Eur. Phys. J. E.*, 37(11), 1–6.
- Hiatt, C., Fernandez, D., Potter, C. (2012). Measurements of fog water deposition on the California Central Coast. *Atmos. Clim. Sci.*, 2(04), 525.
- Jacobs, A.F.G., Heusinkveld, B.G., Berkowicz, S.M. (2008). Passive dew collection in a grassland area. The Netherlands. *Atmos. Res.*, 87(3), 377–385.
- Manea, D., Marin, E., Mateescu, M., Gheorghe, G.V., Baltatu, C., Dumitraşcu, A., Şovăială, Gh. (2021). Innovative system for recovery the moisture from air for irrigation of crops from a vegetable greenhouse. *Proceedings of International Symposium ISB - INMA TEH' 2021 Agricultural and Mechanical Engineering*, 470 - 475.
- Mekonnen, M.M. & Hoekstra, A.Y. (2016). Four billion people facing severe water scarcity. *Sci. Adv.*, 2, e1500323.
- Mircea, C., Manea, D., Marin, E., Mateescu, M. (2019). Experimental research in irrigation by condensation in solarium. *International Scientific Conference Engineering for Rural Development*. Jelgava, Latvia, 94-99.
- Popa, R., Popa, V., Marin, E., Manea, D., Mateescu, M., Gheorghe, G. (2021). Methods of collecting air humidity for the purpose of valorization for crop irrigation. *Acta Technica Corviniensis - Bulletin of Engineering*, 14(3), 35-38.
- Tomaszkiewicz, M., Najm, M.A., Zurayk, R., El-fadel, M. (2017). Dew as an adaptation measure to meet water demand in agriculture and reforestation, *Agricultural and Forest Meteorology*, 232, 411-421.
- Tu, Y., Wang, R., Zhang, Y., & Wang, J. (2018). Progress and Expectation of Atmospheric Water Harvesting. *Joule*, 2, 1452–1475.
- Wahlgren, R.V. (2001). Atmospheric water vapour processor designs for potable water production: a review. *Water Res.*, 35, 1–22.

ZOOTECHNICAL WASTE AS RAW MATERIAL FOR BIOGAS PRODUCTION AND AS FERTILIZER FOR AGRICULTURE

Roxana MITROI¹, Cristina Ileana COVALIU - MIERLĂ¹,
Cristina -Emanuela ENĂȘCUȚĂ², Grigore PSENOVSCHI^{1,2}

¹National University of Science and Technology Politehnica Bucharest,
313 Splaiul Independentei Street, District 6, Bucharest, Romania

²National Institute for Research & Development in Chemistry and Petrochemistry - ICECHIM,
202 Splaiul Independentei Street, Bucharest, Romania

Corresponding author email: cristina_covaliu@yahoo.com

Abstract

In recent times, the anaerobic fermentation process of animal waste has become a promising solution for biogas production through anaerobic digestion. Anaerobic digestion technology is considered not only an environmental solution but also a potential source of energy, contributing to solving economic and social issues. This research has explored the potential of using poultry, cow and pig manure, to produce biogas through the anaerobic digestion process. Animal farming produce significant quantities of waste and thus exert a negative action on the environment. The animal waste resulting from zootechnical activities can represent an important resource to produce renewable. Furthermore, by using animal waste and plant residues as organic materials to produce biogas, we are not only reducing the quantities of waste illegally dumped along riverbanks or in landfills. In this research paper, the objective was to develop an optimal mixture of animal waste and agro-food byproducts to produce biogas.

Key words: anaerobic digestion, biogas, cow manure, pig manure, poultry manure.

INTRODUCTION

Animal farming takes place both in individual households and large specialized farms. A significant aspect of this activity involves the accumulation of substantial quantities of residual organic materials, which can be solid, liquid, or semi-liquid (Artun & Saltuk, 2019). Typically, these residues, which contain significant amounts of organic fertilizers, are used for the fertilization of nearby agricultural lands.

The manure generated from zootechnical activities contains significant levels of nitrogen, such as: fresh poultry manure (1.03%), fresh cow manure (0.35%), and fresh pig manure (0.24%) (Zhang et al., 2013). The nitrogen in this fertilizer is typically in the form of ammonium, which contains enzymes with fast-acting properties. Thus, the use of poultry manure as a fertilizer is easy and doesn't require much care. However, it is important to consider the significant loss of nitrogen in the form of ammonia. Due to this nitrogen loss, it is not recommended to mix poultry manure with alkaline materials such as wood, ash, or

regular lime (Annex 9. Code of Good Agricultural Practice, 2018).

These alkaline materials can easily release ammonia when they meet poultry manure, which can lead to nitrogen loss. Poultry manure can become an excellent fertilizer when mixed with another compost. This can help balance the nutrients and improve the quality of the fertilizer (Annex 9. Code of Good Agricultural Practice, 2018).

The waste generated by the agro-industrial sector could represent a real source of income if it is properly managed. The production of biogas is the most efficient way to utilize this waste (Hălmăciu et al., 2021). Currently, the anaerobic digestion process has become highly sought after in the management of agricultural and animal farming waste, but it also offers numerous advantages, such as reducing pollution and greenhouse gas emissions (Chae et al., 2008; Khalid et al., 2011).

Biogas is an alternative to livestock waste management. However, it leaves a sludge which contains organic composition that can be used as a solid organic fertilizer (Kurnani et al., 2018). Biogas is produced in the absence of

oxygen through the process of anaerobic digestion, which involves various species of microorganisms (Bardeanu et al., 2021; Yaylaci, & Erdal, 2021). This process consists of four phases: hydrolysis, acidogenesis, acetogenesis, and methanogenesis (Khalid et al., 2011; Markowski et al., 2014). Biogas production was influenced by various factors, such as pH, temperature, dry matter content, oxygen, C/N ratio, agitation, time, and activity of microorganisms in a digester (Deublein & Steinhauser, 2008).

The anaerobic digestion process involves the biological transformation of soluble organic matter into biogas, alcohols, volatile fatty acids, and nitrogen-rich organic residues (Anitha et al., 2015).

MATERIALS AND METHODS

Since there are no research studies that use animal waste from different animals in the same biodigester, an experiment with various mixtures containing poultry, cow and pig manure was chosen. In this research paper, the primary objective was to develop an optimal mixture of animal waste and agro-food byproducts to produce biogas.

Equipment description

Using an automatic gas flow measurement system (Gas Endeavour), BPC Instruments AB, Sweden, experiments were carried out on the anaerobic co-digestion process (Figure 1).

Unit A is equipped with the following components: 15 glass bottles, 500 mL as reactors, 15 plastic caps with agitators, 15 plastic screw caps with hole, 15 helical couplings, 14 short motor cables, 1 long motor cable (from Motor Controller to first motor unit), 1 signal cable (from the Gas Volume Measuring Device to Motor Controller), 15 plastic stoppers with 2 tubing ports and rotating shaft for mixing, 1 thermostatic water bath (18 L), 1 plastic glass lid for the water bath, with 15 circular opening, 15 evaporation minimizing rings for the lid and reactors, 15 plastic tubing clamps.

Unit B contains: 1 bottle holder for 15 glass bottles, 15 glass bottles, 100 mL, 15 plastic screw caps with hole, 15 plastic stoppers with 2 tubing ports.

Unit C contains: 1 gas volume measuring device (including 15 flow cell chambers, 15 injection mold flow cells containing magnetic metal pieces, frame, and plastic covering), 30 check valves, 1 plastic syringe, 1 power adapter.

Other components: 1 shielded Ethernet cord, 1 Motor Controller, 1 power adapter, boxes of 15 m flexible Tygon tubing, 1 number markers kit for tubes, 15 plastic lids.

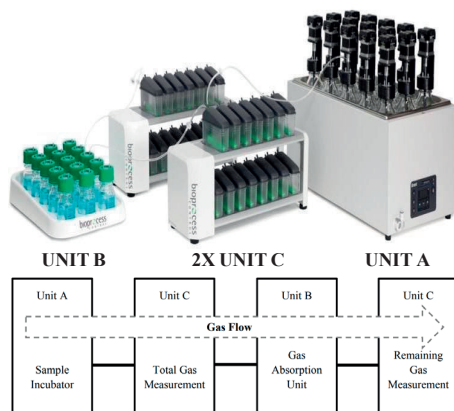


Figure 1. Biogas Production Plant - Gas Endeavour.
 Continuous profile of total gas and CH₄ production
 Source: BPC Instruments AB, 2002

The installation is also equipped with optional equipment: 15 glass bottles, 1 L (bottles with one port designed for continuous pH monitoring during the batch fermentation) and 15 stirrers adjusted for 1 L bottles, 6 glass bottles, 2 L (bottles with one port designed for continuous pH monitoring during the batch fermentation) and 6 stirrers adjusted for 2 L bottles, 1 plastic glass lid for the water bath, with six circular openings for reactors, gas sampling units (BPC Instruments AB, 2002).

With Gas Endeavour, the data analysis and recording are completely automated (Figure 2). The testing vessels (500 mL) from Unit A, containing small quantities of a microbial inoculum sample, are incubated at a temperature of 37°C in the incubation unit, within a thermostatic water bath.

The samples in each vessel are mixed using a slow-rotation agitator, while gas is continuously produced from the material. In the gas absorption unit (Unit B), the gas produced in each flask passes through an individual flask

containing a solution capable of absorbing specific gas fractions. If we use an alkaline solution such as NaOH, acidic fractions like CO₂ and H₂S are retained, and only CH₄ and H₂ will pass to the gas monitoring unit. To monitor the acid-binding capacity of the solution, we can add a pH indicator to each flask. In Unit C, the volume of gas released from either the incubation unit or the gas absorption unit is measured using a wet gas flow measurement device with 15 multiplexed cells. This measurement device operates on the principles of liquid displacement and buoyancy and can monitor ultra-low gas flow rates. When a defined volume of gas flows through the device, it generates a digital pulse, and the data are recorded and displayed, with the apparatus analyzing the results.

The system can measure both the total gas and a specific fraction remaining after absorption, such as CH₄, for seven parallel vessels. This can be achieved by directing the gas produced from a test vessel into a flow cell chamber in Unit C, measuring the total gas, and then connecting the outlet of this chamber to a flask containing an absorption solution, such as NaOH, to remove CO₂ and H₂S. Afterward, the outlet of this flask is connected to a second flow cell (BPC Instruments AB, 2002).



Figure 2. Optimal mixtures of animal waste and agro-food byproducts for biogas production using Gas Endeavour

Operating mode

The animal waste used in this study was collected in August and September 2023 from farms located in Teleorman County. Three different samples of animal waste were characterized to study the anaerobic codigestion process. The physico-chemical properties were assessed through laboratory analyses. The equipment used for the determinations to calculate total nitrogen was the Dionex Aquion Ion Chromatograph and the

CARY60 UV-VIS Spectrophotometer, while for calculating phosphorus and potassium, the equipment used was the PerkinElmer 8300 ICP-OES and the Milestone Ethos Easy System.

Tables 1, 3 and 5 show the calculation of total nitrogen from different samples of animal waste (from poultry, cows and pigs) and Tables 2, 4 and 6 show the calculation of phosphorus and potassium. Animal waste samples were stored at -4°C during the preparation of the mixtures. The inoculum was obtained from a wastewater treatment plant in Teleorman County.

The substrate was a mixture of organic materials with a concentration of 10% solids (animal waste, plant residues, food waste) and the remaining portion is water.

Table 1. Analyses of nitrates, nitrites, nitrogen and total nitrogen (calculated) for poultry waste

Determinations	U/M	Poultry Waste
Nitrites	mg/kg	< 2.5
Nitrates	mg/kg	< 50
Nitrogen Kjeldahl	g/kg	19.1
Total nitrogen (calculated)	mg/kg	19100

Table 2. Analyses of poultry waste

Determinations	U/M	Poultry Waste
Phosphorus	mg/kg	11300
Potassium	mg/kg	27600

Table 3. Analyses of nitrates, nitrites, nitrogen and total nitrogen (calculated) for cow waste

Determinations	U/M	Cow Waste
Nitrites	mg/kg	< 2.5
Nitrates	mg/kg	< 50
Nitrogen Kjeldahl	g/kg	15.6
Total nitrogen (calculated)	mg/kg	15600

Table 4. Analyses of cow waste

Determinations	U/M	Cow Waste
Phosphorus	mg/kg	4760
Potassium	mg/kg	7970

Table 5. Analyses of nitrates, nitrites, nitrogen and total nitrogen (calculated) for pig waste

Determinations	U/M	Pig Waste
Nitrites	mg/kg	< 2.5
Nitrates	mg/kg	< 51.7
Nitrogen Kjeldahl	g/kg	25.0
Total nitrogen (calculated)	mg/kg	25000

Table 6. Analyses of pig waste

Determinations	U/M	Pig Waste
Phosphorus	mg/kg	7760
Potassium	mg/kg	15500

To achieve a uniform distribution of anaerobic bacteria throughout the substrate for the anaerobic co-digestion process, we combined multiple substrates with a 10% solids concentration with 40 g of inoculum (which is a previously prepared culture of anaerobic bacteria) and then introduced them into fermentation reactors with a usable volume of 400 g (Tabel 7). It is advisable for raw material mix recipes to adhere to a C/N ratio ranging from 15 to 25 and to have a moisture content of

at least 90%. The reactors provide the conducive environment in which the anaerobic co-digestion process will take place. The experiments considered are presented in Tables 8, 9, 10 and 11.

Experiment number 5 - Blank test - it involved the use of 40 g of cellulose and 360 g of inoculum (Table 12).

Table 7. The quantities of materials required for the anaerobic co-digestion process

Total volume	500	g
Usable volume	400	g
Substrate	320.0	g
10% solids	40.0	g
Inoculum	40.0	g

Table 8. Experiment number 1 using green organic waste (tomato leaves)

Raw material	C/N	Exp. 1 %	Solid necessity g	Solid requirement %	TO BE FED		
					Fresh plant material	Water	Inoculum
					G	g	g
Green leaves (tomatoes)	20.4	20	8.00	20.00	40.000	172.29	40.00
Pig		40	16.00	22.73	70.392		
Cow		10	4.00	17.00	23.529		
Poultry		30	12.00	22.31	53.786		
TOTAL		100	40.00		187.710	172.29	40.00

Table 9. Experiment number 2 using green organic waste (tomato leaves) and wheat straw

Raw material	C/N	Exp. 2 %	Solid necessity g	Solid requirement %	TO BE FED		
					Fresh plant material	Water	Inoculum
					g	g	g
Green leaves (tomatoes)	25	10	4.00	20.00	20.00	172.29	40.00
Wheat straw		10	4.00	10.00	40.39		
Pig		40	16.00	22.73	70.39		
Cow		10	4.00	17.00	23.53		
Poultry		30	12.00	22.31	53.79		
TOTAL		100	40.00		207.71	172.29	40.00

Table 10. Experiment number 3 using grass as green organic waste

Raw material	C/N	Exp. 3 %	Solid necessity g	Solid requirement %	TO BE FED		
					Fresh plant material	Water	Inoculum
					g	g	g
Grass	17.2	20	8.00	20.00	40.000	172.29	40.00
Pig		40	16.00	22.73	70.392		
Cow		10	4.00	17.00	23.529		
Poultry		30	12.00	22.31	53.786		
TOTAL		100	40.00		187.710	172.29	40.00

Table 11. Experiment number 4 using potato as green organic waste

Raw material	C/N	Exp. 4	Solid necessity	Solid requirement	TO BE FED		
					Fresh plant material	Water	Inoculum
					g	g	g
Potato	15.8	20	8.00	20.00	40.000	172.29	40.00
Pig		40	16.00	22.73	70.392		
Cow		10	4.00	17.00	23.529		
Poultry		30	12.00	22.31	53.786		
TOTAL		100	40.00		187.710	172.29	40.00

Table 12. Experiment number 5 using Blank test

Raw material	cellulose	inoculum
	g	g
	360	40.00
TOTAL	360	40.00

RESULTS AND DISCUSSIONS

Organic fertilizers with a low C/N ratio, such as straw less manure, tend to decompose rapidly. For instance, in the case of pig manure nitrification, this process can occur within a relatively short timeframe, typically ranging from three to five weeks.

On the other hand, fertilizers with a high C/N ratio, such as straw-bedded manure, undergo slower decomposition. This is due, in part, to the type of hydrocarbon substances present in the organic material, which can be degradable. Additionally, the specific nature of the waste (e.g. the chemical composition of animal droppings) can influence the rate of mineralization.

In general, fertilizers with a low C/N ratio tend to release nitrogen more rapidly, while those

with a high C/N ratio can release nitrogen more slowly, which can be beneficial for a gradual and longer-lasting nutrient release. However, proper management of organic fertilizers with different C/N ratios is essential to maximize agricultural benefits and to avoid potential issues related to soil or water pollution.

Experiments were carefully monitored to maintain the best conditions for the development of anaerobic bacteria in the fermentation reactor: optimal temperature, pH level, and continuous substrate feeding. Mixing the substrate with the inoculum accelerated the anaerobic fermentation process.

The maximum biogas level was obtained after 5 days of anaerobic digestion of the animal manure and green grass substrate, reaching approximately 300 m³/day, compared to that derived from the animal manure with green leaves and straw substrate, which was approximately 200 m³/day (Figure 3). The highest recorded flow was 165 m³/day for the green grass and vegetable (potato) substrate (Figure 4).

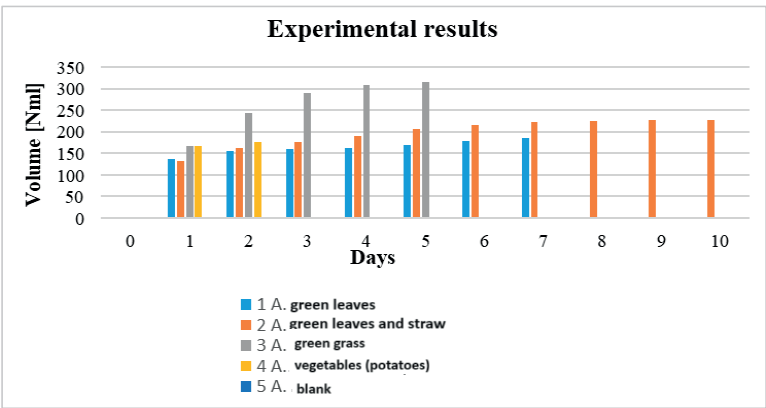


Figure 3. Experiments results - Volume [Nml]

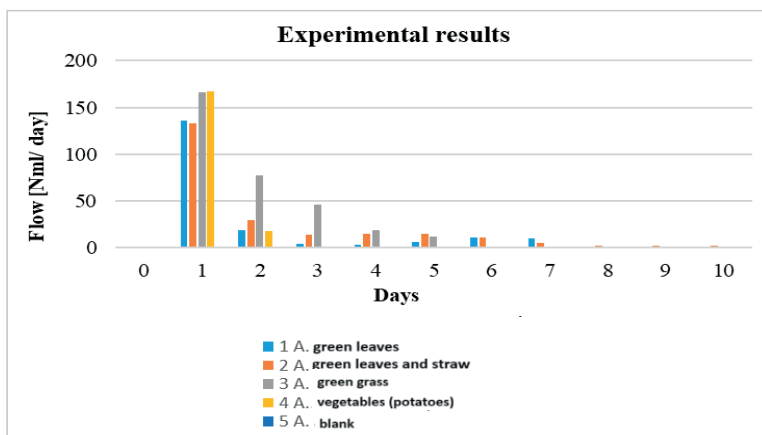


Figure 4. Experiments results - Flow [Nml/day]

CONCLUSIONS

Mixing animal waste with the inoculum is a crucial initial step in biogas production and ensures the efficiency of the anaerobic digestion process.

In this study, we conducted an evaluation of biogas production using poultry waste, cow waste, and pig waste as substrates.

The experiments were conducted using the Gas Endeavour biogas production facility, which is of small capacity, at a temperature of 37°C.

Our goal was to determine when biogas production begins and when the maximum level of production is reached.

In the first days, the installation recorded efficient biogas production, with the optimal mixtures being the mixture with green grass, the mixture with green leaves and straw, and the mixture with vegetables (potatoes).

After ten days of carrying out the experiments, the apparatus no longer recorded any signals, and the experiments were ended. This could indicate the depletion of organic matter resources in the anaerobic digestion process.

ACKNOWLEDGEMENTS

The results presented in this article have been funded by the Ministry of Investments and European Projects through the Human Capital Sectoral Operational Program 2014-2020, Contract no. 62461/03.06.2022, SMIS code 153735. This work was supported by a grant from the Ministry of Research, Innovation and

Digitization through Program 1 - Development of the national research - development system, Subprogram 1.2 - Institutional performance in RDI, Contract no. 15PFE/2021.

REFERENCES

- Annex 9. Code of Good Agricultural Practice, (2018) [in Romanian] https://galdntulcea.ro/wp-content/uploads/2018/01/Anexa_9_Codul_bunelor_practici_agricole-1.pdf
- Anitha, M., Kamarudin, S.K., Shamsul, N.S., Kofli, N.T. (2015). Determination of bio-methanol as intermediate product of anaerobic co-digestion in animal and agriculture wastes, *International Journal of Hydrogen Energy*, 40(35), 11791-11799.
- Artun, O., Saltuk, B. (2019). Investigation of animal origin biogas potential using geographical information systems: east mediterranean region case, *Scientific Papers. Series E. Land Reclamation, Earth Observation & Surveying, Environmental Engineering*, VIII, ISSN 2285-6064, 126-133.
- Bardeanu, H., Matei, F., Popescu, P.-A., Ionescu, O., Jurcoane, S. (2021). Improving a biogas plant parameters in the conversion context of replacing the corn silo with agri-food waste. *Scientific Papers. Series E. Land Reclamation, Earth Observation & Surveying, Environmental Engineering*, X, Print ISSN 2285-6064, 17-23.
- BPC Instruments AB - Gas Endeavour, Automatic Gas Flow Measuring System - Operation and Maintenance Manual, Version 1.2.1 February 2022.
- Chae, K.J., Jang, A., Yim, S.K., Kim, I.S. (2008). The effects of digestion temperature and temperature shock on the biogas yields from the mesophilic anaerobic digestion of swine manure, *Bioresource Technology*, 99, 1-6.
- Deublein D. & Steinhauser A. (2008). Biogas from Waste and Renewable Resources. An Introduction. WileyVCH Verlag GmbH & Co. KGaA.

- Hălmăciu, A.I., Ionel I., Wächter, M.R. (2021). The circular economy in the agro-zootechnical industry. *Journal of Research and Innovation for Sustainable Society (JRISS)*, 3(1), 1-6.
- Khalid, A., Arshad, M., Anjum, M., Mahmood, T., Dawson, L. (2011). The anaerobic digestion of solid organic waste, *Waste Management*, 31, 1737-1744.
- Kurnani, T.B.A., Hamidah, I., Hidayati, Y.A., Marlina, E.T., Harlia, E., Adriani L. (2018). Influence water content of biogas substrate made by dairy cows faeces and rice straw on the quantity and quality of sludge. *Scientific Papers. Series D. Animal Science. LXI(2)*, 177-183.
- Markowski, M., Białobrzewski, I., Zieliński, M., Dębowski, M., Krzemieniewski, M. (2014). Optimizing low-temperature biogas production from biomass by anaerobic digestion. *Renewable Energy, Elsevier*, 69(C), 219-225.
- Yaylaci, C. & Erdal, İ. (2021). Effect of biogas digestate on growth and some potential toxic element concentrations of wheat. *AgroLife Scientific Journal*, 10(2). <https://doi.org/10.17930/AGL2021226>
- Zhang, T., Liu, L., Song, Z., Ren, G., Feng, Y., Han, X., Yang, G. (2013). Biogas production by co-digestion of goat manure with three crop residues. *PLoS ONE*, 8(6), e66845.

RESEARCHES FOR THE PHYSICO-CHEMICAL CHARACTERIZATION OF SOME GRANULAR FERTILIZERS OBTAINED FROM NATIVE WOOL WASTE, IN ORDER TO USE THEM IN AGRICULTURE

Elena Mihaela NAGY¹, Teodor Gabriel FODOREAN¹, Dragos Vasile NICA¹,
Evelin-Anda LAZA¹, Teodor VINTILA²

¹National Institute of Research - Development for Machines and Installations Designed for
Agriculture and Food Industry - INMA Bucharest,

6 Ion Ionescu de la Brad Blvd, District 1, Bucharest, Romania

²University of Life Sciences "King Mihai I" from Timisoara,
119 Calea Aradului, Timisoara, Romania

Corresponding author email: nagy_m2002@yahoo.co.uk

Abstract

Wool waste production cannot be avoided, so reuse and recycling are the best solutions for managing this keratinous waste. At present, in Romania, wool in different forms - raw or washed wool, pelleted wool or wool hydrolysate - is used in agriculture on a relatively small scale, both as a fertilizer and to improve certain physical characteristics of the soil. A good knowledge of the physico-chemical properties of wool-based fertilizer granules will also contribute to increasing the use of this resource. In this research, the characteristics of some wool granules produced in Romania were studied, such as bulk density, granule moisture, water absorption, and the effect of alkaline hydrolysate obtained from them on soil-beneficial bacteria of the Bacillus genus and Rhizobium genus. Among the results obtained, it should be mentioned that the water absorption capacity of the granules is around 200%. Also, the research proved that the alkaline hydrolysate obtained from the wool pellets studied does not show inhibitory effect on the Bacillus and Rhizobium species tested.

Key words: characteristics, granular fertilizer, hydrolysate, wool.

INTRODUCTION

Total world wool production and wool prices have steadily declined over the last decades. According to recent figures, world wool production is 1950 million kg (IWTO, 2021) down 0.6% from 2015, and represents 1.73% of total fibre production (113 million tons) (statista.com).

According to a 2019 report, it is estimated that approximately 10-15% of wool is wasted during sorting and cleaning, and an additional 12-15% is lost during spinning and weaving (Kadam et al., 2014; Sharma et al., 2019).

Disposal of wool waste by incineration and landfilling causes air and soil pollution when the amount of wool is not carefully controlled. (Kumawat, 2018; Marchelli et al., 2021).

In order to overcome these pollution problems and to use this large amount of waste as a resource, it has been proposed over the years to use wool waste for numerous applications such as insulation (Cai et al., 2021), building materials (Buratti et al., 2020), adsorbents (El-

Geundi, 1997), composite materials (Remadevi et al., 2020), mulches or fertilizers for agriculture (Ordiales et al., 2016).

The advantage of wool is given by its amidic structure that can bring benefits to the soil by retaining water and mineralizing nitrogen, wool is also biodegradable within six months under ideal conditions (Haque & Naebe, 2020). The use of wool for plant growth is sustainable and can benefit the soil if used rationally, which can reduce the amount of mineral fertilizer to a minimum, if not replacing it altogether (Wiedemann et al., 2020).

Furthermore, evaluation of cleaned wool residues obtained from textile mills in terms of their effects on soil properties demonstrated that their use improves bulk density, water holding capacity and soil aggregation (Abdallah et al., 2019).

There is also an increased interest in the development of more complex wool-based fertiliser systems that incorporate other components into their structure. One such example is the application of a biostimulant

containing humic acid, lactic acid and *Bacillus subtilis* in the rhizosphere in parallel with the use of unbleached sheep's wool plates as substrate for hydroponic cucumber production (Böhme et al., 2005). Recent studies have also investigated the potential use of arbuscular mycorrhizal fungi in combination with wool pellets for agricultural crops (Larsson, 2022). However, there is no information on the potential of using wool as a carrier for immobilisation of different types of bacteria with important roles in the soil (e.g. nitrifying bacteria, lactic acid bacteria) or on the combined use of wool in various forms in mixture with lyophilisates of these bacterial species for fertilisation, amendment or soil conditioning. Such a research direction is in line with European Circular Economy policies, and from this point of view, coarse wool and other related waste should be treated as a secondary raw material and used as a valuable source of nutrients and organic matter.

In this context, the paper present the research regarding the characteristics of some wool granular fertilizer produced in Romania and the effect of alkaline hydrolysate obtained from them on soil-beneficial bacteria of the *Bacillus* genus and *Rhizobium* genus.

MATERIALS AND METHODS

The wool pellets used for the experiments were purchased directly from the producer, SC Miorita, Ucea de Jos, Brasov. According to the information from the manufacturer the pellets were made from raw, milled wool, with the fibre size being about 6 mm, after which it was processed with a pelleting press. Two types of pellets were made with different diameters, 6 mm (S6) and 9 mm (S9) (Figure 1).



Figure 1. Wool pellets used for experiments

Some of the main quality indicators of wool pellets are presented in Table 1.

Table 1. Wool pellets quality indicators (analysis bulletin Raiffeisen Laborservice)

No.	Quality Indicators	U. M.	Determined values
1	Dry matter	%	89.30
2	pH measured at 20.6 °C	pH units	9.56
3	Density	g/l	0.33
4	Nitrogen	% D.M	12.14
5	P ₂ O ₅	% D.M.	0.18
6	K ₂ O	% D.M	5.08
7	Sulphur	% D.M	2.11
8	CaO	% D.M	0.46
9	MgO	% D.M	0.19
10	Organic matter	g/kg D.M.	847.4
11	Humus-C	g/kg D.M.	460.4
12	Copper	mg/kg D.M	8.1
13	Iron	mg/kg D.M	2296
14	C:N ratio		3.8 :1

To determine the water content, we used samples of about 3 g of granules, which were dried at 70°C, with a thermobalance type AXIS-100 with a weighing accuracy of 0.01%, (Figure 2). At every 30 seconds the masses were recorded until a constant mass has been obtained. Moisture content is given by the difference between the initial and final mass of the samples.

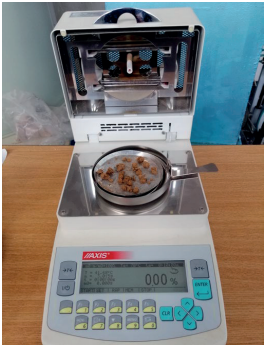


Figure 2. Drying wool pellets with thermobalance Axis-100

To determine the water absorption capacity of the wool pellets, 5 g samples were weighed over which distilled water was added in 10 ml fractions, with a 5-minute break between fractions, until excess water remained. The excess water was removed with absorbent paper and reweighed the saturated sample. The water absorption relative to mass was calculated with the formula (1):

$$a_m = (m_{sa} - m_{us}) * 100 / m_{us} \quad (1)$$

where:

- m_{us} – pellets dry mass, g;
- m_{sa} – pellets saturated mass, g;
- a_m – water absorption relative to mass, %.

To determine the bulk density of the wool pellets we used a calibrated vessel of volume $V = 0.20 \text{ dm}^3$ with mass $m_{vas} = 107.75 \text{ g}$. To obtain the mass m_1 we poured the granules into the vessel from 5 cm height, then we buffered it for around 30 times by a wooden table and weighed again. The measurements were repeated by 5 times to determine the average value of the m_1 . Compact bulk density was calculated using the formula (2):

$$\rho = (m_1 - m_v) / V \quad (2)$$

where:

- m_v – vessel mass, g;
- V – vessel volume, dm^3 ;
- m_1 – mass of the vessel with pellets, g.

In order to increase the fertilizer and soil amendment qualities of wool pellets by the addition of beneficial plant and soil-borne telluric microorganisms, the effect of hydrolysates obtained from the pellets on beneficial bacteria such as *Bacillus* genus and *Rhizobium* genus was studied.

For this the alkaline hydrolysis of wool pellets was carried out and slightly modified according to the previous method described by Berechet and colleagues, which has been declared as suitable for wool by-products and wool itself (Berechet et al., 2018).

For this research bacterial cells of *Bacillus subtilis*, *Bacillus subtilis* USAB, *Bacillus subtilis* B 52, *Bacillus subtilis* B36, and *Bacillus licheniformis* 1, as well as *Rhizobium* Gz 13, *Rhizobium meliloti*, *Rhizobium trifolii*, *Rhizobium meliloti* USAB and *Rhizobium lupini* LP 83 FM, were cultured under aerobic environmental conditions at USV Timisoara.

To assess whether the resulting hydrolysate samples exhibit potential bacterial inhibitory properties, the disc diffusion assay was used for verification, as previously reported (Balta et al., 2021). Briefly, 100 μl of liquid bacterial cultures of *B. subtilis*, *B. subtilis* USAB, *B. subtilis* B 52, *B. subtilis* B36 and *B. licheniformis* 1 were inoculated onto Petri dishes with nutrient agar and spread with a Drigalsky spatula. Similarly,

100 μl of *R. GZ 13*, *R. meliloti*, *R. trifolii*, *R. meliloti* USAB and *R. lupini* LP 83 FM were placed and spread on yeast mannitol agar plates. Next, 6 mm paper discs were placed in each plate and hydrolysate samples at 20 μl were absorbed onto the paper discs at the specified hydrolysate concentration. Plates were left at room temperature for 10 min to allow better absorption of hydrolysates into the blank discs and were incubated inversely at 37°C and 28°C for the appropriate time. Antimicrobial activity of each hydrolysate was measured using the caliper as the diameter of the inhibition zone around the disc.

RESULTS AND DISCUSSIONS

Figure 3 shows graphically the results obtained from the wool pellet drying process. From the analysis of the measured data it was observed that the S6 pellets had a moisture content of 9.6% and the total drying time was 810 s, while for sample S9 the moisture content was 9% and the total drying time was 1020 s. The increase in drying time is due to the larger diameter of the pellets in sample S9.

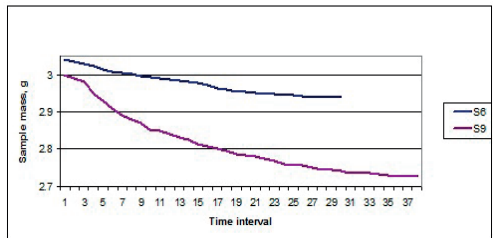


Figure 3. Drying curves at 70°C

The values obtained for the bulk density of the wool pellet's samples are presented in Table 2.

Table 2. Bulk density of wool pellets samples

	S6		S9	
	m_1 , g	ρ , kg/m^3	m_1 , g	ρ , kg/m^3
$V_{vas}=0.20 \text{ dm}^3$ $m_v=107.75 \text{ g}$	231.89	620.05	161.02	270.30
	230.86		162.61	
	231.72		161.63	
	231.95		161.45	
	232.38		162.34	

Sample S9 has a much lower bulk density compared to sample S6 - which can be justified by the appearance of these pellets - much more aerated, probably because the pellet equipment

has been equipped with a sieve with larger orifices (9 mm), but the other working parameters (pressure) remained unchanged as for S6.

Analyzing the data presented in Table 3, obtained from the calculation of water absorbed in relation to mass for the two types of wool pellets, we observe that the two samples show a close water absorption capacity, sample S9 absorbing only 9% more than S6.

Also, during the experiments, it was observed that sample S9 absorbs water much faster - the first 10 ml fraction was absorbed almost instantaneously unlike sample S6 where after 5 minutes water is still observed in the vessel (Figure 4).

Table 3. Water absorption capacity of the wool pellets

Sample	Water added g	Dry pellets m _{sa} , g	Saturated pellets m _{sa} , g	Water absorbed a _m , %
S6	20.02	4.98	15.82	218
S9	19.92	4.99	16.32	227



Figure 4. Water absorption - 5 min. after addition of 10 ml water

When the second 10 ml fraction of water was added, the S9 sample completely disintegrated in the first minute while for the S6 sample after 5 minutes pieces of pellets were still observed (Figure 5). The delay in water absorption is due to the compaction of the pellets - S6 have a much denser structure than S9.

Since the pellets are desired to decompose and release nutrients in a longer time it is obvious that the structure of the S6 sample is more advantageous.



Figure 5. Water saturated samples

After adjusting the pH of the hydrolysate obtained from the pellets to a value as close as possible to 7 (similar to the bacterial growth medium) these conditions were maintained for the next 5 days in order to determine the possible antibacterial effects of the alkaline hydrolysates prepared by the disc diffusion method. The results showed that none of the hydrolysates showed inhibitory effects on the *Bacillus* and *Rhizobium* strains tested. As can be seen in Figure 6 and 7, in all cases the bacteria grew on the agar media up to the discs impregnated with keratin hydrolysates and no zone of inhibition was observed.

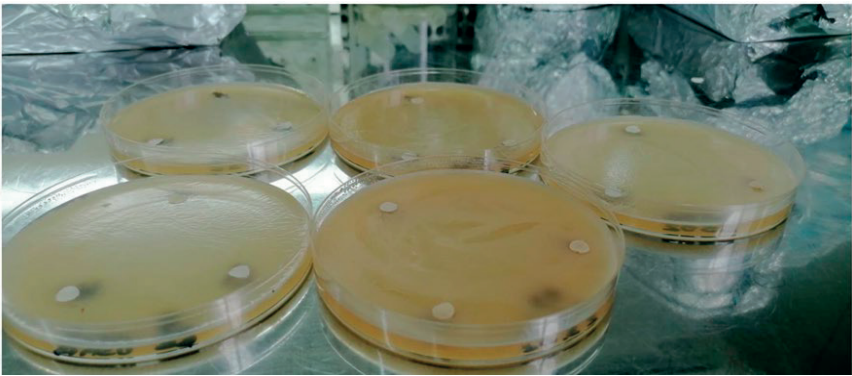


Figure 6. Plates with bacteria of the genus *Bacillus* grown on simple agar with discs impregnated with keratin hydrolysates

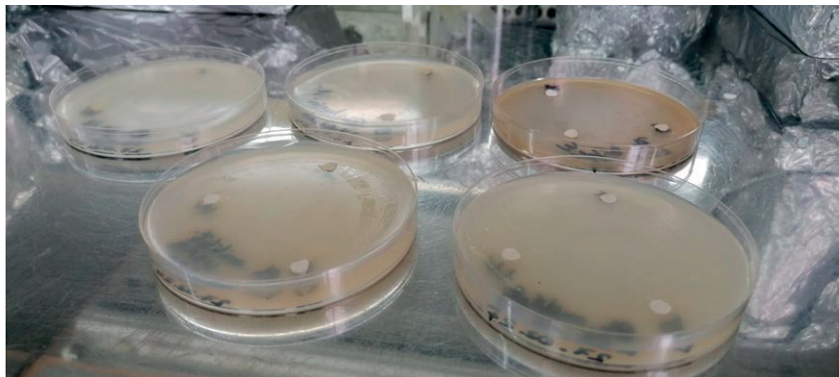


Figure 7. Plates with bacteria of the genus *Rhizobium* grown on YMA medium with discs impregnated with keratin hydrolysates

CONCLUSIONS

The use of wool waste in agriculture is still a relatively new field for Romania, which requires more studies and research.

Knowing the characteristics of wool pellets allows a better management of them, depending on the purpose and the requirements of agricultural crops, and opens new research directions on improving their fertilizer quality.

The results show that:

- the two types of pellets have a similar moisture content, respectively S6 - 9.6% and S9 - 9%;
- S9 pellets, which have a more aerated structure, have a much lower bulk density than S6;

- also, in S9 pellets a higher water absorption rate was observed compared to S6, although the amount of water absorbed had similar values for both samples.

From these results it can be stated that when incorporated into the soil, S9 wool pellets will provide better aeration and lighter soil structure, which is beneficial for plant root growth, but will disintegrate faster which may influence the time of nutrient release into the soil.

In terms of the possibilities of enriching wool pellets with beneficial bacteria it has been observed that the keratin hydrolysates obtained from the wool pellets do not inhibit the growth of the microorganisms tested. The hydrolysates obtained can be used for the development of bacteria of the *Bacillus* and *Rhizobium* genera, which can be applied to agricultural crops to maintain plant health, improve agricultural yields and restore soil biodiversity.

ACKNOWLEDGEMENTS

This work is financed by Ministry of Research, Innovation and Digitalization through Program 1 - Development of the national research-development system, Subprogram 1.2 - Institutional performance - Projects for financing excellence in RDI, Contract no. 1PFE/30.12.2021,, and by NUCLEU programme contr. 9N/01.01.2023, project PN 23 04 02 02

REFERENCES

- Abdallah, A., Ugolini, F., Baronti, S., Maienza, A., Camilli, F., Bonora, L., Martelli, F., Ungaro, F., Primicerio, J. (2019). The potential of recycling wool residues as an amendment for enhancing the physical and hydraulic properties of a sandy loam soil. *Int. J. Recycl. Org. Waste Agric.*, 8, 131–143.
- Balta, I., Marcu, A., Linton, M. *et al.* (2021). Mixtures of natural antimicrobials can reduce *Campylobacter jejuni*, *Salmonella enterica* and *Clostridium perfringens* infections and cellular inflammatory response in MDCK cells. *Gut Pathog.*, 13, 37.
- Berechet, M., Gaidau, C., Niculescu, M., & Stanca, M. (2018). The Influence of Alkaline Hydrolysis of Wool by-Products on the Characteristics of Keratin Hydrolysates. 39-44. 10.24264/icans-2018.1.4.
- Böhme, M., Schevchenko, J., Pinker, I., Herfort, S. (2005). Cucumber grown in sheepwool slabs treated with biostimulator compared to other organic and mineral substrates. *Acta Hort.*, 779, 299–306.
- Buratti, C., Belloni, E. & Merli, F. (2020). Water vapour permeability of innovative building materials from different waste. *Mater. Lett.*, 265, 127459.
- Cai, Z., Al Faruque, M.A., Kiziltas, A., Mielewski, D. & Naebe, M. (2021). Sustainable lightweight insulation materials from textile-based waste for the automobile industry. *Materials*, 14, 1241.

- El-Geundi, M.S. (1997). Adsorbents for industrial pollution control. *Adsorpt. Sci. Technol.*, 15, 777–787.
- Haque A.N.M.A. & Naebe, M. (2022). Waste wool powder for promoting plant growth by moisture retention. *Sustainability*, 14(19), 12267.
- IWTO 2021. Wool Production, International Wool Textile Organization. <https://www.iwto.org/wool-production>
- Kadam, V.V., Meena, L.R., Singh, S., Shakyawar, D.B. & Naqvi, S.M.K. (2014). Utilization of coarse wool in agriculture for soil moisture conservation. *Indian Journal of Small Ruminants*, 20, 83-86.
- Kumawat, T.K., Sharma, A., Sharma, V. & Chandra, S. (2018). Keratin waste: The biodegradable polymers. In *Keratin; IntechOpen*: London, UK.
- Larsson, S. (2022). The potential use of waste wool pellets as a substrate amendment affecting arbuscular mycorrhizal development in container-grown *Allium porrum*, Second cycle, A2E. *Alnarp: SLU, Department of Biosystems and Technology*.
- Marchelli, F., Rovero, G., Curti, M., Arato, E., Bosio, B. & Moliner, C. (2021) An integrated approach to convert lignocellulosic and wool residues into balanced fertilisers. *Energies*, 14, 497.
- Ordiales, E., Gutiérrez, J.I., Zajara, L., Gil, J. & Lanzke, M. (2016). Assessment of utilization of sheep wool pellets as organic fertilizer and soil amendment in processing tomato and broccoli. *Mod. Agric. Sci. Technol.*, 2, 20–35.
- Remadevi, R., Al Faruque, M.A., Zhang, J. & Naebe, M. (2020). Electrically conductive honeycomb structured graphene composites from natural protein fibre waste. *Mater. Lett.*, 264, 127311.
- Sharma, S., Sahoo, A. & Chand, R. (2019) Potential use of waste wool in agriculture: An overview. *Indian J. Small Rumin.*, 25, 1–12.
- Wiedemann, S., Biggs, L., Nebel, B., Bauch, K., Laitala, K., Klepp, I., Swan, P. & Watson, K. (2020) Environmental impacts associated with the production, use, and end-of-life of a woollen garment. *Int. J. Life Cycle Assess.*, 25, 1486–1499.
- www.statista.com/statistics/263154/worldwide-production-volume-of-textile-fibers-since-1975/

IMPROVING PRODUCTIVITY ON DEGRADED LANDS USING A NOVEL TECHNOLOGY OF CULTIVATING CROPS IN BIODEGRADABLE MULTILAYERED STRUCTURES

Florin NENCIU¹, Eugen POPESCU¹, Lorena-Diana POPA²,
Gabriel NAE¹, Andreea MATACHE¹

¹National Institute of Research - Development for Machines and Installations Designed for
Agriculture and Food Industry Bucharest - INMA,
6 Ion Ionescu de la Brad, Bucharest, Romania

²Agricultural Research and Development Station Secuieni, 377 Principala Street,
Secuieni, Neamt, Romania

Corresponding author email: florin_nenciu2000@yahoo.com

Abstract

Integrating degraded or contaminated lands into food production chains poses significant challenges and expenses. This study explores a novel technology for cultivating vegetables on degraded lands employing vegetal substrates in the form of bales. These multi-layered vegetal structures are strategically designed to offer essential support, nutrients, water, warmth, and protection against pests for the cultivated plants. The fertile layer within these structures was produced through composting vegetable waste produced from horticulture. The protective surface of the bale was made from a mixture of agricultural wastes, ensuring both a resilient structure and permeability. The structure was enhanced with two layers made of recycled cotton, aimed at retaining moisture efficiently. The research showed that the adopted technological solution can yield a 30-40% improvement in production of tomato and eggplant. Moreover, it demonstrates high adaptability, being easily applicable for crops establishing in contaminated, degraded environments, or even on concrete surfaces.

Key words: composting, cultivation in bales, degraded soil.

INTRODUCTION

Vast areas of land have experienced degradation as a result of chemical and physical aggressive interventions, while other agricultural soils face constraints in water resources, affecting the quality and suitability of the land for planting. Cultivating vegetables in innovative mediums such as multilayered structures could be a practical solution for establishing food crops in regions with degraded, contaminated, or disease-affected lands (Farag et al., 2015). Extensive research has been undertaken to recycle agricultural residues, including rice straw, into diverse raw materials for the agricultural sector. These materials are often utilized as non-traditional mediums for cultivating specific vegetables. Planting vegetables in straw bales is an alternative and environmentally friendly farming practice that is regaining popularity among gardeners and farmers. This process involves placing seeds or seedlings directly into straw bales as growing

media, thus including agricultural waste in the production cycle.

Studies on straw bale farming have primarily concentrated on vegetable crops with relatively short stature. These include cucumber (El-Aidy 1993; Vatchev 2012), lettuce (Bal et al., 2008; Riad et al., 2017), pepper (El-Marzoky, 2008; Gluntsov et al., 1997), strawberry and tomato (Abdet-Sattar et al., 2008). A research study (Rishead, 2016) evaluated vegetable cultivation on rice bales as growing media, established on a highly saline sodic soil, using treated drainage wastewater. Following one month of bale composting and three months of cultivation, the yields obtained were comparable to the average concurrent production in Egypt cultivated on fertile soils with irrigation.

The productivity of growing crops in rice straw using some pressurized irrigation system (Bakeer, 2013) showed that vegetables grown in as non-traditional media had a better development than the plants that grown in sandy soil. El-Marzoky examined the impact of

cultivating vegetables in rice straw bales versus natural soil, within an area where specific root diseases affecting peppers have been identified. Their objective was to assess the effect of the cultivation medium on disease infection by root pathogens. They found that plants cultivated in rice straw bales show vigorous vegetative growth, higher total yield, and improved fruit quality compared to those grown in naturally infested soil. Studies show that straw bale cultures may it could keep warm during the cold period, thermally protecting the seedlings when they are small.

Crops can develop directly in the straw structure if they are processed before by decomposition actions. However, research has shown that adding a small amount of compost can improve the development of vegetables, especially if they are planted small (Radziemska et al., 2019). A study conducted to enhance the rice straw media for growing eggplant under modified climatic conditions (Sadek et al., 2014), used compost and microbial inoculation solutions to increase productivity. They found that a combination of rice straw and twenty percent compost, inoculated with both *Azotobacter chroococcum* and *Paenibacillus polymyxa*, resulted in the highest crop yield and profit, compared to all the other tested options. However, high air temperature and a relatively high or low humidity may lead to a significant reduction in crop yield and net returns.

Toxic and saline environments pose challenges for optimal plant growth, necessitating the exploration of alternatives or solutions to mitigate the adverse effects of the primary pollutants (Delfine et al., 2000). A food production system supporting the synergic interaction between aquaculture and horticulture, proposed growing vegetables in straw bales in greenhouses (Nenciu et al., 2022). The results were highly favorable, with the bale production system yielding better results than the degraded soils.

The most common advantages identified in the research studies highlight:

- *improved drainage*, straw bales offering excellent drainage capabilities, preventing waterlogging and fostering healthy root development in vegetable plants;
- *weed suppression* is facilitated by the absence of weeds within the straw, while the dense

structure of the bale further aids in inhibiting weed growth. This reduction in weed competition enhances the availability of nutrients and sunlight for vegetable crops, promoting their growth and development;

- *enhanced aeration* within the plant root zone, facilitating efficient gas exchange and supporting the overall health of plants;

- *natural insulation*, bales acting as a natural insulator, regulating temperature;

- *recycling agricultural waste* used in the multilayered structures and mitigating environmental impact;

- *reduced soil-borne diseases* elevating plants above ground level with straw bales can mitigate the risk of soil-borne diseases and pests;

- *enhanced accessibility and versatility*, since cultures may be established in contaminated sites or on areas with poor or degraded soils, on concrete platforms or in greenhouses.

MATERIALS AND METHODS

An experimental plant growth substrate model was used, designed of a multilayered structure, each layer possessing distinct properties to confer specific advantages. The model was constructed using a straw bale, with three longitudinal cuts measuring 30 cm x 30 cm x 500 cm each, forming channels. The central cutting was filled with compost, while the lateral ones were filled with cotton obtained from shredded cotton textile waste (Figure 1).

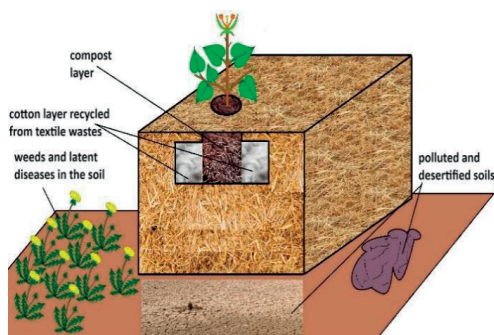


Figure 1. Experimental design for growing vegetables in biodegradable multilayered structures constructed of: straw bales, compost and cotton layer obtained from recycled textile wastes

The traditional methods of planting vegetables in straw bales suffer from a significant

drawback: they require considerable water consumption. The straws within the bales tend to become excessively moist, affecting the insulation benefits during colder periods. Therefore, we conducted tests to reduce the amount of water supplied by incorporating absorbent cotton elements.

While some studies suggest planting vegetables directly into straw, our research has demonstrated that adding a layer of compost can significantly enhance plant growth in these artificial cultivation environments.

The comparative performance assessment of vegetable cultivated in the proposed multilayered substrate versus traditional soil was conducted in an unheated greenhouse from April to August 2022. (Figure 2).



Figure 2. Unheated greenhouse utilized for conducting comparative tests between cultivation on biodegradable multilayered structures and soil under an ecological approach

The greenhouse used for establishing experimental crops is situated within INMA Bucharest Institute, covering an area of 80 square meters. It is equipped with a drip irrigation installation and an automated monitoring system for cultivation parameters.

An ecological growing regime was adopted, where no chemical nutrients or pesticides were added. However, to ensure a fair comparison between the two cultivation methods, an equal amount of compost was added to the seedlings planted on the ground as was introduced into the straw bales.

Three varieties of vegetables were cultivated: tomatoes (*Solanum lycopersicum*, Rila F1 hybrid), long peppers (*Capsicum annuum* L., Kaptur F1 early hybrid), and eggplants (*Solanum melongena*, Kreola F1 hybrid). Planting was conducted on May 15th across all evaluated growing media. The soil was tilled to

a depth of 28-30 cm, and manual weeding was carried out as necessary.

The straw bales were produced by compressing the straw generated from the institute's crops, utilizing the Abbriata M60 square baler. The agricultural waste used for this purpose was generated during the harvesting of crops such as wheat, mustard, and rapeseed (Figure 3).



Figure 3. Straw waste used to produce bales, as the main structure for the multilayer biodegradable structures

The compost was also produced by processing vegetable wastes (leaves, horticultural waste, chopped branches, etc.), for 8 months in compost piles with prismatic shapes. The piles were aerated and mixed using a windrow turner (Figure 4) and were moistened once a week using an irrigation system.



Figure 4. Producing compost from gardening waste, leaves, shredded branches and grass.

To preserve moisture in the straw bales for an extended period and conserve irrigation water, absorbent materials were incorporated at the border between the compost and straws.

Recycled textiles made of cotton were selected to create the absorbent environment for their biodegradability and ability to be composted along with the straws at the end of their lifecycle (Figure 5).

Sensors were installed in both the bales and the soil, activating the irrigation system

independently when low levels of water were detected. Moisture monitoring was carried out with an ATLAS Industrial Monitoring Kit, a MitsubishiFX5U-32MT/DSS PLC, and Arduino soil moisture sensors. The amount of water consumed for the two types of crops was recorded daily, and reported. The objective was to administer a minimal amount of water, in order to reduce consumption (Figure 6).

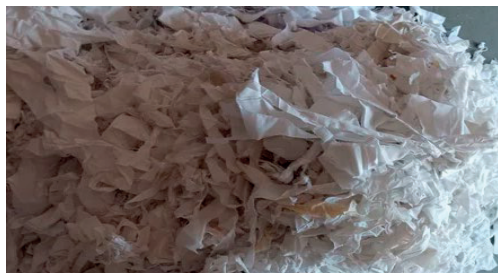


Figure 5. Preparing cotton textile waste for the production of the moisture-retaining layer



Figure 6. Positioning the bales within the greenhouse and establishing the compost and moistening layers

RESULTS AND DISCUSSIONS

The results demonstrated excellent plant performance in the multilayered structures, showing faster seedling growth compared to the soil substrate. That was attributable to the

compost substrate, which had a major effect in the faster growth of plants (Figure 7).

Particularly in the case of tomato development, an enhancement in growth rate was observed, attributed to a combination of factors. The increased height of the plants established on the bales facilitated improved light exposure, while the absence of weeds and diseases in the bales contributed to healthier growth conditions. Additionally, the humidity level was better maintained in the straw bales (Figure 8).



Figure 7. Planting vegetable seedlings in the biodegradable multilayered structures



Figure 8. Caption of a plant growth stage

A reduced water consumption is a primary indicator for the present research, particularly since the experimental design was developed for arid regions with challenging terrain.

Figure 9 illustrates how the bales, equipped with the absorbent cotton layer, successfully maintained a humidity level comparable to that of the soil, but with a more reduced water consumption. Consequently, the cumulative water savings achieved through the implementation of the new technology was recorded at 14.7% per season.

The total amount of recycled textile waste using the technology is 1-1.5 kg per each straw-

bale. Therefore, a greenhouse operating at full capacity (similar to the one employed in the experiment), could potentially recycle up to 144 kg of waste. Consequently, the environmental impact regarding waste reduction could be substantial.

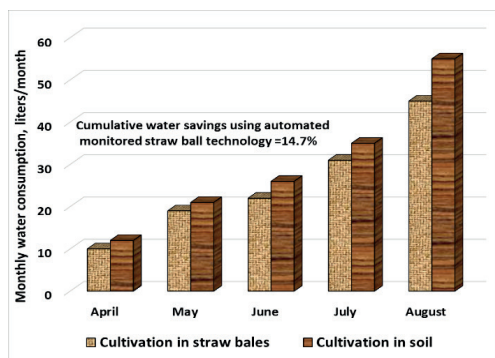


Figure 9. Comparative assessment of water conservation in vegetable cultivation using the evaluated technologies

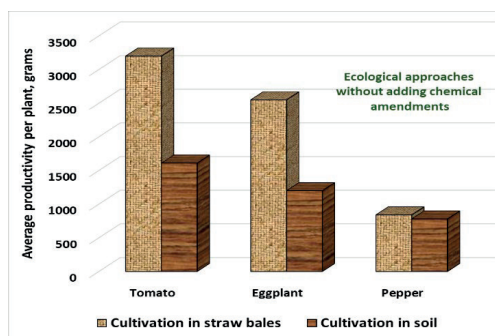


Figure 10. Average productivity under the imposed ecological approach (without chemical amendments)

The temperature inside the straw bale showed an average 0.5-degree higher values than the temperature measured in the soil, during April and May. However, throughout the months June to August, no significant differences were observed. The deviation in findings compared to other research studies can be attributed to the controlled indoor environment (greenhouses). Despite the absence of an active heating source, the greenhouse maintained a high thermal inertia, which led to a stable temperature environment. This stability contrasted with outdoor conditions, where temperature fluctuations are typically more pronounced.

The productivity in both scenarios was relatively low, primarily due to the absence of heating and secondary due to the ecological approach, which avoided chemical interventions. Have been however observed notable differences between the crops planted in soil versus those in straw bales were highlighted (see Figure 10).

CONCLUSIONS

The primary objective, which focused on integrating waste into production activities, was successfully accomplished. The biodegradable multilayered structures, comprised of straw wastes, textile waste, and composted horticultural wastes, demonstrated production of a growth substrate with significant potential. The utilization of biodegradable multilayered structures resulted in a 14.7% reduction in the amount of water required for vegetable cultivation. However, this percentage could potentially increase further with optimization of the shape and dimensions of the moisture-retaining layer.

The straw bales did not bring a significant benefit in maintaining the temperature, but this happened because of the growing environment in the greenhouses. In outdoor space, the variation could be more important.

The productivity was somewhat constrained due to the unheated greenhouse; however, with enhancements to the cultural conditions, higher yields can be achieved.

The experiment succeeded in demonstrating the functionality of biodegradable multilayered structures. Future research includes enhancing the design of these structures and establish more favorable cultivation conditions, to promote vegetable development. Additionally, comparative evaluations with chemically treated crops will be conducted.

ACKNOWLEDGEMENTS

This research was supported by The Romanian Ministry of Research, Innovation and Digitalization, **Project PN 23 04 02 01: Innovative biofertilizer production technology used to restore soil biodiversity and reduce the effects of drought on agricultural lands and MADR ADER 16.1.1 Research on the potential**

for enhanced utilization of the *Cannabis sativa* species for food-related purposes.

REFERENCES

- Abdet-Sattar, M.A., El-Marzoky, H.A. Mohamed, A.I. (2008). Occurrence of Soilborne Diseases and Root Knot Nematodes in Strawberry Plants Grown on Compacted Rice Straw Bales Compared with Naturally Infested Soils. *Journal of Plant Protection Research*, 48(2), 223–235.
- Bakeer, G.A., Hegab, K.K., Attia M.F. (2013). Study of Using Some Pressurized Irrigation Systems for Producing Vegetables on Rice Straw Media. *Misr J. Ag. Eng.*, 30(3), 679 - 700.
- Bal, U., Altintas S. (2008). Effects of *Trichoderma harzianum* on Lettuce in Protected Cultivation. *Journal of Central European Agriculture*, 9(1), 63–70.
- Delfine S., Alvino, A., Villani, M.C., Santarelli, G., Loreto, F., Centritto, M. (2000). Agronomic and physiological aspects of salinity stress on a fieldgrown tomato crop. *Acta Horticulturae*, 537(2), 647-654.
- El-Aidy, F. (1993). Preliminary Results on the Possibility of Using Straw as Natural Substrate for Growing Cucumber under Plastic Greenhouses. *Acta Horticulturae*, 323, 423–427.
- El-Marzoky, H.A., Abdel-Sattar M.A. (2008). Influence of Growing Sweet Pepper in Compacted Rice Straw Bales Compared with Natural Soil, on Infection with Pathogenic Fungi and Nematodes Under Greenhouse Conditions. *Arab Univ. J. Agric. Sci., Ain Shams Univ.*, 16(2), 481-492.
- Farag, A.A., Ahmed, M.S.M., Hashem, F.A., Abdrabbo, M.A.A., Abul-Soud M.A. Radwan H.A. (2015). Utilization of Rice Straw and Vermicompost in vegetable Production Via Soilless Culture, 2(5), 800-813.
- Gluntsov, N.M., Dmitrieva, L.V., Kuts, M.G., Baikova, S.N. (1997). The effect of fertilizers on the yield of cucumbers grown on straw bales, *Trudy Tsentral'nogo Instituta Agrokhim. Obsluzh. S.Kh.*, 3, 54-57.
- Karsten, J. (2015). Straw Bale Gardens Complete: Breakthrough Vegetable Gardening Method. *Quarto Publishing Group USA*, Minneapolis, ISBN 978-1-59186-907-8.
- Nenciu, F., Voicea, I., Cocarta, D.M., Vladut, V.N., Matache, M.G., Arsenoaia, V.-N. (2022). Zero-Waste Food Production System Supporting the Synergic Interaction between Aquaculture and Horticulture. *Sustainability*, 14(20), 13396. <https://doi.org/10.3390/su142013396>.
- Oprescu, M.R., Biris, S.-S., Nenciu, F. (2023). Novel Furrow Diking Equipment-Design Aimed at Increasing Water Consumption Efficiency in Vineyards. *Sustainability*, 15(4), 2861. <https://doi.org/10.3390/su15042861>
- Radziemska, M., Vaverková, M.D., Adamcová, D., Brtnický, M., Mazur, Z. (2019). Valorisation of Fish Waste Compost as a Fertilizer for Agricultural Use. *Waste Biomass Valor*, 10, 2537–2545. <https://doi.org/10.1007/s12649-018-0288-8>
- Riad, G.S., Ghoname, A.A., Hegazi, A.M., Fawzy, Z.F., El-Nemr, M.A. (2017). Cultivation in Rice Straw and Other Natural Treatments as an Eco-Friendly Methyl Bromide Alternative in Head Lettuce Production. *Gesunde Pflanzen* DOI: 10.1007/s10343-017-0381-0.
- Rishead A.A. (2016). Vegetable Production on Rice Bales Using Brackish Treated Drainage Water. *Irrigation and Drainage Wiley Online Library*, 65(5), 664-672. <https://doi.org/10.1002/ird.1994>.
- Sadek I.I., Moursy F.S., Salem E.A., Schüch A.M., Heggi A.M. (2014). Enhancing rice straw media for growing eggplant under modified climatic conditions using compost and bacterial inoculation. *Nature and Science*, 12(4), 8-20.
- Vatchev, T., Maneva. S. (2012). Chemical Control of Root Rot Complex and Stem Rot of Greenhouse Cucumber in Straw-Bale Culture. *Crop Protection*, 42, 16–23.

DETERMINING GREENHOUSE GAS EMISSIONS RESULTING FROM ENERGY AND WATER CONSUMPTION FOR THE DECARBONIZATION OF CORN PRODUCTION AND DEVELOPING STRATEGIES TO REDUCE THE CARBON FOOTPRINT

Hasan Hüseyin ÖZTÜRK¹, Bülent AYHAN², Serdar AYGÜN³,
Ali GÜL⁴, Serkan KARABAĞLI⁴

¹University of Cukurova, Faculty of Agriculture, Sarıcam, Adana, Türkiye

²Ministry of Agriculture and Forestry, Adana Agricultural Production and Agricultural Extension and Training Center, Adana, Türkiye

³General Directorate of Meteorology, Keçiören, Ankara, Türkiye

⁴Ministry of Agriculture and Forestry, Department of Education and Publications, Ankara, Türkiye

Corresponding author email: hhozturk@cu.edu.tr

Abstract

This study aimed to determine greenhouse gas emissions (GHG) resulting from energy and water consumption in corn production and to define carbon footprint (CFP) indicators. As fuel consumption for corn production processes, diesel fuel and engine oil consumed by the tractor engine were taken into account. In the calculations made to determine carbon dioxide (CO₂) emissions resulting from fuel use, the fuel-based CO₂ emission calculation method recommended by the Intergovernmental Panel on Climate Change (IPCC) have been followed. The individual determination of carbon dioxide (CO₂), methane (CH₄) and nitrous oxide (N₂O) emissions related to fuel consumption and their conversion into CO₂ equivalent emissions are explained. The environmental sustainability effectiveness of corn production was evaluated as the carbon footprint (CFP) of energy and water consumption. Carbon footprint indicators for energy and water consumption have been defined.

Key words: carbon footprint, fuel, greenhouse gas emissions.

INTRODUCTION

For sustainable agricultural production, it is necessary to use energy more effectively in agricultural production processes and reduce the use of fossil fuels. For this reason, sustainable production systems that consume less fossil energy, are efficient, and will reduce greenhouse gas emissions (GHGs) should be developed. In order to combat climate change, efforts are being made to control and reduce the increase in GHGs that cause global warming. For this reason, it becomes important to analyze GHGs in agricultural production.

In today's world, the constant increase in the prices of energy resources due to the decrease in energy resources based on fossil fuels and their negative effects on the environment, and the decrease and pollution of water resources are important global problems. Therefore, it is necessary to ensure the sustainability of agricultural practices in order to use energy and water resources efficiently and to reduce the

effects of all inputs used in agricultural production on global climate change. In a global context, the proposed research will contribute to the efficient use of energy and water resources by end users/consumers and to reduce the input costs using these resources.

The agricultural sector is in a position to meet people's nutrition and shelter needs, provide raw materials to industry and therefore have a positive impact on the country's economic development process. Agricultural ecosystems are negatively affected by climate change. This situation causes serious environmental, social and economic impacts. However, in one aspect, the agricultural sector triggers climate change with greenhouse gas emissions (EEA, 2023). In other words, the agricultural sector is in a position to both be affected by and trigger climate change. Harmful substances in exhaust emissions are released into the atmosphere and pollute the environment due to reasons such as the use of fuel and engine oil in agricultural production, not choosing agricultural tools and

machines with power and design suitable for production processes, and overloading of engines. In addition, as the food demand of the ever-increasing population is met by increased agricultural production, it also leads to an increase in GHG emissions.

Reducing the carbon footprint (CFP) is one of the key goals to be achieved in order to limit the overall environmental impact of agriculture. Another important goal is to reduce the use of crop preservative chemicals, which have the negative impact of disrupting essential food webs in and around fields. The agricultural sector contributes significantly to global carbon emissions from a variety of sources, including product and tool and machinery manufacturing, material transportation, and direct and indirect GHG emissions from soil. The agricultural sector is a sector that contributes significantly to global carbon emissions through the production and use of agricultural machinery, crop protection chemicals (pesticides) and fertilizers. The CFP, the total amount of GHG emissions associated with a product throughout the supply chain. Often times, a carbon footprint refers to the amount of GHG something creates, specifically the amount of carbon dioxide (CO₂), methane and nitrous oxide. CO₂ emissions from fertilizer, electricity, machinery, chemicals and fuel production processes are considered to calculate the total carbon footprint. When calculating the CFP, direct and indirect carbon emissions related to the inputs used in agricultural production processes are considered.

There are many methods and practices to reduce the CFP in agriculture. To calculate the total CFP, carbon dioxide This study aimed to determine GHGs emissions resulting from energy and water consumption in corn production and to define some indicators for the CFP. As fuel consumption for corn production processes, diesel fuel and engine oil consumed by the tractor engine were considered.

Justification for the Decarbonisation

The greenhouse gases (GHG) emissions cause climate change. Projected scenarios of the impact of climate change are less water and higher temperatures. These effects mean that more efficient use of water for pasture and livestock farming and radical changes in livestock practices must promote water

conservation and heat tolerance. Adaptation strategies should encourage conservation and efficient consumption of feed. Climate change will also encourage the proliferation of pests and diseases, thereby reducing livestock productivity. As natural ecosystems respond to changing temperatures and precipitation, the ranges of many organisms are expected to expand or change, and new pest and disease combinations are expected to emerge. An increase in the frequency or severity of extreme weather events, such as droughts, heat waves, storms or floods, can also disrupt predator-prey relationships that normally keep pest populations in check. Carbon dioxide (CO₂) concentration has approached more than 50% of the pre-industrial level. Although the CO₂ concentration was 280 ppm in the 1760s, it is now around 410 ppm and is expected to reach 590 ppm by the end of 2100 (Öztürk, 2024a).

The efficiency and profitability of agricultural production depends on energy consumption. Today, agricultural production technologies are developing rapidly and aiming for higher profitability. However, despite all efforts, exhaust emissions from fuel and engine oil consumption of tractors and other agricultural machinery still exceed permissible limits. Inappropriate operating regimes due to improper selection of agricultural tools and machines for the production processes and overloading of engines have negative effects on the environment. In such cases, harmful substances, petroleum products and smoke in exhaust emissions are released into the atmosphere. These emissions cause significant damage to natural environmental ecosystems.

Contribution of Agricultural Production to GHG Emissions

Agriculture has a special importance in terms of climate change. The relationship between agriculture and climate change is bidirectional. Agriculture is a major emitter of greenhouse gases. Research on this subject show that agricultural production is responsible for approximately 16-27% of all anthropogenic emissions. Global emissions from agricultural production are around 21-25% (Öztürk, 2024a). Agricultural emissions are an important component of *food supply chain* emissions.

Direct and indirect fossil fuel consumption causes various greenhouse gas emissions, especially CO₂, N₂O and CH₄. Greenhouse gases from agriculture and other human activities warm the Earth's surface by absorbing atmospheric infrared radiation and heat energy. This warming effect caused the global temperature on earth to increase in the 20th century. Burning fossil fuels causes more than 75% of GHG emissions from human activities. Today, agricultural production is largely based on the consumption of fossil fuels. Fossil energy consumption causes direct negative effects on the environment through the release of CO₂ and other GHGs. In agricultural production, sustainable agricultural product production by reducing the use of fossil energy is very important. Sustainable agricultural production can be achieved by using energy more efficiently in agricultural production processes and reducing the use of fossil fuels. In order to develop sustainable production systems that require less fossil energy and at the same time provide satisfactory efficiency and reduce greenhouse gas emissions, fossil energy must be used efficiently in agricultural systems.

The energy sector makes the largest contribution to global CO₂-eq. emissions. In the energy sector, two-thirds of total CO₂-eq. emissions are caused by the burning of fossil fuels for power generation. While the global total annual CO₂-eq. of food systems for the period 2007-2016 are estimated to be between 21-37%, it is estimated that 21% of the CO₂-eq. emissions in the same period originate only from agricultural production. Industrial processes are responsible for 8% of total GHG emissions (Öztürk, 2024a). The contribution of agricultural production to GHG emissions is gradually decreasing. The contribution of agricultural production to GHG emissions averaged 29% in the 1990s (1990-1999). This contribution was 25% in the 2000s (2000-2009) and 20% in recent years (2010-2017) (Öztürk, 2024a).

CO₂ emissions are a byproduct of the production processes of energy resources such as machinery, fertilizers, electricity and chemicals. Using diesel fuel on the farm also emits large amounts of gas. Average total emissions in wheat and paddy production are reported as 900.9 kg CO₂/ha and 1762.5 kg CO₂/ha, respectively. Diesel fuel use is the highest

emission source in paddy production, accounting for 55.34% of total CO₂ emissions. On the other hand, it is reported that the highest source of CO₂ emissions in wheat production is fertilizer with 49.7% of total emissions (Ashraf et al., 2021).

Emissions from crop and animal production activities continued to increase over the entire period of 2000-2018. These emissions were 14% higher in 2018 compared to 2000. Emissions related to agriculture and land use decreased from 24% to 17% of global GHG emissions from all sectors in 2018. Agricultural activities for crop and animal production emit significant amounts of non-CO₂ emissions such as the potent GHGs CH₄ and N₂O. Agricultural production accounted for 42% of total CH₄ emissions and 75% of N₂O emissions in 2017. CH₄ and N₂O emissions totalled 5.3 GtCO₂-eq. in 2018. Two-thirds of this total comes from animal production. In particular, CH₄ emissions from enteric fermentation in the digestive systems of ruminant animals remained the largest and only component of agricultural emissions (2.1 GtCO₂-eq.) in 2018 (Öztürk, 2024a).

It is estimated that the agricultural sector directly emitted 629 MtCO₂-eq. in 2019. CO₂ accounts for only 1% of GHG emissions directly related to agriculture. N₂O and CH₄ are the main greenhouse gases released from agricultural activities. Agricultural activities originate approximately 60% of the nitrogen dioxide released into the atmosphere and approximately 50% of the methane. Total N₂O emissions from agriculture amount to 364 MtCO₂-eq. This value accounts for 58% of the total agricultural CO₂-eq. in 2019. 28% of the CO₂-eq. released in the agricultural sector in 2019 resulted from the release of CH₄ released from enteric fermentation. 10% of CO₂-eq. in the form of CH₄ comes from manure management (Öztürk, 2024a).

In plant and animal production, the relative contribution of each process to GHG emissions has not changed significantly over the past two decades. N₂O emissions from chemical fertilizers and plant residues had a proportional increase of more than 35% in 2018. These emission values are in line with the increase in crop production globally and the increase in the use of chemical fertilizers worldwide. The

increase in the number of animals increased the increase in emissions from manure and enteric fermentation. These increase rates were 20% and 13%, respectively, in 2018 compared to 2000. Finally, emissions from paddy cultivation, fertilizer management systems and organic soils increased by about 7% in the period 2000–2018 (Öztürk, 2024b).

Energy Consumption in Agriculture

Water, energy and food production are inextricably linked. The agricultural sector uses 11% of the world's land surface, and irrigated farming practices use 70% of the global water resources (Öztürk, 2023a). Drought and reduced agricultural irrigation generally limit production in irrigated areas. As many important food production systems depend on groundwater, poor aquifer levels and groundwater depletion put local and global food production at risk. Increasing food production alone is not enough to ensure food security and eradicate hunger. Efforts to promote food production should be complemented by policies that increase household access to food, either by creating jobs or establishing effective programs.

Approximately 30% of the total water consumption in Europe takes place in the agricultural sector. However, the amount of water consumed in agricultural production in many southern countries of Europe reaches 70% of the total water consumption in these countries. In recent years, regardless of the energy aspect, significant water savings have been achieved and there have been significant increases in energy consumption. In countries such as Spain, the amount of electricity consumed in agricultural irrigation reaches up to 3% of the total national electricity consumption (Öztürk, 2023a).

Essential Measures to Reduce the Impact of the Agricultural Sector on Climate Change in Turkey

Significant progress is being made in reducing greenhouse gas emissions and combating climate change in Turkey. When the policies put forward for various purposes such as the protection of natural resources, sustainable development and protection of the environment, the legal situation, the institutional structure, the projects being implemented and the resources

allocated are examined, it is seen that there is a potential that cannot be underestimated. Steps can be taken by reviewing the current structure regarding climate change and making new regulations.

Measures for the Short Term

The problems that need to be solved in the short term can be summarized as follows:

A unit operating in the monitoring and evaluation of climate change and greenhouse gas emissions should be established within the Ministry of Agriculture and Forestry. This unit should undertake important duties such as determining and collecting data on the subject, creating databases, making and publishing calculations, and coordinating Ministry units. These tasks should be:

- Making and recording phenological (temporal monitoring of vital stages of plants such as germination, tillering, flowering) observations throughout Turkey.
- Monitoring land use changes, especially changes that would be detrimental to agricultural and pasture lands.
- Monitoring the carbon content of soils.
- Ensuring the establishment of the Drought Monitoring System and Drought Early Warning and Management System provided in the Drought Action Plan and operating the system together with climate change policies.
- Determining the sources of greenhouse gas emissions resulting from plant and animal breeding activities and continuing activities to raise awareness in the society.
- Ensuring that R&D activities related to the subject are announced to the relevant units and the public.
- Continuing to work on fulfilling international obligations.
- Establishing geographic information systems-databases where all data are compiled, processing and evaluating the information.
- Carrying out monitoring and evaluation of environmental data related to the sector.
- Keeping inventories regarding agricultural infrastructure projects and determining their effects in the fight against climate change.
- Establishing policies and creating legal regulations (Legal requirement, regulation, instruction).

Measures for the Medium Term

➤ There is no information collection, recording, reporting and monitoring systems in accordance with the Kyoto Protocol and the UN Framework Convention and emission information originating from the agricultural sector.

- There are no emission calculations in the crop production and aviation sectors, which are among the sectors that cause the highest greenhouse gas emissions.
- There are no records and statistics regarding fuel usage preferences and fuel preferences used for crop and animal production.

➤ Incentive policies and practices to expand the use of alternative fuels and environmentally friendly vehicles are insufficient.

- The tax exemption provided to biodiesel for agricultural vehicles is insufficient.
- The recording and monitoring system is insufficient for the policy of increasing the use of biofuels.

➤ Nationally Appropriate Mitigation Action NAMA as a financing source, carbon market and emission trading related activities are few and there is no implementation practice.

➤ There is no mechanism to examine/monitor the contribution of all kinds of investments, whether budget resources, foreign loans or public-private partnerships, to the strategy of preventing climate change and reducing greenhouse gases.

➤ There is a lack of knowledge, awareness of decision makers, experts and planners, as well as all users and the public, on sustainable and environmentally friendly transportation issues.

➤ There is a lack of legal regulation regarding the limitation of CO₂ emissions in all types of motor vehicles used in the agricultural sector.

➤ Studies on creating carbon markets and gaining a share from this market are insufficient.

Measures Precautions for the Long Term

➤ In terms of supporting biofuels, there are no policies for growing products suitable for primary biofuels on vacant lands other than agricultural purposes.

➤ There are no policies regarding the production of biofuel in agricultural areas.

➤ There is a lack of legal regulation in the agricultural sector that clearly sets out emission reduction targets and comprehensively determines the measures.

➤ The current Agricultural Research Stations affiliated with the Ministry do not provide research, development and problems related to local problems such as climate change and greenhouse gas emissions to farmers.

- A certain percentage of farmer supports should be allocated for research studies.
- Areas that are out of use, such as natural meadows, should be used for the cultivation of oil plants such as *jajoba*.
- There are no studies on reforestation of unused areas such as stream banks in agricultural areas. There are no efforts to plant lands that are used for agricultural purposes but are below the economic value threshold with pasture or oil crops such as olives.
- Large *maquis* areas should be reclaimed to increase their sink capacity, and suitable areas should be used for the cultivation of oil plants such as olives, considering biological diversity.
- Studies on the completion of carbon markets and trade are lacking.

MATERIALS AND METHODS

Tillage and Irrigation Methods

Soil tillage and irrigation methods to be applied for second crop corn production are given in Table 1. Experiments will be set up according to the randomized block trial design with two replications. Corn seeds will be planted with a planter at a depth of 4-5 cm in the seed bed prepared with row spacing of 70 cm, row length of 5 m and row width of 20 cm.

The main components that passively save energy in a solar powered drip irrigation system are the energy-saving electric motor due to the low-pressure requirement, high-efficiency photovoltaic (PV) modules and the drip irrigation system. High efficiency electric motors and variable speed irrigation pumps will be used in this research. The electricity required for electric motors will be met from solar radiation with micro inverter PV modules. In this system, the use of energy-saving equipment

and installations within the scope of the passive method will provide energy savings of 10-15%.

Table 1. Soil tillage and irrigation methods for second crop corn production

Methods	Soil Tillage	Irrigation
Traditional method	Tillage once with a rotavator at a depth of 20 cm Tillage once with a cultivator at a depth of 10 cm Pulling a worshiper 2 times	Flood irrigation
Water and energy saving method 1	Tillage once with a combination of rotavator and disc harrow Pulling a worshiper 2 times	Solar powered drip irrigation
Water and energy saving method 2	Tillage once with a disc harrow at a depth of 20 cm Tillage once with a spring harrow Pulling a worshiper 2 times	Solar powered drip irrigation

Calculation of CO₂, CH₄ and N₂O Emission related to Fuel Consumption

CO₂ emissions (kg CO₂/ha) related to diesel fuel and engine oil consumption per unit production area (ha) by the tractor used during corn production operations will be determined as follows:

$$CO_2 = FC \times LHV \times EF_{CO_2} \quad (1)$$

where:

- CO₂ is CO₂ emissions related to fuel consumption (kg CO₂/ha),
 - FC- fuel consumption (L/ha),
 - LHV is lower heating value of diesel (37.1 MJ/L) and engine oil (38.2 MJ/L),
 - EF_{CO₂} is CO₂ emission factor for diesel and engine oil (0.07401 kg CO₂/MJ).
- Methane (CH₄) emissions in corn production will be calculated as follows:

$$CH_4 = (SEV \times EF_{CH_4}) \quad (2)$$

where:

- SEV is the specific energy value of diesel fuel consumed per unit grain product (MJ/kg),
- EF_{CH₄} is CH₄ emission factor for diesel fuel (0.0000039 kg CH₄/MJ).

Nitrous oxide (N₂O) emissions in corn production will be calculated as follows:

$$N_2O = (SEV \times EF_{N_2O}) \quad (3)$$

where:

- EF_{N₂O} is N₂O emission factor for diesel fuel (0.0000039 kg N₂O/MJ).

CO₂ Equivalent Emissions related to Fuel Energy and Water Consumption

The total CO₂-equivalent emissions (CO₂-eq) as a result of diesel fuel consumption in corn

production will be determined by multiplying the CO₂, CH₄ and N₂O emission amounts with the global warming potentials (GWP) for these emissions for the 100-year period as follows:

$$CO_2\text{-eq}_{energy} = (CO_2 \times 1) + (CH_4 \times 28) + (N_2O \times 265) \quad (4)$$

The total CO₂-eq emissions resulting from water consumption in corn production will be determined as follows:

$$CO_2\text{-eq}_{water} = (WC \times EF_{CO_2\text{-eq}}) \quad (5)$$

where:

- WC is the amount of water consumed per unit grain product (L/kg),
- EF_{CO₂-eq} is CO₂-eq emission factor per unit (L) of water consumption (0.000344 kg CO₂-eq/L) (DEFRA, 2022).

Determination of Carbon Footprint related to Energy and Water Consumption

The carbon footprint related to energy consumption (CFP_{Energy}) can be defined as follows

$$CFP_{energy} = \frac{CO_2\text{-eq}_{energy}}{M_{corn}} \quad (6)$$

where:

- CFP_{Energy} is the carbon footprint (kg CO₂-eq/kg_{com}) related to dfuel energy (electricity+Diesel) consumption,
- M_{corn} is mass of grain corn (kg).

Similarly, the carbon footprint related to water consumption (CFP_{water}) can be defined as follows:

$$CFP_{water} = \frac{CO_2\text{-eq}_{water}}{M_{corn}} \quad (7)$$

CONCLUSIONS

Global warming and the resulting climate change problem is a very important environmental problem that covers the whole world and affects all countries. Today, developed or developing countries give priority to using renewable energy sources and implementing energy saving in all production sectors.

In this study, it was aimed to determine the GHGs emissions resulting from energy and water consumption for the decarbonization of second crop grain corn production in Adana province and to develop strategies to reduce the

carbon footprint. The unique value of this research is that in the production of the second product, the details of which are given in the method section, a total of three different applications will be carried out, including the traditional method and two different applications that save energy and water.

Sustainability is defined as the preservation and management of the foundations of institutional changes, technological trends and resources with the aim of continuously meeting and satisfying human needs in present and future generations. In achieving ultimate success in a project, it is important that the results of the project are sustainable. The project is designed to strengthen capacity in evaluating energy consumption in corn production. The main driving force (tool) here is to develop a strategy for studies on technological issues.

A decision support system is needed in order to realize variable rate practices in crop production management. In addition, sensing, monitoring, control and data transfer systems are technologies required for precision agriculture applications.

Variable rate irrigation is to be integrated into irrigation processes at all stages of the agricultural production cycle, using different variables such as soil moisture, effective precipitation and crop evapotranspiration to determine the optimum amount of water and ensure accurate irrigation with climate, weather forecasts and real-time weather data.

The GHGs emissions resulting from energy consumption can be reduced through the development of alternative energy projects such as solar and wind energy, which are renewable sources.

Economic supports paid by the government for the agricultural sector are an important resource that can be used to reduce GHG emissions. Agricultural insurance supports are important for protecting producers in the fight against climate change. However, it is not a tool that can be used directly to reduce greenhouse gas emissions. Organic production support is an important support that can be used to reduce greenhouse gas emissions. It is important not to use chemical fertilizers and chemical pesticides in organic cultivation. In addition, agricultural basin support is one of the most important supports that can be used in greenhouse gas

reductions. Because, with this policy, the right product will be produced in the right quantities in the right basins. In this way, less chemicals will be used, and natural resources will be protected. In general, a resource can be created by supporting good agricultural practices and environmentally friendly production and branding these products.

In order to continue such studies, it should be aimed to minimize the use of smart irrigation systems with sustainable water use in today's world, where the increasing effects of global climate change are experienced globally and the negative effects of drought in the agriculture and food value chain have reached serious levels. In order to increase productivity in agriculture and create a positive impact on the food value chain, protecting and improving plant and soil health should be the main priorities of future studies. Collaboration should be ensured between universities, private sector and government institutions, and joint work should be carried out on research and development projects on relevant technologies.

ACKNOWLEDGEMENTS

This project is supported by Cukurova University Scientific Research Projects Unit with the protocol of FBA-2023-16357.

REFERENCES

- Ashraf, M.N., Mahmood, M.H., Sultan, M., Shamshiri, R.R., Ibrahim, S.M. (2021). Investigation of Energy Consumption and Associated CO₂ Emissions for Wheat-Rice Crop Rotation Farming. *Energies*, 14, 5094. <https://doi.org/10.3390/en14165094>.
- DEFRA (2022). Department for Environment Food & Rural Affairs of UK. Greenhouse gas reporting: Conversion factors 2022.
- EEA (2023). Reduction of greenhouse gas emissions. European Environment Agency. <https://www.eea.europa.eu/tr/themes/climate/intro>
- IPCC (1996). Intergovernmental Panel on Climate Change. Calculating CO₂ Emissions from Mobile Sources Guidance to calculation worksheets. (03/21/05) v1.3. <https://www.ipcc-nggip.iges.or.jp/public/gl/invs1.html>.
- Öztürk, H.H. (2023a). *Energy saving and energy efficiency in agricultural production*. Birsen Publishing House, (In Turkish), pp. 523, ISBN 978-975-511-742-3, Istanbul.
- Öztürk, H.H. (2023b). *Use of technology in agricultural production*. Birsen Publishing House, (In Turkish), pp. 358, ISBN 978-975-511-743-0, Istanbul.

Öztürk, H.H. (2024a). *Greenhouse gas emissions and carbon footprint management in agricultural production*. Academician Publishing House, (In Turkish), pp. 588, ISBN 978-625-399-581-2, Ankara.

Öztürk, H.H. (2024b). *Sustainable agricultural production*. Academician Publishing House, (In Turkish), pp. 506, ISBN 978-625-399-588-1, Ankara.

SUPERIOR CAPITALIZATION OF VEGETABLE WASTE AND NATURAL AGRO-INDUSTRIAL BY-PRODUCTS BY CREATING INNOVATIVE PRODUCTS FOR CONSTRUCTION. SOCIO-ECONOMIC PREDICTIVE ANALYSES

Irina POPA, Vasilica VASILE, Silviu LAMBRACHE

National Institute for Research and Development in Construction,
Urban Planning and Sustainable Spatial Development - URBAN-INCERC,
266 Pantelimon Road, District 2, Bucharest, Romania

Corresponding author email: irinapopa2006@yahoo.com

Abstract

To ensure environmental preservation, it is increasingly necessary to capitalize on waste, both from agriculture and related industries. There is currently research at the worldwide level on the capitalizing of vegetable waste and natural agro-industrial by-products in the field of construction, to obtain innovative materials, which can replace traditional materials. The capitalization of waste ensures not only the reduction of the impact on the environment due to their recovery but also the possibility of cost efficiency compared to the use of traditional materials. Waste recovery is a priority component of sustainable development, aiming to create the conditions for ensuring the well-being of countries and their citizens and implementing global measures to manage natural resources. In this context, our studies focused on determining the economic efficiency of innovative materials, obtained by capitalization of some types of vegetal waste, being necessary to perform a comparative cost analysis. The acquisition costs related to innovative, environmentally friendly materials and those traditionally used in construction were considered, as well as the costs during their use, respectively the maintenance and repair costs.

Key words: agro-industrial by-products, predictive analyses, sustainable development, waste capitalization.

INTRODUCTION

The construction industry, one of the largest consumers of raw materials and energy worldwide and one of the significant sources of global greenhouse gas emissions and waste generation, has led to an increase in demand for new sustainable and environmentally friendly construction solutions. As a result, there is an increasing interest in exploring alternative materials and methods, aiming for the sustainable development of the built environment, while maintaining its structural integrity and functionality, under the conditions of reducing the ecological footprint specific to the field. Also, the negative impact on the environment is recognized because of the improper disposal of waste and even of the agro-industrial by-products.

These aspects end up representing a risk to the ecosystem and human health, causing air and water pollution, soil degradation, loss of biodiversity, and finally the irrational use of resources, given the fact that the respective

materials often contain nutrients and valuable materials that could be reused or recycled. Thus, in general, the improper disposal of waste and agro-industrial by-products has become a waste of resources and a missed opportunity to use them for alternative, value-generating purposes, such as energy production or the creation of new, sustainable construction materials/products (Bakatovich et al., 2018; Binici et al., 2020; Cintura et al., 2021; Fuentes et al., 2021; Yaashikaa et al., 2022).

In this approach, vegetable waste and natural agro-industrial by-products (Popa et al., 2023) represent a notable category in terms of the benefits resulting from their superior valorization. Natural materials like straw, cereal husks, hemp, and low-quality sheep wool are often underutilized waste products from agricultural and industrial processes. By harnessing the potential of these materials for sustainable construction applications it is possible to avoid sending waste to landfills, reduce emissions associated with traditional construction materials and thus contributing to

the development of the circular economy (Cintura et al., 2021).

Current research trends in the field of sustainable construction emphasize the use of natural materials in the development of environmentally friendly construction products. These types of materials offer numerous advantages, including low environmental impact, low energy demand, cost-effectiveness, large-scale availability, biodegradability, low density, and good thermal insulating and mechanical properties (Faruk et al., 2012; Berardi & Iannace, 2015; Sanjay et al., 2018; Nguyen et al., 2020; Popa et al., 2020).

The agricultural and industrial sectors generate large amounts of biodegradable waste which, in the absence of an effective management and without reducing waste production (Bonciu et al., 2021), if not properly collected and utilized, can cause significant damage to the environment and the health of the population. Although currently a way of recycling waste from the two sectors is represented by using it as organic fertilizers, in the short and medium term, the main option for managing biodegradable waste will be the storage, the objective being to promote ways of higher recovery, for example in the construction sector (Şalaru et al., 2013).

Considering the fact that the prevention of waste formation as well as the negative effects caused to the environment and health is much more effective than removing the consequences after they have occurred, by ensuring alignment with European practices of avoiding as much as possible final disposal solutions through storage or incineration, in the long term, the general objective is to find new ways of superior valorizing agro-industrial waste and to replace the permanent storage with a temporary one (Şalaru et al., 2013).

The recycling of agricultural waste can be viewed in terms of three large categories of benefits: social, economic and ecological (Yazid et al., 2020).

The socio-economic (Nath, 2022) and environmental benefits (Omer, 2010) generated by the superior valorization of vegetable waste and natural agro-industrial by-products are multiple:

- The most important benefit is represented by the reduction of the quantity in which these

materials are generated and/or stored. When they are used, they are considered and thus transformed into raw materials for local industries, also raising the degree of local employment (Omer, 2010). By reintegrating them into the economic circuit, a reduction in the consumption of traditional raw materials is achieved, which leads to the conservation of natural resources necessary for production processes, resources obtained by using large amounts of energy. Therefore, recycling reduces energy consumption (Lamma, 2021) and negative effects that occur on the environment integrity (Omer, 2010) and society strong health (Lamma, 2021).

- Waste recycling decreases the need for new raw materials, saving a significant amount of energy in this way. By recycling waste, the energy-consuming industrial activities (Bonciu et al., 2021), the emission of greenhouse gases are mitigated, thus contributing to the reduction of global warming (Lamma, 2021);

- As an essential part of the circular economy, waste recycling leads to the promotion of new industrial processes and ecological products (Nath, 2022), determining the development of new companies, implicitly increasing and diversifying employment opportunities.

- Waste recycling aims to reduce the need for waste deposits and directly lower their volume (Mubaslat, 2021), with beneficial effects on the environmental costs (Halcos & Petrou, 2016) and the health of the population. As a result, on the one hand, it ensures the reduction of costs associated with the uncontrolled disposal of waste (Halcos & Petrou, 2016) and on the other hand, an increased availability of free land is obtained, land that can be used for economic purposes with benefits at the level of entire society (Mubaslat, 2021).

From an ecological and social point of view, an important benefit of recycling is represented by the reduction of the amount of waste sent for incineration, a process that affects the quality of the surrounding air. Referring to the use of vegetable waste and natural agro-industrial by-products by integrating them into different materials/innovative products for constructions, it is becoming increasingly recognized that this approach brings substantial benefits resulting from the specific properties of each natural material.

Agricultural activities generate substantial amounts of valuable waste/by-products, from various sectors:

- The crop sector - such as straw, husks, different types of fibers, substrates in the case of mushroom farms, etc.;
- The livestock sector - such as manure and low-quality wool;
- The agro-industrial processes - such as sunflower seed husks from the edible oil industry, rice husks (RH) from the food industry, etc.

Thus, for example, the use of agro-industrial waste such as rice husks can lead to obtaining new construction materials with good thermal insulation capacity, low moisture content and high thermal power.

The socio-economic benefits of using rice husks are obtained by integrating this material into concrete products, as well as by generating additional income from the sale of rice husk ash and its use as fuel in thermoelectric plants (Nwofoke & Udu, 2019). Also, agro-industrial waste from rice husks can be used in the production of building materials for partitions, such as bricks, ecological products with phonothermal insulating properties, low weight, low transport costs due to reduced weight of products etc. (Chukwudebelu et al., 2015).

In another example, it is shown that ecological building materials, obtained by integrating vegetable waste generated by industrial hemp crops, offer more benefits than traditional materials: durability and light weight, fire resistance, impermeability, moisture, strength, self-insulation, pest resistance and low production costs.

In addition, building materials obtained from hemp (Crini et al., 2020) can capture carbon dioxide, leading to the reduction of carbon emissions (Mausum, 2022), being ideal for protecting the environment.

The increase in the production and consumption of bio-waste worldwide represents a significant challenge for waste management and resource use. In general, but especially for the field of construction materials/products, this challenge also offers an opportunity to transform vegetable waste and natural agro-industrial by-products into valuable resources to produce natural composites.

MATERIALS AND METHODS

The previously specified socio-economic and ecological benefits from a theoretical point of view, regarding the valorization of natural waste and natural agro-industrial by-products in construction, as well as the analysis and quantification of the economic benefits of the valorization of hemp and rice husk waste are presented below.

Determining the economic efficiency of the innovative products, obtained by capitalizing on some types of vegetable waste, requires a comparative analysis of costs. Cost analyses related to construction materials must be carried out in the initial phases of product development so that, during the design of the material, certain changes can be made to obtain an optimal cost.

Starting from the existing regulations in the field of cost estimation for construction works (GD no.907/2016; P91/1-02), after assimilating them from a methodological point of view for determining the economic efficiency of an innovative construction product, the cost estimate for its production can be determined by going through the following stages:

- Estimation of the necessary resources (materials, labor, machinery, transport) for the creation of innovative eco-sustainable products;
- Determination of specific consumption for each considered resource;
- Collection of unit prices at the level of component resources;
- Estimating the cost of the innovative product by aggregating the costs based on multiplying the unit prices with the specific consumptions;
- Carrying out a comparative cost analysis between the innovative product and the traditional product.

Similarly, by extrapolating the Life Cycle Cost (LCC) methodology for estimating the costs during the lifetime of constructions (COSTCONS), it was considered that the cost efficiency of the ecological product can also be quantified through the life cycle cost analysis of the resulting product, to determine its feasibility.

The analysis involved the treatment of cost aspects considering the whole lifetime of the innovative product, the results being

determined mainly by the properties of the component materials considered, the durability of the resulting product and the related costs for manufacturing/repairs/replacements.

The costs involved during the lifetime of the innovative product can be defined as follows:

- The initial acquisition costs - the costs related to the raw materials necessary for the creation of the innovative product;
- Costs for manufacturing the innovative product (e.g. labor, machinery, transport);
- Installing costs - the costs of putting the product into place, estimated on the basis of similar works or by own estimates; if the commissioning allows a selection of the technology based on cost efficiency, the cost optimization will be pursued by ensuring the quality of the works;
- Operating costs - all the costs related to checking and maintaining the product during its use (current and capital repairs);
- Replacement costs - costs resulting from replacing the product.

The lifetime cost expresses the totality of the costs that occur during the use of the analyzed innovative product. Different values of this type of cost for the resulting products, depending on the substitute materials analyzed, can lead to decisions regarding the optimization of costs during the lifetime of use, by selecting the products that present a minimum cost of use during the lifetime.

By summing up the costs related to the acquisition, manufacturing, installation, operation, repair and replacement activities, the total cost over the lifetime of the considered innovative product will be obtained.

RESULTS AND DISCUSSIONS

There is a worldwide interest of the researchers to create, study and promote construction materials/products characterized by comparable properties with those made up of traditional materials, based on synthetic raw materials.

At the international level, many technologies and processes are currently being explored for the valorization of vegetable waste and natural agro-industrial by-products and there are still in the research and development stage.

Considering a first example of the utilization of rice husks in construction, by integrating them into the composition of ecological concrete mixtures (Winarno, 2019), it is found that the strength of the ecological concrete blocks and the resulting costs vary with the proportions of the components of the mixtures, especially with the proportions of cement/rice husks related to the variants of the mixes (Table 1).

Table 1. Overall cost (Indonesian Rupiah, Rp) for 1 m³ of concrete mixture

Mix	% RH to PC	Proportions by weight, kg			Strength kg/cm ²	Cost of 1 m ³ of mix, Rp
		PC	Filler	RH		
V1	67	637	159.25	425.35	19.44	784.40
V2	89	528	132.00	470.09	19.02	662.10
V3	110	451	112.75	501.92	18.61	575.71
V4	134	394	98.50	526.18	17.59	511.81
V5	156	349	87.25	543.76	14.38	461.26
V6	178	314	78.50	559.12	11.51	422.05

Analyzing the data in Table 1 for each of the 6 variants of mixtures V1 to V6, can be noted that, by using the rice husks (RH), the cost of the obtained materials decreased, compared to the initial cost (890 Rp/m³). The cost reductions are between 11.86% and 52.58% depending on the percentage content of husks in the composition of the concrete blocks.

The most efficient variant is V4 (Winarno, 2019), for which optimal cost values are obtained, a 42.5% reduction compared to the traditional concrete block, respectively 890 Rp/m³, with the fulfillment of the resistance standards (Figure 1).

Considering a second example of the valorization of rice husks, this time through the integration of rice husks ash in two road structures (Hossain et al., 2018), the economic efficiency of modified rigid and flexible road structures which contain RHA (rice hull ash) is presented, compared to conventional structure, efficiency assessed through a Life Cycle Cost Analysis (LCCA).

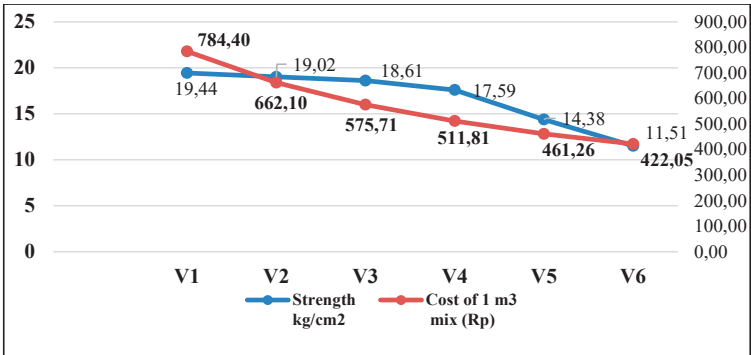


Figure 1. Compressive strength (at 28 days) and cost gained for different percentage of RH

The following scenarios were considered for the LCCA calculation:

- The use of unmodified conventional asphalt mixture (binder) for the realization of the flexible road structure;
- The use of RHA modified asphalt mixture (binder) for the realization of the flexible road structure;

- The use of ordinary unmodified concrete for the realization of the rigid road structure;
- The use of RHA modified concrete for the realization of the rigid road structure (Table 2). In the analysis, the obtained results are detailed in percentage form (processing data from Hossain et al., 2018) for the four variants considered (Figure 2).

Table 2. Present cost (\$/mile) for different pavements

	Initial cost	Resurfacing and structural overlays cost	Recurring maintenance cost	Total cost (\$/mile)
Unmodified Asphalt binder	3,330,845	1,459,982	566,264	5,357,091
RHA-Modified Asphalt binder	3,330,845	918,405	436,605	4,685,855
Unmodified Rigid pavement	3,326,079	1,797,108	730,857	5,854,044
RHA-Modified Rigid pavement	3,150,079	1,042,860	365,428	4,558,367

The results indicated that, for the rigid road structure, the initial installing costs, in the case of using the eco-material, are reduced by 5%, the costs for capital repairs by 42%, and the costs for current repairs by 50%, the total cost for the duration of use being 22% lower compared to the traditional version. For the flexible road structure, the initial installation costs do not show differences, the costs for capital repairs are reduced by 37% in the case of using the asphalt mixture containing RHA, and for current repairs, a lower cost was obtained by 23%. A 13% reduction was obtained for the total cost during the period of use.

Cost analysis is also presented for the materials used in the two constructive variants

considered, rigid structure and flexible structure respectively (Hossain et al., 2018).

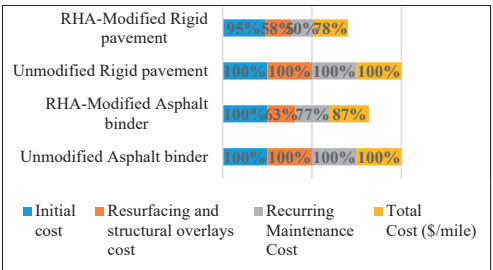


Figure 2. Comparative percentage analysis for the variants considered

For the version with a rigid structure, the cost of the eco-material is 10% lower compared to

the use of the traditional product (Table 3), and for the flexible structure, the necessary costs of installing with the ecological material show a reduction of 46% (Table 4).

Table 3. Cost of cementitious material for 5-mile road construction

Types of Rigid Pavement	Required Cement (Ton)	Unit Price (\$/Ton)	Total Cost (\$)
Unmodified	4,921	113	556,073
RHA-modified	4,428	113	500,364

Table 4. Cost of asphalt binder for 5-mile road construction

Types of Flexible Pavement	Required Cement (Ton)	Unit Price (\$/Ton)	Total Cost (\$)
Unmodified	1,148	901	1,034,348
RHA-modified	1,148	485	556,780

Natural agro-industrial by-products can also be used for other purposes, such for example as solid fuel, in the form of fertilizer for agricultural land or in the livestock industry, the data presented below being the authors' estimates within the research.

If we refer to rice husks and industrial hemp, as natural by-products, in a comparative presentation of the total costs resulting from their recovery (Figure 3), a higher cost is noted for the recovery of the husk, of 561.87 lei/t, the lower cost being obtained for the valorization of the two natural by-products as fertilizers. Comparable costs were obtained to produce hemp-based briquettes, 455.35 lei/t and for the use of husks as bedding in the livestock industry, namely 418.39 lei/t.

Similarly, the total costs for the final disposal of vegetable waste (Figure 4) indicated that, for the final disposal by incineration, the costs are higher compared to the final disposal in ecological deposits, namely 299.50 lei/t compared to 237.13 lei/t.

For all cost categories, regarding the share of direct costs per resource category in the total cost, the highest values were obtained in the "Equipment" chapter, with shares between 50.48% and 88.83% in the total cost, and the

lowest for the "Transport" chapter, with weights between 1.87% and 3.56% (Figure 5). The presented analyzes aimed to estimate the costs regarding the valorization and disposal of vegetable waste and natural agro-industrial by-products. In this sense, the costs for the related resources (materials, labor, equipment, transport) were determined for each option.

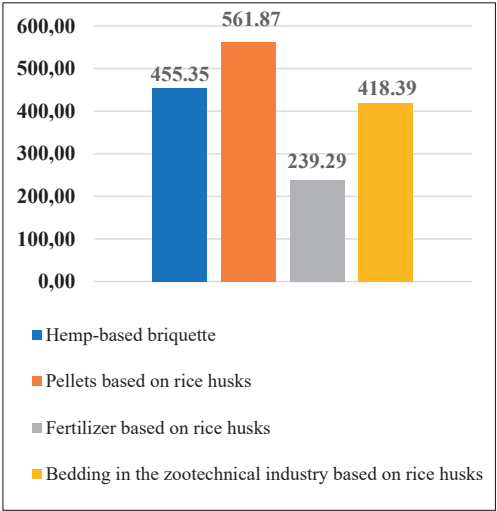


Figure 3. Total costs regarding the capitalization of natural agro-industrial by-products (lei/t)

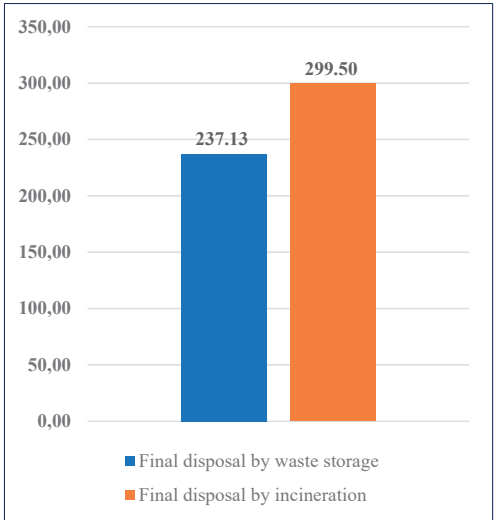


Figure 4. Total costs regarding the final disposal of vegetable waste (lei/t)

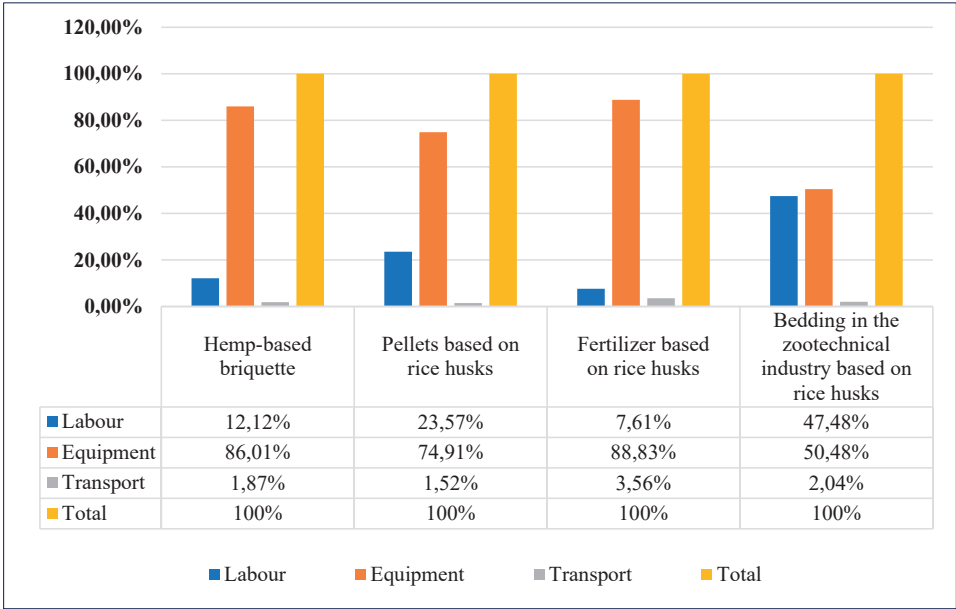


Figure 5. Analysis of direct costs for resources used regarding the capitalization of natural agro-industrial by-products (%)

Based on the results of the analysis, the necessity and opportunity of vegetable waste and natural agro-industrial by-products recovery can be confirmed. This is a process that presents benefits not only from a social but also from an economic point of view compared to disposal processes.

CONCLUSIONS

Generally, the main objectives regarding de management of agro-industrial solid wastes are to protect the health of the population, the environment and to conserve natural resources through waste reduction policies, i.e recycling, valorization, or composting. Capitalizing vegetable wastes and natural agro-industrial by-products offers a promising path for sustainable development, transforming potential waste into valuable resources by respecting the principles of the circular economy.

Minimizing the generation of agro-industrial waste implies reducing their quantities, regardless of the source of production and the type of waste.

Preventing the formation of waste and the negative effects caused to the environment and health is much more effective than removing the consequences after they have occurred.

The recycling of vegetable waste and natural agro-industrial by-products can generate numerous benefits, social, economic, and ecological ones.

The capitalization of waste and natural agro-industrial by-products in the construction sector contributes to the reduction or even to the substitution of the energy-consuming and polluting production of traditional construction materials, having a significant impact in reducing the negative effects on the environment, the innovative products obtained within the circular economy contributing to sustainable development of the built environment.

ACKNOWLEDGEMENTS

This research work was carried out with the support of the Ministry of Research, Innovation and Digitalization and was financed from Project PN 23 35 02 01.

REFERENCES

- Bakatovich, A., Davydenko, N., & Gaspar, F. (2018). Thermal insulating plates produced on the basis of vegetable agricultural waste. *Energy & Buildings*, 180, 72-82.
- Berardi, U. & Iannace, G. (2015). Acoustic characterization of natural fibers for sound absorption applications. *Building and Environment*, 94, 840-852.
- Binici, H., Aksogan, O., Dincer, A., Luga, E., Eken, M., Isikaltun, O. (2020). The possibility of vermiculite, sunflower stalk and wheat stalk using for thermal insulation material production. *Thermal Science and Engineering Progress*, 18, 100567.
- Bonciu, E., Păunescu, R.A., Roșculete, E. & Păunescu G. (2021). Waste management in agriculture. *Scientific Papers Series Management, Economic Engineering in Agriculture and Rural Development*, 21, 219-228.
- Chukwudebelu, J.A., Igwe, C.C., & Madukasi, E.I. (2015). Prospects of using whole rice husks for the production of dense and hollow bricks. *African Journal of Environmental Science and Technology*, 9(5), 493-501.
- Cintura, E., Nunes, L., Esteves, B., & Faria, P. (2021). Agro-industrial wastes as building insulation materials: A review and challenges for Euro-Mediterranean countries. *Ind. Crops Prod.*, 171, 113833.
- Crini, G., Lichtfouse, E., Chanet, G., & Crini, N. (2020). Applications of hemp in textiles, paper industry, insulation and building materials, horticulture, animal nutrition, food and beverages, nutraceuticals, cosmetics and hygiene, medicine, geochemistry, energy production and environment: a review. *Environmental Chemistry Letters*, 18(1), 1451-1476.
- Faruk, O., Bledzki, A. K., Fink, H. P., & Sain, M. (2012). Biocomposites reinforced with natural fibers: 2000–2010. *Progress in polymer science*, 37(11), 1552-1596.
- Fuentes, R.A., Berthe, J.A., Barbosa, S.E. & Castillo, L.A. (2021). Development of biodegradable pots from different agroindustrial wastes and byproducts. *Sustainable Materials and technologies*, 30, e00338
- Halkos, G. & Petrou, K.N. (2016). Efficient waste management practices: A review. *MPRA Munich Personal RePEc Archive*, 1-35.
- Hossain, Z., Elsayed, A., & Islam, T.K. (2018). Use of Rice Hull Ash (RHA) as a Sustainable Source of Construction Material. *Transportation Consortium of South-Central States*, 6. https://repository.lsu.edu/transet_pubs/6.
- Lamma, O.A. (2021). The impact of recycling in preserving the environment. *International Journal of Applied Research*, 7, 297-302.
- Mausum, K.N. (2022). Benefits of Cultivating Industrial Hemp - A Versatile Plant for a Sustainable Future. The 1st International Online Conference on Agriculture - Advances in Agricultural Science and Technology.
- Mubaslat, A. (2021). Introduction to Waste Management, In Jordan, *Sustainability and Waste Management* (pp. 1-42). The Hashemite Kingdom of Jordan. The Deposit Number at The National Library.
- Nath, M.K. (2022). Benefits of Cultivating Industrial Hemp - A Versatile Plant for a Sustainable Future. *Chemistry Proceedings*, 10(14), 14.
- Nguyen, D.M., Grillet, A.C., Diep, T.M.H., Bui, Q.B., & Woloszyn, M. (2020). Characterization of hygrothermal insulating biomaterials modified by inorganic adsorbents. *Heat and Mass Transfer*, 56, 2473-2485.
- Nwofoke, C., & Udu, L.E. (2019). Socioeconomic Determinant of Rice Husk Utilization among Households in Ebonyi State, Nigeria. *Idosr Journal of Banking, Economics and Social Sciences*, 4(1), 34-45.
- Omer, A.M. (2010). The environmental and economical advantages of agricultural wastes for sustainability development in Sudan, *Journal of Brewing and Distilling*, 1, 001-010.
- Popa, I., Petcu, C., Enache, F. & Mureșanu, A. (2020). Using sunflower seed husks waste for sustainable thermal isolating coatings. *Constructii*, (2), 3-9.
- Popa, I., Petcu, C., Alexe, I.-M., Dima, A., Simion, A. & Stoica, D. (2023). *The Research Conference on Constructions, Economy of Buildings, Architecture, Urban and Territorial Development*, 24th Edition, 24. 45.
- Sanjay, M.R., Madhu, P., Jawaid, M., Senthamarakannan, P., Senthil, S. & Pradeep, S. (2018). Characterization and properties of natural fiber polymer composites: a comprehensive re-view. *J. Clean. Prod.* 172, 566–581.
- Șalaru, G., Bahnaru, A., Jolondcovschi, A., Osipov, R., & Golic, A. (2013). *Managementul deșeurilor biodegradabile*. Chisinau, RM: Notograf Prim.
- Winarno, S. (2019). Comparative Strength and Cost of Rice Husk Concrete Block. *MATEC Web of Conferences*, 280, 1-10.
- Yaashikaa, P.R., Senthil Kumar, P., & Varjani, S. (2022). Valorization of agro-industrial wastes for biorefinery process and circular bioeconomy: A critical review. *Bioresour. Technol.*, 343, 126126.
- Yazid, M., Pusfasari, W., & Wildayana, E. (2020). Social, economic and ecological benefits and farmers 'perception of agricultural waste processing in Banyuasin Regency. *IOP Conference Series: Earth and Environmental Science*, 473, 1-5.
- *** Analysis of construction life cycle costs in the context of sustainable development - COSTCONS (in Romanian). Retrieved February 24, <https://incd.ro/proiecte-nationale/>.
- ***<https://legislatie.just.ro/Public/DetaliiDocument/185166>.
- ***https://www.mdpa.ro/userfiles/reglementari/Domeniul_XXV/25_10_P_91_1_2002.pdf.

WATER EROSION OF SOILS IN THE HILLY AREA OF DOLJ COUNTY - ASSESSMENT, CONTROL AND MITIGATION METHODS

Cristian POPESCU, Mihaela BĂLAN, Marius-Nicolae CIOBOATĂ

University of Craiova, Faculty of Agronomy,
19 Libertatii Street, Craiova, Romania

Corresponding author email: mihaela_balancif@yahoo.com

Abstract

Erosion is a process of soil and land degradation, which occurs on a large scale, both in our country and worldwide. Due to its specific characteristics, the study area from the hilly part of Dolj County presents relief, climatic, lithological, hydrological, and vegetation conditions, which have contributed over time and continue to contribute today, to the manifestation of the erosion process, through which the productive capacity of the soils is degraded or diminished. In the reference area, soils subjected to surface water erosion encountered on lands with uniform slope, were identified and evaluated, where slow geological erosion has gradually but permanently removed the solidified surface layer. On slopes with a steep gradient, where deep erosion occurs, strongly eroded soils with gullies and ravines have been identified. By identifying the causes that have produced and continue to produce these shortcomings and based on the morpho-physico-chemical properties of the investigated soils, the most relevant methods of control and combating water-caused erosion were established (agro-improvement works and hydro-ameliorative works).

Key words: control measures, prevention, soil degradation, water erosion.

INTRODUCTION

Erosion, and in particular water erosion, is a degradation process that occurs in large areas of our country, among other processes that degrade soils or reduce their fertility, such as excess phreatic and rainwater moisture, acidity, alkalinity, alluvia, high fine fraction or bedrock content, low organic matter content, compaction, destruction of soil structure, pollution, etc. (Popescu, 2017). Water erosion, landslides, compaction and reduction of humus content, alluvia, are present in the study area. They have been identified as processes that degrade or reduce soil fertility.

In this paper, erosion has been identified and evaluated in both its forms (surface and deep) to establish methods for control, prevention, or mitigation, with the intention of assessing other processes in subsequent research. It should be mentioned from the beginning that water erosion is present in the reference area because of the specific relief, climatic, lithological, hydrological, and vegetation conditions.

On lands with an even slope, surface erosion manifests itself normally on extended surfaces (Figure 1), because it occurs without the anthropic influence intervening and consists in

the gradual and slow detachment and transport of material from the solidified surface (Popescu, 2017; Ciocan et al., 2020).

Gully erosion occurs in the area on the lands with higher inclination, where the intensity of detachment and transport of mineral and organic material are much higher compared to surface erosion. Gully erosion is produced by the concentration of water in a certain direction (Figure 2), causing permanent formations (gullies and ephemeral gullies), with a destructive action (Nicola, 2013).



Figure 1. Natural erosion in the hilly area of Dolj County

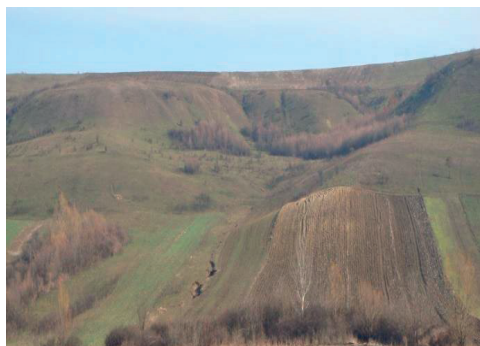


Figure 2. Gully erosion in the hilly area of Dolj County



Figure 3. Landslide in the hilly area of Dolj County

Accelerated erosion occurs together with other forms of degradation listed above: compaction, poor internal drainage, destruction of the structure, acidification (Biali & Cojocaru, 2021).

Losses of soil mineral and organic material, which are imperceptible in the case of slow erosion and produced at a fast pace, through gully erosion, have a negative consequence for agricultural lands and are reflected, in the low level of production (Haidu & Costea, 2012).

Soil erosion also produces other effects on environment, namely the degradation of downstream water (Berghoff et al., 2014), the clogging of rivers, lakes and reservoirs, the degradation of the natural environment, up to desertification (Neamțu, 1996). This explains the fact that worldwide, about 60 million tons of soil are removed annually, from an area of 430 million ha, through water erosion - 31% and wind erosion - 34% (Răuță & Cârstea, 1983).

Having in view these aspects, we can say that we cannot talk about sustainable and efficient development in agriculture, without invoking soil fertility as a decisive factor (Borlan & Hera, 1984). Two major degradation phenomena that occur in the hilly area of Dolj County are soil water erosion and landslides, both diminishing soil fertility (Figure 3).

MATERIALS AND METHODS

In Romania, erosion, in all its degrees of manifestation, on all agricultural lands situated on slopes exceeding 5%, is present on over 6 million hectares, and the intensity of erosion is

assessed by the criterion of "degree of soil profile degradation", especially by the horizons that emerge on the soil surface (Răuță & Cârstea, 1983).

In every area of the country, it is important to know the soil and climate conditions as well as soil properties, to evaluate and develop the most effective measures to control the processes that degrade or reduce their fertility. Laboratory analyses related to the erosion process on soil samples taken from the field soil profiles. Soil profiles of areas subject to natural and accelerated erosion were studied during the field phase. During the field phase, soil profiles were examined, and soil samples were taken in areas of natural morphological variation (Figures 4 and 5).

Laboratory testing consisted of preparing soil samples and conducting physical, hydrophysical and chemical analyses. They were determined according to the IRPA (The Institute of Research for Pedology and Agrochemistry), 1987 methodology:

a) physical-mechanical properties:

- size particle analysis, according to the Kacinski method and the texture was interpreted using the texture triangle;
- bulk density (B_d , g/cm^3) - Nekrasov cylinder method;
- density (D , g/cm^3) - pycnometer method;
- total porosity (P_t , %) - by calculation using the relationship $P_t \% = (1 - B_d/D) \times 100$;

b) hydrophysical properties:

- hygroscopicity coefficient (H_C , %), by the Mitscherlich method;
- wilting point (W_p , %), by calculation with the relationship $W_p \% = H_C \% \times 1.47$;



Figure 4. Soil profile on rupture terrain with natural erosion



Figure 5. Soil profile on rupture terrain with accelerated erosion

- field capacity (FC, %) - by the centrifugation method;

- available water capacity (AWC, %), by calculation using the relationship $AWC \% = FC \% - WP \%$

c) chemical properties:

- humus by the Scholemergher method;

- total nitrogen, by the Kjeldahl method;

- available phosphorus by extraction with ammonium acetate solution and photocolometric dosing;

- available potassium, by extraction with ammonium acetate solution and photocolometric dosing;

- soil reaction (pH), by the potentiometric method, in aqueous extract;

- hydrolytic acidity (SH me/100 g soil), the Kappen method, with sodium acetate and titration with sodium hydroxide;

- the exchange capacity for bases (TEB, me/100 g soil), the Kappen method, modified by Chiriță;

- the total cationic exchange capacity (TEC, meq/100 g soil), indirectly with the relationship $T (meq/100 \text{ g soil}) = BS + HS$;

- degree of saturation in bases (B%), indirectly through the relationship $B \% = BS/TEB \times 100$.

RESULTS AND DISCUSSIONS

Surface and gully erosion in the hilly area of Dolj County are differentiated according to the relief or slope units, the thermal regime of the soil and the vegetation. This process was accentuated in the reference area, especially

after the application of Law 18/1991, when the land was restituted to the owners on the old sites. They have the appearance of belts or strips (Figure 6), with small widths of 10-12 m, which cross the plateau, the slope with southern exposure, the valley, the slope with northern exposure and end in the plateau from the opposite direction, sometimes stretching on a length of 1-2 km. In this way, all the agricultural tillage on the sloping lands were carried out from the hill to the valley, on the line of the greatest slope, and the erosion process manifested itself more intensively.

On land with a uniform slope, where slow geological erosion has gradually but permanently removed the soil formed surface layer, young soils are found which are known as regosoils. (Florea & Munteanu, 2012). These soils have a short profile, made up of the bioaccumulation horizon (Ao) and the parental material C (Popescu, 2019).

On these soils erosion is imperceptible, but there are situations when it can be easily observed where lower genetic horizons appear on the soil surface (Figure 7).

Morphological description

Ao horizon: 0-23 cm; yellowish-brown color (10YR5/6) in wet state and yellow-brown color (10YR6/6) in dry state; clay-clay texture; unstructured or poorly formed granular structure; porous medium; compact environment; dense fibrous roots; rare whitish spots of calcium carbonate; weak effervescence; gradual transition.



Figure 6. The aspect of the terrain in the form of belts (strips) on the line of highest slope in the hilly area of Dolj County



Figure 7. Lower genetic horizons emerged on even-slope slopes in the hilly area of Dolj County

Horizon C: below 23 cm; yellow-brown color (10YR6/6) in wet state and yellow color (10YR7/6) in dry state; clay-clay texture; unstructured or lumpy by drying; fine porous; compact; rare fibrous roots; frequent spots and rare small calcium carbonate concretions; moderate effervescence.

Size composition

The size analysis (Table 1) shows that the soil found on the slopes with a uniform slope has a high content of clay in both horizons, which determines a clay-loamy texture. The high content in clay means that on these lands, especially if the exposure is southern, a more intense expansion and contraction takes place and in this way the detachment of the layer from the solidified surface is more pronounced.

Physical properties

From the analysis of the densities and total porosity of the soil on the slopes with a uniform slope (Table 2), it is constant that the soil is looser in the bioaccumulation horizon, compared to the parent material, as a result of the agricultural tillage carried out.

Hydrophysical properties

The hydrophysical indices of the soil on the slopes with a uniform slope (Table 3), show low values, because of the low content in organic matter, but depending on the percentage of fine fractions there is a specific correlation.

Chemical properties

The soil subjected to natural erosion has a low content of humus (1.54%), very low total nitrogen (0.086%) and medium in mobile phosphorus (33 ppm) and mobile potassium (149 ppm). This higher content in mobile phosphorus and potassium is due to the application of chemical fertilizers.

Table 1. Size composition of the regosoil in the hilly area of Dolj County

Horizon	Depth (cm)	Clay (%)	Coarse sand (%)	Fine sand (%)	Silt (%)	Texture class
Ao	0-23	48.8	2.5	27.1	21.6	AL
C	under 23	50.6	1.6	26.9	20.9	AL

Table 2. The physical properties of the regosoil in the area of Dolj County

Horizon	Depth (cm)	Bulk density (g/cm ³)	Density (g/cm ³)	Total porosity (%)
Ao	0-23	1.35	2.55	47
C	under 23	1.50	2.61	42

Table 3. The hydrophysical properties of the regosoil in the hilly area of Dolj County

Horizon	Depth (cm)	HC %	WP %	FC %	AWC %
Ao	0-23	9.53	14.00	29.54	15.54
C	under 23	10.71	15.74	31.04	15.3

Table 4 The chemical properties of the regosol in the hilly area of Dolj County

Horizon	Depth (cm)	Humus (%)	Total nitrogen (%)	Soluble phosphorus (ppm)	Soluble potassium (ppm)	H ₂ O pH	SH (me /100 g soil)	SB	T	V (%)
Ao	0-23	1.54	0.086	33	149	7.6	-	26.6	26.6	100
C	under 23	0.66	0.039	31	133	8.3	-	31.2	31.2	100

The reaction is maintained in the weak alkaline range (pH 7.6-8.3), which explains the presence of basic elements in the colloidal complex and the degree of saturation in bases 100% (Table 4).

On the steepness lands (over 30%), where accelerated erosion has removed the horizons from the surface, the erodic anthrosol is found. These soils have a poorly developed BC horizon at the surface followed by the parent material. It can be stated that on the basis of the remaining uneroded horizons, the old soil cannot be detected, so that these soils can be called "soil stumps".

Morphological description

BC horizon: 0-17 cm; yellowish-brown color (10YR6/4) in the wet state and yellow-brown color (10YR7/4) in the dry state; clay-clay texture; large or small blocky angular polyhedral structure; fine porous; compact; rare fibrous roots, rare yellowish-whitish spots; very weak effervescence; slow passage.

Horizon C: below 17 cm; yellow-brown color (10YR6/6) in wet state and yellow color (10YR7/6) in dry state; clay-clay texture; unstructured, appearing as a compact mass; fine porous; compact; rare fibrous roots; frequent yellowish-whitish spots; moderate effervescence.

Size composition

And in this eroded soil, the size fraction that predominates is clay, with a percentage of over 50 in both identified horizons. At the opposite pole, it is the coarse sand fraction with only 0.2 %, which makes the soil texturally undifferentiated (Table 5).

Physical properties

The values of the physical properties (density, bulk density, total porosity) show that the soil subjected to accelerated erosion is heavily compacted right from the surface (Table 6).

The bulk density increases from 1.50 g/cm³ in the BC horizon to 1.59 g/cm³ in the parent material. In the same sense, the density of the soil also increases, from 2.68 g/cm³ in the first horizon to 2.71 g/cm³ in the C horizon.

The total porosity has low values in the two horizons of the soil profile, 44% on the surface, in the BC horizon and 41% in depth, in the parent material.

Hydrophysical properties

The hydrophysical indices are characterized by values in the range of clay content that the soil has in both horizons (Table 7).

These measures are needed in order to preseve soil fertility (Bilaşco et al., 2018).

Table 5. Size composition of the erodic anthrosol from the hilly area of Dolj County

Horizon	Depth (cm)	Clay (%)	Coarse sand (%)	Fine sand (%)	Silt (%)	Texture class
BC	0-17	52.1	0.2	24.92	22.78	AL
C	under 17	50.15	0.2	27.98	21.67	AL

Table 6 The physical properties of the erodic anthrosol from the hilly area of Dolj County

Horizon	Depth (cm)	Bulk density (g/cm ³)	Density (g/cm ³)	Total porosity (%)
BC	0-17	1.50	2.68	44
C	under 17	1.59	2.71	41

Table 7 The hydrophysical properties of the erodic anthrosol in the hilly area of Dolj County

Horizon	Depth (cm)	HC %	WP %	AWC %	FC %
BC	0-17	10.97	16.12	32.73	16.61
C	under 17	9.76	14.34	31.96	17.62

Table 8 The chemical properties of the erodic anthrosoil from the hilly area of Dolj County

Horizon	Depth (cm)	Humus (%)	Total nitrogen (%)	Mobile phosphorus (ppm)	Mobile potassium (ppm)	H ₂ O pH	SH (meq / 100 g soil)	SB	T	V (%)
BC	0-17	0.76	0.042	3.9	128	8.2	-	28.1	28.1	100
C	under 17	0.37	0.022	2.15	102	8.5	-	31.3	31.3	100



Figure 8. The seeding operation carried out along contour lines on a uniform slope in the hilly area of Dolj County



Figure 9. Plowing performed along contour lines on a uniform slope in the hilly area of Dolj County



Figure 10. Wheat crop on land with a uniform slope in the hilly area of Dolj County



Figure 11. Terraces with vines on sloping land in the hilly area of Dolj County



Figure 12. Afforestation with acacia, on land with a large slope and in the form of a strip in the hilly area of Dolj County

In this sense, the prevention, combating and conservation of soils with different degrees of erosion can be achieved through agrotechnical and phytotechnical works, especially for soils

affected by natural erosion and through hydro-ameliorative works, complex works to control the development of water leaks on the slope, especially on soils affected by accelerated erosion (Arnaudova et al., 2020).

The execution of all technical works on contour (Figures 8 and 9), the use of crops that are sown in dense rows (Figure 10), the realization of a suitable crop rotation, the administration of organic and chemical fertilizers, are works aimed to preventing erosion by improving the capacity of water infiltration and the reduction of the dispersion of soil particles during precipitation and of course the increase of fertility and the obtaining of higher agricultural productions (Irimuş et al., 2017).

On the lands affected by the accelerated erosion, the efficient works involve the

construction of terraces for the vineyards (Figure 11) and afforestation (Figure 12).

The greatest efficiency in the conservation of lands subject to erosion is the combination of prevention measures and works to combat this process (Biali & Cojocaru, 2020).

CONCLUSIONS

As a result of the geographical location, but also of the natural conditions of relief, climate, vegetation, parent material in the hilly area of Dolj County, surface and gully erosion occur on large areas of land and on smaller areas, landslides.

Generally, the water erosion process involves changes in the properties of the affected soils, being the main degradation process resulting in the mitigating of soil fertility.

By studying in the field and from the laboratory analyzes carried out on the two soils subjected to natural and accelerated erosion processes, there are constant changes regarding the morphological, physical, hydrophysical, chemical and biological properties, as compared to the soils on the unaffected lands.

Both types of eroded soil are compact, compressed, with high density values and low total porosity values, as a result of the high content of fine, clayey fractions, and extremely low humus content. The structure of the soils is also affected, as a result of the decrease in the hydric stability of the structural aggregates, which also explains the compaction of the soils from the surface.

Eroded soils have poor relations with water and air. Being compact soils, permeability to water and air is low. The hydrophysical indices present disadvantages manifested by the increase in the values of the wilting coefficient, the decrease in the values of the field capacity or the moisture equivalent and the useful water capacity.

The chemical properties of the soils subjected to the erosion process are also modified, especially those in the field of organic matter accumulation, reaction and the reserve of nutrients, all as a result of the removal of the mineral and organic soil layer on the surface. Thus, as far as the reaction of the soils is concerned, it was found that it is in the slightly alkaline range, as a result of the presence as

close as possible to the surface or even on the surface, of some horizons rich in basic elements. The content in humus is low and very low, also the supply of total nitrogen is very low and in terms of the reserve of chemical elements, phosphorus and potassium we can say that it is medium to low.

The low content of organic matter and the high compactness determines a weak biological activity in eroded soils.

All these manifestations, reflected in the characteristics of eroded soils, determine their low natural fertility, reflected in the low level of agricultural productions, which is directly proportional to the intensity of the process and the amounts of mineral and organic material detached from the slopes.

In addition to these shortcomings, related to the low productivity of eroded soils, it can be concluded that erosion, as a degradation process of soils and lands, also leads to the disruption of landscape.

The measures to prevent and combat erosion process must be established and applied in the complex, in order to achieve the conservation of soils and lands subject to water erosion in the hilly area of Dolj county.

REFERENCES

- Arnaudova, Z., Bileva, T., Dimka, H. (2020). GIS - based mapping of grasslands and oilseed rapeseeds for ecological data management - case in Bulgaria. *Scientific Papers. Series E. Land Reclamation, Earth Observation and Surveying, Environmental Engineering*, Vol. IX, 199-204.
- Berghoff, A., Berning, A., Wortmann, C., Möller, A., Mahro, B. (2014). Comparative assessment of laboratory and field-based methods to monitor natural attenuation processes in the contaminated groundwater of a former coking plant site. *Environmental Engineering and Management Journal*, 13, 583-596.
- Biali, G. & Cojocaru, P. (2020). Comparison of simulation models of water erosion using GIS. *Scientific Papers. Series E. Land Reclamation, Earth Observation & Surveying, Environmental Engineering*, Vol. IX, 161- 168.
- Biali, G. & Cojocaru, P. (2021). The influence of GIS technology in reclamation solutions for sloping land affected by erosion. *Scientific Papers. Series E. Land Reclamation, Earth Observation & Surveying, Environmental Engineering*, Vol. X, 293-300.
- Bilașco, Șt., Roșca, S., Păcurar, I., Moldovan, N., Vescan, I., Fodorean, I., Petrea, D. (2018). Roads accessibility to agricultural crops using GIS

- technology methodological aproach. *Geographia Technica. Vol 13*(2), 12-30.
- Borlan, Z. & Hera, C. (1984). *Methods of assessing the state of soil fertility in order to use fertilizers rationally*. Bucharest, Romania, Ceres Publishing House.
- Ciocan, V., Moldoveanu, M., Bica, I. (2020). Analysys of the behavior of works to limit water erosion in river basin. *Scientific Papers. Series E. Land Reclamation, Earth Observation & Surveying, Environmental Engineering. Vol. IX*, 118-126.
- Florea, N. & Munteanu, I. (2012). *Romanian Soil System Taxonomy*. Craiova, Sitech Publising House.
- Haidu, I. & Costea, G. (2012). Remote Sensing and GIS for the forest structure assessment at the small basins level in the Apuseni Natural Park. *Studia Universitatis Babes-Bolyia Geographia, I*, 98-112.
- Irimuş, I., Roşca, S., Rus, M.I., Marian, F.L., Bilaşco, Şt. (2017). Landslide susceptibility assessment in alma's basin by means of the frequency rate and GIS techniques. *Geographia Technica. Vol 12*(2), 97-109.
- Neamţu, T. (1996). *Ecology, erosion and anti-erosion agrotechnics*. Editura Ceres, Bucureşti.
- Nicola, O., (2013). *Jurnal for multidimensional Education, 1-2*.
- Popescu, C. (2017). *Reconstrucţia ecologică şi ameliorarea solurilor şi terenurilor degradate*. Editura Sitech, Craiova. (Ecological recovery and improvement of degraded soils and lands. Craiova, Sitech Publishing House), 82 – 86.
- Popescu, C. (2019). *Pedologie II*. Editura Sitech, Craiova, (Pedology II. Craiova, Sitech Publishing House. 38 – 41.
- Răuţă, C., Cârstea, St. (1983). *Prevention and control of soil pollution*. Editura Ceres, Bucureşti.
- ***ICPA (1987) *Pedological studies methodology from Romania*. Vol. I, II and III. Ed. Didactica si Pedagogica, Bucuresti, 53–115.

FOREST DEBRIS-BASED BIOCHAR APPLICATION IN COMPOSTING PROCESS TO REDUCE GREENHOUSE GAS EMISSIONS: A NATURE BASED SUSTAINABLE SOLUTION

Rupesh SINGH^{1,2}, Henrique TRINDADE², João Ricardo SOUSA²

¹University of Trás-os-Montes and Alto Douro (UTAD),
Quinta de Prados - Folhadela, Vila Real, Portugal

²Centre for the Research and Technology of Agro-Environmental and Biological Sciences,
Vila Real, Portugal

Corresponding author email: rupesh@utad.pt

Abstract

Biochar is being produced from biosolids waste of several industrial sectors, including Agri industries by pyrolysis process. Present investigation aims to evaluate the biochar produced from forest debris. Animal farming is a major agri industry and produces huge amounts of waste solids and liquid fractions which are a major source for composting of organic residues. Large amounts of greenhouse gases (carbon dioxide, nitrous oxide) and ammonia are released to the environment during the composting process and become a major concern for environmental health. The solid biowaste from cattle farms was inoculated with biochar and emissions of methane, carbon dioxide, nitrous oxide and ammonia were measured in comparison to control. Present study may develop a sustainable method in the composting process to reduce the greenhouse gas emissions and improve the environmental health for a better tomorrow.

Key words: biochar, greenhouse gases, environmental health, sustainable composting process, nature-based solutions.

INTRODUCTION

Biochar is a nature-based product obtained from different biosolid materials by the thermal conversion process with limited oxygen delivery at temperatures of less than 700°C (Wang et al., 2021).

Biochar exhibits special pores particle structure that facilitates the carbon sequestration, greenhouse gas reduction, increased soil fertility, improved structure, and increased crop production (Lu et al., 2020; Wang et al., 2019). In the past decades, biochar emerged as a potential nature-based material to improve the composting process of organic residues and showed positive effects on multiple issues (Agegnehu et al., 2017; Xiao et al., 2018a; 2018b; Xiao et al., 2023).

Organic wastes are rich sources of organic matter which has been composed by traditional methods since many centuries where the waste residues were piled up in open spaces and left for a long time to decompose by natural process. These traditional practices are very time consuming and produce unpleasant smells to the environment. Additionally, the process releases

the pollutants and eutrophic materials to water bodies and soil (Tang et al., 2020 and 2021).

Increasing global population is leading the pressure on agriculture, where animal farming is a major concern which produces a huge number of organic residues. Management of these organic residues became a major challenge, especially in reference to greenhouse gas emissions during the composting process. Large amounts of greenhouse gases, mainly carbon dioxide, nitrous oxide and ammonia are released to the environment during the composting process and become a major concern for environmental health. Present investigation aimed to evaluate the biochar, produced from forest debris on waste solids from cow farms. Biochar was procured from commercial sources which contained 2-5 mm particle size. The solid biowaste from the cow farm was inoculated with biochar and nano-biochar and emissions of carbon dioxide, nitrous oxide and ammonia were measured in comparison to control.

Present study may develop a sustainable method in the composting process to reduce the greenhouse gas emissions and improve the environmental health for a better tomorrow.

MATERIALS AND METHODS

Forest debris-based Biochar was procured from Portuguese commercial sources. The Biochar was produced from *Acacia* biomass which is an invasive plant species in Portugal and covers the forest land rapidly. This species grows 2-5 m in height as a tree and competes with the native species. Biomass obtained from land cleaning actions, such as water lines and the periphery of plantation areas when they are cut. The plant material was crushed into small pieces and pyrolyzed at 500°C for 14 h, followed by cooling for 20 h at room temperature.

Plastic containers of 135 L total capacity have been used to set up the experiment. The containers were insulated with rock wool to keep the temperature. The bottom part of each container was drilled to place a tube to provide a continuous forced air circulation by connecting to an air pump (KNF, model N010. KN.18) at a rate of 20 L h⁻¹ kg⁻¹ DM (dry matter). Cow slurry was separated into solid and liquid fractions by screw press method. The solid fraction (organic residue from cow slurry) has been collected and treated with biochar (3% w/w) separately while one part of organic residue was kept untreated which serves as control. The experiment was performed in triplicates and is presented in Figure 1.



Figure 1. Apparatus setup for the greenhouse experiments on composting of solid fraction with different additives (control and Biochar). Each treatment and control have 3 replicates

RESULTS AND DISCUSSIONS

The organic matter was observed for microbial growth where high microbial growth was

observed in Biochar treatment while no growth was observed in control upon 7 days (Figure 2a and 2b). The biochar treated material was completely covered with white coloured mycelia growth after 7 days of incubation. The temperature outside was recorded 32°C while inside organic matter was 55°C. The microbial dynamics are needed to characterize by molecular tools in order to obtain the specific community.

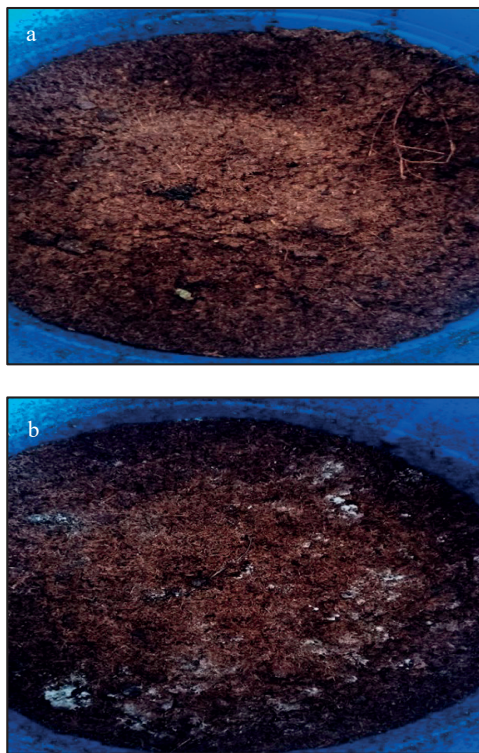


Figure 2. Composting of solid fraction without any treatment after 7 days (a). Treatment with Biochar (b)

The gas emissions were recorded over 7 days by using INNOVA 1412 Photoacoustic Field Gas-Monitor. The tube was placed inside the container and measurements were recorded in triplicates.

NH₃ was reduced by 50% in the biochar treated solid fraction in comparison to control upon 7 days of incubation (Figure 3).

N₂O was reduced by 45% in the biochar treated solid fraction (Figure 4) while emission for CO₂ was recorded 19.05% in the biochar treated fraction (Figure 5).

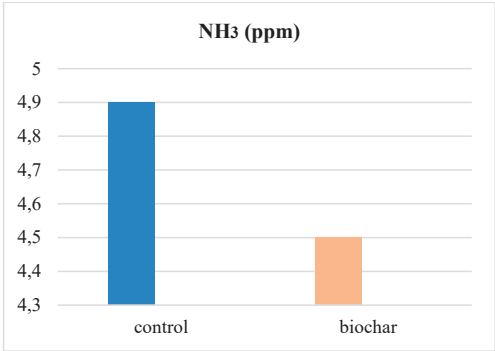


Figure 3. NH₃ mitigation by biochar

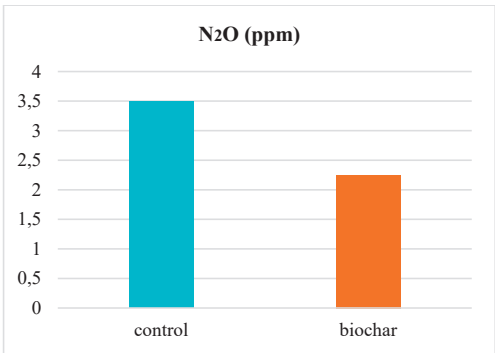


Figure 4. N₂O mitigation by biochar

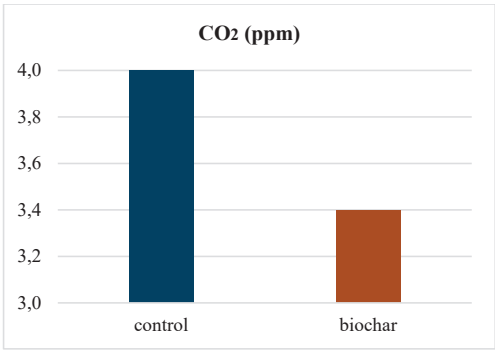


Figure 5. CO₂ mitigation by biochar

Biochar is a nature-based organic material which carries specific functional groups and porosity in structural form and proved as potential mitigation strategy to reduce the greenhouse gas (GHG) emissions during management of waste organic products from the agriculture sector.

Present study demonstrated the reduction of GHGs emissions for methane (CH₄), carbon

dioxide (CO₂), nitrous oxide (N₂O) and ammonia in the initial phases. Previous reports suggested the mitigation of GHGs emissions but largely depends upon the source of Biochar preparation material, pyrolysis temperature and size of the end product (Yin et al., 2021). The Biochar used in present study had small particle size in comparison to previous reports and produced from woody tree species which has been suggested as better material. Amount of Biochar application also affects the mitigation, significant reduction in GHGs emissions were reported by using 10% addition where present study demonstrated significant reduction by 3% addition. More detailed study is required to generate better data and to understand the mechanism behind. Moreover, the improved microbial dynamics may have a correlation between lower emissions, which also need to be investigated.

Accordingly, new methods may be considered by adding microbial cells with biochar as combined formulation should be the new line of research in the upcoming future. Interestingly, the mode of action of GHGs emissions upon Biochar application at molecular level is still not clear and needs attention in near future. The findings observed in the present study may explore the granular biochar application to mitigate GHG emissions from compost.

Emission of Greenhouse gases from soil is not only a major environmental issue, but also leads to huge loss of nutrients and agronomic characteristics of lands (Wang et al., 2018). Biochar application as soil amendment has been investigated intensely since the past decade and suggested a potential positive effect in soil to reduce the emission and increase the nutrients availability (Agyarko-Mintah et al., 2017a; Wang et al., 2018).

CO₂, CH₄ and N₂O are major greenhouse gases which have been investigated in present study. Among three, N₂O is the most important which is being generated upon incomplete nitrification of NH₄⁺ + -N (Czepiel et al., 1996), also by incomplete denitrification of NOX-N at low availability of oxygen. In present study, N₂O has been reduced significantly in biochar and nanobiochar application in comparison to control soil samples. Previous reports suggested that application of biochar potentially increase the aeration and promote the porosity of soil,

reduce the formation of big clumps, followed by reduction in emission of N_2O (He et al., 2017). Previous reports suggested lower total N_2O emission by application of biochar in pig organic matter management (Wang et al., 2013) in later stage of incubation while another report on biochar application in chicken organic waste upon biochar also reduce the N_2O and methane emission (Agyarko-Mintah et al., 2017).

CO_2 is another important Greenhouse gas and biochar addition that showed different results in different studies made in the past. This emission was largely dependent on biochar source material and quantity of application. The report on tobacco stalk biochar at the rate of 10% was effective positive to decrease the CO_2 emissions by 33.90%

(Wang et al. 2018) while biochar derived from bamboo stalks in granular form was applied and observed significant emission reduction (He et al., 2019).

Although, some reports showed a negative result in CO_2 emission upon biochar application

Which was correlated by increasing the temperature and induce the CO_2 synthesis (Czekala et al., 2016). Moreover, biochar addition may improve the aeration in samples and improve the oxygen availability for higher synthesis of CO_2 (Steiner et al., 2010).

Other studies in soils amended with biochar treated compost material demonstrated the lower flux of CO_2 and N_2O in comparison to control and soils amended with chemical fertilizers (Agegnehu et al., 2015). Differential increase in CO_2 while decrease in N_2O in the same experiment was recorded and correlated with weak carbon bonds in biochar which may depend on the source material (Zhang et al., 2012) and (Case et al., 2012). Methane emission has been considered a major concern as well from agriculture industry and biochar application reduced the CH_4 emission by 50.39 % in very later stages of incubation (He et al., 2019).

In brief, biochar application in present study at the rate of 1% showed potential results in N_2O emission reduction while differential emissions were observed for CH_4 and CO_2 emissions. Detailed study with different quantities of biochar and amendments are needed to explore the full potential of this material for longer time incubations. Biochar addition to soil or in

organic matters may be a potential and nature-based strategy to address multiple issues of Greenhouse gas emissions and nutrients recovery from organic matters. Additionally, the instability effect may be a major parameter which depends on soil type and their interaction with biochar material. Biochar pyrolysis temperature and particle size is also a major factor which awaits exploration in the near future. Biochar application in combination with organic matter to the soil is still a major interest which requires the detailed exploration of mechanism behind to answer the insignificant results with different soil types or different organic matters.

FUTURE PERSPECTIVE

Biochar application and results were influenced by type of biochar, raw material or resources for pyrolysis process, pyrolysis temperature and resting conditions, doses of biochar and different organic matter types for composting for different time duration. Detailed studies are still lacking to evaluate all these parameters together to achieve the maximum potential.

Biochar particle size is another important character to influence the maximum output. The biochar may promote aeration in composting process, facilitate the oxygen availability and increased temperature may influence the emission, mainly carbon dioxide gas. Detailed investigation regarding biochar particle size is another interest of research.

Biochar generated from crop residues or waste of plant-based sources contain a significantly higher number of ashes (Zhu et al., 2017). The higher ashes improve the cation exchange capacity upon application in soil and also balance the nutrients availability. Biochar produced from the woody species takes more time during pyrolysis and loses the acidic group in molecular structure. This biochar is recommended to apply in acidic soils to pH correction strategy, followed by reduction in ammonia emission and further improving the nutrients content.

The biochar used in present study was prepared from *Acacia* plants, which is an invasive species in Portugal. This invasive plant is an opportunity which ensures the large number of raw materials for the biochar industry. Further research in

characterizing and investigating the application for longer times with different organic matters may develop a potential sustainable strategy for waste management.

CONCLUSIONS

Biochar treatment was observed to induce the fungal growth in solid fraction after 7 days of incubation. The gases (NH_3 , N_2O , CO_2) were reduced significantly in biochar treatment. The preliminary studies observed significant potential of using biochar for the composting process, although the detailed study is needed for further evaluation. The physiochemical properties of biochar affect the composting process, as well as the agronomic characters upon application of amended compost to soil. Biochar of good quality character may result in value addition in composting as well as nutrients management upon application to the field.

ACKNOWLEDGEMENTS

Funding by The European Union Horizon's Program (HORIZON-CL6-2022-ZEROPOLLUTION-0) under grant agreement number- 101081858 and Centro de Investigação e Tecnologias Agroambientais e Biológicas (CITAB), Universidade de Trás-os-Montes e Alto Douro (UTAD), is gratefully acknowledged.

REFERENCES

- Agegnehu, G., Srivastava, A.K., Michael, I. Bird, M.I. (2017). The role of biochar and biochar-compost in improving soil quality and crop performance: A review. *Applied Soil Ecology*, 119, 156-170, <https://doi.org/10.1016/j.apsoil.2017.06.008>.
- Agegnehu, G., Bass, A.M., Nelson, P.N., Muirhead, B., Wright, G., Bird, M.I. (2015). Biochar and biochar-compost as soil amendments: Effects on peanut yield, soil properties and greenhouse gas emissions in tropical North Queensland, Australia. *Agric. Ecosyst. Environ.* 213, 72–85.
- Agyarko-Mintah, E., Cowie, A., Singh, B.P., Joseph, S., Van Zwieten, L., Cowie, A., Harden, S., Smillie, R. (2017). Biochar increases nitrogen retention and lowers greenhouse gas emissions when added to composting poultry litter. *Waste Manage.* 61, 138–149.
- Case, S.D.C., McNamara, N.P., Reay, D.S., Whitaker, J. (2012). The effect of biochar addition on N_2O and CO_2 emissions from a sandy loam soil – The role of soil aeration. *Soil Biol Biochem.* 51, 125–134.
- Czepiel, P., Douglas, E., Harriss, R., Crill, P. (1996). Measurements of N_2O from composted organic wastes. *Environ. Sci. Technol.* 30, 2519–2525.
- Czekala, W., Malinska, K., Caceres, R., Janczak, D., Dach, J., Lewicki, A. (2016). Composting of poultry manure mixtures amended with biochar - The effect of biochar on temperature and C- CO_2 emission. *Bioresour. Technol.* 200, 921–927.
- He, X., Chen, L., Han, L., Liu, N., Cui, R., Yin, H., Huang, G. (2017). Evaluation of biochar powder on oxygen supply efficiency and global warming potential during mainstream large-scale aerobic composting. *Bioresour. Technol.* 245, 309–317.
- He, X., Yin, H., Han, L., Cui, R., Fang, C., Huang, G. (2019). Effects of biochar size and type on gaseous emissions during pig manure/ wheat straw aerobic composting: Insights into multivariate-microscale characterization and microbial mechanism. *Bioresour. Technol.* 271, 375–382.
- Lu, L.W., Yu, W., Wang, Y., Zhang, K., Zhu, X., Zhang, Y., Wu, Y., Ullah, H., Xiao, X., & Chen, B. (2020). Application of biochar-based materials in environmental remediation: from multi-level structures to specific devices. *Biochar*, 2, 1-31.
- Steiner, C., Das, K.C., Melear, N., Lakly, D. (2010). Reducing nitrogen loss during poultry litter composting using biochar. *J. Environ. Qual.* 39, 1236–1242.
- Tang, J., Zhang, L., Zhang, J., Ren, L., Zhou, Y., Zheng, Y., Luo, L., Yang, Y., Huang, H., Chen, A. (2020). Physicochemical features, metal availability and enzyme activity in heavy metal-polluted soil remediated by biochar and compost. *Science of the Total Environment*, 701, <https://doi.org/10.1016/j.scitotenv.2019.134751>.
- Tang, S., Liang, J., Gong, J., Song, B., Yang, Z., Fang, S., Zhang, P., Cao, W., Li, J., Luo, Y. (2021) The effects of biochar/compost for adsorption behaviors of sulfamethoxazole in amended wetland soil. *Environmental Science and Pollution Research International*, 28(35), 49289–49301. <https://doi.org/10.1007/s11356-021-13959-7>
- Wang, J., Wang, S. (2019). Preparation, modification and environmental application of biochar: a review. *Journal of Cleaner Production*, 227(12). DOI:10.1016/j.jclepro.2019.04.282.
- Wang, L., Rinklebe, J., Sik, O.Y., Daniel, C.W.T. (2021). Biochar composites: Emerging trends, field successes and sustainability implications. *Soil Use and Management*, 38(1), 14-38. DOI:10.1111/sum.12731.
- Wang, Q., Awasthi, M.K., Ren, X., Zhao, J., Li, R., Wang, Z., Wang, M., Chen, H., Zhang, Z. (2018). Combining biochar, zeolite and wood vinegar for composting of pig manure: The effect on greenhouse gas emission and nitrogen conservation. *Waste Manage.* 74, 221–230.
- Wang, C., Lu, H., Dong, D., Deng, H., Strong, P.J., Wang, H., Wu, W. (2013). Insight into the effects of biochar on manure composting: evidence supporting the relationship between N_2O emission and denitrifying community. *Environ. Sci. Technol.* 47, 7341–7349
- Xiao, R., Huang, D., Du, L., Song, B., Yin, L., Chen, Y., Gao, L., Li, R., Huang, H., Zeng, G. (2023). Antibiotic

- resistance in soil-plant systems: a review of the source, dissemination, influence factors, and potential exposure risks. *Sci. Total. Environ.* 15, 869:161855. DOI: 10.1016/j.scitotenv.2023.161855.
- Zhang, A., Liu, Y., Pan, G., Hussain, Q., Li, L., Zheng, J., Zhang, X. (2012). Effect of biochar amendment on maize yield and greenhouse gas emissions from a soil organic carbon poor calcareous loamy soil from central china plain. *Plant Soil* 351, 263–275.
- Zhu, X., Chen, B., Zhu, L., Xing, B. (2017). Effects and mechanisms of biochar-microbe interactions in soil improvement and pollution remediation: a review. *Environ. Pollut.* 227, 98–115.

EVALUATING GREEN AND BLUE INFRASTRUCTURE IN URBAN AREAS IN ROMANIA: A METHODOLOGICAL APPROACH

Teodora UNGUREANU¹, Andreea Cătălina POPA¹, Claudiu-Sorin DRAGOMIR^{1,2}

¹National Institute for Research and Development in Constructions,
Urbanism and Sustainable Spatial Development - URBAN-INCERC,
266 Pantelimon Street, District 2, Bucharest, Romania

²University of Agronomic Sciences and Veterinary Medicine of Bucharest,
59 Marasti Blvd, District 1, Bucharest, Romania

Corresponding author email: teodora.ungureanu@incd.ro

Abstract

This study explores the potential of implementing analysis indicators in the Romanian context to enhance the development and maintenance of green and blue urban infrastructure. Previous studies on GBUI have primarily focused on larger scales, considering cities or territories, to understand connectivity and positive impacts. However, in Romania, green and blue infrastructure in urban areas has received less attention for analysis and development. To understand the impact of GBUI at a neighbourhood level, the study proposes the development of specific indicators that consider the urban form, functional zoning, and the provision of public urban green and blue spaces regarding housing and urban amenities. This research utilises international practice, scientific literature, and national legislation to understand new mechanisms for urban design and sustainable development. It maps indicators for GBUI analysis and design, contributing to a new methodological approach in the Romanian context. This research's findings can guide the design and development of new residential areas, thereby improving the quality of urban life through improved green and blue urban infrastructure.

Key words: green and blue urban infrastructure, sustainable urban development, sustainable housing, urban areas.

INTRODUCTION

Over the last few decades, cities have seen an explosion in growth, both in size and population. The projection is that 68% of the global population will live in cities by 2050 (United Nations, 2018). Consequently, cities must address heightened challenges, including demographic growth and climate change.

In understanding the need to link residential neighbourhoods with green and blue infrastructure, we bring into the discussion the European Commission document The New Leipzig Charter, "The transformative power of cities for the common good". Its importance lies in the holistic understanding of cities as complex cities that need to be understood from multiple perspectives: social, environmental, and economic. One of the land-use policy aspects promoted by the document is the balance between urban density and green and blue infrastructure, addressing both environmental and social needs for a better

quality of life for citizens (European Commission, 2020).

Green infrastructure is becoming an increasingly popular topic in Romania. Civil society is a backer of projects in this area. They believe that investment in green infrastructure can provide numerous benefits, including improved air and water quality, increased biodiversity, and more sustainable and livable communities. Green infrastructure initiatives have been developed in both cities and rural communities ("The Civic Groups of Bucharest", 2022; Sebastian, 2023; Alex Găvan Foundation, 2024). However, there is a lack of coordination among these projects, thus their influence is limited.

Defining urban green and blue infrastructure

The current problems faced by cities, such as global warming, the increase in the number of cars, air pollution, the loss of natural areas, have contributed to the awareness of the

importance of green and blue infrastructure and the benefits they bring.

From the 1990s onward, the term "green infrastructure" has become increasingly prevalent in specialised literature (Popescu & Petrișor, 2020).

In 1994, one of the earliest references to the concept emerged within the efforts of the Florida Greenways Commission, which advocated for a document outlining strategies to advance the development and enhancement of greenways across Florida. In planning new residential developments, alongside transportation and building infrastructure, significant attention should also be directed towards establishing a network of green spaces (Florida Greenways Commission, 1994). A singular park falls short in safeguarding biodiversity, mitigating pollution, facilitating recreation, and fostering social interaction. Therefore, particular emphasis was placed on interconnecting green spaces to optimise the benefits they provide.

Green and blue infrastructures consist of natural and semi-natural areas that offer a large spectrum of ecosystem services (European Commission, 2019). According to the EU, it is vital to support the integration of these infrastructures into strategic urban planning documents. The Natura 2000 sites are a crucial element of the EU's green network. The EU's objectives of environmental conservation, biodiversity, and pollution reduction depend on these areas.

Green and blue infrastructures contribute to economic, ecological, and social well-being, facilitating sustainable urban development and offering spaces that deliver multiple advantages to the local community (Mell, 2009; Town & Country Planning Association, 2004; Pienaru & Rădulescu, 2022).

From a cultural standpoint, green and blue infrastructures fulfil functions such as: direct experience of natural ecosystems, recreation, opportunities for socialisation, environmental education (Ahern, 2007).

MATERIALS AND METHODS

This study is based on an extensive review of Romanian legislation, international documents and policies, and scientific research regarding

green and blue infrastructure, with a focus on urban space. The paper maps GBUI and related concepts in Romania through an analysis of national normative acts. The research used a keyword search of "green infrastructure" and "blue infrastructure" and related elements, such as green spaces, gardens, lakes, rivers, etc., to explore the extent of usage in the legislation. Once the relevant keywords had been determined, they were used to conduct a search on the Romanian Government portal for legislation, JUST (The Romanian Government, 2024). Using a search engine, the syntax "site: legislatie.just.ro keyword" was utilised to conduct broad searches for those laws that contained the searched keywords. An exception to this type of analysis were the Guidelines for the preparation of urban planning documents, which can only be found in scanned digital versions that do not permit optical character recognition (Ministry of Development, Public Works and Administration, 2020).

RESULTS AND DISCUSSIONS

The interest for Green and Blue Urban Infrastructures in European Union

At the level of the European Union, there is a strong interest in reducing pollution levels and achieving sustainable development goals. In this regard, several concepts have been mentioned in official EU documents that can play an important role in improving the quality of the environment. The "European Green Pact" is the document that lays the foundations for transforming the EU economy by reducing the use of non-renewable natural resources and eliminating greenhouse gases by 2050 (European Commission, 2019). At the same time, the document highlights the need for all countries to work together and take action to achieve the proposed targets. It stresses the importance of involving as many countries as possible to achieve the desired results, with the aim of slowing down global warming and its impact on everyone. The document sets out the instruments for making the European economy cleaner. Among the terms used, the term "blue economy" stands out. The term considers the benefits offered by the world's seas and oceans in terms of offshore renewable sources

(European Commission, Joint Research Centre, 2019).

It also considers solutions to mitigate the effects of climate change on specific flora and fauna. Fishing and aquaculture are important economic activities, but they have significant environmental impacts. Such activities need to be carried out, taking into account the impact on local communities in coastal areas. Another concept used in the European Green Deal is "green investment", which aims to reduce environmental impacts. Areas where green investment is strongly encouraged are transport and energy. In addition to environmental impacts, green investments can lead to the creation of new jobs and the development of new technologies (European Commission, 2019).

The increased interest at EU level in reducing pollution is also reflected in the way European funding is allocated. The Regional Operational Programmes allocate significant amounts of funding to the creation of new green infrastructure and the improvement of existing infrastructure. Actions eligible for funding include the conversion of degraded or derelict land into green spaces and the creation of urban forests.

According to the Western Regional Operational Programme, green infrastructure includes forests, ponds and flowering meadows. Green infrastructure is an effective way to improve people's quality of life by reducing the effects of pollution (increasing air quality, reducing noise pollution, mitigating microclimate) (Western Regional Development Agency, 2021). All these benefits make green infrastructure an essential tool in the development of cities. At the community level, green infrastructure can increase local attractiveness by fostering connections between residents (Western Regional Development Agency, 2021). Another advantage is the support of biodiversity through the repopulation and protection of local species, aimed at rejuvenating troubled areas.

The "Guidance on a strategic framework for further supporting the deployment of EU-level green and blue infrastructure" is another European Commission document that highlights the role of green and blue urban infrastructure in halting the trend of declining

air, water, and soil quality and biodiversity loss. In addition to the environmental and health benefits for the population, green and blue infrastructures imply social and economic benefits. At an urban level, GBUI provides the residents with recreational facilities, and children have more places to play. Urban green and blue infrastructures are networks consisting of natural and semi-natural areas that provide ecosystem services, impacting people's quality of life (European Commission, 2022). In addition to these aspects, green and blue infrastructures include highly biodiverse ecosystems, parks, gardens, green roofs, hedgerows, ponds, meadows, as well as abandoned areas given back to local communities. At the heart of these infrastructures are Natura 2000 sites and the network they form across the European Union. In the long term, the aim is to connect these protected areas, as many of them are isolated, which has negative effects on wildlife (European Commission, 2022).

The Green and Blue Urban Infrastructures as urban amenity in Romanian residential areas

Urban planning practice in Romania acknowledges the importance of public green spaces in relation to the development of cities and, implicitly, residential areas (Law No. 350 of 6 July 2001). Socialist planning practice (before the change of political regime in 1989) stresses the importance of designing the new residential estates taking into account green spaces in conjunction with the urban amenities needed for day-to-day life (Lăzărescu, 1977; Laurian, 1965).

In present Romanian practice, the green space area of residential neighbourhoods is not defined by urbanistic indicators in connection with urban density, yet some local urban guidelines suggest percentages of plot area. The General Urban Code, under Annex 6, "Green and Planted Spaces", does not specify the percentage of green space required in residential neighbourhoods, just that at least 2 square metres of green space be provided for each inhabitant (Government Decision No. 525 of 27 June 1996). This annex is defined in paragraph 6.8. for dwellings a minimum of 2 square metres per inhabitant, but it is not

specified for which type of dwelling. It is also not specified what type of green space is taken into account, where it is placed (private courtyards or public parks), and what is the maximum distance green space - dwelling. Nevertheless, this value is well below the European Commission's recommendation of 26 square metres per inhabitant. An additional issue is the process of reporting and measuring the area of green space, due to the lack of adaptation to each individual city targeted for research (Badiu et al., 2016). Although it currently exists in the form of a proposal, it should be noted that the proposed law, "Code of Territorial Planning, Urban Development and Construction" (CATUC), presents a definition of residential areas linking the housing function and green spaces of public character and urban amenities.

The analysis of the 13 normative acts, i.e. 56 articles, sections and annexes, resulted in 28 key words. Some of these keywords were previously established for the identification of normative acts, such as green infrastructures, blue infrastructures, green spaces, waterways, etc. They refer to the type of concepts that are regulated. The second type of key word resulting is that of regulated aspects. Following comparative analyses: definitions of concepts; role of concepts; development of urban

infrastructures: green, blue or both; urban planning documents; norming areas at urban level; norming areas at plot level; norming ancillary functions; norming constructions on GBUI; special situations: protected areas of historical monuments; responsible for maintenance and protection; prohibition of change of use; and contraventions.

Types of Green and Blue Urban Infrastructures

To better understand and analyse the Green and blue urban infrastructure, we examined its urban features. Thus, Table 1 shows the identification of items based on their type: green or blue.

In an urban context, green infrastructure can include parks, gardens, trees, and other natural elements that provide environmental benefits such as air purification and temperature regulation (Czechowski et al., 2018). On the other hand, blue infrastructure can consist of water bodies such as rivers, lakes, and ponds that play a crucial role in managing stormwater and providing recreational opportunities (Brears, 2018). By classifying these items as green and blue, we aim to assess the overall impact of urban infrastructure on the environment and the community in Romanian cities.

Table 1. Identification of types of Green and Blue Urban Infrastructures

GBUI element	Type	Source
lake	blue	Mell & Scott, 2023; Jones et al., 2022
green roof	green	Almaaitah et al., 2021; Mell & Scott, 2023; Abhijith et al., 2017; Castleton et. al., 2010; Baik et al., 2012; Hamel & Tan, 2022; Radinja et al., 2021
permeable pavement	green	Almaaitah et al., 2021; Afonso et al., 2018; CNT, 2010
bioswale	green	Almaaitah et al., 2021; Hamel & Tan, 2022; Jones et al., 2022; Radinja et al., 2021; CNT, 2010
rainwater tanks	blue	Almaaitah et al., 2021
blue roof	blue	Almaaitah et al., 2021; Shafique et al., 2016
rainwater storage under buildings	blue	Almaaitah et al., 2021
public garden	green	Mell & Scott, 2023; Jones et al., 2022
pocket park	green	Mell & Scott, 2023; Hamel & Tan, 2022
river front	green	Mell & Scott, 2023

pond	blue	Mell & Scott, 2023; Jones et al., 2022; Radinja et al., 2021
green wall	green	Mell & Scott, 2023; Abhijith et al., 2017; Jones et al., 2022
trees	green	Abhijith et al., 2017
urban park	green	Mell & Scott, 2023; Jones et al., 2022
hedge	green	Abhijith et al., 2017
urban forest	green	Escobedo et al., 2011; Kuehler et al., 2017; CNT, 2010
green tram tracks	green	O'Donnell et al., 2021; Sikorski et al., 2018; Major et al., 2023; Rendecková et al., 2022;
buffer vegetation strips	green	Wagner et al., 2013
infiltration systems	blue	Wagner et al., 2013
rain garden	green and blue	Hamel & Tan, 2022; Jones et al., 2022; Radinja et al., 2021
amenity areas	green and blue	Jones et al., 2022
canal	blue	Jones et al., 2022
estuary	blue	Jones et al., 2022
green wedges	green	Frey, 1999
sport facilities	green	Lăzărescu, 1977

Analysis Indicators for Green and Blue Urban Infrastructures

The creation of indicators to measure and analyse GBUI can facilitate ongoing monitoring and potential for improvement. The proposed categories of indicators were identified in various studies and existing models that emphasise the significance of GBI in areas such as ecosystem services, health demands (Pakzad & Osmond, 2016), social requirements (Rundle et al., 2013), and cultural aspirations.

Table 2 provides a comprehensive list of indicators we identified and categorized according to their relevance to: economic, health, social, environmental. These indicators can offer valuable insights into the

effectiveness of GBUI interventions and identify areas for improvement for policymakers and stakeholders. The indicators are useful for comparing project outcomes between regions and raise awareness of emerging challenges. Regular monitoring of these indicators will facilitate a more comprehensive approach to GBUI planning and management, ultimately leading to a more sustainable and liveable urban environment. The indicators identified are mostly in the environmental category, with a few related to social, health, and economic aspects as well. Taken as a whole, these indicators provide a comprehensive understanding of the various ways GBUI impacts the environment and society.

Table 2. Analysis Indicators for Green and Blue Urban Infrastructures

Indicator	Measurement	Type	Source
surface of green infrastructure	quantitative	environmental/ health	Dlugonski & Szumanski, 2015
infiltration capacity	quantitative	environmental	Boogaard et al., 2023
air temperature	quantitative	environmental/ health	Bartesaghi Koc et al., 2018

soil temperature	quantitative	environmental	Bartesaghi Koc et al., 2018
relative humidity	quantitative	environmental	Bartesaghi Koc et al., 2018
surface albedo	quantitative	environmental	Bartesaghi Koc et al., 2018
vegetation arrangement	qualitative	environmental	Bartesaghi Koc et al., 2018
plant species	qualitative	environmental	Bartesaghi Koc et al., 2018
evapotranspiration rate	quantitative	environmental	Bartesaghi Koc et al., 2018
soil quality	qualitative	environmental/ health	McKinney, 2006; Zhu & Carreiro, 2004, cited by Pakzad & Osmond, 2016
improve accessibility	qualitative	health/ social	Rundle et al., 2013 cited by Pakzad & Osmond, 2016
noise level	quantitative	environmental/ health	CNT, 2010
potable water use	quantitative	environmental/ health	CNT, 2010
flood risk	qualitative	environmental/ economical/ social/ health	CNT, 2010; Rayan et al., 2021
food production (urban agriculture)	quantitative/ qualitative	social/ economic	Rayan et al., 2021
usage of private car	quantitative	environmental/ economic	Rayan et al., 2021
energy consumption for cooling and heating demands	Quantitative	economic	Rayan et al., 2021
healthcare cost	Quantitative	economic/ health/ social	Rayan et al., 2021
accessibility to public parks gardens and playgrounds	Quantitative	environmental/ social	Wang et al., 2019
pollutants removed by vegetation	Quantitative	environmental/ health	Wang et al., 2019
temperature decrease by tree cover	Quantitative	environmental	Wang et al., 2019
employment resulting from green infrastructure initiatives	quantitative/ qualitative	economic/ social	Wang et al., 2019
semi-natural surfaces providing ecological benefits	quantitative/ qualitative	environmental	Iojă et al., 2014

CONCLUSIONS

Studies have demonstrated that green infrastructure helps to lessen the adverse effects of urbanisation (Tache et al., 2023; Petrișor et al., 2022; Popescu et al., 2022; Badiu et al., 2016). However, efficient coordination and collaboration amongst various stakeholders -

including government agencies, community organisations, and the corporate sector- are essential to realising the full potential of green infrastructure. With the issues brought on by air pollution getting worse (Ilie et al., 2023), there is an increasing need for a healthier environment (Eijck et al., 2017). In order to enhance their general well-being and spend

time in nature in the most enjoyable and healthful setting, city inhabitants require more urban green and blue infrastructure (Hajer et al., 2020).

Cities have the potential to create areas that not only offer recreational possibilities but also enhance air quality and minimise the effects of climate change by incorporating green infrastructure into urban design and development (Mell, 2019).

Although the current Romanian body of legislation contains numerous legislative acts dealing with the subject of green urban infrastructure and related concepts, there is no unified approach and coherent definition. In the absence of a clear definition, the concept of green urban infrastructure is used in several normative acts in different situations: in the context of the digitization and improvement of urban planning documentation (Romania's Urban Policy, 2022), of the motivation for the elaboration of some projects of urban regeneration (Specific Guidelines from 10 May 2022, on conditions for accessing European funds related to the National Recovery and Resilience Plan under calls for projects NRP/2022/C10, component 10. It is noted that it was also used erroneously, with reference to green energies, within Emergency Ordinance No. 183 of 28 December 2022.

One of the biggest problems identified is related to the definition provided by the future Code of Territorial Planning, Urban Development and Construction. The definition offered partially takes over the definition of the European Commission, but the specifications regarding the quality of the environment, the improvement of the lives of the inhabitants, and the advantages offered by the green economy have been eliminated (Ministry of Development, Public Works and Administration, 2023; European Commission, 2022). In this sense, there is a lack of complexity in the definition, with negative effects on the future.

GBUI needs to be considered within the complex urban system, as recent interest in reformulated urban concepts such as the 15-minute city has shown.

Urban strategies developed by cities such as Paris (Cities100, 2019), Milan (Sanesi et al., 2017), or Barcelona (Magrinyà et al., 2023)

emphasise the importance of accessibility and the provision of green and blue spaces. We can therefore observe that GBUI cannot be considered as a whole without taking into account aspects such as housing density in relation to pedestrian mobility, the link between infrastructure and urban amenities, environmental and ecological or economic and cultural needs.

ACKNOWLEDGEMENTS

This work was supported by the PN 23 35: "*Advanced research on the development of eco-innovative solutions, composite materials, technologies and services, in the concept of circular economy and quality of life enhancement, for a sustainable digital infrastructure in a built and urban environment resilient to climate change and disasters*" Acronym: ECODIGICONS, PN 23.35.06.01. project with the title "*Integrated IT-urban planning system for the evaluation of blue-green infrastructure at the level of municipalities and cities in Romania with a view to implementation in urban development plans. Case study: Râmnicu Vâlcea Municipality*", financed by the Ministry of Research, Innovation and Digitalization of Romania.

REFERENCES

- Abhijith, K., Kumar, P., Gallagher, J., McNabola, A., Baldauf, R., Pilla, F., Broderick, B., Di Sabatino, S., & Pulvirenti, B. (2017). Air pollution abatement performances of green infrastructure in open road and built-up street canyon environments – A review. *Atmospheric Environment*, 162, 71-86. <https://doi.org/10.1016/j.atmosenv.2017.05.014>.
- Afonso, M.L., Dinis-Almeida, M., & Fael, C.S. (2018). Permeable pavements – green infrastructures as a flood mitigation measure. *Acta Horti*, 1215, 369-376. <https://doi.org/10.17660/ActaHort.2018.1215.68>
- Ahern, J. (2007). *Green Infrastructure For Cities: The Spatial Dimension*. IWA Publishing, London, UK.
- Alex Găvan Foundation (2024). *Civic Platform Together for the Green Belt*. <https://centuraverde.ro/>.
- Almaaitah, T., Appleby, M., Rosenblat, H., Drake, J., & Joksimovic, D. (2021). The potential of Blue-Green infrastructure as a climate change adaptation strategy: a systematic literature review. *Blue-Green Systems*, 3(1), 223–248. <https://doi.org/10.2166/bgs.2021.016>.

- Badiu, D.L., Ioja, C.I., Pătroescu, M., Breuste, J., Artmann, M., Niță, M.R., Grădinaru, S.R., Hossu, C.A., & Onose, D.A. (2016). Is urban green space per capita a valuable target to achieve cities' sustainability goals? Romania as a case study. *Ecological Indicators*, 70, 53–66. <https://doi.org/10.1016/j.ecolind.2016.05.044>.
- Baik, J.J., Kwak, K.H., Park, S.B., & Ryu, Y.H. (2012). Effects of building roof greening on air quality in street canyons. *Atmospheric Environment*, 61, 48–55. <https://doi.org/10.1016/j.atmosenv.2012.06.076>.
- Bartasaghi Koc, C., Osmond, P., & Peters, A. (2018). Evaluating the cooling effects of green infrastructure: A systematic review of methods, indicators and data sources. *Solar Energy*, 166, 486–508. <https://doi.org/10.1016/j.solener.2018.03.008>.
- Boogaard F., Rooze D., & Stuurman R. (2023). The Long-Term Hydraulic Efficiency of Green Infrastructure under Sea Level: Performance of Raingardens, Swales and Permeable Pavement in New Orleans. *Land*, 12(1), 171. <https://doi.org/10.3390/land12010171>.
- Brears, R.C. (2018). Blue and Green Cities. Palgrave Macmillan UK. <https://doi.org/10.1057/978-1-137-59258-3>.
- Castleton, H.F., Stovin, V., Beck, S.B.M., & Davison, J.B. (2010). Green roofs; building energy savings and the potential for retrofit. *Energy and Buildings*, 42(10), 1582–1591. <https://doi.org/10.1016/j.enbuild.2010.05.004>.
- Cities100. (2019, October). Paris is using blue and green infrastructure to tackle city heat. https://www.c40knowledgehub.org/s/article/Cities100-Paris-is-using-blue-and-green-infrastructure-to-tackle-city-heat?language=en_US.
- CNT (2010). Integrating Valuation Methods to Recognize Green Infrastructure's Multiple Benefits. Center for Neighborhood Technology.
- Czechowski, D., Hauck, T., & Hausladen, G. (Eds.). (2018). Revising Green Infrastructure. CRC Press. <https://doi.org/10.1201/b17639>.
- Dlugonski, A., & Szumanski, M. (2015). Analysis of Green Infrastructure in Lodz, Poland. *Journal of Urban Planning and Development*, 141(3). [https://doi.org/10.1061/\(ASCE\)UP.1943-5444.0000242](https://doi.org/10.1061/(ASCE)UP.1943-5444.0000242).
- Eijck, G. van, Kums, M., Lofvers, W., Naafs, S., Spaandonk, T. van, Steketee, A., & Ziegler, F. (2017). Urban Challenges, Resilient Solutions: Design Thinking for the Future of Urban Regions. TrancityValiz.
- Emergency Ordinance No. 183 of 28 December 2022, on the establishment of measures for the financing of urban regeneration projects, Published in the Official Monitor No. 1268 of 29 December 2022.
- Escobedo, F.J., Kroeger, T., & Wagner, J.E. (2011). Urban forests and pollution mitigation: Analyzing ecosystem services and disservices. *Environmental Pollution*, 159(8–9), 2078–2087. <https://doi.org/10.1016/j.envpol.2011.01.010>.
- European Commission. (2019). Guidance on a strategic framework for further supporting the deployment of EU-level green and blue infrastructure. <https://circabc.europa.eu/ui/group/3f466d71-92a7-49eb-9c63-6cb0fadf29dc/library/dc48dc2a-b87f-4e54-9852-a18c7239260e/details?download=true>.
- European Commission. (2020). New Leipzig Charter-The transformative power of cities for the common good. https://ec.europa.eu/regional_policy/en/information/publications/brochures/2020/new-leipzig-charter-the-transformative-power-of-cities-for-the-common-good?etran=ro.
- European Commission. (2022). Guidance on a strategic framework for further supporting the deployment of EU-level green and blue infrastructure. <https://circabc.europa.eu/ui/group/3f466d71-92a7-49eb-9c63-6cb0fadf29dc/library/dc48dc2a-b87f-4e54-9852-a18c7239260e/details?download=true>.
- Florida Greenways Commission (1994). Creating a Statewide Greenways System. <https://floridadep.gov/sites/default/files/1994FloridaGreenwaysCommissionPlan.pdf>.
- Frey, H. (1999). Designing the City: Towards a More Sustainable Urban Form. Taylor & Francis. <https://doi.org/10.4324/9780203362433>.
- Government Decision No. 525 of 27 June 1996, Approving the General Town Planning Regulation, Published in the Official Monitor No. 856 of 27 November 2002.
- Hajer, M.A., Pelzer, P., van den Hurk, M., ten Dam, C., & Buitelaar, E. (2020). *Neighbourhoods for the future: A plea for a social and ecological urbanism*. Transcity Valiz.
- Hamel, P., & Tan, L. (2022). Blue-Green Infrastructure for Flood and Water Quality Management in Southeast Asia: Evidence and Knowledge Gaps. *Environmental Management*, 69, 699–718. <https://doi.org/10.1007/s00267-021-01467-w>.
- Ilie, A., Vasilescu, J., Talianu, C., Ioja, C., & Nemuc, A. (2023). Spatiotemporal Variability of Urban Air Pollution in Bucharest City. *Atmosphere*, 14(12), Article 12. <https://doi.org/10.3390/atmos14121759>.
- Ioja, C., Niță, M.R., Vănaș, G.O., Onose, D.A., & Gavrilidis, A.A. (2014). Using multi-criteria analysis for the identification of spatial land-use conflicts in the Bucharest Metropolitan Area, *Ecological Indicators*, 42, 112–121. <https://doi.org/10.1016/j.ecolind.2013.09.029>.
- Jones, L., Anderson, S., Læssøe, J., Banzhaf, E., Jensen, A., Bird, D.N., Miller, J., Hutchins, M.G., Yang, J., Garrett, J., Taylor, T., Wheeler, B.W., Lovell, R., Fletcher, D., Qu, Y., Vieno, M., & Zandersen, M. (2022). A typology for urban Green Infrastructure to guide multifunctional planning of nature-based solutions. *Nature-Based Solutions*, 2. <https://doi.org/10.1016/j.nbsj.2022.100041>.
- Kuehler, E., Hathaway, J., & Tirpak, A. (2017). Quantifying the benefits of urban forest systems as a component of the green infrastructure stormwater treatment network. *Ecohydrology*, 10, 1813. <https://doi.org/10.1002/eco.1813>.
- Laurian, R. (1965). *Urbanismul*. Editura Tehnică.
- Law No. 350 of 6 July 2001, on Spatial and Urban Planning, Published in the Official Monitor No. 373 of 10 July 2001.

- Lăzărescu, C. (Ed.) (1977). *Urbanismul în România*. Editura Tehnică.
- Magrinyà, F., Mercadé-Aloy, J., & Ruiz-Apilánez, B. (2023). Merging Green and Active Transportation Infrastructure towards an Equitable Accessibility to Green Areas: Barcelona Green Axes. *Land*, 12(4), Article 4. <https://doi.org/10.3390/land12040919>.
- Major, Z., Szigeti, C., & Czédli, H.M. (2023). "Green" Tram Tracks for the Sustainability of the Urban Environment. *Chemical Engineering Transactions*, 107, 289-294. <https://doi.org/10.3303/CET23107049>
- McKinney, M.L. (2006). Urbanization as a major cause of biotic homogenization. *Biological Conservation*, 127(3), 247-260.
- Mell, I. (2019). *Green infrastructure planning: Reintegrating landscape in urban planning*. Lund Humphries Publishers Ltd.
- Mell, I., & Scott, A. (2023). *Definitions and context of blue-green infrastructure*. In: Washbourne, C.L., Wansbury, C. (Eds.), ICE Manual of Blue-Green Infrastructure, eISBN: 978-0-7277-6543-7, ISBN: 978-0-7277-6542-0.
- Mell, I.C. (2009). Can green infrastructure promote urban sustainability? *Proceedings of the Institution of Civil Engineers - Engineering Sustainability*, 162(1), 23-34. doi:10.1680/ensu.2009.162.1.23.
- Ministry of Development, Public Works and Administration. (2020, May 15). Technical regulations on urban planning documents. <https://www.mdlpa.ro/pages/reglementare29>.
- Ministry of Development, Public Works and Administration. (2023). Draft LAW for the approval of the Code of Territorial Planning, Urbanism and Construction. <https://www.mdlpa.ro/pages/proiectlegeaprobarecodamenajareteritoriurbanismconstructii>.
- National Strategy of 28 December 2022, for Integrated Urban Development towards Resilient, Green, Inclusive and Competitive Cities 2022-2035 - Romania's Urban Policy, Published in the Official Monitor No. 1275 bis of 30 December 2022.
- O'Donnell, E.C., Netusil, N.R., Chan, F.K.S., Dolman, N.J., & Gosling, S.N. (2021). International Perceptions of Urban Blue-Green Infrastructure: A Comparison across Four Cities. *Water*, 13(4), 544. <https://doi.org/10.3390/w13040544>.
- Pakzad, A., & Osmond, P. (2016). Developing a sustainability indicator set for measuring green infrastructure performance. *Procedia - Social and Behavioral Sciences*, 216, 68-79.
- Petrișor, A.-I., Mierzejewska, L., & Mitrea, A. (2022). Mechanisms of Change in Urban Green Infrastructure - Evidence from Romania and Poland. *Land*, 11(5), Article 5. <https://doi.org/10.3390/land11050592>.
- Pienaru, A.-M. & Rădulescu, D. (2022). Opportunities to apply nature-based solutions in Romania in the context of European common agriculture policy. *Scientific Papers. Series E. Land Reclamation, Earth Observation & Surveying, Environmental Engineering*, XI, 511-516, Print ISSN 2285-6064.
- Popescu, O.C., & Petrișor, A.-I. (2020). Originile conectivității infrastructurii verzi în planificarea urbană. *Revista Școlii Doctorale de Urbanism*, 1, 65-84.
- Popescu, O.-C., Tache, A.-V., & Petrișor, A.-I. (2022). Methodology for Identifying Ecological Corridors: A Spatial Planning Perspective. *Land*, 11. <https://doi.org/10.3390/land11071013>.
- Radinja, M., Atanasova, M., & Lamovšek, A.Z. (2021). The water-management aspect of blue-green infrastructure in cities. *Urbani izziv*, 1, 98-110.
- Rayan, M., Gruehn, D., & Khayyam, U. (2021). Green infrastructure indicators to plan resilient urban settlements in Pakistan: Local stakeholder's perspective, *Urban Climate*, 38, 100899, <https://doi.org/10.1016/j.uclim.2021.100899>.
- Rendeková, A., Mičieta, K., Hrabovský, M., Zahradníková, E., Michalová, M., Miškovíc, J., Eliašová, M., & Ballová, D. (2022). Comparison of the differences in the composition of ruderal flora between conventional tram tracks and managed green tram tracks in the urban ecosystem of the city of Bratislava. *Hacquetia*, 21(1), 73-88. <https://doi.org/10.2478/hacq-2021-0020>.
- Rundle, A., Quinn, J., Lovasi, G., Bader, M.D., Yousefzadeh, P., Weiss, C., & Neckerman, K. (2013). Associations between Body Mass Index and Park Proximity, Size, Cleanliness, and Recreational Facilities. *American Journal of Health Promotion*, 27(4), 262-269. <https://doi.org/10.4278/ajhp.110809-QUAN-304>.
- Sanesi, G., Colangelo, G., Laforteza, R., Calvo, E., & Davies, C. (2017). Urban green infrastructure and urban forests: A case study of the Metropolitan Area of Milan. *Landscape Research*, 42(2), 164-175. <https://doi.org/10.1080/01426397.2016.1173658>.
- Sebastian, E. (2023). We're not surrendering IOR Park! The IOR-Titan Civic Initiative Group proposes an action on Saturday to save the Park. 'A city cannot breathe bricks, curbs and concrete'. Ediția de Dimineață. <https://editiadedimineata.ro/nu-cedam-parcul-ior-grupului-de-initiativa-civica-ior-titan-propune-sambata-o-actiune-pentru-salvarea-parcului-un-oras-nu-poate-sa-respire-caramizi-borduri-si-betoane/>.
- Shafique, M., Kim, R., & Lee, D. (2016). The Potential of Green-Blue Roof to Manage Storm Water in Urban Areas. *Nature Environment and Pollution Technology*, 15(2), 715-718. ISSN: 0972-6268.
- Sikorski, P., Wińska-Krysiak, M., Chormański, J., Krauze, K., Kubacka, K., & Sikorska, D. Low-maintenance green tram tracks as a socially acceptable solution to greening a city, *Urban Forestry & Urban Greening*, 35, 148-164. <https://doi.org/10.1016/j.ufug.2018.08.017>.
- Specific Guidelines from 10 May 2022, on conditions for accessing European funds related to the National Recovery and Resilience Plan under calls for projects NRP/2022/C10, component 10 - Local Fund, Published in the Official Monitor No. 467 bis of 10 May 2022.
- Tache, A.-V., Popescu, O.-C., & Petrișor, A.-I. (2023). Conceptual Model for Integrating the Green-Blue Infrastructure in Planning Using Geospatial Tools: Case Study of Bucharest, Romania Metropolitan

- Area. *Land*, 12(7), 1432.
<https://doi.org/10.3390/land12071432>
- The *Civic Groups of Bucharest*. (2022, June 23).
<https://bucuresticivic.ro/>.
- The Romanian Government. (2024). Just - Legiaslative Portal. <https://legislatie.just.ro/>
- Town and Country Planning Association (2004). "Biodiversity by Design: A Guide for Sustainable Communities". TCPA, London, UK.
- United Nations (2018). 68% of the world population projected to live in urban areas by 2050, says UN. <https://www.un.org/sw/desa/68-world-population-projected-live-urban-areas-2050-says-un>.
- Wagner, I., Krauze, K., & Zalewski, M. (2013). Blue aspects of green infrastructure. *Sustainable Development Applications*, 4, 145-155.
- Wang J., Pauleit S., & Banzhaf E. (2019). An Integrated Indicator Framework for the Assessment of Multifunctional Green Infrastructure - Exemplified in a European City. *Remote Sensing*, 11(16), 1869. <https://doi.org/10.3390/rs11161869>.
- Western Regional Development Agency. (2021). PR-Vest-2021-2027_publicat-pe-site.pdf. SFC2021 Programme supported by ERDF (Investment for Employment and Growth), ESF+, Cohesion Fund and EMFF. https://adrvest.ro/wp-content/uploads/2022/10/PR-Vest-2021-2027_publicat-pe-site.pdf.
- Zhu, W.X., & Carreiro, M.M. (2004). Variations of soluble organic nitrogen and microbial nitrogen in deciduous forest soils along an urban-rural gradient. *Soil Biology and Biochemistry*, 36(2), 279-288.

INDUSTRIAL WASTES USED AS ADDITIVES IN BUILDING MATERIALS TO REDUCE ENVIRONMENTAL POLLUTION

Mihai VRABIE^{1,2}, Nicolae APOSTOLESCU¹, Maria HARJA¹

¹“Gheorghe Asachi” Technical University of Iasi, Faculty of Chemical Engineering and
Environmental Protection, 73 Prof. Dimitrie Mangeron Blvd, Iasi, Romania

²S.C. Gemite RO SRL, 52 SF Petru Movila Street, Iasi, Romania

Corresponding author email: maria_harja@yahoo.com

Abstract

Environmental pollution is a major issue that we are dealing with at the moment. The reuse of industrial waste, which is used as raw materials in other industries such as the construction materials industry, is a beneficial way to reduce pollution. This is possible due to the physical, chemical, and mineralogical properties of industrial waste. Examples of industrial waste that can be used for obtaining new building materials are: fly ash, furnace slag, silica fume, and so on. These wastes were analysed in this study using the following techniques: SEM, XRD, and EDAX. After characterization, the wastes were used as additives in cement-based materials. The following properties of the obtained materials were tested: compression strength, flexural strength, adhesion to the substrate, and shrinkage testing. Based on the results of the tests, the percentages used as waste addition were chosen.

Key words: cement-based materials, fly ash, furnace slag, silica fume.

INTRODUCTION

The world is attempting for a circular economy with low carbon emissions. Similarly, the construction industry wants to achieve this goal through alternative large-scale cement-related products, reducing the negative effects of cement production and creating a sustainable and environmentally friendly products (Juang & Kuo, 2023; Swaroop et al., 2013).

The most common building material is cement, whose manufacturing uses a lot of energy and raw materials and produces a lot of greenhouse emissions (Zhang et al., 2023).

Around the world, pozzolanic alternative materials are frequently used in construction as a partial replacement for ordinary Portland cement in mortars and concretes (Rafiza et al., 2022; Durastanti & Moretti, 2020). Fly ash, furnace slag, silica fume, and other industrial wastes are among those that can be used for replacing of regular Portland cement. Reusing these industrial wastes solves the problem of storing them in locations designated for that purpose, such as landfills, which reduces the level of pollution in the environment (He et al., 2019). The addition of waste material to concrete instead of cement helps to meet the grow-

ing demand for concrete while also improving the use of waste materials. Furthermore, it has been noted that the strength and durability of concrete are increased when waste materials are used as pozzolanic (Harja et al., 2022). This lessens the potential damage to the environment (Ahmad et al., 2021; Lee et al., 2016).

The industrial byproduct of burning coal in power plants and thermal power plants is coal fly ash, and practically every country in the world struggles with how to dispose of this material (Harja et al., 2023). However, it should be mentioned that fly ash has a lot of potential for use as a partial substitute for Portland cement because of its excellent pozzolanic activity, fine grain size, and physicochemical characteristics (Golewski & Szostak, 2022; Golewski, 2023; Fu et al., 2022; Wu et al., 2019; Wong et al., 2022).

Furnace slag is a common byproduct of the iron and steel industry and is frequently used as pozzolanic material due to the varying content of reactive silico-aluminate in it. This industrial waste is classified as a pozzolanic material due to its relatively stable chemical properties and high reactivity (Zhao et al., 2024).

Silica fume is a byproduct of the silicon and ferrosilicon alloy manufacturing process. Silica

fume is essential for increasing the strength of cementitious materials because it causes the formation of calcium silicate hydrate, which has a high strength (Mehta & Ashish, 2020; Vrabie et al., 2023; Cotofan et al., 2022). Silica fume increases the hydration level and compressive strength of hardened pastes, mortars and concretes. This increase in strength is due to the bonding of the hardened cement paste to the aggregate. The degree of crystal orientation, crystal size, and calcium hydroxide content at the interface are decreased by the addition of silica fume (Shoubar et al., 2020; Rahmouni et al., 2023).

This study developed a strategy for reusing industrial waste as a partial substitute for cement, reducing CO₂ emissions from cement production and addressing the issue of landfill disposal.

The physical, chemical, and mineralogical properties of the raw materials used have been described, as well as their significant impact on pollution reduction. The prepared materials were mechanically examined to determine the impact of using these wastes instead of cement. The following properties were evaluated: compression strength, flexural strength, adhesion to the substrate, and shrinkage grade of the materials produced.

MATERIALS AND METHODS

In this study, industrial wastes were used as an additive to the mortar. Table 1 shows the compositions of the prepared mixtures. The cement/sand ratio was 1 to 2.5.

Table 1. Mix composition mortar samples

Mix	Compound	Weight (kg)
Mix 0	Portland Cement	571
	Sand 0 – 1 mm	1427.5
	Water	257
Mix 1	Portland Cement	571
	Sand 0 – 1 mm	1427.5
	Fly ash	57,1
	Silica fume	57,1
	Water	300
Mix 2	Portland Cement	571
	Sand 0 – 1 mm	1427.5
	Furnace Slag	57.1
	Silica fume	57.1
	Water	295

Carpatcement Romania (Portland Cement) used in this study was type CEM II/A-LL 42.5 R. Bega Minerale Industriale from Romania supplied the sand used. The fly ash used in this study was obtained from Czech Republic. The furnace slag for this study was supplied by ArcelorMittal of Galați, Romania. The silica fume was supplied by Norchem, from the United States.

Industrial waste was analysed using SEM, XRD, and EDAX.

The compression and flexural strength tests were performed with 40 x 40 x 160 mm molds and the test machine compression/flexural 15/250kN. The adhesion to the substrate was tested using a PoliTest AT tensile adhesion tester. Shrinkage was measured using test machine length comparators.

RESULTS AND DISCUSSIONS

Characterization of fly ash

The SEM presented in Figure 1 shows that fly ash consists of spherical particles with a narrow granulometric spectrum.

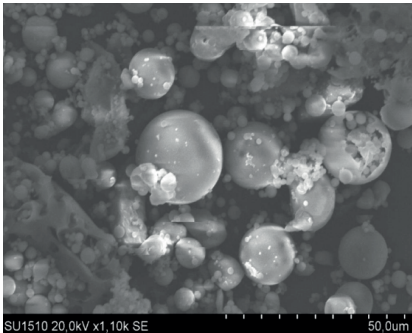


Figure 1. SEM analysis of fly ash

The analysed fly ash has a fine consistency, with particles of various spherical shape sizes, and an off-white colour, indicating a high concentration of CaO. SEM analysis reveals that the ash contains irregularly shaped particles, as well as spherical particles that aggregate into macrospheres. The various forms of silicon result in irregularly shaped particles. In the ash studied, the particles have a spherical shape, and the unburned carbon content is reduced.

Figure 2 depicts an EDAX analysis of fly ash. The ash contains Si, O, Al, Ca, Fe, K, Na, Mg,

and Ti, that determined the physicochemical and technological properties. The elements are found in ash in oxide form.

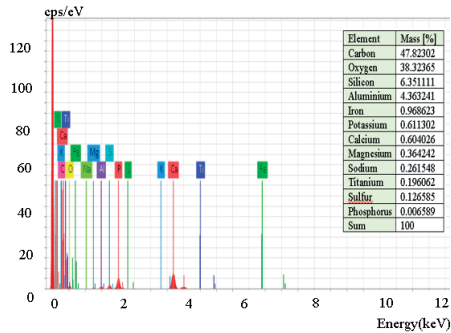


Figure 2. EDAX analysis of fly ash

The EDAX results show that the fly ash contains a high amount of calcium. However, the non-uniform composition of power plant waste and the use of surface EDAX readings at different points may influenced the results.

Figure 3 shows the XRD spectrum of the fly ash, which contains elements (crystalline phases) such as hematite (He), quartz (Q), mullite (M), and a glassy phase.

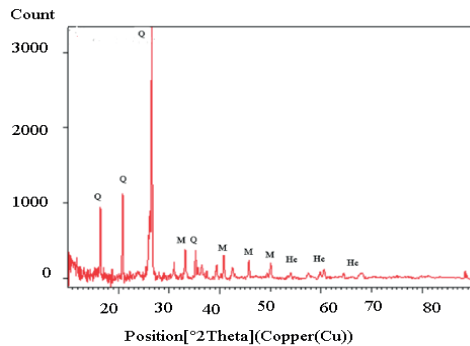


Figure 3. XRD analysis of fly ash

The elements present in the vitreous phase of the ash are estimated using XRD and EDAX analysis, revealing the presence of Si, Al, Ca and K. These elements were found in two main crystals: quartz and calcium-alumino silicates, each in a vitreous phase containing various amounts of K, Na, Ca, Mg and Fe.

Characterization of furnace slag

The data from Figure 4 show that the furnace slag is in the form of a fine powder with

particles of various shapes, which are influence to mechanical grinding.

Furnace slag contains fine particles under 5 μm , accounting for a significant portion of its weight.

The presence of the coarse part indicates open circuit grinding.

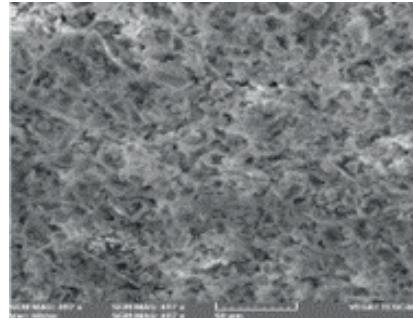


Figure 4. SEM analysis of furnace slag

The chemical elements present in the furnace slag were identified using elementary chemical analysis, with the results shown in Figure 5 and XRD Figure 6.

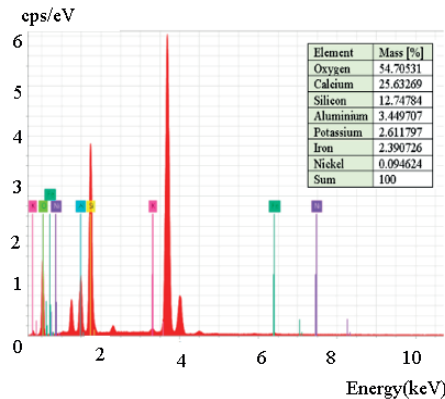


Figure 5. EDAX analysis of furnace slag

Furnace slag is composed of Ca, Si, O, Al, Mg, and Fe, with traces of K, Ti, and Ni found in one area. Chemical analysis reveals a high concentration of calcium oxide and magnesium oxide. In addition, the furnace slag analysed contains a high concentration of aluminium oxide. The XRD analysis shows the presence of alpha cristobalite phases, primarily as $\text{Mg}_3(\text{Fe}, \text{Al}, \text{Si})_2(\text{SiO}_4)_3$. Furnace slag phases and

amorphous content are in accord with literature.

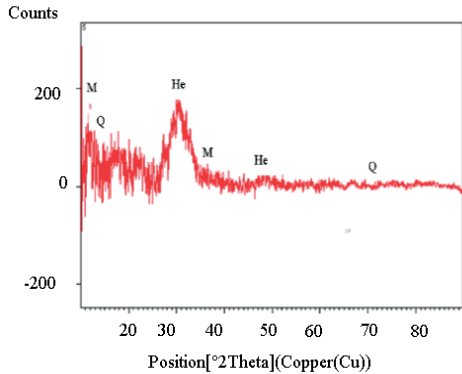


Figure 6. XRD analysis of furnace slag

Based on phase thermal equilibrium relations, the identified compounds form a melilite series that is specific to furnace slag. There are also small CaO and free MgO peaks (Figure 6).

Characterization of silica fume

Figure 7 shows a SEM image performed to emphasise the size and shape of the silica fume particles and Figure 8, the EDAX analysis.

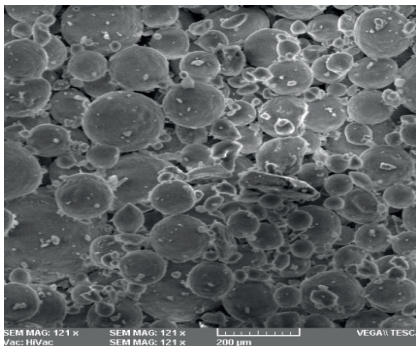


Figure 7. SEM analysis of silica fume

Silica fume is depicted as a grey powder with particles of various sizes and morphologies. Adjacent to these irregularly shaped microparticles are spherical microparticles, whose shape is determined by the temperature at which they are formed and cooled. Silica fume is primarily composed of silicon oxide, but can also contain silicon carbide (less than 3%), free carbon, and impurities from raw materials (Figure 8).

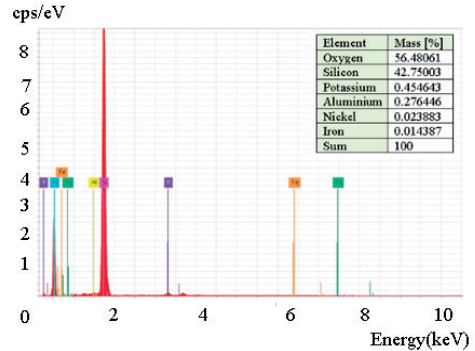


Figure 8. EDAX analysis of silica fume

Figure 9 depicts an XRD diagram of the chemical elements found in silica fume in crystalline form. The XRD analysis shows that quartz (Q) is the primary crystalline phase of silica fume, with minor amounts of muscovite (Ms), kaolinite (K), mullite (M), and other minerals.

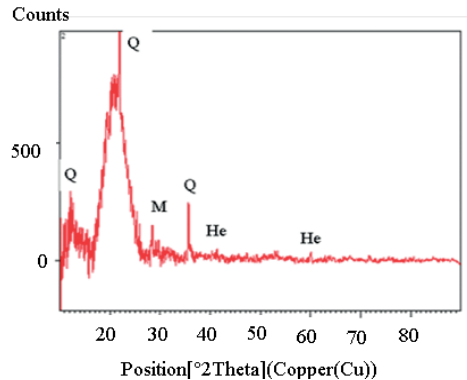


Figure 9. XRD analysis of silica fume

Characterization of mortars

• Compressive strength

Figure 10 shows that the mixture with the highest compressive strength contains silica fume and furnace slag as additives.

The reason for this is the chemical composition, which contains a high concentration of SiO₂ and CaO. Mechanical properties are influenced by the chemical composition of the components as well as the morphology and granulometry of the particles. Mixtures with high SiO₂ and CaO content exhibit higher compression values compared to the blank sample.

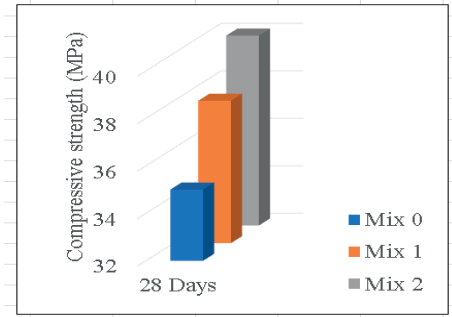


Figure 10. Compressive strength of mortar samples

Despite the fact that more water was required to ensure workability in this study, the prepared materials exhibited excellent properties. Using fly ash and silica fume resulted in lower values than Mix 2, but better than the blank sample (Mix 0). The values obtained ranged from 35 MPa (Mix 0), 38 MPa (Mix 1), and 40 MPa (Mix 2).

- Flexural strength of materials

The same phenomenon occurs with flexural strength as it does with compression strength. Fly ash (Mix 1) and furnace slag (Mix 2) fill in the gaps in silica fume's properties. According to Figure 11, Mix 2 has the highest flexural value at 28 days (10.1 MPa), followed by Mix 1 (9.3 MPa), with the blank sample Mix 0 having the lowest value (8.5 MPa).

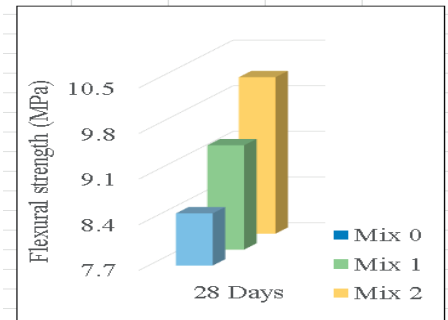


Figure 11. Flexural strength of mortar samples

- Adhesion on substrate of materials

The fineness of the particles, in addition to their chemical composition, is an important factor in adhesion to the substrate. Figure 12 shows that, as with the previously obtained

mechanical characteristics, Mix 2 has the highest adhesion value. This is given that silica fume and furnace slag contain high levels of silicon oxide and calcium oxide. Adhesion values (Figure 12) range from 2.19 MPa (Mix 0), 2.25 MPa (Mix 1), and 2.32 MPa (Mix 2).

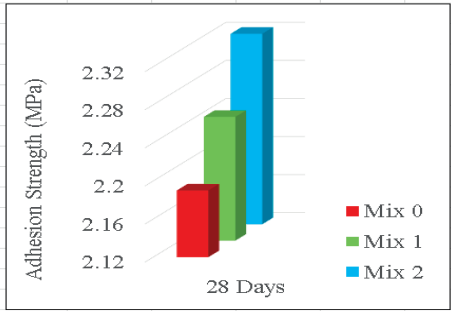


Figure 12. Adhesion strength of mortar samples

- Shrinkage of materials

The best recorded value for material shrinkage can be identified in the blank sample. The consumption of water is an important factor in this determination because it is released when the material matures, which causes the material to shrinkage. Percentages ranged from 0.4% to 0.49%, with a maximum of 0.5% (Figure 13).

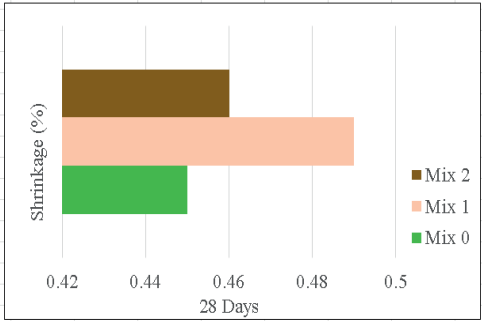


Figure 13. Shrinkage of mortar samples

CONCLUSIONS

After the research conducted or observed, the following conclusions were reached. During performing the analyses, it was found that the chemical, physical, and mineralogical compositions of used wastes such as fly ash, furnace slag, and silica fume are similar to those of cement, indicating that these industrial

wastes have a pozzolanic character and can be used in mortars. From this study, it was determined that they are effective when used as mortar additives.

The mechanical characterization of the obtained materials indicates that the use of industrial waste as additives, resulted in a compressive strength of up to 40 MPa and the flexural strength about 10.1 MPa. The good results were obtained for adhesion to the substrate, values as high as 2.23 MPa. Although the values are within the maximum permitted limit.

It was found that recycling industrial waste has benefits for lowering pollution levels as well as producing materials with superior qualities at comparatively low costs.

ACKNOWLEDGEMENTS

This research was supported by the Gheorghe Asachi Technical University Doctoral School.

REFERENCES

- Ahmad, A., Farooq, F., Niewiadomski, P., Ostrowski, K., Akbar, A., Aslam, F., & Alyousef, R. (2021). Prediction of compressive strength of fly ash based concrete using individual and ensemble algorithm. *Materials*, 14(4), 794.
- Cotofan, A. I., Caftanachi, M., Vrabie, M., Harja, M., (2022), Methods for obtaining of new add-value materials by fly-ash modification, *The bulletin of the polytechnic institute from Iasi*, 68(72), 37-49.
- Durastanti, C., & Moretti, L. (2020). Environmental impacts of cement production: A statistical analysis. *Applied Sciences*, 10(22), 8212.
- Fu, Q., Zhang, Z., Wang, Z., He, J., & Niu, D. (2022). Erosion behavior of ions in lining concrete incorporating fly ash and silica fume under the combined action of load and flowing groundwater containing composite salt. *Case Studies in Construction Materials*, 17, e01659.
- Golewski, G. L. (2023). The effect of the addition of coal fly ash (CFA) on the control of water movement within the structure of the concrete. *Materials*, 16(15), 5218.
- Golewski, G. L., & Szostak, B. (2022). Strength and microstructure of composites with cement matrixes modified by fly ash and active seeds of CSH phase. *Structural Engineering and Mechanics, An Int'l Journal*, 82(4), 543-556.
- Harja, M., Teodosiu, C., Isopescu, D. N., Gencel, O., Lutic, D., Ciobanu, G., & Cretescu, I. (2022). Using fly ash wastes for the development of new building materials with improved compressive strength. *Materials*, 15(2), 644.
- Harja, M., Caftanachi, M., Fanache, M., & Ciobanu, G. (2023). Fly ash waste for obtaining building materials with improved durability. *Scientific Study & Research. Chemistry & Chemical Engineering, Biotechnology, Food Industry*, 24(1), 49-60.
- He, Z., Zhu, X., Wang, J., Mu, M., & Wang, Y. (2019). Comparison of CO₂ emissions from OPC and recycled cement production. *Construction and Building Materials*, 211, 965-973.
- Juang, C.U., & Kuo, W.T. (2023). Properties and Mechanical Strength Analysis of Concrete Using Fly Ash, Ground Granulated Blast Furnace Slag and Various Superplasticizers. *Buildings*, 13(7).
- Lee, M.G., Kang, D., Jo, H., & Park, J. (2016). Carbon dioxide utilization with carbonation using industrial waste-desulfurization gypsum and waste concrete. *Journal of Material Cycles and Waste Management*, 18, 407-412.
- Mehta, A. & Ashish, D.K. (2020). Silica fume and waste glass in cement concrete production: A review. *Journal of Building Engineering*, 29, 100888.
- Rafiza, A.R., Fazlizan, A., Thongtha, A., Asim, N., & Noorashikin, M.S. (2022). The physical and mechanical properties of autoclaved aerated concrete (AAC) with recycled AAC as a partial replacement for sand. *Buildings*, 12(1), 60.
- Rahmouni, Z. E. A., Maza, M., Tebbal, N., & Belouadah, M. (2023). On the Combination of Silica Fume and Ceramic Waste for the Sustainable Production of Mortar. *FDMP-Fluid Dynamics & Materials Processing*, 19(5), 1083-1090.
- Shubbar, A.A., Sadique, M., Nasr, M.S., Al-Khafaji, Z.S., & Hashim, K.S. (2020). The impact of grinding time on properties of cement mortar incorporated high volume waste paper sludge ash. *Karbala International Journal of Modern Science*, 6(4), 7.
- Swaroop, A.H.L., Venkateswararao, K. & Kodandaramarao, P. (2013). Durability studies on concrete with fly ash & Ggbs. *International Journal of Engineering Research and Applications*, 3(4), 285-289.
- Vrabie M., Caftanachi M., Cotofan A.I., Harja, M. (2023), Wastes Used for Obtaining Sustainable Building Materials, *The bulletin of the polytechnic institute from Iasi*, 73, 115-126.
- Wong, L.S., Chandran, S.N., Rajasekar, R.R., & Kong, S.Y. (2022). Pozzolanic characterization of waste newspaper ash as a supplementary cementing material of concrete cylinders. *Case Studies in Construction Materials*, 17, e01342.
- Wu, C.H., Huang, C.H., Kan, Y.C., & Yen, T. (2019). Effects of Fineness and Dosage of Fly Ash on the Fracture Properties and Strength of Concrete. *Applied Sciences*, 9(11), 2266.
- Zhang, Y., Zhao, B., Zhu, J., Wang, Z., Ren, C., Xie, H., & Zhu, D. (2023). Research on Properties of Ash and Slag Composite Cementitious Materials for Biomass Power Plants. *Processes*, 11(6), 1627.
- Zhao, J., Liu, J., Gao, X., Zhang, H., Zhang, H., & Gu, X. (2024). Effect of environment conditions on volume deformation of blended cement mortars containing blast furnace slag and steel slag powder. *Journal of Building Engineering*, 108692.

RECYCLING OF STEEL FURNACE SLAGS (SFS) BY EFFICIENT INTEGRATION IN CONSTRUCTION MATERIALS AS AGGREGATE PARTIAL REPLACEMENT

**Cornelia BAERĂ^{1,2}, Aurelian GRUIN^{1,3}, Ana-Cristina VASILE^{1,3},
Bogdan BOLBOREA^{1,3}, Alexandru ION¹, Gabriela BĂNĂDUC^{2,4}**

¹National Institute for Research and Development in Construction,
Urban Planning and Sustainable Spatial Development - URBAN-INCERC, Timisoara Branch,
2 Traian Lalescu Street, Timisoara, Romania

²Politehnica University Timisoara, Faculty of Management in Construction and Transportation,
14 Remus Street, Timisoara, Romania

³Politehnica University Timisoara, Faculty of Civil Engineering,
2 Traian Lalescu Street, Timisoara, Romania

⁴Caransebes City Hall, Service of Programs, Projects and Strategies, Directorate for Strategies,
Programs and Environmental Protection,
1 Revolution Square, Caransebes, Caras-Severin County, Romania

Corresponding author email: cornelia.baera@upt.ro

Abstract

Slags, mixtures of mainly metal oxides and silicon dioxide, represent by-products or wastes generated by the ore smelting processes. There are several types of slags, but for construction applications as recycling possibilities, there are generally used slags generated by iron and steel making industry. The present study is focused on electric arc furnace slags (EAF), produced, and stored in the western part of Romania, Caransebeș city. The current slag deposit has been operating on this site since 1771, with the establishment of the furnaces to produce cast iron in Reșița. This paper presents a preliminary experimental study on the possibilities of using the Reșița SFS slags as a partial substitute for aggregate in cementitious materials for the construction industry. The opportunity and necessity of the proposed research direction cover several purposes: waste management implementation, environmental protection and natural resources saving, for the Circular Economy (CE) implementation in the Romanian industry. The initial results emphasise the concept's viability applied to the Reșița slag landfill, encouraging further exploration of this environmental engineering topic.

Key words: Circular Economy, construction eco-materials, mineral addition, steel furnace slag (SFS), waste recycling.

INTRODUCTION

As a result of the diverse smelting processes applied to metallic ores generate slags, valuable by-products emerging as a potentially valuable resource for various civil infrastructure applications. The current study focuses on using slags generated from different steelmaking procedures. In the steel production process, the primary refinement takes place at a blast furnace, where iron ore undergoes processing to produce pig iron. The resulting slag from this process, known as blast furnace slag, has applications such as being employed as an aggregate in the form of air-cooled blast furnace slag (ACBFS). However, it is more commonly utilized as a supplementary cementitious material (SCM) in the form of ground

granulated blast furnace slag (GGBFS) (Shi & Qian, 2000; Snellings et al., 2012; Özbay et al., 2016; Wang, 2016; Buddhdev & Timani, 2020). Following the blast furnace, pig iron undergoes refinement to produce crude steel. Additionally, other forms of crude steel are created through the refining of recycled and scrap steel. Various processes can be employed for this purpose, and the resulting slag from these processes is collectively referred to as steel furnace slag (SFS). The steel furnace slag (SFS) includes: a) the electric arc furnace (EAF) slag; b) the basic oxygen furnace (BOF) slag; c) the ladle metallurgy furnace (LMF) slag; and d) the argon oxygen decarburization (AOD) slag (Brand & Fanijo, 2020). (The effective utilization of SFS worldwide is estimated to be around 80% (Branca et al, 2020). Over time various research

studies investigated the different types of SFS materials and their impact on the properties of cementitious composites when used as an aggregate and/or supplementary cementitious material (SCM). The general conclusions indicate that not all SFS additions are identical and consequently, they should be categorized or qualified based on their intended purpose or use, especially when considering applications such as concrete, mortar, alkali-activated material, or soil stabilization (Brand & Fanijo, 2020).

The steel furnace slag (SFS) aggregate can significantly impact the properties of cementitious composites, even when the mixture volumetrics remain constant (Giergiczny, 2014; 2019). For instance, concrete incorporating recycled concrete aggregates (RCAs) typically exhibits strength reductions compared to virgin aggregates, but the extent of this reduction varies widely, depending on several influencing factors, such as microstructure development, adhered mortar, moisture absorption and content, RCA heterogeneity, and overall quality (Li & Herbert, 2012; Snoeck, 2015; Teixeira et al., 2016; Hemalatha & Ramaswamy, 2017; Li, 2008). In the case of SFS aggregates, even when considering the same type of SFS, research indicates that concrete strength can either increase, decrease, or remain similar to that of concrete with virgin aggregates.

Slag possesses a complex chemical composition characterized by elements such as calcium oxide, silicon oxide, aluminium oxide, and others, which determines the physical, mechanical and durability characteristics of materials where used. Slag concretes can develop compressive tensile properties comparable to classic mixes, sometimes even superior. At the same time, the durability performance of slag cement-based materials offers better durability behaviour (Brand & Fanijo, 2020).

Aggregates (sand, gravel and coarse particles), play a pivotal role regarding the mix design of both concrete and mortar, constituting a substantial proportion of their and also determining the future material performance in terms of physical, mechanical and durability. Nevertheless, aggregates are a finite and non-renewable resource sourced from rivers or quarries, and their excessive exploitation, particularly in Romania, poses a considerable

threat to the environment. This overuse can lead to adverse consequences such as shoreline erosion, diminished groundwater levels, destruction of local flora and fauna, landslides, and accidents. The existing legislative framework in Romania is deemed inadequate as it permits excessive and detrimental extraction practices. Furthermore, Romania faces a scarcity of sand, particularly in the fine-grain form, intensifying the urgency for viable solutions to address these pressing issues (Hemalatha & Ramaswamy, 2017).

Valorisation of mineral additions (by-products/residues of industrial flows) in construction materials via innovative inclusion processes, in the context of Circular Economy (CE) strategies in Romania

The current research is applied to steel furnace slags (SFS), specifically electric arc furnace slags (EAF), produced and stored on this site, in the western part of Romania, in Reșita, Caraș-Severin County, since 1771. This paper presents a targeted, theoretical and experimental study on the possibilities of using the identified SFS slags of EAF type, as a partial substitute for aggregate in cementitious materials for the construction industry. The intended major outcome of the study is the increase of the industrial by-product added value concerning the current use. The opportunity and necessity of the proposed research direction were identified by the use of strategic management specific methods, within the research project PN 23 35 04 01 of Nucleu Programme of the National Research Development and Innovation Plan 2022-2027, "ECODIGICONS", supported by the Ministry of Research, Innovation and Digitalization, and it is covering several purposes associated to the project's objectives: waste management implementation, environmental protection and natural resources saving, for the Circular Economy (CE) implementing in the Romanian industry.

The presented research is conducted with respect to the first Axis, the *Development of innovative engineering solutions for eco-intelligent construction products by an efficient capitalization of additions generated by local industries*, of the two fundamental research axes of the PN 23 35 04 The project's objectives include identifying scientific, technical and

applied solutions for the national construction infrastructure, in accordance with the National Strategy regarding the Circular Economy (SNEC 2022), National Strategy for Research, Innovation and Smart Specialization (SNCISI 2022-2027), and the Recovery and Resilience Plan for Romania (PNRR).

The first Axis of the project is concerned with identifying recovery solutions for mineral wastes or by-products as results of local or regional industrial processes, inert, latent hydraulic or with pozzolanic activity materials, with potential applicability in construction materials or products (ADD-S). Targeted mineral additions, in the form of powders, coarse granules, slurries, or mixtures in suspension, are evaluated from this valorising perspective as partial or complete replacement of traditional constituents: aggregates as "skeleton" of concrete or cement as binder.

The research currently aims to identify ADD-S type materials produced by the local industry (Timisoara, Timiș county, the Western region or even Romania) and to assess their potential valorisation in cementitious materials, geopolymers, mixtures asphalt, etc., with diverse applicability areas for the innovative engineering development by the means of eco-intelligent construction products, with advanced functionality (materials, elements and

structures, models and technologies, circular eco-design algorithms and directions, etc.), in the context of SNCISI 2022-2027 regarding the transition to EC and SNEC 2022.

Figure 1 presents the Eco-CP Flowchart, namely the logical scheme for the structural implementation of specific project objectives associated with the first Axis of the project. The considered abbreviations are the following:

- ADD-S: Additions Derived from Waste and Industrial Byproducts (inert/hydraulically latent/pozzolanic, etc.), and/or derived from demolition and/or decommissioning of buildings;
 - AdT: Target Additions (AdT), with high potential for capitalization in circular design for eco-intelligent construction products;
 - Eco-CCM: Eco-intelligent Composite Materials for Constructions, with advanced functionality (Eco-Composite Materials for Constructions);
 - Eco-CP: Eco-intelligent Construction Products, with advanced functionality, made by using Eco-CCM (Eco-Construction Products).
- One of the identified AdT directions is represented by the Steel slag, SFS (EAF and/or BOF), waste/by-product, specifically electric arc furnace slags (EAF), produced and stored in the western part of Romania, in Reșita, Caraș-Severin County.

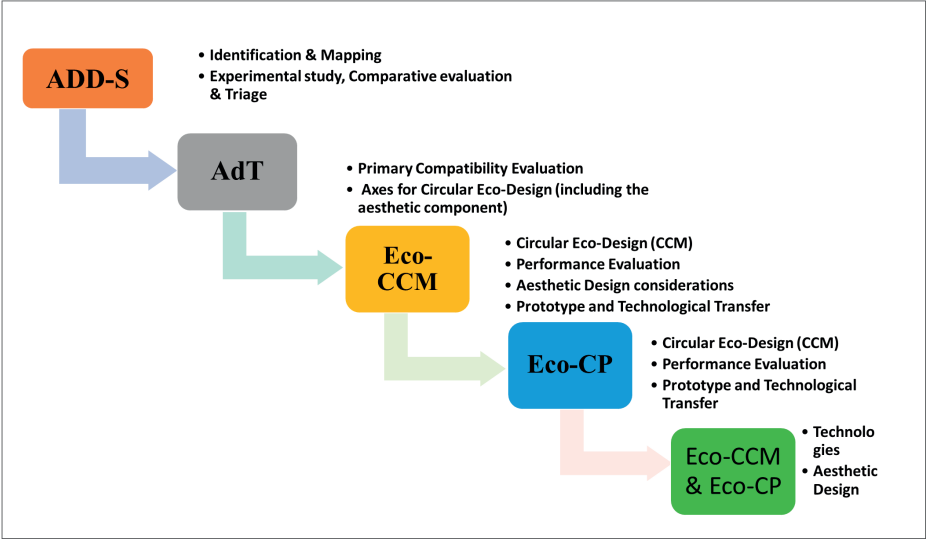


Figure 1. Eco-CP Flowchart: The logical scheme for structural implementation of specific project objectives associated with the first Axis of NIRD URBAN-INCERC research project PN 23 35 04 01

MATERIALS AND METHODS

The present preliminary research is performed to evaluate the opportunity to capitalize on the targeted addition (AdT), namely the EAF slag derived from local industries from the Romanian Western Region (Caraş-Severin County) in cement-based materials for construction. The mineral waste particularly used for the study is abbreviated as RS1, representing the Reşita EAF slag of granular class 0/4 (Figure 2, f). The applied procedure consists in developing of regular mortar mixes, References (R) and also test mortars, RS1 mortars, developed by using RS1 addition. The References (R) mortars represent usual cementitious mixes (mortars) of aggregate (sand), binder (cement) and water. The RS1 test mortars are produced by considering the RS1 addition as a partial substitute for sand in the reference (R), aiming to fast evaluate the elementary compatibility of the RS1 material with the cementitious matrix and thus, the viability of the research direction. The specific comparative analyses of the RS1 mortars with respect to the References (R) are performed in terms of physical and mechanical performance. The control mixes (R1 and R2) represent usual mortars, and the test mixes (RS1 mortars) are developed by considering the RS1 addition as a partial substitute for sand in the

reference (R): 25% and 50% substitution percentage by mass, in accordance with the classical approach of previous studies.

The sequence and duration of the mixing operations are established following the EN 196-1 specifications. The procedure proves viable and is maintained without adjustments throughout the present experimental stage.

Raw materials selective analysis is also performed. The developed mixes (R and RS1) are physically and mechanically evaluated, considering both fresh and hardened state: visual analysis of the mixes, consistency, density, and early age flexural and compressive strength, as critical parameters for further development of the study.

Raw materials

The R and RS1 mixes were produced with locally available raw materials (Figure 2):

- Natural aggregates of granular class 0/4 (sand, S), (Figure 2, a and b);
- Portland Cement, CEM II/A-LL 42.5 R (C), Carpatcement (Figure 2, c and d);
- AdT: EAF slag derived from local industries from the Romanian Western Region (Reşita, Caraş-Severin County), RS1 (Figure 2, e and f).
- Water (tap water).



Figure 2. Raw materials for cement-based mortar mix design: a) and b) Natural sand 0/4 (S 0/4); c) and d) Binder - Carpatcement Portland Cement CEM II/A-LL 42.5 R; e) AdT: EOF (RS) derived from the aggregate crushing line, Caraş-Severin County; f) selected AdT: RS1

Preliminary identification procedures for the RS1 addition

Experimental testing is carried out in order to analyse the RS1 addition inert additions from a physical, mechanical, chemical, mineralogical, etc. aspect, to obtain a preliminary, identification assessment, along with the preliminary compositional integration stage. The EOF crushed aggregate, RS1, was subjected to SEM imaging preliminary determinations, performed by the ISIM Timisoara laboratory. The analysis was done in terms of visual analysis of granule shape and also of chemical analysis performed by energy dispersive spectroscopy (EDS) technique. Table 1 and Figure 3 present the chemical composition of RS1 particles and Figure 4 shows the visual characteristics of the RS1 particles. The experimental sieving analysis of the samples is performed according to EN 933-1

method, and the results are presented in Figure 5. Granulometric analysis by sieving is carried out both, for the usual sand 0/4 (S), for the substitution by-product RS1 and additionally for the S + RS1 mixtures, in the considered substitution proportions: RS1 25% and RS1 50%.

Table 1. SEM analysis: Chemical analysis of RS1

CaSiO			
Element	Signal Type	Wt %	Wt % Sigma
O	EDS	48.78	0.71
Mg	EDS	3.65	0.17
Al	EDS	2.63	0.14
Si	EDS	10.36	0.23
S	EDS	1.71	0.10
Ca	EDS	30.19	0.46
Mn	EDS	0.36	0.11
Fe	EDS	2.31	0.16
Total		100.00	

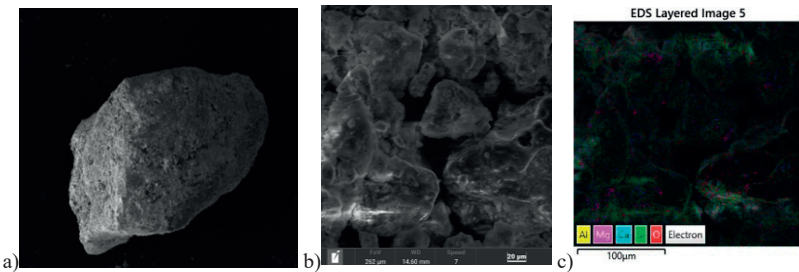


Figure 3. SEM analysis: Visual aspect of ADD-S RS1 grains

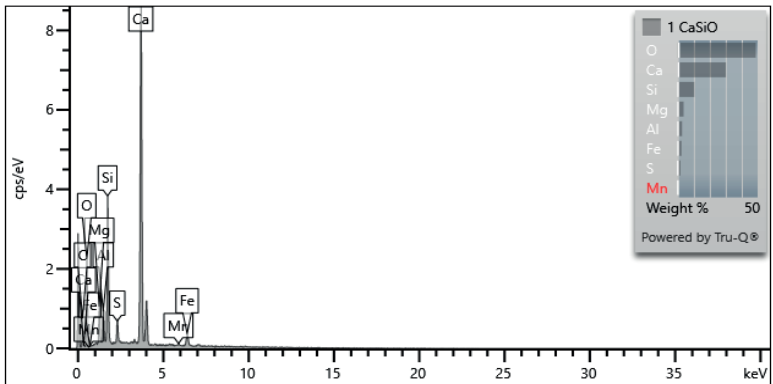


Figure 4. SEM analysis: Chemical analysis of RS1

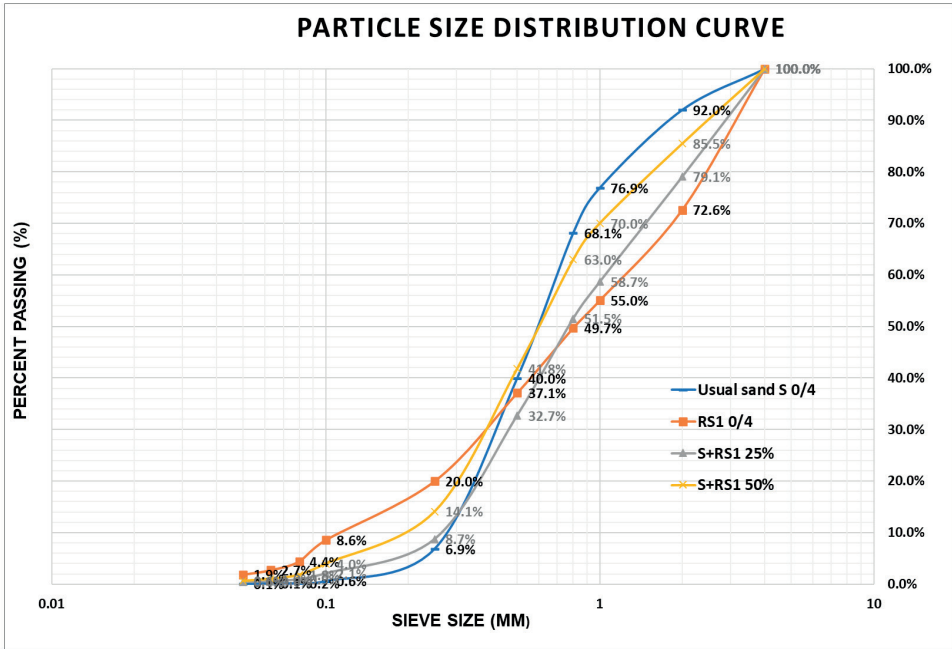


Figure 5. Aggregate grading: Natural sand 0/4 (S), RS1 and aggregate mixes according to the proposed proportions

Mix proportion and specimen preparation

The reference mortar mixes, with classic raw materials: regular sand 0/4 (S), cement and water are produced. The initial reference mix R1, was produced, characterised by the water-to-cement ratio (W/C) 0.56. Further on, considering the dynamics of the research, R2 (W/C = 0.61) was developed. Development of the RS1 mortar mixes implied incremental replacement, by mass, of the usual aggregate (S), with RS1 additions. The considered substitution proportions are RS1 25% and RS1 50%.

The fresh state characteristics of the RS1 mixes show an alteration of workability, especially when using the 50% RS1 substitution, which determined the use of R2 (W/C = 0.61) suitable for relevant specific evaluation. Table 2 presents the mix proportions (established with respect to the cement content, C = 1.0) of all the mixtures used for the preliminary study: the References (R1 and R2) and the RS1 mortars (RS1-25%-0.56; RS1-25%-0.61; RS1-50%-0.61).

The low-volume batch mixing procedure was designed according to EN 196-1 specifications.

Table 2. Mix proportions of the considered mortar mixtures: References and RS1 mixtures

Components	C	S 0/4	RS1	W/C	A/C
Mixtures					
R1	1	3	-	0.56	3
R2	1	3	-	0.61	3
RS1-25%-0.56	1	2.25	0.75	0.56	3
RS1-25%-0.61	1	2.25	0.75	0.61	3
RS1-50%-0.61	1	1.5	1.5	0.61	3

Fresh state evaluation of the preliminary mixes

The mortars were evaluated during and after specific mixture sequences regarding the fresh state mixing behaviour (Figure 6). Further on, the fresh state characteristics are determined: the fresh state density (Figure 7, a and b) and the consistency of the materials (Figure 7, c to l). The fresh state density was determined according to EN 1015-6, by weighing the freshly poured material in a container with a predetermined volume and referring to its volume, respectively 1 l.

The consistency of the fresh mortars was determined by the reference method specified by EN 1015-3, namely the spreading mass.

After mixing and fresh state evaluation (Figure 6), the mortars were casted into the 40 x 40 x 160 (mm) prismatic, metallic molds (Figure 8, a), cured at the temperature $T (20 \pm 1) ^\circ\text{C}$ and relative humidity $RH (90 \pm 5) \%$ for 24 h. The hardened specimens (Figure 8, b) were removed from the molds after 24 hours, visually evaluated and placed in water at the temperature $T (20 \pm 1) ^\circ\text{C}$, until the considered testing age, respectively 7 days.

Hardened state evaluation of the preliminary mixes

The physical-mechanical performance of the mortars is preliminary evaluated by the bending tensile strength, determined on the 40 x 40 x 160 mm prismatic specimens, at an early age,

namely 7 days. The flexural tensile strength and the compressive strength were determined in accordance with EN 1015-11 and EN 196-1. The flexural strength used the three-point bending (3PB) test (Figure 8, c) and the compression was performed on the resulted halve-prisms specimens (Figure 8, d).

RESULTS AND DISCUSSIONS

The visual evaluation of the compositions developed with the RS1 addition indicates an alteration of the workability of the mortar when using the RS1 as sand substitution in the mix. The workability of the fresh mortar alters considerably when increasing the RS1 substitution percent from 25% to 50%.



Figure 6. Fresh state aspect of the mortars: a) R1; b) R2; c) RS1-25%-0.56; d) RS1-25%-0.61; e) RS1-50%-0.61

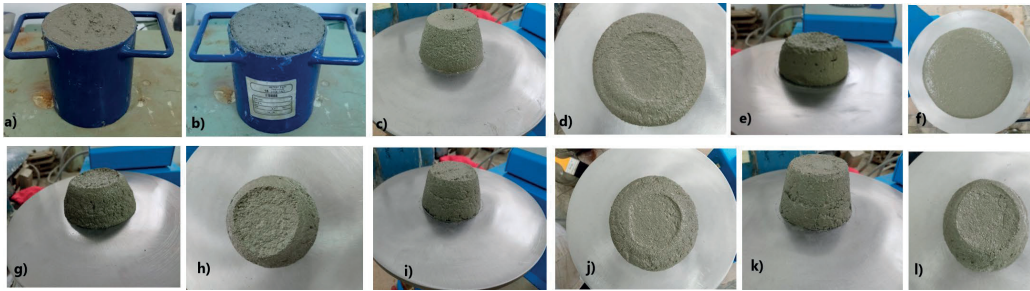


Figure 7. Fresh state characteristics of the mortars: a) and b) determination of fresh state density for RS1-25%-0.56 and RS1-50%-0.61; c) to l) mortar consistency (before and after the shocks): c) and d) R1; e) and f) R2; g) and h) RS1-25%-0.56; i) and j) RS1-25%-0.6; k) and l) RS1-50%-0.61

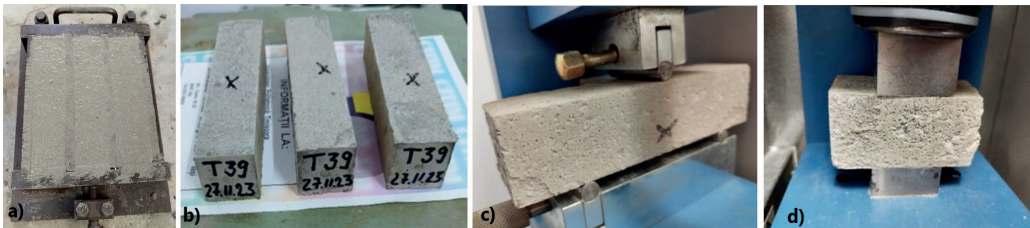


Figure 8. Hardened state characteristics of the mortars: a) and b) specimens' production; c) flexural strength determination by 3PB; d) compressive strength determination on halve-prism specimens

The stiff aspect of the composition RS1-25%-0.56, (A/C ratio = 0.56), similar to the reference composition R1, determines the development of the composition RS1-25%-0.61, with supplementary water addition, respectively A/C ratio = 0.61, and implicitly development of reference R2 with similar A/C ratio, for pertinent performance evaluation. Reference R2, however, presents an extremely fluid consistency (Figure 6, b and Figure 7, e and f), showing early traces of compositional segregation. The composition with high RS1 addition, 50%, was developed with a similar A/C ratio, of 0.61, showing extremely low workability and difficult handling when placed in the prismatic molds (Figure 6, e).

The fresh state determinations lead to the conclusion that the targeted addition, AdT RS1 induces, along with the integration in cementitious compositions, a consistent requirement for mix water increase, in order to regulate the workability. This fact is considered to lead to the deterioration of the mechanical resistances. Therefore, the need to evaluate the RS1 addition, in the field of real densities and masses, as well as the water absorption coefficient, prior to compositional optimization determinations through specific procedures, including addition, is identified.

The apparent fresh state density is determined (Figure 7, a and b) and the results are presented in Table 3.

Table 3. The fresh state apparent density: References and RS1 mixtures

Mixtures	The fresh state apparent density (kg/m ³)
R1	2150
R2	2140
RS1-25%-0.56	2130
RS1-25%-0.61	2120
RS1-50%-0.61	2160

The physical-mechanical performance is evaluated at the early age of 7 days, in order to perform a fast preliminary compositional analysis, namely the RS1 to the cementitious

matrix primary compatibility. Also, identifying further research directions and establishing possible compositional adjustments, as the case may be, are targeted objectives of the early-age evaluation.

The results obtained are presented in Table 5, respectively Figure 9 and Figure 10.

The results of consistency determination for the mortars are shown in Table 4 and representative aspects are shown in Figure 7, c to l. The results are confirming the previous conclusions, namely the workability alteration of the mix when introducing/increasing the RS1 addition as sand partial replacement.

Table 4. Fresh state consistency of the mortars: References and SG mixtures

Mixtures	The fresh state consistency (kg/m ³)
R1	170
R2	210
RS1-25%-0.56	120
RS1-25%-0.61	160
RS1-25%-0.61	130

Table 5. Mechanical performances of RS1 compositions at young ages: flexural strength and compressive strength (7 days)

Mixtures	7-day 3PB Flexural resistance		7- day Compression resistance	
	Strength (MPa)	Strength gain/loss vs R1 (%)	Strength (MPa)	Strength gain/loss vs R1 (%)
R1	7.0	-14.6	23.8	-7.8
R2	5.9	-	22.0	-
RS1-25%-0.56	7.2	3.4	28.5	19.5
RS1-25%-0.61	7.1	1.7	22.8	-4.2
RS1-50%-0.61	6.9	-0.6	22.7	-4.8

The physical and mechanical performances at early ages (7 days), the tensile strength by bending (3PB) and respectively the compressive strength, represent the essential parameters in evaluating the primary compatibility of the considered mineral addition, RS1, to the cementitious matrix. The comparative evaluation of the material performance indicates that the substitution does not induce a strength alteration, but even a slight increase.

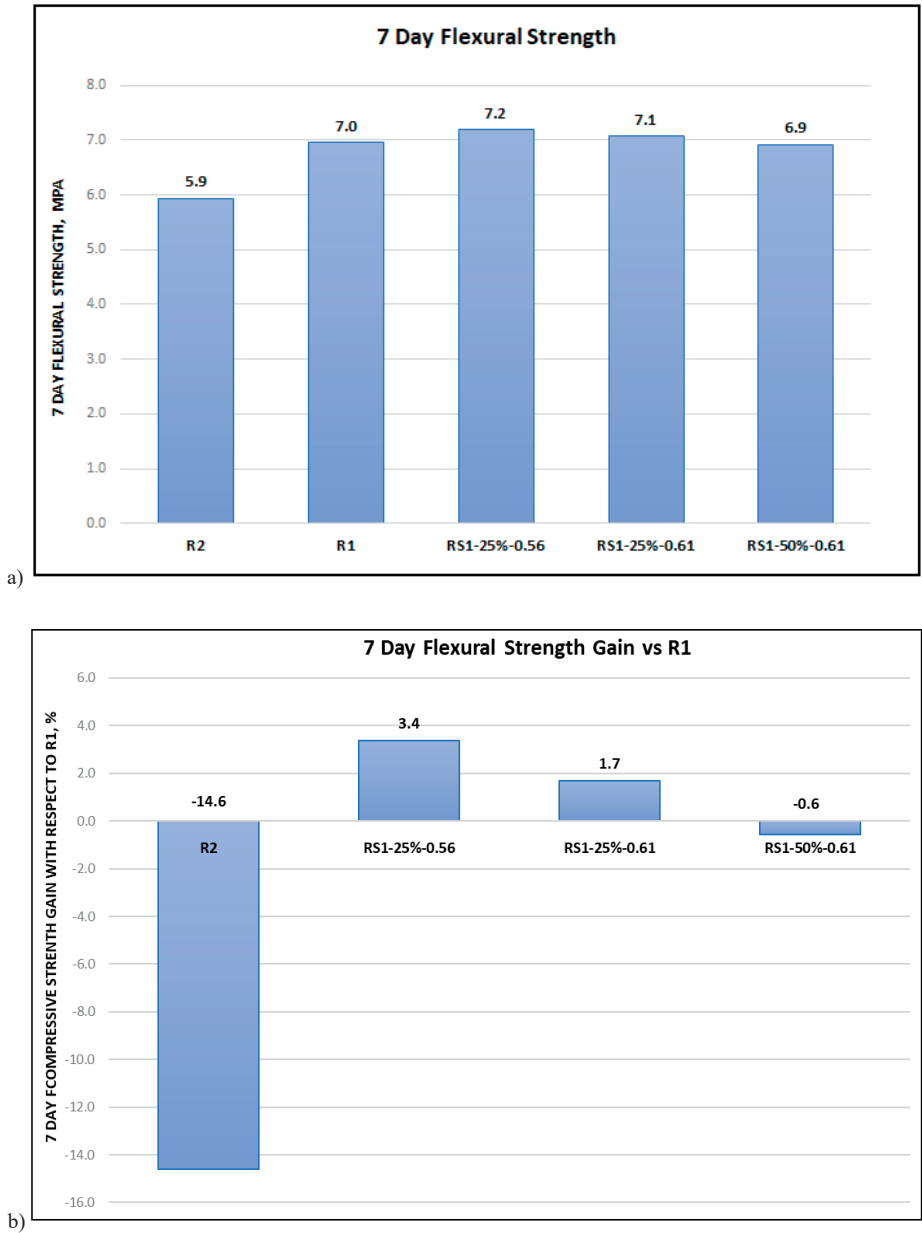
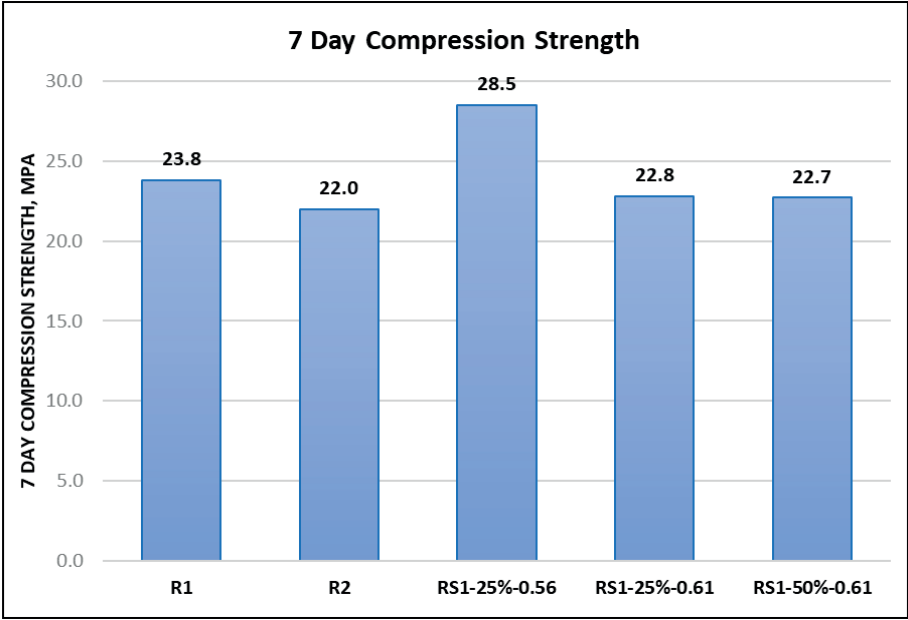
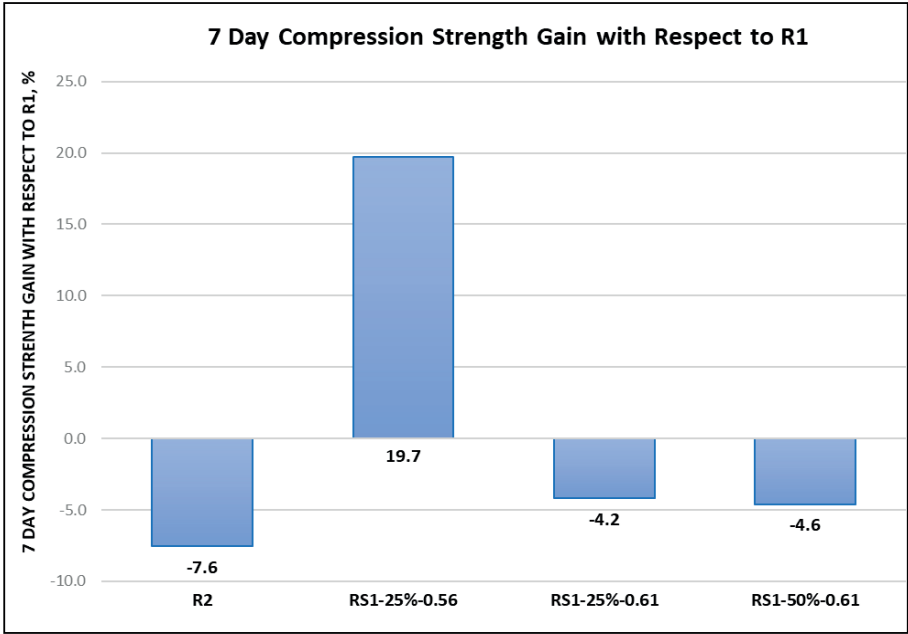


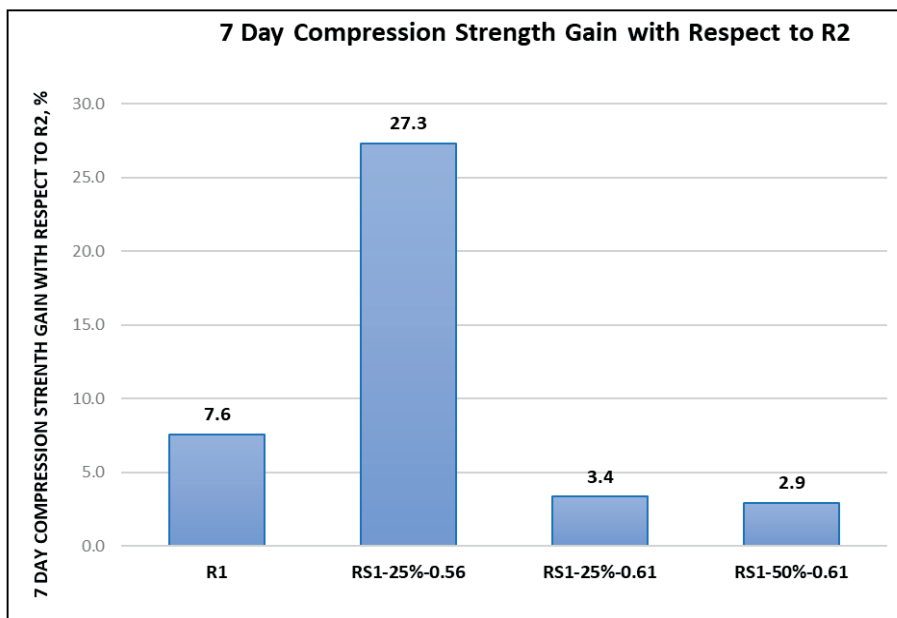
Figure 9. Early age mechanical strength: a) 7-day flexural strength;
b) 7-day flexural strength gain/loss, with respect to R1 (A/C = 0.56)



a)



b)



c)

Figure 10. Early age mechanical strength: a) 7-day compression strength; b) 7-day compression strength gain/loss, with respect to R1 ($A/C = 0.56$); c) 7-day compression strength gain/loss, with respect to R2 ($A/C = 0.61$)

CONCLUSIONS

The preliminary results obtained both in the field of flexural tensile strength, as well as in the field of compressive strength, at the age of 7 days, indicate the possible viability of the proposed substitution.

The comparative analysis of the results allows the following synthetic conclusions to be drawn:

- The increase in the water content, respectively the A/C ratio from 0.56 to 0.61 induces, predictably, the alteration of the mechanical performances, both in the control area (R2 vs. R1) and in the case of the compositions with the addition: RS1-25%-0.56 vs. RS1-25%-0.61. The results after 7 days are conclusive in this regard.
- The compression strength results at 7 days indicate the promising potential of the compositional integration of the RS1 material, namely the electric arc furnace slags (EAF), produced and stored in the western part of Romania, in Reșita, Caraș-Severin County, in cementitious materials.
- Additional tests, to confirm/refute this conclusion, are necessary and they represent ongoing research.

Preliminary testing and corresponding results provide encouraging conclusions regarding the viability of the concept. RS1 waste can be positively integrated into cement-based materials, as it proves to be compatible with the cementitious binder system and also with ordinary sand. The initial physical and chemical testing of RS1 as a potential substitute for ordinary 0/4 local sand, together with the physical and mechanical performance of the proposed initial eco-mortars obtained in this preliminary experimental investigation partially confirms the conclusions of recent studies in the subject and also the potential of the Reșita electric arc furnace slags (EAF) for integration into cement-based construction materials. The compositional behaviour developed with an RS1 sample supports the compatibility of the addition with the usual components of cementitious composites, with a high potential for use in construction products.

At the same time, relevant characteristics of mechanical performance and durability of cement-based composites, together with specific tests regarding the evaluation of contamination with potentially harmful materials for the health of the population, of RS1 additions taken from

several locations of the Resita dump, are critical considerations in the evolution of the subsequent scientific approach, in direct correlation with the applicability guidelines for the valorisation of the electric arc furnace slags (EAF) for valorisation in the circular design for eco-intelligent construction products.

ACKNOWLEDGEMENTS

This work was carried out within the Nucleu Programme of the National Research Development and Innovation Plan 2022-2027, supported by MCID, "ECODIGICONS" project no. PN 23 35 04 01: "Fundamental-applied research into the sustainable development of construction products (materials, elements, and structures, as well as methods and technologies) that utilizes current national resources to enhance the eco-innovative and durable aspects of Romania's civil and transport infrastructure", financed by the Romanian Government.

REFERENCES

- Branca, T.A., Colla, V., Algermissen, D., Granbom, H., Martini, U., Morillon, A., Pietruck, R., Rosendahl, S. (2020). Reuse and recycling of by-products in the steel sector: Recent achievements paving the way to circular economy and industrial symbiosis in Europe. *Metals*, 10, 345.
- Brand, A.S. & Fanijo, E.O. (2020). A review of the influence of steel furnace slag type on the properties of cementitious composites. *Applied sciences*, 10, 8210.
- Buddhdev, B.G., & Timani, K.L. (2020). Critical review for utilization of blast furnace slag in geotechnical application. *Problematic Soils and Geoenvironmental Concerns: Proceedings of IGC 2018*. 87-98.
- EN 196-1. Methods of testing cement - Part 1: Determination of strength.
- EN 1015-3. Methods of test for mortar for masonry - Part 3: Determination of consistence of fresh mortar (by flow table).
- EN 1015-6. Methods of test for mortar for masonry - Part 6: Determination of bulk density of fresh mortar.
- EN 1015-11. Methods of test for mortar for masonry - Part 11: Determination of flexural and compressive strength of hardened mortar.
- Giergiczny, Z. (2014). Fly ash in cement and concrete composition. In *Золышлаки ТЭС: удаление, транспорт, переработка, складирование* (pp. 170-174).
- Giergiczny, Z. (2019). Fly ash and slag. *Cement and concrete research*, 124, 105826.
- Hemalatha, T. & Ramaswamy, A. (2017). A review on fly ash characteristics—Towards promoting high volume utilization in developing sustainable concrete. *Journal of cleaner production*, 147, 546-559.
- Li, V.C. (2008). Engineered cementitious composites (ECC) material, structural, and durability performance.
- Li, V.C., & Herbert, E. (2012). Robust self-healing concrete for sustainable infrastructure. *Journal of Advanced Concrete Technology*, 10(6), 207-218.
- Özbay, E., Erdemir, M. & Durmuş, H.İ. (2016). Utilization and efficiency of ground granulated blast furnace slag on concrete properties—A review. *Construction and Building Materials*, 105, 423-434.
- Romanian Government, Government Decision for the approval of the National Strategy on the circular economy (SNEC 2022), The Official Monitor of Romania, August 7, 2023, <https://dezvoltaredurabila.gov.ro/strategia-nationala-privind-economia-circulara-13409762>.
- Romanian Ministry of European Investments and Projects, Romanian National Recovery and Resilience Plan, 2021, August 7, 2023, <https://mfe.gov.ro/pnrr/> (2023).
- Romanian Ministry of Research, Innovation and Digitalization, National Strategy for Research, Innovation and Smart Specialization 2022-2027 (SNCISI 2022-2027), The Official Monitor of Romania, August 7, 2023, <https://www.mcid.gov.ro/wp-content/uploads/2022/12/strategia-na-ional-de-cercetare-inovare-i-specializare-inteligent-2022-2027.pdf>.
- Shi, C., Qian, J. (2000). High performance cementing materials from industrial slags—A review. *Resources, Conservation and Recycling*. 29, 195–207.
- Snellings, R., Mertens, G., Elsen, J. (2012). Supplementary cementitious materials. *Reviews in Mineralogy and Geochemistry*. 74, 211–278.
- Snoeck, D. (2015). *Self-healing and microstructure of cementitious materials with microfibres and superabsorbent polymers* (Doctoral dissertation, Ghent University).
- Teixeira, E.R., Mateus, R., Camoes, A.F., Bragança, L. & Branco, F. G. (2016). Comparative environmental life-cycle analysis of concretes using biomass and coal fly ashes as partial cement replacement material. *Journal of Cleaner Production*, 112, 2221-2230.
- Wang, G.C. (2016). *The Utilization of Slag in Civil Infrastructure Construction*. Woodhead Publishing: Cambridge, UK.

EFFICACY OF THE SEISMIC ISOLATING SYSTEMS FOR HISTORICAL BUILDINGS UNDER MODERATE SEISMIC FORCES

Stefan Florin BALAN, Bogdan Felix APOSTOL, Anton DANET

National Institute of R-D for Earth Physics,
12 Calugareni Street, Magurele, Ilfov, Romania

Corresponding author email: sbalan@infp.ro

Abstract

National Institute of R-D for Earth Physics is in charge at national level with the task of monitoring the seismicity of the country. For this, it is used a well-developed seismic network with a good coverage of the Romanian territory. Beside the free field network of sensors, there is a number mounted on some buildings, used to evaluate their response to a large range of seismic events. The aim of the paper is to demonstrate the efficacy of the isolation systems of two buildings, situated in Bucharest, during earthquakes. The goals will be achieved through analyzing the seismic response in terms of engineering parameters given by the sensors located at key levels, i.e. under and right above isolating devices. The results show the reduction of the seismic loads above the isolators hence the successful use of this type of technique for older buildings of certain design, exposed to Vrancea seismicity and Bucharest subsoil specificity. Conclusions are drawn about the effectiveness of the isolation system on both structures, as part of a solution in specific cases for seismic risk mitigation.

Key words: base-isolating technique, seismic response analysis, moderate Vrancea earthquakes, seismic isolated buildings.

INTRODUCTION

Because of the Vrancea source, in the aftermath of the November 1940 seismic event of magnitude $MW = 7.4$, civil engineers begun to think of using seismic codes for buildings design and construction. Until this devastating earthquake all buildings were designed after German codes with only considering gravitational and wind forces (Beles, 1941). Things improved even more after the March 4, 1977, earthquake (Vrancea source, $MW = 7.2$) with 1500 casualties and approximately 30 buildings collapsed in downtown Bucharest, and a lot of damage in N-E, E and S-E of the country (Balan et al., 1982; Dilley et al., 2005; Bonjer et al., 2010; Mandrescu, 1982; Trendefiloski et al., 2009). Since 1977 different editions of a modern and scientific seismic code were released, based on recordings from stronger 1977, 1986, 1990 and other seismic events (P. 100-78; P. 100-92; P. 100-1/2006; P. 100-1/2013). Were considered also other different factors linked to buildings: type, shape, function, local conditions of sites, etc., to improve their resilience to earthquakes. With a number of 99 broad band sensors, 184

stations with acceleration sensors (25 are installed in Bucharest-Ilfov) and 2 seismic arrays, the National Institute of R-D for Earth Physics (NIEP) records, archives, processes, interprets and disseminates all seismic data gathered from Romanian territory (Neagoe et al., 2011; Tiganescu et al., 2021).

The recordings from the strongest event of the last (two) years $MW = 4.9$, originating in Vrancea-intermediate depth seismic area are analyzed as they are offered by sensors deployed in certain buildings (ROMPLUS, 2023).

In a previous paper a similar analysis was performed for two tower-type buildings located in different areas, one nearer the epicentre, the other belonging to the Bucharest extended metropolitan area at (roughly) ~ 150 km. The characteristics of these buildings were described, their response and behaviour at this medium seismic solicitation evaluated, by considering the difference in the epicentre distances but similarity in design (Apostol et al., 2023; Balan et al., 2023; Tiganescu et al., 2019). At that time the moment magnitude for the considered seismic event was employed with the value as it was in the Internal Report,

released just in the aftermath of the triggered event, $M_W = 5$ (Internal Report, 2022).

Herein the approach is extended to older buildings that, during reinforcement action they supported, were endowed with base-isolators devices. The motivation was to take advantage from this performance as the structures were equipped with seismic sensors at interest levels. The goal pursued in this paper is to prove the efficacy of this certain type of anti-seismic isolating technique applied to old/historical structures located in the Bucharest downtown. The response of the buildings is considered under medium intensity earthquake and the performance of isolators devices are highlighted in terms of engineering parameters. In Bucharest 3 buildings were seismically isolated: Victor Slavescu building belonging to Bucharest University of Economic Studies (ASE), the Bucharest Town Hall (PMB) and the Triumph Arch (a historic monument). NIEP deployed seismic sensors on all these buildings installed at different times. In this paper only buildings endowed with sensors under and above the isolation system are considered. The point of novelty consists that in one building a sensor under the isolating level was recently installed, hence it exhibits similarity to the other, allowing for an analysis in the same conditions.

MATERIALS AND METHODS

Buildings overview and processed data

The ASE structure, a historical monument was built between 1905 and 1908 of brick masonry with truss roof; it consists of underground, ground floor, two floors and an attic. The building was consolidated after the year 2011, when the seismic isolation system was introduced. It is monitored with two accelerometers, located in the basement below / above the seismic insulators.

The other building, the PMB is also a historical architectonic monument, was built between 1906 and 1908, with brick masonry, reinforced concrete floors with turned caissons. The consolidation procedure started in 2010 and, taking advantage of this, a similar isolated system was introduced. The levels of the structure consist of underground, ground floor, 3 floors and an attic. It is real-time monitored

with 4 accelerometers mounted at ground floor, floors 2, 3 and attic. It should be noted that all of these are placed above the seismic isolation system of the building. Some years ago two accelerometers were added, under and above the seismic isolated system.

This paper attempts to a preliminary evaluation of the recordings on these isolated structures, as offered by the November 3, 2022, Vrancea earthquake.

The characteristics of this seismic event were: data and time triggering 2022/11/03, 04:50:25.81, Latitude: 45.4895°, Longitude: 26.5262°, hypocentral depth $H = 149.0$ km, $M_w = 4.9$ ($M_L = 5.3$) (ROMPLUS, 2023).

The available data belonging to one of the recent strongest earthquakes are analysed and processed in order to highlight the efficacy of the base isolation system at this structural type in Bucharest city area. The level of the hazard assessment parameters, geotechnical features and local effects in terms of site response are compulsory features that have to be taking into consideration when one decides to perform this type of anti-seismic technique. All these issues were referred to in other papers (Aki, 1993; Ishihara, 1996; Bard & Riepl-Thomas, 1999; Panza et al., 2001; Balan et al., 2019; Mandrescu et al., 2004; 2007; Marmureanu et al., 2021; 2020; Marmureanu, 2016) with emphasis on city geophysical local specificity and structural response (Lungu et al., 1999; Moldoveanu and Panza, 2000; Moldoveanu et al., 2004; You et al., 2009; Su et al., 2006).

The processed data are used for elastic response spectra computations which are discussed in terms of peak amplitude parameters and predominant periods or spectral ranges of interest. The outcomes are those related to buildings structural behaviour, health monitoring and resonance phenomenon (Tiganescu et al., 2022; Balan et al., 2020). Also, the data transmission and near-real time assessment are provided and pursued during buildings monitoring process.

The operation is targeted on the possibility to assess the buildings behaviour during and immediately after an earthquake. A rapid response is evaluated, and the output can be implemented in general procedures that can be applied for end-user use-cases and a sustained flow of information is ensured (Balan et al.,

2023; Apostol et al., 2023). Following the rapid evaluation of the engineering parameters, information is obtained about the behaviour of the respective structure or certain type of buildings in the area under the certain seismic

demand. These actions, involving the data collected in free field and on buildings help designers, urban planners and authorities interested in the mitigation of seismic risk in urban areas (Tiganescu et al., 2021; 2022).

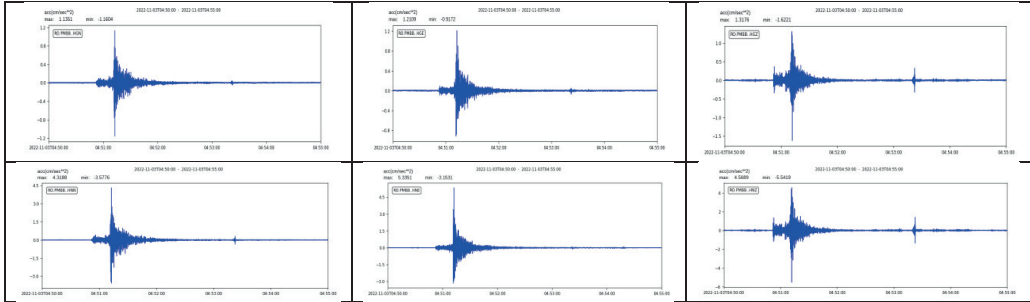


Figure 1. Acceleration on three components (from the left to the right N-S, E-W, Z) at PMB building recorded by sensors located above (upper panel) and below (lower panel) the insulating devices

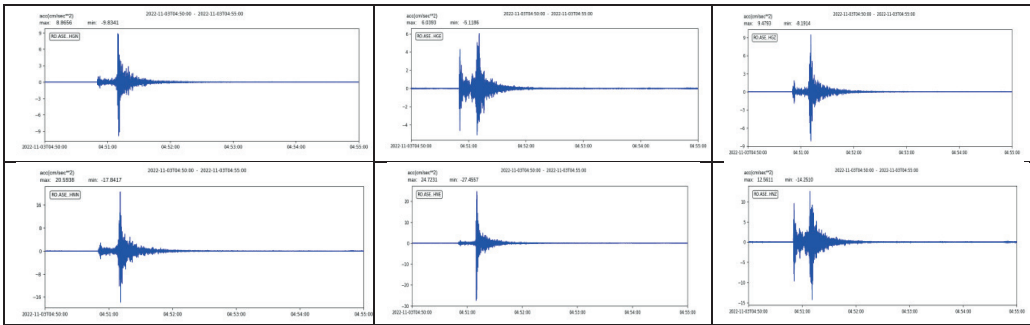


Figure 2. Acceleration on three components (from the left to the right N-S, E-W, Z) at ASE building recorded by sensors located above (upper panel) and below (lower panel) the insulating devices

Figures 1, 2 show the recorded accelerograms at key levels, below and right above the isolating layer, during the 03.11.2022 seismic event, of moment magnitude $M_w = 4.9$, in the retrofitted structures. Accelerometers data recordings on the buildings during earthquakes are near-real time processed, using the same filtering (bandpass 0.2 Hz - 25 Hz, 4th order Butterworth) and the same techniques, in order to keep the results uniform and comparable (BRTT, 2018).

Base - isolated devices performance analysis

In Figures 3, 4 the elastic response spectra are shown with 5% damping for spectral pseudo-acceleration computed at two levels of interest in PMB and ASE buildings. For the computation of the elastic response spectra of

the recorded seismic events the Antelope Environmental Monitoring System is employed herein (BRTT, 2018; Internal Report, 2022). In Table 1 the maximum values are shown, from the recordings on ASE, PMB buildings, under and above the isolated system, on three mutual perpendicular components (two horizontal North-Souths, East-West and one vertical Z). The parameters of engineering interest are maximum acceleration, velocity and spectral acceleration, processed through dedicated software and shown as seismograms and elastic response spectra (Figures 1 to 4).

In Table 2 the reduction of seismic amplitudes is shown in terms of maximum recorded accelerations, in order to have a quantitative representation for the outcome of the employed technique. The reduction coefficient represents

the ratio for under/above values and the reduction percentage stands for its corresponding percent in the considered weight. As seen, the reduction in percentage is over 50% for all components, for both

buildings. One could notice the stronger reduction percentage for the PMB building, for which the recorded values are in general much lower. Also, the reduction is slightly higher on the E-W component, again for both buildings.

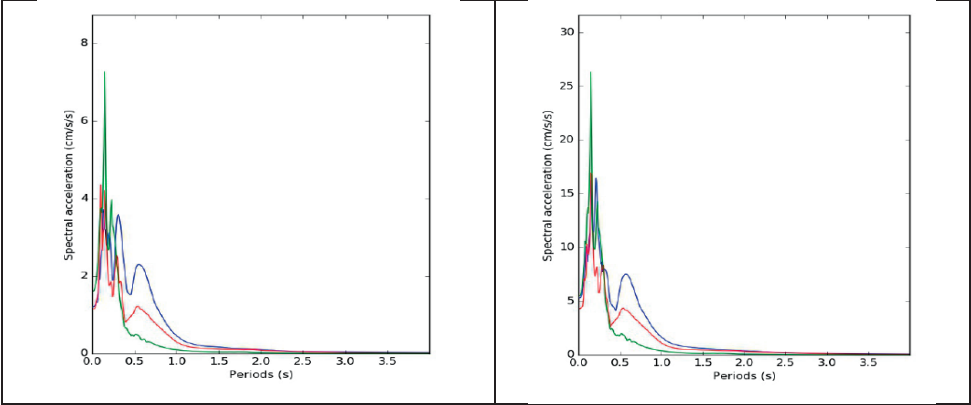


Figure 3. Elastic response spectra for the PMB building above (left) and under (right) isolator layer from recordings of the 03.11.2022 earthquake $M_W = 4.9$

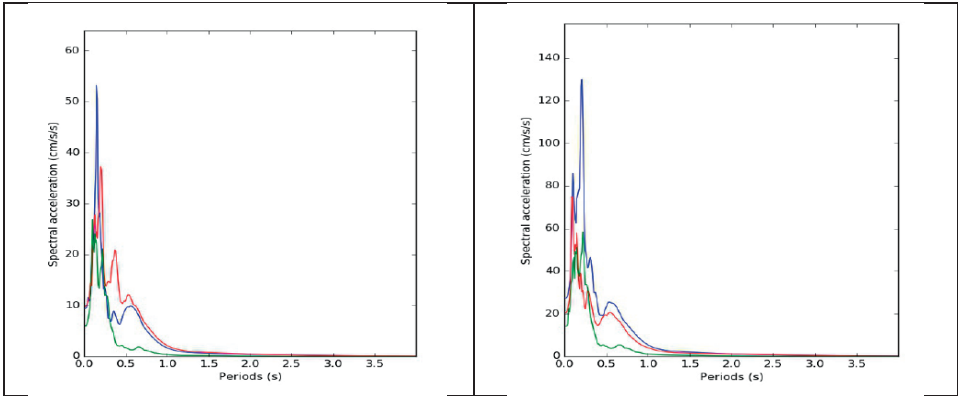


Figure 4. Elastic response spectra for the ASE building above (left) and under (right) isolator layer from recordings of the 03.11.2022 earthquake $M_W = 4.9$

Legend colors: red: N-S, blue: E-W, green: Z (vertical) components of recording

Table 1. Maximum values recorded on ASE and PMB under and above the isolated system. The parameters are maximum acceleration, velocity and spectral acceleration

Buildings code, recorded parameters	Sensor under isolation system			Sensor above isolation system		
	N-S	E-W	Z	N-S	E-W	Z
ASE						
Acceleration [cm/s^2]	20.594	27.456	14.251	9.834	9.479	6.039
Velocity [cm/s]	0.75	1.24	0.39	0.44	0.44	0.16
Spectral Acc. [cm/s^2]	74.95	130.08	58.28	37.29	53.24	26.85
PMB						
Acceleration [cm/s^2]	4.319	5.3351	5.542	1.160	1.211	1.622
Velocity [cm/s]	0.16	0.25	0.17	0.04	0.08	0.04
Spectral Acc [cm/s^2]	19.95	16.45	26.36	4.35	3.72	7.28

Table 2. Base-isolated device performance in terms of reduction coefficient (for acceleration) and corresponding reduction percentage for the two buildings

Buildings	Component N-S		Component E-W		Component Z	
	Reduction coefficient	Reduction percentage	Reduction coefficient	Reduction percentage	Reduction coefficient	Reduction percentage
ASE under/above isolator	2.09	52%	2.89	65.5%	2.35	57.9%
PBM under/above isolator	3.72	73.15%	4.40	77.28%	3.42	70.73%

RESULTS AND DISCUSSIONS

The available seismic recordings for the most recent $M_w \geq 4.9$ earthquake are analysed and processed in order to highlight the efficacy of the base isolation system at this type of structure in Bucharest city area.

The aim is to check the performance of the base isolating solution in the context of soil specificity characteristics and response to seismic forces as induced by the Vrancea earthquakes. The work is based on the data collected on seismic isolated buildings in Bucharest, i.e. the ASE (Victor Slavescu building belonging to Bucharest University of Economic Studies) and the PMB (the building of the Town Hall of Bucharest), from the earthquakes recorded in the Bucharest metropolitan area. The latest sensors installed at PMB as part of a continuous activity through a campaign of structure surveillance across the city offer the possibility to add new data and perform a more appropriate evaluation (from a new perspective).

At the ASE building the larger recorded values under isolation system are on E-W component of recording for accelerations, velocities and spectral accelerations. These values filtered through the isolation system remain the largest on E-W component for velocities and spectral accelerations, though the maximum acceleration is now in N-S component (Table 1).

At the PMB building the largest value under isolation concerning accelerations is in Z direction, E-W direction for velocities and Z direction for spectral accelerations. These values filtered thereby reduced through the isolation system remain the higher for acceleration and spectral acceleration in Z

direction, as for velocities on the E-W direction is recorded the maximum value (Table 1).

The analyzed seismic event being of moderate magnitude also the response in accelerations, velocities and spectral accelerations, on all recorded directions are in accordance with this level of seismic intensity. Their maximum amplitudes are contained in the regular ranges as for many of these types of seismic events. The corresponding spectral domain in which the oscillating periods are attained is also in low range as a typical behavior for the structure's response in the considered area at low-to-medium magnitudes (Figures 3, 4).

The work is intended to bring a contribution to the mitigation of the seismic risk over the city area and in this way to set up a more resilient urban community.

The approximate resemblance of the two structures in regard of age, design, retrofit, anti-seismic devices and seismic sensors deployment led us to perform an evaluation of the behavior under seismic solicitations. According to the expected behavior all data recorded above the isolated system are of lower amplitude than those under the isolation (Table 2). One should conclude that this specific anti-seismic technique, i.e. base isolation has reached its desired initial objective in reducing the solicitations on structures exposed to seismic movement and vibrations.

CONCLUSIONS

This study is restricted to only two structures properly instrumented regarding the sensor deployment, out of three endowed with base isolation system, from Bucharest, the outcomes may support this type of intervening method on such constructions.

One can add the importance of the local effects and uppermost stratified layers and geophysical features as factors of major importance to be considered when deciding for such accomplishments. Also, the avoidance of the dangerous spectral ranges of the higher oscillating periods as they correspond to the fundamental period over the local area is a desirable accomplishment for circumventing possible damage-causing resonance phenomenon.

Comparison was made for maximum values of the recorded accelerations, velocities and spectral acceleration as emerged from processed recordings and elastic response spectra (Figures 1 to 4). A short discussion that can be made regarding the oscillating periods as they correspond to the maximum spectral amplitudes supports the previous findings and related assertions (Apostol et al., 2023; Balan et al., 2020; 2023; Tiganescu et al., 2022) according to which it was found that they show quite a low range (up to 0.22 s for this parameter, see Figures 3 and 4). Therefore, the issue of resonance phenomenon is excluded at this seismic load level. Of course, the dynamic behavior and spectral response for much stronger magnitudes should be considered in the context of actual local soil geology, local effects and hazard level, encountered and generated over the Bucharest area.

ACKNOWLEDGEMENTS

This paper was carried out within Nucleu Program SOL4RISC, contract number 24N/03.01.2023, supported by Ministry of Research, Innovation and Digitization, project no. PN23360202.

REFERENCES

Aki, K. (1993). Local site effects on weak and strong ground motion. *Tectonophysics*, 218, 93-111.
 Apostol, B.F., Balan, S.F., Danet, A. (2023). Post-earthquake assessment for seismic risk mitigation in Romania: case-studies based on recorded data. *Romanian Journal of Physics*, 68(7-8), 804.
 Balan et al. (1982). *Cutremurul de pământ din România din 4 martie 1977*. Editura Academiei Române, București.
 Balan, S.F., Apostol, B.F., Danet, A. (2023). Analysis of seismic data from moderate intensity event of 2022.11.03 recorded on instrumented structures.

Scientific Papers. Series E. Land Reclamation, Earth Observation & Surveying, Environmental Engineering, XII, 205-214, Print ISSN 2285-6064.
 Balan, F., Tiganescu, A., Apostol, B.F., Danet, A. (2019). Post-earthquake warning for Vrancea seismic source based on code spectral acceleration exceedance. *Earthquakes and Structures*, 17(4), 365–372 (<https://doi.org/10.12989/EAS.2019.17.4.365>).
 Balan, F., Tiganescu, A., Apostol, B.F. (2020). Structure Response Analysis of the Seismic Isolated Buildings; in Bucharest City. 2020 IOP Conf. Ser.: *Earth Environ. Sci.* 609012080. Published under licence by IOP Publishing Ltd IOP Conference Series: *Earth and Environmental Science*, 609, 6th World Multidisciplinary Earth Sciences Symposium 7-11 September 2020, Prague, Czech Republic.
 Bard, P.-Y., Riepl-Thomas, J. (1999). Wave propagation in complex geological structures and their effects on strong ground motion. *Wave motion in earthquake engineering*, Chapter 2, E. Kausel, G. Manolis (Eds), WIT Press, Southampton, UK, 38-95.
 Beles, A. (1941). Earthquake and Constructions (in Romanian). *Bull. Polytechnic Soc.*, Year LV, vol. 10 and 11.
 Bonjer, K.-P., Glavcheva, R., Drumea, A., Paskaleva, I., Radulian, M., Radovanovich, S., Gribovszki, K., Weisbrich, W. (2010). Destructive Vrancea (Romania) intermediate depth earthquakes: intensity distribution and isoseismals. *Geophysical Research Abstracts* 12, EGU2010-6159, EGU General Assembly 2010.
 BRTT (2018). *Boulder Real Time Technologies*. Boulder, CO, USA. www.brtt.com
 Dilley, M., Chen, R.S., Deichmann, U., Lerner-Lam, A.L., Arnold, M., Agwe, J., Buys, P., Kjekstad, O., Lyon, B., Yetman, G. (2005). *Natural disaster hotspots: A global risk analysis*. The World Bank Hazard Management Unit, Washington, D.C.
 Internal Seismic Report (2022). National Institute of Research and Development for Earth Physics.
 Ishihara, K. (1996). *Soil behaviour in earthquake geotechnics*. Clarendon Press, Oxford.
 Lungu, D., Cornea, T., Nedelcu, C. (1999). *Hazard assessment and site-dependent response for Vrancea earthquakes*. Vrancea earthquakes: tectonics, hazard and risk mitigation, Wenzel, F., Lungu, D., Novak, O. (eds.), Netherlands: Kluwer Academic Publ. Dordrecht, 251–267.
 Mândrescu, N. (1982). The Romanian earthquake of March 4, 1977; damage distribution. *Rev. Roum. Geol., Geogr. et Geophys.*, 26, 37–44.
 Mândrescu, N., Radulian, M., Marmureanu, G. (2007). Geological, geophysical and seismological criteria for local response evaluation in Bucharest urban area. *Soil Dynamics and Earthquake Engineering*, 27(2007), 367–393.
 Mândrescu, N., Radulian, M., Marmureanu, G. (2004). Microzonation of Bucharest: Geology of the Deep Cohesionless Deposits and Predominant Period of Motion. *Revue Roumaine de Geophysique*, 48, 120-1.
 Marmureanu, G. (2016). *Certainties/ Uncertainties in Vrancea hazard and seismic risk evaluation*.

- Romanian Academy Publishing House, Bucharest, Romania.
- Marmureanu, G., Borcia, I-S. Marmureanu, A., Cioflan, C.O., Toma-Danila, D., Ilies, I., Craiu, G.M. Stoian, I. (2020). Larger peak ground accelerations in extra-Carpathian area than in epicentre. *Romanian Journal of Physics*, 5-6(65), 1-10.
- Marmureanu, G., Cioflan, C.O., Apostol, B.F. (2021). Seismic response analysis for Romanian extra-carpathian sedimentary areas. *Territorium*, 28(II), 83-92.
- Moldoveanu, C.L. & Panza, G.F. (2001). Vrancea source influence on local seismic response Bucharest. *Pure Appl. Geophys.*, 158, 247-2429.
- Moldoveanu, C.L., Radulian, M., Marmureanu, G., Panza, G.F. (2004). *Microzonation of Bucharest: State-of-the-Art*. "Seismic Ground Motion in Large Urban Areas" special issue: Seismic ground motion in large urban areas; Main results of the UNESCO-IUGS-IGCP Project; Panza G.F., Nunziata C., Paskaleva I. (Eds); Birkhauser Verlag, Basel, Switzerland, ISSN 0033-4553, 1125-1147.
- Neagoe, C., Manea, L.M., Ionescu, C. (2011). Romanian complex data centre for dense seismic network. *Annals of Geophysics*, 54(1), 9-16.
- P. 100-78, *Code for the seismic design of dwellings, social-cultural, agro-zoo technical and industrial buildings*. Building Research Institute (INCERC); Bucharest, Romania (in Romanian) 1978.
- P 100-92, *Code for the seismic design of dwellings, social-cultural, agro-zoo technical and industrial buildings*. Ministry of Public Works and Territorial Planning (M.L.P.A.T.); Bucharest, Romania (in Romanian), 1992.
- P 100-1/2006, *Seismic Design Code - Part I: Earthquake Resistant Design of buildings*. Ministry of Transport, Construction and Tourism (M.T.C.T); Bucharest, Romania (in Romanian), 2006.
- P 100-1/2013, *Seismic Design Code - Part I: Earthquake Resistant Design of buildings*, Ministry of Regional Development and Public Administration (M.D.R.A.P.); Bucharest, Romania (in Romanian), 2013.
- Panza, G.F., Romanelli, F., Vaccari, F. (2001). Seismic Wave Propagation in Laterally Heterogeneous Anelastic Media: Theory and Applications to Seismic Zonation. *Advanced in Geophysics*, 43, 1-95.
- ROMPLUS (2023), Romanian earthquake catalogue. National Institute for Earth Physics, Magurele, Romania. www.infp.ro/romplus
- Su, F., Anderson, J.G., Zeng, Y. (2006). *Characteristics of ground motion response spectra from recent large earthquakes and their comparison with IEEE Standard 693*. Proceedings of the 100th Anniversary Earthquake Conference Commemorating the 1906 San Francisco Earthquake. San Francisco, CA, USA.
- Tiganescu, A., Balan, S.F., Toma-Danila, D., Apostol B.F. (2019). *Preliminary Analysis of Data Recorded on Instrumented Buildings from Bucharest Area during the 28th October 2018 Vrancea Earthquake*, Proc. of the 19th International Multidisciplinary Scientific GeoConference SGEM, Albena, Bulgaria, 897-904. doi:10.5593/sgem2019/1.1/S05.111
- Tiganescu, A., Toma-Danila, D., Grecu, B., Craifaleanu, I.-G., Florin Balan, S., and Sorin Dragomir, C. (2021). Current Status and Perspectives on Seismic Monitoring of Structures and Rapid Seismic Loss Estimation in Romania; in: *Proc. of the 1st Croatian Conference on Earthquake Engineering*, S. Lakušić and J. Atalić (Eds.), 81-91 ICroCEE, Zagreb, Croatia. doi:10.5592/CO/ICroCEE.2021.120
- Tiganescu, A., Craifaleanu, I.-G., Aldea, A., Grecu, B., Vacareanu, R., Toma-Danila, D., Balan, S. F., Dragomir, C.S. (2022). Evolution, Recent Progress and Perspectives of the Seismic Monitoring of Building Structures in Romania. *Front. Earth Sci.*, 10, 10:819153, <https://doi.org/10.3389/feart.2022.819153>
- Trendafiloski, G., Wyss, M., Rosset, P., Marmureanu, G. (2009). Constructing city models to estimate losses due to earthquakes worldwide: application to Bucharest, Romania. *Earthquake Spectra.*, 25(3), 665-685.
- You, H.B., Zhao, F.X., Rong, M.S. (2009). Nonlinear seismic response of horizontal layered site due to inclined wave. *Chinese Journal of Geotechnical Engineering*, 31(2), 234-240.

THE INFLUENCE OF EXTREME WEATHER PHENOMENA ON THE MANAGEMENT OF HARDWOOD TREES

Ghiță Cristian CRAINIC¹, Flavius IRIMIE², Flavia Mălina CIOFLAN¹,
Sorin Lucian DOROG¹, Călin Ioan IOVAN¹, Eugenia ȘERBAN¹

¹University of Oradea, 1 Universitatii Street, Oradea, Romania

²"Stefan cel Mare" University of Suceava, 13 Universitatii Street, Suceava, Romania

Corresponding author email: eugeniaserban@yahoo.com

Abstract

The extreme meteorological phenomena, from the date of 17 09 2017, caused a series of destructions especially in the deciduous stands within the Sudrigiu Forest District, Bihor Forest Department stands, in the western part of the country. As a result, a number of stands of species from the deciduous group were affected in the Văratec Forest Management Unit (FMU) VII, with reported windfalls and wind breaks, on compact surfaces of approximately 929 hectares. The volume of the affected trees, which was inventoried as accidental products, is about 94,000 m³. The appearance of these by-products seriously disrupted the management of the stands in the affected forest units, causing a series of major disruptions in the valorization process of the main and secondary wood products, with major implications on the regeneration process of the deciduous stands, which was in progress, at that moment. Although substantial amounts of money were recorded during the valorization of accidental wood products, a relatively high percentage of the wood was depreciated and was not recovered at a level corresponding to the main wood products.

Key words: extreme meteorological phenomena, deciduous stands, accidental products, natural regeneration, secondary wood products.

INTRODUCTION

The concept of sustainable forest management was developed in the 1990s, emphasizing the equal consideration of ecological, economic, and socio-economic ecosystem functions. However, contemporary society is presenting novel and intricate demands on forests, such as those related to climate change, renewable energy, and biodiversity conservation, which may not always align seamlessly. Policy instruments addressing these societal needs and transforming them into legally binding regulations have extensive implications for forest management, challenging the conventional, non-binding structure of international forest policy (Prins et al., 2023). Within the forestry strategies, the establishment of some sustainable management criteria to be applied to obtain the expected effect and a series of indicators to reveal the sustainability of the management were foreseen. These indicators can be divided into two large categories (<https://www.qdidactic.com/>):

- *Quantitative indicators*: the percentage of afforestation, forest area/inhabitant, the volume

of standing wood, possibility, accessibility, the amount of wood released on the market, the number of accessory products offered to the industry, turnover, capacity to receive of the public, etc.

- *Qualitative indicators*: the health and vitality of forest ecosystems, the quality of the factors improved by the forest eco protection, the weight/ratio of intensive treatments, the origin and provenance of stands, the incidence of damaging factors, the fertility of the forest soil, biodiversity indicators (the presence of secular virgin, natural and semi-natural forests, the proportion/rate of mixed stands, the volume of dead wood in the forest, the share/ratio of natural regeneration, the proportion/rate of indigenous and introduced exotic species, rare or endangered species), conservation of forest genetic resources, etc.

Carefully analyzing the two categories of indicators of sustainable management, the differentiation of the two concepts of *conservation* (expressed mainly through qualitative indicators) and *development* (expressed through quantitative indicators), concepts nuanced by the principle

of sustainable evolution can be noticed (<https://www.qdidactic.com/bani-cariera/>).

The intensification of the effects of climate change urgently requires addressing the determinants of this phenomenon, particularly greenhouse gas emissions. Forests provide an efficient solution due to their capacity to store and reduce carbon emissions. In Romania, achieving a balance between forest exploitation and environmental conservation and protection is imperative, considering the significant economic contribution of forestry and wood-based industries to the country's GDP (approximately 5%) and employment for about 300 thousand people, representing 6% of the active workforce (Chivulescu et al., 2024).

The effects of climate change are felt more and more throughout the planet, having an impact on the natural environment, the global and regional economy, but also on people's social life. Among the most obvious effects are listed: the increase in the frequency of droughts and floods, the intensification of extreme weather phenomena, the melting of mountain glaciers and ice caps, the rise of the Planetary Ocean level, etc. Rising global temperatures have contributed to an increase in the frequency and intensity of extreme weather phenomena such as heat waves, thunderstorms, tornadoes, hurricanes, droughts, torrential rains, hail, etc. (Măhăra, 2006).

Extreme weather phenomena can have a major impact on people, both in the short term, through the large number of victims and property damage, and in the medium or long term, through the effect on land degradation and the reduction of its productive potential, through the destruction of natural habitats (Grecu, 2016). Extreme weather phenomena have negative effects in the field of agriculture, forestry, land improvements, water management, environmental protection, etc.

In recent decades, the intensification of extreme weather phenomena has also been observed in Romania, including in the western part of the country (Cristea, 2004; Șerban, 2010; Tudose et al., 2016), where our study area is located. The intensification of storms is also due to local relief conditions, there. The positioning of the Apuseni Mountains range from north to south causes the masses of moist, oceanic air, coming from Western Europe, to suddenly cross the

mountains, which intensifies the storms on the western side of the Apuseni Mountains (where our study area is also located) (Șerban, 2010).

Climate change and environmental pollution are increasingly affecting forest ecosystems (Šimonovičová et al., 2019). Extreme weather phenomena, especially storms, represent a threat to forest ecosystems through the windthrows they generate. This aspect is increasingly studied by many researchers (Ruel, 2020; Giannetti et al., 2021; Konôpka et al., 2021; Ritter et al., 2022; Bozzini et al., 2023; etc.). Many studies focus on the issue of the resistance of stands types to windthrows (Nolet & Béland, 2017; Rukh et al., 2020; Krišāns et al., 2020). Other studies analyze the forest area affected by windthrows and the severity of the damage (Goff et al., 2021; Zhang et al., 2021) or the impact of post-disturbance management on forest stands, presenting various forest regeneration models (Ruel, 2020; Konôpka et al., 2021; Costa et al., 2021).

The storms affected large areas of forest in Romania as well. Such was the severe storm of September 17, 2017, which affected several countries in central and south-eastern Europe, especially Serbia and Romania. Due to the large area of the damage swath (at least 500 km long) and strong wind gusts (up to 40 m/s), it was considered similar to a derecho (Sipos et al., 2021).

In the west of the country, the storm caused windthrows on an area of more than 700 ha of forest only within the Sudrișu Forest District, Bihor County Forest Administration (Sicoe et al., 2023). As a result, these extreme weather phenomena have significantly affected the management of the forest district. In this context, a percentage of the timber volume that was scheduled to be harvested during the 2017-2024 period according to the management plan was affected, and the remaining portion was not harvested (Crainic et al., 2023).

In the current context of global changes and interconnection, forest management needs to present a continuous evolution adapted to contemporary challenges. Consequently, one of the main challenges in forest management is represented by the sustainability of forest resources and the need to preserve the biological diversity of forests (Dinca & Zhiyanski, 2023). Consequently, sustainable forest management

offers long-term benefits, both economically and ecologically (Crişan et al., 2024).

The objectives of the case study refer to the analysis and study of the influence of extreme weather phenomena on forest management within management unit VII Văratec. As a result, the affected stands and the resulting incidental timber products will be identified, evaluated, and analyzed.

MATERIALS AND METHODS

The case study was carried out in the stands affected by extreme weather events within the management unit (PU) VII Văratec, managed by the Sudrigiu Forest District, within the Bihor County Forest Administration. The period during which the research and studies were conducted is from September 2017 to the present. Part of the research activities were carried out in the framework of a research project coordinated by specialists from the Department of Forestry and Forest Engineering, Faculty of Environmental Protection, University of Oradea, in collaboration with the forestry staff of the Sudrigiu Forest District, Bihor County Forest Administration.

In this context, affected stands have been surveyed and analysed, where regeneration works and cultural operations (care felling) are planned, according to the forest management plan in force (Crainic et al., 2023).

The research methods used are: bibliographic documentation, route observation, stationary observation, experimentation, full inventory, comparison, analysis, simulation and digital image recording (Crainic et al., 2022).

For the assessment of the affected stands, a complete inventory of the affected trees was carried out. These are represented by broken trees (partially and fully) and uprooted and fallen trees (Figure 1). The situation of natural regeneration in the stands that are currently being felled for regeneration under the stand and included in the forest management plan was also analysed. As a result, the areas where natural or mixed forest vegetation is needed in these stands have been identified, assessed, and analysed.

Following the complete inventories of all affected trees in the studied stands, the data were processed with the specialized software FOND and SUMAL, within the Sudrigiu Forest

District, Forest Fund Department, thus obtaining the volume of wood related to trees blown down and broken by the wind.



Figure 1. Stand affected by extreme weather events in stand 104 A

The stand damage index i_{as} , according to the total volume of affected wood for each stand, was determined with the formula:

$$i_{as} = \frac{V_{extracted}}{V_{stand}} \quad (1)$$

where:

- i_{as} is the stand damage index;
- $V_{extracted}$ represent the volume of affected trees that has been inventoried and will be extracted;
- V_{stand} is the total volume of the stand at the time of the inventory of affected trees, which represents the volume of the stand when the V_{im} forest management came into force, i.e. in 2014, plus four annual increases (until 2017) i_{va} , when the inventory is carried out (Crainic et al., 2023). As a result,

$$V_{stand} = V_{fm} + 4i_{va} \quad (2)$$

The stand damage index was then used to determine the average degree of damage to the production unit. It was also used to determine the affected areas on which forest vegetation would need to be installed. The stand damage index is applied to the stand area, which is mentioned in the forest management plan, and the following formula is used to obtain the affected area:

$$S_{affected} = S_{fm} \cdot i_{as} \quad (3)$$

where:

- $S_{affected}$ is the area affected;
- S_{fm} represent the area of the plot in the forest management.

The determination of the affected areas, according to the algorithm presented, was carried out in the EXCEL spreadsheet calculation program. After determining the affected areas, the areas on which the regeneration process was carried out, and the areas on which the installation of forest vegetation was necessary, were determined on the basis of field data. These data were recorded in specially prepared sheets, through direct observations in the field and qualitative and quantitative evaluations, analysing in parallel the forest management plan and the forest map. These elements are used for the preparation of the future management plan for the period 2024-2033.

RESULTS AND DISCUSSIONS

The volume of wood that has been determined to be harvested in the period 2014-2023, according to the forest management plan, in the Sudrigiu Forest District is 57855 m³ (Table 1). From the analysis of the data in Table 1, the opportunity for the management unit VII Văratec for the period 2014-2023 is 35761 m³, i.e. 62% of the total opportunity of the forest district for the period mentioned. Up to September 17, 2017, within the P.U. VII Văratec, a volume of approximately 13853 m³ has been harvested (exploited), which represents 38.7% of the total possibility of the production unit. The volume exploited from S.U.P. A by applying regeneration cuts represents 97%, and the difference of 3% was exploited from S.U.P. M by applying conservation cuts (Figure 2).

Table 1. The possibility for the period 2014-2023, related to Sudrigiu Forest District

Management unit		S.U.P.	Possibility (m³)
No.	Designation		
II	Aleu	A	4100
		M	4496
IV	Chișcău	A	8010
		M	5488
VII	Văratec	A	35401
		M	360
		K	0
Total Sudrigiu Forest District			57855

The volume of affected trees was calculated on the basis of their inventories, and classified according to the type of wood products obtained.

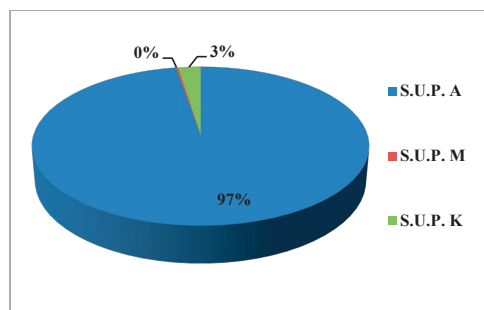


Figure 2. Volume of timber harvested up to September 17, 2017, from P.U. VII Văratec

Volume of Incidental Overlapping Products

Affected trees that have been inventoried in stands that are included in the ten-year primary product plan constitute incidental overlapping wood products. These are assimilated as main wood products (which are harvested during regeneration of stands) and are pre-counted from the possibility of main products (Crainic, 2023; Crainic, 2017) (Figure 3).



Figure 3. Incidental wood products I in the stand of plot 110

The stands in plots 35C and 107 are included in the ten-year forest management plan in regeneration urgency I, with a consistency index $k \leq 0.3$. As a result, the natural regeneration process in these stands is relatively advanced, with the area occupied by natural regeneration being about 70% of the plot area.

The analysis of the results in Table 2 shows that the volume affected in the two strands is 1152 m³ and the total area affected is 8.58 ha.

Table 2. Evidence of overlapping adventitious products in stands included in regeneration urgency I

Plot	V _{amenaj} (m ³ /u.a.)	S _{amenaj} (ha)	V(m ³ /u.a.)		i _{as}
			V _{actual}	V _{extras}	
35C	540	7.29	577.908	95	0.16
107	2356	15.30	2453.920	1057	0.43
Total	2896	22.59	3031.828	1152	0.38

The stands in the plots shown in Table 3 are included in the ten-year main product plan - regeneration, in urgency II, and the consistency index *k* has values in the range 0.4-0.7. The process of natural regeneration is actively dynamic, with natural regeneration installed on about 50% of their area. Analysing the results presented in Table 3 it can be seen that the volume of affected trees in the seven stands is 2962 m³ and the affected area is 11.09 ha.

Table 3. Evidence of overlapping by-products in stands included in regeneration emergency II

Plot	V _{amenaj} (m ³ /u.a.)	S _{amenaj} (ha)	V(m ³ /u.a.)		i _{as}
			V _{actual}	V _{extras}	
97B	1961	6.74	2036.488	155	0.08
99B	105	0.4	109.160	167	1.53
102B	4524	17.07	4776.636	1819	0.38
108A	1028	5.17	1087.972	44	0.04
108B	195	0.84	206.424	46	0.22
113C	8105	28.95	8498.720	365	0.04
114C	2678	14.79	2896.892	366	0.13
Total	18596	73.96	19612.292	2962	0.15

The stands in the plots shown in Table 4 are included in the ten-year plan of main products, in the third urgency, and their consistency index *k* varies between 0.7 and 0.8. In these plots, the natural regeneration process has been triggered, due to abundant fructification in recent years. The volume of affected trees in the six stands analysed is 3573 m³, the affected area being 9.43 ha.

Table 4. Evidence of overlapping by-products in stands included in regeneration emergency III

Plot	V _{amenaj} (m ³ /u.a.)	S _{amenaj} (ha)	V(m ³ /u.a.)		i _{as}
			V _{actual}	V _{extras}	
100B	266	1.00	278.800	104	0.37
110	10537	30.72	11053.10	1954	0.18
114B	201	0.80	213.160	10	0.05
115B	2677	7.52	2824.390	273	0.10
121B	5154	14.94	5416.940	1022	0.19
312A	6476	17.55	6714.68	210	0.03
Total	25311	72.53	26501.070	3573	0.13

The volume of accidental wood products over the stands included in the ten-year regeneration plan, in the three emergencies, is 7687 m³. This represents 21.50% of the volume of wood that has been set to be recovered in the period 2014-2023. Broken down by emergency, the volume

of affected stands included in emergency III represents 46% of the assessed volume, that included in emergency II represents 39%. The volume of affected stands included in Emergency I represents 15% of the assessed volume, as they are in the final stage of application of regeneration felling below the tree stand (Figure 4).

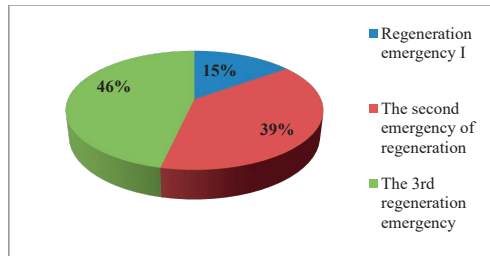


Figure 4. Volume of overlapping accidental products by regeneration urgencies

Volume of Incidental Products

In accordance with the technical rules in force for the national forestry fund, wood products resulting from damage to stands caused by extreme weather events, insect attacks, fires, etc. constitute incidental wood products (Figure 5).



Figure 5. Incidental wood products I in the stand of plot 111

If the age of the affected stands is more than half of the harvestable age (of the production cycle), the resulting incidental wood products are called incidental I products, and are assimilated as main products (Crainic, 2023).

As a result, these wood products are pre-counted from the ten-year possibility of main products, which has been established according to the forest management plan in force.

Volume of Incidental Products I

The affected stands shown in the plots in Table 5 are more than half the age of exploitability.

Accordingly, the timber products assessed in these are considered incidental timber products I and are therefore pre-counted from the possibility of main products (Figure 6).

Table 5. Evidence of incidental products I in affected stands

Plot	V _{amenaj} (m ³ /u.a.)	Samenaj (ha)	V(m ³ /u.a.)		i _{as}
			V _{actual}	V _{extras}	
34B	1270	3.64	1367.552	137	0.10
34C	1124	3.03	1182.176	64	0.05
35A	5235	13.12	5639.096	1254	0.22
35B	750	2.93	810.944	45	0.06
52	882	3.34	951.472	381	0.40
72B	7586	23.56	7896.992	2477	0.31
73B	5075	15.52	5273.656	715	0.14
73C	340	3.24	409.984	13	0.03
94A	5954	22.3	6498.120	1763	0.27
94B	221	0.64	230.984	111	0.48
94C	307	0.89	320.884	145	0.45
95A	6220	16.95	6592.900	2621	0.40
96A	1541	4.27	1640.064	896	0.55
98B	11935	32.61	12417.628	2328	0.19
99A	8160	22.54	8664.896	2654	0.31
100A	7659	22.46	8081.248	1601	0.20
101A	12863	30.92	13506.136	4105	0.30
101B	342	1.23	358.236	137	0.38
102A	3919	9.42	4114.936	1281	0.31
102C	2456	5.47	2585.092	1130	0.44
103A	8861	26.14	9572.008	2806	0.29
104A	11314	35.58	12139.456	5247	0.43
105A	8601	23.63	9215.380	863	0.09
109B	6408	18.79	6911.572	2750	0.40
111	10627	28.19	11258.456	4351	0.39
112A	5316	17.84	5729.888	774	0.14
112B	234	0.55	261.720	220	0.84
113D	579	1.36	637.208	346	0.54
114A	5265	16.35	5709.720	1615	0.28
116A	6330	15.63	6611.340	753	0.11
117A	9654	27.9	10290.120	3058	0.30
118B	3457	12.48	4026.088	1588	0.39
119B	1025	2.14	1146.552	923	0.81
119C	12344	39.82	13427.104	828	0.06
120A	9229	24.81	9814.516	136	0.01
122B	10089	27.49	10979.676	2865	0.26
123A	4602	15.04	5023.120	294	0.06
124A	19567	50.3	21035.760	1573	0.07
124B	746	1.75	834.200	26	0.03
125A	2037	5.46	2279.424	660	0.29
125B	6599	17.74	7017.664	234	0.03
126A	2702	7.34	2857.608	146	0.05
126B	3430	9.42	3641.008	216	0.06
126C	1149	3.29	1234.540	103	0.08
140B	5463	18.21	5725.224	147	0.03
141	5796	18	6055.200	307	0.05
312B	171	0.75	195.000	6	0.03
326	10015	39.9	11148.160	942	0.08
327	12021	42.03	13382.772	2237	0.17
328	3551	15.24	3983.816	421	0.11
329A	9409	32.9	10474.960	202	0.02
329C	519	1.38	562.056	11	0.02
330A	521	2.7	595.520	4	0.01
330B	464	0.97	515.992	18	0.03
330C	9818	36.91	11028.648	19	0.002
331	7713	36.73	8917.744	16	0.002
Total	299465	912.84	322782.216	60563	0.19



Figure 6. Incident wood products I, in the stand of plot 105 A

From the analysis of the records presented in Table 5, the volume of affected trees inventoried in the 56 stands is 60,563 m³ and the actual area affected is 173.44 hectares. The average degree of damage of these stands is $i_{as} = 19\%$ of the total volume at the time of the extreme weather events. The accidental products I (Figure 6) were recovered in several stages, depending on how they were identified, inventoried, and assessed.

Volume of Incident Products II

If the age of the affected stands is less than half of the harvestable age, the resulting incidental wood products are called incidental products II and are not assimilated as main products (Crainic, 2023). The affected stands in the plots shown in Table 6 are less than half of the harvestable age.

Table 6. Record of affected stands in plots from which incidental products are harvested II

Plot	V _{amenaj} (m ³ /u.a.)	S _{amenaj} (ha)	V(m ³ /u.a.)		i _{as}
			V _{actual}	V _{extra} s	
34 A	3075	12.71	3507.14	192	0.05
72 A	808	5.18	990.34	50	0.05
98 A	1847	8.63	2285.40	112	0.05
329 B	942	2.54	1064.94	89	0.08
Total	6672	29.06	7847.82	442	0.06

As a result, the wood products inventoried and evaluated in these stands are considered incidental wood products II (Figures 7 and 8). The volume of incidental wood products II assessed in the affected stands is 442 m³ and the actual area affected is 1.74 ha (Table 6). According to the diagram in Figure 9, it can be seen that the volume of incidental product I has the highest share of 88%, overlapping incidental products account for 11% of the assessed volume and incidental product II has

only 1%. Although spruce stands are vulnerable to the destabilizing actions of prevailing winds, in this study, deciduous stands were considerably damaged.



Figure 7. Incident wood products II in the stand of plot 34A



Figure 8. Incident wood products II in the stand of plot 34A

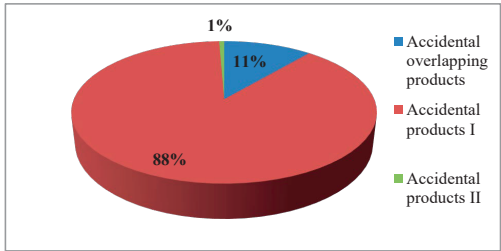


Figure 9. Percentage of valued wood products in affected stands

As a result, beech and gorun trees were uprooted and broken in a relatively high proportion (Figures 10 and 12). Spruce stands, growing in the study area outside the natural range of this species, being mostly artificial stands, were affected to a lesser extent. Most of the spruce trees were broken, at different heights, which shows that they had a consolidated rooting system (Figures 11 and 13). The recovery of the assessed incidental products was carried out under conditions of high economic efficiency. Although most of the time these wood products are of questionable quality, in this study the value obtained is high. Beech wood was valued at an average price of 250 lei/m³ and gorun wood at an average price of 450 lei/m³. A percentage of 15% of the volume of incidental products was recovered on its own account, thus obtaining an average value of 300 lei/m³.



Figure 10. Stand in plot 110, beech, affected by windthrow and windthrow breakage

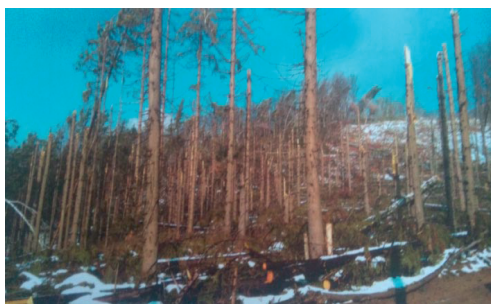


Figure 11. Spruce stand, plot 125A, affected by wind breaks

The high volume of incidental I and overlying products assessed in P.U. VII Văratec has been partially precounted from the unreclaimed volume in the 10-year plan for the period 2014-

2023. As a result, the difference in volume that has not been pre-computed will influence the volume of timber that will be determined to be harvested in the following decades (2024-2033, 2034-2043, etc.).



Figure 12. Stand in plot 110, beech, affected by windthrow and windthrow breakage



Figure 13. Spruce stand, plot 124B, affected by wind breaks

The proposed forest management plan for the period 2024-2033, foresees in most of the affected stands, where regeneration works are needed, only hygienic felling. The volume of wood predicted to be harvested during these interventions is relatively small, about 1 m³/year/ha. In addition, stands that are included in regeneration emergency I, regeneration felling and specific works for the installation and management of natural regeneration are proposed in the decade 2024-2033. Given the considerable areas from which incidental products have been harvested, specific works for the re-establishment of forest vegetation are proposed in the forest management plan for the period 2025-2035. This will ensure that the principle of continuity in time and space is respected.

CONCLUSIONS

The extreme weather events of September 17, 2017 caused considerable damage to the stands in the P.U. VII Văratec, administered by the Sudrigiu Forest District.

As a result, there were windthrow and wind breakages. The incidental wood products that have been identified, assessed and recovered are located in a high proportion in deciduous stands, consisting of beech and hornbeam species. The volume of incidental products I represents 88% of the total volume of incidental products assessed, in P.U. VII, during the case study. Consequently, stands older than half the age of exploitability are found to be vulnerable to the destabilising actions of prevailing winds and strong storms.

In stands that have been coppiced for regeneration, the volume of incidental overlapping products accounts for 11% of the total volume assessed. The volume of by-products II represents 1% of the assessed volume, so that stands less than half the age of exploitability have a high stability to the action of destabilising factors.

Artificial spruce stands in P.U. VII Văratec, although growing outside or at the limit of the range of this species, were affected to a relatively small extent. In this context, they were mostly affected by wind breaks.

The impact of extreme weather events on the management of P.U. VII Văratec is particularly strong. As a result, the volume of timber to be harvested will be considerably reduced in the coming decades. The silvicultural interventions that will be proposed in the management plan for the decade 2024-2033 in the affected stands will be reforestation and hygiene works.

In the stands that have been included in regeneration emergency I during 2014-2023, natural and mixed regeneration works will be completed.

Although incidental wood products have been optimally harvested, the economic efficiency of the activities to be carried out in the P.U. VII Văratec will be affected in the coming decades. As a result, part of the necessary works will be financially supported by the Sudrigiu Forest District and the Bihor County Forest Administration.

ACKNOWLEDGEMENTS

The case study and the related research were carried out within the framework of the research contract with the socio-economic environment: Ecological rehabilitation of the stands affected by the storm of 17.09.2017 in the area of the Sudrigiu Forest District, Bihor Forestry Directorate - Contract no. 12395/ 23.07.2019, University of Oradea - Bihor Forestry Directorate, carried out within the University of Oradea, Faculty of Environmental Protection, Department of Forestry and Forest Engineering, with the collaboration and support of the Bihor Forestry Directorate, Sudrigiu Forest District.

REFERENCES

- Bozzini, A., Francini, S., Chirici, G., Battisti, A., & Faccoli, M. (2023). Spruce Bark Beetle Outbreak Prediction through Automatic Classification of Sentinel-2 Imagery. *Forests*, 14, 1116 (<https://doi.org/10.3390/f14061116>).
- Chivulescu, S., Radu, R.G., Capalb, F., Hapa, M., Pitar, D., Marmureanu, L., Leca, S., Petrea, S., & Badea, O. (2024). Cost Valuation and Climate Mitigation Impacts of Forest Management: A Case Study from Piatra Craiului National Park, Romania. *Land*, 13, 17 (<https://doi.org/10.3390/land13010017>).
- Costa, M., Marchi, N., Bettella, F., Bolzon, P., Berger, F., & Lingua, E. (2021). Biological Legacies and Rockfall: The Protective Effect of a Windthrown Forest. *Forests*, 12, 1141 (<https://doi.org/10.3390/f12091141>).
- Crainic, G.C. (2017). Aspects Relating to The Evaluation Of Accidental Wood Products, In The Period 17 09- 06 11 2017, In The Forestry District Sudrigiu, Bihor Forestry Department. *Annals of the University of Oradea, Forestry Fascicle, University of Oradea Publishing House, XXVIII*, 189-196.
- Crainic, G.C., Sicoe, S., Curilă, M. & Curilă, S. (2020). The influence of structural characteristics on the stability of stands affected by windfalls and windbreaks. *Annals of the University of Oradea, Forestry Fascicle, University of Oradea Publishing House, XXXV*, 153 – 164.
- Crainic G.C., Sicoe S.I., Irimie F, Flavia Irimie (Cioflan) F., Iovan C.I. & Bodog M.F. (2023). The particularities of the ecological rehabilitation works of the sessile oak stands (*Quercus petraea* Matt.) Liebl.), from the seed reserve, Scientific Papers. Series E. Land Reclamation, Earth Observation & Surveying, Environmental Engineering. XII, Print ISSN 2285-6064.
- Crainic, G.C. (2023). *Produse forestiere – Note de curs (Forest products – Course notes)*. Departamentul de Silvicultură și Inginerie Forestieră, Facultatea de Protecția Mediului, Universitatea din Oradea, Romania.
- Cristea, M. (2004). *Riscurile climatice din bazinul hidrografic al Crișurilor (Climatic risks in the*

- Crișurilor hydrographic basin*). Oradea, RO: Abaddaba Publishing House.
- Crișan, V., Dincă, L., Târziu, D., Oneț, A., Oneț, A., & Cântar, I.C. (2024). A Comparison between Uneven-Aged Forest Stands from the Southern Carpathians and Those from the Banat Mountains. *Sustainability*, 16(3), 1109 (<https://doi.org/10.3390/su16031109>).
- Dinca, L., & Zhiyanski, M. (2023). *Forest Management and Biodiversity Conservation*. December 2023, 376 ISBN 978-3-0365-9414-9 (Hardback), ISBN 978-3-0365-9415-6 (<https://doi.org/10.3390/books978-3-0365-9415-6>).
- Giannetti, F., Pecchi, M., Travaglini, D., Francini, S., D'Amico, G., Vangi, E., Coccozza, C., & Chirici, G. (2021). Estimating VAI A Windstorm Damaged Forest Area in Italy Using Time Series Sentinel-2 Imagery and Continuous Change Detection Algorithms. *Forests*, 12, 680. (<https://doi.org/10.3390/f12060680>).
- Goff, T.C., Nelson, M.D., Liknes, G.C., Feeley, T.E., Pugh, S.A., & Morin, R.S. (2021). Rapid Assessment of Tree Damage Resulting from a 2020 Windstorm in Iowa, USA. *Forests*, 12, 555 (<https://doi.org/10.3390/f12050555>).
- Greco, F. (2016). *Hazarde și riscuri naturale, Ediția a V-a cu adăugiri (Natural Hazards and Risks, 5th Edition with Additions)*. Bucharest, RO: University Publishing House. (https://www.researchgate.net/publication/336676748_Hazarde_si_riscuri_naturale_2016).
- Konôpka, B., Šebeň, V., & Merganičová, K. (2021). Forest Regeneration Patterns Differ Considerably between Sites with and without Windthrow Wood Logging in the High Tatra Mountains. *Forests*, 12, 1349 (<https://doi.org/10.3390/f12101349>).
- Krišāns, O., Samariķs, V., Donis, J., & Jansons, Ā. (2020). Structural Root-Plate Characteristics of Wind-Thrown Norway Spruce in Hemiboreal Forests of Latvia. *Forests*, 11, 1143. DOI:10.3390/f11111143.
- Măhăra, Gh. (2006). *Variabilități și schimbări climatice (Climate variability and changes)*. Oradea, RO: University of Oradea Publishing House.
- Nolet, P., & Béland, M. (2017). Long-Term Susceptibility of Even- and Uneven-Aged Northern Hardwood Stands to Partial Windthrow. *Forests*, 8, 128. DOI:10.3390/f8040128.
- Prins, K., Köhl, M., & Linser, S. (2023). Is the concept of sustainable forest management still fit for purpose? *Forest Policy and Economics*, 157, 103072 (<https://doi.org/10.1016/j.forpol.2023.103072>).
- Ritter, T., Gollob, C., Kraßnitzer, R., Stampfer, K., & Nothdurft, A. (2022). A Robust Method for Detecting Wind-Fallen Stems from Aerial RGB Images Using a Line Segment Detection Algorithm. *Forests*, 13, 90. <https://doi.org/10.3390/f13010090>.
- Ruel, J.C. (2020). Ecosystem Management of Eastern Canadian Boreal Forests: Potential Impacts on Wind Damage. *Forests*, 11, 578. DOI:10.3390/f11050578.
- Rukh, S., Poschenrieder, W., Heym, M., & Pretzsch, H. (2020). Drought Resistance of Norway Spruce (*Picea abies* [L.] Karst) and European Beech (*Fagus sylvatica* [L.] in Mixed vs. Monospecific Stands and on Dry vs. Wet Sites. From Evidence at the Tree Level to Relevance at the Stand Level. *Forests*, 11, 639. DOI:10.3390/f11060639.
- Sabău, N.C. & Iovan, C.I. (2018). The influence of climate and pedological droughts on the hydrological drought of the small hydrographic basins from the Northern part of Codru-Moma Mountains, Bihor County. *Natural Resources and Sustainable Development*, 8(2), 87-104. DOI: 10.31924/nrsd.v8i2.011.
- Sicoe, S.I., Crainic, G.C., Iovan, C.I. & Sabău, N.C. (2019). Changes in the common beech stand micro-relief due to windfalls in the Management Unit VII Văratec, Sudrigiu Forest District, Bihor County, Romania. *Natural Resources and Sustainable Development*, 9(2), 203-220. DOI: 10.31924/nrsd.v9i2.037.
- Sicoe, S.I., Crainic, G.C., Samuel, A.D., Bodog, M.F., Iovan, C.I., Curilă, S., Hăruța, I.O., Șerban, E., Dorog, L.S., & Sabău, N.C. (2023). Analysis of the Effects of Windthrows on the Microbiological Properties of the Forest Soils and Their Natural Regeneration. *Forests*, 14, 1200. <https://doi.org/10.3390/f14061200>.
- Šimonovičová, A., Kraková, L., Piecková, E., Planý, M., Globanová, M., Paudišová, E., Šoltys, K., Budiš, J., Szemes, T., Gáfríková, J., & Pangallo, D. (2019). Soil Microbiota of Dystric Cambisol in the High Tatra Mountains (Slovakia) after Windthrow. *Sustainability*, 11, 6851. DOI:10.3390/su11236851.
- Sipos, Z., Simon, A., Csirmaz, K., Lemler, T., Manta, R.D., & Kocsis, Z. (2021). A case study of a derecho storm in dry, high-shear environment. *Quarterly Journal of the Hungarian Meteorological Service*, 125(1), 1-37. DOI:10.28974/idojaras.2021.1.1.
- Șerban, E. (2010). *Hazarde climatice generate de precipitații în Câmpia de Vest situată la nord de Mureș (Climatic hazards generated by precipitation in the Western Plain located north of the Mureș River)*. Oradea, RO: University of Oradea Publishing House.
- Tudose, T., Șerban, E., & Harpa, G.V. (2016). Climate Variability of the Rainy Periods between 1961 and 2013, in Maramureș, Romania. *SGEM Conference Proceedings, Section: Air Pollution and Climate Change*, 4(2), 275-282. Albena, Bulgaria, DOI: 10.5593/SGEM2016/B42/S19.036.
- Zhang, X., Chen, G., Cai, L., Jiao, H., Hua, J., Luo, X., & Wei, X. (2021). Impact Assessments of Typhoon Lekima on Forest Damages in Subtropical China Using Machine Learning Methods and Landsat 8 OLI Imagery. *Sustainability*, 13, 4893. <https://doi.org/10.3390/su13094893>.
- ***Arrangement U.P. VII Văratec, Sudrigiu Forest District, Bihor Forestry Directorate.
- ***Development map of VII Văratec, Sudrigiu Forest District, Bihor Forestry Directorate.
- *** (1997). Ministry of Water, Forests and Environmental Protection (MAPP), National Forest Management (RNP), *Unified time and production norms for works in Forestry*.
- *** (2000). Ministry of Water, Forests and Environmental Protection (MAPP), *Technical norms regarding compositions, schemes and technologies for forest regeneration and afforestation of degraded lands, No. 1*.

- *** (2000). Ministry of Water, Forests and Environmental Protection (MAPP), *Technical rules regarding the annual control of regenerations*, No. 7.
- *** (2019). *Ecological rehabilitation of the stands affected by the storm of September 17, 2017 in the radius of Forest District Sudrigiu, Bihor Forestry Directorate*. Research contract with the socio-economic environment, Partial report.
- *** (2020). *Centralizer regarding the downfalls and wind breaks produced due to special meteorological phenomena recorded in the period 2017-2020, Forest District Sudrigiu, Bihor Forestry Directorate*. No. 1467/06.05. 2020.
- *** (2020). *Ecological rehabilitation of the stands affected by the storm of September 17, 2017 in the radius of Forest District Sudrigiu, Bihor Forestry Directorate*. Research contract with the socio-economic environment, Final report.
- *** <https://www.capital.ro/furtuna-puternica-in-vestul-romaniei-cinci-persoane-au-decedat.html>, 2017.
- *** <https://www.qdidactic.com/bani-cariera/agricultura/silvicultura/conceptul-de-dezvoltare-durabila-a-padurilor483.php>.

THE EVOLUTION OF THE DYNAMIC CHARACTERISTICS OF THE SOIL-STRUCTURE SYSTEM IN CASE OF A UNIVERSITY BUILDING SEISMIC MONITORING

Daniela DOBRE^{1,2}, Claudiu-Sorin DRAGOMIR^{1,3},
Cornelia-Florentina DOBRESCU^{1,4}, Iolanda-Gabriela CRAIFALEANU^{1,2},
Emil-Sever GEORGESCU¹, Marta-Cristina ZAHARIA^{1,3}

¹National Institute for Research and Development in Construction,
Urban Planning and Sustainable Spatial Development - URBAN-INCERC,
266 Pantelimon Road, District 2, Bucharest, Romania

²Technical University of Civil Engineering of Bucharest,
124 Lacul Tei Blvd, District 2, Bucharest, Romania

³University of Agronomic Sciences and Veterinary Medicine of Bucharest,
Faculty of Land Reclamation and Environmental Engineering,
59 Marasti Blvd, District 1, Bucharest, Romania

⁴"Dunarea de Jos" University of Galati, 47 Domneasca Street, Galati, Romania

Corresponding author email: ddobre71@gmail.com

Abstract

In Romania, there are several legislative guidelines regarding the activity of seismic instrumentation/monitoring, which can support this activity in a coherent and effective way (Seismic Design Code, P 100-1/2013, Annex A). The monitoring of the Faculty of Biotechnology building is carried out using 3 Granite triaxial sensors, arranged one each on the top, in the basement and in the free-field. For each of the recordings, the Fourier spectrum, also response and power spectrum, can be represented, using different options related to axes, corrections etc. The processing of the records leads to the determination of the instantaneous maximum values of the accelerations, velocities, displacements. A comparative analysis over time will be presented for the level of vibrations recorded and for the frequency range obtained in free-field, basement, top conditions, as well as an analysis of vibrations from an ambient comfort point of view. Beyond the legislative aspects, this activity responds to the need to know both the characteristics of earthquakes and the structural characteristics of the building.

Key words: ambient comfort, frequencies, vibrations.

INTRODUCTION

In Romania, there are several legislative guidelines regarding the activity of seismic instrumentation/monitoring, which can support it in a coherent and effective way (Seismic Design Code, P 100-1/2013, Annex A, and the Regulation on the management of emergency situations generated by the earthquake, from 2023). Within this complex research activity, the existing concept regarding the location of the sensors for vibration measurement, inside the structural system, but also outside, offers the possibility of obtaining more information about the general structural behaviour (Lungu et al., 2004; Tiganescu et al., 2022). The vulnerability on the one hand and seismic performance of buildings on the other hand are

estimated most of the time considering their structural systems embedded at the base, in which case the sensor located outside the building is not of particular interest, but the studies developed over time try to quantify the effects of the phenomenon of soil-structure interaction (with its kinematic and inertial components), thus requiring the existence of at least one sensor outside, Figure 1.

The effect of the interaction can be an attenuation (dissipation of part of the energy through hysteretic damping, radiation of seismic waves) or an amplification of the dynamic response of the structure (modification of the natural vibration periods of the structural model, longer periods) (Project EUCONS/PN 03 15 02 01, 2004; Project ECOSMARTCONS, 2022). Internationally, there are many provisions

regarding the soil-structure interaction included in several important seismic design standards, such as NEHRP Recommended Provisions for Seismic Regulations for New Buildings and Other Structures 2001, ATC-40: Seismic Evaluation and Retrofit of Concrete Buildings 1996 and A Practical Guide to Soil-Structure Interaction (The Federal Emergency Management Agency, 2020).

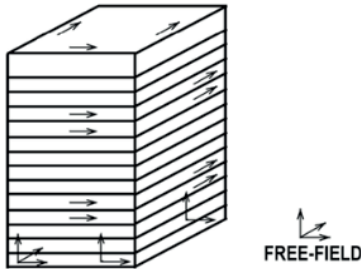


Figure 1. Seismic/ambient vibration monitoring layouts (Celebi, 2000, 2002)

MATERIALS AND METHODS

The defining elements of the soil-structure interaction analysis methods with supporting data from the activity of instrumentation/monitoring (including vibrations data from the near field, or free-field) are:

- the degree of association of interaction components (kinematic, inertial) and the weight of each in the behaviour of the structural system;
- calculation of transfer functions;
- determination of the translational/rotational motion of the foundation;
- estimation of the influence of soil conditions (location effect, vs. structure-soil interaction);
- determination of impedance functions;
- identification of the system from the input-output relationship, or just from output.

Below are presented some methodological concepts for determining the dynamic structural characteristics from the processing of micro vibration recordings and/or moderate/severe earthquake recordings, with/without the effect of the interaction between the structure and the soil, Figure 2-4, given the following:

- in the case of kinematic interaction, in general, a reduction of the motion at the

foundation level is expected in relation to that recorded in the free-field;

- the recorded motion at the foundation level can be evaluated taking into account the superposition of the effects of the two components of the interaction (effective motion);
- the effects of the soil-structure interaction can increase in the bending and torsional moments in the columns and walls on the ground floor (deformation of the building infrastructure, resulting relative rotations at the base of the columns on the ground floor, amplified even more in the case of non-synchronous motions of the foundation soil).

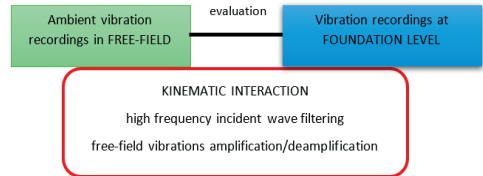


Figure 2. Soil-structure interaction effect: modification of free-field motion characteristics

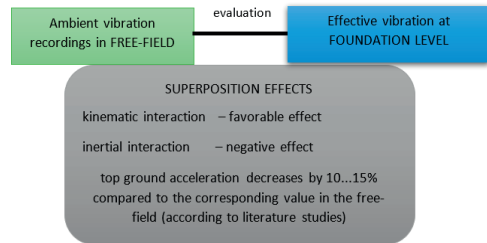


Figure 3. Soil-structure interaction effect: superposition effects

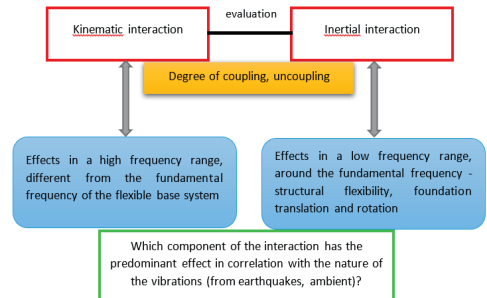


Figure 4. Soil-structure interaction effect: degree of association of interaction components and the weight of each in the behaviour of the structural system

Seismic and vibration monitoring, support tool for soil-structure interaction

The monitoring of the Faculty of Biotechnology building is carried out using 3 Granite triaxial sensors, arranged one each on the top, in the basement and in the free-field (for instance, N-S direction: channel 2 – building exterior; channel 6 – building basement; channel 10 – building top floor), Figure 5. For each of the recordings, the Fourier spectrum, also response and power spectrum, can be represented, using different options related to axes, corrections etc. (Dobre & Dragomir, 2017; Dragomir et al., 2020; Dragomir & Dobre, 2019). The identification of structural dynamic characteristics from ambient vibration measurements as well as according to the simplified formula from P100-1/2023 led to $T_1 = 0.18$ s, according to the seismic zoning map PGA 0.3 g and $T_c = 1.6$ s.



Figure 5. The building of the Faculty of Biotechnologies. Year of construction 2016, S+P+2E, reinforced concrete structural frames and walls, Granite instrument type

From a morphological point of view and geotechnical investigations for the type of soil, layers, stiffnesses, density, damping, the soil's shear wave velocity (Dobrescu & Călărașu, 2015; 2016), the area is located on the Colentina Plain, with an anthropogenically modified relief, flat and stable, with no risk potential regarding flooding phenomena. From a geological point of view, deposits belonging to the Upper Pleistocene, the high level, appear in the area. In order to establish the foundation conditions on the site, a program was developed regarding the analysis of the foundation soil, which included:

- field surveys, with circular boreholes executed on the site with a depth of up to approx. -6.00 m;
- determining the values of the physical characteristics of the samples collected from the borehole (soil granularity; soil moisture; plasticity limits characterized by the plasticity index and the consistency index).

The results of the laboratory tests carried out on the soil samples collected from the boreholes showed the existence of a fill layer with a variable thickness between 0.50-2.50 m, followed by cohesive soils composed of porous clay, with medium plasticity, weakly cohesive soils - dust clay and non-cohesive soils - sand and sand with gravel, starting with a depth of about -3.50 m.

The stratigraphic columns intercepted following the execution of drilling on the investigated site are highlighted by the sequence of soil layers in the lithological profiles of the drilling as follows: 0.00-0.80 m fill from buried soil and gravel; 0.80-1.20 m dusty clay, dark brown, hard; 1.20-2.20 m clay dust, dark brown, hard; 2.20-2.50 m sandy clayey dust, brown, with finely dispersed carbonates, hard; 2.50-3.50 m sandy dust, yellowish, cloudy plastic; 3.50-3.70 m large sand with rare gravel, yellowish, medium density, wet; 3.70-6.00 m sand with wet yellow gravel (data from a first drilling).

Interaction analysis can be made through experimental approaches (field tests), so in order to identify the phenomenon of soil-structure interaction, an analysis of the recordings from two earthquakes in 2021 and of the ambient vibration measurements from the same year was carried out, Figure 6 and Figure 7, later recordings also from 2018-2022 were analysed. The effects are expressed by the difference between the free-field motion, from the basement of the building and the response of the building structure at the top level (assuming that the motion of its base is/is not the same as the free-field motion). This difference depends both on the characteristics of the ground motion in the free-field and on the properties of the structure and the foundation environment.

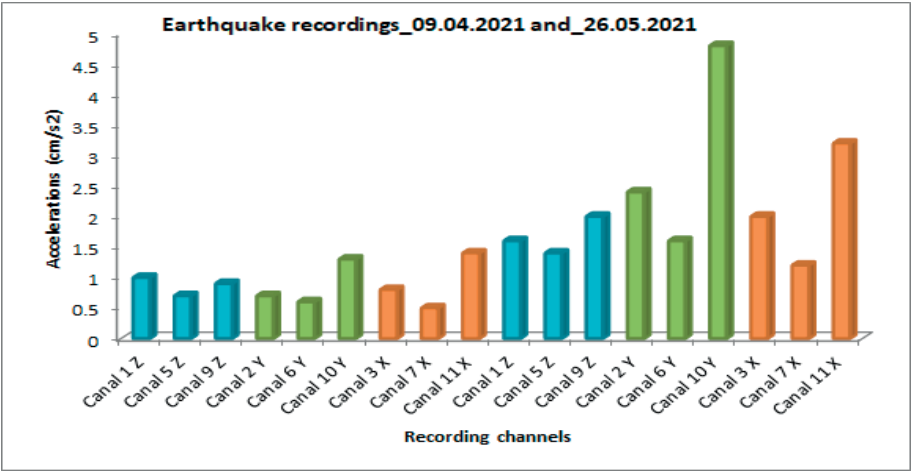


Figure 6. Interaction analysis: seismic acceleration propagation from the free-field to the top level of the building (earthquakes 2021)

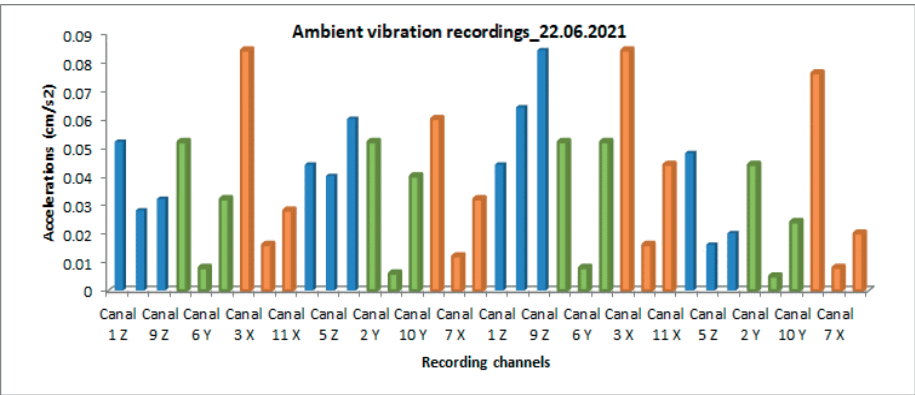


Figure 7. Interaction analysis, ambient acceleration propagation from the free-field to basement and to the top level of the building (2021)

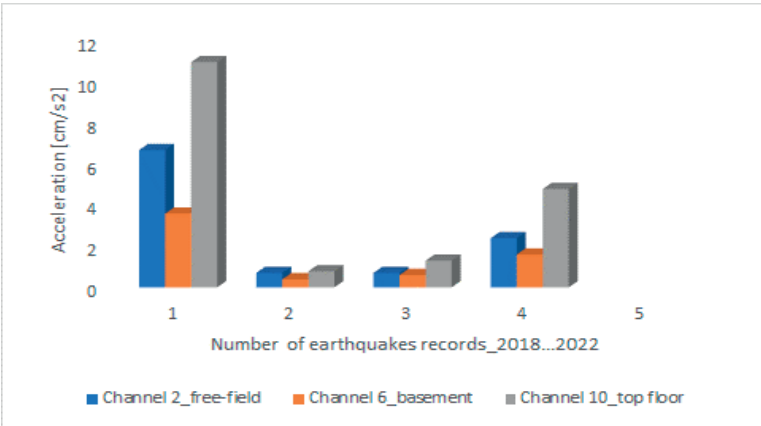


Figure 8. Interaction analysis, seismic acceleration propagation from the free-field to the top level of the building (earthquakes 2018-2022)

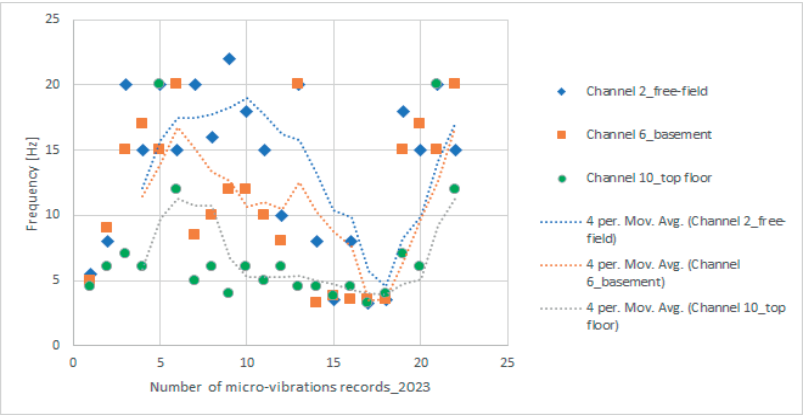


Figure 9. The evolution of the frequency values from the free-field, towards the basement of the building and then vertically towards the top floor

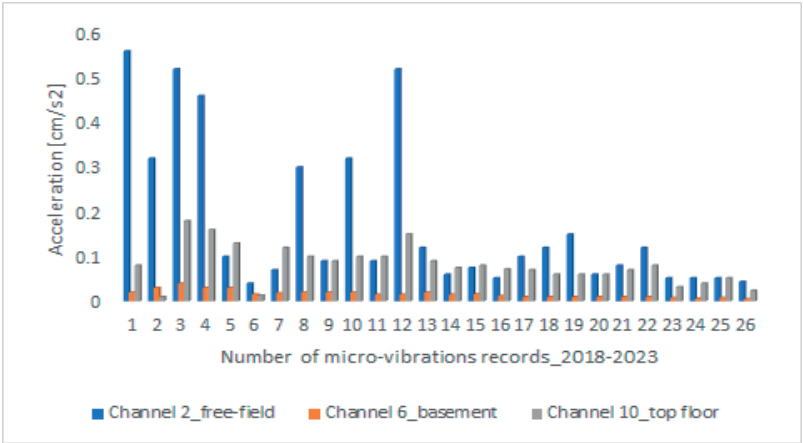


Figure 10. Interaction analysis, ambient acceleration propagation from the free-field to the top level of the building (2018-2022)

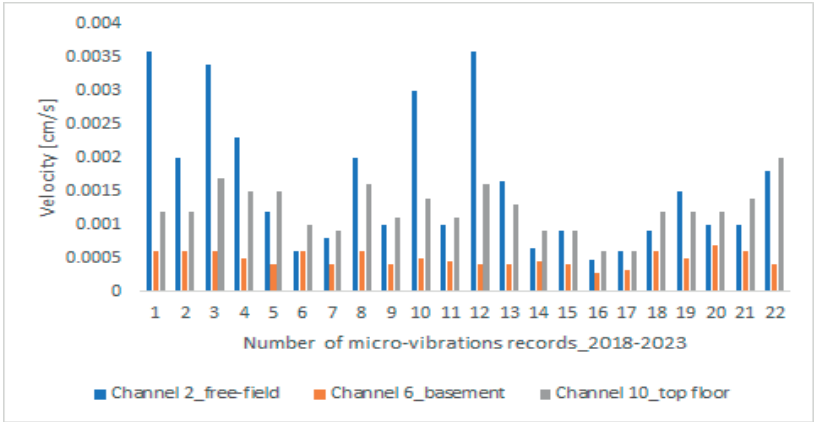


Figure 11. Interaction analysis, ambient velocity propagation from the free field to the top level of the building (2018-2022)

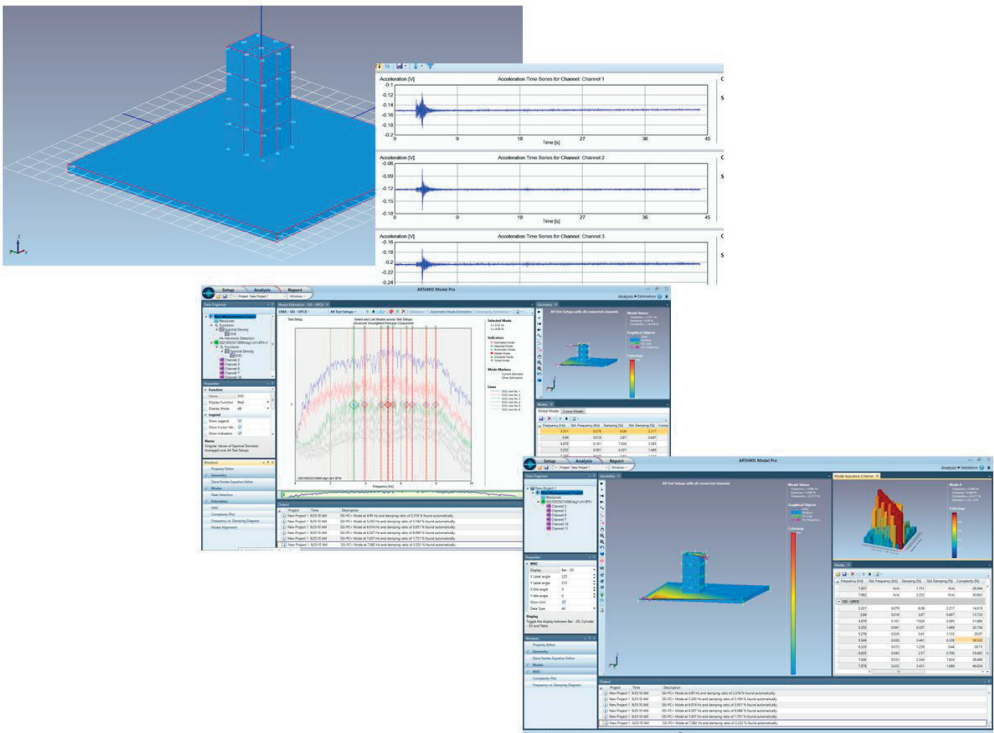


Figure 12. Brief stages of the OMA for the soil-structure assembly (simplified model for the discussed assembly)

The variation of frequencies in relation to 3 measurement points – free-field, basement and top floor, resulting from the ambient micro-vibrations/micro-seismicity recordings (2023) is shown in Figure 8 and Figure 9. The way of propagation of waves and vibrations through the soil conditions specified above highlights the kinematic component of the soil-structure interaction that arises from the presence of the building embedded in the soil (in fact, a disturbance of the free-field vibration due to the presence of structural elements with a stiffness different from that of the soil, at the interface level) and the mechanism differs vertically from the basement to the last level, with an additional displacement at interface caused by the force induced by the motion of the structure (inertial component). Representations for accelerations and velocities are in Figures 10 and 11. Combination of two materials with distinct characteristics and behaviour, the soil and the structure, requires another approach. Using the records obtained over time, the output-only modal analysis in order to get the

dynamic characteristics of the S+P+2E soil-structure assembly is another type of possible analysis, mainly assuming (Figure 12):

- defining the geometry of the structural system;
- entering the file with the data obtained from ambient recordings specifying the sampling interval, specifying the positions and orientations of the sensors on the structure, specifying some parameters for processing the recordings (detrrending, decimation, filtering, estimating the spectral density, detecting harmonic oscillations, iteration in the stochastic subspace);
- the calculation of the power spectral density and the estimation and validation of the natural modes of vibration.

RESULTS AND DISCUSSIONS

The processing of the records leads to the determination of the instantaneous maximum values of the accelerations, velocities, displacements. A comparative analysis was

presented for the level of vibrations recorded and for the frequency range obtained in free-field, basement, top level.

In order to establish a functional model for the study of the soil-structure interaction, based on the processing of the recordings of small earthquakes and ambient vibrations, the time histories recorded in the free-field, at the basement of the building and at the level of the terrace, were compared. In particular, there is a different situation in the case of recorded earthquakes, compared to the one for recorded ambient vibrations:

- in Figure 6 representation of the acceleration recorded on the channel corresponding to the sensor located in free-field decreases on the channel in the basement and then increases (sometimes accentuated) on the channel associated with the sensor on the building terrace; the same trend is observed in the case of both earthquakes;
- in representation Figure 7 is not observed the same variation of accelerations as in the case of ambient vibration recordings; in most situations, the accelerations in free-field are higher than those at the terrace level, showing that there is no amplification of the motion in the building.

Also, the dominant frequencies in the free-field are sometimes comparable to the corresponding ones at the basement level, which does not unequivocally show a filtering effect induced by the building, encountered in other cases. The differences between the motions in the free-field and those in the basement of the building can indicate the existence of soil-structure effects (kinematic interaction component). The range of frequencies in the free-field in this studied case is either between 10 Hz and 20 Hz, or between 40 Hz and 80 Hz (with multiple peaks), in both directions, x and y .

The amplitude spectra and Fourier transforms of the accelerograms of the recordings were determined, and the dynamic characteristics of the soil-structure system were determined. Thus, according to the processing of the two recordings from the earthquakes, at the level of the terrace, the predominant frequencies are included in the following domains: $f_{1x}=4-5$ Hz, $f_{1y}=4-6$ Hz. From ambient vibrations, the predominant frequency values are the same, varying only the f_2 and f_3 frequencies.

The inertial interaction component will be properly highlighted after recordings of moderate or severe earthquakes, the modification of the spectral parameters not being important from recordings of dynamic actions of reduced amplitude.

On the other hand, roughly determined by OMA, the natural period of vibration of the soil-structure assembly is $T_1 = 0.33$ s, and the damping coefficient 9.68% (the main unweighted component).

CONCLUSIONS

Beyond the legislative aspects, this activity responds to the need to know both the characteristics of earthquakes and the structural characteristics of the building.

The importance of the soil-structure interaction phenomenon has been a debated topic for a very long time, showing that it cannot be neglected, but understood in a dynamic context and correlated with a series of aspects regarding the spectral content of the seismic motion and the geotechnical and geological characteristics of a site. On the other hand, in the absence of data from larger earthquakes, micro-vibration/ambient vibration recordings offer an important alternative for structural dynamic analysis and global vulnerability assessment.

The recordings of significant seismic motions, or significant ambient vibrations, obtained both in the free-field (near/far), as well as on the lower, intermediate, or top floor of some buildings, with the possibility of also obtaining other data from the records in their adjacent area, they constitute a valuable source of information for investigating the effect of soil-structure interaction. This investigation also takes into account the type of foundation and soil that properly influence the structural response. The two components of the interaction have a quantified favourable or unfavourable role, once they have been decoupled and properly understood. In principle, the kinematic interaction induces the advantage of reducing the level of motion at the level of the foundation, compared to that in the free-field, but the methods applicable in the studies assume the determination of transfer functions sensitive to the calculations they assume. Regarding the inertial interaction, this involves the preliminary

determination of the translation and rotation motion at the foundation level (coupled/decoupled; shear force and moment that induce displacements of the foundation relative to the ground), then the evaluation of the effect on the fundamental period of vibration and the depreciation coefficient. However, neglecting the effects of soil-structure interaction is another approach accepted in many seismic design codes, in countries with high seismicity, as a conservative simplification. More than that, on a more general scale, some results of the monitoring as new findings are transferable and of special technical and legal importance, the elaborated documents representing the basis for the Technical Book of Building, and the archived information constituting initial records for the future data obtained after a major earthquake. Finding a reliable solution for a quick analysis after an earthquake, by generating a report with the dynamic parameters of the monitored buildings behaviour, is a challenge of a strategic and logistical nature, of acquisition, storage and continuous processing of data, elaboration of analytical models for validation, in context of digital approach for structural engineering.

ACKNOWLEDGEMENTS

This research work was carried out within PN 19-33 01 01-Research on the realization of an integrated system to ensure the security of the built space, with semi-automatic generation of PGA maps from seismic actions or other vibrational sources and rapid assessment of the vulnerability of instrumented buildings, Phase 6 and Phase 9- Evaluation of the vulnerability of instrumented/monitored buildings, with the identification of the soil-building interaction effect (2019-2022) and PN 23 35 01 01- Integrative concept of digital analysis of data from large-scale seismic monitoring of the national territory and the built environment, intended for the rapid identification of the destructive potential of seismic events produced in Romania and in the adjacent regions (2023).

REFERENCES

Celebi, M. (2000). Radiation damping observed from seismic responses of buildings. *12th World Conference on Earthquake Engineering, Auckland, New Zealand*, ISBN 095821543X.

- Celebi, M. (2002). Seismic instrumentation of buildings (with emphasis on Federal buildings). *Special GSA/USGS PROJECT*, An Administrative Report.
- Dobre, D. & Dragomir, C.-S. (2017). Dynamic Characteristics of Buildings from Signal Processing of Ambient Vibration. *IOP Conf. Ser.: Mater. Sci. Eng.*, 245, 022087, DOI: 10.1088/1757-899X/245/2/022087.
- Dobrescu, C.F. & Călărășu, E.A. (2016). Small-scale treatment of clayey soils using chemical stabilization method to support the durability of engineering works. *16th International Multidisciplinary Scientific Geo Conferences SGEM, Albena, Bulgaria, Conference Proceedings*, ISBN 978-619-7105-55-1, ISSN 1314-2704, Book 1, Vol. 1, 981-988.
- Dobrescu, C.F., Călărășu, E.A. & Ungureanu, V.V. (2016). Engineering approach on stability assessment of loess soil structures considering basic geotechnical characteristics. *International Scientific Conference CIBv 2016. Bulletin of the Transylvania University of Brasov. Series I: Engineering Sciences*, 9(58) No. 1 Special Issue, ISSN (CD-ROM): 2065-2127, ISSN (Online): 2971-9364 ISSN-L: 2065-2119.
- Dobrescu, C.F. & Călărășu, E.A. (2015). Overview of expansive soils behaviour based on quantitative geotechnical index achieved from laboratory testing. *15th International Multidisciplinary Scientific Geo Conferences SGEM, Albena, Bulgaria, Conference Proceedings*, (3), 495-502, ISSN 1314-2704.
- Dragomir, C.-S. & Dobre, D. (2019). Structural characteristics from micro-seismic recordings and numerical analysis. *AgroLife Scientific Journal*, 8(1). <https://agrolifejournal.usamv.ro/index.php/agrolife/article/view/421>
- Dragomir, C.-S. & Dobre, D. (2019). Processing data from vibration recordings. *IOP Conf. Ser.: Mater. Sci. Eng.*, 471, 052089, DOI: 10.1088/1757-899X/471/5/052089.
- Dragomir, C.-S., Dobre, D. & Iliescu, V. (2020). A comprehensive approach for the seismic vulnerability of a building of public utility. The 5th World Multidisciplinary Civil Engineering-Architecture-Urban Planning Symposium WMCAUS 2020. *IOP Conf. Series: Materials Science and Engineering*, 960, 042073, DOI 10.1088/1757-899X/960/4/042073.
- Lungu, D., Aldea, A., Demetriu, S. & Craifaleanu, I.-G. (2004). Seismic strengthening of buildings and seismic instrumentation -two priorities for seismic risk reduction in Romania. *Acta Geodaetica et Geophysica Hungarica*, 39(2), 233-258, 2004.
- Tiganescu, A., Craifaleanu, I.-G., Aldea, A., Grecu, B., Vacareanu, R., Toma-Danila, D., Balan, S.-F. & Dragomir, C.-S. (2022). Evolution, Recent Progress and Perspectives of the Seismic Monitoring of Building Structures in Romania. *Frontiers in Earth Science*, 10.
- PN 03-15 02 01 (2004). EUCONS Program - Integration of the construction sector in the European system, Effects of the structure-foundation-soil interaction phenomenon on the dynamic characteristics and mechanisms of seismic damage of buildings (in Romanian, Integrarea sectorului constructii in sistemul European, Efectele fenomenului de

- interacțiune structura-fundatie-teren asupra caracteristicilor dinamice și mecanismelor de avariere seismică ale construcțiilor).
- PN 19-33 01 01 (2022). ECOSMARTCONS Program- Research on the realization of an integrated system to ensure the security of the built space, with semi-automatic generation of PGA maps originating from seismic actions or other vibrational sources and rapid assessment of the vulnerability of instrumented buildings, Phase 6 and Phase 9 (in Romanian, Cercetări privind realizarea unui sistem integrat pentru asigurarea securității spațiului construit, cu generare semi-automată a hărților pga provenite din acțiuni seismice sau alte surse vibratorii și evaluare rapidă a vulnerabilității clădirilor instrumentate).
- PN 23 35 01 01(2023). Integrative concept of digital analysis of data from large-scale seismic monitoring of the national territory and the built environment, intended for the rapid identification of the destructive potential of seismic events produced in Romania and in the adjacent regions.
- Seismic Design Code, P 100-1/2013, Annex A.
- The Regulation on the management of emergency situations generated by the earthquake, approved by the Order nr. 2.061/170/2023 (in Romanian, Regulamentul privind gestionarea situațiilor de urgență generate de cutremur).
- The Federal Emergency Management Agency (2020). A Practical Guide to Soil-Structure Interaction. FEMA P-2091. Federal Emergency Management Agency. December 2020. https://www.fema.gov/sites/default/files/documents/fema_soil-structure-interaction.pdf

THE EFFECT OF URBANIZATION ON CLIMATE CHANGE, THE VULNERABILITY OF URBAN AREAS TO CLIMATE CHANGE AND THEIR CUMULATIVE IMPACT ON STORMWATER

Madalina ENE, Ioan BICA

Technical University of Civil Engineering of Bucharest,
122-124 Lacul Tei Blvd, District 1, Bucharest, Romania

Corresponding author emails: madalina.ene@romair.ro, ioan.bica@utcb.ro

Abstract

Water is an essential factor of the population existence and health and a primordial condition for the evolution of the society. In the context of climate change that determines the reduction of resources, the sustainable use of water, are key factors of sustainable development. The spatial and temporal distribution of water is determined not only by economic activities and the degree of urbanization, but also by natural variations in climate as a result of climate change. In recent decades, there has been a growing awareness of the value of stormwater as a resource that must be considered in urban development. In the context of the deterioration of the ecological conditions of water sources, due to pollution on the one hand, population growth and the influx of people into urban areas, on the other hand, the challenge for cities is to balance the limited supply and the growing demand for water. In recent years, migration is an additional challenge for the urban development strategy. At the same time, water as a resource and related infrastructure are among the most vulnerable sectors during armed conflicts.

Key words: climate change, rainwater, urbanization.

INTRODUCTION

The world is becoming more and more urbanized. Today, more than half of the world's population lives in urban areas, up from about one-third in 1950 and projected to rise to about two-thirds in 2050. In many parts of the world, water resources are declining or depleted, they are contaminated with pollutants and the natural reserves currently in use can no longer meet the growing demands on water supplies. With a steadily growing world population, the consumption of resources, intensive agriculture and climate change, water is becoming a limited resource. These factors can hinder economic development and growth the geographical distribution, density and movement of the population.

Unlike conventional collection/drainage approaches, which treat stormwater as a burden/product to be removed from the urban area as quickly as possible, sustainable stormwater management considers it a multifunctional resource (Mitchell, 2006) with many benefits' potential for society and the environment (Barbosa et al., 2012; Fletcher et al., 2015; Makropoulos et al., 2008; Mitchell, 2006).

A growing awareness of the value of stormwater as a resource to be considered in urban development was determined by various socio-economic aspects, such as:

- population growth and implicitly the demand for water;
- the growth of urban areas and related impervious surfaces;
- increasing awareness of the need for environmental protection;
- the risk/consequences/damage caused by heavy precipitation and storms exacerbated by climate change.

The World Meteorological Organization (WMO) report confirmed that 2023 was the warmest year on record, with the global average near-surface temperature at 1.45°C (with a margin of uncertainty of $\pm 0.12^\circ\text{C}$) above the pre-industrial baseline. It was the warmest ten-year period on record.

In 2023, the impacts of climate change continued to be seen across Europe, with millions of people impacted by extreme weather events, making the development of mitigation and adaptation measurements a priority.

Climate change leads to an increase in the intensity and amount of precipitation, thus

having a direct impact on the behaviour of the sewage system, which, through overloading, can ultimately lead to flooding and material damage in urban areas.

Precipitation is one of the most difficult meteorological elements to forecast. This is because of complex micro-physical processes taking place in clouds, the effect of external factors and geographic conditions and hard to parameterize cloud-forming processes.

Despite these doubts and assuming proper selection of climate change scenario, obtained results may serve as an advisory material supporting long-term development strategy.

For cities, some aspects of climate change may be amplified, including heat, flooding from heavy precipitation events and sea level rise in coastal cities.

The implementation of sustainable stormwater management involves measures at different scales, from urban and regional planning, where different land uses can be determined according to topographic and hydrological conditions, to the construction of individual facilities or the application of best management practices (BMP) (Carmon & Shamir, 2010).

MATERIALS AND METHODS

As part of a scientific research program, the article offers a review of analysis and interpretation of the existing published literature, correlated with the existing worldwide statistical information regarding demographic and climatological data in order to evaluate the cumulative impact of urbanisation, industrialization and climate change on urban area.

Statistical data were taken from United nation - World Social Report 2023, IPCC Reports on Climate Change: Impacts, Adaptation and Vulnerability and also climate change indicators reached record levels in 2023 according to Word Meteorological report.

RESULTS AND DISCUSSIONS

Currently, there is no universal definition of what "urban" means. The oldest cities, which are still inhabited today, testimonies of human and cultural history are considered: Jericho - Palestine (8000 BC), Byblos - Lebanon (6000 BC), Damascus - Syria (5000 BC), Jerusalem, Israel (4500 BC).

In the history of humanity, the development of cities had opposite effects. On the one hand, urbanization brings a positive impact on society as it helps/contributes to improving the social and economic aspects of people's lives. During the development there was a demographic explosion, which generated disruptive phenomena for normal activity: lack of housing and their crowding, lack of food and unemployment.

Urbanization processes dominate not only the history of the last century and a half, but are currently associated with the notion of development, urban equipment indicators being used in any argumentation regarding the quality of life on a national, regional or local scale.

By concentrating the population in big cities following human activity in industry, agriculture, transport, tourism, etc., the elements of biocenosis and biotope in the urban ecosystem fell prey to pollution.

The European Environment Agency declares that "for the first time in human history, more people live in cities than in rural areas. Europe is one of the most urbanized continents. Consequently, the demand for land in and around cities becomes acute, urban expansion reshapes the landscapes and affects people's life quality and the environment. According to the 2022 United Nations World Cities Report, it is predicted that approximately 70% of the world's estimated population will live in urban areas in 2050.

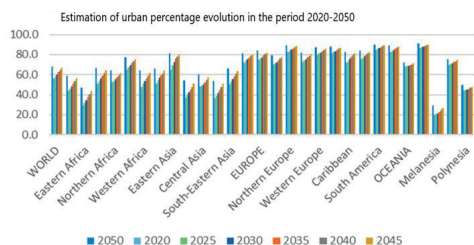


Figure 1. Estimation of urban percentage evolution in the period 2020-2050
<https://ourworldindata.org/urbanization>

The growth rate of the urban population is higher than the population growth rate, both worldwide and at the European level. 80% of the population lives in cities, which therefore generate the majority of greenhouse gas emissions.

Low-density housing, a single family, is preferred rather than multi-family housing even though compact land development is arguably environmentally more sustainable particularly in the face of climate change and demographic shift (immigration) that increase demand for housing and ancillary urban services-water, sewer, and road.

The impact of cities on the environment is not limited to the space within their inner city, the increased needs of such a settlement also require the exploitation of resources from the neighbouring areas and beyond (waste storage, collection of raw materials, etc.).

The high urban density of modern cities and the reduced openings to the sky of the streets contribute to the shading of the canyon surfaces and the decrease in the absorption of solar radiation. On the other hand, the compactness of cities and increased building densities can lead to trapping of long-wave radiation emitted by the ground and building surfaces at night, thus inhibiting urban cooling. In parallel, high surface roughness due to increased building density considerably attenuates the wind flow inside street canyons and the consequent convective heat transfer from urban surfaces to the atmosphere.

Moreover, land and building surfaces in modern cities generally have low values for the relative amount of light that surface reflects compared to the total incoming sunlight (albedo < 0.31), high infrared emissivity, and increased thermal conductivity and specific heat capacity.

Given their thermal and optical characteristics, urban elements absorb and store an important part of the direct solar radiation that reaches their surface, from early morning to late afternoon. The accumulated heat is then dissipated by convective and radiative phenomena during the evening and late night, cooling urban surfaces but increasing the ambient air temperature of adjacent air layers.

Rainwater falling in the atmosphere always contains impurities, even in the absence of human influence.

The results of studies conducted over the past decades, regarding the impact of global climate to changes in albedo showed that increases in albedo cause: decreased land evaporation, decreased land precipitation and increased

precipitation over the sea, in the global change cases (Garratt, 1993).

Other related studies support the statement that increased surface albedo leads to local/regional climatic changes in the direction of greater aridity. Another consequence of urbanisation and industrialisation is acid rain, caused by air pollution, that contributes to climate warming. Acid rain was identified in the 19th century by Robert Angus Smith, a pharmacist from Manchester (England), who measured high levels of acidity in rain falling over industrial regions of England and compared them to the much lower levels he observed in less polluted areas near the coast.

Little attention was paid to his work until the 1950s. Acid rain is one of the consequences of air pollution. The emission of sulphur dioxide, nitrogen dioxide, and carbon dioxide causes acid rain. Carbon dioxide is a primary gas that also leads to the greenhouse effect. Human activities produce these chemicals of acid rain which reach the atmosphere, when their concentration becomes high then the temperature of the atmosphere increases and results in climate warming.

The assessment of the cumulative impact on water, associated with climate change in urban areas, especially the way in which climate systems and urban systems interact, is presented following the study of scientific articles, of which the following aspects are considered representative:

- Globally, increased frequencies and intensities of extreme precipitation from global warming will likely expand the global land area affected by flood hazards (Alfieri et al., 2018; Alfieri et al., 2017; Hoegh-Guldberg et al., 2018);

- Future urban flooding risks increase with the continued increase in surface temperature (IPCC, 2019b; Winsemius et al., 2015; Hoegh-Guldberg et al., 2018);

- Urban flood risks are also increased by urban expansion and their land use due to the increase of the impervious surface, impacting the drainage of flood waters with consecutive sewer overflows (Arnbjerg-Nielsen et al., 2013; Aroua, 2016; Kundzewicz et al., 2014);

- These risks are also determined by the increasing complexity of society, long-term

urban and economic development policy (Berndtsson et al., 2019);

- The economic risks associated with future surface water flooding in cities are considerable. For example, in the UK, annual damage from surface water flooding is predicted to increase by £60-200 million for an estimated warming of 2-4°C scenarios; improved adaptation actions could manage flooding up to 2°C, but will be insufficient beyond this (Sayers et al., 2015);

- The impact of urban flooding can exacerbate the activity of hospital facilities (including the potential occurrence of epidemics, outbreaks of malaria and cholera), which are aggravated by damage to medical facilities (for example, damage to hospitals and disruption of drug supply chains) (Gough et al., 2019);

- Rising sea levels and increased storm surge from tropical cyclones and increased rainfall will increase the likelihood of coastal cities flooding;

- Risks of urban water scarcity and security are compounded by vulnerabilities such as service availability and infrastructure quality (Ahmadalipour et al., 2019; Dong et al., 2020; Reynolds et al., 2019; Thomas et al., 2017; Mullin, 2020);

- Droughts interact and manifest in complex ways in interconnected urban areas by increasing the risk of urban water scarcity (Tapia et al., 2017; Rushforth & Ruddell, 2015);

- Urban interdependencies mean that droughts in one region can limit the availability of water resources in another region (Chuah, Ho, & Chow, 2018; Gober et al., 2016; Srinivasan, Konar, & Sivapalan, 2017; Zhang et al., 2019; Zhao et al., 2020).

Climate change is bringing multiple different changes to different regions – which will all increase with further warming.

These include changes to wetness and dryness, to winds, snow and ice, coastal areas and oceans, like:

- intensifying the water cycle;
- climate change is affecting rainfall patterns. In high latitudes, precipitation is likely

to increase, while it is projected to decrease over large parts of the subtropics;

- coastal areas will see continued sea level rise throughout the 21st century contributing to more frequent and severe coastal flooding in low-lying areas and coastal erosion;

- further warming will amplify permafrost thawing, and the loss of seasonal snow cover, melting of glaciers and ice sheets, and loss of summer Arctic Sea ice;

- changes to the ocean, including warming, more frequent marine heatwaves, ocean acidification, and reduced oxygen levels have been clearly linked to human influence.

During 2023, the majority of Europe was wetter than average; around 7% wetter than average for the continent. The majority of Europe saw wetter-than-average conditions. Drier-than-average conditions were experienced in countries to the west of the Black Sea, and across the southern Iberian Peninsula, where dry conditions occurred from February to April.

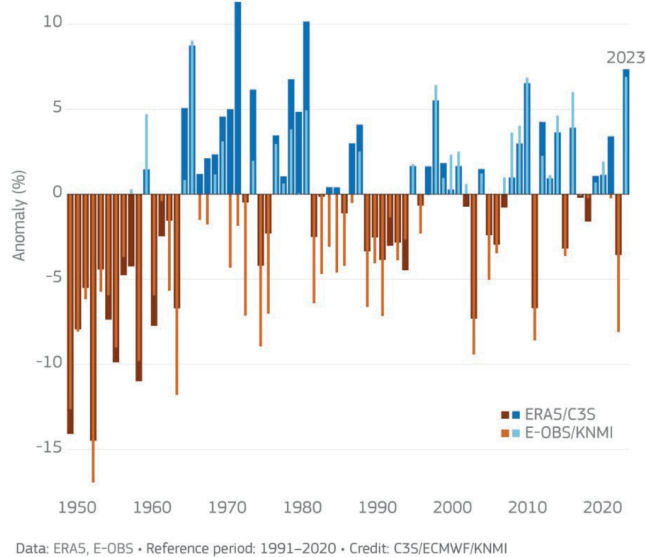
A region between western Europe and Ukraine was wetter than average from October to December, whereas most of Fennoscandia was drier than average in November and December. Figure 2 presents the anomalies expressed as a percentage of the annual average over European land from 1950 to 2023.

Perspectives

As climate change intensifies, the European Union faces more rainfall, stronger storms and rising sea levels. According to the European Environment Agency (EEA), the consequences of fluvial, rainwater and coastal flooding in Europe will worsen overall as a result of the increase, both locally and regionally, in the intensity and frequency of flooding.

Observed climate trends and future climate projections indicate significant regional variations in precipitation across Europe (Figure 3). Forecasts indicate an increase in the amount of annual precipitation in northern Europe. Winter precipitation could increase by more than 25% in the last 20 years of this century in some parts of Europe.

Anomalies in annual precipitation over European land



 Copernicus Climate Change Service
European State of the Climate | 2023  PROGRAMME OF
THE EUROPEAN UNION  

Figure 2. Anomalies (%) in annual precipitation over European land from 1950 to 2023
Data source: E-OBS (light blue and light brown) and ERA5 (dark blue and dark brown)
<https://climate.copernicus.eu/esotc/2023/precipitation>

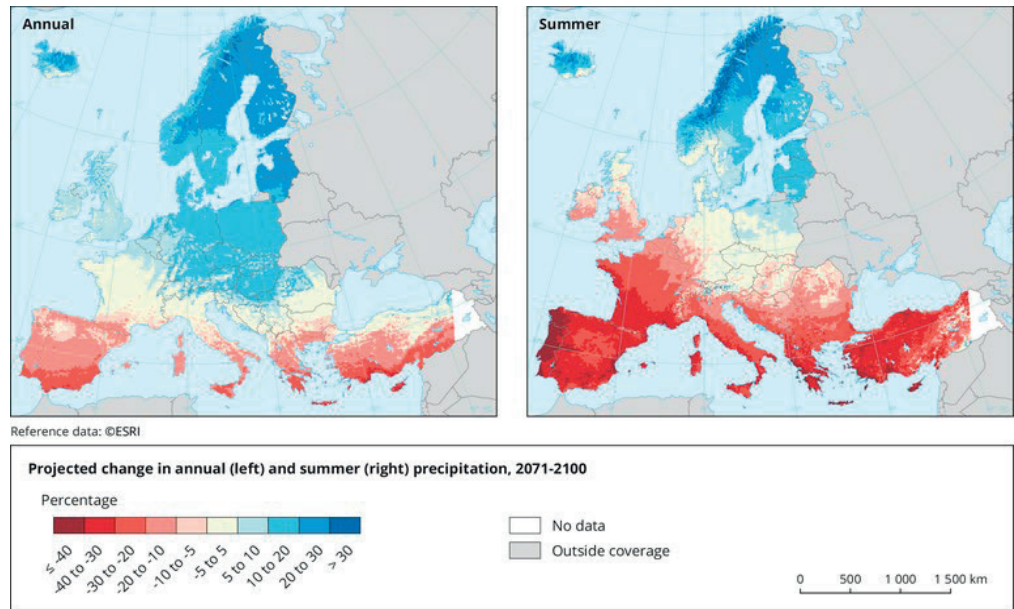


Figure 3. Project change in winter (left) and summer (right), precipitation, in 2071-2100 period (scenario based on a 2°C increase in global temperature), %
<https://www.eea.europa.eu/data-and-maps/figures/projected-changes-in-annual-and-6>

Urbanization is one of the main changes, which has been observed to substantially alter the local environment, especially the soil-atmosphere interaction, resulting in significant diurnal temperature differences (Kalnay, 2003), which could partially contribute to the projected 2°C temperature increase under conditions of potential climate change (Georgescu et al., 2014).

The following changes can be expected in an urbanized watershed:

- The frequency of flood peaks is predicted to increase;
- Increased values of maximum flood flows (by two to five times);
- Increased volume of discharged rainwater;
- Increasing the frequency of summer floods and the severity of floods;
- Reduction of minimum runoff and groundwater levels, because of rapid water drainage;
- Increasing the speed of water flowing on the streets and in the drainage systems and, as a result, increasing the speed of the flow in the emissary during the rain.

Any of the mentioned changes can lead to an increase in the concentration of pollutants in the water discharged into the outfall. At the same time, along with the increase in the maximum flood flows, erosion phenomena and the modification of the emissary bed also occur. Thus, the problems related to pollution are multiplied with the increase of urbanization.

Flood risks are increasing due to the following factors:

- Change of land use destination – excessive cutting of forests and intensive agricultural practices, urbanization and economic activities reduce water retention capacity (natural drainage) during and after rainfall.
- Urbanization and real estate developments in flood risk areas.
- The regularization of natural rivers and the disconnection of the naturally flooded meadows of the watercourses, which increase the flow speeds and reduce the natural retention of water (reducing the time in which the flood propagates in a sector – faster floods.

- The accentuation of extreme hydrometeorological phenomena because of climate change correlated with uncontrolled urban development.

Implementing sustainable stormwater management involves measures at different scales, from urban and regional planning.

In the context of the deterioration/degradation of the ecological conditions of water sources, due to pollution on the one hand, population growth and the influx of people into urban areas, on the other hand, the challenge for cities is to balance the limited supply and the growing demand for water.

Both the infrastructure and the public services, respectively the degree of urbanity that they have tend to measure the suitability or inadequacy of a population to a contemporary way of life.

Increasing urban temperatures will also have a strong influence on evapotranspiration that is largely limited by precipitation.

Thus, there might be increased evapotranspiration in areas with more precipitation but also increased durations of drought in areas with reduced precipitation.

In northern regions there is also an expected seasonal change in precipitation with more winter precipitation falling as rain and higher spring temperatures, leading to increased winter runoff and a reduction in late season snowmelt. Climate change will influence several factors of importance to habitat quality and development of urban biodiversity.

The projected change in temperatures, rainfall, extreme events and enhanced CO₂ concentrations will influence a range of factors related to single species (e.g. physiology), population dynamics, species distribution patterns, species interactions and ecosystem services, as a result of spatial or temporal reorganisation (Bellard et al., 2012).

The perceptivity that both nature and society are at risk drives scientific research to focus on adaptation strategies, to develop mitigation plans, to inspire sustainable solutions and to (re)invent practices how locals and communities, stakeholders and economies, can deal with changing settings and pressures (Walker et al., 2014).

CONCLUSIONS

Extremely dynamic today, contemporary society is increasingly feeling the combined impact of current pressures: urbanization, climate change and the globalization of the economy.

The spatial and temporal distribution of water is determined not only by economic activities and the degree of urbanization, but also by natural variations in climate as a result of climate changes.

Our understanding of the role that urbanization plays in the processes and evolution of the climate system is incomplete.

Adaptation to actual or expected climate change effects involves a range of measures or actions that can be taken to reduce the vulnerability of society and to improve the resilience capacity against expected changing climate.

Due to the climate crisis, the phenomenon of rapid urbanization and the insecurity regarding food and energy, the sustainable management of water resources remains a critical issue. The path towards adaptation and societies' resilience to overcome risks and threats to a more sustainable future entails attentiveness and place-tailored measures and actions (Das et al., 2021).

In recent years, migration is an additional challenge for the urban development strategy. At the same time, water as a resource and related infrastructure are among the most vulnerable sectors during armed conflicts.

Climate change leads to an increase in the intensity and amount of precipitation, thus having a direct impact on the behavior of the sewage system, which, through overloading, can ultimately lead to flooding and material damage in urban areas.

The explosive growth of metropolises and cities, in general, affects territorial structures, impoverishes primary resources and makes it increasingly difficult to manage adaptation processes to current climate conditions.

Change in urban precipitation may be due to interactions of urban heat islands, urban roughness effects, and aerosols, each of which may have a positive, negative, or synergistic impact. Building cities that "work" – green, resilient and inclusive – requires intensive policy coordination and optimal investment choices.

Increasing urban temperatures and changed precipitation dynamics will influence species community development through limiting water availability during the growing season as well as changing the nutrient dynamics.

All these phenomena lead to a chain degradation of the natural balances in an urbanized watershed and to a sharp degradation of the aquatic resources of fauna and flora.

These changes have profound economic and societal implications due to the reduction of significant natural resources and the degradation of their quality.

Acid rain should be considered as one of the important problems derived from the climate change and must be addressed with the importance it has.

Possible adaptation measures to handle climate change can take many forms and be effective at a range of spatial and temporal scales, proactively planned or as a result of socio-political drivers such as new planning regulations, market demand or even social pressure.

With the increasing frequency of human activities and climate change, how to reveal the response of ecosystem water conservation function the changing environment, is a scientific problem that needs to be urgently addressed in ecological hydrology research.

In the context of the deterioration/deterioration of the ecological conditions of water sources, due to pollution on the one hand, population growth and the influx of people into urban areas, on the other hand, the challenge for cities is to balance the limited supply and the growing demand for water. In recent years, migration is an additional challenge for the urban development strategy. At the same time, water as a resource and related infrastructure are among the most vulnerable sectors during armed conflicts.

REFERENCES

- Aguiar, F.C., Bentza, J., Joao, M.N., Ana, S., Fonseca, L., Swarta, R., Duarte Santosa, F., Penha-Lopes, G. (2018). Adaptation to climate change at local level in Europe: An overview. *Environ. Sci. Policy*, 86, 38–63.
- Alfieri, L., Bisselink, B., Dottori, F., Naumann, G., De Roo, A., Salamon, P., Wyser, K., Feyen, L. (2016). Global projections of river flood risk in a warmer world. *Earth's Future*, 5(2), 171–182.

- Alfieri, L., Dottori, F., Betts, R., Salamon, P., Feyen, L. (2018). Multi-Model Projections of River Flood Risk in Europe under Global Warming. *Climate*, 6(1), ISSN 2225-1154, JRC108760.
- Barbosa, A.E., Fernandes, J.N., David, L.M. (2012). Key issues for sustainable urban stormwater management. *Water Research, Special Issue on Stormwater in urban areas*, 46, 6787–6798.
- Bellard, C., Bertelsmeier, C., Leadley, P., Thuiller, W., Courchamp, F. (2012). Impacts of climate change on the future of biodiversity. *Ecology Letters*, 15(4), 365–377.
- Carmon, N., Shamir, U. (2010). Water-sensitive planning: integrating water considerations into urban and regional planning. *Water and Environment Journal*, 24, 181–191.
- Das, J., Goyal, M., Nanduri, U., Eslamian, S. (2021). Water Harvesting, Climate Change, and Variability. In *Handbook of Water Harvesting and Conservation: Basic Concepts and Fundamentals*; Eslamian, S., Ed.; John Wiley & Sons Ltd.: Hoboken, NJ, USA, pp. 427–446.
- Garratt, J.R. (1993). Sensitivity of climate simulations to land-surface and atmospheric boundary-layer treatments. - a review. *J. Climate*, 6, 419–449.
- Georgescu, M., Morefield, P.E., Bierwagen, B.G., & Weaver, C.P. (2014). Urban adaptation can roll back warming of emerging megapolitan regions. *Proceedings of the National Academy of Sciences*, 111(8), 2909–2914.
- Hoegh-Guldberg, O., Poloczanska, E.S., Skirving, W., Dove, S. (2017). Coral Reef Ecosystems under Climate Change and Ocean Acidification. *Frontiers in Marine Science*, 4, 158.
- Makropoulos, C.K., Natsis, K., Liu, S., Mittas, K., Butler, D. (2008). Decision support for sustainable option selection in integrated urban water management. *Environmental Modelling & Software*, 23, 1448–1460.
- Marsalek, J. (2001). Review of Stormwater Source Controls in Urban Drainage, in *Advances in Urban Stormwater and Agricultural Runoff Source Controls*, NATO Science Series, Marsalek, Jiri, Watt, E., Zeman, E., Sieker, H. (eds.). Netherlands, Dordrecht: Springer. p. 1
- Mitchell, V.G. (2006). Applying Integrated Urban Water Management Concepts: A Review of Australian Experience. *Environmental Management*, 37, 589–605.
- Walker, B.J., Adger, W.N., & Russel, D. (2015). Institutional barriers to climate change adaptation in decentralised governance structures: Transport planning in England. *Urban Studies*, 52(12), 2250–2266. <https://doi.org/10.1177/0042098014544759>
- Winsemius, H., Aerts, J., van Beek, L. et al. (2016). Global drivers of future river flood risk. *Nature Climate Change*, 6(4), 381–385.
<https://ourworldindata.org/urbanization>
<https://www.oecd.org/climate-action/ipac/the-climate-action-monitor-2023-60e338a2/chapter-d1e1621#section-d1e1882>
<https://climate.copernicus.eu/esotc/2023/precipitation>
<https://www.eea.europa.eu/data-and-maps/figures/projected-changes-in-annual-and-6>

MODELING THE STRUCTURAL BEHAVIOR OF A CNC BEARING MEMBER SUBJECTED TO STATIC AND DYNAMIC LOADS

Nicoleta-Adaciza IONESCU¹, Daniela DOBRE^{1,2}, Claudiu-Sorin DRAGOMIR^{1,3}

¹National Institute for Research and Development in Construction,
Urban Planning and Sustainable Spatial Development - URBAN-INCERC,
266 Pantelimon Road, District 2, Bucharest, Romania

²Technical University of Civil Engineering of Bucharest,
124 Lacul Tei Blvd, District 2, Bucharest, Romania

³University of Agronomic Sciences and Veterinary Medicine of Bucharest,
59 Marasti Blvd, District 1, Bucharest, Romania

Corresponding author email: adaionescu2002@yahoo.co.uk

Abstract

The paper aims within a multidisciplinary approach (Chemistry, Engineering, Finite element analysis) to highlight the structural behaviour of a computer numerical control (CNC) resistance element from the vibrations point of view and following the deformations and efforts arising from static and dynamic loads. The modelling of the structural bearing member was done with the Finite Element Method, using three-dimensional elements of the Solid type, in specialized software, and considering different types of material (cast iron, reinforced concrete and reinforced concrete with the addition of polymer-coated clinker). Results concerning the variation of the dynamic characteristics (natural periods of vibration) and response spectra in accelerations, velocities and displacements in several points are presented. In conclusion, with regard to the considered materials, the use of concrete with intelligent addition to build the base of a CNC is a good solution. Using a smart reinforced concrete material embedded in the metal box gives greater rigidity to the structural system, the fundamental period having the lowest value, compared to the other two cases.

Key words: concrete, self-repair, modelling, static and dynamic loads.

INTRODUCTION

The support system plays an important role in the correct operation of a numerically controlled (CNC) machine tool because it must ensure stability in the case of a high level of vibrations (vibrations produced within the manufacturing process) and following deformations and structural efforts arising from different types of loads (static, dynamic), Figure 1.



Figure 1. Image of a Computer Numerical Control (CNC) Machine Tool

In order to have a bed structure for a CNC machine tool with a corresponding rigidity as high as possible, it is usually built from cast iron, but in the case of the modelling presented in this work concrete will also be used as a construction material. The considered concrete will have an addition (made of clinker coated with polymer) that improves to a certain extent its properties regarding the density-settlement relationship and the resistance to compression and bending. In addition, this concrete has self-repair properties for a certain area of cracking, thus extending the service life of the concrete.

The concept of self-repair in the case of cementitious materials is fundamentally related to the state of cracking - microcracks in the structure of the material, as a form of inducing degradation in the mass of the material. The self-healing effect is realized by closing the cracks, sealing them, partially or completely.

Most of the time, the recovery initiated is not only at the physical level, related to the microstructure of the material, but also to its

functionality, to the recovery of the initial mechanical characteristics (Zapciu et al., 2021; Voinitchi et al., 2020).

MATERIALS AND METHODS

The finite element analysis carried out is aimed at understanding the behaviour of a structural element (of type support CNC) considering as construction materials for it cast iron, concrete with addition (clinker covered with polymer) and concrete with addition and cast-iron coating. The composition of the cement concrete was developed, according to CP 012-1:2007, depending on the concrete exposure classes. When establishing the concrete recipe, the amount of cement and the water-cement ratio were determined, as well as the amounts of aggregates required. Depending on the granularity of the aggregates, the percentages per granularity class were determined so that they fall within the favourable granularity area of the normative. Tables 1 to 5 are presented comparative the characteristics of cement concrete of class C30/37 with concrete prepared with smart addition of class C30/37.

The degree of crack healing was evaluated on controlled cracked concrete test pieces using a chloride electromigration experiment under the action of an electric field. The degree of repair being the ratio of the relative decrease in current due to the contribution of the crack in the material with smart addition and the classic preparation.

As results presented and discussed will be mainly the dynamic structural characteristics of the CNC machine tool bed structure depending on the material used.

It should be specified that in the case of the modelled CNC machine tool bed structure (with the geometric dimensions of an existing one) there are no known normative provisions that would impose restrictions on the number and maximum value of static and/or dynamic loads, the maximum values of deformations, different safety coefficients (to buckling, breaking or fatigue), minimal execution, assembly or exploitation imperfections, vibration frequencies, rate of deformation in stationary plastic flow, product life, weight, material and moments of inertia, stiffness at different demands, static and/or dynamic stability,

behaviour under different simultaneous loads etc.

Table 1. The compositions of cement concrete and cement concrete with intelligent addition

Component	Concrete (B)	Concrete with intelligent admixture (BAI)
Cement CEM I42.5	450	450
Water	200	200
Air	0	0
Superplasticizer additive	3	3
Aggregate dosages of ballast	1672	1497
Smart addition (polymer coated clinker)	0	200

Table 2. Results of density and settlement determinations for concrete

Sample code	Settling (mm)	Density (kg/m ³)
B	140	2330
BAI	80	2350

Table 3. Results of compressive and flexural strength determinations

Sample code	f_{c7} N/mm ²	f_{c28} N/mm ²	f_{inc7} N/mm ²	f_{inc28} N/mm ²
B	33.8	43.2	4.52	5.34
BAI	35.1	45.7	4.61	5.95

Table 4. Test results for resistance to water penetration under pressure

Sample code	Penetration depth (mm)
B	14
BAI	12

Table 5. Degree of healing after 3 days for cracked and re-cracked self-healing concrete

Concrete condition	Cracked	Re-cracked
Degree of healing after 3 days GV3, %	23.0	14.4

In order to reach the final model for the presented bed structure, the following stages were taken into account:

- the transition from the physical system to a structural model;
- the transition from an infinite number of degrees of freedom to a finite number (situation specific to the mesh grid).

Finite element characteristics are related to 3D finite element dimensions, nodes (identifies the

geometry of the model), degrees of freedom (possible values that the kinematic quantities in the nodes can take), forces applied directly in the nodes. Thus, static force is 18kN, distributed in the nodes of the network on an associated surface, and the dynamic force from the vibrations of the CNC attached to the modelled bed structure is of Time-history type for a certain velocity – $RPM = 60/T$, for 1200 rpm, $T = 0.05$ s the input period.

- constitutive properties: isotropic material with linear elastic behaviour, longitudinal/transversely modulus of elasticity (E or G), Poisson's ratio;

Modulus of elasticity $E_{BAI} = 2.5 \times 10^7$ kN/m², $E_{Cast\ iron} = 115 \times 10^5$ kN/m²; Specific weight_{BAI} = 23.5 kN/m³; Specific weight_{cast iron} = 72.5 kN/m³.

- the solution of the system of equations numerically obtained by the software etc.

In this case, three-dimensional elements of the Solid type were used, with 8 nodes and 6 quadrilateral faces with one joint at each node, Figure 2. This type of element was chosen because the dimensions of bed structure are comparable (there is no negligible dimension in the comparison with the others), this element being able to capture a three-dimensional stress state.

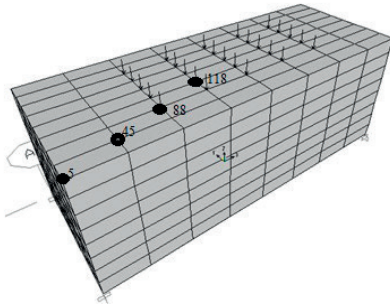


Figure 2. Real dimensions for bed structure of machine tool: 1.321 m x 0.508 m x 0.500 m. The position of the considered nodes (points 5, 45, 88, 118)

RESULTS AND DISCUSSIONS

Table 6 highlights the fact that the use of the BAI material embedded in the metal casing confers greater rigidity to the structural system, the fundamental natural period having the lowest value, compared to the other two cases. For the higher modes, however, the system is more rigid if it is made of BAI without inclusion

in cast iron. It should be specified that the inclusion was made by modelling the shell as a three-dimensional solid structural element of the Shell type, which incorporates both functions, the membrane and the plate (with a thickness of 0.2 m). The results will differ if the thickness of the cast iron casing is changed.

Table 6. The variation of the dynamic characteristics depending on the material used (embedment type support in 4 nodes/support points)

Material for structural system	Dynamic characteristics/ periods of vibration [s]
Cast iron	T1 = 0.04964 T2 = 0.03291 T3 = 0.02944 T4 = 0.01603
Concrete with intelligent addition	T1 = 0.03264 T2 = 0.02108 T3 = 0.01883 T4 = 0.01005
Concrete with intelligent addition in the metal casing (cast iron)	T1 = 0.03123 T2 = 0.02564 T3 = 0.02503 T4 = 0.01313

Figures 3a, 3b, 3c and 3d point out the first 4 modes of vibration, not for all 3 considered materials (embedment-type support on the contour, perimetral support points).

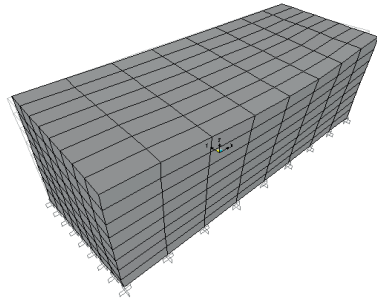


Figure 3a. Fundamental vibration mode, $T_1 = 0.01094s$

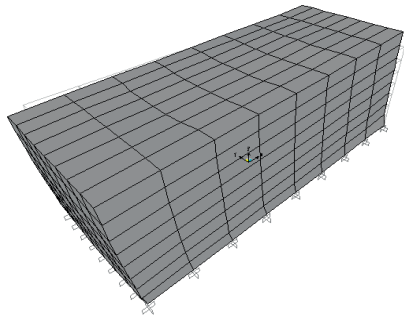


Figure 3b. Vibration mode 2, $T_2 = 0.00773s$

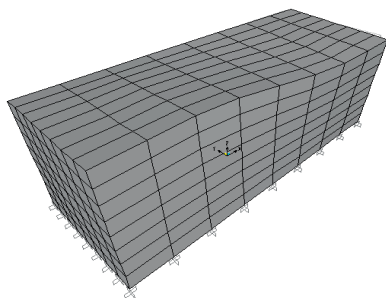


Figure 3c. Vibration mode 3, $T_3 = 0.0068s$

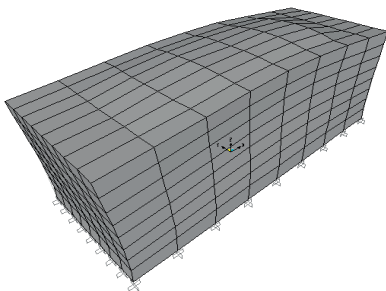


Figure 3d. Vibration mode 4, $T_4 = 0.00622s$

For the situation of a bracing type embedded in 4 nodes (support points), the representation of the vibration modes is approximately the same as the form of representation from Figure 3, but with slightly different values.

The use of BAI material embedded in the metal casing does not confer greater rigidity to the structural system of the batten compared to the second case considered, only BAI, but a better rigidity than in the case of using cast iron.

The same conclusion holds for the higher modes.

Regarding the forms of vibration considering two other materials (cast iron and BAI in the metal case), they do not differ significantly from those in Figure 4 (so that they will not be presented anymore), only the vibration periods differ, as can be seen in Table 7.

Comparatively, the variation of the values of the periods of vibration depending on the material used and the type of support, were also analysed and is found that the bed structure is a more flexible structural element when it is made of cast iron and less flexible when it is made of concrete with intelligent addition, or BAI in the metal case (depending on the type of support).

Table 7. The variation of the dynamic characteristics depending on the material used (embedment-type support on the contour/perimetral support points)

Material for structural system	Dynamic characteristics/periods of vibration [s]
Cast iron	$T_1 = 0.01645$ $T_2 = 0.01179$ $T_3 = 0.01041$ $T_4 = 0.00934$
Concrete with intelligent addition	$T_1 = 0.01094$ $T_2 = 0.00773$ $T_3 = 0.00680$ $T_4 = 0.00622$
Concrete with intelligent addition in the metal casing (cast iron)	$T_1 = 0.01438$ $T_2 = 0.01134$ $T_3 = 0.00980$ $T_4 = 0.00921$

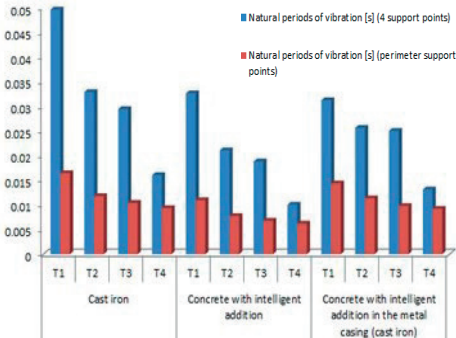


Figure 4. Relation T-Material-Support conditions

On the other hand, the dynamic response is represented by accelerations, velocities, displacements (from the dynamic action type loading), in several points considered of interest, Figures 5a-5c (embedded support in 4 nodes/support points).

The maximum values of the accelerations, velocities, displacements in the nodes considered (with values for damping of 10%, for example) have a small order of magnitude, but the graphic representation is made for the variation of the values in the 3 material situations.

In point 118, for instance, these values are higher in all cases because it is the position closest to the point of application of both static and dynamic force.

In the absence of reference/existing data in codes, standards, norms, or other studies, these values cannot be reported and commented critically.

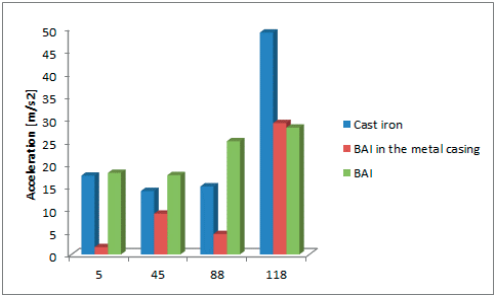


Figure 5a. The maximum values of the accelerations at the specified points, for the materials used

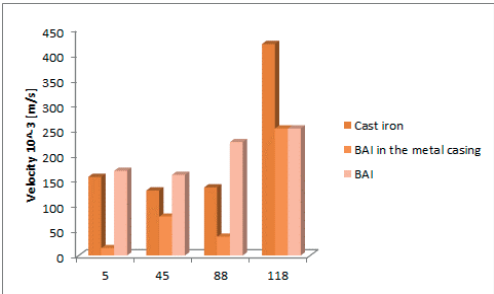


Figure 5b. Maximum velocities values in the specified points, for the materials used

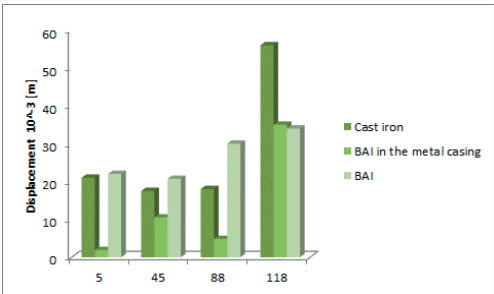


Figure 5c. The maximum values of the displacements in the specified points, for the materials used

It can also be concluded, based on the figure above, that a bed structure made of BAI with a metal casing (cast iron) will have a lower dynamic response than in the case of the other two situations, although its vibration periods were not the littlest.

The answer in terms of kinematic quantities - concrete slab with intelligent addition is presented in Figure 6 and Figure 7.

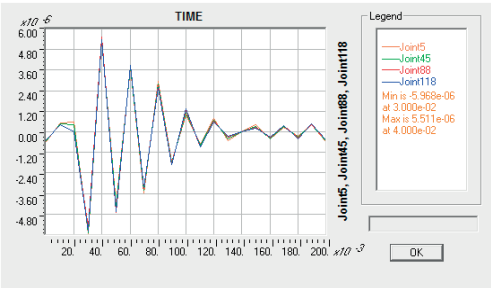


Figure 6. The variation of displacement over time, in several points on the upper surface, from dynamic action

On the other hand, the answer is also represented in terms of kinematic quantities-accelerations, velocities, displacements (from the dynamic action), in several points considered to be of interest (embedded support in 4 nodes/support points), Figure 7 (a-d).

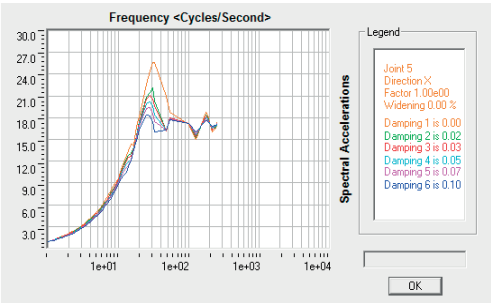


Figure 7a. Point 5

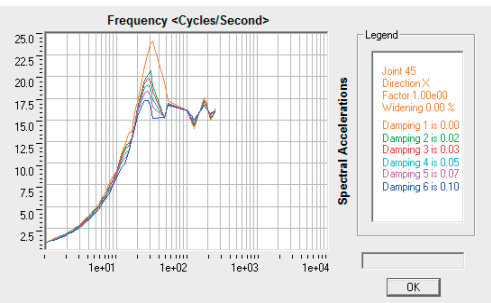


Figure 7b. Point 45

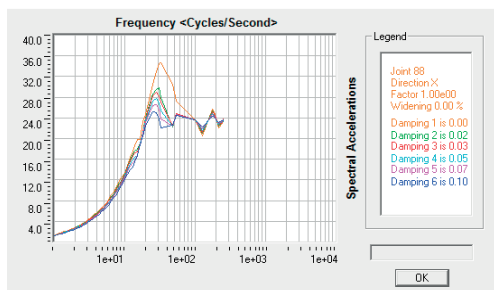


Figure 7c. Point 88

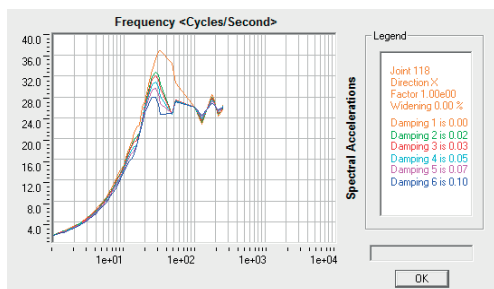


Figure 7d. Point 118

Figure 7. Spectra of response in accelerations, in certain points on the upper surface, from dynamic action

CONCLUSIONS

Concerning to the considered materials, the use of concrete with intelligent addition to build the base of a CNC is a good solution. This is also of interest because, from taking over some loads induced by the operation of the CNC, an opening of cracks of an unfavourable order of magnitude may occur, but the self-repairing capacity of the concrete will be an important element. So, it is highlighted that the use of the BAI material embedded in the metal casing confers greater rigidity to the structural system, the fundamental period having the lowest value, compared to the other two cases. For the higher modes, however, the bed structure is more rigid if it is made of BAI without inclusion in cast iron. By modelling this structural system made of 3 different materials, loaded with static and dynamic forces, in two support situations, we wanted to evaluate the behaviour of a fixed CNC part from the point of view of the dynamic characteristics (natural periods of vibration) and of some kinematic quantities - through response spectra in accelerations, velocities and

displacements. Regarding the modeling method used - Finite element method (in the field of machine, equipment and installation constructions/CNC), the basic component of a system analysed by FEM is the resistance structure defined as a mechanical assembly with a very clearly established functionality, such as taking over some loads, ensuring a certain functionality, ensuring a static and/or dynamic stability, guaranteeing a rigidity imposed by the designer, etc. The article wanted a multidisciplinary approach (Chemistry, Structural Engineering, Finite Element Analysis), but which cannot be related to reference/existing data in codes, standards, norms.

ACKNOWLEDGEMENTS

This research work was carried out within PN 23 35 01 01-Integrative concept of digital analysis of data from large-scale seismic monitoring of the national territory and the built environment, intended for the rapid identification of the destructive potential of seismic events produced in Romania and in the adjacent regions.

REFERENCES

- CP 012-1:2007 Concrete Production Code.
- SAP2000 Integrated Software for Structural Analysis and Design, Computers and Structures Inc., Berkeley, California.
- Voinitchi, C., Baeră, C., Zapciu, M., Matei, C., Szilágyi, H. (2020). Development of Cement-Based Materials Enriched with Polymeric Coated Reactive Grains as Long-Term Promoter of Matrix Continuous Hydration. *IOP Conf. Series: Materials Science and Engineering*, 877, 012028, doi:10.1088/1757-899X/877/1/012028.
- Voinitchi, C., Baeră, C., Zapciu, M., Matei, C., Szilágyi, H., Ionescu, N.-A., Tudorie, F. (2020). Polymeric coated reactive grains as intelligent addition in cementitious composites for generating the self-healing effect. *Annals of the Academy of Romanian Scientists, Series on Engineering Sciences*, 12(1), ISSN 2066-8570.
- Zapciu, M., Voinitchi, C., Ionescu, N.-A., Olteanu, M. (2021). New material using cement-based matrix with self-repair properties based on reactive grains with protective coating. *Studia Ubb Chemia, LXVI*(4), 253-265, doi:10.24193/subbchem.2021.4.18.

TRANSFORMATION MODEL TOWARDS ENERGY POSITIVE PUBLIC BUILDING

Petar KISYOV

University of Food Technologies, 26 Maritza Blvd, Plovdiv, Bulgaria

Corresponding author email: petar.kisyov@yahoo.com

Abstract

Positive Energy Buildings and neighbourhoods are having an important role in the clean energy transition and cities' green energy system transformation. The aim of this paper is to design and evaluate a scenario for the transformation of a single administrative public building located in Plovdiv, Bulgaria into Positive Energy Building. This is achieved through the implementation of set of passive and technological measures, including renewable power, so to decrease building's demand and to fully electrify it and finally to cover buildings total energy demand by renewable mean. This work evaluates the efficiency, impact, investment costs and rate of return of a number of energy conservation measures being designed to be applied. Finally, techno-economic analysis and results are discussed and compared.

Key words: building transformation models, positive energy buildings, renewable energy.

INTRODUCTION

Buildings in the EU are responsible for over 36% of the greenhouse gas emissions and about 40% of the total final energy consumption (European Commission, Energy efficiency in buildings, 2020). Reducing these emissions through energy efficiency measures and renewables is crucial in order to achieve zero-emission buildings stock in 2050. (European Council, 2024; Fit for 55 Infographic). To do so, the EC introduced the Fit for 55 Package, which sets policy actions, so as to decrease greenhouse gas emissions by at least 55% in 2030, while further increasing the share of renewable energy in the final energy consumption. On the other hand, European Commission's 2040 impact assessment, evaluated that electricity should account for 50% of final EU energy consumption to meet climate goals, with 35% by 2030. An important role for achieving these ambitious targets is within the building sector. With the revision of the Energy Performance of Buildings Directive (EPBD), part of the Fit for 55 package, more ambitious energy efficiency standards for building renovations of existing and construction of new buildings are set (European Council, 2023; Fit for 55 package). Bulgaria continues to be one of the most energy-intensive economies in the EU, with a large percentage of greenhouse gas emissions

generation. Thus, opportunities exist for significant energy savings through targeted investment in the building sector, as well as increased investment in clean energy infrastructure. According to the "Energy efficiency" dimension set in the Integrated Energy and Climate Plan of the Republic of Bulgaria 2021-2030, Bulgaria's efforts are aimed at achieving energy savings in the final energy consumption, by improving the energy characteristics of the most inefficient buildings. Within the plan, a goal to reduce the final energy consumption with 11.1% compared to the reference scenario in 2020 is set (Integrated Plan in the Area on Energy and Climate of The Republic of Bulgaria, 2021-2030).

The goal requires the demonstration of cost-effective models for transformation of the existing buildings into highly efficient, such as the Positive Energy Buildings (PEBs). Currently there is a lack of an official definition for a PEB. However, there are range of publications in literature on the PEBs concept, which is considered as evolution of the nearly-zero-energy buildings concept and is introduced as the next level of certification for highly efficient and sustainable buildings (Zhang et al., 2024; Kumar, 2021).

PEB is defined as "an energy-efficient building that produces more energy over the course of a year than the building requires for heating,

cooling, ventilation, domestic hot water and auxiliary systems". Thus, PEBs are requiring the implementation of energy efficiency measures, where a large share of the consumed energy is generated from renewable sources, while there is also excess energy available. Fulfilling the goal, high self-consumption rates and high energy flexibility has also to be achieved (Juusela et al., 2023). It can be summarized that for achieving PEB the implementation of the following three approaches is extremely essential - envelope passive strategies, energy-efficiency measures, highly efficient heating, cooling and ventilation technologies and renewable energy generation.

The first step to reach PEB is to make the building highly energy efficient building with low energy demand (Rehman et al., 2022). Brucks indicates that building envelope retrofitting, such as insulation and multiglazed windows is among buildings optimal technology portfolio and is essential to achieve PEB, especially seen for buildings located in cold climates (Bruck et al., 2022). Retrofitted buildings have a higher self-coverage of the energy demand and react more flexibly to changes in the electricity tariff. This study also determines the value of retrofitting for PEBs is between $1.5 \div 2$ EUR/m²*kWh reduced. In a study by Nundy smart and efficient windows are highlighted as a suitable technology in the PEB transformation (Nundy et al., 2021). Heat pumps with high coefficient of performance (COP) and low environmental impact are among the most suitable technologies for an efficient heating and cooling service for the building sector (Battaglia et al., 2023). PEBs also require photovoltaic systems to achieve energy self-sufficiency. The renewables can be either integrated into the building or supplied as external energy support to the building (Hu, 2016). However, the growing interest in on the on-site energy generation, which has led to the development of numerous research studies on the theme of PV in PEBs. Yang presents a bottom-up dynamic building model based on the implementation of insulation, renewable energy sources, and rooftop PV panels (Yang et al., 2022). The scenario evaluation shows that energy-saving measures together with renewable heat sources can reduce about 2/3 of the energy and 60-90% of GHG emissions for space heating, where

nearly 80% of electricity demand could be met by PVs. In a recent study Zomer provides a performance assessment of the potential of BIPV in enabling energy positive buildings (Zomer et al., 2020). Barrutieta studies a decision-making methodology guiding the different stakeholders towards effective architectural decisions for PV system integration in the PEB design process (Barrutieta et al., 2023).

Special attention is paid on introducing methods for the optimization of the envelope for the best building integrated photovoltaics (BIPV) placement, while balancing roof and facade areas. Finally, an intelligent predictive control schemes, supported by monitoring and networking schemes are seen of high importance in order to achieve generation-consumption matching under real time conditions (Kolokotsa et al., 2011). In recent literature buildings possessing the four main energy functions, such as consumption, generation, storage, and flexibility are also called flexumers (Cai et al., 2024).

PEB topic has been highlighted in several recent researches. Magrini highlights the Positive Energy Building as the next challenge after adopting the Nearly Zero Energy Buildings (NZEBs) concept (Magrini et al., 2020). Bojić investigates a model for three residential buildings powered by electricity from PVs, where the main conclusion sets importance to the size of the PVs as a main element whether to achieve PEBs (Bojić et al., 2011). Johari concludes that net zero energy buildings with high share of PVs have three times more excess power in summer months compared to winter (Johari et al., 2024).

MATERIALS AND METHODS

The case study is an existing inefficient administrative public building - Municipal Administration building - Plovdiv (Figure 1). The building entered into operation in 1969 and currently is occupied by an average of 155 persons serving for administrative purposes. The building functions from Monday to Friday for an average of 11 hours a day.

The aim of this paper is to demonstrate an energy transformation paradigm of a single inefficient administrative public building to a

PEB with zero emission generation by taking into effect the implementation of different energy conservation measures and technologies. To do so, the current energy performance of an administrative pilot building was carefully studied. The study served for the definition of a number energy conservation and renewable measures leading to a transformation towards positive energy and zero emission building.



Figure 1. Photos of the case study

In this publication, the connections between the following fields that are relevant for the PEB design process are carefully studied, so as to design building's transformation model - geometry size, location and climate conditions, current energy consumption and state of the art of buildings heating and cooling systems. In order to evaluate the energy performance of the selected case study and the performance of the formulated scenario, the national energy performance certification methodology was applied. Subsequently, detailed impact evaluation of each of the proposed interventions, part of the transformation scenario, on consumer parameters was conducted.

RESULTS AND DISCUSSIONS

National energy performance policy

The indicators for energy consumption and the energy performance of buildings, as well as the minimum requirements for the energy performance of buildings with a view of achieving the levels of optimal costs, the technical requirements for energy efficiency and nearly zero energy buildings, are determined by (Regulation RD-02-20-3/9.11.2022 on the Technical Requirements for the Energy

Characteristics of Buildings). The ordinance determines:

- the energy performance indicators and the energy requirements characteristics of buildings;
- the national calculation methodology for assessment of the energy characteristics of buildings;
- the scale of energy consumption classes with numerical limits for different purposes categories of buildings and the minimum requirements for energy efficiency in accordance with the scale for the relevant category of buildings;
- the energy efficiency requirements for the establishment of new buildings.

The methodology used for the evaluation of the case study building applies both actual measurements and complied with calculated energy consumption methods, so as to discover baseline scenarios. In this case this approach is applied for calculation of the ventilation demand.

Buildings features and climate conditions

Plovdiv has a humid subtropical climate (Köppen climate classification) with considerable humid continental influences. There are four well established seasons with large temperature amplitudes, requiring implementation of both heating and cooling building infrastructure in order to achieve the all-season regulatory requirements. According to the climatic zoning of the Republic of Bulgaria under (Regulation No. RD-02-20-3/9.11.2022 on the Technical Requirements for the Energy Characteristics of Buildings), the city of Plovdiv belongs to climate zone 6, which is characterized by the following climatic features: a) average duration of the heating season of 175 days, starting October 24 and ending April 6; b) average heating degrees for the city of Plovdiv (DD) – 2400 at an average temperature in the building of 19°C.

Building characteristics

The building is considered as a multi-connected integrated system that consumes energy for heating, cooling, lighting, domestic hot water generation and electrical internal loads needed for its administrative functions.

Building geometry

It is a twelve-floor main building and a two-floor supportive building holding a total heated area of 4876 m² and 12 741 m³ volume.

Envelope characteristics

The building is built of a monolithic reinforced concrete structure ($A_{\text{opaque 1}}$) with walls built of brick masonry of lattice brick, internally plastered and an outside stone cladding made of limestone slabs with no thermal insulation. A small part of the facade walls is reinforced concrete walls with a thickness of 25 cm, with a laid lime-sand plaster ($A_{\text{opaque 2}}$). The window frames of the building are entirely aluminium, filled with transparent glass glazing. The joinery is in poor technical condition and with thermal insulation characteristics that do not meet current national requirements. The poor condition of the joinery leads to a significantly higher infiltration. The roof of the building is a non-insulated cold flat roof built through two reinforced concrete slabs with an unheated non ventilated air gap, the upper one being inclined, covered with waterproofing. The current thermal properties, as well as the total area of the two types of external facades are shown below. The envelope characteristics are presented in Table 1.

Table 1. Current thermal properties of the external facades and windows

Orientation				
	North	South	East	West
$A_{\text{opaque 1}}$ [m ²]	369	370	139	339
U [W/m ² .K]	1.50			
$A_{\text{opaque 2}}$ [m ²]	17	195	212	174
U [W/m ² .K]	2.70			
A_{glazed} [m ²]	767	663	110	255
U [W/m ² .K]	3.59			

Heating, cooling and ventilation

The building is heated by two means – the main heating systems consists of a convective heating installation thermally supplied by an onside substation that is connected to the district heating supply network of the city of Plovdiv. Due to the inefficiency of the main heating mean, in addition to the centralized heat supply, electricity is used through the operation of

individual domestic air conditioners - air-to-air heat pumps supporting the heating in the individual rooms with individual schedules. During the cooling seasons the air-to-air heat pumps are also used for cooling. The building lacks of a centralized ventilation system for the supply of outside air. Fresh air is supplied through the opening of the windows and through the gaps in the window frames, as a result of its wear over time. These practices are leading to high rates of building infiltration and high energy loses.

Lighting

The lighting in the building premises complies with the requirements for minimum illumination. The lighting in the building is solved by means of many different types of lighting fixtures, mostly fluorescent lights. In general, it can be determined that they are inefficient, with reduced light output bringing to higher energy consumption compared to current lighting standards.

Domestic Hot Water (DHW) generation

Hot water for domestic needs in the building is provided by means of electric boilers in the sanitary premises. There are electric instantaneous and volumetric water heaters on 3 floors, and hot water is used only for domestic needs.

Energy consumption

The total energy consumption in the building has a relatively similar character over the 3 years timespan and reflects the loads in the building (Table 2). The electricity has a share of nearly 60%, while the thermal energy holds 40% share. 2021 was chosen as the base year for subsequent analyses.

An analysis of thermal energy and electricity consumption is applied.

Table 2. Energy consumption for the period 2020-2022

	2020		2021		2022	
	MWh	Share, %	MWh	Share, %	MWh	Share, %
Electricity	362.58	61.92	377.72	61.11	330.50	59.59
Thermal energy	223.00	38.08	240.34	38.89	224.13	40.41
Total demand	585.58		618.06		554.63	

Thermal energy consumption

The performed analyses of the monthly thermal energy consumption, demonstrates that the energy changes are adequate to the thermal load profile of the building and they correspondents to the building heating needs during the analysed months (Figure 1).

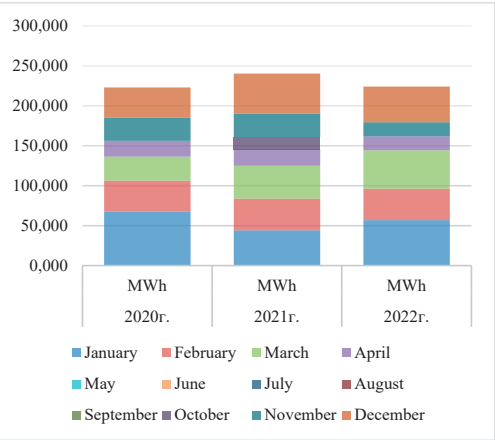


Figure 1. Annual consumption of thermal energy, MWh

Electricity consumption

The analyzes of the monthly electricity consumption demonstrates spikes in winter months when electricity is used for heating and spikes in electricity consumption in summer, when cooling is used (Figure 2 and Figure 3).

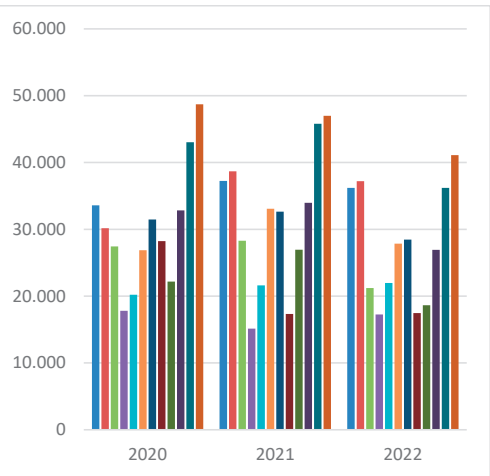


Figure 2. Monthly electricity consumption, kWh

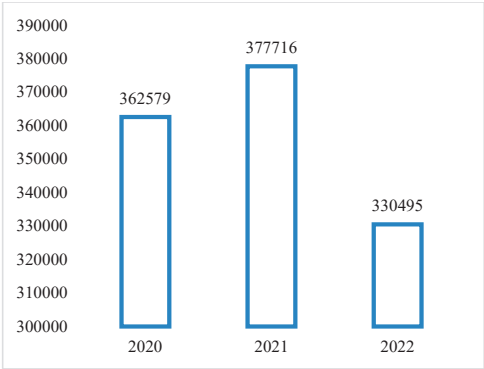


Figure 3. Annual electricity consumption, kWh

Buildings transformation model and related concept

The building can be transformed into PEB with zero emission generation following three main steps. Firstly, through reducing building's energy demand by improving its energy efficiency, following the Energy efficiency first principle, which emphasis reduced and managed demand in a cost-effective way (European Commission, Energy Efficiency First principle, 2023). This can be achieved through very solid passive retrofitting, such as thermal insulation of the building walls, roof and underfloor and window replacements, which is the first step towards highly efficient buildings. Secondly, through building needs electrification by means of implementation of very efficient heat pumps for heating, cooling, ventilation and DHW. And third, by the transition towards high-share of local renewable energy generation for achieving an annual positive energy balance while having net-zero carbon emissions.

Related concept

The following 8 energy conservation measures (ECM) are envisaged, so as to transform the building into PEB:

- ECM-01: Thermal insulation of external walls – the measure envisages the installation of 15cm. stone wool external thermal insulation, coefficient of thermal conductivity $\lambda \leq 0.033$ W/m.K;
- ECM-02: Thermal roof insulation - installation of 15 cm glass wool thermal insulation, $\lambda \leq 0.033$ W/m.K;

- ECM-03: Thermal insulation of the basement - XPS with a thickness of 15 cm, $\lambda \leq 0.035 \text{ W/m.K}$;

- ECM-04: Replacement of existing windows and installation of smart sun protection blinds on the south and west facades;

- Windows: Al windows $U \leq 1.10 \text{ W/m}^2.\text{K}$, with glazing consisted of 4 mm 4-seasons glass, 16 mm argon filling and 4 mm transparent glass.

- Sun protection blinds holding protection with up to 75% dimming capability.

- ECM-05: Implementation of VRV/VRF direct evaporation systems for heating, cooling and heat recovery ventilation;

- Average SEER of units $\geq 6.20 \text{ kW/Kw}$;
- Average SCOP of units: $\geq 4.60 \text{ kW/kW}$;
- Average seasonal heat recovery rate $\geq 75\%$.

- ECM-06: LED lighting - In order to achieve energy savings and to reduce the power consumed for lighting, it is necessary to redesign the lighting in the building, replacing all fluorescent lighting fixtures with high-efficiency LED energy-saving lighting fixtures;

- ECM-07 - Introduction of automation and energy management and monitoring system;

- ECM-08 - Implementation of a PVs (334.2 kWp total capacity) installation for own needs coupled to a lithium-ion energy storage system with a capacity of 60 kWh. The configuration envisages the following roof and facade systems:

a) Total foof capacity - 195.20 kWp (Figure 4)

- Roof system east - 97.60 kWp
- Roof system west - 97.60 kWp

b) Total BIPV capacity - 139.00 kWp (Figure 5, Figure 6 and Figure 7)

- East - 22.14 kWp
- West - 40.18 kWp
- South - 76.68 kWp

In addition to the installation, a lithium-ion energy storage system with a capacity of 60 kWh is planned. The surplus generated in the solar hours will be stored in the batteries, which will have a life of more than 5000 cycles. The stored energy will be fed to the consumers during the hours of no or insufficient production. The battery is sized to cover the building's average nighttime load.

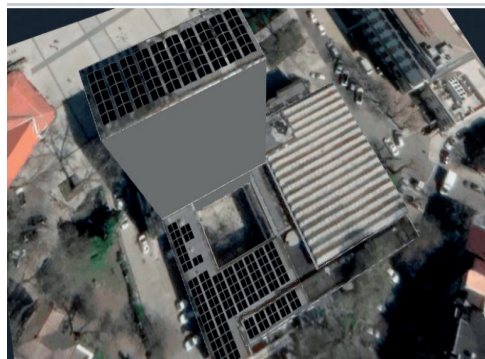


Figure 4. Planned roof system - 195.20 kWp



Figure 5. Layout of BIPV panels - west façade

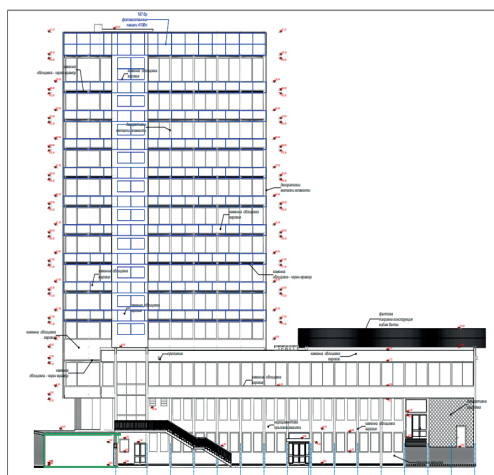


Figure 6. Layout of BIPV panels - south facade

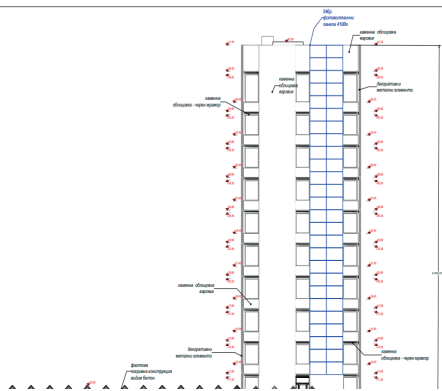


Figure 7. Layout of BIPV panels - east facade

Building energy simulation model

To evaluate the proposed scenario a model study of the energy consumption before and after the conversation measures is applied and tested using the software product EAB (the officially licensed product in Bulgaria). Through the applied computer simulation, a complex model of the energy consumption is created, on the basis of which the compliance of the buildings with the requirements for energy efficiency according to the Law on Energy Efficiency is established. The value of the integrated energy characteristic for energy consumption of the analysed building is defined as integrated (set of energy consumption indicators) according to:

- (Regulation No. RD-02-20-3/9.11.2022 on the technical requirements for the energy performance of buildings)
- (Regulation No. E-RD-04-2/16.12.2022 on energy efficiency auditing, certification and assessment of energy savings in buildings).

When creating the model, the building is considered as an integrated system. The general input data that is entered corresponds to the selection of climatic characteristics (according to the geographical area in which the building is located), type of building, mode of use of the building, characteristics of the enclosing structures. Based on the performed assessment the following distribution of the annual energy consumption per type of consumer was estimated (Table 3).

The main characteristics of the case study over which the model was build are demonstrated on Table 4.

Table 3. Distribution of the annual energy consumption – normalised line

Distribution of the annual energy consumption, %					
Heating	Ventilation	Cooling	DHW	Lighting	Internal loads
63.81	7.96	8.83	0.99	4.17	14.24

Table 4. Main characteristics of the case study before and after implementation of envisaged measures

Parameters	Value before	Value after	Unit
Heating/ Cooling area	4876		m ²
Heating/ Cooling net volume	12741		m ³
External walls area	1814		m ²
Roof area	967		m ²
Floor area	967		m ²
Windows area	1796		m ²
External walls U-value	1.90	0.19	W/m ² .K
Roof U-value	1.44	0.20	W/m ² .K
Floor U-value	0.99	0.28	W/m ² .K
Windows U-value	3.59	1.11	W/m ² .K
Glazing ratio	36.8		%
Warmth from residents	3.20		W/m ²
Av. operational days	256	256	days
Working hours per day	11	11	h
Infiltration rate	0.70	0.50	1/h
Daytime internal heating temperature	22		°C
Nighttime internal heating temperature	18		°C
SCOP	1.60	4.60	W/W
Heating season	175		days
Heating degree days	2400		HDD
Daytime internal cooling temperature	25.0		°C
Nighttime internal cooling temperature	26.0		°C
SEER	3.20	5.00	W/W
Cooling season	184		days
Ventilation rate	1.0	1.0	m ³ /h.m ²
Ventilation temperature	20.0	20.0	°C
Heat recovery	0.0	80.0	%

As a result of the model simulation the following energy consumption forecasts are derived per type of consumer before and after the implementation of the envisaged measures (Table 5).

Table 5. Normalized annual consumption and estimated energy consumption after execution of ECM

System, facility	Normalized annual energy consumption		Annual energy consumption after ECM	
	specific energy use	total energy use	specific energy use	total energy use
	kWh/m ²	kWh	kWh/m ²	kWh
Heating	151.68	739 609	12.60	61 417
Ventilation	18.92	92 249	1.22	5 928
DHW	2.36	11 513	2.36	11 513
Fans, pumps	1.59	7 753	1.59	7 753
Lighting	9.91	48 334	5.10	24 861
Appliances	32.28	157 374	32.28	157 374
Cooling	20.99	102 369	6.58	32 100
Total	237.74	1 159 201	61.72	300 946

The measures applied will bring significant energy savings (74.04%) compared to the baseline scenario, as shown on the Table 6 and Figure 8.

Table 6. Estimation of energy savings

Normalized total consumption	Total consumption after ECM	Energy savings	Energy savings
kWh	kWh	kWh	%
1 159 201	300 946	858 255	74.04

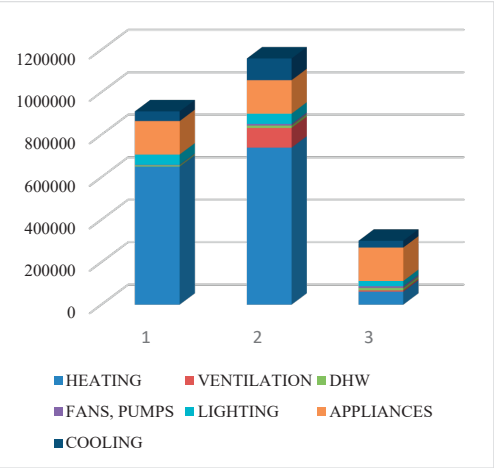


Figure 8. Annual distribution per type of consumer – current situation (1), baseline situation (2) and situation after ECM

The building will demand only electricity since measures are implemented, meaning that this

electricity could be supplied through renewable mean. It is expected that the highest peak of electricity consumption will be during the daytime, which matches with the maximum PV electricity generation, meaning that the self-consumption of the produced energy will be high. Nevertheless, building optimization is highly important, since high PVs penetration levels may result in stress on the electrical grids during hours with high solar power generation. These technical issues can be effectively tackled by coupling PVs and battery energy storage systems (BESSs) on the side of the final consumer to store locally the energy that is not consumed during high generation periods. It has been validated that the deployment BESSs are significantly increasing the self-sufficiency of prosumers, as well as enhancing their autonomy (Kisyov, 2022). Thus, a PVs with a total installed capacity of 334.20 kWp coupled to a lithium-ion energy storage system with a capacity of 60 kWh will be implemented, as avoid large share of unbalanced power to be fed into the grid (Table 7).

Table 7. Estimation of generated energy by the PVs

	Roof PVs generation	Facade PVs generation	Total generation
	195.2 kWp	139.0 kWp	334.2 kWp
	kWh	kWh	kWh
January	8492	7581	16073
February	11120	7771	18891
March	19114	10467	29581
April	25080	10732	35812
May	28918	9956	38874
June	30754	9519	40273
July	32946	10553	43499
August	30550	11916	42466
September	22704	11501	34205
October	15724	10627	26351
November	10020	8676	18696
December	7792	7930	15722
Total	243 214	117 229	360 443

The total estimated generated electricity from both PV installations (facade and rooftop) is estimated at 360 443 kWh per year, meaning an excess electricity of 59 497 kWh is available for different purposes. There are possibilities the excess electricity is trade in the grid or provided

to an adjacent building. Nevertheless, a very coherent load matching management is needed, so as to increase building self-consumption and self-sufficiency rates. The excess electricity available means the building could be considered as a PEB.

Financial estimations

Estimations of the payback period and the total investment required is provided in Table 8, where the payback period is calculated to assess the financial feasibility of the energy transformation model, where a payback period is the length of time it takes to recover the cost of an investment

Table 8. Estimation of payback period and total investment

Package 1	Energy savings	Financial savings	Investment with VAT	Payback
ECM-01	73 069	36 754	368 156	19.59
ECM-02	28 423	14 297	116 137	15.89
ECM-03	16 297	8 197	27 926	6.66
ECM-04	173 791	87 417	696 129	15.57
ECM-05	241 032	121 239	1 032 607	16.66
ECM-06	23 473	17 135	34 279	3.91
ECM-07	17 325	8 714	20 777	4.66
ECM-08	360 443	144 177	528 784	4.91
Total	933 853	437 930	2 824 796	12.62

CONCLUSIONS

The described transformative package of measures was applied to receive funding within the National Plan for Recovery and Sustainability. The project received an excellent score and contract will be signed in the second quarter of 2024. Thus, the envisaged measures will be applied within the next two years.

In overall, the building can be transformed to Positive Energy Building with an investment of 2 824 796 € bringing some 933 853 € of energy improvements. In this case the value of retrofitting for reach PEB is estimated at 3.02 EUR/kWh or 579 EUR/m².

In order to achieve the savings, a management and control system for the HVAC systems will be developed, through which monitoring, parameter settings, switching on/off of the system and/or fan convector and limiting the level of energy consumption will be carried out.

Charging stations for electric cars or electric bicycles can be integrated to the project in for more intelligent utilization of the surplus generated by the PVs.

The next step in the building transformation and PEBs development process is seen in the transformation of districts to Positive Energy Districts (PEDs). The PEDs is consisted of groups of buildings with net zero greenhouse gas emissions generation, who are actively managing an annual surplus production of renewable energy (Guarino et al., 2023). Thus, the pilot case building can set the role model in Plovdiv for the formation of the first Positive Energy District.

REFERENCES

- Barrutieta, X. et al (2023). Decision-making framework for positive energy building design through key performance indicators relating geometry, localization, energy and PV system integration. *Energy and Buildings*, 297, 113442.
- Battaglia, V., Vanoli, L., Verde, C., Nithiarasu, P., & Searle, J.R. (2023). Dynamic modelling of geothermal heat pump system coupled with positive-energy building. *Energy*, 284, 128557.
- Bojić, M., Nikolić, N., Nikolić, D., Skerlić, J., & Miletić, I. (2011). Toward a positive-net-energy residential building in Serbian conditions. *Applied Energy*, 88(7), 2407-2419.
- Bruck, A., Ruano, S.D., Auer, H. (2022). Values and implications of building envelope retrofitting for residential Positive Energy Districts. *Energy and Buildings*, 275, 112493.
- Cai, S., & Gou, Z. (2024). Defining the Energy Role of Buildings as Flexumers: A Review of Definitions, Technologies, and Applications. *Energy and Buildings*, 113821.
- European Commission, Energy efficiency in buildings. (2020). https://commission.europa.eu/news/focus-energy-efficiency-buildings-2020-02-17_en
- European Commission, Energy Efficiency First principle. https://energy.ec.europa.eu/topics/energy-efficiency/energy-efficiency-targets-directive-and-rules/energy-efficiency-first-principle_en
- European Council (2023). Fit for 55 package <https://www.consilium.europa.eu/en/policies/green-deal/fit-for-55-the-eu-plan-for-a-green-transition/>
- European Council. (2024). Fit for 55 Infographic <https://www.consilium.europa.eu/en/infographics/fit-for-55-making-buildings-in-the-eu-greener/>
- Guarino, F., Rincione, R., Mateu, C., Teixidó, M., Cabeza, L. F., & Cellura, M. (2023). Renovation assessment of building districts: Case studies and implications to the positive energy districts definition. *Energy and Buildings*, 296, 113414.
- Hu, M. (2016). Net-positive Building and Alternative Energy in an Institutional Environment. In Summer

- Study on Energy Efficiency in Buildings; *ACEEE: Pacific Grove*, https://www.aceee.org/files/proceedings/2016/data/papers/10_80.pdf
- Integrated Plan in the Area on Energy and Climate of The Republic of Bulgaria 2021 – 2030. https://energy.ec.europa.eu/system/files/2020-06/bg_final_necp_main_en_0.pdf
- Johari, F., Lindberg, O., Ramadhani, U. H., Shadram, F., Munkhammar, J., & Widén, J. (2024). Analysis of large-scale energy retrofit of residential buildings and their impact on the electricity grid using a validated UBEM. *Applied Energy*, 361, 122937.
- Juusela, M., A., Rehman, H., Hukkalainen, M., Reda, F. (2021). Positive Energy Building Definition with the Framework, Elements and Challenges of the Concept. *Energies*, 14(19), 6260.
- Kisyov, P. (2022) Increasing building's self-sufficiency rates through PV plus storage hybrids. *Journal of Physics Conference Series* 2339(1):012023
- Kolokotsa, D.E.K.D., Rovas, D., Kosmatopoulos, E.A., & Kalaitzakis, K. (2011). A roadmap towards intelligent net zero-and positive-energy buildings. *Solar energy*, 85(12), 3067-3084.
- Kumar, G. (2021). State-of-the-Art Review of Positive Energy Building and Community Systems. *Energies*, 14(16), 5046.
- Magrini, A., Lentini, G., Cuman, S., Bodrato, A., & Marengo, L. (2020). From nearly zero energy buildings (NZEB) to positive energy buildings (PEB): The next challenge-The most recent European trends with some notes on the energy analysis of a forerunner PEB example. *Developments in the Built Environment*, 3, 100019.
- Nundy, S., Mesloub, A., Alsolami, B. M., & Ghosh, A. (2021). Electrically actuated visible and near-infrared regulating switchable smart window for energy positive building: A review. *Journal of Cleaner Production*, 301, 126854.
- Rehman, H., Hasan, A., & Reda, F. (2022). Challenges in reaching positive energy building level in apartment buildings in the Nordic climate: A techno-economic analysis. *Energy and Buildings*, 262, 111991.
- Regulation No. RD-02-20-3/9.11.2022 on the Technical Requirements for the Energy Characteristics of Buildings. *Issued by the Ministry of Regional Development and Public Works of Bulgaria*.
- Regulation No. E-RD-04-2/16.12.2022 on Energy Efficiency auditing, certification and assessment of energy savings in buildings. *Issued by the Ministry of Energy and Ministry of Regional Development and Public Works of Bulgaria*.
- Yang, X., Hu, M., Tukker, A., Zhang, C., Huo, T., Steubing, B. (2022). A bottom-up dynamic building stock model for residential energy transition: A case study for the Netherlands. *Applied Energy*, 306, 118060.
- Zhang, W., Deng, M., Xiong, Q. (2024). Evaluation of energy performance in positive energy building: X HOUSE at Solar Decathlon Middle East 2021. *Renewable and Sustainable Energy*, 192, 114163.
- Zomer, C., Custódio, I., Goulart, S., Mantelli, S., Martins, G., Campos, R., & Rüther, R. (2020). Energy balance and performance assessment of PV systems installed at a positive-energy building (PEB) solar energy research centre. *Solar Energy*, 212, 258-274.

CONCEPTUAL ANALYSIS ON DISASTER RESILIENCE IN THE CLIMATE VULNERABLE COMMUNITY CONTEXT

Aurelia NICA¹, Ira-Adeline SIMIONOV^{1,2}, Alina ANTACHE^{1,2}, Catalina ITICESCU^{2,3},
Stefan-Mihai PETREA^{1,2}, Catalin PLATON⁴, Victor CRISTEA⁵

¹"Dunarea de Jos" University of Galati, Food Science and Engineering Faculty,
111 Domneasca Street, Galati, Romania

²"Dunarea de Jos" University of Galati, REXDAN Research Infrastructure,
98 George Cosbuc Street, Galati, Romania

³"Dunarea de Jos" University of Galati, Faculty of Sciences and Environment,
111 Domneasca Street, Galati, Romania

⁴"ROMFISH" National Association of Fish Producers,
12A Nicolae Iorga Blvd, Iasi, Romania

⁵"Dunarea de Jos" University of Galati, Cross-Border Faculty,
47 Domneasca Street, Galati, Romania

Corresponding author email: stefan.petrea@ugal.ro

Abstract

Disaster resilience is the ability of individuals, communities, organizations, and systems to anticipate, prepare for, respond to, and recover from the impacts of hazards, such as natural disasters, extreme weather events, and other emergencies. It encompasses a broad range of factors and capacities that enable communities to withstand and bounce back from adverse events, minimizing their negative impacts and promoting long-term sustainability and well-being. Response efforts focus on the immediate actions taken during and immediately after a disaster to save lives, protect property, and meet the basic needs of affected populations. This includes deploying emergency services, providing medical care, search and rescue operations, and distributing aid to affected areas. Overall, disaster resilience is a dynamic and multidimensional concept that requires a comprehensive and integrated approach to address the complex challenges posed by natural hazards and climate change. By investing in resilience-building measures, communities can enhance their ability to withstand and recover from disasters, ultimately reducing human suffering, economic losses, and environmental degradation.

Key words: adaptation, prevention, preparedness, recovery, response.

INTRODUCTION

The issue of disasters and their management was and remains a necessity and a subject of continuous topicality that requires a joint and multidisciplinary effort, involving human resources and special materials. Improving disaster resilience is used as one of the key approaches to minimise the impact of disasters (Fernando et al., 2023). Disaster resilience in climate-vulnerable communities involves the ability of these communities to anticipate, withstand and recover from the impacts of natural disasters exacerbated by climate change (Parsons et al., 2021). Resilience involves not only the ability to absorb shocks, but also to adapt and transform in response to these events. This encompasses different dimensions,

including social, economic, environmental and institutional aspects. As climate change contributes to increased disaster risk, disaster risk management becomes a vital and urgent component of any climate change adaptation programme (Irshad Ahmad et al., 2024). Climate change has been seen in Europe in the form of higher temperatures, changes in rainfall and runoff patterns, and extreme weather events, prompting reports of an increased incidence of weather-related disasters – such as floods, droughts, fires vegetation, storms and heat or cold waves (Shear et al., 2023).

Climate-vulnerable communities are those disproportionately affected by the impacts of climate change due to factors such as geographic location, socio-economic status, lack of resources and inadequate infrastructure. These

communities are more susceptible to extreme weather events and long-term environmental changes, which can exacerbate existing vulnerabilities and inequalities.

MATERIALS AND METHODS

In this article, we analyzed the specialized literature, identifying the main characteristics and attributes of the concept of resilience to climate change, identifying its antecedents and consequences and their application in the case of vulnerable communities.

To this end we have taken the following steps:

I. We have chosen the concept of "resilience to disasters".

II. We conducted a literature review to obtain information about this concept and identify its different nuances. The Mendeley platform was used as a search engine to define the topic of this review article.

III. We identified the characteristics of the concept.

IV. We examined and evaluated the concept in simpler elements.

V. We characterized the communities at risk from climate change.

RESULTS AND DISCUSSIONS

I. Choosing the concept. In recent years, disasters have occurred more often around the world (Charles et al., 2024). Economic losses from disasters increased by 82% to \$2.97 trillion in 2000-2019, from \$1.63 trillion in 1980-1999 (Elkady et al., 2022). Recent disasters occurring as natural events, industrial incidents and public health crises impose unprecedented challenges on people and communities. The increasing uncertainty and complexity of disasters requires multidisciplinary research efforts due to the various elements involved in a disaster management system (Son, 2023). We chose the concept of "disaster resilience" on the grounds that it is still not clear what it means and how it can be promoted during and after a disruptive event has occurred. The number of those affected by disasters does not appear to be diminishing, and repeated efforts to intervene in the same areas of the world to provide recovery aid have led to a reconsideration of the vulnerabilities that contribute to the triggering of

crisis situations. In 2021, 432 catastrophic events were recorded, which is higher than the average of 357 events that occurred in the last 20 years (Fernando et al., 2023).

Climate change is expected to cause disasters with increasing frequency and expanded impact capacity due to the global connections in contemporary society. Climate change refers to changes in the natural world, including ecosystems, climate patterns and biodiversity, often resulting from both natural processes and human activities.

II. For the literature review, the Mendeley platform was used as a search engine to define the topic of this review article, for the last two years. The first search using the key word "resilience" provided 4,471 relevant results represented by "Conference Proceedings" type documents.

A second search using the key words "disaster resilience" provided 345 results of the same type. We then performed a final search with the key phrase "resilience to disasters and climate change" and obtained the 60 most relevant results from "Conference Proceedings". The increasing frequency of disasters has drawn more attention to the notion of community resilience, which provides society with the ability to prepare for risks, cope with the consequences and recover from the effects (Elkady et al., 2022).

Community resilience has many definitions. Disasters are complex global issues which are inevitable in the community. Community resilience reflects the collective and individual capacity of people to manage and respond adaptively to extreme resource demands and losses caused by disasters. The characteristics of the "resilience to disasters" concept. Natural or man-made disasters can strike at any time or place and can have a catastrophic impact on towns, cities and entire countries. The consequences of natural hazards can be reduced through disaster resilience, even if their prevention is impossible.

Disaster resilience is a comprehensive strategy for disaster management that includes several features such as: preparedness, early warning systems, risk reduction, disaster response, recovery and reconstruction, community involvement, capacity building, adaptability and

flexibility, strong communication and inclusivity. By developing and implementing these features, communities and societies can become better prepared to resist, adapt and recover from disasters. The Disaster Resilience Of Place Model (DROP) is a reliable technique

that supports both disaster resilience development and benchmarking, while supporting local and community practices. The DROP model is presenting the relationship between mitigation, preparedness, event, and adaptive resilience (Figure 1).

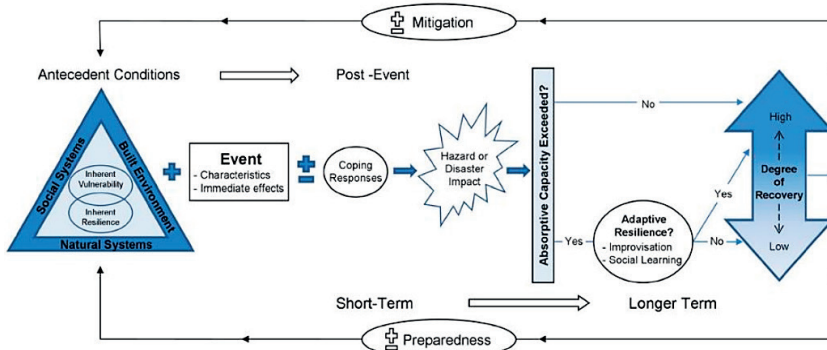


Figure 1. DROP model
 (Cutter et al., 2008, cited by de Fernando et al., 2023)

Two essential components help a community overcome an emergency: the physical and the perceptual. Physical elements include infrastructure, economic resources, availability and access to services. Individuals' perceptions of their community involve factors such as social trust, leadership, and previous experiences with crises (Radu, 2018). This will ultimately reduce the negative effects that natural and man-made disasters have on certain individuals, families and entire communities. Sarker et al. (2020) analyzed the most relevant 21 documents to reveal the potential sources of big data (satellite imagery, aerial imagery and video, wireless sensor web network, simulation and spatial data, crowdsourcing, social media, mobile GPS and call recording (Figure 2).

humanitarian action. But it is still unclear what this concept means and how it can be promoted during and after a disruptive event has occurred (Baltasiu, 2015).

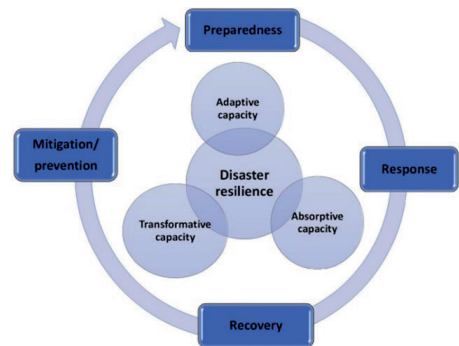


Figure 2. Disaster resilience through big data (after Sarker et al., 2020)

III. Examining the concept in simpler elements.

Resilience is a concept used in many fields of study. Resilience is an important and highly recognised concept within modern-day disaster management initiatives (Dharmadasa et al., 2023). The concept of resilience has gained significant attention among researchers due to the increasing occurrence of natural and man-made disasters worldwide (Boahen et al., 2023). It is at the heart of current discussions about development, climate change adaptation and

In the context of climate change, the resilience of urban communities can be conceptualized as their ability to sustain their social and economic functions. In addition, it involves improving, preparing to address the consequences of climate change, such as floods, droughts and rising temperatures (Sumardjo et al., 2023). The concept of resilience has gained significant attention among researchers due to the increasing occurrence of natural and man-made

disasters worldwide. The resilience of a vulnerable community can be increased by reducing exposure to hazards, reducing its vulnerability and thereby reducing risk, enabling the community to resist, absorb, adapt and recover from hazards and restore its basic functions in a timely and efficient manner. In this way, the respective community will recover from the disaster suffered and improve its resistance.

IV. Below it is a summary of the key points regarding climate change:

1. *Natural processes*: Climate change can occur from natural phenomena such as volcanic eruptions, earthquakes, variations in solar radiation, and geological changes. These processes have occurred throughout Earth's history and have shaped the planet's landscapes, climates and habitats over millions of years.

2. *Human activities*: in the last centuries, human activities have become significant factors of environmental change. Activities such as deforestation, industrialization, urbanization, agriculture, burning fossil fuels, and pollution have profoundly altered Earth's ecosystems and climate systems. These activities have accelerated rates of change far beyond what would occur naturally, leading to widespread environmental degradation and loss of biodiversity.

3. *Climate change*: one of the most pressing environmental changes facing the planet is climate change, caused mainly by the release of greenhouse gases (such as carbon dioxide and methane) from human activities. Climate change is causing global temperature increases, changes in precipitation patterns, more frequent and more severe extreme weather events, melting ice sheets and glaciers, rising sea levels, and disruptions to ecosystems and biodiversity.

4. *Biodiversity loss*: environmental changes have led to significant biodiversity losses, species extinction rates are currently estimated to be tens to hundreds of times higher than the natural background rate. Habitat destruction, pollution, resource overexploitation, invasive species and climate change are major drivers of biodiversity loss, threatening the stability and resilience of ecosystems around the world (Figure 3) (Foden et al., 2013). Taking into account some interdependencies between

regions, along with climate and socioeconomic projections, (Hochrainer-Stigler et al., 2016) estimates that average annual flood losses in Europe could increase from the current level of €4.9 billion to €23.5 billion in 2050.

5. *Ecosystem services*: environmental changes affect the provision of ecosystem services – benefits that people derive from nature, such as clean air and water, fertile soils, pollination, climate regulation, and cultural and recreational opportunities. Disruption of ecosystems can affect their ability to provide these services, compromising human well-being and livelihoods.

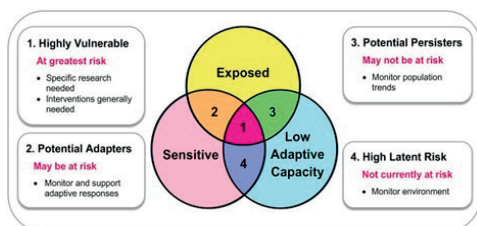


Figure 3. Framework to assess the impacts of climate change on species (Foden et al., 2013)

6. *Adaptation and mitigation*: Addressing environmental change requires both adaptation and mitigation strategies. Adaptation involves adapting to the impacts of environmental change, such as building resilient infrastructure, protecting natural habitats, and implementing agricultural practices that increase resilience to climate variability. Mitigation involves reducing the drivers of environmental change, such as transitioning to renewable energy sources, improving energy efficiency, and implementing policies to reduce greenhouse gas emissions.

7. *Global cooperation*: given the interconnected nature of environmental change and its impacts, addressing these challenges requires coordinated efforts at local, national and global levels. International agreements, such as the Paris Agreement on Climate Change, aim to mobilize collective action to mitigate greenhouse gas emissions and build resilience to the impacts of climate change (Nichersu et al., 2022). We consider the following simple elements particularly important in achieving community resilience: resilience, trust, response and recovery. Human capital (education, physical abilities and skills) has a special role in

increasing individual resilience, and social capital (reciprocity, trust, feeling of belonging to a certain group) includes communication and mutual help.

V. According to the Intergovernmental Panel on Climate Change (IPCC, 2022), vulnerability to climate change is determined by:

- Exposure to climate variability and change: refers to the extent to which an entity (be it a country, community, individual or ecosystem) experiences climate variability and change.
- Sensitivity to climate shocks and stresses: is an assessment of the impact that climate factors have on the entity concerned.
- Adaptive capacity: describes the entity's ability to manage negative impacts and capitalize on any opportunities that arise.

People all over the world are facing the reality of climate change. For some, these just mean changes in weather patterns: slightly higher temperatures, slightly lower temperatures, more uncertainty. For others, however, climate change is already a survival issue: too little or too much water, insufficient food, increased safety and security risks.

Climate change adaptation efforts often focus on adjusting livelihood strategies to respond to new climate conditions. However, these approaches

assume that people have access to the necessary resources to implement these strategies.

Access to and control over critical resources, such as agricultural land, forests and water sources, are key factors in determining vulnerability to climate change. Without access to these vital resources, adaptation options are severely limited and people's ability to respond effectively to climate change is reduced. Thus, to support effective adaptation, it is crucial that policies and financing strategies ensure equitable access to resources for the most vulnerable. This would not only improve the resilience of affected communities, but also help reduce the inequities generated by climate change. Since the most vulnerable, poorest and most marginalized populations are also the most exposed to high risks, increasing the degree of awareness and responsibility regarding the protection of natural resources is essential for survival and implicitly for dealing with disasters. Funding and support should be targeted to the countries, communities and people most in need. The extent of adaptation needs is usually related to the degree of vulnerability to climate change. Vulnerability is a vital factor in resilience to climate change, but there is no universal definition of what constitutes a vulnerable community (Figure 4).

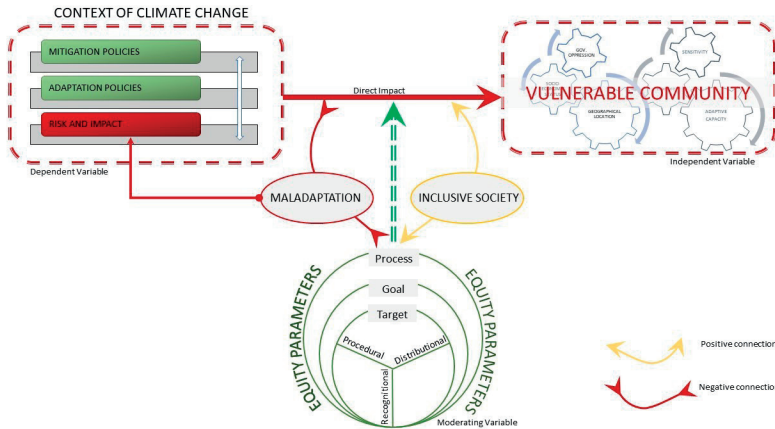


Figure 4. Impact of climate change on vulnerable communities (Hadad, 2020)

The debate is still open because the vulnerability itself is attached to the context of its assessment. Women and girls are more vulnerable to disasters, but that they can also contribute vital

information, skills, resources and experiences to disaster risk reduction and climate change mitigation. Indeed, women and men play different roles in household livelihoods and

therefore experience the impacts of climate change differently.

Following the documentation in the literature, we agree with those authors who consider that the most vulnerable to climate change are the poorest people, who do not have effective strategies to cope with shocks and stresses and who have resorted to ineffective responses. This suggests that we need to look not only at the risks people are exposed to, but also to the quality of their options for dealing with those risks and how they ultimately manage them. Without the resources to safely deal with the worst effects of the pandemic, vulnerable populations have been forced to make impossible choices.

Globally, up to 3.6 billion people live in environments highly vulnerable to climate change, and current unsustainable development patterns increase the exposure of ecosystems and people to climate risks. Romania is also feeling the impact of global warming through the effects of thermal stress, aggravated in large cities by the urban heat island phenomenon, and through the increase in the intensity of precipitation over short periods, which favors floods and urban flooding. These effects will continue to amplify in the future, having multiple socioeconomic implications.

CONCLUSIONS

As the climate continues to change, millions of poor people face increasing challenges in terms of extreme events, health impacts, food, water and livelihood security, migration and forced displacement, loss of identity cultural and other related risks. People in vulnerable situations – due to factors such as geography, poverty, gender, age, indigenous or minority status, national or social origin, birth or other status and disability – may face increased exposure and vulnerability to human rights abuses caused by climate. Understanding the hazards and risks will inform the preparedness and mitigation approaches of local people, authorities and agencies. Poverty becomes the main factor fueling the other vulnerabilities. Therefore, it is imperative to increase the resilience of vulnerable populations in order to mitigate the adverse effects of global warming and to minimize their susceptibility to associated risks

and to strengthen the capacity to identify risks by developing multi-hazard risk information systems, which also include risk exposure and vulnerability data.

ACKNOWLEDGEMENTS

The present research was supported by the project An Integrated System for the Complex Environmental Research and Monitoring in the Danube River Area, REXDAN, SMIS code 127065, co-financed by the European Regional Development Fund through the Competitiveness Operational Programme 2014-2020, contract no. 309/10.07.2021.

REFERENCES

- Baltasiu, R. (2015). Universitatea din Bucuresti, Facultatea de sociologie si asistenta sociala, Scoala doctorala de sociologie. Rezilienta in cazul dezastrelor naturale.
- Boahen, S., Oviroh, P.O., Austin-Breneman, J., Miyingo, E.W., & Papalambros, P.Y. (2023). Understanding resilience of agricultural systems: a systematic literature review. *Proceedings of the Design Society*, 3. <https://doi.org/10.1017/pds.2023.371>
- Charles, M.R., Rodrigues, R.F.T., Miguez, M.G., & Qualharini, E.L. (2024). Analysis of the Variation of Rio de Janeiro City Resilience in Different Scenarios. *Lecture Notes in Civil Engineering*, 444, 417–434. https://doi.org/10.1007/978-3-031-48461-2_37
- Cutter, S.L., Barnes, L., Berry, M., Burton, C., Evans, E.E.T., & Jennifer, W. (2008). A place-based model for understanding community resilience to natural disasters. *Global Environmental Change*, 18(4), 598 – 606. doi:10.1016/j.gloenvcha.2008.07.013
- Dharmadasa, K.H.K., Kulatunga, U., Thayaparan, M., & Keraminiyage, K.P. (2023). Review on the importance of capacity building for enhancing disaster resilience through the effective utilisation of resources. *World Construction Symposium*, 1, 920–929. <https://doi.org/10.31705/WCS.2023.74>
- Elkady, S., Hernantes, J., Muñoz, M., & Labaka, L. (2022). What do emergency services and authorities need from society to better handle disasters? *International Journal of Disaster Risk Reduction*, 72. <https://doi.org/10.1016/j.ijdr.2022.102864>
- Fernando, M.L.S.S., Ranadewa, K.A.T.O., Kulatunga, U., & Keraminiyage, K.P. (2023). Critical assessment of the existing disaster resilience frameworks and their applicability to improve community resilience. *World Construction Symposium*, 1, 432–445. <https://doi.org/10.31705/WCS.2023.36>
- Foden, W.B., Butchart, S.H.M., Stuart, S.N., Vié, J.C., Akçakaya, H.R., Angulo, A., DeVantier, L.M., Gutsche, A., Turak, E., Cao, L., Donner, S.D., Katariya, V., Bernard, R., Holland, R.A., Hughes, A.F., O'Hanlon, S.E., Garnett, S.T., Şekercioğlu,

- Ç.H., & Mace, G.M. (2013). Identifying the World's Most Climate Change Vulnerable Species: A Systematic Trait-Based Assessment of all Birds, Amphibians and Corals. *PLoS ONE*, 8(6). <https://doi.org/10.1371/journal.pone.0065427>
- Haddad, N. (2020). Impact of climate change on vulnerable communities and the role of Equity to reach inclusive societies. (22) Impact of climate change on vulnerable communities and the role of Equity to reach inclusive societies | LinkedIn
- Hochrainer-Stigler, S., Lorant, A., Petrescu, E.-C., Timonina, A., Pflug, G., Ioncica, M., Jongman, B., & Rodrigues, R. (2016). Flood Risk: The EUSF and Romania. In: *Novel Multi-Sector Partnerships in Disaster Risk Management. Results of the ENHANCE project*. Eds. Aerts, Jeroen & Mysiak, Jaroslav, pp. 251-265 Brussels, Belgium: EU FP7 project ENHANCE.
- IPCC Sixth Assessment Report (2022). Climate Change 2022: Impacts, Adaptation and Vulnerability, Climate Change 2022: Impacts, Adaptation and Vulnerability | Climate Change 2022: Impacts, Adaptation and Vulnerability (ipcc.ch)
- Irshad Ahmad, M., Ma, H., Shen, Q., Rehman, A., & Oxley, L. (2024). Climate change variability adaptation and farmers decisions of farm exit and survival in Pakistan. *Climate Services*, 33, 100437. <https://doi.org/10.1016/J.CLISER.2023.100437>
- Nichersu, I., Negrei, C., Livanov, O., Bratfanof, E., Balaican, D. (2022). Local based solutions edaphic-bloom Danube - considerations on the role of organic carbon in reducing greenhouse gases in agriculture. Scientific Papers. Series E. Land Reclamation, Earth Observation & Surveying, Environmental Engineering, Vol. XI, 247-260, Print ISSN 2285-6064.
- Parsons, M., Reeve, I., McGregor, J., Hastings, P., Marshall, G.R., McNeill, J., Stayner, R., & Glavac, S. (2021). Disaster resilience in Australia: A geographic assessment using an index of coping and adaptive capacity. *International Journal of Disaster Risk Reduction*, 62, 102422. <https://doi.org/10.1016/J.IJDRR.2021.102422>
- Radu, B. (2018). Influence of social capital on community resilience in the case of emergency situations in Romania. *Transylvanian Review of Administrative Sciences*, 14(54E), 73-89. <https://doi.org/10.24193/tras.54E.5>
- Sarker, M.N., Peng, Y., Yiran, C., & Shouse, R.C. (2020). Disaster resilience through big data: Way to environmental sustainability. *International journal of disaster risk reduction*, 51, 101769.
- Shear, F., Ashraf, B. N., & Butt, S. (2023). Sensing the heat: Climate change vulnerability and foreign direct investment inflows. *Research in International Business and Finance*, 66. <https://doi.org/10.1016/J.RIBAF.2023.102005>
- Son, C. (2023). Disaster Ergonomics: a Human Factors approach to address escalating challenges from disasters. *Cognition, Technology and Work*, 25(4). <https://doi.org/10.1007/s10111-023-00736-4>
- Sumardjo, Firmansyah, A., & Dharmawan, L. (2023). Peri-urban Community Resilience in Facing the Dynamics of Global Climate-change Impacts toward Sustainable Development. *IOP Conference Series: Earth and Environmental Science*, 1266(1). <https://doi.org/10.1088/1755-1315/1266/1/012045>

RICE HUSKS AND THEIR POTENTIAL FOR USE IN CONSTRUCTION

Irina POPA, Cristian PETCU, Daniela STOICA, Alina DIMA

National Institute for Research and Development in Construction,
Urban Planning and Sustainable Spatial Development - URBAN-INCERC,
266 Pantelimon Road, District 2, Bucharest, Romania

Corresponding author email: irinapopa2006@yahoo.com

Abstract

The growing global demand for agricultural food products has inevitably led to increased amounts of natural agro-industrial by-products. Derived from agricultural and industrial processes, these by-products have traditionally and conservatively been considered waste, and their management represents significant environmental challenges. Currently, the potential of this type of natural materials to be reused in new products with added value is recognized, thus contributing to the development of the circular economy at international level but also in Romania. Current research trends in the field of sustainable construction emphasize the numerous benefits of using natural materials in the development of green building products. The paper presents a series of experimental laboratory research with the aim of studying the potential of rice husk, a natural agro-industrial by-product resulting from the food industry, to be used in construction.

Key words: agro-industrial by-products, sustainable development, waste capitalization.

INTRODUCTION

Globally, rice is a staple food and consumption tends to remain high even during periods of economic turbulence because low-income consumers turn to cost-competitive foods. Global rice production will trend upwards over the next five years, reaching 523.4 million tons in 2025-2026 (International Grains Council Report, 2021).

A natural agro-industrial by-product of rice processing (Figure 1), rice husks are used in constructions in the form of ash, as a pozzolanic filler, in cement-based binders (Xu et al., 2015) as well as for obtaining new composite materials based on natural rubber for the development of supports of vibration isolation (Ubi et al., 2022), of particle boards with various binders (Wilberforce et al., 2022), or as an addition to improve the physicomaterial properties of bricks used as masonry elements (Uderbayev et al., 2022).

The development of new materials that capitalize on natural agro-industrial by-products in the spirit of the circular economy concept requires a better study of their physical, morphological, and microstructural properties so that sustainable, high-performance, and

lasting products can be obtained (Stoica et al., 2020). Starting from the multidisciplinary knowledge of the natural agro-industrial by-products, the future properties of some innovative materials can be modelled to provide a positive response to various requirements specific to the construction field (Thieblisson et al., 2024).



Figure 1. Rice husks

From a theoretical point of view, the potential of rice husks to be exploited by obtaining construction materials and products is supported by the following aspects:

- the international but also national context, which encourages the study of this type of natural materials to minimize the cost of raw materials but also to create innovative products

with comparable or even superior characteristics to those of traditional products;

- the accessibility at the national level of this sustainable eco-material, a natural by-product of the food industry, considering the predominantly agrarian nature of the Romanian economy and the existence of domestic rice crops;

- the specific properties of rice husks, determined in turn by their compositional and structural characteristics, and implicitly the characteristics of the different types of construction materials in the composition of which the husk was integrated (Park et al., 2003; Chabannes et al., 2014; 2016);

- the high potential of creating new eco-materials/construction products with high added value, which leads to new possible ways of superior valorisation of this agro-industrial by-product, in the context of the Romanian circular economy.

The paper presents a series of experimental laboratory research aimed at studying the potential of the rice husks to be used in construction, in the form of new innovative construction materials and products.

MATERIALS AND METHODS

This experimental research involved multidisciplinary testing of rice husks to determine their potential use in construction materials/products.

Preliminary tests were conducted to characterize rice husks in terms of their thermotechnical properties, fire behaviour, water absorption capacity, and resistance to mold development. These aspects are crucial for designing compositional recipes that incorporate plant products.

The experimental study was carried out using methods specific to each field, as follows:

To determine the thermotechnical characteristics of the rice husk, the Guarded Hot Plate (GHP) method was used, to measure the thermal resistance of the material at different densities, according to SR EN 12667. The GHP method is a steady state transfer technique heat which offers a significant advantage due to its high accuracy. This allows the equivalent thermal conductivity to be measured over the entire thickness of relatively large samples,

leading to representative results. In addition, the GHP method is an absolute method that measures thermal conductivity, at an average imposed temperature, without requiring a certified reference material sample.

The process of measuring thermal conductivity for insulating materials involves maintaining a constant and uniform rate of heat transfer, marked as q (in watts per square meter, or W/m^2), and through the material being tested. The measuring area is in the region located near the centre of the test sample, the space where this heat flow is obtained, around the tested area being the marginal guard area.

In a steady-state thermal regime, the heat flux (Q , in watts, W) through the test area (A) is measured. The specific heat transfer intensity is then calculated by dividing the heat flux by the tested area. At the same time, the temperatures (T_1 and T_2) on the two sides of the test specimen are measured using temperature transducers placed on the surfaces of the equipment in contact with the test specimen.

The thermal resistance R of the test specimen can be calculated using the measured values of these physical parameters. This calculation, according to SR EN 12667, is given in formula (1):

$$R = (T_1 - T_2) / Q * A \quad (1)$$

where:

- R , T_1 , T_2 , Q , and A are the parameters previously listed and described.

Instruments based on the GHP method are suitable for determining the thermal resistance and thermal conductivity of both homogeneous and non-homogeneous test specimens, provided that they are flat and plate-shaped. This allows a wide range of materials to be tested for their thermal properties.

Thermal conductivity tests were performed using a LambdaMeter EP500e guarded hot plate apparatus. This high-precision instrument provides a measurement error of less than 1.0% in the range $\lambda = 0.010\text{--}0.060 \text{ W/(m}\cdot\text{K)}$, has a thermal conductivity range between 0.003 and $2\text{ W/(m}\cdot\text{K)}$, and can test samples with thicknesses up to 200 mm, thus allowing a comprehensive analysis of a wide range of materials.

The test protocol strictly adhered to the guidelines described in SR EN 12667, ensuring that the results are consistent, reliable, and

comparable to other tests performed according to the same standard.

To prevent external factors from affecting the measurements, the bulk materials were enclosed in a polyurethane frame during testing. This frame was placed in the thermal guard area, thus eliminating the potential influence of the frame on the test results. This ensures that the thermal conductivity values obtained are solely representative of the material under test, providing accurate and reliable data for further analysis and application.

Due to the polyurethane frame, the tests were conducted at three distinct densities, namely 98.20 kg/m^3 , 113.60 kg/m^3 and 128.20 kg/m^3 respectively. For each density, measurements were made at three different temperature points: 10°C , 25°C and 40°C . Each specimen exhibited distinct physical characteristics, illustrating how density influences the thermal conductivity of bulk materials.

To determine the fire behavior of rice husks, to demonstrate how it will influence a fire when it will be used to make biocomposites, innovative, ecological construction materials, and preliminary tests were carried out on the fire behavior of the rice husks (Stoica D. et al., 2019). The method of determining the higher calorific value (heat of combustion) was used, according to the provisions of the test method standard SR EN ISO 1716. It should be noted that rice husks, if thrown in the garbage, pollute the environment or can even spontaneously ignite, having the potential to generate fires (Dragne et al., 2019).

To know the contribution of this natural agricultural by-product when subjected to the action of fire, its fire reaction was determined. Reaction to fire is defined as the behavior of a material, which, through its decomposition, feeds the fire to which it is exposed, under specified conditions (Stoica et al., 2019).

As part of this experimental research, as a first step, to evaluate the fire behavior of rice husks, the value of their higher calorific value (heat of combustion) was determined through laboratory tests, following the provisions of the SR EN ISO 1716:2018 test method standard and the provisions of the conditioning standard SR EN 13238:2010.

Higher heat of combustion, also known as higher calorific value, represents the total

amount of heat obtained during the complete combustion of a unit mass of fuel, considering also the latent energy of condensation of water vapor produced by the combustion of hydrogen from the fuel.

The determination of the higher heat of combustion was carried out using a calorimeter, designed to measure the heat released during the combustion of a known amount of fuel.

The higher calorific value is expressed in units of energy per unit mass, such as kilojoules per gram (kJ/g) or megajoules per kilogram (MJ/kg). It indicates the energy that can be released during the complete combustion of the fuel.

The standard method used to determine the higher calorific value of a fuel is known as the bomb combustion method or the bomb calorimetry method. This method involves the complete combustion of a known sample of fuel in a bomb calorimeter, and the heat released during combustion is measured and used to calculate the higher heat of combustion. The higher calorific value of rice husks was determined using a British FTT Bomb Calorimeter.

To carry out the determination, a sample of 50 g of rice husks was taken and conditioned until constant weight, for 48 hours before the tests, at a temperature of $(23 \pm 2)^\circ\text{C}$ and a relative humidity of $(50 \pm 5)\%$. Subsequently, three samples of approx. 0.5 g each were taken from the conditioned rice husks.

The water absorption capacity of rice husks, a critical characteristic for formulating compositional recipes with natural products, was determined using the short-term partial immersion method. This method involves calculating the amount of water absorbed by the husk over a 24-hour contact period.

The rice husks were placed in a cylindrical stainless-steel container equipped with a bottom sieve made of inert material. The sieve, featuring an $80 \text{ }\mu\text{m}$ mesh diameter, was essential for allowing the husks to be in contact with the water. The initial mass of the rice husks (m_0) was determined by weighing and then the cylindrical container with the husks was partially immersed in a water tank so that the plant material was immersed $(10 \pm 2) \text{ mm}$ below the surface of the water (Figure 2).

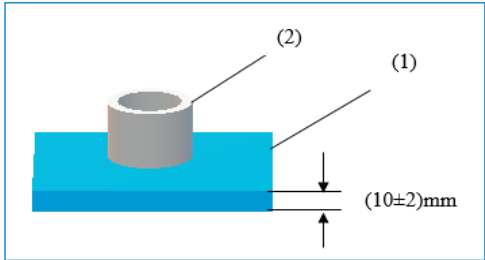


Figure 2. Assembly configuration for determining the water absorption capacity by partial immersion - (1) tank with water; (2) cylindrical stainless-steel container with a sieve

During the determination, the water level was constant. After 24 h, the cylindrical container was removed from the water tank and left to rest for 10 ± 0.5 min on a grid-shaped support, slightly inclined, to allow natural water drainage. The cylindrical container was then weighed to determine the final mass after 24 h of partial immersion, m_{24} . Using equation (2), the short-term (24 h) water absorption by partial immersion corresponding to rice husks, W_p , was calculated, also considering the area (A_p) of the sieve.

$$W_p = \frac{m_{24} - m_0}{A_p} \cdot 10^3 \quad (2)$$

where:

- W_p , m_{24} , m_0 și A_p are the parameters previously listed and described.

For the primary evaluation of the behaviour of rice husks to the development of molds under the action of high humidity ($90 \pm 4\%$) at the normal temperature of $(25 \pm 2)^\circ\text{C}$, previously the sample was dried for 72 h at a temperature of $(70 \pm 2)^\circ\text{C}$ and visually inspected following the development of mold in the product mass and classification according to the standardized criteria mentioned in SR EN 15101-1+A:2019, slightly modified for the current test conditions (Table 1).

A constant amount of plant product of 15 g was used without inoculating the samples with spore suspension. The test assembly was constituted by a desiccator which at the bottom contained a volume of 800 ml of water necessary to create the humidity of $(90 \pm 4)\%$ inside (Figure 3).

The samples were kept for incubation for 28 days and continuously visually monitored to

observe the appearance and degree of mold development.

Table 1. Criteria for classifying mold development

Degree of mold development	Intensity of growth
G0	No visible mold in product mass examined under a reflected light microscope at 50x magnification
G1	Mold growth is visible or barely visible to the naked eye, but clearly visible at 50x magnification
G2	Mold clearly visible to the naked eye

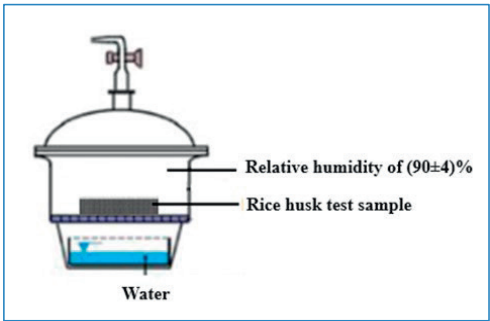


Figure 3. Mold development testing assembly

RESULTS AND DISCUSSIONS

Regarding the thermotechnical characteristics of the rice husks, the obtained experimental results (Figure 4 and Figure 5) indicated the following aspects:

For all samples, thermal conductivity increases with increasing temperature. This is consistent with results obtained on most insulating materials, where thermal conductivity often increases with temperature due to increased molecular motion, leading to greater heat transfer.

The bulk density of the specimens also plays an essential role in determining their thermal properties. Unlike the correlation of the thermal conductivity coefficient of the rice husk with the average temperature of the plates, which appears to be a linear function, the relationship between the rice husk's thermal conductivity and the specimens' average density follows a quadratic function, revealing a local minimum. This local minimum is observed to be around a density of 110 kg/m^3 .

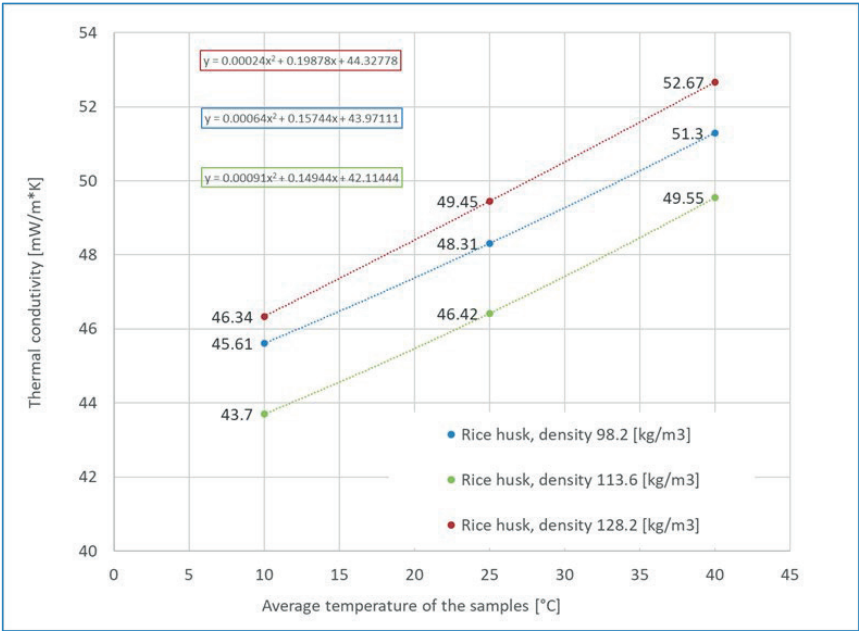


Figure 4. Correlation of the thermal conductivity of the rice husk with the average temperature of the samples during the tests

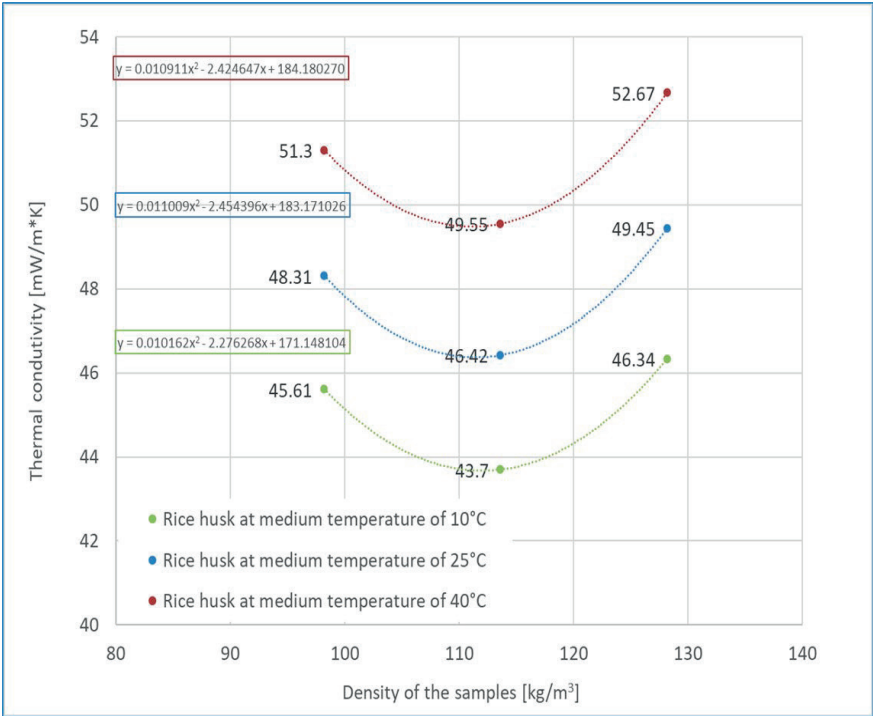


Figure 5. Correlation of the thermal conductivity of the rice husk with the average density of the samples

Using the mathematical relations derived for the interpolation curves, we can determine by derivation and mathematical calculation the exact value of the density for which the lowest thermal conductivity is obtained.

For the average plate temperature of 10°C, this is 112 kg/m³ and the minimum thermal conductivity value is 43,678 [mW/m*K] or 0.043678 [W/m*K], comparable to that of some synthetic heat-insulating materials.

These research results provide an adequate understanding of how the thermal properties of rice husk-based materials respond to changes in temperature and density.

The trends identified here, particularly the positive correlation between temperature and thermal conductivity, are significant considerations in determining the appropriate use of these materials in insulation applications. However, further studies would be beneficial to deepen the interaction of these factors as well as other factors not included in this data set, such as moisture content, to gain a more comprehensive understanding of the behavior of this material under different conditions.

The results obtained after carrying out tests to determine the higher calorific value, to determine the fire behavior of rice husks, according to the provisions of the test method standard SR EN ISO 1716:2018 (Table 2), indicated a superior value of the calorific value /heat of combustion, comparable to that of wood or coal.

Table 2. Results obtained on the determination of higher calorific value/heat of combustion for rice husks

Type of natural agricultural by-product	Equivalent in water, E [J/K]	Superior calorific value, QPCS [MJ/kg]
Rice husks	10137.00	15.34

As previously stated, the calorific value of a product shows the amount of energy that the product can release when completely burned or oxidized and can be a useful indicator in evaluating its potential for use in various applications, including building materials. The higher the calorific value, the more energy the product contains, being likely to fall into a lower, weaker fire reaction class.

Considering the result obtained, relatively high value, it is advisable that, from the point of view of reaction to fire, rice husks are used in the design of new materials natural, sustainable, and ecological biocomposites, such as fire-retardant boards or insulating materials for fire protection (Bode et al., 2023).

The experimental result obtained regarding the capacity of rice husks to absorb water (Table 3), was obtained using equation (2), which was used to calculate the short-term (24 h) absorption of water through partial immersion corresponding to the husks.

Table 3. Water absorption value of rice husks determined by short-term partial immersion

Sieve diameter, D [mm]	Area, A _p [mm ²]	Initial mass, m ₀ [g]	Mass after 24 h of partial immersion, m ₂₄ [g]	Short-term water absorption by partial immersion, W _p [kg/m ²]
190	28.339	134.45	194.99	2.14

The laboratory test carried out on rice husks regarding short-term water absorption revealed a result that slightly exceeds the water absorption value recorded for a synthetic polymer product, namely polyethylene foam (Figure 6), out of which result a material with sound-absorbing properties, foam tested under similar conditions and taken as a reference level (Chiojdoiu et al., 2023).

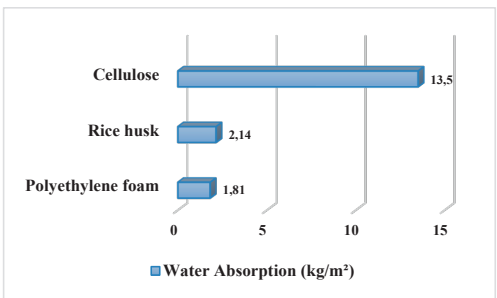


Figure 6. Short-term water absorption by partial immersion for different types of materials

The two values of water absorption are presented in comparison with the corresponding value related to cellulose, a comparison that emphasizes even better the advantage of using rice husks from this point of view in the creation

of innovative eco-materials intended for use in construction.

Regarding the resistance of rice husks to the development of molds, at the end of the 28-day incubation period, in addition to visual observations, the samples were examined under a reflected light microscope at a magnification of 50x and classified based on the specified criteria (Table 1).

On visual examination and on that using the reflected light microscope, at a magnification of 50x, the husks did not show mold in the product mass after 1 day of incubation and after 7 days of incubation, respectively, being classified for these time intervals as having degree 0 mold development (G0). At the end of the 28 days, the rice husks sample presented the appearance of mold visible to the naked eye, spread throughout the plant mass subjected to the test, being included in the 2nd degree of mold development (G2).

As a result, it follows that to develop new building materials incorporating rice husks it is necessary to pre-treat them with anti-mold products so that this inconvenience can be completely eliminated so as not to jeopardize the integrity of the future projected material.

CONCLUSIONS

Internationally, researchers are exploring various technologies and processes to valorize natural agro-industrial by-products, including the use of rice husks, with many processes still in the research and development stage.

The research carried out regarding the study and realization of biocomposite products obtained by the valorization of rice husks, products that can be used in construction, demonstrates worldwide the interest of researchers to create, study, and promote such construction materials/products, having properties comparable to those of materials/products made from synthetic raw materials.

At the national level, due to the predominantly agrarian character of the Romanian economy, the valorization of rice husks represents an opportunity to address the environmental challenges raised by this type of by-product, contributing both to the sustainable development of the built environment and to the consolidation of the circular economy.

Due to the experimental results of the determinations carried out in this research, it is considered that, despite the lack of resistance to the development of molds, the potential of rice husks to be used in construction, through the integration of innovative materials, is reconfirmed as a possibility to contribute to the sustainable development of the built environment.

ACKNOWLEDGEMENTS

This research work was carried out with the support of the Ministry of Research, Innovation and Digitalization and was financed from Project PN 23 35 02 01.

REFERENCES

- Bode, F., Simion, A., Anghel, I., Sandu, M., Banyai, D. (2023). Enhancing Fire Safety: Real-Scale Experimental Analysis of External Thermal Insulation Composite System Façades Behavior in Fire. *Fire*, 6(12), 451.
- Chabannes, M., Bénétet, J.C., Clerc, L. & Garcia-Diaz, E. (2014). Use of raw rice husk as natural aggregate in a lightweight insulating concrete: an innovative application. *Constr. Build. Mater.*, 70. 428–438.
- Chabannes, M., Garcia-Diaz, E., Clerc, L. & Bénétet, J.C. (2016). Effect of curing conditions and Ca(OH)₂-treated aggregates on mechanical properties of rice husk and hemp concretes using a lime-based binder. *Constr. Build. Mater.*, 102. 821–833.
- Chiojdou, A.F., Anghel, I., Safta, C.A., Simion, A. (2023). Influence of water discharge using the „t”, „z”, „o” and „inverted u” letters technique on its distribution in a confined space. Technical University of Cluj-Napoca, ACTA TECHNICA NAPOCENSIS, Series: Applied Mathematics, Mechanics, and Engineering, 66(III), 397–406.
- Dragne, H.G., Simion, A., Stoica, D. (2019). Research on the cladding systems of the buildings from the perspective of the fire reaction of component materials. *Construcții, Journal of Civil Engineering Research*, 20(1-2), 70 – 74.
- Five-year baseline projections of rice supply and demand, Rice Outlook to 2025/26. International Grains Council Report, 11 January 2021. Retrieved from <https://www.igc.int/en/markets/marketinfo-forecasts.aspx>.
- Park, B.-D., Wi, S.G., Lee, K.H., Singh, A.P., Yoon, T.-H. & Kim, Y.S. (2003). Characterization of anatomical features and silica distribution in rice husk using microscopic and micro-analytical techniques. *Biomass Bioenerg.*, 25, 319–327.
- Stoica, D., Simion, A., Dragne, H.G. (2020). Determination of fire performance of silicate decorative plasters. Proceedings of the Construction

- Research Conference, Construction Economics, Town Planning, Spatial Planning, vol.17, 41-47.
- Stoica, D., Simion, A., Dragne, H. (2019). SBI – "key" test in determining the reaction to fire performance of construction products. Proceedings of the Construction Research Conference, Construction Economics, Town Planning, Spatial Planning, vol.16, 5-10.
- Stoica, D., Simion, A., Dragne, H. (2019). Reaction to fire performance of construction products. Proceedings of the Construction Research Conference, Construction Economics, Town Planning, Spatial Planning, vol.15/2019, 27-32.
- SR EN 12667 - "Thermal performance of building materials and products. Determination of thermal resistance by means of guarded hot plate and heat flow meter methods. Products of high and medium thermal resistance", 2002.
- SR EN 13238 – "Fire reaction tests of construction products. How to carry out conditioning and general rules for choosing substrates", 2010.
- SR EN 15101-1+A - "Thermal insulation products for buildings. In-situ formed cellulosic bulk fill (LFCI) products. Part 1: Specification for products before installation", 2019.
- SR EN ISO 1716 - "Fire reaction tests of products. Determination of the gross heat of combustion (calorific value)", 2018.
- Thiebleson, L.M., Calotă, R., Saca, N., Simion, A., Năstase, I., Girip, A., (2024). Reaction to fire, thermal, and mechanical properties of materials based on recycled paper granules bound with starch and clay mortar. *Elsevier Science, Heliyon*, 10(2), e24510.
- Ubi, P.A., Adah, P.U., Ademoh, N.A., Salawu, A.A., Hassan, A.B., Dashe, J.D. & Oyeyemi, S.W. (2022). Rice husk ash reinforced natural rubber composites: effect of benzene diazonium salt treatment. *Nigerian Journal of Technology (NIJOTECH)*, 41, 879 – 886.
- Wilberforce Olupot, P., Menya, E., Lubwama, F., Ssekalu, L., Nabuuma, B. & Wakatuntu, J. (2022). Effects of sawdust and adhesive type on the properties of rice husk particleboards. *Results in Engineering*, 16, 100775.
- Xu, W., Lo, Y.T., Ouyang, D., Memon, S.A., Xing, F., Wang, W. & Yuan, X. (2015). Effect of rice husk ash fineness on porosity and hydration reaction of blended cement paste. *Constr. Build. Mater.*, 89, 90–1.

THE CHALLENGES OF IMPLEMENTING THE GREEN-BLUE INFRASTRUCTURE IN THE METROPOLITAN AREAS OF THE BIG CITIES IN ROMANIA

Oana-Catalina POPESCU, Antonio-Valentin TACHE, Adrian SIMION

National Institute for Research and Development in Construction,
Urban Planning and Sustainable Spatial Development - URBAN-INCERC,
266 Pantelimon Road, District 2, Bucharest, Romania

Corresponding author email: tonytache62@gmail.com

Abstract

This paper aims to demonstrate the necessity of infrastructure planning in the big cities of Romania starting from a theoretical approach to the subject. Green space and green infrastructure have a close connection with topics like urban sprawl, climate change, or nature-based solutions. The present results are based on the research on Google Scholar of the publications that have appeared in recent years. Thus, most scientific papers mostly refer to urban green infrastructure in relation to the field of planning, public health, nature-based solutions and climate change and, in a lower extent, to GIS systems, pandemic and social equity. The conclusions show that an interdisciplinary approach is needed, and that a strategic and priority urban planning must evaluate ecosystem services offered by green infrastructure in order to sustain a healthy city.

Key words: green areas, urban green infrastructure, ecosystem services, NBS, strategic planning.

INTRODUCTION

Urban sprawl increases land fragmentation and decreases connectivity, affecting green space functions and biodiversity, inducing urban growth (Bhatta, 2010; Popescu et al., 2020). Although urban growth can have positive consequences (a greater economic output, new job opportunities), uncontrolled urban sprawl has negative effects, such as a higher cost of infrastructure and services, energy inefficiency, a negative impact on ecosystems, loss of agricultural land, rising temperatures, deterioration of air, water and soil quality.

The most common context of *green space* is the urban context. In cities, although the number of protected green spaces has increased – such as Natura 2000 sites – other green spaces are shrinking, at the expense of the land on which it is being built (European Commission, 2020). The increased interest in green space research is explained by the understanding that nature has a positive impact on human well-being (Frumkin, 2013; Taylor & Hochuli, 2017). Green space is usually considered to be composed of vegetation associated with natural elements (Taylor &

Hochuli, 2017). *Green infrastructure*, a related term, refers to a network of green space, on a city or landscape scale, whose function is in relation to urban inhabitants (Tzoulas et al., 2007; Pienaru & Rădulescu, 2022). Today, the concept of green infrastructure represents a new understanding of the relationship between man and nature and gives a new meaning to the green space planning (Hu et al., 2020). *Urban green (or blue-green) infrastructure* can be defined as a network of natural or nature-based elements located in urban built-up areas. Its elements are increasingly being used for their benefits to humans and wildlife and as a method of adapting to climate change.

Climate change has become a challenge for all of humanity, with negative effects on both natural and socio-economic ecosystems. Coping with climate change requires proactive adaptation actions (Wang & Wang, 2023) for a green, resilient and inclusive development. Planting trees and installing green infrastructure will help to cool urban areas and mitigate the impact of natural disasters. According to the European Commission, *nature-based solutions* (NBS) are essential for reducing emissions and adapting to climate

change. The NBS concept, considered to be an umbrella concept, contains a strong spatial planning dimension and is related to many other concepts and approaches, such as green/blue/urban infrastructure, ecosystem services, urban forestry, etc. (European Commission, 2022).

The benefits of NBS and the promotion of green infrastructure have been focused in European and international frameworks: The EU Green Deal (European Commission, 2019), EU Biodiversity Strategy for 2030 (European Commission, 2020a), The European Union's action plan to reduce air, water and soil pollution to zero (European Commission, 2021), stating that they should be systematically integrated into urban planning – in public spaces, in infrastructure, in buildings and their surroundings.

A recent World Bank study on Romania's development (World Bank, 2023) shows that in Romanian urban areas air pollution often exceeds the limits set by the EU, especially in winter. Rural areas are struggling to manage their forests and increasingly nutrient pollution and chemicals is observed in water bodies. Romania is prone to certain natural disasters induced by climate change, and also the agricultural sector is vulnerable due to the fragmentation of agricultural holdings.

A *green belt* around cities or metropolitan areas can be a way of adapting to climate change. That is why Romania's urban policy foresees the strengthening of green-blue infrastructure to limit and adapt to urban hazards (climate-smart cities). The National Recovery and Resilience Plan (Ministry of European Investments and Projects, 2021) often refers to NBS as a measure to reduce air pollution in large urban agglomerations. NRRP provides the establishment of urban forests as a NBS solution, which can enrich the current green spaces insufficient in surface area and diversity. In this context, the paper presents an analysis of the main topics related to urban green infrastructure as it reflects in recent scientific articles and the necessity to implement this kind of infrastructure in metropolitan areas of the big cities in Romania. The objective of the research is to establish how large cities can create a green-blue infrastructure in a practical

way, because it is a multidisciplinary topic that can be approached from several points of view.

MATERIALS AND METHODS

An exploration of the publications in Google Scholar focusing on green/urban green infrastructure highlights several related topics in close connection on this topic.

To implement the concept of green infrastructure in the big cities in Romania we need to know what the relationship with urban and spatial development is.

The period considered in this study is 2019-2023.

RESULTS AND DISCUSSIONS

The interest on green/urban green infrastructure has grown in recent years, reflected by the large number of scientific publications. A previous analysis (Popescu & Tache, 2023) showed that the number of references about green / urban green infrastructure increased 7 times between 2000 and 2020, with a maximum of interest in the years 2108 and 2019.

Between 2016 and 2023, most publications from Google Scholar having as topic "urban green infrastructure" related to fields such as "urban planning", "public health", "nature-based solutions" and "climate change", and to a lesser extent there were publications approaching "GIS systems", "COVID-19 pandemic" and "social equity". "Metropolitan areas" were also treated in relation to "urban green infrastructure", with emphasis on priority planning through certain changes in land use policies.

In the last 3 years (2021-2023) a slightly downward trend has been observed, a lower interest in the topic of green / urban green infrastructure.

Table 1 presents the main results of the research for the period 2021-2023, in Google Scholar scientific publications.

Based on this table, we can make some observations regarding the possibility of implementing green infrastructure in the metropolitan areas of the big cities in Romania, as a necessity of the present.

Table 1. Bibliographic research on urban green infrastructure planning between 2021 and 2023

Topics addressed	Authors	Key words	Results
1. The concept of green infrastructure - dual and ambiguous	Matsler et al., 2021	GI, ecosystem services urban ecology, urban planing, NBS, rainwater management	The duality of green infrastructure definitions: an ecological network and planning approach vs an engineering technique
2. Evaluation indicators of urban green infrastructure	Hanna et al., 2023	Urban green infrastructure, green areas, vegetation areas	With these indicators, an overview of urban green areas can be obtained
3. Urban green infrastructure and adaptation to climate change	Sánchez & Govindarajulu, 2023	Urbanization, climate change, coastal cities, green-blue infrastructure, changing perception	It is necessary to promote nature-based solutions for climate change adaptation
4. Green infrastructure and efficient use of urban floodplains	Herath et al., 2023	Green-grey infrastructure, SWOT analysis, sustainable and resilient cities	The benefits of urban green infrastructure are multiple
5. Urban green infrastructure and biodiversity	Liu et al., 2023	Urban green infrastructure, urban ecosystems, birds, biodiversity conservation, urbanization	Studying the links and patterns that exist between bird diversity and how they respond to urban green infrastructure can provide the scientific basis for green infrastructure management
6. Urban green infrastructure and the COVID-19 pandemic	Bristowe & Heckert, 2023	Urban green space, parks, nature	It has increased the use of local green infrastructure and its appreciation by people
7. Urban green infrastructure and ecosystem services	Du Toit et al., 2018; Bush et al., 2021	Green space, ecosystem services, biodiversity, climate change, urban planning, regulations, sustainability	Alternative food supply options (e.g. vertical gardens, green roofs, etc.) are needed for urban residents
8. Urban green infrastructure and ecosystem services	Depietri, 2022	Urban green infrastructure, conflicts, synergistic solutions, hybrid infrastructure, stakeholders	There are positive and negative aspects of urban green infrastructure in terms of ecosystem services (services/disservices)
9. Urban green infrastructure and urban and spatial planning	Monteiro et al., 2020; Grabowski et al., 2023	Green infrastructure, spatial planning, planning principles, urban plans, stormwater and sewage systems	If planning procedures are too complex and difficult to implement, policy makers do not consider green infrastructure as a viable planning tool.
10. Inclusion of urban green infrastructure in city plans	Grabowski et al., 2022	Urban planning, urban green infrastructure, integrative concept, rainwater	A synthetic definition of green infrastructure is needed for the future to guide research and planning
11. Metropolitan green infrastructures	Marull et al., 2023; Shen et al., 2023	Metropolitan green infrastructures, land use planning, landscape metabolism, landscape ecology, agricultural management, climate change	Areas of urban/metropolitan infrastructure need to be increased to avoid the ever-increasing ecological risks faced by metropolitan areas

From a theoretical point of view, regarding metropolitan green infrastructures, it is observed that although there is still some ambiguity in the **definition and terminology of the green infrastructure**, there is still an advantage because it allows interdisciplinary approaches, thereby boosting research. No single concept is recommended, but rather recognition of alternative terms and specification of meaning as necessary.

Green infrastructure implementation solutions are needed in the metropolitan areas of Romania because the benefits of urban green infrastructure are multiple. In metropolitan areas, **nature-based solutions** must be promoted for adaptation to climate change, and the local community has an essential role. There is much recent research focusing on green infrastructure in metropolitan areas, especially in countries that want to make the transition to climate-resilient cities.

In the context of the metropolitan areas of the big cities in Romania, the **ecosystem services** offered by the urban green infrastructure must be evaluated. According to the analyzed articles the most representative ecosystem services are those of supply and regulation, and the least attention is paid to those of support. Urban green infrastructure is not evenly distributed in metropolitan areas, so residents do not benefit equally from certain ecosystem services (e.g. recreation service provided by a park), especially in poor areas, slums, where they are sometimes absent and their lack is a health risk. In a metropolitan area, many residents rely on urban green infrastructure for their livelihood, so alternative food supply options are needed (such as vertical gardens, green roofs, etc.).

The latest research shows that there are positive and negative aspects of metropolitan green infrastructure in terms of ecosystem services (services/disservices). Approaching this balance for the implementation of metropolitan green infrastructure requires multidisciplinary teams. The development of a hybrid infrastructure (green-gray) can be a solution to overcome the compromises that may appear.

The literature shows that metropolitan **green infrastructure planning** is based on principles such as connectivity, multifunctionality, multiple scale, integration, diversity, applicability, governance and continuity. Of

course, in the case of the big cities in Romania, there may be different approaches regarding the identification, selection and evaluation of the evaluation principles of the metropolitan green infrastructure due to the different priorities existing in the political agendas, which in turn are also influenced by factors such as geographical location or cultural dynamics.

The implementation of green infrastructure in the metropolitan areas of large cities in Romania is necessary because cities must be **friendly to biodiversity**, they need nature. **Strategic urban planning** must take into account that the requirement of green spaces depends on the socio-economic and temporal gradient (services ecosystems are not a measurable whole, but intertwined with social and political processes). Although urban planning fails to explicitly define what green infrastructure is in metropolitan areas, concepts related to stormwater and less landscape related seem to predominate (most of the ecosystem benefits of urban green infrastructure are related to stormwater).

CONCLUSIONS

After 2020 the interest on urban green infrastructure focused on its benefits – its role to counter the effects on climate change or to increase biodiversity.

In cities and metropolitan areas, planning a green infrastructure is a complex activity, difficult to implement but is still a viable planning tool.

Metropolitan areas face increasingly frequent ecological risks, which cause a decrease in the supply of ecosystem services. In order to avoid risks, the areas of metropolitan green infrastructure must be increased by a priority planning. Future research is needed for the definition of urban green infrastructure to focus on the relationship between ecological, technological and societal infrastructure, and to facilitate the production of the greatest number of social benefits.

ACKNOWLEDGEMENTS

This research is supported by the project PN 23 35 06 01 with the title "Integrated IT-urban planning system for the evaluation of blue-

green infrastructure at the level of municipalities and cities in Romania with a view to implementation in urban development plans. Case study: Râmnicu Vâlcea Municipality", financed by the Ministry of Research, Innovation, Digitalization and carried out under ECODIGICONS Nucleus Program.

REFERENCES

- Bhatta, B. (2010). *Analysis of urban growth and sprawl from remote sensing data*. Springer Science and Business Media, Dordrecht, Germany.
- Bristowe, A., Heckert, M. (2023). How The COVID-19 Pandemic Changed Patterns of Green Infrastructure Use: A Scoping Review. *Urban Forestry & Urban Greening*, 81, 127848.
- Bush, J., Ashley, G., Foster, B., Hall, G. (2021). Integrating green infrastructure into urban planning: Developing Melbourne's green factor tool. *Urban Planning*, 6(1), 20-31.
- Depietri, Y. (2022). Planning for urban green infrastructure: addressing tradeoffs and synergies. Current Opinion in Environmental. *Sustainability*, 54, 101148.
- Du Toit, M.J., Cilliers, S.S., Dallimer, M., Goddard, M., Guenat, S., Cornelius, S.F. (2018). Urban green infrastructure and ecosystem services in sub-Saharan Africa. *Landscape and Urban Planning*, 180, 249-261.
- European Commission (2019). Communication from the Commission to the European Parliament, the European Council, the Council, the European Economic and Social Committee and the Committee of the Regions. The European Green Deal. COM (2019) 640 final, Brussels, Belgium.
- European Commission (2020a). EU Biodiversity Strategy for 2030. Bringing nature back into our lives, COM (2020) 380 final, Brussels, Belgium
- European Commission (2020). Communication from the Commission to the European Parliament, the Council, the European Economic and Social Committee and the Committee of the Regions. EU Biodiversity Strategy for 2030. Bringing nature back into our lives. COM (2020) 380 final, Brussels, Belgium.
- European Commission (2021). Communication from the Commission to the European Parliament, the Council, the European Economic and Social Committee and the Committee of the Regions. Forging a climate-resilient Europe – the new EU Strategy on Adaptation to Climate Change, COM (2021) 82 final, Brussels, Belgium
- European Commission, General Directorate for Research and Innovation (2022). The vital role of nature-based solutions in a nature positive economy. Publications Office of the European Union, 2022.
- Frumkin, H. (2013). The evidence of nature and the nature of evidence. *American journal of preventive medicine*, 44(2), 196-197.
- Grabowski, Z.J., McPhearson, T., Matsler, A.M., Groffman, P., Pickett, S.T. (2022). What is green infrastructure? A study of definitions in US city planning. *Frontiers in Ecology and the Environment*, 20(3), 152-160.
- Grabowski, Z.J., McPhearson, T., Pickett, S.T. (2023). Transforming US urban green infrastructure planning to address equity. *Landscape and Urban Planning*, 229, 104591.
- Hanna, E., Bruno, D., Comín, F.A. (2023). Evaluating naturalness and functioning of urban green infrastructure. *Urban Forestry & Urban Greening*, 80, 127825.
- Herath, H.M.M.S.D., Fujino, T., Senavirathna, M.D.H.J. (2023). A Review of Emerging Scientific Discussions on Green Infrastructure (GI) - Prospects towards Effective Use of Urban Flood Plains. *Sustainability*, 15(2), 1227.
- Hu, T., Chang, J., & Syrbe, R.U. (2020). Green Infrastructure Planning in Germany and China: A comparative approach to green space policy and planning structure. *Research in Urbanism Series*, 6, 99-126.
- Liu, Z., Zhou, Y., Yang, H., Liu, Z. (2023). Urban green infrastructure affects bird biodiversity in the coastal megalopolis region of Shenzhen city. *Applied Geography*, 151, 102860.
- Marull, J., Padró, R., La Rota-Aguilera, M.J., Pino, J., Giocoli, A., Cirera, J., Velasco-Fernández, R. (2023). Modelling land use planning: Socioecological integrated analysis of metropolitan green infrastructures. *Land Use Policy*, 126, 106558.
- Matsler, A.M., Meerow, S., Mell, I.C., Pavao-Zuckerman, M.A. (2021). A 'green'chameleon: Exploring the many disciplinary definitions, goals, and forms of "green infrastructure". *Landscape and Urban Planning*, 214, 104145.
- Ministry of European Investments and Projects (2021). National Recovery and Resilience Plan (NRRP).
- Monteiro, R., Ferreira, J.C., Antunes P. (2020). Green infrastructure planning principles: An integrated literature review. *Land*, 9(12), 525.
- Pienaru, A.-M., Rădulescu, D. (2022). Opportunities to apply nature-based solutions in Romania in the context of European common agriculture Policy. *Scientific Papers. Series E. Land Reclamation, Earth Observation & Surveying, Environmental Engineering*, XI, 511-516, Print ISSN 2285-6064.
- Popescu, O.-C., Tache, A.-V. (2023). Cercetări recente privind infrastructura verde urbană. in: *Lucrările Conferinței de cercetare în construcții, economia construcțiilor, urbanism și amenajarea teritoriului, Ediția a XXIV-a: Cercetări inovative în domeniul construcțiilor, arhitecturii și urbanismului ca răspuns la provocările societale și tehnologice* (Bucharest, November 16, 2023), Vol. 24, Ed. INCD URBAN-INCERC București, 5-14.
- Popescu, O.-C., Tache, A.-V., Petrișor, A.-I. (2020). Methodology for identifying the ecological corridors. Case study: planning for the brown bear corridors in the Romanian Carpathians. *The 2020 International Conference on Sustainable Development (ICSD)*, September 21, 2020, New York, SUA, online.
- Sánchez, F.G., Govindarajulu, D. (2023). Integrating blue-green infrastructure in urban planning for

- climate adaptation: Lessons from Chennai and Kochi, India. *Land use policy*, 124, 106455.
- Shen, J., Peng, Z., Wang, Y. (2023). From GI, UGI to UAGI: Ecosystem service types and indicators of green infrastructure in response to ecological risks and human needs in global metropolitan areas. *Cities*, 134, 104176.
- Taylor, L., Hochuli, D.F. (2017). Defining greenspace: Multiple uses across multiple disciplines. *Landscape and urban planning*, 158, 25-38.
- Tzoulas, K., Korpela, K., Venn, S., Yli-Pelkonen, V., Kaźmierczak, A., Niemela, J., James, P. (2007). Promoting ecosystem and human health in urban areas using Green Infrastructure: A literature review. *Landscape and urban planning*, 81(3), 167-178.
- World Bank (2023). Romania – Systematic Country Diagnostic Update (English). Washington, D.C, World Bank Group.

RESEARCH TRENDS IN WATER MANAGEMENT IN CENTRAL AND EASTERN EUROPE IN THE CONTEXT OF CIRCULAR ECONOMY

Alina-Cerasela ALUCULESEI, Nicoleta GUDANESCU, Sorin IONITESCU,
George Cornel DUMITRESCU, Simona MOAGAR-POLADIAN

Romanian Academy, Institute for World Economy,
13 Calea 13 Septembrie, District 5, Bucharest, Romania

Corresponding author email: alina.cerasela@iem.ro

Abstract

Water resources are highly valuable globally, and their sustainable management has become a top priority for authorities worldwide. Central and Eastern European (CEE) countries, with their extensive history of water usage across various sectors, face significant challenges due to the over-exploitation of these resources. The increasing demand underscores the need for comprehensive management at both national and regional levels. This study examines research trends on water resource exploitation in CEE countries, identifying potential research gaps that academia can address to offer essential a valuable insight for policymakers. By using a bibliometric analysis of 390 articles and proceedings from the Web of Science database, analysed through VosViewer software, the study reveals substantial research interest in areas such as agriculture, water management, wastewater reuse solutions, and sustainable agricultural water use. Despite this, the analysis indicates a notable deficiency in research focused on the new labour market demands associated with emerging water management technologies. These findings highlight the necessity for future research to bridge this gap, providing actionable insights to adapt educational and training programs to the evolving requirements of the water management sector.

Key words: bibliometric analysis, circular economy, circular water, water sustainable, water use, wastewater reuse.

INTRODUCTION

Water is one of the most important resources that allowed urban development, being linked to the agriculture sector, food industry, hospitality, construction or transportation. According to the United Nations, the humanity is facing a water crisis that impacts the economy in many ways, all the countries being affected, no matter their developing degree. For example, in developing states the main issues are related to the water quality and in the developed countries the main concerns are related to the availability of water for irrigation (UNESCO, 2024).

The most water-consuming activity is agriculture, being responsible on 70% of the total water use worldwide (OECD, 2024). In the context of the growing demand for food, there is an unprecedented pressure in this sector, especially in the months when irrigation water can be available only using unsustainable methods (Rosa et al., 2020). According to FAO projections, by 2050 the demand for food will increase by 50% (FAO, 2023) which will maximize the needed quantity of water in agriculture.

The transition towards a circular economy has gained significant momentum in recent years, with environmental legislation and policy plans increasingly incorporating the circular economy concept into business development. This paradigm shift is particularly crucial in the water management sector, where sustainable practices are essential for resource recovery and environmental preservation (Sandu et al., 2023). In Central and Eastern Europe, researchers have been exploring various approaches to enhance the circularity of water management systems. One such approach is the implementation of anaerobic membrane bioreactors (AnMBRs), which have been identified as a promising technology for simultaneous recovery of clean water, renewable energy, and nutrients from municipal wastewater (Robles et al., 2021). Additionally, the concept of sewer mining, which involves extracting wastewater from local sewers for decentralized reuse applications, has garnered significant interest in the region as a means of bridging the gap between household-scale reuse and centralized treatment (Liakopoulou et al., 2020; Mannina et al., 2021).

Wastewater treatment plants (WWTPs) are also undergoing a critical transition, shifting from a linear to a circular economy operation and design concept. This transition involves the recovery of resources, such as water, energy, and materials, from the wastewater stream, with the ultimate goal of minimizing waste and preserving natural resources. Researchers in Central and Eastern Europe have been exploring various strategies to enhance the circularity of wastewater treatment, including the recovery of nutrients, the valorisation of sewage sludge, and the generation of renewable energy from the wastewater stream (Guerra-Rodríguez et al., 2020).

Depending on the location and the weather hazards that take place in a period, there are locations where water may not be available at all for short periods. This is common to the developing countries, arctic regions or isolated rural places. Even though in the last decades the tools for conserving water have developed constantly, in these regions is still common for the citizens to use tankers for preserving water which may represent a health risk for the local population (Salehi, 2022). Water recovery is not so easily to achieve by the citizens, as they do not have the needed infrastructure to recover water and reuse it in household activities. The integration of wastewater in different activities is still limited by the health and environment constraints (Berbel et al., 2023).

Besides the technological issues in recovery wastewater, there are other aspects that should be considered when it comes to a sustainable water management. In tourism, for example, the simplest solution is to increase the awareness among the guests. But messages that make clients more aware about the importance of their behaviour, like saving water when soaping, have limited effects as the tourist's behaviour depends on their culture and their awareness regarding this topic is low (Borys et al., 2023). On the other hand, the hotels can choose to use products that are 99% biodegradable and have a reduced impact on aquatic life (Koseoglu-Imer et al., 2023) or use intelligent devices to doze the water quantity. However, these kinds of initiative are not enough to accomplish a scalable result and higher investments are required which highlights the issues related to the costs that are still too big for the small

business. The change in consumer behaviour is difficult to achieve in the household sector also. As the water demand does not depend on the price in the household sector (European Environment Agency, 2021), it is difficult to constraint the citizen to save water. This puts more pressure on the authorities to find solutions to educate citizens in this regard.

In this context, and in line with the European Green Deal program, water management became one of the European Commission priorities, being an essential part of the transition to the circular economy model (Smol et al., 2020; Sandu & Virsta, 2021) from the linear one, that in this filed involves the disposal of process materials in activities like desalinations and wastewater treatment (Yusuf et al., 2020). In order to assure the circularity in water management, the stakeholders should meet the following five rules: circularity, multiple waters, involving digital tools, using inclusive water and resilient water (infrastructure) (Water Europe, 2024). All these concepts have the role to assure both quality and availability of water resources in Europe. Digital water, for example is a smart way to control water resources involving AI tools to optimize environmental planning and management policies (Nikolaou et al., 2020). The switch to a circular approach in water use is beneficial for the labour field also. In Europe, the implementation of innovative tools and processes for recovering water might provide up to 20000 new jobs (Koseoglu-Imer, 2023).

Starting with 2010, the Water Framework Directive establishes the rules that makes the member states to be more aware about the importance of the quality of water resources and the necessity to implement up-to-date water management solutions (European Commission, 2023). The legal framework was completed in 2023 by the Water Reuse Regulation (European Commission, 2023). This change is a consequence of the need of water in many economic fields, especially agriculture (Zahoor & Mushtaq, 2023), that are highly polluting and that affects both the quality of water and the disposable quantity.

In Europe, many countries are facing issues in water availability, mainly during the summer, when important quantities are used for irrigation. Many studies indicate the urge need for more action from the stakeholder in order to

prevent water pollution and water waste. In South-West Europe, where almost 13,5% of the territory uses water for irrigation and where are located ones of the major EU cities, water management became a necessity (Larraz, 2024). This region is also affected by the increased temperature. The climate-change scenarios indicate that in the next years water availability will continue to be a problem for agriculture (Sordo-Ward et al., 2019). The most affected member states are in the south-western region (Martínez-Valderrama et al., 2023). Even though other European countries seem to not face issues in terms of water availability, like Poland, there is always a risk in terms of quality and temporary interruption. So, innovative solutions should be found, like new shower panels that limit the quantity of water (Czajkowski et al., 2021), renewable water technology (Zhang et al., 2023), behavior-change interventions designed for the citizens (Halabieh & Shu, 2024) or implementing smart water monitoring systems (Alexopoulos et al., 2022).

Water governance is mandatory in the context of the climate change issues, the progress in agriculture and the requirements of the circular economy. So, more action to improve the behaviour of the stakeholders in terms of sustainable use of water resources is needed (Jägermeyr, 2020). In this regard, the first step is to identify the relevant research trends and gaps in research in order to give the decision makers a complex overview in the field. Analysing the most relevant sources in the literature, it can be seen there is many research that focus on the water conservation in specific areas like Mediterranean region (Garcia-Tejero, 2020), (Sismani et al., 2023) and on countries from CEE region, like Romania (Ioja et al., 2021; Timofiti & Pienaru, 2022), Hungary (Gaál & Becsákné Tornay, 2023), Bulgaria (Negm et al, 2020), Poland (Kubiak-Wójcicka, 2021), Czech Republic (Zimková et al., 2023).

The present study completes the literature with a descriptive image about the research trends in water management in the CEE countries, with a focus on the region and less on the individual member states. The novelty of the present research is the geographical approach of the analysis and the aim to investigate if the labour market is considered a mature research topic in

the context of the changes brought by the circular economy requirements. The main objectives of the paper are: **i)** to describe the scientific production of the papers that focused on the way the water resources are used in CEE region and **ii)** to identify the main research trends in the field.

Despite these challenges, numerous European countries are making significant steps forward in water management. For instance, Germany, with its advanced technological infrastructure, has implemented innovative water reuse and conservation strategies. Similarly, Poland has focused on improving water quality and expanding access to clean water in rural areas. China, while not in Europe, serves as a relevant case study due to its large-scale water management projects, such as the South-to-North Water Diversion Project, which aims to address water scarcity in its northern regions. Spain and the USA, with their diverse climates and water-intensive agricultural sectors, offer valuable insights into water management practices in different contexts. These examples highlight the importance of tailored solutions and collaborative efforts in addressing the multifaceted water crisis.

In regions of the world affected by water scarcity, economic activities can be constrained by water availability, leading to competition both among sectors and between human uses and environmental needs. While the commodification of water remains a contentious political issue, the valuation of this natural resource is sometimes viewed as a strategy to avoid water waste. Likewise, water markets have been invoked as a mechanism to allocate water to economically most efficient uses. However, the value of water remains difficult to estimate because water markets and market prices exist only in few regions of the world. Despite numerous attempts at estimating the value of water in the absence of markets, a global spatially explicit assessment of the value of water in agriculture is still missing. This lack of comprehensive data on the economic value of water in agriculture presents a significant challenge in transitioning towards a circular water economy, as it hinders effective decision-making and resource allocation (D'Odorico et al., 2020).

MATERIALS AND METHODS

In order to achieve a comprehensive image about the use of water resource in CEE countries, a bibliometric analysis was performed. The research was based on the simplified PRISMA protocol that is used in systematic review to describe the research stages in a transparent way (Page et al., 2021). The systematic review of the literature is one of the research methods that have a high contribution to knowledge in a field (Rowe et al., 2023), being used to describe bibliometric indicators and research trends in many domains, like agriculture (Pradhan et al., 2023), tourism (Huang et al., 2023), engineering (Nwaogu et al., 2023), education science (Oliveira & Bonito, 2023) and others.

The data was extracted from Web of Science database, one of the most relevant bibliometric databases worldwide that contains documents

since 1900 (Web of Science, 2024) and which in countries like Romania is considered the baseline in academic publishing evaluation. The results were interpreted using VosViewer software, a validated tool used for bibliometric mapping (van Eck et al., 2010). In order to unify different variations of the same items, a Thesaurus file was built and used.

The research design is presented in Figure 1 and the data was filtrated to include in the topic (title, abstract and key words) the following items:

- water and
- resource*/management/consume/ supply and
- CEE/Central and Eastern Europe/ Central and Eastern Countries/ Central Europe/Eastern Europe.

The interrogation focused on CEE as a region, so the name of the countries from this area were not included in the search phase.

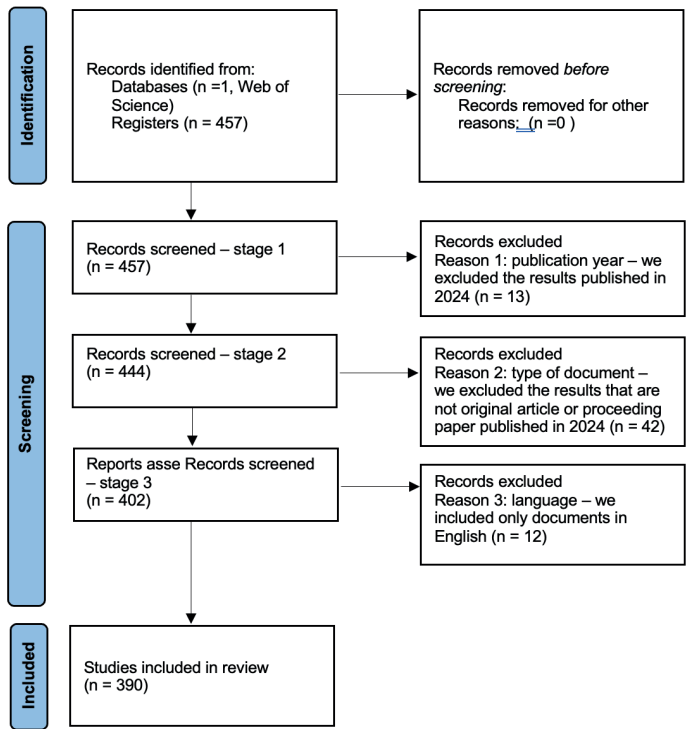


Figure 1. The research stages based on PRISMA protocol
(Source: Author elaboration based on Page et al., 2021)

The research included only original articles and proceedings papers written in English, as the

novelty in research is the highest in these two types of documents. There were excluded

review articles as they are not considered relevant for the present investigation. There were included the documents published up to 2024. As the research was performed during 2024 and one of the objectives of the study is to describe the scientific production, analysing only a half of a year would not be relevant. To enhance the validity and reliability of the findings, the research also incorporated a qualitative analysis of selected articles and proceedings papers. This analysis aimed to identify emerging themes, trends, and research gaps that may not be fully captured by bibliometric indicators alone. The qualitative analysis involved a close reading of the selected documents, with a focus on their research questions, methodologies, findings, and implications. The qualitative findings were then triangulated with the bibliometric results to provide a more comprehensive and nuanced understanding of the conducted research.

RESULTS AND DISCUSSIONS

The scientific production of the studies related to the water use in CEE region started to increase after 2010, the same year when the EU framework related to water management

changed (Figure 2). The increase in published articles and proceedings is not exponential from one year to another, except 2020, the year when Green Deal Program started to be populated, and the trend is marked by ups and downs. This shows that the subject is of interest for the academic community and even though there is a change in the legislation framework in the member states, and the EU makes efforts to improve the circularity in this field, the topic was not artificially pushed by the EU Directives. Moreover, 56% of the total papers included in the study received funding for research, showing the high interest for the topic at national and international level from both funding bodies and research teams to access grants.

Overall, the research trends in water management in Central and Eastern Europe in the context of circular economy suggest a growing interest and commitment to addressing the complex challenges in this domain, though significant work remains to be done to achieve a truly circular water economy in the region (Díaz-García et al., 2020; OECD, 2022; Implementing Water Economics in the EU Water Framework Directive, 2023; Trică et al., 2019).

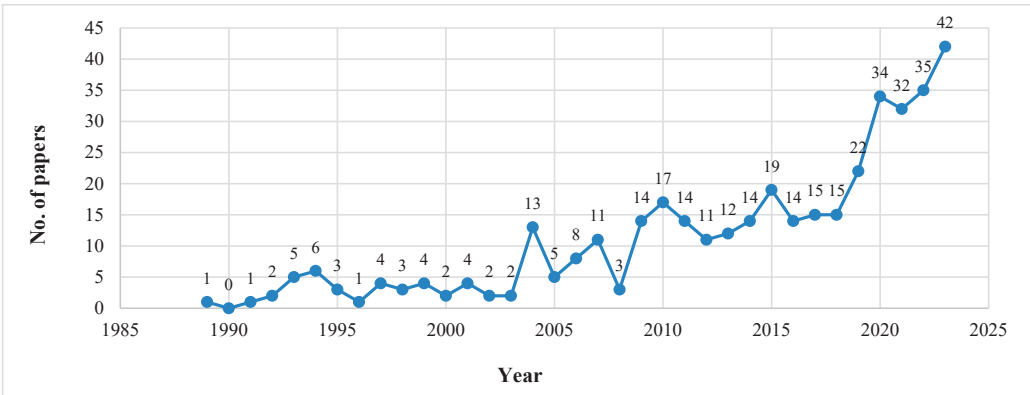


Figure 2. Scientific production

The countries that focus the most on this research topic are Germany (86 documents), Poland (43 document), China (40 documents), Spain (37 documents) and the USA (33 documents). Even though the investigated subject is related to the situation from the CEE region, except Poland, the other states from the

CEE recorded a low scientific production in terms of studying the use of water resources in the region (Figure 3). Czech Republic had 26 documents, Hungary recorded 22 documents, Slovakia 12 documents, Romania 8 documents and Slovenia 7 documents. The highest impact of the published papers recorded Germany

(4611 citations), USA (3916 citations), England (3062 citations), Switzerland (2744 citations) and Netherlands (2700 citations).

The research interest in water management in CEE countries has been growing steadily, as evidenced by the increasing number of publications over time. This trend can be attributed to several factors, including:

- **Heightened awareness of water scarcity and climate change:** the escalating impacts of climate change, such as droughts, floods, and extreme weather events, have underscored the vulnerability of water resources in the region. This has prompted researchers and policymakers to prioritize water management research and develop adaptive strategies.
- **Policy and regulatory frameworks:** the implementation of the EU Water Framework

Directive and the Water Reuse Regulation has created a regulatory environment that encourages research and innovation in water management. These frameworks have set ambitious targets for water quality and reuse, stimulating research activities aimed at achieving these goals.

- **Technological advancements:** the development of new technologies, such as smart sensors, remote sensing, and data analytics, has opened up new avenues for water management research. These technologies enable more accurate monitoring of water resources, better forecasting of water availability, and more efficient management of water use.

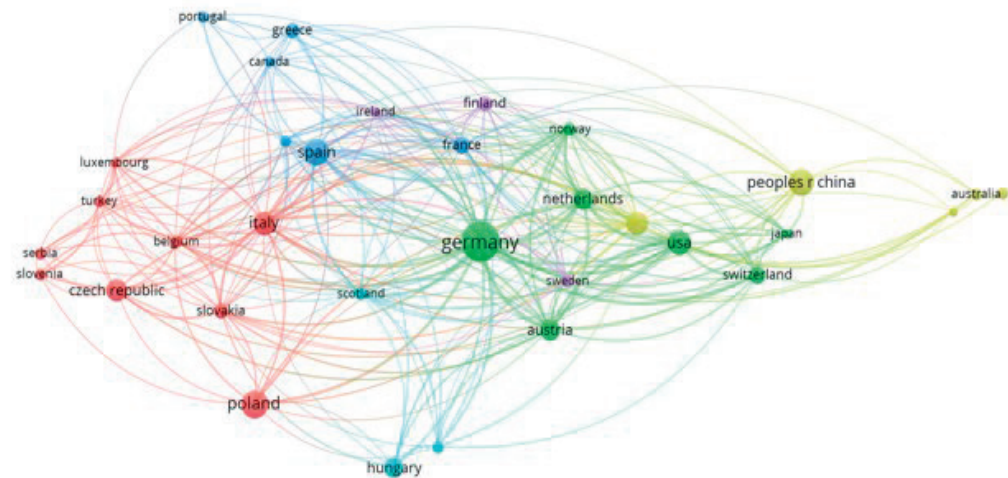


Figure 3. The affiliation map of the documents based on country
(* minimum number of documents of a country = 5)

Related to the interest for studying the sustainable ways to use water resources in CEE region, it can be observed (Figure 4) that the institutions that recorded the most articles and proceedings that met the present selection criteria are Chinese Acad Sci with 10 documents, University Kassel with 9 documents, Polish Academy of Science with 8 documents and University Utrecht and University Freiburg with 7 documents each. The impact of the published papers changes the rank of the research institutions. University Kassel

recorded the highest number of total citations of the published papers (1704) followed by Potsdam Inst Climate impact res (1543 citations) and Chinese Acad Sci (11172 citations). In order to eliminate plural forms of the resulted items and similar format of the key words (ex: climate change and climate-change), a Thesaurus file was used. After the unification step of the terms, resulted 110 key words that grouped the research interest regarding the sustainable use of water resources in CEE countries into six clusters (Figure 5).

The highly used items are climate change (occurrence = 70), management (42), impact (37), model (36) and drought (27).

The red cluster contains 28 items that are related to water management. The most relevant items, that are used in the most papers are: river basin management (occurrence = 20), management (42), pollution (12), quality (26), water framework directive (14), water quality (12).

The green cluster contains 27 items that are connected to climate change issues. The most common key words in the investigated papers are climate change (occurrence = 70), groundwater (18), precipitation (12), variability (18), water resource management (26).

The blue cluster consists of 20 items related to the consequences of climate change. The key

words with the highest occurrence are climate (20), drought (27), emissions (19), irrigation (13).

The yellow cluster contains 18 items that are related to agriculture field. The most common key words are agriculture (occurrence = 14), impact (37), water management (12), temperature (12).

The purple cluster has 13 items connected to the water governance. The most common key words are system (18), consumption (8), ecosystem services (7), framework (8), water footprint (9), water scarcity (9).

The light blue cluster contains only 2 terms: adaptation (occurrence = 9) and projection (7), both of them having links with all the other clusters.

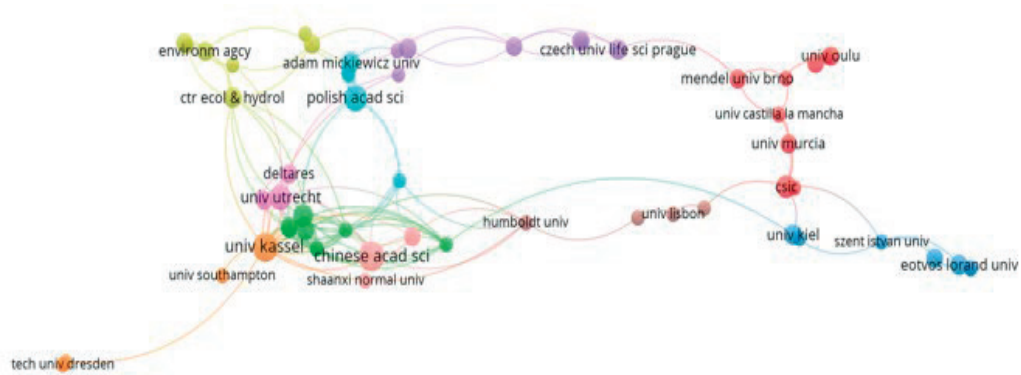


Figure 4. The affiliation map based on institution
(* minimum number of documents of a country = 3)

The analysis shows the research interest related to labour issues is low in this field and no cluster indicated directly the concerns related to the new requirements of the circular water in terms of job creation.

The terms that are indirectly connected to the labour market are framework, governance, adaptation, water framework directive, water governance, water management, water use efficiency.

The most research is focused on issues related to the climate change impact on the agriculture and the lack of water for irrigation, on sustainable

ways to recover waste water and ecosystem services.

The analysis of the countries and institutions involved in this research reveals a diverse landscape with both regional and international collaborations. While Germany, Poland, China, Spain and the USA are leading contributors to the research output, there is a clear need for increased research capacity and collaboration within the CEE region itself. This is essential to ensure that research findings are relevant to the specific challenges and opportunities faced by these countries.

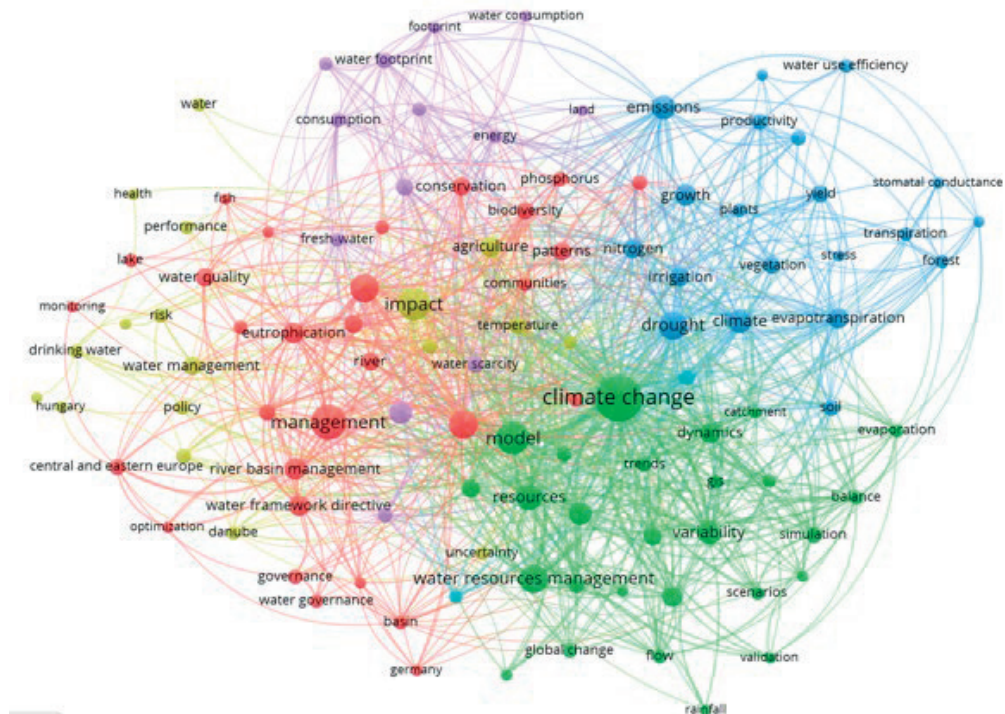


Figure 5. The affiliation map based on keywords
 (* minimum number of documents of a country = 5)

CONCLUSIONS

Water management is an actual topic in research and the EU agenda underlines the urge to find innovative ways to recover water and accelerate the switch from the linear model to the circular one. The present bibliometric analysis showed the research in the field is encouraged more by the impact of the socio-economic factors and climate change issues than by the legislative framework. This tendency illustrates the research related to the use of water resources in various field is dependent on previous studies and the scientific production has in general a gradual increase.

Regardless, water management is an actual trend in research, there is less interest in studying the use of water resources in CEE countries, despite their focus on agriculture and the need for irrigation, than in other EU regions, like the Mediterranean area. This can be noticed from the limited studies in the field that concentrated the present study on 390 documents. Even though the present study illustrates the research

trends in a specific EU area, the highest research interest for this region comes from developed countries like Germany and USA and less from the CEE countries. Poland was the only CEE country that recorded a significant number of research documents that investigated the use of water resources in the region. Moreover, the strongest research institutions in terms of scientific production are mainly located in countries from other geographical regions than from CEE area. This illustrates that research related to the water use doesn't depend on the geographical aspects and the results are useful for the stakeholders from another region too.

Ultimately, the transition towards a circular economy in water management requires a multifaceted approach that integrates technological innovations, policy frameworks, and stakeholder engagement.

While the progress in Central and Eastern Europe is promising, significant barriers still exist, including outdated infrastructure, limited financial resources, and regulatory challenges. Overcoming these barriers will require a

multifaceted approach, involving the collaboration of policymakers, researchers, and industry stakeholders.

The research related to water use in CEE region focus on specific topics like agriculture, climate-change consequences, water management, water governance and the need of change and adaptation in the field. The most mature interest in research is related to the agriculture field which shows that the change in assuring circularity in water use should start from this sector. Moreover, the other research topics that are grouped in clusters are highly linked to the agriculture. For example, the cluster that contains aspects about the impact of climate change on the water use has items that describe activities with impact on agriculture, like drought or irrigation. This indicates that on the one hand, the stakeholders from this region should concentrate their efforts to other activities also, as increasing the awareness of the involved population. On the other hand, it shows the highest problems in this region about the water use and availability are in agriculture.

The lack of direct interest on the impact of water uses on the labour market in the context of the new changes of the Green Deal Program and circular economy adoption shows the progress in using sustainable ways to treat water is still low. Such a switch would bring new requirements for the employees as green jobs involves new skills and a high capacity of adaptation. As no cluster illustrates a direct interest in this regard, it is clear that the circularity in water management is still at the beginning and Academia should focus more on this topic.

The present research has several limitations. Firstly, the study is based on the selection of articles and proceeding from only one database. Secondly, the research didn't consider reports and legislative documents that would give a more comprehensive image about the use of water resources in CEE region. In order to complete the present results and to offer the stakeholders a more complex image on the topic, the future research will analyse the results from more bibliometric databases (ex: SCOPUS and PubMed) and will complete the analysed documents with reports, legislative frameworks and case studies.

ACKNOWLEDGEMENTS

The work in this article was carried out with the contribution and during co-author Sorin Ionitescu's second-year doctoral research activities at the Romanian Academy, Institute for World Economy, School of Advanced Studies of the Romanian Academy, Doctoral School of Economic Sciences, National Institute for Economic Research "Costin C. Kirițescu", Institute for World Economy.

REFERENCES

- Alexopoulos, T., Marsh, J., Llewellyn, G., & Packianather, M. (2022). An adaptive water consumption monitoring and conservation system. In International Conference on Sustainable Design and Manufacturing (pp. 191-200). Singapore: Springer Nature Singapore.
- Berbel, J., Mesa-Pérez, E., & Simón, P. (2023). Challenges for circular economy under the EU 2020/741 wastewater reuse regulation. *Global Challenges*, 7(7), 2200232.
- Borys, T., Bugdol, M., Puciato, D., Szromek, A.R., & Geryk, M. (2023). Motivations for hotels to undertake pro-ecological activities—opinions of hotel guests. *Economics and Environment*, 87(4), 673-21.
- Czajkowski, V.A., Remiorz, L., Pawlak, S., Remiorz, E., Szygula, J., Marek, D., ... & Antemijczuk, O. (2021). Global water crisis: Concept of a new interactive shower panel based on IoT and cloud computing for rational water consumption. *Applied Sciences*, 11(9), 4081.
- D'Oro, P., Chiarelli, D.D., Rosa, L., Bini, A., Zilberman, D., & Rulli, M.C. (2020). The global value of water in agriculture. *National Academy of Sciences*, 117(36), 21985-21993. <https://doi.org/10.1073/pnas.2005835117>.
- Diaz-Garcia, C., Moreno, A.G., & Sáez-Martínez, F.J. (2020). *Circular economy and SMEs: insights and EU situation*. Edward Elgar Publishing. <https://doi.org/10.4337/9781839109690.00008>
- European Commission. (2023). *Water reuse regulation*. European Commission. 2023. Water Framework Directive. Available at: https://environment.ec.europa.eu/topics/water/water-framework-directive_en
- European Environment Agency. 2021. Water management in Europe: price and non-price approaches to water conservation. Available at: <https://www.eea.europa.eu/publications/water-management-in-europe-price>.
- FAO. (2023). FAO land and water 2021 annual overview.
- Gaál, M., & Becsákné Tornay, E. (2023). Drought events in Hungary and farmers' attitudes towards sustainable irrigation. IDŐJÁRÁS/QUARTERLY. *Journal of the Hungarian meteorological service*, 127(2), 143-165.
- García-Tejero, I.F., Carbonell, R., Ordoñez, R., Torres, F.P., & Durán Zuazo, V.H. (2020). Conservation agriculture practices to improve the soil water

- management and soil carbon storage in Mediterranean rainfed agro-ecosystems. *Soil health restoration and management*, 203-230.
- Guerra-Rodríguez, S., Oulego, P., Rodríguez, E., Singh, D., & Rodríguez-Chueca, J. (2020). Towards the Implementation of Circular Economy in the Wastewater Sector: Challenges and Opportunities. *Multidisciplinary Digital Publishing Institute*, 12(5), 1431-1431. <https://doi.org/10.3390/w12051431>
- Halabieh, S., & Shu, L. H. (2024). Reducing waste outflow to motivate water conservation. *Journal of Mechanical Design*, 146(2).
- Huang, G.L., Karl, M., Wong, I.A., & Law, R. (2023). Tourism destination research from 2000 to 2020: A systematic narrative review in conjunction with bibliographic mapping analysis. *Tourism management*, 95, 104686.
- Iojă, C.I., Badiu, D.L., Haase, D., Hossu, A.C., & Niță, M.R. (2021). How about water? Urban blue infrastructure management in Romania. *Cities*, 110, 103084.
- Jägermeyr, J. (2020). Agriculture's historic twin-challenge toward sustainable water use and food supply for all. *Frontiers in Sustainable Food Systems*, 4, 35.
- Koseoglu-Imer, D.Y., Oral, H.V., Calheiros, C.S.C., Krzeminski, P., Güçlü, S., Pereira, S.A., Surmacz-Górska, J., Plaza, E., Samaras, P., Binder, P.M., Van Hullebusch, E.D. & Devolli, A. (2023). Current challenges and future perspectives for the full circular economy of water in European countries. *Journal of Environmental Management*, 345, 118627.
- Kubiak-Wójcicka, K., & Kielik, M. (2021). The State of Water and Sewage Management in Poland. Quality of Water Resources in Poland, 375-397.
- Larraz, B., García-Rubio, N., Gámez, M., Sauvage, S., Cakir, R., Raimonet, M., & Pérez, J. M. S. (2024). Socio-Economic Indicators for Water Management in the South-West Europe Territory: Sectorial Water Productivity and Intensity in Employment. *Water*, 16(7), 959.
- Liakopoulou, A., Makropoulos, C., Nikolopoulos, D., Monokrousou, K., & Karakatsanis, G. (2020, August 11). An Urban Water Simulation Model for the Design, Testing and Economic Viability Assessment of Distributed Water Management Systems for a Circular Economy. <https://doi.org/10.3390/environsciproc2020002014>
- Mannina, G., Badalucco, L., Barbara, L., Cosenza, A., Trapani, D.D., Gallo, G., Laudicina, V.A., Marino, G., Muscarella, S.M., Presti, D., & Helness, H. (2021, March 30). Enhancing a Transition to a Circular Economy in the Water Sector: The EU Project WIDER UPTAKE. *Multidisciplinary Digital Publishing Institute*, 13(7), 946-946. <https://doi.org/10.3390/w13070946>
- Martínez-Valderrama, J., Olcina, J., Delacámara, G., Guirado, E., & Maestre, F. T. (2023). Complex Policy mixes are needed to cope with Agricultural Water demands under Climate Change. *Water Resources Management*, 37(6), 2805-2834.
- Negm, A.M., Romanescu, G., & Zeleňáková, M. (Eds.). (2020). Water resources management in Balkan countries. Springer International Publishing.
- Nikolaou, G., Neocleous, D., Christou, A., Kitta, E., & Katsoulas, N. (2020). Implementing sustainable irrigation in water-scarce regions under the impact of climate change. *Agronomy*, 10(8), 1120.
- Nwaogu, J.M., Yang, Y., Chan, A.P., & Chi, H.L. (2023). Application of drones in the architecture, engineering, and construction (AEC) industry. *Automation in Construction*, 150, 104827.
- OECD. (2022, July 13). Closing the loop in the Slovak Republic. <https://doi.org/10.1787/acadd43a-en>
- OECD. (2023, March 21). Implementing Water Economics in the EU Water Framework Directive. Organization for Economic Cooperation and Development. <https://doi.org/10.1787/d6abda81-en>
- OECD. 2024. Water and agriculture. Available at: <https://www.oecd.org/agriculture/topics/water-and-agriculture/>
- Oliveira, H., & Bonito, J. (2023, May). Practical work in science education: a systematic literature review. In *Frontiers in Education*, 8, 1151641.
- Page, M.J., McKenzie, J.E., Bossuyt, P.M. et al. (2021). The PRISMA 2020 statement: an updated guideline for reporting systematic reviews. *Syst Rev*, 10, 89. <https://doi.org/10.1186/s13643-021-01626-4>.
- Pradhan, P., Callaghan, M., Hu, Y., Dahal, K., Hunecke, C., Reußwig, F., ... & Kropp, J. P. (2023). A systematic review highlights that there are multiple benefits of urban agriculture besides food. *Global Food Security*, 38, 100700.
- Robles, Á., Serralla, J., Martí, N., Ferrer, J., & Seco, A. (2021, January 1). Anaerobic membrane bioreactors for resource recovery from municipal wastewater: a comprehensive review of recent advances. *Royal Society of Chemistry*, 7(11), 1944-1965. <https://doi.org/10.1039/d1ew00217a>.
- Rosa, L., Chiarelli, D. D., Rulli, M.C., Dell'Angelo, J., & D'Odorico, P. (2020). Global agricultural economic water scarcity. *Science Advances*, 6(18), eaaz6031.
- Rowe, F., Kanita, N., & Walsh, I. (2023). The importance of theoretical positioning and the relevance of using bibliometrics for literature reviews. *Journal of Decision Systems*, 1-16.
- Salehi, M. (2022). Global water shortage and potable water safety; Today's concern and tomorrow's crisis. *Environment International*, 158, 106936.
- Sandu, M.A., Vladasel (Pasarescu), A.C., Pienaru, A.M. (2023). Embedding low carbon emission into the water infrastructure. *Scientific Papers. Series E. Land Reclamation, Earth Observation & Surveying, Environmental Engineering*, 12, Print ISSN 2285-6064, 52-59.
- Sandu, M.A., Virsta, A. (2021). The water footprint in context of circular economy. *AgroLife Scientific Journal*, 10(2).
- Sismani, G., Pisinaras, V., & Arampatzis, G. (2024). Water Governance for Climate-Resilient Agriculture in Mediterranean Countries. *Water*, 16(8), 1103.
- Smol, M., Adam, C., & Preisner, M. (2020). Circular economy model framework in the European water and wastewater sector. *Journal of Material Cycles and Waste Management*, 22, 682-697.
- Sordo-Ward, A., Granados, A., Iglesias, A., Garrote, L., & Bejarano, M. D. (2019). Adaptation effort and

- performance of water management strategies to face climate change impacts in six representative basins of Southern Europe. *Water*, 11(5), 1078.
- Timofti, M., & Pienaru, A.M. (2022). The current state of water in circular economy in Romania. *Scientific Papers. Series E. Land Reclamation, Earth Observation & Surveying, Environmental Engineering*, 11, Print ISSN 2285-6064.
- Trică, C.L., Bănașu, C.S., & Bușu, M. (2019, February 20). Environmental Factors and Sustainability of the Circular Economy Model at the European Union Level. Multidisciplinary Digital Publishing Institute, 11(4), 1114-1114. <https://doi.org/10.3390/su11041114>
- United Nations. (2024). The United Nations World Water Development Report 2024: Water for Prosperity and Peace. UNESCO, Paris.
- Van Eck, N.J., Waltman, L., Dekker, R., van den Berg, J. (2010). A comparison of two techniques for bibliometric mapping: Multidimensional scaling and VOS. *Journal of the American Society for Information Science and Technology*, 61(2), 2405-2416.
- Water Europe. (2024). <https://watereurope.eu/water-vision>, accessed on 25.05.2024.
- Web of Science. (2024). Web of Science platform.
- Yusuf, A., Sodiq, A., Giwa, A., Eke, J., Pikuda, O., De Luca, G., ... & Chakraborty, S. (2020). A review of emerging trends in membrane science and technology for sustainable water treatment. *Journal of cleaner production*, 266, 121867.
- Zahoor, I., & Mushtaq, A. (2023). Water pollution from agricultural activities: A critical global review. *Int. J. Chem. Biochem. Sci.*, 23(1), 164-176.
- Zhang, S., Wu, Y., & Xu, B. (2023). Rational utilization of water resources to promote sustainable development of rural ecotourism. *Water Supply*, 23(9), 3844-3855.
- Zimková, E., Gurčíková, P., Vidiečanová, M., Pintér, L. U., & Lawson, C. (2023). Efficiency Evaluation of Water Sector in the Czech Republic: Two-Stage Network Dea. *Statistika*, 103(4), 462-475.

TEMPORAL VARIATION AND RELATIONSHIP BETWEEN HYDROLOGICAL PARAMETERS AND WATER POLLUTANTS ON THE LOWER DANUBE, ROMANIA

Maxim ARSENI^{1,3}, Valentina-Andreea CALMUC³, Madalina CALMUC³,
Stefan-Mihai PETREA^{2,3}, Adrian ROSU^{1,3}, Eugen BUSILA⁴,
Catalina ITICESCU^{1,3}, Puiu-Lucian GEORGESCU^{1,3}

¹"Dunarea de Jos" University of Galati, Faculty of Sciences and Environment,
111 Domneasca Street, Galati, Romania

²"Dunarea de Jos" University of Galati, Faculty of Food Science and Engineering,
111 Domneasca Street, Galati, Romania

³"Dunarea de Jos" University of Galati, REXDAN Research Infrastructure,
98 George Cosbuc Street Galati, Romania

⁴Trigen S.R.L., 36 Otelarilor Street, Galati, Romania

Corresponding author email: maxim.arseni@ugal.ro

Abstract

The interaction between hydrological parameters and aquatic quality parameters is important nowadays for integrated analysis of the status of an aquatic ecosystem. Discharge, flow speed, current direction, and water level represent some of the most important river parameters that can provide valuable information about the health and integrity of the ecosystem. At the same time, through an interdisciplinary approach that includes water pollution parameters, the status of the ecosystem can be analyzed in an integrated manner. A river's flow can influence how pollutants are transported and dispersed. The study carried out on the Lower Danube River part aims for an integrated analysis of these parameters, to establish the behavior of water pollutants according to hydrological parameters. The results show an accumulation of high values of CCO and NH_4^+ in areas where the hydrological regime of the river is attenuated, water flow decreases and where the banks are less steep. By integrating data on hydrological parameters with water quality results we can contribute to the development of effective environmental management strategies to protect and conserve natural resources.

Key words: ADCP, pollutants dispersion, river discharge, Sound Velocity Profiler, water quality.

INTRODUCTION

The application of traditional methods of assessing the quality of water and the correspondence with hydrological parameters, through determining chemical, biological, and physical parameters cannot fully cover all the questions (Albaggar, 2021). From this perspective, different methods are developed based on the interconnection and interdependence of the biotic indicators of the aquatic ecosystem and the characteristics of the habitat of the aquatic biota. The methods of estimating the quality of water and the ecological state of water ecosystems, used in the practice of water management, are based on the determination of chemical, biological, and physical indicators. The joint application of physical, chemical, and biological methods

allows for a quantitative analysis of the state of the ecosystem as a whole. However, in many cases, it is impossible, for example, when planning measures for the use and protection of water resources on a large-scale area, where the strategy of using water parameters for a perspective period is considered in the scale of river section, river basin or country region (Salih et al., 2021). Due to its scale and multifactorial nature, this task is quite complex. A large amount of initial data is required, especially those that characterize the quality of water (concentrations of pollutants, hydrobiological indicators, hydrological parameters), while the information is necessary for different models of the water quality in different years (Islam et al., 2021). The situation is exacerbated by the necessity of forecasting the influence of

anthropogenic activity on water ecosystems, especially trans-border water systems.

For this study, a proper water body is given by the lower course of the Danube River. This river section allows analysis of the correlation between physicochemical parameters and hydromorphological indicators, in terms of anthropogenic influence on a cross-border area (Iticescu et al., 2019; Radu et al., 2020).

The presented method allows for predicting the quality of water and the environmental condition of rivers using available information about the discharge, water velocity, and some river pollutants.

The study area is situated between 45°15'20" and 45°28'35" North Latitude and 28°00'29" 28°30'2" East Longitude. The total length of the river section is 57 km, with a medium width of 650m. For the water quality and hydromorphological assessment, 10 sampling points were established in the field (Figure 1). To assess the influence of tributaries, two points were established on the Siret and Prut rivers.

MATERIALS AND METHODS

Sampling and survey step

Water was sampled from all 10 points and was made hydrological transects for discharge and flow velocity.

Water sampling was made with a telescopic surface water sampler with a biodegradable bottle (Figure 2). The Swing Sampler enables it to reach out up to 3 m from river banks to take a 1.0 L surface water sample. At the same time, different in-situ parameters were recorded: ph, conductivity, salinity, turbidity, and dissolved oxygen (DO).

Discharge measurement

Bathymetry is a branch of hydrology and is defined as a method that deals with the determination of depths in seas, lakes, rivers, streams, and canals, resulting in the creation of maps and bathymetric sections similar to topographical maps, highlighting the underwater relief (Banescu et al., 2020; Bănescu et al., 2019).

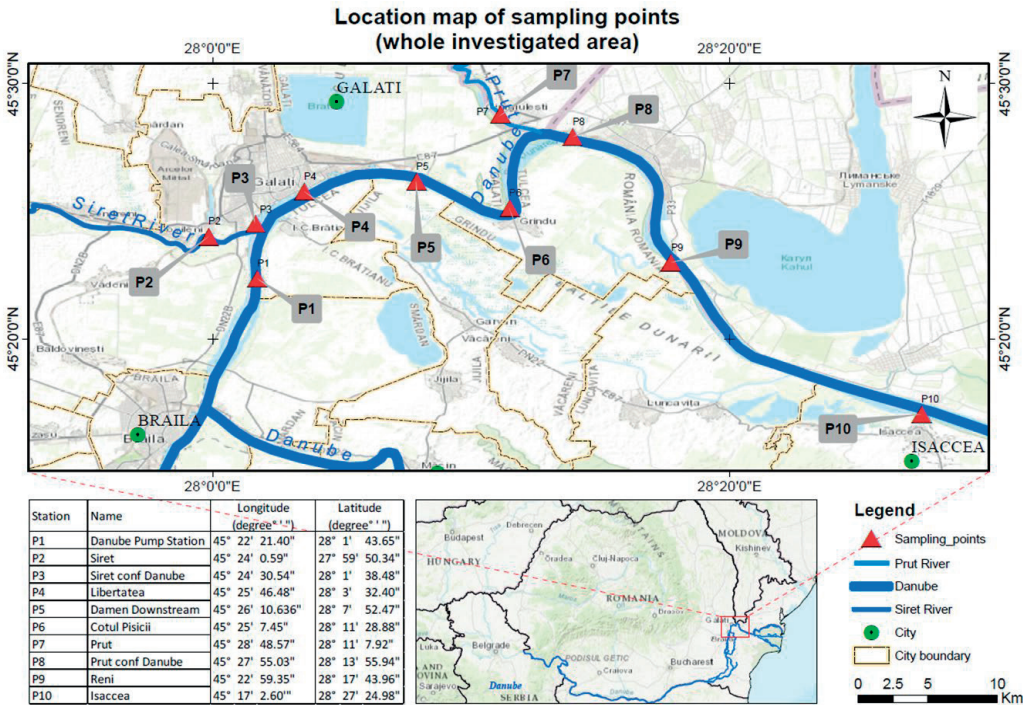


Figure 1. Location map of sampling and surveyed points



Figure 2. Water sampling and in situ water quality measurements

Currently, single-beam and multibeam sonar systems are used for bathymetric measurements. Sonar sends an acoustic wave from the bottom of a boat to the bottom of the water. One is reflected in the transponder. The time required for the sound wave to be sent and received determines the topography of the water bottom. The longer the time, the deeper water.

ADCP (Acoustic Doppler Current Profile) equipment is used to perform simultaneous measurements of discharge, flow velocities, and depth (Iuliana et al., 2022). This type of equipment is specially intended for measuring the flow rates, currents, depths, and bathymetry of rivers, channels, in various aquatic environments. The equipment can be used both from stationary vessels and from small and medium-sized boats in motion. One such equipment is the RiverSurveyor M9 ADCP system (Moradi et al., 2019), which is used to carry out the bathymetric measurement activity within the project (Figure 3). This equipment offers the possibility of determining the previously specified hydrological parameters. The system combines the acoustic Doppler mode for velocity profiles with a Windows-compatible software package that can be used on a personal computer (PC) or mobile device (smartphone).



Figure 3. The M9 ADCP principal components

The bathymetric system is composed of the following basic components:

1) The M9 ADP complex system – represents a system with nine fascicles with two sets of four fascicles each for profiling (each set with its frequency) and one vertical fascicle. The M9 has a profiling range for velocities up to 40 m depth and a flow measurement range up to 80 m (when using GPS and vertical beam) (Arseni et al., 2022). Using the acoustic multi-frequency with precise band control, high-precision measurements are obtained and measurements can be made both on rivers and canals, starting from small depths (< 25 cm) to large depths (> 70 m). The M9 ADP module is equipped with a specialized microcontroller that automatically selects the appropriate acoustics and pulse schemes as it is crossed, or the transversal profile of a channel (bad) is created. The 9th beam is the fast-sampling, low-frequency vertical beam that extends the maximum measuring depth of the equipment and provides a superior definition of the channel surface for flow and bathymetry measurements.

2) The PCM module – represents the Power Supply and Communication Module that connects directly to the M9 ADP instrument, through a battery pack. It supplies power to the ADP and allows remote communication with a PC or a mobile device via a radio signal.

3) GNSS receiver - represents the equipment that allows positioning with a precision of less than 50 cm, using SBAS technology, through connection with the DGPS option. It is also connected to the PCM module. The DGPS data is received by the PCM at a frequency of 10 Hz and transferred to the internal memory of the ADP system for integration and processing.

4) Hydroboard II – represents the floating board that was specially created to be used together with the M9 ADP system and components. It is provided with a vertical mounting system for the M9 ADP system and the PCM mode.

A measurement in a transect made by a boat crossing from one bank to the other is divided into two key components: the starting edge, the transect, and the ending edge. So the total flow is calculated by summing the Start Edge, Top Estimate, Measured Area, Bottom Estimate, and

End Edge values (Figure 4) (Rennie & Rainville, 2008; Vermeulen et al., 2014).

Only the Measured Area is measured by the acoustic Doppler system, with the Start Edge and End Edge areas being estimated by automatic calculations (Figure 4).

The measurement limitations of the ADP system are imposed by several factors, such as the existence of a minimum depth at which the profiler can operate (for depths lower than the minimum operating value, the water speed and implicitly the flow must be estimated, based on the speed and the depth from the banks); the mounting depth plus a small distance (called the blind distance) from the instrument to the profile where the velocity measurement starts, leave a section of water from the surface (Figure 5), unmeasured (this surface is called the Top Estimate); possible contamination of the data from the last cell (e.g. the cell partially or completely touches the river bed) or the possible appearance of interference at the end of the profile, leaves a section from the bottom of the water unmeasured (called Bottom Estimate).

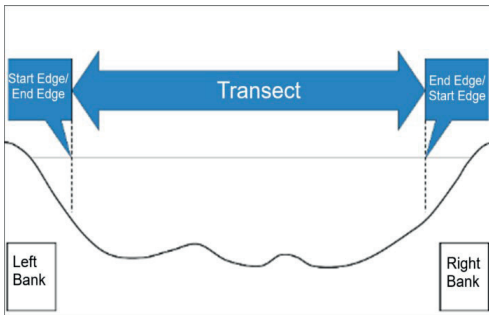


Figure 4. The generally divided sections of an M9 ADCP survey from an entire river cross-section

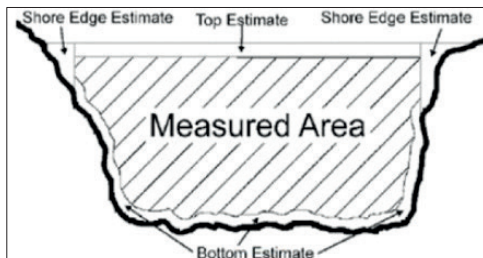


Figure 5. The measured area representation with Top, Bottom, and left/right Edge estimation

The measurement of flows, speed, and depth with RiverSurveyor M9 ADCP equipment consists of the following work steps:

a) mounting/attaching the RiverSurveyor equipment to a boat - the equipment can be mounted directly on the boat or attached to its side, to take measurements (Figure 6).

b) configuring the main settings of the equipment - this stage consists of checking all the basic settings and functional parameters of the equipment (checking the power supply, DGPS connection, and radio transmission, calibrating the compass, making a recording in test mode, checking the water temperature measurement, checking the records given by each cell, the introduction after pre-measurement tests of the initial data of the project).

The Velocity Profile Extrapolation technique is used to estimate the unmeasured values and is used to estimate the unmeasured areas from the base and surface. Velocity Profile Extrapolation uses an accredited velocity profile, proposed by Chen (1991), for the calculation of velocities above and below the Measured Area. The extrapolation is calculated using the next equation:

$$\frac{u}{u_*} = 9.5 * \left(\frac{z}{z_0}\right)^b \quad (1)$$

where:

- u represents the velocity at height z , measured from the base of the channel;
- u^* is the bottom shear velocity; z_0 is the height of the base roughness;
- b is a constant (equal to 1/6, according to Chen, 1991).

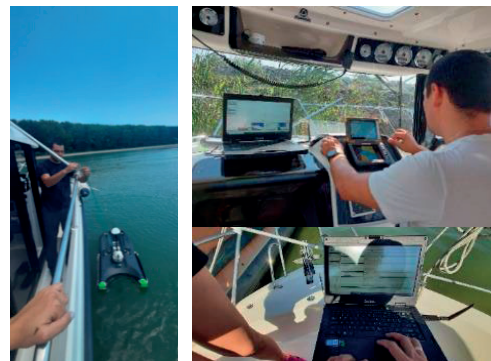


Figure 6. Basic configuration for data collecting of M9 ADCP system

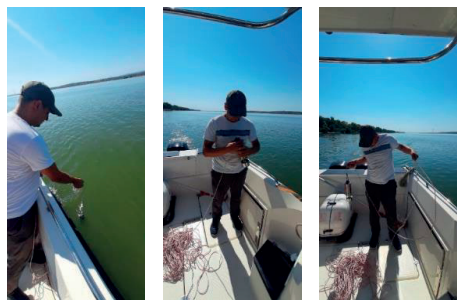


Figure 7. The survey with Swift SVP equipment

Sound velocity in water measurements

The ADCP survey was calibrated and adjusted with an in-situ survey of the following parameters: Sound velocity in water, Pressure, Temperature, Salinity, Conductivity, and Density. All these parameters were measured in situ with a Sound Velocity Profiler, produced by Valeport, model SVP Swift Profiler (Figure 7). The SWiFT profiler is available for survey in two main forms – SVP and CTD. The SVP is fitted with sound velocity, temperature, and pressure sensors, the CTD is fitted with conductivity, temperature, and pressure sensors. Configuration and data download is via dedicated Valeport Ocean software to a PC or mobile device. The downcast mode of survey was used, by 1m trigger interval (Figure 8).

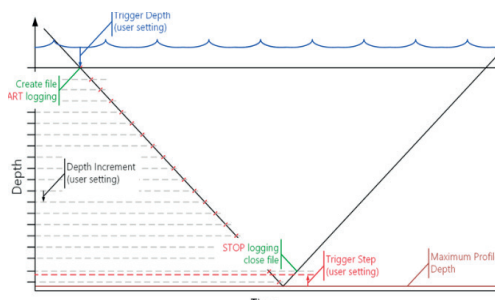


Figure 8. The downcast method of the SVP survey

RESULTS AND DISCUSSIONS

For the validation of the discharge measurements and the final flow rate, a series of at least 4 measurements were made in the same transect profile. Thus, those measurements were chosen that are very close, eliminating determinations with high deviation from the compared profiles.

For the determination of discharges and flow velocities, measurements were made with the ADCP equipment at each sampling point P1-P10, during 2 periods: July 2022 and October 2022. Next, the main results expressed graphically, for both bathymetric measurement campaigns, of flow velocities and flow rates for each sampling point are presented (Figure 9).

Table 1 presents the values data of discharge (Q), water level at Galati and Isaccea hydrometric station (WL_{GL}, WL_{IS}), maximum water velocity (V_{max}), mean water velocity (V_{avg}), maximum measured depth (D_{max}) and measured cross-section width (W).

The normalization of distance from the streambed, by separating each segment of the cross-section into 5 percent, ranging from 0.05 to 1, shows the deviation of discharge and depth data (Figures 10 and 11). The median value was used to represent each discharge section. Only medians with sufficient points were utilized to compute extrapolation for non-measured depth cells, using the 20% thresholds (Roşu et al., 2022). By breaking the cross-section into smaller parts and normalizing the distance, we effectively create a consistent framework for comparing data regardless of the section's exact size. The result of normalization show a deviation from median between 0.1 to 0.8.

The results of the 10 physico-chemical parameters of water quality (BOD₅, CCO, Cl⁻, Fe²⁺, N-total, NH₄⁺, N-NO₂, N-NO₃, P-PO₄, SO₄²⁻) analyzed ex situ using electrochemical and spectrophotometric methods following the standards in force and combined with the results of in-situ parameters (pH, conductivity, turbidity, dissolved oxygen,) were introduced in a mathematical model and computed for dispersion in the entire river section. By applying the ADCP survey results the dispersion model was calibrated.

The hydrological dispersion of water quality parameters shows how these move across a river channel. It takes into consideration both advection (moving with the flow of the river) and dispersion (spreading caused by turbulence or mixing) (Ciucure et al., 2023; Simionov et al., 2023).

The equation can be expressed as:

$$\frac{\partial P}{\partial t} + v_{avg} \frac{\partial P}{\partial d} = D \frac{\partial^2 P}{\partial d^2} \quad (2)$$

where:

- P is the physico-chemical parameter concentration being transported;
- t is time; d is the distance along the river channel;
- v_{avg} is the mean velocity of the flow;

- D is the dispersion coefficient.

The maps from Figures 12 to 22 represent the geospatial dispersion of water quality parameters for the July and October survey campaigns (left respectively right image).

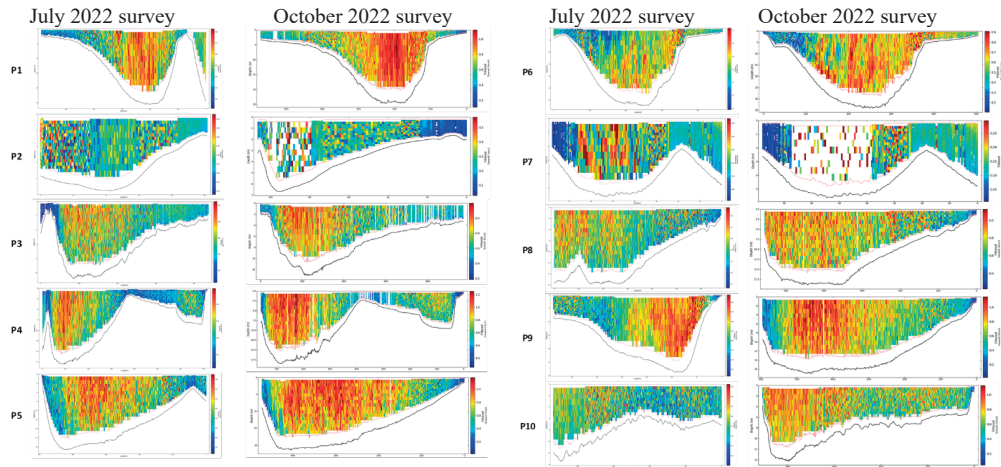


Figure 9. The flow velocity graphs obtained after the ADCP M9 transects was adjusted with SVP info

Table 1. The main surveyed hydromorphological parameters for the July and October 2022 campaign

Station	July 2022 campaign							October 2022 campaign						
	Q [mc/s]	WL_{GL} [m]	WL_{IS} [m]	V_{max} [m/s]	V_{avg} [m/s]	D_{max} [m]	W [m]	Q [mc/s]	WL_{GL} [m]	WL_{IS} [m]	V_{max} [m/s]	V_{avg} [m/s]	D_{max} [m]	W [m]
P1 (Danube)	2916	0.79	0.80	1.080	0.518	25.827	569	4839	2.28	1.76	1.291	0.766	24.628	590
P2 (Siret)	53			0.607	0.242	4.814	98	91			0.750	0.234	6.869	109
P3 (Danube)	2854			1.460	0.520	24.011	952	4851			1.547	0.703	13.071	1041
P4 (Danube)	2943			1.302	0.485	18.428	715	4968			1.556	0.719	18.649	775
P5 (Danube)	2944			1.132	0.495	20.917	424	5138			1.326	0.745	21.377	491
P6 (Danube)	2851			1.002	0.386	32.380	525	4640			1.127	0.536	33.838	559
P7 (Prut)	30			0.645	0.115	5.701	74	33			0.648	0.119	5.786	77
P8 (Danube)	2949			1.048	0.481	17.509	617	4926			1.318	0.729	18.850	581
P9 (Danube)	3002			1.078	0.511	29.498	344	4908			1.366	0.718	16.941	545
P10(Danube)	2976			1.310	0.530	13.867	773	4941			1.357	0.662	14.255	895

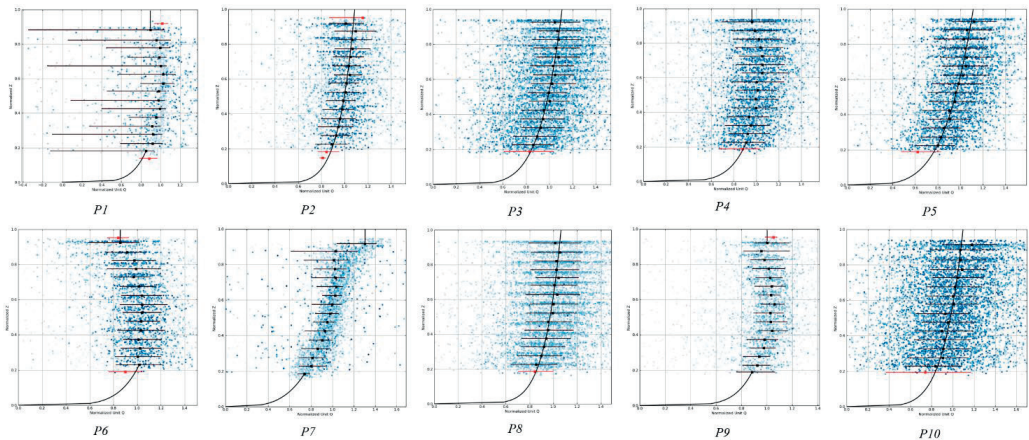


Figure 10. The extrapolation statistical analysis depends on medians for depth data of each beam cell, for transects measured in the July 2022 survey campaign for P1 to P10 sampling station

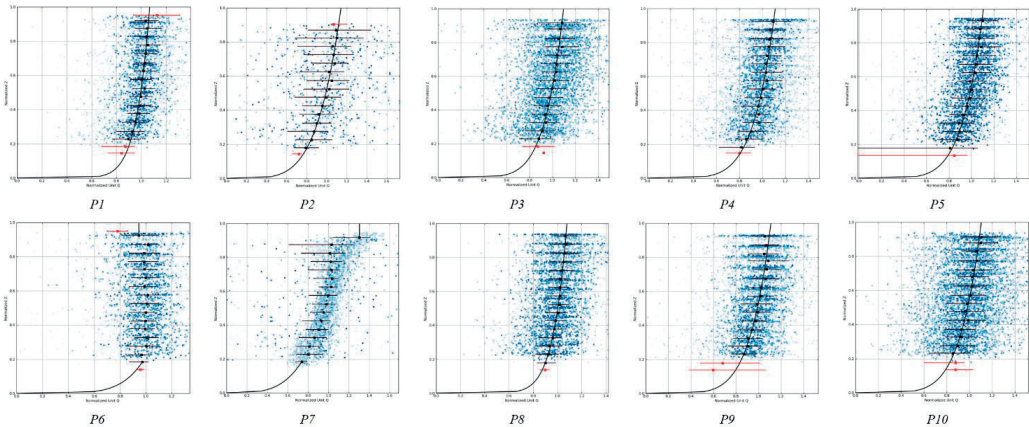


Figure 11. The extrapolation statistical analysis depends on medians for depth data of each beam cell, for transects measured in the October 2022 survey campaign for P1 to P10 sampling station

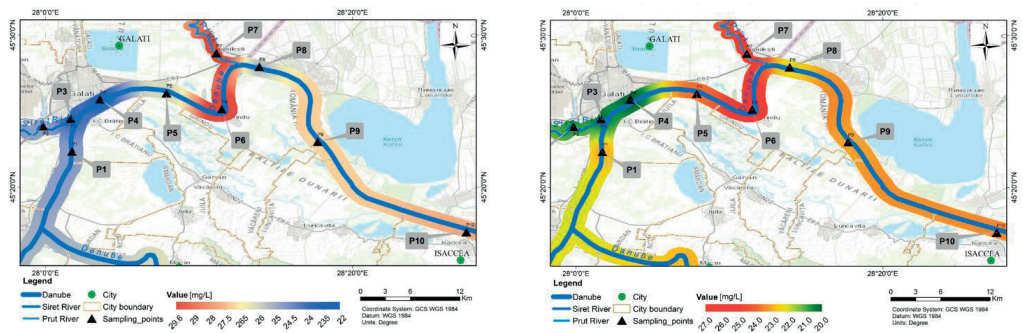


Figure 12. The dispersion map of BOD₅

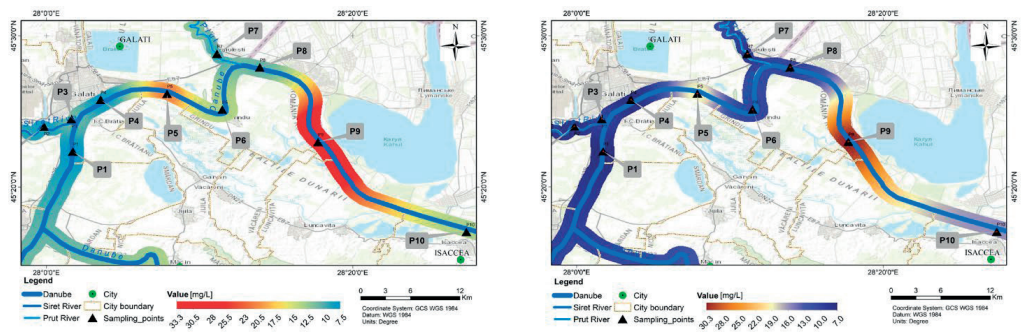


Figure 13. The dispersion map of CCO

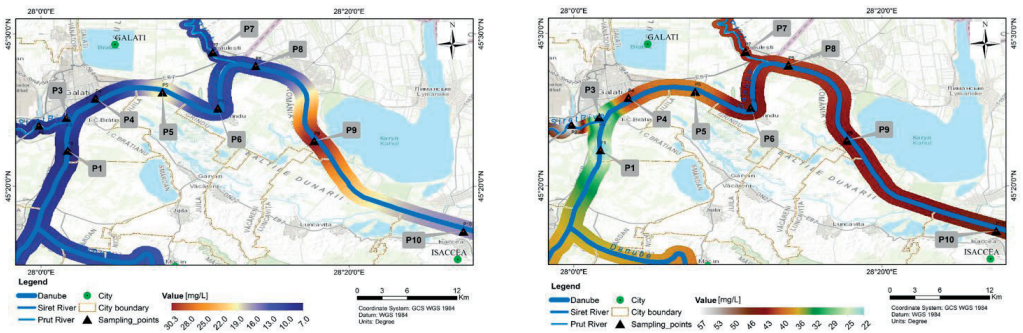


Figure 14. The dispersion map of Cl⁻

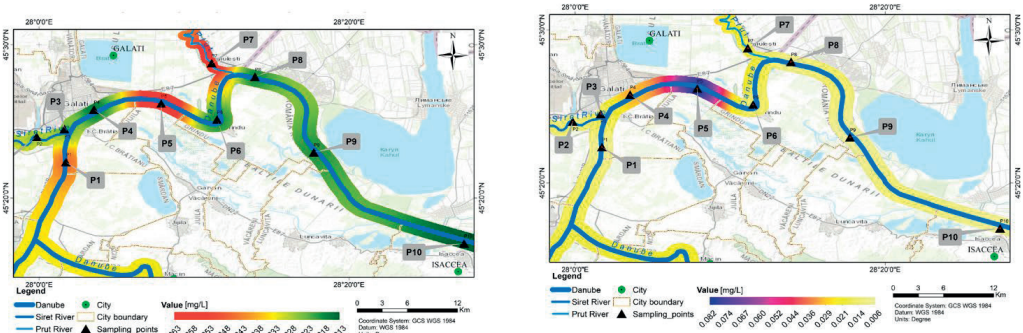


Figure 15. The dispersion map of Fe₂⁺

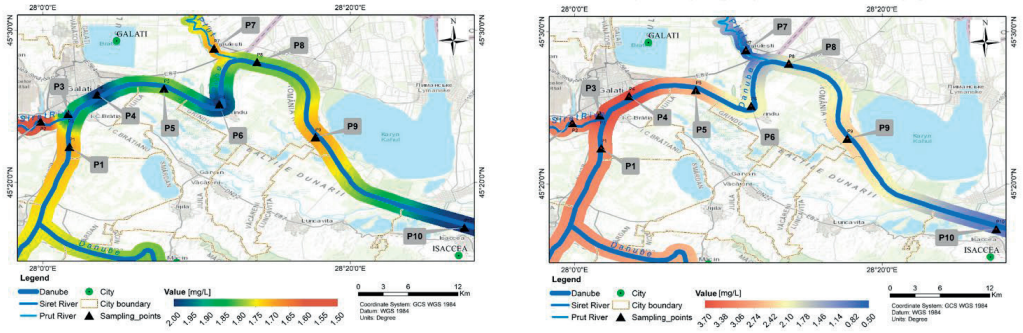


Figure 16. The dispersion map of N-total

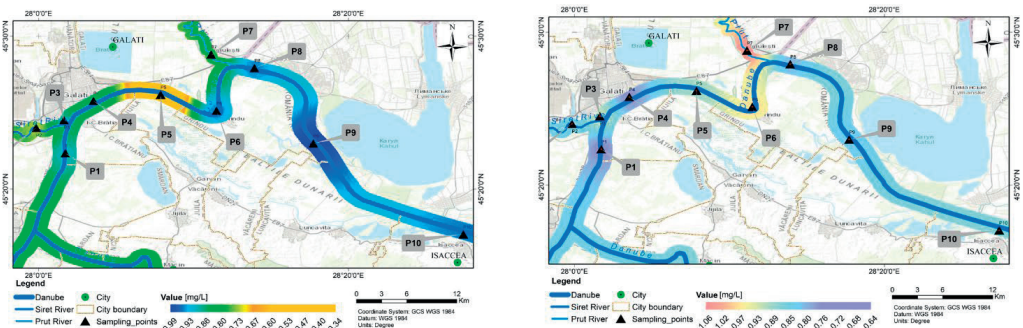


Figure 17. The dispersion map of NH_4^+

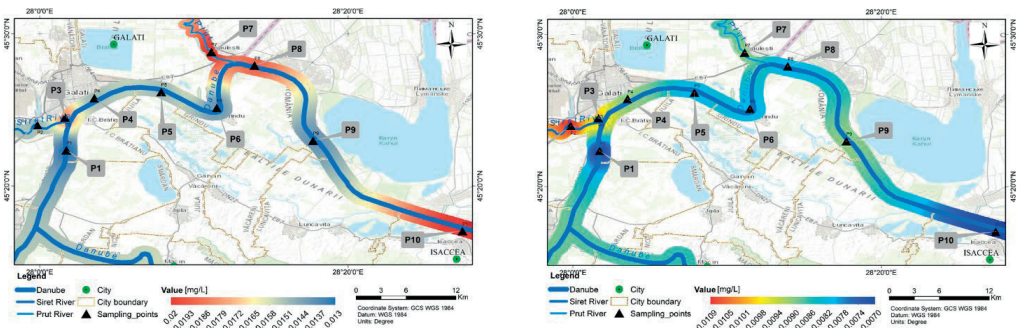


Figure 18. The dispersion map of N-NO_2

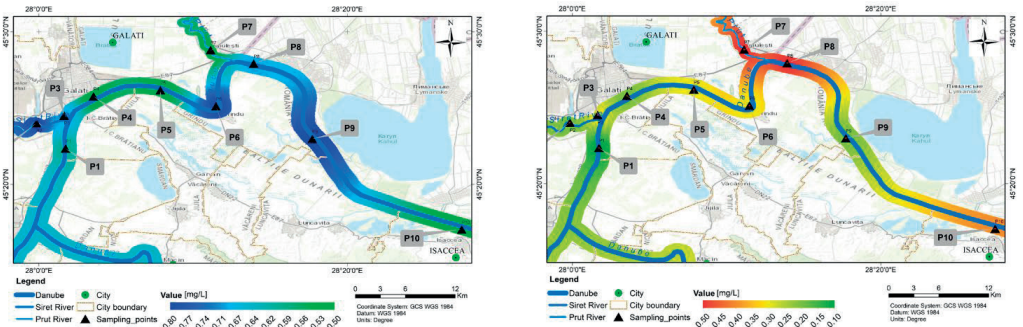


Figure 19. The dispersion map of N-NO_3

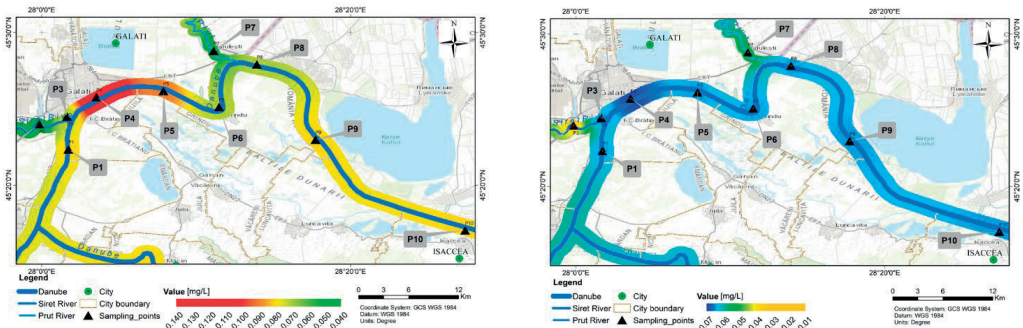


Figure 20. The dispersion map of P-PO_4

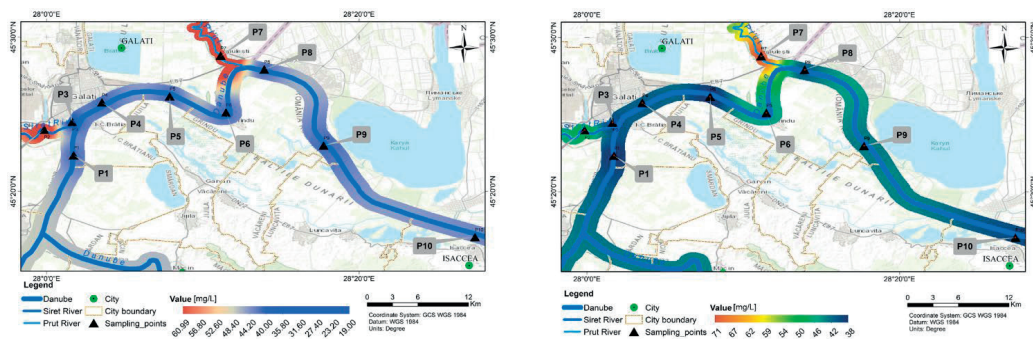


Figure 21. The dispersion map of SO_4^{2-}

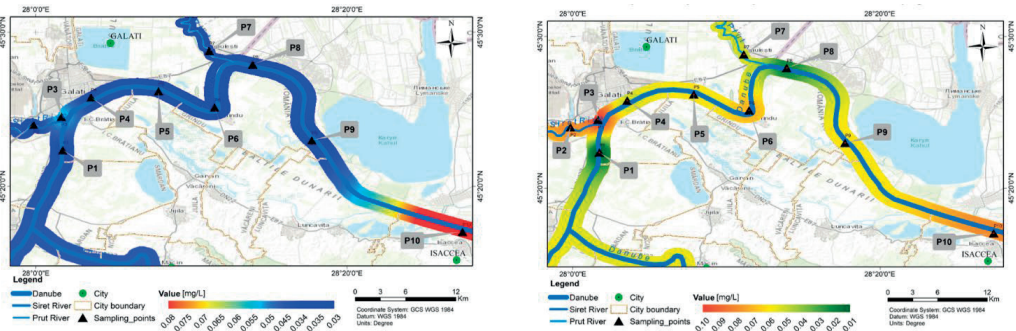


Figure 22. The dispersion map Phenols

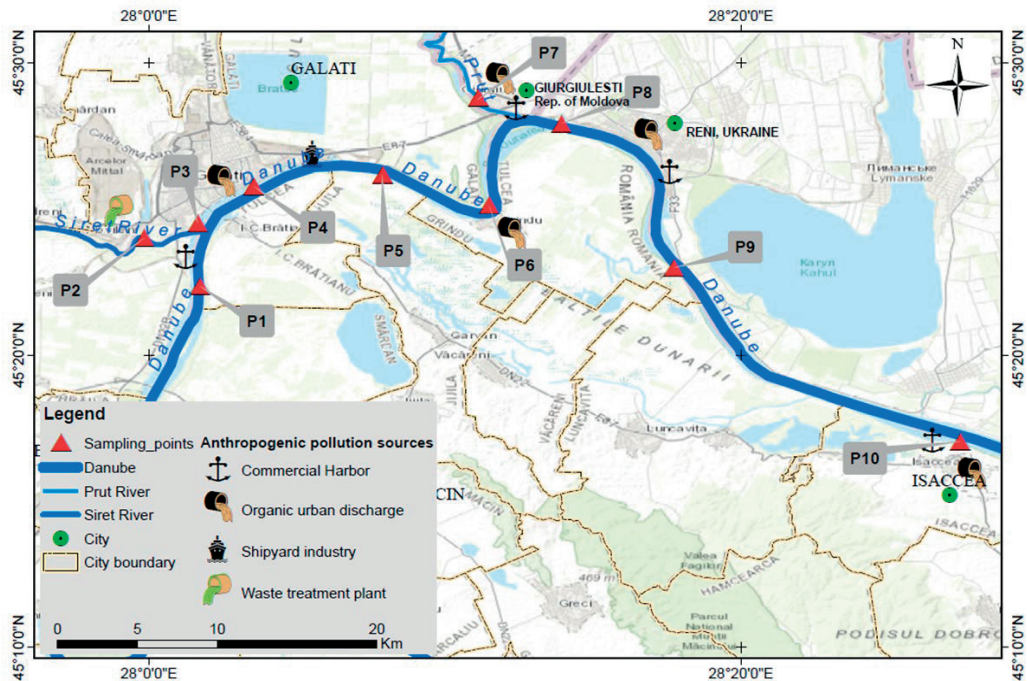


Figure 23. Location map of anthropogenic pollution sources

CONCLUSIONS

By analyzing the deviation of discharge and depth data within each segment, we can identify patterns such as areas of high variability or consistency vertically within the stream. This information can be crucial for understanding the flow dynamics and geomorphology of the stream, which is valuable for various applications such as hydraulic engineering, ecology, and water resource management.

ADCP system can measure water currents at multiple depths simultaneously, providing a comprehensive picture of current profiles over a vertical section. At the same time, it can provide real-time or near-real-time data, allowing researchers and scientists to monitor and respond to changes in current patterns promptly. Calibrating discharge measurements with a speed of sound in a water profiler is essential for improving the accuracy, reliability, and interpretability of hydrological data. From the calibrated results the maximum depth was at cross-section P9 (29.498m). The maximum discharge was recorded at the P9 cross-section in July campaign, and at P8 in October campaign. The hydromorphological form of cross-section shows that the speed of water decreases near banks, which means that the water pollutants accumulate more in these areas.

The dispersion map of physico-chemical parameters indicates fluctuation of values between stations. These are influenced by the anthropogenic activities (Figure 22). At the same time there are fluctuations between values caused by seasonal time variation. These seasonal variations are influenced by the climate change indicator (Voiculescu et al., 2020), such as water and air temperature, humidity, air pressure.

In conclusion, the dispersion map shows a direct correlation between water velocity and pollutant transport. The slower water velocities result in longer retention times, allowing pollutants more time to settle or be taken up by aquatic organisms, potentially reducing dispersion. However, stagnant or slow-moving water can also lead to localized accumulation of pollutants. On the other hand, higher water velocities can carry pollutants further downstream, increasing the spatial extent of pollution.

ACKNOWLEDGEMENTS

The work of Adrian ROSU, Madalina CALMUC, Eugen BUSILA, Catalina ITICESCU, Puiu-Lucian GEORGESCU and Mihai-Stefan PETREA was supported by the project *An Integrated System for the Complex Environmental Research and Monitoring in the Danube River Area*, REXDAN, 309/10.07.2021, and the work of Maxim ARSENI, Valentina-Andreea CALMUC, was supported by the project *Advanced nanotechnology based approaches to waste water purification from organic pollutants and their monitoring in water bodies*, 2SOFT/1.2/139.

REFERENCES

- Albaggar, A.K.A. (2021). Investigation of some physical, chemical, and bacteriological parameters of water quality in some dams in Albaha region, Saudi Arabia. *Saudi Journal of Biological Sciences*, 28(8), 4605–4612.
- Arseni, M., Rosu, A., Petrea, Ș.-M., Calmuc, M., Rosu, B., Constantin, D.-E., Iticescu, C., & Georgescu, P.-L. (2022). The positive effects of channels restoration in the Danube Delta Biosphere Reserve. *Scientific Papers. Series E. Land Reclamation, Earth Observation & Surveying, Environmental Engineering*, 11. <https://www.landreclamationjournal.usamv.ro/pdf/2022/Art39.pdf>
- Bănescu, A., Arseni, M., Georgescu, L.P., Rusu, E., & Iticescu, C. (2020). Evaluation of different simulation methods for analyzing flood scenarios in the Danube Delta. *Applied Sciences*, 10(23), 8327.
- Bănescu, A., Georgescu, L.P., Iticescu, C., & Rusu, E. (2019). Use of GIS technology in flood risk analysis. Case study Mila 23 locality from the Danube Delta. *Analele Universității "Dunărea de Jos" Din Galați. Fascicula II, Matematică, Fizică, Mecanică Teoretică/Annals of the "Dunarea de Jos" University of Galati. Fascicle II, Mathematics, Physics, Theoretical Mechanics*, 42(1), 77–84.
- Chen, C. (1991). Unified Theory on Power Laws for Flow Resistance. *Journal of Hydraulic Engineering*, 117(3), 371–389. [https://doi.org/10.1061/\(ASCE\)0733-9429\(1991\)117:3\(371\)](https://doi.org/10.1061/(ASCE)0733-9429(1991)117:3(371))
- Ciucure, C.T., Geana, E.-I., Arseni, M., & Ionete, R.E. (2023). Status of different anthropogenic organic pollutants accumulated in sediments from Olt River Basin, Romania: From distribution and sources to risk assessment. *Science of The Total Environment*, 886, 163967.
- Islam, Md.S., Idris, A.M., Islam, A.R. Md.T., Ali, M.M., & Rakib, Md. R.J. (2021). Hydrological distribution of physicochemical parameters and heavy metals in surface water and their ecotoxicological implications in the Bay of Bengal coast of Bangladesh. *Environmental Science and Pollution Research*,

- 28(48), 68585–68599. <https://doi.org/10.1007/s11356-021-15353-9>
- Iticescu, C., Georgescu, L.P., Murariu, G., Topa, C., Timofti, M., Pintilie, V., & Arseni, M. (2019). Lower Danube water quality quantified through WQI and multivariate analysis. *Water*, 11(6), 1305.
- Iuliana, N.I., Simionov, M., Constantinescu, A., & Nichersu, I. (2022). *Water circulation system data analysis in fluvio-maritime Danube Delta*. 25. http://www.ddniscientificannals.ddni.ro/images/25_15.pdf
- Moradi, G., Vermeulen, B., Rennie, C.D., Cardot, R., & Lane, S.N. (2019). Evaluation of aDcp processing options for secondary flow identification at river junctions. *Earth Surface Processes and Landforms*, 44(14), 2903–2921. <https://doi.org/10.1002/esp.4719>
- Radu, V.-M., Ionescu, P., Deak, G., Diacu, E., Ivanov, A.A., Zamfir, S., & Marcus, M.-I. (2020). Overall assessment of surface water quality in the Lower Danube River. *Environmental Monitoring and Assessment*, 192(2), 135. <https://doi.org/10.1007/s10661-020-8086-8>
- Rennie, C.D., & Rainville, F. (2008). Improving Precision in the Reference Velocity of ADCP Measurements Using a Kalman Filter with GPS and Bottom Track. *Journal of Hydraulic Engineering*, 134(9), 1257–1266. [https://doi.org/10.1061/\(ASCE\)0733-9429\(2008\)134:9\(1257\)](https://doi.org/10.1061/(ASCE)0733-9429(2008)134:9(1257))
- Roșu, A., Arseni, M., Roșu, B., Petrea, Ștefan-M., Iticescu, C., & Georgescu, P.L. (2022). Study of the influence of manning parameter variation for waterflow simulation in Danube Delta, Romania. *Scientific Papers. Series E. Land Reclamation, Earth Observation & Surveying, Environmental Engineering*, 11. <https://www.landreclamationjournal.usamv.ro/pdf/2022/Art46.pdf>
- Salih, S.Q., Alakili, I., Beyaztas, U., Shahid, S., & Yaseen, Z.M. (2021). Prediction of dissolved oxygen, biochemical oxygen demand, and chemical oxygen demand using hydrometeorological variables: Case study of Selangor River, Malaysia. *Environment, Development and Sustainability*, 23(5), 8027–8046. <https://doi.org/10.1007/s10668-020-00927-3>
- Simionov, I.-A., Călmuc, M., Iticescu, C., Călmuc, V., Georgescu, P.-L., Faggio, C., & Petrea, Ș.-M. (2023). Human health risk assessment of potentially toxic elements and microplastics accumulation in products from the Danube River Basin fish market. *Environmental Toxicology and Pharmacology*, 104, 104307.
- Vermeulen, B., Sassi, M.G., & Hoitink, A.J.F. (2014). Improved flow velocity estimates from moving-boat ADCP measurements. *Water Resources Research*, 50(5), 4186–4196. <https://doi.org/10.1002/2013WR015152>
- Voiculescu, M., Constantin, D.-E., Condurache-Bota, S., Călmuc, V., Roșu, A., & Dragomir Bălănică, C.M. (2020). Role of meteorological parameters in the diurnal and seasonal variation of NO₂ in a Romanian urban environment. *International Journal of Environmental Research and Public Health*, 17(17), 6228.

EVALUATION OF MICROBIAL AND CHEMICAL INDICATORS AS A MEASURE OF THE DEGREE OF POTABILITY OF WATER

Aurica Breica BOROZAN¹, Sorina POPESCU¹, Delia Gabriela DUMBRĂVĂ¹,
 Diana Nicoleta RABA¹, Mirela Viorica POPA¹, Corina Dana MIȘCĂ¹,
 Carmen Daniela PETCU², Despina Maria BORDEAN¹, Camelia MOLDOVAN¹

¹University of Life Sciences "King Mihai I" from Timisoara,
 119 Calea Aradului, Timisoara, Romania

²University of Agronomic Sciences and Veterinary Medicine of Bucharest,
 Faculty of Veterinary Medicine, 105 Splaiul Independentei, Bucharest, Romania

Corresponding author email: miscacorina@gmail.com

Abstract

The quality of drinking water is a challenge for consumers and scientists in our century. The bacterial diseases and deaths recorded in recent years, as a result of the consumption of fecal-contaminated water, are reasons for concern and microbiological evaluation of water in all populated areas on Earth. In this paper, microbiological and chemical analyses were performed for ten samples of water from wells drilled in households in the perimeter of Timis County, Romania. The analyses included the range of microbial groups and species considered indicators of water quality. Their isolation and identification were carried out on specific nutrient media and were completed with determinations of nitrates, phosphates and pH. According to the analysis reports, faecaligenous enterococci were not identified, instead clostridia were observed in most of the samples and a contamination with Escherichia coli. The microbial load is high in the majority of samples. The chemical analyses indicated the presence of phosphates and nitrates in most of the evaluated samples. The nitrates in the analyzed water samples did not exceed the value of 50 mgL⁻¹ stipulated in the standard. The obtained results suggest the presence of some sources of faecal contamination and require taking measures to treat the waters in question.

Key words: Clostridia, Escherichia coli, faecaligenous enterococci, fountain water, nitrates.

INTRODUCTION

Water is one of the essential elements of life (Mitrănescu et al., 2007; Petcu, 2015). The United Nations supports the sustainable development of drinking water resources and wants to implement the project of access to sewage and drinking water for all nations with limited resources by 2030 (WHO, 2015). Chemical and biological monitoring is a concern for scientists in the 21st century due to the importance of water quality in human health. WHO (2022) points out that 1.2 billion people do not have access to drinking water services. Biological, chemical (WHO, 2017a), and physical pollutants can cause degradation in water quality. Among these pollutants, microorganisms (Figure 1) cause the most health problems worldwide (WHO, 2011). Microorganisms have a negative impact on children, the elderly, and immunodeficient individuals (Freeman et al., 2012).

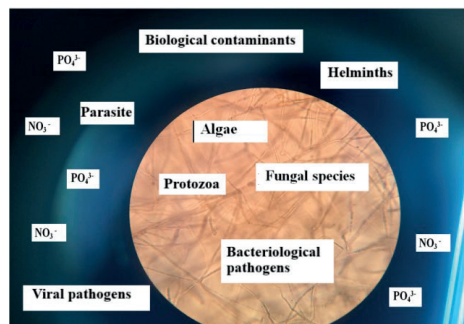


Figure 1. Table of biological and chemical water contaminants

Studies show that over 829,000 deaths are caused by pathogens present in water (Cabral, 2010; WHO, 2022). Diseases caused by microbiologically contaminated water are diarrhea (Baker, 2016; Ercumen et al., 2017), dysentery, cholera, poliomyelitis and typhoid. Among these diseases, diarrhea causes around 505.000 deaths annually (WHO, 2022). Among

the most incriminated bacteria are coliforms (Bai et al., 2022), enterococci (Boehm & Sassoubre, 2014) and *E. coli*, also called "faecal indicators". Besides these, there are other new pathogens that are causing waterborne diseases.

These biological contaminants reach the environment (water, soil, food) through faeces, appear in the form of microbial biofilms in water systems because of their stagnation or the use of small amounts of disinfectant (Farhadkhani et al., 2014). Nitrates and phosphates are among the chemical pollutants that create major problems worldwide (Borozan et al., 2021). Nitrogen and phosphorus in moderate amounts support the growth of living organisms (Grzyb et al., 2021), but at high levels they cause eutrophication and deterioration of water quality, and have a negative impact on ecosystems and human health (Dodds & Smith, 2016; Ward et al., 2018). Animal, human, industrial, and agricultural waste are all potential sources of pollution. Sources of drinking water for consumers are represented by bottled water, automatic sources, tap water and water from dug or drilled wells (Hile Dama et al., 2023). Some studies show that water from individual wells is increasingly used, because access to groundwater is easy, well construction costs are reduced and it does not involve any additional fees. In developed regions, bottled water has a high percentage. In Romania there are several sources of drinking water, including drilled or dug wells. They are located in urban and rural areas. The water is intended to be consumed by humans, as well as for animals and irrigation. In every situation, ensuring water quality is essential, as it has the potential to affect the health of plants, animals, and humans. There is currently a lack of analysis concerning the quality of drinking water and available information regarding its potability in peri-urban and rural areas. Wells in these areas are often shallowly drilled or dug, raising the possibility of microbial contamination. Additionally, there is a growing percentage of septic tanks that could potentially contaminate water sources. According to the Ministry of Health, 30% of Romania's population uses water that is not monitored from a qualitative point of view, the water

coming from traditional or drilled individual wells (<https://www.asro.ro>).

This study aims to examine the impact of well depth (ranging from 16 to 62 meters) and household pollution sources on the microbiological and chemical properties of water from peri-urban drilled or dug wells. Its objectives include informing consumers about the chemical and biological risks they face, identifying pollution sources, highlighting relevant regulations, determining distances between water sources and critical pollution points, and tracing pollutants along trophic chains. Therefore, the study's objective is to promote sustainability and efficiency in managing underground water resources and constructing wells that minimize water degradation.

MATERIALS AND METHODS

Study area

The drinking water samples come from the northwestern part of Timis county (20°16'22"33'E, 45°11'46"11'N), from a locality (VA) located near the Mures river, characterized through a plain climate, where three types of climates intersect. The community consists of over 6000 inhabitants.

Sampling

The collection of water samples was carried out in accordance with the regulations in force. The amount of water collected was 1 L for each fountain. The water level in the bottle was about 1 cm below the edge. Each sampling bottle was accompanied by sample identification data (date, time, place). The samples were transported to the laboratory under optimal temperature conditions (4°C) (Castilla et al., 2008). The water samples were processed in a maximum time of 6 hours.

Microbiological analyses

Microbiological analyses of drinking water were carried out by conventional methods. For the determination of mesophilic bacteria, faecal enterococci, clostridia and *E. coli*, the method of plate cultures was used, and for the evaluation of coliform bacteria, the method of serial dilutions was used. A number of 10 water samples were analyzed. Culture methods are preferred to qPCR, because they involve lower costs (Stelma, 2018). Water has legal

regulations regarding the absence of bacteria or the numerical limitation of other microbial groups (Table 1).

Table 1. Microbiological parameters according to Law No.96/2024

Parameter	Maximum value allowed
<i>Escherichia coli</i>	0/100 mL
Intestinal enterococci	0/100 mL
Coliform bacteria	0/100 mL
<i>Pseudomonas aeruginosa</i>	0/250 mL
<i>Clostridium perfringens</i>	0/100 mL
Number of colonies at 22°C	100/mL
Number of colonies at 37°C	20/mL

For the isolation of mesophilic bacteria, 1 mL of undiluted water was inoculated in Petri plates with nutrient agar. The plates inoculated by the embedding technique were incubated at 37°C for 48 hours. The colonies developed on the surface of the medium were counted, and the results obtained were expressed as Colony Forming Units per milliliter (CFU·mL⁻¹) (Zamorska et al., 2023).

For the isolation of coliform bacteria, the presumptive test was applied (Rahayu et al., 2020). The inoculation of undiluted and diluted water samples (10⁻¹ and 10⁻²) was carried out on Tryptose-Lauryl-Sulphate medium, in three repetitions. In each medium test tube, a Durham tube was inserted to capture the gases resulting from the fermentation process. Incubation was carried out at a temperature of 37°C for 24 hours. To confirm *E. coli* bacteria, positive test tubes from the presumptive test were confirmed on Levine medium (EMB agar). The growth of *E. coli* bacteria took place at a temperature of 37°C, for 18 hours. *E. coli* produced metallic sheen colonies on EMB medium.

C. perfringens is a species that is anaerobic, sporogenous, bacillary, Gram-variable, motile, and can occur either solitarily or in pairs (UK Standards). The monitoring of this bacterium is mandatory in drinking water, especially in drilled wells, but it is not mandatory in surface waters subject to drinking water Law 96/2024. It is present in the faeces of animals and humans. It can contaminate water, soil, air and food (Petcu et al., 2007; WHO, 2011). To isolate the bacterium *C. perfringens*, undiluted water was inoculated on the basic medium,

Clostridium. Incubation was carried out under anaerobic conditions, at a temperature of 37°C, for 24 hours. Enterococci or group D streptococci, represent another group of bacteria that indicate faecal water pollution. These bacteria are common in nosocomial infections and present a high risk, because they can transfer resistance genes to other Gram-positive and Gram-negative pathogenic bacteria. *Enterococcus faecalis* is a group D bacterium, common in mineral, flat and spring water, which causes infections (Wei et al., 2017). For the isolation of enterococci in a single step, a solid medium, Azida-Bila-Esculina was used, a selective medium used for counting and confirming enterococci in water. The incubation temperature was 37°C for 24 hours.

Chemical analyses

To conduct an initial screening for areas of fecal contamination, the nitrate (NO₃⁻) concentration was also assessed.

The concentration of phosphate ions (PO₄³⁻) and the pH value were also established in several wells, chosen according to the depth. NO₃⁻ was quantified using 4500-NO₃⁻ E. Cadmium Reduction Method (https://www.edgeanalytical.com/wp-content/uploads/Waste_SM4500-NO3-.pdf) and PO₄³⁻ was quantified using ammonium molybdate and antimony potassium tartrate (catalyst) under acidic conditions, in order to form to form a blue heteropoly compound (12-molybdophosphoric acid complex) and measured spectrophotometrically at wavelength 660 nm (<https://assets.thermofisher.com/TFS-Assets/CMD/manuals/PI-D09244-DA-Phosphate-PID09244-EN.pdf>).

RESULTS AND DISCUSSIONS

The mesophilic bacteria

The results obtained were reported to the regulations of Law No.96/2024. This law includes the requirements of European legislation regarding the quality of drinking water. This was made possible by Ordinance No. 7/2023 on the quality of water intended for human consumption, issued by the Government of Romania and published in the Official Gazette, Part I No. 63 of January 25, 2023, effective from January 28, 2023.

The results of the microbiological evaluation of the water from the ten wells demonstrate that in the analyzed water samples, most of the bacteriological indicators have high values and exceed the values provided by the standards in force. For example, mesophilic bacteria register a high number in almost all samples. The number of mesophilic bacteria is between $0.4 \times 10^2/\text{mL}$.

In the same samples, the number of *C. perfringens* bacteria (which falls between $0.5.85 \times 10^2/\text{mL}$) and coliform bacteria (whose number was between 36-110 germs/ cm^3) also increased. According to Law 96/2024, the number of mesophilic bacteria, grown at a temperature of 37°C , must be 20/mL. Our research shows that after 48 hours of incubation, mesophilic bacteria exceeded this limit in most samples, apart from sample 4, which comes from a 43 m deep well (Figure 2 and Figure 3). These results are supported by other studies showing that shallow groundwater systems are prone to fecal and chemical contamination (Islam et al., 2016; Lorentz et al., 2015; UNICEF, 2019).

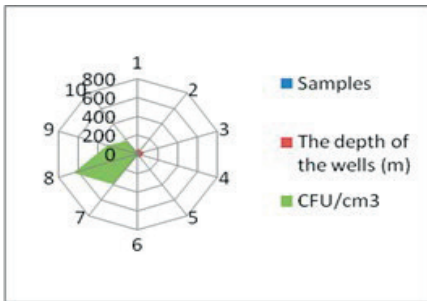


Figure 2. Estimation of mesophilic bacteria

Depending on the bacterial load (UFC/mL), the samples can be grouped in the following descending order: 6.5×10^2 (in sample 8) > 4.02 (in sample 7) 3.08×10^2 (in sample 9) > 2.61 (in sample 2) 1.77×10^2 (in sample 10) > 1.05 (in sample 5).

Wells analyzed microbiologically and chemically have different depths. The depths of the 10 wells are between 16-62 m. Maran et al. (2016) claim that the contamination with microorganisms is also correlated with the depth of the wells. The highest number was discovered in the well with a depth of 55 m. Samples 1 (the depth of the well is 60 m) and 6

(the depth of the well is 16 m) have a low concentration of bacteria compared to the other samples, but nevertheless exceed by 2.5-12.5% the value provided by the standard. The absence of pollution sources from households or the greater distance from the wells may be the reason for the lower number of bacteria in some wells. Some studies mention that the microbiological quality of water also depends on the season (Zamorska et al., 2023). The studies on the water from the wells were carried out in the spring.

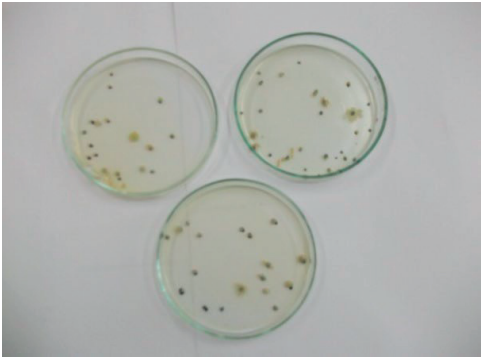


Figure 3. Mesophilic bacterial cultures

The load of *Clostridium perfringens* and faecal enterococci

C. perfringens spores are reliable indicators of polluted waters and are a stable ecological indicator (Stelma, 2018). They are widely distributed in sewage and constantly associated with faeces (Bisson, 1980). They are the parameters of contamination with human feces (Stelma, 2018). A genomic analysis claims that this bacterium is demanding from a nutritional point of view, because it prefers certain amino acids and is not present in the fecal of herbivores (Vierheilg et al., 2013) (Figure 4).

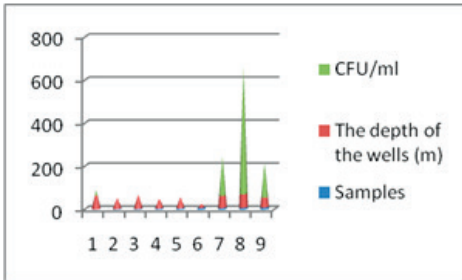


Figure 4. Estimation of bacteria *Clostridium perfringens*

According to the data presented in Figure 4, clostridia are found in large numbers in sample number 8 (5.85×10^2), followed in descending order by samples 10 (2.2×10^2), 7 (1.78×10^2), 9 (1.56×10^2) and 1 (0.25×10^2). *Clostridium* can be found in high numbers due to multiple factors. *C. perfringens* is an anaerobic bacterium, a condition that can be fulfilled by a drilled well. It is a sporogenous bacterium that easily survives through spores. It can also withstand lower temperatures.

Furthermore, the presence of animals and agricultural activities in rural areas contributes to the proliferation of clostridia and enterococci. Our studies are also supported by the research carried out by Hiroyuki and co-workers (2021). These authors demonstrated that *C. perfringens* is an effective indicator for water contamination with human faeces. The lowest number of *C. perfringens* was observed in samples 3 and 4. Clostridia were absent in samples 2, 4 and 6.

While enterococci are commonly present in fecal material, specific researchers suggest that the viability of *E. faecalis* might fluctuate based on the methodology of analysis utilized (Pourcher et al., 1991). Compared to clostridia, enterococci did not have such a high percentage. According to the Law 96/2024, enterococci and *C. perfringens* bacteria must be absent in drinking water.

Coliform bacteria and *Escherichia coli*

Coliform bacteria are facultatively anaerobic, Gram-negative bacilli, capable of fermenting glucose and producing acid and gases. They are present in the environment and in human and animal faeces (Martin et al., 2016). The regulations in force show that coliform bacteria and *E. coli* must be absent/100 mL drinking water.

Contrary to these norms, high levels of coliforms were observed in some water samples (Figure 5 & Figure 6). This refers to the same samples in which a high load of mesophilic bacteria and clostridia was detected. The highest number of coliforms was reported in sample no. 8 (1.10×10^2), followed by samples 9, 10 and 6. Inadequate sanitation systems and unhygienic human practices (Wright et al., 2004; Mahmud et al., 2019) contributes to a large extent of water sources

the pollution. Mahmud and his team (2019), observed that in the water samples from tube wells the contamination with coliforms was 28%, and with *E. coli* 10.5%. Our research is also supported by other authors, who showed that vulnerability to contamination is also linked to the use of septic tanks placed at small distances from wells (Allevi et al., 2013; Back et al., 2018; Nayebare et al., 2020; Gumoteyo et al., 2021), improper management of household waste, improper maintenance of wells (Jimmy et al., 2013) presence of animals, unless they are kept in paddocks located a considerable distance from the water source (Navab-Daneshmand et al., 2018). Also, the mobility of faecal bacteria and chemical contaminants can be caused by anthropogenic activities in households, the depth and diameter of the well (Hynds, 2014), the type of well and the method of construction, buckets or motor pumps that come into contact with the water from the well (Maran et al., 2016), the properties of the soil and the underground water source.

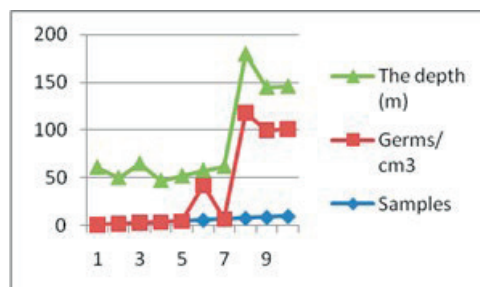


Figure 5. Estimation of coliform bacteria

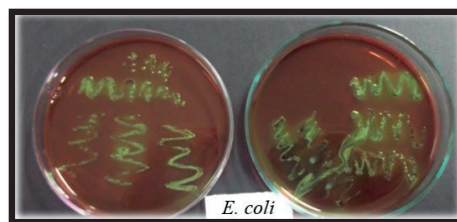


Figure 6. *E. coli* on EMB medium

Assessment of pH, nitrates and phosphates

pH plays a crucial role in affecting both the chemical and biological parameters that ultimately define water quality (Saalidong et al., 2022). Some researchers have proven that

pH influences microorganisms and the availability of substances in water (Pal, 2017). According to Saalidong et al. (2022), "the relationship between water pH and other water quality parameters are different in different water systems and can be influenced by the presence of other parameters".

The pH values influence the microbiological quality of the water (WHO, 2024). In the acidic pH range, the growth of *E. coli* bacteria can be inhibited (WHO, 1996).

According to The Directive (EU) 2020/2184 of the European Parliament and of The Council, of 16 December 2020 on the quality of water intended for human consumption and Law 96/2024 shows that the pH value must be 6.5-9.5 pH units or ≥ 6.5 and ≤ 9.5 pH units (Senaldi et al., 2021).

In our research, the pH values in the four wells are close and are in the range of 6.25-6.65 (Figure 7).

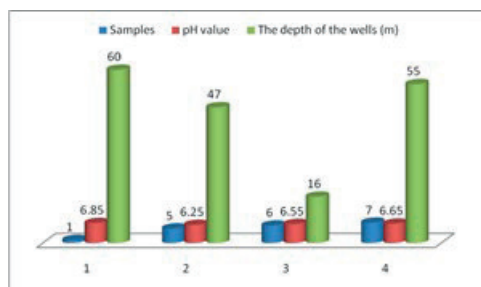


Figure 7. pH in wells drilled at different depths

Nitrogen and phosphorus are two essential elements for the growth of living organisms, but the excessive amount turns them into chemical contaminants, which depreciate the water quality and affect health (Chen et al., 1999; Davidson et al., 2012; Ward et al., 2018). Application of nitrogen and phosphorus fertilizers can result in groundwater pollution, potentially contaminating drinking water sources (Akiyama et al., 2006; Wang et al., 2019). The level of nitrates can increase in agricultural areas by applying manure in large amounts.

Nitrates ($0 \div 2 \text{ mg} \cdot \text{L}^{-1}$) and phosphates ($0 \div 0.01 \text{ mg} \cdot \text{L}^{-1}$) were noticed in most of the water samples (Figure 8). In his studies, Fones et al. (2020), discovered that phosphate ($0.62 \text{ mg} \cdot \text{L}^{-1}$) exceeded the average values allowed.

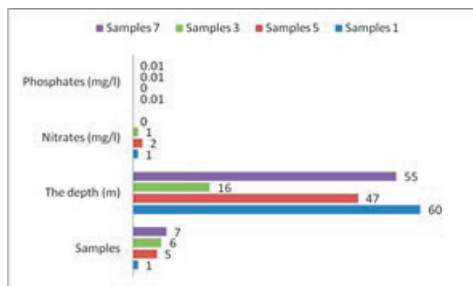


Figure 8. Estimation of nitrates and phosphates from wells drilled at different depths

According to the European drinking water regulations, nitrate maximum allowable value is $50 \text{ mg} \cdot \text{L}^{-1}$ while there is no specific limit for phosphate. The maximum allowed concentration of nitrates in drinking water in Romania is set at $50 \text{ mg} \cdot \text{L}^{-1}$, this limit is aligned with the European Union standard. This reference value is also mentioned in the World Health Organization guidelines (WHO, 2016; 2017), with the aim of protecting the health of more vulnerable population groups. For example, infants are protected against methemoglobinemia. Many authors have observed that exceeding the allowed concentration causes thyroid hypertrophy (Van Maanen et al., 1996), macular degeneration (Klein et al., 2013), bladder and ovarian cancers (Ward et al., 2018). In our studies, the concentration of nitrates is low, below the limit imposed by the standards in force, which is why we consider that nitrates do not endanger the health of consumers. In addition, some authors mention that the reduced intake of nitrates has as potential benefits the lowering of blood pressure and immunoregulatory effects (Ahluwalia et al., 2016).

CONCLUSIONS

As a result of the fact that the water comes from the countryside and there are animals, septic tanks and inorganic fertilizers and chemical treatments for weeds, diseases and pests are used there, it is necessary to periodically evaluate the physico-chemical and microbiological parameters.

Overall quantitative water analysis has higher accuracy compared to qualitative analysis, but the latter confirms us the identity of the

contaminants. Most waters have a high microbial load of mesophilic bacteria, *C. perfringens*, respectively coliform bacteria and *E. coli* which makes the water unfit for consumption. All these microorganisms cause health problems. Nitrates were below standard limits ($0\div2\text{ mg}\cdot\text{L}^{-1}$).

Each consumer was informed about the microbiological and chemical characteristics of the water. To avoid health risks, preventive and treatment measures were recommended for correcting water properties, boiling water, cleaning wells, limiting the access of animals to wells, connecting to a centralized distribution system (where applicable) and observing the optimal distance between septic tanks and wells. Also, septic tanks must meet standard construction requirements.

REFERENCES

- Ahluwalia, A., Gladwin, M., Coleman, G.D., Hord, N., Howard, G., Kim-Shapiro, D.B., Lajous, M., Larsen, F.J., Lefer, D.J., McClure, L.A. et al. (2016). Dietary nitrate and the epidemiology of cardiovascular disease: Report from a national heart, lung, and blood institute workshop. *Journal of the American Heart Association* 5, 003402.
- Akiyama, H., Yan, X., Yagi, K. (2006). Estimations of emission factors for fertilizer-induced direct N_2O emissions from agricultural soils in Japan: Summary of available data. *Soil Science and Plant Nutrition*, 52, 774–787.
- Allevi, R.P., Krometis, L.A.H., Hagedorn, C., Benham, B., Lawrence, A.H., Ling, E.J., Ziegler, P.E. (2013). Quantitative analysis of microbial contamination in private drinking water supply systems. *Journal of Water and Health* 11(2), 244–255.
- Back, J.O., Rivett, M.O., Hinz, L.B., Mackay, N., Wanangwa, G.J., Phiri, O.L., Songola, C.E., Thomas, M.A.S., Kumwenda, S., Nhlema, M., Miller, A.V.M. & Kalin, R.M. (2018). Risk assessment to groundwater of pit latrine rural sanitation policy in developing country settings. *Science of the Total Environment* 613, 592–610.
- Baker, K.K., O'Reilly, C.E., Levine, M.M., Kotloff, K.L., Nataro, J.P., Ayers, T.L., Farag, T.H., Nasrin, D., Blackwelder, W.C., Wu, Y., Alonso, P.L., Breiman, R.F., Omere, R., Faruque, A.S., Das, S.K., Ahmed, S., Saha, D., Sow, S.O., Sur, D., Zaidi, A.K., Quadri, F., Mintz, E.D. (2016). Sanitation and hygiene-specific risk factors for moderate-to-severe diarrhea in young children in the global enteric multicenter study, 2007–2011: case-control study. *Plos Medicine*, 13: e1002010.
- Bai, V.R., Kit, A.C., Kangadharan, G., Gopinath, R., Varadarajan, P., Hao, A.J. (2022). Experimental study on total coliform violations in the complied NH_2CL , O_3 , and UV treated municipal water supply system. *The European Physical Journal Plus*, 137(6), 689.
- Bisson, J.W., Cabelli, V.J. (1980). *Clostridium perfringens* as a water quality indicator. *Journal of the Water Pollution Control Federation*, 52, 241–248.
- Boehm, A.B., Sassoubre, L.M. (2014). Enterococci as Indicators of Environmental Fecal Contamination. In: Gilmore MS, Clewell DB, Ike Y, et al., editors. *Enterococci: From Commensals to Leading Causes of Drug Resistant Infection*. Boston: Massachusetts Eye and Ear Infirmary.
- Borozan, A.B., Bordean, D.M., Poiana, M.A., Alexa, E., Caba, I.L., Pirvulescu, L., Raba, D.N., Obistioiu, D., Morar, A., Misca, C.D., Petcu, C.D. (2021). Soil Pollution with Heavy Metals and Bioremediation Methods. *AgroLife Scientific Journal*, 10(1), 54–66. <https://doi.org/10.17930/AGL202115>.
- Cabral, J.P. (2010). Water microbiology. Bacterial pathogens and water. *International Journal of Environmental Research and Public Health*, 7(10), 3657–703.
- Castilla, J., Barricarte, A., Aldaz, J., Garcí a Cenoz, M., Ferrer, T., Pelaz, C., et al., (2008). A large Legionnaires' disease outbreak in Pamplona, Spain: early detection, rapid control and no case fatality. *Epidemiology & Infection*, 136(6), 823832.
- Chen S., Wu Z., Yu W., Lu Y. (1999). Formation, harmfulness, prevention, control and treatment of waters eutrophication. *Environmental Science and Technology*, 2, 12–16.
- Davidson, E.A., David, M.B., Galloway, J.N., Goodale, C.L., Haeuber, R., Harrison, J.A., Howarth, R.W., Jaynes, D.B., Lowrance, R.R., Nolan, B.T., et al. (2012). Excess nitrogen in the U.S. environment: Trends, risks, and solutions. In *Issues in Ecology*, Ecological Society of America: Washington, DC, USA.
- Dodds, W. & Smith, V. (2016). Nitrogen, phosphorus, and eutrophication in streams. *In land Water*, 6, 155–164.
- Ercumen, A., Arnold, B.F., Naser, A.M., Unicomb, L., Colford, J. M., Luby, S.P. (2017). Potential sources of bias in the use of *Escherichia coli* to measure waterborne diarrhoea risk in low-income settings., *Tropical Medicine and International Health*, 22, 2–11.
- Farhadkhani, M., Nikaeen, M., Adergani, B.A., Hatamzadeh, M., Nabavi, B.F., Hassanzadeh, A. (2014). Assessment of drinking water quality from bottled water coolers. *Iranian Journal of Public Health*, 43(5), 674.
- Fones, G.R., Bakir, A., Gray, J., Mattingley, L., Measham, N., Knight, P., Bowes, M.J., Greenwood, R., Mills, G.A. (2020). Using high-frequency phosphorus monitoring for water quality management: a case study of the upper River Itchen, UK. *Environmental Monitoring and Assessment*, 18, 192(3), 184.
- Freeman, M.C., Trinies, V., Boisson, S., Mak, G., Clasen, T. (2012). Promoting household water treatment through women's self-help groups in rural

- India: Assessing impact on drinking water quality and equity. *PLoS ONE*, 7, e44068.
- Grzyb, A., Wolna-Maruwka, A., Niewiadomska, A. (2021). The Significance of Microbial Transformation of Nitrogen Compounds in the Light of Integrated Crop Management. *Agronomy*, 11(7), 1415.
- Gumoteyo, Nayebare J., Owora, M., Kulabakob, R., Taylor, R.G. (2021). Faecal contamination pathways of shallow groundwater in low-income urban areas: implications for water resource planning and management. *Water Practice and Technology*, 17(1), 285.
- Hile Dama, T., Dunbar, G., Stephen Ryan, G. (2023). Sinclair, Microbial contamination analysis of drinking water from bulk dispensers and fast-food restaurants in the Eastern Coachella Valley, California. *Water Supply*, 23(9), 3578–3596.
- Hiroyuki, S., Kenji, O., Atsushi Hashimoto, A. (2021), Evaluation of *C. perfringens* cpe-positive Strain as a Source Tracking Indicator of Human Contamination in Freshwater Environments, *Journal of Water and Environment Technology*, 19(1), 1–12.
- Hynds, P., Misstear, B.D., Gill, L.W., Murphy, H.M. (2014). Groundwater source contamination mechanisms: Physicochemical profile clustering, risk factor analysis and multivariate modelling. *Journal of Contaminant Hydrology*, 159, 47–56.
- Klein, B.E.K., McElroy, J.A., Klein, R., Howard, K.P., Lee, K.E. (2013). Nitrate-nitrogen levels in rural drinking water: Is there an association with age-related macular degeneration? *Journal of Environmental Science and Health, Part A*, 48, 1757–1763.
- Islam, M.S., Mahmud, Z.H., Islam, M.S., Saha, G.C., Zahid, A., Ali, A.Z., Hassan, M.Q., Islam, K., Jahan, H., Hossain, Y., Hasan, M.M., Cairncross, S., Carter, R., Luby, S.P., Cravioto, A., Endtz, H.P., Faruque, S.M. & Clemens, J.D. (2016). Safe distances between groundwater-based water wells and pit latrines at different hydrogeological conditions in the Ganges Atrai floodplains of Bangladesh. *Journal of Health, Population, and Nutrition* 35(1), 26.
- Jimmy, D.H., Sundufu, A.J., Malanoski, A.P., Jacobsen, K.H., Ansumana, R., Leski, T.A., Bangura, U., Bockarie, A.S., Tejan, E., Lin, B., et al. (2013). Water quality associated public health risk in Bo, Sierra Leone. *Environmental Monitoring and Assessment*, 185, 241–251.
- Lorentz, S.A., Wickham, B., Still, D. (2015). Investigation Into Pollution From On-Site Dry Sanitation Systems. Report (No. 2115/1, 15). *Report to the Water Research Commission*, University of KwaZulu-Natal, South Africa.
- Mahmud Z.H., Islam M.S., Imran K.M., Syed Adnan Ibna Hakim, Martin Worth, Alvee Ahmed, Shanewaz Hossan, Maliha Haider, Mohammad Rafiqul Islam, Ferdous Hossain, Dara Johnston, Ahmed, N. (2019) Occurrence of *Escherichia coli* and faecal coliforms in drinking water at source and household point-of-use in Rohingya camps, Bangladesh, *Gut Pathogens*, 11, 52.
- Maran, N.H., Crispim, B.D.A., Iahnn, S.R., Araújo, R.P., Grisolia, A.B., Oliveira, K.M.P. (2016). Depth and Well Type Related to Groundwater Microbiological Contamination. *International Journal of Environmental Research and Public Health*. 13(10), 1036.
- Machado, A., Bordalo, A.A. (2014). Prevalence of antibiotic resistance in bacteria isolated from drinking well water available in Guinea-Bissau (West Africa). *Ecotoxicology and Environmental Safety*, 106, 188–194.
- Martin, N.H., Trmcic, A., Hsieh, T., Boor, K.J., Wiedmann, M. (2016). The evolving role of coliforms as indicators of unhygienic processing conditions in dairy foods. *Frontiers in Microbiology*, 7, 1549.
- Mitrănescu, E., Furnaris, F., Tudor, L., Tăpăloagă, D., Petcu, C., Simion, V., Pârnu, M. (2007). Research regarding the quality of used waters in Târgoviște area. *Bulletin of University of Agricultural Sciences and Veterinary Medicine Cluj-Napoca*, 64(1-2), 184–187.
- Nayebare, J.G., Owor, M.M., Kulabako, R., Campos, L.C., Fottrell, E., Taylor, R.G. (2020). WASH conditions in a small town in Uganda: how safe are on-site facilities? *Journal of Water Sanitation and Hygiene for Development*, 10(1), 96–110.
- Navab-Daneshmand, T., Friedrich, M.N.D., Gächter, M., Montealegre, M.C., MLambo, L.S., Nhiwatiwa, T., Mosler, H.J., Julian, T.R. (2018). *Escherichia coli* Contamination across Multiple Environmental Compartments (Soil, Hands, Drinking Water, and Handwashing Water) in Urban Harare: Correlations and Risk Factors. - *American Journal of Tropical Medicine and Hygiene*, 98(3), 803–813.
- Pal, P. (2017). Industrial water treatment process technology: Butterworth-Heinemann.
- Petcu, C.D., Savu, C., Mitrănescu, E., Chirilă, S. (2007). The implementation of the integrated quality and food safety management system in the food industry units. *Lucrări Științifice Medicină Veterinară*, XL, 545–51.
- Petcu, C.D. (2015). *Calitatea și tehnologia cărnii*. Editura Granada, București.
- Pourcher, A.M., Devriese, L.A., Hernandez, J.F., Delattre, J.M. (1991). Enumeration by a miniaturized method of *Escherichia coli*, *Streptococcus bovis* and enterococci as indicators of the origin of faecal pollution of waters. *Journal of Applied Bacteriology*, 70(6), 525–530.
- Rahayu, D., Anggoro, S., Soeprbowati, T. (2020). Water quality assessment based on microbiological parameter indicators for drinking water criteria on the Wadaslintang Reservoir E3S *Web of Conferences*, 202, 05019, ICENIS.
- Said, M.D. & Mahmud, A.M. (2013). Spectrophotometric determination of nitrate and phosphate levels in drinking water samples in the vicinity of irrigated farmlands of Kura Town, Kano State-Nigeria. *ChemSearch Journal*, 4(1), 47–50.
- Saalidong, B.M., Aram, S.A., Otu, S., Lartey, P.O. (2022). Examining the dynamics of the relationship between water pH and other water quality parameters

- in ground and surface water systems. *PLoS One*, 17(1), e0262117.
- Senaldi, C., Crutzen, H., & Hoekstra, E. (2021). Review of standards related to materials in contact with drinking water. <https://publications.jrc.ec.europa.eu/repository/handle/JRC125733>.
- Stelma, G.N.Jr. (2018). Use of bacterial spores in monitoring water quality and treatment. *Journal of Water and Health*, 16(4), 491-500.
- Vierheilig, J., Frick, C., Mayer, R.E., Kirschner, A.K. T., Reischer G.H., Derx J., Mach, R.L., Sommer, R., Farnleitner, A.H. (2013). *Clostridium perfringens* Is Not Suitable for the Indication of Fecal Pollution from Ruminant Wildlife but Is Associated with Excreta from Nonherbivorous Animals and Human Sewage. *Applied and Environmental Microbiology*, 79.
- Van Maanen, J.M., Welle, I.J., Hageman, G., Dallinga, J.W., Mertens, P.L., Kleinjans, J.C. (1996). Nitrate contamination of drinking water: Relationship with HPRT variant frequency in lymphocyte DNA and urinary excretion of N-nitrosamines. *Environmental Health Perspectives*, 104, 522-528.
- Wang, P., Zhang, W., Li, M., Han, Y. (2019). Does fertilizer education program increase the technical efficiency of chemical fertilizer use? Evidence from wheat production in China. *Sustainability*, 11, 543.
- Ward, M.H., Jones, R.R., Brender, J.D., De Kok, T.M., Weyer, P.J., Nolan, B.T., Villanueva, C.M., Van Breda, S.G. (2018). Drinking Water Nitrate and Human Health: An Updated Review. *International Journal of Environmental Research and Public Health*, 15(7), 1557.
- Washington, C.W. (1996). *Medical microbiology*. In: Baron, S. (Ed.), *Legionella*, Chapter 40, fourth ed University of Texas Medical Branch, Galveston (TX)
- Wei, L., Wu Q., Zhang, J., Guo, W., Chen, M., Xue, L., Wang, J., Ma, L. (2017). Prevalence and Genetic Diversity of *Enterococcus faecalis* Isolates from Mineral Water and Spring Water in China. *Frontiers in Microbiology*, 16(8), 1109.
- Wright, J., Gundry, S., Conroy, R. (2004). Household drinking water in developing countries: a systematic review of microbiological contamination between source and point-of-use. *Tropical Medicine and International Health*, 9, 106-17.
- Zamorska, J., Karwowska, E., Przysaś, W. (2023). Assessment of Microbiological Quality of Water Using Culture Methods, Flow Cytometry and Luminometry. *Water*, 15(23), 4077.
- ***European Parliament and Council of the European Union. "Directive (EU) 2020/2184 on the Quality of Water Intended for Human Consumption." Official Journal of the European Union, L 435, 16 Dec. 2020, pp. 1-62.
- ***Ordinance No. 7/2023 on the quality of water intended for human consumption, issued by the Government of Romania and published in the Official Gazette, Part I No. 63.
- ***UK Standards for Microbiology Investigations identification of *Clostridium* species, Public Health England, London NW9 5EQ/
- ***UNICEF (2019). Global Framework for Urban Water, Sanitation and Hygiene. UNICEF, New York.
- ***World Health Organization (WHO), (1996). Guidelines for Drinking-Water Quality, World Health Organization, Geneva, Switzerland.
- ***World Health Organization (WHO), (2004). Guidelines for Water Quality, 3rd ed. World Health Organization (WHO), Geneva.
- ***World Health Organization. (2011). Guidelines for Drinking-Water Quality; WHO Press: Geneva, Switzerland, 1-541.
- ***World Health Organization (WHO), (2015). Water, Sanitation and Hygiene in Health Care Facilities Status in Low- and Middle-Income Countries and Way Forward. WHO, Geneva, 52.
- ***World Health Organization (WHO), (2016). Guidelines for Drinking-water Quality, Nitrate and Nitrite in Drinking-water Background document for development of WHO/SDE/WSH/7.01/16/Rev/1
- ***World Health Organization (WHO), (2017). Guidelines for Drinking-Water Quality: 4th edn, Incorporating the 1st Addendum. World Health Organization, Geneva.
- ***World Health Organization (WHO), (2022). *Drinking-Water Geneva* WHO, Geneva, Switzerland. Available from: <https://www.who.int/news-room/fact-sheets/detail/drinking-water>.
- ***World Health Organization (WHO), (2024). Guidelines for drinking-water quality: small water supplies.
- ***<https://delmarvawatersolutions.com/ph-in-your-water-what-is-it-how-it-affects-your-health>
- ***https://osse.ssec.wisc.edu/curriculum/earth/Minifact2_Phosphorus.pdf
- ***<https://www.asro.ro/calitatea-apei-standarde-si-legislatie/>
- ***[https://www.uvm.edu/bwrl/lab_docs/protocols/4500-NO3-AandE_Nitrate_by_cadmium%20reduction_\(SM\).PDF](https://www.uvm.edu/bwrl/lab_docs/protocols/4500-NO3-AandE_Nitrate_by_cadmium%20reduction_(SM).PDF)
- ***https://www.edgeanalytical.com/wp-content/uploads/Waste_SM4500-NO3-.pdf
- ***<https://assets.thermofisher.com/TFS-Assets/CMD/manuals/PI-D09244-DA-Phosphate-PID09244-EN.pdf>

PHYSIOLOGICAL AND BIOCHEMICAL RESPONSE OF TWO DURUM WHEAT VARIETIES TO WATER STRESS COMBINED WITH A SLUDGE AMENDMENT

Sonia BOUDJABI^{1,2}, Nawal ABABSA^{2,3}, Haroun CHENCHOUNI^{3,4},
Aya DEBAB^{1,2}, Amna BRAHMI^{1,2}

¹University of Tebessa, Faculty of Exact Sciences and Nature and Life Sciences,
Department of Nature and Life Sciences, Laboratory "Water and Environment", Tebessa, Algeria

²University of Khenchela, Faculty of Nature and Life Sciences, Department of Ecology and
Environment, El-Hamma, Khenchela, Algeria

³University of Oum-El-Bouaghi, Laboratory of Natural Resources and Management of Sensitive
Environments 'RNAMS', Oum-El-Bouaghi, Algeria

⁴Higher National School of Forests, Department of Forest Management, Khenchela, Algeria

Corresponding author emails: soniabeida@yahoo.fr, sonia.boudjabi@univ-tebessa.dz

Abstract

Sewage sludge, as biosolids, can improve the fertility of degraded soils in arid and semi-arid regions. The use of these biosolids reduces reliance on increasingly expensive chemical fertilizers. They also limit carbon emissions and promote soil microbial growth, while stimulating plant growth. The objective of this study is to investigate the physiological and biochemical response of two durum wheat varieties (Hedba and BiDi) to the application of residual sludge (D0 = control, D1 = 30 g and D2 = 60 g of sludge per pot) under water stress conditions (S0 = 100%, S1 = 40%, S2 = 25% FC). The analyses indicated a linear and significant accumulation in the biochemical variables (sugars, proline and N) under the effect of stress and residual sludge. Contrary to the physiological variables with (WRC, Cell Integrity). However, chlorophyll a content accumulates with stress and residual sludge. Hedba variety is more resistant to stress compared to BD.

Key words: *biochemistry, Durum wheat, physiology, residual sludge, water stress.*

INTRODUCTION

Agriculture plays a crucial role in economic and social development by providing food, raw materials, and generating employment (Lallaoua et al., 2023). This role is even more important given that global food demand is expected to increase by 70% by 2050, driven by rapid population growth, bringing the world population to over 9 billion people, thus threatening human food security (Hunter et al., 2020). Faced with this imminent challenge, ensuring future food security requires a multidimensional approach that includes assessing and improving soil quality, optimizing agricultural productivity, and strategic food planning (El Behairy et al., 2024). Environmental stresses, particularly droughts, cause significant decreases in cereal crop yields, affecting durum wheat particularly, an essential crop in North Africa and the main staple food in Algeria (Boudjabi et al., 2023).

Indeed, in arid and semi-arid regions, durum wheat cultivation faces the constant challenge of recurring water stress (Boudjabi et al., 2023). This alarming situation threatens the food security of North African populations, making the search for sustainable solutions to optimize durum wheat production in these challenging environments all the more urgent. The use of residual sludge as an amendment emerges as a promising alternative to mineral fertilizers (Singh et al., 2011; Ababsa et al., 2023; Boudjabi & Chenchouni, 2023). Indeed, these biosolids, rich in organic matter and nutrients (Sharma et al., 2017; Vera-García et al., 2023; Boudjabi et al., 2019), contribute to soil quality improvement and increased yields (Boudjabi & Chenchouni, 2023). They offer an economic, ecological, and more efficient solution to restore soil fertility and sustainably boost agricultural yields. Moreover, the use of residual sludge as an amendment aligns with the principles of the circular economy by

encouraging waste reuse and reducing dependence on non-renewable resources. In this study, we simulated water stress conditions frequently encountered in semi-arid regions of Algeria. Our objective was to assess the effect of soil amendment with residual sludge on the response of two durum wheat genotypes (Hedba and BD) to variable water stress. To achieve this, we analyzed various physiological and biochemical parameters of Hedba and BD plants, such as cellular integrity, relative water content, proline and sugar content, leaf nitrogen content, and chlorophyll a, under different doses of residual sludge (D0 = 0, D1 = 30, and D2 = 60 g/pot) and three levels of water stress (S0 = 100%, S1 = 40%, and S2 = 25% FC). Our hypothesis is that water stress will negatively affect physiological parameters and induce an increase in biochemical variables. However, our hypothesis regarding the amendment of residual sludge is that the effect of stress will be paradoxically corrected and mitigated by the application of sludge, and this correction will be linear with the doses of sludge applied.

MATERIALS AND METHODS

Experimental Site

To study the physiological and biochemical response of two durum wheat varieties to increasing doses of residual sludge under water deficit conditions, an experiment was conducted in a plastic greenhouse at the Biology Department of the Cheikh Larbi Tebessi, Tébessa University during the academic year 2021-2022.

Experimental Design

The experiment was carried out in identical plastic pots with a capacity of 3 kg, considering three factors. The first factor is the variety effect, with two varieties selected Hedba and BIDI(BD). The varieties used were obtained from the OAIC of Tébessa (Algeria). The application of residual sludge and water stress were applied at three levels: S0 = 100% FC, 40% FC, and 25% FC for water stress, and D0 = control (without sludge), D1 = 30 g of residual sludge, D2 = 60 g for residual sludge. The residual sludge used was urban sludge, brought from the wastewater treatment plant located in Ain Beida (a region in eastern

Algeria). It underwent air drying, grinding, and sieving through a 2 mm sieve. Before its application in the pots, a fraction of this residual sludge was taken for chemical analysis, and a fraction of the soil used was also analyzed at the same time. Their physicochemical characteristics are shown in Table 1.

Table 1. Physicochemical characteristics of soil and sewage sludge used in experiments

Physico chemical parameters	Soil	Sewage sludge
Organic carbon [%]	1.60	30.47
Total nitrogen [%]	0.18	5.88
Assimilable phosphorus [$\mu\text{g/g}$]	2.67	19.34
Total CaCO_3 [%]	14.68	–
Active CaCO_3 [%]	2.32	–
Electrical conductivity [dS/cm]	0.323	1.58
pH	7.45	7.68
Nitrate [mg/kg]	14.3	52.28
Iron [ppm]	4.6	7.6
Zinc [ppm]	1.86	22.19
Copper [ppm]	7.24	12.69
Soil texture	Silt-clay	–

Description of the experiment

Six seeds of each durum wheat variety (Hedba and BD) were sown in pots filled with soil from Tébessa. The pots were then amended with sludge according to the defined doses and placed in a greenhouse. Water stress was applied to the plants at the jointing stage. The experiment was repeated three times for each treatment combination (sludge and water stress), for a total of 54 pots (27 per variety).

Plant analyses

Determination of Biochemical parameters

The method of Dubois et al. (1956) was used to quantify sugars in durum wheat leaves. 100 mg of fresh leaves are macerated in 80% ethanol for 48 hours, then the ethanol was evaporated. The volume is brought up to 20 ml with distilled water. 1 ml of the extract is reacted with phenol and sulfuric acid. The optical density (OD) is measured at 496 nm, and soluble sugars are calculated according to the equation $Y = 0.0029 \text{ OD} - 0.323$. The method of Troll and Lindsley in Pérez-Alfocea (1995) is used to measure proline content in durum wheat leaves. 100 mg of leaves are macerated in 40% methanol heated to 85°C for one hour.

1 ml of the extract is then reacted with acetic acid, ninhydrin, and a mixture of distilled water and orthophosphoric acid. The solution is boiled for 30 minutes, cooled, and toluene is added. The upper organic phase, containing proline, is recovered and its optical density (OD) is measured at 528 nm. Proline content is calculated using the equation $y = 0.913 \text{ OD} + 0.004$. The Kjeldahl method (Sáez-Plaza et al., 2013) was used to determine the nitrogen (N) content of the samples. 1 g of dry plant material was mineralized with concentrated sulfuric acid and a catalyst ($\text{CuSO}_4 + \text{K}_2\text{SO}_4$) to convert organic nitrogen into ammonium sulfate $[(\text{NH}_4)_2\text{SO}_4]$. Ammonia was then released from the ammonium sulfate with sodium hydroxide and titrated with a standard solution of sodium hydroxide to quantify the nitrogen content.

Determination of physiological parameters

The leaf cell turgor was measured according to the method of Barrs (1968). Leaf segments of 1 cm are weighed fresh (FW), then placed in water for 24 hours to obtain the turgid weight (TW). They are then dried at 80°C for 48 hours and weighed dry (DW). The relative water content (RWC) is calculated using the formula $\text{RWC (\%)} = (\text{FW} - \text{DW}) / (\text{TW} - \text{DW}) \times 100$. Membrane integrity was assessed by measuring electrolyte leakage using the method of Matos et al. (2002). Leaf discs were immersed in water for 4 hours to obtain the free conductivity (EC), and then autoclaved to obtain the total conductivity (TC). The percentage of membrane integrity (CI) was calculated using the formula $\text{CI (\%)} = (1 - \text{EC}) / \text{TC} \times 100$. Chlorophyll (a) was extracted using the methods of Luo (2023), employing acetone and anhydrous ethanol. Fresh leaf material (0.1 g) was cut and placed in a graduated test tube. Then, 10 mL of a 95% ethanol and 80% acetone mixture (1:1 v/v) was added, and the mixture was incubated in the dark for 48 hours until the green leaves became colorless. A blank control was prepared using the same solvent mixture. Absorbance values were measured at 645 nm and 663 nm using a UV spectrophotometer. Chlorophyll (a) concentration was calculated using the following equations: **Chlorophyll a** = $(12.72 \times \text{A663} - 2.59 \times \text{A645}) \times V \times N / W$, where V represents

the extract volume, N represents the dilution factor, and W represents the fresh weight of the sample (g).

Statistical Analysis

The values obtained for the physiological and biochemical traits of the plants observed between the combinations of residual sludge doses and water stress levels were subjected to ANOVA testing. For all variables that presented significant differences, the analysis was complemented with Tukey's post-hoc tests (HSD) to perform multiple comparisons of means between residual sludge doses, water stress levels, and their combinations by groups. The statistical significance threshold was set at $p < 0.05$. All statistical operations were done using Statistica 13.0 software.

RESULTS AND DISCUSSIONS

Analysis of variance for the results related to sugar content in the plants indicated a significant genotype effect ($p = 0.001$) (Table 2), showing a higher accumulation for the Hedba variety with a content of $0.56 \pm 0.030 \mu\text{g/g DW}$, compared to BD with a content of $0.51 \pm 0.039 \mu\text{g/g DW}$ (Figure 1). The application of water stress also induced a highly significant increase in sugars ($p < 0.001$) (Table 2) in the plants used. The Tukey HSD test for mean comparison indicated two groups: S2, S1 > S0. The sugar content at the S0 moisture level was $0.48 \pm 0.054 \mu\text{g/g DW}$, while the highest content of $0.57 \pm 0.035 \mu\text{g/g DW}$ was obtained with the S2 stress level (Figure 1).

Amending the soil with residual sludge showed the same trend, with a highly significant increase in sugars ($p < 0.001$). The highest sugar content of $0.72 \pm 0.018 \mu\text{g/g DW}$ was observed with the highest sludge dose, D2, followed by D1 with a content of $0.54 \pm 0.023 \mu\text{g/g DW}$, and finally, the control plants, D0, with a content of $0.35 \pm 0.030 \mu\text{g/g DW}$ (Figure 1).

Regarding proline content, the statistical analysis showed a highly significant accumulation ($p < 0.001$) in the Hedba variety with a value of $0.10 \pm 0.018 \mu\text{g/g DW}$ compared to the BD variety, which had a content of $0.35 \pm 0.048 \mu\text{g/g DW}$ (Figure 1). The effect of water stress was also significant ($p = 0.02$) (Table 2). The proline content at the S0 stress level was

0.15±0.051 µg/g DW, while at the S2 level; it was 0.28±0.057 µg/g DW (Figure 1). The Tukey HSD test indicated two groups: S0, S1 < S2.

According to the results obtained in this study, amending the soil with residual sludge significantly favored the formation and accumulation of proline (p < 0.001), indicating the following two groups: D2 > D1, D0. With the dose D2, a proline content of 0.34±0.052

µg/g DW was obtained, while the lowest content of 0.16±0.062 µg/g DW (Figure 1) was observed with D0. Nitrogen content in the plants showed no significant difference (p = 0.09) (Table 2) between the two varieties used. The Hedba variety had a slightly lower content of 0.53±0.045 µg/g DW compared to BD, which had a content of 0.56±0.059 µg/g DW (Figure 1).

Table 2. Tow-way Anova testing the effects of Sewage Sludge doses (D0 = 0 g of Sewage sludge /kg of soil, D1 = 30 g of Sewage sludge/kg of soil, D2 = 60 g de Sewage sludge /Kg of soil), and drought stress levels (S0 = 100%, S1 = 40%, et S2 = 25% of field capacity) on the variation of physiological plants parameters

Factors	df	SS	<i>p</i> -value	Sig	SS	<i>p</i> -value	Sig	SS	<i>p</i> -value	Sig
		Sugar			Proline			Nitrogen		
G	1	0.032	=0.001	**	0.792	<0.001	***	0.012	0.093	ns
S	2	0.091	<0.001	***	0.213	<0.01	**	1.054	<0.001	***
D	2	1.254	<0.001	***	0.436	<0.001	***	2.442	<0.001	***
GxS	2	0.118	<0.001	***	0.035	0.320	ns	0.002	=0.790	ns
GxD	2	0.029	<0.05	*	0.155	0.010	**	0.118	<0.001	***
SxD	4	0.148	<0.001	***	0.153	0.055	ns	0.067	<0.01	**
GxSxD	4	0.032	<0.05	*	0.262	<0.01	**	0.067	<0.01	**

df: degrees of freedom, SS: Sum of Squares, Sig: statistical significance, ***: p < 0.001, **: p < 0.01, *: p ≤ 0.05, ns: p > 0.05)

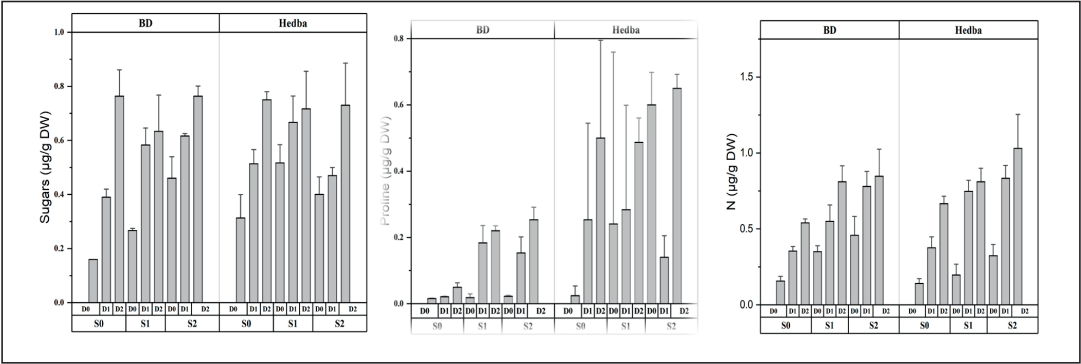


Figure 1. Bares with SD representing the variation of wheat plant biochemical parameters for different sludge amendments D0 = 0 g of Sewage sludge /kg of soil, D1 = 30 g of Sewage sludge /kg of soil, D2 = 60 g de Sewage sludge/kg of soil and drought stress treatments (100%, 40%, and 25%FC).

Contrary to the genotype effect, the application of water stress and the amendment of residual sludge induced a highly significant increase in nitrogen content (p < 0.001) for both factors. With water stress, the nitrogen content at the S0 level was 0.37±0.046 µg/g DW, and it increased to a higher value of 0.71±0.061 µg/g DW for S2. However, the S1 level noted a content of 0.57±0.058 µg/g DW (Figure 1).

Nitrogen content in the plants increased linearly with the increasing doses of residual sludge applied. Indeed, the highest nitrogen content of 0.78±0.040 µg/g DW (Figure 1) was observed with the highest dose, D2, while the lowest content of 0.27±0.029 µg/g DW (Figure 1) was obtained with the lowest dose, D0. The Tukey HSD test indicated three groups in ascending order: D0<D1<D2. The difference in

the accumulation of sugars and proline in the leaves of the two varieties used indicates that the Hedba variety is more resistant compared to the BD variety. This is confirmed by the strong capacity for the synthesis of both osmoticums analyzed (sugars and proline). Several authors (Chaib et al., 2015) report that the accumulation of osmoticums in the leaves of durum wheat varieties is a criterion that allows the selection of the most resistant varieties or genotypes. In our case study, the evolution of sugar and proline content follows the same trend with increasing stress levels. Our results concur with those of Chaib et al. (2015), who, by using several durum wheat genotypes subjected to multiple stress levels, obtained a similar trend in the evolution of sugars and prolines for 75% FC, 35% FC, and 25% FC. With 75% FC as an example, the highest proline content was observed with the Hedba variety, reaching $3.75 \mu\text{mol/mg DW}$.

The more a plant accumulates sugars or proline, the better it can resist and maintain life for as long as possible under stress conditions (Akçay et al., 2023). Soluble sugars and proline are believed to play a major role in osmotic adjustment by contributing to the change in the plant's osmotic potential, enabling it to cope with adverse environmental stress conditions.

It is clear that the accumulation of sugars and proline increases with the severity of water stress, and this observation is consistent with the literature. Indeed, several authors (Bekka, 2021) report in their research a linear accumulation of sugars and proline as water stress becomes more severe. In the same vein, our results corroborate the findings of Chahbar & Belkhodja (2016), who state that the effect of water deficit translates into a marked increase in the concentration of certain constituents, which can be nitrogenous compounds, carbohydrates, or organic acids.

The accumulated proline plays a role in regulating cytoplasmic pH or serves as a nitrogen reserve for the plant. Additionally, sugars are considered an energy source that promotes various metabolic reactions within the cell (Bajji et al., 2000).

The enhanced synthesis of sugars and prolines tested in the leaves of plants under the influence of residual sludge can be attributed to the fertilizing role of this bio-solid, which acts

as a source of several mineral elements, primarily nitrogen and carbon (Hao et al., 2024). Indeed, the analysis of this bio-solid in our laboratory reveals its richness in nitrogen and carbon, aligning with the findings of several authors (Souza Filho et al., 2023), who report that residual sludge is a source of nitrogen. Amending the soil with this fertilizer allows for the release of nitrogen into the soil and its subsequent incorporation into the existing nitrogenous compounds in the plant. Additionally, the applying of this fertilizer in the soil facilitates the utilization of mineral elements (nitrogen and carbon) and their integration into the formation of sugars and proline within the plant. This is supported by the observations in this study, which show that the increase in leaf nitrogen content under stress conditions is positively correlated with the increase in proline content.

Under stress conditions, plants absorb nitrogen to concentrate on proline synthesis (Mahdid & Simonneau, 2023). The decrease in RWC is significant with the increase in water stress. It appears that BD retains water in its leaves better than the Hedba variety, and this difference in behavior can be explained by the variation in leaf surface area. The larger the leaf surface, the greater the effect of water evaporation through the pores (Semida et al., 2020). Indeed, in this study, the leaf surface area of the BD variety is smaller than that of Hedba, which explains its superior water retention capacity compared to the latter (El Yamani et al., 2020).

Analysis of variance for the values obtained for leaf water content revealed a highly significant genotype, stress, and sludge amendment effect ($p < 0.001$) (Table 2). The Hedba variety retained more water in its leaves $60.29 \pm 3.410\%$ compared to BD $51.48 \pm 3.809\%$ (Figure 2). Overall, according to the results, leaf water content decreased with increasing water stress. At the control level, S0, the water reserve in the leaves was $68.68 \pm 3.716\%$, and it decreased to the lowest content of $45.81 \pm 3.146\%$ with S2 (Figure 2). It appears from the obtained values that the application of residual sludge negatively affects the water content of the plants. Indeed, it is noticeable that WRC decreases as the doses increase, ranging from $71.82 \pm 2.719\%$ for D0 to $38.77 \pm 2.810\%$ (Figure 2).

The statistical analysis of cell integrity in the plants revealed highly significant effects ($p < 0.001$) for genotype, water stress, and residual sludge amendment. It appears that the membrane of the BIDI variety is more resistant compared to Hedba. The integrity observed for BD $21.18 \pm 0.811\%$, is higher than that of Hedba, $17.66 \pm 0.691\%$ (Figure 2).

According to the obtained averages, it is clear that the increase in water stress leads to a loss and a decrease in cell integrity. The Tukey HSD test indicated two groups: S0 with a value of $(21.22 \pm 0.930\%)$ followed by a second group, S2 ($18.66 \pm 0.709\%$), and S1 ($18.38 \pm 1.223\%$). The amendment of residual sludge showed the same trend as water stress, with a decrease in integrity as the amendment doses increased. The value obtained for D0 $22.83 \pm 0.833\%$, decreased to $15.61 \pm 0.583\%$ for the highest sludge dose, while D1 had a value of $19.83 \pm 0.755\%$. The following groups were obtained: $D0 > D1 > D2$.

The evolution of chlorophyll a content was significant ($p = 0.0003$) (Table 3) between the two varieties used in this study. Hedba revealed chlorophyll a content of 0.86 ± 0.066 mg/g DW, while BIDI noted a lower content of 0.69 ± 0.565 mg/g DW (Figure 2). Water stress induced a significant increase in the pigment ($p < 0.0001$) (Table 3). The comparison of means showed two groups: S1, S2 > S0. At the S0 level, the content was 0.64 ± 0.059 mg/g DW, while the highest content of 0.88 ± 0.700 mg/g DW (Figure 2) was observed at the S2 level. The variance analysis of the results obtained for the amendment of residual sludge indicated a highly significant effect ($p < 0.001$), showing an improvement in chlorophyll a content from 0.48 ± 0.037 mg/g DW for D0 to 1.00 ± 0.089 mg/g DW for S2 (Figure 2).

The decrease in RWC of plants under water stress conditions was correlated with the increase in water stress levels. This observation is entirely logical; the less irrigation the soil receives, the less water will be available to the plants (Ahmad et al., 2023). Several authors who report similar observations further support these results. Regarding the effect of residual sludge, it is evident that it negatively influences plant water restoration. This effect can be attributed to the role of this amendment as an adsorbent matrix that retains water in its

interstices, limiting the water passage to the plants (Glaab et al., 2020), leading to a decrease in leaf water content. Contrary to our findings, several studies (Benalioua, 2023) indicate that residual sludge improves plant water reserves. These authors report that plants amended with residual sludge exhibit a significantly higher relative water content compared to control plants because this organic fertilizer establishes sufficient moisture in the soil and enhances its water-holding capacity (Delibacak et al., 2020). Boudjabi & Chenchouni (2021) also reported an improvement in soil water retention after amending the soil with residual sludge.

The accumulation and synthesis of proline and sugars in the plant require the utilization and integration of water molecules, leading to an increase in their concentration and a consequent elevation in osmotic potential. In contrast, there is a decrease in leaf water content. The Hedba variety exhibits higher cell membrane integrity compared to the BD variety. This observation confirms that Hedba is more resistant than BD. Furthermore, according to the observed results, it is evident that the synthesis of proline and sugars is more pronounced in Hedba, and these elements, one based on nitrogen (proline) and the other on carbon (sugars), play a role in the formation of the cell membrane, contributing to its resistance to water stress (Khan et al., 2020). In the same vein, it is worth mentioning that the accumulation of osmolytes, particularly proline, glycine betaine, and soluble sugars, can protect membranes from desiccation (Abasi et al., 2024). Sugars contribute to maintaining phosphorylation reactions and energy production (Loretto et al., 2001). They protect enzyme synthesis processes, which could enhance plant tolerance to drought (Ahmad et al., 2021). However, it is observed that cell membrane integrity decreases with increasing water stress. This finding corroborates the existing literature and the findings of several authors (Harsha et al., 2024), who mention a loss of cell membrane integrity under severe water stress. As previously noted for WRC, the amendment of residual sludge limits water passage to the plants, and this effect negatively influences the synthesis of essential components for all the biochemical reactions necessary for cell membrane synthesis

(Quilambo, 2004). It is worth mentioning that this decrease becomes more pronounced with increasing doses of residual sludge applied to the soil. Indeed, as the doses increase, water retention intensifies, and plants are less able to restore essential elements for biochemical reactions. Valentovič et al. (2006) reported that

the application of water stress on two maize varieties for 24 hours, induced by 0.3 M sorbitol (-1.4 MPa), resulted in cell membrane damage, which they attributed to the effect of lipid peroxidation observed in their experiment. Stressed plants responded by increasing the amount of chlorophyll (a).

Table 3. Tow-way Anova testing the effects of Sewage Sludge doses (D0 = 0 g of Sewage sludge/kg of soil, D1 = 30 g of Sewage sludge/kg of soil, D2 = 60 g of Sewage sludge/kg of soil), and drought stress levels (S0 = 100%, S1 = 40%, S2 = 25% of field capacity) on the variation of biochemical plants parameters

Factors	Df	SS	p-value	Sig	SS	p-value	Sig	SS	p-value	Sig
WRC				CI				Chlo (a)		
G	2	1045.9	<0.001	***	167.13	<0.001	***	0.391	<0.001	***
S	2	4707.7	<0.001	***	87.81	<0.001	***	0.565	<0.001	***
D	2	9866.5	<0.001	***	473.93	<0.001	***	2.520	<0.001	***
G×S	4	468.7	<0.01	**	25.15	<0.05	*	0.319	<0.01	**
G×D	4	228.5	0.071	ns	13.48	0.180	Ns	0.086	0.192	Ns
S×D	4	383.4	0.069	ns	31.63	0.100	ns	0.615	<0.001	***
G×S×D	8	1053.2	<0.001	***	3074	0.108	ns	0.729	<0.001	***

df: degrees of freedom, SS: Sum of Squares, Sig: statistical significance, ***: $p < 0.001$, **: $p < 0.01$, *: $p \leq 0.05$, ^{ns}: $p > 0.05$)

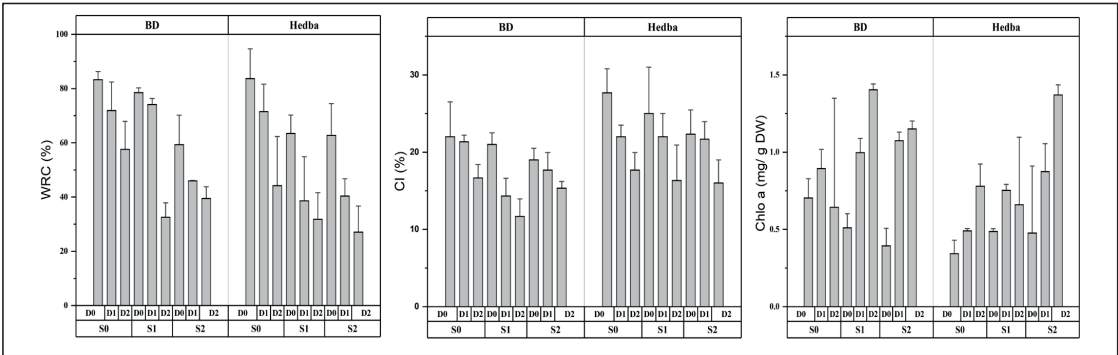


Figure 2. Bares with SD representing the variation of wheat plant physiological parameters for different sludge amendments (D0 = 0 g of Sewage sludge/kg of soil, D1 = 30 g of Sewage sludge/kg of soil, D2 = 60 g de Sewage sludge/kg of soiland drought stress treatments (100%, 40%, and 25% FC).

This increase is linked to a rise in nitrogen content in the leaves, as this mineral is an essential element for the formation of this pigment. According to the results, it appears that nitrogen content increases linearly with the level of stress. As previously noted, amending the soil with sludge is an effective source of nitrogen for the plant. This bio-solid releases all forms of nitrogen into the soil, and once this mineral is taken up by the plant, it is incorporated into the synthesis of chlorophyll a (Kaya et al., 2024). Contrary to our findings, Gai et al. (2024) obtained a decrease in chlorophyll content in water-stressed sugarcane plants.

CONCLUSIONS

In conclusion, amending the soil with low doses of residual sludge in combination with water stress enables the plant to counter the effects of stress through a good accumulation of sugars, proline, and nitrogen. This observation is confirmed by the green color of the plant leaves, indicating a high content of chlorophyll (a), an essential pigment in energy reactions required by the plant. However, further experimentation with additional precautions is warranted. It is crucial to diagnose the heavy metal content in residual sludge to thoroughly understand and control the

effects of this bio-solid amendment on both the soil and the plant.

REFERENCES

- Ababsa, N., Boudjabi, S., & Chenchouni, H. (2023). Biochar amendments changed soil properties and improved cereal crop growth under salt stress. *Journal of Soil Science and Plant Nutrition*, 23(4), 4912-4925. <https://doi.org/10.1007/s42729-023-01453-7>
- Abasi, F., Ehsan, M., Raja, N.I., Sohail, M., Iqbal, M., Shahbaz, M., & Raza, M.U. (2024). Physiological and molecular pathways of crop plants in response to heat stress. In *Improving Stress Resilience in Plants* (pp. 459-479). Academic Press. <https://doi.org/10.1016/B978-0-443-18927-2.00020-0>
- Ahmad, F., Singh, A., & Kamal, A. (2020). Osmoprotective role of sugar in mitigating abiotic stress in plants. *Protective chemical agents in the amelioration of plant abiotic stress: Biochemical and molecular perspectives*, 53-70. <https://doi.org/10.1002/9781119552154.ch3>
- Ahmad, R., Alsahli, A.A., Alansi, S., & Altaf, M.A. (2023). Exogenous melatonin confers drought stress by promoting plant growth, photosynthetic efficiency and antioxidant defense system of pea. *Scientia Horticulturae*, 322, 112431.
- Akcay, U.C., & Okudan, N. (2023). Exogenous serotonin improves drought and salt tolerance in tomato seedlings. *Plant Growth Regulation*, 101(1), 239-249. <https://doi.org/10.1007/s10725-023-01016-x>
- Bajji, M., Lutts, S., & Kinet, J.M. (2000). Physiological changes after exposure to and recovery from polyethylene glycol-induced water deficit in callus cultures issued from durum wheat (*Triticum durum* Desf.) cultivars differing in drought resistance. *Journal of Plant Physiology*, 156(1), 75-83. [https://doi.org/10.1016/S0176-1617\(00\)80275-8](https://doi.org/10.1016/S0176-1617(00)80275-8)
- Barrs, H.D. (1968). *Determination of water deficit in plant tissues*. In: *Water Deficit and Plant Growth* (T.T. Kozlowski, ed.). Academy Press, New York, pp.235-368.
- Bekka, S. (2021). Amélioration de la tolérance du blé tendre au stress hydrique par apport de la proline BEKKA. *Revue Agrobiologia*, 11(2), 2651-2659. <https://www.asjp.cerist.dz/en/article/173037>
- Benalioua, B.K. (2023). *Évaluation de l'effet de Trichoderma sp. sur la résistance du blé dur (Triticum durum Desf. Var. Vitron) au stress hydrique simulé par le PEG6000 au stade germination* (Doctoral dissertation).
- Boudjabi, S., & Chenchouni, H. (2021). On the sustainability of land applications of sewage sludge: how to apply the sewage biosolid in order to improve soil fertility and increase crop yield? *Chemosphere*, 282, 131122. <https://doi.org/10.1016/j.chemosphere.2021.131122>
- Boudjabi, S., & Chenchouni, H. (2023). Comparative effectiveness of exogenous organic amendments on soil fertility, growth, photosynthesis and heavy metal accumulation in cereal crops. *Heliyon*, 9(4). <https://doi.org/10.1016/j.heliyon.2023.e14615>
- Boudjabi, S., Ababsa, N., & Chenchouni, H. (2023). Enhancing soil resilience and crop physiology with biochar application for mitigating drought stress in durum wheat (*Triticum durum*). *Heliyon*, 9(12). <https://doi.org/10.1016/j.heliyon.2023.e22909>
- Boudjabi, S., Kribaa, M., & Chenchouni, H. (2019). Sewage sludge fertilization alleviates drought stress and improves physiological adaptation and yield performances in Durum Wheat (*Triticum durum*): a double-edged sword. *Journal of King Saud University-Science*, 31(3), 336-344. <https://doi.org/10.1016/j.jksus.2017.12.012>
- Chahbar, S., & Belkhdja, M. (2016). Effet du déficit hydrique sur certains osmolytes chez cinq variétés de blé dur (*Triticum durum*) [Water deficit effects on osmolytes traits in five durum wheat varieties (*Triticum durum*)]. *International Journal of Innovation and Applied Studies*, 17(3), 757-767. <http://www.ijias.issr-journals.org/>
- Chaib, G., Benlaribi, M., & Hazmoune, T. (2015). Accumulation d'osmolytes chez le blé dur (*Triticum durum* Desf.) sous stress hydrique. *European Scientific Journal*, 11(24).
- Delibacak, S., Voronina, L., & Morachevskaya, E. (2020). Use of sewage sludge in agricultural soils: Useful or harmful. *Eurasian Journal of Soil Science*, 9(2), 126-139. <https://doi.org/10.18393/ejss.687052>
- DuBois, M., Gilles, K.A., Hamilton, J.K., Rebers, P.T., & Smith, F. (1956). Colorimetric method for determination of sugars and related substances. *Analytical chemistry*, 28(3), 350-356. <https://doi.org/10.1021/ac60111a017>
- El Behairy, R.A., El Arwash, H.M., El Baroudy, A.A., Ibrahim, M.M., Mohamed, E.S., Rebouh, N.Y., & Shokr, M.S. (2024). An Accurate Approach for Predicting Soil Quality Based on Machine Learning in Drylands. *Agriculture*, 14(4), 627. <https://doi.org/10.3390/agriculture14040627>
- El Yamani, M., Boussakouran, A., & Rharrabti, Y. (2020). Leaf water status, physiological behavior and biochemical mechanism involved in young olive plants under water deficit. *Scientia Horticulturae*, 261, 108906. <https://doi.org/10.1016/j.scienta.2019.108906>
- Gai, J., Wang, J., Xie, S., Xiang, L., & Wang, Z. (2024). Spectroscopic determination of chlorophyll content in sugarcane leaves for drought stress detection. *Precision Agriculture*, 25(2), 543-569. <https://doi.org/10.1007/s11119-023-10082-0>
- Głąb, T., Żabiński, A., Sadowska, U., Gondek, K., Kopeć, M., Mierzwa-Hersztek, M., & Stanek-Tarkowska, J. (2020). Fertilization effects of compost produced from maize, sewage sludge and biochar on soil water retention and chemical properties. *Soil and Tillage Research*, 197, 104493. <https://doi.org/10.1016/j.still.2019.104493>
- Hao, J., Tan, J., Zhang, Y., Gu, X., Zhu, G., Wang, S., & Li, J. (2024). Sewage sludge-derived nutrients and biostimulants stimulate rice leaf photosynthesis and root metabolism to enhance carbohydrate, nitrogen and antioxidants accumulation. *Chemosphere*, 352,

141335. <https://doi.org/10.1016/j.chemosphere.2024.141335>
- Harsha, S.G., Girish, B., Dinsha, M., Patil, M.I., Singh, T. H., & Prathibha, M.D. (2024). Comparative study on physiological intricacies and sugar accumulation dynamics in brinjal (*Solanum melongena* L.) under drought stress. *Scientia Horticulturae*, 325, 112633.
- Hunter, M.C., Smith, R.G., Schipanski, M.E., Atwood, L.W., & Mortensen, D.A. (2017). Agriculture in 2050: recalibrating targets for sustainable intensification. *Bioscience*, 67(4), 386-391. <https://doi.org/10.1093/biosci/bix010>
- Kaya, C., Akin, S., Sarioglu, A., Ashraf, M., Alyemeni, M. N., & Ahmad, P. (2024). Enhancement of soybean tolerance to water stress through regulation of nitrogen and antioxidant defence mechanisms mediated by the synergistic role of salicylic acid and thiourea. *Plant Physiology and Biochemistry*, 207, 108320.
- Khan, N., Ali, S., Zandi, P., Mehmood, A., Ullah, S., Ikram, M., & Babar, M. A. (2020). Role of sugars, amino acids and organic acids in improving plant abiotic stress tolerance. *Pak. J. Bot.*, 52(2), 355-363.
- Lallaouna, R., Ababsa, N., Della, Y., & Boudjabi, S. (2023). Soil respiration as an indicator of soil quality under agrochemical treatment in a semi-arid area of southern Mediterranean. *Arabian Journal of Geosciences*, 16(9), 531. <https://doi.org/10.1007/s12517-023-11649-x>
- Loretti E, De Bellis L, Alpi A, Perata P. (2001). Why and how do plant cells sense sugars? *Ann Bot.*, 88, 803-812.
- Luo, Q., Xie, H., Chen, Z., Ma, Y., Yang, H., Yang, B., & Ma, Y. (2023). Morphology, photosynthetic physiology and biochemistry of nine herbaceous plants under water stress. *Frontiers in Plant Science*, 14, 1147208. <https://doi.org/10.3389/fpls.2023.1147208>
- Mahdid, M., & Simonneau, T. (2023). Rapid responses and physiological events of leaf growth in response to water stress induced by poly ethylene glycol in maize (*Zea mays* L.). *Algerian Journal of Environmental Science and Technology*, 9(1).
- Matos, M.C., Campos, P.S., Ramalho, J.C., Medeira, M.C., Maia, M.I., Semedo, J.M., & Matos, A. (2002). Photosynthetic activity and cellular integrity of the Andean legume *Pachyrhizusahipa* (Wedd.) Parodi under heat and water stress. *Photosynthetica*, 40(4), 493-501.
- Pérez-Alfocea, F., & Larher, F. (1995). Sucrose and proline accumulation and sugar efflux in tomato leaf discs affected by NaCl and polyethylene glycol 6000 iso-osmotic stresses. *Plant Science*, 107(1), 9-15.
- Quilambo, O.A. (2004). Proline content, water retention capability and cell membrane integrity as parameters for drought tolerance in two peanut cultivars. *South African Journal of Botany*, 70(2), 227-234. [https://doi.org/10.1016/S0254-6299\(15\)30239-8](https://doi.org/10.1016/S0254-6299(15)30239-8)
- Sáez-Plaza, P., Navas, M.J., Wybraniec, S., Michałowski, T., & Asuero, A.G. (2013). An overview of the Kjeldahl method of nitrogen determination. Part II. Sample preparation, working scale, instrumental finish, and quality control. *Critical Reviews in Analytical Chemistry*, 43(4), 224-272.
- Semida, W.M., Abdelkhalik, A., Rady, M.O., Marey, R.A., & Abd El-Mageed, T.A. (2020). Exogenously applied proline enhances growth and productivity of drought stressed onion by improving photosynthetic efficiency, water use efficiency and up-regulating osmoprotectants. *Scientia Horticulturae*, 272, 109580.
- Sharma B., Sarkar A., Singh P., Singh R.P. (2017). Agricultural utilization of biosolids: A review on potential effects on soil and plant grown. *Waste Manag.* 64, 117-132.
- Singh, R.P., Singh, P., Ibrahim, M.H., Hashim, R. (2011). Land application of sewage sludge: physicochemical and microbial response. *Rev Environ Contam Toxicol.*, 214, 41-61.
- Souza Filho, E.J., Barros, K.K., Bezerra Neto, E., Gavazza, S., Florencio, L., & Kato, M.T. (2023). Effect of reclaimed water and dehydrated sludge on the morpho-physiology and yield of sorghum. *Environmental Technology*, 1-17.
- Valentovic, P.S.A.V., Luxova, M.S.A.V., Kolarovic, L.S.A.V., & Gasparikova, O.S.A.V. (2006). Effect of osmotic stress on compatible solutes content, membrane stability and water relations in two maize cultivars. *Plant Soil and Environment*, 52(4), 184.
- Vera-García, S.L., Rodríguez-Casasola, F.N., Barrera-Cortés, J., Albores-Medina, A., Muñoz-Páez, K.M., Cañizares-Villanueva RO, Montes-Horcasitas MC. (2023). Enhancing Phosphorus and Nitrogen Uptake in Maize Crops with Food Industry Biosolids and *Azotobacter nigricans*. *Plants (Basel)*. 12(17), 3052. doi: 10.3390/plants12173052. PMID: 37687299; PMCID: PMC10489705.

ASSESSMENT OF THE SURFACE WATER QUALITY DATA COLLECTED SEASONALLY AT THE DANUBE RIVER BIFURCATIONS (CEATAL IZMAIL AND CEATAL SF. GHEORGHE)

Irina CATIANIS, Adriana Maria CONSTANTINESCU, Dumitru GROSU,
Gabriel IORDACHE, Florin DUȚU, Ana-Bianca PAVEL

National Institute for Research and Development for Marine Geology and GeoEcology
(GeoEcoMar), 23-25 Dimitrie Onciul Street, Bucharest, Romania

Corresponding author email: irina.catianis@geoecomar.ro

Abstract

This study was carried out in the Danube Delta, at Ceatal Izmail and Ceatal Sfântu Gheorghe. The investigated sectors are of great importance, being essential key points related to the hydrological connectivity between the Danube River distributary branches and interdistributary channels, streams, and lakes of the Danube Delta. Thereby, six stations were selected to provide seasonal water quality data, collected biannually, from 2018 to 2023, in different hydrodynamic conditions (high and low waters). To assess the conditions of the investigated surface waters, several physical in-situ measurements (T, pH, DO, EC, TDS, Transp.) were taken at all sampling locations. Additionally, water samples were collected for laboratory analysis ($N-NH_4^+$, $N-NO_2^-$, $N-NO_3^-$, $P-PO_4^{3-}$, Chla, SiO_2 , TOC, SO_4^{2-} , Turb., TSS, ORP). The criteria used to assess the water quality in the investigated sites include the current Romanian national legislation (Ord. 161/2006) and other international environmental standards. Most of the investigated physical-chemical parameters were in line with correlated criteria, and only incidentally, the objectives were exceeded at single or multiple locations. According to this assessment, permanent monitoring of water quality is mandatory at these important hydrological nodes, by analyzing the status and trends in physical and chemical characteristics of the surface water environment.

Key words: ecosystems, environment, physical-chemical parameters, seasonal, water quality.

INTRODUCTION

Nowadays, water pollution is a general concern worldwide. Preserving surface water quality is essential for daily demand everywhere. The freshwater which is stored in rivers, lakes, reservoirs, creeks, and streams, represents the major source of water for the human population, animal and plant communities, as well as for irrigation water demands and other socio-economic requirements.

Since the beginning of industrialization and the expansion of modern civilization, the Danube River water quality has been persistently declining because of anthropogenic inputs and the discharging of untreated or poorly treated sewages (Ilie et al., 2014; Simionov et al., 2020). Even if, lately, a series of measures have been taken regarding the environmental conservation and preservation of surface waters (EU-WFD, 2000), the river is still subject to natural and anthropogenic pressures due to its function as an environmental resource and economic potential, such as navigable transport, water regulation, commercial fishing, recreational activities etc.

(Gasparotti, 2014). In addition, the consequences of the Iron Gate dam constructions (1972 and 1985), hydro-technical works, water abstractions, and associated impoundments, regulations etc. (Panin et al., 1999), resulted in considerable changes in physical, chemical, and biological characteristics of the downstream Danube River water (Gasparotti et al., 2013).

The Danube is one of the world's most international rivers and is regarded as a pan-European river, not only because of its length and large drainage basin area, but especially due to its pan-European character in socio-economic and cultural aspects (Padlo et al., 2021).

The Danube River is the second-longest river in Europe after the Volga (in Russia), regarding length (2857 km) and area (801463 km²), shaping one of the most important and large European water system consisting of the Danube River - Danube Delta - Black Sea (Panin et al., 2016; Calmuc et al., 2023).

The river is subdivided into three main sections: the Upper Danube (1060 km), the Middle Danube (725 km), and the Lower Danube (1075

km). The Lower Danube (1075 km) represents a natural border between Romania and states such as Serbia, Bulgaria, Ukraine, and the Republic of Moldova (Gâstescu & Țuchiu, 2012). Before reaching the Black Sea, the Danube River splits into three main branches: Chilia to the North (with a length of 104 km, transporting 60% of the Danube's flow), Sulina in the middle (with a length of 71 km and carrying 18% of the Danube's flow) and Sf. Gheorghe in the South (with a length of 112 km and 22% of the Danube's flow). The areas between these branches shape the distinct specific environments of the Danube Delta.

The Danube's alluvial inputs, distributed by the three branches, loaded with solid particulate material and other associated contaminants, is considerably the main source of the local potential pollution, being currently accountable for the environmental impairments within the river and the north-western region of the Black Sea (Păun et al., 2017).

Due to its large catchment and the anthropic pressures, the Danube water is affected by pollution from multiple sources (Jitar et al., 2015; Pavlović et al., 2016; Simionov et al., 2021). As mentioned before, the Danube River water quality is vulnerable to contamination as a consequence of anthropogenic inputs such as discharges of industrial and agricultural effluents or untreated wastewaters which can have both allochthonous, as well as autochthonous origin. These potential contaminants may lead to severe changes in the physical-chemical and biological parameters not only of the Danube River but also of the Danube Delta ecosystems. Maintaining good water quality and proper ecosystems is imperative for the favorable functioning of the Danube River Delta region (Kyle, 2006).

In this context, the purpose of the study was to assess the surface water quality at the Danube River bifurcations, i.e., *Ceatal Izmail* and *Ceatal Sf. Gheorghe*, the two main distribution nodes for water and sediment throughout the Danube Delta.

Regular water quality assessment of the Danube River, especially in these specific "key" locations is critical for sustaining viable water criteria for the unique aquatic biodiversity and migratory birds (Rose, 1992; Rose, 1993; Zöckler et al., 2003) as well as ecosystem

services of the Danube Delta (Cazacu & Adamescu, 2017; Gómez-Baggethun et al., 2019; Lazăr et al., 2022). This study contributes to covering a gap in published data on water quality in these specific locations (Burt et al., 2013; Myroshnychenko et al., 2015; Chapman et al., 2016).

MATERIALS AND METHODS

Study area

This study was carried out at the main two bifurcations of the Danube River within its Delta, i.e., *Ceatal Izmail* and *Ceatal Sf. Gheorghe* (Figure 1). At the first bifurcation of the Delta - *Ceatal Izmail*, the Danube River splits into two distributaries: Chilia (the northern Arm) and Tulcea (the southern Arm). Branching in the right direction at *Ceatal Izmail* (Mile 43), the Tulcea Arm extends farther south to 17 km to the second bifurcation at *Ceatal Sf. Gheorghe* (Mile 34).

Here, the Tulcea Arm separates into two main branches: Sulina Arm (on the left) and Sf. Gheorghe Arm (on the right) (Duțu et al., 2022). The investigated sectors i.e., *Ceatal Izmail* and *Ceatal Sf. Gheorghe*, are of great importance, being essential key points related to the hydrological connectivity between the Danube River distributary branches and interdistributary channels, streams and lakes of the delta. As well, these bifurcations are characterized as very dynamic hydro morphological areas.

The purpose of the investigations was to emphasize the potential impact on the investigated ecosystems, due to the surplus of available contaminants that comes from different upstream and local anthropogenic activities, considering that the pollution point sources leakages are increased in the lower sector contrary to the upper Danube area (Gasparotti, 2014).

Sample collection

Distinct control sections (sampling stations) were selected (Figure 1) to provide seasonal data on the dynamics of different physical-chemical environmental indicators. The sampling activities occurred at the R/V "Istros" of the National Institute for Research and Development of Marine Geology and Geoecology-GeoEcoMar, Romania.

An overall number of 57 water samples were collected seasonally, from 2018 to 2023, in

different hydrodynamic conditions (high and low Danube levels) (Figure 2).

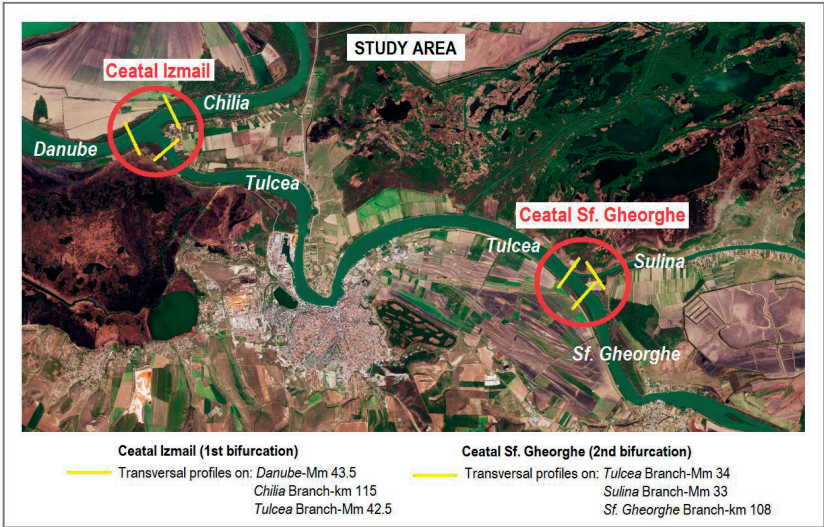


Figure 1. Map of the Danube River bifurcations (Base map source: <https://www.esa.int/>)

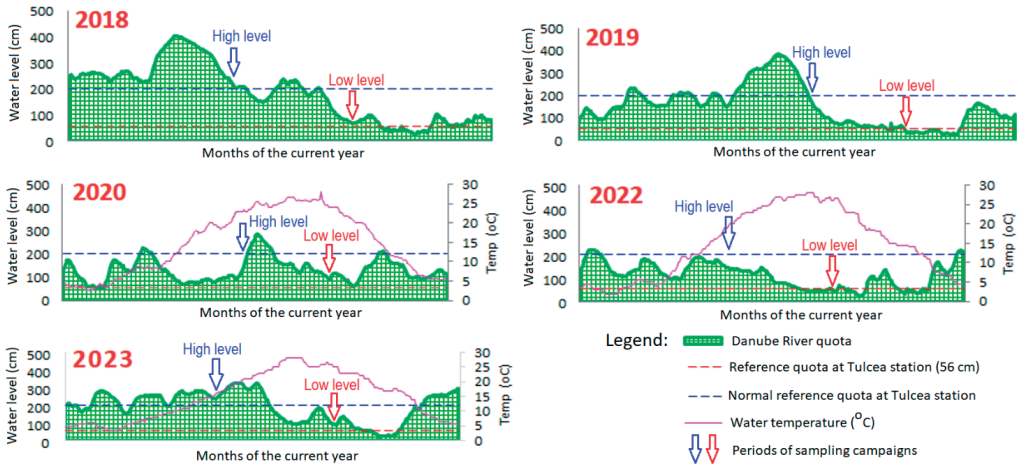


Figure 2. Danube River flow variations recorded at the Tulcea Port (<https://www.afdj.ro/cotele-dunarii>)

The periods of sampling campaigns with wet season conditions (seasonal rains) and high-water Danube levels were: *May 2018* (04.05-13.05), *July 2019* (01.07-14.07), *June 2020* (15.06-28.06), *May 2022* (09.05-17.05) and *May 2023* (16.05-23.05). Then, the periods of sampling campaigns with dry season conditions (no significant rain recorded) and low-water Danube levels were: *August 2018* (08.08-27.08), *September 2019* (24.09-04.10), *August 2020*

(25.08-05.09), *August 2022* (22.08-31.08) and *September 2023* (06.09-15.09).

The exact location of the stations was recorded every single time, and the samples were gathered from the middle of each distributary, at a depth of 0.5 m.

From the *Ceatal Izmail bifurcation*, the following samples were gathered as: *Dunărea-Mm 43.5* (wet season: DD18-02, DD19-18, DD20-18, DD23-02; dry season: DD18-79,

DD19-119, DD20-101, DD22-67, DD23-97), *Chilia-km 115* (wet season: DD18-05, DD19-15, DD20-15, DD23-05; dry season: DD18-86, DD19-122, DD20-104, DD22-70, DD23-100) and *Tulcea-Mm 42.5* (wet season: DD18-08, DD19-21, DD20-21, DD23-08; dry season: DD18-82, DD19-125, DD20-110, DD22-73, DD23-104). From the *Sf. Gheorghe bifurcation*, the following samples were collected as: *Tulcea-Mm 34* (wet season: DD18-14, DD19-27, DD20-27, DD22-05, DD23-14; dry season: DD18-132, DD19-131, DD20-113, DD22-79, DD23-109), *Sulina-Mm 33* (wet season: DD18-17, DD19-29, DD20-32, DD22-07, DD23-16; dry season: DD18-135, DD19-133, DD20-115, DD22-81, DD23-111) and *Sf Gheorghe-Km 108* (wet season: DD18-11, DD19-31, DD20-30, DD22-02, DD23-11; dry season: DD18-138, DD19-135, DD20-117, DD22-76, DD23-106). It is worth mentioning that navigable waterways are expressed in nautical miles (i.e. Mm), and natural courses in km.

Parameters such as temperature, pH, dissolved oxygen, electrical conductivity and total dissolved solids were acquired *in situ*, at each sampling location, using the WTW Multiparameter Field Meter-3630 IDS. Subsequently, laboratory analysis was achieved to identify the contents of ammonium, nitrite, nitrate, phosphate, chlorophyll "a", silica, total organic carbon, sulfates, turbidity, total suspended solids, water transparency and oxidation-reduction potential using a Hach-DR6000 UV-VIS Spectrophotometer and a Hach-2100 Portable Turbidimeter. The analysis protocol is established according to standard methodologies of the laboratories of NIRD GeoEcoMar.

RESULTS AND DISCUSSIONS

Throughout time, the Danube River aroused interest in the scientific community that has been manifested by different investigations and research studies under several aspects, such as the environmental impacts of hydroelectric power (Panin & Jipa, 2002; Vukovic et al., 2014; Habersack & Bradley, 2022), the significant impact of anthropogenic organic and inorganic substances (Cozzi et al., 2019; Mănoiu & Crăciun, 2021; Lazăr et al., 2024), the impacts of the heavy metals (Vignati et al., 2013; Rico et

al., 2016; Saeed et al., 2023) etc. Anywise, there are not many environmental quality evaluations strictly dedicated to *Ceatal Izmail* and *Ceatal Sf. Gheorghe*. Taking into account the multitude of anthropogenic and natural factors that can contribute to Danube River water degradation, a first step within this study was made in the sense of the investigation of some selected physical-chemical parameters at the two bifurcations. So, this paper focused on assessing the physical-chemical parameters impacting water quality, and the seasonal, temporal and spatial variations of water quality in these Danube River's sections.

The results acquired within this study may improve the available water-quality database with relevant information in terms of the Water Framework Directive guidelines (EU-WFD, 2000) by combining water-quality data from multiple sources. The EU-WFD instructions, stipulate EU countries to implement water quality no less than the category "good status" in rivers, lakes, groundwater, estuaries and coastal waters, by 2027 at the latest.

The obtained results and interpretations were related to the current national legislation (Order 161/2006), in addition to other international reference standards referring to the quality classification of surface water.

Generally, the average values of data sets related to the physical-chemical parameters investigated in sampling points at *Ceatal Izmail bifurcation* (Danube-Mm 43.5, Chilia-Km 115, Tulcea-Mm 42.5) and *Ceatal Sf. Gheorghe bifurcation* (Tulcea-Mm 34, Sulina-Mm 33, Sf. Gheorghe-Km 108) are relatively good. Generally speaking, no critical increments/abatements were noticed, apart from some specific cases that will be discussed hereinafter.

The variations (the minimum, maximum and average values) of the considered physical-chemical parameters between sampling stations are presented in Table 1 and Table 2.

Water temperature (°C), water reaction levels (pH units) and dissolved oxygen contents (mg O₂/L) did not register significant differences. The water temperature's fluctuations were mainly related to the evolution of air temperature trends attributable to climatic seasons (www.accuweather.com/ro/) and the dynamic action of the wind. Consequently,

significant differences between upstream (*Ceatal Izmail*) and downstream (*Ceatal Sf. Gheorghe*) were not registered in the investigated sampling points (Table 1) neither seasonal nor annual.

Regarding the reaction of water (pH units), it was noticed that the slightly alkaline pH values (Table 1) have the largest preponderance (Order 161/2006). Transitional waters (rivers, lakes etc.) generally range between acidic (5) and

alkaline (9) on the pH scale, cumulating the results of diverse circumstances (microbial activity, microbial sulfate reduction, ammonification, water evaporation closely related to high contents of sodium and magnesium carbonates (Grant, 2004). Accordingly, there is no evident sign of acidity or alkalinity in the upstream (*Ceatal Izmail*) and downstream (*Ceatal Sf. Gheorghe*) probed waters, neither seasonal nor annual (Figure 3).

Table 1. Synthesis of the results obtained after the analysis of the parameters such as temperature, water reaction, dissolved oxygen, nutrients, chlorophyll and silica

Location		Value	T (°C)	pH (unit)	DO ₂ (mg O ₂ /L)	N-NH ₄ ⁺ (mg/L)	N-NO ₂ ⁻ (mg/L)	N-NO ₃ ⁻ (mg/L)	P-PO ₄ ³⁻ (mg/L)	Chla (µg/L)	SiO ₂ (mg/L)
Ceatal Izmail	Danube – Mm 43.5 (n = 9)	Min.	16.7	7.56	5.75	0.019	0.007	0.010	0.080	7.50	0.64
		Max.	27.7	8.56	9.26	0.064	0.035	0.330	1.666	24.06	5.23
		Average	23.62	8.03	7.68	0.041	0.013	0.134	0.350	14.42	2.74
	Chilia – Km 115 (n = 9)	Min.	17.3	7.24	5.72	0.003	0.007	0.050	0.053	8.06	1.08
		Max.	28.5	8.26	9.24	0.200	0.020	0.320	1.100	27.12	5.36
		Average	23.78	7.96	7.69	0.060	0.010	0.143	0.271	16.87	2.50
	Tulcea – Mm 42.5 (n = 9)	Min.	17.2	7.4	5.76	0.019	0.007	0.040	0.080	6.77	1.21
		Max.	28.2	8.24	9.53	0.080	0.023	0.320	1.660	28.60	4.72
		Average	23.49	7.96	7.69	0.040	0.012	0.144	0.439	13.58	2.69
Ceatal Sf Gheorghe	Tulcea – Mm 34 (n = 10)	Min.	17.1	7.83	4.44	0.009	0.001	0.010	0.060	5.26	0.02
		Max.	26.8	8.2	9.39	0.070	0.032	0.330	1.650	20.39	5.03
		Average	22.74	8.03	7.41	0.030	0.011	0.144	0.458	11.41	2.50
	Sulina – Mm 33 (n = 10)	Min.	17.1	7.54	4.16	0.006	0.007	0.070	0.056	5.26	0.02
		Max.	27.1	8.27	9.36	0.110	0.025	0.300	1.850	20.67	4.80
		Average	22.80	7.99	7.32	0.045	0.010	0.142	0.711	12.11	2.44
	Sf. Gheorghe – Km 108 (n = 10)	Min.	17.5	7.35	4.73	0.008	0.008	0.050	0.046	3.91	0.75
		Max.	27	8.23	9.26	0.100	0.026	0.320	1.686	34.12	4.06
		Average	22.78	7.96	7.45	0.045	0.011	0.157	0.326	12.67	2.46

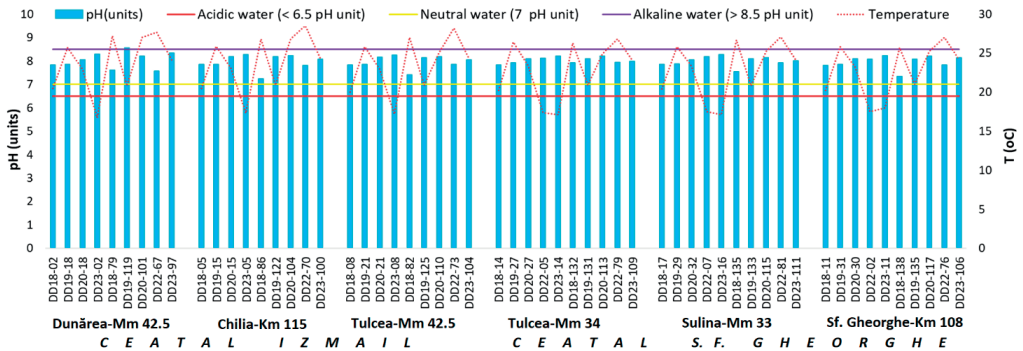


Figure 3. Seasonal and spatial variation of pH (water reaction) in investigated sites

The dissolved oxygen (DO) contents showed slight variations (Table 1) (Figure 4). Generally,

the investigated sampling sites showed well-oxygenated surface waters (8 mgO₂/L),

subsequently followed by moderate-oxygenated surface waters (5-7 mg O₂/L) (Order 161/2006), and poor-oxygenated surface waters (< 5 mg/L) (www.niwa.co.nz). Incidentally, poor-oxygenated surface waters were encountered in the year 2022 (in May) at *Ceatal Sf. Gheorghe* (Table 1), where some lower values were noticed, such as Tulcea-Mm 34 (DD22-05 = 4.4 mg O₂/L), Sulina-Mm 33 (DD22-07 = 4.16 mg

O₂/L), and Sf. Gheorghe-Km 108 (DD22-02 = 4.73 mg O₂/L). The DO decreases could be related to local specific circumstances as a result of the increased organic load in the upstream urban section of the Danube River. Significant variations were not registered between the upstream and downstream sites (Table 1) neither seasonal nor annual, except *Ceatal Sf. Gheorghe* during 2022 (May).

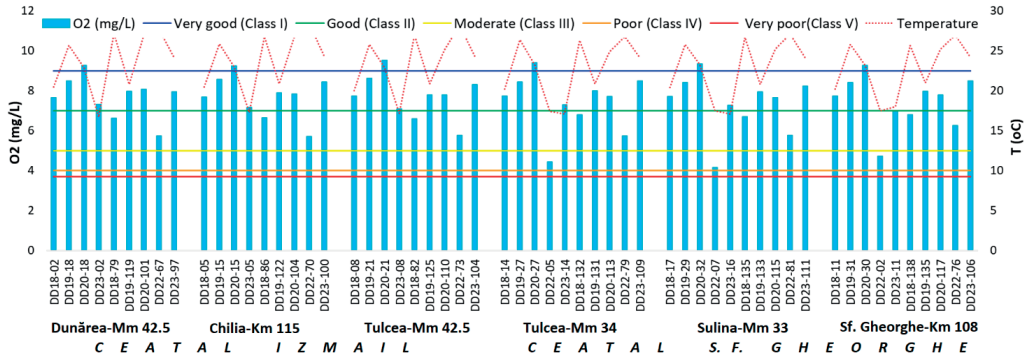


Figure 4. Seasonal and spatial variation of dissolved oxygen in investigated sites

In this study, the dynamic of the nutrient's regime (Nitrogen and Phosphorus compounds) showed an interesting situation and great variability. For instance, the concentration of different nitrogen compounds (such as ammonium, nitrite and nitrate) in the water samples did not show threatening changes. The concentrations of ammonium (N-NH₄⁺) showed lower values (Table 1), below the imposed limit (0.4 mg/L) settled for the first-class water quality (very good) (Order 161/2006).

In the case of nitrite-nitrogen (N-NO₂⁻), a similar situation was noticed in the sense that the majority of values (Table 1) were included in the first-class water quality (very good) (0.01 mg/L) (Order 161/2006). However, during 2022 (August) two sampling sites detected values pertaining to the second-class water quality (good) (0.03 mg/L), such as Danube-Mm 43.5 (DD22-67 = 0.035 mg/L), Tulcea-Mm 34 (DD22-79 = 0.032 mg/L) (Figure 5).

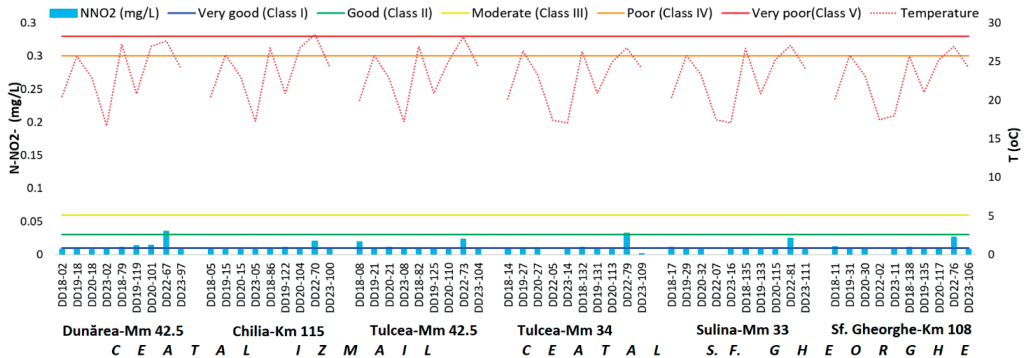


Figure 5. Seasonal and spatial variation of nitrite in investigated sites

In terms of nitrate-nitrogen (N-NO_3^-) very low values were noticed (Table 1), below the threshold (1 mg/L) settled for first-class quality (very good) (Order 161/2006).

Instead, the orthophosphate (P-PO_4^{3-}) contents showed great spatial, seasonal, and temporal variability (Table 1) (Figure 6). Values that cover the entire spectrum of all types of water quality categories were encountered, such as first-class water quality (very good) (0.1 mg/L), second-class water quality (good) (0.2 mg/L), third-class water quality (moderate) (0.4 mg/L), forth-class water quality (poor) (0.9 mg/L) and fifth-class water quality (very poor) (> 0.9 mg/L) (Order 161/2006). The values, varied randomly between upstream and downstream sites, from wet season to dry season, from one year to another year, all that independent of the spatial-temporal variation of the Danube water flow, so no relationship was found between them. Further seasonal analysis is required to untangle the influencing factors and spatial patterns of this variability.

Probably, the P-PO_4^{3-} exceeding could be linked to local specific environments because of the increased contaminant load with phosphorus compounds (i.e., domestic effluents, agricultural inputs, industrial waste) in the upstream urban section of the Danube River. Additionally, natural sources may contribute to water contamination as a consequence of atmospheric deposition, natural decomposition of rocks and minerals, dissolution of soluble inorganic materials, decomposition of plant or animal biomass, re-sedimentation from the bottom substrate etc.

Given the large differences (one order of magnitude) between the highest (over 1 mg/L -

class V) and the normal or low P-PO_4^{3-} concentrations (class I and II) and the predominance of most high values to the Sulina Channel, another potential explanation for the large variability in nutrients concentration may be related to an overlooked local point source: enlarged contamination with residual water due to increased maritime navigation on the Danube. Among the three Danube's arms, Sulina Channel is the only one used for maritime commercial navigation with the end destination being the Brăila Harbor. Through their journey up or down between Sulina and Brăila, large commercial ships can often be found not only in designated harbors but also standing in line, anchored along the Danube's shore. This is especially true for the last years and mostly since the war in Ukraine started which caused a dramatic increase in the maritime navigation activities on the Danube. Such increased point-source pollution issues related to the intensified maritime traffic can affect the quality of the water for the Black Sea shore near the Sulina port area where nowadays, at any time somewhere between one and a few hundred ships, anchored in the port road, are awaiting long periods (even months) for their permission to navigate upstream on the river. However, the impact of increased navigation activities on the water quality of the Danube and the Black Sea has yet to be determined.

Generally, about the chlorophyll "a" ($\text{Chla} - \mu\text{g/L}$) content, lower values were obtained (Table 1), below the imposed limit (25 $\mu\text{g/L}$) settled for the first-class water quality (very good) (Order 161/2006). However, infrequently, three samples slightly exceeded this limit.



Figure 6. Seasonal and spatial variation of orthophosphates in investigated sites

The silica concentrations (SiO_2 - mg/L) varied more between the investigated stations (Table 1). Despite that, the values were low, below the conventional limit established for rivers and lakes (5-25 mg/L) (Chapman, 1996). Under these circumstances, the concentration of nutrient compounds identified within this study (ammonium, nitrite, and nitrate), did not pose a serious stress on the aquatic biodiversity (variety of plants and animals) existent in the upstream (*Ceatal Izmail*) and downstream sites (*Ceatal Sf. Gheorghe*). Appropriately, the results obtained for chlorophyll "a" and silica content are not conducive to a phenomenon of excessive

nutrient enrichment in the investigated freshwater samples.

As regards the orthophosphates, spatiotemporal variations were recorded, as well as some extreme values that were encountered randomly. In this context, it is recommended that a periodical monitoring program should be carried out, considering the impact of phosphates exceeding on aquatic environments (i.e., eutrophication, oxygen deficiency, and the reduction of biodiversity).

As concerns to total organic carbon (TOC - mg/L) levels, lower values were detected (Table 2).

Table 2. Synthesis of the results obtained after the analysis of the parameters such as total organic carbon, electrical conductivity, total dissolved solids, sulphates, turbidity, total suspended solids, transparency and oxidation-reduction potential

Location		Value	TOC (mg/L)	EC ($\mu\text{S}/\text{cm}$)	TDS (mg/L)	SO_4^{2-} (mg/L)	Turb. (mg/L)	TSS (mg/L)	Transp. (m)	ORP (mV)
C e a t a l I z m a i l	Danube – Mm 43.5 (n = 9)	Min.	2.27	345	173	24	7.93	9	0.15	-19
		Max.	9.20	425	213	37	57.2	52	1	80
		Average	4.43	386.63	192.31	30.56	23.80	27.89	0.54	25.71
	Chilia – Km 115 (n = 9)	Min.	1.97	345	173	26	15.5	14	0.1	-76
		Max.	24.90	420	210	45	56.5	70	1	92
		Average	7.95	390.50	194.19	32.00	30.37	33.11	0.52	17.50
	Tulcea – Mm 42.5 (n = 9)	Min.	1.98	345	173	27	9.41	11	0.2	-22
		Max.	11.10	417	209	33	47.5	232	1.1	74
		Average	5.17	385.63	191.75	29.33	22.31	48.33	0.52	23.38
C e a t a l S f G h e o r g h e	Tulcea – Mm 34 (n = 10)	Min.	2.03	347	174	23	7.92	13	0.3	-22
		Max.	32.60	417	209	44	73.7	68	0.9	93
		Average	10.15	386.78	193.56	30.10	23.80	25.50	0.53	25.22
	Sulina – Mm 33 (n = 10)	Min.	1.87	348	174	24	8.81	13	0.15	-36
		Max.	22.40	417	209	34	51.5	60	0.7	90
		Average	9.15	388.22	194.22	29.00	24.23	27.50	0.48	25.56
	Sf. Gheorghe – Km 108 (n = 10)	Min.	2.05	347	174	23	7.55	11	0.15	-55
		Max.	22.90	417	209	49	69.7	69	0.8	94
		Average	8.53	386.78	193.56	30.70	22.88	24.70	0.48	24.67

The results did not overpass the typical limits of natural water variations (1-30 mg/L) (www.for.gov.bc.ca), except one sample collected during 2023 (May) from Tulcea-Mm 34 (DD23-14 = 32.6 mg/L) that could be related to local environmental environs (i.e., excessive amounts of organic load). Admittedly, there is no evident sign of potential organic contamination between upstream (*Ceatal Izmail*) and downstream sites (*Ceatal Sf. Gheorghe*), neither seasonal nor annual. The data set results related to the electrical conductivity (EC) ($\mu\text{S}/\text{cm}$) (Figure 7), total

dissolved solids (TDS) (mg/L), and sulfate levels (SO_4^{2-}) (mg/L) investigated at *Ceatal Izmail* and *Ceatal Sf. Gheorghe* revealed lower values (Table 2), below the threshold settled for the first-class quality (very good), as follows: EC (500 $\mu\text{S}/\text{cm}$) (Order 161/2006), TDS (0 - 1000 mg/L) (Lehr et al., 1980; De Zuane, 1997) and SO_4^{2-} (60 mg/L) (Order 161/2006). As a result, in terms of these parameters (i.e., EC, TDS and SO_4^{2-}) there is no evidence of poor water quality upstream (*Ceatal Izmail*) and downstream sites (*Ceatal Sf. Gheorghe*).

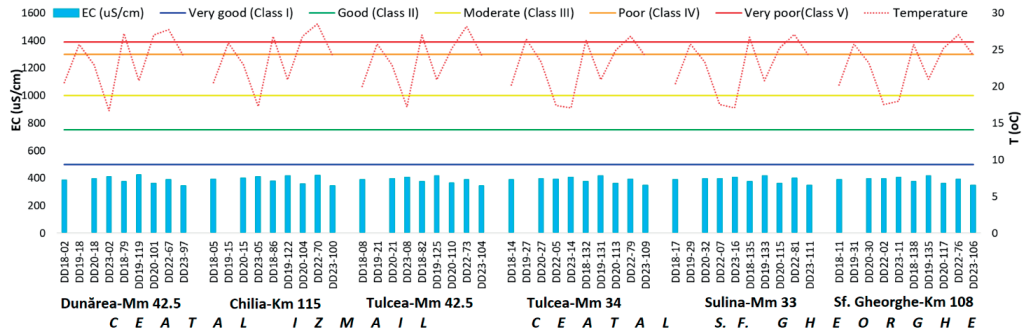


Figure 7. Seasonal and spatial variation of water electrical conductivity in investigated sites

In the case of turbidity, a small variation was recorded between the investigated stations (Table 2). Many values categorized the investigated water samples as low turbidity waters (< 10 NTU) and moderate turbidity waters (10 - 50 NTU) during the investigations (Figure 8). Despite that, the relatively highest values, which categorized the investigated water samples as high turbidity waters (50-100 NTU) were noticed during 2019 (July) at stations as

Dunărea-Mm 43.5 (DD19-18 = 57.2 NTU), Chilia-Km 115 (DD19-15 = 56.5 NTU), Tulcea-Mm 34 (DD19-27 = 73.7 NTU), Sulina-Mm 33 (DD19-29 = 51.5 NTU), Sf. Gheorghe-Km 108 (DD19-31 = 69.7 NTU). These relatively higher values may result from several factors, such as the variation of Danube River water levels, disintegration and resuspension of bottom sediments, rapid algal bloom etc.

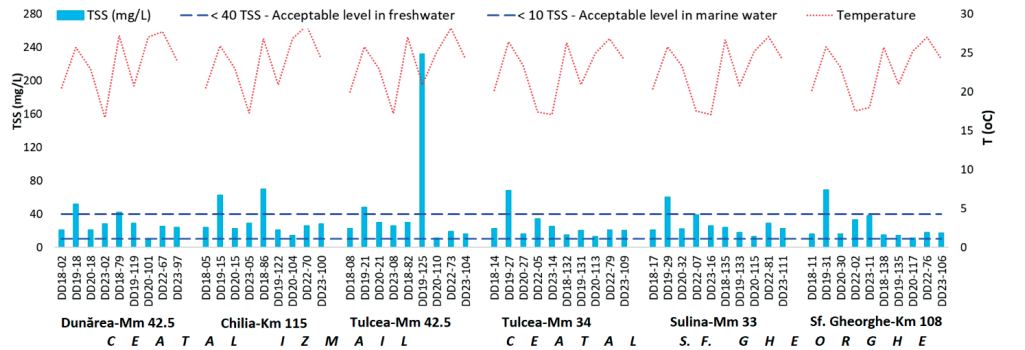


Figure 8. Seasonal and spatial variation of turbidity in investigated sites

Largely, in terms of the total suspended solids (TSS) (mg/L) it was noticed TSS values enclosed in the acceptable category of the freshwater environment (< 40 mg/L) (ANZECC 2000 Guidelines) (Table 2). Irregularly, relatively higher TSS contents (> 40 mg/L) were identified (Figure 9) during 2018 (August) at samplings as Chilia-Km 115 (DD18-86 = 70

mg/L), and 2019 (July) at sites as Dunărea-Mm 43.5 (DD19-18 = 52 mg/L), Chilia-Km 115 (DD19-15 = 63 mg/L), Tulcea-Mm 34 (DD19-27 = 68 mg/L), Sulina-Mm 33 (DD19-29 = 60 mg/L), Sf. Gheorghe-Km 108 (DD19-31 = 69 mg/L), including 2019 (September-October) at the station as Tulcea-Mm 42.5 (DD19-125 = 232 mg/L).

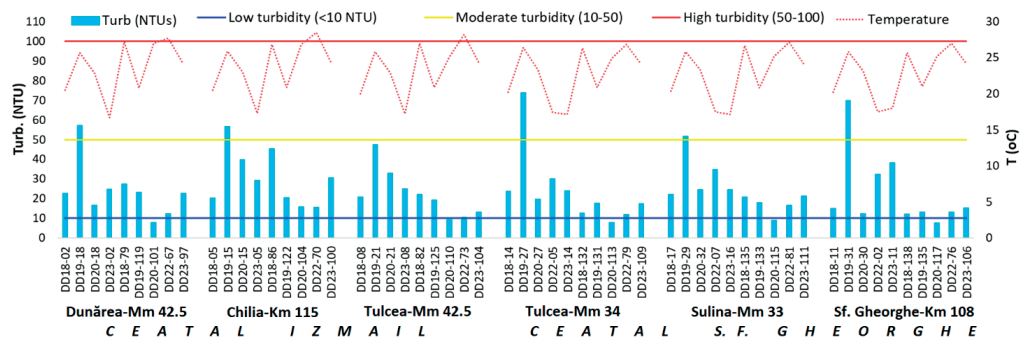


Figure 9. Seasonal and spatial variation of total suspended solids in investigated sites

The TSS higher concentrations are only recorded locally and may have several causes linked to both the natural variation of the suspended materials in the water (erosion of banks, content of organic matter) or anthropic (e.g. sources of pollution, waste, etc.).

On the subject of the oxidation-reduction potential, both positive and negative values were recorded (Table 2) with slight variations since the results were included in the broad range of natural waters from - 500 mV to + 700 mV (Chapman, 1996).

CONCLUSIONS

The results of this study present a general overview related to the status of the surface water quality investigated at the Danube River bifurcations (*Ceatal Izmail* and *Ceatal Sf. Gheorghe*). The physical-chemical conditions of these investigated key points are mainly controlled by the seasonal variations in the hydrological regime of the Danube River, as well as climatic changes and to a slight extent by the spatial variations. Most of the investigated environmental indicators showed very little seasonal fluctuations (i.e., water temperature, transparency, pH, dissolved oxygen, ammonium, nitrite, nitrate, chlorophyll "a", silica, total organic carbon, electrical conductivity, total dissolved solids and oxidation-reduction potential) which are included in the range of natural waters and are characteristic for the fluvial environments. Slight fluctuations and/or incidental exceeding of certain parameters from the trend lines (i.e., orthophosphates, turbidity and total suspended solids) were observed. These exceedances are

probably related to the ongoing environmental circumstances (i.e., the impact of climate change and socio-economic development, that mask or enhance natural processes).

Conclusively, in terms of parameters such as pH, DO, N-NH_4^+ , N-NO_2^- , N-NO_3^- , Chla, SiO_2 , TOC, EC, TDS and ORP the investigated water samples indicate categories as very good and good water quality. But when it comes to P-PO_4^{3-} , turbidity and TSS, quite a few water samples indicate categories as moderate or poor water quality.

Even if, generally, biota have adapted to the variation in the physical-chemical variables, this study contributed with pieces of evidence that a continuous monitorization of multiple water quality environmental indicators is required for biodiversity conservation and ecosystem services in the Danube Delta.

ACKNOWLEDGEMENTS

This research work was carried out through the support of the Romanian Ministry of Research, Innovation and Digitalization of the Research Core Program, within the National Plan for Research, Development and Innovation 2022-2027, implemented with the support of MCID, Project – PN 23 30 03 02 and PN 23 30 03 04. The authors would like to thank Dr. Cristian Teodoru for useful suggestions and remarks.

REFERENCES

- ANZECC 2000 Guidelines. (2000). Australian and New Zealand Guidelines for Fresh and Marine Water Quality, <http://www.mfe.govt.nz/fresh-water/tools-and-guidelines/anzecc-2000-guidelines>

- Burt, T., Howden, N., Worrall, F. (2013). On the importance of very long-term water quality records. *Wiley Interdiscip. Rev. Water*, 1, 41–48.
- Calmuc, V.A., Calmuc, M., Maxim Arseni, M., Simionov, I.-A., Antache, A., Milea, S.-A., Iticescu, C., Georgescu, P.L. (2023). Spatial distribution of pharmaceuticals in the lower Danube River water. *Scientific Papers. Series E. Land Reclamation, Earth Observation & Surveying, Environmental Engineering, Vol. XII*, 92-97, Print ISSN 2285-6064.
- Cazacu, C., Adamescu, M.C. (2017). Ecosystem services provided by the bio-physical structure of natural capital in the Danube Delta Biosphere Reserve Romania, *Conference Volume of 6th Symposium for Research in Protected Areas*, 2 to 3 November 2017, Salzburg, 97-102.
- Chapman, D. (1996). *Water Quality Assessments, A Guide to Use of Biota, Sediments and Water in Environmental Monitoring* - Second Edition, Published on behalf of UNESCO, WHO, UNEP. E /FNSPON. London. Great Britain, University Press, Cambridge, 626 p.
- Chapman, D.V., Bradley, C., Gettel, G.M., Hatvani, I.G., Hein, T., Kovács, J., Liska, I., Oliver, D.M., Tanos, P., Trásy, B., Várbiro, G. (2016). Developments in water quality monitoring and management in large river catchments using the Danube River as an example. *Environ. Sci. Policy*, 64, 141-154.
- Cozzi, S., Ibáñez, C., Lazar, L., Raimbault, P., Giani, M. (2019). Flow Regime and Nutrient-Loading Trends from the Largest South European Watersheds: Implications for the Productivity of Mediterranean and Black Sea's Coastal Areas. *Water* 2019, 11, 1. <https://doi.org/10.3390/w11010001>.
- De Zuane, J. (1997). *Handbook of Drinking Water Quality (2nd ed.)*, John Wiley and Sons, 592 p. ISBN 0-471-28789-X.
- Duțu, F., Duțu, L., Catianis, I., Iordache, G. (2022). Morphology and water dynamics of channel bifurcation in deltaic environment, *The XXIIth International Multidisciplinary Scientific GeoConference Surveying, Geology and Mining, Ecology and Management – SGEM 2022*, 22 (1.1) DOI:10.5593/sgem2022/L1/s01.003
- European Union Council. (2000). Directive 2000/60/EC of the European Parliament and of the Council of 23 October 2000 establishing a framework for Community action in the field of water policy. *Official Journal of the European Communities*, 2000, 43 (L327), 1-73.
- Gasparotti, C. (2014). The main factors of water pollution in Danube River basin, *EuroEconomica*, Danubius University of Galati, 1(33), 91-106.
- Gasparotti, C., Rusu, E., Dragomir, S. (2013). The impact of anthropogenic activities on the water quality in the Danube River Basin, *Conference Bulgaria, Ecology, Economics, Education and Legislation*, 1, DOI: 10.5593/sgem, 2013, 987-994
- Gâstescu, P., Ţuchiu, E. (2012). The Danube River in the lower sector in two hydrological hypostases—high and low waters, *Riscuri si Catastrofe*, Edit. Casa cărţii de ştiinţă, Cluj-Napoca, 10 (1), 1-19.
- Gómez-Baggethun, E., Tudor, M., Doroftei, M., Covaliov, S., Năstase, A., Onăra, D.F., Mierlă, M., Marinov, M., Dorosencu, A.-C., Lupu, G., Teodorof, L., Tudor, I.-M., Köhler, B., Museth, J., Aronsen, E., Johnsen, S.I., Ibram, O., Marin, E., Crăciun, A., Cioacă, E. (2019). Changes in ecosystem services from wetland loss and restoration: An ecosystem assessment of the Danube Delta (1960–2010), *Ecosystem Services*, 39, 100965
- Grant, W.D. (2004). Introductory chapter: Half a Lifetime in Soda Lakes. In A.Ventosa (Ed.) *Halophilic Microorganisms*, Springer-Verlag Berlin Heidelberg, 17-31.
- Habersack, H., Bradley, C. (2022). Hydropower in the Danube River Basin: Current Status and Emerging Challenges, Editor(s): Thomas Mehner, Klement Tockner, *Encyclopedia of Inland Waters* (Second Edition), Elsevier, 126-133.
- Ilie, M., Marinescu, F., Ghita, G., Deak, G., Tanase, G.S., Raischi, M. (2014). Assessment of heavy metal in water and sediments of the Danube River, *Journal of Environmental Protection and Ecology*, 15, 825-833.
- Jitar, O., Teodosiu, C., Oros, A., Plavan, G., Nicoara, M. (2015). Bioaccumulation of heavy metals in marine organisms from the Romanian sector of the Black Sea, *New Biotechnology*, 32 (3), 369-378.
- Kyle, J. (2006). *Romania: The Fragile Danube Delta is Under Increasing Threat*, 2006, on line at: <http://www.dw.com/en/romania-the-fragile-danube-delta-is-under-increasing-threat/a-2143418>
- Lazăr, L., Rodino, S., Pop, R., Tiller, R., D'Haese, N., Viaene, P., De Kok, J.-L. (2022). Sustainable Development Scenarios in the Danube Delta-A Pilot Methodology for Decision Makers. *Water* 2022, 14, 3484.
- Lazăr, N.N., Simionov, I.-A., Petrea, S.-M., Iticescu, C., Georgescu, P.-L., Dima, F., Antache, A. (2024). The influence of climate changes on heavy metals accumulation in *Alosa immaculata* from the Danube River Basin, *Marine Pollution Bulletin*, 200, 116145.
- Lehr, J.H., Gass, T.E., Pettyjohn, W.A., De Marre, J. (1980). *Domestic water treatment*, New York, NY: McGraw-Hill Book Co., 655.
- Mănoiu, V.-M., Crăciun, A.-I. (2021). Danube river water quality trends: A qualitative review based on the open access web of science database, *Ecology & Hydrobiology*, 21 (4), 613-628.
- Myroshnychenko, V., Ray, N., Lehmann, A., Giuliani, G., Kideys, A., Weller, P., Teodor, D. (2015). Environmental data gaps in Black Sea catchment countries: INSPIRE and GEOSS State of Play. *Environ. Sci. Policy*, 46, 13–25.
- Order no. 161/2006. (2006). Normative concerning the classification of surface water quality to establish the ecological status of water bodies (Romanian Order MEWM no. 161/2006), Annex C-Elements and physico-chemical quality standards in water, published in *Romanian Official Monitor*, part I, no. 511 bis, from 13th of June, 2006.
- Padlo, T., Struś, P., Gil, A. (2012). Danube as a symbol of Europe. Perception of the river from varied geographical perspectives. *PLoS One*. 2021 Dec 2;16(12): e0260848. doi:

- 10.1371/journal.pone.0260848. PMID: 34855880; PMCID: PMC8638847.
- Panin, N., Jipa, D. (2002). Danube River Sediment Input and its Interaction with the North-western Black Sea, *Estuarine, Coastal and Shelf Science*, 54, (3), 551-562.
- Panin, N., Jipa, D.C., Gomoiu, M.T., Secrieru, D. (1999). Importance of sedimentary processes in environmental changes: Lower River Danube-Danube Delta-Western Black Sea system, in *Environmental Degradation of the Black Sea: Changes and Remedies*, edited by S.T. Besiktepe et al., 1999, 23-42, NATO Sci. Ser., Springer, New York
- Panin, N., Tiron Duțu, L., Duțu, F. (2016). The Danube Delta: An overview of its Holocene evolution. *Méditerranée*, 126, 37-54.
- Păun, I., Chiriac, F.L., Marin, N.M., Cruceru, L.V., Pascu, L.F., Lehr, C.B., Ene, C. (2017). Water Quality Index, a useful tool for evaluation of Danube River raw water. *Rev. Chim.*, 68, 1732–1739.
- Pavlović, P., Mitrović, M., Đorđević, D., Sakan, S., Slobodnik, J., Liška, I., Csanyi, B., Jarić, S., Kostić, O., Pavlović, D., Marinković, N., Tubić, B., Paunović, M. (2016). Assessment of the contamination of riparian soil and vegetation by trace metals-A Danube River case study, *Science of The Total Environment*, 540, 396-409.
- Rico, A., Van den Brink, P.J., Leitner, P., Graf, W., Focks, A. (2016). Relative influence of chemical and non-chemical stressors on invertebrate communities: a case study in the Danube River, *Science of The Total Environment*, 571, 1370-1382.
- Rose, P.M. & Taylor, V. (1993). Western Palearctic and South West Asia Waterfowl Census 1993. IWRB, Slimbridge, UK, 1993
- Rose, P.M. (1992). Western Palearctic Waterfowl Census 1992. IWRB, Slimbridge, UK, 1992
- Saeed, O., Székács, A., Jordán, G., Mörtl, M., Abukhadra, M.R., Eid, M.H. (2023). Investigating the impacts of heavy metal(loid)s on ecology and human health in the lower basin of Hungary's Danube River: A Python and Monte Carlo simulation-based study. *Environ Geochem Health*, 45(12), 9757-9784.
- Simionov, I.-A., Cristea, D.S., Petrea, S.-M., Mogodan, A., Nicoara, M., Plavan, G., Baltag, E.S., Jijie, R., Strungaru, S.-A. (2021). Preliminary investigation of lower Danube pollution caused by potentially toxic metals, *Chemosphere*, 264 (1), 128496.
- Simionov, I.-A., Cristea, V., Petrea, S.M., Mogodan, A., Nica, A., Strungaru, S.-A., Ene, A., Sarpe, D.A. (2020). Heavy metal evaluation in the lower sector of Danube River. *Scientific Papers. Series E. Land Reclamation, Earth Observation & Surveying, Environmental Engineering, Vol. IX*, 11-16, Print ISSN 2285-6064.
- Vignati, D.A.L., Secrieru, D., Bogatova, Y.I., Dominik, J., Cérégino, R., Berlinsky, N.A., Oaic, Gh., Szobotka, S., Stanica, A. (2013). Trace element contamination in the arms of the Danube Delta (Romania/Ukraine): Current state of knowledge and future needs, *Journal of Environmental Management*, 125, 169-178.
- Vukovic, D., Vukovic, Z., Stankovic, S. (2014). The impact of the Danube Iron Gate Dam on heavy metal storage and sediment flux within the reservoir, *CATENA*, 113, 18-23.
- Zöckler, C., Delany, S., Hagemeijer, W. (2003). Wader Populations Are Declining-How Will We Elucidate the Reasons? *Wader Study Group Bulletin*, 100, 202-211.
- <https://www.accuweather.com/ro/>
- <https://www.for.gov.bc.ca>
- <https://www.niwa.co.nz>
- <https://www.esa.int/>
- <https://www.afdj.ro/ro/cotele-dunarii>

ESTIMATION OF RIVERBANK SOIL EROSION RATE - A CASE STUDY

Mihai Teopent CORCHES

"1 Decembrie 1918" University of Alba Iulia,
5 Gabriel Bethlen Street, Alba Iulia, Romania

Corresponding author email: corchesmihai@yahoo.com

Abstract

Erosion of riverbanks is a natural phenomenon, which leads to the loss of important agricultural land areas. At the same time, riverbank erosion can be considered a natural risk that can cause major damage to road and railway infrastructure, flood management infrastructure, biodiversity and even the population located in flood risk areas. This phenomenon is generally more pronounced in the meanders of the rivers and in regions with higher flow rates, but it can be accentuated due to climate change which can lead to changes in watercourse flows. This study aimed to estimate the net annual soil loss due to riverbank erosion on the Siret River, Romania, using aerial photogrammetry and GIS analysis.

Key words: climate change, riverbank erosion, soil erosion.

INTRODUCTION

Erosion of riverbanks is a natural phenomenon, which leads to the loss of important land areas, but also to the accumulation of sediments in rivers and to the damage to aquatic biodiversity. At the same time, riverbank erosion can be considered a natural hazard, when the riverbank erosion rate is higher than normal, and this phenomenon is causing major damage to infrastructure. Riverbank erosion can affect the local community, in some situations, residents are forced to move to safer areas (Mahmoodzada et al., 2023), with higher altitudes.

Riverbank erosion has a short-term impact on local communities through the loss of housing and land, but also an indirect long-term impact on the living conditions and health of the displaced population, especially in areas with high population density and low economic development. At the same time, in areas affected by riverbank erosion, local authorities can impose certain restrictions on the use of land, thus affecting the economic development (Leng et al., 2023).

Considering the above, it is necessary to predict the magnitude of the erosion of the riverbank, to prevent the occurrence of certain damages caused by this phenomenon. Tracking and forecasting the evolution of riverbank erosion phenomena can help to improve water management practices and the use of spatial

analysis can help to study larger areas (Benavidez et al., 2018).

Riverbank erosion is a natural geological process that can occur slowly or with a higher erosion rate, which depends on several factors such as: hydraulic characteristics of the watercourse, soil properties, soil erodibility or soil resistance to erosion (Nur et al., 2024). The phenomenon of riverbank erosion is accelerated with rising water levels and the loss of soil matric suction, or the force with which the soil holds water, which occurs in soils that are partially saturated with water (Nardi et al., 2012).

The severity of the consequences of riverbank erosion can be correlated with the hazard exposure of the potentially affected areas, being higher in areas exposed to flood risks with a high population density and in built-up areas (Tha et al., 2022).

Riverbank erosion rates increase greatly during periods of high river flow, when high flow of water hits the riverbank with force, causing the riverbank to collapse due to pressure differences (Hasanuzzaman et al., 2023).

The importance of roughness induced by the topography of the watercourse in limiting the phenomenon of riverbank erosion must also be considered (Darby et al., 2010). Riverbank erosion varies greatly over time, with the shape of banks changing radically, especially after floods, increasing the likelihood of riverbank

erosion. For example, by doubling the duration of bank flooding from 10 to 20 days, leads to a 50% increase in the probability of riverbank erosion (Vietz et al., 2016).

According to a study carried out over a period of 3 months, which investigated the lateral erosion rate of riverbank using the erosion pins method, the erosion rate was between 0.05-0.51 cm/day, and was influenced by the flow velocity of water, and the degree of vegetation coverage of the riverbank (Nur et al., 2021).

Riverbank erosion is higher on unvegetated riverbanks than on vegetated riverbanks, so the presence of vegetation increases the stability of the riverbank, thus reducing riverbank mass failure, and decreasing the water velocity in the bank area (Li et al., 2023).

Climate change significantly impacts riverbank erosion, exacerbating the natural processes that cause it. Future climate changes will affect the rainfall pattern in certain areas of the world; thus, they will play a significant role in increasing the risk of floods in the coming years, and at the same time in intensifying the riverbank erosion rate. That is why assessing the impact of climate change on bank erosion is essential for planning the timing of climate change mitigation actions (Aktar, 2023). Riverbank erosion protection strategies must consider the vulnerability of the population and infrastructure to flood risk. Protection measures against riverbank erosion in flood risk areas can be combined with measures to reduce river flows during floods such as the construction of lateral non-permanent accumulations (polders).

MATERIALS AND METHODS

A growing trend in the research community is to use various high-tech techniques to identify and solve the problems of people. GIS is an important tool which can be of assistance in the identification of river changes and bank erosion situations. To study the fluvial geomorphology of a river, the identification of the channel migration pattern of rivers from satellite images of different years using GIS and remote sensing technology is found to be very useful.

This study aimed to quantify the riverbank erosion rate using aerial photography and GIS analysis, on a 1 km long sector of the Siret River, Galați County, Romania. On the right bank of

the river there is a flood protection dike that protects important areas of agricultural land and several different localities. The riverbank erosion rate analysis can be used as an argument in decision-making by the competent authorities for water management.

There are several methods for quantifying bank erosion: high-resolution traditional photogrammetry, SFM photogrammetry, UAV photogrammetry, satellite imagery (with certain cost limitations), highly accurate total station measurements, direct measurements with erosion probes, terrestrial laser scanning, airborne laser scanning and dendrogeomorphological studies (de Souza Dias et al., 2022).

Aerial photographs publicly available on the website of the National Agency for Cadastre and Land Registration were used to carry out this study (N.A.C.L.R. Romania, 2024), from 2005, 2016, as well as an aerial photograph made with a drone in 2023. These data were processed in GIS to calculate riverbank areas lost through erosion. To calculate the daily rate of riverbank erosion, the riverbank length in centimetres lost through erosion obtained between different years were divided by the number of days between the years of study.

All the figures were made in QGIS, and the photos are original.

RESULTS AND DISCUSSIONS

The study was carried out on a 1 km sector of the Siret River, Galați County in Romania, the location being presented in Figures 1 and 2. Galați County is in the eastern part of Romania on the border with Moldova. The Siret River originates in the forested Carpathian Mountains (Ukraine). The Siret River has a length of 559 km, a catchment area of 42890 square km, and the sinuosity coefficient is 1.86. In practical terms, it is the river basin with the highest hydro-energy potential and with the largest supply of fresh water in the country. The total theoretical water resource of the Siret river basin is 6,868 million m³/year, which is above the average for Romania (Ministry of the Environment, 1992).

This study aimed to identify the riverbank daily erosion rate in the study area, in the period 2005-2023, to serve as a basis for decision-making regarding the implementation of works to

prevent riverbank erosion phenomena in the area.

In Figures 4 and 5 present the riverbank erosion from Siret River.

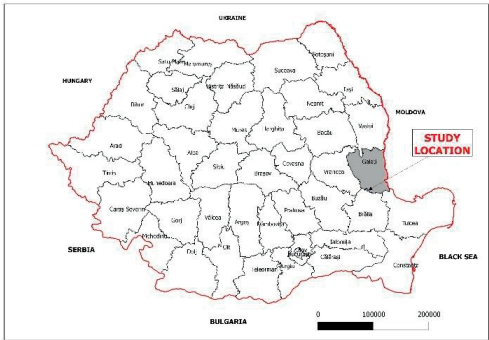


Figure 1. Study location in Romania



Figure 4. Riverbank erosion in the study area (original)

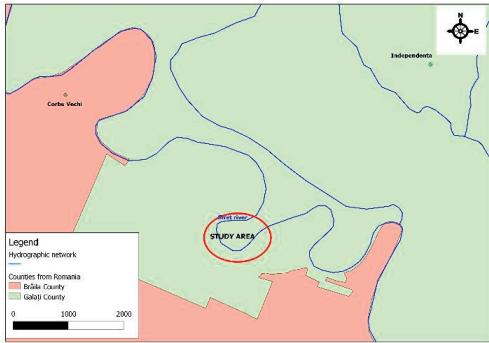


Figure 2. Study location



Figure 5. Riverbank erosion in the study area

Taking the construction decision of riverbank erosion prevention works must balance the need to secure the Nămolosa-Măxineni flood protection dike (Figure 3) to prevent the risk of floods.



Figure 3. The flood protection dike Nămolosa-Măxineni

As a result of this study, the riverbank surface lost due to erosion in the study area was calculated, and it was found that during the period 2005-2016, approximately 3,313 hectares were lost (approx. 0.3 hectares/year) (Figures 6, 7 and 9). In this interval, riverbank erosion was between 10.5 and 81 meters, resulting in an erosion rate between 0.26 cm/day and 2.02 cm/day. The land areas lost through erosion were calculated by measuring the areas lost in the interval between the study years using the QGIS software, and the results obtained were divided by 11 years between the study intervals. To calculate the daily riverbank erosion rate, the distances by which the erosion advanced between the years of the study were measured, and the results obtained in centimetres were divided by the number of days between the years of study (approx. 4015 days).



Figure 6. The riverbank line in 2005

Also in this interval, the water management authorities carried out a lower-bank riprap erosion prevention construction, which stopped riverbank erosion on a section on a section of 380 m (Figure 8). Following the evolution of erosion in the period 2016-2023, it was found that the erosion phenomena continued upstream and downstream of the riverbank anti-erosion construction, while in this area the phenomenon of riverbank erosion stopped (Figures 9 and 10).

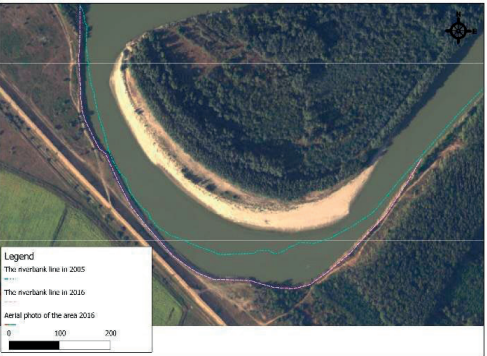


Figure 7. The riverbank line in 2016



Figure 8. Anti-erosion works carried out in the area

During this period, approximately 1.328 hectares were lost (approx. 0.19 hectares/year) (Figure 10). In this interval, the erosion of the riverbank advanced by 1 to 32.5 meters, thus resulting in an erosion rate between 0.04 cm/day and 1.27 cm/day. The riverbank surfaces lost through river erosion were calculated by measuring the areas lost in the interval between the study years using the QGIS software, and the results obtained were divided by 7 years between the study intervals. To calculate the riverbank daily erosion rate, the distances by which the erosion advanced between the years of the study were measured, and the results obtained in centimetres were divided by the number of days between the years of study (approx. 2555 days).

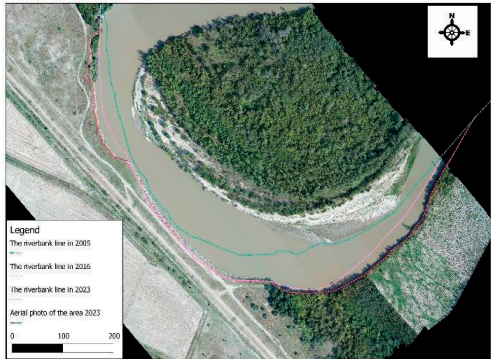


Figure 9. The riverbank line in 2023

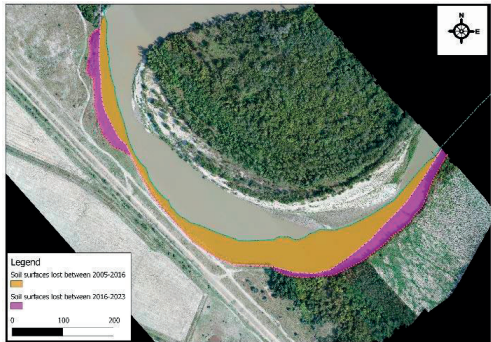


Figure 10. Riverbank surfaces lost between 2005 and 2023

CONCLUSIONS

This study aimed to identify the riverbank daily erosion rate in the study area, in the period 2005-2023, to serve as a basis for decision-making

regarding the implementation of works to prevent riverbank erosion phenomena in the area. After carrying out this study, it was found that the vegetation on the riverbanks protects the riverbank against erosion, and that the areas most exposed to this phenomenon are those without riparian vegetation and those in the meanders of the watercourse, where an erosion rate between 0.04 and 2.02 cm/day. At the same time, it was found that the erosion prevention construction of the lower-bank riprap type was effective and that it should be extended upstream and downstream to protect the flood protection dike in the area.

At the same time, an accelerated increase in the areas with sediment deposits was observed in various areas of the watercourse, which exerts additional pressure on the opposite riverbank, contributing to the accentuation of the erosion phenomena, but these were not quantified in this study and can be the subject of further research. The study confirmed that the flood protection dike is at risk due to the intensification of erosion phenomena and that urgent measures must be taken.

Riverbank monitoring using aerial photograms is a simple and easily accessible method, the accuracy of which depends on the quality of the images used. This method does not require complicated calculations and can be quickly applied to large areas and can be used to monitor the evolution of riverbank erosion phenomena over time and to make quick decisions.

REFERENCES

- Aktar, M.N. (2013). Impact of climate change on riverbank erosion. *International Journal of Sciences: Basic and Applied Research*, 7(1), 36-42. <https://environmentalsystemsresearch.springeropen.com/articles/10.1186/s40068-020-00214-0>
- Benavidez, R. Jackson, B., Maxwell, D., Norton, K. (2018). A review of the (Revised) Universal Soil Loss Equation ((R)USLE): with a view to increasing its global applicability and improving soil loss estimates. *Hydrol. Earth Syst. Sci.*, 22, 6059–6086, <https://hess.copernicus.org/articles/22/6059/2018/>
- Darby, S.E., Trieu, H.Q., Carling, P.A., Sarkkula, J., Koponen, J., Kumm, M., Conlan, I., Leyland, J. (2010). A physically based model to predict hydraulic erosion of fine-grained riverbanks: The role of form roughness in limiting erosion. *Journal of Geophysical Research*, 115, F04003, 1-20. <https://agupubs.onlinelibrary.wiley.com/doi/10.1029/2010JF001708>
- Hasanuzzaman, M., Bera, B., Islam, A., Shit, P.K. (2023). Estimation and prediction of riverbank erosion and accretion rate using DSAS, BEHI, and REBVI models: evidence from the lower Ganga River in India. *Natural Hazards*, 118, 1163–1190. <https://link.springer.com/article/10.1007/s11069-023-06044-4>
- De Souza Dias, V., de Faria, K.M.S., da Luz, M.P., Formiga, K.T.M. (2022). Investigation and Quantification of Erosions in the Margins of Water Bodies: A Systematic Review. *Water*, 14, 1693. <https://www.mdpi.com/2073-4441/14/11/1693>
- Leng, S.T.K., Bin Jafar, M., Ata, F.M., Bin Modh Jamil, M.R. (2023). Socio-Economic Impact of Riverbank Failure at Kg. Pohon Celagi in Pasir Mas, Kelantan, Malaysia. *Akademika*, 93(1), 307 - 316. <https://ejournals.ukm.my/akademika/article/view/62253/14159>
- Li, Q., Wang, L., Ma, X., Nie, R. (2023). Experimental study of the effects of riverbank vegetation conditions on riverbank erosion processes. *Environmental Fluid Mechanics*, 23, 621–632. <https://link.springer.com/article/10.1007/s10652-023-09924-2>
- Mahmoodzada, A.B., Varade, D., Shimada, S., Okazawa, H., Aryan, S., Gulab, G., Abd. El-Zaher, M.A.M., Rizwana, H., Ahlawat, Y.K., Elansary H.O. (2023). Quantification of Amu River Riverbank Erosion in Balkh Province of Afghanistan during 2004–2020. *Land*, 12(10), <https://www.mdpi.com/2073-445X/12/10/1890>
- Ministry of the Environment (1992). *Atlasul cadastrului apelor din Romania – Partea 1 – Date morfo-hidrografice asupra retelei hidrografice de suprafață*, pp. 654 <https://pdfslide.net/documents/184635870-atlasul-cadastrului-apeilor-din-romaniapdf.html?page=1>
- Mou, M.A., Tusar, M.K., Haque, M.R., Chakraborty, S., Ahmed, S. (2023). Assessment of Riverbank Erosion and Accretion and its Impact on the People of Chairman Ghat, Noakhali, Bangladesh. *Journal of Sustainability and Environmental Management*, 2(4), 220-230.
- N.A.C.L.R - National Agency for Cadastre and Land Registration, (2024), <https://renns.ancpi.ro/renns-public/>
- Nardi, L., Rinaldi M., Solari, L., and Schleiss, A.J. (2012). An experimental investigation on mass failures occurring in a riverbank composed of sandy gravel. *Geomorphology - ISSN 0169-555X. - Stampa*, 56-69. <https://www.sciencedirect.com/science/article/abs/pii/S0169555X11004041>
- Nur, A.M.R., Saerahany, L.I., Siti, H.Y. (2024). Effects of soil erodibility on riverbank erosion and failures. *IJUM Engineering Journal*, 25(1), 115 - 127. <https://journals.iium.edu.my/ejournal/index.php/iiumej/article/view/2959>
- Nur, A.M.R., Saerahany, L.I., Rabitah, H., Md, N.S. (2021). Measurement of Riverbank Erosion Rates of Pusu River Using Erosion Pins Method. *IJUM International Journal of Integrated Engineering*, 13(3), 142 - 147. <https://publisher.uthm.edu.my/ojs/index.php/ijie/article/view/8911>

- Tha, T., Piman, T., Bhatpuria, D., Ruangrassamee, P. (2022). Assessment of Riverbank Erosion Hotspots along the Mekong River in Cambodia Using Remote Sensing and Hazard Exposure Mapping. *Water*, 14, 1981. <https://www.mdpi.com/2073-4441/14/13/1981>
- Vietz, J.G., Lintern, A., Webb, J.A., Sraccione, D. (2018). River Bank Erosion and the Influence of Environmental Flow Management. *Environmental Management*, 61, 454–468. <https://link.springer.com/article/10.1007/s00267-017-0857-9>

PRINCIPAL COMPONENT ANALYSIS: AN APPROPRIATE TOOL FOR TROPHIC PARAMETERS INTERACTION - APPLICATION IN LARGEST LAKE IN BALKAN

Erdona DEMIRAJ, Irena DUKA, Ferdi BRAHUSHI, Seit SHALLARI

Agricultural University of Tirana, Department of Environment and Natural Resources,
1029 Pajsi Vodica Street, Tirana, Albania

Corresponding author email: edemiraj@ubt.edu.al

Abstract

The Lake of Shkodra is the largest lake in the Balkans with Ramsar status, which offers a variety of important ecosystem services such as water sources for agriculture, rich biodiversity and providing habitat and nesting grounds for wildlife, and tourism development for Albania and Montenegro. During the last decade, different studies reported an increase in macronutrient content, reporting the increase in the eutrophication in this lake which may reduce the biodiversity of the species. The aim of this study is to use the Principal Component Analysis (PCA) as a tool to define the relation of water quality parameters with the TN: TP ratio. According to PCA, the TN: TP molar observed ratio can be related to the anthropogenic activities and agricultural land use patterns around the catchment area indicating a high possibility of untreated waste entering the lake through the active inlets.

Key words: PCA, Shkodra Lake, TN: TP ratio, TSI.

INTRODUCTION

Monitoring of water quality is of high importance as water pollution and its irrational use represent two risk factors for the sustainable development of human society. The chemical composition of surface waters is related to natural and anthropogenic processes (Bojarczuk et al., 2018). Natural sources can be found in microbial activity, geological structures, and naturally existing pollutants found in water supplies. On the other side, anthropogenic causes are caused by human activities such as industrial operations, agricultural practices, inappropriate waste disposal, and insufficient sewage systems (Babuji et al., 2023). The preservation of water quality can be attained through the establishment of indicators that are systematically monitored and tailored specifically to freshwater ecosystems. The Agriculture, Forestry, and Other Land Uses (AFOLU) sector contributes about 13-21% of global total anthropogenic GHG emissions (IPCC, 2022), meanwhile the agriculture sector contributes to nitrate pollution (inland and coastal waters e.g. eutrophication) which represent the main chemical contaminant in the world's groundwater aquifers (WWAP, 2013). In the European Union, 38 % of water bodies are

significantly under pressure from agricultural pollution (WWAP, 2015). Diffuse pollution from agriculture is the most common pressure causing less-than-good groundwater chemical status and affects 19% of the total groundwater body area in the EU-27 (EEA, 2021).

Albania's average quantity of fresh water is estimated at about 8,700 cubic meters per capita per year, which is one of the highest in Europe (MPWT, 2011). In this regard, one of the largest water catchments is the Drini River where an important water body in this basin is Shkodra Lake, the largest in the Balkan Peninsula (Kashta et al., 2001). The Shkodra lake has also been part of the Ramsar Wetlands Convention since 2005 (Demiraj et al., 2018). These areas are threatened by urban, industrial, and agricultural activities from water courses that discharge into them by contributing to trophic status, water quality deterioration, and diminishing the biodiversity index (Demiraj et al., 2018; Rakočević, 2018; Pešić et al., 2018; Bacu et al., 2011; Sulçe et al., 2018). Several indicators represent different aspects of water quality that vary in their significance in different geographical regions (Walsh & Wheeler, 2012). Furthermore, in some cases it can be difficult to convey relevant water quality information to

policymakers and the public regions (Walsh & Wheeler, 2012).

The aim of current study was:

- (i) to have full data of water quality parameters for the highest pollution pressure spring-summer-autumn;
- (ii) to evaluate the importance of water parameters in water quality evaluation by using statistical modelling such as Principal Component Analysis (PCA) after data collection.

MATERIALS AND METHODS

The Shkodra lake is laid in the northern part of Albania with a surface of approximately 360-

540 km² part of Drin - Buna River basin, the largest one with typical karstic origin. The main tributary is Morača River in the northern part of the Lake and the total water flow is about 210 m³/sec. The watershed of Shkodra lake is characterised by concave topography, steep slopes, high annual rainfall (IGEWE, 2016) and high erosion processes. This lake is a host ecosystem for a diverse number of species: 52 species of fish, 240 species of aquatic plants and 283 bird species. The physio-geography classifies the watershed as mainly composed of geologically limestone with 330.000 inhabitants where about 85% of their activity is related to the lake such as intensive agricultural and tourism activities.



Figure 1. A map from Shkodra Lake and sampling stations

Due to this a program of monitoring was established with a total of 13 sampling expeditions, from May - October 2022. During this expedition some water quality parameters were evaluated in situ: Temperature (T, °C), pH (pH unit), dissolved oxygen (DO, mgL⁻¹), electrical conductivity (EC, μScm^{-1}) by using a Parametric multi-probe WTW 340 instrument. Meanwhile, sampling was transported at Agriculture University of Tirana to perform the: Total suspended solids (TSS, mg/L), Total dissolved solids (TDS, mg/L), nitrate nitrogen (N-NO_3^- , mgNL⁻¹), phosphate-phosphorus (P-PO_4^{3-} , mgPL⁻¹), p-alkalinity and *Chlorophyll a* in mgL⁻¹. The sampling process was performed

before 12:00 PM since ISO 10260:1992 was followed.

Nutrient phosphorus and nitrogen species were assessed by spectrophotometric means as follows: phosphate-phosphorus (P-PO_4^{3-}) when using the molybdenum blue method (DIN EN 16169, 2012; Murphy & Riley, 1962); nitrate nitrogen (N-NO_3^-) when using 2,4-phenoldisulphonic acid in a basic medium (Sandu et al., 2023a; 2023b). Appropriate calibrations of the devices employed in analyses were performed before determinations to ensure the quality of the analytical procedures and correctness of the obtained data. The sampling process was performed before 12:00 PM since

ISO 10260:1992 was followed. Total P was analyzed using the ascorbic acid molybdenum blue method (DIN EN 16169, 2012; Murphy & Riley, 1962). N-NO_3^- was determined within 24 h, by using a spectrophotometer. The data collected was statistically elaborated by using JMP 11 software. Principal Component Analysis (PCA) is a robust technique utilised for identifying patterns that elucidate the variance within extensive datasets comprising interrelated variables, subsequently facilitating their transformation into smaller sets of independent variables, known as principal components (Zela et al., 2020).

RESULTS AND DISCUSSIONS

Studies show that the premises for eutrophication are not the specific amounts of each element soluble in water but the molar ratios between TN:TP. The first result was elaborated for nutrient parameters to estimate the TN:TP ratio. This ratio was used by Downing, J.A. & E. McCauley in 1992 to examine the form of the relationship of total N (TN) to total P (TP) in some world's lakes. The lakes with a high concentration of TP are usually often rich in TN (Sakamoto, 1966), therefore

there is a positive correlation between the TN and TP concentrations of lakes. Furthermore, it is observed that if the slope of this relationship is constant, then TN:TP might not be related to lake trophic status, whereas if the reverse occurs, then nutrient sources of oligotrophic and eutrophic lakes have differing TN:TP ratios (Ahl, 1979).

In ratios $> 16:1$, TP is the limiting factor for algae growth, in lower ratios the limiting factor is TN. In this regard in our study, the results show that during the late spring (May) with the high number of freshwater flows, the TN:TP ratio is between 1.40-3.63, respectively higher in the stations of Vrake and Shtojt, indicating a presence of nitrogen in the discharges that come mainly from agricultural lands and which dictates that the limiting element for the development of the eutrophication process is phosphorus (Figure 2). The same results were obtained in all the stations during August and September where the amount of freshwater decreased. The increase in rainfall during the October season returns the decreased amount of phosphate due to the low amount of fertiliser used in agriculture areas and the low solubility of phosphorus from sediment of the lake.

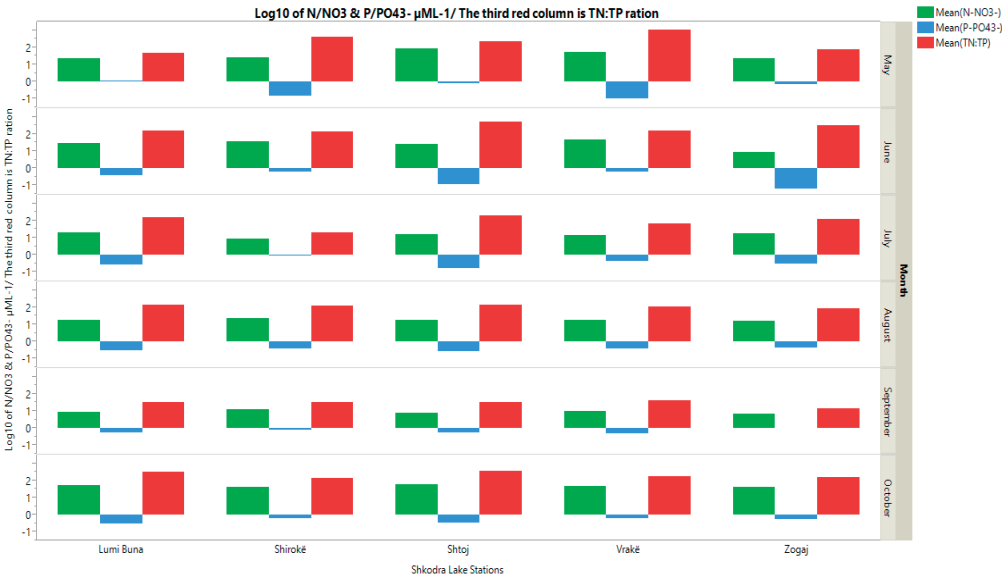


Figure 2. The value is calculated in molar concentration of N/NO_3^- and P/PO_4^{3-} , while their report is represented as TN:TP

Principal Component Analysis (PCA) is a methodology to elucidate alterations within datasets and explain the interrelationships among variables, thereby discerning their significance across distinct groups by down weighting the least influential variables. In PCA, the comprehensive index of transformation analysis is usually called the principal component. The principal component is a linear combination of the original variables and is not correlated with each other (Zhang et al., 2019). In this study, PCA was applied to process data for each season across multiple years. The PCA approach hinges upon scrutinizing correlation structures utilizing Pearson distribution, thereby establishing links and directing factors towards the original variables to facilitate comprehensible interpretation.

Figure 3 shows the obtained results from the PCA analysis of the measurements performed during the May were the component 1 describe the 43% of total variation and was comprised by Temperature, N/NO_3^- , $CaCO_3$, DO, pH, TDS and TN:TP while the component 2 explained the 24 % of the variance and significantly consisted of P/PO_4^{3-} , TSS and *Chlorophyll a*. Another situation was observed during June (Figure 4) where component 1 describes the 40% of total variation Temperature, N/NO_3^- , $CaCO_3$, DO, pH, and TN:TP. Component 2 estimated by 20% of total variation between TDS, TSS, $CaCO_3$, P/PO_4^{3-} , TSS and *Chlorophyll a*.

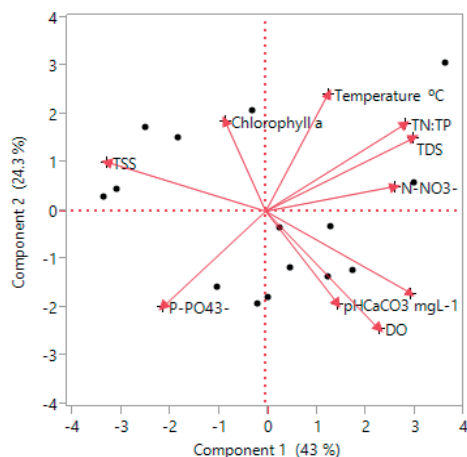


Figure 3. PCA of TN:TP and of the physicochemical parameters as 10 variables and their influence during May

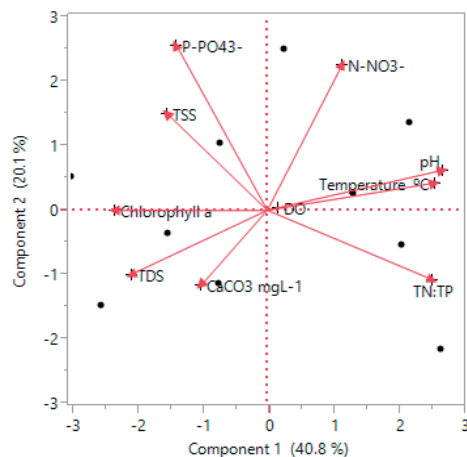


Figure 4. PCA of TN:TP and of the physicochemical parameters as 10 variables and their influence during June

As we expected in July (Figure 5) the reduction of rainfall helps that physical and chemical processes develop more intensively in water. In this regard the Component 1 represented by P/PO_4^{3-} , TSS, TDS, pH, DO, Temperature, N/NO_3^- , $CaCO_3$ cover 52% of total variation and strongly correlated with TN:TP and *Chlorophyll a* in component 2 with 21% of total variation.

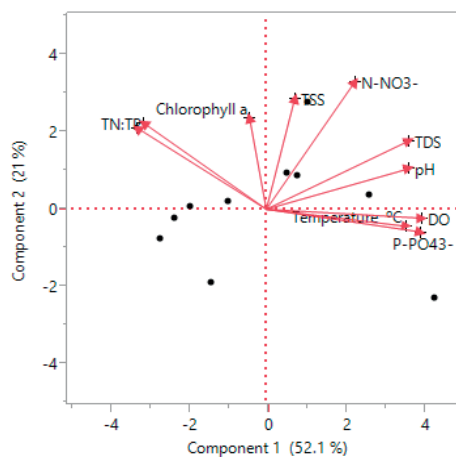


Figure 5. PCA of TN:TP and of the physicochemical parameters as 10 variables and their influence during July

After the consumption of DO during the August (Figure 6) the water system has decrease the pH which is in correlation with DO, Temperature, TN:TP, TSS, TDS and *Chlorophyll a* in

component 1 with 42% but the component 2 about 33% represented by N/NO_3^- and P/PO_4^{3-} , $CaCO_3$.

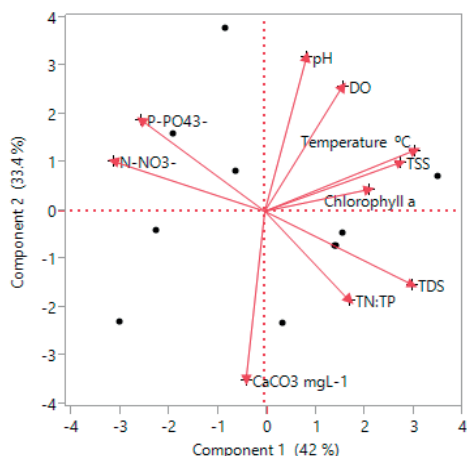


Figure 6. PCA of TN:TP and of the physicochemical parameters as 10 variables and their influence during August

During the September (Figure 7) the component 1 describes the 48% of total variation represented by TSS, DO, pH, Temperature, P/PO_4^{3-} , *Chlorophyll a*. In the other hand the component 2 describe the 23% of total variation by considering the TDS, TN:TP, N/NO_3^- and $CaCO_3$.

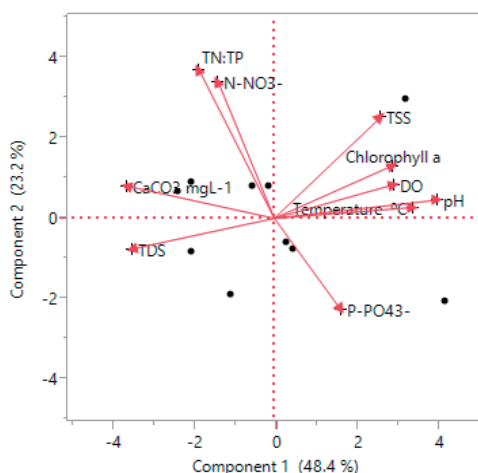


Figure 7. PCA of TN:TP and of the physicochemical parameters as 10 variables and their influence during September

The last period of data collation has increased the interaction between factors so the component 1 in October (Figure 8) represents 46% of total variation by involving the TN:TP, N/NO_3^- and $CaCO_3$, TDS, TSS. Component 2 represents 26 % of the variation with a correlation between pH, DO, Temperature, P/PO_4^{3-} and *Chlorophyll a*.

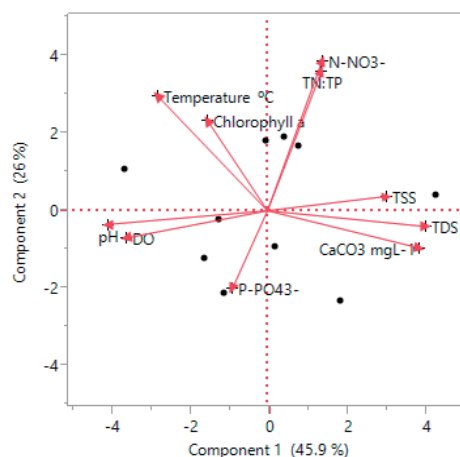


Figure 8. PCA of TN:TP and of the physicochemical parameters as 10 variables and their influence during October

CONCLUSIONS

The eutrophication of the Shkodra lake represented by the PCA helps in the determination of the factors that interact between each other that implicate the status. The decrease of freshwater quantity as well as the consequent decrease of dissolved oxygen implies the physico-chemical reactions that lead to the eutrophication of the lake, which is also assessed by the TN:TP ratio in this study. Our results underline the fact that extending these assessments over a longer period would help to determine more precisely the sources of eutrophication of this lake.

ACKNOWLEDGEMENTS

This research work was performed with the support of the Department of Environment and Natural Resources, Agricultural University of Tirana.

REFERENCES

- Ahl, T. (1979). Natural and human effects on trophic evolution. *Ergeb. Limnol.*, 13, 259-277.
- Babuji, P.; Thirumalaisamy, S.; Duraisamy, K.; Periyasamy, G. (2023). Human Health Risks due to Exposure to Water Pollution: A Review. *Water*, 15, 2532.
- Bojarczuk, A., Jelonkiewicz, L., Lenart-Boron, A. (2018) The effect of anthropogenic and natural factors on the prevalence of physicochemical parameters of water and bacterial water quality indicators along the river Bialka, southern Poland. *Environ. Sci. Pollut. Res.* 25, 10102–10114.
- Demiraj, E., Libutti, A., Malttezi, J., Brahushi, F., Rroço, E., Monteleone, M., & Sulçe, S. (2018). Effect of organic amendments on nitrate leaching mitigation in a sandy loam soil of Shkodra district, Albania. *Italian Journal of Agronomy*, 93-101.
- Downing, J.A. & McCauley, E. (1992). The nitrogen: phosphorus relationship in lakes. *Limnol. Oceanogr.* 37, 936–945.
- EEA (2021). European Environment Agency. Europe's groundwater — a key resource under pressure.
- IGWE, 2016. Institute of GeoSciences, Energy, Water and Environment.
- IPCC. (2022). Summary for Policymakers. In: Climate Change 2022: Mitigation of Climate Change. *Contribution of Working Group III to the Sixth Assessment Report of the Intergovernmental Panel on Climate Change*.
- Kashta, L., Dhora, D., Sokoli, F., Rakaj, M., Hoti, M., Beka, I., & Žižić-Velimirović, O. (2001). Bibliography on Shkodra/Shkadar Lake. Checklist of species. *The Regional Environmental Center for Central and Eastern Europe, Activity*, 1(1), 12.
- MPWT. (2011). (Ministry of Public Works and Transport of Albania). *National water supply and sewerage services sector strategy 2011-2017*, Tirane, 8-11.
- Pešić, V., Karaman, G., Kostianoy, A., & Vukašinović-Pešić, V. (2018). Conclusions: Recent Advances and the Future Prospects of the Lake Skadar/Shkodra Environment. In *The Skadar/Shkodra Lake Environment. The Handbook of Environmental Chemistry*, 80.
- Rakočević, J. (2018). The Phytoplankton and Trophic State of Lake Skadar/Shkodra. In *The Skadar/Shkodra Lake Environment. The Handbook of Environmental Chemistry*, 80.
- Sakamoto, M. (1966). Primary production by phytoplankton community in some Japanese lakes and its dependence on lake depth. *Arch. Hydrobiol.* 62, 1-28.
- Sandu, M.A., Madjar, R.M., Preda, M., Virsta, A., Stavrescu-Bedivan, M.-M., Vasile Scăteanu, G. Assessment of Water Quality and Parasitofauna, and a Biometric Analysis of the Prussian Carp of the Romanian Lentic Ecosystem in Moara Domnească, Ilfov County. *Water*. 15(22), 3978. <https://doi.org/10.3390/w15223978>
- Sandu, M.A., Virsta, A., Vasile Scăteanu, G., Iliescu, A.-I., Ivan, I., Nicolae, C.G., Stoian, M., & Madjar, R.M. (2023). Water quality monitoring of Moara Domnească Pond, Ilfov County, using UAV-Based RGB Imaging. *AgroLife Scientific Journal*, 12(1), 191–201.
- Sulçe, S., Rroço, E., Malttezi, J., Shallari, S., Libohova, Z., Sinaj, S., & Qafoku, N. (2018). Water quality in Albania: An overview of sources of contamination and controlling factors. *Albanian Journal of Agriculture Science* (Special edition – Proceedings of ICOALS, 2018), 279-297.
- Walsh P., Wheeler, W. (2012) Water Quality Index Aggregation and Cost Benefit Analysis. *US Environmental Protection Agency*, Washington, DC.
- WWAP. (2013). The United Nations World Water Development Report 2013. *United Nations World Water Assessment Programme (WWAP)*. Paris, United Nations Educational, Scientific and Cultural Organization.
- WWAP. (2015). The United Nations World Water Development Report 2015: *Water for a sustainable world. United Nations World Water Assessment Programme (WWAP)*. Paris, United Nations Educational, Scientific and Cultural Organization.
- Zela, G., Demiraj, E., Marko, O., Gjipalaj, J., Erebara, A., Malttezi, J., Zela, E. & Bani, A. (2020). Assessment of the Water Quality Index in the Semani River in Albania. *Journal of Environmental Protection*, 11, 998-1013.
- Zhang, L., Zhong, M. F., Xu, Y. X., Wang, Z. Y., & Huang, H. (2019). The Water Quality Evaluation in Balihe Lake Based on Principal Component Analysis. *Journal of Geoscience and Environment Protection*, 7, 38-48.

ASSESSMENT OF PHYSICOCHEMICAL AND BACTERIOLOGICAL QUALITY OF WELL WATER USED FOR DRINKING AND DOMESTIC PURPOSES IN AN INDUSTRIAL AREA OF ELBASAN DISTRICT, ALBANIA

Ariola DEVOLLI¹, Edlira SHAHINASI¹, Enkeleida SALLAKU²,
Marilda OSMANI³, Belinda HOXHA³, Frederik DARA⁴

¹Agricultural University of Tirana, Faculty of Biotechnology and Food,
Department of Chemistry, Kodër Kamëz, 1025 Pajsi Vodica, Tirana, Albania

²Agricultural University of Tirana, Faculty of Agriculture and Environment, Department
of Ecology and Natural Resources, Kodër Kamëz, 1025 Pajsi Vodica, Tirana, Albania

³"Aleksandër Xhuvani" University, Faculty of Natural Sciences, Department of Chemistry,
Ismail Zyma, Elbasan, Albania.

⁴University of Tirana, Faculty of Natural Sciences, Department of Applied Mathematics,
4 Sheshi Nënë Tereza, Tiranë, Albania

Corresponding author email: adevolli@ubt.edu.al

Abstract

Rapid population growth, urbanization, and unsustainable water management practices have all contributed to the depletion of freshwater resources. Groundwater is considered an important source for drinking and domestic purposes. In most cases, groundwater is threatened by physical, chemical, and microbiological contamination. The sources of groundwater contamination are numerous and have severe implications for public health. This study aims to assess the physicochemical and bacteriological quality of well water used for drinking and domestic purposes in the industrial area of the Elbasan district. Samples were collected from 57 wells and analysed for bacteriological (Total Coliforms and Escherichia coli) and physicochemical quality (pH, Electrical conductivity, total phosphorus, sulfate, ammonia, etc.) using standard methods. The collected data were subject to statistical analysis using the SPSS software ver. 22. Physicochemical results revealed that 65% of wells did not meet WHO standards and Albanian guidelines set for drinking water. In terms of bacteriological analysis, 80% of the samples were contaminated with total coliforms and 19% with E. coli. Based on analysis of heavy metals some samples exceeded the limits of iron and lead content.

Key words: bacteriological quality, groundwater, physicochemical quality, well water.

INTRODUCTION

Groundwater is a significant water supply source, which constitute about 20% of the world's supply (Jyothilekshmi et al., 2019). It is considered an essential source of human development, for a range of different sectors, and environmental flows (Velis et al., 2017). Recently, scientists and decision-makers have been paying more attention to sustainable water resource development and management due to limited water resources and rapid socioeconomic development (Tang et al., 2021). Freshwater has vital importance, and for many years its availability in urban areas has been a priority objective of the world (WWAP, 2019); therefore strategic importance for global water and food security is being intensified under

climate change as more frequent and intense climate extremes increase precipitation, soil moisture, and surface water availability variability (Vadiati et al., 2018)

Due to increasing population growth, human water demand for drinking, domestic, industrial, and agricultural purposes increases as well (UNDP, 2006), and water is becoming a scarce commodity in most of the world. On the other hand, an increase in population affects the quantity and quality of water, and any physical or chemical pollution causes changes to the quality of the receiving water body (Aremu et al., 2011).

Groundwater is an indispensable resource for our planet, considered the most preferred source of drinking water worldwide, more reliable than surface water, and more accessible (Naomi et

al., 2019; Marggat, 2013). According to Jakeman et al. (2016), groundwater provides over 97% of accessible freshwater, half of the drinking water, and approximately half of the irrigation water for agriculture.

Wells are one of the major sources of groundwater and have long been considered one of the purest forms of water in nature and meet the overall demand of rural and semi-urban residents (Nair et al., 2013).

As mentioned in the work of Devolli et al. (2017), approximately 70 % of Albanian cities use groundwater to fulfil their needs. Furthermore, the wells in the Elbasan district provide a reliable and ample water supply for drinking, domestic, and agricultural irrigation purposes (Osmani et al., 2023). However, water is a critical component of public health and failure to supply safe water places a heavy burden on humanity, industrial pollution (toxic elements), agricultural residues (runoff fertilizers), and microbial contamination are major concerns of groundwater sources which can affect the water quality and consequently human health (Yasin et al., 2015). These contaminants are further categorized as microorganisms, inorganics, organics, radionuclides, and disinfectants (Nollet, 2000). Albanian public water system uses water treatment and monitoring to protect consumers from such contaminants, but generally, the water quality of private wells is not covered by Albanian legislation and regulations of drinking water quality monitoring. Well-owners are responsible for protecting and monitoring water quality and must be aware of the potential of well-water contamination and the possible health effects (Osmani et al., 2023; Devolli et al., 2017).

Although private well-owners, unlike public water supplies, are legally obliged to test their water quality frequently (Schuitema 2020), however in practice, they rarely follow these recommendations and mostly test their well water only if problems arise (Hooks et al., 2019; Devolli et al., 2017).

As a result, the water quality of private wells is a major concern and there is an inevitable need for regular water testing and monitoring.

Recently, the implementation of instrumentation such as GPRS (General Packet Radio Service) destined for water quality evaluation (testing

and monitoring of chemical parameters) allows using a mobile device to view results and receive text warnings via SMS about the quality of groundwater and potable water in a real-time (Ionel et al., 2015).

The current study aims to assess private well water quality used to fulfil the drinking, domestic, and irrigation needs of the rural community in an industrial area of Elbasan district. Analyzing physicochemical parameters, heavy metal content, and bacteriological quality of well water was the main objective of this study. WHO guidelines and Albanian standards were used to assess the overall well water quality for drinking and household purposes.

MATERIALS AND METHODS

Description of Study Area

The study was conducted in 2022 at Bradashesh village, located in the industrial area of Elbasan district. Geographically, the study area is situated 4 km from Elbasan city between 41°06'09.3"N and 20°01'29.4"E (Figure 1).

This City suffers from problems related to overpopulation, such as waste management, high levels of air pollution, and significant noise pollution (Lazo et al., 2021).

According to the data of INSTAT 2022, the economy of this community is predominantly based on livestock farming and heavy industry (metallurgic plant and metal processing factory). The metallurgical complex considered as the biggest industry in the country is situated in the vicinity of the Bradashesh village (Shtiza et al., 2009).

Sample collection

About 75% of the total rural community is dependent only on their private well water to fulfil domestic consumption and drinking needs (Devolli et al., 2017; Osmani et al., 2023). A total of 57 well-water samples from 7 representative selected stations within the study area (Figure 1) were collected. Water wells ranged from 35 to 50 meters deep. Samples collection and treatment were carried out in accordance with the standard methods ISO 5667-5:2006; APHA, 2017; WHO, 2017.

Water samples should be representative of well water quality. Initially, the water was allowed to run at full flow from the pump for 10 minutes to

ensure that the water sample represented the quality of groundwater that feeds the deep well before sampling.

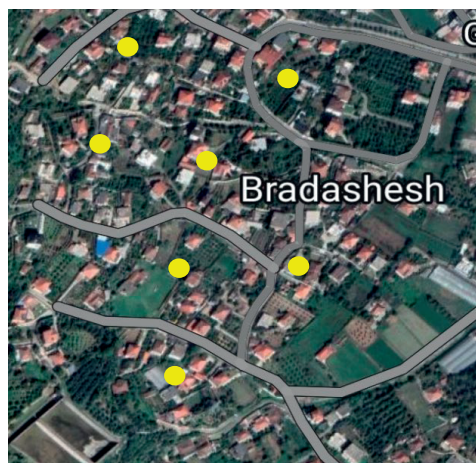


Figure 1. Map of the study area (yellow circles specify sampling stations) (Source: Google Maps)

The samples were collected in 1-liter polyethylene (PET) bottles and were immediately transported to the laboratory in a thermo-box to avoid any contamination. There were used 250 mL sterile plastic bottles for microbiological analysis.

Physicochemical analysis

The collected water samples were analysed for various physicochemical parameters such as temperature, pH, turbidity, electrical conductivity (EC), total dissolved solids (TDS), total suspended solids (TSS), biological oxygen demand (BOD), chemical oxygen demand (COD), total alkalinity (TA), total hardness (TH), calcium, magnesium, chloride, sulphate, phosphate, ammonium, nitrite, and nitrate according to the standard analytical methods for the examination of water and wastewater (APHA, 2017).

Temperature, pH, electric conductivity (EC), and total dissolved solids (TDS) were determined in situ using a multi-parameter water analyser WTW 3620 IDS. The measurement of TSS in water samples was carried out according to the standard APHA (2017) method by the filtration process.

The total alkalinity was determined using titrimetric method. Total hardness, calcium and

magnesium hardness were determined using EDTA titrimetric method. Chloride concentration was determined using argentometric titration method (AWWA, 2011). BOD content in well water samples was determined by the Winkler method as described by APHA (2017), while the COD concentration was determined according to the standard method 5220D with an accuracy of 0.1 mg COD per litre (APHA, 2012).

The anions sulphate, phosphate, ammonium, nitrite and nitrate were determined by using a WTW Spectrophotometer 7100 VIS.

Acidified well water samples ($\text{pH} = 2$) were analysed for the presence of heavy metals (lead, zinc, copper, iron and cadmium) by using a Flame Atomic Absorption Spectrometer (Analytik Jena GmbH - novAA 400 P).

All chemicals and reagents were of the analytical grade, and doubly distilled water was used for dilutions.

Bacteriological analysis

Microbiological load (Total Coliforms and *Escherichia coli*) in well-water was carried out through the membrane filtration method (ISO 9308-1:2014).

The plate count was conducted by pouring the plate technique on Plate Count Agar (PCA) and counting the colonies developed after the incubation. Enumeration of colonies was done as described by Rodier et al., (2009) and results were expressed as colony forming units (CFU)/100ml. M-Endo Agar LES medium was used for enumeration of *Escherichia coli* in water using a two-step membrane filter method. Inoculation temperature was 44°C for 24 hours. Violet Red Bile Agar medium was used for the detection of Total Coliforms at an incubation temperature of 37°C for 48 hours.

Statistical analysis

Analyses of water samples were conducted with 3 replications. The collected data were subject to statistical analysis and analysis of variance (ANOVA) at a 5% level of significance to determine the physicochemical and bacteriological quality variations among all site stations of private well-water sources using the SPSS software ver.22.

The relationships between the physicochemical parameters and bacteriological quality in the

water samples were established using Pearson correlation, and also there was utilized the multivariate analysis of Cluster Analysis (CA).

RESULTS AND DISCUSSIONS

Table 1 represents analytical results of the physical parameters of private well water samples collected from seven stations (E1 to E7).

The obtained results were evaluated and compared with WHO guidelines and Albanian standards for drinking water quality (WHO 2017; STASH 1998).

The pH values of well water samples ranged from 6.98 to 8.05, within the recommended limits of WHO guidelines and national standards for drinking water quality.

Mean values of EC varied from 660 to 1182.3 (µS/cm). It was evaluated that 90% of well water samples exceeded the threshold value allowed for drinking water according to WHO guidelines and Albanian standards (400-600 µS/cm). High conductivity in water can occur due to natural sources such as minerals, or as a result of industrial activity. The lowest and highest content of electric conductivity was registered in the E1 and E2 water sample stations, respectively. TDS content in analysed water samples ranged from 246 to 1020 mg/L. 10 % of water samples exceeded the WHO standard and 30% exceeded the maximum concentration of TDS specified in the Albanian standard (500 mg/L). Higher values of TSS and turbidity were recorded at station E4, 44 mg/L, and 7.66 NTU, respectively.

The alkalinity of well water is due to the presence of mineral salts, primarily carbonate and bicarbonate ions. It does not play a significant role in human health, but it makes water tasteful and helps in coagulation (Hussain et al., 2021). The minimum value should be 30 mg HCO₃⁻/L, and the maximum permitted level should not exceed 100 mg HCO₃⁻/L.

As is noticed in Figure 2, all analysed water samples exceeded the maximum permitted level according to WHO guidelines for drinking water quality.

Regarding TH, most of the well water samples exceeded the maximum level set by WHO and STASH (300 mg/L) for drinking and domestic purposes, while the samples of stations E1 and E2 resulted within the hardness standard.

Table 1. Results of physical parameters of well water samples

pH				EC (µS/cm)		
site code	Mean	SD	Range	Mean	SD	Range
E.1	7.617	0.217	0.53	660.0	83.77	205.0
E.2	7.263	0.221	0.54	1182.3	57.41	129.0
E.3	7.610	0.297	0.71	954.0	74.55	174.0
E.4	7.950	0.082	0.20	691.0	55.36	134.0
E.5	7.597	0.097	0.23	961.7	82.04	200.0
E.6	7.600	0.147	0.35	943.7	81.08	192.0
E.7	7.687	0.152	0.34	967.3	154.6	378.0
WHO*	6.5-8.5			400.00		
site code	TDS (mg/l)			TSS (mg/l)		
E.1	352.0	76.7	179.0	9.50	2.68	6.50
E.2	772.8	77.0	188.6	17.53	1.91	4.60
E.3	679.9	129.2	313.4	8.37	1.03	2.50
E.4	437.0	50.3	123.0	44.00	6.98	17.00
E.5	757.2	207.2	506.4	6.87	0.78	1.90
E.6	552.9	52.8	125.2	8.47	1.91	4.40
E.7	710.7	154.2	356.0	12.93	3.02	7.40
WHO*	500-1000			25		
site code	Turbidity (NTU)			Temperature (°C)		
E.1	0.70	0.14	0.33	16.17	0.74	1.70
E.2	1.08	0.45	1.09	15.83	0.45	1.10
E.3	0.96	0.21	0.49	15.03	0.31	0.70
E.4	7.66	0.70	1.71	15.03	0.40	0.90
E.5	1.94	0.21	0.48	16.07	0.31	0.70
E.6	0.76	0.15	0.35	15.57	0.17	0.40
E.7	2.12	0.56	1.33	15.57	0.77	1.80
WHO*	5			25		

WHO* - World Health Organization 2017 Guidelines for Drinking Water Quality (2017).

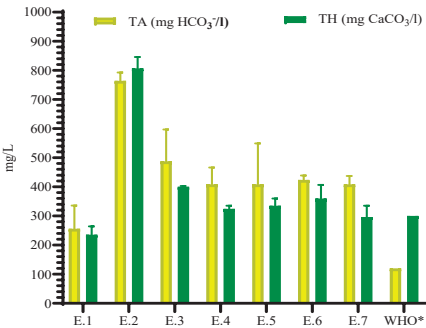


Figure 2. Variation of Total Alkalinity (TA) and Total Hardness (TH) of well water samples in 7 stations compared with WHO guidelines

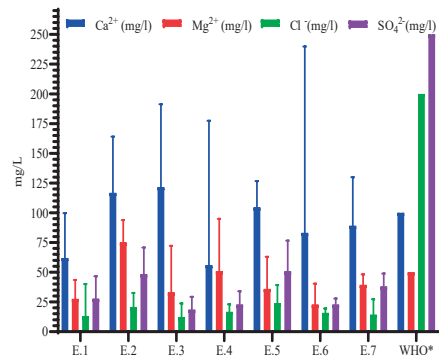


Figure 3. Variation of ions Ca^{2+} , Mg^{2+} , Cl^- and SO_4^{2-} of well water samples in 7 stations compared with WHO guidelines

Principally, the Ca and Mg presence is responsible for the hardness of the water, and their permitted limits are 100 mg/L and 50 mg/L, respectively (WHO, 2017). The high amount of magnesium imparts a repulsive taste to drinking water (Worako, 2015). In the current study, the concentration of magnesium in all the analysed water samples was within WHO guidelines (Figure 3). The chloride and sulphate concentrations were below the WHO guidelines, 200 mg/L and 250 mg/L, respectively. In the case of sampling stations (E2, E3, and E6), the concentration of Ca^{2+} exceeded the allowed limitation set by WHO guidelines for drinking water quality (Figure 3).

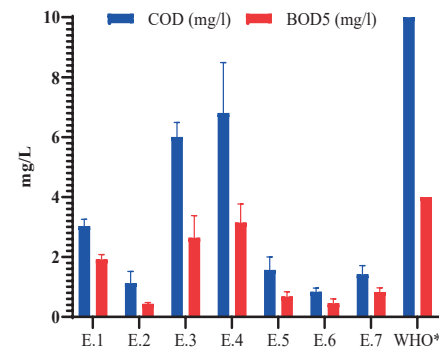


Figure 4. Variation of COD and BOD of well water samples in 7 stations compared with WHO guidelines

BOD is an indicator of the organic pollution of water, while the COD indicates the organic matter present in a water sample (Clair, 2003). As shown in Figure 4, the content of BOD and COD in all analysed water samples was beyond the permissible limits of WHO guidelines 4 mg/l and 10 mg/L, respectively. As noted in Table 2, the concentrations of nitrites, nitrates, ammonia, and phosphates in all analysed water samples were within the WHO guidelines and Albanian standards recommended for drinking water quality.

Table 2. Results of chemical parameters of well water samples

PO ₄ ³⁻ (mg/L)				NO ₃ ⁻ (mg/l)		
Site code	Mean	SD	Range	Mean	SD	Range
E.1	0.102	0.077	0.19	1.373	0.928	2.27
E.2	0.460	0.207	0.47	12.187	5.185	12.70
E.3	0.727	0.214	0.52	1.864	0.980	2.11
E.4	0.330	0.164	0.40	3.109	1.480	3.22
E.5	0.830	0.234	0.52	5.767	2.027	4.85
E.6	0.490	0.219	0.47	12.20	3.048	7.42
E.7	0.523	0.296	0.66	8.383	1.579	3.85
WHO*	2.00			50.00		
Site code	NO ₂ ⁻ (mg/L)			N-NH ₄		
E.1	0.005	0.003	0.01	0.045	0.012	0.03
E.2	0.000	0.000	0.00	0.483	0.143	0.35
E.3	0.002	0.000	0.00	0.061	0.021	0.05
E.4	0.031	0.022	0.05	0.136	0.030	0.07
E.5	0.007	0.001	0.00	0.189	0.077	0.18
E.6	0.018	0.004	0.01	0.033	0.012	0.03
E.7	0.007	0.002	0.00	0.147	0.064	0.16
WHO*	0.1000			0.5000		

The presence of heavy metals in drinking water higher than a certain concentration can have detrimental impacts on human health (Shehu, 2022). Water quality assessment concerning heavy metals was based on the safe limits set by WHO and Albanian legislation. In the present study, the mean values of heavy metals (Fe, Cu, Zn, Cd, Pb) analysed in well water samples are presented in Table 3. In the case of stations (E3, E4, E6, and E7), the values of Cd concentration exceeded the allowed limitation of 0.005 ppm. The concentration of lead in stations E3, E4, and E6 exceeded safe limits due to nearby industrial activity in the study area.

Table 3. Concentration of heavy metals (mg/L) in well water samples

Site code	Fe (m/L)	Cu (mg/L)	Cd (mg/L)	Pb (mg/L)	Zn (mg/L)
E.1	0.0502	1.0078	0.0067	0.00629	0.3072
E.2	1.0263	2.067	0.0032	0.0281	0.7601
E.3	0.0802	1.1064	0.0458	0.8405	0.4025
E.4	2.0675	3.7862	0.0764	1.0561	1.8602
E.5	0.0903	0.9247	0.0027	0.0421	0.5162
E.6	0.1501	1.0628	0.0163	0.1283	0.6407
E.7	0.5604	0.0965	0.0241	0.0367	0.5405
WHO*	0.1	1.000	0.005	0.05	5.000

Iron is present in significant amounts in soils, principally in insoluble forms, and therefore may be present in groundwater by causing harmful effects on human health (EPA 2001). Four sampling stations (E2, E4, E6, and E7) of well water showed higher iron content exceeding the maximum level of WHO standards for drinking water quality.

A higher content of Cu was also observed in sampling stations (E2, E4, and E6). Various studies have raised concerns about the impact of high levels of air pollution and significant river water pollution in the Elbasan district due to industrial activity (metallurgical plant and metal processing factory) and the discharge of industrial waste without being pre-treated (Bekteshi, 2023). This includes heavy metal levels such as Fe, Cu, Pb, Zn, etc.

Table 4. Results of bacteriological analyses

Site code	Total coliforms (cfu/100 mL)	Escherichia coli (cfu/100 mL)
E.1	<100	0.00
E.2	<100	3.00
E.3	50-100	0.00
E.4	50-100	0.00
E.5	>10	0.00
E.6	>10	3.00
E.7	50-100	2.00
WHO*	0.00	0.00

Table 4 presents the results of microbiological analyses of well water samples collected from seven sampling stations for the presence of Total Coliforms and *Escherichia coli*. Results are expressed in cfu/100ml. Most of the analysed water samples show the presence of coliform bacteria in high concentrations. *E. coli* was detected in three sampling stations (E2, E6, and E7).

The presence of coliform bacteria in drinking water is a potential health hazard. Numerous diseases can be caused by water pollution with pathogenic bacteria, such as diarrhea and gastrointestinal illnesses (Pandey, 2014).

The evaluated microbiological indicators were found to be well above the permissible limits of WHO and STASH (zero/100 mL) for the drinking, household, irrigation, and recreational uses.

In terms of bacteriological analysis, 80 % of well water samples were contaminated with total coliforms and 19 % with *E. coli* (Figure 5).

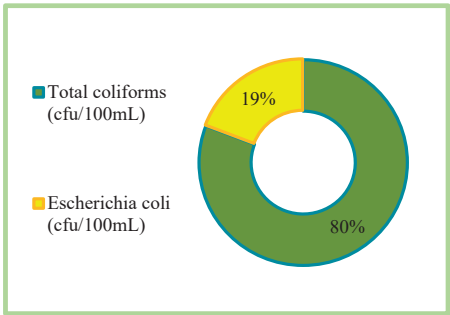


Figure 5. Percentage of Total Coliforms and *E. coli* presence in all analyzed wells

Our study points to possible fecal or surface runoff contamination of the well water sources in all sampling stations of Bradashesh village, as indicated by microbiological indicators (Total Coliform and *E. coli*).

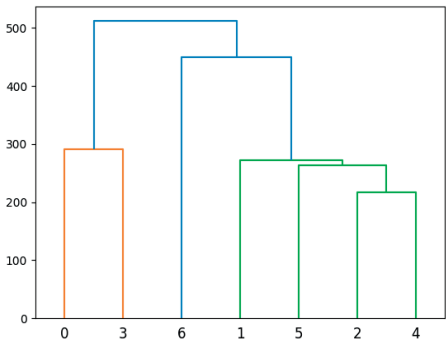


Figure 6. Dendrogram showing spatial similarities of sampling stations produced by cluster analysis

A dendrogram of the location pattern resulting from the cluster analyses (CA) is presented in Figure 6.

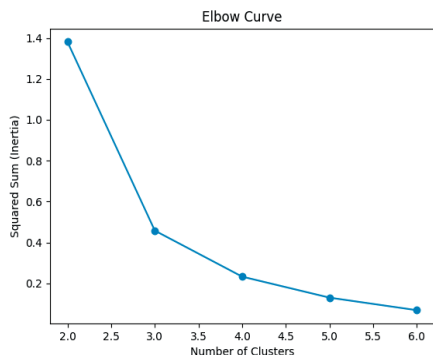


Figure 7. Elbow curve for optimal cluster number

The dendrogram shows that all the monitoring stations may be grouped into three main clusters. Cluster I is formed by stations (E1 and E4), Cluster II is formed by stations (E2, E3, E5, and E6) and Cluster III is formed by station E7. The Elbow curve also shows that the optimal number of clusters was three (Figure 7).

CONCLUSIONS

Based on the bacteriological analysis and referred to the standards set by WHO and STASH, well water quality characteristics of all collected samples from different stations of Bradashes village in Elbasan district were considered unsuitable for drinking/domestic uses without treatment.

Most of the physical data indicated marginally tolerable quality to pH, TDS, TSS, turbidity, and temperature but poor quality concerning conductivity, with values higher than permissible standards.

From the obtained results, nitrites, nitrates, ammonia, phosphates, chlorides, sulphates, BOD, and COD concentrations of well water samples were found to be within the maximum permitted level of WHO for drinking/household water quality.

The analysed wells were found to have moderately hard and hard water from the total hardness, total alkalinity, and calcium measure, hence undesirable for drinking and domestic uses.

The study concluded that in four of seven sampling stations, the concentrations of heavy metals (Fe, Cu, Cd, and Pb) exceeded the safe limits set by WHO and Albanian legislation.

This study employed multivariate statistical techniques to classify seven sampling stations located in the study area into groups of similar water quality characteristics. Cluster Analysis (CA) and Elbow curve showed that the optimal number of clusters was three.

Based on the results of this study, it is highly recommended that the wells' waters in this study area should be treated and continuously monitored to satisfy the Albanian standards and WHO guidelines recommended for drinking water quality. Treatment and hygienic practices should be improved to prevent or reduce contamination.

Water sources must be protected from contamination by human activity and animal wastes. Regular monitoring of water quality is needed to protect if further polluted. Water quality should be controlled to minimize acute problems of water-related diseases, which are endemic to human health.

Elbasan municipal council should ensure proper sanitation and water safety plans for these drinking and household water sources. They should encourage and obligate well owners to monitor water quality regularly and to test water quality frequently.

ACKNOWLEDGEMENTS

The authors would like to thank the staff of Laboratory of Water and Wastewater Analysis at the Agricultural University of Tirana for their continuous help and support for the analysis of well water samples.

REFERENCES

- American Water Works Association (AWWA, 2011). *Standard methods for examination of water and waste*. American public Health Association, American Water Works Association Water Environment Federation PART 9000.
- APHA (2017). *Standard Methods for the Examination of Water and Waste Water*, 23th ed. (Clesceri, L.S., Greenberg, A. E. & Eaton, A. D. eds.). America Public Health Association, Washington, DC.
- APHA-AWWA-WEF (2012). *Standard methods for the examination of water and wastewater*, 22th ed., Washington DC, USA.
- Aremu, M.O., Olaofe, O., Ikokoh, P.P., & Yakubu, M.M. (2011). Physicochemical characteristics of stream, well and borehole water sources in Eggon, Nasarawa State, Nigeria. *Journal Chemical Society Nigeria*, 36(1), 131-136.

- Bekteshi, L., Hoxha, B., Gega, N., Karamelo P. (2023). The impact of urban and industrial activity in the pollution of Shkumbini River. *5th International Conference on Applied Engineering and Natural Sciences. All Sciences Proceedings*, 1066-1070.
- Carrard, N., Foster, T., & Willetts, J. (2019). Groundwater as a Source of Drinking Water in Southeast Asia and the Pacific: A Multi-Country Review of Current Reliance and Resource Concerns. *Water*, 11, 1605, <https://www.mdpi.com/journal/water>.
- Council Directive 98/83/EC of 3 November 1998 on the quality of water intended for human consumption.
- Devolli, A., Kodra, M., Shahinasi, E., Stafasani, M. (2017). A survey of private well water quality in suburb of Albanian capital city. *ITEMA*, 808-821.
- EPA, (2001). *Parameters of Water Quality: Interpretation and Standards*, ISBN 1- 84096-015-3.
- Hussain, M., Jamir, L., Singh, M.R. (2021). Assessment of physico-chemical parameters and trace heavy metal elements from different sources of water in and around institutional campus of Lumami, Nagaland University, India. *Applied Water Science*, 11(76), 2-21.
- INSTAT, (2022) <https://www.instat.gov.al/media/11851/tregu-i-punes-2022.pdf>.
- Ionel, R., Pitulice, L. Vasiua, G., Mischie, S., Spiridon, O.B. (2015). Implementation of a GPRS based remote water quality analysis instrumentation. *Measurement*, 65, 81–93.
- ISO 5667-5:2006. Water Quality-Sampling-Part 5. Guidance on Sampling of Drinking Water from Treatment Works and Piped Distribution Systems. International Organization for Standardization, Geneva.
- ISO 9308-1:2014. Water quality — Enumeration of *Escherichia coli* and coliform bacteria — Part 1: Membrane filtration method for waters with low bacterial background flora.
- Jakeman, A., Barreteau, O., Hunt, R.J., Rinaudo, J.D., Ross, A. (2016). *Integrated Groundwater Management*. Springer. <https://doi.org/10.1007/978-3-319-23576-9>
- Jyothilekshmi, S., Sajan, S., Anjali, P., Yadhu Krishnan, R., Amal Kumar, S., Reshmi Sudhakaran, Neethu, F., Pratap Chandran, R. (2019). Physicochemical and Microbiological analysis of well water samples collected from North of Punnappa village, Alappuzha district, Kerala state, India. *Int. J. Adv. Res. Biol. Sci.* 6(6), 104-113.
- Lazo, P., Qarri, F., Allajbeu, Sh., Kane, S., Bekteshi, L., Frontasyeva, M., Stafilov, T. (2021). *The Evaluation of Air Quality in Albania by Moss Biomonitoring and Metals Atmospheric Deposition*. Springer Cham, ISBN 978-3-030-62357-9, Series 2191-5555.
- Margat, J., van der Gun, J. (2013) *Groundwater Around the World: A Geographic Synopsis*. CRC Press Taylor & Francis Group: Boca Raton, FL, USA.
- Nair, G.A., Chandran, P.R., Sukumar, B., Santhosh, S., Vijayamohan, Sobha, V. (2013). Assessment of well water quality in Tsunami affected regions of south-west coast of Kerala, India. *J. Environ. Biol.* 34(4), 771 - 777.
- Nollet, L.M.L. (2000) *Handbook of Water Analysis*. Marcel Dekker, New York.
- Osmani, M., Hoxha, B., Mazrreku, A., Kucaj, E., Gjoni, A. (2023). Assessment of Physicochemical Properties of Drinking Water Quality in Elbasan District. *International Journal of Chemistry and Chemical Engineering Systems*, 8, 16-23.
- Pandey, P.K., Kass, P.H., Soupir, M.L., Biswas, S., Singh, V.P. (2014). Contamination of water resources by pathogenic bacteria. *Amb Express* 4, 51.
- Rodier, J., Legube, B., Merlet, N. (2009) *L'Analyse de l'eau (Water Analysis)*, 9th ed. Dunod, Paris, France.
- Sawyer, C.N., McCarty, L.P., Parkin, G.F. (2003). *Chemistry for Environmental Engineering and Science*, 5th ed. New York: McGraw-Hill. ISBN 0-07-248066-1.
- Schuitema, G., Hooks, T., McDermott, F. (2020). Water quality perceptions and private well management: The role of perceived risks, worry and control. *Journal of Environmental Management*, 267, 110654.
- Shehu, A., Vasjari, M., Duka, S., Vallja, L., Broli, N., Cenolli, S. (2022). Assessment of health risk induced by heavy metal contents in drinking water. *Journal of Water, Sanitation and Hygiene for Development*, 12(11), 816-827.
- Shtiza, A., Tashko, A., Swennen, R., Van den Brande, A. (2009). Impact of metallurgy on the geochemical signature of dusts, soils and sediments in the vicinity of Elbasan complex (Albania). *Cent. Eur. J. Geosci.*, 1(1), 63-83.
- Standardi shqiptar i ujit të pijshëm STASH 3904:1997, Botimi i dytë datë 1.03.1998.
- Tang, B., Mao, R., Song, J., Sun, H., Kong, F., Cheng, D., Gao, X. (2021). Assessing the Impact of Optimization Measures on Sustainable Water Resource Management in the Guanzhong Area, China. *Front. Environ. Sci.*, 9, <https://doi.org/10.3389/fenvs.2021.805513>
- UNDP - United Nations Development Programme, (2006). *Human Development Report 2006*. Beyond Scarcity: power, poverty and the global water crisis.
- Vadiatia, M., Adamowska, J., Beynaghi, A. (2018). A brief overview of trends in groundwater research: Progress towards sustainability? *Jenvman*, 223, 849-851
- Velis, M.; Conti, K.; Biermann, F. (2017). Groundwater and human development: Synergies and trade-offs within the context of the sustainable development goals. *Sustain. Sci.* 12, 1007–1017.
- Velis, M.; Conti, K.; Biermann, F. (2017). Groundwater and human development: Synergies and trade-offs within the context of the sustainable development goals. *Sustain. Sci.* 12, 1007–1017.
- WHO (2017). *Guidelines for Drinking Water Quality*, 4th ed. World Health Organization, Geneva, Switzerland.
- Worako, A.W. (2015). Physicochemical and biological water quality assessment of lake Hawassa for multiple designated water uses. *Journal of Urban and Environmental Engineering*, 9(2), 146-157.
- Yasin, M., Ketema, T., Bacha, K. (2015). Physico-chemical and bacteriological quality of drinking water of different sources, Jimma zone, Southwest Ethiopia. *BMC Res Notes*, 8, 541, <https://doi.org/10.1186/s13104-015-1376-5>

USING HYDROGRAPHIC SURVEYS IN THE STUDY OF WATER BODIES DEPTHS

Levente DIMEN, Silvia Alexandra DREGHICI, Tudor BORȘAN

"1 Decembrie 1918" University of Alba Iulia,
5 Gabriel Bethlen, Alba Iulia, Romania

Corresponding author email: ldimen@uab.ro

Abstract

More than 70% of Earth's surface is covered by water bodies. The underwater relief is very diverse, from continental shelf to deepest trenches and is mostly insufficient known. Water bodies play an important role for our planet and human life, mainly because of helping to regulate the mass and energy transfer between Earth's layers, being source of food and supporting transportation. Due to the high importance of the water bodies, a better knowledge of the water bodies depths and protecting the underwater environment are vital. Though reaching the seabed for exploration could be difficult, modern technologies based on acoustic, optical or radio methods and bathymetric equipment allows hydrographic surveying in order to study the underwater relief. Therefore, strategies concerning climate change, reducing water pollution and environmental negative impact could be elaborated, ensuring sustainability.

Key words: bathymetric equipment, depth, hydrographic survey, underwater body.

INTRODUCTION

Natural phenomena (such as geological, hydrological, geotechnical, and environmental), as well as human activities, are causing deformations of the Earth surface (subsidence, landslides, floods, sinking, tectonic activity). These deformations take place at an increasing rate. Water bodies cover more than two thirds of our planet's surface; therefore, many changes are due to extreme events, most likely to be driven by climate change (Geomatics Research & Development SRL, 2021).

Knowing the depth and shape of the water bodies is fundamental for understanding ocean circulation, tides, tsunami forecasting, fishing resources, sediment transport, environmental change, underwater geo-hazards, infrastructure construction and maintenance, cable and pipeline routing and much more (<https://www.gebco.net/>).

The before-mentioned aspects can lead to negative and sometimes even destructive impacts on the Earth surface covered by water, and could even eventually be leading to a collapse. The sensitivity to different hazards puts forward the need for an integrated and cost-effective bathymetric monitoring capability (Geomatics Research & Development SRL, 2021).

An important role in the study of water bodies is played by the spatial measuring and monitoring. Spatial measurements offer precise observations and correlated data that can be used in monitoring our planet and the impacts of climate change. Therefore, Earth monitoring programmes using spatial observations are considered key-elements in adaptation strategies. As an example, the analysis of the sea level rise due to global warming require high-precision monitoring of tide gauges. This can be achieved using conventional levelling techniques combined with GPS positioning and bathymetric surveys (Hannah, 2014). Earth monitoring programmes require spatial information management, referring to (Hannah, 2014): databases for relevant data collection and storage and data integration into a common coordinate framework.

A corresponding spatial information management allows data mining, interpretation, and visualization of different climate change mitigation and adaptation strategies. A range of adaptation strategies and disaster risk management can be embedded into Earth monitoring programmes so as to reduce water pollution and environmental negative impacts, ensuring sustainability (Hannah, 2014).

Earth monitoring programmes can be achieved based on collections of large volumes of data

spread over long periods of time, expressing the complex interactions within the Earth system.

Such global, comprehensive, detailed, reliable and consistent data are collected both by Earth fixed and space borne instrumentation (Hannah, 2014). Longer time series of observation data allows better changing analysis and more reliable results interpretation. For a global approach concerning climate change and sustainable development, data collection and integration from multiple sources and multiple platforms is required (Hannah, 2014).

According to the monitored objectives, Earth observations are divided into nine areas such as disaster, health, energy resources, climate, water, weather, ecosystems, agriculture and biodiversity. The assessment of climate change and its evidences can be found in nearly all these areas: storms frequency and intensity, ice cap melt, sea level rise, etc. Long time series of data show the association of natural changes with anthropogenic forcing (Hannah, 2014).

In turn, the large amount of reliable spatial data requires stable, consistent reference systems, which themselves rely upon Earth observations on the variable shape, gravity field and rotation, allowing the definition of time dependent coordinates – an indispensable foundation for all sustainable Earth observations. Time dependent coordinates provide the spatial location of the analysed data to assess important elements of climate change processes (Hannah, 2014).

MATERIALS AND METHODS

Research and monitoring of the water bodies have a great role in scientific fields, leading scientists to innovation and progress, by discovering and improving new underwater resources. The more accurate information and educational programs are, the better understanding of the changing Earth surface, including water functions. The main objectives for ensuring a sustainable future for humanity are to educate the public concerning environmental aspects, climate change and its impacts, as well as reaching awareness of the population about the ecosystem's vulnerability. Only then, actions for environmental protection and responsible use and conservation of the water resources can be taken (Elhassan, 2015;

<https://www.gebco.net/>; Chişbac & Dreghici, 2023).

Data Acquisition

The datasets collected and used for climate change studies include trigonometric data, tide gauge data, meteorological data, ocean temperature data, gravity data, ice core data, salinity and currents data. Hydrographic data collection refers to the usage of bathymetric equipment, such as single- and multi-beam, side scan sonar, sound velocity profilers etc. Data collection tools allow the monitoring of Earth surface and features very accurately. The collected datasets, when accurately geo-referenced and integrated, allow detailed analyses of continuous global change (Hannah, 2014).

Nowadays, we face a continuous technological development, that bring surveyors in front of modern technologies, complex surveying equipment and methods, leading to a better accuracy and efficiency. Depending on the main goal and the type and depth of the water body to be surveyed, there are different bathymetric surveying methods and equipment, based on acoustic, optical and radio pulses and their propagation through water (Figure 1) (Dreghici, 2023; Chişbac & Dreghici, 2023).

Data Integration and Analysis

Spatial data integration represents combining different geospatial datasets into a complete heterogeneous one. These datasets correspond to natural or artificial phenomena or information and should be homogenous. The new dataset can then be used for analysis or information retrieval purposes, enabling object-based image analysis, multi-scale and multi-dimensional phenomena analysis, impact visualization, and the assessment of ecosystem dynamics. Finally, the analysis can lead to better decision-making. Spatial data integration can be carried out in order to establish relationships amongst corresponding object instances represented by different, autonomously produced spatial datasets of the same geographic space. Such an approach is essential for assessing and achieving sustainable development and climate change scenarios (Hannah, 2014).

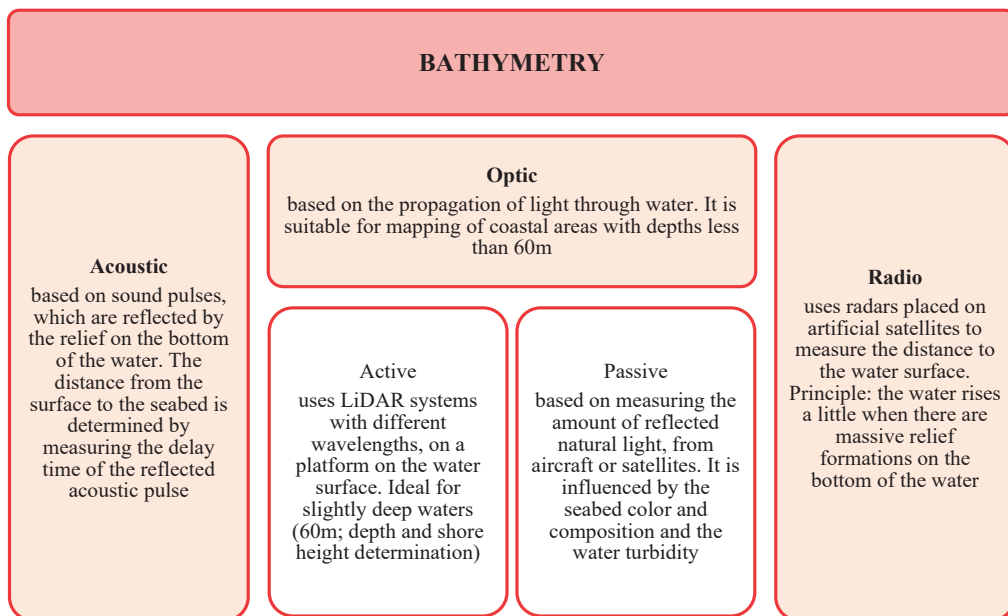


Figure 1. Bathymetric surveying methods (Chişbac & Dreghici, 2023)

Spatial data integration consists of three stages (Hannah, 2014):

- Pre-Integration: choosing the common schema for the geospatial datasets used;
- Matching and Modelling: results in global or local reciprocal modelling framework for the different datasets;
- Integration: may involve vector or raster data (images, raster maps and digital terrain models), or a mixture of both. This involves the use of image-processing and image-recognition techniques, spatial data registration, matching and transformation.

Datasets analytical tools are used in determining the extent of climate change and its impacts, to quantify changes or to monitor motions or changes from satellite-based measurement data. Analysing integrated datasets can lead to a better understanding of climate change processes expressed by environmental indicators, quantitative climatic conditions, numerical model simulations, etc. (Hannah, 2014).

Climate change should not be treated as a local geographical problem which can be solved by local or regional means. On the contrary, it should raise global awareness and seek global solutions in an integrated manner (Hannah, 2014).

Bathymetric Observation Programmes

Worldwide there are research institutions, extend and organizations dealing with Earth monitoring on local, regional or global level, offering products and services support for public sector, holding key roles in shaping global policies, helping to better understand our natural world and to protect its precious resources extends beyond national borders to monitor global weather and climate, and working with partners around the world (<https://www.noaa.gov/>).

Nowadays, water bodies are covered with bathymetric open source data. Using this data, underwater representations can be created, as well as high definition bathymetric maps. The so created bathymetric products can then be used for a wide range of applications. The modeling workflow, weather using self-collected data or open source data, is the same: data collection, data preliminary processing (preparatory works), data conversion (main processing, interpolation, drawing up the bathymetric map), data interpretation, quality assessment (checking if the results reach the high-quality requirements) and data usage in different applications (further research can be carried out) (Dumpis & Lagzdīņš, 2020).

European Space Agency and EU member states are implementing the world's largest Earth observation programme, Copernicus, under the coordination of the European Commission. In achieving the objectives of the programme, global, continuous, autonomous, high quality, wide range data is collected from a constellation of artificial satellites, called Sentinels. Radar equipment is mounted on artificial satellites, and then radar data collected is correlated with data from sensors on board and on the ground. Monitoring the Earth surface and the environment includes the assessment and management of water resources. There are time-series parameters, such as water body surface, the number of micro-algae in suspension, temperature, ice cover, etc., that can indicate the pollution degree of studied areas (<https://www.esa.int/>; Elhassan, 2015; <https://argans.co.uk/>; Chişbac & Dreghici, 2023).

General Bathymetric Chart of the Oceans, GEBCO, is an organization aiming to provide bathymetric data sets and products of the world's oceans: global gridded bathymetric data sets, undersea feature names, world map, web map services and a reference manual on how to build bathymetric grids. Data acquisition is mainly based on acoustic measuring systems, such as multibeam echosounders. Data acquisition also relies on crowdsourced bathymetry (CSB), a collection of bathymetric data collected from vessels, using standard navigation instruments, while engaged in routine maritime operations. GEBCO uses CSB to supplement the more rigorous and scientific bathymetric coverage done by hydrographic offices, industry, and researchers around the world. Bathymetric data collected by other than conventional means are examined how best to be incorporated, managed, and used (<https://www.gebco.net/>).

NOAA is an agency whose objectives are observing, measuring, assessing, protecting, and managing coastal areas and oceans. Their mission is to understand and predict changes in climate, weather, ocean, and coasts, to share that knowledge and information with others, and to conserve and manage coastal and marine ecosystems and resources (<https://www.noaa.gov/>).

Mare Nigrum is a Romanian multifunctional marine research vessel of pan-European interest,

involved in many researches and monitoring European projects. It provides various research activities in the fields of geology and geophysics, marine biology and ecology, being equipped with modern research equipment (bathymetric multibeam, seismo-acoustic, magnetometric, gravimetric equipment, various sensors etc.). Mare Nigrum carried out over 2400 scientific expeditions in the Black Sea: exploration campaigns in Romania's national waters (high-resolution geophysical surveys and geological surveys) and in international waters (Bulgaria, Georgia, Ukraine, Turkey) (<https://geoecomar.ro/nave/mare-nigrum/>).

In the present article, for the purposed case study, open-source data for the Black Sea was used.

The Black Sea, as one of the most important seas in the Euro-Asian region, oriented from East to West, even if it is small, arouses significant interest in terms of the study and mapping of its seabed. Six countries lie on its shores: Bulgaria and Romania to the west, Ukraine to the north, the Russian Federation to the northeast, Georgia to the east, and Turkey to the south. The Black Sea Basin is characterized by a significant depth and an elongated shape, located between parallels 40°56' and 46°33' north latitude. The Crimean Peninsula and the convexity of the Anatolian Coast divide the Black Sea into two distinct sub-basins. From a bathymetric perspective, the Black Sea basin is segmented into four distinct elements: shelf (continental plateau), slope, piedmont and abyssal plain, with a relatively uneven distribution between them, thus approximately 50% of the basin's surface is in the abyssal plain, located below -2000m, while 25% represents the area of continental shelves. The remaining 25% is distributed between continental slopes and continental glaciations (Vespremeanu, 2005).

The generation of a digital model of the Black Sea is an essential component of this effort, having significant implications in areas such as navigation, geological research and protection of the marine environment (Vespremeanu, 2005). For the proposed modeling of the digital model, there was used open-source data provided by GEBCO (General Bathymetric Chart of the Oceans). The data consists in a raster of sea depths globally. This raster is a valuable resource for marine mapping, with a

resolution of 15 arcseconds, with elevation values recorded in the center of the grid cells. GEBCO's global elevation models are generated by assimilating heterogeneous data, assuming that they are all referenced to mean sea level (<https://www.gebco.net/>).

RESULTS AND DISCUSSIONS

After importing the raster into the GIS environment, using the Arc GIS Desktop 10.6.1 solution, a pre-processing was performed to eliminate possible errors or discontinuities thus ensuring the coherence and reliability of the data, essential in the development of a precise elevation model (Figure 2) (Miller et al., 2010).

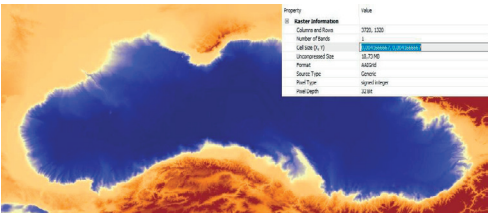


Figure 2. Pre-processing the image

The global integration of the data set is considered appropriate, provided that a vector layer containing a single object is imposed, the spatial constraint vector being in the form of an irregular polygon, in which its limits coincide with the limits given by the average water surface unaffected by the presence of waves (tide) (Figure 3).

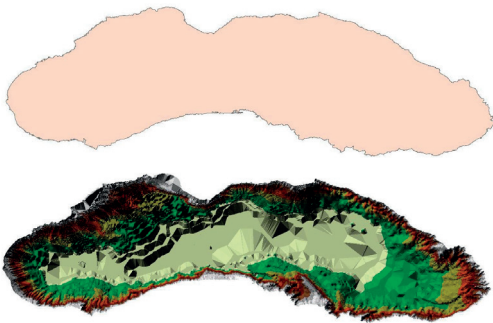


Figure 3. Applying the constraint vector in the model delineation

By construction, a value field signifying the maximum elevation can be attached to it, so that

the resulting model is based on two altimetric sources. In this way, the outer portions of the Black Sea basin are cancelled, attention being directed to its submerged relief (Miller et al., 2010).

The symbology was applied aiming at a classification of depths on equal intervals, omitting the isobaths and the filling aspect automatically included in the model generation; several classification methods can be used, the most common being those user-defined (by imposing quota ranges) (Figure 4). It is also possible to highlight or exclude certain interest data or that led to the generating of an erroneous model (Miller et al., 2010).

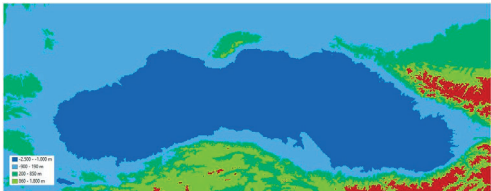


Figure 4. Symbology usage in defining elevation ranges

The performed delineation also affects the actions intended to prepare the three-dimensional model in the sense of applying the height base in relation to the modeled surface, and in the case of vertical exaggeration, the same constraining factor is necessarily applied to the vector entity, delineation tool (Figure 5) (Miller et al., 2010).

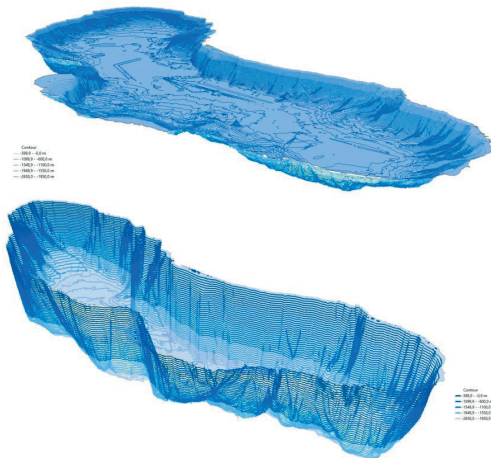


Figure 5. Three-dimensional models of the Black Sea basin

CONCLUSIONS

The Black Sea has been a key element for human lives since ancient times, being the mean of transportation, trade, migration and war. The water body helps regulating our climate and weather patterns, supports marine transportation, supports water-dependent businesses, provides us with many unique activities, from fishing to boating, provides seafood and food ingredients, as well as medicinal products.

Due to the great importance and impact of water into human lives, it is vital to know and understand the underwater world. Bathymetric data collection technologies (acoustics, optics and radar) and processing methods developed and improved rapidly in the last century. Lately, bathymetric products began to be used more and more often in a large variety of applications. Acquisition methods via radio bathymetry are characterized to be less accurate comparing to other methods, therefore acoustic bathymetric surveys are required to validate gravimetric bathymetry in remote regions of the world. Also, open source data play an important role in bathymetric researches, offering users high-resolution data.

Drawing the bottom line, bathymetry has a high potential in studying still unknown areas covered by water, which could be the key in ensuring sustainability.

REFERENCES

- Chişbac, L.R., Dregheci, S.A. (2023). Improving Human Living Using Bathymetric Methods, *Rev CAD Journal of Geodesy and Cadastre*, 34, 71-76.
- Dregheci, A., (2023). Underwater Mapping, *Blended Intensive Programme on Scientific Research: Young Researchers Academy with Specific Case Studies*, “1 Decembrie 1918” University of Alba Iulia
- Dumpis, J., Lagzdīns, A. (2020). Methodology for Bathymetric Mapping Using Open-Source Software, *Environmental and Climate Technologies*, 24(3), 239–248, <https://doi.org/10.2478/rtuct-2020-0100>
- Elhassan, I., (2015). Bathymetric Techniques, FIG Working Week, Sofia, Bulgaria
- Geomatics Research & Development SRL, (2021). GIMS Final Project Report, Grant agreement ID: 776335, DOI 10.3030/776335
- Hannah, J. (2014). *The Surveyor's Role in Monitoring, Mitigating, and Adapting to Climate Change*, FIG Task Force on Surveyors and Climate Change, FIG Publication, 65.
- Miller, F.P., Vandome, A.F., McBrewster, J. (2010). *Bathymetry*. VDM Publishing House Ltd., 68, ISBN: 6130704542
- Vespremeanu, E. (2005). *Geografia Mării Negre*, Editura Universitara, Bucuresti, pp. 256, ISBN 973-749-017-7. 913
- <https://argans.co.uk/>, accessed 15.08.2023
- <https://www.esa.int/>, accessed 13.09.2023
- <https://www.gebco.net/>, accessed 02.02.2024
- <https://geoecomar.ro/nave/mare-nigrum/>, accessed 17.02.2024
- <https://www.noaa.gov/>, accessed 17.02.2024

ASSESSMENT OF THE SEDIMENT (DIS)CONNECTIVITY IN A DELTAIC SYSTEM, DANUBE DELTA, ROMANIA

Florin DUȚU, Bogdan-Adrian ISPAS, Irina CATIANIS, Ana-Bianca PAVEL, Laura DUȚU

National Institute for Research and Development for Marine Geology and GeoEcology
(GeoEcoMar), 23-25 Dimitrie Onciul Street, Bucharest, Romania

Corresponding author email: florin.dutu@geoecomar.ro

Abstract

Delta systems, as final receptors of the fluvial systems are under considerable and increasing influence of multiple anthropogenic stresses, such as hydropower plant developments in the basins, extraction of groundwater in delta plains, embankment of banks, dredging of the navigation channel, the land use change, channel engineering, that affect the sediment connectivity. Along the Sulina Canal, the cut-off program and construction of the groins and dikes had important responses in grain size distribution between the main channel, the rectified meanders, and the lakes of the Danube Delta. Two field campaigns (at high and low waters) were made in May and October 2023, focusing on the bed sediment composition and lithological constituents. Sediment samples were acquired throughout several cross-sections, to investigate the bed sediment characteristics. Grain size parameters (such as Median, Standard deviation, and Skewness) show the predominance of fine fraction (medium and fine sand, and silt), moderately and poorly sorted. The data were compared and larger modifications were found between the two analysed periods in the distribution of sediments.

Key words: connectivity, Danube Delta, grain size, lithology, riverbed sediment.

INTRODUCTION

Recently, a special consideration has been devoted to the relationship between the concept of connectivity and the sediment transport and delivery to the coastal areas (Crema & Cavalli, 2018; Mishra et al., 2019). The sediment connectivity is assessed as the degree of linkage between the sediment source to downstream area, representing one of the most important factors controlling the landscape evolution (Mishra et al., 2019). The loss of the lateral and longitudinal sediment connectivity affects river systems generally, and mainly the functionality of the deltaic systems (Bunn & Arthington, 2022; Baldan et al., 2023). Sediment (dis)connectivity is governed by the spatial distribution of the sediment sources and the geomorphic conditions of the transfer pathways, as showed by many authors as Poepl et al., 2017; 2020.

In the deltaic systems, the meander cutoffs play an important role in river morphodynamics by increasing local channel slope, decreasing river sinuosity, and reducing floodplain access (Schwenk & Foufoula-Georgiou, 2016).

The reduction of the sediment load has been recorded in the majority of the deltaic systems around the world (Walling & Fang, 2003;

Syvitski, 2011) and is generally due to the human activities, such as landscape engineering, construction of reservoirs, hydrotechnical works, dredging (Zaharia et al., 2011; Habersack et al., 2016; Nistor et al., 2021; Duțu et al., 2022; 2023; Constantinescu et al., 2023). In the Danube Delta, the period of major anthropic interventions began after the establishment of the Danube Commission in 1856 with the meander belt cut-off programme of the Sulina branch (between 1858-1902) shortening this arm by about 25% (of the initial 83 km length). Besides other important transformations affecting the delta, such as cutting and dredging of shallow canals, construction of jetties and new channels, many sinuosities have been corrected. Along the Sulina distributary, a number of 27 belts and sinuosities were cut-off. Only a few meander belts of the former Sulina Canal remained connected to the main channel (such as Maliuc meander (connected to the main channel at Mile 23.7), and the "Big M" meander belt, connected at Mile 13.5 and Mile 8.4). The regulation of the Sulina Canal consisted in the construction of 167 submerged groins and the protection of the banks with rock blocks (along 91.8 km) (Panin, 1999; Panin et al., 2016; Duțu et al., 2022).

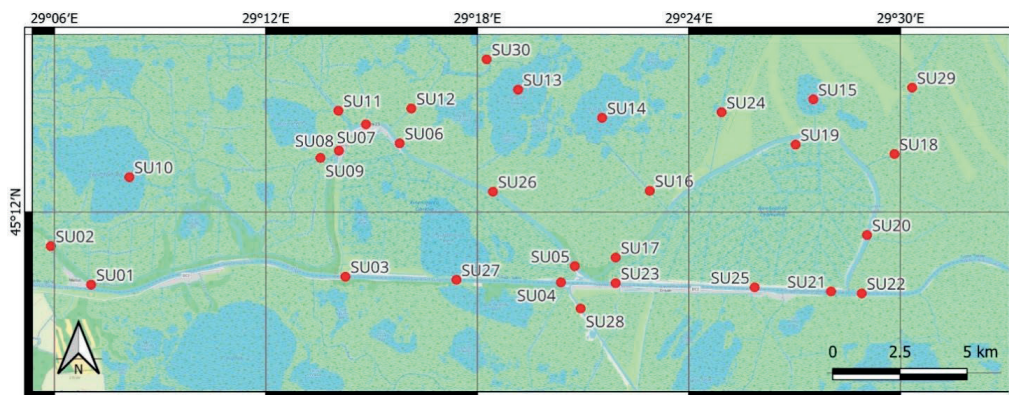


Figure 1. The Sulina Canal with the rectified meander "Big M" and the position of the investigated locations (Global Mapper v17)

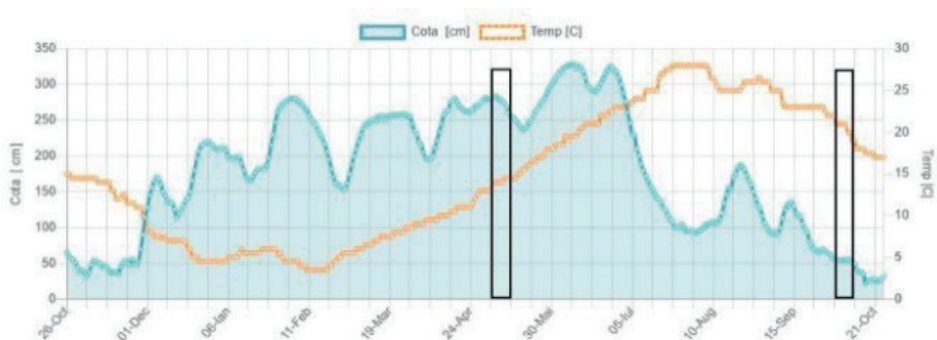


Figure 2. The water level (in blue) and the water temperature (in yellow) at the hydrometrical station Tulcea with the position of the two field campaigns in May and October 2023 (<https://edelta.ro/cote-dunare-365-de-zile>)

The results are consisting in changes of the river bed morphology, water and sediment fluxes and thus, a perturbation of the sediment transit from the main distributary to the delta depressions through the former meanders and canals, affecting the hydrological connectivity (Pacioglu et al., 2022; Duțu et al., 2023).

The objective of this paper was to investigate the distribution of the bed sediments in the former meanders during two different hydrological conditions (high and low waters, in May and October 2023), and to assess the sediment (dis)connectivity between the main distributary, the former meanders and the interdistributary depressions connected by lateral (natural or man-made) canals.

MATERIALS AND METHODS

The sedimentological data were acquired in May and October 2023, at high and low waters (the

water discharge on Profile P03 was $1490 \text{ m}^3 \cdot \text{s}^{-1}$ in May and $641 \text{ m}^3 \cdot \text{s}^{-1}$ in October) (Figure 1 and Figure 2). During the measurements, the water level stage had large variations (at the hydrometrical station Tulcea) with a total of 31 cm in May and 21 cm in October. Reported water depths are expressed in local values.

Bottom samples were collected with a grab sediment sampler, on 30 sediment sampling stations distributed along the main Sulina channel, the former meanders "Big M" and Maliuc) on the lateral canals and connected lakes (Crânjală, Gârla lui Eracle, Dovnica, Șontea, Gârla Ledianca, Magearu, Bogdaproste, Eracle, Caraorman Canals and Fortuna, Răducu, Bogdaproste, Trei Iezere Lakes) (Figure 1).

Grain size was done for all of the sediment samples by diffractometry. The texture categories (sand, silt, and clay) were separated using the Udden-Wentworth logarithmic scale while the classification of sediments was done

according to the Shepard diagram (Udden, 1914, Wentworth, 1922, Shepard, 1954). Based on the primary data the following granulometric parameters were extracted from the distribution curve (expressed in Φ units): *the median* (M_d), *the standard deviation* (σ) and *the asymmetry coefficient* Sk_1 (Folk & Ward, 1957; Visher, 1969). Technical approaches regarding the grain size analyses were developed by Duřu et al., (2018). *The lithological content* of the sediments was determined using the Loss On Ignition (LOI) method. Primarily, the sediment sub-samples were oven-dried at 105°C (Memmert Etuve) to determine the moisture content (%) by Loss On Drying (LOD) method (Smith & Mullins, 2000). After oven drying, the samples were weighed and exposed to sequential heating (Snol 8.2/1100 Calcination Furnace) and measuring weight loss between heating stages (%) by Loss On Ignition (LOI) method. The loss in mass by combustion at 550°C (Dean, 1974), confers an assessment of the total organic matter (TOM%). The loss in mass by calcination at 950°C (Digerfeldt et al., 2000; www.geog.cam.ac.uk), imparts an estimation associated with the total carbonate content (CAR%). The residual material is ascribed to the siliciclastic fraction (SIL%). The results are expressed as percentages of the total sample mass.

RESULTS AND DISCUSSIONS

Granulometric analyses of the sediments. In May 2023, during high waters, two types of sediments were found: sandy sediments, dominated by the fine subfraction, and silty-clay sediments, consisting of silt and clay, with the clayey fraction subordinate to the silty one. Along with the inorganic material, in most cases, there is also a content of biogenic origin, composed of shells and fragments and/or debris. Some samples had soft pebbles and blackish, unctuous clay with decomposed organic matter. Along the Sulina Canal the sediments are composed of sands (with more than 90%), with subordinated fractions of clay and shelly material. Among the subfractions of sand, fine and medium sand is dominant (Photo 1, Figure 3). The mean and median values are positive (maximum 2.48 Φ). The standard deviation, which has values between 0.56 and 0.63, indicates a relatively good sorting of the particles. The asymmetry has predominantly

negative values, covering the range between -0.25 – +0.20 and Kurtosis is in the platykurtic – very leptokurtic range.

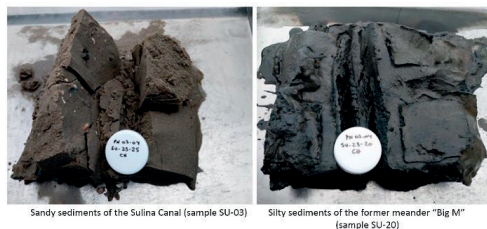


Photo 1. Bottom sediments sampled from the Sulina Canal in May 2023 (sample SU-23-03) and the former meander "Big M" (sample SU-23-20)

The sediments of the former meanders are generally composed of sandy silts, with the clayey fraction subordinate to the silty one. Samples SU-23-05 and SU-23-17 are the only ones with a sand content above 50% due to their position near the main stream where the sediments can be mixed by the strong water currents. The most common textural categories are silt and sandy silt. Among the silt subfractions, medium and coarse silt is the most representative, and in the case of sands, the fine subfraction. The mean and median values are positive (with a maximum of 6.57 Φ). The standard deviation, which has values between 1.26 and 2.29, indicates weak to very weak particle sorting. The asymmetry has predominantly positive values, covering the range between -0.26 and +0.52, and Kurtosis is platykurtic – mesokurtic.

The sediment samples taken from lakes are composed of sandy mud, in which the silty fraction is predominant. For the silts, medium and coarse silt subfractions are more frequent. Among the silt subfractions, coarse and medium silt is the most representative. The mean and median values are positive (maximum 5.81 Φ). The standard deviation, which has values between 1.59 and 1.88, indicates poor particle sorting. Asymmetry has positive values, covering the range between +0.01 and +0.12, and Kurtosis is leptokurtic.

Along the lateral natural or man-made canals, the sediments are sandy silts, with the clayey fraction subordinate to the silty one. Sample SU-23-28, situated on the Caraorman Canal, is the only sample with a sand content of more than 50% (Figure 3). The most common textural

category is sandy silt. Among the silt subfractions, coarse and medium silt is the most representative, and in the case of sands, the fine subfraction. The mean and median values are positive (maximum 6.80 Φ). The standard deviation, which has values between 1.68 and 2.32, indicates from weak to very weak particle sorting. The asymmetry has positive values, covering the range between +0.05 and +0.52; Kurtosis is platykurtic – leptokurtic. In October 2023, during the low water levels, two types of sediments were found: medium sand (with plant fibers), and sandy clay-silty sediments (sandy muds), consisting of mud and sand, with the clayey fraction subordinate to the silty one, present in areas where the water velocity is low. Along with the inorganic material, in most cases, there is also a content of biogenic origin, generally made up of shells, fragments, and/or plant remains. Also, some sediments have soft pebbles (sample SU-23-18)

and blackish, unctuous mud with decomposed organic matter. The sediments of the Sulina Canal are composed of sands, with subordinate fractions of mud and shelly material. Sand percentages exceed 70% in most cases (Figure 4, Photo 2). Among the subfractions of sand, fine and medium sand predominate. The mean and median values are positive (maximum 6.20 Φ). The standard deviation, which has values between 0.64 and 2.43, indicates relatively good sorting to very poor particle sorting. The asymmetry has predominantly positive values, covering the range between -0.10 and +0.36, and the Kurtosis is in the platykurtic-extremely leptokurtic range. Considering that some samples are composed of high clay percentage (SU-23-04 and SU-23-05), formed by compact material, it is very likely that the samples were collected from the bed substrate.

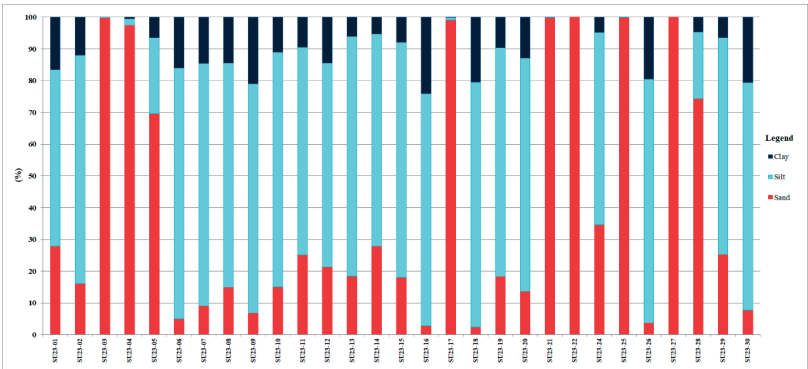


Figure 3. The texture diagram of the sediments in May 2023

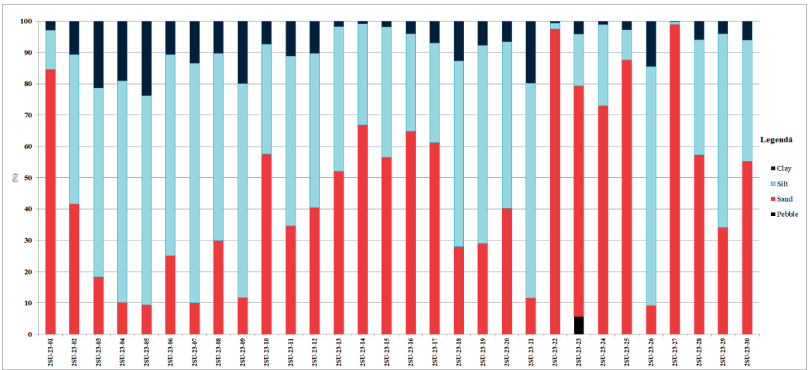


Figure 4. The texture diagram of the sediments in October 2023

Along the former meanders the sediments are composed of sandy silts, with the clayey fraction subordinate to the silty one. Sample SU-23-17 is the only one with a sand content above 50%. The most common textural category is sandy silt. Among the silt subfractions, medium silt is the most representative, and in the case of sands, the medium sand subfraction. The mean and median values are positive (maximum of 6.45Φ). The standard deviation, which has values between 1.74 and 2.51, indicates weak to very weak particle sorting. The asymmetry has predominantly positive values, covering the range between -0.02 and +0.47, and the Kurtosis is platykurtic – mesokurtic.

In the lakes, the sediments are composed of sands, with subordinate fractions of mud and shelly material. The sand percentages are mostly due to existing plant fibres. Among the sand subfractions, very fine sand predominates. The mean and median values are positive (maximum of 4.16Φ). The standard deviation, which has values between 1.67 and 2.15, indicates relatively good sorting to poor particle sorting. The asymmetry has predominantly positive values, covering the range between -0.03 and +0.31 and the Kurtosis is in the platykurtic – leptokurtic interval.



Silty sediments of the Bogdaproste lake (sample SU-14) Sandy sediments of the Sulina Canal (sample SU-27)

Photo 2. Bottom sediments sampled in October 2023 from the Bogdaproste canal (sample SU-23-14) and the from the Sulina Canal (sample SU-23-27)

Along the canals, sandy silts have been identified, with the clayey fraction subordinate to the silty one, but also from silty sands, in fewer cases. The most common textural categories are sandy silt and silty sand. Among the silt subfractions, in general, medium silt is the most common, and in the case of sands, the very fine and coarse subfractions are the most representative, in most cases. The mean and median values are positive (maximum 6.22Φ). The standard deviation, which has values between 1.47 and 2.65, indicates weak to very

weak particle sorting. The asymmetry has predominantly positive values, covering the range between -0.05 and +0.38. The Kurtosis is platykurtic to extremely leptokurtic.

The lithological content of the bottom sediments. The overall composition of sediments includes several primary constituents such as water (moisture) content, organic matter, carbonates, and inorganic (minerogenic) content. Lithological identification of the main sediment components (total organic matter, carbonate content, and siliciclastic fraction) is essential for studying aquatic sediments, providing relevant complementary information on a variety of factors related to environmental changes (hydrology, watershed weathering, water level, pollution, human activities), including evidence about the formation, deposition, and evolution of the sedimentary environment (sedimentation dynamics).

In May 2023, the sediment samples taken from the Sulina Canal (SU-23-03, SU-23-04, SU-23-21, SU-23-22, SU-23-25, and SU-23-27), from the former meanders (SU-23-05, SU-23-08, and SU-23-17) and lateral channels (SU-23-01, SU-23-09, SU-23-16, SU-23-18, SU-23-28, and SU-23-30) are characterized by a relatively higher level of siliciclastic content (SIL%), with values more than 30% of the total dry sediment weight (Table 1, Figure 5). The siliciclastic component (SIL%) has values included in a wide range, respectively 6.05-90.35%, and the average value is 51.43%. The highest value (90.35% SIL) was recorded in station SU-23-25 (Sulina Canal at Mm 10 + 800), and the lowest value (6.05% SIL) was observed in station SU-23-15 (Răducu Lake).

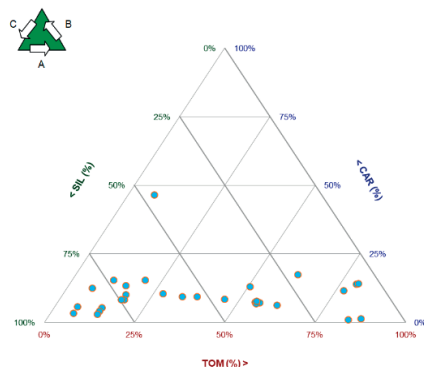


Figure 5. The lithological constituents (%) of the sampled sediments in May 2023 (siliciclastic fraction - SIL, total carbonates - CAR and total matter - TOM)

Instead, the sediment samples taken from various locations along the former meanders (SU-23-06, SU-23-07, SU-23-08, SU-23-19, SU-23-20, and SU-23-26), canals as Gârla lui Eracle, Magearu Canal (SU-23-11, SU- 23-12, SU-23-29), and lakes (SU-23-10, SU-23-13, SU-23-14, and SU-23-15), are characterized by a very high contribution of organic matter, with values over 30% of the total weight of the dry sediment (Table 1, Figure 5).

Table 1. The results of the lithological analyses, May 2023

Sample	WC (%)	DM (%)	TOM (%)	CAR (%)	SIL (%)
SU-23-01	18.77	81.23	17.54	10.03	72.43
SU-23-02	14.56	85.44	33.49	9.43	57.08
SU-23-03	10.16	89.84	13.21	5.37	81.41
SU-23-04	12.82	87.18	11.42	15.44	73.14
SU-23-05	29.25	70.75	7.10	12.40	80.50
SU-23-06	16.23	83.77	54.64	7.28	38.08
SU-23-07	24.25	75.75	45.64	8.53	45.83
SU-23-08	26.42	73.58	37.64	9.32	53.04
SU-23-09	28.30	71.70	15.87	13.43	70.70
SU-23-10	23.51	76.49	61.51	17.41	21.08
SU-23-11	20.69	79.31	61.21	6.30	32.49
SU-23-12	23.93	76.07	50.35	13.08	36.57
SU-23-13	26.07	73.93	79.43	13.89	6.68
SU-23-14	28.02	71.98	77.08	11.49	11.42
SU-23-15	23.10	76.90	79.83	14.12	6.05
SU-23-16	18.48	81.52	27.52	10.53	61.94
SU-23-17	17.67	82.33	7.19	46.58	46.23
SU-23-18	25.04	74.96	20.25	15.42	64.34
SU-23-19	25.73	74.27	56.09	7.10	36.80
SU-23-20	22.44	77.56	55.21	6.84	37.95
SU-23-21	11.28	88.72	13.16	4.12	82.73
SU-23-22	12.78	87.22	6.35	5.68	87.97
SU-23-24	18.18	81.82	83.67	0.90	15.43
SU-23-25	16.31	83.69	6.36	3.29	90.35
SU-23-26	18.79	81.21	54.90	7.77	37.33
SU-23-27	9.34	90.66	13.22	2.88	83.90
SU-23-28	12.98	87.02	18.05	8.19	73.76
SU-23-29	24.89	75.11	86.97	1.40	11.63
SU-23-30	19.45	80.55	17.10	8.21	74.70
Minimum value					
Maximum value					

The distribution of organic matter in the investigated samples has values within a wide range of variation, namely 6.35-86.97% TOM and an average value of 38.35% TOM. The highest value (86.97% TOM) was measured in station SU-23-25 (Magearu Canal), and the lowest value (6.35% TOM) was observed in station SU-23-25 (Sulina Canal Mm 8 +500). The variation range of carbonates is wide, presenting different values ($\text{CaCO}_3 \leq 10\%$; $10\% < \text{CaCO}_3 \leq 30\%$) of the total dry sediment weight, respectively, values in the range 0.90-

46.58% CAR, with an average value of 10.22% CAR.

The highest value (46.58% CAR) was recorded in station SU-23-25 (meander “Big M”), and the lowest value (0.90%CAR) was observed in station SU-23-25 (Dovnica Canal). Based on the results obtained, the analyzed sediments evidenced mixed sediments ranging from mineral-rich sediments ($>15\text{-}30\%$ SIL), subsequently followed by organic-rich sediments and a variable carbonate content, as non-carbonated sediments ($\text{CaCO}_3 \leq 10\%$) or low calcareous sediments ($10\% < \text{CaCO}_3 \leq 30\%$). The high carbonate content found in a single sample in the station SU-23-25 is attributed to the abundant biogenic material (shells, shell fragments and shelly detritus).

In October 2023, it was observed that the sediment samples from the locations located on the bed of the Sulina Canal (SU-23-03, SU- 23-04, SU-23-21, SU-23-22, SU-23-23, SU-23-25, and SU-23-27), channels as Crânjălă (SU-23-01, SU-23-02), Șontea (SU-23-09), Dovnica (SU-23-24), and Caraorman (SU-23-28), “the Big M” meanders (SU-23-05, SU-23-08, and SU-23-17) and Fortuna Lake (SU-23-10), are characterized by a relatively higher level of siliciclastic content (SIL%), with values more than 30% of the total dry sediment weight (Table 2, Figure 6). The siliciclastic component (SIL%) has values in a wide range, respectively 4.57-90.96%, and the average value is 51.30%. The highest value (90.96 %SIL) was measured on the Sulina Canal at Mm 16+000 (SU-23-27), and the lowest value (4.57 %SIL) was identified on the Răducu Lake (SU-23-25).

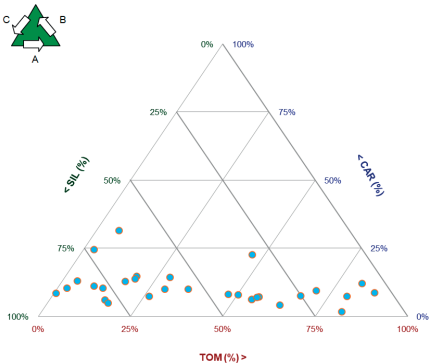


Figure 6. The lithological constituents (%) of the sampled sediments in October 2023 (siliciclastic fraction - SIL, total carbonates - CAR and total matter - TOM)

Carbonates have a wide range of variation, presenting different values ($\text{CaCO}_3 \leq 10\%$; $10\% < \text{CaCO}_3 \leq 30\%$) of the total dry sediment weight, respectively, values in the range of 1.72-31.52% CAR, and an average value of 10.73 %CAR. The highest value (31.52% CAR) was recorded in station SU-23-25 (on the Sulina Canal), and the lowest value (1.72% CAR) was found in station SU-23- 29 (Măgearu Canal).

Table 2. The results of the lithological analyses in October 2023

Sample	WC (%)	DM (%)	TOM (%)	CAR (%)	SIL (%)
SU-23-01	20.45	79.55	2.53	10.40	87.08
SU-23-02	16.47	83.53	17.03	12.89	70.07
SU-23-03	16.88	83.12	15.00	6.03	78.97
SU-23-04	15.79	84.21	2.79	24.68	72.53
SU-23-05	24.98	75.02	26.30	7.33	66.38
SU-23-06	19.03	80.97	47.25	8.22	44.53
SU-23-07	25.08	74.92	50.14	8.07	41.79
SU-23-08	23.36	76.64	35.57	10.15	54.28
SU-23-09	24.33	75.67	19.29	14.79	65.92
SU-23-10	21.68	78.32	9.43	11.28	79.29
SU-23-11	15.73	84.27	54.57	6.32	39.11
SU-23-12	14.73	85.27	46.53	22.63	30.84
SU-23-13	18.89	81.11	81.58	12.15	6.27
SU-23-14	14.25	85.75	70.46	9.44	20.09
SU-23-15	14.86	85.14	86.68	8.75	4.57
SU-23-16	16.99	83.01	67.19	7.65	25.16
SU-23-17	16.62	83.38	29.23	10.09	60.68
SU-23-18	14.78	85.22	79.84	7.34	12.82
SU-23-19	14.54	85.46	54.67	6.24	39.09
SU-23-20	14.12	85.88	56.09	7.24	36.67
SU-23-21	21.14	78.86	19.25	13.85	66.90
SU-23-22	9.52	90.48	16.46	4.92	78.62
SU-23-23	19.73	80.27	6.01	31.52	62.47
SU-23-24	29.11	70.89	28.42	14.48	57.10
SU-23-25	19.60	80.40	4.04	13.16	82.80
SU-23-26	20.93	79.07	55.60	7.13	37.27
SU-23-27	22.87	77.13	0.44	8.60	90.96
SU-23-28	16.84	83.16	12.23	10.40	77.36
SU-23-29	21.64	78.36	81.32	1.72	16.96
SU-23-30	27.12	72.88	63.29	4.29	32.43
Minimum value					
Maximum value					

The content of total organic matter (TOM%) suggests a spatial variability correlated with the location of the sampling stations and the specific local conditions of the transition area between the fluvial and lacustrine environment. For example, the sediment samples situated along the former meanders (SU-23-06, SU-23-07, SU-23-08, SU-23-19, SU-23-20, and SU-23-26), canals (SU-23-11, SU- 23-12, SU-23-16, SU-23-18, SU-23-29, and SU-23-30), and lakes (SU-23-13, SU-23-14, and SU-23-15), are characterized by a very high amount of organic matter, with values over 30% of the total weight of dry sediment (Table 2, Figure 6).

The distribution of organic matter in the investigated samples has values within a wide range of variation, respectively 0.44-86.68% and an average value of 37.97% TOM. The highest value (86.68% TOM) was recorded in station SU-23-15 (Răducu Lake), and the lowest value (0.44% TOM) was observed in station SU-23-25 (Sulina Canal, at Mm 16 +000).

Based on the results obtained (Figure 6), it can be appreciated that the superficial sediments (sediment-water interface) can be included in the domain of mineral-rich sediments ($>15\text{-}30\%$ SIL), subsequently followed by organic rich-sediments and a variable carbonate content, as non-carbonated sediments ($\text{CaCO}_3 \leq 10\%$) or low calcareous sediments ($10\% < \text{CaCO}_3 \leq 30\%$). The results of these investigations allowed the recognition of some types of mixed sediments: mineral-rich sediments ($>15\text{-}30\%$ SIL) and organic-rich sediments ($>15\text{-}30\%$ TOM), resulting from the local sedimentation conditions, specific to the transition from fluvial to lacustrine environment (sediments with a high content of lithoclastic material – sand, silt, clay and with a subordinate content of organic material). Along with the organic and inorganic content, a bioclastic content is also present, consisting of shells, shell fragments and shelly detritus.

The higher siliciclastic contribution ($>15\text{-}30\%$) can be attributed to the allochthonous source (high input of fluvial sedimentary material). Instead, the lower organic matter input ($<15\text{-}30\%$) can be attributed to the fluvial, dynamic, active, energetic, dominant natural conditions of the Danube water, which characterize these areas, and do not facilitate a significant accumulation of organic material. In addition, well-aerated/oxygenated waters (high levels of dissolved oxygen content) influence the rate of decomposition of organic matter. Organic matter decomposes much faster when the waters are well aerated, and much more slowly in stagnant waters. On the other hand, it can be appreciated that the superficial sediments taken from certain locations located on tributaries, side channels, and lakes, can be included in the field of organic-rich sediments ($>15\text{-}30\%$ TOM), subsequently followed by mineral-rich sediments and a variable carbonate content, as non-carbonated sediments ($\text{CaCO}_3 \leq 10\%$) or low calcareous sediments ($10\% < \text{CaCO}_3 \leq 30\%$).



Figure 7. The assessment of the sediment (dis)connectivity in the study area (the main stream in green, in yellow the former meanders and the lateral canals, occasionally disconnected for the main stream at very low discharge and, in red the areas disconnected when the lateral connectivity is lost)

At the Sulina Canal, hydrotechnical works to improve navigation led to disruptions in the exchange of fresh water and sediments between the river arm and the entire delta. The effects were widespread erosion of the main channel and aggradation of the former meanders and side channels. Now, a large number of natural and man-made channels are currently heavily clogged and the sediments accumulated in the bed create sediment blockages and disruptions in the sedimentary transit, especially with the closest lakes as Fortuna, Bogdaproste, Lideanca, Trei Iezer, Răduci Lakes) (Figure 7). Those effects are observed and amplified by climate changes and the anthropic works located upstream, in the basin area.

The lateral connectivity exhibits significant variations both spatially and temporally, in relationship mainly with the water level. Therefore, at low water levels, many areas are isolated from the main distributary producing interruptions of the sedimentary fluxes transfer. Over time, this process tends to separate the former meander channel from the main branch and isolate the interdistributary areas, as is the case of the middle part of the "Big M" meander (Figure 7) where at low waters the connectivity can be completely interrupted. As in a chain process/effect, the partial or complete disconnection of the lateral natural channels from the former meander (red line in Figure 7)

can lead to the physical separation of the interdistributary depressions (deltaic lakes).

CONCLUSIONS

The results show the complex distribution of the bottom sediments in the study area. The superficial sediments (sediment-water interface) can be included in the category of mineral-rich sediments ($>15\text{-}30\%$ SIL), subsequently followed by organic rich-sediments and variable carbonate content, as non-carbonated sediments ($\text{CaCO}_3 \leq 10\%$) or low calcareous sediments ($10\% < \text{CaCO}_3 \leq 30\%$). That might be the result of the complexity of the deltaic environment characterized by the transition from fluvial to the lacustrine environment (sediments with a high content of lithoclastic material – sand, silt, clay, and with a subordinate content of organic material). An important factor must be related to past human intervention, especially the shortening of the natural course of the river, which led to an increase in the angle of inclination of the anhydrous surface and thus the inability of the mainstream to distribute the water and sediment flows to the delta area. To understand the sedimentological (dis)connectivity in this complex environment, complementary analyses during different hydrological regimes are required.

ACKNOWLEDGEMENTS

This research was financially supported by the Romanian Ministry of Research, Innovation, and Digitization in the framework of the National CORE Programme projects: PN23300304 and PN23300302 (Contract no. 4N/30.12.2022).

The authors thank Stănescu Ion from GeoEcoMar for collecting the sediment samples.

REFERENCES

- Baldan, D., Cunillera-Montcusi, D., Funk, A., & Hein, T. (2022). Introducing 'riverconn': an R package to assess river connectivity indices. *Environmental Modelling and Software*, 156, 105470.
- Bunn, S.E. & Arthington, A. H. (2002). Basic principles and ecological consequences of altered flow regimes for aquatic biodiversity. *Environmental Management* 30, 492–507.
- Constantinescu, A.M., Tyler, A.N., Stanică, A., Spyarakos, E., Hunter, P.D., Catianis, I., Panin, N. (2023). A century of human interventions on sediment flux variations in the Danube-Black Sea transition zone. *Front. Mar. Sci.* 10:1068065. doi: 10.3389/fmars.2023.1068065
- Crema, S., & Cavalli, M. (2018). SedInConnect: a stand-alone, free and open source tool for the assessment of sediment connectivity. *Computers & geosciences* 111, 39-45.
- Dean, W.E. Jr. (1974). Determination of carbonate and organic matter in calcareous sediments and sedimentary rocks by loss on ignition: Comparison with other methods. *J. Sediment. Petrol.*, 44(1), 242–248.
- Digerfeldt, G., Olsson, S., Sandgren, P. (2000). Reconstruction of lake-level changes in lake Xinias, central Greece, during the last 40000 years. *Palaeogeography, Palaeoclimatology Palaeoecology*, 158(1-2), 65-82.
- Duțu, F., Panin, N., Ion, G & Tiron Duțu, L. (2018). Multibeam bathymetric investigations of the morphology and associated bedforms, Sulina channel, Danube Delta. *Geosciences*, 8(7) 8010007.
- Duțu, F., Duțu, L., Catianis, I., & Ispas, B-A. (2022). Sediment dynamics and hydrodynamical processes in the Danube Delta (Romania): A response to hydrotechnical works. *Zeitschrift für Geomorphologie*, 64(4), 365-378.
- Duțu, F., Tiron Duțu, L., Catianis, I. (2023). Dramatic reduction of the water and sediment fluxes in a human modified meandering ecosystem from the Danube Delta, Romania. *Scientific Papers. Series E. Land Reclamation, Earth Observation & Surveying, Environmental Engineering. Vol. XII*, 267-274.
- Folk, R.L. & Ward, W.C. (1957). Brazos River bar, a study in the significance of grain-size parameters. *Journal of Sedimentary Petrology*, 27, 3-26.
- Habersack, H., Hein, T., Stanică, A., Liska, I., Mair, R., Jager, E., Hauer, C., & Bradley, C. (2016). Challenges of river basin management: Current status of, and prospects for, the River Danube from a river engineering perspective. *Science of the Total Environment*, 543, 828-845.
- Mishra, K., Sinha, R., Jain, V., Nepal, S., & Uddin, K. (2019). Towards the assessment of sediment connectivity in a large Himalayan river basin. *Science of the Total Environment*, 661, 251-265.
- Nistor, C., Savulescu, I., Mihai, B-A., Zaharia, L., Virghileanu, M., & Cacablaia, S. (2021). The impact of the large dams on fluvial sedimentation; the Iron gates reservoir on the Danube River. *Acta geographica Slovenia*, 61(1), 41–55.
- Pacioglu, O., Duțu, L., Duțu, F., & Pavel, A.B. (2022). Habitat preferences and trophic interactions of the benthic invertebrate communities inhabiting depositional and erosional banks of a meander from Danube Delta (Romania). *Global Ecology and Conservation*, 38, e02213.
- Panin, N. (1999). Global changes, sea level rising and the Danube Delta. *GeoEcoMarina*, 4, 19-29.
- Panin, N., Tiron Duțu, L. & Duțu, F. (2016). The Danube delta an overview of its Holocene evolution. *Mediterranée*, 126, 37-54.
- Poepl, R.E., Keesstra, S.D., & Maroulis, J. (2017). A conceptual connectivity framework for understanding geomorphic change in human-impacted fluvial systems. *Geomorphology*, 277, 237–250.
- Poepl, R.E., Fryirs, K.A., Tunnicliffe, J., & Brierley, G.J. (2020). Managing sediment (dis)connectivity in fluvial systems. *Science of the Total Environment*, 736, 139627.
- Shepard, F.P. (1954). Nomenclature based on sand-silt-clay ratios. *J. Sediment. Petrol.*, 24, 151–158.
- Schwenk, J., & Foufoula-Georgiou, E. (2016). Meander cutoffs nonlocally accelerate upstream and downstream migration and channel widening. *Geophys. Res. Lett.*, 43, doi:10.1002/2016GL071670.
- Smith K.A. & Mullins C.E. (2000). Soil and Environmental Analysis: Physical Methods. Revised and Expanded. New York, NY, USA: Marcel Dekker, Inc. Soil Survey Division Staff (1993). Soil Survey Manual. Washington, DC, USA: United States Department of Agriculture, pp. 651.
- Syvitski, J.P.M. (2011). Global sediment fluxes to the earth's coastal ocean. *Appl. Geochemistry*, 26, S373–S374.
- Udden, J.A. (1914). Mechanical composition of clastic sediments. *Geol. Soc. Am. Bull.* 25(1), 655–744
- Visher, G.S. (1969). Grain-Size Distribution and Depositional Processes. *Journal of Sedimentary Petrology*, 39, 1074-1106.
- Walling, D.E., & Fang, D. (2003). The changing sediment loads of the world's rivers. *Global Planetary Change* 39, 111–126.
- Wentworth, C.K. (1922). A scale of grade and class terms for clastic sediments, *J. Geol.* 30(5), 377–392.
- Zaharia, L., Grecu, F., Toroiac, I.G., & Neculau, G., (2011). Sediment Transport and River Channel Dynamics in Romania – Variability and Control Factors. In: Manning, A. J., editor. *Sediment Transport in Aquatic Environments*. London: IntechOpen. doi: 10.5772/2141.
- <https://edelta.ro/cote-dunare-365-de-zile>

IMPACT OF PHYSICOCHEMICAL PARAMETERS ON ZOOPLANKTON AND BIOCOENOLOGICAL ANALYZES ON ZOOPLANKTON OF MANDRA RESERVOIR, IN SOUTHEASTERN BULGARIA

Eleonora FIKOVSKA, Dimitar KOZUHAROV

Sofia University "St. Kliment Ohridski",
8 Dragan Tzankov Blvd, Sofia, Bulgaria

Corresponding author email: e_fikovska@abv.bg

Abstract

The aim of this paper is to present some unpublished data from studies of zooplankton complexes in Mandra Reservoir during the period 2020-2021 at 7 research sites. It analyses whether physicochemical parameters pH, dissolved oxygen and conductivity significantly influence the occurrence of zooplankton in a reservoir. At the time of the investigation, 33 taxa of rotifers, 18 taxa of Cladocera, and 12 taxa of Copepoda were noted, and 4 taxa from Protozoa too. Canonical Correspondence Analysis (CCA) and biocoenological analyses were performed. In conclusion, we can say that in this shallow holopolymictic basin, no strong correlation was found between the grouping of zooplankton and the measured values for pH, dissolved oxygen and electrical conductivity. The dominant analysis reflects the dynamics in the dominant complexes of zooplankton in accordance with the conditions in the ecotonic zones between the Mandra Reservoir and the inflowing rivers.

Key words: zooplankton, biocoenological analyzes, Mandra Reservoir.

INTRODUCTION

The results in this paper are a continuation and upgrade of the work and analysis about zooplankton of Mandra Reservoir published by Fikovska et al., 2022. During the period February 2020 - January 2021, 67 zooplankton components were found - 33 taxa of rotifers, 18 taxa of Cladocera, and 12 taxa of Copepoda were noted, and 4 Protozoan taxa too. A complete list of the species found in Reservoir Mandra and their values of pF – frequency of occurrence for the studied period is presented by Fikovska et al., 2022, Table 1.

Ecotone effects in river-reservoir systems, as well as the influence of environmental factors on the dynamics of zooplankton, have been studied for a number of water bodies in Bulgaria, such as Zhrebchevo Reservoir (Naidenow, 1981; Stanachkova et al., 2010; Kozuharov & Stanachkova, 2015), Iskar Reservoir (Stefanova et al., 2015; Kozuharov et al., 2016; Stanachkova et al., 2017; Stefanova et al., 2020), Pchelina Reservoir (Kozuharov et al., 2007; Kozuharov, 2019).

Zooplankton organisms occupy a fundamental position in aquatic food webs because of the fact that they have the role of primary consumers and are an energy link between primary producers such as phytoplankton and higher consumers such as fish (Lampert & Sommer, 1997; Haberman & Haldna, 2014; Zhikharev et al., 2024). They are an important element in the structure and functioning of aquatic ecosystems. In addition, zooplankton can rapidly respond to changes in trophic cascades, such as phytoplankton blooms, and to the physicochemical conditions of the habitat, changing species richness, increasing or decreasing their number (Naselli-Flores & Rossetti, 2010). These characteristics make them suitable indicators of water quality and changes in trophic conditions (Anas et al., 2013).

To expand the understanding of the relationship between environmental factors and the quantitative development of zooplankton in different trophic conditions, Zhikharev et al. (2024) used several environmental parameters measured at each zooplankton sampling station.

Authors choose the following parameters as the most relevant: specific electrical conductivity of water (EC), pH value (pH), water temperature (WT), content of chlorophyll-pigment in water (Chlorophyll a) and dissolved oxygen (DO) in water (Zhikharev et al., 2024).

This paper also aims to assess the influence of some physicochemical factors of the environment on the distribution of zooplankton in Mandra Reservoir. It is considered that zooplankton biomass is affected by temporal and spatial changes of water quality parameters (Ahmad et al., 2011; Fakioglu et al., 2018; Paturej et al., 2017).

Dissolved oxygen (DO) is an important aquatic parameter whose measurement is vital in the context of culture of any aquatic animal as oxygen plays a crucial role in its life processes (Rajagopa et al., 2010).

MATERIALS AND METHODS

The study was carried out in the coastal reservoir Mandra, which is located in southeastern Bulgaria, at 7 sampling points, which are indicated in Figure 1.

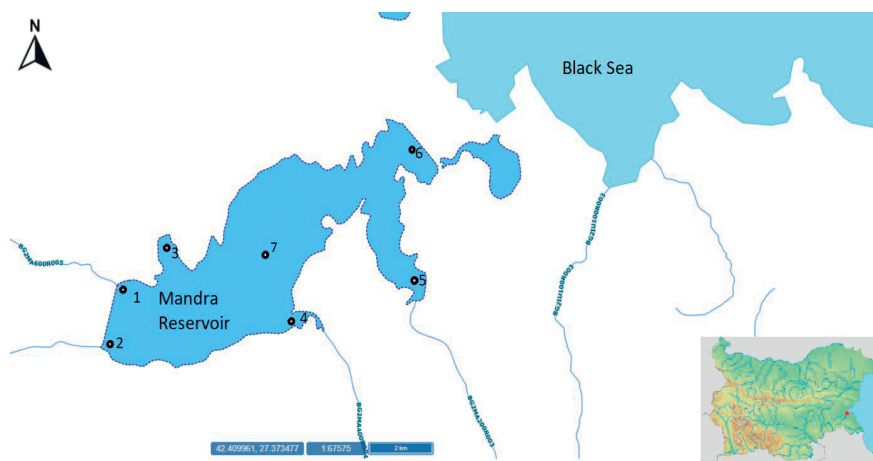


Figure 1. Location of the sampling points in Mandra Reservoir: 1 - mouth of Rusokastrenska River; 2 - mouth of Sredetska River; 3 - northern dike; 4 - mouth of Fakiyska River; 5 - mouth of Izvorska River; 6 – Dam; 7 - central part

The reservoir is a shallow holo-polymictic water body with maximum depth of 7 m, surface of 13000 hectares and maximal volume of 165 000 000 m³. Most of the sampling points were situated in the ecotone zones between the inflowing rivers and the reservoir. The reason was to find out the eventual influence of the contamination from the inflowing wastes on the reservoir plankton. The methods of collecting the samples, the used equipment, as well as the subsequent processing of the information, are standard to the international hydrobiological practice and were described in detail by Fikovska et al. (2022).

The data on the parameters of the environment is presented in Table 1.

Biocoenological analyzes were then conducted on the basis of several widely used indexes such

as frequency of dominance (DF) and order of dominance (DT) after De Vries - (Pielou, 1975; Odum & Barrett, 2005; Kumar & Mina, 2018). The frequency of dominance, like the frequency of occurrence, is directly proportional to the importance of the given species for the biocoenosis.

The order of dominance is an indicator of the evenness of the distribution of the species in time and space. These indexes were used for analysis of the zooplankton community status, together with structural indexes such as Shannon - Weaver individual diversity, index of domination after Simpson, and evenness index after Pielou (1975) (Fikovska et al., 2022).

Table 1. Values of hydrological parameters measured in Mandra Reservoir during the studied period, pH, dissolved oxygen (DO, mg/l), oxygen saturation (DOS, %) and electrical conductivity (COND, μ S)

Date-sampling point	pH	DOS (%)	DO (mg/l)	COND (μ S)
Feb 20-S4	8.5	58	6.9	662
Feb 20-S5	8.85	56	6.5	630
Feb 20-S6	9.26	50	6	600
Feb 20-S7	8.73	57	7.12	638
June 20-S1	7.99	102	8.23	1039
June 20-S2	7.48	88	7.2	691
June 20-S3	7.5	86	7.5	560
June 20-S4	7.51	61	5.35	936
June 20-S5	7.94	65	5.65	523
June 20-S6	9.16	115	9.29	508
Sep 20-S1	8.85	99	9	585
Sep 20-S2	8.6	61	5.7	483
Sep 20-S3	8.85	75	6.8	229
Sep 20-S4	9	75	6.8	214
Sep 20-S5	8.9	57	5.2	194
Sep 20-S6	8.89	41	3.7	583
Sep 20-S7	8.8	53	4.8	193
Jan 21-S1	8.69	53	6	494
Jan 21-S2	8.59	50	5.7	671
Jan 21-S3	8.7	61	6.8	535
Jan 21-S4	8.66	61	6.9	625
Jan 21-S5	8.67	59	6.5	639
Jan 21-S6	8.33	52	6	428
Jan 21-S7	8.36	63	7.12	470

RESULTS AND DISCUSSIONS

The analysis of zooplankton in assessing its response to different trophic conditions should start with basic indicators, namely species richness and dominant species (Zhikharev et al., 2024).

For the entire study period, Nauplii and Copepodites of Copepoda with the highest frequency of occurrence are with $pF = 97.22$, while the values for adult copepods do not exceed 50%. In general, the larval stages of Copepoda – Nauplii and Copepodites numerically outnumber the adult Copepodites (Fikovska et al., 2022). A possible reason is the better survival of juvenile forms under unfavorable conditions, which is observed in some other species (Fakioglu et al., 2018).

Permanent representatives of the zooplankton complexes can also be considered *Keratella cochlearis* with $pF = 100\%$, *Bosmina coregoni* with $pF = 83\%$. Both *Pompholyx complanata* and *Chydorus sphaericus* have the same $pF = 79\%$. With the present publication, we have set out to complement the dominant community analysis and to compare it with previous ones. When calculating dominance frequency (DF) and dominance order (DT) of the zooplankton elements we prefer to use their abundance, rather than their biomass. The reason is that the numerical value is more representative and is used more often in this type of research (Kozuharov et al., 2009).

The dynamic conditions of the environment, as well as the ecotone effects and the processes taking place in the ecotone zones are the reason for the frequent dynamic changes of species composition and in the zooplankton dominant complexes. In Mandra reservoir, for the entire period of study, the frequency of dominance varied between 21 and 42% (Table 2). Examined by sampling sessions/seasons, DF reaches 100% in the coldest months - January and February, when only 1 species is present in the dominant complexes. During the study period the reservoir doesn't freeze in winter – the lowest registered temperature was 4.5°C. In the other seasons, the dominant complex includes two or three components, on which the dynamics of the zooplankton complexes in the Mandra reservoir and the replacement of some dominants with others can be traced. A typical example is the dominant complex in September 2020 (Table 2). The perennial dominant zooplankton element was Nauplii of Copepoda. The established dominant zooplankton organisms are typical for the eutrophic and hypertrophic water bodies. This result confirms these from the use of the RCC index which presents correlation between three main taxonomic groups in the zooplankton – Rotifera, Cladocera and Copepoda (Kozuharov et al., 2013). Both types of analysis show the advanced process of eutrophication, which is illustrated by high abundance of Rotifera species – *Polyarthra vulgaris*, *Keratella cochlearis* and partly *Pompholyx complanata*. The high numbered presence of Cladocera Chydoridae species *Ch. sphaericus* is also a demonstration of this eutrophication process.

Table 2. Frequency of dominance (DF) and order of dominance (DT) of zooplankton in Mandra reservoir by seasons and for the whole study period (2020-2021), values are in %

Date	Taxa	DF	DT
Feb. 2020	Nauplii	100	100
Jun. 2020	Nauplii	50	50
	<i>Polyarthra vulgaris</i>	33	50
	<i>Chydorus sphaericus</i>	17	25
Sep. 2020	Nauplii	43	43
	<i>Polyarthra vulgaris</i>	43	43
	<i>Keratella cochlearis</i>	14	14
Jan. 2021	<i>Keratella cochlearis</i>	100	100
For the whole period	Nauplii	42	42
	<i>Keratella cochlearis</i>	33	33
	<i>Polyarthra vulgaris</i>	21	25

Dominance order indicates whether a dominant is local or not, whether it dominates throughout the study period or only for a particular season. The order of dominance has high values for species that occur rarely, but when they do occur, they dominate the other species. The DT value was between 25 and 42% for the entire period, with the three components of the dominant complex showing close values. This

illustrates unstable dominant complexes. Stable communities cannot practically exist in the ecotone zone between the reservoir and the inflowing rivers because of the frequently changing conditions there.

Nauplii and Copepodites of Copepoda are zooplankton components but they are not taxa. They are also included in the dominant complex, but to the extent that they cannot be determined, they are reported separately as quantitative components of the plankton important for self-purification processes in the basin and as an important trophic resource for fish.

A CCA analysis was performed to show the correlation between zooplankton distribution and measured values for pH, dissolved oxygen (DO), oxygen saturation (DOS) and electrical conductivity. Species that were numerically dominant for the period between February 2020 and January 2021 are included in the analysis.

The CCA (Figure 2) shows that the first axis, which represents a total variance of 82.1 %, has a positive correlation with pH, and a negative correlation with dissolved oxygen, oxygen saturation and electrical conductivity. Axis 2 showed 17.4% variance and was positively related to DO, DOS and conductivity and negatively related to pH.

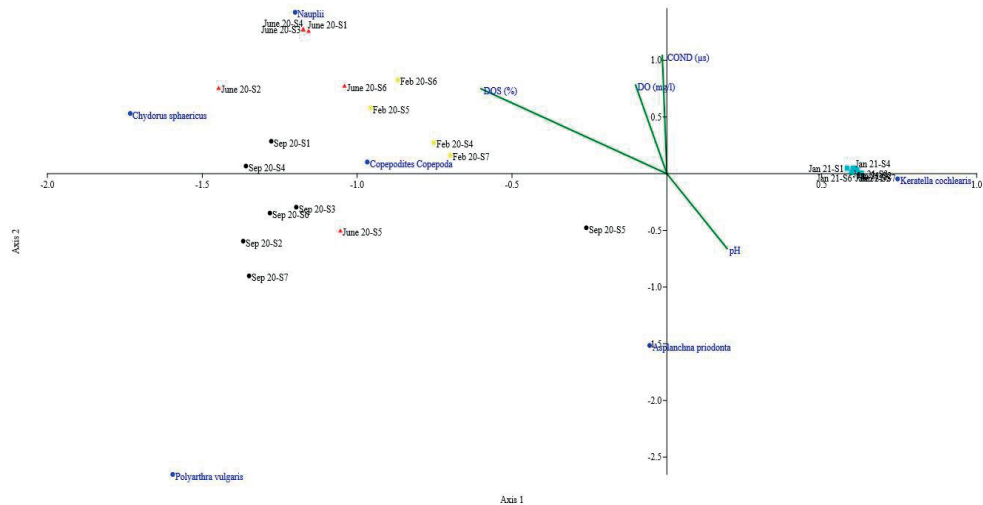


Figure 2. Canonical correspondence analysis (CCA) triplot for the ecological correlations between dominant zooplankton taxa in Mandra Reservoir and pH, dissolved oxygen (DO, mg/l), oxygen saturation (DOS, %) and electrical conductivity (COND, μ S) of water measured in the period February 2020 - January 2021 (S1, S2, S3, S4, S5, S6, S7 - sampling points)

These results indicate an equal distribution of dissolved oxygen in the water body because of its mixing regime, and that this factor is not a determinant of the distribution of zooplankton communities in Mandra Reservoir. This is due to the small depth of the reservoir and its comparatively high surface area, frequent mixing, as a result of which good aeration of the water is ensured and dissolved oxygen is not a limiting factor.

CONCLUSIONS

In the study presented here, no distinct trends of zooplankton grouping depending on a given environmental parameter were observed. This can be explained by the specific conditions in the eutrophic Mandra Reservoir and the presence of eurybiont species that have a high tolerance to changes in the environment. A typical example species is *K. cochlearis*. Our study also proves that shallow water bodies exhibit deviations from some regularities described by the authors. This is due to the specific conditions, especially in the coastal lakes, subjected to multiple mixings caused by the blowing of permanent comparatively strong winds, higher average temperatures even in winter, thanks to the milder climate and other factors. If you compare obtained results with these from Iskar Reservoir - the biggest reservoir in Bulgaria (Stefanova et al., 2020), the dominant complexes and whole species composition of Mandra reservoir are poorer. This tendency is typical for the Bulgarian eutrophic reservoirs and coastal lakes which are eutrophic too (Kozuharov, 2019).

REFERENCES

- Ahmad, U., Parveen, S., Khan, A.A., Kabir, H.A., Mola, H.R.A., Ganai, A.H. (2011). Zooplankton population in relation to physico-chemical factors of a sewage fed pond of Aligarh (UP), India. *Biology and Medicine*, 3, 336-341.
- Anas, M.U., Scott, K.A., Wissel, B. (2013). Suitability of presence vs. absence indicator species to characterize stress gradients: Lessons from zooplankton species of boreal lakes. *Ecological Indicators*, 30, 90-99.
- Fakioglu, O., Kokturk, M., Uzundumlu, A., Arslan, H., Atamanalp, M. (2018). Planktonic-based assessment of the landside-dammed lake (Erzurum-Turkey). *Iranian Journal of Fisheries Sciences*, 17, 503-515. DOI: 10.22092/IJFS.2018.115504
- Fikovska, E., Kozuharov, D., Stanachkova, M. (2022). Influence of some environmental factors on the distribution of zooplankton complexes in Mandra Reservoir, in Southeastern Bulgaria. In: Chankova S, Peneva V, Metcheva R, Belcheva M, Vassilev K, Radeva G, Danova K (Eds) *Current trends of ecology. BioRisk*, 17, 343-355. <https://doi.org/10.3897/biorisk.17.77368>
- Haberman, J. & Haldna, M. (2014). Indices of zooplankton community as valuable tools in assessing the trophic state and water quality of eutrophic lakes: long term study of Lake Vörtsjärv. *Journal of Limnology*, 73, 263-273.
- Kozuharov, D., Evtimova, V., Zacharieva, D. (2007). Long-Term Changes of Zooplankton and Dynamics of Eutrophication in the Polluted System of the Struma River-Pchelina Reservoir (South-West Bulgaria). *Acta zoologica bulgarica*, 59(2), 191-202.
- Kozuharov, D., Trichkova, T., Borisova, P., Stanachkova, M. (2009). The zooplankton Composition in two reservoirs in the North-west Bulgaria in relation to Dreissena spp., occurrence. *Biotechn. & Biotechn. Equipment*, 23, 271-275, Special edition, On-line.
- Kozuharov, D. & Stanachkova, M. (2015). Long-term Changes in Zooplankton Community in Zhrebchevo Reservoir, Central Bulgaria. *Acta Zoologica Bulgarica*, 67, 541-552.
- Kozuharov, D., Raikova, G., Stefanova, M., Fikovska, E. (2016). Dynamics of the zooplankton composition of the system Iskar River – Iskar Reservoir in relation to some environmental factors, *C. R. Acad. Bulg. Sci.*, 69(8), 1029-1038.
- Kozuharov, D. (2019). *Lymnology*. Sofia, BG: Pensoft Publishers (In Bulgarian).
- Kumar, P., & Mina, U. (2018). *Fundamentals of Ecology and Environment*. New Delhi, India: Pathfinder Publication.
- Lampert, W. & Sommer, U. (1997). *Limnecology: The Ecology of Lakes and Streams*. Oxford, UK: Oxford University Press.
- Naidenow, W. (1981). Changes of zooplankton structure in the Zhrebchevo Reservoir as a result of pollution and hydrotechnical devices. *Hydrobiology*, 15, 22-43. (In Bulgarian, German summary).
- Naselli-Flores, L. & Rossetti, G. (2010). Fifty years after the homage to santa rosalia: Old and new paradigms on biodiversity in aquatic ecosystems. In S. Rosalia *50 Years on Developments in Hydrobiology*. Cham, Switzerland: Springer.
- Odum, E., & Barrett, G. W. (2005). *Fundamentals of Ecology*. Belmont, CA: Thomson Brooks/Cole.
- Paturej, E., Gutkowska, A., Koszałka, J., Bowszys, M. (2017). Effect of physicochemical parameters on zooplankton in the brackish, coastal Vistula Lagoon. *Oceanologia*, 59(1), 49-56. <https://doi.org/10.1016/j.oceano.2016.08.001>.
- Pielou, E. C. (1975). *Ecological Diversity*. N.Y., USA :J. A Wiley – Interscience Publication.
- Rajagopal, T., Thangamani, A., Sevakodiyone, S. P., Sekar, M., Archunan, G. (2010). Zooplankton diversity and physico-chemical conditions in three perennial ponds of Virudhunagar district, Tamilnadu.

- Journal of environmental biology / Academy of Environmental Biology, India, 31, 265-72.*
- Stanachkova, M., Kozuharov, D., Trichkova, T., Botev, I., Tyufekchieva, V. (2010). Changes in Zooplankton Community of Jrebchevo Reservoir Before and After Infestation by *Dreissena polymorpha* (Pallas, 1771). In: *Youth Scientific Conference "Kliment's Days"*, 22-23 November, Sofia.
- Stanachkova, M., Stefanova, M., Kozuharov, D., Raikova, G., Fikovska, E. (2017). Community structure of zooplankton as key factor for self-purification capacity of Iskar reservoir. *Ecological Engineering and Environment Protection*, 9(1), 39-46.
- Stefanova, M., Kozuharov, D., Rajkova, G. (2015). Changes in the zooplankton community of the ecotone zone between Iskar River and Iskar Reservoir and the pelagial of the reservoir. *Annuaire de l'Université de Sofia "St. Kliment Ohridski" Faculte De Biologie 2015, 100(4)*, 304–313.
- Stefanova, M., Kozuharov, D., Stanachkova, M., Andreev, S., Rajkova-Petrova, G. (2020). Zooplankton community response to the ageing of Iskar reservoir (Bulgaria). *Comptes rendus de l'Académie bulgare des sciences: sciences mathématiques et naturelles*, 73, 829-838. DOI: 10.7546/CRABS.2020.06.11.
- Zhikharev, V., Gavrilko, D., Zolotareva, T., Kudrin, I., Shurganova, G. (2024). Chapter 5. Methods for assessing the response of zooplankton communities to different trophic conditions. In book: *The textbook "Environmental Monitoring. Part XI"* Publisher: Nizhny Novgorod State University. (In Russian).

MODERN PROTECTION SOLUTIONS AGAINST COASTAL EROSION

Iulian IANCU, Alexandru DIMACHE, Oana-Stefania BUCUR, Daniel CORNEA

Technical University of Civil Engineering of Bucharest,
122-124 Lacul Tei Blvd, Bucharest, Romania

Corresponding author email: alexandru.dimache@utcb.ro

Abstract

Romania is one of the countries that experience the coastal erosion phenomenon, a natural process found along shorelines worldwide, caused by the action of waves and currents that entrain sediments. In the context of climate change, a significant intensification of coastal erosion has been observed in our country, especially due to increased wave heights resulting from severe storms. Reducing wave energy using traditional coastal protection structures is not always effective, besides being factually inefficient, it is also extremely costly, both in terms of investment and maintenance. In recent years, modern technologies for wave energy dissipation have been developed, such as the use of floaters, submerged air cushions, and even the use of sound waves to attenuate the force of waves. The paper presents a solution to reduce wave energy using submerged mats, with direct benefits on reducing the erosive power of waves and ensuring coastal protection. The goal is to optimize the solution of submerged mats, ensuring maximum efficiency at minimum cost by adjusting the structural characteristics of the mat (length, thickness, elasticity, permeability) to the characteristics of the waves.

Key words: coastal erosion, submerged mats, wave energy.

INTRODUCTION

Coastal erosion is a natural process that occurs in coastal areas, mainly caused by the action of waves and currents, which leads to the entrainment of sediments into the sea or ocean. In the context of the increasingly pronounced effects of climate change, as well as human activities, the phenomenon of beach erosion has intensified in recent decades, especially due to the increase in wave height and the severity of weather events. The effect of coastal protection structures and the turbulence that occurs as waves break in the surf zone add an additional layer of complexity to the phenomenon of coastal erosion. As a result of this phenomenon, beaches loose sediment through longshore transport, due to longitudinal marine currents, but also through offshore transport due to wave action (Coveianu, 2016).

The Romanian coastal area is facing this problem, especially in the southern part where there is a developed tourist area and where it has been found that up to tens of centimeters of beach disappear annually. The economic effects of this phenomenon are extremely serious, ranging from the reduction of the tourist potential of the beaches to the undermining of

the stability of important buildings that are at risk of collapsing. (Tatu et al., 2015). The phenomenon of beach erosion was previously counteracted by the alluvial input from the Danube, which has now been drastically reduced with the construction of the Iron Gates I and II hydroelectric power plants. In this situation, it is necessary to protect the beaches by limiting the erosive power of the waves, correlated with the beach widening projects that are currently being implemented on the Romanian coast.

The mechanism of beach erosion by waves is well known: waves that reach the shore continuously "bite" from the beach sand, and it has been scientifically established that in the withdrawal phase (descending phase) of the wave, a greater amount of sand is drawn into the sea compared to the amount of sand pushed by the wave towards the beach in the ascending phase (Tatu et al., 2015).

The mechanism of wave propagation that reaches the shore is a complicated one, the wave motion without mass transport transforming into one with mass transport, with breaking and with the last phase, the run-up, that is with ascension on the slope of the shore (Holthuijsen, 2007). However, the erosive action of waves depends

on their energy in the vicinity of the shore, energy that must be reduced as much as possible. The main methods of protecting coastal areas against the erosion process can be grouped into two main categories: coastal protection structures and beach nourishment works. There are several types of coastal protection structures: dikes (breakwaters), groynes, seawalls, spurs and sills. The reduction of wave energy using classic coastal protection structures has proven to be ineffective over time. This is mainly because the current structure of the dikes does not substantially reduce the water velocity or the velocity of the currents, respectively the oscillatory motion due to wave action (Tatu et al., 2016). Beach nourishment, on the other hand, in the absence of other protective measures, would only slow down the erosion phenomenon.

In recent years, modern technologies have been developed, such as the use of air wave attenuators, submerged mattresses, wave energy conversion into mechanical energy, vegetation and even the use of sound waves to attenuate the force of waves (Dalrymple et al., 1990; Yu et al, 2021).

Air-Filled Wave Attenuators (AFWA) are in fact floating air-filled breakwaters used to absorb wave energy. These types of breakwaters are popular because they have a lower environmental impact than traditional breakwaters, which can disrupt marine ecosystems (Pereira et al., 2022). Air-Filled Wave Attenuators are made of flexible waterproof materials, the main body consisting of a floating module in the form of a rectangular prism filled with air. This is ballasted with sandbags placed all around. The volume of air acts as a hydraulic shock absorber, absorbing the energy of the waves. Wave attenuators are very efficient, capable of attenuating up to 95% of the incoming wave height and do not affect marine ecosystems like traditional breakwaters.

Submerged mattresses are structures that use a flexible porous membrane filled with water to dissipate wave energy (Koley et al., 2022; Collins et al., 2021). The principle of wave energy dissipation by submerged mattresses is based on two mechanisms: the deformation of the mattress as the waves passes over the mattress membrane, and the formation of turbulence and vortices as the water passes

through the porous membrane. Submerged mattresses represent a promising and innovative approach to coastal protection, offering a balance between cost and wave attenuation performance.

Vegetation, such as seagrass, can attenuate and dissipate wave energy, acting as a natural barrier (Ikha et al., 2022). Vegetation can have a stabilizing effect on sediment transport, keeping them in shallow water areas, leading to energy dissipation. Wave energy attenuation by vegetation is the process by which waves are reduced in height and energy as they pass over or through vegetation. The amount of wave energy attenuated by vegetation depends on a number of factors, including the type of vegetation, its density, the water depth and the wave characteristics (Bradley et al., 2009).

An emerging alternative to traditional wave energy attenuation methods is the use of sound waves. This technology is still under development, but it has the potential to be more efficient and less costly than traditional methods. There are several ways in which sound waves can be used to attenuate wave energy. One method is to use a system of speakers to generate underwater sound, which propagates and interacts with the waves, reducing their energy. Another method is to use a system of air bubbles to create an underwater sound field that dissipates wave energy.

In the context of modern coastal protection solutions against the phenomenon of erosion, and for wave energy dissipation, the article aims to study the effectiveness of submerged breakwaters for reducing energy, and implicitly wave amplitude, with a direct beneficial effect on the erosive power of waves. The paper proposes a mathematical model to determine the mechanical energy consumed from the energy of a wave with certain characteristics, which passes over a submerged mattress made of a homogeneous material, deforming it.

The use of submerged mattresses has clear advantages over the classic breakwaters used today. The most important of these are the much lower investment costs, practically zero maintenance costs (being submerged, they do not deteriorate the marine landscape and do not affect surface activities such as navigation, in general, and marine sports, in particular), and

they fix the sand on the seabed, preventing its entrainment by longitudinal currents.

MATERIALS AND METHODS

To develop a mathematical model for the energy dissipated from wave energy by a submerged mattress, the determining parameters of the waves were first determined. These parameters will be used to evaluate the efficiency of the mattress both on the mathematical model developed and on the physical model that will be developed later for the calibration and validation of the mathematical model.

The submerged mattress will be made of a homogeneous permeable material, filled with water, and waterproofed with an elastic membrane on all sides.

The determination of the wave characteristics was conducted in the wave channel (Figure 1), within the Hydraulics Laboratory of the Technical University of Civil Engineering Bucharest (UTCB). The wave channel has a length of 16 m and a width of 1 m, the maximum water depth being 0.9 m. The channel, which has a fixed slope, is equipped at one end with a wave generator and at the opposite end with an attenuator designed to dissipate wave energy and prevent the occurrence of the reflection phenomenon, which would alter the characteristics of the incident waves.

The wave generating system consists of a flat, movable flap that is hinged at the bottom of the channel and is set in motion at the top by a crank-slider system (Figure 2).



Figure 1. Wave Channel - Hydraulics Laboratory, UTCB

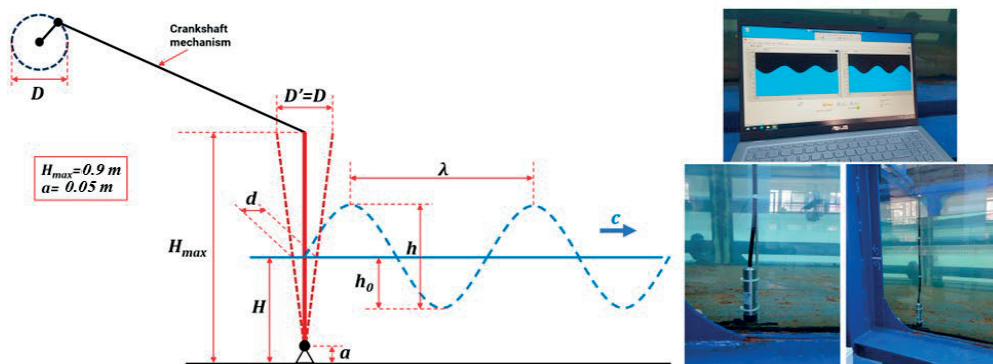


Figure 2. Schematic of the wave generation system and level transducers

The determination of the wave characteristics was conducted considering a water depth $H = 0.5$ m. The determining parameters of the measured waves were the wave height h , the period T and the wavelength λ . To determine the amplitude of the waves, two level sensors placed

at 4 m from each other were used. The wavelength, respectively the wave period, was measured between two successive crests of the waves. The results of the measurements are presented in Table 1.

Table 1. Measured waves characteristics

Wave height h (m)	Wavelength λ (m)	Period T (s)	Celerity c (m/s)
0.14	1.65	1.06	1.56
0.13	1.23	0.90	1.37
0.12	1.10	0.83	1.33
0.10	0.94	0.74	1.27
0.09	0.72	0.66	1.09

Based on the measurements, the propagation speed (celerity) of the waves was calculated. The physical model of the wave energy mitigation device - the submerged mattress - that will be tested later in the wave channel will have the following dimensions: length $L_s = 4$ m, width $b = 1$ m and height $h_s = 0.1$ m. The permeability characteristics and elasticity of the submerged mattress will be established at the time of making its physical model. Based on the measured characteristics of the waves and the proposed characteristics of the submerged

mattress, the following mathematical model was developed.

MATHEMATICAL MODEL

A submerged mattress with the following dimensions is considered: L_s – mattress length, b – mattress width and h_s – mattress height (thickness), made of a homogeneous material with permeability coefficient k . The mattress is waterproofed on all sides and filled with water.

A wave passes over the submerged mattress with the following characteristics: wave height h (the vertical distance between the crest and the base of the wave), the oscillation period T (the time between two successive maxima or minima), respectively the wavelength λ .

The wavelength λ is the distance travelled by the wave, when it travels (propagates) with speed c (the celerity or speed of propagation of the wave), during a period T . Therefore, $\lambda = c \cdot T$ and is equal to the distance between two adjacent crests.

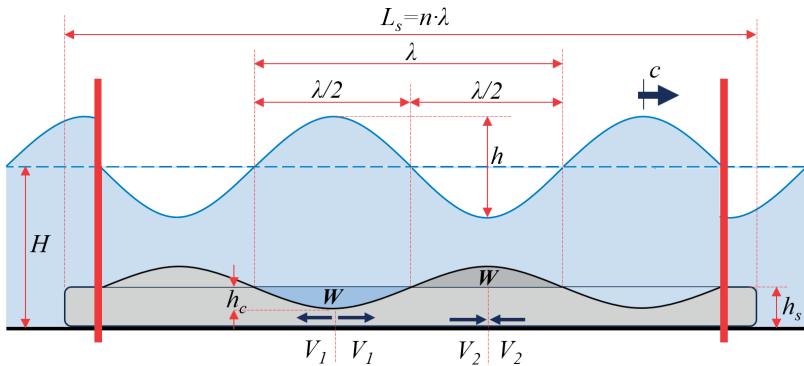


Figure 3. Mathematical model for wave energy attenuation using a submerged mattress of homogeneous material

Function of the height of the wave, respectively of the elasticity of the mattress, at the moment in Figure 3, it will compress over a distance $\lambda/2$, respectively it will decompress over the same length $\lambda/2$, on a section of the mattress having the length L_s/n , where n is the number of sections of the mattress of length equal to the wavelength λ . The maximum value of the height compression, respectively of the mattress decompression, is h_c . With cc was noted the compression coefficient of the mattress $cc = h_c/h_s$.

At other moments in time, the deformation of the mattress will have a different shape (Figure 4) but, overall, the compressed or decompressed volumes remain the same.

To evaluate the energy consumed from the wave energy to compress the mattress, a calculation scheme is used that is based on the evaluation of the average speed of water flow in the mattress, at the time of its compression and decompression under the action of the wave, using Darcy's calculation formula of the flow velocity in a permeable medium.

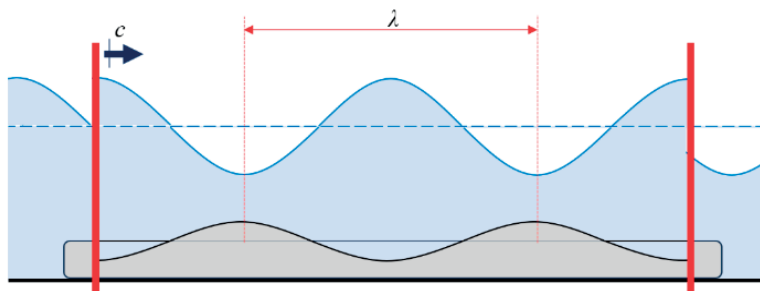


Figure 4. Deformation of the submerged mattress

To estimate the average flow speed in the mattress, the water flow speed in the mattress will be evaluated first to the maximum, V_{1max} in the area where the mattress compresses to the maximum, respectively V_{2max} in the area where the mattress decompresses.

The volume with which the mattress is compressed, respectively decompressed, along the length $\lambda/2$ is W :

$$W = \frac{2}{3} \cdot \frac{\lambda}{2} \cdot h_c \cdot b = \frac{\lambda \cdot h_c \cdot b}{3}$$

Then, the maximum water flow velocity in the mattress in the compressed area is:

$$V_{1max} = \frac{1}{2} \cdot \frac{W}{h_c \cdot b} \cdot \frac{1}{\Delta t} = \frac{1}{2} \cdot \frac{\lambda \cdot h_c \cdot b}{3 \cdot h_c \cdot b} \cdot \frac{1}{\Delta t} = \frac{\lambda}{6 \cdot \Delta t}$$

where Δt is the time interval in which the wave travels a distance Δs , and the mattress is compressed, respectively decompressed by the moving volume W . To obtain the average speed of water flow in the compressed area of the mattress, it will be averaged between 0 and V_{1max} .

$$V_1 = \frac{0 + V_{1max}}{2} = \frac{\lambda}{12 \cdot \Delta t}$$

In the area where the mattress decompresses the speed is:

$$V_{2max} = \frac{1}{2} \cdot \frac{W}{(h_s + h_c) \cdot b} \cdot \frac{1}{\Delta t}$$

$$V_{2max} = \frac{1}{2} \cdot \frac{\lambda \cdot h_c \cdot b}{3 \cdot \left(\frac{1}{c} \cdot h_c + h_c \right) \cdot b} \cdot \frac{1}{\Delta t}$$

$$V_{2max} = \frac{\lambda \cdot c_c}{6 \cdot (c_c + 1) \cdot \Delta t}$$

and the average speed of water flow in the area where the mattress decompresses is:

$$V_2 = \frac{0 + V_{2max}}{2} = \frac{\lambda \cdot c_c}{12 \cdot (c_c + 1) \cdot \Delta t}$$

The average water flow rate in the mattress is:

$$V_m = \frac{V_1 + V_2}{2} = \frac{1}{2} \cdot \left(\frac{\lambda}{12 \cdot \Delta t} + \frac{\lambda \cdot c_c}{12 \cdot (c_c + 1) \cdot \Delta t} \right)$$

$$V_m = \frac{1}{24} \cdot \frac{\lambda}{\Delta t} \cdot \left(1 + \frac{c_c}{c_c + 1} \right) = \frac{1}{24} \cdot \frac{\lambda}{\Delta t} \cdot \left(\frac{2 \cdot c_c + 1}{c_c + 1} \right)$$

The average water flow rate in the mattress is reduced in relation to those presented previously:

- the material from which the mattress is made is not perfectly elastic and does not deform as soon as it is subjected to the pressure force of the wave;
- the flow of water in the mattress (through the permeable medium) is "braked" by the inertia of the liquid mass. Darcy's law used is for a permanent, stabilized flow regime; in fact, in reality, the flow has a strong non-permanent flow regime;
- the mattress has a finite length, being closed at both ends, where the flow is blocked.

As a result, in the calculation of the average hydraulic gradient, from Darcy's law, to determine the head loss, the attenuation

coefficient of the water flow speed c_{at} was introduced.

$$I_m = \frac{c_{at} \cdot V_m}{k} = \frac{1}{24} \cdot \frac{\lambda}{\Delta t} \cdot \left(\frac{2 \cdot c_c + 1}{c_c + 1} \right)$$

$$I_m = \frac{c_{at}}{24 \cdot k} \cdot \frac{\lambda}{\Delta t} \cdot \left(\frac{2 \cdot c_c + 1}{c_c + 1} \right)$$

The head loss Δh_r over a length Δl will be:

$$\Delta h_r = I_m \cdot \Delta l$$

The head loss on a part of mattress length will be:

$$h_r = \frac{c_{at}}{24 \cdot k} \cdot \frac{\lambda}{\Delta t} \cdot \left(\frac{2 \cdot c_c + 1}{c_c + 1} \right) \cdot \lambda$$

The head loss on a mattress length equal to λ , for a wave of period T (during a period T the wave travels the length λ) is:

$$h_r = \frac{c_{at}}{24 \cdot k} \cdot \frac{\lambda^2}{T} \cdot \left(\frac{2 \cdot c_c + 1}{c_c + 1} \right)$$

To evaluate the energy loss from head loss, the motion in the mattress is equated to a unilinear flow with velocity:

$$V_{echiv} = \frac{W}{b \cdot h_s \cdot T} = \frac{\frac{\lambda \cdot h_c \cdot b}{3} \cdot c_c}{b \cdot h_c \cdot T} = \frac{1}{3} \cdot \frac{c_c \cdot \lambda}{T}$$

The mass carried by the water in the interval T is:

$$m = Q_m \cdot T = \rho \cdot b \cdot h_s \cdot V_{echiv} \cdot T$$

$$m = \rho \cdot b \cdot \frac{h_c}{c_c} \cdot \frac{1}{3} \cdot \frac{c_c \cdot \lambda}{T} \cdot T = \frac{1}{3} \cdot \rho \cdot b \cdot h_c \cdot \lambda$$

The energy consumed (dissipated) by the mattress from the wave energy is:

$$E_r = h_r \cdot m \cdot g$$

$$E_r = \frac{c_{at}}{72} \cdot \frac{\lambda^3}{k \cdot T} \cdot \left(\frac{2 \cdot c_c + 1}{c_c + 1} \right) \cdot \rho \cdot g \cdot b \cdot h_c$$

The wave mechanical energy corresponding to unit length of wave crest with wavelength λ is (Luca & Luca, 2002):

$$E = \frac{\rho \cdot g \cdot h^2 \cdot \lambda}{8}$$

The mechanical energy of the wave across the entire width of the mattress is:

$$E_v = E \cdot b = \frac{\rho \cdot g \cdot h^2 \cdot b \cdot \lambda}{8}$$

To determine the height h_f of the wave at the exit from the mattress, from the initial energy of the wave E_v we subtract the energy dissipated by the mattress E_r and then from the resulting final energy E_f we get the height of the wave h_f .

$$E_f = E_v - E_r$$

$$E_f = \frac{\rho \cdot g \cdot h_f^2 \cdot b \cdot \lambda}{8}$$

$$h_f = \sqrt{\frac{8 \cdot E_f}{\rho \cdot g \cdot b \cdot \lambda}}$$

RESULTS AND DISCUSSIONS

The mathematical model created for the calculation of the energy dissipated by the mattress from the wave energy, was applied to the characteristic values of the waves measured in the wave channel, considering a mattress having the length equal to the wavelength of the wave, the unit width ($b = 1$ m) and height $h_s = 0.1$ m. The coefficient of permeability of the material from which the mattress is made was considered $k = 1$ m/s. The attenuation coefficient of the water flow velocities in the mattress was considered to be $c_{at} = 0.30$. This coefficient depends on the elasticity of the material from which the mattress is made and the material that waterproofs the mattress. It was considered that the mattress is compressed by half of its height, the compression coefficient of the mattress being $c_c = 0.5$.

For a wave of known characteristics (h, λ, T), the variation in wave height, between the entry and exit of a mattress with the characteristics ($L_s = \lambda, h_s, b, k$), depends on two parameters: the ratio between the attenuation coefficient and the permeability coefficient, c_{at}/k , respectively on the compression coefficient c_c . The compression coefficient is specific to the mattress, depending on its elasticity and permeability coefficient. The only unknown coefficient is the attenuation

coefficient of the speeds c_{at} . To determine it, an inverse calculation can be made considering that the wave height is reduced by 10% by the mattress, to be able to determine the order of magnitude of the coefficient. Thus, doing the calculation for the wave characteristics in Table 1, it is obtained that the attenuation coefficient of the speeds varies between 0.21 and 0.27. Considering the attenuation coefficient as having the value $c_{at} = 0.3$, the obtained results (Table 2) indicate an attenuation of the wave energy on average by approximately 24%, and of the wave height by approximately 13%. The efficiency of the submerged mattress in reducing wave energy, respectively the parameters that condition the efficiency will have to be determined experimentally on a physical model. These parameters are the permeability coefficient of the mattress material

and the compression coefficient that will have to be measured, respectively the attenuation coefficient of the water flow speed in the submerged mattress that will have to be determined experimentally.

Considering the characteristics of the wave with the height $h = 0.12$ m and changing only the compression coefficient of the mattress between 0.05 and 0.6, in Figure 5 is presented the variation of the height of the wave at the exit from the mattress and of the energy dissipated by it, according to this coefficient.

The mathematical model made provides the anticipated results, but without a calibration and validation of it on a physical model it will not be able to be used for a constructive optimization of submerged mattresses made of homogeneous materials and filled with water.

Table 2. Application of the mathematical model to calculate the energy dissipated by the mattress and the wave height at the exit from the mattress

Wave characteristics	Height h_s (m)	0.14	0.13	0.12	0.10	0.09
	Wavelength λ (m)	1.65	1.23	1.10	0.94	0.72
	Period T (s)	1.06	0.90	0.83	0.74	0.66
Features of the submerged mattress	Length L_s (m)	1.65	1.23	1.10	0.94	0.72
	Width b (m)	1.00	1.00	1.00	1.00	1.00
	Height h_s (m)	0.10	0.10	0.10	0.10	0.10
	Permeability coefficient k (m/s)	1.00	1.00	1.00	1.00	1.00
	Attenuation coefficient of the water flow speed c_{at}	0.30	0.30	0.30	0.30	0.30
	Compression coefficient c_c (-)	0.50	0.50	0.50	0.50	0.50
	Compressed/uncompressed height h_c (m)	0.05	0.05	0.05	0.05	0.05
	Energy consumed (dissipated) by the mattress E_r (j)	11.55	5.63	4.37	3.06	1.54
	The energy of the wave upon entering the mattress E (j)	39.66	25.49	19.42	11.53	7.15
	The energy of the wave at the exit from the mattress E_f (j)	28.11	19.86	15.05	8.47	5.61
	The height of the wave at the exit from the mattress h_f (m)	0.118	0.115	0.106	0.086	0.080

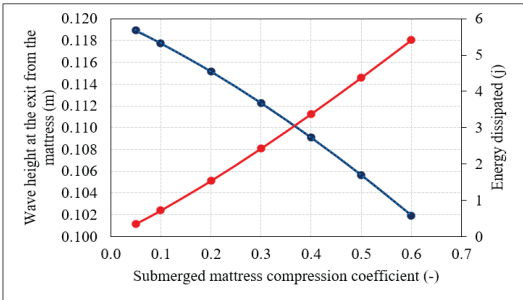


Figure 5. The variation of the wave height at the exit from the submerged mattress and the dissipated energy, as a function of the compression coefficient of the submerged mattress

On the physical model of the submerged mattress, it will be possible to study several constructive variants of the mattress (length,

thickness, elasticity, permeability) to obtain a maximum yield at a minimum cost. Various physical modelling scenarios will be developed,

modifying the determining parameters of the waves, to evaluate the efficiency of the mattress, depending on its constructive characteristics.

CONCLUSIONS

The reduction of wave energy using innovative solutions can lead to reliable results if these solutions are well based and studied on scale physical models and/or through numerical simulation.

The article proposes a mathematical model for the optimization of a submerged mattress, made of a homogeneous material, waterproofed and filled with water, for the mitigation of waves in the coastal area and protection against beach erosion. The mathematical model made must be calibrated and validated on a physical model in the wave channel.

From the application of the mathematical model, an important decreasing of the mechanical energy, respectively of the height of a wave of known characteristics is observed, which lead to the demonstration of the concept regarding the functionalities and characteristics of the submerged mattress solutions in laboratory conditions, respectively to the validation and demonstration of the functionality of the solution under relevant operating conditions.

The final goal of this research regarding the effectiveness of submerged mattresses, is to calibrate and validate the mathematical model on a scaled physical model, tested in a wave channel.

Various constructive and location variants of the submerged mattress will be studied, aiming, through optimization, a maximum efficiency with minimum cost, by correcting the constructive characteristics of the mattress (length, thickness, elasticity, permeability) to various wave characteristics (amplitude, period, wavelength).

To the extent that the results of measurements on the physical model will prove their effectiveness in mitigating waves and protecting against beach erosion, the impact of the project can be an important one in terms of coastal protection solutions, socio-economic and environmental implications.

ACKNOWLEDGEMENTS

This work is supported by a National Research Grants of the Technical University of Civil Engineering Bucharest, project number UTCB-09/2023.

REFERENCES

- Bradley, K. & Houser, C. (2009). Relative velocity of seagrass blades: Implications for wave attenuation in low-energy environments, *Journal of Geophysical Research*, 114.
- Collins, I., Hossain, M., Dettmer, W., Masters, I. (2021). Flexible membrane structures for wave energy harvesting: A review of the developments, materials, and computational modelling approaches, *Renewable and Sustainable Energy Reviews*, 151.
- Coveianu, A.L. (2016). *Marine Hydraulics Research*, Bucharest, RO: PhD Thesis.
- Dalrymple, R.A., Martin, M.W., (1990). Wave attenuation by air-filled flexible membranes, *Journal of Waterway, Port, Coastal, and Ocean Engineering*, 116(1), 36-52.
- Holthuijsen, H.L. (2007). *Waves in Oceanic and Coastal Waters*, Delft University of Technology and UNESCO – IHE, Cambridge University Press.
- Koley, S., Vijay, K.G., Nishad, C.S., Sundaravadivelu, R. (2022). Performance of a submerged flexible membrane and a breakwater in the presence of a seawall, *Applied Ocean Research*, 124.
- Ikha, M., Andadari, G.R., Reeve, D. (2022). An integrated study of wave attenuation by vegetation, *Wave Motion*, 110.
- Luca, O., Luca B.A. (2002). *Construction Hydraulics*, Timisoara, RO: Orizonturi Universitare.
- Pereira, E.J., Teh, H.M., Ma, Z. (2022). Hydrodynamic Performance of Air-Filled Wave Attenuator for Wave Control: Experimental Study, *J. Shanghai Jiao Tong Univ. (Sci.)*, 27(3), 316-325.
- Tatu, G., Dimache, A.N., Iancu, I., Coveianu, A.L., Ciugulea, O. (2015). A new vision on the marine dikes' structure, *Ecology, Economics, Education and Legislation*, II, 27-34.
- Tatu, G., Dimache, A.N., Iancu, I., Mateescu, R., Mârzali, I. (2016). Studies on continuous and oscillating currents through breakwaters, *Ecology, Economics, Education and Legislation Conference Proceedings*, I, 629-636.
- Yu, Y., Zhang, X., Yan, X., Wu, G. (2021). Numerical study on wave attenuation by a flexible air cushion breakwater, *Applied Ocean Research*, 108.

ANALYSIS OF SOME PARAMETERS OF THE HYDROGRAPHIC BASINS IN THE FOREST FUND

Calin Ioan IOVAN¹, Nicu Cornel SABĂU¹, Lucian Sorin DOROG¹,
Florin COVACI¹, Agneta Rodica IOVAN², Ghiță Cristian CRAINIC¹

¹University of Oradea, 1 University Street, Oradea, Romania

²Diosig Gymnasial School, 53 Orchards Street, Diosig, Bihor, Romania

Corresponding author email: gccrainic@yahoo.com

Abstract

The forestry sector, due to its binary nature (biologically specific but also technical), must participate in solving some problems regarding the conservation and improvement of hydrological resources, the inventory and sustainable exploitation of all resources, the research of the structures and compositions of stands in hydrographic basins, in order to improve the hydrological functions of forests and soil protection. The paper presents a series of characteristics and parameters of the Aleu Valley watercourse and at the same time of the hydrographic and forest basin in which it is located. For this purpose, a series of determinations of water flows, parameters of the hydrographic basin (type of longitudinal profile of the course, shape, surface, maximum length and width, perimeter, shape index, average slope of the basin, length of the hydrographic network), as well as the analysis of the degree of total afforestation and partial areas in the Aleu Valley basin. The results of these analyzes may be of interest in order to capitalize on the potential of small watercourses in the forestry sector in the fisheries or energy fields.

Key words: forest fund, hydrographic basin, parameters.

INTRODUCTION

Due to the relatively limited values of water resources, compared to the growing needs, the development of human society requires an intensive and well-coordinated management, capitalization of all these resources (Șmuleac et al., 2017; Sandu et al., 2021).

From this perspective, scientific research in forestry must propose changing its attention to the various problems related to:

- inventory of all forms of water resources existing in the forest fund (including energy ones);
- researching the structures and compositions of forests in the hydrographic basins, in order to improve the hydrological functions of forests and soil protection;
- investigation and evaluation of the potential of small water courses, present in the forest fund;
- capitalizing on hydro potential in order to obtain alternative energy sources in production processes (Arion et al., 2023);
- measurements in the field in order to obtain some parameters and characteristics of the hydrographic basins, relevant under different aspects;

- evaluation of climatic and hydrographic factors, which influence the dynamics of water flows (Costin, 2003);

- analyzes and comparisons of the characteristic parameters of hydrographic and forest basins (Lee, 1980);

The main objective of this paper is the analysis and presentation of a small water course in northwestern Romania, namely from the Aleu Valley hydrographic basin, located in the Crișul Negru river basin, which presents a real potential for its development and exploitation. This course is a flowing water, formed by springs (which are points of discharge of the phreatic layers), shallow water layers, where the water is not under pressure, and/or precipitation, which under the influence of gravity and the slope, moves downstream along the line of greatest slope.

The exploitation of the hydro potential of the rivers and streams in Romania must be viewed with maximum interest, in the perspective of its sustainable management and conservation (Călmuc et al., 2022). Hydraulic resources represent one of the natural riches, characterized by the fact that they are practically inexhaustible and have numerous and varied uses, in all branches of human activity. In view of the special

interest that water presents, both for agriculture, forestry, industry, and for human settlements, it is necessary that when using these resources, all these needs should be taken into account, in order to ensure a complex and integral utilization of water courses (Păcurar, 2005; Iovan, 2012).

It is known that the forest directly, strongly, and complexly influences the water regime, regardless of the state of water aggregation (De Azagara et al., 1996), and the simultaneous presence of the two in mountain and hill regions, where I find most springs and watercourses. Due to these connections and influences of the forest on water, the ancient saying "the forest is the house of water" is very well known (Mancia & Mancia, 2003). The phenomena through which the forest intervenes on the water regime are: interception of water through the tree crown, evapotranspiration, water infiltration into the soil, water runoff and definitely its quality (Dumitru et al., 2004).

MATERIALS AND METHODS

The studied water course Aleu Valley originates from the Bihor Mountains and runs on their south-western side (Figures 1 and 2). It is a right tributary of the Crișul Pietros river, has a length of 9.5 km and crosses a forest floor area of 2456 ha after the Arrangement Forest District Sudrigiu.



Figure 1. The location of the water course Aleu Valley (<https://www.forajeapa.ro/bihor-oradea>)



Figure 2. Satellite image of Aleu Valley (<https://www.google.com/maps>)

The hydrographic basin (reception basin, water collection basin) represents the surface that includes the hydrographic network, from which it collects its waters (Man et al., 2010). Aleu Valley has a hydrographic basin with an area of 3619 ha, it is characterized by a longitudinal profile with an average slope of 95‰, as well as natural slope breaks.

The research method used in the first stage was the experiment, respectively the measurement of the morphometric elements of the sections studied (S1 downstream, respectively at the spillway, S2 in the central part of the basin and S3 in the upper part of the basin), based on which they established, through analytical calculation, the velocities and flow rates of the water course. For the hydrological characterization of a watercourse, the most important element to be determined is the *flow rate* (Q) (Helsel et al., 1992). Thus, this determination of the flow rates of the water courses was carried out in parallel with the help of the method based on the speed measured with floats, and respectively with the hydrometric mill. The method of calculating flows based on velocities measured with floats is a convenient method (Hersch, 1995), and which must meet certain conditions, respectively:

- lack of wind, which can influence the speed of the floats;
- the water level during the determinations should be stable, in order not to influence the trajectory of the floats towards the banks;
- lack of vegetation on the respective portion of the river;
- the most rectilinear shape of the course in the measured portion;

With the help of this method, the speed at the surface of the water current was determined, a

speed considered close to the value of the average speed.

After choosing the river sector targeted for measurements, the three sections were established, respectively: the hydrocanate (the

main section), the upper section (inlet of the floats), the lower section (outlet of the floats); Figure 3 shows the layout of the profiles, for calculating the morphometric elements of the measured cross-sections.

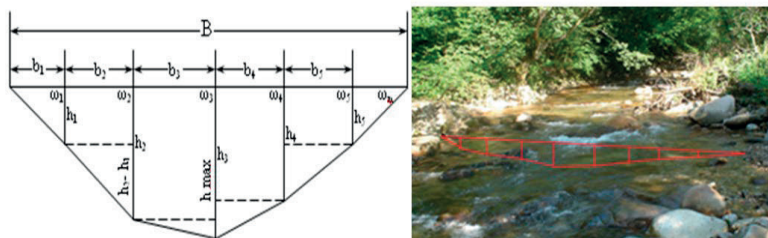


Figure 3. Helping profile to calculate the morphometric elements of the transversal section:
 $\omega_1 \dots \omega_n$ - surface of the active section; $b_1 \dots b_n$ - distance between the verticals; $h_1 \dots h_n$ - depth of the test verticals;
 h_{max} - maximum depth; B - width of the river

The most used is the method for determining the flow rate of water courses, it is related to the method of determining velocities with the hydrometric mill.

Through this method, the flow rate is determined as follows:

- the transverse profile of the bed is represented at a suitable scale;
 - calculate the surface of the section occupied by water (watered section);
 - the average speed of the water is determined using one of the previously presented methods;
- The water flow results from relation 1:

$$Q = \omega \cdot V_{med} \text{ [m}^3/\text{s or l/s]} \quad (1)$$

where:

- ω is watered section;
- V_{med} is the average speed of the water.

The hydrometric mill is a powerful, light, convenient and widely used device for measuring water velocities at different points in the stream. The name comes from the paddles, which rotate around an axis, under the influence of water currents. To obtain the magnitude of the speed of the water current, at a certain point, the number of rotations of the paddle in a unit of time, n , must be determined, knowing the relationship between the speed of the current (V) and the number of rotations of the paddle per second (n):

$$V = f(n) \quad (2)$$

For these measurements, the OTT type hydrometric mill was used (Figure 4), which works according to the Faraday principle (the induction of a uniform magnetic field is a

physical vector quantity, whose mode is equal to the ratio between the force with which that magnetic field acts on of a rectilinear conductor, perpendicular to the lines of the magnetic field, and the product of the current intensity in the conductor and the length of the conductor, located in the magnetic field) to determine the speed of the water at the measuring point.



Figure 4. OTT type of hydrometric micro mill

In order to detect the volume of water, this hydrometric mill has a cylindrical sensor included in the body of the dug. The equipment is functional in any fluid with minimal conductivity, and measures the water velocity twice in one second, calculating it as the average of the two readings.

Next, we moved on to processing the data obtained by the surface float method. For the flow calculation, with the help of this method, the calculation relations proposed by Morariu et al. (1970) were used: the surface of the active section (ω), was determined with the help of relation 3:

$$\omega = \frac{h_1}{2} b_1 + \frac{h_1+h_2}{2} b_2 + \dots + \frac{h_{n-1}+h_n}{2} b_{n-1} + \frac{h_n}{2} b_n \quad (3)$$

Based on the measurements made, the flow of the valley in the respective sections was subsequently calculated, as follows: in the first phase the fictitious flow rate Q_Φ , based on relation 4:

$$Q_\Phi = \omega V_m \quad (4)$$

and then the real flow rate Q , on the vase of relation 5:

$$Q = K Q_\Phi [m^3/s] \quad (5)$$

where:

- V_m is average speed;
- K represent transition or reduction coefficient, which is obtained as a ratio between the flow rate measured with the drill and the flow rate calculated based on surface velocities, but in the absence of these data, the value of K is roughly between 0.86 and 0.89.

The method used to measure the flow rates with the hydrometric trowel was the analytical one, which consists in determining the partial flow rates for the surfaces between the velocity verticals and summing them up according to the SEBA Hydrometry user manual, by going through the following steps:

- determining the average speeds for each vertical (V_1, V_2, \dots, V_n);
- calculation of the partial surfaces ($\omega_0, \omega_1, \omega_2, \dots, \omega_n$) between the speed verticals;
- the calculation of the average speeds for each of the partial surfaces, as the arithmetic mean of the average speeds of the neighboring verticals; for the first and last portion of the section, the average speed is considered to be 2/3 of the speed of the first, respectively the last vertical;
- determining the partial flow rate by multiplying each area by the average speed;
- adding up the partial flows for the entire section using relation 6, recommended by Morariu et al., 1970, and obtaining the total flow:

$$Q = \frac{2}{3} \omega_0 V_1 + \omega_1 \frac{V_1+V_2}{2} + \omega_2 \frac{V_2+V_3}{2} + \dots + \omega_{n-1} \frac{V_{n-1}+V_n}{2} + \frac{2}{3} \omega_n V_n \quad (6)$$

After the effective determination of the measurements on the watercourses, the data was downloaded into the computer system, and with the help of the software provided by the CamdR program, the measured flows and respectively all the elements of the watercourse were obtained, according to the model presented in Figure 6.

Next, the parameters of the hydrographic basin studied were determined, starting from their topographic maps (scale 1:50000 and equidistance of 20m) on which, after delimiting their perimeter, the level curves were introduced (by vectorization), with the help of the MapSys program.

Later, the hydrographic basin surface was divided into partial hydrographic basin surfaces, by means of sections depending on the sections where flow measurements and confluences with tributaries were made. Finally, with the help of the facilities offered by the Surfer program, the spatial model of the terrain (3D) was created.

RESULTS AND DISCUSSIONS

The 3D representation of the Aleu Valley hydrographic basin shows the form in Figure 5, which later determined all the values of the characteristic parameters of the basin, presented in Table 1.

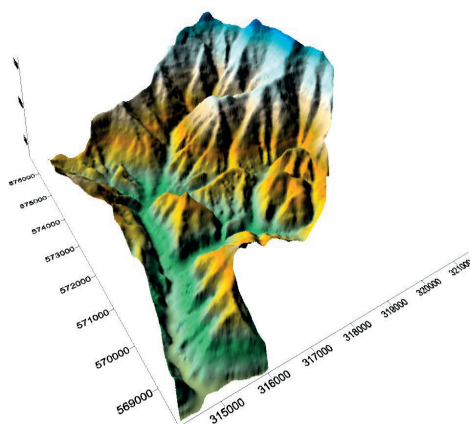


Figure 5. The space model of the field (3D) in the hydrographic basin of Aleu Valley

It is found that for the months of July, August and September (2018-2022) the correlations between the measured flow (with floats and hydrometric mill) and the forested area are significant, which means that the variation of the flows is really influenced by the forested area. So, we can say that during these months the forest intervenes significantly and decisively in the process of water retention from precipitation. At the same time, it can be observed that the same correlation for the month of June in the studied interval is insignificant. This fact can be explained by the influence of other factors that lead to relatively close flow rates regardless of the forested area. Even though the correlation is insignificant, the calculated t -test still has a value very close to the theoretical t -test.

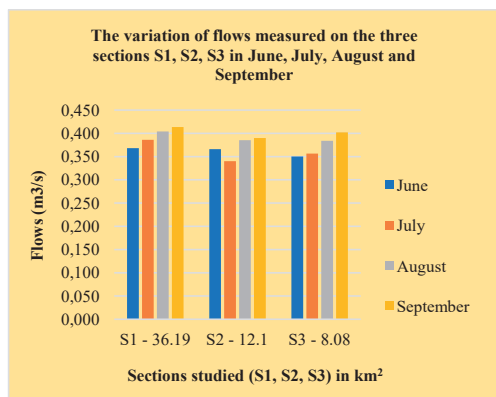


Figure 7. The variation of flows measured on the three sections S1, S2, S3 in the months of June, July, August and September in the interval 2018-2022

In order to analyze the existence of correlations between flows and the characteristic parameters of the hydrographic basin (basin form index, basin length, basin width and forested area), a comparative study was carried out with several hydrographic basins (Iada Valley, Brătuța Valley, Crăiasa, Galbena Valley, Crișul Pietros Valley, Finiș Valley, Tărcăița Valley and Văratec Valley) from the large hydrographic basins of the Crișul Repede and Crișul Negru rivers. This resulted in significant correlation coefficients between flow rates, the shape index, and the length of the hydrographic network of the basin, respectively between flow rates, the shape index and the surface of the hydrographic basin. At the same time, the correlation between the form

index and the multiannual average flows taken from the hydrological station was not relevant. In another vein, the connection between the average monthly rainfall in l/m^2 (taken from the ANMH-Weather station Stâna de Vale, which is the closest) and the average flows per calendar month (taken from the Cadastral Atlas of Romanian Waters) was tested in the period 2003-2022. From Figure 8 the equation of the distribution of correlation coefficients by calendar months (period 2003-2022) is a polynomial type of the 6th degree, with the coefficient of determination $R^2 = 0.6761$. Previous determinations for other types of regressions resulted in coefficients of determination with values below 0.5.

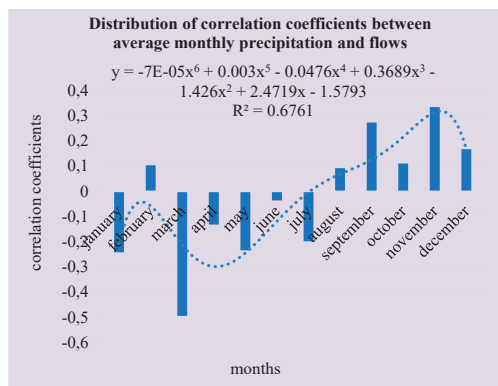


Figure 8. Distribution of correlation coefficients between average monthly precipitation and flows for the period 2003-2022 per calendar month

From the analysis of some correlations between the partial and total flows measured in the three sections (S1-S3) from June-September 2018-2022 (Figure 9), the existence of significant correlations between the calculated t and the theoretical t was found. This fact is normal due to the influence of flow rates measured upstream on those downstream.

Due to the small amounts of precipitation in the warm season, the flow variation is influenced by the forested surface of the basin. Also, some variations of these flows in the hydrographic and forest basin studied can be explained by the influence of other factors, such as: tree species, the consistency of the forest, the inclination and exposure of the slopes, etc.

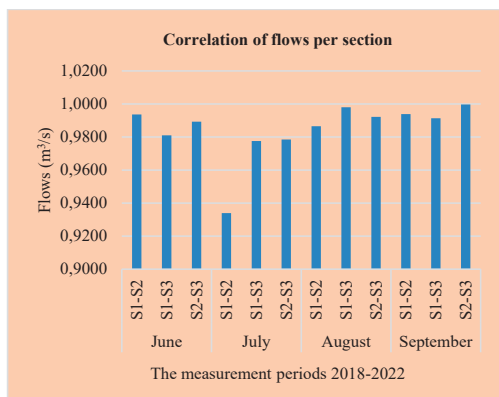


Figure 9. Correlations between partial and total flow rates measured in the three sections

CONCLUSIONS

Through the multivariate statistical analysis of flows according to a series of variables (characteristic parameters), the aim was to establish the degree of similarity (dissimilarity) between them and the partial and total subsurface of the hydrographic basin studied.

The identification of the variables considered to be more strongly correlated led to the conclusion that there are significant correlation coefficients between flow rates, the form index, and the length of the hydrographic network of the basin, respectively between flow rates, the form index and the area of the hydrographic basin.

From the multitude of types of correlative links, those with a higher correlation ratio and statistical significance were selected. Thus, the correlative links with statistical significance selected were those of the polynomial and linear type. Correlative links with statistical significance of the polynomial type suggested a stronger correlation in relation to the linear ones, but the corresponding regression curve indicates a certain reduction in the flow value before its increase, which is more difficult to explain.

The presentation of a flow analysis method was achieved by dividing the hydrographic basins into smaller areas and by characterizing them separately.

In the end, some recommendations can be made, respectively: directing attention to the hydrological resources available in the hydrological forest basins; awareness of the fact that the existence of small constructions (for example, troutery, artificial waterfalls, etc.)

contribute to the oxygenation of water in warm periods, when there is a risk of its temperature increasing and negatively affecting fauna (especially fish) or flora; the exploitation of all flowing waters with a low flow in order to obtain some forms of clean energy to serve isolated consumers (troutery, locations for forest management activities) existing in the forest fund, or of some small isolated localities.

Based on the research presented in this paper, it can be recommended to draw attention to the problems related to ensuring the permanence of the water flow, the presence or absence of torrential phenomena, the impact on the environment, etc. during the installation of constructions intended for the exploitation of water energy.

We can say with certainty that the evolution and variation of the flows of a watercourse located totally or partially in the forest floor are influenced by a much larger series of factors than those presented in the paper, such as the variation of the flows of tributaries of different degrees, the permanent or periodic operation of some works of the type of captures and others.

The last conclusion that can be drawn is that the flows of the studied watercourse reach the highest values in the winter-spring period, while the lowest flows are recorded in the warm season.

ACKNOWLEDGEMENTS

The case study and the related research were carried out on the ground within the Forest District Sudrigiu with the collaboration and support of the Bihor Forestry Directorate and Romanian Waters, Directorate of Crişuri Waters, to whom we thank in this way.

REFERENCES

- Arion, I.D., Arion, F., Morar, I.M. (2023). The efficiency of hydrotechnical works in the Gurghiu hydrographic basin, Series E. *Land Reclamation, Earth Observation & Surveying, Environmental Engineering, XII*, 281-289, Print ISSN 2285-6064.
- Călmuc, M., Călmuc, V.A., Arseni, M., Simionov, I.-A., Antache, A., Apetrei, C., Georgescu, P.L., Iticescu, C. (2022). Identification and characterization of plastic particles found in the lower danube river, Series E. *Land Reclamation, Earth Observation & Surveying, Environmental Engineering, XI*, 332-337, Print ISSN 2285-6064.
- Costin, A. (2003). The forest, a determining factor in reducing floods, *Forest Magazine*, 2, 35-37, Bucharest.

- De Azagara, A.M., Hevia, J.N. (1996). *Forest Hydrology- The hydrological cycle*, Valladolid, Secretariat of 14. Publications and Editorial Exchange University of Valladolid.
- Dumitru, I. & Daia, M. (2004). The role of forests in water management and measures to combat soil erosion, *Forest Magazine*, 3, 41-46, Bucharest.
- Helsel, D.R., Hirsch, R.M. (1992). *Statistical methods in water resources*, Elsevier Science Publishers, NY, USA, ISBN 0-444-81463-9
- Herschey, W.R. (1995). *Streamflow measurement*, London, UK, E&FN Spon, An Imprint of Chapman & Hall, ISBN 0 419 19490 8, second edition.
- Iovan, C.I. (2012). Research on the use of troutery feed water for energy and economic purposes, Transylvania University of Braşov, Romania, Doctoral Thesis.
- Lee, R. (1980). *Forest hidrology*, Elsevier Publishers, ISBN 0-231-04718-9
- Man, T.E., Sabău, N.C., Cimpan, G., Bodog, M. (2010). *Hydroimprovements*, Timişoara, RO: Aprilia Print Publishing House, ISBN 973-99452-0-1, 258.
- Mancia, A. & Mancia, M. (2003). The arrangement and management of the waters of the Criş hydrographic basin, *Annals of the University of Oradea*, Fascicle Constructions and Hydro-development Installations, V, 129-132, ISSN 1454-4067.
- Morariu, T., Pişota, I., Buta, I. (1970). *General hydrology*, Bucharest, RO: Didactic and Pedagogical Publishing House.
- Păcurar, V.D. (2005). A new method of hydrological mapping of forest lands using geographic information systems, *Forest Magazine*, 2, 28-31.
- Sandu, M.A. & Vîrsta, A. (2021). The water footprint in context of circular economy. *AgroLife Scientific Journal*, 10(2), 170-177.
- Şmuleac, L., Imbrea, F., Corodan, I., Ienciu, A., Şmuleac, A., Manea, D. (2017). The influence of anthropic activity on some river water quality, *AgroLife Scientific Journal*, 6(2), 178-182.
- Timofte, A.I. & Dorog S. (2011). *Forest biostatistics*, Oradea, RO: Oradea University Publishing House, ISBN 978-606-10-0442-3.
- ***Arrangement Forest District Sudrigiu, Bihor Forestry Directorate
- ***Cadastral Atlas, Romanian Waters, Directorate of Crişuri Waters
- ***National Agency of Meteorology and Hydrology (ANMH), Weather station Stâna de Vale
- ***SEBA HYDROMETRIE - Portable equipment for determining water velocity, User's Manual
- ***CamdR program
- ***<https://www.forajecapa.ro/bihor-oradea>
- ***<https://www.google.com/maps>

IRRIGATION CHANGES IN THE MARITSA RIVER BASIN: A CASE STUDY FROM THE PLOVDIV REGION

Krasya KOLCHEVA

National Institute of Geophysics, Geodesy and Geography - Hydrology and Water Management
Research Center, Bulgarian Academy of Sciences,
Acad. Georgi Bonchev Street, Sofia, Bulgaria

Corresponding author email: kolchevakrasi@abv.bg

Abstract

In the context of the policy of securing and protecting water resources for growth and sustainable development, agriculture must, through adequate planning of land use, cultivated crops and water infrastructure and taking into account climate changes and the needs of ecosystems, have a responsible managing role. The changes in Bulgaria after 1989 have brought for agriculture many risks and challenges. Therefore, the present study aims at making a general overview of the state of irrigation in the region of Plovdiv, as an example of the Maritsa River watershed in the period 2017-2021. On the basis of the obtained results, major problems and their possible solutions for agriculture and irrigation will be defined, such as recommendations for improving the agricultural policy and integrated water management in Bulgaria.

Key words: irrigation system (IS), river water intake (RWI), water source.

INTRODUCTION

Bulgaria, as a country, rich in diverse and fertile soils and relatively significant water resources, has its traditions in irrigation, with a well-developed hydro-meliorative fund, amounting at 1.2 million ha irrigation area at the end of 1980s. Political changes after 1989 led to various but still not entirely successful reforms in the agricultural sector. The introduced in 1991 private ownership of the agricultural fields and not sufficiently clear vision of the agricultural development completely changed the organization of the irrigation process, the size of the irrigated areas and the water supply. Thus, a large part of the existing large-scale irrigation infrastructure lost its purpose and suffered a significant decline in the last 30 years.

Meeting the demand for irrigation water depends on the type of crops, the size of the arable areas, the climatic factors and the good technical condition of the irrigation systems. Therefore, this paper aims at evaluating the irrigation changes, including the crops, grown in the period 2017÷2021 in Plovdiv region, in the Maritsa River basin (the main unit for water management in the East Aegean Sea region).

Based on the obtained results and on previous water balance assessments, the main problems

will be marked, and recommendation will be made for the development of agriculture and irrigation in Bulgaria.

MATERIALS AND METHODS

Study area

The basin of the River Maritsa (with a length of 524.6 km and an area of 53 000 km², of which 21 083.5 km² on Bulgarian territory, i.e., almost half of this is the Aegean sea watershed) occupies the central part of the Aegean drainage area (Hristova, 2012). The river takes its source from two high-mountain lakes in Marishka circus and after the town of Belovo enters the Upper Thracian lowland, covering the middle part of its watershed. The Thracian lowland is the most extensive and fertile lowland in Bulgaria with an area of 6032 km², an average altitude of 168 m and a transitional continental to Mediterranean climate on its southern slopes. The morpho-hydrographic and physical-geographic features of the lowland determine its division into two sub-regions – Western (Pazardzhik - Plovdiv field) and Eastern – (Stara Zagora field).

The Pazardzhik-Plovdiv field (with a length of up to 105 km, a width in the middle part > 50 km and an altitude of 300 m at the town of Belovo

to 100 m at the town of Parvomai) is a plain in southern Bulgaria, covering the territory of the districts of Pazardzhik and Plovdiv. The average annual temperature in the field is 12.5°C (for Plovdiv 12.2°C). The winter season is relatively mild and warm with an average January temperature of 0°C to 1°C (for Plovdiv 0.2°C), and the summer is hot with an average July temperature of 23-24°C (for Plovdiv 23.6°C).

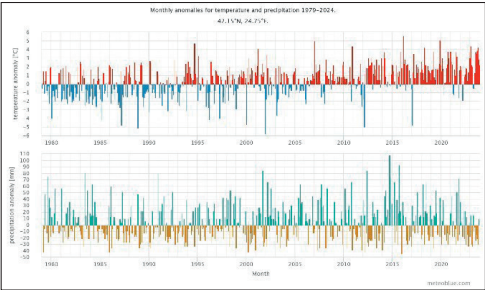


Figure 1. Monthly deviations from the 30-year average climatic value of temperature and precipitation for the Plovdiv City in the period 1979÷2021, <https://www.meteoblue.com>

The upper graph in Figure 1 shows the temperature anomaly, while the lower one illustrates the precipitation anomaly for each month from 1979 to 2021 for the city of Plovdiv. i.e., the corresponding deviations from the 30-year average climate values of temperature and precipitation for the period 1980÷2010. The months in red are warmer, in blue – colder, in green – wetter and the months in brown are drier than the climatic norm for the period. The increase in the number of warmer and less humid months over the years confirms the climatic trends in Bulgaria towards warming since the late 1970s and increasingly milder winters since the second half of the 20th century. This will compromise to a certain extent the production of the main agricultural crops by lowering their yield (Veselin, 2020). Therefore, the change in multi-year precipitation totals is an important regional indicator for various economic sectors, and especially for agriculture (Shopova et al., 2022).

The fertile soils and the relatively good water resources and climatic conditions in the Pazardzhik-Plovdiv field, and more specifically in the region of Plovdiv, are decisive for the development of vegetable farming, viticulture,

fruit-growing, and above all rice production (which dates back to the 14-15th century), and, respectively, are decisive also for the large irrigation systems in Bulgaria.

The demand for irrigation water in the studied region is mainly satisfied by surface waters – rivers and the 11 dams, built on them, which almost always guarantee the water needs. Three of the dams (Vacha, Topolnitsa and Pyasachnik) are complex and significant according to Annex №1 to the Water Act (2000), and the rest are managed by "Irrigation systems" EAD.

The irrigation systems Plovdiv and Stryama – Chirpan receive water through river water intake (RWI), respectively Polatovo and Manole from the Maritza River and Chernozemen and Ivan Vazovo – from the Stryama River. Water reaches the irrigated fields through the main irrigation canal (MIC) Eni Ark for the first system and through the main irrigation canal "Stryama-Chirpan" - for the second one. The main water sources of the remaining irrigation systems are the dams, given in Table 1.

Table 1. Irrigation systems (IS) in The Region of Plovdiv

Location IS	Water source	Constructed area, ha
IS Vacha - Parts of the Stara (Peshterska) River and Vacha River, Stamboliiski and Krichim municipalities	Dam Vacha	15456
IS Topolnitsa - Part between the rivers Piasachnik and Stryama, Maritsa, Kaloyanovo and Saedinenie municipalities	Dam Topolnitsa and Dam Pyasachnik	36586
IS Plovdiv - Part of the Maritza River basin, Maritsa and Saedinenie municipalities	Maritza river	6857
IS Asenitsa - Part of the Cherkezitsa River catchment, Asenovgrad municipality	Dams - 40-te isvora and Shushitza	15456
IS Stryama - Chirpan - Part of the Stryama River catchment, Kaloyanovo municipality	Stryama River	13280
IS Domlyan - Part of the Stryama River catchment, Karlovo municipality	Dam Domlyan	7082
IS Dondukovo - Part of the Stryama River catchment Srebra river catchment, Brezovo municipality	Dam Dondukovo	42
IS Karavelovo - Part of the Stryama River catchment, Karlovo municipality	Dam Kliment and Dam Sinyata reka	1955
IS Parvomai - Part of the Mechka River and the Kayaklika River catchments, Asenovgrad and Parvomai municipalities	Dams - Ezerovo, Lenovo, Mechka and Bryagovo	12597

The only irrigation system, not considered in the studied region, is the IS Rosino, the 720 da built irrigation areas of which on the Stryama river catchment, are not functional in practice. In the years of change, smaller farms increasingly use underground water sources for irrigation.

Data and methodology

Basic data on the irrigated areas, used water masses and cultivated crops for the period 2017÷2021 have been provided by "Irrigation systems" EAD for the ongoing project "Research on the security of water needs in the Maritsa river basin" carried out by the author. For performing a statistical analysis of the data, concerning the irrigated and built areas, the cultivated crops and the used water volumes, as well as for establishing trends, the program MS EXCEL was used. Summarizing spreadsheets were created to analyze the mentioned data. Calculation procedures were carried out on an annual basis for the period 2017÷2021, regarding: the size of the arable areas; the share of the irrigated from the total of the built areas; the sewn areas by types of crops out of the total of the irrigated areas; the used water volumes from the total volume by irrigation systems; the used water volumes by irrigation systems and types of crops. The results are graphically represented and analyzed, taking into account the dynamics and the trend.

With the aim of assessing the degree of securing the irrigation in the Maritsa river basin, various balance methods have been applied, generally based on a comparison between the inflow and the water consumption in certain nodes of the water management system (WMS). For example, with the help of the imitation (simulation) model SIMYL, transforming the physical scheme of the WMS into a directional graph, and solving the network flow problem, a scientific team from the Bulgarian Academy of Sciences assessed the security of water consumption by volume, months and years, and by the presence of water shortage (WPI-BAS, 2000). Currently, this assessment, with an already upgraded model, is being updated, including for irrigation under the above-mentioned project.

Another example of a balance method is the modeling system MIKE 11, which, through the rainfall/runoff module (MIKE 11-RR) determines the quasi-natural runoff for the hydrographic unit (NAM-catchment) and

through the hydrodynamic module (MIKE 11-HD) simulates the change of the river runoff from the water intake (JICA Project, 2006-2008). And in the second river basin management plan (RBMP) for the East Aegean District, the assessment of the water intake pressure, including from irrigation at the water body level in a 6-level classification system, is also based on a balance method (calculated by the National Institute of Meteorology and Hydrology - RBMP, the East Aegean District, 2016-2021).

RESULTS AND DISCUSSIONS

Statistical analysis of the irrigation in Plovdiv District for the period 2017÷2021 - Irrigation Systems Analysis

The size of the irrigated areas in Vacha IS during the studied period has a downward trend with a sharp decrease in 2018 compared to 2017 by 49.6% and a subsequent smooth decrease by 14.9% in 2021. The irrigated areas of Topolnitsa IS as of 2018 decreased by 37.1% compared to the first year of the period, then increased by 31.1% as of 2020, and, compared to this year, decreased by 89.7% at the end of the period (Figure 2).

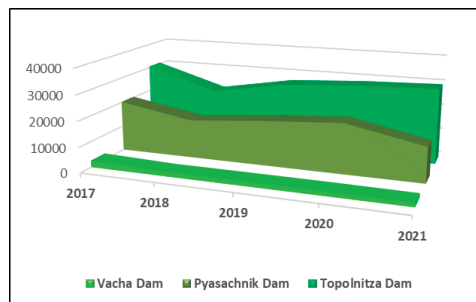


Figure 2. Irrigation Systems Vacha and Topolnitsa - Irrigated Area (da)

The change for the IS Asenitzia and IS Parvomai is similar but with more pronounced peaks of decrease. The first peak of decrease is in 2018, with almost 20 times for IS Asenitzia and 57.3% for the IS Parvomai, compared to 2017; and the second peak is in 2021 with 61.5% for the first irrigation system and twice for the second one, compared to 2020. A growth of 12.7% and 4.5 times for the entire period marked the irrigated areas, respectively, of the IS Plovdiv and IS

Karavelovo (Figure 3). For the irrigation system Stryama-Chirpan and the irrigation systems Dondukovo and Domlyan considered combined, an increase in the size of the areas after 2019 is

reported - 2.5 times for the first system and by 56% for the other two systems combined (Figure 4).

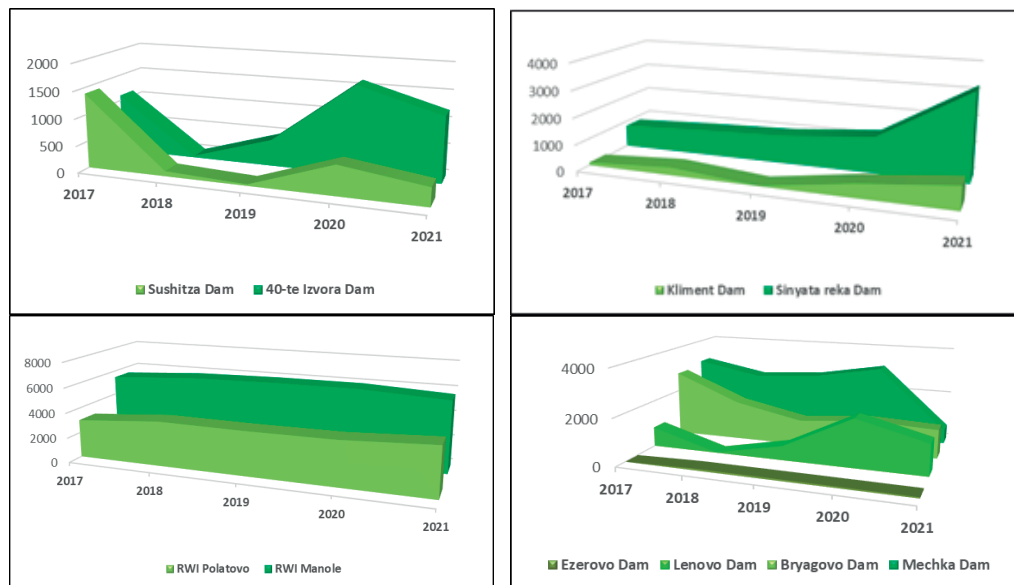


Figure 3. Irrigation Systems Asenitza, Plovdiv, Karavelovo and Parvomai - Irrigated Area (da)

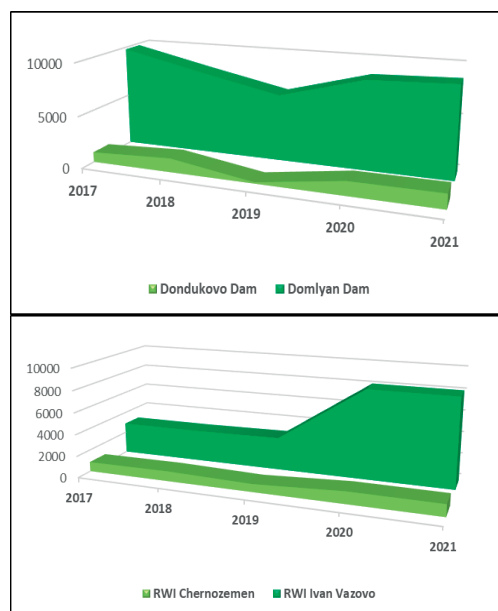


Figure 4. Irrigation Systems Stryama-Chirpan, Dondukovo and Domlyan - Irrigated Area (da)

Given what has been stated about the dynamics of the irrigated areas in the region of Plovdiv during the studied period, the following generalizations can be made: a downward trend for Vacha Irrigation System and a general upward trend for the irrigation systems of Plovdiv and Karavelovo; growth in the middle of the period and decline at its beginning and end for the irrigation systems Topolnitsa, Asenitza and Parvomai; two clearly expressed trends – a downward trend as of 2019 and an upward one as of 2021 for the IS Domlyan and Dondukovo and alternating upward and downward trends for the IS Stryama-Chirpan.

The share of the irrigated areas out of the built-up ones, presented in Figure 5, reached only 17% for the IS Vacha in 2017. And on average for the period 2017÷2021, the largest share of 13.6% belongs to Plovdiv IS, followed by the irrigation systems of Domlyan and Dondukovo with 13.1% and the irrigation systems Topolnitsa and Vacha with 12.3% each, whereas the smallest share of 0.9% belongs to Asenitza IS.



Figure 5. Share of the irrigated areas from the total amount of built-up areas, by irrigation systems, in %

Cultivated crops

Regarding the cultivated crops: rice is characteristic of the irrigation systems Topolnitza (80.9%), Plovdiv (67.9%), Domlyan (53%) and Stryama-Chirpan (5.5%); corn - of all systems without the IS Plovdiv, with a share of 62.7% belonging to Asenitza IS; tobacco is typical for five irrigation systems, of which the IS Parvomai has the largest share of 52.6%; and permanent plantations are present in all systems except for the irrigation systems Plovdiv and Stryama-Chirpan, with the IS Vacha having the largest share of 24.3%. Vegetable production is the least represented, with a share of 17.5% for Vacha IS, followed by 2.3% to 5% for the irrigation systems Asenitza, Parvomai, Domlyan/ Dondukovo and Karavelovo, and only 0.3% for the irrigation system Topolnitza.

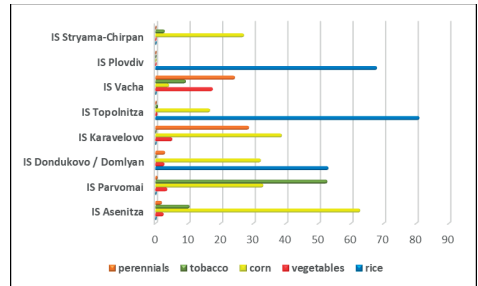


Figure 6. Share of the areas, sown by crops, from the total amount of irrigated areas, by irrigation systems, in %

Water volumes used for irrigation

The volume of the water used for irrigation is determined by the size of the irrigated areas and cultivated crops, and therefore their dynamics is similar. The share of the main water sources for the irrigation systems, comprising more than one water source, is presented in Table 2.

Table 2. Share of the main water sources for the irrigation systems, in %

IS Asenitza		IS Plovdiv	
40-te Izvora Dam	65.06	RWI Manole	62.35
IS Parvomai		IS Topolnitza	
Mechka Dam	47.33	Topolnitza Dam	61.30
IS Karavelovo		IS Stryama-Chirpan	
Sinyata reka Dam	81.23	RI Ivan Vazovo	84.32

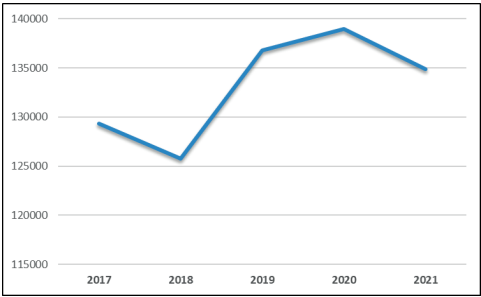


Figure 7. Total used water volume in the period 2017-2021

In the period 2017-2021, the total consumption of water for irrigation (reported by invoice) amounts to $665724 \cdot 10^3 \text{ m}^3$ with a minimum in 2018 and a maximum in 2020 and compared to 2020 it decreases by 3% as of 2021 (Figure 7). The largest share of this expenditure belongs to the irrigation systems Topolnitza and Plovdiv, with 67% and 17%, respectively (Figure 8).

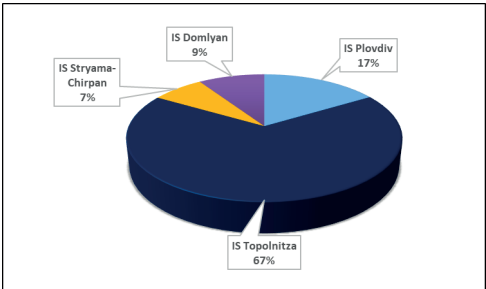


Figure 8. Share of used water volumes for the more significant irrigation systems out of the total volume (%)

Regarding the distribution of the water volume, consumed by crops, cultivation of rice takes the largest share - 95.9%, while vegetables and perennial plants are with the smallest share of 0.1% each.

Modeling and Impact Assessment

The results of the experimental study with the SIMYL model, according to four scenarios - basic, pessimistic, realistic and optimistic, with the inclusion in the latter of the areas constructed for irrigation, show the presence of a water deficit in the catchments of the rivers Stryama and Chepelarska due to the lack of regulating volumes (WPI-BAS, 2000).

The results obtained from the study with the modeling system MIKE11 show a possible risk for the irrigation in the watersheds of the rivers Stara reka (Peshterska) and Pyasachnik after the dam (JICA Project, 2006-2008).

The assessment of the pressure from the water intakes in the RBMP (2016-2021) ascertains a significant pressure of more than 30% in the Maritsa River basin from intakes for irrigation, of which in the studied area are: Kayakliika River – 67%, Pyasachnik River – 78% and Stara (Peshterska) River – 61% (RBMP, the East Aegean District, 2016-2021). Individual sections of the irrigation systems Vacha, Topolnitsa and Parvomai are generally at risk of water shortage as of 2021.

Main problems and possible solutions

The main problems and their possible solutions for the "Agriculture" sector and for the irrigation in Bulgaria, are:

- uncertainty due to the lack of a strategy with clear objectives for the development of the sector, including for irrigation, in compliance with the objectives of the Common Agricultural Policy of the European Union (EU). The "General Strategy for the Management and Development of Hydromelioration and Protection from the Harmful Effects of Water" developed by a World Bank team and approved by the Council of Ministers in 2016, remained without application and currently needs updating;

- legal uncertainty - the multitude of regulations in the sector create difficulties for the farmers, and in the field of the hydromelioration activities there is a need for new ones, for example,

development and adoption of a Law on Hydromelioration and a methodology for determining the price of the service for supplying water for irrigation;

- management uncertainty based on unclear demarcation of the management levels and responsibilities, lack of inter-institutional coherence and poor infrastructure management and water supply service quality. What is needed is a new model for management of the hydromelioration fund and new activities, reforming both the management and the operation of the networks and facilities;

- uncertainty in achieving the goals of integrated water management through the RBMP, overcoming which is possible through targeted sectoral coherence and activities such as: re-evaluation of: - the water sources; - the irrigation standards; - the permitted water intakes and the irrigation systems in terms of their water supply, size of irrigated areas and irrigation techniques and technologies with determination of the priorities for reconstruction. In addition, the presence of monitoring and effective control of water use, including in real-time, water balance assessments and the promotion of organized irrigation through irrigation associations are important for the water provision for consumers;

- climate uncertainty, i.e. agricultural production will be increasingly affected by climate change - a decrease in the amount of precipitation leads to a decrease in the river runoff and hence to a water deficit in the agricultural areas. In addition to the measures mentioned above, the following could be listed: - new genomic techniques for selecting drought-resistant agricultural crops; - introduction of water-saving irrigation techniques and compilation of irrigation options, adequate to the different climate scenarios, while protecting the water resources and the environment;

- uncertainty for the regional planning related to determining the type of the grown crops and the relevant irrigation infrastructure to provide water. The restoration and modernization of the irrigation systems should be linked to a methodically justified prioritization to determine the significant ones for the sector by classifying them according to certain criteria. For example, in the strategy mentioned above, the following four criteria with different weights are proposed: - system/technical priority; -

regional priority; - and a criterion according to the type of water source;

– uncertainty for the small and medium-sized farms, growing, for example, vegetables and orchards, which negatively affects irrigation and the infrastructure, related to it. This is due to the incorrect subsidy model, determining the creation of large conglomerates for the cultivation of grain crops, competing for the consolidation of the agricultural lands.

CONCLUSIONS

Regarding the cultivated crops, the tradition of rice production is preserved, though on a smaller scale, on the one hand, and vegetable production and fruit growing are too poorly developed. The differences in the irrigated areas and used water volumes are mainly due to the lack of maintenance and absence of measuring equipment for reporting the actual water consumption.

The defined problems provide insight into the state and the challenges facing the agriculture and irrigation, and the proposed measures for their overcoming are important for policy reform and support of decision makers. In conclusion, the present paper proposes a way of studying other regions as well, which will expand and clarify the issues and improve the recommendations for irrigation development,

including the infrastructure, in the context of the productive agriculture in Bulgaria, resilient to the changing climate and water resources.

REFERENCES

- Hristova, N. (2012). River waters of Bulgaria. 1st Edition, Publ. House Tip-Top, Sofia, ISBN: 978-954-723-08-04, pp. 830. (in Bulgarian with English Summary);
- JICA Project. (2006-2008). "Study on Integrated Water Management in the Republic of Bulgaria", contract between the Ministry of Environmental and Water of the Republic of Bulgaria and Japan International Cooperation Agency (JICA).
- River Basin Management Plan for the East Aegean District (2016-2021). <https://www.bta.bg/en/green-BTA/21025-Project-for-Updating-River-Basin-Management-Plans-in-East-Aegean-Region-Presente>
- Shopova, N., Alexandrov, V., Tsaikin, N., (2022). Hydrothermal conditions in the agricultural areas of Bulgaria expressed by the indices of Ped and De Martonne. In: Proceedings of the Climate, atmosphere and water resources in the face of climate change, Sofia, Volume 4, 2022, ISSN: 2683-0558, 85-92.
- Veselin, A. (2020). Climate change in the past and nowadays, causes and scenarios, impacts and vulnerability, Conference Proceedings "Climate, atmosphere and water resources in the face of climate change", Volume 2, pp. 70-79.
- Water Problems Institute at the Bulgarian Academy of Sciences (WPI-BAS). (2000). Project - "General schemes for the use of water in the basin management areas" under a contract between the WPI and the Ministry of Environment and Water. <https://www.meteoblue.com>

SUSTAINABLE MANAGEMENT OF WATER RESOURCES

Aurelia NICA¹, Stefan-Mihai PETREA^{1,2}, Ira-Adeline SIMIONOV^{1,2}, Alina ANTACHE^{1,2},
Catalina ITICESCU^{2,3}, Catalin PLATON⁴, Victor CRISTEA⁵

¹"Dunarea de Jos" University of Galati, Faculty of Food Science and Engineering,
111 Domneasca Street, Galati, Romania

²"Dunarea de Jos" University of Galati, REXDAN Research Infrastructure,
98 George Cosbuc Street, Galati, Romania

³"Dunarea de Jos" University of Galati, Faculty of Sciences and Environment,
111 Domneasca Street, Galati, Romania

⁴ROMFISH National Association of Fish Producers,
12A Nicolae Iorga Blvd, Iasi, Romania

⁵"Dunarea de Jos" University of Galati, Cross-Border Faculty,
47 Domneasca Street, Galati, Romania

Corresponding author email: anica@ugal.ro

Abstract

The sustainable management of water resources involves the careful stewardship, conservation, and equitable distribution of water to meet current and future needs while preserving the integrity of ecosystems and ensuring social and economic development. Here are some key principles and strategies for sustainable water management: Integrated Water Resource Management, Water Conservation and Efficiency, Protecting Ecosystems, Climate Resilience, Water Governance and Institutions, Investment in Infrastructure and Technology and Cross-Sectoral Collaboration. Sustainable water management requires collaboration and coordination across sectors such as agriculture, energy, industry, and urban development, as water is interconnected with various aspects of socio-economic development. Integrated planning and decision-making processes can help balance competing water demands and identify synergies and trade-offs among different sectors. By adopting these principles and strategies, communities, governments, and organizations can work towards ensuring the sustainable management of water resources, safeguarding water security, supporting ecosystem health, and promoting equitable access to clean and reliable water for present and future generations.

Key words: management, resources, sustainable, waters.

INTRODUCTION

Water is essential and vital for sustaining human life on earth. Water is one of the most precious natural resources, vital for human survival and for maintaining any form of socio-economic activity. Although about 71% of the earth is covered by water, only 3% of the world's water is fresh water, and two-thirds of this water is hidden in glaciers that are frozen or unavailable for use. In addition, most people in the world do not have clean and safe drinking water (Mezni et al., 2022; Popa et al., 2022). The world's drinking water resources are under increasing pressure.

Even though the total amount of water in the world remains the same, we see a constant deterioration of water quality, aquatic ecosystems and the environment of watercourses and reservoirs (Zyder et al., 2023). The purpose of

this article is to highlight the critical need for sustainable management of water resources considering increasing demand, impacts of climate change and pollution. Once perceived as limitless, this invaluable resource is now understood to be finite and increasingly scarce. Water resources management involves the monitoring and management of water quality as well as the monitoring and management of water quantity (Zoga et al., n.d.-a). Water resources were and are resources for society, regardless of region, with a direct economic value using water for drinking, agriculture, transport, obtaining energy. According to national legislation, water is a renewable, vulnerable and limited natural resource, an indispensable element for life and society, a determining factor in maintaining the ecological balance, a raw material for productive activities, a source of energy and a means of transport, a heritage natural, which

must be protected, treated and defended as such, being part of the public domain of the state, and any natural or legal person has the right to use water Constantin et al. (2009).

Proper water and wastewater management is essential for a healthy society, prosperous economy and a sustainable environment.

MATERIALS AND METHODS

The Mendeley platform was used as the search engine to define the subject of this review article. The first search using the keyword water resources provided 3,162 relevant results for the last two years (2023 and 2024). The flow of bibliographic references could provide a wide range of information to ensure the accuracy of the review article.

A second search using the keywords agriculture, energy, industry and urban development:

1. water resources and agriculture provided 407 results;
2. water resources and energy provided 688 results;
3. water resources and industry provided 337 results;
4. water resources and urban development provided 100 results;
5. conservation of water resources - 20 results.

The above search provides new ideas such as definition, conception, strategy, implementation, objectives, principles and indicators of the sustainable management of water resources in the world, but a single work is missing to incorporate and unify all these scattered information found in different references bibliographic. Thus, the work develops the following key areas (areas): integrated management of water resources, water conservation and efficiency, ecosystem protection, water governance and institutions, investments in infrastructure and technology and intersectoral collaboration.

RESULTS AND DISCUSSIONS

1. *Integrated management of water resources.*

The integrated management of water resources is exposed to the effects of several risks: climatic, socio-economic and political. Integrated Water Resources Management is a methodology that can help countries in their efforts to deal with water problems in a

sustainable and cost-effective way (TAC-Documente informative nr. 4 Managementul integrat al resurselor de apă, n.d.).

Climate change is currently one of the biggest risks for many countries around the world and for the agricultural sector (El Ouadi & Ouarda, 2023). Climate change itself can best be described as the average change in weather. Although climate is intertwined and closely related to weather, there are important differences.

A common distinction is the difficulty scientists have in predicting the weather for a few weeks, while confidently predicting the climate 50 years from now (Banouar & Bouslihim, 2024). Both inter- and intra-annual rainfall variability affects the outcome of cropping systems during any season. Increasing climate variability will jeopardize the sustainability of agricultural production (Boutracheh et al., 2024).

Current approaches to the problem of water quality in the world, especially those in the EU and the US, are based on the application of integral analysis, including all river basins (Zoga et al., n.d.-b.). The European approach was implemented through the Water Framework Directive (Directive, 2000/60/EC) integrating many previous directives. The Water Framework Directive contains a series of recommendations that Member States should implement in their regulatory framework to achieve the objective - "good water quality". These recommendations relate to water quality standards as well as effluent discharge limitations.

Adaptive water resource management has been suggested as a strategy to better coordinate surface water and groundwater resources (ie, conjunctive water use) to address drought (Josef et al., n.d.).

For areas at risk, alternative water sources have been identified as important options to maintain water supply security in the coming years, alongside centralized surface water and desalinated water sources.

This could help not only to identify the potential of existing rainwater and recycled water supply systems to reduce drinking water demand and return water to the environment, but also to identify additional opportunities at different parts of the water cycle and planning scales (Figure 1) (Ashbolt & Kularathna, 2023).

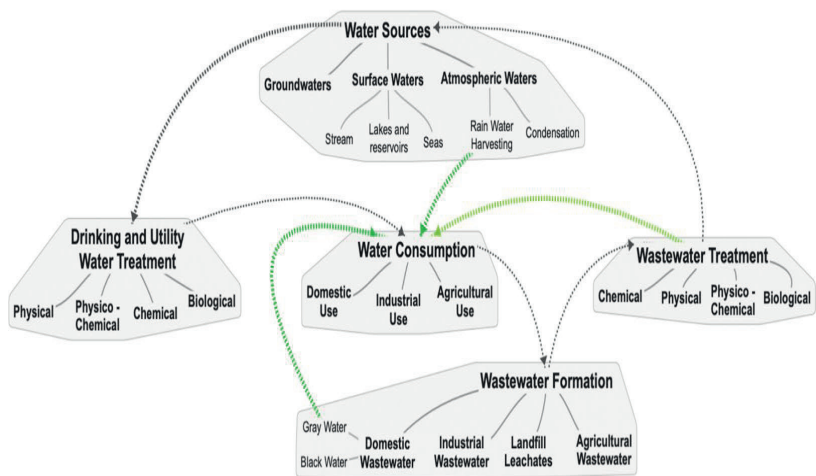


Figure 1. Urban water cycle and CE pathways (green arrows)

2. Water conservation and efficiency. Water security is a broad concept that encompasses ensuring the sustainable use of water resources, providing accessible services for all and mitigating water-related risks in the context of continuous change - the objective being to build a better future from the point of view of the security of water resources for people, economy and environment in the context of global changes. Using water only when needed and in the right amount is the most effective strategy. It is essential to choose the best technology for a job to save water (Kalyanapu et al., 2023). In the coming decades, climate change issues, increasing constraints on water resources, population growth and natural hazards will force hydrologists around the world to adapt and develop strategies to maintain security related to water resource management (Ghobadi & Kang, 2023). Effective management of water resources is essential for promoting sustainable development, reducing water-related conflicts and protecting aquatic ecosystems (Kamyab et al., 2023).

3. Protecting ecosystems. Aquatic ecosystems are generators of goods and services. A general classification of the services provided by aquatic ecosystems is presented in Table 1 (Durabil Al Apelor, n.d.). Ecosystems depend on water flows, seasonality and water level fluctuations, both surface and underground, and on water quality as a fundamental element. Water and land manage-

ment must ensure that fundamental ecosystems are preserved and that adverse effects on other natural resources are considered and where possible ameliorated when management and development decisions are made (TAC-Documente informative nr. 4 Managementul integrat al resurselor de apă, n.d.).

Tabel 1. Services generated by aquatic ecosystems

		Supply services:
		- Food
		- Water
		- Wood
		- Combustible
		Regulation services:
		- Climate stabilization
Support services:		- Flood control (storage and retention)
- Nutrient cycle		- Retention of nutrients
- Ground		- Water processing (detoxification).
- Primary producers		
		Socio-cultural services:
		- Spiritual, religious and cultural heritage
		- Education
		- Recreation and ecotourism
		- Landscaping and leisure

The complex interactions between human society and water resource systems, as well as the rapid growth of water resource use, forces many countries to face the task of reaching higher levels in water management planning and control of ongoing hydrological processes (Banouar & Bouslihim, 2024).

Engineering (or structural) measures such as dams, ponds, reservoirs, diversion channels, pumping stations can reallocate water in terms of time and space and are the operational tools to deal with water-related problems such as floods, drought and water pollution; Complementarily, non-engineering (or non-structural) measures, such as data acquisition, hydrometeorological forecasting, evacuation programs and risk awareness education, are the means to ensure the operation and effective use of engineering measures. The trend of urbanization and unsustainable consumption causes a rapid decrease in the limited water resources, which represent a strategic source of sustainable development of the city (Šulyová & Kubina, 2022).

Since the 1990s, population growth and competition in water use (private commercial water companies, state water distributors, and tourism) have frequently resulted in water access problems for irrigating agricultural communities and private households (Hamdani et al., 2021).

4. *Water governance and institutions.* Water planning aims to ensure sustainable results for human-technical-ecological systems. The factors that influence water planning are (bio)physical, technological, economic, socio-cultural and political (Rosello et al., 2023).

Water planning must consider the uncertainties of the future. Often, past development strategies are not suitable for planning future water supply and sanitation systems. Climate change and population growth are factors that cannot be controlled. The growing population of the globe also means increasing water consumption in industry, agriculture and energy production.

Increasing flexibility and reducing dependence on external factors in the planning of water systems will improve their response to developments and unforeseen events. Decisions and actions in the field of integrated management of water resources must be taken by all those who may be affected at the most appropriate level (principle of subsidiarity) (Pisleaga et al., 2019).

5. *Investments in infrastructure.* Investments are needed not only in new infrastructure, but also in the maintenance and operation of existing stock to improve their efficiency and reduce water losses.

Investments in water security face a number of barriers, including (HIGH LEVEL PANEL ON WATER Recommendations Headline Recommendation Report of the High Level Panel on Financing Infrastructure for a Water-Secure World. Water Infrastructure and Investment, n.d.):

- Water is often under-assessed and under-priced, leading to poor cost recovery for investments in this area.

- Water infrastructure is capital intensive, having high sunk costs and a long payback period, requiring a large initial investment.

- Water improvements provide a combination of public and private benefits, such as valuable goods and services and reduced water-related risks. Many of these benefits are difficult to monetize or their positive effects occur outside the investment project.

- The lack of appropriate analytical tools and data for evaluating complex water-related investments and the history of these investments can deter funders.

- Water projects are sometimes too small and too specific, which increases transaction costs and makes it difficult to scale up innovative emerging financing models.

6. *Technology and cross-sectoral collaboration.*

The choice of appropriate water management operations depends mainly on its quality and the hardware capabilities of the water areas. In each zone, water sensors and monitoring hubs collect useful data such as pH, water temperature, turbidity, conductivity, dissolved and chemical oxygen demand, NH₃-N, hardness, solids, chloramines, the number of sulfates, electrical conductivity, organic carbon, trihalomethanes, potability, etc.

Using this real-time data, managers of distributed autonomous services can decide on appropriate water management policy (Mezni et al., 2022).

Pollution limits for wastewater treatment plants of all types are constantly being tightened, which increases the already high costs of their operation and often adds to the increased prices for wastewater. One of the possible solutions to reduce these costs, or at least maintain them at the current level, is to invest in new technologies that allow reaching tighter limits at identical or lower costs (Zyder et al., 2023).

Automation allows farmers to increase efficiency through prudent consumption of resources, making farm management smarter. The use of smart irrigation technology spans a wide range with benefits for consumers (Armando, 2023). An efficient intelligent water management system is a must to avoid the severe repercussions of water scarcity (Mezni et al., 2022).

CONCLUSIONS

Water supply can be improved through management and technological approaches. Water resource management is a multifaceted endeavor that requires careful consideration of numerous environmental, social, and economic factors.

Water management approaches include immediate or future construction activities or those intended for long-term sustainability (Peña-Guzmán et al., 2021). Harnessing water means recognizing and considering all the benefits and risks it provides, including economic, social, ecological and security dimensions, as well as its cultural and religious meanings.

This process promotes efficiency and good practice by highlighting the short- and long-term costs of pollution, waste and misallocation. In this paper, it is highlighted that the lack of water is a major problem in the modern world and a rigorous management of water resources is required throughout the world.

Due to the significant increase in global industrial production and the overexploitation of terrestrial and marine resources, the quality of drinking water has deteriorated considerably.

Also, many water supply systems serving growing human populations are currently facing shortages as many rivers, lakes and aquifers dry up due to global climate change.

Water conservation has become an urgent necessity given the ever-increasing demand of the population for this vital resource, which is increasing by the minute. An adequate management of water resources neutralizes the threats and serious diseases that can be caused to the global population by water scarcity, both in terms of its availability and quality.

ACKNOWLEDGEMENTS

The present research was supported by the project An Integrated System for the Complex Environmental Research and Monitoring in the Danube River Area, REXDAN, SMIS code 127065, co-financed by the European Regional Development Fund through the Competitiveness Operational Programme 2014–2020, contract no. 309/10.07.2021.

REFERENCES

- Armando, M.T. (2023). Water Shortages in Monterrey. Analysis and Technological Solutions: Thermoelectric Power Generation and Technological Recommendations to Reduce Water Consumption. *PICMET 2023 - Portland International Conference on Management of Engineering and Technology. Managing Technology, Engineering and Manufacturing for a Sustainable World, Proceedings*. <https://doi.org/10.23919/PICMET59654.2023.10216841>.
- Ashbolt, S.C., & Kularathna, M.D.U.P. (2023). *The role of water resource planning models in integrated water management: A Melbourne Water case study*. <https://waterforlifestrategy.com.au/>
- Banouar, A., & Bouslihim, A. (2024). Integrated water resource management in the decision-making of large firms in Morocco: Case of Managem group (Hydraulic basin of Tensift AL Haouz). *E3S Web of Conferences*, 489. <https://doi.org/10.1051/e3sconf/202448905001>.
- Boutracheh, H., El Bouhaddioui, M., & Moumen, A. (2024). Current research priorities on fog harvesting as a clean water resource: a bibliometric approach. *E3S Web of Conferences*, 489. <https://doi.org/10.1051/e3sconf/202448905002>.
- Constantin, E., Mărăcineanu, F., Luca, E., & Mărăcine, N. (2009). Strategia globală a gospodăririi resurselor de apă. *Agricultura-Știință și practică* nr. 1-2 (69-70). DOI:10.15835/arspa.v69i1-2.3518.
- Directive 2000/60/EC of the European Parliament and of the Council of 23 October 2000 establishing a framework for Community action in the field of water policy, OJ L 327, 22.12.2000.
- Durabil Al Apelor, M. (n.d.). *Managementul Resurselor Naturale (Păduri, Ape și Planificare Strategică) suport de curs*. www.propark.ro.
- El Ouadi, I., & Ouarda, T.B.M.J. (2023). Climate Uncertainty Modelling in Integrated Water Resources Management: Review. *E3S Web of Conferences*, 364. <https://doi.org/10.1051/e3sconf/202336401013>.
- Ghobadi, F., & Kang, D. (2023). Application of Machine Learning in Water Resources Management: A Systematic Literature Review. *Water*, 15(4). <https://doi.org/10.3390/w15040620>.

- Hamdani, A., Kartiwa, B., & Sosiawan, H. (2021). Improving irrigated agriculture through integrated water resources management in Pusur Watershed, Central Java. *IOP Conference Series: Earth and Environmental Science*, 648(1).
- HIGH LEVEL PANEL ON WATER Recommendations
 Headline Recommendation report of the High Level Panel on Financing Infrastructure for a Water-Secure World. *Water Infrastructure and Investment*. (n.d.). <http://www.oecd.org/>.
- Josef, E., Parteli, R., Welsh, K., Sardooi, E. R., Zhao, M., Gov, M. Z., & Boll, J. (n.d.). *Adaptation of water resources management under climate change*.
- Kalyanapu, S., Kandula, A.R., Movva, S.R.K.D., Potharlanka, S.M.C., Yakkala, P., & Pittu, M. (2023). An Automatic Water Flow Management System for Agriculture. *Proceedings - 5th International Conference on Smart Systems and Inventive Technology, ICSSIT 2023*.
- Kamyab, H., Khademi, T., Chelliapan, S., SaberiKamarposhti, M., Rezanian, S., Yusuf, M., Farajnezhad, M., Abbas, M., Hun Jeon, B., & Ahn, Y. (2023). The latest innovative avenues for the utilization of artificial Intelligence and big data analytics in water resource management. *Results in Engineering*, 20.
- Mezni, H., Driss, M., Boulila, W., Atitallah, S. Ben, Sellami, M., & Alharbi, N. (2022). SmartWater: A Service-Oriented and Sensor Cloud-Based Framework for Smart Monitoring of Water Environments. *Remote Sensing*, 14(4). <https://doi.org/10.3390/rs14040922>.
- Peña-Guzmán, C., Domínguez-Sánchez, M.A., Rodríguez, M., Pulicharla, R., & Mora-Cabrera, K. (2021). The urban water cycle as a planning tool to monitor sars-cov-2: A review of the literature. *Sustainability*, 13(16). <https://doi.org/10.3390/su13169010>.
- Pisleaga, M., Eles, G., Badaluta-Minda C., & Popescu, D. (2019). Sustainable Water Resources Development as Part of the Integrated Water Resource Management for Mureş River. *IOP Conference Series: Materials Science and Engineering*, 603(4). <https://doi.org/10.1088/1757-899X/603/4/042022>.
- Popa, M., Glevitzky, I., Dumitrel, G.-A., Dorin POPA, Virsta, A., Glevitzky, M. (2022). Qualitative analysis and statistical models between spring water quality indicators in Alba County, Romania. *Scientific Papers. Series E. Land Reclamation, Earth Observation & Surveying, Environmental Engineering, Vol. XI*, 358-366, Print ISSN 2285-6064.
- Rosello, C., Guillaume, J.H.A., Pollino, C., & Jakeman, A.J. (2023). Identifying factors influencing water planning: Benefits of a capability approach? *Proceedings of the International Congress on Modelling and Simulation, MODSIM*. <https://doi.org/10.36334/modsim.2023.rosello103>.
- Šulyová, D., & Kubina, M. (2022). Integrated management of limited water resources in Smart Cities. *IOP Conference Series: Earth and Environmental Science*, 1077(1). <https://doi.org/10.1088/1755-1315/1077/1/012003>
- TAC-Documente informative nr. 4 Managementul Integrat al Resurselor De Apă. (n.d.).
- Zoga, P., Bode, A., Tirana, S., Kodhelaj, N., Kucaj, S., Balla, R., & Kučaj, S. (n.d.-a). *Water resources systems planning and management Water resources systems planning and management Ramiz Balla Water resources systems planning and management*. <https://knowledgecenter.ubt-uni.net/conference>.
- Zoga, P., Bode, A., Tirana, S., Kodhelaj, N., Kucaj, S., Balla, R., & Kučaj, S. (n.d.-b). *Water resources systems planning and management Water resources systems planning and management Ramiz Balla Water resources systems planning and management*. <https://knowledgecenter.ubt-uni.net/conference>.
- Zyder, V., Hubáček, J., Ameir, O., & Piecha, M. (2023). Wastewater reuse and recycling strategic management. *International Multidisciplinary Scientific GeoConference Surveying Geology and Mining Ecology Management, SGEM*, 23(5.1). <https://doi.org/10.5593/sgem2023/5.1/s20.39>.

DRIP IRRIGATION EFFICIENCY IN SOYBEAN CULTIVATION IN SOUTHEAST ROMANIA, A SUSTAINABLE APPROACH TO WATER MANAGEMENT

Oana Alina NIȚU¹, Ionuț Ovidiu JERCA¹, Mihaela BĂLAN²

¹University of Agronomic Sciences and Veterinary Medicine of Bucharest,
Faculty of Land Reclamation and Environmental Engineering,
59 Marasti Blvd, District 1, Bucharest, Romania

²University of Craiova, Faculty of Agronomy,
19 Libertatii Street, Craiova, Romania

Corresponding author email: oanaalinanitu1111@gmail.com

Abstract

Cultivating soybeans holds significant importance in ensuring food security and economic stability. In the context of climate challenges and limited resources, efficient water resource management becomes crucial. This article explores the sustainable approach of drip irrigation in soybean cultivation, specifically in Southeast Romania. Drip irrigation proves effective in Southeast Romania by delivering water directly to the soybean roots, minimizing losses from evaporation and runoff. This contributes to the conservation of water resources in the region. The precise water distribution of drip irrigation ensures uniformity in water supply, preventing both over-irrigation and under-irrigation, with significant benefits for soybean crops in Southeast Romania. Drip irrigation systems are tailored to the soil types and climate conditions present in Southeast Romania, ensuring optimal water usage efficiency. Given the variable weather patterns in the region, the ability of drip irrigation to adapt and respond to changes in climate contributes to the resilience of soybean crops. Through the use of advanced technology and local expertise, customized drip irrigation configurations are implemented to suit the specific needs of soybean cultivation in Southeast Romania.

Key words: advanced technology, crop efficiency, uniform water distribution.

INTRODUCTION

Over the years, it has been proven that people adapt easily to climate change, while ecological systems are more vulnerable and less flexible to such changes (Burghila et al., 2015). Water resources at a global level represent one of the most pressing challenges in ensuring food security. Scenarios indicate that the agricultural sector will need to increase its production by 60% worldwide and by 100% in developing countries by the year 2050 (Alexandratos & Bruinsma, 2012). It is very important to correctly use irrigation strategies and available technologies to use water efficiently and save energy since irrigation systems are large energy consumers (Drăcea et al., 2003). These measures should be implemented at the level of large agricultural farms to achieve significant improvements in terms of water use efficiency and crop productivity.

Thus, we will be able to achieve higher yields using the same amount of water, thereby

reducing the pressure on limited water resources (Odhiambo et al., 2012). Water stress is one of the most significant factors limiting yield in soybean production in many regions of the world, and the way soybean productivity responds to different levels of water.

Stress under various sowing epochs and irrigation norms is not fully understood. In the absence of weeds, diseases, nutrient deficiencies, or other stress factors, the effect of yield reduction due to lack of water is determined by the development stage of the plant. Some studies have highlighted the sensitivity of soybeans to water stress at different stages of development (vegetative, flowering, pod formation, and seed filling) (Brevedan & Egli, 2003). The application of fertilizers at the beginning of the vegetation period plays an essential role in achieving significant agricultural production and in protecting the soil against erosion (Balan & Patru, 2014). According to research, the application of supplementary or deficit

irrigation during the growing season or at a specific growth stage can significantly increase water use efficiency and the yield of the soybean crop (Giménez et al., 2017; Jha et al., 2018).

The response to irrigation is influenced by climatic conditions, the amount of rainfall during the growing season, soil characteristics, soybean variety, agronomic practices, and the experimental methods used (Evetts et al., 2000). Research has shown that by applying a single irrigation at different critical water stages, both the yield and its quality can increase in early soybean varieties, compared to the non-irrigated crop (Sweeney & Kirkham, 2003). It has been found that in soybeans, the leaf water potential is sensitive to soil moisture variations, so the leaf water potential, which is relatively easy to determine, can be used to schedule the necessary irrigations for the crop (Jovanovici et al., 1993).

Limited irrigation can have a significant impact on crop productivity in various environments. According to studies, deficit irrigation can be useful under conditions of decreasing water availability. Additionally, understanding how the crop responds to water stress throughout the growing season is important for better predicting and managing crop performance in various conditions. This information can be useful for making water management decisions and for improving its use in agriculture (Djaman et al., 2013; Akcay & Dagdelen, 2016). Drip irrigation holds particular importance in the solutions proposed for the water crisis. The average daily evapotranspiration will increase by about 6% if the average air temperature rises by 2°C and by about 15% at an average temperature of over 5°C (Nitu et al., 2023). Confidence in the water-saving potential of drip irrigation is often supported by impressive statistics and measurements. Drip irrigation has the potential to double the yield of agricultural crops, including most vegetables, cotton, sugarcane, and grapevines. The higher efficiency of water application and increased yields result in a doubling or even tripling of water productivity (Postel, 2000). Drip irrigation is an advanced and water-efficient method, ensuring that plant roots maintain optimal moisture conditions over extended periods, thereby favoring both

physiological activity and crop development (Yan et al., 2022). It has been observed that drip irrigation, compared to furrow irrigation, not only increases production but also significantly improves the quality of squash fruits (Amer, 2011). This irrigation method minimizes electrolyte loss from leaves, thus contributing to a notable improvement in physiological activity and corn yield (Cakmakci & Sahin, 2021). Other studies have indicated that drip irrigation helps reduce the levels of salt ions in the soil near the dripper, creating a conducive environment for plant growth in the root zone and mitigating the negative effects of soil salinization on crop development (Zhang et al., 2019). Some studies have also found that salt ions in crop root zone soil can migrate to the wetting front under the action of high-frequency drip irrigation, thus reducing the salt ion concentration and pH value of root zone soil and ensuring the normal growth of crops in saline-alkali land (Dong et al., 2021; Liu et al., 2012). In addition, drip irrigation can regulate soil nutrient cycling by affecting root-soil-microorganism interactions (Wang et al., 2022). The objective of establishing an irrigation schedule is to precisely determine the volume and optimal timing of water application to crops (Salata et al., 2022), based on at least one parameter from the soil-plant-atmosphere system (Kang et al., 2021). Choosing an appropriate irrigation scheduling strategy is crucial for supporting the physiological processes of plants and, consequently, for maximizing production (Kumar Jha et al., 2019).

Additionally, efficient irrigation scheduling contributes to reducing water and energy consumption (Souza & Rodrigues, 2022). On the other hand, over-irrigation, or under-irrigation, resulting from an inadequate or poorly designed irrigation plan, has generally led to reduced grain production and decreased efficiency in the use of irrigation water (Irrigation Water Productivity), as well as issues such as land flooding, soil salinization, and elevated groundwater levels (Yohannes et al., 2019; Almeida et al., 2022; Quiloango-Chimarro et al., 2022). Scientific and field development initiatives aimed at optimizing irrigation scheduling for soybeans have focused more on climate-based approaches than those

related to soil or plant characteristics. Recent research has examined the accuracy of crop coefficients specific to the southern region of Brazil (da Silva et al., 2019) and assessed crop evapotranspiration using the eddy covariance method in the United States (Anapalli et al., 2022). However, the challenges in choosing an appropriate irrigation strategy for soybeans stem from the wide variations in the amount of irrigation water used and the different levels of irrigation water productivity (IWP) among soybean genotypes, influenced by their maturity group. Differences have been identified between maturity groups V and VI, both in terms of the volume of irrigation water used and IWP, namely 65 mm and 0.6 kg m⁻³, respectively (Garcia et al., 2010). Similarly, in other legume species, the efficiency of irrigation scheduling has been correlated with variations in growth patterns (Rowland et al., 2010) and genetic differences in water use strategies (Farooq et al., 2019). Therefore, it is imperative to conduct studies that investigate various irrigation scheduling strategies, tailored to the specific characteristics of different soybean varieties.

MATERIALS AND METHODS

To achieve the purpose and objectives pursued within the research, a bifactorial experiment of the 2 x 2 type in three repetitions was set up at Fundulea, Calarasi County, during the period 2022-2023 (Figure 1).

Factor A was represented by the two soybean varieties P21T45 and PR92B63, while factor B was the cultivation technology with the following gradations:

- b₁ - non-irrigated,
- b₂ - irrigated 50% I.U.A at 0-80 cm with m = 400 m³/ha N0P60K60,
- b₃ - irrigated 50% I.U.A at 0-40 cm, with ½ m = 200 m³/ha N60P60K60 (Table 1).

Table 1. Experimental Variants

Factor A	Factor B		
a ₁ P21T45	b ₁ - non-irrigated	b ₂ - irrigated 50% I.U.A at 0-80 cm with m=400m ³ /ha N0P60K60	b ₃ - irrigated 50% I.U.A at 0-40 cm, with ½ m=200 m ³ /ha N60P60K60
a ₂ PR92B63			

The experiment was conducted on a site uniform in terms of fertility and micro relief. Irrigation was applied at various growth stages, ensuring that soil moisture did not fall below the minimum threshold of 50% I.U.A, regardless of the irrigation variant. In calculating the drip irrigation rate, it was necessary to know the distance between drippers and the distance between drip hoses to obtain the value of the percentage of moistened soil (P).

$$m_{brut} = 1/\eta c \cdot H \cdot Da \cdot (CC - P_{min}) \cdot P \text{ (m}^3/\text{ha)}$$

m_{brut} = drip irrigation norm;

H = irrigation depth;

Da = soil bulk density;

CC = field water capacity;

P_{min} = minimum soil moisture threshold;

P = percentage of moistened soil.

$$P = 100 \frac{Su}{dp \cdot dc} \%$$

For the calculation of the irrigation norm, the weighted values of the physical and hydrophysical indices of the soil from Fundulea for the active layer of 0.8 m and 0.4 m were used.

Calculation of irrigation norms for depths of 0.8 m and 0.4 m.

$$m_{brut} = 1/0.95 \cdot 100 \cdot 0.8 \cdot 1.38 \cdot (26.45 - 19.69) \cdot 0.50 = 396 \approx 400 \text{ m}^3/\text{ha}$$

$$m_{brut} = 1/0.95 \cdot 100 \cdot 0.4 \cdot 1.38 \cdot (26.9 - 19.75) \cdot 0.50 = 209 \approx 200 \text{ m}^3/\text{ha}$$



Figure 1. Image from the field

From a climatic point of view, Fundulea is characterized by the appearance of a transition between the dry steppe climate and the sub-humid forested zone. The year 2022 has a strong warming character in terms of

temperature in January and February. Starting from September, monthly average temperatures close to the multi-year average have been recorded at Fundulea. Thus, in terms of temperature, we can say that the year 2022 can be considered excessively warm, with an annual average temperature of 12.7°C exceeding the multi-year average by 2.1°C. The lowest multi-year average temperature is recorded in January, at -2.6°C, while the highest is in July, at 22.4°C (Figure 2). In terms of the annual average temperature, the year 2023 recorded a difference of only 0.2°C compared to the multi-year average of 10.6°C and can be considered a drought year in terms of temperature (Figure 3).

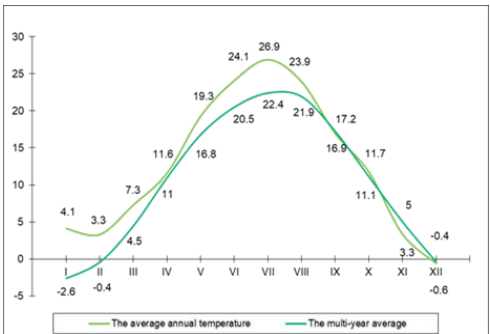


Figure 2. Monthly average air temperature recorded in the year 2022 and the multi-year average at the Fundulea meteorological station

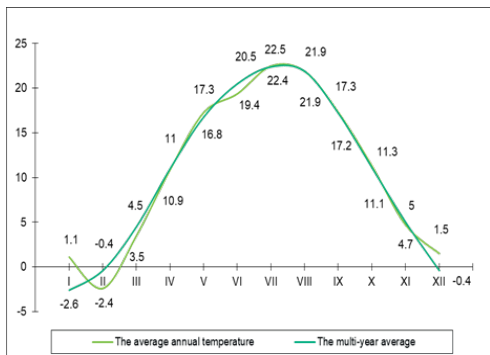


Figure 3. Monthly average air temperature recorded in the year 2023 and the multi-year average at the Fundulea meteorological station

Regarding the precipitation regime in 2022, it is deficient starting from the first month of the year. During the period from January to July 2022, the precipitation level was approximately

50% lower than normal, characterizing this interval as extremely dry. During the warm period of the year, the precipitation value recorded a decrease of approximately 32.5% compared to the multi-year average value in this area. In terms of precipitation, the year 2022 can be considered a drought year, with an interval of prolonged extreme drought throughout almost the entire growing season of spring crops (Figure 4). The year 2023 can be considered a drought year, with a drought interval from May to August. During the cold period of the year, the precipitation value recorded a decrease of 37% compared to the multi-year average value for this period, while during the warm period of the year, there was a decrease of 10% (Figure 5).

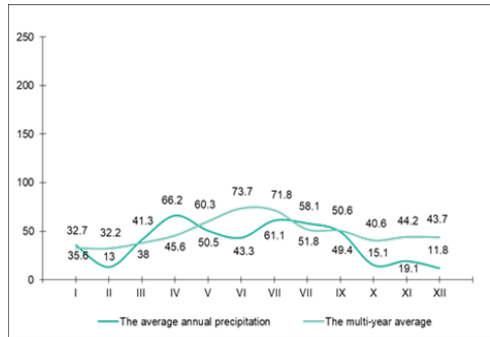


Figure 4. Monthly average precipitation recorded in the year 2022 and the multi-year average at the Fundulea meteorological station

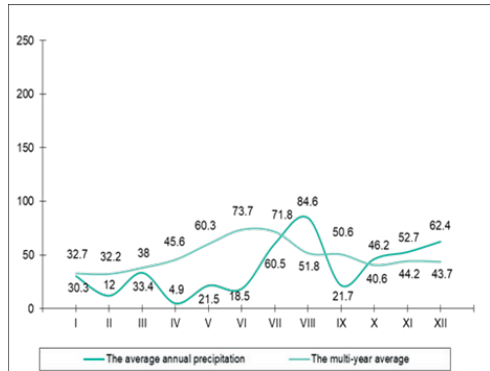


Figure 5. Monthly average precipitation recorded in the year 2023 and the multi-year average at the Fundulea meteorological station

After the maintenance works, drip hoses were also permanently positioned. The length of the

irrigation pipe was 300 meters, with 1.40 meters between pipes. Irrigation was carried out according to the established experimental variants, in line with the water needs of the crop, the level of precipitation during the growing season, and the soil moisture at that time.

RESULTS AND DISCUSSIONS

Variety PR92B63 obtained a higher yield, with 36.31 q/ha, compared to variety P21T45, which had a yield of 25.17 q/ha. The production difference between the two varieties is 11.14 q/ha, statistically ensured to be very significant (Table 2).

Table 2. The influence of soybean varieties on average yield

Factor A	Production (q/ha)	Difference from Ct	Significance
a ₁ P21T45	25.17	Ct	
a ₂ PR92B63	36.31	11.14	***

DL= 5% 1.2; DL =1% 1.7; DL = 0.1% 2.3

Table 3. The effect of different cultivation technologies on average yield for the two soybean varieties

Factor B	Production (q/ha)	Difference from Ct	Significance
b ₁ - non-irrigated	18.56	Mt	
b ₂ - irrigated 50% I.U.A at 0-80 cm with m=400m ³ /ha N ₆₀ P ₆₀ K ₆₀	33.63	15.07	***
b ₃ - irrigated 50% I.U.A at 0-40 cm, with ½ m=200 m ³ /ha N ₆₀ P ₆₀ K ₆₀	40.03	21.47	***

DL= 5% 1.0; DL =1% 1.4; DL = 0.1% 1.9

The production obtained under non-irrigated conditions was 18.56 q/ha, serving as the baseline level (Ct) for comparison. The introduction of irrigation and a fertilization regimen increased the production to 33.63 q/ha, resulting in a production increase of 15.07 q/ha compared to non-irrigated. Reducing the irrigation depth and intensifying fertilization led to the highest increase in production, reaching 40.03 q/ha, resulting in a highly significant production increase of 21.47 q/ha compared to non-irrigated (Table 3).

From the interaction of factors, it is evident that irrigation and fertilization significantly increase production compared to non-irrigated crops. Transitioning from non-irrigated (b₁) to irrigated with 50% IUA at 0-80 cm and irrigation with 400 m³/ha of water together with the application of N₆₀P₆₀K₆₀ fertilizers (b₂) resulted in a significant production increase of 4.12 q/ha. The application of irrigation at 50% IUA at 0-40 cm and with a rate of 200 m³/ha, but with a fertilization regimen of N₆₀P₆₀K₆₀ (b₃), resulted in a statistically very significant production increase of 9.89 q/ha compared to the control variant. For the PR92B63 variety, the results showed a very significant increase in production under the influence of irrigation and fertilization. Compared to the non-irrigated variants, irrigation and fertilization according to technology b₃ resulted in an increase in production of 30.94 q/ha.

This result shows that the PR92B63 variety exhibits an enhanced capacity to respond to irrigation and fertilization strategies, indicating better adaptation to optimizing water and nutrient resources (Table 4, Figure 6).

Table 4. The impact of irrigation and fertilization on varieties P21T45 and PR92B63

Factor B	Factor A	Production (q/ha)	Difference from Ct	Significance
b ₁ - non-irrigated	a ₁ P21T45	16.50	Ct	
b ₂ - irrigated 50% I.U.A at 0-80 cm with m=400m ³ /ha N ₆₀ P ₆₀ K ₆₀	a ₁ P21T45	20.62	4.12	*
b ₃ - irrigated 50% I.U.A at 0-40 cm, with ½ m=200 m ³ /ha N ₆₀ P ₆₀ K ₆₀	a ₁ P21T45	26.39	9.89	***
b ₁ - non-irrigated	a ₂ PR92B63	40.86	24.37	***
b ₂ - irrigated 50% I.U.A at 0-80 cm with m=400m ³ /ha N ₆₀ P ₆₀ K ₆₀	a ₂ PR92B63	32.62	16.13	***
b ₃ - irrigated 50% I.U.A at 0-40 cm, with ½ m=200 m ³ /ha N ₆₀ P ₆₀ K ₆₀	a ₂ PR92B63	47.43	30.94	***

DL= 5% 3.70; DL = 0.1% 5.08; DL = 0.1% 6.95

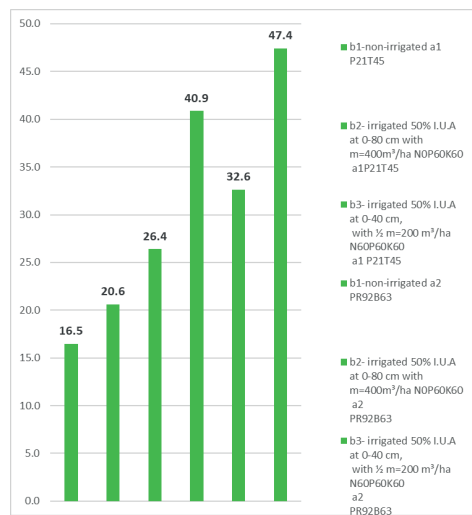


Figure 6. The impact of irrigation and fertilization on varieties P21T45 and PR92B63

CONCLUSIONS

The results demonstrate that the introduction of irrigation and an appropriate fertilization regimen has a significantly positive effect on crop production. Compared to non-irrigated conditions, where production was 18.56 q/ha, the implementation of these practices increased production to 33.63 q/ha and even 40.03 q/ha, highlighting the decisive role of water and nutrient management in optimizing crop yields. Reducing irrigation depth combined with increase in production, highlighting the importance of optimizing resource utilization. This suggests that a precise and well-established approach to irrigation and fertilization can lead to significant improvements in the efficiency of water and nutrient resource utilization. The PR92B63 variety has demonstrated an enhanced capacity to respond to irrigation and fertilization compared to the P21T45 variety, indicating significant genetic variability between varieties regarding adaptability and resource utilization efficiency. The production increases were statistically ensured to be highly significant indicating that the observed differences are not the result of random variations but rather real effects of the applied technology. The results underline the potential of well-managed irrigation and fertilization to contribute to sustainable agriculture.

ACKNOWLEDGEMENTS

The present paper and the research work included is supported by the Faculty of Land Reclamation and Environmental Engineering, University of Agronomic Sciences and Veterinary Medicine of Bucharest

REFERENCES

- Akcaay, S., & Dagdelen, N. (2016). Water use efficiency, yield and yield components of second crop sunflower under deficit irrigation. *Turkish Journal of Field Crops*, 21(2), 190-199.
- Alexandratos, N., & Bruinsma, J. (2012). World agriculture towards 2030/2050: *The 2012 revision*.
- Amer, K.H. (2011). Effect of irrigation method and quantity on squash yield and quality. *Misr Journal of Agricultural Engineering*, 28(1), 87-111.
- Anapalli, S.S., Pinnamaneni, S.R., Reddy, K.N., Sui, R., & Singh, G. (2022). Investigating soybean (*Glycine max* L.) responses to irrigation on a large-scale farm in the humid climate of the Mississippi Delta region. *Agricultural Water Management*, 262, 107432.
- Balan, M., & Patru, F. (2014). The influence of fertilizers on hay production on sloppy soils affected by surface EROSION. *Annals of the University of Craiova-Agriculture, Montanology, Cadastre Series*, 43(1), 25-30.
- Brevedan, R.E., & Egli, D.B. (2003). Short periods of water stress during seed filling, leaf senescence, and yield of soybean. *Crop Science*, 43(6), 2083-2088.
- Burghila, D., Bordun, C.E., Doru, M., Sarbu, N., Badea, A., & Cimpeanu, S.M. (2015). Climate change effects—where to next? *Agriculture and Agricultural Science Procedia*, 6, 405-412.
- Cakmakci, T., & Sahin, U. (2021). Improving silage maize productivity using recycled wastewater under different irrigation methods. *Agricultural Water Management*, 255, 107051.
- da Silva, E.H., Gonçalves, A.O., Pereira, R.A., Júnior, I.M.F., Sobenko, L.R., & Marin, F.R. (2019). Soybean irrigation requirements and canopy-atmosphere coupling in Southern Brazil. *Agricultural Water Management*, 218, 1-7.
- de Almeida, A.M., Coelho, R.D., da Silva Barros, T.H., de Oliveira Costa, J., Quiloango-Chimarro, C.A., Moreno-Pizani, M.A., & Farias-Ramírez, A.J. (2022). Water productivity and canopy thermal response of pearl millet subjected to different irrigation levels. *Agricultural Water Management*, 272, 107829.
- Djaman, K., Irmak, S., Rathje, W. R., Martin, D.L., & Eisenhauer, D.E. (2013). Maize evapotranspiration, yield production functions, biomass, grain yield, harvest index, and yield response factors under full and limited irrigation. *Transactions of the ASABE*, 56(2), 373-393.
- Dong, S., Wan, S., Kang, Y., & Li, X. (2021). Establishing an ecological forest system of salt-tolerant plants in heavily saline wasteland using the

- drip-irrigation reclamation method. *Agricultural Water Management*, 245, 106587.
- Drăcea, D., Tronac, A.S., Mustață, S. (2023). Are there opportunities of using solar energy in irrigation systems? *Scientific Papers. Series E. Land Reclamation, Earth Observation & Surveying, Environmental Engineering, Vol. XII*, Print ISSN 2285-6064, 194-198.
- Evett, S.R., Howell, T.A., Schneider, A.D., Upchurch, D.R., & Wanjura, D.F. (2000). Automatic drip irrigation of corn and soybean. In *Proceedings of the 4th decennial national irrigation symposium*, 401-408.
- Farooq, M., Hussain, M., Ul-Allah, S., & Siddique, K.H. (2019). Physiological and agronomic approaches for improving water-use efficiency in crop plants. *Agricultural Water Management*, 219, 95-108.
- Giménez, L., Paredes, P., & Pereira, L.S. (2017). Water use and yield of soybean under various irrigation regimes and severe water stress. Application of AquaCrop and SIMDualKc models. *Water*, 9(6), 393.
- Jha, P.K., Kumar, S.N., & Ines, A.V. (2018). Responses of soybean to water stress and supplemental irrigation in upper Indo-Gangetic plain: Field experiment and modeling approach. *Field crops research*, 219, 76-86.
- Jovanovic, N., Stricevic, R., & Pocuca, V. (1993). A simple plant water stress criteria for irrigation schedule [soybean crop]. *Review of research work at the Faculty of Agriculture (Yugoslavia)*, 38(1).
- Liu, S., Kang, Y., Wan, S., Wang, Z., Liang, Z., Jiang, S., & Wang, R. (2012). Germination and growth of *Puccinellia tenuiflora* in saline-sodic soil under drip irrigation. *Agricultural water management*, 109, 127-134.
- Nițu, O.A., Ivan, E.S., & Nițu, D.S. (2023). Climate change and its impact on water consumption in the main agricultural crops of the Romanian plain and Dobrogea. *Scientific papers. series A. Agronomy*, 66(1).
- Odhiambo, L.O., & Irmak, S. (2012). Evaluation of the impact of surface residue cover on single and dual crop coefficient for estimating soybean actual evapotranspiration. *Agricultural Water Management*, 104, 221-234.
- Postel, S. (2000). Redesigning irrigated agriculture. In *National irrigation symposium. Proceedings of the 4th Decennial Symposium*, Phoenix, Arizona, USA, November 14-16, 2000, 1-12. *American Society of Agricultural Engineers*.
- Quiloango-Chimarro, C.A., Coelho, R.D., Heinemann, A.B., Arrieta, R.G., da Silva Gundim, A., & França, A.C.F. (2022). Physiology, yield, and water use efficiency of drip-irrigated upland rice cultivars subjected to water stress at and after flowering. *Experimental Agriculture*, 58.
- Rowland, D.L., Beasley Jr. J.P., & Faircloth, W.H. (2010). Genotypic differences in current peanut (*Arachis hypogaea* L.) cultivars in phenology and stability of these traits under different irrigation scheduling methods. *Peanut Science*, 37(2), 110-123.
- Souza, S.A., & Rodrigues, L.N. (2022). Increased profitability and energy savings potential with the use of precision irrigation. *Agricultural Water Management*, 270, 107730.
- Sweeney, D.W., Long, J.H., & Kirkham, M.B. (2003). A single irrigation to improve early maturing soybean yield and quality. *Soil Science Society of America Journal*, 67(1), 235-240.
- Wang, J., Du, Y., Niu, W., Han, J., Li, Y., & Yang, P. (2022). Drip irrigation mode affects tomato yield by regulating root-soil-microbe interactions. *Agricultural Water Management*, 260, 107188.
- y Garcia, A.G., Persson, T., Guerra, L.C., Hoogenboom, G. (2010). Response of soybean genotypes to different irrigation regimes in a humid region of the southeastern USA. *Agricultural water management*, 97(7), 981-987.
- Yan, S., Wu, Y., Fan, J., Zhang, F., Guo, J., Zheng, J., Wu, L. (2022). Quantifying grain yield, protein, nutrient uptake and utilization of winter wheat under various drip fertigation regimes. *Agricultural Water Management*, 261, 107380.
- Yohannes, D.F., Ritsema, C.J., Eyasu, Y., Solomon, H., Van Dam, J.C., Froebrich, J., Meressa, A. (2019). A participatory and practical irrigation scheduling in semiarid areas: the case of Gumselassa irrigation scheme in Northern Ethiopia. *Agricultural Water Management*, 218, 102-114.
- Zhang, T., Zhan, X., He, J., & Feng, H. (2019). Moving salts in an impermeable saline-sodic soil with drip irrigation to permit wolfberry production. *Agricultural water management*, 213, 636-645.

BIODIVERSITY AND ECOLOGICAL ASSESSMENT OF THE CHEPELARSKA RIVER, BULGARIA

Georgi PATRONOV¹, Diana KIRIN^{2,3}

¹University of Plovdiv "Paissii Hilendarski", Department of Chemical Technology,
24 Tsar Assen Street, Plovdiv, Bulgaria

²Agricultural University-Plovdiv, Department of Agroecology and Environmental Protection,
12 Mendeleev Street, Plovdiv, Bulgaria

³National Institute of Geophysics, Geodesy and Geography, Hydrology and Water
Management Research Centre, Bulgarian Academy of Sciences,
Acad. Georgi Bonchev Street, Sofia, Bulgaria

Corresponding author email: gipatronov@abv.bg

Abstract

The results of research on biological diversity in a section of the Chepelarska River and the territories adjacent to it, subjected to anthropogenic pressure, are presented. The studied area (water body code BG3MA500R103, river type R5Semi-mountainous type in Ecoregion 7 Eastern Balkans) falls entirely within protected area BG0000194 "Chaya River". It is located along the lower section of the river before it flows into the Maritsa River (Eastern White Sea Basin). The types of natural habitats and their ecological status are presented. Regarding the registered 45 species of higher plants and 22 animal species, the nature protection status and the species with resource importance have been determined. The results from the ecological monitoring of the freshwater ecosystem based on physicochemical elements (dissolved O₂, pH, electrical conductivity, P_{total}, N-NH₄, N-NO₂, N-NO₃, P-orthoPO₄, Zn, Cu, Pb, Cd) and ecological quality element macrozoobenthos, after applying the established standards are discussed. Measures to improve the ecological condition of the studied area are indicated.

Key words: chemical state, ecological condition, ecological indices, protected habitats, protected species.

INTRODUCTION

River Chepelarska (86 km) is a right tributary of the Maritsa River in Central Southern Bulgaria. It springs from 1550 m above sea level, from the mountain resort of Pamporovo, the Rhodope Mountains. It flows into the Maritsa River at 148 m above sea level. The Chepelarska River occupies 1.9% of the watershed of the Maritsa River. Refers to river type R5: Semi-montane type in Ecoregion 7: Eastern Balkans (Belkinova et al., 2013). The waters of the Chepelarska River are used for electricity production, irrigation, and industrial water supply. For a long time, the river has been subjected to pollution from industrial, agriculture and domestic wastewater (withdrawal of water for irrigation; pollution with heavy metals, pesticides; deposition of construction and household waste; removal of ballast substances (Interim overview of the significant water management issues in East Aegean river basin management district.

https://earbd.bg/indexdetails.php?menu_id=84). All of them have provoked the performance of a number of studies on the state and management of the river ecosystem (Radeva, Seymenov, 2021; Gartsyanova et al., 2023; Gecheva et al., 2023; Kolcheva, 2020; Kolcheva et al., 2023; Park et al., 2023; Zaharieva, 2023), as well as for the successful management of agricultural areas and generated waste, according to the Law on Waste Management (Kehajov et al., 2016; Zahariev and Kehajov, 2016; Kehayov et al., 2017; Kehayov et al., 2022; Kehajov et al., 2023). The adjacent coastal and surrounding water ecosystems, the object of the present study, fall entirely within the boundaries of the protected area (SCI) BG0000194 "Chaya River" (650.62 ha), declared under Directive 92/43/EEC for the protection of natural habitats and wild flora and fauna (Decision No. 122/02.03.2007 of the Council of Ministers and Order No RD-688/ 25.08.2020 of the Ministry of Internal Affairs and Communications). The purpose of the research is to present the results

of research on biological diversity in a section of the Chepelarska River and adjacent territories subject to anthropogenic pressure, as well as the results of ecological monitoring research.

MATERIALS AND METHODS

The researched territory is located in the land of Katunitsa village, Popskoto area, Plovdiv region (42005'59.98"N 24051'52.09"E; 42006'00.86"N 25051'46.79"E). The territory has been subject to intense and long-lasting anthropogenic impacts related to removing ballast substances and depositing large amounts of construction waste.

Biodiversity studies were carried out using the method of observation and the method of test plots (Gusev & Bancheva, https://eea.government.bg/bg/bio/nsnbr/praktichesko-rakovodstvo-metodiki-za-monitoring-i-otsenka/Metodika_monitoring_Rastenia.pdf; Coulloudon et al., 1999)

The species identification was carried out according to Delipavlov et al., 2003; Marinov, 2000; Chineri, 1999; Karapetkova, Zhivkov, 2006; Kottelat & Freyhof, 2007.

The basic abiotic characteristics of the water habitat in the region under research were determined (temperature, pH, dissolved oxygen, electrical conductivity, calcium-carbonate hardness, biological oxygen demand (BOD₅), biogenic substances, and heavy metals). The methods of analysis used are as follows: - basic physicochemical indicators: temperature – BSS 17.1.4.01:1977, pH – BSS EN ISO 10523:2012, dissolved oxygen – BSS EN ISO 5814:2012, electrical conductivity – BSS EN 27888:2000, calcium carbonate hardness - BSS ISO 6059:2002, BOD₅ - BSS EN 1899-2:2004 - biogenic substances: P_{total} – BSS EN ISO 6878:2005, P_{ortho}-PO₄ – BSS EN ISO 6878:2005, N-NH₄ – BSS ISO 7150-1:2002, N-NO₂ – BSS EN 26777:1997, N-NO₃ – BSS EN ISO 10304-1:2009; - priority substances and specific pollutants: Zn – BSS EN ISO 17294-2:2016, Cu – BSS EN ISO 17294-2:2016, Pb – BSS EN ISO 17294-2:2016, Cd – BSS EN ISO 17294-2:2016. The evaluation was carried out according to the accepted European quality standards. The main physicochemical indicators and biogenic substances have been evaluated according to Ordinance № H-4/2012 on the

characterization of surface waters and heavy metals - according to the Ordinance on environmental quality standards for priority substances of 11.12.2015. A hydrobiological monitoring and ecologic assessment of the state of the Chepelarska River was carried out on the basis of the macrozoobenthos biological quality element (BSS EN ISO 10870:2012 Water quality - Guidelines for the selection of sampling methods and devices for benthic macroinvertebrates in fresh waters; BSS EN ISO 5667-1:2022 Water quality - Sampling - Part 1: Guidance on the design of sampling programmes and sampling techniques; EN ISO 5667-3:2003/AC:2007 Water quality - Sampling - Part 3: Guidance on the preservation and handling of water samples).

RESULTS AND DISCUSSIONS

Biodiversity and nature habitats

Bulgaria occupies part of the European-West Siberian biogeographic region of the Palearctic kingdom. It is located in the biome of the northern hemisphere's broad-leaved and mixed forests of temperate latitudes. The studied territory is located in the South Bulgarian province, the Central Bulgarian biogeographic region, and the subregion of the Upper Thracian Lowland (Gruev & Kuzmanov, 1994). The types of habitats subject to protection in the protected area are:

1) 92A0 Riverside galleries of *Salix alba* and *Populus alba*/06G1 Willow-poplar galleries in southern Bulgaria. Nature protection status: included in Appendix 1 of the Biodiversity Act, item 3. Natural habitats of the Red Book of the Republic of Bulgaria with the category Vulnerable (VU; IUCN), the Habitats Directive - part of the European ecological network NATURA 2000. The following negative factors are indicated: afforestation with exotic species and cultivars; you cut; waste disposal and water pollution; the invasion of atypical species (*Acer negundo* L., *Amorpha fruticosa* L., etc.); Parasitism (*Viscum album* Linnaeus, 1753 and *Loranthus europaeus* Jacq.); agricultural activities related to converting riparian forests into cultivated areas; grazing; corrections and cleaning of riverbeds, etc. (Red Book of the Republic of Bulgaria, item 3, Natural habitats). The protected habitat occupies 50.21 ha of the

territory of the protected area BG0000194 "Chaya River" (7.72% of the area).

2) 92D0 Southern riverside galleries and shrubs (Nerio-Tamaricetea and Securinegietinctoriae) are in the Red Book of the Republic of Bulgaria, vol. 3. Natural habitats as natural habitat 31F9 Riparian heather (*Tamarix* spp.) communities. Nature protection status: included in Appendix 1 of the Biodiversity Act, item 3. of the Red Book of the Republic of Bulgaria with the endangered category (EN; IUCN), the Habitats Directive - part of the European ecological network NATURA 2000, the Bern Convention. On the territory of the "Chaya River", both types of natural habitats are in good ecological condition

(http://natura2000.moew.government.bg/PublicDownloads/Auto/PS_SCI/BG0000194/BG0000194_PS_16.pdf).

A total of 45 species of higher plants have been established in the aquatic ecosystems of the Chepelarska River (Table 1). They refer to 13 groups of flora elements. The group of European-Asian species (Eur-As; 10 species) is distinguished by the most significant number of species, followed by the groups of European-Mediterranean species and cosmopolitans (Eur-Med and Kos; 5 species each); of adventitious species (Adv; 4 species), etc. Of the established species of resource importance, the largest share is medicinal plants (L; 29 species), followed by weeds (P; 16 species), honey plants (M; 13 species), dye plants (Bg; 11 species), and its. These species are widespread in the terrestrial habitats of the zone and are represented in high numbers. There are no established plant species that are protected by the Biodiversity Act or other national and international legislative documents. Some species of animals were also found, including protected (Table 2).

A total of one species of higher plant, 10 species of invertebrates, and 12 species of vertebrates (8 species of fish, 7 species of amphibians, 7 species of reptiles, and 9 species of mammals) are protected in the protected area (Standard form of Protected area 'Chaya'). None of these species were found in the studied biotopes. The removal of the waste and the improvement of the ecological condition of the studied territory leads to the creation of conditions for the distribution and habitation of species

represented in the area, the increase of biological diversity, and the improvement of the ecological potential in the anthropogenic part of the area.

Ecological assessment of the condition of the Chepelarska River

The Chepelarska River belongs to the Eastern White Sea Basin, river type R5: Semi-mountainous rivers in Ecoregion 7: Eastern Balkans. The results of the performed physicochemical and hydrobiological monitoring are presented (Tables 3 and 4).

Physicochemical monitoring

Basic physicochemical parameters were analysed: temperature, pH, electrical conductivity (Multi parameter instrument, WTW Multi 340 i), dissolved oxygen (Microprocessor oximeter, Orion Star A223), N-NH₄, N-NO₂, N-NO₃, P-ortho-PO₄ (Spectrophotometer, DR 3900), total phosphorus (UV-VIS Spectrophotometer, Thermo Scientific UV-Visible), calcium-carbonate hardness (Water Hardness Meter PCE-CP 21), BOD₅ (Manometric method BOD₅ analyzer LH-BOD601SL), zinc, copper, lead and cadmium (ELEMENT HR-ICP-MS system) (Table 3).

Hydrobiological monitoring

As a result of the biomonitoring on the base, 10 taxa of bioindicator macrozoobenthos were established, represented by a total of 231 specimens. *Hydropsyche* sp. (Hydropsichidae; Trichoptera) is represented with the highest number - 79 specimens, followed by *Gammarus* spp. (Gamaridae; Malacostraca) - 38 specimens; *Herpobdella stagnalis* (L.) (Glossiphoniidae; Hirudinea) and *Ephemerella ignita* (Poda) (Ephemerellidae; Ephemeroptera) - 27 specimens each; *Tubifex* sp. (Tubificidae; Oligochaeta) - 25 specimens, etc. The lowest number is *Lymnaea stagnalis* (L.) (Lymnaeidae; Gastropoda) - one specimen. The established taxa are distributed by sensitivity groups. Groups B (fewer sensitive forms), C (relatively tolerant forms) and D (tolerant forms) are represented by 3 taxa each, but the taxa of group B are the most numerous (110 specimens; Table 4).

Table 1. Biological diversity, floral elements and economic importance of plant taxa

№	Taxa Plants	Conservation status	Floral elements	Economic importance
Trees				
1	<i>Salix alba</i> L. (Salicaceae)	LC (IUCN)	Eur-As	Fr, Ho, De, Dy, Nt, Fd, He, Ta
2	<i>Populus alba</i> L. (Salicaceae)	LC (IUCN)	Eur-As	Fr, V, Ho, He, Ta
3	<i>Juglans regia</i> L., 1753 (Juglandaceae)	Not evaluated (IUCN)	Eur-As	Fr, Cu, He, M, Dy, Fr
4	<i>Fraxinus ornus</i> L. (Oleaceae)	LC (IUCN)	subMed	Fr, De, Ho, Dy, Fd, He
5	<i>Ailanthus altissima</i> Swingle (Simaroubaceae) – China	Not evaluated (IUCN)	Adv	I, De, Ho
6	<i>Alnus glutinosa</i> (L.) Gaertner (Betulaceae)	LC (IUCN)	Med-CAs	Fr, He, Ho, Dy
7	<i>Ulmus minor</i> Miller (Ulmaceae)	Not evaluated (IUCN)	Eur-Med	Fr, He, Ta, Ho
8	<i>Robinia pseudoacacia</i> L. (Robiniaceae) – North America	-	Adv	I, Ta, De, Ho, Fr, Ae
Bushes				
9	<i>Paliurus spina-christi</i> Millet (Rhamnaceae)	Not evaluated (IUCN)	Eur-As	He, Ho, Dy, De, Ta
10	<i>Rubus caesius</i> L., 1753 (Rosaceae)	LC (IUCN)	Eur-As	V, Nt, He, Ho
Grasses				
11	<i>Cynodon dactylon</i> (L.) Pers. (Poaceae)	Not evaluated (IUCN)	Kos	Fd, He, We
12	<i>Glyceria fluitans</i> (L.) Br. (Poaceae)	LC (IUCN)	Kos	Fd
13	<i>Sorghum halepense</i> Pers., 1805 (Poaceae)	Not evaluated (IUCN)	subMed-As	We, Fd
14	<i>Phragmites australis</i> (Cav.) Trin. Ex Steudel (Poaceae)	LC (IUCN)	Kos	Te
15	<i>Festuca pratensis</i> Hudson, 1762 (Poaceae)	Not evaluated (IUCN)	Boreal	Fd
16	<i>Hordeum murinum</i> L. (Poaceae)	LC (IUCN)	Boreal	We
17	<i>Persicaria hydropiper</i> (L.) Opiz (Polygonaceae)	LC (IUCN)	Eur-As	He, Dy
18	<i>Xanthium strumarium</i> L. (Asteraceae)	Not evaluated (IUCN)	Eur	We, He, Po
19	Обикновена синя жълчка (<i>Cichorium intybus</i> L.; Asteraceae)	LC (IUCN)	Eur-Sib	Nt, He, We
20	<i>Artemisia vulgaris</i> L., 1753 (Asteraceae)	LC (IUCN)	subBoreal	He
21	<i>Lactuca serriola</i> L. (Asteraceae)	LC (IUCN)	Eur-As	We, He
22	<i>Xeranthemum annuum</i> L. (Asteraceae)	Not evaluated (IUCN)	subMed	He
23	<i>Silybum arianum</i> (L.) Gaerner (Asretaceae)	LC (IUCN)	Med	He
24	<i>Sonchus arvensis</i> L. (Asteraceae)	Not evaluated (IUCN)	Eur-As	We
25	<i>Conyza canadensis</i> (L.) Cronq. (Asteraceae) – North America	Not evaluated (IUCN)	Adv	We
26	<i>Lapsana communis</i> L. (Asteraceae)	Not evaluated (IUCN)	Eur-Sib	We
27	<i>Centaurea solstitialis</i> L. (Asteraceae)	Not evaluated (IUCN)	Eur-Med	He
28	<i>Convolvulus arvensis</i> L., 1753 (Convolvulaceae)	Not evaluated (IUCN)	Kos	We, He
29	<i>Chenopodium album</i> L. (Amaranthaceae)	Not evaluated (IUCN)	Kos	We, He
30	<i>Silene vulgaris</i> (Moench) Garcke (Caryophyllaceae)	Not evaluated (IUCN)	Eur-As	-
31	<i>Teucrium pollium</i> L. (Lamiaceae)	Not evaluated (IUCN)	Pont-Med	He, Dy, Ta, Ho
32	<i>Urtica dioica</i> L., 1753 (Lamiaceae)	LC (IUCN)	Boreal	Nt, He, Dy
33	<i>Lamium purpureum</i> L. (Lamiaceae)	Not evaluated (IUCN)	Eur-Med	We, Nt, He, Ho
34	<i>Anthriscus caucalis</i> Bieb. (Apiaceae)	Not evaluated (IUCN)	Eur-Med	Po
35	<i>Eryngium campestre</i> L. (Apiaceae)	Not evaluated (IUCN)	Pont-Med	He, We
36	<i>Daucus carota</i> L. (Apiaceae)	LC (IUCN)	Eur-As	We
37	<i>Foeniculum vulgare</i> Mill., 1768 (Apiaceae)	Not evaluated (IUCN)	subMed	Eo, Dy, He, Sp
38	<i>Knautia arvensis</i> (L.) Colt. (Caprifoliaceae)	Not evaluated (IUCN)	Eur-Sib	Dy, He, Ho
39	<i>Verbascum sinuatum</i> L. (Scrophulariaceae)	Not evaluated (IUCN)	Med	-
40	<i>Verbascum phlomoides</i> L. (Scrophulariaceae)	LC (IUCN)	Eur	He, D, Dy, Nt
41	<i>Cynoglossum creticum</i> Miller (Boraginaceae)	Not evaluated (IUCN)	Med-CAs	-
42	<i>Euphorbia cyparissias</i> L. (Euphorbiaceae)	Not evaluated (IUCN)	Eur	We, He
43	<i>Datura stramonium</i> L., 1753 (Solanaceae) – America	Not evaluated (IUCN)	Adv	Po, We, He, Ru
44	<i>Lotus corniculatus</i> L. (Papilionaceae)	LC (IUCN)	Eur-Med	He
45	<i>Sinapis arvensis</i> L. (Brassicaceae)	LC (IUCN)	Med	We

Legend conservation status: LC – non-threatened species; IUCN – International Union for Conservation of Nature; RbBG – Red Book Republic of Bulgaria, vol. 1.

Legend flora elements: Eur-As – European-Asian; Adv – Adventitious; subMed– Sub-Mediterranean; Med – Mediterranean; subMed– Sub-Mediterranean; subMed-As – Sub-Mediterranean-Asian; Pont-Med – Pontic-Mediterranean; Boreal – Boreal; Eur-Med – European-Mediterranean; subBoreal–Subboreal; Med-CAs – Mediterranean-Central Asian; Kos – Cosmopolitan; Eur – European; Eur-Sib – European-Siberian.

Legend resource value: Fr – forestry species; Ho – honeyed; De – decorative; Dy – dyed; Nt – nutritionally; Fd – fodder; He – healing; Ta – tanned; V – vitaminic; I – introduced; Ae – anti-erosion; Fr – fruity; Cu – cultivated; Po – poisonous; Te – technical; We – weed; Sp – spice; Eo – essential oil; Ru – rudely.

Table 2. Biological diversity of established species of animals

№	Species of Animals	Consevation status
1	<i>Calopteryx splendens</i> (Harris, 1780) (Calopterygidae)	LC (IUCN)
2	<i>Tettigonia viridissima</i> Linnaeus, 1758 (Tettigoniidae)	LC (IUCN)
3	<i>Saturnia pyri</i> (Denis & Schiffermüller, 1775) (Lepidoptera)	Biodiversity Act-II; Not evaluated (IUCN)
4	<i>Ciconia ciconia</i> (Linnaeus, 1758) (Ciconiidae)	LC (IUCN); VU (Vulnerable; RbBg, vol. 2); 3BP-II
5	<i>Squalius orphaeus</i> (Kottelat & Economidis, 2006)	LC (IUCN)
6	<i>Barbus cyclolepis</i> (Heckel, 1837)	LC (IUCN)

Legend: Biodiversity Act-II – Biodiversity Act - Appendix II; IUCN - International Union for Conservation of Nature and Natural Resources; LC – non-threatened species; Not evaluated – not evaluated; RbBg, vol. 2 – Red Book of Republic of Bulgaria, volume 2; VU – vulnerable species.

Table 3. Basic abiotic indices of the studied fresh water ecosystems from the Chepelarska River

Abiotic indices	Unit of measure	Mean \pm SD	Standard
Temperature	$^{\circ}\text{C}$	3.5 ± 0.4	-
pH	-	8.02 ± 0.03	$6.5 - 8.5$
Dissolved oxygen	mg/l	12.7 ± 0.6	6.00
Electrical conductivity	$\mu\text{S/cm}$	343 ± 9	750
Calcium carbonate hardness	mg CaCO_3/l	177 ± 7	-
BOD ₅	mg/l	< 1	3
Ptotal	mg/l	0.046 ± 0.005	0.075
P-ortho-PO₄	mg/l	0.040 ± 0.004	0.04
N-NH ₄	mg/l	0.19 ± 0.02	0.4
N-NO ₂	mg/l	0.0070 ± 0.0006	0.03
N-NO ₃	mg/l	0.51 ± 0.03	1.5
Zn	$\mu\text{g/l}$	56 ± 3	75
Cu	$\mu\text{g/l}$	2.6 ± 0.1	10
Pb	$\mu\text{g/l}$	1.7 ± 0.1	14
Cd	$\mu\text{g/l}$	1.8 ± 0.1	0.9

Table 4. Number of bioindicative taxa, specimens, sensitive and saprobity groups

Sensitive groups, No. taxa (No. specimens)				
B	C	D	E	
3(110)	3(61)	3(35)	1(25)	
Saprobity groups, No. taxa (No. specimens)				
β	$\chi\text{-}\beta$	0- β	$\beta\text{-}\alpha$	p
5(116)	1(38)	1(21)	1(4)	1(25)
Biotic indices				
Total N0. of Taxa (Specimens)	10 (231)			
RETI	0.48			
BI(EQR)	3(0.6)			

Legend: No. taxa – Number of taxa; No. sps. – Number of specimens; B – less sensitive forms; C – relatively tolerant forms; D – tolerant forms; E – most tolerant forms; RETI – Rhithron Feeding Type Index; BI – Adapted Biotic Index.

With one taxon and the smallest number of specimens is group E (most tolerant forms; 25 specimens).

Five saprobic groups are distinguished: β -mesosaprobic organisms; $\chi\text{-}\beta$ -mesosaprobic; 0- β -mesosaprobic; $\beta\text{-}\alpha$ -mesosaprobic and p-saprobic organisms.

The group of β -mesosaprobic organisms is represented with the largest number of taxa and number of specimens - 5 taxa with 116 specimens. All other saprobic groups are represented by one specimen each. The Rhithron

Feeding Type Index was 0.48, and the determined adapted biotic index (BI) was 3, which corresponds to a moderate (medium) ecological condition (Table 4).

Compared to previous studies (Boyanov et al., 2011; Boyanov et al., 2011a), an increase in the abundance of bioindicators from the sensitive B group was observed, as well as a decrease in the abundance of organisms from the other sensitivity groups, as well as more good environmental condition (BI = 3). The reasons for the state of the taxonomic compositions and

the dominant structure of the macrozoobenthos in the lower section of the Chepelarska River are arable agricultural lands, fishing, poaching, waste disposal (Park et al., 2023).

Leading for determining the ecological condition are the biological elements. The complex assessment, however, is determined according to the lowest indicator. The provisions of the Water Act of 1999, Ordinance № H-4/2012, etc. are implemented. The state of the water body for the period 2012-2021 is presented (Table 5).

Based on the environmental monitoring studies carried out by the Regional Laboratory Complex, Plovdiv, and the reports on the state of water bodies on the territory of the Eastern White Sea region for the period 2012-2021 with the presentation of an integrated ecological assessment, the general state of the river ecosystem for the water body is as bad as in 2021 in terms of biological and physicochemical indicators, as well as in terms of ecological status/potential, an improvement of the status is observed to moderate, in contrast to that for the previous periods (poor). In 2022, our biological and physicochemical indicators (macrozoobenthos) studies confirm the 2021 ecological assessment.

The main groups as shifting indicators exceeding the permissible concentrations can be

united into three groups - biological elements (macrozoobenthos), biogenic (nitrites - NO_2^- , phosphates - PO_4^- , total phosphorus, etc.), and heavy metals (cadmium - Cd, lead - Pb, etc.). Based on the ecological monitoring studies carried out with an integrated ecological assessment presentation, the ecological status of the studied section of the river ecosystem is moderate (average).

According to the Plan for the Management of River Basins in the Eastern White Sea Region and the Reports on the Status of Water Bodies in the Eastern White Sea Basin for the period 2012-2021, the Chepelarska River is polluted after the confluence of the Yugovska River with lead, where the source of pollution is the metal enrichment factory ores and the tailings storage facility of "Gorubso", the town of Laki and before flowing into Maritsa river - after "Plant for non-ferrous metals 2000 Group", the town of Plovdiv with lead and cadmium. The discharges of domestic and industrial water from the town of Asenovgrad and other settlements are also indicated as sources: withdrawal of water for irrigation and electricity production; small outflow; pressure from settlements; cosmetic factory Rosa Impex; ISA 2000 Ltd.; "Plant for non-ferrous metals 2000 Group"; "Agria".

Table 5. Condition of surface water body BG3MA500R103 "Chepelarska River" from the town of Asenovgrad to the mouth and "Krumovskiy collector"

Year	Biological indicators	Physicochemical indicators	Ecological condition	Chemical condition	Total condition	Shifting metrics
2012	bad	moderate	bad	bad	bad	-
2013	bad	bad	bad	bad	bad	NH_4 , NO_2 , PO_4 , Zn, Cu
2014	bad	moderate	bad	bad	bad	macrozoobenthos, NH_4 , NO_2 , PO_4 , Cd
2015	bad	moderate	bad	bad	bad	PO_4 , Zn, Cd
2016	bad	moderate	bad	bad	bad	NO_2 , NO_3 , PO_4 , Ptotal, Ntotal, Mn, Zn, Cd, Pb
2017	bad	moderate	bad	bad	bad	macrozoobenthos, NO_2 , PO_4 , Ptotal, Ntotal, Mn, Zn, Cd, Pb
2018	bad	moderate	bad	bad	bad	NH_4 , NO_2 , PO_4 , Ptotal, Ntotal, Mn, Cd, Pb
2019	bad	moderate	bad	bad	bad	macrozoobenthos, NH_4 , NO_2 , PO_4 , Ptotal, Ntotal, Mn, Cd, Pb
2020	bad	moderate	bad	bad	bad	macrozoobenthos, electroconductivity, NO_3 , NO_2 , PO_4 , Ntotal, Mn, Cd, Pb
2021	moderate	moderate	moderate	bad	bad	macrozoobenthos, phytobenthos, NO_2 , PO_4 , Ptotal, Ntotal, Cd, Pb

Optimizing the hydrological regime can restore the river's self-purification ability. For industrial enterprises, a measure for the modernization of an industrial wastewater treatment plant ("Agria") is foreseen collection and removal of industrially polluted waters of "Plant for non-ferrous metals 2000 Group" to the industrial wastewater treatment plant and study of the bioaccumulation of priority and dangerous substances in fish (fish from the Chepelarska River near the collector of "Plant for non-ferrous metals 2000 Groupv). As a result of the measures taken, the implemented plans, and programs from 2021 to the present, improvements have been established in the ecological condition of the Chepelarska River from the town of Asenovgrad to its mouth. The Eastern White Sea Basin River Basin Management Plan for 2022-2027 is also expected to achieve this.

CONCLUSIONS

As a result of the inventory studies on the biological diversity of the anthropogenically influenced section of the Chepelarska River, the restoration of the natural vegetation was established. Still, the protected species characteristic of the protected area BG0000194 "Chaya River" was absent. The performed physicochemical and biological monitoring gives reason to define the ecological condition of the studied section of the river ecosystem as poor.

REFERENCES

- Belkinova, D., Gecheva, G., Cheshmedzhiev, S., Dimitrova-Dyulgerova, I., Mladenov, R., Marinov, M., Teneva, I., Stoyanov, P., Ivanov, P., Michov, S., Pehlivanov, L., Varadinova, E., Karagyozyova, Z., Vasilev, M., Apostolu, A., Velkov, B., Pavlova, M. (2013). *Biological analysis and ecological assessment of surface water types in Bulgaria*. University Publishing House "Paisii Hilendarski", 235.
- Bondev, I. (1991). *Vegetation of Bulgaria*. Univ. Publishing "Kliment Ohridski", Sofia.
- Boyakov, B., Kirin, D., Manolova, I. (2011). Physicochemical and Hydrobiological Monitoring of the Chepelarska River, Bulgaria. (2021). *8th Simpozium "Reciklažne Tehnologije I. Održivi Razvoj"*, Soko Banja, 353-359.
- Boyakov, B., Kirin, D., Manolova, I. (2011a). Ecological appraisal for the condition of the Chepelarska river, Bulgaria. *11th ICOBTE, Congress Center*, Florence, Italy, July 3-7, 2011.
- BDS EN ISO 10870:2012 Water quality - Guidelines for the selection of sampling methods and devices for benthic macroinvertebrates in fresh waters.
- BDS EN ISO 5667-1:2022 Water quality - Sampling - Part 1: Guidance on the design of sampling programmes and sampling techniques.
- Biodiversity Act. DB, 77, 2002.
- BSS 17.1.4.01:1977 Nature protection. Hydrosphere. Water quality indicators. A method for determining smell, color and temperature.
- BSS EN ISO 10523:2012 Water quality - Determination of pH.
- BSS EN ISO 5814:2012 Water quality - Determination of dissolved oxygen - Electrochemical probe method.
- BSS EN 27888:2000 Water quality - Determination of electrical conductivity.
- BSS ISO 6059:2002 Water quality - Determination of the sum of calcium and magnesium - EDTA titrimetric method.
- BSS EN 1899-2:2004 Water quality - Determination of biochemical oxygen demand after n days.
- BSS EN ISO 6878:2005 Water quality - Determination of phosphorus - Ammonium molybdate spectrometric method.
- BSS ISO 7150-1:2002 Water quality - Determination of ammonium - Part 1: Manual spectrometric method.
- BSS EN 26777:1997 Water quality - Determination of nitrite - Molecular absorption spectrometric method.
- BSS EN ISO 10304-1:2009 Water quality - Determination of dissolved anions by liquid chromatography of ions - Part 1: Determination of bromide, chloride, fluoride, nitrate, nitrite, phosphate and sulfate.
- BSS EN ISO 17294-2:2016 Water quality - Application of inductively coupled plasma mass spectrometry.
- Chinery, M. (1999). *Insects*. Harper Collins Publishers, 256.
- Coulloudon, B. et al. (1999). Sampling Vegetation Attributes, Technical Reference 1734-4, Bureau of Land Management. Denver, Colorado. BLM/RS/ST-96/002+1730 online @ www.blm.gov/nstc/library/pdf/sampleveg.pdf.
- Decision No. 122/02.03.2007 of the Council of Ministers Directive 92/43/EEC.
- Delipavlov, D., Cheshmedzhiev, I., Popova, M., Terzijski, D., & Kovachev, I. (2003). *Handbook of Plants in Bulgaria*. Academic Publishing House of Agricultural University, Plovdiv, 592.
- EN ISO 5667-3:2003/AC:2007 Water quality - Sampling - Part 3: Guidance on the preservation and handling of water samples (ISO 5667-3:2003).
- Ganeva, A., Rusakova, V., Gogushev, G., Dimitrov, M., Zhelev, P., Ivanov, P., Tsonev, R., Ivanova, T., Belev, T., Gusev, Ch. (2005). Guide for the designation of habitats of European importance in Bulgaria. World Wildlife Fund, Danube-Carpathian Program, Green Balkans Federation, Sofia.
- Gartsyanova, K., Genchev, S., Kitev, A., & Varbanov, M. (2023). Assessment of physic-chemical status of waters in selected sampling sites of Chepelarska River, Bulgaria. *Forestry Ideas*, 29, 2(66), 216-225.

- Gecheva, G., Stankova, S., Varbanova, E., Kaynarova, L., & Georgieva, D. (2023). Macrophyte-Based Assessment of Upland Rivers: Bioindicators and Biomonitorers. *Plants*, 12, 1366.
- Gruev, B., & Kuzmanov, B. (1994). *General biogeography*. UI "St.Kliment Ohridski", Sofia.
- Gusev, Ch., & Bancheva S. Methodology for monitoring higher plants.https://eea.government.bg/bg/bio/nsnbr/praktichesko-rakovodstvo-metodiki-za-monitoring-i-otsenka/Metodika_monitoring_Rastenia.pdf
- Interim overview of the significant water management issues in East Aegean river basin management district. https://earbd.bg/indexdetails.php?menu_id=845
- Karapetkova, M., & Zhivkov, M. (2006). *Fish in Bulgaria*. GeaLibris, Sofia, 216.
- Kehajov, D., Zahariev I., Komitov G. (2016). Development of machine for removing rose rods from area between rows. *European Journal of Technical and Natural Sciences*, 4, 27-29.
- Kehayov, D., Zahariev, I., & Mitkov, I. (2017). Technologies for the use of residual biomass from the production of oil rosen Bulgaria. *Proceedings of University of Ruse*, 56(1.1.), 67-72.
- Kehayov, D., Zahariev I., & Genkova P. (2022). Influence of the Type of the spraying on same technological and economic indicators in Pesticide Treatment of Vineyards. *Scientific Papers. Series B, Horticulture, LXVI*(1), 807-811.
- Kehajov, D., Bojkov, I., Zahariev, I., & Hristova, G. (2023). Electric drive to the sowing apparatus of the Saxonia A200seeder. *Agricultural Science & Technology*, 15(1), 60-64.
- Kolcheva, K. (2020). *Water policy and management of water resources in the world and in Bulgaria*. Plovdiv University Publishing House "Paisii Hilendarski", 262.
- Kolcheva, K., Varbanov M., & Gartsyanova K. (2023). Status, problems and solutions concerning surface water management in Bulgaria. *Scientific Papers. Series E. Land Reclamation, Earth Observation & Surveying, Environmental Engineering, XII*, 258-266.
- Kottelat, M., & Freyhof, J. (2007). *Handbook of European freshwater fishes*. Publications Kottelat, Cornol and Freyhof, Berlin, 646.
- Marinov, M. (2000). Pocket Field Guide of Dragonflies in Bulgaria. Publishing house "Eventus", Sofia, 104.
- NATURA 2000. http://natura2000.moew.government.bg/PublicDownloads/Auto/PS_SCI/BG0000194/BG0000194_PS_16.pdf
- Order No. RD-688/ 25.08.2020 of the Ministry of Internal Affairs and Communications
- Ordinance No. H-4 of 14.09.2012 Sugar characterization of surface waters. SG No. 22/2012
- Park, J., Sakelariava L., Varadinova E., Evtimova E., Evtimova V., Vidinova Y., Tyufekchieva V., Georgieva G., Ihtimanska M., & Todorov M. (2023). Taxonomic Composition and Dominant Structure of the Macrozoobenthos in the Maritsa River and Some Tributaries, South Bulgaria. *Acta Zool. Bulg., Supplement*, 16, 61-74.
- Plan for the management of the river basins of the Eastern White Sea region, 2022-2027.
- Radeva, K., & Seymenov, K. (2021). Surface Water Pollution with Nutrient Components, Trace Metals and Metalloids in Agricultural and Mining-affected River Catchments (A Case Study for Three Tributaries of the Maritsa River, Southern Bulgaria). *Geographica Pannonica*, 25(3), 214-225.
- Red Book of the Republic of the Republic of Bulgaria, item 1. Plants and mushrooms. <http://e-ecodb.bas.bg/rdb/bg/vol1/>
- Red Book of the Republic of Bulgaria, item 2. Animals. <http://e-ecodb.bas.bg/rdb/bg/vol2/>
- Red Book of the Republic of Bulgaria, item 3. Natural habitats. <http://e-ecodb.bas.bg/rdb/bg/vol3/>
- Reports on the state of water bodies on the territory of the IDB for the period 2012-2021.
- Standard Form Protected Area BG0000194 "Chaya River" https://natura2000.egov.bg/EsriBg.Natura.Public.Web.App/PublicDownloads/SDF/Site_BG0000194.pdf
- Waste Management Law. State Gazette, 6p.53/ 2012 г.
- Zahariev, I., & Kehayov, D. (2016). Determining the Location of the Assembly Center for Extrusion the waste from Rose production in Republic of Bulgaria. *Scientific Papers. Series A. Agronomy, LIX*, 552-558.
- Zaharieva, R. (2023). Parasites and Parasite communities of *Squalius orpheus* Kottelat & Economidis, 2006 from the Chepelarska River. *Scientific Papers. Series D. Animal Science, LXVI*(2), 696-705.

VARIATIONS OF PHYSICO-CHEMICAL PARAMETERS IN SULINA BRANCH AND ADJACENT MEANDERS DURING TWO SEASONS IN 2023

Ana Bianca PAVEL, Florin DUTU, Gabriel IORDACHE,
Catalina GAVRILA, Irina CATIANIS, Laura DUTU

National Institute for Research and Development on Marine Geology and Geo-ecology
(GeoEcoMar), 23-25 Dimitrie Onciul Street, Bucharest, Romania

Corresponding author email: laura.dutu@geocomar.ro

Abstract

The Sulina Branch, situated in the Delta's midpoint, features a distinct straight course requiring continuous dredging for maritime navigation. Stretching 71 km, it conveys 18% of the Romanian lower sector of Danube's water and historically served as a pivotal fluvial transport route, despite navigational challenges posed by sinuities. It underwent a significant transformation that shortened it by 21.2 km (25.30%), converting it into a nearly straight navigable canal. This led to adverse effects like benthic habitat destruction, increased turbidity, and altered flooding patterns, impacting local ichthyofauna and avifauna. Navigation along the now straight Sulina Branch faced disruptions from sediment shoals at the mouth, due to the synergistic action of fluvial and coastal currents. In spring and autumn 2023, we measured physico-chemical parameters at 30 stations along Sulina Branch and adjacent Meanders, correlating them with bathymetry, water flow, and currents. Clear distinctions were observed, especially between upstream and downstream locations. Oxygen measurements both in spring and autumn, indicated good status water quality. Results demonstrated a good status in water quality at most stations during the study period.

Key words: meanders, physico-chemical parameters, Sulina branch, water quality.

INTRODUCTION

The Black Sea is the main recipient of liquid and solid contributions from Central Europe (via the Danube) and Eastern Europe (Ukrainian rivers like the Dniester, Dnieper, Southern Bug, Don, and Kuban). The catchment basin covers approximately 1864000 km², predominantly consisting of river basins from the northwest, notably the Danube (43.8%), Dniester, Bug, Dnieper, and Kuban. These rivers have a total discharge of about 276 km³/year, with the Danube contribution of approximately 70%. Current sedimentary processes on the continental shelf of the northwest Black Sea are significantly influenced by sediment contributions from rivers discharging into this area (Panin and Jipa, 1998), with the Danube playing a predominant role in the sedimentation of the northwest shelf of the Black Sea (Panin, 1999). These rivers transport and deposit around 61×10^6 tons of sediment on the continental shelf annually, with the Danube accounting for about 81% of this (Wong et al., 1994). Other tributaries are not as significant in providing water and sediment to the northwest Black Sea, mainly because they deposit their

sediment load into lagoon, separated from the sea by coastal barriers (Panin, 1999). In the last century, numerous rivers have been impacted by dam construction, affecting morphology, hydrology, and sediment transfer (Williams and Wolman, 1984; Knox, 2006; Assani and Petit, 2004). Furthermore, anthropogenic interventions on rivers, such as embankments, meander cuts, caused significant changes of their longitudinal profiles (Keller, 1972). On the Danube, flood control, navigation improvement, irrigation systems, and energy production have driven engineering works since the 17th century, involving the construction of dams, reservoirs, dikes, bank protections, canals, dredging, and meander straightening. The Danube's entire course has a hydroelectric potential of 29,000 MW, achieved by constructing numerous dams (850, including 700 on tributaries), such as at Bad Abbach, KM 2041, Regensburg KM 2381, Geisling KM 2354, and Gabčíkovo KM 1842. Post-1970, hydroelectric developments in Romania, notably the Iron Gates I and II dams and hydrotechnical arrangements on Romanian tributaries (Jiu, Olt, Vedea, Siret) disrupted the Danube's lower course hydrological and

sedimentary functions. The average long-term liquid discharge measured at the delta's entrance (Tulcea hydrometric station) is $6,550 \text{ m}^3/\text{s}$, resulting from the catchment's water balance (average precipitation of 816 mm, average evaporation of 547 mm) (Almazov et al., 1963). Anthropogenic alterations in the river's upper and middle basin have reduced the downstream sediment flow. Since 1970, the construction of the Iron Gates I and II dams and hydrotechnical works on Romanian Danube tributaries have affected the regime of liquid and solid discharges downstream. These works have led to a significant reduction in sediment discharge at the Danube's mouths. Over 130 years, Bondar et al. (1991) have estimated the Danube's average sediment discharge at its mouths at $51.7 \times 10^6 \text{ tons/year}$, with a progressive decrease over time. Later, Panin and Jipa, 2002; Walling, 2003 have estimated that sediment discharge has decreased from $67.5 \times 10^6 \text{ tons/year}$ to $25\text{-}30 \times 10^6 \text{ tons/year}$. The Danube River, besides its natural biodiversity component, holds significant economic and political importance for Europe. The delta formed at its mouth reflects the evolution of climatic and anthropogenic conditions that have intensely transformed the natural state of the watershed over the last centuries. These basin-scale changes (morphological, hydrological, sedimentological, etc.) have been amplified by climate changes within the delta, causing variations in liquid and solid fluxes and local adjustments in channel morphology, significantly affecting local hydro-sedimentary dynamics. At its sea outflow, the Danube has created one of Europe's most significant deltas over an area of 5800 km^2 , the Danube Delta, designated a UNESCO World Heritage Site and a biosphere reserve. Its geographical location, acting as a "buffer zone" for the Danube-Delta-Black Sea system, begins at the first bifurcation of the Danube (at Ceatal Izmail) 83.8 kilometres from the mouth (Gâstescu, 2009). Here, the Danube splits into two branches, the northern Chilia and the southern Tulcea, which further divides into the Sulina and Sfântu Gheorghe branches. The Chilia branch forms a secondary delta at its mouth. The Sulina branch, the central and navigable channel thanks to rectification works, is extended into the sea, with shores consolidated against erosion to

maintain the maritime navigation. The Sfântu Gheorghe branch, morphodynamically active at its mouth, forms a secondary delta. Among the main distributaries, the Danube has created a network of primary and secondary channels, both natural and artificial, facilitating water and sediment circulation from the main branches to inter-distributary depressions, vital for the existence and evolution of deltaic ecosystems (Panin and Jipa, 2002). Important developments began with the establishment of the European Commission of the Danube at Galați in 1856 (Gâstescu & Știucă, 2008). Early in the 20th century, the Romanian Fishing Authority initiated delta channel regularization works to improve internal navigation. These anthropogenic interventions have influenced the Danube's flow regime, the sediment balance in the coastal area between Sulina and Sf. Gheorghe, and the morphology of the northwest Black Sea shelf (Rose, 1992; Rose et al., 1993).

MATERIALS AND METHODS

Study area

The Sulina Branch, the Danube's central distributary within the delta, has garnered special interest due to meander cuts and developments for navigation between 1858 and 1902. Initially sinuous and 83 km long with varying widths and depths, hydraulic works deepened the channel from less than 2.5 m in 1857 to at least 9.5 m by 1959, altering the Danube's flow regime through increased discharge (Bondar & Papadopol, 1972; Bondar & Panin, 2000). Major rectifications, including cutting two meanders known as the "Big M" (Figure 1), shortened the river and facilitated navigation by ensuring a constant width and depth (Bondar & Panin, 2000; David, 2010).

These interventions increased the liquid flow from 7-9% to 16-17% by 1921, and up to 18-20% presently, significantly changing the hydrological and sedimentary conditions, affecting the annual distribution of liquid and solid discharges (Bondar & Papadopol, 1972). This led to adverse effects like benthic habitat destruction, increased turbidity, and altered flooding patterns, impacting local ichthyofauna and avifauna (Gâstescu, 2009).

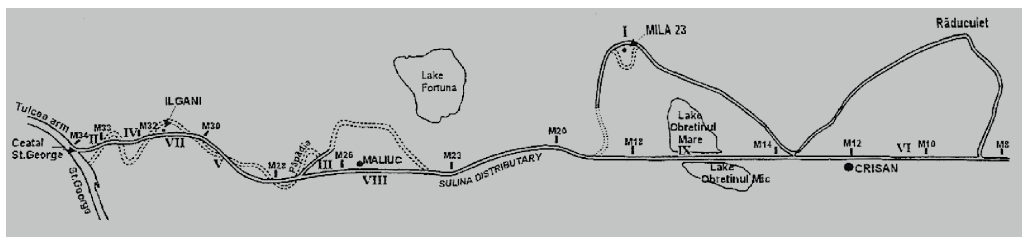


Figure 1. Rectified meanders of the Sulina arm in the period 1968-1902, after Panin, 1999

Navigation along the now straight Sulina Branch faced disruptions from sediment shoals at the mouth, due to the synergistic action of fluvial and coastal currents (Dutu et al., 2023).

In spring and autumn 2023, we measured physico-chemical parameters at 30 stations along Sulina Branch and adjacent Meanders, analysing them in relation with hydrodynamic measurements that were performed with an Acoustic Doppler Current Profiler (ADCP) across 18 profiles (Table 1, Figure 2). Water

samples were collected from various locations, including the Sulina Branch, straightened meanders, natural channels, and lakes, as well as areas upstream and downstream of the bifurcation with the main distributary. Measurements were also made on the artificial channel, the cut meanders of Maliuc and the "Big M" (Old Danube), and the connecting channels to the deltaic lakes (Caraorman Channel and Sontea Channel).

Table 1. Sampling stations collected from the studied areas

Station	Location	Depth (m)	Coordinates	
			Lat. (φ)	Long. (λ)
SU23-01	Cârjălă Channel	2	45°10'31.2"N	29°07'02.6"E
SU23-02	Cârjălă Channel	3.5	45°11'18.3 "N	29°05'53.9"E
SU23-03	Sulina Branch Mm 18+300	14	45°10'41.0"N	29°14'15.4"E
SU23-04	Sulina Branch, Upstream Crișan, Mm 14+700	11.4	45°10'34.1"N	29°20'22.3"E
SU23-05	Old Danube, Downstream Lebăda	5.4	45°10'53.9"N	29°20'45.8"E
SU23-06	Old Danube, Downstream Mila 23 (Meander)	8.4	45°13'23.8"N	29°15'47.8"E
SU23-07	Old Danube, Downstream Mila 23 (Meander)	6.4	45°10'49.8"N	29°21'51.6"E
SU23-08	Old Danube, Downstream Mila 23 (Meander)	3.8	45°13'14.9"N	29°14'04.4"E
SU23-09	Șonțea Channel	3.5	45°13'06.1"N	29°13'32.9"E
SU23-10	Fortuna Lake	1.9	45°12'42.5"N	29°08'07.7"E
SU23-11	Ledianca Channel (Olguța)	4	45°14'03.6"N	29°14'03.4"E
SU23-12	Eracle Channel	3	45°14'06.3"N	29°16'07.6"E
SU23-13	Trei Ozere lake	3	45°14'29.3"N	29°19'09.4"E
SU23-14	Bogdaproste lake	1.5	45°13'54.9"N	29°21'32.3"E
SU23-15	Raducu Lake	1.9	45°14'17.5"N	29°27'31.9"E
SU23-16	Bogdaproste Channel	4	45°12'25.9"N	29°22'53.5"E
SU23-17	Old Danube (Meander)	3.5	45°10'41.2 "N	29°21'21.3"E
SU23-18	Magearu Channel	1.9	45°13'10.8 "N	29°29'49.9"E
SU23-19	Old Danube (Meander)	7.4	45°13'22.2"N	29°27'01.7"E
SU23-20	Old Danube (Meander)	5.7	45°11'31.8"N	29°29'03.2"E
SU23-21	Sulina Branch, Mm 8+700	15	45°10'23.0"N	29°28'02.0"E
SU23-22	Sulina Branch, Mm 8+500	14.8	45°10'20.5"N	29°28'54.2"E
SU23-23	Sulina Branch, Downstream Lebăda, Mm 13+000	11.9	45°10'23.7"N	29°28'45.3"E
SU23-24	Canton Dovnica Channel	1.9	45°14'01.7"N	29°24'55.8"E
SU23-25	Sulina Branch, Mm 10+800	14.4	45°10'28.0"N	29°25'52.0"E
SU23-26	Old Danube (Meander)	7.7	45°12'24.8"N	29°18'26.6"E
SU23-27	Sulina Branch Mm 16+000	15.3	45°10'37.2"N	29°17'24.4"E
SU23-28	Caraorman Channel	2	45°10'02.1"N	29°20'55.8"E
SU23-29	Magearu Channel	2.5	45°14'31.8"N	29°30'20.0"E
SU23-30	Eracle Channel	4	45°15'06.3"N	29°18'15.8"E

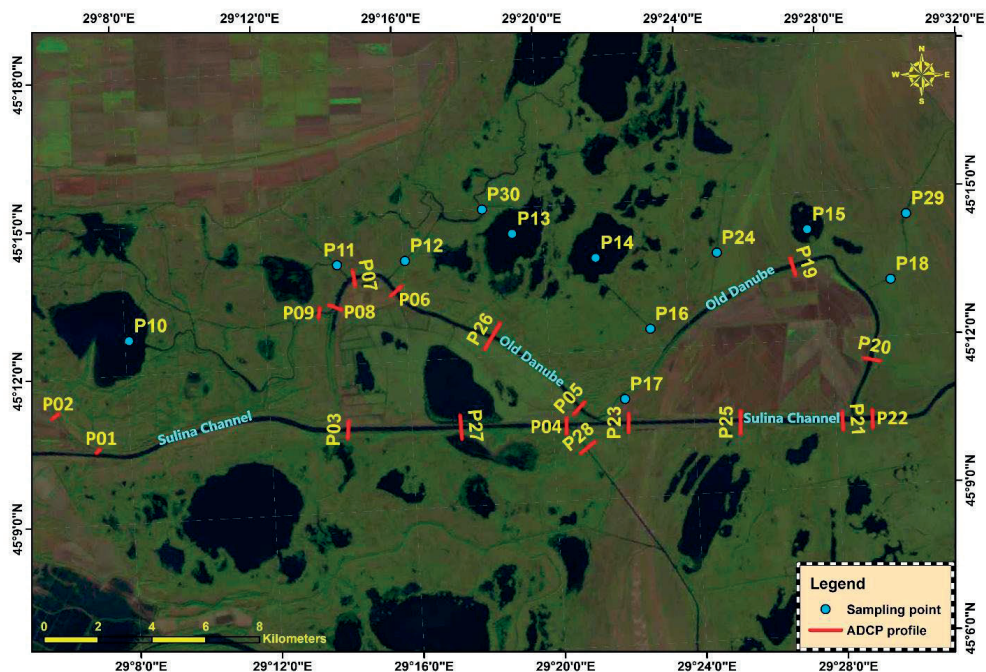


Figure 2. Sampling stations on the Sulina Branch, the straightened meanders of "Maliuc" and "The Big M", the lateral connection channels, and in deltaic lakes

Methodology for analyzing the physico-chemical parameters of water

To evaluate the physico-chemical parameters of aquatic environments within the study area, the following measurements were conducted: Chlorophyll (RFU), Conductivity ($\mu\text{S}/\text{cm}$), Dissolved Oxygen (DO, mg/L), Oxygen saturation (ODO, %), Salinity psu, Total Algal Content (TAL) PC RFU, Total Dissolved Solids (TDS) mg/L , Turbidity (FNU), pH and Temperature ($^{\circ}\text{C}$).

For these measurements, the multiparameter instrument model EX02, produced by YSI – USA, was used (Figure 3 left).

Methodology for hydrodynamic measurements (velocities, currents, and water discharges)

The measurements of water flow velocity, discharges, and currents (speeds and directions) were conducted using a high-accuracy ADCP (Acoustic Doppler Current Profiler) system. This system utilizes the Doppler Effect (Acoustic Doppler Current Profiler River Ray 600 kHz produced by Teledyne RD Instruments (Figure 3 right).



Figure 3. Multiparameter instrument model EX02 (left); ADCP River Ray 600 kHz (right)

RESULTS AND DISCUSSIONS

The lotic ecosystem complexes represented by the Danube River and the Danube Delta, according to Annex XI of the WFD, belong to the Pontic Ecoregion (12). Based on the parameters described in the Synthesis of the Project Management Plans at the Basin/Hydrographic Areas level (2022), for the Danube and the Danube Delta, 19 types of natural watercourses have been defined. The areas studied are included in RO15 The Danube River - Isaccea - The Danube Delta.

Hydrological regime during the measurement period

During the measurement period, the water levels of the Danube showed significant fluctuations at both hydrometric stations located near the measurement area, Tulcea and Sulina. In May, a

decrease in water level of up to 31 cm in Tulcea and 9 cm in Sulina was recorded. In October, there was a decrease in water level of up to 21 cm at Tulcea, while at Sulina, the level varied, initially increasing by 15 cm followed by a decrease of 10 cm (Table 2, Figure 4).

Table 2. Water levels (cm) of the Danube at the Tulcea and Sulina hydrometric stations during the measurement period

Date	Hydrometric Stations		Date	Hydrometric Stations	
May	Tulcea	Sulina	October	Tulcea	Sulina
08.05.2023	277	103	09.10.2023	56	40
09.05.2023	274	105	10.10.2023	54	50
10.05.2023	269	98	11.10.2023	52	50
11.05.2023	261	92	12.10.2023	49	55
12.05.2023	255	90	13.10.2023	41	49
13.05.2023	254	89	14.10.2023	37	50
14.05.2023	250	90	15.10.2023	38	50
15.05.2023	246	94	16.10.2023	35	45

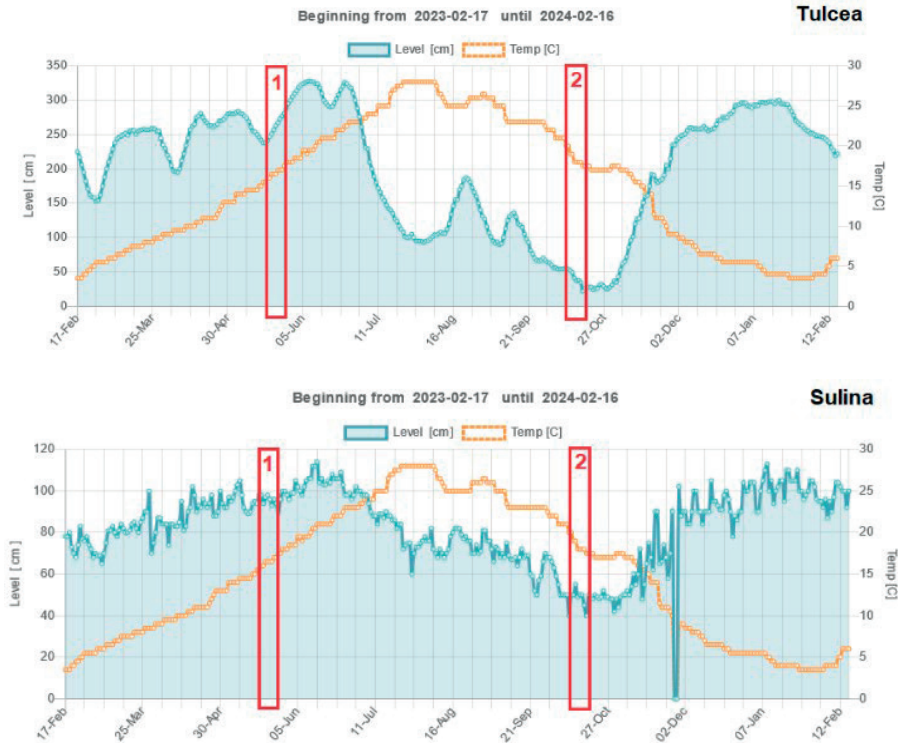


Figure 4. Water Levels of the Danube at the Tulcea and Sulina Hydrometric Stations During the Measurement Periods in May and October
(<https://edelta.ro/cote-dunare-365-de-zile>)

Hydrodynamic measurements (velocities, currents, and water discharges)

In May, a total of 18 hydrometric profiles were conducted. At the time of measurement, the Sulina Branch was transporting a discharge of approximately 1490 m³/s before entering in the "Big M" meander area (profile SU23-03). Downstream, the discharge increased to 1720 m³/s (profile SU23-22) due to water exchanges within the delta. Water flow in the old Maliuc meander channel proceeds from the Sulina Branch. In the "Big M" meander, the discharge is significantly reduced (between 177 and 269 m³/s). The average water velocities ranged between 0.14 and 1.3 m/s, with maximum

velocities reaching their highest at profile SU23-21, at 2.67 m/s. In October, Sulina Branch was transporting a measured discharge of approximately 641 m³/s before entering in the "Big M" meander area (profile SU23-03). Downstream, the discharge decreased to 626 m³/s (profile SU23-22). Water flow in the old Maliuc meander channel, even at low water levels, proceeds from the Sulina Branch with a discharge of 5-6 m³/s. In the "Big M" meander, the discharge is also significantly reduced (between 13.6 and 42.9 m³/s). The average water velocities ranged between 0.01 and 0.54 m/s, with maximum velocities reaching their highest at profile SU23-23, at 2.18 m/s (Figures 5 and 6).

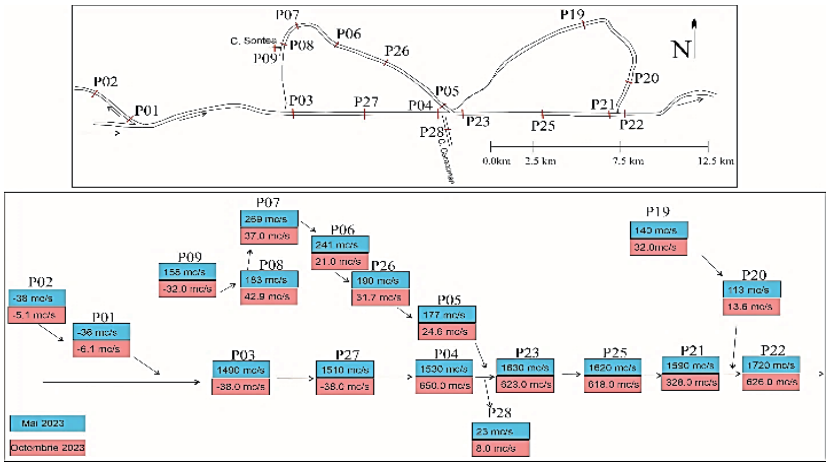


Figure 5. Water Discharge Distribution on the Sulina Branch and the Straightened Meanders During the Two Study Periods

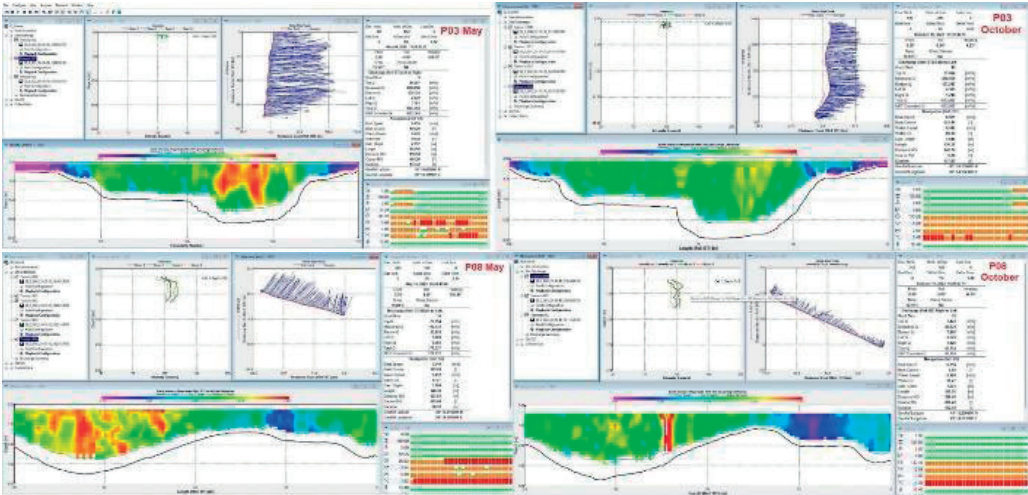


Figure 6. Examples of hydrometric profiles

Analysis of the physico-chemical parameters of water

Water serves as a nexus, integrating diverse environmental concerns and strategies across various human activities, including agriculture, economy, transport, energy, industry, and environmental protection. It is a pivotal factor in development, indispensable for the survival of aquatic life and the well-being of humans, encompassing needs such as sustenance, hygiene, comfort, and health. Water quality is significantly impacted by industrial and agricultural development, energy production, and domestic activities (Vasilii et al., 2021). The advent of climate change necessitates a resilient and unified approach to water management (Poff et al., 2002; Capon et al., 2013). The EU Water Framework Directive (WFD, 2000/60/EC) mandates both qualitative and quantitative water management to preserve healthy aquatic

ecosystems and achieve "good status" for water quality. Conformity with Romanian National Environmental Standards, specifically Normative No. 161/2006 (Approval of the Norm Concerning the Reference Objectives for the Surface Water Quality Classification, Official Journal of Romania, Part 1, No 511 bis), guides the assessment of surface water quality, employing environmental standards to measure indicators like total dissolved solids (https://en.wikipedia.org/wiki/Total_dissolved_solids) and turbidity (STAS 6323 – 88). The evaluation process also aligns with Normative 161/2006, which sets the criteria for classifying surface water quality and assessing ecological status. The aggregated physico-chemical data of sampling sites are shown in Table 3, representing the range (minimal and maximal) and average (\pm standard deviation) values of each parameter per season.

Table 3. A synopsis of the physico-chemical parameters of water surface samples

The physico-chemical parameters in the studied areas, .					
May 2023					
	Chlorophyll RFU	ODO % sat	ODO mg/L	Sal psu	TAL PC RFU
Min	0.34	42.94	4.28	0.17	0.21
Max	5.16	99.32	9.77	0.24	5.52
Mean \pm SD	1.14 \pm 1.11	85.57 \pm 14.55	8.24 \pm 1.29	0.19 \pm 0.01	0.72 \pm 0.95
	TDS mg/L	Turbidity FNU		pH	Temp. °C
Min	230.59	0.30		7.55	15.18
Max	318.69	14.89		8.31	16.12
Mean \pm SD	260.86 \pm 13.07	7.24 \pm 4.23		8.04 \pm 0.22	15.71 \pm 0.26

The physico-chemical parameters in the studied areas,					
October 2023					
	Chlorophyll RFU	ODO % sat	ODO mg/L	Sal psu	TAL PC RFU
Min	0.34	54.80	5.70	0.17	0.08
Max	4.45	106.53	11.16	0.21	2.41
Mean \pm SD	0.97 \pm 0.79	90.05 \pm 9.79	8.70 \pm 0.93	0.19 \pm 0.01	0.55 \pm 0.51
	TDS mg/L	Turbidity FNU		pH	Temp °C
Min	228.04	1.02		7.79	12.95
Max	277.53	20.27		8.64	19.66
Mean \pm SD	257.69 \pm 9.29	8.07 \pm 4.62		8.21 \pm 0.18	17.04 \pm 2.25

The physico-chemical parameters values generally varied within the limits set by the environmental standards. The average temperature distribution observed during sampling periods matched anticipated seasonal fluctuations (Radan et al., 2000). Oxygen levels in most sampling locations either exceeded or fell below of the environmental standards' maximum allowable concentrations. Notably,

reduced oxygen concentrations were recorded within the stations SU23-24 Canton Dovnica Channel (4.28 mg/l) and the SU23-30 Eracle Channel (5.31 mg/l) and SU23-11 Ledianca Channel (Olguța) (5.41 mg/l) in May, and a concentration of 5.70 mg/l was observed in October only in one station SU23-24 Canton Dovnica Channel. Dissolved Oxygen (DO) levels at these stations categorize them within

water quality Classes III and IV, as they exhibit values below 9.00 mg/l threshold requisite for Class I status. Conversely, the rest of the stations are classified within Classes I and II. A high concentration of dissolved oxygen (DO) is critical for the sustenance of aquatic ecosystems. It is recommended that a minimum DO concentration of 5 mg/l be maintained to support aquatic life effectively. Optimal fish health is also associated with this DO threshold. Different species exhibit varying levels of sensitivity to low DO concentrations; however, it is generally observed that fish experience distress when DO levels decline to between 2 and 4 mg/l. Mortality in fish populations is commonly observed when DO concentrations fall below 2 mg/l (https://niwa.co.nz/our-science/freshwater/tools/kaitiaki_tools/impacts/dissolved-oxygen).

Salinity and total dissolved solids measurements fell within the limits set by environmental guidelines. In the water samples evaluated, the Total Dissolved Solids (TDS), encompassing both organic and inorganic matter, ranged within the following values: 230.59 to 318.69 mg/l with a mean value of 260.86 ± 13.07 mg/l in May; and from 228.04 to 277.53 mg/l with a mean value of 257.69 ± 9.29 mg/l in October. pH levels across the study areas varied, indicating a gradual increase towards slightly alkaline water

conditions, as depicted in Table 2. The turbidity of water samples yielded a range from 0.30 to 14.89 Formazin Nephelometric Units (FNU), with an average value of 7.24 ± 4.23 FNU in May. In October, the measured turbidity spanned from 1.02 to 20.27 FNU, with an average of 8.07 ± 4.62 FNU. The observed increase in turbidity in some stations, in surface waters may be attributed to factors such as phytoplankton activity, organic detritus, and resuspended bottom sediments. The average values of water quality parameters varied according to local environmental conditions, sampling locations, and seasonal water budget changes. The values recorded for the physical-chemical parameters in the present study are generally comparable with other previous investigations acquired at different water bodies from the DDBR area (Radan et al. 2000, Munteanu et al. 2012). Based on the Euclidian similarity index (Figure 7), it can be observed that the stations were grouped according to the variation in water discharge. Three clusters were formed: one with stations on the Sulina Branch (SU23-21, SU23-22, SU23-23, SU23-25, SU23-03, SU23-04, SU23-27), one with stations on the Old Danube - Meanders (SU23-20, SU23-05, SU23-08, SU23-26, SU23-09, SU23-19, SU23-06, SU23-07), and a third with the channels (SU23-28, SU23-02, SU23-01).

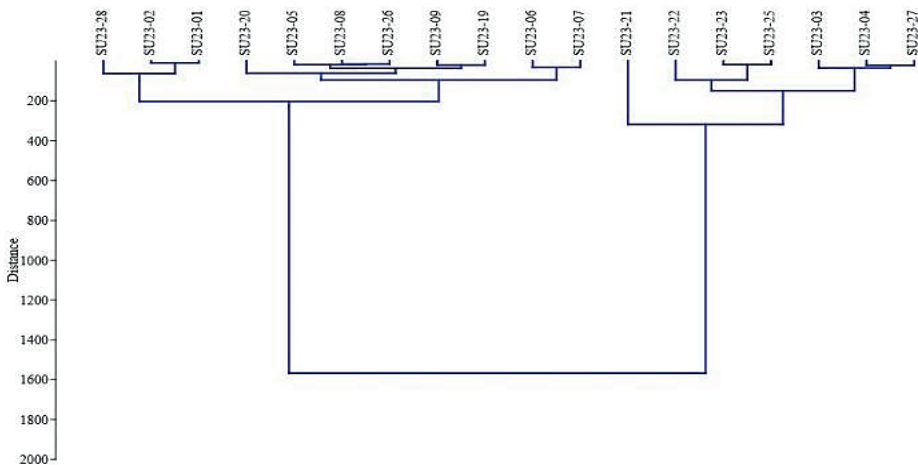


Figure 7. Similarity index based on Euclidian transformed data

The highest discharge in both periods was recorded on the Sulina Branch, followed by the Old Danube-Meanders area, with the lowest

discharge on the channels connecting the meander lakes. Water discharge was not measured for the lake stations and several

channel stations (SU23-10, SU23-11, SU23-12, SU23-13, SU23-14, SU23-15, SU23-16, SU23-17, SU23-18, SU23-24, SU23-29, SU23-30). High turbidity values were recorded at the Sulina Branch, where high discharge was observed, and also at the Carjala channel in two stations, in both seasons, where a negative discharge was recorded. As expected, high concentrations of dissolved oxygen, pH, and chlorophyll were found in the Caraorman and Carjala channel stations, followed by the meander area, where the water discharge was lower. The lowest dissolved oxygen concentration was recorded on the Sulina Branch in both periods, May and October.

CONCLUSIONS

This investigation aims to address an existing deficiency in the scientific literature by documenting the physicochemical attributes of the surface water within the study area's water-rich ecosystems. The quality of water in the analyzed regions is influenced by a confluence of unique and localized factors, such as variations in the water level of the Danube River, the flood regime, meteorological dynamics, as well as diurnal and seasonal changes. Additionally, anthropogenic activities in the vicinity of the Danube Delta, particularly around the Sulina Branch, meanders, channels, and selected lakes, also play a significant role.

The study's findings indicate that the majority of the evaluated physico-chemical parameters conform to the standards of Classes I and II, which correspond to very good and good ecological statuses, respectively. However, at certain stations, the parameters were consistent with the criteria for Classes III and IV, denoting moderate and poor ecological conditions.

The analysis based on the Euclidian similarity index reveals a clear correlation between water flow and the distribution of physico-chemical parameters across different locations in the studied areas. The formation of three distinct clusters suggests that hydrodynamic conditions significantly influence water quality. The Sulina Branch, with the highest water discharge, exhibited elevated turbidity levels, indicating a strong association between flow dynamics and sediment transport. Conversely, the channels connecting meander lakes, characterized by the lowest discharge rates, showed variations in

water quality parameters, including dissolved oxygen, pH, and chlorophyll concentrations. Notably, areas with no water discharge measurements, such as some lake and channel stations, underscore the complexity of hydrodynamic impacts on water quality. High turbidity in the Carjala channel, despite negative discharge rates, further underscores this complexity. The findings suggest that water management strategies in the Danube Delta should consider the intricate relationships between hydrodynamics and water quality to ensure ecological health and sustainability.

ACKNOWLEDGEMENTS

This work was carried out as part of the project "Analysis of the potential for sustainable use of vegetation specific to the Danube-Delta system Danube-Black Sea - D3MN" POC/78/1/2. The research leading to these results was financed from the Romanian National Authority for Scientific Research and Innovation - ANCSI - "Nucleu Program, PN 23 30 03 04 - Development of an Intelligent System for Monitoring Hydrological Connectivity in the Humanized Fluvial Ecosystems of the Danube Delta and PN 23 30 03 02 – The impact of anthropogenic and climate changes, vulnerabilities and adaptation measures to increase resilience in the lakes of the Danube Delta Biosphere Reserve.

The authors also thank the anonymous reviewers for all suggestions provided for improving the manuscript.

REFERENCES

- Almazov, A.A., Bondar, C., Diaconu, C., Ghederim, V., Mihailov, A.N., Mita, P., Nichiforov, I.D., Rai, I.A., Rodionov, N.A., Stanescu, S., Stanescu, V., Vaghin, N.F. (1963). *Zona de vărsare a Dunării. Monografie hidrologică*. pp. 396, Ed. Tehnică, București. [in Romanian]
- Assani, A.A., Petit, F. (2004). Impact of hydroelectric power releases on the morphology and sedimentology of the bed of the Warche River (Belgium). *Earth Surface Processes and Landforms*, 29(2), 133-143.
- Bondar, C., Panin, N. (2000). The Danube Delta Hydrologic Database and Modeling, *Geo-Eco-Marina*, 5-6, 5-53.
- Bondar, C., Papadopol, A. (1972). Evoluția albiei Canalului Sulina. *Transporturi auto, navale și aeriene, Vol. II (19)*, Nr. 3, 144-147. [in Romanian]
- Bondar, C., State, I., Cernea, D., Harabagiu, E., (1991). Water flow and sediments transport of the Danube at its

- outlet into the Black Sea. *Meteorol. si Hidrol.*, 21(1), 21-25.
- Capon, S.J., Chambers, L.E., Mac Nally, R., Naiman, R.J., Davies, P., Marshall, N., Pittcock, J., Reid, M. et al. (2013). Riparian ecosystems in the 21st century: Hotspots for global change adaptation. *Ecosystems*, 16, 359–381.
- David, A. (2010). Lucrările tehnice efectuate pe dunărea maritimă în perioada 1918-1938. *Analele Universității „Dunărea de Jos” Galați, Seria 19, Istorie*, 119-144. [in Romanian]
- Dutu, F., Tiron Dutu, L., Catianis, I. (2023). Dramatic Reduction of The Water and Sediment Fluxes in A Human Modified Meandering Ecosystem from The Danube Delta, Romania, *Scientific Papers-Series E-Land Reclamation Earth Observation & Surveying Environmental Engineering*, 12, 267-274.
- Gâstescu, P. (2009). The Danube Delta biosphere reserve. Geography, biodiversity, protection, management, *Rev Roum Géogr.*, 53(2), 139–52.
- Gâstescu, P. & Știucă, R. (2008). *The Danube Delta - A Biosphere Reserve*. CD Press Publishing House, Bucharest, 400. [in Romanian, with Contents and Introduction in English]
- Keller, E.A., (1972). Development of alluvial stream channels. *Bulletin of the Geological Society of America*, 83, 1531-1536.
- Knox, J.C. (2006). Floodplain sedimentation in the Upper Mississippi Valley: Natural versus human accelerated. *Geomorphology*, 79, 286–310.
- Munteanu, I., Tuzlaru, C., Cioroiu, L., Vasilescu, G., Raicu, M., Bascau, F., Raileanu, G, Nitu, M., Varzaru, E. (2012). *Report on the Danube Delta Biosphere Reserve - State of the Environment in 2012*, elaborated by the Ministry of Environment and Climate Change [in Romanian]
- Order no. 161/2006 - Standard on surface water quality classification for determination of the ecological status of Water bodies, Annex C - Elements and physico-chemical quality standards in water, published in Romanian Official Monitor, part I, no. 511 bis, from 13th of June, 2006.
- Panin, N. (1999). Danube Delta: Geology, Sedimentology, Evolution. Association des Sédimentologues Français, Maison de la Géologie, Paris, pp. 66.
- Panin, N., Jipa, D. (1998). Danube river sediment input and its interaction with the north-western Black Sea: results of EROS-2000 and EROS-21 projects. *Geo-Eco-Marina*, 3, 23-35.
- Panin, N., Jipa, D. (2002). Danube river sediment input and its interaction with the North - western Black Sea. *Estuarine, Coastal and Shelf Science*, 54, 551 – 562
- Poff, N.L., M.A. Brinson, M.A., Day, J.W. (2002). Aquatic ecosystems and global climate change: potential impacts on inland freshwater and coastal wetland ecosystems in the United States. Report of PEW Center on Global Climate Change, Arlington, Virginia, VA: 44.
- Rădan, S., Ganciu, A., Strechie, C. (2000). *Overview of the Long-term Ecological Research performed by GeoEcoMar in the Danube Delta, Romania*. In: Lajtha K. and Vanderbilt K., eds. 2000 - Cooperation in Long Term Ecological Research in Central and Eastern Europe, Oregon State University, Corvallis, OR, 101-112.
- Romanian Standard – STAS 6323 – 88 – Determination of turbidity
- Rose, P.M. (1992). Western Palearctic Waterfowl Census, IWRB, Slimbridge, UK
- Rose, P.M. and Taylor, V. (1993). Western Palearctic and South West Asia Waterfowl Census. IWRB, Slimbridge, UK.
- Vasiliu, D., Tiron Dutu, L., Bucse, A., Lupascu, N., Dutu, F. (2021), *Scientific Papers-Series E-Land Reclamation Earth Observation & Surveying Environmental Engineering*, 10, 258-264.
- Walling, D.E., Fang, D. (2003). Recent trends in the suspended sediment loads of the world's rivers. *Global and Planetary Change*, 39, 111– 126.
- Williams, G.P., Wolman, G.P. (1984). Downstream effects of dams on alluvial rivers. USGS circular, 781, 48.
- Wong, H. K., Panin, N., Dinu, C., Georgescu, P., Rahn, C. (1994). Morphology and post-Chaudian (Late Pleistocene) evolution of the submarine Danube fan complex. *Terra Nova*, 6, 502-511.
- <https://edelta.ro/cote-dunare-365-de-zile>
https://en.wikipedia.org/wiki/Total_dissolved_solids
https://niwa.co.nz/ourscience/freshwater/tools/kaitiaki_to_ols/impacts/dissolved-oxygen.

ENABLING SOFT SENSORS FOR WATER QUALITY MONITORING IN MULTI-TROPHIC AQUACULTURE SYSTEMS

**Stefan-Mihai PETREA^{1,2,4}, Ira-Adeline SIMIONOV^{1,2,5}, Alina ANTACHE^{1,2,6},
Aurelia NICA¹, Madalina CALMUC^{2,3}, Valentina CALMUC^{2,3}, Dragos CRISTEA⁴,
Puiu Lucian GEORGESCU^{2,3}**

¹"Dunarea de Jos" University of Galati, Food Science and Engineering Faculty,
111 Domneasca Street, Galati, Romania

²"Dunarea de Jos" University of Galati, REXDAN Research Infrastructure,
98 George Cosbuc Street, Galati, Romania

³"Dunărea de Jos" University of Galati, Faculty of Sciences and Environment,
111 Domneasca Street, Galati, Romania

⁴"Dunărea de Jos" University of Galati, Faculty of Economics and Business Administration,
59-61 Nicolae Balcescu Street, Galati, Romania

⁵"Dunărea de Jos" University of Galati, Faculty of Automatic Control, Computers,
Electrical Engineering and Electronics, 2 Stiintei Street, Galati, Romania

⁶"Alexandru Ioan Cuza" University of Iasi, 11 Carol I Blvd, Iasi, Romania

Corresponding author email: stefan.petrea@ugal.ro

Abstract

The paper aims to use machine-learning-based algorithms in order to enable and empower the integration of soft sensors for improving the economic sustainability of integrated multi-trophic recirculating aquaculture systems (IMRAS) through efficient and accurate water quality monitoring of nitrate (NO₃), the main key parameter for maintaining the sustainability of the IMRAS in various production scenarios. A 30-day trial was conducted in a sturgeon-tarragon IMRAS to develop a NO₃ soft sensor, based on a series of predictors such as pH, temperature, NH₄, NO₂, NO₃, conductivity (EC), P₂O₅, Ca and Mg, as well as to identify the prediction model peculiarities in various exploitation scenarios generated by the crops culture density. The results reveal the effectiveness of different learning algorithms as MLR and XGBoost (>80% accuracy) in developing solutions for supporting the water quality monitoring process in IMRASs, concluding that the intensity of production technologies must be considered as a determinant factor in upscaling the solutions to industrial level.

Key words: soft sensor, machine-learning, nitrate, water quality, multi-trophic aquaculture.

INTRODUCTION

The European Committee (EC) policy strategies, through its plan of transition from a Blue to a Green economy, emphasize the strategic orientation towards sustainable and competitive aquaculture within the European Union (EU) borders, which is targeted to be implemented within the period 2021-2030.

In order to support this desideratum, research oriented towards the identification of scalable and replicable innovative technical and technological solutions, based on artificial intelligence, which are able to support the maximization of sustainability degree associated with the emergent integrated production technologies, a multi-disciplinary analytical

framework must be considered and research niches that can improve various peculiar processes with the technology must be tackled. Since aquaculture is a major part of Blue Economic - Development, the shift toward a Green Economy imposes the extent of sustainable aquaculture systems and practices, limiting therefore their negative impact on the environment, mostly associated with the degree of production intensity. Thus, previous studies (Paepae et al., 2021; Petrea et al., 2023a) present integrated aquaponics as a feasible solution for limiting aquaculture wastes by using circular economy principles that consist of valorizing the wastes for obtaining a second crop production that can also be commercialized and, therefore, can contribute to the increase of economic

competitiveness, a fact confirmed by Bosma et al. (2017), Petrea et al. (2019), Asciuto et al. (2019) and Costache et al. (2021).

However, integrating aquaponics into already existing aquaculture conventional or recirculating aquaculture systems-based farms is a complex process, both from technical and technological perspectives, as resulting from various studies (Yildiz et al., 2017; Goddek et al., 2019). The most important process within an aquaponic system is related to nutrient management – thus, continuous water quality monitoring is imposed to limit potential dysfunctions which can have fatal impacts both for fish and plant production.

According to a previous study (Petrea et al., 2023b), nitrate is considered one of the most important water quality parameters in aquaculture systems and has an accumulation trend – this situation can be efficiently exploited by aquaponics technologies since nitrate is an essential nutrient during the plants culture process.

Petrea et al. (2023a) confirmed that soft sensors can be successfully used in aquaponics multi-trophic systems in order to accurately predict the concentration of essential water quality parameters.

However, since each integrated aquaponic technology has its peculiarities related to various variables such as plant and fish species used, technology production intensity (e.g. feed input, fish stocking density, plant production density etc.) or aquaponics techniques used (e.g. floating rafts, nutrient film technique, substrate techniques etc.), the develop of artificial intelligence (AI) - based soft sensors cannot have yet, a universal applicability.

Thus, if the generative character of AI will be exploited in future, considering the soft sensors' analytical frameworks, this limitation will be overcome.

The present research targets to apply machine-learning-based algorithms in order to enable and empower the integration of soft sensors for improving the economic sustainability of integrated multi-trophic recirculating aquaculture systems (IMRAS) through efficient and accurate water quality monitoring of nitrate, considering a series of predictors, specific for IMRAS and various technological scenarios.

MATERIALS AND METHODS

Experimental design, data collection and dataset description

In order to create the dataset used for developing the soft sensor for determining water NO₃ concentration in an aquaponic system, a 30-day trial was conducted in a sturgeon (*A. baeri*) – tarragon (*Artemisia dracuncululus* L.) IMRAS where light expanded clay aggregate (LECA) aquaponic substrate was used as plant growing substrate and 3 different tarragon culture densities were applied, together with the control variant, as follows:

- D1 – culture density of tarragon - 80 plants/m²;
- D2 – culture density of tarragon - 60 plants/m²;
- D3 – culture density of tarragon - 40 plants/m²;
- C – Control variant – no plants were used, only LECA plants' culture substrate.

During the experimental trial, the following water quality parameters concentrations were monitored: NH₄ (ammonium), NO₂ (nitrites), NO₃ (nitrates), EC (electroconductivity), P₂O₅ (phosphorus pentoxide), Ca (calcium) and Mg (magnesium). Thus, all parameters were determined using Libelium® Smart Water Sensor Platform Adds Ion Monitoring (Zaragoza, Spain) - the equipment is fully described by Petrea et al., 2023a. However, P₂O₅ was the only parameter determined by using laboratory analytical procedures – sensors were calibrated before the trial and validation of the data was performed by crosschecking the sensor results with the results obtained by applying the classical analytical determination procedures. The sampling points were both at the inlet (*In*) and outlet (*Out*) of the aquaponics modules, for each experimental variant, to create a decision-support analytical framework, oriented towards NO₃, that can be developed, further on, in order to serve as a solution for determining the real-time NO₃ removal rate.

The resulting dataset was divided into 2 groups, as follows: the 1st group contains 70% of the data allocated for training, while the 2nd group has the rest 30% of data, that are to be used for the validation process. Database pre-processing is described by Petrea et al. (2023a), while the

predictor's standardization was performed as presented by Petrea et al. (2020).

Machine learning data-processing methods and workflow

In order to perform the analytical framework of the present study, the workflow diagram described in Figure 1 was applied.

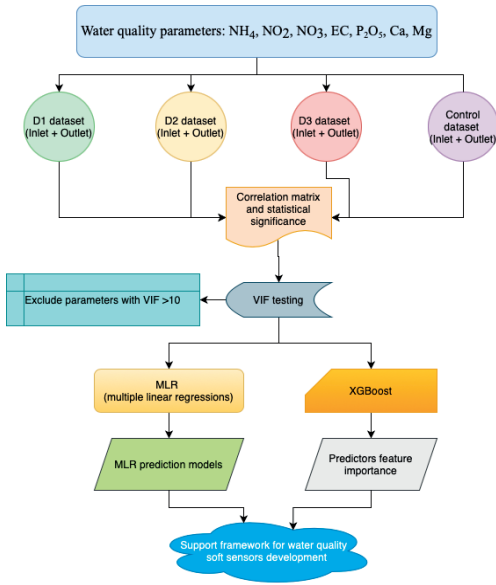


Figure 1. The workflow for enabling and empowering the integration of soft sensors in IMRAS, considering various technological scenarios

Thus, a number of 2 machine learning-based supervised algorithms were used, namely multiple linear regression (MLR) and XGBoost (XGB), in order to generate high-metrics predictions of NO_3 concentration in water, considering 6 main predictors, associated with each of the 4 technological scenarios ($D1$, $D2$, $D3$, C), both at the inlet (In) and outlet (Out) of the aquaponic units.

The Python NumPy library was used for obtaining the correlation matrix and Seaborn library to visualize it, as presented by Petrea et al., 2023b.

The MLR model equation is presented below (eq. 1), according to Petrea et al. (2023a):

$$y_{\text{predict}} = a_1x_1 + a_2x_2 + \dots + a_nx_n + b + \epsilon \quad (1)$$

where:

- y_{predict} is the dependent variable;

- x_1, x_2, \dots, x_n are the n independent variables;
- b is the intercept indicating the Y value when all the predictors are zeros;
- a_1, a_2, \dots, a_n are the coefficients of predictors, reflecting the contribution of each independent variable in predicting the dependent variable; ϵ is the residual term indicating the difference between the actual and the fitted response value.

The XGBoost core-concept is presented in eq. 2.

$$Obj = \sum_{i=1}^n l(y_i - \hat{y}_i) + \sum_{k=1}^K \Omega(f_k) \quad (2)$$

where:

- y_i is the measured value; y
- \hat{y}_i is the predicted value of each tree; l is the loss function, which is used to measure the total prediction error;
- $\sum \Omega(f_k)$ is the regularization term.

RESULTS AND DISCUSSIONS

Correlation matrix

The matrixes reveal that, in the case of $D1$, the highest significant ($p < 0.05$) positive correlations are recorded between the pH and EC, P_2O_5 and NO_3 , respectively, while the significant ($p < 0.05$) high negative correlations are observed between EC – P_2O_5 , P_2O_5 – NO_3 and EC – NO_3 (Figure 2).

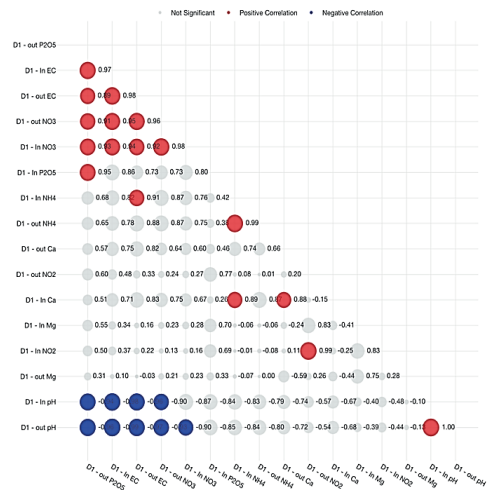


Figure 2. Correlation matrix for water quality parameter dataset associated with $D1$ technological scenario

In the case of D2, the highest significant ($p < 0.05$) positive correlations encountered at D1 are confirmed, the pH dynamics conditioning the EC, P_2O_5 and NO_3 , fact valid both for *In* and *Out* sampling points (Figure 3). In terms of significant ($p < 0.05$) high negative correlations, outside EC – P_2O_5 – NO_3 conditioning triangle, Ca – NH_4 and Mg – NO_3 relations are also pointed out as negative and significant ($p < 0.05$) (Figure 3).

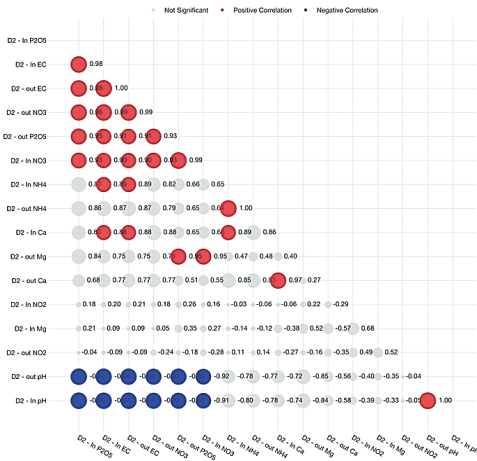


Figure 3. Correlation matrix for water quality parameter dataset associated with D2 technological scenario

The matrixes in the case of D3 reveal the highest significant ($p < 0.05$) positive correlations recorded between the pH and EC, P_2O_5 and NO_3 , while the significant ($p < 0.05$) high negative correlations are observed between EC – P_2O_5 – NO_3 – NH_4 conditioning nexus, Ca- EC and Mg, NO_2 and pH *In* – *Out* (Figure 4).

In the case of the C experimental variant correlation matrix (Figure 5), the highest significant ($p < 0.05$) positive correlations were recorded, similar to D1, D2 and D3, between the pH and EC, P_2O_5 and NO_3 , while the significant ($p < 0.05$) high negative correlations are observed between EC, NH_4 , P_2O_5 , Mg, Ca *In* – *Out*, EC – NO_3 , EC- NH_4 , Ca – NO_3 and P_2O_5 – NO_3 . It can be observed that D1, D2 and D3 experimental variants present less correlation between the concentration of the parameter in *In* vs. *Out* sampling points, respectively, compared to C, a fact that can be due to tarragon dynamics to absorb nutrients that cannot be structured in a pattern based on correlation matrixes. Thus, to

perform an in-depth analysis of the dataset conditionalities as a base tool for future development of soft sensors, AI-based machine learning algorithms must be applied.

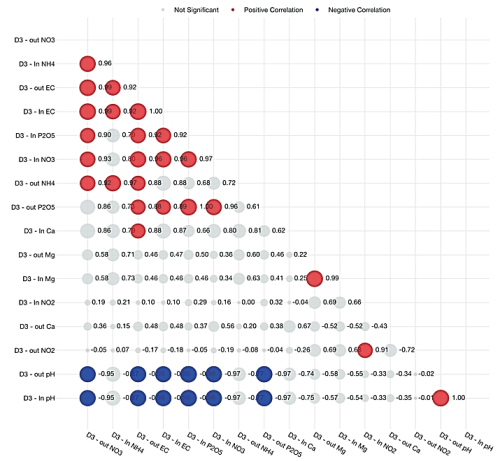


Figure 4. Correlation matrix for water quality parameter dataset associated with D3 technological scenario

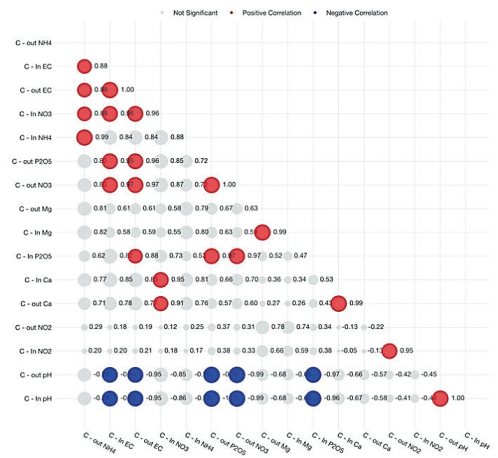


Figure 5. Correlation matrix for water quality parameter dataset associated with D4 technological scenario

MLR prediction models

In the case of D1, the MLR-based prediction models reveal that NH_4 and Mg can be considered the main predictors for determining the NO_3 concentration in IMRAS technological water, both for *In* (eq. 3) and *Out* (eq. 4) sampling points, since they are associated with the highest coefficient values within the model.

All parameters were used as predictors since their VIF values were lower than 10.

The models' metrics reveal good accuracy, with an Rsq value of 83.24 for the NO_3 D_{1in} prediction model (eq. 3) and 80.45 for the NO_3 D_{1out} prediction model (eq. 4). However, a positive predictive relation can be observed between NO_3 and the predictors EC and NH_4 , while negative predictive weight is associated to Ca and Mg, a fact valid for both *In* and *Out* sampling points.

$$\circ \text{NO}_3 D_{1in} = 1059.48 - 30.69 \text{ Ca } D_{1in} + 2.75 \text{ EC } D_{1in} - 46.96 \text{ Mg } D_{1in} + 1325.72 \text{ NH}_4 D_{1in} \quad (3)$$

$$\circ \text{NO}_3 D_{1out} = 951.23 - 25.92 \text{ Ca } D_{1out} + 2.25 \text{ EC } D_{1out} - 38.93 \text{ Mg } D_{1out} + 1301.42 \text{ NH}_4 D_{1out} \quad (4)$$

In the case of D2, the MLR-based prediction models reveal that most of the NO_3 dynamics can be explained by NH_4 , a fact valid for both *In* and *Out* sampling points (eq.5 and eq.6). However, the Ca and Mg predicting weight increases in the case of NO_3 D_{2in} (eq.5), compared to NO_3 D_{2out} (eq.6). All parameters were used as predictors since their VIF values were lower than 10. The models' metrics reveal good accuracy, with an Rsq value of 86.12 for the NO_3 D_{2in} prediction model (eq.5) and 81.87 for the NO_3 D_{2out} prediction model (eq.6).

$$\circ \text{NO}_3 D_{2in} = -632.16 - 12.55 \text{ Ca } D_{2in} + 2.12 \text{ EC } D_{2in} - 16.5 \text{ Mg } D_{2in} - 199.77 \text{ NH}_4 D_{2in} \quad (5)$$

$$\circ \text{NO}_3 D_{2out} = -422.30 - 1.38 \text{ Ca } D_{2out} + 0.83 \text{ EC } D_{2out} - 3.28 \text{ Mg } D_{2out} - 157.13 \text{ NH}_4 D_{2out} \quad (6)$$

In the case of D3, the MLR-based prediction models reveal that NO_3 prediction is mostly conditioned by NH_4 concentration in the technological water, in both *In* and *Out* sampling points (eq. 7 and eq. 8). However, the NO_3 D_{3in} model emphasizes the low weight of Ca in the prediction equation (eq. 7), compared to NO_3 D_{3out} . Also, it can be concluded that both EC and Mg share a similar trend of predictive weight (eq. 7 and eq. 8). The models' metrics reveal good accuracy, with an Rsq value of 83.34 for the NO_3 D_{3in} prediction model (eq.7) and 80.52 for the NO_3 D_{3out} prediction model (eq.8). The NH_4 has a direct trend in relation to the predicted variable, in the case of *Out* sampling point, while in the *In* sampling point, the relation is indirect (negative). This can be explained by the autoregulation capacity of the aquaponic unit, in terms of the water quality matrix.

$$\circ \text{NO}_3 D_{3in} = -585.46 + 0.06 \text{ Ca } D_{3in} + 0.77 \text{ EC } D_{3in} + 3.05 \text{ Mg } D_{3in} - 421.42 \text{ NH}_4 D_{3in} \quad (7)$$

$$\circ \text{NO}_3 D_{3out} = -239.95 + 0.55 \text{ Ca } D_{3out} + 0.41 \text{ EC } D_{3out} + 1.86 \text{ Mg } D_{3out} + 33.54 \text{ NH}_4 D_{3out} \quad (8)$$

The C experimental variant presents good accuracy metrics, with an Rsq value of 89.58 for the NO_3 C_{in} prediction model (eq. 9) and 84.32 for the NO_3 C_{out} prediction model (eq. 10). In both cases, the NH_4 has the highest weight in predicting the NO_3 , followed by Ca and Mg. However, it can be pointed out that Ca has an indirect trend in relation to the predicted variable, in the case of *Out* sampling point, while in the *In* sampling point, the relation is direct (positive).

$$\circ \text{NO}_3 C_{in} = -318.82 + 4.40 \text{ Ca } C_{in} + 0.18 \text{ EC } C_{in} + 3.49 \text{ Mg } C_{in} - 155.86 \text{ NH}_4 C_{in} \quad (9)$$

$$\circ \text{NO}_3 C_{out} = -574.48 - 1.83 \text{ Ca } C_{out} + 0.89 \text{ EC } C_{out} + 2.41 \text{ Mg } C_{out} - 241.66 \text{ NH}_4 C_{out} \quad (10)$$

In the end, it can be partially concluded that the MLR models emphasize that NH_4 has a considerable weight, being recommended to be used as the main predictor for the development of the NO_3 soft sensors, applicable in IMRAS, in various technological scenarios.

XGBoost prediction models

The XGBoost prediction models, applied by using the D1 dataset, reveal that for *In* sampling point (Figure 6), the In-EC and In-Ca are the only predictors that present future importance associated with the prediction of the In- NO_3 concentration in the technological water matrix. However, in the case of the *Out* sampling point (Figure 7), the Ca has the highest future importance, followed by EC.

The metrics of both D1 prediction models (Figures 6, 7) indicate good accuracy, as follows: Rsq of 91.37 for the *In* sampling point and 89.34 for the *Out* sampling point, respectively.

The XGBoost prediction models, applied by using the D2 dataset, reveal that for *In* sampling point (Figure 8), the In-EC, In- P_2O_5 and In-Ca are the only predictors that present future importance in predicting the In- NO_3 concentration at the level of technological water. However, in the case of the *Out* sampling point (Figure 9), the Ca has the highest future importance, followed by EC, while the P_2O_5 has no associated value for feature importance.

Thus, it can be concluded that the variation of tarragon culture density from 80 plants/m² to 60 plants/m² has an impact on predictors feature importance when predicting the NO₃ concentration from aquaponics modules inlet sampling point, recommending, therefore, to consider P₂O₅ among EC and Ca, as main predictors.

The metrics of both D2 prediction models (Figures 8, 9) indicate good accuracy, better than D1 models, as follows: Rsq of 93.12 for the *In* sampling point and 90.44 for the *Out* sampling point, respectively.

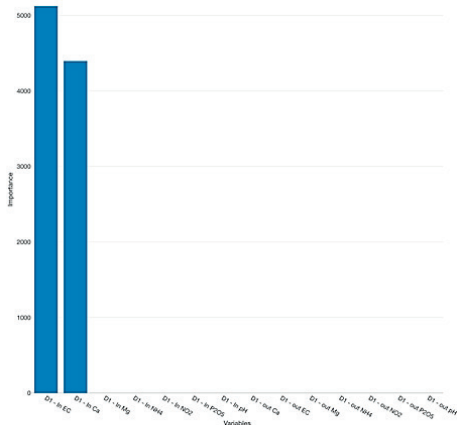


Figure 6. The predictors feature importance in predicting NO₃ concentration at D1-In

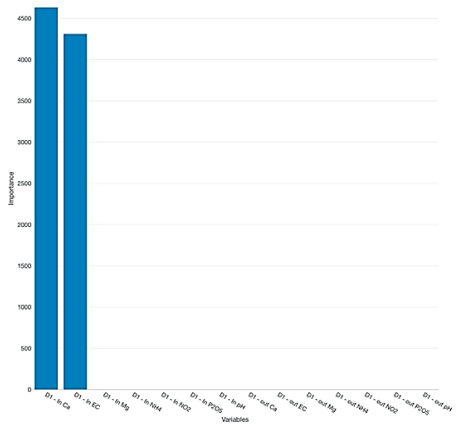


Figure 7. The predictors feature importance in predicting NO₃ concentration at D1-Out

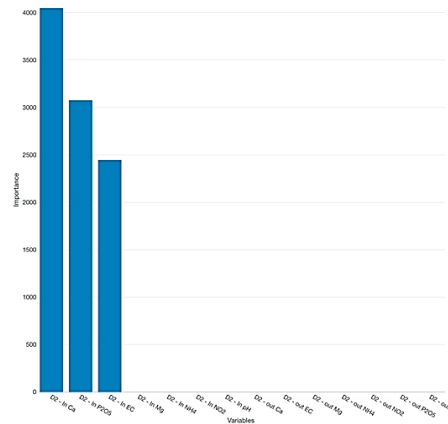


Figure 8. The predictors feature importance in predicting NO₃ concentration at D2-In

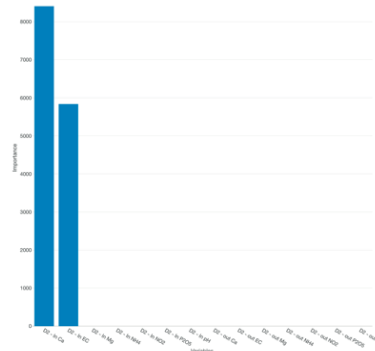


Figure 9. The predictors feature importance in predicting NO₃ concentration at D2-Out

The NO₃ - XGBoost prediction models applied by using the D3 dataset reveal that, for both sampling points, the EC is considered as the main predictor, followed by Ca (Figures 10, 11). Thus, the findings confirm, generally, the predictors ranking resulted from MLR models, presented above. However, the metrics of both D3 prediction models (Figures 10, 11) indicate good accuracy, better than D1 and D2 models, as follows: Rsq of 95.55 for the *In* sampling point and 93.12 for the *Out* sampling point, respectively.

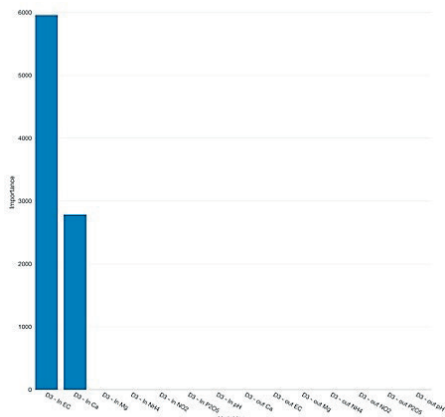


Figure 10. The predictors feature importance in predicting NO_3 concentration at D3-In

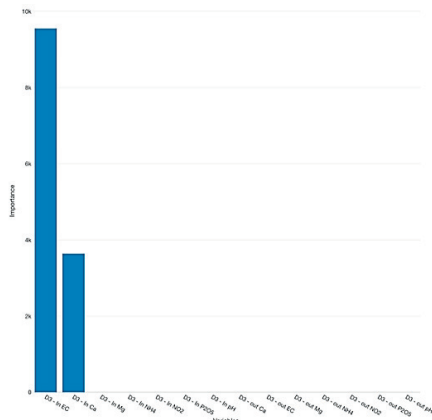


Figure 11. The predictors feature importance in predicting NO_3 concentration at D3-Out

The C experimental variant confirms the Ca feature importance, as a predictor, in predicting the NO_3 concentration of technological water, in the *In* sampling point (Figure 12). However, at the *Out* sampling point, the situation is different, with the EC recording the highest feature importance among the predictors (Figure 13). Also, compared to *In* sampling point, the model for predicting the NO_3 concentration in water at the aquaponics units outlet attributes a feature importance value, also, to P_2O_5 , outside EC and Ca.

The metrics of both C prediction models (Figure 12, 13) indicate good accuracy, better than D1, D2 and D3 models, as follows: Rsq of 97.10 for the *In* sampling point and 95.14 for the *Out* sampling point, respectively. This can be

explained by the lack of plant biomass at the level of control variant aquaponics modules – thus, this makes the model more stable and emphasizes the complexity degree in identifying high-accuracy models for various aquaponics culture density scenarios.

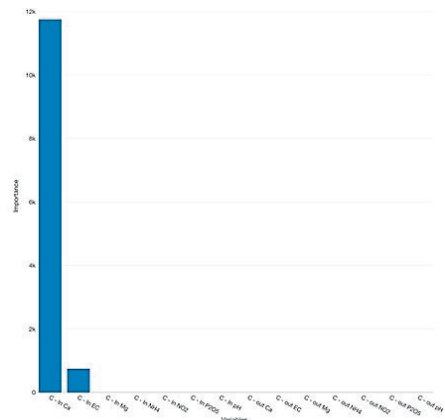


Figure 12. The predictors feature importance in predicting NO_3 concentration at C-In

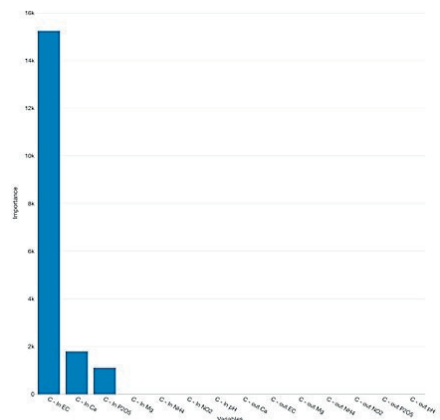


Figure 13. The predictors feature importance in predicting NO_3 concentration at C-Out

The metrics of both C prediction models (Figures 12, 13) indicate good accuracy, better than D1, D2 and D3 models, as follows: Rsq of 97.10 for the *In* sampling point and 95.14 for the *Out* sampling point, respectively. This can be explained by the lack of plant biomass at the level of control variant aquaponics modules – thus, this makes the model more stable and emphasizes the complexity degree in identifying

high-accuracy models for various aquaponics culture density scenarios.

Also, it can be concluded that for all experimental variants, the accuracy metrics recorded by applying XGBoost algorithms are superior compared to the metrics resulting because of applying MLR algorithms.

Similar to other studies, this study has its own limitations in terms of dataset dimension, as well as experimental framework. However, the study results (prediction models) are associated with high accuracy metrics, a fact that makes them reliable for upscaling in real industrial conditions.

CONCLUSIONS

The results reveal the effectiveness of different learning algorithms as MLR and XGBoost (>80% accuracy) in developing solutions for supporting the water quality monitoring process in IMRASs, concluding that the intensity of production technologies must be considered as a determinant factor in upscaling the solutions to industrial level.

It is recommended that future research should take into consideration the application of other machine learning algorithms such as GAM, SVM, Random Forest, GBM, CNN, Stacked ensemble, DRF or Naïve Bayesian in order to have a complete background of the technical aspects that may be used for future development of the analytical framework for black-box and grey-box soft sensors.

ACKNOWLEDGEMENTS

The present research was supported by the project: "An Integrated System for the Complex Environmental Research and Monitoring in the Danube River Area", REXDAN, SMIS code 127065, co-financed by the European Regional Development Fund through the Competitiveness Operational Programme 2014–2020, contract no. 309/10.07.2021. The present research was supported by the project "Integrated research and sustainable solutions to protect and restore Lower Danube Basin and coastal Black Sea ecosystems, (ResPonSE)", 760010/30.12.2022, component C9. PRIVATE SECTOR SUPPORT, RESEARCH, DEVELOPMENT AND INNOVATION,

Investment "I5. Establishment and operationalization of Competence Centers". (specific project no.1 - Decision Support Solutions based on mathematical modeling, for complex ecological systems – CESMoSS).

REFERENCES

- Asciuto, E.S., Cottone, C. & Borsellino, V. (2019) A financial feasibility study of an aquaponic system in a Mediterranean urban context. *Urban For. Urban Green*, 38, 10.1016/j.ufug.2019.02.001.
- Bosma, R.H., Lacambra, L., Landstra, Y., Perini, C., Poulie, J., Schwaner, M.J. & Yin, Y. (2017). The financial feasibility of producing fish and vegetables through aquaponics. *Aquac. Eng.*, 78, 10.1016/j.aquaeng.2017.07.002
- Costache, M., Cristea, D.S., Petrea, S.-M., Neculita, M., Rahoveanu, M.M.T., Simionov, I.-A., Mogodan, A., Sarpe, D. & Rahoveanu, A.T. (2021). Integrating aquaponics production systems into the Romanian green procurement network. *Land Use Policy*, 108, 105531.
- Goddek, S. & Körner, O.A. (2019). Fully Integrated Simulation Model of Multi-Loop Aquaponics: A Case Study for System Sizing in Different Environments. *Agricultural Systems*, 171, doi:10.1016/j.agsy.2019.01.010.
- Paepae, T., Bokoro, P.N. & Kyamakyia, K. (2021). From fully physical to virtual sensing for water quality assessment: A comprehensive review of the relevant state-of-the-art. *Sensors*, 21, 6971.
- Petrea, Ș.-M., Simionov, I.A., Antache, A.; Nica, A., Oprica, L., Miron, A., Zamfir, C.G., Neculiță, M., Dima, M.F. & Cristea, D.S. (2023a). An Analytical Framework on Utilizing Various Integrated Multi-Trophic Scenarios for Basil Production. *Plants*, 12, 540. <https://doi.org/10.3390/plants12030540>
- Petrea, Ș.-M., Bandi, A.C., Cristea, D. & Neculiță, M. (2019). Cost-benefit analysis into integrated aquaponics systems. *Custos E Agronegócio Line*, 15, 239–269.
- Petrea, Ș.-M., Simionov, I. A., Antache, A., Cristea D. S., Nica, A. & Cristea V. (2023b). Analytical framework for the development of water quality virtual sensors in integrated aquaculture systems based on various aquaponics techniques. *IEEE 28th International Conference on Emerging Technologies and Factory Automation (ETFA)*, Sinaia, Romania, pp. 1-5. doi: 10.1109/ETFA54631.2023.10275350.
- Petrea, Ș.-M., Costache, M., Cristea, D., Strungaru, Ș.-A., Simionov, I.-A., Mogodan A., Oprica, L. & Cristea V. (2020). A Machine Learning Approach in Analyzing Bioaccumulation of Heavy Metals in Turbot Tissues. *Molecules*, 25, 4696
- Yildiz, H.Y., Robaina, L., Pirhonen, J., Mente, E., Domínguez, D. & Parisi, G. (2017). Fish Welfare in Aquaponic Systems: Its Relation to Water Quality with an Emphasis on Feed and Faeces-A Review. *Water (Switzerland)*, 9.

VIRTUAL SENSOR FOR AMMONIA ESTIMATION IN AQUACULTURE TECHNOLOGICAL WATER FROM CAMBODIA

Ira-Adeline SIMIONOV¹, Lin KONG^{2,3}, Samnang PEL^{2,3}, Catalin PLANTON⁴,
Domenico CARUSO^{2,3}, Jacques SLEMBROUCK^{2,3}, Stefan-Mihai PETREA¹

¹"Dunărea de Jos" University of Galati, 47 Domneasca Street, Galati, Romania

²Institute of Evolutionary Science of Montpellier (ISEM), University De Montpellier, CNRS, IRD,
Bâtiment 39 – CC57, 300 Avenue du Professeur Emile Jeanbrau, Montpellier, France

³Royal University of Agriculture, Dongkor District, Phnom Pehn, Cambodia

⁴ROMFISH - National Association of Fish Producers, 12A Nicolae Iorga Blvd, Iasi, Romania

Corresponding author email: ira.simionov@ugal.ro

Abstract

In Cambodia, the aquaculture sector registers as one of the fastest-growing food sectors, with a mean annual growth of more than 18% between 2002 and 2020. The main challenge associated with the intensification of aquaculture is the discharge of untreated effluents, which contain large amounts of organic matter, nutrients, minerals, and other chemicals. Among these, ammonia (NH₃) is of the highest interest to monitor and measure in the technological water since it directly influences the survival and growth performance of the fish biomass. At the same time, the discharge of aquaculture wastewaters, containing high concentrations of ammonia, can generate water eutrophication in the natural aquatic environments receiving the effluents. The present study aimed to develop a virtual sensor capable of estimating the concentration of NH₃ in the technological water of a typical earthen aquaculture pond from Phnom Penh – Cambodia. Multiple decision tree algorithms were employed for the prediction analysis and the accuracy was established based on RMSE (root mean square error) and R squared values.

Key words: soft-sensor, ammonia, aquaculture, Cambodia.

INTRODUCTION

Mekong River (MR) is one of the largest rivers in the world, with a total length of 4800 km (Meur et al., 2021). The Lower MR supports highly valuable economic activities such as fisheries and aquaculture (Sor et al., 2021). The water resources provided by the Lower MR are crucial for the well-being of the riparian communities from Cambodia, Vietnam Laos, and Thailand respectively (Chea et al., 2016). For instance, in Cambodia, the aquaculture sector registers one of the fastest growth among all the food sectors, with a mean annual growth of more than 18% between 2002 and 2020 (Larson et al., 2023). Aquaculture in Cambodia is dominated by fish farming in freshwater, in small-scale production systems such as cage culture and pond culture respectively (Larson et al., 2022). Fish and derived fish products account for 76% of the total animal protein intake of Cambodian people, with an average fish consumption of 63 kg/person/year (Chea et al., 2023). In 2018, the total annual fish

production was 910,153 tons, with inland capture fisheries accounting for 59%, followed by aquaculture (28%) and marine capture fisheries (13%) (Chea et al., 2023). In terms of economic importance, Cambodia's total aquaculture sector value was \$200 million in 2022 and is forecasted to reach \$500 million by 2027. In this context of Cambodia's intensification of aquaculture, special care should be paid to water quality. Water quality directly influences growth performance and aquatic livestock production (Nguyen et al., 2022). The main challenge associated with the intensification of the aquaculture sector is the discharge of untreated effluents, which contain large amounts of organic matter, nutrients, minerals, and other chemicals. Among these, ammonia (NH₃) is of the highest interest to monitor and measure in the technological water since it directly influences the survival and growth performance of the fish biomass. At the same time, the discharge of aquaculture wastewaters, containing high concentrations of ammonia, can generate water eutrophication in

the natural aquatic environments receiving the effluents. Therefore, continuous monitoring of water physicochemical parameters is mandatory to maintain the optimum and safe levels of various indicators (Hong & Giao, 2022). Assessment of water quality is a practice that involves high financial resources allocated to specialized human resources and expensive equipment, and reagents respectively. During the last years, the development of the Internet of Things (IoT), artificial intelligence (AI) technologies, and predictive modeling techniques such as machine learning have become assistance for monitoring water quality in different aquatic ecosystems (Ahmed et al., 2019; Sankaran, 2019). The objective of virtual sensors is to identify mathematical connections between the variables within an aquatic ecosystem and to develop models able to predict the parameters that are difficult to measure based on those that are easy to measure (Zhou et al., 2022).

The present study aimed to develop a virtual sensor capable of estimating the concentration of NH_3 in the technological water of a typical earthen aquaculture pond from Phnom Penh – Cambodia. Multiple decision tree algorithms were employed for the prediction analysis and the accuracy was established based on RMSE (root mean square error) and R squared values.

MATERIALS AND METHODS

The water quality data was obtained daily, based on *in situ* measurements and laboratory analysis during April and December 2023. The measurements were determined in the technological water of a nursery pond from the National Aquaculture Research and Development Institute (NARDI) – Phnom Penh, Cambodia. The following physicochemical parameters were analyzed: dissolved oxygen (DO), temperature, pH, electroconductivity (EC), and ammonia (NH_3). Temperature, DO, EC, and pH were measured using portable sensor devices, while ammonia (NH_3) was calculated based on the HN_4 concentration value determined spectrophotometrically.

The database was further used to predict the value of NH_3 in the technological water based on the values of DO, EC, pH, and temperature respectively. Multiple decision tree algorithms

were employed (random forest, decision tree, and XGBoost) for the prediction analysis and the accuracy was established based on RMSE (root mean square error) and R-squared values. As well, a multi-linear regression model was used in the prediction analysis to compare accuracy.

RESULTS AND DISCUSSIONS

1. *Random forest analysis*

The RF analysis for the prediction of NH_3 generated an R-squared of 0.62 and an RMSE of 0.07 (Figures 1 and 2).

The feature importance highlighted that the most important variable for the prediction of NH_3 was temperature, followed by pH (Figure 3). The least important variable in the prediction analysis was EC (Figure 3).

2. *Decision tree analysis*

The decision tree analysis for the prediction of NH_3 generated an R-squared of 0.55 and an RMSE of 0.078 (Figures 4 and 5).

The feature importance highlighted that the most important variable for the prediction of NH_3 in the decision tree analysis was temperature, followed by pH (Figure 6). The influence of DO and EC in the prediction analysis through the decision tree technique was limited.

3. *XGBoost analysis*

The HGBost analysis for the prediction of NH_3 generated an R-squared of -0.01 and an RMSE of 0.11 (Figure 7). This technique was not performant in the prediction of HN_3 .

4. *Multi-linear regression model*

The first step in the multi-linear regression analysis was to test the collinearity of the data (Figure 8), to ensure there is no overlaying.

As can be seen in Figure 8, the variance inflation factor was below 10, which indicates that the data is not overlaying.

The multi-linear regression analysis for the prediction of NH_3 generated an R-squared of 0.5 and an RMSE of 0.08 (Figures 9 and 10).

As can be observed in Figure 10, the significant parameters in the prediction NH_3 were temperature, pH, and EC, while DO was not significant in the prediction analysis.

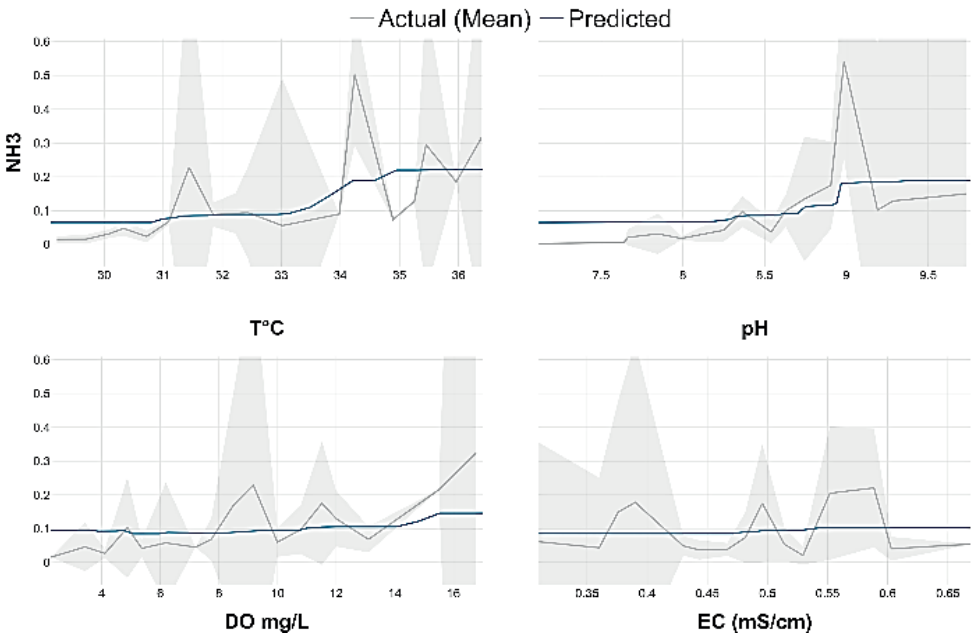


Figure 1. Performance of RF analysis for the prediction of NH_3

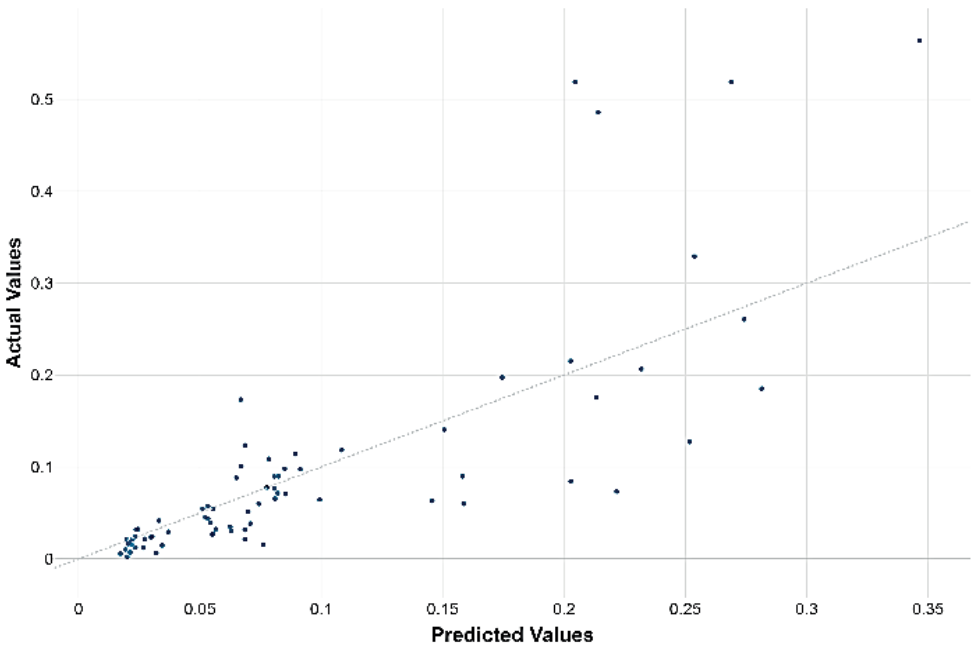


Figure 2. Performance of RF analysis for the prediction of NH_3

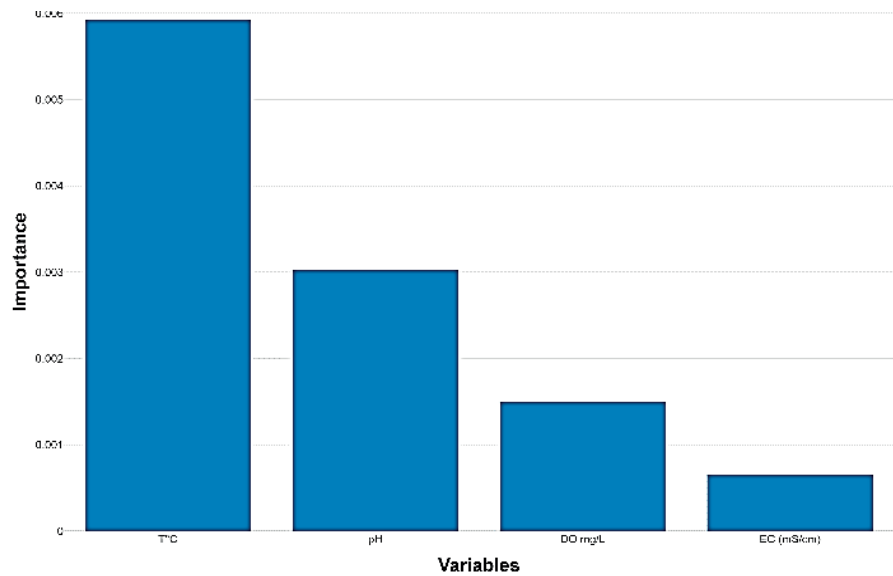


Figure 3. The FI of dependent variables in the RF analysis

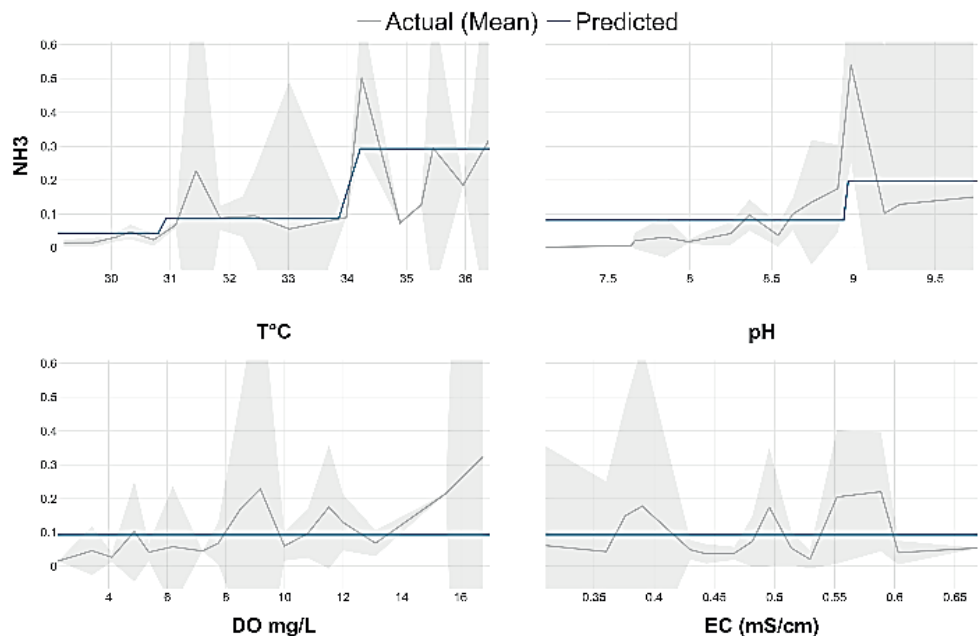


Figure 4. Performance of decision tree analysis for the prediction of NH₃

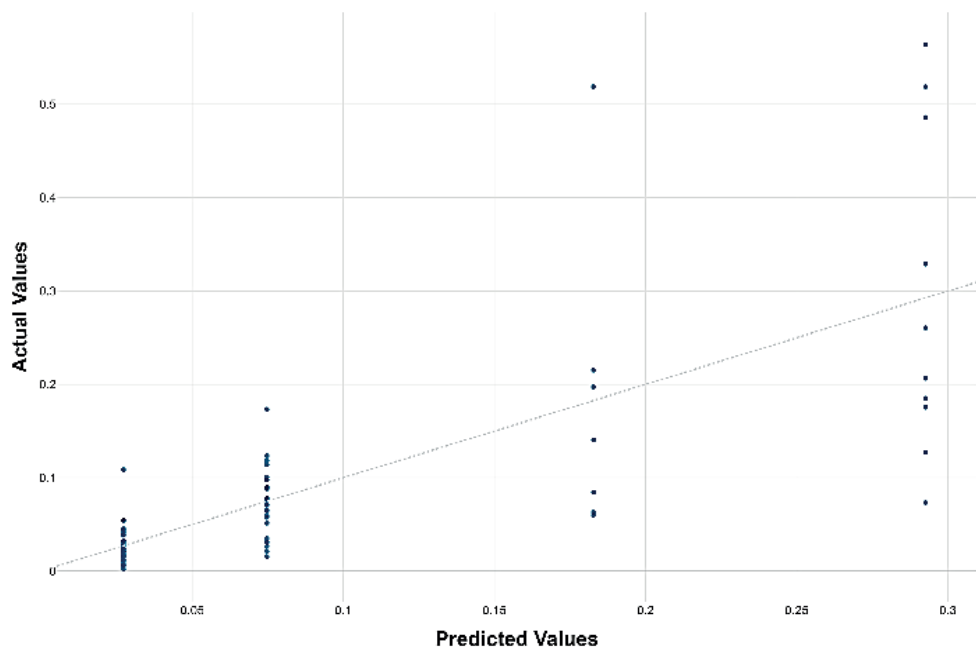


Figure 5. Performance of decision tree analysis for the prediction of NH_3

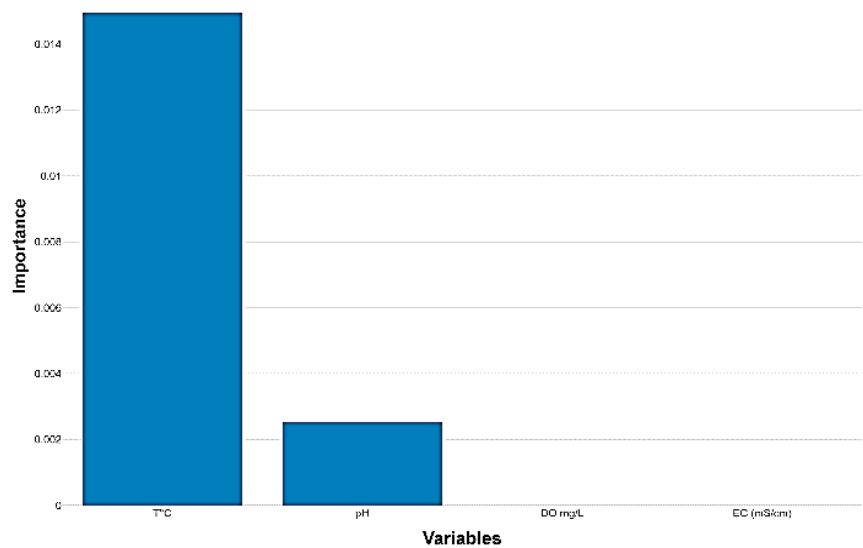


Figure 6. The FI of dependent variables in the decision tree analysis

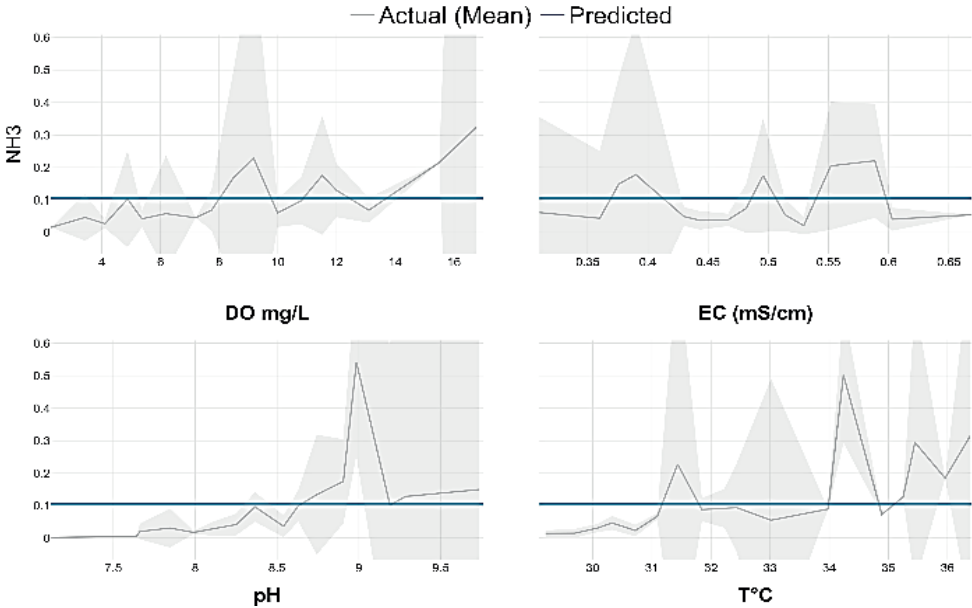


Figure 7. Performance of HGBBoost analysis for the prediction of NH_3

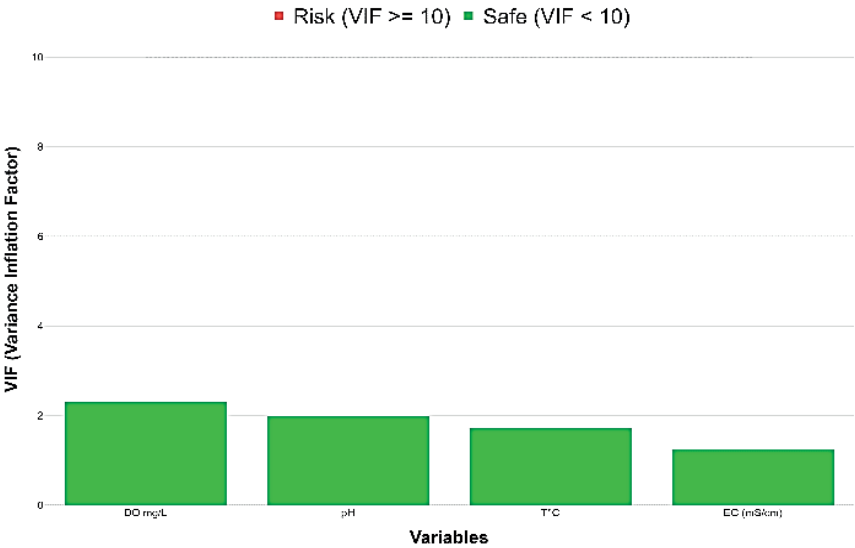


Figure 8. Data collinearity

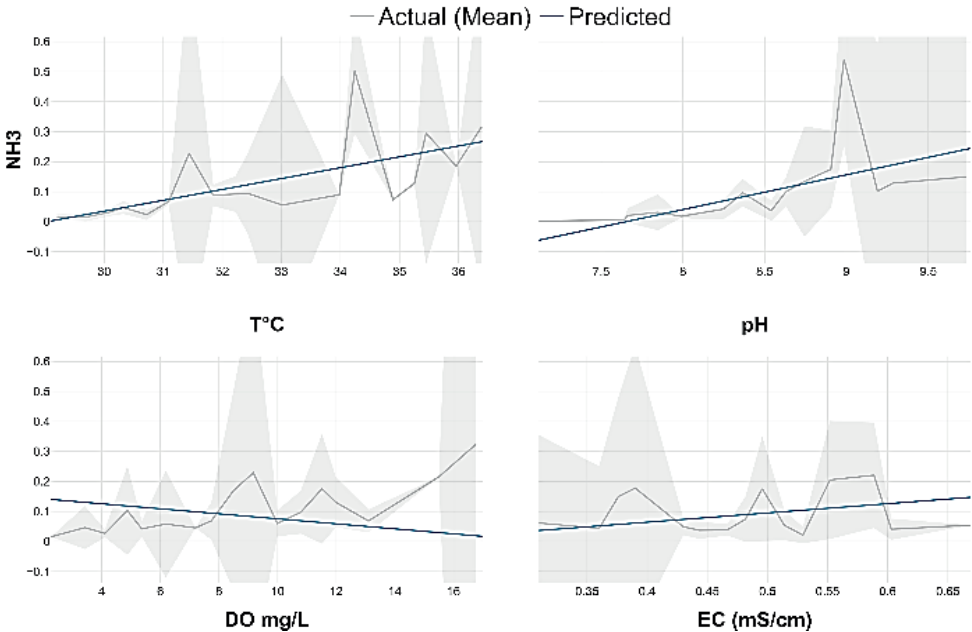


Figure 9. Performance of multi-linear regression analysis for the prediction of NH_3

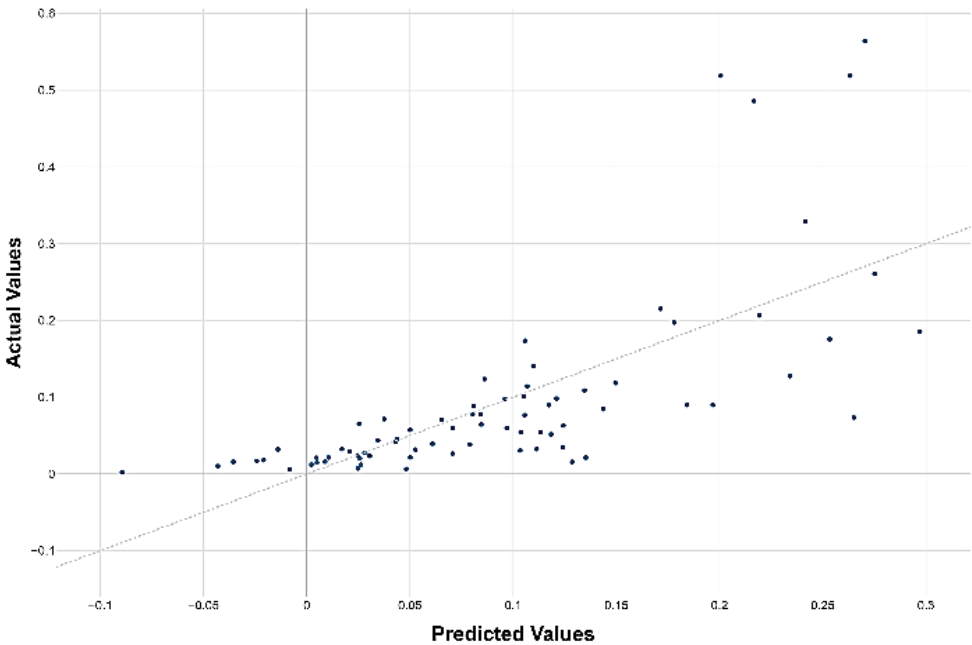


Figure 10. Performance of multi-linear regression analysis for the prediction of NH_3

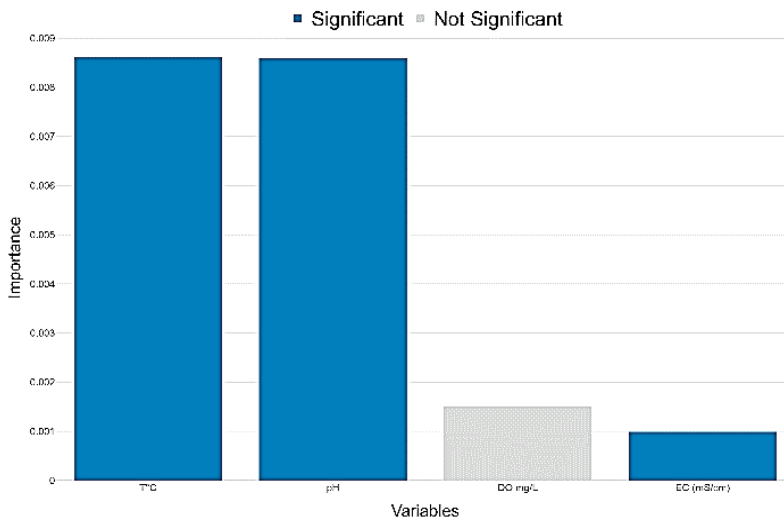


Figure 11. The FI of dependent variables in the multi-linear regression analysis

CONCLUSIONS

The present study demonstrated that the use of aquatic soft sensors for the determination of ammonia compounds in aquaculture facilities is feasible. Random forest performed the best in the prediction analysis, followed by the multi-linear regression analysis. This solution can be applied not only in areas lacking financial resources but also in more developed areas, thus increasing economic and environmental sustainability.

ACKNOWLEDGEMENTS

This work has been carried out within the framework of the CaPFish Aquaculture project and has been jointly carried out by researchers from the IT1 team and FIA. This project is supported by the European Union. The authors are grateful for the technical support provided by Hang Savin – deputy director of the National Aquaculture Research and Development Institute (NARDI) and Hav Viseth – general director of The Freshwater Aquaculture Research and Development Centre (FARDeC).

REFERENCES

Ahmed, U., Mumtaz, R., Anwar, H., Mumtaz, S., & Qamar, A.M. (2019). Water quality monitoring: From conventional to emerging technologies. *Water Supply*, 20(1), 28–45. <https://doi.org/10.2166/ws.2019.144>

Chea, R., Ahsan, D., García-Lorenzo, I., & Teh, L. (2023). Fish consumption patterns and value chain analysis in north-western Cambodia. *Fisheries Research*, 263, 106677. <https://doi.org/10.1016/j.fishres.2023.106677>

Chea, R., Grenouillet, G., & Lek, S. (2016). Evidence of water quality degradation in lower Mekong Basin revealed by self-organizing map. *PLOS ONE*, 11(1), e0145527. <https://doi.org/10.1371/journal.pone.0145527>

Hong, T.T.K., & Giao, N.T. (2022). Analysis of surface water quality in upstream province of Vietnamese Mekong Delta using Multivariate Statistics. *Water*, 14(12), <https://doi.org/10.3390/w14121975>.

Larson, S., Hoy, S., Thay, S., & Rimmer, M.A. (2023). Sustainable and inclusive development of finfish mariculture in Cambodia: Perceived barriers to engagement and expansion. *Marine Policy*, 148.

Larson, S., Rimmer, M.A., Hoy, S., & Thay, S. (2022). Is the marine finfish cage farming value chain in Cambodia inclusive? *Aquaculture*, 549, 737782.

Meur, M.L., Phu, V.L., Gratiot, N., Meur, M.L., Phu, V.L., & Gratiot, N. (2021). What is the future of the Lower Mekong Basin struggling against human activities? A Review. In *River Deltas Research—Recent Advances*. IntechOpen.

Nguyen, T.G., Phan, K.A., & Huynh, T.H.N. (2022). Major concerns of surface water quality in south-west coastal regions of Vietnamese Mekong Delta. *Sustainable Environment Research*, 32(1).

Sankaran, M. (2019). *Why wastewater quality monitoring matters*. Wastewater Digest.

Sor, R., Ngor, P.B., Soum, S., Chandra, S., Hogan, Z.S., & Null, S.E. (2021). Water quality degradation in the Lower Mekong Basin. *Water*, 13(11).

Zhou, M., Zhang, Y., Wang, J., Shi, Y., & Puig, V. (2022). Water quality indicator interval prediction in wastewater treatment process based on the improved BES-LSSVM Algorithm. *Sensors*, 22(2).

ASPECTS REGARDING THE ESTIMATION OF THE FLOOD LIMITS USING AN UAV IN ORDER TO HYDRAULIC DESIGN WATER MANAGEMENT WORKS

Alexandru SÎNTU-LĂSAT^{1,2}

¹University of Agronomic Sciences and Veterinary Medicine of Bucharest,
59 Marasti Blvd, District 1, Bucharest, Romania

²National Administration of Romanian Waters,
11 Ion Campineanu Street, District 1, Bucharest, Romania

Corresponding author email: alex.lasat@gmail.com

Abstract

The present paper aims to highlight a more efficient and safer way to estimate the flood limits especially in hard-to-reach areas (hill-mountain) in order to reduce the calamities caused by flash-floods through water management works. It was used an UAV (drone) with D-RTK technology together with a GPS station with which there were captured elevation points on the ground. The study area is located in Alba County on the Răchita Valley near the Sebeș city, area having a strong torrential character, especially during short-term and high-intensity rains. In 2019-2020 winter, a flood of 106 m³/s was recorded, representing a huge value compared to the multiannual flow of the main water course of 8.88 m³/s. The estimation of the flood limits is fully computerized, obtaining the most accurate results in order to be able to design hydraulic specifications for hydrotechnical schemes and structures needed considering both structural and environmental sides.

Key words: D-RTK, flash-flood, flood limit, hydraulic works, UAV.

INTRODUCTION

As known, or rather, as felt, the climate changes, are present, the most efficient way to response is immediate adaptation. Over the past 20 years, Romania has experienced increasingly extreme phenomena such as extreme drought or rapid floods. Unfortunately, engineering works for flood defense or irrigation to combat those phenomena are outdated in the current context. Through this paper, it is highlighted the fact that technological expansion is as useful as it can be. Located in the South-Eastern Europe, on the lower course of Danube and at the Black Sea seaside, the Romania territory (237,502 km²) presents a unique diversity of natural conditions and resources, long processes and climatic changes generated during various geological periods, a large complexity of relief forms appeared on the Romanian territory, characterized however by proportionality and harmony (Marinescu, 2000).

Following the new trend of 21st century technology and at the same time seeing how efficient a UAV has become in the processes of sizing/designing/executing engineering works,

it is important to present a series of aspects related to how the flood limit can be graphically represented.

Data acquisition using the principles of aerial photogrammetry is a modern method that allows surveying a large amount of data in a short time compared to classical topography methods. The data can be retrieved using opto-electronic or optical-mechanical sensors that are located on board aircraft. In this case, UAV (unmanned aircraft vehicle) technology was used, also called a drone, equipped with an RTK module that allows real-time corrections (Vorovencii, 2010; Carvajal, 2011; Raeva, 2016).

MATERIALS AND METHODS

The study area is located in Alba County on the Răchita Valley near the Sebeș city (Figure 1). The Răchita stream (cadastral code IV-1.102.14) is 5 km long with 10 km² hydrographic basin and an altitude of 550 m. In this sector, the stream has a slope of 1%, thus the floods propagate at high speed with an accentuated destructive effect. The climate of the Răchita valley belongs to the continental hill

and plateau climate with altitudes of 300-600 m. The average annual air temperature varies between 8 and 21°C.

From geo-morphological and structural point of view, Răchita valley belongs to the Secase Plateau. The particularities of the relief in the area are closely related to the evolution over time of the great unit of the Transylvanian Basin, the South-South East Zone.

The field survey took place in August 2023, where we captured various scenarios with the help of the UAV.

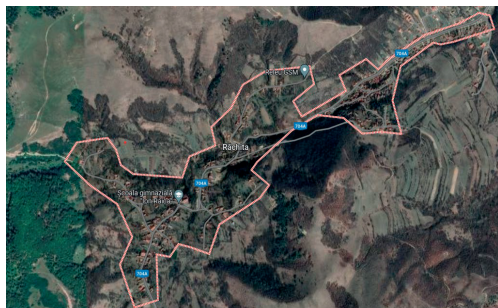


Figure 1. Aerial representation of area of study- source Google Earth

The equipment's used to carrying this work are DJI D-RTK 2 Mobile Station and the DJI Mavic 3 Enterprise. Stonex 980+ base station and Stonex 990+ we use as an over.

The DJI D-RTK 2 mobile station is a high quality and easy to use electronic station with high-precision GNSS receiver that supports all GPS, GLONASS, Beidou and GALILEO signals providing real-time accuracy. This equipment was used to collect ground points to have a good accuracy, optionally it could be used the GPS subscription offered by ROMPos, but in that area, there wasn't sufficient GPRS signal, which is why it was used the D-RTK station.

The DJI Mavic 3 Enterprise RTK UAV system has an RTK module and can receive signals from GNSS systems: GPS, Galileo, Glonass, and Beidou. With this module it is possible to position in real time with very high accuracy, requiring a small number of ground control points. In this case it was turned on the obstacle sensor because the drone reaches a speed of 90 km/h and 45 minutes flying operate with one battery.

The Stonex 980+ was used as a base station and Stonex 990+ as a rover, this equipment helped to compare the accuracy of the ground points that was collected with D-RTK Mobile Station. Positioning using GNSS technology was used to determine the photogrammetric landmarks. The real-time kinematic method Real Time Kinematic (RTK) radio rover base was used, which allows the transmission of real-time corrections and ensures centimeter accuracy. (Dierwechter, 2008; Lwin, 2012)

Software applications to obtain the data were:

- DJI Pilot 2 for flight mission;
- GStar Cad 2023 for marking plans;
- Pix4D Mapper we used to process images and orthophotoplan;
- GlobalMapper used for photogrammetric data processing;
- TransDatRO for transforming the coordinates taken with the UAV.

To initiate the aerial photography project, it is necessary to establish the direction of the UAV flight path, flight altitude, elevation plan, longitudinal and transversal coverage of the frame, total number of photographs taken, distance between the axes of photography, and the time required for the aerial photography mission. The UAV controller (DJI Rc Plus) comes pre-installed with the control application, namely DJI Pilot 2, which was used for flight planning and execution. A flight covering the entire valley was conducted. With the RTK module functioning on GPS frequencies: L1/L2, GLONASS: L1/L1, BeiDou: B1/B2, and Galileo: E1/E5a, the UAV ensures a positional accuracy of ± 1.5 cm + 1ppm RMS vertically and ± 1 cm + 1 ppm horizontally.

The mapping area was determined by the flight plan, which was automatically set based on manually input boundaries. The flight was set at a variable altitude of 100 m, following the natural terrain, with a frontal and lateral image overlap of over 80%, resulting in the collection of 738 images covering 37 ha of land. The integrated camera is housed within a gimbal with automatic image stabilization and mechanical shutter, leading to highly precise image stabilization. The sensor has a resolution of 20 megapixels and a 24 mm lens. Due to the use of the integrated RTK module along with the mobile D-RTK station, the number of ground

control points was relatively low, and the error did not exceed 1 cm. Throughout the mission, the UAV remained connected to the mobile D-RTK station, receiving corrections to improve its coordinates. The D-RTK station was connected to the UAV via the RC Plus remote controller, and, upon connection, significant improvements in elements such as latitude, longitude, and altitude were observed. The coordinates were taken from

the WGS84 projection system (World Geodetic System 1984) and were trans-calculated in the TransDatRO application, then reintroduced into the software as in Stereo 70 (Figure 2). Following data processing, the Pix4D Mapper application generated a processing report containing details about the camera's location, residual errors, camera orientation errors, etc. The process of collecting the photos lasted 3 hours and 18 minutes.

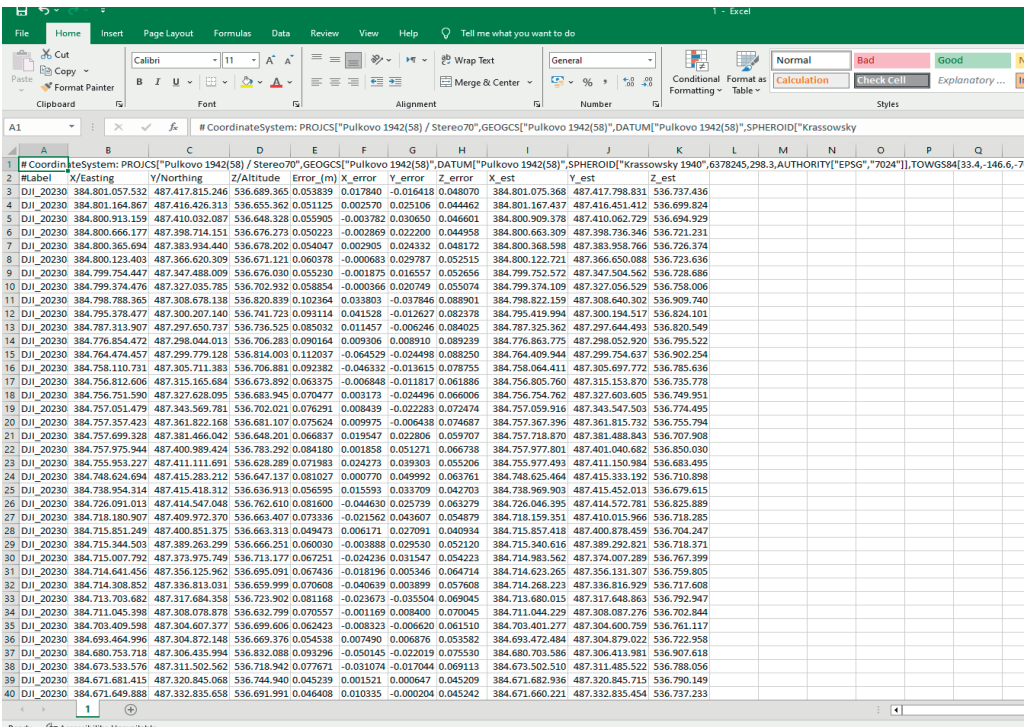


Figure 2. Print Screen of Converting coordinates from WGS84 to Stereo 70

RESULTS AND DISCUSSIONS

For image processing, as mentioned earlier, it is used a specialized software package. For the basic stages, Pix4D Mapper was used, the post-processing steps being: - the first step - alignment - it includes aerial triangulation (AT) and bundle block adjustment (BBA). At this stage Pix4D Mapper searches for feature points on the images and matches them across images into tie points. The program also finds the position of the camera for each image and refines camera calibration parameters (estimates interior - IO

and exterior - EO camera orientation parameters) (Figure 3). - the second step - generation of a surface in 3D (mesh) and/or 2.5D (DEM). Polygonal model (mesh) can be textured for photorealistic digital representation of the object/scene and exported in numerous formats compatible with processing software, both for CAD and 3D modelling workflows. The digital elevation model (DEM) is generated based on the point cloud data, and it can include either both terrain and all the objects above the ground, like trees, buildings and other man-made structures (digital surface model, DSM,

only show the landscape of the territory, digital terrain model, DTM).

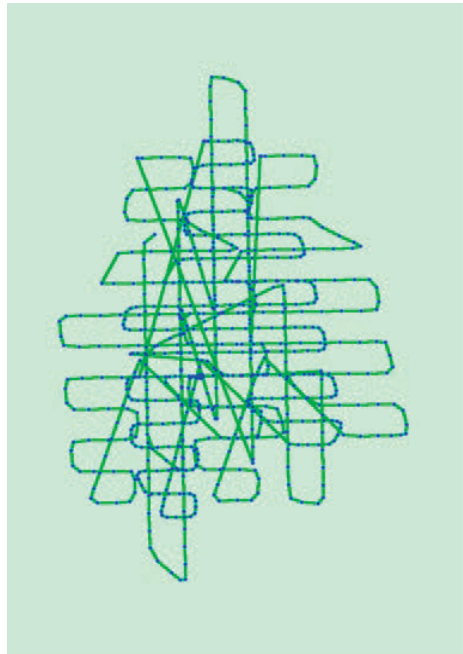


Figure 3. Top view of the initial image position. The green line follows the position of the images in time starting from the large blue dot

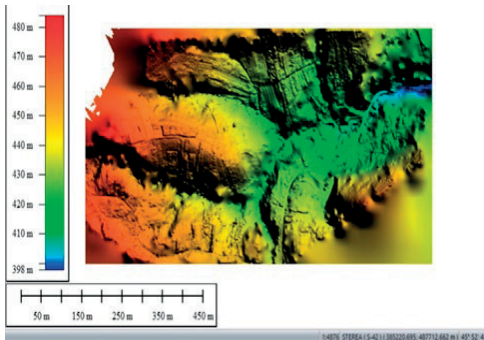


Figure 4. DEM Model

For the DEM model the error on the X coordinates is 0.020271 cm, for Y 0.022106 cm and for Z 0.045698 cm. For the X and Y coordinates, the error is represented by the root mean square of the ground control points and is 0.054662 cm, while the total error is given by the average of all ground control points and is 0.032691 cm. The elevations presented in Figures 3, 4, and 6 are represented by

progressive colors, namely: blue represents the lowest elevation, while red represents elevations up to 120 m. Following the establishment of the flight path, the digital elevation model (DEM) has a resolution of 7.31 cm/pixel, and the point density is 35.7 points/m².

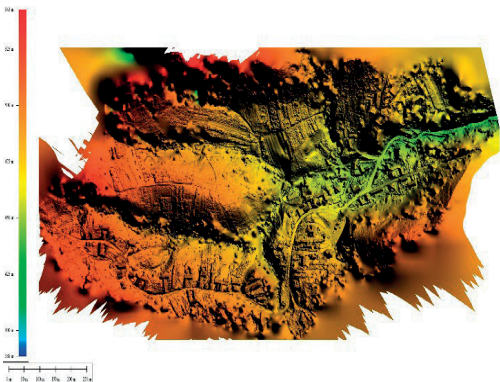


Figure 5. DTM Without Vegetation

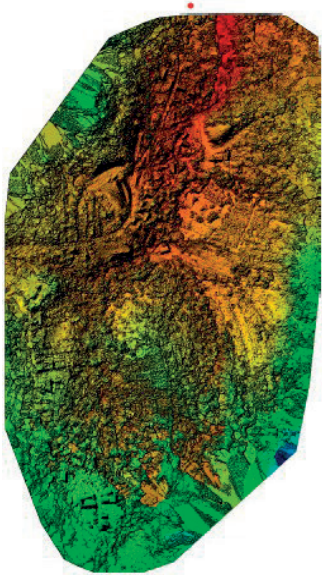


Figure 6. DSM Model with Vegetation

- *the third step* - creating of orthomosaic, which can be georeferenced and used as a base layer for various types of maps and further post processing analysis and vectorization. Orthomosaic is generated by projecting the images according to their EO/IO data on a surface of the user's choice: DEM or mesh (Figure 7).



Figure 7. Orthomosaic Model

The overlapping model shows the number of overlapping images computed for each pixel of the orthomosaic (Figure 8). Red and yellow areas indicate low overlap only 1 photo for which poor results may be generated. Green areas indicate an overlap of over 5 images for every pixel. Good quality results will be generated as long as the number of key-points matches is also sufficient for these areas.

The UAV working altitude was 100 m with the terrain tracking function activated, and the ground sampling distance (GSD) being of 2.11 cm/pixel. The analyzed area covers 0.37 km², the number of aligned frames was 708. To identify the connection points, at least two images from the point cloud are required. In this case, there are a total of 2,357,685 connection points, along with an error of 0.185 cm/pixel, which represents the error between the distance to the projected point and the measured one. Based on the aforementioned steps, it can be

developed the flood hazard boundary associated with the Rachita Valley. Subsequently, it is designed a reservoir in the pasture area of the village where it is possible to store the water volume from rapid floods.



Figure 8. Overlap Model

Based on the Digital Elevation Model and Digital Surface Model it was built the flood limit using GlobalMapper software. For the graphical representation of the limit, in concordance with the hydrological flows recorded and elaborated by the National Institute of Water Management (Tabel 1), where, based on the respective section of the studied basin surface, a maximum calculated flow of 52.4 m³/s was obtained with various probabilities of exceedance, resulting in a water level elevation of 487 m.

As observed in the graphical processing, at the computational flow rate $Q_{1\%}=52.4 \text{ m}^3/\text{s}$ the water blade formed, flooding the Rachita village to the extent of 95% (Figure 9).

Table 1. Hydrological data (source: National Institute of Hydrology and Water Management)

Water Course	Section	F (km ²)	Hmed (m)	Q1% (m ³ /s)	ρ %	γ	Grow time (h)	Total Time (h)
Rachita (IV.1.102.14)	x-386412.50 y-488058.88	4.50	487	52.4	27.1	0.24	4.5	18

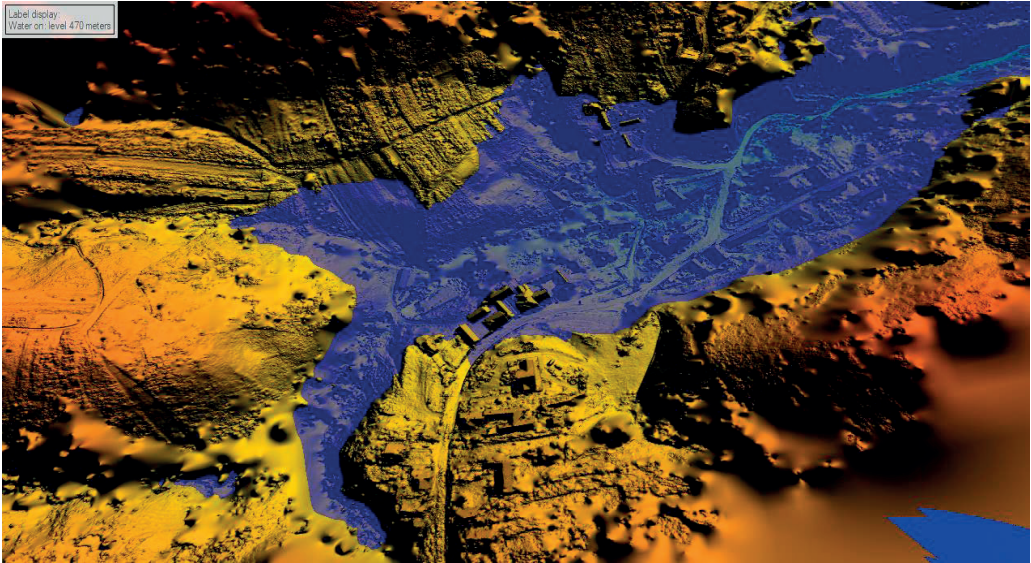


Figure 9. Flood Limit formed in Rachita Village

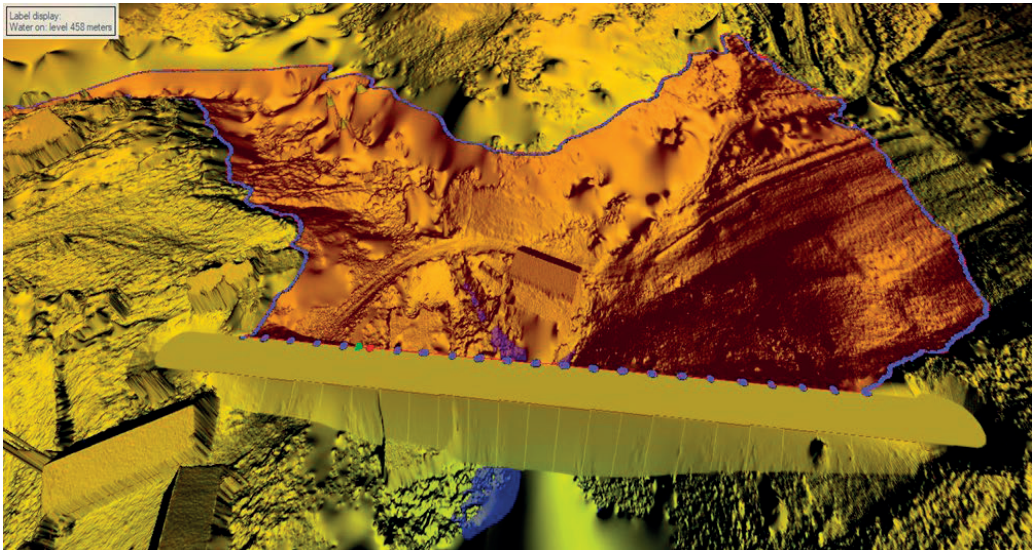


Figure 10. The Dam

It can be observed what disaster a flash flood can cause when the flows from the slopes cannot be controlled. At a flash flood discharge of approximately $50 \text{ m}^3/\text{s}$, 90% of the commune is submerged, represents approximately 0.20 km^2 . Analyzing the flood limit obtained it is obvious that the hole locality is under water, meaning it is necessary to find a technical solution to avoid this situation.

To prevent such disaster, it is appropriate to allocate a temporary space for the flood that does not endanger the adjacent population, and after the critical period has passed, it could safely transit the stored volume, working as a temporary reservoir.

On the previously obtained details and in accordance with the flow rates provided by the National Institute of Water Management, it is graphically designed a dam capable of withstanding the volume of water during the flood. The dam was designed upstream of the village of Răchita, where the village pasture is located. Based on the graphic processing and the input data, the dam has the following technical characteristics: the crest elevation reaches 438 m above sea level, while the riverbed elevation is at 412.50 m above sea level, resulting in a dam height of 26 m at the axis. The collected flow rates will be gradually released in line with the transit flow supported by the riverbed (Figure 10).

To properly dimension the temporary reservoir, the assistance of GlobalMapper software is needed, where using the Create Area function based on contour lines, the result is a storage volume of 55.291 m^3 .

CONCLUSIONS

After analyzing the methods and results obtained through this study, it can be concluded that UAV equipment can significantly reduce

the time needed to establish the flood limit, and furthermore, with the help of exported data, it is possible to design certain engineering works intended to protect the population against flooding.

ACKNOWLEDGEMENTS

This research work was carried out with the support of Doctoral School of Engineering and Management of Plant and Animal Resources within the University of Agronomic Sciences and Veterinary Medicine of Bucharest, of National Administration "Romanian Waters" and of the National Institute of Hydrology and Water Management.

REFERENCES

- Carvajal, F., Aguera, F., Perez, M. (2011). Surveying a Landslide in a Road Embankment Using Unmanned Aerial Vehicle Photogrammetry. (4) ISPRS, XXXVIII-1/C22: 201–206
- Dierwechter, Y., Carlson, T. (2008). Effects of urban growth boundaries on residential development in Pierce County, Washington. *The Professional Geographer*, 59(1), 207–220.
- Lwin, K.K., Murayama, Y., Mizutani, C. (2012). Quantitative versus Qualitative Geospatial Data in Spatial Modelling and Decision Making. *Journal of Geographic Information System*, 1, 235–241.
- Marinescu, P., Lefter, L., Tecuci, I. (2000). Objectives of Romanian's Resources Development (Chapter 1)- Romanian National Committee on Large Damns, Bucharest, Romania.
- Raeva, P.L., Filipova, S.L., Filipov, D.G. (2016). Volume computation of a stockpile – a study case comparing GPS and UAV measurements in an open pit quarry. The International Archives of the Photogrammetry, Remote Sensing and Spatial Information Sciences, XXIII ISPRS Congress, Prague, Czech Republic, XLI-B1(4) 999–1004.
- Vorovencii, I. (2010). *Photogrammetry*. Matrixrom Publishing House, Bucharest, Romania

THE INFLUENCE OF THE LAKE HYPOLYMNON DISCHARGE ON THE PHYSICO-CHEMICAL PARAMETERS OF THE RIVER

Lavinia TATARU, Florian STĂTESCU, Nicolae MARCOIE

"Gheorghe Asachi" Technical University of Iasi,
67 Dimitrie Mangeron Blvd, Iasi, Romania

Corresponding author email: lavinia.tataru@student.tuiasi.ro

Abstract

The analysis of the evolution of water quality parameters over time is of interest to researchers and authorities because it provides information on long-term changes in the river basin and allows the evaluation of the effectiveness of pollution control measures in the context of national and international commitments. This study describes eutrophication as a process of degradation of Lake Kortowskie, Poland, summarizes the effects of lake hypolimnion discharge on the water quality of the Kortówka River, and presents, in tabular form, the statistical principles specific to factor analysis (ANOVA). Water quality was assessed by comparing temperature, pH, changes in oxygen concentration (DO), conductivity (EC) and redox potential (ORP) before the experiment, during and after the experiment.

Key words: eutrophication, nutrients, restoration techniques, statistical analysis, water quality.

INTRODUCTION

Eutrophication has become the main water quality issue for most of the world's freshwater ecosystems (Tandyrak et al., 2016). Research shows that eutrophication occurs mainly in lakes where water circulation is reduced during the summer, when nutrient concentrations (total nitrogen and total phosphorus) increase at high temperatures (Şalaru et al., 2007).

In general, increasing the concentration of nitrogen and phosphorus causes a massive development of aquatic vegetation and, therefore, an increase in the amount of organic matter (Szymanski et al., 2013) which decomposes and accumulates in sediments (Ilechukwu et al., 2020) leading to the depletion of oxygen in hypolimnion and, at the same time, to the decrease of water quality (Bryant et al., 2011).

Improving water quality in lakes can be achieved by discontinuing external sources of pollution, but in most cases this method is not sufficient (Mientki & Teodorowicz, 1996), and the use of restoration techniques that include methods to reduce the phosphorus recycling rate is necessary, without physically removing phosphorus from the lake, dredging sediment or evacuating hypolimnion (Dunalska et al., 2007; Dunalska et al., 2014). Discharged hypolimnion

should be aerated and mechanically treated before discharge into downstream rivers (Nürnberg et al., 1987).

The first restoration technique was used by Olszewski in Lake Kortowskie, Poland, in 1956 and continues to this day. This method is based on removing the hypolimnion, a deep layer of oxygen-free, low-light, low-phytoplankton water. Removal of hypolimnion is an efficient, simple method that works without consuming electricity, does not affect epilimnion, and the effects of eutrophication on the lake are eliminated to restore a normal oxygen concentration (Mientki & Teodorowicz, 1996), but downstream the effects of the eutrophication are felt, depletion of oxygen and release of toxic substances (hydrogen sulphide, ammonia) from the air into the air which influence the formation of the characteristic odour by microbiological processes of decomposition of organic matter (Tandyrak et al., 2016).

The effects of hypolimnion evacuation on physicochemical conditions suggest that this method restores nutrient balance, directly influencing the growth of phytoplankton biomass and increasing the water temperature in hypolimnion, weakening the thermal stratification (Dunalska et al., 2014). Moreover, this method is suitable for lakes that are stratified during the summer when favorable

conditions for sulfate reduction are created, under anaerobic conditions and in the presence of organic substances. In the case of lakes these conditions are created in hypolimnion (Tandyrak et al., 2016).

In some lakes, the evacuation of hypolimnion is used to prevent the warming of downstream waters (Nürnberg, 2007), because the high temperature affects the photosynthesis process of aquatic plants and the metabolic rates of aquatic organisms, increases the energy consumption of living things and reduces dissolved oxygen levels (Sandu, 2018). Due to low oxygen levels and high ammonia levels in the hypolimnion, it is necessary to treat the discharged water to prevent adverse effects downstream, especially in low flow rivers. (Nürnberg, 2007).

We consider that there is limited information regarding how the discharge of the hypolimnion may influence the water quality of the downstream river and how parameters vary before and after discharge. Our objective is to understand how these processes interact with the river ecosystem. This information can be utilized for developing strategies to protect aquatic ecosystems.

MATERIALS AND METHODS

Study Site

Lake Kortowskie is located in the town of Olsztyn, Poland, covers an area of 89.7 ha and is fed by five streams. The maximum length of the lake is 1,660 m and the maximum width is 715 m (Rybak & Rybak, 1985). In the south-east, the Parkowy stream collects water from the nearby valley, but with a very low flow the amount of nutrients introduced into the lake is negligible.

The Starodworski stream has a catchment area of 0.55 km² and receives pollutants from a section of a building, feeding the lake to the south. In the southwest it flows into the Leśny stream, collecting water from an area of 11.3 km² (64.5% of this area includes forests, 18.5% arable land and 17% pastures and meadows). To the south, 300 m from the entrance of the Leśny stream, a drainage pipe discharges the collected water from an area of 0.5 km² (Dunalska, 2002). The only surface outlet of the reservoir is the Kortówka River

(Szymanski et al., 2013) which is also the outlet of the pipe for the removal of hypolimnion (Dunalska, 2002).

The aim of the study was the Kortówka River, which crosses the campus of the University of Warmia and Mazury in Olsztyn, from where the river has its source in Lake Kortowskie (the exit of the Olszewski pipeline) to the confluence with the Lyna River (Figure 1). The river has a maximum width of 2 m. It is very shallow, about 0.3 m, and slow flowing.

The measurements were performed at a distance of 1,695 m at six points as follows: 30 m downstream of the hypolimnion exhaust pipe (P1), gymnasium bridge (260 m) (P2), stadium bridge (425 m) (P3), bridge of the Faculty of Environmental Sciences, Department of Environmental Engineering (605 m) (P4), Volvo service bridge (1,220 m) (P5) and the last point 10 m upstream of the confluence with the river Lyna (1,685 m) (P6).

Two measurements were made on the Lyna River: upstream (30 m) (P7) and downstream (55 m) (P8) confluence.

The following parameters were measured in situ using the YSI 6600 V2 probe: temperature, dissolved oxygen (DO), pH, redox potential (ORP) and conductivity (EC). Additional measured parameters include: flow, salinity, turbidity, total dissolved solids, chlorophyll and blue-green algae, but these will not be discussed in this article.

Description of the "Kortowskie" experiment

One of the methods used to restore the lakes is the Olszewski method, also called the Kortowskie experiment, used to improve the water quality of Lake Kortowskie in Olsztyn (Wysocka et al., 2014). The method involves the selective discharge of water from the deep part of the lake together with the decanted organic particles, as well as the substances and microorganisms released from the sediments (Tandyrak et al., 2016).

In 1950, studies of Lake Kortowskie showed significant degradation of the water body, and in 1952 water in the southern section of the lake was deficient in oxygen for 134 days and hydrogen sulphide was present 5 m below the water surface.

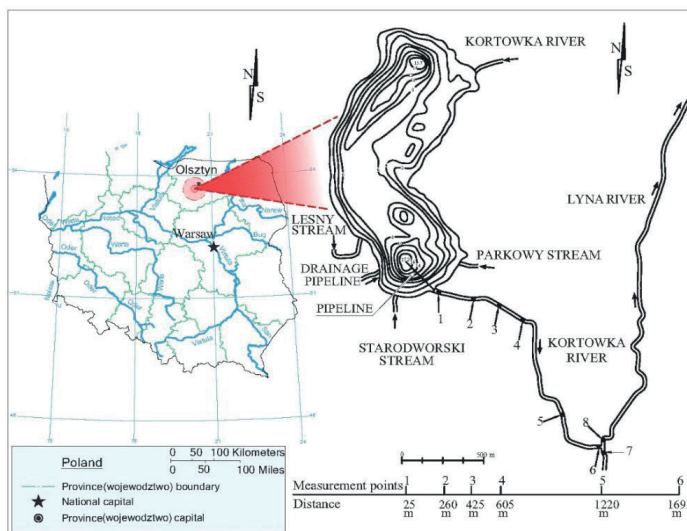


Figure 1. Lake Kortowskie and the location of the measurements at the Kortowka River

Between 1956 and 1967, the hypolimnion was evacuated in the summer, and in 1968 it was evacuated in the summer and winter (Dunalska et al., 2007).

Due to technical problems in 1973, the experiment was closed. Since then, the years 1956-1973 have been considered the first stage in the process of restoring Lake Kortowskie. The second stage began in 1976, and the new pipeline was built of fiberglass and polyester (Mientki & Teodorowicz, 1996).

The parameters of the pipeline are as follows: length 250 m, diameter 600 mm and maximum flow 0.25 m³/s. It is located in the southern section of the lake, being equipped with a device set on the outlet flow that allows the closure, opening and regulation of the amount of water discharged, because hypolimnion must be eliminated when the amounts of nutrients that accumulate are maximum (Dunalska, 2002).

Highly polluted waters are directed to the Kortowka River, which disturbs the chemical and biological balance in the original part of the river (Dunalska et al., 2007).

Changes in environmental factors lead to the development of aquatic plant and animal communities, the structure and functions of aquatic ecosystems with a number of different responses depending on the nature of these changes, their intensity and duration of action. Aquatic ecosystems, through their internal self-regulation mechanisms, succeed in a self-

purification process involving filtration, sedimentation, dissolution, dilution and oxygenation, to restore the affected components naturally (Momeu et al., 2018).

RESULTS AND DISCUSSIONS

The measurements performed for this study were divided into three stages as follows: before the experiment - stage I (March-June 2018), during the experiment - stage II (July-September 2018) and after the experiment - stage III (October 2018-May 2019).

From Figure 2 it can be seen that the water temperature changes with the season. The maximum temperature is 10.2°C in stage I, 18.6°C in stage II and 10.3°C in stage III; the lowest temperature is 9.7°C in stage I, 14.5°C in stage II and 8.2°C in stage III.

The effects of climatic conditions varied considerably from one season to another, and the greatest influences on the thermal regime of the water were observed in summer and autumn. The discharge of the cold water of the hypolimnion from the lake is discharged with an accentuated thermal exchange, weakening the thermal stratification and facilitating the mixing of the water column (Ying et al., 2012; Weber et al., 2017).

The increase in temperature in P7 and P8, measurements made on the Lysa River, may be due to the fact that the studied river segment is

lighter and deeper, thus allowing more heat exchange with the atmosphere (Chatanga et al., 2019).

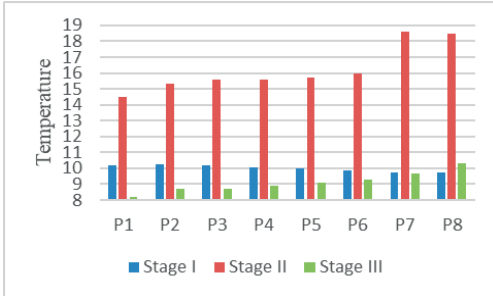


Figure 2. Seasonal temperature fluctuations in the Kortowka River and the Lyna River

The values of EC varied before the experiment from 401 $\mu\text{S}/\text{cm}$ to 480 $\mu\text{S}/\text{cm}$, during the experiment from 367 $\mu\text{S}/\text{cm}$ to 547 $\mu\text{S}/\text{cm}$, and after the experiment from 387 $\mu\text{S}/\text{cm}$ to 524 $\mu\text{S}/\text{cm}$. EC values are useful for estimating the concentration of total dissolved solids (TDS) in water (Rostom et al., 2017).

TDS values ranged from 260 mg/L to 312 mg/L before the experiment, from 239 mg/L to 356 mg/L during the experiment, and from 263 mg/L to 365 mg/L after the experiment.

From Figure 3, in the Kortowka River higher values can be observed during the experiment than before the experiment. Usually, the EC in surface waters is influenced by dissolved ions of natural and anthropogenic origin. Higher EC values during the experiment are a likely indication that significant proportions of dissolved ions were transported to the river during the evacuation of the hypolimnion from Lake Kortowskie (Chatanga et al., 2019; Miyittah et al., 2020).

As shown in Figure 4, during the experiment the pH values ranged from 7.07 to 7.98. The highest pH value was recorded at measurement P2, 260 m downstream of the hypolimnion discharge line, and the lowest at P6 and P8.

Before the experiment the maximum pH (7.32) was recorded in P2, while the minimum pH (7.26) was recorded in P5, and after the experiment the pH values increase, varying from 7.57 downstream of the hypolimnion drainage pipe, up to 7.63 downstream of the confluence of the Kortowka and Lyna rivers.

ORP values ranged from 32.47 mV to 53.77 mV before the experiment, from -158.08 mV to 5.27 mV during the experiment, and from -31.54 mV to 36.41 mV after the experiment, as shown in Figure 5.

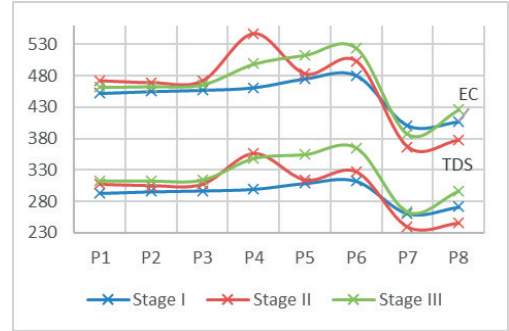


Figure 3. Seasonal changes in EC and TDS recorded in the Kortowka River and the Lyna River

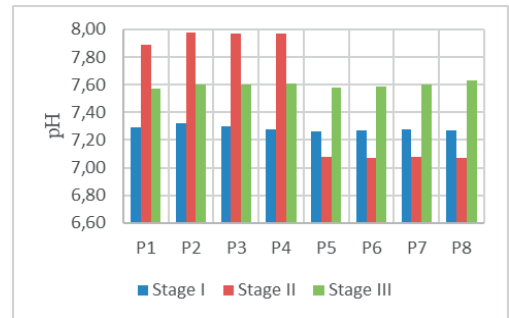


Figure 4. Seasonal variations in pH recorded in the Kortowka River and the Lyna River

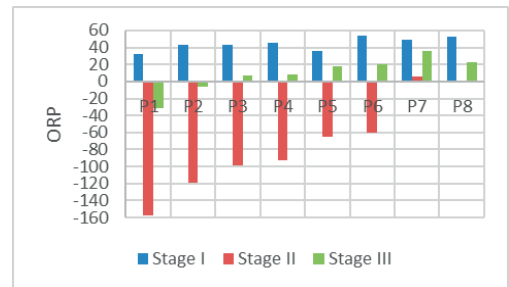


Figure 5. Seasonal variations in ORP in the Kortowka River and the Lyna River

The ORP is measured in addition to dissolved oxygen, as it can provide additional information about water quality and pollution (Rostom et al., 2017). In healthy waters, the ORP should be between 300 and 500 mV (Selim et al., 2023). In

this study, low ORP values were obtained in the waters of the Kortowka River due to the removal of hypolimnion from Lake Kortowskie. The values obtained for the DO index measured in the eight points for the experimental period, respectively March 2018 - May 2019, recorded averages located in the intervals:

- 8.1-11.2 mg/L for measurements made in the first stage;
- 0.4-1.91 mg/L for measurements made in the second stage;
- 4.66-10.81 mg/L for measurements made in the last stage.

As shown in Figure 6, before the experiment, the dissolved oxygen values showed a decreasing trend, except for the values in P4 (Kortowka river) and P8 (Lyna river), where an upward trend is observed.

The lowest values are recorded during the experiment. The decrease in DO concentration is closely linked to the increase in and accumulation of organic matter in water and is caused by the evacuation of hypolimnion from Lake Kortowskie (Kunz et al., 2013; Momeu et al., 2018).

It is observed that after the experiment the DO values showed an upward trend along the Kortowka River. On the Lyna River at P8, downstream of the Kortowka River, the value of DO decreases, being associated with the presence of nutrients such as nitrates and phosphates (Ying et al., 2012).

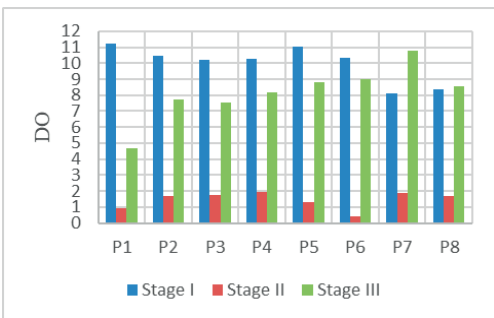


Figure 6. Seasonal variations in DO recorded in the Kortowka River and the Lyna River

The data set analysis was performed using correlation analysis to assess the relationship between the analyzed variables (Ilechukwu et al., 2020). A coefficient close to -1 or 1 means a strong negative or positive relationship between

two variables, and its value closest to 0 means that there is no linear relationship between them at a significant level with p-values less than 0.05 (Kothari et al., 2021; Sadeghi, 2022; Mehmood et al., 2024). As we can see, between the variables, occurs both a positive and a negative correlation, due to the significance of each variable analyzed. The correlation analysis is presented in Table 1.

Table 1. Correlation coefficient for the analyzed parameters

Parameters	T	EC	pH	ORP	DO
T	1				
EC	-0.151	1			
pH	-0.418	0.089	1		
ORP	-0.603	-0.354	0.291	1	
DO	-0.842	-0.071	0.467	0.835	1

The data were further verified by performing the Kaisere Meyere Olkin (KMO) and Bartlett tests to verify that the variables could be factorized efficiently (Table 2) (Balata et al., 2022).

The KMO index compares the values of the correlations between the variables and those of the partial correlations. In general, this index should be greater than 0.5 for a satisfactory analysis of the factors (Lyon et al., 2012; Samian et al., 2015).

In this study, the KMO had a value of 0.629. The value of the Bartlett's Test of Sphericity (66.742, Sig = 0.000) is small enough to reject the hypothesis that the variables are uncorrelated, as a result there is a strong relationship between the data (Ajtai et al., 2023; Chen et al., 2023; Xue et al., 2023). These values indicate the presence of one or more common factors which motivate the application of a factor reduction procedure.

Table 2. KMO test and Bartlett test

Kaiser-Meyer-Olkin Measure of Sampling Adequacy		0.629
Bartlett's Test of Sphericity	Approx. Chi-Square	66.724
	df	10
	Sig.	0.000

Table 3 shows the Rotated Component Matrix, which transforms the principal factors to find the relationship between them and reduce the data variability. When all component rotations are performed, a new cycle of rotations begins, and the process repeats until a maximum number of

iterations is reached; in our case, rotation converges in just 3 iterations (Weide & Beauducel, 2019; Rahman et al., 2021; Tiwari et al., 2023).

Table 3. Rotated Component Matrix

	Component	
	1	2
Dissolved oxygen	0.951	-0.178
Temperature	-0.903	-0.097
ORP	0.780	-0.523
pH	0.643	0.245
Electrical conductivity	0.062	0.944
Extraction Method: Principal Component Analysis.		
Rotation Method: Varimax with Kaiser Normalization.		
a. Rotation convergent in 3 iterations.		

The factor structure for the analyzed variables is:

- the first factor is made up of the variables DO (0.951), ORP (0.780) and pH (0.643);
- the second factor consists only of the variable EC (0.944).

Using this type of factor analysis, we can obtain useful information on the factors that have a great influence on water quality, giving statisticians the opportunity to track its upward or downward evolution (Elkorashey, 2022).

CONCLUSIONS

This study highlights the usefulness of applying the method of analyzing key components in the field of water and environmental sciences, with the ultimate goal of identifying those factors that significantly influence water quality in the current context of globalization and accelerated development.

The immediate effect of this type of application may be the ability to analyze, test and improve those factors that are directly responsible for the level of water quality. Knowing and analyzing these factors, programs can be initiated to bring water quality to a higher level.

DO values were, on average, less than 6.5 mg/L throughout the experimental period, suggesting that the river was in low oxygen conditions, leading to anaerobic decomposition of excess organic matter.

Significant changes in all parameters except pH can be attributed to the evacuation of hypolimnion from Lake Kortowskie.

ACKNOWLEDGEMENTS

This research work was carried out with the support of Prof. Dr. Hab. Katarzyna Glińska-Lewczuk, Ph.D. Katarzyna Sobczyńska-Wójcik, Ph.D. Eng. Szymon Kobus, and Andrzej Rochwerger from the Department of Water Resources, Climatology, and Environmental Management, Faculty of Environmental Management and Agriculture, University of Warmia and Mazury in Olsztyn, Poland.

Special thanks are extended to Lect. Ph.D. Eng. Marius Telișcă from the Faculty of Hydrotechnics, Geodesy, and Environmental Engineering, "Gheorghe Asachi" Technical University of Iasi, Romania, for guidance within the Erasmus+ program.

REFERENCES

- Ajtai, I., Ștefănie, H., Maloș, C., Botezan, C., Radovici, A., Bizău-Cârstea, M., & Băciu, C. (2023). Mapping social vulnerability to floods. A comprehensive framework using a vulnerability index approach and PCA analysis. *Ecological Indicators*, 154, 110838.
- Balata, E.E., Pinto, P., & Moreira da Silva, M. (2022). Latent dimensions between water use and socio-economic development: A global exploratory statistical analysis. *Regional Sustainability*, 3(3), 269–280.
- Bryant, L.D., Gantzer, P.A., & Little, J.C. (2011). Increased sediment oxygen uptake caused by oxygenation-induced hypolimnetic mixing. *Water Research*, 45(12), 3692–3703.
- Chatanga, P., Ntuli, V., Mugomeri, E., Keketsi, T., & Chikowore, N.V.T. (2019). Situational analysis of physico-chemical, biochemical and microbiological quality of water along Mohokare River, Lesotho. *The Egyptian Journal of Aquatic Research*, 45(1), 45–51.
- Chen, K., Liu, Q., Peng, W., Liu, Y., & Wang, Z. (2023). Source apportionment of river water pollution in a typical agricultural city of Anhui Province, eastern China using multivariate statistical techniques with APCS-MLR. *Water Science and Engineering*, 16(2), 165–174, ISSN 1674-2370.
- Dunalska, J.A. (2002). Influence of limited water flow in a pipeline on the nutrients budget in a lake restored by hypolimnetic withdrawal method. *Polish Journal of Environmental Studies*, 11(6), 631–637.
- Dunalska, J.A., Wisniewski, G., & Mientki, C. (2007). Assessment of multi-year (1956–2003) hypolimnetic withdrawal from Lake Kortowskie, Poland. *Lake and Reservoir Management*, 23, 377–387.
- Dunalska, J.A., Stach, P.A., Jaworska, B., Górnica, D., & Gomulka, P. (2014). Ecosystem metabolism in a lake restored by hypolimnetic withdrawal. *Ecological Engineering*, 73, 616–623.

- Elkorashey, R.M. (2022). Utilizing chemometric techniques to evaluate water quality spatial and temporal variation. A case study: Bahr El-Baqar drain — Egypt. *Environmental Technology & Innovation*, 26, 102332, ISSN 2352-1864.
- Ilechukwu, I., Olusina, T.A., & Echeta, O.C. (2020). Physicochemical analysis of water and sediments of Usuma Dam, Abuja, Nigeria. *Ovidius University Annals of Chemistry*, 31(2), 80–87.
- Kothari, V., Vij, S., Sharma, S.K., & Gupta, N. (2021). Correlation of various water quality parameters and water quality index of districts of Uttarakhand. *Environmental and Sustainability Indicators*, 9, 100093, ISSN 2665-9727.
- Kunz, M.J., Senn, D.B., Wehrli, B., Mwelwa, E.M., & Wüest, A. (2013). Optimizing turbine withdrawal from a tropical reservoir for improved water quality in downstream wetlands. *Water Resources Research*, 49, 5570–5584.
- Lyon, S.W., Nathanson, M., Spans, A., Grabs, T., Laudon, H., Temnerud, J., Bishop, K.H., & Seibert, J. (2012). Specific discharge variability in a boreal landscape. *Water Resour. Res.*, 48, W08506.
- Mehmood, K., Anees, S.A., Luo, M., Akram, M., Zubair, M., Khan, K.A., & Khan, W.R. (2024). Assessing Chilgoza pine (*Pinus gerardiana*) forest fire severity: remote sensing analysis, correlations, and predictive modeling for enhanced management strategies. *Trees, Forests and People*, 100521.
- Mientki, C., & Teodorowicz, M. (1996). Assessment of the effects of hypolimnion water removal from the Kortowskie lake. *Chemistry for the Protection of the Environment*, 2, 361–374.
- Miyittah, M.K., Tulashe, S.K., Tsyawo, F.W., Sarfo, J.K., & Darko, A.A. (2020). Assessment of surface water quality status of the Aby Lagoon System in the Western Region of Ghana. *Heliyon*, 6(7), e04466.
- Momeu, L., Cimpean, M., & Battes, K. (2018). Hidrobiologie. *Presa Universitară Clujeană*, 1–131, ISBN: 978-606-37-0321-8.
- Nürnberg, G.K., Hartley, R., & Davis, E., (1987). Hypolimnetic withdrawal in two north american lakes with anoxic phosphorus release from the sediment. *Water Research*, 21(8), 923–928.
- Nürnberg, G.K. (2007). Lake responses to long-term hypolimnetic withdrawal treatments. *Lake and Reservoir Management*, 23(4), 388–409.
- Rahman, A., Jahanara, I., & Jolly, Y.N. (2021). Assessment of physicochemical properties of water and their seasonal variation in an urban river in Bangladesh. *Water Science and Engineering*, 14(2), 139–148.
- Rostom, N.G., Shalaby, A.A., Issa, Y.M., & Afifi, A.A. (2017). Evaluation of Mariut Lake water quality using Hyperspectral Remote Sensing and laboratory works. *The Egyptian Journal of Remote Sensing and Space Science*, 20(1), S39–S48.
- Rybak, I., & Rybak, M. (1985). Development of Lake Kortowskie in relation to the climatic changes in three Holocene periods. *Hydrobiologia*, 124(2), 151–166.
- Sadeghi, B. (2022). Chatterjee Correlation Coefficient: A robust alternative for classic correlation methods in geochemical studies- (including “TripleCpy” Python package). *Ore Geology Reviews*, 146, 104954.
- Samian, M., Naderi Mahdei, K., Saadi, H., & Movahedi, R. (2015). Identifying factors affecting optimal management of agricultural water. *Journal of the Saudi Society of Agricultural Sciences*, 14(1), 11–18.
- Sandu, A.V. (2018). Managementul de Mediu în Ingineria Materialelor, I. Teorie și aplicații pentru studenți. *Ed. Pim*, 164.
- Selim, A., Shuvo, S.N.A., Islam, M.M., Moniruzzaman, M., Shah, S., & Ohiduzzaman, M. (2023). Predictive models for dissolved oxygen in an urban lake by regression analysis and artificial neural network. *Total Environment Research Themes*, 7, 100066.
- Szymanski, D., Dunalska, J.A., Jaworska, B., Bigaj, I., Zielinski, R., & Nowosad, E. (2013). Seasonal variability of primary production and respiration of phytoplankton in the littoral zone of an eutrophic lake. *Rocznik Ochrona Srodowiska*, 15, 2573–2590.
- Șalaru, V., Dudnicenco, T., & Tincu, A. (2007). Troficitatea unor lacuri din municipiul Chișinău. *Biologie, Științe ale naturii*, 1, 1857–1735.
- Tandyrak, R., Golaś, I., Parszuto, K., Bowszys, M., Szymański, D., Harnisz, M., Brudniak, A., & Wysocka, I. (2016). The effect of lake restoration by the hypolimnetic withdrawal method on the intensity of ambient odour. *Journal of limnology*, 75(3).
- Tiwari, N.K., Mohanty, T.R., Das Gupta, S., Roy, S., Swain, H.S., Baitha, R., Ramteke, M.H., & Das, B.K. (2023). Hemato-biochemical alteration in the bronze featherback *Notopterus notopterus* (Pallas, 1769) as a biomonitoring tool to assess riverine pollution and ecology: a case study from the middle and lower stretch of river Ganga. *Environ Sci Pollut Res*, 30, 46826–46846.
- Weber, M., Rinke, K., Hipsey, M.R., & Boehrer, B. (2017). Optimizing withdrawal from drinking water reservoirs to reduce downstream temperature pollution and reservoir hypoxia. *Journal of Environmental Management*, 197, 96–105.
- Weide, A.C., & Beauducel, A. (2019). Varimax rotation based on gradient projection is a feasible alternative to SPSS. *Frontiers in Psychology*, 10.
- Wysocka, I., Brudniak, A., & Kowalczyk, J. (2014). Odor nuisance related to Lake Kortowskie restoration by the hypolimnetic withdrawal. *Ochrona Srodowiska*, 36, 29–32.
- Xue, Y., Ma, Y., Long, G., He, H., Li, Z., Yan, Z., Wan, J., Zhang, S., & Zhu, B. (2023). Evaluation of water quality pollution and analysis of vertical distribution characteristics of typical Rivers in the Pearl River Delta, South China. *Journal of Sea Research*, 193, 102380.
- Ying, L., Jiao, M., & Yong, L. (2012). Analysis of eutrophication of Yangtze River Yibin section. *Energy Procedia*, 16(A), 203–210.

SUSTAINABLE APPROACH OF NUTRIENT FILM TECHNOLOGY BASED ON EFFICIENT WATER AND ENERGY USE - INTERMEDIATE RESULTS

**Augustina Sandina TRONAC, Dragoș DRĂCEA,
Sebastian MUSTĂȚĂ, Oana Alina NIȚU**

University of Agronomic Sciences and Veterinary Medicine of Bucharest,
59 Marasti Blvd, District 1, Bucharest, Romania

Corresponding author email: augustina.tronac@yahoo.com

Abstract

The paper approach the greenhouse plant yield analyzing water and energy resources embedded in product when Nutrient Film Technology (NFT) is applied. Examining the process, identifying the phases, the intervening components, calibrating the model, it is possible, as intermediate results, to determine for each growth element the water and energy consumption, in order to offer solutions for reducing water, nutrients, electricity content, diminishing production costs and being environmentally friendly. The consequences are important for functional engineering of plant growth as well as for technological developments to make natural resources more efficient in a sustainable manner. The research will continue and will try to define the moment in the evolution of the culture in which harvesting is optimal from the point of view of the included resources, the resulting nutritional value, the minimum impact on the environment.

Key words: nutrient film technology (NFT); greenhouse plant yield; water and energy use; efficiency; sustainability.

INTRODUCTION

Climate change as extreme phenomena, global population growth, global energy crisis related to resources or pollution, water shortages identified at certain points in time or in certain territories, all of these have major implications in the field of agriculture. General food safety, with a special emphasis on vegetables and fruits due to their beneficial effects on human health, represents the desired for which the manner of designing and managing agricultural activities needs to be adapted (Liantas et al., 2023). Improvements in horticultural breeding technologies that lead to quality, sustainable, and economically efficient products are valuable (Dobrin et al., 2018).

For the constraints listed, cultivation in protected spaces is a solution provided that it is carried out with the evaluation of the efficiency of water and energy use, the control of environmental factors (temperature, humidity, light, CO₂ concentration) imposes pressure on these two resources (Khan et al., 2018), cultivation in greenhouses being an example of horticultural practice with high quantitative and qualitative productions, which, however, involves high initial costs and during the exploitation period important consumption of water and energy.

The horticultural production (especially protected) - environment interaction is biunivocal: the resources included in the production affect the climate, it changes and alters the future conditions of plant growth; for example, waves of high and low temperatures strongly influence the operating parameters of a greenhouse because they require adaptation processes to maintain constant indoor plant growth conditions regardless of the values recorded in the external environment, such as: choosing genetic material resistant to water stress, natural ventilation for cooling and necessary humidity, the introduction of renewable energy sources, optimal exposure to light, horticultural technologies to reduce the duration of growth, etc., which would lead to sustainable options (Gruda et al., 2019). It is necessary to evaluate the efficiency of water and energy used per unit or kg of product obtained - kg product/m³ water - WUE (water use efficiency), respectively kg of product/kWh - EUE (energy use efficiency) (Pennisi et al., 2020) as well as the impact on the general production environment in the greenhouse depending on the chosen hydroponic system, the season in which the culture is carried out, the energy mix, the temperature maintained at the

plant root level and in the greenhouse atmosphere (Liantas et al., 2023).

The carbon footprint is a valuable indicator for evaluating the impact on, being able to be established for the entire process or for its components (water consumption, energy consumption). The European Commission (EU, 2021) recommends the environmental footprint in the form of PEF (Product Environmental Footprint) and OEF or EF (Organization Environmental Footprint) as a method based on LCA (Life Cycle Assessment) to quantify the environmental impact of products and organizations. For representative products and companies that have complied in determining the environmental footprint, data can be found in the EU LCA database (EPLCA, 2023). If production in greenhouses is considered the most conservative solution in terms of water use, much diminished compared to cultivation in open spaces, energy consumption represents the most important component of the environmental impact (Hirich, Choukr-Allah, 2017). Thus, according to the public data of FAO (2022), the share of CO₂-eq emissions from agri-food systems caused by energy use in 2020 in Romania was 83.1091% (FAO, 2023), the total CO₂- emissions eq from the use of energy in agriculture being 68496.7 ktons, respectively from the use of energy in farms 1647.321 ktons. By comparison, Portugal has a share of 41.3315%, with 36676.6 ktons and from energy use in farms 1256.6124 ktons, while Great Britain registers 72.5315%, with 298558.85 ktons, and from energy use in farms 2353.0178 ktons. Analyzing the variation in the share of CO₂-eq emissions in the period 2001-2020 (Figure 1), Romania had a slight upward trend, while Portugal has a strong decreasing trend, UK a slight downward trend as EU and Europe, with the specification that at the level of the EU and Europe as a whole, peaks were recorded during this period, higher than the end values, in 2011.

Although greenhouse crops are an important part of agricultural production, and this way of cultivation is very energy-intensive, there are only a few researches dedicated to this field (Paris et al., 2022), the Netherlands having a research department of Wageningen University which is dedicated to identifying solutions to reduce the dependence on gas in energy production, to reduce the amount of energy, to

achieve sustainable productions, to reduce costs so that Dutch horticulture survives (Wageningen University & Research, 2020).

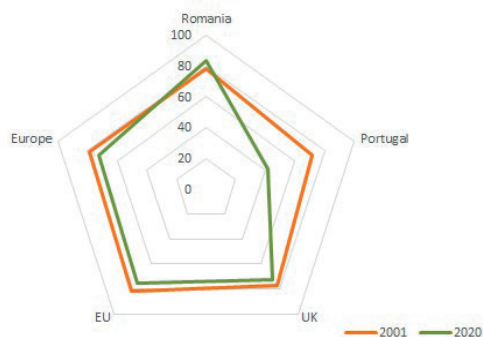


Figure 1. Share of CO₂-eq emissions for Romania, Portugal, UK, EU, Europe, years 2001 and 2020

Control includes temperature, humidity, water and fertilizer, light, CO₂ concentration, horticultural technologies leading to impressive increases in yields, up to 6 times (Paris et al., 2022). Options for greenhouse heating include air heaters, district heating through pipes, boilers, cogeneration systems, natural gas, heat pumps, with energy sources that can be based on fossil fuels, coming from the national energy system, own plants that provide both heat as well as electricity, respectively heat pumps, any combination of these variants being possible. It could be noticed that the literature consulted covers either warm areas, where cooling is the main concern, or cold areas, where, on the contrary, heating is predominant; in temperate zones, both aspects occur, making it more difficult to choose the solution and requiring temperature regulation almost throughout the year!

In order to determine the embodied energy in the case of protected crops, energy inputs from the production of fertilizers, for pumping the water-nutrient mixture, for the production of the growth support, for water recirculation, etc., are included, the age of the greenhouse being directly proportional to its consumption (Paris et al., 2022).

The elimination of energy based on fossil fuel to protect the environment and achieve a sustainable process is the subject of the European project AgroFossilFree (EU, 2020) started in October 2020 which addresses impro-

ving the efficiency of energy use; none of the scientific articles that are uploaded on the project platform on the topic of "resource conservation agriculture/energy efficiency" address the growth of horticultural products in controlled environments.

MATERIALS AND METHODS

In order to define the NFT water and energy use it is needed to identify the process stages, to establish the component activities, the flows, inputs and outputs, the influence factors and the way of estimating the weights, the definition of the functional units. The steps are:

- the choice and purchase of seeds, in this case being the Lollo Bionda and Lollo Rosa varieties from Holland Farming - 90% germination, i.e. a total of 1340 seeds for a number of 1200 germinated plants;
- planting them in pressed peat pellets 33 mm Jiffy - 1200 pieces;
- placing in the Jiffy-pot and maintaining it until the root system develops;
- replanting of seedlings with Jiffy pots in 6 troughs with NFT system from the greenhouse compartment whose dimensions are 8 m wide, 20 m long, 6.2 m height at the crest, with an area of 160 m² and a volume of 912 m³;
- all plants are permanently fed with nutrient solution that is formed with 1 m³ of water in which 10 l of nutrient solution A and 10 l of nutrient solution B are added; for nutrient solution A and the nutrient solution B the recipes at 0.25 m³ are shown in Tabel 1.

Nutrient solutions contain different chemical compounds, each of those needed: nitrogen (nitrate, NO₃, ammonium nitrate, NH₄NO₃) is essential for leaf growth and general plant development, Potassium (Potassium oxide, K₂O, Potassium nitrate, KNO₃, Potassium sulfate, K₂SO₄) contributes to the health of the plants vascular system and helps to regulate enzymatic processes, Iron, Fe is vital for the synthesis of chlorophyll and the efficient functioning of the photosynthesis process, Mono Potassium Phosphate, KH₂PO₄ and Magnesium sulfate, MgSO₄ are important for cellular energy, microelements (Zinc sulfate, ZnSO₄, Copper sulfate, CuSO₄, Sodium molybdate, MoNa₂O₄, Borron, B) are essential for biochemical processes at the cellular level.

Tabel 1. Nutrient solutions recipes

Nutrient solution A		Nutrient solution B	
Component	Quant (kg)	Component	Quant (kg)
water	250.00	water	250.00
NO ₃	18.75	KH ₂ PO ₄	7.50
K ₂ O	12.50	KNO ₃	12.50
NH ₄ NO ₃	1.25	K ₂ SO ₄	2.50
HNO ₃ (1.4 kg/l; 63.7% conc)	1.59 (1.75l)	MgSO ₄	2.50
Fe (6% conc)	6.50	KCl	1.25
		HNO ₃ (1.4 kg/l; 54.6% conc)	1.37 (1.5l)
		ZnSO ₄	12.50.10 ⁻³
		CuSO ₄	10.00.10 ⁻³
		B	5.00.10 ⁻³
		MoNa ₂ O ₄	5.00.10 ⁻³

A quantity of approx. 95 l/day is used (result as an average of a period of 3 weeks from the location - 2000 l being prepared).

- recirculation is done permanently, the pump being LOWARA SHE 32-160/22/C with a flow rate of 27 m³/h, a variable pumping height between the minimum admissible of 18 m and the maximum admissible of 32.5 m, a power of 2.2 kW;

- the water used comes from the precipitation captured and stored in an underground tank of 100 m³ from which it is taken with a vertical mixing pump GRUNDFOS CR 20-03 A-F-A-E-HQQE with a flow rate of 21 m³/h, H_{pumping min} 34.6 m, H_{pumping max} = 43.9 m, power 4 kW; the water mixed with the nutrient solution is then transmitted to the compartment tank from where it is permanently transmitted to the gutters;

- the compartment is heated with the help of a 1162 kW power plant (serves the entire assembly, which has an area of 2756 m²) which is fueled by methane gas; in the premises, the heat agent with a temperature of 70°C circulates through pipes, where it reaches by using a GRUNDFOS MAGNA 32-80 180 pump with a minimum power of 10 W and a maximum of 140 W;

- the 6 troughs are divided as follows:

2 - control - receive only nutrient;

2 - sample 1 - they receive nutrients and are oxygenated with an air pump with 4 channels, 4 membranes and Sera Precision air 550 R plus regulation, having the characteristics: maximum 550l/h, 150 mbar, power 12 W;

2 - sample 2 - receive nutrients, are oxygenated, are subjected to LED light max 12 h/day, depending on the lighting data provided by the meteorological station; the LED light is provided by 4 Kathay Waterproof Plant Grow

lamps with a wavelength of 380-840 nm and a power of 100 W;
 - the compartment monitors the CO₂ concentration and "corrects" it by bringing it to a general constant by operating the ventilation hatches, according to the graph provided by the PRIVA software; 2 T56B4 type engines are used with a maximum power of 0.11 kW;
 - to protect the crop in case of solar radiation exceeding the value of 500 W/m², the side curtains are automatically activated by means of a T56B4 motor with a maximum power of 0.11 kW;
 - to protect the crop in case of outside temperatures lower than 5°C, the thermal barrier type curtains are activated automatically by means of 2 tubular motors 230 W and actuation time 10 min per direction.

Tests prior to the experiments, determination of the empty operation values associated with the system, establishment of calculation relationships and correlations - prior to the experiments, the compartment was emptied, sanitized and sterilized, so as to avoid the effects on the plants generated by pathogenic factors. For this activity, 500 l and 15 l of aqueous solution with 150 ml of MEMOCLEAN disinfectant were used, the washing being carried out with a pressure washer with a power of 2.8 kW.

RESULTS AND DISCUSSIONS

The operating values are derived from the characteristics of the equipment involved, as summarized in Figure 2, analyzing every process involved in production.

The number of hours of equipment operation is shown in Figure 3, dividing the type into permanent, periodic, or occasional categories. For preparation of nutritious materials – (approx. 95 l/zi) values listed in Tabel 2 are to be taken into consideration.

Estimation by measurement and calculation of values for water and energy consumption - The energy measuring meters were installed quite late, so that only the periods of vegetation in which the heating, administration of nutrient solution, pump were constantly used were captured of air, LED lighting and an average value of 91 kW/day was determined, of low relevance given the small number of records, to be recalculated after each week and correlated as

far as possible with the growth stages of the lettuce plants.

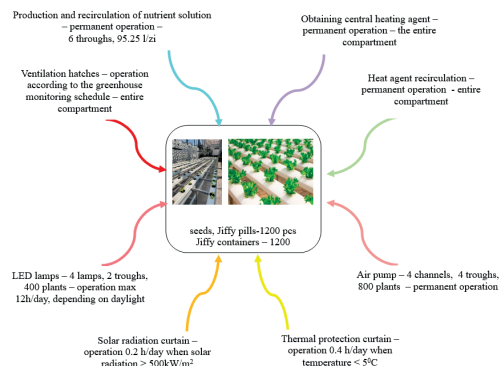


Figure 2. Embedded values in NFT system lettuce production

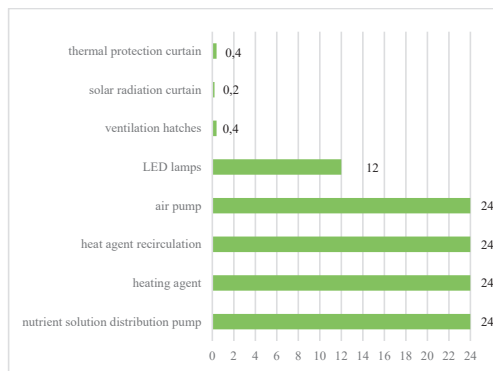


Figure 3. Equipment operation hours

Tabel 2. Nutrient solutions intake per day

Solution A		Solution B	
Component	Quant (l/day)	Component	Quant (l/day)
Water	82.00	Water	82.00
NO ₃	6.15	KN ₂ PO ₄	2.46
K ₂ O	4.10	KNO ₃	4.1
NH ₄ NO ₃	0.41	K ₂ SO ₄	0.82
Fe	1.968	MgSO ₄	0.82
HNO ₃	0.52234	KCl	0.41
Total	95.15034	ZnSO ₄	4.1
		CuSO ₄	0.00328
		B	0.00164
		MoNa ₂ O ₄	0.00164
		HNO ₃	0.44772
		Total	95.6428

Regarding the calculation estimation of water and energy consumption, it is considered that:

- water for making the thermal agent is used in a closed circuit, so it is not considered
- the water for the nutrient solution is approx. 90 l/day;

- water for sanitizing the compartment before the experiment 0.5 m³, meaning 16.67 l/day, if the value were uniformly distributed during the experiment;
- energy consumption for every activity is detailed in Figure 4.

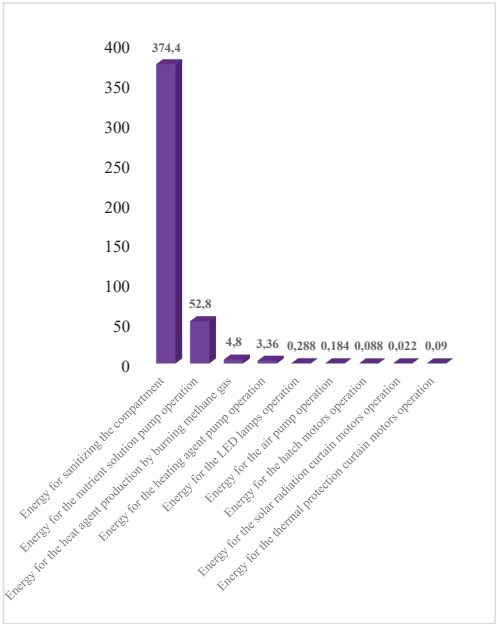


Figure 4. Energy consumption (kWh/day)

Considering that the entire amount of energy is obtained from Thermo-Electric Plants based on methane gas, at a conversion of 1 kWh * 0.2 = 1 kg CO₂ then the CO₂ emission values will result per day as in Figure 5, and for the entire experiment it is estimated of 2.616 tons CO₂ emission.

The highest CO₂ emission value comes from the heating system, followed by the system administrating the nutrient solution.

In percentage terms, 85.86% represents the heat agent production by burning methane gas and the other 12.11% the nutrient solution pump operation, only 2.03% being targeted for any other activity.

For efficiency of using energy, it could be analysed the graph in Figure 6.

It seems to be suggested that the period with the maximum efficiency of energy use is the maturity, its earlier harvesting leading to less judicious use.

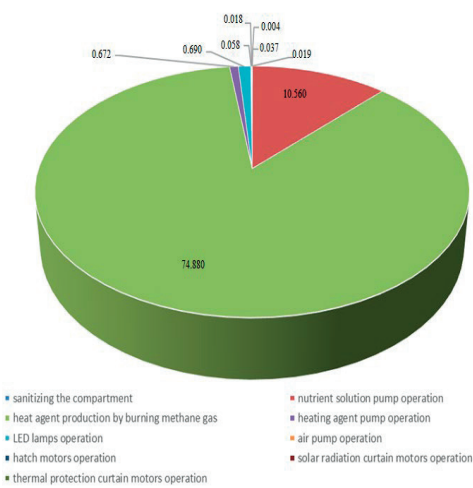


Figure 5. CO₂ emission (kg CO₂/day)

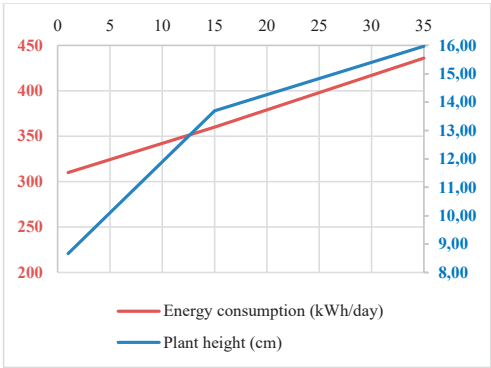


Figure 6. Energy consumption over lettuce growth in time

CONCLUSIONS

Global warming, the increase in energy demand, the change in food preferences with a preponderance of plant-based food, the increase in the incidence of obesity, all of these are arguments for augmentation of protected areas vegetable production, in a sustainable manner. The research presents lettuce planting in NFT system of a reasonable density value, returning to 7.5 plants/m²; the amount of energy is about and a consumption of 436 kWh and approx 95 l/day of water represents 80 ml/day.plant, and 178 m³/ha.month, only 12% compared to classic irrigation systems in unprotected spaces or field crops, where the value is about 1500 m³/ha month of water.

Next research stage will address the impact of the values in the process, the elements that lead to the highest values in correlation with the stages of development of lettuce plants in the NFT system will be followed, making the connection between the lettuce nutritional value and the efficiency of energy use, respectively plant dimensions.

ACKNOWLEDGEMENTS

This research work was carried out with the support of the University of Agronomic Sciences and Veterinary Medicine of Bucharest and is financed through Internal Project no. 850/30.06.2023.

REFERENCES

- Dobrin, A., Ivan, E.S., Jerca, I.O., Bera, I.R., Ciceoi, R., Samih, A.A. (2018). The accumulation of nutrients and contaminants in aromatic plants grown in a hydroponic system, "Agriculture for Life, Life for Agriculture" Conference Proceedings, 1(1), 284-289, <https://doi.org/10.2478/alife-2018-0042>
- EU (oct. (2020) *AgroFossilFree project*. <https://www.agrofossilfree.eu/project-structure/>
- EU, Commission recommendation 2021/2279 of 15 (December 2021) *on the use of the Environmental Footprint methods to measure and communicate the life cycle environmental performance of products and organisations*. <https://eur-lex.europa.eu/legal-content/EN/TXT/PDF/?uri=OJ:L:2021:471:FULL>
- EU, European Platform on LCA, EPLCA. (2023). <https://eplca.jrc.ec.europa.eu/EF-node>
- Food and Agriculture Organization of the United Nations, *FAO, faostat – Statistics*. (2022). <https://www.fao.org/faostat/en/#data/EM>
- Gruda, N.S., Bisbis, M., Tanny, J. (2019). Influence of climate change on protected cultivation: impacts and sustainable adaptation strategies - a review. *Journal of Cleaner Production*, 225, 481-495, <https://doi.org/10.1016/j.jclepro.2019.03.210>
- Hirich, A., Choukr-Allah, R. (2017). *Water and energy efficiency of greenhouse and nethouse under desert conditions of UAE: agronomic and economic analysis*. Chapter in Water resources in arid areas: the way forward. Ed. Abdalla et al., Springer Water, pp. 481-499, https://doi.org/10.1007/978-3-319-51856-5_28
- Khan, F.A., Kurklu, A., Ghafoor, A., Ali, Q., Umair, M., Shahzaib (2018). A review on hydroponic greenhouse cultivation for sustainable agriculture. *International Journal of Agriculture, Environment and Food Sciences*, 2(2), 59-66, <https://doi.org/10.31015/iaefs.18010>
- Liantas, G., Chatzigeorgiou, I., Ravani, M. Koukounaras, A., Ntinis, G. (2023). Energy use efficiency and carbon footprint of greenhouse hydroponic cultivation using public grid and PVs as energy providers. *Sustainability*, 15, 1024, 1-14, <https://doi.org/10.3390/su15021024>
- Paris, B., Vandroou, F., Balafoutis, A.T., Vaiopoulos, K., Kyriakarakos, G., Manollakos, D., Papadakis, G. (2022). Energy use in greenhouses in the EU: a review recommending energy efficiency measures and renewable energy sources adoption. *Applies Sciences*, 12, 5150, 1-19, <https://doi.org/10.3390/app12105150>
- Pennisi, G., Pistillo, A., Orsini, A., Cellini, A., Spinelli, F., Nicola, S., Fernandez, J.A., Crepaldi, A., Gianquinto, G., Marcelis, L.F.M. (2020). Optimal light intensity for sustainable water and energy use in indoor cultivation of lettuce and basil under red and blue LEDs. *Scientia Horticulturae*, 272, 1-10, <https://doi.org/10.1016/j.scienta.2020.109508>
- Wageningen University & Research, *Greenhouse 2030: Sustainable production for the future – project* (2020). <https://www.wur.nl/en/research-results/research-institutes/plant-research/greenhouse-horticulture/show-greenhouse/greenhouse2030.htm>

ADVANCE HYDRAULIC MODELING FOR IRRIGATION SYSTEMS, CASE STUDY SPP15 IRRIGATION PLOT HOTĂRANI - ROMANIA

**Daniela-Cristina UNTARU, Teodor-Eugen MAN, Robert BEILICCI,
Mircea VISESCU, Erika BEILICCI, Antonia-Mariana PASC**

Politehnica University of Timisoara,
1A Splaiul Spiru Haret, Timisoara, Romania

Corresponding author email: mircea.visescu@upt.ro

Abstract

The numerical models commonly used for pressurized water distribution networks can also be adapted for modeling underground irrigation networks, which has also been done in this paper. Software packages such as Epanet, Mike Urban, etc. are usually designed for drinking water supply applications thus requiring adaptation of boundary conditions specific to underground irrigation networks. In this case study the hydraulic modelling of the irrigation network was done with the advanced Mike Urban software package. Following the modelling, the sizing of the newly designed pipeline network, the diagrams of pressures, speeds, flows, as well as the evolution in time in various operating scenarios were performed. The investment of the modernization and rehabilitation of OUA Hotarani was financed currently through the 2023-2027 Strategic Program, intervention DR-25. In our paper we present the current nonfunctional and proposed rehabilitated functional situation of the SPP15 Hotarani irrigation system. Modernization by using new/modern mobile irrigation by sprinkling equipment ensures the operation at superior technical parameters, water, and energy saving.

Key words: head loss, hydraulic modelling, irrigation sprinkler system, pressure diagram, rehabilitation.

INTRODUCTION

Through its rural development policy, the European Union (EU) aims to help rural areas meet the multiple economic, social, and environmental challenges that the twenty-first century brings. This policy forms the second pillar of the Common Agricultural Policy (CAP), which includes specific measures and funding programs dedicated to rural development. DR-25, as outlined in Regulation (EU) 2021/2115 of the European Parliament and of the Council dated 2 December 2021, pertains to the upgrading of irrigation infrastructure. It aligns with the stipulations laid out in Articles 73 and 74 and supports the attainment of Specific Objective 5, which focuses on advancing sustainable development and effective management of natural resources like water, soil, and air. This objective includes endeavors to diminish reliance on chemicals. (AFIR, 2024).

Climate change poses significant challenges to existing water resources with implications for agricultural productivity, water security, and community well-being (UN, 2016; Sandu &

Virsta, 2021). The adverse effects of climate change manifest through diminished crop yields and cultivated land, disruptions to both living and non-living components of ecosystems, financial setbacks, heightened labor demands, and escalated expenses for equipment. Agricultural irrigation stands as the primary consumer of water, representing over 70% of global water withdrawals, and plays a critical role in nourishing the world's populace. Water management in agriculture is very complex. Options in agricultural water management include a wide range of technical, economic, social and infrastructure factors (Çetin, 2023; Iglesias & Garroteb, 2015). Given the poor adaptation of existing infrastructure to new agricultural structures, the sector remains vulnerable to climatic conditions (frequent alternation, drought, and flooding), with significant economic effects on the economic viability of farms. Although the area arranged for irrigation has not decreased, the area irrigated differs from year to year, due to various causes, such as: weather conditions, lack of capital for investments in modernizing irrigation infrastructure, and implicitly lack of

access to new technologies leading to improved energy efficiency and reduced water losses, as well as the cost of water due to the liberalization of electricity prices for irrigation. The adaptation of infrastructure to the new agricultural structure, as well as its efficient use, requires investments for modernization and development. Droughts, floods, and other threats related to climate change have a significant impact on production stability and national food security (Ivanescu et al., 2016). The lack of adequate infrastructure contributes to limiting opportunities for economic development despite the existence of agricultural potential. In order to adapt to the effects of climate change and protect the environment and for competitive reasons, it is necessary to modernize irrigation facilities to ensure efficient water use, using new technologies leading to a reduction in water consumption at investment level, and to reduce pressure on surface water bodies (ANIF, 2024). Numerous mathematical models have been created to evaluate water resources management, such as MIKE SHE (Sandu & Virsta, 2015), RIBASIM (Van der Krogt, 2004), WEAP (Demertzi et al., 2013), and MIKE 11 (Madsen 2000; Ivanescu et al., 2014). These models play a crucial role in decision support systems for managing water resources. Investment in modernizing irrigation infrastructure is necessary to improve the efficiency of these systems (reduced water losses, improved energy efficiency), reduce the dependence of agricultural production on weather conditions, increase farmers' competitiveness, and help the sector meet the long-term challenges posed by the effects of climate change (Cojocinescu, 2023). In this context, it is important that the rehabilitation solution is dimensioned so as to ensure the flow and pressure in the underground irrigation network, necessary for the efficient operation of the equipment.

MATERIALS AND METHODS

The paper presents the solutions for modernization and refurbishment of the irrigation arrangement in plot SPP15 belonging to OUAI Hotarani, Mehedinti County (DALI, 2024). The study method is based on the use of

Mike Urban software for hydraulic modeling of the underground irrigation pipeline network and the use of new / modern sprinkler irrigation equipment.

MIKE URBAN is a powerful water distribution modeling package that can analyze entire systems under various flow conditions and provide water quality analysis as needed. MIKE URBAN offers flexibility in water distribution model development, allowing users to import data from GIS databases, schematically draw pipe networks, or directly enter data using program editors. MIKE URBAN enables users to create network models for water distribution systems without detailed maps by defining components in interactive dialog boxes, allowing for accurate model definition when accurate maps are unavailable.

MIKE URBAN water distribution views the water distribution network as a collection of links connected by nodes, identified by ID numbers, and can be arranged in any way. The pipe data includes pipe length, diameter, roughness coefficient and minor loss coefficient, while the junction node data includes the water demand and elevation of the node for each network node. Control components consist of pumps, check valves, regulating valves, sustaining valves, flow control valves, and storage tanks. With the data entered, MIKE URBAN Water Distribution can perform a comprehensive check of the input data and geometric verification of the network connectivity after it has been entered (DHI, 2014). The pipe network can be analyzed after verification of the input data, ensuring that the results accurately define the model and appear reasonable.

The infrastructure owned and managed by O.U.A.I. SPP15 Hotarani, is part of the irrigation arrangement Crivina - Vinju Mare and serves the land area afferent to the plot SPP15 Hotarani, respectively a gross area of 1785 ha and a net area of 1605 ha (Figure 1) (Untaru et al., 2020).

The SPP15 Hotarani pump station is a pressure pump station, which sucks water from the CD5 irrigation channel and discharges it into the network of pressure pipes, main, secondary, and antennas located in the arranged agricultural area (Figure 1).

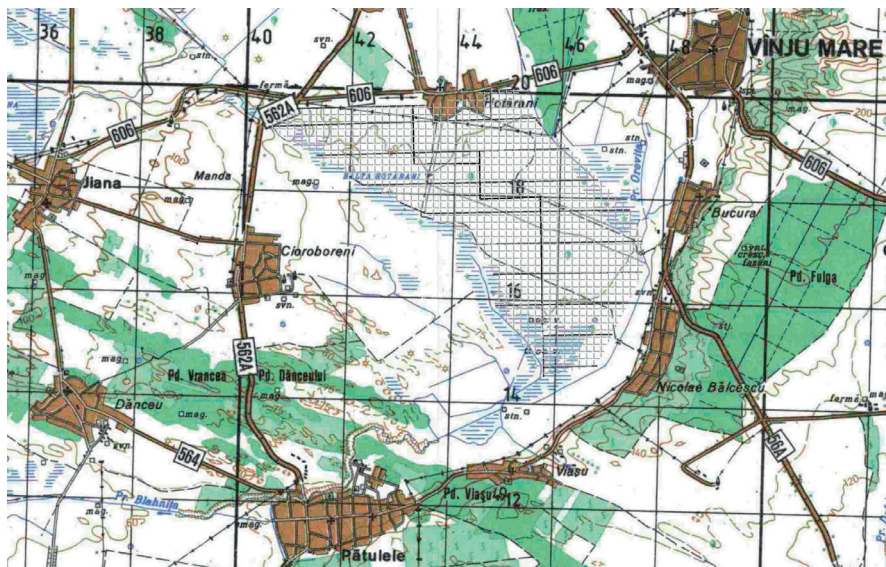


Figure 1. Location of the irrigation plot adjacent to the pumping station "SPP15 Hotarani", Mehedinti County

Within technical expertise, two variants of technical solutions for intervention works for the modernization and refurbishment of the irrigation system related to the OAU plot "SPP 15 Hotarani" were analyzed, regarding:

1. Modernization and renovation of the SPP15 pressure station belonging to OUA1 SPP15 Hotarani, Mehedinti County;
2. Modernization and renovation of the irrigation pipeline network.

The recommended option involves the rehabilitation of the pumping station "SPP 15 Hotarani", of the suction basin and repairs to the distribution pipe network, metering the water consumption on discharge, keeping the utility of the building "SPP 15 Hotarani", which involves carrying out important repair works to the existing building (missing roof, exterior and interior plastering, repairs of the floor access staircase, new low voltage electrical installations, metal joinery (doors, windows), purchase of a new transformer station and medium voltage cells, purchase and installation of pump control and automation panels, replacement of existing pumping units to ensure: total installed flow: $1,238 \text{ m}^3/\text{sec}$ and total installed station power: 1567.9 KW , installation of two ultrasonic flow meters for water metering on the two main pipes, new suction and discharge pipes from the pumping station, fencing.

Regarding the underground network of irrigation water transmission and distribution pipes, the main and secondary pipes and antennas will be replaced with new PEHD high-density polyethylene pipes, the ventilation installations will be replaced, the nodes on the main / secondary pipes, the anchorage massifs, manholes with line valves will be restored.

SPP15 is located on the CD5 bypass channel having the following characteristics: pumping units 9 pcs of which 7 type 8 NDS, with motor 200 kW speed 1500 rpm and 2 pcs type Cris125 with motor 75 kW speed 3000 rpm, post power supply 1600 kVA, 20/0 4kV, with an installed power 1550 kW specific consumption 350, ensuring a total flow of 1.24 m³/s, at a pumping height of 62 mCA.



Figure 2. Overview of the SPP15 pumping station OUAH
Hotarani Mehedinti County

The SPP15 pressure station SPP15 (Figure 2) is a pumping station with a closed above-ground building, with a ground floor and dry tank height regime and upstairs the energy annex transformer point. The station is of the type of closed reinforced concrete bowl with an eraser.

The procedure for the modernization / rehabilitation of an existing irrigation plot, which is in the patrimony of the OUA, includes the following steps (Man et al., 2023):

- drawing up expertise (with photo documentary and two proposed variants);
- preparation of intervention work authorization documentation (DALI, 2023);
- topographic studies in Stereo 70 coordinates;
- geotechnical studies;
- hydrological and/or hydrogeological studies;
- urbanism certificate, land book extract;
- environmental permit;
- opinions, as appropriate, from National Land Improvement Agency/Basin Water Administration (ANIF/ABA);
- PT + DTAC for building permit.

Based on the expert report, DALI documentation is developed, of which for the case study plot SPP15 Hotarani, for the recommended version, requires the following modernization works:

- reconstruction of the tank and roof at the SPP15 Hotarani pressure station SPP15 Hotarani;
- procurement and installation of new pumping technological lines (pumping aggregates, euisment aggregate), with improved parameters to ensure the necessary flow and projected pressure;
- electric pumps shall be equipped with frequency converters to take over flow variations and to protect electric motors and their economic operation;
- restoration of the electrical connection and installation of newly designed electrical installations;
- repair of the electrical attachment;
- installation of new PVC doors and windows, with wire mesh protection grilles on the outside;

- installation of capture (suction) and discharge installations from pumping aggregates;
- mounting two ultrasonic flow meters on the main discharge pipes;
- electrical and automation installations will be replaced with new high-performance installations;
- fence with mesh fence on metal poles of the station enclosure, including access ridges.

Due to the superior efficiencies of new pumps installed in the station, the specific consumption of electricity with water pumping will be reduced, which will eliminate the payment of reactive current, and the automation of operation leading to the reduction of unnecessary water losses. The use of frequency converters to equip electric pumps has been proposed to take over flow variations and protect electric motors and their economical operation. The proposed technical solution ensures the functional safety of the entire irrigated area of the current irrigation system, starting from the distribution pipe network, necessary for water transport, and up to ensuring the operation of watering installations to its terminal end.

RESULTS AND DISCUSSIONS

In order to carry out the modeling, the simulation model was created by introducing coordinates in stereo system 70, network nodes, and introducing pipe sections, specifying materials and diameters. This results in the situation plan shown in Figure 3.

The SPP15 pumping station was returned, supplied from the ANIF channel, with an installed flow of 3000 m³/h. Following the calibration and running the model we obtained flow (Figure 4), speed (Figure 5), headloss (Figure 6), and pressure (Figure 7) on all pipes and nodes resulting in diagrams.

Therefore, we were able to make the pressure/velocity/headloss diagram in all sections which is presented in Figures 8 and 9 we in the directions SPP15 – A01 and SPP15 – A18, respectively.

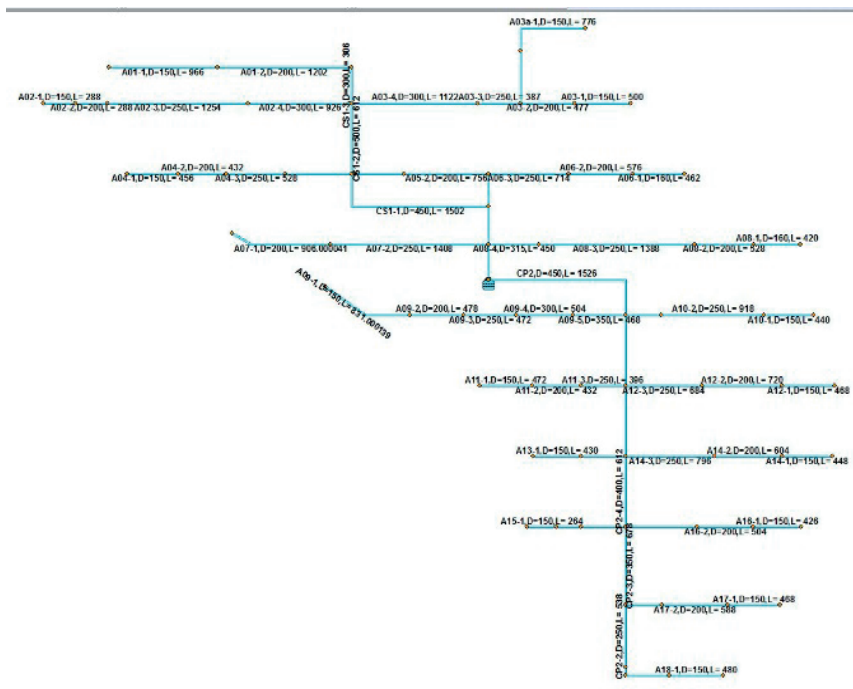


Figure 3. Plan view model

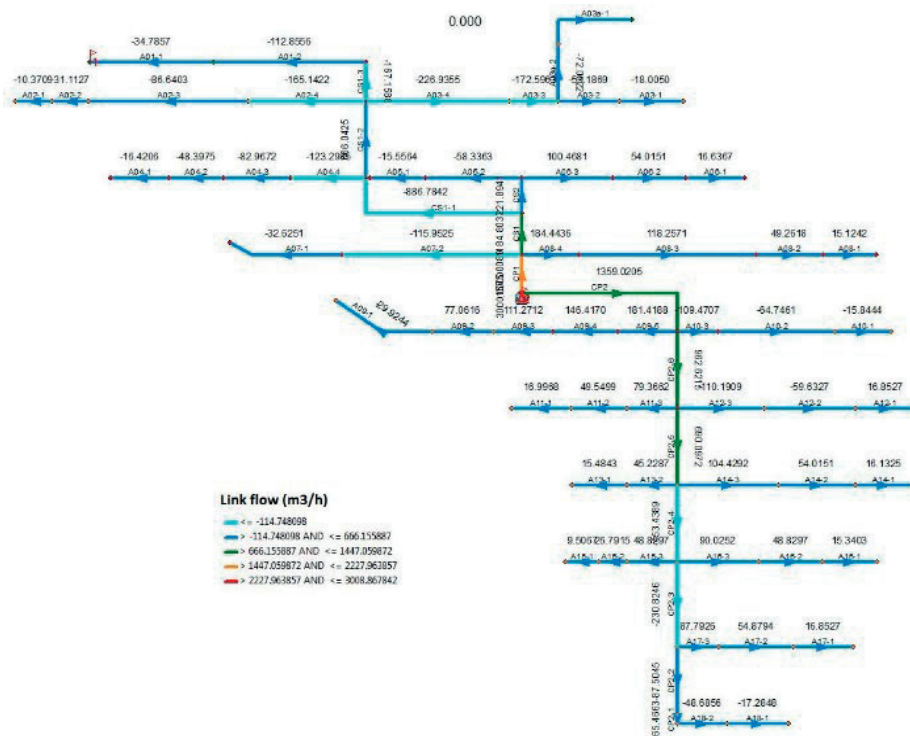


Figure 4. Pipe flows

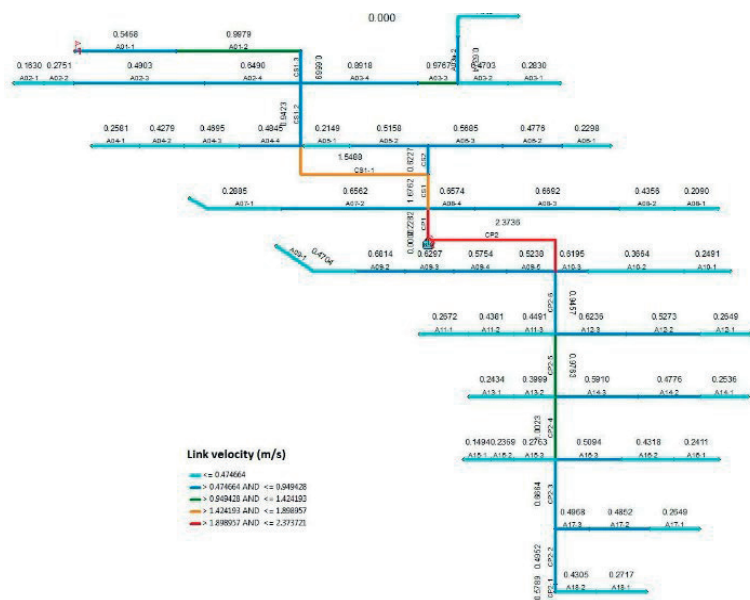


Figure 5. Pipe velocity

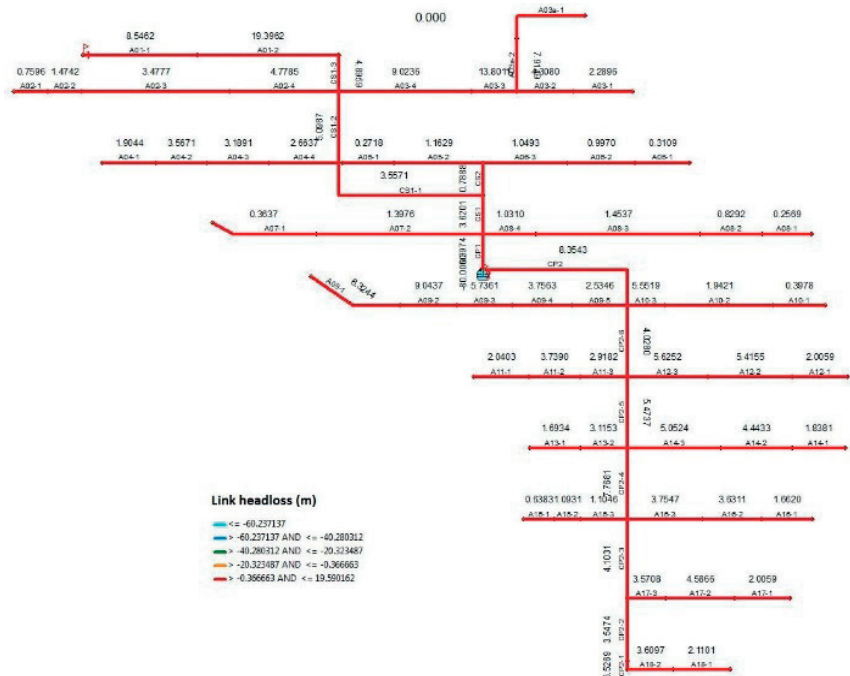


Figure 6. Pipe headloss

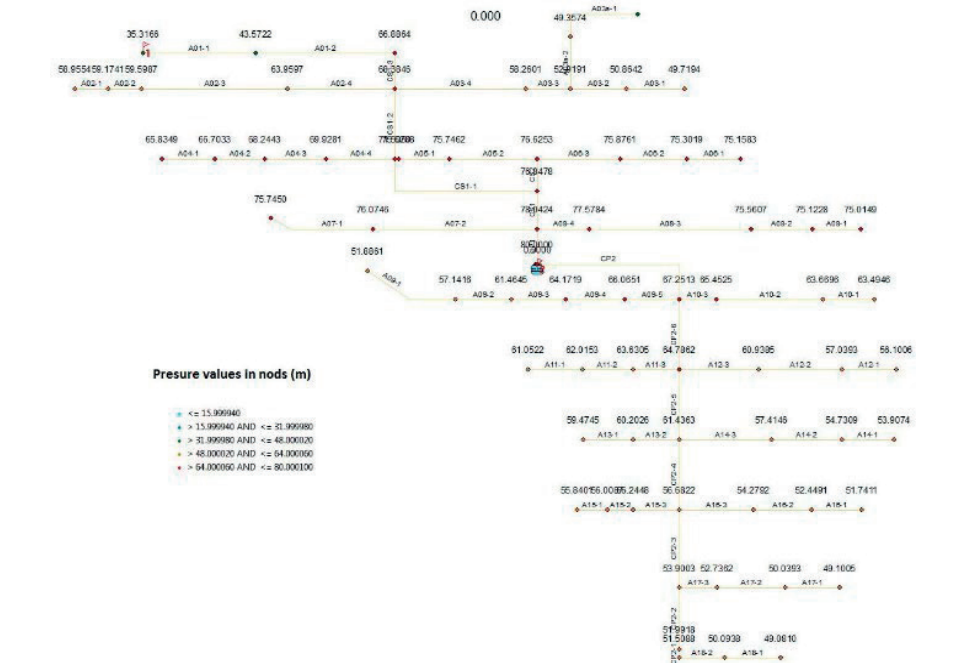


Figure 7. Pipe pressure

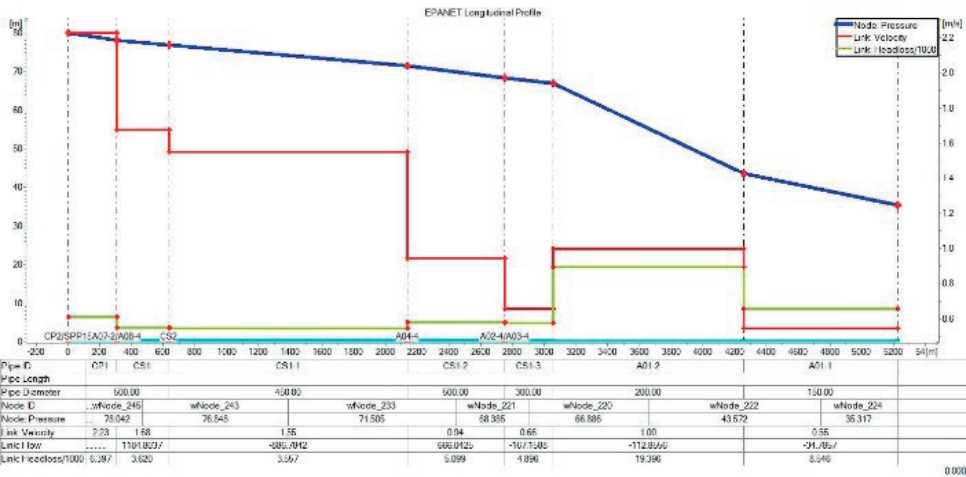


Figure 8. Section pressure diagram SPP15 – A01

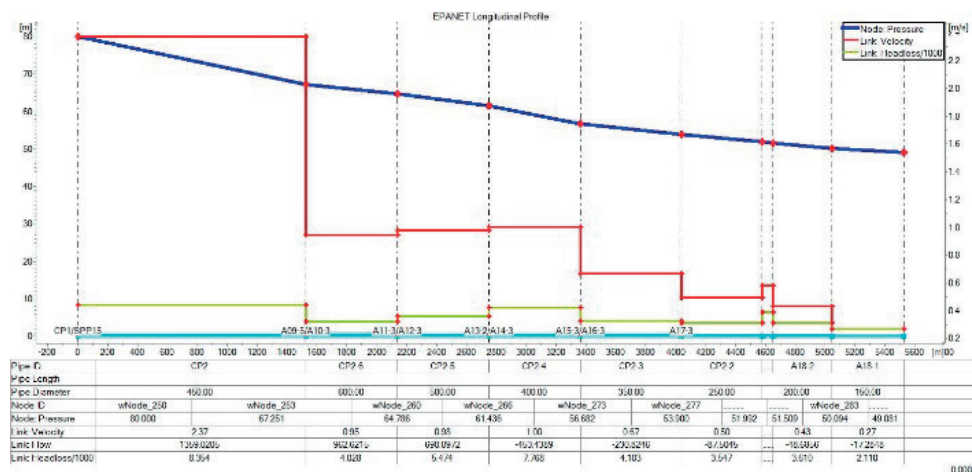


Figure 9. Section pressure diagram SPP15 – A18

CONCLUSIONS

The application of hydraulic modelling led to the pressure diagram diagrams from Figures 8 and 9 which are fundamental to dimensioning underground pipeline network for irrigation and ensuring the pressure and flow necessary for the efficient operation of sprinkler watering equipment.

Modernization scenarios proposed for the optimal operation of the irrigation system are mainly concerned with the SPP15 pressure pumping station and the irrigation pipe network for the transport of water that supplies the irrigation installations of landscaped agricultural land.

The installation of new equipment to measure flows and volume of water distributed for watering agricultural plants will allow a correct relationship based on the contract between the water supplier, the ANIF Territorial Branch for Land Improvements Mehedinti and its user OUA1 SPP15 Hotarani, eliminating possible conflicts in the event of lack of measuring equipment.

State-of-the-art efficient automation is proposed, so that during the exploitation period of the irrigation system, it is necessary to have as little staff as possible in the pumping station.

REFERENCES

Çetin, Ö., Doğanay, K.H., Bezdin, J. (2023). Adaptation strategies to climate change with sustainable irrigation. *Scientific Papers. Series E. Land*

Reclamation, Earth Observation & Surveying, Environmental Engineering, Vol. XII, 176-180, Print ISSN 2285-6064.

Cojocinescu, M.I. (2023). *Evolution over time of land improvement arrangements in Romania*. Doctoral thesis, Politehnica University Timisoara.

Demertzi, K.A., Papamichail, D.M., Georgiou, P.E., Karamouzis, D.N., Aschonitis, V.G. (2013). Assessment of rural and highly seasonal tourist activity plus drought effects on reservoir operation in a semi-arid region of Greece using the WEAP model. *Water Int*, 39,23–34.

DHI (2014). Mike Urban. Training guide.

Iglesiasa, A., Garroteb, L. (2015). Adaptation strategies for agricultural water management under climate change in Europe. *Agricultural Water Management* 155, 113–124, <https://doi.org/10.1016/j.agwat.2015.03.014>

Ivanescu, V., Drobot, R. (2020). Deriving rain threshold for early warning based on a coupled hydrological-hydraulic model. *Mathematical Modelling in Civil Engineering*, 12(4), 10-21.

Ivanescu, V., Mocanu, P., Sandu, M.A. (2014). Application of a hydrodynamic MIKE 11 model for Argesel River. *14th International Multidisciplinary Scientific GeoConference SGEM 2014*, Conference Proceedings. Geoconference on water resources, forest, marine and ocean ecosystems, 65-72, Albena, Bulgaria. DOI: 10.5593/SGEM2014/B31/S12.009

Madsen, H. (2000). Automatic calibration of a conceptual rainfall runoff model using multiple objectives. *J Hydrol*, 235, 276–288.

Man, T.E., Beilicci, R., Cojocinescu, M., Untaru, D., Pasc, A., Ilca, M. (2023) Arrangement of sprinkler irrigation made using water from drainage canals in Romania, Timiş county. *Scientific Bulletin of Politehnica University Timisoara, Transactions on Hydrotehnics*, 68(82), Issue 1, Timisoara, Romania.

Sandu, M.A., & Virsta, A. (2015). Applicability of MIKE SHE to Simulate Hydrology in Argesel River

- Catchment. *Agriculture and Agricultural Science Procedia*, 6, 517-524, ISSN 2210-7843, <https://doi.org/10.1016/j.aaspro.2015.08.135>
- Sandu, M.A., & Virsta, A. (2021). The water footprint in context of circular economy. *AgroLife Scientific Journal*, 10(2). <https://doi.org/10.17930/AGL2021221>
- Untaru, D., Man, T.E., Beilicci, R., Cojocinescu, M.I., Pasc, A.M. (2020). Modernization and rehabilitation of secondary irrigation infrastructure Plot SPP 10, Crivina-Vanju Mare, Mehedinti County. *Scientific Bulletin of Politehnica University Timisoara, Transactions on Hydrotehnics*, 64(78), Issue 1, Timisoara, Romania.
- Van der Krogt WNM (2004) RIBASIM version 6.32. Technical reference manual. WL Delft Hydraulics, Delft
- xxx – Agentia Nationala de Imbunatatiri Funciare (ANIF), Technical Archive - Territorial Branch of Land Improvements Mehedinti, Available online: <https://www.anif.ro>
- xxx - Agentia pentru Finantarea Investitiilor Rurale (AFIR), DR-25 - Modernization of irrigation infrastructure, (2024). Available online: www.afir.ro
- xxx - DALI (2023). Documentation for approval of intervention works – "Modernization and refurbishment of the SPP15 Hotarani pressurization station belonging to OUAI SPP15 Hotarani, Mehedinti County", S.C. Roxad Cioclov, SRL
- xxx - United Nations, UN, (2016). Available online: <https://www.un.org/development/desa/en/key-issues/population.html>.

DROUGHT MONITORING IN SOUTHEASTERN ROMANIA BASED ON THE COMPARISON AND CORRELATION OF SPEI AND SPI INDICES

Sara VENTURI¹, Elena MATEESCU², Ana VIRSTA³,
Nicolae PETRESCU⁴, Daniel DUNEA⁴, Stefano CASADEI¹

¹Università degli Studi di Perugia, 93 Via Duranti, Perugia, Italy

²National Administration of Meteorology, 97 Bucuresti-Ploiești Road, Bucharest, Romania

³University of Agronomic Sciences and Veterinary Medicine of Bucharest,
59 Marasti Blvd, District 1, Bucharest, Romania

⁴Valahia University of Targoviste, 13 Sinaia Alley Street, Targoviste, Romania

Corresponding author email: dan.dunea@valahia.ro

Abstract

The main aim was to assess the drought phenomena by comparing two relevant indicators i.e., the standardized precipitation index (SPI) and the standardized precipitation evaporation index (SPEI) using long time series of precipitation and temperature starting from 1961 up to 2020 gauged and validated in the land monitoring system of the Ialomita district located in the southeast of Romania at Grivita station. The obtained results suggested that SPEI can provide better insights regarding the drought phenomena concerning the occurrence of drought events and trend estimation. In the next years, drought events are expected to rise in frequency, duration, and intensity. In our opinion, it would be necessary to exceed the prevailing use of the SPI to assess the drought phenomena and improve the environmental monitoring systems to have robust data both of rainfall and temperature in a high number of gauging stations that could be utilized also for a spatially distributed evaluation of SPEI index.

Key words: climate trend, drought indices, Grivita meteorological station, Ialomita district, SPEI-SPI correlation.

INTRODUCTION

In the last decade, large areas of Europe experienced a persistent deficit of precipitation from winter to summer. Higher-than-average temperatures combined with this deficit, led to severe to extreme droughts more frequently. These droughts significantly affected various European regions causing severe socio-economic impacts on sectors such as agriculture and on the natural systems (European Commission, Copernicus Climate Change Service, 2022; Casadei et al., 2020; Vicente, 2022). Short-term drought effects can also include lower water levels in lakes and reservoirs and consequent deterioration of water quality (Di Francesco et al., 2023; Çetin, 2023). The *standardized precipitation index* (SPI), first developed by McKee et al. (1993), was proposed by the World Meteorological Organization and the Lincoln Declaration on Drought as a reliable standard index for worldwide application (Hayes et al., 2011). Later on, it was selected in the set of common indicators for water scarcity and drought by the Water Scarcity and Drought

Expert Group of the European Commission (Faergemann, 2012). Considering global climate warming, air temperature variations are expected to become particularly the new primary driver of droughts, at the level of high-latitude cold catchments.

Assessment of the evapotranspiration (ET) processes is a key element for providing updated information for water resources management, weather forecasts, climate studies, agriculture, and other applications (Dunea et al., 2021; Casadei et al., 2021). Easy access to reliable estimations of ET is important within these sensitive domains. ET has an important role in examining and forecasting drought occurrence and drought severity both at local and global scales. Consequently, ET should be used together with precipitation in developing reliable drought indices (Khoshnazar et al., 2022).

Vicente-Serrano et al. (2010) developed the *standardized precipitation evapotranspiration index* (SPEI) based on SPI by including the temperature in its computation with input parameters such as the monthly precipitation and temperature data. A complete dataset is

required with no missing months in the time series.

SPEI has been employed in different areas of the world to analyze the drought incidence, its characteristics, and its relationship with water scarcity. The utility of SPEI in drought studies is demonstrated, but the requirement of a complete dataset for both temperature and precipitation can be challenging and may limit the use of SPEI due to data unavailability.

In this context, the present study aims to explore the correlation SPEI vs. SPI using long time series (from 1961 to 2020) recorded at Grivita station in Ialomita district, Romania, an area located in a plain with temperate-continental climate characterized by very hot summers and cold winters, and a relatively large annual and diurnal thermal amplitude and by precipitation in small amounts (the average annual thermal amplitude is 25.1°C, and the maximum amplitude exceeded 70°C). The *SPEI-SPI correlation* is expected to provide useful insights to overcome the potential lack of temperature dataset. Ialomita district is one of the most important agricultural regions for cropping maize, and sunflower in Romania. Therefore, the presented results may provide useful outcomes for future assessments and better management in these regions and elsewhere, also improving the agrometeorological forecasting. So far, this type of study has been conducted by a small number of researchers with incomplete results, and thus the knowledge is still at the beginning (191 results in the Web of Science database using the string "*SPEI SPI correlation*").

For Romania, only two papers were retrieved with case studies for the Carpathian Region (Spinoni et al., 2013) and Eastern Romania (Minea et al., 2022). Furthermore, the European Drought Observatory mentions SPEI as a widely-used drought index, but it produces updated data only for the SPI index (<https://edo.jrc.ec.europa.eu/edov2/php/index.php?id=1010>).

The current study is the first applied for a region located in the South of Romania by employing long time series derived from data collected at a gauging station (60 years period), rather than available gridded datasets, to have a more reliable indication for the study of climatic trends and the comparison between SPI and SPEI.

MATERIALS AND METHODS

Study area

The Ialomita district (Muntenia region, Romania, Figure 1) is located in the plain and it has a temperate continental climate with excessive nuance that is characterized by the presence of hot summers and very cold winters, with a high thermal amplitude of 76.5°C (the absolute minimum was -32.5°C in Armășești, Jan. 25, 1942, and the absolute maximum until +44°C, Amara, in August 1951), low precipitation and unevenly distributed both in time and territory and an atmospheric circulation predominantly from the east and northeast.

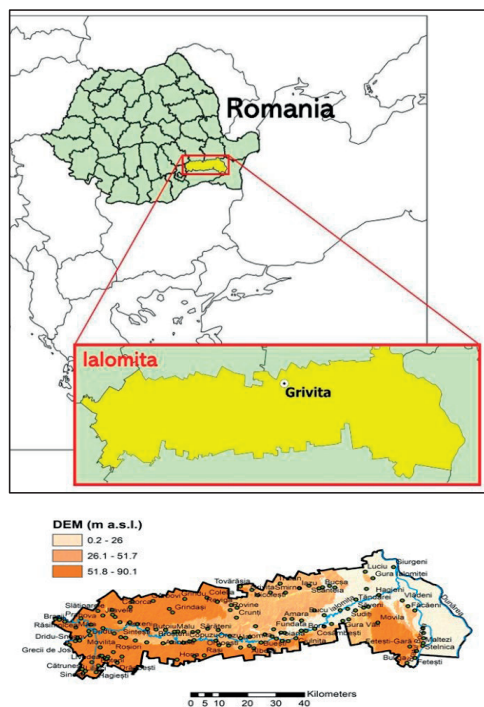


Figure 1. Area of study in southeastern Romania: Ialomita District with Grivita meteorological station; Altimetry of the Ialomita District (Romania) based on the EU-DEM v1.1 (<https://land.copernicus.eu/imagery-in-situ/eu-dem/eu-dem-v1.1/view>) and the Grivita station

Among the characteristic climatic phenomena stand out frost and blizzards, in the cold period, and drought, dew, and hail, in the warm periods of the year. The Grivita meteorological station (27.294E; 44.748N; 45 m a.s.l.) is representative in the area.

Datasets

The computation for both SPI and SPEI requires at least thirty years of data to achieve credible results, and consequently longer samples can assure improved accuracy in drought estimations (Wu et al., 2005). Usually, SPEI and SPI indices are computed at different time scales from 1 month to 48 months allowing the estimation of the drought's impact on various types of water resources. For example, agricultural droughts, mainly conditioned by soil moisture, are typically defined at a time scale shorter than hydrologic droughts, linked to groundwater, streamflow, and reservoirs (Svoboda et al., 2012). There are seven SPI classes (generally considered valid also for the SPEI index) according to WMO's SPI User Guide from *extremely wet* to *extremely dry* with various probabilities of occurrence. In this study, we have selected an annual time period for presentation (SPI12 and SPEI12) to provide a clear general image of the drought trends. The monthly rainfall data used for SPI (SPEI) calculation has been obtained as cumulative daily rainfall, and the mean, maximum, and minimum monthly temperature as an average of mean, maximum, and minimum daily temperature, respectively.

Computations and data analysis

The selected indices were calculated in the R-environment using the SPEI package <https://cran.r-project.org/package=SPEI>.

In this study, the drought events were retrieved using the run theory as described in Yevjevich (1967). SPI (SPEI) values were characterized as time series functions and specify the intensity (I) of drought (or wet) conditions. Continuous negative values of the index under the threshold value $SPI (SPEI) = 0$ indicate that a drought event occurs (Sharafati et al., 2020).

Trend detection was performed using the Mann-Kendall (MK) method (Mann, 1945; Kendall, 1975), which is a non-parametric test to analyze the trend in time series, and the Innovative-Sen trend (IST) method (Sen, 2012).

The Pearson correlation coefficient r was computed to evaluate the correlation.

RESULTS AND DISCUSSIONS

Precipitation and temperature: the trend detection

The annual cumulative precipitation (ACP) was between 287.1 mm and 775.9 mm and the annual average temperature (AAT) ranged between 9.3°C and 13.1°C at Grivita station. Table 1 provides the slope of linear regression (m), the standardized variable Z_{MK} , slope s , and the correspondent confidence limit determined using the IST test. First, considering the linear regression slope, Grivita presents a decreasing tendency of ACP ($m = -1.24$) and an increasing trend of AAT ($m = 0.0308$). The MK test evaluated the trend of the ACP of Grivita not significant for a significance level of 5%. Differently, the increasing trend of AAT was evaluated both by the MK test ($Z_{MK} = 4.95$) and IST method as significant, for the same significance level.

It is possible to conclude that, both for precipitation and temperature, the Grivita dataset presented a monotonic trend, decreasing for precipitation and increasing for temperature.

SPI (SPEI) 12 trend

The tendency of the annual time series of SPI (SPEI) 12 is shown in Figure 2 where, in the same chart, both the indices' temporal series (the red line for SPI and the blue line for SPEI) are represented.

For SPEI (SPI) 12, Figure 3 (a) illustrates the linear regression analysis with the correspondent regression equation, and Figure 3 (b) the results of the IST method.

Table 2 allows the comparison of the results of regression analysis, MK, and IST methods. First, it is possible to observe that the slope of linear regression m is negative for both indices, but the value of SPEI is more negative than SPI. MK test provides a significant negative monotonic trend only for the SPEI 12, not for the SPI 12; differently, the IST method provides a significant negative monotonic trend both for SPI 12 and SPEI 12.

Comparing the trend of SPI 12 and SPEI 12, it is clear that SPEI shows generally a decreasing tendency more significant than SPI, both in terms of regression slope m and IST test results.

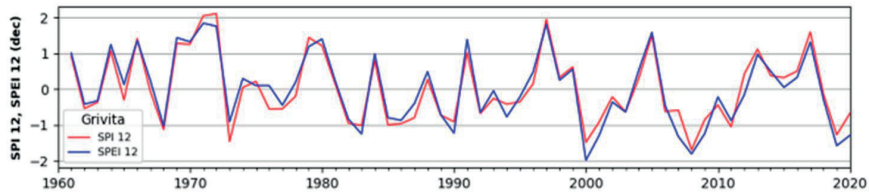


Figure 2. SPI 12, SPEI 12 time series recorded for Grivita station between 1961 and 2020

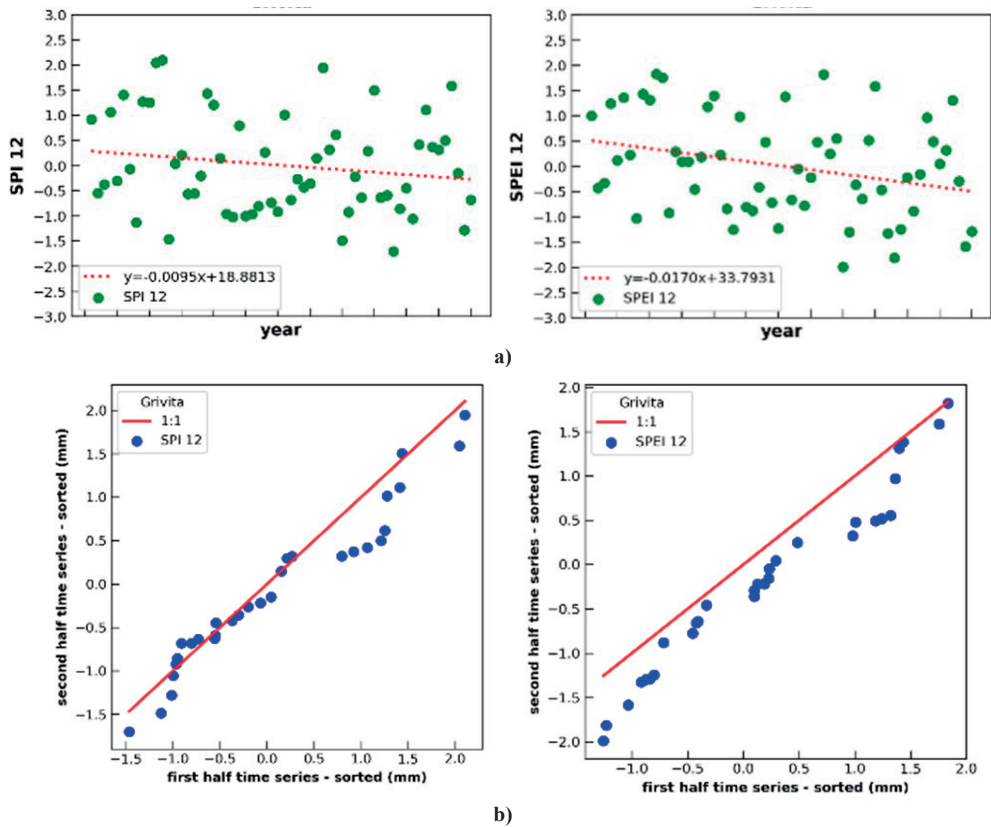


Figure 3. Linear regression (a); IST method - SPI 12 and SPEI 12 (b)

Run Test

The run test has been used to identify the drought features based on the SPI (SPEI) 12-time series; in particular, the first half part of the time series (first period: FP - 1961-1990) and the second half part (second period: SP - 1991-2020) have been considered.

In Table 3, drought events have been characterized using the following parameters: number of events, maximum, average, and

standard deviation (SD) of the duration expressed in years, maximum peak and severity value, and their occurrence.

In Figure 4, the boxplot charts of peak and intensity magnitudes of SPI (SPEI) 12 for each drought event, in the first and second periods, are shown. It is possible to observe that both the median and average peak and intensity are always lower in the first period than in the second period.

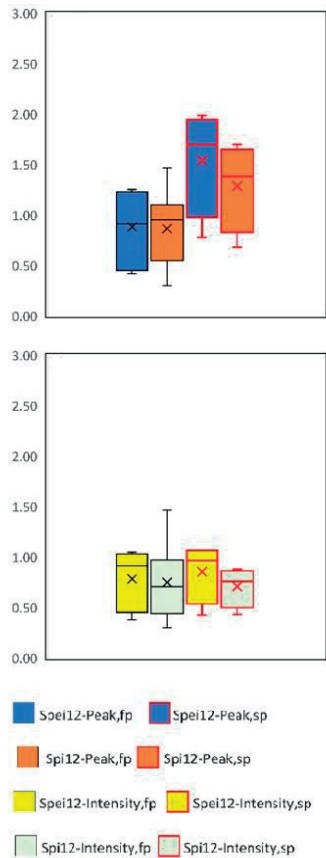


Figure 4. Boxplot of the absolute value of peak and intensity for SPI(SPEI) 12 for Grivita station. Boxplot elements: box = values of 25th and 75th percentiles; horizontal line = median; cross = average; whiskers limit = minimum/maximum value; interquartile range (IQR) = difference between 25th and 75th percentile

Then, in particular, in the second period, it is clear that the trend of the median (average) of SPEI overcomes the one of SPI.

Previous considerations are according to the trend test analysis of SPI (SPEI) and can be because SPEI, which considers the temperature, can catch, better than SPI, the increasing tendency of drought phenomena.

In Figure 5, the peak magnitude values derived from run test analysis have been arranged in four classes, from 0 to 3, following the WMO guidelines (Svoboda et al., 2012): "0" identifies the normal level, "1" the moderately dry, "2" the severely dry and "3" the extremely dry level.

First, we observe that SPEI gives a percentage of critical events (falling in the second and third

class) higher than SPI (27% against 8%); then, only for SPEI, the percentage of critical events that fall in the first period is lower than in the second period (9% against 27%) whereas this trend is not confirmed for SPI (25% against 8%).

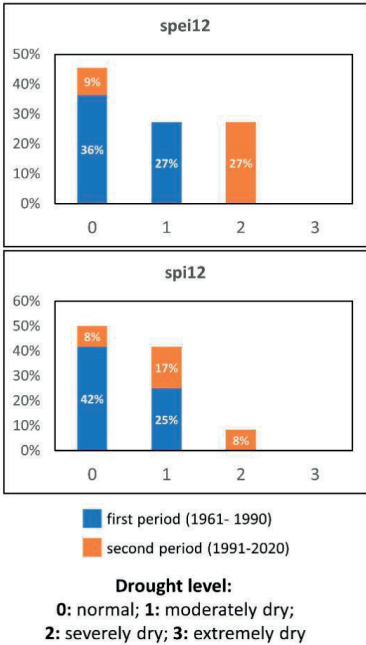


Figure 5. Distribution of drought levels (WMO, 2012) in the first and second periods (SPI 12, SPEI 12)

SPEI and SPI correlation

Hereafter, we consider the relationship, based on the method of least squares, between SPEI and SPI indices, to compare the eventual change of trend in the last sixty years.

The linear correlation between SPI and SPEI 12 is shown in Figure 6. In each graph, the linear regression equation and the determination coefficient (R^2) are indicated, which specifies how well the regression equation explains the relationship between the variables.

The goodness of fit of the linear regression can be also expressed by the Pearson correlation coefficient r , with $r = \sqrt{R^2}$.

In Table 4, it is possible to observe that r is always relatively high; however, there is a certain difference between the first and the second periods: in fact, r is lower in the second period than in the first (0.961 against 0.973).

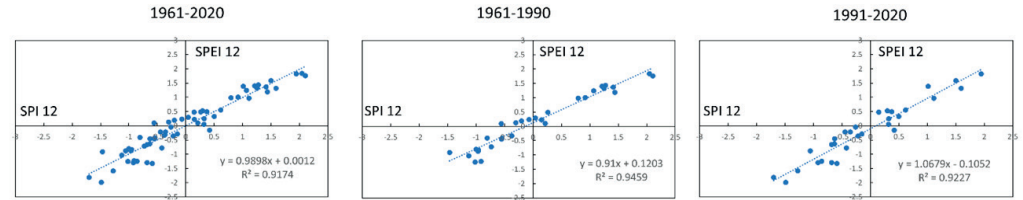


Figure 6. Relationships related to the drought trends: SPEI 12-SPI 12 correlations

Table 1. Linear regression, MK test and IST method applied to annual cumulative precipitation and average annual temperature at the Grivita station

Station	Variable	Linear regression (slope m)	Mann Kendal test (Standardized variable Z_{MK})	IST - trend slope	
				Confidence limit $CL_{1-\alpha}$	Trend slope (s)
Grivita	annual cumulative precipitation (ACP)	-1.24	-0.86	± 0.256	-0.743*
	average annual temperature (AAT)	0.0308	4.95*	± 0.002	0.031*

*Statistically significant at a 5% level

Table 2. SPI, SPEI 12 (linear regression, Mann Kendall test, IST)

Station	Indicator	Linear regression (slope m)	Mann Kendall test (Standardized variable Z_{MK})	IST - trend slope	
				Confidence limit $CL_{1-\alpha}$	Trend slope (s)
Grivita	SPI 12	-0.0095	-0.86	± 0.00195	-0.00537*
	SPEI 12	-0.0170	-1.96*	± 0.00120	-0.01279*

*statistically significant at a 5% level

Table 3. Characterization of drought events for Grivita time series: SPI12, SPEI12

Parameters	Grivita			
	SPI12		SPEI12	
	FP	SP	FP	SP
Droughts number	8	4	7	4
Max droughts duration (years)	3	6	3	7
Average droughts duration (years)	2.00	4.25	1.71	4.50
SD droughts duration (years)	0.76	1.26	0.76	1.73
Max Peak Value	1.70		1.99	
Max Peak Value - occurrence	2008		2000	
Max Severity Value	5.28		6.10	
Max Severity Value - occurrence	2006-2011		2006-2012	

Table 4. Correlation SPI-SPEI: r values

SPI 12 - SPEI 12		
r12	r12-1	r12-2
1961-2020	1961-1990	1991-2020
0.958	0.973	0.961

CONCLUSIONS

The study aims to compare the efficacy of SPI and SPEI indices in monitoring drought events in southeastern Romania areas, in particular verifying the correlation between the two indicators and the consequential possibility of using SPI instead of SPEI. In fact, SPI, based only on precipitation, requires less availability of data concerning SPEI, which needs the estimation of evapotranspiration.

For this purpose, we have considered a long-time series at Grivita Station (Southeastern Romania) of precipitation and temperature data, gauged and validated through the environmental monitoring systems.

The analysis of SPI (SPEI) 12 shows a general decreasing tendency of the indices both in terms of regression slope, MK, and IST test results. In particular, this trend was confirmed by the run theory applied to the first part (1961-1990) and second part (1991-2020) of the SPEI time series: in fact, the percentage of drought events that fall in the first period is lower than in the second period; moreover, it is observed that SPEI gives a percentage of critical events higher than SPI. Finally, the possible estimation of SPEI from

SPI has been correlated to the Pearson coefficient: its value is generally high, but it tends to decrease passing from the first part to the second part of the time series.

This could be explained by the increase in the mean temperature in the last thirty years, which negatively affects the quality of the correlation between the two indices.

Given this, it could be convenient to overcome the prevailing use of the SPI index to assess droughts, improving the environmental monitoring systems to have reliable data both of rainfall and temperature in a high number of gauging stations.

An increased number of stations could be also useful for a spatially distributed evaluation of the SPEI index.

REFERENCES

- Casadei, S., Peppoloni, F., Pierleoni, A. (2020). A New Approach to Calculate the Water Exploitation Index (WEI+). *Water*, 12(11), 3227, 1-16.
- Casadei, S., Peppoloni, F., Ventura, F., Teodorescu, R., Dunea, D., Petrescu, N. (2021). Application of smart irrigation systems for water conservation in Italian farms. *Environ Sci Pollut Res*, 28, 26488–26499.
- Çetin, Ö., Doğanay, K.H., Bezdan, J. (2023). Adaptation strategies to climate change with sustainable irrigation. *Scientific Papers. Series E. Land Reclamation, Earth Observation & Surveying, Environmental Engineering*, *VXII*, 176-180.
- Di Francesco, S., Venturi, S., & Casadei, S. (2023). An integrated water resource management approach for Lake Trasimeno, Italy. *Hydrological Sciences Journal*, 68(4), 630-644.
- Dingman, S.L. (2014). *Physical Hydrology*. Waveland Press, Inc.; 3rd edition.
- Dunea, D., Bretean, P., Purcoi, L., Tanislav, D., Serban, G., Neagoe, A., Iordache, V., Iordache, S. (2021). Effects of riparian vegetation on evapotranspiration processes and water quality of small plain streams. *Ecohydrology & Hydrobiology*, 21(4), 629-640.
- European Commission - Drought European State of the Climate 2022
<https://climate.copernicus.eu/esotc/2022/drought>
- Faergemann, H. (2012). Update on Water Scarcity and Droughts indicator development. In EC Expert Group on Water Scarcity & Droughts; European Environment Agency: Brussels, Belgium, 1–23.
- Hayes, M., Wall, N., Widhalm, M. (2011). The Lincoln declaration on drought indices: universal meteorological drought index recommended. *American Meteorological Society*, 92, 485–488, <https://doi.org/10.1175/2010BAMS3103.1>
- Kendall, M.G. (1975) Rank Correlation Methods; Griffin: London, UK.
- Khoshnazar, A., Corzo Perez, G.A., Diaz, V., Aminzadeh, M., Cerón Pineda, R.A. (2022). Wet-environment Evapotranspiration and Precipitation Standardized Index (WEPSI) for drought assessment and monitoring. *Hydrology Research*, 53(11), 1393–1413, <https://doi.org/10.2166/nh.2022.062>.
- Mann, H.B. (1945). Nonparametric tests against trend. *Econometrica: Journal of the econometric society*, 245-259.
- Minca, I., Iosub, M., Boicu, D. (2022). Multi-scale approach for different type of drought in temperate climatic conditions. *Natural Hazards*, 110(2), 1153-1177.
- Sen, Z. (2012). Innovative trend analysis methodology. *Journal of Hydrologic Engineering*, 17(9), 1042-1046.
- Sharafati, A., Nabaei, S., & Shahid, S. Spatial assessment of meteorological drought features over different climate regions in Iran. (2020). *International Journal of Climatology*, 40(3), 1864-1884, <https://doi.org/10.1002/joc.6307>.
- Spinoni, J., Antofie, T., Barbosa, P., Bihari, Z., Lakatos, M., Szalai, S, Szentimrey, T., Vogt, J. (2013). An overview of drought events in the Carpathian Region in 1961-2010. 12th EMS Annual Meeting/9th European Conference on Applied Climatology (ECAC), *Advances in Science and Research*, 10, 21-32.
- Svoboda, M., Hayes, M., Wood, D. (2012). Standardized Precipitation Index User Guide. World Meteorological Organization, Geneva.
- Vicente, O. (2022). Improving agricultural production and food security under climate change conditions. *AgroLife Scientific Journal*, 11(1), <https://doi.org/10.17930/AGL2022128>.
- Vicente-Serrano, S.M., Beguería, S., López-Moreno, J.I. (2010). A multiscalar drought index sensitive to global warming: the standardized precipitation evapotranspiration index. *Journal of climate*, 23(7), 1696-1718.
- Wu, H., Hayes, M.J., Wilhite, D.A., Svoboda, M.D. (2005). The effect of the length of record on the standardized precipitation index calculation. *Int J Climatol*, 25(4), 505–520.
- Yevjevich, V.M. (1967). Objective approach to definitions and investigations of continental hydrologic droughts, Doctoral dissertation, Colorado State University Libraries.

PHYTOREMEDIATION OF CHROMIUM BY BAD BIRNBACH ROSES IN URBAN AREAS

Aysen AKAY

University of Selcuk, Agriculture Faculty, Department of Soil Science and Plant Nutrition,
Konya, Türkiye

Corresponding author email: aakay@selcuk.edu.tr

Abstract

Chromium is a heavy metal that is toxic to plants and other living things. It is known that plants can be used to remove heavy metals from the environment if they accumulate in the soil. Various ornamental plants are used in urban areas due to their decorative properties. In this study, the effectiveness of the Bad-Birnbach rose variety in removing excess chromium in the soil was investigated. To determine its effect on the vegetative and generative development states of roses and Cr uptake from the soil, different doses of Cr^{+6} (0, 25, 50 mg/kg soil) and 0-5-10-20 mmol EDTA were applied to the plant growth medium. At the end of the experiment, the dry weight of the stem and root decreased significantly with the applications of Cr^{+6} . With EDTA application, the dry weight of roots and flowers increased. Cr concentrations in stem, root and rose are between 3.63-55.04, 14.53-314.77 and 2.31-13.44 mg/kg, respectively. Cr concentrations in the plant are above the permissible limit values and Cr^{+6} has accumulated significantly in the root zone.

Key words: chromium, EDTA, heavy metal, ornamental plants, phytoremediation.

INTRODUCTION

In recent years, chromium (Cr) has reached increasingly toxic levels in the environment as a result of various industrial and agricultural activities. Cr cause concern as an environmental pollutant (Zayed & Terry, 2003). In various countries such as China, Iran and Russia, Cr pollution is intensely encountered around the places where chromium mines are processed (Vodyanitskii, 2009; Solgi & Parmah, 2015; Zhang et al., 2016). In our country, it was found in the soils of the Karamenderes Basin (Sümer et al., 2013), in the wastewater of Trabzon province (Topcuoglu et al., 2002), in the agricultural lands around Hatay (Özkan et al., 2017) and in the areas irrigated with water from the wastewater treatment system in Konya (Akay et al., 2009), Cr concentrations are above the limit values.

In addition to various remediation methods, the phytoremediation technique is also recommended to remediate Cr-polluted soils and waters. The toxic effect of Cr in Cr^{3+} and Cr^{6+} forms depend on the oxidation state (Vodyanitskii, 2009). Cr^{6+} is the toxic and persistent form of Cr in the soil (Srivastava et

al., 2021). Cr retards plant growth (Han et al., 2004); seed germination, root elongation and plant development are negatively affected (Shahid et al., 2017).

Cleaning Cr-contaminated areas using plants is a good and environmentally friendly technology (Thakur et al., 2016). The use of ornamental plants in areas where pollution treatment is applied can be preferred in remediation studies due to their various advantages (Rocha et al., 2022). It has been determined that periwinkle and oleander flowers have the capacity to remove Cr and Pb minerals (Al-Anbari et al., 2018). Among the ornamental plants *Mirabilis jalapa*, *Impatiens balsamin* (I. Balsamin) and *Tagetes erecta* L., it was observed that *Mirabilis jalapa* was more effective in Cr uptake than the other two plants (Miao & Yan, 2013). It has been stated that marsh iris (*I. pseudacorus* L.) also retains Cr in its roots (Caldelas et al., 2012). Cr^{+6} stress causes early flowering in *Zinnia elegans* L. (Panda et al., 2020); *Cosmos bipinnatus* Cav. and *Celosia cristata* L. belongs to Asteraceae and Amaranthaceae family plants showed morphological changes when grown in Cr^{+6} polluted soils, and *C. bipinnatus* Cav. was stated to be able to adapt and withstand harsh

conditions (Karthik & Sharavanan, 2016). Various chelating substances can be used to increase the heavy metal uptake of plants (Saifullah et al., 2009). Thus, it is stated that some chemicals and various chelators will be effective to increase the effectiveness of the remediation study (Liu et al., 2009). Synthetic chelates such as ethylene diamine tetraacetate (EDTA), diethylene triamine pentaacetic acid (DTPA), and hydroxy ethylene diamine triacetic acid (HEDTA) are widely used chemicals that solubilize metals in soil (Sabir et al., 2014). Chelating substances dissolve heavy metals in the soil, making them available to the plant and allowing remediation plants to absorb more metal (Salt et al., 1998).

EDTA is stated as the most effective chelate in extracting metals from soil (Hsiao et al., 2007). In the study where the solubility of Cr^{3+} in the presence and absence of EDTA was calculated as a function of pH, it was found that in the absence of the chelator, Cr^{3+} would form inorganic $\text{Cr}(\text{OH})_3$ complexes, and thus precipitated in solution between pH > 3-4. In the presence of EDTA, it was observed that Cr^{3+} maintained its solubility as a Cr^{3+} -EDTA complex in the pH range of 3-7.

Cr precipitation in the form of $\text{Cr}(\text{OH})_3$ could be prevented up to pH 9. Soluble Cr concentration and therefore the amount of plant-available Cr was five times higher in the presence of EDTA (Erenoglu et al., 2007). EDTA disrupts the concentration balance of Cr^{6+} in the liquid and solid phase of the soil and can form mobile compounds that can be absorbed by plants by chelating or coordinating some difficult-to-transport Cr (Ebrahimi, 2015). In such conditions, some resistant plants can still grow (Ram et al., 2019).

In this study, it was aimed to determine the Cr heavy metal uptake capacity of Bad Birnbach rose grown in soil contaminated with different concentrations of Cr. It was also aimed to determine the effectiveness of EDTA chelate in the solubility of Cr applied to the soil and in Cr uptake by the plant.

MATERIALS AND METHODS

Certified Bad Birnbach rose was used in the study. The roses were obtained from a certified production company in Turkey. The sandy soil

used in the greenhouse experiment was sieved through a 4 mm sieve and then filled into 6 litter pots. Chromium ($\text{K}_2\text{Cr}_2\text{O}_7$) in the Cr^{+6} form, which was the subject of the experiment, was applied to the pots at doses of 0, 25, 50 mg Cr kg^{-1} soil and 0-5-10-20 mmol EDTA chelate. After the Cr application, the pots were incubated for 2 months. At the end of the incubation period, bare-rooted rose seedlings were pruned in stem and root and immediately planted in pots. The experiment was carried out in the greenhouse in three replicates, according to the randomized plots factorial trial design. Macro and micronutrient need of plants were calculated according to soil analysis results and applied regularly using Hogland's solution (The content of the Hoagland solution is as follows: Fe-EDTA, H_3BO_4 , MnSO_4 , $\text{CuSO}_4 \cdot 5\text{H}_2\text{O}$, Zn-EDTA, $(\text{NH}_4)_6\text{Mo}_7\text{O}_{24} \cdot 4\text{H}_2\text{O}$, CaNO_3 , KH_2PO_4 , KNO_3 , MgSO_4 (16.50, 2.86, 1.29, 0.393, 1.33, 0.018, 590, 219.5, 443.5, 492 mg L^{-1}).

The soil used in the experiment was analyzed. The soil was slightly alkaline (pH 7.78) and sandy. It had an EC of $382 \mu\text{S cm}^{-1}$ (salt-free), CaCO_3 content was 4.96% (calcareous). The P concentration of soil was very little (1.76 mg kg^{-1}), Ca and Mg concentrations were sufficient (respectively 3972 and 207 mg kg^{-1}), and K concentration was little (71 mg kg^{-1}). The soil had 8.72 mg kg^{-1} available Fe (high), 1.62 mg kg^{-1} available Zn (sufficient), 1.06 mg kg^{-1} available Cu (sufficient), 0.80 mg kg^{-1} available B (little), and 4.27 mg kg^{-1} available Mn (little). Organic matter content was 0.38% (very little). Plant material: Bad Birnbach rose is a disease-resistant rose belonging to the Kordes' Klima-Rosen collection, which has awards from international rose competitions. It is a bushy vertical plant that can reach 50 cm in height and 50 cm in crown width. It is appropriate to plant 4 pieces per 1 m^2 in mass plantings. The average diameter of its flower is 4-5 cm. The plant, which is heat resistant, suitable for balcony boxes, semi-shades, hanging and growing in pots, is resistant to weather conditions (Anonymous, 2024). It was first introduced to the public in 2000 with its plump salmon and pink flowers (Anonymous, 2024a). This rose variety is widely used in pavements with heavy traffic and in various landscaping

applications in Konya, where the trial was carried out.

After bloomed throughout the experiment, flowers were collected regularly weekly, and their fresh and dry weights were recorded. At the end of the experiment, flower yield (taking into account the applications in all pots) were calculated according to the values obtained. Harvesting was done, when the flowering rate of the plants decreased, after the 10-month development period. During the harvesting process, the roots, stems and rose parts were weighed separately, and their fresh weights were taken. Then, to determine the dry weights, the root, stem and flower parts were kept at 65°C for 2 days and their weight was determined by weighing on a precision scale.

Cr concentration in stem, flower, and root samples:

Cr analysis in plants was done using the modified wet burning method (Zheljazkov & Nielsen, 1996; Hseu, 2004). Cr concentrations were determined with the ICP-OES (Agilent Technologies (SPS3) 5100 model) device. 1000 mg/L (Merck, New Jersey, USA) was used as internal standard. STD IPE 952 (grass (mixture)/Poaceae) standard certified plant sample was used to verify the readings by the elemental analysis. The concentration of Cr for IPE 952 was 3810 µg kg⁻¹.

The amount of Cr removed from the soil by plant parts was calculated according to the following formula:

Cr removed by plant organ (µg kg⁻¹) = [(plant organ Cr concentration (mg/kg) × plant organ dry weight (g/pot)/1000]*1000.

The translocation factors (TF) were calculated as the ratio of plant aerial part metal concentration to root metal concentration (Ghosh & Singh, 2005; Zurayk et al., 2002).

TF = MS/MR*100

were:

- MR = Cr concentration in root (mg kg⁻¹)
- MS = Cr concentration in stem (mg kg⁻¹)

Tolerance index (ToI) was calculated by dividing the dry weight of the trial plant to the dry weight of the control plant.

The bioaccumulation factor (BCF) for Cr was calculated according to Zayed et al. (1998).

Bioaccumulation factor (BCF) = Cr concentration in plant/ Cr concentration applied to the plant initially

Cr concentration in plant = (Stem Cr concentration*stem weight) + (Flower Cr concentration*flower weight) + (Root Cr concentration*root weight).

The data obtained as a result of the pot experiment were carried out with the MINITAB 18 statistical package program and the significant differences were subjected to the Tukey multiple comparison test.

RESULTS AND DISCUSSIONS

It was observed that the effect of Cr and EDTA applications on the fresh and dry weights of the stem, root and flower parts of the Bad Brinbach rose was statistically significant (p < 0.05) (Table 1 and Figure 1). Both fresh and dry weight values of stems and roots were higher in the Cr control application compared to the 25 mg kg⁻¹ Cr and 50 mg kg⁻¹ Cr applications. Also flower dry weight was higher (5.34 g) in the 25 mg kg⁻¹ Cr application compared to the control and 50 mg kg⁻¹ Cr applications. When the effect of EDTA applications was examined, there was no statistical difference in both fresh and dry weights of the stem and root compared to the control. In general, application of 20 mmol EDTA was reduced the stated weight data. When the effect of Cr*EDTA interaction was examined, the highest data was in the Cr0*E10 application in the stem wet weight (37.71 g). In generally, increasing doses of Cr caused a decrease in stem and root weights. Increasing doses of EDTA at Cr0 control application reduced stem and root weight. Flower dry weight, the average value (5.34 g) increased in the 25 mg kg⁻¹ Cr application compared to the control (3.22 g), while it decreased in the 50 mg kg⁻¹ Cr (4.08 g) application. When the Cr*EDTA interaction was examined, no statistical difference was generally observed between EDTA applications. The highest flower dry weight (8.98 g) was obtained only in the Cr25E10 application. Cr generally negatively affected the development of the plant.

The effect of EDTA and Cr applications on the stem, root and flower Cr concentration values were presented in Table 2 and Figure 2. When

the Figure 2 was examined, the highest Cr concentrations were generally in the root (14.53 - 314.77 mg kg⁻¹). The root was followed by the stem (3.63 - 55.04 mg kg⁻¹) and flower parts (2.31-13.44 mg kg⁻¹). Between stem, root and flower chromium concentrations with increasing Cr applications were observed significant differences. Similarly, Cr*EDTA interaction was also statistically significant ($p < 0.05$). While the average Cr concentration in the stem is 6.61 mg kg⁻¹ in the control, it is 40.86 mg kg⁻¹ at the 25 mg kg⁻¹ Cr dose. The Cr concentration of the root increased with increasing Cr doses ($p < 0.05$), and the highest value was observed at the 50 mg kg⁻¹ Cr dose (275.8 mg kg⁻¹). The Cr concentration of the flower at the 25 mg kg⁻¹ Cr (8.54 mg kg⁻¹) was higher compared to control and 50 mg kg⁻¹ Cr applications.

When Cr*EDTA interaction was examined, the Cr concentration in the stem was higher than Cr25*E10 and Cr50*E10 applications (55.04 and 53.73 mg kg⁻¹, respectively) compared to other applications. The Cr concentration in the root was higher at the 50 mg kg⁻¹ Cr dose compared to the control and 25 mg kg⁻¹ Cr doses, and the highest values were obtained in the Cr50*E10 and Cr50*E20 treatments (314.77 and 312.99 mg kg⁻¹, respectively) ($p < 0.05$) (Figure 2).

When the effect of EDTA and Cr applications on the amount of chromium removed from the soil by stem, root and flower parts is examined, the highest Cr removed from the soil was from the root and the values were between 0.348-6.111 mg kg⁻¹ (Table 3). The root was followed by the Cr values removed from the soil by the stem (0.071-0.749 mg kg⁻¹) and flower parts (0.007-0.121 mg kg⁻¹).

Considering the average values, the amount of chromium taken up by the root increased significantly with increasing Cr doses ($p < 0.05$). Similarly, in the Cr*EDTA interaction, there were statistically significant differences in the amount of Cr taken up by the root ($p < 0.05$).

When the average amount of Cr taken by the stem was examined, the values at 50 mg kg⁻¹ Cr and 25 mg kg⁻¹ Cr doses are higher than the control (0.514 and 0.492 mg kg⁻¹, respectively). In the Cr*EDTA interaction, the amount of Cr taken up by the stem increased with increasing doses of EDTA, up to the 10 mmol dose, and the highest values were in Cr50*E10 and Cr25*E10 applications ($p < 0.05$). EDTA application positively affected the amount of Cr taken from the soil. The values for the amount of Cr taken from the flower varied between 0.007-0.121 mg kg⁻¹, and the highest values were observed in 25 mg kg⁻¹ Cr applications.

Transfer Factor, tolerance index and Bioaccumulation Factor (BCF) values were presented in Table 4. In our Bad Brinbach rose, TF values are $TF > 1$ and generally varied between 9.88 and 55.98. The highest values were at the Cr0 control dose and there were significant differences between the values ($p < 0.05$). Tolerance index (ToI) values also varied between 42.85 and 100 ($p < 0.05$). While the ToI value decreased with increasing Cr doses, it increased with increasing EDTA doses. The plant's BCF factor values were >1 , but when these values were taken into consideration, it was noteworthy that the plant was more resistant to the 25 mg kg⁻¹ Cr dose than the 50 mg kg⁻¹ Cr dose ($p < 0.05$) (Figures 3, 4 and 5).

Table 1. The effect of Cr and EDTA applications on the dry weight of the stem, root and flower of Bad Brinbach rose (Different letters indicate comparison of mean values according to Tukey test; $p < 0.05$)

Cr and EDTA doses	Stem wet weight (g)	Stem dry weight (g)	Root wet weight (g)	Root dry weight (g)	Flower dry weight (g)
Cr0	32.59 a	17.55 a	70.54 a	32.70 a	3.22 c
Cr25	24.94 b	11.85 b	38.24 b	19.03 b	5.34 a
Cr50	29.50 ab	13.86 b	36.71 b	16.41 b	4.08 b
E0	31.31 ab	15.93 a	45.56 b	23.33 ab	3.79 b
E5	27.82 ab	14.22 ab	48.99 ab	22.44 ab	3.88 b
E10	32.62 a	16.53 a	55.60 a	26.27 a	6.07 a
E20	24.29 b	10.99 b	43.85 b	18.80 b	3.12 b

Table 2. The effect of the application of Cr and EDTA on the concentration of Cr in the stem, root and flower of Bad Birnbach rose (Different letters indicate comparison of mean values according to Tukey test; $p < 0.05$)

Cr doses	Stem Cr (mg kg ⁻¹)	Flower Cr (mg kg ⁻¹)	Root Cr (mg kg ⁻¹)
Cr0	6.61 c	4.47 c	16.11 c
Cr25	40.86 a	8.54 a	171.2 b
Cr50	37.00 b	6.83 b	275.8 a
E0	22.88 b	5.39 b	123.49 c
E5	24.39 b	7.65 a	155.73 b
E10	39.31 a	8.87 a	172.97 a
E20	26.05 b	4.53 b	165.34 ab

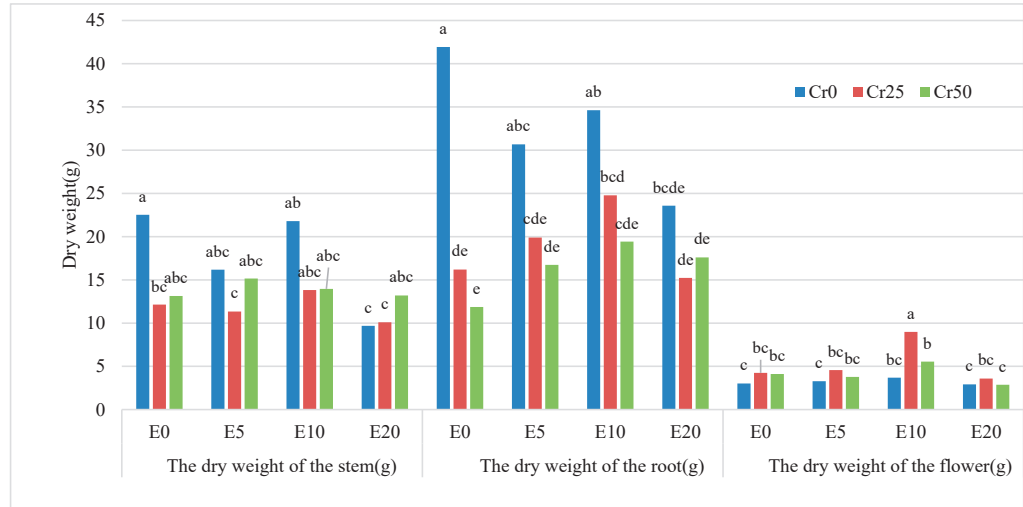


Figure 1. The effect of Cr and EDTA applications on the dry weight of the stem, root and flower of Bad Birnbach rose (Different letters on the bar plots indicate comparison of mean values according to Tukey test; $p < 0.05$)

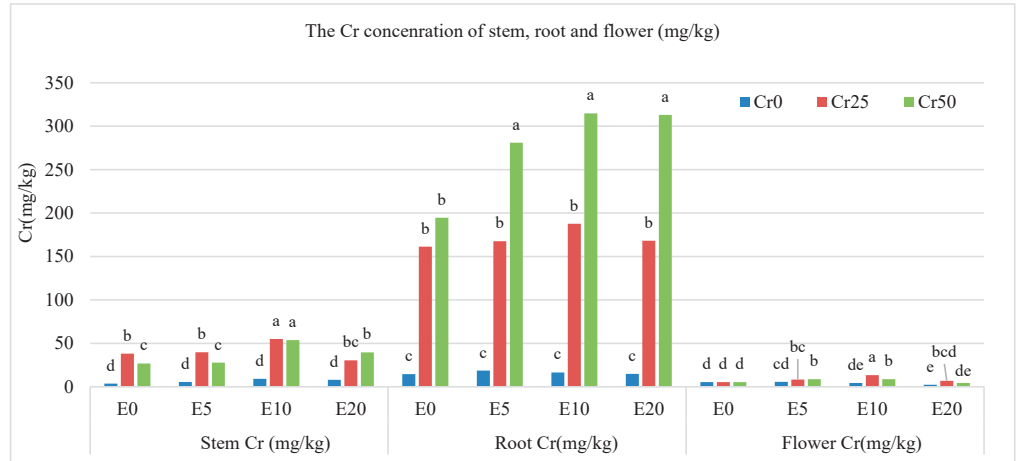


Figure 2. The effect of the application of Cr and EDTA on the concentration of Cr in the stem, root and flower of Bad Birnbach rose (Different letters indicate comparison of mean values according to Tukey test; $p < 0.05$)

Table 3. The effect of Cr and EDTA applications on the amount of Cr removed by the stems, roots, and flowers of Bad Birnbach rose (Different letters indicate comparison of mean values according to Tukey test; $p < 0.05$)

Cr and EDTA doses	Stem removed Cr (mg kg ⁻¹)	Flower removed Cr (mg kg ⁻¹)	Root removed Cr (mg kg ⁻¹)
Cr0	0.110 b	0.015 c	0.524 c
Cr25	0.492 a	0.052 a	3.294 b
Cr50	0.514 a	0.029 b	4.666 a
E0	0.299 b	0.021 bc	1.852 c
E5	0.323 b	0.030 b	2.882 b
E10	0.566 a	0.062 a	3.776 a
E20	0.300 b	0.015 c	2.802 b
Cr0xE0	0.081 d	0.016 cde	0.610 d
Cr0XE5	0.089 d	0.019 cde	0.572 d
Cr0XE10	0.199 cd	0.016 cde	0.566 d
Cr0XE20	0.071 d	0.007 e	0.348 d
Cr25xE0	0.464 abc	0.023 cde	2.627 c
Cr25XE5	0.451 abc	0.039 bc	3.336 bc
Cr25XE10	0.748 a	0.121 a	4.649 ab
Cr25XE20	0.303 bcd	0.025 bcde	2.561 c
Cr50xE0	0.351 bcd	0.022 cde	2.318 c
Cr50XE5	0.428 abc	0.033 bcd	4.738 ab
Cr50XE10	0,749 a	0,048 b	6,111 a
Cr50XE20	0,527 ab	0,013 de	5,497 a

Table 4. The effect of Cr and EDTA applications on Transfer Factor, Tolerance index and Bioaccumulation Factor of Bad Birnbach rose (Different letters indicate comparison of mean values according to Tukey test; $p < 0.05$)

Cr and EDTA doses	Transfer Factor	Tolerance index	BCF
Cr0	41.55 a	79.25 a	0
Cr25	23.78 b	53.68 b	8.82 a
Cr50	13.36 c	50.91 b	6.39 b
E0	20.83 b	63.82 ab	6.37 c
E5	21.23 b	60.08 b	7.49 b
E10	34.15 a	72.44 a	8.89 a
E20	28.71 ab	48.79 c	762 b

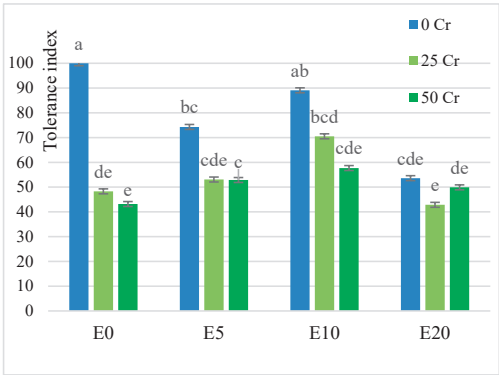


Figure 3. The effect of the application of Cr and EDTA on the tolerance index
(Different letters indicate comparison of mean values according to Tukey test; $p < 0.05$)

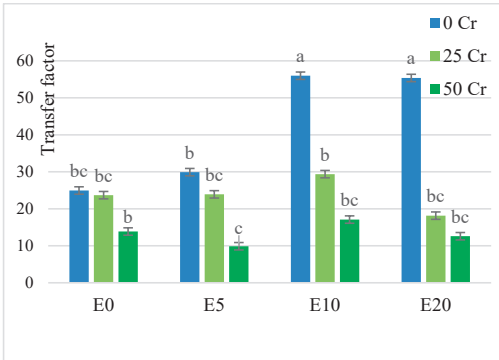


Figure 4. The effect of the application of Cr and EDTA on the transfer factor
(Different letters indicate comparison of mean values according to Tukey test; $p < 0.05$)

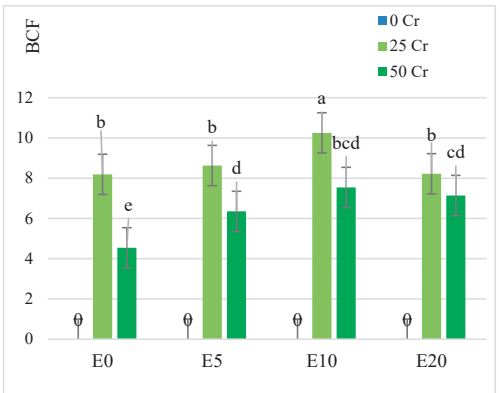


Figure 5. The effect of the application of Cr and EDTA on BCF (Different letters indicate comparison of mean values according to Tukey test; $p < 0.05$)

DISCUSSIONS

In this study, increasing doses of chromium reduced the dry weights of stems, roots and flowers. It was observed that 5-10-15 mmol application doses of EDTA did not change these data, while 20 mmol EDTA application decreased it ($p < 0.05$) (Table 1). In various studies on Cr toxicity, it had been determined that the Cr^{+6} form was more toxic, more mobile, and soluble than the Cr^{+3} form (Sunitha et al., 2014; Oliveira, 2012; Sępniewska & Wolińska, 2005). Although the symptoms seen in plants in case of Cr^{+6} toxicity were various, it is generally stated that plant growth is inhibited and the development of some plant organs was limited (Were et al., 2017).

In this study, Bad Birnbach roses did not lose their vigour, but overall, there were partial decreases in stem root and flower weights compared to the control. Considering the concentration of chromium in plant organs, the concentration values were listed in root>stem>flower parts respectively. EDTA applications increased the Cr concentration in the plant (Table 2). A similar situation was valid for the amount of Cr taken from the soil. The plant accumulated the most Cr in its roots, followed by the stem (Table 3). In a similar study, it was stated that Cr accumulation was mostly in the roots of four bamboo species (Were et al., 2017).

The bioconcentration factor is considered as the ratio of the metal concentration in the aboveground part of the plant to the metal concentration in the soil, and the translocation factor (TF) is the ratio of the metal concentration in the stem part of the plant to the metal concentration in the root part. These two factors must be >1 in accumulator plants. Tolerance index (ToI) is the ratio of the dry weight of the plant, which indicates its growth status, to the dry weight of the control plant (McGrath & Zhao, 2003; Turner et al., 1991).

The TI value (Ghosh & Singh, 2005; Zurayk et al., 2002), which calculates the transport of heavy metal from the root zone of the plant to the above-ground stem parts, is greater than 1 in the study plant. In the study, the highest BCF value was observed at the 25 mg kg^{-1} Cr dose and the highest tolerance index was observed at the 50 mg kg^{-1} Cr dose. In EDTA applications,

the highest TI, ToI and BCF values were observed in 10 mg kg⁻¹ applications.

Similarly, in case of heavy metal stress, increasing doses of EDTA applications increased TI values in the *Echinochloa crus galii* plant (Ebrahimi, 2013). In another study, 5 mmol EDTA kg⁻¹ of soil dose was the most appropriate dose for remediation of heavy metal (Ali & Chaudhury, 2016). In this study, considering the average TF values, it was noteworthy that Bad Brinbach rose may be a Cr hyperaccumulator. There are various studies in which plants with TF >1 is classified as hyperaccumulators (Arshad et al., 2008; Faridah et al., 2017; Aghelan et al., 2022). It has been stated that *Vinca rosea* L. plant has chromium levels between 10 and 60 mg kg⁻¹, plant height, fresh and dry weight values decreased at high doses of Cr, and TF value is greater than 1 at 30 and 60 mg kg⁻¹ Cr concentrations (Ehsan et al., 2016).

It will provide an advantage, because of this plant is not included in the human and animal food chain and this plant can be used in regions with Cr pollution up to 50 mg kg⁻¹. It is known that growing plants consumed as food, especially in soil contaminated with Cr, has various health risks. In the restoration of areas exposed to various heavy metal pollution, the advantage of the plant is that it reduces Cr pollution in the soil and can be used visually in landscaping. More research is needed on such ornamental plants in the phytoremediation technique to be used in the improvement of such areas.

CONCLUSIONS

The study showed that the Bad Birnbach rose variety can tolerate Cr-polluted environments and remove chromium from the soil. The plant can easily grow in areas with heavy traffic, on roadsides, on pavements and median strips, without requiring special care. It is a species that can be used to reduce areas contaminated with low and medium levels of Cr. The plant can be recommended for phytostabilization of Cr-contaminated areas.

ACKNOWLEDGEMENTS

Project financially supported by the BAP Coordinator of Selcuk University of Türkiye (Proje No. 21401051)

REFERENCES

- Aghelan, N., Sobhan Ardakani, S., Cheraghi, M., & Lorestani, B. (2022). A Comparative study on valuation of efficiency of EDTA, citric acid and salicylic acid chelating agents in phytoremediation enhancing of two ornamental plant species for elimination of Cr (III) and Cu (II) from contaminated soils. *Journal of Research in Environmental Health*, 8(3), 280-299.
- Akay, A., Bas, M. & Duran, S. (2009). Determination of heavy metal concentration in agricultural soil and sewage sludge of main wastewater system collected from Çengilti site in Konya. *International Conference, Lakes and Nutrient Loads Alblakes09*, Tirana, 278-284.
- Al-Anbari, R., Al-Obaidy, A.H., Al-Khafaji, M. & Al-Imari, T. (2018). Removing chromium and lead metals using phytoremediation technique. *MATEC Web of Conferences*, 05004.
- Ali, S.Y., & Chaudhury, S. (2016). EDTA-enhanced phytoextraction by *Tagetes* sp. and effect on bioconcentration and translocation of heavy metals. *Environmental Processes*, 3(4), 735-746.
- Anonymous (2024). <https://www.rosen.de/en/garden-roses/shop-by-type/adr-roses-roselax/bad-birnbach>
- Anonymous (2024a). <https://www.badbirnbach.de/en/stories/rose-bad-birnbach>
- Arshad, M., Silvestre, J., Pinelli, E., Kallerhoff, J., Kaemmerer, M., Tarigo, A. & Dumat, C. (2008). A field study of lead phytoextraction by various scented *Pelargonium* cultivars. *Chemosphere*, 71(11), 2187-2192.
- Caldelas, C., Araus, J., Febrero, A. & Bort, J. (2012). Accumulation and toxic effects of chromium and zinc in *Iris pseudacorus* L. *Acta Physiologiae Plantarum*, 34(3), 1217-1228.
- Ebrahimi, M. (2013). Effect of EDTA application on heavy metals uptake and germination of *Echinochloa crus galii* (L.) Beave in contaminated soil. *Int J Agric Crop Sci*, 6, 197-202.
- Ebrahimi, M. (2015). Effect of EDTA treatment method on leaching of Pb and Cr by *Phragmites australis* (Cav.) Trin. Ex Steudel (common reed). *Caspian Journal of Environmental Sciences*, 13(2), 153-166.
- Ehsan, N., Nawaz, R., Ahmad, S., Khan, M. M. & Hayat, J. (2016). Phytoremediation of chromium contaminated soil by an ornamental plant *Vinca (Vinca rosea L.)*. *Journal of Environmental and Agricultural Sciences*, 7, 29.
- Erenoglu, B.E., Patra, H.K., Khodr, H., Römheld, V. & Von Wirén, N. (2007). Uptake and apoplastic retention of EDTA-and phytosiderophore-chelated

- chromium (III) in maize. *Journal of Plant Nutrition and Soil Science*, 170(6), 788-795.
- Ghosh, M., & Singh, S.P. (2005). A review on phytoremediation of heavy metals and utilization of it's by products. *Asian J Energy Environ*, 6(4), 18.
- Han, F.X., Sridhar, B.M., Monts, D.L. & Su, Y. (2004). Phytoavailability and toxicity of trivalent and hexavalent chromium to *Brassica juncea*. *New Phytologist*, 162(2), 489-499.
- Hseu, Z.Y. (2004). Evaluating heavy metal contents in nine composts using four digestion methods. *Bioresource Technology*, 95(1), 53-59.
- Hsiao, K.H., Kao, P.H. & Hseu, Z.Y. (2007). Effects of chelators on chromium and nickel uptake by *Brassica juncea* on serpentine-mine tailings for phytoextraction. *Journal of Hazardous Materials*, 148(1-2), 366-376.
- Karthik, K. & Sharavanan, P. S. (2016). Effects of hexavalent chromium on growth, phytotoxicity, tolerance index of *Cosmos bipinnatus*, Cav. and *Celosia cristata*, L.-Phytoremediation. *Journal of Aridland Agriculture*, 2, 18-21.
- Liu, J.N., Zhou, Q.X., Wang, S. & Sun, T. (2009). Cadmium tolerance and accumulation of *Althaea rosea* Cav. and its potential as a hyperaccumulator under chemical enhancement. *Environ. Monit. Assess.*, 149, 419-427. [https:// doi. org/ 10. 1007/s10661- 008- 0218-5](https://doi.org/10.1007/s10661-008-0218-5)
- McGrath, S.P. & Zhao, F.J. (2003). Phytoextraction of metals and metalloids from contaminated soils. *Current Opinion in Biotechnology*, 14(3), 277-282.
- Miao, Q. & Yan, J. (2013). Comparison of three ornamental plants for phytoextraction potential of chromium removal from tannery sludge. *Journal of Material Cycles and Waste Management*, 15(1), 98-105.
- Oliveira H. (2017). Chromium as an environmental pollutant: insights on induced plant toxicity. *J Bot* [Internet] 2012 [cited 2017 Nov 22];1-8. Article ID 375843. doi:10.1155/2012/375843. Available from: <https://www.hindawi.com/journals/jb/2012/375843/>
- Özkan, A., Özkan, V., Sungur, Ş. & Birses, H. (2017). Heavy metal pollution around international Hatay airport. *Natural and Engineering Sciences*, 2(1), 18-24.
- Panda, A., Patra, D.K., Acharya, S., Pradhan, C. & Patra, H.K. (2020). Assessment of the phytoremediation potential of *Zinnia elegans* L. plant species for hexavalent chromium through pot experiment. *Environmental Technology & Innovation*, 20, 101042.
- Ram, B.K., Han, Y., Yang, G., Ling, Q. & Dong, F. (2019). Effect of hexavalent chromium [Cr (VI)] on phytoremediation potential and biochemical response of hybrid Napier grass with and without EDTA application. *Plants*, 8(11), 515.
- Rocha, C.S., Rocha, D.C., Kochi, L. Y., Carneiro, D.N. M., Dos Reis, M.V. & Gomes, M.P. (2022). Phytoremediation by ornamental plants: a beautiful and ecological alternative. *Environmental Science and Pollution Research*, 1-19.
- Sabir, M., Hanafi, M.M., Zia-Ur-Rehman, M., Saifullah, Ahmad, H.R., Hakeem, K.R. & Aziz, T. (2014). Comparison of low-molecular-weight organic acids and ethylenediaminetetraacetic acid to enhance phytoextraction of heavy metals by maize. *Communications in Soil Science and Plant Analysis*, 45(1), 42-52.
- Saifullah, Ghafoor, A. & Qadir, M. (2009). Lead phytoextraction by wheat in response to the EDTA application method. *International Journal of Phytoremediation*, 11(3), 268-282.
- Salt, D.E., Smith, R.D. & Raskin, I. (1998). Phytoremediation. *Annual Review of Plant Biology*, 49(1), 643-668.
- Shahid, M., Shamshad, S., Rafiq, M., Khalid, S., Bibi, I., Niazi, N.K., Dumat, C. & Rashid, M.I. (2017). Chromium speciation, bioavailability, uptake, toxicity and detoxification in soil-plant system: a review. *Chemosphere*, 178, 513-533.
- Solgi, E. & Parmah, J. (2015). Analysis and assessment of nickel and chromium pollution in soils around Baghejar chromite mine of Sabzevar Ophiolite Belt, Northeastern Iran. *Transactions of Nonferrous Metals Society of China*, 25(7), 2380-2387.
- Srivastava, D., Tiwari, M., Dutta, P., Singh, P., Chawda, K., Kumari, M. & Chakrabarty, D. (2021). Chromium stress in plants: toxicity, tolerance and phytoremediation. *Sustainability*, 13(9), 4629.
- Stępniewska, Z. & Wolińska, A. (2005). Soil dehydrogenase activity in the presence of chromium (III) and chromium (VI). *Int Agrophys*, 19, 79-83.
- Sümer, A., Adiloğlu, S., Çetinkaya, O., Adiloğlu, A., Sungur, A. & Akbulak, C. (2013). An investigation of some heavy metals (Cr, Ni, Pb) pollution of Karamenderes basin soils in Çanakkale. *Journal of Tekirdag Agricultural Faculty*, 10(1), 83-89.
- Sunitha, R., Mahimairaja, S., Bharani, A. & Gayathri, P. (2014). Enhanced phytoremediation technology for chromium contaminated soils using biological amendments. *International Journal of Science and Technology*, 3(3), 153-162.
- Thakur, R., Sharma, G., Dwivedi, B. & Khatik, S. (2016). Chromium: as a pollutant. *Journal of Industrial Pollution Control*, 23(2), 197-203.
- Topcuoğlu, S., Kırbasoğlu, Ç. & Güngör, N. (2002). Heavy metals in organisms and sediments from Turkish Coast of the Black Sea, 1997-1998. *Environment international*, 27(7), 521-526.
- Turner, A.P., Dickinson, N.M. & Lepp, N.W. (1991). Indices of metal tolerance in trees. *Water, Air, and Soil Pollution*, 57, 617-625.
- Vodyanitskii, Y.N. (2009). Chromium and arsenic in contaminated soils (review of publications). *Eurasian Soil Science*, 42, 507-515.
- Were, F.H., Wafula, G.A. & Wairungu, S. (2017). Phytoremediation using bamboo to reduce the risk of chromium exposure from a contaminated tannery site in Kenya. *Journal of Health and Pollution*, 7(16), 12-25.
- Zayed, A.M. & Terry, N. (2003). Chromium in the environment: factors affecting biological remediation. *Plant and soil*, 249, 139-156.
- Zayed, A., Gowthaman, S. & Terry, N. (1998). Phytoaccumulation of trace elements by wetland plants: I. duckweed. *Journal of Environmental*

- Quality*, 27(3), 715–721. <https://doi.org/10.2134/jeq1998.00472425002700030032x>
- Zhang, X., Zhong, T., Liu, L., Zhang, X., Cheng, M., Li, X. & Jin, J. (2016). Chromium occurrences in arable soil and its influence on food production in China. *Environmental Earth Sciences*, 75, 1-8.
- Zheljazkov, V.D. & Nielsen, N.E. (1996). Studies on the effect of heavy metals (Cd, Pb, Cu, Mn, Zn and Fe) upon the growth, productivity and quality of lavender (*Lavandula angustifolia* Mill.) production. *Journal of Essential Oil Research*, 8(3), 259-274.
- Zurayk, R., Sukkariyah, B., Baalbaki, R. & Abi Ghanem, D. (2002). Ni Phytoaccumulation in *Mentha aquatica* L. and *Mentha sylvestris* L. *Water, Air, and Soil Pollution*, 139, 355-364.

SILPHIUM PERFOLIATUM A PROMISING ENERGY CROP FOR PHYTOREMEDIATION OF HEAVY METAL CONTAMINATED SOILS

Violina ANGELOVA, Vera KOLEVA

Agricultural University - Plovdiv, 12 Mendelev Blvd, Plovdiv, Bulgaria

Corresponding author email: vileriz@abv.bg

Abstract

*Comparative studies have been carried out to determine the quantities and depositions of heavy metals, macro, and microelements in the vegetative organs of *Silphium perfoliatum*, the efficiency for phytoremediation and the quality of the biomass as a renewable energy source for the combustion process. The field experiment was conducted on an agricultural field contaminated by the Non-Ferrous Metals Plant near Plovdiv, Bulgaria. *Silphium perfoliatum* is tolerant to heavy metals and can be grown on highly contaminated soils (1671.6 mg/kg Zn, 1694.8 mg/kg Pb, and 54.8 mg/kg Cd). Pb, Zn, Hg, Cu, Fe, Mn, Ca and Mg accumulated in leaves, Cd and P - in roots, and K in stems. Cup plant can be classified as a excluder plant with bioconcentration factor < 1 and can also be used in phytoremediation of contaminated soils. *Silphium perfoliatum* can be a significant source of good-quality raw material in producing solid biofuels. The biomass studied is of high quality (high in C and H and low in ash, N, Cl, and S) and has high energy potential. Biomass of *Silphium perfoliatum* from highly contaminated soils could be used as a source of energy.*

Key words: cup plant, polluted soils, proximate and ultimate analysis, combustion.

INTRODUCTION

The cup plant (*Silphium perfoliatum* L.) is a honey-bearing herbaceous perennial plant of the Asteraceae family. The plant was brought to Europe from North America in the 18th century because of the plant's ornamental value. *Silphium perfoliatum* L. is cold hardy (withstanding winter temperatures down to minus 30-35°C), disease and pest-resistant, undemanding to soils, tolerant to droughts, and can be grown effectively throughout Europe (Gansberger et al., 2014). Due to its phenotypic plasticity, it can be cultivated on degraded soils (Zhang et al., 2010; Gansberger et al., 2014). In the first year, it forms a 60-70 cm diameter rosette of leaves, and in the 2nd year, the plant forms numerous flowering stems up to 1.5 m tall, which secrete a resinous sap with a strong odor similar to that of turpentine. It has many leaves (8-14 pairs of opposite leaves with an area of 85-120 cm²) arranged alternately at 10-18 cm (Peni et al., 2020).

The biomass can be harvested twice during the growing season (Cumplido-Marin et al., 2020; Stolarski et al., 2020). The plant is characterized by a high regrowth ability maintained for up to 15-20 years. Sunflower-

like yellow flower heads form in branched corymbs.

Phytoremediation is a process by which plants effectively remove heavy metals by absorbing them from the contaminated substrate (Chaney et al., 1997). It is desirable for plants to have a rapid growth rate with high biomass production potential, a deep and branching root system, and to be tolerant to biotic and abiotic stress. Recommended plant species for heavy metal extraction should have translocation factor and bioaccumulation factor values above 1. *S. perfoliatum* L. is one of the proposed species for remediation of heavy metal contaminated soils as it has an intensive growth rate, is tolerant to biotic and abiotic stress, produces a significant amount of plant biomass that can be harvested and used in biogas production, and direct combustion (Sumala et al., 2020; Nescu et al., 2022; Sumalan et al., 2023).

Figas et al. (2015) indicate that the plant can potentially rehabilitate degraded land through phytoremediation. Preliminary studies suggest cup plant is a good candidate for phytoremediation of Cd-impacted soils (Zhang et al., 2010). However, according to Sumalan et al. (2023), *Silphium perfoliatum* is a potential hyperaccumulator.

The purpose of this study is to conduct systematic research that will allow us to determine the quantities and the deposits for accumulation of heavy metals, macro- and microelements in the vegetative organs of cup plants, the quality of biomass as a biofuel, as well as the possibilities to use the plant for phytoremediation of heavy metal contaminated soils.

MATERIALS AND METHODS

The experiment was carried out on an agricultural field contaminated with Zn, Pb, and Cd, located 0.5 km from the source of contamination - a non-ferrous metals plant (NMP) near Plovdiv, Bulgaria. The soil used in this experiment was slightly alkaline (pH 7.6) with moderate in organic matter (2.5%). The total Zn, Pb, and Cd contents were high (1671.6 mg/kg Zn, 1694.8 mg/kg Pb, and 54.8 mg/kg Cd, respectively) and exceeded the maximum allowable concentrations (MAC) (400 mg/kg Zn, 100 mg/kg Pb, 3.0 mg/kg Cd) (Table 1). The Hg content in soils is lower than the MAC.

Table 1. The total content of Pb, Zn, Cd (mg/kg), and Hg (ng/g) in soil sampled from NFMW-Plovdiv

Element	Pb	Zn	Cd	Hg
x±sd	1671.6±3.1	1694.8±3.5	54.8±0.9	574.8±10

x - average value (mg/kg) from 5 repetitions; sd - mean standard deviation

MAC (pH >7.4) - Pb - 100 mg/kg, Cd - 3.0 mg/kg, Zn - 400 mg/kg, Hg - 1.5 mg/kg

The field tests with the cup plant were set after the block method in four replications. The size of the test plot was 100 m². Plants were planted in May by planting the seedlings at 0.75 m intra-row and inter-row spacing. Whole plants (3 plants from each replicate) were taken for analysis in mid-November before frost fall.

The plants were collected, and the content of heavy metals and macro and trace elements in their different parts - roots, stems, and leaves, was analyzed separately. The samples were dried at room temperature to obtain an air-dry mass and then dried at 105°C.

The total metal composition of the soils was determined according to ISO 11466.

Plant samples were processed by the microwave mineralization method. An

inductively coupled emission spectrometer (Jobin Yvon Horiba "ULTIMA 2", France) was used to determine the content of heavy metals, micro- and macroelements in plant and soil samples.

Heating value, ultimate and proximate analysis, are among the main parameters in the evaluation of biomass in the direct combustion process.

Proximate analysis. The samples were characterized according to standard methods: moisture content (EN 14774-2:2009), ash (EN 14775:2009), fixed carbon (by difference), and volatile matter (EN 15148:2009).

Ultimate analysis. Total C, H, N, and S were determined by dry combustion in a Vario Macro CHNS analyzer (Elementar Analysen systeme GmbH, Germany), according to the protocols (EN 15104:2011) and (EN 15289:2011). The O content was calculated by difference.

Heating value. The heating value was determined by the ISO method (EN 14918:2010) using an IKA C200 oxygen bomb calorimeter (IKA Analysentechnik GmbH, Heitersheim, Germany).

RESULTS AND DISCUSSIONS

Accumulation of heavy metals in vegetative organs of cup plant

Table 2 presents the results obtained for the content of heavy metals in the vegetative organs of the study energy crop.

Significant differences were found in the content of the elements in the different parts of the cup plant. Pb, Zn, Hg, Cu, Fe, Mn, Ca and Mg accumulated in leaves, Cd and P - in roots, and K in stems.

Sumalan et al. (2023) found good absorption and selective accumulation capacity of cup plant. Cu and Zn mainly accumulate in the stems, Cd in the roots and stems, while Pb primarily accumulates in the roots.

The heavy metal contents of Pb, Zn, and Hg were lower compared to the leaves, while the opposite trend was found for Cd. The Pb content of the roots reached 42.1 mg/kg, Zn - 172.1 mg/kg, Cd - 20.3 mg/kg, and Hg- 41.0 µg/kg. The contents of micro- and macro elements (except P) were also lower in the root system.

Table 2. Content of heavy metals, macro- and microelements in vegetative organs of cup plant

	Roots	Stems	Leaves
Pb, mg/kg	42.1	40.3	268.2
Cd, mg/kg	20.3	0.66	3.3
Zn, mg/kg	172.0	73.7	291.0
Cu, mg/kg	12.0	13.5	51.4
Fe, mg/kg	261.6	77.9	681.7
Mn, mg/kg	27.8	20.2	120.2
P, mg/kg	1438.3	383.2	847.2
Ca, mg/kg	2487.1	4758.2	28052.6
Mg, mg/kg	1064.0	726.2	2710.7
K, mg/kg	5760.7	8589.4	6016.5
Hg, µg/kg	41.0	23.0	215.9

A probable reason for this is that the root system of the cup plant is fibrous, consisting of a central main root that reaches a penetration depth of 80 cm and shallow rhizomes that help the vegetative spread of the plant.

However, studies conducted by Fitzgerald et al. (2003) have shown that the level of heavy metal accumulation in plants is directly related to their concentration in the soil and that the root system of plants is their main storage organ. Similar results were also obtained by Sumalan et al. (2020), who found that heavy metal accumulation in *S. perfoliatum* was higher in the roots compared to the leaves in the early stages of vegetative growth. The amount of metals absorbed depends on the metal content of the soil as well as the developmental stage of the root system. The content of heavy metals and micro and macro elements in the stems was lower compared to the root system (except K), which showed that their movement through the conductive system was strongly restricted. The content of Pb in the stems of cup plants grown at 0.5 km from NFMW reached 40.3 mg/kg, Zn - 73.7 mg/kg, Cd - 0.66 mg/kg, and Hg - 23.0 µg/kg.

The movement of Pb from the roots to the aboveground parts of plants is typically limited. Once Pb enters the plant's roots, it promptly interacts with phosphates, carbonates, and bicarbonates in high concentrations within the intercellular spaces. This interaction causes Pb to precipitate as phosphates or carbonates, preventing its transportation through the xylem (Kabata Pendias, 2001).

Cd is a very mobile element that moves from the roots to the aboveground mass, but this was not observed in our studies. Probably, Cd is mainly bound to the cell walls and stored in

vacuoles of the root cortex and not transported to the shoots (Zhang et al., 2010).

The content of Pb in the leaves of cup plants grown at 0.5 km from NFMW reached 268.2 mg/kg, Zn - 291.3 mg/kg, Cd - 3.25 mg/kg, and Hg - 215.9 µg/kg. A probable reason is that the leaves of the cup plant are rough, hairy, large, and deeply feathery with a coarse texture, which is a prerequisite for their aerosol contamination. The accumulation values and heavy metal concentrations in *S. perfoliatum* plants during rosette leaf formation are significantly lower than those for hyperaccumulators (Sumalan et al., 2020), which is confirmed by obtained results. Studies by Sumalan et al. (2023) showed that Zn and Pb mainly accumulate in leaves. The ability of the aboveground mass to accumulate greater amounts of heavy metals compared to the root system has been confirmed by Nouri et al. (2009) on various species of the Asteraceae family grown on contaminated soils.

Translocation factor and bioconcentration factors were calculated to determine the phytoremediation potential of the plant.

The translocation factor (TF) provides information on the ability of plants to absorb heavy metals through the roots and translocate them to the aboveground mass (stems and leaves). For Pb and Hg, the TF values are more significant than 1 (6.37 and 5.27, respectively). for Zn about 1 (1.69) and for Cd less than 1 (0.16). $TF > 1$ were also found by Sumalan et al. (2020), which follow the order $Pb > Zn > Cr$. $TF > 1$ for plants growing on soils contaminated with heavy metals were also found by Zhang et al. (2010) and Nescu et al. (2022).

The bioconcentration factor (BCF) determines the effectiveness of phytoremediation. BCF root is a ratio of the content of heavy metals in roots to soil content ($BCF_{roots} = [Metal]_{roots} / [Metal]_{soils}$). The results show that BCF_{roots} reaches up to 0.025 for Pb, 0.37 for Cd, 0.10 for Zn, and 0.07 for Hg.

BCF_{shoot} is defined as the ratio of the metal concentration in the aboveground mass of the plant (stems and leaves) and in the soil ($BCF_{shoot} = [Metal]_{shoots} / [Metal]_{soils}$) and is a measure of the plant's ability to absorb and move the metals to the aboveground mass, which can be easily harvested.

The results show that the BCF_{root} for Pb reaches 0.16, Cd from 0.09 to 0.26, Zn 0.17, and Hg 0.38. A plant is an excluder if $BCF < 1$, an accumulator if $1 < BCF < 10$, and if $BCF > 10$, the plant is a hyperaccumulator.

The study results show that the cup plant can be classified as an excluder since BCF is less than 1. This confirms the results obtained by Zhang et al. (2010) which found that *S. perfoliatum* is a Cd excluder.

Table 3. Translocation factor (TF) and bioconcentration coefficients (BCF_{roots}, BCF_{shoots}) of cup plant

Coefficient	Pb	Cd	Zn	Hg
TF	6.37	0.16	1.69	5.27
BCF _{root}	0.025	0.37	0.10	0.07
BCF _{shoot}	0.16	0.069	0.17	0.38

$BCF_{root} = [Metal]_{shoots} / [Metal]_{soil}$, $TF = [Metal]_{shoots} / [Metal]_{roots}$,
 $BCF_{shoot} = [Metal]_{shoot} / [Metal]_{soil}$

The cup plant accumulates a small amount of heavy metals in the leaves and has no potential for phytoextraction. This is in contradiction to the results of Sumalan et al. (2020), according to which *S. perfoliatum* has the potential to bioaccumulate heavy metals in soils contaminated with Cu, Zn, Cr and Pb Mockeviciene et al. (2023) found an accumulative capacity of the cup plant concerning Cu and Zn, while the BCF (for Cr, Ni and Pb) was relatively low, indicating that the plant could only absorb but not accumulate these heavy metals.

Heating value, ultimate and proximate analysis

Moisture content (MC), ash content (AC), volatile matter (VM), nitrogen (N), sulphur (S) and oxygen (O) are undesirable components in biomass, in contrast to fixed carbon (FC), carbon (C), hydrogen (H) and lower heating value (LHV), whose higher levels improve biomass quality when it comes to direct combustion. The lower heating value (LHV), moisture and ash contents depend on the harvesting time of *Silphium perfoliatum*, while the higher heating value (HHV), C, H and S contents are less affected by these factors (Stolarski et al., 2018).

The results obtained for the plant biomass of cups grown on heavy Metal-contaminated soils are presented in Tables 4 and 5. The tables also present the values of the solid fuels standard EN ISO 17225-6 for non-wood pellets and data

from the analysis of cup plant biomass grown in different countries.

Table 4. Proximate analyses and lower heating value of cup plant biomass

Parameter	Moisture %	Ash, %	FC, %	VM, %	LHV, MJ/kg
Cup plant	9.1	6.1	16.56	77.34	16.49
Reference	3.84-13.0	2.04-9.22	9.28	77.45	15.7-16.61
Standard	≤12	≤6-10	-	-	≥14.5

Table 5. Ultimate analysis of *Miscanthus x giganteus* biomass

	N, %	C, %	S, %	H, %	O, %	Cl, %
Cup plant	0.846	40.5	0.052	5.7	46.03	0.074
Reference	0.37-0.68	42.94-45.44	0.02-0.07	5.28-5.30	38.57-50.92	0.026
Standard	≤1.5	-	≤0.2	-	-	≤0.1

The moisture content is influenced by the environmental conditions, in particular by, temperature, and humidity, but also by soil properties (soil type and altitude), genetic characteristics, the applied agrotechnique (mainly fertilization), as well as the development and phenophase of the plant (Kowalska et al., 2020). The results show that the moisture content reaches 9.1%, which are in accordance with the standard EN ISO 17225-6 (≤12). The moisture content of the biomass varies from 3.84% to 13.0% (Fraczek et al., 2011; Bury et al., 2020; Stolarski et al., 2020).

The ash content is one of the main factors determining biomass quality. In direct combustion, it is desirable to have as low ash content as possible since ash has no calorific value and thus reduces the efficiency of the combustion system. The results show that the ash content reaches up to 6.1%, which is in accordance with the standard for solid fuels EN ISO 17225-6 (6 to 10%). The ash content in cup plant biomass varies from 2.84% to 14.54% (Stolarski et al., 2004; Fraczek et al., 2011; Wever et al., 2019; Bury et al., 2020; Suric et al., 2022).

Higher values of fixed carbon affect biomass quality due to the higher heating values. The fixed carbon content is calculated by the formula Fixed Carbon (%) = 100 - Ash (% Dry Basis) - Volatile Matter (% Dry Basis).

The results show that the fixed carbon varies reaching 16.56%. Significantly lower results were obtained by Suric et al. (2022) (9.28%).

Volatile matters are the components released at high temperatures when the fuel is heated, without considering the moisture that is part of the combustible gases (C_xH_y gases, CO or H₂) and non-combustible gases (CO₂, SO₂ or NO_x) (Garcia et al., 2012). The results obtained show that volatile matter reaches up to 77.34%.

Heating values decrease with higher moisture content, with higher levels leading to lower combustion temperatures and affecting quality (Garcia et al., 2012). The net calorific value of biomass depends on the chemical composition, moisture content, and carbon (C), hydrogen (H) and ash contents, with moisture content being the main cause of variation in results.

The results show that the net heat of combustion on a dry basis reaches up to 16.49 MJ/kg. According to this parameter in the EN ISO 17225-6 standard, the biomass from cup plant is characterised as a valuable energy raw material suitable for use in the combustion process. Similar results for LHV for cup plant biomass were found by Stolarski et al. (2020) (15.7 MJ/kg) and Bury et al. (2020) (16.61 MJ/kg). The calorific value of cup plant biomass is in the same range as the energy crop *M. x giganteus* (Stolarski et al., 2020). Carbon is the main and most important element in all types of fuels, and its content determines their quality, i.e. higher carbon levels increase fuel quality. Cup plant biomass contains carbon in the range of 42.0-51.9%, indicating a high potential for thermal energy. 51.9% (Peni et al., 2020). Similar results were obtained in this research (40.5% carbon).

Hydrogen, together with nitrogen, forms the basic fuel composition of any fuel, and increased hydrogen content improves fuel quality by positively affecting oxygen levels. Peni et al. (2020) found H content of 5.75%, which agrees with the obtained results (5.7%). The oxygen content is calculated by the formula $\text{Oxygen (\%)} = 100 - \text{Carbon (\% Dry Basis)} - \text{Hydrogen (\% Dry Basis)} - \text{Nitrogen (\% Dry Basis)} - \text{Sulphur (\% Dry Basis)} - \text{Ash (\% Dry Basis)}$. The oxygen content reaches up to 46.03%. According to the Siaudinis et al. (2015) and Suric et al. (2022) the content of O varies from 38.57% to 50.92%.

From an environmental point of view, N and S contribute to the increase of greenhouse gases and are considered unfavourable elements in biomass. The content of N reaches up to 0.846% and of S up to 0.0524%. The values obtained are below the permissible values in the standard for solid fuels EN ISO 17225-6 (N is less than 1.5%, and for S is 0.2%). The low levels of S in the cup plant, is an indicator of the potential of the plant for direct combustion. Chlorine content reaches 0.074%, values below the permissible values in the standard for solid fuels EN ISO 17225-6 (<0.1%). Lower values were also found by Peni et al. (2022) (0.026%).

CONCLUSIONS

The cup plant is tolerant to heavy metals and can be grown in heavy metal polluted soils (1671.6 mg/kg Zn, 1694.8 mg/kg Pb, and 54.8 mg/kg Cd), and can be successfully used in the phytoremediation of heavy metal polluted soils. Significant differences were found in the content of the elements in the different parts of the cup plant. Pb, Zn, Hg, Cu, Fe, Mn, Ca and Mg accumulated in leaves, Cd and P - in roots, and K in stems.

Cup plant can be classified as an excluder plant with BCF < 1. The moisture content of biomass in cup plant is low and within the standard.

Ash content as an indicator of fuel quality is also low, highlighting the good quality of the biomass studied.

The cup plant biomass studied is of high quality (high in C and H and low in ash, N, Cl, and S) and has high energy potential.

ACKNOWLEDGEMENTS

This research work was carried out with the support of Bulgarian National Science Fund and also was financed from Project KP-06-H54/7 "Possibilities for limiting the impact of mercury on the environment and human health".

REFERENCES

- Bury, M., Mozdzer, E., Kitzak, T., Siwek, H., Włodarczyk, M. (2020). Yields, calorific value and chemical properties of cup plant *Silphium perfoliatum* L. biomass, depending on the method of establishing the plantation. *Agronomy*, 10, 851-872.

- Chaney, R.L., Malik, M., Li, Y.M., Brown, S.L., Brewer, E.P., Angle, J.S. (1997). Phytoremediation of soils metals. *Current Opinion in Biotech.*, 8, 279–284.
- Cumplido-Marin, L., Graves, A.R., Burgess, P.J., Morhart, C., Paris, P., Jablonowski, N.D. (2020). Two novel energy crops: *Sida hermaphrodita* (L.) Rusby and *Silphium perfoliatum* L. - state of knowledge. *Agronomy*, 10, 928.
- EN 14774-2 (2009). Solid biofuels - Determination of moisture content - Oven dry method - Part 2: Total moisture - Simplified method.
- EN 14775 (2009). Solid biofuels - Determination of ash content).
- EN 14918 (2010). Solid biofuels - Determination of calorific value
- EN 15104 (2011). Solid biofuels - Determination of total content of carbon, hydrogen and nitrogen - Instrumental methods.
- EN 15148 (2009). Solid biofuels - Determination of the content of volatile matter
- EN 15289 (2011). Solid biofuels - Determination of total content of sulfur and chlorine.
- Figas, A., Rolbiecki, R., Tomaszewska-Sowa, M. (2015). Influence of drip irrigation on the height of the biennial cup plant (*Silphium perfoliatum* L.) from the micropropagation seedlings. *Infrastructure and Ecology of Rural Areas*, 3, Polska Akademia Nauk, Oddział w Krakowie, 779-786.
- Fitzgerald, E.J., Caffrey, J.M., Nesaratnam, S.T., McLoughlin, P. (2003). Copper and lead concentrations in salt marsh plants on the Suir Estuary, Ireland. *Environmental Pollution*, 123(1), 67-74.
- Frączek, J., Mudryk, K., Wrbel, M. (2011). Cup plant *Silphium perfoliatum* L. biomass source for the production of solid fuels. *Inżynieria Rol.*, 6, 21–27 (In Polish).
- Gansberger, M., Montgomery, L.F.R., Liebhard, P. (2015). Botanical characteristics, crop management and potential of *Silphium Perfoliatum* L. as a renewable resource for biogas production: a review. *Ind Crop Prod.*, 63, 362–372.
- Garcia, R., Pizarro, C., Lavín, A.G., Bueno, J.L. (2012). Characterization of Spanish biomass wastes for energy use. *Biore. Technol.*, 103(1), 249-258.
- ISO 11466 (1995). Soil Quality-Extraction of Trace Elements Soluble in Aqua Regia.
- ISO 17225-6 (2021). Solid biofuels - Fuel specifications and classes Part 6: Graded non-woody pellets
- Kabata-Pendias, A. (2001). Trace elements in soils and plants. 3rd ed. CRC Press LLC, Boca Raton, 2001.
- Kowalska, G., Pankiewicz, U., Kowalski, R. (2020). Evaluation of chemical composition of some *Silphium* L. species as alternative raw materials. *Agriculture*, 10, 132.
- Mockeviciene, I., Siaudinis, G., Karcauskiene, D., Repsiene, R., Barcauskaite, K., Anne, O. (2023). The evaluation of the phytoremediation potential of the energy crops in acid soil by sewage sludge fertilization. *Land*, 12(4), 866.
- Nescu, V., Ciulca, S., Sumalan, R.M., Berbecea, A., Velicevici, G., Negrea, P., Gaspar, S., Sumalan, R.L. (2022). Physiological aspects of absorption, translocation, and accumulation of heavy metals in *Silphium perfoliatum* L. plants grown in a mining-contaminated soil. *Minerals*, 12, 334.
- Nouri, J., Khorasani, N., Lorestani, B.B., Karami, M., Hassani, H.A., Yousef, N. (2009). Accumulation of heavy metals in soil and uptake by plant species with phytoremediation potential. *Environ. Earth Sci.*, 59, 315–323
- Peni, D., Stolarski, M.J., Dębowski, M. (2022). Green biomass quality of perennial herbaceous crops depending on the species, type and level of fertilization. *Industrial Crops and Products*, 184(3), 115026.
- Peni, D., Stolarski, M.J., Bordiean, A., Krzyzaniak, M., Debowski, M. (2020). *Silphium perfoliatum* - A herbaceous crop with increased interest in recent years for multi-purpose use. *Agriculture*, 10, 640.
- Siaudinis, G., Jasinskas, A., Sarauskis, E., Steponavicius, D., Karcauskiene, D., Liaudanskiene, I. (2015). The assessment of Virginia mallow (*Sida hermaphrodita* Rusby) and cup plant (*Silphium perfoliatum* L.) productivity, physico-mechanical properties and energy expenses. *Energy*, 93(1), 606-612.
- Stolarski, M. (2004). Production and harvesting of biomass from long-term energy crops. *Probl. Inżynierii Rol.*, 3, 47–56.
- Stolarski, M.J., Krzyzaniak, M., Olba-Zięty, E. (2020). Biomass yield and quality of perennial herbaceous crops in a double harvest in a continental environment. *Ind Crop Prod.*, 180, 114752.
- Stolarski, M.J., Snieg, M., Krzyzaniak, M., Tworowski, J., Szczukowski, S., Graban, L.; Lajszner, W. (2018). Short rotation coppices, grasses and other herbaceous crops: Biomass properties versus 26 genotypes and harvest time. *Ind. Crop. Prod.*, 119, 22–32.
- Sumalan, R.L., Muntean, C., Kostov, A., Krzanovic, D., Jucor, N.L., Ciulca, S.I., Sumalan, R.M., Gheju, M., Cernicova-Buca, M. (2020). The cup plant (*Silphium perfoliatum* L.) - A viable solution for bioremediating soils polluted with heavy metals. *Not. Bot. Horti Agrobot. Cluj-Napoca*, 48, 2095–2113.
- Sumalan, R.L., Nescu, V., Berbecea, A., Sumalan, R.M., Crisan, M., Negrea, P., Ciulca, S. (2023). The Impact of heavy metal accumulation on some physiological parameters in *Silphium perfoliatum* L. plants grown in hydroponic systems. *Plants*, 12, 1718.
- Suric, J., Sic Zlabur, J., Peter, A., Brandic, I., Voca, S., Dujmovic, M., Leto, J., Voca, N. (2022). Energy vs. nutritional potential of virginia mallow (*Sida hermaphrodita* L.) and cup plant (*Silphium perfoliatum* L.). *Plants*, 11, 2906.
- Wever, C., Holler, M., Becker, L., Biertumpfel, A., Köhler, J., van Inghelandt, D., Westhoff, P., Pude, R., Pestsova, E. (2019). Towards high-biomass yielding bioenergy crop *Silphium perfoliatum* L.: Phenotypic and genotypic evaluation of five cultivated populations. *Biomass Bioenergy*, 124, 102–113.
- Zhang, X., Xia, H., Li, Z., Zhuang, P., Gao, B. (2010). Potential of four forage grasses in remediation of Cd and Zn contaminated soils. *Bioresour. Technol.*, 101, 2063–2066.

IMPACT ASSESSMENT REGARDING POLLUTION WITH NUTRIENTS OF WATER RESOURCES DUE TO THE USE OF FERTILIZERS WITH MICROBIAL BIOMASS

Mihaela BEGEA¹, Nicoleta RADU^{2,3}, Mariana CONSTANTIN³, Roxana ZAHARIA⁴

¹National University of Sciences and Technology Politehnica Bucharest,
313 Splaiul Independentei, District 6, Bucharest, Romania

²University of Agronomic Sciences and Veterinary Medicine of Bucharest,
59 Marasti Blvd, District 1, Bucharest, Romania

³National Institute for Research & Development in Chemistry and Petrochemistry - ICECHIM
Bucharest, 202 Splaiul Independentei, Bucharest, Romania

⁴Institute of Plant Protection R & D, 8 Ion Ionescu de la Brad Blvd, District 1, Bucharest Romania

Corresponding author email: nicoleta.radu@biotehnologii.usamv.ro

Abstract

A way of valorise the solid by-products resulting from industrial biosyntheses is to use them as such to fertilize agricultural soils or to obtain new types of fertilizers. Two types of fertilizers obtained with spent microbial biomass were evaluated regarding the impact generated on the waters as a result of potential nutrient loss processes through washing throughout rainwater. The tests were carried out in the lab, in glass columns filled with a mixture of red-brown soil, sand, and fertilizers, the last one added in quantities corresponding to a fertilization norm of 200 kg SA/ha. For each experimental variant, an average pluviometry flow rate of 14 L/m² was simulated; in each column, water was added at intervals of 1; 4; 7, and 15 days. The nutrients lost by leaching were assessed after each interval. The obtained results showed that fertilizers formulated with microbial biomass lose (77.9-85.11)% P₂O₅ and (76.2-90)% K₂O in 24 h, compared to classic fertilizers, which lose 75% P₂O₅ through leaching, respectively 86.5% K₂O. Because the behaviour of fertilizers formulated with microbial biomass is similar to that of complex fertilizers, was estimated that the impact generated by the use of fertilizers with microbial biomass on the water is insignificant.

Key words: fertilizer, microbial biomass.

INTRODUCTION

In the current context, biotechnological processes (white or red biotechnologies) generate large quantities of by-products (microbial biomass) that are stored in dumps (Sullivan et al., 2017; Halter et al., 2020). These deposits often cause environmental problems, because they block large areas of land, from where the wind and rainfall can transport it in air, soil, water or groundwater polluting all environmental factors (Gowariker et al., 2009; Jayanta et al., 2028) Over time, the valorisation of spent microbial biomass has been made in three main directions: 1) obtaining absorbents used to reduce the load of metal cations present in industrial wastewater (Radu et al., 2006; Radu et al., 2007a; Dima et al., 2006; Migahed et al., 2017; Chwastowski, et al., 2023); 2) conditioning them in the form of organic fertilisers, after thermal or chemical inactivation

(Andersen et al., 2001; Halter et al., 2020; Stikane et al., 2022; Stikane et al., 2023; Vurukonda et al., 2024) or using them in the formulation of fertiliser type NP/NK/NPK/NPK with microelements (Radu & Meghea, 2007b; Radu et al., 2020) and 3) combustion under controlled conditions to obtain the biochar (Meng et al., 2023). Actual environmental legislation together with the reduction of available land for the storage of spent microbial biomass, has forced large biotech companies to look for profitable ways to capitalize on this waste. A sustainable way of valorising the by-products resulting from biotechnological processes is to use them to obtain new fertilizers, which can be used in agriculture (Radu et al., 2006; Meghea et al., 2007; Radu et al., 2020). The products obtained with microbial biomass combine two qualities: they have fertilization properties, thanks to the nutrients in the biomass (Arrieche-Luna, 2010; Černý et al., 2023), and

they act as precursors for humic compounds, which improve the agrochemical properties of the soil (Azizah et al., 2023; Wang et al., 2023). The main purpose of the conducted studies was to evaluate the impact generated on water sources (surface water; underground water) as a result of the use of NP/NPK/NK type fertilizers formulated with microbial biomass functionalized with microelements.

The studied fertilizers were obtained in the lab according to the methodology presented by Radu et al. (Radu et al., 2007b; Meghea et al., 2007; Radu et al., 2020).

MATERIALS AND METHODS

To evaluate the impact on water resources generated by fertilizers with microbial biomass, the leaching tests were performed with fertilizers formulated with two spent microbial biomass types: *Penicillium* sp. (PB) and *Streptomyces* sp., (SB) resulting from the current pharma bioprocesses. Elemental composition of the two types of microbial biomass is shown in the Table 1.

Table 1. Elemental composition of microbial biomass

Element	C %	Ca %	Mg %	N %	P ₂ O ₅ %	Co μg/g	Cu μg/g	Fe μg/g	Mn μg/g	Zn μg/g
Concentration										
Biomass 1 (SB)	36.8	3.73	0.013	6.24	0.11	30.47	1.71	938.3	24.3	26.6
Biomass 2 (PB)	30.3	0.32	0.001	1.84	1.44	1.73	28.74	705.2	5.11	52.3

The two types of microbial biomass were tested alone (PB and SB) or as a fertilizers type NPK (9:8:4; 11:22:5; 13:13:7; 17:41:9), obtained with biomass of SB. The tests were carried out in glass columns, in which were introduced a mixture of red-brown soil and sand (mass ratio: 1:1). Fertilizers were introduced in columns in amounts corresponding to the fertilization norm of 200 kg SA/ha, after which an average pluviometry flow rate of 14 L/m² was simulated at each watering.

The water was added in columns used in the experiment at four intervals: 24h; 96h; 168h and 360h. Nutrients lost by leaching were made from the effluents obtained in the collector vessel, after each interval.

Each experiment was performed in three times, and results were presented as average value, with corresponding standard deviation. The loss

of microelements and macroelements by washing were measured after removing of organic compounds from aqueous effluents (Radu et al., 2020), using an ICP AES spectrometer type VARIAN Liberty 110.

RESULTS AND DISCUSSIONS

Results obtained after measurements done after 24 h show that in the case of SB, this generally retains much better their constituents, in comparison to the PB. In the case of main (or major) macronutrients, results obtained show the following:

- for magnesium: the biomass derived from SB loses 4.6% of this in comparison with the PB, which loses 25.4% (Figure 1 and Figure 2);
- in the case of calcium, the SB loses 19.5% Ca while the PB loses 48.8% Ca (Figure 1 and Figure 2);
- regarding P₂O₅, the SB loses 1.1% in comparison with the PB, which loses 2.9% (Figure 1 and Figure 2).

Potassium (expressed as K₂O), from SB, loses 30.4% in comparison with the PB, which loses 66.7% (Figure 1 and Figure 2).

Regarding the macroelements lost by leaching, it is found that the PB loses 2 times more nutrients in comparison with SB.

In the terms of microelements, the amount lost by leaching is much higher for PB except the Fe, where the SB loses 1.7%, more than PB, which loses only 0.5% (Figure 3 and Figure 4).

In the case of the PB, this loses its microelements in greater quantities, respectively 47.6% Co, 34.3% Cu, 46.3% Mn, 100% Mo, and 3.1% Zn, in comparison with the SB (Figure 3 and Figure 4), which loses microelements in smaller quantities: 28.7% Co, 7.1% Cu, 28.4% Mn, 100% Mo, 0.6% Zn, except Mo, for which they both subproducts lost Mo in the same quantities (100%).

Keeping into account the concentration levels of macroelements and microelements in the effluents tested, we consider that the environmental risk due to lost macroelements and microelements leached from both microbial biomasses is insignificant (Table 2), because the concentration levels in each effluent are smaller than intervention limits imposed by legislation in force (NTPA 011).

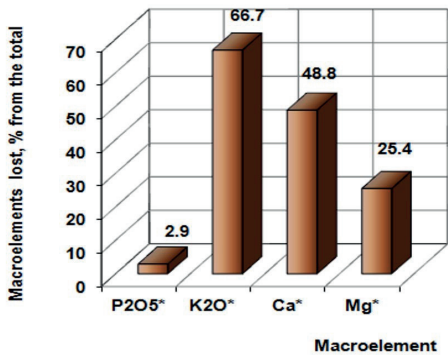


Figure 1. Macronutrients lost by leaching from the PB after 24 hours

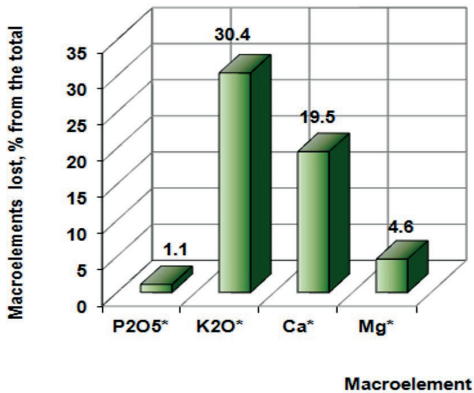


Figure 2. Macronutrients lost by leaching from the SB after 24 hours

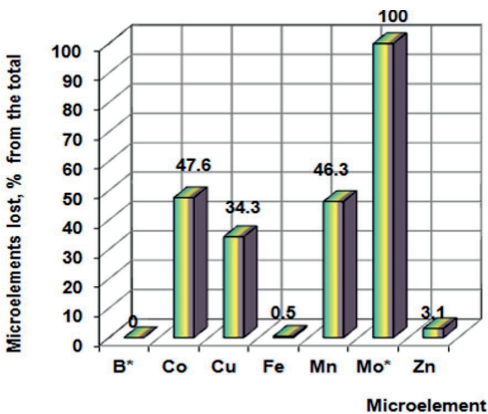


Figure 3. Micronutrients lost through leaching from microbial biomass of PB after 24 h

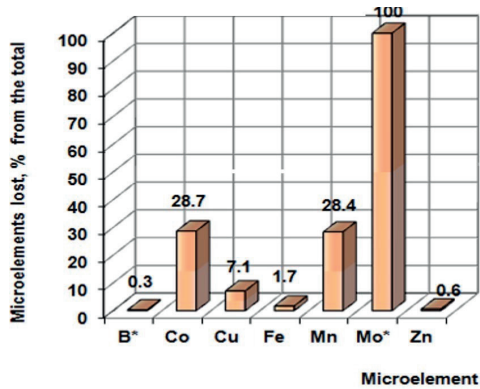


Figure 4. Micronutrients lost through leaching from microbial biomass of SB after 24 h

Table 2. Risk assessment regarding water pollution with elements from microbial biomass

Element (ppm)	Maximum permissible concentration (admissible level, ppm)		Elements lost due to leaching from SB	Elements lost due to leaching from PB	Environmental impact
	Household receivers (sewage)	Natural receptors			
Ca	-	300	0.4296	0.0332	INSIGNIFICANT
Mg	-	100	0.0868	0.0053	
P	5	1(2)	0.0280	0.0545	
Cu	0.2	0.1	0.0998	0.0657	
Co	-	1	0.0339	0.0136	
Fe	-	5	0.0479	0.0017	
Zn	1	0.5	0.0046	0.0041	
Mn	2	1	0.0445	0.0145	
Mo	-	0.1	0.0200	0.0038	

Regarding the leachability in time of fertilizers with microbial biomass, the results obtained until 360 hours with the four types of fertilizers studied, (two fertilizers formulated with microbial biomass respectively A: NPK 9:8:4 and B: NPK 11:22:5 and two types are conventional fertilizers C: NPK 11:22:5 and D: NPK 17:41:9) showed the following:

- in the case of P₂O₅, the fertilizers formulated with microbial biomass lose about (77.9-85.11)% P₂O₅ on the first day (24 h) (Figure 5), in comparison with classical fertilizers, where the degree of loss is below 75%;
- after 360 h, the P₂O₅ loss by leaching is in the proportion of (96-98)%;

- the potassium loss (expressed as K_2O) is situated in the range of (76.2-90)% in 24 h (Figure 6), in the case of fertilizers formulated with microbial biomass, while for the classic fertilizers, the K_2O loss is situated below 86.5%;

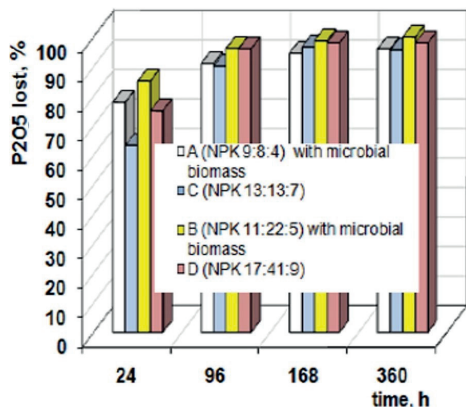


Figure 5. P_2O_5 loss through leaching in time

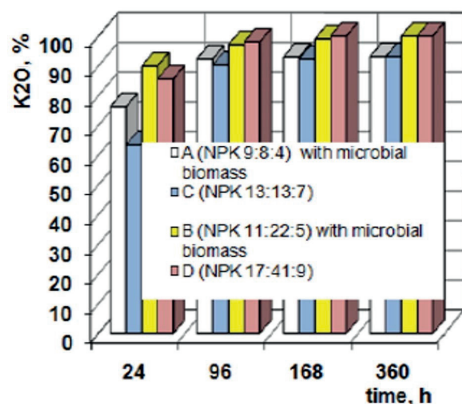


Figure 6. K_2O loss through leaching in time

- at 360 h, a proportion of (93-100%) from K_2O is lost by leaching in the case of fertilizers with microbial biomass, and respectively 93-100% is lost by leaching in the case of classic NPK fertilizers. Regarding the Ca element: this is loosed totally by leaching at 24 h for all types of fertilizers that contain microbial biomass (Figure 7). In the case of Mg, at 24 h, this is lost in the proportion of 63% for mixed fertilizers (variant A), and in the proportion of 42% for classic NPK.

At 96 h, the losses of Ca and Mg are almost total 99-100%. Taking into account the fact that the

lost nutrients from both types of fertilizers (mixed fertilizers formulated with microbial biomass and classic fertilizers type NPK) have similar values, we consider that the environmental impact generated by leaching nutrients from fertilizers with microbial biomass in waters is insignificant.

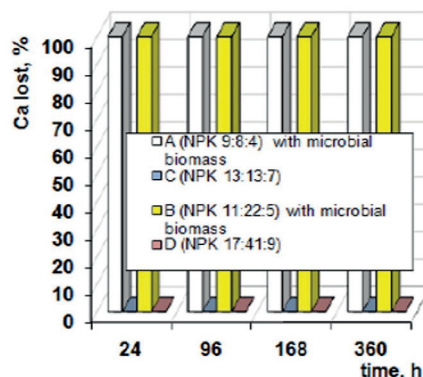


Figure 7. Ca loss through leaching in time

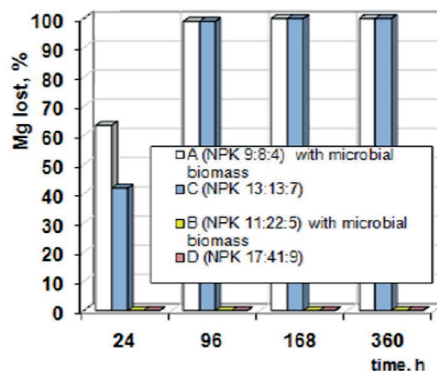


Figure 8. Mg loss through leaching in time

Similar results have been reported in other studies regarding the environmental impact of using microbial biomass generated as by-products from biotechnological processes in agriculture. Thus, Andersen and colab. (Andersen et al., 2001) have demonstrated through their studies carried out in Denmark on soils fertilized for 7 years with inactive spent biomass, derived from genetically modified microorganisms used in pharma biosyntheses, that this fertilization technique does not affect the soil microbiome. The molecular analyses performed on to microorganisms isolated from these soils did not reveal the existence of

genes/gene fragments similar to those existing in the microorganisms from the inactive spent microbial biomass (Andersen et al., 2001). Similar results were also obtained in the research carried out in the USA by Sullivan et al., on the soils cultivated with *Zea mays*, fertilized with inactivated spent microbial biomass (Sullivan et al., 2017), in the sense that in the microorganisms present in the soil fertilized in this way, were not highlighted gene transfer from the spent inactivated biomass used as fertilizer. Instead, in all cases where biomass-based products were used for fertilization, positive effects were reported regarding the growth and development of crop plants, the yields obtained per hectare in the case of the use of these bioproducts being similar to those obtained by applying the fertilizers obtained throughout chemical synthesis (urea) (Sullivan et al., 2017; Wang et al., 2023). Moreover, Halter and colab. (Halter et al., 2020) the tests carried out in Tennessee, USA, found that at a fertilization rate of 7.5 t/ha with inactive biomass, the soil microbiota is characterized by copiotrophic microorganisms (microorganisms specific to soil sites rich in nutrients).

In addition, under the influence of microbial biomass, as well as vegetal biomass, the soil microbiome and microbial activity improve (Nakhro et al., 2010; Wang et al., 2023); the content of organic C and N in the soil increases; the physical-chemical parameters of the soil (pH; respiration; enzymatic activity) is improved and the agrochemical quality of the soil increases (Meng et al., 2023; Azizah et al., 2023). According to the European Union, the transition from an oil-based economy to a biomass-based economy (Bioeconomy) will represent a characteristic of the 21st century due to the exhaustion of natural resources. The transition will bring back to the fore microbial biotechnologies and generate the huge amounts of biomass that must be capitalized (Stikane et al., 2023). An advantageous option is the re-use of these bioresources in sustainable agriculture to obtain fertilizers (Radu et al., 2020; Stikane et al., 2023) or biochar (Manolikaki & Diamadopoulos, 2020). These options of valorisation will supply nutrients for crops (Manolikaki et al., 2020; Radu et al., 2020; Vukuonda et al., 2024), will improve the agrochemical properties of the soil and most

importantly aspect, will affect insignificantly water resources. In this regard, innovative companies in the field of biotechnologies have made more industrial processing scenarios, with spent microbial biomass as a raw material, with concepts of economic sustainability and environmental protection (Stikane et al., 2023; He-Lambert et al., 2019).

CONCLUSIONS

In terms of resistance at leachability for the fertilizers with microbial biomass, is found that the materials which contain biomass of *Streptomyces sp.* are more resistant to loss by leaching in comparison with fertilizers that contain the biomass of *Penicillium sp.* For this reason, only the *Streptomyces* biomass was used as raw materials for obtaining fertilizers. The leachability tests conducted at the lab scale indicate that the leaching behaviour of fertilizer with microbial biomass of *Streptomyces sp.* is comparable to that of complex NPK fertilizers. Consequently, it is estimated that the impact on water resources from the use of these new types of fertilizers is insignificant.

ACKNOWLEDGEMENTS

The research was carried out with funding support from Project ADER 5.1.6/17.07.2023.

REFERENCES

- Andersen, J. T., Schäfer, T., Jørgensen, P. L., Møller, S. (2001). Using inactivated microbial biomass as fertilizer: the fate of antibiotic resistance genes in the environment. *Research in Microbiology*, 152(9), 823-833.
- Arrieche-Luna, E., Ruiz-Dager, M. (2010). Influence of inorganic and organic fertilization on microbial biomass carbon and maize yield in two soils of contrasting pH. *Agrociencia*, 44, 249-260.
- Assandri D., Bianco A., Pampuro N., Cavallo E., Zara G., Bardi L., Coronas R., Budroni M. (2023). Enhancing Fertilizer Effect of Bioprocessed Brewers' Spent Grain by Microbial Consortium Addition. *Agronomy*. 13(10), 2654.
- Azizah, F. R., Prayogo, C., Kurniawan, S., Rowe, R. L. (2023). Microbial Biomass and Soil Respiration Response to Pruning and Fertilization Practices in Coffee Pine Agroforestry. *Journal of Ecological Engineering*, 24(8), 329-342.
- Černý, J., Balík, J., Pavlíková, D., Zitková, M., Sýkora K. (2003). The influence of organic and mineral nitrogen fertilizers on microbial biomass nitrogen and

- extractable organic nitrogen in long-term experiments with maize. *Plant Soil Environ.*, 49(12), 560–564.
- Chwastowski, J., Guzik, M., Bednarz, S., & Staroń, P. (2023). Upcycling Waste Streams from a Biorefinery Process-A Case Study on Cadmium and Lead Biosorption by Two Types of Biopolymer Post-Extraction Biomass. *Molecules (Basel, Switzerland)*, 28(17), 6345.
- Dima, G., Radu, N., Chirvase, A.A., Pena, E.L. (2006). Studies concerning fungal residual biomass use for the removal of heavy metals from the residual waters. *Revista de Chimie*, 58(6), 561-565.
- Gowariker, V. Krishnamurthy, N., Gowariker, S. (2009). *The Fertilizer Encyclopedia*. Technology & Engineering, John Wiley & Sons, USA.
- Halter, M., Vaisvil, B., Kapatral, V., & Zahn, J. (2020). Organic farming practices utilizing spent microbial biomass from an industrial fermentation facility promote transition to copiotrophic soil communities. *Journal of Industrial Microbiology & Biotechnology*, 47(11), 1005–1018.
- He-Lambert, L., Shylo, O., English, B.C., Eash, N.S., Zahn, J.A. Lambert D.M. (2019). Supply chain and logistic optimization of industrial Spent Microbial Biomass distribution as a soil amendment for field crop production. *Resources, Conservation and Recycling*, 146, 218-231.
- Jayanta, K.P., Gitishree, D., Han-Seung S. (2018). Microbial Biotechnology, vol.2. *Application in Food and Pharmacology*, Springer Nature, Singapore.
- Manolikaki, I., Diamadopoulos, E. (2020). Agronomic potential of biochar prepared from brewery byproducts, *Journal of Environmental Management*, 255, 109856.
- Meghea, A., Radu, N., Rau, I., Lucia, S., Marica E. (2007). Fertilizers with microbial biomass. *Patent RO 121557 (B1)-2007-11-30*.
- Meng, F., Yang, H., Fan, X. et al. (2023). A microbial ecosystem enhanced by regulating soil carbon and nitrogen balance using biochar and nitrogen fertiliser five years after application. *Sci Rep.*, 13, 22233.
- Migahed, F., Abdelrazak, A., Fawzy, G. (2017). Batch and continuous removal of heavy metals from industrial effluents using microbial consortia. *Int. J. Environ. Sci. Technol.*, 14, 1169.
- Nakhro, N., Dkhar, M.S. (2010). Impact of Organic and Inorganic Fertilizers on Microbial Populations and Biomass Carbon in Paddy Field Soil. *Journal of Agronomy*, 9, 102-110.
- Radu N., Chirvase A.A., Babeanu N., Popa O., Cornea P., Pirvu L., Bostan M., Ciric A., Mathe E., Radu E. (2020). Study Regarding the Potential Use of a Spent Microbial Biomass in Fertilizer Manufacturing. *Agronomy*, 10(2), 299.
- Radu, N., Bondar, E., Meghea, A. Rau, I. (2006). Removal cooper and cobalt from dilute aqueous system by biosorption process. *Revista de Chimie*, 7, 711-717.
- Radu, N., Lanyi, L., Meghea, A (2007a). Studies concerning the recovery of nutrient from industrial wastewaters as fertilisers. *Journal of Environmental Protection and Ecology*, 8(4), 866-874.
- Radu, N., Meghea, A. (2007b). Studies concerning the use of microbial biomass by fertilisers manufacture. *Journal of Environmental Protection and Ecology*, 8(4), 824-834.
- Sullivan, C.T., Harman, R.M., Eash, N.S., Zahn, J.A., Goddard, J.J., Walker, F.R., Saxton, A.M., Lambert, D.M., McIntosh, D.W., Hart, W.E., Freeland, R.S. Morrison, J.E. (2017). Utilization of Spent Microbial Biomass as an Alternative Crop Nitrogen Source. *Agronomy Journal*, 109, 1870-1879.
- Stikane A, Baumanis M.R., Muiznieks R., Stalidzans E. (2023). Impact of Waste as a Substrate on Biomass Formation, and Optimization of Spent Microbial Biomass Re-Use by Sustainable Metabolic Engineering. *Fermentation*, 9(6), 531.
- Stikane, A., Elina Dace, E., Stalidzans, E. (2022). Closing the loop in bioproduction: Spent microbial biomass as a resource within circular bioeconomy, *New Biotechnology*, 70, 109-115.
- Technical Norms on Urban Waste Disposal, NTPA 011. Pollutant loading limits of industrial and urban wastewater discharged into natural receptors - *HG 188/2002* updated in 2016.
- Vurukonda S.S.K.P., Fotopoulos V, Saeid A. (2024) Production of a Rich Fertilizer Base for Plants from Waste Organic Residues by Microbial Formulation Technology. *Microorganisms*, 12(3), 541.
- Wang Y., Li Q. Li C. (2023). Organic fertilizer has a greater effect on soil microbial community structure and carbon and nitrogen mineralization than planting pattern in rainfed farmland of the loess plateau. *Front. Environ. Sci.*, 11, 1232527.

ACCUMULATION OF HEAVY METALS IN *DACTYLIS GLOMERATA* L. PLANTS IN CORRELATION WITH SOIL IN PERMANENT MEADOWS IN THE COPȘA MICĂ AREA OF ROMANIA

Vera CARABULEA¹, Dumitru-Marian MOTELICĂ¹, Nicoleta Olimpia VRÎNCEANU¹, Georgiana PLOPEANU¹, Bogdan Ștefan OPREA¹, Mihaela COSTEA¹, Vasilica LUCHIAN²

¹National Research and Development Institute for Soil Science, Agrochemistry and Environment - ICPA Bucharest, 61 Marasti Blvd, District 1, Bucharest, Romania

²University of Agronomic Sciences and Veterinary Medicine of Bucharest, 59 Marasti Blvd, District 1, Bucharest, Romania

Corresponding author email: oprea.bogdan95@yahoo.com

Abstract

This study aims to estimate the accumulation of heavy metals (Cd, Pb, Zn and Cu) from soil in Dactylis glomerata L. plants from permanent meadows in the polluted area of Copșa Mică, Romania. The estimation of heavy metal accumulation in Dactylis glomerata L. plants was carried out based on a data set collected from permanent meadows used for grazing and hay production. The logarithmic power-type regression plots estimating the stochastic dependence between the total cadmium content in the aerial part of Dactylis glomerata L. plants and soil is statistically significant, and for Cu, Pb and Zn they are less significant. The variation of the total metal content (Cd, Cu, Pb and Zn) determined in the soil samples in the 0–20 cm layer according to the distance from the pollution source is statistically significant. The results of this study are important for the estimation of heavy metal (Cd, Cu, Pb and Zn) accumulation in Dactylis glomerata L. plants from permanent grasslands, which are consumed by animals.

Key words: heavy metals, pollution, soil, *Dactylis glomerata* L.

INTRODUCTION

Soil pollution with heavy metals is an increasingly discussed problem all over the world because, in addition to high toxicity, they persist for a long time in the soil altering the ecosystem (Anaman et al., 2022; Patra, 2022; Senila et al., 2022; Chaplygin et al., 2020; Cai et al., 2015). High concentrations of heavy metals in soil are largely due to anthropogenic sources that heavily affect the soil, resulting in a high level of toxicity (Gupta et al., 2021). The main sources of soil pollution are metal processing and mining industries, burning of fossil fuels, exhaust gases from traffic, etc. (Bartha, 2021; Massa et al., 2010; Popa, 2005; Remon et al., 2005). Smelting activities are considered to produce polluting wastes and account for 40–70% of the heavy metals around those areas (Anaman et al., 2022).

Some heavy metals (Zn, Cu), which are essential micronutrients for plants, when in high concentrations become toxic, and others such as Cd, Pb are also dangerous in low concentrations.

These metals can accumulate in plant parts used in human and animal nutrition, which become toxic to living organisms (Pietrelli et al., 2022; Sabir et al., 2022; Castro-Bedriñana et al., 2021; Kachou et al., 2011).

The translocation of zinc and copper from soil to above-ground parts of plants are not surprising, as they are essential nutrients for many physiological processes, including photosynthesis and growth hormone production; therefore, plants tend to translocate them into leaves (Murtic, 2021; Roschztardt et al., 2019).

Studies by Gawryluk et al. (2020) show that grass species can be considered accumulators of Cu and Zn because the levels of these elements in the aboveground biomass of plants were higher than in the analysed soil (0–20 cm layer) and they are not high bioaccumulators of Pb.

The high content of cadmium in the soil has harmful effects on both organisms in the soil, as well as on the vegetation, which leads to the limitation of the growth of roots and shoots, can prevent breathing, photosynthesis, water

absorption and other (Quezada-Hinojosa et al., 2015).

Simple correlations between total metal content (Cd, Pb and Zn) and plant showed that the increasing content of heavy metals causes stress and death of metal-sensitive plants and the appearance of those tolerant to metals (Woch et al., 2016).

Studies are showing that the uptake and bioaccumulation of heavy metals in plants it depends, among other factors, on the plant species (Sharma & Dubey, 2005).

Dactylis glomerata L. is a perennial species with high fodder value, fast growing in spring, and resistant to drought, and low temperatures, but also to frequent mowing and pests, which makes it a common species in meadows and pastures (Malinowska et al., 2023; Nefed'eva et al., 2020).

Piertelli et al. (2022) showed that the accumulation of heavy metals (Cd, Cu, Ni, Pb, Zn) in *Dactylis glomerata* L. plants has a higher proportion in urban than in rural environments and higher accumulations in roots and basal leaves than in leaves, stems and flowers in both environments. The exception is chromium, which accumulates more in flowers than the other metals.

The most well-known areas polluted with heavy metals in Romania, over large areas, are located near the former metallurgical plants near Copșa Mică - Sibiu County, Zlatna - Alba County, Baia Mare-Maramureș County and Neferal-Acumulatorul near Bucharest (Sur et al., 2017; Manea et al., 2015; Gamenț et al., 2010; Vrînceanu et al., 2010).

Our study refers to the Copșa Mică area, where the main activity was the non-ferrous metallurgy of the two industrial platforms: S.C. SOMETRA S.A. with a profile of non-ferrous and ferrous metals and CARBOSIN S.A. with chemical profile (Vrînceanu et al., 2009). Even though metallurgical activities have been stopped, the soil remains loaded with heavy metals and local communities continue their agricultural activities.

From the studies carried out by Bartha et al. (2021), the soil pollution index according to the degree of pollution in the Copșa Mică area shows that 20% of the investigated soils have maximum pollution, 46% in the category of very strong pollution, 7% - strong pollution, 7% -

medium pollution, 7% - low pollution and 13% fall into the minimal pollution category.

MATERIALS AND METHODS

The present paper presents a study carried out in 2023, regarding the accumulation of heavy metals (Cd, Pb, Zn and Cu) in *Dactylis glomerata* L. plants in correlation with the polluted soil from the permanent meadows in the Copșa Mică area. This area is recognized with a high degree of historical pollution.

The estimation of the accumulation of heavy metals in *Dactylis glomerata* L. plants was carried out based on a set of data collected from permanent meadows in Copșa Mică, Axente Sever, Târnava, Micăsasa and Valea Viilor (Figure 1).



Figure 1. View from the field, Copșa Mică area

The soil samples were collected using the agrochemical probe at a 0-20 cm depth (by homogenizing 13 subsamples), then dried at room temperature, mortared, and passed through a 0.2 mm sieve. From these samples, the content of heavy metals (Cd, Pb, Zn, and Cu) was determined by atomic absorption spectrometry, after extraction by the aqua regia - microwave digestion method.

Plant samples were identified and harvested in the field, then oven-dried, chopped, and ground. Plant samples were treated with nitric acid in a microwave digestion system. Total heavy metal content was determined using atomic absorption spectrometry (Flame GBC 932AA or graphite furnace GBC SavanataAZ).

Microsoft Excel 2010 was used for statistical data processing.

RESULTS AND DISCUSSIONS

The accumulation of the total heavy metal content in the 0-20 cm soil layer, from the permanent meadows in the Copșa Mică area, is presented in Table 1.

The values of the total cadmium content in the soil, at the depth of 0-20 cm, varied between $2.50 \text{ mg}\cdot\text{kg}^{-1}$ and $48.29 \text{ mg}\cdot\text{kg}^{-1}$, with a standard deviation of $11.77 \text{ mg}\cdot\text{kg}^{-1}$ and a coefficient of variation of 104%. Total lead content ranges from $87 \text{ mg}\cdot\text{kg}^{-1}$ to $955 \text{ mg}\cdot\text{kg}^{-1}$ with a standard deviation of $256.9 \text{ mg}\cdot\text{kg}^{-1}$ and a coefficient of variation of 76.3%. Zinc has values between $168 \text{ mg}\cdot\text{kg}^{-1}$ and $2015 \text{ mg}\cdot\text{kg}^{-1}$, with a standard deviation of $486.45 \text{ mg}\cdot\text{kg}^{-1}$ and a coefficient of variation of 76.9%, and copper between $22 \text{ mg}\cdot\text{kg}^{-1}$ and $182 \text{ mg}\cdot\text{kg}^{-1}$, with a standard deviation of $49.88 \text{ mg}\cdot\text{kg}^{-1}$ and 70.2%.

According to Order 756/1997 on soil pollution, the arithmetic mean values ($11.32 \text{ mg}\cdot\text{kg}^{-1}$) of the cadmium content exceed the intervention threshold for the use of several sensitive, and regarding the lead content ($336.7 \text{ mg}\cdot\text{kg}^{-1}$) and zinc ($632.8 \text{ mg}\cdot\text{kg}^{-1}$) exceed the intervention threshold for sensitive uses. The average values

of the copper content ($71.1 \text{ mg}\cdot\text{kg}^{-1}$) fall within the alert threshold for sensitive use types.

Table 2 shows the values of the statistical parameters characterizing the variability of the content of Cd, Pb, Zn and Cu in the soil - the extractable forms with DTPA, where are the minimum and maximum values, as well as the arithmetic mean concentrations. The extractable cadmium content varied between $1.71 \text{ mg}\cdot\text{kg}^{-1}$ and $33.55 \text{ mg}\cdot\text{kg}^{-1}$, with an arithmetic mean of $8.14 \text{ mg}\cdot\text{kg}^{-1}$ and a coefficient of variation of 102.2%. Lead ranges between $23 \text{ mg}\cdot\text{kg}^{-1}$ and $301 \text{ mg}\cdot\text{kg}^{-1}$ with an arithmetic mean of 129.3 mg/kg , standard deviation of $93.7 \text{ mg}\cdot\text{kg}^{-1}$, and coefficient of variation of 72.5%. Zinc content values range from $24 \text{ mg}\cdot\text{kg}^{-1}$ to $336 \text{ mg}\cdot\text{kg}^{-1}$ with a mean of $131.4 \text{ mg}\cdot\text{kg}^{-1}$ with a standard deviation of $106 \text{ mg}\cdot\text{kg}^{-1}$ and a coefficient of variation of 80.7%, and copper between $2.46 \text{ mg}\cdot\text{kg}^{-1}$ and $23.4 \text{ mg}\cdot\text{kg}^{-1}$ with a mean of $8.22 \text{ mg}\cdot\text{kg}^{-1}$ and the coefficient of variation of 70.8%.

The average concentration of total and extractable forms in the 0-20 cm soil layer increases in the following order: $\text{Cd} < \text{Cu} < \text{Pb} < \text{Zn}$.

Table 1. Values of statistical parameters that characterize the central tendency and the variability of the total cadmium, lead, zinc, copper contents in soil (n = 14)

Variable	Minimum	Maximum	Median	Geometric mean	Arithmetic mean	Standard deviation	Coefficient of variation
$\text{mg}\cdot\text{kg}^{-1} \text{ DW}$							
Cd_{soil}	2.50	48.29	8.43	7.99	11.32	11.77	104.0%
Pb_{soil}	87	955	271.0	258.7	336.7	256.9	76.3%
Zn_{soil}	168	2015	552.5	496.4	632.8	486.5	76.9%
Cu_{soil}	22	182	57.5	57.8	71.1	49.9	70.2%

DW - Dry Weight

Table 2. Values of statistical parameters that characterize the central tendency and the variability of the cadmium, lead, zinc, copper contents in soil - DTPA-extractable forms (n = 14)

Variable	Minimum	Maximum	Median	Geometric mean	Arithmetic mean	Standard deviation	Coefficient of variation
$\text{mg}\cdot\text{kg}^{-1} \text{ DW}$							
Cd_{DTPA}	1.71	33.55	6.29	5.66	8.14	8.32	102.2%
Pb_{DTPA}	23	301	115	95.3	129.3	93.7	72.5%
Zn_{DTPA}	24	336	87	96.2	131.4	106.0	80.7%
Cu_{DTPA}	2.46	23.41	6.30	6.71	8.22	5.82	70.8%

DW - Dry Weight

Dactylis glomerata L. is one of the most common grasses in the Gramineae family found in the study area. The heavy metal content found in *Dactylis glomerata* L. plants from permanent grasslands is shown in Table 3.

The cadmium content of the plants ranged from $0.05 \text{ mg}\cdot\text{kg}^{-1}$ to $1.21 \text{ mg}\cdot\text{kg}^{-1}$, the mean value was $0.51 \text{ mg}\cdot\text{kg}^{-1}$ and the coefficient of variation of 78.4%. Quezada-Hinojosa shows that *Dactylis glomerata* L. is a plant known for its

pastoral value and accumulates higher levels of cadmium in roots than in shoots. In the shoots, it accumulates cadmium concentrations up to 0.8 $\text{mg}\cdot\text{kg}^{-1}$, which does not pose a major risk.

Table 3. Values of statistical parameters that characterize the central tendency and the variability of the cadmium, lead, zinc, copper contents in the *Dactylis glomerata* plants (n = 14)

Variable	Minimum	Maximum	Median	Geometric mean	Arithmetic mean	Standard deviation	Coefficient of variation
$\text{mg}\cdot\text{kg}^{-1}\text{ DW}$							
Cd_{plant}	0.05	1.21	0.41	0.33	0.51	0.40	78.4%
Pb_{plant}	0.15	4.38	1.15	0.78	1.27	1.22	96.1%
Zn_{plant}	34.7	122.4	60.3	58.7	63.4	25.9	40.9%
Cu_{plant}	2.80	5.30	4.01	3.99	4.07	0.83	20.4%

DW - Dry Weight

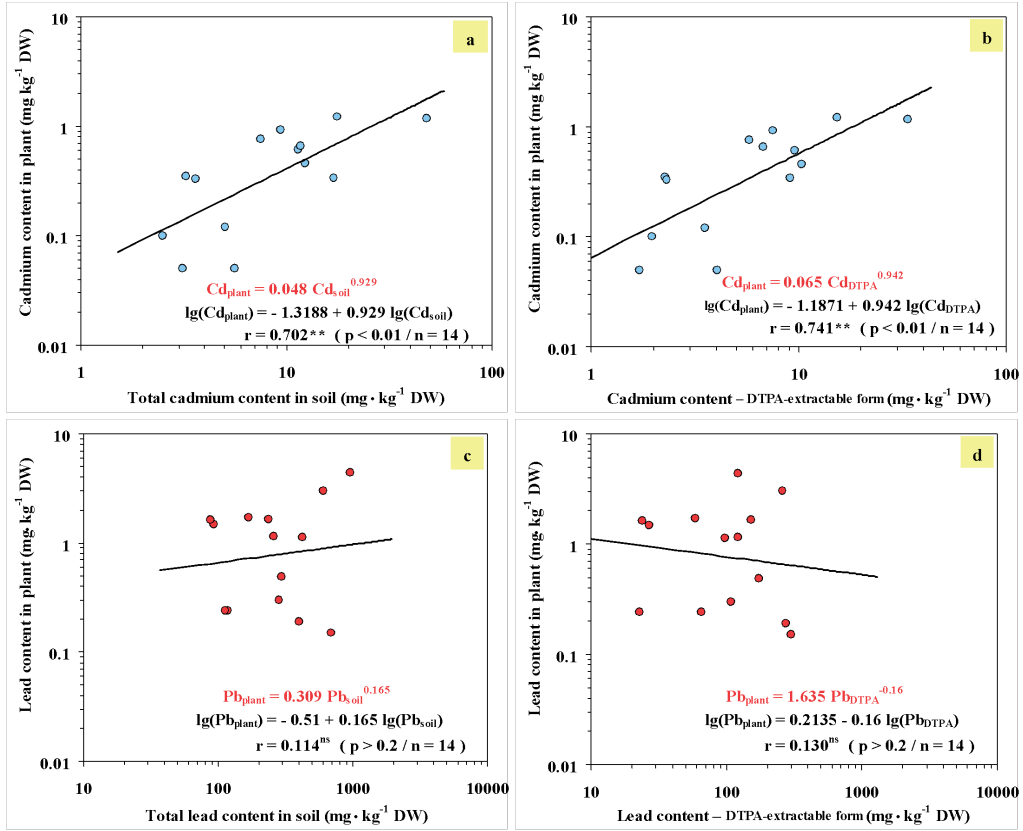


Figure 2. Log-log diagrams for power regression curves that estimate the stochastic dependency between total cadmium content in soil (a), soil cadmium content - DTPA-extractable form (b), total lead content in soil (c), soil lead content - DTPA-extractable form (d) and cadmium/lead contents in *Dactylis glomerata* L. plants

Lead values were between 0.15 $\text{mg}\cdot\text{kg}^{-1}$ and 4.38 $\text{mg}\cdot\text{kg}^{-1}$, with a standard deviation of 1.22 $\text{mg}\cdot\text{kg}^{-1}$ and a coefficient of variation of 96.1%. The zinc content was between 34.7 $\text{mg}\cdot\text{kg}^{-1}$ and 122.4 $\text{mg}\cdot\text{kg}^{-1}$, with the arithmetic mean - 63.4 $\text{mg}\cdot\text{kg}^{-1}$, and the copper between 2.80 $\text{mg}\cdot\text{kg}^{-1}$ and 5.30 $\text{mg}\cdot\text{kg}^{-1}$.

Logarithmic plots for power-type regression curves, estimating the stochastic dependence between total soil heavy metal content (Cd, Pb, Zn, and Cu), soil heavy metal content - extractable form DTPA from *Dactylis glomerata* L. plants are shown in Figure 2 and Figure 3.

The value of the linear correlation coefficient obtained for the dependence between the total cadmium content in the soil and the plant (Figure 2a) and the extractable cadmium content in the soil and the cadmium content in the plant (Figure 2b) is distinctly significantly different from zero indicating a close correlation between the two variables, the value of the linear correlation coefficient ($r = 0.702^{**}$) and respectively ($r = 0.741^{**}$) for extractable forms.

For lead, the value of the linear correlation coefficient is not significantly different from zero, for total forms $r = 0.114^{ns}$ (Figure 2c) and for extractable forms $r = 0.130^{ns}$ (Figure 2d), which indicates that the estimation of lead accumulation in plants of *Dactylis glomerata* L. cannot be described by simple power regressions.

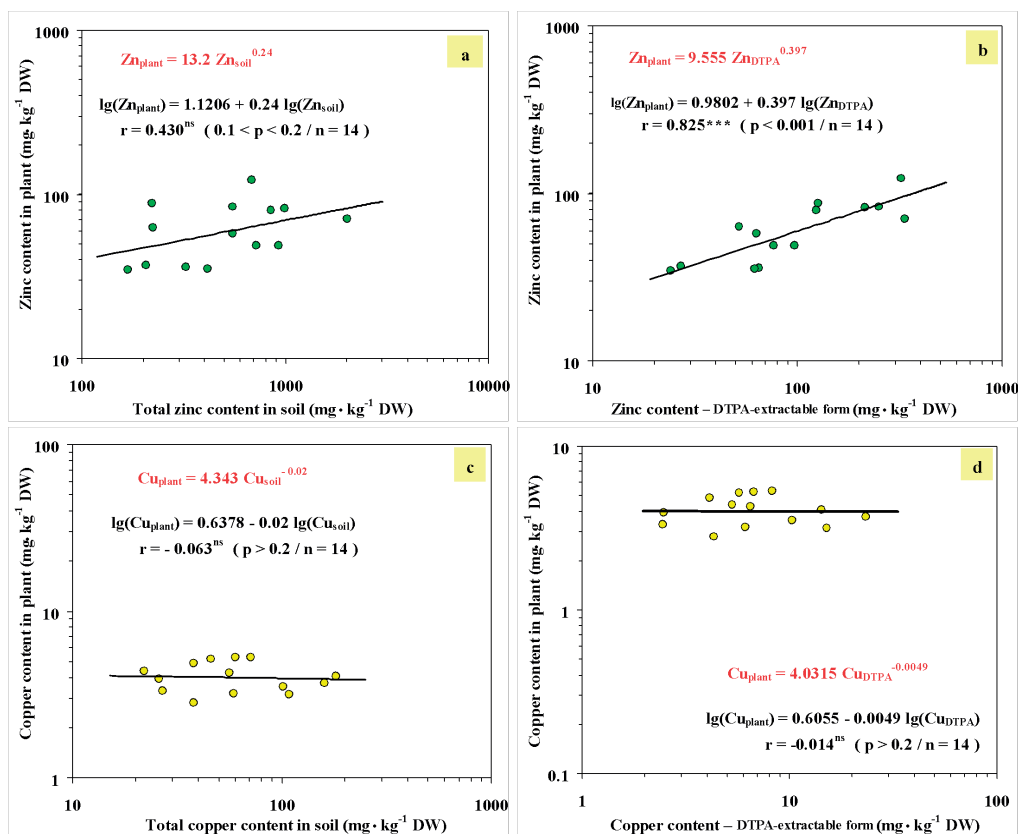


Figure 3. Log-log diagrams for power regression curves that estimate the stochastic dependency between total zinc content in soil (a), soil zinc content - DTPA-extractable form (b), total copper content in soil (c), soil copper content - DTPA-extractable form (d) and zinc/copper contents in *Dactylis glomerata* L. plants

The power regression curves estimating the stochastic dependence between the total zinc content of the soil (0-20 cm layer) and the aerial part of the *Dactylis glomerata* L. plant (Figure 3a) is insignificant ($r = 0.430^{ns}$). The dependence between the extractable zinc content in the soil and the total zinc content in the plant (Figure 3b) shows a strong correlation between the two variables and a distinctly significant linear

correlation index ($r = 0.825^{***}$), which proved to be the better estimation of bioaccumulation in *Dactylis glomerata* L. plants.

For both total copper and extractable copper, the linear correlation coefficient value is $r = -0.063^{ns}$ and $r = -0.014^{ns}$, which shows that the estimation of copper accumulation in *Dactylis glomerata* L. plants cannot be described by equations simple power type (Figure 3c and Figure 3d).

The copper content of the aerial part of the plant is not a good indicator of copper toxicity due to the immobilization of this element in plant roots (Vrinceanu et al., 2010).

Figure 4 shows the logarithmic plots for the power-type regression curves that estimate the variations in the total content of heavy metals

(Cd, Pb, Zn, and Cu) in the soil as a function of the distance from the pollution source - S.C. SOMETRA S.A. The linear correlation index between the total soil cadmium content and the distance from the pollution source is very significant ($r = -0.823^{***}$).

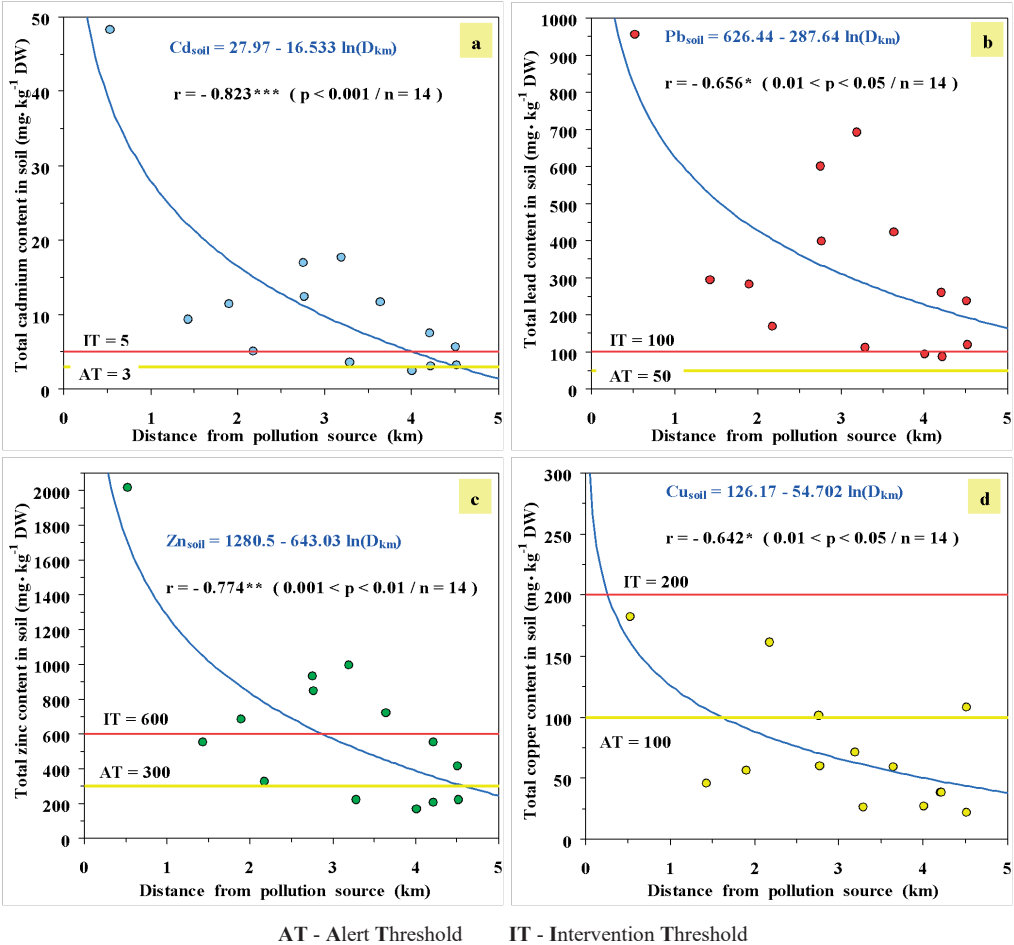


Figure 4. Total cadmium (a), lead (b), zinc(c) and copper(d) contents in soil as functions of the distance from the pollution source - S.C. SOMETRA S.A. (Copșa Mică, 0-20 cm layer)

The values of the cadmium content of soil are greater than the alert threshold for sensitive uses (3 mg·kg⁻¹) and fall below this limit at distances of 4 km. The highest value of the total cadmium content in the soil was found in samples collected approximately 0.5 km from the pollution source (Figure 4a).

In Figure 4b, between total soil lead content and distance from the pollution source, the linear

correlation index is significant ($r = -0.656^*$). The values of lead content in the soil are above the alert threshold for sensitive uses (50 mg·kg⁻¹) and are increasing above the intervention threshold for sensitive uses (100 mg·kg⁻¹).

In the study by Jankowski et al. (2019), the largest amounts of Pb (13.52 mg·kg⁻¹) and Cd (0.333 mg·kg⁻¹) were found in the soil at a distance of 5 m from roadworthy lead and

cadmium content varied significantly and were dependent both the plant species (*Dactylis glomerata* L., *Arrhenatherum elatius* and *Alopecurus pratensis*) and the distance from the road. *Dactylis glomerata* L. accumulated the lowest content ($3.246 \text{ mg} \cdot \text{kg}^{-1}$) of lead and the greatest amount of cadmium ($0.286 \text{ mg} \cdot \text{kg}^{-1}$), and the highest concentrations were in plants growing at a distance of 5 m from the road, while at distances greater than 10 and 15 m, the concentrations decreased systematically.

The linear correlation index for zinc is distinctly significant ($r = -0.774^{**}$), with values below the alert threshold between 3 and 5 km and less than 50%, above the intervention threshold (Figure 4c).

Copper content values from the soil are lower than the intervention threshold for sensitive use ($200 \text{ mg} \cdot \text{kg}^{-1}$) over the entire studied area. Variance estimated by power regression equations indicates that total copper values in the 0-20 cm layer fall below the alert threshold at greater distances of 1 km from the pollution source. About 80% of the copper content values are below the alert threshold for sensitive uses. The values of the linear correlation coefficient ($r = -0.642^{*}$) are significant (Figure 4d).

CONCLUSIONS

The current study shows the potential for the accumulation of heavy metals from polluted soils in *Dactylis glomerata* L. plants from permanent meadows.

The results showed that the value of the linear correlation coefficient obtained for the dependence between the total and extractable content of cadmium plants from the soil and *Dactylis glomerata* L. is significantly significant and shows a close correlation between the two variables. The dependence between the content of extractable zinc in the soil and the content of zinc in the plant shows a strong correlation between the two variables.

In addition, the linear correlation coefficient values are not significant for lead and copper.

The index of linear correlation between total soil cadmium content and distance from the pollution source is strongly significant, for zinc distinctly significant, and for lead and copper significant.

ACKNOWLEDGEMENTS

This work was funded by two projects of the Ministry of Research, Innovation and Digitalization from Romania, project number PN 23 29 04 01, entitled: "Assessment of the heavy metals bioaccumulation in meadows vegetation using the regression analysis to develop a guide of good practices for grazing and animal feedstock in areas affected by industrial pollution" and project number 44 PFE /2021, Program 1 - Development of the national research and development system, Subprogram 1.2 - Institutional performance - CDI Excellence Funding Projects.

REFERENCES

- Anaman, R., Peng, C., Jiang, Z., Liu, X., Zhou, Z., Guo, Z., Xiao, X. (2022). Identifying sources and transport routes of heavy metals in soil with different land uses around a smelting site by GIS based PCA and PMF. *Science of the Total Environment*, 823, 153759.
- Bartha, S., Tăut, I., Goji, G., Vlad, I.A., Burescu, L.I. N., Muresan, C. (2021). Evaluation of soil pollution degree in the Copșa Mică area (Romania) by means of relative indices. *Scientific Papers. Series A. Agronomy*, 64(1), 15-22.
- Blagodatskaya, E.V., Pampura, T.V., Dem'yanova, E.G., Myakshina, T.N. (2006). Effect of lead on growth characteristics of microorganisms in soil and rhizosphere of *Dactylis glomerata*. *Eurasian Soil Science*, 39, 653-660.
- Cai, L., Xu, Z., Bao, P., He, M., Dou, L., Chen, L., Zhou, Y., Zhu, Y.G. (2015). Multivariate and geostatistical analyses of the spatial distribution and source of arsenic and heavy metals in the agricultural soils in Shunde, Southeast China. *Journal of Geochemical Exploration*, 148, 189-195.
- Castro-Bedriñana, J., Chirinos-Peinado, D., Garcia-Olarte, E., Quispe-Ramos, R. (2021). Lead transfer in the soil-root-plant system in a highly contaminated Andean area. *Peer J*, 9, e10624.
- Chaplygin, V., Mandzhieva, S., Minkina, T., Barahov, A., Nevidomskaya, D., Kizilkaya, R., Rajput, V. (2020). Accumulating capacity of herbaceous plants of the Asteraceae and Poaceae families under technogenic soil pollution with zinc and cadmium. *Eurasian Journal of Soil Science*, 9(2), 165-172.
- Gament, E., Carabulea, V., Ploeanu, G., Vrinceanu, N., Ulmanu, M., Anger, I. (2010). Hot areas polluted with heavy metals. *Annals of the University of Craiova-Agriculture, Montanology, Cadastre Series*, 40(1), 391-398.
- Gawryluk, A., Wylupek, T., Wolański, P. (2020). Assessment of Cu, Pb and Zn content in selected species of grasses and in the soil of the roadside embankment. *Ecology and Evolution*, 10(18), 9841-9852.

- Jankowski, K., Malinowska, E., Ciepiela, G. A., Jankowska, J., Wiśniewska-Kadžajan, B., Sosnowski, J. (2019). Lead and cadmium content in grass growing near an expressway. *Archives of environmental contamination and toxicology*, 76, 66-75.
- Malinowska, E., Wiśniewska-Kadžajan, B., Ostaszewska, U., Horaczek, T. (2023). The Effects of Various Organic Materials on *Dactylis glomerata* Yield and Content of Selected Macroelements. *Journal of Ecological Engineering*, 24(7).
- Manea, A., Dumitru, S., Vrinceanu, N. (2015). Spatial distribution of copper content in soils from Zlatna area, Romania. In *15th International Multidisciplinary Scientific GeoConference SGEM 2015* (pp. 317-324).
- Massa, N., Andreucci, F., Poli, M., Aceto, M., Barbato, R., Berta, G. (2010). Screening for heavy metal accumulators amongst autochthonous plants in a polluted site in Italy. *Ecotoxicology and environmental safety*, 73(8), 1988-1997.
- Mawari, G., Kumar, N., Sarkar, S., Daga, M. K., Singh, M. M., Joshi, T. K., Khan, N. A. (2022). Heavy metal accumulation in fruits and vegetables and human health risk assessment: findings from Maharashtra, India. *Environmental Health Insights*, 16, 1-10, 11786302221119151.
- Ministry Order No. 756 from November 3, (1997) for approval of Regulation concerning environmental pollution assessment published in Official Monitor No. 303/6 November 1997.
- Murtic, S., Zahirovic, C., Civic, H., Sijahovic, E., Podrug, A. (2021). Phytoaccumulation of heavy metals in native plants growing on soils in the Spreča river valley, Bosnia and Herzegovina. *Plant, Soil & Environment*, 67(9).
- Nefed'eva, E.E., Sevriukova, G.A., Zheltobryukhov, V.F., Gracheva, N.V., Abdulabbas, A.Y.A. (2020). Assortment of herbaceous plants for remediation of soils contaminated with oil products and heavy metals. In *IOP Conference Series: Earth and Environmental Science*, 421(6), 062008. IOP Publishing.
- Patra, D.K., Acharya, S., Pradhan, C., Patra, H.K. (2021). *Poaceae* plants as potential phytoremediators of heavy metals and eco-restoration in contaminated mining sites. *Environmental Technology & Innovation*, 21, 101293.
- Pietrelli, L., Menegoni, P., Papetti, P. (2022). Bioaccumulation of heavy metals by herbaceous species grown in urban and rural sites. *Water, Air, & Soil Pollution*, 233(4), 141.
- Popa, M. (2005). Modern methods and techniques for the determination of environmental pollution with heavy metals. Case studies reviews and analyses in Zlatna area. *Casa Cărții de Știință Publishing House*.
- Quezada-Hinojosa, R., Föllmi, K.B., Gillet, F., Matera, V. (2015). Cadmium accumulation in six common plant species associated with soils containing high geogenic cadmium concentrations at Le Gurnigel, Swiss Jura Mountains. *Catena*, 124, 85-96.
- Remon, E., Bouchardon, J.L., Cornier, B., Guy, B., Leclerc, J.C., Faure, O. (2005). Soil characteristics, heavy metal availability and vegetation recovery at a former metallurgical landfill: Implications in risk assessment and site restoration. *Environmental Pollution*, 137(2), 316-323.
- Roschztardt, H., González-Guerrero, M., Gomez-Casati, D.F. (2019). Metallic micronutrient homeostasis in plants. *Frontiers in Plant Science*, 10, 478369.
- Sabir, M., Baltrėnaitė-Gedienė, E., Ditta, A., Ullah, H., Kanwal, A., Ullah, S., Faraj, T.K. (2022). Bioaccumulation of heavy metals in a soil-plant system from an open dumpsite and the associated health risks through multiple routes. *Sustainability*, 14(20), 13223.
- Senila, M., Cadar, O., Senila, L., Angyus, B.S. (2022). Simulated bioavailability of heavy metals (Cd, Cr, Cu, Pb, Zn) in contaminated soil amended with natural zeolite using diffusive gradients in thin-films (DGT) technique. *Agriculture*, 12(3), 321.
- Sharma, P., & Dubey, R.S. (2005). Lead toxicity in plants. *Brazilian journal of plant physiology*, 17, 35-52.
- Sur, I.M., Cimpean, A., Micle, V., Tanaselia, C. (2017). Physical-chemical properties analysis of the soil contaminated with heavy metals from Copșa Mica area. *Scientific Papers. Series E. Land Reclamation, Earth Observation & Surveying, Environmental Engineering, Vol. V*, 51-56, Print ISSN 2285-6064.
- Vrinceanu, N., Motelica, D.M., Dumitru, M., Gament, E., (2009). Zinc accumulation in soils and vegetation of polluted area Copșa Mică. *Annals Food Science and Technology*, 10(2), 630-634.
- Vrinceanu, N., Motelica, D.M., Dumitru, M., Preda, M., Tănase, V. (2010). Copper accumulation in soil and vegetation of polluted area Copșa Mică. *Annals: Food Science and Technology*. 11(1), 100-104.
- Woch, M.W., Kapusta, P., Stefanowicz, A.M. (2016). Variation in dry grassland communities along a heavy metals gradient. *Ecotoxicology*, 25, 80-90.

GREEN-SYNTHESIZED ZnO NPs AS SUSTAINABLE PHOTOCATALYSTS FOR THE DEGRADATION OF ACETAMINOPHEN

Alexandra Corina COSTANDACHE¹, Leon Dumitru COVALIU¹,
Anca Andreea ȘĂULEAN¹, Cristina Ileana COVALIU-MIERLA¹, Ecaterina MATEI¹,
Razvan TEODORESCU², Valerica TUDOR²

¹National University of Science and Technology Politehnica Bucharest,
313 Splaiul Independentei Street, District 6, Bucharest, Romania

²University of Agronomic Sciences and Veterinary Medicine of Bucharest,
59 Marasti Blvd, District 1, Bucharest, Romania

Corresponding author email: leon.covaliu@yahoo.com

Abstract

Water contamination is a growing concern with profound implications for public health and ecosystems. The advent of nanotechnology has expanded the utility of nanoparticles (NPs) in diverse fields. These biogenic ZnO nanostructures offer an eco-friendly alternative for photocatalysis. The research aims to (i) employ a green synthesis method for ZnO nanostructure production using a grapefruit extract, (ii) thoroughly characterize these nanostructures using optical microscopy (OM), X-ray diffraction (XRD), Zeta potential and pH_{pzc}, and (iii) evaluate the photocatalytic efficiency in degrading acetaminophen from water solutions. The findings display a sustainable approach to water purification, addressing the challenges of water contamination and emerging pollutants by utilizing green-synthesized ZnO nanoparticles.

Key words: acetaminophen, green synthesis, photodegradation, zinc oxide.

INTRODUCTION

Water contamination is a pressing environmental issue that significantly challenges public health and ecosystems (Aragaw et al., 2021; Sandu et al., 2023). In recent years, the proliferation of nanotechnology has led to a dramatic increase in the use of nanoparticles (NPs) and their potential applications. These NPs differ from their bulk or dissolved counterparts in various aspects, such as particle size, dispersion, morphology, surface area, and shape, offering a wide range of possibilities in industries like catalysis, medicine, biology, and cosmetics (Bundschuh et al., 2018). Over the past few years, researchers have extensively explored the performance of nanomaterials in various aqueous environments, including oceans, rivers, lakes, and wetlands. A collective concern among research organizations has been to discover environmentally friendly remediation agents to promote a green economy for soil and water remediation (Saleem & Zaidi, 2020). Some nanomaterials exhibit a significant adsorption effect on organic substances and

metal ions because of the hydroxyl groups present on the nanoparticle surfaces, which bind to certain cations. For instance, carbon nanoparticles, when compared to traditional wastewater treatment agents, demonstrate exceptional stability under alkaline and acidic conditions, boasting a high specific surface area and porous structure (Negroiu et al., 2021). Consequently, the utilization of nanomaterials in wastewater treatment not only overcomes the limitations of conventional technology but also displays outstanding remediation performance (Kayastha et al., 2022). Moreover, with the advancement of analytical tools, pharmaceuticals and chemicals originating from their metabolism have been detected in various environmental media. The accumulation of these compounds in wastewater is attributed to patient dosages and the rate of metabolism. Even at modest concentrations, these pollutants can adversely influence ecosystems. Acetaminophen (AMP), also referred to as paracetamol, is a popular analgesic and antipyretic medication. It exits the body either unmodified by excretion in the urine and feces or transformed into hazardous metabolites (such

N-Acetyl-p-benzoquinone imine, or NAPQ). Through the aquatic media, these metabolites enter the food chain (Avramescu et al., 2022). Paracetamol exposure over an extended length of time has been proven in numerous studies to have chronic effects on aquatic creatures, which can impair their growth or reproductive rates (Acevedo-Barrios, & Severiche-Sierra, 2017; Koagouw et al., 2021). Drinking water has been shown to contain traces of AMP, which may cause someone to consume more than is advised daily (Pereira et al., 2021).

Measures have been suggested to reduce drug contamination, including changing the law, strengthening ERA (Environmental Risk Assessment), limiting emissions, and classifying pharmaceuticals as hazardous wastes (Palma et al., 2020). However, these actions are insufficient, and new pollutants continue to accumulate in the environment (Akkari, 2018). Because of this, wastewater treatment facilities have started using advanced oxidation processes (AOPs) that may break down soluble organic contaminants (Richardson, 2009; Vilhunen & Sillanpää, 2010).

Photocatalysis, relying on semiconductors like TiO_2 or ZnO activated by light, is a powerful technique for initiating chemical reactions (Abebe et al., 2020). However, the widespread use of TiO_2 has raised cost concerns, leading to a growing interest in alternative photocatalysts. ZnO has emerged as a promising alternative due to its similar attributes, versatility, and photodegradation mechanism, which, in some cases, offers superior photocatalytic performance (Swati et al., 2020). ZnO NPs have been widely used as semiconductor photocatalysts due to their high reaction rate, large number of available reactive sites, high efficiency in hydrogen peroxide generation, low cost, and environmentally friendly nature.

In recent years, the concept of "green synthesis" has gained prominence in materials science, focusing on environmentally friendly methods for producing nanomaterials (Akhter et al., 2018). This approach aims to reduce chemical by-products, use less hazardous chemicals, employ eco-friendly solvents, and utilize renewable precursors. Various biological materials, including plant extracts, microorganisms, and bioregenerable substances, have been employed in green synthesis,

particularly for metal/metal oxide nanoparticles. Nanomaterials synthesized through such methods are often termed "biogenic".

Among these green methods, the use of plant extracts for synthesizing metal oxide nanoparticles has gained attention. This method offers several advantages, such as the ready availability of plant sources, safety, non-toxicity, ease of processing, and the presence of necessary chemical components for the reduction process during synthesis (Jamdagni et al., 2018). Large-scale synthesis using plant extracts is economical and straightforward, with no associated health risks or concerns regarding dangerous microorganisms.

These plant-based synthesis procedures rely on the use of various plant parts, including leaves, stems, fruits, flowers, and roots. Extracts can be easily obtained by exposing the plant material to solvents like distilled water or ethanol. Leaves are often preferred due to their rich deposit of active phytochemicals, offering a renewable, abundant, and non-destructive option. Fruits and seeds are also cost-effective choices.

The synthesis of ZnO nanoparticles via a green method, typically involves mixing plant extracts rich in phytochemicals with a zinc precursor solution, with variations in precursor concentrations, pH, and temperature (Paulkumar et al., 2014). The synthesized nanoparticles are typically annealed to enhance their crystalline nature. Notably, plants are known to contain substantial amounts of polyphenols and flavonoids, which exhibit antioxidant activity. Several studies have demonstrated the successful fabrication of ZnO nanoparticles using plant extracts rich in polyols, phenolic acids, flavonoids, and other bioactive compounds (Dahoumane et al., 2017).

Considering the above context, the primary objectives of this research are (i) to employ green synthesis methods to obtain ZnO nanostructures; (ii) to comprehensively characterize these nanostructures; and (iii) to assess their efficacy as photocatalysts in the degradation of emerging pollutants present in water samples. This research aims to contribute to developing eco-friendly solutions for water purification, harnessing the potential of green-synthesized ZnO nanoparticles to address the challenges posed by water contamination and emerging pollutants.

MATERIALS AND METHODS

Reagents and fruit-based materials

Zinc sulfate heptahydrate (CAS 7446-20-0) $\text{ZnSO}_4 \cdot 7\text{H}_2\text{O}$ and sodium hydroxide (CAS 1310-73-2) NaOH are the reagents used for the synthesis of zinc oxide and were purchased from Sigma Aldrich Romania. The fruit peels (grapefruit) used for the preparation of the extracts were purchased commercially from Romania.

ZnO_g NPs characterization

A detailed analysis of the morpho-structural characteristics of eco-materials obtained from waste as well as those integrated into biopolymer matrices was carried out. This analysis was carried out through an exhaustive research program that highlighted parameters impacting the retention processes of emerging compounds from aqueous solutions using the developed eco-materials. Characterization techniques used included optical microscopy (OM) using an Olympus (BX 51 M), X-ray diffraction (XRD) analysis was performed using a PANalytical X'Pert PRO MPD spectrometer (Almelo, The Netherlands) with a Cu anode, and zeta potential and pH_{pzc} were determined with a ZetaNanosizer (Malvern, Model: Zetasizer Nano ZSP).

Photodegradation experiments

The photocatalytic experiment was performed in the presence of two different dosages of ZnO used as a photocatalyst and acetaminophen (AMP) under UV irradiation. The pollutant solutions are obtained by diluting stock solutions of AMP.

Pollutant analysis

Synthetic wastewater pollutant residues were effectively assessed using the Total Organic Carbon (TOC) technique. The TOC method features specific performance parameters: a detection limit of 0.1 mg/L, a quantification limit of 0.3 mg/L, and an extended uncertainty of the analysis method amounting to 12%. The experimental equipment utilized in these investigations goes by the name of Shimadzu Analyzer TOC TN LCPN.

The removal efficiency (RE) can be determined using the following equation:

$$RE\% = \left(\frac{C_i - C_t}{C_i} \right) \times 100 \quad (1)$$

where:

- C_t and C_i are the concentration AMP at t moment and the initial moment.

RESULTS AND DISCUSSIONS

ZnO_g NPs preparation

The ZnO NPs (ZnO-grapefruit) were synthesized using a green synthesis method presented in previous research (Constandache et al., 2023). Still, instead of grapes for the “green” extract, grapefruit peels were used. In essence, the aqueous extract of Citrus Paradisi (grapefruit) was prepared by boiling 50 g of outer peel in 200 mL of distilled water for 30 minutes at 80°C. For further experiments, the extract was filtered using a Whatman No. 1 paper and stored at 4°C in the refrigerator. Boiling 50 g of peel in 200 mL of water yielded 150 mL of extract and 40 g of waste.

ZnO NPs were prepared using a solution of 3 mM $\text{ZnSO}_4 \cdot 7\text{H}_2\text{O}$. In a typical preparation, 30 ml of aqueous grapefruit peel extract was added to 30 ml of 3mM $\text{ZnSO}_4 \cdot 7\text{H}_2\text{O}$, and the pH was adjusted to 11 using 3 Mm NaOH. The mixture was mixed for 3 h at 75°C at 300 rpm. The resulting ZnO nanoparticles were separated by decanting overnight, and the next day they were washed five times with distilled water, then dried in a hot air oven at 100°C and calcined at 150°C for 1 hour. After calcination, the resulting nanoparticles were ground in a pistil mill.

Flavonoid, limonoid, and carotenoid molecules include free OH/COOH groups that can react with ZnSO_4 to generate a flavonoid/ limonoid/ carotenoid zinc complex. During drying, the zinc flavonoids/ limonoids/ carotenoids are transformed into ZnO nanoparticles.

ZnO_g NPs characterization

Optical Microscopy (OM)

Nanoparticles obtained by the green method were characterized using optical microscopy analysis at 50x magnifications, and the image obtained is shown in Figure 1. It can be seen that the material is in the form of a fine, pale pink powder, and the dimensions of ZnO_g are in the range of 50-150 nm, which are characteristic of nanoparticle agglomerates.

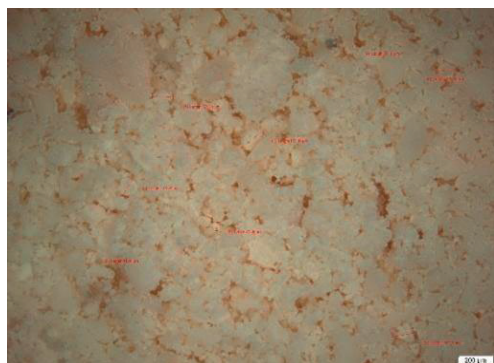


Figure 1. Optical microscopy image of ZnO NPs at 50x magnification

XRD analysis

The resultant diffractogram (Figure 2) demonstrates that the examined ZnO_g contains zinc oxide components, with characteristic diffraction peaks at 2θ of 31.7° , 34.5° , and 36.5° which correspond to the lattice planes of (100), (002), and (101), respectively, were found by analysis. These peaks agreed with the hexagonal zincite structure of ZnO (Naqvi et al., 2014).

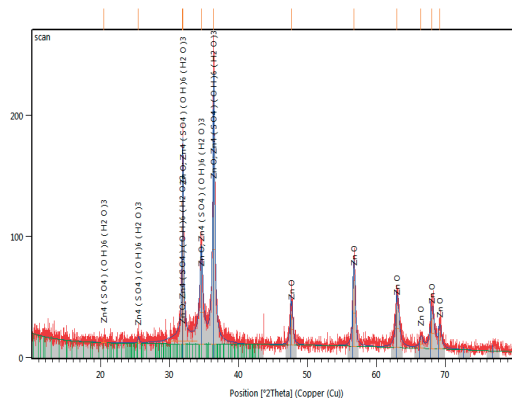


Figure 2. XRD pattern of ZnO NPs

Other diffraction peaks were observed at 2θ of 47.5° , 56.6° , 63.7° , 66.3° , 67.9° , and 69.10° , corresponding to lattice planes of (102), (110), (103), (200), (112), and (201), respectively (JCPDS: 36-1451) (Madhumitha et al., 2019). These findings demonstrated the hexagonal wurtzite structure of the ZnO NPs.

Zeta potential and pH_{Hpzc}

Determination of zeta potential (ζ) and isoelectric point (IEP) or pH_{Hpzc} were carried out

at 25°C using 1 M NaOH and 1 M HCl solutions respectively for measurement at basic and acidic pH. The samples to be analyzed were prepared by preparing a dispersion in distilled water, ultrasonicing it, and then adding a few drops of this dispersion in a 1 mM NaCl solution.

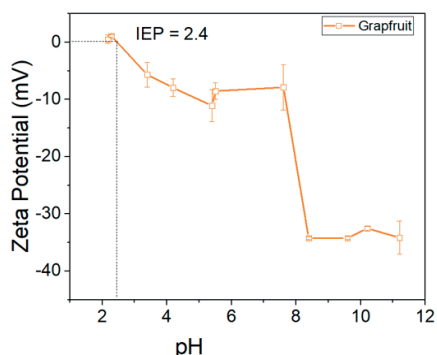


Figure 3. Zeta potential evolution as a function of pH value for ZnO_g

From Figure 3 it can be seen that the isoelectric point values for ZnO nanoparticles prepared in the laboratory are around 2.6. The difference between the IEP of ZnO NPs prepared in the laboratory and that reported in the literature may be due to several factors, including nanoparticle size, surface chemistry, and synthesis method. In the case of ZnO nanoparticles synthesized using grapefruit extracts the specific pH of 2.6 as isoelectric point may be due to surface functional groups or coating agents in the form of organic compounds in the extracts used. The size and shape of the nanoparticles may affect their isoelectric point. Larger nanoparticles may have lower isoelectric points.

Photodegradation tests

By observing the amount of paracetamol that was degraded in water samples, the photocatalytic efficiency of the ZnO_g was determined. In a typical experiment, different dosages of ZnO_g NPs were placed in contact with two 150 mL vessels of 10 mg/L solutions of AMP. During the experiment, the surfactant solution was homogenized by mixing with a magnetic stirrer, and the UV lamp was positioned laterally. All experiments were performed at room temperature. To determine the concentration of AMP removed, samples were taken at intervals of 15 minutes in the first

part of the experiment and at longer intervals in the second part. The samples collected were stored at 4°C until analysis.

The photodegradation efficiency was determined using TOC analyses, an invaluable method for gauging organic constituents within wastewater, particularly when dealing with low concentrations, involving the introduction of a known sample quantity into a high-temperature furnace or chemically oxidizing environment. Within this controlled setting, organic carbon undergoes oxidation to become carbon dioxide, in the presence of a catalyst.

The resulting carbon dioxide is meticulously quantified using an infrared analyzer. By preparing the sample through acidification and aeration before analysis, any potential errors stemming from the presence of inorganic carbon are effectively mitigated. This method boasts swift execution and is steadily gaining popularity. Figures 4 and 5 present the photodegradation efficiency for AMP when using 0.1 g of ZnO and 0.2 g, respectively.

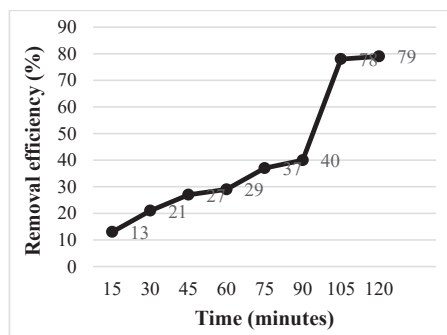


Figure 4. Removal efficiency versus time for acetaminophen contained by wastewater for 0.1 g of ZnO_g

It was observed that the photodegradation in the first 90 minutes increased at a slower rate for both dosages of ZnO₂, reaching only 40% at this time for 0.1g photocatalyst and 53% for 0.2 g, respectively. After this time, the efficiency increased rapidly and stabilized at 79% and 88% after 120 minutes of contact time.

At higher ZnO dosages, the photodegradation efficiency for AMP is higher due to the increased number of active sites on the photocatalyst surface resulting from the higher ZnO₂ dosage. With the increase in dosage, the number of free radicals ($\bullet\text{OH}$ and O_2^{2-}) in the

solution is also increased, consequently leading to enhanced photodegradation of the wastewater sample (Aisien et al., 2014).

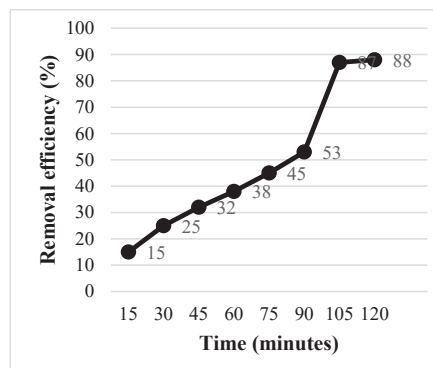


Figure 5. Photodegradation efficiency versus time for acetaminophen contained by wastewater for 0.2 g of ZnO_g

CONCLUSIONS

A ZnO photocatalyst was prepared via a green synthesis precipitation method, using a grapefruit extract as the reducing agent. The structural and morphological analyses suggested that the material was in the form of a fine powder, with aggregates sized in the range of 50-150 nm. The XRD pattern confirmed the presence of ZnO characteristic diffraction peaks, suggesting the successful preparation of ZnO. The ZnO photocatalyst had the highest degradation efficiency of 88% after 120 minutes of contact with 200 mg of material, for a solution with the concentration of 10 mg AMF. These findings confirm the possibility of using an eco-friendly method to produce an efficient "green" ZnO photocatalyst, with potential application in the removal of emerging pollutants from water.

ACKNOWLEDGEMENTS

This work was supported by a grant of the Romanian Education Ministry, UEFISCDI, project number 86PTE/2022, "Advanced technology for purging industrial wastewaters by using environmentally friendly products, in the context of climate changes" (CHITOMAG), within PNCDI III. The results presented in this article has been funded by the Ministry of Investments and European Projects through the Human Capital Sectoral Operational Program

2014-2020, Contract no. 62461/03.06.2022,
 SMIS code 153735.

REFERENCES

- Abebe, B., Zereffa, E.A., Tadesse, A., & Murthy, H.C.A. (2020). A Review on Enhancing the Antibacterial Activity of ZnO: Mechanisms and Microscopic Investigation. *Nanoscale Research Letters*, 15(1), 19.
- Acevedo-Barrios, R.L., Severiche-Sierra, C.A., Jaimes Morales, J.D.C. (2017). Efectos tóxicos del paracetamol en la salud humana y el ambiente. *Revista de Investigacion. Agraria y Ambiental* 8(1), 139-149.
- Aisien, F., Amenaghawon, A., Ekpenisi, E. (2014). Photocatalytic decolourisation of industrial wastewater from a soft drink company. *Journal of Engineering and Applied Sciences*, 9, 11-16.
- Akhter, S.M.H., Mahmood, Z., Ahmad, S., Mohammad, F. (2018). Plant-mediated green synthesis of zinc oxide nanoparticles using *Swertia chirayita* leaf extract, characterization and its antibacterial efficacy against some common pathogenic bacteria. *Bionanoscience*, 8, 811-817.
- Akkari, M., Aranda, P., Belver, C., Bedia, J., Amara, A.B., & Ruiz-Hitzky, E. (2018). Reprint of ZnO/sepiolite heterostructured materials for solar photocatalytic degradation of pharmaceuticals in wastewater. *Applied Clay Science*, 160, 3-8.
- Aragaw, T.A., Bogale, F.M., Aragaw, B.A. (2021). Iron-based nanoparticles in wastewater treatment: A review on synthesis methods, applications, and removal mechanisms. *Journal of Saudi Chemical Society*, 25(8), 101280.
- Avramescu, S.M., Fierascu, I., Fierascu, R.C., Brazdis, R. I., Nica, A.V., Butean, C., Olaru, E.A., Ulinici, S., Verziu, M.N., Dumitru, A. (2022). Removal of Paracetamol from Aqueous Solutions by Photocatalytic Ozonation over $\text{TiO}_2\text{-Me}_x\text{O}_y$ Thin Films. *Nanomaterials*, 12(4), 613.
- Bundschuh, M., Filser, J., Lüderwald, S., McKee, M.S., Metreveli, G., Schaumann, G.E., Wagner, S. (2018). Nanoparticles in the environment: where do we come from, where do we go to? *Environmental Sciences Europe*, 30, 17.
- Constandache, A.C., Favier, L., Covaliu, L., Saulean, A. A., Predescu, A.M., Predescu, C., Matei, E. (2023). Morphological and Structural Investigations of ZnO Resulted from Green Synthesis. *University Politehnica of Bucharest Scientific Bulletin Series B-Chemistry and Materials Science*, 85(2), 275-283.
- Dahoumane, S.A., Mechouet, M., Wijesekera, K., Filipe, C.D., Sicard, C., Bazylinski, D.A., Jeffries, C. (2017). Algae-mediated biosynthesis of inorganic nanomaterials as a promising route in nanobiotechnology—a review. *Green Chemistry*, 19(3), 552-587.
- Jamdagani, P., Khatri, P. Rana, J. (2018). Green synthesis of zinc oxide nanoparticles using flower extract of *Nyctanthes arbor-tristis* and their antifungal activity. *Journal of King Saud University-Science*, 30, 168-175.
- Kayastha, V., Patel, J., Kathrani, N., Varjani, S., Bilal, M., Show, P.L., Kim, S.H., Bontempi, E., Bhatia, S.K., Bui, X.T. (2022). New Insights in factors affecting ground water quality with focus on health risk assessment and remediation techniques. *Environmental Research*, 212, 113171.
- Koagouw, W., Stewart N.A., Ciocan, C. (2021). Long-term exposure of marine mussels to paracetamol: is time a healer or a killer? *Environmental Science and Pollution Research*, 28(35), 48823-48836.
- Madhumitha, G., Fowsiya, J., Gupta, N., Kumar, A., Singh, M. (2019). Green synthesis, characterization and antifungal and photocatalytic activity of *Pithecellobium dulce* peel-mediated ZnO nanoparticles, *Journal of Physics and Chemistry of Solids*, 127, 43-51.
- Naqvi, S.M.A., Soleimani, H., Yahya, N.B., Irshad, K. (2014). Structural And Optical Properties Of Chromium Doped Zinc Oxide Nanoparticles Synthesized by Sol-Gel Method. *AIP Conference Proceedings*, 1621(1), 530-537.
- Negroiu, M., Turcanu, A.A., Matei, E., Rapă, M., Covaliu, C.I., Predescu, A.M., Pantilimon, C.M., Coman, G., Predescu, C. (2021). Novel Adsorbent Based on Banana Peel Waste for Removal of Heavy Metal Ions from Synthetic Solutions. *Materials*, 14, 3946.
- Palma, P., Fialho, S., Lima, A., Novais, M.H., Costa, M.J., Montemurro, N., Pérez S, de Alda, M.L. (2020). Pharmaceuticals in a Mediterranean Basin: The influence of temporal and hydrological patterns in environmental risk assessment. *Science of the Total Environment*, 709.
- Paulkumar, K., Gnanajobitha, G., Vanaja, M., Rajeshkumar, S., Malarkodi, C., Pandian, K., Annadurai, G. (2014). Piper nigrum leaf and stem assisted green synthesis of silver nanoparticles and evaluation of its antibacterial activity against agricultural plant pathogens. *The Scientific World Journal*, 2014.
- Pereira, A., Silva, L., Laranjeiro, C., Pena, A., (2021). Assessment of Human Pharmaceuticals in Drinking Water Catchments, Tap and Drinking Fountain Waters. *Applied Sciences-Basel*, 11(15).
- Richardson, S.D. (2009), Water Analysis: Emerging Contaminants and Current Issues. *Analytical Chemistry*, 81(20), 8654-8654.
- Saleem, H., & Zaidi, S.J. (2020). Developments in the Application of Nanomaterials for Water Treatment and Their Impact on the Environment. *Nanomaterials*, 10(9), 39.
- Sandu, M.A., Vladasel (Pasarescu) A.C., Pienaru, A.M. (2023). Embedding low carbon emission into the water infrastructure. *Scientific Papers. Series E. Land Reclamation, Earth Observation & Surveying, Environmental Engineering*, 12, 52-59.
- Swati, Verma, R., Chauhan, A., Shandilya, M., Li, X., Kumar, R., Kulshrestha, S. (2020). Antimicrobial potential of ag-doped ZnO nanostructure synthesized by the green method using moringa oleifera extract. *Journal of Environmental Chemical Engineering*, 8(3), 103730.
- Vilhunen, S. & M. Sillanpää, (2010). Recent developments in photochemical and chemical AOPs in water treatment: a mini review. *Reviews in Environmental Science and Bio-Technology*, 323-330.

ECOLOGICAL TREATMENT OF WASTEWATER CONTAINING A CATIONIC SURFACTANT POLLUTANT

Leon Dumitru COVALIU¹, Iuliana PAUN^{1,2}, Vasile Ion IANCU², Ecaterina MATEI¹,
Razvan TEODORESCU³, Valerica TUDOR³, Gigel PARASCHIV¹,
Cristina Ileana COVALIU-MIERLA¹

¹National University of Science and Technology POLITEHNICA Bucharest,
313 Splaiul Independentei Street, District 6, Bucharest, Romania

²National Research and Development Institute for Industrial Ecology – ECOIND,
71-73 Drumul Podu Dambovitei Street, District 6, Bucharest, Romania

³University of Agronomic Sciences and Veterinary Medicine of Bucharest,
59 Marasti Blvd, District 1, Bucharest, Romania

Corresponding author email: cristina_covaliu@yahoo.com

Abstract

Increasing pollution from organic substances that are difficult to biodegrade has led scientists to search for solutions to prevent them from entering the environment. A type of pollutant widely found in the environment is quaternary ammonium compounds, with benzalkonium chlorides being the main representative. Among the benzalkonium chlorides class, was chosen to study the method of removal of benzyldimethyldodecylammonium chloride (C12-BAC) from wastewater. One efficient method for the removal of organic compounds from wastewater is by using adsorbent material. For this reason, this paper presents the treatment of wastewater containing benzyldimethyldodecylammonium chloride (C12-BAC) by activated carbon material.

Key words: activated carbon powder, benzalkonium chloride, quaternary ammonium salt, wastewater treatment.

INTRODUCTION

One of the major challenges in wastewater treatment is the treatment of emerging contaminants such as surfactants. The reason for that lies in the fact that tensides are used extensively and widely and that they have an adverse effect on the wastewater treatment process and, above all, on the environment. This requires continuous improvement of wastewater treatment technologies (Dracea et al., 2022) and constant monitoring of water quality (Sandu et al., 2023). Various techniques including physical, chemical, biological and membrane treatment are used to remove surfactants from wastewater. The use of adsorbent materials has proven to be the most effective and cost-efficient approach for eliminating organic pollutants from wastewater. A significant advantage of this method is its ability to prevent the generation of additional pollutants, which can sometimes be even more toxic than the substances being removed. Surfactants are very persistent and water-soluble contaminants. They can pose a serious health risk to humans, animals

and aquatic life by passing through wastewater treatment processes (Bautista-Toledo et al., 2008). One crucial class of pollutants that find their way into the environment includes organic compounds like cationic surfactants (Marković et al., 2017). Among these, benzalkonium chlorides are extensively utilized due to their dual attributes as both biocides and surfactants. They primarily serve as active ingredients in disinfection and cleaning products, with applications extending to surface disinfection, equipment sanitation, and device cleaning in hospitals and the food industry. Furthermore, they are employed in wood preservation. Notably, during the COVID-19 pandemic, there has been a significant surge in the use of these products, resulting in their detection in wastewater.

Benzalkonium chloride boasts a wide array of applications, serving as a versatile cationic surfactant, disinfectant, and bactericide. Additionally, its synergy with natural zeolites has given rise to organozeolites that are effectively employed for the adsorption and

elimination of various non-polar organic substances, including drugs and mycotoxins.

In one study, natural zeolite clinoptilolite was subjected to modification with three different concentrations of benzalkonium chloride, with the resulting material being utilized for the in vitro adsorption of mycotoxins, specifically ochratoxin A and zearalenone (Marković et al., 2017). In another context, zeolites were modified with varying quantities of benzalkonium chloride and cetylpyridine chloride to facilitate the adsorption of the mycotoxin zearalenone (Daković et al., 2013). Furthermore, the combined use of natural zeolite-clinoptilolite and benzalkonium chloride demonstrated efficacy in adsorbing a range of substances, including two drugs, sulfamethoxazole, and metronidazole (Rivera & Farias, 2005), aspirin (Lam & Rivera, 2006), diclofenac diethylamine (Krajišnik et al., 2011), and in conjunction with natural kaolinite, they formed an adsorbent material for the removal of the pesticide diazinon from wastewater (Tilakia et al., 2020).

A tailored zeolite material was engineered by combining natural mordenite zeolite with benzalkonium chloride, and this composite was effectively employed for the removal of Congo red dye (Astuti et al., 2020).

Functionalized zeolites were crafted through the synergistic combination of cationic surfactants (cetylpyridinium chloride, tetrapropylammonium chloride, and benzalkonium chloride) with two zeolites of the FAU zeotype, enabling them to be utilized for the adsorption of tannic acid and the insecticide acetamiprid (Jevremović et al., 2020).

Given the coexistence of pesticides, heavy metals, and cationic surfactants in wastewater, a study focused on the adsorption of benzalkonium chloride surfactant, paraquat cationic herbicide, and cadmium metal onto montmorillonite. Notably, it was observed that the cationic surfactant augmented the adsorption capacity of the herbicide without affecting the metal's adsorption capacity (Ilari et al., 2014).

A comparative investigation involving montmorillonite phyllosilicate clay was carried out to assess the adsorption of benzyl dodecyldimethyl ammonium chloride and benzyl tetradecyldimethyl ammonium chloride (Zanini et al., 2013). A zeolitic tuff with a Si/Al

ratio of 2/4 was used to absorb the cationic surfactant benzyldimethyldodecyl ammonium chloride (Leone & Iovino, 2016; Covaliu et al., 2017; Paun & Covaliu-Mierla, 2023).

Due to its bactericidal properties, benzalkonium chloride together with kaolinite produced an absorbent material with bactericidal properties that was used against *Staphylococcus aureus* by inactivating 60% of the bacteria in 10 minutes (Zhang et al., 2023).

Modified zeolites with bactericidal properties against *Bacillus subtilis* bacteria were derived from synthetic zeolites A, X, and Y in combination with quaternary ammonium compounds, specifically hexadecyltrimethyl ammonium bromide and benzalkonium chloride (Maleka & Maleka, 2012).

Activated carbon exhibits a negative charge when submerged in water, making it capable of removing only cations from the water. Activated carbon is a non-toxic material to the environment and can be regenerated and reused in wastewater treatment technology.

The introduction of quaternary ammonium compounds, primarily benzalkonium chloride, transforms the charge from negative to positive in the resulting activated carbon material modified with cationic surfactant. This newly developed material can effectively eliminate anions from water, including substances like fluorides (Liang et al., 2022), perchlorates (Hou et al., 2013), hexavalent chromium compounds (Tilaki & Motlagh, 2017), and even non-polar compounds such as volatile organic substances Li et al., 2020).

Hospital wastewater containing benzalkonium chloride was successfully treated by adsorption using granular activated carbon (Tanada et al., 1991). Additionally, powdered activated carbon was employed for the removal of binary and ternary combinations of BAC12, BAC14, and BAC16 from water (Kim et al., 2022).

The removal of benzalkonium chloride was achieved using four ion exchange resins, comprising three strongly acidic resins with sulfonate functional groups and one weakly acidic resin with a carboxylic functional group. Across all ion exchange resins, removal rates exceeded 80%, with contact times ranging from 40 to 60 minutes (Klimonda et al., 2019).

The hydrophobic polymer adsorbent Amberlite XAD-16 was applied for the removal of

benzalkonium chloride (BAC), which is a commercial product containing mixtures of C12-BAC and C14-BAC counterparts (Turku & Sainio, 2009).

Adsorbent materials, like zeolites, find application in the removal of benzalkonium chlorides from wastewater. In a related context, two natural zeolites, smectite, and kaolinite, were employed as adsorbents for two quaternary alkylammonium compounds, namely benzyl dimethyl dodecyl ammonium chloride (C12-BAC) and dodecyl dimethyl ammonium chloride. Simultaneously, the study delved into the bacterial growth of eight bacterial taxa on adsorbent materials containing quaternary alkylammonium compounds. It was revealed that the adsorbent material plays a pivotal role in mitigating the toxicity of quaternary ammonium salts to bacteria (Fortunato et al., 2019).

For a deeper understanding of the adsorption mechanisms of C12-BAC, C14-BAC, and C16-BAC from water, powdered activated carbon was employed. Following the adsorption of BACs onto powdered activated carbon, a partial detoxification of water was observed, as indicated by a Microtox assay (Kim et al., 2022). The removal of cationic surfactants primarily revolves around adsorption methods, employing a variety of adsorbent materials, including silica gel (Zhu et al., 2010), bentonites (Banerjee et al., 2006), fly ash (Zanini et al., 2013), clays (Mykola et al., 2016), montmorillonite, charcoal (Kozak & Domka, 2004), as well as nanomaterials like carbon nanotubes (Mahmoud et al., 1999), untreated multi-walled carbon nanotubes (Lopez-Lopez et al., 2016), and nano zero-valent iron (Ncibi et al., 2015). Increasingly, natural zeolites are being used as eco-friendly adsorbents to extract cationic surfactants from wastewater (El-Lateef et al., 2018; Hasan & El-Gawad, 2014; Liu et al., 2015).

This study addresses the removal of the prevalent benzalkonium chloride, specifically benzyl dodecyl dimethyl ammonium chloride (C12-BAC) presented in Figure 1, using environmentally friendly adsorbent materials like activated carbon. It explores the influence of experimental parameters such as pH, contact time, C12-BAC concentration, and the quantity of adsorbent material on the process.

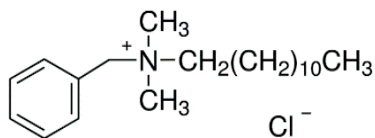


Figure 1. Molecular structure of C12-BAC

MATERIALS AND METHODS

Reagents and adsorbent materials

Benzyl dimethyl dodecyl ammonium chloride (C12-BAC) was purchased from Sigma-Aldrich, and Figure 1 shows its molecular structure.

The activated carbon was purchased from Trace Elemental Instruments with a particle size between 10 and 50 μm . The adsorbent material (activated carbon) presents a specific surface area of 256 m^2/g , a pore size of 12.7 \AA , and a total pore area of 870 m^2/g .

C12-BAC analysis

The chromatographic method used to determine the concentrations of C12-BAC was developed in another paper (Covaliu et al., 2017) and the equipment used was an Agilent 1200 liquid chromatograph equipped with a DAD detector operating at a wavelength of 262 nm, and an Acclaim Surfactant chromatographic column Plus, 3 μm , length 150 mm, inner diameter 3 mm. The operating parameters of the method were column temperature of 30°C, injection volume of 20 μL , mobile phase of ammonium acetate 0.2 M: acetonitrile in the ratio 50:50 (v/v), mobile phase flow of 0.5 mL/min, elution time for C12-BAC was 2.4 minutes.

The kinetic studies

Kinetic studies were performed by adding: 250 mg of PAC to 500 mL synthetic wastewater with C12-BAC concentrations of 50 mg/L, 100 mg/L and 250 mg/L.

The mixtures were shaken at 250 rpm for 60 minutes. The samples were taken every 10 minutes and analyzed.

pH influence

To investigate the effect of pH on C12-BAC adsorption, the experiments were carried out at the same concentration of 50 mg/L of C12-BAC and two different amounts of the adsorbent

material, respectively 200 mg and 250 mg at three pH values: pH=4, pH=6 and pH=10.

The adsorption studies

C12-BAC is absorbed on adsorbent material, namely PAC (powder activated carbon).

The experiments were carried out in 500 mL of synthetic wastewater with a concentration of 50 mg/L of C12-BAC. The three amounts of adsorbent material were used for the adsorption of C12-BAC: 100 mg, 200 mg and 250 mg. The experiments were performed at pH=10. The mixtures were homogenized at 250 rpm for 60 minutes. The samples were taken every 10 minutes and analyzed.

The removal efficiency (RE) can be determined using the following equation:

$$RE\% = 100 \times \left(1 - \frac{C_t}{C_i}\right) \quad (1)$$

where:

- C_t and C_i are the concentration of C12-BAC at t moment and initial moment.

The amount of C12-BAC adsorbed on the adsorbent material at equilibrium used was calculated using the following equation:

$$Q_e = \frac{(C_i - C_e) \cdot V}{m} \quad (2)$$

where:

- Q_e - adsorption capacity at equilibrium, mg/g;
- C_i and C_e - the C12-BAC concentrations in the initial wastewater and at equilibrium (mg/L);
- m - the mass of adsorbent material (g);
- V - the C12-BAC volume initially used in the study (L).

Sorption isotherms are used to explain adsorption processes, and in addition calculate the adsorption capacity of the adsorbent material used using mathematical modelling. The most used adsorption isotherm models are Langmuir (Langmuir, 1918; Allen et al., 2004) and Freundlich (Freundlich, 1906) isotherms.

Langmuir isotherm is based on the following mathematical equation:

$$Q_e = \frac{Q_{max} K_L C_e}{1 + K_L C_e} \quad (3)$$

where:

- C_e is concentration of C12-BAC at equilibrium (mg/L);
- K_L is the equilibrium constant of the Langmuir model (L/mg);
- Q_e is the adsorption capacity at equilibrium (mg/g);

- Q_{max} is the maximum adsorption capacity (mg/g);

- 1 is the maximum capacity occupied by adsorption for a given set of conditions to balance the entire monomolecular layer, mg/g.

The Freundlich isotherm equation is based on the following mathematical equation (Freundlich, 1906):

$$Q_e = K_F \times C_e^{\frac{1}{n}} \quad (4)$$

where:

- K_F is adsorption capacity determined from Freundlich equation (mg/g);

- $1/n$ represents Freundlich parameter with respect to adsorption intensity;

- C_e is the concentration of C12-BAC at equilibrium (mg/L).

RESULTS AND DISCUSSIONS

The kinetic studies

The calculated removal efficiency for each concentration of C12-BAC was 92.3% for the concentration of 50 mg C12-BAC/L, 67.5% for the concentration of 100 mg C12-BAC/L and 39.92% for the concentration of 250 mg/L as seen in Figure 2.

For wastewater containing 50 mg/L C12-BAC and PAC adsorbent material, after 60 minutes of contact time the determined concentration was 0.40 mg C12-BAC/L. The adsorption capacity of PAC was 0.20 mg C12-BAC/mg PAC. For the concentration of 100 mg C12-BAC/L in wastewater, the concentration remaining in the treated wastewater was 0.38 mg C12-BAC/mg PAC, and the adsorption capacity of PAC was 0.38 mg C12-BAC/mg PAC. For the wastewater containing 250 mg C12-BAC/L, 26 mg C12-BAC/L was determined in the wastewater, which corresponds to a PAC adsorption capacity of 0.90 mg C12-BAC/mg PAC.

As can be seen in Figure 2, the removal yields are over 90% for all three concentrations of wastewater used in the experiments.

Influence of pH

The effects of pH on the removal efficiency of C12-BAC using powdered activated carbon, was determined by the interaction of 200 mg and 250 mg of adsorbent material with a concentration of 50 mg/L of C12-BAC at three pH values, namely pH=4, pH=6 and pH=10. The

results of the quantitative dosing of C12-BAC showed that at pH=4 the removal efficiency was below 50%, at pH=6 the removal efficiency was over 50%, and at pH=10 the removal efficiency was over 90%, as seen in Figure 3.

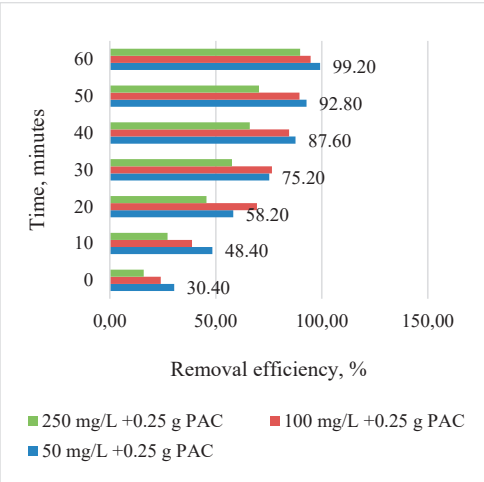


Figure 2. The removal efficiency for C12-BAC when using 0.25 g PAC adsorbent material

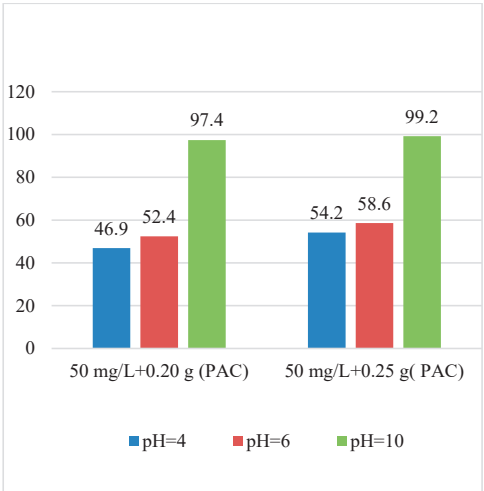


Figure 3. The influence of pH in the removal efficiency of C12-BAC by powdered activated carbon (PAC)

The adsorption studies

The removal efficiency of C12-BAC on different amounts of PAC material increased with the amount of adsorbent material as can be seen in Figure 4. The experimental data obtained in the adsorption study were used to calculate

the adsorption isotherms for each adsorbent material used.

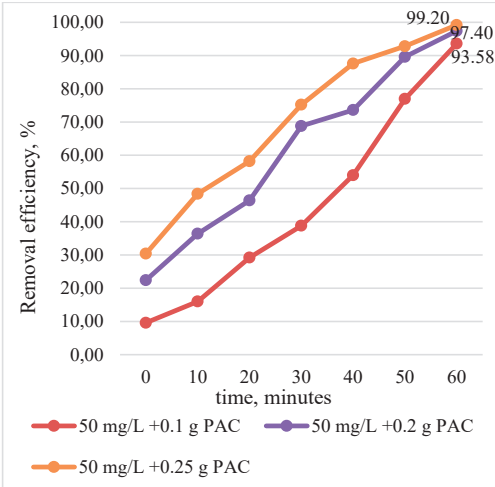


Figure 4. Removal efficiency of C12-BAC as a function of time for different amounts of PAC material

The adsorption capacity of PAC material increased depending on the contact time, as can be seen in Figure 5.

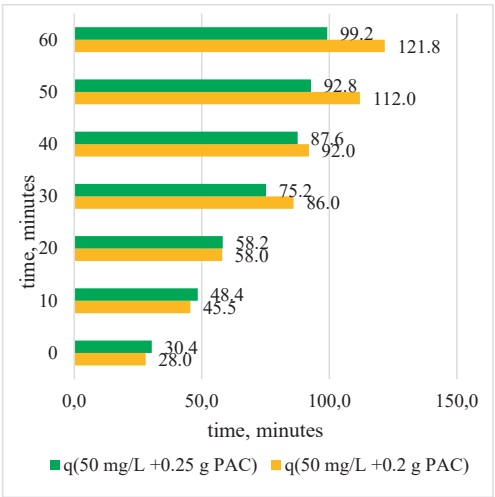


Figure 5. Adsorption capacity of PAC ecomaterial in time

The Langmuir isotherm proposes that adsorption occurs on homogeneous active sites of a monolayer adsorption surface with a finite number of identical sites, with no interactions between adsorbed molecules. Freundlich

isothermal model can be used for multilayer adsorption on heterogeneous sites. Heterogeneous adsorption is when the pollutant enters the adsorbent material in such a way that the adsorption is continuously increased, and the adsorption equilibrium is not reached.

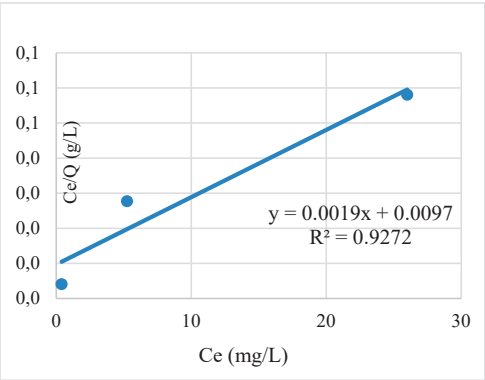


Figure 6. Langmuir isotherm for PAC

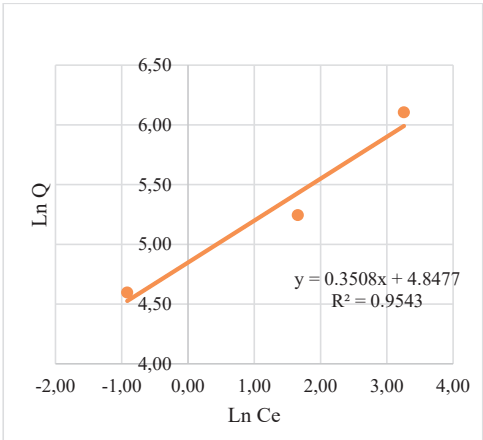


Figure 7. Freundlich isotherm for PAC ecomaterial

Table 1. Langmuir and Freundlich adsorption parameters

	Langmuir parameters			Freundlich parameters		
Adsorbent material	Q_{\max} (mg/g)	K_L (L/mg)	R^2	K_F (L/g)	$1/n$	R^2
PAC	526	0.196	0.9272	2.85	127	0.9543

As can be seen from Figures 6 and 7 and Table 1, the correlation coefficients (R^2) and the values of the isotherm parameters used show that all the adsorption data for the PAC

adsorbent material fit better with the Freundlich model.

CONCLUSIONS

The adsorption of C12-BAC increases with the increase in the pH of the wastewater and the maximum adsorption of C12-BAC is obtained at a pH of 10. The PAC adsorbent ecomaterial had the highest adsorption capacity of 526 mg/g, and the removal efficiency was 99.2% for 250 mg of adsorbent material, for the concentration of 50 mg C12-BAC/L and pH =10. The correlation coefficients (R^2) and the values of the isotherm parameters for the PAC adsorbent ecomaterial fit better with the Freundlich model which is applied to explain the adsorption for the heterogeneous surface.

ACKNOWLEDGEMENTS

The results presented in this article have been funded by the Ministry of Investments and European Projects through the Human Capital Sectoral Operational Program 2014-2020, Contract no. 62461/03.06.2022, SMIS code 153735.

REFERENCES

Allen, S.J., McKay, G., Porter, J.F. (2004). Adsorption isotherm models for basic dye adsorption by peat in single and binary component systems'. *Journal of Colloid and Interface Science*, 280, 322-333.

Astuti, D.W., Aprilita, N.H., Mudasir, M. (2020). Adsorption of the anionic dye of congo red from aqueous solution using a modified natural zeolite with benzalkonium chloride. *RASĀYAN Journal of Chemistry*, 13, 845 – 853.

Banerjee, S.S., Joshi, M.V., Jayaram, R.V. (2006). Effect of quaternary ammonium cations on dye sorption to fly ash from aqueous media. *J. Colloid Interface Sci*, 303, 477–483.

Bautista-Toledo M.I., Méndez-Díaz J.D., Sánchez-Polo M., Rivera-Utrilla J., Ferro-García M.A. (2008). Adsorption of sodium dodecylbenzenesulfonate on activated carbons: Effects of solution chemistry and presence of bacteria. *Journal of Colloid and Interface Science*, 317(1), 11-17.

Covaliu, C., Paraschiv, G., Vasile, E., Matei, E. (2017). Nanostructured zeolites for heavy metals removal from wastewater. In *Proceedings of the Applied Nanotechnology and Nanoscience International Conference*, Rome, Italy, 151.

- Daković, A., Kragović, M., Rottinghaus, G.E., Marković, M., Milić, J., Krajišnik D. (2013). Zearalenone adsorption on a natural zeolite modified with different surfactants, *Proceedings of the 5th Serbian-Croatian-Slovenian Symposium on Zeolites*, 120-123.
- Dracea, D., Tronac, A., Mustata, S. (2022). Continuous adjustment within wastewater treatment plants operation to meet natural receptors discharge conditions. *Scientific Papers. Series E. Land Reclamation, Earth Observation & Surveying, Environmental Engineering*, XI, 344-349.
- El-Lateef, H.M.A., Ali, M.M.K., Saleh, M.M. (2018). Adsorption and removal of cationic and anionic surfactants using zero-valent iron nanoparticles. *J. Mol. Liq.*, 268, 497-505.
- Fortunato, M.S., Baroni, S., González, A.J., Roncancio, J.D.A., Storino, A., Parise, C., Planes, E., Gallego, A., Koro, S.E. (2019). Biodegradation and Detoxification of Benzalkonium Chloride in Synthetic and Industrial Effluents in Upflow Biofilm Aerobic Reactors, *Water Air Soil Pollut.*, 230, 79.
- Freundlich, H.M.F. (1906). Über die adsorption in lösungen. *Z. Phys. Chem.*, 57, 385-470.
- Hasan, S., El-Gawad, A. (2014). Aquatic Environmental Monitoring and Removal Efficiency of Detergents. *Water Research*, 28, 305-311.
- Hou, P., Cannon, F.S., Brown, N.R., Byrne, T., Gu, X., Delgado, C.N. (2013). Granular activated carbon anchored with quaternary ammonium/epoxide-forming compounds to enhance perchlorate removal from groundwater. *Carbon*, 53, 197-207.
- Ilari, R., Etcheverry, M., Zenobi, C., Zanini, G. (2014). Effect of the surfactant benzalkonium chloride in the sorption of paraquat and cadmium on montmorillonite. *International Journal of Environment and Health*, 7(1).
- Jevremović, A., Božinović, N., Arsenijević, D., Marmakov, S., Vasiljević, B.N., Uskoković-Marković, S., Bajuk-Bogdanović, D., Milojević-Rakić, M. (2020). Modulation of cytotoxicity by consecutive adsorption of tannic acid and pesticides on surfactant functionalized zeolites. *Environmental Science: Processes & Impacts*, 22, 2199-2211.
- Kim, T.K., Choe, W.S., Kim, T., Chae, S.H., Hwang, Y.S., Zoh, K.D. (2022). Adsorption of benzalkonium chlorides onto powdered activated carbon: mechanisms and detoxification. *Environ. Eng. Res*, 27, 210496.
- Klimonda, A., Kowalska, I. (2019). Removal of quaternary ammonium compounds in ion exchange process. *E3S Web of Conferences*, 116, 00034.
- Krajišnik, D., Daković, A., Malenović, A., Milić, J. (2011). Comparison of cationic surfactants-modified zeolites as a potential drug carrier for diclofenac diethylamine. *Proceedings of the 4th Slovenian-Croatian Symposium on Zeolites*, 65-68.
- Kozak, M., Domka, L. (2004). Adsorption of the quaternary ammonium salts on montmorillonite. *J. Phys. Chem. Solids*, 65, 441-445.
- Lam, A., Rivera, A. (2006). Theoretical study of the interaction of surfactants and drugs with natural zeolite. *Microporous and Mesoporous Materials*, 91, 181-186.
- Langmuir, I. (1918). The adsorption of gases on plane surfaces of glass, mica and platinum. *J. Am. Chem. Soc.*, 40, 1361-1403.
- Leone, V., Iovino, P. (2016). Sorption of a Cationic Surfactant Benzyl dimethyldodecyl Ammonium Chloride onto a Natural Zeolite. *Water Air Soil Pollut.*, 227, 2-8.
- Li, X., Zhang, L., Yang, Z., Wang, P., Yan, Y., Ra, J. (2020). Adsorption materials for volatile organic compounds (VOCs) and the key factors for VOCs adsorption process: A review. *Separation and Purification Technology*, 235, 116213.
- Liang, D., Yu, F., Zhu, K., Zhang, Z., Tang, J., Xie, Q., Liu, J., Xie, F. (2022). Quaternary ammonium salts targeted regulate the surface charge distribution of activated carbon: A study of their binding modes and modification effects. *Environmental Research*, 214, 114103.
- Liu, B., Wattanaprayoon, C., Oh, S.C., Emdadi, L., Liu, D. (2015). Synthesis of Organic Iillared MFI Zeolite as Biofunctional Acid-Base Catalyst. *Chem. Mater.*, 27, 1479-1487.
- Lopez-Lopez, M., Bernal, E., Moy, M.L., Sanchez, F., Lopez-Cornejo, P. (2016). Study of ionic surfactants interactions with carboxylated single-walled carbon nanotubes by using ion-selective electrodes. *Electrochem. Commun.*, 67, 31-34.
- Mahmoud, M., Saleh, I., Atia A.A. (1999). Removal of Some Surfactants from Dilute Aqueous Solutions Using Charcoal. *Adsorption Science & Technology*, 17, 53-63.
- Maleka, N.A.N.N., Maleka, N.S. (2012). Modification of Synthetic Zeolites by Quaternary Ammonium Compounds and Its Antibacterial Activity against *Bacillus Subtilis*, ICCCP 2012: 5-6 May 2012, Kuala Lumpur, Malaysia.
- Marković, M., Daković, A., Rottinghaus, G. E., Petković, A., Kragović, M., Krajišnik, D., Milić, J., Ochrotxin, A., (2017). Zearalenone adsorption by the natural zeolite treated with benzalkonium chloride. *Colloids and Surfaces A: Physicochemical and Engineering Aspects*, 529, 7-17.
- Mykola, S., Olga, N., Dmitry, M. (2016). The influence of alkylammonium modified clays on the fungal resistance and biodeterioration of epoxy-clay nanocomposites. *Int. Biodeterior. Biodegrad.*, 110, 136-140.
- Ncibi, M.C., Gaspard, S., Sillanpaa, M. (2015). As-synthesized multi-walled carbon nanotubes for the removal of ionic and non-ionic surfactants. *J. Hazard Mater*, 286, 195-203.
- Paun, I., Covaliu-Mierla, C.I. (2023). Determination of benzalkonium chlorides from wastewater using HPLC-DAD method, *U.P.B. Sci. Bull.*, Series B, 85, ISSN 1454-2331.
- Rivera, A., Farias, T. (2005). Clinoptilolite-surfactant composites as drug support: A new potential application. *Microporous and Mesoporous Materials*, 80, 337-346.
- Sandu, M.A., Virsta, A., Scaeteanu, G.V., Iliescu, A.I., Ivan, I., Nicolae, C.G., Stoian, M., Madjar, R.M. (2023). Water quality monitoring of Moara

- Domnească pond, Ilfov county, using uav-based rgb imaging. *Agrolife Science Journal*, 12(1), 191-20.
- Tanada, M., Miyoshi, T., Nakamura, T., Tanada, S. (1991). Adsorption Removal of Benzalkonium Chloride by Granular Activated Carbon for Medical Waste Water Treatment. *Asia Pacific Journal of Public Health*, 5, 27-31.
- Tilaki, R.D., Kalakeshb, L.R., Bavandia, S., Babanejada, I., Charatic, J.Y., Rodriguez-Couto, S. (2020). Surfactant modified kaolinite (MK-BZK) as an adsorbent for the removal of diazinon from aqueous solutions. *Desalination and Water Treatment*, 196, 137–145, 2020.
- Tilaki, R.D., Motlagh, S.S.H. (2017). Removal of Chromium (VI) from Aqueous Solution by Activated Carbon Modified with Cationic Surfactant Benzalkonium Chloride, J Mazandaran. *Univ Med Sci*, 27, 122-135.
- Turku, I., Sainio, T. (2009). Modeling of adsorptive removal of benzalkonium chloride from water with a polymeric adsorbent. *Separation and Purification Technology*, 69, 185–194.
- Zanini, G.P., Ovesen, R.G., Hansen, H.C.B. (2013). Bjarne W. Strobel, Adsorption of the disinfectant benzalkonium chloride on montmorillonite. Synergistic effect in mixture of molecules with different chain lengths. *Journal of Environmental Management*, 128, 100-105.
- Zhang, X., Li, S., Deng, Y., Zuo, Z., Sun, Z., Li, C., Zheng, S. (2023). Benzalkonium chloride modified kaolinite with rapid bactericidal activity for the development of antibacterial films. *Materials Today Communications*, 35, 106152.
- Zhu, R., Wang, T., Zhu, J., Ge, F., Yuan, P., He, H. (2010). Structural and sorptive characteristics of the cetyltrimethylammonium and polyacrylamide modified bentonite. *Chem. Eng. J.*, 160, 220–225.

ENVIRONMENT CONTAMINATION WITH PETROLEUM HYDROCARBONS

Cristian Mugurel IORGA¹, Puiu Lucian GEORGESCU¹, Mihaela Marilena STANCU²

¹"Dunarea de Jos" University of Galati, Faculty of Sciences and Environment,
European Centre of Excellence for the Environment, 111 Domneasca Street, Galati, Romania

²Institute of Biology Bucharest of Romanian Academy,
296 Splaiul Independentei, Bucharest, Romania

Corresponding authors emails: cristian.iorga@ugal.ro, mihaela.stancu@ibirol.ro

Abstract

Important quantities of petroleum hydrocarbons are frequently spilled into the environment harming the environment, as well as human health. Furthermore, the interaction of petroleum hydrocarbons with the environment significantly disturbs the activity of the microorganisms, including bacteria that exist in petroleum hydrocarbons polluted environments. Using two different microbiological methods four groups of bacteria, such as heterotrophic, hydrocarbon-tolerant, hydrocarbon-degrading, as well as enterobacteria were detected in the analyzed samples collected from an old petroleum products storage. The detection of these bacteria, especially hydrocarbon-degrading, as well as hydrocarbon-tolerant bacteria was not unexpected since the concentration of the petroleum hydrocarbons in the analyzed samples was above the limit allowed by international environmental standards. Up to now, different treatment technologies have been developed to remove toxic hydrocarbons from environments contaminated with petroleum products. Therefore, because of the use of different remediation strategies, like bioremediations, the affected areas can be recovered and returned to their natural circuit.

Key words: bacteria, bioremediation, contamination, environment, petroleum hydrocarbon.

INTRODUCTION

Petroleum and petroleum products (e.g., diesel, gasoline, lubricants) are all over the world the principal source of energy for many industries and our daily lives. Consequently, accidents, leaks, and spills occur during petroleum exploration, production, transport, and storage, and petroleum hydrocarbons are frequently released into the environment (Onutu & Tita, 2018). As a result of the contamination of soil and groundwater with petroleum hydrocarbons diversity and activity of indigenous microorganisms are frequently perturbed. Furthermore, petroleum hydrocarbon contamination also has a negative impact on human health, animals, and plants (Das & Chandran, 2010; Chikere et al., 2011; Xu et al., 2018; Logeshwaran et al., 2018; Petruta & Drăcea, 2023). Nowadays, different physical, chemical, and biological methods are used for the remediation of environments contaminated with petroleum and petroleum products. Biological methods are considered eco-friendly, cost-effective, and more efficient in

the complete degradation of petroleum hydrocarbons, as compared with other methods. Furthermore, strategies that ensure adequate concentration of oxygen and nutrients can create suitable environmental conditions for the growth of bacteria capable of degrading petroleum and petroleum products. Analyzing the effects of petroleum hydrocarbons on bacterial community diversity and dynamics in contaminated sites has been reported to be valuable for remediation practices and to help in evaluating the recovery potential of petroleum and petroleum products contaminated sites (Logeshwaran et al., 2018). As bacteria play a significant role in the degradation of petroleum hydrocarbons investigations into the bacterial communities within contaminated samples are essential to find adequate strategies for bioremediation of the petroleum hydrocarbon contaminated sites (Truskewycz et al., 2019). The purpose of this research was to investigate the presence of several bacterial groups, such as heterotrophic, hydrocarbon-tolerant, hydrocarbon-degrading, and enterobacteria in two environmental

samples collected from an old site contaminated with petroleum products.

MATERIALS AND METHODS

Samples collection

The groundwater and soil samples analyzed in the present study were collected from an old site contaminated with petroleum products (Figure 1) located in Constanta County. The water table level at the time of taking the aquifer sample was located at a depth of -4.73 m, and the soil sample was taken from the vicinity of the monitoring well at a depth of about -0.8 m. We observed that in the soil sample, an advanced degree of degradation of petroleum products was found, and in the groundwater sample, a film of petroleum hydrocarbons was observed, which indicates an

old pollution. Petroleum and petroleum products that are accidentally released into the environment due to different human activities can often contaminate the soil, and by vertical migration, they reach the groundwater (Ossai et al., 2020). When petroleum hydrocarbons contaminate the environment, they undergo a variety of weathering that involves physicochemical processes (e.g., dispersion, evaporation, dissolution, adsorption, photolysis) and biological processes (biodegradation and biotransformation). According to the literature data, environmental factors, for instance, temperature, humidity, and precipitation affect the biodegradation process of petroleum hydrocarbons (Abena et al., 2019; Truskewycz et al., 2019; Ossai et al., 2020).

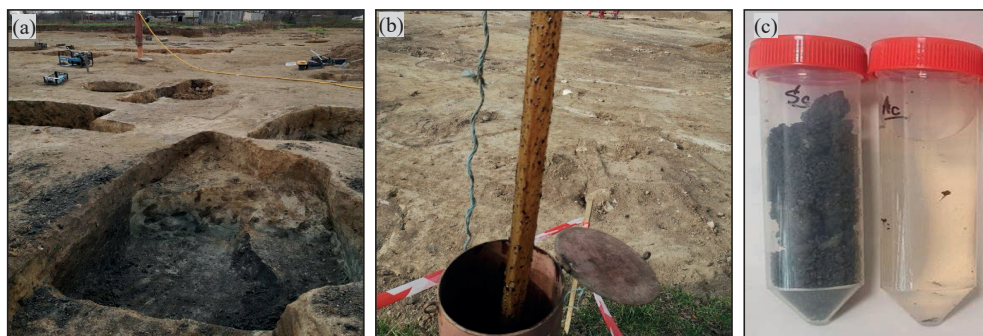


Figure 1. Samples collection from an old petroleum products storage:
(a) groundwater; (b) soil; (c) samples

Microbiological analysis of samples

The microbiological analysis of the samples was made by the agar plate method and the most probable number method. The pH of the samples was measured by using a Hanna pH 213 (Woonsocket, Rhode Island, USA).

Plate count agar (PCA) method. Serial dilutions (10^{-1} - 10^{-6} in phosphate buffer saline or PBS) of each sample were inoculated on different culture media, such as LB agar (Sambrook et al., 1989) for heterotrophic bacteria, LB agar with 5% (v/v) diesel for hydrocarbon-tolerant bacteria, minimal agar (Stancu, 2023) with 5% diesel for hydrocarbon-degrading bacteria, and EMB agar for enterobacteria. Petri dishes were incubated at 30°C for 1-5 days. Then, it was determined the number of bacteria present per ml or g (CFU ml⁻¹, CFU g⁻¹).

The most probable number (MPN) method. Serial dilutions (10^{-1} - 10^{-12} in PBS) of each sample were inoculated into 96-multiwall plates (Stancu & Grifoll, 2011) containing different culture media, such as LB broth (Sambrook et al., 1989) for quantification of heterotrophic bacteria, LB broth with 5% diesel for hydrocarbon-tolerant bacteria, and minimal broth (Stancu, 2023) with 5% diesel for quantification of hydrocarbon-degrading bacteria. Multiwall plates were incubated at 30°C for 1-14 days. The growth of bacteria was determined (cell ml⁻¹, cell g⁻¹) using 0.3% triphenyl tetrazolium chloride (TTC) dye as a redox indicator of cellular respiration (Stancu & Grifoll, 2011).

Isolation of hydrocarbon-tolerant, hydrocarbon-degrading bacteria

The hydrocarbon-tolerant, hydrocarbon-degrading bacteria were isolated by the enrichment culture method (Stancu, 2020; Stancu, 2023). Each sample (5% v/v) was used to initiate enrichment cultures in LB broth as well as in minimal broth supplemented with 5% diesel as a sole carbon source. The tubes were incubated at 30°C on a rotary shaker (200 rpm) for 14 days. Then, the enrichment cultures (5% v/v) were transferred into fresh LB broth with 5% diesel for the isolation of hydrocarbon-tolerant bacteria and minimal broth with 5% diesel for the isolation of hydrocarbon-degrading bacteria. The tubes were incubated under the same conditions for another 14 days. Then, the growth of isolated bacteria in the presence of diesel was determined by measuring the optical density at 660 nm (OD_{660}), as well as by the spot method (Stancu, 2020; Stancu, 2023) using LB agar, EMB agar, and LB with diesel. The biodegradation of diesel by the isolated bacterial population was confirmed by diesel film fragmentation, as well as by monitoring the free carbon dioxide (CO_2 mg l^{-1}) (Stancu, 2023).

Chemical analysis of samples

The extraction of petroleum hydrocarbons from the aquifer sample was made using perchloroethylene, while the extraction of hydrocarbons from the soil was done by using S-316 solvent. Polar compounds were removed from extracts by adding activated aluminum oxide. To determine the hydrocarbon concentration in the aquifer (mg l^{-1}) and soil (mg kg^{-1}), the non-polar solvent extracts were analyzed by Fourier transform infrared spectroscopy (FTIR) (Falkova et al., 2016).

RESULTS AND DISCUSSIONS

Microbiological analysis of samples

In the aquifer and soil samples which had an alkaline pH (7.8, 8.6), we revealed by plate count agar (PCA) method (Figure 2) the

presence of the following groups of bacteria: heterotrophic, hydrocarbon-tolerant, hydrocarbon-degrading, and enterobacteria. The number of these bacteria varied from one sample to another (10^5 - 10^7 CFU ml^{-1} or g^{-1}) (Table 1). Heterotrophic bacteria were present in high numbers in both the aquifer (10^6 CFU ml^{-1}) and soil (10^7 CFU g^{-1}) samples. Most of the bacteria present in the analyzed samples proved to be hydrocarbon-tolerant bacteria (10^5 , 10^7 CFU ml^{-1} or g^{-1}). Also, enterobacteria were present in both the analyzed (10^5 , 10^6 CFU ml^{-1} or g^{-1}) samples.

By the most probable number method (MPN) (Figure 2) the existence of the following groups of bacteria was highlighted: heterotrophic bacteria, hydrocarbon-tolerant bacteria, and hydrocarbon-degrading bacteria, and their number varied from one sample to another (10^7 - 10^{12} cells ml^{-1} or g^{-1}) (Table 1). Heterotrophic and hydrocarbon-tolerant (HCT) bacteria were present in higher numbers (10^{11} - 10^{12} cells ml^{-1} or g^{-1}) in the two analyzed samples. Unlike these two groups of bacteria, the hydrocarbon-degrading (HCD) bacteria were present in lower numbers (10^7 cells ml^{-1} or g^{-1}) both in the soil and aquifer samples. These results can be explained because not all bacteria present in natural samples can degrade petroleum hydrocarbons which generally are very toxic for most microorganisms, including bacteria.

Isolation of hydrocarbon-tolerant, hydrocarbon-degrading bacteria

Previously it was observed (Stancu, 2020; Stancu, 2023), that the enriched culture method is a very effective technique for the isolation of bacteria that exist in environments polluted with petroleum and petroleum products. Consequently, we use the enriched culture method for the isolation of hydrocarbon-tolerant and hydrocarbon-degrading bacteria from soil and groundwater samples (Figure 2).

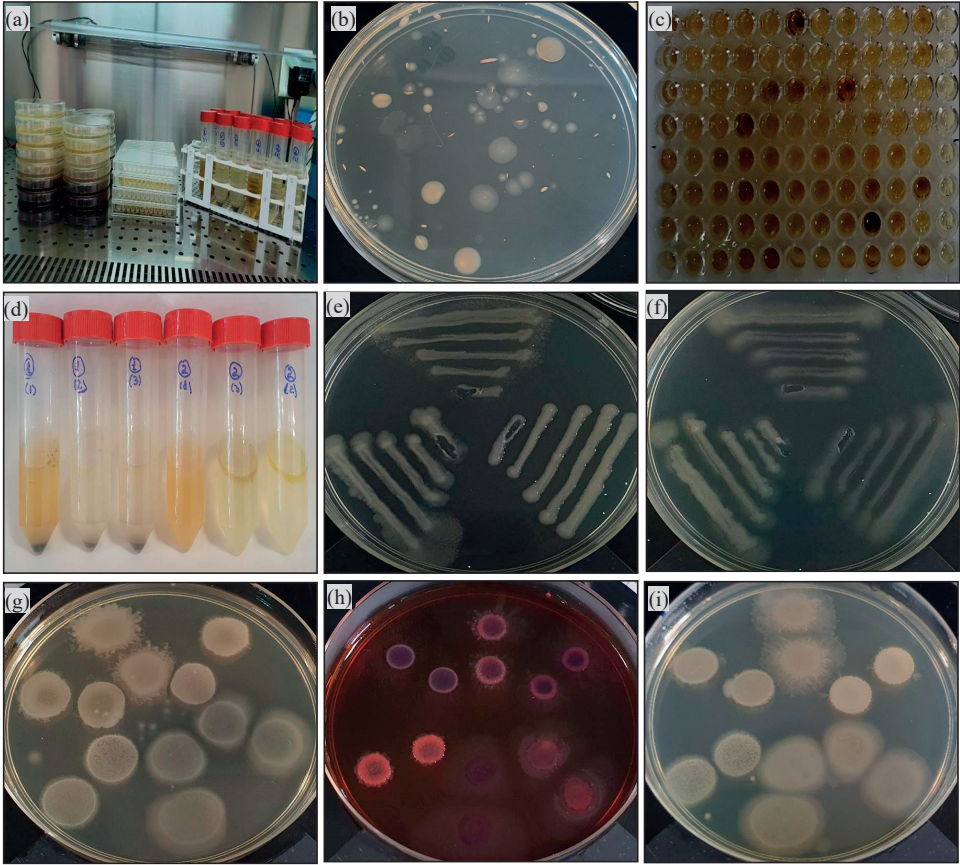


Figure 2. Enumeration and isolation of hydrocarbon-tolerant and hydrocarbon-degrading bacteria:
(a) microbiological analysis of samples; (b) plate count agar method; (c) most probable number method;
(d) bacteria isolation by enrichment culture method; (e, f) bacteria purification; (g) bacteria growth on LB agar;
(h) bacteria growth on EMB agar; (i) bacteria growth on LB agar with diesel

Table 1. Microbiological analysis of aquifer and soil samples

Samples	Number of bacteria by					
	PCA method (CFU ml ⁻¹ or g ⁻¹)			MPN method (cells ml ⁻¹ or g ⁻¹)		
Ground water	Heterotrophic	HCT	Enterobacteria	Heterotrophic	HCT	HCD
Soil	4.5·10 ⁶	1.6·10 ⁵	5.3·10 ⁵	4.0·10 ¹¹	1.6·10 ¹¹	2.0·10 ⁷
	5.9·10 ⁷	6.5·10 ⁷	5.6·10 ⁶	1.6·10 ¹²	1.2·10 ¹²	9.5·10 ⁷

As expected, in the soil and groundwater samples, the presence of both hydrocarbon-tolerant and hydrocarbon-degrading bacteria was observed. The growth of these bacteria varied from one sample to another depending on the culture conditions (DO₆₆₀ 0.99-2.21) (Table 2). In the case of hydrocarbon-tolerant bacteria, we observed better growth (DO₆₆₀ 1.45, 2.21), compared to that of hydrocarbon-

degrading bacteria (DO₆₆₀ 0.99, 1.84). All these bacteria showed good viability on the LB agar, EMB agar, and LB agar with diesel (Figure 2). The fragmentation of the diesel film, because of the biodegradation of the hydrocarbons, was observed for both the hydrocarbon-tolerant bacteria and hydrocarbon-degrading bacteria. The amount of free CO₂ released varied from one sample to another (1012, 1110 mg l⁻¹).

Table 2. Characterization of the isolated bacterial populations

Samples	Hydrocarbon-tolerant				Hydrocarbon-degrading			
	(DO ₆₆₀)	Viability	Diesel degr.	CO ₂ (mg l ⁻¹)	(DO ₆₆₀)	Viability	Diesel degr.	CO ₂ (mg l ⁻¹)
Groundwater	1.45	100	+	1012	0.99	100	+	1100
Soil	2.21	100	+	1110	1.84	100	+	1210

Chemical analysis of samples

The isolation of hydrocarbon-tolerant and hydrocarbon-degrading bacteria from soil and aquifer was not surprising since both these samples were highly contaminated with petroleum hydrocarbons.

Based on the FTIR spectroscopy analysis, in the aquifer sample, the concentration of total petroleum hydrocarbons (TPH) was 273 mg l⁻¹, while in the soil their concentration was 17300 mg kg⁻¹ (Table 3).

Table 3. Petroleum hydrocarbon in aquifer and soil samples

Samples	Petroleum hydrocarbons
	Concentration (mg l ⁻¹ or mg kg ⁻¹)
Groundwater	273
Soil	17300

The TPH parameter is used as the first element in identifying sites contaminated with petroleum products, being an indicator of petroleum hydrocarbon contamination of the environment.

Based on the evaluation of this parameter, measures can be taken to remediate a contaminated site (Pinedo et al., 2013). As observed, the petroleum hydrocarbon concentrations were over the limit allowed by international environmental standards in both samples.

These results were not surprising, since in the past there was a deposit of petroleum products, such as gasoline, lighter liquid fuel, engine, and transmission oils in this area.

CONCLUSIONS

In groundwater and soil samples, the presence of heterotrophic, hydrocarbon-tolerant, hydrocarbon-degrading, and enterobacteria was highlighted by using two classical microbiological methods.

All these bacteria were detected in lower numbers (10⁵-10¹¹ CFU or cells ml⁻¹) in the aquifer sample, compared with their numbers in the soil sample (10⁶-10¹² CFU or cells g⁻¹).

The isolation of hydrocarbon-degrading bacteria, as well as hydrocarbon-tolerant bacteria from the analyzed samples, was not unexpected, since both aquifer and soil samples were highly contaminated with petroleum

hydrocarbons (273 mg l⁻¹, 17300 mg kg⁻¹) because of different human activities.

ACKNOWLEDGEMENTS

The study was funded by project no. 769/2022 from the "Dunarea de Jos" University of Galati and project no. RO1567-IBB05/2022 from the Institute of Biology Bucharest of Romanian Academy.

REFERENCES

- Abena, M.T.B., Tongtong, L., Shah, M.N., Zong, W. (2019). Biodegradation of total petroleum hydrocarbons (TPH) in highly contaminated soils by natural attenuation and bioaugmentation. *Chemosphere*, 234, 864-874.
- Chikere, C.B., Okpokwasili, G.C., Chikere, B.O. (2011). Monitoring of microbial hydrocarbon remediation in the soil. *3 Biotech*, 1, 117-138.
- Das, N., Chandran, P. (2011). Microbial degradation of petroleum hydrocarbon contaminants: An overview. *Biotechnology Research International*, 941810, doi:10.4061/2011/941810.
- Falkova, M., Vakh, C., Shishov, A., Zubakina, E., Moskvina, A., Moskvina, L., Bulatov, A. (2016). Automated IR determination of petroleum products in water based on sequential injection analysis. *Talanta*, 148, 661-665.
- Logeshwaran, P., Megharaj, M., Chadalavada, S., Bowman, M., Naidu, R. (2018). Petroleum hydrocarbons (PH) in groundwater aquifers: An overview of environmental fate, toxicity, microbial degradation and risk-based remediation approaches. *Environmental technology & innovation*, 10, 175-193.

- Onutu I., Tita, M. (2018). Soil contamination with petroleum compounds and heavy metals - case study. *Scientific Papers. Series E. Land Reclamation, Earth Observation & Surveying, Environmental Engineering, VII*, 140-145, Print ISSN 2285-6064.
- Ossai, I.C., Ahmed, A., Hassan, A., Hamid, F.S. (2020). Remediation of soil and water contaminated with petroleum hydrocarbon: A review. *Environmental Technology & Innovation*, 17, 100526. doi:10.1016/j.eti.2019.100526.
- Petruta, A.M., Drăcea, D. (2023). The risk assessment for the management of petroleum product storage & distribution site. *Scientific Papers. Series E. Land Reclamation, Earth Observation & Surveying, Environmental Engineering, XII*, 142-149, Print ISSN 2285-6064.
- Pinedo, J., Ibáñez, R., Lijzen, J.P.A., Irabien, Á. (2013). Assessment of soil pollution based on total petroleum hydrocarbons and individual oil substances. *Journal of Environmental Management*, 130, 72-79.
- Sambrook, J., Fritsch, E.F., Maniatis, T. (1989). *Molecular Cloning*, A Laboratory Manual. 2nd ed. Cold Spring Harbor Laboratory Press, Cold Spring Harbor, New York.
- Stancu, M.M. (2020). Kerosene tolerance in *Achromobacter* and *Pseudomonas* species. *Annals of Microbiology*, 70(8), doi:10.1186/s13213-020-01543-2.
- Stancu, M.M. (2023). Characterization of new diesel-degrading bacteria isolated from freshwater sediments. *International Microbiology*, 26(1), 109-122.
- Stancu, M.M., Grifoll, M. (2011). Multidrug resistance in hydrocarbon-tolerant Gram-positive and Gram-negative bacteria. *The Journal of General and Applied Microbiology*, 57, 1-18.
- Truskewycz, A., Gundry, T.D., Khudur, L.S., Kolobaric, A., Taha, M., Aburto-Medina, A., Ball, A.S., Shahsavari, E. (2019). Petroleum hydrocarbon contamination in terrestrial ecosystems-fate and microbial responses. *Molecules*, 24, 3400.
- Xu, X., Liu, W., Tian, S., Wang, W., Qi, Q., Jiang, P., Jiang, P., Gao, X., Li, F., Li, H., Yu, H. (2018). Petroleum hydrocarbon-degrading bacteria for the remediation of oil pollution under aerobic conditions: a perspective analysis. *Frontiers in Microbiology*, 9, 2885. doi:10.3389/fmicb.2018.02885.

SOIL AND SLUDGE SAMPLES CHEMICAL PROPERTIES AND VEGETATION MINERAL COMPOSITION MONITORIZATION ON THE IAȘI SEWAGE TREATMENT-PLANT PONDS PRECINCT (TOMEȘTI)

Mihaela LUNGU, Radu LĂCĂTUȘU, Andrei VRÎNCEANU,
Rodica LAZĂR, Ilie CALCIU

National Research and Development Institute for Soil Science,
Agrochemistry and Environment - ICPA Bucharest,
61 Marasti Blvd, District 1, Bucharest, Romania

Corresponding author email: mihaelalungu.icpa@gmail.com

Abstract

Sludge quality resulted from the Iași sewage treatment-plant and deposited in the Tomești ponds has been studied over several years, starting 2005, with the aim of land greening. The main general chemical properties of the sewage treatment sludge in process of soil formation showed that it offers normal conditions for vegetation development even though upper horizons salinization was detected that year due to drought occurrence. Zinc contents were very high in the upper horizons. The sampled plants accumulated normal macro elements quantities and only zinc out of the heavy metals in higher concentrations, especially in the roots, without prejudice to vegetation development. As compared to this situation the Tomești sewage treatment pond had reached an incipient soil formation stage in 2020 following several greening measures and the draining phenomenon which had a certain intensity and determined vegetal cover changes, from a mainly hygrophytic vegetation to a less humidity loving one.

Key words: sewage treatment sludge, soil quality, macro elements, salinization, heavy metals.

INTRODUCTION

For several years, from 2005 to 2020, research has been carried out on the sludge produced by the Iași wastewater treatment plant and deposited in the Tomești sludge pond.

Their purpose was to draw up level II environment balance and risk assessment (2005), ponds phyto-rehabilitation (2007), environment impact assessment and monitoring of the soil heavy metals contents in samples from ponds bordering soil, ponds mud, and vegetation grown on the pond's precinct (2012, 2013, and 2014).

Further research continued soil chemism monitorization, especially that of salinization and heavy metals contents, of the zinc one by choice, from the pond mud, soils around it, and vegetation grown on them.

This paper presents the evolution of pond bordering soil quality as influenced by the phyto-rehabilitation operations during the 2015-2020 period.

MATERIALS AND METHODS

In 2015 observations were made after completing the garbage heap arrangement and greening works which aimed at changes monitoring of the water condition, flora composition, surface aspect and morphometry of the deposited material within the pond consisting of urban sludge. A retrenchment of the water covered areas was ascertained. Also, the water volume in the precinct south and east edging drainage was reduced as compared to the observations made in the previous years. The only drainage branch still in an overflow state was that of the north side.

As ascertained in the previous years starting 2010 it was noticed that the material stratum deposited in the pond, consisting of urban waste, evolved in a slow and lengthy process towards outlining a soil material. At the same time the botanic composition of the Tomești urban waste pond's specific surface continues to progressively change towards a natural wild

flora similar to that which existed before changing the land use and creating the pond. The presence of some shrubs specimens was identified in 2014 consisting of elderberry arboreal (*Sambucus nigra*) around the dams' ramps, where the slightly higher ground offered a better drained soil material stratum. This eutrophic, mezophytic - mezo hygrophytic species developed very well and occupied a significant area in the pond's precinct centre (Lăcătușu et al., 2017b).

Thenceforth arboreal species number enhancement could be identified beside the elderberry one not only around dams' banks but also in the areas where the slightly higher pond surface levels offered a better drained soil material stratum.

The general direction of the material stratum consisting of urban waste was thenceforth that of levelling and equalization of the specific surface, even if small depressions will still exist randomly disseminated on the whole precinct surface which would be filled with water in times of excessive water inputs, which is frequently encountered in the river's major beds and as natural as it gets.

The mud pond greening process and the mud material development towards a soil one also influenced the bordering area. The quality of these soils was also monitored over time, in five soil profiles (SE1-SE5) located in Figure 1.

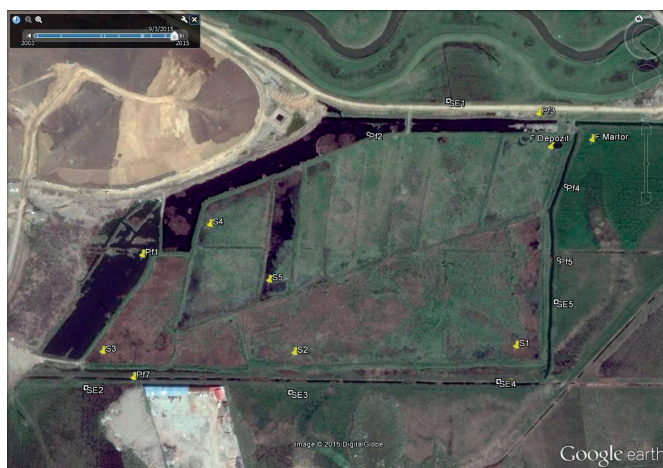


Figure1. The mud, vegetation, soil and water sampling points within the Tomești, Iași County, urban sludge deposit

Soil samples were taken by geometric horizons, by the 0-20; 20-40; and 40-60 cm depths. They were dried and grounded according to specific technical procedures and analytical determinations were carried out according to dedicated methodology and standards commonly used in the laboratories for pedological and agrochemical studies (Lăcătușu et al., 2017a), as follows:

- Water content was determined gravimetrically by drying the samples in a stove at 105°C.
- Soil reaction (pH) was determined through potentiometric analysis, in aqueous suspension, using a combined glass-calomel electrode.
- Organic carbon content was assessed by the Walkley-Black method modified by Gogoasă.
- The nitrate nitrogen (N-NO₃) mobile form was determined by potentiometric analysis with ion-

selective electrode. The nitrogen total content was determined by the Kjeldhal method.

- The mobile phosphorus (PAL) and potassium (KAL) contents were determined in an ammonium acetate lactate solution with 3.7 pH (after Egnér-Riehm-Domingo) by spectrophotometry and flame photometry respectively.
- The totals soluble salts contents were determined through conductometric analysis.
- Total heavy metals contents (cadmium - Cd, cobalt - Co, chromium - Cr, copper - Cu, iron - Fe, manganese - Mn, nickel - Ni, lead - Pb, and zinc - Zn) were determined by atomic absorption spectrometry in the solution obtained after digesting the samples with a concentrated perchloric, nitric, and sulphuric acids).

RESULTS AND DISCUSSIONS

Water content, reaction, and macroelements contents of the soil samples from around the purging mud ponds

The dry climate accompanied by high temperatures contributed to the water content spectacular decrease in soils. The very low soil water content, up to 44% in 2015 (Table 1) clearly shows the drought period through which the area was going at the time. Actually, the whole water content range of 18-44% with a 29

± 9% average is significant in this respect. In 2016 the soil had, down to 60 cm depth, an average 33% water content, a relatively constant value as the 6% standard deviation shows.

In July 2017 the soil also had a high aridity degree, the water content didn't go beyond 32% of the water holding capacity.

Worth noticing that the grouping centre parameters (\bar{x} , Me, Mo) varied in a narrow range (18-32%) and the higher values were specific for the 40-60 cm layer.

Table 1. Average values of water content, reaction, and macro elements contents in the soil samples from around the purging mud ponds

Year of study	Water content at 105°C %	pH	C _{org.}	N _t	C/N	N-NO ₃	P _{AL}	K _{AL}
			%			mg/kg		
2015	29	8.02	3.15	0.31	11.1	70	61	132
2016	33	7.94	3.20	0.26	11.1	5	58	633
2017	23	8.12	3.14	0.25	15.2	13	30	473
2018	54	8.11	3.18	0.21	17.5	85	81	550
2020		8.19	2.16	0.22	11.1	10	26	318

The arid sludge water content also reflected on the pond mud samples water content values so that in 2018 the bordering soil water content was similar to the pond mud one which demonstrates a balanced state existence between the two. It's enough to say that the average values were 58% and 56%, respectively.

The **reaction** (Table 1) varied very little along the research years and was constantly slightly alkaline due to the intrinsic chemical characteristics of the Calcaric Fluvisol strongly salinized in-depth. Alkalinity is also brought about by the carbonates and soluble salts presence. The pH varied in 2015 between 7.55 and 8.22 with an average 8.02 ± 0.15 .

By comparing the statistical parameters of the pond sludge and the surrounding soil, it can be concluded that there is no influence of the former on the chemical and physical condition of the latter. A slight pH increase was noticed in-depth with approximately 0.2 units.

The **organic carbon** and **total nitrogen** contents (Table 1) of the bordering soil are normal for that Calcaric Fluvisol. The analytical data signify a low – average organic carbon content and an average total nitrogen one. It contains 4timesless organic carbon and 4.4 times less total nitrogen than the pond's mud. So, neither

the soil organic carbon nor its total nitrogen content is influenced by the pond's mud.

In 2017 the soil had, in its upper horizon (0-20 cm), a high organic carbon content (4.81%) but much lower (2.5 times) than the mud. Worth noticing that in the soil underlying horizons the organic carbon content decreases by 45 and 61%, respectively.

The organic carbon statistical data in 2018 though presented high contents ranges with 3.18% average values. The values of the other two grouping centre parameters (Me, Mo) and of the dispersion indices were also close to one another showing thus a levelling of the land around the pond from this point of view.

A depletion of the organic carbon was noticed in 2020 down to an average content of 2.20% in the upper horizon which was 5.4 times lower than that of the soil from inside the precinct. It also decreased in-depth.

Total nitrogen contents in the pond's bordering soil were medium in 2015 with an average value of 0.31%. In 2016 the values ranged from 0.34% in the 0-20 cm layer to 0.17% below 60 cm depth with a $0.29 \pm 0.14\%$ average value in the upper horizon which shows a high total nitrogen content soil. And it continued to be high in 2017 with 0.19 and 0.46% values in the upper horizon

and a 0.33% average. Although the values decrease in the lower layers to 0.24 and 0.18% respectively, they belong to the same content class. These high contents are characteristic for the Calcaric Fluvisol which the pond lies on and there's no question about being influenced by the neighbouring mud.

Alike the total nitrogen contents ranged between 0.29 and 0.45% in the upper horizon with a 0.37% average value.

The values and statistical parameters of the **nitrogen mobile forms: $N-NO_3$ (nitrate) and $N-NH_4$ (ammonium)** (Table 1) stand proof that no ammonium nitrification reactions take place in the soil. The fact that ammonium nitrate can't be detected in soil samples by the analytical method in use shows that the main factor for triggering this phenomenon is missing. Furthermore, the nitrate nitrogen contents are also low, at the limit of soils unfertilized with nitrogen.

In 2016 the soil had a very low nitrates content, normal for a soil on which no fertilizers were spread, and it was 25.4 times lower than the purging mud nitrates content.

The soil C/N ratio (Table 1), 10.8 ± 2.0 in the upper horizon (0-20 cm) in 2015, shows a normal organic matter mineralization rate (Davidescu & Davidescu, 1999). In 2018 though the 16-18 average values and also 9-12 singular ones show a diversity of the soil organic matter mineralization degree.

Mobile forms of macro elements are sufficient for plants nutrition. Thus, nitrate nitrogen ranged in 2015 between 55 and 188 mg/kg with a 67 ± 34 mg/kg average value. Mobile phosphorus, soluble in the al solution (Table 1), ranged between 25 and 245 mg/kg with a 61 ± 53 mg/kg average value, showing a high supply level with this plant nutrition macro element and also a great variability of it. The mobile potassium values soluble in the same conventional reagent ranged between 70 and 314 mg/kg with a 132 ± 73 mg/kg average value showing a medium supply level with this chemical element. In 2016 mobile phosphorus and potassium supply was still very good although the soil contained 20 times less mobile phosphorus and 1.3 times less mobile potassium than the purging mud.

Analytical data in 2017 highlighted, on an average, a high mobile phosphorus supply in the

first layer (0-20 cm), average in the next one (20-40 cm) a lower in the third. Accordingly, a normal distribution for this type of soil. Mobile potassium supply is very high, with 363 mg/kg average values in the 40-60 cm layer and up to 606 mg/kg in the first one. Again, the very good supply of these two elements is not influenced by the neighbouring pond mud. The average values in 2018 were higher than agricultural soil normal contents namely: $N-NO_3$ 2 times, P_{AL} 1.1 times, and K_{AL} 1.8 times.

Salinization level of the soil samples from around the purging mud ponds

Data regarding conductometric residue analysis (Table 2) highlight a moderate salinization below 60 cm depth of the Calcaric Fluvisol and below that, at 80-100 cm depth, the salinization level is very strong, with a 1.574 mg/100 g soil value of the conductometric residue. High contents of soluble salts, in the hundreds and thousands of mg/100 g soil, were registered in the samples collected from around the pond which signify a strong salinization. This salinization could have two causes: the capillary water rising loaded with salts proceeded from the strongly salinized soil base or the saline influence of the neighbouring purging mud deposit.

Sulphates predominate in the soluble salts composition in other proportions than in the mud, namely: 32% sodium sulphate (Na_2SO_4), 24% Calcium sulphate ($CaSO_4$), and 19% magnesium sulphate ($MgSO_4$); chlorides: 12% sodium (NaCl) and 5% potassium (KCl). Bicarbonates also occur in significant quantities: calcium 14% and occasionally magnesium or sodium.

The accented salinization of the soil bordering the ponds didn't negatively influence the area's characteristic vegetation development.

The total soluble salts contents in 2016 were 115 mg/100 g soil in the 0-20 cm layer and 1.088 mg/100 g soil in the 120-140 cm layer of the control profile. That is because of the vicinity of the pool with levigated water from the waste deposit. Another cause for the high soluble salt's contents of the bordering soil, starting even with the 20-40 depth, could be the scraping of the soil surface horizon to build the pond surrounding the dam.

Table 2. Average values of the total soluble salts contents in the soil samples collected from around the purging mud ponds

Year of study	Conductometric residue mg/100 g sol
2015	801
2016	1.098
2017	810
2018	364
2020	550

The salts also consist of mostly sulphates, this time the sodium one (Na_2SO_4) is predominant. The sulphates range in a decreasing order as follows: 44% Na_2SO_4 , 21.4% MgSO_4 , 10.0% CaSO_4 . The difference is completed by 11.5% calcium bicarbonate ($\text{Ca}(\text{HCO}_3)_2$) and sodium (NaCl) and potassium chloride (KCl).

Data regarding the total soluble salt's contents in the pond bordering soils clearly highlight the strongly in-depth soil salinization reaching up to 2.275 mg/100 g soil values 40-60 cm deep as compared to 66 mg/100 g soil which was determined in the 0-20 cm layer which is consistent with a non-salinized soil material. The sulphate anion (SO_4^{2-}) is predominant and the Na^+ cation, followed by magnesium (Mg), calcium (Ca), and sometimes potassium (K) in much lower quantities. Consequently, the dominant salt is sodium sulphate (Na_2SO_4) with a $42 \pm 22\%$ average content. The magnesium sulphate (MgSO_4) has a $22 \pm 8\%$ average content, and the calcium one (CaSO_4) $21 \pm 10\%$. The other soluble salts: potassium sulphate (K_2SO_4), calcium bicarbonate ($\text{Ca}(\text{HCO}_3)_2$), sodium chloride (NaCl), and potassium chloride (KCl) have much lower contents.

So, if calcium sulphate (CaSO_4) was the predominant salt in the mud, sodium sulphate (Na_2SO_4) is to be found in the largest quantities in the bordering soil. But then their sources differ too, anthropic in the first case and natural in the latter.

Considering that high soluble salts concentrations are in the soil depth and in the upper layer the salinization degree is practically null, a specific grassland vegetation developed with plants whose root system didn't penetrate below 40-45 cm depth.

The same slight salinization of the upper layer is noticed in 2018 and a very strong one in the deep ones. But the pond bordering soil salinization is 36 times lower in the upper horizons and 7 times

lower in the deep horizons than that of the mud. The predominant anion is sulphate.

The predominant anion is the sulphate (SO_4^{2-}), decreasingly followed by bicarbonate (HCO_3^-), and chlorine (Cl^-). Among the cations sodium is predominant (Na^+), followed by magnesium (Mg^{2+}) and calcium (Ca^{2+}) with similar values, and finally potassium (K^+) with the lowest content. The predominance of sodium resulted in its salts predominance namely the sulphate (Na_2SO_4), the bicarbonate (NaHCO_3), and the chloride (NaCl). The sulphates and the bicarbonates come next in the soluble salts hierarchy in the purging mud pond bordering soil represented by CaSO_4 , MgSO_4 , $\text{Ca}(\text{HCO}_3)_2$ and $\text{Mg}(\text{HCO}_3)_2$. The smallest contribution to the total soluble salts content comes from the potassium chloride (KCl). The total soluble salts contents reach 2.114 mg/100 g soil in 2020 in the 80-100 cm layer of the control profile as compared to a minimum 60 mg/100 g soil determined in the 0-20 cm layer and which shows a non-salinized soil material. But salts percentage composition differs, qualitatively in the first place: magnesium ($\text{Mg}(\text{HCO}_3)_2$) and sodium bicarbonates (NaHCO_3) occur. The sulphate anion (SO_4^{2-}) and sodium cation (Na^+) predominate, followed by calcium (Ca) and magnesium (Mg), and potassium (K) in extremely low quantities.

The calcium bicarbonate ($\text{Ca}(\text{HCO}_3)_2$) is the predominant salt which has a $59.2 \pm 25.9\%$ concentration in the first layer; the sodium chloride is next ($29.8 \pm 17.8\%$), magnesium sulphate ($\text{Mg}(\text{SO}_4)_2$) with $16.9 \pm 3.6\%$ values, sodium sulphate (Na_2SO_4) with 18.6 ± 14.5 , and potassium chloride (KCl) with $7.7 \pm 7.3\%$. The great variability of the salt's percentage composition is to be noticed reflected in the very high standard variation values and in the fact that some of the salts are not to be found in all the collected samples (the magnesium and sodium bicarbonates, the calcium and magnesium sulphates).

Consequently, if calcium sulphate (CaSO_4) was predominant in the samples collected from inside the precinct the calcium bicarbonate ($\text{Ca}(\text{HCO}_3)_2$) is to be found in the largest quantity in the bordering soil. And again, their source differs, anthropic in the first case, natural in the latter.

Heavy metals contents of the soil samples from around the purging mud ponds

Analytical data regarding total heavy metals of the pond bordering soils (Table 3) highlight the fact that the mud heavy metals contents didn't

influence the same elements concentration in the bordering soil. Thus in 2015 the zinc content of the bordering soil is much lower than the alert threshold, although it outruns the soil normal value by 86 mg/kg. Its concentration can be seen as normal for this kind of soil.

Table 3. Average values of total heavy metals contents in the soil samples from around the purging mud ponds

Year	Zn	Cu	Fe	Mn	Pb	Cd	Cr	Co	Ni
	mg·kg ⁻¹								
2015	3.937	77.9	26.990	470	98.2	4.00	69.4	12.7	38.0
2016	142	51.1	33.591	560	19.1	0.80	52.6	5.6	43.9
2017	182	38.7	31.788	573	29.3	0.82	57.0	14.7	35.0
2018	196	38.6	28.615	490	18.9	0.48	45.1	9.5	49.8
2020	83.3	28.5	29.685	420	14.7	0.34	49.8	7.8	3.8

The other determined heavy metals (copper, nickel, lead) all have lower contents than the alert thresholds although they have higher values, sometimes double as compared to the normal soil contents. It's worth noticing that the cadmium and manganese average

concentrations are lower than the normal values encountered in soils.

Consequently, the Tomești Calcaric Fluvisol on which the purging mud ponds are placed has normal heavy metals contents not influenced by the pond's mud.

Out of the analysed heavy metals range only the zinc concentrated to a higher degree in the purging, namely 27 times more than in the pond surrounding soil and 91 times more than the general soil average content. As long as the pond surface was covered with *Phragmites* sp. it absorbed important zinc quantities from the mud, namely 2.000-3.000 mg/kg. But as the *Phragmites* plants were not harvested the zinc absorbed quantities returned to the mud in the process of soil formation along with the plants which were mineralized and contributed to the new zinc content increase. Actually, the phenomenon is ongoing although not at the same intensity as during the *Phragmites* plants mineralization. In spite of these high zinc content values the present vegetation growth is not negatively influenced.

The described phenomenon took place for other heavy metals too (copper and cadmium) but at much lower intensities. Thus, the copper content of the mud in the process of soil formation is 2.6

times higher than in the bordering soil and 6.4 times higher than the general soils average concentration. The mud lead concentration is 5.6 times higher than that of the pond surrounding soil and 11.7 times higher than the soils average content. Finally, the cadmium concentration in the mud is 9.5 times higher than the surrounding soil average content and 14 times higher than the general soils average concentration. It must be mentioned that heavy metals mobility in the neutral - slightly alkaline soil is much lower than in acid soils so these elements absorption in plants will be much reduced and will have no effect on plants growth and development on the purging mud in the process of soil formation.

Zinc content decrease was registered in the following years below the maximum allowable limit (MAL). Concentrations decrease with the profile depth. The low level of the other heavy metals (copper, iron, manganese, cadmium, chromium, cobalt, nickel) contents in the bordering soil is a consequence of these elements' presence in the purging mud at low levels too.

The heavy metals concentrations in the Tomești Calcaric Fluvisol on which the purging mud ponds are located were already around soil normal contents by 2018.

Although slightly increased average values were sometimes registered between 2010 and 2018, as in 2014-2016, a sure influence of the mud deposited in the pond can't be ascertained. Likewise it can be noticed that other heavy metals (copper, nickel) have average concentration values double as compared to the

general average values reported for common soils.

Other heavy metals (cobalt, chromium, lead) have the determined average values practically equal to those known from literature (Baker & Brooks, 1989; Filep, 1999; Kabata-Pendias & Pendias, 2001; Kim Tan, 1993), while others (cadmium and manganese) have average content values lower than these.

A slight increase of zinc and chromium contents was noticed in 2020 in the upper layer (0-20 cm) but without outrunning MAL. The concentrations generally decrease down the soil profile. It might be possible that this slight increase is due to the vicinity of the mud or to the diffusion phenomenon occurring once the drain water levels in the ditch around the pond increase, the more so that the contents values in the deeper horizons are higher than those at the surface.

The slightly increased zinc abundance in the pond bordering soil didn't impede the development of a vegetation consistent with the Calcaric Fluvisol strongly salinized in-depth in the area existing conditions.

CONCLUSIONS

The Calcaric Fluvisol on which the Tomești mud deposit lies has a slightly alkaline reaction, average organic carbon, total nitrogen, nitrate nitrogen contents, high mobile phosphorus content and average mobile potassium one. So, it offers good conditions for plant nutrition with macro elements.

It is slightly salinized in the upper horizons and very strongly salinized in the deep ones. The dominant salt is sodium sulphate (Na_2SO_4), while calcium sulphate (CaSO_4) dominates in the mud.

From these points of view the Calcaric Fluvisol strongly salinized in-depth is a fertile soil, not influenced by the Tomești pond purging mud presence.

The Calcaric Fluvisol strongly salinized in-depth contains heavy metals at concentrations levels around the known normal values for soils. The slightly increased zinc abundance in the pond bordering soil didn't impede the development of a vegetation consistent with the Calcaric Fluvisol strongly salinized in-depth and with the environment conditions existing in the area.

ACKNOWLEDGEMENTS

This work was supported by project no. 44 PFE/2021, Program 1 – Development of national research-development system, Subprogram 1.2 – Institutional performance – RDI Excellence Financing Projects.

REFERENCES

- Baker, A.J.M. & Brooks, R.R. (1989). Terrestrial higher plants which hyperaccumulate metallic elements – a review of their distribution, ecology and phytochemistry. *Biorecovery*, 1, 81-126.
- Davidescu, V. & Davidescu, D. (1999). *Agrochemical Compendium*. Ed. Acad. Romane, Bucuresti [in Romanian].
- Filep, G. (1999). *Soil chemistry. Processes and Constituents*, Akadémiai Kiadó, Budapest.
- Kabata-Pendias, A. & Pendias, H. (2001). *Trace Elements in Soils and Plant*. CRC Press, Boca Raton, London, New York, Whashington DC.
- Kim Tan, H. (1993). *Principle of Soil Chemistry, Second Edition*. Marcel Dekker Inc., New York, Basel, Hong Kong.
- Lăcătușu, R., Lungu, M., Rizea, N. (2017a). *Soil Global Chemistry. Processes, Determinations, interpretations*. Terra Nostra Publishing House, Iasi, ISBN 978-606-623-074-2 [in Romanian].
- Lăcătușu, R., Lăcătușu, A-R., Vrinceanu, A., Lungu, M., Rizea, N., Lazăr, D.R., Trofin, O., Catrina V. (2017b). Evolution of the Tomești (Iași County) Calcaric Fluvisol chemical soil characteristics lying beneath the Iași Municipality waste water purging mud deposit. *Lucr. Conf. Soc. Naț. A Moldovei de Știința Solului*, 54-64, Chișinău [in Romanian].

SOIL HEAVY METALS CONTENT VARIATION DEPENDING ON THE DISTANCE FROM POLLUTION SOURCE AND UPTAKE BY THE *TRIFOLIUM PRATENSE* L. SPECIES HARVESTED FROM COPȘA MICĂ AREA, CENTRAL ROMANIA

Bogdan Ștefan OPREA, Nicoleta Olimpia VRÎNCEANU, Vera CARABULEA, Dumitru-Marian MOTELICĂ, Mihaela COSTEA, Georgiana Iuliana PLOPEANU

National Research and Development Institute for Soil Science,
Agrochemistry and Environment, - ICPA Bucharest,
61 Marasti Blvd, District 1, Bucharest, Romania

Corresponding author email: carabulea_vera@yahoo.com

Abstract

Heavy metals pollution has always been a significant problem for human, animal, and plant health. Copșa Mică, Romania, stands out as one of the most polluted areas with heavy metals, mainly due to emissions from two factories (Carbosin and Sometra), which have been operating in the past for about 60 years. In 2023, soil and plant (*Trifolium pratense* L.) samples were collected from the polluted meadows in the researched area to analyze and determine cadmium, lead, zinc, and copper concentrations. Cd recorded the lowest concentration in both soil and plant samples with values of 5.17 mg·kg⁻¹ dry weight (d.w.) and 0.52 mg·kg⁻¹ d.w., respectively. The highest content in both soil and plant samples was recorded by Zn, with values of 334.5 mg·kg⁻¹ d.w. (soil) and 69.67 mg·kg⁻¹ d.w. (plant). Soil heavy metals content variation depending on the distance from the pollution source showed significant values only for Cd and Zn, while the values for Pb and Cu were insignificant. The results obtained from this study will be used to raise awareness of the population living in the affected areas on the risks that arise from using the meadows for grazing and harvesting hay.

Key words: accumulation, heavy metals, meadow, pollution, *Trifolium pratense* L.

INTRODUCTION

Worldwide, the *Fabaceae* family is one of the most economically important plant families, comprising more than 700 genera and about 20.000 species (Kaurinovic et al., 2012; Schrire et al., 2005). Red clover (*Trifolium pratense* L.) is one of the common species of this family, mostly used as a source of fodder in animal feed. In addition to its use as feed, Savirant et al. (2007) demonstrated that the aerial parts of this plant, especially the leaves, contain high amounts of isoflavones, which can enhance the use of the plant in the food and pharmaceutical industries. Pollution of soil, water, and air with heavy metals from industrial activities, agriculture, and transport affects the whole world, and finding effective and cheap solutions is a challenge for mankind (Borozan et al., 2021). Heavy metals are a serious threat to human life because, through the food chain, they can enter the body causing a range of health problems.

Ali et al. (2012), Bidar et al. (2007), and Liu et al. (2018) cited by Pescatore et al. (2022)

reported that forage plants, including red clover, can be successfully used in phytoremediation of polluted soils due to their increased adaptability, rapid growth, high biomass production and resistance to pollution.

Liu et al. (2018) demonstrated that clover plants have high resistance to lead (Pb) pollution.

In a study by Bidar et al. (2009) on the bioaccumulation of heavy metals and their transfer in *T. repens* and *L. perenne* plants grown on polluted soil showed that metals accumulated mainly in the roots as follows: Cd>Zn>Pb, and their transfer to the aerial parts was limited.

Memić et al. (2023) reported high concentrations of Cu and Pb in clover roots, while more Cd and Zn accumulated in leaves, they demonstrated that heavy metals content depended on area and season.

A study by Kujawska et al. (2018) on the effects and transfer of heavy metals in red clover grown on substrates produced from mixtures of different materials showed that the plants

accumulated high contents of Cu, Zn, and Ni, but did not present a risk in the use of the plants as feed.

Studies have shown that heavy metals soil pollution has an inhibitory effect on the development of clover plants (Stravinskienė & Račaitė, 2014). Cajak et al. (2023) reported high concentrations of heavy metals in *T. pratense* cultivated in different locations in western Poland, concluding that this species of plant can be utilized as a bioindicator of contamination with these types of metals in urban areas. Heavy metals like Zn and Cu accumulate mainly in roots and leaves and less in the shoots.

Different levels of soil heavy metals (Zn and Cu) contamination affect the leaf surface area of red clover (Sakal et al., 2019).

Heavy metals negatively affect plant development, producing biochemical and physiological changes in their vegetative organs (Asati et al., 2016).

Meng et al. (2022) demonstrated that *T. pratense* plants had a positive response to low concentrations of Pb (500 mg/kg), but double or higher concentrations of Pb are toxic and damage metabolic processes in the plant.

In a study by Malizia et al. (2012), using herbaceous and leguminous plants (*T. pratense*) to monitor heavy metal content in soil, reported higher concentrations in roots compared to leaves, but the difference between the two species was insignificant. However, soil heavy metals concentrations were directly proportional to the levels in plants.

Lambrechts et al. (2014) showed that *Trifolium repens* has a lower tolerance to heavy metal pollution compared to *Lolium perenne*. They demonstrated that exposure of white clover to Cd resulted in decreased biomass production and inhibition of root growth.

According to Sotiriou et al. (2023) in a study regarding growing white clover on heavy metals contaminated soil using zeolite, they demonstrated that the plants accumulated heavy metals in the dry biomass above normal consumption limits. They indicated that this species accumulated higher amounts of Cd and Zn compared to Pb.

This study aims to assess the accumulation of Cd, Pb, Cu, and Zn by *T. pratense* species harvested from polluted natural meadows in Copșa Mică area and soil heavy metals content

variation depending on the distance from the pollution source.

MATERIALS AND METHODS

Soil and plant samples (*T. pratense*) were collected in 2023, from 5 localities affected by pollution (Copșa Mică, Axente Sever, Micăsasa, Târnava, and Valea Viilor) in Sibiu County, to analyze the heavy metals content (Cd, Cu, Pb, and Zn). Soil samples were collected from the first soil layer (0-20 cm). A soil sample was composed of 13 sub-samples, dried at room temperature, grounded, and sieved to remove stones and plant waste. Atomic absorption spectrometry, after the extraction by the aqua regia - microwave digestion method was used to determine heavy metals content from soil samples. DTPA- extractable heavy metals were extracted from soil (10 g) with 20 ml of extracting solution (0.05 M DTPA, 0.01 M CaCl_2 and 0.1 M tetraethylammonium adjusted to pH 7.3), according to SR ISO 14870:2002. Red clover plant samples (aerial part) collected were oven dried then milled and treated with nitric acid in a microwave digestion system. Atomic absorption spectrometry (Flame GBC 932AA or Graphite furnace GBC SavanataAZ) method was used to determine the heavy metals content. The statistical processing of the data was done using Microsoft Excel 2010.

RESULTS AND DISCUSSIONS

Analyzing the values of statistical parameters that characterize the central tendency and the variability of the soil heavy metal total contents (Table 1) for the minimum and maximum values, they varied as follows: Cd ($0.38 \text{ mg} \cdot \text{kg}^{-1} \text{ d.w.}$ - $16.9 \text{ mg} \cdot \text{kg}^{-1} \text{ d.w.}$), Pb ($25 \text{ mg} \cdot \text{kg}^{-1} \text{ d.w.}$ - $599 \text{ mg} \cdot \text{kg}^{-1} \text{ d.w.}$), Zn ($89 \text{ mg} \cdot \text{kg}^{-1} \text{ d.w.}$ - $930 \text{ mg} \cdot \text{kg}^{-1} \text{ d.w.}$ and Cu ($15 \text{ mg} \cdot \text{kg}^{-1} \text{ d.w.}$ - $161 \text{ mg} \cdot \text{kg}^{-1} \text{ d.w.}$).

In terms of average soil metal concentration, the lowest value was obtained for Cd ($5.15 \text{ mg} \cdot \text{kg}^{-1} \text{ d.w.}$) while Zn had the highest value ($334.5 \text{ mg} \cdot \text{kg}^{-1} \text{ d.w.}$). Also, Pb recorded an average value of $177.4 \text{ mg} \cdot \text{kg}^{-1} \text{ d.w.}$ and $53.7 \text{ mg} \cdot \text{kg}^{-1} \text{ d.w.}$ for Cu. Biasoli et al. (2006) obtained similar results for heavy metals contents in urban samples. The coefficient of variation of the heavy metals contents in the soil samples

analyzed ranged from 68.3% for Zn to 84.7% for Cd. The values recorded for Pb and Cu contents were 80.4% and 75.8% respectively. The standard deviation ranged from 4.38 $\text{mg}\cdot\text{kg}^{-1}$ d.w. for Cd to 228.3 $\text{mg}\cdot\text{kg}^{-1}$ d.w. for Zn. Analyzing the median and geometric mean, Cd content recorded the lowest value for both statistical parameters, Pb had the highest value (132 $\text{mg}\cdot\text{kg}^{-1}$ d.w.) for the median, while Zn obtained the highest value for the geometric mean (277.9 $\text{mg}\cdot\text{kg}^{-1}$ d.w.). The heavy metals' total content in the soil was in the following order: $\text{Zn} > \text{Pb} > \text{Cu} > \text{Cd}$. Cd and Pb content in soil exceeded alert and intervention thresholds for sensitive land use. Zn content exceeded only the alert threshold, while Cu was within the limits (Ministerial Order 756/1997). The values of statistical parameters that characterize the central tendency and the variability of the Cd, Pb, Zn, and Cu contents in soil - DTPA-extractable forms were presented in Table 2. The Cd content recorded the lowest mean value (3.42 $\text{mg}\cdot\text{kg}^{-1}$ d.w.) while the highest mean content (80.1 $\text{mg}\cdot\text{kg}^{-1}$ d.w.) was obtained by Zn.

Analyzing the heavy metals contents (extractable forms) of the soil following the minimum and maximum values were as follows: Cd (0.23-9.53 $\text{mg}\cdot\text{kg}^{-1}$ d.w.), Pb (4-260 $\text{mg}\cdot\text{kg}^{-1}$ d.w.), Zn (7-323 $\text{mg}\cdot\text{kg}^{-1}$ d.w.), and Cu (2.46-23.41 $\text{mg}\cdot\text{kg}^{-1}$ d.w.). Median values ranged from 2.28 $\text{mg}\cdot\text{kg}^{-1}$ d.w. for Cd to 52 $\text{mg}\cdot\text{kg}^{-1}$ d.w. for Zn. Following the geometric mean values for the content of heavy metals in the soil, it is observed that the lowest value was obtained for Cd (2.41 $\text{mg}\cdot\text{kg}^{-1}$ d.w.) while Zn had the highest value (49.5 $\text{mg}\cdot\text{kg}^{-1}$ d.w.), the content of Pb and Cu recorded values of 42.6 $\text{mg}\cdot\text{kg}^{-1}$ d.w., respectively 69.1 $\text{mg}\cdot\text{kg}^{-1}$ d.w. Cd recorded the lowest value for the standard deviation (2.93 $\text{mg}\cdot\text{kg}^{-1}$ d.w.) followed by Cu with a value of 5.65 $\text{mg}\cdot\text{kg}^{-1}$ d.w. and Pb (72.9 $\text{mg}\cdot\text{kg}^{-1}$ d.w.). Analysing the values of the coefficient of variation they ranged from 71.8% for Cu to 112.9% for Zn content. The Cd and Pb contents had values of 87.5 $\text{mg}\cdot\text{kg}^{-1}$ d.w. and 105.5 $\text{mg}\cdot\text{kg}^{-1}$ d.w., respectively. The heavy metals content in the soil (DTPA-extractable forms) was in the following order: $\text{Zn} > \text{Pb} > \text{Cu} > \text{Cd}$.

Table 1. Values of statistical parameters that characterize the central tendency and the variability of the total cadmium, lead, zinc and copper contents in soil (n = 15)

Variable	Minimum	Maximum	Median	Geometric mean	Arithmetic mean	Standard deviation	Coefficient of variation
----- $\text{mg}\cdot\text{kg}^{-1}$ d.w. -----							
Cd _{soil}	0.38	16.92	3.91	3.67	5.17	4.38	84.7%
Pb _{soil}	25	599	132	135.5	177.4	142.7	80.4%
Zn _{soil}	89	930	270	277.9	334.5	228.3	68.3%
Cu _{soil}	15	161	38	42.8	53.7	40.7	75.8%

Table 2. Values of statistical parameters that characterize the central tendency and the variability of the cadmium, lead, zinc, copper contents in soil - DTPA-extractable forms (n = 15)

Variable	Minimum	Maximum	Median	Geometric mean	Arithmetic mean	Standard deviation	Coefficient of variation
----- $\text{mg}\cdot\text{kg}^{-1}$ d.w. -----							
Cd _{DTPA}	0.23	9.53	2.28	2.41	3.42	2.93	85.7%
Pb _{DTPA}	4	260	35	42.6	69.1	72.9	105.5%
Zn _{DTPA}	7	323	52	49.5	80.1	90.4	112.9%
Cu _{DTPA}	2.46	23.41	5.73	6.45	7.87	5.65	71.8%

Table 3. Values of statistical parameters that characterize the central tendency and the variability of the cadmium, lead, zinc, and copper contents in the red clover (*Trifolium pratense*) (n = 15)

Variable	Minimum	Maximum	Median	Geometric mean	Arithmetic mean	Standard deviation	Coefficient of variation
----- mg·kg ⁻¹ d.w. -----							
Cd _{red clover}	0.08	1.68	0.38	0.313	0.52	0.509	98.8%
Pb _{red clover}	0.13	1.68	0.56	0.498	0.67	0.486	73.1%
Zn _{red clover}	33	169	48	58.24	69.67	48.89	70.2%
Cu _{redclover}	6	13.5	8.2	8.28	8.5	2.14	25.2%

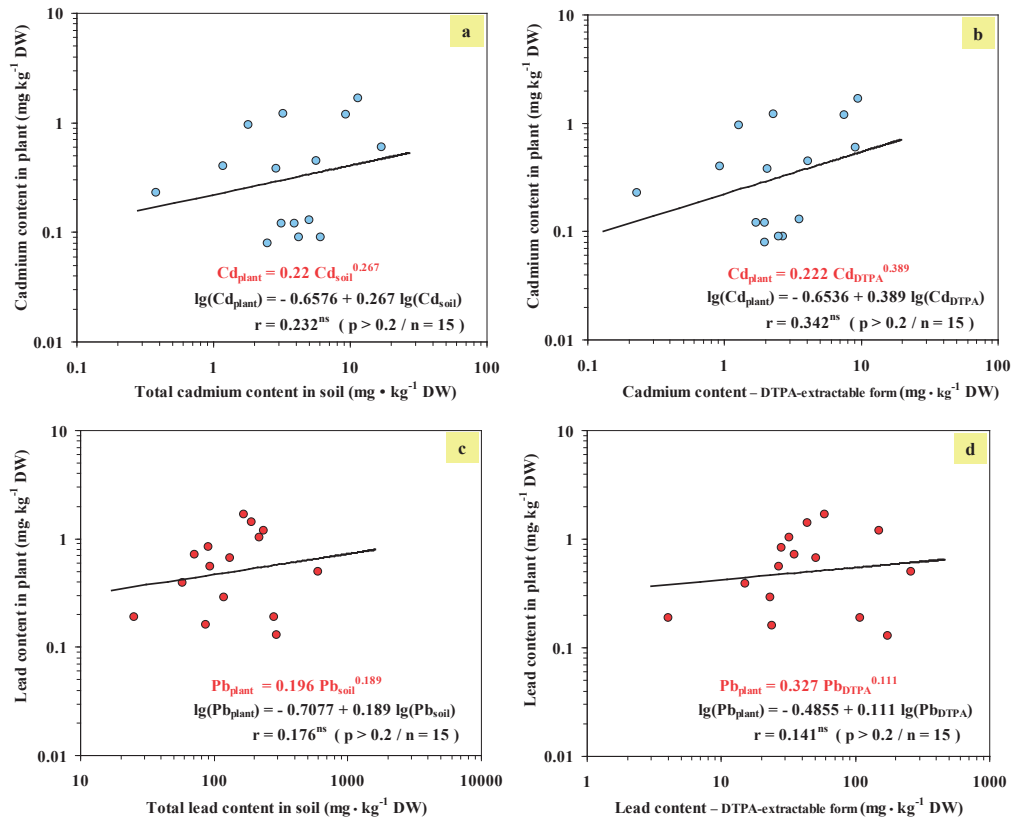


Figure 1. Log-log diagrams for power regression curves that estimate the stochastic dependency between total cadmium content in soil (a), soil cadmium content - DTPA-extractable forms (b), total lead content in soil (c), soil lead content - DTPA-extractable forms (d) and cadmium/lead contents in *Trifolium pratense* plants

Regarding the values of statistical parameters that characterize the central tendency and the variability of the Cd, Pb, Zn, and Cu contents in the red clover (*T. pratense*) (Table 3), it shows that the total Cd content recorded the lowest mean value (0.52 mg·kg⁻¹ d.w.), while the Zn content (69.67 mg·kg⁻¹ d.w.) was the highest. The mean values of Pb and Cu

contents were 0.67 mg·kg⁻¹ d.w. and 8.5 mg·kg⁻¹ d.w., respectively.

Analyzing the geometric mean values of the heavy metal contents, Cd content obtained the lowest value (0.313 mg·kg⁻¹ d.w.) while the highest value was obtained for Zn (58.24 mg·kg⁻¹ d.w.). The median values for heavy metals content in red

clover plants were: 0.38 mg·kg⁻¹ d.w. Cd, 0.56 mg·kg⁻¹ d.w. Pb, 8.28 mg·kg⁻¹ d.w. Cu and 48 mg·kg⁻¹ d.w. Zn, respectively. The standard deviation for heavy metal contents in the plant samples analyzed ranged from 0.486 mg·kg⁻¹ d.w. for Pb to 48.09 mg·kg⁻¹ d.w. Zn. Liu et al. (2018) demonstrated that the content of heavy metals in plants depends on their concentration in the soil.

Pricop et al. (2010) showed that red clover can be successfully used to remediate Pb polluted soils.

The heavy metals contents in the red clover were in the following order: Zn>Cu>Pb>Cd.

The logarithmic diagrams for power regression curves that estimate the stochastic dependency between total contents and DTPA- extractable

forms of Cd and Pb in soil, and the contents of those heavy metals in *T. pratense* plants (Figure 1) show that the values obtained were insignificant for both metals. However, in the case of Cd content (Figure 1a, 1b) the correlation coefficient value was higher for the extractable forms ($r = 0.342$) compared to the total content ($r = 0.232$). Figure 1c, 1d shows that the correlation coefficient value for Pb content was higher for total forms ($r = 0.176$).

Figure 2 shows the logarithmic plots for power regression curves that estimate the stochastic dependency between the total contents and DTPA- extractable forms of Zn, and Cu in soil and the amounts of those metals in *T. pratense* plants.

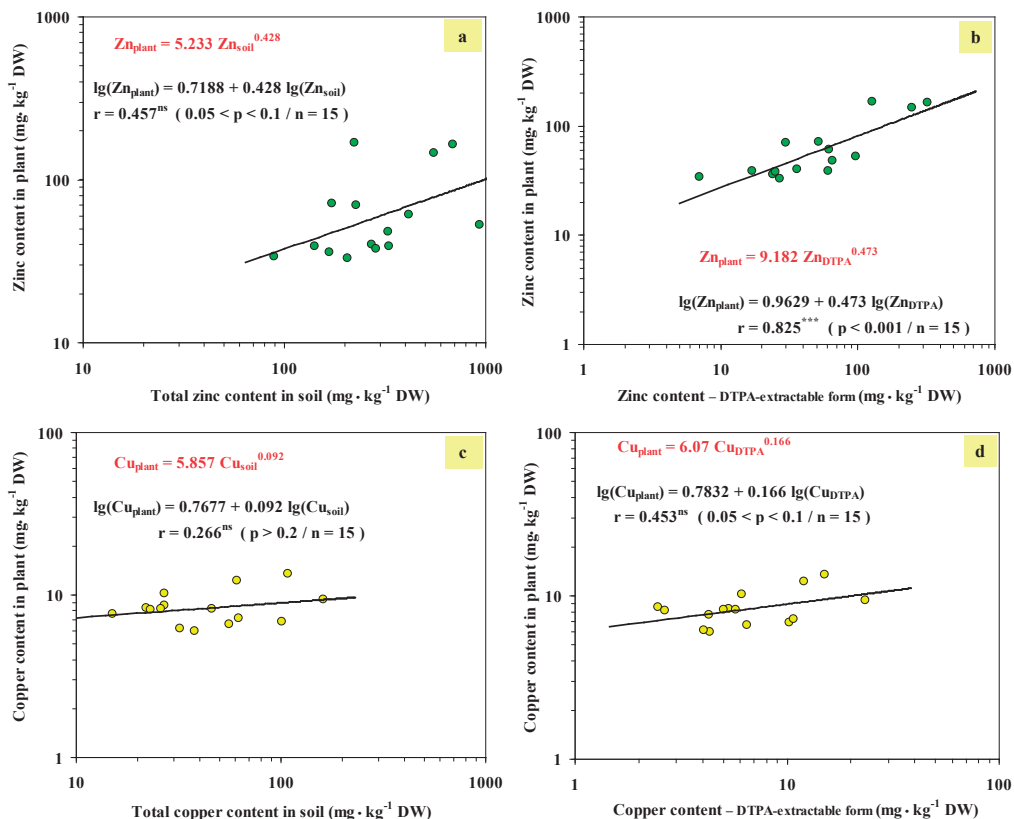


Figure 2. Log-log diagrams for power regression curves that estimate the stochastic dependency between total zinc content in soil (a), soil zinc content - DTPA-extractable forms (b), total copper content in soil (c), soil copper content - DTPA-extractable forms (d) and zinc/copper contents in *Trifolium pratense* plants.

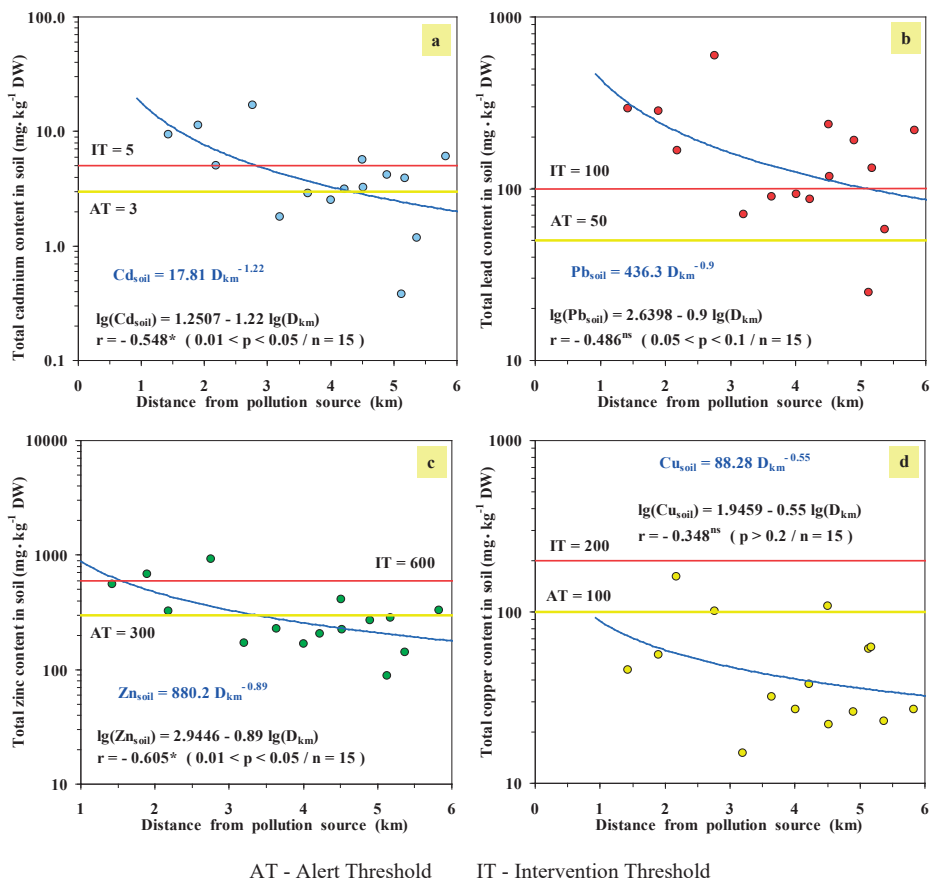


Figure 3. Total cadmium (a), lead (b), zinc (c) and copper (d) contents in soil depending on the distance from the pollution source - S.C. SOMETRA S.A. (Copșa Mică, 0-20 cm layer)

Analyzing Figure 2a, 2b shows that the correlation coefficient recorded a very significant value in the case of the DTPA-extractable form of Zn in soil ($r = 0.825$) compared to the total content which had an insignificant value. In the case of Cu content (Figure 2c, 2d), the value of the linear correlation coefficient does not differ significantly from zero for both forms of metal and therefore there is no dependence between the two variables considered. However, the correlation coefficient value for the DTPA-extractable form was higher (0.453) compared to total content (0.266). Figure 3 shows that the Cd and Zn variation contents in soil depending on the distance from the pollution source recorded

significant values ($r = -0.548$, respectively $r = -0.605$) compared to Pb and Cu variation contents whose values ($r = -0.486$, respectively $r = -0.348$) were insignificant. Wang et al. (2018) demonstrated that the length of the roads around the sample site has a great impact on the concentrations of heavy metals. They showed that the 1-2 km range influences the concentrations of heavy metals in the soil in the study area. Cd and Pb are harmful heavy metals that should be constantly monitored due to their high concentrations in soil with a negative impact on human, animal, and plant health (Chen et al., 2015). Marrugo-Negrete et al. (2017) demonstrated that heavy metals follow an ascending order

depending on the land use (rice>pasture>cotton). They showed that there are significant differences for Cu, Cd and Zn contents in soils cultivated with paddy compared to those cultivated with pasture or cotton.

CONCLUSIONS

Heavy metals contents in soil, plant (aerial part), and soil pollution content variation depending on the distance from the pollution source were analyzed in this study. The Zn content obtained the highest value both in soil (total soil content = $228.3 \text{ mg} \cdot \text{kg}^{-1} \text{ d.w.}$; DTPA-extractable form = $90.4 \text{ mg} \cdot \text{kg}^{-1} \text{ d.w.}$), and in plant ($48.99 \text{ mg} \cdot \text{kg}^{-1} \text{ d.w.}$). The lowest content in the soil was obtained by Cd, and the lowest content in the plant was obtained by Pb. However, according to Ministerial Order 756/1997, the Zn, Cd, and Pb content exceeded the alert and intervention thresholds for sensitive land use, only Cu had concentrations within the permitted limits. The heavy metal contents in the soil were as follows: $\text{Zn} > \text{Pb} > \text{Cu} > \text{Cd}$. The heavy metal contents in the plant were in the following order: $\text{Zn} > \text{Cu} > \text{Cd} > \text{Pb}$. Soil pollution content variation depending on the distance from the pollution source recorded significant values only for Cd and Zn. However, in addition to the distance from the pollution source, there are other factors such as precipitation, wind direction, and slope inclination that can influence the degree of metal pollution in certain areas. The value of the linear correlation coefficient obtained for the dependence between the DTPA-extractable form of Zn in the soil and that in the plant differs statistically significantly from zero indicating a strong correlation between the two variables. The results from this study and future data will be used to increase people's awareness of the risks they are exposed to by using meadows for grazing animals or harvesting hay.

ACKNOWLEDGEMENTS

This work was financed by project number PN 23.29.04.01 entitled: "Assessment of

heavy metals bioaccumulation in meadows vegetation using the regression analysis to develop a guide of good practices for grazing and animal feedstock in areas affected by industrial pollution" and project number 44 PFE /2021, Program 1 – Development of national research development system, Subprogramme 1.2 – Institutional performance – RDI Excellence Financing Projects.

REFERENCES

- Ali, H., Naseer, M., & Sajad, M.A. (2012). Phytoremediation of heavy metals by *Trifolium alexandrinum*. *International Journal of Environmental Sciences*, 2(3), 1459-1469.
- Asati, A., Pichhode, M., & Nikhil, K. (2016). Effect of heavy metals on plants: an overview. *International Journal of Application or Innovation in Engineering & Management*, 5(3), 56-66.
- Biasioli, M., Barberis, R., & Ajmone-Marsan, F. (2006). The influence of a large city on some soil properties and metals content. *Science of the Total Environment*, 356(1-3), 154-164.
- Bidar, G., Garçon, G., Pruvot, C., Dewaele, D., Cazier, F., Douay, F., & Shirali, P. (2007). Behavior of *Trifolium repens* and *Lolium perenne* growing in a heavy metal contaminated field: plant metal concentration and phytotoxicity. *Environmental Pollution*, 147(3), 546-553.
- Bidar, G., Pruvot, C., Garçon, G., Verdin, A., Shirali, P., & Douay, F. (2009). Seasonal and annual variations of metal uptake, bioaccumulation, and toxicity in *Trifolium repens* and *Lolium perenne* growing in a heavy metal-contaminated field. *Environmental Science and Pollution Research*, 16, 42-53.
- Borozan, A.B., Bordean, D-M., Poiana, M-A., Alexa, E., Caba, I.L., Pîrvulescu, L., Raba, D.N., Obistoiu, D., Morar, A., Misca, C.D., & PETCU, C.D. (2021). Soil pollution with heavy metals and bioremediation methods. *AgroLife Scientific Journal*, 10(1).
- Cakaj, A., Hanč, A., Lisiak-Zielińska, M., Borowiak, K., & Drapikowska, M. (2023). *Trifolium pratense* and the Heavy Metal Content in Various Urban Areas. *Sustainability*, 15(9), 7325.
- Chen, H., Teng, Y., Lu, S., Wang, Y., & Wang, J. (2015). Contamination features and health risk of soil heavy metals in China. *Science of the total environment*, 512, 143-153.
- Denchylia-Sakal, H.M., Gandzyura, V.P., & Kolesnyk, A.V. (2019). Accumulation of zinc and copper compounds and their effect on assimilation system in *Trifolium pratense* L. *Ukrainian Journal of Ecology*, 9(3), 247-254.

- Kaurinovic, B., Popovic, M., Vlaisavljevic, S., Schwartzova, H., & Vojinovic-Miloradov, M. (2012). Antioxidant profile of *Trifolium pratense* L. *Molecules*, 17(9), 11156-11172.
- Kujawska, J., & Pawłowska, M. (2018). Effects of soil-like materials mix from drill cuttings, sewage sludge and sawdust on the growth of *Trifolium pratense* L. and transfer of heavy metals. *Journal of Ecological Engineering*, 19(6).
- Lambrechts, T., Lequeue, G., Lobet, G., Godin, B., Bielders, C.L., & Lutts, S. (2014). Comparative analysis of Cd and Zn impacts on root distribution and morphology of *Lolium perenne* and *Trifolium repens*: implications for phytostabilization. *Plant and soil*, 376, 229-244.
- Liu, C., Lin, H., Dong, Y., Li, B., & Liu, Y. (2018). Investigation on microbial community in remediation of lead-contaminated soil by *Trifolium repens* L. *Ecotoxicology and Environmental Safety*, 165, 52-60.
- Malizia, D., Giuliano, A., Ortaggi, G., & Masotti, A. (2012). Common plants as alternative analytical tools to monitor heavy metals in soil. *Chemistry Central Journal*, 6, 1-10.
- Marrugo-Negrete, J., Pinedo-Hernández, J., & Díez, S. (2017). Assessment of heavy metal pollution, spatial distribution and origin in agricultural soils along the Sinú River Basin, Colombia. *Environmental research*, 154, 380-388.
- Memić, S., Bektić, S., & Huseinović, S. (2023). Effect of Soil Composition on Heavy Metal Uptake and Distribution in White Clover (*Trifolium repens* L.). *Journal of Applied Life Sciences International*, 26(5), 87-95.
- Meng, L., Yang, Y., Ma, Z., Jiang, J., Zhang, X., Chen, Z., Cui, G., & Yin, X. (2022). Integrated physiological, transcriptomic and metabolomic analysis of the response of *Trifolium pratense* L. to Pb toxicity. *Journal of Hazardous Materials*, 436, 129128.
- Ministry Order No. 756 from November 3, 1997 for approval of Regulation concerning environmental pollution assessment published in Official Monitor No. 303/6 November 1997.
- Pescatore, A., Grassi, C., Rizzo, A.M., Orlandini, S., & Napoli, M. (2022). Effects of biochar on berseem clover (*Trifolium alexandrinum* L.) growth and heavy metal (Cd, Cr, Cu, Ni, Pb, and Zn) accumulation. *Chemosphere*, 287, 131986.
- Pricop, A., Lixandru, B., Dragomir, N., Bogatu, C., Mășu, S., & Morariu, F. (2010). Phytoextraction of heavy metals from soil polluted with waste mining by using forage plants in successive cultures. *Animal Science and Biotechnologies*, 43(2), 129-32.
- Saviranta, N.M., Anttonen, M.J., von Wright, A., & Karjalainen, R.O. (2008). Red clover (*Trifolium pratense* L.) isoflavones: determination of concentrations by plant stage, flower colour, plant part and cultivar. *Journal of the Science of Food and Agriculture*, 88(1), 125-132.
- Schrire, B., Lewis, G. and Lavin, M. (2005) *Biogeography of the Leguminosae*. In: Lewis, G.P., Schrire, B.D., MacKinder, B. and Lock, M., Eds., *Legumes of the World*, Kew Publishing, 21-54.
- Sotiriou, V., Michas, G., Xiong, L., Drosos, M., Vlachostergios, D., Papadaki, M., Mihalakakou, G., Kargiotidou, A., Tziouvalekas, M., Salachas, G., & Giannakopoulos, E. (2023). Effects of heavy metal ions on white clover (*Trifolium repens* L.) growth in Cd, Pb and Zn contaminated soils using zeolite. *Soil Science and Environment*, 2(1).
- Stravinskienė, V., & Račaitė, M. (2014). Impact of cadmium and zinc on the growth of white clover (*Trifolium repens* L.) shoots and roots. *Pol J Environ Stud*, 23(4), 1355-1359.
- Wang, N., Guan, Q., Sun, Y., Wang, B., Ma, Y., Shao, W., & Li, H. (2021). Predicting the spatial pollution of soil heavy metals by using the distance determination coefficient method. *Science of the Total Environment*, 799, 149452.

WASTE CLASSIFICATION USING VISION TRANSFORMERS

Dan Constantin PUCHIANU

Valahia University of Targoviste, 13 Sinaia Alley Street, Targoviste, Romania

Corresponding author email: author_email@gmail.com

Abstract

Effective identification of recyclable waste is a major challenge in resource management and environmental protection. The present study explores the integration of transformer-based architectures for the accurate classification of recyclable waste, including plastic, glass, metal, and paper. A dataset consisting of digital images of different types of waste was used to train and evaluate the proposed architectures. To improve the generalization of the model a division of the data set was pursued for training, validation, and testing areas, as well as the implementation of data augmentation and transfer-learning techniques. Compared to traditional methods and different convolutional neural network architectures, transformer-based architectures have demonstrated superior performance both in terms of accuracy and computational efficiency. Analyzing the experimental results, the proposed models demonstrated accuracy values of over 95%. The study finally notes that the use of transformer-based architectures for the classification of waste from digital images presents a major potential in the development of efficient waste management practices and for reducing the impact of waste on the environment.

Key words: deep learning, image classification, sustainability, vision transformers, waste management.

INTRODUCTION

Pollution is one of the most pressing problems of modern society. Inefficient administration of waste management and pollution reduction solutions have a negative impact on the environment (Alrayes et al., 2023). The growth of the global population influences both the demand for and production of goods and services (Virsta et al., 2020; Agafitei & Pavel, 2023). Consequently, there is a greater risk of waste accumulation. Most of the time, the precise identification of waste resulting from the consumption and activities of modern society is based on manual work, being inefficient and time-consuming (Chen et al., 2023; Dong et al., 2022).

The field of Deep Learning and Computer Vision has experienced considerable advancement during the previous five-to-six-year period (Boldeanu et al., 2023). The advance of deep learning technologies and convolutional neural networks has brought to the fore innovative solutions in the field of detection and identification of objects illustrated in digital images and videos (An & Zhang, 2022). The processing and analysis of this data is a strong point of these architectures and at the same time an important research

topic that is also applied in the field of waste management (Dookhee, 2022; Hu et al., 2022).

In this context and part of the present study, the automatic detection and classification of waste becomes a crucial step for its efficient management. The advanced technologies of convolutional neural networks (CNN) and vision transformers (VIT) offer modern solutions to this challenge (Huang et al., 2021; Kumar et al., 2023).

Because of their ability to analyse and understand digital images, convolutional neural networks have revolutionized the field of computer vision (Mao et al., 2021; Qin et al., 2024). These architectures consist of a multitude of convolutional layers and can extract relevant features from the input data. In the context of waste management, CNNs are used to identify and classify images containing waste of various categories (Kurz et al., 2022). These models can be trained on large data sets and their performance can be improved as the models are exposed to more examples (Ma et al., 2024).

Using Vision Transformer models, research is observed that capitalizes on the performance, features and popularity of these models. In the study carried out, the authors (Alrayes et al., 2023) discuss the rapid progress of deep

learning, facilitating the implementation of modern solutions for waste classification. To solve problems and limitations related to low accuracy and slow processing, the authors proposed a model based on the VIT architecture that was integrated with a hybrid multilayer network: VT-MLH-CNN. The developed model demonstrated remarkable performance with accuracy values up to 95.5%, outperforming state-of-the-art models and being effective for waste classification. Other key approaches presented the implementation of the model on a cloud service, highlighting the potential of the method to be integrated into real-time applications.

In the same context, another model, called WMC-Vit, was the basis of the authors' research (Kurz et al., 2022). The study proposes an efficient waste classification model using a combination of VIT structures and convolutional neural network models. The training and testing of the model was done based on a public dataset called TrashNet, the same being true for the case of the previous study. In this case, the model analyzes the images and achieves a maximum accuracy of 94.27%, integrating a Multi-Head block with parallel processing for transformer blocks. The authors note in the study the problem of constant growth of waste that can be effectively managed using carefully implemented deep learning models.

In another study, the authors (Huang et al., 2021), present an innovative method for waste identification, using the TrashNet dataset, transfer-learning techniques, and vision transformer-based architectures. The authors note the problem of manual sorting of waste, being expensive, time-consuming, and inefficient. To solve these limitations the authors proposed a VIT model, based on self-attention mechanisms to improve the accuracy of waste classification, finally obtaining an accuracy score of 96.98%. It was observed that the proposed model outperformed classical CNN and machine learning models. Moreover, to extend the applicability of the model, it was implemented on a cloud server that allows the automatic classification of waste using mobile devices.

The authors' study (Dong, Chen & Lu, 2022) explores the use of deep learning techniques

and VIT models for the accurate identification of construction waste. The study proposes a model called BAT - Boundary-Aware Transformer for the precise identification of hard-to-classify waste. The key innovations of this model include a transformer structure with cascaded decoder and a careful edge processing model based on machine learning. The research also contributes to the implementation of a deep learning model for the semantic segmentation of construction waste with implementations aimed at waste sorting using systems with robotic arms and circular economy.

The present study proposes the implementation and optimization of architectures based on vision transformers for the automatic classification of various types of waste. The following sections detail the materials and methods used to implement the study, the experimental results obtained for waste classification, and finally the discussions and conclusions that note the relevance of the research.

MATERIALS AND METHODS

This part of the paper presents the materials used to implement the study, covering the dataset, the architectures used for the classification task, and the hardware and software details.

Creating a dataset is an important step for training and evaluating classification models as part of deep learning, especially for waste identification. For the present work, a dataset of RGB digital images was attached to the proposed classification models. Considering these details, it was aimed to divide the dataset into representative subsets for training, validation, and testing after a ration of 70%, 20% and 10% respectively. The dataset division process summed 1960 images for the training part, 560 images for the validation part, and 280 images for the test part. In total 2800 images were used.

The images in the dataset illustrate various types of waste, under varying conditions and from real contexts. Representative images taken from the dataset are illustrated in Figure 1.

No artificially generated images were used for the dataset of the present work, only pre-processing and augmentation processes were involved. Color transformations and geometric transformations have been implemented, as well as image resizing for an entry point standard specific to classification models (224x224px).

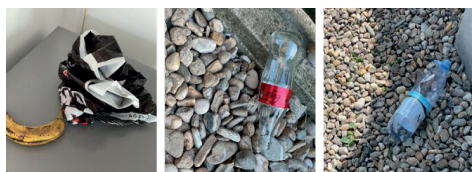


Figure 1. Example images from the dataset

Several vision transformer-based models were implemented and optimized for waste classification, following the dataset presented. The first model used for the present study, ViT Base (Dosovitskiy et al., 2020), represents a modern architecture for image classification tasks. ViT uses a transformer-type architecture adapted from natural language processing that divides digital images into patches of fixed size for their analysis as sequences. At the same time, the architecture offers self-attention mechanisms to capture the global characteristics of the entire image. The next model, DeiT (Touvron et al., 2021), is an optimized version of the Vision Transformer. The core feature of this optimized architecture involves a teacher-student training strategy developed to improve classification performance and efficiency with less data. At the same time, the architecture presents structures of distillation tokens for improving accuracy and generalization, having applicability in real-time scenarios. Another model used, the MaxViT Nano (Tu, Z. et al., 2022), completes the features of the vision transformer architectures, present as a compact version of the MaxViT family. The main characteristic of this model is the combination of CNN and ViT strategies, using multi-axis self-attention mechanisms. This hybrid approach to the architecture translates into lightweight features that can be successfully applied in resource-constrained environments. Finally, the present study also used the Swin Transformer v2 (SwinV2) (Liu et al., 2022), an

advanced architecture developed from the original Swin Transformer model. The present model represents a state-of-the-art architecture developed to improve image classification performance. The architecture stands out for the introduction of hierarchical shifted window structures that allow the model to capture spatial relationships at different scales and an improvement in the analysis of digital images. Other structures such as window-based attention mechanisms reduce the complexity of the architecture, increase the stability of training and the ability to generalize in various visual domains.

The last model used for this work, XCiT Small, represents another state-of-the-art architecture designed for image classification tasks based on Vision Transformer structures (Ali et al., 2021). The full name of the Cross-Covariance Image Transformer model brings key innovations compared to the ViT model and introduces new cross-covariance attention modules instead of the classic self-attention ones. In the same vein, the model introduces instead of spatial tokens modules that use channel-level attention, a key point to compute feature relationships, to reduce model complexity and optimize speed and accuracy. Key points of the architecture include feed-forward networks and multi-head attention to satisfy these features. For the present study, the small version of the model was used, being suitable for environments with low computing resources.

The hardware and software part of the system used in this study consisted of a customized setup with a Windows 10 Pro operating system, an AMD Ryzen 9 5900HS CPU, and a GeForce RTX 3060 6GB GPU. The selected programming language was Python v3.9, with PyTorch chosen as the framework.

RESULTS AND DISCUSSIONS

Analyzing the architectures used as well as the structure of the digital image dataset, the obtained results demonstrate the effectiveness of the proposed methodologies. For most of the models, accuracy values above 94-98% are noted, the metrics resulting from the evaluation of the models being presented in Table 1, using test images.

Each model demonstrated state-of-the-art classification performances for the waste dataset. The performance evolution for training and validation, loss and accuracy plots are presented in Figures 2-5, for each model.

Table 1. Waste classification performances for the proposed vision transformers models

Model	Accuracy
VIT Base	96.73%
MaxVit Nano	98.70%
SwinV2	97.39%
DeiT Base	93.46%
XCiT Small	94.10%

The presented results bring to the fore the stability of modern, optimized, and lightweight models such as SwinV2, XCiT or MaxViT. The proposed architectures demonstrate notable performance for the task of the present study, focused on waste classification, being a good choice for the implementation of automatic identification applications.

For the present study, vision transformer-based models demonstrated very good accuracy values. Following the experimental results, all models show a good and fast convergence both in the case of the precision and accuracy functions. MaxViT Nano and XCiT Small demonstrate the best and balanced performance, indicating a good generalization ability. The next top-performing model, SwinV2, shows slight fluctuations in validation accuracy, close to the results of the VIT Base model. DeiT performs below the previously presented models, an architecture that can highlight slight overfit/underfit issues, with a noticeable gap between validation and training

performance. These features may indicate signs of considerable improvement, optimized for this task.

It can be noted that transformer models such as MaxViT and SwinV2 are effective for the task of waste classification due to advanced architectures that combine innovative elements such as CNNs and Transformers to capture detailed features from digital images. Although performing well, the VIT Base and DeiT models can have difficulty generalizing, indicating a sensitivity to the analyzed data set.

The XCiT Small model shows remarkable performance during training and validation. It is observed that the accuracy during training and validation increases rapidly in the first 10-15 epochs, reaching values of about 0.94 and remaining constant with small fluctuations. At the same time, the stability observed on validation indicates that the model generalizes well and does not suffer from overfitting.

Another observation highlights the fact that a complex architecture is not always more performing and efficient, the analysis capacity and optimization being key points of these architectures, including for basic models and in relation to the proposed dataset. Following the evolution of the VIT Base model, a slight instability in the generalization capacity can be observed, but it notes a good learning capacity according to the evaluation results. The MaxViT model achieves the best results and with a trend that suggests very efficient learning, observing accuracy and loss during training and validation.

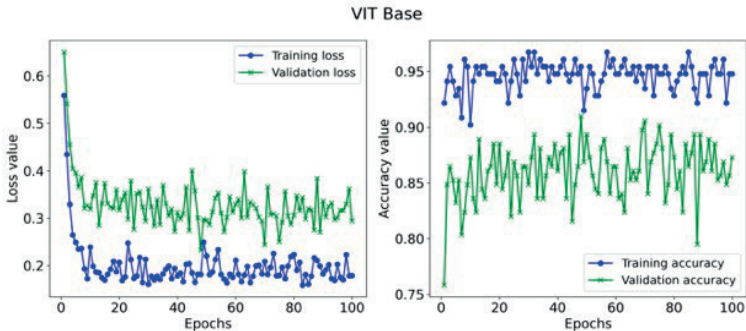


Figure 2. Training and Validation Metrics Over Epochs for VIT Base Model

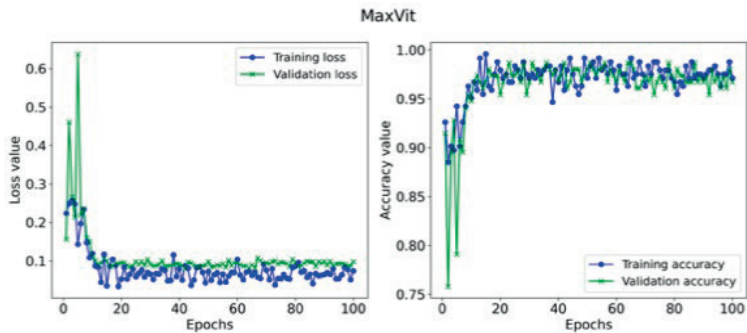


Figure 3. Training and Validation Metrics Over Epochs for MaxVit Model

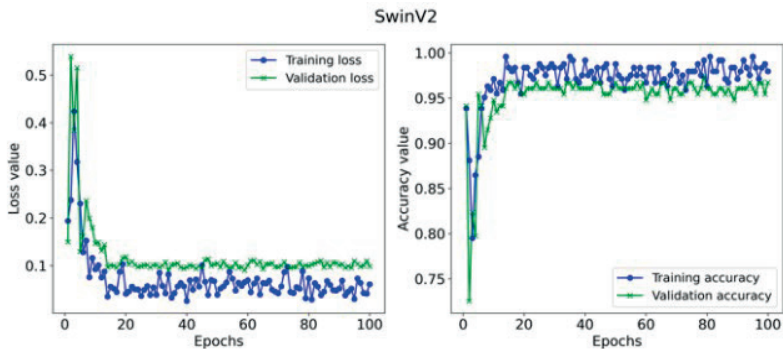


Figure 4. Training and Validation Metrics Over Epochs for SwinV2 Model

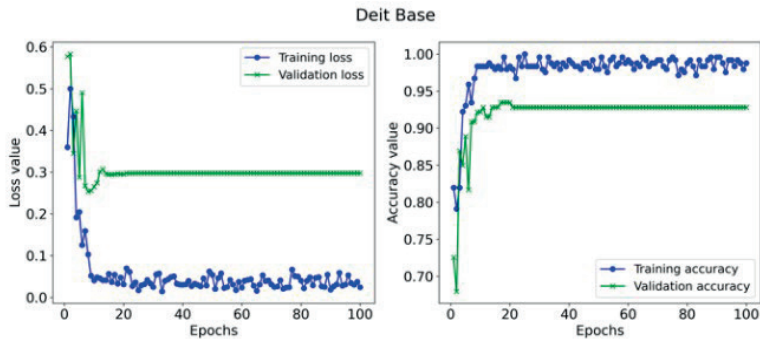


Figure 5. Training and Validation Metrics Over Epochs for DeiTBase Model

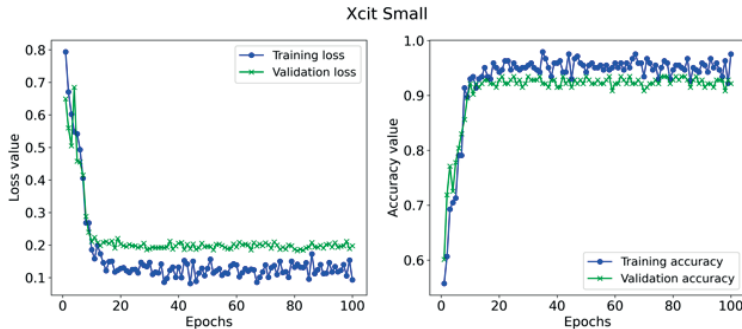


Figure 6. Training and Validation Metrics Over Epochs for XCiT Small Model

The training and validation metrics for DeiT Base suggest a possible complexity or under-training of the model, being more unstable than the other models and which may suggest room for improvement. The loss during training and evaluation decreases rapidly in the first epochs and stabilizes around 0.1-0.3, and the accuracy is lower compared to other analyzed models.

The SwinV2 model shows remarkable performance, both on the training and validation side, with low losses and high accuracy. It can be seen that the loss decreases rapidly in the first 10 epochs and stabilizes below the value of 0.1. The training and validation accuracies increase rapidly and suggest effective learning with very good values above 97%.

In the end, the analyzed models note a reasonable efficiency and performance, contributing to the development of modern solutions for automatic classification of waste, based on deep-learning techniques. According to the experiments and the comparative study, the MaxViT Nano and SwinV2 models stand out for their high accuracy and stability. These metrics and features observed among top models may pave the way for implementations in real-time waste sorting applications, contributing to recycling and sustainability efforts.

CONCLUSIONS

Automated waste detection is essential for efficient waste management, sustainability, and a cleaner future. In the present study, modern

and innovative solutions for this problem were presented, leveraging the characteristics of vision transformer architectures for automated image classification.

The results obtained in this study note the efficiency and performance of vision transformer, deep learning architectures for automatic waste classification. The method proposed in the present study was based on phases of training and evaluation of the implemented models in relation to transfer learning and fine-tuning techniques.

In this sense notable performances were observed, with waste classification accuracy values over 94%, even 97-98% for the top models, which can contribute to the implementation of high-performance and robust detection systems. The analyzed models included state-of-the-art architectures optimized for the classification task, the best and most stable models observed being MaxViT, SwinV2, and XCiT. Notable results, but with small fluctuations in the metrics, were observed for the ViT Base and DeiT models, but which still provided notable accuracy values.

The practical development of these systems can significantly contribute to efficient recycling solutions and environmental protection. As part of future developments, recent vision transformer models can be implemented for waste classification and optimized accordingly. Furthermore, the best models can be developed as part of automated waste identification systems using various real-time and lightweight platforms.

REFERENCES

- Agafitei, A., Pavel, V.L. (2021). Researches regarding the impact of waste landfill in Sibiu county, Romania on the environment and measures to reduce it. *Scientific Papers. Series E. Land Reclamation, Earth Observation & Surveying, Environmental Engineering, X*, 11-16, Print ISSN 2285-6064.
- Ali, A., Touvron, H., Caron, M., Bojanowski, P., Douze, M., Joulin, A., & Jégou, H. (2021). XcIT: Cross-covariance image transformers. *Advances in neural information processing systems*, 34, 20014-20027.
- Alrayes, Fatma S., Mashael M. Asiri, Mashael S. Maashi, Mohamed K. Nour, Mohammed Rizwanullah, Azza Elneil Osman, Suhandar Drar & Abu Sarwar Zamani. (2023). Waste Classification Using Vision Transformer Based on Multilayer Hybrid Convolution Neural Network. *Urban Climate*, May, 101483. <https://doi.org/10.1016/j.uclim.2023.101483>.
- An, Kang & Yanping Zhang. (2022). LPViT: A Transformer Based Model for PCB Image Classification and Defect Detection. *IEEE Access*, 42542–53. <https://doi.org/10.1109/access.2022.3168861>.
- Boldeanu, G., Gheorghe, M., Moise, C., Dana Negula, I., Tudor, G. (2023). Earth observation techniques applied for land waste detection and monitoring. *Scientific Papers. Series E. Land Reclamation, Earth Observation & Surveying, Environmental Engineering, Vol. XII*, 383-388, Print ISSN 2285-6064.
- Chen, Jinxiang, Yiqun Cheng & Jianxin Zhang. (2023). Anti-Local Occlusion Intelligent Classification Method Based on MobileNet for Hazardous Waste. *International Journal of Modelling, Identification and Control*, 4, 333–40. <https://doi.org/10.1504/ijmic.2023.131203>.
- Dong, Zhiming, Junjie Chen, and Weisheng Lu. (2022). Computer Vision to Recognize Construction Waste Compositions: A Novel Boundary-Aware Transformer (BAT) Model. *Journal of Environmental Management*, 114405. <https://doi.org/10.1016/j.jenvman.2021.114405>.
- Dookhee, Surajsingh. (2022). Domestic Solid Waste Classification Using Convolutional Neural Networks. 2022 IEEE 5th International Conference on Image Processing Applications and Systems (IPAS), December. <https://doi.org/10.1109/ipas55744.2022.10052971>.
- Dosovitskiy, A., Beyer, L., Kolesnikov, A., Weissenborn, D., Zhai, X., Unterthiner, T., Dehghani, M., Minderer, M., Heigold, G., Gelly, S., Uszkoreit, J., & Houlsby, N. (2020). An Image is Worth 16x16 Words: Transformers for Image Recognition at Scale. *ArXiv*, abs/2010.11929.
- Hu, Fan, Pengjiang Qian, Yizhang Jiang, and Jian Yao. (2022). An Improved Waste Detection and Classification Model Based on YOLOV5. In *Intelligent Computing Methodologies*, 741–54. Springer International Publishing. http://dx.doi.org/10.1007/978-3-031-13832-4_61.
- Huang, Kai, Huan Lei, Zeyu Jiao & Zhenyu Zhong. (2021). Recycling Waste Classification Using Vision Transformer on Portable Device. *Sustainability*, 21 11572, <https://doi.org/10.3390/su132111572>.
- Kumar, Avan, Bhavik R. Bakshi, Manojkumar Ramteke, & Hariprasad Kodamana. (2023). Recycle-BERT: Extracting Knowledge about Plastic Waste Recycling by Natural Language Processing. *ACS Sustainable Chemistry & Engineering*, 32, 12123–34. <https://doi.org/10.1021/acssuschemeng.3c03162>.
- Kurz, Aidan, Ethan Adams, Arthur C. Depoian, Colleen P. Bailey & Parthasarathy Guturu. (2022). WMC-ViT: Waste Multi-Class Classification Using a Modified Vision Transformer. *IEEE MetroCon*, November. <https://doi.org/10.1109/metrocon56047.2022.9971136>.
- Liu, Ze, Han Hu, Yutong Lin, Zhuliang Yao, Zhenda Xie, Yixuan Wei, Jia Ning, et al. (2022). Swin Transformer V2: Scaling Up Capacity and Resolution. 2022 IEEE/CVF Conference on Computer Vision and Pattern Recognition (CVPR), June. <https://doi.org/10.1109/cvpr52688.2022.01170>.
- Ma, Wanqi, Hong Chen, Wenkang Zhang, Han Huang, Jian Wu, Xu Peng & Qingqing Sun. (2024). DSYOLO-Trash: An Attention Mechanism-Integrated and Object Tracking Algorithm for Solid Waste Detection. *Waste Management*, 46–56. <https://doi.org/10.1016/j.wasman.2024.02.014>.
- Mao, Wei-Lung, Wei-Chun Chen, Chien-Tsung Wang & Yu-Hao Lin. (2021). Recycling Waste Classification Using Optimized Convolutional Neural Network. *Resources, Conservation and Recycling*, 105132. <https://doi.org/10.1016/j.resconrec.2020.105132>.
- Qin, Hai, Liye Shu, Li Zhou, Songyun Deng, Haihua Xiao, Wei Sun, Qiaokang Liang, Dan Zhang & Yaonan Wang. (2024). Active Learning-DETR: Cost-Effective Object Detection for Kitchen Waste. *IEEE Transactions on Instrumentation and Measurement*, 1–15. <https://doi.org/10.1109/tim.2024.3368494>.
- Touvron, H., Cord, M., Douze, M., Massa, F., Sablayrolles, A., & Jégou, H. (2021). Training data-efficient image transformers & distillation through attention. In *International conference on machine learning*, 10347-10357.
- Tu, Z., Talebi, H., Zhang, H., Yang, F., Milanfar, P., Bovik, A., & Li, Y. (2022). Maxvit: Multi-axis vision transformer. In *European conference on computer vision*, 459-479. Cham: Springer Nature Switzerland.
- Virsta, A., Sandu M.A., Daraban A.E. (2020). Dealing with the transition from in line economy to circular economy - public awareness investigation in Bucharest. *AgroLife Scientific Journal*, 9(1), 355–362.

GOOD PRACTICES FOR REDUCING LAND POLLUTION IN THE AREA OF SWINE FARMS WITH LIQUID MANURE

Mihaela Alexandra ROTARU, Loredana VĂDUVA,
Olimpia Alina IORDĂNESCU, Ioan PETROMAN

University of Life Sciences "King Mihai I" from Timisoara,
119 Aradului Avenue, Timisoara, Romania

Corresponding authors emails: olimpia.iordanescu@yahoo.com, loredana_heber@yahoo.com

Abstract

The pollution of surface or underground water sources is done by physical, chemical, and biological means, the ecological effects manifesting themselves through the modification of abiotic factors and implicitly all trophic levels. Evacuated unprocessed, untreated and accidentally ending up in emissions or on the ground, the liquid wastes contribute to the heating of the water and the decrease of oxygenation degree determined by the acceleration of the organic mass decomposition phenomena and on the soil by degrading its quality by increasing the amount of nitrogen. These effects the more visible in the researched area, Arad County in the vicinity of swine farms and especially in the area of former treatment plants belonging to disused farms, where the waters of the area, due to the activity of aerobic microorganisms, flourished and some species of fauna and flora even disappeared if the discharged faeces, after a certain processing the CBO5 parameter had 45.1-55.0 mg·L⁻¹.

Key words: environmental pollution, good practices, manure, swine.

INTRODUCTION

Swine holdings as production units are equipped with accommodation spaces, utility annexes, and specific means of transport, in which coordination is ensured by managers, specialists, and highly qualified workforce. To be functional, holdings must be in areas authorized by environmental bodies, and, outside the fenced premises, they may also have areas of land intended for crop production. The mechanism of operation of the management system is based on a set of laws, principles, methods, and procedures that make up the methodological elements. The technical, economic, and social organization of pork production takes place in the conditions of a great diversity of types and forms, so farms can be classified by:

- orientation of production and nature of activity;
- integration of production by branch;
- technical-economic profile.

The establishment of a performing professional pig holding requires, from the point of view of Integrated Production Management, investments in land procurement for the construction of shelters, investments in

exploitation technology, mechanization and automation of farm activities, control of the microclimate in shelters, provision of fodder resources, water and energy, manure management (Deviney et al., 2021), and implementation of measures to protect natural environmental factors and avoidance of environmental risk. Major investments are needed for the construction of modern wastewater and slurry treatment plants, for the avoidance of environmental risk, as well as in the management of the environment and the qualification of the human resource, and the development of procedures related to:

- management of environmental risk;
- integration in the management of the environment and Total Quality Management;
- implementation of the best management in the meat industry, production, processing, distribution, and capitalization on the market.

To achieve the most efficient investment in professional integrated pig farms, it is necessary to analyse some elements that condition the technological processes of production, and the viability and economic efficiency of the holding. For the establishment of an integrated performance pig holding, it is necessary to follow the following steps (Das et al., 2023):

- knowing the climate and economic factors around the holding;
- choosing the location: road network, electricity, source of water supply, and feed resources;
- using efficiently manure and waste water as organic fertilizers;
- elaborating the technological project;
- conducting technical, economic, and social studies;
- elaborating the execution project;
- constructing shelters and utilities;
- equipping the holding with performing means;
- implementing the integrated management system;
- populating with genetic material.

The choice of area and location of the holding is an important decision considering that, once built, the shelters can no longer be moved to another site. For a good site and with few environmental risks, it is necessary to know the factors that can influence the evolution of the farm:

Technical and technological factors:

- risk of pollution, which needs measures of optimal dimensioning of the farm and of the systems of collection, storage, treatment, and disposal of manure;
- climate factors, of which minimum and maximum air temperatures, daytime and nighttime temperatures per periods and seasons (Ahmed et al., 2013), and relative humidity will be analysed. The direction of the prevailing winds is analysed to establish the thickness of the shelter walls, the orientation of shelter placement, and the need for the formation of protective curtains;
- quality of the site: the soil must be compact, stable, sloping, and away from emissaries to avoid accidental leakage;
- drinking water, which is necessary for the pigs and for technological and human consumption and must be sufficient and at great depths to avoid pollution;
- pluviometric regime;
- feed resources, which depend on the size and method of procurement (purchase or own production) (Andretta et al., 2021);
- national power grid or own sources;
- transport network.

Socio-economic factors:

- availability of human and feed resources;

- competition in the area;
- traditions regarding the consumption of pork;
- market trends;
- possibilities of capitalization of finished production.

The main objectives of this scientific approach are: finding new methods of managing waste from pig farms to avoid environmental degradation in the farm area; the regulation of the livestock according to the affordability of the environmental factors and the monitoring of the quality of the environment in the area of the pig farms to avoid their degradation.

MATERIALS AND METHODS

Because pig farms with classic production technologies involve low investments in manure management, they have environmental problems caused by the exceeded values of nitrites and nitrates in surface and deep water (Luo et al., 2019), by their administration on the lands around the farms as organic fertilizers in large quantities unprocessed properly by separation to increase the production. In this scientific approach, the authors sought solutions for the implementation of modern processing and management technologies by incorporation into the soil in controlled dilutions to reduce their negative effects on the environmental (Yost et al., 2022). Statistical data obtained in this scientific approach represent the results of the samples from 4 drills made during the years 2020, 2021, and 2022, twice a year, in the first and second semester: they represent the database subjected to statistical processing using SAS Studio [SAS]. Although the values of the samples are within the parameters, to test the differences between the values determined by two groups, the T-two sample test was used, respectively the Mann-Whitney nonparametric equivalent.

For the data distributed in three groups (annual series) and four groups (determined by drilling in different locations), the One-Way ANOVA procedure and the Kruskal Wallis nonparametric test were used. Multiple post hoc comparisons were performed using the Tukey test for the parameters followed, pH values, chemical oxygen consumption - potassium permanganate method (CCOMn), ammoniacal nitrogen, nitrite

and nitrate quantity, phosphorus, and chlorides (Chen et al., 2020).

RESULTS AND DISCUSSIONS

Quality indicators for groundwater and surface water around the pig farms highlight the degree of pollution and the management of solid and liquid manure management over a certain period

(Abrantes Pinto De Brito et al., 2022). The evolution of the water quality parameters at the control drills, around the farms where solid manure was administered and near the wastewater management stations from the farm are presented over a period of three years in the tables below.

Groundwater quality in the farm area is presented in Tables 1 to 4.

Table 1. Groundwater quality at drilling (F1) in the manure storage area

Item	UM	2020		2021		2022	
		1 st Semester	2 nd Semester	1 st Semester	2 nd Semester	1 st Semester	2 nd Semester
Water pH	pH	7.40	7.45	7.30	7.50	7.20	7.45
Chemical oxygen consumption - potassium permanganate method	mg-O ₂ ·L ⁻¹	6.35	4.50	2.20	5.80	2.00	3.20
Ammoniacal nitrogen	mg·L ⁻¹	0.25	0.10	0.20	0.10	0.20	0.30
Nitrites	mg·L ⁻¹	0.50	0.40	0.40	0.30	0.10	0.20
Nitrates	mg·L ⁻¹	2.40	2.20	0.40	2.30	0.50	1.50
Total phosphorus	mg·L ⁻¹	0.01	0.03	0.20	0.10	0.20	0.47
Chlorides	mg·L ⁻¹	9.50	36.50	22.50	12.40	22.30	28.30

Table 2. Groundwater quality at drilling (F2) in the area where slurry was used in 2020 to increase agricultural production on sole 1 (S1)

Item	UM	2020		2021		2022	
		1 st Semester	2 nd Semester	1 st Semester	2 nd Semester	1 st Semester	2 nd Semester
Water pH	pH	7.10	7.00	7.20	7.40	7.40	7.50
Chemical oxygen consumption - potassium permanganate method	mg-O ₂ ·L ⁻¹	3.30	4.20	1.50	1.70	1.70	1.80
Ammoniacal nitrogen	mg·L ⁻¹	0.40	0.30	0.20	0.35	0.20	0.35
Nitrites	mg·L ⁻¹	0.45	2.50	0.35	0.20	0.38	0.18
Nitrates	mg·L ⁻¹	3.30	0.80	2.60	0.50	0.90	0.30
Total phosphorus	mg·L ⁻¹	0.06	0.04	0.10	0.10	0.08	0.15
Chlorides	mg·L ⁻¹	40.50	38.20	13.50	19.30	17.30	22.20

Table 3. Groundwater quality at drilling (F3) in the area where slurry was used in 2020 to increase agricultural production on sole 2 (S2)

Item	UM	2020		2021		2022	
		1 st Semester	2 nd Semester	1 st Semester	2 nd Semester	1 st Semester	2 nd Semester
Water pH	pH	7.20	7.20	7.30	7.60	7.10	7.40
Chemical oxygen consumption - potassium permanganate method	mg-O ₂ ·L ⁻¹	11.50	12.20	2.00	1.70	1.70	1.60
Ammoniacal nitrogen	mg·L ⁻¹	0.50	0.30	0.08	0.03	0.03	0.22
Nitrites	mg·L ⁻¹	0.10	1.80	0.08	0.08	0.10	0.30
Nitrates	mg·L ⁻¹	1.45	0.85	3.20	3.80	0.60	0.20
Total phosphorus	mg·L ⁻¹	0.008	0.007	0.090	0.33	0.20	0.38
Chlorides	mg·L ⁻¹	88.40	40.20	28.80	22.40	20.20	13.10

Table 4. Groundwater quality at drilling (F₄) in the area where slurry was used in 2020 to increase agricultural production - on sole 3 (S₃)

Item	UM	2020		2021		2022	
		1 st Semester	2 nd Semester	1 st Semester	2 nd Semester	1 st Semester	2 nd Semester
Water pH	pH	7.20	7.50	7.10	7.40	7.00	7.30
Chemical oxygen consumption - potassium permanganate method	mgO ₂ ·L ⁻¹	2.20	3.80	2.60	3.50	2.00	1.85
Ammoniacal nitrogen	mg·L ⁻¹	0.45	0.30	0.20	1.60	0.70	0.95
Nitrites	mg·L ⁻¹	0.50	2.70	0.20	0.09	0.40	1.22
Nitrates	mg·L ⁻¹	0.40	0.70	13.44	5.20	0.60	0.10
Total phosphorus	mg·L ⁻¹	0.07	0.09	0.10	0.25	0.20	0.30
Chlorides	mg·L ⁻¹	56.20	67.20	12.50	23.50	17.80	24.20

Table 5. Evolution of nitrate values at control drillings (S₁, S₂, S₃)

Item	Indicator analysed	UM	Value determined	
			1 st Semester (mg·L ⁻¹)	2 nd Semester (mg·L ⁻¹)
Storage pools	Nitrates	mg·L ⁻¹	0.10- 2.40	0.20-2.30
Control drill sole 1			0.35- 3.30	0.18-2.50
Control drill sole 2			0.08- 3.20	0.08-3.80
Control drill sole 3			0.20-13.44	0.09-5.20

Evolution of nitrate values at control drillings

The evolution of nitrate concentrations from control drills on soils fertilized with pig manure to increase agricultural production highlights the influence of fertilizers from slurry on groundwater, as shown by the data presented in Table 5.

Comparing the results obtained based on the measurements made per semesters over 3 years around the pig farm from Arad County, it follows that, although the surveyed area is in "a vulnerable and potentially vulnerable to pollution area" in both semesters:

- there were no exceeding permissible limits of pollution: the pH of the water reached values of 7.00-7.50 (the allowed pH limits are between 6.50-8.50) although they used pig manure to increase agricultural production on the investigated soils, with a crop rotation every 3 years;
- there were no exceeding permissible limits of pollution due to compliance with dilutions to avoid pollution of the environmental;
- there was mechanical separation of coarse manure while maintaining it in the drying beds and of the liquid manure in storage pools until using them as fertilizers; they were discharged after processing 45.1-55.0 mg·L⁻¹ CBOs;
- there was variation of nitrites during the analysis period due to weather conditions (high number of precipitations), which determined the increase of groundwater concentrations;

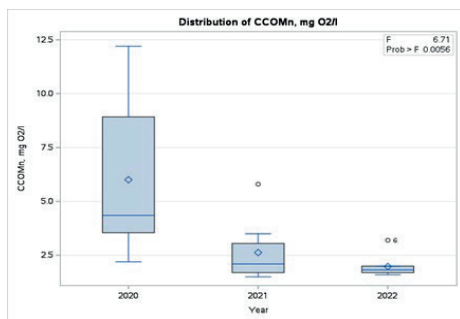
- there was a permeable soil that favoured the rapid accumulation of nitrates in the water;

- there was a variation of the level of chlorides in water during the semesters of the analysed period, reaching values between 6.20-88.40 mg·L⁻¹, the highest quantities being in 2020 in all 3 control drills on the soils where liquid manure from pigs had been administered.

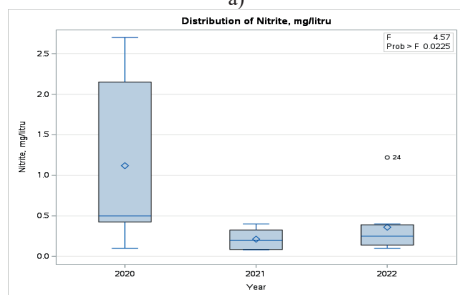
The statistical processing regarding the values of the measured parameters with the ANOVA test produced statistically significant differences during the three years (2020, 2021 and 2022) in the case of CCOMn values with $p = 0.0056$, $F = 6.71$ (Figure 1a), nitrites $p = 0.0225$, $F = 4.57$ (Figure 1b), nitrates $p = 0.0376$, $F = 3.85$ (Figure 1c), phosphorus $P = 0.0008$, $F = 10.24$ (Figure 1d) and chlorides $P = 0.0011$, $F = 9.57$ (Figure 1e).

The significant differences between the groups determined in the three years are also confirmed by the application of the Kruskal Wallis nonparametric test. Thus, the values obtained were $p = 0.002$ with a.m. 2 = 11.90 for CCOMn, $p = 0.018$ with a.m. 2 = 9.06 for nitrites, $p = 0.019$ with a.m. 2 = 7.87 for nitrates, $p = 0.0004$ with a.m. 2 = 15.54 for phosphorus and $p = 0.013$ with a.m. 2 = 8.66 for chlorides. If in the case of CCOMn, nitrites and chlorides there is a decreasing trend in value, in the case of phosphorus there was an increase in value during the three years (2020, 2021 and 2022).

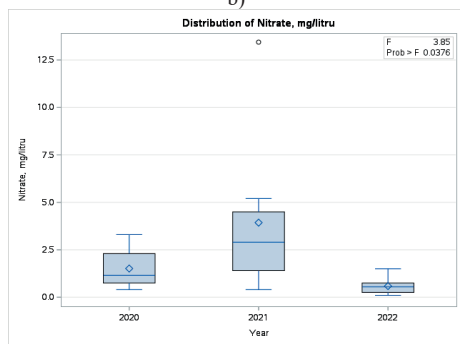
Specifically, in 2020, the average value of phosphorus content was about $0.03 \text{ mg}\cdot\text{L}^{-1}$.



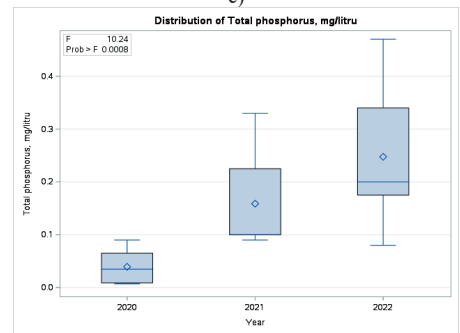
a)



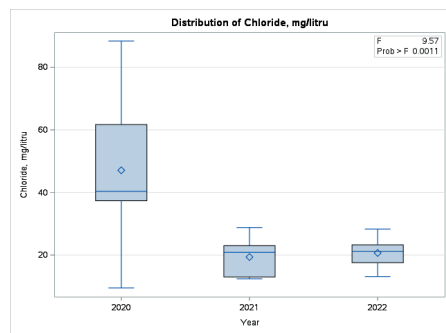
b)



c)



d)



e)

Figure 1. Boxplot charts showing the variation of the value of the parameters followed over the three years (2020, 2021, 2022). *Source:* authors' own representation of statistical data using SAS Studio-One Way ANOVA

Multiple comparisons using the Tukey test show significant differences between the phosphorus value of 2020 and the other years, each individually. Regarding the nitrite value, it was about $1.18 \text{ mg}\cdot\text{L}^{-1}$ in 2020, being significantly lower in 2021, when the average value reaches about $0.21 \text{ g}\cdot\text{L}^{-1}$ ($p = 0.026$, according to the Tukey post hoc test).

For the other parameters, namely the values of the pH and NH_4^+ , respectively, no significant differences were observed between the groups determined by the three years in which the statistical observations were made. Differences between the groups determined for the 4 drills were also tested and, in all situations, except NH_4^+ , there were no statistically significant differences between the values of the parameters monitored. In the case of NH_4^+ , ANOVA showed values such as $p = 0.015$, $F = 4.41$ (Figure 2). Significant differences were also confirmed by the Kruskal-Wallis nonparametric Test, $p = 0.0038$ with $\chi^2 = 8.39$. To concretely track the differences in NH_4^+ values, multiple comparisons between groups were additionally applied, using the Tukey test. Samples from drilling 4 show higher significantly different values from those from drilling 1 and 3. The other values, even if they show slight differences in NH_4^+ content, have no statistical significance regardless of which drill they come from.

The authors also examined whether the values of the measured parameters in the first part of the year differ from those in the second part. Thus, aggregating all the data of the period 2020-2022 relating to the first semester and then, all the data

measured in the second semester, the differences between the groups have no statistical significance, with one exception. We refer here to the pH values which for the first semester had an average value of 7.20 significantly different from the average value of 7.39 for the data of the second semester during the three years (Figure 3). The T-two sample test indicates the value $p = 0.0049$, i.e. significantly different values. Also, the Mann Whitney nonparametric test confirms the existence of differences between semesters, $p = 0.01$.

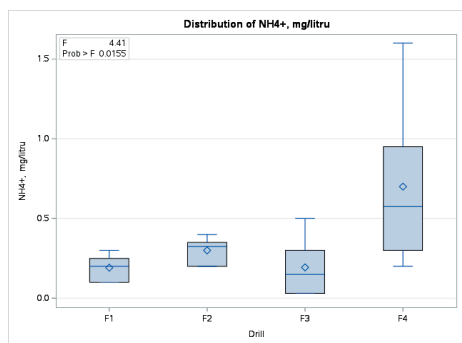


Figure 2. Boxplot diagram of NH_4^+ values in the four drills. *Source:* authors' own representation of statistical data using SAS Studio-One Way ANOVA

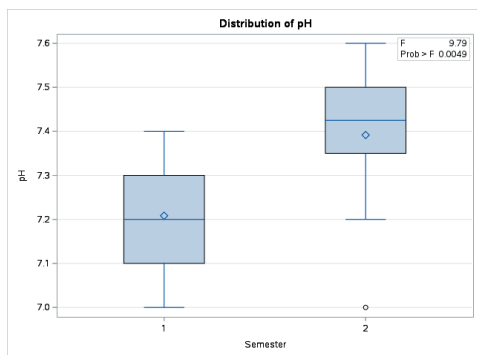


Figure 3. Boxplot diagram of the pH values between the two semesters, cumulative for the period 2020-2022. *Source:* authors' own representation of statistical data using SAS Studio-One Way ANOVA

Studies show that the concentration of pig herds in the past in large units in the past, without analysing the degree of environmental tolerability, determined over time the deterioration of the quality of groundwater and surface waters, the causes of the deterioration of

the environmental factors in the farms being multiple:

- concentration and high density of pigs in farms, in relation to the soils existing around them;
- location of farms near surface water sources and on permeable soils, with groundwater web at shallow depth;
- positioning farms on sloping sites that favour runoff;
- improper management of manure in particular quantities stored and administered as organic fertilisers;
- use of solid uncontrolled swine manure resulting in massive accumulation of nitrates in soil and groundwater;
- lack of investment in production technologies, where water management must be controlled to reduce the quantities of liquid manure (Yang et al., 2020);
- hydraulic discharge of slurry corresponding to pollution of surface and underground waters;
- lack of efficient plants for treatment, storage, and management of manure.

Reducing the negative effects of pollution requires environmental management risk measures; in this regard, the authors propose the following for the implementation of management measures to reduce the pollution of soil and surface and groundwater for the pig farms in the investigated area:

- Applying codes of good practices for the use as fertilizers of solid or liquid manure, to stimulate crop production:
 - establishing the optimal period of soil integration of liquid swine manure;
 - controlling the maximum quantities of solid manure administered as fertilisers;
 - using swine manure according to soil quality: creditworthiness, texture, permeability;
 - refusing to use slurry on sloping land or near water resources.
- Using modern methods of storing liquid or solid manure from pigs by:
 - designing pools with sufficient storage capacities until treatment, dilution, and administration;
 - sealing storage platforms for solid manure;
 - preventing purine infiltration on land near sewage treatment plants, and treatment and storage of manure;

- reducing the amount of manure by controlling the nutritive level of water, using biological material that produces less manure.

- Monitoring the quantities of manure by:

- optimizing the size of farms and categories of pigs;

- investing in the treatment, storage, and distribution of manure;

- Improving the way of evacuation and storage at the treatment and storage stations for manure:

- transport logistics;

- evacuation, storage, treatment, and dilution techniques;

- analysis of manure composition;

- Using environmentally friendly production technology systems by:

- using species that restore soil structure (Jiménez-de-Santiago et al., 2022);

- cultivating plants that restore soil quality;

- rotating fertilized soils with solid or liquid organic fertilizers incorporated into the soil;

- controlling dilution, scattering, or embedding mode;

- reducing the risk of pollution by nitrite reduction methods through: periodic analyses of manure to be used as fertiliser; controlled application according to the amount of precipitation and optimal season; use on high permeability land and surface water table;

- Environmental risk management to reduce pollution by:

- controlling soil nitrate by mapping;

- fertilizing by GIS;

- differentiating soil fertilization by nitrate load;

- setting the optimum nitrogen and phosphorus levels depending on: soil quality in the area where swine manure is used; the degree of tolerability of environmental factors depending on the period of use in time of swine manure for the growth of plant productions;

- monitoring the quantity and quality of water from manure;

- applying solid manure on soil by controlling the quantities and quality of manure;

- improving irrigation methods with diluted manure, depending on: soil permeability and water retention capacity; period of administration and type of culture;

- controlling the amounts of nitrates, which can be processed by plants used in the previous crop and reserves in the soil.

- Independent monitoring of environmental factors, tracking their evolution and their effects over time:

- air quality - the amount of ammonia and hydrogen sulphide on the farms, treatment plants and land fertilized with manure as organic fertilizers;

- quality of manure distributed as fertilizer and possible effects on agricultural land;

- water protection against nitrate pollution by grassed protective curtains;

- physico-chemical measurements through the analysis of samples from the monitoring of control drills, to know the degree of pollution and pollution prevention measures;

- analysis of soil quality indicators around treatment plants, manure storage and soils where solid or liquid manure from pigs was distributed to increase production;

- Implementing the best management to improve environmental risk management through:

- periodic quality control of natural environmental factors on the farms;

- improvement of production technologies to reduce the quantities of manure;

- reduction of the quantities of manure used as organic fertilizers by using them to obtain biogas.

- Improving the management of the flow of information on the quality of environmental factors, through:

- monitoring the activities of pig farms;

- controlling the quantity and quality of manure;

- checking the management of manure by administrative bodies.

CONCLUSIONS

The research carried out per semester during the three years, in the area of a pig farm, highlights the fact that, although the area under analysis is in a vulnerable and potentially vulnerable area to pollution of surface or underground water sources, the permissible limits of pollution have not been exceeded. The use of liquid pig manure to increase agricultural production on the investigated soils, with a rotation of application every 3 years and compliance with dilutions, made it possible not to exceed the permissible limits of the pH of the water, reaching values of 7.00-7.50. The pH values which, for the first

semester, had an average value of 7.20 significantly different from the average value of 7.39 for the data of the second semester during the three years, the T test indicates the value $p = 0.0049$, i.e. significantly different values; likewise, the Mann Whitney nonparametric test confirms the existence of differences between semesters, $p = 0.01$, due to the use in the past of mechanically separated solid manure as organic fertilizers with concentrations of $45.1\text{--}55.0 \text{ mg}\cdot\text{L}^{-1}$ CBO5 to increase plant yields. Testing the differences between the groups determined for the 4 drills in all situations, except NH_4^+ , did not reveal statistically significant differences between the values of the parameters followed only in the case of NH_4^+ , $p = 0.015$, $F = 4.41$, the significant differences being confirmed by the Kruskal-Wallis nonparametric Test, $p = 0.0038$ with $\chi^2 = 8.39$, differences of NH_4^+ values, for multiple comparisons between groups, resulting that the samples of drilling 4, sole 3, indicate higher values and significantly different from those drills 1 and 3, the other values, even though they have slight differences in NH_4^+ content, they have no statistical significance regardless of the drill they come from. Studies show that the concentration of pig herds in the past in large units, without analysing the degree of environmental tolerability determined over time the deterioration of the quality of environmental factors. The causes of the presented situation are: (a) multiple high density of pigs on farms, (b) improper location of farms near surface water sources and on permeable soils and improper management of manure especially the quantities stored and administered as organic fertilizers and the lack of efficient treatment, (c) storage and management stations for manure.

REFERENCES

- Abrantes Pinto De Brito, S., Diniz Duarte, G., da Silva Sobral, F.E. & Lindsey Christoffersen, M. (2020). Environmental impacts of swine farming. *Environmental Smoke*, 5(3), 1-6. <https://doi.org/10.32435/envsmoke.2022531-6>.
- Ahmed, S., Mickelson, S.K., Pederson, C.H., Baker, J.L., Kanwar, R.S., Lorimor, J.C. & Webber, D.F. (2013). Effects of swine manure rate, timing, and method of application on post-harvest soil nutrients and crop yield in a corn-soybean rotation. *Transactions of the American Society of Agricultural and Biological Engineers*, 56(22), 395-408. <https://doi.org/10.13031/2013.42678>.
- Andretta, I., Hickmann F.M.W., Remus, A., Franceschi, C.H., Mariani, A.B., Orso, C., Kipper, M., Létourneau-Montminy, M.P. & Pomar, C. (2021). Environmental impacts of pig and poultry production: Insights from a systematic review. *Frontiers in Veterinary Science*, 8, 1-14. <https://doi.org/10.3389/fvets.2021.750733>.
- Chen, B., Koziel, J.A., Banik, C., Ma, H., Lee, M., Wi, J., Meir Khanuly, Z., O'Brien, S.C., Li, P., Andersen, D.S., Białowiec, A., Parker, D.B. (2020). Mitigation of odor, NH_3 , H_2S , GHG, and VOC emissions with current products for use in deep-pit swine manure storage structures. *Frontiers in Environmental Science*, 8, 1-17. <https://doi.org/10.3389/fenvs.2020.613646>.
- Das, S., Liptzin, D. & Maharjan, B. (2023). Long-term manure application improves soil health and stabilizes carbon in continuous maize production system. *Geoderma*, 430, 1-14. <https://doi.org/10.1016/j.geoderma.2023.116338>.
- Deviney, A., Classen, J., Bruce, J. & Sharara, M. (2021). Sustainable swine manure management: A tale of two agreements. *Sustainability*, 13(1), 15. <https://dx.doi.org/10.3390/su13010015>
- Jiménez-de-Santiago, D.E., Almendros, G., Bosch-Serra, A.D. (2023). Structural changes in humic substances after long-term fertilization of a calcareous soil with pig slurries. *Soil Use and Management*, 39(4), 1-13. <https://doi.org/10.1111/sum.12896>.
- Luo, W., O'Brien, P.L., Hatfield, J.L. (2019). Crop yield and nitrous oxide emissions following swine manure application: A meta-analysis. *Agricultural & Environmental Letters*, 4(1), 1-5. <https://doi.org/10.2134/acl2019.07.0024>.
- Yang, F., Han, B., Gu, Y., Zhang, K. (2020). *Scientific Reports*, 10, 1-10. <https://doi.org/10.1038/s41598-020-72149-6>.
- Yost, J.L., Schmidt, A., Koelsch, R. & Schott, L.R. (2022). Effect of swine manure on soil health properties: A systematic review. *Soil Science Society of America Journal*, 86, 450-486. <https://doi.org/10.1002/saj2.20359>.

COMPARATIVE ANALYSIS ON AIR POLLUTION LEVEL OF BUCHAREST URBAN AREA DURING THE COVID-19 PANDEMIC

Vasilica VASILE, Cristian PETCU, Alina DIMA, Mihaela ION

National Institute for Research and Development in Construction,
Urban Planning and Sustainable Spatial Development - URBAN-INCERC,
266 Pantelimon Road, District 2, Bucharest, Romania

Corresponding author email: vasile@incd.ro

Abstract

The pollution level of urban area is often high, mainly due to the traffic conditions that can lead to pollutant emissions such as nitrogen dioxide (NO₂) and particulate matter (PM), negatively affecting inhabitant's health. However, this level of traffic had a strong decrease, given the lockdown of the population imposed by the COVID-19 pandemic. Thus, the present paper is a comparative analysis on air pollution level, before and during the two periods of lockdown. For this, the concentrations of specific traffic pollutants, suspended particles (PM_{2.5}) and nitrogen dioxide (NO₂), were monitored. According to the obtained results, PM_{2.5} values have been lowering with 37.5% and 54.8 %, in trend with those from San Jose (45%) or Los Angeles (41%). Likewise, NO₂ concentrations decreased with 62.3% in the first month and with 57.0% in the second month of the lockdown, similar with values recorded in London (40%) or Barcelona (70%). The analysis showed that air pollution can be reduced and considering the importance of health for inhabitants, long-term solutions must be found.

Key words: air pollution, COVID-19 pandemic, environmental monitoring, health effects.

INTRODUCTION

According to the United Nations Environment Programme (UNEP), the leading global authority on the environment, "air pollution is the greatest environmental threat to public health globally" (unep.org), and is responsible for around seven million premature deaths, worldwide, every year (Siouti et al., 2024; WHO, 2021; unep.org).

The urban area seems to be the most affected by air pollution, mainly due to human activities, such as industrial activities, energy generation and transportation (Roşu et al., 2023; Feng et al., 2023). Among the most important air pollutants monitored in urban areas are particles with a diameter lower than 2.5 µm (PM_{2.5}) (Siouti et al., 2024; Roşu et al., 2023; Cherecheş et al., 2023; Feng et al., 2023), and nitrogen dioxide (NO₂) (Cherecheş et al., 2023; Roşu et al., 2023; Velayarce et al., 2022; Zoran et al., 2020). All the mentioned studies described the well-known PM_{2.5} - aerosol particles, with chemical compositions, shapes and different origins, and NO₂, a chemical substance in gaseous state, yellowish-brown, irritating and toxic.

The main ambient sources of NO₂ are fuel burning, especially from means of transport, off-road equipment, housing heating systems, energy sector (power plants), etc. (Velayarce et al., 2022; Cherecheş et al., 2023; Fuller et al., 2020). The reasons for their monitoring are mainly linked to the harmful effects on health of inhabitants, especially respiratory, cardiovascular, and neurological or skin problems, presented extensively in a lot of research papers (Cherecheş et al., 2023; Zoran et al., 2022; Velayarce et al., 2022; Siouti et al., 2024).

Nevertheless, in the first part of 2020, internationally, a severe epidemiological situation occurred, because of the spread of SARS-CoV-2 in more than 150 countries, on March 11, 2020, the World Health Organization declaring the Pandemic State, being infected, at that moment, about 160,000 people and more than 5,800 dead.

In Romania, the first case of infected person appeared on February 26, 2020, and due to rapid evolution of coronavirus, the President of Romania declared throughout the territory, for a period of 30 days, between March 16 to April

15, the health emergency state (HES1), by (Decree no. 195 of March 16, 2020). The ascending evolution of SARS-CoV-2 epidemic, quantified by the number of infected persons and the registered number of deaths, after the entry into force of the mentioned decree, has led to extend by another 30 days, between April 16 to May 15, of the health emergency state (HES2) throughout Romania, by (Decree no. 240 of April 14, 2020).

The measures established by the two decrees had as their main purpose the limitation of the spread of the disease, but they also led to the limitation of people's movement, with the reduction of most economic activities and implicitly also of transports. This resulted in a considerable reduction in traffic and, as a consequence, a commensurate reduction in levels of urban pollution (Tobias et al., 2020).

This article presents a comparative analysis on urban air pollution level of Bucharest in terms of PM_{2.5} and NO₂ monitored concentrations, in three period of time from the beginning of 2020, namely before the establishment of the state of health emergency, between February 18 and March 15 (bHES), during the first decree

(HES1) and during the second decree (HES2), the periods being above-mentioned. Images of Bucharest streets during the first period of health emergency state are presented in Figure 1 (<https://visitbucharest.today/coronavirus-lockdown-the-fascinating-deserted-streets-of-bucharest/>).

MATERIALS AND METHODS

The HAZ-SCANNER EPAS equipment for monitoring air quality parameters of the atmospheric environment is positioned within the platform of INCD - URBAN-INCERC, Bucharest, Romania near two boulevards with intense urban traffic (Figure 2). The mentioned instrument has data logging capabilities, and renders, in real-time, direct readings. The technical characteristics of HAZ SCANNER EPAS, manufacturer SKC, UK, are presented in the Table 1.

The concentrations of the two pollutants were monitored continuously, at 1-minute intervals, and, simultaneously the climate parameters, temperature and relative humidity.



Figure 1. Images from Bucharest streets during the first period of health emergency state (<https://visitbucharest.today/coronavirus-lockdown-the-fascinating-deserted-streets-of-bucharest/>)



Figure 2. HAZ-SCANNER equipment position compared to the two boulevards

Table 1. Details of HAZ-SCANEER EPAS equipment

Pollutant/ Climate parameter	Principle	Values range	Resolution
Particulate matter, PM2.5	Optical	0 - 5000 $\mu\text{g}/\text{m}^3$	1 $\mu\text{g}/\text{m}^3$
Nitrogen Dioxide, NO ₂	Electrochemical	0 to 5000 ppb (0 to 5 ppm)	1ppb
Temperature, degree C	NTC thermistor	-4 to 140 F (-20 to 60 C)	1 degree F or C
Relative humidity, %	Thin-film capacitive	0 to 100%	1%

RESULTS AND DISCUSSIONS

The obtained results in the three periods of early 2020 - bHES, HES1 and HES2, were analysed to quantify the influence of lockdown measures on air pollution level of urban area of Bucharest. Regarding the PM2.5 concentration levels, it can be seen that they varied during the bHES period between 20.6 and 225.7 $\mu\text{g}/\text{m}^3$, with an average of 46.9 $\mu\text{g}/\text{m}^3$ and a median value of 39.3 $\mu\text{g}/\text{m}^3$; in the HES1 period, between 10.04 and 54.8 $\mu\text{g}/\text{m}^3$, with an average of 29.3 $\mu\text{g}/\text{m}^3$ and a median value of 29.6 $\mu\text{g}/\text{m}^3$; and in the HES2 period, between 12.01 and 33.8 $\mu\text{g}/\text{m}^3$, with an average of 21.2 $\mu\text{g}/\text{m}^3$, and 20.1 $\mu\text{g}/\text{m}^3$ median value. There is a decrease in PM2.5 concentrations during the two periods HES1 and HES2, both in the minimum values recorded, as well as in the maximum and average values, the average being between 37.5 and 54.8%.

The trend is similar to that recorded in cities like San Jose, with 45%, or Las Vegas and Los Angeles, with 41% (Antony Chen et al., 2020), in Milan between 37.1% and 47.4% (Collivignarelli et al., 2020), Delhi by 20.8%,

Mumbai by 20.2%, Wuhan by 21.1%, Bangalore by 33.6%, Lima by 23.79%, London by 21.1% and Moscow by 30.5% (Kumari and Toshniwal, 2020). However, in some cities increases in PM2.5 concentrations were found, namely in United Kingdom of Great Britain (UK) by 28.2% (Ropkins and Tate, 2021), by 47% in Indianapolis and by 44% in Seattle (Chen et al., 2020). The summary of concentration variation for PM2.5 is shown in Table 2.

Nitrogen dioxide (NO₂) concentration values, recorded during the bHES period, varied between 21.8 $\mu\text{g}/\text{m}^3$ and 108.9 $\mu\text{g}/\text{m}^3$, with an average of 67.9 $\mu\text{g}/\text{m}^3$ and 66.7 $\mu\text{g}/\text{m}^3$ median value; in the HES1 period, between 5.6 $\mu\text{g}/\text{m}^3$ and 54.0 $\mu\text{g}/\text{m}^3$, with an average of 25.6 $\mu\text{g}/\text{m}^3$, a median value of 22.0 $\mu\text{g}/\text{m}^3$ and in the HES2 period, between 8.8 $\mu\text{g}/\text{m}^3$ and 78.4 $\mu\text{g}/\text{m}^3$, with an average of 29, 2 $\mu\text{g}/\text{m}^3$ and 28.4 $\mu\text{g}/\text{m}^3$ median value.

The findings are similar to those reported in other studies in large European cities, for example Barcelona or London, with reductions in NO₂ concentrations of 51% (Tobias et al., 2020) and 40% (Brown et al., 2021), Milan, with

64.7% (Zoran et al., 2020), cities in India such as New Delhi or Mumbai, with 60% and 78% respectively (Kumari and Toshniwal, 2020) or in the USA such as Las Vegas, Salt Lake City or New York, with 49%, 43% and 40% respectively (Chen et al., 2020). The values of concentration variation for NO₂ are summarized in Table 3.

The recorded values for climate parameters, temperature and relative humidity are represented in graphic form in Figures 3 and 4, and the summary of them in Table 4. From the data presented in Table 4, it can be observed that the temperature values varied in the analysed periods between 5.6⁰C and 15.0⁰C in bHES, between 2.8⁰C and 17.5⁰C in HES1 and between 9.7⁰C and 24.1⁰C in HES2, and the relative

humidity had values between 32.8% and 98.6% in bHES, between 15.4% and 88.4% in HES1 and between 20.5% and 90.7% in HES2

Also, it was carried out a comparative analysis of the results obtained by monitoring the ambient air quality, with the levels provided by specific documents (Table 5), in force at European and international level, namely:

- Directive 2008/50 / EC of the European Parliament and of the Council of 21 May 2008 on ambient air quality and cleaner air for Europe.

- World Health Organization (WHO) (2021). WHO global air quality guidelines. Particulate matter (PM_{2.5} and PM₁₀), ozone, nitrogen dioxide, sulfur dioxide and carbon monoxide.

Table 2. Variation of PM_{2.5} levels in different cities of the world

Pollutant level Decrease (-)/ Increase (+) %	City/ Reference	Pollutant level Decrease (-)/ Increase (+) %	City/ Reference
-45	San Jose/ Chen et al., 2020	-23.79	Lima/Kumari and Toshniwal, 2020
-41	Las Vegas/ Chen et al., 2020	+28.2	Londra/Ropkins and Tate, 2021
-41	Los Angeles/Chen et al., 2020	+47	Indianapolis /Chen et al., 2020
-47.4	Milano/ Collivignarelli et al., 2020	+44	Seattle/Chen et al., 2020
-21.1	Wuhan/Kumari and Toshniwal, 2020	-18.84	Cluj-Napoca/Cherecheș et al., 2023
-33.6	Bengalore/Kumari and Toshniwal, 2020	-37.5; -54.8	Bucharest/Current study

Table 3. Summary of values levels for NO₂ around the world

Pollutant level Decrease (-)/ Increase (+) %	City/ Reference	Pollutant level Decrease (-)/ Increase (+) %	City/ Reference
-51	Barcelona/ Tobias et al., 2020	-43	Salt Lake City/Chen et al., 2020
-40	London/ Brown et al., 2020	-40	New York/Chen et al., 2020
-64.7	Milan/Zoran et al., 2020	-15	Atlanta/Chen et al., 2020
-78	Mumbai/Kumari and Toshniwal, 2020	-13; -23.4	Cities from Ecuador/Pacheco et al., 2020
-60	New Delhi/Kumari and Toshniwal, 2020	-60; -40	Lima/Velayarce et al., 2022
-20.1	Vienna/Brancher, 2020	-33.45	Cluj-Napoca/Cherecheș et al., 2023
-49	Las Vegas/Chen et al., 2020	-57; -62.3	Bucharest/Current study

Table 4. Values levels of climate parameters in the three periods of 2020

Period	Climate parameters Average (min/max/median)	
	Temperature, °C	Relative humidity, %
bHES	10.0 (5.6/15.0/9.5)	67.9 (32.8/98.6/67.9)
HES1	11.1 (2.8/17.5/11.2)	35.3 (15.4/88.4/32.6)
Variation, %	+11.0	-48.0
HES2	16.5 (9.7/24.1/16.5)	44.5 (20.5/90.7/42.9)
Variation, %	+65.0	-34.5

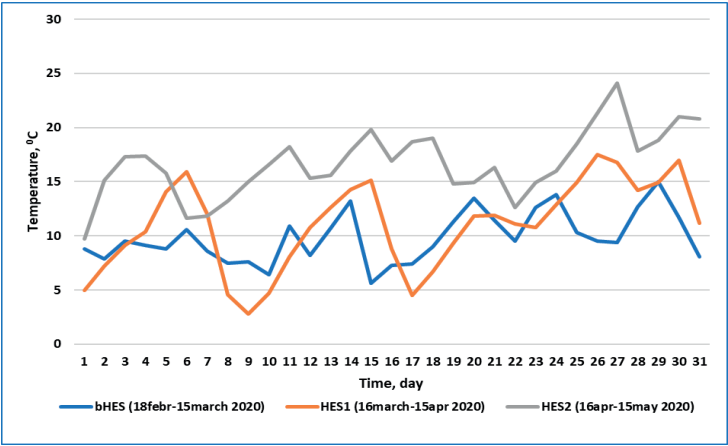


Figure 3. Variation of one of climate parameters – temperature in the analysed periods

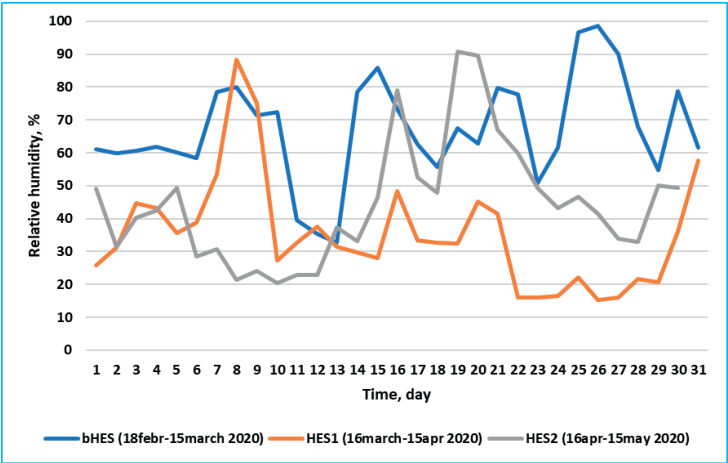


Figure 4. Graphical form of recorded values for relative humidity during the three periods

Table 5. The levels of PM2.5 and NO₂ concentrations, from two specific documents

Pollutant	Averaging time	Admissible level
WHO global air quality guidelines 2021		
PM2.5, $\mu\text{g}/\text{m}^3$	Annual	5
	24-hour	15
NO ₂ , $\mu\text{g}/\text{m}^3$	Annual	10
	24-hour	25
Directive 2008/50/EC		
PM2.5, $\mu\text{g}/\text{m}^3$	Annual	20
NO ₂ , $\mu\text{g}/\text{m}^3$	Annual	40

Figures 5 and 6 represent in graphic form the comparative analysis of the monitored values of the two pollutants, PM2.5 and NO₂, with the limits provided by the two specific documents mentioned, during the three periods studied. Thus, from the analysis of the recorded levels for PM2.5, it is found that they exceeded the limit value of 20 $\mu\text{g}/\text{m}^3$, provided by Directive 2008/50/EC, for a period of one year, on all days of the bHES period, in a proportion of 80% of the days of the HES1 period and in 55% of the days of the HES2 period.

The limit of 5 $\mu\text{g}/\text{m}^3$, for one year, provided by the WHO Guideline 2021, was exceeded in all three studied periods, and the limit of 15 $\mu\text{g}/\text{m}^3$, provided by the same document for 24 hours was exceeded in a proportion of 100% on the days of bHES period, on 95% of the days of the HES1 period and 95% of the days of the HES2 period.

The comparative analysis of NO₂ levels with the annual limit of 40 $\mu\text{g}/\text{m}^3$, provided by Directive 2008/50/EC, reveals that in the period February-March 2020 (bHES) most of the average values were above the specified limit, while during the two periods, HES1 and HES2, the average values of NO₂ levels exceeded this limit in only a few days.

Comparing the recorded values of NO₂ concentrations with limit of 10 $\mu\text{g}/\text{m}^3$ for one year period from WHO Guideline 2021 it can be observed that the obtained results are over this limit in all three studied periods, and comparing with the limit of 25 $\mu\text{g}/\text{m}^3$ for averaging time of 24-h, in the bHES period all values are over the mentioned limit, and in HES1 and HES2 periods, a proportion of about 50% of monitored values are over the limit.

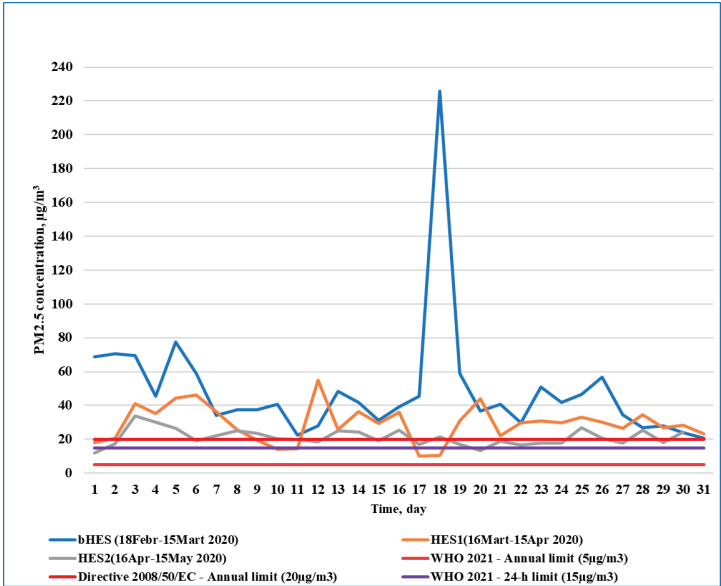


Figure 5. Comparative analysis of PM2.5 concentrations with the limits given in the specific documents

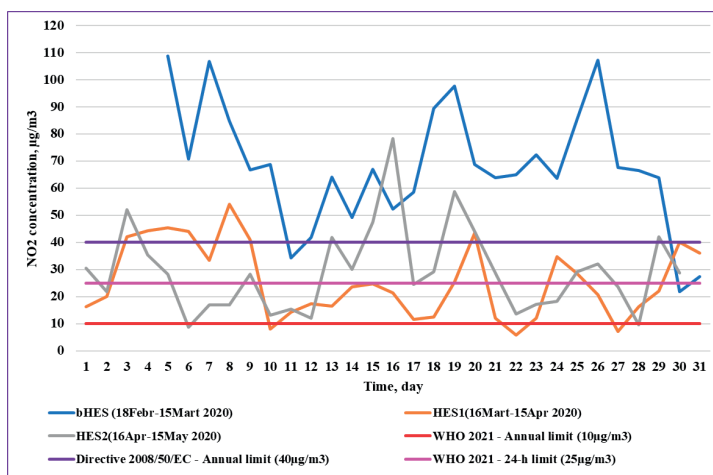


Figure 6. NO₂ concentrations analysis compared to the thresholds from the specific documents

CONCLUSIONS

The industrial development of human societies has brought a lot of advantages to ease daily life, but some activities have become generators of problems for the health of people and the environment. The COVID-19 pandemic proved to be the hard way for humanity to learn that pollution problems can be mitigated through various short-term measures. Thus, our paper carried out a comparative analysis of the levels of PM_{2.5} and NO₂, two pollutants with sources from different types of human activities, levels recorded both before the establishment of the state of health emergency (bHES) due to the upward evolution of the COVID-19 pandemic, and during the two periods of lockdown (HES1 and HES2). Moreover, the obtained results were compared with the levels provided by specific documents, in force at European and international level, namely: Directive 2008/50/EC of the European Parliament and of the Council of 21 May 2008 on ambient air quality and cleaner air for Europe, and World Health Organization (WHO) global air quality guidelines, updated in 2021. Regarding the levels of PM_{2.5} it was observed that there was a significantly decrease in PM_{2.5} concentrations during the two periods HES1 and HES2, both in the minimum values recorded, as well as in the maximum and average values, the average being between 37.5 and 54.8%, the findings being similar to those reported in other studies carried out in European or international

cities. For NO₂ concentrations, there was a decrease of 62.3% in the first month and of 57.0% in the second month of the lockdown, also similar with values recorded worldwide.

From the comparison of the PM_{2.5} recorded values with the limit value of 20 µg/m³, provided by Directive 2008/50/EC, for a period of one year, an overshoot of this limit can be seen on all days of the bHES period, in a proportion of 80% of the days of the HES1 period and in 55% of the days of the HES2 period. Also, the limit of 5 µg/m³, for one year, provided by the WHO Guideline 2021, was exceeded in all three studied periods, and the limit of 15 µg/m³, provided by the same document for 24 hours was exceeded in a large proportion in all studied periods.

The annual limit of 40 µg/m³, provided by Directive 2008/50/EC, NO₂ levels was exceeded in the period February-March 2020 (bHES), while during the HES1 and HES2 periods, the average values of NO₂ levels exceeded this limit in only a few days. Comparison of the recorded values of NO₂ concentrations with limit of 10 µg/m³ for one year period from WHO Guideline 2021 lead to the conclusion that obtained results are over this limit in all three studied periods, and comparing with the limit of 25 µg/m³ for averaging time of 24-h, in the bHES period all values are over the mentioned limit, and in HES1 and HES2 periods, a proportion of about 50% of monitored values are over the limit.

The conclusions of this analysis showed that air pollution can be reduced, one of the lessons of

COVID-19 pandemic being the possibility to implement, for health reasons, major measures in human societies, changes that seemed impossible having become reality in a few days. We can only hope that mankind will have learnt from this sad experience, and keeping of urban pollution at a low level, will become an essential concern of inhabitants.

ACKNOWLEDGEMENTS

This research work was carried out within Projects PN 23 35 02 01 and PN 19 33 04 02, financed by the Ministry of Research, Innovation and Digitalization.

REFERENCES

- Brancher, M. (2021). Increased ozone pollution alongside reduced nitrogen dioxide concentrations during Vienna's first COVID-19 lockdown: Significance for air quality management. *Environmental Pollution*, 117153.
- Brown, L., Barnes, J., & Hayes, E. (2021). Traffic-related air pollution reduction at UK schools during the Covid-19 lockdown. *Science of the Total Environment*, 780, 1-7.
- Chen, A.; Chen, L.-W. A.; Chien, L.-C.; Li Y.; & Lin G. (2020). Nonuniform impacts of COVID-19 lockdown on air quality over the United States. *Science of the Total Environment*, 745, 1-4.
- Chereches, I.A., Arion, I.D., Muresan, I. C., & Gaspar, F. (2023). Study of the Effects of the COVID-19 Pandemic on Air Quality: A Case Study in Cluj-Napoca, Romania. *Sustainability*, 15, 2549. <https://doi.org/10.3390/su15032549>.
- Collivignarelli M.C. et al. (2020). Lockdown for COVID-2019 in Milan: What are the effects on air quality?, *Science of the Total Environment*, 732, 139280.
- DECREE no. 195 of March 16, 2020, regarding the establishment of the state of emergency on the Romanian territory (in Romanian - DECRET nr. 195 din 16 martie 2020, privind instituirea stării de urgență pe teritoriul României).
- DECREE no. 240 of April 14, 2020 regarding the extension of the state of emergency on the Romanian territory (in Romanian - DECRET nr. 240 din 14 aprilie 2020 privind prelungirea stării de urgență pe teritoriul României)
- Directive 2008/50 / EC of the European Parliament and of the Council of 21 May 2008 on ambient air quality and cleaner air for Europe, retrieved from <https://eur-lex.europa.eu/eli/dir/2008/50/oj>
- Feng, J., Fan, F., Feng, Y., Hu, M., Chen, J., Shen, Y., Fu, Q., & Wang, S. (2023). Effects of COVID-19 Control Measures on the Concentration and Composition of PM_{2.5}-Bound Polycyclic Aromatic Hydrocarbons in Shanghai. *Atmosphere*, 14, 95. <https://doi.org/10.3390/atmos14010095>.
- Fuller, C.H., Jones, J.W., & Roblin, D. (2020). Evaluating changes in ambient ozone and respiratory-related healthcare utilization in the Washington, DC metropolitan area. *Environmental Research*, 186. <https://www.unep.org/interactives/air-pollution-note>, accessed on 14 February 2024
- Kumari P., & Toshniwal D. (2020). Impact of lockdown on air quality over major cities across the globe during COVID-19 pandemic. *Urban Climate*, 34, 1-19.
- Pacheco, H., Díaz-López, S., Jarre, E., Pacheco, H., Méndez, W., & Zamora-Ledezma, E. (2020). NO₂ levels after the COVID-19 lockdown in Ecuador: A trade-off between environment and human health. *Urban Climate*, 34, 1-6.
- Ropkins, K. & Tate, J. (2021). Early observations on the impact of the COVID-19 lockdown on air quality trends across the UK. *Science of the Total Environment*, 754, 142374.
- Roșu, A., Arseni, M., Constantin, D.-E., Roșu, B., Petrea, S.-M., Voiculescu, M., Iticescu, C., & Georgescu, L.P. (2023). Study of air pollution level in an urban area using low-cost sensor system onboard mobile platform. *Scientific Papers. Series E. Land Reclamation, Earth Observation & Surveying, Environmental Engineering, Vol. XII*, 124.
- Siouti, E., Skyllakou, K., Kioutsioukis, I., Patoulas, D., Apostolopoulos, I.D., Fouskas, G., & Pandis, S.N. (2024). Prediction of the Concentration and Source Contributions of PM_{2.5} and Gas-Phase Pollutants in an Urban Area with the SmartAQ Forecasting System. *Atmosphere*, 15, 8.
- Tobías, A., Carnerero, C., Reche, C., Massagué, J., Via, M., Minguillón, M.C., Alastuey, A., & Querol, X. (2020). Changes in air quality during the lockdown in Barcelona (Spain) one month into the SARS-CoV-2 epidemic. *Science of the Total Environment*, 726, 1-4.
- Velayarce, D., Bustos, Q., García, M.P., Timaná, C., Carbajal, R., Salvatierra, N., Horna, D., & Murray, V. (2022). Air Quality Analysis in Lima, Peru Using the NO₂ Levels during the COVID-19 Pandemic Lockdown. *Atmosphere*, 13, 373. <https://doi.org/10.3390/atmos13030373>.
- World Health Organization (WHO) (2021). WHO global air quality guidelines. Particulate matter (PM_{2.5} and PM₁₀), ozone, nitrogen dioxide, sulfur dioxide and carbon monoxide. Retrieved from <https://www.who.int/publications/i/item/9789240034228>.
- Zoran, M.A., Savastru, R.S., Savastru, D.M., & Tautan M.N. (2020). Assessing the relationship between ground levels of ozone (O₃) and nitrogen dioxide (NO₂) with coronavirus (COVID-19) in Milan, Italy. *Science of the Total Environment*, 740, 1-10.
- Zoran, M.A., Savastru, R.S., Savastru, D.M., & Tautan M.N. (2022). Cumulative effects of air pollution and climate drivers on COVID-19 multiwaves in Bucharest, Romania. *Process Safety and Environmental Protection*, 166, 368-383. <https://visitbucharest.today/coronavirus-lockdown-the-fascinating-deserted-streets-of-bucharest/>

RELATIONSHIPS BETWEEN SPECTRAL VEGETATION INDICES (SVIs) AND GROWTH STAGES IN A TABLE GRAPE VINEYARD

Zhulieta ARNAUDOVA, Boyan STALEV

Agricultural University - Plovdiv, 12 Mendelev Blvd, Plovdiv, Bulgaria

Corresponding author email: julieta_arnaudova@abv.bg

Abstract

Table grape is a crop with a high nutritional value and frequent control is a guarantee of high quality and yields. The application instruments and methods for remote monitoring in obtaining information on the status of the vineyard will allow farmers to respond adequately to changes in plant development and grape quality. The aim of this study is to use non-destructive methods, such as satellite monitoring in the prediction of phenological changes that occur in the vine crop. The object of the study is a commercial table grape vineyard Vitis vinifera cv Velika in the land of village Granit, Stara Zagora district, Bulgaria in the period 2021-2023. NDVI was calculated using data from Sentinel 2 satellite in the main growth stages. The physiological state of the vines and the growth behaviour in the crop were monitored. An analysis was made of the relationship between the dynamics of the growth and NDVI to predict the yields.

Key words: NDVI, remote sensing, vineyards, vegetation indices.

INTRODUCTION

Climate change poses a significant challenge to the global grape industry as it has the potential to disrupt vineyard growth. The profitability and growth of the wine industry in different regions can be affected by climate change, as the development of plantations is highly dependent on weather conditions in the short-term and climate conditions in the long-term (Sun et al., 2023).

Environmental conditions play a crucial role in determining not only yield but also the potential quality of grapes. Furthermore, profitability for growers in certain regions may be stimulated by optimizing yields and reducing production costs, while in other regions it may be stimulated by producing higher quality grapes. The factors that influence profitability include market access and growing conditions. This information is based on a study by Dr. Qun Sun published in 2023.

The growth conditions of vines during critical phenological stages can significantly affect the quality and quantity of grapes. Field observations of vine growth stages are insufficient to capture the spatial variability of vine conditions. Predicting grape yield using traditional methods requires many grape samples. Satellite imagery analysis is used more and more in many domains, from micro - to

macro scale (Herbei et al., 2021) and remote sensing data can provide detailed spatial and temporal information on vine development, which is useful for vineyard management (Liang et al., 2017; Sabbatini et al., 2016).

The size and distribution of the sample are determined by the rows and spacing between the vines, which means that spatial variability must be considered. Yield estimation systems are based on sampling: (a) the number of grapevines per hectare; (b) the number of grape berries per vine, with most of them; and (c) the weight of the grape (Clingeffer, 2016; Wolpert et al., 1992; Tarara et al., 2013). Manufacturers must determine whether, when, and how many fruits to remove during thinning. Therefore, daily observation for optimal vineyard management through ground measurements is unlikely to be representative of field conditions and is expensive to install and maintain, especially for large and distributed production systems.

Remote sensing data has significant advantages over other monitoring techniques as it provides a timely, synoptic, and up-to-date overview of actual crop growing conditions over large areas at several stages during the growing season.

Strong relationships have been found to exist between satellite-based vegetation indices, such as NDVI, and vine development in vineyards (Cunha et al., 2010; Johnson et al., 2003; Hall et al., 2002).

Remotely sensed data can be used to infer vine shape and size (Hall et al., 2001), predict phenols and grape colour (Lamb et al., 2004), and differentiate cultivars in vineyards (Brady et al., 2000; Arkun et al., 2001). Different approaches exist for using vegetation indices and their relationships with analytical measurements. These can be classified into two main categories: using empirical relationships between vegetation indices or by inverting a physical radiative transfer mode (Ganguly et al., 2012; Dong et al., 2016; Huang et al., 2015).

The aim of this study is to use non-destructive methods, such as satellite monitoring for establishing a relationship between analytical measurement and vegetation indices in the prediction of phenological changes that occur in the vine crop.

MATERIALS AND METHODS

This study focuses on the open field situated in the South-Central region of Bulgaria, specifically in the village of Granit, municipality of Bratya Daskalovi, Stara Zagora district (Figure 1).



Figure 1. Location of study area
 (Google Earth 17.06.2022)
 L42°14'51.69"N B25° 9'6.36"E

Experimental design and treatments

NDVI was obtained from Copernicus Land Monitoring Service as a daily update of Normalised Difference Vegetation Index provided at pan-European level and in near real time. The data were available at 10 m x 10 m spatial resolution from Sentinel-2 HR multispectral satellite imagery (according to Data viewer - Copernicus Land Monitoring Service).

The Normalized Difference Vegetation Index (NDVI) is an effective index for quantifying green vegetation. It is a measure of the state of vegetation health based on how plants reflect light at certain wavelengths. The value range of the NDVI is -1 to 1. Negative values of NDVI (values approaching -1) correspond to water. Values close to zero (-0.1 to 0.1) generally correspond to barren areas of rock, sand, or snow. Low, positive values represent shrub and grassland (approximately 0.2 to 0.4), while high values indicate good health and growth of the vegetation (values approaching 1).

The formula of the NDVI is:

$$NDVI = \frac{NIR - RED}{NIR + RED}$$

where:

- NIR is near-infrared light;
- RED is red light.

For Sentinel-2, the index looks like this:

$$NDVI = \frac{B8 - B4}{B8 + B4}$$

where:

- B8 = 842 nm;
- B4 = 665 nm.

In the event of the plant becoming dehydrated, diseased, afflicted by a disease etc., the spongy layer will deteriorate, resulting in a change in the plant's ability to reflect rather than absorb near-infrared light.

Using the NDVI data in the study regions, the changes in vegetation cover present in the area and the trend in occurrence of agricultural drought can be studied (Sruthi et al., 2015).

The images and sample raster values from NDVI imagery were processed by QGIS 3.10.

Time series imageries were downloaded for the main stages of the vine plant in the experimental field and in situ data collection for 2021-2023. The growth stages are calculated in the Days Of the Year (DOY). The correlations between the studied variables were obtained by regression analysis in Excel Microsoft 365 and were valid within the time range studied.

In situ data collection was conducted between 2021 and 2023 in a 30-hectare vineyard. Observations were made on a 1-hectare experimental plot. Phenology and growth of 40 vines, arranged in 4 replicates of 10 vines in two rows, were monitored within the target field.

The planting distance is 2.80 m between the rows and 1.20 m between the vines in each row and stem Gyuyo formation. Pruning involved leaving two fruit canes and two spurs. The climate data for temperature and precipitation has been recorded by the Meteobot climate station in the plantation. The vineyard is cultivated under irrigation.

In situ measurements were carried out during six main stages of grape development: budding, appearance of first leaf, flowering, veraison, technological maturity, and leaf fall. The plants on which the growth dynamics were monitored were not pruned to account for the maximum length of the shoots. Linear growth was recorded until the shoots reached their maximum height. Measurements began when the shoots were 15-20 cm long and were taken every 10-15 days.

The growth dynamics of the shoots have been traced and a correlation has been established between the values of NDVI and the length of the shoots, based on the DOY.

RESULTS AND DISCUSSIONS

The object of the study is a typical table grape variety Velika, created in 1997 in the IASS "Obraztsov chiflik", Rousse. The main distribution area is in Bulgaria, Italy, Macedonia, Morocco. It belongs to the early ripening grape varieties with ripening period from 15 to 20 August. It is suitable for growing in warm regions with a lack of late spring and early autumn frosts. The development of the vines from forced dormancy to vegetation occurs when the average daily temperature is 10°C In the frame of the experiment, this temperature occurred in late March and early April in all three years. The selected cultivar and vineyard are in a transitional-continental zone, where we have periods of irregular precipitation and large temperature amplitude. The experimental years had a growing season length of 208-215 days (Table 1.)

Table 1. Phenological development of the Velika cultivar (Granit)

Year	Budding	First leaf	Flowering	Veraison	Maturity	Fall leaf	Vegetation period
2021	10.04	28.04	8.06	30.07	15.09	4.11	208
2022	28.03	10.04	31.05	20.08	19.09	28.10	215
2023	26.03.	5.04	14.06	28.08	16.09	26.10	215

The Meteobot station's meteorological model data is used to determine the vineyard's stages. The results indicate a direct correlation between the availability of minimum temperatures required for phenological growth and the development of the winter buds and dormant buds in the vine during the experimental years. In 2022, a climatic anomaly was observed in terms of vine phenology. The data from soil and atmosphere temperature sensors showed that growth stage development was primarily temperature dependent. However, in 2022, less precipitation was recorded in the spring, leading to budding as early as 10 April. The lack of rainfall caused the vines to stop developing, resulting in a delay in the following phenophases (Figures 2 and 3).

The application of satellite imagery in the early stages of grapevine development and the values of the vegetation index (NDVI) from the beginning of active vegetation (130 DOY) would provide practical information to grape producers for conducting measures that

reactivate growth processes and transition to subsequent phenophases. The growth of shoots in viticulture indicates the physiological state of the vineyard and its readiness to produce high-quality grape raw material.

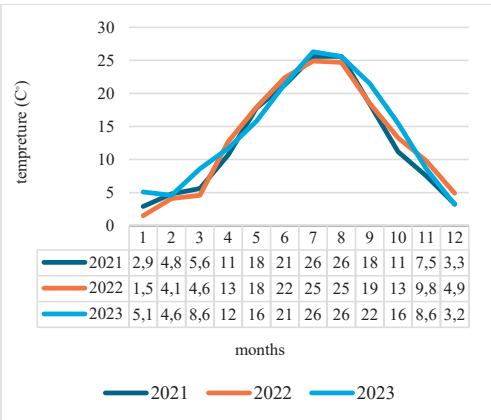


Figure 2. Climate characteristics for the experimental period

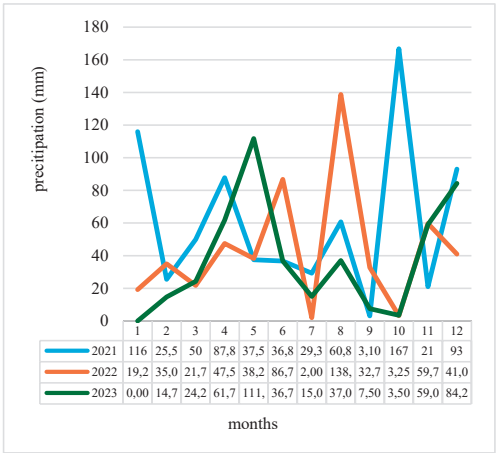


Figure 3. Precipitation for the experimental period

The results of our three-year experiment show that the formation of leaf mass on the shoot depends on environmental factors and the care provided by the producer. The growth in the first measurement dates indicates lower activity, which is due to temperature fluctuations and cold soil.

With the increase in the average daily temperature, the growth rate accelerates and reaches 4-5 cm per day. The observation indicates that most of the new vegetative growth is formed within 160-180 days from the beginning of vegetation (200-220 DOY) (Figure 4).

The obtained dependencies between the length of the shoots in the active vegetation period have a high degree of multiple correlation. During the first two years of the study period, the growth is described with a second-degree polynomial curve and equation due to the delayed growth. However, for the year 2023, the relationship is linear. The multiple correlation coefficient R^2 is 0.96-0.98 for the three years.

The relationship between NDVI values during the active vegetation period and the occurrence of the four main stages in the vineyard was investigated.

The relationships found showed very high and high correlation coefficients throughout the active period. For 2021 $R^2 = 0.98$, $R^2 = 0.78$ for 2022. The lowest value of the coefficient is recorded in 2023, which is characterized by the lowest shoot growth and high temperatures (Figure 5).

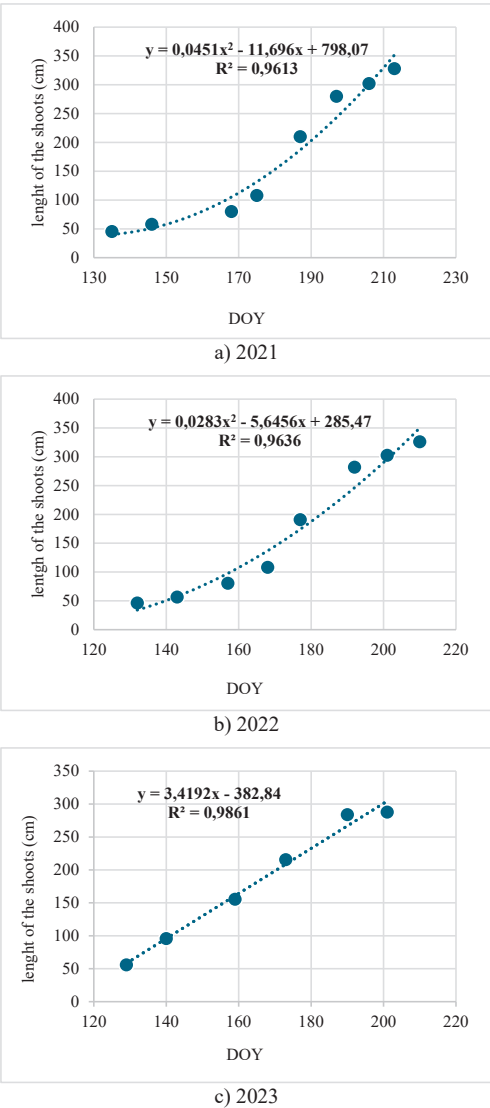


Figure 4. Shoot growth dynamics over the three experimental years

To reduce the duration of analytical in situ measurements, a correlation was discovered between shoot growth and reported NDVI values. This enables in situ observations to be limited to the main vegetation stages, with the remaining data interpreted by predicting vegetation index and shoot length data.

The downloaded images from the NDVI time series cover only the four main phases from April to mid-September. The measured shoot lengths are for a period of active growth from

May to July, over an average of 15 days, based on the occurrence of the phenophases. The equations that relate NDVI and DOY to vegetation stages have a wider validity than the measured shoot lengths. They can be used to predict results and derive a mathematical model for the relationship between NDVI values and shoot length.

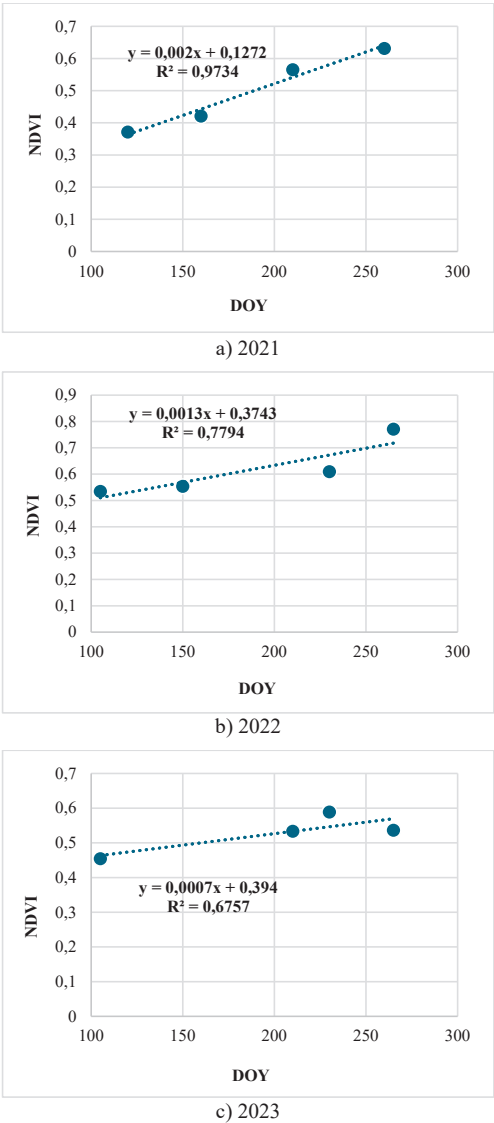


Figure 5. Relationship between NDVI values and active vegetation stages

The resulting models have a high degree of multiple correlation and are a reliable indicator

for relating satellite data to in situ measurements.

The growth processes are demonstrated based on the satellite images and NDVI values.

Figure 6 presents the mathematical models for the three experimental years.

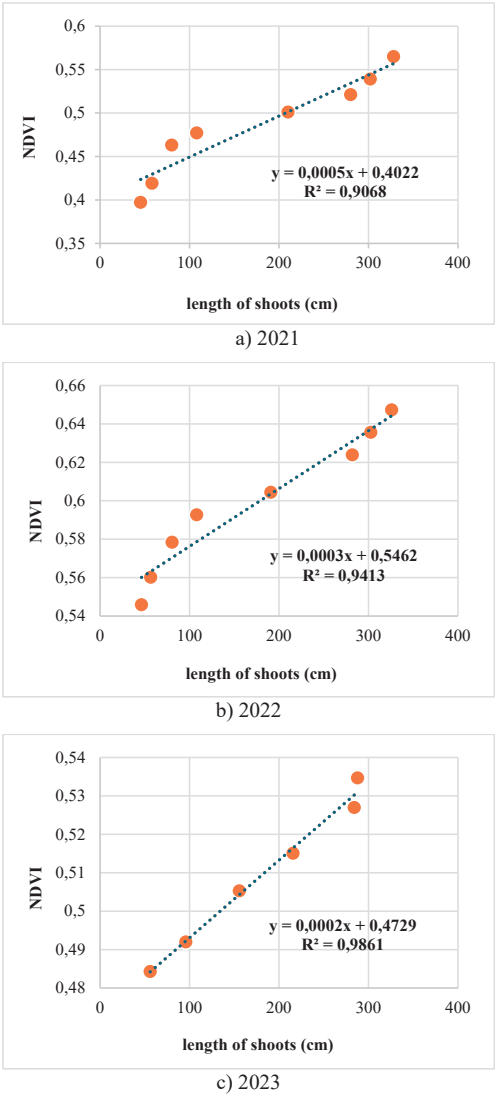


Figure 6. Mathematical model of dependence between NDVI value and length of the shoots

CONCLUSIONS

The study presents information on the phenological and growth processes of the vine during its annual development cycle.

The prediction of growth dynamics and NDVI values will enable the optimization of pruning timing in vineyards.

The use of digital tools, such as satellite images, enables us to apply appropriate agronomic practices to restore the growth and vigour potential of the vine crop in the event of a delay in the phenological phases and the formation of vegetative mass.

ACKNOWLEDGEMENTS

This work is supported by the Bulgarian Ministry of Education and Science under the National Research Program "Smart Crop Production", Grant D01-65/19.03.2021, approved by Decision of the Ministry Council No 866/ 26.11.2020.

REFERENCES

- Arkun, S., Dunk, I.J., Ranson, S.M. (2001). Hyperspectral remote sensing for vineyard management. In *Proceedings of the 1st National Conference on Geospatial Information & Agriculture*, Sydney, Australia, 586–599.
- Brady, J., Wiley, S. (2000). Tading AIMS amongst the vines. *Aust. Grapegrow. Winemak.* 441, 73–75.
- Clingeffer, P. (2016). Crop Development, Crop Estimation and Crop Control to Secure Quality and Production of Major Wine Grape Varieties: A National Approach. <http://research.wineaustralia.com/wp-content/uploads/2012/09/CSH-96-1.pdf>.
- Cunha, M., Marçal, A.R.S., Silva, L. (2010). Very early prediction of wine yield based on satellite data from vegetation. *Int. J. Remote Sens.*, 31, 3125–3142.
- Data viewer – Copernicus Land Monitoring Service
- Dong, T., Liu, J., Qian, B., Zhao, T., Jing, Q., Geng, X., Wang, J., Huffman, T., Shang, J. (2016). Estimating winter wheat biomass by assimilating leaf area index derived from fusion of Landsat-8 and MODIS data. *Int. J. Appl. Earth Obs. Geoinf.*, 49, 63–74.
- Ganguly, S., Nemani, R.R., Zhang, G., Hashimoto, H., Milesi, C., Michaelis, A., Wang, W., Votava, P., Samanta, A., Melton, F., et al. (2012). Generating global Leaf Area Index from Landsat: Algorithm formulation and demonstration. *Remote Sens. Environ.*, 122, 185–202.
- Hall, A., Lamb, D.W., Holzappel, B., Louis, J. (2002). Optical remote sensing applications in viticulture—A review. *Aust. J. Grape Wine Res.*, 8, 36–47.
- Hall, A., Louis, J., Lamb, D. (2001). A method for extracting detailed information from high resolution Multispectral images of vineyards. In *Proceedings of the 6th International Conference on Geocomputation*, Brisbane, Australia, 24–26 September 2001.
- Herbei, M.V., Bertici, R., Sala, F. (2021). Geomatic methods for management planning of protected areas. case study: Paniova forest, Timis County, Romania. *Scientific Papers. Series E. Land Reclamation, Earth Observation & Surveying, Environmental Engineering*, X, 301–310, Print ISSN 2285-6064
- Huang, J., Tian, L., Liang, S., Ma, H., Becker-Reshef, I., Huang, Y., Su, W., Zhang, X., Zhu, D., Wu, W. (2015). Improving winter wheat yield estimation by assimilation of the leaf area index from Landsat TM and MODIS data into the WOFOST model. *Agric. For. Meteorol.*, 204, 106–121.
- Johnson, L.F., Roczen, D.E., Youkhana, S.K., Nemani, R.R., Bosch, D.F. (2003). Mapping vineyard leaf area with multispectral satellite imagery. *Comput. Electron. Agric.*, 38, 33–44.
- Lamb, D., Weedon, M.M., Bramley, R.G.V. (2004). Using remote sensing to predict grape phenolics and colour at harvest in a Cabernet Sauvignon vineyard: Timing observations against vine phenology and optimising image resolution image. *Aust. J. Grape Wine Res.*, 10, 46–54.
- Sabbatini, P., Dami, I., Howell, G.S. (2016) Predicting Harvest Yield in Juice and Wine Grape Vineyards. Predicting_Harvest_Yield_in_Juice_and_Wine_Grape_Vineyards_(E3186).pdf (msu.edu)
- Sruthi, S., M.A. Mohammed Aslam (2015). Agricultural Drought Analysis Using the NDVI and Land Surface Temperature Data; a Case Study of Raichur District. *International Conference on Water Resources, Coastal and Ocean Engineering (ICWRCOE 2015)*, Aquatic Procedia, 4, 1258 – 1264.
- Sun, L., Gao, F., Anderson, M.C., Kustas, W.P., Alsina, M.M., Sanchez, L., Sams, B., McKee, L., Dulaney, W., White, W.A., et al. (2017). Daily Mapping of 30 m LAI and NDVI for Grape Yield Prediction in California Vineyards. *Remote Sensing*, 9(4), 317. <https://doi.org/10.3390/rs9040317>
- Sun, Q., Granco, G., Groves, L., Voong, J., Van Zyl, S. (2023). Viticultural Manipulation and New Technologies to Address Environmental Challenges Caused by Climate Change. *Climate*, 11(4), 83, <https://doi.org/10.3390/cli11040083>
- Tarara, J.M., Chaves, B., Sanchez, L.A., Dokoozlian, N.K. (2013). Analytical determination of the lag phase in grapes by remote measurement of trellis tension. *HortScience*, 48, 453–461.
- Wolpert, J.A., Vilas, E.P. (1992). Estimating Vineyard Yields: Introduction to a Simple, Two-Step Method. *Am. J. Enol. Vitic.*, 43, 384–388.
- http://msue.anr.msu.edu/uploads/resources/pdfs/Predicting_Harvest_Yield_in_Juice_and_Wine_Grape_Vineyards_%28E3186%29.pdf.

DETERMINATION OF LAI AT DIFFERENT GROWTH STAGES OF PEPPER PLANTS GROWN IN FIELD

Zhulieta ARNAUDOVA, Dimka HAYTOVA

Agricultural University - Plovdiv, 12 Mendelev Blvd, Plovdiv, Bulgaria

Corresponding author email: julieta_arnaudova@abv.bg

Abstract

The leaf area index (LAI) is important for monitoring and assessing crop vigor. It is used in the evaluation of plant condition, as inputs in various models to predict productivity. The main aim of this study was to identify the changes in LAI between major growth stages of pepper. In situ measurements and time series imagery from Copernicus Land Monitoring services were used. In situ data collection was carried out in a production pepper plantation, cv. Slonsko uho is grown under open field conditions in the village of Katunitsa, Plovdiv region, Bulgaria. Measurements were carried out in different stages of the development of plants. The destructive determination of LAI was conducted after collection of plant samples. The leaf area was determined using an electronic plotter Image Analysis Systems "WinDias 3". The leaf area index was calculated as the ratio of plant leaf area covering a unit of land area. The LAI images were downloaded for two years (2022 and 2023), between different stages of the development of pepper. A correlation between satellite data and in situ measurements was established. The dependence of LAI on the time series for the two years was determined.

Key words: pepper, productivity, vegetation indices.

INTRODUCTION

Remote sensing and vegetation indices are fast and efficient methods of crop assessment. Satellite and remote sensing images can identify crop classes, predict crop yield, and make inferences about the status of plants and their environmental conditions on an almost real-time basis (Schuler, 2002; Mihailescu & Cimpeanu, 2023). Remote sensing data can be very useful for detecting the phenological variability of a crop (Poenu et al., 2017). Zhang et al. (2006) applied mathematical models to Moderate Resolution Imaging Spectroradiometer (MODIS) time series to determine vegetation phenology on a global scale. They establish that the spatial distribution of phenological indicators estimated from MODIS data is qualitatively more realistic and shows strong agreement with climatic conditions in agricultural regions. The economic benefits of using remote sensing for crop monitoring include scientific, technological, methodological, and economic efficiency (Badarch, 1990). According to Liu et al. (2016), leaf area index (LAI) derived from hyperspectral imagery has been successfully used for more than 20 years.

The leaf area index is calculated as the ratio of the unilateral (illuminated) leaf area to the soil surface area they can cover (Chen & Black, 1992). Determining LAI for an agricultural crop and tracking its dynamics is very important for a wide range of research as well as for continuous monitoring of the crop and real-time diagnostics (Fang et al., 2011). The ratio of the leaf area covering a land surface unit describes the potential active photosynthetic leaf area, which plays an important role in the basic life processes of the plant organism - photosynthesis, autotrophic respiration, transpiration, stomatal conductance etc. In its wider interpretation, LAI is an index reflecting the physiological and biochemical processes occurring in the plant organism (Viña et al., 2011; Liu et al., 2014). According to Viña et al. (2011), most vegetation indices (including LAI) are species-specific, and need to be determined individually according to the leaf structure and morphological characteristics of the plants and the vegetative growth rate.

In the scientific literature, information on LAI determination in pepper is limited. Li et al. (2017) determined LAI in pepper for stand evaluation using satellite data from Sentinel-2. They recommend the use of remote sensing in

precision agriculture. In their future research, they put the focus on the comparison of LAI and NDVI to build a comprehensive model for remote monitoring of pepper grown in open areas. LAI is not only an important parameter used to describe the geometry of the vegetation canopy but also a key indicator for understanding the ecological processes at the global and regional scale. The growth dynamics and seasonal progression of vegetation can also be timely reflected by the LAI (Qiao et al., 2019). The use of remote sensing and the possibilities of LAI as an active indicator of ongoing plant processes (Soudani et al., 2006; Kobayashi et al., 2007; Wu et al., 2015; He Y. et al., 2016; He L.I. et al., 2016) are the main motivation for this publication.

The main aim of this study was to identify the changes in LAI between major growth stages of pepper.

MATERIALS AND METHODS

The open field is located in the Sout-Central region of Bulgaria in the village of Katunitsa, municipality Sadovo, Plovdiv district (Figure 1). Leaf Area Index was obtained from Copernicus Land Monitoring Servies by Sentinel-2 HR multispectral satellite imagery. The LAI images are available at a spatial resolution of 10m x 10m and daily updates of Leaf Area Index are provided at pan-European level and in near real-time (Data Viewer/ Bio-geophysical parameters /Vegetation/LAI,Europe,daily <https://land.copernicus.eu/en/map-viewer>).

This index is used to forecast crop growth and yield and estimate foliage cover. LAI uses the empirical formula developed by Boegh et al. (2002):

$$LAI = (3.618 * EVI - 0.118)$$

where:

- EVI is Enhanced Vegetation Index value.

The images and sample raster values from LAI were processed by QGIS 3.10. Time series images were downloaded for the same period of experimental in situ data collection. The main growth stages are calculated in the days after transplanting the pepper on the open field. The correlations between the studied variables were obtained by regression analysis in Excel Microsoft 365 and were valid within the time range studied.



a) L42°6'49.69"N B24°52'38.77"E
 (Goggle Earth 3.07.2022)



b) L42°8'16.77"N B24°52'17.84"E
 (Google Earth 29.06.2023)

Figure 1. Location of study areas and target fields

In situ data collection was carried out in the period 2022-2023 on a production pepper plantation. A randomized block design was used. Five target fields were determined. These elementary plots are 50 m² with 400 plants in each (Figure 2).

In situ measurements were carried out in four main stages of pepper development - flower buds, flowering, before maturity, and maturity. Destructive determination of LAI was made after the collection of plant samples. The number of leaves per plant was established. Leaf area per plant (cm²) and total leaf area (m²/ha) were determined. Leaf area meter, WinDias3 system of the company WinDias Image Analysis System of the company Delta-T Devices, Cambridge, UK was used. The leaf area index was calculated as the ratio of plant leaf area covering a unit of land area (Arnaudova et al., 2022).

The pepper was grown according to conventional technology for middle-early field production in open fields (Cholakov, 2009; Shaban et al., 2014). The scheme used is 90+70/15 with a population of 833.3 plants per hectare and drip irrigation.



Figure 2. Methodological plan of the experiment

RESULTS AND DISCUSSIONS

The variety 'Elephant ear' belongs to the species *Capsicum annum* ssp. *macrocarpum* ser. var. Leaf formation the intensified setting of reproductive organs and fruit formation is staged and their number increases during all observed phases (Figure 3). This feature was found in both vegetation periods (2022 and 2023).

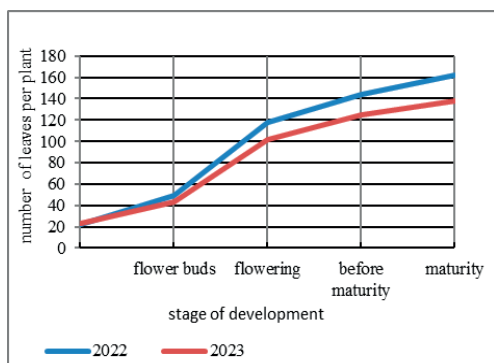


Figure 3. Dynamics of leaf formation during the stage of pepper development

The most intense leaf formation is recorded between the flower buds and flowering phases. In the following stages of development, the rate slows down, which is most likely due to longum var. *kapia*. It is characterized by large dark green leaves with a broadleaved shape (Panayotov & Jadchak, 2020). As the number of leaves formed on a single plant increases, the leaf area also increases (Figure 4.). In 2022, the change was from 426.86 cm² at the bud stage to 2088.36 cm² at the botanical maturity stage. In 2023, the change was from 375.64 cm² to 1775.11 cm². The results obtained from the in-situ field data for both experimental years highlight a trend of

balanced development of pepper plants without any sharp deviations or lag in their development. The formed leaf assimilation surface is a prerequisite for the normal establishment of generative organs and the formation of economic yield (Mihov et al., 2014; Sandhu et al., 2020).

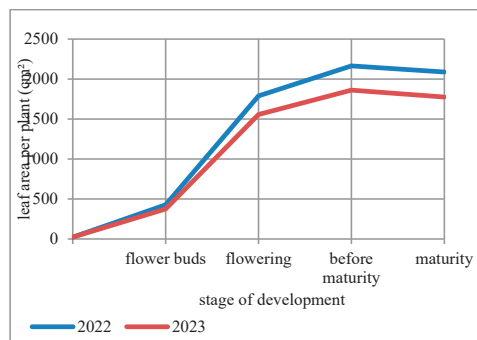


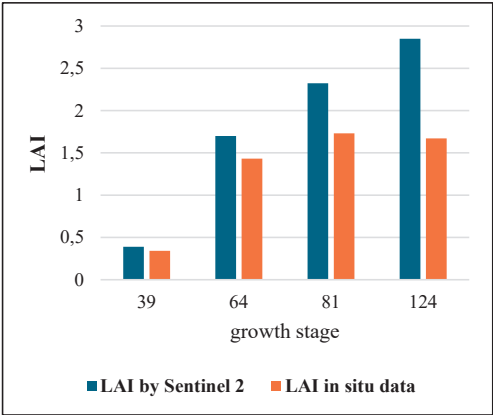
Figure 4. Formation of leaf area per plant during the different stages of grow

In 2022, the LAI calculated by the destructive method increases to the technological maturity phase from 0.34 in the flower buds stage to 1.73, and in the botanical maturity stage decreases to 1.67. This feature is most likely due to physiological senescence and scaling of some of the earliest leaves. The results are similar in 2023 (Figure 5).

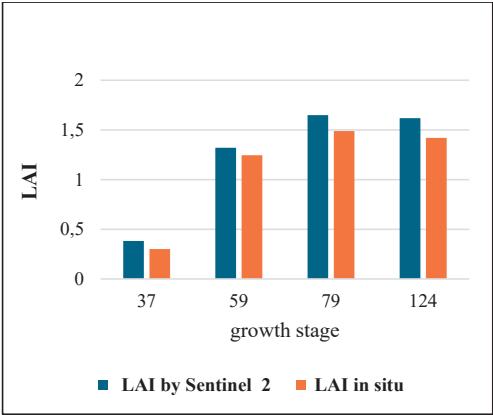
The LAI values obtained from the images of the experimental plots compared with the in-situ data increased through all stages of pepper, from 0.39 at the flower bud stage to 2.85 at the botanical maturity stage for 2022. The differences in the constant increase of LAI are due to weeding in the crop.

The values for 2023 increased from 0.38 at the flower bud stage to 1.65 and decreased to 1.61 at the botanical maturity stage due to drought or physiological senescence and leaf scaling of pepper (Figure 5 and Figure 6).

Figure 6 a depicts maps with 10-meter spatial resolution generated by the Copernicus Land Service of the LAI for growth stages in 2022, with the phases occurring at 39, 64, 81, and 124 days after transplanting. The same growth stages are depicted for 2023 in Figure 6 b, occurring at 37, 59, 79, and 124 days after transplanting. The LAI values from the sample points at the five target sites were averaged and compared to the *in situ* data.



a) 2022



b) 2023

Figure 5. LAI value by satellite and in situ data

To analyze the values thus obtained, a comparative regression analysis was performed between the satellite data and the analytical ones. The coefficient of multiple correlations is very high $R^2 = 0.90$ for 2022 and $R^2 = 0.99$ for 2023 (Figure 7). Two-year dependencies of LAI were identified through investigations, and mathematical models were constructed to describe the difference between LAI values and in situ data by the main pepper stage of development.

The derived equations were used to fit satellite data to the analytically determined indices, allowing for the prediction of expected LAI values. The multiple correlation coefficients were $R^2 = 0.99$ for 2022 and $R^2 = 0.85$ for 2023.

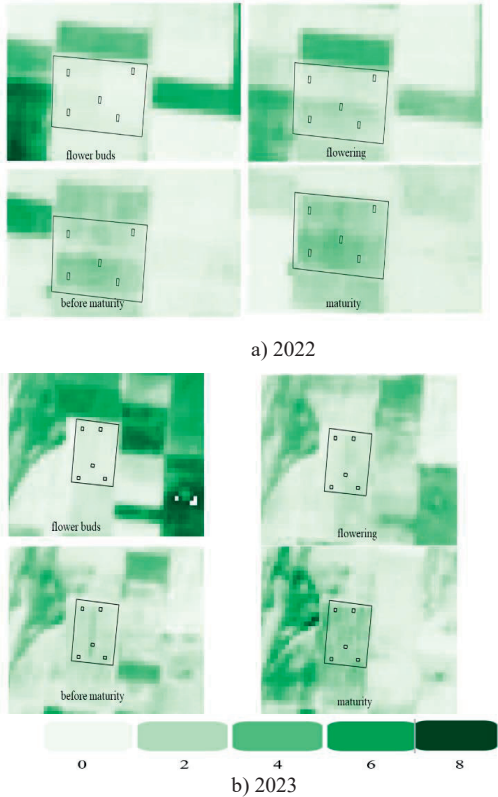
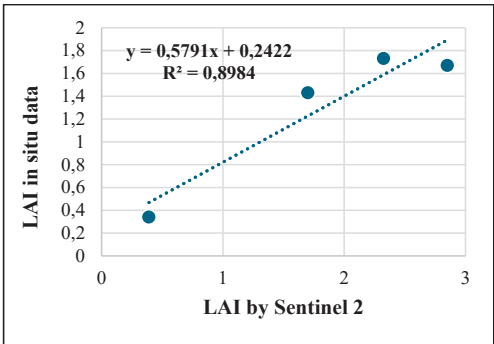
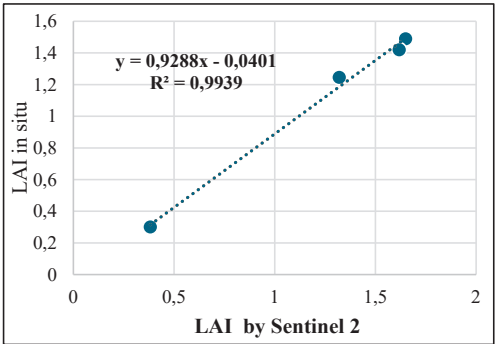


Figure 6. Satellite images of LAI for the main growth stages

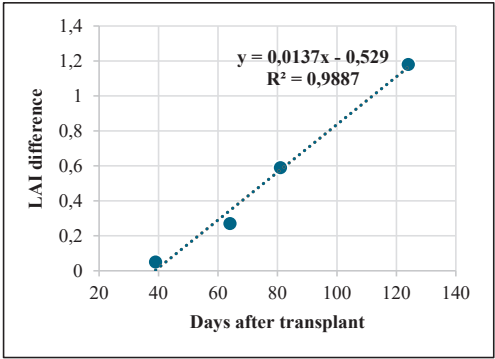
The data from both years confirm that using imaging and extracting LAI values from the time series is a reliable method for estimating the stages of pepper development (Figure 8).



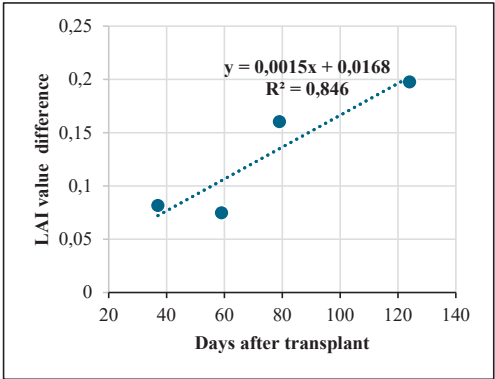


b) 2023

Figure 7. Relationship between LAI value from satellite and in situ data



a) 2022



b) 2023

Figure 8. Mathematical models of the difference between LAI values and *in situ* data by main growth stages

Our results are in line with the research conducted by Li et al. (2017) to use satellite images for determining bio-geophysical parameters and establish the correlation between field data and remote sensing data.

CONCLUSIONS

The investigation results indicate that using 10x10 m spatial resolution time-series imagery for the Sentinel 2 LAI is highly useful.

The robust correlation between the LAI values determined by in-situ and LAI values derived from satellite imagery can be evidenced by the high values of the multiple correlation coefficient $R^2 = 0.90$ for 2022, and $R^2 = 0.99$ for 2023.

The mathematical model developed for the discrepancies between LAI estimates obtained from in situ observations and satellite imagery can be utilised to predict the development of pepper plants with high accuracy.

The use of remote sensing data to estimate the LAI is more cost-effective and timesaving compared with other methods and is suitable for large-scale and long-term monitoring of vegetation with minimum effort.

For future pepper plantations remote sensing monitoring research, a relationship between LAI and other vegetation indices for example as NDVI and SAVI can be explored based on the results obtained.

ACKNOWLEDGEMENTS

This work is supported by the Bulgarian Ministry of Education and Science under the National Research Program "Smart Crop Production", Grant D01-65/19.03.2021, approved by Decision of the Ministry Council No 866/ 26.11.2020.

REFERENCES

- Arnaudova, Z., Haytova, D., Panayotov, N., & Petrova, S. (2022). Methodological approach for assemble data from vegetable crops for use in remote sensing. *Agribalkan*, 470.
- Badarch, M. (1990). An Assessment of the Economics of Remote Sensing Applications to Natural Resources and Environment Development in Mongolia. *The Economics of Remote Sensing. Report of Regional Conference on the Assessment of Economics of Remote Sensing Applications to Natural Resources and Environment Development Projects in the ESCAP Region*, 62–64.
- Boegh, E., Soegaard, H., Broge, N., Hasager, C. B., Jensen, N. O., Schelde, K. & Thomsen, A. (2002). Airborne multispectral data for quantifying leaf area index, nitrogen concentration, and photo-synthetic

- efficiency in agriculture. *Remote Sens. Environ.*, 81, 179–193, doi:10.1016/S0034-4257(01)00342-x.
- Chen, J.M., Black, T.A. (1992). Defining Leaf-Area Index for Non-Flat Leaves. *Plant Cell. Environ.*, 15, 421–429.
- Cholakov, D. (2009). *Technology for cultivation pepper in Vegetable-growing*. Academic publishers of Agricultural University-Plovdiv, pp. 130-150 (in Bulgarian).
- Fang, H., Liang, S., Hoogenboom, G. (2011). Integration of MODIS LAI and vegetation index products with the CSM-CERES-Maize model for corn yield estimation. *International Journal of Remote Sensing*. 32(4), 1039–1065.
- He, L.I., Zhongxin, C., Zhiwei, J., Wenbin, W.U., Jianqiang, R.E.N., Bin, L.I.U., Tuya, H. (2016). Comparative analysis of GF-1, HJ-1, and Landsat-8 data for estimating the leaf area index of winter wheat. *Journal of Integrative Agriculture*, 16(2), 266–285, Doi: 10.1016/S2095-3119(15)61293-X.
- He, Y., Bo, Y., Chai, L., Liu, X., Li, A. (2016). Linking in situ LAI and fine resolution remote sensing data to map reference LAI over cropland and grassland using geostatistical regression method. *International Journal of Applied Earth Observation & Geoinformation*, 50, 26–38.
<https://land.copernicus.eu/en/map-viewer>
- Kobayashi, H., Suzuki, R., Kobayashi, S. (2007). Reflectance seasonality and its relation to the canopy leaf area index in an eastern Siberian larch forest: Multi-satellite data and radiative transfer analyses. *Remote Sensing of Environment*, 106(2), 238–252.
- Li, D., Jiang, H., Chen, S., Wang, C., Huang, S., & Liu, W. (2016). Leaf area index estimation of winter pepper based on canopy spectral data and simulated bands of satellite. In *International Conference on Geo-Informatics in Resource Management and Sustainable Ecosystems*, pp. 515–526. Springer Singapore.
- Liu, K., Zhou, Q.-B., Wu, W.-B., Xia, T., Tang, H.-J. (2016) Estimating the crop leaf area index using hyperspectral remote sensing. *Journal of Integrative Agriculture*, 15(2), 475–491.
- Liu, Q., Liang, S., Xiao, Z., Fang, H. (2014). Retrieval of leaf area index using temporal, spectral, and angular information from multiple satellite data. *Remote Sensing of Environment*, 145(8), 25–37.
- Mihailescu, D. & Cimpeanu, S.M. (2023). Monitoring the vegetation state in Oltenia plain, using Copernicus land products. *Scientific Papers. Series E. Land Reclamation, Earth Observation & Surveying, Environmental Engineering*, XII, 458–466, Print ISSN 2285-6064.
- Mihov, Kr., Panayotov, N., Filipov, St., Babrikov, T., Kostadinov, K., Haytova, D. (2014). *Exercise Guide to Vegetable Production with Seed Production*. Academic publishers of Agricultural University - Plovdiv, pp.108. (in Bulgarian).
- Panayotov, N. & Jachak D. (2020). Genotype response of different pepper varieties to the accelerated aging test of the seeds. *Scientific Papers. Series B. Horticulture*, LXIV(2), 207–214, Print ISSN 2285-5653.
- Poenaru, V., Badea, A., Dana Negula, I., Moise, C. (2017). Monitoring vegetation phenology in the Braila plain using Sentinel 2 data. *Scientific Papers. Series E. Land Reclamation, Earth Observation & Surveying, Environmental Engineering*, V, 175–180, Print ISSN 2285-6064.
- Qiao, K., Zhu, W., Xie, Z., Li, P. (2019). Estimating the Seasonal Dynamics of the Leaf Area Index Using Piecewise LAI-VI Relationships Based on Phenophases. *Remote Sens.*, 11, 689. <https://doi.org/10.3390/rs11060689>.
- Sandhu, R.K., Boyd, N.S., Qiu, Q., Guan, Z. (2020). Optimization of planting dates of Jalapeno pepper (*Capsicum annuum* 'Jalapeño' L.) and cantaloupe (*Cucumis melo* var. *cantalupensis* Ser.) relay cropped with strawberry (*Fragaria* × *ananassa* Duchesne). *PLoS ONE* 15(7), e0236677. <https://doi.org/10.1371/journal.pone.0236677>
- Schuler, R.T. (2002). Remote Sensing Experiences in Production Fields. <http://alfi.soils.wisc.edu/extension/FAPM/2002proceedings/Schuler.pdf>.
- Shaban, N., Bistrichanov, N., Kadum, E., Tityanov, M., Moskova, TSV., Mitova, I., Bumov, P. (2014). *Vegetable-growing*. Academic publishers House of University of forestry pp. 59–87 (in Bulgarian)
- Soudani, K., François, C., Maire, G.L., Dantec, V.L., Dufrêne, E. (2006). Comparative analysis of IKONOS, SPOT, and ETM+ data for leaf area index estimation in temperate coniferous and deciduous forest stands. *Remote Sensing of Environment*, 102(1–2), 161–175.
- Viña, A., Gitelson, A.A., Nguy-Robertson, A.L. & Peng, Y. (2011). Comparison of different vegetation indices for the remote assessment of green leaf area index of crops. *Remote sensing of environment*, 115(12), 3468–3478.
- Wu, M., Wu, C., Huang, W., Niu, Z., Wang, C. (2015). High-resolution Leaf Area Index estimation from synthetic Landsat data generated by a spatial and temporal data fusion model. *Computers & Electronics in Agriculture*, 115, 1–11.
- Zhang, X., Friedl, M.A. & Schaaf, C. (2006). Global Vegetation Phenology from Moderate Resolution Imaging Spectroradiometer (MODIS): Evaluation of Global Patterns and Comparison with *in situ* Measurements, *Journal of Geophysical Research*, 111, G04017, Doi: 10.1029/2006JG000217.

PAST AND FUTURE - A PERSPECTIVE OF THE EVOLUTION OF INEU'S FORESTS

Marinela BODOG, Alexandru RACZ, Nicu Cornel SABĂU

University of Oradea, 1 Universitatii Street, Oradea, Romania

Corresponding author email: mbodog@uoradea.ro

Abstract

This paper aims to investigate the evolution of the land base by land use categories: arable land, grassland, forests, and other wooded land. Specifically, the case study will analyse the evolution of the areas occupied by forest vegetation, included in the National Forest Fund, and managed by the Bihor Forestry Directorate through the Oradea Forestry Office, within the U.P.U.III Ineu, according to forest management plans referring to period 2007-2016 and 2017-2026. The research focuses on the evolution of the structural and qualitative characteristics of the stands, respectively the implementation and the results of the forest management plans for the studied stands, during the mentioned period, using the QGIS software. A comparative analysis will also be made of the ten-year plans for harvesting wood products and carrying out natural and artificial regeneration. The importance of these analyses lies in their ability to provide quick solutions to various problems encountered in current practical activities in the forestry sector.

Key words: geographic information system, forestry, forest regime, trees.

INTRODUCTION

Today, Geographic Information Systems (GIS) represent a crucial tool in advancing and implementing contemporary urban and regional research within planning processes. Recent developments in GIS focus primarily on improving its technical functionality as a tool for storing, processing, integrating, and representing spatial data. Additionally, a diverse range of applications in planning has emerged (Bilaşco et al., 2017; Wieslaw, 1993; Pica et al., 2022).

GIS serves as a modern approach for the continuous improvement of services and decisions, essential to confront current trends of globalisation and European integration efforts. The ability to manage, to correlate, to model, to predict and to disseminate geographical information makes GIS an analytical tool par excellence (Băduţ, 2007; Franch-Pardo et al., 2020).

The applicability of GIS is practically limitless, considering that the significant trait of most human activities is spatial location (Şmuleac et al., 2020). The purpose of information technology is to produce information for analysis by individuals and decision-making based on it for the implementation of any action.

The synergistic use of remotely sensed images and GIS vector data has gained significant interest in recent years (Gancz & Pătrăşcoiu, 2000).

Analysing the historical evolution of forests over the past 10 years, we aim for a closer integration of remote sensing and GIS technologies, along with the requirements of integrated software systems, for facilitating the combination of remote sensing data with vector datasets for maximum impact.

The main categories of software include system programs, application programs, and software development tools. System programs primarily include operating systems that ensure the interaction of all other programs with hardware and the user's interaction with personal computer programs. Utilities or service programs are also included in this category (Roşca et al., 2017).

QGIS is a multi-platform, free, and open-source GIS application that supports the visualisation, editing, printing, and analysis of geospatial data. QGIS functions as a GIS software, allowing users to analyse and edit spatial information, as well as compose and export graphical maps (<https://qgis.org/ro/site/>).

Modern land mapping technologies, which replace traditional mapping techniques, enable

the development of GIS, essential for the collection and processing of data required for land and forest assessment. Geographic reference and base maps serve as frameworks for the geographic reference and coordination of all data entering the GIS, mutual alignment of informational layers, and subsequent analysis using overlay procedures. New types of digital and electronic maps promise to be created using automated mapping systems and GIS for mapping purposes (Anji Reddy, 2018).

GIS typically provides spatial analysis tools for calculating statistics for entities and conducting geoprocessing activities such as data interpretation. In this case, we will analyse a forest area, emphasising the importance of tree analysis, age, distribution of forest species to better understand the modelling in the studied space. We will also highlight access routes, topographic height, and water circulation in this area.

GIS is experiencing exponential growth, being applied in various fields, from navigation systems in automobiles (Park et al., 2020) to analyses of urban crime (Ristea & Leitner, 2020), disease spread (Murad & Khashoggi, 2020), archaeological research (Dell'Unto & Landeschi, 2022), and forest studies (Soubry, 2021).

GIS proves indispensable when seeking answers related to location, territorial modelling, local trends, and conditions. GIS cannot be conceived without a database linked on a map to a specific geographical position. Data sources can be obtained through satellite imagery processing, orthophoto plans, statistics from surveys or censuses, data collected through Global Navigation Satellite Systems (GNSS), and field research and measurements.

This paper aims to highlight both the evolution of the forest in Ineu, Bihor County, as described in the forest management plans, and the implementation of proposed works to achieve the established management objectives.

The commune of Ineu is situated in the central part of Bihor County, being the easternmost locality within the Oradea Metropolitan Area. The total area of the Ineu commune is 49,51 km², located 20 km away from the city of Oradea (<https://zmo.ro/componenta/comuna-ineu>).

MATERIALS AND METHODS

The selected area for this analysis is the forest within the administrative-territorial unit of Ineu, under the administration of the National Forest Administration ROMSILVA (Figure 1).

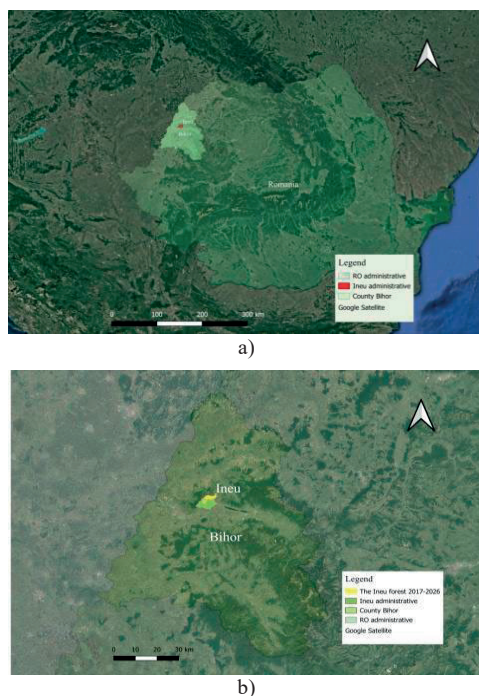


Figure 1. The location of the Ineu forest: a) national level location; b) location at the level of Bihor County

The geographic coordinates of the forest under study are 47°06'05"N - 22°06'10"E.

Within the territory of the Ineu commune, there are two Natura 2000 sites: ROSCI0050 Crișul Repede and ROSCI0267 Valea Roșie. In the Crișul Repede site, upstream of Oradea, the habitat of White Willow (*Salix alba*) and White Poplar (*Populus alba*) groves is present and the Valea Roșie site is representative of beech forests of the Asperulo-Fagetum type, part of which is included in the Valea Roșie Hay Meadow Natural Reserve.

The Natura 2000 network can become effective and properly managed if the financial sustainability of forests is ensured through compensation systems covering all types and categories of property rights (Winter et al., 2014).

The method used to highlight administrative data, location, composition, topography, species distribution, and a comparative analysis of the two forestry plans used as data sources (DSB, 2007; DSB, 2017) involves the use of a GIS, graphics, tables, and their correlation using the QGIS software after creating, managing, analysing, and mapping all types of data.

The QGIS software connects data to a map, integrating location with all types of descriptive information. This provides a basis for mapping and analysis used in science and nearly every industry. Regarding forest management, QGIS is an extremely useful tool as it can assist foresters with information about the status, location, development, and future trends necessary in decision-making.

According to the current Forest Code regulations (Law no. 46/2008):

- "The management of the national forest fund is regulated through forest management plans, which constitute the basis of the specialised cadastre and the state property title for the state-owned forest fund.

- The objectives of forest management are established through forest management plans, in accordance with ecological and socio-economic objectives and with respect to the property rights exercised over the forests, in accordance with the provisions of this code.

- The drafting of forest management plans is mandatory for forest properties larger than 10 hectares."

Forestry is defined as "the art and science of controlling and establishing the growth, composition, health, and quality of forests and other lands with forest vegetation for the purpose of achieving sustainable values and needs imposed by the owner and society on a sustainable basis" (FAO, 2015).

The implementation of the concept of sustainable forest management reflects the social perception of realities, a perception determined culturally and varying in relation to historical and institutional contexts (Schanz, 1997).

The ecological and functional diversity of the forest fund, the management goals set by forest management plans, and the technical-economic conditions for forest management require the application of the selection forest regime, based on seed regeneration and the management of stands at old ages.

At the level of the forest fund in Romania, the selection forest regime is applied to 91%, justified by silvicultural and economic reasons to produce large and medium-sized timber for industrial and commercial purposes.

The silvicultural practices analysed are regulated by the forest management plan (forest management plan), in accordance with current legislation (Sîngeorzan et al., 2022).

Due to the desire to ensure the permanence of forests by avoiding interventions that could strip the soil on large surfaces, as these forests serve a protective function, the management of forests towards multiple protection and production structures is necessary.

Treatment is the set of silvicultural interventions carried out in stands reaching maturity to ensure their regeneration, constituting the main tool for normalising the forest structure (Duduman & Drăgoi, 2019). The treatment of progressive cuttings is part of the group of treatments with repeated cuttings and regeneration under the stand.

In the case of the Ineu forest, the adopted treatment is that of progressive cuttings (in gaps) with long periods of regeneration in oak, hornbeam, and slope clearings (SDLI, 2020).

Regeneration works are carried out in gaps of variable sizes depending on the temperament of the species and site conditions. The aim is to ensure natural regeneration under the standby applying successive uneven-aged cuttings placed irregularly throughout the stand.

The treatment of progressive cuttings in the wood harvesting process, correlated with the regeneration process, separates three types of cuttings:

- opening cuts;
- thinning and widening cuts;
- connecting cuts.

RESULTS AND DISCUSSIONS

The non-agricultural land area in the commune is 1960 hectares, of which 1631 hectares (83.21% of the non-agricultural area) consist of forests and other forest lands, 160 hectares (8.16% of the non-agricultural area) are properties and yards, 50 hectares (2.55%) are water bodies, and 109 hectares (5.56%) are occupied by communication routes. The length of forest roads is 2.5 km (Figure 2).

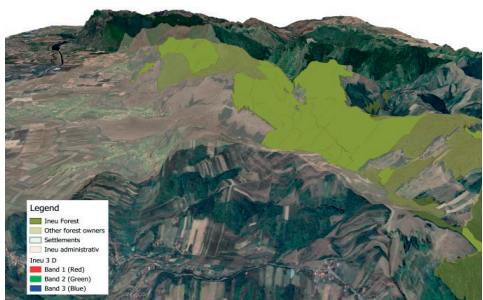


Figure 2. Ineu Forest
(3D view performed in QGIS 3.34 PRIZEREN)

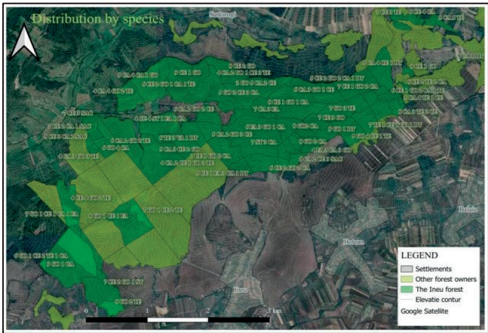


Figure 3b. Production Unit III, Ineu Forest District:
2017-2026
(3D view performed in QGIS 3.34 PRIZEREN)

The forest management plans of the Oradea Forestry Department, Bihor Silvicultural Direction, U.P. III Ineu, for the periods 2007-2016 and 2017-2026, respectively, highlight differences in terms of area, number of plots, and subplots (Table 1, Figure 3 a,b) due to the land restitution processes carried out based on:

- Law no. 18 of February 19, 1991 - The Land Fund Law, with subsequent amendments, for an area of 3 hectares.
- Law no. 1 of January 11, 2000, for the re-establishment of ownership rights over agricultural and forest lands, in its updated form, for an area of 103.72 hectares.

Table 1. Differences in Forest Management Plans of the Oradea Forestry Department, U.P. III Ineu

Period	Surface (ha)	No. of parcels	No. sub-parcels
2007-2016	883.0	72	162
2017-2026	776.28	64	136

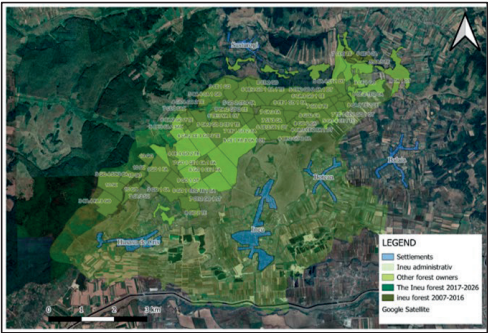


Figure 3a. Production Unit III, Ineu Forest District:
2007-2016

It is important to mention that the individuals who received property rights were obligated to manage the forest under silvicultural regulations, based on forest management plans, either through their own structures or through management contracts with specialized forestry entities, in accordance with the applicable legislation.

The main structural characteristics of the forest stands, compared between the two analysed periods, are highlighted in Table 2, Figure 4 and Figure 5. For differentiating forest management and the regulation of the production process comparative management units were established during the analysed periods (Table 3, Table 4). Quantitative indicators, crucial for characterising the dynamics of forest fund development in comparative periods, are presented in Table 5.

These quantitative indicators are comparable for the analysed periods, the differentiated values being justified by alterations in the forest area, primarily due to land restitutions as per legal provisions. The forest structure, composition, and average age are easily identifiable in the two management plans used for comparison.

The graphical representation of forest management activities has adhered to the specific care needs outlined in the management plans, ensuring the conservation of valuable timber resources.

Table 2. Tree structure

Pr.	Parameters	CE	CA	GO	TE	FA	ST	SAC	DR	DT	DM	UP
2007-2016	Composition %	35	25	27	3	4	1	2	-	3	-	100
	Consistency	0.77	0.81	0.74	0.83	0.77	0.82	0.83	-	0.82	-	-
	Average Age (years)	57	47	65	32	62	41	25	-	31	-	-
2017-2026	Composition %	40	27	19	6	3	1	1	-	3	-	100
	Consistency	0.75	0.82	0.72	0.87	0.79	0.74	0.90	0.70	0.77	0.88	0.77
	Average Age (years)	63	51	71	31	75	66	14	50	43	23	59

Note: CE - *Quercus cerris*, CA - *Carpinus betulus*, GO - *Quercus petraea*, TE - *Tilia cordata*, FA - *Fagus sylvatica*, ST - *Quercus robur*, SAC - *Robinia pseudoacacia*, DR - Various conifers, DT - Various hardwoods, DM - Various softwoods, UP - Production Unit

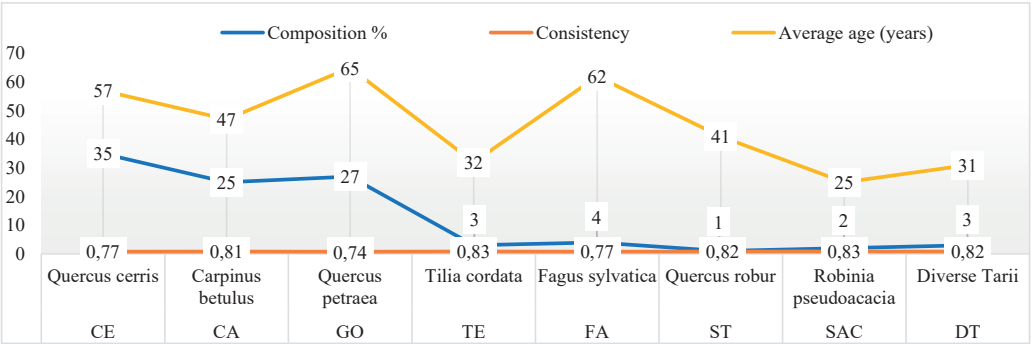


Figure 4. Structure of the management plan for Production Unit Ineu, 2007-2016

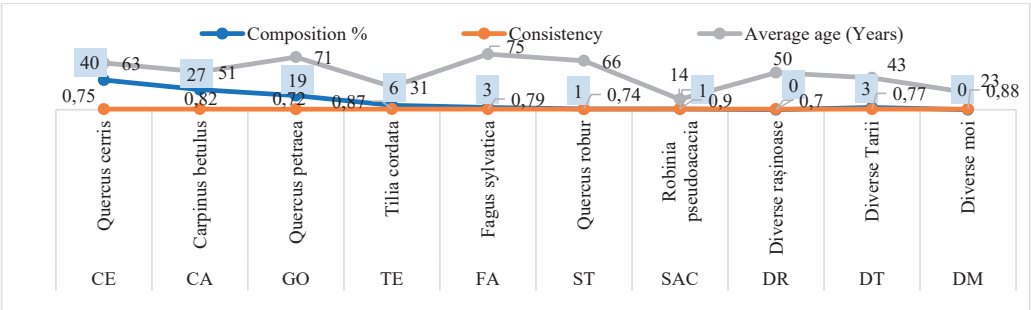


Figure 5. Structure of the management plan for Production Unit Ineu, 2017-2026

The utilisation of QGIS has significantly contributed to the forest inventory, emerging as a crucial management tool for the forests. It has provided valuable information related to monitoring, planning, research, evaluation, timber production, and sales. The spatial inventory of trees offers essential insights from both economic and ecological perspectives, projecting the intended changes in the forest structure over time. The Forest Management Plan for the Oradea Forestry Department, Bihor Silvicultural Direction, U.P. III Ineu for the

period 2017-2026 outlines the intention to replace certain fewer valuable species with more economically valuable ones, thus modifying the production structure by species from 42CE 28CA 16GO 6TE 3FA 1ST 1SAC 3DT to 28CE 27GO 13ST 8GI 8TE 5FA 1FR 10DT. The use of GIS facilitates forest inventory and provides both qualitative and quantitative information about the forests in the Ineu region. The obtained data can be used to formulate long-term forest plans aimed at the protection and conservation of wildlife.

Table 3. Comparative forest management

Decade	Type	Regime	Composition goal	Treatment	Exploitability	Cycle
2007-2016	S.U.P. "A"	regular forest common assortments - 825.4 ha	corresponding to the fundamental natural types of forest improved with valuable species of mixtures (maple Acer, ash Fraxinus, cherry Prunus)	progressive cuttings, clearcut regeneration cutting, thinning cutting	for protection, all trees being in group I	100 years for the trees in Production Unit A
	S.U.P. "K"	seed reserves - 28.0 ha				
2017-2026	S.U.P. "A"	regular forest common assortments – 719.53 ha	corresponding to the fundamental natural types of forest improved with valuable species of mixtures (maple Acer, ash Fraxinus, cherry Prunus)	progressive cuttings	technique for trees in group II	100 years for the trees in Production Unit A
	S.U.P. "K"	seed reserves 28.83 ha				

Table 4. The annual area covered by care works

	L.P	D.	C.	R.	T.ig.	L. im
2007-2016	Area (ha)	7.5	5.5	27.9	253.4	30.04
2017-2026	Area (ha)	1.96	12.8	24.37	245.86	24.17

Note: L.P - proposed works, D - clearings, C - cleanings, R - thinning, T.ig. - hygiene cuttings, L.im. - reforestation works

Table 5. Quantitative indicators

No.	Quantitative indicators	U.M	Values 2007-2016	Values 2017-2026
1	The proportion of forests in the total area of the forest fund	%	97	96
2	Standing timber volume - total	m ³	153525	140046
3	Standing timber volume - average	m ³ /year	179	187
4	Average production class	-		II a
5	Total production class	m ³	4892	4408
6	Average production class	m ³ /year/ha	5.7	5.9
7	Total current increment - production fund	m ³	4814	4333
8	Total current growth - production fund	m ³ /year	5.8	6.0
9	Increment indicators - total	m ³ /year	2466	2075
10	Increment indicators - average	m ³ /year/ha	3.0	2.9
11	Possibility of main products - total	m ³ /year	1320	1215
12	Possibility of main products - hectares	m ³ /year	120	144
13	Possibility of secondary products - total	m ³ /year	495	545
14	Possibility of secondary products - hectares	m ³ /year	15	15

CONCLUSIONS

The comparative analysis of the forest fund in Production Unit III, Ineu Forestry Department, for the two management plans has highlighted the location, topography, and the structure of the Ineu forest stand and shed light on the undertaken activities for the maintenance,

valorisation, and conservation of valuable tree species.

Furthermore, it emphasised comparable indicators for the two analysed periods, except for changes in the secondary forest area, which were retroceded to former owners.

The use of QGIS has significantly enhanced the quality of forest inventory data, enabling a

strategic and long-term vision for forest improvement, short and long-term planning and for dynamic development of the forest found, estimating the forest growth, and replacing less valuable tree species with other competitive valuable species.

The versatility of QGIS allowed for the expansion of its application beyond forest inventory, encompassing the evaluation of wildlife populations, flora, and soil resources, facilitating a holistic approach to climate changes and biodiversity monitoring.

Although QGIS significantly improves data quality, we must consider whether the granularity of the data suffices for all study aims. The analysis has temporal limitations because only comparing two periods and additional temporal checkpoints could provide a more dynamic and continuous understanding of forest evolution.

In the future the continuation of the study could cover various components like wildlife and flora, or other crucial factors such as hydrological impacts or non-native invasive species that could influence forest health.

Also, local community interaction with the forest (eg, logging, recreation) could provide insights into human influence on forest dynamics.

By addressing these areas, the study could enhance its impact and provide a more robust framework for managing and conserving the Ineu forest in a sustainable and scientifically informed manner.

REFERENCES

- Anji Reddy, M. (2018). *Remote Sensing and Geographical Information Systems*, BS Publications, pp. 1895.
- Băduț, M. (2007). *Sisteme Informatice Geografice (GIS). Fundamente practice*, Editura Albastră, Seria 181 PC.
- Bilașco, Șt., Moldovan, M.-O., Roșca, S. (2017). *Aplicații GIS în administrația publică locală*, Editura Rosoprint Cluj Napoca, pp. 210.
- Commune of Ineu. Oradea Metropolitan Area (n.d.). Retrieved from <https://zmo.ro/componenta/comuna-ineu>
- Dell'Unto, N., Landeschi, G. (2022). *Archaeological 3D GIS*, Taylor & Francis, pp. 176.
- DSB (2007). *Amenajamentul Ocolului Silvic Oradea, Direcția Silvică Bihor, U.P. III Ineu 2007-2016*.
- DSB (2017). *Amenajamentul Ocolului Silvic Oradea, Direcția Silvică Bihor, U.P. III Ineu 2017-2026*.
- Duduman, G., Drăgoi, M. (2019). *Amenajarea padurilor*, vol. 1, Editura Universității Ștefan cel Mare din Suceava.
- FAO (Food and Agriculture Organization of the United Nations) (2015). *Forest Resources Assessment*, Working Paper, pp. 180.
- Franch-Pardo, I., Napoletano, B.M., Rosete-Verges, F., Billa, L. (2020). Spatial analysis and GIS in the study of COVID-19. A review. *Science of The Total Environment*, 739, 140033, <https://doi.org/10.1016/j.scitotenv.2020.140033>
- Gancz, V., Patrascoiu, N. (2000). Cartografierea ecosistemelor forestiere din România prin mijloace GIS și de teledetectie. *Revista Padurilor*, 2, 35-40. <https://qgis.org/ro/site/>
- Law No. 1 of January 11, 2000, for the restitution of property rights over agricultural and forestry lands, updated version.
- Law No. 18 of February 19, 1991 - The Land Fund Law, updated version.
- Law No. 46/2008 on the Forest Code, Official Gazette of Romania, Part I, No. 611 of August 12, 2015.
- Murad, A., Khashoggi, B.F. (2020). Using GIS for Disease Mapping and Clustering in Jeddah, Saudi Arabia. *ISPRS International Journal of Geo-Information*, 9(5), 328, <https://doi.org/10.3390/ijgi9050328>
- Park, G., Lee, B., Kim, D.G., Jae, Y., Sung, S. (2020). Design and Performance Validation of Integrated Navigation System Based on Geometric Range Measurements and GIS Map for Urban Aerial Navigation. *Int. J. Control Autom. Syst.*, 18, 2509–2521, <https://doi.org/10.1007/s12555-019-1059-4>;
- Pica, A., Boja, F., Foră, C., Moatar, M., Boja, N. (2022). Advantages of using GNSS technology and QGIS software in inventory stands exploiters. *Scientific Papers. Series E. Land Reclamation, Earth Observation & Surveying, Environmental Engineering*, XI, 434-443, Print ISSN 2285-6064.
- QGIS User Manual, Version: 2.0.
- Ristea, A., Leitner, M. (2020). Urban Crime Mapping and Analysis Using GIS. *ISPRS. International Journal of Geo-Information*, 9(9), 511, <https://doi.org/10.3390/ijgi9090511>
- Roșca, C.F., Harpa, G.V., Croitoru, A.E., Herbel, I., Imbroane, A.M., Burada, D.C. (2017). The impact of climatic and non-climatic factors on land surface temperature in southwestern Romania. *Theoretical and Applied Climatology*, 130, 775-790.
- Schanz, H. (1997). Sustainable Forest management—on the meanings and functions of a central term in forestry. In Voluntary Paper for XI. *World Forest Congress*, Antalya.
- SDLI (Strategia de dezvoltare locală a comunei Ineu), (2020), Zona Metropolitană Oradea 2021-2017. https://zmo.ro/download/SDD%20INEU_2021_2027_FINAL.pdf
- Șingeorzan, S.-M., Holonec, L., Truta, A.M., Morar, I.M., Dan, C., Colișar, A., Viman, O., Negrușier, C., Borsai, O., Criveanu, H., Vlasin, H.D., Păcurar, I. (2022). Influence of Physical Treatments on Seed Germination and Seedling Development of Spruce

- (*Picea abies* [L.] Karst.). *Forests*, 13, 1498, <https://doi.org/10.3390/f13091498>.
- Șmuleac, A., Șmuleac, L., Man, T.E., Popescu, C.A., Imbrea, F., Radulov, I., Adamov, T., Pașcalău, R. (2020). Use of Modern Technologies for the Conservation of Historical Heritage in Water Management. *Water*; 12(10), 2895-2901, <https://doi.org/10.3390/w12102895>
- Soubry, I., Doan, T., Chu, T., Guo, X. (2021). A systematic review on the integration of remote sensing and GIS to forest and grassland ecosystem health attributes, indicators, and measures. *Remote Sensing*, 13(16), 3262-3268.
- Wieslaw, Z.M. (1993). GIS in land use change analysis: integration of remotely sensed data into GIS, *Applied Geography*, 13(1), 28-44, [https://doi.org/10.1016/0143-6228\(93\)90078-F](https://doi.org/10.1016/0143-6228(93)90078-F)
- Winter S., Borrass, L., Geitzenauer, M., Blondet, M., Breibeck, R., Weiss, G., Winkel, G. (2014). The impact of Natura 2000 on forest management: a socio-ecological analysis in the continental region of the European Union. *Biodiversity and Conservation*, 23, 3451-3482.

EXPLORING THE TOP 5 DRONES FOR LAND MEASUREMENTS: A REVIEW

Alexandru CĂLIN

University of Agronomic Sciences and Veterinary Medicine of Bucharest,
Faculty of Land Reclamation and Environment Engineering,
59 Marasti Blvd, District 1, Bucharest, Romania

Corresponding author email: alexcalin@fifim.ro

Abstract

In the paper titled "Exploring the Top 5 Drones for Land Measurements", we conduct a comprehensive analysis of the latest drone technology applied in the field of geospatial surveying. The study evaluates five leading drone models based on their accuracy, efficiency, and cost-effectiveness in land measurement tasks. Through a series of field tests and data comparisons, the paper highlights the strengths and limitations of each drone, providing insights into their suitability for various surveying contexts. The findings aim to guide professionals in selecting the most appropriate drone technology for their specific land measurement needs, ultimately contributing to more informed decision-making in the industry. This abstract summarizes the paper's intent to bridge the gap between drone technology and practical application in land surveying.

Key words: AI, drones, future, land, measurements.

INTRODUCTION

Globalization has been driven by technological integration, and drone technology has been one of its most prominent technological advancements.

The Evolution of Land Surveying

Land surveying, once reliant on traditional methods that were often time-consuming and labor-intensive, is undergoing a revolutionary transformation. Today, improvements and new tools have emerged for land survey, remote sensing, hydrography, map data processing and data transmission (Bryan et al., 2023). The fusion of drones (unmanned aerial vehicles - UAVs) and artificial intelligence (AI) is reshaping the landscape of surveying practices, propelling the industry into an era of unparalleled efficiency, accuracy, and innovation.

Historical Perspectives: From Theodolites to Drones

Surveying, deeply rooted in human history, has evolved from early theodolite measurements to satellite-based systems. The limitations of these traditional methods have spurred the quest for technological alternatives. Drones, equipped with advanced sensors and AI capabilities, have emerged as the vanguards of this technological

evolution. While drone technology is evolving, advances in sensor technology will drive further innovation and expand the potential of UAVs in many areas, shaping the future of aerial intelligence and disrupting industries around the world (Emimi et al., 2023).

The Rise of Drones in Land Surveying

The integration of drones into land surveying practices has marked a seismic shift in the industry. Drones offer agility and accessibility, enabling surveys of terrains that were once arduous to navigate. These aerial marvels have become indispensable tools for capturing high-resolution imagery and collecting geospatial data with unprecedented speed and precision.

Due to their low cost, ease of use, vertical take-off and landing, and ability to operate in high-risk or hard-to-reach areas, drones have found many applications (Quamar et al., 2023). The use of drones in various fields, especially in areas such as mapping, surveying (Jiang et al., 2022) disaster management (Tonti et al., 2023), agriculture (Fareed & Rehman, 2020), healthcare and the military, has seen a remarkable increase.

AI's Role in Revolutionizing Land Surveying

The symbiotic relationship between drones and AI unlocks a realm of possibilities for surveyors. AI algorithms process vast datasets collected by

drones, unraveling patterns, detecting anomalies, and making real-time decisions. This marriage of technologies enhances the analytical capacity of surveying, transforming raw data into actionable insights.

Advancements in Drone Technology

Modern surveying drones transcend their predecessors. They boast longer flight endurance, allowing for extensive coverage in a single mission. Enhanced payload capacities accommodate sophisticated sensors, including LiDAR and multispectral cameras, elevating the quality and scope of data acquisition (Popescu et al., 2019). Obstacle avoidance features contribute to safer and more efficient surveying operations (Croitoru et al., 2023).

Precision and Accuracy Redefined

The hallmark of drone and AI integration lies in the unprecedented precision it brings to land surveying. Real-time kinematic (RTK) technology, combined with AI-enhanced data processing, delivers centimeter-level accuracy. This level of precision not only surpasses traditional surveying methods but also reduces the margin of error, instilling confidence in survey outcomes.

Efficiency and Cost-Effectiveness

Efficiency is the heartbeat of modern surveying. Drones, guided by AI, execute surveys swiftly, reducing project timelines significantly. The cost-effectiveness of drone surveys, stemming from quicker data acquisition and fewer operational expenses, positions this technology as an economic boon for surveying projects of varying scales.

Challenges and Ethical Considerations

While the integration of drones and AI brings transformative benefits, it is not without challenges. Regulatory complexities, privacy concerns, and ethical considerations surrounding data usage necessitate a thoughtful approach. Striking a balance between innovation and responsible implementation becomes imperative for the sustainable growth of the industry.

Future Trends and Innovations

The trajectory of land surveying points towards a future laden with innovations. Ongoing research in AI algorithms, sensor technologies, and drone design promises continuous enhancements. The advent of 5G connectivity holds the potential to further elevate real-time

data transmission, allowing for even more dynamic and responsive surveying practices.

Environmental Monitoring and Sustainability

Drones equipped with AI extend their utility beyond traditional surveying applications. Environmental monitoring becomes a focal point as these technologies aid in assessing ecological health, tracking changes in vegetation, and contributing to sustainable land management practices. The marriage of surveying, AI, and environmental stewardship emerges as a powerful force for sustainable development.

Case Studies: Showcasing Success Stories

Examining real-world case studies provides a tangible understanding of the impact of drone and AI integration. Projects ranging from large-scale infrastructure surveys to environmental conservation efforts highlight the transformative outcomes and lessons learned from adopting this innovative approach.

TOP 5 DRONES

1. DJI Phantom 4 RTK

The DJI Phantom 4 RTK (Figure 1) has earned its place as a stalwart in the realm of land measurements. Known for its high-precision RTK (Real-Time Kinematics) capabilities, this drone offers unparalleled accuracy, making it a preferred choice for professionals engaged in precise topographic surveys.

Key Features:

- RTK Technology: The integration of RTK technology ensures centimeter-level accuracy, vital for detailed land measurements.
- Obstacle Avoidance: With obstacle sensors on all sides, the Phantom 4 RTK excels in navigating challenging terrains, enhancing data collection in complex environments.
- High-Quality Camera: The drone boasts a high-resolution camera, capturing detailed imagery essential for topographic mapping (https://dl.djicdn.com/downloads/phantom_4_rtk/20200721/Phantom_4_RTK_User_Manual_v2.4_EN.pdf).

Pros:

- Exceptional accuracy due to RTK technology.
- Robust obstacle avoidance capabilities.
- Reliable and widely used in professional surveying applications.

Cons:

- The price point might be a deterrent for smaller-scale projects.

Overall Impression:

The Phantom 4 RTK stands out for its reliability and precision. While the initial investment may be substantial, its performance justifies the cost for projects demanding utmost accuracy.



Figure 1. DJI Phantom 4 RTK
(<https://www.appia-drones.ro/echipament/p4-m-rtk/>)

2. SenseFly eBee X

The senseFly eBee X (Figure 2) caters to the demands of large-scale land surveys, offering an impressive combination of flight endurance and versatility. This fixed-wing drone has garnered attention for its interchangeable payloads, allowing professionals to adapt to diverse mapping needs (<https://ageagle.com/wp-content/uploads/2022/06/AgEagle-eBee-X-EN-2022-2.pdf>).

Key Features:

- Long Flight Endurance: The eBee X boasts extended flight times, facilitating coverage of extensive areas in a single flight session.
- Payload Flexibility: The ability to swap payloads ensures adaptability, making it suitable for varied mapping applications.
- Professional-Grade Data: Its precision and reliability make it a favorite for mapping professionals handling extensive projects.

Pros:

- Long flight endurance.
- Interchangeable payloads for versatile data collection.
- Well-suited for large-scale land surveys.

Cons:

- Initial setup may be complex, particularly for beginners.

Overall Impression:

The senseFly eBee X impresses with its capacity for large-scale surveys. While setup complexity might pose a challenge initially, its performance justifies the learning curve for professionals engaged in expansive mapping projects.



Figure 2. SenseFly eBee X
(<https://www.lewisinstruments.com/products/sensefly-ebee-x>)

3. Parrot Anafi USA

The Parrot Anafi USA (Figure 3) stands out in the world of land measurements for its compact design and high-resolution imaging capabilities. Ideal for smaller-scale projects and inspections, this drone is a cost-effective yet reliable choice (<https://www.parrot.com/assets/s3fs-public/2023-02/ANAFI-USA-user-manual.pdf>).

Key Features:

- Compact and Portable: The Anafi USA's lightweight design makes it highly portable, ideal for on-the-go land measurements and inspections.
- High-Resolution Imaging: Equipped with a high-quality camera, it provides detailed imagery for accurate mapping and analysis.
- Thermal Imaging Options: The inclusion of thermal imaging enhances its utility for diverse surveying applications.

Pros:

- Portability is a significant advantage.
- Competitive pricing for the features offered.
- Suitable for smaller-scale land measurements and inspections.

Cons:

- Limited flight time compared to other professional drones.

Overall Impression:

The Parrot Anafi USA shines as a portable and cost-effective solution for smaller-scale land measurements. Its versatility, combined with

thermal imaging options, adds a layer of functionality for various applications.



Figure 3. Parrot Anafi USA
(<https://pilotinstitute.com/course/parrot-anafi-usa-deep-dive/>)

4. DJI Matrice 300 RTK

The DJI Matrice 300 RTK (Figure 4) is an industrial-grade drone designed to meet the demanding requirements of topographic surveys. With triple redundancy systems and the ability to carry multiple payloads simultaneously, it offers unmatched reliability and flexibility (https://dl.djicdn.com/downloads/matrice-300/20200507/M300_RTK_User_Manual_EN.pdf).

Key Features:

- Triple Redundancy Systems: The drone incorporates redundant sensors and systems, ensuring robust performance in challenging environments.
- Multiple Payloads: Its capacity to carry multiple payloads simultaneously enhances its versatility for different surveying needs.
- High-Performance RTK: The Matrice 300 RTK maintains high accuracy through advanced RTK technology.

Pros:

- Industrial-grade reliability.
- Capability to carry multiple payloads.
- High precision with RTK technology.

Cons:

- Complexity may be overwhelming for beginners.
- Higher price point compared to consumer-grade drones.

Overall Impression:

The Matrice 300 RTK caters to professionals requiring industrial-grade performance. Its robustness and capacity for multiple payloads

make it a top choice for complex topographic surveys.



Figure 4. DJI Matrice 300 RTK
(<https://www.dsrlrpros.com/matrice-350-rtk-agriculture-package.html>)

5. Autel Robotics EVO Lite+

The Autel Robotics EVO Lite+ (Figure 5) strikes a balance between affordability and functionality. With a 6K camera resolution and versatility for mapping and inspection, it offers a compelling option for those seeking a cost-effective yet capable drone (<https://www.vertigodrones.com/assets/images/EVO%20Lite%20Series%20User%20Manual%20-%20EN.pdf>).

Key Features:

- Affordability: The EVO Lite+ offers competitive pricing without compromising on essential features.
- High-Resolution Camera: A 6K camera resolution ensures detailed imagery for accurate land measurements.
- Versatility: Suitable for both mapping and inspection applications, making it a versatile choice.

Pros:

- Cost-effective option for the features offered.
- Competitive camera resolution.
- Versatile for different surveying needs.

Cons:

- May lack some advanced features found in higher-end models.

Overall Impression:

The Autel Robotics EVO Lite+ provides a cost-effective entry point for professionals and educational purposes. While it may not have all the advanced features of premium drones, its functionality and affordability make it a valuable choice.

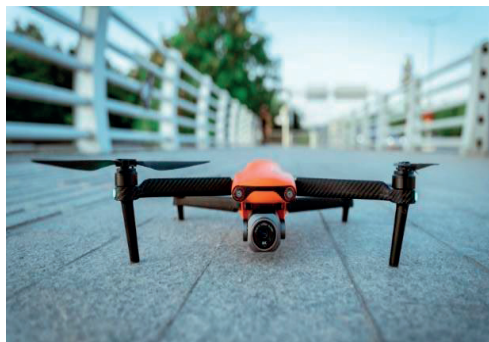


Figure 5. Autel Robotics EVO Lite+
(<https://www.thedronegirl.com/2022/01/06/autel-evo-nano-and-lite-drones-have-arrived/>)

THE FUTURE OF DRONE TECHNOLOGY IN LAND MEASUREMENTS

1. AI Integration

The integration of artificial intelligence (AI) into drone technology is poised to revolutionize land measurements. AI algorithms can analyze real-time data during flights, enabling drones to make instantaneous decisions for more efficient and accurate mapping.

2. Improved Sensors

Continued advancements in sensor technologies are expected to enhance the precision and range of data collection. From LiDAR (Light Detection and Ranging) to more sophisticated environmental sensors, the future will see drones equipped with sensors capable of capturing a broader spectrum of data.

3. Extended Flight Endurance

Researchers and engineers are actively working on developing longer-lasting batteries and more energy-efficient drone designs. Extended flight endurance will allow drones to cover larger areas in a single flight, reducing the need for multiple take-offs and landings during extensive land measurements.

4. Autonomous Operations

The future holds increased autonomy for drones. Advancements in artificial intelligence and machine learning will empower drones to navigate complex terrains independently, minimizing the need for constant manual control. This autonomy will streamline surveying processes and enhance overall efficiency.

5. Environmental Monitoring Features

As environmental concerns grow, future drones used in land measurements are likely to

incorporate advanced sensors for monitoring factors such as air quality, vegetation health, and soil conditions. This expansion of capabilities will contribute to a more holistic understanding of the land's health and sustainability.

CONCLUSIONS

The current array of drones for land measurements caters to a diverse range of needs, from high-precision surveys to cost-effective solutions for smaller-scale projects. Each drone reviewed has its unique strengths, addressing different requirements within the field of topography.

The future of land surveying propelled by drones and artificial intelligence is a compelling narrative of progress and promise. As industry navigates uncharted territories, the synergy between technological advancements and the evolving needs of surveyors charts a skyline of possibilities. The collaboration between drones and AI transcends the limits of traditional surveying, ushering in an era where precision, efficiency, and sustainability converge to redefine the very essence of land surveying.

The journey ahead promises not only technological breakthroughs but a transformative impact on how we perceive, analyze, and safeguard the landscapes that shape our world.

REFERENCES

- Alicaway, B.K., Castillo, T.A., Gonzales, A., Loyola, D., Quizeo, A.J., Uytensu, B.I.Y. (2023). The Developments of Land Surveying Techniques and Equipment, *International Journal of Research Publication and Reviews*, 4(12), 3060-3066.
- Croitoru, A., Babuca, N.I., Călina, J., Călina, A., Bădescu, G. (2023). Modern and precise solutions for making orthophotos with the topographic drone, necessary for obstacle studies. *Scientific Papers. Series E. Land Reclamation, Earth Observation & Surveying, Environmental Engineering*, XII, 358-363.
- Emimi, M., Khaleel, M., Alkrash, A. (2023). The Current Opportunities and Challenges in Drone Technolog. *International Journal of Electrical Engineering and Sustainability*, 1(3), 74-89.
- Fareed, N., Rehman, K. (2020). Integration of remote sensing and GIS to extract plantation rows from a drone-based image point cloud digital surface model. *ISPRS Int. J. Geo Inf.*, 9, 151.
- Jiang, Y., Huang, Y., Liu, J., Li, D., Li, S., Nie, W., Chung, I.H. (2022). Automatic volume calculation and mapping of construction and demolition debris using drones, deep learning, and GIS. *Drones*, 6, 279.

- Popescu, G., Balota, O.L., Iordan, D., Ilie, D. (2019). Advantages of realistic representation of a geographic area by combining optical and LiDAR data captured with UAVs. *Scientific Papers. Series E. Land Reclamation, Earth Observation & Surveying, Environmental Engineering, VIII*, 169-174.
- Quamar, M.M., Al-Ramadan, B., Khan, K., Shafiullah, M., El Ferik, S. (2023). Advancements and Applications of Drone-Integrated Geographic Information System Technology - A Review. *Remote Sensing*. 15(20), 5039. doi:10.3390/rs15205039.
- Tonti, I., Lingua, A.M., Piccinini, F., Pierdicca, R., Malinverni, E.S. (2023). Digitalization and spatial documentation of post-earthquake temporary housing in Central Italy: An integrated geomatic approach involving UAV and a GIS-based system. *Drones*, 7, 438.
https://dl.djicdn.com/downloads/phantom_4_rtk/20200721/Phantom_4_RTK_User_Manual_v2.4_EN.pdf
- <https://www.appia-drones.ro/echipament/p4-m-rtk/>
<https://ageagle.com/wp-content/uploads/2022/06/AgEagle-eBee-X-EN-2022-2.pdf>
<https://www.lewisinstruments.com/products/sensefly-ebec-x>
<https://www.parrot.com/assets/s3fs-public/2023-02/ANAFI-USA-user-manual.pdf>
<https://pilotinstitute.com/course/parrot-anafi-usa-deep-dive/>
https://dl.djicdn.com/downloads/matrice-300/20200507/M300_RTK_User_Manual_EN.pdf
<https://www.dslrpros.com/matrice-350-rtk-agriculture-package.html>
<https://www.vertigodrones.com/assets/images/EVO%20Lite%20Series%20User%20Manual%20-%20EN.pdf>
<https://www.thedronegirl.com/2022/01/06/autel-evo-nano-and-lite-drones-have-arrived/>

GIS METHODS FOR ESTIMATING SOIL EROSION AND ITS IMPACT ON THE ENVIRONMENT. CASE STUDY: CRIȘUL ALB HYDROGRAPHIC BASIN

Loredana COPĂCEAN^{1,2}, Eugen Teodor MAN¹, Sorin HERBAN¹,
Luminița COJOCARIU^{2,3}, Cosmin POPESCU²

¹Politehnica University of Timisoara, 2 Victoriei Square, Timisoara, Romania

²University of Life Sciences "King Mihai I" from Timisoara,
119 Calea Aradului, Timisoara, Romania

³Agricultural Research and Development Station Lovrin,
200 Principală Street, Lovrin, Romania

Corresponding author email: luminita_cojocariu@usvt.ro

Abstract

In Romania, in recent decades, many facilities to combat soil erosion have been abandoned, which leads to the amplification of the effects of this phenomenon, with repercussions on the environment. In this context, through this study, it is aimed to apply a spatial analysis model to identify areas susceptible to soil erosion, to establish the intensity of this phenomenon, but also to analyze its impact on the environment, at the level of the Crișul Alb basin. GIS technique and Universal Soil Loss Equation (USLE) were used. Through this equation, the following factors, participants /determinants of soil erosion were taken into account: climatic aggressiveness, land topography, soil characteristics, vegetation cover, land improvement measures. The soil erosion map at basin level, was classified into five classes, respectively areas with very low, low, moderate, high and very high susceptibility to soil erosion. The results show that 74% of the territory belongs to the class of susceptibility to very low erosion, and 4% with high and very high erosion rates, these being the main "hot spots" that must be taken into account in the development strategies of the hydrographic basin.

Key words: GIS models, impact, USLE, watershed.

INTRODUCTION

Soil erosion is one of the severe land degradation phenomena in many areas of the globe (Kim et al., 2005; Spalevic et al., 2020; Biali & Cojocaru, 2021) and varies depending on natural and/or anthropic factors. Balabathina et al. (2020) consider that approximately 85% of degraded lands globally are due to soil erosion, a phenomenon with significant implications for crop productivity due to soil fertility reduction (Singh & Panda, 2017; Copacean et al., 2019; Popescu et al., 2022; Patriche, 2023), also considered a major environmental issue.

In Romania, approximately 43% of agricultural lands exhibit erosion potential, which takes various forms depending on specific local conditions (Nistor & Nistor, 2002). The critical erosion season is generally from May to August, against a backdrop of heavy, torrential rainfall (Nistor & Nistor, 2002).

At the level of Romania, in the last decades, many of the arrangements for combating soil

erosion (originally existing on the surface of 2,231,356 ha) have been abandoned or are in a precarious state, which leads to the amplification of the effects of erosion on other components of the environment, such as groundwater and surface waters, agricultural lands and so on (Mircea, 2011; Man, 2014).

Classical methods for assessing soil loss through erosion at the watershed level are very difficult to implement and apply, requiring financial and time resources and a large volume of data, sometimes unavailable. In this context, various spatial and temporal assessment and computerized modeling techniques can be chosen to evaluate soil loss through erosion at different spatial and temporal scales (Borrelli et al., 2015; Greiner et al., 2017; Todisco et al., 2022).

One of the most well-known and widely used methods for estimating the susceptibility to erosion of a territory is the Universal Soil Loss Equation (USLE) developed by the United States Department of Agriculture (USDA), an

equation revised by RUSLE, with several variants (Foster et al., 2003; Panagos et al., 2015). These methods are easily applied through Geographic Information Systems (GIS) under various conditions and at different spatiotemporal scales, both internationally and in Romania (Diodato & Bellocchi, 2007; Estifanos, 2014; Roșca et al., 2014; Golosov et al., 2017; Asnake & Amare, 2019; Mengie et al., 2019; Niacsu et al., 2021; Patriche, 2023).

In the elaboration of the present study, we have exploited the possibility of applying the USLE model to estimate the average soil erosion in the Crișul Alb watershed, using remote sensing

tools and GIS technologies. Therefore, this study aims to apply a spatial analysis model to identify areas susceptible to soil erosion and to determine the intensity of this phenomenon in different subzones of the Crișul Alb river basin.

MATERIALS AND METHODS

1. Study area

The study area is represented by the hydrographic basin (H.B.) of the Crișul Alb River (Figure 1), located in western Romania, mostly within the territory of Arad County. The basin area covers 422,798 hectares.

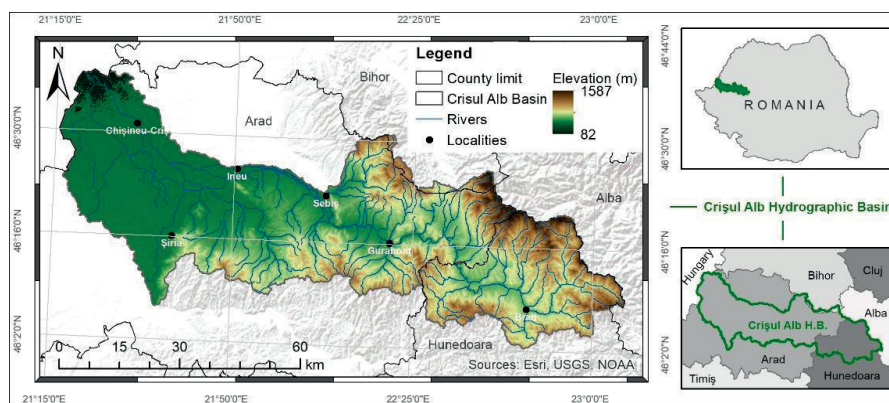


Figure 1. Location of the study area (processing after EEA, 2016; Geospatial, 2022)

The relief of the study area is varied, with altitudes ranging from 1587 meters, in the mountainous region, to 82 meters in the plain areas and river valleys. The average altitude of the Crișul Alb H.B. is 323 meters. In terms of land use, the eastern half is predominantly covered by forest areas interspersed with grasslands, while in the western half and in depressions, agricultural lands predominate. The relief units with significant presence in the analyzed territory are: the Bihorul Mountains, the Metaliferi Mountains, the Cigherului Hills, the Brad - Hălmaș Depression, the Low Plains of the Criș Rivers and the Mureș Plain (Posea & Badea, 1984; Rusu, 2007; Simon et al., 2022).

2. Materials used

The study area, respectively the territory of the Crișul Alb basin, was delimited according to the Crișuri Water Basin Administration.

In the case of the present study, the following materials were used:

- climatic data, specifically annual precipitation amounts from the period 2013-2022, recorded at 11 meteorological stations near the area of interest (Climatic databases, 2023; Open Source data): Alba Iulia, Cămpeni (Bistra), Chișineu-Criș, Deva, Gurahonț, Roșia Montană, Sănnicolau Mare, Sebeș (Alba), Șiria, Ștei (Petru Groza), Vărădia de Mureș. Since the level of precipitation is very variable, from one year to another, in the study we took the multiannual average over ten years;
- pedological data, in vector format (Geospatial, 2022);
- the Digital Elevation Model (DEM), with a spatial resolution of 25 m (EEA, 2016), a hybrid product based on SRTM and ASTER GDEM data; based on the DEM, flow direction and flow accumulation maps, as well as the map of the slopes, were generated;

- Sentinel 2 satellite images, from the year 2021, from the months of March, May, July, October and November (Copernicus Open Hub, 2023); based on them, the NDVI map was generated, with average values, at the level of 2021. The year 2021 was chosen based on the availability of Sentinel images from the selected periods (images without clouds or noise). Based on the working models from the specialized literature, but also the fact that all evolutionary stages of the vegetation were captured, 5 satellite images were used to calculate the average NDVI.

3. The working methodology

The Universal Soil Loss Equation (USLE) formulated by Wischmeier and Smith (1978) was used to estimate the annual amount of soil lost through erosion and to generate a map of soil erosion susceptibility in the analyzed territory. This equation involves the product of five factors: Rainfall erosivity factor (R), Soil erodibility factor (K), Topographic Factor (LS), Land cover management factor (C), and Conservation Support Practice Factor (P) (Balabathina et al., 2020; Selmy et al., 2021; Ge

et al., 2023). The five USLE factors were spatialized in GIS as raster maps (Figure 2) with a spatial resolution of 25 meters. The spatial resolution at which the results were obtained was conditioned by the available geospatial data, especially DEM.

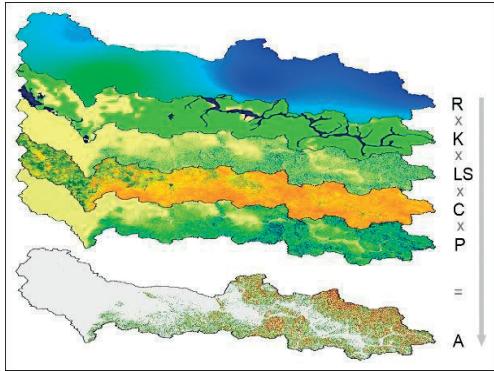


Figure 2. The USLE factors in the Crișul Alb H.B.

The calculation relations from Table 1 were used to determine the USLE factors.

Table 1. Calculation relations of the USLE factors

Factor	Calculation relation		Meaning
Rainfall erosivity factor ¹ (MJ mm ha ⁻¹ h ⁻¹ year ⁻¹)	$R = 0.55 \times P - 4.7$	(1)	P - average annual precipitation (mm).
Soil erodibility factor ² (t ha ⁻¹ MJ ⁻¹ mm ⁻¹)	$100K = 2.1M^{1.14} \times 10^{-4} \times (12 - a) + 3.25 \times (b - 2) + 2.5(c - 3)$	(2)	M - calculated as [very fine sand (%) + silt (%)] × [100 - Clay (%)]; a - soil organic matter (%); b - soil structure code; c - soil profile permeability class.
Topographic Factor ³ (adimensional)	$LS = \left(\frac{FA \times cell\ size}{22.13} \right)^m \times \left(\frac{\sin(slope\ angle \times 0.01745)}{0.9} \right)^n$	(3)	FA - flow accumulation; cell size - 25 × 25 m; slope angle – map of slope, in radians; m = 0.5; n = 1.3 - the exponent values
Land cover management factor ⁴ (adimensional)	$C = \exp \left[-\alpha \times \frac{NDVI}{(\beta - NDVI)} \right]$	(4)	NDVI - Near-infrared band; R - Red band; α = 2; β = 1
Conservation Support Practice Factor ⁵ (adimensional)	$P = 0.2 + 0.03 \times S$	(5)	S - the slope grade (%).
Average annual soil loss (t ha ⁻¹ year ⁻¹) ⁶	$A = R \times K \times LS \times C \times P$	(6)	

Resource: ¹Hurni, 1985, cited by Balabathina et al., 2020; ²Wischmeier et al., 1971, cited by Selmy et al., 2021; ³Mitasova, 1996, cited by Zisu, 2014; ⁴Van der Knijff et al., 2000, cited by Balabathina et al., 2020; ⁵Wener approach, cited by Allafta & Opp, 2022; ⁶Balabathina et al., 2020; Selmy et al., 2021; Ge et al., 2023

In the initial approach, Wischmeier (1959) calculated the rainfall erosivity index (EI, in MJ/ha) as the product of the total kinetic energy of rain (E, in t/ha) and the maximum intensity of

rainfall in 30 minutes (I₃₀, in mm/h) (Zisu, 2014; Balabathina et al., 2020). Considering the lack of climatic data over time, various methods have been developed for determining the R factor

(Choudhury & Nayak, 2003; Fathizad et al., 2014). In this study, the R factor was calculated based on equation (1), and for the spatialization of the results, the Inverse Distance Weighted (IDW) interpolation method was applied (ArcGIS Documentation, 2022).

The K factor, calculated on the basis of equation (2), refers to the soil's susceptibility to erosion, or in other words, it expresses the soil's resistance to erosion, a characteristic given by its physical and chemical properties. In the quantification of the K factor, the texture, structure, permeability and organic matter content of the soil are considered in particular (Balabathina et al., 2020; Selmy et al., 2021; Allafta & Opp, 2022).

The LS factor (equation 3) shows the contribution of topography to soil erosion and represents one of the most complex and difficult-to-estimate factors of the USLE (Ligonja & Shrestha, 2015). Based on this consideration, over time, several algorithms for calculating the LS factor have been developed, which generally involve the slope of the terrain, the flow direction, and flow accumulation (Zhang et al., 2013; Pham et al., 2018).

The C factor expresses the effect of land use and their management on soil erosion (Renard et al., 1997; Balabathina et al., 2020). Parameters that have the highest impact on the C factor are represented, especially by the degree of soil cover with vegetation, the canopy of trees, the roughness of the terrain, and its previous land use (Zisu, 2014; Cojocariu et al., 2024; Măgureanu et al., 2024).

In this study, the C factor was obtained based on the NDVI map, according to relation (4). Although different algorithms for determining the P factor are described in the specialized literature (Foster et al., 2003; Fu et al., 2005; Robert et al., 2012), this is considered one of the "uncertain" factors of USLE, considering given the lack of data on the practices applied in the territory.

Due to this consideration, an algorithm based on slope terrain (equation 5) was chosen for calculating P, highlighting areas at major risk of soil erosion. The five raster images obtained for each factor were multiplied according to equation (6), resulting in the map of soil erosion susceptibility for the analyzed territory (Figure 2).

Soil erosion map was classified, based on the intensity of the phenomenon, into five classes: very low rate (tolerable) below $3 \text{ t ha}^{-1} \text{ year}^{-1}$; low rate between $3.1\text{-}10 \text{ t ha}^{-1} \text{ year}^{-1}$; moderate rate between $11\text{-}20 \text{ t ha}^{-1} \text{ year}^{-1}$; high rate, between $21\text{-}40 \text{ t ha}^{-1} \text{ year}^{-1}$ and very high rate, above $41 \text{ t ha}^{-1} \text{ year}^{-1}$ (Sestras et al., 2023).

RESULTS AND DISCUSSIONS

1. Rainfall erosivity factor (R)

Rainfall erosivity (R) refers to the capacity of raindrops to cause erosion by detaching and mobilizing soil particles (Allafta & Opp, 2022). In this study, the map of the R factor (Figure 3) was determined based on the equation proposed by Hurni (1985), as cited by Balabathina et al., 2020.

In the study area, the multi-year average precipitation over the period 2013-2022 is distributed unevenly; precipitation amounts varied between 247 mm (Alba Iulia, 2013) and 1739 mm (Rusca Montană, 2021). Based on the multi-year average precipitation values, the map of the R factor was generated, with minimum values of $275.85 \text{ MJ mm ha}^{-1} \text{ h}^{-1} \text{ year}^{-1}$, in the southwest, in the lowland area, and maximum values of $571.59 \text{ MJ mm ha}^{-1} \text{ h}^{-1} \text{ year}^{-1}$, in the central and mountainous areas (Figure 3).

2. Soil erodibility factor (K)

The soil erodibility factor (Figure 4) depicts the soil particles' predisposition to detachment and transportation by runoff. The soils in the analyzed area are distributed in accordance with physico-geographical factors: in mountainous and hilly areas, districambosols and luvisols predominate, while in low-lying areas, chernozems, eutricambosols, and alluvial soils prevail.

In the study area, the values of the K factor range between $0.04 \text{ t ha}^{-1} \text{ MJ}^{-1} \text{ mm}^{-1}$, for sandy soils and $0.6 \text{ t ha}^{-1} \text{ MJ}^{-1} \text{ mm}^{-1}$, for clayey soils (Figure 4).

3. Topographic Factor (LS)

The LS factor refers to the impact of topography on erosion processes. In this context, the most important elements are the length and inclination (angle) of the slope (Simon et al., 2020; Allafta & Opp, 2022), the impact of erosion phenomena increasing proportionally with them (Liu et al., 2000; Lastoria et al., 2008).

In the study area, the terrain is complex and varies between 82 and 1587 meters in elevation,

and the slope ranges from 0 to 59 degrees. Under these conditions, LS values range from 0 to 16.56 (Figure 5). The minimum LS values are

specific to low-lying, plain areas, while the maximum values are found on the slopes of mountainous areas.

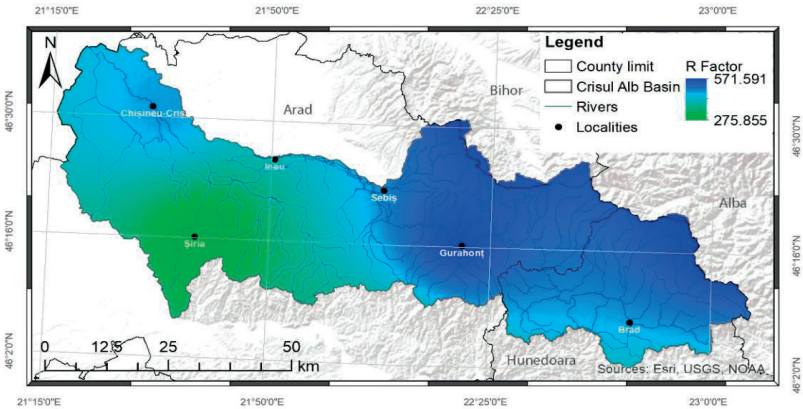


Figure 3. The R factor distribution map ($\text{MJ mm ha}^{-1} \text{h}^{-1} \text{year}^{-1}$) in the study area

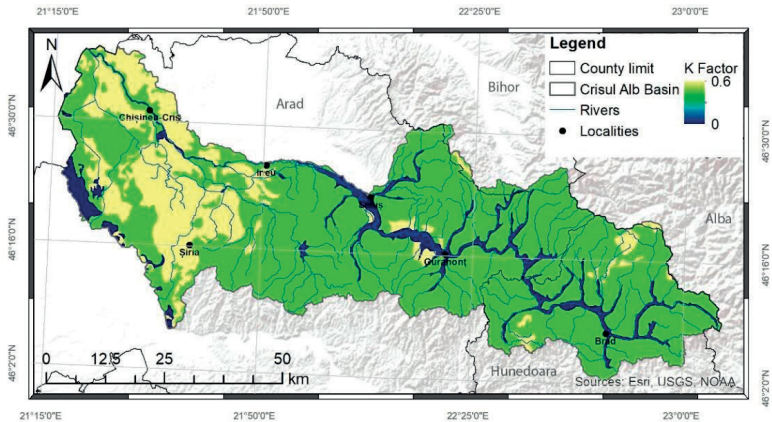


Figure 4. The K factor distribution map ($\text{t ha}^{-1} \text{MJ}^{-1} \text{mm}^{-1}$) in the study area

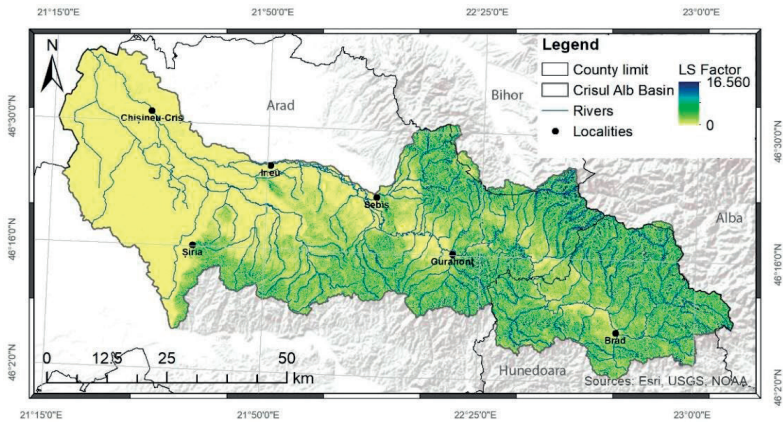


Figure 5. The LS factor distribution map in the study area

4. Land cover management factor (C)

In the case of this study, the C factor (Figure 6) was determined based on the NDVI derived from satellite images, a method applied through various algorithms in other studies (Durigon et al., 2014). In the hydrographic basin of the Crișul Alb River, in the year 2021, the average NDVI values ranged from -0.21 to 0.63. The minimum values are specific to areas not covered by vegetation (water bodies, roads, or plowed or harvested agricultural land), while the maximum values characterize forested areas in mountainous regions. The C factor, calculated based on satellite images, ranged from 0.03 to 1.41, in the hydrographic basin of the Crișul Alb River. The maximum values of

the C factor correspond to plain areas dominated by agricultural land with a lower degree of soil cover and therefore lower potential protection against erosion.

The C values decrease towards higher altitudes, where forested areas prevail, providing a higher degree of soil erosion protection.

5. Conservation Support Practice Factor (P)

The P factor defines the impact of land use and agricultural and non-agricultural practices on soil erosion, thus quantifying the influence of conservation strategies in the emergence and manifestation of erosion processes (Allafta & Opp, 2022).

In the case of the area of interest, P had values ranging from 0.2 to 5.2 (Figure 7).

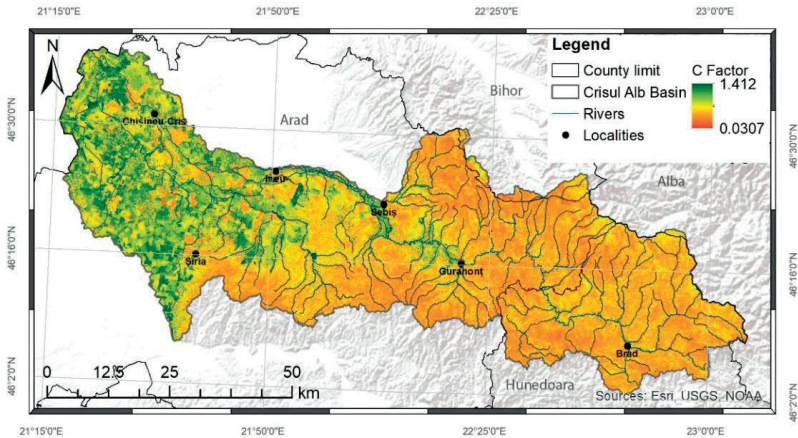


Figure 6. The C factor distribution map in the study area

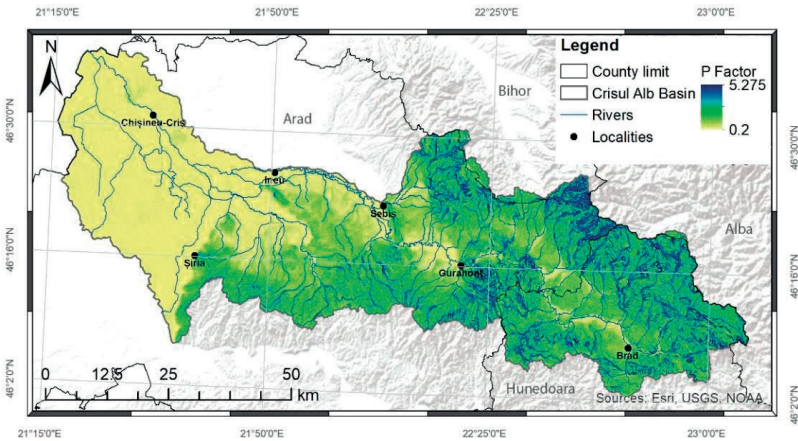


Figure 7. The P factor distribution map in the study area

Assessing the vulnerability of the territory to soil erosion

At the level of the study area, the soil erosion rate falls between 0 - >41 t ha⁻¹ year⁻¹.

Based on the severity level, the soil erosion map of the Crișul Alb watershed has been divided into five classes: very low rate (tolerable) of less than 3 t ha⁻¹ year⁻¹; low rate between 3.1-10 t ha⁻¹ year⁻¹; moderate rate between 11-20 t ha⁻¹ year⁻¹; high rate, between 21-40 t ha⁻¹ year⁻¹ and very high rate of over 41 t ha⁻¹ year⁻¹ (Sestras et al., 2023).

From Figure 8 and Table 2, it can be observed that 74% of the territory falls into the class of

very low susceptibility to soil erosion (below 3 t ha⁻¹ year⁻¹), which are areas located in low-lying plains, river valleys, and depressions, at the base of slopes. In the class with a low rate (3.1-10 t ha⁻¹ year⁻¹), 14% of the land is classified; 7% have been classified with moderate rates, while 4% have high (21-40 t ha⁻¹ year⁻¹) and very high erosion rates (over 41 t ha⁻¹ year⁻¹).

High rates of soil loss through erosion generally characterize areas with high amounts of precipitation, with clay soils and high values of slopes, in premontane and mountainous areas.

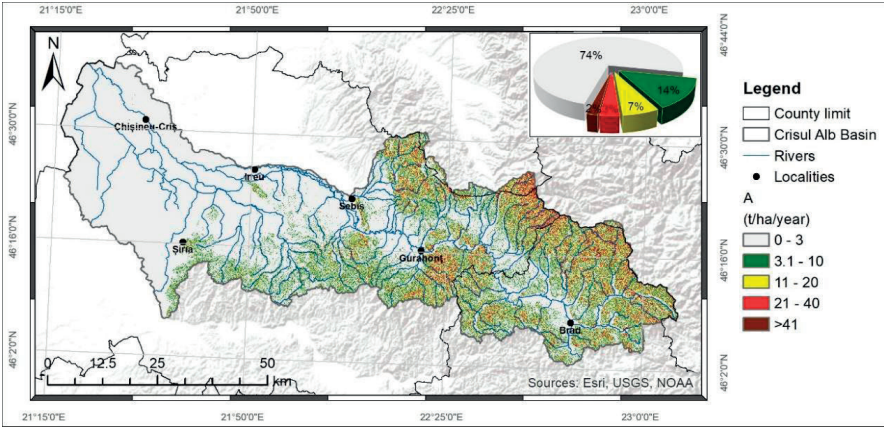


Figure 8 Soil erosion susceptibility map (t ha⁻¹ year⁻¹), of the Crișul Alb H

Table 2 Erosion modeling by severity classes (erosion rates), at the sub-basin level

Sub-basin	Classes of erosion susceptibility (t ha ⁻¹ year ⁻¹)					Sub-basin	Classes of erosion susceptibility (t ha ⁻¹ year ⁻¹)				
	0-3	3.1-10	11-20	21-40	>41		0-3	3.1-10	11-20	21-40	>41
Crișul Alb	78	11	6	4	2	Topasca	92	7	1	0	0
Valea Satului	40	27	18	11	5	Chisindia	60	28	9	3	1
Birtin	50	27	14	7	2	Cleja	92	6	1	0	0
Vata	52	27	13	6	1	Sebis	60	20	12	6	2
Obarsa	70	18	7	4	1	Hodis	93	6	0	0	0
Pravaleni	51	27	14	7	2	Potoc	97	3	0	0	0
Ociu	84	13	3	1	0	Trei Holamburi	99	1	0	0	0
Banesti	44	22	16	12	7	Gut	97	3	1	0	0
Leasa	89	11	1	0	0	Cigher	87	11	2	0	0
Valea de la Lazuri	55	17	11	10	7	Luncoiu	61	24	10	4	1
Valea Mare	41	30	17	9	3	Valea Noua Chiser	100	0	0	0	0
Tacasele	69	20	7	3	1	Canalul Morilor	100	0	0	0	0
Artan	38	26	20	12	4	Brad	57	27	11	5	1
Grulet	59	25	10	4	1	Junc	52	25	14	7	2
Sighisoara	48	28	15	8	2	Ribita	40	24	18	12	6
Zimbru	61	25	9	4	1	Tebea	58	26	11	5	1
Mustesti	77	18	4	1	0	Baldovin	63	24	9	3	1
Fenis	80	16	3	1	0	Valea Laptelui	35	25	19	13	7
Crocna	64	21	9	5	1	Plai	31	24	22	14	9
Bodesti	72	20	6	2	0	Bucuresci	52	27	13	6	2
Dumbravita	69	17	9	4	1						
Craicova	77	13	7	3	1						
Almas	67	26	6	1	0						
						Total	315417	58786	27446	14628	5811
						% of total	74	14	6	3	1

The soil erosion susceptibility map (Figure 8) illustrates that the spatial distribution of annual average soil loss in the analyzed hydrographic basin was variable, with minimum values in the western half, corresponding to the plains and low hills, and maximum values in the eastern half, in the highland areas.

The precision and accuracy of the results is conditioned by the average resolution of the data used. This aspect is also a limitation in using the data for large-scale analyses. However, such studies are accepted in the specialized literature and practices in the field, given the fact that they provide an overview of the phenomena in the territory.

CONCLUSIONS

In this study, USLE, the empirical soil erosion estimation method, was used, implemented through GIS tools and remote sensing data. By applying this method, accessible from the point of view of the involved data and working methods, both the quantitative evaluation of the average annual soil losses and the classification of the area of interest, according to the risk of soil erosion, was achieved.

The research results in the hydrographic basin of Crișul Alb have revealed a significant spatial variability in the soil erosion potential, influenced by intrinsic and extrinsic factors. Estimated soil loss varies from 0 t ha⁻¹ year⁻¹, in low-slope plain areas to over 41 t ha⁻¹ year⁻¹, in mountainous areas with steep slopes or in degraded and unvegetated lands.

Attention is drawn to areas where the erosion rate is high and very high (approximately 4% of the territory), which should be considered a priority for implementing soil erosion control measures (excess moisture removal, slope stabilization, proper agricultural management, and so on).

The results regarding the identification and classification of erosion-prone areas support the development of H.B. management plans aimed at soil conservation.

The spatial distribution of erosion rates, according to the severity of the phenomenon, along with other individual factors, helps in understanding the primary processes that cause and sustain erosion and can provide support in

recommending measures for preventing and controlling soil erosion.

REFERENCES

- Allafta, H., & Opp, C. (2022). Soil Erosion Assessment Using the RUSLE Model, Remote Sensing, and GIS in the Shatt Al-Arab Basin (Iraq-Iran). *Appl. Sci.*, 12, 7776. <https://doi.org/10.3390/app12157776>.
- ArcGIS Documentation. (2022). <https://desktop.arcgis.com/en/documentation/> (accessed on 25.10.2022).
- Arhiva Administrației Bazinale de Apă Crișuri, 2023.
- Asnake, Y., & Amare, B. (2019). Soil erosion mapping and severity analysis based on RUSLE model and local perception in the Beshillo Catchment of the Blue Nile Basin, Ethiopia. *Environ. Syst. Res.*, 8, 17.
- Balabathina, V.N., Raju, R.P., Muluallem, W., & Tadele, G. (2020). Estimation of soil loss using remote sensing and GIS-based universal soil loss equation in northern catchment of Lake Tana Sub-basin, Upper Blue Nile Basin, Northwest Ethiopia. *Environ. Syst. Res.*, 9, 35. <https://doi.org/10.1186/s40068-020-00203-3>.
- Biali, G. & Cojocaru, P. (2021). The influence of gis technology in reclamation solutions for sloping land affected by erosion. *Scientific Papers. Series E. Land Reclamation, Earth Observation & Surveying, Environmental Engineering*, X, 293-300, Print ISSN 2285-6064.
- Borrelli, P., Märker, M., & Schütt, B. (2015). Modelling post-tree-harvesting soil erosion and sediment deposition potential in the Turano River basin (Italian Central Apennine). *Land Degrad. Dev.*, 26, 356–366.
- Choudhury, M.K., & Nayak, T. (2003). Estimation of soil erosion in Sagar Lake catchment of Central India. In *Proceedings of the International Conference on Water and Environment*, Bhopal, India, 15–18 December; pp. 387–392.
- Climatic Database. (2023) https://rp5.ru/Weather_in_Romania.
- Cojocariu, L.L., Copăcean, L., Ursu, A., Sărățeanu, V., Popescu, C.A., Horablaga, M.N., Bordean, D.-M., Horablaga, A., & Bostan, C. (2024). Assessment of the Impact of Population Reduction on Grasslands with a New "Tool": A Case Study on the "Mountainous Banat" Area of Romania. *Land*, 13, 134. <https://doi.org/10.3390/land13020134>.
- Copăcean, L., Zisu, I., Mazăre, V., & Cojocariu, L. (2019). Analysis of land use changes and their influence on soil features. Case study: Secaș village, Timiș County (Romania). *PESD*, 13(2), Doi: 10.2478/pesd-2019-0032.
- Copernicus Open Access Hub. (2023). Available online: <https://scihub.copernicus.eu/dhus/#/home> (accessed on 11.01.2023).
- Diodato, N., & Bellocchi, G. (2007). Estimating monthly R factor USLE climate input in a Mediterranean region using limited data. *J. Hydrol.*, 345, 224–236.
- Durigon, V.L., Carvalho, D.F., Antunes, M.A.H., Oliveira, P.T.S., & Fernandes, M.M. (2014). NDVI time series for monitoring RUSLE cover management

- factor in a tropical watershed. *Int. J. Remote Sens.*, 35(2), 441–453.
- Estifanos, A. (2014). Assessment of Micro-Watershed Vulnerability for Soil Erosion in Ribb Watershed using GIS and Remote Sensing. MSc Thesis. Mekelle University, Ethiopia.
- European Environment Agency (EEA). (2016). Digital Elevation Model (DEM), <https://www.eea.europa.eu/data-and-maps/data/copernicus-land-monitoring-service-eu-dem> (accessed on 13.12.2016).
- Fathizad, H., Karimi, H., & Alibakhshi, S.M. (2014). The estimation of erosion and sediment by using the RUSLE model and RS and GIS techniques (Case study: Arid and semi-arid regions of Dohra, Ilam province, Iran). *Int. J. Agric. Crop Sci.*, 7, 304–314.
- Foster, G.R., Toy, T.J., & Renard, K.G. (2003). Comparison of the USLE, RUSLE1.06c, and RUSLE2 for application to highly disturbed lands. In *Proceedings of the First Interagency Conference on Research in the Watersheds*, Benson, AZ, USA, 27–30 October; pp. 154–160.
- Fu, B.J., Zhao, W.W., Chen, L.D., Zhang, Q.J., Lü, Y.H., Gulinc, H., & Poesen, J. (2005). Assessment of soil erosion at largewatershed scale using rusle and GIS: A case study in the Loess Plateau of China. *Land Degrad. Dev.*, 16, 73–85.
- Ge, Y., Zhao, L., Chen, J., Li, X., Li, H., Wang, Z., & Ren, Y. (2023). Study on Soil Erosion Driving Forces by Using (R)USLE Framework and Machine Learning: A Case Study in Southwest China. *Land*, 12, 639. <https://doi.org/10.3390/land12030639>.
- Geospatial. (2022). România: seturi de date vectoriale generale – <http://geospatial.org/vechi/download/romania-seturi-vectoriale> (accessed on 10.01.2022).
- Golosov, V., Gusarov, A., Litvin, L., Yermolaev, O., Chizhikova, N., Safina, G., & Kiryukhina, Z. (2017). Evaluation of soil erosion rates in the southern half of the Russian Plain: Methodology and initial results. *Proc. Int. Assoc. Hydrol. Sci.*, 375, 23.
- Greiner, L., Keller, A., Grêt-Regamey, A., & Papritz, A. (2017). Soil function assessment: review of methods for quantifying the contributions of soils to ecosystem services. *Land Use Policy*, 69, 224–237. <https://doi.org/10.1016/j.landusepol.2017.06.025>.
- Kim, J.B., Saunders, P., John, T.F. (2005). Rapid assessment of soil erosion in the Rio Lempa Basin, Central America, using the universal soil loss equation and geographic information systems. *Environ. Manage.*, 36(6), 872–885.
- Lastoria, B., Miserocchi, F., Lanciani, A., & Monacelli, G. (2008). An estimated erosion map for the Aterno-Pescara river Basin. *Eur. Water*, 21/22, 29–39.
- Ligonja, P.J., & Shrestha, R.P. (2015). Soil erosion assessment in Kondoeroded area in Tanzania using Universal Soil Loss Equation, geographic information systems and socioeconomic approach. *Land Degrad. Dev.*, 26, 367–379.
- Liu, B.Y., Nearing, M.A., Shi, P.J., & Jia, Z.W. (2000). Slope length effects on soil loss for steep slopes. *Soil Sci. Soc. Am. J.*, 64, 1759–1763.
- Măgureanu, M., Sfircoci, M., Copacean, L., & Cojocariu, L. (2024). Monitoring the vegetation coverage of the grasslands in the Poiana Ruscă Mountains using different remote sensing indices. *Present Environment and Sustainable Development*, 17, 189–199. [10.47743/pesd2023172014](https://doi.org/10.47743/pesd2023172014).
- Man, E.T. (2014). *Drenaje*, Vol. I., Editura Orizonturi universitare, Timișoara, Romania.
- Mengie, B., Teshome, Y., & Dereje, T. (2019). Potential soil erosion estimation and area prioritization for better conservation planning in Gumara watershed using RUSLE and GIS techniques. *Environ Syst. Res.*, 8, 20.
- Mircea, S. (2011). *Impactul ravenarii asupra mediului in B.H. Slanic/Buzau*, Editura BREN, Bucuresti, Romania.
- Niacsu, L., Ionita, I., Samoila, C., Grigoras, G., & Blebea-Apostu, A.M. (2021). Land Degradation and Soil Conservation Measures in the Moldavian Plateau, Eastern Romania: A Case Study from the Racova Catchment. *Water*, 13, 2877. <https://doi.org/10.3390/w13202877>.
- Nistor, D., & Nistor, D. (2002). Land Degradation by Erosion and Its Control in Romania, *12th ISCO Conference, Beijing*, <https://topsoil.nserl.purdue.edu/isco/isco12/Volumell/LandDegradationbyErosion.pdf>
- Panagos, P., Ballabio, C., Borrelli, P., Meusburger, K., Klik, A., Rousseva, S., Tadić, M.P., Michaelides, S., Hrabalíková, M., Olsen, P., Aalto, J., Lakatos, M., Rymaszewicz, A., Dumitrescu, A., Beguería, S., & Alewell, C. (2015). Rainfall erosivity in Europe. *Sci. Total Environ.*, 511, 801–814.
- Patriche, C. (2023). Applying RUSLE for soil erosion estimation in Romania under current and future climate scenarios. *Geoderma Regional*, 34, e00687. [10.1016/j.geodrs.2023.e00687](https://doi.org/10.1016/j.geodrs.2023.e00687).
- Pham, T.G., Nguyen, H.T., & Kappas, M. (2018). Assessment of soil quality indicators under different agricultural land use and topographic aspects in Central Vietnam. *Int Soil Water Conserv. Res.*, 6(4), 280–288.
- Popescu, E., Nenciu, F., Vladut, V. (2022). A new strategic approach used for the regeneration of soil fertility, in order to improve the productivity in ecological systems. *Scientific Papers. Series E. Land Reclamation, Earth Observation & Surveying, Environmental Engineering*, XI, 277–284, Print ISSN 2285-6064.
- Posea, G., & Badea, L. (1984). *România. Unitățile de relief (Regiunea geomorfologică)*. Ed. Științifică și Enciclopedică, București, Romania.
- Renard, K.G., Foster, G.R., Weesies, G.A., McCool, D.K., & Yoder, D.C. (1997). *Predicting soil erosion by water: A guide to conservation planning with the revised universal soil loss equation (RUSLE)*. In *USDA Agricultural Handbook*; U.S. Department of Agriculture: Washington, DC, USA; No. 703.
- Robert, P., Stone, P., & Don, H. (2012). Universal Soil Loss Equation (USLE); Ministry of Agriculture, Food and Rural Affairs: Ontario, ON, Canada. Available online:

- <http://www.omafra.gov.on.ca/english/engineer/facts/12-051.htm> (accessed on 20.01.2024).
- Roșca, S., Bilașco, Ș., Petrea, D., Vescan, I., Fodorean, I., & Filip, S. (2014). Application of soil loss scenarios using the ROMSEM model depending on maximum land use pretability classes. A case study. *Studia UBB Geographia*, 59, 101-116.
- Rusu, R. (2007). *Organizarea spațiului geografic în Banat*, Ed. Mirton, Timișoara, Romania.
- Selmy, S.A.H., Abd Al-Aziz, S.H., Jiménez-Ballesta, R., García-Navarro, F.J., & Fadl, M.E. (2021). Modeling and Assessing Potential Soil Erosion Hazards Using USLE and Wind Erosion Models in Integration with GIS Techniques: Dakhla Oasis, Egypt. *Agriculture*, 11, 1124.
- Sestras, P., Mircea, S., Rosca, S., Bilașco, S., Salagean, T., Dragomir, L., Herbei, M., Bruma, S., Sabou, C., Marković, R., & Kader, S. (2023). GIS based soil erosion assessment using the USLE model for efficient land management: A case study in an area with diverse pedo-geomorphological and bioclimatic characteristics. *Notulae Botanicae Horti Agrobotanici Cluj-Napoca*, 51, 10.15835/nbha51313263.
- Simon, M., Copăcean, L., & Cojocariu, L. (2022). Techniques for identification, mapping and analysis of grasslands. Case study: Arad county. *PESD*, 16(2), 39-49. <https://doi.org/10.47743/pesd2022162004>.
- Simon, M., Popescu, C.A., Copăcean, L., & Cojocariu, L. (2020). Complex model based on UAV technology for investigating pastoral space. *PESD*, 14(2), 139 – 150. <https://doi.org/10.15551/pesd2020142011>.
- Singh, G., & Panda, R.K. (2017). Grid-cell-based assessment of soil erosion potential for identification of critical erosion-prone areas using USLE, GIS and remote sensing: a case study in the Kapgari watershed, India. *Int Soil Water Conserv. Res.*, 5(3), 202–211.
- Spalevic, V., Barovic, G., Vujacic, D., Curovic, M., Behzadfar, M., Djurovic, N., & Billi, P. (2020). The impact of land use changes on soil erosion in the river basin of Miocki Potok, Montenegro. *Water*, 12(11), 2973. <https://doi.org/10.3390/w12112973>.
- Todisco, F., Vergni, L., Ortenzi, S., & Di Matteo, L. (2022). Soil Loss Estimation Coupling a Modified USLE Model with a Runoff Correction Factor Based on Rainfall and Satellite Soil Moisture Data. *Water*, 14, 2081. <https://doi.org/10.3390/w14132081>.
- Wischmeier, W.H., & Smith, D.D. (1978). *Predicting rainfall erosion losses- a guide to conservation planning*. Agriculture Handbook No. 537, Department of Agriculture, US
- Zhang, H., Yang, Q., Li, R., Liu, Q., Moore, D., He, P., Ritsema, C.J., & Geissen, V. (2013). Extension of a GIS procedure for calculating the RUSLE equation LS factor. *J. Comput. Geosci.*, 52, 177–188.
- Zisu, I. (2014). *Studiu pedogeografic al Dealurilor Lugojului cu privire specială asupra calității terenurilor Agricole*. Teză de doctorat, Universitatea de Vest Timișoara. Romania.

3D MODELING OF THE CAMPUS OF THE UNIVERSITY OF AGRICULTURAL SCIENCES AND VETERINARY MEDICINE CLUJ-NAPOCA USING ARCGIS PRO

**Iulia COROIAN, Diana FICIOR, Tudor SĂLĂGEAN, Silvia CHIOREAN,
Ioana Delia POP, Mircea-Emil NAP, Elemer-Emanuel SUBA**

University of Agricultural Sciences and Veterinary Medicine Cluj-Napoca,
3-5 Manastur Street, Cluj-Napoca, Romania

Corresponding author emails: silvia.chiorean@usamvcluj.com, diana.ficior@usamvcluj.ro

Abstract

The 3D modeling process consists of a three-dimensional representation of an object or a surface using certain specialized software. The 3D modeling was done by using a point cloud resulting from a drone flight. GIS applications enable the analysis of spatial locations by creating and layering information through maps or 3D scenes. In order to create a 3D model of the land, the orthophotomap resulting from a photogrammetric drone flight was used. The generation of the orthophotomap and the dense point cloud offers the possibility of making digital measurements, exporting and creating a database for making applications and drawing up interactive maps according to the user's wishes. The purpose of this work is to use the latest methods of obtaining photogrammetric data with the help of drones, but also to create interactive maps that allow studies and spatial analysis to be carried out. The case study was carried out on the campus of the University of Agricultural Sciences and Veterinary Medicine Cluj-Napoca using the photogrammetric method and GIS analysis. To obtain the orthophotomap and photogrammetric data, it was decided to fly with the DJI Phantom 4 RTK drone. The analysis of the orthophotomap of the campus and the dense point clouds allowed the graphical representation of the cartographic elements in the ArcGIS PRO application, respectively ArcGIS Online, offering the possibility of accessing them in real time, which represents an up-to-date process and to be considered for conducting studies and spatial analyses. The maps created, both in 2D and 3D format, as well as the WEB applications have the purpose of providing users with data regarding the shape, location, character and arrangement within the campus of the University of Agricultural Sciences and Veterinary Medicine Cluj-Napoca of the most important component buildings, taking into account their character.

Key words: 3D modeling, databases, GIS, Photogrammetry, Web map.

INTRODUCTION

The main goal is to create a 3D model of the University of Agricultural Sciences and Veterinary Medicine campus in Cluj-Napoca using photogrammetry and GIS techniques. The analysis of the ortophotomaps of the campus and the point cloud data enabled the digitization of campus features within the ArcGIS PRO application and ArcGIS Online. This process resulted in the development of interactive real-time maps, ensuring that the data remains current.

The University of Agricultural Sciences and Veterinary Medicine is located within the Cluj-Napoca municipality, which is situated in the northwestern region of Romania, specifically in the central part of Transylvania, covering an approximate area of 23,000 square meters (Figure 1).

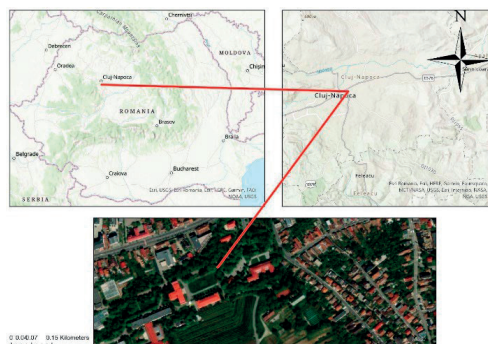


Figure 1. Location of USAMV in Romanian
and Cluj-Napoca

MATERIALS AND METHODS

To achieve the desired results, logistical and technical support was necessary, included the use of two drones, one for making the flight for

the orthophotomap and the second for capturing aerial photographs of the building facades. Also, a suite of software applications in the field of photogrammetry and geographic information systems played a crucial role. These applications were used in processing the raw images, generating the orthophotomap, creating the database, and georeferencing the campus buildings in 3D format.

To conduct the planned study, a photogrammetric flight was executed using the DJI Phantom 4 RTK drone. This drone is a popular choice for photogrammetric flights due to its high-quality camera and the assistance of various sensors, which together deliver excellent performance and superior image quality.

The technology incorporated in this drone enables data acquisition with centimeter-level accuracy, eliminating the requirement for additional ground control points. The drone is equipped with an integrated RTK module that offers real-time positioning data, ensuring the absolute geotagging for the images.

In addition to ensure optimized flight safety and precise data collection, the DJI Phantom 4 RTK also stores satellite observation data that can be Post Processed (PPK). The DJI Mavic Air 2S drone is an ideal choice for capturing high-quality imagery. Despite its compact size, the drone is equipped with a 20-megapixel camera capable of producing professional-grade photos and videos, making it well-suited for content creators, but also for photogrammetric missions. It comes equipped with a 1-inch sensor and can record videos at 5.4K/30 fps and 4K/60 fps.

The photogrammetric data was processed with Agisoft MetaShape software. This supposed processing the previously captured images, resulting in the generation of a dense point cloud. To conduct the planned study, the orthophotomap was overlaid with the point cloud data using Global Mapper. Subsequently, measurements were taken, and the coordinates of the buildings within the campus were obtained.

For the georeferencing and 3D construction of the main campus buildings, the ArcGIS Pro software was used. This software enables the creation of a geographic information system that includes a database, a data set, and various

layers of different types, such as point, line, polygon, 3D objects, and others.

ArcGIS Online platform facilitates the viewing of interactive maps in an online environment, enabling users to customize the maps based on their specific needs and analyses. Additionally, ArcGIS Online enables the creation of applications using various widgets with multiple functionalities, offering real-time creation, visualization, and analysis of data both in office and field. For optimal drone performance, a camera calibration is preconfigured at start-up, ensuring that all the equipped sensors are functional and ready to execute their tasks during the mission.

Following this, the specific area of interest, the flight path, and the band overlap were chosen, with the software providing estimates for the flight duration, optimal drone altitude, speed, and the number of captured images.

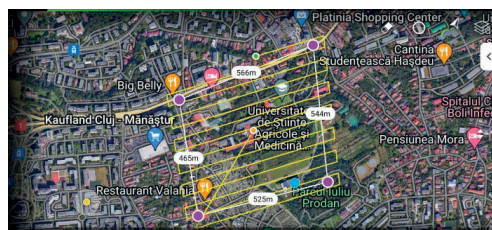


Figure 2. UAV Mission planning

Post-flight, the software automatically generates a comprehensive mission report, detailing all technical settings, including camera calibration and parameters used, along with a mission summary. During the mission, a total of 413 photos were captured at a medium altitude of 97.6 meters. The photogrammetric flight, aimed at mapping the designated area of interest, was conducted from within the university campus and lasted approximately 20 minutes.

RESULTS AND DISCUSSIONS

The processing report indicates, as shown in the blue-coloured image above, the optimal alignment of the images captured during the flight, represented by points denoting the camera positions at the time of shooting (Figure 3). Additionally, subsequent to the flight, a digital elevation model is created,

illustrating the variations in elevation across the surveyed region.

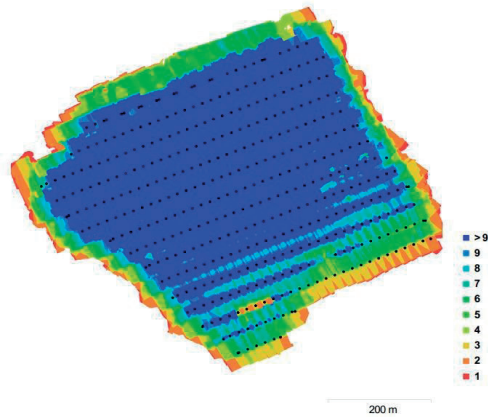


Figure 3. Camera Locations and image overlap

The higher altitude section of the campus is represented in red, the lower portion of the campus is blue, while the green-coloured area represents the middle heights zone. Lastly, the red-tinted lower section of the image represents the ICHAT area, the highest altitude points of the campus, situated at an approximate altitude of 427 meters (Figure 4).

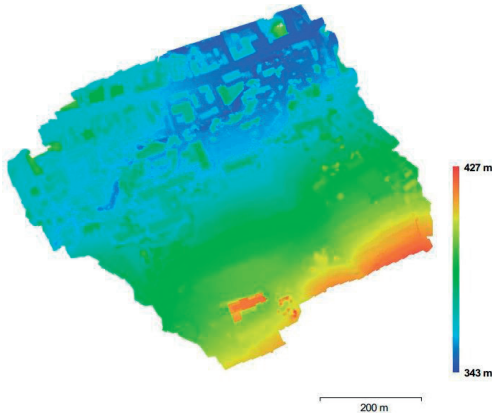


Figure 4. Digital Elevation Model

After the drone flight, a series of crucial steps were taken to obtain the orthophotomap and the dense point cloud. These steps should be executed chronologically and in a systematic manner to achieve the best quality results. The steps include creating the project, importing the raw images, generating tie points using a

specific method, adjusting tie points, compensating the block aerial triangulation, conducting precise aerial triangulation, generating and selecting the digital elevation model, and obtaining the orthophotomap. Ground control points (Figure 5) are used in georeferencing the model both from planimetric and altimetric point of view.



Figure 5. Ground Control points locations

The accuracy of the aerotriangulation is determined as mean squared error, which is calculated based on the disparities between the control points and the actual model. The drone flight and processing in Agisoft MetaShape contributed to the creation of a dense point cloud enabling the identification of points even in challenging areas, such as buildings near trees (Figure 6).

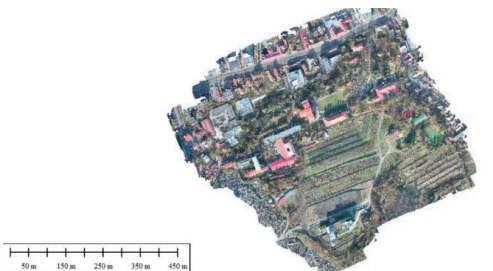


Figure 6. Dense point Cloud

Figure 7 displays the digital elevation model, illustrating the variations in elevation across the surveyed area (Sălăgean et al., 2018). After completing all the requisite procedures, the

resulting orthophotomap (Figure 7) is suitable for mapping, conducting analyses, and performing complex measurements.

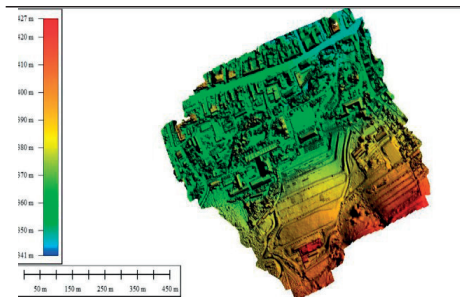


Figure 7. Digital Elevation Model in Global Mapper

After completing all the requisite procedures, the resulting orthophotomap (Figure 8) is suitable for mapping, conducting analyses, and performing digital measurements. We accomplished significant progress using Global Mapper software, especially in implementing key steps to achieve our intended objectives, such as integrating the point cloud over the orthophotomap (Jayaraj et al., 2018).

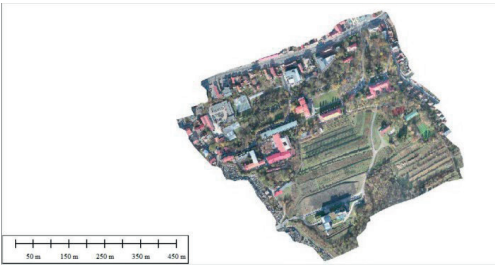


Figure 8. The USAMV Cluj-Napoca Campus Orthophotomap

Through the imported data, the coordinates of both the base of the buildings and the top of the buildings were extracted. Creating area features for each facade of the buildings is an essential step for a detailed and comprehensive analysis of the structures. The use of the Create Area Feature function to delineate the shapes of the buildings on the point cloud ensures accuracy and facilitates the creation of polygons. With the polygons generated for the Rectorate building, the Faculty of Horticulture building, and the Aula Magna building, we can conduct a more thorough study as intended. The most important aspect for the data processing part in

ArcGIS PRO is the creation of the database (Figure 9). Raster data and vector data such as line, point and polygon were inserted into the project, which were used to fulfill the problem addressed.



Figure 9. Geodatabase of the USAMV Cluj-Napoca Campus in Arcgis Pro

To create the 3D model of the buildings on the USAMV Cluj-Napoca campus, the coordinates of the points at the base of the main buildings were determined, namely the Rectorate building, the Faculty of Horticulture building and the Mihai Șerban Magna Hall building.(Figure 10).



Figure 10. Geodatabase with the buildings

GIS applications find use in various fields related to the processing of spatial information, including urban planning, cadastral management, and cartography. In urban planning, GIS tools optimize urban transport, aid in locating housing space, establish zoning based on diverse criteria, support urban planning studies, facilitate the issuance of construction and demolition permits, and enable the inventory of land uses. In the realm of cadastral management, GIS applications are employed for the comprehensive integration of the entire cadastral process, from land measurements to the editing of plans and cadastral records. Moreover, in cartography, GIS applications are instrumental in the

creation and maintenance of maps and topographic plans. They also integrate terrain, photogrammetric, and satellite data into map content to generate thematic maps. ([https://www.academia.edu/19674635/Curs_Sisteme Informale Geografice](https://www.academia.edu/19674635/Curs_Sisteme_Informale_Geografice)).

As shown in Figure 11 in the created application, a part of the points at the base of the campus component buildings are represented, together with a selection of the green space.

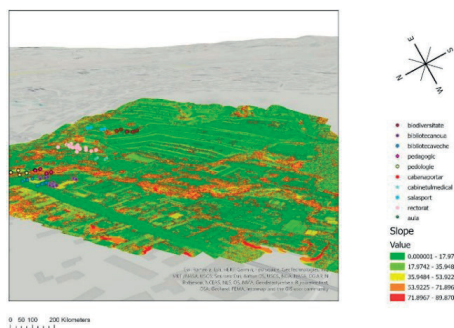


Figure 11. The ArcGIS PRO Application

As can be seen in Figure 12, a 3D map of the area of interest was generated, taking into account the location and shape of the buildings, and also taking into account the differences in height and the Ground area (Song, et al., 2018).



Figure 12. 3D Visualization of the USAMV Cluj-Napoca Campus

In Figure 13 the contour lines across the USAMV Cluj-Napoca Campus are represented. To render the contours, the digital elevation model was inserted as an input file and an interval of 8 contours were added.

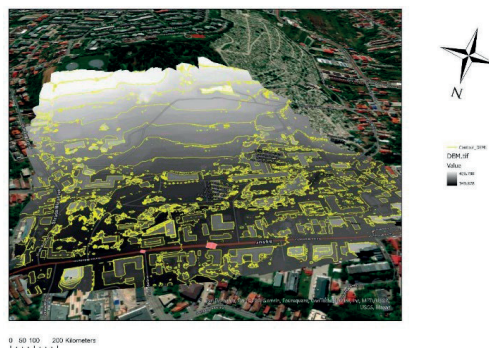


Figure 13. Contour lines în ArcGIS PRO

In the last part of the study, several online applications were made using the Arcgis Online platform. Within the interactive map in Figure 14, buildings of interest are included, each with an individual color. Also, two layers that form the database have been inserted within the map. The first layer, titled 3D buildings, is the actual representation of the buildings, and the halls layer is a symbolic representation of the location of several halls where student, administrative and festive activities are carried out.



Figure 14. Interactive map of the USAMV Cluj-Napoca campus in ArcGIS Online

Figure 15 shows an innovative concept of the ArcGIS platform, namely allowing real-time localization of the user. The interactive map was accessed and by allowing the use of location and the phone's built-in GPS module, real-time positioning was possible. Thus, the position of the user in the center of the lawn can be observed.

This applicability can be exploited for example by any user who wants to reach a certain building within the campus. Within the scene of the interactive map represented in Figure 16, some information is presented in a succinct way (Sugianto et al., 2023).

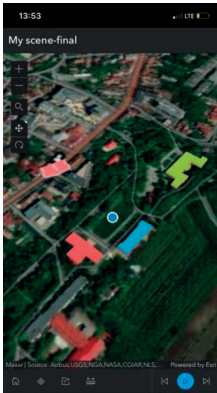


Figure 15. Accessing the interactive map from the mobile version of ArcGIS Online

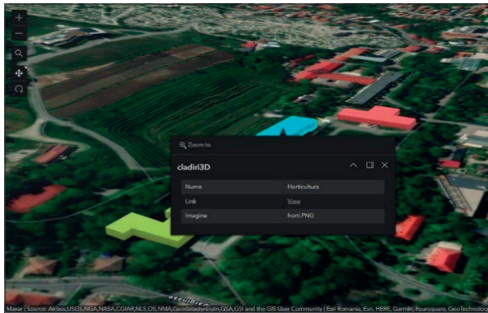


Figure 16. Accessing informations regarding the inserted buildings

By simply pressing the cursor on the surface of any represented building, a table is displayed that includes some information about the building of interest, such as the name, a link that redirects the user to the official website, namely to the Faculty website of Horticulture, and a representative picture of the objective in question (Xu et al., 2012).

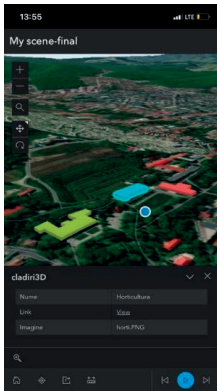


Figure 17. Accessing information from the phone

Similarly, the interactive map allows access for information in the phone version of the program as well (Figure 17), being important or the user to know where they need to go within the campus.



Figure 18. Path lenght measurement function

As can be seen in Figure 18, the length measurement function has been introduced within the interactive map. On the right side of the image, all the available functionalities are displayed, and for the measurement function, both the measurement of lengths and the measurement of the area of the desired polygon have been added. Thus, according to the figure, it can be seen that the length from the entrance point to the campus of the University of Agricultural Sciences and Veterinary Medicine Cluj-Napoca to the front of the Faculty of Horticulture building is approximately 245.85 meters.

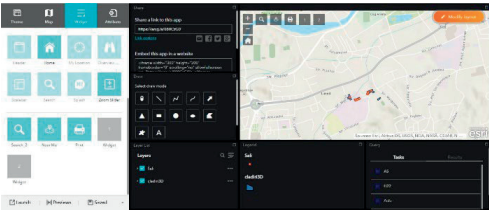


Figure 19. Editing the interactive map

Figure 19 shows all the elements that can be added to the display of an interactive map. Applications are in the form of widgets and can be added according to the user's desire. All the available widgets are presented on the left side, and on the right side are those inserted in the map composition.

Thus, in the presented map (Figure 20) widgets such as:

- The Share function that offers the possibility of distributing the interactive map to any user.

Sharing is done via a link and can be sent to social media applications allowed and agreed to by ArcGIS Online developers.

- The drawing function allows the graphic representation of elements such as point, line, polyline, curved line, or geometric elements such as triangles, rectangles, circles and textural elements.

- The Layers function provides the display of all layers included in the interactive map, and allows their selection or de-selection.

- The map legend displays all the elements represented in the map composition

- Query is the function to query the map by displaying the rooms that have been entered into the map database.

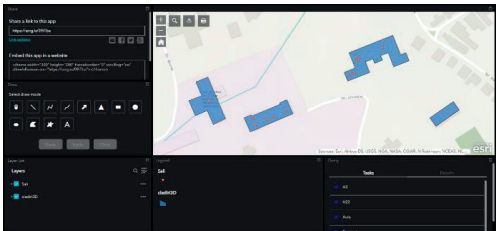


Figure 20. Viewing loaded widgets

Figure 21 shows the result of a query. A query was made within the created map, by accessing a point in the building of the Rectorate of the University of Agricultural Sciences and Veterinary Medicine Cluj-Napoca.

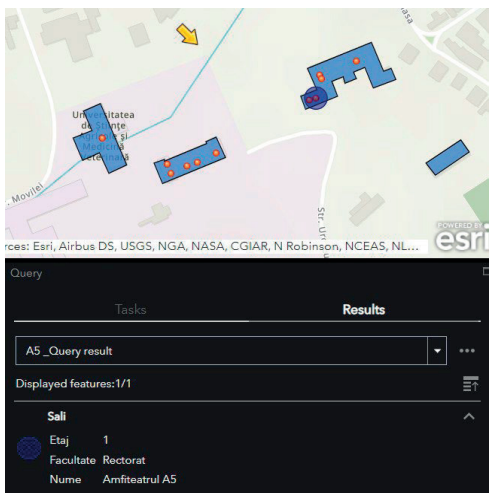


Figure 21. Performing a query

Thus, the performed application immediately rendered the location of the A5 Amphitheater. In the displayed table the A5 Amphitheater is located in the Rectorate building on the 1st floor.

CONCLUSIONS

The advantages of performing photogrammetric flights instead of classical measurements consists in the speed of mission execution and the high accuracy of the obtained data. For the economic sector, execution costs are significantly reduced compared to classic methods and with the help of drones accessibility is possible in dangerous areas or inaccessible to human operators.

At the same time, the data obtained from the photogrammetric works are accessible for use. They are easy to manage from the storage point of view and can generate many subsequent exports in correlation with the requirements of the project. For processing, certain programs such as Agisoft MetaShape or Global Mapper facilitates the principle of operation or the execution of scanning or cadastral works.

Using the Geographic Information System, through the ArcGIS PRO and ArcGIS Online programs, the functionalities and permeability of the creation of various types of applications, represent an advantage for all users who want to carry out studies or spatial analyses. Also, another advantage of the programs developed by ESRI is the implementation of functions for creating interactive maps in 3D format that are used to reproduce the details of a surface in the highest possible quality.

The advantages of the Geographical Information Systems are its use in fields of activity such as cadastre, through the storage, management and permanent updating of cadastral data. Also, the GIS offers a plus to geography, being possible to represent any surface of land regardless of the current position.

Also, the work addressed is a topical one, in that it presents contemporary procedures and state-of-the-art methods, through these programs and applications that facilitate the principle of operation in the field of photogrammetry and GIS.

Using the drone to generate digital data was imperially needed to make measurements on the USAMV campus. Through the resulting data, it was possible to create specific maps for the objective proposed in the work.

The maps created, both in 2D and 3D format, as well as the WEB applications have the purpose of providing users with data regarding the shape, location, character and arrangement within the campus of the University of Agricultural Sciences and Veterinary Medicine Cluj-Napoca of the most important component buildings, taking into account their character.

The generated WEB applications can be accessed from any device which is an important advantage of viewing the campus as well as various functionalities through the user's location.

REFERENCES

- Jayaraj, P., & Ramiya, A. M. (2018). 3D CityGML building modelling from lidar point cloud data. *The International Archives of Photogrammetry, Remote Sensing and Spatial Information Sciences*, 42, 175-180.
- Sălăgean T., Şuba E.E, (2018) *Fotogrammetrie şi Fotointerpretare I*, Cluj-Napoca.
- Song, P., Sun, G., Liu, X. (2021). Research on 3D campus integrated management based on ArcGIS Pro and CityEngine. In *Proceedings of the 2021 5th International Conference on Electronic Information Technology and Computer Engineering*, 355-360.
- Sugianto E, Hoseaa J.F, Jabara B.A, Irwansyaha E., Fitriana D. (2023). 3D Modelling Building of District Johar Baru Using ArcGIS Pro and CityEngine. *Procedia Computer Science*, 227, 623–631.
- Xu, Z., & Coors, V. (2012). Combining system dynamics model, GIS and 3D visualization in sustainability assessment of urban residential development. *Building and Environment*, 47, 272-287.

ISSUES RELATED TO THE IMPLEMENTATION OF GEOMATIC APPLICATIONS IN THE NATIONAL FORESTRY FUND

Ghiță Cristian CRAINIC

University of Oradea, 1 Universitatii Street, Oradea, Romania

Corresponding author email: gccrainic@yahoo.com

Abstract

The development of various geomatic applications in the forest requires advanced technologies for collecting, transferring, and processing data from the field, related to the spatial positioning of various topographic details. Special software is also required to report the coordinates of detail points and obtain various graphical products. In the forestry sector, planning maps, in analogue and/or digital format as appropriate, are used for various practical applications. The exploitation of cartographic material in digital format, with high accuracy, involves a process of spatial transformation or georeferencing, for which a few at least four points of known coordinates, are required in the two working systems. The positioning of the points required for the georeferencing process is performed with Global Navigation Satellite System (G.N.S.S.) technology, with a G.P.S system and/or with total station (TS), as appropriate. The MapSys 10.0 software can be used to perform the spatial transformation process. The results obtained in this case study ensure that the georeferenced raster is used with optimal accuracy to solve various current problems in the forestry sector.

Key words: forest fund, forest map, geomatic applications, GNSS technology, GPS system, MapSys 10 program.

INTRODUCTION

Sustainable management and administration of forest resources, regardless of ownership, is one of the objectives of the forestry strategy at national level. For the successful implementation of the various current and future activities in the national forestry fund, it is necessary to create and use an appropriate infrastructure for the spatial positioning of topographical details on forest areas and their representation on plans and maps.

Giurescu (2004) mentions that the maps of the 18th and early 19th centuries, compared with those of today, are of the greatest use for the study of the evolution of the country's forest area. For decades, plans and maps in analogue format have been used for several research and production activities specific to forestry.

Nowadays, thanks to modern working technologies and state-of-the-art equipment related to the land measurement sector, new, efficient possibilities (opportunities) have been created to obtain graphical representations of forest details in digital format, allowing high flexibility in their use and exploitation. Consequently, the application of various positioning technologies - such as the Global Navigation Satellite System (G.N.S.S.),

different satellite systems, conventional total stations, and combined positioning methods—has enabled more efficient spatial positioning of various details within the forest fund. As a result, the use of the Global Navigation Satellite System (G.N.S.S.), conventional technology represented by total stations, combined positioning technologies, has made it possible to spatially position various details of the forest fund with greater efficiency (Crainic, 2011). In this context, the logistical basis for collecting, recording, verifying, transferring, and processing field data has significantly enhanced the efficient production of diverse alphanumeric and graphical digital outputs (Tereşneu & Tereşneu, 2023).

In principle, the positioning of detailed topographic points, with the GPS, in the national forest fund, can be carried out using various methods and procedures of data acquisition and processing, each with many peculiarities related to the equipment and calculation algorithms used (Pica et al., 2022; Crainic et al., 2023). In this context, by considering some specific conditions of the forest sector frequently encountered, an attempt was made to analyse, by comparison, the opportunities offered by the various working procedures of GNSS technology.

Only under these conditions can specific proposals for the forestry fund be formulated, ensuring adequate accuracy, higher yield, and increased efficiency of the national geodetic network (Crainic et al., 2011).

In this context, a new direction of activity has been outlined, concerning the acquisition and processing of data necessary for the spatial positioning of topographic details on forest areas, using specific state-of-the-art technologies, namely Forest Geomatics. As a result, Geomatics is a modern discipline that integrates the acquisition, processing, modeling, analysis, and management of geo-referenced spatial data, based on the scientific support of geodetic and terrestrial, aerial and satellite records (Boş, 2011). Thus, Geomatics provides specific (spatial) information related to an investigated area on the earth's crust.

Accordingly, forest geomatics is a component of general geomatics, whose objectives are the study and knowledge of forests in terms of their extent, geographical location, structure, condition etc. These objectives are achieved through the integrated use of modern geo-topo-photogrammetric, aerial and satellite remote sensing techniques (used for the acquisition, storage, transfer, and processing of spatial data) (Boş, 2011; Petrila et al., 2010), and the archiving of the final products obtained.

A series of remote sensing applications in the forestry sector have been aimed at studying forest habitat fragmentation and the effects of forest management practices. Analysis of environmental conditions in protected areas has also been successfully carried out using these high-performance technologies (Olariu et al., 2022; Sabău & Crainic, 2006a).

The use of forest maps in analog format is currently restricted in the forestry sector, but there are still several current activities where these special graphical representations are used. Scanning produces the digital conversion or raster of the analogue forestry map format, which is defined by a specific extension, jpg, tif, ecw etc. As a result, it is possible to use them in digital format, thus ensuring their efficient and rigorous exploitation (Crainic et al., 2021; Crainic et al., 2022).

For the use of forest maps in analogue and implicitly in digital format, and for their differentiated exploitation, a series of specific

work steps are required, which are conditioned by the final product required. If the digital format of the landscape map is requested for exploitation and evaluation in the national reference system - Stereographic-1970, topographic points of known coordinates in this system are required. If the digital format map is intended for surface evaluations (to scale), the topographic points used for transformation do not need to be positioned within the national reference system (Crainic et al., 2021; Sabău, 2010).

MATERIALS AND METHODS

The case study was carried out in the forest fund of Sălard Commune, Bihor County, which is managed by the Production Unit (PU) I - Sălard, Săcuieni Forest District, under the Bihor County Forest Administration.

The area on which the research was carried out is approximately 120.70 ha and is represented by several 21 stands (plots), which are shown in Figure 1.



Figure 1. Location of the case study-Toros Forest (after the Forest Map of the U.P. I Sălard, 2015)

The objectives of the case study are: to carry out integrated geomatic applications in the forestry background; and differentiated exploitation of forestry maps in analogue and digital format, according to the requirements imposed by the activities in the forestry sector.

The integrated geomatic applications carried out in the forestry background concern: the determination of a regional datum from the geodetic points in the study area; its verification

by repositioning known geodetic points, and the spatial positioning with the G.P.S. system of characteristic topographic points of detail, in the studied stands.

Two research and study options were approached for the differentiated exploitation of forest maps. In the first variant, the raster of the forest maps in analogue format at a scale of 1:20000 was georeferenced to a local coordinate system, represented by the corners of its rectangular A3 format (Cioflan et al., 2023). In the second variant, vector data was used for georeferencing, represented by the spatial coordinates, in the national reference system, of the characteristic points corresponding to the corners of the plots.

The research methods used are: bibliographic documentation, observation, pilot experiment, simulation, comparison, and analysis.

The bibliographic documentation involves the study and analysis of specialized treatises, research and scientific papers related to topographic applications in the forestry sector. Technical standards related to the land measurement sector were also analysed.

The observation was carried out in the field, on the route and at the stationary, when identifying the study location (Figure 2). The pilot experiment is a research method based on a preliminary experiment, whereby methods and techniques are tested.

Table 1. Inventory of coordinates of geodetic points used to obtain the regional datum, in STEREO 70 projection system and Black Sea 1975 coordinate system

Topographic point		X (m)	Y (m)	Z (m)
Code	Order			
7	IV	641,143.150	275,370.096	109.517
11	IV	641,359.879	287,730.401	138.411
41	IV	648,959.326	274,488.095	111.925
16401	II	648,424.902	285,780.343	218.360
42401	I	623,315.749	273,944.933	294.259
43101	I	613,159.578	258,199.448	132.740
52401	IV	674,298.698	284,124.563	145.516

As a result, methods for spatial positioning of topographic points in the forestry sector were tested and verified with modern working technologies.

To obtain the regional datum, the geodetic points in the working area were analysed, positioned, and spatially repositioned with the G.N.S.S. technology, G.P.S. system, using the traditional static method (Tables 1 and 2). The spatial coordinates of the geodetic points used for the experiment are shown in Tables 1 and 2 and Figure 2.

Table 2. Known geodetic points in the area positioned in the global geocentric system on the WGS-84 ellipsoid

Topographic point		X(m)	Y(m)	Z(m)
Code	Order			
7	IV	4022080.269	1627582.127	4659390.965
11	IV	4016997.393	1638839.045	4659866.580
41	IV	4017227.959	1624350.434	4664669.252
16401	II	4013124.326	1634882.839	4664668.344
42401	I	4034621.346	1631844.383	4647376.578
43101	I	4047548.519	1620516.059	4639923.201
52401	IV	3996465.545	1625304.068	4682066.904

Figure 2 shows the location of known geodetic points in the study area.

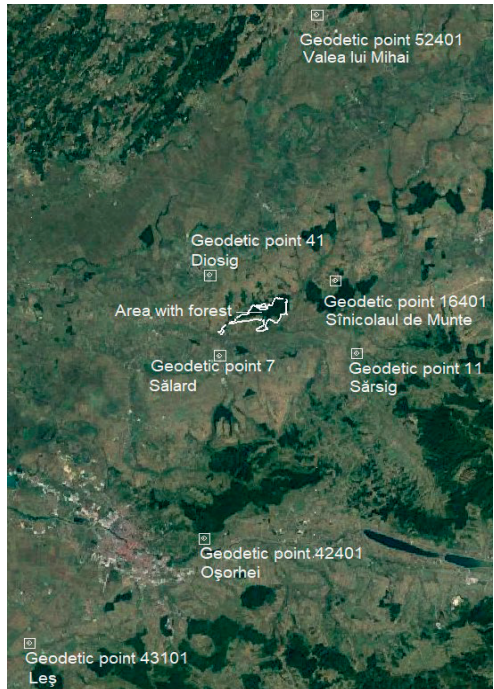


Figure 2. Location of known geodetic points in the study area

The analysis of the elements in Figure 2 shows that there are seven geodetic points in the working area. Simulation is a modern research tool. For the georeferencing of the raster related

to the forest map, two working variants were simulated, with common transformation points in the national reference system and in the local system, respectively. In this context, the raster georeferencing process was carried out with the Mapsys 10.0 software. The software used is licensed.

For this process, transformation points in the local system and respectively points in the national reference system, Stereographic - 1970, were used.

The comparison contributes to a deeper study and knowledge of the methods of spatial positioning of details, georeferencing, as well as the accuracy and precision of the final products obtained. In this context, the spatial coordinates of some geodetic points that have been redetermined with the GPS system, using the regional datum, have been compared with those of the inventory of Cadastre and Real Estate Publicity Office Bihor. Also, the areas of vectorized stands on the two rasters (which were georeferenced using topographic points in different reference systems), were compared. Content analysis was used to test and verify the working technologies and the quality of the results obtained. Consequently, the working methods and the results obtained were analysed to optimise the exploitation of the final products, and enhance the proposed technical solutions.

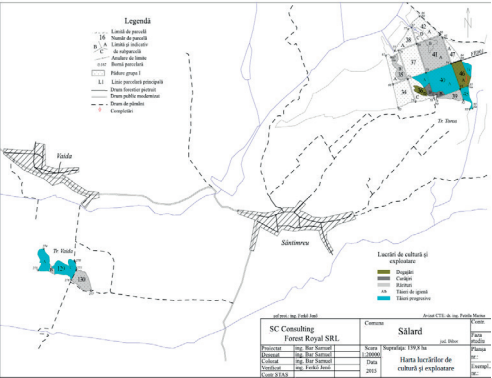


Figure 3. Forest Map of Production Unit (PU) I Sălărd (2015)

The logistics used include analogue and rasterised landscape maps, Trimble R3 GPS receivers, A3 antennas, specialised software for data collection - RawDataEditor, and for data processing - Trimble Total Control (T.T.C.).

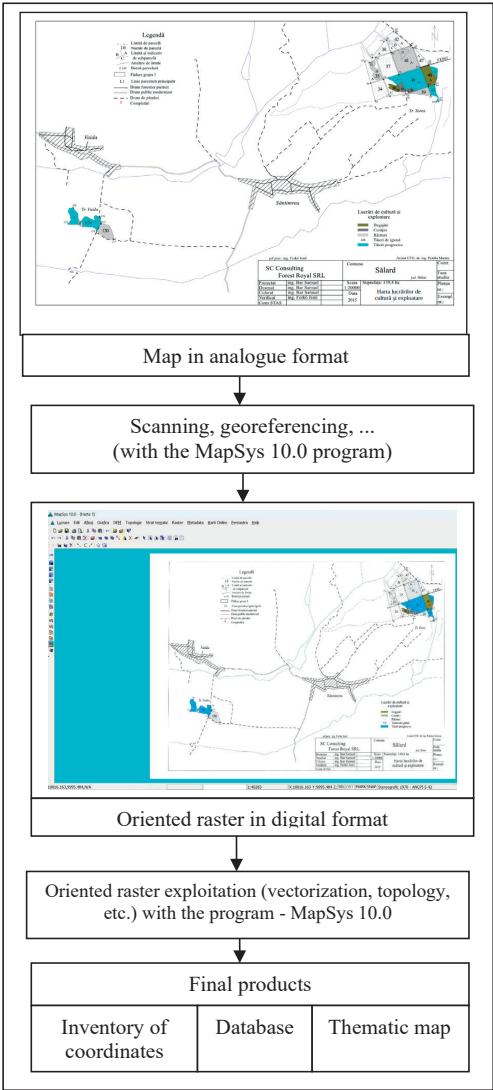


Figure 4. Work steps for exploiting cartographic material in digital format, with MapSys 10.0 software

MapSys 10 software was also used for: reporting the coordinates of the positioned points, georeferencing the raster, making the geographic information system and making the related database (Marton, 2007). For a complete analysis of the possibilities of exploitation of the cartographic material related to the forest background, the orthophoto plan of the study location was also used (Bodog & Crainic, 2016). The spatial coordinates of the characteristic points that represent the outline of the parcels

were determined with G.N.S.S. technology, the G.P.S. system, using the fast static positioning method. To obtain the final coordinates, the regional datum was used, which was determined by a spatial transformation with seven parameters. The transformation parameters are a rotation and a translation on the three axes, OX, OY and OZ and respectively the scale factor (Figure 5).

This transformation relied on four geodetic points, accurately determined within the study location, and was then applied to the national reference system (Table 1). The planimetric standard deviation of the geodetic points is $s_{xy} \leq 5$ cm.

The geodetic points 7 Sălard, 41 Diosig and 16401 Sinicolaul de Munte, 42401 Oșorhei, 43101 Leș and 52401 Valea lui Mihai are in a very good technical condition and point 11 Sărsig shows a 20% deterioration.

The georeferencing of the raster for the forest maps, in the two working variants, was carried out with the MapSys 10 program, using four common coordinate points in the two reference systems (local and national). Consequently, the stages presented in Figure 4 were completed for each variant.

RESULTS AND DISCUSSIONS

The results obtained in this case study are ranked and presented in turn, according to the stages completed.

Since 2001, research and studies conducted in the case study location (Crainic, 2011) have confirmed that using a regional datum for satellite positioning of various topographic details in the forestry sector, based on highly accurate geodetic points, achieves high accuracy. With the Trimble Total Control (T.T.C.) calculation system, the transformation of coordinates from the WGS 84 global reference system to national coordinates - planimetric and altimetric - was performed. In principle, this is carried out according to the conditions imposed by specific working algorithms.

The computation steps are: determination of the common points on which the transformation will be performed; implementation of the coordinates in the national reference system under the Control Coordinates option; selection of the type of transformation (planar or spatial);

the processing of the selected transformation and obtaining the transformation parameters; analysis of the accuracy indicators of the performed transformation; implementation of the transformation parameters in the database of the computation system (Coordinate System Manager) related to the national datum.

The set of transformation parameters (Figure 5) that has been implemented in the database of the computing system - in the Coordinate System Manager section (Figure 6), together with the reference ellipsoid, the map projection system, the coordinate reference system, constitutes the regional datum for the working area. It is properly archived to keep and use (access) it, as needed, in the appropriate database (Figure 6).

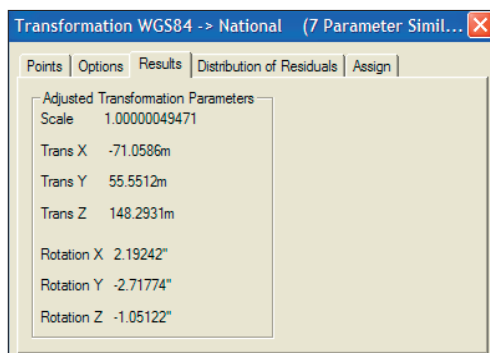


Figure 5. Set of transformation parameters on four known points obtained with the T.T.C. program

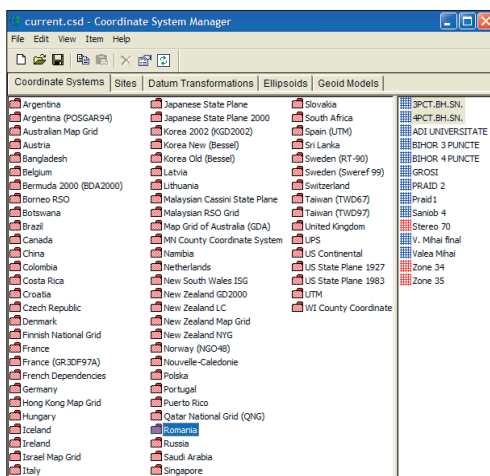


Figure 6. Database of datums related to the Trimble Total Control calculation system with the datums determined for the case study, implemented

As a result, in the Trimble Total Control calculation system, the regional datum can be used, by setting, to configure the worksheet for a new project.

Consequently, the use of the regional datum, (obtained from the transformation parameters shown Figure 5), when using the T.T.C. (program for processing satellite records), facilitates the obtaining of final coordinates, rigorously compensated in the national reference system. As a result, no further transformation in the national reference system will be necessary to obtain them.

Three geodetic points in the study area were repositioned to verify the datum. Processing of the recorded satellite data with the T.T.C. software, to obtain the final coordinates in the Stereographic 1970 system, involves the following steps: initialization of the program and opening of a new working project; setting of the corresponding processing parameters; transfer of the records into the computer system; primary verification and processing of the recorded data; verification of the triangle mismatches and the type of solution adopted; recalculation of the verified data and obtaining the provisional (3D) spatial coordinates; rigorous compensation of the provisional spatial coordinates and obtaining the final spatial coordinates with the related statistical accuracy indicators (Figure 7).

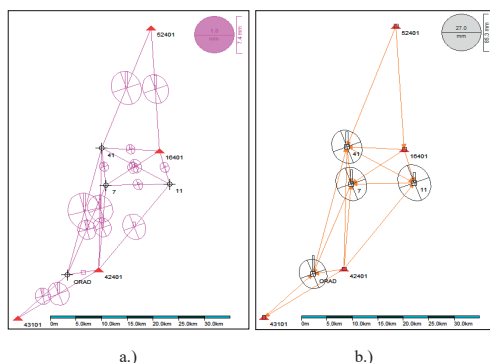


Figure 7. Sketch of vectors processed for compensation, a) primary processing; b) rigorous compensation

In the preliminary operations, comprising the first five positions above, the possibility of

checking the recorded data is ensured, including the elimination of some inappropriate ones, affected by disturbing factors, by deactivating certain intervals of records. Thus, in the case of records from the points to be repositioned, following the primary processing of the data, the inappropriate solutions, of the *float* type, will be eliminated and only the *fixed* type solutions will be kept. Fixed solutions result from the processing of primary data with a specific algorithm, and the results fall within an established tolerance. Consequently, positioning with centimeter precision is ensured.

From the analysis of the coordinates presented in Table 3, the planimetric standard deviations vary between 49 and 53 mm, and those for the elevations vary between 68 and 90 mm.

Table 3. Inventory of coordinates of geodetic points repositioned with regional datum, in 1970 Stereographic projection system and 1975 Black Sea coordinate system

Point	X (m)	Y (m)	s _{xy} (mm)	Z (m)	s _z (mm)
7	641,143.200	275,370.173	50	109.202	86
11	641,359.990	287,730.395	53	138.188	68
41	648,959.360	274,488.137	49	111.554	90

s_{XY} - planimetric standard deviation, s_z - altimetric standard deviation.

Consequently, geodetic points 7, 11, and 41 have been repositioned with high accuracy, using the regional datum.

In order to obtain the spatial coordinates of the characteristic points of detail, of the corners of the plots, successive stages of positioning with the GPS system were carried out (Crainic, 2011), aspects that are presented in the Figures 8-11.

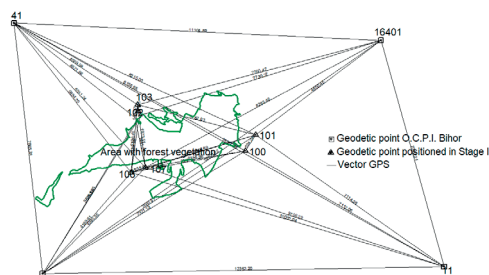


Figure 8. Stage I of the creation of the net of control points, from the case study location (Crainic, 2011)

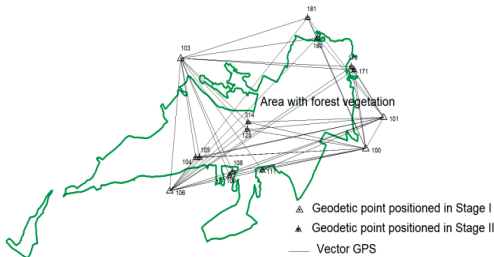


Figure 9. Phase II of the creation of the net of control points, from the case study location (Crainic, 2011)

As a result, point couplings were determined in the working area to optimise the satellite positioning process. In this context, within the framework of the fast static method, the prerequisites were created for reducing the positioning time and ensuring a higher accuracy (Crainic, 2011).

Satellite data recording in the field was performed by the fast static method, with TRIMBLE R3 receivers, A3 antenna, with a single L1 frequency. The dwell time at each point was 15-30 minutes, with recording epochs of 15 seconds, using Trimble Digital Fieldbook software.

The field data were recorded in RINEX files and processed in a similar way to the data processing shown for geodetic point repositioning. The spatial coordinates, in the national reference system, are shown in Table 4.

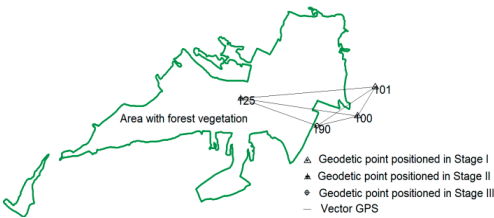


Figure 10. Stage III of the creation of the net of control points, from the case study location (Crainic, 2011)

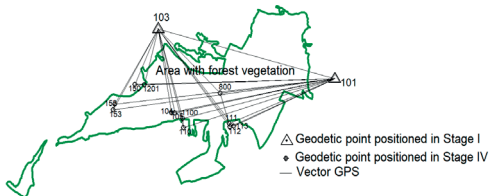


Figure 11. Phase III of the creation of the net of control points, from the case study location (Crainic, 2011)

Table 4. Inventory of coordinates of topographic detail points in the 1970 STEREOGRAPHIC System and the 1975 Black Sea Elevation System

Point	X (m)	Y (m)	Z (m)
134	644,584.550	278,203.908	181.286
234	644,939.695	278,112.170	171.015
334	645,023.830	278,368.765	157.488
434	644,674.220	278,464.376	188.085
135	644,945.487	278,111.532	171.006
235	645,372.203	277,995.343	150.68
335	645,461.943	278,218.134	150.633
435	645,031.728	278,366.624	158.325
137	645,033.838	278,372.179	159.337
237	645,463.709	278,223.065	150.465
337	645,563.133	278,513.615	156.778
437	645,130.634	278,657.004	183.237
141	645,132.388	278,663.880	183.938
241	645,565.867	278,519.434	156.734
341	645,659.912	278,921.284	164.783
441	645,263.970	279,063.858	185.715
542	645,695.198	278,886.566	161.832
145	644,693.770	279,261.232	183.484
245	644,865.868	279,205.283	175.01
345	645,010.838	279,629.022	179.204
445	644,678.617	279,735.686	180.764
146	644,871.401	279,203.777	175.771
246	645,261.477	279,072.244	185.082
346	645,395.497	279,492.996	181.909
4460	645,017.111	279,627.817	178.463
147	645,265.558	279,070.387	185.429
247	645,654.991	278,926.764	165.169
347	645,580.324	279,428.708	185.993
447	645,402.790	279,490.095	182.45
547	645,590.356	279,102.534	176.347

Exploitation of digital cartographic material related to the case study location.

For the exploitation of the raster cartographic material, obtained by converting the landscape map from analogue to digital format, the MapSys 10.0 software was used, going through the following steps which are summarised in Figure 3 (Tămăioagă G. & Tămăioagă D., 2007; Crainic et al., 2022; Matei et al., 2022).

In the first variant for georeferencing, four common feature points were used, which have spatial coordinates referenced in a local reference system (Cioflan (Irimie) et al., 2023). These points are the corners of a planning map sheet at a scale of 1:20000, on which the 21 plots studied are represented - Figure 1, in A3 format, i.e. a rectangle with length $L = 42.0$ cm and width $l = 29.7$ cm. (Crainic et al., 2022; Sabău & Crainic, 2006 b).

In this case, the width of the sheet is parallel to the direction of geographic North, and the width is oriented East. Therefore, based on the A3 size, $\Delta X = 29,7$ cm, and $\Delta Y = 42,0$ cm. If the scale of the map is taken as 1:20000, then the relative coordinates of the format shown are $\Delta X = 5940$ m and $\Delta Y = 8400$ cm.

Finally, the feature point in the S-V corner of the format will be given the number 1, and assigned arbitrary coordinates, in the case of this study, $X_1 = 10000$ m, and $Y_1 = 10000$ m. Next, the other minutiae, have the following characteristics:

- point 2 in the N-W corner, $X_2 = X_1 + \Delta X = 10000$ m + 5940 m = 15940 m, and $Y_1 = 10000$ m;
- point 3 in the N-E corner, $X_3 = 15940$ m, and $Y_3 = Y_1 + \Delta Y = 10000 + 8400$ m = 18400 m;
- point 4 in the S-E corner, $X_4 = X_1$ 10000 m, and $Y_4 = Y_3 = 18400$ m.

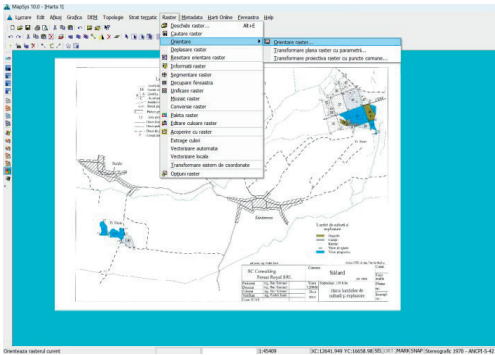


Figure 12. Starting the raster orientation and georeferencing process on four points in the local projection system with MapSys 10.0 software

Consequently, the coordinates of these four points will be used for georeferencing the raster of the forest management map used by transforming to common points. After georeferencing the raster, it was vectorized, thus obtaining the polygons corresponding to the plots and implicitly to the studied and analysed stands.

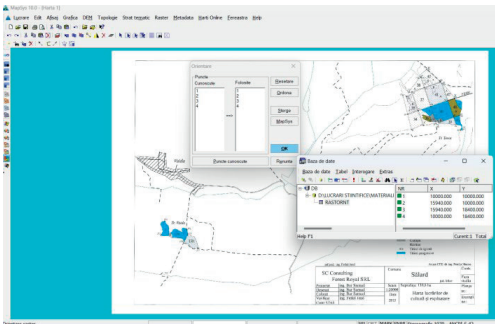


Figure 13. Implementation of common points and raster georeferencing in the local projection system with MapSys 10.0 software

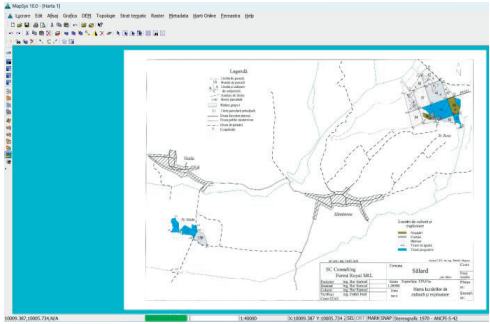


Figure 14. Geo-referenced raster in local projection system with MapSys 10.0 software



Figure 15. Vector of the georeferenced raster in the local projection system

As a result, the areas of the stands were determined and compared with their values presented in the forestry plan in force. In the second version of the study, the raster will be georeferenced according to the coordinates of the characteristic points that have been determined by satellite positioning, with the GPS system (using the fast static method), which are shown in Table 5. These feature points were located near the (forest) boundary markers that delimit the adjacent plots. The steps of the raster georeferencing process, in the variant using coordinates in the national reference system, are like those followed in variant I of the study.

Table 5. Inventory of coordinates of topographic points, which were used for raster georeferencing

Nr. point	X (m)	Y (m)	Z (m)
1/134	644,584.550	278,203.908	181.286
2/235	645,372.203	277,995.343	150.68
3/247	645,654.991	278,926.764	165.169
4/146	644,871.401	279,203.777	175.771

The georeferenced raster is shown superimposed on the orthophoto map of the study area in Figure 16.

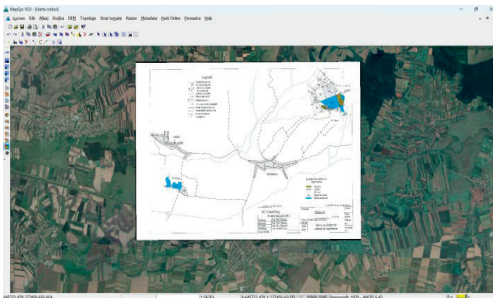


Figure 16. Screenshot of a geo-referenced raster in the national reference system with MapSys 10.0 software

Following the raster vectorisation process, the vector obtained is presented relative to the orthophoto plan.

On the vectors obtained in the two study variants, quantitative assessments were carried out on the stand area of the plots surveyed and analysed. As a result, the values obtained from the two calculation methods were compared to each other and to the area in forest management, using formulas 1 and 2 for the analysis.

$$\Delta S_I = S_{mp} - S_I; \quad (1)$$

$$\Delta S_{II} = S_{mp} - S_{II}; \quad (2)$$

where: ΔS_I - area difference for calculation variant I, ΔS_{II} - area difference for calculation variant II, S_{mp} - the surface from the management plan, S_I - area determined on the raster vector oriented in calculation variant I, S_{II} - area determined on the raster vector oriented in calculation variant II (Figure 17).



Figure 17. Vector obtained in the second study variant

Table 6. Evidence of assessed areas and differences reported to the forest management area in the two study variants

Plot nr.	S_{mp} (ha)	S_I (ha)	S_{II} (ha)	ΔS_I (ha)	ΔS_{II} (ha)
34	10.7	8.81	9.67	1.89	1.03
35A	5.7	5.08	5.56	0.62	0.14
35B	3.7	3.96	4.35	-0.26	-0.65
36A	3.2	2.54	2.89	0.66	0.31
36B	1.4	1.37	1.51	0.03	-0.11
36C	6.2	4.49	5.00	1.71	1.20
36D	1.7	1.89	2.06	-0.19	-0.36
37	14.4	12.14	13.54	2.26	0.86
38A	5.9	4.98	5.48	0.92	0.42
39	4.2	2.98	3.40	1.22	0.80
40A	16.6	14.12	15.42	2.48	1.18
40B	1.2	1.00	1.12	0.20	0.08
41A	17.6	15.12	16.73	2.48	0.87
41B	2.6	1.76	1.95	0.84	0.65
42A	6.4	6.04	6.62	0.36	-0.22
42C	1.3	1.18	1.28	0.12	0.02
42D	2.3	1.99	2.18	0.31	0.12
45	2.2	2.33	2.63	-0.13	-0.43
46A	7.4	6.64	7.34	0.76	0.06
46B	1.8	1.63	1.74	0.17	0.06
47A	4.2	3.40	3.71	0.80	0.49
Total	120.7	103.45	114.17	17.25	6.53

Figure 18 shows the correlation between the differences ΔS_I and the areas in the forest management, corresponding to the plots evaluated in variant I of the study.

The analysis of the elements in Figure 18 shows that there is a strong linear correlation between the ΔS_I area differences and the forest management areas.

The coefficient of determination $R^2 = 0.8065$ and the correlation coefficient $R = 0.898$. As a result, the regression line has a positive slope.

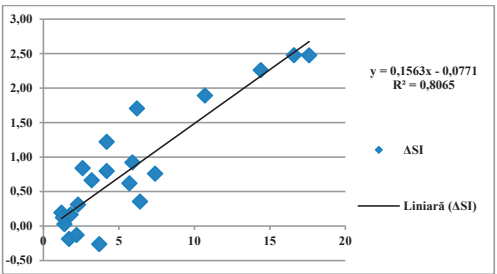


Figure 18. Correlation between ΔS_I differences and forest management areas, stands studied

For the ΔS_{II} area differences, no significant correlation was found between these and the areas in the forest management for the 21 stands studied in Figure 19.

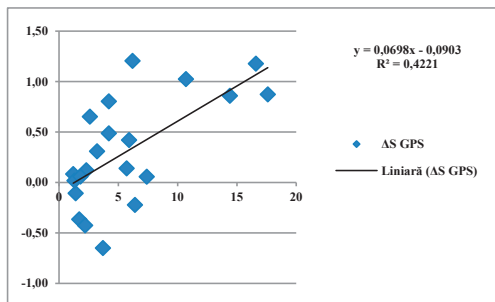


Figure 19. Correlation between ΔS_{II} differences and forest management areas, stands studied

From the comparison and analysis of the total areas evaluated by the two variants of research, the total value of the area differences in the two variants is as follows: $\Sigma \Delta S_I = 17.25$ ha, $\Sigma \Delta S_{II} = 6.53$ ha. The surface difference for the first study option represents 14.3% of the surface in the management plan. For the second variant of the study, the surface difference represents 5.4% of the surface in the management plan. As a result, it is found that the II working variant provides superior precision for the quantitative exploitation of analogue forest maps, converted into a raster format.

CONCLUSIONS

The use of G.N.S.S. technology and the G.P.S. system for the positioning of detailed topographic points in the forest fund, by static method, ensures superior accuracy in determining their coordinates.

The use of the regional datum for processing satellite records for positioning by static methods, ensures the optimization of the calculation steps, and the achievement of a superior precision and accuracy.

The coordinates of the geodetic points, which were recalculated using the regional datum, have a high precision and accuracy.

The georeferencing of the raster for the forest management map of the case study area, through the two variants, offers the possibility of differentiated exploitation of the forest map material.

The differences in area ΔS_I and ΔS_{II} respectively highlight the particularities of the georeferencing and vectorization process of the raster used.

The use of topographical points positioned with the GPS system, with high precision, for the

georeferencing of the rasters, ensures a relatively high precision in the process of their quantitative exploitation.

Also, the readability and accuracy of the analogue forest management map influence the georeferencing accuracy and thus the quantitative exploitation process of the obtained raster and vector data.

ACKNOWLEDGEMENTS

Thanks to the collective of the Săcueni Forestry District, Bihor County Forest Administration, for their collaboration and support given during the field stage of this research.

REFERENCES

- Bodog, M.F., & Crainic, G.C. (2016). Some Specific Characteristics of the Geomatic Applications in the Agro-Forestry Sector. *Annals of the University of Oradea, Environmental Protection Fascicle*, University of Oradea Publishing House, Vol. XXVII, 2016, ISSN - 1224-6255, 337-346.
- Boş, N. (2011). Geomatics and the realization of the cartographic base of the forest fund in Romania. *Forest Magazine*, No. 6, 126, 27-36.
- Cioflan (Irimie), F., Crainic, G.C., Iovan, C., Irimie, F. & Covaci, F. (2023). Aspects relating to quantitative and qualitative assessments of topographic details, on map material, in analog and digital format. *Annals of the University of Oradea, Fascicle: Environmental Protection*, 85 - 94.
- Crainic, G.C., Covaci, F., Sabău, N.C., Sicoe, S.I., Irimie (Cioflan), F., Bodog, M.F. & Iovan, C.I. (2023). Works specific to the introduction of silvopastoral systems in the forest fund. *Scientific Papers. Series E. Land Reclamation, Earth Observation & Surveying, Environmental Engineering, Vol. XII*, 74-85, Print ISSN 2285-6064.
- Crainic, G.C., Bodog, M., Iovan, C., Cioflan (Irimie), & Flavius, I. (2022). Differentiated use of cartographic material in the forestry sector, in the plain area. *Annals of the University of Oradea, Fascicle: Environmental Protection*, Vol. XXXIX, 79 - 86. doi.org/10.5281/zenodo.4362307, ISSN 2065-3484.
- Crainic, G.C., Irimie, F., & Irimie, F.M. (2021). Realization of a geographical informatic system for inaccessible forest fund. *Annals of the University of Oradea, Fascicle: Environmental Protection*, Vol. XXXVII, 185 - 196. doi.org/10.5281/zenodo.4362307.
- Crainic, G.C., Bodog, M., Sicoe, S., Bungău, D., Druță, N., Ardelean, R. & Bar, I. (2018). Aspects relating to technology topographic details G.N.S.S. positioning system G.P.S. in the forestry massive. *Annals of the University of Oradea, Fascicle: Environmental Protection*, Vol. XXXI, 121-132, ISSN 1224-6255.
- Crainic, G.C., Damian, V.L. & Spilca, M. (2011). Possibilities of realisation of the minor control network

- with gnss tehnology in the occupied areas with forest vegetation in mountain areas. *Research Journal of Agricultural Science, University of Agricultural Science and Veterinar Medicine of the Banat Timișoara*, 43(3). ISSN - 2066-1843, 283-291.
- Crainic, G.C. (2011). *Research on the modernization of topographical works in the forestry sector*. Ministry of Education, Research, Youth and Sports, Transilvania University of Brasov, Faculty of Forestry and Forestry, Department of Forestry, Forest Management, Land Surveys, Brasov, PhD Thesis.
- Damian, V.L. & Crainic, G.C. (2016). Possible use of geomatics for the analysis of spatial distribution of chestnut (*Castanea sativa* Mill) populations in Romania. *Annals of the University of Oradea, Fascicle: Environmental Protection, Vol. XXVI*, 185-194, ISSN 1224-6255.
- Giurescu, C.C. (2004). *The history of the Romanian forest from the earliest times to today*. Third edition, revised and added. Bucharest, RO: Orion Publishing House.
- Marton, G., Albotă, M., Filotti, D., Molea, O., Șalariu, I. (1976). *Polyglot dictionary of geodesy, photogrammetry and cartography*. Bucharest RO: Tehnical Publishing House.
- Marton, H. (2007). *MapSys, TopoSys - User manual*. Odorheiu Secuiesc, Romania.
- Matei, L., Crainic, G.C., Curilă, S. & Curilă, S. (2022). *Designing and creating a related database current activities in the forestry sector*, Analele Universității din Oradea, Fascicula: Protecția Mediului, Vol. XXXIX, 113 – 120, ISSN 2065-3484. doi.org/10.5281/zenodo.4362307.
- Olariu, B., Virghileanu, M, Mihai, B.A., Săvulescu, I., Toma, L. & Săvulescu, M.G. (2022). Forest Habitat Fragmentation in Mountain Protected Areas Using Historical Corona KH-9 and Sentinel-2 Satellite Imagery. *Remote Sens.*, 14(11), 2593. <https://doi.org/10.3390/rs14112593>.
- Petrila, M., Apostol, B., Gancz, V., Loreț, A. (2010). *Applications of geomatic technologies in forestry*. Silvic Publishing House.
- Pica, A., Boja, F., For a, C., Moatar ,M., & Boja, N. (2022). Advantages of using gnss technology and QGIS software in inventory stands exploiters. *Series E. Land Reclamation, Earth Observation & Surveying, Environmental Engineering, Vol. XI*, 434 -443, Print ISSN 2285-6064.
- Sabău, N.C. (2010). *Terrestrial measurements*. Oradea University Publishing House.
- Sabău, N.C., Crainic, Gh.C. (2006 a). *Remote sensing and forest cadastre*. Publishing House of the University of Oradea, 318 pages, ISBN (10) - 973 - 759 - 203 - 4, ISBN (13) - 978 - 759 - 203 - 3. Recognized by CNCISIS, code. 149.
- Sabău, N.C., Crainic, Gh.C. (2006 b). *Applications of remote sensing in forest cadastre*. Publishing House of the University of Oradea, 156 pages, ISBN (10) - 973 - 759 - 203 - 4, ISBN (13) - 978 - 759 - 203 - 3. Recognized by CNCISIS, cod. 149.
- Tămăioagă, G. & Tămăioagă, D. (2007). *Automation of cadastre works*. Bucharest RO: Matrix Rom Publishing House.
- Tereșneu, C.C. & Tereșneu, C.S. (2023). GIS facilities for the automation of cadastral documentations. *Scientific Papers. Series E. Land Reclamation, Earth Observation & Surveying, Environmental Engineering, Vol. XII*, 371-376, Print ISSN 2285-6064.
- ****Forest management of Production Unit I Sălard, Bihor County*. (2018).
- ****Forestry map of Production Unit I Sălard, Bihor County*. (2018).

ANALYSIS OF LANDSAT AND SENTINEL SATELLITE IMAGES FOR ROȘIA POIENI QUARRY AND VALEA ȘESII DECANTATION POND

Sorin HERBAN¹, Clara-Beatrice VÎLCEANU¹, Andrei CRIȘAN²,
Livia NISTOR-LOPATENCO³

¹Politehnica University Timisoara, Civil Engineer Faculty, Department of Overland Communication Ways, Foundations and Cadastral Survey, 1 Ioan Curea Street, Timisoara, Romania

²Politehnica University Timisoara, Civil Engineer Faculty, Department of Steel Structures and Structural Mechanics, 2 Traian Lalescu Street, Timisoara, Romania

³Technical University of Moldova, Faculty of Construction, Geodesy and Cadastre, 41 Dacia Blvd, Chisinau, Republic of Moldova

Corresponding author email: beatrice.vilceanu@upt.ro

Abstract

Taking into consideration the valuable spectral information and its wide coverage, satellite remote sensing is an efficient and accurate instrument to analyse and monitor the Earth's surface over time, even the negative consequences of anthropic activities. The present paper aims at monitoring in time the Roșia Poieni quarry and the negative effects resulting from the copper and gold exploitation, which led to the existence of the Valea Șesii tailing pond. To this purpose, Landsat satellite images were analysed over a 30-year period from platforms that offer free downloads. Image processing consisted of cropping the images according to the area of interest, applying the RGB combination and classifying them in order to obtain the surfaces. Moreover, indices for vegetation and water were applied for the images taken in 2018, 2020 and 2022. In order to obtain a more realistic image and to observe the differences, for the specified years, namely 2018, 2020 and 2022, Sentinel satellite images were processed in parallel. Despite the small size of the study area, satellite remote sensing has succeeded in delivering plausible, noteworthy results with great emphasis on hard-to-reach areas.

Key words: image processing, mining, monitoring, remote sensing, tailing pond.

INTRODUCTION

The Roșia Poieni quarry (Figures 1 and 2) is a surface copper mine in the Apuseni Mountains, located in Lupșa commune, Alba County, Transylvania area, Romania. The main storage location for tailings from mining is the Valea Șesii pond (Figure 2). The area's topography is characterized by rocky relief, deep valleys, and hanging platforms caused by the presence of facies formations that highlight specific volcanic regimes. On the slopes of the valley, there are several irregularities, including some negative shapes and sloughs, both on the platforms and in the meadows or on the terraces of the valley. The lands are regularly damaged by erosions, due to the high value of relief energy, displayed mainly altitudes starting from 400 m to 900 m, and the poor consistency of the clays and Senonian marls that mostly cover the surrounding region of deposit.



Figure 1. Location of the study area
(<https://geoportal.ancpi.ro/geoportal/imobile/Harta.html>,
https://harti.wansait.com/ro_ro/2012/judetul-alba-harta-administrativa-interactiva/)

The pond does not have a drainage system, so the quality indicators of the discharged water are frequently exceeded. Thus, the entire area is affected by both the quality of the water and the solvents found in the tributaries that flow into the Aries River and affect. In addition to this phenomenon, there are also negative effects in the area at the exit of the tailings, through

which sulfuric acid and heavy metal sulphates end up in water and soil, generating intense pollution of the Aries River Basin (Moldovan et al., 2021; Popa et al., 2015).



Figure 2. Roșia Poieni quarry (top photo <https://mapio.net/pic/p-26288806/>) and Valea Șesii tailing pond (bottom photo <https://adevarul.ro/stiri-locale/alba-iulia/foto-satul-idilic-din-apuseni-disparut-sub-o-1883658.html>)

The exploitation of the quarry began in 1978, the copper production in 1983 and the storage of the residues resulting from the exploitation was carried out in the village of Geamăna, due to its proximity and relief. In almost 40 years of waste storage, the village of Geamăna was transformed into a colourful and toxic desert of chemical sludge and heavy metals, of which only the steeple of the sunken village church remains (Toderaș, 2021) (Figure 3).

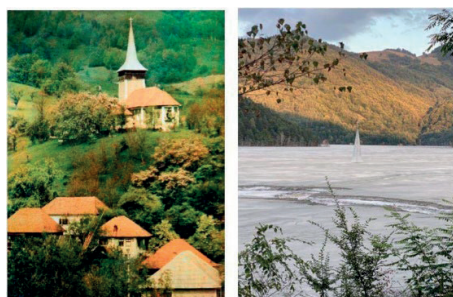


Figure 3. The steeple of the sunken church in Geamăna village (before and after)

https://www.dailymail.co.uk/travel/travel_news/article-4596446/Amos-Chapple-captures-Romanian-s-Geamana-village.html

MATERIALS AND METHODS

Remote sensing from satellites of parameters waters has been extensively applied to lakes', rivers, seas' studies. Water remote sensing is based on the examination of the spectrum of optical active components of the upper layer of the water body, such as mineral content, turbidity, total suspended particles, and chlorophyll-a. Earth observation satellite data (e.g. Landsat, Sentinel) available for free can provide valuable information for evaluating huge areas, however, the quality and frequency of data transmission can vary (Makri, 2016).

In order to download the necessary satellite images (Mendez Garzón & Valánszki, 2020), the Earth Explorer platform - USGS (United States Geological Survey) was used (<https://www.usgs.gov/landsat-missions>).

Firstly, the study area was specified, then the criteria of interest, namely the period, the type of satellite, and the degree of cloud coverage. For the processing, the following images from the summer-autumn period have been downloaded:

- year 1992, Landsat 4-5 satellites data;
- year 2000, Landsat 7 satellite data;
- year 2014, Landsat 8 satellite data;
- year 2018, Landsat 8 satellite data;
- year 2020, Landsat 8 satellite data;
- year 2022, Landsat 9 satellite data.

To download the satellite images from the Copernicus platform, the study area was first chosen by drawing a polygon to include it, then the following criteria were selected: the period, the type of satellites and the degree of cloud coverage. Images that were not available at the time were added to the cart and downloaded shortly after they were available.

The following images were taken and processed:

- the years 2016, 2018, 2020 and 2022, data taken with Sentinel 1 to apply corrections and orthorectifications.
- the years 2018, 2020 and 2020, data retrieved with Sentinel 2 for their classification and application of water and vegetation indices (<https://sentinels.copernicus.eu/web/sentinel/home>).

Landsat and Sentinel data have been used in this case study as satellite sensors operate on various spatial, spectral, and temporal

resolutions. In particular, the Copernicus Emergency Management Service (CEMS) makes substantial use of Sentinel-1 data, as SAR equipment' ability to identify flooded areas, see through clouds or dense smoke, and detect land changes is especially important in emergency situations. Sentinel-1 SAR data eases the identification of alterations in topography and infrastructure damage after urban disasters, allowing for more precise assessments that are critical for recovery planning and community impact evaluation.

Landsat images processing

The Landsat satellite images have been further processed. In order to achieve the RGB combination, it was necessary to know the correspondence between the bands of the Landsat satellites and the area of the electromagnetic spectrum. Thus, bands 3, 2 and 1 were used for images taken with Landsat 4, 5 and 7 satellites, and bands 4, 3 and 2 were used for images taken with Landsat 8 and 9 satellites.

The steps before performing the RGB combination (Badulescu et al., 2019) consisted of importing the downloaded images in tiff format and cropping them according to the area of interest. Applying the RGB combination to all the data that correspond to each year of the change monitor (Hila et al., 2018) produces the Figure 4.

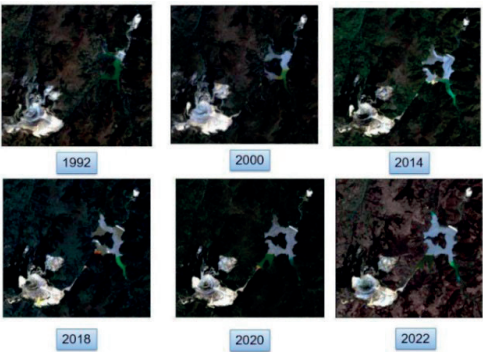


Figure 4. RGB combination for Landsat images

To achieve the supervised classification, the following steps are followed:

- Sampling - the stage in which the operator intervenes to identify and define each sample;

- Classification - involves placing each pixel in the right class. This step is the most important because the computer uses predefined decision rules to identify each pixel in the image (Basayigit & Ersan, 2015);

- Obtaining the final product or presenting the result in the form of thematic maps or tables corresponding to the recording of the scene (Iosub, 2012).

Choosing samples was realized based on the classification scheme (Table 1), by choosing the class categories that contain the number, type of information classes and their description.

Table 1. Images classification scheme

No.	Sample	Sample description
1	forest	Area with dense tree layer
2	pasture land	Area covered with grassy vegetation
3	quarry	Exploitation area
4	water	The amount of water resulting from settling
5	tailings	The amount of acidic water with high content of toxic substances
6	sludge	The amount of toxic mineral sediments

The creation of the samples was carried out using the cropped true colour RGB 321 and RGB 432 composite images for each year. From the "Supervised" menu, the "Signature Editor" window was opened, and the samples were vectorized using the "polygon" function (Figure 5).

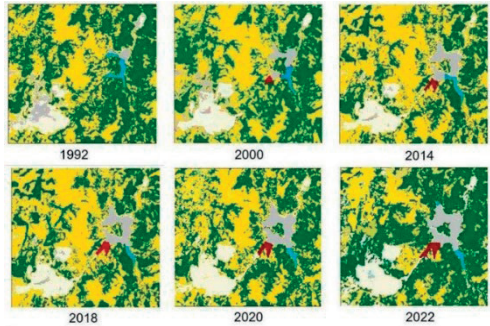


Figure 5. Supervised classification for Landsat images

Unsupervised classification is based on spectral classes (pixel values) or clusters in a multi-band image or individual pixel values. The more classes there are, the number of iterations for the algorithm increases.

In the Erda's Imagine 2015 program, the unsupervised classification was realized from

the "Raster" menu, the sequence "Classification - Unsupervised - Unsupervised Classification". The total area of the study that was covered by Landsat satellite images is 4158 ha. To determine surface changes over the years

(Vorovencii, 2015), the number of pixels corresponding to each class was multiplied by 0.09 ha. The surfaces that resulted are presented in Table 2.

Table 2. Surfaces obtained from processing Landsat satellite images

	1992	2000	2014	2018	2020	2022
	(Hectares)					
Forest surface	1930.48	1970.04	2060.59	2026.48	2025.46	2102.95
Pastureland surface	1854.77	1747.01	1716.90	1658.03	1657.19	1586.44
Quarry surface	302.38	342.95	323.22	310.56	301.47	284.58
Water surface	57.41	22.54	28.19	17.80	18.06	16.36
Tailings surface	0	10.06	16.76	20.81	26.09	24.29
Sludge surface	12.95	65.38	102.51	124.30	129.71	143.36

Sentinel images processing

Pre-processing Sentinel1 images using SNAP software involved, firstly, identifying the study area in the image and cutting it according to a drawn rectangle that includes the entire studied area. The image pre-processing process (Herbei et al., 2023) involved the following steps: radiometric calibration - betaO type calibration; Earth curvature correction and noise removal (Figure 6), for the image that was previously calibrated, resulting the final image (Figure 7) after the orthorectification.

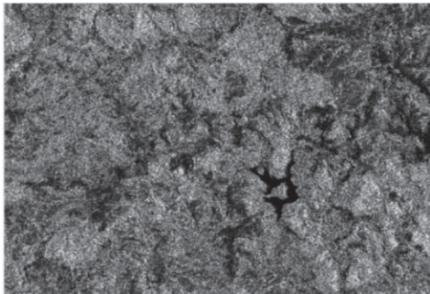


Figure 6. The 2022 Sentinel image after noise removal

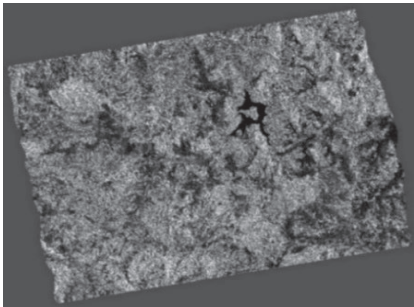


Figure 7. The 2022 Sentinel image after applying all corrections

To achieve the RGB combination of satellite images taken with Sentinel 1, the Gamma_VH band is used for the red band, the Gamma_VV band for the green band and Gamma_VH/Gamma_VV band was used for the blue band. For a better processing of the images and obtaining better quality results, images taken with the Sentinel 2 satellite were also downloaded, the continuation of the study being based on the results obtained after their processing. In this case, the combination of bands that correspond to RGB consists of bands 4, 3, and 2, respectively (Figure 8).

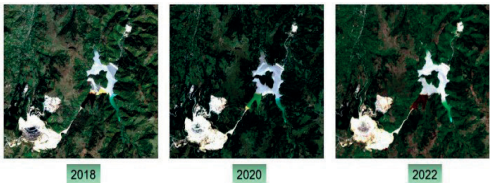


Figure 8. RGB combination for the years 2018, 2020, 2022

For the supervised classification of Sentinel satellite images, the Maximum Likelihood algorithm was used, which assumes that pixels are assigned to the class with the highest probability. To create the samples, the classes described in the classification scheme in Table 1 were used. The sampled areas represent groups of pixels that include the characteristic elements necessary to identify and separate the classes (Figure 9). Vector layers were created for each class and areas defining the class were vectorized and then assigned to them. Figure 10 shows the result of the supervised classification. Unsupervised Media - K classification was used for this study. This algorithm combines

"observations" (pixels) and places them into discrete groups. Pixel placement is realized by creating nodes that are placed in the center of the cluster.

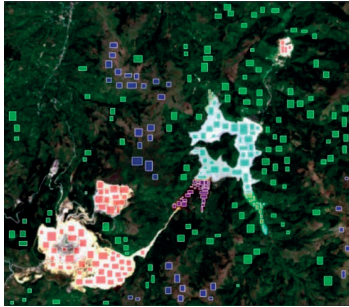


Figure 9. Sampling creation

The node is positioned so that the distance between the node and the closest point is less than the distance between these points and the next node. A number of 14 classes were chosen that were automatically customized based on algorithms. The difference between this method and supervised classification is that in the latter spectral signatures chosen by the user are used (Figure 11).

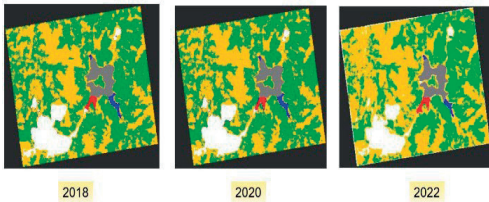


Figure 10. Supervised classification for images corresponding to the years 2018, 2020 and 2022

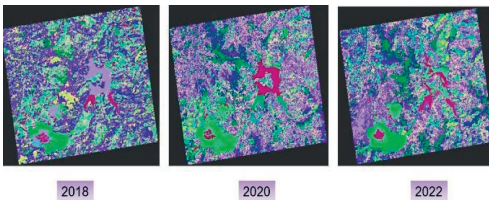


Figure 11. Unsupervised classification for images corresponding to the years 2018, 2020 and 2022

For the Sentinel images, the surfaces were also determined, from which the percentages representing the degree of coverage of each class were taken (Table 3).

Table 3. Surfaces obtained from processing Sentinel satellite images

	2018	2020	2022
	(Hectares)		
Forest surface	2322.39	2325.74	2427.83
Pasture land surface	1917.90	1912.38	1815.61
Quarry surface	309.22	300.12	283.98
Water surface	17.98	18.35	17.02
Tailings surface	20.96	26.35	24.68
Sludge surface	124.68	130.21	144.02

RESULTS AND DISCUSSIONS

Once the surfaces have been obtained, the following were concluded:

- throughout the 30 years, the forest surface has increased, and the forest area has started to gain ground over the pastures;
- the tailings surface in the settling pond and the sludge surface have increased significantly, the result being worrying;
- the surface of the quarry at the ground level decreases since exploitation is concentrated on depth and nature recovers land.

The next step consisted of studying the settling pond's surfaces, as well as the elements that make it up: tailings, water, and sludge (Figure 12). The surface of the tailing pond has increased considerably (Table 4), which has caused the compromise of people's habitat in the area.

Table 4. The evolution of the settling pond surfaces

	1992	2000	2014	2018	2020	2022
	(Hectares)					
Water surface	57.41	22.54	28.19	17.80	18.06	16.36
Tailing surface	0	10.06	16.76	20.81	26.09	24.29
Sludge surface	12.95	65.38	102.51	124.3	129.71	143.36
Tailing pond's surface	70.36	97.98	147.46	162.91	173.86	184.01

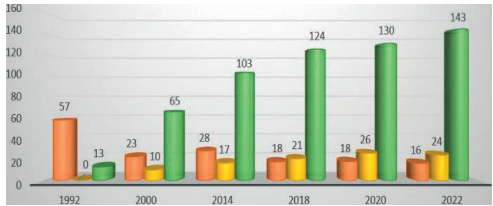


Figure 12. Time evolution of the Valea Șesii decantation pond (Red - Water surface, Orange - Tailing pond surface, Green - Sludge surface)

Normalized Difference Vegetation Index

The differential reflection between the red band and the near-infrared band allows density and intensity of green vegetation monitoring using the spectral reflectivity of solar radiation.

(Rouse et al.) Green leaves show a better reflection in the near infrared wavelength than in the visible spectrum. Leaves that are water-deficient or diseased or dead turn yellow and their reflectivity decreases greatly for the infrared wavelength.

For near-infrared and red, the corresponding bands are 4 and 3 for images taken with Landsat 4-5 and 7, and for images taken with Landsat 8 and 9 satellites, bands 5 and 4. The NDVI index was applied to images taken in 2018, 2020 and 2022, and after applying the formula, the resulting images were automatically generated. For the images resulted after applying the NDVI index to be interpretable, it was necessary to reclassify them. This was realized from the GIS Analysis menu, the Database Query - Reclass sequence. The images presented in Figure 13 and classification categories were thus obtained. As regards the images taken with Sentinel satellites, the bands used for the NDVI index are band 8 and band 4 (Figure 14).

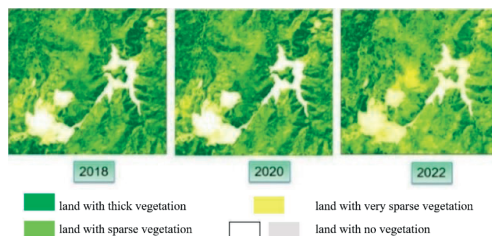


Figure 13. The Landsat images after applying the NDVI index and reclassified for the years 2018, 2020 and 2022

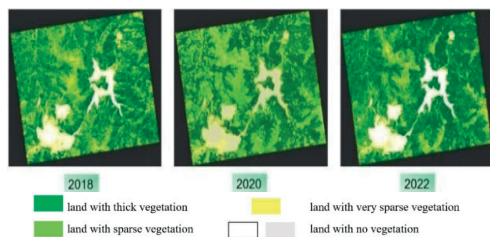


Figure 14. Sentinel images after applying the NDVI index and reclassified for the years 2018, 2020, 2022

Normalized Difference Water Index

The corresponding near-infrared and green bands are 4 and 5 for Landsat 4-5 and 7 images. Bands 5 and 6 were chosen for Landsat 8 and 9 images (Figures 15 and 16) (McFeeters, 1996).

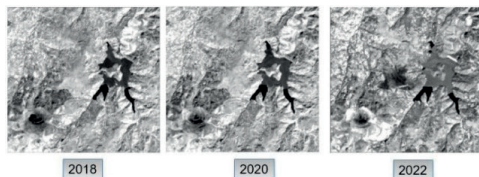


Figure 15. Landsat images resulting after applying the NDWI index for the years 2018, 2020 and 2022

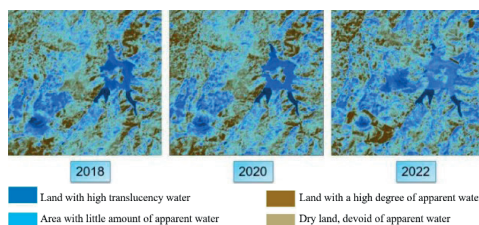


Figure 16. Landsat images after applying the NDWI index and reclassified for the years 2018, 2020 and 2022

For Sentinel satellite images, the appropriate bands for applying the NDWI index are band 8 and band 9 (Figure 17). The sequence used in the SNAP program is Raster - Band Maths. The specific formula, respectively $(B8 - B9) / (B8 + B9)$ is written in the dialog box. The values of the NDWI index are between -1 and +1, are presented in Figure 18 and are as follows:

- dark tons (values <0) express the sheen of the water;
- light tons (values >0) represent dry land.

A comparison of the processed images, both those taken with Landsat satellites and those taken with Sentinel satellites, was followed and presented in Figures 19, 20, 21 and 22.

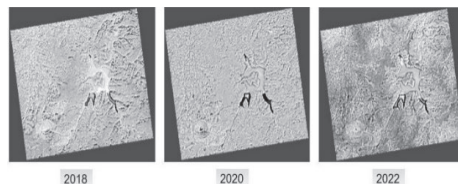


Figure 17. Sentinel images resulting after applying the NDWI index for the years 2018, 2020 and 2022

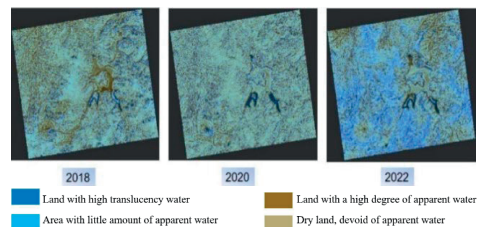


Figure 18. Sentinel images after applying the NDWI index and reclassified for the years 2018, 2020 and 2022

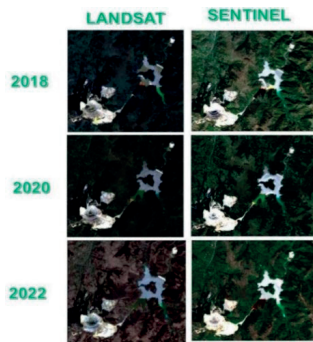


Figure 19. RGB combination for Landsat and Sentinel images

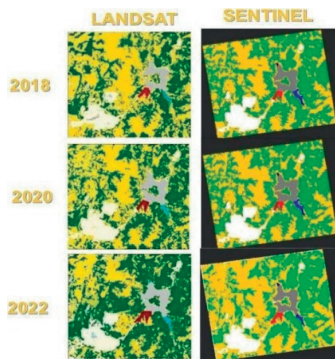


Figure 20. Classification of Landsat and Sentinel images

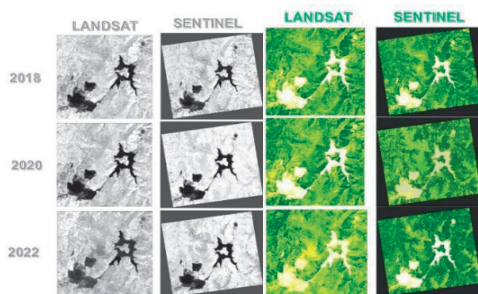


Figure 21. NDVI index and reclassified for the years 2018, 2020, 2022

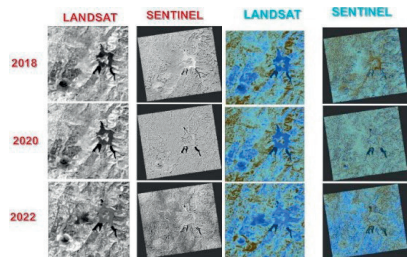


Figure 22. NDWI index and reclassified for the years 2018, 2020, 2022

The comparison of the Figure 23 with Figure 24 from the point of view of the surfaces concerned strictly the surface rendered by the settling pond.

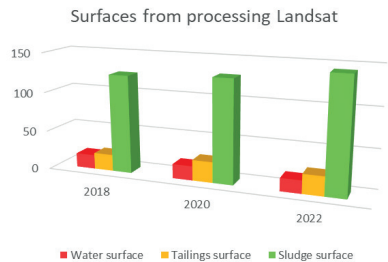


Figure 23. Tailings pond surfaces comparison for Landsat images

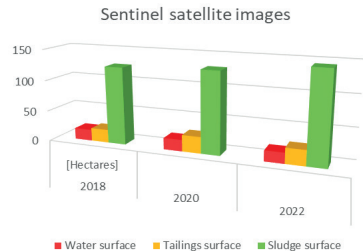


Figure 24. Tailings pond surfaces comparison for Sentinel images

CONCLUSIONS

The present article is a brief description of the workflow followed for the analysis of Landsat and Sentinel satellite images for Roşia Poieni quarry and Valea Şesii decantation pond. Regarding the performance of combining multispectral and SAR (Sentinel and Landsat) satellite data for estimating both volumes and areas in the study area, Valea Sesii decantation pond, following the research carried out, it was found that:

- ✓ The quarry's surface at the ground level for the studied area has decreased in recent years because mining is focused on depth and nature is reclaiming land.
- ✓ The surface of the Valea Şesii settling pond has increased significantly, from 70.36 ha in 1992, to 184.01 ha in 2022.
- ✓ The number of tailings has increased considerably, currently occupying an area of 24.29 ha. This fact exerts a huge influence on the area, both now and in the future.
- ✓ Compared to Landsat images, those taken with Sentinel satellites have a slightly better spatial resolution, facilitating their processing.
- ✓ To obtain a higher quality of the processing results of the Sentinel 1 images, they must be pre-processed by applying various corrections.

From the analysed data it can be clearly seen that by using Sentinel SAR images it was possible to determine and continuously monitor the forest, pasture, water, tailing pond, quarry and sludge surface. The accuracy of the SAR water surface estimation was comparable to the NDWI given by Landsat. This data was validated by physical observations in the field, confirming that the protocols followed can be reliably applied and can be repeated.

Despite the small area of the study area, satellite remote sensing succeeds brilliantly in providing plausible results, worthy of consideration and of great importance over hard-to-reach areas.

REFERENCES

- Badulescu, B., Matache, A.M., Vrancuta, L., Musat, S., Mircea, S., Petrescu, N. (2019). Shadows correction methods for Landsat satellite images. *Scientific Papers. Series E. Land Reclamation, Earth Observation & Surveying, Environmental Engineering, VIII*, 162-168, Print ISSN 2285-6064.
- Basayigit, L., Ersan, R. (2015). Comparison of pixel-based and object-based classification methods for separation of crop patterns. *Scientific Papers. Series E. Land Reclamation, Earth Observation & Surveying, Environmental Engineering, IV*, 148-153, Print ISSN 2285-6064.
- Herbei, M.V., Popescu, C.A., Bertici, R., Sala, F. (2023). Estimation of sunflower crop production based on remote sensing techniques. *Agrolife Scientific Journal*, 12(1), 87-96.
- Hila, A.S., Ferencz, Z., Cimpeanu, S. M. (2018). Land surface temperature monitoring through GIS technology using satellite Landsat images. *Scientific Papers. Series E. Land Reclamation, Earth Observation & Surveying, Environmental Engineering, VII*, 163-167, Print ISSN 2285-6064.
- Iosub, F. (2012). Extracting spatial information from satellite images using supervised and unsupervised classifications, Geospatial seminars, geo-spatial.org.
- Makri, S. (2016). Sentinel-2 and Landsat-7 satellite images qualitative comparison for evaluating advances in detecting lakes' quality parameters, Complementary certificate in Geomatics, Université de Geneve, Institut de Sciences de L'Environnement.
- McFeeters, S.K. (1996). The use of the Normalized Difference Water Index (NDWI) in the delineation of open water features. *Intern J of Remote Sensing*, 17(7), 1425-1432, <https://doi.org/10.1080/01431169608948714>.
- Mendez Garzón, F.A., Valánszki, I. (2020). Remote sensing tendencies in the assessment of areas damaged by armed conflicts. *Scientific Papers. Series E. Land Reclamation, Earth Observation & Surveying, Environmental Engineering, IX*, 223-234, Print ISSN 2285-6064.
- Moldovan, A., Török, A.I., Cadar, O., Roman, M., Roman, C., Micle, V. (2021). Assessment of toxic elements contamination in surface water and sediments in a mining affected area. *Studia Universitatis Babes-Bolyai Chemia*, 66(2), 181-196, DOI10.24193/subbchem.2021.2.16.
- Popa, M., Bostan, R., Ilie, N., Varvara, S. (2015). Natural sorbents used for the removal of heavy metals from acidic wastewaters generated at 'Valea Sesei' tailing pond from Rosia Poeni mining perimeter (Romania). *J Environ Prot & Ecology*, 16(3), 839-849.
- Rouse, J. W., R. H. Haas, J. A. Schell, and D. W. Deering (1973). Monitoring vegetation systems in the Great Plains with ERTS, Third ERTS Symposium, NASA SP-351 I, 309-317.
- Toderaş, M. (2021). Mining risks at exploitation in Roşia Poieni open pit mine, Romania. *Mining Revue*, 27(1), 1-11, ISSN-L 1220-2053 / ISSN 2247-8590, DOI: 10.2478/minrv-2021-0001.
- Vorovencii, I. (2015). Habilitation Thesis: Identification, assessing and monitoring of environmental changes using remote sensing methods, available online at https://www.unitbv.ro/documente/cercetare/doctorat-postdoctorat/abilitare/teze-de-abilitare/vorovencii-iosif/05-vorovencii_iosif-Teza_de_abilitare_RO.pdf
- <https://www.earthdata.nasa.gov/>
- <https://sentinels.copernicus.eu/web/sentinel/home>
- <https://www.usgs.gov/landsat-missions>
- <https://static.eos.com/wp-content/uploads/2020/11/how-NDVI-works-EN.jpg>
- [https://ro.wikipedia.org/wiki/Valea_%C8%98esii_\(Lup%C8%99a\)_Alba](https://ro.wikipedia.org/wiki/Valea_%C8%98esii_(Lup%C8%99a)_Alba)
- <https://mapio.net/pic/p-26288806/>
- <https://adevarul.ro/stiri-locale/alba-iulia/foto-satul-idilic-din-apuseni-disparut-sub-o-1883658.html>
- <https://static.eos.com/wp-content/uploads/2020/11/how-NDVI-works-EN.jpg>
- https://harti.wansait.com/ro_ro/2012/judetul-alba-harta-administrativa-interactiva/
- <https://geoportal.ancpi.ro/geoportal/imobile/Harta.html>

EXPLORING THE COSMOS: A WEB-BASED APPLICATION FOR POLLUTION, CONSTELLATION AND MOON PHASE RECOGNITION

Mihai MAFTEI, Iuliana MARIN

National University of Science and Technology Politehnica Bucharest,
313 Splaiul Independentei, District 6, Bucharest, Romania

Corresponding author email: marin.iuliana25@gmail.com

Abstract

Throughout human history, the fascination with celestial objects and the night sky has persisted. This article introduces a web-based application designed to assist users in identifying constellations, light pollution that obscures stars in the night sky, along with moon phases in astronomical photographs. The application utilizes image processing techniques and template matching to achieve this recognition, enabling users to explore the cosmos independently. The article outlines the methodology, including the creation of constellation templates and the process of image normalization and matching. It also discusses the mathematical calculations involved in star recognition and moon phase determination. The application's user-friendly interface and feedback from users are presented, indicating a positive response. The article concludes by highlighting the potential for further development, including the conversion of the application into a mobile version and the addition of features such as air pollutants indices, a moon phase calendar, and zodiacal data. The application is poised to be a valuable tool for astronomy enthusiasts, navigators, and those interested in exploring the mysteries of the night sky.

Key words: constellations, image processing, moon phase, stars, template matching.

INTRODUCTION

Since the dawn of humanity until these days, the idea of evolution has been understood. People always searched for methods that would make their lives easier and learn as much as they could in the shortest amount of time. Modernity, technology, and tools make life easier wherever we turn, but when we turn off the switch and the power go out, we become aware of the mysteries of the sky, a blue map covered with shining dots that stand in for the past, present and future.

Known as stars, they are essential elements of the cosmos that can be connected and represent constellations, often used by navigators for guidance or even for mythical storytelling. Even so, only a skilled and experienced stargazer with sufficient background knowledge will be able to identify constellations.

Numerous guidebooks, websites, and cell phone apps have been developed to assist non-professionals in locating the constellations (Contreras-Koterbay & Mirocha, 2016; Gomez & Fitzgerald, 2017; McKee et al., 2022; Molnar & Kiss, 2023). Even though these options appear to be useful, they can only make suggestions and cannot take environmental

factors into account. However, the question remains how a human can look up at the sky and identify the stars and constellations by himself. Everything may now be streamlined and made feasible thanks to technological advancements (Modeling, Systems Engineering, and Project Management for Astronomy III | Request PDF, n.d.), and the only things that are required are a clear desire to study and hard work. Searching for an answer to this question and thinking about the preceding catch-up regarding the process of cosmic reaching (Hall, 2022), the current research wanted to create something that will assist people who share interest in cosmic exploration. The present paper is about a constellation recognition application which will allow the user to scan the sky and identify unfamiliar celestial objects. The application includes features such as constellation recognition, by using a pattern matching algorithm, but also a moon phase detector, using its circularity. The important steps in this process, that will be discussed in the next chapters, are similar applications, along with the creation of the template coordinates file, the processing of the test images and the detection algorithm for both constellation and moon phase

recognition. The last chapter outlines the conclusions and future work.

MATERIALS AND METHODS

An early scientific tool for keeping time and performing observations was the astrolabe (Raposo, 2022). This instrument was a popular astronomical equipment in the Middle Ages, and it is one of the first instruments used for sky searching. The astrolabe has origins in antiquity, but it was widespread in the 17th century, being used for astronomical observations, such as determining the height or distance from the zenith of the sun, moon, planets, or stars, but also the heights of mountains and towers, as well as the depths of wells. But it was more important when the astrolabe was used as an additional computational tool, meaning that the locations of the sun and other bright stars in relation to the meridian and the horizon, as well as the astronomer's geographic latitude and true north orientation, were all possible by using this equipment (Edney, 2023).

Another tool used in astronomy, the sextant, was made by John Bird in the 18th century (Kelly & Gráda, 2022). A sextant is a device used to calculate an object's height above the horizon. The angle and time of measurement can be used to create a location line on a nautical or aeronautical chart, in that way a sextant is often used to find one's latitude by observing the sun and moon. It can also be used to determine the angle between any two objects when held horizontally, such as stars or even planets.

From Galileo until now, the telescope has played and continues to play an important part in our understanding of the cosmos, and its continuing growth and refinement will no doubt lead to many new discoveries and insights into the future (Zubairy, n.d.). A telescope is an optical equipment used to examine distant celestial objects such as stars, planets, and galaxies. It collects and focuses light from these objects, which is then amplified and brought into focus to generate a picture.

The use of optical instruments such as telescopes, cameras, and image processing techniques to automatically identify and locate stars and constellations in the night sky is referred to as optical star and constellation recognition (Rettberg, n.d.). This method is

frequently employed in astronomical research, surveying, and navigation.

One common method of optical star recognition is to use a star catalog as a reference, which contains the positions and brightness of known stars (Savanevych et al., 2023). The positions and brightness of the stars in the image are identified and measured after images of the night sky are compared to the catalog.

In the field of artificial intelligence known as computer vision, it is possible for machines to gather useful data starting with digital photos, movies, and other visual inputs, and then act or offer ideas in response to that data (Utama et al., 2023). Computer vision requires a large amount of data since it performs data analysis repeatedly until it begins to distinguish distinctions and ultimately images. In the current research are involved computer vision methods like thresholding, contour detection, and star extraction from astronomical photos. This procedure includes several phases, including picture preparation, segmentation, feature extraction, and classification.

When referring to constellation searching, a solution to this problem could be using Deep Learning (Khajuria et al., n.d.). This represents a machine learning approach that trains computers to do what people do naturally: learn. Deep Learning is an area of artificial intelligence that focuses on creating large neural network models that can make accurate data-driven decisions, its technologies, such as speech recognition and facial detection on digital cameras, being available on all current smart phones. This machine learning type is a search method aimed at selecting the optimal function from a collection of functions to explain the connections between characteristics in a dataset (Mehta et al., 2022).

A common deep learning model for image analysis tasks like object identification and recognition is the convolutional neural network (CNN) (Zhao et al., 2022; Lubura et al., 2022). In a CNN, each neuron only analyzes data in its receptive field, like the neurons from a biological vision system that respond to inputs only in the constrained region of the visual field. Simpler patterns, such lines, or curves, are identified first in the layers, then more distinct patterns, like objects (Kyselica et al., 2022). Consequently, CNN could be a solution for

constellation detection. Automatic learning and extracting relevant features from images are an example of how in the context of constellations searching, CNN learns to identify key patterns and structures that correspond to different stars connections (Song et al., 2023). Translation invariance or robustness to noise and variability are other examples of features that could help in night sky searching (Ramos-Alcaraz et al., 2023).

Another solution for constellation detection is called template matching. While template matching is sometimes seen as a very basic, restricted approach to the most fascinating issues in computer vision, it does touch on many old and new techniques in the field (Jordan et al., n.d.). In this technique, templates are built to reflect the intended pattern or object and they encapsulate the fundamental properties and qualities of the item to be detected (Doukari et al., 2022). The template is then moved over different sections of the input picture. The similarity measure, matching score, thresholding, and localization are computed next, followed by iterative search, because the template matching procedure may entail numerous iterations.

Image processing is critical in template matching because it provides the required techniques and procedures to improve the input pictures, extract significant characteristics, and efficiently complete the matching process. Important factors such as preprocessing, feature extraction, feature representation, template creation, matching algorithm, and post-processing must be highlighted since in the current research all of them are used to get the desired outcome.

RESULTS AND DISCUSSIONS

The proposed solution for gaining the constellation detector involves template matching, technique in which are built templates that reflect the intended pattern or object, and they encapsulate the fundamental properties and qualities of the topic to be detected. The template is then moved over different sections of the input picture. The similarity measure, matching score, thresholding, and localization are next computed, followed by iterative search,

because the template matching procedure may entail numerous iterations.

Another method that was involved was image processing, a technique that represents the manipulation and analysis of digital pictures using algorithms and procedures with the objective of increasing their visual quality, extracting relevant information, or changing them into new forms.

Image processing in template matching provides the required techniques and procedures to improve the input pictures, extract significant characteristics, and efficiently complete the matching process. Factors such as preprocessing, feature extraction, feature representation, template creation, matching algorithm, and post-processing are highlighted since all of them are identified to get the desired outcome. As mentioned, there are a few steps of the process that need to be developed before, to make sure that the application will work as planned.

Templates

The production of the used template establishes the initial section of the program. The AstronomyOnline website graphics of all 88 constellations were used to map out the complete celestial sphere in alphabetical order and according to International Astronomical Union (IAU) rules (Observation - 88 Constellations, n.d.).

After obtaining the constellation photos (Figure 1), they were preprocessed using the Python programming language to obtain the coordinates of the stars in each of them. Therefore, an iteration of each file in the template directory was performed to extract the required characteristics.

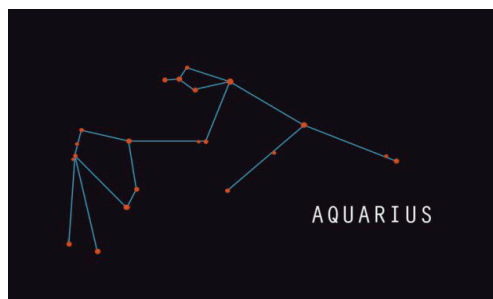


Figure 1. Example of Downloaded Template

Distances and normalization

The constellations in images are represented using the red color to depict the stars and with blue to determine the connections between them. Thus, after reading the images with the function 'cv2.imread()', the red and blue color channels are obtained using the 'get.red()' and 'get.blue()' methods. The results are illustrated in Figures 2 and 3.

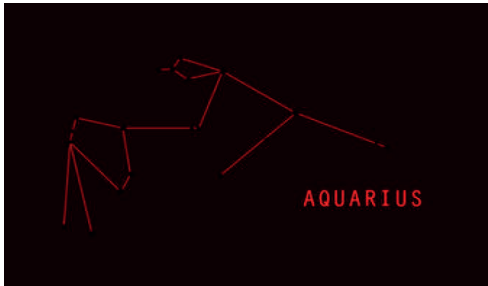


Figure 2. Application of the Red Channel



Figure 3. Application of the Blue Channel

The 'binarise_image()' method was used to threshold the red and blue channels, with any extraneous items being deleted once the binary pictures of stars and lines are converted to grayscale. The use of the 'cv2.bitwise_not()' function to invert the stars binary picture for boosting star areas is followed by edge detection using the 'cv2.Canny()' function.

The Hough line transformation was applied to detect and extract lines from a binary picture. The contours on the edge picture are filtered to remove noise once they have been detected, as in Figures 4 and 5.

To extract the normalized coordinates of stars and lines from contours and drawn lines, the iterate function is used. In the iterate function, it is gone through all the contours of the stars and the centroid for each one of them is calculated,

so that it is obtained the brightness (size) of every dot.

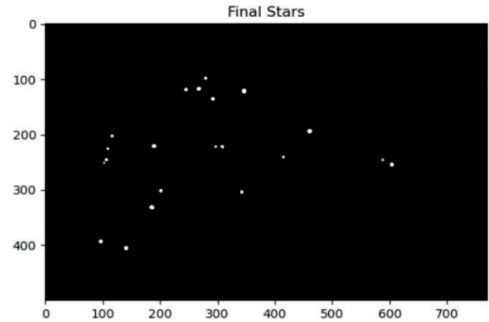


Figure 4. The Found Stars

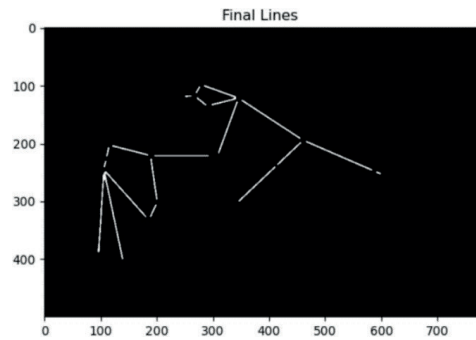


Figure 5. The Found Connections between Stars

The list of coordinates of every point is sorted in descending order, such that there are obtained the first two brightest stars. After getting the first two biggest stars, there can be passed through all the stars and calculate the normalized coordinates by calling the 'get_normalised_coordinates()' function. This takes the x and y coordinates of the stars and lines, then shifts them with respect to the brightest star, before replacing it in the origin of the coordinate system. It is calculated the distance and angle between the first and second brightest stars and then the distance between all the stars is normalized, as well as the coordinates for points and lines are updated.

The extracted coordinates, as well as the number of contours and normalized lines, are saved in the 'templates_coordinates' dictionary, and then a visualization of the normalized stars and lines is created using the 'matplotlib.pyplot' library and the output is saved as an image (Figure 6), in which there can be seen the first two brightest stars, such that the user can clearly see the

connections and how the constellation was found.

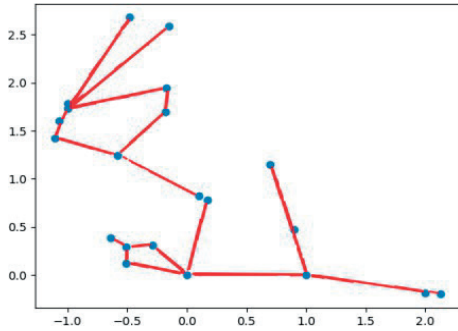


Figure 6. Normalized template example

Following the processing of all template pictures, the 'template_coordinates' dictionary is serialized and stored as a binary file using the 'pickle.dump()' method, so that it may be used in testing to validate the matching with additional photos.

Template matching

After the dictionary with the coordinates of the template for all constellations is triggered, new images of the night sky can be examined to see if there are any similar scenarios.

When a new image is uploaded by the user, the path to it is sent to the 'test_normaliser' function. Then it does the same processing operations that were outlined in the template file creation process, such as normalization and extraction of the coordinates of the stars discovered in the image, which are saved and returned as a list.

The 'similarity_error' function calculated the similarity error between the normalized coordinates of the test picture and the template image to ensure that there was discovered the perfect match of the stars pattern. The function analyzes the distances between comparable star coordinates and calculates the error depending on the threshold, then returns the count of matched stars and the error value. The constellation with the greatest score is then chosen as the anticipated label. The user may observe the visualization of the matching stars since it is created and saved in a local directory.

Moon phase

The moon, the nearest big celestial body, and the only natural satellite of planet Earth, has been

recognized since prehistoric times and is the second-brightest object in the sky after the Sun. The Moon's nature and genesis have been the subject of centuries of observation and scientific research. Early investigations into the Moon's motion and position enabled tide prediction and sparked the creation of calendars.

The major benefit of researching the history of astronomy is that ancient people observed the same patterns in the sky as today, unlike the study of most historical events, which are singular occurrences. The most significant advances in comprehending Moon phases and eclipses were placed in the explanations provided by Aristotle in his well-known work "On the Heavens" in the fourth century BC is the result of his research in the cities of Babylonia and ancient Greece (Belmonte & Lull, 2023).

Although these discoveries were made very early, they were fought for, and they provide guidance on how to effectively arrange activities for pupils. Aside from a constellation recognition form, the user may scan the moon in a separate form to determine its phase (Figure 7) and the number of days till a new or full moon.



Figure 7. Cycle of the Moon (Phases of the Moon, n.d.)

The idea is like the stars pattern in that when the user enters a photo of the moon, the algorithm analyzes it and looks for the largest item in the image. After locating it, the image is binarized, and the algorithm calculates the circularity of the object, allowing us to determine the stage of the moon phase. After the moon's circularity is determined, there is identified which side is present, left or right, or if the moon is at its fullest. The object's y minimum and maximum points were computed as a solution to this problem. Next, there was drawn a line between these two points and counted the pixels on the line's left and right sides that make up the

contoured object. In this method, the circularity is on the left side if there were discovered more pixels there; else, the right side is similarly affected. The moon phase in the image is determined based on these characteristics.

Mathematics behind the overall computation

Some important equations in astronomy, particularly in the field of star recognition and normalization, are used to calculate the distance between two points and the angle between three stars (Mathematical Handbook for Scientists and Engineers: Definitions, Theorems ... - Granino A. Korn, Theresa M. Korn - Google Books, n.d.). These computations aid in the identification and normalization of star locations in the night sky.

Distance between two points (used to determine the distance between two stars)

$$d = \sqrt{[(x_2 - x_1)^2 + (y_2 - y_1)^2]} \quad (1)$$

where:

- (x_1, y_1) and (x_2, y_2) are two coordinate points.
 The angle is formed by three points (used to determine the angle of rotation of three stars)

$$\text{angle} = \arccos\left(\frac{c^2 + b^2 - a^2}{2cb}\right) \quad (2)$$

where:

- a, b and c represent the distances between three points. In this example, there was calculated the angle in point A.

The circularity formula (used to determine the circularity of the moon contour)

$$\text{circularity} = 4 \cdot \pi \cdot (A/P^2) \quad (3)$$

where:

- P represents the perimeter of the contour;
 - A represents the area of the same contour.

Interface

The application of the current paper was built for anyone who wishes to learn about the constellations visible in the night sky (Figure 8). Users may upload photos or photographs taken by themselves and then see what the software detects and shows as a result. The application may be a valuable learning tool for instructors, professors, and students, as it can motivate them to be outgoing and understand how the connections between stars are discovered on their own.

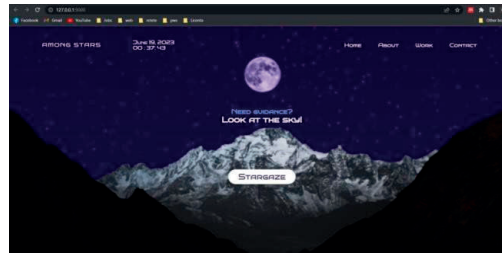


Figure 8. The interface available for the user

The interface is represented by a web application that contains some information about constellations, some appealing visuals, and, most importantly, a slide containing two forms that allow the user to upload the desired picture (Figure 9), scan it with the help of the program behind the application, and view the results. The two forms rely on a backend application that processes and tests the uploaded picture to produce the desired outcome.

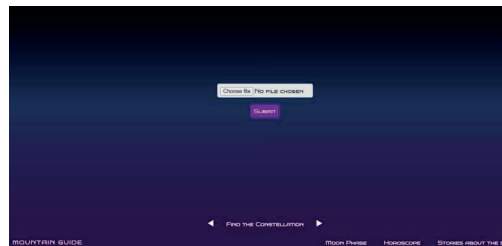


Figure 9. upload of the wanted file to be analyzed

In the current chapter it is explained how the application was tested, how it works, what should be uploaded, and what the outputs are. The feedback that was received while giving the application to various users to test it and see how they reacted is also included. Furthermore, there are presented the conditions in which the application may, or may not, work and the details about light pollution.

Testing and results

As previously mentioned, the program operates as follows: the application is launched, running the main.py file, and accessing the address printed in the console, the program is available to the user. In the graphical user interface, the tester may examine the interface's visuals and read some information about the sky, while as the user scrolls down, he will be able to see two

forms: one for constellation recognition and one for moon phase recognition.

If the user selects to upload and inspect an image in the constellation form, the application will display the provided image, the stars of the identified constellation in a coordinate system so the user can see how they were found (Figure 10), and finally a picture of the template used.

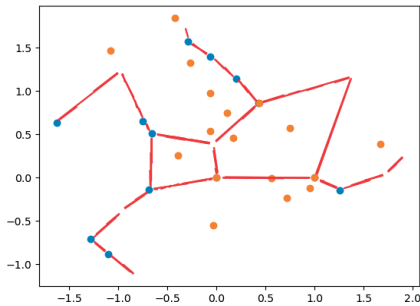


Figure 10. Example of predicted image of a constellation

The coordinate system image will show the first two brightest stars in the locations (0.0) and (1.0), as well as the lines connecting the stars that make up the constellation. Aside from these images, there will be some information about the discovered constellation (Figure 11).

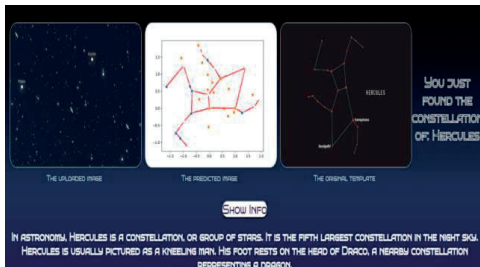


Figure 11. Output of the constellation detection form

The same approach applies to recognizing moon phases. The user submits a picture of the moon, presses the button, and then a picture of the moon, contoured with a red line and having crossed a blue line between the y min and y max of the contour (Figure 12; that will be used for calculating the number of the pixels), will be displayed, along with a picture representing the phases of the moon, to help the user understand the concept.

In addition to constellation recognition, the user will receive information about the current moon phase, as well as the anticipated time until the

next new/full moon phase, as illustrated in Figure 13.

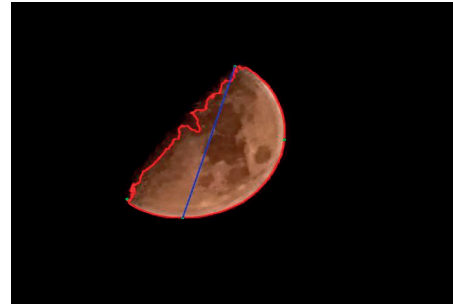


Figure 12. Example of detection image for the Moon

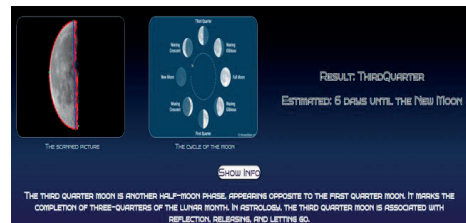


Figure 13. Output of the Moon Phase recognition form

In what concerns the feedback for the application, 20 individuals answered a survey. When asked if they were pleasantly surprised by the application's interface, most users (55% replied yes), with three not so delighted with the offered visual effects, indicating that they can be improved in the future updates. When looking for constellations, most users (40%) like the high accuracy feature of the results, while 20% prefer the application to be user pleasant, therefore it must include interactive elements that capture the user's attention. A free tool is more of an approved application for users, as 17.8% consider that a costly one is unappealing. Another characteristic is that the employed tool should not have any advertisements, as this will prevent the user from being upset and bored by the annoying commercials. Therefore, the overall opinion regarding the proposed software solution was positive.

Light pollution

There is a lot of pollution, and as a result, the stars are not as visible, the major reason being that there are a lot of different illumination sources that fill the night sky with artificial light. Light pollution is the intentional change of

outdoor light levels from those that occur naturally, or, due to excessive artificial light. Light pollution, like noise pollution, is a type of waste energy that can have negative consequences and impair environmental quality. Furthermore, because light (delivered as electromagnetic waves) is normally created by electricity, which is typically generated by the burning of fossil fuels, a link between light pollution and air pollution (from fossil-fuelled power plant emissions) may be established.

This kind of pollution has a negative impact on professional and amateur astronomers, as well as casual night sky viewers since it diminishes the visibility of stars and other celestial objects. The decrease in night sky visibility is caused by skyglow, which is upward-directed light emitted by poorly built or aimed lighting and security floodlights. This squandered light is dispersed and reflected by solid or liquid particles in the atmosphere before returning to people's eyes from the ground, obliterating their view of the night sky. This is a concern not just for astronomers and those who simply wish to gaze at the stars because the glare from streetlamps, business security lights and signage, or even a neighbor's bright and misdirected yard illumination can cause pain and distraction, lowering many people's quality of life (Figure 14) (Light Pollution | Definition, Causes, & Facts | Britannica, n.d.).



Figure 14. Process of light pollution

Light pollution is also harmful to birds and other creatures. Many migrating birds, for example, fly at night, when the light from the stars and Moon aids in navigation. The glare of artificial light causes these birds to get disoriented when they fly over urban and suburban regions (Light Pollution | Definition, Causes, & Facts | Britannica, n.d.). There is multiple advice for

how to reduce light pollution, from turning off the lights when not in use, to pointing our lights towards the ground when going out and even unplugging from devices as the sun sets (10 Simple Ways to Reduce Light Pollution | Visit Durango, CO | Official Tourism Site, n.d.). In Figure 15 provided by (Light Pollution Map, n.d.), can be observed the locations where the light pollution is at its highest values (Barentine, 2019).

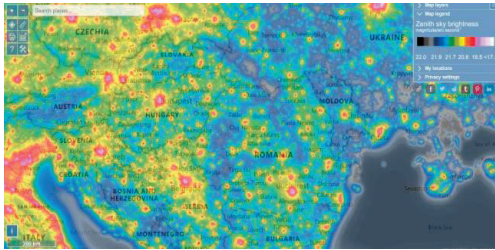


Figure 15. Map of light pollution

There are areas where light pollution exists but is not recorded or even known. The current program was improved so that it can compare photos of the same point in the sky taken at different times of the night or of the year. External data from specialized sources can be integrated into the program to provide information on light pollution in various regions. This data can be used in tandem with photographs to provide a more complete picture of light pollution levels. Light sensors in mobile devices are taken into consideration if users use their phones to capture photos. The sensors directly measure the level of ambient light when the photo is captured and how blurred is the taken photo (Mander et al., 2023).

Image processing techniques are used to determine the level of light pollution in the night sky, for example contrast stretching or histogram equalization to enhance the features in the image and convert the image to a suitable color space, such as LAB (CIELAB) or HSV (Hue, Saturation, Value).

Another solution that could work is the luminance calculation by converting the image to grayscale to simplify processing and then calculate the luminance of each pixel. This can be done using different methods, such as a weighted sum of RGB (Red, Green, Blue) channels, which we are already familiar with. In Figures 16 and 17, can be observed a case of

light pollution, the picture being taken in different moments, but in the same place, this highlighting that the problem is real.



Figure 16. Light polluted night sky

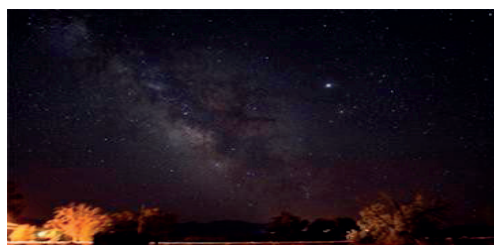


Figure 17. Clear night sky

CONCLUSIONS

The proposed program is a web-based application for constellation and moon phase recognition. After technical improvements, image processing techniques may now be used to locate and identify constellations in astronomical photographs automatically. Therefore, even without Internet connectivity, the proposed program can automatically recognize constellations in photos.

The application has the potential to become an even more powerful tool for studying the stars, discovering the universe, and even calculating the level of light pollution with ongoing development and upgrades. Aside from stargazing and pollution detection, the application can also serve as an educational guide, explaining in detail the algorithm of constellation detection and teaching students every step of the way.

As future work, the software solution will be converted into a mobile application for users to be able to utilize it for real-time sky scanning. In this manner, users can immediately scan the celestial objects or point the phone's camera at the sky and capture a photo.

To make the program more appealing to users and maintain their attention, the user interface will be improved to be friendlier and include additional functions like a moon phase calendar, user-specific zodiacal data, and information on how planetary alignments affect people's behavior.

Finally, the application has the potential to be a valuable tool for stargazers, navigators, volunteers who want to support the fight against light pollution, and anyone else interested in the night sky. Its success is due to the combination of superior technology, precision, and user-friendliness.

REFERENCES

- Barentine, J.C. (2019). Methods for Assessment and Monitoring of Light Pollution around Ecologically Sensitive Sites. *Journal of Imaging* 2019, 5(5), 54.
- Belmonte, J.A., & Lull, J. (2023). *Mapping the Stars: The Skies of Ancient Egypt*. 193–306.
- Contreras-Koterbay, S., & Mirocha, L. (2016). The New Aesthetic and Art: Constellations of the Postdigital. *The New Aesthetic and Art: Constellations of the Postdigital*.
- Doukari, O., Greenwood, D., Rogage, K., & Kassem, M. (2022). Object-Centred Automated Compliance Checking: A Novel, Bottom-Up Approach. *Journal of Information Technology in Construction (ITcon)*, 27, 336.
- Edney, M.H. (2023). Latitude, Longitude, and Geospatial Technologies to 1884. *The Routledge Handbook of Geospatial Technologies and Society*, 7–22.
- Gomez, E.L., & Fitzgerald, M.T. (2017). Robotic Telescopes in Education. *Astronomical Review*, 13(1), 28–68.
- Hall, E.D. (2022). Cosmic Explorer: A Next- Generation Ground-Based Gravitational-Wave Observatory. *Galaxies*, 10(4), 90.
- Jordan, J., Posada, D., Zuehlke, D., Radulovic, A., Malik, A., & Henderson, T. (n.d.). (Preprint) AAS 22-775 *Satellite Detection in Unresolved Space Imagery for Space Domain Awareness using Neural Networks*, from https://www.researchgate.net/publication/362252394_Satellite_Detection_in_Unresolved_Space_Imagery_for_Space_Domain_Awareness_Using_Neural_Networks
- Kelly, M., & Gráda, C. (2022). Connecting the Scientific and Industrial Revolutions: The Role of Practical Mathematics. *The Journal of Economic History*, 82(3), 841–873.
- Khajuria, T., Tulver, K., Luik, T., & Aru, J. (n.d.). *Constellations: A Novel Dataset for Studying Iterative Inference in Humans and AI*.
- Kyselica, D., Jurkasová, L., Ďurikovič, R., & Šilha, J. (2022). Astronomical Objects Classification by Convolutional Neural Network Algorithms Layers.

- Proceedings of the International Conference on New Trends in Signal Processing, NTSP.
- Light pollution | Definition, Causes, & Facts | Britannica. (n.d.). Retrieved 30 November 2023, from <https://www.britannica.com/science/light-pollution>.
- Light pollution map. (n.d.). Retrieved 30 November 2023, from [https://www.lightpollutionmap.info/#zoom=5.21&lat=45.1575&lon=23.0716&state=cyJiYXNlbWFWljoitGF5ZSJCW5nUm9hZCIsIm9mZ2ZsYXkiOiJ3YV8yMDE1Iiwib3ZlcmxheWNvbG9yIjpmYWxzZW5wb3ZlcmxheW9wYWNpdHkiOiJyYwLCJmZW50dXJlc29wYWNpdHkiOiJlQ=](https://www.lightpollutionmap.info/#zoom=5.21&lat=45.1575&lon=23.0716&state=cyJiYXNlbWFWljoitGF5ZSJCW5nUm9hZCIsIm9mZ2ZsYXkiOiJ3YV8yMDE1Iiwib3ZlcmxheWNvbG9yIjpmYWxzZW5wb3ZlcmxheW9wYWNPdHkiOiJyYwLCJmZW50dXJlc29wYWNpdHkiOiJlQ=)
- Lubura, J., Pezo, L., Sandu, M.A., Voronova, V., Donsi, F., Šic Žlabur, J., Ribić, B., Peter, A., Šurić, J., Brandić, I., et al. (2022). Food Recognition and Food Waste Estimation Using Convolutional Neural Network. *Electronics*, 11(22), 3746. <https://doi.org/10.3390/electronics11223746>
- Mander, S., Alam, F., Lovreglio, R., & Ooi, M. (2023). How to Measure Light Pollution—A Systematic Review of Methods and Applications. *Sustainable Cities and Society*, 92, 104465.
- Mathematical Handbook for Scientists and Engineers: Definitions, Theorems – Granino, A. Korn, Theresa M. Korn - Google Books. (n.d.). Retrieved 30 November 2023, from https://books.google.ro/books/about/Mathematical_Handbook_for_Scientists_and.html?id=A4XCAGAAQBAJ&redir_esc=y
- McKee, P., Kowalski, J., & Christian, J.A. (2022). Navigation and star identification for an interstellar mission. *Acta Astronautica*, 192, 390–401.
- Mehta, T., Bhuta, N., & Shinde, S. (2022). Experimental Analysis of Stellar Classification by using Different Machine Learning Algorithms. 2022 International Conference on Industry 4. Technology (I4Tech).
- Modeling, Systems Engineering, and Project Management for Astronomy III | Request PDF. (n.d.). Retrieved 30 November 2023, from https://www.researchgate.net/publication/234224661_Modeling_Systems_Engineering_and_Project_Management_for_Astronomy_III
- Molnar, Z., & Kiss, D. (2023). Constellation Recognition on Digital Images. *SACI 2023 - IEEE 17th International Symposium on Applied Computational Intelligence and Informatics, Proceedings*, 443–447.
- Observation - 88 Constellations. (n.d.). Retrieved 10 November 2023, from https://astronomyonline.org/Observation/Cons_tellations.asp.
- Phases of the Moon. (n.d.). Retrieved 30 November 2023, from <https://www.timeanddate.com/astronomy/moon/phases.html>
- Ramos-Alcaraz, G.E., Alonso-Arévalo, M.A., & Nuñez-Alfonso, J.M. (2023). Star-Identification System Based on Polygon Recognition. *Aerospace* 2023, 10(9), 748.
- Raposo, P.M.P. (2022). The Astrolabe: From “Mathematical Jewel” to Cultural Connector. *Migrants Shaping Europe, Past and Present*, 19–40.
- Rettberg, J.W. (n.d.). *Machine Vision: How Algorithms are Changing the Way we see the World*. Retrieved 10 November 2023, from <https://www.wiley.com/en-cn/Machine+Vision+%3A+How+Algorithms+are+Changing+the+Way+We+See+the+World-p-9781509545247>
- Savanevych, V., Khlamov, S., Briukhovetskyi, O., Trunova, T., & Tabakova, I. (2023). Mathematical Methods for an Accurate Navigation of the Robotic Telescopes. *Mathematics* 2023, 11(10), 2246.
- Song, S., Sun, H., & Xu, W. (2023). Modulation Recognition with Enhanced Constellation Based on Convolutional Neural Network. *IEEE Vehicular Technology Conference, 2023-June*.
- Utama, J.A., Zuhudi, A.R., Prasetyo, Y., Rachman, A., Sugeng Riadi, A.R., Nandi, & Riza, L.S. (2023). Young Lunar Crescent Detection Based on Video Data with Computer Vision Techniques. *Astronomy and Computing*, 44.
- Zhao, Z., Wei, J., & Jiang, B. (2022). Automated Stellar Spectra Classification with Ensemble Convolutional Neural Network. *Advances in Astronomy*, 2022.
- Zubairy, M. S. (n.d.). *A Mysterious Universe: Quantum Mechanics, Relativity, and Cosmology for Everyone*. Retrieved 30 November 2023, from https://books.google.com/books/about/A_Mysterious_Universe.html?id=0lbgzwEACAAJ
- 10 Simple Ways to Reduce Light Pollution | Visit Durango, CO | Official Tourism Site. (n.d.). Retrieved 30 November 2023, from <https://www.durango.org/blog/post/ways-reduce-light-pollution/>

REMOTE ASSESSMENT OF THE FRACTION OF ABSORBED PHOTOSYNTHETICALLY ACTIVE RADIATION (fAPAR) FOR MOUNTAIN GRASSLANDS

Margareta MAGUREANU¹, Loredana COPACEAN¹,
Despina-Maria BORDEAN¹, Luminita COJOCARIU^{1,2}

¹University of Life Sciences “King Mihai I” from Timisoara,
119 Calea Aradului Street, Timisoara, Romania

²Agricultural Research and Development Station Lovrin,
200 Principala Street, Lovrin, Romania

Corresponding author email: luminita_cojocariu@usvt.ro

Abstract

The work focused on the analysis of the vegetation cover of the grasslands according to the Fraction of Absorbed Photosynthetically Active Radiation (fAPAR index), in five different stages, during the same year (2022), on altitudinal levels, from three groups of mountains. 110 grasslands located in different environmental conditions were studied, from: the Banat Mountains, the Poiana Ruscă Mountains and part of the Southern Carpathians. Five Sentinel 2 satellite scenes were used, acquired on the following dates: 22.03, 16.05, 15.07, 08.09, 18.10 and the Digital Elevation Model, classified into 8 altitudinal levels, from 53-2473 m. The results show that the fAPAR values are different, lower in March when the vegetation is still stagnant and does not use solar radiation, maximum in July when the vegetation is very well represented and uses maximum solar radiation, and from August, a downward trend, along with the reduction of the physiological activity of the plants in the grasslands. Also, differences in average fAPAR values by mountain groups and similarities in altitudinal steps between mountain groups were noticed.

Key words: fAPAR, grasslands, seasonal variation, spatial variation.

INTRODUCTION

fAPAR, acronym for *Fraction of Absorbed Photosynthetically Active Radiation* (Myneni & Williams, 1994; Epiphanio & Huete, 1995), is the remote sensing index that expresses the fraction of solar radiation absorbed by living leaves (Wang et al., 2016), in the electromagnetic spectrum ranging between 400-700 nm, for photosynthetic activity, meaning it refers only to the green and living elements of the vegetation canopy. In this context, previous research (Field et al., 1995; Zhang et al., 2015) has demonstrated that the primary productivity, gross or net, of plants is closely related to the fAPAR values.

fAPAR is one of the Essential Climate Variables (ECV) recognized by the Global Climate Observing System (GCOS) (GCOS, 2006), and when applied to satellite images, fAPAR, with values between 0 and 1 (Yang et al., 2014), is a biophysical variable used in ecosystem analysis, in various climate models, in estimating primary productivity of vegetation or crop yield (Sellers

et al., 1996; Fensholt et al., 2004; Viña & Gitelson, 2005; Qin et al., 2018), at regional or global scales (Xiao et al., 2016).

In recent decades, both fAPAR and other remote sensing indices have been successfully applied in pasture analysis, with various objectives, among the most important being the assessment of vegetation status, spatiotemporal monitoring of surfaces, analysis of vegetation cover distribution, productivity estimation and so on (Rossini et al., 2012; Chen et al., 2017; Pu et al., 2020; Noumonvi & Ferlan, 2020; Šandera & Štych 2020; Xu et al., 2023).

In this context, the aim of the study was to analyze pasture vegetation based on fAPAR index values and identify developmental patterns over time and space under different environmental conditions.

MATERIALS AND METHODS

Study area

The study area (Figure 1) is located in southwestern Romania, covering parts of five

counties: Caraș-Severin (with the largest share), Hunedoara, Gorj, Mehedinți, and Timiș. Geographically, according to the geomorphological zoning conducted by Posea & Badea (1984), the study area overlaps with the Retezat - Godeanu Group in the Southern Carpathians (Retezat Mountains, Godeanu Mountains, Țarcu Mountains, Cernei Mountains, Mehedinți Mountains, Vâlcău Mountains), Poiana Ruscă Mountains, and

Banat Mountains (Almăj Mountains, Semenici Mountains, Locva Mountains, Anina Mountains, Dognecei Mountains, and the associated depression areas). The altitude varies between 54 and 2473 m; the complexity of relief conditions (Rusu, 2007; Caluseru et al., 2015) imposes variability in environmental factors across the territory, which is reflected in the distribution of pasture vegetation.

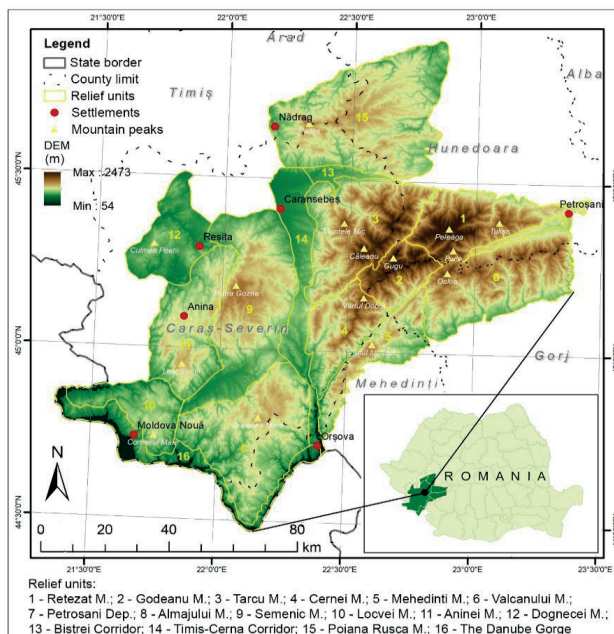


Figure 1. The location of the study area (processing after Posea & Badea, 1984; EEA-DEM, 2023; Geospatial, 2023)

In the analyzed area, with a total surface of 1,112,683 hectares (11,126.83 km²), forested areas predominated, covering approximately 70% of the territory, followed by grasslands, accounting for 14.75% (CLC, 2023). The other land use categories have proportions below 5%. Grasslands, totaling 164,092 hectares, are spread across the entire analyzed area, in all forms and relief units, with the largest areas found in hilly and mountainous regions.

The working methodology

For the analysis of the area of interest through remote sensing, Sentinel 2 satellite images from the year 2022 were used, downloaded for free from the Copernicus Open Access Hub platform. Five Moments of observation (M)

were established, noted as M1...M5: on 22.03, 16.05, 15.07, 08.09, and 18.10. Considering the large extent of the study area, four satellite scenes were downloaded for each M, with the indicators 34TER, 34TFR, 34TEQ, and 34TFQ. In the first stage, the satellite scenes were processed in the SNAP software, and the following operations were applied (Figure 2):

1. Mosaicking the four scenes from each Moment (M);
2. Extracting the area containing the area of interest (Subset);
3. Resizing the spatial resolution to 20 meters for all spectral bands (Resampling);
4. Generating fAPAR images using the algorithm implemented in the software.

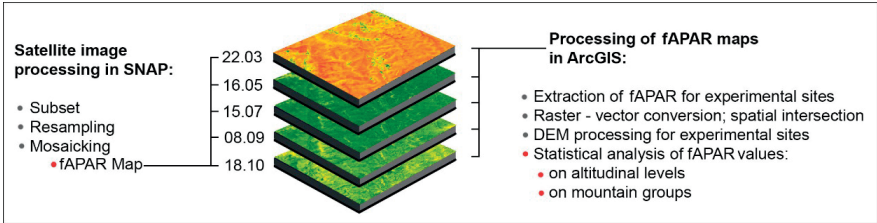


Figure 2. The workflow (Original diagram)

The second stage of the workflow involved processing geospatial data in ArcGIS according to the following algorithm:

1. Extraction of the area of interest from the fAPAR images based on a specific contour for each observation moment;
2. Classification of the Digital Elevation Model (DEM) with a spatial resolution of 25 meters (EEA, 2023) into 8 altitude classes: 53-300 m, 301-600 m, 601-800 m, 801-1000 m, 1001-1200 m, 1201-1400 m, 1401-1600 m, 1601-2473 m;
3. Selection of grassland test surfaces - from the Corine Land Cover database (2018 edition), 110 representative grassland surfaces were selected, located in areas with different environmental conditions and relief units;
4. Extraction of images and numerical values of fAPAR from each Moment for the selected grassland surfaces, which were subsequently used in the statistical analysis of the results;
5. Conversion of fAPAR maps for grasslands into vector format and spatial intersection of two datasets;

6. Statistical analysis of fAPAR values on altitude classes and mountain groups. The data were statistically evaluated using PAST Version 2.17c software (Hammer et al., 2001).

RESULTS AND DISCUSSIONS

Although fAPAR can be applied through in situ procedures, one of the most efficient ways to determine this index is the determination and representation on high spatial resolution photogrammetric images (Copăcean et al., 2020; Simon et al., 2020) or on satellite images, on a global or regional scale, depending on the needs of the studies (Liang & Wang, 2019; Jin et al., 2022; Cojocariu et al., 2024).

The analysis of grassland vegetation dynamics across the temporal moments M1 - M5 is based on the fAPAR values

For the study area, in the year 2022, five fAPAR images were generated; the images from the beginning (22.03) and from the end of the period (18.10) are presented in Figure 3.

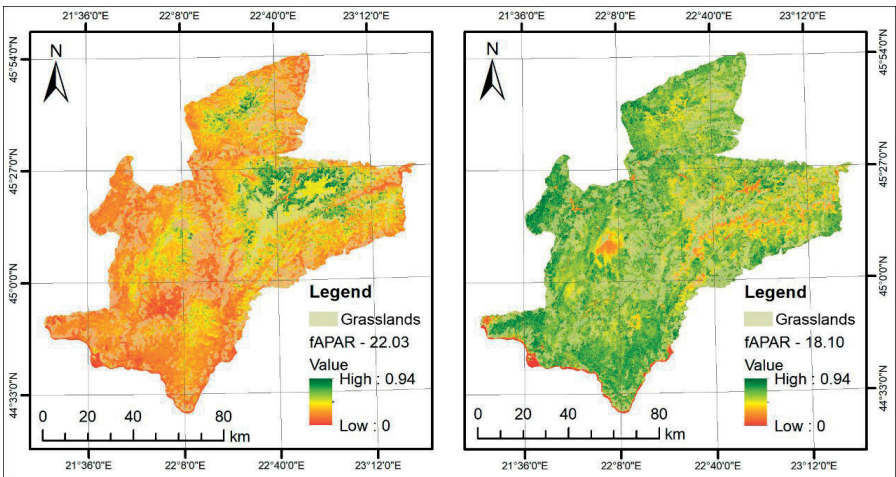


Figure 3. The spatial distribution of fAPAR values across different temporal moments

To analyze the changes produced during the considered period, the fAPAR values were classified into four equal classes, depending on the minimum and maximum value of the index. In M1 (March), for the selected grasslands, the fAPAR index ranged from 0 to 0.93, with the average value being very low at 0.15. In M1,

77% of the fAPAR values were between 0 and 0.25 (Figure 4), indicating that plants utilized only 25% of visible light to produce biomass. This suggests a low vegetation cover. The obtained results also agree with other studies (Jarocinska & Zagajewski, 2009).

The transitions matrix 22.03 - 16.05					
fAPAR	0.00-0.25	0.26-0.50	0.51-0.75	0.76-1.00	Total (ha)
0.00-0.25	138	2246	5101	1134	8619
0.26-0.50	193	1387	712	201	2493
0.51-0.75	0	5	36	5	47
0.76-1.00		0	4	0	5
Total (ha)	331	3639	5853	1341	11164

The transitions matrix 16.05 - 15.07					
fAPAR	0.00-0.25	0.26-0.50	0.51-0.75	0.76-1.00	Total (ha)
0.00-0.25	20	51	186	74	331
0.26-0.50	99	1445	1795	303	3642
0.51-0.75	188	1605	3456	605	5854
0.76-1.00	17	127	454	753	1351
Total (ha)	324	3228	5891	1735	11164

The transitions matrix 15.07 - 08.09					
fAPAR	0.00-0.25	0.26-0.50	0.51-0.75	0.76-1.00	Total (ha)
0.00-0.25	40	184	98	2	324
0.26-0.50	33	2155	1022	21	3230
0.51-0.75	2	873	4939	82	5896
0.76-1.00	0	26	966	738	1731
Total (ha)	74	3239	7025	843	11164

The transitions matrix 08.09 - 18.10					
fAPAR	0.00-0.25	0.26-0.50	0.51-0.75	0.76-1.00	Total (ha)
0.00-0.25	26	47	2	0	74
0.26-0.50	45	1317	1860	15	3237
0.51-0.75	23	1509	5243	249	7024
0.76-1.00	14	158	548	115	835
Total (ha)	108	3032	7652	380	11164

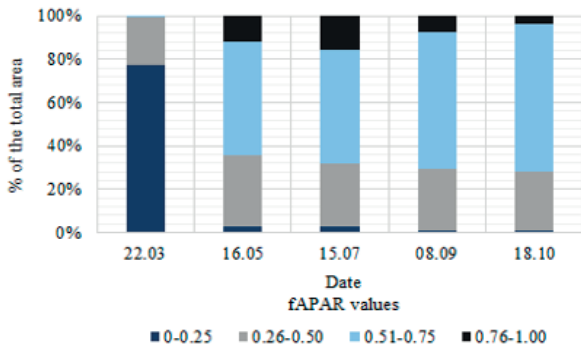


Figure 4. The variation of fAPAR values across M1 – M5

In M2 (May), in the analyzed grasslands, fAPAR values ranged from 0 to 0.94, with an average of 0.55. At this moment, compared to M1, there is an increase in the percentage of radiation utilized by plants, indicating a higher biomass "quantity" and consequently a higher degree of soil cover. In this scenario, 32% of fAPAR values fell between 0.26 and 0.50, and 52% fell within the range of 0.51-0.75. In M3 (July), the fAPAR index ranged from 0 to 0.94, with an average of 0.57. This period corresponds to the peak vegetation period in grasslands. In grasslands, vegetation is mosaic, and therefore in M3, there are four classes of fAPAR index values: 0-0.25 (3%); 0.26-0.50 (29%); 0.51-0.75 (53%); and 0.76-1.0 (16%).

In September (M4), it is observed that the fAPAR index values remain within the same limits as in M3, as a result of vegetation recovery after the rains at the end of summer. Surprisingly, for the analyzed area, in October (M5), 69% of fAPAR index values fell between 0.51-0.75, indicating that plants use visible radiation to a large extent (between 51-75%). This suggests a good state of grassland vegetation. To analyze the variations in fAPAR values in the defined temporal moments, Principal Component Analysis (PCA) was applied. This was done using the correlation matrix, without considering the grouping of the data values. The main components, with a Joliffe cut-off at 0.7, are presented in Table 1.

Table 1. Distribution of principal components based on PCA

PC	Eigenvalue	% variance
1	2.62473	52.495
2	1.61062	32.212
3	0.482899	9.658
4	0.217262	4.3452
5	0.0644861	1.2897

From Figure 5, it can be observed that the M1 vector exhibits the highest influence on the polygonal area described by the data values corresponding to the Southern Carpathian

Mountains (CM), indicating that in M1 (March), the greatest variation of the fAPAR index is observed, regardless of the altitude class.

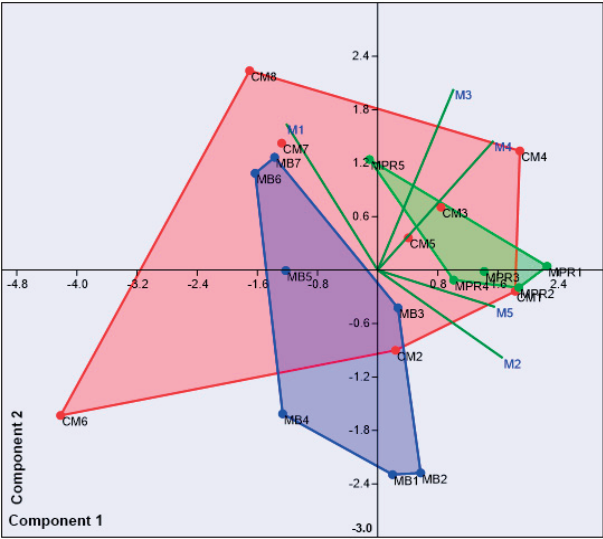


Figure 5. Graphical representation of the distribution of data values on principal components - PCA

The fAPAR index remained quite stable during intensive vegetative growth and with the onset of senescence, a situation also noted in other studies (Viña & Gitelson, 2005; Zhang et al., 2014; Sakowska et al., 2016).

The analysis of the fAPAR index across altitude classes within the analyzed mountain groups

Between the three mountain groups analyzed in the study, there are differences and many similarities across altitude classes, as presented in Figure 6.

Cluster analysis was performed using the Ward algorithm, with Euclidean distances as the similarity measure. As a result of the cluster analysis, a significantly strong correlation coefficient of 0.7886 was obtained.

The cluster analysis (Figure 6) highlights two large groups, A and B:

- Group A consists of CM6, CM8, CM7, MB6, MB7 – they are the upper floors of the high mountains, where the fAPAR values are similar and suggest that the vegetation has similar "behavior", independent of the mountain groups (CM and MB);
- Group B includes three different subgroups of which: B1 (MPR3, CM1, MPR2, CM4 and MPR1); B2 (MB4, MB1, MB2); B3, consisting of B3.1 (CM3, CM2, MB3, MPR4) and B3.2 (MB5, CM5, MPR5).

According to the cluster analysis, similarities were observed between different altitudinal steps, within the three groups of mountains. Within the same mountain group, the fAPAR index has similar values on several altitudinal levels.

The results show that the fAPAR values present a high degree of similarity from altitudes above 1001 m, in all the considered mountain units. Below the altitude of 1000 m, the grouping

based on similarity is different, most likely under the influence of local conditions, which influence the vegetation of the grasslands.

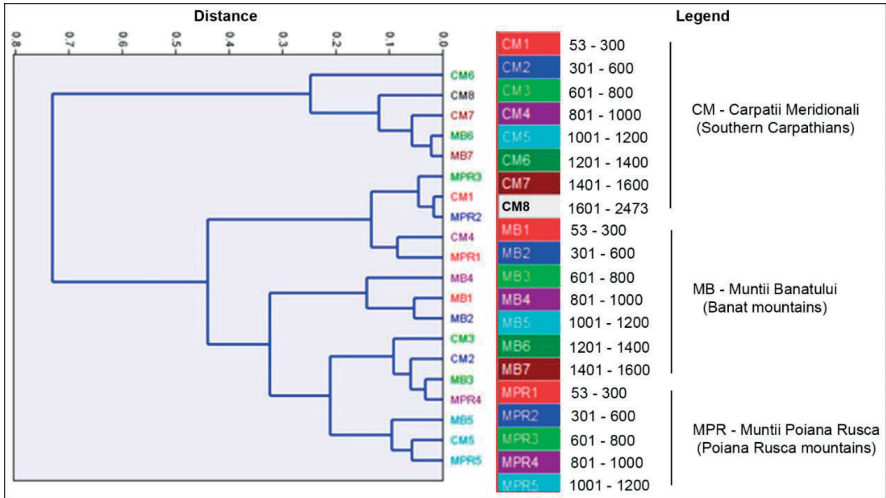


Figure 6. Cluster analysis based on the selection of altitude classes for all mountain groups

CONCLUSIONS

The fAPAR remote sensing index, applied through specific techniques, on satellite images, has demonstrated its usefulness in pratology through the analysis of grassland vegetation. Although they are data conditioned by the spatial resolution, they can be applied on extended surfaces, on altitudinal levels, vegetation seasons, in different periods of time. The analysis of the fAPAR index, between March and October, shows that the vegetation is very well represented and uses solar radiation to the maximum, in July (average values of 0.57) and that the vegetation is still stagnant and uses solar radiation to a reduced extent, in March (average of 0.15).

In the analyzed area, represented by the Retezat-Godeanu Group, the Poiana Ruscă Mountains and the Banatului Mountains, the fAPAR values showed variations, both from one time point to another, and on altitudinal levels, from one mountain group to another.

Such studies can be used, at different scales, to monitor the state of vegetation, to analyze the degree of vegetation coverage of grasslands and can be included in rural development or management programs, at the regional level.

REFERENCES

- ArcGIS Documentation. (2022). <https://desktop.arcgis.com/en/documentation/> (accessed on 25.10.2022)
- Caluseru, A.L., Cojocariu, L., Borlea, F., Bordean, D.-M., & Horablaga, A. (2015). Rural Development of Mountain Areas in Romania, Challenges and Targets for the Year 2020. In *Proceedings of the SGEM 2015 Conference Proceedings*, Albena, Bulgaria, 2, 791–798.
- Chen, B.X., Zhang, X.Z., Sun, Y.F., Wang, J.S., & He, Y.T. (2017). Alpine grassland fPAR change over the Northern Tibetan Plateau from 2002 to 2011. *Adv. Climate Change Res.*, 8, 108–116.
- Cojocariu, L.L., Copăcean, L., Ursu, A., Sărățeanu, V., Popescu, C.A., Horablaga, M.N., Bordean, D.-M., Horablaga, A., & Bostan, C. (2024). Assessment of the Impact of Population Reduction on Grasslands with a New “Tool”: A Case Study on the “Mountainous Banat” Area of Romania. *Land*, 13, 134.
- Copăcean, L., Cojocariu, L., Simon, M., Zisu, I., & Popescu, C. (2020). Geomatic techniques applied for remote determination of the hay quantity in agro-silvo-pastoral systems. *PESD*, 14(2), 89 – 101,
- Copernicus Land Monitoring Service - Corine Land Cover (CLC) Database, 2018 Edition, Available online: <https://land.copernicus.eu/pan-european/corine-land-cover> (accessed on 15.09.2022)
- Copernicus Open Access Hub, Available online: <https://scihub.copernicus.eu/dhus/#/home> (accessed on 11.10.2022)

- Epiphany, J.C.N., & Huete, A.R. (1995). Dependence of NDVI and SAVI on Sun/Sensor Geometry and Its Effect on fAPAR Relationships in Alfalfa. *Remote Sensing of Environment*, 51, 351-360.
- European Environment Agency (EEA), 2023, Digital Elevation Model (DEM), <https://www.eea.europa.eu/data-and-maps/data/copernicus-land-monitoring-service-eu-dem> (accessed on 13.11.2022)
- Fensholt, R., Sandholt, I., Rasmussen, M.S. (2004). Evaluation of MODIS LAI, fAPAR and the relation between fAPAR and NDVI in a semi-arid environment using in situ measurements. *Remote Sens Environ.*, 91(3-4), 490-507.
- Field, C.B., Randerson, J.T., & Malmström, C.M. (1995). Global net primary production: combining ecology and remote sensing. *Remote Sens Environ*, 51, 74-88.
- GCOS. (2006). Satellite-Based Products for Climate, Supplemental Details to the Satellite Based Component of the Implementation Plan for the Global Observing System for Climate in Support of the UNFCCC; Report GCOS-107 (WMO/TD No. 1338); World Meteorological Organization (WMO): Geneva, Switzerland
- Geospatial, 2023, România: seturi de date vectoriale generale – <http://geo-spatial.org/vechi/download/romania-seturi-vectoriale> (accessed on 18.08.2022).
- Hammer, O., Harper, D.A.T., Paul, D.R. (2001). Past: Paleontological statistic software package for education and data analysis. *Palaeontol. Electron*, 4(9). Available online: https://palaeo-electronica.org/2001_1/past/issue1_01.html.
- Jarocinska, A., & Zagajewski, B. (2009). Remote sensing tools for analysis of vegetation condition in extensively used agricultural areas. *International journal*, 1-6.
- Jin, H., Li, A., Liang, S., Ma, H., Xie, X., Liu, T., & He, T. (2022). Generating high spatial resolution GLASS FAPAR product from Landsat images. *Science of Remote Sensing.*, 6, 100060, 10.1016/j.srs.2022.100060.
- Liang, S., & Wang, J. (2019). Advanced Remote Sensing: Terrestrial Information Extraction and Applications (2e ed.), Academic Press/Elsevier, Cambridge, UK (accessed on 02.02.2024).
- Myneni, R.B., & Williams, L.D. (1994). On the Relationship between FAPAR and NDVI. *Remote Sensing of Environment*, 49, 200-211.
- Noumonvi, K.D., & Ferlan, M. (2020). Empirical vs. light-use efficiency modelling for estimating carbon fluxes in a mid-succession ecosystem developed on abandoned karst grassland. *PLoS One*, 15(8):e0237351. doi: 10.1371/journal.pone.0237351.
- Posea, G., & Badea, L. (1984). România. *Unitățile de relief (Regiunea geomorfologică)*. Ed. Științifică și Enciclopedică, București.
- Pu, J., Yan, K., Zhou, G., Lei, Y., Zhu, Y., Guo, D., Li, H., Xu, L., Knyazikhin, Y., & Myneni, R.B. (2020). Evaluation of the MODIS LAI/fPAR Algorithm Based on 3D-RTM Simulations: A Case Study of Grassland. *Remote Sens.*, 12, 3391.
- Qin, H., Wang, C., Zhao, K., & Xi, X. (2018). Estimation of the fraction of absorbed photosynthetically active radiation (fPAR) in maize canopies using LiDAR data and hyperspectral imagery. *PLoS ONE*, 13(5), e0197510. <https://doi.org/10.1371/journal.pone.0197510>.
- Rossini, M., Cogliati, S., Meroni, M., Migliavacca, M., Galvagno, M., Busetto, L., et al. (2012). Remote sensing-based estimation of gross primary production in a subalpine grassland. *Biogeosciences*, 9, 2565-84. 10.5194/bg-9-2565-2012.
- Rusu, R. (2007). *Organizarea spațiului geografic în Banat*. Ed. Mirton, Timișoara.
- Sakowska, K., Juszczak, R., & Gianelle, D. (2016). Remote Sensing of Grassland Biophysical Parameters in the Context of the Sentinel-2 Satellite Mission. *Journal of Sensors*, 16, 10.1155/2016/4612809.
- Șandera, J., & Ștych, P. (2020). Selecting Relevant Biological Variables Derived from Sentinel-2 Data for Mapping Changes from Grassland to Arable Land Using Random Forest Classifier. *Land*, 9, 420. <https://doi.org/10.3390/land9110420>.
- Sellers, P.J., Randall, D.A., Collatz, G.J., Berry, J.A., Field, C.B., Dazlich, D.A., et al. (1996). A revised land surface parameterization (SiB2) for atmospheric GCMs. Part I: Model formulation. *J. Climate*, 9(4), 676-705.
- Simon, M., Popescu, C.A., Copăcean, L., & Cojocariu, L. (2020). Complex model based on UAV technology for investigating pastoral space. *PESD*, 14(2), 139 – 150.
- Viña, A., & Gitelson, A.A. (2005). New developments in the remote estimation of the fraction of absorbed photosynthetically active radiation in crops. *Geophys Res. Lett.*, 32, L17403.
- Wang, Y., Xie, D., Liu, S., Hu, R., Li, Y., & Yan, G. (2016). Scaling of FAPAR from the Field to the Satellite. *Remote Sens.*, 8, 310.
- Xiao, Z., Liang, S., Wang, T., & Jiang, B. (2016). Retrieval of Leaf Area Index (LAI) and Fraction of Absorbed Photosynthetically Active Radiation (FAPAR) from VIIRS Time-Series Data. *Remote Sens.*, 8, 351. <https://doi.org/10.3390/rs8040351>.
- Xu, X., Tang, J., Zhang, N., Zhang, A., Wang, W., & Sun, Q. (2023). Remote Sensing Classification of Temperate Grassland in Eurasia Based on Normalized Difference Vegetation Index (NDVI) Time-Series Data. *Sustainability*, 15, 14973.
- Yang, F., Ren, H., Li, X., Hu, M., & Yang, Y. (2014). Assessment of MODIS, MERIS, GEOV1 FPAR products over Northern China with ground measured data and by analyzing residential effect in mixed pixel. *Remote Sens.*, 6(6), 5428-51.
- Zhang, Q., Cheng, Y., Lyapustin, A., Wang, Y., Gao, F., Suyker, A., Verma, S., & Middleton, E. (2014). Estimation of crop gross primary production (GPP): fAPAR_{chl} versus MOD15A2 FPAR. *Remote Sensing of Environment*, 153, 1-6, 10.1016/j.rse.2014.07.012.
- Zhang, F., Zhou, G., & Nilsson, C. (2015). Remote estimation of the Fraction of Absorbed Photosynthetically Active Radiation for a maize canopy in Northeast China. *Journal of Plant Ecology*, 8(4), 429-435, <https://doi.org/10.1093/jpe/rtu027>.

APPLICATION OF MACHINE LEARNING APPROACHES FOR LAND USE CHANGE MODELLING IN SURINAME

Tamara MYSLYVA¹, Marciano DASAI¹, Christiaan Max HUISDEN²,
Petro NADTOCHIY³, Yurii BILYAVSKIY⁴

¹Ministry of Spatial Planning and Environment of Suriname,
22 Prins Hendrikstraat, Paramaribo, Republic of Suriname

²Anton de Kom University of Suriname, Leysweg, 86 Paramaribo, Republic of Suriname

³Institute of Agriculture of Polissia NAAS of Ukraine,
132 Kyiv highway, Zhytomyr, Ukraine

⁴Zhytomyr Agricultural Technical Professional College,
96 Pokrovska Street, Zhytomyr, Ukraine

Corresponding author email: byrty41@yahoo.com

Abstract

Machine learning (ML) algorithm-based models represent cutting-edge techniques used for mapping, quantifying, and modelling changes in land use and land cover (LULC) over time. In this study, a comparative analysis was conducted on the multilayer perceptron neural network (MLP) and support vector machine classification (SVM) applied to LULC change detection and forecasting within the coastal plain territory of Suriname. Sentinel-2A satellite data covering the period from 2017 to 2022 was utilised, along with additional variables such as the distance from rivers, roads, and administrative cities in each district and slope and digital elevation models in the prediction models. The SVM algorithm based predictive model, incorporating an urbanization transition sub-model, exhibited an impressive accuracy of 83.85%, surpassing the MLP algorithm-based model, which did not exceed 64.63%. Consequently, this model is recommended for generating LULC change prediction maps. These maps can serve as a crucial baseline for the Surinamese government, providing valuable insights for policy development and sustainable land use management.

Key words: detection, machine learning, modelling, remote sensing, Suriname.

INTRODUCTION

Analysing spatiotemporal trends in land use and land cover (LULC) change is crucial for gaining insights into effective and sustainable land management (Girma et al., 2022; Devi & Shimrah, 2023). This is particularly pertinent given the widespread prevalence of extensive LULC changes globally, especially in developing countries, where such transformations have become notably common in recent decades (Kafy et al., 2021). Similarly, Suriname has experienced pronounced LULC changes in the last decades, marked by a significant expansion of built-up areas at the expense of other LULC types, predominantly forest-covered and agricultural lands. Specifically, Suriname is struggling with illegal artisanal gold mining, causing large-scale contamination in the environment (Huisden et al., 2020a), as well as illegal deforestation that endangers biodiversity, degrades air and water quality, and leads to undesirable land use

changes (Huisden et al., 2020b). LULC change modelling is an innovative technique for monitoring and managing land resources (Anurag & Pradhan, 2018) and has proven to be an essential tool for land use forecasting (Rozario et al., 2017). Modelling demonstrates the capability to efficiently represent and forecast complex LULC systems by incorporating multiple variables (Wang et al., 2021). These driving variables are represented by various geospatial data, which can be acquired through the use of satellite remote sensing data and geographical information system techniques (Kafy et al., 2021). Frequently employed models for predicting changes in land use encompass statistical models (Hyandye 2015; Yeh & Liaw, 2021), evolutionary models (Aitkenhead & Alders, 2009), cellular models (Muhammad et al., 2021), Markov models (Mohamed & Worku, 2020), hybrid models (Marquez et al., 2019), and multi-agent-based models (Ralha et al., 2013). Among these, the most widely utilised

are cellular and Markov chain analyses, along with their amalgamated form known as the CA-Markov model (Dey et al., 2021). Markov chain analysis, a random stochastic modelling method discrete in both time and state (Myslyva et al., 2021), outlines LULC transitions from one time period (t_1) to the next (t_2), enabling the projection of future changes (Rongqun et al., 2011). While Markov analysis is widely employed for simulating and predicting land use changes, it does have some drawbacks, making it more suitable for short-term projections (Sinha & Kumar, 2013). Notably, it lacks consideration for the spatial allocation of information within each class, and the probabilities of change between landscape states are not constant. As a result, while it can provide accurate magnitudes of change, it may not accurately indicate the direction of land use and land cover (LULC) changes (Wang et al., 2021). To augment the predictive capabilities of the Markov chain model, various techniques are implemented. Among these, a promising approach involves incorporating machine learning techniques, such as artificial neural networks or support vector machines, to complement the Markov model (Gharaibeh et al., 2020; Girma et al., 2022). This integration aims to enhance the model's capacity to capture intricate relationships and non-linear patterns in land-use change dynamics, thereby facilitating more accurate predictions of future land-use scenarios (Wang et al., 2021).

Despite the apparent occurrence of land use changes in the Suriname context, a notable gap exists in studies specifically addressing the detection of current trends and the prediction of future dynamics in the country's land use and land cover. This research void impedes a comprehensive understanding of the dynamic land use patterns in Suriname, limiting the ability to make informed decisions for sustainable development. Taking into account the aforementioned challenges, this study pursues a threefold objective: (1) to collect and process initial geospatial data on land use and land cover; (2) to evaluate the accuracy and reliability of two machine learning algorithms (MLP - multilayer perceptron neural network; SVM - support vector machine classification) in predicting future land use changes within Suriname; and (3) to develop a robust simulation

model using the most effective machine learning algorithm identified from the comparative analysis. The simulation model is specifically designed to predict LULC changes over the upcoming 10-year period, aiming to provide valuable insights for strategic planning and decision-making in the context of Suriname's sustainable development.

MATERIALS AND METHODS

Study area. The studies were conducted in Suriname, a country situated north of the equator on the north-eastern coast of South America. Suriname's geographical coordinates extend from 1°50.45' N to 6°0.35' N and 53°59.08' W to 54°33.49' W. Geologically, over 80% of Suriname comprises the deeply weathered, rainforest-covered Precambrian Guiana Shield, extending east and south to the Amazon River in Brazil and west to the Orinoco River in Venezuela. Major rivers in the country include the Marowijne River, Commewijne River, Suriname River, Saramacca River, Coppename River, Nickerie River, and Corantijn River.

Suriname covers an area of approximately 16.4 million hectares and is divided into ten administrative districts, eight of which fall within the study area: Marowijne, Commewijne, Wanica, Paramaribo, Para, Saramacca, Coronie, and Nickerie (Figure 1). The study area, covering 25,755 km², is located in the northern part of Suriname within the Young Coastal Plain. This area ranges in width from about 20 km in the east to about 100 km in the west, with elevation variations of 0–4 m above mean sea level (MSL). Additionally, the study area includes the Old Coastal Plain, formed on remnants of ridges, gullies, and mud flats, with elevation variations of 4–10 m above MSL, and the Cover Landscape (also known as the Savannah Belt), ranging from 10 to 100 m above MSL (Ouboter & Jairam, 2012).

The climate of the study area is tropical-equatorial (Af), tropical monsoon (Am) and tropical savanna climate (Aw/As) (due to Köppen-Geiger climate classification). The average daily temperature varies from 26°C in January to 31°C in October. Average annual rainfall within the coastal plains ranges from 1500 to 1700 mm. The soil cover of the study area is represented by Umbric Glaysols, Albic

Arenosols, Albic Plintosols and Fibric Histosols according to the international soil classification system (WRB, 2014) (Gardi et al., 2015).

digital elevation model (DEM) was downloaded from the freely accessible 30-meter SRTM Tile Downloader (Table 1).

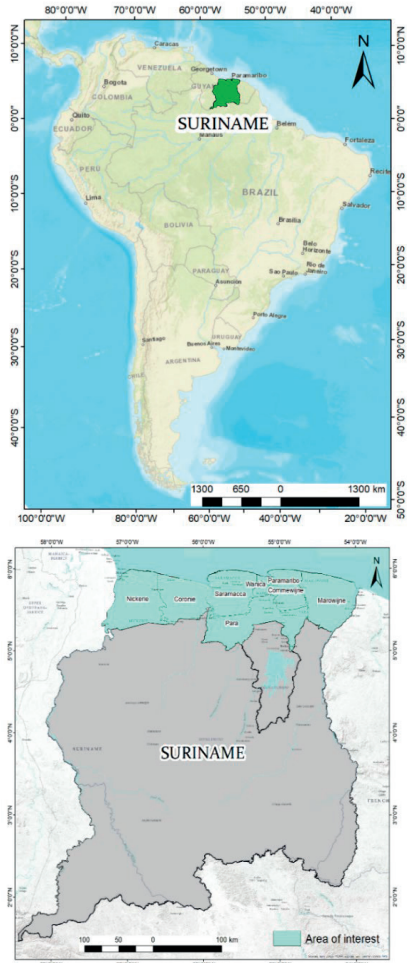


Figure 1. Location of the study area

Datasets used. In this study, three remotely sensed satellite images were employed to analyze LULC change dynamics. The Sentinel-2 L2A image scenes, which were classified and converted into LULC maps, were obtained from the freely accessible Esri land cover data portal. The downloaded raster images were pre-geo-referenced in a latitude/longitude projection (EPSG:4326) with a datum and ellipsoid of WGS84. Additionally, the road-river network map and administrative cities of the district locations within the study area were acquired from OpenStreetMap (www.openstreetmap.org). The

Table 1. Characteristics of data collected

Data	Source	Acquisition year	Scale/Resolution
Multispectral satellite imagery	Esri Land Cover: https://livingatlas.arcgis.com/landcover/	2017 2021 2022	10 m
Digital Elevation Model	30-Meter SRTM Tile Downloader: https://dwtkns.com/srtm30m/	2018	1-arcsecond (3601x3601 pixels)

Slope, distance from rivers, distance from roads, and distance from urban datasets were developed through individual elaboration in 2023 with a resolution of 10 m.

These datasets underwent processing in QGIS 3.34 and ArcGIS 10.8 packages, involving operations such as projection to WGS 84 UTM Zone 21N, data conversion, DEM masking, and separation of road networks from other features (rivers) using the Query tool. The Euclidean distance function was employed to generate distance maps from roads, rivers/creeks, and urban areas using vector data of the features (Gharaibeh et al., 2020; Kafy et al., 2021). The DEM was manipulated in ArcGIS spatial analyst tools to create elevation and slope maps.

LULC change detection and simulation. Land Change Modeler (LCM) built in TerrSet software version 18.31 was utilized to detect and simulate future LULC changes. This empirically driven, stepwise process involves change analysis, transition potential modelling, and change prediction (Eastman, 2016), based on historical changes from time 1 ($t_1 = 2017$) to time 2 ($t_2 = 2021$). The Markov probability matrix was employed to determine the probability of converting from the current state (LULC class) to another state in the next period. Low and high transitions were assigned probabilities near 0 and 1, respectively (Sinha & Kumar, 2013; Wang et al., 2021). Gains and losses to each LULC category were identified, and transitions from one land cover state to another were used to generalize the spatial changing pattern (Dey et al., 2021; Leta et al.,

2021). Recognizing the need to incorporate the potential influence of independent variables in simulating LULC changes (Gharaibeh et al., 2020), this study considered six key driver variables. These variables include distances from rivers/creeks, roads, and administrative centres within the district, as well as terrain relief and slope represented by the DEM. Land cover transition potentials, indicating the likelihood of land transitioning from one class to another in the future, were determined using various methodologies, including a multi-layer perceptron neural network and support vector machine learning algorithms. Driver variables were inputted into the LCM transition sub-model, and machine learning algorithms were employed to generate potential transition maps using the dependent variables (2017 and 2021 imagery). Subsequently, hard predictions for the LULC changes in the year 2022 were generated. For every modelling approach, four transition sub-models were tested.

Validation of model outputs. The validation process was conducted to assess the agreement and disagreement between the actual and simulated LULC maps of 2022, ensuring the reliability and acceptance of different model approaches in predicting the future scenario in 2026 and 2031 (Dey et al., 2021; Kafy et al., 2021). Two distinct validations were carried out using the VALIDATE module in TerrSet and the ROC Tool of ArcSDM. The VALIDATE module computed kappa index statistics using the hard prediction as a comparison map, including kappa for no information (K_{no}), kappa for grid cell level location ($K_{location}$), kappa for stratum-level location ($K_{locationStrata}$), and kappa standard ($K_{standard}$) (Mishra et al., 2018; Girma et al., 2022). A strong and acceptable Kappa value is typically associated with values around 80% and above (Gharaibeh et al., 2020; Girma et al., 2022). The second method employed for estimating LULC change model performance was the Receiver Operating Characteristic (ROC). The area under the ROC curve (AUC) was calculated, representing the discriminatory power of the model in accurately predicting the occurrence or non-occurrence of land use change (Arabameri et al., 2019; Arora et al., 2021). AUC values were interpreted as follows: <0.6 (poor), 0.6-0.7 (moderate), 0.7-0.8 (good), 0.8-0.9 (very good), and >0.9 (excellent) model

performance (Nhu et al., 2020). For future predictions, the images of 2017 and 2021 were considered as the dependent variables to simulate the LULC maps of 2026 and 2031. Figure 2 illustrates the modelling and validation processes employed in this study.

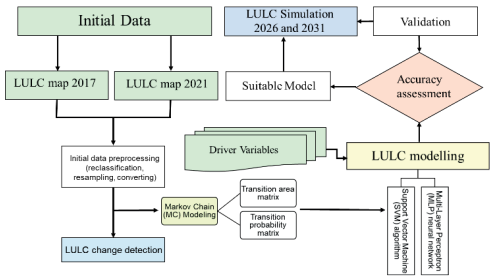


Figure 2. Research design flowchart

RESULTS AND DISCUSSIONS

Analyzing and comprehending the historical alterations in LULC dynamics is essential for predicting forthcoming trends in the coming decades (Regasa et al., 2021; Girma et al., 2022). The study area underwent landscape modifications, and diverse land use changes were observed during the period spanning from 2017 to 2021, as illustrated in Table 2 and Figure 3. Despite the overall stability in the structure of land cover, with over 80% of the territory remaining forested, a discernible trend was noted in the increase of flooded areas, constituting a net change of 25.7% of the total area.

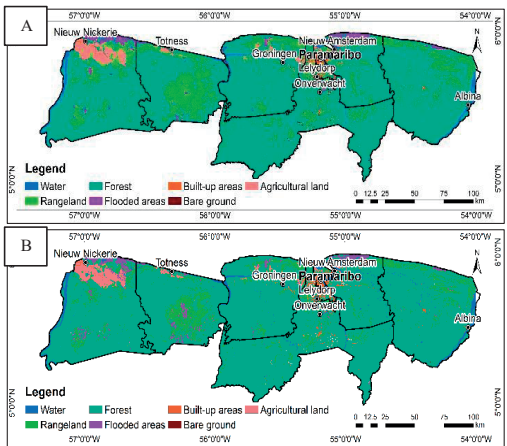


Figure 3. LULC maps for 2017 (A) and 2021 (B)

Several factors may contribute to the increase in flooded areas in Suriname: (a) changes in precipitation patterns and increased rainfall intensity due to global climate change; (b) human activities, such as deforestation, urbanization, or changes in agricultural practices, can alter or block natural waterways; (c) poorly designed or maintained drainage and flood control infrastructure.

Table 2. Area and net change of LULC classes

LULC class	Area, ha		Annual change, ha/year	Net change, % of area
	2017	2021		
Water	63755.9	66927.6	792.9	5.0
Forest	2112756.7	2146469.8	8428.3	1.6
Flooded areas	42030.8	52824.5	2698.4	25.7
Agricultural land	64147.9	59966.0	-1045.5	-6.5
Built-up areas	33765.8	37060.2	823.6	9.8
Bare ground	7370.4	266.9	-1775.9	-96.4
Rangeland	251705.8	212018.2	-9921.9	-15.8

Anthropogenic activities related to the development of buildings and constructions, especially intensive in coastal regions, coupled with uncontrolled and unjustified impacts on the hydrological regime, have played a crucial role in the rise of flooded areas. This is evidenced by a rapid annual increase in built-up areas, exceeding 820 hectares during the observation period. Gains and losses for the respective study period were acquired from the TerrSet LCM change analysis module and represented by a graph in Figures 4 and 5. The most significant increase occurred in forest-covered areas, while rangeland experienced a notable decrease throughout the entire period. The transitional area matrix contains the pixel number that is expected to change from each LULC class over the specified time frame (Eastman, 2016). Table 3 represents the detailed transition area matrix of each LULC class between 2017 and 2021.

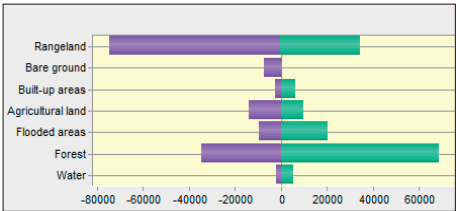


Figure 4. Gains and losses graph between 2017 and 2021 (ha)

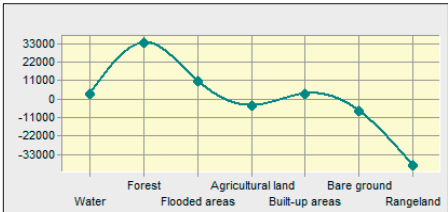


Figure 5. Net change graph between 2017 and 2021 (ha)

Table 3. Transition area matrix (thousand ha) of LULC between 2017 and 2021

	2021							Total
	Water	Forest	Flooded areas	Agricultural land	Built-up areas	Bare ground	Rangeland	
2017								
Water	61.5	1.2	0.6	0.1	0.0	0.0	0.3	63.8
Forest	2.2	2078.0	5.4	2.3	1.8	0.0	23.1	2112.8
Flooded areas	0.9	5.7	32.4	0.3	0.0	0.0	2.7	42.0
Agricultural land	0.7	3.7	2.5	50.1	0.5	0.0	6.7	64.1
Built-up areas	0.0	1.7	0.0	0.3	31.1	0.0	0.6	33.8
Bare ground	1.2	2.0	0.1	0.2	2.4	0.2	1.4	7.4
Rangeland	0.4	54.3	12.0	6.6	1.3	0.0	177.2	251.7
Total	66.9	2146.5	52.8	60.0	37.1	0.3	212.0	2575.5

In summary, there are notable changes in forest-covered and flooded areas, agricultural land, built-up areas, bare ground, and rangeland over the specified period. Rangeland, in particular, stands out with a considerable reduction, while forest and agricultural land show substantial increases. The outcomes of the LULC change analysis serve as the foundation for constructing transition sub-models. Based on these results, considering the most significant gains and losses for each land use class, four sub-transition models are identified (Table 4). The factors influencing changes in land use are identified through spatial analysis and incorporated into the model as either static or dynamic components to enhance its accuracy (Leta et al., 2021). This study utilized topography and proximity factors for predicting LULC changes. Before integrating these drivers into the predictive model, selected driver variables underwent testing to assess their explanatory power, with Cramer's V used to

measure the strength of association and P values used for statistical significance evaluation (Table 5).

Table 4. Transition sub-models and their descriptors

Transition sub-model	Description	Land cover transition
Afforestation	Other land classes are converted to forest	Rangeland to forest Agricultural land to forest Bare ground to forest
Urbanization	Other land classes are converted to built-up areas	Bare ground to built-up areas Rangeland to built-up areas Agricultural land to built-up areas Forest to built-up areas
Flood intensification	Other land classes are converted to flooded areas or flooded areas are converted to water	Rangeland to flooded areas Agricultural land to flooded areas Flooded areas to water
Desolation	Agricultural land converted into other land classes	Agricultural land to flooded areas Agricultural land to built-up areas Agricultural land to forest Agricultural land to water

Table 5. Cramer’s V and p-value for each of the explanatory variables

Driver variables	Cramer’s V	p-value
Elevation	0.388	0.0000
Slope	0.379	0.0000
Distance from rivers	0.149	0.0000
Distance from roads	0.140	0.0000
Distance from urban	0.214	0.0000
Evidence Likelihood	0.763	0.0000

According to Eastman (2016), Cramer’s V values of 0.15 or higher are considered ‘useful,’ while values of 0.4 or higher are deemed ‘good.’ Variables such as elevation, slope, and distance from rivers and urban areas are considered useful for predicting transitions. On the other hand, variables like distance from roads have low Cramer’s V values, indicating that their effect on LULC change in the study area is not critical. The assessment of evidence likelihood serves as a means to determine the relative frequency of pixels representing various LULC classes within changing areas. This approach is particularly recommended in instances where Cramer’s V values are low (Gibson, 2018). The results obtained from evidence likelihood are deemed satisfactory in this study, serving as a quantitative measure of the frequency of change observed between rangeland and all other land classes.

The skill measures and accuracy rates of each sub-model were calculated using MLP and SVM, and the results are summarized in Tables

6 and 7. Despite numerical data indicating a higher accuracy rate for MLP (Girma et al., 2022; Leta et al., 2021; Gharaibeh et al., 2020; Gibson et al., 2018, and others), SVM demonstrated a higher predictive ability in the current study. For the MLP sub-model, accuracy varies from 20.06% to 64.63%, while for SVM, its value fluctuates from 47.82% to 83.85%.

Table 6. Sub-models included in MLP with associated performance indicators

		M i n i s s u i c e l l s t h a t r a n s i t i o n	C l a s s i f i c a t i o n	S u b - m o d e l	Sub- model skill	RMSE	
						T r a n s i t i o n	T e s t i n g
A f f o r e s t a t i o n	Transition to the forest-covered land: Agricultural land Bare ground Rangeland Persistence: Agricultural land Bare ground Rangeland	195508 15514	 0 4 2 3 3	 5 1 9 4	0.0628 0.1816 0.4124 0.3957 0.9090 0.5762	0 3 8 0	0 3 8 3
U r b a n i z a t i o n	Transition to built-up areas: Forest Agricultural land Bare ground Rangeland Persistence: Forest Agricultural land Bare ground Rangeland	48112 15514	 0 4 7 4	 5 4 3 6	-0.1429 0.5596 0.7525 0.9157 0.4597 0.5038 0.0304 0.7410	0 2 6 9	0 2 6 6
F l o o d i n t e n s i f i c a t i o n	Transition to water and flooded areas: Flooded areas* Agricultural land** Rangeland** Persistence: Flooded areas Agricultural land Rangeland	94899 3237518	 0 5 7 6	 6 4 6 3	0.5851 0.7067 0.7825 0.4308 0.5319 0.4182	0 2 8 2	0 2 8 6
D e s o l a t i o n	Transition: Agricultural land to water Agricultural land to forest Agricultural land to flooded areas Agricultural land to built-up areas Persistence: Agricultural land	48112 12133	 0 0 0 8	 2 0 6	-0.2500 1.0000 -0.2500 -0.2500 -0.2500	0 4 4 2	0 4 4 2

Note: * - transition to water; ** - transition to flooded areas.

Table 7. Sub-models included in SVM with associated performance indicators

Sub-model	Transition/Persistence class	Su b m o d e l	CV a c c u r a c y	Out- of- sam ple a c c u r a c y	Skil l m e a s u r e
Agricultural land	Transition to the forest-covered land:				
	Agricultural land	1637	0.7248	0.7345	0.4689
	Bare ground	1063	0.6540	0.6656	0.3312
	Rangeland	1863	0.6824	0.6716	0.3432
	Persistence:				
	Agricultural land	1648	0.6348	0.6300	0.2600
Urbanization	Bare ground	1080	0.9264	0.9111	0.8223
	Rangeland	1881	0.5468	0.5294	0.0588
	Transition to built-up areas:				
	Forest				
	Agricultural land	840	0.9056	0.9149	0.8299
	Bare ground	1664	0.9104	0.9005	0.8010
Flooded areas	Rangeland	490	0.8400	0.8486	0.6972
	Persistence:				
	Forest	735	0.9100	0.9150	0.8301
	Agricultural land	879	0.7652	0.7772	0.5544
	Bare ground	1664	0.5924	0.5841	0.1683
	Rangeland	502	0.9700	0.9664	0.9328
Intercropping		736	0.8148	0.8036	0.6072
	Transition to water and flooded areas:				
	Flooded areas*	1519	0.8268	0.8266	0.6533
	Agricultural land**	894	0.8088	0.8013	0.6026
	Rangeland**	1328	0.7816	0.7862	0.5724
	Persistence:				
Decision	Flooded areas	1530	0.5712	0.5707	0.1414
	Agricultural land	904	0.8448	0.8355	0.6709
	Rangeland	1369	0.6932	0.6759	0.3517
	Transition:				
	Agricultural land to water	2200	0.2900	0.2474	0.0593
	Agricultural land to forest	2293	0.6208	0.6170	0.5213
Sol	Agricultural land to flooded areas	1623	0.6212	0.6963	0.6204
	Agricultural land to built-up areas	1836	0.6100	0.5855	0.4819
	Persistence:				
	Agricultural land	2292	0.2492	0.2501	0.0626

Both SVM and MLP are commonly used machine learning algorithms for classification tasks, including LULC change prediction. The choice of algorithm can depend on various factors, and the fact that SVM demonstrated higher accuracy than MLP may be influenced by several reasons: (1) SVM is known for its effectiveness in handling high-dimensional data and complex decision boundaries. Considering that our LULC change prediction task involves a non-linear and complex relationship between input features, SVM performs better than MLP; (2) SVM can be more robust when dealing with small datasets. In the current study, the dataset is limited (considering dependent variables for 5 years), and due to this, SVM generalizes better than MLP, which could be more prone to overfitting; (3) the performance of both SVM and MLP heavily depends on parameter tuning. It's possible that the hyperparameters of the SVM were tuned more effectively for this specific dataset, leading to better performance; (4) SVM is effective in high-dimensional spaces and excels in capturing complex relationships, while MLP might require more data to effectively train its parameters, especially when dealing with a high-dimensional feature space; (5) SVM is generally robust to outliers present

in the dataset, and it can utilize the kernel trick to transform the input space into a higher-dimensional space, making it more adaptable to non-linear relationships. It's important to note that the performance of machine learning algorithms is highly dataset-dependent, and utilizing SVM is more effective for small datasets than employing MLP. The higher accuracy is demonstrated by the model with the following parameters (Table 8).

Table 8. Model parameters and accuracy

Parameter	Value
Modelling approach	SVM learning algorithm
Sub-model	Urbanization
Kernel type	Radial Basis Function
Epsilon (ϵ)	0.0100
Class number	8
Total CV number	7510
Total sample number	20000
Overall CV accuracy	0.8385
Overall out-of-sample accuracy	0.8388
Overall skill measure	0.6776

Note: CV - cross-validation.

To validate the model, the Kappa statistic (k-index) for quantity and location was computed by comparing the hard simulation with the reference map of 2022 (Table 9).

Table 9. The k-index values of the simulated LULC map of 2022

Index	Value
K _{no}	0.9695
K _{location}	0.9724
K _{locationStrata}	0.9724
K _{standard}	0.9547

The statistics reveal that all kappa index values surpass the satisfactory range ($\geq 80\%$). The overall disagreement between the reference and predictive maps is generally low, primarily attributed to allocation errors (0.0160) rather than quantity errors (0.0107). Despite the presence of allocation errors, the overall agreement between the actual and simulated maps is high, reaching 97.34% (Figure 6). The validation and assessment of the results from the simulation of (LULC) changes were conducted using the ROC curve to evaluate prediction accuracy. The area under the ROC curve serves as an indicator of the forecasting model's ability to correctly anticipate the occurrence or non-occurrence of pre-defined 'events' (Arora et al., 2021; Myslyva et al., 2023).

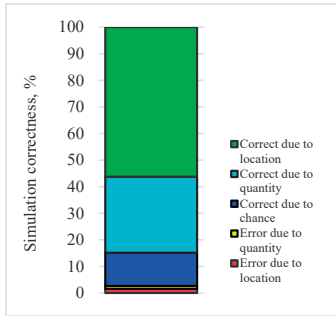


Figure 6. Successes and errors of the simulation

The model's prediction rate has been computed and is depicted in Figure 7.

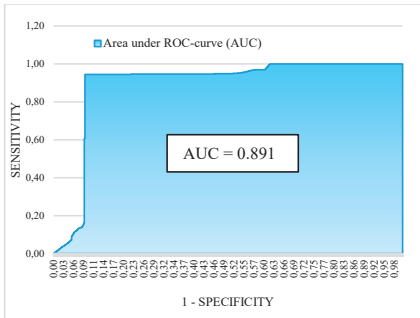


Figure 7. Performance of the model based on SVM for the LULC change prediction

The predictive model demonstrates an accuracy of 89% ($AUC = 0.891$), indicating a 'very good' performance level. The developed model was then used to predict future land use and land cover (LULC) changes in 2026 and 2031 under the business-as-usual (BAU) scenario.

The simulated area extent, gains, losses, and net change (in hectares) are depicted in Figures 8-10.

Notably, in the context of land use land cover modelling, a business-as-usual scenario involves projecting future land use patterns based on the assumption that current trends and practices persist without significant alterations. Considering this, the expansion of built-up areas (8.6% and 8.3%) is expected by 2026 and 2031, respectively. In contrast, the forest-covered area (0.1%), agricultural land (0.7%), and rangeland (0.4%) are expected to decrease, while bare ground will experience a decrease until 2026 (23.4% of the area) and subsequent growth of 3.7% by 2031.

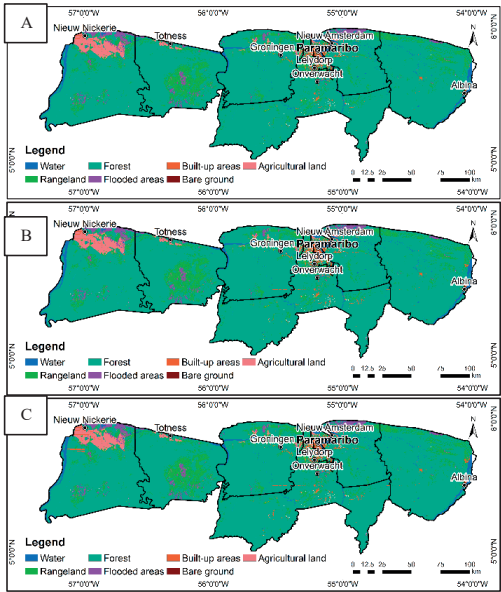


Figure 8. Existing (A) LULC map for 2022 and projected LULC maps for 2026 (B) and 2031 (C)

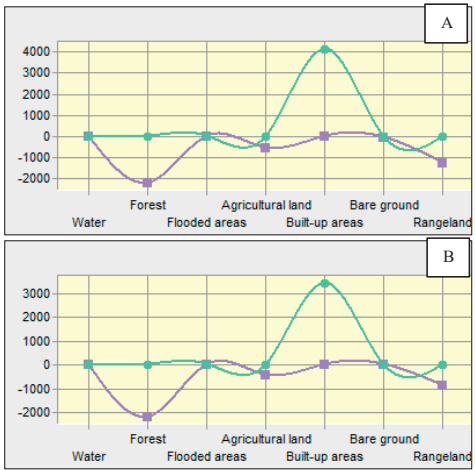
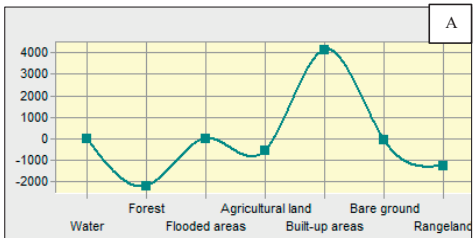


Figure 9. Gains and losses (ha) graph between 2022-2026 (A) and 2026-2031 (B)



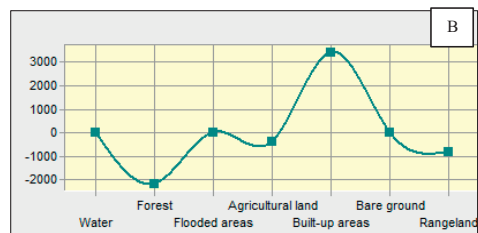


Figure 10. Net change (ha) graph between 2022-2026 (A) and 2026-2031 (B)

The forecast indicates that the Wanica and Nickerie districts will experience the most significant changes, while minor LULC changes are expected in Para and Marowijne. In general, two significant trends will be observed in the upcoming 10-year period. One involves the drastic expansion of urbanization, and the second is associated with deforestation and the shortage of agricultural land (Table 10).

Table 10. Descriptions and explanations for observed trends in LULC changes (2022-2031 predictions)

LULC class	Trend	Explanation	Required activities
Water and flooded areas	The water area will remain constant	A stable water area indicates a consistent presence of water bodies, such as rivers, lakes, and coastal areas. This stability is vital for maintaining ecosystem health and supporting various aquatic life forms	Sustainable water management practices are crucial to support wetland ecosystems
Forest	The forest area will gradually decline (net changes will amount to 0.1%)	Forest reduction is influenced by logging and infrastructure development	Sustainable forestry management practices are crucial to balance conservation efforts and economic activities
Agricultural land	Agricultural land will decrease slightly (net changes will amount to 0.7%)	This trend indicates a shift in land use due to urbanization	Supporting the balance between food production needs and environmental conservation is essential
Built-up areas	Built-up areas will significantly increase (net changes will amount to more than 8.0%)	The substantial growth in built-up areas signals urbanization and infrastructural development which drives the expansion of residential, commercial, and industrial spaces	Implementing crucial measures, such as sustainable urban planning practices, enforcing zoning regulations and engaging local communities in decision-making, is essential
Bare ground	The bare ground will fluctuate (an annual decrease of 23% for 2022–2026 and an annual increase of 4% for 2026-2031)	Fluctuations in bare ground could result from natural processes like erosion, reforestation efforts, or human activities	Monitoring and managing bare ground are essential for preventing soil degradation and maintaining ecosystem health
Rangeland	Rangeland will gradually decrease (net changes will amount to more than 0.4%)	The decline in rangeland is influenced by factors such as urban expansion or changes in land use practices	Sustainable land management strategies are crucial to balance urban expansion with the preservation of natural habitats

Considering that Suriname faces a significant shortage of land resources suitable for building, infrastructure development, and agricultural activity, coupled with the continued use of the most productive land parcels for building construction, there is a pressing need to implement an urgent land management plan.

Such a plan will help mitigate the negative consequences of irrational land use during the last decade.

CONCLUSIONS

The transformation in land use and land cover within the coastal plain area of Suriname from 2017 to 2031 was simulated using various geospatial methodologies alongside the SVM machine learning algorithm. This research utilized a range of dependent/driver and independent spatial datasets. TerrSet software was employed for assessing LULC changes, including statistical and graphical analyses of gains, losses, and net changes.

Topographical features, proximity variables, and evidence likelihood (related to the transition from rangeland to other land classes) were identified as the primary drivers of LULC change. Evidence likelihood is the most influential parameter, while distance from roads has the least effect in this study. To enhance the accuracy of future predictions, it is advisable to expand the list of independent variables to include additional information, such as weather data. When considering scenarios other than business-as-usual, it becomes necessary to augment the list of driving variables with geospatial data corresponding to the distance from deforested areas and areas with illegal mining.

Two machine learning algorithms, MLP and SVM, were tested for their ability to predict LULC change. To evaluate the accuracy and reliability of MLP and SVM algorithms-based predictive models, skill measures and accuracy rates were utilized. The SVM algorithm-based predictive model, which included the urbanization transition sub-model (bare ground, agricultural land, rangeland, and forest converted to built-up areas), demonstrated an overall skill of 0.7 and an accuracy of 83.85%. It's important to note that the performance of machine learning algorithms can be highly dataset-dependent, and the superiority of one algorithm over another may vary across different applications and datasets.

The prediction results for 2022 from the SVM algorithm-based model were further validated using the VALIDATE and ArcSDM modules, based on the actual reference image (2022). The

derived Kappa statistics (95%) and AUC value (89%) ensure the reliability of the SVM algorithm-based model in predicting land use changes. Future LULC changes for 2026 and 2031 were forecasted, considering the business-as-usual scenario. The model predicts an expansion of built-up areas between 2026 and 2030, accompanied by a reduction in forest, agricultural land, and rangeland.

Given that individual districts in Suriname possess distinct characteristics that can significantly influence future land use change predictions, forthcoming studies should undertake an examination to develop more detailed tailored predictive models. These models should encompass specific driving variables that are highly significant for each respective district

REFERENCES

- Aitkenhead, M. J., Aalders, I. H. (2009). Predicting land cover using GIS, Bayesian and evolutionary algorithm methods. *Journal of Environmental Management*, 90(1), 236–250.
- Anurag, Saxena, A., & Pradhan, B. (2018). Land use/ land cover change modelling: issues and challenges. *Journal of Rural Development*, 37(2), 413–424.
- Arabameri, A., Rezaei, K., Cerda, A., Conoscenti, C., Kalantari, Z. (2019). A comparison of statistical methods and multi-criteria decision-making to map flood hazard susceptibility in Northern Iran. *Science of the Total Environment*, 660, 443–458.
- Arora, A., Pandey, M., Siddiqui, M. A., Haoyuan, H., Mishra, V. N. (2021). Spatial flood susceptibility prediction in Middle Ganga Plain: comparison of frequency ratio and Shannon's entropy models. *Geocarto International*, 36(18), 2085–2116.
- Devi, A. R., Shimrah, T. (2023). Modelling LULC using Multi-Layer Perceptron Markov change (MLP-MC) and identifying local drivers of LULC in the hilly district of Manipur, India. *Environmental Science and Pollution Research International*, 30(26), 68450–68466.
- Dey, N. N., al Rakib, A., al Kafy, A., Raikwar, V. (2021). Geospatial modelling of changes in land use/land cover dynamics using multi-layer perception Markov chain model in Rajshahi City, Bangladesh. *Environmental Challenges*, 4, 100148.
- Eastman, J. R. (2016). *TerrSet Manual, Geospatial Monitoring and Modeling System*. Clark University, Worcester, USA. Clark University, Worcester, USA.
- Gardi, C., Angelini, M., Barceló, S., Comerma, J., Cruz Gaistardo, C. and all (2015). *Soil Atlas of Latin America and the Caribbean*. European Commission, Luxembourg, 176.
- Gharaibeh, A., Shaamala, A., Obeidat, R., Al-Kofahi, S. (2020). Improving land-use change modelling by integrating ANN with cellular automata-Markov chain model. *Heliyon*, 6.
- Gibson, L., Munch, Z., Palmer, A., Mantel, S. (2018). Future land cover change scenarios in South African grasslands – implications of altered biophysical drivers on land management. *Heliyon*, 4 (7).
- Girma, R., Fürst C., Moges A. (2022) Land use land cover change modelling by integrating the artificial neural network with cellular Automata-Markov chain model in Gidabo river basin, main Ethiopian rift. *Environmental Challenges*, 6, 100419.
- Huisden, C. M., Kanhai, S., Bogor, D. (2020). An assessment of volatile organic compound pollution in relation to the petroleum industry in Suriname. *Academic Journal of Suriname*, (11)1, 33–44.
- Huisden, C. M., Landburg, G., Niram, A., Algoe, S., Dakriet, N. (2020) Mercury toxicity through fish consumption in Paramaribo, Suriname. *Academic Journal of Suriname*, (11)1, 25–32.
- Hyandye, C., Geoffrey Mandara, C., Safari, J. (2015). GIS and logit regression model applications in land use/land cover change and distribution in Usangu catchment. *American Journal of Remote Sensing*, 3(1), 6–16.
- Kafy, A.-A., Naim, M. d. N. H., Subramanyam, G., Faisal, A.-A., Ahmed, N. U., al Rakib, A., Kona, M. A., Sattar, G. S. (2021). Cellular Automata approach in dynamic modelling of land cover changes using RapidEye images in Dhaka, Bangladesh. *Environmental Challenges*, 4, 100084.
- Leta, M. K., Demissie, T. A., Tränckner, J. (2021). Modelling and prediction of land use land cover change dynamics based on land change modeller (Lcm) in Nashe watershed, upper Blue Nile basin, Ethiopia. *Sustainability*, 13.
- Marquez, A.M., Guevara, E., & Rey, D. (2019). Hybrid model for forecasting of changes in land use and land cover using satellite techniques. *IEEE Journal of Selected Topics in Applied Earth Observations and Remote Sensing*, 12, 252–273.
- Mishra, V. N., Rai, P. K., Prasad, R., Punia, M., Nistor, M.–M. (2018). Prediction of spatiotemporal land use/land cover dynamics in rapidly developing Varanasi district of Uttar Pradesh, India, using geospatial approach: a comparison of hybrid models. *Applied Geomatics*, 10(3), 257–276.
- Mohamed, A., Worku, H. (2020). Simulating urban land use and cover dynamics using cellular automata and Markov chain approach in Addis Ababa and the surroundings. *Urban Climate*, 31, 100545.
- Muhammad, R., Zhang, W., Abbas, Z., Guo, F., Gwiazdzinski L. (2021). Spatiotemporal change analysis and prediction of future land use and land cover changes using QGIS MOLUSCE plugin and remote sensing big data: A case study of Linyi, China. *Land*, 11(3), 419.
- Myslyva, T., Nadtochiy, P., Bilyavskiy, Y., & Trofymenko, P. (2023). Intra-field spatial heterogeneity prediction for the purposes of precision farming: Comparison of frequency ratio and Shannon's entropy models. *Scientific Papers. Series A. Agronomy*, LXVI (1), 138–147.

- Myslyva, T., Sheliuta, B., Bushueva, V. (2021) Use of medium and high-resolution remote sensing data and Markov chains for forecasting productivity of non-conventional fodder crops. *Scientific Papers. Series A. Agronomy*, LXIV (1), 478–485.
- Nhu V.-H., Shirzadi A., Shahabi H., S. K., Al-Ansari N., Clague J. J. and all (2020). Shallow landslide susceptibility mapping: a comparison between logistic model tree, logistic regression, naïve Bayes tree, artificial neural network, and support vector machine algorithms. *Environmental Research and Public Health*, 17, 2749.
- Ouboter, P. E., Jairam, R. (2012). Geography of Suriname. In *Amphibians of Suriname*. Leiden, Netherlands: Brill, 376 pp.
- Ralha, C. G., Abreu, C. G., Coelho, C. G. C., Zaghetto, A., Macchiavello, B., Machado R. B. (2013). A multi-agent model system for land-use change simulation. *Environmental Modelling and Software*, 42, 30–46.
- Regasa, M. S., Nones, M., Adeba, D. (2021). A review on land use and land cover change in Ethiopian basins. *Land*, 10 (10), 585.
- Rongqun Z., Chengjie T., Suhua M., Hui Y., Lingling G., Wenyu F. (2011). Using Markov chains to analyze changes in wetland trends in arid Yinchuan Plain, China. *Mathematical and Computer Modelling*, 54 (3–4), 924–930.
- Rozario, P. F., Oduor, P., Kotchman, L. and Kangas, M. (2017) Transition modelling of land-use dynamics in the Pipestem Creek, North Dakota, USA. *Journal of Geoscience and Environment Protection*, 5, 182–201.
- Sinha, P., Kumar, L. (2013). Markov land cover change modelling using pairs of time series satellite images. *Photogrammetric Engineering and Remote Sensing*, 79, 1037–1051.
- Wang, S. W., Munkhnasan, L., Lee, W.K. (2021). Land use and land cover change detection and prediction in Bhutan's high-altitude city of Thimphu, using cellular automata and Markov chain. *Environmental Challenges*, 2, 100017.
- Yeh, C. K., Liaw, S. C. (2021). Applying spatial autocorrelation and logistic regression to analyze land cover change trajectory in a forested watershed. *Terrestrial, Atmospheric and Oceanic Sciences*, 32, 35–5.

THE EFFECT OF THE ALTITUDE GRADIENT ON THE VEGETATION OF THE GRASSLANDS IN THE POIANA RUSCĂ MOUNTAINS, BASED ON NDVI

Monica SFÎRCOCI¹, Loredana COPĂCEAN¹, Luminița COJOCARIU^{1,2}

¹University of Life Sciences "King Mihai I" from Timisoara,
119 Calea Aradului Street, Timisoara, Romania

²Agricultural Research and Development Station Lovrin,
200 Principala Street, Lovrin, Romania

Corresponding author email: lorecopacean@yahoo.com

Abstract

The relief is the main factor that determines the "vertical" arrangement of the vegetation. Starting from this hypothesis, the aim of the study is to quantify the influence of the altitudinal gradient on the vegetation cover of the grasslands and to test the condition of maintaining this influence over time. The Normalized Difference Vegetation Index (NDVI) was used, applied to Sentinel 2 images from March, May, July, August, October. It was established that, in grasslands, the average values of NDVI are minimum in spring, beginning of the vegetation season (0.3743), increase in May (0.6775) and reach the maximum in July (0.8233 - high degree of coverage). In autumn, the vegetation cover decreases (NDVI = 0.6258). On the altitudinal gradient, in spring, vegetation cover decreases with increasing altitude ($r = -0.85$), in summer, it is "uniformly" distributed, and in autumn, it increases simultaneously with altitude ($r = 0.5831$), against the background of maintaining a temperature-precipitation ratio optimal on the upper floors. The use of NDVI in the analysis of grassland provides a global picture and the possibility of expanding the analysis in different research directions.

Key words: altitudinal variation, grasslands, NDVI, vegetation.

INTRODUCTION

It is well known that relief, through altitude, slope, or the exposure of slopes, is the main factor determining the "vertical" zoning of other environmental factors, which influences the typology and distribution of vegetation cover, including grassland entities (Bennie, 2003; Lieffers & Larkin-Lieffers, 2011; Lieffering et al., 2019; Wang et al., 2023). Altitude, as an abiotic factor, is reflected in the distribution, composition of plant species, and the structure of grassland habitats, both directly and indirectly, by modifying climate and soil conditions (Austrheim, 2002; Mayor et al., 2017; Bagousse-Pinguet et al., 2019).

In recent years, numerous remote sensing applications and Geographic Information Systems (GIS) have been developed for analyzing grasslands in correlation with relief factors or other environmental factors, surpassing the limitations of traditional methods and offering the possibility of complex analyses with multidisciplinary significance (Pyke et al., 2002; Li et al., 2014; Zlinszky et al., 2015;

Hatfield et al., 2019; Soubry et al., 2021; Bobric et al., 2023). Understanding the distribution and evolution of vegetation, as well as monitoring grassland areas, is an important issue, especially for local communities dependent on these natural resources (Thomas et al., 2013; Caluseru et al., 2015; Mokarram et al., 2015; Copăcean et al., 2020; Simon et al., 2020).

An extremely useful tool in investigating grasslands in relation to environmental factors, with multiple applications, is the Normalized Difference Vegetation Index (NDVI). This index has been widely used for assessing the vegetation growth status of grasslands (Fensholt et al., 2009; Boori et al., 2020), temporal and spatial changes in vegetation cover (Gandhi et al., 2015), estimating biomass quantity, and the health status of grasslands (Bento et al., 2020; Soubry et al., 2021; Wang et al., 2022).

The hypothesis for this study, supported by numerous specialized studies in different areas, is that vegetation distribution varies according to altitude (Piao et al., 2011; Zhang et al., 2021; Hua et al., 2022). Furthermore, the idea of seasonal variation in grasslands, located in

extensive areas under variable environmental conditions, has sparked interest. Based on these considerations, the question arose: *"What is the behavior of vegetation at different altitudes at distinct moments of the growing season?"* From this point, a new challenge emerged: whether the NDVI index could be a theoretically and practically applicable solution under the conditions of the area of interest.

In this regard, the aim of the study was, on one hand, to quantify the influence of the altitudinal gradient on vegetation cover in grasslands, and on the other hand, to test the condition of maintaining this influence over time during the growing season.

MATERIALS AND METHODS

Study area

The research was conducted in the Poiana Ruscă Mountains, located in southwestern Romania, within the administrative territories of three counties: Hunedoara, Caraș-Severin, and Timiș (Figure 1).

The study area is intersected by the 45°N parallel and the 22°E meridian. It has the shape of a quadrilateral with an area of 167,084 hectares. Along the N-S direction, the length of the area of interest is approximately 46 km and along the W-E direction, it is about 54 km.

From a geological perspective, the Poiana Ruscă Mountains are predominantly composed of crystalline schists, limestones, and crystalline dolomites (Rusu, 2007). Altitudinally, they

range between 188 to 1374 meters, with the maximum altitude reached at Padeș Peak. The average elevation of the terrain is 706 meters.

The Poiana Ruscă Mountains belong to the transitional temperate continental climate sector. The multiannual average temperature varies between 9-11°C in the low, marginal areas and between 2-8°C in the mountainous area. The average annual amount of precipitation, due to oceanic influences, increases with altitude, from values of approximately 700 mm, in the marginal areas, to over 1000 mm, in the mountainous areas.

The eastern half of the Poiana Ruscă Mountains belongs to the Mureș watershed (the main rivers being Cerna and Strei), and the western part to the Bega river watershed. In the south, the Bistra river basin is individualized.

In terms of land use, the Poiana Ruscă Mountains are covered by forests to over 75% of their area, particularly in the western half (Rusu, 2007).

Human settlements were formed both on the interfluvies (in the areas with narrow valleys and thermal inversions), and on the valleys, in the depression basins in the northwest.

Materials used in research

The regionalization carried out by Posea and Badea was considered for delimiting the Poiana Ruscă Mountains (1984).

For the conduct of the research, the following geospatial data were utilized:

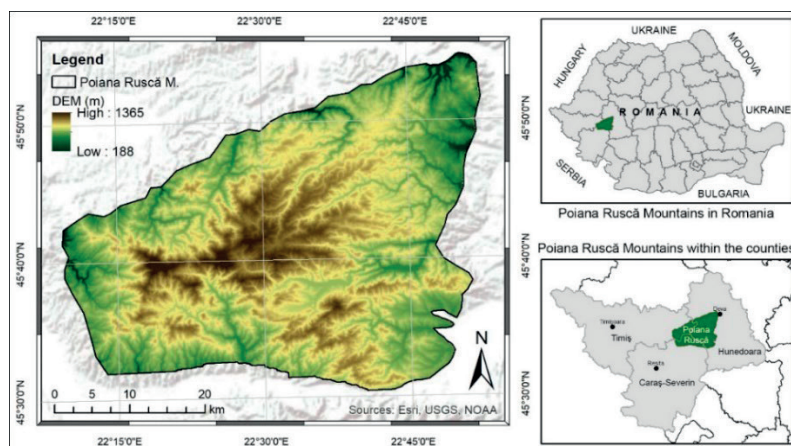


Figure 1 The location and the physical and geographical characteristics of the studied area (processing after EEA, 2016 2023; Geospatial, 2023; Posea & Badea, 1984)

- Sentinel 2A satellite imagery - for obtaining NDVI maps, downloaded from the Copernicus Open Access Hub platform;
- The Digital Elevation Model (DEM), in raster format, with a spatial resolution of 25 m, hybrid product based on SRTM and ASTER GDEM data, available for free on the platform of the European Environment Agency - for extracting altimetric information (EEA, 2016);
- Corine Land Cover (CLC) database, 2018 edition - for identifying grassland areas.

The geospatial datasets were processed using the SNAP and ArcGIS 10.4 software.

The methodology employed

The workflow involved several stages, as depicted in Figure 2:

1. **The satellite imagery download.** In the case of this study, for the application and testing of the work algorithm, the "experimental year" 2019 was chosen, in which five temporal moments of the vegetation season were selected, marked T₀...T₄, respectively 28.03, 11.05, 01.07, 10.08 and 09.10. We opted for the analysis over different periods, considering the fact that the vegetation has different "behavior" and characteristics, depending on the vegetation phases. For each of these moments in time, two Sentinel 2A MSI satellite scenes were downloaded, with the atmospheric corrections

and georeferenced in the UTM (Universal Transverse Mercator) system, from the areas with the code 34TER and 34TFR (taking into account the fact that the area of interest is partially overlaps both scenes).

2. **Processing satellite scenes in SNAP** involved mosaic creation, band conversion to the same spatial resolution (20 m), approximate extraction of the area of interest, and generation of NDVI maps for the five temporal moments considered.

3. **The processing of the DEM** involved extracting the area of interest and classifying it into 11 altitude classes with an altitude range of 100 meters (between 188 and 1374 m);

4. **The identification of grassland areas** utilized the CLC 2018 database, from which the secondary grasslands class (code 231) and natural grasslands class (code 321) were extracted. The spatial entities were validated based on cadastral maps, orthophotoplanes, and GPS points collected in the field (Table 1).

5. **The extraction of NDVI values for grassland areas** involved retrieving both spatial entities and numerical values required for statistical data processing from the NDVI maps.

6. **Spatial analysis, for grasslands**, involved correlating NDVI with altitude to identify the trend of NDVI values as altitude values change.

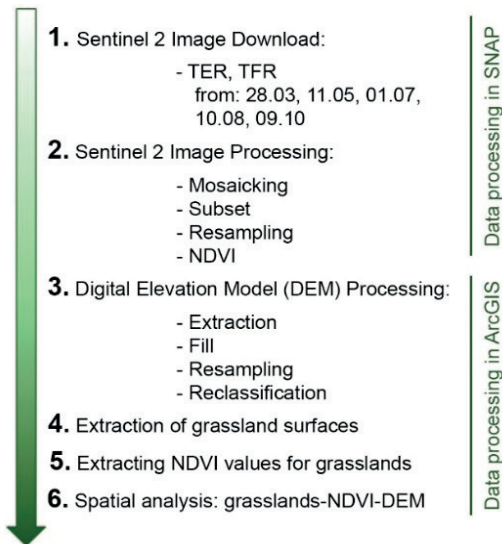


Figure 2. Workflow

Table 1. The accuracy assessment of geospatial data through ground control points

	Grasslands	Others	Total	Accuracy (%)	Prediction (%)
Grasslands	31	4	35	88.57	86.11
Others	5	0	5	100.00	13.89
Total	36	4	40		
	Grasslands	Others	Total	Commision	Producers accuracy
Grasslands	31	0	31	0.00	1.00
Others	4	5	9	0.44	0.56
Total	35	5	40		
Commision	0.11	0.00			
Producers accuracy	0.89	1.00			
Overall accuracy	0.90	0.90			
K	0.56				
p(r)	0.78				

For the analysis of climatic conditions in the area of interest, climatic data (Climatic Databases, 2023) were retrieved, including monthly average temperatures and monthly precipitation amounts for the year of 2019, from 26 nearby meteorological stations, located at different altitudes.

RESULTS AND DISCUSSIONS

According to the Corine Land Cover (CLC) database, 2018 edition, grassland areas have been identified covering 21,890 hectares, which represents 14.74% of the total surface of the study area (Figure 3).

The grasslands of the Poiana Ruscă Mountains are extremely varied from the point of view of the floristic composition, respectively they are characterized by a great biodiversity. Thus Maruşca et al. (2020) in the representative grasslands of the Poiana Ruscă Mountains identify several phytosociological alliances: Al. *Festucion rupicolae* (As. *Agrostideto capillaris* - *Festucetum rupicolae*, As. *Botriochloetum ischaemi*, As. *Brometum fibrosi*); Al. *Cynosurion* (As. *Festuco rubrae* - *Agrostietum capillaris*); Al. *Violo declinatae* - *Nardion* (As. *Violo declinatae* - *Nardetum*); Al. *Trifolion medii* (As. *Clinopodio* - *Pteridietum*); Al. *Agropyro* - *Rumicion* (As. *Trifolio repenti* - *Lolietum perennis*); Al. *Molinion coerulae* (As. *Peucedano* - *Molinietum*), respectively Al. *Potentillion anserinae* (As. *Junco inflexi* - *Menthetum longifoliae*). The variety of species in the meadows also have different periods of

initiation into vegetation, respectively growth, fruiting and senescence during the vegetation period, an aspect that influences the values of the NDVI index.

In the case of the vegetation cover of the grasslands, the analysis based on the NDVI values (Figure 3), highlighted significant variations, during a sequence of the vegetation season, an aspect also noticed by other studies (Copacean et al., 2023).

The expeditious analysis of the NDVI maps (Figure 3) shows that in addition to the "horizontal" variation, from one sequence of the vegetation season to another, there is also a "vertical" variation, under the influence of altitude.

The analysis of environmental factors directly influencing the spatial distribution of grassland vegetation

The analysis of grasslands in relation to the relief shows their uneven distribution in the vertical plane, indicating different conditions for the formation and evolution of vegetation (Figure 4). Among the grasslands in the study area, 78% are located at altitudes between 400-800 m, with an average altitude of 718 m. Of the total grassland areas, 61% are situated on terrain with slopes between 5-15° (Figure 4), suggesting variability in the vegetation cover along the altitudinal gradient, considering that the relief is the main determining factor of vegetation spatial distribution. The average slope of the grassland areas is 10.3°

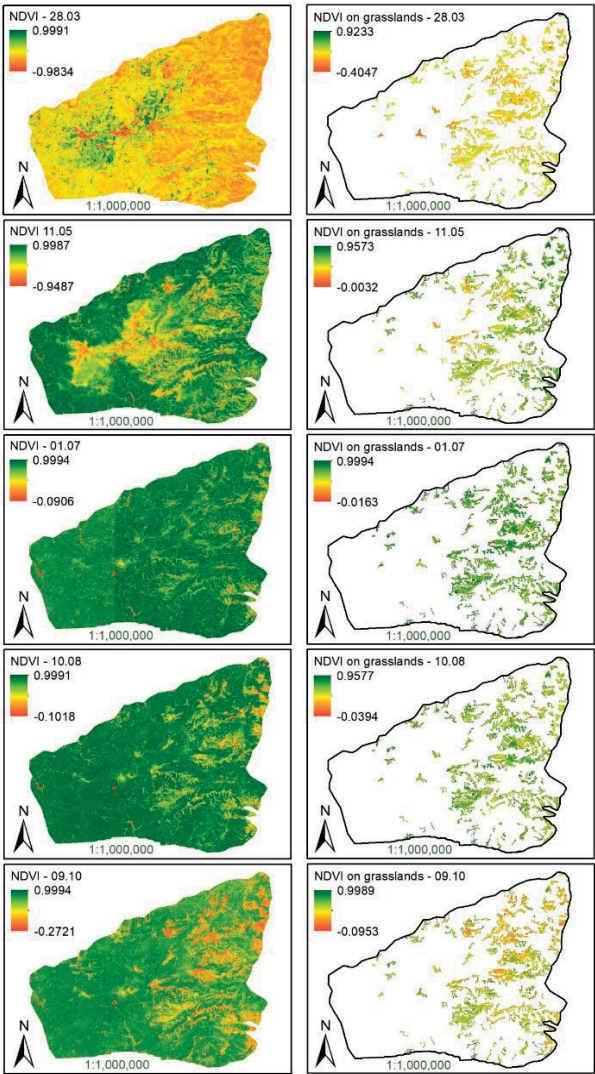


Figure 3 The distribution of the NDVI values in the study area for T₀-T₄ (processing after: Geospatial, 2023; Copernicus Open Hub, 2022)

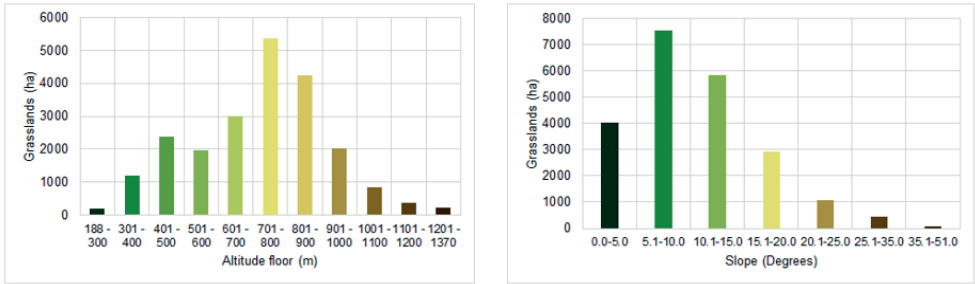


Figure 4 The distribution of grassland areas by altitude zones (left) and slope classes (right)

Furthermore, relief directly and indirectly influences the "behavior" of climatic factors, which in turn determine the characteristics and distribution of vegetation (Gonga et al., 2008). In the case of the study area, based on climatic data recorded at 26 nearby meteorological stations, it was found that air temperature decreases with increasing altitude ($r = -0.9711$), following a vertical thermal gradient of $0.53^{\circ}\text{C}/100\text{ m}$ altitude. Regarding precipitation, a weak to moderate correlation with altitude was determined ($r = 0.5332$), with values increasing vertically but being influenced by local conditions (Figure 5).

The analysis of the relief and climatic factors, in correlation with grasslands, which are altitude-dependent variables, supports the hypothesis of variability in the vegetation cover degree along the altitudinal gradient.

The analysis of the vegetation cover variation in grasslands during the period from March to October, by altitude zones

To highlight the variation in grassland vegetation cover degree vertically, NDVI values in grasslands located at different altitudes were analyzed at different time points. In T_0 , the first considered stage (March), the grassland cover degree was low since plants had not started growing yet due to restrictive

climatic conditions. At this stage, the influence of altitude is evident (Table 2, Figure 6), with a strongly negative correlation established with NDVI values ($r = -0.8406$, $ts = -0.0100$). This is explained by the fact that most grassland plants start growing at temperatures above 10°C , for at least 7 consecutive days, a condition not met at higher altitudes (Figure 5).

The NDVI calculated for T_0 has low values with a similar trend across all altitude thresholds except for grasslands located between 1200-1370 meters (Figure 6), where the lowest values are observed (0.2680). The fact that NDVI is maintained at low values, on all altitudinal levels (does not show significant variations) suggests that the plants in the grasslands have not entered vegetation, with few exceptions.

At T_1 , compared to T_0 , as temperatures rise and moderate precipitation occurs (700-1000 mm/year), the grassland vegetation cover degree increases. There is a variation in vegetation growth with altitude, with a strong negative linear correlation with NDVI values ($r = -0.9600$, $ts = -0.0300$), indicating a reduction in cover degree towards the high mountain zone, where vegetation grows later. Although higher values are observed compared to T_0 , restrictive climatic conditions for grassland plant growth and development still persist (Figure 5).

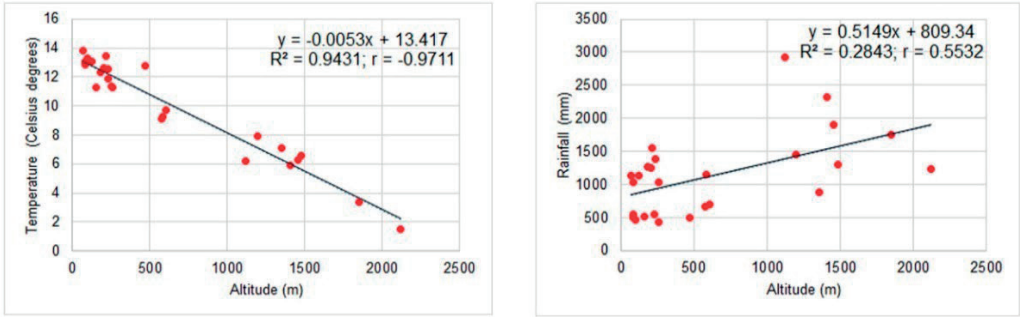


Figure 5. Correlation between temperature and altitude (left) and precipitation and altitude (right)

Table 2. Values of correlation coefficients in T_0 - T_4 (March - October interval)

Specification	T_0	T_1	T_2	T_3	T_4
The regression equation	$y = -0.0001x + 0.456$	$y = -0.0003x + 0.8878$	$y = -0.0001x + 0.8255$	$y = 0.0025x + 0.7598$	$y = 0.0063x + 0.5763$
R^2	0.7067	0.9216	0.0044	0.2807	0.3346
r	-0.8406	-0.9600	-0.0665	0.5298	0.5784
Theil Sen (ts)	-0.0100	-0.0300	0.0000	0.0000	0.0100

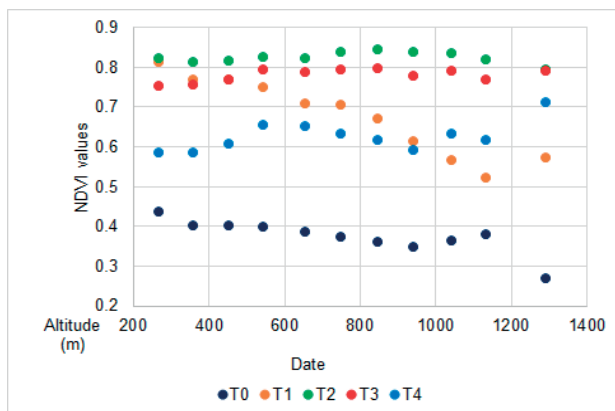


Figure 6 Correlation between NDVI (average) and altitude in T₀-T₄ (March - October interval)

In T₂, the NDVI values show the maximum degree of vegetation cover (Figure 6), with an average value of 0.8233. A dependency relationship between NDVI and altitude was not established ($r = -0.0665$, $ts = 0.0000$), indicating vegetation uniformity along the altitudinal gradient. At this moment, both in the lower and upper altitudes, plants meet optimal development conditions (above 17°C) and cover the ground to a very high extent. For the specific conditions in the Poiana Ruscă Mountains, T₂ is the moment when a “growth peak” is observed, a situation also noted in other studies for different environmental conditions (Hu et al., 2009; Bickford et al., 2011; Spasojevic et al., 2013).

Translated into practice, in the month of July the largest amount of vegetable mass is recorded for the animals that use the grassland.

In Romania, similar to the Poiana Ruscă Mountains, the month of August (T₃) generally has similar thermal conditions to July (T₂), but with reduced precipitation amounts, which translates into reduced physiological activity of plants in the pastoral landscape. Growth stagnates, and seed formation occurs, leading to reduced chlorophyll activity and a decrease in NDVI. Altitudinal trends and vegetation cover uniformity remain similar to T₂ but with lower NDVI values (Figure 6), except for the upper elevation range (1200 - 1370 m), which benefits from greater amounts of precipitation (over 1000 mm/year).

Both in T₂ and T₃, the NDVI variation with altitude follows a similar pattern: values

increase from the lower part up to about 1000 m, likely due to increased precipitation.

In recent years, global climate change (Allamano et al., 2009; Rogora et al., 2018; Șmuleac et al., 2020; Losapio et al., 2021; Sărățeanu et al., 2023), has influenced the vegetation period.

In Romania, this period extends until the end of September or early October, which is reflected in the NDVI values for the study area. The NDVI-altitude correlation in T₄, weak to moderately positive ($r = 0.5784$, $ts = 0.0100$), indicates a high vegetation cover degree in the upper elevations, where optimal conditions for grassland plants persist even at the beginning of October. Compared to T₃, the average NDVI values decrease from 0.7787 to 0.6258.

The variation in NDVI values with altitude is explained by topoclimatic conditions: values are influenced by local conditions. NDVI values may differ where grasslands are bordered by large forested areas, creating locally humid microclimates and/or if the grasslands are located on north-facing slopes with reduced insolation and excess water balance (Barnard et al., 2017; Lieffering et al., 2019). In both situations, a prolongation of the vegetation season can occur.

The management practices of grasslands can also influence NDVI values: grazed grasslands typically exhibit greener vegetation compared to hayfields at harvest time, where plants are in a different phenophase and are senescing, reflecting electromagnetic radiation differently.

CONCLUSIONS

The relief, characterized by altitude, slope, or aspect, along with climate factors such as temperature and precipitation, are the main drivers of the vertical "zoning" of grassland vegetation and its behavior throughout a growing season.

In the case of grasslands, NDVI variation during the growing season indicates fluctuations in vegetation cover: minimum average values in spring (0.3743), as plants begin their growth phase, increasing in May (0.6775), and reaching a peak in July (0.8233). During this time, the vegetation cover of the grasslands is dense and covers the ground almost entirely. By August, some species from the upper vegetation layer and those left uneaten by animals have dried, leading to a slight change in NDVI values (0.7787). In autumn, the vegetation cover decreases (NDVI = 0.6258).

Regarding the altitude, the extent of vegetation coverage in grasslands fluctuates both over different time periods and vertically, at various altitudes. NDVI values suggest that in T_0 , regardless of altitude, vegetation cover is low, indicating unsuitability for grazing. In May (T_1), NDVI values show an increasing trend from lower to higher altitudes, indicating the possibility of grazing. Both T_2 and T_3 show extensive vegetation cover across all altitude ranges, with minor exceptions. T_4 also exhibits slight variations in altitude and marks the end of the summer season.

The correlation between NDVI and altitude indicated an uneven distribution of vegetation cover across different altitudes during the spring season, diminishing as altitude increased. Values become more uniform during the summer when, even at higher altitudes, plants find optimal conditions for development. In autumn, NDVI reveals a distribution of vegetation in altitude with a higher coverage degree in the upper elevations, under the conditions of the year 2019.

In a multidisciplinary perspective, NDVI can be a valuable tool not only in agricultural practice but also in ecology and natural sciences. Assessing grassland vegetation cover is crucial for marking the beginning of grazing and the duration of the grazing season, determining the degree of degradation, or maintaining long-term

stability of the grassland ecosystem in the context of ongoing climate change.

REFERENCES

- Allamano, P., Claps, P., & Laio, F. (2009). Global Warming Increases Flood Risk in Mountainous Areas. *Geophys. Res. Lett.*, 36, L24404.
- ArcGIS Documentation. (2022). <https://desktop.arcgis.com/en/documentation/>
- Austrheim, G. (2002). Plant diversity patterns in semi-natural grasslands along an elevational gradient in southern Norway. *Plant Ecology*, 161, 193-205.
- Bagousse-Pinguet, Y., Soliveres, S., Gross, N., Torices, R., Berdugo, M., & Maestre, F.T. (2019). Phylogenetic, functional, and taxonomic richness have both positive and negative effects on ecosystem multifunctionality. *Proceedings of the National Academy of Sciences of the United States of America*, 116(17), 8419–8424.
- Barnard, D.M., Barnard, H.R., & Molotch, N.P. (2017). Topoclimate effects on growing season length and montane conifer growth in complex terrain, *Environ. Res. Lett.*, 12, 10.1088/1748-9326/aa6da8.
- Baze de date climatică, (2023). https://rp5.ru/Weather_in_Romania.
- Bennie, J.J. (2003). The ecological effects of slope and aspect in chalk grassland. Doctoral thesis, Durham University, <http://etheses.dur.ac.uk/4017/>.
- Bento, V.A., Gouveia, C.M., DaCamara, C.C., Libonati, R., & Trigo, I.F. (2020). The roles of NDVI and Land Surface Temperature when using the Vegetation Health Index over dry regions. *Glob. Planet. Change*, 190, 103198.
- Bickford, C.P., Hunt, J.E., & Heenan, P.B. (2011). Microclimate characteristics of alpine bluff ecosystems of New Zealand's South Island, and implications for plant growth New Zealand. *J. Ecol.*, 35, 273-279.
- Bobric, E.D., Stoleriu, A.P., Niacșu, L., Alion, G.S., & Breabăn, I.G. (2023). The use of spectral techniques to monitor the vegetation status in a protected area in the Iasi county. *PESD*, 17(1), 109-125.
- Boori, M., Choudhary, K., & Kupriyanov, A. (2020). Crop growth monitoring through Sentinel and Landsat data based NDVI time-series. *Computer Optics*, 44, 409-419, 10.18287/2412-6179-CO-635.
- Caluseru, A.L., Cojocariu, L., Borlea, F., Bordean, D-M., & Horablagă, A. (2015). Rural Development of Mountain Areas in Romania, Challenges and Targets for the Year 2020. In Proceedings of the SGEM 2015 Conference Proceedings, Bulgaria; Vol 2, pp. 791–798.
- Copăcean, L., Popescu, C., Bărliba, L.L., Simon, M., & Cojocariu, L., (2023). Analysis of vegetation coverage of grasslands based on NDVI values. Case study: Poiana Ruscă Mountains, International Multidisciplinary Scientific GeoConference: SGEM; Section Advances in Biotechnology.
- Copăcean, L., Cojocariu, L., Simon, M., Zisu, I., & Popescu, C. (2020). Geomatic techniques applied for remote determination of the hay quantity in agro-silvo-

- pastoral systems. *PESD*, 14(2), 89 – 101. <https://doi.org/10.15551/pesd2020142006>.
- Copernicus Land Monitoring Service - Corine Land Cover (CLC) Database, 2018 Edition, <https://land.copernicus.eu/pan-european/corine-land-cover> (accessed on 15.09.2022).
- Copernicus Open Access Hub, Available online: <https://scihub.copernicus.eu/dhus/#/home>.
- European Environment Agency (EEA), 2016, Digital Elevation Model (DEM), <https://www.eea.europa.eu/data-and-maps/data/copernicus-land-monitoring-service-eu-dem> (accessed on 18.10.2022).
- Fensholt, R., Rasmussen, K., Nielsen, T.T., & Mbaw, C. (2009). Evaluation of earth observation based long term vegetation trends—Intercomparing NDVI time series trend analysis consistency of Sahel from AVHRR GIMMS, Terra MODIS and SPOT VGT data. *Remote Sens. Environ.*, 113, 1886–1898.
- Gandhi, G.M., Parthiban, S., Thummalu, N., & Christy, A. (2015). NDVI: Vegetation Change Detection Using Remote Sensing and Gis—A Case Study of Vellore District. *Procedia Comput. Sci.*, 57, 1199–1210.
- Geospatial, 2023, România: seturi de date vectoriale generale – <http://geospatial.org/vechi/download/romania-seturi-vectoriale> (accessed on 18.08.2022).
- Gong, X., Brueck, H., Giese, K.M., Zhang, L., Sattelmacher, B., & Lin, S. (2008). Slope aspect has effects on productivity and species composition of hilly grassland in the Xilin River Basin, Inner Mongolia, China. *J. Arid Environ.*, 72(4), 483 - 493, <https://doi.org/10.1016/j.jaridenv.2007.07.001>.
- Hatfield, L.J., Prueger, H.J., Sauer, J.T., Dold, C., O'Brien, P., & Wacha, K. (2019). Applications of Vegetative Indices from Remote Sensing to Agriculture: Past and Future. *Inventions*, 4, 71. <https://doi.org/10.3390/inventions4040071>.
- Hu, Z., Zhengwei, Y., Liping, D., Lin, L., & Haihong, Z. (2009). Crop phenology date estimation based on NDVI derived from the reconstructed MODIS daily surface reflectance data," 2009 17th International Conference on Geoinformatics, pp. 1-6, doi: 10.1109/GEOINFORMATICS.2009.5293522.
- Hua, X., Ohlemüller, R., & Sirgucy, P. (2022). Differential effects of topography on the timing of the growing season in mountainous grassland ecosystems. *Environmental Advances*, 8, 100234. <https://doi.org/10.1016/j.envadv.2022.100234>.
- Li, Z., Xu, D., & Guo, X. (2014). Remote Sensing of Ecosystem Health: Opportunities, Challenges, and Future Perspectives. *Sensors*, 14, 21117–21139.
- Lieffering, M., Newton, P.C.D., Brock, C.S., & Theobald, W.P. (2019). Some effects of topographic aspect on grassland responses to elevated CO₂. *Plant Production Science*, 22(3), 345–351.
- Lieffers, V., & Larkin-Lieffers, P. (2011). Slope, aspect, and slope position as factors controlling grassland communities in the coulees of the Oldman River, Alberta. *Can. J. Botany*, 65, 1371–1378. <https://doi.org/10.1139/b87-189>
- Losapio, G., Cerabolini, B.E.L., Maffioletti, C., Tampucci, D., Gobbi, M., & Caccianiga, M. (2021). The consequences of glacier retreat are uneven between plant species. *Front. Ecol. Evol.*, 8, 616562.
- Marușca, T., Arsene, G.G., & Taulescu, E. (2020). Assessment of Permanent Grassland Productivity in Poiana Ruscă Mountains (Southwest Romanian Carpathians). *Annals of the Academy of Romanian Scientists Series Agriculture, Silviculture and Veterinary Medicine Sciences* (1), Available at SSRN: <https://ssrn.com/abstract=3699189>
- Mayor, J., Sanders, N., Classen, A. et al. (2017). Elevation alters ecosystem properties across temperate treelines globally. *Nature*, 542, 91–95.
- Mokarram, M., & Sathyamoorthy, D. (2015). Modeling the relationship between elevation, aspect and spatial distribution of vegetation in the Darab Mountain, Iran using remote sensing data. *Model. Earth Syst. Environ.*, 1, 30.
- Piao, S., Cui, M., Chen, A., Wang, X., Ciais, P., Liu, J., & Tang, Y. (2011). Altitude and temperature dependence of change in the spring vegetation green-up date from 1982 to 2006 in the Qinghai-Xizang Plateau. *Agricultural and Forest Meteorology*, 151(12), 1599–1608
- Posea, G., & Badea, L. (1984). *România. Unitățile de relief (Regiunea geomorfologică)*. Ed. Științifică și Enciclopedică, București
- Pyke, D.A., Herrick, J.E., Shaver, P., & Pellant, M. (2002). Rangeland Health Attributes and Indicators for Qualitative Assessment. *J. Range Manag.*, 55, 584–597
- Rogora, M et al. (2018). Assessment of climate change effects on mountain ecosystems through a cross-site analysis in the Alps and Apennines. *Science of The Total Environment* 624, 1429-1442. doi:<https://doi.org/10.1016/j.scitotenv.2017.12.155>
- Rusu, R. (2007). *Organizarea spațiului geografic în Banat*. Ed. Mirton, Timișoara.
- Sărățeanu, V., Cotuna, O., Paraschivu, M., Cojocariu, L.L., Horablagă, N.M., Rechișean, D., Mircov, V.D., Sălceanu, C., Urică, A.A., & Copăcean, L. (2023). Features of Natural Succession of Ex-Arable Forest Steppe Grassland (from Western Romania) under the Influence of Climate. *Plants*, 12, 1204. <https://doi.org/10.3390/plants12061204>
- Simon, M., Popescu, C.A., Copăcean, L., & Cojocariu, L. (2020). Complex model based on UAV technology for investigating pastoral space. *PESD*, 14(2), 139 – 150. <https://doi.org/10.15551/pesd2020142011>.
- Soubry, I., Doan, T., Chu, T., & Guo, X. (2021). A Systematic Review on the Integration of Remote Sensing and GIS to Forest and Grassland Ecosystem Health Attributes, Indicators, and Measures. *Remote Sens.*, 13, 3262.
- Spasojevic, M.J., Bowman, W.D., Humphries, H.C., Seastedt, T.R., & Suding, K.N. (2013). Changes in alpine vegetation over 21 years: are patterns across a heterogeneous landscape consistent with predictions? *Ecosphere*, 4, 10.1890/es13-00133.1.
- Șmuleac, L., Rujescu, C., Șmuleac, A., Imbrea, F., Radulov, I., Manea, D., & Pașcalău, R. (2020). Impact of Climate Change in the Banat Plain, Western Romania, on the Accessibility of Water for Crop Production in Agriculture. *Agriculture*, 10(10), 437.

- Thomas, J., Duff, T.L., & York, A. (2013). Recognising fuzzy vegetation pattern: the spatial prediction of floristically defined fuzzy communities using species distribution modelling methods. *J. Veg. Sci.*, 25, 323–337. doi:10.1111/jvs.12092.
- Wang, K., Cao, C., Xie, B., Xu, M., Yang, X., Guo, H., & Duerler, R.S. (2022). Analysis of the Spatial and Temporal Evolution Patterns of Grassland Health and Its Driving Factors in Xilingol. *Remote Sens.*, 14, 5179. <https://doi.org/10.3390/rs14205179>
- Wang, Y., Sun, J., Lee, & T.M. (2023). Altitude dependence of alpine grassland ecosystem multifunctionality across the Tibetan Plateau. *J. Environ. Manage.*, 332, 117358.
- Zlinszky, A., Heilmeyer, H., Balzter, H., Czúcz, B., & Pfeifer, N. (2015). Remote Sensing and GIS for Habitat Quality Monitoring: New Approaches and Future Research. *Remote Sens.*, 7, 7987–7994.
- Zhang, L., Yan, H., Qiu, L., Cao, S., He, Y., & Pang, G. (2021). Spatial and Temporal Analyses of Vegetation Changes at Multiple Time Scales in the Qilian Mountains. *Remote Sens.*, 2021, 13.

THE USE OF GEOMATICS FOR THE PLANNING OF A SPORTS COMPLEX

Cornel Cristian TEREȘNEU

Transilvania University of Brasov, 25 Eroilor Street, Brasov, Romania

Corresponding author email: cteresneu@unitbv.ro

Abstract

In this paper, a topographical survey was carried out and the resulting data were processed for the development of the Zănoaga area in Bran, as a multifunctional sports complex. For the existing ski slope, all field data were collected, and a corresponding database was constructed. For the rest of the area, a comprehensive survey was conducted to establish the routes for a summer toboggan run, a tubing installation, and a bike trail (with multiple variants). A ComNav T300 GNSS equipment was used. Field data were initially processed in AutoCAD Civil 3D and then imported into ArcGIS. In this latter program, the initial 3D profile, and the possible profiles for optimal operation of the mentioned facilities were created. A program model was built in GIS through which the user can choose the suitable slope according to their experience, and the construction mode of the summer slope was simulated, based on projected speed.

Key words: sports complex, GIS, geomatics, VBA sequences.

INTRODUCTION

The need to relax is becoming more and more acute as life has become very demanding, or rather far too stressful. Thus, all tourist resorts aim to create and offer the widest possible range of leisure opportunities (Câdea & Erdeli, 2001). It is a well-known fact that Romania offers a multitude of leisure options (Erdeli and Istrate, 1996), the differentiation between the different locations (tourist resorts) being given by the way they are managed, and the range of services offered (Ganea, 2006). Tourism in Romania (Glăvan, 2000) has ancient roots (Epuran, 1958), but this aspect should motivate us to increase the quality of the services offered and the appropriate arrangement of the various locations. In addition, another great advantage of tourist resorts in our country is their location in diverse regions, each offering in a unique way other values (Posea et al., 1974).

Unfortunately, it can be observed that the tourist potential (Ielenicz & Comănescu, 2006), although it is a great one, does not always stimulate those who want to exploit it in one way or another, as there are no qualitative concerns but only quantitative ones, although it is known that tourism, in most cases, directly influences the quality of life (Barbu, 1980).

Each stage in the historical development of society has its own imprint on what tourism means (Hossu Longin, 1980), and the way in which the reality of time is seen is also absorbed into the tourism industry. We could even say that tourism is not only a social phenomenon, but also an economic and cultural one (Ionescu, 1999).

The development of certain regions located within landscapes (Barabas and Rusu, 1979) should not only be inspiring for the rest of the country (Ciangă, 2001), but should be an imperative that leads to the co-interest of decision-makers and local factors. The food industry can also be closely linked to the development of tourism (Bărbănescu, 1975), given that (especially) rural areas offer traditional products of great value and quality, and sometimes the beauty of places is appreciated together with the quality of gastronomic products. Of course, a tourist location requires certain minimum amenities (Ilieș, 2007), with mountain areas having a special note in this respect (Bălțeanu, 1975).

In recent times there has been a particular rise in rural tourism (Petrea & Petrea, 2000), with an increasing demand for the lifestyle and conditions that characterized the Romanian peasant of the last century. Moreover, time spent outdoors is trying to be oriented in a certain direction, giving it also a sporting

emphasis. In this context, it is becoming increasingly necessary to set up a sports center (Monea & Yamora, 1998), which would provide the sedentary majority population with the necessary skills.

For mountain resorts, a ski slope is an essential part of the landscape. This is why there are many materials which try to arouse the interest of tourists (Bâră, 1983; Ionescu, 2004; Matei, 1982), as well as materials aimed at those who have some experience in this field (Barabas & Ganea, 1995; Cârstocea, 1998; Grigoraș, 2002). The tourist resort of local interest Bran also belongs to the ranks of all self-respecting resorts and aims to develop the sports base in the Zănoaga area. There has been a ski slope here since the 2000s, but the intention is to extend it. This expansion concerns both the ski slope, which will have a new trail and therefore a new ski lift, and other facilities for winter sports (tubing trail) and summer sports (bicycle trail).

MATERIALS AND METHODS

The following materials were used for this work:

- A ComNav T300 GNSS equipment providing an accuracy of 8 mm + 1 ppm Root Mean Square (RMS) in the horizontal plane and 15 mm + 1 ppm RMS in the vertical plane;
- A Dell Latitude 5411 laptop with an Intel Core i7-10850H CPU @ 2.70GHz 2.71 GHz; and 16MB RAM;
- ArcMap software;
- Microsoft Office software package (namely Excel and Word applications);
- AutoCAD Civil 3D software;
- A topographical survey totalling over 2500 points.

Regarding the research methods, the following were used:

- Direct measurement method by which the coordinates of the points of interest were taken;
- Statistical methods of filtering the points whose coordinates have been determined;
- Geographic Information Systems (GIS) methods (georeferencing and vectorization of cadastral plans; use of Visual Basic for Applications (VBA) programming sequences to carry out various analyses).

RESULTS AND DISCUSSIONS

The measurements were carried out in several stages as the beneficiary's requirements were fragmented (Figure 1). The *.rw5 files were analyzed and only the coordinates of the points that were recorded as a fixed solution and with corresponding dilution of precision (PDOP) values were kept.



Figure 1. Study area

Subsequently these coordinates were imported into AutoCAD Civil 3D, the 3D model was created (Figure 2) and contour lines were drawn (Figure 3) to highlight the terrain's configuration.

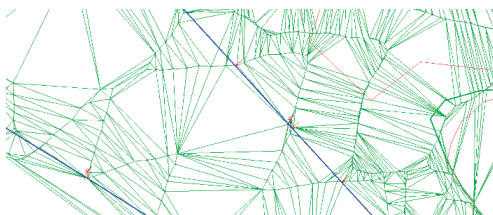


Figure 2. The 3D model

Subsequently the problems were addressed separately, according to the objective in mind. Since in all cases the 3D profile of the area is of interest, it was also created in the ArcMap environment. For this purpose, the *.txt file was transformed into *.xls format. This sheet was in turn transformed into *.shp format using the ArcCatalog module, following the sequence: right click on *Sheet1* → *Create Feature Class* → *From XY Table* (Figure 4).

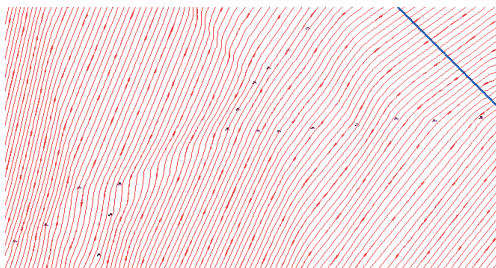


Figure 3. Drawing level curves

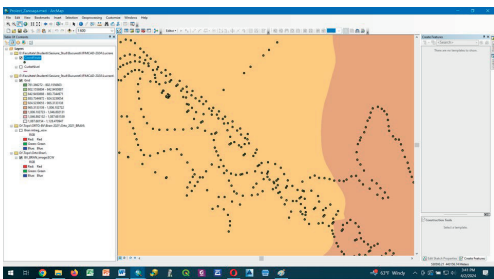


Figure 6. Creating the grid

FID	Shape	839	443488.248	530349.011	906.670	Statie
48	Point ZM	42	443370.503	530509.504	931.02	RIGOLA
49	Point ZM	43	443370.946	530500.465	930.26	RIGOLA
50	Point ZM	44	443371.116	530495.789	929.83	RIGOLA
51	Point ZM	45	443373.134	530481.94	928.37	RIGOLA
52	Point ZM	46	443374.922	530472.088	927.84	RIGOLA
53	Point ZM	47	443374.271	530468.408	927.35	RIGOLA
54	Point ZM	48	443373.574	530464.382	927.15	RIGOLA
55	Point ZM	49	443374.444	530461.935	927.16	POD
56	Point ZM	50	443373.012	530461.275	926.75	POD
57	Point ZM	51	443374.531	530457.651	926.6	POD
58	Point ZM	52	443375.749	530458.018	926.67	POD
59	Point ZM	53	443395.264	530460.603	926.03	GL
60	Point ZM	54	443391.086	530463.455	926.33	GL
61	Point ZM	55	443386.379	530472.548	926.59	GL
62	Point ZM	56	443383.255	530472.549	927.29	GL
63	Point ZM	57	443380.594	530478.406	927.9	GL
64	Point ZM	58	443379.527	530483.668	928.41	GL
65	Point ZM	59	443377.999	530489.935	929.1	GL
66	Point ZM	60	443377.665	530495.567	929.52	GL
67	Point ZM	61	443377.088	530501.278	930.41	GL

Figure 4. Stereographic coordinates in ArcMap

Next, a Geodatabase File is created in which a Feature Dataset is created. The *.shp file containing the coordinates of the points is transformed into a File Geodatabase by following the sequence: *points.shp* → *Export* → *To Geodatabase (single)* (Figure 5). Then the contour lines are created. To do this, a raster was first created from point Z-values, resulting in the grid layer (Figure 6). The last step is the actual creation of the contour lines, following the sequence: *Arc Toolbox* → *3D Analyst Tools* → *Raster Surface* → *Contour*, using the previously created grid (Figure 7).

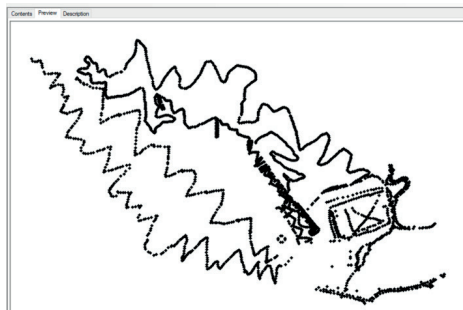


Figure 5. Coordinates in ArcCatalog

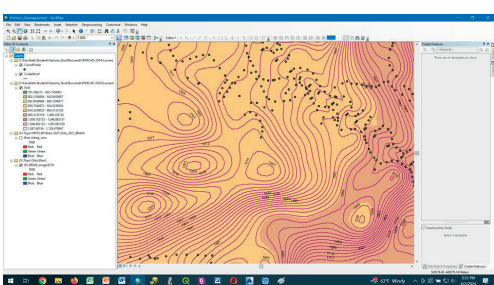


Figure 7. Creating contours

Next (GIS) facilities were used to perform the complex study considered (Tereşneiu et al., 2016), the main directions of action being:

- For the case of the chairlift, the aim was to achieve the optimal conditions for the commissioning of route 3 and the development of modules that would help the users to find out various information on the possibilities of skiing according to their experience. Three ski lift routes will be put into operation, with the following characteristics:
 - Route 1 has a topographic length of 253 m and is intended for children and those less initiated in the sport. For this route we can find a lot of useful information, such as the starting point (Figure 8) and the end point (Figure 9). Having the coordinates of the end points (including Z), we can find out the difference in altitude and the actual skiable distance. For this route the following values were found by querying the map (Tereşneiu et al., 2009): the elevation of the downstream point 941.42 m and the elevation of the upstream point 969.84 m. Therefore, the difference in elevation is 28.42 m. The slope of this route is $m = (y_2 -$

$y_1/(x_2-x_1) = -2.85$. Also, the skiable length is 254.6 m and the difference in elevation = 28.42 m. All these values can be found from the 3D model made in ArcGis by creating (VBA) sequences (Tereşneu & Tereşneu, 2023, Tereşneu & Vasilescu, 2013, Tereşneu et al., 2013) (Figure 10);

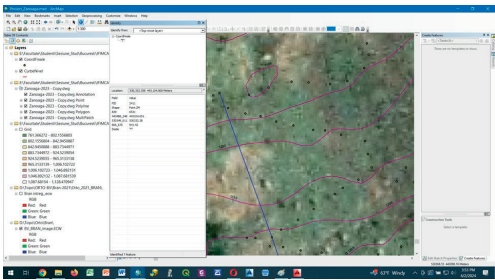


Figure 8. Elevation of the downstream point for the first ski lift route

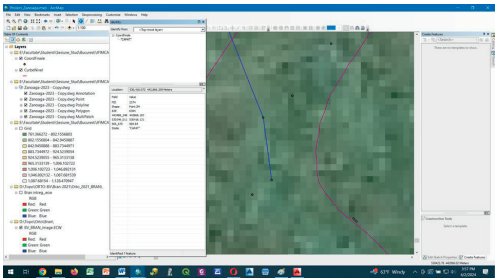


Figure 9 Elevation of the upstream point for the first ski lift route

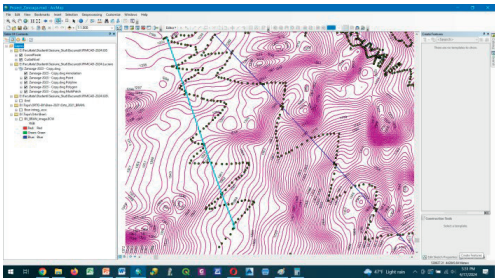


Figure 10 Determination of the actual length of the route of the first ski slope by VBA sequence

- Route 2 is 619 m long, has a downstream point elevation of 944.03 m and an upstream point elevation of 1087.06 m. This results in a slope $m = -0.90$, an elevation difference = 143.03 m and a skiable length of 635.3 m;

- For route 3 we have a topographic length of 539 m, an elevation of the downstream point of 967.44 m and an elevation of the upstream point of 1118.09 m, slope $m = -0.63$, elevation difference = 150.65 m, skiable distance of 577.65 m.
- b. The same characteristics were similarly determined for the tubing route:
 - Topographic length = 177.85 m;
 - The elevation of the downstream point = 945.42 m;
 - The elevation of upstream point = 979.64 m;
 - Elevation difference = 34.22 m;
 - Effective distance = 181.1 m;
- c. For the summer sledge route the following were determined:
 - Topographic length = 780 m;
 - The elevation of the downstream point = 948.43 m;
 - Elevation of upstream point = 983.30 m;
 - Effective distance = 811.35 m;
 - Branch with the steepest slope;
 - Branch with the lowest slope;
- d. For the cycle routes several variants are being studied, but it is not yet possible to simulate all the possible variants because the documentation is still being submitted to the forest protection service pending approval. Only after this approval has been given can the simulation of the 5 trails with different degrees of difficulty begin.

As far as the ski area is concerned, a program has been drawn up to guide skiers to the most suitable slope. For this purpose ArcMap software was used and a (VBA) sequence was created which takes into account: the skier's weight (a scale was created from 5 to 5 kg), the age of the skier (a scale was created that took into account certain coefficients that had higher values at younger and older ages - here also specifying certain aspects related to the individual's health), the skier's courage or degree of fear (a scale was created from 1 to 10) and the skier's skiing experience (on a scale from 1 to 10) (Figure 11). The (VBA) sequence created considers all these criteria (with the values indicated by the skier) and outputs one of the 3 possible routes,

also specifying the possible travel speed (or the maximum speed allowed for the skier's experience) (Figure 12). A specific interface has been created for this program where the user is asked to answer the 4 questions and, depending on the answers given, will be guided to the most suitable route for him.

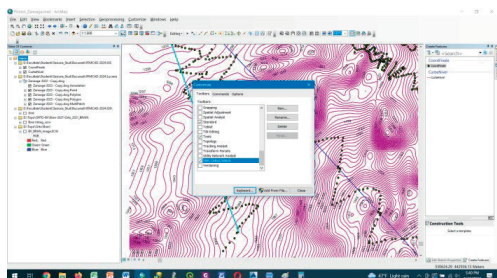


Figure 11. Creating the VBA sequence for choosing the appropriate slope

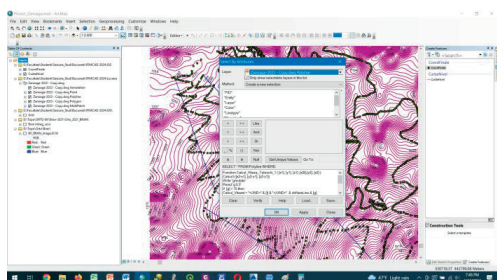


Figure 12. VBA sequence for setting the travel speed

For the part that considers the route of the summer sled, (GIS) facilities were used to design the route and to establish the fundamental elements in the design of the speed at which the sleds will move. It was observed that it is necessary to establish the main points of the route (those points that influence the projected speed the most), the height of the main pillars (those pillars that change the speed of travel to the lowest) and of the less important ones, the number and twist of the spirals (a very important element in controlling speed), the degree of opening of the curves. For a design speed of 40 km/h all these values were determined by a Visual Basic for Applications (VBA) sequence (Figure 13).

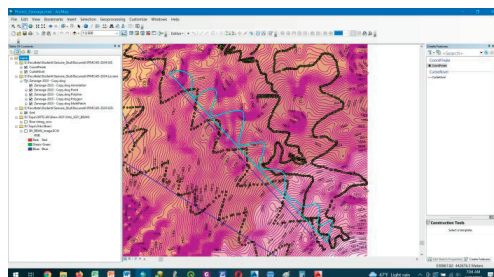


Figure 13. VBA sequence for determining the optimal route of the summer sled

CONCLUSIONS

The use of geographical information systems in the management of sports complexes is proving to be very beneficial in many ways. In addition to very clear and efficient management and the possibility of producing highly accurate maps, it is also possible to use (VBA) programming sequences to simulate certain situations or to facilitate all the calculations required for the design of various facilities. As part of this work, a small program called UNDE SCHIEZ has been created, which allows any skier to calculate, according to weight, age, courage and experience, which slope is best suited. Simulations have also been carried out on the speed of the summer sledging route, considering: the essential points of the route, the height of the pylons, the number and twist of the spirals, the degree of openness of the bends. With the help of (GIS), the appropriate values for the above parameters were established, based on predicted speed.

REFERENCES

- Barabaș, N., Rusu, T., (1979). *Curs de turism*. FEFS, Cluj Napoca, pp. 256.
- Barabaș, N. & Ganea I.V. (1995). *Schi alpin-Caiet de lucrări practice*. Universitatea Babeș-Bolyai, Cluj Napoca, pp. 187.
- Bălțeanu, D. (1975). *Piatra Mare, Ghid turistic*. Editura Sport turism, București, pp. 168.
- Bărănescu, R. (1975). *Turism și alimentație publică*. Editura Didactică și Pedagogică, București, pp. 220.
- Barbu, Ghe. (1980). *Turismul și calitatea vieții*. Editura Politică, București, pp. 189.

- Bără, M. (1983). *Schiul pentru toți*. Editura Stadion, București, pp. 236.
- Cândea, M. & Erdeli, G. (2001). *România. Potențialul turistic și turism*, Editura Universității București, pp. 268.
- Ciangă, N. (2001). *România, Geografia turismului*. Editura Presa Universitară Clujeană, Cluj Napoca, pp. 269.
- Cârstocea, V. (1998). *Schiul alpin*. Editura IEFS, București, pp. 175.
- Erdeli, G. & Istrate, I. (1996). *Potențialul turistic al României*. Editura Universității din București, pp. 229.
- Epuran, Ghe., (1958). *Urme de schi peste veacuri*. Editura Tineretului, București, pp. 195.
- Ganea, I.V. (2006). *Managementul agrementului în natură*. Editura Napoca Star, Cluj Napoca, pp. 221.
- Grigoraș, P. (2002). *Schi alpin, Snowboard, Carving*. Editura Accent, Cluj Napoca, pp. 237.
- Glăvan, V. (2000). *Turismul în România*. Editura Economică, București, pp. 184.
- Hossu Longin, V. (1980). Momente din istoria turismului românesc. În *România Pitorească 6*, București, pp. 28-32.
- Ielenicz, M., Comănescu, L. (2006). *România: potențial turistic*. Editura Universitară, București, pp. 226.
- Ilieș, M. (2007). *Amenajare turistică*. Editura Casa Cărții de Știință, Cluj-Napoca, pp. 174.
- Ionescu, I. (1999). *Turismul-fenomen economic, social și cultural*. Editura Oscar Print, București, pp. 258.
- Ionescu, Ghe. (2004). *Predeal. Istoria schiului*. Editura Ecran Magazin, Brașov, pp. 159.
- Matei, I. (1982). *Marea aventură a schiului*. Editura Albatros, București, pp. 283.
- Monea, Ghe. & Yamora, E. (1998). *Amenajări baze sportive*, Universitatea Babeș Bolyai, Cluj Napoca, pp. 311.
- Petrea, R. & Petrea, D. (2000). *Turism rural*. Editura Presa Universitară Clujeană, Cluj Napoca, pp. 299.
- Posea, G., Popescu, N., Ielenicy, M. (1974). *Relieful României*. Editura Științifică, București, pp. 273.
- Teodorescu, A.B. (1998). *Turism și orientare sportivă*. Editura Fundației România de Măine, București, pp. 236.
- Tereșneu, C.C. & Tereșneu, C.S., (2023), GIS facilities for the automation of cadastral documentations. *Scientific papers – series E – Land reclamation Earth observation & surveying environmental engineering. XII*, 371-376.
- Tereșneu, C.C., Tamaș, Șt., Vasilescu, M.M., Ionescu, M., Hanzu, M., Cîrștian D.G. (2009). Possibilities of automated solving of some representative surveying-related problems by means of AutoCAD and Scilab software. În *Pădurea și dezvoltarea durabilă*, Editura Universității Transilvania din Brașov, pp. 503-510.
- Tereșneu, C.C. & Vasilescu, M.M. (2013): Possibilities to automatize the process of elaboration the cadastral documentation. *RevCAD*, 14, 179-188.
- Tereșneu, C.C., Cîrștian, D.G., Hanganu, H., Vlad-Drăghici, H.G. (2013). Using Geographical Information System for the Automatic Creation of Topographic Maps. În *Pădurea și dezvoltarea durabilă*, Editura Universității Transilvania din Brașov, pp. 117-122.
- Tereșneu, C.C., Clinciu, I., Vasilescu, M.M., Biali, G. (2016). Using the GIS Tools for a sustainable forest management. *Environmental Engineering and Management Journal*, 15(2), 461-472.

REDUCING THE ENVIRONMENTAL IMPACT BY USING A SUSTAINABLE PROTEIN SOURCE IN FISH DIET - INSECT MEAL. A REVIEW

Alina ANTACHE^{1,2,3}, Ira-Adeline SIMIONOV^{1,3}, Stefan-Mihai PETREA^{1,3}, Aurelia NICA³,
Catalina ITICESCU^{1,4}, Puiu Lucian GEORGESCU^{1,4},
Catalin PLATON⁵, Alin-Stelian CIOBÎCĂ^{2,6,7,8}

¹"Dunarea de Jos" University of Galati, REXDAN Research Infrastructure,
98 George Cosbuc Street, Galati, Romania

²"Alexandru Ioan Cuza" University of Iasi, Faculty of Biology,
20A Carol I Blvd, Iasi, Romania

³"Dunarea de Jos" University of Galati, Faculty of Food Science and Engineering,
111 Domneasca Street, Galati, Romania

⁴"Dunarea de Jos" University of Galati, Faculty of Sciences and Environment,
111 Domneasca Street, Galati, Romania

⁵"ROMFISH" - National Association of Fish Producers,
12A Nicolae Iorga Blvd, Iasi, Romania

⁶Centre of Biomedical Research, Romanian Academy,
8 Carol I Blvd, Iasi, Romania

⁷Academy of Romanian Scientists, 54 Splaiul Independentei Street,
District 5, Bucharest, Romania

⁸Apollonia University, Preclinical Department,
11 Pacurari Street, Iasi, Romania

Corresponding author email: alina.antache@ugal.ro

Abstract

Due to the growth intensification in the aquaculture industry it is desirable to ensure fish production and improve it in a sustainable manner. It is known that the protein source from fish diet is represented by the fish meal which is very expensive. Obtaining fishmeal requires quite a lot of pressure on fish stocks in the natural environment due to overfishing, which leads to a drastic reduction of stocks. For this reason, it is desirable to find sustainable alternative sources that can replace the protein from fish meal. Therefore, was tried the replacement with soy, sorghum or wheat meal, but their production involves a very large cultivation area. Recently, was made some research on the fish growth and welfare effect in case of replacement of fish meal with insect meal. In conclusion, it has been demonstrated that the insect meal has a much higher nutritional value and has a low impact on the environment (low footprint, less water and feed consuming), but the selection of optimal insect species for the production of protein for fish feed represents a considerable challenge.

Key words: environmental impact, insect meal, overfishing, sustainable protein source.

INTRODUCTION

In recent years the aquaculture sector has experienced an intensive production in a very rapid way in the worldwide to contribute to food security. The world population has consumed more farmed fish than captured fish (FAO, 2016).

Fisheries and aquaculture production reaches an all-time high of 214 million tons in 2020 (FAO, 2022). Also, aquaculture production has a huge potential for expansion for increased fish

supply, which is an important high-quality source of animal protein for human food (Munguti et al., 2021). This exponential growth has also led to the experimentation of certain aspects related to the economic and ecological issues as the supply of fishmeal and fish oil included in fish diet which is constantly decreasing (Tschirner & Kloas, 2017). Therefore, putting a lot of pressure on the fish population contributes to the production of fish meal and oil that goes into fish feed endangers the sustainability of wild fish fauna. This leads

to an increased costs related to the production of fish feed, with a direct effect on the economic profitability of fish farming (FAO, 2016). But, the consistent use of fish meal in aquaculture has not only threatened the sustainability of fisheries ecosystems but has also increased fish demand, and thus affecting profit margins of the fish farmers (Ogello et al., 2014).

Research on novel ingredients for fish feeds, such as microalgae and other single cell proteins, macroalgae, and insect meals, has proliferated recently and will continue to expand (Naylor et al., 2021; Dumitrache et al., 2022). Over time, plants have been introduced into the diet of fish, to replace a part of fish meal, as a source of protein such as soybeans, peas, etc. However, it is known that the composition of the fish diets can have a very big impact on the environmental sustainability as it is necessary to evaluate feed materials and whether or not an alternative is possible that would be more effective and have less impact on the environment.

Therefore, the marine stocks harvested from the wild for fishmeal production are decreasing and from ecologic and economic points of view, the plant-based protein sources are no longer sustainable (FAO, 2016). From this reason, was made different research to look an alternative source of protein to replace fish meal in fish diet, more exactly to improve fish production but also to maintain environmental sustainability.

In fish nutrition were used different plant meals such as SBM, copra meal, sunflower meal, cotton meal and pea meal, but are not parts of natural fish diets, and therefore, their protein contents and AA profiles are not well balanced for fish. Animal by-products such as blood meal, hydrolysed feather meal, bone meal and meat meal have also been used in fish nutrition (Campos et al., 2017; Moutinho et al., 2017). Also, it is known that the protein source from fish diet is represented by the fish meal which is very expensive. Obtaining fishmeal requires quite a lot of pressure on fish stocks in the natural environment due to overfishing, which leads to a drastic reduction of stocks. For this reason, it is desirable to find sustainable alternative sources that can replace the protein from fish meal.

The aim of these paper is to present the alternative protein sources used to replace the

fish meal from fish diet with that from vegetable plants or insects and the effect of this on the fish growth and welfare.

VEGETABLE PLANTS USED AS PROTEIN SOURCE IN FISH DIET AND THEIR IMPACT

Over the years, attempts have been made to replace fish meal with meal from terrestrial plants more precisely in order to find an alternative source of protein for fish feed as a strategy to contribute to aquaculture sustainability and to reducing the production costs. But in recent years, research has shown that replacing fishmeal with plant-based meal can have negative effects on fish growth and welfare.

Most plant used as protein source contain a variety of biologically active antinutritional elements, which may negatively affect the feed intake, digestion and absorption of nutrients, and fish health status (Hardy, 2010; Glencross et al., 2020).

In 2011, Montero & Izquierdo, but also Merrifield et al., reported that a high level of vegetable ingredients present in fish diet have a negative impact on the fish health and growth performance due to the nutritional imbalances or to the presence of some antinutritional elements. In some study was showed that soybean meal can induce the enteritis in case of fish meal replacement strategies from fish diet.

For example, based on the morphological alterations found in the liver and distal intestine of gilthead seabream juveniles, a possible negative effect of long-term feeding with diets containing more than 34% of carob seed germ meal was suggested (Martínez-Llorens et al., 2012), due to content in tannins in carob seed germ.

Studies in other species, like common carp and gilthead seabream reveal a similar pattern of soybean-induced enteritis but at much higher levels of inclusion when compared to Atlantic salmon (Uran, 2008), suggesting a different species susceptibility towards vegetal ingredients. The symptoms described for fish in which the diet have a high inclusions of soybean meal were: a decrease in digestive enzymes activities, an inhibition of adsorption of brush border enzymes, alterations on the intestinal

morphology (shortening of the intestinal mucosa folds, supranuclear vacuoles in enterocytes), inflammation process, fat deposition in liver and enterocytes, loss of intestine selectivity and lower resistance to diseases due to the decrease in the immunity (Ribeiro et al., 2014).

In 2020, Johny et al. reported that the introduction of wheat meal in 30% concentration in fish diet affected the intestinal and liver health of Atlantic salmon after 63 days of feeding. The symptoms were similar to gluten sensitivity in humans.

In case of *Lates calcarifer* species, fed with a diet in which the fish meal was replaced with 75% by lupin meal for 60 days, was observed a liver steatosis, a necrosis in kidney and a low growth performance (Siddik et al., 2021). This is because lupine contains phytic acid, tannins, saponins and lectins, substances considered to be antinutritional factors.

Fishmeal replacement, by a mix of plant proteins negatively affected the immune status of the turbot juveniles (mix: wheat gluten, soybean meal, and soy protein concentrate, the replacement was up to 50%) (Bonaldo et al., 2015) and decreased the plasma immunoglobulins, blood monocytes, and gut interleukin-10 (IL-10) mRNA expression in case of European seabass (mix: meal, wheat meal, wheat gluten and corn gluten) (Azeredo et al., 2017).

Unlike to land plants, the macro- and microalgae have been considered alternative ingredients, due to their high growth rates and non-competition of arable lands for cultivation. Macroalgae encompass algae that are multicellular and macroscopic and, depending on the species, their nutritional value is quite different (Aragao et al., 2022).

Generally, plant-based protein derivatives are limited regarding to the essential amino acids' composition, presence of endogenous antinutritional factors that reduce their efficiency of utilization in fish (Hossain et al., 2003). Also, they have low palatability (Refstie et al., 2000), high ash and fibre contents (Olvera-Novoa et al., 2002), which in high levels inclusions in fish diet reduces digestibility and protein conversion by fish as well as pellet quality of the feed (Mugo-Bundi et al., 2013; Ogello & Munguti, 2016). For example sunflower has inadequate lysine, phenylalanine, methionine, phosphorus,

high fibre levels, low energy and poor palatability (Ogello et al., 2017) and soybean is limited due to the low levels of methionine and cost ineffectiveness (Gamboa-Delgado et al., 2013).

All these aspects contribute to the reduction the bioavailability of nutrients in the fish, decrease the efficiency of utilization, increase the feed conversion ratio, culminating with the reduction in economic success (Hossain et al., 2003). Therefore, non-conventional protein sources, such as insect meal, have gained interests to provide an alternative protein source due to its nutritional values that are close to that of fish meal (Fadaee, 2012).

INSECT MEAL USED AS ALTERNATIVE PROTEIN SOURCE IN FISH DIET AND THEIR IMPACT

Unlike to the plants used in fish nutrition, insects which are farmed under controlled conditions can be a viable alternative protein source in fish diets.

Insects, as well as other animals, are good sources of protein, lipids, vitamins and minerals (sodium, iron, potassium and zinc), but the amounts of these nutrients will vary according to the diet and the stage of the animal (Nogales-Merida et al., 2019). This makes the use of insects, in the fish diet, a sustainable source.

Insects are an excellent source of protein due to content in amino acids; their levels of protein range from 25% to 75 % (Finke et al., 2015). From all insects, those from *Orthoptera* has the maximum protein values, ranging from 60% to 77% (Barroso et al., 2014). When insect protein is compared with plant and meat proteins, it is found that insects contain a substantial amount of good-quality protein due to balanced amino acid proportions (Rumpolds et al., 2013).

Insect used in fish diet

Black Soldier Fly

The black soldier fly (*Hermetia illucens*) represents one of the best options currently used as an alternative source of protein in the fish diet and due to his nutritional value is one of the most investigated insect species (Chen et al., 2021). They balanced nutritional composition makes it

an ideal and possibly significant alternative to fish meal.

The content in bioactive compounds such as lauric acid, chitin and antimicrobial peptides, make them to have nutraceutical properties which contribute to improve the fish growth (Surendra et al., 2020). Also, the protein of black soldier fly has a good protein solubility, water binding capacity, and lipid binding capacity (Bußler et al., 2016). The introduction of BSFL meal in fish diet did not show any adverse impact on fish development (Cummins et al., 2017; Dumas et al., 2018).

The use of this insect makes it sustainable due to the fact that it can utilize organic wastes as the substrate, such as animal dung (Moula et al., 2018; Parodi et al., 2021) and plant waste, which includes vegetables and fruit wastes (Meneguz et al., 2018) and algae (Liland et al., 2017). In case of Nile tilapia BSFL meal was found to have a greater growth response and feed conversion ratio than fish meal (Aini et al., 2018).

Common Housefly

Housefly (*Musca domestica*) maggot meal has a high nutritional value as an insect protein source. The housefly contains a substantial number of proteins, lipids, and carbohydrates similar to fishmeal, improving fish growth (Makkar et al., 2014). Housefly larvae are less expensive, have healthy nutritional contents, and are easier to produce.

Houseflies can quickly digest food waste and cattle dung waste, which is organic, using nutrients from waste to reduce the volume of waste in its entirety. Wang et al. (2017), observed that the supplemented diet of Nile tilapia with 75% maggot meal had no substantial adverse effects on the fish growth and development. But, in other study the replacement of fish meal with maggot meal (100%) had no any negative impact on Nile tilapia fingerlings (Ogunji et al., 2008) and African catfish (Okey Aniebo et al., 2009) without damaging growth or nutrient utilization ability or causing oxidative stress fingerlings (Ogunji et al., 2008). Also, several feeding studies on various fish species have shown that adding housefly maggots meal in fish diets may boost growth and FCR while limiting physiological stress, also the fish diet which

contain housefly meal is also less expensive (Ogunji et al., 2021).

Cricket

Cricket (*Acheta domesticus*) meal contains a significant amount of crude protein (64.9%) and lipids (17.4%) with a good proportion of amino acids, including lysine and methionine, which are deficient in a plant-based diet (Jeong et al., 2021). Recent studies reported that 8.7% of chitin is present in cricket meals, and its supplementation in the fish diet can improve the interaction of chitosan glucosamine with bacterial cell walls (Phesatcha et al., 2022).

In fish diet cricket meal has the potential to partially or completely replace the fish meal (Jeong et al., 2021). In case of African catfish, the replace of fish meal with cricket meal in 100% proportion in concentration show better growth performance than the control diet (Taufek et al., 2018). In other study the substitute of fish meal with 50% cricket meal in red Nile tilapia diet not significantly affecting growth performance or feed consumption (Finke et al., 2015).

Locust

Locusts are among the most commonly consumed insect species, they are a protein source for the chickens and fish (Van Huise et al., 2013) because they have up to 70% protein content in dry matter basis. Several studies have shown that replacing 20% fish meal with locust meal did not influence digestibility and growth performance of catfish and Nile tilapia (Alegbeleye et al., 2012). But the replacement with 50% locust meal has led to optimal results in terms of growth.

Mealworm

Mealworms (*Tenebrio molitor* - TM) are simple to produce, have a low environmental impact, are easily to manipulate, have a good nutritional content and are highly efficient.

Research shows that TM meal is an innovative protein source that can partially substitute fish meal in rainbow trout (Belforti et al., 2015), European sea bass (Gasco et al., 2016), gilthead seabream (Piccolo et al., 2017) and blackspot seabream (Jeong et al., 2021). Also, a 100% replacement of fish meal with yellow mealworm meal enhances the Pacific white shrimp lipid content but does not affect the growth rate and feed conversion ratio (Panini et al., 2017). But it must be considered that the meal worm has a

low concentration of calcium so primarily feeding fish with mealworms might result in calcium deficiencies and body deformities, despite this, the mealworm insect is an excellent choice to replace fishmeal (Makkar et al., 2014).

Silkworm

Silkworm meal contains 56% protein and is obtained by drying and grinding the larvae uncoiled boiled cocoons (Tomotake et al., 2010). Researches showed that replacing fish meal with 10% silkworm meal can be successfully substituted in the diet of salmon and olive flounder (Lee et al., 2012), and with 50% in African catfish fingerlings diet conduct to an increase in growth rate and feed utilization efficiency (Kurbanov et al., 2015).

The supplemented fish diet with 30-50% silkworm pupae registered a successful in case of some fish species (rohu, common carp, mahseer, and rainbow trout) (Sawhney et al., 2014). Also, silkworm meal was found to be an advantageous sustainable feed element in carp (Wan et al., 2017) and rainbow shark (Raja et al., 2020) diets, with benefits for boosting growth performance and specific physiological markers.

But in Jian carp and Nile tilapia the replacement of fish meal with silkworm meal in different concentrations show negative responses as: reduced digestive enzyme activity, heat shock protein activities, and increased oxidative stress (Boscolo et al., 2002; Ji et al., 2015).

Advantages of using insects in aquaculture

Insect production requires six times less feed than conventional livestock to produce the same number of proteins (Randazzo et al., 2021). The greenhouse gas emission from the insects is much less compared to the conventional livestock in the production of food/feed. In the same time the insects can be mass produced using organic waste streams (Gaudioso et al., 2021).

In the wild, fish consume insects, omnivorous fish species eat insects from the bottom of water, while carnivorous fish species consume juvenile life stages of insects (Lopez-Pedrouso et al., 2020). Insects such as the housefly, mealworm, grasshopper, black soldier fly and cricket have been identified as good alternatives to fishmeal (Gasco et al., 2018).

Some research studies with fish fed diets with varying inclusion levels of black soldier fly larvae meal have reported good growth performances similar to those from fish fed on common protein sources such as fish meal. Fingerlings of *Ictalurus punctatus* had a similar weight gain when the diets were supplemented with up to 30% of full-fat black soldier fly larvae meal (BM) (Newton et al., 2005). In case of *Oncorhynchus mykiss* a replacement of fish meal with 25% black soldier fly meal not have any negative effect on the fish weight gain (St-Hilaire et al., 2007).

Regarding to the investment and the cost-benefit ratio was similar across the diets, suggesting that black soldier fly meal is a suitable and cost-equivalent dietary supplement of fish meal up to 100% in aquafeed for growing tilapia fish in earthen ponds for the market (Wachira et al., 2021).

In case of African catfish supplemented diet with 22% black soldier fly meal conduct to an improvement of growth performance and restored gut microbioma equilibrium. Also enhanced development performance and optimized feed utilization, accompanied by increased antioxidant enzyme activity and contribute to reduced lipid peroxidation in the fish fillet (Fawole et al., 2020).

Benefits of insect meal in aquaculture

Nutritional value - Research has shown that insect – based feeds can provide a balanced amino-acid profile, essential fatty acids, vitamins and minerals necessary for optimal fish health (Chen et al., 2021).

Environmental sustainability - Insects require less land, water and feed resources, emit lower greenhouse gas emissions and generate fewer nutrient-rich effluents. The environmental impact can be reduced by correspondingly increasing insect production, and as a result, insects can compete with conventional ingredients (Smetana et al., 2019). Environmental impact categories of *T. molitor* (Le Feon et al., 2019), *M. domestica* (Roffeis et al., 2020) and *H. illucens* (Maiolo et al., 2020) largely contribute to the food produced in the insect farming industry. Therefore, providing the right substrate for insect growth and increasing plant efficiency will be major

contributors to achieving the environmental benefits of insect meal (Smetana et al., 2019; Thevenot et al., 2018). Bioconversion technique for insect production is one of the sustainable solutions to food security. In this sense, waste is a valuable resource for high-quality production protein (insect meal) for the food system. As a result, the technology produces zero waste and reduces the need for expensive protein sources such as soybean meal and fish meal in aqua feed (IPIFF, 2019).

Disease control - Insects possess innate antimicrobial properties, making them potentially valuable in disease prevention and control in aquaculture (Wang et al., 2019).

Economic viability - The cost-effectiveness of insect cultivation for aquaculture feeds is gaining traction (Moreki et al., 2012).

In future must be support the use of insect meal into large scale commercial feed manufacturing and enhance sustainable intensification in aquaculture production.

CONCLUSIONS

In conclusion, it has been demonstrated that the insect meal has a much higher nutritional value and has a low impact on the environment (low footprint, less water and feed consuming), but the selection of optimal insect species for the production of protein for fish feed represents a considerable challenge.

Compared to traditional fish-based feeds, insect cultivation has a significantly lower environmental impact. Insects are highly efficient in converting organic waste materials into valuable biomass.

The replacement of fish meal with insect meal can conduct to the increase of fish growth performance and immunity status improving the welfare status.

ACKNOWLEDGEMENTS

The present research was supported by the project An Integrated System for the Complex Environmental Research and Monitoring in the Danube River Area, REXDAN, SMIS code 127065, co-financed by the European Regional Development Fund through the Competitiveness Operational Programme 2014–2020, contract no. 309/10.07.2021.

REFERENCES

- Aini, N., Nugroho, R.A., Hariani, N. (2018). Growth and Survival Evaluation of *Oreochromis Sp Fed Hermetia Illucens Larva and Manihot Esculenta Leaves Meal*. Biosaintifika. *J. Biol. Biol. Educ.*, 10, 565–573.
- Alegbeleye, W.O., Obasa, S.O., Olude, O.O., Otubu, K., Jimoh, W. (2012). Preliminary Evaluation of the Nutritive Value of the Variegated Grasshopper (*Zonocerus variegatus* L.) for African Catfish *Clarias gariepinus* (Burchell. 1822) Fingerlings. *Aquac. Res.*, 43, 412–420.
- Aragão, C., Gonçalves, A.T., Costas, B., Azeredo, R., Xavier, M.J., Engrola, S. (2022). Alternative Proteins for Fish Diets: Implications beyond Growth. *Animals* 12, 1211. <https://doi.org/10.3390/ani12091211>.
- Azeredo, R., Machado, M., Kreuz, E., Wuertz, S., Oliveira-Teles, A., Enes, P., Costas, B. (2017). The European seabass (*Dicentrarchus labrax*) innate immunity and gut health are modulated by dietary plant-protein inclusion and prebiotic supplementation. *Fish Shellfish Immunol.*, 60, 78–87.
- Barroso, F.G., de Haro, C., Sánchez-Muros, M.J., Venegas, E., Martínez-Sánchez, A., Pérez-Bañón, C. (2014). The Potential of Various Insect Species for Use as Food for Fish. *Aquaculture*, 422–423, 193–201.
- Belforti, M., Gai, F., Lussiana, C., Renna, M., Malfatto, V., Rotolo, L., De Marco, M., Dabbou, S., Schiavone, A., Zoccarato, I., et al. (2015). Tenebrio molitor Meal in Rainbow Trout (*Oncorhynchus mykiss*) Diets: Effects on Animal Performance, Nutrient Digestibility and Chemical Composition of Fillets. *Ital. J. Anim. Sci.*, 14, 670–676.
- Bonaldo, A., di Marco, P., Petochi, T., Marino, G., Parma, L., Fontanillas, R., Koppe, W., Mongile, F., Finoia, M.G., Gatta, P.P. (2015). Feeding turbot juveniles *Psetta maxima* L. with increasing dietary plant protein levels affects growth performance and fish welfare. *Aquac. Nutr.*, 21, 401–413.
- Boscolo, W.R., Hayashi, C., Meurer, F. (2002). Digestibilidade Aparente Da Energia e Nutrientes de Alimentos Convencionais e Alternativos Para a Tilápia Do Nilo (*Oreochromis niloticus*, L.). *Rev. Bras. Zootec.*, 31, 539–545.
- Bußler, S., Rumpold, B.A., Jander, E., Rawel, H.M., Schlüter, O.K. (2016). Recovery and Techno-Functionality of Flours and Proteins from Two Edible Insect Species: Meal Worm (*Tenebrio molitor*) and Black Soldier Fly (*Hermetia illucens*) Larvae. *Heliyon*, 2, e00218.
- Campos, I., Matos, E., Marques, A., Valente, L.M.P. (2017). Hydrolyzed feather meal as a partial fishmeal replacement in diets for European seabass (*Dicentrarchus labrax*) juveniles. *Aquaculture*, 476, 152–159.
- Chen, H.Y., Li, H.L., Pang, H., Zhu, C.D., Zhang, Y.Z. (2021). Investigating the Parasitoid Community Associated with the Invasive Mealybug *Phenacoccus Solenopsis* in Southern China. *Insects*, 12, 290.
- Cummins, V.C., Rawles, S.D., Thompson, K.R., Velasquez, A., Kobayashi, Y., Hager, J., Webster, C.D. (2017). Evaluation of Black Soldier Fly

- (*Hermetia illucens*) Larvae Meal as Partial or Total Replacement of Marine Fish Meal in Practical Diets for Pacific White Shrimp (*Litopenaeus vannamei*). *Aquaculture*, 473, 337–344. [CrossRef]
- Dumas, A., Raggi, T., Barkhouse, J., Lewis, E., Weltzien, E. (2018). The Oil Fraction and Partially Defatted Meal of Black Soldier Fly Larvae (*Hermetia illucens*) Affect Differently Growth Performance, Feed Efficiency, Nutrient Deposition, Blood Glucose and Lipid Digestibility of Rainbow Trout (*Oncorhynchus mykiss*). *Aquaculture*, 492, 24–34. [CrossRef]
- Dumitrache, C., Mihai, C., Frîncu M. (2022). Yeast - sustainable nutrient source for fish feed - review. *Scientific Papers. Series E. Land Reclamation, Earth Observation & Surveying, Environmental Engineering, Vol. XI*, 464-469, Print ISSN 2285-6064.
- Fadace, R. (2012). A review on earthworm *Eisenia foetida* and its applications. *Annals of Biological Research*, 3(5), 2500–2506.
- FAO, The State of World Fisheries and Aquaculture 2022. Towards Blue Transformation, 2022.
- Fawole, F.J., Adeoye, A.A., Tiamiyu, L.O., Ajala, K.I., Obadara, S.O., & Ganiyu. I.O. (2020). Substituting fishmeal with *Hermetia illucens* in the diets of African catfish (*Clarias gariepinus*): effects on growth, nutrient utilization, haematophysiological response, and oxidative stress biomarker. *Aquaculture*, 518, 73484.
- Finke, M.D. (2015). Complete Nutrient Content of Four Species of Commercially Available Feeder Insects Fed Enhanced Diets during Growth. *Zoo Biol.*, 34, 554–564.
- Gamboa-Delgado, J., Rojas-Casas, M.G., Nieto-López, M.G., & Cruz-Suárez, L.E. (2013). Simultaneous estimation of the nutritional contribution of fish meal, soy protein isolate and corn gluten to the growth of Pacific white shrimp (*Litopenaeus vannamei*) using dual stable isotope analysis. *Aquaculture*, 380–383, 33–40. <https://doi.org/10.1016/j.aquaculture.2012.11.028>.
- Gasco, L., Henry, M., Piccolo, G., Marono, S., Gai, F., Renna, M., Lussiana, C., Antonopoulou, E., Mola, P., Chatzifotis, S. (2016). Tenebrio molitor Meal in Diets for European Sea Bass (*Dicentrarchus labrax* L.) Juveniles: Growth Performance, Whole Body Composition and in Vivo Apparent Digestibility. *Anim. Feed Sci. Technol.*, 220, 34–45.
- Gaudio, G., Marzorati, G., Faccenda, F., Weil, T., Lunelli, F., Cardinaletti, G., Marino, G., Olivotto, I., Parisi, G., Tibaldi, E., et al. (2021). Processed Animal Proteins from Insect and Poultry By-products in a Fish Meal-free Diet for Rainbow Trout: Impact on Intestinal Microbiota and Inflammatory Markers. *Int. J. Mol. Sci.*, 22, 5454. [CrossRef]
- Glencross, B.D., Bailly, J., Berntssen, M.H.G., Hardy, R., MacKenzie, S., Tocher, D.R. (2020). Risk assessment of the use of alternative animal and plant raw material resources in aquaculture feeds. *Rev. Aquac.*, 12, 703–758.
- Hardy, R.W. (2010). Utilization of plant proteins in fish diets: Effects of global demand and supplies of fishmeal. *Aquac. Res.*, 41, 770–776. [CrossRef]
- Hossain, M.A., Focken, U., & Becker, K. (2003). Antinutritive effects of galactomannan rich endosperm of sesbania (*Sesbania aculeate*) seeds on growth and feed utilization in tilapia, *Oreochromis niloticus* L. *Aquaculture Research*, 43(3), 1171–1179. <https://doi.org/10.1046/j.1365-2109.2003.00924.x>
- IPIFF. The European Insect Sector Today: Challenges, Opportunities and Regulatory Landscape; IPIFF Vision Paper on the Future of the Insect Sector towards 2030; IPIFF: Brussels, Belgium, 2019; p. 16.
- Jeong, S.M., Khosravi, S., Mauliasari, I.R., Lee, B.J., You, S.G., Lee, S.M. (2021). Nutritional Evaluation of Cricket, *Gryllus bimaculatus*, Meal as Fish Meal Substitute for Olive Flounder, *Paralichthys Olivaceus*, Juveniles. *J. World Aquac. Soc.*, 52, 859–880.
- Jeong, S.M., Khosravi, S., Yoon, K.Y., Kim, K.W., Lee, B.J., Hur, S.W., Lee, S.M. (2021). Mealworm, *Tenebrio molitor*, as a Feed Ingredient for Juvenile Olive Flounder, *Paralichthys Olivaceus*. *Aquac. Rep.*, 20, 100747.
- Ji, H., Zhang, J.L., Huang, J.Q., Cheng, X.F., Liu, C. (2015). Effect of Replacement of Dietary Fish Meal with Silkworm Pupae Meal on Growth Performance, Body Composition, Intestinal Protease Activity and Health Status in Juvenile Jian Carp (*Cyprinus carpio* var. jian). *Aquac. Res.*, 46, 1209–1221.
- Kurbanov, A.R., Milusheva, R., Rashidova, S., Kamilov, B. (2015). Effect of Replacement of Fish Meal with Silkworm (*Bombyx mori*) Pupa Protein on the Growth of *Clarias Gariepinus* Fingerling. *Int. J. Fish. Aquat. Stud.*, 2, 25–27.
- Le Féon, S., Thévenot, A., Maillard, F., Macombe, C., Forteau, L., Aubin, J. (2019). Life Cycle Assessment of Fish Fed with Insect Meal: Case Study of Mealworm Inclusion in Trout Feed, in France. *Aquaculture*, 500, 82–91.
- Lee, J., Choi, I.C., Kim, K.T., Cho, S.H., Yoo, J.Y. (2012). Response of Dietary Substitution of Fishmeal with Various Protein Sources on Growth, Body Composition and Blood Chemistry of Olive Flounder (*Paralichthys olivaceus*, Temminck & Schlegel, 1846). *Fish Physiol. Biochem.*, 38, 735–744.
- Liland, N.S., Biancarosa, I., Araujo, P., Biemans, D., Bruckner, C.G., Waagbø, R., Torstensen, B.E., Lock, E.J. (2017). Modulation of Nutrient Composition of Black Soldier Fly (*Hermetia illucens*) Larvae by Feeding Seaweed-Enriched Media. *PLoS ONE*, 12, e0183188.
- López-Pedrouso, M., Lorenzo, J.M., Cantalapiedra, J., Zapata, C., Franco, J.M., Franco, D. (2020). Aquaculture and By-Products: Challenges and Opportunities in the Use of Alternative Protein Sources and Bioactive Compounds. *Adv. Food Nutr. Res.*, 92, 127–185.
- Maiolo, S., Parisi, G., Biondi, N., Lunelli, F., Tibaldi, E., Pastres, R. (2020). Fishmeal Partial Substitution within Aquafeed Formulations: Life Cycle Assessment of Four Alternative Protein Sources. *Int. J. Life Cycle Assess.*, 25, 1455–1471.
- Makkar, H.P.S., Tran, G., Heuzé, V., Ankers, P. (2014). State-of-the-Art on Use of Insects as Animal Feed. *Anim. Feed Sci. Technol.*, 197, 1–33.
- Martínez-Llorens, S., Baeza-Ariño, R., Nogales-Mérida, S., Jover-Cerdá, M., Tomás-Vidal, A. (2012). Carob seed germ meal as a partial substitute in gilthead sea

- bream (*Sparus aurata*) diets: Amino acid retention, digestibility, gut and liver histology. *Aquaculture*, 338–341, 124–133. [CrossRef]
- Meneguz, M., Gasco, L., Tomberlin, J.K. (2018). Impact of PH and Feeding System on Black Soldier Fly (*Hermetia illucens*, L.; Diptera: Stratiomyidae) Larval Development. *PLoS ONE*, 13, e0202591.
- Merrifield, D.L., Olsen, R.E., Myklebust, R., Ringø, E. (2011). Dietary Effect of Soybean (Glycine max) Products on Gut Histology and Microbiota of Fish, Soybean and Nutrition. Prof. Hany El-Shemy (Ed.), ISBN: 978-953-307-536-5, InTech, Available from: <http://www.intechopen.com/books/soybean-and-nutrition/dietary-effect-of-soybeanglycine-max-products-on-gut-histology-and-microbiota-of-fish>.
- Montero, D., Izquierdo, M.S. (2011). Welfare and health of fish fed vegetable oils as alternative lipid sources to fish oil. In: Turchini, G., Ng, W., Tocher, D. (Eds.), *Fish Oil Replacement and Alternative Lipid Sources in Aquaculture Feeds*. CRC Press, Cambridge, UK, pp. 439-485.
- Moreki, J.C., Tiroesele, B., & Chiripasi, S.C. (2012). Prospects of utilizing insects as alternative sources of protein in poultry diets in Botswana. *Journal of Animal Science Advance*, 2, 649-58.
- Moula, N., Scippo, M.L., Douny, C., Degand, G., Dawans, E., Cabaraux, J.F., Hornick, J.L., Medigo, R.C., Leroy, P., Francis, F., et al. (2018). Performances of Local Poultry Breed Fed Black Soldier Fly Larvae Reared on Horse Manure. *Anim. Nutr.*, 4, 73–78.
- Moutinho, S., Martinez-Llorens, S., Tomas-Vidal, A., Jover-Cerda, M., Oliva-Teles, A., Peres, H. (2017). Meat and bone meal as partial replacement for fish meal in diets for gilthead seabream (*Sparus aurata*) juveniles: growth, feed efficiency, amino acid utilization, and economic efficiency. *Aquaculture*, 468, 271–277.
- Mugo-Bundi, J., Oyoo-Okoth, E., Ngugi, C.C., Manguya-Lusega, D., Rasowo, J., Chepkirui-Boit, V., Njiru, J. (2013). Utilization of *Caridina nilotica* (Roux) meal as a protein ingredient in feeds for Nile tilapia (*Oreochromis niloticus*). *Aquaculture Research*, 46, 346–357.
- Naylor, R.L., Hardy, R.W., Buschmann, A.H., Bush, S.R., Cao, L., Klinger, D.H., Little, D.C., Lubchenco, J., Shumway, S.E., Troell, M. (2021). A 20-year retrospective review of global aquaculture. *Nature*, 591, 551–563. [CrossRef] [PubMed]
- Newton, L., Sheppard, C., Watson, D.W., Burtle, G., Dove, R. (2005). Using the Black Soldier Fly, *Hermetia illucens*, as a Value-Added Tool for the Management of Swine Manure; Report for Mike Williams; Director of the Animal and Poultry Waste Management Center, North Carolina State University: Raleigh, NC, USA.
- Nogales-Merida, S., Gobbi, P., Jozefiak, D., Mazurkiewicz, J., Dudek, K., Rawski, M., Kieronczyk, B., Jozefiak, A. (2019). Insect meals in fish nutrition. *Reviews in Aquaculture* 11, 1080–1103 doi: 10.1111/raq.12281.
- Ogello, E.O., & Munguti, J.M. (2016). Aquaculture: A promising solution for food insecurity, poverty and malnutrition in Kenya. *Africa Journal of food Agriculture Nutrition Development*, 16, 4.
- Ogello, E.O., Kembenya, M., Githukia, M., Aera, N., Munguti, M., & Nyamweya, S. (2017). Substitution of fish meal with sunflower seed meal in diets for Nile tilapia (*Oreochromis niloticus* L.) reared in earthen ponds. *Journal of Applied Aquaculture*, 29, 81–99. <https://doi.org/10.1080/10454438.2016.1275074>
- Ogello, E.O., Munguti, J.M., Sakakura, Y., & Hagiwara, A. (2014). Complete replacement of fish meal in the diet of Nile tilapia (*Oreochromis niloticus*) grow-out with alternative protein sources: A review. *International Journal of Advanced Research*, 2(8), 962–978.
- Ogunji, J., Schulz, C., Kloas, W. (2008). Growth Performance, Nutrient Utilization of Nile Tilapia *Oreochromis niloticus* Fed Housefly Maggot Meal (Maggot) Diets. *Turkish J. Fish. Aquat. Sci.*, 8, 141–147.
- Ogunji, J.O., Iheanacho, S.C., Mgbabu, C.N., Amaechi, N.C., Evulobi, O.O.C. (2021). Housefly Maggot Meal as a Potent Bioresource for Fish Feed to Facilitate Early Gonadal Development in *Clarias gariepinus* (Burchell, 1822). *Sustainability*, 13, 921. <https://doi.org/10.3390/su13020921>.
- Okey Aniebo, A., Erundu, E.S., Owen, O.J. (2009). Replacement of Fish Meal with Maggot Meal in African Catfish (*Clarias gariepinus*) Diets. *Rev. UDO Agricola*, 9, 666–671.
- Olivotto, I. (2021). Physiological Response of Rainbow Trout (*Oncorhynchus mykiss*) to Graded Levels of *Hermetia illucens* or Poultry by-Product Meals as Single or Combined Substitute Ingredients to Dietary Plant Proteins. *Aquaculture*, 538, 736550. [CrossRef]
- Olvera-Novoa, M., Olivera-Castillo, L., & Martínez-Palacios, C.A. (2002). Sunflower seed meal as a protein source in diets for Tilapia *rendalli* (Boulanger 1896. Fingerlings). *Aquaculture Research*, 33, 223–229. <https://doi.org/10.1046/j.1365-2109.2002.00666.x>.
- Parodi, A., Gerrits, W.J.J., Van Loon, J.J.A., De Boer, I.J.M., Aarnink, A.J.A., Van Zanten, H.H.E. (2021). Black Soldier Fly Reared on Pig Manure: Bioconversion Efficiencies, Nutrients in the Residual Material, Greenhouse Gas and Ammonia Emissions. *Waste Manag.*, 126, 674–683. [CrossRef]
- Phesatcha, B., Phesatcha, K., Viennaxay, B., Matra, M., Totakul, P., Wanapat, M. (2022). Cricket Meal (*Gryllus bimaculatus*) as a Protein Supplement on In Vitro Fermentation Characteristics and Methane Mitigation. *Insects*, 13, 129.
- Piccolo, G., Iaconisi, V., Marono, S., Gasco, L., Loponte, R., Nizza, S., Bovera, F., Parisi, G. (2017). Effect of *Tenebrio molitor* Larvae Meal on Growth Performance, in Vivo Nutrients Digestibility, Somatic and Marketable Indexes of Gilthead Sea Bream (*Sparus aurata*). *Anim. Feed Sci. Technol.*, 226, 12–20.
- Raja, P.K., Aanand, S., Sampathkumar, J.S., Padmavathy, P. (2020). Effect of Silkworm (*Bombyx mori*) Pupae on the Growth and Maturation of Rainbow Shark *Epalzeorhynchus frenatum* (Fowler, 1934) under Captive Rearing. *Indian J. Fish.*, 67, 89–96.

- Randazzo, B., Zarantonello, M., Gioacchini, G., Cardinaletti, G., Belloni, A.; Giorgini, E.; Faccenda, F., Cerri, R., Tibaldi, E. (2021). Physiological response of rainbow trout (*Oncorhynchus mykiss*) to graded levels of *Hermetia illucens* or poultry by-product meals as single or combined substitute ingredients to dietary plant proteins. *Aquaculture*, 538, 736550. <https://doi.org/10.1016/j.aquaculture.2021.736550>.
- Refstie, S., Korsoen, O.J., Storebakken, T., Baeverfjord, G., Lein, I., & Roem, A.J. (2000). Differing nutritional responses to dietary soybean meal in rainbow trout (*Oncorhynchus mykiss*) and Atlantic salmon (*Salmo salar*). *Aquaculture*, 190, 49–63. [https://doi.org/10.1016/S0044-8486\(00\)00382-3](https://doi.org/10.1016/S0044-8486(00)00382-3)
- Ribeiro, L., Moura, J., Santos, M., Colen, R., Rodrigues, V., Bandarra, N., Soares, F., Ramalho, P., Barata, M., Moura, P., Pous̃ao-Ferreira, P., Dias, J. (2014). Effect of vegetable based diets on growth, intestinal morphology, activity of intestinal enzymes and haematological stress indicators in meagre (*Argyrosomus regius*). *Aquaculture*, doi:10.1016/j.aquaculture.2014.12.017
- Roffeis, M., Fitches, E.C., Wakefield, M.E., Almeida, J., Alves Valada, T.R., Devic, E., Koné, N.G., Kenis, M., Nacambo, S., Koko, G.K.D., et al. (2020). Ex-Ante Life Cycle Impact Assessment of Insect Based Feed Production in West Africa. *Agric. Syst.*, 178, 102710.
- Rumpold, B.A. & Schlüter, O.K. (2013). Potential and Challenges of Insects as an Innovative Source for Food and Feed Production. *Innov. Food Sci. Emerg. Technol.*, 17, 1–11. [CrossRef]
- Sawhney, S. (2014). Effect of Partial Substitution of Expensive Ingredient 1e Fishmeal on the Growth of *Tor putitora* Fed Practical Diets. *J. Int. Acad. Res. Multidiscipl.*, 2, 482–489.
- Siddik, M.A.B., Pham, H.D., Francis, D.S., Vo, B.V., Shahjahan, M. (2021). Dietary supplementation of fish protein hydrolysate in high plant protein diets modulates growth, liver and kidney health, and immunity of barramundi (*Lates calcarifer*). *Aquac. Nutr.*, 27, 86–98.
- Situation and Alternative Sources. In *Feeds for the Aquaculture Sector*. Springer International Publishing: New York, NY, USA, 2018; pp. 1–103. ISBN 9783319779409.
- Smetana, S., Schmitt, E., Mathys, A. (2019). Sustainable Use of *Hermetia illucens* Insect Biomass for Feed and Food: Attributional and Consequential Life Cycle Assessment. *Resour. Conserv. Recycl.*, 144, 285–296.
- St-Hilaire, S., Sheppard, C., Tomberlin, J.K., Irving, S., Newton, L., McGuire, M.A., Mosley, E.E., Hardy, R.W., Sealey, W. (2007). Fly Prepupae as a feedstuff for rainbow trout, *Oncorhynchus mykiss*. *J. World Aquac. Soc.*, 3, 59–67. [CrossRef]
- Surendra, K.C., Tomberlin, J.K., van Huis, A., Cammack, J.A., Heckmann, L.H.L., Khanal, S.K., Rethinking (2020). Organic Wastes Bioconversion: Evaluating the Potential of the Black Soldier Fly (*Hermetia illucens* (L.)) (Diptera: Stratiomyidae) (BSF). *Waste Manag.*, 117, 58–80.
- Taufek, N.M., Muin, H., Raji, A.A., Md Yusof, H., Alias, Z., Razak, S.A. (2018). Potential of Field Crickets Meal (*Gryllus bimaculatus*) in the Diet of African Catfish (*Clarias gariepinus*). *J. Appl. Anim. Res.*, 46, 541–546.
- Thévenot, A., Rivera, J.L., Wilfart, A., Maillard, F., Hassouna, M., Senga-Kiesse, T., Le Féon, S., Aubin, J. (2018). Mealworm Meal for Animal Feed: Environmental Assessment and Sensitivity Analysis to Guide Future Prospects. *J. Clean. Prod.*, 170, 1260–1267.
- Tomotake, H., Katagiri, M., Yamato, M. (2010). Silkworm Pupae (*Bombyx mori*) are new sources of high quality protein and lipid. *J. Nutr. Sci. Vitaminol.*, 56, 446–448.
- Uran, P.A. (2008). *Etiology of soybean-induced enteritis in fish*. University of Wageningen. 176 pp.
- Van Huis, A., Van Itterbeek, J., Klunder, H., Mertens, E., Halloran, A., Muir, G., Vantomme, P. (2013). *Edible Insects: Future Prospects for Food and Feed Security*; Food and Agriculture Organization of the United Nations: Rome, Italy; ISBN 9251075964.
- Wachira, M.N., Osuga, I.M., Munguti, J.M., Ambula, M.K., Subramanian, S., Tanga, C.M. (2021). Efficiency and Improved Profitability of Insect-Based Aquafeeds for Farming Nile Tilapia Fish (*Oreochromis niloticus* L.). *Animals*, 11, 2599. <https://doi.org/10.3390/ani11092599>
- Wan, A.H.L., Snellgrove, D.L., Davies, S.J. (2017). A Comparison between Marine and Terrestrial Invertebrate Meals for Mirror Carp (*Cyprinus Carpio*) Diets: Impact on Growth, Haematology and Health. *Aquac. Res.*, 48, 5004–5016.
- Wang, G., Peng, K., Hu, J., Yi, C., Chen, X., & Wu, H. (2019). Evaluation of defatted black soldier fly (*Hermetia illucens* L.) larvae meal as an alternative protein ingredient for juvenile Japanese seabass (*Lateolabrax japonicus*) diets. *Aquaculture*, 507, 144e54. <https://doi.org/10.1016/j.aquaculture.2019.04.023>
- Wang, L., Li, J., Jin, J.N., Zhu, F., Roffeis, M., Zhang, X.Z. (2017). A Comprehensive Evaluation of Replacing Fishmeal with Housefly (*Musca domestica*) Maggot Meal in the Diet of Nile Tilapia (*Oreochromis niloticus*): Growth Performance, Flesh Quality, Innate Immunity and Water Environment. *Aquac. Nutr.*, 23, 983–993.

OPTIMISATION OF CULTURE MEDIA FACTORS FOR ACTIVE WINE YEAST BIOMASS PRODUCTION

Iuliana Diana BĂRBULESCU¹, Raluca Ștefania RĂDOI-ENCEA¹, Corina DUMITRACHE²,
Mihaela Violeta GHICA³, Mihai FRÎNCU⁴, Mihaela BEGEA⁵, Valerica TUDOR²,
Elena-Mirela BOROIU², Răzvan Ionuț TEODORESCU²

¹University of Agronomic Sciences and Veterinary Medicine of Bucharest, Faculty of Biotechnology, 59 Marasti Blvd, District 1, Bucharest, Romania

²University of Agronomic Sciences and Veterinary Medicine of Bucharest, Faculty of Land Reclamation and Environmental Engineering, 59 Marasti Blvd, District 1, Bucharest, Romania

³"Carol Davila" University of Medicine and Pharmacy, Faculty of Pharmacy, 6 Traian Vuia Street, Bucharest, Romania

⁴University of Agronomic Sciences and Veterinary Medicine of Bucharest, Research Center for Studies of Food Quality and Agricultural Products Bucharest, 59 Marasti Blvd, District 1, Bucharest, Romania

⁵National University of Science and Technology Politehnica Bucharest, Faculty of Biotechnical Systems Engineering, 313 Splaiul Independentei, District 6, Bucharest, Romania

Corresponding author email: corina_dumitrache17@yahoo.com

Abstract

*The present work describes the optimization of the composition of liquid culture medium in sub-merged fermentation in batch system by varying 7 factors, according to a Hadamard matrix. The work aimed to determine the optimal values of the varied factors (sugar content, yeast extract, KCl, medium volume (V_w/V_t), inoculation ratio, $MgSO_4 \times 7H_2O$, vitamins) that conducted to a maximum value of the system response, namely the yeast biomass cell weight, (6.61 g) a parameter relevant from technical and economic point of view. The temperature, stirring rate and air flow rate for the Hadamard matrix were maintained constant for each process variant. Applying the process, an active yeast biomass with a protein content of 36.45 g% was obtained. The active yeast biomass of *S. cerevisiae* PFE-II-3 was used in a further study to obtain wines at the Pietroasa Viticulture and Winemaking Research and Development Station.*

Key words: bioprocess, Hadamard matrix, optimisation, *S. cerevisiae*, yeast.

INTRODUCTION

The establishment of the culture media composition and the cultivation conditions in batch fermentation process requires the study of the largest possible number of experimental variants, depending on the environmental factors used. The use of the optimization techniques allows to study a larger number of factors and to determine their interaction, optimizing one or more experimental responses. The factor is a defined parameter (e.g., the constituent of a culture medium, the physical-chemical conditions etc.) that can have an influence on the experimental response (Srivastava et al., 2017; Chai, 2024; Michel et al., 2019; Carsanba et al., 2023). The response is the result of an experiment (e.g., biomass

concentration obtained) (Vieira et al., 2013). The purpose of optimization consists in determining the optimal values of the factors leading to a maximum value of the system response, provided that the parameter that quantifies the system response is relevant from technical and economic point of view (Bărbulescu et al., 2010).

Saccharomyces cerevisiae (*S. cerevisiae*) is one of the most intensively studied microorganisms and, as a cell factory, has a long history of successful application in industrial applications (Wronska, 2022; Chuo et al., 2011; Radoi-Encea et al., 2023; Dumitrache et al., 2019; Mihai et al., 2022).

Several optimization techniques are used to find the best operational fermentation conditions, mentioned by different authors in their research

studies: Taguchi design (Barbulescu et al., 2021), Latin square method, one-factor-at-a-time (OFAT) experiments (Gonzalez et al., 1995), Response surface methodology (RSM) was performed in the study of the optimization fermentation process by Chen et al. (2022) and Morteza et al. (2016).

During the medium optimization it must be considered that a minimal growth requirement of the microorganism must be fulfilled to obtain a maximum production of metabolite(s) (Singh et al., 2017). By performing a fed-batch cultivation of *K. marxianus* in lactose-based culture medium at varying initial lactose concentrations (10–60 g L⁻¹) at 30°C, pH 5.0, dissolved oxygen concentrations greater than 20%, the study elaborated by Lukondeh et al. (2005) led to a final biomass concentration of up to 105 g·L⁻¹.

In general, the carbon and nitrogen sources present in the medium can influence the production of metabolites. Carbon source is the meaningful medium component, as it is an energy source for the microorganisms and plays an important role in the growth as well as in the production of yeast cell biomass. The rate at which the carbon source is metabolized can influence the formation of the yeast cell biomass (Bărbulescu et al., 2022). The selection of nitrogen source and its concentration in the culture media fermentation also have an important role in metabolite production. The microorganism can use both inorganic and/or organic sources of nitrogen (Marwick et al., 1999).

Concerning the potassium source, Dubencovs (2021), determined the optimal component (glucose, phosphorus, nitrogen, and potassium) concentration relations for the *K. marxianus* DSM5422 synthetic growth medium to maintain the mentioned components in appropriate amounts during fed-batch cultivations in order to obtain high cell densities. Potassium is also important players in cell physiology. In yeasts, the plasma-membrane H1-ATPase encoded by the PMA1 gene has an essential role in ion homeostasis (Morsomme et al., 2000).

Regarding the media volume, from the data presented by Frîncu et al. (2022) it is observed that the highest amount of wet and dry biomass was obtained when working on a volumetric ratio of 200 mL / 500 mL.

Regarding the *inoculation ratio*, Vieira et al. (2013) grown yeast in a PDA slant for 24 h at 32°C, followed by resuspension in sterilized water and inoculated at a 10% concentration of the total volume of the fermentation medium for biomass obtainment. The authors incubated the flasks in a shaker for 24 h at 32°C and 150 rpm. Magnesium as sulphate salts, source, is important for culture media fermentation (Barbulescu et al., 2010). In accordance with the literature, the main factors affecting yeast biomass growth and protein content, are pH, temperature, time of cultivation and requirements for carbon, nitrogen, and vitamins. Barbulescu et al. (2010) in their study supplemented the media culture with a nitrogen source and vitamins for optimal growth. It is known that vitamin is an organic compound that an organism needs in small quantities to properly run its metabolic functions (Wronska, 2022).

Referring to vitamins, biotin and pantothenate are required for the proper growth of brewing yeast strains (Łukaszewicz et al., 2024). Biotin (vitamin B7) is an important nutrient for many fermentations (Han et al., 2019) used 0.002 mg as growth factor for aerobic growth to produce glutamic acid.

The goal of the present work was the evaluation of the influence of different media factors (sugar content; yeast extract; KCl; media volume; inoculation ratio; MgSO₄ × 7H₂O, and biotin) on wet cells weight development (WCW, g/100 mL), using a Hadamard matrix for seven factors.

MATERIALS AND METHODS

Biotechnological process optimization

The purpose of optimization consisted in the determination of the optimal fermentation parameters values in batch system that lead to a maximum value of the system response, which are relevant from technical and economic point of view (Bărbulescu et al., 2010).

The Hadamard matrix used in the optimization of culture media factors for obtaining active wine yeast biomass is presented in Table 1.

A molecularly identified *S. cerevisiae* strain, coded as *PFE-II-3*, formerly isolated in UASMV Bucharest vineyard, was used for liquid inoculum development.

Table 1. Experimental matrix for K = 7 and N = 8

Exp. variant	Factor							Response
	X ₁	X ₂	X ₃	X ₄	X ₅	X ₆	X ₇	
1	+	+	+	-	+	-	-	y ₁
2	-	+	+	+	-	+	-	y ₂
3	-	-	+	+	+	-	+	y ₃
4	+	-	-	+	+	+	-	y ₄
5	-	+	-	-	+	+	+	y ₅
6	+	-	+	-	-	+	+	y ₆
7	+	+	-	+	-	-	+	y ₇
8	-	-	-	-	-	-	-	y ₈
9	0	0	0	0	0	0	0	Control

The response of the optimisation “y” is represented by a function (polynomial) in the form:

$$y = b_0 + b_1X_1 + b_2X_2 + \dots b_kX_k$$

where:

- b_0 = the average value of the response “y”
 - X_i = value of variable factors (culture medium factors)
 - b_i = linear coefficients to be determined ($i=1; 2; 3; \dots; k$)
- we have:

$$b_0 = \sum \frac{y_i}{N} \text{ and } b_i = \sum \frac{x_i y_i}{N}$$

where:

- X_i is the transposition of the matrix.
- To calculate the linear coefficients (b_i) it is sufficient to assign the sign to each answer (y_i),

corresponding sign in the column related to the factors for which we want to calculate the coefficient, then the algebraic sum is made and divided by the number of experiences ($N = 8$). The response is represented by a polynomial in the form:

$$y = b_0 + b_1X_1 + b_2X_2 + b_3X_3 + b_4X_4 + b_5X_5 + b_6X_6 + b_7X_7$$

where:

$$b_0 = \sum \frac{y_i}{8} = \frac{(y_1 + y_2 + y_3 + y_4 + y_5 + y_6 + y_7 + y_8)}{8}$$

The interpretation of the results consists in ranking the factors with a significant influence on the response, depending on their sign:

- $b_i > 0$ – positive influence;
- $b_i < 0$ – negative influence

$$\begin{aligned}
 b_1 &= (y_1 - y_2 - y_3 + y_4 - y_5 + y_6 + y_7 - y_8) / 8 & \rightarrow & \sum_1^8 \frac{x_1 y_i}{8} \\
 b_2 &= (y_1 + y_2 - y_3 - y_4 + y_5 - y_6 + y_7 - y_8) / 8 & \rightarrow & \sum_1^8 \frac{x_2 y_i}{8} \\
 b_3 &= (y_1 + y_2 + y_3 - y_4 - y_5 + y_6 - y_7 - y_8) / 8 & \rightarrow & \sum_1^8 \frac{x_3 y_i}{8} \\
 b_4 &= (-y_1 + y_2 + y_3 + y_4 - y_5 - y_6 + y_7 - y_8) / 8 & \rightarrow & \sum_1^8 \frac{x_4 y_i}{8} \\
 b_5 &= (y_1 - y_2 + y_3 + y_4 + y_5 - y_6 - y_7 - y_8) / 8 & \rightarrow & \sum_1^8 \frac{x_5 y_i}{8} \\
 b_6 &= (-y_1 + y_2 - y_3 + y_4 + y_5 + y_6 - y_7 - y_8) / 8 & \rightarrow & \sum_1^8 \frac{x_6 y_i}{8} \\
 b_7 &= (-y_1 - y_2 + y_3 - y_4 + y_5 + y_6 + y_7 - y_8) / 8 & \rightarrow & \sum_1^8 \frac{x_7 y_i}{8}
 \end{aligned}$$

Depending on the results, and the number of studied factors, the step of the variation can then

be modified, and a new matrix of the same type is set up, or following the objectives, other

matrices are used for a final study, observing the interactions between different factors.

The processing of the resulting fermentation medium was performed in 2 steps:

- separation of the yeast biomass by centrifugation at 4500 rpm for 5 minutes;
- purification of the yeast cells biomass using successive washing with sterile water by centrifugation at 4500 rpm.

For the determination of wet weight biomass (WCW) (g/100 mL), 10 mL of samples were centrifugated at 4500 rpm for 5 minutes and then weighed. For the determination of dry cell weight (DCW) (g/100 mL), the resulted wet biomass was subjected to a drying process at a Pheonix BM-60 moisture analyser (Lukondeh et al., 2005). Dry cell weight (DCW) was determined through gravimetric measurement after harvesting, washing, and lyophilization of a 2 mL culture sample (Awad et al., 2019).

Physico-chemical analyses

The determination of the *protein content* for yeast biomass was performed according to the Kjeldahl method. The crude protein is obtained based on the nitrogen content determined by the Kjeldahl method multiplied by the factor 6.25. As equipment a digestion Unit Buchi K-426, a titration unit Titrino Plus 877, a distillation unit Kjelflex 360, and an analytical balance OHAUS AX224M (OHAUS Corporation; New Jersey, USA) were used.

The determination of the *ash content* was performed by calcination at 550-600°C. As equipment, a Nabertherm L9 / 11/ B410 oven (Lilienthal, Germany) and an analytical balance (SHIMADZU ATX224R; Kyoto, Japan) were used.

The *moisture content* was determined through drying the samples at 103°C for four hours. As equipment, a Memmert UN55 drying oven (Schwabach, Germany) and an analytical balance (SHIMADZU ATX224R; Kyoto, Japan) were used.

Total soluble solids (TSS) were used as of-line parameter in fermentation bioprocess.

Microbiological analyses

The determination of *yeast and moulds* was performed in accordance with the standard SR ISO 21527-2:2009 - Microbiology of food and animal feeding stuffs - Horizontal method for

the enumeration of yeasts and moulds - Part 2: Colony count technique in products with water activity less than or equal to 0.95. As cultivation medium Dichloran Rose-Bengal Chloramphenicol (DRBC) agar was used and the incubation was performed at $25 \pm 1^\circ\text{C}$ for 5 days.

The determination of *E. coli* was performed in accordance with the standard SR ISO 16649-2:2007 - Microbiology of food and animal feeding stuffs - Horizontal method for the enumeration of beta-glucuronidase-positive *E. coli* - Part 2: Colony-count technique at 44°C using 5-bromo-4-chloro-3-indolyl beta-D-glucuronide. As cultivation medium tryptone-bile-glucuronide medium (TBX) agar was used and the incubation was performed at $44 \pm 1^\circ\text{C}$ for 18-24 h.

The determination of *coliform bacteria* was performed in accordance with the standard SR ISO 4832:2009 - Microbiology of food and animal feeding stuffs - Horizontal method for the enumeration of coliforms - Colony-count technique. As cultivation medium crystal violet neutral red bile lactose agar was used and the incubation was performed at $37 \pm 1^\circ\text{C}$ for 24 ± 2 h.

Optimizing the culture medium and cultivation parameters for obtaining active yeast biomass of *S. cerevisiae* PFE II-3

Step 1 optimization

Fermentation costs could be reduced by replacing expensive components with cheaper sources, such as food sugar, and/or with increased productivity, and these could contribute to a successful optimization strategy. The strain used in liquid media fermentation in different ratio has been proved to be another valuable optimization strategy toward the enhancement of the product yield (WCW) and the process improvement.

Optimizing the fermentation medium at laboratory level (using Erlenmeyer flasks) involves large number of experiments regardless of the chosen formula and is an open-ended experiment (Table 2).

The data generated by the shaker flask media seldom matches the fermentation behavior at the fermenter level (Kennedy et al., 1994; Kennedy et al., 1999). Vitamin solution - 0.002 g biotin was dissolved in 50 mL sterile distilled water at

50°C for 1 h, with stirring. The inoculation ratio was established based on the previous experiments as the salts, C and N source and vitamin source.

Fermentation using the strain *S. cerevisiae* PFE-II-3 for the of optimization biotechnological process

*Obtaining the pure culture of *S. cerevisiae* yeast strain.*

The preinoculum of yeast cultures of *S. cerevisiae* PFE II-3 were grown and developed on YPG (yeast extract, peptone hy-soy, and glucose) (Barbulescu et al., 2024) or YPS (yeast extract, hy-soy peptone, and sucrose) agar slant medium - 48 h at 30°C. This yeast was previously isolated from the Tămăioasă Românească grape by Barbulescu et al. (2024) and identified in 2023 by MALDI-TOF techniques and was validated by PCR molecular technique.

Obtaining the liquid inoculum. The liquid inoculum was obtained in 100 mL of YPG medium/500 ml Erlenmeyer flasks, (yeast

extract were purchased from Sigma - Aldrich, peptone hy-soy were purchased from VWR Chemicals, and glucose were purchased from VWR Chemicals), inoculated with 2 tubes of previously developed pre-inoculum and left to incubate for a maximum of 14-16 h, at 240 rpm overnight at 30°C (Figure 1).

The experimental matrix for $K = 7$ and $N = 8$ media is shown in Table 3 and the factors tested for optimisation in Table 4.



Figure 1. Experimental variants at the laboratory level

Table 2. Concentration level taken in the experiment - optimization step 1

Media factors		Concentration level (g %)		
		-1	0	1
X ₁	Sugar	7	8	9
X ₂	Yeast extract E.D.	0.5	0.7	0.9
X ₃	KCl	0.04	0.05	0.06
X ₄	Medium volume Vw/Vt ratio	100/500	150/500	200/500
X ₅	Vitamin	0.5	1	1.5
X ₆	Inoculation ratio (%)	5	10	15
X ₇	MgSO ₄ × 7H ₂ O	0.04	0.05	0.06

Table 3. Experimental matrix for $K = 7$ and $N = 8$

Optimization factors							Response (y _i)
Sugar g%	E.D. g%	KCl g%	Media volume from Erlenmeyer flasks Vw/Vt ratio	Vitamin g%	Inoculation ratio (%) (v/v)	MgSO ₄ × 7H ₂ O g%	WCW (wet weight cell) g/100 mL
X1	X2	X3	X4	X5	X6	X7	
+	+	+	-	+	-	-	y ₁
-	+	+	+	-	+	-	y ₂
-	-	+	+	+	-	+	y ₃
+	-	-	+	+	+	-	y ₄
-	+	-	-	+	+	+	y ₅
+	-	+	-	-	+	+	y ₆
+	+	-	+	-	-	+	y ₇
-	-	-	-	-	-	-	y ₈
0	0	0	0	0	0	0	Control

Table 4. Media factors tested for optimization

Exp. no.	Exp. variant	Optimization factors						Response		y
		Sugar (g %)	YE (Yeast extract) (g %)	KCl (g %)	Medium volume (mL) Vw/Vt ratio	Vitamin (mL)	Inoculation ratio (%) (v/v)	MgSO ₄ ×7H ₂ O (g %)	WCW (g/100 mL)	
		X1	X2	X3	X4	X5	X6	X7		
1	1	9	0.9	0.06	100/500	1.5	5	0.04	4.02	y1
2	2	7	0.9	0.06	200/500	0.5	15	0.04	4.09	y2
3	3	7	0.5	0.06	200/500	1.5	5	0.06	2.67	y3
4	4	9	0.5	0.04	200/500	1.5	15	0.04	3.58	y4
5	5	7	0.9	0.04	200/500	1.5	15	0.06	4.33	y5
6	6	9	0.5	0.06	100/500	0.5	15	0.06	3.30	y6
7	7	9	0.9	0.04	200/500	0.5	5	0.06	4.11	y7
8	8	7	0.5	0.04	100/500	0.5	5	0.04	2.89	y8
9	Control	8	0.7	0.05	150/500	1	10	0.05	3.28	Control

RESULTS AND DISCUSSIONS

By performing fed-batch cultivation of *S. cerevisiae* PFE-II-3 in a complex medium it was possible to achieve a final biomass concentration of up to 50 g/L. The results for fermentation for obtaining active yeast biomass of *S. cerevisiae* PFE-II-3 are presented in Table 5. The response obtained represented the answer for the following optimization calculation, as is presented in Table 6.

Optimization Step 2

In accordance with the most influent factor from the Table 6 were established the next step of optimisation in the Table 7, based on the results: (u) * (c). Following the optimization method, the variation step of the most influent factor is chosen within a more reduced space compared

to the preceding factorial plan. This allows a better settlement of the optimal regions. A new experimental plan was established (Table 7) in which variable factors are: sugar, yeast extract, inoculation ration and vitamin, the rest of the ingredients remaining unchanged.

The results from step one goes to improve the results and that is why in the next step 3 variants were selected which are presented in Tables 8 and 9. For the next step, the liquid yeast inoculum *S. cerevisiae* PFE -II-3 was obtained. The results concerning the pH and TSS, Brix for the fermentation process is described in Table 9. According with the optimization method, the variation step of the most influent factor is chosen in a smaller space compared to the previous factorial plan, and this allows a better placement of the optimal regions.

Table 5. Results for fermentation for obtaining active yeast biomass of *S. cerevisiae* PFE-II-3

Cultivation time (h)	Analyses/ Variants	V1	V2	V3	V4	V5	V6	V7	V8	M
0	pH	5.5	5.5	5.5	5.5	5.5	5.5	5.5	5.5	6
	TSS, Brix	8.9	7.4	7.7	8.4	7.2	8.3	9.3	7.4	8.6
16	pH	5.1	5.1	5.1	5.1	5.1	5.1	5.1	5.1	4.8
	TSS, Brix	2.5	1.5	1.5	1.7	1.4	1.6	1.4	1.6	1.7
18	pH	5	5	5	5	5	5	5	5	4.5
	TSS, Brix	1.3	1.3	1.2	1.1	1.3	1.6	1.3	1.2	1.5
20	pH	4.5	4.5	4.5	4.5	4.5	4.5	4.5	4.5	4.5
	TSS, Brix	1.3	1.1	1.2	1.0	1.3	1.6	1.3	1.1	1.5

Legend: TSS = Total Soluble Solids

Otherwise: $b_1 = (y_1 - y_2 - y_3 + y_4 - y_5 + y_6 + y_7 - y_8) / 8 \rightarrow \sum_{i=1}^8 \frac{x_1 y_i}{8} = 0.13$

$b_2 = (y_1 + y_2 - y_3 - y_4 + y_5 - y_6 + y_7 - y_8) / 8 \rightarrow \sum_{i=1}^8 \frac{x_2 y_i}{8} = 0.51$

$$\begin{aligned}b_3 &= (y_1 + y_2 + y_3 - y_4 - y_5 + y_6 - y_7 - y_8) / 8 \quad \rightarrow \quad \sum_1^8 \frac{x_3 y_i}{8} = -0.10 \\b_4 &= (-y_1 + y_2 + y_3 + y_4 - y_5 - y_6 + y_7 - y_8) / 8 \quad \rightarrow \quad \sum_1^8 \frac{x_4 y_i}{8} = -0.01 \\b_5 &= (y_1 - y_2 + y_3 + y_4 + y_5 - y_6 - y_7 - y_8) / 8 \quad \rightarrow \quad \sum_1^8 \frac{x_5 y_i}{8} = 0.03 \\b_6 &= (-y_1 + y_2 - y_3 + y_4 + y_5 + y_6 - y_7 - y_8) / 8 \quad \rightarrow \quad \sum_1^8 \frac{x_6 y_i}{8} = 0.20 \\b_7 &= (-y_1 - y_2 + y_3 - y_4 + y_5 + y_6 + y_7 - y_8) / 8 \quad \rightarrow \quad \sum_1^8 \frac{x_7 y_i}{8} = -0.02\end{aligned}$$

where:

$$b_0 = \sum \frac{y_i}{8} = (y_1 + y_2 + y_3 + y_4 + y_5 + y_6 + y_7 + y_8) / 8 = 4.03$$

bi > 5.76

Table 6. Step 2 of optimisation

Environmental factors	X_1	X_2	X_3	X_4	X_5	X_6	X_7
Base level	8	0.7	0.05	150	1	10	0.05
Variation unity (u)	1	0.2	0.01	50	0.5	5	0.01
Linear coefficient (c)	0.13	0.51	-0.1	-0.01	0.03	0.2	-0.02
(u) * (c)	0.13	0.102	-0.001	-0.5	0.015	1	-0.0002

Table 7. Concentration level taken in the experiment - optimization step 2

Media factors		Experimental variants		
		M-V10	V11	V12
X_1	sugar	8	8.13	8.26
X_2	Yeast extract	0.7	0.802	0.904
X_3	KCl	0.05	0.049	0.048
X_4	Media volume: Vw/Vt ratio	150	149.5	149
X_5	Vitamins	1	1.015	1.03
X_6	Inoculation ratio (%) (v/v)	9	10	11
X_7	MgSO ₄ × 7 H ₂ O	0.05	0.0498	0.0496

Table 8. The answer of the experimental variants by varying the experimental factors

Exp. variant	Optimization factors							Response
	Sugar (g%)	Yeast extract (g%)	KCl (g%)	Media volume (ml) Vw/Vt ratio	Vitamin (mL)	Inoculation ratio (%) (v/v)	MgSO ₄ × 7H ₂ O (g%)	WCW (g/100 mL)
	X1	X2	X3	X4	X5	X6	X7	
V10	8	0.7	0.05	150	1	9	0.05	4.07
V11	8.13	0.802	0.049	149.5	1.015	10	0.0498	4.63
V12	8.26	0.904	0.048	149	1.015	11	0.0496	4.78

Table 9. Fermentation to obtain yeast biomass of *S. cerevisiae* PFE-II-3

Cultivation time (h)	Analyses	V10	V11	V12
0	pH	6	6	6
	TSS, °Brix	9.3	10.4	11.4
16	pH	4.5	4.5	4.5
	TSS, °Brix	2.3	2.5	3.2
18	pH	4.5	4.5	4.5
	TSS, °Brix	1.8	2.4	2.8
20	pH	4.5	4.5	4.5
	TSS, °Brix	1.8	2.4	2.8

Optimization Step 3

A new experimental plan was established (Table 10), in which variable factor is the media volume Vw/Vt ratio (mL) X₄, and the rest of the parameters are unchanged.

The static cultivation of the microorganism was developed in tubes with a slant medium incubated at 30°C – 48 h, to obtain the maintenance strain and the static *S. cerevisiae* PFE-II-3 culture preinoculum;

Cultivation to obtain the inoculum was carried out in a discontinuous system by shaking 500 ml

Erlenmeyer flasks with 149 mL YPG liquid media, in a closed incubator shaking system at 240 rpm, 30°C for 12-18 hours overnight.

The liquid inoculum of *S. cerevisiae* PFE-II-3 was obtained further in a shaker with stirring at 240 rpm, at a temperature of 30°C, overnight.

In the next phase, the fermentation was carried out for step 3 of optimization to improve the concentration of wet weight biomass by growing the inoculation ratio because has the highest positive influence (Tables 10 and 11).

Table 10. The response of media factors for the development of *S. cerevisiae* PFE -II-3 yeast biomass

Experimental variants	Experimental media factors							Answer
	Sugar (g %)	Yeast extract (g %)	KCl (g %)	Media volume Vw/Vt ratio (mL)	Vitamin (mL)	Inoculation ratio (%) (v/v)	MgSO ₄ × 7H ₂ O (g %)	WCW (g/100 mL)
	X1	X2	X3	X4	X5	X6	X7	
V13	8.26	0.904	0.048	149	1.015	10	0.0496	4.6
V14	8.26	0.904	0.048	149	1.015	15	0.0496	5.24
V15	8.26	0.904	0.048	149	1.015	20	0.0496	5.35

Table 11. Obtaining active yeast biomass for optimization step 3

Cultivation time (h)	Analyses	V13	V14	V15
0	pH	6	6	6
	TSS, Brix	10	10.1	9.1
20	pH	4	4	4
	TSS, Brix	1	1.1	0.7

It is observed that the best experimental variant was obtained for V3 based on the WCW yield. Biomass study of Torrellas et al. (2023) were performed by using molasses provided by Lessafre Iberica (60 g/L of sucrose for batch experiments, 100 g/L of sucrose for fed-batch phase and 20 g/L in diluted molasses experiments), supplemented with 7.5 g/L (NH₄)₂SO₄, 3.5 g/L KH₂PO₄, 0.75 g/L MgSO₄, and 10 mL/L vitamin solution.

The vitamin solution contained 0.5 mg/L D-biotin, 1 mg/L calcium pantothenate and 1 mg/L

thiamine hydrochloride (Torrellas et al., 2023). The optimized variant V3 has the following performance parameters: 5.35 g/ 100 mL WCW (as active wet yeast biomass) and 1.33 g/100 mL DCW (as active dry yeast biomass).

The obtained active yeast biomass of *S. cerevisiae* PFE II-3 was analyzed from physical-chemical and microbiological point of view (Table 12), and it is observed that the sample was free of microbiological contamination and the cell viability decreases over time after 8-14 months.

Table 12. Physico-chemical and microbiological characterization of active dry yeast biomass for winemaking testing

Sample	<i>S. cerevisiae</i> PFE II-3 active yeast biomass
Physico-chemical analyses	
Protein	36.45 g %
Ash	3.19 %
Humidity	5.62 %
Microbiological analyses	
Yeasts and Molds after optimisation	3.2x10 ⁸ UFC/g
Yeasts and Molds after 8-14 months	3.2x10 ⁴ UFC/g
<i>E. coli</i>	under 10 UFC/g
Coliforms	under 10 UFC/g

CONCLUSIONS

The technology for the production of the active yeast biomass of *S. cerevisiae* PFE II-3 was optimized using a Hadamard matrix by varying 7 factors:

The best variant was for V₃ which consists in varying of the following process parameters: sugar content - 8.26 g %; yeast extract - 0.904 g %; KCl -0.048 g %; media volume 149.5 mL/500 mL Erlenmeyer flasks, inoculation ratio 20%; MgSO₄ × 7H₂O - 0.0496 g %; vitamins - 1.015 mL.

It is noticed that the cell viability for the active yeast biomass decreases over time after 8-14 months.

ACKNOWLEDGEMENTS

This work was supported by the project 7PFE/2021 “Circular economy in USAMV farms - whole use of by-products resulting from fermentation processing”, Program 1 - Development of the national research-development system, Subprogram 1.2 - Institutional performance - Institutional development projects - Projects to finance excellence in RDI.

REFERENCES

Awad, D., Bohnen, F., Mehlmer, N. & Brueck, T. (2019). Multi-Factorial-Guided Media Optimization for Enhanced Biomass and Lipid Formation by the Oleaginous Yeast *Cutaneotrichosporon oleaginosus*. *Front. Bioeng. Biotechnol.*, 7, 54. DOI: 10.3389/fbioe.2019.00054

Bărbulescu, I.D., Dumitrache, C., Diguță, C.F., Begea, M., Matei, P.M., Frincu, M., Mărculescu, S.I., Cîrîc, A.I., Tudor, V., Boroiu, E.M., Teodorescu, R.I.

(2022). Evolution at the microfermenter level of the growth dynamics of *Saccharomyces cerevisiae* and *Starmella bacillaris* yeasts with potential for use in winemaking at the Pietroasa Winery. *AgroLife Scientific Journal*, 11(2), DOI: <https://doi.org/10.17930/AGL202221>

Bărbulescu, I.D., Ghica, M.V., Begea, M., Albu Kaya, M.G., Teodorescu, R.I., Popa, L., Mărculescu, S.I., Cîrîc, A.I., Dumitrache, C., Lupuliasa, D., Matei, F., Dinu-Pîrvu, C.E. (2021). Optimization of the fermentation conditions for brewing yeast biomass production using the response surface methodology and Taguchi Technique. *Agriculture* 11(12), 1237, <https://doi.org/10.3390/agriculture11121237>

Bărbulescu, I.D., Rusu, N., Rughinis, R., Popa, O., Stefaniu, A. Casarica, A. (2010). Obtaining yeast biomass enriched with copper, zinc and manganese. *Romanian Biotechnological Letters*, 15(1).

Barbulescu, I.D., Teodorescu, R.I., Dumitrache, C., Begea, M., Dragotoiu, D., Frincu, M., Marculescu, S.I., Cîrîc, A.I., Banita, D.C., Tudor, V. & Boroiu, E.M. (2024). Influence of inoculum on the dynamics of *Saccharomyces cerevisiae* yeast biomass development. *International Symposium on Beverage Crops* Eds.: E. Gómez Plaza et al. DOI 10.17660/ActaHortic.2024.1387.35 Proc. III.

Carsanba, E., Agirman, B., Papanikolaou, S., Fickers, P., Erten, H. (2023). Valorisation of Waste Bread for the Production of Yeast Biomass by *Yarrowia lipolytica* Bioreactor Fermentation. *Fermentation*, 9, 687. <https://doi.org/10.3390/fermentation9070687>

Chai, W.Y., Tan, M.K., Teo, K.T.K., Tham, H.J. (2024). Optimization of Fed-Batch Baker’s Yeast Fermentation Using Deep Reinforcement Learning. *Process Integration and Optimization for Sustainability*, 8(2), 1-17, DOI:10.1007/s41660-024-00406-6.

Chen, J., Lan, X., Jia, R., Hu, L., Wang, Y. (2022). Response Surface Methodology (RSM) Mediated Optimization of Medium Components for Mycelial Growth and Metabolites Production of *Streptomyces alfalfae* XN-04. *Microorganisms*, 10, 1854. <https://doi.org/10.3390/microorganisms10091854>

Chuo, H.S.E., Tan, M.K., Tham HJ., Teo, K.T.K. (2011). Optimization of fed-batch baker’s yeast fermentation process using learning algorithm, *Proceedings of 18th*

- regional symposium on Chemical Engineering (RSCE2011).*
- Dubencovs, K., Liepins, J., Suleiko, A., Suleiko, A., Vangravs, R., Kassaliete, J., Scerbaka, R., Grigs. (2021). Optimization of Synthetic Media, Composition for *Kluyveromyces marxianus* Fed-Batch Cultivation. *Fermentation*, 7, 62. <https://doi.org/10.3390/fermentation7020062>
- Dumitrache, C., Matei, F., Barbulescu, D.I., Frincu, M., Tudor, V., Hirjoaba, L.N., Teodorescu, R.I. (2019). Protein sources for animal feed: yeast biomass of beer and/or wine - review. *Scientific Papers. Series E. Land Reclamation, Earth Observation & Surveying, Environmental Engineering, VIII*, 175-182, Print ISSN 2285-6064.
- Frincu, M., Dumitrache, C., Begea, M., Teodorescu, R.I., Diguță, C.F., Baniță, C.D., Tudor, V., Cîrc, A.I., Mărculescu, S.I., Bărbulescu, I.D. (2022). Active wine yeast biomass obtained through biotechnological process. *Journal of Agroalimentary Processes and Technologies*, 28(1), 20-26.
- Gonzalez, R., Islas, L., Obregon, A.-M., Escalante, L., & Sanchez, S. (1995). Gentamicin formation in *Micromonospora purpurea*: stimulatory effect of ammonium. *J. Antibiot.*, 48, 479-483. DOI: 10.7164/antibiotics.48.479
- Han, X., Li, L., Bao, J. (2019). Microbial extraction of biotin from lignocellulose biomass and its application on glutamic acid production. *Bioresource Technology*, 288, 121523, ISSN 0960-8524.
- Kennedy, M., & Krouse, D. (1999). Strategies for improving fermentation medium performance: a review. *J. Ind. Microbiol. Biotechnol.*, 23, 456-475. DOI: 10.1038/sj.jim.2900755
- Kennedy, M., Reader, S., Davies, R.J., Rhoades, D. & Silby, H. (1994). The scale up of mycelial shake flask fermentations: a case study of gamma linolenic acid production by *Mucor hiemalis* IRL 51. *J. Ind. Microbiol.*, 13, 212-216. DOI: 10.1007/BF01569750
- Łukaszewicz, M., Leszczynski, P., Jabłonski, S.J., Kawa-Rygielska, J. (2024). Potential Applications of Yeast Biomass Derived from Small-Scale Breweries. *Appl. Sci.*, 14, 2529. <https://doi.org/10.3390/app14062529>
- Lukondeh, T., Ashbolt, N.J., Rogers, P.L. (2005). Fed-batch fermentation for production of *Kluyveromyces marxianus* FII 510700 cultivated on a lactose-based medium. *J. Ind. Microbiol. Biotechnol.* 32(7), 284-8. DOI: 10.1007/s10295-005-0245-y.
- Marwick, J.D., Wright, P.C., Burgess, J.G. (1999). Bioprocess intensification for production of novel marine bacterial antibiotics through bioreactor operation and design. *Mar. Biotechnol.*, 1, 495-507. DOI: 10.1007/PL00011806
- Michel, M., Meier-Dörnberg, T., Jacob, F., Schneiderbanger, H., and Hutzler, M. (2020). Optimisation of yeast vitality measurement to better predict fermentation performance. *J. Inst. Brew.*, 126, 161-167. <https://doi.org/10.1002/jib.604>
- Mihai, C., Frincu, M., Dumitrache, C. (2022). Isolation and characterization of new yeasts strains from barley samples. *Scientific Papers. Series E. Land Reclamation, Earth Observation & Surveying, Environmental Engineering, XI*, 499-504. Print ISSN 2285-6064.
- Morsomme, P., Slayman, C.W. & Goffeau, A. (2000). Mutagenic study of the structure, function and biogenesis of the yeast plasma membrane H1-ATPase. *Biochim Biophys Acta*, 1469, 133-157.
- Morteza, M.A., Mohammad, R.F., Mohsen, A., Nasim, H.R., Nasrin, S. (2017). Optimization of Culture Conditions for Enrichment of *Saccharomyces cerevisiae* with Dl- α -Tocopherol by Response Surface Methodology. *Iranian Journal of Pharmaceutical Research* 16(4), 1546-1554.
- Rădoi-Encea, R.-Ș., Pădureanu, V., Diguță, C.F., Ion, M., Brîndușe, E., Matei, F. (2023). Achievements of Autochthonous Wine Yeast Isolation and Selection in Romania - A Review. *Fermentation*, 9(5), 407. <https://doi.org/10.3390/fermentation9050407>.
- Singh, V., Haque, S., Niwas, R., Srivastava, A., Pasupuleti, M., Tripathi, C.K.M. (2017). Strategies for Fermentation Medium Optimization: An In-Depth Review. *Front. Microbiol.*, 7, 2087. DOI: 10.3389/fmicb.2016.02087.
- Torrellas, M., Pietrafesa, R., Ferrer-Pinós, A., Capece, A., Matallana, E., Aranda, A. (2023). Optimizing growth and biomass production of *non-Saccharomyces* wine yeast starters by overcoming sucrose consumption deficiency. *Front. Microbiol.* 14, 1209940. DOI: 10.3389/fmicb.2023.1209940
- Vieira, E.D., Andrietta, MdaG, Stupiello, Andrietta, S.R. (2013). Yeast biomass production: a new approach in glucose-limited feeding strategy. *Brazilian Journal of Microbiology*, 44(2), 551-558, ISSN 1678-4405.
- Wronska, A.K. (2022). Engineering biotin synthesis; towards vitamin independency of *Saccharomyces cerevisiae*. Degree granting institution, doctoral thesis, 978-94-6423-708-5, <https://doi.org/10.4233/uuid:bd748c70-2cda-4094-945f-0f0577700367>

TRENDS IN "FETEASCĂ REGALĂ" GRAPES YIELD AND SUGAR CONTENT IN SITE SPECIFIC CLIMATE

Octav-Mihai CISMAȘIU¹, Ioan OROIAN¹, Marcel DÎRJA²,
Cristian IEDERAN¹, Antonia ODAGIU¹

¹University of Agricultural Sciences and Veterinary Medicine Cluj-Napoca, Faculty of Agriculture,
3-5 Calea Manastur, Cluj-Napoca, Romania

²University of Agricultural Sciences and Veterinary Medicine Cluj-Napoca,
Faculty of Silviculture and Cadastre, 3-5 Calea Manastur, Cluj-Napoca, Romania

Corresponding author email: antonia.odagiu@usamvcluj.ro

Abstract

In this article we analyse the evolution of the grapes yield and their sugar content belonging to "Fetească Regală" vineyard variety cultivated in climatic conditions of Transylvanian region, Romania, covering the time period 2020–2022. In each experimental year, daily temperatures and precipitations were recorded during the grapevine vegetation period. Grapevine yield and sugar content was recorded at the end of each vegetation period. Averages were calculated yearly and by entire experimental period. Descriptive statistics and multi regression approach were implemented to calculate de averages, dispersion parameters, significance of differences, and relationships between the climatic factors and production traits. Overall datasets concerning grapes yields and their sugar content expressed a normal distribution. Our study emphasizes that precipitations have low influence on grapes yields and their sugar content, while temperature is positively associated with both above mentioned quantitative traits. When expressed by experimental years, increased temperatures led to higher yields and sugar content, significant differences are reported among yearly values.

Key words: *precipitations, production, temperature, vineyard, quantitative traits.*

INTRODUCTION

The yield of "Fetească Regală" grapes and the sugar content are significantly influenced by the climatic conditions specific to the wine-growing site. The variety "Fetească Regală" is known to produce aromatic and pleasant wines, and the aspects related to the yield and the chemical composition of the grapes are essential for the final quality of the wine (Mirošević & Karoglan-Kontić, 2015; Ollat et al., 2002).

The variety "Fetească Regală" grows well in a temperate climate, with mild winters and warm, but not excessively hot, summers. Well-drained and moderately fertile soils are preferred, as they allow adequate root development and ensure good nutrient absorption. The variety "Fetească Regală" thrives in a moderate temperature range, with warm summers and mild winters (Colibaba et al., 2024).

Grape yields can vary depending on many factors, including vineyard management, vine health, and weather conditions during the growing season (Borca et al., 2019; Bărbulescu et al., 2022). The site-specific climate has a

major impact on the ripeness of the grapes and their sugar content. Temperature is a key factor in the development of grapes and the accumulation of sugar in the fruit (Block et al., 2013; Bucur et al., 2019; Carroquino et al., 2020; Van Leeuwen & Darriet, 2016; Ollat et al., 2002).

High temperatures during the growing season can accelerate the ripening process of the grapes, causing a faster accumulation of sugar. However, temperatures that are too high can lead to water stress and loss of acidity in the grapes, which can negatively affect the quality of the wine.

The amount and distribution of rainfall are essential for the healthy development of the vines and the production of quality grapes. Excessive rainfall can cause the grapes to crack and promote fungal diseases such as mold and rot. Conversely, a lack of rainfall can lead to water stress, which can reduce the size and quality of grapes and negatively influence their sugar content. Temperature variations between day and night can significantly influence the quality of the grapes. Cooler nights can help

maintain acidity in the grapes, while warm days favor sugar build-up and flavor development (Hannah et al., 2013; Mendez- Costabel et al., 2014; Spayd et al., 2002).

Vine management techniques such as the proper administration of fertilizers and phytosanitary treatments can significantly influence grape yield and quality. Proper management can help maintain a healthy balance between vegetative growth and grape development.

The aim of the present study is to emphasize the "Fetească Regală" grape yield and sugar content function of specific climatic conditions of Geoagiu area, Hunedoara County, characterized by appropriate environmental conditions for vineyard development.

MATERIALS AND METHODS

The experiments took place during the period 2021-2022, respectively in two experimental years, in Geoagiu Basin, Hunedoara County, according to a bifactorial experiment (2 x 3), in randomized blocks, with different graduations, the factors being represented by the year experimental with its two graduations, respectively 2021 and 2022 and the phytosanitary treatment scheme with the 3 graduations, represented by the untreated control experimental variant and the experimental variants I and II treated according to different schemes.

Three repetitions were performed for each experimental variant. For each experimental variant, 8 treatments were applied. The experimental area, which covers an area of 3600 m², was divided into plots (1200 m² each plot), corresponding to the 3 experimental variants. Phytosanitary treatment was applied function of vegetation period with phytosanitary products homologated in Romania (<https://aloe.anfd.ro/>): 1 - control, where no treatments were applied; 2 - complex treatment scheme, which includes 12 sprinkles (with a mixture of 12 active substances), and 3 - medium treatment scheme with 8 sprinkles (with a mixture of 11 active substances).

Fertilization administered to the soil was carried out with NPK complex mineral fertilizer (16-16-16). On each plot (40 m x 30 m), the distance between the stumps is equal to 1 m (1.5 m on the edge), and between the rows 1.5 m. On each of

the 11 rows (2 m on the edge) there are 25 rows cones, of which, on average, 21 cones per fruit. The biological material used in the present study is represented by the "Fetească Regală" vine variety, which has an important tradition in culture at the level of the Geoagiu Basin area and produces white grapes. The grape variety "Fetească Regală" (syn. Königstraube, Dănașană, Kirayleanca, Galbenă de Ardeal) is a hybrid between the Fetească albă and Francușe varieties. This variety is part of the category of semi-aromatic varieties and has a good capacity to exploit the vast majority of soil types (https://www.horticultorul.ro/vita-de-vi_e/feteasca-regala/).

The environmental temperature and precipitations data were obtained from the meteorological station iMETOS 3.3 placed in the experimental field, which performs daily recordings. Grapes yields and sugar contents data were collected, by weighing and laboratory analysis, respectively. The sugar content was realized refractometrically.

In order to statistically process the raw data, the program STATISTICA v.8.0 for Windows was used, both for the monitored environmental factors and for the grapes yield and sugar content of the grapes.

The "Descriptive statistics" program component was used with the aim of calculating the following parameters of the basic statistics: mean, standard deviation, coefficient of variability, values of maximum and minimum. With the help of the "t - test independent by variables" component of the program, the significance of the differences between the means was calculated, at the significance thresholds of 5%, 1% and 0.1% (Merce & Merce, 2009).

With the help of the components of the "Multiple Regression" program, the multiple correlations, the related coefficients of determination and the regression lines were calculated, which highlighted the interdependencies between the characteristics analyzed and the climatic factors. The component of the "Multivariate Exploratory Techniques" program, through its option Cluster analysis, was used to rank the productions and the content of the sugar, depending on the experimental variant.

RESULTS AND DISCUSSIONS

Analyzing the climatic indices, we find that in 2022 the averages of the environmental parameters characterized by growing season

significantly increased compared to 2021. By entire experimental field, the temperature increased by 8.57%, while relative humidity and precipitations decreased by 16.31%, and 19.72%, respectively (Table 1).

Table 1. The basic statistics for environmental temperature, air humidity and rainfall regimen in experimental site located in Geoagiu area, 2021-2022

Issue	Year	N	X	S	Minimum	Maximum	s
Temperature (°C)	2021	183	18.04 ^a	3301.80	6.20	24.70	3.44
Air humidity (%)		183	72.39 ^c	13250.80	39.60	98.10	11.36
Precipitations (mm)		96	4.87 ^e	468.00	0.50	25.00	5.28
Temperature (°C)	2022	183	19.73 ^b	3538.00	7.00	30.20	9.31
Air humidity (%)		183	60.53 ^d	11077.00	28.00	90.00	13.16
Precipitations (mm)		94	3.91 ^f	368.00	0.50	25.00	4.82

N - number of days; X - mean; S - sum; s - standard deviation; the differences between any two yield averages are significant, if their values are followed by letters, or groups of different letters.

The average grapes' yield recorded statistically significant variation, function of phytosanitary treatment and climatic conditions, in a wide range. The lowest average production (0.53 t/ha) corresponds to no phytosanitary treatment, lowest average temperature and highest relative humidity, and precipitations of the growing period, and largest (0.93 t/ha) to the Ist treatment scheme applied in conditions of the year 2022, characterized by highest average temperature and lowest relative humidity and precipitations, reported to the growing season of the entire experimental period (Tables 1, and 2). Higher productions and evolutions according to temperature and precipitations regimes are

reported by Bădulescu et al. (2020), who in climatic conditions of Ștefănești, Arges County obtained an average "Fetească Regală" grapes' production of 17.32 t/ha in 2019, and 18.71 t/ha, in 2020, growth in the same conditions, in two successive years characterized by higher temperature, and lower rainfall regimen in 2020, compared with 2019. Similar productions with majority of those reported in this study, were obtained by Băjenaru et al. (2022), 14.39 t/ha in 2020, and 14.48 t/ha, in 2021, in pedo-climatic conditions of Dăbuleni, Dolj County, with a light increase reported in 2021, year characterized by higher temperature and lower rainfall regimen, compared with 2020.

Table 2. The basic statistics for the yield recorded in Fetească Regală grapes variety, when different phytosanitary schemes are applied, 2021-2022 (t/ha)

Experimental variant	Year	N	X	Minimum	Maximum	s	CV
I	2021	10	10.20 ^{ab}	0.40	0.83	0.11	20.75
II		10	15.01 ^{ab}	0.65	0.90	0.09	11.53
III		10	12.32 ^a	0.50	0.80	0.07	10.93
I	2022	10	11.74 ^b	0.55	0.80	0.08	13.11
II		10	17.91 ^b	0.70	1.05	0.14	16.86
III		10	15.21 ^b	0.50	0.90	0.15	18.98

I - control not treated; II - Ist pattern of phytosanitary treatment; III - IInd pattern of phytosanitary treatment; X - arithmetic mean (%); s - standard deviation (%); CV - variation coefficient (%); the differences between any two yield averages are significant, if their values are followed by letters, or groups of different letters.

Concerning sugar content, we find the same evolutions as for grapes' yield, function of phytosanitary treatment and climatic conditions, but statistically significant differences are reported only between control, and sugar content corresponding to Ist treatment scheme, by each year. In this case, low variations are recorded, and they frame within 176.17 g/L-198.50 g/L (Table 3). Bădulescu et al. (2020), in climatic conditions of Ștefănești, Arges County

reported similar "Fetească Regală" grapes sugar content, corresponding to 2019 (230 g/L) and 2020 (230.08 g/L), but higher compared to results emphasized in this study. Băjenaru et al. (2022), reported an average sugar content of 178 g/L by a 9 years period (2013-2020), in Fetească regală grapes, in pedo-climatic conditions of Dăbuleni, Dolj County, which is similar to majority of those reported in this study.

Table 3. The basic statistics for the sugar content recorded in Fetească Regală grapes variety, when different phytosanitary schemes are applied, 2021-2022 (g/L)

Experimental variant	Year	N	X	Minimum	Maximum	s	CV
I	2021	10	176.17 ^{ab}	160.00	183.00	5.88	3.34
II		10	192.00 ^b	170.00	200.00	5.05	2.63
III		10	180.27 ^{ab}	173.00	192.00	8.31	4.61
I	2022	10	179.33 ^{ab}	167.00	184.00	7.47	4.17
II		10	198.50 ^b	189.00	205.00	4.07	2.05
III		10	189.00 ^{ab}	178.00	200.00	8.24	4.35

I - control not treated; II - Ist pattern of phytosanitary treatment; III - IInd pattern of phytosanitary treatment; X - arithmetic mean (%); s - standard deviation (%); CV - variation coefficient (%); the differences between any two yield averages are significant, if their values are followed by letters, or groups of different letters.

Trials conducted in Dealul Silagiului, Timiș County during 2018-2019, by Borca et al. (2019) to control the efficacy of different phytosanitary treatment schemes on "Fetească Regală" grapes yield and sugar content emphasizes similar evolutions like our study, with best performances when complex scheme of treatment was applied, and lowest for minimal treatment scheme. Their results show lower values of grapes yield, framing in the range of 11.42 t/ha-14.85 t/ha, but higher sugar content corresponding to complex scheme of phytosanitary fight, framing in the range of 176 g/L-203 g/L, compared with those reported by our study.

The multiple regression analyze was conducted to predict both grapes' yield and sugar content based on the evolutions of environmental temperature, relative humidity, and precipitations recorded in experimental site. The increase of grapes' yield and sugar content

function of phytosanitary treatments is multiple corelated with analyzed environmental parameters in a strong manner as the values of multiple correlations coefficients show. They frame within the ranges of $R = 0.661$ (accounting for 43.7% of variance) corresponding to moderate treatment scheme - 0.778 (accounting for 60.5% of variance) corresponding to control, for grapes' yield (Table 4), and within the ranges $R = 0.512$ (accounting for 34% of variance) corresponding to moderate treatment scheme, and $R = 0.623$ (accounting for 38.8% of variance) corresponding to control without treatment, for sugar content (Table 5).

Very strong simple correlation is reported by Cogato et al. (2019) between relative humidity in June ($R = 0.939$ accounting for 88.2% of variance) and sugar content, for several withe, grey and red wines growth in North-East of Italy.

Table 4. The relationship between Fetească Regală grapes yield environmental temperature (°C), relative humidity (%) and precipitations (mm), 2021-2022

Experimental variant	Year	R	R ²	Regression line
I	2021	0.778	0.605	$Y = 1.387 + 1.143X_1 - 0.378X_2 - 1.036X_3$
II		0.680	0.462	$Y = 1.875 + 0.843X_1 - 0.234X_2 - 0.643X_3$
III		0.661	0.437	$Y = 1.346 + 0.799X_1 - 0.130X_2 - 0.711X_3$
I	2022	0.749	0.561	$Y = 2.178 + 1.265X_1 - 0.318X_2 - 1.499X_3$
II		0.695	0.483	$Y = 3.603 + 0.904X_1 - 0.219X_2 - 0.639X_3$
III		0.662	0.438	$Y = 1.875 + 0.843X_1 - 0.234X_2 - 0.743X_3$

Analysing the dendrogram obtained for the grapes yields, we find two clusters. One is made of two branches and corresponds to experimental variants, with highest yields, and the other with a single branch, corresponding to control yield, which is lower compared to experimental yields (Figure 1a). The

dendrogram corresponding to sugar content also has two clusters (Figure 1b). One corresponds to sugar content obtained when the first treatment scheme is applied, which is the highest by entire experiment, and the second with two branches corresponding to control and second treatment scheme.

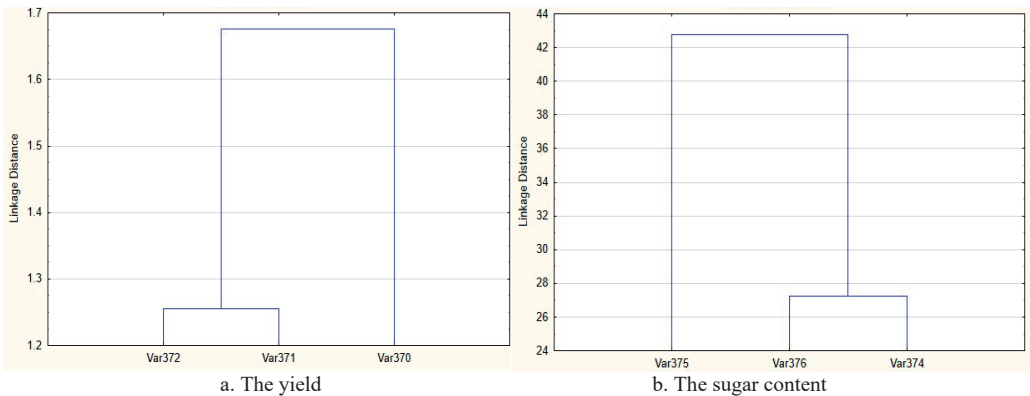


Figure 1. The cluster analysis for grape yields and sugar content
(Var 370 - control; Var 371 - 1st experimental scheme; Var 372 - 2nd experimental scheme; Var 374 - control; Var 375 - 1st experimental scheme; Var 376 - 2nd experimental scheme)

These results show that grapes yield corresponding to both experimental schemes are similar, but different compared with control, much higher in our case, while the first experimental scheme led to a much higher sugar content compared with control and second experimental scheme. Bucur and Dejeu (2014) reported moderate to strong simple positive correlations between

average summer temperature on one hand, yield ($R = 0.549$ accounting for 30.2% of variance) and sugar content ($R = 0.554$ accounting for 30.8% of variance), for "Fetească Regală" variety growth in Bucharest - Băneasa areal. They also reported a negative strong correlation between sum of precipitations in spring and grapes' yield ($R = -0.723$ accounting for 52.3% of variance).

Table 5. The relationship between Fetească Regală grapes sugar content, and environmental ($^{\circ}\text{C}$), relative humidity (%) and precipitations (mm), 2021-2022

Experimental variant	Year	R	R ²	Regression line
I	2021	0.623	0.388	$Y = 133.864 + 0.489X_1 - 0.123X_2 - 0.201X_3$
II		0.525	0.346	$Y = 191.776 + 0.323X_1 - 0.026X_2 - 0.153X_3$
III		0.541	0.366	$Y = 184.945 + 0.387X_1 - 0.029X_2 - 0.161X_3$
I	2022	0.602	0.362	$Y = 102.409 + 0.517X_1 - 0.123X_2 - 0.229X_3$
II		0.512	0.340	$Y = 238.169 + 0.315X_1 - 0.091X_2 - 0.129X_3$
III		0.535	0.354	$Y = 183.621 + 0.382X_1 - 0.094X_2 - 0.180X_3$

According to our analyse, the largest grapes' yields and sugar content corresponds in both experimental years to the phytosanitary complex scheme (I), if no influence of environmental factors would be considered. As regression lines show, in all cases, temperature positively influences both grapes' yields and sugar content, while precipitations and relative humidity contribute to their decrease. When the control scheme is applied, the influence of all environmental parameters is more consistent compared to that observed as corresponding to the other schemes of treatment in sugars' yield, and slightly superior for sugar content (Tables 4 and 5). It suggests that the application of phytosanitary treatments reduces, to some

extent, the dependence of grapes' yields of environmental factors influence.

CONCLUSIONS

The results of our study show that both climatic conditions expressed by environmental temperature, relative humidity, and precipitations and phytosanitary treatments are factors that significantly affects the grapes' yield and sugar content, but not with at same extent. The lowest average yield and sugar content correspond to no phytosanitary treatment, lowest average temperature and highest relative humidity, and precipitations expressed by the growing period, and highest to the complex

phytosanitary treatment (1st experimental scheme) in conditions of the year 2022, characterized by highest average temperature and lowest relative humidity and precipitations. For both analyzed traits (grapes' yield, and sugar content), temperature positively influences their increase, while precipitations and relative humidity has a negative influence.

ACKNOWLEDGEMENTS

This study was supported by funds from the National Research Development Projects to finance excellence (PFE)-14/2022–2024 granted by the Romanian Ministry of Research and Innovation.

REFERENCES

- Bădulescu, A., Sumedrea, D.I., Florea, A., Onache, A., Tănase, A. (2020). Influence of climate factors on yield and quality of some vine cultivars from the Ștefănești Center. *Romanian journal of Horticulture* 1(1), 149–156. DOI 10.51258/RJH.2020.20.
- Bărbulescu, I.D., Matei, P.M., Frîncu, M., Baniță, C.D., Teodorescu, R.I., Tudor, V., Dumitrache, C. (2022). Tămâioasă Românească and Busuioacă de Bohotin grapes - valuable sources for wine production, *Scientific Papers. Series B, Horticulture, LXVI*(2), 171 – 176.
- Block, A., Sparks, T.H., Estrella, N., Menel, A. (2013). Climate-Induced Changes in Grapevine Yield and Must Sugar Content in Franconia (Germany) between 1805 and 2010. *PLoS ONE*, 8(7), e69015. <https://doi.org/10.1371/journal.pone.0069015>.
- Borca, F., Nan, R.D., Nistor, E., Dobrei, A. (2019). Effect of different phytosanitary treatment schemes on the yield and quality of some wine grape varieties. *Journal of Horticulture, Forestry and Biotechnology*, 23(4), 8–13.
- Bucur, G.M., Cojocaru, G.A., Antocea A.O. (2019). The climate change influences and trends on the grapevine growing in Southern Romania: A long-term study, *BIO Web Conf.*, 15, 01008, <https://doi.org/10.1051/bioconf/20191501008>.
- Bucur, G.M., Dejeu, L. (2014). Influence of climate variability on growth, yield and quality of grapes in the south part of Romania. *Scientific Papers, Series B, Horticulture, LVIII*, 133–138.
- Carroquino, J., Garcia-Casarejos, N., Gargallo, P. (2020). Classification of Spanish wineries according to their adoption of measures against climate change. *J. Clean. Prod.*, 244, 142–155.
- Cogato, A., Meggio, F., Pirotti, F., Cristante, A., Marinello, F. (2019). Analysis and impact of recent climate trends on grape composition in north-east Italy, *BIO Web of Conferences*, 04014, DOI:10.10 51 /bio conf/ 20191304014.
- Colibaba, L.C., Bosoi, I., Pușcalău, M., Bodale, I., Luchian, C., Rotaru, L., Cotea, V.V. (2024). Climatic projections vs. grapevine phenology: a regional case study. *Notulae Botanicae Horti Agrobotanici Cluj-Napoca*, 52(1), 13381. <https://doi.org/10.15835/nbha52113381>.
- Hannah, L., Roehrdanz, P.R., Ikegami, M., Shepard, A.V., Shaw, M.R., Tabor, G., Zhi, L., Marquet, P.A., Hijmans, R.J. (2013). Climate change, wine, and conservation. *Proc. Natl. Acad. Sci. USA*, 110, 6907–6912.
- Mendez-Costabel, M., Wilkinson, K., Bastian, S., Jordans, C., McCarthy, M., Ford C., Dokoozlian, N. (2014). Effect of winter rainfall on yield components and fruit green aromas of Vitis vinifera L. cv. Merlot in California. *Aust. J. Grape Wine Res*, 20, 100–110.
- Merce, E., Merce, C.C., (2009). *Statistics – consecrated paradigms and complementary paradigms*. Academic Pres Publishing House, Cluj-Napoca, pp. 457.
- Mirošević, N., Karoglan-Kontić, J. (2008). *Viticulture*. Faculty of Agriculture, Zagreb.
- Ollat, N., Diakou-Verdin, P., Carde, J., Barrieu, F., Gaudillère J., Moing, A. (2002). Grape berry development: a review, *J. Int. Sci. Vigne Vin*, 36, 109–131.
- OIV (2009). Descriptor List for Grape Varieties and Vitis species, 2nd edition. <http://oiv.int>. (Accessed: 26.01.2024).
- Spayd, S., Tarara, J., Mee, D., Ferguson, J. (2002). Separation of sunlight and temperature effects on the composition of Vitis vinifera cv. Merlot berries. *Am. J. Enol. Vitic.*, 53, 171–182.
- Van Leeuwen, C., Darriet, P. (2016). The Impact of Climate Change on Viticulture and Wine Quality. *J. Wine Econ.*, 11, 150–167. [https://aloe.anfd.fr/\(Accessed: 24.01.2024\)](https://aloe.anfd.fr/(Accessed: 24.01.2024)). <https://www.horticultorul.ro/vita-de-vi e/feteasca -regala/> (Accessed: 24.01.2024).

TRADITIONAL ROMANIAN CULINARY PRACTICES AND THEIR HISTORICAL AND CULTURAL SIGNIFICANCE – A REVIEW

Carlo Marius DRAGOMIR¹, Simona-Maria ILIE¹, Mariana-Atena POIANA¹,
Corina Dana MISCA¹, Ileana COCAN¹, Delia-Gabriela DUMBRAVĂ¹,
Camelia MOLDOVAN¹, Viorica-Mirela POPA¹, Carmen Daniela PETCU²,
Claudia ROMAN³, Diana-Nicoleta RABA¹

¹University of Life Sciences "King Mihai I" from Timisoara,
119 Calea Aradului, Timisoara, Romania

²University of Agronomic Sciences and Veterinary Medicine of Bucharest,
59 Marasti Blvd, District 1, Bucharest, Romania

³Universidad de Huelva, Campus de "El Carmen", Huelva, Spain

Corresponding author emails: carmen28petcu@gmail.com, diana.raba@usvt.ro

Abstract

Food symbols, along with other important values in different aspects of life, individualize Romanian folk culture in relation to other cultures. Research in the field of traditional Romanian food has increased greatly in last year's resulting in many books, studies and articles that approach the changing complexities of taste and the world of food and its cooking. In this paper are presented the main traditional Romanian culinary practices in the context of their historical and cultural characteristics. Results of the study shown that, Romania is noted for many traditional foods and drinks. Romanian culinary practices are mainly determined by regional distinctions. In last years, because of industrialization, Romanian culinary practices have undergone a general trend of transformation and alignment to the imposed production and distribution standards, society has witnessed undermining of traditional food cultures.

Key words: culinary practices, cultural aspects, Romanian gastronomy, traditional dishes.

INTRODUCTION

Romania is a country located in south-central Europe, north of the Balkan Peninsula, in the north-western part of the Black Sea, along the lower Danube River. This geographical location places Romania at a crossroads of Central, Eastern, and Southeastern Europe (Figure 1), making it a country with a diverse cultural heritage and significant historical importance (Salanță et al., 2015).

The earliest written evidence of inhabitants in present-day Romania, the Getae, is found in Herodotus' Histories, Book I. The territories north of the Danube were inhabited by the Dacians. They are considered part of the Getae tribes mentioned by Herodotus. The Getae were an ancient group that inhabited the regions along the lower Danube River and the areas that are now part of Romania and Bulgaria. The Getae are often mentioned in historical sources alongside the Dacians, with whom they shared many cultural and linguistic traits (Păucean, 2013).



Figure1. Romania on the Europe map
(<https://www.quora.com/Why-does-Romania-count-as-a-Balkan-country-and-why-does-Hungary-not>)

Gastronomy, defined as "the art or science of eating well", encompasses the study of food and beverage production and preparation, as well as the context in which they are consumed, with attention to natural resources, including water resources (Virsta et al., 2020). Gourmet tourism, according to other authors, involves tourists

purchasing or consuming regional products and beverages, and engaging in food production activities, from agriculture to cooking trainings (Björk & Kauppinen-Räsänen, 2014; Jeroscenkova et al., 2016). Also, gastronomy has played a crucial role in uniting cultures. Romania boasts a rich heritage of traditional food products and authentic preparation methods. Local cuisines significantly contribute to sustainable tourism by enhancing the authenticity of destinations, boosting the local economy, supporting environmentally friendly infrastructure, and increasing tourist's awareness of a region's cultural richness (Sava & Cleșiu, 2013; Salanță et al., 2015; Dobre & Mocuța, 2022).

Romanian gastronomy throughout its history, highlights the influences of historical aspects, and socio-cultural factors.

Romanian cuisine is notable for its originality and the ingenious combination of traditional peasant recipes (from shepherding and fishing) with Oriental, Polish, Russian, Ukrainian, and French-Austrian-Hungarian influences. It encompasses both everyday meals and festive dishes, including those associated with Christian traditions, such as fasts and feasts. Romania's historical regions, represented by: Moldavia with Bucovina, Transylvania, with Maramureș, Crișana, and Banat, Muntenia, with Oltenia and Dobrogea, boasts a distinct historical, socio-cultural, economic, and gastronomic identity (Simoni, 2017; Simoni et al., 2021).

MATERIALS AND METHODS

Gastronomy is a significant aspect of cultural identity and heritage, deeply rooted in the traditions and practices of a region's people. This paper explores how the unique culinary traditions of Romania's ethnographic regions play a vital role in both preserving cultural heritage and fostering economic development. The study is based on comprehensive research of bibliographic sources, including specialty books and papers, as well as publications and information from relevant web pages. The gathered information is thoroughly analyzed and processed to draw pertinent conclusions regarding the economic and cultural importance of gastronomic differences between traditional products of the ethnographic regions in

Romania. However, there are currently no works entirely dedicated to the Romanian history of gastronomy, and this work is an attempt to collect information from various sources.

RESULTS AND DISCUSSIONS

History of Romanian Cuisine

The main information is provided by archaeological discoveries: charred seeds, osteological remains, household inventory (ceramics, metal vessels, kitchen utensils) (Iordan, 2013). The diet of the population in Dacia, both in the pre-Roman period and after the arrival of the Romans, included a wide and varied range of foods: cereals, vegetables, fruits, meat, dairy products, wines, and beer. Products could be consumed raw, in case of vegetables and fruits, most of them boiled, such as vegetables, cereals and meat, ground into flour and turned into bread, as in the case of the cereals, roasted and fried, in case of fish and meat (Chelariu, 2023). There are certainly differences in the diet of different social classes. In addition to domestic plants and animals, wild ones were also consumed. Diet is constantly influenced by social status, local customs and traditions, specific foods or animals available in the area, and the intensity of trade relations with other areas. Food, dishes, culinary customs, and recipes of the ancient world are a great fascination for modern people (Voinea et al., 2020).

After the founding of Rome, during the time of Romulus, the cuisine was military, lacking elegance or refinement. After marrying the Sabine women, the Romans remained soldiers during wartime, but in peacetime, they began to cultivate vegetables. Daily food consisted of cereals, pulses, and vegetables (Pop, 2020; Chelariu, 2023).

During the Republican era, the Romans conquered vast territories, especially for their fertile agricultural lands. Greek cuisine had a significant influence on Roman cuisine. By conquering the western Mediterranean, the Romans also took control of trade routes to India and China, introducing spices to Rome.

Roman cuisine gradually abandoned the virtues of rural simplicity, making way for the cosmopolitanism of Imperial Rome (Djuvara, 2016; Florescu, 2022).

Many changes occurred with the advent of Christianity. Roman gastronomy did not collapse due to dietary laws, and the transformation of a culture that had developed over more than a thousand years did not happen overnight. In Christianity, delicacies were considered the path to hell and damnation (Djuvara, 2016; Florescu, 2022).

Ancient cuisine was quite varied. Various species of fish were consumed, along with meat (pork, lamb, goat, chicken, duck, goose, pigeon, rabbit, wild boar, partridge, pheasant, deer, roe deer, thrush, snails, bacon, many types of sausages, ham), vegetables (asparagus, beetroot, cabbage, carrots, artichokes, horseradish, onions, leeks, cucumbers, mushrooms and truffles, beans, lupin, lentils, peas, chickpeas), milk, cheese, dairy products, fruits (apples, pears, pomegranates, quinces, plums, blackberries, mulberries, cherries, watermelons and melons, walnuts, hazelnuts, almonds, dates, olives, berries, figs, grapes), cereals (barley, spelt, wheat, millet, oats, rye, rice), the famous puls, and bread (Ghinea & Prisacaru, 2023). The Latin word for cook was "coquus" or "cocus," but "coctor" also appeared. The head cook was called "archimagirus" or "praepositus cocorum," and sometimes "supra cocos" (Ghinea & Prisacaru, 2023).

With the spread of luxurious meals, the popularity of specialized cooks grew. The culinary extravagances of the imperial era allowed cooks to showcase their skills, turning cooking into a true art.

Plautus provides information about the profession of cooking. Pliny, Plautus, and Terentius tell us that professional cooks were hired from the macellum, also known as the "forum coquinum". The characteristics of cooks were often those presented in Greek comedies: boastful, thieving, proud of their profession, and in rivalry with each other. Roman cooks were also boastful, proud of their profession, thieves who took food home and tasted all the ingredients during preparation, lovers of jokes, capable of deceiving with their culinary talents (preparing one type of food to resemble another that was requested by their master but not available), and quarrelsome with other cooks (Mulcahy, 2021).

In the context of ancient Roman cuisine, two vital elements in the cooking process were water

and fire. These foundational resources facilitated a sophisticated culinary culture that greatly influenced subsequent European gastronomic traditions. These aqueducts allowed many Roman houses to be connected to the city's water network, ensuring a consistent flow of running water for kitchens and baths. This innovation not only improved sanitation and daily living conditions but also enabled more efficient and varied cooking practices. In addition, fire was central to Roman cooking, utilized in various forms such as fixed stoves and portable stoves and ovens. The availability of both fixed and portable cooking equipment allowed for a versatile approach to meal preparation, whether at home or during communal gatherings. Some had water vessels and grills to prepare both vegetables and meat. Roman cooks had numerous cooking tools: knives, cutting boards, meat forks, soup spoons, sieves, graters, skewers, nutcrackers, measuring cups, and all sorts of pots and pans (Templeman, 2013). The basic flavors were the ones we know today: sour (lemon, vinegar), salty (salt, brine, various fish sauces), sweet (honey), and bitter. Among these four flavors, sweet was the most common. The bitter flavor was not very popular. Cooks usually tried to mask or soften it. There is a multitude of herbs mentioned in Latin literature, including lovage, cumin, rue, mint, basil, celery, parsley, marjoram, thyme, dill, fennel, anise, bay, myrtle, mustard, poppy, saffron, sage, rosemary, and sesame (Kocevski & Risteski, 2020). The scientific difference between herbs and spices is not clear. The most used spices were pepper, cinnamon, cassia, cardamom, and ginger. Other ingredients used in Roman cuisine included olive oil, animal fats, perfumes, and cheese (Kocevski & Risteski, 2020).

Ensuring a constant and sufficient food supply for armies has always been an important issue. The basic diet during peacetime seems to have included: cereals, bacon, cheese, vegetables, sour wine, with access to salt and olive oil. A certain amount was deducted from the soldiers' pay for these basic foods. A greater variety of foods were available on military calendar holidays. Meat was a constant part of the soldiers' diet, sourced from provincials, acquisitions, hunting, unit vivariums, and sacrifices. Domestic animals, wild game,

poultry, fish, and shellfish were consumed. Milk and cheese were also consumed, as were fruits and nuts. Among vegetables, beans and lentils were the most frequently consumed. All evidence indicates a very good diet for Roman soldiers, both qualitatively and quantitatively (Templeman, 2013; Kocevski & Risteski, 2020).

The gastronomic landscape of Romania is a rich mosaic created by centuries of cultural interactions and historical events. From the introduction of borscht with meat by the Slavs (7th-8th century AD) to the significant influence of Hungarian (12th-13th century), Ottoman, Greek, Arabic, Armenian, and Byzantine culinary traditions (13th to the 19th century), Romanian cuisine reflects a diverse heritage. These influences have not only added to the variety and richness of Romanian food but also helped shape the country's culinary identity, making it a unique and flavorful part of European gastronomy (Smaranda, 2017). During this last period, tomatoes, eggplants, onions, peppers, corn, quince, and melon were introduced and cultivated. Consequently, the Romanian menu was enriched with Turkish dishes (such as meatball "perişoare" soup, meatballs, pilaf, stuffed bell peppers, "kebab," "ciulama," "tuslama," "baklava," "sarailie"), Greek moussaka, and Bulgarian vegetable stews like "zacusca" and "ghiveci." In the 18th century, Romanian cuisine was further influenced by neighboring ethnic groups: Ukrainians in Maramureş, Lippovans in Northern Dobruja, and Serbians, Austrians, Germans, Hungarians, and Ukrainians in Banat. Following the formation of the Romanian state in the late 19th and early 20th centuries, many restaurants featuring fine Western dishes (French, Italian, Austrian) opened in major cities (Simoni, 2017; Nacu, 2021; Raba et al., 2021).

Over the years, Romania's population remained predominantly rural until the latter half of the twentieth century: 88% were rural in 1912, 68% in 1960, 50% in 1985, and 46% today. Throughout history, most Romanians were poor peasants whose livelihoods were primarily rooted in agriculture. This agrarian lifestyle was supplemented by various local activities that were closely tied to the natural environment, including forestry, fishing, hunting, and beekeeping. These activities not only provided

essential resources but also contributed to the cultural and economic fabric of rural communities. The period after 1960 marked a significant transformation in Romania, characterized by industrialization, agricultural mechanization, and urbanization. These changes modernized the food industry, increased agricultural productivity, and led to significant socio-economic shifts. While these developments brought about economic growth and improved living standards, they also introduced new challenges and changes to traditional lifestyles. Prior to this, everything from clothing to food was homemade using agricultural products from local farms (Simoni, 2017).

The gastronomy of Romania is a testament to the country's rich history, diverse geography, and cultural resilience. Shaped by natural factors, historical influences, and socio-economic changes, traditional Romanian cuisine continues to evolve while retaining its unique identity. It serves as a source of pride and connection to the past, offering insights into the cultural fabric of the nation. On the other hand, historically, Romania's division between various empires exposed its people to a variety of cultural traditions, leading them to adopt and adapt numerous dishes from Turkish, Arabic, Greek, Hungarian, Austrian, French, Russian, Jewish, Polish, Serbian, and Italian cuisines. This resulted in a unique culinary tradition characterized by the creative fusion of old peasant recipes. Western cooks began to appear in major cities (Smaranda, 2017; Dumitrache & Nae, 2023).

The traditional gastronomy of Romanian regions

The regional specificities in Romanian cuisine highlight the country's cultural diversity and culinary richness. Despite its size, Romania's various regions offer a wide array of flavors and dishes that reflect historical influences and local ingredients. These culinary traditions not only satisfy the diverse preferences of the population but also serve as a source of cultural pride and identity (Morăraşu & Drugă, 2015; Smaranda, 2017; Dumitrache & Nae, 2023). Exploring the nuances of Romanian cuisine across different regions provides a deeper understanding of the country's vibrant gastronomic heritage. In

Romania, as small as it may be, different regions have their own specificities. The cuisine of Dobrogea or that of the Delta, where fish predominates, differs significantly from that of Transylvania, where pork fat and dishes with roux predominate, or that of the southern regions, based on cornmeal and soups, and broths. The Moldovans also have their specialties, such as "tochitura", "poale-n brau", or "parjoale" (Salață et al., 2015).

However, it can be said that some dishes are equally popular in all regions, such as polenta, grills, "mititei" (grilled minced meat rolls), pork aspic, stuffed cabbage rolls ("sarmale"), and among pickles, pickled cucumbers and pickled cabbage, not to mention that bread is the staple of the diet in all regions at this time (Teodoroiu, 2015). As the connection between different regions of the country intensifies, numerous dishes that were once specific to a certain area are found throughout Romania. Furthermore, globalization is also felt in gastronomy, with the exchange of recipes and culinary customs between different parts of the world becoming increasingly intense (Sohodoleanu, 2020).

Moldovan Cuisine

Considered by some specialists as the most "elaborate" cuisine in the country, it is characterized by creamy sauces or light sauces, with or without a little flour. Minced meat is preferred in the preparation, and lard is used in many dishes. Renowned are the pies with meat, with mushrooms, with cabbage (cabbage pies), vegetable soups, pumpkin dishes, beans, homemade noodles, chicken or beef, giblet soup (gizzards, livers, wings, heads, feet), etc. (Ghinea & Prisacaru, 2023).

Other Moldovan specialties include "alivenci" (a dish made from polenta and cottage cheese baked in the oven), "tochitura" (made from pork and organs fried in lard), Moldovan meatballs and one of the most appreciated meal, forest mushroom "hribi and opintici" stew. Among desserts, the most famous is the "cozonac" (made from leavened dough with walnut, poppy or Turkish delight filling). Also, we should mention "invartita" (thin pastry sheets sprinkled with nuts and rolled, baked in the oven and syruped), Moldovan "mucenici" (made from sweet bread dough, baked in the oven, coated with honey and sprinkled with nuts), "poale-n

brau" (another sweet bread dough, rolled out and cut into squares, filled with cottage cheese, baked in the oven), and "tocmagei" with nuts (<https://sadova.ro/mancare-sadova-bucovina/>).

The most representative wines produced and consumed in Moldova include: "Grasa de Cotnari", "Galbenă de Odobești", "Feteasca alba", "Feteasca neagră", "Zgihara de Huși", "Frâncușa", "Băbeasca neagră", "Busuioaca de Bohotin" and "Tămâioasa Românească" (Nedelcu, 2017; Petcu C.D. et al., 2019).

Transylvanian Cuisine (including Crișana and Maramureș)

Transylvanian cuisine is strongly influenced by Austro-Hungarian traditions and offers rich and hearty dishes.

Transylvanian cuisine is also characterized by sweet fruit sauces and garnishes, thick sauces bound with plenty of flour, and soups with roux. Sweet paprika is used more here than in other regions (Păucean, 2013).

Pork is predominant in dishes, and lard is frequently used for cooking. Borscht and sour soups are less common, often replaced by soups (broth), and souring is often done with sour milk (yogurt). Among soups, cumin, sorrel, lettuce, bean, or bean pod soups with smoked ribs, beef soup with noodles (lăște), and sausage soup are notable. Renowned sour soups include pork with tarragon and potato soup (Păucean, 2013).

In Maramureș, dishes have an „ancestral taste” influenced by Romanians, Saxons and Hungarians. Polenta with cheese (with lard), baked in the oven, and "balmoș" (boiled cornmeal with "jintuială" - the fatty whey from making sweet cheese), Cluj-style cabbage "varza a la Cluj" and larger-sized Transylvanian stuffed cabbage rolls are highly esteemed (Mitu, 2021).

Crișana cuisine is influenced by Hungarian and German culinary traditions, prominently features pork and vegetable dishes. Some notable examples of traditional dishes are pork stew, stuffed peppers, liver dumplings, goulash, vegetable stew and beans with Sausage (Raba et al., 2021). Other specific dishes include Banat-style pork chop, pork roast with fruit sauce (especially sour cherries). Desserts include pancakes with jams or preserves, and in urban areas, "cremes" (cream cakes) and tortes. Related to the drinks, the most popular wines

are: "The White Feteasca", "The Royal Feteasca", "Muscat Ottonel", "Babeasca" and "Feteasca Neagră" (Păucean, 2013).

Muntenian and Oltenian Cuisine

Muntenian cuisine is influenced by French cuisine but also by Turkish cuisine. Generally, it is refined and subtle, reflecting the capital's influence. The dishes highlight the richness and variety of Muntenian cuisine, characterized by robust flavors, hearty ingredients, and traditional cooking techniques that have been passed down through generations (<https://www.romanian-places.com/muntenia-oltenia.html>). In all Muntenian regions, many similar or identical dishes can be found, such as sour soups, broths, grilled roasts, and "mititei" (grilled minced meat rolls).

Among broths, we can mention those made with orach, sorrel, nettles, porcini mushrooms with beans, and the classic meatball broth. Among sour soups, notable ones include the potato soup from Câmpulung, bean soup, pork bone soup, stuffed zucchini soup, and rustic chicken soup. Tomato and lentil soups are also prepared. Salads include eggplant salad, green bean salad with garlic, cucumber salad, and mushroom salad (<https://www.romanian-places.com/muntenia-oltenia.html>).

Various dishes are prepared, including pilafs, stews, and "ciulama" (a creamy dish), with different vegetables or mushrooms, small stuffed cabbage rolls, and a wide range of fish dishes (Danube herring, carp), chicken dishes (with various vegetables), beef, and pork dishes, including various vegetables stuffed with meat (zucchini, eggplants, potatoes). The national vegetable stew ("ghiveci") is also a specialty from the southern part of the country (<https://bucatarianationala.wordpress.com/>).

Oltenian cuisine is characterized by heavily spiced dishes – dominated by hot peppers – and simple culinary operations. Boiling is the most used cooking method. Especially in Oltenia, leek holds a place of honor and is prepared in various forms. Olives are also found in numerous dishes. Desserts include donuts, puddings, and pancakes (<https://www.romanian-places.com/muntenia-oltenia.html>). The wines which are produced in this region of the Romania are: "Feteasca regală", "Băbeasca neagră", Sangiovese,

"Roşioara", "Pinot noir", and "Zaibăr" a local sort considered the pride of Oltenia (Nedelcu, 2017; Smaranda, 2017).

Dobrogea Cuisine

Dobrogea cuisine is based on the natural resources of the area: freshwater and marine fish, particularly tasty lamb, and it is strongly influenced by Oriental cuisine, featuring dishes characterized by the presence of raisins, nuts, and concentrated syrups. A specific culinary method is spit-roasting (Nedelcu, 2017).

Among the soups, notable ones include tripe soup, fish soup (with a creamy consistency, made from various species of small and large fish, the latter served separately with garlic sauce), and carp head soup. The Lipovans, originally from Russia, cook a fisherman's soup called "uha" following old 18th-century Russian recipes. A renowned specialty is the Dobrogean pie (with grated sheep's cheese, wrapped in puff pastry) served with yogurt. Similar are the "merdenele" also prepared with sheep's cheese (Nedelcu, 2017, <https://www.info-delta.ro/retete-culinare-31/>).

Unique to this region are the stuffed cabbage rolls with rice and raisins. Fish dishes are numerous: baked carp, carp stuffed with nuts and raisins, carp with rice, and especially spit-roasted carp, to name a few. Lamb and mutton are prepared in various ways, including lamb drob (a type of haggis), ostropel (a type of stew), ghiveci (vegetable stew), and shashlik (skewered meat), with mutton often baked with a rice garnish.

The most famous sweet dishes are baklava (two layers of nuts sandwiched between three layers of pastry, brushed with butter, baked, and soaked in a fragrant syrup), "sarailii" (similar to baklava), homemade halva, and gingerbread (Nedelcu, 2017).

The wines from Dobrogea are among the best known and appreciated wines in the world and come from the Murfatlar winery, including Chardonnay, Pinot, Riesling and Muscat Ottonel (Nedelcu, 2017).

Trend of Romanian culinary practices

The accelerating global industrialization in recent decades has led to a clear tendency to adapt the food system to production and distribution standards imposed by current

legislation, resulting in the systematic undermining of traditional food cultures everywhere. In addition, the emergence of the concept of "world cuisine", dominated by the rationale of quantity, has led to the supremacy of standardized products and uniformity of taste (Petrini, 2015).

Traditional Romanian culinary practices have also been affected by the changes that have also taken place in our society. Globalization, urbanization, modernization of production and packaging technologies (Petcu, 2014) and migration have profoundly impacted how modern Romanian consumers consumes food, leading to significant changes in culinary practices and the emergence of a "world cuisine" (Privitera et al., 2018). Despite this, in Romania, traditional foods continue to garner significant interest, particularly within the context of the growing economic importance of gastronomic rural tourism. This trend underscores a desire to preserve and promote local culinary traditions, which play a pivotal role in attracting tourists and maintaining the cultural identity of different regions (Tanasa, 2014).

However, the adoption by Romanian consumers of the new model of food behavior, with an emphasis on seasonal vegetables and fruits of local origin, on reducing meat consumption and access to sustainable methods of food preparation, while preserving the most representative characteristics of the Romanian ancestral food culture would have the effect of improving consumer health and at the same time protecting the environment (Voinea et al., 2020).

CONCLUSIONS

Romania's culinary history has its origins in pre-Roman times and has undergone a number of cultural influences over the centuries, reflecting the diverse heritage and rich agricultural landscape of the country. From ancient times to the present day, Romanian cuisine has evolved, incorporating elements from various civilizations and neighboring regions.

Romania's regional specificities in cuisine indeed underscore the country's cultural diversity and culinary richness. Each region boasts distinct flavors and dishes, shaped by historical influences and local ingredients,

which together create a vibrant culinary tapestry and embody cultural pride and identity.

New trends in global food culture have also influenced Romanian culinary preferences and practices.

REFERENCES

- Björk, P. & Kauppinen-Räsänen, H. (2014). Culinary-gastronomic tourism - a search for local food experiences. *Nutrition & Food Science*, Emerald Publishing, Bingley, UK. 44(4), 294-309.
- Chelariu, A.R. (2023). *Romanian Folklore and Its Archaic Heritage: A Cultural and Linguistic Comparative Study*. London, New York: Palgrave, MacMillan, Springer.
- Djuvara, N. (2016). *A brief illustrated history of Romanians*. Humanitas SA.
- Dobre, L. & Mocuța, D.N. (2022). The risks of land fragmentation over the quality of life in rural areas in romania. *Scientific Papers. Series E. Land Reclamation, Earth Observation & Surveying, Environmental Engineering*, XI, 213-221.
- Dumitrache, L. & Nae, M. (2023). Romanian Food on an International Plate: Exploring Communication, Recipes, and Virtual Affect in Culinary Blogs. *Berichte. Geographie und Landeskunde*, 96(1), 54-72.
- Florescu, R.R. (2022). Essays on Romanian history. *Histria Books*.
- Ghinea, C. & Prisacaru, A.E. (2023). Romanian Traditional Dishes and Certified Food Products. *Food and Environment Safety Journal*, 22(2).
- Jordan, V. (2013). Ghidul Gastronomic al României: Bucătăria Tradițională. *House of Guides*, Bucuresti, Romania.
- Jeroscenkova, L., Kruzmetra, M., Rivza, B., Foris, D. (2016). Similarities and differences in the value manifestations and management of cultural heritage. *Management Theory and Studies for Rural Business and Infrastructure Development*, 38(1), 18-27.
- Kocevski, J. & Risteski, M. (2020). Defining cuisine and types of cuisine. *Horizons International Scientific Journal Series A Social Sciences and Humanities*, 26, 291-302.
- Mitu, S. (2021). Traditional Food and Gastronomy in Maramureș. *Memoria Ethnologica*, 78-79, 82-101.
- Morărașu, N.N. & Drugă, L. (2015). The symbolic functions of culinary practices shaping Romanian gastronomic identity. *Cultural Perspectives*, 20, 98-115.
- Mulcahy, J.D. (2021). Historical evolution of gastronomic tourism. *The Routledge handbook of gastronomic tourism*. Routledge, 24-31.
- Nacu, F. (2021). A Survey of Romanian Culinary Heritage in the Second Half of the Nineteenth Century. *Transylvanian Review*, 30(2), 79-102.
- Nedelcu, A. (2017). Gastronomic and wine tourism – key elements for local economic development. Case study Romania. *Second International Thematic Monograph, Modern Management Tools and Economy of Tourism Sector in Present Era*, Belgrade, 142-160.

- Păucean, A. (2013). A geographical and historical overview of the Transylvanian cuisine. *Bulletin UASVM Food Science and Technology*, 70(1), 1-7.
- Petrini, C. (2015). *Food & Freedom: How the slow food movement is changing the world through gastronomy*. Rizzoli Ex Libris Publishing House. New York, NY, USA, ISBN 978-0-8478-4685-6.
- Petcu, C.D. (2014). Ambalaje utilizate în industria alimentară. *Editura Granada Bucuresti*.
- Petcu, C.D., Deleanu, C., Matei, I., Cotan, Ș.D., Viziteu, G., Andronic, V. (2019). Contributions concerning the study of the antiseptic effect of sulfur dioxide on the yeasts present in two wines provided by Cotnari vineyard. *Lucrări Științifice*, 62(4) seria Medicină Veterinară, Iași, 317-322.
- Pop, I.A. (2020). A Short-illustrated history of Romanians. *Grup Editorial Litera*, Bucharest.
- Privitera, D., Nedelcu, A., Nicula, V. (2018). Gastronomic and food Tourism as an economic local resource: case studies from Romania and Italy. *Geo Journal of Tourism and Geosites*, 1(21), 143 -157.
- Raba, D.N., Cassian, A.G., Dincu, A.M., Moldovan, C., Borozan, A.B. (2021). The influence of the cuisine of ethnic communities on the Banatians' eating habits. *Agricultural Management, Lucrări Științifice, Seria I*, 23(1), 240-250.
- Salanță, L.C., Păucean, A., Tofană, M., Man, S., Pop, C. (2015). Romanian Cuisine: Culinary Habits and Local Produce. *Journal of Agroalimentary Processes and Technologies*, 21(2), 186-191.
- Sava, C. & Cleșiu, S.R. (2013). Romanian gastronomy between traditionalism, commerce, business and rural tourism. *Knowledge Horizons. Economics*, 6(3), 66-69.
- Simoni, S. (2017). Traditional Romanian Food as the result of history, nature, way of life and human ingenuity. *Lucrări Științifice Management Agricol*, 19(1), 221-228.
- Simoni, S., Teodoroiu, F., Țală, M.L., Țigu, G. (2021). Cultural and economic aspects of promoting Romanian traditional gastronomy. *The Bucharest University of Economic Studies, Romania, Basiq International Conference*, 582-589.
- Smaranda, S. (2017). Traditional Romanian food-as the result of history, nature, way of life and human ingenuity. *Agricultural Management, Lucrări Științifice Seria I*, 19(1), 221- 228.
- Sohodoleanu, A. (2020). The production of the 'New Romanian cuisine': Elite local taste and globalisation. *Journal of Comparative Research in Anthropology and Sociology*, 11(02), 49-64.
- Tanasa, L. (2014). Benefits of short food supply chains for the development of rural tourism in Romania as emergent country during crisis. *Agricultural Economics and Rural Development*, 11, 181–193.
- Templeman, S.J. (2013). *Cooks, cooking, and food on the early modern stage*. University of Exeter, United Kingdom.
- Teodoroiu, F. (2015). Traditional food. Case study: Romanian local food. *Revista de Management Comparat Internațional*, 16(2), 256-268.
- Virsta, A., Sandu, M.A., Daraban, A.E. (2020). Dealing with the transition from in line economy to circular economy - public awareness investigation in Bucharest. *AgroLife Scientific Journal*, 9(1).
- Voinea, L., Popescu, D.V., Bucur, M., Negrea, T.M., Dina, R., Enache, C. (2020). Reshaping the traditional pattern of food consumption in Romania through the integration of sustainable diet principles. A qualitative study. *Sustainability*, 12(14), 5826.
- <https://bucatarianationala.wordpress.com/>
<https://sadova.ro/mancare-sadova-bucovina/>
<https://www.info-delta.ro/retete-culinare-31/>
<https://www.quora.com/Why-does-Romania-count-as-a-Balkan-country-and-why-does-Hungary-not>
<https://www.romanian-places.com/muntenia-oltenia.html>.

SIR JOSEPH WILLIAM BAZALGETTE - THE INGENIOUS CIVIL ENGINEER WHO HAS CHANGED LONDON

Elena NISTOR

University of Agronomic Sciences and Veterinary Medicine of Bucharest,
59 Marasti Blvd, District 1, Bucharest, Romania

Corresponding author email: elena_nistor@yahoo.com

Abstract

The year 2024 marks the 205th anniversary of the birth of Sir Joseph William Bazalgette (1819-1891), the English civil engineer best known as the mastermind behind the sewerage system for Central London which he devised in the second half of the 19th century, in response to the Great Stink. In the summer of 1858, the hot weather increased the stench of the untreated human and industrial waste deposited on the banks of the Thames and into the river, resulting in about 12,000 fatalities due to contagious diseases. As Chief Engineer of the Metropolitan Board of Works, Bazalgette's solution was to build a sewer network that would collect the waste water and waste matter flowing freely on the London streets. Proposed in 1858, his project was completed in 1875. The complex infrastructure, consisting of 132 km (82 miles) of underground sewers, about 2,100 km (1,300 miles) of street sewers, and four pumping stations (Deptford, Crossness, Abbey Mills and Chelsea Embankment) has fundamentally reshaped the sewage system of the English capital and is still in use, making London the city it is today.

Key words: London, pumping station, sewage system, the Great Stink, the Thames.

INTRODUCTION

A period marked by contrasts and differences, the Victorian Age left an impressive heritage to Britain. Throughout almost 64 years of reign, Queen Victoria ruled a large empire that was to become the world's industrial power, and encouraged the development of knowledge under its most revolutionary forms, which ultimately led to a rapid change in the essence of the British society and an unprecedented evolution of science, technology and the arts. Creative imagination and masterly skills, doubled by innovative vision and high ideals, have generated various types of masterpieces that were then regarded as groundbreaking discoveries and even today are clearly acknowledged as not only factual and social achievements but also prominent cultural symbols of a nation at its very best moment in its history.

This paper is intended as a celebration of the life and work of one particular personality of the time: Sir Joseph William Bazalgette, the English civil engineer who is remembered as the creator of the first sewerage system for Central London in the mid-1800s. It is a descriptive-interpretive approach primarily

based on specialist literature and the engineer's own report, 'On the Metropolitan System of Drainage and the Interception of the Sewage from the River Thames', presented at the Institute of Civil Engineers on the 14th of March 1865 (Bazalgette, 1865). The analysis focuses primarily on the scientific aspects of the project, minutely advocated by facts and data, and also emphasizes the profoundly human nature of such an unprecedented enterprise. The boldness and complexity of the work stand as ultimate proof that civil engineering is a profession that successfully combines systematic knowledge based on evidence with creativity and resourcefulness for the sake of progress, of creating healthier and happier communities in safer and more secure environments.

THE SETTING

At the time of Queen Victoria's coronation on the 28th of June 1838, London was the capital of the British Empire and the largest city in the world, about to reach two million inhabitants consisting of locals as well as migrants from Ireland and continental Europe, Africa and

America, and colonists returning from North America and later Australia.

The emerging hub of the world was far from being ‘the flower of cities all’ (Dunbar, 2012). As personal stories were absorbed into the collective urban narrative, geographic and demographic expansion resulted in overcrowding and low living standards. Divided between the affluent West districts and the poverty-stricken East, the city was heavily dependent on coal heating to keep its buildings warm, manual pumps to provide clean water to its increasing population, a rainwater system to wash the dirt and filth off its streets, and human waste collectors (euphemistically called ‘night soil men’) to help maintain somewhat decent conditions in its domestic households. Nevertheless, what the individual dwelling place was striving to gain in comfort, the whole congregation was losing in safety: the air was unbreathable, the water was undrinkable.

The dark reality of Victorian London was exquisitely chronicled by Charles Dickens, the famous novelist who depicted the baffling incongruities between cynical prosperity on the one hand and despondent poverty on the other. The devout Londoner often placed his characters against the memorable landscape of a dynamic yet desolate urban agglomeration. In his first novel, *The Posthumous Papers of the Pickwick Club* (1836-1837), he refers to ‘the climate of London, which is extremely disagreeable’ (Dickens, 1992) and, six years later, he opens the first chapter of *Bleak House* (1852-1853) with an indelible image of the English capital:

“As much mud in the streets as if the waters had but newly retired from the face of the earth, and it would not be wonderful to meet a Megalosaurus, forty feet long or so, waddling like an elephantine lizard up Holborn Hill. Smoke lowering down from chimney-pots, making a soft black drizzle, with flakes of soot in it as big as full-grown snow-flakes - gone into mourning, one might imagine, for the death of the sun” (Dickens, 2003).

The muddy streets and the smoke contribute to the general sense of discomfort and frustration generated by an oppressively grim environment, emphasised by the pervasive presence of fog, which adds an aura of mystery to easily recognisable geographic locations and,

at the same time, enhances mental anguish and emotional distress:

“Fog everywhere. Fog up the river, where it flows among green aits and meadows; fog down the river, where it rolls defiled among the tiers of shipping and the waterside pollutions of a great (and dirty) city. Fog on the Essex marshes, fog on the Kentish heights. Fog creeping into the cabooses of collier-brigs; fog lying out on the yards, and hovering in the rigging of great ships; fog drooping on the gunwales of barges and small boats. Fog in the eyes and throats of ancient Greenwich pensioners, wheezing by the firesides of their wards; fog in the stem and bowl of the afternoon pipe of the wrathful skipper, down in his close cabin; fog cruelly pinching the toes and fingers of his shivering little ‘prentice boy on deck” (Dickens, 2003).

Dense and dark, the description has repeatedly been anthologised not only for the literary value of the accumulation of tenebrous emotions forged by the dramatic exposition, but also for the oblique critique of the striking consequences of the fast industrial development on people and their surroundings. It is an inescapable trap that suffocates all living creatures and their ideals, since ‘the raw afternoon is rawest, and the dense fog is densest, and the muddy streets are muddiest.’ (Dickens, 2003).

The vicious circle metaphorically chronicled by the writer in many of his works was much harsher in reality, as the overcrowded and under-supplied boroughs were in imminent danger. The naturally occurring fog was becoming more dense due to the smoke, soot and ash resulting from coal burning in both homes and factories. The mud on the streets was thickened with dung from the hundreds of thousands of horses pulling the carriages and wagons on the streets. The human waste produced by 2.5 million Londoners was disposed of straight in the river, alongside animal carcasses and other rotting materials.

No wonder that more and more people were falling ill, with no hope of recovery. At first they blamed the odour emanating from decomposing organic matter but it soon became clear that it was the *Vibrio cholerae* that was proliferating in the city’s watercourse and passing into the pumps that supplied the

boroughs with water from the river. The bacteria caused three major cholera outbreaks: in 1831, when 6,536 people died; between 1848 and 1849, when 14,136 deaths were recorded; and between 1853 and 1854, when the disease claimed 10,738 lives. In 1854 the English physician John Snow identified the source of the epidemic as the public water pump located on Broad Street (today Broadwick Street) in Soho and persuaded the local council to disable it, subsequently noting the decline in the number of cases (Klein, 2015).

Nevertheless, as Londoners continued to pollute the river and its banks with their waste, the threat of hazards was critical. The year 1858 recorded a particularly hot summer, with temperatures of 35-36°C in the shade which caused a rapid decrease in the water level and a consequent increase in pollutant concentration. The unbearable smell rising from the river was to be remembered as 'The Great Stink', one of the major environmental crises in the history of the metropolis.

Dickens had given a worrying account of the life-threatening waterway passing through the heart of the city in *Little Dorrit* (1855-1857). In the third chapter of the novel, ironically titled 'Home', he contemplated the undergoing hardships of the Londoners forced to live in unhealthy conditions: "Miles of close wells and pits of houses, where the inhabitants gasped for air, stretched far away towards every point of the compass. Through the heart of the town a deadly sewer ebbed and flowed, in the place of a fine fresh river" (Dickens, 2004). The juxtaposition of the two images, the previously glamorous waters and the contemporary Styx slithering across the urban area, deepens the state of grimness. Even the rain adds to the decay and unpleasantness of the city: far from giving it new strength and energy, it "developed only foul stale smells, and was a sickly, lukewarm, dirt-stained, wretched addition to the gutters" (Dickens, 2004).

The newspapers of the time lamented over the infernal stench and the reprehensible condition of the river. On the 28th of June 1858, *The Standard* (today *The Evening Standard*) painted a grotesque picture of the Thames, ironically personified as a disgraced father figure: "Dirty Old Father Thames reached, on Wednesday last, a point of infamy which we firmly believe

was never before attained by any being, animate or inanimate, whose misdeeds fill up the chronicle of British wickedness. His noisome qualities have been execrated by the passengers of our bridges and the travellers in our penny steam boats; people have not only turned up, but stopped their noses, whenever they have approached his unsavoury banks; his foulness has supplied matter for many a smart leader in our journals whenever parliamentary debates have been uninteresting and foreign intelligence has been scant; "constant readers" have vied with each other in describing their particular sufferings under the influence of his abominable exhalations" (*The Standard*, 1858). The news of the severe situation generated by the dry weather was spreading outside the capital. *The Leeds Intelligencer and Yorkshire General Advertiser* reported the degradation of the river in its urban sector and its severe hazardous potential: "In London the concurrence of neap tides with the excessive heat has rendered the Thames an insupportable nuisance, and it seems probable that at last something or other will be done towards its purification, in spite of the Conservators of the Thames and the Board of Works. Indeed serious alarm is beginning to be felt lest some form of malignant fever should break out with all the violence of a pestilence" (*The Leeds Intelligencer and Yorkshire General Advertiser*, 1858).

Back in the city, *The Morning Chronicle* highlighted the ineffectiveness of the immediate bureaucratic measures in addressing the issue, focussing on the urgent need for effective procedures to control pollution: "The Board of Works - "Words" it has been irreverently termed - has exercised its function for nearly four years. Each year, as the summer heat has returned, the Thames has given off reeking filthy stench, which have become on each occasion more and more intolerable, till at last we see a fleet of barges lying off the banks pitching lime into the river to prevent members of Parliament from being poisoned; and canvas, chemically steeped, stretched across all the windows, in order that the air for the assembled Commons may be purified to some extent of the deleterious matters with which it is loaded by the pestiferous exhalations from the Thames" (*The Morning Chronicle*, 1858).

On a lighter note, the inglorious event was conferred enduring fame in verse, as this ‘Poem about Father Thames’ personifies the river as a repulsive creature, raising concerns about the devastating impact of industrialisation upon the natural world:

“And from the cloud a perfume rose,
That might be smelt but never sung;
And every member to his nose,
The guardian bandana flung;
Slowly the cloud took form, and slow
The perfume to a centre grew,
And on the deck before them, lo!
A grisly form appear to view!
A trailing robe of sludge and slime,
Fell o’er his limbs of muddy green,
And now and then, a streak of lime
Showed where the Board of Works had been;
From out his mouth’s mephitic well,
Poured fetid stench and sulphurous flames,
And - was it sight, or was it smell? -
All there, somehow, knew Father Thames.”
(*The Morning Chronicle*, 1858).

However gloomy or light-hearted the approach was, the circumstances were extreme and action was mandatory. And, in times of crisis, a hero is needed.

THE MASTERMIND

Joseph William Bazalgette was born in a family of French descent. His grandfather, Jean-Louis Bazalgette, left France for the Americas and ended up a landowner in Jamaica. He arrived in England in 1775, and established himself as a merchant in London, building up a considerable fortune. He had three children from his first marriage, the first of which was Joseph William Bazalgette, the father of the future engineer. Born in 1783, he enrolled in the Royal Navy and was wounded in an engagement and retired in 1809. He married Teresa Philo Pilton with whom he had thirteen children, of which only four survived: three daughters (Theresa Philo, Louiza and Julia) and a boy, born on the 28th of March 1819 and named after his father: Joseph William (*Hourly History*, 2018).

The family lived in the residential area of Clay Hill in the north of Enfield Town until 1827, then moved to Hamilton Terrace in St John’s Wood, where eight-year old Joseph spent his

teenage and young adult years. He was privately educated and, at the age of 17, was already an apprentice of Sir John Benjamin Macneill, a distinguished Irish civil engineer. Between 1836 and 1838 he was involved in railway projects in Northern Ireland, and gained experience in land drainage and reclamation, partly in China and Ireland. In 1842 he moved to London, where he set up a private consultancy to provide expert advice on the expansion of the city’s railways. From his office in Westminster, he took part in various engineering projects, such as the Tame Valley Canal in Birmingham, Portsmouth Dockyard and railway surveys.

In 1845 he married Maria Kaugh and over the next 16 years they had 11 children, six sons and four daughters, born between 1846 and 1861. The following year he became a full member of the Institute of Civil Engineers, the independent professional association for civil engineers in the United Kingdom. At 28, he was the head of a team of engineers who carried out a wide variety of transport-related works across the country, from ship canals and railways, water supply and sewage treatment processes to land reclamation from the sea to the construction of a tunnel between Dover and Calais.

Despite his personal and professional success, the young engineer collapsed under the pressure of increasingly demanding responsibilities (*Hourly History*, 2018). In 1847, he left London for the countryside to recover and returned two years later, when the second cholera epidemic was devastating the capital. He was appointed assistant surveyor to the Metropolitan Commission of Sewers, a public institution established with the declared purpose to unify, adapt and develop the existing structures into a coherent sewer and drainage infrastructure. The debates and dissensions divided and eventually dissolved the group, leading to the formation of three subsequent advisory bodies. The fifth Commission, to which Bazalgette was chief engineer, was set up in 1852 but the lack of funding forced its members to resign in 1854. The crisis was solved the following year, when the Metropolis Management Act provided for the foundation of the Metropolitan Board of Work, the first central government for the City of London that was granted power to carry out

construction projects including roads, bridges, parks, and sewers. On the 1st of January 1856, Joseph Bazalgette was formally asked to become chief engineer to the new board, a position that was to become crucial for the future of the city. Zealous and meticulous, he dedicated himself to the work that would bring him immortality.

THE MASTER PLAN

In only 59 years, London's population had doubled, reaching about 2-2.5 million people, which resulted in a massive rise in human waste that its outdated drainage systems could not support. Although the fish and fauna in the Thames were killed by the sewage dumped into it, the majority of Londoners were still using water from the river for domestic consumption, which posed a major health to the population.

Fully aware of the precarious situation, in 1856 Bazalgette submitted a plan including the construction of sewers that would prevent waste matter from flowing into the Thames in or near the metropolis. According to his scheme, the area north of the river would be drained by three low-level intercepting sewers collecting the wastes at Beckton, while the area south of the river would be served by two high-level intercepting sewers emptying into the river at Crossness during high tide. The five sewers would be fully encased in brick subterranean tunnels stretching along 82 miles to which 1,300 miles of sewers would be added above the ground to transfer rainwater and wastewater from dwellings and street level.

The plan raised various concerns, such as the distance from the Palace of Westminster to keep the effluvium far from the Members of Parliament, and the total funds necessary for the construction and maintenance of such a system.

And then came the Great Stink of 1858, with the record-breaking summer temperatures decomposing the waste in the river and releasing the legendary unbearable malodour plaguing the city. The acute environmental and public health crisis prompted the adoption of the Metropolis Local Management Amendment Act that stipulated the urgent provision of funding for sewage disposal as far away from the city as practically possible, so work on the

new sewage system began in 1859. What became known as the most expensive work of modern times, at a cost of £4.1 million (roughly between £160 million and £1.7 billion today), was going to last for about 16 years, until 1875. Bazalgette's genius consisted not only in his overview but especially in his perspective regarding the viability of his project beyond his times. He calculated the number of people living in each area of London and the approximate amount of waste matter they could produce, and doubled the figure. He also analysed the existing water supply and estimated it for the increasing population, together with the amount of rainfall predicted for the next decades. Then he used the huge figures anticipating the considerable expansion of the metropolis to provide the foundations of the mega project that was designed to last for at least one century ahead.

The three main intercepting lines of sewers were constructed on each side of the Thames, and were named considering the terrain elevation to be crossed: the High Level, the Middle Level, and the Low Level. The first two sewers were planned to discharge by gravitation, whereas the third only by the aid of pumping. North of the river the sewers converged at Abbey Mills, where the contents would be carried on a concrete embankment across the marshes to Barking Creek, and discharged into the river by gravitation. According to Bazalgette, Abbey Mills Pumping Station was planned to be "the largest establishment of the kind on the Main Drainage Works, providing, as it does, engine power to the extent of 1,140 H.P., for the purpose of lifting a maximum quantity of sewage and rainfall of 15,000 cubic feet/minute a height of 36 feet" (Bazalgette, 1865). South of the river, the three intercepting lines united at Deptford Creek, where Deptford Pumping Station was planned to lift the sewage from the Low-Level Sewer into the Outfall Sewer at a height of 18 feet. Subsequently, the contents would flow in one channel through Woolwich to Crossness Reservoir and Pumping Station, where four engines would lift the sewage from the deep sewers into a reservoir with a capacity of 25 million gallons and covering an area of over six acres, then discharge it in Erith Marshes at high tide. According to Bazalgette, "The maximum

quantity of sewage to be lifted by these engines will ordinarily be about 10,000 cubic feet/minute” (Bazalgette, 1865).

The southern system was the first stage of the project and was completed in 1865, when it was inaugurated by Edward, Prince of Wales. The northern system would be completed in 1868, ten years after the first works began, and the whole project would come to an end in 1875 (Figure 1).



Figure 1. Crossness Pumping Station
(© 2023 Elena Nistor All Rights Reserved)

As works on the southern system were nearing completion, Bazalgette prepared a report that highlighted the importance of developing a modern system for the well-being of both the city and its citizens, based on the history of London's drainage system since medieval times. On the 14th of March 1865, he defended his views expressed in the document, titled 'On the Metropolitan System of Drainage, and the Interception of the Sewage from the River Thames', before his fellow members of the Institute of Civil Engineers. In a formal and cautiously measured tone, he warned of the consequences of neglecting proper waste management and emphasised the urgent necessity of sewage systems and proper sanitation in urban areas:

“The majority of the inhabitants and towns are frequently unconscious of the magnitude, intricacy, and extent of the underground works, which have been designed and constructed at great cost, and are necessary for the maintenance of their health and comfort. It is, however, impossible for large numbers of the human species to congregate and live upon a

limited space, without provision being made for the rapid removal of the refuse thereby produced. This necessity is perhaps most forcibly illustrated, by the fearful destruction of life from malaria produced amongst troops suddenly encamped upon ground not previously so prepared for human habitation” (Bazalgette, 1865).

In his address, the engineer pointed out the negative impact of population growth and urban development on the environment, specifically on the use of cesspools and the pollution of the sewers due to human activities. He commented on the excessive changes made to the natural landscape and the environmental degradation caused by human intervention in the natural environment, stressing the importance of sustainable practices and responsible urban planning in managing the increasing population density: “As the population of London increased, its subsoil became thickly studded with cesspools, improved household appliances were introduced, and overflow drains from the cesspools to the sewers were constructed; thus the sewers became polluted, and covered brick channels were unnecessarily substituted for existing open streams” (Bazalgette, 1865).

Naturally, his exposition included the recent cholera outbreaks and their catastrophic consequences - “The metropolis had suffered severely in the cholera visitation of 1831-2, again in 1848-8, and lastly in 1853-4. In 1849 the deaths were 18,036, and in 1854 nearly 20,000...” (Bazalgette, 1865), which prompted the consideration of developing an updated disposal network for the metropolitan area. The engineer advocated for goals and benefits of implementing a new drainage system to rectify the deficiencies of the existing infrastructure and to achieve specific objectives related to sewage management and pollution prevention, concluding that “It is easier and more economical to originate a new and complete system of drainage having these objects in view, than to adapt existing and defective sewers to a uniform and more perfect system” (Bazalgette, 1865).

The introduction was followed by a minutely detailed description of the main sewers, including technical specifications and locations, accompanied by numerous appendices, and was illustrated by a map of London, together with

models and enlarged diagrams of some of the principal works, as well as a complete set of specifications and contract drawings, in tune with the engineer's meticulous nature. The precise details and accurate explanations render the reasoning behind the construction process very clearly and easily to understand even by non-specialists. The descriptive-argumentative account, although abundant in technical terms, is highly visual, developing each phase shot by shot, as in a motion picture, highlighting the exquisite professionalism of the 19th century specialist.

Concluding his elaborated communication with a systematic summary of the logistics and resources required for such an extensive engineering endeavour, he called attention to the massive scale of the project, highlighting the cost and amounts of the materials and resources involved in the construction project: "Three hundred and eighteen millions of bricks, and 880,000 cubic yards of concrete have been consumed, and 3½ million cubic yards of earth have been excavated in the execution of Main Drainage Works. The total pumping power employed is 2,380 nominal H.P.; and if at full work night and day, 44,000 tons of coals per annum would be consumed, but the average consumption if estimated at 20,000 tons" (Bazalgette, 1865).

Despite the definitive facts and figures, the over-scrupulous genius concluded his presentation with a focus on the remaining work to be done on the Low Level Sewer north of the river, detailing the timeline for its completion in relation to yet another project, the walkway along the Thames:

"The whole of the Main Drainage scheme is now completed, with the exception of the Low Level Sewer on the North side of the Thames, which is being formed in conjunction with the Thames Embankment and the new street to the Mansion house, and will therefore probably not come into operation for a couple of years. The proportion of the area drained by that Sewer is one seventh of the whole" (Bazalgette, 1865).

The construction of the 82 miles of main sewer running parallel to the Thames to the outflows at Barking and Crossness and the additional 1,300 miles of subsidiary tunnels was carefully supervised by the perfectionist engineer. Bazalgette personally chose a particular type of brick for the sewer tunnel, as he considered that

the high crushing strength and low water absorption of Staffordshire blue brick were able to resist the scouring effect of water falling through the system from high to low level. He also insisted on the use of the relatively recently invented Portland cement, that had been patented in 1825, owing to its water resistance and unique capacity to strengthen when constantly exposed to water. He substantiated his choice on carefully detailed tests, and it was for the first time that this material was used in any large-scale public project.

However, Bazalgette's capabilities went beyond inflexible engineering tasks. Together with architect Charles Henry Driver, he turned the two main pumping stations, Abbey Mills and Crossness, into genuine artworks. The 'cathedrals of sewage', as they are sometimes labelled, are conspicuous through their stunning Victorian industrial architecture combining Italian Venetian, French Gothic, Flemish, Byzantine/Moorish, Russian Orthodox and Celtic styles (Abbey Mills), and ancient Roman and Byzantine styles (Crossness) (Figure 2).



Figure 2. The Octagon, Crossness Pumping Station
(© 2023 Elena Nistor All Rights Reserved)

The interiors featuring intricately wrought iron patterns and cast iron columns, and the colorful paintings of naturalistic motifs alluding to sacred and symbolic spaces reveal the engineer's artistic side, stressing both the

practical effectiveness and the aesthetically pleasing design of the two buildings.

Bazalgette and Driver continued their collaboration after the completion of the massive engineering project that changed the history of London and the Thames, as they united their creative efforts in shaping The Embankment. To avoid digging off central London in order to incorporate the huge pipes of the main sewers, they proposed raised structures along the Thames, which also helped protect the low-lying districts from flooding, and eventually created an important green space in one of the busiest part of the English capital. Over one mile long, the wide promenade was lined with trees and decorated with bronze mooring rings cast in the shape of lion heads; originally lit with dolphin-shaped, cast iron lamps, it became the first London street to be electrified in December 1878.

LEGACY

Joseph Bazalgette remained chief engineer with the Metropolitan Board of Works until the institution was replaced by the London County Council in 1889. His outstanding skills as a surveyor, planner, and engineer received national acknowledgment, and he was made a Commander of the Bath in 1871 and knighted by Queen Victoria at Windsor in 1874. Towards the end of this life, he was appointed the 24th President of the Institution of Civil Engineers, a position that he held for only two year, between 1882 and 1884. He retired in 1889, after a long and illustrious career.

He died at his home near Wimbledon on the 15th of March 1891, less than two weeks before his 72nd birth anniversary. His death was marked by a lengthy obituary in the Proceedings of the Institution of Civil Engineers, the organisation of which he had been a member for more than 40 years and to which he had served as president for two years. Many national newspapers paid their respects to the genius who had undertaken engineering work on an unprecedented scale. On the 17th of March 1891, *The Leeds Mercury* wrote:

“The death of Sir Joseph Bazalgette removes from this generation one who must ever be memorable on its annals. What Baron Haussmann was to Paris Sir Joseph Bazalgette

was to London. He drained and purified London, and he did much to beautify it by giving the Thames a swifter course, by building embankments planted in boulevard fashion with trees, and by constructing bridges. [...] There is one monument of his skill as an engineer that will endure as long as any monument in Venice. That is the Embankment between Blackfriars Bridge and Westminster. The health of London was advanced immensely by this great work and its consequent enterprises” (*The Leeds Mercury*, 1891).

Bazalgette was interred alongside his wife Maria and five of their children in the family mausoleum in the grounds of St Mary's Church, Wimbledon, in the London Borough of Merton. The simplicity of the Grade II listed structure made of Portland stone is given by the rusticated base and the obelisk atop, stating the names of the family members laid to rest inside. At present the deteriorating mausoleum is at risk of internal collapse due to water ingress but the church is taking steps for restoration work in partnership with a south-west London based charity.



Figure 3. Sir Joseph Bazalgette bust, Victoria Embankment
(© 2024 Elena Nistor All Rights Reserved)

In 1899, sculptor George Blackall Simonds created a memorial to the Victorian engineer. The bronze bust set in a decorative stone wall can be found on the Victoria Embankment, a few steps away from Hungerford and Golden Jubilee Bridges (Figure 3). The inscription above the bust reads “*Flumini vincula posuit*” (“He put the river in chains”).

In 1974, Greater London Council erected a blue plaque at 17 Hamilton Terrace, St John's

Wood, the North-West London home of Bazalgette between 1827 and 1845, to remember the notable resident of the brick double house.

In 2006, a BBC survey nominated Bazalgette's sewers as one of the nation's favourite wonders ever created by humans in the UK. The "triumph of Victorian engineering", as it is often called, was included in the ten episodes' TV series named *Seven Man-Made Wonders of London* that ran throughout the summer of that year.

Ten years later, on the occasion of the 200-year anniversary of the Institute of Civil Engineers, the exhibition "Invisible Superheroes" paid tribute to some of the past and present champions of civil engineering whose innovative work changed lives and shaped the world. Among others, it honoured the engineer nicknamed "Drainy Jo" in his lifetime as Captain Sanitation, for his groundbreaking project and its environmental effects.

On the 1st of November 2023, to mark National Engineering Day, Transport for London joined the Royal Academy of Engineering to draw up an Engineering Icons Tube Map of London as a means to "inspire people of all backgrounds to study science, technology, engineering (in particular) and mathematical subjects, and then pursue them professionally", as stated on the TfL blog. The map showcased 274 engineers across 11 themes such as Life and Health, Environment, Infrastructure, Energy and Power, Materials and Manufacturing, and others. Sir Joseph Bazalgette was featured at Blackfriars Underground Station on the Circle and District Lines, in celebration of the public space next to Blackfriars Bridge that had been named after the 'King of Sewers' three years earlier.

His memory still lives on through his descendants, great-great-grandsons Peter and Edward. Peter Lytton Bazalgette, a television executive and producer better known for bringing the American TV show *Big Brother* to the UK, was invited to present a documentary about the Great Stink for Channel Five in 2002 and set up Crossness Engines Trust in 1985, raising £4.5 million to restore the pumping station built by his ancestor. In 2015, as Chair of Arts Council England, he was also invited by King's College London to discuss his great-

great-grandfather's accomplishments in a public meeting with the academic community. His third cousin, Edward Bazalgette, a television director and former musician, directed and produced the drama-documentary 'The Sewer King' broadcast by BBC Two in March 2003, as part of the series called *The Seven Wonders of the Industrial World*.

CONCLUSIONS

Sir Joseph Bazalgette will be forever remembered as the Victorian engineer, city planner, bridge builder and landscape architect who shaped London into the city of today. Many of his master creations are confined to the depths of the metropolis, winding under its streets and parks. And yet, what can be seen still amazes with the fineness of the engineering, architectural and artistic details: Abbey Mills and Crossness Pumping Stations have been included on the Grade I list of sites, owing to their exceptional national importance and those who have the opportunity to visit their exhibition centres can only bow to the English engineer's extraordinary ability to think ahead and turn his vision into a reality that transcends centuries. He anticipated population growth and planned the sewage system to serve twice as many inhabitants as was necessary in his times.

For about 150 years, Bazalgette's network has been functional for millions of Londoners. Today, with the city approaching 10 million inhabitants, it has reached its full capacity, so a consortium of investors proposed a new super-sewage to meet the present and future demands of the ever-expanding conurbation. The construction of Thames Tideway Tunnel, a 16 miles' long combined tunnel extending from Acton, Ealing, to Beckton Sewage Treatment Works in Newham, started in 2016 and ended in March 2024, and is currently followed by a testing and handover phase expected to conclude in 2025.

Building on Bazalgette's achievements, the new project preserves his legacy in the 21st century, addressing some of the environmental challenges posed by the new Millennium and maintaining the Thames one of the cleanest metropolitan rivers in the world.

ACKNOWLEDGEMENTS

Part of the research work was carried out with the support of the Special Collections of Senate House Library, University of London, and Crossness Museum Store at Crossness Pumping Station.

REFERENCES

- Bazalgette, J. W. (1865). 'On the Metropolitan System of Drainage and the Interception of the Sewage from the River Thames'. Charles Manby and James Forrest (Eds.) Excerpt minutes of proceedings of the Institution of Civil Engineers, Vol. XXIV, Session 1864-65. London: William Clowes and Sons, Stamford Street and Charing Cross
- Dunbar, W. (2012). "In Honour of the City of London". *London. A History in Verse*. Ed. Mark Ford. Cambridge, Massachussets and London, England: The Belknap Press of Harvard University Press, pp. 56-58
- Dickens, C. (1992). 'Chapter 21. In which the old man launches forth into his favourite theme, and relates a story about a queer client'. *The Posthumous Papers of the Pickwick Club*. Ware, Hertfordshire: Wordsworth Editions Ltd., illustrated edition
- Dickens, C. (2003). 'Chapter 1. In Chancery'. *Bleak House*. London: Penguin Classics, reissued edition
- Dickens, C. (2004). 'Chapter 3. Home'. *Little Dorrit*. London: Penguin Classics, revised edition, 2004.
- Hourly History (2018). *Joseph Bazalgette. A Life From Beginning to End* (Biographies of Engineers). CreateSpace Independent Publishing Platform
- Klein, G. (2015). 'The Broad Street Pump'. *Seeing What Others Don't. The Remarkable Ways We Gain Insights*. New York: PublicAffairs, pp. 69-75
- Roberts, B. *Sir Joseph Bazalgette and London's Intercepting Sewers*. (www.hevac-heritage.otg/built_environment/pioneers_revisited/sur_names_a-o/bazalgette.pdf) Accessed: 9 February 2024
- ***'Dirty Old Father Thames' "abominable exhalations". *The Standard* (London, Greater London, England), Monday, 18 June 1858, p. 4 (https://www.newspapers.com/image/401650478/?clipping_id=23502734&fcfToken=eyJhbGciOiJIUzI1NiIsInR5cCI6IkpXVCJ9.eyJmcmVILXZpZXctaWQiOiJQwMTY1MDQ3OCwiaWF0IjoxNzEzMDkwODU2LCJleHAiOiE3MTMxNzcyNTZ9.Fb3ZoC6SmCdCABUbl41jny2xxBuSh8JTHpOXripBB6g) Accessed: 12 January 2024
- ***'Each summer the stench is more intolerable'. *The Morning Chronicle* (London, Greater London, England), Monday, 21 June 1858, p. 4 (https://www.newspapers.com/image/392645577/?clipping_id=23498918&fcfToken=eyJhbGciOiJIUzI1NiIsInR5cCI6IkpXVCJ9.eyJmcmVILXZpZXctaWQiOiJmM5MjY0NTU3NywiaWF0IjoxNzEzMDkwNzZlLCJleHAiOiE3MTMxNzcyNTZ9.B1Ughv0-AL7OFcJNXKOo84KLD3IylWamySwQHhtaBdE) Accessed: 12 January 2024
- ***'Engineering Icons Tube Map'. (<https://londonblog.tfl.gov.uk/2023/11/01/engineering-icons-tube-map/>) Accessed: 17 November 2023
- ***'Poem about Father Thames', *The Morning Chronicle* (London, Greater London, England), Thursday, 29 July 1858, p. 6 (https://www.newspapers.com/image/392665114/?clipping_id=23499032&fcfToken=eyJhbGciOiJIUzI1NiIsInR5cCI6IkpXVCJ9.eyJmcmVILXZpZXctaWQiOiJmM5MjY2NTEwNzEzMDkwNjU0LCJleHAiOiE3MTMxNzcyNTZ9.BBPeDwnQ_bHNZ-mdZiZj9OyQ5FOptb6URr5yH-Vvw8E) Accessed: 12 January 2024
- ***'Sir Joseph Bazalgette, civil engineer, 1819-1891'. (<https://www.ice.org.uk/what-is-civil-engineering/who-are-civil-engineers/sir-joseph-bazalgette>) Accessed: 23 January 2024
- ***'Sir Joseph Bazalgette's Contribution'. *The Leeds Mercury* (Leeds, West Yorkshire, England), Tuesday, 17 March 1891, p. 5 (<https://www.newspapers.com/image/390665950/?fcfToken=eyJhbGciOiJIUzI1NiIsInR5cCI6IkpXVCJ9.eyJmcmVILXZpZXctaWQiOiJmM5MDY2NTk1MCwiaWF0IjoxNzEzOTI4NDkzLCJleHAiOiE3MTMwMTQ4OTN9.G1JRxESEOYX6z-DS8BVwd7NtkCneqd1zdmk1J24bSg>) Accessed: 12 January 2024
- ***'Thames is "an insupportable nuisance" in the excessive heat'. *The Leeds Intelligencer and Yorkshire General Advertiser* (Leeds, West Yorkshire, England), Saturday, 19 June 1858, p. 5 (https://www.newspapers.com/image/396799163/?clipping_id=23498947&fcfToken=eyJhbGciOiJIUzI1NiIsInR5cCI6IkpXVCJ9.eyJmcmVILXZpZXctaWQiOiJmM5Njc5OTE2MywiaWF0IjoxNzEzMDkwODE0LCJleHAiOiE3MTMxNzcyMTR9.GIN5Z2Ewul69_5Ld5YwPkZyTP8wqMXBNe13mLCebCo) Accessed: 12 January 2024

A REFINEMENT OF THE SECOND CRITERIA OF COMPARISON FOR THE COVERAGE OF SERIES OR IMPROPER INTEGRALS

Cosmin-Constantin NIȚU

University of Agronomic Sciences and Veterinary Medicine of Bucharest,
 59 Marasti Blvd, District 1, Bucharest, Romania

Corresponding author email: cosmin.nitu@ffim.ro

Abstract

The second criterion of comparison for the convergence of series or improper integrals, also called the limit comparison test, is a little bit unnatural and difficult for students when it comes to finding the comparison term. In this paper we give a refinement of this criteria via equivalents, which is more natural. We say that two sequences or two functions are equivalent if their quotient tends to 1 at some point. When two sequences or two integrable functions are equivalent, then their associated series or integrals have the same nature. We also present different applications of this method for both series and improper integrals.

Key words: equivalent, limit comparison test, improper integrals, series.

INTRODUCTION

The notion of series

In mathematics, a series represents a sum with an infinite number of terms. We are interested in such a sum can be correctly defined, that is if it has a limit, and, if possible, to calculate its sum. A series with a finite sum is called *convergent*.

Definition 1. Let $(x_n)_{n \geq 1}$ be a positive sequence of real numbers (Colojară, 1983). A series with positive terms is a sum with an infinite number of terms of the form:

$$x_1 + x_2 + \dots + x_n + \dots$$

which can be written in a more compact way:

$$\sum_{n=1}^{\infty} x_n \text{ or } \sum_{n \geq 1} x_n$$

Remark 1.

$$\sum_{n \geq 1} x_n \neq \lim_{n \rightarrow \infty} x_n$$

Remark 2. x_n is called the *general term* of the series.

Observation. A series may start from any natural index, for example:

$$x_k + x_{k+1} + \dots + x_n + \dots = \sum_{n=k}^{\infty} x_n = \sum_{n \geq k} x_n$$

We will write in a simpler manner $\sum x_n$ for series or (x_n) for sequences when the starting index is not important.

The convergence of a series with positive terms

We denote $S_n = x_k + x_2 + \dots + x_n$ the partial sum of order n of a series:

$$\sum_{n \geq k} x_n$$

Remark 3. A sequence of real numbers (a_n) is called *convergent* to a number $L \in \mathbb{R}$ if:

$$\lim_{n \rightarrow \infty} x_n = L$$

Definition 2. The series $\sum x_n$ is convergent if and only if the sequence (S_n) is convergent, more exactly:

$$\sum x_n = a \stackrel{\text{def}}{\Leftrightarrow} \lim_{n \rightarrow \infty} S_n = a$$

where:

- a is called the *sum* of the series.

Remark 4. The convergence of a series is not affected by its starting term.

A theorem of Weierstrass states that a monotonous sequence (i.e. increasing or decreasing) and bounded is convergent.

Therefore, the *nature (convergence)* of a series with positive terms is:

$$\begin{cases} \text{convergent (if bounded): } \sum x_n = a \in \mathbb{R} \\ \text{divergent (if unbounded): } \sum x_n = \infty \end{cases}$$

Remark 5. In general, it is easier to study the convergence of a series, because there exist certain criteria, than to calculate its sum.

Classical series

There are two important series that can be used in the comparison tests:

1) *The generalized harmonic series:*

$$\sum_{n \geq 1} \frac{1}{n^\alpha} = 1 + \frac{1}{2^\alpha} + \frac{1}{3^\alpha} + \dots$$

is $\begin{cases} \text{conv}, & \alpha > 1 \\ \text{div}, & \alpha \leq 1 \end{cases}$

Example 1.

$$\sum_{n \geq 1} \frac{1}{n^2} = 1 + \frac{1}{2^2} + \frac{1}{3^2} + \dots = \frac{\pi^2}{6}$$

is convergent because $\alpha = 2 > 1$.

Remark 6. The fact that its sum is $\frac{\pi^2}{6}$ can be proved with advanced techniques of trigonometry and complex analysis. This shows that a series' sum is sometimes hard or even impossible to calculate.

Example 2.

$$\sum_{n \geq 1} \frac{1}{n} = \sum_{n \geq 1} \frac{1}{n^1} = 1 + \frac{1}{2} + \frac{1}{3} + \dots = \infty$$

is divergent because $\alpha = 1 \leq 1$.

Remark 7. The divergence of this series is a little bit unnatural for a beginner, as its general term becomes smaller and smaller ($\frac{1}{n} \rightarrow 0$).

2) *The geometric series:*

$$\sum_{n \geq 0} a^n = 1 + a + a^2 + \dots$$

is $\begin{cases} \text{conv} = \frac{1}{1-a}, & \text{for } a < 1 \\ \text{div}, & \text{for } a \geq 1 \end{cases}$

Example:

$$\sum_{n \geq 0} \frac{1}{3^n} = \sum_{n \geq 0} \left(\frac{1}{3}\right)^n$$

is convergent because $a = \frac{1}{3} < 1$, and its sum is:

$$\sum_{n \geq 0} \left(\frac{1}{3}\right)^n = \frac{1}{1-a} = \frac{1}{1-\frac{1}{3}} = \frac{1}{\frac{2}{3}} = \frac{3}{2}$$

Improper integrals

The classical Riemann integral of an integrable function $f: [a, b] \rightarrow \mathbb{R}$ can be called a *proper integral*.

$$\int_a^b f(x) dx = \int_{[a,b]} f(x) dx$$

Definition 3. Let $a \in \mathbb{R}$. We define *improper integrals* of the form:

$$\int_I f(x) dx$$

where:

- $I \subset \mathbb{R}$ is an interval and $f(x)$ is a function Riemann integrable.

1) $I = [a, \infty)$

$$\int_{[a,\infty)} f(x) dx = \int_a^\infty f(x) dx = \lim_{t \rightarrow \infty} \int_a^t f(x) dx$$

2) $I = (-\infty, a]$

$$\int_{(-\infty,a]} f(x) dx = \int_{-\infty}^a f(x) dx = \lim_{t \rightarrow -\infty} \int_t^a f(x) dx$$

3) $I = \mathbb{R}$

$$\begin{aligned} \int_{\mathbb{R}} f(x) dx &= \int_{-\infty}^\infty f(x) dx \\ &= \int_{-\infty}^a f(x) dx + \int_a^\infty f(x) dx \end{aligned}$$

where:

- a can be any real number, most commonly 0 or 1.

Remark 8. Notations for lateral limits of a function in one variable at a point $a \in \mathbb{R}$:

The limit to the left:

$$l_s = f_s(a) = \lim_{x \rightarrow a^-} f(x) = f(a-0) = f(a-)$$

The limit to the right:

$$l_a = f_a(a) = \lim_{x \rightarrow a^+} f(x) = f(a+0) = f(a+)$$

4) $I = [a, b)$

$$\int_{[a,b)} f(x) dx = \int_a^{b-} f(x) dx = \lim_{t \rightarrow b^-} \int_a^t f(x) dx$$

5) $I = (a, b]$

$$\int_{(a,b)}^{\square} f(x)dx = \int_{a+}^b f(x)dx = \lim_{\substack{t \rightarrow a \\ t > a}} \int_t^b f(x)dx$$

6) $I = (a, b)$

$$\begin{aligned} \int_{(a,b)}^{\square} f(x)dx &= \int_{a+}^{b-} f(x)dx \\ &= \int_{a+}^c f(x)dx + \int_c^{b-} f(x)dx \end{aligned}$$

where:

- $c \in (a, b)$ can be chosen arbitrary, most commonly $c = \frac{a+b}{2}$.

7) $I = (a, \infty)$

$$\begin{aligned} \int_{(a,\infty)}^{\square} f(x)dx &= \int_{a+}^{\infty} f(x)dx \\ &= \int_{a+}^c f(x)dx + \int_c^{\infty} f(x)dx \end{aligned}$$

where:

- $c \in (a, \infty)$ can chose arbitrary.

8) $I = (-\infty, a)$

$$\begin{aligned} \int_{(-\infty,a)}^{\square} f(x)dx &= \int_{-\infty}^{a-} f(x)dx \\ &= \int_{-\infty}^c f(x)dx + \int_c^{a-} f(x)dx \end{aligned}$$

where:

- $c \in (-\infty, a)$ can chosen arbitrary.

Definition 4. An improper integral is called *convergent* if it is finite and *divergent* if it is infinite or does not exist.

There are many connections between series and improper integrals: the terminology for convergence, similar criteria, the integral criterion for series, etc.

Theorem 1. The integral criterion for positive series (Boboc, 1999; Miculescu, 2010).

Let $f: [a, \infty) \rightarrow \mathbb{R}_+$ be a positive and decreasing function (i. e. $x \leq y \Rightarrow f(x) \geq f(y)$). Then:

$$\sum_{n \geq a}^{\square} f(n) \sim \int_a^{\infty} f(x)dx$$

The series has the same nature with the integral.

Remark 9. The nature of the integral $\int_a^{\infty} f(x)dx$ doesn't depend on the number a .

MATERIALS AND METHODS

When studying the convergence of a series or improper integral, the classical comparison test with inequalities is sometimes difficult to apply and very sensitive to signs. There is a more practical second comparison test that uses limits.

Theorem 1. Limit comparison criterion for series (Boboc, 1999; Goleț et al., 2014).

If $\lim_{n \rightarrow \infty} \frac{x_n}{y_n} = l$ then if:

$$a) l \in (0, \infty) \Rightarrow \sum x_n \sim \sum y_n$$

The two series have the same nature.

$$b) l = 0 \Rightarrow \begin{cases} a) \sum y_n \text{ conv} \Rightarrow \sum x_n \text{ conv} \\ b) \sum x_n \text{ div} \Rightarrow \sum y_n \text{ div} \end{cases}$$

$$c) l = \infty \Rightarrow \begin{cases} a) \sum x_n \text{ conv} \Rightarrow \sum y_n \text{ conv} \\ b) \sum y_n \text{ div} \Rightarrow \sum x_n \text{ div} \end{cases}$$

Remark 10. In this form, the limit comparison criterion may be difficult to apply, because the comparison term y_n may be difficult and artificial to find. Thus, we propose a more natural way to find the comparison term, using the language of equivalents.

Definition 5.

We say that two sequences (x_n) and (y_n) are *equivalent* and we write:

$$x_n \sim y_n \stackrel{\text{def}}{\iff} \lim_{n \rightarrow \infty} \frac{x_n}{y_n} = 1$$

(Stănășilă, 1981; Martin, 2008).

Remark 11. Any expression is equivalent to its dominant term (if it has one!).

For example, $3n^2 - n + 5 \sim 3n^2$, because by the "degree rule" one has

$$\frac{3n^2 - n + 5}{3n^2} \rightarrow \frac{3}{3} = 1$$

Remark 12. The order of the elementary sequences at infinity ($n \rightarrow \infty$):

$$\ln n \ll n^k \ll a^n \ll n! \ll n^n$$

where:

$$k > 0, a > 1.$$

By " $x \ll y$ " we mean that x is "a lot smaller" than y , which imply fundamental limits such:

$\lim_{n \rightarrow \infty} \frac{\ln n}{n^k} = 0, \lim_{n \rightarrow \infty} \frac{n^k}{a^n} = 0, \lim_{n \rightarrow \infty} \frac{a^n}{\ln n} = \infty$ etc.

Definition 6. Let $f, g: \mathbb{R} \rightarrow \mathbb{R}$. We $f(x)$ and $g(x)$ are *equivalent* at a point $a \in \mathbb{R} = [-\infty, +\infty]$ and we write:

$$\begin{matrix} \square \\ f(x) \sim g(x) \\ a \end{matrix}$$

if:

$$\lim_{x \rightarrow a} \frac{f(x)}{g(x)} = 1.$$

Remark 13. If $f(x) \sim g(x)$ we simply write:

$$\begin{matrix} \square \\ f(x) \sim g(x) \\ \infty \end{matrix}$$

Remark 14. The order of the elementary functions at infinity ($x \rightarrow \infty$):

$$\ln x \ll x^k \ll a^x \ll x^x$$

where: $k > 0, a > 1$,

which imply fundamental limits such:

$$\lim_{n \rightarrow \infty} \frac{\ln x}{x^k} = 0, \lim_{n \rightarrow \infty} \frac{x^k}{a^x} = 0, \lim_{n \rightarrow \infty} \frac{a^x}{\ln x} = \infty \text{ etc.}$$

Theorem 2. For two series with positive terms:

$$\begin{matrix} \square \\ x_n \sim y_n \Rightarrow \sum x_n \sim \sum y_n \end{matrix}$$

Proof. This is a particular case written in the language of *equivalents* for the main case a) of Theorem 1.

If $x_n \sim y_n$, then $\lim_{n \rightarrow \infty} \frac{x_n}{y_n} = 1$.

Thus, the two series have the same nature:

$$\begin{matrix} \square \\ \sum x_n \sim \sum y_n \end{matrix}$$

Theorem 3. Limit comparison criterion for improper integrals defined on an infinite interval (Nicolescu et al., 1971).

Let f and g be two positive and integrable functions with $\lim_{x \rightarrow \infty} \frac{f(x)}{g(x)} = l$.

Then if:

$$a) l \in (0, \infty) \Rightarrow \int_a^\infty f(x) dx \sim \int_a^\infty g(x) dx$$

The two integrals have the same nature.

b) $l = 0$

$$\Rightarrow \begin{cases} a) \int_a^\infty g(x) dx \text{ conv} \Rightarrow \int_a^\infty f(x) dx \text{ conv} \\ b) \int_a^\infty f(x) dx \text{ div} \Rightarrow \int_a^\infty g(x) dx \text{ div} \end{cases}$$

c) $l = \infty$

$$\Rightarrow \begin{cases} a) \int_a^\infty f(x) dx \text{ conv} \Rightarrow \int_a^\infty g(x) dx \text{ conv} \\ b) \int_a^\infty g(x) dx \text{ div} \Rightarrow \int_a^\infty f(x) dx \text{ div} \end{cases}$$

Remark 15. A similar criterion can be defined at $-\infty$. We leave that to the reader.

Remark 16. The theorem is valid even if f and g are positive on a neighbourhood of ∞ .

Theorem 4. The limit comparison criterion with equivalents for improper integrals is defined on an infinite interval.

Let f and g be two positive and integrable functions. If $f(x) \sim g(x)$, then:

$$\int_a^\infty f(x) dx \sim \int_a^\infty g(x) dx$$

The integrals have the same nature.

Proof. The fact that $f(x) \sim_\infty g(x)$ means that:

$$l = \lim_{x \rightarrow \infty} \frac{f(x)}{g(x)} = 1$$

And we apply case a) of the Theorem 3.

Theorem 5. Limit comparison criterion for improper integrals defined on a finite interval.

Let f and g be two positive and integrable functions with $\lim_{x \rightarrow a} \frac{f(x)}{g(x)} = l$.

Then if:

$$a) l \in (0, \infty) \Rightarrow \int_{a+}^b f(x) dx \sim \int_{a+}^b g(x) dx$$

The two integrals have the same nature.

b) $l = 0$

$$\Rightarrow \begin{cases} a) \int_{a+}^b g(x) dx \text{ conv} \Rightarrow \int_{a+}^b f(x) dx \text{ conv} \\ b) \int_{a+}^b f(x) dx \text{ div} \Rightarrow \int_{a+}^b g(x) dx \text{ div} \end{cases}$$

c) $l = \infty$

$$\Rightarrow \begin{cases} a) \int_{a+}^b f(x) dx \text{ conv} \Rightarrow \int_{a+}^b g(x) dx \text{ conv} \\ b) \int_{a+}^b g(x) dx \text{ div} \Rightarrow \int_{a+}^b f(x) dx \text{ div} \end{cases}$$

Remark 17. A similar criterion can be defined at $b -$.

Theorem 6. Limit comparison criterion with equivalents for improper integrals defined on a finite interval.

Let f and g be two positive and integrable functions:

$$\text{i) } f(x) \sim g(x) \Rightarrow \int_{a+}^b f(x) dx \sim \int_{a+}^b g(x) dx$$

$$\text{ii) } f(x) \sim g(x) \Rightarrow \int_a^{b-} f(x) dx \sim \int_a^{b-} g(x) dx$$

The integrals have the same nature.

RESULTS AND DISCUSSIONS

Applications for series of the limit comparison criteria with equivalents

Example 1. Find the nature of the series:

$$\sum_{n \geq 1} \frac{1}{2\sqrt{n} + 1}$$

Solution. By Theorem 2

$$\sum_{n \geq 1} \frac{1}{2\sqrt{n} + 1} \sim \sum_{n \geq 1} \frac{1}{2\sqrt{n}} = \frac{1}{2} \sum_{n \geq 1} \frac{1}{n^{\frac{1}{2}}} \quad \begin{matrix} \text{div} \\ (\alpha = \frac{1}{2} < 1) \end{matrix}$$

Example 2. Study the convergence of the series:

$$\sum_{n \geq 1} \frac{2n + n^2}{n^5 - 2n^3 + 1}$$

Solution.

$$\sum_{n \geq 1} \frac{2n + n^2}{n^5 - 2n^3 + 1} \sim \sum_{n \geq 1} \frac{n^2}{n^5} = \sum_{n \geq 1} \frac{1}{n^3} \quad \begin{matrix} \text{conv} \\ (\alpha = 3 > 1) \end{matrix}$$

Example 3.

$$\sum_{n \geq 2} \frac{n - 2}{\sqrt{n^2 + 1}}$$

Solution.

$$\sum_{n \geq 2} \frac{n - 2}{\sqrt{n^2 + 1}} \sim \sum_{n \geq 2} \frac{n}{\sqrt{n^2}} = \sum_{n \geq 2} \frac{n}{n} = \sum_{n \geq 1} 1$$

$$= 1 + 1 + \dots = \infty \text{ (div)}$$

Example 4.

$$\sum_{n \geq 2} \frac{n + 7}{n(n + 1)(n + 2)}$$

Solution.

$$\sum_{n \geq 1} \frac{n + 7}{n(n + 1)(n + 2)} \sim \sum_{n \geq 1} \frac{n}{n \cdot n \cdot n} = \sum_{n \geq 1} \frac{1}{n^2} \quad \begin{matrix} \text{conv} \\ (\alpha = 2 > 1) \end{matrix}$$

The equivalence criterion can be mixed with other criteria, as in:

Example 5.

$$\sum_{n \geq 1} \frac{n + 3\sqrt{n} + 1}{2^n + \ln n}$$

Solution.

$$\sum_{n \geq 1} \frac{n + 3\sqrt{n} + 1}{2^n + \ln n} \sim \sum_{n \geq 2} \frac{n}{2^n}$$

Now, we leave to the reader to show that the series of the equivalent is convergent via *D'Alembert's quotient criterion (the ratio test)*:

If $\lim_{n \rightarrow \infty} \frac{x_{n+1}}{x_n} = l$

$$\Rightarrow \begin{cases} l < 1 \Rightarrow \sum x_n \text{ conv} \\ l > 1 \Rightarrow \sum x_n \text{ div} \\ l = 1 \Rightarrow ? \text{ (apply other criteria) } \end{cases}$$

In are some situations, the application of the equivalence criteria is surprising.

Example 6.

$$\sum_{n \geq 1} \ln\left(\frac{n + 1}{n}\right)$$

Solution. Because $\lim_{x \rightarrow 0} \frac{\ln(1+x)}{x} = 1$, it results:

$$\ln(1 + x) \sim x \quad \begin{matrix} \text{conv} \\ 0 \end{matrix}$$

Taking $x = \frac{1}{n} \rightarrow 0$, we obtain:

$$\ln\left(1 + \frac{1}{n}\right) \sim \frac{1}{n}$$

Therefore,

$$\sum_{n \geq 1} \ln\left(1 + \frac{1}{n}\right) \sim \sum_{n \geq 1} \frac{1}{n} \quad \begin{matrix} \text{div} \\ (\alpha = 1 \leq 1) \end{matrix}$$

Sometimes, applying the equivalence criterion is impossible, as in:

Example 7.

$$\sum_{n \geq 2} \frac{n^2}{2^{3n+5}}$$

Remark 18. $\frac{n^2}{2^{3n+5}}$ is not equivalent with $\frac{n^2}{2^{3n}}$, because their quotient does't tend to 1.

Solution. The series is written in minimal form, so no simpler equivalent can be found (it is self-equivalent!). We leave to the reader to prove that the series is convergent using D'Alembert's criterion.

Remark 19. Equivalents can successfully be applied situations such:

$$\sum_{n \geq 2} \frac{F(n)}{G(n)}, \quad \sum_{n \geq 2} \left(\frac{F(n)}{G(n)} \right)^k, \quad \sum_{n \geq 2} \sqrt[k]{\frac{F(n)}{G(n)}}$$

where:

- $F(n)$ și $G(n)$ are polynomials, and $k \in \mathbb{N}$ is fixed, but it cannot be applied, for example, for:

$$\sum_{n \geq 2} \left(\frac{F(n)}{G(n)} \right)^k$$

because 1^∞ is indetermination case for function limits.

Applications for improper integrals of the limit comparison criteria with equivalents

Example 1. Find the nature of the integral:

$$\int_1^\infty \frac{x}{x^5 + 2x^4 - x^3 + 7} dx$$

Solution. We apply Theorem 4:

$$\int_1^\infty \frac{x}{x^5 + 2x^4 - x^3 + 7} dx \sim \int_1^\infty \frac{x}{x^5} dx = \int_1^\infty \frac{1}{x^4} dx$$

(conv, $\alpha = 4 > 1$).

Remark 20. Be easy calculus, it can be shown that:

$$\int_1^\infty \frac{1}{x^\alpha} dx = \begin{cases} \text{conv}, & \alpha > 1 \\ \infty (\text{div}), & \alpha \leq 1 \end{cases}$$

Example 2.

$$\int_0^\infty \frac{1}{\sqrt{x^2+1}} dx \sim \int_1^\infty \frac{1}{\sqrt{x^2+1}} dx \sim \int_1^\infty \frac{1}{\sqrt{x^2}} dx = \int_1^\infty \frac{1}{x} dx$$

(div, $\alpha = 1 \leq 1$).

Example 3.

$$\int_3^\infty \frac{(x+1)^2}{x^4 + \sin^2 x} dx \sim \int_3^\infty \frac{x^2}{x^4} dx \sim \int_3^\infty \frac{1}{x^2} dx$$

(conv, $\alpha = 2 > 1$).

Remark 21. Be easy calculus, it can be shown that:

$$\text{i) } \int_{a+}^b \frac{1}{(x-a)^\lambda} dx = \begin{cases} \text{conv}, & \lambda < 1 \\ \infty (\text{div}), & \lambda \geq 1 \end{cases}$$

$$\text{ii) } \int_a^{b-} \frac{1}{(b-x)^\lambda} dx = \begin{cases} \text{conv}, & \lambda < 1 \\ \infty (\text{div}), & \lambda \geq 1 \end{cases}$$

Example 4. Study the convergence:

$$\int_0^1 \frac{1}{\sqrt{1-x^2}} dx.$$

Solution. We apply Theorem 6:

$$\begin{aligned} \int_0^1 \frac{1}{\sqrt{1-x^2}} dx &= \int_0^1 \frac{1}{\sqrt{(1-x)(1+x)}} dx \\ &\sim \int_0^1 \frac{1}{\sqrt{(1-x)(1+1)}} dx = \frac{1}{\sqrt{2}} \int_0^1 \frac{1}{(1-x)^{\frac{1}{2}}} dx \\ &(\text{conv}, \lambda = \frac{1}{2} < 1). \end{aligned}$$

Remark 22. The integral is improper because the numerator is undefined at 1. Generally, authors don't specify the limit to the right or to the left, it can be deduced from the context.

Example 5.

$$\int_1^3 \sqrt{\frac{1}{(3-x)^5(x-1)}} dx.$$

$$\begin{aligned} \text{Solution. } \int_1^3 \sqrt{\frac{1}{(3-x)^5(x-1)}} dx &= \\ \underbrace{\int_1^2 \sqrt{\frac{1}{(3-x)^5(x-1)}} dx}_{I_1} &+ \underbrace{\int_2^3 \sqrt{\frac{1}{(3-x)^5(x-1)}} dx}_{I_2} \end{aligned}$$

We have:

$$\begin{aligned} \sqrt{\frac{1}{(3-x)^5(x-1)}} &\sim \sqrt{\frac{1}{(3-1)^5(x-1)}} = \frac{1}{4\sqrt{2}} \cdot \sqrt{\frac{1}{x-1}} \\ &= \frac{1}{4\sqrt{2}} \cdot \frac{1}{(x-1)^{\frac{1}{2}}} \end{aligned}$$

Thus:

$$\begin{aligned} I_1 &= \int_1^2 \sqrt{\frac{1}{(3-x)^5(1-x)^3}} dx \sim \int_2^3 \frac{1}{(x-1)^{\frac{1}{2}}} dx, \\ &(\text{conv}, \lambda = \frac{1}{2} < 1). \end{aligned}$$

We have:

$$\sqrt{\frac{1}{(3-x)^5(x-1)}} \sim \sqrt{\frac{1}{(3-x)^5(3-1)}} = \frac{1}{\sqrt{2}} \cdot \sqrt{\frac{1}{(3-x)^5}}$$

$$= \frac{1}{\sqrt{2}} \cdot \frac{1}{(3-x)^{\frac{5}{2}}}$$

$$I_2 = \int_2^3 \sqrt{\frac{1}{(3-x)^5(1-x)^3}} dx \sim \int_2^3 \frac{1}{(3-x)^{\frac{5}{2}}} dx,$$

$$(\text{div} = \infty, \lambda = \frac{5}{2} > 1).$$

Therefore,

$$I = I_1 + I_2 = \text{conv} + \infty = \infty (\text{div})$$

Some applications of series or improper integrals in or outside mathematics

Zeno's arrow paradox in philosophy

Zeno of Elea (490-430 b.Ch.) was a pre-Socratic greek philosopher.

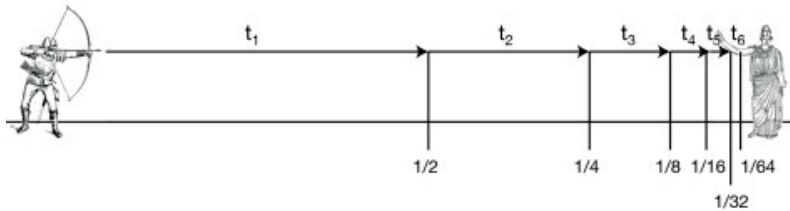


Figure 1. Zeno's paradox

<http://www.naturphilosophie.co.uk/zenos-paradoxes-or-what-happened-when-achilles-and-the-hare-decided-to-outfox-the-legendary-tortoise>

In fact, this paradox shows that time is infinitely divisible, and can be better understood with the series:

$$\frac{1}{2} + \frac{1}{4} + \frac{1}{8} + \dots = 1$$

which explains that, when adding all the segments, the arrow reaches its target.

Taylor series

Every elementary function can be locally approximated around the point a by a sum of its derivatives of the form:

$$f(x) = \sum_{n \geq 0} \frac{f^{(n)}(a)}{n!} (x-a)^n$$

For example:

$$\sin x = x - \frac{x^3}{3!} + \frac{x^5}{5!} - \frac{x^7}{7!} + \dots, \quad x \in \mathbb{R}$$

Taking a sufficient number of terms, one may approximate any functions at a point with a convenient number of decimals.

Taylor series are the main tool for approximating the values of elementary functions on any ordinary scientific calculator,

In the arrow paradox (Huggett, 2024), Zeno states that for motion to occur, an object must change its position. He gives an example of an arrow in flight (Figure 1). He states that at instant of time, the arrow is neither moving to where it is, nor to where it is not. It cannot move to where it is not, because no time elapses for it to move there; it cannot move to where it is, because it is already there. In other words, at every instant of time there is no motion occurring. If everything is motionless at every instant, and time is entirely composed of instants, then motion is impossible.

although there are some additional methods of improving the accuracy.

Graphical interpretation of Riemann and improper integrals

It is well known that the Riemann integral of a positive function $f: [a, b] \rightarrow \mathbb{R}$ is the area of the subgraph above the abscissa. This property can also be extended to improper integrals. Thus, an important role of integrals is in calculating areas, volumes, and lengths.

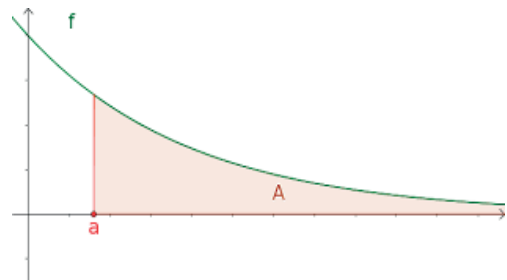


Figure 2. Geometric interpretation of the improper integral

The area of the subgraph of a positive function represented in Figure 2 is:

$$A = \int_a^{\infty} f(x) dx$$

For example, in physics, if $f(x)$ represents the value of a force, the integral represents the mechanical work of the force.

Fourier series

They were first used in the early 1800's by Joseph Fourier in order to find solutions to the heat equation.

Nowadays they have applications in physics, signal processing, image processing, conversion of special data into frequency data etc. (Budău et al., 2023; Calmuc et al., 2022).

A usual Fourier series is a representation of a periodic function $f(x)$ on $[-\pi, \pi]$ as a series of sines and cosines of the form:

$$f(x) = \frac{1}{2}a_0 + \sum_{n \geq 1} a_n \cos nx + \sum_{n \geq 1} b_n \sin nx$$

The coefficients have the following formulas:

$$\begin{aligned} a_0 &= \int_{-\pi}^{\pi} f(x) dx \\ a_n &= \frac{1}{\pi} \int_{-\pi}^{\pi} f(x) \cos nx dx \\ b_n &= \frac{1}{\pi} \int_{-\pi}^{\pi} f(x) \sin nx dx \end{aligned}$$

CONCLUSIONS

Integrals and series play an important role in, or outside mathematics and they are closely related to the overall progress of science and humanity. The limit comparison criteria with equivalents for series with positive terms or improper integrals are very useful and natural techniques.

Of course, as other convergence criteria, they can't be used for computing sums or integrals in case of convergence.

ACKNOWLEDGEMENTS

The present paper and the research work included is supported by the Faculty of Land Reclamation and Environmental Engineering, University of Agronomic Sciences and Veterinary Medicine of Bucharest.

REFERENCES

- Boboc, N. (1999). *Analiză matematică* (2 vol), Ed. Universității din București.
- Budău, L., Pescari, S., Chendeș, R., Vilceanu, C.B., Herban, S. (2023). Comparative study on digital image processing for 3d modeling. *Scientific Papers. Series E. Land Reclamation, Earth Observation & Surveying, Environmental Engineering*, Vol. XII, Print ISSN 2285-6064, 364-370.
- Calmuc, M., Calmuc, V.A., Arseni, M., Simionov, I.-A., Antache, A., Apetrei, C., Georgescu, P.L., Iticescu, C. (2022). Identification and characterization of plastic particles found in the lower Danube River. *Scientific Papers. Series E. Land Reclamation, Earth Observation & Surveying, Environmental Engineering*, Vol. XI, Print ISSN 2285-6064, 332-337.
- Colojoară, I. (1983). *Analiză matematică*, Ed. D.P. București.
- Goleț I., Hedrea C., Petrișor C. (2014). *Analiză Matematică – sinteze teoretice și aplicații*, Ed. Politehnica.
- Huggett, N. (2024). *Zeno's Paradoxes, The Stanford Encyclopedia of Philosophy* (Spring 2024 Edition), Ed. Edward N. Zalta & Uri Nodelman.
- Martin, O. (2008). *Calcul diferențial și integral în tehnică*, Ed. Politehnica, București.
- Miculescu, R. (2010). *Analiză Matematică – note de curs*, Ed. Universității din București.
- Nicolescu, M., Dinculeanu, N., Marcus, S. (1971). *Analiză Matematică*, Ed. D.P. București.
- Stănășilă, O. (1981). *Analiză Matematică*, Ed. D.P. București.

THE INFLUENCE OF TECHNOLOGY ON CULTURE IN THE PRODUCTION OF LETTUCE IN THE NUTRIENT FILM TECHNIQUE SYSTEM: A REVIEW

Oana Alina NIȚU¹, Emanuela JERCA², Elene Ștefania IVAN³, Marinela GHEORGHE¹

¹University of Agronomic Sciences and Veterinary Medicine of Bucharest,
Faculty of Land Reclamation and Environmental Engineering,
59 Marasti Blvd, District 1, Bucharest, Romania

²University of Agronomic Sciences and Veterinary Medicine of Bucharest,
Faculty of Horticulture, 59 Marasti Blvd, District 1, Bucharest, Romania

³University of Agronomic Sciences and Veterinary Medicine of Bucharest,
Research Center for Studies of Food Quality and Agricultural Products,
59 Marasti Blvd, District 1, Bucharest, Romania

Corresponding author email: elena.ivan@qlab.usamv.ro

Abstract

The NFT (Nutrient Film Technique) technology is one of the hydroponic methods used for cultivating plants, including lettuce. In this system, the plant roots are suspended in a continuous flow of nutrient solution, which is pumped through an inclined channel or a thin tray. This thin flow of nutrient solution allows the roots to receive essential nutrients such as nitrogen, phosphorus, and potassium, along with other necessary substances for healthy plant growth. The system utilizes a minimal amount of water because the water and nutrients are constantly recirculated within the system, thus reducing waste and the need for irrigation. By precisely monitoring and adjusting the composition of the nutrient solution, growers can ensure that plants receive the optimal amount of nutrients to grow healthily and produce quality yields.

Key words: hydroponic system, green salad, optimizing water input, recycling and resource conservation.

INTRODUCTION

Lettuce, scientifically known as *Lactuca sativa* L., is a vegetable plant belonging to the Asteraceae family (previously known as Compositae). This plant family encompasses a variety of genera and species found worldwide. Among other plants in the same family, we can mention chicory (*Cichorium intybus* L.), sunflower (*Helianthus annuus*), and dandelion (*Taraxacum officinale*). Although numerous studies have demonstrated the superior performance of hydroponic systems compared to traditional ones, to date, only a few studies have compared different growth models in hydroponic systems. Additionally, hydroponic systems are often associated with protected cultivation, making it difficult to identify specific growth trends for these systems (de Anda & Shear, 2017). Researchers have concluded that hydroponic production can vary significantly depending on crops and environmental conditions (Gashgari et al.,

2018). Lettuce is a cool-season crop with significant economic importance due to its capacity to generate income and is extensively cultivated worldwide, especially in temperate and subtropical regions (Mou, 2008; Kumar et al., 2010). Because of its nutritional value, lettuce can fetch higher prices in the market and, therefore, is traded extensively internationally (Abu-Rayyan et al., 2004). Despite the recent promotion of lettuce cultivation in protected conditions, production techniques have not yet been standardized (Kadayifci et al., 2004; Spehia et al., 2018).

The main challenge in lettuce production in greenhouses is standardizing growth systems to improve the quality and quantity of production while ensuring efficient water management and reducing environmental impact (Schwarz et al., 2009; Acharya et al., 2013).

Studies have shown that hydroponic growth systems can lead to an increase in leaf production (Barbosa et al., 2015; Petropoulos et al., 2016). However, there are concerns among

consumers regarding nutritional quality, water consumption, and economic aspects that may hinder the expansion of hydroponics in the commercial sector. While the cultivated areas for lettuce have decreased in Romania, the interest in soilless cultivation systems remains high due to their numerous advantages. These include the ability to carry out multiple cropping cycles per year, achieving higher yields, improving economic efficiency, and ensuring food safety and phytosanitary standards (Drăghici et al., 2021). Circulating hydroponic systems are classified into three distinct categories. These include the Nutrient Film Technique (NFT), the Drip Flow Technique (DFT), and the New Growing System (NGS) (Resh, 2013; Goddek et al., 2019). The name of the NFT system derives from the abbreviation of the term "Nutrient Film Technique". This hydroponic system was developed in the late 1960s by Dr. Allan Cooper at the Glasshouse Crops Research Institute in Littlehampton, United Kingdom (Roberto, 2003). Over time, the NFT system has demonstrated its effectiveness and has been considered the most versatile in the field (Resh, 2022). The NFT cultivation system can be characterized as a network of channels (Shanmugabhavatharani et al., 2021), preferably made of plastic. Through these channels, the nutrient solution circulates in the form of a thin film, with a thickness of approximately 1-2 cm (Van Os et al., 2008), hence the name "nutrient film." In the channels of the NFT system, plant roots are integrated. In addition to plastic, the walls of these channels can also be made from other flexible materials to prevent light penetration and nutrient solution evaporation. The NFT system is designed as a closed-loop system, where the nutrient solution is recirculated within the culture using a supply reservoir (Sardare & Admane, 2013).

In the NFT system, plant roots are maintained in direct contact with the nutrient solution, which is constantly distributed using a submersible pump from the supply reservoir (Pradhan & Deo, 2019). In 1920, Dennis R. Hoagland developed a formula that forms the basis of the nutrient compositions used today, providing all the essential nutrients required for a nutrient solution compatible with the NFT

system (Spehia et al., 2018). In modern times, soilless crops stand out due to their advanced technology and the diversity of systems used, which gives them versatility and the ability to produce remarkable results across a variety of plant cultures. The benefits of soilless systems are numerous and include efficient water usage, the possibility of water recycling, efficient fertilizer utilization, the creation of a controlled growing environment, increased disease and pest management capability, and reduced water consumption through recycling (Wignarajah, 1995; Jensen, 1981; Bradley & Marulanda, 2000; Resh, 2013).

The growing medium plays a crucial role in influencing production, leaf texture, and physiological characteristics of plants, as well as the importance of interaction between substrate and nutrient solution (Samarakoon et al., 2020). In unconventional cultivation systems, it is crucial for the nutrient solution to contain all essential nutrients for lettuce plant growth. A deficiency of these elements can lead to the onset of physiological issues that ultimately affect the quality of lettuce plants (Henry et al., 2019).

Various research studies have highlighted the adverse effects of salinity on lettuce plants, manifested by decreased leaf density (Al-Maskri et al., 2010), reduced leaf surface area and even photosynthetic capacity, as well as decreased fresh plant mass and root system impairment (Neocleous et al., 2014). Additionally, it has been found that the pH of the nutrient solution has a significant impact on plant development and growth (Al Meselmani, 2022). In cases where the temperature of the nutrient solution exceeds or falls below the permissible limits, it is observed that the growth and development of lettuce plants are affected (Thakulla et al., 2021).

In the context of hydroponic lettuce cultivation, it is recommended that nutrients be present in the nutrient solution at the following concentrations: 200 mg/L (ppm) of nitrogen (N), 50 mg/L (ppm) of phosphorus (P), 300 mg/L (ppm) of potassium (K), 200 mg/L (ppm) of calcium (Ca), and 65 mg/L (ppm) of magnesium (Mg) (Schon, 1992).

Lettuce plants develop optimally when the dissolved oxygen content in the nutrient solution reaches at least 6 ppm. Oxygenation of

the nutrient solution can be achieved through its recirculation or by aeration using air pumps. The amount of dissolved oxygen in the nutrient solution can be monitored using specialized sensors. The absence or decrease in the level of oxygen in the nutrient solution can lead to the disruption of root respiration, causing their suffocation and ultimately the death of the plants (Libia et al., 2016). There are several factors that influence the root respiration of plants, including high temperature and salinity (Zinnen, 1988). In hydroponic crops, high temperatures of the nutrient solution and periods of elevated temperatures have a negative impact on plant development (Al-Rawahy et al., 2023). The oxygen deficiency in the root zone is a crucial factor (Fagerstedt et al., 2023). The lack or insufficiency of oxygen can affect the development of the root system and may even lead to its deterioration, resulting in plant drying (Boru et al., 2003). The additional addition of oxygen to the nutrient solution has increased the yields of plants cultivated in hydroponic systems (Soffer et al., 1991). A low oxygen content in the root zone can create favorable conditions for the occurrence of plant diseases (Cherif et al., 1997) and can promote infestation of the root system with pathogens such as *Phytophthora infestans* (Lal et al., 2018). It has been demonstrated that there is a direct connection between increasing the flow rate of the nutrient solution and increasing the concentration of oxygen in the root zone of plants.

MATERIALS AND METHODS

This literature review covers publications related to lettuce cultivation in hydroponic systems and is based on the Science Direct, Scopus, and Web of Science databases, as well as relevant books. The main criteria for selecting publications focused on the topic of improving modern technologies used to enhance production per unit area, including the use of vertical farming techniques.

RESULTS AND DISCUSSIONS

Head, romaine, and leaf lettuce varieties are successfully cultivated in hydroponic systems (Kaiser & Ernst, 2012). Lettuce is the most

cultivated plant in the greens category in hydroponic systems (Ohse et al., 2009; Ryder, 1999). In these systems, the lifespan of lettuce is shorter compared to traditional cultivation systems.

The NFT cultivation system is ideal for growing lettuce (*Lactuca Sativa* L.), even allowing for up to eight harvests within a calendar year (Fussy & Papenbrock, 2022). Research has shown that using the NFT cultivation system can lead to a 6% - 10% increase in lettuce yield (Frasetya et al., 2021). Various studies demonstrate that the lettuce plant is remarkably adaptable to different hydroponic cultivation systems (Jones, 2005; 2007 & Ryder, 1999). Additionally, it is important to note that in recent years, the areas dedicated to lettuce cultivation in soilless systems have seen a significant increase globally, according to data provided by the Food and Agriculture Organization of the United Nations (FAO).

The NFT hydroponic system is the most widespread in growing greens. Lettuce is particularly well-suited for cultivation in the NFT system. This system helps reduce problems associated with excessive water uptake by the plant, which is especially important for lettuce, a plant sensitive to salinity, regardless of the cultivation system used (Tabaglio et al., 2020). The presence of the nutrient solution at the root level can act as a barrier to gas exchange between roots and the environment (Suhl et al., 2019). Although oxygen deficiency may affect only certain parts of the root, it can disrupt its function (Morard & Silvestre, 1996). However, based on the results obtained, there is no justification for using a higher flow rate of the nutrient solution than 2.5 l/min (Stoica et al., 2022).

Considering the continuous flow of the nutrient solution in the NFT system, changes in the concentration of dissolved salts in the solution can occur. One of the advantages of the NFT system is its ability to allow plant cultivation at higher concentrations of salts compared to traditional soil-based crops (Dias et al., 2011; Burrage, 1998).

For growing lettuce in a hydroponic system, it is feasible to use nutrient solutions prepared with low-quality water or to recycle nutrient solutions. The use of alternative water sources

and fertilizers can lead to a reduction in production costs in the hydroponic system (Azad et al., 2013), but there is a lack of information regarding proper nutrient solution management (Bugbee, 2003). Although liquid residues contain macro and micronutrients, the contents found can be limiting for plant growth,

CONCLUSIONS

In the context of modern agriculture, soilless cultivation systems, especially the Nutrient Film Technique (NFT) hydroponic system, represent an increasingly attractive solution for growing plants such as lettuce. Interest in these systems remains high as they offer numerous advantages, including the ability to conduct multiple cultivation cycles per year, achieving higher yields, increasing economic efficiency, and ensuring food and phytosanitary safety. In the NFT system, the nutrient solution circulates in the form of a thin film within the channels where plant roots are integrated. This system allows for efficient distribution of nutrients while maintaining a controlled growing environment. Furthermore, the recirculation of the nutrient solution contributes to efficient water usage and reduces fertilizer consumption. However, proper management of the nutrient solution is crucial for achieving quality production. The concentration of dissolved salts in the solution must be monitored and adjusted accordingly to avoid the adverse effects of salinity on plants. In conclusion, soilless cultivation systems, especially the NFT system, represent a promising technology for modern agriculture, offering significant benefits in terms of efficiency and sustainability of agricultural production. However, it is important to pay attention to aspects related to managing the nutrient solution and controlling the growing environment to ensure the success of growing plants such as lettuce. Cultivating lettuce in a hydroponic system offers multiple advantages, including the possibility of using nutrient solutions prepared with low-quality water or recycling nutrient solutions, which can reduce production costs. Indeed, there are still deficiencies in the proper management of the nutrient solution, which can have an impact on plant development. It is crucial to give special

attention to this aspect to guarantee optimal plant growth and to prevent excessive accumulation or deficiency of nutrients. In conclusion, studies highlight the importance of proper management of the nutrient solution in hydroponic lettuce crops. Temperature, nutrient concentration, and oxygen level are critical factors for healthy plant development. The lack or decrease of oxygen level can lead to serious root system problems and can negatively affect plant growth and production. Additionally, it is essential for the nutrient solution to be adequately oxygenated to ensure optimal nutrient absorption by the roots. The study also highlights that a nutrient solution flow rate greater than 2.5 L/min is not justified and may lead to resource wastage. Overall, proper management of the growing environment and nutrient solution is crucial for achieving high-quality lettuce production in hydroponic systems.

ACKNOWLEDGEMENTS

This work was supported by a grant from the University of Agronomic Sciences and Veterinary Medicine of Bucharest, project number 2023-0004, nr. 848/30.06/2023, within IPC 2023

REFERENCES

- Al Meselmani, M.A. (2022). *Nutrient solution for hydroponics*. IntechOpen. <https://doi.org/10.5772/intechopen.101604>
- Al-Maskri, A.H.M.E.D., Al-Kharusi, L., Al-Miqbali, H., & Khan, M.M. (2010). Effects of salinity stress on growth of lettuce (*Lactuca sativa*) under closed-recycle nutrient film technique. *Int. J. Agric. Biol.*, 12(3), 377-380.
- Almuktar, S.A.A.A.N., Scholz, M., Al-Isawi, R.H.K., & Sani, A. (2015). Recycling of domestic wastewater treated by vertical-flow wetlands for irrigating chillies and sweet peppers. *Agricultural Water Management*, 149, 1-22.
- Al-Rawahy, M.S., Al-Abri, W.S., Al-Hinai, A.S., Al-Abri, H.A., Al-Mahrooqi, S.H., Al-Shmali, N.M., & Al-Subhi, K.S. (2023). Response of Ozone Treatment on Disease Incidence, Dissolved Oxygen Levels, Growth and Yield of Cucumber Crop Grown in Hydroponics in Cooled Green House. Season: Summer (June-August) at DGALR, Rumais. *Journal of Agricultural Science*, 15(3), 85.
- Azad, A.K., Ishikawa, K., Diaz-Perez, J.C., Eaton, T.E. J., & Takeda, N. (2013). Growth and development of komatsuna (*Brassica rapa* L. Nothovar) in NFT

- (nutrient film technique) system, as influenced by natural mineral. *Agricultural Sciences*, 4(7A).
- Benton Jones, J. (2005). *Hydroponics. A practical guide for the soilless grower*. Boca Raton, 440, <https://doi.org/10.1201/9780849331671>
- Bradley, P., & Marulanda, C. (2000). Simplified hydroponics to reduce global hunger. In *World Congress on Soilless Culture: Agriculture in the Coming Millennium*, 554, 289-296.
- Bugbee, B. (2003). Nutrient management in recirculating hydroponic culture. In *South Pacific Soilless Culture Conference-SPSCC*, 648, 99-112.
- Burrage, S.W. (1998). Soilless culture and water use efficiency for greenhouses in arid, hot climates. *International Workshop on Protected Agriculture in the Arabian Peninsula*, Doha (Qatar).
- Chérif, M., Tirilly, Y., & Bélanger, R.R. (1997). Effect of oxygen concentration on plant growth, lipidperoxidation, and receptivity of tomato roots to Pythium F under hydroponic conditions. *European Journal of Plant Pathology*, 103, 255-264.
- Dias, N.D.S., Jales, A.G.D.O., Sousa Neto, O.N.D., Gonzaga, M.I.D.S., Queiroz, Í.S.R.D., & Porto, M.A. F. (2011). Hydroponic lettuce production on coconut fiber using desalination wastewater. *Revista Ceres*, 58, 632-637.
- Drăghici, E.M., Jerca, O.I., Cîmpeanu, S.M., Teodorescu, R.I., Țiu, J., & Bădulescu, L. (2021). Study regarding the evolution of high-performance cultivation technologies in greenhouses and hight tunnels in Romania. *Scientific Papers. Series B, Horticulture, LXI*(1).
- Fagerstedt, K. V., Pucciariello, C., Pedersen, O., & Perata, P. (2023). Recent progress in understanding the cellular and genetic basis of plant responses to low oxygen hold promise for developing flood-resilient crops. *Journal of Experimental Botany*, 75(5), 1217-1233, <https://doi.org/10.1093/jxb/erad457>
- Frasetya, B., Harisman, K., & Ramdaniah, N.A.H. (2021). The effect of hydroponics systems on the growth of lettuce. In *IOP Conference Series: Materials Science and Engineering*, 1098(4), 042115. IOP Publishing.
- Fussy, A., & Papenbrock, J. (2022). An overview of soil and soilless cultivation techniques Chances, challenges and the neglected question of sustainability. *Plants*, 11(9), 1153.
- Goddek, S., Joyce, A., Kotzen, B., & Burnell, G.M. (2019). *Aquaponics food production systems: combined aquaculture and hydroponic production technologies for the future*. Springer Nature, 619.
- Henry, J.B., Vann, M.C., & Lewis, R.S. (2019). Agronomic practices affecting nicotine concentration in flue-cured tobacco: A review. *Agronomy Journal*, 111(6), 3067-3075.
- Jensen, K. (1981). Coloured Petri nets and the invariant-method. *Theoretical computer science*, 14(3), 317-336.
- Kaiser, C., & Ernst, M. (2012). Hydroponic lettuce. *University Of Kentucky College of Agriculture, Food and Environment*.
- Kratky, B.A. (2005). Growing lettuce in non-aerated, non-circulated hydroponic systems. *Journal of vegetable science*, 11(2), 35-42.
- Lal, M., Luthra, S.K., Gupta, V. K., & Yadav, S. (2018). Evaluation of potato genotypes for foliar and tuber resistance against *phytophthora infestans* causing late blight of potato under subtropical plains of India. *Int J Curr Microbiol Appl Sci*, 7(3), 1234-42.
- Morard, P., & Silvestre, J. (1996). Plant injury due to oxygen deficiency in the root environment of soilless culture: a review. *Plant and soil*, 184, 243-254.
- Neocleous, D., Koukounaras, A., Siomos, A.S., & Vasilakakis, M. (2014). Assessing the salinity effects on mineral composition and nutritional quality of green and red "baby" lettuce. *Journal of Food Quality*, 37(1), 1-8.
- Ohse, S., Ramos, D.M.R., Carvalho, S.M.D., Fett, R., & Oliveira, J.L.B. (2009). Composição centesimal e teor de nitrato em cinco cultivares de alface produzidas sob cultivo hidropônico. *Bragantia*, 68, 407-414.
- Pradhan, B., & Deo, B. (2019). Detection of phytochemicals and in vitro propagation of Banana (Musa variety Gaja Bantal). *Journal of Medicinal Plant Studies*, 7(1), 46-49.
- Resh, H.M. (2013). Water culture: microgreens. *Hydroponic food production*. CRC Press, Boca Raton, FL, 135-142.
- Resh, H.M. (2022). *Hydroponic food production: a definitive guidebook for the advanced home gardener and the commercial hydroponic grower*. CRC press.
- Resh, M.D. (2013). Covalent lipid modifications of proteins. *Current Biology*, 23(10), 431-435.
- Roberto, K. (2003). How-to Hydroponics; Futuregarden. Inc.: Lindenhurst, NY, USA.
- Ryder, E.J. (1999). *Lettuce, endive and chicory*. Cab International.
- Samarakoon, U., Palmer, J., Ling, P., & Altland, J. (2020). Effects of electrical conductivity, pH, and foliar application of calcium chloride on yield and tipburn of *Lactuca sativa* grown using the nutrient-film technique. *Hort Science*, 55(8), 1265-1271.
- Sardare, M.D., & Admane, S.V. (2013). A review on plant without soil-hydroponics. *International Journal of Research in Engineering and Technology*, 2(3), 299-304.
- Schon, M. (1992, April). Tailoring nutrient solutions to meet the demands of your plants. In *Proceedings of the 13th Annual Conference on Hydroponics, Hydroponic Society of America, Orlando, FL, USA*, 9-12.
- Shanmugabhavatharani, R., Priya, R.S., Kaleeswari, R.K., & Sankari, A. (2021). Performance assessment of mint on growth and yield attributes supplied with three nutrient combinations under two modified nutrient film technique (NFT). *The Pharma Inno. J.*, 10, 17-22.
- Soffer, H., Burger, D.W., & Lieth, J.H. (1991). Plant growth and development of Chrysanthemum and Ficus in aero-hydroponics: response to low dissolved oxygen concentrations. *Scientia horticultrae*, 45(3-4), 287-294.

- Spehia, R.S., Devi, M., Singh, J., Sharma, S., Negi, A., Singh, S. & Sharma, J.C. (2018). Lettuce growth and yield in hoagland solution with an organic concoction. *International Journal of Vegetable Science*, 24(6), 557-566.
- Stoica, C.M., Velcea, M., Chira, L., Jerca, O.I., Velea, M. A., & Drăghici, E.M. (2022). The nutrient solution oxygenation influences the growth of the species *lactuca sativa* l. root system cultivated in the nutrient film technique (nft) system. *Scientific papers. series B. horticulture*, 66(1).
- Suhl, J., Oppedijk, B., Baganz, D., Kloas, W., Schmidt, U., & van Duijn, B. (2019). Oxygen consumption in recirculating nutrient film technique in aquaponics. *Scientia Horticulturae*, 255, 281-291.
- Tabaglio, V., Boselli, R., Fiorini, A., Ganimede, C., Beccari, P., Santelli, S., & Nervo, G. (2020). Reducing nitrate accumulation and fertilizer use in lettuce with modified intermittent Nutrient Film Technique (NFT) system. *Agronomy*, 10(8), 1208.
- Thakulla, D., Dunn, B., Hu, B., Goad, C., & Maness, N. (2021). Nutrient solution temperature affects growth and Brix parameters of seventeen lettuce cultivars grown in an NFT hydroponic system. *Horticulturae*, 7(9), 321.
- Van Os E.A., Gieling T.H., Lieth J.H. (2008). *Technical equipment in soilless production systems*. In: Raviv, Lieth (eds) *Soilless culture, theory and practice*. Elsevier, Amsterdam, 157-207.
- Wignarajah, K. (1995). Mineral nutrition of plants. *Handbook of plant and crop physiology*.
- Zinnen, T. M. (1988). Assessment of plant diseases in hydroponic culture. *Plant disease*, 72(2), 96-99.

EXPLORING THE USE OF WEB APPLICATIONS AND NEURAL NETWORKS FOR CAR PARKING SERVICES

Dan Constantin PUCHIANU

Valahia University of Targoviste, 13 Sinaia Alley Street, Targoviste, Romania

Corresponding author email: pdantgv@yahoo.com

Abstract

Intelligent parking systems that capitalize on the characteristics of deep-learning architectures have become an important point of research due to their ability to improve efficiency, reduce traffic congestion and improve the experience of drivers. The availability and ineffective management of parking spaces is a major problem in most cities, leading to traffic congestion and pollution. This study aims to introduce a state-of-the-art implementation of intelligent parking systems using neural networks and web application development. The optimization of neural networks enables careful analysis of images and videos from surveillance cameras to quickly identify available parking spaces in real time. These implementations offer innovative solutions for drivers looking for parking spaces, thus reducing the time spent searching for them and reducing traffic congestion. The development of a web application was proposed to complete the implementation part of the study using trained neural networks to provide a useful user interface for displaying available parking spaces. This study aims to open the way to automated parking, predictive parking availability and smart parking systems. Compared to other architectures, the proposed models have demonstrated superior performance, and the effective use of these technologies can improve smart-city practices and reduce the impact of traffic pollution on the environment.

Key words: deep learning, image processing, intelligent parking, neural networks, sustainability.

INTRODUCTION

Technological development has significantly changed modern society by providing useful solutions for critical problems of the environment in which we live. The field of deep learning has witnessed a notable advancement during the preceding period (Boldeanu et al., 2023). Among these, deep learning technologies and object detection architectures stand out as having applications in different fields such as computer vision, medical and smart city. Among these areas, the range of deep learning technologies and models is a key point for intelligent parking systems, having the role of contributing to sustainability and more efficient traffic (An et al., 2022; De Luelmo et al., 2022). Deep learning is a field that involves using neural networks to extract key features from visual data such as images and videos (Lubura et al., 2022). In this context, object detection architectures such as YOLO, Faster R-CNN or RetinaNet stand out, which demonstrate notable performance in the identification and localization of objects from these visual data (Goumiri et al., 2021; Hwang et al., 2023; Xie et

al., 2015). Leveraging these features detection models are successfully integrated into traffic monitoring applications, autonomous systems, and smart-city solutions (Gkolias & Vlahogianni, 2019; Gören et al., 2019). A popular area that has brought continuous research in recent years is represented by the implementation of intelligent parking solutions where these models can quickly identify the status of these reference areas (Deruytter & Anckaert, 2013; Ellis et al., 2021). Intelligent parking systems are using video cameras to monitor parking spaces in an efficient way (Amato et al., 2017; Çiçek & Gören, 2020). Based on these, the system manages to capture key visual information that can represent the entry point of deep learning detection models. Based on these monitoring and visual data, the systems can quickly identify available parking spaces in real time, providing drivers with quick data and reducing the time it takes to search for a parking space (Nurullayev & Lee, 2019). Following these characteristics, intelligent parking systems have a positive impact on sustainability and overall traffic. Reducing the time spent in traffic looking for a parking space

reduces fuel consumption, provides safety for drivers, and has a major impact on efficient traffic solutions (Satyanath et al., 2022). Moreover, with the reduction of time spent in traffic, searching for parking, gas emissions that endanger health and the environment are also reduced. In addition, intelligent systems can provide drivers with fast, real-time information, reducing the added stress that comes with congested traffic (Thakur et al., 2023).

These features have the role of managing smart-city solutions by generating real traffic information. The analysis of collected data can bring to the fore not only smart parking solutions but also appropriate measures for the management of heavily trafficked areas, management of parking spaces and sustainable urban development (Ng et al., 2018; Truong et al., 2022).

As technologies evolve and their documentation is well defined, various studies note key features of deep learning to contribute to a sustainable and well-informed future of traffic. Their integration represents areas of ongoing research solving problems as urban areas become increasingly congested and difficult to manage (Hwang et al., 2023; Zhang et al., 2018).

This paper presents the implementation of detection models of the YOLO family for the automatic detection of parking spaces from digital images, an important first step in the development of intelligent systems related to this task. Moreover, the models are optimized to extract important features from the input data, and finally they are tested to export a model capable of making accurate and high-confidence detections. Additionally, a React.js web application is developed to use the trained and validated models in making automatic detections for data uploaded to the web interface.

A solution of this type aims to demonstrate the remarkable performance of deep learning technologies integrated with modern web technologies. Apart from the introductory chapter, chapters are attached that present the materials and methods used for the development of the study, as well as a part of experimental results and discussions that capitalize on the characteristics of the implemented detection models. Finally, the conclusion section presents the key points of the study.

MATERIALS AND METHODS

Implementing an automatic vehicle parking management system using visual data starts with building a large, robust dataset that includes relevant examples so that the detection model presents a solid foundation for training and testing. Following the previously presented characteristics and state-of-the-art analysis, a digital image dataset was collected, using various sources that included open-source datasets and images taken from nearby urban areas (Blanderbuss-Kaggle, 2024). The images in the dataset of the present study are of RGB type and include files with the extension PNG or JPEG, with varying resolutions and illustrating different real-world conditions and contexts.

The total number of images in the dataset is 1100. They have been structured into subfolders that include the information needed to train and evaluate a detection model - training, validation, and testing. The division of the dataset followed a structure of 70% for training (770 images), 20% validation (220 images) and 10% testing (110 images). Each part of the dataset contains the images and annotations relevant to the detection process, the implemented annotation format is YOLO, with files in the .txt extension. They will be attached to the chosen detection model, from the YOLO family, to be presented in this chapter. Example images of the dataset are shown in Figure 1.

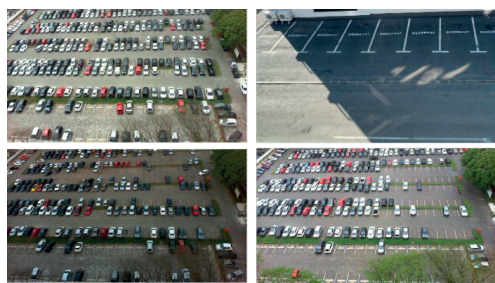


Figure 1. Examples of digital images of the dataset for car parking detection

Starting from the attached examples, it is observed within the dataset variations and various conditions present in the dataset images. The dataset also includes marginal examples with various lighting, blur, contrast conditions to present the detection model with learning examples close to real conditions. The images in

the dataset went through an online augmentation process, typical of YOLO models. At the same time, a part of pre-processing was followed so that the size of the input image is the one expected by the used YOLO model - 640x640px.

Online augmentation involves a series of transformations applied to the training data set during the training process of the detection model. These transformations are random and are not applied before the training process, which allows the model to see different examples in each training epoch. This adopted process is essential to increase the detection and generalization ability of the model and included various types of transformations - rotation, scaling, translation, brightness and contrast changes, noise, cutout and mosaic, a type of augmentation that combines 4 images examples that are presented to the model during training. The detection model chosen for the development of the present study was YOLOv8 (Jocher, 2023), being one of the new, advanced versions of this family (You Only Look Once). The YOLOv8 model brings significant improvements over previous variants and is distinguished by several key features. Studying the code attached to this variant allows the extraction of these key innovations, for the present variant there is no official paper.

YOLOv8 introduces improved backbone and neck architectures. The backbone structure responsible for extracting the information of interest presents changes to the CSP Darknet network. The representative blocks of this Cross-Stage Partial Connections structure improve the flow of useful information to the detection model and significantly reduce the computational complexity footprint. PANet (Path Aggregation Network) represents the basis of the neck structure for a precise detection of objects of various sizes, a module that facilitates the integration of image features at different resolutions. The YOLOv8 capabilities describe the one-stage network detection process characteristic of the YOLO family and are successfully applied for multi-scale detection capabilities similar to state-of-the-art structures such as Feature Pyramid Networks. The head structures of the new YOLOv8 variant are specialized for the classification and regression part and support clear separation of tasks and

overall model accuracy. In this way, the predictions are optimized, and the localization and classification of objects is accurate. The architecture improvements also include new optimization techniques at the core, with advanced data augmentation that ultimately brings fast convergence and diverse hardware performance. Tasks for using YOLOv8 include detection, classification, and segmentation of digital images.

The hardware and software part that was the basis of the implementation of the solutions in the present study included a dedicated system with Windows 11 operating system. From a hardware point of view, the system features a dedicated NVIDIA GeForce RTX 4070 8GB video card for the successful management of deep learning architectures, CUDA support, to which is added an Intel Core i7-14700HX CPU, 32 GB RAM, 1 TB SSD. The chosen programming language was Python version 3.10, and the chosen deep learning framework was PyTorch, for the basis of the implementation of the chosen detection architectures, in relation to the YOLOv8 code.

RESULTS AND DISCUSSIONS

This chapter presents the experimental results and discussions based on the performances obtained from the training and evaluation of the detection models. The methodologies and metrics used are exposed throughout this chapter highlighting the strengths and limitations of each proposed model in relation to the attached data set.

For the present work transfer learning and fine-tuning techniques were adopted in using the YOLOv8 model (Jocher, 2023). To describe fast detection systems, the motivation of the present study included choosing optimized models of YOLOv8, small and medium in terms of complexity and export on resource-constrained platforms: YOLOv8 versions n (nano), s (small), and m (medium). For the present case hyperparameter fitting techniques were also pursued. These can have a positive impact on performance and include learning rate, optimal batch size, number of training epochs, early stopping, and size of anchors for detections of various sizes. In principle, a balance between convergence and performance was followed and

analyzed. Table 1 shows the detection metrics resulting from model evaluation on the test dataset, with new images from the previously presented dataset split. Based on these test images, the best saved weights of each model are run to observe the behavior on new data.

Table 1. Parking lot detection performance on the test set (ALL Class)

Model	Precision	Recall	mAP@50	mAP@50:95
YOLOv8n	0.977	0.935	0.974	0.810
YOLOv8s	0.971	0.952	0.956	0.780
YOLOv8m	0.959	0.964	0.983	0.809

Version 8.2 of the YOLOv8 model was used from the base of the ultralytics library (Jocher, 2023) that supports this part of the code. The optimizer was AdamW with a learning rate of 0.00125 and momentum 0.9. The number of epochs was 500. The models were evaluated using common object detection metrics: Precision, Recall, and IoU (Intersection Over Union) for calculating mAP@50, mAP@50:95. The composition of the dataset presents two reference classes, related to the availability of parking spaces: free or occupied, with the annotations created and attached to each image of the dataset. A class called "ALL" is typical for detection tasks in relation to the YOLO family model and involves an averaging of the results obtained for each class separately, treating them with equal importance and defining a common point for evaluating the overall performances, the model being trained to recognize correct the two availability statuses in the illustration of the parking spaces.

According to the metrics obtained (Table 1), the models implemented for the present study achieve remarkable results. The characteristics and performances demonstrated are based on the settings attached to the training and evaluation steps. The evolution of the metrics for these cases are presented in Figures 2, 3 and 4, graphs resulting from the YOLOv8 code and organized in the typical YOLO format.

The first chosen model, YOLOv8n, describes a good performance in terms of accuracy and mAP@50, and highlights the model's ability to detect available parking spaces, generating few false detections. Outside of these metrics, recall is lower compared to the other models, missing instances of interest. YOLOv8s presents itself as

a balanced model in terms of Precision and Recall. This notes that the model is quite good at correctly detecting parking spaces and minimizing false detection errors. However, mAP@50:95 is lower with poor performance over a wide range of precision-recall and at different IoU thresholds. YOLOv8m is the model with the highest recall value, indicating the remarkable performance of the model in detecting parking spaces. However, the accuracy value decreases indicating that the model may generate more false predictions, but the model shows superior performance in terms of overall accuracy.

Each model implemented presented weaknesses and strengths. YOLOv8m can be noted as the top model with high overall accuracy and good coverage marked by the highest recall. YOLOv8n is good in terms of precision, while YOLOv8s is the most balanced model implemented. The choice of the desired, optimal model depends on the characteristics of the application for which these deep learning models are implemented, based on prioritization of various categories: hardware, general accuracy, maximum accuracy, or detection speed.

The context presented in the dataset illustrates areas with parking spaces starting from favorable to slightly unfavorable environmental conditions. As a first step in the further development of the present work, it is desired to collect data that complements the existing data set with a series of unfavorable conditions, which could make such implemented detection models difficult. The motivation for this is related to testing in various conditions that can successfully cover detection systems that want to respond even in the most difficult conditions, without being affected by false detections.

According to the study carried out, a series of limitations of the implemented models were observed that contribute to the decrease in performance. First, there is a small problem of detecting dark-colored cars occupying parking spaces, which often do not have clearly visible details to result in correct detections. This is because the color of the material paving the parking areas is similar.

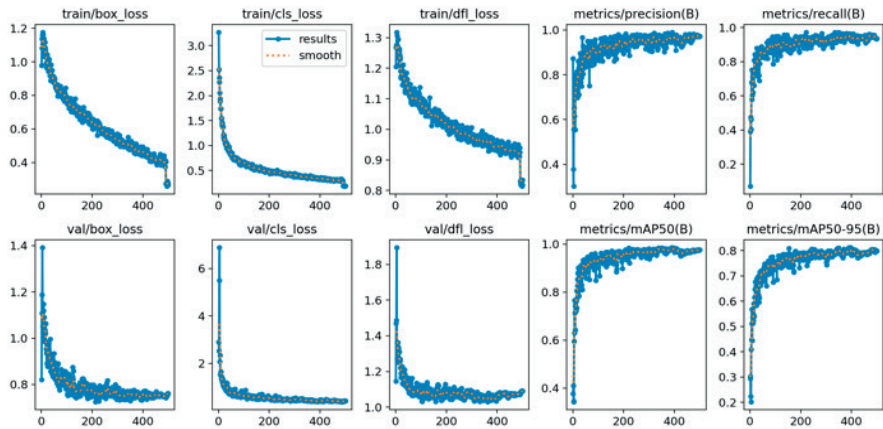


Figure 2. YOLOv8n training and validation results

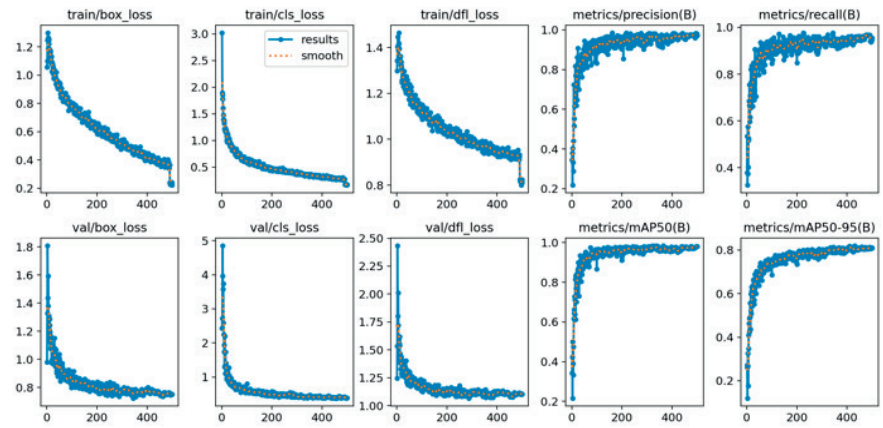


Figure 3. YOLOv8s training and validation results

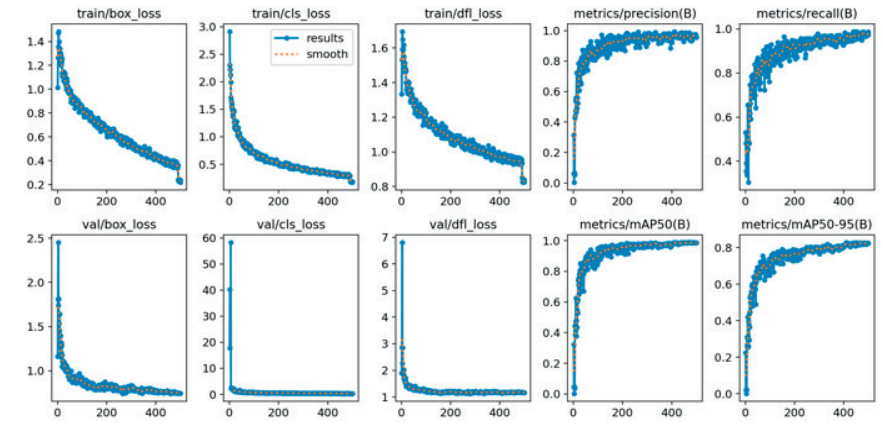


Figure 4. YOLOv8m training and validation results

Another problem is described by false detections of models arising from inappropriate parking lots, with vehicles parked in two or more spaces or vehicles oriented differently. The detection model was observed to be very reliable in predictions of where parking spaces are correctly occupied and the (usually white) boundary lines are clearly visible. Other problems observed are in the case of shaded areas, partially or totally covered by objects other than those of vehicles, and parking lots with blurred or hardly visible boundary lines. For these marginal cases the data set can be supplemented later, and the models re-trained accordingly. At the same time, the models can be adapted to define these cases, for better management of parking spaces and for their quick identification and release. With all these characteristics, the present study marks an initial direction of solid development, with satisfactory results, which finally support the performance of deep learning in such tasks, useful for the management of public or private parking lots and urban traffic.

CONCLUSIONS

Deep learning, especially detection models based on convolutional neural networks, demonstrate remarkable performance in the detection and estimation of the state of parking spaces as part of intelligent systems. Manually inspecting parking spaces using authorized personnel is expensive and time-consuming. In this sense, the development of deep learning solutions for automatic detection and continuous monitoring represents key points of research and development.

In the present work, three optimized models of the YOLOv8 architecture were implemented for automated parking detection. The obtained results demonstrate the effectiveness of these implementations and open the way to new research directions, in the direction of automatic parking management and monitoring systems. The performances obtained were based on a carefully collected and annotated data set that tends to illustrate the various conditions that may be present in real scenarios. Key metrics demonstrated Precision and mAP@50 values above 95%, recall values between 92-96% and overall mAP@50:95 performance above 75%.

The optimization of the chosen detection models using transfer learning techniques, fine-tuning and the adoption of online augmentation, had a positive impact on the obtained performances. However, there are limitations and observations that emerge from the performances obtained and prove critical steps through which the study carried out can be developed further, to be adapted to different environmental conditions. The collected data set can be increased by adding new scenarios and areas to analyze the ability of the detection models in much more complicated scenarios, as often happens in real cases. Detection models can be improved by integrating new key feature capture modules and can pursue their implementation in lightweight platforms to create autonomous systems, testing the speed of inference and detection. However, the performances obtained are notable and can be seen as important research that can materialize in customer-oriented, sustainability and smart-city systems.

REFERENCES

- Amato, G., Carrara, F., Falchi, F., Gennaro, C., Meghini, C., & Vairo, C. (2017). Deep Learning for Decentralized Parking Lot Occupancy Detection. *Expert Systems with Applications*, 327–334. <https://doi.org/10.1016/j.eswa.2016.10.055>.
- An, Q., Wang, H. & Chen, X. (2022). EPSDNet: Efficient Campus Parking Space Detection via Convolutional Neural Networks and Vehicle Image Recognition for Intelligent Human–Computer Interactions. *Sensors*, 24, 9835. <https://doi.org/10.3390/s22249835>.
- Blanderbuss. (n.d.). Parking Lot Dataset. Kaggle. Retrieved [May, 2024], from <https://www.kaggle.com/datasets/blanderbuss/parking-lot-dataset/data>
- Boldeanu, G., Gheorghe, M., Moise, C., Dana Negula, I., Tudor, G. (2023). Earth observation techniques applied for land waste detection and monitoring. *Scientific Papers. Series E. Land Reclamation, Earth Observation & Surveying, Environmental Engineering, Vol. XII*, Print ISSN 2285-6064, 383–388.
- Çiçek, E., & Gören, S. (2020). Fully Automated Roadside Parking Spot Detection in Real Time with Deep Learning. *Concurrency and Computation: Practice and Experience*, 23. <https://doi.org/10.1002/cpe.6006>.
- De Luelmo, S.P., Giraldo Del Viejo E., Montemayor A.S. & Pantrigo, J.J. (2022). Visual Parking Space Estimation Using Detection Networks and Rule-Based Systems. In *Bio-Inspired Systems and Applications: From Robotics to Ambient Intelligence*, 583–592. Springer International Publishing. http://dx.doi.org/10.1007/978-3-031-06527-9_58.

- Deruytter, M. & Anckaert, K. (2013). *Video-Based Parking Occupancy Detection*. Edited by Robert Paul Locc, Eli Saber, and Sreenath Rao Vantaram. SPIE Proceedings, <https://doi.org/10.1117/12.2003884>.
- Ellis, J.D., Harris, A., Saquer N. & Iqbal, R. (2021). An Analysis of Lightweight Convolutional Neural Networks for Parking Space Occupancy Detection. *IEEE International Symposium on Multimedia (ISM)*, <https://doi.org/10.1109/ism52913.2021.00052>.
- Gkolas, K. & Vlahogianni E.I. (2019). Convolutional Neural Networks for On-Street Parking Space Detection in Urban Networks. *IEEE Transactions on Intelligent Transportation Systems*, 12, 4318–4327. <https://doi.org/10.1109/tits.2018.2882439>.
- Gören, S., Öncevarlık, D.-F., Yldz K.D., & Hakyemez, T.Z. (2019). On-Street Parking Spot Detection for Smart Cities. *IEEE International Smart Cities Conference (ISC2)*, <https://doi.org/10.1109/isc246665.2019.9071760>.
- Goumiri, S., Benboudjema, D. & Pieczynski, W. (2021). One convolutional layer model for parking occupancy detection. *IEEE International Smart Cities Conference (ISC2)*, Manchester, United Kingdom, 1–5, doi: 10.1109/ISC253183.2021.9562946. <https://doi.org/10.1109/isc253183.2021.9562946>.
- Hwang, J.-H., Cho, B. & Choi, D.-H. (2023). Feature Map Analysis of Neural Networks for the Application of Vacant Parking Slot Detection. *Applied Sciences*, 13, 10342. <https://doi.org/10.3390/app131810342>.
- Jocher, G., Chaurasia, A., & Qiu, J. (2023). Ultralytics YOLO (Version 8.0.0) [Computer software]. <https://github.com/ultralytics/ultralytics>
- Lubura, J., Pezo, L., Sandu, M.A., Voronova, V., Donsi, F., Šic Žlabur, J., Ribić, B., Peter, A., Šurić, J., Brandić, I., et al. (2022). Food Recognition and Food Waste Estimation Using Convolutional Neural Network. *Electronics*, 11(22), 3746. <https://doi.org/10.3390/electronics11223746>.
- Ng, C., Cheong, S., & Foo, Y.-L. (2018). Lightweight Deep Neural Network Approach for Parking Violation Detection. *Proceedings of the 2018 VII International Conference on Network, Communication and Computing*, December. <https://doi.org/10.1145/3301326.3301387>.
- Nurullayev, S. & Lee, S.-W. (2019). Generalized Parking Occupancy Analysis Based on Dilated Convolutional Neural Network. *Sensors*, 19, 277. <https://doi.org/10.3390/s19020277>.
- Satyanath, G., Sahoo, J.K. & Roul, R.K. (2022). Smart Parking Space Detection under Hazy Conditions Using Convolutional Neural Networks: A Novel Approach. *Multimedia Tools and Applications*, 82(10), 15415–15438. <https://doi.org/10.1007/s11042-022-13958-x>.
- Thakur, N., Bhattacharjee, E., Jain, R., Acharya B., & Hu, Y.-C. (2023). Deep Learning-Based Parking Occupancy Detection Framework Using ResNet and VGG-16. *Multimedia Tools and Applications*, 1, 1941–1964. <https://doi.org/10.1007/s11042-023-15654-w>.
- Truong, L.N.H., Clay, E., Mora, O.E., Cheng, W., Singh, M. & Jia, X. (2022). Rotated Mask Region-Based Convolutional Neural Network Detection for Parking Space Management System. *Transportation Research Record: Journal of the Transportation Research Board*, 2677(1), 1564–1581. <https://doi.org/10.1177/03611981221105066>.
- Xie, H., Wu, Q., Chen, B., Chen, Y. & Hong, S., (2015). Vehicle Detection in Open Parks Using a Convolutional Neural Network. *Sixth International Conference on Intelligent Systems Design and Engineering Applications (ISDEA)*, Guiyang, China, 927–930, doi: 10.1109/ISDEA.2015.233, <https://doi.org/10.1109/isdea.2015.233>.
- Zhang, L., Huang, J., Li, X. & Xiong, L. (2018). Vision-Based Parking-Slot Detection: A DCNN-Based Approach and a Large-Scale Benchmark Dataset. *IEEE Transactions on Image Processing*, 11, 5350–5364. <https://doi.org/10.1109/tip.2018.2857407>.

ROMANIA TOWARDS A GREEN TRANSITION: CARBON BORDER ADJUSTMENT MECHANISM (CBAM) REGULATIONS

Cristiana SÎRBU

University of Agronomic Sciences and Veterinary Medicine of Bucharest,
59 Marasti Blvd, District 1, Bucharest, Romania

Corresponding author email: cris_sirbu@yahoo.com

Abstract

The paper aims to highlight the steps our country needs to take to achieve green economy and industry, defining the new adopted regulations regarding the greenhouse gas emissions embedded in goods imported. The Carbon Border Adjustment Mechanism (CBAM) is a price adjustment dedicated to goods carrying CO₂ emissions that enter the European Union. The main purpose of CBAM is to prevent the risk of carbon leakage and by encouraging the reduction of emissions by operators in third countries (countries outside the EU), global carbon emissions should be reduced. Carbon Border Adjustment Mechanism is an instrument used to achieve a greener industry, economy and life, a tool to a green transition. The paper presents the basis and decisions made in time and seeks to identify the measures that need to be taken so that we can all contribute to what it means to decarbonize the European Union.

Key words: carbon, European Union, emissions, green transition, regulations.

INTRODUCTION

Extreme climate events in increasing numbers perfectly define global warming although there are thesis and theories that do not accept "global warming" and place numerous phenomena like floods, droughts, extreme precipitation, heat waves, forest fires, shifting and melting glaciers, rising sea levels, etc., on the cycle of periods from glaciations to overheating, over 4.6 billion years. Clearly the scientific evidence shows that the risks of irreversible and catastrophic changes would increase significantly if global warming were to exceed pre-industrial levels by 2°C or at least 1.5°C (The Ministry of Research, Innovation and Digitalization, 2023).

MATERIALS AND METHODS

The year 2024 puts the European Union as a global economic power to actively engage in tackling greenhouse gas (GHG) emissions, maintaining a 31% decrease from previous years' levels.

Human activities such as fuel burning, haphazard agriculture forcing deforestation have become unhindered producers of carbon, methane, nitrous oxide and fluorocarbon emissions (Borzykh et al., 2023; Cadar et al., 2023).

These greenhouse gases store heat from the earth's surface and prevented it from being released, causing global warming. The global warming is a continuous temperature rise in Earth's temperature. Studies have shown that each year, we register a higher average temperature.

The Sixth IPCC Climate Change Synthesis Report (IPCC) published in March 2023 shows that projections of an increased global temperature average from 1.4°C to 4.4°C.

The rise in global average temperature is putting freshwater resources at major risk through accelerated melting of glaciers. The prolonged drought of the last 10 years has caused large financial losses to all countries with developed agriculture and reduced possibilities to recover water reserves in the soil to ensure good or average yields for the global food supply over time.

Reducing pollution, conserving carbon dioxide in the soil by 2030 are just some of the projects on the UN Agenda 2020-2030.

RESULTS AND DISCUSSIONS

In order to create a greener and more prosperous future, legislative initiatives by individual countries are needed, which in theory should create a robust and well-defined resilience plan.

Climate change is of interest to all. It affects almost every socio-economic sector, from agriculture to tourism, from infrastructure to health. It impacts on strategic resources such as water, food and energy. They slow down and even threaten sustainable development, and certainly not only in developing countries. The cost of inaction is high and will become even higher if we do not act immediately and decisively.

Climate change is an imminent threat to the world we live in, but we can all do something about it: combat it and build a better future. Under the Kyoto Protocol, the European Commission has presented the Green Deal as the most ambitious White Paper proposal of the entire globe with clear measures to reduce greenhouse gas emissions by 55%, decarbonising the EU economy by 2030, according with the Paris Agreement (EC, 2019). Ensuring a balance between the economic and social situation must consider the essential aspects of governance and civil society, inclusiveness and recognition of the necessary interconnections between its goals and targets, make the Green Deal a precise guide to reducing the pressures posed by global warming worldwide.

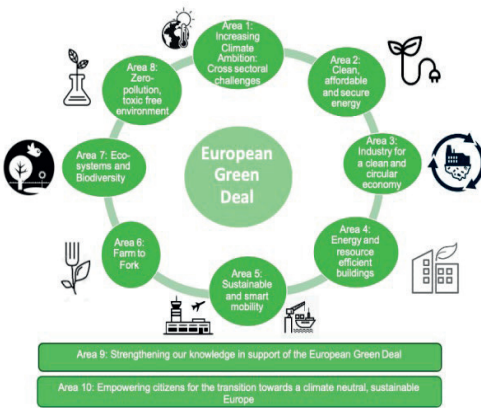


Figure 1. The EU Green Deal Structure
<https://prod5.assets-cdn.io/event/5366/assets/8399064725-d9f9a42933.pdf>

The Stern review (2006) shows that the fight against global warming would cost around 1% of global GDP each year. But if urgent action is not taken, the cost would rise to 5% of global GDP every year.

Estimates in 2024 under climate action show that financial efforts to combat global warming could amount to 20% of global GDP.

It would take much less of the world's total GDP to invest in a low-emission economy.

In December 2015 at the 12th Conference of the Parties (COP 21) the first agreement on climate change was adopted. Carbon emissions are the main drivers in climate changes and the biggest impact on climate.

CBAM (Carbon Border Adjustment Mechanism) is a European Union mechanism that aims to prevent the risk of greenhouse gas leakage that can occur when EU companies move their production to countries with less stringent climate policies or when products of European origin are replaced by similar imported products, but whose production has directly or indirectly incorporated greenhouse gas emissions (Deloitte Romania, 2023). This mechanism is also part of the EU's efforts to encourage decarbonization abroad, and push for the global pricing of greenhouse gas (GHG) emissions.

The main industries that are polluting are the production of cement, fertilizers, iron, steel chemicals, energy. These types of industries are required, that starting with 2026, to pay a tax under the name of "CBAM Certificate" in order to cover the carbon dioxide emissions.

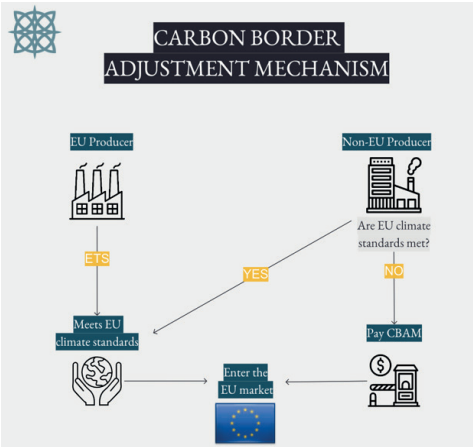


Figure 2. How CBAM works
<https://www.apalagroup.com/angles/eus-carbon-border-adjust-mechanism-cbam-impact-on-asia>

This mechanism should guarantee that importers of pollutant-intensive products into the EU pay

the same price for carbon as domestic EU producers.

The CBAM rules will be implemented in several stages, starting with a transitional period that came into force from 1 October 2023. The period from 1 October 2023 to 31 December 2025 is defined as a transitional period with no obligation to pay a fee. After completion of the transition period, the CBAM is fully operational as of 2026. The major concern will be what CBAM reporting entails and which products are covered. There is a CBAM fee which brings with it the methodology of calculation. Priority will be given to those technologies that will lead over time to a reduction in carbon emissions. Perception of the readiness of the socio-economic space to implement CBAM, "Fit for 55" contains a set of rules, directions and proposals to meet the European Union's climate goal of at least 55% emission reductions by 2030.

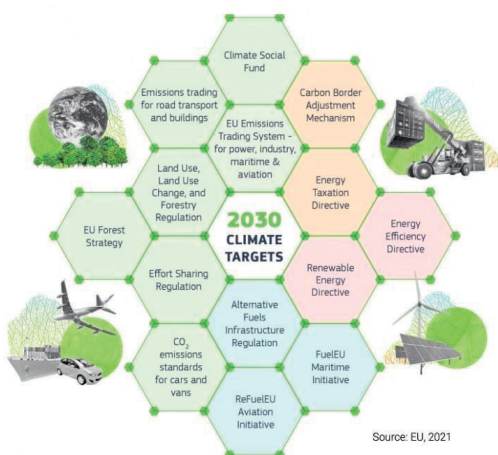


Figure 3. Understanding "Fit-for-55", (EU, 2021)

The "Fit for 55" package is a set of proposals to revise and update legislation to ensure that EU policies are in line with the climate targets agreed by the Council and the European Parliament. "Fit for 55" is defined as the European Union's objective to reduce net greenhouse gas emissions at least 55% by 2030. "Fit for 55" is considered a tool used by the European Union to a greener transition. The main purpose of "Fit for 55" is to turn the goals into laws.

The package of proposals aims to put in place a coherent and balanced framework to achieve the climate targets, as follows:

1. Providing an equitable and socio-balanced transition;
2. Innovation and competitiveness in EU industry and with third country operators;
3. European Union is recognised as a leader in climate change fight.

The proposals in the "Fit for 55" package were first presented and discussed at technical level in the Council working groups responsible for the specific policy area. Subsequently, they were discussed by Member States' ambassadors to prepare the ground for the agreements to be reached by the 27 Member States. Under the ordinary legislative procedure, the Council then engages in negotiations with the European Parliament to reach a common agreement with a view to the final adoption of the legislative acts. The "Fit for 55" legislative package:

1. Reform of the EU Emissions Trading Scheme (EU ETS) - is a carbon market based on a cap-and-trade system for energy-intensive industries and the power generation sector.

This is the main instrument used by the European Union to reduce emissions. Since 2005, EU emissions have fallen by 41%.

The "Ready for 55" package aims to reform the EU ETS to make it more ambitious, so the proposals are as follows:

- Extension to emissions from shipping;
- Faster reduction of emission allowances in the scheme and phasing out of free allowances for certain sectors;
- Implementation of the Carbon Offsetting and Reduction Scheme for International Aviation (CORSIA) worldwide through the EU ETS;
- Increased funding for the Modernisation Fund and the Innovation Fund;
- Review of the Market Stability Reserve.

The programme "Fit for 55" is considered to be a support for most affected citizen and industries and to boost renewable sources for life, energy, transport and industry.

A new stand-alone emissions trading system has been created for buildings, road transport and fuels for other sectors. The Environment

Council adopted a general approach on the EU ETS review in June 2022.

The Parliament of the European Union and the Environment Council reached an agreement to reduce emissions in the EU ETS sectors to 62% by 2030, compared to the proposed 61% target. A (provisional) political agreement was also reached on the revision of the rules of the EU Emissions Trading Scheme for aviation.

The agreement is a guarantee that aviation is committed to and guarantees the EU objectives that are part of the EU ETS.

In December 2022, the Council adopted a decision on the notification of offset requirements under CORSIA. CORSIA (Carbon Offset and Reduction Scheme for International Aviation) is a global scheme to offset CO₂ emissions from international aviation.

For the period 2024-2027, Romania wants to increase the national perspective of balanced economic development through the funding negotiated under the National Recovery and Resilience Plan (NRRP). Romania will have at its disposal almost €80 billion (€46.3 billion in non-reimbursable funds from the EU Multiannual Budget for 2024-2027 and €33.5 billion from the NextGenerationEU (economic recovery fund). Priorities are projects for: Cohesion, agriculture and infrastructure (Cohesion policy €18.57 billion), Common Agricultural Policy (€12.5 billion for direct payments and €6.22 billion for rural development), Fair Transition Fund (€7.6 billion). Our future is looking closely at the open and developed economies of the world.

In a world where EU carbon regulations are constantly evolving, it is important to have clear information and support in complying with the new regulations.

Expectations are very high as we all want economic predictability, fair and concrete partnerships, a return to normality, if we can still hope for that.

CONCLUSIONS

A memorandum has been signed by all countries of the world that every five years each country will submit a transparent report showing the nationally determined contributions to economic

and social climate change that have resulted in climate change mitigation.

Measures, such as financial support from each country under the Climate Change Plan should highlight water conservation, crop rotation, public planning, public awareness, raising the height of dams, increasing renewable energy, forest conservation, associated with the negative effects of climate change (CCS, 2023)

Ratification of the agreement requires that at least 55% of total global GHG emissions be formally ratified after Paris, globally.

Of course, the Paris Agreement of 5 October 2016 ratified the effort of all countries in the world with the ambition to decrease global GHG emissions by more than 50%.

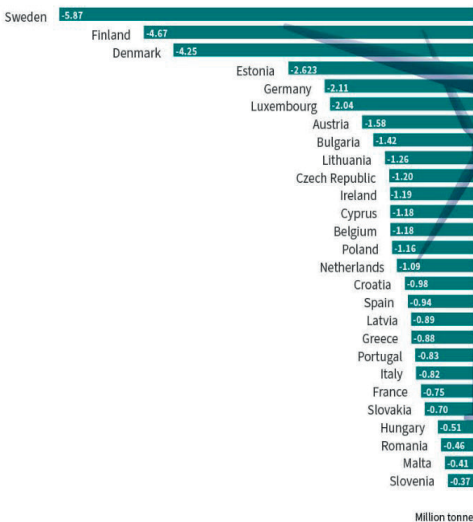


Figure 4. Quantity of emissions avoided due to renewable energy, million tons of CO₂
Fit for 55: how the EU plans to boost renewable energy - Consilium (europa.eu)

We are today in 2024 in front of clear evidence that every country has received the financial contribution dedicated to climate change under the Paris Agreement. In the countless conferences I have attended in many of the world's countries, I have found that the Renewable Energy Directive by 2030 appears to be the most ambitious with reversible results.



Figure 5. EU targets for 2030

Fit for 55: how the EU plans to boost renewable energy - Consilium (europa.eu)

A large part of Romania's carbon emissions is produced by the coal industry, which is causing our country to reconfigure this type of industry. Cars and trucks produce around 15% of the EU's CO₂ emissions, so reducing them can make a significant contribution to fighting climate change. EU legislation sets clear emission limits that manufacturers must respect.

Studies on the influence of climatic factors on the various modes of transport as well as on new technologies resilient to the effects of climate change are essential to ensure that Romania's transport system will not be affected by expected or unexpected climate change.

Mobility planning policies need to be improved and alternative and environmentally friendly means of transport need to be supported, especially in urban areas.

Romania's green economy transition needs to focus on sustainable energy. The country has signed up to the Paris Agreement and targets a 40% reduction in greenhouse gas emissions by 2030.

Romania was the first EU country to achieve the bloc's target of 20% renewables share ahead of the 2020 deadline, but investment in renewable energy has stalled in recent years due to a lack of commitment (EBRD, 2022).

Soil energy, hydropower, wind energy, biomass energy contributes at least one third of total EU energy consumption for electricity generation, transport, heating and cooling.

Now, more than ever, we need to realise that the climate and environmental crisis is intensifying year by year.

The droughts of recent years have dramatically reduced agricultural production, putting great obstacles in the way of future agricultural planning. Devastating fires in European countries, as well as around the world, have

brought the resilience of global climate disasters into focus. Floods, too, have posed serious problems in Southern European countries (Greece, Italy, Cyprus, Spain). The danger is common and as a result every country must contribute to our adaptation, that of all mankind. Climate neutrality is no longer just a story with frothy declarations, it needs a White Carta of the Responsibilities of all countries in the world.

I hope we can all contribute to what decarbonisation of the European Union means. Of course, this is not easy, but Romania is easily and safely on the path to achieving the "Fit for 55" targets.

Sustainable Development is about ensuring a balance between the economic and social dimensions considering the essential aspects of Government and Civil Society, inclusive and recognising the necessary interconnections between its objectives and targets.

The essence of the sustainable development of human society lies in the current and future management of its natural, energy, material, and information resources in relation to the objectives of economic growth and ensuring an increasingly high quality of environment and life.

ACKNOWLEDGEMENTS

Year after year, the Foundation "Group for Ecological Initiative and Sustainable Development", a public utility organization under the auspices of the Ministry of Environment, headed by its President, PhD. Eng. Cristiana Sirbu and Mr. Ion Iliescu, the Founding President, campaigns for better environmental protection and the fight against climate change. In almost 20 years of activity, we have carried out reforestation campaigns, forums for sustainable development with partners from civil society, academia, the Romanian Government, the European Union, World Watch Institute, Earth Policy.

The paper is a sum of all themes and subjects of discussion approached in the conferences, seminars and online events attended in the last years.

REFERENCES

Borzykh O., Chaika, V., Schevchuk, O., Borysenko, V. & Janse, L. (2023). Long-term (2005-2020) winter wheat

- pest population dynamics in Ukraine in response to effects of acreage treated with insecticides and climate change. *AgroLife Scientific Journal*, 12(2), 35–45. <https://doi.org/10.17930/AGL202325>
- Cadar, N., Pitar, D., Iacoban, C., Căntar, I.-C. (2023). The influence of forests from lunca Mureșului natural park on greenhouse gases levels. *Scientific Papers. Series E. Land Reclamation, Earth Observation & Surveying, Environmental Engineering, XII*, Print ISSN 2285-6064, 31-37.
- Climate Change Summit, CCS (2023). *Social Innovation Solutions*. Available online: <https://www.socialinnovationsolutions.org/climate-change-summit>
- Deloitte Romania (2023). *Webinar: CBAM reporting and charging - what does it mean and how does it apply?* Available online: <https://www2.deloitte.com/ro/ro/pages/about-deloitte/events/raportarea-si-taxarea-cbam-ce-inseamna-si-cum-se-aplica.html>
- EBRD in Romania (2022). *Green Economy Transition*. Available online: <https://2022.tr-ebrd.com/>
- European Commission, EC. (2019). *Communication From The Commission, The European Green Deal*. Available online: <https://eur-lex.europa.eu/legal-content/EN/TXT/?uri=CELEX:52019DC0640>
- European Union, EU (2021). *European Green Deal*. Available online: https://ec.europa.eu/info/strategy/priorities-2019-2024/european-green-deal_en
- European Union, EU (2023). *Fit for 55: how the EU plans to boost renewable energy*. Available online: Fit for 55: how the EU plans to boost renewable energy - Consilium (europa.eu)
- Intergovernmental Panel on Climate Change, IPCC. (2023). *Global Warming of 1.5°C*. Available online: <https://www.ipcc.ch/sr15/>
- Stern, N. (2006). *Stern Review: The Economics of Climate Change*. Cambridge University Press, Cambridge.
- The Ministry of Research, Innovation and Digitisation (2023). "Danube and Black Sea Lighthouse" event as part of the EU Mission "Restore our Ocean and Waters by 2030" under the Horizon Europe programme. <https://prod5.assets-cdn.io/event/5366/assets/8399064725-d9f9a42933.pdf>
- <https://www.apalagroup.com/angles/eus-carbon-border-adjust-mechanism-cbam-impact-on-asia>

PHYTOCHEMICAL PROFILE OF LEMON BASIL GROWN IN AQUAPONIC CULTURE

**Irina TOMASU, Simona MARCU SPINU, Mihaela DRAGOI CUDALBEANU,
Constanta MIHAI, Petronela ROSU, Raluca PASCU, Alina ORTAN**

University of Agronomic Sciences and Veterinary Medicine of Bucharest,
59 Marasti Blvd, District 1, Bucharest, Romania

Corresponding author email: rosupetronelamihaela@yahoo.com

Abstract

*A traditional aromatic culinary plant, basil (*Ocimum spp.*) also offers a wide range of potential health benefits, including antioxidant, anti-inflammatory and anticarcinogenic effects. Multiple varieties cultivated around the world, ranging from the traditional *Ocimum basilicum* - sweet basil to Genovese basil, cinnamon basil, purple basil, holy basil, etc, were investigated for their therapeutic properties due to their high content of antioxidant compounds. The aim of this study was the phytochemical analysis of a lemon-flavored basil, with seeds procured from Kiepenkerl. To promote a circular economy, the lemon basil was grown together with yeast biomass fed fish in an aquaponic system. The samples consisted of basil grown with: different percentages of yeast biomass added to conventional fish feed, regular fish feed, and traditional soil-based technologies. The phytochemical composition of the samples was assessed following microwave-assisted extraction. The evaluation included antioxidant activity (DPPH, FRAP, ABTS assays), as well as total phenolic and flavonoid contents. Among the 14 compounds identified in the UPLC investigation, caffeic acid and rosmarinic acid had the highest content in all the samples.*

Key words: aquaponic culture, antioxidant activity, flavonoid content, *Ocimum basilicum*, UPLC, total phenolic count.

INTRODUCTION

Food production depends on the availability of resources and nutrients, which are currently depleting faster than they can be generated for a global population that is estimated to reach 10 billion people by 2050 (FAO, 2017). This growth is expected to occur in a world where climate change, biodiversity decline, and the degradation of arable land are already leaving a mark, which makes providing the appropriate food production levels worldwide an even bigger challenge. In order to combat this situation, alternative ways to soil based plant cultivation are currently being researched and practiced, among which aquaponics systems represent a viable option (Goddek et al., 2019). Aquaponics systems work on the basis of nutrient exchange between a hydroponic unit and an aquaculture unit with the help of the nitrification process initiated by nitrifying bacteria. Metabolites resulting from the food digestion of various fish species are transformed in a two-step nitrification process. Ammoniac is oxidized to nitrites by *Nitrosomonas* type of bacteria, being further

oxidized to nitrates by *Nitrobacter*, which leads to an easier access to nitrogen, an essential component for plant growth and its protein synthesis (Rana et al., 2019).

The simultaneous cultivation of both plants and fish can lead to economic benefits since two types of cultures are obtained and production can increase because of nutrient recycling and the reduced consumption of water. Advantages include a reduced impact on the environment, a continuous plant production throughout the year, as well as the end result of organic cultures with a minimum amount of added chemical substances (Joyce et al., 2019; Greenfeld et al., 2022; Albadwawi et al., 2022). The foremost characteristics among the fish species used in this type of cultivation system consist of their capacity to tolerate higher densities of population and increased values of solid particles, nitrogen, phosphorus and potassium. Often utilized fish species include Nile tilapia, carp and African catfish (Lennard et al., 2019; Yep & Zheng, 2019).

Plant cultures with a high tolerance towards disease and pests, that develop well in water with high concentrations of nitrogen with

shorter growth periods and without high nutritional requirements are preferable in the case of aquaponics systems. Among the most used plants grown in aquaponics systems, Love et al. (2015) mention *Ocimum basilicum* (81%), *Solanum lycopersicum* (68%), *Lactuca sativa* (68%), *Brassica oleracea* (56%), *Beta vulgaris* (55%), *Brassica rapa* subsp. *chinensis* (51%), *Capsicum annuum* (piper) (48%) and *Cucumis sativus* (45%).

O. basilicum renders itself as a suitable plant for aquaponics, which is an advantage given its potential as a medicinal plant and its historically demonstrated therapeutic effects. Part of the aromatic *Lamiaceae* family, it has a variety of over 65 cultivars, such as sweet basil, purple basil, Genovese basil, holy basil, cinnamon basil, that mostly prefer subtropical climate (Makri & Kintzios, 2008). It is an Asian native plant traditionally used in the treatments of fever, coughing, headaches and digestive problems (Shahrajabian et al., 2020). Its high content in polyphenols and flavonoids determines a wide array of anti-inflammatory, anticancer, antioxidant, antiviral and antibacterial properties. In a 2019 study, Singh et al (2019) found that ethanol extracts from basil leaves inhibited Zika virus replication in Vero E6 cells, with a maximum inhibitory concentration (IC₅₀) of 1:134. Other studies have also demonstrated antiviral activity against viruses, such as herpes, adenovirus, hepatitis B, and enterovirus 71 (Azizah et al., 2023). In a 2022 study, Dharsono et al. (2022) observed inhibition zones of 20-40 mm of essential oils from various basil species against both Gram-positive and Gram-negative bacteria. In a 2021 study, Ciotea et al. (2021) tested basil essential oil obtained by steam distillation against bacteria, which displayed a strong antibacterial activity against *S. pyogenes*, *S. viridans*, and moderate to low one for the *S. pneumoniae*, *K. pneumoniae*, *E. coli*, *E. faecalis* bacteria.

Basil's anti-inflammatory effects are attributed to compounds like linalool, estragole, methyl cinnamate, and methyl eugenol. Basil essential oil inhibits lipogenesis at low concentrations, while plant extracts suppress nitric oxide (NO) production (Brandão et al., 2022). Additionally, basil extracts exhibit stronger anti-inflammatory activity than aspirin by

preventing egg albumin denaturation (Akoto et al., 2020). Plant extracts of *O. basilicum* can act against cancer by inducing cytotoxicity in MCF7 mammary cancer cells (Koolamchal et al., 2022). All these properties display the high nutraceutical potential basil possess.

The present study aims to investigate the phytochemical profile of a lemon flavoured basil grown in an aquaponic culture following a differentiated diet regime for the fish, consisting of a combination between industrial feed and various proportions of *Saccharomyces cerevisiae*, in order to highlight the differences between the antioxidant properties of the various methods of cultivation.

MATERIALS AND METHODS

The aquaponic system was composed of a reservoir with dimensions of 47x37x42 cm and a volume of 73 cm³ (Figure 1). The biofilter used for the development of nitrifying bacteria consisted of expanded clay granules. The system was complemented by an EHEIM compact 300 pump with a capacity of 150-300 l/h and 5W power, as previously implemented in a 2016 study (Frincu & Dumitrache, 2016). The fish species present in the aquaponic system were *Carassius auratus* and *Hypostomus plecostomus*.

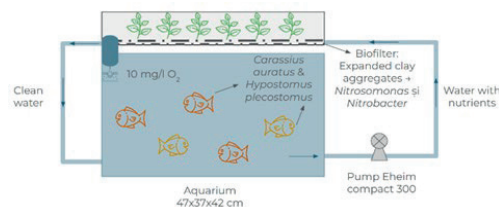


Figure 1. Schematic representation of the aquaponics system

The lemon-flavored basil seeds “Sweet Lemon” were obtained from the Kiepenkerl company and sown using sterilized Jiffy peat pellets with a diameter of 50 mm. Basil samples were obtained through different dietary regimes for the fish: one sample was raised by feeding the fish industrial feed – further utilised in the experiment with the M1 code, another by providing experimental feed with 3% yeast biomass – marked as P1, and a third by feeding with 5% yeast biomass – marked as P2. As a

control, basil plants were grown in soil and marked with the M2 code. The feed and yeast biomass mixture were prepared by incorporating *Saccharomyces cerevisiae* yeast into pellet feed. A total of 1000 g of commercial feed pellets were transformed into dough, pelletized, and dried for 24 hours at 40°C. The fish were fed a daily amount equivalent to 2.5% of their total body weight. The basil extracts were prepared using the Milestone ETHOS X microwave extraction system (Milestone, Sorisole, Italy). The mature, freeze-dried basil plant was finely ground into a homogenous powder at 4500 rpm using the Grindomix GM mill (Retsch, Dusseldorf, Germany). From each of the four basil samples, approx. 1.5 g of plant material was weighed and mixed with ethanol at varying concentrations (50%, 70%, and 100%) in plant-to-solvent ratios of 1:20 and 1:40. This resulted in a total of 24 hydroalcoholic extracts (as detailed in Table 1). The extraction process involved maintaining a temperature of 100°C for 60 minutes with a power output of 500W. Subsequently, the plant-solvent mixture underwent vacuum filtration using Whatman filter paper No. 1. The resulting extract was then utilized for various analyses, including DPPH, ABTS, FRAP, determination of total phenolic and flavonoid content, and UPLC chromatographic analysis.

Table 1. Hydroalcoholic extracts

Sample code	Plant mass (g)	Plant: solvent ratio	EtOH (%)
P1.1, P2.1, M1.1, M2.1	1.5	1:20	50
P1.2, P2.2, M2.1, M2.2	1.5	1:20	70
P1.3, P2.3, M1.3, M2.3	1.5	1:40	50
P1.4, P2.4, M1.4, M2.4	1.5	1:40	70
P1.5, P2.5, M1.5, M2.5	1.36	1:20	100
P1.6, P2.6, M1.6, M2.6	1.36	1:40	100

The extraction yield of hydroalcoholic extracts was obtained by weighing the mass of the plant material and the solvent before and after filtration.

Total content of phenolic acids

The content of phenolic acids was determined using the Folin-Ciocalteu method, adapted for microspectrophotometer method according to a previous study published in 2023 by Marchidan et al. The reference standard used was gallic acid and the results were expressed in

milligrams of gallic acid equivalents per kilogram of plant material (mg GAE/kg). All extracts were analysed in triplicate by absorbance measurements at 760 nm.

Total flavonoid content

The total flavonoid content was determined using the microspectrophotometer method. (Marchidan et al., 2023) After incubation in the dark for 15 minutes, the absorbance was read at 415 nm and the results were expressed in milligrams of quercetin equivalents per kilogram of sample (mg EqQ/kg).

Antioxidant activity

The antioxidant activity was assessed using the microspectrophotometer method with DPPH (2,2-diphenyl-1-picrylhydrazyl) reagent, as presented in a previous paper by Marchidan et al. (2023), the absorbance of each sample was measured at a wavelength of 517 nm. The inhibition percentage, indicative of antioxidant activity, was calculated using the equation:

$$\text{Inhibition percentage} = \frac{\text{Control absorbance} - \text{Sample absorbance}}{\text{Control absorbance}} \times 100$$

The antioxidant content was also calculated using the ABTS⁺ cation radical solution, using the method presented earlier in a study in 2023 (Marchidan et al., 2023). The absorbance was measured at 734 nm and the inhibition percentage was calculated using the following formula:

$$\text{Inhibition percentage} = \frac{\text{Control absorbance} - \text{Sample absorbance}}{\text{Control absorbance}} \times 100$$

The FRAP (Ferric Reducing Antioxidant Power) solution was prepared using an adapted microspectrophotometer method and the absorbance was measured at 593 nm. The antioxidant capacity was calculated using the following equation:

$$\text{Antioxidant capacity} = \frac{\text{Sample absorbance after 20 minutes} - \text{Initial absorbance}}{\text{Positive control absorbance} - \text{Initial absorbance}} \times 2$$

The results were expressed in milligrams of ascorbic acid equivalents per kilogram of sample (mg EqAA/kg).

Chromatographic assay

The separation, identification and quantification the polyphenolic compounds

present in the extracts were analysed using Acquity UPLC I Class system (Waters Corporation, Milford, Massachusetts, U.S.), with a Zorbax Eclipse Plus C18 column (100 mm x 4.6 mm, with a 5 µm sized particles) and an injection volume of 10 µl. The temperature was set at 30°C, and the mobile phases consisted of (A) 0.1% formic acid in water and (B) 0.1% formic acid in acetonitrile. The elution gradient spanned 0-100% B over 30 minutes, with a flow rate of 0.8 mL/min. 14 reference compounds were used, including caffeic acid, rosmarinic acid, chlorogenic acid, epicatechin, p-coumaric acid, rutin, isoquercetin, ferulic acid, naringin, myricetin, luteolin, quercetin, and naringenin. Detection wavelengths of 280 nm, 320 nm, and 370 nm were employed. Identification and quantification were performed by comparing retention times with reference compounds. Stock solutions of reference compounds were prepared at a concentration of 12 mg/ml, and linear concentrations of 5-150 µg/ml were used to create calibration curves.

RESULTS AND DISCUSSIONS

Microwave-assisted extraction was chosen due to its reduced operating time compared to classical methods such as maceration or ultrasonication, which allows for improved efficiency and cost-effectiveness, as well as reduced degradation of the compounds of interest. Heating the solvents and samples enhances the transition of compounds from the plant matrix into the solvent. Ethanol was selected as the extraction solvent due to its low toxicity, enabling integration of the extract into food or pharmaceutical products. The presence of water in the hydroalcoholic extract alongside the polar solvent determines more efficient heating and facilitates the extraction process (Sonar & Rathod, 2020).

The extraction yield obtained (Table 2) indicate the highest values for the EtOH extraction of 50% and 70% with a plant: solvent ratio of 1: 40 for both concentrations. The extraction yield range varies between 53.98% and 86.17%, the highest yield being observed in the control group cultivated in soil (86.17% for M2.3, 83.75% for M2.4, and 84.59% for M2.1). Following this, the samples obtained through

3% yeast biomass feeding at a 1:40 ratio and using EtOH concentrations of 50% and 70% exhibit yields of 81.68% (P1.3) and 79.90% (P1.4), respectively.

Table 2. Extraction yield

Sample	Plant (g)	Plant:solvent ratio	EtOH (%)	Yield (%)
P1.1	1.50	1:20	50	65.65
P1.2	1.50	1:20	70	68.85
P1.3	1.50	1:40	50	81.68
P1.4	1.50	1:40	70	79.90
P1.5	1.36	1:20	100	62.22
P1.6	1.36	1:40	100	80.53
P2.1	1.50	1:20	50	64.84
P2.2	1.50	1:20	70	55.57
P2.3	1.50	1:40	50	76.29
P2.4	1.50	1:40	70	77.25
P2.5	1.36	1:20	100	63.73
P2.6	1.36	1:40	100	53.98
M1.1	1.50	1:20	50	67.57
M1.2	1.50	1:20	70	63.77
M1.3	1.50	1:40	50	78.73
M1.4	1.50	1:40	70	77.19
M1.5	1.36	1:20	100	61.72
M1.6	1.36	1:40	100	72.74
M2.1	1.50	1:20	50	84.59
M2.2	1.50	1:20	70	75.35
M2.3	1.50	1:40	50	86.17
M2.4	1.50	1:40	70	83.75
M2.5	1.36	1:20	100	62.81
M2.6	1.36	1:40	100	73.63

Total content of phenolic acids

TPC was performed using a calibration curve with a known standard. Based on the absorbances measured at concentrations of 0.20, 0.39, 0.78, 1.56, 3.15, 6.25, 12.50, 25, 50, and 100 µg/ml, a calibration curve was constructed using gallic acid as the reference standard. The total polyphenol content was expressed in milligrams of gallic acid equivalents per kilogram (mg GAE/kg) using the arithmetic mean of the three readings performed for each individual sample. Higher values were observed in the extracts obtained from basil cultivated in aquaponic systems and fish fed with a combination of industrial feed and 3% yeast biomass, as seen in Figure 2.

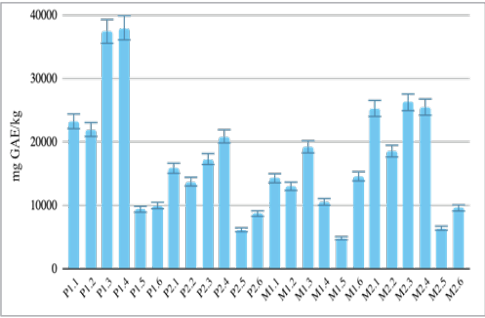


Figure 2. Total polyphenolic content of the basil samples expressed as mg GAE/kg

The best results were achieved through microwave-assisted extraction using 50% and 70% ethanol (EtOH) in a plant:solvent ratio of 1:40. Specifically, the concentrations of active compounds (expressed as gallic acid equivalents, GAE) were P1.3 = 37403 mg/kg and P1.4 = 37970 mg/kg. Notably, relatively high values ranging from 25271 to 26226 mg were also found in the control group of basil grown in soil, particularly at the 1:20 ratio with 50% EtOH concentration and the 1:40 ratio with both 50% and 70% EtOH concentrations. Compared to the highest value obtained for TPC in this study, 37.403 mg/g GAE, Nadeem et al (2022) reported a higher content of 191.2 mg GAE/g in basil extracted with ethanol and lower TPC of 29.7 mg/g in basil extracted with *n*-hexane. In a 2022 study, Romano et al obtained for supercritical CO₂ extracts from “Italiano Classico” and “Genovese” cultivars TPC values of 72.15 and 79.62 mg GAE/g, respectively, while the ethanol extraction method yielded TPC values of 91.66 and 98.99 mg GAE/g for the same cultivars. These findings suggest a possible difference in TPC values due to different extraction methods and different cultivars. According to Albadwawi et al. (2022), total phenols of aquaponic grown basil displayed higher values than soil grown plant, which is different compared to the control TPC values obtained in the present study.

Total flavonoid content

The quantification of total flavonoids was expressed in correlation with a standard calibration curve having quercetin as a reference. The calibration curve was plotted

using a series of decreasing concentrations starting with 100 µg/ml and ending with 1.56 µg/ml. Figure 3 indicates the highest value as 2958.40 mg QE/kg obtained for the control basil grown in soil and extracted with EtOH 70% in plant: solvent ratio of 1:40. All the basil samples showed higher values for a EtOH concentration of 70% in a plant solvent ratio of 1:40.

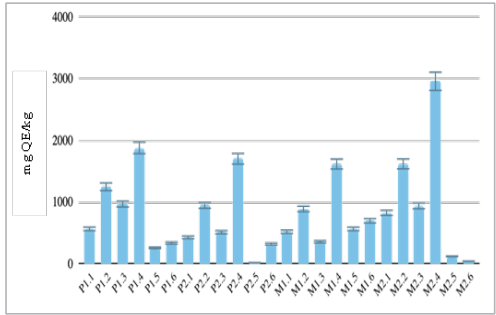


Figure 3. Total flavonoid content of the basil samples expressed as mg QE/kg

Antioxidant activity

The antioxidant activity determined by the inhibition of the DPPH radical was superior for the samples prepared in a 1:20 plant: solvent ratio, as can be observed in Figure 4, regardless of the concentration levels of ethanol (50% or 70%), which suggests that the antioxidant activity is not dependant on the total polyphenolic content in the case of the investigated basil species.

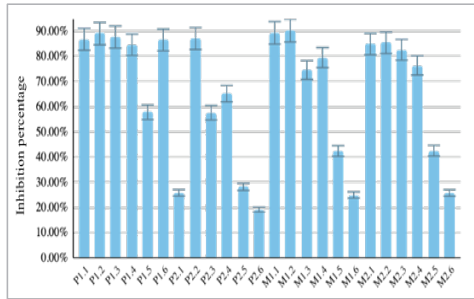


Figure 4. Antioxidant activity obtained following the inhibition of the DPPH radical

Highest values ranged between 86% and 89% for the basil grown with fish fed with a 3% yeast biomass, while the maximum value of 90.21% was registered for the sample grown

with fish fed with just industrial feed, results similar in range to those obtained by DPPH assay by Nadeem et al for ethanolic extracts (82.4%). Figure 4 also indicates lower numerical results for the samples obtained with 100% EtOH and a plant:solvent ratio of 1:40.

The antioxidant potential of the samples was expressed as a percentage of ABTS^{•+} cationic radical inhibition and ranged for almost all samples between 90-100%, as shown in Figure 5, with maximum values of approx. 96% obtained by the sample grown with fish fed with 5% yeast biomass and a plant: solvent ratio of 1:20. Similarly to the results of the DPPH test, the lowest values were found for the 100% EtOH concentration and a 1:40 ratio, where the inhibition percentage ranged from 20-45%. These results suggest that the extraction made with a binary solvent leads to superior results regarding the antioxidant activity. The higher percentage of inhibition for ABTS assay compared to DPPH is similar to the results obtained by in 2022 by Romano et al., suggesting the ABTS assay exhibits distinct reactivity with various components and follows different pathways compared to the DPPH assay.

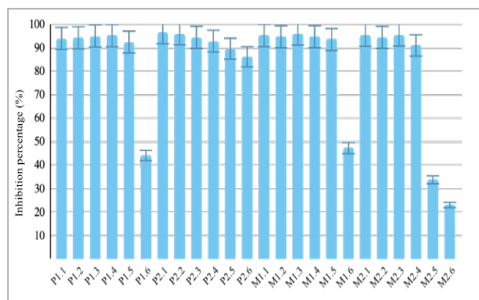


Figure 5. Antioxidant activity obtained following the inhibition of the ABTS radical

For the FRAP assay, the antioxidant potential of basil extracts was expressed in terms of antioxidant activity equivalents, specifically in

milligrams of ascorbic acid equivalent per kilogram of plant material. The results are shown in Figure 6. The highest values are observed for sample P1.3 = 38800.07 mg AA/kg and P1.4 = 40233.39 mg AA/kg, corresponding to basil cultivated in an aquaponic system with fish fed a mixture of industrial feed and 3% yeast biomass, a plant: solvent ratio of 1:40 and 50% and 70% EtOH concentrations. Other values fall within the range of 14000 to 28000 mg AA/kg, except for the samples extracted with 100% EtOH which feature lower values.

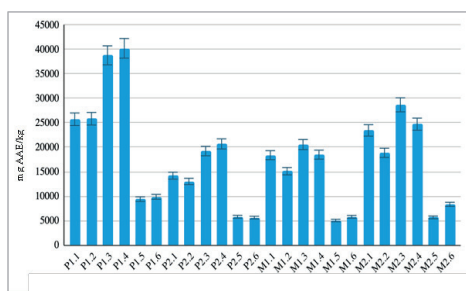


Figure 6. Antioxidant activity resulted from FRAP analysis expressed in mg AAE/kg

Chromatographic assay

To identify and quantify polyphenolic compounds in the hydroalcoholic basil extracts, 14 reference compounds were used, as mentioned in the Materials and Methods subsection. For identification, the retention times of these reference compounds were compared with those obtained during the separation of each basil extract.

The hydroalcoholic basil extracts were analyzed at three fixed wavelengths (280 nm, 320 nm, and 370 nm), selected based on the λ_{max} value obtained from molecular absorption spectra in the 200–400 nm range and relevant literature. Figure 7 represent an exemplification of the chromatograms obtained in case of P1.3 sample, for all three λ values considered.

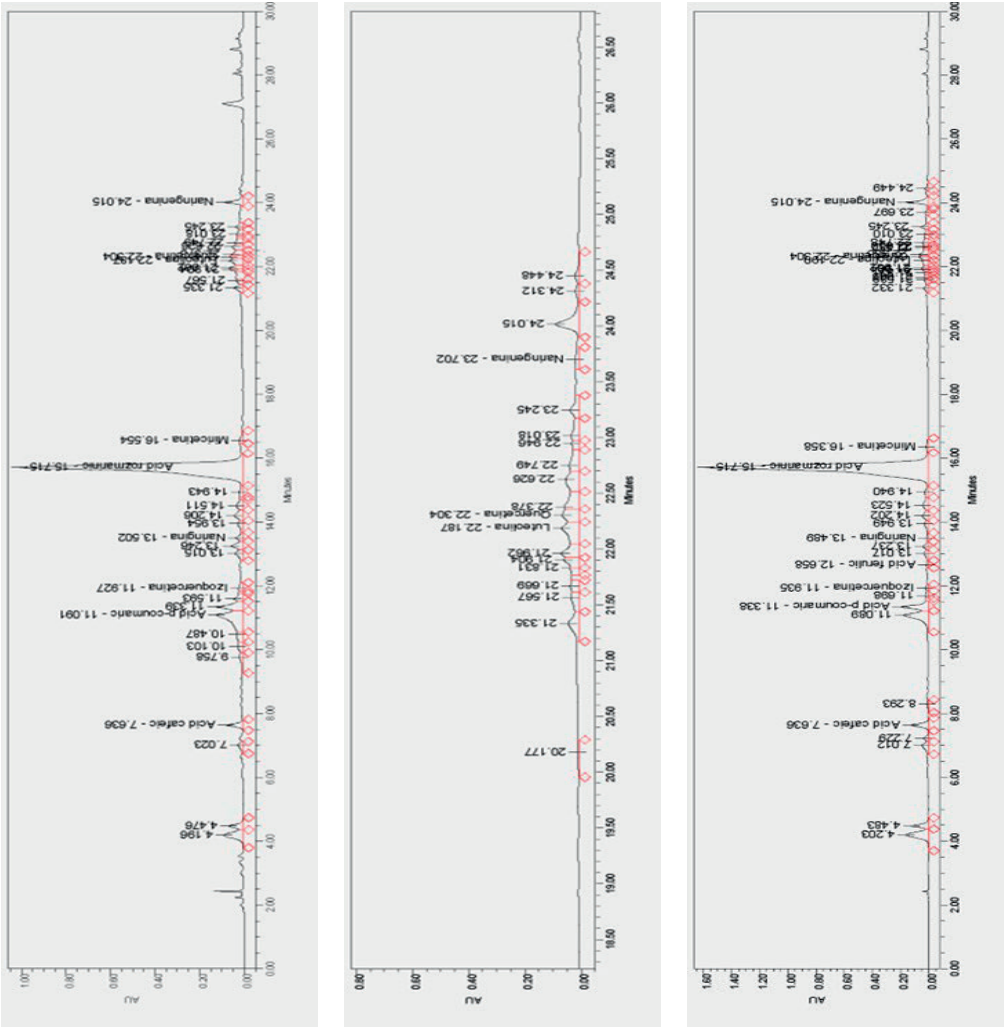


Table 3. Quantification of compounds in the basil extracts at λ_{max} expressed in mg of compound/kg of plant

Sample	GA	CH	CA	CF	EP	PC	IS	FA	NA	RS	MY	LU	QE	NR
P1.1	910.66	76.83	24.64	4684.55	35.21	325.68	52.99	70.14	380.28	115.05	61.71	163.41	126.79	124.65
P1.2	1145.69	117.83	ND	4454.50	26.49	322.01	31.39	99.01	384.22	108.40	64.79	212.12	119.37	95.03
P1.3	ND	95.06	165.77	6352.63	71.33	599.30	105.25	135.90	495.86	20288.80	146.08	556.88	273.51	123.93
P1.4	ND	107.98	45.70	5708.33	67.45	539.82	58.46	175.91	493.68	107.76	144.24	727.54	266.41	175.15
P1.5	ND	22.95	36.23	36.71	22.58	31.88	14.78	47.70	44.40	22.84	ND	120.11	80.43	40.70
P1.6	47.52	53.19	58.44	123.93	53.60	48.66	32.804	110.59	51.73	3897.44	ND	255.74	196.74	94.97
P2.1	473.73	71.53	19.34	3821.31	27.27	356.28	54.35	56.84	56.70	7883.78	61.94	206.04	111.56	54.46
P2.2	981.68	67.40	ND	2594.03	18.80	195.55	19.60	73.49	24.99	56.15	52.58	156.30	85.66	42.47
P2.3	ND	72.45	47.46	2542.86	55.83	385.95	56.07	103.08	88.77	7688.73	135.33	332.19	211.47	105.24
P2.4	1711.23	91.45	6579.96	1805.22	590.33	387.20	44.99	127.82	218.32	6432.85	138.52	317.12	262.69	102.46
P2.5	ND	21.26	20.90	39.72	21.84	47.47	25.91	43.93	19.12	2265.98	ND	101.30	74.30	39.71
P2.6	45.94	45.47	45.00	50.53	45.76	44.41	39.55	94.74	43.47	48.03	ND	211.90	167.88	204.00
M1.1	ND	26.47	94.21	1196.11	22.18	137.72	24.81	48.87	32.20	11513.20	57.05	228.39	80.70	103.40
M1.2	ND	23.32	25.92	729.32	24.90	99.04	17.80	43.88	25.72	6537.94	55.40	178.22	76.19	77.29
M1.3	ND	49.97	58.44	963.34	43.82	171.57	39.55	95.75	58.22	12348.20	124.53	333.38	165.04	141.31
M1.4	ND	49.08	ND	463.34	40.68	153.13	32.82	101.70	48.92	7954.32	128.13	320.91	164.39	140.95
M1.5	ND	14.09	12.84	17.96	143.30	13.98	ND	30.02	13.42	2774.76	ND	79.07	52.77	29.32
M1.6	35.03	ND	46.99	81.90	32.52	32.33	21.42	71.16	32.70	3246.43	ND	170.64	127.76	75.69
M2.1	2393.43	130.22	ND	3469.53	25.47	477.8	144.7	106.05	54.16	10393.50	77.81	484.14	123.88	748.56
M2.2	ND	92.35	ND	2444.76	353.05	700.47	76.53	81.93	329.38	5506.41	70.03	259.18	134.11	183.22
M2.3	2539.07	78.18	61.2	2430.4	542.74	852.18	134.29	156.83	515.60	10745.8	166.14	481.04	279.73	133.04
M2.4	ND	71.20	ND	1169.64	51.52	862.42	95.54	149.32	392.06	6292.58	161.19	582.82	257.76	172.43
M2.5	22.42	22.49	33.70	33.37	20.34	28.81	13.49	46.07	19.31	1810.47	ND	134.31	77.47	434.55
M2.6	45.82	50.09	70.53	52.85	43.50	43.32	34.24	94.18	43.76	48.24	132.29	251.88	168.06	645.12

ND - unidentified polyphenolic compound. TA - tannic acid; GA - gallic acid; CA - catechin; CF - caffeic acid; CH - chlorogenic acid; EP - epicatechin; PC - p-coumaric acid;
FA - ferulic acid; IS - isosquercetin; MY - myricetin; RS - rosmarinic acid; NA - naringin; QE - quercetin; LU - luteolin; NR - naringenin.

The Table 3 displays the maximum concentration for each compound identified in basil extracts obtained from the aquaponic environment through feeding with industrial feed and 3% yeast biomass, the most quantitatively significant being caffeic acid, reaching a maximum value of 6352.63 mg/kg for the sample extracted with EtOH 50% and 5708.33 mg/kg for the sample extracted with EtOH 70% in a plant solvent ration of 1:40 and rosmarinic acid with 20288.75 mg/kg and 3897.44 mg/kg in for the same extraction conditions. Gallic acid was not detected in several samples (P1.3, P1.4, or P1.5), while myricetin was absent in EtOH 100% samples. For the sample grown with 5% yeast biomass fed fish, high values were obtained for the catechin in the case of the EtOH 70% and 1:40 ratio with a value of 6579.96 mg/kg. Highest value of caffeic acid (3821.31 mg/kg) was found in the EtOH 50%, 1:20 ratio, while rosmarinic acid held high values in the range of 6000-7000 mg/kg for almost all samples resulted from extraction with EtOH 50% and 70%.

In the case of the aquaponic control sample, overall lower values of the compounds were detected, compared to the sample supplemented with yeast biomass, with caffeic acid and rosmarinic acid being the highest in the case of the EtOH 50% and 1:20 ratio and EtOH 50% and 1:40 ratio, respectively.

The sample developed in soil presented the same pattern of higher values in the case of rosmarinic acid and caffeic acid, with almost halved values compared to the 3% yeast biomass fed sample, while catechin remained undetected in more than one case.

The high value of the rosmarinic acid is consistent with another study on lemon flavoured basil conducted by Majdi et al in 2020 and several studies conducted on *Ocimum basilicum* (Makri & Kintzios, 2008; Romano et al, 2022).

CONCLUSIONS

Aquaponic culture is an alternative solution to the current challenges generated by climate change and pollution, presenting several advantages, such as obtaining better production with fewer but better managed

resources. Basil, which has many beneficial health properties, is a crop that lends itself to aquaponic production because it grows well in water with high nitrogen concentrations, has low susceptibility to diseases and pests, and has minimal nutritional requirements.

The highest total polyphenol content was obtained from hydroalcoholic extraction assisted by microwaves, using EtOH as the solvent, with a plant:solvent ratio of 1:40 for the sample obtained by feeding fish with 3% yeast biomass.

The highest extraction yield was achieved from basil grown in soil and extracted with EtOH concentrations of 50% and 70%, respectively, with a plant:solvent ratio of 1:40.

Antioxidant activity, determined by DPPH radical inhibition, was superior for samples prepared with a plant:solvent ratio of 1:20, regardless of the EtOH concentration (50% or 70%).

In the ABTS test, all samples showed inhibition percentages in the range of 90-100%, except for samples extracted with 100% ethanol at a plant: solvent ratio of 1:40, where inhibition percentages were in the range of 20-45%.

HPLC analysis identified rosmarinic acid as the major phenolic compound in all basil samples studied. The aquaponically grown basil sample, obtained by feeding fish with 3% biomass, had the highest quantity, consistent with existing literature.

In conclusion, the species grown in the aquaponic system, by feeding the fish with a mixture of industrial feed and yeast biomass (3%), has been proven superior in terms of total polyphenol content, the maximum content being obtained in the case of microwave-assisted hydroalcoholic extraction (70% EtOH) and a plant: solvent ratio of 1:40, and rosmarinic acid with the maximum content in the 50% EtOH, 1:40 plant: solvent ratio sample.

ACKNOWLEDGEMENTS

This research was funded by the University of Agronomic Sciences and Veterinary Medicine of Bucharest - Romania, Research Project 846/30.06.2023, acronym EnterGreenFood in the Competition IPC 2023.

REFERENCES

- Akoto, C.O., Acheampong, A., Boakyee, Y.D., Naazo, A.A., & Adomah, D.H. (2020). Anti-Inflammatory, Antioxidant, and Anthelmintic Activities of *Ocimum basilicum* (Sweet Basil) Fruits. *Journal of Chemistry*, Article ID 2153534, 91.
- Albadwawi, M.A.O.K., Ahmed, Z.F.R., Kurup, S.S., Alyafei, M.A., & Jaleel, A. (2022). A Comparative Evaluation of Aquaponic and Soil Systems on Yield and Antioxidant Levels in Basil, an Important Food Plant in *Lamiaceae*. *Agronomy*, 12(12), 3007.
- Azizah, N.S., Irawan, B., Kusmoro, J., Safriansyah, W., Farabi, K., Oktavia, D., Doni, F., & Miranti, M. (2023). Sweet Basil (*Ocimum basilicum* L.)—A Review of Its Botany, Phytochemistry, Pharmacological Activities, and Biotechnological Development. *Plants*, 12(24), 41482.
- Brandão, L.B., Santos, L.L., Martins, R.L., Rodrigues, A.B.L., Costa, A.L.P., Faustino, C.G., & Almeida, S.S.M.S. (2022). The Potential Effects of Species *Ocimum basilicum* L. On Health: A Review of the Chemical and Biological Studies. *Pharmacog Rev*, 16(31), 22-26.
- Ciotea, D., Shamtzyan, M., & Popa, M.E. (2021). Antibacterial Activity of Peppermint, Basil, and Rosemary Essential Oils Obtained by Steam Distillation. *Agrolife Scientific Journal*, 10(1).
- Dharsono, H.D.A., Putri, S.A., Kurnia, D., Dudi, D., & Satari, M.H. (2022). *Ocimum* Species: A Review on Chemical Constituents and Antibacterial Activity. *Molecules*, 27(19), 6350.
- FAO. (2017). The State of Food and Agriculture: Leveraging Food Systems for Inclusive Rural Transformation. Rome: FAO.
- Frincu, M., & Dumitrache, C. (2016). Study regarding nitrification in experimental aquaponic system. *Journal of Young Scientist*, 4, 27-32.
- Goddek, S., Joyce, A., Kotzen, B., & Dos-Santos, M. (2019). Aquaponics and Global Food Challenges. In S. Goddek, A. Joyce, B. Kotzen, & G. M. Burnell (Eds.), *Aquaponics Food Production Systems*. Springer, Cham.
- Greenfeld, A., Becker, N., Bornman, J.F. et al. (2022). 'Is aquaponics good for the environment?—evaluation of environmental impact through life cycle assessment studies on aquaponics systems', *Aquacult Int*, 30, 305–322. doi: 10.1007/s10499-021-00800-8.
- Joyce, A., Goddek, S., Kotzen, B., & Wuertz, S. (2019). Aquaponics: Closing the Cycle on Limited Water, Land and Nutrient Resources. In Goddek, S., Joyce, A., Kotzen, B. & Burnell, G.M. (Eds.), *Aquaponics Food Production Systems*. Springer, Cham.
- Koolamchal, M.A., Mundakani, A., Job, J.T., Narayanankutty, A., Benil, P.B., Rajagopal, R., Alfarhan, A., & Barcelo, D. (2022). Phytochemical analysis, antioxidant, anti-inflammatory, antigenotoxic, and anticancer activities of different *Ocimum* plant extracts prepared by ultrasound-assisted method. *Physiological and Molecular Plant Pathology*, 117, 101746.
- Lennard, W., & Goddek, S. (2019). *Aquaponics: The Basics*. In S. Goddek, A. Joyce, B. Kotzen, & G. M. Burnell (Eds.), *Aquaponics Food Production Systems*. Springer, Cham.
- Love, D.C., Fry, J.P., Li, X., Hill, E.S., Genello, L., Semmens, K., & Thompson, R.E. (2015). Commercial aquaponics production and profitability: findings from an international survey. *Aquaculture*, 435, 67–74.
- Makri, O., & Kintzios, S. (2008). *Ocimum* sp. (Basil): Botany, Cultivation, Pharmaceutical Properties, and Biotechnology. *Journal of Herbs, Spices & Medicinal Plants*, 13(3), 123–150.
- Majdi, C., Pereira, C., Dias, M.I., Calhelha, R.C., Alves, M.J., Rhourri-Frih, B., Charrouf, Z., Barros, L., Amaral, J.S., & Ferreira, I.C. (2020). Phytochemical Characterization and Bioactive Properties of Cinnamon Basil (*Ocimum basilicum* cv. 'Cinnamon') and Lemon Basil (*Ocimum* × *citriodorum*). *Antioxidants*, 9(5).
- Marchidan, I.G., Ortan, A., Spinu, S.M., Avramescu, S. M., Avram, I., Fierascu, R.C., & Babeanu, N. (2023). Chemical Composition and Biological Properties of New Romanian *Lavandula* Species. *Antioxidants*, 12(12), 2127.
- Nadeem, H.R., Akhtar, S., Sestili, P., Ismail, T., Neugart, S., Qamar, M., & Esatbeyoglu, T. (2022). Toxicity, Antioxidant Activity, and Phytochemicals of Basil (*Ocimum basilicum* L.) Leaves Cultivated in Southern Punjab, Pakistan. *Foods*, 11(9), 1239.
- Rana, A., Pandey, R.K., & Ramakrishnan, B. (2019). Chapter 3 - Enzymology of the nitrogen cycle and bioremediation of toxic nitrogenous compounds. In P. Bhatt (Ed.), *Smart Bioremediation Technologies*. Academic Press, 45-61. ISBN: 9780128183076. DOI: 10.1016/B978-0-12-818307-6.00003-2.
- Romano, R., De Luca, L., Aiello, A., Pagano, R., Di Pierro, P., Pizzolongo, F., & Masi, P. (2022). Basil (*Ocimum basilicum* L.) Leaves as a Source of Bioactive Compounds. *Foods*, 11(12), 3212. DOI: 10.3390/foods11203212
- Shahrajabian, M.H., Sun, W., & Cheng, Q. (2020). Chemical components and pharmacological benefits of Basil (*Ocimum basilicum*): a review. *International Journal of Food Properties*, 23(1), 1961–1970.
- Singh, P., Chakraborty, P., He, D.-H., & Mergia, A. (2019). Extract prepared from the leaves of *Ocimum basilicum* inhibits the entry of Zika virus. *Acta Virologica*, 63, 316–321.
- Sonar, M.P., & Rathod, V.K. (2020). Microwave-assisted extraction (MAE) used as a tool for rapid extraction of Marmelosin from *Aegle marmelos* and evaluations of total phenolic and flavonoids content, antioxidant, and anti-inflammatory activity. *Chemical Data Collections*, 30, 100545.
- Yep, B., & Zheng, Y. (2019). Aquaponic trends and challenges—A review. *Journal of Cleaner Production*, 228, 1586.

SUSTAINABILITY OF SOME FOREST SPECIES' ASSOCIATIONS ESTABLISHED ON DEGRADED LANDS FROM THE TRANSYLVANIA PLAIN, IN THE CONTEXT OF CLIMATE CHANGE

Alexandru COLISAR¹, Marcel DÎRJA¹, Vasile SIMONCA¹, Steluta Maria SINGEORZAN¹,
Victor SFECLA², Horia Dan VLASIN¹, Cornel NEGRUSIER³, Alina Maria TRUTA¹,
Florin Alexandru REBREAN¹, Vasile CEUCA¹

¹University of Agricultural Sciences and Veterinary Medicine Cluj-Napoca,
Faculty of Forestry and Cadastre, 3-5 Manastur Street, Cluj-Napoca, Romania

²Technical University of Moldova, Faculty of Agriculture, Forestry and Environmental Sciences,
48 Mircești Street, Chisinau, Republic of Moldova

³University of Agricultural Sciences and Veterinary Medicine Cluj-Napoca,
Faculty of Agriculture, 3-5 Manastur Street, Cluj-Napoca, Romania

Corresponding author email: vasile.ceuca@usamvcluj.ro

Abstract

*This research was carried out based on a wide range of knowledge and research results reported due to previous studies on afforestation of degraded lands and forest species associations, in the southwestern part of the Transylvanian Plain. The existing knowledge made it possible to deepen and analyze different forest management practices, such as forest stand improvement, restoration of degraded lands through afforestation in the context of climate change. Therefore, the main objective of this research was to restore a degraded land in the south-western part of Transylvania. To achieve this goal, different forest plant communities were proposed, established and monitored over 9 years. During the research period, the development of forest plant communities was monitored in a fixed area in Vișoara, in order to determine the influence of soil type and plant community composition on the survival rate of the plants. For this purpose, the survival rates after 3, 5, 7 and 9 years after planting were calculated in relation to forest biometric data such as tree height and crown diameter. The results show that both soil type and forest plant community composition influenced the development of the species. The highest survival rates (96-99.5%) were recorded in *Pinus sylvestris*, *Acer campestre*, *Hippophaë rhamnoides* and *Crataegus monogyna* preluvosol, erodisol and luvosol. Among the 12 forest species tested, *Tilia cordata*, *Quercus petraea* and *Acer campestre* had the highest biometric values in terms of plant height, which ranged from 357.33 cm (*Acer campestre*) to 412.42 cm (*Tilia cordata*) along the diameter of the trunk, which varied from 6.27 cm (*Quercus petraea*) to 11.65 cm (*Tilia cordata*).*

Key words: afforestation; degraded lands; ecosystem; natural hazards; turkey oak; scots pine.

INTRODUCTION

A lot of previous research has already shown that the restoration of soil is a very slow and long process in comparison to the degradation of soil (Ibrahim, 2008; Bastida et al., 2015; Farrell et al., 2020). Afforestation as a forest management practice can be usefully applied to degraded lands unsuitable for agricultural crops to transform them into productive stands (Reyer et al, 2009; El-Beltagy, 2000). On the one hand, afforestation creates a close-knit forest community that helps restore ecological goods and services. On the other hand, these degraded lands are restored and put back into productive circulation (Duan & Abduwali, 2021).

In addition to afforestation, reforestation is another important tool for improving degraded lands. Previous reports have shown that most agricultural land was covered by forests, but due to global population growth and the transition from extensive to intensive agriculture, forest cover has decreased significantly (Rudel et al., 2005). According to Ritchie et al. (2023), the entire world lost about one-third of the world's forests within a few millennia. It has been observed that when an agricultural land is abandoned or becomes unsuitable for crops, the number of pests, except for the beneficial entomofauna, for certain types of crops (agricultural, meadows and hayfields or plantations) increases exponentially (over

several tenfold) in the abandoned areas, leading to real disasters (Visockiene et al., 2019; Bonan, 2008). Within the studied area, an intense activity of the pest *Corythucha arcuata* is observed, a fact that has also been observed in other similar situations (Bălăcenoiu et al., 2021). Unsustainable resource management practices leave degraded lands vulnerable to soil erosion and environmental damage, leading to a decline in biodiversity. This degradation also diminishes the land's capacity to store carbon and retain usable water, further impacting the ecosystem's health and resilience (Alig et al., 1997; Alcamo et al., 2005; Goebel et al., 2005). To effectively combat the negative consequences of land degradation on ecosystems, it's crucial to understand the intricacies and potential impacts of restoration efforts. By implementing targeted ecological restoration activities, we can rehabilitate degraded lands, safeguard biodiversity, and ultimately restore essential ecosystem services that benefit both the environment and human well-being (Govers et al., 2017). While ecological theory provides a valuable framework for restoring degraded land, putting these theories into practice isn't always straightforward. There's a gap between theoretical knowledge and real-world application, and in many cases, restoration efforts require ongoing adaptation, refinement, and persistence to achieve the desired outcomes (Lazar et al., 2017). In general, these areas are found in extreme conditions, the development of species is much more difficult and requires more work, while the range of forest species is broader than in the case of some basic natural forest types (Costandache et al., 2006; Giannini et al., 2017). The importance of reforesting degraded lands is widely recognized and supported by extensive research. Scientists have explored various reforestation methods, but there's no one-size-fits-all solution. Each degraded area presents unique challenges that require careful planning and adaptive management strategies (Pawson et al., 2013). To effectively restore degraded land through afforestation, we need to equip forestry professionals with the right resources, tools, and knowledge. This includes ongoing training and access to the latest research and technology, allowing them to adapt their

strategies as needed. Successful afforestation also demands a deep understanding of each site's unique characteristics, including its soil, microclimate, and existing vegetation. This detailed assessment will inform the development of tailored reforestation strategies. While species like pine and white sea buckthorn were once popular choices for land improvement due to their hardiness, a more nuanced approach is now required. However, recent experience and updated best practices show that these species may decline after an initial period of growth, highlighting the need for more nuanced and site-specific approaches to reforestation (Untaru et al., 1993; Ayan et al., 2020). In recent years, the choice of the right species for reforestation of degraded lands has become a major challenge in terms of guidelines and increasing risks or disasters (drought, frozen rains, insect or rodent attacks) that require a longer time for research and understanding of the phenomena (Costandache et al., 2010; Hartanto et al., 2003; Täut, et al., 2018). In this context, the afforestation of this type of land consists mainly in reducing the intensity of land degradation processes and gradually improving them, under the direct effect of protective forest crops, and mitigating climate change. It also protects human settlements against landslides, wind or snow, provides timber in areas where it is scarce, creates melliferous bases, improves the landscape and, finally, improves the living conditions of the inhabitants of the area (Bowen et al., 2007; Dalling, 2008; Liu et al., 2018; Untaru et al., 2012).

The main function of forest plant species that are established on degraded lands is the mitigation or cessation of land degradation processes and the improvement of environmental conditions. Considering the function of these forest ecosystems, it can be said that forest stands have a temporary role, after fulfilling their role of protection and improvement, they will be replaced, naturally or artificially, by other stands of valuable species' characteristic of the basic natural type, and their protective function will change, taking its place of production (Schuler et al., 2017).

The main objective of the present research was to increase the knowledge about the planting of

forest species on degraded lands unsuitable for agriculture, located in the south-western part of the Transylvanian Plain, with the knowledge of the difficulties encountered due to the physical-geographical conditions (nature of the land, climatic factors and harmful factors), including their vegetation state in the first years after planting. The research aims to specify the circumstances regarding the current state of the plantations, the sustainability of the forest species associations and the interspecific relationships within the plant communities. Another objective is the efficiency of the ecological reconstruction of the land within the perimeters of improvement, and the other is the effect and intensity of the disasters found in these areas.

MATERIALS AND METHODS

To conduct this experiment, several research methods were used. Observation as a research method was used for the recognition of the study area, the description of the land configuration, the characteristics of land degradation, and the soil preparation technology in the establishment of crops. In addition, the viability of the forest seedlings was monitored after several growing seasons. During the growing seasons, their adaptation and vegetation condition were assessed. To determine the biometric characteristics of the forest plants, actual measurements were made. Thus, the associations of forest species established in the Viisoara area were inventoried on soil types and forest compositions, in percentage of success at different intervals since planting (3 years, 5 years, 7 years, 9 years), with the specification that in the 5th, 7th and 9th years, the percentage of filling carried out previously (in the first 3 years after planting) was also taken into account. At the same time, biometric data (tree height and trunk diameter) were measured, and the vegetation status of forest species and the impact of harmful factors and their intensity were determined.

Study area

The study area is located near the village of Urca, which is part of UAT Viisoara, located in the southwestern part of the Transylvanian Plain

(Figure 1). The study area consists of a grassland with different degrees of surface and deep erosion, as well as landslides, with different landforms, from steep but short slopes, with slopes of more than 35°, to those with very little inclination, plateaus, as well as numerous ravines and bones. In the usual morphological aspect, the study area is located in the Hilly Plain of Transylvania, consisting of a complex of slow peaks, separated by wide valleys with an altitude between 25 - 640 m. Physically - geographically, the improvement perimeter is located on the southern and western slopes of the hills Vomirul Mare and Vomirul Mic with an altitude between 320 meters and 470 meters.

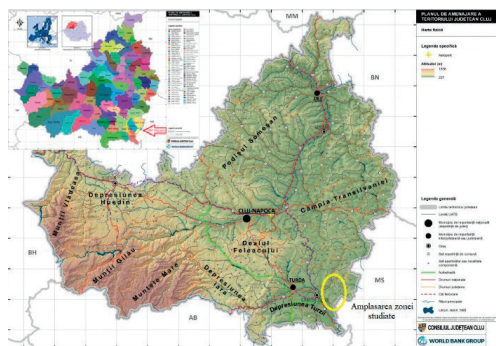


Figure 1. Location of the survey area
 (Source: <https://www.patjcluj.ro>)

It is worth mentioning that out of the total area of 123.37 ha, only 122.15 ha were covered with ecological forest reconstruction works, while the remaining 1.21 ha were non-productive lands, namely a very high slope ravine - 0.81 ha, as well as two bush areas, where the close crop was already formed and where no deforestation and reforestation intervention was appropriate. In this situation, it was intended that the replacement of the current vegetation would take place in time and naturally, the areas being relatively small - 0.4 ha. Prior to the actual reforestation work, a pedostratigraphic mapping of the area was carried out in order to carefully match the reforestation solutions with the soil type and its requirements.

Climate and site conditions

As far as the climatic conditions of the studied area are concerned, Viisoara is situated in the

climatic province Dfbx, in the climatic sector Ibp, that is, in the provincial sector with continental-moderate climate, in the country of the hill climate, in the subdivision of the Transylvanian Plain. This land is characterized by a relatively constant higher humidity than in the eastern sector of the country, but also by an uneven distribution of all-weather elements. In this climatic country, the studied area is part of the plain area, which, especially in its southern part, feels the influence of the föhn, which leads to a general increase in air temperature, especially during clear skies, and a decrease in the amount of precipitation (less than 600 mm annually), therefore the studied area is atypical to the general characterization.

The climate of the area is characterized by mild winters, with an annual precipitation of about 550-600 mm, but with an aridity index of about 34, which gives the area a transitional character towards the forest-steppe. Thus, the area under study is one of the driest of the Transylvanian Plain, with atypical climatic conditions. The rainfall regime is characterized by annual average values between 560 and 610 mm per year, but in recent years the average values recorded in the study area did not exceed 580 mm. This area experiences a Mediterranean climate, with rainfall peaking in June (averaging 96.5 mm) and reaching its lowest point in March (averaging 29.1 mm). Winter is the driest season (90-95 mm), while summer brings the most rain (240-250 mm). Although this rainfall level generally supports healthy forest growth, the high temperatures lead to significant evapotranspiration, exceeding precipitation, particularly in July and August. This water deficit can create challenging conditions for vegetation during the summer months. The area around Viisoara is facing increasing challenges due to climate change. Recent years have seen more frequent and severe droughts, particularly on sunny, steep slopes, causing significant damage to existing forest vegetation. While the region lacks natural forests, there is a small, artificially planted stand about 40 years old. Although it initially helped with land

improvement, this stand is now insufficient to meet the area's needs for tree cover and does little to influence the local microclimate. Essentially, the area is struggling with a lack of forest cover to mitigate the effects of drought and improve the local environment. The existing forest stand is composed of black pine on the south-facing slopes, with a mix of oak species at the base, along with scattered hawthorn, blackthorn, and black locust trees. However, this stand is showing clear signs of decline due to the increasingly dry conditions. Between 2020 and 2024, a significant portion of the pines have died, and the oaks are also suffering, exhibiting dieback in their crowns and producing stunted shoots because of prolonged water stress. The soil within the study area is diverse and includes preluvosols, luvosols, and alluviosols. Significantly, there are also areas with moderate to severe erosion, classified as erodisols (Figure 2). This variety in soil types is likely influenced by the topography and past land use within the study area.

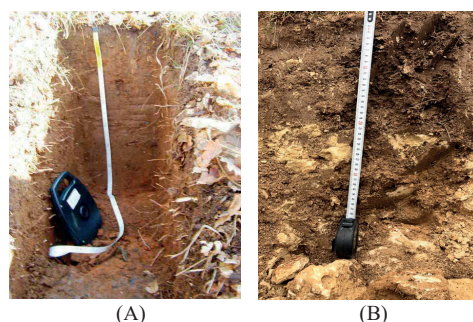


Figure 2. Soil types found within the perimeter of Viisoara. (A) – alluviosol; (B) – luvosol.
(source: original)

Table 1 provides a helpful guide for matching the right trees to the right soil conditions within the study area. It outlines the different soil types found in the area (preluvosols, luvosols, alluviosols, and erodisols) and identifies suitable site types for various ecological groups of trees. Essentially, it recommends the types of vegetation best suited to thrive in each specific soil type, aiding in successful reforestation efforts.

Table 1. Soil types and forest sites characteristics by ecological groups

Ecological group / Sites group (GE/GS)	Soil Type	Site Type (TS) Proposed afforestation compositions	UA/US	Surface	
				ha	%
GE 56	Preluvosol	TS 1 - GE 56 - Quercus hills site, high edaphic volume 3St(Gi)3Ce(Str)2Te(Ci)2Ci(Ju,Lc)	11, 18A, 3, 9B	12.27	10.0.
GE 57	Preluvosol	TS 2 - GE 57 Hill mixed hardwood forest, medium-large edaphic volume 3Go(Gi)3Ce(Str)2Te(Ci)2Ju(Lc)	14A, 14B, 1A, 24	17.55	14.4.
GS 54	Alluviosol	TS 3 - GS 54 - Slippery land with a moderately kneaded slip mass, with a thickness of over 75 cm, without prolonged excess water 25Str(Ec)25Fr25Te(Ci)25Lc(Ju)	13A, 15B, 15C, 19A, 1C, 22A, 4B, 5, 7B, 8A	38.79	31.8.
GS 9	Luvosol	TS 4 - GS 9 - High slope soil, moderate erosion, 25Pi25Ci(Mj)25Mi(Vi.t)25Pd(Lc)	10, 15A, 15D, 17, 20A, 23A, 23B, 25, 4D, 7A	28.25	23.1.
GS 11	Erodisol	TS 5 - GS 11 - Large slope land with very strong and excessive erosion, clay texture, without rocks 50Pi50Ct(Mj)	12, 13B, 16, 19F, 19G, 20B, 21A, 22B, 22C, 22D, 22E, 22F, 2A, 4A, 4C, 6A, 8B, 8D, 9A	23.17	19.0.
GS 29	Erodisol	TS 6 - GS 29 - Slopes of ravines and gully on erodisols, without rocks 100Ct(100Sl)	15E, 15F, 18B, 18C, 19E, 21B, 21C, 21D, 21E, 21F, 21G, 2B, 2C, 6C, 7C, 8E, 8F, 8G, 9C, 9D, 9E, 9F, 9G, 9H,	2.12	1.7.

Biometric measurements

In order to achieve these objectives, at the end of the growing seasons in the years indicated in Table 2, 100 m² sample plots were placed homogeneously in the field on the surface of the site units inventoried at each crossing perimeter. Inventories of seedlings were conducted within the sample plots to determine seedling recruitment or failure rate by determining the percentage of success at the end of the growing season. Collar diameter and plant height measurements were also made. Height was measured to the end bud of each seedling using the roulette in centimeters, and when measuring with the roulette became difficult, a graduated pole was used. Collar diameter was measured in centimeters with a caliper. By differentiating the measurements over the years, annual increases in diameter and height were determined.

Statistical analyzes

All recorded data were analyzed using IBM SPSS Statistics 19 (IBM). One-way analysis of variance (ANOVA) was performed at 95% confidence level to determine statistically

significant differences between the means of the same species but different soil types and their adaptability to different climatic and site conditions. When the ANOVA null hypothesis was rejected, Duncan's multiple range test was used to determine significant differences between the means.

RESULTS AND DISCUSSIONS

The climatic factors (temperatures, precipitation and potential evapotranspiration), together with the landscape conditions, give the studied area a topo-climate different from the normal representative one. The phenological data of the main species (oak and sessile oak) show that, for them and for other species of the mixture in the mixed hardwood of the hills, the normal climate favors their development, but the typical extreme climate of the area cancels this advantage (Mette et al., 2013; Černý et al., 2024), an aspect that can be observed in the case of the present study (Figure 3).

Although the perimeter was established in 2012-2013, due to the calamities to which it was exposed (prolonged drought and attacks of

rodents), in the spring of 2014 it went into full recovery, therefore, the experiments started in 2015, with regular return and consisted in the follow-up of forest crops, determining the

growth of trees, the vitality and resistance to disruptive factors. This research will continue until the close crops is achieved, which has not been fully achieved by 2024.



Figure 3. Restoration of the ecosystem through afforestation. Changing the landscape 2012-2016-2024 in the perimeter of Viisoara (Source: original)

Table 2 presents the findings of our measurements, reflecting the factors discussed earlier. The initial success of the seedlings planted in 2013 depended heavily on the weather conditions that year, particularly temperature and rainfall, and the seedlings' ability to adapt to those conditions. While planting was done manually in prepared strips along the slopes, mechanized site preparation could have been more efficient and cost-effective, potentially improving seedling survival rates, as suggested by Wronski & Murphy (1994). After one growing season, with annual monitoring of species regeneration, it was found that the species survival rate was low, so that in the spring of 2014, the reestablishment of the stands took place at a rate of 80%.

Regarding the percentage of success recorded after five years of establishment, it can be observed that for turkey oak (*Quercus cerris*) the percentage of survival varied between 68.5% (u.s. 1A) and 73% (u.s. 7B), a rather low percentage considering that the gaps were filled over three years, this percentage being lower than that recorded for oak (*Quercus robur*) 77.5% and sessile oak (*Quercus petraea*) 81%. At 9 years after planting, the percentage of survival had the following proportion, with the specification that from the fourth year no filling the gaps have been made, turkey oak (*Quercus cerris*) the percentage of maintenance is between 47.5% (u.s. 11) and 58.75% (u.s. 1A) the percentage being lower than before, this percentage is below the percentage recorded by

sessile oak (*Quercus petraea*) 68.5%, with the exception of oak (*Quercus robur*) 58%.

This aspect is somewhat surprising, since the turkey oak (*Quercus cerris*) is a relatively thermophilic and xerophytic species that grows in lowlands and forest-steppe areas with warm climates, tolerating well drought and aridity, and which, due to its strong roots and ability to reduce its sweat, also vegetates well on clay and compact soils with variable humidity, aspects also reported by (De Rigo et al., 2013; Di Filippo et al., 2010). On the one hand, these low survival rates of forest species are mainly due to the attack of biotic pests (invasion of field mice, which gnaw the roots and the collar of the seedlings, and the action of deer, which gnaw the annual growth of the seedlings). On the other hand, the lack of rainfall and the above-average temperatures led to a withered state of the vegetation, which subsequently led to the desiccation of the planted crops (Figure 4). Figure 4 also shows that the vegetation on the southeastern slopes remained much weaker than on the northwestern slopes.

For the mixed species studied, it is noted that the corresponding success is recorded for the common ash (*Fraxinus excelsior*), 81% at 5 years and 75% at 9 years, and European white linden (*Tilia tomentosa*), which is well adapted to the soil and climatic conditions at the base of slopes, achieving a success percentage between 81% and 91% at 5 years, respectively 62.75% and 74.5% at 9 years (Clark et al., 2013; Frischbier et al., 2019).

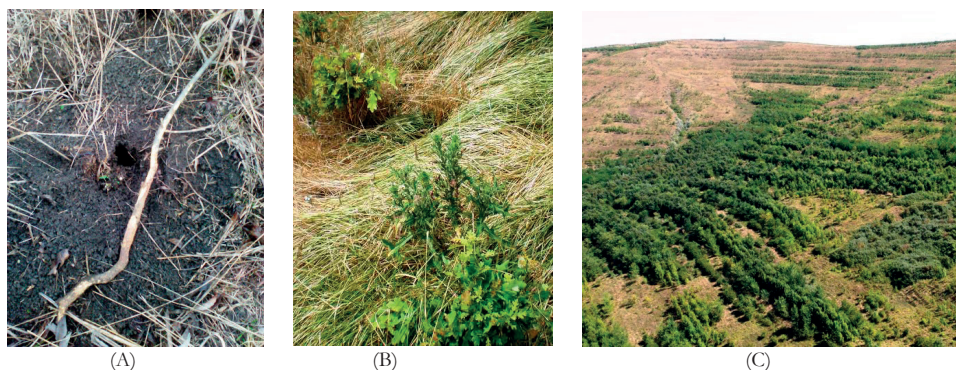


Figure 4. Factors leading to low crop success. (A) - Attack of rodents; (B) - Appearance of bush at the sessile oak due to the gnawing of annual growths by the roe deer; (C) - Development of vegetation according to the exhibition of slopes. (source: original)

Among the complementary species of deciduous trees and shrubs, the best survival rates were as follows: bird cherry (*Prunus padus*) with 77.5%, sea buckthorn (*Hippophaë rhamnoides*) with 99% and hawthorn (*Crataegus monogina*) with 99.5%. In the case of coniferous species, Scots pine (*Pinus sylvestris*), showed a higher ecological amplitude (Rehfeldt et al., 2002; Silvestru-Grigore et al., 2018), at least for the moment, have adapted to the pedostasis conditions of the area with a normal development and an optimal survival and development percentage, 96% and 97.5%, respectively, in the ninth year of vegetation.

For seven test areas installed in the Viisoara improvement perimeter, Table 2 summarizes the measurements, and the elements studied.

Appreciation of vegetation status and harmful factors (climatic, biotic and abiotic factors) was made using a symbol scale according to the following specifications:

Abiotic pests

1. Injuries due to climatic factors

- a. high temperatures in the growing season;
- b. lack of precipitation.

Biotic pests

2. Leaf diseases

- a. oak powdery mildew (*Microsphaera abbreviata* Peck);
- b. purple staining of cherry leaves (*Coccomyces hiemalis*).

3. Animal pests

- a. roe deer (*Capreolus capreolus*);

b. rabbit (*Lepus europaeus*);

c. field mouse (*Microtus arvalis*);

d. oak lace bug (*Corythucha arcuata*).

The intensity of injuries was assessed according to the following scale:

I. very weak (up to 25 %);

II. weak (26-50);

III. medium (51-75%);

IV. strong (over 75%).

For the assessment of the vegetation status of the crops, the notations mentioned in Technical Norms 7/2000 and the best practice guide approved in OM 2357/28.09.2022 were used as follows:

a. very vigorous;

b. vigorous;

c. normal;

d. poor;

e. very weak.

The biometric dimensions of individuals and species are very varied, due to the soil conditions mainly and the climate conditions in secondary. Thus, very varied heights were measured, the average dimensions being in the main deciduous species between 73 cm in the turkey oak (*Quercus cerris*) and 97 cm in the sessile oak (*Quercus petraea*) in year 5 respectively between 43 and 47 cm in the scots pine (*Pinus sylvestris*). At year 9 the measured values recorded 245.33 cm in the turkey oak (*Quercus cerris*) and 362 cm in the sessile oak (*Quercus petraea*), the coniferous being between 120.33 and 137.5 cm (Figures 5 and 6).

Table 2. The centralization of the measurements and elements studied

u.s		Afforestation composition		Succeeded After				Biometric characteristics by				Vegetation status Age 9	Factors of injury Age 9
No.	Soil Type	Species	Proportion %	Age 3 %	Age 5 %	Age 7 %	Age 9 %	Age 5		Age 9			
								Height - cm-	Collar diameter -cm-	Height - cm-	Collar diameter -cm-		
11	preluposol	St	30	60	77.5	72	58	85	1.5	278	5.8	c-d	1.a.b.2.a.3.a.c.d.III
		Ce	30	58	72	66	47.5	73	1.3	245	5.4	c-d	1.a.b.2.a.3.a.c.d.III
		Te	20	72	81	76.5	62.75	115	2.1	386	11.2	b-c	1.b.3.c.II
		Ci	20	40	63.5	51	32.5	121	2.5	321	8.1	d	1.b.2.b.3.c.III
1A	preluposol	Go	30	57	81	76.75	68.5	97	1.5	362	6.2	c-d	1.a.b.2.a.3.c.d.II
		Ce	30	52	68.5	65	58.75	75	1.2	276	5.8	c	1.a.b.2.a.3.c.III
		Te	20	83	91	88	73	124	2.3	412	11.7	b-c	1.b.3.c.II
		Ju	20	92	100	96	96	115	1.9	357	7.8	b	1.b.I
7B	alluviosol	Ce	25	68	73	71	68.75	91	1.2	278	4.9	c-d	1.a.b.3.c.III
		Fr	25	80	81	78	75	78	1.9	319	4.6	b	1.a.b.2.c.3.c.II
		Te	25	86.75	89.5	82.75	74.5	71	1.8	357	8.4	b-c	1.b.3.c.II
		Le	25	90	87.5	86	81	62	0.7	211	2.8	b	1.b.II
15D	luvosol	Pi	25	90	100	99	97.5	47	1.4	121	3.9	b	1.a.b.II
		Ci	25	68	63	57	48.75	89	2.3	235	6.9	c	1.b.2.b.3.c.III
		MI	25	72	84	79	77.5	104	1.4	297	3.6	b	1.b.II
		Pd	25	98	100	100	99.5	83	0.8	211	2.3	b	1.b.I
19G	erodisol	Pi	50	91	97	96.5	96	43	1.1	137	3.6	b	1.a.II.
9F	erodisol	Ct	50	100	99	98	99	86	1.3	201	3.1	b	1.a.b.I
		Ct	100	98	99.5	99	99	103	1.5	227	3.4	b	1.a.b.I
21C	erodisol	SI	100	87	89.75	87.5	84	87	1.7	248	3.7	b-c	1.b.I.

- the notations of vegetation status and the action of harmful factors are illustrated in the following paragraph
- the notation of species is: St (oak – *Quercus robur*); Go (sessile oak – *Quercus petraea*); Ce (Turkey oak – *Quercus cerris*); Te (European white lime – *Tilia tomentosa*); Fr (common ash – *Fraxinus excelsior*); Ci (wild cherry – *Prunus avium*); Ju (Field maple – *Acer campestre*) Pi (scots pine – *Pinus sylvestris*); MI (bird cherry – *Prunus padus*); Le (privet – *Ligustrum vulgare*); Pd (hawthorn – *Crataegus monogyna*); Ct (buckthorn – *Hippophaë rhamnoides*); SI (oleaster – *Eleagnus angustifolia*);

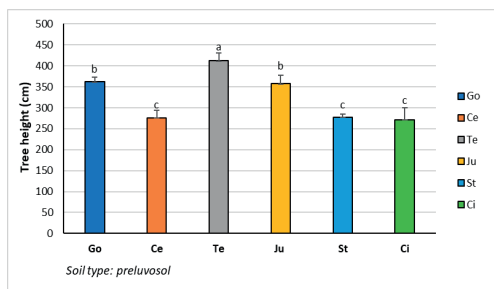


Figure 5. Average tree heights of the investigated species after 9 years of growth. Lowercase letters above the bars indicate significant differences between the species studied according to Duncan's multiple range test at $p < 0.05$. * Go (sessile oak - *Quercus petraea*); Ce (turkey oak - *Quercus cerris*); Te (European white lime - *Tilia tomentosa*); Ju (field maple - *Acer campestre*); St (oak - *Quercus robur*); Ci (wild cherry - *Prunus avium*).

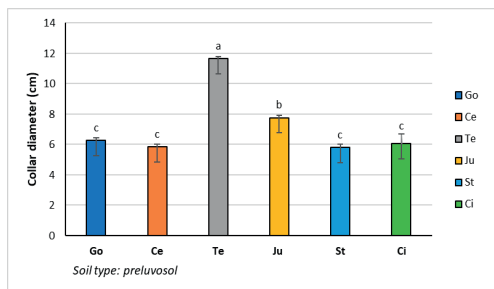


Figure 6. Average collar diameter of the investigated species after 9 years of growth. Lowercase letters above the bars indicate significant differences between the species studied according to Duncan's multiple range test at $p < 0.05$. Go (sessile oak - *Quercus petraea*); Ce (turkey oak - *Quercus cerris*); Te (European white lime - *Tilia tomentosa*); Ju (field maple - *Acer campestre*); St (oak - *Quercus robur*); Ci (wild cherry - *Prunus avium*).

After nine years, there's a clear difference in height between the tree species planted. *Tilia tomentosa* emerged as the top performer in terms of growth, reaching an average height of 412.42 cm. It was followed by *Quercus petraea* at 361.67 cm and *Acer campestre* at 357.33 cm. These species showed the strongest growth, increasing in size by 69-80% over a 5-year period. Their crown diameters also followed a similar pattern. Based on the results obtained, a positive correlation between tree height and crown diameter was observed in all species studied.

Tilia tomentosa and *Quercus cerris* have been proposed and grown on two different soil type to test their adaptability and survival rate. The

results show that the growth parameters recorded in *Quercus cerris* including average tree height and collar diameter were slightly influenced by the soil type, but no statistically significant differences were detected according to Duncan's multiple range test at $p < 0.05$. In this context, it was observed that the maximum average tree height was recorded on aluviosol, while the collar diameter of *Quercus cerris* was larger in trees grown on preluvosol (Figure 7 and Figure 8). On the contrary, the growth of *Tilia tomentosa* species was significantly higher than that of *Quercus cerris*, both in terms of tree height and diameter at breast. The highest mean values for *Tilia tomentosa* were recorded for trees grown on preluvosol (Figure 7 and Figure 8).

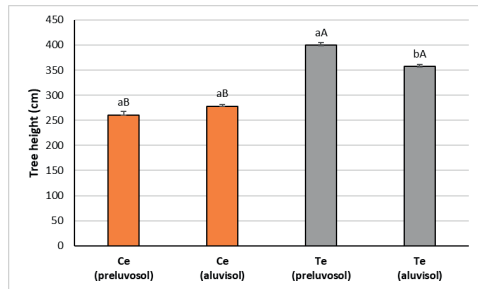


Figure 7. Average tree heights in Ce (turkey oak - *Quercus cerris*) and Te (European white lime - *Tilia tomentosa*) grown on different soil types after 9 years of growth. Lowercase letters above the bars indicate significant differences between soil types within the same species, while capital letters indicate significant differences between tree species grown on the same soil type according to Duncan's multiple range test at $p < 0.05$.

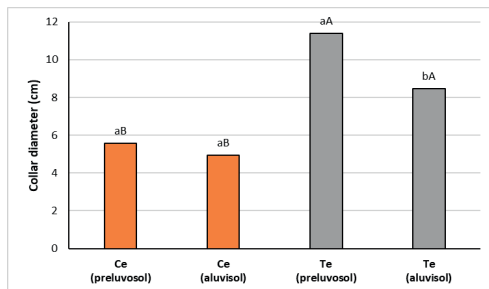


Figure 8. Average collar diameter in Ce (turkey oak - *Quercus cerris*) and Te (European white lime - *Tilia tomentosa*) grown on different soil types after 9 years of growth. Lowercase letters above the bars indicate significant differences between soil types within the same species, while capital letters indicate significant differences between tree species grown on the same soil type according to Duncan's multiple range test at $p < 0.05$.

Besides soil, the mix of tree species planted also affects how well individual species grow (Tănase, 2012). Some species can help or hinder the growth of others. Both *Quercus cerris* and *Tilia tomentosa* grew taller and had thicker trunks when planted alongside *Quercus petraea* (and *Acer campestre*). Specifically, *Quercus cerris* reached an average height of 276.33 cm and a trunk diameter of 5.83 cm, while *Tilia tomentosa* reached an impressive 412.42 cm in height and 11.65 cm in diameter. Lower values of these growth parameters were recorded when *Quercus cerris* and *Tilia tomentosa* were planted in a community with *Quercus robur* L. and *Prunus avium* L. (245.33 cm height; 5.3 cm collar diameter and 386.25 cm height; 11.12 collar diameter).

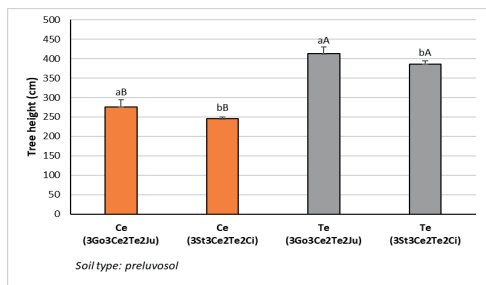


Figure 9. Average tree height in Ce – *Quercus cerris* and Te – *Tilia tomentosa* grown in different plant communities after 9 years of growth. Lowercase letters above the bars indicate significant differences between soil types within the same species, while capital letters indicate significant differences between tree species grown on the same soil type according to Duncan's multiple range test at $p < 0.05$.

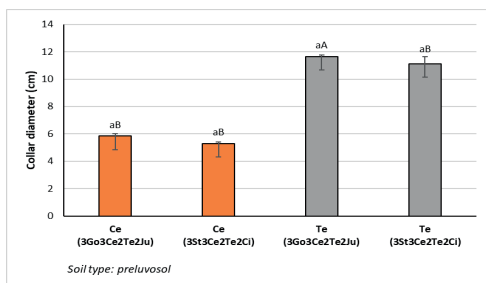


Figure 10. Average collar diameter in Ce – *Quercus cerris* and Te – *Tilia tomentosa* grown in different plant communities after 9 years of growth. Lowercase letters above the bars indicate significant differences between soil types within the same species, while capital letters indicate significant differences between tree species grown on the same soil type according to Duncan's multiple range test at $p < 0.05$.

Other species, such as *Pinus sylvestris*, exhibited different growth rates which appeared to be influenced by the soil type along slope exposure (Vlasin, 2010; Stoll et al., 1994; Ayan et al., 2021). It appears that *Pinus sylvestris* grew better on erodisol, reaching an average height of 137.50 cm, compared to 120.33 cm on luvosol. This difference in growth based on soil type was statistically confirmed and is clearly illustrated in Figure 11.

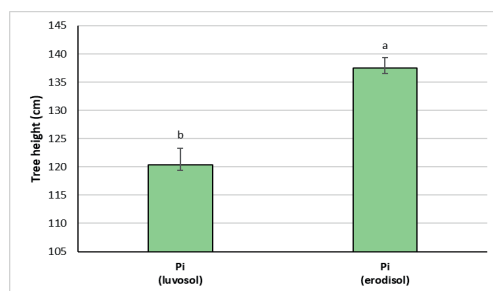


Figure 11. Average tree height of Pi – *Pinus sylvestris* grown on different soil types

In respect to collar diameter of *Pinus sylvestris*, the same growing tendency was observed: erodisol stimulated more collar diameter as well than luvosol (Figure 12).

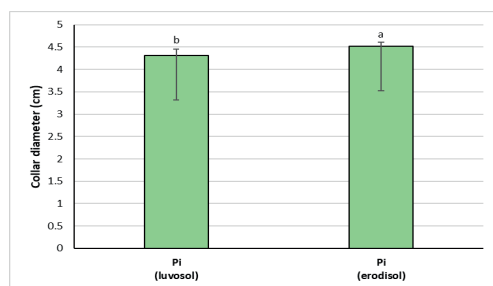


Figure 12. Average collar diameter of Pi – *Pinus sylvestris* grown on different soil types

Hippophaë rhamnoides L. also known as sea buckthorn is an indigenous species with high ecological adaptability. This species is cultivated first, in forest plant communities due to its role in preventing soil erosion, and second, for its fruits which are rich in bioactive compounds and Vitamin C. The roots of this species are rich in root nodules and thus very effective in nitrogen fixation (Chen et al., 2019). In this study, this

species has been suggested and planted for pure and mixed plant communities to improve degraded lands by conserving the soil and water for longer time. Therefore, the results show that sea buckthorn reached higher values in terms of plant height when planted and grown in pure communities (227.23 cm) than associated with *Pinus sylvestris* (201.6 cm) as presented in Figure 13.

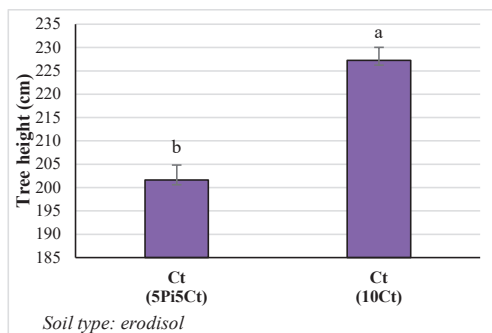


Figure 13. Average plant height of Ct – *Hippophaë rhamnoides* L. grown in different species associations

However, the collar diameter was slightly bigger (3.32 cm) when planted in mixed communities in comparison to pure communities (3.14 cm) as shown in Figure 14.

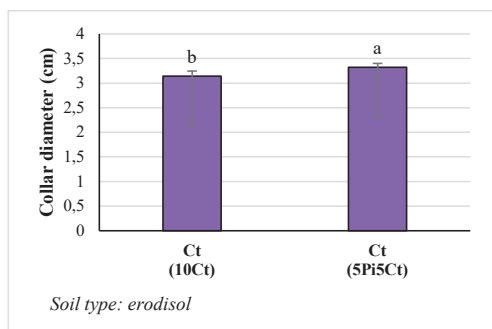


Figure 14. Average collar diameter of Ct – *Hippophaë rhamnoides* L. grown in different species associations

Among the aiding species, the common ash (*Fraxinus excelsior*) reached 319 cm, and the European white lime (*Tilia tomentosa*) reached between 357 and 412 cm in year 9 after planting. The field maple (*Acer campestre*) is a thermophilic species but with certain demands on the soil, vegetating well on the slopes and at

the base of the slopes on dry soils and with a higher degree of compaction, a highlighted aspect and by (Zecchin et al., 2016).

From the point of view of the collar diameter, the situation is as follows: the cvercinees recorded values between 1.2 and 1.5 cm and the pine between 1.1 and 1.4 cm in year 5. These differences between values were maintained in year 9 after planting, with the cvercinees between 4.9 and 6.2 cm and the pine between 3.6 and 3.9 cm.

Of the aiding species, common ash (*Fraxinus excelsior*) reached 4.6 cm and European white lime (*Tilia tomentosa*) ranging between 8.4 and 11.7 cm in diameter in year 9 after planting, with the specification that these dimensions were recorded at specimens that developed mainly at the base of the slopes, on the banks of some ravines or on the north-western slopes. As shown in Figure 15 on the southern and south-eastern slopes, the tree vegetation is almost non-existent (except for common ash and pine trees), with only shrub vegetation developing.

Forest crops have developed differently during the research period, depending on the foresting composition of each variant. Differences can thus be observed for each species, which allows some useful conclusions to be drawn for the future, regarding the choice of species associations according to the soil and climatic conditions and the characteristic type of microsite.



Figure 16. Development of forest associations 10 years after planting in the Viișoara improvement perimeter (Source: original)

CONCLUSIONS

Water is the limiting factor in the development of plants, therefore a potential trophicity is

distinguished, expressed by the nutrient fund used by plants. In the months with lower humidity compared to the optimal level, the soil trophicity attainment is lower and due to the potential evapotranspiration, namely the lower humidity, the dryness or aridity phenomenon will occur. Linking the ecological requirements of the species to the stationary conditions in the area under consideration, the following species associations were established: oak, sessile oak and turkey oak as the main basic species in the case of deciduous trees, or Scots pine in the case of coniferous trees, used as an association with European white lime and common ash as the main secondary species, field maple, bird cherry and wild cherry as supporting species, and hawthorn, buckthorn and oleaster as shrubby species. The period of adaptation and growth of the forest seedlings is quite long, as the percentages of success and survival during the study period and the measured values show.

Thus, taking into account the soil type, the slope exposure, the composition of the afforestation species, the recorded temperatures and rainfall, it can be said that the forest species planted at the foot of the slopes had an optimal survival percentage and development, similar to those established on the northwestern slopes. However, both in the middle and in the lower third of the slope, optimal values of plant growth were recorded, the survival rate of the species decreased. In addition, on the south-eastern slopes almost, as well as in the upper third of all slopes, the survival rates were lower (in some cases close to zero), and certain species grew inadequately or desolate. Due to the lack of rainfall, the studied area was affected by various disturbing factors (calamities), among which the rodent attack was the most devastating. From November to April, the roots and some of the annual shoots of the trees were gnawed by rodents, while in the spring, the deer came to severely stunt the growth of the young tree, which eventually led to the death of the plant. The turkey oak, a very important forest species with a greater capacity to adapt to extreme conditions, being considered a thermophilic and xerophytic species, did not register a better growth than the sessile oak or the oak. This could be explained by the fact that the turkey

oak was used on the slopes, while the other *Quercus* species were planted in the lower part of the slopes. In addition, Scots pine and sea buckthorn were planted in different species associations on different types of soil, these two had an optimal growth and development, resulting also in a high survival rate. Overall, the results of this research are satisfactory in terms of plant growth and development, but future improvements are still needed to increase their survival rate from 66% to over 90%. In this regard, due to the increasing temperatures in recent years and the increased potential of evapotranspiration, it is recommended to introduce also other species in the studied area, such as black locust (*Robinia pseudoacacia* L.), which can grow and form forest protective curtains for other species such as downy oak (*Quercus pubescens*), sea buckthorn and Scots pine or others, in order to form a forest massif and reach high levels of degraded land improvement.

REFERENCES

- Alcamo, J., van Vuuren, D., Ringler, C., Cramer, W., Masui, T., Alder, J., & Schulze, K. (2005). Changes in nature's balance sheet: model-based estimates of future worldwide ecosystem services. *Ecology and society*, 10(2), <https://www.jstor.org/stable/26267733>
- Alig, R., Adams, D., McCarl, B., Callaway, J.M., & Winnett, S. (1997). Assessing effects of mitigation strategies for global climate change with an intertemporal model of the US forest and agriculture sectors. *Environmental and Resource Economics*, 9(3), 259-274.
- Ayan, S., Civek, E., Çelik, E.N.Y., Gülseven, O., Özel, H. B., Eshaibi, J.A.H., Akin, Ş.S., & Yılmaz, E. (2020). Farklı yaşlardaki tüplü Fıstıkçamı (*Pinus pinea* L.) fidanlarının morfolojik kalite özellikleri. *Bartın Orman Fakültesi Dergisi*, 22(2), 633-641.
- Ayan, S., Yücedağ, C., & Simovski, B. (2021). A major tool for afforestation of semi-arid and anthropogenic steppe areas in Turkey: *Pinus nigra* JF Arnold subsp. *pallasiana* (Lamb.) Holmboe. *Journal of Forest Science*, 67(10), 449-463 | DOI: 10.17221/74/2021-JFS.
- Bălăcenoiu, F., Simon, D.C., Nețoiu, C., Toma, D., & Petrișan, I.C. (2021) The seasonal population dynamics of *Corythucha arcuata* (Say, 1832) (Hemiptera: Tingidae) and the relationship between meteorological factors and the diurnal flight intensity of the adults in Romanian oak forests. *Forests*, 12(12), 1774.
- Bastida, F., Selevsek, N., Torres, I.F., Hernández, T., & García, C. (2015). Soil restoration with organic

- amendments: linking cellular functionality and ecosystem processes. *Scientific Reports*, 5(1), 15550.
- Bonan, G.B. (2008). Forests and climate change: fortbacks, and the climate benefits of forests. *Science*, 320, 1444-1449, doi: 10.1126/science.1155121.
- Bowen, M.E., McAlpine, C.A., House, A.P., & Smith, G.C. (2007). Regrowth forests on abandoned agricultural land: a review of their habitat values for recovering forest fauna. *Biological Conservation*, 140(3-4), 273-296.
- Černý, J., Špulák, O., Kománek, M., Žižková, E., & Sýkora, P. (2024). Sessile oak (*Quercus petraea* [Matt.] Liebl.) and its adaptation strategies in the context of global climate change: a review. *Central European Forestry Journal*, 70(2), 77-94, <https://doi.org/10.2478/forj-2024-0012>
- Chen, J., Li, Y., Luo, Y., Tu, W., & Wan, T. (2019). Drought differently affects growth properties, leaf ultrastructure, nitrogen absorption and metabolism of two dominant species of Hippophae in Tibet Plateau. *Acta Physiologiae Plantarum*, 41(1), 10.1007/s11738-018-2785-6.
- Clark, J.R. (2013). Adaptation of Ash (*Fraxinus Exelsior* L.) to Climate Change (Doctoral dissertation, Bangor University (Environment, Natural Resources and Geography)).
- Constandache, C., Nistor, S., & Ivan, V. (2006). Împădurirea terenurilor degradate ineficiente pentru agricultura din sud-estul țării. *Annals of Forest Research*, 49, 187-204.
- Constandache, C., Blujdea, V., & Nistor, S. (2010). Achievements and perspectives on the improvement by afforestation of degraded lands in Romania. *Land Degradation and Desertification: Assessment, Mitigation and Remediation*, 547-560.
- Dalling, J.W. (2008). Pioneer species. In the Encyclopedia of Ecology, Five-Volume Set (pp. 2779-2782). Elsevier Inc.
- De Rigo, D., Enescu, C.M., Houston Durrant, T., & Caudullo, G. (2016). *Quercus cerris* in Europe: distribution, habitat, usage and threats. European Atlas of Forest Tree Species; San-Miguel-Ayanz, J., de Rigo, D., Caudullo, G., Houston Durrant, T., Mauri, A., Eds., 148-149.
- Di Filippo, A., Alessandrini, A., Biondi, F., Blasi, S., Portoghesi, L., & Piovesan, G. (2010). Climate change and oak growth decline: Dendroecology and stand productivity of a Turkey oak (*Quercus cerris* L.) old stored coppice in Central Italy. *Annals of Forest Science*, 67, 706-706.
- Duan, J., & Abdulwali, D. (2021). Basic Theory and Methods of Afforestation. In *Silviculture*. IntechOpen.
- El-Beltagy, A. (2000). Land Degradation: A Global and Regional Problem; in: Conference Proceeding for the International Conference United Nations and Global Governance in the New Millennium, 19-21 January 2000, Tokyo, <http://www.unu.edu/millennium/environment.html>.
- Farrell, H.L., Léger, A., Breed, M.F., & Gornish, E.S. (2020). Restoration, soil organisms, and soil processes: emerging approaches. *Restoration Ecology*, 28, S307-S310.
- Frischbier, N., Nikolova, P.S., Brang, P., Klump, R., Aas, G., & Binder, F. (2019). Climate change adaptation with non-native tree species in Central European forests: early tree survival in a multi-site field trial. *European Journal of Forest Research*, 138(6), 1015-1032.
- Giannini, T.C., Giulietti, A.M., Harley, R.M., Viana, P.L., Jaffe, R., Alves, R., Pinto, C.E., Mota, N.F.O., Caldeira, C.F., Imperatriz-Fonseca, V.L., et al. (2017). Selecting plant species for practical restoration of degraded lands using a multiple-trait approach. *Austral Ecology*, 42(5), 510-521, <https://doi.org/10.1111/aec.12470>.
- Goebel, P.C., Wyse, T.C., & Corace III, R.G. (2005). Determining reference ecosystem conditions for disturbed landscapes within the context of contemporary resource management issues. *Journal of Forestry*, 103(7), 351-356.
- Govers, G., Merckx, R., van Wesemael, B., Van Oost, K. (2017). Soil conservation in the 21st century: Why we need smart agricultural intensification. *Soil*, 3, 45-59, <https://doi.org/10.5194/soil-3-45-2017>.
- Hartanto, H., Prabhu, R., Widayat, A.S., Asdak, C. (2003). Factors affecting runoff and soil erosion: Plot-level soil loss monitoring for assessing sustainability of forest management. *For. Ecol. Manag.*, 180, 361-374, [https://doi.org/10.1016/S0378-1127\(02\)00656-4](https://doi.org/10.1016/S0378-1127(02)00656-4).
- Ibrahim, A. (2008). *Soil Pollution: Origin, Monitoring & Remediation*, 2nd ed.; Springer, Berlin, Germany, pp. 35-55.
- Lazar, M., Faur, F.G., Dunca, E., Ciolea, D.-I. (2017). New methodology for establishing the optimal reuse alternative of degraded lands. *Environ. Eng. Manag. J.*, 16, 1301-1308, <https://doi.org/10.30638/eemj.2017.138>.
- Liu, C.L.C., Kuchma, O., & Krutovsky, K.V. (2018) Mixed-species versus monocultures in plantation forestry: Development, benefits, ecosystem services and perspectives for the future. *Global Ecology and Conservation*, 15, e00419.
- Mette, T., et al. (2013). Climate turning point for beech and oak under climate change in Central Europe. *Ecosphere*, 4(12), 1-19.
- Pawson, S.M., Brin, A., Brockerhoff, E.G. et al. (2013). Plantation forests, climate change and biodiversity. *Biodivers. Preserve*, 22, 1203-1227, <https://doi.org/10.1007/s10531-013-0458-8>.
- Rehfeldt, G.E., Tchebakova, N.M., Parfenova, Y.I., Wykoff, W.R., Kuzmina, N.A., & Milyutin, L.I. (2002). Intraspecific responses to climate in *Pinus sylvestris*. *Global Change Biology*, 8(9), 912-929.
- Reyer, C., Guericke, M., & Ibisch, P.L. (2009). Climate change mitigation via afforestation, reforestation and deforestation avoidance: and what about adaptation to environmental change?. *New Forests*, 38, 15-34.
- Ritchie, H., & Roser, M. (2023). Deforestation and forest loss. Our world in data.
- Rudel, T.K., Coomes, O.T., Moran, E., Achard, F., Angelsen, A., Xu, J., & Lambin, E. (2005). Forest transitions: towards a global understanding of land use change. *Global environmental change*, 15(1), 23-31.
- Schuler, L.J., Bugmann, H. & Snell, R.S. (2017). From monocultures to mixed-species forests: is tree

- diversity key for providing ecosystem services at the landscape scale? *Landscape Ecol.* **32**, 1499-1516, <https://doi.org/10.1007/s10980-016-0422-6>
- Silvestru-Grigore, C.V., Dinulică, F., Spârchez, G., Hălălișan, A.F., Dincă, L.C., Enescu, R.E., & Crișan, V.E. (2018). Radial growth behavior of pines on Romanian degraded lands. *Forests*, **9**(4), 213.
- Stoll, P., Weiner, J., & Schmid, B. (1994). Growth variation in a naturally established population of *Pinus sylvestris*. *Ecology*, **75**(3), 660-670.
- Tănase, P. (2012). The relation between the diameter of the stalk and the height at the species of greyish oak installed on lands which are unsuitable for agriculture and situated on the hills of Tulcea (northern Dobrogea). *Analele Universității din Oradea, Fascicula Protecția Mediului*, Vol. XVIII, 187-192.
- Tăut, I., Moldovan, M. C., Simonca, V., Colișar, A., Boca, L. C., & Lungu, T. I. (2018). Control of pathogens and pests from stands located in degraded lands in north west of Romania. *Current Trends in Natural Sciences*, **7**(14), 22-27.
- Untaru, E. (1993). *Ameliorarea terenurilor degradate, din Istoricul și activitatea Institutului de Cercetari si Amenajari Silvice*. Editura Tehnica Silvica, Bucuresti, pp 78-84.
- Untaru, E., Constandache, C., & Nistor, S. (2012). Starea actuală și proiectii pentru viitor în privința reconstrucției ecologice prin împădurire a terenurilor degradate din România (I). *Rev. Păd.* **127**, 28-34.
- Visockiene, J.S., Tumeliene, E., & Maliene, V. (2019). Analysis and identification of abandoned agricultural land using remote sensing methodology. *Land Use Policy*, **82**, 709-715
- Vlasin, H.D. (2010). Structural and biometrical specific features of some black pine stands on eroded degraded lands in the Transylvanian Plain. *Bulletin UASVM Horticulture*, **67**(1).
- Wronski, E.B., & Murphy, G. (1994). Responses of forest crops to soil compaction. *Developments in Agricultural Engineering*, **11**, 317-342. Elsevier.
- Zecchin, B., Caudullo, G., & de Rigo, D. (2016). *Acer campestre in Europe: distribution, habitat, usage and threats*. European Atlas of Forest Tree Species; San-Miguel-Ayán, J., de Rigo, D., Caudullo, G., Houston Durrant, T., Mauri, A., Eds, e012c65.
- *** Norme tehnice privind compoziții, scheme și tehnologii de regenerare a pădurilor și de împădurire a terenurilor degradate. Ministerul Apelor, Pădurilor și Protecției Mediului Inconjurător, 2000

OPTIMIZING RESOURCES IN AGRICULTURE: A BIBLIOMETRIC ANALYSIS OF ECONOMIC STRATEGIES AND TECHNOLOGICAL ADVANCEMENTS

Iuliana Mirela PINȚĂ

University of Agronomic Sciences and Veterinary Medicine of Bucharest,
59 Marasti Blvd, District 1, Bucharest, Romania

Corresponding author email: mirela.pinta@usamv.ro

Abstract

This paper investigates the optimization of resources and activities in agriculture, focusing on increasing efficiency and productivity through modern technologies and resource management practices. Precision agriculture, crop rotation, and integrated pest management are highlighted as key methods for improving yields while minimizing environmental impacts. Bibliometric analysis was conducted on 1,366 academic publications using tools such as citation analysis and keyword co-occurrence analysis. The results show a significant growth in research on economic optimization in agriculture, with sustainability and technological advancements driving the field. Key areas of focus include resource efficiency, automation, and multi-objective optimization, with water management emerging as a critical topic. The study provides insights into the evolving research landscape, emphasizing the integration of advanced technologies such as AI, IoT, and machine learning in future agricultural practices. Although bibliometric methods offer valuable assessments, the limitations of these approaches, such as citation biases, should be considered when interpreting results. The analysis underscores the growing importance of sustainable agricultural practices and resource optimization in addressing global challenges like climate change and resource scarcity

Key words: resources, efficiency, productivity, technologies, agriculture

INTRODUCTION

The optimization of resources and activities on farms, whether crop and/or livestock production, is an important process to increase agricultural efficiency and productivity. This process of optimization involves the rational use of the resources used, including land, seeds, fertilizers, equipment, but especially water, all to maximize yield and profitability by reducing costs and environmental impact.

Integrating modern technologies as they have been developed and refined, such as precision agriculture, has become a key aspect of optimization. New technologies allow crop monitoring and management using sensors and data, and enable farmers to adjust resources in real time according to their specific needs. Other aspects practiced to reduce excessive pesticide use and contribute to soil revitalization are crop rotation and integrated pest management. In addition, economic optimization involves financial planning including cost analysis, identifying opportunities to diversify production and accessing new markets. In a nutshell,

optimization not only supports environmental sustainability but also ensures the long-term economic viability of farms.

With the mechanization of agriculture and its industrialization, resource inputs have increased exponentially to increase yields. In this respect, farmers, but especially researchers, have tried to create models for optimizing crop technologies so as to rebalance the effect-effort balance, or more specifically to achieve the optimal correlation between production and resources used.

Bibliometric analysis is a quantitative method used to measure and evaluate scientific research, its impact and collaboration between researchers. The term was introduced by Pritchard (1969), describing the use of statistics to analyse books and other forms of written communication. The main purpose of bibliometric analysis is to schematize research in a field, assess scholarly impact and identify trends and gaps in the field.

Methods and tools used include citation analysis, co-citation and keyword co-occurrence analysis. Citation analysis measures the number

of citations a paper receives, providing a clear quantification of its impact (Garfield, 1979). Co-citation, introduced by Small (1973), examines how frequently two papers are cited together, revealing conceptual links between them. In addition, co-authorship analysis can highlight scholarly collaborations (Newman, 2001).

Frequently used data sources include databases such as Scopus and Web of Science, which provide access to scholarly publications and impact assessment tools. Scopus is a preferred platform for citation analysis and assessment of international collaborations (Elsevier, 2023), while Web of Science allows the analysis of co-citation networks (Clarivate Analytics, 2023).

Bibliometric indicators include: the number of publications, the total number of citations and the h-index, an index that combines the productivity and impact of a researcher's work (Hirsch, 2005). While these indicators are useful, bibliometric analysis also has limitations. Dissensions in bibliometric assessments can arise due to the predominance of papers published in English and in open access journals, which may influence the frequency with which they are cited (van Raan, 2005). In addition, citations do not always reflect the quality of research, but rather its visibility.

Consequently, bibliometric analysis is a tool for evaluating academic research, providing an overview of scientific impact and collaborative networks. However, its results should be interpreted with caution, given the inherent limitations of this method.

MATERIALS AND METHODS

For this bibliometric analysis, we used the keywords "economic optimization in agriculture" in the Scopus search engine. This provided a starting point for identifying all relevant publications. Initially, the search returned a total of 1604 publications on this topic. Next, we applied a series of filters to refine the results and ensure that the study focused on the most relevant academic papers in the areas of interest.

Filtering publications

In the first stage of refining the results, we restricted the list to publications that include articles in academic journals, papers presented

at conferences, books and book chapters. This filter was applied to ensure a dataset composed of papers with significant scientific impact. Other types of publications, such as technical notes or review articles, were excluded to maintain a rigorous approach.

Subsequently, we applied additional filters to focus on specific areas of interest that are directly related to economic optimization in agriculture. The selected areas were:

- Environmental sciences - to include studies related to the sustainability of resource use and the impact of economic optimization on the environment;

- Agricultural and Biological Sciences - the main area addressing agricultural practices and technologies underlying economic optimization;

- Engineering - to cover technical aspects and innovations that can contribute to resource optimization;

- Energy - covering the essential role of energy in agriculture, including energy efficiency solutions;

- Business, Management and Accounting - to examine the economic, management and planning dimensions of optimization in agriculture;

- Economics, Econometrics and Finance - this area was selected to understand the economic modeling and financial viability studies of different strategies used both in agricultural practices and in informing decisions;

- Multi-disciplinary - we included this category to capture publications that do not fall strictly within a single field, but make contributions to a holistic understanding of the topic.

Applying these filters reduced the number of publications to 1366 relevant papers, which will be analyzed in detail in this chapter. After refining the results, the 1366 publications represent a significant selection of papers exploring economic optimization from diverse perspectives, ranging from technological innovations and management practices to energy solutions and economic models. A detailed analysis of these papers can contribute to an integrated understanding of economic optimization in agriculture and its impact on

sustainability and efficiency in the agricultural sector.

RESULTS AND DISCUSSIONS

The number of publications on economic optimization in agriculture has shown significant growth between 2012 and 2022 (Figure 1). Initially, there was a gradual increase in the number of publications from 2012 to 2016, indicating an emerging interest in the topic. The pace of growth accelerated from 2017 onwards, reaching 181 publications in 2020. This can be attributed to advancements in technology and the digitalization of agriculture, which have created new opportunities for optimizing resources and production. The COVID-19 pandemic and its impact on supply chains and agricultural systems have also fueled research on more resilient solutions. Additionally, global issues such as climate change, sustainability, dwindling resources, and EU regulations have contributed to the increased focus on economic optimization in agriculture. The growing need for research is driven by the implementation of policies supporting sustainable agriculture and the reorganization of agricultural practices to align with these policies.

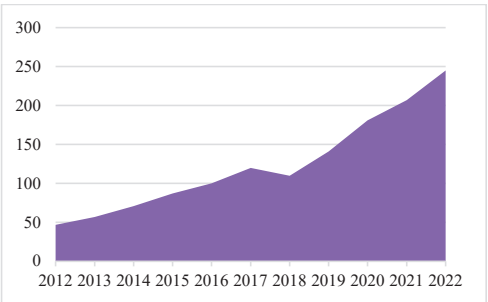


Figure 1. The evolution in number of publications in the period 2012-2022

Source: own processing based on data extracted from Scopus

Analysis of the number of publications shows that economic optimization in agriculture has become increasingly important in scientific literature. The steady increase in the number of publications over the last decade, especially after 2017, reflects the growing concerns about the efficiency and sustainability of agriculture in

the face of global challenges. This trend suggests that the topic will continue to be widely explored in the years to come, given the ongoing need to optimize agricultural resources and processes.

The top 10 journals with the highest number of publications related to economic optimization in agriculture is dominated by Nongye Gongcheng Xuebao/Transactions of the Chinese Society of Agricultural Engineering, which includes 77 publications. This is followed by Journal of Cleaner Production with 54 publications and Science of the Total Environment with 41 publications. Other relevant journals include Agricultural Water Management with 38 publications and IOP Conference Series: Earth and Environmental Science, along with Agricultural Systems, both with 33 publications each. Journal of Environmental Management stands out with 29 publications, while Sustainability (Switzerland) and Water (Switzerland) contributed with 24 and 22 publications respectively. Finally, Computers and Electronics in Agriculture published 19 papers. These journals are essential sources of research on economic optimization in agriculture. The 10 journals contain a total of 370 publications (Table 1). This number represents about 27.09% of the total 1366 publications on economic optimization in agriculture.

Table 1. Ranking of journals by number of publications

Journal title	Publication number	Percentage of total (%)
Nongye Gongcheng Xuebao/Transactions of the Chinese Society of Agricultural Engineering	77	5.64
Journal of Cleaner Production	54	3.95
Science of the Total Environment	41	3
Agricultural Water Management	38	2.78
IOP Conference Series: Earth and Environmental Science	33	2.42
Agricultural Systems	33	2.42
Journal of Environmental Management	29	2.12
Sustainability (Switzerland)	24	1.76
Water (Switzerland)	22	1.61
Computers and Electronics in Agriculture	19	1.39
Total	370	27.09

Most research publications in the field of economic optimization in agriculture consist of scientific articles, which account for about 81.7% of all publications, with a total of 1116 articles. Conference papers follow, representing approximately 14.2% of the total, with 194 publications. These findings suggest that a significant portion of research and findings in this field are initially presented and discussed at academic conferences. Book chapters constitute about 3.5% of the total publications, with 48 chapters. These chapters often explore specific topics in greater detail within a broader or interdisciplinary context and are commonly found in reference works. Books have the smallest share, with only 8 publications, making up about 0.6% of the total. This indicates that while there is interest in the field, research in the area is primarily published in shorter formats like articles and conference papers, as opposed to longer works like treatises or books.

The 8 books identified as part of the bibliometric analysis related to economic optimization in agriculture cover a wide range of topics relevant to sustainable development and agricultural efficiency at the global and regional level. Here is a brief overview of each paper:

- *Biogas Systems in China* (Deng et al., 2014) - This book analyzes the use of biogas in China, highlighting the economic and environmental benefits of this system for agriculture. It is an important resource for energy optimization and reducing dependence on conventional energy sources in agriculture.
- *Climate Smart Agriculture in South Asia: Technologies, Policies and Institutions* (Hossain & Awasthi, 2019) - This paper focuses on the implementation of climate smart agriculture in South Asia, discussing technologies and policies aimed at optimizing agricultural resources and reducing the impact of climate change on production.
- *The Economy in Romania and the Need for Optimization of Agricultural Production Structures* (Popescu, 2017) - This book discusses the need for optimization of agricultural production structures in Romania, highlighting the importance of economic adjustments to increase the efficiency and competitiveness of agriculture in the Romanian economic context.

- *Modeling and Optimization of Biomass Supply Chains: Top-down and Bottom-up Assessment for Agricultural, Forest and Waste Feedstock* (Gonzalez-Sanchez & Elbersen, 2016) - This paper addresses the modeling and optimization of biomass supply chains, with a focus on the assessment of agricultural, forest and waste feedstock. It is particularly relevant for developing sustainable and economical solutions in agriculture.

- *Plant Genetic Resources, Inventory, Collection and Conservation* (Engels & Ramanatha Rao, 2002) - This book explores the management of plant genetic resources, with a focus on inventory, collection and conservation, which are essential aspects for optimizing agricultural production and maintaining the genetic diversity necessary for sustainable agriculture.

- *Process Management in Spinning* (Chakraborty, 2018) - This paper presents information on process management in the textile industry, with direct applications in streamlining production in textile fiber-related agriculture, such as cotton and other technical crops.

- *Specifications of Photovoltaic Pumping Systems in Agriculture: Sizing, Fuzzy Energy Management and Economic Sensitivity Analysis* (Alahmed & Cherkaoui, 2020) - The book discusses the specificities of photovoltaic systems in agriculture, providing solutions for their efficient energy management and economic sensitivity analysis. It is a relevant work for optimizing energy resources on modern farms.

- *Structural Change, Productivity, and Climate Nexus in Agriculture: An Eastern European Perspective* (Csaki & Forgacs, 2021) - The paper addresses the relationship between structural change, productivity, and climate change in agriculture, focusing on the Eastern European perspective. It analyzes how structural adaptations can lead to more efficient and sustainable agriculture.

Keyword link analysis

This paper discusses the central terms and their link strength in the scientific literature on economic optimization in agriculture. The terms "agriculture" and "optimization" are the most central, indicating that these topics are frequently correlated with other topics in the

literature. The term "Economics" and related terms such as "economic and social effects" and "sustainable development" are also central, highlighting the importance of economic aspects and social effects in the context of sustainable agriculture. Additionally, the terms "water supply" and "water management" are central in discussions on optimizing water resources in agriculture, particularly considering the increasing droughts in recent years. The total link strength of a term represents the strength of its relationships with other terms in the network, indicating its centrality and importance in the field (Table 2 and Figure 2).

Table 2. Links between terms and total strength of links

Terms	Links	Total strength of links
Agriculture	441	8104
Optimization	439	7448
Economics	427	3132
Economic and social effects	426	3455
Sustainable development	423	3276
Article	416	3931
Water supply	399	3376
Decision making	397	2675
Water management	396	3693
Crops	391	2534

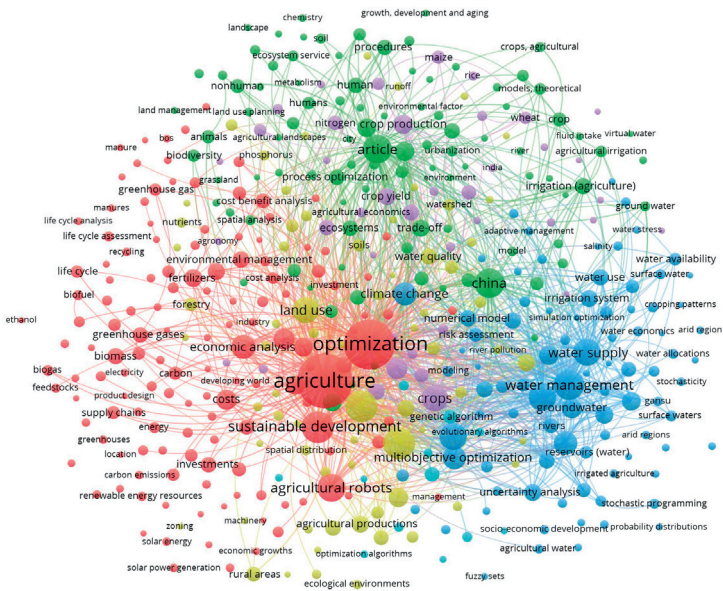


Figure 2. Map of links between terms
Source: own processing with VOS Viewer based on data extracted from Scopus

The future of research in economic optimization in agriculture will be driven by advanced technologies like deep learning, machine learning, and the Internet of Things (IoT). These technologies will play a crucial role in the transformation of agriculture towards precision agriculture. They enable real-time data collection and analysis, allowing for automated decision-making on farms. Precision agriculture will be achieved through the use of autonomous cars and drones equipped with IoT sensors, which will monitor soil and plant health. Deep learning will be utilized for problem recognition and management, including detecting crop

diseases, monitoring environmental factors, and optimizing irrigation. This integration of technology and smart solutions in agriculture will enable farmers to maximize crop yields and minimize resource losses. Sustainability and resource efficiency in agriculture are also of growing concern, with issues related to water resource management and multi-objective optimization being key areas for research. Overall, the future of agricultural research will be characterized by the integration of advanced technologies and the focus on sustainability (Figure 3).

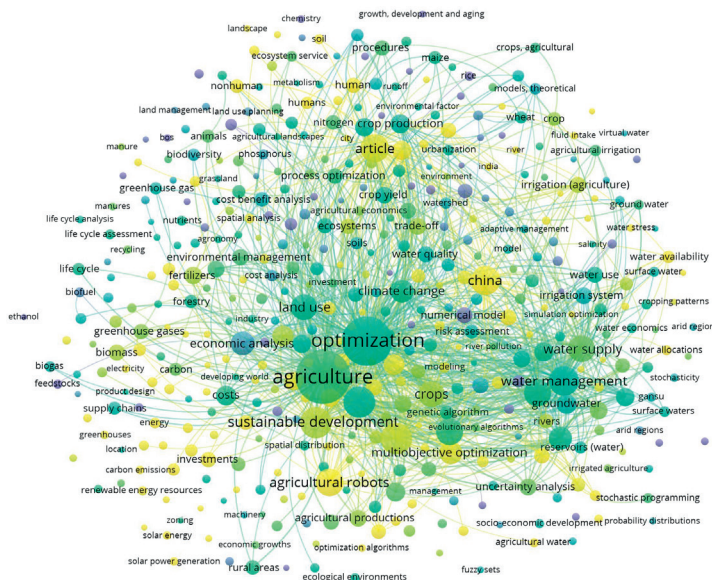


Figure 3. Map of terms by year of publication
 Source: own processing with VOS Viewer based on data extracted from Scopus

Research in water resources is crucial due to climate pressures and global water scarcity. The future of agriculture depends on efficient water management, which will be supported by research in irrigation, water harvesting, and reuse technologies. To address limited water and space resources, innovative systems like vertical farms and controlled environment farming will be developed for more sustainable and efficient agriculture.

Multi-objective optimization and predictive models will play a significant role as well. We can expect a deeper integration of these methods into agricultural processes. Multi-objective models enable decisions that optimize multiple criteria simultaneously, such as crop yield, costs, and environmental impact. Advanced optimization algorithms will provide tailored solutions for different regions and climatic conditions. Moreover, advanced predictive models will be developed to anticipate extreme events like floods and droughts, with suggestions for optimal preventive measures. Integration with machine learning technologies will allow real-time updates based on new data, enhancing the accuracy and reliability of these models.

The future of agriculture will largely be focused on automation, with the aim of reducing manual

labour and increasing efficiency through the use of autonomous machines, robots, and artificial intelligence. Agricultural robotics will play a significant role in transforming the sector, with robots being utilized for tasks such as planting, harvesting, and plant care. Additionally, there will be a growing emphasis on sustainability and reducing carbon footprints, leading to an increase in research into regenerative agriculture practices. These practices, like carbon sequestration and resource recycling, will become mandatory in efforts to minimize environmental impact. Achieving carbon neutrality will be a key objective for farmers, and agriculture will be at the forefront of implementing initiatives to reduce greenhouse gas emissions. Integrated digital platforms will also become more prevalent in the agricultural industry, aggregating data from various sources such as IoT, drones, and predictive modelling. This real-time information will enable farmers to make data-driven decisions on planting, fertilizing, and harvesting.

CONCLUSIONS

The bibliometric analysis carried out, based on 1366 publications, highlighted the main research directions in economic optimization in

agriculture. Based on the distribution of terms, co-occurrences and clusters identified, we can draw the following conclusions supported by concrete figures:

- Sustainability and natural resource management: cluster 1, the largest, contains 138 terms and is centred on sustainability. Terms such as agriculture (with 441 links and a total strength of 8104) and sustainable development (423 links, strength of 3276) highlight the importance of research on sustainability in agriculture. Research focuses on the efficient use of resources, especially water and land, to meet the challenges of climate change.
- Emerging technologies and automation in agriculture: Cluster 6, which includes 12 terms, focuses on advanced technologies such as genetic algorithms (274 links, total strength of 765) and machine learning (97 links, strength of 147). These terms show a growing interest in agricultural automation through artificial intelligence and optimization algorithms. This line of research is supported by advances in deep learning and artificial neural networks, which enable more accurate decision-making and optimization of complex agricultural processes.
- The economic and social importance of decisions in agriculture: Cluster 4 (68 terms) is centred on the economic efficiency and social impact of decisions in agriculture. Terms such as economics (427 links, strength 3132) and economic and social effects (426 links, strength 3455) emphasize that research focuses on the economic and social analysis of agricultural decisions, assessing their impact on costs, efficiency and regional development.
- Multi-objective optimization and increasing productivity: Cluster 5, with 40 terms, reflects efforts to maximize agricultural productivity. The terms crops (391 links, strength 2534) and crop yield (290 links, strength 967) show a significant focus on improving the yield and efficiency of agricultural crops. In addition, the term multi-objective optimization (292 links, strength 803) indicates the use of advanced optimization techniques to balance cost, yield and sustainability in agriculture.
- Water resources management and strategic decision making: Cluster 3 (88 terms) is centred on water resources management and decision making. The terms water supply (399 links,

strength 3376), water management (396 links, strength 3693) and decision making (397 links, strength 2675) emphasize that optimizing water use is a crucial topic in agriculture.

REFERENCES

- Alahmed, Z., & Cherkaoui, R. (2020). *Specifications of Photovoltaic Pumping Systems in Agriculture: Sizing, Fuzzy Energy Management and Economic Sensitivity Analysis*. Springer.
- Chakraborty, P. (2018). *Process management in spinning*. CRC Press.
- Clarivate Analytics. (2023). Web of Science Core Collection: Overview.
- Csaki, C., & Forgacs, C. (2021). *Structural Change, Productivity, and Climate Nexus in Agriculture: An Eastern European Perspective*. Springer.
- Deng, Y., Zhang, Y., & Yuan, Z. (2014). *Biogas systems in China*. Springer.
- Despommier, D. (2013). Future food-production systems: Vertical farming and controlled-environment agriculture. *Environmental Health Perspectives*, 121(11-12), 795-800. <https://doi.org/10.1289/ehp.1205690>
- Elsevier. (2023). *Scopus: Content Coverage Guide*. Elsevier Publishing.
- Engels, J.M.M., & Ramanatha Rao, V. (2002). *Plant Genetic Resources, Inventory, Collection and Conservation*. CABI Publishing.
- Garfield, E. (1979). *Citation Indexing – Its Theory and Application in Science, Technology, and Humanities*. New York: Wiley.
- Gonzalez-Sanchez, R., & Elbersen, B. (2016). *Modeling and optimization of biomass supply chains: Top-down and bottom-up assessment for agricultural, forest and waste feedstock*. Elsevier.
- Hirsch, J.E. (2005). An index to quantify an individual's scientific research output. *Proceedings of the National Academy of Sciences*, 102(46), 16569-16572.
- Hossain, A., & Awasthi, L.P. (2019). *Climate Smart Agriculture in South Asia: Technologies, policies and institutions*. Springer.
- Newman, M.E.J. (2001). The structure of scientific collaboration networks. *Proceedings of the National Academy of Sciences*, 98(2), 404-409.
- Popescu, G.H. (2017). *Economy in Romania and the need for optimization of agricultural production structures*. Nova Science Publishers.
- Pritchard, A. (1969). Statistical bibliography or bibliometrics? *Journal of Documentation*, 25(4), 348-349.
- van Raan, A.F.J. (2005). Fatal attraction: Conceptual and methodological problems in the ranking of universities by bibliometric methods. *Scientometrics*, 62(1), 133-143.
- Small, H. (1973). Co-citation in the scientific literature: A new measure of the relationship between two documents. *Journal of the American Society for Information Science*, 24(4), 265-269.

IMPLEMENTATION OF METHODS AIMED AT SUSTAINABLE DEVELOPMENT THROUGH BIONICS

Cristian-George DRAGOMIRESCU¹, Victor ILIESCU²

¹National University of Science and Technology POLITEHNICA Bucharest,
313 Splaiul Independentei, District 6, Bucharest, Romania

²University of Agronomic Sciences and Veterinary Medicine of Bucharest, 59 Marasti Blvd,
District 1, Bucharest, Romania

Corresponding author email: victor.iliescu@ymail.com

Abstract

Given the significance of the concept of sustainability and the methods used to fulfil its objectives, the paper aims to highlight the possibility of utilizing Bionics to find and implement methods aimed at sustainable development.

In the authors' opinion, the mentioned methods and means can be complemented by using Bionics as a source of documentation and implicitly applying models aimed at increasing sustainability.

Considering the specificity of this science to decode the "inventions of living nature" by observing natural phenomena, mathematical modelling, prototyping, and verifying theoretical results with practical outcomes, the paper presents several classic examples that contribute to the effort for sustainable development: the drag reduction effect in all fluid flows, based on the shark skin model, used in creating a coating for aircraft to reduce energy consumption, or swarm intelligence of bees and ant algorithms that transfer the behaviour of insects and other animals living in larger communities into technical areas.

Key words: Bionics, sustainable development, method, biological models.

INTRODUCTION

The introduction is based mainly on four papers (European Commission, 2019; European Commission, 2021; European Commission, 2023; European Environment Agency, 2023). Accordingly, sustainability is a highly relevant concept in contemporary society and broadly refers to the ability to perpetuate a process continuously over a defined period.

In the context of business policies and practices, sustainability denotes the capacity to operate and produce without depleting the planet's resources, with the intent of preserving them for as long as possible.

Sustainability, or sustainable development, was first defined by the United Nations in the Brundtland Report over 30 years ago as the capacity to exist and progress without exhausting natural resources. Consequently, sustainability involves meeting humanity's present needs without compromising the resources designated for future generations.

The concept of sustainable development originates from the understanding that Earth's resources are finite, thus limited, and must be

utilized responsibly and conservatively to mitigate the negative effects that could adversely affect the environment. The sustainability concept is built upon three pillars: environmental, economic, and social—colloquially referred to as planet, profit, and people.

Currently, there are two principal categories of sustainability: economic sustainability and financial sustainability.

Economic sustainability refers to growth based on well-structured plans and projects, in which medium- and long-term resources intended for core activities are clearly delineated. Additionally, these plans detail the manner in which resources will be utilized, as well as how waste will be collected, stored, transported, and reused, ensuring these operations contribute to the economic prosperity of the business and align with sustainable development goals.

Financial sustainability is closely related to economic sustainability, in that all projects for sustainable development can attract various funding sources and financial instruments. Simultaneously, financial sustainability leads to

reduced raw material costs by optimizing production or service expenditures.

The concept of sustainable development encompasses all forms and methodologies available to both the general population and businesses for utilizing natural resources, aiming to establish a balance between social, economic, and environmental considerations, with a focus on environmental protection.

A developed society must exhibit a high degree of sustainability to achieve harmonious development. Sustainable behaviour is characterized by efforts to protect the environment and the incorporation of ecosystem-friendly practices into daily life.

The notion of sustainable development is supported by current legislation, which has been aligned with the latest European regulations in this field. These regulations pertain to environmental monitoring, selective collection and recycling of resources, environmental legislation, and the adoption of green energy technologies.

The United Nations has outlined sustainable development goals (SDGs) aimed at ensuring a better and more sustainable future. These seventeen goals tackle global challenges related to sustainability, including poverty eradication, zero hunger, clean water and sanitation, affordable and clean energy, and responsible consumption and production. The objective is to achieve these targets by 2030.

In 2018, the European Commission introduced six key transformations, which, if properly implemented, will enable improved sustainability by 2050:

- Enhancing education and healthcare to achieve higher income levels and make more informed environmental decisions.
- Responsible consumption and production, emphasizing doing more with fewer resources to support the adoption of a circular economy and reduce demand.
- Decarbonising the energy industry through the use of clean and renewable energy resources to provide affordable and sustainable energy.
- Ensuring clean food and water through the protection of the biosphere and oceans by fostering efficient and sustainable food systems. This can be achieved by increasing

agricultural productivity and reducing meat consumption.

- Developing smart cities through intelligent infrastructure and internet connectivity.
- Promoting a digital revolution in science, technology, and innovation to support sustainable development.

In conclusion, a sustainable society must be socially responsible, focusing on environmental protection and maintaining a dynamic equilibrium between human and natural systems.

MEANS OF ACHIEVING PROPOSED OBJECTIVES

Considering a recent work (Ioniță, 2023) and common knowledge popularised on several media channels (twi-global.com, 2023; spotmedia.ro, 2023; ecosynergy.ro, 2023) we may describe the means of achieving proposed objectives as follows.

In the last decade, several methods have been analyzed for society to achieve sustainability, ensuring that the environment is adequately protected. Humanity can develop without depleting or excessively exploiting planetary resources, nor should they be degraded or destroyed.

One of the most salient examples involves the ever-increasing quantity of waste, which affects both terrestrial and aquatic environments, significantly impacting the quality of life for humans and animals and contributing to pollution. Thus, a business can become economically sustainable in terms of waste collection by devising a sustainable development plan, which ensures compliance with reporting, collection, and valorisation obligations for packaging waste until legal requirements are met. These obligations may also attract financial support.

When addressing waste collection, economic sustainability can be achieved by creating short- and medium-term plans that implement various recycling solutions for packaging. The ultimate goal is to reduce costs associated with collecting, sorting, storing, and transporting waste to specialized companies that can transform it into reusable resources.

Selective collection and the reuse of packaging and waste represent some of the most effective

concepts of sustainability, enabling companies to contribute to sustainable development. Waste collection and transformation should form the foundation of all societies aiming to achieve prosperity and healthy development. By expanding the process of waste collection and recycling, pollution levels can be reduced.

In many regions of the world, massive pollution causes numerous problems. *Factories release chemicals into the air or discharge pollutants into rivers, seas, and oceans*, affecting both flora and fauna, as well as human health. It is crucial *to reduce pollution levels* in order to safeguard public health and secure a future that is not jeopardized by more severe environmental problems.

In addition to air pollution, there are other pressing environmental challenges. For instance, *waste that enters rivers, lakes, seas, and oceans* severely impacts aquatic flora and fauna, leading to ecological imbalances. Aquatic life is endangered, and *many plant and fish species are on the brink of extinction*. Moreover, *chemical spills into the soil* compromise the quality of agricultural crops, leading to poor crop development.

To mitigate these challenges, humanity must turn toward methods to prevent and combat pollution in these environments. In addition to *proper waste collection and secure storage that minimizes environmental impact*, *waste must also be recycled*. Furthermore, citizens can support sustainable businesses that utilize *biodegradable products or packaging*, cloth bags that can be washed and reused, and *eco-friendly cutlery*. Additionally, clothing made *from eco-friendly materials* should be adopted. *Waste must be disposed of in specially designated bins in central or residential areas*, which are equipped with separate compartments for plastic, paper, glass, and metal. Food waste should be disposed of in spaces reserved for organic waste.

A sustainable lifestyle can be adopted at both the individual and corporate level by engaging in selective waste collection and the valorisation of all waste that can generate reusable raw materials, by conserving resources, and by using clean energy wherever possible. It is widely recognized that *fossil fuels take significantly longer to regenerate than the time it takes for humans to consume them*,

which means they are not a sustainable energy source. Solar and wind energy, by contrast, are renewable resources available almost continuously, depending on the region, making them viable for indefinite energy supply.

Sustainability is a vital component of any economic activity, as it involves reintegrating primary resources and raw materials obtained from recovered elements through selective collection. This leads to sustainable development, and natural resources can thus be protected, conserved, or preserved for future generations. Sustainable development also involves a commitment to reducing the negative environmental impacts, particularly through the extensive use of renewable energy sources.

Significant financial savings can be achieved, and these savings can be reinvested in modernizing equipment, production facilities, and logistics, or even transitioning to a more advanced level through automation or robotic systems, improving overall labour efficiency.

By considering *tidal and wave energy*, we already possess enough renewable resources to achieve global energy independence.

With *the ongoing climate crisis*, sustainability is increasingly becoming a priority for businesses, as people are becoming more aware of these phenomena and adapting their lives to align with legislative standards. It is likely that in the future, the positive impact on the climate throughout the entire value chain, the enhanced impact on the environment, the improvement in human health, and the productive contribution to society will become the responsibility of companies across all industrial sectors. Environmental damage and harmful emissions must be either reduced or eliminated from production processes.

Moreover, there is a focus on reusing resources to accommodate the global population growth through the implementation of a *circular economy*, allowing one person's waste to become another person's resource. This would drastically reduce waste and create a more efficient supply chain.

By recycling old products—such as aluminium, gold, or copper, which cannot be replaced with alternative materials—we can extend the lifespan of these resources, contributing to sustainability.

Reducing the carbon footprint across all sectors, better water resource management, and even developing solutions to create new potable water reserves for vulnerable areas are essential. Meeting energy demands without releasing harmful emissions is crucial to achieving healthy living, energy independence, and ecosystem preservation.

In the authors' view, the aforementioned methods and solutions can be supplemented through the use of Bionics as a documentation source and implicitly applying models aimed at enhancing sustainability.

PRINCIPLES OF BIONICS

Speaking about Bionics (Rechenberg, 1973; Schwessinger, 1994) we may say that Bionics - alternatively termed biomimetic or biomimesis - is the discipline concerned with the systematic deconstruction of the "inventions" of living nature and their innovative implementation into technological applications. The foundational premise is that natural structures, processes, and systems have been (relatively) optimized through evolutionary mechanisms.

Bionics operates as an interdisciplinary field, where researchers from diverse domains such as biology, engineering, and, when necessary, architecture, philosophy, and design collaborate to develop novel solutions.

The term BIONIK (originating from the German language) is derived from a combination of the words "biology" and "technology." This reflects the discipline's central objective - harnessing principles derived from biological systems and applying them to technical challenges. Bionics goes beyond mere natural inspiration by systematically identifying and decoding these principles for direct technological implementation.

There are two primary pathways in bionics:

Analogical Bionics (a "top-down" approach), where solutions to engineering problems are specifically sought within biological systems. This method involves identifying biological analogies, analyzing them, and utilizing these insights to solve technical challenges. In this case, the biological model is retained and applied to the design or problem in question.

Abstraction Bionics (a "bottom-up" approach), where biological principles are abstracted and

detached from their natural context. These principles are then used as templates to conceptualize solutions for technological issues that may not have a clear biological counterpart. This involves recognizing a fundamental principle within a biological model, abstracting it into general scientific terms, and then developing applications in collaboration with engineers, designers, and other technical experts.

Bionics is a highly interdisciplinary field, enriched by new and enhanced investigative methodologies, including advanced computing, modern manufacturing processes, and cross-disciplinary input. While engineers developing functional technical elements were not always aware of corresponding biological solutions, bionics explicitly searches for structures, processes, and systems within nature that are potentially significant from a technical perspective.

This search for biological analogies is not an accidental discovery, but a systematic and intentional exploration.

Bionic's *main domains of application*:

- Bionics has found utility across a wide spectrum of domains, each reflecting the versatility and applicability of biological solutions.
- Construction Bionics: Investigates biological structural elements and compares them with engineering constructions to optimize load distribution, stability, and material efficiency.
- Sensor Bionics: Examines biological sensor systems for the reception and processing of stimuli, such as vision, olfaction, or auditory systems, and applies these principles to improve technological sensors.
- Motion Bionics: Focuses on the study of locomotive systems in nature, such as propulsion mechanisms and flow control in animals. For instance, studying the surface structures and flow regulation mechanisms of marine animals can lead to advancements in aerodynamics and hydrodynamics.
- Neurobionics: Investigates the natural transfer and processing of information in biological neural systems, translating these mechanisms into information systems and robotics.

- **Process Bionics:** Analyzes biological processes, such as photosynthesis, with the goal of optimizing energy transfer, resource utilization, and efficiency in industrial processes.
- **Anthropobionics:** Studies biological movement—particularly in animals—for applications in robotics and artificial intelligence. This includes replicating animal behaviours or movement mechanics in machines and automation systems.
- **Climatic Bionics:** Engages with natural systems for ventilation, cooling, and heating, using biological models to develop passive and efficient systems in architecture and climate control technologies.

Bionic approaches can be categorized into two methods for addressing technical problems. First we mention *Bionics as a "Top-Down" Process (Analogical Bionics)*: In this approach, biological analogies are sought in nature, thoroughly analyzed, and then applied to technical challenges. By leveraging biological knowledge, this method mirrors the principles observed in nature within technical contexts.

Examples:

- **Bird flight:** The vortex structures observed at the tips of bird wings, such as those of condors and vultures, have led to the design of winglets on aircraft. These winglets reduce the large vortices created at the wingtips, which are responsible for significant fuel consumption. By mimicking the multi-vortex structure of bird wings, engineers achieved a reduction in aircraft fuel consumption by 5-6%.
- **Cat paw biomechanics:** When changing direction, the cat's paws expand, increasing the contact area with the ground, thus improving stability. This observation inspired the development of advanced tire profiles that improve vehicle grip, stability, and safety in various driving conditions.
- **Spider leg mechanics:** Autonomous control mechanisms observed in spider legs have led to the creation of spider-like robots, which exhibit greater productivity and efficiency compared to centrally controlled robots.

Secondly, *Bionics as a "Bottom-Up" Process (Abstraction Bionics)*: This method starts with fundamental biological research, identifying

underlying principles in biological systems, abstracting them, and then seeking possible technical applications.

Examples:

- **Lotus leaf effect:** The water-repellent and self-cleaning properties of lotus leaves—where water droplets roll off without adhering—have inspired patented technologies for non-wettable and self-cleaning surfaces. These are now used in products such as facade paints that remain clean over time by mimicking the lotus effect.
- **Shark skin structure:** The study of shark skin, which consists of tiny, closely packed scales with fine grooves aligned parallel to the flow of water, has led to the development of riblet films. These films, applied to the surface of aircraft, reduce drag by minimizing air resistance and thus lead to significant reductions in fuel consumption.
- **Swarm intelligence:** The behaviour of bee swarms and ant colonies - specifically how they self-organize and solve complex problems - has been transferred into technical systems such as information processing algorithms. These swarm-based models are used to optimize various technical applications, including distributed computing and network management.

A possible conclusion: Bionics reflects the study of the biologic evolution results from the engineer perspective.

CLASSICAL APPLICATIONS OF BIONICS RELATED TO SUSTAINABILITY IN TECHNICAL FIELD

Discoveries derived from observing nature (Rechenberg, 1973; Schwessinger, 1994; Niedner, 2017), which are subsequently transformed into technical solutions, align with the strategic objectives of sustainable development, regardless of the methods employed.

The following section reviews various technical applications that illustrate the significance of bionics, particularly from the perspective of sustainability.

In the materials science domain, several notable advancements have been made such as:

- **Solar Paint (BRESOPAN):** A novel material used in the production of energy through photovoltaic processes, contributing to cleaner energy solutions.
- **Self-structuring bridges (Ossit):** Inspired by biological systems, the structural design of bridges can adaptively reinforce itself, enhancing load-bearing capacity. This increases durability and promotes material efficiency, thus contributing to sustainability by reducing the amount of material needed.
- **Self-healing materials (NovoOssit):** Drawing on biological mechanisms, these materials have the ability to automatically repair damage, such as filling potholes in roads. This innovation not only extends the lifespan of infrastructure but also reduces the demand for new material production, which is energy-intensive. Additionally, the decrease in infrastructure failures contributes to accident prevention, further emphasizing its importance in the sustainable development context.
- **Resilin-based rubber (Resilindex):** Inspired by resilin, a highly elastic protein found in the joints of insect wings, this nearly perfect synthetic rubber offers superior resilience and energy efficiency. Its application in various mechanical systems reduces energy loss and increases overall durability.

In the transportation sector, innovations stemming from biological observations have led to significant advances in energy efficiency:

- **Shark-inspired micro-longitudinal grooves:** The development of specialized surface textures mimicking the dermal denticles of shark skin has resulted in a reduction of drag, significantly improving the aerodynamic performance of aircraft. These grooves help to streamline airflow, contributing to a reduction in fuel consumption by up to 80%.
- **Flexible surfaces and dolphin-like propulsion:** Borrowing from the hydrodynamic efficiency of dolphins, flexible surfaces that mimic their skin dynamics are applied in aircraft and submarines to further enhance energy

efficiency. This innovation leads to a 90% reduction in fuel consumption for submarines by utilizing biologically inspired damping properties.

- **Medusa-inspired propulsion:** Mimicking the motion of jellyfish, this system offers efficient propulsion for submarines by reducing energy losses and improving underwater manoeuvrability.

In the domain of waste management, the implementation of protein-based mechanisms (PROMIM) offers a biologically inspired solution for waste reduction and material recovery. Regarding neuro-bionic applications, the coupling of artificial sensory organs with parallel neural networks (PNN) presents groundbreaking advancements in neural systems, contributing to enhanced sensor technology and neural communication.

In the field of agriculture, innovative bionic applications offer biological pest control solutions. For instance, the bionic cleaning beetle and dragonfly-based models are employed to eliminate agricultural pests, such as the Colorado potato beetle, reducing the need for harmful chemical pesticides.

Swarm engineering draws inspiration from the behaviour of bees, utilizing their collective intelligence in various technical domains, including construction and distributed system management. This bio mimetic approach allows for optimized structural designs and resource-efficient construction techniques.

The key to these bionic applications lies in their energy-saving potential, enhanced material longevity, and reduction of resource consumption. By adopting nature's optimized strategies, technological developments benefit from increased sustainability, which aligns with long-term economic efficiency and environmental protection goals.

These examples underscore the transformative potential of bionics in driving sustainable innovation. By reducing the reliance on non-renewable resources, enhancing energy efficiency, and creating systems that can self-repair or self-regulate, bionic applications contribute significantly to minimizing environmental impact while maximizing technological performance.

CLASSICAL APPLICATIONS OF BIONICS RELATED TO SUSTAINABILITY IN ECONOMIC AND MANAGEMENT FIELDS

Nature serves as a model for management systems, particularly in the optimization of process flows and communication between organizations (Niedner, 2017; Futur, 2022; Futur, 2023). A classic example lies in the behaviour of ants, which locate food sources efficiently because ants that have already found the food leave a pheromone trail behind. Other ants can then follow these trails, ensuring a highly efficient process for locating resources. This biological behaviour has been replicated in logistics, where companies utilize algorithmic models based on the ants' pheromone tracking system to design optimal transport routes, thereby reducing transit times, lowering costs, and minimizing carbon dioxide emissions.

Researchers working within the domain of economic bionics also study the communication strategies of colony-forming insects, seeking insights that can be applied to team management and organizational behaviour. In this context, swarm intelligence offers a model for solving complex problems through decentralized interaction. Just as individual ants or bees contribute to the collective decision-making process, companies can emulate this model by encouraging collaborative problem-solving, where new ideas are pursued and developed through group participation. This also suggests that managers should be willing to invest time in exploring and implementing innovative concepts, much as nature optimizes survival through gradual adaptations and mutations.

In the realm of evolutionary economics, it becomes evident that companies should not seek to impose constant technological progress by force, but rather engage in a more adaptive approach, akin to natural selection processes. In nature, mutations and variations arise organically, leading to breakthroughs in survival and efficiency. Similarly, companies should not only focus on generating new products but also revisit and refine existing solutions that have proven effective. This evolutionary perspective on management

supports the idea that businesses must be agile and responsive to external changes, avoiding a linear or rigid trajectory.

The field of evolutionary economics proposes techniques that assist organizations in preventing and managing future economic crises, drawing on the premise that companies are dynamic and complex systems rather than mechanistic and predictable entities. One key insight from this field is that the complexity and unpredictability of a company's growth mirrors the fluctuating patterns seen in nature. Much like the evolutionary process, businesses experience phases of expansion and contraction, and these cycles of growth and crisis are inherent to their development. Consequently, economic bionics suggests that crises are not abnormal phenomena but are part of the natural lifecycle of organizations. The focus should be on developing adaptive strategies to manage these crises, rather than attempting to prevent them entirely.

Biological systems in nature are well-equipped to handle adverse conditions by evolving over time. Plants and animals anticipate challenges, developing traits that enable rapid adaptation. Similarly, companies need to have robust early warning systems in place to detect and respond to impending crises. In this context, corporate strategy should prioritize long-term sustainability rather than short-term profit margins, as relying solely on quarterly financial results is an insufficient measure of corporate health. For organizations to grow sustainably, they must continuously adapt to evolving external conditions, not just when they face immediate threats. This concept is mirrored in natural ecosystems, where organisms are in a constant state of adaptation to ensure survival. Similarly, companies should embrace evolutionary strategies that allow them to shift business models as needed, which is often essential for long-term viability.

Furthermore, each organization must develop its own tailored solutions for the challenges it faces, rather than focusing solely on eliminating competitors. Internal cooperation among departments should be encouraged, rather than fostering internal competition, just as cooperation within natural communities - such as those in bee hives or ant colonies - leads to increased productivity and survival. In

such biological systems, the collective effort is always greater than the sum of individual actions.

In responding to crises, companies should not limit their strategies to cost-cutting, restructuring, or process optimization. These measures are often insufficient on their own. Instead, what is required are soft management skills, such as leadership, the development of cooperative abilities, and the flexibility to embrace change within an organization.

In summary, the bionic approach in economics emphasizes that recurring crises and periods of change are an inherent part of organizational growth. Thus, companies must develop the flexibility to leverage both opportunities and risks, using evolutionary principles to manage periods of turbulence effectively.

Nature, while not inherently more equitable or just, does provide an invaluable framework of flexibility and innovation from which organizations can learn. Nature's adaptive processes, honed over millions of years, offer a blueprint for understanding how complex systems survive and thrive. By adopting these strategies, companies can enhance their sustainability, resilience, and long-term success.

Biological diversity, with its millions of species, ecosystems, and landscapes, represents a vast repository of natural wealth that has direct implications for human existence. However, in national budgets and corporate balance sheets, the conservation of nature is often seen primarily as a cost, rather than as an investment that yields economic returns. The role of nature as a productive force - one that contributes to economic growth, value creation, and job markets - is systematically undervalued. Yet, biodiversity provides solutions to nearly every imaginable problem, and while precise quantitative data on its benefits may not yet be available, numerous applications of biological models have demonstrated innovative and economic advantages.

One of the fastest-growing sectors globally is ecotourism, which includes travel and recreation based on experiencing nature. This vast industry, encompassing a wide range of activities, engages nearly the entire population. Ecotourism responds to diverse individual

lifestyle preferences, from tranquil forest retreats to the appreciation of unique landscapes, encounters with wilderness, and outdoor sporting activities. In this context, the economic necessity of nature conservation becomes particularly evident, as it provides direct economic benefits. The revenues of private tourism companies and related industries often depend on maintaining intact natural environments, and any tourism model that disregards environmental concerns runs the risk of self-destruction.

CONCLUSIONS

For these paper we intentionally used more open bibliographic sources in order to show that sustainable development using bionics is at hand with huge potential to boost the sustainability because nature is the most efficient developer and manager.

This paper seeks to underscore the pivotal role that Bionics currently plays, and can continue to play, in fostering sustainable development, as articulated by contemporary legislative frameworks.

Bionics leverages scientific methodologies to "learn from nature" in the pursuit of solving both technical and economic problems. It represents a comprehensive approach to research and development, where solutions, inventions, and innovations are derived from the observation and analysis of biological systems and subsequently transferred to technical systems and economic models.

By conceptualizing living organisms as highly advanced technological systems, bionics enables a paradigm shift that resolves the perceived dichotomy between nature and technology. This suggests that a technology more in harmony with nature - or more efficiently adapted to natural cycles - can be realized through bionic approaches. Such an approach would yield technologies characterized by enhanced properties, improved adaptation to ecological cycles, lower risk profiles, higher tolerance for errors, and greater environmental compatibility.

This paper, through a review of pertinent literature, highlights the potential for applying bionic principles across a wide range of disciplines, including but not limited to

construction, device engineering, process optimization, material sciences, locomotion systems, and management strategies. Bionics, thus, provides a promising avenue for innovation and sustainable development across diverse fields of human activity.

Nevertheless, there are considerable barriers hindering the broader integration of bionics within current innovation ecosystems. These include extended development timelines for bionic products and processes, resistance from industrial sectors, disparities between academic and industrial stakeholders, limited but increasing funding for research, the absence of bionics from formal educational curricula, and communication gaps between key sectors.

Despite these obstacles, the successful application of bionic innovations in a range of technical fields, combined with the existence of management frameworks inspired by natural systems and the growing academic interest in this domain (universities started to introduce bionics in the curricula, i.e. National University of Science and Technology POLITEHNICA Bucharest), strongly supports the notion that Bionics offers the tools and perspectives necessary for achieving sustainable development.

By providing actionable solutions for implementing the concept of sustainability across various industries, Bionics emerges as an essential instrument in the realization of environmentally sound, economically viable, and socially equitable practices.

REFERENCES

- European Commission (2019). The European Green Deal, Brussels, <https://eurlex.europa.eu/legal-content/EN/TXT/?uri=COM%3A2019%3A640%3AFIN>.
- European Commission (2021). Proposal for a Council Implementing Decision on the approval of the assessment of the recovery and resilience plan for Romania and Annex, Brussels, https://commission.europa.eu/publications/proposal-council-implementing-decision-approval-assessment-recovery-and-resilience-plan-romania-and_en.
- European Commission (2012). Regulation (EU) No. 2018/2066 on the monitoring and reporting of greenhouse gas emissions pursuant to Directive 2003/87/EC of the European Parliament and of the European Council and amending Commission Regulation (EU) No.601/2012, <https://eurlex.europa.eu/legal-content/EN/TXT/PDF/?uri=CELEX:32018R2066> (accessed 19 August 2023).
- European Environment Agency (2023). Emissions and energy use in large combustion plants in Europe, <https://www.eea.europa.eu/ims/emissions-and-energy-use-in>.
- Ioniță, M.- C. (2023). Sustenabilitatea. Ce este și de ce trebuie să devenim sustenabili. *Industry & Environment*, <https://jurnaldesustenabilitate.ro/sustenabilitate/>, 6.02.2023.
- <https://www.twi-global.com/locations/romania/ce-facem/intrebari-frecvente-faq/ce-este-sustenabilitatea> (2023)
- <https://spotmedia.ro/stiri/mediu/sustenabilitatea-ce-inseamna-de-ce-este-importanta-intr-o-societate-si-de-ce-este-necesara-o-dezvoltare-sustenabila-lmt> (2023)
- <https://ecosynergy.ro/ce-reprezinta-sustenabilitatea/> (2023)
- Rechenberg, I. (1973). Evolutionsstrategie '94: Enthält zugleich: Evolutionsstrategie (Werkstatt Bionik und Evolutionstechnik, Band 1).
- Schwessinger, G.K. (1994). *Werkstatt Bionik und Evolutionstechnik*. Deutsch, Gebunden ISBN 978-3-7728-1641-3.
- Niedner, B. (2017). Agil ohne Planung: Wie Unternehmen von der Natur lernen können (Haufe Fachbuch), ASIN: 3648101641, Publisher: Haufe; 1. Auflage 2017 (24 Nov. 2017), ISBN-10: 9783648101643 ISBN-13: 978-3648101643.
- Futur, Das Magazin aus dem Produktionstechnischen Zentrum Berlin, Fraunhofer-Institut für Produktionsanlagen und Konstruktionstechnik IPK, 2022.
- Futur, Das Magazin aus dem Produktionstechnischen Zentrum Berlin, Fraunhofer-Institut für Produktionsanlagen und Konstruktionstechnik IPK, 2023.

THE LINK BETWEEN CARBON FOOTPRINT SIZE AND PV ENERGY SYSTEM INITIAL INVESTMENT, ESPECIALLY REGARDING STORAGE ELEMENTS AND THEIR EXPLOITATION MODALITY

Mihaita Nicolae ARDELEANU¹, Emil Mihail DIACONU¹,
Otilia NEDELICU¹, Sorin IONITESCU²

¹University Valahia Targoviste, 13 Alea Sinaia, 130004, Targoviste, Romania

²Romanian Academy, School of Advanced Studies of the Romanian Academy, Doctoral School of Economic Sciences, National Institute for Economic Research "Costin C. Kirițescu", Institute for World Economy, 13 Calea 13 Septembrie, District 5, Bucharest, Romania

Corresponding author email: otilia.nedelcu@valahia.ro

Abstract

The carbon footprint is inherent in any production process, even more so in the case of the production of batteries for the storage of electrical energy. The structure of the photovoltaic (PV) energy system determines the initial investment and, with it, the way of exploitation of the storage elements is outlined. The idea of reducing the investment usually determines an intensive exploitation of the batteries, which leads to the shortening of their exploitation period and implicitly their replacement with new ones. In addition to the problem of fitting the new batteries to the group of existing ones, it goes without saying that their purchase involves another manufacturing exercise that inherently requires a new carbon footprint. By optimizing the way batteries are used, their life is extended up to double, which means that the environmental impact of the production process is halved. The simulation exercise carried out, based on the concrete data provided by the specialized literature and the data of the LIFEP04 battery manufacturers, demonstrated that it is possible to reduce the mentioned carbon footprint through an optimal structuring of the PV system starting from the very initial investment.

Key words: PV system, initial investment, batteries exploitation, batteries production, carbon footprint.

INTRODUCTION

A photovoltaic system with electrical energy storage requires batteries. Electric batteries are chemical products resulting from highly polluting production processes. In this context, the use of batteries requires a prior analysis that allows a choice process with very precise optimization criteria to allow a maximum possible exploitation time for a given set of conditions. The European Union has regulated the choices of specific elements for PV systems, within a directive generically called Ecodesign by which it establishes carbon footprint thresholds with a minimum qualification for the European market.

The carbon footprint calculation methodology imposes a number of different parameters that are considered, but the most important are the lifetime of a photovoltaic module as well as the degradation rate (Khan et al., 2024)). The Ecodesign Directive thus eliminates those least sustainable PV modules, with the precise aim of

reducing the carbon footprint associated with all the constituent elements of the designed PV system. The systemic carbon footprint is determined by adding together all the individual elemental carbon footprints, resulting in a cumulative total (Polverini et al., 2023).

The environmental cost of PV system production includes all carbon emissions generated from all specific phases of the production supply chain, and work is currently underway on dynamic data tracking systems that allow the exact calculation of the carbon footprint related to the purchase of a PV module (You et al., 2017). The life cycle assessment of PV modules is based on statistical analyzes of case studies on the net energy produced and the associated carbon footprint (Cellura et al., 2023).

The concept of the 'Big Data Value Chain' provides a comprehensive framework for managing data, from acquisition to utilization, enabling more accurate and efficient calculations of carbon footprints in photovoltaic

systems (Ionitescu et al., 2024). The carbon footprint of the photovoltaic cells that make up the PV capture part, as a module of the energy system, depends on the materials and methods specific to their manufacturing technologies (Stylos & Koroneos, 2014). The type of PV cell and its production technology is directly related to the lifetime and energy efficiency, so the higher the two parameters in absolute value, the lower the manufacturing effort and the frequency of replacement to maintain the capability of the system over time will be reduced, both aspects leading to a substantially reduced carbon footprint. The carbon footprints generated by the establishment and operation of PV energy systems are much reduced compared to those involved in an energy system based on a Diesel plant, but even in this advantageous context for the renewable resource, the optimal structural system must be consistently pursued. The issue of the carbon footprint involves many socio-economic aspects, in all cases the modelling of polluting systemic states is essential to correlate the cause with the effect. Carbon emissions increase 25 times when idling for a stationary and starting car, or, in acceleration/braking situations, there is an increase of 1.5-2 times higher than during constant driving (Ruscă et al., 2022).

Following the same reasoning of determining the cause-and-effect vector in the case of carbon emissions, in PV systems, the systemic composition and the way of exploitation of the elements can lead to an unnecessary increase in the carbon footprint throughout the life of use, as in the case of to a vehicle in traffic, if an automatic engine shutdown system is added and/or the driver approaches a driving style without unnecessary acceleration/deceleration, the carbon footprint over the lifetime of the vehicle's operation will be substantially lower than the careless case of working with the same system.

The electrification strategies of some areas with undeveloped national grids require mini grids based on PV, and in this case, precise calculations have highlighted a reduced carbon footprint of $200\text{gCO}_2/\text{KWh}$ (Chamarande et al., 2024). To produce each KWh of capacity for a LiFePo₄ battery, a carbon footprint of between 100 and 200 Kg CO₂ is estimated, depending on the materials, the manufacturing technology and

its energy efficiency. This dimensioning of the carbon emission was considered for the simulations carried out in this work, respectively the average of $\text{CFP}_{1\text{KWh}}=150\text{ KgCO}_2$.

Simulating the structure of a PV system is essential to determine from the design phase the technical-economic benefits, the calculation model having to consider all socio-economic aspects, including incentives per KWh offered by society to encourage the production and storage of renewable energy. (Hassan et al., 2017). Storage in batteries involves a different calculation in the case of small PV system energy capacities compared to large PV power plants. In a mini-grid application the group of batteries will work as a unit, in PV plants the battery degradation model becomes essential for replacing the required ones and accommodating the new ones in the large groups to maintain the nominal energy storage capacities (Yao & Cai, 2021).

Recycling of Li-ion Cathodes (Or et al., 2020) and Direct Regeneration of Cathode Materials from Used Electric Batteries (Lan et al., 2024) represent concrete actions to reduce pollutant emissions generated by the function of electric energy storage in PV systems, but optimizing the way the battery works and modeling the initial investment to ensure a long life cycle for the entire system is a source of significant carbon footprint reduction, as demonstrated by the simulations presented in this paper.

PV SYSTEM LIFETIME PARADIGM

Simulating the amount of energy produced during the lifetime of a PV system is a complex problem, which takes into account many factors such as: the energy characteristics of the geographical place for which the estimate is made, the geoclimatic conditions, the probability density applied to the annual predictions regarding the amount of solar energy for each season, degradation rates of system modules, uncertainties applied to energy production, energy prediction risks, module reliability, maintenance requirement induced by integrated modules (Georgitsioti et al., 2019). Having accurately estimated the energy result of the investment, for the case where the PV system is made, decisions can be made in a well-founded way. For these calculations to follow

the reality throughout the operating life, it is necessary that the predominant technical factors are set to the values that allow maximum durability of the modules of the PV system. In this paper we focused our attention on the storage module, namely the battery. The reliability of the battery is a decisive factor enabling a long lifetime of the PV system. In addition to reliability, the way the battery is operated produces irreversible effects on the electrochemical mechanisms, accentuating or reducing the degree of its degradation. To create a measure of system reliability, we consider a first parameter of the simulation, namely the operating time of a module of the PV system until the first maintenance intervention, namely the operating time without maintenance abbreviated TWM (Time Without Maintenance), expressed in months. Figure 1 illustrates the flow of energy captured by a photovoltaic (PV) system and circulated through an energy storage module. Three scenarios are depicted – Cases A, B, and C – each with an increasing number of battery groups within the storage module, while maintaining a constant input of PV-generated energy.

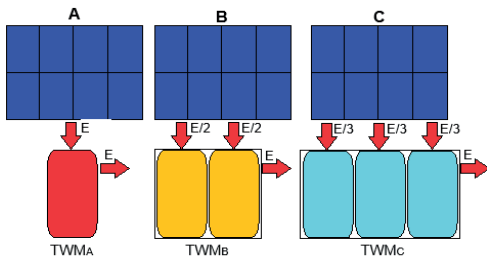


Figure 1. The same energy captured by the PV system, transited through storage groups with different capacities

The operational lifespan of batteries in a photovoltaic (PV) system, represented by the Time Without Maintenance (TWM) parameter, is significantly influenced by the stress levels experienced due to various chemical processes. Consequently:

$$TWM_A < TWM_B < TWM_C \quad [1]$$

The initial investment in a photovoltaic (PV) system plays a crucial role in determining both its operational lifespan and the cost of energy production throughout its service life. A well-

planned initial investment minimizes the need for major maintenance, repairs, or replacements of modules or critical components, which can incur significant expenses. A reduced reliability of a system component induces a lower initial price but a higher maintenance cost, while an increased reliability of the same component transfers the cost of quality into its price, eliminating subsequent maintenance costs for considerable periods of time, so a higher TWM. The decision on investment must quantify the mentioned aspects, as a result we introduced a ratio between the total investment involved over the entire lifetime and the operating time until the first major maintenance intervention on any of the basic components of the PV system. This ratio is called OIDF (Optimal Investment Decision Factor) and represents a way of quantifying the return on investment. Figure 2 shows the method of calculating OIDF, with only the values with the green arrow being active for calculation. The inclusion of the red arrow values leads to a global analysis factor during the operation of the PV system.

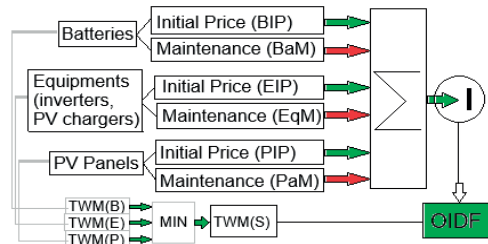


Figure 2. OIDF calculation scheme

The meanings of the notations in figure 2:

- BIP – Batteries Initial Price;
- Bam – Batteries Maintenance cost;
- EIP – Equipements Initial Price;
- EqM – Equipements Maintenance cost;
- PIP – PV panels Initial Price;
- PaM – PV panels Maintenance cost;
- TWM(B) – TWM for batteries;
- TWM(E) – TWM for equipements;
- TWM(P) – TWM for PV panels;
- I – Investment for PV system.

The calculation formula for OIDF is:

$$OIDF = \frac{(BIP+EIP+PIP)}{\text{MIN}(TWM(B),TWM(E),TWM(P))} \quad [2]$$

The meaning of the unit of measure of this factor is monetary unit for unit of time of good

operation: Euro/Month. The lower the OI DF, the more profitable the investment for the PV system. The paradigm of the lifetime of the PV system is reduced to obtaining the longest operating times until the first major maintenance intervention, for the same amount of initial investment.

BATTERY. EXPLOITATION MODALITY

The battery is essential, having the function of storing the energy captured by the PV system at certain times of the day, and making it available to the distribution network at other times of the day, when the sun is no longer geographically active in the photovoltaic production area.

Depending on the internal chemical mechanisms, batteries are of several types. For the exercise of this paper, we have chosen the LiFePo₄ battery type, as it is the most widely used in residential energy systems. The LiFePO₄ battery is part of the Li-ion battery family. The cathode is made by the lithium-iron-phosphate chemical structure, and the anode is geophytized carbon on a metal support. Manufacturing costs are low, with low toxicity, no fire risk, and a long-life cycle, all of which propel this type of battery to the top of the energy storage battery charts. Even the Tesla Company has turned to this type of batteries, 68% of the LiFePo₄ batteries produced in 2022 being purchased by it. In the same year, LiFePo₄ batteries reached, as a market share, 31% of the battery sector for electric vehicles.

Among the characteristics of a battery, we present those relevant to the study undertaken:

- DoD – Depth of Discharge (%)
- C - Nominal Capacity (Ah)
- CC – Charge Capacity (Ah)
- DC – Discharge Capacity (Ah)
- DL_{25°C} – Design Life at @25°C (Years)
- CL- Cycle Life at @25°C & @DOD 80% (number of charge-discharge cycles)
- SoC – State of Charge (%)

After a study of the technical documentation provided by major brands of LiFePo₄ batteries, we define below the optimal operating condition that provides the longest battery life (over 10 years lifetime):

- Exploitation temperature: 25°C
- DoD: 80%
- SoC (maximum charge): 90%

- SoC (minimum discharge): 10%
- CC: 0.2C (Ah)
- DC: 0.2C (Ah)

Figure 3 shows a graph from the technical documentation of the EV-Lithium battery manufacturer (<https://www.evlithium.com/>), respectively the EVL battery with C=5KWh, in which the dependence between the battery discharge mode and battery life in number of charge-discharge cycles, at constant operating temperature of 25°C.

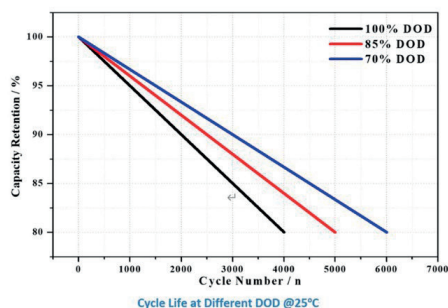


Figure 3. Storage capacity of EV-Lithium's LiFePo₄ battery, according to DoD. Web source of original graphic: <https://www.evlithium.com/home-energy-storage-system.html>

Thorough and in-depth research has been carried out by a team of researchers funded by a large Belgian manufacturer of industrial LiFePo₄ battery electric storage groups, and the results of this research are presented in the paper (Omar et al., 2014). The graph shown in Figure 4 is built based on the original data presented in the work (Omar, 2014), a graph that shows the dependence between the Operating Temperature (OT) of the battery and its lifetime in the number of charge-discharge cycles. The reproduced data were processed to determine the polynomial regression function necessary to approximate the evolution determined experimentally in the work mentioned above. Using this retrieved data, the percentage increase or decrease of the lifetime of a LiFePo₄ battery depending on OT was modeled and simulated. Through the data presented in Figures 3 and 4, characteristics of some ways of operating LiFePo₄ batteries were presented, with consequences on the variation of the life span, a fact that influences their premature replacement and the increase of the carbon footprint determined by the new purchase of these modules of PV system.

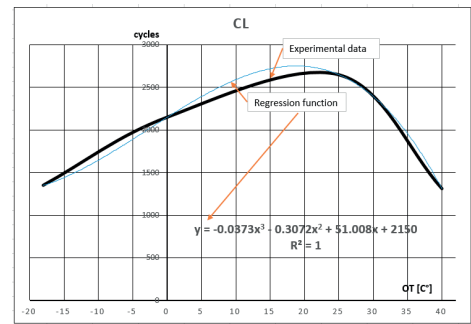


Figure 4. LiFePO4 battery storage capacity relative to OT

MODELING SIMULATION RESULTS

This study investigated a 5kWh off-grid photovoltaic (PV) system with an EVL5KWh battery for energy storage. Using manufacturer data (Figure 3) and a mathematical model, Table 1 presents a simulation of the system's performance with a 300-kWh average monthly consumption. Interestingly, the relationship between the battery's Depth of Discharge (DOD) and its lifespan, as depicted by the model, is linear. This linear relationship can be expressed through the following equations:

$$CL = -DOD \cdot 66,667 + 10667 \quad [3]$$

$$Storage = 5 \cdot CL \quad [4]$$

$$Lifetime = \frac{Storage}{AMC} \quad [5]$$

$$Increase = \frac{Lifetime_k - Lifetime_{100}}{Lifetime_{100}} \cdot 100 \quad [6]$$

$$CFP = C \cdot \left(1 - \frac{increase}{100}\right) \cdot CFP_{1KWh} \quad [7]$$

This study further explored the performance of an off-grid PV energy system under varying temperature conditions. Utilizing data from Figure 4 and a mathematical model, Table 2 presents a simulation where the ambient temperature fluctuates around 25°C. The specified temperature was meticulously chosen as it aligns perfectly with the optimal operational parameters for the LiFePO4 battery integrated within the system. This value is also consistently documented within the technical specifications provided by leading manufacturers of these batteries, serving as a benchmark temperature. This temperature is a critical prerequisite for establishing the applicability of other operational characteristics (DoD, CC, DC, SoC) that guarantee the

extended lifespan of the products marketed. It is noted that the mathematical model describing the dependence between OT and battery life is a 3rd order polynomial, expressed by the relation [8] below.

$$CL = -0,0373 \cdot OT^3 - 0,3072 \cdot OT^2 + 51,008 \cdot OT + 2150 \quad [8]$$

To assess the impact of temperature on battery performance, the percentage variation in lifespan compared to the maximum lifetime at 25°C is determined using equation [9]. Subsequently, the corresponding effect on the carbon footprint is calculated using equation [10].

$$Variation = \frac{CL_{25} - CL_k}{CL_{25}} \cdot 100 \quad [9]$$

$$CFP = \frac{Variation_{25} - Variation_k}{100} \cdot CFP_{1KWh} \quad [10]$$

Simulation analysis reveals the relationship between LiFePO4 battery Depth of Discharge (DoD) and carbon footprint within a photovoltaic system

Table 1. Battery lifetime depending on DOD & CFP

DoD	CL	Storage	Lifetime	Increase	CFP
%	cycles	KWh	months	%	KgCO2/KWh
100	4000	20002	67	0	750
95	4334	21668	72	8	688
90	4667	23335	78	17	625
85	5000	25002	83	25	563
80	5334	26668	89	33	500
75	5667	28335	94	42	438
70	6000	30002	100	50	375
65	6334	31668	106	58	313
60	6667	33335	111	67	250
55	7000	35002	117	75	188
50	7334	36668	122	83	125

Table 2. Battery lifetime depending on OT & CFP

OT	CL	Variation	CFP
°C	cycles	%	KgCO2/KWh
-5	1647	-40	60
0	1892	-31	47
5	2150	-22	33
10	2393	-13	19
15	2592	-6	9
20	2720	-1	2
25	2749	0	0
30	2650	-4	5
35	2397	-13	19
40	1960	-29	43
45	1312	-52	78

CONCLUSIONS

Any PV system has an operating optimum that battery manufacturers indicate very precisely through customized values of specific parameters (DoD, SoC, CC, DC, OT). Without

systems to control battery temperature and operating parameters, achieving optimal efficiency is challenging. This optimal state, representing minimal pollution, serves as a benchmark for calculating the carbon footprint of a PV system. Any deviation from this ideal state increases the carbon footprint, measured as a percentage increase from the baseline optimal value.

The initial investment can ensure a greater reserve for the storage capacity of the PV system, this fact leading to a decrease in the demand for the chemical mechanisms in the batteries and implicitly extending life and postponing the moment of their replacement with new ones. It can be seen in Figure 1 that tripling the storage capacity leads to a relaxation of the batteries, and purchasing three times the number of batteries does not necessarily mean tripling the price.

Equation [2] highlights the importance of maximizing battery lifespan to optimize the initial investment in a PV system. This can be achieved by adhering to the optimal operating practices recommended by battery manufacturers. Table 1 demonstrates that reducing the Depth of Discharge (DoD) to 50% significantly decreases the carbon footprint (CFP) by a factor of six, while simultaneously extending battery life by 1.82 times. This extended lifespan enhances convenience by delaying maintenance and replacement needs within the battery storage system. Furthermore, Table 2 reveals that a temperature increase of 15°C above the optimal operating temperature results in a 20% rise in CFP. This finding underscores the need for PV system operators to prioritize optimal battery management practices to minimize environmental impact.

ACKNOWLEDGEMENTS

This research was carried out with the support of University Valahia Targoviste, Institute of Scientific and Technological Multidisciplinary Research.

REFERENCES

Cellura, M., Le Quyen, L., Guarino, F., & Longo, S. (2023, November). Net Energy Analysis and Carbon Footprint of Solar Cells. 2023 *Asia Meeting on*

- Environment and Electrical Engineering (EEE-AM)*, Hanoi, Vietnam, 2023, pp. 01-06.
- Chamarande, T., Hingray, B., & Mathy, S. (2024). Carbon footprint of solar based mini-grids in Africa: Drivers and levers for reduction. *Renewable Energy*, 121480.
- Georgitsioti, T., Pearsall, N., Forbes, I., & Pillai, G. (2019). A combined model for PV system lifetime energy prediction and annual energy assessment. *Solar Energy*, 183, 738-744.
- Hassan, A. S., Cipcigan, L., & Jenkins, N. (2017). Optimal battery storage operation for PV systems with tariff incentives. *Applied Energy*, 203, 422-441.
- Ionitescu S., Popescu A., Moagar-Poladian S., Gudanescu N.L., Aluculesci A.C. (2024). Value chains in raw materials, high-tech and agricultural products. international, European and Romanian perspectives. *Scientific Papers. Series "Management, Economic Engineering in Agriculture and Rural Development"*, 24(2), 537-548, PRINT ISSN 2284-7995.
- Khan, A.A., Molina, P., Reichel, C., Protti, A.A., Neuhaus, D.H., Rentsch, J., & Nold, S. (2024). The European Union's Ecodesign Directive-Analysis of Carbon Footprint Assessment Methodology and Implications for Photovoltaic Module Manufacturers. *Solar RRL*, 2301011.
- Lan, Y., Li, X., Zhou, G., Yao, W., Cheng, H. M., & Tang, Y. (2024). Direct Regenerating Cathode Materials from Spent Lithium-Ion Batteries. *Advanced Science*, 11(1), 2304425.
- Omar, N., Monem, M.A., Firouz, Y., Salminen, J., Smekens, J., Hegazy, O., & Van Mierlo, J. (2014). Lithium iron phosphate based battery-Assessment of the aging parameters and development of cycle life model. *Applied Energy*, 113, 1575-1585.
- Or, T., Gourley, S. W., Kaliyappan, K., Yu, A., & Chen, Z. (2020). Recycling of mixed cathode lithium-ion batteries for electric vehicles: Current status and future outlook. *Carbon energy*, 2(1), 6-43.
- Polverini, D., Espinosa, N., Eynard, U., Leccisi, E., Ardente, F., & Mathieux, F. (2023). Assessing the carbon footprint of photovoltaic modules through the EU Ecodesign Directive. *Solar Energy*, 257, 1-9.
- Ruscă, M., Dimen, L., & Mărcuță, L. (2022). environmental pollution due to road vehicles, alternative solutions (electric vehicles, hybrids, bicycles) sustainability of crowded centers of cities. *Scientific Papers. Series E. Land Reclamation, Earth Observation & Surveying, Environmental Engineering*, 11. Print ISSN 2285-6064.
- Stylos, N., & Koroneos, C. (2014). Carbon footprint of polycrystalline photovoltaic systems. *Journal of Cleaner Production*, 64, 639-645.
- Tu, M., Chung, W. H., Chiu, C. K., Chung, W., & Tzeng, Y. (2017). A novel IoT-based dynamic carbon footprint approach to reducing uncertainties in carbon footprint assessment of a solar PV supply chain. 2017 *4th International Conference on Industrial Engineering and Applications (ICIEA)*, 249-254.
- Yao, M., & Cai, X. (2021). Energy storage sizing optimization for large-scale PV power plant. *IEEE*, 9, 75599-75607.

MODERN STRATEGIES FOR REDUCING POLLUTION IN TRAFFIC CONGESTIONS: A REVIEW OF CARBON FOOTPRINT-BASED METHODS

Mihaita Nicolae ARDELEANU¹, Emil Mihail DIACONU¹, Otilia NEDELCU¹,
Marius-Alexandru DINCA², Petru NICOLAE³, Sorin IONITESCU³

¹Valahia University of Targoviste, 13 Alea Sinaia Street, Targoviste, Romania

²National University of Sciences and Technology Politehnica Bucharest,
313 Splaiul Independentei, District 6, Bucharest, Romania

³Romanian Academy, School of Advanced Studies of the Romanian Academy, Doctoral School
of Economic Sciences, National Institute for Economic Research "Costin C. Kirițescu",
Institute for World Economy, 13 Calea 13 Septembrie, District 5, Bucharest, Romania

Corresponding author email: emy_diaconu@yahoo.com

Abstract

The development of deep learning technologies and digital image processing have brought innovative solutions for various fields of activity. One area that has benefited from these technological innovations is urban traffic analysis. Architectures based on convolutional neural networks are used in a wide variety of intelligent systems that rely on image detection and analysis. This micro-review aims to provide a comprehensive overview of strategies for reducing pollution in traffic congestions through carbon footprint-based methods. The emphasis is on methodologies that quantify and mitigate the environmental impact of traffic congestion, combining advances in technology with authority measures. Examining current methodologies, new trends and case studies, this study seeks to highlight modern and effective strategies that can be implemented to provide practical solutions for more efficient and sustainable urban transport and pollution reduction.

Keywords: sustainability, carbon footprint, deep learning, image processing, remote sensing

INTRODUCTION

Urbanization and the rapid growth of motorized transport have led to significant increases in traffic congestion worldwide. According to several research studies, the world's population breathes air containing high levels of pollutants, much of which is attributed to vehicle emissions in congested urban areas. Congested traffic causes delays and economic losses but contributes substantially to environmental degradation by increasing carbon dioxide and harmful emissions (Rusca et al., 2022). As cities continue to expand, addressing the environmental impact of traffic congestion has become a pressing concern and an area of massive research and development.

The concept of carbon footprint has emerged as an important measure for quantifying the environmental impact of various activities, including transportation (Kousoulidou et al., 2013). In the context of traffic management and monitoring, carbon footprint methods provide a

systematic approach to assess and mitigate the environmental impact of vehicle emissions (Gao et al., 2023; Rafique et al., 2023). By quantifying emissions, important courses of action can be identified, the effectiveness of mitigation strategies can be assessed, and informed decisions can be made to reduce pollution (Kuneva et al., 2023; Rosu et al., 2023).

The development of sensor technologies and the field of deep learning supported by modern digital image processing techniques have brought to the fore major changes in this direction. For traffic analysis and monitoring, modern society today enjoys a series of best practices and continuous research directions aimed at solving major problems in this context (Zaharia et al., 2023; Dunea et al., 2016).

The ongoing analysis of contexts of this type, research focused on carbon-footprint documentation and the major impact of deep learning described the significant impact of models such as traffic analysis and Intelligent Transportation Systems (ITS). Traditional

strategies to alleviate traffic congestion have focused on infrastructure expansion, such as building new roads or widening existing ones. Although these solutions are initially feasible, they quickly become problematic resulting in continuous agglomerations based on the population encouraged to adopt personal vehicles for any type of travel, eventually leading back to congestion. Infrastructure projects are capital-intensive and may be impractical in heavily populated urban areas.

The present work presents a systematic review of modern strategies and techniques for reducing traffic pollution based on carbon-footprint methods. The importance of this review is described by the interdisciplinary approach, bringing to the stage methodologies from environmental science, transport engineering, smart-city and cutting-edge technologies. The key areas that are explored are described by ITS in optimizing traffic flow to reduce emissions, the application of the field of deep learning and image processing in the prediction and management of traffic congestion and the analysis of the impact of these modern strategies. In the same framework, challenges and limitations associated with these strategies and best practices are discussed.

MATERIALS AND METHODS

In order to observe the important research directions and the impact in this field, several impact specialist works were analyzed and focused on an important direction - new trends and the role of deep learning and image processing in reducing the carbon footprint. The extraction and analysis of specialized papers focused on this topic, published between the years 2019 and 2024, was pursued. The databases used for this study were IEEE and Web of Science. The papers were selected based on several criteria oriented towards innovation, number of citations, impact factor and new period. The extraction of specialized papers from the mentioned databases was done by using some key terms, connected by *AND* / *OR* operators, including deep learning, image processing, traffic management, carbon footprint, pollution, artificial neural networks, intelligent transport systems.

The addressed research topic underlines a

considerable evolution of research in recent years (Figure 1). The effectiveness of different strategies was analyzed based on case studies, research papers and experimental results or simulations. From the extensive list of works, studies that did not provide concrete data or that were not relevant to the objectives of the present research were excluded.

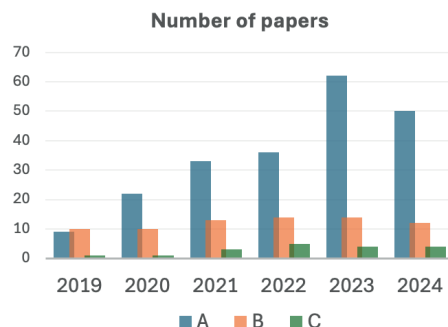


Figure 1. Search results for important terms in the Web of Science database, between the years 2019-2024:

- A) (deep learning) AND (traffic emissions),
- B) (image processing) AND (traffic emissions),
- C) (vehicle detection) AND (neural networks) AND (traffic emissions)

KEY METHODOLOGIES AND NEW TRENDS

The processing of digital images, the integration of deep learning techniques and remote sensing areas have allowed the creation of modern methods for evaluating the carbon footprint in congested urban traffic. In this sense, we distinguish a series of key methodologies as part of the new trends, resulting from the analysis of the current state and the specialized works extracted. Various essential methodologies can be noted in this case: vehicle detection and counting, traffic flow and speed estimation, and emissions calculation and analysis (Rafique et al., 2023).

Convolutional neural networks have revolutionized the field of visual data analysis by extracting essential features from it. Notable studies applying vehicle identification and classification techniques from images and video streams are observed (Petrea et al., 2023).

Architectures of this type can extract complex data and features from images enabling the detection of different types of vehicles. CNNs

are trained and evaluated on vast and comprehensive datasets, divided into training, validation and testing subsets. Common metrics for performance evaluation are attached to classification, segmentation or object detection tasks and include precision, recall, accuracy, F1 or mAP scores, calculated using indices of the so-called confusion matrix (Adi et al., 2024).

An important research direction involves the use of CNNs or combinations thereof for the detection and identification of important features in traffic optimization. The authors (Adi et al., 2024) proposed a method based on fusion algorithms for the identification of free parking spaces. The system uses a YOLOv7 model to segment vehicle instances and detect objects using algorithms such as Euclidean distance, intersection over reference (IoR), and intersection over union (IoU).

An intelligent and modern system to detect vehicles was proposed by the authors (Rafique et al., 2023). The system uses data sets comprising aerial images and CNNs, detecting vehicles in different conditions, classifying them and tracking their path using advanced digital image processing areas. A Pyramid Pooling Vehicle Detection module was used to improve detection accuracy by comparing performance using various established datasets such as VAID, VEDAI and DLR3K. The system developed based on new deep learning techniques can identify and track vehicles even in conditions of variable lighting or partial occlusion.

The utility and efficiency of a system based on CNN and deep learning algorithms used on a large scale was presented in the authors' study (Velesaca et al., 2020) to describe an urban video analysis system. The proposed system aims to extract essential information about traffic and pedestrians using urban surveillance cameras, ultimately generating key statistics on detected vehicles and the number of people. The tests were carried out on a university campus, demonstrating the usefulness and efficiency of the system. It is observed in this case that the integration of object detection architectures with advanced digital image processing algorithms (YOLO, SORT) has the role of creating modular

and flexible traffic management and carbon footprint estimation systems.

In this way, intelligent systems are developed that can distinguish vehicles in different conditions and contexts (Figure 2). Automatic detection based on these techniques facilitates accurate vehicle identification in real time by providing important data about the context, volume and typology of traffic. Applied technological methods include the use of traditional cameras, thermal cameras or LiDAR in visual data collection.



Figure 2. Vehicle detection examples using YOLO models

Among the more advanced methods are research directions that use modified, hybrid or combined CNN architectures to create intelligent systems for detection and analysis of digital images (Zhang & Fu, 2025). Some of the advanced modifications made to CNNs aim to improve accuracy, efficiency, and scalability. By aggregating the predictions of several models, the ensemble method can achieve better accuracy and generalization than any individual CNN in the ensemble (Figure 3). In the same framework, modifications to existing architectures can improve the accuracy of models in various tasks, starting from basic models and exploring various architectural modifications and parameter optimization. In general, ensemble methods are based on the idea that combining the outputs of multiple models leads to better predictions because different models may capture different aspects of the data.

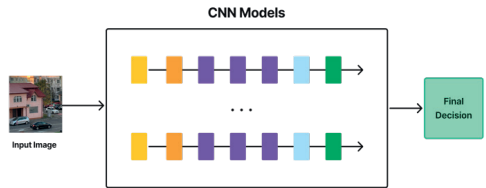


Figure 3. Example of CNN Ensemble

The study (Zhang & Fu, 2025) presents an efficient method for traffic estimation in congested intersections using a combination of neural networks and attention mechanisms. The proposed system uses the power of the SSD model for the object detection task and the ResNet architecture for the feature extraction part. A SENet attention mechanism is integrated to improve performance by emphasizing relevant features and suppressing others. On the other hand, a feature fusion model is used to improve the detection of small objects, a major challenge in traffic scenes with crowded contexts. The method was tested in real intersections, outperforming traditional methods and achieving an accuracy of 88.5% and a latency of only 12 milliseconds. The paper points out that the method can be applied in real intersection scenes for adaptive traffic light management and traffic risk detection, providing a fast and accurate solution for traffic density monitoring. For applications of estimating traffic conditions and determining flow density, advanced image analysis techniques and specially designed algorithms for object location and tracking are used (Figure 4).



Figure 4. Traffic flow detection

The article (Chen et al., 2021) proposes a traffic flow detection system based on deep learning and edge computing. For the proposed system, the authors used the YOLOv3 architecture for vehicle detection and DeepSORT for real-time tracking. Both areas have been optimized to run efficiently on edge devices such as the Jetson TX2. Compared to classic cloud computing models, it is observed that the proposed

approach improves the speed and accuracy of video data processing for traffic monitoring systems. Experimental results show an average accuracy of 92.0% and a processing speed of 37.9 frames per second on the edge device, which enables real-time detection of traffic flow. The study highlights the robustness of the method under varying lighting and occlusion conditions, highlighting its importance for intelligent monitoring management systems. The work contributes to the field of traffic monitoring systems by providing an efficient and accurate solution using advanced computer vision techniques with potential application in real-world intelligent transportation systems. The paper also highlights the potential of such methods to create intelligent systems, ultimately helping to reduce traffic congestion and pollution.

By applying architectures based on neural networks and models based on optical flow one can track the movement of vehicles in different frames. These ultimately allow estimation of vehicle speed and general flow. On the other hand, the analysis of such data brings to the fore important information regarding traffic patterns, congestion areas, and a deep understanding traffic dynamics in various areas and under various natural conditions (Labib et al., 2018). An important framework in this research uses data obtained from the previously mentioned detection and classification applications to develop models for estimating emissions of CO₂ or other types of pollutants. By correlating the types of vehicles with the behavior observed in traffic, speed or various conditions, the specific emissions can be calculated (Zaharia et al., 2023). This framework lays the foundations for methods focused on carbon-footprint assessment. Modern methods and new trends highlight models such as COPERT, PEMS or similar ones successfully used to estimate emissions based on relevant factors (Kousoulidou et al., 2013; Rešetar et al., 2024). On the other hand, the authors' study (Gao et al., 2023) brings to the forefront a clear picture of the limitations and opportunities related to the reduction of carbon emissions in the life cycle of electric cars. Although electric vehicles have the role of reducing carbon emissions from transport, their negative impact is found in the production area, during the manufacture of

batteries, compared to vehicles with internal combustion engines. Finally, the authors note solutions for reducing the carbon footprint through various best practices.

Integrating such models with the power of deep learning and digital image processing architectures enables accurate and real-time assessment of the carbon footprint generated by various traffic conditions. Considering these features, the studies highlight the robustness of the approaches under varying illumination and occlusion conditions, highlighting their importance for intelligent traffic management systems. Each work contributes to the field of traffic monitoring systems by providing efficient and accurate solutions using advanced computer vision techniques with potential application in real-world intelligent transportation systems.

RESULTS AND DISCUSSIONS

Continued, relevant research and the impact of deep learning techniques and advanced image processing for carbon footprint analysis and calculation note both significant opportunities and notable challenges.

For the topic of using deep learning architectures, one of the main obstacles is represented by the quality and availability of data. To train and develop accurate deep learning models, a considerable volume of high-quality data covering various scenarios and traffic conditions is required. Moreover, the collection of this data can be problematic when we bring up various aspects related to the existing infrastructure and restrictions related to video surveillance and personal data protection. The complexity of digital image analysis and processing models as well as carbon footprint and emission estimation models are other major challenges. The increased complexity associated with these techniques can make interpretation of results difficult and bring high implementation and operating costs.

In this context, the observed future research directions include new methods of visual data analysis and techniques to improve the accuracy of the developed models. Efficient architectures, model compression and optimization techniques, or advanced vision transformer models are key steps in achieving these goals.

Validation and limitations of studies may also include issues such as data generalizability - differences between urban environments and challenges in transferring models between them, data quality - impact of datasets, bias and class imbalances, and computational resources. Advanced deep learning models require significant computational power to train and deploy in real time. This can lead to high implementation costs, both in terms of the hardware required and the associated power consumption.

On the other hand, the set of available information can be improved by integration with other data sources. Data from various sensors, air quality sensors and IoT areas can provide a more complete picture of the impact of traffic on the environment. This multimodal approach can provide new insights and research directions ultimately contributing to the accuracy of estimates and precise modeling of the relationship between traffic and pollution.

The concept of the 'Big Data Value Chain' can significantly enhance the management of data in efforts to reduce pollution in traffic congestions. This framework, which includes stages such as data acquisition, storage, processing, analysis, and utilization, enables a comprehensive approach to managing the vast amounts of data generated by traffic systems. By leveraging this framework, cities can optimize traffic flow, reduce emissions, and make informed decisions to improve urban air quality (Ionitescu et al., 2024). Addressing privacy issues for large-scale deployment may include local processing techniques, data encryption and anonymization as well as edge computing devices.

CONCLUSIONS

As urban areas continue to face the dual challenges of transport congestion and environmental pollution, there is an important requirement for policies that address both concerns simultaneously. Carbon footprint-based methods offer a viable approach to measuring and mitigating the environmental effects of traffic congestion and aims to outperform or assist existing traditional methods. Their applications are diverse, and they manage to offer fast and efficient solutions in relation to existing problems.

Following the details presented in this study, the new trends in advanced image processing, deep learning and best practices associated with the topic of carbon footprint reduction strategies can create systems and techniques successfully applied in the modern and continuously developing society. Current research initiatives comprise upon the efficiency of ensembles and integrating CNNs with other architectures, resulting in a variety of hybrid and optimal deep learning systems for advanced image processing. Despite the considerable challenges in using image processing and deep learning for carbon footprint assessment in congested urban transport, future research avenues present encouraging possibilities.

REFERENCES

- Adi, G.S., Nugroho, H., Rahmatullah, GM., Fadhlán, M.Y., & Mutamaddin, D. (2024). Fusion Algorithms on Identifying Vacant Parking Spots Using Vision-Based Approach. *Indonesian Journal of Electrical Engineering and Computer Science*, 36(3), 1640. <https://doi.org/10.11591/ijeecs.v36.i3.pp1640-1654>.
- Chen, C., Liu, B., Wan, S., Qiao, P., & Pei, Q. (2021). An Edge Traffic Flow Detection Scheme Based on Deep Learning in an Intelligent Transportation System. *IEEE Transactions on Intelligent Transportation Systems*, 3 (March), 1840–1852. <https://doi.org/10.1109/tits.2020.3025687>.
- Dunea, D., Savu, T., & Marsteen, L. (2016). Monitoring of Size-Segregated Particulate Matter Fractions with Optical Instruments in Urban Areas. *Scientific Papers. Series E. Land Reclamation, Earth Observation & Surveying, Environmental Engineering*, 5, 99–104. Print ISSN 2285-6064.
- Gao, Z., Xie, H., Yang, X., Zhang, L., Yu, H., Wang, W., Liu, Y., et al. (2023). Electric Vehicle Lifecycle Carbon Emission Reduction: A Review. *Carbon Neutralization*, 5 (August), 528–50. <https://doi.org/10.1002/cnl2.81>.
- Kousoulidou, M., Fontaras, G., Ntziachristos, L., Bonnel, P., Samaras, Z., & Dilara, P. (2013). Use of Portable Emissions Measurement System (PEMS) for the Development and Validation of Passenger Car Emission Factors. *Atmospheric Environment*, January, 329–38.
- Kuneva, V. & Dallev, M. (2023). An Optimization Model for the Delivery of Plants to Nurseries. *Scientific Papers. Series E. Land Reclamation, Earth Observation & Surveying, Environmental Engineering* 12, 489–494. Print ISSN 2285-6064.
- Ionitescu, S., Popescu, A., Moagar-Poladian, S., Gudanescu, N.L., Aluculesei, A.C. (2024). Value chains in raw materials, high-tech and agricultural products. international, European and Romanian perspectives. *Scientific Papers. Series "Management, Economic Engineering in Agriculture and rural development"*, 24(2), PRINT ISSN 2284-7995, 537–548.
- Labib, S.M., Neema, M.N., Rahaman, Z., Patwary, S.H., & Shakil, S.H. (2018). Carbon Dioxide Emission and Bio-Capacity Indexing for Transportation Activities: A Methodological Development in Determining the Sustainability of Vehicular Transportation Systems. *Journal of Environmental Management*, October, 57–73. <https://doi.org/10.1016/j.jenvman.2018.06.010>.
- Petrea, S.-M., Simionov, I.-A., Antache, A., Nica, A., Antohi, C., Cristea, D.S., Arseni, M., Calmuc, M., & Iticescu, C. (2023). Machine Learning-Based Modeling Framework for Improving Romanian Resilience Strategy to Greenhouse Gas Emissions in Relation to Visegrad Group. *Scientific Papers. Series E. Land Reclamation, Earth Observation & Surveying, Environmental Engineering*, 12, 150–157. Print ISSN 2285-6064.
- Rafique, A.A., Al-Rasheed, A., Ksibi, A., Ayadi, M., Jalal, A., Alnowaiser, K., Meshref, H., Shorfuazzaman, M., Gochoo, M., & Park, J. (2023). Smart Traffic Monitoring Through Pyramid Pooling Vehicle Detection and Filter-Based Tracking on Aerial Images. *IEEE Access*, 2993–3007. <https://doi.org/10.1109/access.2023.3234281>.
- Rešetar, M., Pejić, G., Ilinčić, P., & Lulić, Z. (2024). An Estimate of the NOX Emissions of Euro 6 Diesel Passenger Cars with Manipulated Emission Control Systems. *Sustainability*, 5, 1883.
- Rosu, A., Arseni, M. Constantin, D.-E., Rosu, B., Petrea, S.-M., Voiculescu, M., Iticescu, C., & Georgescu, L.-P. (2023). Study of Air Pollution Level in an Urban Area Using Low-Cost Sensor System Onboard Mobile Platform. *Scientific Papers. Series E. Land Reclamation, Earth Observation & Surveying, Environmental Engineering*, 12, 124–133. Print ISSN 2285-6064.
- Rusca, M., Dimen, L., & Mărcuță, L. (2022). Environmental Pollution Due to Road Vehicles, Alternative Solutions (Electric Vehicles, Hybrids, Bicycles), Sustainability of Crowded Centers of Cities. *Scientific Papers. Series E. Land Reclamation, Earth Observation & Surveying, Environmental Engineering*, 11, 172–180. Print ISSN 2285-6064.
- Velesaca, H.O., Araujo, S., Suarez, P.L., Sanchez, A., & Sappa, A.D. (2020). Off-The-Shelf Based System for Urban Environment Video Analytics. *2020 International Conference on Systems, Signals and Image Processing (IWSSIP)*, 459–64. <https://doi.org/10.1109/iwssip48289.2020.9145121>.
- Zaharia, M.C., & Voloaca G. (2023). Evaluation of the Influence of Green Space in the Process of Reducing Urban Noise, on the Transversal Profiles of Traffic Roads. *Scientific Papers. Series E. Land Reclamation, Earth Observation & Surveying, Environmental Engineering*, 12, 349–357. Print ISSN 2285-6064.
- Zhang, Q., & Fu, Y. (2025). Effective Traffic Density Recognition Based on ResNet-SSD with Feature Fusion and Attention Mechanism in Normal Intersection Scenes. *Expert Systems with Applications*, 261, 125508, Available online 5 October 2024, <https://doi.org/10.1016/j.eswa.2024.125508>



ISSN 2285 – 6064
ISSN-L 2285 – 6064